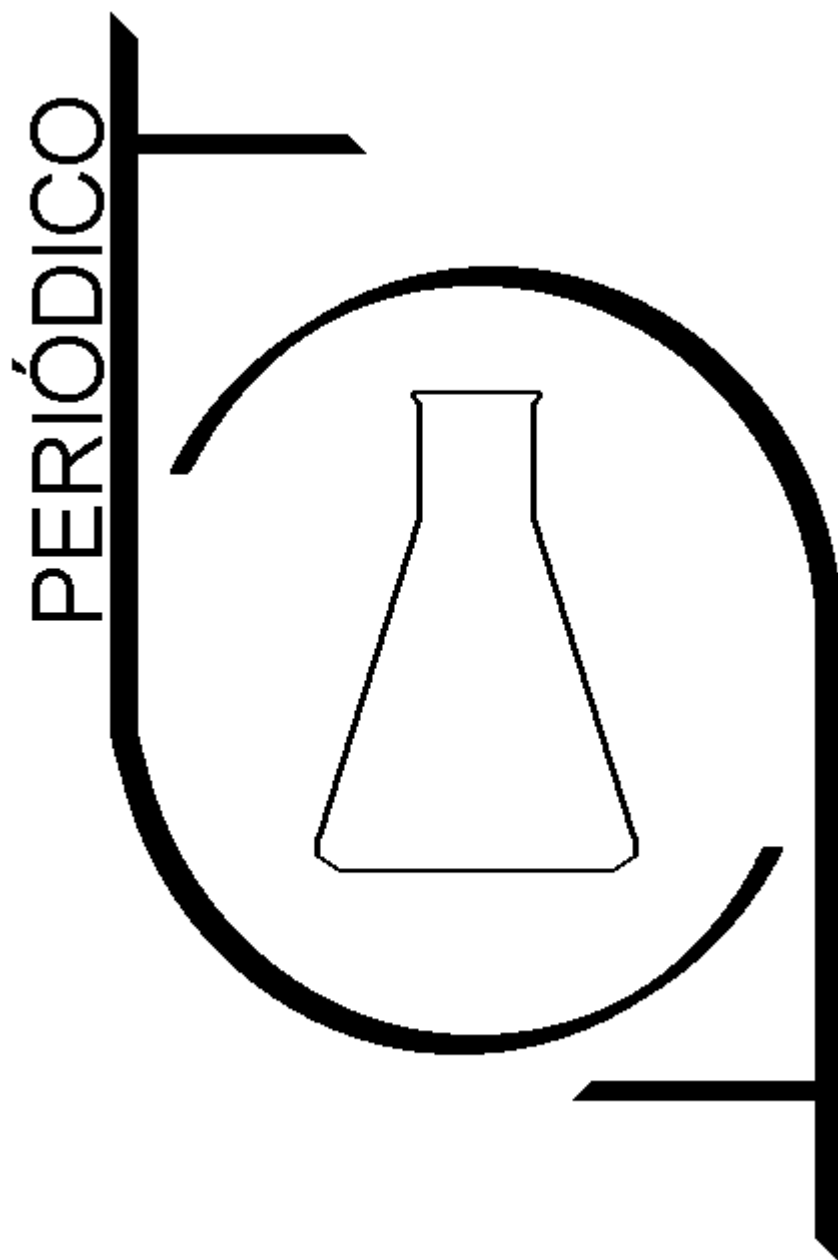


# PERIÓDICO TCHÊ QUÍMICA



Volume 17

-

Número 35

-

2020 ISSN 2179-0302

**Órgão de divulgação científica e informativa**

**[www.periodico.tchequimica.com](http://www.periodico.tchequimica.com)**

# PERIÓDICO TCHÊ QUÍMICA

ISSN - 1806-0374 (Impresso) - ISSN - 2179-0302 (Online)

Volume 17

Número 35 – 2020

ISSN 2179 - 0302

Órgão de divulgação científica e informativa.

## Dados Internacionais de Catalogação na Publicação (CIP)

Periódico Tchê Química: órgão de divulgação científica e informativa [recurso eletrônico] / Grupo Tchê Química – Vol. 1, n. 1 (Jan. 2004)- . – Porto Alegre: Grupo Tchê Química, 2005 - Semestral.

Sistema requerido: Adobe Acrobat Reader.

Modo de acesso: World Wide Web:

<<http://www.tchequimica.com>>

Descrição baseada em: Vol. 14, n. 28 (ago. 2017).

ISSN 1806-0374

ISSN 2179-0302

1. Química. I. Grupo Tchê Química.

CDD 540

## Bibliotecário Responsável

Ednei de Freitas Silveira

CRB 10/1262



## Welcome to the TCHÊ QUÍMICA JOURNAL

*International multidisciplinary scientific journal*

*The Tchê Química Journal publishes original research papers, review articles, short communications (scientific publications), book reviews, forum articles, technical reports, articles on chemical education, interviews, announcements or letters. Articles suitable for publication in the Tchê Química Journal are those that cover the traditional fields of **Chemistry, Physics, Mathematics, Biology, Pharmacy, Medicine, Engineering and Agriculture**. We are especially interested in those submissions that are highly relevant to theoretical and applied contributions in the area of chemistry and related disciplines.*



# PERIÓDICO TCHÊ QUÍMICA

Volume 17

Número 35 – 2020

ISSN 2179 - 0302

Órgão de divulgação científica e informativa.

## Comissão Editorial

### Editores-chefe

- Dr. Luis Alcides Brandini De Boni,  
[deboni@tchequimica.com](mailto:deboni@tchequimica.com)
- Dr. Eduardo Goldani,  
[goldani@tchequimica.com](mailto:goldani@tchequimica.com)

### Editores técnicos

- Ednei de Freitas Silveira  
– *Bibliotecário Responsável*
- Dr. Francisco José Santos Lima,  
[lima@tchequimica.com](mailto:lima@tchequimica.com), Brasil, UFRN.
- Dr. Carlos Eduardo Cardoso,  
[cardoso@tchequimica.com](mailto:cardoso@tchequimica.com), Brasil, USS.
- Dr. Sérgio Machado Corrêa,  
[correa@tchequimica.com](mailto:correa@tchequimica.com), Brasil, UERJ.

## Corpo Editorial

### Membros

- Teresa M. Roseiro Maria Estronca, Dr.,  
[roseiro@tchequimica.com](mailto:roseiro@tchequimica.com), Portugal, UC.
- Monica Regina da Costa Marques, Dr.,  
[aguiar@tchequimica.com](mailto:aguiar@tchequimica.com), Brasil, UERJ.
- Ketevan Kapatadze, Dr.,  
[kapatadze@tchequimica.com](mailto:kapatadze@tchequimica.com), Geórgia, ISU.
- Márcio von Mühlen, Dr.,  
[vonmuhlen@tchequimica.com](mailto:vonmuhlen@tchequimica.com), EUA, MIT.
- Élcio Jeronimo de Oliveira, Dr.,  
[elcio@tchequimica.com](mailto:elcio@tchequimica.com), Brasil, CTA.

- José Carlos Oliveira Santos, Dr.,  
[zecarlosufcg@tchequimica.com](mailto:zecarlosufcg@tchequimica.com), Brasil, UFCG.
- Alcides Wagner Serpa Guarino, Dr.,  
[guarino@tchequimica.com](mailto:guarino@tchequimica.com), Brasil, UNIRIO.
- Roseli Fernandes Gennari, Dr.,  
[gennari@tchequimica.com](mailto:gennari@tchequimica.com), Brasil, USP.
- Rafael Rodrigues de Oliveira, Dr.,  
[oliveira@tchequimica.com](mailto:oliveira@tchequimica.com), Brasil, Brava Biosciences.
- Lívio César Cunha Nunes, Dr.,  
[nunes@tchequimica.com](mailto:nunes@tchequimica.com), Brasil, UFPI.
- João Guilherme Casagrande Jr, Dr.,  
[casagrande@tchequimica.com](mailto:casagrande@tchequimica.com), Brasil, EMBRAPA.
- Denise Alves Fungaro, Dr.,  
[fungaro@tchequimica.com](mailto:fungaro@tchequimica.com), Brasil, IPEN.
- Murilo Sérgio da Silva Julião, Dr.,  
[juliao@tchequimica.com](mailto:juliao@tchequimica.com), Brasil, UVA.
- Amit Chaudhry, Dr.,  
[chaudhry@tchequimica.com](mailto:chaudhry@tchequimica.com), Índia, Panjab University.
- Hugo David Chirinos Collantes, Dr.,  
[chirinos@tchequimica.com](mailto:chirinos@tchequimica.com), Peru, UNI.
- Carlos E. de Medeiros J., Dr.,  
[jeronimo@tchequimica.com](mailto:jeronimo@tchequimica.com), Brasil, PETROBRAS.
- Walter José Peláez, Dr.,  
[pelaez@tchequimica.com](mailto:pelaez@tchequimica.com), Argentina, UNC.
- Rodrigo Brambilla, Dr.,  
[brambilla@tchequimica.com](mailto:brambilla@tchequimica.com), Brasil, UFRGS.
- Joan Josep Solaz-Portolés, Dr.,  
[solaz@tchequimica.com](mailto:solaz@tchequimica.com), Espanha, UV.
- José Euzébio Simões Neto, Dr.,  
[simoes@tchequimica.com](mailto:simoes@tchequimica.com), Brasil, UFRP.
- Aline Maria dos Santos Teixeira, Dr.,  
[santos@tchequimica.com](mailto:santos@tchequimica.com), Brasil, UFRJ.

- César Luiz da Silva Guimarães, Me., [guimaraes@tchequimica.com](mailto:guimaraes@tchequimica.com), Brasil, IBAMA.
- Daniel Ricardo Arsand, Dr., [arsand@tchequimica.com](mailto:arsand@tchequimica.com), Brasil, IFSul.
- Paulo Sergio Souza, Dr., [souza@tchequimica.com](mailto:souza@tchequimica.com), Brasil, Fundação Osorio.
- Moisés Rômolos Cesário, Dr., [romolos@tchequimica.com](mailto:romolos@tchequimica.com), França, ULCO.
- Andrian Saputra, Dr., [saputra@tchequimica.com](mailto:saputra@tchequimica.com), Universidade de Lampung, Indonésia.
- Vanessa Barbieri Xavier, Dr., [xavier@tchequimica.com](mailto:xavier@tchequimica.com), Brasil, PUCRS.
- Danyelle Medeiros de Araújo Moura, Dr., [moura@tchequimica.com](mailto:moura@tchequimica.com), Brasil, UFRN.
- Shaima R. Banoon, Me., [shimarb@uomisan.edu.iq](mailto:shimarb@uomisan.edu.iq), Iraque, Universidade de Misan.
- Gabriel Rubensam, Me., [grubensam@tchequimica.com](mailto:grubensam@tchequimica.com), Brasil, UFRGS.
- Masurquede de Azevedo Coimbra, Me., [coimbra@tchequimica.com](mailto:coimbra@tchequimica.com), Brasil, Sec. de Saúde do Estado - RS.
- Oana-Maria Popa, Me., [popa@tchequimica.com](mailto:popa@tchequimica.com), IPN, Romênia.

Esta revista é indexada e resumida pelo CAS, EBSCO, Latindex, Sumários, Index Copernicus, Scopus, OAIJ, CAB Abstracts, EuroPub e Reaxys.

### Missão

O Periódico Tchê Química (PTQ) publica artigos de pesquisa originais, artigos de revisão, notas curtas (publicações científicas), revisões de livros, artigos de fórum, editoriais e entrevistas. Pesquisadores de todos os países são convidados a publicar nas páginas do PTQ.

A responsabilidade sobre os artigos é de exclusividade dos autores.

### Correspondências

Rua Anita Garibaldi, 359/603.  
Bairro Mon't Serrat. CEP: 90450-001  
Porto Alegre – RS. Brasil.  
Skype: tchequimica  
[www.periodico.tchequimica.com](http://www.periodico.tchequimica.com)  
[tchequimica@tchequimica.com](mailto:tchequimica@tchequimica.com)

### Periódico Tchê Química

ISSN - 1806-0374 (Print)  
ISSN - 2179-0302 (Online)

LCCN: 2010240735

Divulgação *on-line* em  
<http://www.periodico.tchequimica.com>  
<http://www.journal.tchequimica.com>  
<http://www.tchequimica.com>

# Índice

## 1- Artigo / Article

SEIDAKHMETOVA, Roza B.; ARYSTAN, Leila I.; MULDAEVA, Gulmira M.; HAYDARGALIEVA, Leila S.; NURMAGANBETOV, Zhangel'dy S.

KAZAKHSTAN

### AVALIAÇÃO DE EFEITOS NEUROPROTETIVOS DE COMPOSTOS ALCALÓIDES

ASSESSMENT OF NEUROPROTECTIVE EFFECTS OF ALKALOID COMPOUNDS

Página – 1

## 3- Artigo / Article

SALIKOVA, NATALYA S.; BEKTEMISOVA, AINASH U.; NAZAROVA, VALENTINA D.; BEGENOVA, BAHYT E.; OSTAFEICHUK, NATALYA V.;

KAZAKHSTAN

### OBTENÇÃO DE HIDROGELS MISTOS BASEADOS EM BIOPOLÍMEROS E ESTUDO DE SUAS PROPRIEDADES REOLÓGICAS

PREPARATION OF MIXED HYDROGELS BASED ON BIOPOLYMERS AND THE STUDY OF THEIR RHEOLOGICAL PROPERTIES

Página – 23

## 5- Artigo / Article

NUGRAHA, Dewanta Arya; CARI, C.; SUPARMI, A.; SUNARNO, Wídha

INDONESIA.

### INVESTIGAÇÃO DO ENTENDIMENTO CONCEITUAL DE ESTUDANTES DE GRADUAÇÃO SOBRE MOVIMENTO HARMÔNICO SIMPLES EM SISTEMA DE MASSA-MOLA

INVESTIGATION OF UNDERGRADUATE STUDENTS CONCEPTUAL UNDERSTANDING ABOUT SIMPLE HARMONIC MOTION ON MASS-SPRING SYSTEM

Página – 55

## 2- Artigo / Article

KYDYRALIYEVA, Aziza D.; BESTEREKOV, Uilesbek; BOLYSBEK, Aidarbek A.; YESKENDIROVA, Marina M.; URAKOV, Kinis N.

KAZAKHSTAN

### OTIMIZAÇÃO DA TECNOLOGIA DE PRODUÇÃO DE FERTILIZANTES NPK

OPTIMIZATION OF AN NPK-FERTILIZER PRODUCTION TECHNOLOGY

Página – 12

## 4- Artigo / Article

AVDARSOL, SAILAUGUL; RAKHIMZHANOVA, LYAZZAT B.; BOSTANOV, BEKTAS G.; SAGIMBAEVA, AINUR YE.; KHAKIMOVA, TIYSHTIK

KAZAKHSTAN

### AVALIAÇÃO BASEADA EM CRITÉRIOS COMO MODO DE FORMAÇÃO DA ALFABETIZAÇÃO FUNCIONAL DOS ESTUDANTES EM CIÊNCIA DA COMPUTAÇÃO

CRITERIA-BASED ASSESSMENT AS THE WAY OF FORMING STUDENTS' FUNCTIONAL LITERACY IN COMPUTER SCIENCE

Página – 41

## 6- Artigo / Article

AL-ZUHAIRY, Noor AL-Huda Salah1; AL-ALI, Zainab Abudal Jabbar Ridha

IRAQ

### MARCADORES ÓSSEOS METABÓLICOS BIOQUÍMICOS E HORMÔNIO DA PARATIREOIDE EM PACIENTES COM B - TALASSEMIA MAIOR NA PROVÍNCIA DE MISAN / IRAQUE

PARATHYROID HORMONE AND BIOCHEMICAL METABOLIC BONE MARKERS IN PATIENTS WITH B-THALASSEMIA MAJOR IN MISAN PROVINCE / IRAQ

Página – 65

---

**7- Artigo / Article**

---

MOHAMMED, Samar Jasim; NULIT, Rosimah

IRAQ / MALAYSIA.

**A PREPARAÇÃO DE SEMENTES MELHORA A GERMINAÇÃO E O CRESCIMENTO PRECOCE DE MUDAS DE NABO SOB ESTRESSE DE SALINIDADE**

*SEED PRIMING IMPROVES THE GERMINATION AND EARLY GROWTH OF TURNIP SEEDLINGS UNDER SALINITY STRESS*

**Página - 73**

---

**9- Artigo / Article**

---

QASIM, Mohammed Jasim; AL-NORRI, Mustafa Adnan

IRAQ.

**TOXOPLASMOSE E PERTURBAÇÃO CONGENITA**

*TOXOPLASMOSIS AND CONGENITAL DISTURBANCE*

**Página – 93**

---

**11- Artigo / Article**

---

JABBAR, Adel Ismael, RAWI, Rehab Ayal, RADHI, Ahmed H.

IRAQ

**NOVA SÍNTESE E CARACTERIZAÇÃO DE ESTRUTURAS MACROMOLECULARES**

*NEW MACROMOLECULAR STRUCTURES SYNTHESIS AND CHARACTERIZATION*

**Página – 109**

---

**13- Artigo / Article**

---

HASSANZADEH, SARA; ADABI, MOHAMMAD HOSSEIN; KOHANSAL GHADIMVAND, NADER; JALALI, MAHMOOD

IRAN

**ANÁLISE DE FÁCIES E ARQUITETURA ESTRATIGRÁFICA DE SEQUÊNCIA EM UMA BACIA DE ARCO TRASEIRO NO IRÃ CENTRAL: UM ESTUDO DE CASO DO MIOCENO INICIAL DA FORMAÇÃO QOM**

*FACIES ANALYSIS AND SEQUENCE STRATIGRAPHIC ARCHITECTURE IN A BACK-ARC BASIN IN CENTRAL IRAN: A CASE STUDY FROM THE EARLY MIOCENE OF THE QOM FORMATION*

**Página – 135**

---

**8- Artigo / Article**

---

MIRONOVA, Irina; GALIEVA, Zul'fiya; GAZEEV, Igor; BELOUSOV, Alexander; GALIMOVA, Venire

RUSSIA

**ALTERAÇÃO DA COMPOSIÇÃO QUÍMICA, GORDURA E ÁCIDA E PROPRIEDADES FÍSICAS E TÉCNICAS DE GORDURA DE CORDEIRO SOB INFLUÊNCIA DE VÁRIAS FORRAGENS**

*CHANGE OF THE CHEMICAL, FAT AND ACID COMPOSITION AND PHYSICAL AND TECHNICAL PROPERTIES OF LAMB FAT UNDER INFLUENCE OF VARIOUS FODDER BACKGROUND*

**Página – 83**

---

**10- Artigo / Article**

---

FANIANDARI, Suci; SUPARMI, A; CARi, C.

INDONESIA

**SOLUÇÃO ANALÍTICA DA EQUAÇÃO DO SCHRÖDINGER PARA O POTENCIAL DE YUKAWA COM MASSA VARIÁVEL EM COORDENADA TOROIDAL USANDO MECÂNICA QUÂNTICA SUPERSIMÉTRICA**

*ANALYTICAL SOLUTION OF SCHRÖDINGER EQUATION FOR YUKAWA POTENTIAL WITH VARIABLE MASS IN TOROIDAL COORDINATE USING SUPERSYMMETRIC QUANTUM MECHANICS*

**Página – 100**

---

**12- Artigo / Article**

---

FADIAWATI, Noor; DIAWATI, Chansyanah; SYAMSURI, M. Mahfudz Fauzi

INDONESIA

**USANDO O APRENDIZADO BASEADO EM PROBLEMAS PARA MELHORAR AS HABILIDADES CRÍTICAS DOS ESTUDANTES PARA LIDAR COM INFORMAÇÕES ENGANOSAS EM QUÍMICA**

*USING PROBLEM-BASED LEARNING TO IMPROVE STUDENTS' CRITICAL THINKING SKILLS TO DEAL HOAX INFORMATION IN CHEMISTRY*

**Página – 120**

---

**14- Artigo / Article**

---

NIKOLAEVA, LIUDMILA

RUSSIA

**MEDULA ÓSSEA DE OSSOS TUBULARES NO PROCESSO ONCOLÓGICO**

*BONE MARROW OF TUBULAR BONES IN THE ONCOLOGICAL PROCESS*

**Página – 155**

---

**15- Artigo / Article**

---

HAMIL, Muslim Idan, KHALAF, Mohammed K, AL-SHAKBAN, Mundher

IRAQ

**PULVERIZAÇÃO POR MAGNETRON DE FILMES FINOS  
NANOCRISTALINOS DE TIN E PROPRIEDADES DE  
CORROSÃO**

*MAGNETRON SPUTTERED NANOCRYSTALLINE TIN THIN  
FILMS AND CORROSION PROPERTIES*

**Página – 164**

---

**17- Artigo / Article**

---

JASIM, Ekhlas Qanber; ALASADI, Erfan A.; MOHAMMAD-ALI, Munther Abduljaleel

IRAQ

**EXTRATO DE SEMENTES DE ABÓBORA COMO INIBIDOR DE  
CORROSÃO DE LIGA DE AÇO LEVE EM SOLUÇÃO ÁCIDA**

*THE EXTRACT OF PUMPKIN SEEDS AS A CORROSION  
INHIBITOR OF MILD STEEL ALLOY IN ACIDIC SOLUTION*

**Página – 181**

---

**19- Artigo / Article**

---

LIMA, SARAH GIOVANNA MONTENEGRO; CRUZ, THIAGO JACKSON TORRES; PEREIRA, FRANCISCO CLAUDECE; SILVA, ADEMIR OLIVEIRA DA; LIMA, FRANCISCO JOSÉ SANTOS

BRASIL

**MODELAGEM MOLECULAR, MEDIDAS CONDUTIMÉTRICAS E  
ESPECTROS UV-VIS DO ÁCIDO ASCÓRBICO PARA  
FORMAÇÃO DE SISTEMAS QUÍMICOS COMPLEXOS**

*MOLECULAR MODELING, CONDUCTIVE MEASUREMENTS,  
AND UV-VIS SPECTERS OF ASCORBIC ACID FOR FORMATION  
OF COMPLEX CHEMICAL SYSTEMS.*

**Página – 203**

---

**21- Artigo / Article**

---

AL NAQEEB, Neran A.; MASHEE, Fouad K.; AL HASSANY, Jinan S.

IRAQ

**ESTIMATIVA DOS FATORES QUE AFETAM O CRESCIMENTO  
DE ALGAS NO LAGO DE UM EL-NAAJ USANDO TÉCNICAS DE  
SENSORIAMENTO REMOTO**

*ESTIMATION THE FACTORS AFFECTING ON GROWTH OF  
ALGAE IN UM EL-NAAJ LAKE BY USING REMOTE SENSING  
TECHNIQUES*

**Página – 227**

---

**16- Artigo / Article**

---

FARAJ, Salah H.; AYIED, Asaad Y.; SEGER, D. K.

IRAQ

**POLIMORFISMO DO GENE DGAT1 E SUAS RELAÇÕES COM  
RENDIMENTO DO LEITE DE GADO E SUA COMPOSIÇÃO  
QUÍMICA**

*DGAT1 GENE POLYMORPHISM AND ITS RELATIONSHIPS WITH  
CATTLE MILK YIELD AND CHEMICAL COMPOSITION*

**Página – 174**

---

**18 - Artigo / Article**

---

NASIYEV, Beybit; BEKKALIYEV, Askhat; ZHANATALAPOV, Nurbolat; SHIBAIIKIN, Vladimir YELESHEV, Rakhimzhan

KAZAKHSTAN / RUSSIA

**ALTERAÇÕES NOS PARÂMETROS FÍSICO-QUÍMICOS DOS  
SOLOS CASTANHOS DO CAZAQUISTÃO OCIDENTAL SOB A  
INFLUÊNCIA DAS TECNOLOGIAS DE PASTAGEM**

*CHANGES IN THE PHYSICOCHEMICAL PARAMETERS OF  
CHESTNUT SOILS IN WESTERN KAZAKHSTAN UNDER THE  
INFLUENCE OF THE GRAZING TECHNOLOGIES*

**Página – 192**

---

**20- Artigo / Article**

---

RUDIBYANI, RATU BETTA

INDONESIA

**IMPLEMENTAÇÃO DO MODELO DE APRENDIZAGEM  
BASEADO EM PROBLEMAS PARA AUMENTAR A AUTO-  
CONFIANÇA E COMPREENSÃO DE ESTUDANTES DE  
GRADUAÇÃO ACERCA DO CONCEITO DE ELETROQUÍMICA  
NA EDUCAÇÃO QUÍMICA**

*IMPLEMENTATION OF PROBLEM-BASED LEARNING MODEL  
TO INCREASE SELF-CONFIDENCE AND UNDERGRADUATE  
STUDENTS UNDERSTANDING OF THE ELECTROCHEMISTRY  
CONCEPT IN CHEMICAL EDUCATION*

**Página – 216**

---

**22- Artigo / Article**

---

IZTAYEV, Auyelbek; BAIBATYROV Torebek; MUKASHEVA Tarbiye; MULDABEKOVA, Bayan; YAKIYAYEVA, Madina

KAZAKHSTAN

**ESTUDOS EXPERIMENTAIS DO GRÃO DE CEVADA DE  
BAISHESHEK PROCESSADO PELA MISTURA DE ION-OZÔNIO**

*EXPERIMENTAL STUDIES OF THE BAISHESHEK BARLEY  
GRAIN PROCESSED BY THE ION-OZONE MIXTURE*

**Página – 239**

---

**23- Artigo / Article**

---

ASYLBAEV, Ilgiz; NIGMATZYANOV, Almas; KHABIROV, Ilgiz;  
SERGEEV, Vladislav; KURMASHEVA, Nadezhda

RUSSIA

**COMPOSIÇÃO, PROPRIEDADES E USO DE RECURSOS  
SECUNDÁRIOS COMO FERTILIZANTES ORGÂNICOS DE  
SOLOS**

*COMPOSITION, PROPERTIES, AND USE OF SECONDARY  
RESOURCES AS ORGANIC SOIL FERTILIZERS*

**Página - 259**

---

**25- Artigo / Article**

---

SUNYONO, Sunyono; TANIA, Lisa; SAPUTRA, Andrian

INDONESIA

**ANÁLISE DE FATORES EXPLORATÓRIOS DO INTERESSE DE  
CARREIRA DE CIÊNCIA, TECNOLOGIA, ENGENHARIA E  
MATEMÁTICA PARA FUTUROS PROFESSORES DE  
MATEMÁTICA E CIÊNCIA: UM CASO DA UNIVERSIDADE DE  
LAMPUNG, INDONÉSIA**

*EXPLORATORY FACTOR ANALYSIS OF SCIENCE,  
TECHNOLOGY, ENGINEERING AND MATHEMATICS CAREER  
INTEREST FOR PRE-SERVICE MATH AND SCIENCE  
TEACHERS: A CASE OF LAMPUNG UNIVERSITY, INDONESIA*

**Página - 282**

---

**27- Artigo / Article**

---

E SOUZA, MARCELO KEHL; KLUNK, MARCOS ANTÔNIO;  
XAVIER, SOYANE JUCELI SIQUEIRA; DAS, MOHULI;  
DASGUPTA, SUDIPTA

BRASIL

**MÉTODOS ESPECTROSCÓPICOS PARA A DETERMINAÇÃO  
DE GEOTITA EM CAULINITA**

*SPECTROSCOPIC METHODS TO DETERMINATION OF  
GEOTHITE IN KAOLINITE*

**Página - 303**

---

**29- Artigo / Article**

---

VOSTRIKOVA, TATIANA V.; KALAEV, VLADISLAV N.;  
MEDVEDEVA, SVETLANA M.; NOVICHKHINA, NADEZHDA P.;  
SHIKHALIEV, KHIDMET S.

RUSSIA

**COMPOSTOS ORGÂNICOS SINTESIZADOS UTILIZADOS  
COMO ESTIMULANTES DE CRESCIMENTO PARA PLANTAS  
LENHOSAS**

*SYNTHESIZED ORGANIC COMPOUNDS AS GROWTH  
STIMULATORS FOR WOODY PLANTS*

**Página - 327**

---

**24- Artigo / Article**

---

LEKOMTSEV, Alexander Viktorovich; ILIUSHIN, Pavel Yurjevich;  
KOROBOV, Grigory Yurievich

RUSSIA

**MODELAGEM E PROVA DE SOLUÇÕES DE PROJETO PARA A  
RECONSTRUÇÃO DA ESTAÇÃO DE TRATAMENTO DE ÓLEO E  
ÁGUA**

*MODELING AND PROVING OF DESIGN SOLUTIONS FOR THE  
RECONSTRUCTION OF TREATMENT FACILITY OF OIL AND  
WATER*

**Página – 269**

---

**26- Artigo / Article**

---

SILVA, Ednilson Barros; ROCHA, José Roberto Caetano da

BRASIL

**AVALIAÇÃO ANTRÓPICA NO LITORAL PARANAENSE  
ATRAVÉS DA DETERMINAÇÃO DA CONCENTRAÇÃO DO ÍON  
FOSFATO EM RECURSOS HÍDRICOS**

*ANTHROPIC EVALUATION IN THE PARANÁ COAST THROUGH  
THE ION PHOSPHATE CONCENTRATION DETERMINATION IN  
WATER RESOURCES*

**Página – 293**

---

**28- Artigo / Article**

---

MADHI, QUSAI HATTAB; ABASS, MOHAMMED HAMZA;  
MATROOD, ABDULNABI ABDUL AMEER

IRAQ

**POLUIÇÃO POR METAIS PESADOS EM CAMPOS DE TRIGO  
(SOLO E FOLHAS) AMOSTRADOS NAS PROVÍNCIAS DE  
BASRAH E MAYSAN**

*HEAVY METALS POLLUTION OF WHEAT FIELDS (SOIL AND  
LEAVES) SAMPLED FROM BASRAH AND MAYSAN PROVINCES*

**Página – 315**

---

**30- Artigo / Article**

---

;RUCHIN, ALEXANDER B.

RUSSIA.

**EFEITO DA ILUMINAÇÃO NO CRESCIMENTO E  
COMPORTAMENTO DO BARRIGUDINHO, POECILIA  
RETICULATA**

*EFFECT OF ILLUMINATION ON GROWTH AND BEHAVIOUR OF  
GUPPY, POECILIA RETICULATA*

**Página – 338**

---

**31- Artigo / Article**

---

KUPATADZE, KETEVAN

GEORGIA

**MONITORAMENTO DA COMPOSIÇÃO QUÍMICA DO RIO IORI**

*MONITORING OF THE CHEMICAL COMPOSITION OF IORI RIVER*

**Página – 346**

---

**33- Artigo / Article**

---

WAFI K. ESSA; NAJLAA K. ISSA; WALAA H. ABDULQADER; IBTESAM M. KAMAL

IRAQ

**USO DE EXTRATO DE CEBOLA SELVAGEM ECOLÓGICA (URGINEA MARITIMA) COMO INIBIDOR DE CORROSÃO PARA AÇO CARBONO EM ÁCIDO CLORÍDRICO**

*THE USE OF ECO-FRIENDLY WILD ONION EXTRACT (URGINEA MARITIMA) AS CORROSION INHIBITOR FOR CARBON STEEL IN HYDROCHLORIC ACID*

**Página - 367**

---

**35- Artigo / Article**

---

GAVRILOVA, YEKATERINA N.; SEITOVA, SABYRKUL M.; KOZHASHEVA, GULNAR O.; ALDABERGENOVA, AIGUL O., KYDYRBAEVA, GALIYA T.;

RUSSIA

**RESULTADOS DO ESTUDO PARA O TREINAMENTO METODOLÓGICO DE PROFESSORES DE MATEMÁTICA EM CONDIÇÕES DE INOVAÇÃO**

*STUDY RESULTS FOR METHODOLOGICAL TRAINING OF TEACHERS OF MATHEMATICS IN CONDITIONS OF INNOVATION*

**Página - 391**

---

**37- Artigo / Article**

---

SKVORTSOV, ARKADIY A.; GNATYUK, EVGENIYA O.; RYBAKOVA, MARGARITA R.; BURUKIN, IVAN V.;

RUSSIA

**MÉTODOS PARA ENDURECIMENTO E MELHORIA DAS CARACTERÍSTICAS DE FADIGA DE AMOSTRAS DE LIGAS DE NÍQUEL CROMO-FERRO E TITÂNIO**

*METHODS FOR HARDENING AND IMPROVEMENT OF FATIGUE CHARACTERISTICS OF TITANIUM AND IRON-CHROMIUM NICKEL ALLOY SAMPLES*

**Página - 425**

---

**32- Artigo / Article**

---

BRYKIN, VENIAMIN A.; VOROSHILIN, ANTON P.; RIPETSKIY, ANDREY V.; UHOV, PETR A.;

RUSSIA

**IMPLEMENTAÇÃO DA PROTOTIPAGEM RÁPIDA NA RESOLUÇÃO DE PROBLEMAS APLICADOS NA PRODUÇÃO**

*INTRODUCTION OF RAPID PROTOTYPING IN SOLVING APPLIED PROBLEMS IN PRODUCTION*

**Página – 354**

---

**34- Artigo / Article**

---

SEVBITOV, ANDREI; DAVIDYANTS, ALLA; BALKIN, ROMAN; TIMOSHIN, ANTON; KUZNETSOVA, MARIYA

RUSSIA

**ANÁLISE DA EFICÁCIA DA IMUNOTERAPIA USANDO UM COMPLEXO AUTOLOGICO DE IMUNOPEPTÍDEOS NO TRATAMENTO CIRÚRGICO DA PERIODONTITE**

*ANALYSIS OF THE EFFECTIVENESS OF IMMUNOTHERAPY USING AN AUTOLOGOUS COMPLEX OF IMMUNOPEPTIDES IN THE SURGICAL TREATMENT OF PERIODONTITIS*

**Página - 381**

---

**36- Artigo / Article**

---

KOZHAGUL, AIDOS; BIDAIBEKOV, YESSEN; BOSTANOV, BEKTAS; PAK, NIKOLAY; KOZHAGULOVA, ZHANAR;

KAZAKHSTAN

**INTEGRAÇÃO DE PROJETO ROBÓTICO NO PROCESSO DE APRENDIZAGEM NA ESCOLA**

*INTEGRATION OF ROBOTICS DESIGN INTO THE LEARNING PROCESS AT SCHOOL*

**Página – 404**

---

**38- Artigo / Article**

---

FARHAN, Ahmed Jadah

IRAQ

**ESTUDO DA CINÉTICA DA DEGRADAÇÃO TÉRMICA DE COMPOSTOS DE NANOPARTÍCULAS NÃO-SATURADAS DE POLIÉSTER E POLIÉSTER / SILICA POR TÉCNICAS DE ANÁLISE TGA E DSC**

*STUDY OF THE KINETICS OF THERMAL DEGRADATION OF UNSATURATED POLYESTER AND POLYESTER/ SILICA NANOPARTICLES COMPOSITES BY TGA AND DSC ANALYSIS TECHNIQUES*

**Página – 437**

---

**39- Artigo / Article**

---

SAEED, NOOR HAZIM MOHAMMEDTHALJI; ABBAS, AHMED MAJED

IRAQ

**CINÉTICA E MECANISMO DE OXIDAÇÃO DO TETRA-HIDROFURANO PELA CLORAMINA-T EM MEIOS ACIDICOS**

*KINETICS AND MECHANISM OF TETRAHYDROFURAN OXIDATION BY CHLORAMINE-T IN ACIDIC MEDIA*

**Página - 449**

---

**41- Artigo / Article**

---

ALAM, ASHRAF

INDIA

**TESTE DE CONHECIMENTO DE CONCEITOS DE VETORES ELEMENTARES ENTRE ESTUDANTES DO PRIMEIRO SEMESTRE DE BACHARELADO EM ENGENHARIA E DE TECNOLOGIA**

*TEST OF KNOWLEDGE OF ELEMENTARY VECTORS CONCEPTS AMONG FIRST-SEMESTER BACHELOR OF ENGINEERING AND TECHNOLOGY STUDENTS*

**Página - 477**

---

**43- Artigo / Article**

---

COMINOTE, MARINA; SILVA, GABRIEL LIBARDI; HERINGER, NETALIANNE MITCHELLE FAGUNDES; GAZEL, FAIÇAL; OLIVEIRA, RENATO CÉSAR DE SOUZA

BRASIL

**AVALIAÇÃO DE TRATAMENTO DE EFLUENTE TÊXTIL POR ELETROFLOCULAÇÃO COM MONITORAMENTO E CONTROLE AUTOMÁTICO CONSIDERANDO ESTUDO DE VIABILIDADE DE USO DE GERAÇÃO FOTOVOLTAICA**

*EVALUATION OF TREATMENT OF TEXTILE EFFLUENT BY ELECTROFLOCCULATION WITH MONITORING AND AUTOMATIC CONTROL CONSIDERING A FEASIBILITY STUDY OF THE USE OF PHOTOVOLTAIC GENERATION*

**Página - 507**

---

**45- Artigo / Article**

---

AL-JABERI, AHMED K., HAMEED, EHSAN M., ABDUL-WAHAB, MOHAMMED S.

IRAQ

**UM NOVO MÉTODO ANALÍTICO PARA RESOLVER A EQUAÇÃO DE TELEGRAFIA LINEAR E NÃO-LINEAR**

*A NOVEL ANALYTIC METHOD FOR SOLVING LINEAR AND NON-LINEAR TELEGRAPH EQUATION*

**Página – 536**

---

**40- Artigo / Article**

---

ANISHCHENKO, Lidia; MOSKALENKO, Igor; AVRAMENKO, Marina; VOROCHAY, Yuliya; PLAKHOTIN, Aleksey

RUSSIA

**ESPECIFICAÇÕES BIOINDICATIVAS, ECOLÓGICAS E ANALÍTICAS DE FLUXOS MENORES SOB A INFLUÊNCIA DE OBJETOS ARTIFICIAIS PERIGOSOS**

*BIOINDICATIVE, ECOLOGICAL AND ANALYTICAL SPECIFICATIONS OF MINOR STREAMS UNDER THE INFLUENCE OF HAZARDOUS MAN-MADE OBJECTS*

**Página – 462**

---

**42- Artigo / Article**

---

DAKHNO, LARYSA; LOGVYNENKO, IRYNA;

UKRAINE

**EFEITO DA OSTEOTOMIA SEGMENTAR ISOLADA DO QUEIXO (SCO) NO ESPAÇO DAS VIAS AÉREAS FARÍNGEAS**

*THE EFFECT OF ISOLATED SEGMENTAL CHIN OSTEOTOMY (SCO) ON THE PHARYNGEAL AIRWAY SPACE*

**Página – 495**

---

**44- Artigo / Article**

---

UNNES, SUDARMIN; SUMARNI, WORO; DILIAROSTA, SKUNDA; RAMADANTY, ISABELA

INDONESIA

**A RECONSTRUÇÃO DO CONHECIMENTO CIENTÍFICO SOBRE A BIOATIVIDADE DE BAJAKAH KALALAWIT (UNCARIA GAMBIR ROXB) COMO ETNOMEDICINA**

*THE RECONSTRUCTION OF SCIENTIFIC KNOWLEDGE ABOUT BAJAKAH KALALAWIT (UNCARIA GAMBIR ROXB) BIOACTIVITY AS ETHNOMEDICINE*

**Página – 524**

---

**46- Artigo / Article**

---

AL-JABERI, AHMED K., HAMEED, EHSAN M., ABDUL-WAHAB, MOHAMMED S.

IRAQ

**UM NOVO MÉTODO ANALÍTICO PARA RESOLVER A EQUAÇÃO DE TELEGRAFIA LINEAR E NÃO-LINEAR**

*A NOVEL ANALYTIC METHOD FOR SOLVING LINEAR AND NON-LINEAR TELEGRAPH EQUATION*

**Página – 536**

SHA, MINGGONG; PROKUDIN, OLEG A.; SOLYAEV, YURY O.; VAKHNEEV, SERGEY N.

Republic of China and RUSSIA

**DEPENDÊNCIA DOS MECANISMOS DE DESTRUIÇÃO “GLARE” DA EXTENSÃO DE AMOSTRAS EM TESTES DE FLEXÃO DE TRÊS PONTOS**

*DEPENDENCE OF GLARE DESTRUCTION MECHANISMS ON THE ELONGATION OF SAMPLES IN TESTS TO THREE-POINT FLEXURAL*

**Página – 549**



---

**47- Artigo / Article**

---

NIGMATZYANOV, VLADISLAV V.; POGODIN, VENIAMIN A.;  
RABINSKIY, LEV N.; SITNIKOV, SERGEY A.; ZIN HEIN, THANT

RUSSIA

**PRECURSORES POLIMÉRICOS PARA A CRIAÇÃO DE UMA  
CÂMARA DE DESCARGA DE GÁS DO MOTOR DE FOGUETE  
ELÉTRICO**

*POLYMER PRECURSORS FOR CREATING GAS DISCHARGE  
CHAMBER FOR ELECTRIC ROCKET ENGINE*

**Página - 560**

---

**49- Artigo / Article**

---

EMAN A. M. AL-JAWADI; MOHAMMED I. MAJEED

IRAQ

**SENSORES ELETROQUÍMICOS À BASE DE FILME POLI (L-  
FENIL ALANINA) EM MWCNT PARA DETERMINAÇÃO DE TPS**

*ELECTROCHEMICAL SENSORS BASED ON POLY (L-PHENYL  
ALANINE) FILM ON MWCNT FOR DETERMINATION OF TPS*

**Página – 579**

---

**51- Artigo / Article**

---

OREKHOV, ALEXANDER A.; UTKIN, YURI A.; PRONINA, POLINA  
F.

RUSSIA

**DEFINIÇÃO DE DEFORMAÇÕES NA ESTRUTURA COMPOSTA  
DE GRADE SOB A AÇÃO DE CARGAS COMPRESSIVAS**

*DETERMINATION OF DEFORMATION IN MESH COMPOSITE  
STRUCTURE UNDER THE ACTION OF COMPRESSIVE LOADS*

**Página – 599**

---

**53- Artigo / Article**

---

UMRAN, MAY ALI HUSSEIN; AL-KHATEEB, SUMAYA NAJIM

IRAQ

**PADRÃO DE PRODUÇÃO DE CÁPSULAS DE ESCHERICHIA  
COLI UROPATOGÊNICAS DE PACIENTES COM INFECÇÃO DO  
TRATO URINÁRIO EM HOSPITAIS DE KIRKUK**

*CAPSULE PRODUCTION PATTERN OF UROPATHOGENIC  
ESCHERICHIA COLI OF URINARY TRACT INFECTION  
PATIENTS IN KIRKUK HOSPITALS*

**Página – 621**

---

**48- Artigo / Article**

---

HALBOOS, MOHANAD HAZIM; HUSSEIN, BAYAN JABR;  
SAYHOOD, AAYAD AMMAR

IRAQ

**PREPARAÇÃO DE UM NOVO COMPOSTO AZO (HAZM)  
UTILIZADO PARA DETERMINAÇÃO ESPECTROFOTOMÉTRICA  
ANALÍTICA DE GLICOSE NO SANGUE E NA SALIVA**

*PREPARATION OF A NEW AZO COMPOUND (HAZM) USED FOR  
ANALYTICAL SPECTROPHOTOMETRIC DETERMINATION OF  
GLUCOSE IN BLOOD AND SALIVA*

**Página – 569**

---

**50- Artigo / Article**

---

LI, YULONG; DOBRYANSKIY, VASILII N.; OREKHOV,  
ALEXANDER A.

CHINA and RUSSIA

**MODELAGEM DE PROCESSOS DE DESENVOLVIMENTO DE  
FISSURAS EM ELEMENTOS COMPOSITOS BASEADOS NOS  
MODELOS “VIRTUAL CRACK CLOSURE TECHNIQUE” E  
“COHEZIVE ZONE MODE”**

*MODELLING OF CRACK DEVELOPMENT PROCESSES IN  
COMPOSITE ELEMENTS BASED ON VIRTUAL CRACK  
CLOSURE TECHNIQUE AND COHESIVE ZONE MODEL*

**Página – 591**

---

**52- Artigo / Article**

---

SALTABAYEVA, ULBOSSYN SH.; MORENKO, MARINA A.;  
ROZENSON, RAFAIL I.

KAZAKHSTAN

**ESTUDO COMPARATIVO DA PREVALÊNCIA DA REATIVIDADE  
DE IGE A ALÉRGENOS RECOMBINANTES**

*COMPARATIVE STUDY OF THE PREVALENCE OF IGE  
REACTIVITY TO RECOMBINANT ALLERGENS ON THE  
BACKGROUND OF ALLERGEN-SPECIFIC IMMUNOTHERAPY*

**Página – 609**

---

**54- Artigo / Article**

---

SHAHEED, IHSAN MAHDI; HATAM, RAGHAD SAAD; KUDHAIR,  
AHMED F., AND MOHAMMED, NOOR JAMAL

IRAQ

**EXTRAÇÃO DE PONTO DE NÉVOA ECO-AMIGÁVEL  
ACOPLADA COM UM MÉTODO ESPECTROFOTOMÉTRICO  
PARA A DETERMINAÇÃO DO HIDROCLORETO RANITIDINA EM  
AMOSTRAS FARMACÊUTICAS**

*ECO-FRIENDLY CLOUD POINT EXTRACTION COUPLED WITH A  
SPECTROPHOTOMETRIC METHOD FOR THE DETERMINATION  
OF RANITIDINE HYDROCHLORIDE IN PHARMACEUTICAL  
SAMPLES*

**Página – 628**

---

**55- Artigo / Article**

---

TLEBAYEV, MANAT B.; BIIBOSUNOV, BOLOTBEK I.; TASZHUREKOVA, ZHAZIRA K.; BAIZHARIKOVA, MARINA A.; AITBAYEVA, ZAMIRA K.

REPUBLIC OF KAZAKHSTAN AND KYRGYZ REPUBLIC

**CRIAÇÃO DO MODELO MATEMÁTICO DE COMPUTADOR DO PROCESSO BIOTECNOLÓGICO DO PROCESSAMENTO DE MATÉRIAS-PRIMAS**

*CREATION OF A COMPUTER-ASSISTED MATHEMATICAL MODEL FOR THE RAW MATERIALS BIOLOGICAL PROCESSING LINE*

**Página – 640**

---

**57- Artigo / Article**

---

MOLDABAYEVA, GULNAZ; SULEIMENOVA, RAIKHAN; KARIMOVA, AKMARAL; AKHMETOV, NURKEN; MARDANOVA, LYAILYA

KAZAKHSTAN

**PROJETO DE ENSAIO EXPERIMENTAL DE TECNOLOGIA DE INUNDAÇÃO DE POLÍMEROS EM DEPÓSITOS DO CAZAQUISTÃO OCIDENTAL**

*EXPERIMENTAL SUPPORT OF FIELD TRIAL ON THE POLYMER FLOODING TECHNOLOGY SUBSTANTIATION IN THE OIL FIELD OF WESTERN KAZAKHSTAN*

**Página – 663**

---

**59- Artigo / Article**

---

SHIGALUGOV, STANISLAV H.; TYURIN, YURIY I.; DUBROV, DMITRIY V.; BOROVITSKAYA, ANNA O.; DERIABINA, LARISSA B.

RUSSIA

**LUMINESCÊNCIA DE A-WILLEMITE NA OXIDAÇÃO CATALÍTICA DE MONÓXIDO DE CARBONO**

*LUMINESCENCE OF A-WILLEMITE IN THE CATALYTIC OXIDATION OF CARBON MONOXIDE*

**Página – 691**

---

**61- Artigo / Article**

---

GIZATOV, ALBERT; GIZATOVA, NATALIA; MIRONOVA, IRINA; GAZEYEV, IGOR; NIGMATYANOV, AZAT

RUSSIA

**CRIAÇÃO E USO DO CONSÓRCIO DE MICROORGANISMOS NA PRODUÇÃO DE CARNES**

*CREATION AND USE OF MICROORGANISM CONSORTIUM IN MEAT PRODUCTION*

**Página – 713**

---

**56- Artigo / Article**

---

BABAYTSEV, ARSENIY V.; KYAW, YE KO; VAKHNEEV, SERGEY N.; ZIN HEIN, THANT

RUSSIA

**ESTUDO DA INFLUÊNCIA DE INCLUSÕES ESFÉRICAS EM CARACTERÍSTICAS MECÂNICAS**

*STUDY OF THE INFLUENCE OF SPHERICAL INCLUSIONS ON MECHANICAL CHARACTERISTICS*

**Página – 654**

---

**58- Artigo / Article**

---

HASSAN, BAYDAA ABOOD; LAWI, ZAHRAA KAMIL KADHIM; BANOON, SHAIMA RABEEA

IRAQ

**DETECÇÃO DA ATIVIDADE DE NANOPARTÍCULAS DE PRATA, PSEUDOMONAS FLUORESCENS E BACILLUS CIRCULANS NA INIBIÇÃO DO CRESCIMENTO DE ASPERGILLUS NIGER ISOLADO A PARTIR DE FRUTAS ALARGADAS**

*DETECTING THE ACTIVITY OF SILVER NANOPARTICLES, PSEUDOMONAS FLUORESCENS AND BACILLUS CIRCULANS ON INHIBITION OF ASPERGILLUS NIGER GROWTH ISOLATED FROM MOLDY ORANGE FRUITS*

**Página – 678**

---

**60- Artigo / Article**

---

SADRITDINOV, AYNUR R.; KHUSNULLIN, AYGIZ G.; PSYANCHIN, ARTUR A.; ZAKHAROVA, ELENA M.; ZAKHAROV, VADIM P.

RÚSSIA

**PROPRIEDADES FÍSICO-MECÂNICAS E TERMOFÍSICAS DE COMPOSITOS POLÍMEROS À BASE DE POLIPROPILENO SECUNDÁRIO PREENCHIDOS DE CASCA DE ARROZ**

*PHYSICAL AND MECHANICAL AND THERMOPHYSICAL PROPERTIES OF POLYMER COMPOSITES BASED ON RECYCLED POLYPROPYLENE FILLED WITH RICE HUSK*

**Página – 703**

---

**62- Artigo / Article**

---

ASTAPIEVA, OLHA M.; GRUSHKA, GANNA V.; PASKEVYCH, OLGA I.; FEDULENKOVA, YULIIA YA.; MAKSIMISHYN, OLEKSII V.

UKRAINE

**ANÁLISE RETROSPECTIVA DO CURSO DE CÂNCER DE TIREÓIDE COM METÁSTASES NOS PULMÕES APÓS RADIOTERAPIA**

*RETROSPECTIVE ANALYSIS OF THE COURSE OF THYROID CARCINOMA WITH LUNG METASTASES AFTER RADIOIODINE THERAPY*

**Página – 728**

---

**63- Artigo / Article**

---

ABDULRAHMAN, HAYDER J.; MOHAMMED, SUZAN B.

IRAQ

**DESENVOLVIMENTO DE LASERS DE ALTA INTENSIDADE  
ULTRACURTOS PARA A FAIXA DE ESPECTROS VISÍVEIS**

*DEVELOPMENT OF ULTRA-SHORT HIGH INTENSITY LASERS  
FOR THE VISIBLE SPECTRA RANGE*

**Página – 739**

---

**65- Artigo / Article**

---

MYRZASHEVA, AIGUL N.; KENZHEGULOV, BEKET;  
SHAZHEDEKEEVA, NURGUL K.; TULEUOVA, RAIGUL U.

KAZAKHSTAN

**MÉTODO NUMÉRICO PARA DETERMINAR A DEPENDÊNCIA  
DO ESTADO DE TENSÃO TÉRMICA DA HASTE DA  
TEMPERATURA DO MEIO AMBIENTE NA PRESENÇA  
SIMULTÂNEA DE PROCESSOS TÉRMICOS**

*A NUMERICAL METHOD FOR DETERMINING THE  
DEPENDENCE OF THE THERMALLY STRESSED STATE OF A  
ROD ON AMBIENT TEMPERATURE WITH THE SIMULTANEOUS  
PRESENCE OF THERMAL PROCESSES*

**Página – 765**

---

**67- Artigo / Article**

---

ISMAGILOV, RAFAEL; ASYLBAEV, ILGIZ; URAZBAKHTINA,  
NURIYA; ANDRIYANOV, DENIS; AVSAKHOV, FIRDAVIS

RUSSIA

**CRESCIMENTO DE TUBERCULOS DE SEMENTE DE BATATA  
SEM VÍRUS EM PLANTIO AEROPÔNICO**

*GROWING OF VIRUS-FREE POTATO SEED TUBERS IN THE  
AEROPONIC PLANT*

**Página – 791**

---

**69- Artigo / Article**

---

ERMOLOVA, NATALYA VICTOROVNA; PETROV, YURIY  
ALEKSEEVICH; LEVKOVICH, MARINA ARKADEVNA;  
KOLESHNIKOVA, LUDMILA VALERIEVNA; DRUKKER, NINA  
ALEKSANDROVNA

RUSSIA

**INFLUÊNCIA DA PRODUÇÃO DE CITOCINAS, METABOLITOS  
DE ÓXIDO DE NITROGÊNIO E TROCA DE LÍPIDOS NA  
FORMAÇÃO DE ESTÁGIOS EXTERNOS DE ENDOMETRIOSE  
GENITAL NOS PACIENTES EM IDADE REPRODUTIVA**

*INFLUENCE OF CYTOKINES PRODUCTION, NITROGEN OXIDE  
METABOLITES AND LIPIDS EXCHANGE ON THE FORMATION  
OF EXTERNAL GENITAL ENDOMETRIOSIS STAGES IN  
PATIENTS OF REPRODUCTIVE AGE*

**Página – 813**

---

**64- Artigo / Article**

---

PRONINA, POLINA F.; TUSHAVINA, OLGA V.; STAROVOITOV,  
EDUARD I.

RUSSIA

**ESTUDO DA SITUAÇÃO DE RADIAÇÃO EM MOSCOU POR  
MEIO DA PESQUISA DOS ORGANISMOS ELASTOPLÁSTICOS  
NO FLUXO DE NÊUTRONS, CONSIDERANDO OS EFEITOS DO  
CALOR**

*STUDY OF THE RADIATION SITUATION IN MOSCOW BY  
INVESTIGATING ELASTOPLASTIC BODIES IN A NEUTRON  
FLUX TAKING INTO ACCOUNT THERMAL EFFECTS*

**Página – 753**

---

**66- Artigo / Article**

---

VOSTRIKOVA, TATIANA V.; KALAEV, VLADISLAV N.; POTAPOV,  
ANDREY YU. POTAPOV, MICHAIL A.; SHIKHALIEV, KHMIDMET S.

RÚSSIA

**USO DE NOVOS COMPOSTOS DA SÉRIE QUINOLINA COMO  
ESTIMULANTES EFICAZES DOS PROCESSOS DE  
CRESCIMENTO**

*USE OF NEW COMPOUNDS OF THE QUINOLINE SERIES AS  
EFFECTIVE STIMULANTS OF GROWTH PROCESSES*

**Página – 781**

---

**68- Artigo / Article**

---

DOLININ, ILGIZ; BAZEKIN, GEORGE; SKOVORODIN, EVGENY;  
SHARIPOV, ALMAZ; CHUDOV, IVAN

RÚSSIA

**O USO DE BIOSTIMULANTE PARA AUMENTAR O GANHO DE  
PESO CORPORAL DE FRANGOS**

*THE USE OF BIOSTIMULANT FOR INCREASING THE BODY  
WEIGHT GAIN OF CHICKENS*

**Página – 800**

---

**70- Artigo / Article**

---

MARDIYANA; USODO, BUDI; BUDIYONO; JINGGA, ANISA  
ASTRA; FAHRUDIN, DWI

INDONISIA

**ANÁLISE DOS ERROS DE CONEXÃO MATEMÁTICA DOS  
ALUNOS NA RESOLUÇÃO DE PROBLEMAS DE IDENTIDADE  
TRIGONOMÉTRICA**

*ANALYSIS OF STUDENTS' MATHEMATICAL CONNECTION  
ERRORS IN TRIGONOMETRIC IDENTITY PROBLEM SOLVING*

**Página – 825**

---

**71- Artigo / Article**

---

ALI, SAFAA HUSSEIN; ABD ALREDHA, HASSAN MWAZI; ABDULHUSSEIN, HAIDER SABAH

IRAQ

**ATIVIDADE ANTIBIÓTICA DE NOVAS ESPÉCIES DE COMPLEXOS DE METAIS DE BASE DE SCHIFF**

*ANTIBIOTIC ACTIVITY OF NEW SPECIES OF SCHIFF BASE METAL COMPLEXES*

**Página – 837**

---

**73- Artigo / Article**

---

MASHFUFUFAH, AYNIN; NURKAMTO, JOKO; SAJIDAN; WIRANTO.

INDONESIA

**A EFICÁCIA DO MODELO DE APRENDIZAGEM EM LABORATÓRIO BASEADO EM ETNOSOCIOECOLOGIA PARA APLICAR A ALFABETIZAÇÃO AMBIENTAL EM PROFESSORES DE BIOLOGIA EM TREINAMENTO**

*THE EFFECTIVENESS OF INQUIRY LABORATORY-BASED ETHNOSOCIOECOLOGY LEARNING MODEL TO EMPOWER ENVIRONMENTAL LITERACY IN PRESERVICE BIOLOGY TEACHERS*

**Página – 877**

---

**75- Artigo / Article**

---

AITKELDIYEVA, Svetlana; DAUGALIYEVA, Saule; ALIMBETOVA, Anna; FAIZULINA, Elmira; SADANOV, Amankeldi

KAZAKHSTAN

**DIVERSIDADE MICROBIANA DE SOLOS CONTAMINADOS NOS CAMPOS PETRÓLÍFEROS DO CAZAQUISTÃO**

*MICROBIAL DIVERSITY OF THE CONTAMINATED SOILS IN KAZAKHSTAN OILFIELDS*

**Página – 908**

---

**77- Artigo / Article**

---

GHAFIYEHSANJ, ELHAM; DILMAGHANI, KAMALADDIN; CHAPARZADEH, NADER; SAADATMAND, SARA

IRAN

**ESTUDO SOBRE COMPOSIÇÕES DE ÓLEO ESSENCIAL DE SALVIA (SALVIA NEMOROSA L.) COLHIDA DO NOROESTE DO IRÃ EM DIFERENTES ESTÁGIOS DE CRESCIMENTO**

*STUDY ON ESSENTIAL OIL COMPOSITIONS OF SAGE (SALVIA NEMOROSA L.) COLLECTED FROM THE NORTH WEST OF IRAN AT DIFFERENT GROWTH STAGES*

**Página – 934**

---

**72- Artigo / Article**

---

ARSANI, IDA AYU ANOM; SETYOSARI, PUNAJI; KUSWANDI, DEDI; DASNA, I WAYAN

INDONESIA

**ESTRATÉGIAS DE APRENDIZAGEM BASEADAS EM PROBLEMAS USANDO VÁRIAS REPRESENTAÇÕES E ESTILOS DE APRENDIZAGEM PARA MELHORAR AS COMPREENSÕES CONCEITUAIS DA QUÍMICA**

*PROBLEM-BASED LEARNING STRATEGIES USING MULTIPLE REPRESENTATIONS AND LEARNING STYLES TO ENHANCE CONCEPTUAL UNDERSTANDINGS OF CHEMISTRY*

**Página – 860**

---

**74- Artigo / Article**

---

AUYEZKHANOVA, ASSEMGUL S.; TALGATOV ELDAR T.; AKHMETOVA SANDUGASH N.; KAPYSHEVA UNZIRA N.; ZHARMAGAMBETOVA ALIMA K.

KAZAKHSTAN

**SÍNTESE E PROPRIEDADES DE PROTEÇÃO DOS COMPOSTOS DE PECTINA / MONTMORILONITA CONTRA A ENTEROCOLITE INDUZIDA POR ASPIRINA**

*SYNTHESIS AND PROTECTIVE PROPERTIES OF PECTIN/MONTMORILLONITE COMPOSITES AGAINST ASPIRIN-INDUCED ENTEROCOLITIS*

**Página – 897**

---

**76- Artigo / Article**

---

ROMANOVA, LUBOV; TOLMATCHEVA, NATALIA; MASLOVA, ZHANNA; KAPITOVA, IRINA; SHAMITOVA, ELENA

RUSSIA

**USO DE BIOCORRETORES NA ESTIMULAÇÃO DA REGENERAÇÃO HEPÁTICA FETAL DE RATOS LESIONADOS MECANICAMENTE**

*USING OF BIOCORRECTORS IN REGENERATION PACING OF MECHANICALLY INJURED RATS' FETAL HEPATIC*

**Página – 924**

---

**78- Artigo / Article**

---

ALBERTON, MATHEUS BORGHEZAN; LINDINO, CLEBER ANTONIO.

BRASIL

**ADSORÇÃO DO HORMÔNIO 17 $\alpha$ -METILTESTOSTERONA EM SOLOS**

*ADSORPTION OF HORMONE 17 $\alpha$ -METHYLTESTOSTERONE IN SOILS*

**Página – 948**

---

**79- Artigo / Article**

---

UTAMI, DEKA DYAH; SETYOSARI, PUNAJI; KAMDI, WARAS; ULFA; SAIDA; KUSWANDI, DEDI

INDONÉSIA

**O EFEITO DA ESTRATÉGIA DE APRENDIZAGEM SMART-PBL E DA APRENDIZAGEM ACADÊMICA AUTORREGULADA SOBRE AS HABILIDADES METACOGNITIVAS E DE RESOLUÇÃO DE PROBLEMAS NA APRENDIZAGEM EM QUÍMICA**

*THE EFFECT OF SMART-PBL LEARNING STRATEGY AND ACADEMIC-SELF REGULATED LEARNING ON METACOGNITIVE & PROBLEM-SOLVING SKILLS IN LEARNING CHEMISTRY*

**Página – 960**

---

**81- Artigo / Article**

---

SHA, MINGGONG; UTKIN, YURI A.; TUSHAVINA, OLGA V.; PRONINA, POLINA F.

CHINA and RUSSIA

**ESTUDOS EXPERIMENTAIS DE TRANSFERÊNCIA DE CALOR E MASSA DE MODELOS DE PONTAS PRODUZIDOS A PARTIR DE MATERIAL COMPÓSITO DE CARBONOCARBONO (MCCC) SOB CONDIÇÕES DE CARGA DE CALOR DE ALTA INTENSIDADE**

*EXPERIMENTAL STUDIES OF HEAT AND MASS TRANSFER FROM TIP MODELS MADE OF CARBON-CARBON COMPOSITE MATERIAL (CCCM) UNDER CONDITIONS OF HIGH-INTENSITY THERMAL LOAD*

**Página – 988**

---

**83- Artigo / Article**

---

BBABASKIN, D.V.; LITVINOVA, T.M.; BABASKINA, L.I.; OVAKIMYAN, A.K.; KOLEVATOVA, K.Y.

RUSSIA

**AVALIAÇÃO DE MARKETING DAS PREFERÊNCIAS DO CONSUMIDOR NO USO DE APLICATIVOS MÓVEIS PARA CUIDADOS DE SAÚDE PARA APOIAR A ADERÊNCIA AO MEDICAMENTO**

*MARKETING EVALUATION OF CONSUMER PREFERENCES IN USING MOBILE APPS FOR HEALTHCARE TO SUPPORT DRUG ADHERENCE*

**Página – 1013**

---

**85- Artigo / Article**

---

GONÇALVES, THÁIS PAULA RODRIGUES; PARREIRA, ADRIANO GUIMARÃES; LIMA, LUCIANA ALVES RODRIGUES DOS SANTOS

BRASIL

**ESTUDO DA ATIVIDADE ANTIMICROBIANA DE *Tecoma stans* (L.) ex Kunth (BIGNONIACEAE)**

*STUDY OF THE ANTIMICROBIAL ACTIVITY OF *Tecoma stans* (L.) ex Kunth (BIGNONIACEAE)*

**Página – 1037**

---

**80- Artigo / Article**

---

BEREZINA, TATIANA N.; CHUMAKOVA, ELIZAVETA

RUSSIA

**HÁBITOS COMPORTAMENTAIS DE DOENÇA CARDIOVASCULAR EM PENSIONISTAS DE VÁRIOS PERFIS PROFISSIONAIS**

*BEHAVIORAL BACKGROUND OF CARDIOVASCULAR DISEASE IN PENSIONERS OF VARIOUS PROFESSIONAL TYPES*

**Página – 977**

---

**82- Artigo / Article**

---

NAZAROVA, VALENTINA D.; SALIKOVA, NATALYA S.; BEKTEMISOVA, AINASH U.; BEGENOVA, BAHYT E.; AUBAKIROVA, GULSIM B.

KAZAKHSTAN

**PRODUÇÃO DE FRAÇÕES DE MIRICETINA DE PLANTA DE *LYNOSYRIS VILLOSA* E ESTUDO DE SUA ATIVIDADE BIOLÓGICA**

*ISOLATION OF MIRICETINE-CONTAINING FRACTIONS FROM *LYNOSYRIS VILLOSA* PLANT AND THEIR APPLICATION AS ANTIANEMIC AGENT*

**Página – 998**

---

**84- Artigo / Article**

---

BOITSOVA, TATYANA MARYANOVNA; PROKOPETS, ZHANNA GEORGIEVNA; ZHURAVLEVA, SVETLANA VALEREVNA; LYAKH, VLADIMIR ALEKSEEVICH

RUSSIA

**CONTROLE DE ODORES EM PRODUTOS ALIMENTARES USANDO FIBRAS ALIMENTARES**

*ODOR CONTROL IN FOODS USING DIETARY FIBERS*

**Página – 1028**

---

**86- Artigo / Article**

---

KHUDYAKOVA, ELENA V.; KHUDYAKOVA, HATIMA K.; SHITIKOVA, ALEKSANDRA V.; SAVOSKINA, OLGA A.; KONSTANTINOVICH, ANASTASIIA V.

RUSSIA

**TECNOLOGIAS DA INFORMAÇÃO PARA DETERMINAR O PERÍODO ÓTIMO DE PREPARAÇÃO DE ALIMENTOS A PARTIR DE ERVAS DE CEREALIS PERENES**

*INFORMATION TECHNOLOGIES FOR DETERMINATION THE OPTIMAL PERIOD OF PREPARING FODDER FROM PERENNIAL GRASSES*

**Página – 1044**

---

**87- Artigo / Article**

---

BUGERO, NINA VLADIMIROVNA; ILYINA, NATALYA ANATOLYEVNA; ALEXANDROVA, SVETLANA MIKHAYLOVNA

RUSSIA

**POTENCIAL DE PERSISTENCIA DOS PROTOZOÁRIOS  
BLASTOCYSTIS SPP.**

*PERSISTENT POTENTIAL OF PROTOZOA BLASTOCYSTIS SPP.*

**Página – 1057**

---

**89- Artigo / Article**

---

MELNYK, OLEKSANDR V.; SOVHIRA, SVITLANA V.; DUSHECHKINA, NATALIYA YU.; AVRAMENKO, OLEG B.; DUBOVA, NATALIYA V.

UKRAINE

**AValiação OPERACIONAL DOS PARÂMETROS DE  
CONTAMINAÇÃO QUÍMICA**

*RAPID ASSESSMENT OF CHEMICAL CONTAMINATION  
PARAMETERS*

**Página – 1084**

---

**91- Artigo / Article**

---

SALIM, BADRAN JASIM; JASIM, ODAY AHMED

IRAQ

**MÉTODO CAS WAVELETS PARA RESOLVER O SISTEMA DE  
DIFUSÃO DE REAÇÃO E COMPARAR COM O MÉTODO (G.F.E)**

*CAS WAVELETS METHOD TO SOLVE REACTION-DIFFUSION  
SYSTEM AND COMPARE IT WITH (G.F.E) METHOD*

**Página – 1110**

---

**93- Artigo / Article**

---

BAKHTIYAROVA, SHOLPAN; ZHAKSYMOM, BOLATBEK; KAPYSHEVA, UNZIRA; CHEREDNICHENKO, OKSANA

KAZAKHSTAN

**ALTERAÇÕES CITOGENÉTICAS EM CRIANÇAS RESIDENTES  
EM REGIÕES ECOLOGICAMENTE ADVERSAS DO  
CAZAQUISTÃO**

*CYTOGENETIC CHANGES IN SCHOOLCHILDREN RESIDING IN  
ECOLOGICALLY ADVERSE REGIONS OF KAZAKHSTAN*

**Página – 1137**

---

**88- Artigo / Article**

---

LISOVSKAYA, S. B.; KARGIN, V. S.; MATYUSHIN, A. A.; TITOVA, N. A.; BELOV, A. V.

RUSSIA

**AValiação DA BIOEQUIVALÊNCIA EM VOLUNTÁRIOS  
SAUDÁVEIS DE TABLETS ORODISPERSÍVEIS COM  
OLANZAPINA**

*ASSESSMENT OF OLANZAPINE ORODISPERSIBLE TABLETS  
BIOEQUIVALENCE IN HEALTHY VOLUNTEERS*

**Página – 1070**

---

**90- Artigo / Article**

---

SYZDYKOV, Kuanysh N.; NARBAYEV, Serik; ASSYLBEKOVA, Ainur S.; BARINOVA, Gulnaz K.; KUANCHALEYEV, Zhaxygali B.

KAZAKHSTAN

**EXPERIÊNCIA DA INTRODUÇÃO DE TILÁPIA NAS FONTES  
GEOTÉRMICAS DO CAZAQUISTÃO**

*EXPERIENCE OF TILAPIA INTRODUCTION AT GEOTHERMAL  
SOURCES OF KAZAKHSTAN*

**Página – 1096**

---

**92- Artigo / Article**

---

KOZLIAKOVA, IRINA; KOZHEVNIKOVA, IRINA; EREMINA, OLGA; ANISIMOVA, NADEZHDA

RUSSIA

**ENGENHARIA DE TIPIFICAÇÃO GEOLÓGICA DE TERRITÓRIOS  
PARA ALOCAÇÃO DE INSTALAÇÕES MUNICIPAIS DE  
GERENCIAMENTO DE RESÍDUOS SÓLIDOS**

*ENGINEERING GEOLOGICAL TYPIFICATION OF TERRITORIES  
FOR ALLOCATION OF MUNICIPAL SOLID WASTE  
MANAGEMENT FACILITIES*

**Página – 1124**

---

**94- Artigo / Article**

---

JABBAR, MOHAMMED L.; AL-SHEJAIRY, KADHUM J.

IRAQ

**UMA NOVA GEOMETRIA FRACTAL DOPING PARA  
NANOFIBRAS DE GRAFENO E A OTIMIZAÇÃO DE CRISTAL:  
UM ESTUDO DA TEORIA DA DENSIDADE FUNCIONAL (DFT)**

*A NOVEL FRACTAL GEOMETRY DOPING FOR GRAPHENE  
NANORIBBON AND THE OPTIMIZATION OF CRYSTAL: A  
DENSITY FUNCTIONAL THEORY (DFT) STUDY*

**Página – 1148**

---

**95- Artigo / Article**

---

SOZONTOVA, ELENA A.; PRODANOVA, NATALIA A.; ZEKIY, ANGELINA O.; RAKHMATULLINA, LEILA V.; KONOVALOVA, ELENA V.

RUSSIA

**EFICIÊNCIA DAS TECNOLOGIAS REMOTAS NA ABORDAGEM DO CONTEÚDO DE UM CURSO DE MATEMÁTICA E-LEARNING USANDO O SISTEMA MOODLE: ESTUDO DE CASO**

*EFFICIENCY OF REMOTE TECHNOLOGIES ON THE APPROACHING THE CONTENT OF A E-LEARNING MATHEMATICS COURSE USING MOODLE SYSTEM: CASE STUDY*

**Página – 1159**

---

**97- Artigo / Article**

---

BUTOV, A. V.; ZUBKOVA, T. V.

RUSSIA

**SISTEMA DE PROTEÇÃO DA BATATA CONTRA PRAGAS E DOENÇAS PARA OBTENÇÃO DE PRODUTOS ECOLÓGICAMENTE LIMPOS**

*SYSTEM OF PROTECTION FOR POTATO FROM PESTS AND DISEASES TO GET ECOLOGICALLY CLEAN PRODUCTS*

**Página – 1186**

---

**99- Artigo / Article**

---

PUTRANTO, TERAWAN AGUS., IKRAR, TARUNA., WASKITO, PUJO

INDONESIA

**MACRÓFAGOS REGENERATIVOS: UMA NOVA ESPERANÇA PARA CARDIOMIOPATIA**

*REGENERATIVE MACROPHAGES: A NEW HOPE FOR CARDIOMYOPATHY*

**Página – 1207**

Instructions to authors

**Página – 1231**

---

**96- Artigo / Article**

---

ISMAGILOV, RAPHAEL; SOTCHENKO, ELENA; AKHIYAROV, BULAT; ISLAMGULOV, DAMIR; NURLYGANOV, RAZIT

RUSSIA

**PRODUTIVIDADE DE NOVOS HÍBRIDOS DE MILHO NAS CONDIÇÕES DOS URAIS**

*PRODUCTIVITY OF NEW MAIZE HYBRIDS IN CONDITIONS OF THE URALS*

**Página – 1175**

---

**98- Artigo / Article**

---

VAKHRUSHEVA, LYUDMILA P.; ABDULGANIEVA, ELVIRA F.; AKHKIYAMOVA, GUZELIYA R., SHICHYAKH, RUSTEM A.; AVDEEV, YURI M.

RUSSIA

**CARACTERÍSTICAS MORFOLÓGICAS E ANATÔMICAS DOS ESTADOS ETÁRIOS DE *Scutellaria stevenii* Juz. (*Scutellaria orientalis* subsp. *orientalis*) EM FITOCENÓSES DA CRIMEIA DE ENCOSTAS**

*MORPHOLOGICAL AND ANATOMICAL FEATURES OF AGE STATES OF *Scutellaria stevenii* Juz. (*Scutellaria orientalis* subsp. *orientalis*) IN PHYTOCENOSES OF THE CRIMEA FOOTHILLS*

**Página – 1196**

---

**100- Artigo / Article**

---

MEDVEDSKIY, ALEKSANDR L.; MARTIROSOV, MIKHAIL I.; KHOMCHENKO, ANTON V.; DEDOVA, DARINA V.

RUSSIA

**AVALIAÇÃO DA FORÇA DE UM PACOTE COMPOSTO COM DEFEITOS INTERNOS DE ACORDO COM VÁRIOS CRITÉRIOS DE FALHAS SOB A INFLUÊNCIA DE CARGA INDEPENDENTE**

*ASSESSMENT OF THE STRENGTH OF A COMPOSITE PACKAGE WITH INTERNAL DEFECTS ACCORDING TO VARIOUS FAILURES CRITERIA UNDER THE INFLUENCE OF UNSTEADY LOAD*

**Página – 1218**

**AVALIAÇÃO DOS EFEITOS DE MITIGAÇÃO DE *GLOMUS MOSSEAE* EM *TRITICUM AESTIVUM* L., CV. CHAMRAN SOB ESTRESSE SECA**

**EVALUATION OF MITIGATION EFFECTS OF *GLOMUS MOSSEAE* ON *TRITICUM AESTIVUM* L., CV. CHAMRAN UNDER DROUGHT STRESS**

**ارزیابی اثرات بهبود دهنده *GLOMUS MOSSEAE* روی *TRITICUM AESTIVUM* L., CV. CHAMRAN تحت تنش خشک**

BITARAF, Negin<sup>1</sup>; SAADATMAND, Sara\*<sup>2</sup>; MEHREGAN, Iraj<sup>3</sup>; AHMADVAND, Rahim<sup>4</sup>; EBADI, Mostafa<sup>5</sup>

<sup>1,4</sup>Islamic Azad University, Science and Research Branch, Faculty of Science, Biology Department

<sup>5</sup>Seed and Plant Improvement Institute, Agricultural Research, Education and Extension Organization

**Citation:** Bitaraf, N., Saadatmand, S., Mehregan, I., Ahmadvand, R and Ebadi, M. (2020). Evaluation of mitigation effects of *Glomus mosseae* on *Triticum aestivum* L., cv. Chamran under drought stress. Journal of Tchê Química, 17 (34): 1033-1145.

The affiliations of the authors are not in the correct order and affiliation of the last author is missing. The correct affiliations are as follows:

BITARAF, Negin<sup>1</sup>; SAADATMAND, Sara\*<sup>2</sup>; MEHREGAN, Iraj<sup>3</sup>; AHMADVAND, Rahim<sup>4</sup>; EBADI, Mostafa<sup>5</sup>

<sup>1,3</sup>Islamic Azad University, Science and Research Branch, Faculty of Science, Department of Biology, Iran

<sup>4</sup>Seed and Plant Improvement Institute, Agricultural Research, Education and Extension Organization, Iran

<sup>5</sup>Islamic Azad University, Damghan Branch, Faculty of Science, Department of Biology, Iran



## AVALIAÇÃO DE EFEITOS NEUROPROTETIVOS DE COMPOSTOS ALCALÓIDES

## ASSESSMENT OF NEUROPROTECTIVE EFFECTS OF ALKALOID COMPOUNDS

## ОЦЕНКА НЕЙРОПРОТЕКТОРНЫХ ЭФФЕКТОВ АЛКАЛОИДНЫХ СОЕДИНЕНИЙ

SEIDAKHMETOVA, Roza B.<sup>1\*</sup>; ARYSTAN, Leila I.<sup>2</sup>; MULDAEVA, Gulmira M.<sup>3</sup>;  
HAYDARGALIEVA, Leila S.<sup>4</sup>; NURMAGANBETOV, Zhangel'dy S.<sup>5</sup>;

<sup>1</sup> JSC "International Research and Production Holding "Phytochemistry", Laboratory of Pharmacology, Karaganda – Republic of Kazakhstan

<sup>2,3,4</sup> Karaganda Medical University, Department of Family Medicine, Karaganda – Republic of Kazakhstan

<sup>5</sup> Karaganda Medical University, Department of Biochemistry, Karaganda – Republic of Kazakhstan

\* Corresponding author  
e-mail: rozabat@mail.ru

Received 22 January 2020; received in revised form 20 March 2020; accepted 25 April 2020

### RESUMO

Os alcaloides beta-carbolina mostram uma ampla gama de efeitos psicofarmacológicos (por exemplo, alguns alcaloides beta-carbolina facilitam a transmissão dopaminérgica e interagem com os receptores dopaminérgicos D1 e D2 no corpo estriado). Este artigo apresenta dados sobre os efeitos neuroprotetores de compostos alcaloides usando métodos de simulação em computador, triagem virtual baseada em *docking* e farmacologia experimental. O objetivo do estudo foi investigar a ação neuroprotetora / protetora contra o estresse de novos derivados de compostos alcaloides usando os métodos de simulação computacional, triagem virtual baseada em *docking* e farmacologia experimental. Com o auxílio dos programas *ChemDraw* e *MGLTools*, foram utilizados os métodos de modelagem computacional das moléculas de derivados alcaloides, triagem virtual baseada em *docking*, receptor DRD2 e modelos tridimensionais das moléculas de ligantes. A energia de ligação de uma conformação individual foi usada como resultado final, o que mostra a força da interação entre o ligante e a molécula alvo. Foram estudados 22 compostos de alcaloides e seus derivados. A modelagem virtual de moléculas foi realizada para compostos e receptores, a ligação da molécula "ligante-alvo" foi realizada e os compostos candidatos foram selecionados. Estudos experimentais *in vivo* dos efeitos neuroprotetores desses compostos foram conduzidos no modelo de estresse emocional. Foram estudados os efeitos dos alcaloides harmina, norharmane e guanina no tempo de imobilidade no teste de natação forçada em camundongos, um modelo de depressão em animais. Um teste de natação forçada e um labirinto positivo elevado foram utilizados para determinar os efeitos antidepressivos e ansiolíticos da harmina em ratos. De acordo com os resultados do *docking*, as moléculas apresentadas de compostos alcaloides apresentaram interações com o receptor de dopamina D2. Os resultados obtidos no teste "Elevated Plus Maze (labirinto positivo elevado)" mostraram que os animais tratados com 9-metoxi-2-fenil-11H-indolisino [8,7-β] indol, lappaconitina e citisina na dose de 5 mg/kg, comparados em ratos do grupo controle, experimentaram uma ação ansiolítica (anti-ansiedade) no estresse emocional experimental.

**Palavras-chave:** beta-carbolina, teste de natação forçada, triagem virtual baseada em *docking*, atividade neurotrópica.

### ABSTRACT

Beta-carboline alkaloids show a wide range of psychopharmacological effects (for example, some beta-carboline alkaloids facilitate dopaminergic transmission and interact with dopaminergic receptors D1 and D2 in the striatum). This article presents data on neuroprotective effects of alkaloid compounds using computer simulation methods, docking-based virtual screening, and experimental pharmacology. The purpose of the study was to investigate the neuroprotective/stress-protective action of new derivatives of alkaloid compounds using the methods of computer simulation, docking-based virtual screening, and experimental pharmacology. Through *ChemDraw*, *MGLTools* programs, they have used computer modeling of the molecules of alkaloid derivatives, docking-based virtual screening, DRD2 receptor, and three-dimensional models of the ligand molecules. The binding energy of an individual conformation was used as a final result, which shows the strength of the interaction between the ligand and the target molecule. 22 compounds of alkaloids and their derivatives were studied. Virtual

molecule modeling was performed for compounds and receptors, "ligand-target" molecule docking was carried out, and candidate compounds were selected. *In vivo* experimental studies of the neuroprotective effects of these compounds were conducted in the emotional stress model. The effects of harmine, norharmane, and guanine alkaloids on immobility time in the forced swimming test in mice, a model of depression in animals, were studied. A forced swimming test and an elevated plus-maze were used to determine the antidepressant and anxiolytic effects of harmine in rats. According to the docking results, the presented molecules of alkaloid compounds showed interactions with dopamine receptor D2. The results obtained in the "Elevated Plus Maze" test showed that the animals treated with 9-methoxy-2-phenyl-11H-indolizino[8,7-β]indole, lappaconitine and cytisine at a dose of 5 mg/kg, compared to rats in the control group, experienced an anxiolytic (anti-anxiety) action in the experimental emotional stress.

**Keywords:** *beta-carboline, forced swimming test, docking-based virtual screening, neurotropic activity.*

## АННОТАЦИЯ

Бета-карболиновые алкалоиды проявляют широкий спектр психофармакологических эффектов (например, некоторые алкалоиды бета-карболина облегчают дофаминергическую передачу и взаимодействуют с дофаминергическими рецепторами D1 и D2 в полосатом теле). В этой статье представлены данные о нейропротекторном действии алкалоидных соединений с использованием методов компьютерного моделирования, виртуального скрининга на основе докинга и экспериментальной фармакологии. Цель исследования – изучение нейропротекторного/стресс-протекторного действия новых производных алкалоидных соединений с применением методов компьютерного моделирования, виртуального докинга и экспериментальной фармакологии. В ходе исследования использовались следующие методы: компьютерное моделирование молекул производных алкалоидов, виртуальный скрининг на основе докинга, рецептор DRD2, трехмерные модели молекул лигандов, которые были сконструированы с использованием программы ChemDraw с использованием набора программ. Autodock (Исследовательский институт Скриппса, США), MGLTools (Исследовательский институт Скриппса, США). В качестве конечного результата была использована энергия связи индивидуальной конформации, которая показывает силу взаимодействия между лигандом и молекулой-мишенью. Было изучено 22 соединения алкалоидов и их производных. Моделирование виртуальных молекул выполняли для соединений и рецепторов, проводили стыковку молекул «лиганд-мишень» и отбирали соединения-кандидаты. Экспериментальные исследования нейропротекторных эффектов этих соединений в естественных условиях проводились в модели эмоционального стресса. Исследовано влияние алкалоидов гуарена, норхармана и гуанина на время неподвижности в тесте принудительного плавания на мышах, модели депрессии на животных. Тест на принудительное плавание и лабиринт с повышенным уровнем плюс были использованы для определения антидепрессивного и анксиолитического действия гуанина у крыс. По результатам проведенного докинга установлено, что представленные молекулы алкалоидных соединений проявили взаимодействие с рецептором дофамин D2. Результаты, полученные в тесте «Приподнятый крестообразный лабиринт», показали, что в группе животных, получавших вещества 9-Метокси-2-фенил-11Н-индолизин [8,7-β] индол, лаппаконитин и цитизин в дозе 5 мг/кг по сравнению с крысами контрольной группы в условиях экспериментального эмоционального стресса, проявлялось анксиолитическое (противотревожное) действие.

**Ключевые слова:** *бета-карболин, тест принудительного плавания, виртуальный скрининг на основе докинга, нейротропная активность.*

## 1. INTRODUCTION:

Beta-carboline alkaloids show a wide range of psychopharmacological effects through binding to benzodiazepine, imidazoline, serotonin and opiate receptors, as well as monoamine oxidase (MAO) inhibition (Herraiz *et al.*, 2010; Liu *et al.*, 2017; Xiong *et al.*, 2018; Costanzi *et al.*, 2019). Neurochemical and behavioral studies have shown that some beta-carboline alkaloids facilitate dopaminergic transmission and interact with dopaminergic receptors D1 and D2 in the striatum (Farzin *et al.*, 2011; Li *et al.*, 2017; Ye *et*

*al.*, 2017; Liu *et al.*, 2019). Most beta-carboline alkaloids are known to be potent inhibitors that metabolize catecholamine neurotransmitters (Yonezawa *et al.*, 2011; Taborskaya *et al.*, 2017; Axen *et al.*, 2017; Moore *et al.*, 2018). Harmine, an indole alkaloid, shows antidepressant activity, interacting with MAO-A and several cell surface receptors, including serotonin 2A receptor (5-hydroxytryptamine receptor 2A, 5-HT2A) (Réus *et al.*, 2010; Nasehi *et al.*, 2018; Kwon *et al.*, 2018; Li *et al.*, 2018; Long *et al.*, 2019; Sun *et al.*, 2019).

The effects of harmine, norharmane, and guanine alkaloids on immobility time in the forced

swimming test (FST) in mice, a model of depression in animals, were studied. It was concluded that harmine, norharmane and guanine shorten immobility time in this test, suggesting an antidepressant effect, due to the inverse agonistic mechanism located in benzodiazepine receptors (Farzin and Mansouri, 2006; Dai *et al.*, 2018; Xi *et al.*, 2018). A forced swimming test (FST) and an elevated plus maze (EPM) were used to determine the antidepressant and anxiolytic effects of harmine in rats compared to a known antidepressant, imipramine (30 mg/kg ip). Administration of harmine resulted in a dose-dependent reduction of the immobility time in the FST and increased the time spent in the open arms in the EPM, compared to the group which received saline (dos Santos and Hallak, 2017; Herraiz and Guillén, 2018). Therefore, as an endogenous substance, it has anti-anxiety and anti-depressant effects (Arıcıoglu and Altunbas, 2003; Chen *et al.*, 2017; Wang *et al.*, 2018; Ferraz *et al.*, 2019).

Several potential molecular targets that have been identified for the central pharmacological effects of harmine include zinc-dependent kinases CDK (CDK1, 2 and 5), MAO-A, 5-HT<sub>2A</sub> sites, and imidazoline receptors I1 and I2. Harmine is a potent, double specific tyrosine phosphorylation inhibitor regulated by kinase (DYRK) (Song *et al.*, 2004; Egusa *et al.*, 2011; Ueda *et al.*, 2019). Harmine has been reported to show antidepressant effects in rodents (Réus *et al.*, 2012; Deng *et al.*, 2017; Zhang *et al.*, 2019). Harmine has anxiolytic, behavioral effects and antitumor potential both *in vitro* and *in vivo* (Hamsa and Kuttan, 2011; Cui *et al.*, 2019a). Harmine has a high inhibitory affinity to the kinase activity of DYRK1A, which indicates that harmine can modify tau phosphorylation (Frost *et al.*, 2011; Zhao *et al.*, 2019). Harmine also has a dual effect on the upstream potential of the atrial muscle (Carpentier, 1982). Also, a cytotoxic activity against human tumor cell lines has been reported in humans (Cao *et al.*, 2005; Freire *et al.*, 2018).

At the International Research and Production Holding "Phytochemistry" (Karaganda, Kazakhstan), a phytochemical study of an individual compound obtained from the roots of harmel peganum (*Peganum harmala* L.) growing in the southern regions of the Republic of Kazakhstan was carried out. Harmine, an indole alkaloid, was isolated and processed, and a water-soluble form, harmine hydrochloride, was synthesized. Studies of harmine hydrochloride pharmacological activity show edits potential antiparkinsonian activity (Turmukhambetov, 2009;

Turmukhambetov *et al.*, 2009). Further toxicological studies showed that harmine hydrochloride had no toxic effects on the internal organs or brain in a chronic three-month experiment in rats at the studied doses of 2.5 and 5 mg/kg (Lou *et al.*, 2017; Zhanaidarova *et al.*, 2019; Cui *et al.*, 2019b; Krüzselyi *et al.*, 2019).

The antiparkinsonian effects of harmine hydrochloride were studied in the experiments. To achieve this goal, the authors used haloperidol-induced catalepsy and MPTP-induced Parkinson's disease. It was found that harmine hydrochloride at a dose of 2.5 mg/kg eliminated haloperidol-induced catalepsy in rats and reduced hypokinesia and rigidity in the test for parkinsonism in C57BL/6 mice (Nurmaganbetov *et al.*, 2019). Based on the results, the search for new harmine derivatives with neuroprotective activity was continued.

The purpose of the study was to investigate the neuroprotective/stress-protective action of new derivatives of alkaloid compounds using the methods of computer simulation, docking-based virtual screening, and experimental pharmacology.

## 2. MATERIALS AND METHODS:

The following compounds were presented for the study: harmine N-oxide, 6-bromoharmine; 8-bromoharmine; 6,8-dibromoharmine; 6-iodoharmine; 6,8-dichloroharmine; 9-methoxy-2-phenyl-11*H*-indolisino[8,7- $\beta$ ]indole; 9-methoxy-2-(4-methoxyphenyl)-11*H*-indolisino[8,7- $\beta$ ]indole; 2-(3,4-dichlorophenyl)-9-methoxy-11*H*-indolisino[8,7- $\beta$ ]indole; 2-(4-methoxy-phenyl)-3,10-bis-formyl-11*H*-indolisino[8,7- $\beta$ ]indole; 3-acetyl-9-methoxy-2-phenyl-11*H*-indolisino[8,7- $\beta$ ]indole; 8-acetylharmine; 8-formylharmine; chalcone derivative of harmine; pyrazoline derivative of harmine; 4-methoxychalcone derivative of harmine; 4-methoxy-pyrazoline derivative of harmine; 2,4-dimethoxy-chalcone derivative of harmine; 2,4-dimethoxy-pyrazoline derivative of harmine; 2,3,4-trimethoxy-chalcone derivative of harmine; 2,3,4-trimethoxy-pyrazoline derivative of harmine; 2-F-chalcone derivative of harmine; 2-F-pyrazoline derivative of harmine.

Computer modeling of the molecules of alkaloid derivatives and docking-based virtual screening with an estimated biological target, DRD2 receptor, one of the five known types of dopamine receptors belonging to the class of D<sub>2</sub>-like receptors which inhibit adenylate cyclase, were performed (Arıcıoglu and Altunbas, 2003). Three-dimensional models of the ligand molecules were constructed using the ChemDraw program,

using a set of programs Autodock (The Scripps Research Institute, USA), MGLTools (The Scripps Research Institute, USA). The binding energy of an individual conformation was used as a final result, which shows the strength of the interaction between the ligand and the target molecule.

The experimental part was carried out following the "Rules of the European Convention for the Protection of Vertebrate Animals Used for Experimental and Other Scientific Purposes" (European Convention..., 1986) and under the requirements for the studies of new pharmacological substances in sexually mature rats (60 animals), equal amounts of females and males, with initial body weight of 240-370 g. The animals were kept in standard vivarium conditions on a regular diet and free access to water and food. Besides, general conditions of the animals were evaluated: changes in the animal's body weight, motor activity, appetite and reaction to external stimuli.

Emotional stress was modeled by placing the rats in tight plastic cylinders with their subsequent immersion in water to the neck level (20-22°C) for 2 hours daily for four days (Razueva *et al.*, 2014). The studied substances were administered to the animals at doses of 5 mg/kg for seven days before modeling emotional stress followed by a daily administration 1 hour before placing the animals in the plastic cylinders. Piracetam (JSC "BZMP", Republic of Belarus) was used as a reference drug, which was administered to the animals according to a similar scheme. All drugs were administered daily orally in the form of an aqueous solution at a dose of 1 ml/kg. The animals of the control and intact groups received purified water in the same volume.

On the fourth day after emotional stress modeling, the behavioral effects of the studied compounds were assessed using generally accepted methods in the following tests: "Open Field" and "Elevated Plus Maze" (Koplik *et al.*, 1995). Statistical processing of the results was carried out using the "Statistica 8.0" software package. The results are presented as "mean values  $\pm$  standard error of the mean". The differences were considered significant at a significance level of  $p < 0.05$ .

### 3. RESULTS AND DISCUSSION:

According to the docking results, the presented molecules of alkaloid compounds showed interactions with dopamine receptor D2. According to the docking results, the following alkaloid derivatives showed the maximum binding

to dopamine receptor D2: 9-methoxy-2-phenyl-11H-indolisino[8,7- $\beta$ ]indole (BE = -11.6); 2-(3,4-dichlorophenyl)-9-methoxy-11H-indolisino[8,7- $\beta$ ]indole (BE = -10.7); 2-F-chalcone derivative of harmine (BE = -10.7) (Table 1). The spatial structures of the ligands and a schematic representation of the ligand-target interactions are presented in Figures 1-3.

During the experiment to assess an *in vivo* neurotrophic activity, it was noted that body weight data in the rats from all groups remained within baseline parameters; there were no significant changes in body weight gain in the animals from all groups (Table 2).

Administration of the studied compounds, harmine, 8-acetylharminine, delcosine and lappaconitine, to rats reduced the number of entries into the closed arms; administration of 8-acetylharminine and lappaconitine increased the number of peeps. The number of leaning overincreased in the 8-acetylharminine and delcosine groups. The number of defecations and urinations decreased in the groups of 8-acetylharminine, ((E)-1-(7-methoxy-1-methyl-9H-pyrido[3,4-b]indole-8-yl)-3-(2,4-dimethoxyphenyl)prop-2-en-1-on, (E)-1-(7-methoxy-1-methyl-9H-pyrido[3,4-b]indole-8-yl)-3-(2-fluorophenyl)prop-2-en-1-on and echinopsine (Tables 3, 4).

According to the docking results, the following alkaloid derivatives showed the maximum binding to dopamine receptor D2: 9-methoxy-2-phenyl-11H-indolisino[8,7- $\beta$ ]indole (BE = -11.6); 2-(3,4-dichlorophenyl)-9-methoxy-11H-indolisino[8,7- $\beta$ ]indole (BE = -10.7); 2-F-chalcone derivative of harmine (BE = -10.7). This experimental study showed that indole alkaloids, 8-acetylharminine, 9-methoxy-2-phenyl-11H-indolisino[8,7- $\beta$ ]indole, diterpene alkaloid lappaconitine and cytosine at a dose of 5 mg/kg exhibit neurotropic effects, increase the levels of orientation and research activity, normalize emotional state and decrease anxiety and fear levels in animals.

### 4. CONCLUSIONS:

The results obtained in the "Elevated Plus Maze" test showed that the animals treated with 9-methoxy-2-phenyl-11H-indolisino[8,7- $\beta$ ]indole, lappaconitine and cytosine at a dose of 5 mg/kg, compared to rats in the control group, experienced an anxiolytic (anti-anxiety) action in the experimental emotional stress.

In particular, the time spent in the closed

arms was reduced by 23.9% in the lappaconitine group, by 12.5% in the 9-methoxy-2-phenyl-11H-indolisino[8,7- $\beta$ ]indole group, by 12.4% in the 8-acetylgermine group and by 5.6% in the cytosine group, compared to the control group. The time spent by the animals in the open arms increased by 78% in the 9-Methoxy-2-phenyl-11H-indolisino[8,7- $\beta$ ]indole group, by 76.4% in the lappaconitine group, by 76.1% in the 8-acetylgermine group and by 64.1% in the cytosine group, compared to the control group. The time spent on the central site increased by 37.8% in the lappaconitine group, compared to the control group.

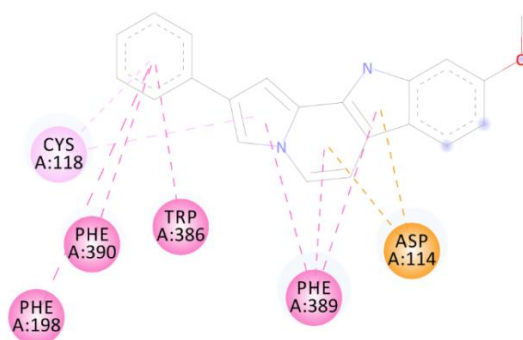
Therefore, 9-methoxy-2-phenyl-11H-indolisino[8,7- $\beta$ ]indole, which had the highest binding energy during ligand-target docking, is a candidate substance as a stress-protective agent for further in-depth studies, as well as indole alkaloids, 8-acetylgermine, 9-methoxy-2-phenyl-11H-indolisino[8,7- $\beta$ ]indole, and diterpene alkaloid lappaconitine, which showed an anxiolytic effect in the stress test.

## 5. REFERENCES:

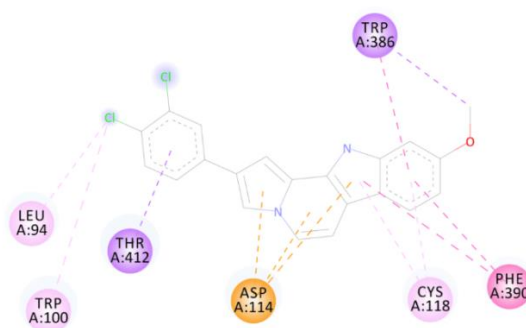
1. Aricioglu, F., Altunbas, H. *Annals of the New York Academy of Sciences*, **2003**, 1009, 196–201.
2. Axen, S.D., Huang, X.-P., Cáceres, E.L., Gendele, L., Roth, B.L., Keiser, M.J. *Journal of Medicinal Chemistry*, **2017**, 60(17), 7393–7409.
3. Cao, R., Peng, W., Chen, H., Ma, Y., Liu, X., Hou, X., Guan, H., Xu, A. *Biochemical and Biophysical Research Communications*, **2005**, 338(3), 1557–1563.
4. Carpentier, R.G. *British Journal of Pharmacology*, **1982**, 75(1), 207–212.
5. Costanzi, S., Cohen, A., Danfora, A., Dolatmoradi, M. *Journal of Chemical Information and Modeling*, **2019**, 59(7), 3177–3190.
6. Cui, G., Shu, B., Veeran, S., Yuan, H., Yi, X., Zhong, G. *Pesticide Biochemistry and Physiology*, **2019a**, 154, 67–77.
7. Cui, Y., Jiang, L., Yu, R., Shao, Y., Mei, L., Tao, Y. *Journal of Ethnopharmacology*, **2019b**, 243, article number 112096.
8. Chen, S., Feng, Z., Wang, Y., Ma, S., Hu, Z., Yang, P., Chai, Y., Xie, X. *Journal of Chemical Information and Modeling*, **2017**, 57(5), 1101–1111.
9. Dai, J., Dan, W., Schneider, U., Wang, J. *European Journal of Medicinal Chemistry*, **2018**, 157, 622–656.
10. Deng, Y., Wang, Q.-R., Wang, J.-H., Li, C.-H., Wang, X.-Z. *Chinese Traditional and Herbal Drugs*, **2017**, 48(11), 2353–2364.
11. dos Santos, R.G., Hallak, J.E.C. *Journal of Psychoactive Drugs*, **2017**, 49(1), 1–10.
12. Egusa, H., Doi, M., Saeki, M., Fukuyasu, S., Akashi, Y., Yokota, Y., Yatani, H., Kamisaki, Y. *Bone*, **2011**, 49(2), 264–274.
13. European Convention for the Protection of Vertebrate Animals Used for Experiments or for Other Scientific Purposes. **1986**. <https://rm.coe.int/168007a6a8>, accessed 20 December 2019.
14. Farzin, D., Haghparast, A., Motaman, S., Baryar, F., Mansouri, N. *Pharmacology Biochemistry and Behavior*, **2011**, 98(2), 215–219.
15. Farzin, D., Mansouri, N. *European Neuropsychopharmacology*, **2006**, 16(5), 324–328.
16. Ferraz, C.A.A., de Oliveira Júnior, R.G., Picot, L., da Silva Almeida, J.R.G., Nunes, X.P. *Fitoterapia*, **2019**, 137, article number 104196.
17. Freire, V.F., Silva, G.R., Yariwake, J.H. *Journal of the Brazilian Chemical Society*, **2018**, 29(4), 775–781.
18. Frost, D., Meechoovet, B., Wang, T., Gately, S., Giorgetti, M., Shcherbakova, I., Dunckley, T. *PLoS One*, **2011**, 6(5), article number e19264.
19. Hamsa, T.P., Kuttan, G. *Chinese Medicine*, **2011**, 6(1), 11.
20. Herraiz, T., González, D., Ancín-Azpilicueta, C., Arán, V.J., Guillén, H. *Food and Chemical Toxicology*, **2010**, 48(3), 839–845.
21. Herraiz, T., Guillén, H. *BioMed Research International*, **2018**, 2018, article number 4810394.
22. Koplik, E.V., Salieva, R.M., Gorbunova, A.V. *Journal of Higher Nervous Activity*, **1995**, 45(4), 775–781.
23. Krüzselyi, D., Vetter, J., Ott, P.G., Darcsi, A., Béni, S., Gömöry, Á., Drahos, L., Zsila, F., Móricz, Á.M. *Fitoterapia*, **2019**, 137, article number 104180.

24. Kwon, H.S., Lee, H., Lee, J.S., Lee, K., Choi, J.-H. *Archives of Pharmacal Research*, **2018**, 41(5), 513-518.
25. Li, S., Zhang, Y., Deng, G., Wang, Y., Qi, S., Cheng, X., Ma, Y., Xie, Y., Wang, C. *Frontiers in Pharmacology*, **2017**, 8(AUG), article number 541.
26. Li, S.-P., Wang, Y.-W., Qi, S.-L., Zhang, Y.-P., Deng, G., Ding, W.-Z., Ma, C., Lin, Q.-Y., Guan, H.-D., Liu, W., Cheng, X.-M., Wang, C.-H. *Frontiers in Pharmacology*, **2018**, 9(APR), article number 346.
27. Liu, F., Wu, J., Gong, Y., Wang, P., Zhu, L., Tong, L., Chen, X., Ling, Y., Huang, C. *Progress in Neuro-Psychopharmacology and Biological Psychiatry*, **2017**, 79, 258-267.
28. Liu, Y.-P., Guo, J.-M., Wang, X.-P., Liu, Y.-Y., Zhang, W., Wang, T., Qiang, L., Fu, Y.-H. *Bioorganic Chemistry*, **2019**, 92, article number 103278.
29. Long, S., Resende, D.I.S.P., Kijjoa, A., Silva, A.M.S., Fernandes, R., Xavier, C.P.R., Vasconcelos, M.H., Sousa, E., Pinto, M.M.M. *Molecules*, **2019**, 24(3), <https://www.mdpi.com/1420-3049/24/3/534>, accessed 21 December 2019.
30. Lou, L.-L., Liu, S., Yan, Z.-Y., Lin, B., Wang, X.-B., Huang, X.-X., Song, S.-J. *Phytochemistry Letters*, **2017**, 22, 107-112.
31. Moore, A., Beidler, J., Hong, M.Y. *Molecules*, **2018**, 23(9), article number 2197.
32. Nasehi, M., Shahini, F., Ebrahimi-Ghiri, M., Azarbayjani, M., Zarrindast, M.-R. *Physiology and Behavior*, **2018**, 194, 239-245.
33. Nurmaganbetov, Zh.S., Arystan, L.I., Muldaeva, G.M., Haydargalieva, L.S., Adekenov, S.M. *Pharmacological Reports*, **2019**, 71(6), 1050-1058.
34. Razueva, Ya.G., Kukharensko, N.S., Ivanova, Yu.L., Nikolaev, S.M., Verlan, N.V., Ubeeva, I.P. *Medical Journal*, **2014**, 6, 125-127.
35. Réus, G.Z., Stringari, R.B., de Souza, B., Petronilho, F., Dal-Pizzol, F., Hallak, J.E., Zuardi, A.W., Crippa, J.A., Quevedo, J. *Oxidative Medicine and Cellular Longevity*, **2010**, 3(5), 325-331.
36. Réus, G.Z., Stringari, R.B., Gonçalves, C.L., Scaini, G., Carvalho-Silva, M., Jeremias, G.C., Jeremias, I.C., Ferreira, G.K., Streck, E.L., Hallak, J.E., Zuardi, A.W., Crippa, J.A., Quevedo, J. *Depression Research and Treatment*, **2012**, 2012, article number 987397.
37. Song, Y., Kesuma, D., Wang, J., Deng, Y., Duan, J., Wang, J.H., Qi, R.Z. *Biochemical and Biophysical Research Communications*, **2004**, 317(1), 128-132.
38. Sun, Q., Liu, F., Sang, J., Lin, M., Ma, J., Xiao, X., Yan, S., Benjamin Naman, C., Wang, N., He, S., Yan, X., Cui, W., Liang, H. *Marine Drugs*, **2019**, 17(2), article number 121.
39. Taborskaya, K.I., Belinskaya, D.A., Avdonin, P.V., Goncharov, N.V. *Journal of Evolutionary Biochemistry and Physiology*, **2017**, 53(5), 384-393.
40. Turmukhambetov, A.Zh. *Alkaloids of plants of Kazakhstan. Isolation, chemical modification and biological activity*. Karaganda: Glasir, **2009**.
41. Turmukhambetov, A.Zh., Agedilova, M.T., Nurmaganbetov, J.S. *Chemistry of Natural Compounds*, **2009**, 4, 504-507.
42. Ueda, S., Ikeda, H., Namba, T., Ikejiri, Y., Nishimoto, Y., Arai, M., Nihira, T., Kitani, S. *Journal of Industrial Microbiology and Biotechnology*, **2019**, 46(5), 739-750.
43. Wang, Z.-X., Xiang, J.-C., Cheng, Y., Ma, J.-T., Wu, Y.-D., Wu, A.-X. *Journal of Organic Chemistry*, **2018**, 83(19), 12247-12254.
44. Xi, J., Zhang, Z., Zhu, Q., Zhong, G. *International Journal of Molecular Sciences*, **2018**, 19(12), article number 4044.
45. Xiong, H., Li, R.-R., Liu, S.-Y., Wu, F.-X., Yang, W.-C., Yang, G.-F. *ACS Applied Bio Materials*, **2018**, 1(2), 310-317.
46. Ye, Y., Zhang, B., Mao, R., Zhang, C., Wang, Y., Xing, J., Liu, Y.-C., Luo, X., Ding, H., Yang, Y., Zhou, B., Jiang, H., Chen, K., Luo, C., Zheng, M. *Organic and Biomolecular Chemistry*, **2017**, 15(17), 3648-3661.
47. Yonezawa, T., Hasegawa, S., Asai, M., Ninomiya, T., Sasaki, T., Cha, B.Y., Teruya, T., Ozawa, H., Yagasaki, K., Nagai, K., Woo, J.T. *European Journal of Pharmacology*, **2011**, 650(2-3), 511-518.
48. Zhanaidarova, G.U., Yessimova, R.Zh., Nurseitova, K.T., Seidakhmetova, R.B., Arystan, L.I., Adekenov, S.M., Nauryzov, N.N., Berikbaeva, B.Kh. *Bangladesh Journal of Medical Science*, **2019**, 18, 598-606.
49. Zhang, J., Wang, C.-X., Song, X.-J., Li, S., Fan, C.-L., Chen, G.-D., Hu, D., Yao, X.-S.,

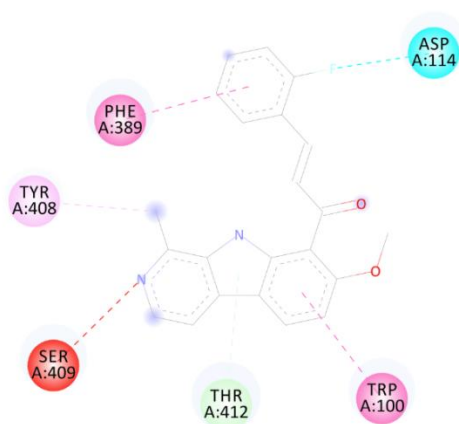
50. Zhao, W.-Y., Chen, J.-J., Zou, C.-X., Zhou, W.-Y., Yao, G.-D., Wang, X.-B., Lin, B.,



**Figure 1.** Interaction between 9-methoxy-2-phenyl-11H-indolizino[8,7-β]indole (Gar-13) and DRD2 receptor; BE = -11.6 kcal/mol<sup>1</sup>

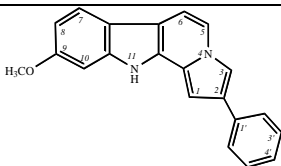
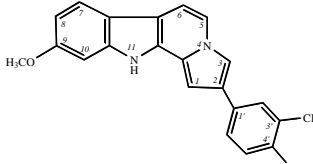
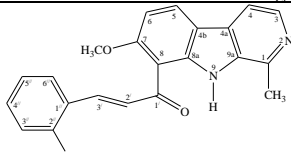
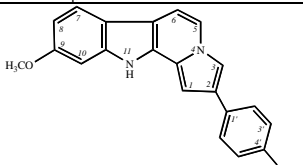
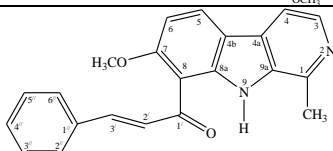
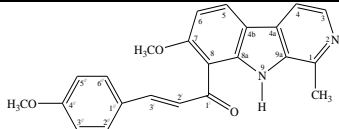
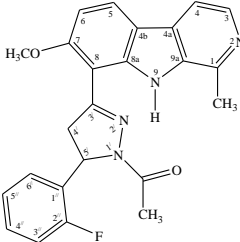
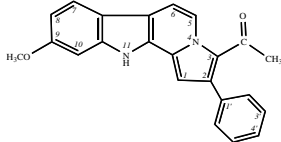
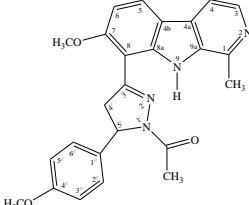
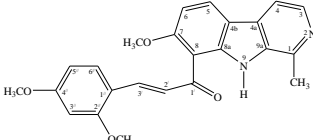


**Figure 2.** Interaction between 2-(3,4-dichlorophenyl)-9-methoxy-11H-indolizino[8,7-β]indole (Gar-17) and DRD2 receptor; BE = -10.7 kcal/mol<sup>1</sup>

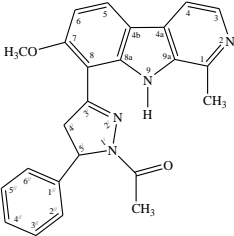
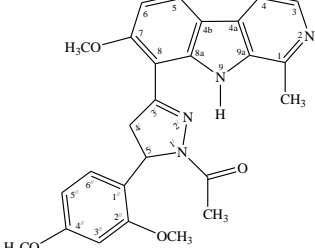
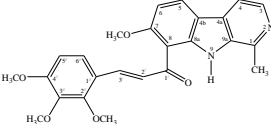
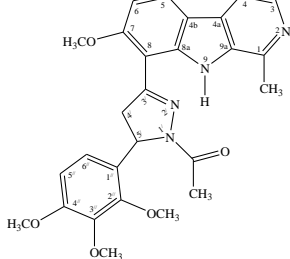
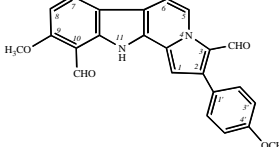
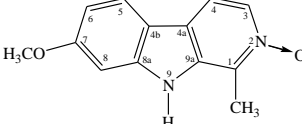
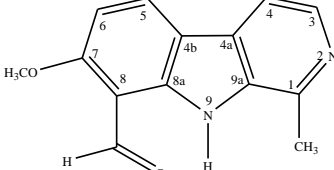
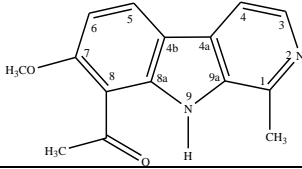
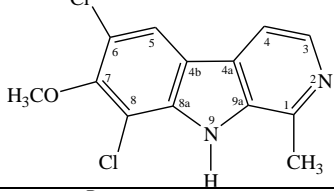
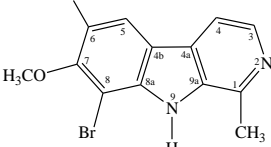


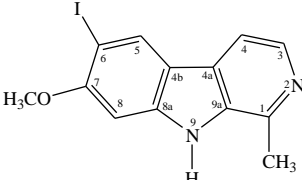
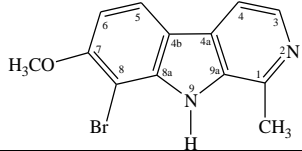
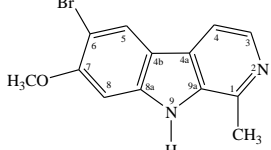
**Figure 3.** Interaction between 2-F-chalcone derivative of harmine (Gar-116) and DRD2 receptor; BE = -10.5 kcal/mol<sup>1</sup>

**Table 1.** The results of the interaction between the molecules of alkaloid compounds and DRD2 receptor

| Position | Name   | Code    | Chemical formula   | Binding Energy – kcal/mol <sup>-1</sup> |
|----------|--|---------|--|---|
| 1        | 9-methoxy-2-phenyl-11H-indolisino[8,7-β]indole<br>C <sub>21</sub> H <sub>16</sub> N <sub>2</sub> O                               | Gar-13  |    | -11.6                                   |
| 2        | 2-(3,4-dichlorophenyl)-9-methoxy-11H-indolisino[8,7-β]indole<br>C <sub>21</sub> H <sub>14</sub> Cl <sub>2</sub> N <sub>2</sub> O | Gar-17  |    | -10.7                                   |
| 3        | 2-F-chalcone derivative of harmine<br>C <sub>22</sub> H <sub>17</sub> FN <sub>2</sub> O <sub>2</sub>                             | Gar-116 |    | -10.5                                   |
| 4        | 9-methoxy-2-(4-methoxyphenyl)-11H-indolisino[8,7-β]indole<br>C <sub>22</sub> H <sub>18</sub> N <sub>2</sub> O <sub>2</sub>       | Gar-15  |   | -10.4                                   |
| 5        | Chalcone derivative of harmine<br>C <sub>22</sub> H <sub>18</sub> N <sub>2</sub> O <sub>2</sub>                                  | Gar-105 |  | -10.3                                   |
| 6        | 4-methoxychalcone derivative of harmine<br>C <sub>23</sub> H <sub>20</sub> N <sub>2</sub> O <sub>3</sub>                         | Gar-107 |  | -10.3                                   |
| 7        | 2-F-pyrazoline derivative of harmine<br>C <sub>24</sub> H <sub>21</sub> FN <sub>4</sub> O <sub>2</sub>                           | Gar-117 |  | -10.3                                   |
| 8        | 3-acetyl-9-methoxy-2-phenyl-11H-indolisino[8,7-β]indole<br>C <sub>23</sub> H <sub>18</sub> N <sub>2</sub> O <sub>2</sub>         | Gar-24  |  | -10.2                                   |
| 9        | 4-methoxy-pyrazoline derivative of harmine<br>C <sub>25</sub> H <sub>24</sub> N <sub>4</sub> O <sub>3</sub>                      | Gar-108 |  | -10.2                                   |
| 10       | 2,4-dimethoxy-chalcone derivative of harmine<br>C <sub>24</sub> H <sub>22</sub> N <sub>2</sub> O <sub>4</sub>                    | Gar-113 |  | -10.2                                   |



|    |  |           |  |      |
|----|--|-----------|--|------|
| 11 | Pyrazoline derivative of harmine<br>$C_{24}H_{22}N_4O_2$                                 | Gar-106   |    | -9.9 |
| 12 | 2,4-dimethoxy-pyrazoline derivative of harmine<br>$C_{26}H_{26}N_4O_4$                   | Gar-115   |    | -9.6 |
| 13 | 2,3,4-trimethoxy-chalcone derivative of harmine<br>$C_{25}H_{24}N_2O_5$                  | Gar-110   |    | -9.4 |
| 14 | 2,3,4-trimethoxy-pyrazoline derivative of harmine<br>$C_{27}H_{28}N_4O_5$                | Gar-111   |   | -8.6 |
| 15 | 2-(4-methoxy-phenyl)-3,10-bis-formyl-11H-indolisino[8,7-β]indole<br>$C_{24}H_{18}N_2O_4$ | Gar-23    |  | -8.5 |
| 16 | Harmine N-oxide<br>$C_{13}H_{12}N_2O_2$  | Gar-N-O   |  | -8.1 |
| 17 | 8-Formylharmine  | 8-FGar    |  | -7.5 |
| 18 | 8-Acetylharmine<br>$C_{15}H_{14}N_2O_2$  | 8-AcGar   |  | -7.4 |
| 19 | 6,8-Dichloroharmine<br>$C_{13}H_{10}Cl_2N_2O$  | Gar-6,8Cl |  | -7.4 |
| 20 | 6,8-Dibromoharmine<br>$C_{13}H_{10}Br_2N_2O$   | Gar-6,8Br |  | -7.3 |

|    |  |         |  |      |
|----|--|---------|--|------|
| 21 | 6-Iodoharmine<br>$C_{13}H_{11}IN_2O$   | Gar-6I  |  | -7.2 |
| 22 | 8-Bromoharmine<br>$C_{13}H_{11}BrN_2O$ | Gar-8Br |  | -7.2 |
| 23 | 6-Bromoharmine<br>$C_{13}H_{11}BrN_2O$ | Gar-6Br |  | -7.1 |

**Table 2.** Weight gain in rats

| Group  | Weight, g     |               |
|--|---------------|---------------|
|  | Before        | After         |
| Intact rats, n=6   | 296.3 ± 20.3* | 297.0 ± 20.8  |
| Control (no treatment) n=6   | 367.8 ± 8.5   | 373.3 ± 10.2  |
| Reference group (Piracetam) n=6  | 328.0 ± 12.0  | 324.5 ± 22.7  |
| Harmine (Gar), n=6   | 303.3 ± 53.0* | 307.3 ± 49.6* |
| 8-Acetylharminen=6   | 287.5 ± 18.6  | 291.3 ± 24.3  |
| 9-Methoxy-2-phenyl-11H-indolisino[8,7-β]indole   | 243.0 ± 10.2  | 241.8 ± 6.0*  |
| (E)-1-(7-Methoxy-1-methyl-9H-pyrido[3,4-b]indole-8-yl)-3-(2-fluorophenyl)prop-2-en-1-onn=6 | 287.5 ± 18.6  | 258.0 ± 32.3  |
| Delcosinen=6   | 295.3 ± 45.5  | 298.0 ± 47.6  |
| Lappaconitinen=6   | 298.0 ± 6.5   | 301.0 ± 7.7   |
| Cytisinen=6  | 245.0 ± 8.4*  | 243.3 ± 6.7*  |
| Echinopsinen=6   | 264.3 ± 26.2  | 262.3 ± 27.9  |

Note: \* – p < 0.05 compared to the control group, n – number of animals in the group.

**Table 3.** Effects of the studied compounds on behavior of the rats in the "Elevated Plus Maze" test

| Group   | Time spent in the closed arms, (sec.) | Time spent in the open arms, (sec.) | Number of entries into the closed arms, (n) | Number of entries into the open arms, (n) | Number of peeps, (n) |
|---|---------------------------------------|-------------------------------------|---|---|----------------------|
| Intact rats, n=6  | 59.5 ± 11.8*                          | 77.3 ± 19.3                         | 3.3 ± 1.9                                   | 1.5 ± 1.3                                 | 3.0 ± 2.4            |
| Control (no treatment) n=6  | 161.0 ± 15.6                          | 8.0 ± 1.2                           | 1.5 ± 0.6                                   | 2.0 ± 1.4                                 | 2.0 ± 2.3            |
| Reference group (Piracetam) n=6   | 152.0 ± 32.0                          | 20.5 ± 9.8                          | 0.8 ± 1.0                                   | 1.5 ± 0.6                                 | 5.0 ± 2.2            |
| Harmine (Gar), n=6  | 167.0 ± 8.7*                          | 13.0 ± 8.7                          | 1.5 ± 0.6                                   | 1.5 ± 0.6                                 | 0.3 ± 0.5            |
| 8-Acetylharminen=6  | 141.3 ± 40.1                          | 33.5 ± 15.4                         | 1.0 ± 0.8                                   | 1.3 ± 0.5                                 | 3.0 ± 3.2            |
| 9-Methoxy-2-phenyl-11H-indolisino[8,7-β]indole  | 140.8 ± 32.3*                         | 36.3 ± 17.9                         | 1.5 ± 0.6                                   | 2.0 ± 1.2                                 | 1.8 ± 1.0            |
| (E)-1-(7-Methoxy-1-methyl-9H-pyrido[3,4-b]indole-8-yl)-3-(2-fluorophenyl)prop-2-en-1-on n=6 | 167.5 ± 5.6*                          | 9.5 ± 3.9                           | 1.0 ± 0.0                                   | 1.3 ± 0.5                                 | 0.8 ± 1.0            |
| Delcosinen=6  | 164.5 ± 11.5                          | 9.8 ± 4.2                           | 1.3 ± 0.5                                   | 1.3 ± 1.0                                 | 1.8 ± 2.4            |
| Lappaconitinen=6  | 125.5 ± 80.4                          | 35.4 ± 10.8                         | 1.3 ± 0.5                                   | 1.5 ± 1.0                                 | 2.5 ± 1.3            |
| Cytisinen=6   | 152.0 ± 23.6*                         | 22.3 ± 6.3                          | 1.3 ± 0.5                                   | 2.0 ± 0.8                                 | 1.3 ± 0.5            |

|                |             |          |         |         |         |
|----------------|-------------|----------|---------|---------|---------|
| Echinopsinen=6 | 167.3±12.2* | 12.0±2.0 | 0.8±0.5 | 1.3±0.5 | 0.5±0.6 |
|----------------|-------------|----------|---------|---------|---------|

Note: \* – p <0.05 compared to the animals in the control group, n – number of animals in the group.

**Table 4.** Effects of the studied compounds on behavior of the rats in the "Elevated Plus Maze" test

| Group   | Number of leaning over, (n) | Number of stands, (n) | Time spent on the central site, (sec.) | Number of defecations | Number of urinations |
|---|-----------------------------|-----------------------|--|-----------------------|----------------------|
| Intact rats, n=6  | 9.0±2.1                     | 2.5±1.3               | 34.5±12.1                              | 1.3±0.5*              | 0.5±0.6              |
| Control (no treatment) n=6  | 2.5±2.1                     | 0                     | 11.5±8.3                               | 3.3±1.2               | 0.3±0.6              |
| Reference group (Piracetam) n=6   | 2.5±1.0                     | 0.3±0.5               | 6.3±2.3                                | 0                     | 0.3±0.5              |
| Harmine (Gar), n=6  | 1.8±1.7                     | 8.0±3.2               | 0.5±1.0                                | 0.3±0.5               | 0.3±0.5              |
| 8-Acetylharmin n=6  | 4.3±1.5                     | 0                     | 3.5±1.9                                | 0                     | 0.3±0.5              |
| 9-Methoxy-2-phenyl-11H-indolizino[8,7-β]indole  | 1.0±0.2                     | 0                     | 5.0±3.1                                | 0                     | 0.3±0.5              |
| (E)-1-(7-Methoxy-1-methyl-9H-pyrido[3,4-b]indole-8-yl)-3-(2-fluorophenyl)prop-2-en-1-on n=6 | 0.8±0.5                     | 0                     | 3.0±1.6                                | 0                     | 0                    |
| Delcosinen=6  | 3.0±2.2                     | 0                     | 5.3±2.2                                | 0.8±0.5               | 0.5±0.6              |
| Lappaconitinen=6  | 2.8±1.5                     | 0                     | 18.5±9.7                               | 0.3±0.5               | 0.3±0.5              |
| Cytisinen=6   | 2.5±1.7                     | 0                     | 1.3±0.10                               | 0.3±0.5               | 0.3±0.5              |
| Echinopsinen=6  | 3.3±1.8                     | 0                     | 0.8±0.10                               | 0                     | 0.3±0.5              |

Note: \* – p <0.05 compared to the animals of the control group, n – number of animals in the group.

## OTIMIZAÇÃO DA TECNOLOGIA DE PRODUÇÃO DE FERTILIZANTES NPK

## OPTIMIZATION OF AN NPK-FERTILIZER PRODUCTION TECHNOLOGY

## ОПТИМИЗАЦИЯ ТЕХНОЛОГИИ ПОЛУЧЕНИЯ NPK-УДОБРЕНИЯ

KYDYRALIYEVA, Aziza D.<sup>1\*</sup>; BESTEREKOV, Uilesbek<sup>2</sup>; BOLYSBEK, Aidarbek A.<sup>3</sup>;  
YESKENDIROVA, Marina M.<sup>4</sup>; URAKOV, Kinis N.<sup>5</sup>;

<sup>1,2,3,4,5</sup> M. Auezov South Kazakhstan State University, The Higher School of Chemical Engineering and Biotechnology, Department of Chemical Technology of Inorganic Substances, Shymkent – Republic of Kazakhstan

\* Correspondence author  
e-mail: aziza\_kydyralieva@mail.ru

Received 22 January 2020; received in revised form 20 March 2020; accepted 30 April 2020

### RESUMO

O nitrato de amônio é o fertilizante de nitrogênio mais comum e eficaz do mundo. No entanto, o nitrato de amônio tem uma desvantagem muito séria – o risco de incêndio e o risco de explosão, o que causa certas dificuldades e limitações tanto para seus consumidores quanto para seus fabricantes. O objetivo deste trabalho foi estudar a possibilidade de produzir os fertilizantes NPK com propriedades agroquímicas melhoradas e com uma proporção controlada de nutrientes N/P<sub>2</sub>O<sub>5</sub>/K<sub>2</sub>O, obtidos com base em uma solução de nitrato de amônio, rocha fosfática moída e cloreto de potássio. Os experimentos laboratoriais e industriais foram realizados usando um método de planejamento rotativo – o método de modelagem de segunda ordem Box-Hunter. O artigo apresenta os resultados de estudos sobre a regulação da proporção de nutrientes (N/(P<sub>2</sub>O<sub>5</sub> + K<sub>2</sub>O)) em fertilizantes contendo NPK, obtidos com base em uma solução de nitrato de amônio, rocha fosfática moída e cloreto de potássio. Foi estudada a influência de variáveis independentes – consumo específico de nitrato de amônio, fósforo moído e cloreto de potássio. Foi obtida uma equação de regressão adequada da influência desses fatores na proporção N/(P<sub>2</sub>O<sub>5</sub> + K<sub>2</sub>O) nos produtos finais. Os valores-limite do consumo específico de nitrato de amônio, fósforo moído e cloreto de potássio nas misturas iniciais foram encontrados, nos quais o conteúdo total de nutrientes nos produtos-alvo é de 30% a 33%, e o coeficiente N/(P<sub>2</sub>O<sub>5</sub> + K<sub>2</sub>O) possui um valor ótimo (1,14 - 3,50).

**Palavras-chave:** *nitrato de amônio, farinha fosfórica, cloreto de potássio, nutrientes, composição química.*

### ABSTRACT

Ammoniac saltpeter is the most widespread in the world and effective nitric fertilizer. However, ammonia saltpeter has a severe disadvantage – fire risk and explosion hazard that causes some difficulties and restrictions of both its consumers and its manufacturers. The purpose of the present work consisted in the studying the possibility of production of NPK-fertilizers with improved agrochemical properties and a controlled ratio of nutrients N/P<sub>2</sub>O<sub>5</sub>/K<sub>2</sub>O produced based on an ammonia saltpeter solution, ground phosphate rock, and potassium chloride. The laboratory and industrial experiments were continued using a rotatable planning method – the Box-Hunter second-order modeling technique. The article contains the research results on the regulation of nutritious elements (N/(P<sub>2</sub>O<sub>5</sub>+K<sub>2</sub>O)) ratios in the NPK-containing fertilizers produced based on an ammonia saltpeter solution, a ground phosphate rock, and potassium chloride. The effect of independent variables – specific consumptions of ammonia saltpeter, a ground phosphate rock, and potassium chloride – was studied. The adequate regression equation of influence of these factors on an N/(P<sub>2</sub>O<sub>5</sub>+K<sub>2</sub>O) ratio in the end products was obtained. Boundary values of the ammonia saltpeter, a ground phosphate rock and potassium chloride specific consumptions in the initial mixtures were found at which the total content of nutritious elements in the target products is from 30% to 33% and the N/(P<sub>2</sub>O<sub>5</sub>+K<sub>2</sub>O) ratio has the optimum value (1.14 - 3.50).

**Keywords:** *ammonium nitrate, phosphorus flour, potassium chloride, nutrients, chemical composition.*

### АННОТАЦИЯ

Аммиачная селитра является наиболее распространенным в мире и эффективным азотным

удобрением. Однако аммиачная селитра имеет очень серьезный недостаток – риск возникновения пожара и опасность взрыва, что вызывает определенные трудности и ограничения как у ее потребителей, так и у ее производителей. Цель настоящей работы состояла в изучении возможности получения NPK-удобрений с улучшенными агрохимическими свойствами и контролируемым соотношением питательных веществ  $N/P_2O_5/K_2O$ , получаемых на основе раствора аммиачной селитры, измельченной фосфоритовой породы и хлорида калия. Лабораторные и промышленные эксперименты были проведены с использованием вращающегося метода планирования – метода моделирования второго порядка Box-Hunter. В статье приведены результаты исследований по регулированию соотношений питательных элементов ( $N/(P_2O_5 + K_2O)$ ) в NPK-содержащих удобрениях, полученных на основе раствора аммиачной селитры, измельченной фосфатной породы и хлорида калия. Было изучено влияние независимых переменных – удельного расхода аммиачной селитры, молотого фосфорита и хлорида калия. Получено адекватное регрессионное уравнение влияния этих факторов на отношение  $N/(P_2O_5 + K_2O)$  в конечных продуктах. Найдены граничные значения удельных расходов аммиачной селитры, молотого фосфорита и хлорида калия в исходных смесях, при которых общее содержание питательных элементов в целевых продуктах составляет от 30% до 33%, а  $N/(P_2O_5 + K_2O)$  коэффициент имеет оптимальное значение (1,14 - 3,50).

**Ключевые слова:** аммиачная селитра, фосфорная мука, хлорид калия, питательные вещества, химический состав.

## 1. INTRODUCTION:

Ammoniac saltpeter is the most widespread in the world and effective nitric fertilizer (Ivanov *et al.*, 1990; Chernyshev *et al.*, 2009). It is used in agriculture for all kinds of crops and any types of soils (Maltas *et al.*, 2018; Besterekov *et al.*, 2019). However, ammonia saltpeter has a severe disadvantage – fire risk and explosion hazard that causes some difficulties and restrictions of both its consumers and its manufacturers (Oxley *et al.*, 2002; Dechy *et al.*, 2004; Lavrov and Shedov, 2004; Sinditskii *et al.*, 2005). For this reason, to obtain rich and qualitative harvests, it is necessary to apply balanced mineral fertilizers, i.e., containing nitrogen, phosphorus, potassium and other nutrients in reasonable ratios (Skydanenko *et al.*, 2017; Daitx *et al.*, 2019; Ramadhani *et al.*, 2019). These are so-called complex fertilizers whose major characteristic is their high agrochemical value (Abramov *et al.*, 2002; Levin and Sokolov, 2004; Pavlova, 2007; Ovchinnikov *et al.*, 2008; Akhmad *et al.*, 2018).

At present, there is a great demand for the fertilizers containing nitrogen, phosphorus and potassium that promotes numerous researches on introduction of phosphorus and potassium-containing components, be it natural minerals, the products obtained at their industrial processing or technogenic phosphorus and potassium-containing waste, in ammonia saltpeter melt (Belova and Ryabtseva, 2007; Dmitrieva and Ovchinnikov, 2007; Botirov and Beglov, 2008; Kiiski, 2009; Reymov *et al.*, 2013; Taran and Taran, 2016; Tugalukov *et al.*, 2017; Zhang *et al.*, 2018; Hirzel *et al.*, 2019; Yan *et al.*, 2019).

The only manufacturer of ammonia

saltpeter in the Republic of Kazakhstan is “KazAzot” JSC (Aktau, Kazakhstan). To solve the above-mentioned problem on the improvement of ammonia saltpeter agrochemical value and consumer properties, the own phosphate ores of the Republic of Kazakhstan can be successfully applied (Directory of deposits..., 2014). According to a draft proposal of the “KazAzot” JSC concerning to determination of new possibilities of improvement of agrochemical and consumer properties of ammonia saltpeter, the scientific personnel of the chair “Chemical technology of inorganic substances” of M. Auezov South Kazakhstan State University (Shymkent, Kazakhstan) (Official site..., 2019) has implemented the research on production of new NPK fertilizers on the basis of the following initial components: the ammonia saltpeter solution produced by “KazAzot” JSC, State Standard 2-2013; the ground phosphate rock of FM-2 grade (TS 930640000252-01-2011, 17% of  $P_2O_5$ ), produced by “Temir-service” LP (Aktyubinsk, Kazakhstan) from the Chilisay phosphorite (The mining company..., 2014); potassium chloride – the most available potassium salt – meeting to technical requirements 2184-048-00203944-2014. Under the agreement with the customer, the 64-71 % ammonia saltpeter solution obtained in accordance with the traditional ammonia saltpeter technology at the first evaporation stage was applied as the initial component. The agreed content of nitrogen, phosphorus pentoxide and potassium oxide in the end products were 10-28%, 2.5-10%, and 2.5-10%, respectively.

The purpose of the present work consisted in the studying the possibility of production of NPK-fertilizers with improved agrochemical properties and a controlled ratio of nutrients  $N/P_2O_5/K_2O$  produced based on an ammonia saltpeter

solution, ground phosphate rock and potassium chloride.

## 2. MATERIALS AND METHODS:

The research was carried out under the laboratory conditions of M. Auezov SKSU. The experimental results were tested at a trial plot of the operating ammonia saltpeter manufacture of "KazAzot" JSC. During the experiments, the individual volumes of 64-71% ammonia saltpeter solution with temperature of 110-130°C were mixed with calculated weights of the ground phosphate rock and potassium chloride (Dier *et al.*, 2018; Galliou *et al.*, 2018; Sigurnjak *et al.*, 2019). Insignificant quantities of a modifying mineral additive were also added in the mixture. The obtained suspension was carefully agitated and fed at the temperature of 120-130°C in sprayers of a granulating drum where the mixture was sprayed and dried by a direct-flow drying agent and granulated at the observance of technological parameters of the operating ammonia saltpeter manufacture (Ivanov *et al.*, 1990; Technological regulations..., 2012; Artyukhov and Ivaniia, 2017; Boyandin *et al.*, 2017; Gorbovskiy *et al.*, 2017; Lombardo *et al.*, 2017; Churov *et al.*, 2018; Rus *et al.*, 2019).

The analysis of composition and properties of the initial components and the obtained NPK-fertilizer samples was implemented according to the methods given in the standard documentation on the fertilizers:

- the total nitrogen content in the obtained NPK fertilizer according to State Standard 30181;
- the total and assimilable phosphorus pentoxide content ( $P_2O_5$ total,  $P_2O_5$ assim.) – in accordance with State Standard 20851.2-75;
- the potassium chloride mass fraction – in accordance with State Standard 20851;
- moisture content – in accordance with State Standard 20851.4;
- strength of the fertilizer granules on a device IPG-1M;
- pH on a device I-160 MI (Raposo *et al.*, 2017; Gezerman and Çorbacioğlu, 2017; Bamatov *et al.*, 2019; Macholdt *et al.*, 2019).

## 3. RESULTS AND DISCUSSION:

Tables 1 and 2 contain the results of the experimental research carried out at the laboratory and industrial conditions. Specific consumptions of the ammonia saltpeter, ground phosphate rock,

and potassium chloride were calculated in terms of 1 tonne of the target product.

First of all, the influence of specific consumptions of ammonia saltpeter, ground phosphate rock and potassium chloride, and also content of nutritious elements in them on the ratio of  $N/(P_2O_5+K_2O)$  in the target products was studied. The results of the research are represented in Figures 1-3.

As follows from the obtained results, the change of the  $N/(P_2O_5+K_2O)$  ratio in the products depends on two opposite processes: its growth at the increase in the nitrogen content, i.e. the specific ammonia saltpeter consumption, and its decrease at the increase in the phosphorus and potassium content, i.e., specific consumptions of the phosphorite and potassium chloride. In this connection, the further research was performed using a rotatable second-order experiment's planning technique (the Box-Hunter method) (Akhazarova and Kafarov, 1985; Zečević *et al.*, 2017; Silver *et al.*, 2018; Jameel and Al-Tai, 2017; Bijarniya *et al.*, 2019). The ratio of  $N/(P_2O_5+K_2O)$  in the product was the optimization parameter. Table 3 contains the information about domains of variation of the independent variables calculated based on data of Table 1. The experiments' planning matrix and results are represented in Table 4.

Using the data of Table 4 and (Inkov *et al.*, 2000) we obtained the regression equations of influence of ammonia saltpeter, phosphorite and potassium chloride amounts in the initial mixture on the  $N/(P_2O_5+K_2O)$  ratios in the coded and natural kinds (Equations. 1-2):

Determination of the coefficients in regression equation (2) was carried out using the Student's test, and the adequacy of the equation – using the Fisher's test. In our case, the Fisher's test tabular value makes 5.10, and its calculated value taking into account a 5% error of the experiment is 5.00. As  $F_{tab} > F_{cal}$ , the obtained regression equation is adequate. The experimental and calculated according to (2) values of  $N/(P_2O_5+K_2O)$  ratios in the NPK fertilizers produced are represented in Table 5.

On the basis of equation (2) using the MathCAD program (Ochkov, 2007) the 3D images of response surfaces of  $N/(P_2O_5+K_2O)_{nat} = f(AS, GPR \text{ at } KCl = \text{const} = 0.097; 0.063; 0.131; 0.154; 0.352 \text{ (according to data of Table 4)})$  and their horizontal sections were constructed (Figures 4-8).

Besides the  $N/(P_2O_5+K_2O)$  ratio, modern

fertilizers should meet the following requirements: the size of fertilizer's granules – 2-4 mm, their mass fraction – not less than 83-89%, the granules' strength – not more than 60 N/g. As follows from Table 2 data, these requirements are fulfilled if the  $N/(P_2O_5+K_2O)$  ratio  $\geq 1.14$ . Figures 1-5 show the areas *mnpj*, *xyzh*, *abcd*, *qwvf*, *rusk*, for which this ratio is 1,14-3.50.

Table 6 contains the information about the boundary values of optimization parameters and variable factors for  $N/(P_2O_5+K_2O) \geq 1.14$ .

As follows from Figures 1-5 and table 6, the least value of the optimization parameter – the  $N/(P_2O_5+K_2O)$  ratio – is characteristic for the technological area *rusk*. Therefore, the optimization of the process studied should be carried out within the *rusk* area. The values of technological parameters in the *rusk* area are represented in Table 7.

Judging by the data of Figure 5 and Table 7, the optimum values of ammonia saltpeter and ground phosphate rock specific consumptions at the maximum allowed particular potassium consumption chloride equal to 0.154 t and the  $N/(P_2O_5 + K_2O)$  ratio in the NPK-fertilizer obtained within 1.14-1.73 are situated on lines *ks* (ammonia saltpeter) and *su* (phosphorite). That is the specific consumption of ammonia saltpeter can change from 0.47 t to 0.71 t, and for the phosphorite – from 0.23 t to 0.47 t.

#### 4. CONCLUSIONS:

Based on the results obtained at the modeling the influence of ammonia saltpeter, ground phosphate rock and potassium chloride specific consumptions on the nutrients ( $N/(P_2O_5 + K_2O)$ ) ratio in the NPK-containing products it is possible to draw the following conclusions:

- the change of the  $N/(P_2O_5+K_2O)$  ratio in the target products depends on two opposite processes: its growth at the increase in the nitrogen content, i.e., the specific ammonia saltpeter consumption, and its decrease at the increase in the phosphorus and potassium content, i.e., specific consumptions of the phosphorite and potassium chloride;

- to produce the NPK-containing fertilizers of required quality and with the  $N/(P_2O_5 + K_2O)$  ratio within 1.14-3.50 based on the 64-71% ammonia saltpeter solution (State Standard 2-2013), the Chilisay ground phosphate rock of FM-2 grade (TS 930640000252-01-2011, 17% of  $P_2O_5$ ) and potassium chloride meeting to technical requirements 2184-048-00203944-2014, the

consumptions of the components should be maintained in the following limits: ammonia saltpeter – 0.4-0.71 t, Chilisay ground phosphate rock – 0.23-0.47 t, potassium chloride – 0.040-0.131 t. At the maximum allowed potassium chloride rate (0.154 t), the corresponding consumptions of ammonia saltpeter and Chilisay phosphorite are in the limits of 0.47-0.71 t and 0.23-0.47 t, respectively. In this case, it is possible to produce many nitrogen, phosphorus, and potassium-containing fertilizers in which the total content of nutritious elements will make: 33%; 32%; 31%; 30%; that convincingly enough prove their high agrochemical value.

#### 5. ACKNOWLEDGMENTS:

The authors are grateful to the management of the "KazAzot" JSC for the material, technical, and financial support of the research.

#### 6. REFERENCES:

1. Abramov, O.B., Afanasen, E.V., Vandyshev, S.A., Zakharova, O.M. Patent No. 2216526, Russian Federation, IPC C05B 11/06, C05B 11/04, C05G 1/00. *A method for producing complex NPK-fertilizer with an adjustable ratio of nutrients*. KCHKhK OJSC (RU), No. 2002125154/12, Declared September 19, 2002.
2. Akhmad, A., Dewi, W.S., Sagiman, S., Suntoro, S. *IOP Conference Series: Earth and Environmental Science*, **2018**, 142(1), article number 012078.
3. Akhnazarova, S.A., Kafarov, B.V. *Methods for optimizing an experiment in the chemical industry*. Moscow: Vysshaya shkola, **1985**.
4. Artyukhov, A.E., Ivaniia, A.V. *Naukovyi Visnyk Natsionalno Hirnychoho Universytetu*, **2017**, 6, 68-75.
5. Bamatov, I.M., Rumyantsev, E.V., Bamatov, D.M. *Journal of Physics: Conference Series*, **2019**, 1399(4), article number 044029.
6. Belova, N.P., Ryabtseva, I.Yu. *Obtaining complex fertilizer based on ammonium nitrate*. Stavropol: SevKavSTU, **2007**.
7. Besterekov, U., Yeskendirova, M.M., Kydyralieva, A.D., Bolysbek, A.A., Petropavlovskiy, I.A., Nazarbekova, S.P. *International Journal of Engineering Research and Technology*, **2019**, 12(12), 2964-2971.

8. Bijarniya, H., Khura, T.K., Mani, I., Kushwaha, H.L., Lande, S.D., Sarkar, S.K. *Indian Journal of Agricultural Sciences*, **2019**, 89(1), 22-27.
9. Botirov, B.B., Beglov, B.M. *Control and Management*, **2008**, 6, 12-24.
10. Boyandin, A.N., Kazantseva, E.A., Varygina, D.E., Volova, T.G. *Journal of Agricultural and Food Chemistry*, **2017**, 65(32), 6745-6752.
11. Chernyshev, A.K., Levin, B.V., Tugolukov, A.V., Ogarkov, A.A., Iljin, V.A. *Ammonium nitrate: Properties, Production, and Application*. Moscow: INFOKHIM, **2009**.
12. Churov, V.A., Sidorchik, V.A., Kupreichik, S.N., Shcherbich, A.V. *Gornyi Zhurnal*, **2018**, 8, 109-112.
13. Daitx, T.S., Giovanela, M., Carli, L.N., Mauler, R.S. *Polymers for Advanced Technologies*, **2019**, 30(3), 631-639.
14. Dechy, N., Bourdeaux, T., Ayrault, N., Kordek, M., Le Coze, J. *AZF Plant*, **2004**, 111(1-3), 131-138.
15. Dier, M., Meinen, R., Erbs, M., Kollhorst, L., Baillie, C.-K., Kaufholdt, D., Kücke, M., Weigel, H.-J., Zörb, C., Hänsch, R., Manderscheid, R. *Global Change Biology*, **2018**, 24(1), e40-e54.
16. Directory of deposits of Kazakhstan, **2014**, <http://info.geology.gov.kz/ru/informatsiya/spravochnik-mestorozhdenij-kazakhstana>, accessed 21 November 2019
17. Dmitrieva, O.A., Ovchinnikov, V.M. *New technologies for the production of fertilizers based on ammonium nitrate at EuroChem Chemical and Chemical Complex OJSC Nevinnomysskaya Azot*. Stavropol: SevKavSTU, **2007**.
18. Gallioui, F., Markakis, N., Fountoulakis, M.S., Nikolaidis, N., Manios, T. *Waste Management*, **2018**, 75, 305-311.
19. Gezerman, A.O., Çorbacioğlu, B.D. *International Journal of Energetic Materials and Chemical Propulsion*, **2017**, 16(4), 295-307.
20. Gorbovskiy, K., Kazakov, A., Norov, A., Malyavin, A., Mikhaylichenko, A. *International Journal of Industrial Chemistry*, **2017**, 8(3), 315-327.
21. Hirzel, J., Donnay, D., Fernández, C., Meier, S., Lagos, O., Mejias-Barrera, P., Rodríguez, F. *Biological Agriculture and Horticulture*, **2019**, 35(3), 197-213.
22. Inkov, A.M., Tapalov, T., Umbetov, U.U., Hu Ven Price, V., Akhmetova, K.T., Dyakova, E.T. *Optimization methods*. Shymkent: SKSU, **2000**.
23. Ivanov, M.E., Olevskii, V.M., Polyakov, N.N., Strizhevskii, I.I., Ferd, M.L., Tsekhanskaya, Yu.V. *Ammonium Nitrate Production Technology*. Moscow: Khimiya, **1990**.
24. Jameel, D.A., Al-Tai, A.A.S. *Journal of Global Pharma Technology*, **2017**, 9(12), 341-348.
25. Kiiski, H. *Properties of ammonium nitrate based fertilizers*. Helsinki: University of Helsinki, **2009**.
26. Lavrov, V.V., Shedov, K.K. *INFOKHIM*, **2004**, 2, 44-49.
27. Levin, B.V., Sokolov, A.N. *World series: N, P and K*, **2004**, 2, 13-21.
28. Lombardo, S., Pandino, G., Mauromicale, G. *Food Research International*, **2017**, 100, 95-99.
29. Macholdt, J., Piepho, H.-P., Honermeier, B. *European Journal of Agronomy*, **2019**, 102, 14-22.
30. Maltas, A., Kebli, H., Oberholzer, H.R., Weisskopf, P., Sinaj, S. *Land Degradation and Development*, **2018**, 29(4), 926-938.
31. Ochkov, V.F. *Mathcad 14 for students, engineers, and designers*. St. Petersburg: BKHV-Peterburg, **2007**.
32. Official site of LP "Kazazot", **2019**, <http://kazazot.kz>, accessed 22 November 2019.
33. Ovchinnikov, L.N., Tyurenkin, S.V., Korolyov, D.A. *News of Higher Educational Institutions*, **2008**, 51, 96-98.
34. Oxley, J., Smith, J., Rogers, E., Yu, M. *Thermochim Acta*, **2002**, 384(1), 23-45.
35. Pavlova, G.S. *Machinery and Equipment for the Village*, **2007**, 2, 6-10.
36. Ramadhani, I., Suliasih Widawati, S., Sudiana, I.M., Kobayashi, M. *IOP Conference Series: Earth and Environmental Science*, **2019**, 308(1), article number 012045.
37. Raposo, S., Constantino, A., Rodrigues, F., Rodrigues, B., Lima-Costa, M.E. *Applied*



- Biochemistry and Biotechnology*, **2017**, 181(2), 827-843.
38. Reymov, A.M., Namazov, Sh.S., Beglov, B.M. *Journal of Chemical Technology and Metallurgy*, **2013**, 48(4), 391-395
  39. Rus, D.C., Gabriel, V., Kovacs, A., Jan Gheorghiosu, E., Jitea, I.C. *International Multidisciplinary Scientific GeoConference Surveying Geology and Mining Ecology Management, SGEM*, **2019**, 19(1.3), 293-300.
  40. Sigmundjak, I., Brienza, C., Snauwaert, E., De Dobbelaere, A., De Mey, J., Vaneeckhaute, C., Michels, E., Schoumans, O., Adani, F., Meers, E. *Waste Management*, **2019**, 89, 265-274.
  41. Silver, M., Knöller, K., Schlögl, J., Kübeck, C., Schüth, C. *Applied Geochemistry*, **2018**, 97, 71-80.
  42. Sinditskii, V.P., Egorshv, V.Yu., Levshenkov, A.I., Serushkin, V.V. *Propellants, Explosives, Pyrotechnics*, **2005**, 4, 269-280
  43. Skydanenko, M., Sklabinskyi, V., Saleh, S., Barghi, S. *Processes*, **2017**, 5(3), article number 37.
  44. Taran, Yu.A., Taran, A.V. *University News. Chemistry and Chemical Technology*, **2016**, 59(3), 49-54.
  45. Technological regulations for the production of ammonium nitrate, **2012**, [https://studwood.ru/1106062/matematika\\_himiya\\_fizika/tehnologiya\\_proizvodstva\\_ammiachnoy\\_selitry](https://studwood.ru/1106062/matematika_himiya_fizika/tehnologiya_proizvodstva_ammiachnoy_selitry), accessed 21 November 2019.
  46. The mining company "Temir-Service" LLP, **2014**, <https://temir-servis.satu.kz/>, accessed 20 November 2019.
  47. Tugalukov, A.V., Valyshev, D.V., Elin, O.L., Lekhotsky, P. Patent No. 2626947 Russia, IPC CO5C 1/100 (2006.01), CO5G 1/100 (2006.01), A01P 21/00 (2006/01). *Phosphorus potassium-nitrogen-containing NPK fertilizers and a method for producing granular phosphocalium-nitrogen-containing NPK fertilizers: EuroChem MCC*, (105064, Moscow, PO Box 88, OOO Patent Attorneys Kvashnin, Sapelnikov and Partners). No. 2016107776: Stated 03.03.2016; Published on August 2, **2017**.
  48. Yan, L., Xu, X., Xia, J. *Science of the Total Environment*, **2019**, 686, 1010-1018.
  49. Zečević, N., Ljubičić, M., Bjelić, J., Lisac, H., Valkov, S. *Kemija u industriji/Journal of Chemists and Chemical Engineers*, **2017**, 66(9-10), 457-466.
  50. Zhang, W., Jiang, L., Xu, C., He, X., Geng, Z. *International Journal of Agriculture and Biology*, **2018**, 20(7), 1555-1561.

$$N/(P_2O_5+K_2O)_{\text{cod}} = 4.449 \cdot Z_1^2 - 0.3251 \cdot Z_1 \cdot Z_2 - 26.631 \cdot Z_1 \cdot Z_3 + 1.362 \cdot Z_1 - 2.189 \cdot Z_2^2 + 8.07 \cdot Z_2 \cdot Z_3 - 0.722 \cdot Z_2 + 47.803 \cdot Z_3^2 - 7.214 \cdot Z_3 + 1.462 \quad (\text{Eq. 1})$$

$$N/(P_2O_5+K_2O)_{\text{nat}} = 1.462 + 1.362 \cdot AC - 0.722 \cdot \Phi M - 7.214 \cdot KCl + 4.449 \cdot AC^2 - 2.189 \cdot \Phi M^2 + 47.803 \cdot KCl^2 - 0.3251 \cdot AC \cdot \Phi M - 26.631 \cdot AC \cdot KCl + 8.07 \cdot \Phi M \cdot KCl \quad (\text{Eq. 2})$$

**Table 1.** Specific consumptions of the initial components, contents and ratios of nutrients in the end products

| Fertilizer sample | Specific consumption, tonne |                               |                             | Content of a nutrient (N, P <sub>2</sub> O <sub>5</sub> , K <sub>2</sub> O) in the end product, % | Ratio of the nutrients (N/P <sub>2</sub> O <sub>5</sub> /K <sub>2</sub> O) in the end product |
|-------------------|-----------------------------|-------------------------------|-----------------------------|---|---|
|                   | Ammonia saltpeter, t (AS)   | Ground phosphate rock, t(GPR) | Potassium chloride, t (KCl) |   |   |
| 1                 | 0.814                       | 0.146                         | 0.040                       | 28.0/2.5/2.5  | 11.2/1/1  |
| 2                 | 0.639                       | 0.283                         | 0.078                       | 22.0/5.0/5.0  | 4.4/1/1   |
| 3                 | 0.553                       | 0.351                         | 0.096                       | 19.0/6.0/6.0  | 3.1/1/1   |
| 4                 | 0.466                       | 0.412                         | 0.113                       | 16.0/7.0/7.0  | 2.28/1/1  |
| 5                 | 0.437                       | 0.442                         | 0.121                       | 15.0/7.5/7.5  | 2.00/1/1  |
| 6                 | 0.290                       | 0.557                         | 0.153                       | 10.0/10.0/10.0  | 1.05/1/1  |

**Table 2.** Basic physical and chemical properties of the fertilizers obtained

| Fertilizer sample | pH of the 10 % solution | Humidity of the product, % | Strength of the fertilizer granules, N/g | The ratio in the end product                      |   | Mass fraction of 2-4 mm granules in the end product, mass % |
|-------------------|-------------------------|----------------------------|--|---|---|---|
|                   |                         |                            |  | N:P <sub>2</sub> O <sub>5</sub> :K <sub>2</sub> O | N/(P <sub>2</sub> O <sub>5</sub> +K <sub>2</sub> O) |   |
| 1                 | 6.38                    | 0.17                       | 50.58                                    | 11.2:1:1  | 5.60  | 85-95   |
| 2                 | 6.40                    | 0.17                       | 55.70                                    | 4.4:1:1   | 2.20  | 85-94   |
| 3                 | 6.47                    | 0.17                       | 58.68                                    | 3.1:1:1   | 1.50  | 84-89   |
| 4                 | 6.50                    | 0.15                       | 60.65                                    | 2.28:1:1  | 1.14  | 83-89   |
| 5                 | 6.55                    | 0.16                       | 62.47                                    | 2.00:1:1  | 1.00  | 81-88   |
| 6                 | 6.65                    | 0.15                       | 66.15                                    | 1.05:1:1  | 0.52  | 78-80   |

**Table 3.** Variation intervals of the variables

| Variation interval | Variables                |                                      |  |                        |
|--------------------|--------------------------|--------------------------------------|--|------------------------|
|                    | Code kind X <sub>i</sub> | Natural kind                         |  |                        |
|                    |                          | Ammonia saltpeter consumption, tonne | Ground phosphate rock consumption, tonne | KCl consumption, tonne |
| Basic level        | 0                        | 0.552                                | 0.352                                    | 0.097                  |
| Variation interval | Δ                        | 0.156                                | 0.123                                    | 0.034                  |
| Upper level        | +1                       | 0.708                                | 0.475                                    | 0.131                  |
| Lower level        | -1                       | 0.396                                | 0.229                                    | 0.063                  |
| Upper star arm     | +1.68                    | 0.814                                | 0.557                                    | 0.153                  |
| Lower star arm     | -1.68                    | 0.290                                | 0.146                                    | 0.040                  |

**Table 4.** The planning matrix and results of studying the effect of ammonia saltpeter, ground phosphate rock and potassium chloride in the initial mixture on the nutrients' ratio in the end products

| No. | Variables      |                |                |           |            |            | N/(P <sub>2</sub> O <sub>5</sub> +K <sub>2</sub> O)<br>ratio in the<br>fertilizer |
|-----|----------------|----------------|----------------|-----------|------------|------------|---|
|     | Code kind      |                |                | Code kind |            |            |   |
|     | X <sub>1</sub> | X <sub>2</sub> | X <sub>3</sub> | AS, tonne | GPR, tonne | KCl, tonne |   |
| 1   | +1             | +1             | +1             | 0.708     | 0.475      | 0.131      | 1.50  |
| 2   | -1             | +1             | +1             | 0.396     | 0.475      | 0.131      | 0.84  |
| 3   | +1             | -1             | +1             | 0.708     | 0.229      | 0.131      | 2.00  |
| 4   | -1             | -1             | +1             | 0.396     | 0.229      | 0.131      | 1.18  |
| 5   | +1             | +1             | -1             | 0.708     | 0.475      | 0.063      | 2.50  |
| 6   | -1             | +1             | -1             | 0.396     | 0.475      | 0.063      | 1.14  |
| 7   | +1             | -1             | -1             | 0.708     | 0.229      | 0.063      | 3.00  |
| 8   | -1             | -1             | -1             | 0.396     | 0.229      | 0.063      | 1.75  |
| 9   | +1.68          | 0              | 0              | 0.814     | 0.352      | 0.097      | 2.90  |
| 10  | -1.68          | 0              | 0              | 0.290     | 0.352      | 0.097      | 0.80  |
| 11  | 0              | +1.68          | 0              | 0.552     | 0.557      | 0.097      | 1.20  |
| 12  | 0              | -1.68          | 0              | 0.552     | 0.146      | 0.097      | 1.70  |
| 13  | 0              | 0              | +1.68          | 0.552     | 0.352      | 0.153      | 1.20  |
| 14  | 0              | 0              | -1.68          | 0.552     | 0.352      | 0.040      | 2.20  |
| 15  | 0              | 0              | 0              | 0.552     | 0.352      | 0.097      | 1.58  |
| 16  | 0              | 0              | 0              | 0.552     | 0.352      | 0.097      | 1.68  |
| 17  | 0              | 0              | 0              | 0.552     | 0.352      | 0.097      | 1.65  |
| 18  | 0              | 0              | 0              | 0.552     | 0.352      | 0.097      | 1.55  |
| 19  | 0              | 0              | 0              | 0.552     | 0.352      | 0.097      | 1.53  |
| 20  | 0              | 0              | 0              | 0.552     | 0.352      | 0.097      | 1.52  |

**Table 5.** Comparative data of experimental and calculated values of nutrients ratios in the NPK-fertilizers

| No. | N/(P <sub>2</sub> O <sub>5</sub> +K <sub>2</sub> O) experimental | N/(P <sub>2</sub> O <sub>5</sub> +K <sub>2</sub> O) calculated | Error, % |
|-----|--|--|----------|
| 1   | 1.50   | 1.62   | -7.87    |
| 2   | 0.84   | 0.79   | 5.09     |
| 3   | 2.00   | 1.97   | 1.42     |
| 4   | 1.18   | 1.12   | 4.59     |
| 5   | 2.50   | 2.49   | 0.02     |
| 6   | 1.14   | 1.11   | 2.32     |
| 7   | 3.00   | 2.99   | 0.40     |
| 8   | 1.75   | 1.58   | 9.88     |
| 9   | 2.90   | 2.83   | 2.57     |
| 10  | 0.80   | 0.95   | -18.62   |
| 11  | 1.20   | 1.14   | 4.70     |
| 12  | 1.70   | 1.83   | -7.69    |
| 13  | 1.20   | 1.18   | 1.93     |
| 14  | 2.20   | 2.29   | -4.44    |
| 15  | 1.58   | 1.58   | -0.06    |
| 16  | 1.68   | 1.58   | 5.90     |
| 17  | 1.65   | 1.58   | 4.19     |
| 18  | 1.55   | 1.58   | -2.00    |
| 19  | 1.53   | 1.58   | -3.33    |
| 20  | 1.52   | 1.58   | -4.01    |

**Table 6.** Boundary values of optimization parameters and variable factors

| Technological area | AS specific consumption, t | Phosphorite specific consumption, t | KCl specific consumption, t | Optimization parameter N/(P <sub>2</sub> O <sub>5</sub> +K <sub>2</sub> O) |
|--------------------|----------------------------|-------------------------------------|-----------------------------|--|
| mpj                | 0.4-0.71                   | 0.23-0.47                           | 0.040                       | 1.30-3.50  |
| xyzh               | 0.4-0.71                   | 0.23-0.47                           | 0.063                       | 1.15-3.00  |
| abcd               | 0.4-0.71                   | 0.34-0.47                           | 0.097                       | 1.14-2.43  |
| qwvf               | 0.41-0.71                  | 0.23-0.47                           | 0.131                       | 1.14-1.95  |
| rusk               | 0.47-0.71                  | 0.23-0.47                           | 0.154                       | 1.14-1.73  |

**Table 7.** Ranges of technological parameters in the rusk area (Figure 5)

| Points in Figure 5 | Ammonia saltpeter specific consumption, t | Ground phosphate rock specific consumption, t | KCl specific consumption, t | N/(P <sub>2</sub> O <sub>5</sub> + K <sub>2</sub> O) ratio in the end product |
|--------------------|---|---|-----------------------------|---|
| r                  | 0.61                                      | 0.47  | 0.154                       | 1.14  |
| u                  | 0.71                                      | 0.47  | 0.154                       | 1.40  |
| s                  | 0.71                                      | 0.23  | 0.154                       | 1.73  |
| k                  | 0.47                                      | 0.23  | 0.154                       | 1.14  |

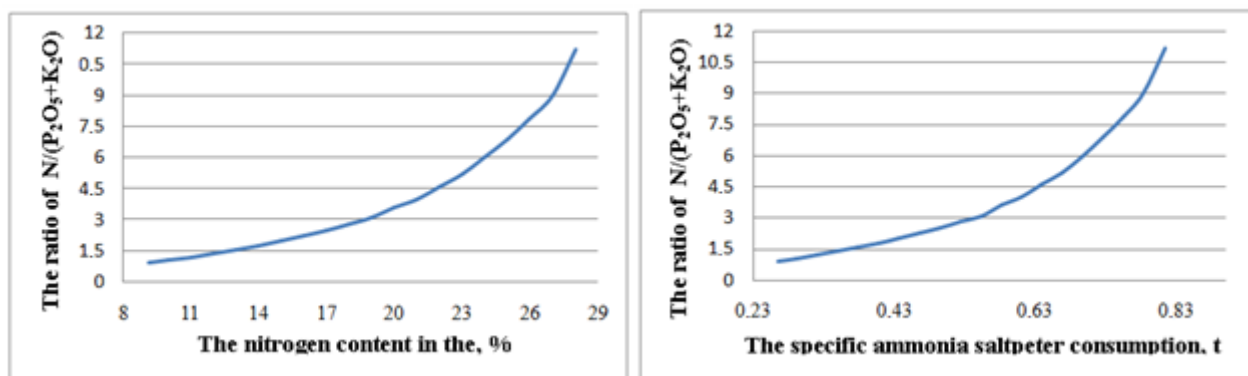


**Figure 1.** Change of the ratio of  $N/(P_2O_5+K_2O)$  in the end product depending on the nitrogen content and specific consumption of ammonia salt peter

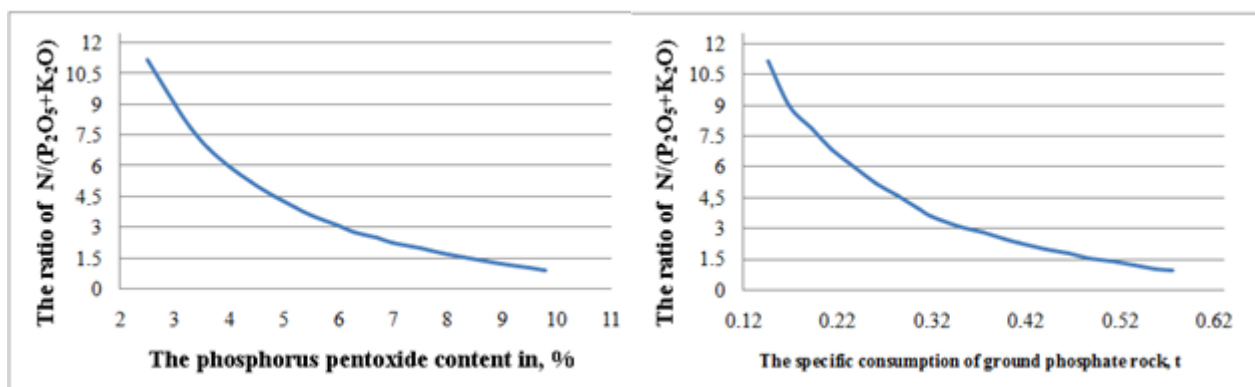


**Figure 2.** Change of the ratio of  $N/(P_2O_5+K_2O)$  in the end product depending on the phosphorus pentoxide content and specific consumption of ground phosphate rock

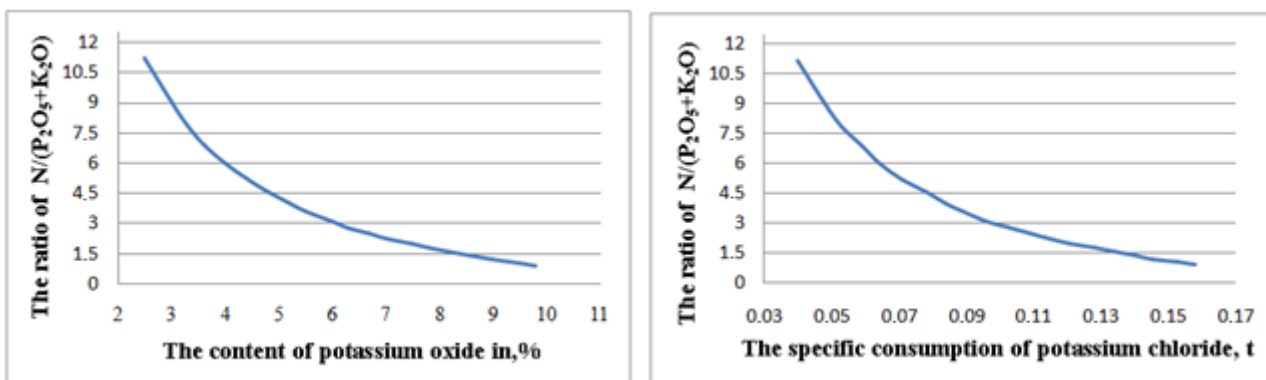


**Figure 3.** Change of the ratio of  $N/(P_2O_5+K_2O)$  in the end product depending on the potassium oxide content and specific consumption of potassium chloride

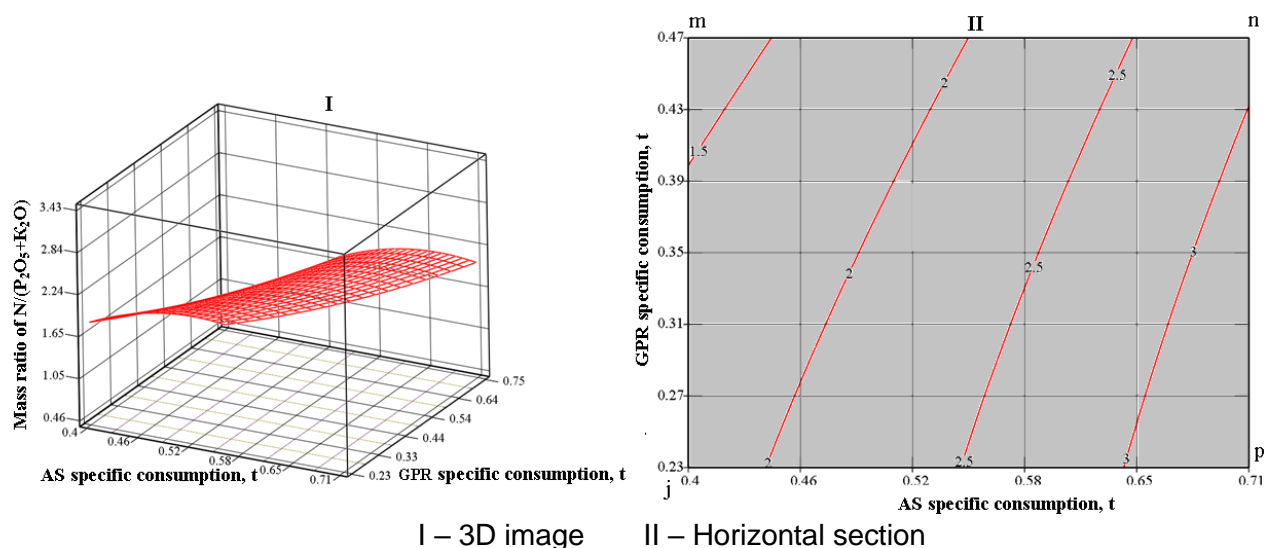


**Figure 4.** Influence of the ammonia salt peter and ground phosphate rock rates on the  $N/(P_2O_5+K_2O)$  ratio in the target product at  $KCl = 0.04 \text{ t}$

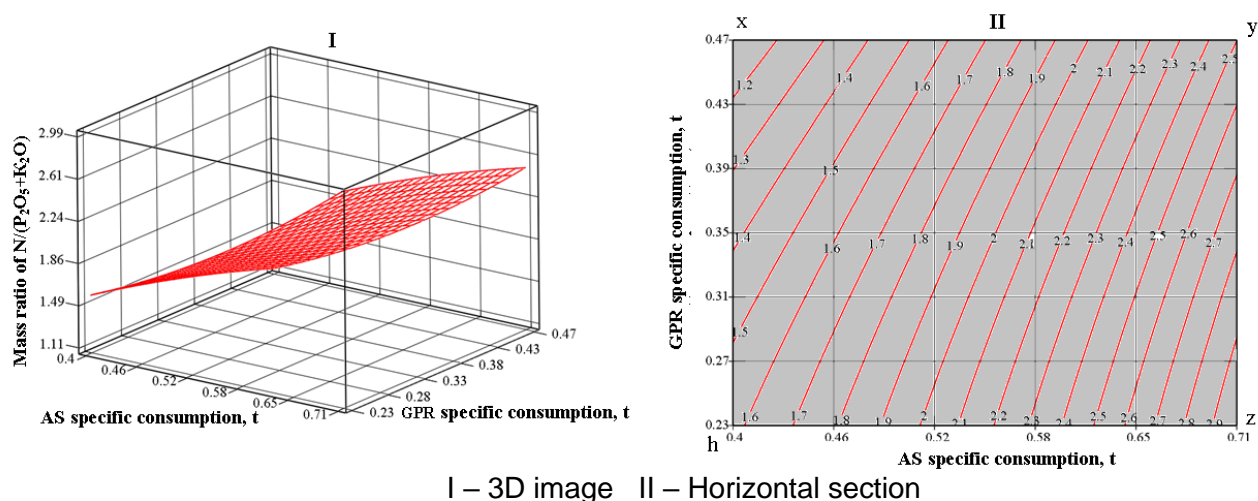


**Figure 5.** Influence of the ammonia salt peter and ground phosphate rock rates on the  $N/(P_2O_5+K_2O)$  ratio in the target product at  $KCl = 0.063 \text{ t}$

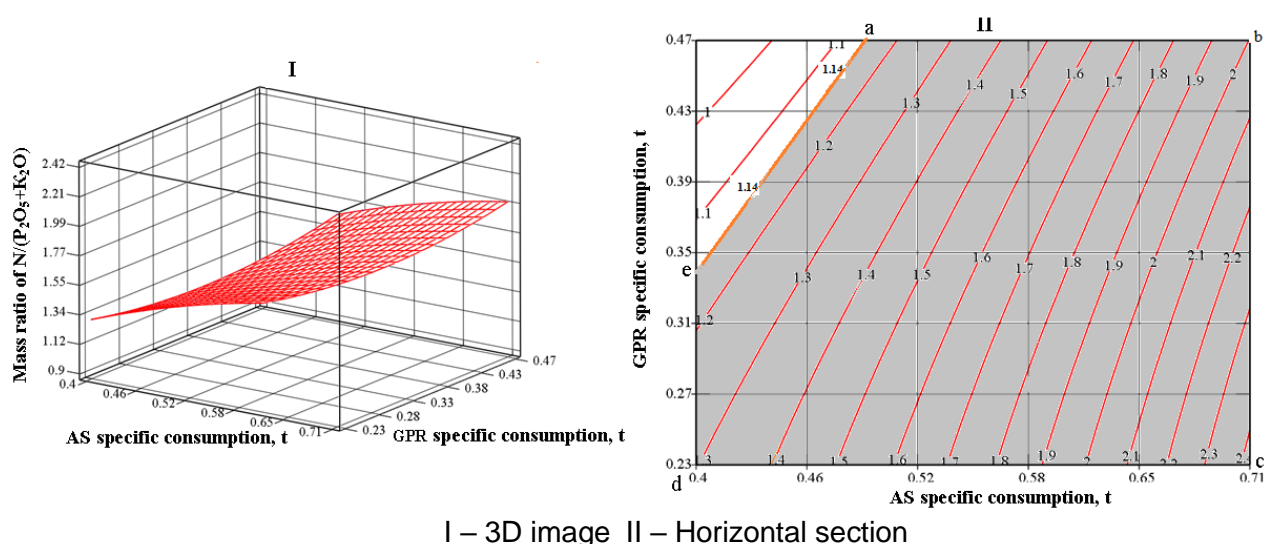


**Figure 6.** Influence of the ammonia salt peter and ground phosphate rock rates on the  $N/(P_2O_5+K_2O)$  ratio in the target product at  $KCl = 0.097 \text{ t}$

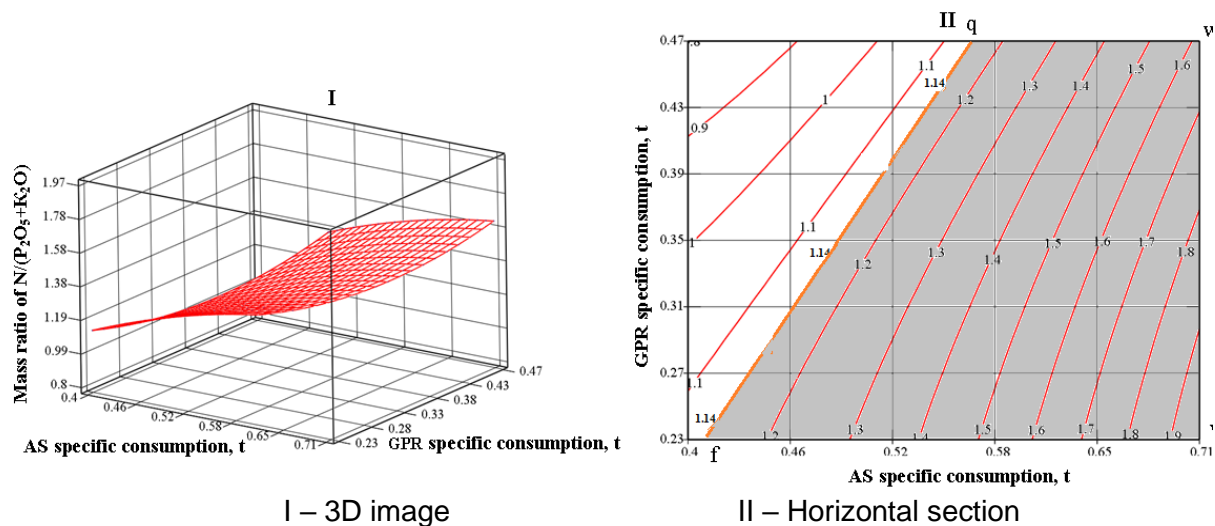


**Figure 7.** Influence of the ammonia salt peter and ground phosphate rock rates on the  $N/(P_2O_5+K_2O)$  ratio in the target product at  $KCl = 0.131\ t$

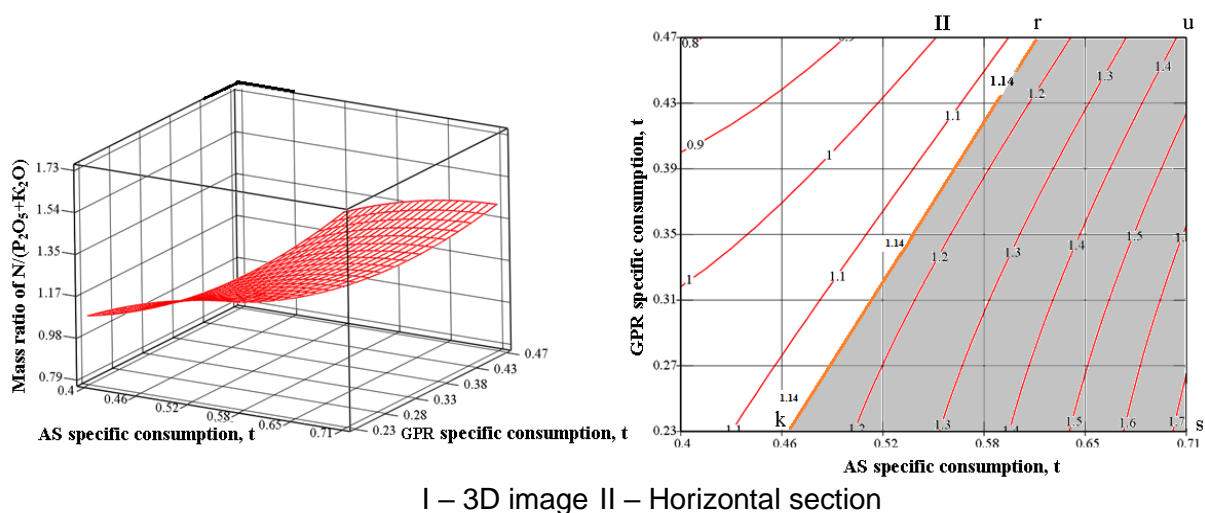


**Figure 8.** Influence of the ammonia salt peter and ground phosphate rock rates on the  $N/(P_2O_5+K_2O)$  ratio in the target product at  $KCl = 0.154\ t$

## OBTENÇÃO DE HIDROGELS MISTOS BASEADOS EM BIOPOLÍMEROS E ESTUDO DE SUAS PROPRIEDADES REOLÓGICAS

## PREPARATION OF MIXED HYDROGELS BASED ON BIOPOLYMERS AND THE STUDY OF THEIR RHEOLOGICAL PROPERTIES

## ПОЛУЧЕНИЕ СМЕШАННЫХ ГИДРОГЕЛЕЙ НА ОСНОВЕ БИОПОЛИМЕРОВ И ИЗУЧЕНИЕ ИХ РЕОЛОГИЧЕСКИХ СВОЙСТВ

SALIKOVA, Natalya S.<sup>1\*</sup>; BEKTEMISOVA, Ainash U.<sup>2</sup>; NAZAROVA, Valentina D.<sup>3</sup>; BEGENOVA, Bahyt E.<sup>4</sup>; OSTAFEICHUK, Natalya V.<sup>5</sup>;<sup>1</sup>Abay Myrzakhmetov Kokshetau University; Department of Ecology, Life Safety and Environmental Protection; Kokshetau – Republic of Kazakhstan<sup>2,3,4,5</sup>M. Kozybayev North Kazakhstan State University; Department of Chemistry and Chemical Technology; Petropavlovsk – Republic of Kazakhstan\* Corresponding author  
e-mail: natsal66@mail.ru

Received 22 January 2020; received in revised form 25 March 2020; accepted 10 May 2020

## RESUMO

Um método bem conhecido, acessível e barato de modificação de biopolímeros é simplesmente sua mistura com polímeros sintéticos e naturais. Como resultado, semelhante às ligas metálicas, é possível obter complexo interpolímeros com propriedades predeterminadas. Apesar do fato de que os complexos interpolímeros terem sido estudados e aplicados há muito tempo, na prática doméstica o estudo de biopolímeros naturais é limitado. O objetivo deste estudo é apresentar e estudar o problema de estruturação em soluções de biopolímeros e polímeros sintéticos, uma vez que, com baixo teor de matéria seca, essas estruturas têm muitas propriedades do corpo sólido. Polímeros anfóliticos naturais são polieletrólitos, o que também é de grande importância para estudos futuros. Ao analisar os resultados de estudos de complexos formados por um polieletrólito linear sintético com o parceiro carregado – a proteína, torna-se possível criar novos complexos de polieletrólitos “inteligentes” que podem sofrer alterações de fase em faixas estreitas e controladas de pH. Foi estabelecido o efeito positivo da carboximetilcelulose de sódio na gelificação de hidrogéis de gelatina a 5%. Foi estabelecido que a presença de aditivos de sais inorgânicos leva a um aumento na expansão de géis de gelatina. Foi também estabelecido que os géis mais duráveis são menos propensas ao envelhecimento. A importância prática desses estudos é determinada pelo fato de que em várias indústrias de alimentos, sabão, tinta e verniz e outras, é necessário obter estruturas com as propriedades desejadas. A formação dos géis também pode ser um fenômeno indesejável que deve ser evitado, por exemplo, na produção de fibras químicas, colas e soluções de bronzeamento. Além disso, na maioria dos casos, os próprios objetos biológicos são os géis de proteínas com certas propriedades mecânicas.

**Palavras-chave:** *estrutura e dinâmica de gel de gelatina, gelificação de gelatina, colapso de redes heterogêneas, expansão de gel de gelatina, adsorção de gelatina.*

## ABSTRACT

A well-known, affordable, and cheap method of modifying biopolymers is their simple mixing with synthetic and natural polymers. As a result, similar to metal alloys, polymer-polymer complexes with predetermined properties can be obtained. Although interpolymers complexes became a subject of study and application a long time ago, in domestic practice, the study of natural biopolymers is limited. The purpose of this study was to present and study the issue of structuring in solutions of bio- and synthetic polymers, as with a low dry matter content such structures have many properties of a solid. Natural ampholytic polymers are polyelectrolytes, which is also of great importance for their further study. By analyzing the results of studies of complexes formed by a synthetic linear polyelectrolyte with a charged partner – protein, it becomes possible to create new “smart” polyelectrolyte complexes that can undergo phase changes in narrow, controlled pH ranges. The positive effect of sodium carboxymethyl cellulose on the gelation of 5% gelatine hydrogels was established. It was determined that the presence of additives of inorganic salts leads to an increase in the swelling of gelatine gels. It was established

that more durable gels are less prone to aging. The practical significance of these studies is determined by the fact that in many industries (food, soap, paint, and varnish), it is necessary to obtain structures with tailor-made properties. Gel formation may also be an undesirable phenomenon that must be prevented, for example, in the production of chemical fibers, glues, and tanning solutions. Furthermore, biological objects themselves in most cases, by their nature, are protein gels with specific mechanical properties.

**Keywords:** *structure and dynamics of gelatine mixed hydrogels, adsorption on solid surfaces, collapse of heterogeneous networks, swelling and aging of mixed gelatine hydrogels.*

## АННОТАЦИЯ

Хорошо известным, доступным и дешевым методом модификации биополимеров является их простое смешение с синтетическими и природными полимерами. В результате, подобно сплавам металлам, можно получить полимер-полимерные комплексы с заранее заданными свойствами. Несмотря на то, что интерполимерные комплексы начали изучаться и применяться давно, в отечественной практике изучение природных биополимеров ограничено. Цель данного исследования – представить и изучить проблему структурирования в растворах био- и синтетических полимеров, так как при незначительном содержании сухого вещества такие структуры обладают многими свойствами твердого тела. Природные амфолитные полимеры являются полиэлектролитами, что также имеет огромное значение для их дальнейшего изучения. Анализируя результаты исследований комплексов, образованных синтетическим линейным полиэлектролитом с заряженным партнером – белком, становится возможным создание новых «умных» полиэлектролитных комплексов, способных претерпевать фазовые изменения в узких, контролируемых диапазонах pH. Установлено положительное влияние натрийкарбоксиметилцеллюлозы на гелеобразование 5% гидрогелей желатина. Установлено, что присутствие добавок неорганических солей приводит к увеличению набухания студней желатина. Установлено, что более прочные студни менее подвержены старению. Практическое значение этих исследований определяется, тем, что в ряде отраслей промышленности пищевой, мыловаренной, лакокрасочной и других надо получать структуры с заданными свойствами. Образование студней может оказаться и нежелательным явлением, которое надо предотвращать, например, в производстве химических волокон, клеев, растворов дубителей и т.д. Кроме того, сами биологические объекты в большинстве случаев по своей природе представляют собой студни белков с определенными механическими свойствами.

**Ключевые слова:** *структура и динамика смешанных желатиновых гидрогелей, адсорбция на твердых поверхностях, коллапс гетерогенных сеток, набухание и старение смешанных желатиновых гидрогелей.*

## 1. INTRODUCTION:

The possibility of a directed change in the properties of biopolymers due to external influences, such as the formation of stable association products with macromolecules and low molecular weight compounds (alcohols, carbohydrates, salts, etc.), makes them one of the most promising materials. In addition, another relevant study is of the effect of the interaction of the mixture components on the rheological and conformational properties of macromolecules due to non-covalent polymer interactions. The study of interpolymer complexes based on natural biopolymers is necessary for the further development of the technology for the production of environmentally friendly products that are promising for agriculture, medicine, food industry, cosmetology, etc. (Lanik, 1986; Tsereteli and Smirnova, 1991; Irshak and Varyukhin, 1995; Shandryuk *et al.*, 2002).

Feature of the formed biopolymer systems

is the mechanical properties of the resulting interpolymer complexes, allowing their use in technical industries. For example, mixed systems of polysaccharide-based biopolymers are used in the oil industry as reagents as drilling agents and flushing fluids. It is proved that the inclusion of small amounts of mixed systems based on gelatine and polyvinyl alcohol, sodium caseinate and polyvinyl alcohol in the feed composition increases the biological value of feed and increases the productivity of animal and poultry product, which makes it promising to apply mixed systems based on natural polymers in animal husbandry (Izmailova *et al.*, 1964; Pchelin, 1972; Vasiliev, 1981).

The mechanism and laws of formation, deformation, and destruction of dispersed structures of various types from liquid-like to high-strength materials of modern technology are the subject of the physicochemical mechanics of dispersed systems. From literature data (Gurevich, 1975; Busk, 1984; Deryagin, 1990; Katsuyoshi, 1993) it is known that an important



condition for the formation of a gel is the lack of the ability of the polymer to dissolve in a solvent unlimitedly. This condition, reduction of the interaction of the polymer and the solvent, can be achieved by changing the temperature, the nature of the solvent, the introduction of precipitators, specific additives. The fact that the loss of solubility does not lead to demixing is connected with the fact that the polymer chain molecules bind in solution during gelation into a single spatial structure that covers the entire volume.

An essential condition for gelation is the achievement of a specific, so-called critical concentration of the solution. Gelation can also occur when certain additives are introduced into polymer solutions, which lead to the formation of intermolecular or chemical bonds between different polymer macromolecules (Karásek and Meissner, 1992). The gelation process is also affected by the structure of the macromolecule itself. Gel formation also depends on the flexibility of the polymer chain and its conformation in solution (Yiebke *et al.*, 1994). Some ordering in the arrangement of polymer molecules is necessary for the emergence of secondary structures. However, with a large ordering of polymer macromolecules relative to each other, a precipitate forms. It should be noted that the gel state is the usual state of natural substances. Gels of various nature arouse the interest of researchers due to the emergence of the frame, which determines the mechanical properties of gels in the structure (Irshak and Varyukhin, 1995).

By definition of S.P. Papkov (1971), the gel phase is a matrix in which the second, low-concentrated polymer equilibrium phase is located. Such structures are characterized by the practical absence of irreversible deformation of the gel as a whole. Studying the rheological properties of jellies and their dependence on the type of stresses, temperature, duration of various influences, including the composition of the components allows to indirectly judge on the structure of gels, in particular, on their affiliation to a certain type (Valevsky, 1983; Hidekazu and Yoshihito, 1993; Kuleznev, 1993).

The purpose of this study was to present and study the issue of structuring in solutions of bio- and synthetic polymers, as with a low dry matter content such structures have many properties of a solid.

## 2. LITERATURE REVIEW:

In recent years, the principle of molecular recognition, which is based on steric effects,

electrostatic interaction, and hydrogen bonding, has been widely used in organic and polymer chemistry as a way to create new supramolecular materials. In the work of Shandryuk (Shandryuk *et al.*, 2002), a directed modification of systems is performed by introducing additives capable of hydrogen bonding with a polymer matrix. Rheological studies demonstrated that liquid crystal hydrogen-bonded networks are capable of large reversible deformations (up to 4-5-fold degrees of extension). Relatively many works are devoted to gelation of aqueous gelatine solutions. Most of these works are collected in Veys' monograph (Veys, 1971). It follows that the minimum concentration of gelatine gel formation is 0.5% and does not depend on pH in the region of 4-8 at temperatures below 18°C; at temperatures above 25°C, the gelation concentration increases and becomes dependent on the pH of the medium: in the region  $\text{pH} = 4.6 \div 4.8$  and at a temperature of 0°C 0.6% gelatine solution does not gelate for 20 hours.

Gelatine gels were repeatedly subjected to structural and mechanical studies due to having solid-like properties. However, there are very conflicting ideas in the matter of the structure of gelatine gels. In particular, the fact that gelatine gels belong to two- or single-phase gels causes controversy and doubts among researchers. Two possible assumptions are made regarding the cause of gelation of gelatine solutions after the conformational transition of its molecules from a coil to a spiral. The first is that there is a mechanism of local crystallization of spiralized macromolecules upon the formation of gel of the first type. According to the second hypothesis, due to the transition of gelatine to a rigid conformation, the polymer loses its solubility and forms a gel. In his work, A. Veys points out the unlikelihood of the gelation mechanism based on the renaturation of the structure of tropocollagen. Research conducted by G.I. Tsereteli and O.I. Smirnova (Tsereteli and Smirnova, 1991) points at the formation of metastable collagen-like structures in the process of gelation.

In his work, V.G. Vasiliev, having studied the effect of chemical crosslinking on the elastic modulus, concluded that a substantial increase does not occur in the latter. Crosslinking fixes the glomerular conformation of macromolecules, which prevents the formation of intermolecular bonds and, consequently, structure formation (Vasiliev, 1981). A series of works is devoted to the study of the rheological properties of gelatine solutions and jellies of various concentrations in a narrow temperature range and the replacement of

water with organic solvents (Rogovina *et al.*, 1971; Grigoryeva, 1975; Lanik, 1986). The properties of gelatine-water gels were experimentally studied at various temperatures, gelatine concentrations and frequencies of mechanical stresses. The relationship between the properties of gels and the shape and structure of polymer molecules was evaluated (Ross-Murphy, 1992; Hsu and Jamilison, 1993; Golfen and Borhard, 1994; Bocchard, 1998). An increase in high elasticity is also observed due to a possible change in both the nature of the bond in the spatial network and the conformations of macromolecules and a significant dependence of the elastic modulus of gelatine on the nature of the solvent. Authors believe that the Ferry-Eldridge equation is applicable to the researched systems with sufficient accuracy.

The study of the structure and dynamics of gelatine gels during temperature jumps by method of holographic relaxation spectroscopy was considered by Chi and Wolfgang (Chi and Wolfgang, 1990). The authors determined that in the process of normal cooling at a speed of 2 K/min two types of grids are formed. One type refers to a coarse structure formed by aggregation of collagen-like triplet standard helices, and the other – to a fine structure formed by links between gelatine molecules. Some works are devoted to the study of gelatine gels near the gelation threshold and in the immediate vicinity of the sol-gel transition point (Takahiro and Masayuki, 1990).

The published data on the thermal effect of gelation of gelatine are contradictory. Thus, having examined the sol-gel similarly to glass-liquid, absence of phase transition upon gelation is indicated (Nikolaev and Neumann, 1957). In contrast, other authors demonstrated that gelation of gelatine solutions is similar to crystallization and is accompanied by a thermal effect (Bobrova *et al.*, 1970; Gordovsky, 1971).

Many works cover the research of swelling and collapse of heterogeneous networks, including gelatine gels in an aqueous medium, as one of the characteristics of the void ratio of the formed structures. Patlazhan's (2002) work displayed that when polymer networks swell with an inhomogeneous crosslinking distribution, local internal stresses arise, the magnitude of which depends on the degree of swelling, the type and structure of the network. The effective swelling coefficient of such networks is less than the corresponding average value. Its relative change, including the statistical properties of internal stresses, are determined by the structural features

of the network, expressed through the correlation function of fluctuations of macromolecular chains connecting the neighboring nodes. The dependence of light scattering on the degree of swelling is investigated. It is concluded: with increasing degree of swelling, the scattering intensity passes through a maximum.

In the work of (Xion and Zheng Pei, 1997), research on the change in the volume of gelatine gels depending on the pH and ionic strength of aqueous solutions was conducted. The dependence of the swelling gel force (the force exerting pressure on the polymer network when it is enclosed in a cell of constant volume) is noted on these factors. The influence of changes in the volume of gels and swelling forces on chemomechanical energy, including on changes in rheological properties, is pointed out. V.V. Klepko and co-workers studied the kinetics and equilibrium of swelling of gelatine gels in a good solvent (Klepko and Melnichenko, 1994). It was demonstrated that in the studied range of ripening times (1÷5) hours, sol-gel transition temperatures (4÷22)°C and gelatine concentration in the initial solution (0.02÷0.13), the equilibrium degree of swelling depends on the initial concentration gel as  $F_0 - 0.4$ , which corresponds to Flory's theory.

Proceeding from the consideration of swelling as a diffusion-controlled process, it was concluded that the use of first-order kinetics is valid only at the initial and middle stages of the swelling process. At the stage of extensive swelling, first-order kinetics is not applicable. The explanation for this observation was made on the basis of the assumptions that the swelling rate is directly proportional to the relative swelling in time  $\tau$  and the specific area  $S_{int}$ , which limits the places of the polymer network that have not yet reacted with water in time  $\tau$ , but will be hydrated (Hans, 1992). The use of a new interferometric sensor and a special interferometer allowed the authors of the work (Chi and Chui-Sing, 1994) to study the kinetics of swelling of thin gelatine films. In situ measurements were performed both at times of several minutes and several days. It is noted that the data on swelling are well-suited for the kinetics of the first-order reaction, which contradicts the previous work. The discrepancies were explained by the significant difference in the processes in the solvent and in air, including the specificity of gelatine gels. The presence of a correlation between the shear modulus, the longitudinal modulus of elasticity, and the cooperative diffusion coefficient is noted.

The subject of the study is also the nature

of the bonds responsible for gelatine gelation. Some data give preference to nonpolar groups; according to other data, hydrogen and hydrophobic bonds play an important part in gelatine gelation (Izmailova *et al.*, 1964; Pchelin, 1972). The study of the interaction between water-soluble polymers, in particular proteins and surfactants, is necessary in connection with the expanding use of such joint systems in a number of biological and industrial processes. The work (Fruhner and Kzetzschmar, 1989; Roe *et al.*, 1998) researches the interaction between gelatine and ionic surfactant-alkyl sulfates and alkyl trimethylammonium ions by the direct method of surface-active selective electrolysis with a liquid membrane of o-nitrotoluene containing a complex of cetyltrimethylammonium dodecyl. The interaction of polyphenols with gelatine amino acids was studied in (Shi *et al.*, 1994). It was demonstrated that such an interaction is largely determined by hydrophobic forces.

In connection with the widespread use of gelatine in the pharmaceutical and food industries, adsorption of this fibrillar protein on solid adsorbents is being studied. The general regularities of the kinetics of gelatine adsorption at the solid-liquid border are discussed in (Bajpai, 1994). In (Bajpai, 1995), kinematic measurements of gelatine adsorption on alumina were performed. To analyse the adsorption process and its kinetic parameters, the magnetic formalism technique was used. The effect of gelatine pH, salt concentration in solution, and anion valency on the adsorption process is noted. The study of gelatine adsorption on small particles of magnetic iron oxide is the subject of work of (Hirotooshi *et al.*, 1997). The authors investigated the adsorption of gelatine depending on various parameters (temperature, pH, salt concentration). It indicates an increase in the adsorption and molecular weight of gelatine with an increase in the initial concentration of gelatine.

Some works are devoted to the study of polymer complexes containing gelatine as one of its components. P.N. Gilsenan, R.V. Richardson investigated the gelatine-pectin cogels (Gilsenan and Richardson, 1998). The effect of the structure of gelatine micellar solutions in the isooctane-water (bis-2-ethylhexyl) sodium sulfosuccinate system on gelation was considered in (Krasovskii and Andreeva, 1996). A number of works covers aqueous systems of gelatine-sodium alginate. The authors (Mukhin and Tolstoguzov, 1980), upon studying the compatibility of proteins and polysaccharides, found that aqueous mixtures of gelatine and sodium alginate at single ionic

strength and pH above the isoelectric point of gelatine are single-phase. An assumption was put forward that the compatibility of gelatine with anionic polysaccharides is conditioned by the formation of complexes of different nature between them. A study of mixed gels of gelatine and calcium alginate (Tolstoguzov, 1980) indicates the existence of two independent spatial networks.

The authors I.V. Fedusenko, T.E. Eryshkanova, V.I. Klenin (Fedusenko *et al.*, 2001) studied the gelation process in the gelatine-sodium alginate-water system with a total polymer concentration of 3 wt. %. It was demonstrated that gelation in the system is conditioned by local crystallization of polymers. When the gelatine content in the polymer mixture is 90%, a complex is formed. Gels of this composition have a higher melting (gelation) point and a greater value of the elastic modulus. Works of I.V. Fedusenko, L.I. Khomutov deal with the rheological behaviour of gelatine + sodium alginate + water system depending on the ratio of gelatine and sodium alginate at a total polymer concentration of (2-4) %. The dependence of the tensile strength of the forming structural formations depending on the content of sodium alginate in the mixture and temperature is shown. The appearance of spatially cross-linked thermoreversible structures in such ternary polymer systems is also discussed (Fedusenko and Khomutov, 1996).

In the work of E.A. Reshetnyak (Reshetnyak *et al.*, 2005), properties of gelatine are compared to modified gelatine (degree of modification of 10, 30 and 85%). Using the method of capillary viscometry, it was demonstrated that upon hydrophobization of gelatine, its macromolecular tangles become more compact and symmetrical. At the maximum degree of hydrophobization of gelatine, its adsorption activity increases by approximately 4 times. Methods were developed for the preparation of a polymer complex of phthaloyl gelatine with proxanol and other additives (Pobedimsky *et al.*, 2000; Elin *et al.*, 2002), characterized by the presence of a significant number of functional groups, large size, and the possibility of being used as a sorbent for wastewater treatment in such industries as petrochemical, pharmaceutical, etc.

A large role is given to the introduction of small additives of gelatine in composite materials, which enables the increase in the physicomechanical properties of composites and reduces their cost. In this regard, the work (Kudaibergenova *et al.*, 2008) studied the possibility of obtaining homogeneous and

interconnected composites on the basis of gelatine and bentonite clay with insignificant amounts of clay (0.2-2%). The degree of swelling of various compositions was determined using a scanning microscope, the morphology and structure of composite gels were determined using a scanning electron microscope, and the rheological properties of the compositions were studied using a Brookfield DV-II+PRO device (USA). An assumption on the formation of complexes through hydrogen bonds is put forward. It is shown that the compositions obtained in terms of homogeneity, stability, interoperability and structure-forming properties correspond to the requirements for carriers of medicinal and biologically active compounds.

The rheological properties of gelatine-calcium and sodium alginates system are also considered in detail in the dissertation of Evtushenko (2008). The work of A.V. Varlamov, A.N. Zuev, E.E. Latinsky (Varlamov *et al.*, 2008) displays that upon hydrophobizing gelatine with succinylauril, the macromolecular tangles become more compact and symmetrical. At the maximum degree of hydrophobization of gelatine, its adsorption activity increases by approximately 4 times. Chemical modification of gelatine with lauric acid succinimide ester changes the rheological properties, greatly changes the hydrodynamic parameters of protein macromolecules.

The structure formation of solutions of various protein molecules was studied in Kazakhstan by A. Zholbolsynova (Kozlov *et al.*, 1984; Zholbolsynova *et al.*, 1992). The process of structure formation in aqueous solutions of edible gelatine in the presence of organic additives (carbohydrates) was studied, the bonds determining the strength of the structure and the conformational transformations of macromolecules were determined. The conformation of gelatine macromolecules was studied by measuring the specific optical rotation. It is shown that the addition of carbohydrates increases the strength of the resulting structure, reduces the induction period. A conformational change in macromolecules accompanies the process of gel formation. It is assumed that the stabilization of the resulting structure is conditioned by hydrophobic bonds and an increase in the number of intermolecular bonds.

Further studies examined the effect of synthetic and biopolymers on the structuring and rheological properties of gelatine (polyvinyl alcohol, polyvinylpyrrolidone, sodium humate and nitrohumate, salts of inorganic acids, carbohydrates, organic alcohols, surfactants)

(Salikova *et al.*, 1999; Salikova and Zholbolsynova, 1999; Salikova and Zholbolsynova, 2000; Salikova *et al.*, 2000; Salikova *et al.*, 2001; Zholbolsynova and Salikova, 2001; Salikova *et al.*, 2002; Bektemisova *et al.*, 2009a; Bektemisova *et al.*, 2009b; Zhakina, *et al.*, 2009; Bektemisova *et al.*, 2009c; Salikova *et al.*, 2014).

### 3. MATERIALS AND METHODS:

Here we consider the effect of sodium carboxymethyl cellulose on the processes of structure formation, the rheological properties of mixed gels and the adsorption processes of gelatine. To clarify the gelation mechanism, we used the kinetic approach, since this allows us to consider the processes of nucleation and formation of spatial structures.

The object of the research in this part of the study was gelatine, on the basis of which experiments were carried out to determine the structure formation in its mixed systems with sodium carboxymethyl cellulose. We used edible gelatine, purified and reduced to an isoelectric state. The moisture content of the preparation is 15%, the ash content is 12%, and the molecular weight is 70.000. Proceeding from the analysis, all previous studies, a working gelatine concentration of 5% was selected. The process of structure formation was studied through the following parameters: structuring time, melting point, ultimate shear stress at different pH.

As in most cases, the polymer-polymer-low molecular weight liquid systems are incompatible with a wide range of component composition changes, the effect of the polymer volume ratio on the structuring process was studied. It was established that mixed gelatine gels are formed at certain optimal ratios. The compatibility criterion was the shape of the viscosity – composition curves. A linear relationship was observed, which signifies the formation of a homogeneous system when the selected components are mixed up to 50% NaCMC in the mixture; when a share of NaCMC in the mixture is above 50% vol., system demixing is observed. As a result of determining the conditions for the formation of mixed solutions, the range of variation of the NaCMC fraction in the mixture of 0÷50 (vol%) was chosen. It was suggested that during the formation of crystalline nuclei, the process will occur at different rates depending on the content of NaCMC. Table 1 presents data on the effect of the NaCMC content in a mixture with gelatine on the structuring time of mixed systems as an indicator of the rate of

formation of three-dimensional structures.

The identification of the structuring time demonstrated that, appropriately, the pH of the medium affects the structure formation of mixed gels. pH = 5, as the isoelectric state of gelatine, due to the lack of resistance to structuring from the side of its charged chains, leads to the shortest time for structuring mixed gels. Because of the change in the properties of gelatine aqueous solutions due to modification of properties of the solvent by the presence of NaCMC, an increase in the content of the modifier in the mixture (up to the previously established limit of 50% vol.) leads to an acceleration of the structure formation process. Kinetic studies of the ultimate shear stress of 5% mixed gelatine gels and NaCMC allowed to identify the time interval necessary to achieve the equilibrium strength of systems equal to 4 days (Figure 1).

To identify the effect of pH of the medium, the composition of the mixture on the melting temperature, measurements were performed for 5% concentrations formed in gel in the course of four days (Table 2).

#### 4. RESULTS AND DISCUSSION:

Since collagen folding is a cooperative phenomenon characterized by high activation energy; therefore, the melting points should be the same regardless of the gel composition. Our results show an increase in  $T_{mel}$ . With an increase in the content of NaCMC, which proves the participation of NaCMC in the stabilization of the network structure. It is necessary to note the distinct melting temperature during the measurement, which is evidence of the network structure of the gel stabilized by secondary forces.

This is because the value of  $T_{mel}$  depends on the relative number of hydrogen and hydrophobic bonds involved in each series of interacting chain segments; the melting temperature rises with an increase in the number of bonds per segment and becomes more defined. The distinctness of  $T_{mel}$  is directly related to the fact that the rupture of interacting pairs of chain segments involves the simultaneous rupture of several bonds. Adding NaCMC to the system does not change the effect of pH. Gels have the highest melting point at pH corresponding to the isoelectric state of gelatine. In parallel with measurements of the melting temperature in the same gels, their tensile strength was identified (Table 3).

It was concluded that the presence of a charge in gelatine macromolecules at a pH other

than the isoelectric state impairs the rheological properties of mixed gelatine gels and sodium carboxymethyl cellulose. Studying the adsorption of biopolymers at the liquid-solid interface is of great practical and theoretical importance. The extremely important role of proteins as biological objects is well known. Proteins provide cell adhesion and tissue formation. For the functional properties of biological systems, the surface activity of proteins is of no small importance. The part of surface phenomena in protein systems is very great in natural and technological processes.

Thus, the study of structure formation in mixed 5% gelatine and sodium carboxymethyl cellulose gels suggests that the synthetic polymer has a positive effect on gelation of gelatine. An increase in the content of NaCMC leads to an acceleration of the gelation process and the formation of stronger spatial structures.

Concentration of proteins at the phase boundaries, technological stages of emulsification and stabilization are widespread in the food, chemical, pharmaceutical industries. In animal husbandry, the use of biopolymers as fillers is known. In addition, surface phenomena involving proteins are often accompanied by structure formation or phase transitions; therefore, the study of adsorption provides additional information on the structuring of aqueous solutions. With that, the adsorption of macromolecular compounds from solutions on a solid surface is most important, since polymer adhesion, structural and mechanical properties of the high molecular weight compound boundary layers, the structure and the most important characteristics of monolayers and various composite materials are associated with it.

An analysis of the literature data shows that most of the experimental work on the study of polymer adsorption was performed using dilute polymer solutions, when intermolecular interaction in solutions can be neglected. However, even in this case it is impossible to draw unambiguous conclusions about the influence of various factors on the adsorption of polymers. Adsorption of biopolymers, in particular gelatine, is devoted to a small amount, especially for the adsorption of mixed solutions of gelatine with artificial polymers. Therefore, we studied the kinetics of adsorption of a mixture of gelatine with sodium carboxymethyl cellulose (NaCMC), the dependence of the adsorption on the amount and nature of the adsorbent, the specific surface of the adsorbent, and the concentration of the mixture. Preliminary studies of the rheological properties established the optimal ratio of gelatine and NaCMC in the

mixture – 1:1. Based on initial experiments, the optimum adsorption temperature was determined – 50°C; lowering the temperature below the optimum value leads to undesirable gelation of the system.

The study of the kinetics of adsorption is important from the standpoint of identifying factors determining the duration of the formation of adsorption layers. A study of the kinetics of gelatine adsorption with NaCMC displayed that the maximum contact time of the studied mixed aqueous solutions is 8-10 hours, the adsorption equilibrium is achieved within 2-3 hours and is practically independent of the mixture concentration; with an increase in the mixture concentration, the adsorption equilibrium is reached faster (Figure 2). The contour of the curves indicates that the experimental points fit well on the Langmuir adsorption equilibrium curve. Achieving equilibrium within a few hours, unlike pure gelatine, when equilibrium is reached faster (30 min-1 hour) (Zholbolsynova *et al.*, 1986), proves structural changes in NaCMC-modified gelatine. Gelatine macromolecules lose their flexibility, the diffusion rate to the surface of a solid decreases.

The established range of variation in the concentration of the adsorbent (0.5-3) g/dl of the solution is optimal for the adsorption of gelatine. The study of adsorption at such amounts of adsorbent (Table 4) allowed to establish the working concentration of the adsorbent equal to 0.5 g/dl of the solution. The decrease in adsorption with increasing adsorbent content can be explained by a decrease in their effective specific surface area due to adsorbent aggregation. The effect of the mixture concentration on the adsorption value of the gelatine and NaCMC mixture is provided in Table 5.

The data indicates that an increase in the concentration of the mixture leads to a larger adsorption value. An increase in the concentration of the mixture above 1% causes system structuring. At a given concentration of the mixture (1%) in the solution, the process of formation of large aggregates begins, including up to several hundred macromolecules of gelatine bonded with NaCMC. The effect of the specific surface area on the adsorption of a mixture of gelatine with NaCMC is presented in Table 6.

With an increase in the specific surface area of the adsorbent, which facilitates adsorption of large aggregates, the specific adsorption of gelatine with NaCMC increases. To identify the effect of the nature of the adsorbent on the specific

adsorption value, a mixed solution of gelatine with NaCMC was adsorbed on alumina oxide, activated carbon, ground brick, bentonite and silica gel (Table 7).

The results indicate that the adsorption of the test mixture depends on the chemical nature of the substrate, which is explained by the influence of the formed adsorption layer, which completely shields the surfaces of any solids. The results show that the best adsorption properties for mixed gelatine systems with NaCMC are hydrophilic surfaces with a well-developed macro- and microstructure of pores, such as silica gel and ground brick (significant intermolecular interactions in the adsorption layer are observed). Non-polar adsorbents with an activated surface, such as activated carbon, are also good adsorbents for gelatine aggregates with NaCMC. Adsorption on charged surfaces of alumina oxide is characterized by a significant energy barrier. The specific adsorption on such surfaces is significantly smaller.

A study of the adsorption of gelatine with NaCMC proves rheological studies, the results display structural changes in NaCMC-modified gelatine. When gelatine is mixed with NaCMC, larger structures and aggregates are formed in the solution, which lead to an increase in the time for the establishment of adsorption equilibrium, which is explained by spatial difficulties in the formation of adsorption layers. It should be noted that the specific adsorption value depends on the quantity and nature of the adsorbent. It was established that hydrophilic and activated surfaces are good adsorbents for gelatine with NaCMC.

Gels of various nature arouse the interest of researchers because of the emergence of the framework in the structure, determining their mechanical properties. Furthermore, a gelatinous state is a common state of natural polymers. The study of the formation of spatial structures of various types in disperse systems, their properties and the management of this process opens up unlimited possibilities for obtaining materials with tailor-made properties.

One of the essential conditions for gelation is to achieve a specific concentration of the solution, the so-called critical concentration, including the limited solubility of the polymer in this solvent. Reducing the interaction of the polymer and the solvent can be achieved by changing the temperature, the nature of the solvent, including the introduction of specific additives into the solvent. Thus, gelation can be enhanced when some additives (alcohols, various salts, heavy

metal oxides, etc.) are introduced into the polymer solution, which lead to the formation of intermolecular or chemical bonds between different polymer macromolecules (Asaubekov *et al.*, 1996). Indirect evidence of the hardening gel structure is its ability to swell. The stabilization of the gel structure can be analysed by its resistance to aging.

The object of research, in this case, was also gelatine, based on which experiments were carried out to determine the swelling and aging of its gels using inorganic salts, such as sodium chloride, calcium chloride, aluminum chloride. In this work, edible gelatine is used, purified, and reduced to isoelectric state. The moisture content of the preparation is 15%, the ash content is 12%, and the molecular weight is 70.000. Based on the analysis of literature data (Zholbolsynova, 1973), the working concentration of gelatine and the amount of sodium, calcium, and aluminum chloride additives were selected. In the research, selective nature of the swelling process (gelatine swells in water and in aqueous solutions and does not swell in liquid organic substances) was considered; therefore, water was used as a solvent for swelling gelatine gels.

The obtained experimental data are presented in Tables 8-10. From the provided data, it follows that the presence of additives of inorganic salts leads to an increase in the swelling of gelatine gels. Thus, the degree of swelling increased by 100% with the addition of sodium chloride, by 73% with the addition of calcium chloride, and by 60% with the addition of aluminum chloride. Investigation of the effect of the pH of the medium on the degree of gelatine swelling in the presence of inorganic salts suggests that a deviation of the pH of the medium from the isoelectric state also leads to a change in swelling degree. At pH = 9 and pH = 3, an increase in the degree of swelling is observed compared to the isoelectric point. With that, at pH = 3, the degree of swelling is somewhat greater than at pH = 9. This is due to the influence of a charge that is distributed throughout the gelatine gel chain at pH = 3 and is localized in certain regions at pH = 9. A similar dependence is observed for gelatine gels both in the presence of sodium chloride and of calcium and aluminum chlorides.

The results also display that aluminum chloride has the greatest effect on increasing the degree of swelling. It turned out that the maximum degree of gelatine gel swelling is observed with the introduction of NaCl, average – with CaCl<sub>2</sub>, minimum – with AlCl<sub>3</sub>. The results on the effect of the anion charge on the gelatine gel swelling

correlate with the results of studying their influence on the ultimate shear stress. With an increase in the anion charge, an increase in the ultimate shear stress (gel strength) occurs, which manifests itself, in this case, in a decrease in the gel swelling, which may be due to an increase in the osmotic pressure inside the network because of the different amounts of low molecular weight ions (Bekturov *et al.*, 1999). Measurement of the degree of swelling of 5% gelatine gel with the introduction of sodium, calcium, and aluminum chlorides allowed to graphically consider the dependence of the kinetics of its swelling on the cation charge at pH = 5 (Figure 3).

Figure 4 demonstrates a characteristic curve of gelatine gel swelling in the presence of NaCl additive depending on pH. From Figure 4 it follows that the degree of swelling depends on the pH of the medium and increases with a shift in pH to the acidic and alkaline regions. At the isoelectric point swelling is minimum.

Gels of macromolecular compounds are not subject to the process of their aging, and a change in some of their properties during prolonged standing is conditioned by the slow action of foreign substances capable of oxidation present in them. It was suggested that the presence of low molecular weight additives in the polymer hydrogel, contributing to the structure formation and hardening of gels, will destabilize the spatial system and contribute to its aging. In this case, we determined the aging of 5% gelatine gel with the introduction of 0.5M sodium, calcium, aluminum chlorides at different pH. The study of aging was carried out through studying changes in the size and mass of the initial sample (gel height,  $\Delta h$ , mm), changes in mass  $\Delta m$ , g.

Measurements were also taken over time. The results are presented in Tables 11-13. The procured data indicate that the presence of salts accelerates the aging process with a content of sodium, calcium, and aluminum chlorides at a concentration of 0.5 mol/L; the procured data correlate with the results of a study of the swelling process. The results of a study of the aging processes in gelatine in the presence of inorganic salts suggests the greater the charge of the anion the greater the presence of salts affects the strength of the gel. The aging process of gelatine hydrogels in the presence of inorganic salts depends on the pH of the medium. Stronger gels are less prone to aging.

## 5. CONCLUSIONS:

The positive effect of sodium

carboxymethyl cellulose on the gelation of 5% gelatine hydrogels was established. An increase in the content of NaCMC in a mixture with gelatine leads to an acceleration of the gelation process and the formation of stronger spatial structures. The participation of NaCMC in stabilizing the network structure was indirectly noted by the distinct melting temperature upon measurement.

The study of surface phenomena at the phase division boundary "mixed gelatine hydrogels – solid medium" indicated that quantitatively the adsorption of the test mixture depends on the chemical nature of the supporting medium, which is explained by the influence of the formed adsorption layer. The best adsorption properties for mixed gelatine systems with NaCMC was established – hydrophilic surfaces with well-developed macro- and microstructure of pores, such as silica gel and ground brick. Non-polar adsorbents with an activated surface, such as activated carbon, are also good adsorbents for gelatine aggregates with NaCMC. Adsorption on charged surfaces of alumina oxide is characterized by a significant energy barrier. The value of specific adsorption on such surfaces is set to be much smaller. The effect of pH on the structuring processes, the adsorption of mixed hydrogels of gelatine as a polyampholytic polymer is confirmed.

The gelation process of gelatine-based hydrogels was also studied from the standpoint of its stability over time in the presence of inorganic salts. It was established that the presence of additives of inorganic salts leads to an increase in the swelling of gelatine gels. The presence of inorganic salts also accelerates the aging process of gelatine hydrogels with a content of sodium, calcium, and aluminum chlorides at a concentration of 0.5 mol/l. The higher the charge of the salt anion, the greater the modification of gelatine hydrogels with inorganic salts affects the strength of the gel. It is established that more durable gels are less prone to aging. The process of swelling and aging of gelatine hydrogels in the presence of inorganic salts also depends on the pH of the medium.

## 6. ACKNOWLEDGEMENTS:

Authors extend their thanks to the professor, Doctor in Chemistry Amina S. Zholbolsynova for assistance with writing this paper.

## 7. REFERENCES:

1. Asaubekov, M.A., Bekturov, E.A., Shaikhutdinov, E.M. *Report of the Academy of Sciences of the Republic of Kazakhstan*, **1996**, 1, 61-65.
2. Bajpai, A.K. *Journal of Macromolecular Science*, **1995**, 32(3), 467-478.
3. Bajpai, A.K. *Polymer International*, **1994**, 33(3), 315-319.
4. Bektemisova, A.U., Salikova, N.S., Zholbolsynova, A.S., Abdykashev, A.F. *Bulletin of KarSU. Series: Chemistry*, **2009a**, 3(55), 60-63.
5. Bektemisova, A.U., Salikova, N.S., Zholbolsynova, A.S., Akkulova, Z.G. *Bulletin of the National Academy of Sciences of the Republic of Kazakhstan*, **2009c**, 1, 23-26.
6. Bektemisova, A.U., Salikova, N.S., Zholbolsynova, A.S., Akkulova, Z.G. *News of the National Academy of Sciences of the Republic of Kazakhstan. Series: Chemistry*, **2009b**, 1, 43-47.
7. Bekturov, E.A., Bimendina, L.A., Kozlov, V.A., Suleimenov, I.E. *Self-Organization of Organic and Inorganic Polymers in Water*. Almaty: Nauka, **1999**.
8. Bobrova, L.E., Izmailova, V.E., Holler, V.A. *Colloid Journal*, **1970**, 32(5), 662-666.
9. Bocchard, W. *Berichte der Bunsengesellschaft für physikalische Chemie*, **1998**, 102(11), 1580-1588.
10. Busk, G.C. *Food Technician*, **1984**, 38(5), 59-62.
11. Chi, W., Chui-Sing, Y. *Macromolecules*, **1994**, 27(16), 4516-4520.
12. Chi, W., Wolfgang, S. *Macromolecular Symposia*, **1990**, 40, 153-156.
13. Deryagin, B.V. *Bulletin of the USSR Academy of Sciences*, **1990**, 9, 68-75.
14. Elin, A.Ya., Elin, G.Ya., Elina, V.A., Popovich, P.R., Sherstnev, M.P., Yachmenev, N.I. *The catalyst for wastewater treatment from organic substances and salts of heavy metals*. Patent No. 2189949 of the RF. Published on May 24, **2002**.
15. Evtushenko, A.M. *Protective polymer coatings with a special set of properties for biological objects*. Moscow: Moscow State University, **2008**.



16. Fedusenko, I.V., Eryshkanova, T.E., Klenin, V.I. *Polymer Science*, **2001**, 43(10), 1861-1866.
17. Fedusenko, I.V., Khomutov, L.I. Features of the rheological behaviour of the gelatine + sodium alginate + water system. *Materials of the 18th Symposium on Rheology* (pp. 111), A.V. Topchiev Institute of Petrochemical Synthesis of the Russian Academy of Sciences, Karacharovo, Russian Federation, **1996**.
18. Fruhner, H., Kzetzschmar, G. *Colloid and Polymer Science*, **1989**, 267(9), 839-843.
19. Gilsenan, P.M., Richardson, R.V. Gelatine-pectin cogels. *Proceedings of the 14th Polymer Networks Group International Conference* (pp. 56), Trondheim, Norway, **1998**.
20. Golfen, H., Borhard, W. *Acta Polymerica*, **1994**, 45(4), 325-329.
21. Gordovsky, Yu.K. *Polymer Science*, **1971**, 13(12), 2768-2776.
22. Grigoryeva, V.A. *VMS*, **1975**, 17(1), 143-147.
23. Gurevich, I.Ya. *VMS*, **1975**, 115(11), 823-825.
24. Hans, S. *Journal of Macromolecular Science Part B*, **1992**, 31(1), 1-9.
25. Hidekazu, Y., Yoshihito, O. *Journal of High Polymer*, **1993**, 42(4), 336-339.
26. Hirotooshi, T., Ken, I., Koichi, T., Hidefumi, H. *Polymer Science and Technology*, **1997**, 54(7), 427-433.
27. Hsu, S.H., Jamilson, A.M. *Polymer*, **1993**, 34(12), 2602-2608.
28. Irshak, V.I., Varyukhin, S.E. Relaxation properties of polymer gels and concept of physical networks. *Proceedings of the Europhysics Conference Macromolecules Physics* (pp. 69), Balatonszeplak, Hungary, **1995**.
29. Izmailova, V.N., Pchelin, V.A., Samir Abu Ali. *Polymer Science*, **1964**, 6(12), 2197-2199.
30. Karásek, L., Meissner, B. *Abstract Book*, **1992**, S1, 531-543.
31. Katsuyoshi, H. *Fiber*, **1993**, 49(3), 84-93.
32. Klepko, V.V., Melnichenko, Yu.B. *Polymer Science*, **1994**, 36(3), 461-465.
33. Kozlov, A.S., Zholbolsynova, A.S., Bekturov, E.A. *News of the Academy of Sciences of the Kazakh SSR. Series: Chemistry*, **1984**, 3, 44-47.
34. Krasovskii, A.N., Andreeva, A.I. The structure of micellar solutions of gelatine in the system izooctan-water-bis(2-ethylhexyl) sodium sulfosuccinate on the threshold of gel. In: 2-nd International *Materials of the symposium "Molecular Order and Mobility Polymer Systems"* (pp. 163), St. Petersburg, Russian Federation, **1996**.
35. Kudaibergenova, B.M., Beisebekov, M.K., Zhumagalieva, Sh.N., Abilov, Zh.A. *Chemical Journal of Kazakhstan*, **2008**, 21, 197-202.
36. Kuleznev, V.N. *Polymer Science*, **1993**, 35(8), 1391-1402.
37. Lanik, N.A. *Structuring Processes in Polymer Systems*. Saratov: Saratov State University, **1986**.
38. Mukhin, M.A., Tolstoguzov, V.B. *Structuring Processes in Polymer Solutions*. Saratov: Saratov University, **1980**.
39. Nikolaev, A.V., Neyman, R.E. *Colloid Journal*, **1957**, 19(1), 121-124.
40. Papkov, S. *Physicochemical Basics of the Processing of Polymer Solutions*. Moscow: Khimiya, **1971**.
41. Patlazhan, S.A. *Polymer Science*, **2002**, 44(6), 1029-1037.
42. Pchelin, V.A. *Colloid Journal*, **1972**, 34(3), 432-437.
43. Pobedimsky, D.G., Akhmadullina, F.Yu., Gabutdinov, M.S., Asadullin, A.Z., Gibaeva, L.G., Kavieva, R.R., Volkova, L.A. *A method of biochemical wastewater treatment from organic substances*. Patent No. 2026827 of the RF, 1995. Published on August 24th, 2000.
44. Reshetnyak, E.A., Nikitina, N.A., Loginova, L.P., Mchedlov-Petrosyan, N.O., Svetlova, N.V. *Bulletin of Kharkiv National University. Chemistry*, **2005**, 13(36), 48-52.
45. Roe, J.A., Griffith, P.C., Fallis, I.A. Interaction of gelatine anionic surfactants. *Materials of the 216th American Chemist Social Natural Meeting and Explosion Program*. (pp. 104), Boston, USA, **1998**.
46. Rogovina, L.Z., Slonimsky, G.L., Aksenova, L.A. *Polymer Science*, **1971**, 13(7), 1451-1455.
47. Ross-Murphu, S.B. *Polymer*, **1992**, 33(12), 2622-2627.

48. Salikova, N.S., Bektemisova, A.U., Zholbolsynova, A.S., Sheiko, T.A. *Chemical Journal of Kazakhstan*, **2014**, 1(45), 239-249.
49. Salikova, N.S., Zholbolsynova, A.S. *Collection of Deposited Scientific Works*, **2000**, 2, 175-186.
50. Salikova, N.S., Zholbolsynova, A.S. The effect of some organic compounds on the structure formation of aqueous solutions of gelatine with polyvinyl alcohol. *Materials of the Republican Scientific-Theoretical Conference dedicated to the 100th anniversary of Academician K.I. Satpayev* (pp. 239-242), E.A. Buketov Karaganda State University, Karaganda, Russian Federation, **1999**.
51. Salikova, N.S., Zholbolsynova, A.S., Bekturov, E.A. *Bulletin of Kazakhstan National University. Series: Chemistry*, **2001**, 1(18), 130-134.
52. Salikova, N.S., Zholbolsynova, A.S., Bekturov, E.A. *Bulletin of Kazakhstan National University. Series: Chemistry*, **2002**, 2(26), 97-101.
53. Salikova, N.S., Zholbolsynova, A.S., Bekturov, E.A. *Poisk*, **1999**, 3, 16-19.
54. Salikova, N.S., Zholbolsynova, A.S., Bekturov, E.A. *Poisk*, **2000**, 1, 19-22.
55. Shandryuk, G.A., Koval, M.V., Kuptsov, S.A., Sasnovsky, G.M., Talrose, R.V., Plate, N.A. *Polymer Science*, **2002**, 44(3), 434-442.
56. Shi, B., He, X., Haslam, E. *American Leather Chemists Association*, **1994**, 89(4), 98-104.
57. Takahiro, I., Masayuki, T. *Japanese Journal of Applied Physics*, **1990**, 28(1). <https://iopscience.iop.org/article/10.1143/JJA.P.28.1639/meta>, accessed 21 December 2019.
58. Tolstoguzov, V.B. *Structuring Processes in Polymer Solutions*. Saratov: Saratov University, **1980**.
59. Tsereteli, G.I., Smirnova, O.I. *Polymer Science*, **1991**, 33(10), 2243-2249.
60. Valevsky, V.I. *Strength Study of Dispersed Systems by Rheology Methods*. Kyiv: Naukova Dumka, **1983**.
61. Varlamov, A.V., Zuev, A.N., Latin, E.E. *Chemical Industry*, **2008**, 85(3), 135-137.
62. Vasiliev, V.G. *Physical Properties of Viscoelastic Polymers*. Sverdlovsk: Scientific Training Center of the Academy of Sciences of USSR, **1981**.
63. Veys, A. *Macromolecular Chemistry of Gelatine*. Moscow: Pishchevaya promyshlennost', **1971**.
64. Xion, Y.J., Zheng Pei, J. *British Polymer Journal*, **1997**, 44(4), 448-452.
65. Yiebke, Ch., Piculell, L., Nilsson, S. *Macromolecules*, **1994**, 27(15), 4160-4166.
66. Zhakina, A.Kh., Bektemisova, A.U., Satymbaev, A.S., Akkulova, Z.G., Zholbolsynova, A.S. Study of gelatine-humate sorbents. *Proceedings of the international scientific-practical conference "Pure water-2009"* (pp. 403-407), Kemerovo Institute of Food Technology, Kemerovo, Russian Federation, **2009**.
67. Zholbolsynova, A.S. *News of the Academy of Sciences of the Kazakh SSR*, **1973**, 5, 87-89.
68. Zholbolsynova, A.S., Kozlov, A.S., Bekturov, E.A., Bolatbaev, K.N. *News of the Academy of Sciences of the Kazakh SSR. Series: Chemistry*, **1986**, 5, 79-82.
69. Zholbolsynova, A.S., Morinets, P.G., Martin, V.G., Bekturov, E.A. *News of the Academy of Sciences of the Republic of Kazakhstan. Series: Chemistry*, **1992**, 4, 39-42.
70. Zholbolsynova, A.S., Salikova, N.S. On the matter of swelling of mixed biopolymer systems. *Materials of the International Scientific and Practical Conference "Modern Problems of Education and Science at the Beginning of the Century"* (pp. 68-70), E.A. Buketov Karaganda State University, Karaganda, Russian Federation, **2001**.

**Table 1.** The effect of the composition and pH of 5% mixed gelatine-based aqueous systems on sodium carboxymethyl cellulose on the structuring time

| Content of NaCMC, % | Structuring time, min. at pH: |    |    |
|---------------------|-------------------------------|----|----|
|                     | 3                             | 5  | 9  |
| 0                   | 53                            | 32 | 35 |
| 5                   | 52                            | 31 | 34 |
| 15                  | 50                            | 31 | 33 |
| 25                  | 48                            | 30 | 32 |
| 35                  | 47                            | 29 | 32 |
| 50                  | 45                            | 28 | 31 |

**Table 2.** Effect of the composition and pH of 5% of mixed aqueous systems based on gelatine and NaCMC on the melting temperature

| Content of NaCMC, % | Melting temperature, $t_{mel}$ , °C, at pH: |      |      |
|---------------------|---|------|------|
|                     | 3   | 5    | 9    |
| 0                   | 30.1  | 34.5 | 32.5 |
| 15                  | 31.6  | 35.6 | 33.0 |
| 25                  | 32.5  | 36.0 | 34.1 |
| 35                  | 33.1  | 36.5 | 35.2 |
| 50                  | 34.2  | 37.8 | 36.6 |

**Table 3.** Dependence of the maximum strength of 5% mixed gelatine gels and NaCMC on the composition at different pH

| Content of NaCMC, % | Critical shear stress, $P_m$ , kg/m <sup>2</sup> , at pH: |       |       |
|---------------------|---|-------|-------|
|                     | 3   | 5     | 9     |
| 0                   | 150.0   | 250.1 | 250.2 |
| 5                   | 153.3   | 254.3 | 253.6 |
| 15                  | 158.1   | 260.4 | 258.7 |
| 25                  | 163.8   | 268.6 | 263.8 |
| 35                  | 169.1   | 276.1 | 270.2 |
| 50                  | 177.2   | 287.2 | 277.5 |

**Table 4.** Dependence of the specific adsorption of a mixture of gelatine and NaCMC on the mass of silica gel, the concentration of the mixture = 1 %;  $S_{sp} = 14 \text{ m}^2/\text{g}$ ;  $t = 50^\circ\text{C}$

| Adsorbent mass, m, g         | 0.5 | 1.0 | 1.5 | 2.0 | 2.5 | 3.0 |
|------------------------------|-----|-----|-----|-----|-----|-----|
| Specific adsorption, G, mg/g | 423 | 385 | 340 | 290 | 255 | 210 |

**Table 5.** Dependence of the adsorption value of a mixture of gelatine and NaCMC on silica gel on the concentration of the mixture,  $m$  (adsorbent) = 0.5 g;  $S_{sp} = 14 \text{ m}^2/\text{g}$ ;  $t = 50^\circ\text{C}$

| Mixture concentration, C, %  | 0.2 | 0.3 | 0.5 | 0.7 | 0.9 | 1.0 |
|------------------------------|-----|-----|-----|-----|-----|-----|
| Specific adsorption, G, mg/g | 78  | 140 | 223 | 318 | 405 | 423 |

**Table 6.** Dependence of the specific adsorption of a mixture of gelatine and NaCMC on the specific surface of silica gel,  $m$  (adsorbent) = 0.5 g;  $C_{mix} = 1\%$ ;  $t = 50^\circ\text{C}$

| Silica gel specific surface, $S_{sp}$ , m <sup>2</sup> /g | 12  | 14  | 18  | 25  |
|---|-----|-----|-----|-----|
| Specific adsorption, G, mg/g                              | 363 | 423 | 544 | 755 |

**Table 7.** Dependence of the specific adsorption of a mixture of gelatine and NaCMC on the nature of the adsorbent,  $m$  (adsorbent) = 0.5 g;  $S_{sp} = 14 \text{ m}^2/\text{g}$ ;  $C_{mix} = 1 \%$ ;  $t = 50^\circ\text{C}$

| Adsorbent        | Specific adsorption, G, mg/g |
|------------------|------------------------------|
| Alumina oxide    | 366                          |
| Bentonite        | 377                          |
| Silica gel       | 423                          |
| Activated carbon | 646                          |
| Ground brick     | 753                          |

**Table 8.** Kinetics of the degree of swelling of 5% gelatine gels ( $\text{pH} = 5$ ) in the presence of salts

| Concentration of salts, mol/l | Time, h | Swelling degree, $\alpha$ , % |                   |                   |
|-------------------------------|---------|-------------------------------|-------------------|-------------------|
|                               |         | NaCl                          | CaCl <sub>2</sub> | AlCl <sub>3</sub> |
| 0                             | 0       | 0                             | 0                 | 0                 |
|                               | 1       | 18                            | 18                | 18                |
|                               | 3       | 25.6                          | 25.6              | 25.6              |
|                               | 5       | 31.2                          | 31.2              | 31.2              |
|                               | 7       | 37.8                          | 37.8              | 37.8              |
|                               | 9       | 38                            | 38                | 38                |
|                               | 0       | 0                             | 0                 | 0                 |
| 0.5                           | 1       | 36                            | 31.2              | 28.8              |
|                               | 3       | 51.2                          | 44.4              | 40.9              |
|                               | 5       | 62.4                          | 54.2              | 49.9              |
|                               | 7       | 75.6                          | 65.6              | 60.5              |
|                               | 9       | 76                            | 65.9              | 60.8              |

**Table 9.** Kinetics of the degree of swelling of 5% gelatine gels ( $\text{pH}=3$ ) in the presence of salts

| Concentration of salts, mol/l | Time, h | Swelling degree, $\alpha$ , % |                   |                   |
|-------------------------------|---------|-------------------------------|-------------------|-------------------|
|                               |         | NaCl                          | CaCl <sub>2</sub> | AlCl <sub>3</sub> |
| 0                             | 0       | 0                             | 0                 | 0                 |
|                               | 1       | 22                            | 22                | 22                |
|                               | 3       | 46.6                          | 46.6              | 46.6              |
|                               | 5       | 58                            | 58                | 58                |
|                               | 7       | 60.4                          | 60.4              | 60.4              |
|                               | 9       | 60.8                          | 60.8              | 60.8              |
|                               | 0       | 0                             | 0                 | 0                 |
| 0.5                           | 1       | 44                            | 38                | 36.3              |
|                               | 3       | 93.2                          | 80.9              | 76.8              |
|                               | 5       | 116                           | 100.6             | 95.7              |
|                               | 7       | 120.8                         | 104.8             | 99.6              |
|                               | 9       | 121.8                         | 105.5             | 100.3             |

**Table 10.** Kinetics of the degree of swelling of 5% gelatine gels (pH=9) in the presence of salts

| Concentration of salts, mol/l | Time, h | Swelling degree, $\alpha$ , % |                   |                   |
|-------------------------------|---------|-------------------------------|-------------------|-------------------|
|                               |         | NaCl                          | CaCl <sub>2</sub> | AlCl <sub>3</sub> |
| 0                             | 0       | 0                             | 0                 | 0                 |
|                               | 1       | 20                            | 20                | 20                |
|                               | 3       | 30                            | 30                | 30                |
|                               | 5       | 37                            | 37                | 37                |
|                               | 7       | 41.6                          | 41.6              | 41.6              |
|                               | 9       | 41.8                          | 41.8              | 41.8              |
| 0.5                           | 0       | 0                             | 0                 | 0                 |
|                               | 1       | 40                            | 34.7              | 32                |
|                               | 3       | 60                            | 52.1              | 48                |
|                               | 5       | 74                            | 64.2              | 59.2              |
|                               | 7       | 83.2                          | 72.2              | 66.6              |
|                               | 9       | 83.6                          | 72.5              | 66.8              |

**Table 11.** The kinetics of aging of 5% gelatine gels (pH=5) in the presence of salts

| Concentration of chlorides, mol/l | Time, h | NaCl           |                 | CaCl <sub>2</sub> |                 | AlCl <sub>3</sub> |                 |
|-----------------------------------|---------|----------------|-----------------|-------------------|-----------------|-------------------|-----------------|
|                                   |         | $\Delta m$ , g | $\Delta h$ , mm | $\Delta m$ , g    | $\Delta h$ , mm | $\Delta m$ , g    | $\Delta h$ , mm |
| 0                                 | 0       | 0              | 0               | 0                 | 0               | 0                 | 0               |
|                                   | 24      | 0.9            | 1.3             | 0.9               | 1.3             | 0.9               | 1.3             |
|                                   | 48      | 1.58           | 2.3             | 1.58              | 2.3             | 1.58              | 2.3             |
|                                   | 72      | 1.98           | 2.9             | 1.98              | 2.9             | 1.98              | 2.9             |
|                                   | 96      | 2.23           | 3.2             | 2.23              | 3.2             | 2.23              | 3.2             |
|                                   | 120     | 2.47           | 3.5             | 2.47              | 3.5             | 2.47              | 3.5             |
| 0.5                               | 0       | 0              | 0               | 0                 | 0               | 0                 | 0               |
|                                   | 24      | 1.86           | 2.6             | 1.56              | 2.3             | 1.08              | 2.03            |
|                                   | 48      | 3.16           | 4.6             | 2.74              | 4               | 1.85              | 2.66            |
|                                   | 72      | 3.96           | 5.8             | 3.43              | 5.03            | 2.3               | 3.3             |
|                                   | 96      | 4.46           | 6.4             | 3.87              | 6               | 2.5               | 3.6             |
|                                   | 120     | 4.94           | 7               | 4.2               | 6.1             | 2.7               | 4               |

**Table 12.** The kinetics of aging of 5% gelatine gels (pH=3) in the presence of salts

| Concentration of chlorides, mol/l | Time, h | NaCl           |                 | CaCl <sub>2</sub> |                 | AlCl <sub>3</sub> |                 |
|-----------------------------------|---------|----------------|-----------------|-------------------|-----------------|-------------------|-----------------|
|                                   |         | $\Delta m$ , g | $\Delta h$ , mm | $\Delta m$ , g    | $\Delta h$ , mm | $\Delta m$ , g    | $\Delta h$ , mm |
| 0                                 | 0       | 0              | 0               | 0                 | 0               | 0                 | 0               |
|                                   | 24      | 1.35           | 1.93            | 1.35              | 1.93            | 1.35              | 1.93            |
|                                   | 48      | 2.37           | 3.39            | 2.37              | 3.39            | 2.37              | 3.39            |
|                                   | 72      | 2.97           | 4.25            | 2.97              | 4.25            | 2.97              | 4.25            |
|                                   | 96      | 3.34           | 4.77            | 3.34              | 4.77            | 3.34              | 4.77            |
|                                   | 120     | 3.69           | 5.27            | 3.69              | 5.27            | 3.69              | 5.27            |
| 0.5                               | 0       | 0              | 0               | 0                 | 0               | 0                 | 0               |
|                                   | 24      | 2.7            | 3.86            | 2.35              | 3.35            | 2.16              | 3.1             |
|                                   | 48      | 4.74           | 6.78            | 4.1               | 5.88            | 3.8               | 5.42            |
|                                   | 72      | 5.94           | 8.15            | 5.15              | 7.37            | 4.75              | 6.8             |
|                                   | 96      | 6.68           | 10              | 5.8               | 8.7             | 5.3               | 8               |
|                                   | 120     | 7.38           | 10.5            | 6.4               | 9.1             | 5.6               | 8.4             |

**Table 13.** The kinetics of aging of 5% gelatine gels (pH=9) in the presence of salts

| Concentration of chlorides, mol/l | Time, h | NaCl           |                 | CaCl <sub>2</sub> |                 | AlCl <sub>3</sub> |                 |
|-----------------------------------|---------|----------------|-----------------|-------------------|-----------------|-------------------|-----------------|
|                                   |         | $\Delta m$ , g | $\Delta h$ , mm | $\Delta m$ , g    | $\Delta h$ , mm | $\Delta m$ , g    | $\Delta h$ , mm |
| 0                                 | 0       | 0              | 0               | 0                 | 0               | 0                 | 0               |
|                                   | 24      | 0.99           | 1.42            | 0.99              | 1.42            | 0.99              | 1.42            |
|                                   | 48      | 1.74           | 2.49            | 1.74              | 2.49            | 1.74              | 2.49            |
|                                   | 72      | 2.19           | 3.13            | 2.19              | 3.13            | 2.19              | 3.13            |
|                                   | 96      | 2.46           | 3.61            | 2.46              | 3.61            | 2.46              | 3.61            |
|                                   | 120     | 2.72           | 3.89            | 2.72              | 3.89            | 2.72              | 3.89            |
| 0.5                               | 0       | 0              | 0               | 0                 | 0               | 0                 | 0               |
|                                   | 24      | 1.98           | 2.84            | 1.71              | 2.46            | 1.58              | 2.27            |
|                                   | 48      | 3.48           | 2.98            | 3.02              | 4.3             | 2.8               | 3.9             |
|                                   | 72      | 4.38           | 6.26            | 3.8               | 5.4             | 3.5               | 5               |
|                                   | 96      | 4.92           | 7.22            | 4.27              | 6.3             | 3.9               | 5.7             |
|                                   | 120     | 5.4            | 7.5             | 4.5               | 6.6             | 4                 | 6               |

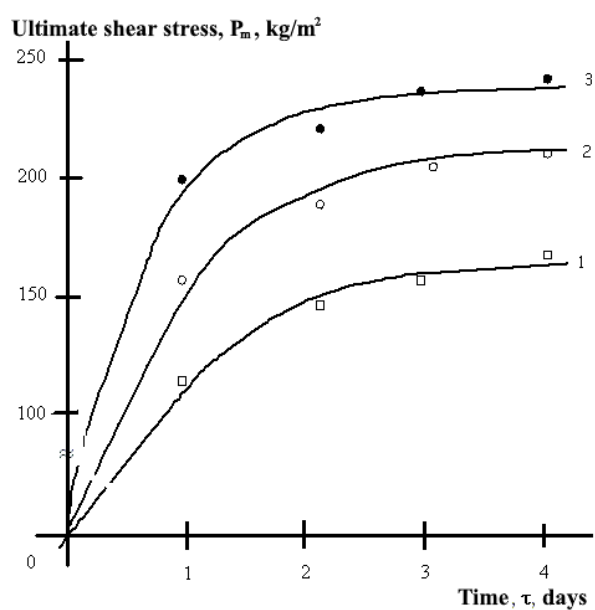


**Figure 1.** Kinetics of changes in the ultimate shear stress of 5% mixed systems of gelatine and NaCMC in a ratio of 85:15 of pH. Designation of curves, pH: 1– 3; 2 – 9; 3 – 5

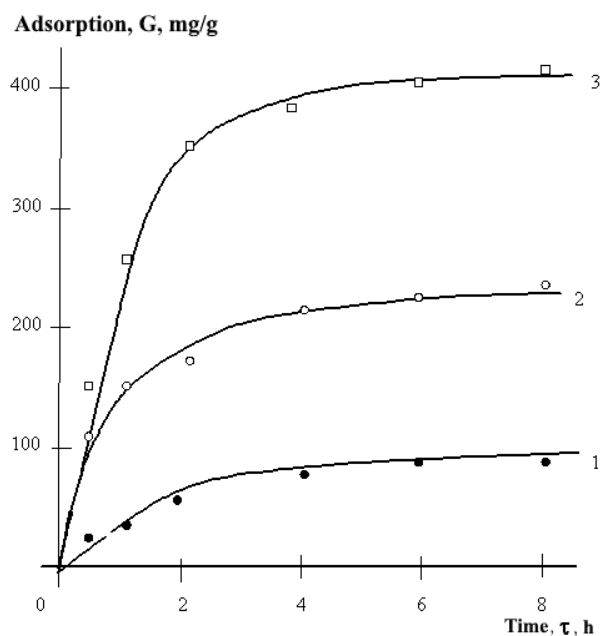


**Figure 2.** Kinetics of changes in the adsorption of a mixture of gelatine and NaCMC on silica gel, the adsorbent mass is 0.5 g;  $S_{sp} = 14 \text{ m}^2/\text{g}$ . The designation of the curves, the concentration of the mixture, %: 1 – 0.2; 2 – 0.5; 3 – 1.0

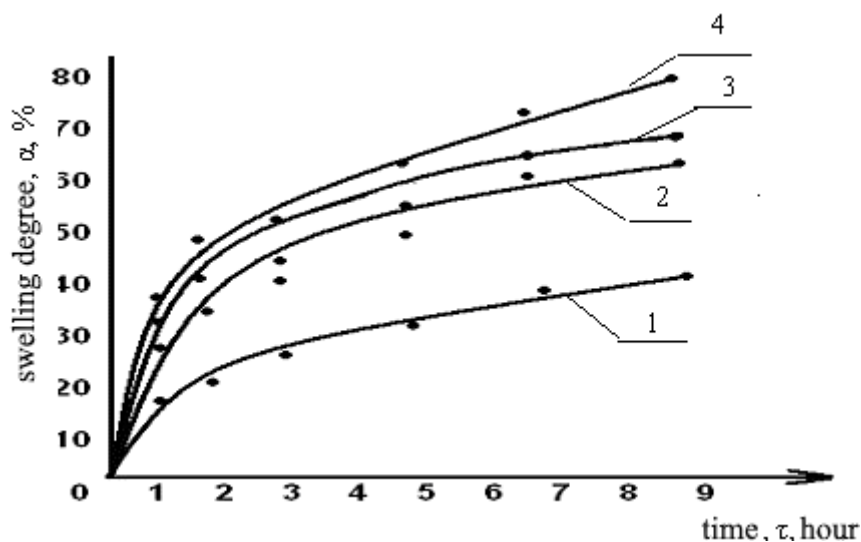


**Figure 3.** The dependence of the kinetics of swelling of 5% gelatine gel (pH=5) on the cation charge. Designation of curves: additive: 1 – absent; 2 –  $\text{AlCl}_3$ ; 3 –  $\text{CaCl}_2$ ; 4 –  $\text{NaCl}$

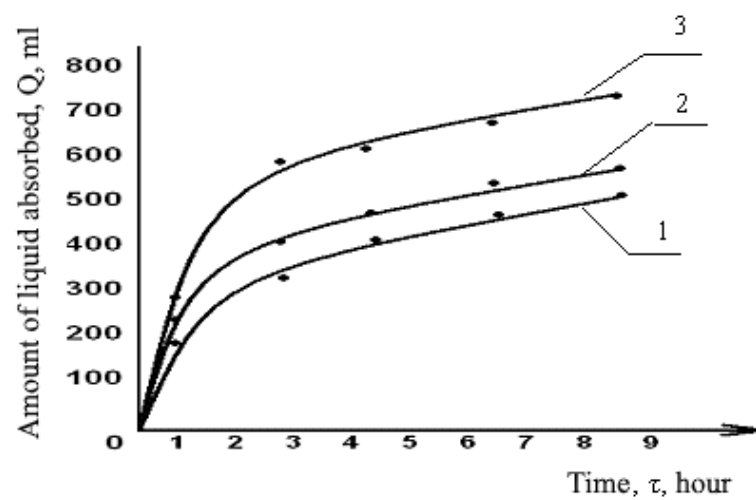


**Figure 4.** Swelling kinetics of 5% gelatine gel in the presence of sodium chloride depending on pH.  
 Note: Curve designations, pH: 1 – 5; 2 – 9; 3 – 3



**AVALIAÇÃO BASEADA EM CRITÉRIOS COMO MODO DE FORMAÇÃO DA ALFABETIZAÇÃO FUNCIONAL DOS ESTUDANTES EM CIÊNCIA DA COMPUTAÇÃO****CRITERIA-BASED ASSESSMENT AS THE WAY OF FORMING STUDENTS' FUNCTIONAL LITERACY IN COMPUTER SCIENCE****КРИТЕРИАЛЬНОЕ ОЦЕНИВАНИЕ КАК СПОСОБ ФОРМИРОВАНИЯ ФУНКЦИОНАЛЬНОЙ ГРАМОТНОСТИ УЧАЩИХСЯ ПО ИНФОРМАТИКЕ**

AVDARSOL, Sailaugul<sup>1\*</sup>; RAKHIMZHANOVA, Lyazzat B.<sup>2</sup>; BOSTANOV, Bektas G.<sup>3</sup>; SAGIMBAEVA, Ainur Ye.<sup>4</sup>; KHAKIMOVA, Tiyshtik<sup>5</sup>;

<sup>1,3,4</sup> Abai Kazakh National Pedagogical University, Institute of Mathematics, Physics and Informatics, Department of Informatics and Informatization of Education – Republic of Kazakhstan

<sup>2,5</sup> Al-Farabi Kazakh National University, Department of Computer Science – Republic of Kazakhstan

*\* Corresponding author  
e-mail: sailau-abai@mail.ru*

Received 14 February 2020; received in revised form 03 April 2020; accepted 24 April 2020

**RESUMO**

Durante muito tempo, a principal abordagem da avaliação foi a abordagem normativa, quando as realizações individuais dos estudantes foram comparadas com uma determinada norma (os resultados da maioria dos estudantes). Recentemente, a pesquisa pedagógica doméstica tem desenvolvido uma abordagem baseada em critérios para avaliar o desempenho acadêmico, de acordo com que as realizações dos estudantes são comparadas com o escopo de conhecimento que deve ser adquirido em um estágio específico do treinamento. Este estudo teve como objetivo determinar o papel da avaliação baseada em critérios na formação da alfabetização funcional dos estudantes em ciência da computação e construir um modelo de avaliação baseada em critérios no desenvolvimento da alfabetização funcional além de demonstrar a eficácia dos métodos de formação dos alunos. 'alfabetização funcional em ciência da computação. Os principais métodos de pesquisa foram a metodologia de avaliação baseada em critérios desenvolvida pelos autores e a metodologia de avaliação formativa. Foram analisados alguns elementos da metodologia de avaliação formativa. Para o desenvolvimento adicional da metodologia para a formação da alfabetização funcional dos estudantes em ciência da computação, foi construído um modelo de avaliação baseada em critérios. A introdução da avaliação baseada em critérios permitirá mudar para uma avaliação formativa destinada ao desenvolvimento da competência do estudante. A avaliação, composta por critérios que o estudante entende, o estimula e torna o processo de aprendizado lógico. Com base nos experimentos práticos e na avaliação proposta com base em critérios, foi comprovada a eficácia de métodos para a formação da alfabetização funcional dos estudantes em ciência da computação.

**Palavras-chave:** *avaliação crítica, educação, resultados, avaliação, ciência da computação.*

**ABSTRACT**

For a long time, the primary approach to assessment was the normative approach when the individual achievements of students were compared with a particular norm (the results of most students). Recently, domestic pedagogical research has been developing a criteria-based approach to assessing academic achievement when students' achievements are compared with the amount of knowledge that needs to be acquired at a particular stage of training. This study aimed to determine the role of criteria-based assessment in the formation of students' functional literacy in computer science and to build a criteria-based assessment model in the development of functional literacy beyond to demonstrate the effectiveness of the methods of formation of students' functional literacy in computer science. The leading research methods were the criteria-based assessment methodology developed by the authors and the method of formative assessment. Some elements of the methodology of forming evaluation were considered. For further development of the methods for the formation of students' functional literacy in computer science, a criteria-based assessment model has been built. The introduction of criteria-based assessment will allow to switch to a formative evaluation aimed at developing student competence. The evaluation, consisting of criteria that a student understands, stimulates him and makes the learning process meaningful. Based on practical experiments and the proposed criteria-based assessment, the effectiveness of

methods for the formation of students' functional literacy in computer science has been proved.

**Keywords:** *critical assessment, education, results, assessment, computer science.*

## АННОТАЦИЯ

На протяжении долгого времени основным подходом к оцениванию был нормативный подход, когда индивидуальные достижения учащихся сравнивались с определенной нормой (результатами большинства обучающихся). В последнее время в отечественных педагогических исследованиях разрабатывается критериальный подход к оценке успеваемости, когда достижения учащихся сравниваются с объемом знаний, который подлежит усвоению на определенном этапе обучения. Целью данного исследования было определить роль критериального оценивания при формировании функциональной грамотности учащихся по информатике и построить модель критериального оценивания для развития функциональной грамотности, чтобы показать эффективность методов формирования функциональной грамотности учащихся по информатике. Ведущими методами исследования стали разработанная авторами методика критериального оценивания и методика формирующего оценивания. Рассмотрены некоторые элементы методики формирующего оценивания. Для дальнейшей разработки методики формирования функциональной грамотности учащихся по информатике, построена модель критериального оценивания. Внедрение критериального оценивания позволит перейти к формативному оцениванию, направленному на развитие компетентности учащегося. Оценка, состоящая из критериев, понятных ученику, стимулирует его и делает процесс обучения смысловым. На основании практических экспериментов и предложенного критериального оценивания доказана эффективность методов формирования функциональной грамотности учащихся по информатике.

**Ключевые слова:** *критическое оценивание, образование, результаты, оценивание, информатика.*

## 1. INTRODUCTION:

For a long time, the main approach to assessment was the normative approach, when the individual achievements of students were compared with a particular norm (the results of most students) (Yang *et al.*, 2017; Yang *et al.*, 2019). Recently, domestic pedagogical research (Krasnoborova, 2009; Sokolova, 2017; Shalashova *et al.*, 2018; Totikova *et al.*, 2019) has been developing a criteria-based approach to assessing academic achievement, when students' achievements are compared with the amount of knowledge that needs to be acquired at a certain stage of training since there is a need for assessment, the results of which would allow to determine what educational goals a student has achieved. This led to the advancement of such an aspect of assessing as comparing an individual result with predetermined criteria.

Evaluation systems in different countries show that a five-point grading system with vague indicators is traditional and does not satisfy modern educational needs (Müller *et al.*, 2017; Cencelj *et al.*, 2019; Guo and Yan, 2019; Kim, 2019). A multi-point system is conventional, but different countries practice different points; the most optimal, in authors' opinion, is the letter designation of achievements, which means a certain number of points (Haber and Mitchell, 2017; Lookadoo *et al.*, 2017; Buchholtz *et al.*,

2018; Sagimbaeva *et al.*, 2019).

Kazakhstani school education is being developed in accordance with the State Program for the Development of Education of the Republic of Kazakhstan for 2011-2020. The updated educational program is aimed at developing a wide range of functional literacy of students, following international practice, enables students to develop functional literacy and critical thinking. In the program of Kazakhstan on the development of the functional literacy of students for 2012-2016, the results of the development of functional literacy of students and the application of acquired knowledge in practice are indicated as the main competencies.

Currently, Nazarbayev Intellectual Schools JSC, together with the Cambridge University Board of Examiners is developing experimental learning outcomes for each section and topic of the subject in innovative integrated training programs, and ways to assess their achievement. In a primary school (7–10th grades), students learn the same program material over a different period, depending on their abilities, and by the end of the 10th grade, they must achieve the same learning goals. This approach to the organization of the educational process, as it is seen, gives a high result (Sagimbaeva *et al.*, 2019) of training, and in the future, leads to a successful adult life.

In the curriculum for assessing the performance of students of other secondary

schools, in educational materials, practical experience systematically affecting the formation of educational and cognitive competence of students, the established criteria for assessing the achievements of students, who have interdisciplinary sciences, are not defined in advance. Criteria-based assessment in the educational process is not fully understood. Existing assessments and monitoring do not allow to determine whether achievements in the field of education are fully used since the subjective assessment tools used (tests, theoretical questions, control issues, etc. are not criteria for determining the level of knowledge acquisition) (Broadbent *et al.*, 2018; Sagimbaeva *et al.*, 2019)

The establishment of various approaches to assessing competence, personal orientation, the development of a general pedagogical concept based on the development of relationships – all this determines the current trends in the development of the assessment system, and some criteria for assessing the level of required competence are based on a comparison of students' achievements, methodological problems of criteria-based assessment (Carter and Bathmaker, 2017; Sanchez *et al.*, 2017; Alt, 2018; Mohamadi, 2018; Astriawati and Djukri, 2019; Basera, 2019; Palmiero and Cecconi, 2019; Mirmotahari *et al.*, 2019).

Thus, based on the theoretical and practical foundations of world and domestic experience, it can be concluded that as part of the educational process, assessment and control and evaluation activities as a whole act as an independent element of the content of education, requiring development (Azmy and Mokhtar, 2017; Marinkovich *et al.*, 2018; Mohamadi Zenouzagh, 2019; Pastore *et al.*, 2019; Silseth and Gilje, 2019). At the same time, the assessment system allows to receive integral and differentiated information about the educational process, track individual student progress in achieving the planned results, provide feedback for teachers, students, and parents, track the effectiveness of the educational program (Luckin *et al.*, 2017; Meek *et al.*, 2017; Houston and Thompson, 2017; Black and Wiliam, 2018; Tienson-Tseng, 2019).

This study aimed to determine the role of criteria-based assessment in the formation of students' functional literacy in computer science and to build a criteria-based assessment model in the development of functional literacy beyond to demonstrate the effectiveness of the methods of formation of students' functional literacy in computer science.

## 2. LITERATURE REVIEW:

A.A. Krasnoborova (2009), in her article, proposes the author's definition of pedagogical technology for criteria-based assessment. The authors call the pedagogical technology of criteria-based evaluation of students in the framework of educational and cognitive activity a process-effective meta-technology that provides a system of interconnected control and assessment of actions of all participants in the educational process to achieve the goals and objectives of the training.

In the study of E.A Sokolova. (2017) a methodology is developed in which criteria-based internal assessment is included in all stages of the activity-oriented design of teaching the topic of the school geometry course developed in this study. Studies suggest different approaches to assessing results.

The study by M.M. McGill (McGill and Decker, 2019) introduces a Resource Centre (csedresearch.org) designed to provide resources for researchers in primary and secondary computer education. The center has a primary function to provide a centralized location for assessment tools, many of which focus on computing.

Y. Ohashi (Ohashi and Yamachi, 2017) used participant observation and group interviews as research methods, as well as a case code matrix and a qualitative data analysis method. The authors developed assessment criteria for an information volunteer for a training course launched in 1997, in which students participated in educational activities based on information from nearby schools. The study generated 30 cases, which were organized in the following three categories: problems, support, and what they learned from this activity. Each of these categories was further divided into the following subcategories: communication, office work, and training. It was discovered that students could not solve all the problems. Also, students demonstrated different levels of performance, which, according to their conclusion, may be associated with differences in students' academic abilities, as well as with the diversity of activities from school to school.

When determining functional online literacy in the study by K. Dolenc (Dolenc *et al.*, 2015), it is demonstrated that there are differences in reading comprehension when reading offline and online, when using electronic school material in their educational process. The study involved 78

students of the 8th grade of primary school, studying the course "Technology and Science." The authors used individual and adaptive intelligent learning systems (ITS) and, using the assessment of the results, showed that for this form of ITS there is still enough room for optimization, which is a constant method of improvement and updating in such systems.

Priscilla Haring (Haring *et al.*, 2018), examining information on the relationship between game design and player's cognitive processes, explores the use of Bloom's taxonomy in describing a psychotherapeutic game in terms of knowledge and cognitive processing.

The study by Valerie J. Shute (Shute *et al.*, 2011) examines the research literature on the relationship between parental involvement (PI) and academic performance, with a particular emphasis on high school (middle and high school). The results first show how individual PI variables relate to academic achievement, and then move on to a more sophisticated analysis of several variables of the general design described in the literature.

Yuan Wang (Wang *et al.*, 2018), in his studies, showed that assessing the skills of information literacy students is extremely important. This article explores an improved compression criterion, which is based on the entropy of a population in an objective space and the maximum distance in a decision-making space and is used to make a decision about starting a local search. The authors argue that the modified model-based population reinitialisation strategy is designed to enhance the ability of HDEM (hybrid differential evolution with model-based reinitialisation) to search globally for solving complex problems.

Panagiotis Psomos (Psomos and Kordaki, 2011) presents a new model for assessing the pedagogical validity of educational digital storytelling environments (EDSE). This model is based on modern social and constructivist views on learning and consists of sixteen dimensions. The model has the shape of a star called the "Digital Storytelling Pedagogical evaluation star," consisting of sixteen peaks as the number of aspects of the assessment above model. The proposed model can help researchers and designers in the pedagogical analysis of the existing EDSE and in making appropriate decisions for the design of the future EDSE. Besides, this model can help teachers choose the right EDSE so that they can complete specific pedagogical tasks in their classrooms.

Rosário R. (Rosário *et al.*, 2011) analyses the role played by some homework variables in student achievement (proximal and distal), as well as their mediating role in using self-regulatory learning strategies and perceived self-efficacy in the subject area. The focus is on English as a Foreign Language (EFL), and a sample of 591 Portuguese fifth and sixth-grade students is used. The data they obtained confirm the indirect effect of homework on school achievement with the help of the mentioned cognitive and motivational variables (the use of self-regulatory learning strategies and self-efficacy).

Inga Glogger (Glogger *et al.*, 2013) shows in her study teacher preparation for evaluating important components of self-regulatory learning, such as learning strategies, which is an essential aspect of integrating self-regulatory knowledge in the school. The authors argue that training journals can be used to evaluate learning strategies per models of the cyclic process of self-regulatory learning and provide precious formative feedback. A computer-based learning environment (CBLE) has been developed that educates teachers in evaluating learning strategies using instructional journals.

The goal of Manuela Leidinger (Leidinger and Perels, 2012), based on Zimmermann's theory of self-regulation, was to promote a robust learning environment to support self-regulatory learning using teaching materials. Learning materials have been developed that focus on the specific (meta) cognitive and motivational components of self-regulatory learning and are divided into six blocks, with which students from the experimental group worked weekly. In total, 135 fourth-graders took part in the study.

The article by A. Vernon (2011) reviews a model developed by the authors to evaluate non-traditional teaching methods, such as group learning. This model was applied to group training courses, which included innovative enhancements such as group exams and group-based role-playing games. The model required a balanced presentation among the set of learning criteria, grouped into six sets of target criteria; all of them are taken from the literature on group learning. The authors developed a test tool based on this model and presented it to 85 students at the end of three business strategy courses.

Many topical questions were asked by teachers in a study by Vreda Pieterse (Pieterse and du Toit, 2009) in a closed electronic survey to identify possible causes for misrepresentation of questions in assessing knowledge, due to the

students' inability to sufficiently understand their essence. In this study, they tried to extrapolate aspects that could lead to computer science students misunderstanding instructions and scientific research. As a result, they would not be able to solve the very questions that the lecturer wants to evaluate. The authors sought to compile a set of guidelines to address issues related to misunderstanding of the issues raised.

Functional literacy consists of language, legal, environmental, computer, information, and activity literacy. During the current continuous development of the information society, everyone has the opportunity to master information technology and use it according to their own needs, that is, forms their own computer literacy, which is one of the components of students' functional literacy, and it is also known that computer science plays a huge role in the formation of information and technological competencies, which are an integral part of the competencies indicated above.

The expected results of students in computer science provide an opportunity to objectively evaluate their educational achievements and determine their development paths, considering the abilities of each student, also help stimulate students' skills and expect improvement in the quality of the educational process.

In reflecting the assessment of computer science for K-8 teachers, Hannah E. Chipman (Chipman *et al.*, 2019) concluded that one area that has not been fully explored is how grades can affect student confidence and attitudes to CS. It was shown that the threat of stereotype and modality of a test affect the performance of the tested CS.

As a result of studying the functional literacy of students in the work of Anatoly Veryaev (Veryaev *et al.*, 2012), it was shown that functional literacy reflects practical ideas about adaptation to social conditions, and cannot be considered as one of the leading educational goals. It is concluded that the natural-scientific direction of training, in comparison with the humanities, has a more favorable effect on the test results in the framework of tasks proposed by international organizations. As a result, the identification of computer and information literacy levels allowed to test the developed test tasks focused on the Federal State Educational Standard to adjust lectures and practical classes for first-year students at the Computer Science course.

The monograph by H.S. Bhola (1979)

considers assessment as a link in the "ideology for technology" chain, assessment models and approaches, an assessment model for a specific situation, providing assessment in functional literacy programs, classic change measurement protocols, some newly discovered change measurement protocols, implementation data for management and evaluation, particular assessment tasks for employees of functional literacy, data verification, and analysis, design of assessment and interpretation of evaluation results for decision making.

### 3. MATERIALS AND METHODS:

Criteria-based self-assessment: at the beginning of work with this technique, a teacher needs to determine the criteria for assessment with students. A teacher should show by example the levels of achievement of these criteria and how the assessment process will take place. It is also useful to practice evaluating works. Examples of criteria-based self-assessment tools are systems of conditional signals and designations of the level of understanding or mastering by a student of a particular knowledge or skill (for example, "color tracks", "traffic lights", "rulers", "cards +/-").

For criteria-based mutual assessment, maps or sheets of assessment are developed with criteria and levels of achievement or forms of feedback on a work. Weekly reports are sheets that students fill out at the end of the week, containing three questions: What have I learned this week? What questions remained unclear for me? What questions would I ask students if I were a teacher to check if they understood the material?

The mind map (intellect map, concept map) consists of the names of concepts placed in frames; they are connected by lines fixing the relations of these concepts from general to particular. A map is considered from top to bottom, a teacher will be able to determine how well students see the overall picture of an entire course or a single topic.

The introduction of criteria-based assessment will allow switching to a formative evaluation aimed at developing student competence. The assessment, consisting of criteria that a student understands, stimulates him, and makes the learning process meaningful. The criterion approach to assessing students consists in comparing the student's achievements with well-defined, collectively developed criteria well known to all participants in the process. Criteria of assessment are developed for each subject. With proper preparation of the criteria scale, the student

can independently assess the quality of their work, which stimulates the achievement of a higher educational result and the formation of educational independence. The use of criteria-based assessment in the educational system makes it possible to identify and improve the method for assessing student performance with the objective goals of an individual subject, as well as using specific parameters (criteria) that allow students to compete in high school.

#### 4. RESULTS AND DISCUSSION:

Criteria assessment consists of formative and summative assessments. The training manual of the Ministry of Education and Science of the Republic of Kazakhstan (Methodological and educational..., 2017) indicates that formative assessment is an assessment of the current work in the classroom, which is mandatory for this stage of training and the cognitive process. This is the student's current performance indicator, providing feedback between a student and teacher. It helps to identify student difficulties and increase the ability to achieve good results. A student should be able to fill current gaps in learning, considering the recommendations of a teacher, with the advice of other students, completing the remaining or additional tasks.

Summative assessment is a cumulative form of assessment that is carried out at the end of a specific training period (quarter, trimester, academic year), and also after mastering the section (Methodological and educational ..., 2017). Following the curriculum, the criteria-based assessment is conducted continuously by a teacher, provides feedback between a teacher and students, and allows timely correction of learning processes, not only scores, grades. A total assessment of sections/general topics is carried out by a teacher 2-3 times a quarter. The final quarterly assessment is carried out by a teacher at the end of each quarter. Summative assessment to determine the level of knowledge is carried out at the end of the primary, principal, senior grade. The funded system records only the achievements of students; therefore, actively encourages students to self-study and cognitive activity, to the full mastery of the curriculum. Standards, methods, and means of assessment vary depending on the type of assessment and subject specificity. The authors present the developed criteria-based evaluation model in the form of a scheme (Figure 1). Consider the techniques of formative assessment (Figure 2). Each of them is based on different criteria.

Computer science training mainly involves the development of user skills, in particular computer skills and new technologies. Therefore, when studying some topics, practical work on the computer is conducted. When developing and testing experimental integrated educational programs in subjects, the authors partially began to use the approach used by Nazarbayev Intellectual Schools in conjunction with the Examination Council of the University of Cambridge.

The authors want to focus on the practice of preparing assignments and carrying out SAS (summative assessment of a section) and SAQ (summative assessment of a quarter) when teaching computer science. When developing tasks of SAS and SAQ with the use of criteria-based assessment at computer science lessons and meeting the requirements of the modern system of updated content in training, it is necessary to strive to develop students' thinking, to provide an opportunity to analyse the proposed situations, thereby students learn to analyse and evaluate their critical thinking. When developing test tasks in the SAQ, it is necessary to adhere to the test specification (ST), where the learning objectives and tested skills are predefined.

For example, consider the topic "Measuring information and a task" in the "Computer" section (Table 1). It is possible to accept tasks in the form of tests (Table 2).

For an objective and evidence-based verification of the validity of the pedagogical hypothesis, a pedagogical experiment was conducted using the following methodology. As a result of measuring the same indicator using the same measurement procedure, the following data are obtained:  $x = (x_1, x_2, \dots, x_n)$  – sample for the experimental group and  $y = (y_1, y_2, \dots, y_m)$  – for the control group, where  $x_i$  – the sample element – is the value of the studied indicator (feature1) for the  $i$ -th member of the experimental group,  $i = 1, 2, \dots, n$ , and  $y_j$  is the value of the studied indicator for the  $y_j$ -th member of the control group,  $j = 1, 2, \dots, m$ . The number of sample elements is called its size — for example, the size of sample  $x$  is  $N$ , and the size of sample  $y$  is  $M$  (Novikov, 2004).

Measurements were made on the *ratio scale* (time, number, etc.),  $\{x_i\}$  and  $\{y_j\}$  – positive, including natural numbers, for which all arithmetic operations make sense. The measurement consists in determining the level of knowledge by conducting a test that includes 20 tasks. It is assumed that the characteristic of a student (sign) is the number of correctly solved problems.

The authors use an *ordinal scale* (rank scale) with  $L$  gradations; it is assumed that  $\{x_i\}$  and  $\{y_j\}$  are natural numbers that take one of  $L$  values. A set of values (points) is a set of numbers from one to  $L$ . A characteristic of a group will be the number of its members who have gained a given score. That is, for the experimental group, the point vector is  $n = (n_1, n_2, \dots, n_L)$ , where  $n_k$  is the number of members of the experimental group who received the  $k$ -th point,  $k = 1, 2, \dots, L$ . For the control group, the point vector is  $m = (m_1, m_2, \dots, m_L)$ , where  $m_k$  is the number of control group members who received the  $k$ -th point,  $k = 1, 2, \dots, L$ . Obviously,  $n_1 + n_2 + \dots + n_L = N$ ,  $m_1 + m_2 + \dots + m_L = M$ .

Here are the formulas for calculating the main indicators. The arithmetic mean  $\bar{x}$  of the sample  $\{x_i\}_{i=1}^N$  (sample mean) is calculated as follows (Equation 1) and the sample dispersion  $D_x$  (Equation 2). For the data measured in the ratio scale, to test the hypothesis that the characteristics of the two groups coincide, it is advisable to use the Cramer-Welch criterion. The Cramer-Welch criterion is designed to test the hypothesis of equality of means (strictly speaking, mathematical expectations) of two samples.

The empirical value of this criterion is calculated on the basis of information about the volumes  $N$  and  $M$  of samples  $x$  and  $y$ , sample means  $\bar{x}$  and  $\bar{y}$ , and sample dispersions  $D_x$  and  $D_y$  of the compared samples (these values can be calculated manually using formulas (1)-(2) or using the tool "Descriptive statistics" in the computer program Microsoft Excel according to the following formula (Equation 3):

Descriptive statistics, firstly, allows presenting the results of a pedagogical experiment in a compact and informative form, which makes it possible to conduct a qualitative analysis of the objects studied. Secondly, several indicators of descriptive statistics are used in quantitative analysis (when applying statistical criteria). The algorithm for determining the accuracy of coincidences and differences in the characteristics of the compared samples for the experimental data measured in the ratio scale using the Cramer-Welch criterion is as follows:

1. To calculate for the analyzed samples the  $T_{\text{emp}}$  – the practical value of the Cramer-Welch criterion according to formula (3).

2. To compare this value with the critical value  $T_{0.05} = 1.96$ : if  $T_{\text{emp}} \leq 1.96$ , then conclude: "the characteristics of the compared samples coincide at a significance level of 0.05"; if  $T_{\text{emp}} > 1.96$ , then conclude "the reliability of differences in

the characteristics of the compared samples is 95%".

Experimental training was conducted in several schools in Almaty. Students were divided into experimental and control groups. The purpose of the pedagogical experiment was to verify the effectiveness of the developed system of tasks and tests and the authors' proposed methodology for the formation of students' functional literacy in computer science.

In the experimental and control groups, the SAQ was carried out according to the authors' tasks and tests. The experimental group consisted of  $N = 15$  people, and the control group consisted of  $M = 20$  people. The results of measurements of the level of knowledge in the control and experimental groups before and after the experiment are shown in Table 3.

The experimental results are also obtained in the ordinal scale. For  $N = 15$ ,  $M = 20$ , there are three levels of knowledge  $L = 3$ : low (the number of solved problems is less than or equal to 10), medium (the number of solved problems is strictly bigger than 10, but less than or equal to 15) and high (the number of solved problems is strictly bigger than 15). The authors form Table 4, in which the upper limits of the ranges are indicated (Figure 3).

For the measurement results in the ratio scale (Table 4), the descriptive statistics indicators were divided into several groups: position indicators describing the position of the experimental data on the numerical axis; scatter indicators describing the degree of spread of data relative to its center (average value). These include sample dispersion, the difference between the minimum and maximum elements (range, sampling interval), etc.; asymmetry indicators: the position of the median relative to the average, etc.

These indicators were used for visual representation and primary ("visual") analysis of the results of measurements of the characteristics of the experimental and control groups. Descriptive statistics for the first column of Table 3 (the number of correctly solved problems in the control group before the start of the experiment) are shown in Table 5.

The authors review the algorithm for determining the accuracy of coincidences and differences in the characteristics of the compared samples for the data from Table 1, measured in the ratio scale, using the Cramer-Welch criterion (Table 6). To do this, first, it is needed to compare the number of correctly solved problems in the

control and experimental groups before the experiment. The authors calculate by the formula (3) the value of  $T_{\text{emp}} = 0.84 \leq 1.96$ . Therefore, the hypothesis that the characteristics of the control and experimental groups coincide before the start of the experiment is accepted at a significance level of 0.05.

Now compare the characteristics of the control and experimental groups after the end of the experiment. The authors calculate by the formula (3) the value of  $T_{\text{emp}} = 2.04 > 1.96$ . Therefore, the reliability of differences in the characteristics of the control and experimental groups after the end of the experiment is 95%.

So, the initial (before the start of the experiment) states of the experimental and control groups coincide, and the final ones (after the end of the experiment) are different. Therefore, it can be concluded that the effect of changes is due precisely to the application of the experimental teaching methodology.

## 5. CONCLUSIONS:

The study of criteria-based assessment as a way of forming students' functional literacy in computer science and the results of experimental work have led to many conclusions:

1. The necessity to ensure the mastery of the primary content of the subjects studied and the formation of functional literacy among schoolchildren in seven key competencies require the development of a new system for assessment by criteria.

2. The basic content of education involves objective results aimed at enhancing the functional, including practical, focus of training. Despite the different number of points in the assessment and the divergence of opinions on this issue in different countries, in all of these systems the unifying core is the criterion of assessment and the differentiation of the levels of assimilation of educational material of students.

3. The process of developing functional literacy among schoolchildren determines the introduction of a new assessment system that takes into account the effectiveness of all types of educational activities, the procedural side of learning material, and the manifestation of individual and personal qualities of students.

4. When studying in the elementary school (7–10th grades), the same program material for a different period, depending on individual abilities, by the end of the 10th grade, students should

achieve the same learning goals. This approach to the organizing the educational process gives a high learning outcome, and in the future, leads to a successful adult life.

5. The assessment system allows to receive integrated and differentiated information about the educational process, track individual student progress in achieving the planned results, provide feedback for teachers, students, and parents, track the effectiveness of the educational program.

As a result of the study, the following results were obtained:

1. For further development of the methodology for the formation of students' functional literacy in computer science, a criteria-based assessment model has been built.

2. Based on practical experiments and the proposed criteria-based assessment, the effectiveness of methods for the formation of students' functional literacy in computer science has been proved.

## 6. REFERENCES:

1. Alt, D. *Learning Environments Research*, **2018**, 21(3), 387-406.
2. Astriawati, F., Djukri. *Journal of Physics: Conference Series*, **2019**, 1397(1), article number 012049.
3. Azmy, A., Mokhtar, H. *International Journal of Engineering Education*, **2017**, 33(2), 629-638.
4. Basera, C.H. *Journal of Education and e-Learning Research*, **2019**, 6(2), 76-81.
5. Bhola, H.S. (Ed.). *Evaluating Functional Literacy*. London: Hulton, **1979**.
6. Black, P., Wiliam, D. *Assessment in Education: Principles, Policy and Practice*, **2018**, 25(6), 551-575.
7. Broadbent, J., Panadero, E., Bouda, D. *Assessment and Evaluation in Higher Education*, **2018**, 43(2), 307-322.
8. Buchholtz, N.F., Krosanke, N., Orschulik, A.B., Vorhölter, K. *ZDM – Mathematics Education*, **2018**, 50(4), 715-728.
9. Carter, A., Bathmaker, A.-M. *Journal of Further and Higher Education*, **2017**, 41(4), 460-474.
10. Cencelj, Z., Aberšek, M.K., Aberšek, B., Flogie, A. *Journal of Baltic Science*



*Education*, **2019**, 18(1), 132-142.

11. Chipman, H.E., Rodríguez, F.J., Boyer, K.E. "I Impressed Myself with How Confident I Felt": Reflections on a Computer Science Assessment for K-8 Teachers. *Proceedings of the 50th ACM Technical Symposium on Computer Science Education* (pp. 1081-1087), Minneapolis, USA, **2019**.
12. Dolenc, K., Aberšek, B., Aberšek, M.K. *Journal of Baltic Science Education*, **2015**, 14(2), 162-171.
13. Glogger, I., Holzäpfel, L., Kappich, J., Schwonke, R., Nückles, M., Renkl, A. *Education Research International*, **2013**, 2013, article ID 785065.
14. Guo, W.Y., Yan, Z. *Assessment in Education: Principles, Policy and Practice*, **2019**, 26(6), 675-699.
15. Haber, N., Mitchell, T.N. *Journal of Library and Information Services in Distance Learning*, **2017**, 11(3-4), 300-313.
16. Haring, P., Warmelink, H., Valente, M., Roth Ch. *International Journal of Computer Games Technology*, **2018**, October, article ID 8784750.
17. Houston, D., Thompson, J.N. *Journal of University Teaching and Learning Practice*, **2017**, 14(3), article number 2.
18. Kim, P.H. *Asia Life Sciences*, **2019**, 20(2), 119-126.
19. Krasnoborova, A.A. *Criteria assessment as a means of improving the quality of education in the logic of the competency-based approach*. Perm: Perm State Pedagogical University, **2009**.
20. Leidinger, M., Perels, F. *Education Research International*, **2012**, 2012, article ID 735790.
21. Lookadoo, K.L., Bostwick, E.N., Ralston, R., Elizondo, F.J., Wilson, S., Shaw, T.J., Jensen, M.L. *Journal of Science Education and Technology*, **2017**, 26(6), 597-612.
22. Luckin, R., Clark, W., Avramides, K., Hunter, J., Oliver, M. *Interactive Learning Environments*, **2017**, 25(1), 85-97.
23. Marinkovich, J., Sologuren, E., Shawky, M. *Circulo de Linguística Aplicada a la Comunicación*, **2018**, 74, 195-220.
24. McGill, M.M., Decker, A.B. *CSeDResearch.org: Resources for primary and secondary computer science education research*. Aberdeen: University of Aberdeen, **2019**.
25. Meek, S.E.M., Blakemore, L., Marks, L. *Assessment and Evaluation in Higher Education*, **2017**, 42(6), 1000-1013.
26. Methodological and educational-methodical foundations for the implementation of a system of criteria-based assessment of educational achievements of students. Toolkit. Astana: NAO named after I. Altynsarin, **2017**, <https://nao.kz/blogs/download/117>, accessed 25 December 2019.
27. Mirmotahari, O., Berg, Y., Fremstad, E., Damsa, C. *IEEE Global Engineering Education Conference, EDUCON*, **2019**, April-2019, 1152-1157.
28. Mohamadi Zenouzagh, Z. *Asia Pacific Education Review*, **2019**, 20(3), 343-359.
29. Mohamadi, Z. *Studies in Educational Evaluation*, **2018**, 59, 29-40.
30. Müller, W., Rebholz, S., Libbrecht, P. *Lecture Notes in Computer Science (including subseries Lecture Notes in Artificial Intelligence and Lecture Notes in Bioinformatics)*, **2017**, 10108 LNCS, 480-489.
31. Novikov, D.A. *Statistical methods in pedagogical research (typical cases)*. Moscow: MZ-Press, **2004**.
32. Ohashi, Y., Yamachi, H. Developing evaluation criteria for a service-learning course in computer science education. *Proceeding of the 5th International Conference on Information and Education Technology* (pp. 53-57), Tokyo, Japan, **2017**.
33. Palmiero, C., Cecconi, L. *Journal of E-Learning and Knowledge Society*, **2019**, 15(3), 89-99.
34. Pastore, S., Manuti, A., Scardigno, A.F. *European Journal of Teacher Education*, **2019**, 42(3), 359-374.
35. Pieterse, V., du Toit, C.M. You asked for IT!: phrasing questions for computer science assessment, **2009**, <https://dl.acm.org/doi/abs/10.1145/1562741.1562762>, accessed 26 December 2019.
36. Psomos, P., Kordaki, M. *Proceedings of E-Learn*, **2011**, 37(4), 17-21.

37. Rosário, P., Mourão, R., Trigo, L., Suárez, N., Fernández, E., Tuero-Herrero, E. *Psicothema*, **2011**, 23(4), 681-687.
38. Sagimbaeva, A.E., Zaslavskaya, O.Yu., Avdarsol, S. *Criteria for assessing academic achievement in the Republic of Kazakhstan*. Moscow: Moscow State Pedagogical University, **2019**.
39. Sanchez, C.E., Atkinson, K.M., Koenka, A.C., Moshontz, H., Cooper, H. *Journal of Educational Psychology*, **2017**, 109(8), 1049-1066.
40. Shalashova, M.M., Shevchenko, N.I., Mahotin, D.A. *Espacios*, **2018**, 39(30), 1-13.
41. Shute, V.J., Hansen, E.G., Underwood, J.S., Razzouk, R.A. *Education Research International*, **2011**, 2011, article ID 915326.
42. Silseth, K., Gilje, Ø. *Assessment in Education: Principles, Policy and Practice*, **2019**, 26(1), 26-42.
43. Sokolova, E.V. *Criteria internal assessment of educational achievements of students in grades 7-9 in teaching geometry*. Moscow: Moscow State Pedagogical University, **2017**.
44. Tienson-Tseng, H.L. *ACS Symposium Series*, **2019**, 1337, 219-243.
45. Totikova, G., Aldabergenov, N., Salmirza, J., Nazarova, G., Gurbanova, A., Madiyarov, N., Yessaliyev, A. *Elementary Education Online*, **2019**, 18(2), 461-471.
46. Vernon, A. *Innovative Higher Education*, **2011**, 26(1), 59-77. DOI: 10.1023/A:1010938521365.
47. Veryaev, A., Nechunaeva, M., Tatarnikova, H. *Izvestiya of Altai State University*, **2012**, 2(2), article number P13-17 2013.
48. Wang, Y., Li, H., Ding, Z. *Computational Intelligence and Neuroscience*, **2018**, 2018, article ID 9745639.
49. Yang, S.-C., Luo, Y.-F., Chiang, C.-H. *Journal of Medical Internet Research*, **2017**, 19(1), article number e15.
50. Yang, S.C., Luo, Y.F., Chiang, C.-H. *Journal of Medical Internet Research*, **2019**, 21(11), article number e13140.

$$\bar{x} = \frac{1}{N} (x_1 + x_2 + x_3 + \dots + x_{n-1} + x_n) = \frac{1}{N} \sum_{i=1}^N x_i \quad (\text{Eq. 1})$$

$$D_x = \frac{1}{N-1} \sum_{i=1}^N (x_i - \bar{x})^2 \quad (\text{Eq. 2})$$

$$T_{sim} = \frac{\sqrt{M \cdot N} |\bar{x} - \bar{y}|}{\sqrt{M \cdot D_x + N \cdot D_y}} \quad (\text{Eq. 3})$$

**Table 1.** SAS assignments on the topic “Measuring information and computer memory”

| The objective of learning | 7.1.3.1 Classification of computer networks  |
|---------------------------|--|
| Criteria of assessment    | <p>Student:</p> <ul style="list-style-type: none"> <li>– determines the types of computer networks, information devices;</li> <li>– computer networks determine large-scale and local networks;</li> <li>– divides computer networks into wired and wireless networks;</li> <li>– is able to use types of networks in life;</li> <li>– types of networks, topology, information</li> </ul> |
| Level of thinking skills  | <p>Use</p> <p>Skills of high level</p>   |

|                |            |
|----------------|------------|
| Execution time | 20 minutes |
|----------------|------------|

**Table 2.** Test questions on classification of computer networks

| Criteria of assessment                         | Tasks No. | Descriptor Student   | Grade |
|--|-----------|--|-------|
| 7.1.3.1<br>Classification of computer networks | 1         | Determines the types of computer networks, information devices   | 1     |
|  | 2         | Is able to write names of network topology   | 1     |
|  | 3         | Provides examples of using the topology of a network of schools, classes, buildings, institutions  | 1     |
|  | 4         | Identifies advantages and disadvantages of computer network  | 1     |
|  | 5         | Determines characteristics of definitions of local, big, global, zipping, text, table, regional, state, algorithm, package, image, format, wireless, cable, etc. | 1     |
|  | 6         | In order to unite several cellphones, choses a type of network, defines in practice  | 1     |
| In total                                       |           |  | 6     |

**Table 3.** The results of measurements of the level of knowledge in the control and experimental groups before and after the experiment

| No. | The control group (the number of correctly solved problems before the start of the experiment) | The experimental group (the number of correctly solved problems before the start of the experiment) | The control group (the number of correctly solved problems after the end of the experiment) | The experimental group (the number of correctly solved problems after the end of the experiment) |
|-----|--|---|---|--|
| 1   | 15   | 12  | 16  | 15   |
| 2   | 13   | 11  | 12  | 18   |
| 3   | 11   | 15  | 14  | 12   |
| 4   | 18   | 17  | 17  | 20   |
| 5   | 10   | 18  | 11  | 16   |
| 6   | 8  | 6   | 9   | 11   |
| 7   | 20   | 8   | 15  | 13   |
| 8   | 7  | 10  | 8   | 7  |
| 9   | 8  | 16  | 6   | 14   |
| 10  | 12   | 12  | 13  | 17   |
| 11  | 15   | 15  | 17  | 19   |
| 12  | 16   | 14  | 19  | 16   |
| 13  | 13   | 19  | 15  | 12   |
| 14  | 14   | 13  | 11  | 15   |
| 15  | 14   | 19  | 9   | 19   |
| 16  | 19   |   | 19  |  |
| 17  | 7  |   | 8   |  |
| 18  | 8  |   | 6   |  |
| 19  | 11   |   | 9   |  |
| 20  | 12   |   | 12  |  |

**Table 4.** The results of the experiment by level of knowledge

| The level of knowledge | Before the experiment |    | After the experiment |    |
|------------------------|-----------------------|----|----------------------|----|
|                        | CG                    | EG | CG                   | EG |
| Low                    | 6                     | 3  | 7                    | 1  |
| Medium                 | 10                    | 8  | 8                    | 7  |
| High                   | 4                     | 4  | 5                    | 7  |

**Table 5.** The numbers of correctly solved problems in the control group before the experiment

| Parameters       | Control group before the start of the experiment | Control group after the end of the experiment | Experimental group before the start of the experiment | Experimental group after the end of the experiment |
|------------------|--|---|---|--|
| Size of a sample | 20   | 15  | 20  | 15   |
| Minimum          | 7  | 6   | 6   | 7  |
| Maximum          | 20   | 19  | 19  | 20   |
| Interval (range) | 13   | 13  | 13  | 13   |
| Sum              | 251  | 205   | 246   | 224  |
| Average          | 12.55  | 13.6667                                       | 12.3  | 14.9333  |
| Median           | 12.5   | 14  | 12  | 15   |
| Dispersion       | 15.31  | 15.24   | 16.75   | 12.49  |

**Table 6.** Criterion Method of Cramer-Welch

|                       |          |    |          |
|-----------------------|----------|----|----------|
| 15                    | 6.0025   | 15 | 0.004444 |
| 13                    | 0.2025   | 18 | 9.404444 |
| 11                    | 2.4025   | 12 | 8.604444 |
| 18                    | 29.7025  | 20 | 25.67111 |
| 10                    | 6.5025   | 16 | 1.137778 |
| 8                     | 20.7025  | 11 | 15.47111 |
| 20                    | 55.5025  | 13 | 3.737778 |
| 7                     | 30.8025  | 7  | 62.93778 |
| 8                     | 20.7025  | 14 | 0.871111 |
| 12                    | 0.3025   | 17 | 4.271111 |
| 15                    | 6.0025   | 19 | 16.53778 |
| 16                    | 11.9025  | 16 | 1.137778 |
| 13                    | 0.2025   | 12 | 8.604444 |
| 14                    | 2.1025   | 15 | 0.004444 |
| 14                    | 2.1025   | 19 | 16.53778 |
| 19                    | 41.6025  |    |          |
| 7                     | 30.8025  |    |          |
| 8                     | 20.7025  |    |          |
| 11                    | 2.4025   |    |          |
| 12                    | 0.3025   |    |          |
| number                | 20       |    | 15       |
| average               | 12.55    |    | 14.93333 |
| dispersion            | 15.31316 |    | 12.49524 |
| value of a criterion: | 1.884972 |    |          |

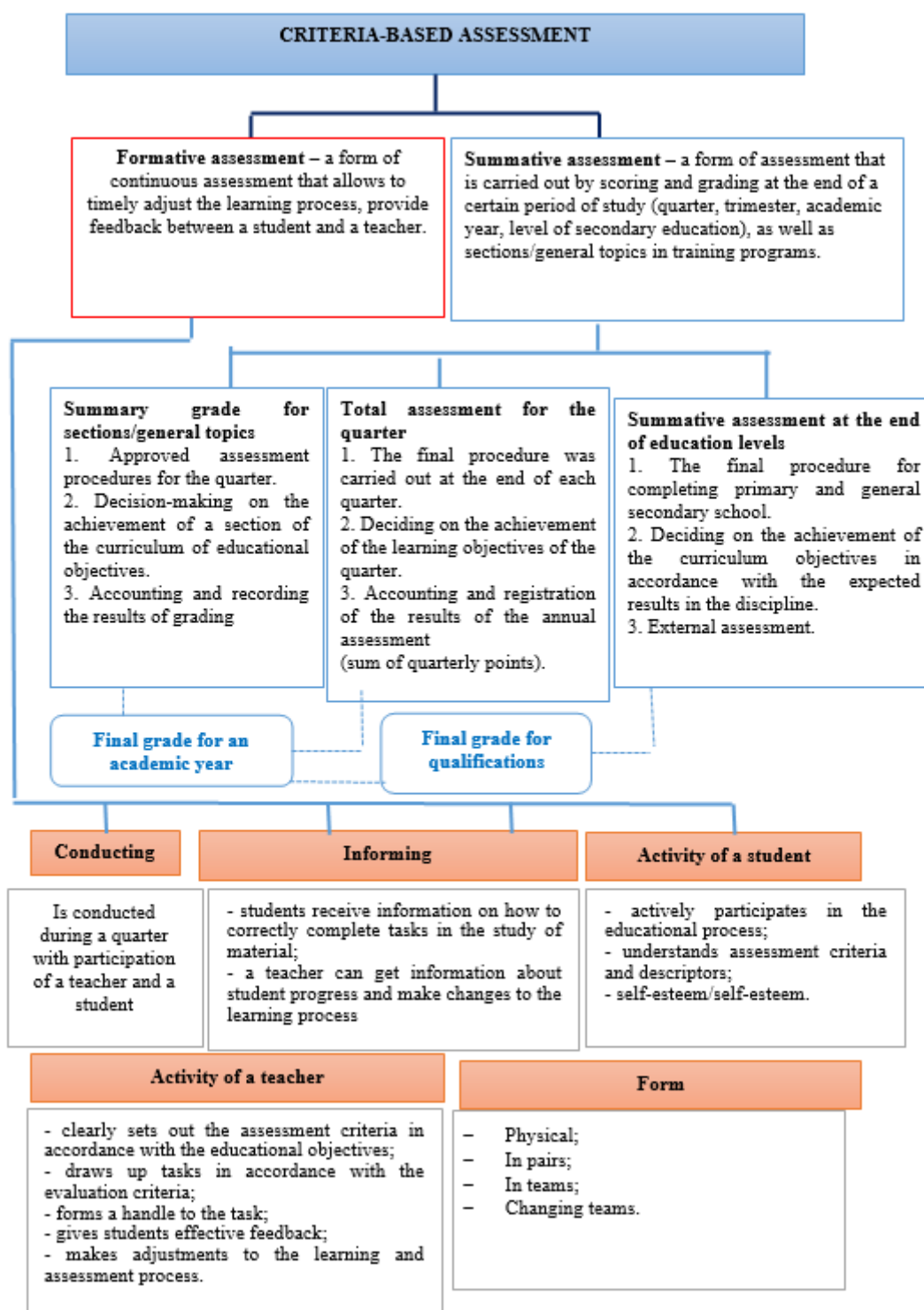


**Figure 1.** The model of criteria-based assessment

Reference: developed by the authors.

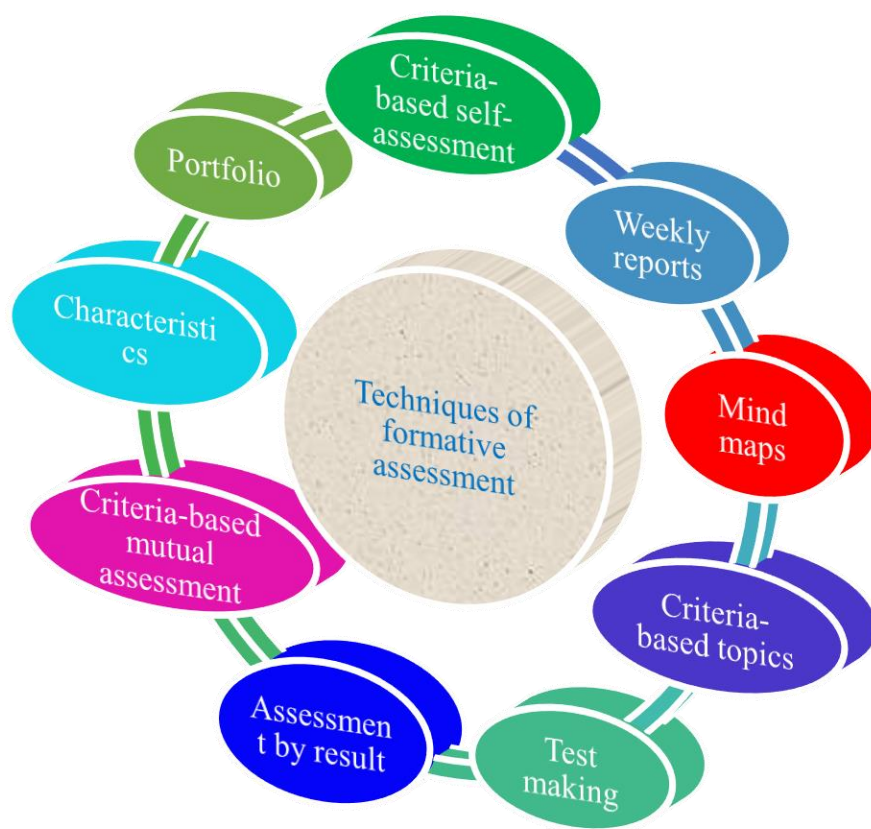


**Figure 2.** Formative assessment methods

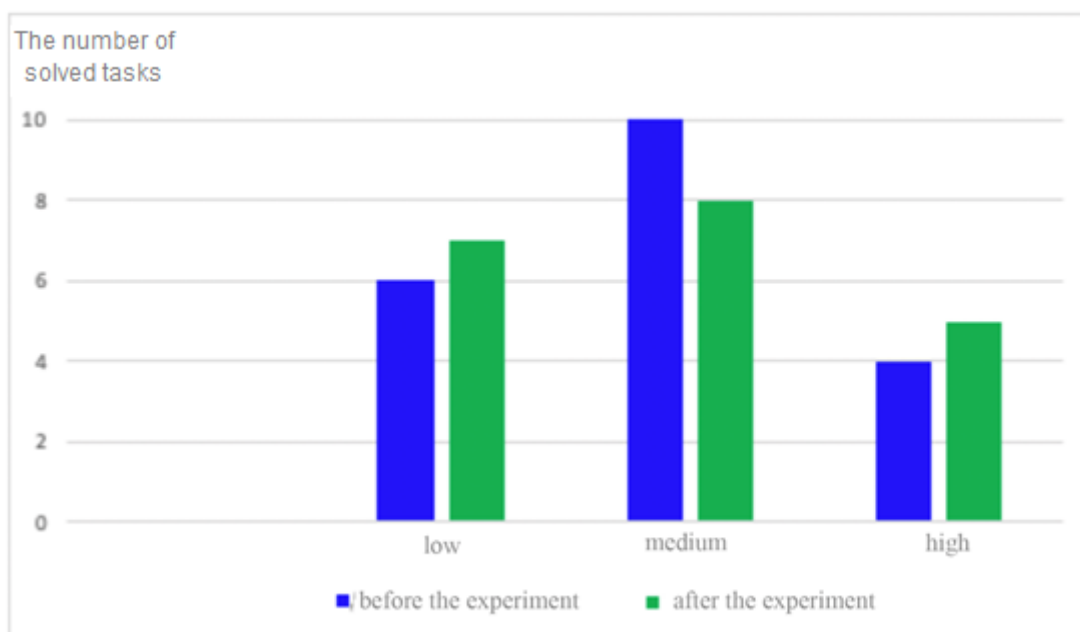


**Figure 3.** Chart of knowledge levels

## INVESTIGAÇÃO DO ENTENDIMENTO CONCEITUAL DE ESTUDANTES DE GRADUAÇÃO SOBRE MOVIMENTO HARMÔNICO SIMPLES EM SISTEMA DE MASSA-MOLA

### INVESTIGATION OF UNDERGRADUATE STUDENTS CONCEPTUAL UNDERSTANDING ABOUT SIMPLE HARMONIC MOTION ON MASS-SPRING SYSTEM

NUGRAHA, Dewanta Arya<sup>1\*</sup>; CARI, C.<sup>2</sup>; SUPARMI, A.<sup>3</sup>; SUNARNO, Widha<sup>4</sup>

<sup>1,4</sup>Doctorate Program of Science Education, Universitas Sebelas Maret, Surakarta, Central Java, Indonesia.

<sup>2,3</sup>Physics Department, Universitas Sebelas Maret, Surakarta, Central Java, Indonesia.

\* Corresponding author

e-mail: dewanta.an@student.uns.ac.id

Received 18 March 2020; received in revised form 21 April 2020; accepted 24 May 2020

#### RESUMO

O Movimento Harmônico Simples (SHM) é um dos tópicos básicos da física que subjaz a outros conceitos e está intimamente relacionado à vida cotidiana e à tecnologia. É usado para entender os fenômenos de movimento mecânico, som, luz e teoria quântica, em particular, osciladores harmônicos. O objetivo do estudo foi investigar a compreensão conceitual dos alunos sobre o movimento harmônico simples no sistema massa-mola. A coleta de dados foi realizada por meio de testes e entrevistas. Os sujeitos da pesquisa consistiram em 49 estudantes em uma universidade em Jacarta. Os instrumentos utilizados foram tarefas de múltipla escolha. Os resultados da investigação mostraram que a maioria dos estudantes não conseguiu dominar bem os conceitos básicos do movimento harmônico simples, determinar a magnitude da aceleração dos objetos devido à oscilação e encontrar o escopo do período de oscilação. Os resultados mostram que o desempenho médio dos alunos é inferior a 50%. A falta de compreensão da concepção do aluno é causada pelo fato de os alunos não conseguirem relacionar conteúdos anteriores (como a lei de Newton e a lei de Hooke) com estratégias para resolver problemas.

**Palavras-chave:** *Investigação, compreensão de conceitos, Lei de Hooke, movimento harmônico simples, sistema de massa-mola.*

#### ABSTRACT

Simple Harmonic Motion (SHM) is one of a primary physics topic that underlies other concepts and is closely related to everyday life and technology. It is used to understand the phenomena of mechanical motion, sound, light, and quantum theory, in particular, harmonic oscillators. This study aimed at investigating students' conceptual understanding of simple harmonic motion on the mass-spring system. Data collection was made using tests and interviews. The research subjects consisted of 49 students at a university in Jakarta. The instruments used were multiple-choice tasks. The results of the investigation showed that most students have not been able to name the basic concepts of simple harmonic motion, determine the magnitude of the acceleration of objects due to oscillation, and find the scope of the oscillation period. The results show that the average achievement of students is less than 50%. Lack of understanding of student conception is caused by students not being able to relate previous insights (such as Newton's law and Hooke's Law) with strategies for solving problems.

**Keywords:** *Investigation, Concepts Understanding, Hooke's Law, Simple Harmonic Motion, Mass-spring System.*

#### 1. INTRODUCTION:

Nowadays, research in the field of physics education, in particular, understanding student concepts, is a research trend that is studied in depth. Understanding concepts is one of the main objectives in learning physics (Adolphus, Alamina, Aderonmu, Education, and State, 2013; Arista and

Kuswanto, 2018; Eldy and Wui, 2019; Krinks, 2016; Maison and Syamsurizal, 2019; Ogundéji, Madu, and Onuya, 2019; Olmstead, 2019; Somroob and Wattanakasiwich, 2017; Son, 2017), so that with a good understanding of the concept students can apply it in everyday life (Dimas, Suparmi., Sarwanto., and Nugraha., 2018; Nugraha, Suparmi, Masykuri, and Cari, 2016).

Physics is the study of matter, energy, and its interactions. Physics plays a key role in the progress of humanity; in this case, physics, as a basic concept for technological advancements needed to drive the world economy (Adolphus *et al.*, 2013). Simple Harmonic Motion (SHM) is one of the physical materials that is closely related to everyday phenomena; it is used to understand the phenomena of mechanical motion, sound and light, and quantum theory in particular harmonic oscillators (Adolphus *et al.*, 2013; Alho, Silva, Teodoro, and Bonfait, 2019; Greene, Gill, and Eyerly, 2016; Parnafes, 2010).

The application of SHM concepts in daily life can help students identify and shape their knowledge (Khowatim, Mahardika, and Alex, 2017). Some real-world phenomena, such as simple harmonic motion, require an understanding of the concepts of coordinates in various wave functions (Parnafes, 2010). So it can be said that the understanding of SHM concepts that must be understood by students both in theory and mathematical calculations (Adolphus *et al.*, 2013). By learning how students understand physics, and their attitude towards learning physics is something interesting to study (Angell, Guttersrud, Henriksen, and Isnes, 2004; Son, 2017). It aims to improve the quality of physics learning.

The quality of physics learning has a positive correlation between teacher mastery of physics material and better pedagogical practices (Dandare, 2018). The results of research conducted by Dandare (2018), revealed that there are gaps in physics teachers regarding simple harmonic motion material.

Therefore, the aim of this study was to investigate students' conceptual understanding of simple harmonic motion on the mass-spring system.

## 2. LITERATURE REVIEW:

Understanding the concept is a process of adaptation and transformation of science (Gardner, 1999). Concept mastery is the result of student learning in the form of achieving the competence of physics courses in the cognitive domain. A scientific concept is expressed in various levels and presented or generalized in curriculum standards (OECD, 1999). The concepts of students are explored and developed using logical reasoning skills, training, formulating theories, and participation in problem-solving so that students can create an accurate conclusion (Nurhuda, Rusdiana, and Setiawan, 2017).

Physics learning aims to make students obtain many concepts and apply or apply flexibly (Reif, 1995). To represent the concept of physics requires an exceptional understanding of the idea. In other words, the multi-representation ability is closely related to understanding student concepts. The representation can be interpreted as a description of the relationship between objects and symbols (Hwang, Chen, Dung, and Yang, 2007). The connection with learning physics representation aims to describe a concept/object/phenomenon using specific symbols, including words/verbal symbols, diagrams/pictures, graphs, and mathematical symbols.

While multi-representation is a way to represent a concept in the form of different representations. Waldrip *et al.* (2006: 87) define multiple representations as practices to describe the same idea through various ways, which include descriptive descriptions (verbal, graphs, tables), experimental, mathematical, figurative (pictorial, analogy, and metaphorical), kinesthetic, visual and operational-operational (Waldrip, Prain, and Carolan, 2006). Merging these representations complement each other, making it easier for students to understand concepts and solve problems.

Multirepresentations have three main functions, namely as a complementary, limiting interpretation, and understanding builder (Ainsworth, 2006). Multirepresentations support the inculcation of concepts by providing supplementary information about an idea, limiting the possibility of errors in the use of other representations, and helping to build deeper understanding by increasing abstraction, helping generalization, and building relationships between representations. Learning process by using multi representation models effectively to enhance students' understanding of concepts (Fatmaryanti and Nugraha, 2019).

Simple harmonic motion (SHM) is one of the materials taught in basic physics courses. Some research has been done on understanding concepts and learning from SHM material. Research by Somroob (Somroob and Wattanakasiwich, 2017) shows most students have misconceptions about the recovery style, and they have problems connecting mathematical solutions with real movements, especially phase angles. Also, they have issues with interpreting mechanical energy from charts and motion diagrams (Somroob and Wattanakasiwich, 2017).



### 3. MATERIALS AND METHODS:

#### 3.1. Research Design

This research method was surveying with qualitative analysis. The instrument used in this research was developed from some source such as the Serway and Jewett physics textbook, AP Physics SHM test, and SHM-CS (Hammer, 1996; Nugraha, Cari, Suparmi, and Sunarno, 2019; Serway and Jewett, 2004; Somroob and Wattanakasiwich, 2017). The instrument have been validated before use. The tool consists of twelve items. The distribution of items used is presented in Table 1. The topic discussed in this study is the mass-spring system with six items. The data was analyzed qualitatively compared with the result of unstructured interviews with students. The interviews conducted to clarify student reasoning due to their answer (Lee and Park, 2013; Waldrup, Prain, and Sellings, 2013).

#### 3.2. Research Subject

The sample used in the study were students in the physics education program at Indraprasta University. This study held in indraprasta with permission from the lecturer or physics education at Indraprasta University in 2019. The sample selection uses a purposive sampling technique with a total sample of 49 students. Purposive sampling is sampling based on specific considerations based on researchers' criteria (Patton, 2014; Teddlie and Tashakkori, 2009).

#### 3.3. Instrument

The instrument was a conceptual survey that is used to determine the level of students' understanding after they have completed a series of physics learning. The instrument used was in the form of a reasonable multiple choice that was adopted. The instrument is developed from a daily phenomenon and combine with the theories. The validated instrument consists of some concepts about simple harmonic motion. The concepts included (1) Direction of the normal force vector and the gravity; (2) Basic concepts of simple harmonic motion; (3) Acceleration of the object due to oscillation, and (4) System oscillation period. The distribution of items in each concept is presented in Table 1.

**Table 1.** Distribution of Question Items for Concept Understanding Instrument

| No | Sub Concept Material Mass-Spring System              | Number of Items |
|----|--|-----------------|
| 1  | Direction of the normal force vector and the gravity | 1               |
| 2  | Basic concepts of simple harmonic motion             | 2               |
| 3  | Acceleration of the object due to oscillation        | 2               |
| 4  | System oscillation period                            | 1               |

Before an analysis of students' conceptual understanding is carried out, a study of the characteristics of the instrument is conducted. The features of the instruments used, referring to the modern test theory. Analysis of instrument characteristics using the Quest program, the results of the study are presented in Table 2.

**Table 2.** Characteristics of Concept Understanding Assessment Instruments

| No | Review                                 | Estimates for Items | Estimates for Testees |
|----|--|---------------------|-----------------------|
| 1  | Average values and standard deviations | .00 ± .26           | .03 ± .40             |
| 2  | Reliability                            | .65                 | .79                   |
| 3  | Average values and standard deviations | 1.00 ± .10          | 1.00 ± .39            |

The assessment instrument has a mean INFIT MNSQ of 1.00 and a standard deviation (SD) of 0.10, meaning that overall the items developed are fit with the Rasch model. This is following the opinion of Aminah (2017), which states that the mean INFIT MNSQ 1.01 and SD 0.09. It means that overall the items are under the Rasch model (Aminah, 2017). While the reliability estimation results obtained the value of person reliability 0.79, and item reliability 0.65. It can be concluded that the consistency of the answers both from the TESTEE (a person subjected to a test/One who takes or has taken a test) or from the item has high reliability.

### 4. RESULTS AND DISCUSSION:

#### 4.1. Overall Performance

Investigating students' understanding of concepts is carried out on students who have to learn fundamental physics courses, especially simple harmonic motion (SHM). The results of the student answer analysis, in general, presented in

Figure 1.

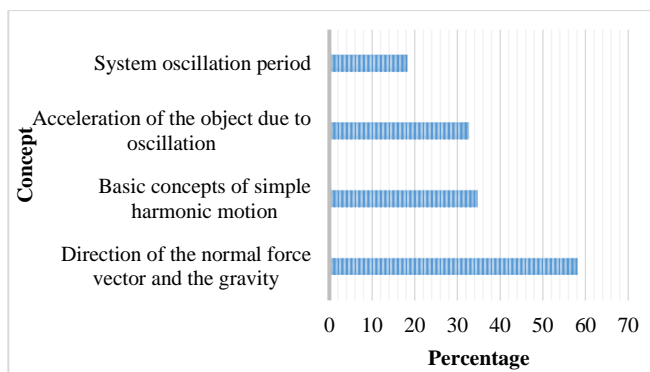


**Figure 1. Investigations on the Student Concepts Understanding in the Mass-Spring System Material.** Source: The author

Figure 1 shows that the four aspects which consist of the basic concepts of simple harmonic motion, determining the magnitude of the acceleration of objects due to oscillation, and finding the importance of the system oscillation period are still below 50%. In contrast, the concept of the normal force and gravity vector is above 50%. These results indicate that most students have not been able to understand the concept of SHM in an elaborate manner. These results are consistent with Ambrose's research, which shows that students have difficulty mastering basic concepts to hamper their understanding of more complex ideas (Ambrose, 2007).

#### 4.2. Normal force vector and the gravity

The investigation results of students' conceptual understanding in determining the direction of normal force and gravity vectors get an average percentage of about 58.16%. The items used were two items, in the first item as many as 19 (38.77%) students answered correctly, and in the second item as many as 38 (77.55%), students answered correctly. This result shows that most students have difficulty in answering the first problem. The basic concept in the first problem can be solved by knowing the concept of force resultant.

The resultant force on blocks placed on the floor is zero. Based on Newton's second law, there are two quantities of force that balance each other. For example, a block rests on the floor, and then the floor exerts a force upward. The upward (normal) force applied by the floor to the block is often called the touch force because it occurs in two objects that touch. When the normal force is perpendicular to the surface of the touch plane, the force is usually called the normal force. There are three types of the "zero" meaning in the equation

of Newton first law. Zero as (1) the "zero intuitive", which means "nothing", (2) a "zero number" which used to represent numbers and (3) a "mathematical zero" according to modern mathematics (Qiang and Dong, 2007). The problem given is in the form of two blocks connected by a massless spring when in a stationary position, which presented in Figure 2.

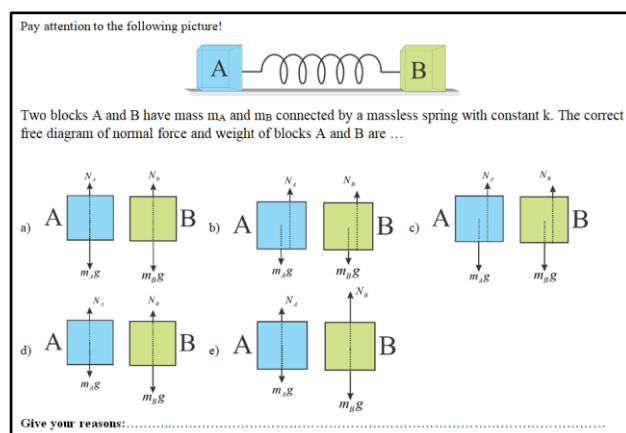


**Figure 2. Item Problem about Concept of Gravity and Normal Force.** Source: The author

Normal Force is a force acting on a plane that touches between two surfaces of an object, whose direction is always perpendicular to the touch plane. The normal force symbol is  $N$  and the International System unit is  $\text{kg m/s}^2$  or Newton. Most students are able to answer this problem correctly. Examples of student answers are presented in Figure 3.

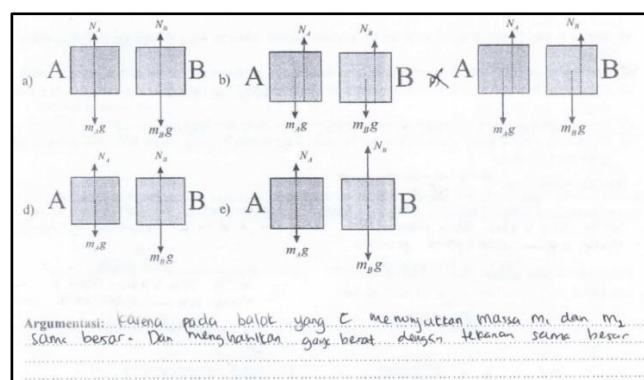


**Figure 3. Examples of Student Answers on Item about Concepts of Gravity and Normal Force.** Source: The author

Figure 3 is an example of a student who is unable to answer this problem well. This can be seen in the answers the student chooses the answer C. The reason given by the student is because the option C block shows masses of  $m_A$  and  $m_B$  as equal, and produces a force with equal pressure. These results indicate that the student is not able to master the basic concepts of the gravity

well. This finding proved that the mathematical presentation of students' understanding can be used to identify the zero intuition experienced of students (Handhika, Cari, and Suparmi, 2017). In any case some students can interpret that no forces are acting on the object on the Newton first law concepts (Hsu, 2001).

These results are consistent with Ambrose's research, which shows that students have difficulty mastering basic concepts to hamper their understanding of more complex concepts (Ambrose, 2007). Other research conducted Nugraha, *et al.* (2019) shows that the student's inability to master the basic concepts of the simple harmonic motion is in determining the relationship between distance, speed, and acceleration.

The concept of normal force direction is always perpendicular to the touchpad (Giancoli, 2019; Serway and Jewett, 2004). If the touch plane between two objects is horizontal, the direction of the normal force is vertical. If the plane of the touch is vertical, then the direction of the normal force is horizontal. If the plane of the tilt is tilted, then the direction of the normal force will also be tilted. The base or vector capture point starts from the point where two surfaces of objects touch and then draw a perpendicular line through the center of mass of the object.

#### 4.3. Basic concepts of simple harmonic motion

The investigating results of students' understanding of concepts about basic concepts of simple harmonic motion get a percentage of 34.65% or as many as 17 students who managed to answer correctly. These results indicate that most students have difficulty in determining the basic concepts of simple harmonic motion. Oscillation motion is the movement of an object back and forth over the same path. An example of a simple case is the oscillation motion of an object with mass  $m$  placed at the end of spring, as in Figure 4.

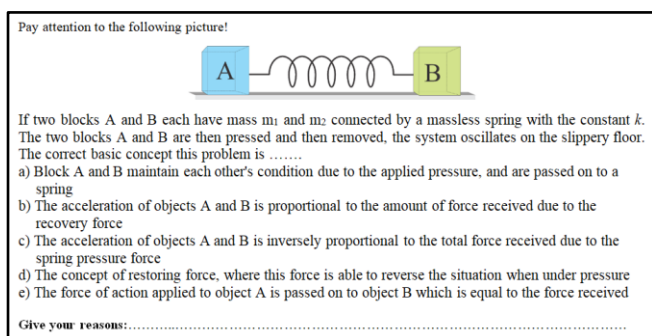


**Figure 4.** Item of Basic Concepts of Spring Oscillation. Source: The author

Figure 4 is an example of an item that visualizes the concept of oscillating motion on a spring on a slippery floor so that there is no friction. If the spring is pushed to the left or right with a displacement of  $x$ , after the thrust is removed, the spring will try to return to the equilibrium position. The force applied by the spring to return to its original position is called the restoring force. Because the force acting on an object is not constant, the acceleration of the object is also not constant but is proportional to the magnitude of the restoring force. The acceleration is directly proportional to the position of the block, and the direction is opposite to the displacement from the equilibrium position. An object experiences simple harmonic motion when its acceleration is directly proportional to its position and in the opposite direction to its movement from equilibrium

The results showed that most students answered correctly on this item. However, there are still some students who have difficulty understanding the basic concepts of spring oscillations. One example of students who cannot solve this problem properly is presented in Figure 5.

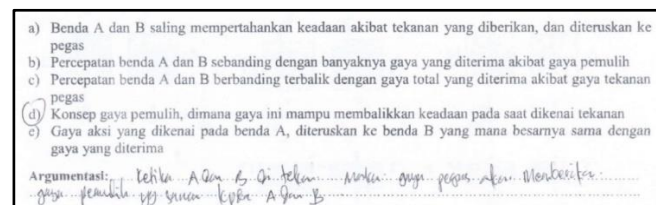


**Figure 5.** Examples of Student Answers on Item Basic Concepts of Spring Oscillation. Source: The author

Figure 5 is an example of a student who is unable to answer this problem well. This can be seen in the answers students choose the answer choice D. The reason given by the student is that when A and B are pressed, the spring force will give the same restoring force to A and B.

These results indicate that the student is not able to master the basic concepts of the gravity well. These results are consistent with Ambrose's research, which shows that students have difficulty learning basic concepts to hamper their understanding of more complex concepts (Ambrose, 2007). This is in line with the results of the study (Parnafes, 2010) that in some problems, students have not been able to understand the basic concepts of mechanical motion as a basis for understanding simple harmonic motion. These concepts include the concept of instantaneous speed, frequency, and average speed.

#### 4.4. Acceleration of the object due to oscillation

The results of investigating students' understanding of concepts in determining the magnitude of the acceleration of objects due to oscillation, with an average percentage of 32.65%. The items used were two items, in the first item as many as 18 (36.73%) students answered correctly, and in the second item as many as 14 (28.57%), students answered correctly. These results indicate that most students have difficulty in answering the second question. The basic concept in the second problem can be solved by knowing Newton's second law concept.

The restoring force is the force that leads to an equilibrium position and is, therefore, the opposite of the displacement of an object from its equilibrium. By using Newton's second law  $\sum F_x = ma_x$ ,  $F_x$  is Hooke's law that is the force produced by a spring on a block is directly proportional to its position. The item used to determine the students' understanding of the concept of accelerating the oscillation of the mass-spring system is presented in Figure 6.

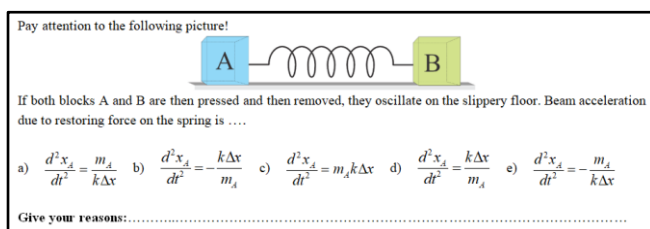


**Figure 6.** Item about the Concept of Acceleration of Mass-Spring System Oscillation. Source: The author

The results showed that most students answered correctly on this item. But there are still some students who have difficulty understanding the concept of accelerating the oscillation of the mass-spring system. One example of students who cannot solve this problem properly is presented in Figure 7.

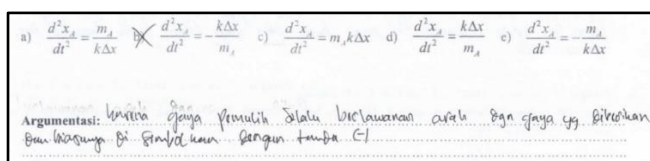


**Figure 7.** Example of Student Answers on the Concept of Acceleration on Mass-Spring System Oscillation. Source: The author

Figure 7 is an example of a student who is unable to answer this problem well. This can be seen in the answers students choose the answer choice B. The reason given by the student is

because the recovery style is always in the opposite direction to the force given and is usually symbolized by a negative sign (-). This finding shows that the student answers the item using his perception without using the correct theoretical basis.

These results indicate that students have not been able to use mathematical equations in solving problems. They need guidance on mathematical operations, and which factors affect the acceleration of the oscillation of the mass-spring system (Ambrose, 2007). When block A moves at any time at the reference point symbolized by  $x_{1A}$  and Block B moves at all times at the reference point symbolized by  $x_{2B}$ . Then the length of the spring at any given moment is:

$$x_{2B} - x_{1A} \quad (1)$$

If the difference is the length of the spring  $x_{2B} - x_{1A}$ , then there is a long increase in the spring. The addition of spring length can be written:

$$X = (x_{2B} - x_{1A}) - x_0 \quad (2)$$

or

$$x_{2B} - x_{1A} = X + x_0 \quad (3)$$

Where  $x_0$ , is the initial length of the spring, based on Newton's Second Law, the magnitude of

restoration force is obtained  $F_p = m_A \frac{d^2 x_{1A}}{dt^2}$ .

Remember that FP is a restorer style, by entering the Hooke Law equation, obtained:

$$\frac{d^2 x_{1A}}{dt^2} = \frac{kX}{m_A} \quad (4)$$

The results obtained are functions  $x(t)$  that satisfy the second-order differential equation. This function is a mathematical representation of the position of objects as a function of time. Most of the students have not been able to master the mathematical representation of the concept of a mass-spring system.

#### 4.5. Find the magnitude of the system oscillation period

The results of investigating students' understanding of the concept in determining the period of system oscillation get a percentage of



18.36%. Students who managed to answer correctly on this item were nine people. These results indicate that most students have difficulty in determining the period of system oscillation. The motion period (T) is the time interval required for the particle to go through one full cycle of its motion. The items used to find the magnitude of the system oscillation period is presented in Figure 8.

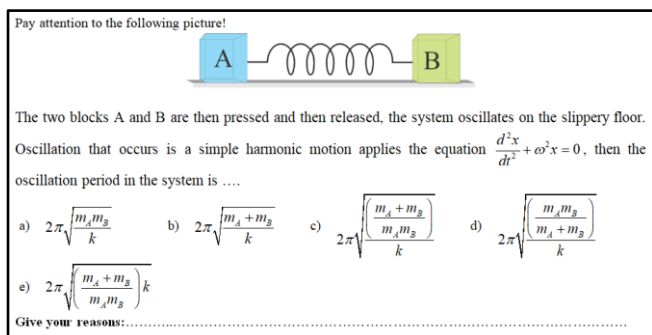


**Figure 8.** Item about Oscillation Period Mass-Spring System. Source: The author

The item in Figure 8 requires students to be able to find the system oscillation period. Based on the results obtained in the previous problem, obtained acceleration of object A. In the same way, the acceleration of object B is:

$$\frac{d^2 x_2}{dt^2} = -\frac{k \Delta x}{m_B} \quad (5)$$

A negative value on the recovery force indicates the opposite direction of the force. Equations (4) and (5) are substituted:

$$\frac{d^2 x_{2B}}{dt^2} - \frac{d^2 x_{1A}}{dt^2} = -\frac{kX}{m_B} - \left( \frac{kX}{m_A} \right)$$

$$\frac{d^2 (X + x_0)}{dt^2} = -k \left( \frac{m_A + m_B}{m_A m_B} \right) X$$

Since  $\frac{d^2 x_0}{dt^2} = 0$ , then we get:

$$\frac{d^2 X}{dt^2} + \frac{k}{\left( \frac{m_A m_B}{m_A + m_B} \right)} X = 0$$

Because the motion that occurs is a simple

harmonic motion, it applies  $\frac{d^2 x}{dt^2} + \omega^2 x = 0$ , then we get:

$$\omega^2 = \frac{k}{\left( \frac{m_A m_B}{m_A + m_B} \right)}$$

$$T = 2\pi \sqrt{\frac{\left( \frac{m_A m_B}{m_A + m_B} \right)}{k}} \quad (6)$$

The mathematical representation of the simple harmonic motion of the period of motion (T) is the time interval required for a particle to go through one full cycle of its motion. The size of the period depends on the mass of the block and the magnitude of the force of the bag and has no effect on the motion parameters (Triana and Fajardo, 2012). Like, amplitude A or phase angle  $\phi$ . The results showed that most students were not able to answer correctly on this item. One example of students who cannot solve this problem properly is presented in Figure 9.

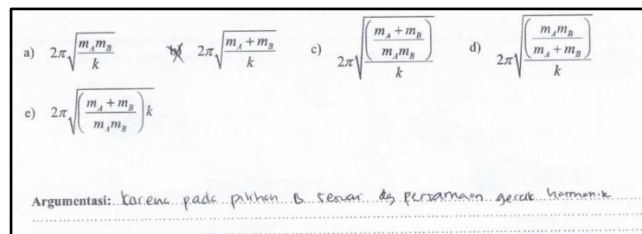


**Figure 9.** Examples of Student Answers in determining the Mass-Spring System Oscillation Period. Source: The author

Figure 9 is an example of an inability of students to answer this problem well. This can be seen in the answers students choose the answer choice B. The reason given by the student is because the choice B matches the harmonic motion equation. These results indicate that most students are not able to grasp the meaning or meaning of a concept. While the concept is an abstraction that represents an object or event obtained based on one's experience. Learning concepts is one of the main objectives of learning.

One of the goals of learning physics is to improve the understanding of student concepts through a quality teacher or lecturer teaching system. Thus, an effective teacher is one who must have a teacher who is more rooted in knowledge about the subjects being taught, the sharpness of teaching skills in the classroom,

following developments in the topic (field) and in education in general, generating and contributing new knowledge to the profession (Adolphus *et al.*, 2013).

The results of the study are generally based on four concepts: direction of the normal force vector and the gravity, basic concepts of simple harmonic motion, acceleration of the object due to oscillation, and system oscillation period is still below 50%. On the other hand, the concept of normal force and gravity vector is above 50%. These results indicate that most students have not been able to understand the concept of SHM in a complex manner. These results are consistent with Ambrose's research, which shows that students have difficulty mastering basic concepts to hamper their understanding of more complex concepts (Ambrose, 2007). The concepts students have can be obtained from daily experiences, learning processes, media, and so on (Aretz, Borowski, and Schmeling, 2016).

## 5. CONCLUSIONS:

Most students have not been able to master the concept well. The students' understanding of concepts is not good, namely, the basic concepts of simple harmonic motion, determine the magnitude of the acceleration of objects due to oscillations, and find the magnitude of the oscillation period. Based on the result, it shows that understanding concepts isn't as simple as it said. Lack of understanding of student concepts is caused by students not being able to relate previous insights (such as Newton's law concepts, and Hooke's Law) with strategies for solving problems. This is shown from the results of the average achievement below 50%. The low understanding of student concepts is due to the inability of students to interpret mathematical equations, and how to operate these equations in solving problems. The students' concepts understanding correlated with the students' basic concept of the basic concepts as required concepts, daily conception, multirepresentations (especially mathematical representation), and the students' intuition. Besides, it can be caused by the traditional learning process has not made students understand the concept well.

## 6. ACKNOWLEDGEMENTS:

This research was partly supported by Universitas Sebelas Maret - Hibah Unggulan Terapan with contract No. 516/UN27.21/PP/2019.

## 7. REFERENCES:

1. Adolphus, T., Alamina, J., Aderonmu, T., Education, T., and State, R. (2013). *The Effects of Collaborative Learning on Problem Solving Abilities among Senior Secondary School Physics Students in Simple Harmonic Motion*. 4(25), 95–101.
2. Ainsworth, S. (2006). DeFT: A conceptual framework for considering learning with multiple representations. *Learning and Instruction*, 16(3), 183–198.
3. Alho, J., Silva, H., Teodoro, V., and Bonfait, G. (2019). A simple pendulum studied with a low-cost wireless acquisition board. *Physics Education*, 54(1). <https://doi.org/10.1088/1361-6552/aaea9d>
4. Ambrose, B. S. (2007). Probing student reasoning and intuitions in intermediate mechanics: An example with linear oscillations. *AIP Conference Proceedings*, 883(2007), 30–33. <https://doi.org/10.1063/1.2508684>
5. Aminah, N. S. (2017). *Assesmen Pembelajaran Fisika* (1st ed.). Surakarta: UNS Press.
6. Angell, C., Guttersrud, Ø., Henriksen, E. K., and Isnes, A. (2004). Physics: Frightful, but fun - Pupils' and teachers' views of physics and physics teaching. *Science Education*, 88(5), 683–706. <https://doi.org/10.1002/sce.10141>
7. Aretz, S., Borowski, A., and Schmeling, S. (2016). A fairytale creation or the beginning of everything: Students' pre-instructional conceptions about the Big Bang theory. *Perspectives in Science*, 10, 46–58. <https://doi.org/10.1016/j.pisc.2016.08.003>
8. Arista, F. S., and Kuswanto, H. (2018). Virtual Physics Laboratory Application Based on the Android Smartphone to Improve Learning Independence and Conceptual Understanding. *International Journal of Instruction*, 11(1), 1–16.
9. Dandare, K. (2018). A study of conceptions of preservice physics teachers in relation to the simple pendulum. *Physics Education*, 53(5). <https://doi.org/10.1088/1361-6552/aac92f>
10. Dimas, A., Suparmi., Sarwanto., and Nugraha., D. A. (2018). Analysis multiple representation skills of high school students on simple harmonic motion. *AIP Conference Proceedings, ICSAS 2018, 020131–*

- 1(September), 020131–020136.  
<https://doi.org/10.1063/1.5054535>
11. Eldy, E. F., and Wui, C. H. (2019). Inverted Classroom Improves Pre-University Students Understanding on Basic Topic of Physics: The Preliminary Study. *Journal of Technology and Science Education*, 9(3), 420–427.
  12. Fatmaryanti, S. D., and Nugraha, D. A. (2019). Using multiple representations model to enhance student's understanding in magnetic field direction concepts. *Journal of Physics: Conference Series*, 1153(1), 12147. IOP Publishing.
  13. Gardner, H. (1999). *The Discipline Mind: What All Students Should Understand*. New York: Simon and Schuster Inc.
  14. Giancoli, D. C. (2019). *Physics; Principle with Applications* (Seventh). California: Pearson Education.
  15. Greene, N. R., Gill, T., and Eyerly, S. (2016). Finding the Effective Mass and Spring Constant of a Force Probe from Simple Harmonic Motion. *The Physics Teacher*, 54(3), 138–141.
  16. Hammer, D. (1996). Misconceptions or P-Prims: How May Alternative Perspectives of Cognitive Structure Influence Instructional Perceptions and Intentions? *Journal of the Learning Sciences*, 5(2), 97–127. [https://doi.org/10.1207/s15327809jls0502\\_1](https://doi.org/10.1207/s15327809jls0502_1)
  17. Handhika, J., Cari, C., and Suparmi, A. (2017). Students' representation about Newton law: consequences of "zero intuition." *Journal of Physics: Conference Series*, 795(1), 12057. IOP Publishing.
  18. Hsu, L. (2001). Teaching Newton's laws before projectile motion. *The Physics Teacher*, 39(4), 206–209.
  19. Hwang, W., Chen, N., Dung, J.-J., and Yang, Y.-L. (2007). Multiple Representation Skills and Creativity Effects on Mathematical Problem Solving using a Multimedia Whiteboard System. *Journal of Educational Technology and Society*, 10(2), 191–212.
  20. Khowatim, S. K., Mahardika, I. K., and Alex, H. (2017). Study of Simple Harmonic Motion's Subject Assisted Worksheet Based on MGR with Learning Setting of Poe. *Pancaran Pendidikan*, 6(3), 110–119. <https://doi.org/10.25037/pancaran.v6i3.57>
  21. Krinks, K. D. (2016). *Integrating Digital Games and Modeling in K-12 Science Classrooms*. Vanderbilt University.
  22. Lee, H. S., and Park, J. (2013). Deductive reasoning to teach Newton's law of motion. *International Journal of Science and Mathematics Education*, 11(6), 1391–1414.
  23. Maison, S., and Syamsurizal, T. (2019). Learning Environment, Students' Beliefs, And Self-Regulation In Learning Physics: Structural Equation Modeling. *Journal of Baltic Science Education*, 18(3), 389.
  24. Nugraha, D. A., Cari, C., Suparmi, A., and Sunarno, W. (2019). Physics students' answer on simple harmonic motion. *Journal of Physics: Conference Series*, 1153(1). <https://doi.org/10.1088/1742-6596/1153/1/012151>
  25. Nugraha, D. A., Suparmi, S., Masykuri, M., and Cari, C. (2016). Survei Pemahaman Mahasiswa Fisika Pada Materi Kalor Dan Temperatur. *Prosiding SNPF (Seminar Nasional Pendidikan Fisika)*, 24–28.
  26. Nurhuda, T., Rusdiana, D., and Setiawan, W. (2017). Analyzing Students' Level of Understanding on Kinetic Theory of Gases. *Journal of Physics: Conference Series*, 812, 12105. <https://doi.org/10.1088/1742-6596/812/1/012105>
  27. OECD. (1999). *Measuring Student Knowledge and Skills*. France.
  28. Ogundeji, O. M., Madu, B. C., and Onuya, C. C. (2019). Scientific Explanation of Phenomena and Concept Formation as Correlates of Students' Understanding of Physics Concepts. *European Journal of Physics Education*, 10(3), 10–19.
  29. Olmstead, M. (2019). Using Games to Understand Physics Concepts. *The Physics Teacher*, 57(5), 304–307.
  30. Parnafes, O. (2010). When Simple Harmonic Motion is not That Simple: Managing Epistemological Complexity by Using Computer-based Representations. *Journal of Science Education and Technology*, 19(6), 565–579. <https://doi.org/10.1007/s10956-010-9224-9>
  31. Patton, M. Q. (2014). *Qualitative research and evaluation methods: Integrating theory and practice*. Sage publications.
  32. Qiang, W. C., and Dong, S. H. (2007). Arbitrary I-state solutions of the rotating Morse potential through the exact quantization rule method. *Physics Letters, Section A: General*,

*Atomic and Solid State Physics*, 363(3), 169–176.  
<https://doi.org/10.1016/j.physleta.2006.10.091>

33. Reif, F. (1995). Understanding and teaching important scientific thought processes. *Journal of Science Education and Technology*, 4(4), 261–282.  
<https://doi.org/10.1007/BF02211259>
34. Serway, R. A., and Jewett, J. W. (2004). *Physics 6th*. <https://doi.org/013613923X>
35. Somroob, S., and Wattanakasiwich, P. (2017). Investigating student understanding of simple harmonic motion. *Journal of Physics: Conference Series*, 901, 012123.
36. Son, J. (2017). The Effects of Physics Teaching-Learning Method Using Storytelling on Scientific Attitudes and Perception of Concepts Understanding. *Journal of Science Education*, 41(2), 213–225.
37. Teddlie, C., and Tashakkori, A. (2009). *Foundations of Mixed Methods Research; Integrating Quantitative and Qualitative Approaches in the Social and Behavioral Sciences*. United States of America: Sage Publications.
38. Triana, C. A., and Fajardo, F. (2012). The influence of spring length on the physical parameters of simple harmonic motion. *European Journal of Physics*, 33(1), 219–229.  
<https://doi.org/10.1088/0143-0807/33/1/019>
39. Waldrip, B., Prain, V., and Carolan, J. (2006). Learning junior secondary science through multi-modal representations. *Electronic Journal of Science Education*, 11(1).
40. Waldrip, B., Prain, V., and Sellings, P. (2013). Explaining Newton's laws of motion: Using student reasoning through representations to develop conceptual understanding. *Instructional Science*, 41(1), 165–189.



## MARCADORES ÓSSEOS METABÓLICOS BIOQUÍMICOS E HORMÔNIO DA PARATIREOIDE EM PACIENTES COM $\beta$ -TALASSEMIA MAIOR NA PROVÍNCIA DE MISAN / IRAQUE

### PARATHYROID HORMONE AND BIOCHEMICAL METABOLIC BONE MARKERS IN PATIENTS WITH $\beta$ -THALASSEMIA MAJOR IN MISAN PROVINCE / IRAQ

هرمون جار الدرقية وعلامات العظام الايضية الكيموحيوية عند مرضى بيتا فقر دم حوض البحر الأبيض المتوسط في محافظة ميسان/ العراق

AL-ZUHAIRY, Noor AL-Huda Salah<sup>1</sup>; AL-ALI, Zainab Abdul Jabbar Ridha<sup>1\*</sup>

<sup>1</sup>Department of Biology, College of Science, University of Misan, Maysan, Iraq

\* Corresponding author  
e-mail: zainab.alali@yahoo.com

Received 18 March 2020; received in revised form 21 April 2020; accepted 24 May 2020

### RESUMO

A beta-talassemia é um grupo heterogêneo de doenças hereditárias do sangue caracterizadas por defeitos na síntese das cadeias  $\beta$  da hemoglobina, resultando em fenótipos variáveis que variam de anemia grave a indivíduos clinicamente assintomáticos. Este estudo tem como objetivo avaliar os níveis séricos de PTH, vitamina D, cálcio, fósforo, fosfatase alcalina e magnésio nos principais pacientes com  $\beta$ -talassemia. Um total de 50 (30 homens e 20 mulheres) pacientes com  $\beta$ -talassemia maior com idades entre 11 e 16 anos e um número igual de adolescentes saudáveis pareados por sexo como grupo controle foram incluídos neste estudo. Um total de 52% dos pacientes residia em área urbana e não houve diferença significativa entre os pacientes e o grupo controle em relação à residência. Pacientes do sexo masculino apresentaram baixos níveis estatisticamente significativos ( $P < 0,05$ ) de PTH sérico, vitamina D e níveis de cálcio, mas os níveis séricos médios de fósforo e fosfatase alcalina foram significativamente mais altos ( $P < 0,05$ ) quando comparados ao grupo controle masculino. No entanto, as pacientes do sexo feminino apresentaram nível médio de PTH sérico baixo, mas sem significância estatística ( $P > 0,05$ ), enquanto os níveis de vitamina D e cálcio foram altamente significativos ( $P < 0,05$ ). Os níveis de fósforo e ALP aumentaram significativamente ( $P < 0,05$ ) quando comparados aos controles femininos. Em relação ao grupo principal da  $\beta$ -talassemia, o presente estudo mostrou que pacientes do sexo masculino apresentaram níveis elevados não significativos ( $P > 0,05$ ) de PTH, cálcio, fósforo e ALP. Por outro lado, o nível de vitamina D não foi significativamente ( $P > 0,05$ ) baixo em pacientes do sexo masculino em comparação com pacientes do sexo feminino. O nível sérico médio de PTH teve uma correlação negativa com fósforo, mas teve uma associação positiva com vitamina D, cálcio, ALP e magnésio. Em conclusão, esse estudo demonstrou que os principais pacientes com  $\beta$ -talassemia têm um perfil ósseo metabólico bioquímico marcadamente perturbado. Também é recomendado o monitoramento regular do PTH e do perfil mineral bioquímico.

**Palavras-chave:**  $\beta$ -talassemia maior, PTH, marcadores ósseos metabólicos.

### ABSTRACT

Beta-thalassemia is a heterogeneous group of hereditary blood disorders characterized by defects in the synthesis of the  $\beta$ - chains of hemoglobin, resulting in variable phenotypes ranging from severe anemia to clinically asymptomatic individuals. This study aims to assess the serum PTH, vitamin D, calcium, phosphorus, alkaline phosphatase, and magnesium levels in  $\beta$ -thalassemia major patients. A total of 50 (30 male and 20 female) patients with  $\beta$ -thalassemia major with ages range 11- 16 years and an equal number of sex-matched healthy adolescents as a control group were included in this study. A total of 52% of patients were lived in an urban area, and there was no significant difference between patients and the control group regarding residency. Male patients showed low statistically significant ( $P < 0.05$ ) mean serum PTH, vitamin D, and calcium levels, but mean serum phosphorus and alkaline phosphatase levels were significantly higher ( $P < 0.05$ ) as compared to the male control group. However, female patients had low, but without statistical significant ( $P > 0.05$ ) mean serum PTH level, whereas vitamin D and calcium levels were highly significant ( $P < 0.05$ ) reduced. The phosphorus and ALP levels were highly significantly ( $P < 0.05$ ) increased as compared to female controls. Regarding  $\beta$ -thalassemia major group, the current study showed male patients had non-significant ( $P > 0.05$ ) higher levels of PTH, calcium, phosphorus, and ALP. In contrast, vitamin D level was non-significantly ( $P > 0.05$ ) low in male patients as compared

to female patients. Mean serum level of PTH had a negative correlation with phosphorus, but it had a positive association with vitamin D, calcium, ALP, and magnesium. In conclusion, this study demonstrated that  $\beta$ -thalassemia major patients have a markedly deranged biochemical metabolic bone profile. Regular monitoring of PTH and biochemical mineral profile is also recommended.

**Keywords:**  $\beta$ -thalassemia major, PTH, Metabolic Bone Markers.

## المخلص

بيتا فقر دم البحر الابيض المتوسط (الثلاسيميا) هي مجموعة غير متجانسة من اضطرابات الدم الوراثية تتميز بخلل في تخليق سلاسل بيتا في الهيموغلوبين، مما يؤدي الى انماط ظاهرية متغيرة تتراوح بين فقر الدم الشديد الى بدون اعراض مرضية عند الافراد. تهدف الدراسة الى تقييم مستويات هرمون جار الدرقية، فيتامين D، الكالسيوم، الفسفور، أنزيم الفوسفاتيز القاعدي والمغنسيوم في مصل الدم لمرضى بيتا ثلاسيميا الكبرى. شملت الدراسة 50 مريضاً (30 ذكر و 20 أنثى) مصابين بمرض بيتا ثلاسيميا الكبرى والذين تراوحت اعمارهم من 11 – 16 سنة، وعدد متساو من المراهقين الاصحاء المطابقين للجنس كمجموعة ضابطة في هذه الدراسة. يسكن 52% من المرضى في المناطق الحضرية ولم يلاحظ اختلافات معنوية بين المرضى ومجموعة السيطرة فيما يتعلق بمنطقة الإقامة. المرضى الذكور لوحظ لديهم انخفاض معنوي ( $p < 0.05$ ) في مستويات هرمون جار الدرقية، فيتامين D والكالسيوم، ولكن مستويات الفسفور وأنزيم الفوسفاتيز القاعدي مرتفعة معنويًا ( $p < 0.05$ ) بالمقارنة مع المجموعة الضابطة من الذكور. ومع ذلك، هرمون جار الدرقية انخفض لدى المرضى من الإناث لكن لم يصل الى مستوى المعنوية ( $p > 0.05$ )، بينما مستوى فيتامين D والكالسيوم انخفض معنويًا ( $P < 0.05$ )، مستويات الفسفور وأنزيم الفوسفاتيز ارتفعت معنويًا ( $p < 0.05$ ) بالمقارنة مع المجموعة الضابطة من الإناث. فيما يتعلق بمجموعة مرضى فقر دم البحر الابيض المتوسط (الثلاسيميا) الكبرى، بينت الدراسة الحالية ان المرضى من الذكور لديهم مستويات مرتفعة غير معنوية ( $p > 0.05$ ) من هرمون جار الدرقية، الكالسيوم، الفسفور وأنزيم الفوسفاتيز القاعدي ومستوى منخفض غير معنوي ( $p > 0.05$ ) من فيتامين D عند مقارنتهم مع المرضى من الإناث. أظهر هرمون جار الدرقية علاقة ارتباط سلبية مع الفسفور وعلاقة ارتباط موجبة مع فيتامين D، الكالسيوم، أنزيم الفوسفاتيز القاعدي والمغنسيوم. في الختام، أثبتت هذه الدراسة ان مرضى فقر دم البحر الابيض المتوسط (الثلاسيميا) الكبرى لديهم اضطراب بشكل ملحوظ في صورة العظام الايضية والكيموحيوية. توصي الدراسة الحالية بالمراقبة المنتظمة لمستوى هرمون جار الدرقية ومعايير العظام الكيوكيوية.

**الكلمات المفتاحية:** بيتا ثلاسيميا الكبرى، هرمون جار الدرقية، معايير العظم الايضية.

## 1. INTRODUCTION:

Beta-thalassemia is a heterogeneous group of hereditary blood disorders characterized by defects in the synthesis of the  $\beta$ - chains of hemoglobin, resulting in variable phenotypes ranging from severe anemia to clinically asymptomatic individuals. It has been estimated that about 1.5% of the global population (80 to 90 million people) are carriers of  $\beta$ - thalassemia, with about 60,000 symptomatic individuals born annually, the vast majority in the developing world (Galanello and Origa, 2010). In Iraq, the prevalence of thalassemia syndrome is 37.1/100.000 inhabitants, and  $\beta$ -thalassemia major represents 73.9% of all types of thalassemia (Kadhim *et al.*, 2017).  $\beta$ -thalassemia major is more severe transfusion-dependent anemia result from homozygosity or compound heterozygosity for a mutant  $\beta$ - globin gene and, occasionally, from heterozygosity for dominant mutations (Cao and Galanello, 2010; Olivieri, 1999).

The combination of transfusion and chelation therapy has dramatically extended the life expectancy of  $\beta$ -thalassemia major patients but is complicated by subsequent iron overload resulting in a high incidence of endocrine complication in children, adolescents, and young adults (Shamshirsaz *et al.*, 2003). Endocrine and metabolic bone disorders that are caused by repeated blood transfusions are of higher importance in  $\beta$ -thalassemia major patients. They are the second leading cause of mortality, after heart disorders, in these individuals (Chahkandi *et al.*, 2017).

Disturbance of calcium and phosphorus hemostasis due to parathyroid dysfunction, as well as metabolic bone diseases with various skeletal

complications including osteopenia, osteoporosis, scoliosis, rickets, spinal deformities, and spontaneous fractures, are a significant cause of morbidity and regularly reported in transfusion-dependent  $\beta$ -thalassemia major patients (Saboor *et al.*, 2017; Salama *et al.*, 2006). These complications are mainly due to repeated blood transfusion results in citrate toxicity and iron overload with deposition in parathyroid cells and tissue fibrosis, and chronic anemia (Galanello and Origa, 2010; Hamidi, 2016).

Bone turnover is assessed with several specific and sensitive serological markers, and serum PTH, calcium, phosphorous, alkaline phosphatase, vitamin D, and magnesium are characteristically altered with bone impairment in patients with thalassemia (Saboor *et al.*, 2017; Salama *et al.*, 2006; Khaleel, 2018).

This study aimed to assess the serum levels of PTH, vitamin D, calcium, phosphorus, alkaline phosphatase, and magnesium in  $\beta$ -thalassemia major patients.

## 2. MATERIALS AND METHODS:

Over six months, from 1<sup>st</sup> of December 2018 to the 31<sup>st</sup> of May 2019, a total 50 (30 male and 20 female) patients with  $\beta$ - thalassemia major with ages range between 11 to 16 years attended Misan Thalassemia Center along with 50 age and sex-matched healthy adolescents as control group were included in this case control study. Informed consent was obtained from parents or guardians of patients, and the Ethical Committee approved this study protocol at the College of Medicine, Misan University, Iraq. The diagnosis of  $\beta$ -thalassemia major was based on clinical history and examination in addition to the usual hematological data

(complete blood count, and Hb electrophoresis). The cases and control individuals were investigated for serum PTH, vitamin D, calcium, phosphorus, alkaline phosphatase, and magnesium levels. The assay principle for PTH based on competitive radioimmunoassay (RIA) (Cavalier *et al.*, 2015), combines an enzyme immunoassay sandwich method with a final fluorescent detection Enzyme Linked Fluorescent Assay (ELFA) was used for serum vitamin D measurement (Holick, 2007), serum calcium was determined by colorimetric method using methylmol blue indicator (Finley and Tietz, 1996), serum phosphorus level was determined by ammonium molybdate end point method (Drewes, 1972), ALP was also measured by colorimetric method using p-nitrophenylphosphate (Belfield and Goldberg, 1971), while spectrophotometric determination employing Calmagite was used to measured serum magnesium (Ingman and Ringbom, 1966).

Statistical analyses were reports as mean estimation  $\pm$  standard error, t test, and correlation using Statistical Package for Social Science (SPSS) version 23 for windows. Comparison of categorical data was carried by Chi-square test. *P* value of  $<0.05$  was considered as statistically significant.

### 3. RESULTS AND DISCUSSION:

A total 50 patients consisted of 30 (60%) male and 20 (40%) female  $\beta$ -thalassemia major patients and 50 healthy children matched for age and sex were studied as control group were enrolled in this study, see Table 1. In present study (52%, 26 patients) of thalassemia major patients lived in urban areas, while (38%, 19 patients) of control individuals were lived in rural area, and there was no significant difference between control and patients group regarding residency (*P* value 0.31), as shown in Table 2.

Regarding biochemical bone markers, data analysis showed that male patients have a highly significant ( $p < 0.05$ ) low serum PTH ( $35.01 \pm 5.19$  pg/ml), vitamin D ( $12.22 \pm 0.67$  ng/ml), and calcium ( $7.90 \pm 0.19$  mg/dL) levels in comparison to male control subjects ( $74.76 \pm 7.30$  pg/ml,  $54.30 \pm 4.69$  ng/ml, and  $9.84 \pm 0.23$  mg/dL respectively), but serum phosphorous ( $4.97 \pm 0.32$  mg/dL) and ALP ( $212.20 \pm 19.40$  U/L) were highly statistically significant ( $p < 0.05$ ) increased in male patients compared with male control ( $1.96 \pm 0.14$  mg/dL and  $83.62 \pm 7.11$  U/L respectively), also serum magnesium ( $2.18 \pm 0.38$  mg/dL) was increased but without statistical significant (*P* value=0.386) in male patients compared with control ( $1.83 \pm 0.09$  mg/dL), see Table 3.

In comparison female patients with female control results revealed that serum PTH level ( $31.39 \pm 5.69$  pg/ml) decreased without statistical significant (*P* value=0.549), but vitamin D ( $12.70 \pm 0.84$  ng/ml) and calcium ( $7.55 \pm 0.23$  mg/dL) levels were highly significant ( $p < 0.05$ ) decreased in patients compared with control females ( $40.38 \pm 4.66$  ng/ml and  $9.59 \pm 0.24$  mg/dL). Phosphorus ( $4.61 \pm 0.52$  mg/dL),

ALP ( $210.30 \pm 33.54$  U/L), and magnesium ( $2.04 \pm 0.36$  mg/dL) levels were measured higher. Still, only phosphorus level and ALP were highly significant ( $P < 0.05$ ) in female patients in comparison to the female control group ( $2.75 \pm 0.21$  mg/dL,  $91.36 \pm 4.55$  U/L, and  $1.76 \pm 0.12$  mg/dL respectively), as shown in Table 3.

Table 4, demonstrated that the serum levels of bone metabolic biochemical markers in male  $\beta$ -thalassemia major patients group including PTH ( $35.01 \pm 5.19$  pg/ml), calcium ( $7.90 \pm 0.19$  mg/dL), phosphorus ( $4.97 \pm 0.32$  mg/dL), ALP ( $212.20 \pm 19.40$  U/L), and magnesium ( $2.18 \pm 0.38$  mg/dL) were measured higher than in female patients ( $31.39 \pm 5.69$  pg/ml,  $7.55 \pm 0.23$  mg/dL,  $4.61 \pm 0.52$  mg/dL,  $210.30 \pm 33.54$  U/L, and  $2.04 \pm 0.36$  mg/dL respectively), but without significant difference, while vitamin D levels in male ( $12.22 \pm 0.67$  ng/ml) was lower without statistical significant difference than that in female patients ( $12.70 \pm 0.84$  ng/ml).

The results showed that the level of PTH had a negative correlation with phosphorus (-0.137), while it had a positive correlation with vitamin D (0.205), calcium (0.111), ALP (0.097) and magnesium (0.091). Vitamin D had an inverse correlation with phosphorus (-0.147) but is positively correlated with ALP (0.060), and magnesium (0.238), and significantly positive ( $P < 0.05$ ) with calcium (0.287). While calcium in our study results reported a negative correlation with ALP (-0.091) and a highly significant negative correlation with phosphorus (-0.583), but it had a highly significant positive ( $P < 0.01$ ) with magnesium (0.430). The level of phosphorus had an inverse correlation with magnesium level (-0.028), but it had a positive correlation with ALP (0.019) in our patient's results. Lastly, the level of serum ALP in our study showed a positive correlation with the level of serum magnesium (0.073) (Table 5).

In this study, 52% of  $\beta$ -thalassemia major patients lived in an urban area, and there was no significant difference between patients and the control group regarding residency. In agreement with our findings, Al-Ali and Faraj (2016) observed the incidence of  $\beta$ -thalassemia was significantly unchanged between the urban and rural populations, and so a study designed by Qurat-ul-Ain *et al.*, (2011) found the incidence of  $\beta$ -thalassemia was significantly higher in urban population than rural. In contrast, Tunç *et al.*, (2002) noticed the low frequency of  $\beta$ -thalassemia in the city center than in neighboring areas. The findings might be due to the same rate of consanguineous marriages among our population wherever they live, lack of effective prevention programs and poor legislation in our governorate.

Analysis of study results demonstrated that male patients in  $\beta$ -thalassemia major group have low statistically significant mean serum PTH, vitamin D, and calcium levels, but mean serum phosphorus and alkaline phosphatase levels significantly higher as compared to the male control group. However, in comparison to female  $\beta$ -thalassemia major patients with female control individuals, we observed low but without statistically significant ( $P < 0.05$ ) serum PTH

level. In contrast, vitamin D and calcium levels were highly significantly reduced, but phosphorus and ALP levels were highly significantly increased. Regarding  $\beta$ -thalassemia major group, the current study show male patients have non-significant higher levels of PTH, calcium, phosphorus, and ALP. In contrast, vitamin D level was non-significantly low in male patients as compared to female patients.

In agreement with our results, De Sanctis *et al.*, (1992) and Aleem *et al.* (2000) observed low PTH among  $\beta$ -thalassemia major patients. Low, PTH level among our patients is mainly due to the involvement of the parathyroid gland by iron overload, as well as its oxidative damage. Gutteridge and Halliwell (1998) and Goyal *et al.*, (2010) mentioned that parathyroid gland involvement by iron overload occurs particularly after ten years of age in  $\beta$ -thalassemia major patients, and a number of possible mechanisms have been described to be responsible for the damage of parathyroid glands through iron overload, which includes free radical formation and lipid peroxidation resulting in mitochondrial, lysosomal and sarcolemmal membrane damage. Also, Aleem *et al.*, (2000) found that parathyroid gland dysfunction in  $\beta$ -thalassemia major with iron overload is due to chelation therapy.

Parathyroid hormone is essential in calcium and phosphorus hemostasis and also plays a role in the conversion of vitamin D to its active form (1, 25 dihydroxycholecalciferol) in the kidney. A decrease in extracellular calcium concentrations or an increase in phosphorus concentrations leads to a PTH release from the parathyroid gland, which in turn increases renal reabsorption of calcium, renal activation of vitamin D, urinary phosphorus excretion, and bone resorption. In turn, vitamin D increases intestinal absorption and renal reabsorption of calcium and phosphorus (Penido and Alon, 2012; Kliegman, 2020). Documented abnormalities in PTH and biochemical metabolic bone markers values have been observed among  $\beta$ -thalassemia major (Hamidi, 2016; Dejkhamron *et al.*, 2018).

In agreement with our findings, Shetty and Shenoy, (2014), in their case-control study, found a significant decrease in serum PTH, and calcium, but significant increase in serum phosphorus and ALP in  $\beta$ -thalassemia major patients when compared to control. However, Goyal *et al.*, (2010) noticed serum PTH and serum calcium significantly reduced in  $\beta$ -thalassemia major patients that are similar to our results. Still, their serum ALP and phosphorus were not significantly altered when compared to the respective mean values for the control group. Also, Anju and Jain (2017) found serum calcium level was statistically significantly low, whereas serum phosphorus had no significant difference as compared  $\beta$ -thalassemia major patients to the control group. In contrast to our findings, Agrawal *et al.* (2016) observed that mean serum PTH was significantly higher and so calcium level but without significant difference, while phosphorus level was non-significantly lower in thalassemia patients compared to control. However, vitamin D value in their study is in agreement with our results was significantly lower in

patients compared to the control group. Still, there was no significant correlation found between vitamin D level and sex. In contrast, in our study, we found a significantly reduced level of vitamin D in male and female patients group compared to male and female control groups. However, in another study by Aggarwal *et al.*, (2018) found significant low vitamin D levels, despite serum PTH levels were not significantly different between cases and controls, while the serum level of calcium was found in the normal range in both groups, although the phosphorus and ALP levels were found to be significantly high in cases in comparison to controls.

The lower serum levels of vitamin D among  $\beta$ -thalassemia major patients can be due to decreased serum PTH level in our patients as a result of parathyroid gland involvement by iron overload. (Penido and Alon, 2012) documented PTH is one of the strongest stimulators of 1, 25 (OH)<sub>2</sub> D<sub>3</sub> production by increasing proximal tubular expression of 25(OH) D 1 $\alpha$ -hydroxylase, resulting in increased production of 1, 25(OH)<sub>2</sub> D<sub>3</sub>. Moreover, Soliman *et al.*, (2013) mentioned that both defective synthesis of 25 (OH) vitamin D and/ or hypoparathyroidism had been described in  $\beta$ -thalassemia major patients.

Our results were consistent with that of (Khaleel *et al.*, 2018; Ridha *et al.*, 2018) when they observed serum magnesium level was significantly higher in patients than normal control. At variance with our findings, Arcasoy and Cavdar (1975) and Fahmy *et al.*, (2019) observed a normal serum magnesium level in  $\beta$ -thalassemia patients, while Al-Samarrai *et al.*, (2008) and Nafady *et al.*, (2018) in their study showed that serum magnesium level was significantly lower in patients than the healthy control group. Hyman *et al.*, (1980) had been speculated that hypomagnesemia could be due to chelation by citrate in chronically transfused patients, or could just be a consequence of the cellular iron overload, but, Genc *et al.*, (2016) observed that level of magnesium had no significant difference between controls and patients with  $\beta$ -thalassemia major regardless type of chelating therapies. The finding of serum magnesium in our thalassemia patients may result from diet, chelation therapies, bone involvement (as 50% of total body magnesium resides in the bone), an increased rate of hemolysis among our patients (as magnesium is one of the major intracellular ions). In our study PTH had no significant correlation with calcium and phosphorus; that's similar to El-Deen *et al.*, (2014) observation.

In agreement with our results (Ridha *et al.*, 2018) noticed vitamin D had a significant correlation with calcium and ALP, while no significant association between PTH with the vitamin D, calcium, phosphorus, ALP, and magnesium.

#### 4. CONCLUSIONS:

There was no significant difference between control and  $\beta$ -thalassemia major patients groups regarding residency.  $\beta$ -thalassemia major patients

have markedly deranged biochemical metabolic bone markers. Male  $\beta$ -thalassemia major patients have highly significant decreased levels of serum PTH, vitamin D, and calcium. While serum phosphorous and ALP was a highly statistically significant increase in male patients compared with control. Female patients have highly significant decreased serum vitamin D and calcium levels, but phosphorus and ALP levels were highly significant in comparison to control. Regular monitoring of PTH and biochemical mineral profiles, as well as nutritional support and calcium/vitamin D supplementation, are highly recommended for these patients.

## 5. ACKNOWLEDGEMENTS:

Much obliged to Dr. Assad Yahia, Muntaha Yacoub, and Dr. Hummod Madhi for their assistance in performing the statistical analysis.

## 6. REFERENCES:

- Aggarwal, V. A., Popli, V., and Uppal, V. (2018). Assessment of Vitamin D levels and Parathyroid Hormone levels in children with Beta Thalassemia major, and to compare their respective values with age and sex matched controls. *IOSR Journal of Dental and Medical Sciences*, 17(3), 17.
- Agrawal, A., Garg, M., Singh, J., Mathur, P., and Khan, K. (2016). A comparative study of 25 hydroxy vitamin D levels in patients of thalassemia and healthy children. *International Journal of Pediatric Research*, 3(9): 652-656.
- Al-Ali, Z. A., and Faraj, S. H. (2016). Prevalence of  $\beta$ -thalassemia Patients in Missan Province. *Global Journal of Biology, Agriculture and Health Science*, 5(1):68-70.
- Aleem, A., Al-Momen, A. K., Al-Harakati, M. S., Hassan, A., and Al-Fawaz, I. (2000). Hypocalcemia due to hypoparathyroidism in  $\beta$ -thalassemia major patients. *Annals of Saudi medicine*, 20(5-6), 364-366.
- Al-Samarrai, A. H., Adaay, M. H., Al-Tikriti, K. A., and Al-Anzy, M. M. (2008). Evaluation of some essential element levels in thalassemia major patients in Mosul district, Iraq. *Saudi medical journal*, 29(1), 94-97.
- Anju, R., and Jain, S. (2017). Study of Serum Calcium and Serum Phosphorus Levels in Patients of Thalassemia Receiving Repeated Blood Transfusion. *International Journal of Science and Research*, 6(1), 1355-1357.
- Arcasoy, A., and Cavdar, A. O. (1975). Changes of trace minerals (serum iron, zinc, copper and magnesium) in thalassemia. *Acta haematologica*, 53(6), 341-346.
- Belfield, A., and Goldberg, D. M. (1971). Revised assay for serum phenyl phosphatase activity using 4-amino-antipyrine. *Enzyme*, 12, 561-573.
- Cao, A., and Galanello, R. (2010). Beta-thalassemia. *Genetics in medicine*, 12(2), 61-76.
- Cavalier, E., Delanaye, P., Nyssen, L., and Souberbielle, J. C. (2015, May). Problems with the PTH assays. In *Annales d'endocrinologie* (Vol. 76, No. 2, pp. 128-133). Elsevier Masson.
- Chahkandi, T., Norouzasl, S., Farzad, M., and Ghanad, F. (2017). Endocrine disorders in beta thalassemia major patients. *International Journal of Pediatrics*, 5(8), 5531-5538.
- De Satictis, V., Vullo, C., Bagni, B., and Chiccoli, L. (1992). Hypoparathyroidism in beta-thalassemia major. *Acta haematologica*, 88(2-3), 105-108.
- Dejkharnon, P., Wejaphikul, K., Mahatumarat, T., Silvilairat, S., Charoenkwan, P., Saekho, S., and Unachak, K. (2018). Vitamin D deficiency and its relationship with cardiac iron and function in patients with transfusion-dependent thalassemia at Chiang Mai University Hospital. *Pediatric hematology and oncology*, 35(1), 52-59.
- Drewes, P. A. (1972). Direct colorimetric determination of phosphorus in serum and urine. *Clinica Chimica Acta*, 39(1), 81-88.
- El-Deen, Z. M. M., Ismail, A. M., Meguid, M. M. A., and Harb, M. T. (2014). Some endocrinal changes in children with  $\beta$ -thalassemia major. *The Egyptian Journal of Haematology*, 39(3), 103.
- Fahmy, E. M., Salama, E. H., and Mohammed, N. A. (2019). Copper, zinc, and magnesium status among patients with thalassemia attending pediatric hematological unit at Sohag University Hospital. *The Egyptian Journal of Haematology*, 44(2), 98.
- Finley, P. R., and Tietz, N. W. (Eds.). (1996). *Clinical guide to laboratory tests*. WB Saunders company.
- Galanello, R., and Origa, R. (2010). Beta-thalassemia. *Orphanet journal of rare diseases*, 5(1), 11.

19. Genc, G. E., Ozturk, Z., Gumuslu, S., and Kupesiz, A. (2016). Mineral levels in thalassaemia major patients using different iron chelators. *Biological trace element research*, 170(1), 9-16.
20. Goyal, M., Abrol, P., and Lal, H. (2010). Parathyroid and calcium status in patients with thalassemia. *Indian Journal of Clinical Biochemistry*, 25(4), 385-387.
21. Gutteridge, J. M., and Halliwell, B. (1989). 1 Iron toxicity and oxygen radicals. *Bailliere's clinical haematology*, 2(2), 195-256.
22. Hamidi, Z. (2016). Endocrine disorders in thalassemia major patients: a review. *KUWAIT MEDICAL JOURNAL*, 48(1), 4-11.
23. Holick, M. F. (2007). Vitamin D deficiency. *New England Journal of Medicine*, 357(3), 266-281.
24. Hyman, C. B., Ortega, J. A., Costin, G., and Takahashi, M. (1980). The clinical significance of magnesium depletion in thalassemia. *Annals of the New York Academy of Sciences*, 344, 436-443.
25. Ingman, F., and Ringbom, A. (1966). Spectrophotometric determination of small amounts of magnesium and calcium employing calmagite. *Microchemical Journal*, 10(1-4), 545-553.
26. Kadhim, K. A., Baldawi, K. H., and Lami, F. H. (2017). Prevalence, incidence, trend, and complications of thalassemia in Iraq. *Hemoglobin*, 41(3), 164-168.
27. Khaleel, K. J. (2018). Biomarkers and trace elements in beta thalassemia major. *Iraqi Journal of Cancer and Medical Genetics*, 6(1).
28. Kliegman, R. M., St Geme, J. W., Blum, N. J., Shah, S. S., Tasker, R. C., and Wilson, K. M. (2020). Hormones and peptides of calcium homeostasis and bone metabolism. *Nelson Textbook of Pediatrics*. 21st ed. Philadelphia, PA: Elsevier.
29. Nafady, A., Nasreldin, E., Nafady-Hego, H., Nasif, K. A., Abd-Elmawgoud, E. A., and Sayed, M. M. (2018). Alteration of trace elements and T-cell subsets in patients with  $\beta$ -thalassemia major: influence of high ferritin level. *The Egyptian Journal of Haematology*, 43(2), 55.
30. Olivieri, N. F. (1999). The  $\beta$ -thalassemias. *New England journal of medicine*, 341(2), 99-109.
31. Penido, M. G. M., and Alon, U. S. (2012). Phosphate homeostasis and its role in bone health. *Pediatric nephrology*, 27(11), 2039-2048.
32. Qurat-ul-Ain, L. A., Hassan, M., Rana, S. M., and Jabeen, F. (2011). Prevalence of  $\beta$ -thalassemic patients associated with consanguinity and anti-HCV-antibody positivity—a cross sectional study. *Pak J Zool*, 43(1), 29-36.
33. Ridha, M.A., Mohammed, Z.H., and Al-Hakeim, H.K. (2018). Calcium Status In Sever Iron Overload Iraqi Thalassemia Major Patients. *Biochem. Cell. Arch*, 18(1):1-5.
34. Saboor, M., Qudsia, F., Qamar, K., and Moinuddin, M. (2014). Levels of calcium, corrected calcium, alkaline phosphatase and inorganic phosphorus in patients' serum with  $\beta$ -thalassemia major on subcutaneous deferoxamine. *J Hematol Thromb Dis*, 2(130), 2.
35. Salama, O. S., Al-Tonbary, Y. A., Shahin, R. A., and Sharaf Eldeen, O. A. (2006). Unbalanced bone turnover in children with  $\beta$ -thalassemia. *Hematology*, 11(3), 197-202.
36. Shamshirsaz, A. A., Bekheirnia, M. R., Kamgar, M., Pourzahedgilani, N., Bouzari, N., Habibzadeh, M., ... and Larijani, B. (2003). Metabolic and endocrinologic complications in beta-thalassemia major: a multicenter study in Tehran. *BMC endocrine disorders*, 3(1), 4.
37. Shetty, B., and Shenoy, U. V. (2014). Prevalence of hypoparathyroidism (HPT) in beta thalassemia major. *Journal of clinical and diagnostic research: JCDR*, 8(2), 24.
38. Soliman, A., De Sanctis, V., and Yassin, M. (2013). Vitamin D status in thalassemia major: an update. *Mediterranean journal of hematology and infectious diseases*, 5(1).
39. Tunc, B., Cetin, H., Gümrük, F., Istanbulu, B., Yavrucuoğlu, H., Kurt, U., and Genc, H. (2002). The prevalence and molecular basis of beta-thalassemia in Isparta province and region. *The Turkish journal of pediatrics*, 44(1), 18-20.

**Table 1.** Number and percentage of control and  $\beta$ -thalassemia major patients according to gender

| Gender | Control No. (%) | Patient No. (%) | Total No. (%) |
|--------|-----------------|-----------------|---------------|
| Male   | 30 (60)         | 30 (60)         | 60 (60)       |
| Female | 20 (40)         | 20 (40)         | 40 (40)       |
| Total  | 50 (100)        | 50 (100)        | 100 (100)     |

**Table 2.** Comparison between control and  $\beta$ -thalassemia major patients regarding residency

| Residency | Control No. (%) | Patients No. (%) | Total | $\chi^2$ | P. value |
|-----------|-----------------|------------------|-------|----------|----------|
| Urban     | 31(62)          | 26 (52)          | 57    | 1.02     | 0.31     |
| Rural     | 19 (38)         | 24(48)           | 43    |          |          |
| Total     | 50 (100)        | 50 (100)         | 100   |          |          |

**Table 3.** Comparison of biochemical bone markers in control and  $\beta$ -thalassemia patients regarding gender

| Variables          | Gender | Control Group    | Patients Group     | P Value | T test |
|--------------------|--------|------------------|--------------------|---------|--------|
| PTH (pg/ml)        | Male   | 74.76 $\pm$ 7.30 | 35.01 $\pm$ 5.19   | 0.000   | 4.434  |
|                    | Female | 36.64 $\pm$ 6.57 | 31.39 $\pm$ 5.69   | 0.549   | 0.604  |
| Vitamin D (ng/ml)  | Male   | 54.30 $\pm$ 4.69 | 12.22 $\pm$ 0.67   | 0.000   | 8.867  |
|                    | Female | 40.38 $\pm$ 4.66 | 12.70 $\pm$ 0.84   | 0.000   | 5.842  |
| Calcium (mg/dL)    | Male   | 9.84 $\pm$ 0.23  | 7.90 $\pm$ 0.19    | 0.000   | 6.408  |
|                    | Female | 9.59 $\pm$ 0.24  | 7.55 $\pm$ 0.23    | 0.000   | 6.085  |
| Phosphorus (mg/dL) | Male   | 1.96 $\pm$ 0.14  | 4.97 $\pm$ 0.32    | 0.000   | 8.730  |
|                    | Female | 2.75 $\pm$ 0.21  | 4.61 $\pm$ 0.52    | 0.002   | 3.300  |
| ALP (U/L)          | Male   | 83.62 $\pm$ 7.11 | 212.20 $\pm$ 19.40 | 0.000   | 6.223  |
|                    | Female | 91.36 $\pm$ 4.55 | 210.30 $\pm$ 33.54 | 0.001   | 3.515  |
| Magnesium (mg/dL)  | Male   | 1.83 $\pm$ 0.09  | 2.18 $\pm$ 0.38    | 0.386   | 0.874  |
|                    | Female | 1.76 $\pm$ 0.12  | 2.04 $\pm$ 0.36    | 0.486   | 0.704  |

Value represented mean  $\pm$  SE.

**Table 4.** Biochemical bone markers according to gender and age groups in  $\beta$ -thalassemia patients

| Variables          | Male (30 patients) | Female (20 patients) | P Value | T test |
|--------------------|--------------------|----------------------|---------|--------|
| PTH (pg/ml)        | 35.01 $\pm$ 5.19   | 31.39 $\pm$ 5.69     | 0.51    | 0.460  |
| Vitamin D (ng/ml)  | 12.22 $\pm$ 0.67   | 12.70 $\pm$ 0.84     | 0.94    | 0.442  |
| Calcium (mg/dL)    | 7.90 $\pm$ 0.19    | 7.55 $\pm$ 0.23      | 0.89    | 1.187  |
| Phosphorus (mg/dL) | 4.97 $\pm$ 0.32    | 4.61 $\pm$ 0.52      | 0.24    | 0.644  |
| ALP (U/L)          | 212.20 $\pm$ 19.40 | 210.30 $\pm$ 33.54   | 0.34    | 0.052  |
| Magnesium (mg/dL)  | 2.18 $\pm$ 0.38    | 2.04 $\pm$ 0.36      | 0.33    | 0.252  |

Value represented mean  $\pm$ SE.

**Table 5.** Correlation between serum PTH and biochemical bone markers in  $\beta$ -thalassemia major patients

| Variables  | PTH   | Vitamin D | Calcium | Phosphorus | ALP  |
|------------|-------|-----------|---------|------------|------|
| PTH        | 1     |           |         |            |      |
| Vitamin D  | .205  | 1         |         |            |      |
| Calcium    | .111  | .287*     | 1       |            |      |
| Phosphorus | -.137 | -.147     | -.583** | 1          |      |
| ALP        | .097  | .060      | -.091   | .019       | 1    |
| Magnesium  | .091  | .238      | .430**  | -.028      | .073 |

\* Correlation is significant at the 0.05 level (2-tailed), \*\* Correlation is significant at the 0.01 level (2-tailed).



## A PREPARAÇÃO DE SEMENTES MELHORA A GERMINAÇÃO E O CRESCIMENTO PRECOCE DE MUDAS DE NABO SOB ESTRESSE DE SALINIDADE

### SEED PRIMING IMPROVES THE GERMINATION AND EARLY GROWTH OF TURNIP SEEDLINGS UNDER SALINITY STRESS

إعداد البذور يحسن الإنبات والنمو المبكر لشتلات اللفت تحت ضغط الملوحة

MOHAMMED, Samar Jasim<sup>1\*</sup>; NULIT, Rosimah<sup>2</sup>

<sup>1</sup>Department of Biology, College of Science, University of Misan, Maysan, Iraq

<sup>2</sup>Department of Biology, Faculty of Science, Universiti Putra Malaysia, Putrajaya, Malaysia

\* Correspondence author

e-mail: samarjasim@uomisan.edu.iq

Received 15 March 2020; received in revised form 02 May 2020; accepted 03 May 2020

#### RESUMO

Um experimento foi conduzido para melhorar o desempenho das sementes de nabo sob condições de estresse de salinidade. O impacto da priming com uma dosagem otimizada (5 g/l) de KCl e NaCl foi avaliado para aumentar o vigor das mudas e a tolerância ao estresse salino em mudas de nabo. Sementes preparadas com (5 g/l) de soluções de KCl e NaCl foram examinadas em diferentes níveis de salinidade (0, 50, 100, 150, 200) mM de NaCl em relação ao estágio inicial de crescimento. Os dados foram analisados no Windows SPSS versão 23 (ANOVA de uma via  $p < 0,05$ ) para determinar a diferença significativa entre os tratamentos e os teste de Duncan,  $p < 0,05$  para comparação das médias. Os resultados mostraram que o priming com KCl e NaCl foi eficaz na redução dos efeitos adversos da salinidade. Um aumento significativo ( $P < 0,05$ ) na porcentagem de germinação, vigor das sementes, comprimento do hipocótilo e radícula, tolerância ao sal e peso seco das mudas de semente que iniciaram com (5 g/l) de KCl e NaCl em comparação com as sementes não preparadas foi gravado. Por outro lado, neste experimento, concluiu-se que se descobriu que o priming de sementes com KCl e NaCl era um melhor tratamento, especialmente na alta concentração de sais em comparação com as sementes não preparadas em caso de nabo para aumentar o vigor das sementes. e crescimento de plântulas sob condições estressantes ao sal.

**Palavras-chave:** *germinação, plântulas, nabo, preparação de sementes, sal.*

#### ABSTRACT

An experiment was conducted to enhance the turnip seed performance under salinity stress conditions. The impact of priming with an optimized dosage (5 g/l) of KCl and NaCl had been evaluated for enhancing seedling vigor and salt stress tolerance in seedlings of the turnip. Seeds prepared with (5 g/l) of KCl and NaCl solutions were examined at different salinity levels (0, 50, 100, 150, 200)mM of NaCl concerning the early growth stage. The data were analyzed using SPSS windows version 23 (one way ANOVA  $p \leq 0.05$ ) to determine the significant difference between treatments and followed Duncan test,  $p < 0.05$  for means comparison. The results have shown that priming with KCl and NaCl were effective in reducing the adverse effects of salinity. A significant ( $P < 0.05$ ) increase in germination percentage, seed vigor, hypocotyl and radicle length, salt tolerance, and dry weight of the seedlings of seed that priming with (5 g/l) of KCl and NaCl compared to non-primed seeds was recorded. On the other hand, In this experiment, it was concluded that seed priming with KCl and NaCl had been discovered to be better treatment, especially in the high concentration of salts as compared to non-primed seeds in case of turnip for rising the seeds vigor and seedling growth under salt-stressed conditions.

**Keywords:** *germination, seedling, turnip, seed priming, salt.*

#### المخلص:

أجريت تجربة لتحسين أداء بذور اللفت تحت ظروف إجهاد الملوحة. تم تقييم تأثير التحضير بجرعة محسنة (5 جم / لتر) من (KCl) و (NaCl) لتعزيز قوة الشتلات وتحمل الإجهاد الملحي في شتلات اللفت. تم فحص البذور المحضرة بمحلول (5 جم / لتر) من محلول كلوريد البوتاسيوم و كلوريد الصوديوم

بمستويات ملوحة مختلفة (0، 50، 100، 150، 200) ملي مولار من كلوريد الصوديوم فيما يتعلق بمرحلة النمو المبكر. تم تحليل البيانات باستخدام نافذة الحزمة الإحصائية للعلوم الاجتماعية (SPSS) الإصدار 23 (تحليل التباين باتجاه واحد ANOVA قيمة  $p \leq 0.05$ ) لتحديد الفروق المعنوية بين المعاملات والمتبع بأختبار دنكن ذو المدى المتعدد، قيمة  $p < 0.05$  للمقارنة. أوضحت النتائج أن الإعداد باستخدام كلوريد البوتاسيوم و كلوريد الصوديوم كان فعالاً في تقليل التأثيرات السلبية للملوحة. تم تسجيل زيادة معنوية ( $P < 0.05$ ) في نسبة الإنبات وقوة البذور وطول السويق وطول الجذير وتحمل الملح والوزن الجاف لشتلات البذور التي تم معاملة بـ (5 جم / لتر) من KCl و NaCl مقارنة بالبذور غير المعاملة. من ناحية أخرى، في هذه التجربة، تم الاستنتاج إلى أن إعداد البذور باستخدام KCl و NaCl قد تم اكتشافه على أنه أفضل معاملة، خاصة في التراكيز العالية للأملاح بالمقارنة مع البذور غير المعاملة في حالة اللفت لتحسين قوة البذور و نمو الشتلات تحت ظروف الإجهاد الملحي.

**الكلمات المفتاحية:** الإنبات، الشتلات، اللفت، تحضير البذور، الملح.

## 1. INTRODUCTION:

Turnip (*Brassica rapa*) belongs to family Cruciferae, and It is one of the most important dicotyledonous, cross-pollinated, and cool-season vegetable crops grown both for its enlarged roots and for the foliage (Pink, 1993). *Brassica* species are distinguished by their immense intraspecific diversity, exemplified by leafy plants, oilseeds, and crops with extended inflorescences and above-ground storage organs (Liu *et al.*, 2019). Soil salinity is one of the abiotic adversely influence on seed germination, seedling establishment, and efficiency of numerous harvests by creating an osmotic potential outside the seed inhibiting the absorption of water, or by the toxic effect (Mustafa *et al.*, 2017; Bose *et al.*, 2017). Osmotic and saline stresses are in charge of the inhibition and declines of seed germination and plant development (Yohannes and Abraha, 2013).

The water absorption decreases during the imbibition stage, and salinity leads to excessive absorption of toxic ions by the seed (Abraha and Yohannes, 2013; Murillo-Amador *et al.*, 2002). From the beginning of agriculture, the man established contact with seed physiology and realized that many seeds do not germinate easily and uniformly. The capacity of seemingly (dead seed) to regenerate and grow a viable young and healthy seedling after germination had been fascinated by the ancient civilization, therefore, the scientists for decades trying to figure out several methods of seed priming in order to activate seeds and alleviate environmental stresses and common technique its water-based priming techniques, which is a pre-sowing treatment that partially hydrates seeds without allowing emergence (Evenari, 1984; Chen and Arora, 2011).

Seed priming is a pre-germination seed treatment that leads to a physiological state that enables the seed to germinate more efficiently mean seeds are held at water potential that permits imbibition but prevents radicle extensions (Ashraf and Foolad, 2005; Gupta *et al.*, 2008;

Lutts *et al.*, 2016). Seed priming enhances seed performance by rapid and uniform germination, healthy and vigor seedlings, which resulted in faster and better germination and development in various harvests, this also helps seedlings to grow in stressed conditions (Mohammadi, 2009; Safdar *et al.*, 2019). Priming-induced increase in germination may be associated with a change in plant hormone biosynthesis and signaling. Priming has been reported to increase the gibberellins (GA)/abscisic acid (ABA) ratio, and this may be a direct consequence of a priming impact in gene expression pattern (El-Araby *et al.*, 2006; Schwember and Bradford, 2010). Several variables influence the priming performance and are highly on handled plant species and the priming technique selected. Physical and chemical factors such as osmotic and water capacity, priming agent, length, temperature, presence or absence of light, aeration and seed condition also affect the priming performance and decide the time and rate of germination, seedling vigor, and further plant growth (Hussain *et al.*, 2006; Varier, 2010).

Osmopriming means soaking seeds with low water content in an osmotic solution, rather than pure water. Because of the low water capacity of osmotic solutions, water enters seed gradually, which allows gradual impregnation of seed and activation of early germination phases but prevents radicular protrusion (Girolamo and Barbanti, 2012).

However, values of water potential, together with the duration of the priming treatment, should always be adjusted to species, cultivar, and sometimes seed lot. Different compounds are used in osmopriming procedures, including polyethylene glycol (PEG), mannitol, sorbitol, glycerol, and inorganic salts such as NaCl, KCl, KNO<sub>3</sub>, K<sub>3</sub>PO<sub>4</sub>, KH<sub>2</sub>PO<sub>4</sub>, MgSO<sub>4</sub>, and CaCl<sub>2</sub>. Priming with salt solutions is often referred to as "halopriming" (Yacoubi *et al.*, 2013).

Seed priming with various salts, especially KCl and NaCl, has appeared to improve the germination and development of numerous

harvests under stressed conditions (Naz *et al.*, 2014). The present study was carried out to investigate the impact of KCl and NaCl priming on germinations of seeds and seedling growth of turnip (*Brassica rapa rapa*) under salinity conditions.

## 2. MATERIALS AND METHODS:

### 2.1. Experiment site

In order to determine the effects of different salinity levels and Osmo priming on germination and seedling growth, the experiment was carried out in botany Laboratory, Department of Biology, University of Misan. The laboratory was approximately at 21°C, and the experiment was carried out inside safety cabins, the materials were used seeds, deionized distilled water, 5 g/l iter of NaCl and KCl, (50,100,150, 200mM) of NaCl, 70% ethanol, 5% Na<sub>2</sub>HCl, the equipment was used Petri dishes, filter paper, and parafilm.

### 2.2. Seed sterilization and soaking

Healthy turnip seeds were surface sterilized with 70% ethanol for 30 seconds and then with 5% sodium hypochlorite (Na<sub>2</sub>HCl) solution for 20 min and then thoroughly washed three times with sterilized distilled water (sterilized by using autoclave). Subsequently, the seeds were soaking with 5 g/l KCl and NaCl solution separately for 24 hours at 21°C. After priming. The seeds were washed with sterilized distilled water after priming and dried at room temperature on filter paper for 24 h to their original moisture level, utilizing sensor balance before being used in germination tests. (Yohannes and Abraha, 2013).

### 2.3. Experimental design

The study was carried out in November/2019. A complete random design (CRD) used to study the effect of seed priming on germination and seedling growth of turnip under salt stress. This part of the experiment was carried out in the laboratory in 45 Petri dishes, that is, 15 for KCl, 15 for NaCl primed seeds, and 15 for unprimed (control) seeds and repeated thrice. Primed and unprimed seeds were placed in 9 cm diameter Petri dishes on two layers of filter papers (Whatman No. 1). 15<sup>th</sup> seeds were placed in each Petri dishes were containing 5 ml of five different saline solutions (0, 50, 100, 150, 200 mM of NaCl). The Petri dishes were closed with par-film to prevent evaporation and kept in

the growth chamber at 21 ± 2°C. The experiment was conducted in a completely randomized design with six replications and 15<sup>th</sup> seeds per replicate. Seed germination was recorded daily up to day ten after the start of the experiment. When the radicle emerges by around 2 mm in length, a seed was considered germinated (Mohammed and Nulit, 2019<sup>a</sup>). The length of the hypocotyl and radicle of seedling were measured by selecting three seedlings randomly from each Petri dish, the seedlings were dried at 60°C for 48 h and then weighed (Li, 2008; Oliveira *et al.*, 2019). Germination percentage (GP %) was calculated according to Equation 1 by (Kandil *et al.*, 2012).

$$GP\% = \frac{\text{Number of germinated seeds}}{\text{Total number of seeds sown}} \times 100 \quad (\text{Eq. 1})$$

Seed vigor was calculated according to (Gebremedhn and Berhanu, 2013) Equation 2, which is:

$$\text{Seed vigor} = \frac{(L1 + L2) \times \text{germination percentage}}{100} \quad (\text{Eq. 2})$$

whereas: L1= length of hypocotyls

L2= length of radical

### 2.4. Statistical analysis

Statistical analysis was performed using SPSS window version 23. One-way confidence-level variance analysis (ANOVA) (Naz, 2014),  $p \leq 0.05$  was performed to find the significance deference among treatments followed by Duncan's multiple range test (DMRT) at  $p \leq 0.05$  for mean comparison.

## 3. RESULTS AND DISCUSSION:

### 3.1. Germination percentage (GP %)

Figure 1 shows the impact of NaCl and KCl priming on turnip (GP %) at different saltiness concentrations, respectively, in 10 days. From both primed and unprimed seeds diminished significantly ( $P \leq 0.5$ ) with increasing NaCl salinity level. However, this reduction in (GP %) was lower for primed seeds compared to unprimed seeds. Salinity reduced germination percentage for more than half due to an increase in salinity level from 0 mM to 200 mM. A similar decrease in germination percentage has been

recorded with rising salt levels in turnip (Mohammed and Nulit, 2019a; Mohammed and Nulit, 2019b). Seed generally, increasing salinity causes a decrease in turnip germination; this might be due to the toxic effects of  $\text{Na}^+$  and  $\text{Cl}^-$  in the process of germination (Tobe *et al.*, 2004; Osman, 2018). It changes the imbibitions of water by seeds due to decline osmotic capacity of germination media (Ibrahim *et al.*, 2019), it causes toxicity which changes the activity of certain enzymes of DNA metabolism, changes the metabolism of protein, breaks down the hormonal balance, and reduce the usage of seed reserve food (Ashraf and McNeilly, 2004; Ashraf *et al.*, 2010). Primed seeds of turnip might have better competency for water absorption from the growing media that enabled metabolic activities in seeds during the germination process of a start much earlier than radical and hypocotyl appearance (Elouaer and Hannachi, 2012; Zaghdani, 2002).

Similarly, increased solubility of seed storage proteins such as the beta subunit of the globulin and enhanced antioxidative reduction in lipid peroxidation and activity in primed seeds facilitated germination (Patade *et al.*, 2009; Kazemi and Eskandari, 2012). According to Soeda *et al.* (2005), the faster germination was due to the synthesis of protein, DNA, and RNA during seeds priming. A high positive correlation between seed germination and the amount of total soluble protein, Tania *et al.* (2019), reported the increased germination ability and total protein in areas with low pollution levels of anthropogenic pressure in *Betula pendula* plant.

### 3.2. Turnip seedlings length

Shoot and root lengths are the essential factors in the plant for salt stress because roots absorb water due to direct contact with soil, and then shoots enable its supply in the whole plant. For this reason, shoot and root lengths provide important indications of a plant's response to salt stress (Dinnyeny, 2019). Figure (2) shows an increase in the concentration of salts caused the reduction in the early growth of turnip seedlings. The length of seedling (radicle+ hypocotyl) significantly declined with increasing salts concentration in both primed and un-primed seeds. However, this influence was more distinguished in radicle (Figure 3) and hypocotyl (Figure 4) lengths from unprimed seeds when compared to the primed ones. A similar study shows that the adverse impact of salinity on *Pisum sativum* was overcome by the application of potassium nutrient through seed priming with KCl (Naz *et al.*, 2014). Seedlings' growth was

affected by both osmotic and specific ionic of salinity (Nawaz *et al.*, 2010; Tabatabaei and Naghibalghora, 2014). Nasim *et al.* (2008) and Petropoulos *et al.* (2017) investigated that salinity inhibits the absorption of essential nutrients such as P and K, which could negatively affect seedlings growth. In this study, seed priming significantly improved turnip seedling growth at different salinity levels. The improvement in radicle and hypocotyl length in the primed seeds may be attributed to earlier germination induced by priming (Farooq *et al.*, 2005). During the period of priming, the embryo expands and compresses the endosperm, the compaction force of the embryo and the water activity on the walls of endosperm cell may alter the tissues to be flexible when dehydrated, Produce free space and facilitate rapid projection of root and seedlings after rehydration (Mohammadi, 2009; Yohannesu and Abraha, 2013).

### 3.3. Seed vigor

Seed vigor is the characteristics of seed that determine the level of activity and performance of seeds during germination and emergence of seedling under a wide range of field conditions. Seedlings of high-activity seeds are expected to develop more uniformly than seedlings of low-activity seeds (Talai and Sen-Mandi, 2010; Egli and Rucker, 2012). Figure (5) shows both primed with (NaCl or KCl) and unprimed seeds diminished significantly with increasing salinity levels. However, this reduction in vigor was lower for primed seeds compared to unprimed seeds. Similar past investigation on Canola (*Brassica napus* L.) and tomato (*Lycopersicon esculentum* Mill.) showed that seed priming significantly improved shoot and radicle length (Nawaz *et al.*, 2010).

### 3.4. Dry Biomass of turnip

Salinity treatments were applied on turnip showed a significant reduction in dry seedling biomass with the rise of stress level as compared with control in both unprimed and primed seeds (Figure 6). For primed seeds, dry biomass was higher than for unprimed ones at different levels of salinity stress. Mohammed and Nulit (2019a; 2019b) showed that salt stress decreases the weight of turnip seedling. They suggested that the decrease in growth of turnip seedling is due to ionic stress and osmotic stress of salts. By increasing salinity, the biomass of seedling decreased, which might be attributed to a decrease in the remobilization of the seed reserves from cotyledons to the embryonic axis

(Yohannes and Abraha, 2013). The factors that affected the growth rate of the embryonic axis also affected transfer from cotyledons to the embryonic axis and reserve remobilization (Sedghi *et al.*, 2010; Naz *et al.*, 2014). The efficiency of seed priming with KCl or NaCl in improving biomass weight under stressful conditions was also reported in sunflower, melon (Matias *et al.*, 2018; Oliveira *et al.*, 2019).

#### 4. CONCLUSIONS:

This investigation provided useful knowledge on seed priming using a NaCl and KCl. Turnip's primed and unprimed seeds have different responses to saline solutions, especially in high concentrations. Seed priming with NaCl and KCl overcame these adverse effects of salinity. This priming significantly improved the germination and seedling growth of these plants. In unprimed seeds, declines in germination percentage and seedling growth with rising salinity levels were more apparent than in the primed seeds. Pretreatment with NaCl and KCl lead to a substantial improvement in the percentage of germination seed vigor seedling radical length, hypocotyl seedling length, and dry seedling biomass. Therefore, this research highlighted the benefit of applying seed priming techniques in salty stressful environments to reduce the adverse effects of salinity stress on germination and early development of seedlings under controlled conditions. However, more work is required to assess crop production (NaCl and KCl) on vegetative growth and yield under field conditions.

#### 5. ACKNOWLEDGMENTS:

The authors wish to acknowledge the College of Science staff at the University of Misan in supporting this work in their laboratories.

#### 6. REFERENCES:

1. Abraha, B., and Yohannes, G. (2013). The role of seed priming in improving seedling growth of maize (*Zea mays* L.) under salt stress at field conditions. *Agricultural Sciences*, 4(12), 666-672.
2. Ashraf, M., Akram, N. A., Arteca, R. N., and Foolad, M. R. (2010). The physiological, biochemical, and molecular roles of brassinosteroids and salicylic acid in plant processes and salt tolerance. *Critical Reviews in Plant Sciences*, 29(3), 162-190.
3. Ashraf, M., and Foolad, M. R. (2005). Pre-sowing seed treatment—A shotgun approach to improve germination, plant growth, and crop yield under saline and non-saline conditions. *Advances in agronomy*, 88, 223-271.
4. Ashraf, M., and McNeilly, T. (2004). Salinity tolerance in Brassica oilseeds. *Critical Reviews in Plant Sciences*, 23(2), 157-174.
5. Bose, B., Kumar, M., Singhal, R. K., and Mondal, S. (2018). Impact of seed priming on the modulation of physico-chemical and molecular processes during germination, growth, and development of crops. In *Advances in seed priming* (pp. 23-40). Springer, Singapore.
6. Chen, K., and Arora, R. (2011). Dynamics of the antioxidant system during seed osmopriming, post-priming germination, and seedling establishment in spinach (*Spinacia oleracea*). *Plant Science*, 180(2), 212-220.
7. Di Girolamo, G., and Barbanti, L. (2012). Treatment conditions and biochemical processes influencing seed priming effectiveness. *Italian Journal of Agronomy*, e25-e25.
8. Dinnyen, J. R. (2019). Developmental Responses to Water and Salinity in Root Systems. *Annual review of cell and developmental biology*, 35, 239-257.
9. Egli, D. B., and Rucker, M. (2012). Seed vigor and the uniformity of emergence of corn seedlings. *Crop Science*, 52(6), 2774-2782.
10. El-Araby, M. M., Moustafa, S. M. A., Ismail, and A. I., and Hegazi, A. Z. A. (2006). Hormone and phenol levels during germination and osmopriming of tomato seeds, and associated variations in protein patterns and anatomical seed features. *Acta Agronomica Hungarica*, 54(4), 441-457.
11. Elouaer, M. A., and Hannachi, C. (2012). Seed priming to improve germination and seedling growth of safflower (*Carthamus tinctorius*) under salt stress. *Eurasian Journal of BioSciences*, 6(1), 76-84.
12. Evenari, M. (1984). Seed physiology: its history from antiquity to the beginning of the 20th century. *The Botanical Review*, 50(2), 119-142.
13. Farooq, M. S. M. A., Basra, S. M. A.,

- Saleem, B. A., Nafees, M., and Chishti, S. A. (2005). Enhancement of tomato seed germination and seedling vigor by osmopriming. *Pak. J. Agri. Sci*, 42, 3-4.
14. Gupta, A., Dadlani, M., Arun Kumar, M. B., Roy, M., Naseem, M., Choudhary, V. K., and Maiti, R. K. (2008). Seed priming: the aftermath. *Int J Agric Environ Biotechnol*, 1, 199-209.
  15. Hussain, M. U. B. S. H. A. R., FArooq, M., Basra, S. M., and Ahmad, N. (2006). Influence of seed priming techniques on the seedling establishment, yield, and quality of hybrid sunflower. *International Journal of Agriculture and Biology*, 8(1), 14-18.
  16. Ibrahim, M. H., Abas, N. A., and Zahra, S. M. (2019). Impact of Salinity Stress on Germination of Water Spinach (*Ipomoea aquatica*). *Annual Research and Review in Biology*, 1-12.
  17. Kandil, A. A., Sharief, A. E., and Ahmed, S. R. H. (2012). Germination and seedling growth of some chickpea cultivars (*Cicer arietinum* L.) under salinity stress. *Journal of Basic and Applied Sciences*, 8(2), 49.
  18. Kazemi, K., and Eskandari, H. (2012). Does priming improve seed performance under salt and drought stress. *Journal of Basic and Applied Scientific Research*, 2(4), 3503-3507.
  19. Li, Y. (2008). Effect of salt stress on seed germination and seedling growth of three salinity plants. *Pak. J. Biol. Sci*, 11(9), 1268-1272.
  20. Liu, M., Bassetti, N., Petrasch, S., Zhang, N., Bucher, J., Shen, S., Zhao, J. and Bonnema, G. (2019). What makes turnips: anatomy, physiology and transcriptome during early stages of its hypocotyl-tuber development. *Horticulture Research*, 6(1), 1-14.
  21. Lutts, S., Benincasa, P., Wojtyla, L., Kubala, S., Pace, R., Lechowska, K., Quinet, M., and Garnczarska, M. (2016). Seed priming: new comprehensive approaches for an old empirical technique. *New challenges in seed biology-Basic and translational research driving seed technology. InTechOpen, Rijeka, Croatia*, 1-46.
  22. Matias, J. R., Torres, S. B., Leal, C. C., Leite, M. D. S., and Carvalho, S. (2018). Hydropriming as inducer of salinity tolerance in sunflower seeds. *Revista Brasileira de Engenharia Agrícola e Ambiental*, 22(4), 255-260.
  23. Mohammadi, G. R. (2009). The influence of NaCl priming on seed germination and seedling growth of canola (*Brassica napus* L.) under salinity conditions. *American-Eurasian Journal of Agricultural and Environmental Sciences*, 5(5), 696-700.
  24. Mohammed, S. J. and Nulit, R. (2019a). Impact of NaCl, MgCl<sub>2</sub> and CaCl<sub>2</sub> on seed germination and seedling growth on turnip (*Brassica rapa rapa*). *Plant Arch*, 19(1):1041-1047.
  25. Mohammed, S. J. and Nulit, R. (2019b). Impact Of NaCl, KCl , MCl<sub>2</sub>, MgSO<sub>4</sub>, and CaCl<sub>2</sub> On The Seed Germination And Seedling Growth Of Cucumber ( *Cucumis Sativus* cv . mti2). *Plant Arch*, 19(2):3111–3117.
  26. Murillo-Amador, B., López-Aguilar, R., Kaya, C., Larrinaga-Mayoral, J., and Flores-Hernández, A. (2002). Comparative effects of NaCl and polyethylene glycol on germination, emergence and seedling growth of cowpea. *Journal of Agronomy and Crop Science*, 188(4), 235-247.
  27. Mustafa, H. S. B., Mahmood, T., Ullah, A., Sharif, A., Bhatti, A. N., Muhammad Nadeem, M., and Ali, R. (2017). Role of seed priming to enhance growth and development of crop plants against biotic and abiotic stresses. *Bull Biol Allied Sci Res*, 2, 1-11.
  28. Nasim, M. U. H. A. M. M. A. D., Qureshi, R., Aziz, T. A. R. I. Q., Saqib, M., Nawaz, S. H. A. F. Q. A. T., Sahi, S. T., and Pervaiz, S. (2008). Growth and ionic composition of salt stressed *Eucalyptus camaldulensis* and *Eucalyptus teretecornis*. *Pakistan Journal of Botany*, 40(2), 799-805.
  29. Nawaz, K., Talat, A., Hussain, K., and Majeed, A. (2010). Induction of salt tolerance in two cultivars of sorghum (*Sorghum bicolor* L.) by exogenous application of proline at seedling stage. *World Applied Sciences Journal*, 10(1), 93-99.
  30. Naz, F., Gul, H., Hamayun, M., Sayyed, A., Khan, H., and Sherwani, S. (2014). Effect of NaCl stress on *Pisum sativum* germination and seedling growth with the influence of seed priming with potassium (KCL and KOH). *American-Eurasian Journal of Agricultural and Environmental Sciences*, 14(11), 1304-1311
  31. Oliveira, C. E. D. S., Steiner, F., Zuffo, A.

- M., Zoz, T., Alves, C. Z., and Aguiar, V. C. B. D. (2019). Seed priming improves the germination and growth rate of melon seedlings under saline stress. *Ciência Rural*, 49(7). Osman, K. T. (2018). Saline and Sodic Soils. In *Management of Soil Problems* (pp. 255-298). Springer, Cham.
32. Patade, V. Y., Bhargava, S., and Suprasanna, P. (2009). Halopriming imparts tolerance to salt and PEG induced drought stress in sugarcane. *Agriculture, ecosystems and environment*, 134(1-2), 24-28.
  33. Petropoulos, S. A., Levizou, E., Ntatsi, G., Fernandes, Â., Petrotos, K., Akoumianakis, K., Barros, L., and Ferreira, I. C. (2017). Salinity effect on nutritional value, chemical composition and bioactive compounds content of *Cichorium spinosum* L. *Food chemistry*, 214, 129-136.
  34. Pink, D. A. C., and KEANE, E. M. (1993). Lettuce: *Lactuca sativa* L. In *Genetic improvement of vegetable crops* (pp. 543-571). Pergamon.
  35. Safdar, H., Amin, A., Shafiq, Y., Ali, A., Yasin, R., Shoukat, A., Hussan, M. U. and Sarwar, M. I. (2019). A review: impact of salinity on plant growth. *Nat Sci*, 17(1), 34-40.
  36. Schwember, A. R., and Bradford, K. J. (2010). A genetic locus and gene expression patterns associated with the priming effect on lettuce seed germination at elevated temperatures. *Plant molecular biology*, 73(1-2), 105-118.
  37. Sedghi, M., Nemati, A., and Esmailpour, B. (2010). Effect of seed priming on germination and seedling growth of two medicinal plants under salinity. *Emirates Journal of Food and Agriculture*, 130-139.
  38. Soeda, Y., Konings, M. C., Vorst, O., van Houwelingen, A. M., Stoop, G. M., Maliepaard, C. A., Kodde, J., Bino, R.J., Groot, S. P.C., and van der Geest, A. H. (2005). Gene expression programs during *Brassica oleracea* seed maturation, osmopriming, and germination are indicators of progression of the germination process and the stress tolerance level. *Plant Physiology*, 137(1), 354-368.
  39. Tabatabaei, S. A., and Naghibalghora, S. M. (2014). The effect of salinity stress on germination characteristics and changes of biochemically of sesame seeds. *Cercetari Agronomice in Moldova*, 47(2), 61-68.
  40. Talai, S., and Sen-Mandi, S. (2010). Seed vigour-related DNA marker in rice shows homology with acetyl CoA carboxylase gene. *Acta physiologiae plantarum*, 32(1), 153-167.
  41. Tania, L., Diawati, C., Setyarini, M., Kadaritna, N., and Saputra, A. (2019). USING POTENTIOMETRIC ACID-BASE TITRATION TO DETERMINE PKA FROM MANGOSTEEN PERICARPS EXTRACT. *Periodico Tchê Química*, 16(32 (2)), 768-773.
  42. Tobe, K., Li, X., and Omasa, K. (2004). Effects of five different salts on seed germination and seedling growth of *Haloxylon ammodendron* (Chenopodiaceae). *Seed Science Research*, 14(4), 345-353.
  43. Varier, A., Vari, A. K., and Dadlani, M. (2010). The subcellular basis of seed priming. *Current Science*, 450-456.
  44. Yacoubi, R., Job, C., Belghazi, M., Chaibi, W., and Job, D. (2013). Proteomic analysis of the enhancement of seed vigour in osmoprimed alfalfa seeds germinated under salinity stress. *Seed Science Research*, 23(2), 99-110.
  45. Yohannes, G., and Abraha, B. (2013). The role of seed priming in improving seed germination and seedling growth of maize (*Zea mays* L.) under salt stress at laboratory conditions. *African Journal of Biotechnology*, 12(46), 6484-6490.
  46. Zaghdani, A. S. (2002). *Effect of pre-sowing seed treatments for quality of cucumber, pepper, tomato and pea seed* (Doctoral dissertation, Szent István Egyetem).

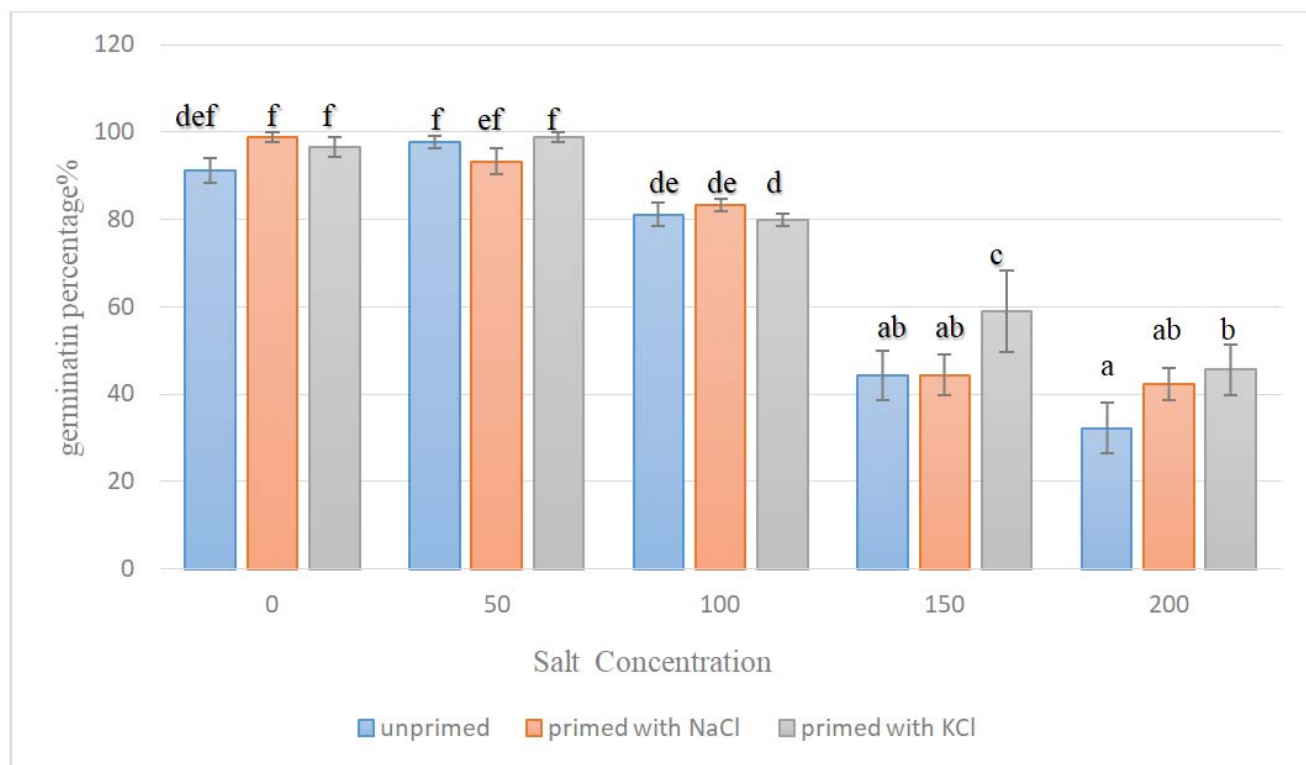


**Figure 1.** Effect of seed priming with NaCl and KCl on germination percentage of *Brassica rapa rapa* under different concentrations of salt. Different letters indicate significant difference among means (Duncan's test,  $p < 0.05$ ).

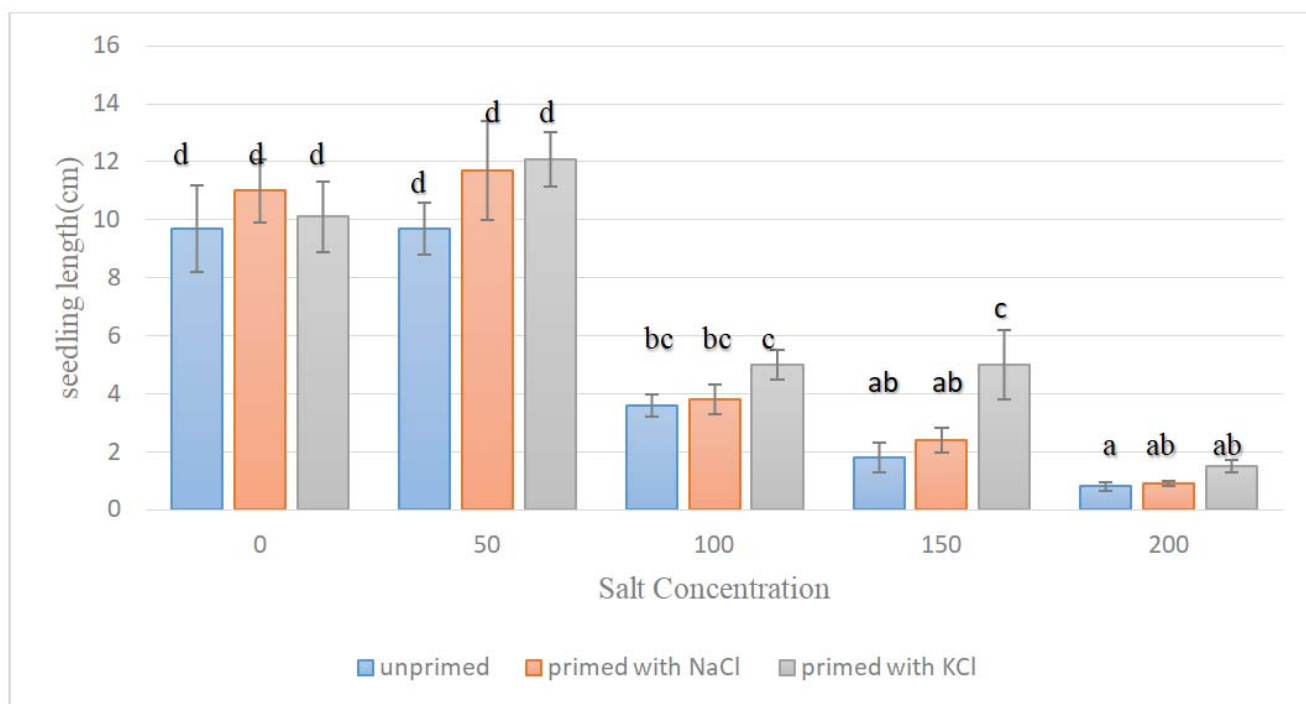


**Figure 2.** Effect of seed priming with NaCl and KCl on seedling length of *Brassica rapa rapa* under different concentrations of salt. Different letters indicate significant difference among means (Duncan's test,  $p < 0.05$ ).



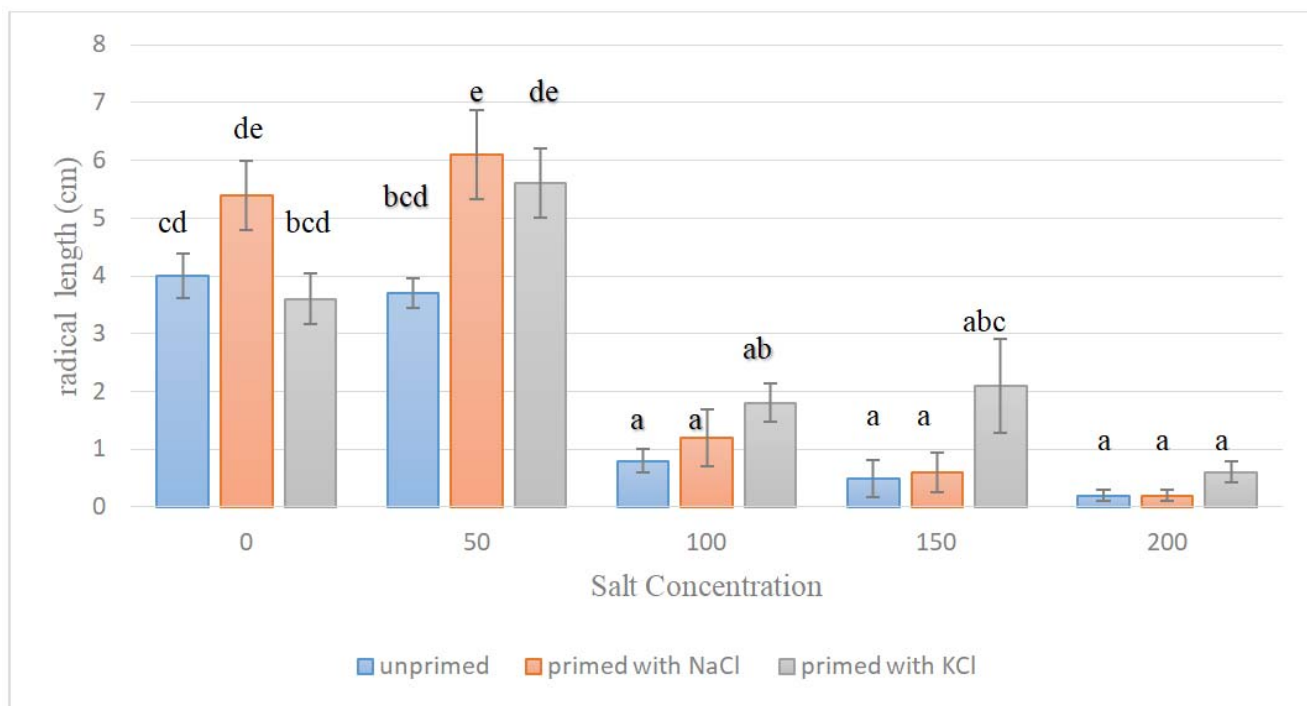


**Figure 3.** Effect of seed priming with NaCl and KCl on radical length of *Brassica rapa rapa* under different concentrations of salt. Different letters indicate significant difference among means (Duncan's test,  $p < 0.05$ ).

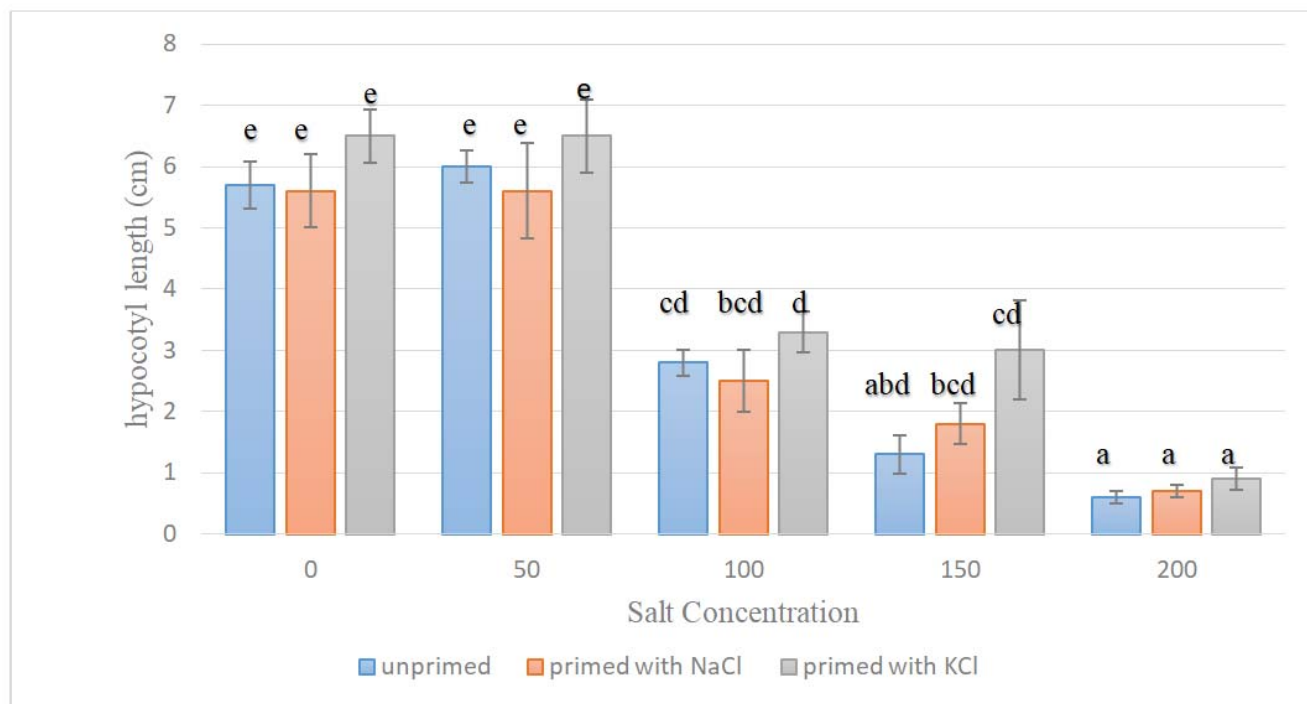


**Figure 4.** Effect of seed priming with NaCl and KCl on hypocotyl length of *Brassica rapa rapa* under different concentrations of salt. Different letters indicate significant difference among means (Duncan's test,  $p < 0.05$ ).

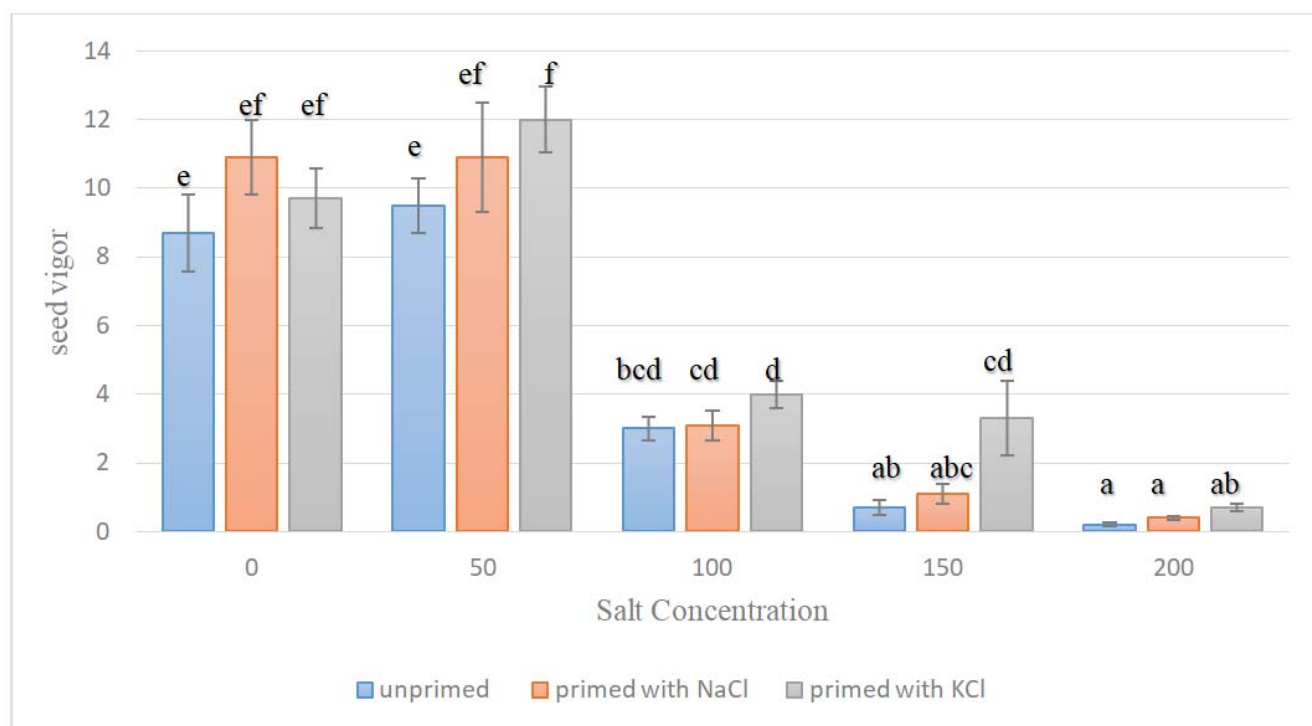


**Figure 5.** Effect of seed priming with NaCl and KCl on seed vigor of *Brassica rapa rapa* under different concentrations of salt. Different letters indicate significant difference among means (Duncan's test,  $p < 0.05$ ).

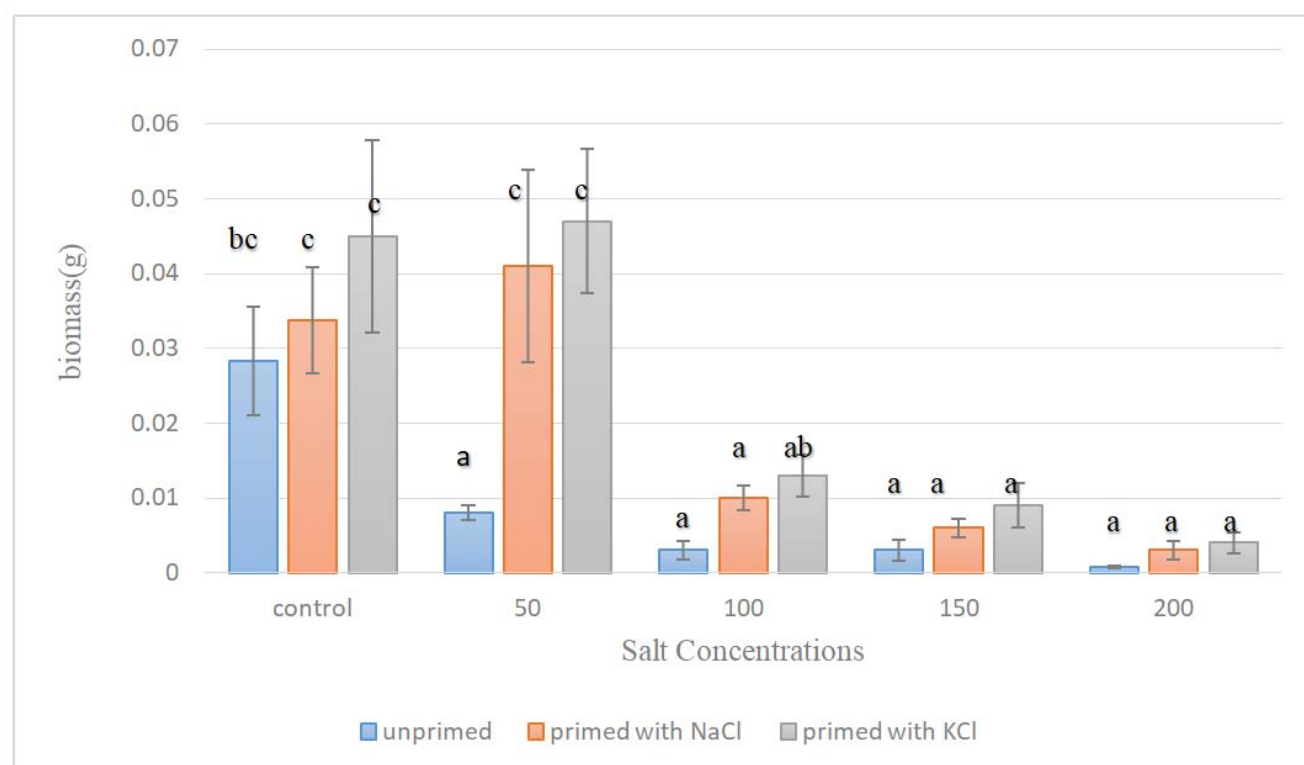


**Figure 6.** Effect of seed priming with NaCl and KCl on germination percentage of *Brassica rapa rapa* under different concentrations of salt. Different letters indicate significant difference among means (Duncan's test,  $p < 0.05$ ).

**ALTERAÇÃO DA COMPOSIÇÃO QUÍMICA, GORDURA E ÁCIDA E PROPRIEDADES FÍSICAS E TÉCNICAS DE GORDURA DE CORDEIRO SOB INFLUÊNCIA DE VÁRIAS FORRAGENS****CHANGE OF THE CHEMICAL, FAT AND ACID COMPOSITION AND PHYSICAL AND TECHNICAL PROPERTIES OF LAMB FAT UNDER INFLUENCE OF VARIOUS FODDER BACKGROUND**

MIRONOVA, Irina<sup>1\*</sup>; GALIEVA, Zul'fiya<sup>1</sup>; GAZEEV, Igor<sup>2</sup>; BELOUSOV, Alexander<sup>3</sup>; GALIMOVA, Venire<sup>1</sup>

<sup>1</sup> Federal State Budgetary Educational Establishment of Higher Education "Bashkir State Agrarian University", Department of Technologies of Meat, Dairy Products and Chemistry. Russian Federation

<sup>2</sup> Federal State Budgetary Educational Establishment of Higher Education "Bashkir State Agrarian University", Department of Life Safety and Process Equipment. Russian Federation

<sup>3</sup> Federal State Budgetary Educational Establishment of Higher Education "Orenburg State Agrarian University", Department of Livestock Production and Processing Technologies. Russian Federation

*\* Corresponding author  
e-mail: mironova.irina.v@rambler.ru*

Received 03 April 2020; received in revised form 04 May 2020; accepted 05 June 2020

**RESUMO**

O papel das gorduras na nutrição é determinado pelo seu alto teor calórico e participação na construção dos tecidos do corpo, juntamente com proteínas e carboidratos. A nutrição enriquecida é de grande importância no complexo de questões que determinam sua utilidade. Assim, a questão do efeito dos probióticos e sorventes na dieta do organismo animal tornou-se muito relevante. O objetivo do trabalho foi uma avaliação comparativa da composição e propriedades do tecido adiposo de carneiros, consumindo juntos e separadamente preparações com efeito de sorção e probiótico. Os estudos foram realizados em duas etapas. Na primeira, durante o experimento científico e econômico, 80 carneiros recém-nascidos cresceram e se desenvolveram até um ano de idade, seguidos pelo abate de três animais de cada grupo. Na segunda etapa, as amostras de gordura interna foram examinadas de acordo com vários indicadores. A análise sensorial revelou que todas as amostras internas de gordura atendiam aos requisitos estabelecidos, enquanto a cor e consistência das amostras experimentais melhoraram. O teor de matéria seca, incluindo gordura nas amostras experimentais de tecido adiposo, aumentou e a umidade diminuiu. Os parâmetros físicos e técnicos da gordura interna também mudaram no aspecto intergrupo. Na amostra controle, o número de iodo diminuiu e o número de saponificação, ponto de fluidez e ponto de fusão aumentaram. O cálculo do valor energético indica que, na primeira amostra, o indicador aumentou 0,08 MJ (0,23%); Grupo II - por 0,16 MJ (0,45%) e grupo III - por 0,25 MJ (0,70%). De acordo com a soma de ácidos graxos monoinsaturados, o grupo jovem III estava na liderança. O conteúdo de ácidos graxos poliinsaturados foi o oposto. A eficácia biológica das gorduras é determinada pela proporção que foi melhor nas amostras experimentais. Assim, a inclusão de aditivos forrageiros na dieta dos carneiros da raça Romanov ajuda a melhorar a qualidade das matérias-primas.

**Palavras-chave:** *composição, gordura interna, probiótico, raça Romanov, aditivo de sorção.*

**ABSTRACT**

The role of fats in nutrition is determined by their high-calorie content and participation in the construction of body tissues, together with proteins and carbohydrates. Enriched nutrition is of great importance in the complex of issues that determine its usefulness. Thus, the question of the effect of probiotics and sorbents in the diet on the animal organism has become very relevant. The purpose of the work was a comparative assessment of the composition and properties of adipose tissue of rams, consuming together and separately preparations with sorption and probiotic effect. The studies were carried out in two stages. In the first, during the scientific and economic experiment, 80 newborn rams grew and developed up to a year of age, followed by the slaughter of three animals from each group. In the second stage, samples of internal fat were examined according to some indicators. Sensory analysis revealed that all internal fat samples met the established requirements, while the

color and consistency of the experimental samples improved. The dry matter content, including fat in the experimental samples of fat tissue, increased, and moisture decreased. The physical and technical parameters of internal fat also changed in the intergroup aspect. In the control sample, the iodine number decreased, and the saponification number, pour point, and melting point increased. Calculation of energy value indicates that in the first sample, the indicator increased by 0.08 MJ (0.23%); Group II – by 0.16 MJ (0.45%) and group III – by 0.25 MJ (0.70%). According to the sum of monounsaturated fatty acids, young group III was in the lead. The content of polyunsaturated fatty acids was the opposite. The biological effectiveness of fats is determined by the ratio that was better in the experimental samples. Thus, the inclusion of fodder additives in the diet of the rams of the Romanov breed helps to improve the quality of raw materials.

**Keywords:** *composition, internal fat, probiotic, Romanov breed, sorption additive*

## 1. INTRODUCTION:

Fats, including animal fats, are an essential component of food. The significance of fats consists, first of all, in their high energy value, since the caloric content of 1 g of fat is 9 kcal, which is more than two times exceeds the caloric content of proteins and carbohydrates. The biological value of animal fat lies in the presence of vitamins A, D, E, K and polyunsaturated fatty acids in it (Bagautdinov *et al.*, 2018; Creemers, Van Passel, and Vigani, 2019; Dementyev *et al.*, 2018; Khaziakhmetov *et al.*, 2018a, 2018b; Kick, Zering, and Classen, 2017; Lamanov *et al.*, 2020; Sharipova *et al.*, 2017a).

The global trend indicates that the consumption of fats and butter has quadrupled compared with the level recorded 50 years ago. This was due to an increase in population, an increase in fat intake, and a change in cooking methods (Aslanova, Derevitsckaya, and Dydikin, 2018; Igenbayev *et al.*, 2019; Mironova, Nigmatyanov, Radchenko, and Gizatova, 2019a; Okuskhanova *et al.*, 2019; Sydykova *et al.*, 2019).

In 1950, the number of animal fats on the market was only slightly lower than vegetable oils. In 1970, animal fats accounted for only a quarter, and currently – only 15% (Gavrilova *et al.*, 2019; Gubaidullin, Mironova, and Islamgulova, 2010; Kalasov, Andrienko, Galieva, and Kasimova, 2019; Kosilov, Gazeev, and Yuldashbaev, 2016; Mironova, Nigmatyanov, Grunina, Sepiashvili, and Strigulina, 2019; Shkilev, Gazeev, and Nikonova, 2011).

The UN Food and Agriculture Organization estimated the total mean energy intake from plant and animal sources to be around 3380 kcal in Europe and the US with the animal source energy intake accounting for 943 kcal (27.9%). In developing countries, a similar figure is 2,261 kcal, and 331 kcal (14.6%) of energy is supplied through animal feed. In countries with transition economies, which include Russia, the total energy

supply is 2,906 kcal, and 671 kcal (23.1%) comes from animal feed. In recent years, there has been an accumulation of critical knowledge about the predominance of vegetable fats in the human diet. A study of the role of individual fatty acids in biochemical transformations indicates that animal fats are necessary for the normal functioning of the body, and possible negative consequences are reduced or even eliminated by the presence of individual fatty acids or other biologically active substances (Kuzmicheva, 2013; Khaziev *et al.*, 2018; Obolentsev, 2018; World Health Organization, 2003; Ziyangirova, Mironova, Gazeev, Galieva, and Galieva, 2019).

By analyzing data from the FAO report, a specific food production concept has been outlined. The idea is a point aimed at expanding the use of biological resources, thereby diversifying the nutritional composition of foods to satisfy the physiological needs of the population (Tagirov *et al.*, 2018; World Health Organization, 2003).

One of the approaches to expanding the species diversity of raw materials in the conditions of the Southern Urals is the use of mutton. The volume of its production in the Russian Federation is not more than 3% of the total mass of raw meat. Even though the Volga Federal District is the leader in the number of sheep, the volume of output is much less than the needs of the domestic market. Therefore, the development of sheep breeding will allow, firstly, to partially eliminate the shortage of meat raw materials and secondly to expand the range of products, including those with new properties (Gabitov *et al.*, 2018; P. Kornienko, Yusupov, Eremanenko, and R. Kornienko, 2008; Ponomarenko, Grishina, and Bekturov, 2017; Traisov, Sultanova, Yuldashbayev, and Esengaliyev, 2014; Traisov *et al.*, 2015).

Besides, the development of the sheep industry allows, in addition to food products, which include milk and meat, to supply the light industry with raw materials, such as wool and sheepskin

(Bogolyubova, Korotky, Zenkin, Ryzhov, and Buryakov, 2017; Sharipova *et al.*, 2017b; V. Vorobyev, D. Vorobyev, Zakharkina, Polkovnichenko, and Safonov, 2019).

Russia is famous for its more than century-old history of breeding Romanov sheep with a meat-and-wool direction of productivity. A distinctive feature of this breed is its good adaptability to sharply continental climate conditions, unpretentiousness to feeds, fecundity, early maturity, and polyestricity. The resulting lamb is characterized by good taste, the absence of a specific taste, high biological, and low energy value (Bogolyubova *et al.*, 2017; Chernitskiy, Shabunin, Kuchmenko, and Safonov, 2019; Dvalishvili and Vinogradov, 2015).

Although the animals of the Romanov breed are unpretentious to the feeding conditions, they can still maximize the productive potential of the sheep with a full and balanced diet (Okuskhanova *et al.*, 2019; Sedykh *et al.*, 2018). It is recommended to enrich the diet with feed additives of sorption action and probiotic. Then the choice of the object of study is since fats, like protein components of meat, play an important role in human life, provided they are reasonably consumed. Meat is the main source of animal fats, which supply vitamins A and D to the body and contribute to their absorption (Zabelina and Lushnikov, 1999).

The optimal total norm of consumption of animal and vegetable fats in the diet is 100-150 g per day, while animal fats should account for 70-75 g, vegetable fats – 30 g. For the organization of the herodietic ration, this ratio should be at the level of 1:1 (Andrienko, 2018; Efimova and Antonenko, 2016).

It is known that the composition of fat is represented by carbon, hydrogen, and oxygen, and by the chemical structure, they are complex substances. The fat molecule contains glycerin and fatty acids, which are classified as saturated and unsaturated. The group of saturated lamb fatty acids is represented by palmitic, stearic, and unsaturated – by oleic acids. According to their properties, palmitic and stearic acids at 15-20 °C retain their hardness, and oleic acid is in liquid form. Stearic acid, which is part of lamb fat, undergoes melting at a temperature of 69.2 °C, and upon solidification, it crystallizes.

According to the organoleptic properties, lamb fat should have white matte color and a specific smell. It is important to note that the fat of

adult animals has a more saturated and dark color than the fat of young animals.

The studies of domestic and foreign scientists indicate that if the nutrients of the diet are not used as a building material, then they are transported and stored in the body in the form of a reserve – fat. Not only lipids but also unused nitrogenous substances and carbohydrates turn into fat (Gadiev *et al.*, 2019; Erochin *et al.*, 2013; Khabibullin *et al.*, 2019).

Sheep are characterized by having a certain sequence in the deposition of fat: first – on the internal organs (kidneys, intestines, stomach), then – at the root of the tail, on the lower back, brisket (subcutaneous) and between the muscles (intramuscular). Fat accumulated in animals, in many respects, affects the taste, appearance, and calorie content of meat (Andrienko, 2018).

The purpose of this study was to study the physicochemical parameters, as well as the fatty-acid balance of the internal sheep's fat, obtained from animals consuming various supplements.

## 2. MATERIALS AND METHODS:

The studies were carried out according to the thematic plan of Bashkir State Agrarian University No. 01860076873. To obtain fat raw materials at the initial stage in the conditions of the Republic of Bashkortostan, scientific and economic experience was organized on rams of the Romanov breed, which were divided into four groups of 20 animals each. The number of animals was selected, taking into account the possibility of ensuring the reliability of the data. Groups were formed according to the principle of analogs from among newborn lambs. Feeding the young of the control group consisted of giving the main diet adopted on the farm. The diet of animals from the experimental groups additionally included additives that were added at the rate of 0.10 g / kg of live weight. For the sheep of group I, a sorption additive was used, group II was probiotic, group III used both together. The experiment lasted until the animals reached the age of one year. To conduct the second stage of research with the aim of comparative studying the chemical composition of internal fat at 12 months of age, a control slaughter of three animals from each group was organized according to the All-Russian Institute for Animal Breeding method (1978).

Sensory assessment of fat was carried out by the organoleptic method, which is based on the perception of the senses – vision, smell, hearing,

touch, taste. Color and consistency were analyzed at a temperature of 15-20 °C, and the degree of transparency was established in the molten state of fat. To study the chemical composition of adipose tissue, an average sample was taken, and the All-Russian Institute for Animal Breeding method (1978) was applied. The mass fraction of moisture was determined according to State Standard 9793-74, the protein was established by the Kjeldahl total nitrogen determination method, the iodine number was determined by the Güble method, the melting point was determined by the capillary method, and the energy value was established by the Aleksandrov formula (1951); the amount of fatty acids – on a “Crystal-2000M” gas-liquid analytical chromatograph according to State Standard R-51.483-99.

The animals were kept according to the instructions and recommendations of Russian Regulations, 1987 (Order No.755 on 08/12/1977 the USSR Ministry of Health), as well as “The Guide for Care and Use of Laboratory Animals (Institute of Laboratory Animal Resources, Commission on Life Sciences, National Research Council, National Academy Press Washington, DC 1996)” (Institute of Laboratory Animal Resources, 1996; The USSR Ministry of Health, 1987). In the course of the research, efforts were made to minimize animal suffering and the least number of samples used.

The digital material obtained in the experiment was processed by the variation method of statistics Microsoft Office with determining the reliability of the difference at three levels of probability, according to Student.

### 3. RESULTS AND DISCUSSIONS:

The assessment of the quality of fat by organoleptic indicators showed that regardless of the type of additive used, all samples of internal fat met the established requirements (Table 1).

At the same time, some intergroup differences in the consistency of the samples are noted. In particular, the best consistency of fat is noted in the sample obtained from animals of groups I and II, which is characterized as dense. The introduction of feed additives into the diet positively affected the color of the product. The fat of the experimental samples was characterized by white color, without a clear yellowish tint, which meets the requirements of normative and technical documentation.

Because its constituent components

determine the quality of fat, a chemical analysis was carried out (Figure 1).

It was found that the highest solids content was observed in experimental samples of adipose tissue. So, the advantage of the rams of the first experimental group over the young ones of the control group was 0.30%; group II – 0.47%; group III 0.72%. A similar distribution between groups is also noted in the content of chemically pure fat. It is enough to note that the difference in favor of the experimental young rams of the I, II, and III groups was 0.20%; 0.39% and 0.60%. In all cases, in the lead were the rams consuming the tested additives together.

By a mass fraction of moisture, the intergroup difference was the opposite. In animals of the control group, the studied indicator increased by 0.23%; 0.47 and 0.69%, respectively. For a more accurate analysis of the influence of the feed additive on the qualitative characteristics of the fat of rams, physicochemical studies of internal fat were carried out (Table 2).

The previously established differences in the chemical composition of adipose tissue of different localization affected the energy value. In experimental samples of fat (I, II, III), compared with the baseline, the energy value of 1 kg fat increased by 0.08 MJ (0.23%), 0.16 MJ (0.45%), and 0.25 MJ (0.70%), respectively.

Saponification number is an indicator for determining the authenticity of fatty oils. Fats containing mainly triglycerides are analyzed by the average molecular weight of the fatty acids included in them. Moreover, fats rich in saturated acids have a high melting point, while unsaturated fats have a low melting point.

The introduction of test additives in the diet of animals contributed to the improvement of technological parameters of internal fat.

The results of the study indicate that the introduction of additives into the diet did not adversely affect the pour point of the internal fat of ram carcasses of all the samples studied. The intergroup differences in the value of the melting temperature and the Güble number were insignificant within the physiological norms.

In assessing the quality of fat, significant importance is given to the qualitative composition of fatty acids. In this regard, the fat-acid gas-chromatographic analysis of the triglycerides that make up the internal (omentum + perinephric) adipose tissue of sheep fat was carried out. The

analysis of these studies indicates an increase in the content of many saturated fatty acids in the experimental samples compared with the control (Table. 3). The superiority of young rams from I-III groups in the content of capric fatty acid over peers of the control group was 0.01–0.02%, myristic – 0.03-0.07%, palmitic – 0.06-0.08%, stearic – 0.05-0.06%. Among monounsaturated fatty acids, oleic predominates. The value of the studied indicator in young animals of the first experimental group was higher than in control by 0.04%, II – by 0.2%, III – by 0.21%.

The indicators of polyunsaturated arachinic and arachidonic fatty acids did not change and were in the range of 0.25-0.26% and 0.27%, respectively. The indices of linoleic fatty acid in rams of the first experimental group decreased by 0.06% compared to the control group, of the second experimental group – by 0.1%, the third experimental group – 0.03%; linolenic – by 0.05%; 0.03% and 0.03%, respectively. When analyzing the total mass fractions of the fatty acid content, certain intergroup differences are noted (Table 4).

According to the amount of monounsaturated fatty acids, young rams from group III were in the lead. Its superiority over control peers in terms of the studied indicator was 0.37%, over analogs of the first group – 0.09%, II – 0.33%. The content of polyunsaturated fatty acids was the opposite. It is enough to note that in young animals, this indicator was higher than in experienced peers of the I, II, and III groups – by 0.1%, 0.12%, and 0.06%, respectively.

It should be noted that the amount of saturated fatty acids was higher in animals consuming test supplements. So, they have this indicator increased by 0.14%, 0.16%, and 0.21%, compared with the control peers.

A comparative analysis of the ratio characterizing the biological effects of fats indicates a similar dynamics in young animals of all experimental groups. Thus, the introduction of sorption and probiotic additives into the diet of rams did not have a significant effect on the biological effectiveness of fats. However, there was a slight positive tendency in the experimental samples.

The search for measures to provide the population with full-fledged food products, due to the species diversity of raw materials, is a strategic task of the agricultural sector (Andreeva *et al.*, 2018; Andrienko, 2018; Filippova *et al.*, 2017; Gadiev *et al.*, 2019; Gubaidullin, Kanareykina, and

Timerbulatova, 2014; Khabibullin *et al.*, 2019; Khaziahmetov *et al.*, 2018; Kosilov, Nikonova, Wilver, and Kubatbekov, 2016; Zabelina and Lushnikov, 1999). It is proposed to intensify the sheep breeding industry by improving the feeding system of Romanov rams with subsequent analysis of the quality of the obtained raw materials. The organoleptic assessment revealed intergroup differences in the consistency of samples with the best characteristics, characterized by density, in samples I and II. In this case, the fat of the test samples was white, without a clear yellowish tint.

The chemical analysis of internal mutton fat revealed a decrease in the proportion of moisture (by 0.23-0.69%), an increase in the share of solids (by 0.30-0.72%), fat (by 0.20-0.60%) and therefore, the energy value of 1 kg of fat (0.08-0.25 MJ (0.23-0.70%) in experimental samples of adipose tissue.

The physical-technical properties of the fat of all the studied samples when sorption and probiotic additives were added to the diet of rams did not have a negative effect. At the same time, specific differences between the groups in connection with the use of different fodder backgrounds were insignificant and did not go beyond the normative.

The study of the qualitative composition of fatty acids revealed an increase in the proportion of some saturated fatty acids (capric, myristic, palmitic, stearic) in the experimental samples, compared with the control. Among monounsaturated fatty acids, oleic predominates. Indicators of polyunsaturated fatty acids of arachinic and arachidonic did not change, but the content of linoleic and linolenic fatty acids in the rams of the experimental groups decreased.

The comparative analysis of the ratio characterizing the biological effectiveness of fats indicates its improvement in animals consuming test supplements.

#### 4. CONCLUSIONS:

Thus, the chemical composition and physical properties of the internal raw fat tended to change in the intergroup aspect. At the same time, its energy saturation increased due to the accumulation of chemically pure fat, and the biological value decreased due to a decrease in the total amount of polyunsaturated fatty acids. However, the changes occurring in the adipose tissue of young sheep were within the



physiological norm and corresponded to breed characteristics. The data obtained indicate that only a differentiated approach to the quality of raw materials, taking into account a balanced feed background of sheep, makes it possible to choose the most optimal variant of its rational use.

## 5. REFERENCES:

1. Andreeva, A. V., Nikolaeva, O. N., Ismagilova, E. R., Tuktarov, V. R., Fazlaev, R. G., Ivanov, A. I., ... and Khakimova, A. Z. (2018). Effect of probiotic preparations on the intestinal microbiome. *Journal of Engineering and Applied Sciences*, 13(S8), 6467-6472.
2. Andrienko, D. A. (2018). The nature of the distribution of adipose tissue in the body of young sheep of the Stavropol sheep breed in the Southern Urals. In *Ways to implement the Federal Scientific and Technical Program for the Development of Agriculture for 2017-2025* (pp. 346-350). Lesnikovo.
3. Aslanova, M. A., Derevitskaya, O. K., and Dydikin, A. S. (2018). Functional meat products: problems and perspectives. *Meat Industry*, 3, 38-42.
4. Bagautdinov, A. M., Baimatov, V. N., Gildikov, D. I., Kozlov, G. N., Chudov, I. V., Tagirov, K., ... and Mukminov, M. N. (2018). Assessment of the antioxidant properties of plant and chemical origin dietary supplements in the model test system. *Journal of Engineering and Applied Sciences*, 13(S8), 6576-6583.
5. Bogolyubova, N. V., Korotky, V. P., Zenkin, A. S., Ryzhov, V. A., and Buryakov, N. P. (2017). Digestion and Metabolism Indices of Sheep When Using Activated Charcoal Supplement. *OnLine Journal of Biological Sciences*, 17(2), 121-127.
6. Chernitskiy, A., Shabunin, S., Kuchmenko, T., and Safonov, V. (2019). On-farm diagnosis of latent respiratory failure in calves. *Turkish Journal of Veterinary and Animal Sciences*, 43(6), 707-715.
7. Creemers, S., Van Passel, S., and Vigani, M. (2019). Relationship between farmers' perception of sustainability and future farming strategies: A commodity-level comparison. *AIMS Agriculture and Food*, 4, 613-642.
8. Dementyev, E. P., Bazekin, G. V., Tokarev, I. N., Lobodina, G. V., Karimov, F. A., Andreeva, A. V., ... and Bliznetsov, A. V. (2018). The Application of physical and biological stimulants in livestock breeding. *Journal of Engineering and Applied Sciences*, 13(S10), 8325-8330.
9. Dvalishvili, V. G., and Vinogradov, S. (2015). Productivity of young sheep of the Romanovskaya breed of different origin. *Newsletter of the National Union of Sheep Breeders*, 2, 58-62.
10. Efimova, N. I., and Antonenko, T. I. (2016). Fattening meat and indicators of soviet merino sheep young with different shares of thorough-breediness by Australian meat merino. *Science and the World*, 4, 116-119.
11. Erochin, A. I., Karasyov, E. A., Yuldashbayev, Y. A., Magomadov, T. A., Medvedyev, M. V., and Razumeyev, K. E. (2013). The productivity of kuibyshevskaya sheep breed and its crossbreds with the rams of Romney marsh and north Caucasian-texel breeds. *News of the Timeryazev Agricultural Academy*, 7, 67-78.
12. Filippova, O. B., Zazulya, A. N., Frolov, A. I., and Vigdorovich, V. I. (2017). Natural sorbent in calf feed. *Science in Central Russia*, 1(25), 63-68.
13. Gabitov, I. I., Mudarisov, S. G., Gafurov, I. D., Ableeva, A. M., Negovora, A. V., Davletshin, M. M., ... and Yukhin, G. P. (2018). Evaluation of the efficiency of mechanized technological processes of agricultural production. *Journal of Engineering and Applied Sciences*, 13(S10), 8338-8345.
14. Gadiev, R. R., Khaziev, D. D., Galina, C. R., Farrakhov, A. R., Farhutdinov, K. D., Dolmatova, I. Y., ... and Latypova, G. F. (2019). The use of chlorella in goose breeding. *AIMS Agriculture and Food*, 4, 349-361.
15. Gavrilova, N., Rebezov, M., Harlap, S., Nigmatyanov, A., Peshcherov, G., Bychkova, T., ... and Karapetyan, I. (2019). Biotechnology of specialized fermented product for elderly nutrition. *International Journal of Pharmaceutical Research*, 11(1), 545-550.
16. Gubaidullin, N. M., Kanareykina, S. G., and Timerbulatova, A. T. (2014). The dynamics of milk productivity of Bashkir mares when feeding probiotic feed additives "Biogumitel". *Bulletin of Bashkir State Agrarian University*, 4(32), 51-54.
17. Gubaidullin, N. M., Mironova, I. V., and Islamgulova, I. N. (2010). The effect of feeding aluminosilicates to castrate gobies on the



- nutritional and energy value of meat products. *News of the Orenburg State Agrarian University*, 1, 198-200.
18. Igenbayev, A., Okuskhanova, E., Nurgazezova, A., Rebezov, Y., Kassymov, S., Nurymkhan, G., ... and Rebezov, M. (2019). Fatty Acid Composition of Female Turkey Muscles in Kazakhstan. *Journal of World's Poultry Research*, 9(2), 78-81.
  19. Institute of Laboratory Animal Resources (1996). *The Guide for Care and Use of Laboratory Animals. Institute of Laboratory Animal Resources, Commission on Life Sciences, National Research Council*. Washington, DC: National Academy Press.
  20. Kalasov, M. B., Andrienko, D. A., Galieva, Z. A., and Kasimova, G. V. (2019). The results of growing young sheep of the Kazakh fat tail sheep breed. *Science and Education*, 4, 100-103.
  21. Khabibullin, R., Khabibullin, I., Yagafarov, R., Bakirova, A., Fazlaev, R., Karimov, F., ... and Tuktarov, V. (2019). The influence of dietary supplements on the adaptive processes in animals after physical stress. *Bulgarian Journal of Agricultural Science*, 25(2), 105-118.
  22. Khaziakhmetov, F. S., Khabirov, A. F., Avzalov, R. K., Tsapalova, G. R., Rebezov, M. B., Tagirov, K., ... and Yessimbekov, Z. S. (2018a). Effect of probiotics on calves, weaned pigs and lamb growth. *Research Journal of Pharmaceutical, Biological and Chemical Sciences*, 9(3), 866-870.
  23. Khaziakhmetov, F. S., Khabirov, A. F., Avzalov, R. K., Tsapalova, G. R., Tagirov, K., Giniyatullin, S., ... and Gafarov, F. A. (2018b). Effects of Paenibacillus-based probiotic (baxispecin) on growth performance, gut microflora and hematology indices in goslings. *Journal of Engineering and Applied Sciences*, 13(S8), 6541-6545.
  24. Khaziev, D. D., Gadiev, R. R., Dolmatova, I. Y., Farrakhov, A. R., Galina, C. R., Akhmetgareeva, N. N., ... and Sharipova, A. F. (2018). Chemical composition and functional-technological properties of mulard meat. *Journal of Engineering and Applied Sciences*, 13(S8), 6413-6418.
  25. Kick, E. L., Zering, K., and Classen, J. (2017). Approaches to agricultural innovation and their effectiveness. *AIMS Agriculture and Food*, 2, 370-373.
  26. Kornienko, P. P., Yusupov, Sh. Y., Eremenko, E. P., and Kornienko, R. P. (2008). Modern approach in sheep breeding management in central-chernozem region. *Achievements of Science and Technology of Agribusiness*, 9, 38-41.
  27. Kosilov, V. I., Gazeev, I. R., and Yuldashbaev, Yu. A. (2016). Growth and development of young people of the edilbai breed. *Bulletin of the Bashkir State Agrarian University*, 4, 40-46.
  28. Kosilov, V. I., Nikonova, E. A., Wilver, D. S., and Kubatbekov, T. S. (2016). The effect of probiotic supplement Biogumitator 2G on the efficiency of the use of nutrients in feed rations. *Agribusiness of Russia*, 23, 1016-1021.
  29. Kuzmicheva, M. B. (2008). Development trends of the Russian lamb market. *Meat Industry*, 2, 4-5.
  30. Lamanov, A., Ivanov, Y., Iskhakov, R., Zubairova, L., Tagirov, K., and Salikhov, A. (2020). Beef quality indicators and their dependence on keeping technology of bull calves of different genotypes. *AIMS Agriculture and Food*, 1, 1-10.
  31. Mironova, I., Nigmatyanov, A., Grunina, O., Sepiashvili, E., and Strigulina, E. (2019). Role of chicken meat in human diet. *International Journal of Pharmaceutical Research*, 4, 701-703.
  32. Mironova, I., Nigmatyanov, A., Radchenko, E., and Gizatova, N. (2019). Effect of feeding haylage on milk and beef quality indices. In *E3S Web of Conferences* (Vol. 135, p. 01100). EDP Sciences.
  33. Obolentsev, I. (2018). Interview with the head of the RSPP commission on agribusiness. *Meat Market*, 2, 19.
  34. Okuskhanova, E., Rebezov, Ya., Khayrullin, M., Nesterenko, A., Mironova, I., Gazeev, I., ... and Goncharov, A. (2019). Low-calorie meat food for obesity prevention. *International Journal of Pharmaceutical Research*, 11(1), 1589-1592.
  35. Ponomarenko, I. N., Grishina, L. A., and Bekturov, A. B. (2017). The effectiveness of the use of local feed additives for glauconite in winter diets of ewes of the Kyrgyz fine-wool breed. *Bulletin of the Kyrgyz National Agrarian University*, 3, 52-57.
  36. Sedykh, T. A., Gizatullin, R. S., Kosilov, V. I., Chudov, I. V., Andreeva, A. V., Giniyatullin, M.

- G., ... and Kalashnikova, L. A. (2018). Adapting australian hereford cattle to the conditions of the southern urals. *Research Journal of Pharmaceutical, Biological and Chemical Sciences*, 9(3), 885-898.
37. Sharipova, A., Khaziev, D., Kanareikina, S., Kanareikin, V., Rebezov, M., Okuskhanova, E., ... and Yessimbekov, Z. (2017a). The effects of a probiotic dietary supplementation on the livability and weight gain of broilers. *Annual Research and Review in Biology*, 19(6), 1-5.
  38. Sharipova, A., Khaziev, D., Kanareikina, S., Kanareikin, V., Rebezov, M., Kazanina, M., ... and Bykova, O. (2017b). The effects of a probiotic dietary supplementation on the amino acid and mineral composition of broilers meat. *Annual Research and Review in Biology*, 21(6), 1-7.
  39. Shkilev, P. N., Gazeev, I. R., and Nikonova, E. A. (2011). Biological value of sheep meat in Tsigaysky, South Ural and Stavropol breeds taking into account age, sex and castration. *News of the Orenburg State Agrarian University*, 1, 181-185.
  40. Sydykova, M., Nurymkhan, G., Gaptar, S., Rebezov, Y. M., Khayrullin, M., Nesterenko, A., and Gazeev, I. (2019). Using of lactic-acid bacteria in the production of sausage products: modern conditions and perspectives. *International Journal of Pharmaceutical Research*, 11(1), 1073-1083.
  41. Tagirov, K., Gubaidullin, N. M., Fakhretdinov, I. R., Khaziakhmetov, F. S., Avzalov, R. K., Mironova, I. V., ... and Gizatova, N. V. (2018). Carcass quality and yield attributes of bull calves fed on fodder concentrate" Zolotoi Felutsen". *Journal of Engineering and Applied Sciences*, 13(S8), 6597-6603.
  42. The USSR Ministry of Health (1987). *Order No.755 on 08/12/1977*.
  43. Traisov, B. B., Sultanova, A. K., Yuldashbayev, Y. A., and Esengaliyev, K. G. (2014). Meat productivity and characteristics of carcasses of young animals born from different selection options of akzhaik meat-wool sheep. *Biosci. Biotechnologies Biotechnology Research Asia*, 11, 1431-1437.
  44. Traisov, B. B., Yuldashbayev, Y. A., Sultanova, A. K., Esengaliyev, K. G., and Bozymova, A. K. (2015). Growth and development of lambs of the akzhaik sheep depending on selection *Biology and Medicine (Aligarh)*, 7, BM-074-15.
  45. Vorobyev, V. I., Vorobyev, D. V., Zakharkina, N. I., Polkovnichenko, A. P., and Safonov, V. A. (2019). Physiological status of king squab pigeon (*Columba Livia* gm. CV 'King') in biogeochemical conditions of low iodine, selenium and cobalt levels in the environment. *Asia Life Sciences*, 28(1), 99-110.
  46. World Health Organization (2003). *Diet, nutrition, and the prevention of chronic diseases: report of a joint WHO/FAO expert consultation* (Vol. 916). World Health Organization.
  47. Zabelina, V. V., and Lushnikov, V. P. (1999). Using sheep of different breeds for the production of lamb *Zootechnics*, 1, 29-31.
  48. Ziyangirova, S. R., Mironova, I. V., Gazeev, I. R., Galieva, Z. A., and Galieva, Ch. R. (2019). Morphological composition of half husbands of romanovsky breeds when using sorption and probiotic additives. *Morphology*, 2, 122.

**Table 1.** *Organoleptic indicators of internal fat of rams*

| Group   | Indicator                   |  |              |             |
|---------|-----------------------------|--|--------------|-------------|
|         | Color                       | Smell and taste  | Transparency | Consistency |
| Control | White with a yellowish tint | Characteristic for this species, recessed from fresh raw materials | Transparent  | Solid       |
| I       | White matte                 | Characteristic for this species, recessed from fresh raw materials | Transparent  | Dense       |
| II      | White matte                 | Characteristic for this species, recessed from fresh raw materials | Transparent  | Dense       |
| III     | White matte                 | Characteristic for this species, recessed from fresh raw materials | Transparent  | Solid       |

**Table 2.** *Properties of internal fat of rams*

| Indicator                       | Group       |             |             |             |
|---------------------------------|-------------|-------------|-------------|-------------|
|                                 | control     | I           | II          | III         |
| Iodine number, g/%              | 30.59±0.14  | 30.65±0.21  | 30.72±0.04  | 30.78±0.23  |
| Saponification number, mg/%     | 190.3 ±0.20 | 189.0 ±0.14 | 191.2 ±0.14 | 191.9 ±0.11 |
| Pour point, °C                  | 37.1 ±0.17  | 36.8 ±0.13  | 36.8 ±0.15  | 36.2 ±0.20  |
| Melting point, °C               | 42.36±0.16  | 42.31±0.23  | 42.23±0.17  | 42.14±0.22  |
| Energy value of 1 kg of fat, MJ | 35.50       | 35.58       | 35.66       | 35.75       |

**Table 3.** *Results of fatty acid analysis of samples of internal adipose tissue, %*

| Protein component                  | Group       |             |             |             |
|------------------------------------|-------------|-------------|-------------|-------------|
|                                    | control     | I           | II          | III         |
| <b>Monounsaturated fatty acids</b> |             |             |             |             |
| Palmitoleic C <sub>16:1</sub>      | 1.36±0.025  | 1.39±0.049  | 1.43±0.044  | 1.44±0.015* |
| Heptadecene C <sub>17:1</sub>      | 0.62±0.021  | 0.64±0.044  | 0.69±0.025* | 0.70±0.025* |
| Oleic C <sub>18:1</sub>            | 33.26±0.222 | 33.30±0.199 | 33.46±0.156 | 33.47±0.057 |
| <b>Polyunsaturated fatty acids</b> |             |             |             |             |
| Linoleic C <sub>18:2</sub>         | 4.86±0.076  | 4.80±0.135  | 4.76±0.067  | 4.83±0.122  |
| Linolenic C <sub>18:3</sub>        | 1.06±0.037  | 1.01±0.022  | 1.03±0.111  | 1.03±0.016  |
| Arachinic C <sub>20:0</sub>        | 0.25±0.007  | 0.26±0.007  | 0.26±0.015  | 0.25±0.007  |
| Arachidonic C <sub>20:4</sub>      | 0.27±0.004  | 0.27±0.007  | 0.27±0.007  | 0.27±0.004  |
| <b>Saturated fatty acids</b>       |             |             |             |             |
| Capric C <sub>10:0</sub>           | 0.20±0.015  | 0.22±0.011  | 0.21±0.011  | 0.22±0.011  |
| Lauric C <sub>12:0</sub>           | 0.33±0.011  | 0.31±0.023  | 0.32±0.011  | 0.32±0.019  |
| Myristine C <sub>14:0</sub>        | 7.25±0.022  | 7.28±0.018  | 7.31±0.014* | 7.32±0.023* |
| Palmitic C <sub>16:0</sub>         | 24.74±0.054 | 24.81±0.047 | 24.80±0.043 | 24.82±0.082 |
| Stearic C <sub>18:0</sub>          | 22.19±0.074 | 22.24±0.067 | 22.25±0.074 | 22.25±0.049 |

**Table 4.** Fatty acid composition of internal adipose tissue, % of the total content

| Indicator   | Group       |             |             |             |
|---|-------------|-------------|-------------|-------------|
|   | control     | I           | II          | III         |
| Amount of monounsaturated fatty acids (MUFA)                | 35.24±0.215 | 35.33±0.153 | 35.57±0.170 | 35.61±0.078 |
| Amount of polyunsaturated fatty acids (PUFA), including     | 6.44±0.102  | 6.34±0.157  | 6.32±0.064  | 6.38±0.135  |
| Linoleic C <sub>18:2</sub>                                  | 4.86±0.076  | 4.80±0.135  | 4.76±0.067  | 4.83±0.122  |
| Linolenic C <sub>18:3</sub>                                 | 1.06±0.037  | 1.01±0.022  | 1.03±0.111  | 1.03±0.016  |
| Arachinic C <sub>20:0</sub>                                 | 0.25±0.007  | 0.26±0.007  | 0.26±0.015  | 0.25±0.007  |
| Arachidonic C <sub>20:4</sub>                               | 0.27±0.004  | 0.27±0.007  | 0.27±0.007  | 0.27±0.004  |
| Amount of saturated fatty acids (SFA)                       | 54.72±0.145 | 54.86±0.049 | 54.88±0.100 | 54.93±0.072 |
| Ratios characterizing the biological effectiveness of fats: |             |             |             |             |
| MUFA: PUFA: SFA   | 1:0.2:1.6   | 1:0.2:1.6   | 1:0.2:1.5   | 1:0.2:1.5   |
| PUFA: SFA   | 0.12        | 0.11        | 0.11        | 0.11        |
| Ratio ω-6:ω-3   | 4.8         | 5.0         | 5.0         | 5.0         |

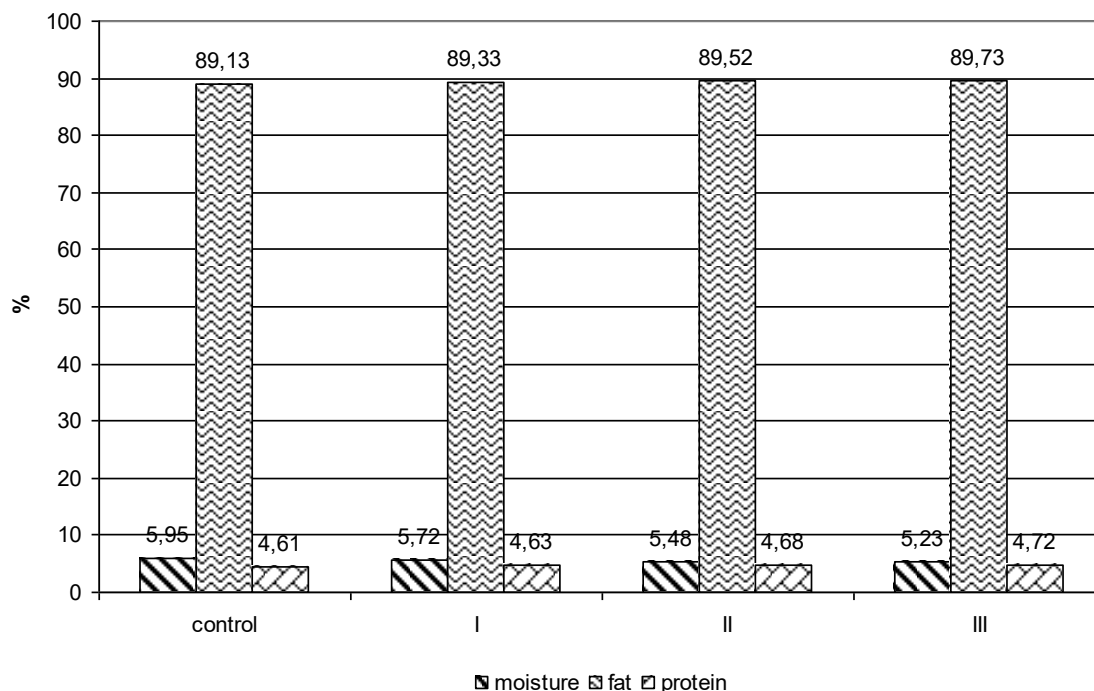


**Figure 1.** Chemical composition of internal sheep fat

# TOXOPLASMOSE E PERTURBAÇÃO CONGENITA

## TOXOPLASMOSIS AND CONGENITAL DISTURBANCE

داء المقوسات والاضطرابات الخلقية

QASIM, Mohammed Jasim<sup>1\*</sup>; NAMA, Mustafa Adnan<sup>2</sup>

<sup>1,2</sup> Department of Basic science, College of Nursing, University of Misan, Maysan, Iraq

\* Corresponding author

e-mail: mohammed\_j82@uomisan.edu.iq

Received 19 March 2020; received in revised form 04 May 2020; accepted 18 May 2020

### RESUMO

A infecção da toxoplasmose é causada por parasitas protozoários intracelulares chamados *Toxoplasma gondii*. O animal e o humano podem sofrer as infecções por diferentes vias. Algumas pessoas com status imunocomprometido estão em alto risco de infecção; exemplos desses grupos são gestantes, fetos e recém-nascidos. Este estudo teve como objetivo avaliar o papel da infecção por toxoplasma na manifestação de abortos e outros distúrbios congênitos entre mulheres casadas com idades entre 18 e 45 anos na cidade de Maysan (no sul do Iraque). Os critérios de inclusão incluem o grupo de estudo com histórico de infecção por *Toxoplasma gondii* (100 mulheres) e, para controles, aqueles que estavam livres de toxoplasmose (100 mulheres). Os critérios de exclusão foram gestantes, solteiras e portadoras de doenças imunossupressoras. As amostras de soro foram testadas quanto a IgG e IgM contra antígenos de *Toxoplasma gondii* usando o sistema de imunoenensaio automático Biomerieux Mini VIDAS, que dependia do princípio da tecnologia *Enzyme Linked Fluorescent Assay* (ELFA). O estudo revelou que as mulheres não abortadas infectadas eram 14 (14%), enquanto as mulheres não abortadas não infectadas eram 24 (24%). As mulheres infectadas com um caso de aborto foram sessenta (60,0%), enquanto as mulheres não infectadas com um caso de aborto foram 40 (40,0%). As mulheres infectadas que tiveram dois casos de aborto e aquelas infectadas que tiveram mais de dois casos de aborto foram 26 (26%) e 14 (14%), respectivamente. Houve diferença estatisticamente significativa entre mulheres infectadas e não infectadas em relação ao aborto ( $p < 0,01$ ). Verificou-se que houve diferenças altamente significativas entre mulheres infectadas e não infectadas em relação a anomalias e partos por cesariana (valor de  $p = 0,001$ ). Houve diferença estatisticamente significativa (valor de  $p = 0,01$ ) entre mulheres infectadas e não infectadas em relação ao parto com ou sem bebês prematuros.

**Palavras-chave:** *Toxoplasma gondii*, abortos, anomalias, cesarianas, bebês prematuros

### ABSTRACT

Toxoplasmosis is a disease caused by intracellular protozoan parasites called *Toxoplasma gondii*. The animal and human could suffer from infections through different routes involving diets, non-hygienic habit, contacts to soil, as well as blood transfusions and organs grafting. Some people with immune-compromised status are at a high risk of infection; examples of these groups are pregnant women, fetuses, and newborns. This study aimed to evaluate the role of Toxoplasma infection in the manifestation of abortions and other congenital disturbances among married women aged 18 to 45 years in Maysan city (in the south of Iraq). Inclusion criteria include the study group with a history of infection with *Toxoplasma gondii* (100 females) and for controls, those who were free from toxoplasmosis (100 females). Exclusion criteria were pregnant women, unmarried women, and those suffering from immunosuppressive diseases. The serum samples were tested for IgG and IgM against *Toxoplasma gondii* antigens by using the Biomerieux Mini VIDAS automated immunoassay system, which depended on the principle of Enzyme-Linked Fluorescent Assay (ELFA) technology. The study revealed that infected non-aborted women were 14 (14%), while non-infected non-aborted women were 24 (24%). Infected women with one case of abortion were sixty (60.0%), while non-infected women with one case of abortion were 40 (40.0%). The infected women who had two abortion cases and those infected ones who had more than two cases of abortions were 26 (26%) and 14 (14%), respectively. There was a statistically significant difference between infected and uninfected women regarding abortion ( $p < 0.01$ ). It has been found that there were highly significant differences between infected and non-infected women concerning anomalies and deliveries by cesarean sections ( $p$ -value = 0.001). There was a statically significant difference ( $p$ -value = 0.01) between infected and non-infected women concerning their deliveries with or without premature babies.

**Keywords:** *Toxoplasma gondii*, abortions, anomalies, cesarean sections, premature babies.

## المخلص:

داء المقوسات هو مرض تسببه طفيليات البروتوزا الداخلية الخلوية والتي تدعى المقوسات الكوندية. تصيب هذه الطفيليات كل من الانسان والحيوان من خلال العديد من الطرق وتشمل الغذاء ، العادات غير الصحية ، التماس مع التربة بالإضافة الى نقل الدم وزراعة الاعضاء . اكثر الاشخاص عرضة للإصابة هم الذين تكون مناعتهم ضعيفة ومن الأمثلة على ذلك النساء الحوامل ، الأجنة ، وكذلك حديثي الولادة. تهدف هذه الدراسة الى تقييم دور الإصابة بداء المقوسات في حصول الاجهاض وبقيّة الاضطرابات الخلقية لدى النساء المتزوجات للأعمار من 18 الى 45 في مدينة ميسان (في جنوب العراق). المعايير المتضمنة شملت مجموعة الدراسة والتي كانت مكونة من الاناث المصابات بالمقوسات الكوندية وعددهن 100 امرأة ، وشملت ايضاً مجموعة السيطرة والتي هي الاخرى مكونة من 100 امرأة ولكنهن غير مصابات بهذه الطفيليات. المعايير المستثناة من الدراسة هي النساء الحوامل ، غير المتزوجات ، وكذلك النساء الاتي يعانين من الأمراض المثبطة للمناعة. عينات مصل الدم فحصت للتحري عن وجود الاجسام المناعية المضادة للمقوسات الكوندية من نوع (IgM) و (IgG) وذلك باستخدام جهاز (Biomerieux Mini VIDAS) بنظام الطرق المناعية الآلية والتي تعتمد على تقنية الفحص المتألق المرتبط مناعياً (ELFA). اظهرت الدراسة ان النساء المصابات غير المجهاضات كانت اعدادهن 14 (14%) بينما غير المصابات من اللواتي لم يحدث عندهن اجهاض كانت اعدادهن 24 (24%). النساء المصابات مع حالة اجهاض واحدة كانت اعدادهن 60 (60%) بينما غير المصابات مع حالة اجهاض واحدة كانت اعدادهن 40 (40%). المصابات مع حالتها اجهاض والمصابات مع اكثر من حالتها اجهاض كانت اعدادهن 26 (26%) و 14 (14%) على التوالي ، مع فرق معنوي احصائي بين أعداد المصابات وغير المصابات حيث كانت p-value اصغر من 0.01 ( $p < 0.01$ ). كما قد وجد ان هناك فرق معنوي عالي بين أعداد النساء المصابات وغير المصابات فيما يخص التشوهات وحالات الوضع بواسطة العمليات القيصرية ( $p\text{-value} = 0.001$ ). كما ان هناك فرق معنوي احصائي ( $p\text{-value} = 0.01$ ) بين أعداد المصابات وغير المصابات فيما يتعلق بولادة النساء لحديثي الولادة غير المكتملين (الخدج)

**الكلمات المفتاحية:** مقوسة كوندية ، الاجهاضات ، التشوهات ، العمليات القيصرية ، أطفال الخدج

## 1. INTRODUCTION:

Toxoplasmosis is a disease caused by *Toxoplasma gondii* that can infect animal and human (Lu *et al.*, 2015; Robert-Gangneux and Darde, 2012).

*T. gondii* divided into three stages: tachyzoites, bradyzoites (tissue cysts), and sporozoites (in cats' feces). It can be transmitted by ingestion of contaminated fruit, vegetable, under-cooked meats, unpasteurized milk as well as low hygiene around food and cook-ware. Another route of transmission is through contact with contaminated soil or by changing the cat litter box (Kaakour *et al.*, 2019 ; Soares and Caldeira, 2019). Around 30% of the world's population is assumed to be infected with *T. gondii* (Montoya and Liesenfeld, 2004).

In immune-competent humans, the toxoplasmosis is commonly asymptomatic. Still, it can be fatal in immune-compromised persons, such as patients with HIV and cancer in addition to organ transplant recipients and pregnant women (Lu *et al.*, 2015; Agrawal *et al.*, 2014).

*T. gondii* causes encephalitis and neurologic defects, and it can affect the heart, inner ears, eyes (chorioretinitis), and liver. Although rare, congenital toxoplasmosis (infection of the infant) leads to ocular (retinochoroiditis) or severe permanent neurological disease, as well as brain and cardiac anomalies (Montoya, 2002). The clinical effects of toxoplasmosis among pregnant women are various. Such women may suffer from spontaneous abortions, stillbirth, intrauterine

growth retardation, deliveries of premature babies and anomalies in fetus. Furthermore, it has been suggested that *Toxoplasma* infections have some undesired implications on the capacity of the reproductive organ in both males and females (Flegr, 2013).

The infection of pregnant women with the *Toxoplasma* parasite is linked to exposure to cats and the age. This infection can lead to delivery with cesarean section and to *Toxoplasma* infected newborn (Kaakour *et al.*, 2019).

The study aimed to investigate the possible association between toxoplasmosis and some congenital disturbances among women who attended at Al. Sadr Teaching Hospital in Maysan city.

## 2. MATERIALS AND METHODS:

After finding the female eligible for the present study, she was explained the nature of the study and consent was sought. Those willing to give the consent and able to cooperate brief history were taken from them in the college of Nursing.

### 2.1. Study design

A case-control research was conducted in Al. Sadr Teaching Hospital, from July 2019 to February 2020. The study applied to married women aged 18 to 45 years with the exclusion of pregnant and unmarried women and those suffering from immunosuppressive diseases. A total number of 200 females were categorized into

two groups: Study group included 100 females who were infected with *Toxoplasma gondii*, another (control) group including 100 non-infected women, and without previous history of infection with toxoplasmosis.

## 2.2. Procedure

Five milliliters of antecubital venous blood was collected from each female in a sterile test tube and left for 30 minutes at room temperature until the clot has appeared in the blood. Then these blood samples were centrifuged to 4000 round/minute (for 10 minutes) to separate the serum. Sera were stored at -20°C till tested.

The serum samples were tested for IgG and IgM against *Toxoplasma gondii* antigens by using Biomerieux Mini VIDAS automated immunoassay system, which depended on the principle of Enzyme Linked Fluorescent Assay (ELFA) technology.

## 2.3. Statistical analysis

Statistical analysis was done using the statistical package for social sciences (SPSS version 18). Chi-square tests and descriptive statistics were applied to measure the frequencies and levels of significance—the values considered to be significant if P value < 0.05.

## 3. RESULTS AND DISCUSSION:

According to the findings in Table 1, it was revealed that the majority of infected women were located in the 21-25 years age group (38%). Almost more than half numbers of infected women were found in the first two groups compared to other groups. These results indicated that toxoplasmosis has occurred at an early age, more than the old ages of women in the current study. The findings have disagreed with many studies which found out that, the raised level of *Toxoplasma* infection was among 35-45 age groups, in comparison with a reduced rate of toxoplasmosis at 15-19 age groups (Al-Kalaby *et al.*, 2016; Sroka *et al.*, 2010; Jassam, 2010; AL-Ani, 2012; Al-Harthi *et al.*, 2006).

The indication of Table 1 was in agreement with findings of other studies, which demonstrated that the infection of *Toxoplasma* parasite was higher in the younger ages (Suhaila, 2008; Tasawar *et al.*, 2012). More upper infections that occur in young individuals may be due to the association with poor sanitary habits

and lower immunity against this *Toxoplasma gondii* (Jones *et al.*, 2008).

Table 2 revealed that infected non-aborted women were 14 (14%) while non-infected women who had not any abortion history were 24 (24%). Sixty (60.0%) positive women had a history of one case of abortion while 40 (40.0%) negative women had a previous one abortion. According to the table, the infected women with a history of two abortion cases were 26 (26%), while those non-infected women who had the same number of abortions were 18 (18%). In the case of more than two abortion histories, the number of infected women was 14 (14%), while negative women for toxoplasmosis were 4 (4%). The comparative evaluation of these results indicates that there was a significant difference ( $p < 0.01$ ) between non-infected and infected women with abortion.

The present study demonstrated that there was statically significant ( $p$ -value = 0.01) when applied cross-tabulation between infection and abortion (Table 2). Simultaneously, Table 3 showed that 35 (35.0%) of infected women had newborns with different anomalies compared to 14 (14.0%) of non-infected women ( $p$ -value = 0.001). These results were in line with several studies which indicated a correlation between infection with toxoplasmosis and congenital anomalies as well as previous history of abortion (Al-Kalaby *et al.*, 2016; Al-haris *et al.*, 2014; Muqbil *et al.*, 2014; Amin *et al.*, 2012; Mohamed *et al.*, 2012).

The findings of data analysis, as showed in Table 4 revealed that infected women with cesarean section deliveries were 17 (17.0%) in compared to 9 (9.9%) non-infected women who had deliveries by cesarean section. Contrarily, the infected women with standard deliveries were noticeably less than non-infected women 29, 49, respectively. Hence, the  $p$ -value was highly significant (0.005). These findings were approximately in agreement with the study that achieved in Lebanon (Kaakour *et al.*, 2019).

The correlation between toxoplasmosis premature babies was determined in Table 5 which revealed that there were 28 (28.0%) of infected women had premature babies while non-infected women were 11 (11.0%) only. The significant difference was high ( $p$ -value = 0.01). These findings were supported by another study, which indicated that the associations between prematurity and severity of congenital toxoplasmosis, including severe eye and brain disease (McLeod *et al.*, 2012).

#### 4. CONCLUSIONS:

According to the study, it has been found that the Infection of women with *T.gondii* is associated with abortions and different anomalies that occur in fetuses and newborns. This infection may lead to cesarean section deliveries and preterm births.

#### 5. ACKNOWLEDGMENTS:

We would like to thank each technician in the laboratory of Al-Sadr Teaching Hospital for their help to complete this study. A special thanks to Shaima R. Banoon and Hadi Hussein Mahdi for his valuable and constructive suggestions during the development of this research work.

#### 6. REFERENCES:

1. Lu, N.; Liu, C.; Wang, J.; Ding, Y.; Ai, Q. (2015). Toxoplasmosis complicating lung cancer: a case report. *Int. Med. Case Rep. J.*, 8, 37–40.
2. Robert-Gangneux, F.; Darde, M. L. (2012). Epidemiology of and diagnostic strategies for toxoplasmosis. *Clin. Microbiol. Rev.*, 25, 264–296.
3. Kaakour, F.; Farhat, L.; Dia, Widad.; Kadry, Seifedine. (2019). Risk Factors and Altered Parameters in Pregnant Women Infected by *Toxoplasma gondii* in Lebanon. *Global Journal of Health Science*, 11(12), 65-79.
4. Soares, J. A. S.; Caldeira, A. P. (2019). Congenital toxoplasmosis: the challenge of early diagnosis of a complex and neglected disease. *Rev Soc Bras Med Trop.*, 52, e20180228.
5. Montoya, J. G. ; Liesenfeld, O. (2004). Toxoplasmosis. *Lancet* 363, 1965–1976.
6. Agrawal, S.; Singh, V.; Ingale, S.; Jain, A. P. (2014). Toxoplasmosis of spinal cord in acquired immunodeficiency syndrome patient presenting as paraparesis: a rare entity. *J. Glob. Infect. Dis.*, 6, 178–181.
7. Montoya, J.G. (2002). Laboratory diagnosis of *Toxoplasma gondii* infection and toxoplasmosis. *J. Infect. Dis.*, 185, S73-S82.
8. Flegr, J. (2013). How and why *Toxoplasma* makes us crazy. *Trends Parasitol.*, 29 (4),156–163.
9. Kaakour, F.; Farhat, L.; Dia, W.; Kadry, S. (2019). Risk Factors and Altered Parameters in Pregnant Women Infected by *Toxoplasma gondii* in Lebanon. *Global Journal of Health Science*, 11, 12.
10. Al-Kalaby, R. F.; Sultan B. A.; AL-Fatlawi S. N. (2016). Relationship between *Toxoplasma gondii* and abortion in aborted women in Najaf province. *Journal of Kerbala University*,14( 1), 177-185.
11. Sroka, S.; Nina, B.; Andreas, W.; Jörg, H.; Liana, A.; Heliane, R.; *et al.*(2010). Prevalence and Risk Factors of Toxoplasmosis among Pregnant Women in Fortaleza, Northeastern Brazil. *Am J Trop Med Hyg.*, 83(3), 528–533.
12. Jassam, F. S. (2010). Relationship between toxoplasmosis and testosterone hormone among schizophrenic patients in Baghdad. M.Sc. thesis, College of Health and Medical Technology, Foundation of Technical Education. Iraq.
13. AL-Ani, R. T. (2012). Study of Toxoplasma infection in women recurrent abortion in First trimester of pregnancy by Indirect immunofluorescent antibody test (IFAT), 8 (2) DJPS.
14. Al-Harhi, S. A.; Manal, B.; Jamjoom; Hani, O.; Ghazi; (2006). Seroprevalence of Toxoplasma Gondii Among Pregnant Women in Makkah, Saudi Arabia. *Umm Al-Qura Univ. J. Sci. Med. Eng.*, 18(2), 217 - 227.
15. Suhaila, S.K.; (2008). Prevalence, serodiagnosis and some immunological aspects of toxoplasmosis among women in Baghdad province. M.Sc. thesis, College of Health and Medical Technology, Foundation of Technical Education. Iraq.
16. Tasawar, Z.; Aziz, F.; Lashari, M.H.; Shafi, S.; Ahmad, M.; Lal, V.; Hayat, C. S. (2012). Seroprevalence of Human toxoplasmosis in Southern Punjab, Pakistan. *Pak. j. life soc. Sci.*, 10(10), 1-5.
17. Jones, J.L.; Kruszon-Moran, D.; Won, K.; Wilson, M.; Schantz, P.M. (2008). *Toxoplasma gondii* and *Toxocara* spp. co-infection. *American Journal of Tropical Medical Hygiene*, 78, 35-39.
18. Al-haris, F. M.; Hulal, S. S.; Karar, M. A. (2014). Investigation of Toxoplasmosis in Cord Blood of Newborns at Al-Najaf Province, Iraq by Searching for IgG and



- IgM Antibodies. Journal of New Science Biotechnology, 1(1), 1-10.
19. Muqbil, N. A.; Alqubatii, M. A. (2014). Seroprevalence of toxoplasmosis among women in Aden city, Yemen. Archives of Biomedical Sciences, 2 (2), 42-50.
  20. Amin, Y. K.; Hataw, J. T.; Mustafa H.A. R. (2012). Screening of IgM and IgG against cytomegalovirus, rubella and toxoplasma infections among spontaneous miscarriages in Maternity Teaching Hospital- Erbil Province. Medical Sciences Proceeding Book, Vol, (I).
  21. Mohamed, K; Kodym, P.; Maly, M.; Rayah, I. E. L. (2012) Socio-economical Risk Factors Associated with *Toxoplasma gondii* Infection in Rural Women at Childbearing Age in Sudan, 1,488.
  22. McLeod, R.; Boyer, K. M.; Lee, D.; Mui, E.; Wroblewski, K.; Karrison, T.; Noble, G. A.; Withers, S.; Swisher, C. N.; Heydemann, P.T.; Sautter, M. ; Jane Babiarz, ; Peter Rabiah,; Meier, P.; Grigg, M. E. (2012). The Toxoplasmosis Study Groupb Prematurity and Severity are Associated with *Toxoplasma gondii* Alleles (NCCCTS, 1981–2009). Clinical Infectious Diseases, 54(11), 1595–605.

**Table 1.** Distribution of the Women According to Toxoplasmosis and the ages

| Age (years) |   | Toxoplasmosis |            | P-value                                |
|-------------|---|---------------|------------|--|
|             |   | Infected      | Uninfected |  |
| 20 and Less | F | 14            | 22         | Pearson<br>Chi-Square<br>= 0. 07<br>Ns |
|             | % | 14.0%         | 22.0%      |  |
| 21-25       | F | 38            | 24         |  |
|             | % | 38.0%         | 24.0%      |  |
| 26-30       | F | 16            | 26         |  |
|             | % | 16.0%         | 26.0%      |  |
| 31-35       | F | 10            | 14         |  |
|             | % | 10.0%         | 14.0%      |  |
| 36-40       | F | 18            | 12         |  |
|             | % | 18.0%         | 12.0%      |  |
| 41-45       | F | 4             | 2          |  |
|             | % | 4.0%          | 2.0%       |  |
| Total       | F | 100           | 100        |  |
|             | % | 100%          | 100%       |  |

F = Frequencies; % = Percentages; Ns = Non-Significant;

**Table 2.** Demonstration of the association between *Toxoplasma* infections and the Number of Abortions

| Number of Abortion |   | Infected | Uninfected | P-value                                 |
|--------------------|---|----------|------------|---|
| None               | F | 14       | 24         | Pearson Chi-Square<br>= 0.01<br><br>(S) |
|                    | % | 14.0%    | 24.0%      |   |
| One                | F | 60       | 40         |   |
|                    | % | 60.0%    | 40.0%      |   |
| Twice              | F | 26       | 18         |   |
|                    | % | 26.0%    | 18.0%      |   |
| Three and more     | F | 14       | 4          |   |
|                    | % | 14.0%    | 4.0%       |   |

F = Frequencies; % = Percentages; S = Significant;

**Table 3.** Demonstration of the Association between *Toxoplasma* infections and the Anomalies

| Anomalies |   | Toxoplasmosis |            | P-value                               |
|-----------|---|---------------|------------|---------------------------------------|
|           |   | Infected      | Uninfected |                                       |
| Yes       | F | 35            | 14         | Pearson Chi-Square<br>= 0.001<br>(Hs) |
|           | % | 35.0%         | 14.0%      |                                       |
| None      | F | 34            | 51         |                                       |
|           | % | 34.0%         | 51.0%      |                                       |

F = Frequencies; % = Percentages; Hs = Highly Significant;

**Table 4.** Demonstration of the Association between *Toxoplasma* infections and Cesarean Sections

| Cesarean Sections |   | Toxoplasmosis |            | P-value                               |
|-------------------|---|---------------|------------|---------------------------------------|
|                   |   | Infected      | Uninfected |                                       |
| Yes               | F | 17            | 9          | Pearson Chi-Square<br>= 0.005<br>(Hs) |
|                   | % | 17.0%         | 9.0%       |                                       |
| None              | F | 29            | 49         |                                       |
|                   | % | 29.0%         | 49.0%      |                                       |

F = Frequencies; % = Percentages; Hs = Highly Significant;

**Table 5.** *Demonstration of the Association between Toxoplasma infections and Premature Babies*

| Premature Baby |   | Toxoplasmosis |            | P-value                            |
|----------------|---|---------------|------------|------------------------------------|
|                |   | Infected      | Uninfected |                                    |
| Yes            | F | 28            | 11         | Person Chi-Square<br>= 0.01<br>(S) |
|                | % | 28.0%         | 11.0%      |                                    |
| None           | F | 37            | 56         |                                    |
|                | % | 37.0%         | 56.0%      |                                    |

F = Frequencies; % = Percentages; S = Significant;

## SOLUÇÃO ANALÍTICA DA EQUAÇÃO DO SCHRÖDINGER PARA O POTENCIAL DE YUKAWA COM MASSA VARIÁVEL EM COORDENADA TOROIDAL USANDO MECÂNICA QUÂNTICA SUPERSIMÉTRICA

## ANALYTICAL SOLUTION OF SCHRÖDINGER EQUATION FOR YUKAWA POTENTIAL WITH VARIABLE MASS IN TOROIDAL COORDINATE USING SUPERSYMMETRIC QUANTUM MECHANICS

FANIANDARI, Suci<sup>1</sup>; SUPARMI, A<sup>2\*</sup>; CARI, C<sup>3</sup>

<sup>1</sup>Graduate student at Physics Department, Sebelas Maret University, Indonesia

<sup>2,3</sup>Faculties member of Physics Department, Sebelas Maret University, Indonesia

*\*Corresponding author*

*e-mail: soeparmi@staff.uns.ac.id*

Received 24 March 2020; received in revised form April 2020; accepted 14 May 2020

### RESUMO

A equação de Schrödinger em uma coordenada toroidal foi proposta na física teórica para obter as informações e o comportamento do sistema de partículas. Foi resolvido recentemente, no caso de uma partícula escalar carregada interagindo com um campo magnético uniforme, um campo elétrico uniforme e uma carga neutra restringida à superfície. A metodologia usada no referido trabalho foi resolver a equação de Schrödinger usando uma abordagem descrita no tratado Whittaker-Watson que lida com um problema de valor próprio infinito-dimensional e com valores particulares específicos do campo aplicado para o problema de função própria, enquanto no problema da mecânica quântica um tinha um problema de autovalor generalizado de dimensão infinita. Este estudo teve como objetivo obter o valor próprio de energia não-relativística e a função de onda radial da equação de Schrödinger sob a influência do potencial de Yukawa. O método da Mecânica Quântica Supersimétrica (SUSY QM) foi usado como base para abordar o objetivo principal deste artigo, estudar o problema de uma partícula com massa variável em coordenadas toroidais. O super potencial adequado foi usado para lidar com a forma hiperbólica do potencial efetivo e os espectros de energia foram calculados para diferentes números quânticos, profundidade potencial e parâmetros potenciais. A equação da função de onda radial para o solo e o estado excitado foi obtida. Os resultados mostraram que o valor crescente dos números quânticos fez com que os espectros de energia do sistema aumentassem para o valor mais alto quando o número quântico era igual ao parâmetro potencial, o que significa que o valor energético mais eficaz foi produzido e depois diminuiu. Enquanto o valor da energia não dependia da alteração do parâmetro potencial. Essa propriedade poderia ser usada para produzir essa equação como uma aplicação dos resultados anteriores. A função própria de Schrödinger foi usada como ponto de partida para resolver a outra equação no mesmo cenário e potencial geométrico.

**Palavras-chave:** *Valor próprio da energia, espectros de energia, função de onda no estado fundamental*

### ABSTRACT

Schrodinger equation on a toroidal coordinate was proposed in theoretical physics to get the information and the behavior of the system of particle. It was solved just recently in case of a charged scalar particle interacting with a uniform magnetic field, a uniform electric field, and a neutral charge constrained to the surface. The methodology used in the referred work was to solve the Schrodinger equation using an approach outlined in the Whittaker-Watson treatise, which deals with an infinite-dimensional eigenvalue problem and specific particular values of the applied field for eigenfunction problem. In contrast, in the quantum mechanical problem, one had an infinite-dimensional generalized eigenvalue problem. This study aimed to obtain the non-relativistic energy eigenvalue and the radial wave function of the Schrodinger equation under the influence of Yukawa potential. The Supersymmetric Quantum Mechanics (SUSY QM) method was used as a basis to tackle the primary objective of this paper to study the problem of a particle with variable mass in toroidal coordinate. The proper super potential was used to deal with the hyperbolic form of effective potential, and the energy spectra were calculated for different quantum numbers, potential depth, and potential parameters. The radial wave function equation for ground and excited state were obtained. The results showed that the increasing value of the quantum numbers caused the energy spectra of the system to increase to the highest value when the quantum number was equal to the potential parameter, which means the most effective energy value was produced, then it was decreased

afterward. While the energy value did not depend on the change of the potential parameter. This property could be used to produce this equation as an application of the previous results, the Schrödinger eigenfunction was used as the starting points to solve the other equation in the same geometrical setting and potential.

**Keywords:** Energy eigenvalue, energy spectra, ground-state wave function

## 1. INTRODUCTION:

There had been increasing interest in theoretical physics to obtain the exact solution of the Schrodinger equation in spacetimes with non-spherical topology and negative cosmological constant (Krisch and Glass, 2003). The main purposes of this interest were to obtain the energy eigenvalue and the wave function. It was important to understand because it contained all the information about the quantum system. However, SUSY QM allowed one to determine eigenvalues and eigenstates of known analytically solvable potentials using algebra operator formalism without ever had to solve the Schrödinger differential equation by standard series method (Cari *et al.*, 2014). The other methods have been used to solve the Schrodinger equation, such as the Hypergeometric method (Dianawati *et al.*, 2018), Nikiforov-Uvarov method (Onate *et al.*, 2018), and Asymptotic Iteration Method (Elviyanti *et al.*, 2018).

The method of separation of variables in various coordinate systems was a classic approach to find the exact solutions of the Schrodinger equation that had been thoroughly studied. One such set of coordinates was the toroidal system, but it will be argued that some of the usefulness of this coordinate system had been hidden. It was because, while the usual way of separating the variables was appropriate for some situations, there was another way that more suited to a certain class of problems, in particular, some interesting problems in electrostatics (Andrews, 2006)

The toroidal coordinates (Moon and Spencer, 1971) of any point were given by the intersection of a torus, a sphere with its center on the axis of the torus (the z-axis), and an azimuthal half-plane (terminated by the z-axis). A toroid with a circular cross-section was a torus, so a torus was a toroid, and tori were toroids (Lucht, 2016). The radius and center of the sphere were determined by the spherical coordinate  $\mu$ , the major and minor radii of the torus were given by the toroidal coordinate  $\eta$ , and the particular half-plane was specified by its azimuthal angle  $\phi$ .

The solutions for the Schrodinger equation with a position-dependent mass lie at the center of

interest of the professional public because it helped us to understand the behavior of quantum particles in the cases in which their mass varies spatially (Bednarik and Cervenka, 2017). For instance, the variable mass Schrodinger equation played an essential role in the study of the electronic properties of inhomogeneous crystals, quantum dots, and quantum liquids (Golubov and Mazin, 1997). A suitable choice of a mass position function of the exponential-like form had been devised (Meyur, *et al.*, 2014). However, the application of variable mass in the Schrodinger equation was needed to be studied in a significant way.

Energy eigenvalue and wave function of non-relativistic particle have been solved using Schrodinger equation in the presence of many potentials such as Eckart potential (Goudarzi and Vahidi, 2011), Poschl-Teller (Suparmi *et al.*, 2012), Hylleraas (Suparmi *et al.*, 2017), and ring-shaped pseudo-harmonic oscillatory (Oliveira and Schmidh, 2019). The energy eigenvalue and wave function also could be used to determine other properties and further information of the system such as thermodynamics properties (Adebimpe *et al.*, 2019), entropy information (Faniandari *et al.*, 2019; Ma'arif *et al.*, 2019) and optical properties (Falkovsky, 2008).

The hyperbolic form of Yukawa potential was put into the formulation of the radial part of the Schrodinger equation in toroidal coordinates. The supersymmetric quantum mechanics method and variable mass were used. Therefore, this study aimed to obtain the energy eigenvalue, the un-normalized ground state wave function, and the exciting wave function of the system.

## 2. MATERIALS AND METHODS:

### 2.1. Schrödinger Equation with Variable Mass

The Laplacian in this coordinate was given by:

$$\nabla^2 \Psi = \frac{1}{h_\mu^3} \left[ \frac{1}{\sinh \mu} \frac{\partial}{\partial \mu} \left( h_\mu \sinh \mu \frac{\partial \Psi}{\partial \mu} \right) + \frac{\partial}{\partial \eta} \left( h_\eta \frac{\partial \Psi}{\partial \eta} \right) + \frac{h_\mu}{\sinh^2 \mu} \frac{\partial^2 \Psi}{\partial \phi^2} \right] \quad (\text{Eq. 1})$$

where

$$\Psi = \sqrt{\cosh \mu - \cos \eta} F(\mu, \eta, \phi) \quad (\text{Eq. 2})$$

$$h_\mu = h_\theta = \frac{a}{\cosh \mu - \cos \eta} \quad (\text{Eq. 3a})$$

$$h_\phi = \frac{a \sinh \mu}{\cosh \mu - \cos \eta} \quad (\text{Eq. 3b})$$

After applying the general wave function and scaling factors, the Laplacian could be simplified, so the Schrodinger equation with energy eigenvalue and potential was defined as

$$\left\{ \frac{(\cosh \mu - \cos \eta)^2}{a^2} \left[ \frac{1}{\sinh \mu} \frac{\partial}{\partial \mu} \left( \sinh \mu \frac{\partial F}{\partial \mu} \right) + \frac{\partial^2 F}{\partial \eta^2} \right] + \frac{1}{\sinh^2 \mu} \frac{\partial^2 F}{\partial \phi^2} + \frac{1}{4} F \right\} - \frac{2m}{\hbar^2} V F(\mu, \eta, \phi) = - \frac{2m}{\hbar^2} E F(\mu, \eta, \phi) \quad (\text{Eq. 4})$$

The variable mass was proposed as

$$m \approx \frac{m_0 (\cosh \mu - \cos \eta)^2}{a^2} \quad (\text{Eq. 5})$$

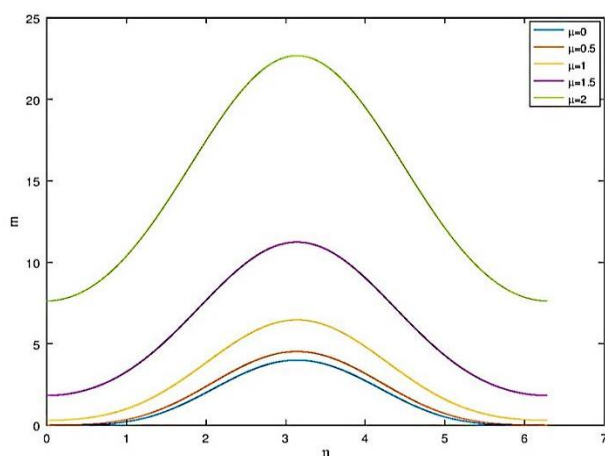


**Figure 1.** Plot for mass function  $m$  with the variation of  $\eta$ ,  $m_0 = 1$ ,  $a = 1$

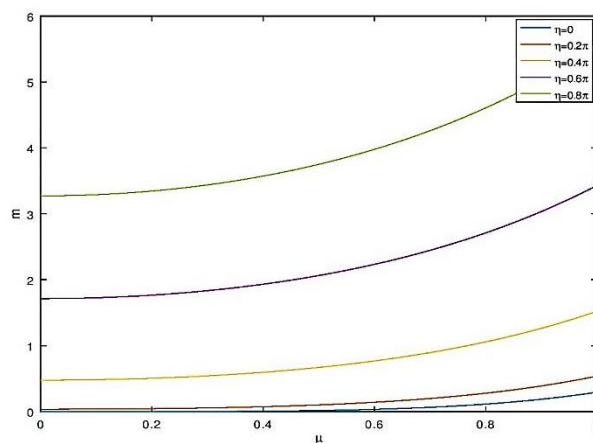


**Figure 2.** Plot for mass function  $m$  with the variation of  $\mu$ ,  $m_0 = 1$ ,  $a = 1$

The non-central potential was applied to Eq. (4) which expressed by

$$V(\mu, \eta, \phi) = V(\mu) + V(\eta) + \frac{V(\phi)}{\sinh^2 \mu} \quad (\text{Eq. 6})$$

Generally, the Schrodinger equation could be solved by reducing the system of particles to the second-order differential equation. For the wave function

$$F = M(\mu) H(\eta) P(\phi) \quad (\text{Eq. 7})$$

The angular parts were

$$\frac{\partial^2 H}{\partial \eta^2} - \frac{2m_0}{\hbar^2} V(\eta) H = \lambda_1 H \quad (\text{Eq. 8})$$

$$\frac{\partial^2 P}{\partial \phi^2} - \frac{2m_0}{\hbar^2} V(\phi) P = \lambda_2 P \quad (\text{Eq. 9})$$

and the radial part was

$$\begin{aligned} & -\frac{1}{\sinh \mu} \frac{\partial}{\partial \mu} \left( \sinh \mu \frac{\partial M}{\partial \mu} \right) + \frac{2m_0}{\hbar^2} V(\mu) M \\ & - \lambda_1 M - \left( \frac{1}{4} + \frac{2m_0 E}{\hbar^2} \right) M = \frac{\lambda_2}{\sinh^2 \mu} M \end{aligned} \quad (\text{Eq. 10})$$

The solution was simplified to be

$$\left\{ -\frac{\hbar^2}{2m_0} \frac{\partial^2 K}{\partial \mu^2} + \frac{\hbar^2}{2m_0} \frac{-\lambda_2 - \frac{1}{4}}{\sinh^2 \mu} K \right\} \quad (\text{Eq. 11})$$

$$+V(\mu)K - \lambda_1 \frac{\hbar^2}{2m_0} K - EK = 0$$

where  $M = \frac{K}{\sqrt{\sinh \mu}}$ .

## 2.2. Supersymmetric Quantum Mechanics Method

Quantum mechanics, in its development, had brought the concept of symmetry as a foundation for thinking to simplify physical systems. The concept of symmetry mathematically means the invariant nature of a system when subject to a particular transformation. Closed algebra under the anti-commutation relationship was introduced in the supersymmetry system. The Supersymmetry system in quantum mechanics was defined as a system consisting of a supercharge operator  $Q_i$  which was commutative towards Hamiltonian Supersymmetry ( $H_{SS}$ ) (Witten, 1981).

$$[Q_i, H_{SS}] = 0 \text{ and } i = 1, 2, \dots, N \quad (\text{Eq. 12})$$

where  $N$  was the number of generators and meets the anti-commutation relationship below

$$\{Q_i, Q_j\} = \delta_{ij} H_{SS} \quad (\text{Eq. 13})$$

Hamiltonian Supersymmetry ( $H_{SS}$ ) was defined as the sum of squares of the supercharge operator ( $Q_i$ ):

$$H_{SS} = 2Q_1^2 = 2Q_2^2 \quad (\text{Eq. 14})$$

The simplest SUSY QM system, where  $N = 2$  with supercharge operators  $Q_1$  and  $Q_2$  could be associated with spin 1/2 particles moving in a straight line.  $Q_1$  and  $Q_2$  in this simple system were defined as follows:

$$Q_1 = \frac{1}{\sqrt{2}} \left( \sigma_1 \frac{p}{\sqrt{2m}} + \sigma_2 \phi(x) \right) \quad (\text{Eq. 15a})$$

$$Q_2 = \frac{1}{\sqrt{2}} \left( \sigma_2 \frac{p}{\sqrt{2m}} - \sigma_1 \phi(x) \right) \quad (\text{Eq. 15b})$$

where  $\sigma_1$  and  $\sigma_2$  were matrices from Pauli (Suparmi, 2011).

$H_{SS}$  was Hamiltonian supersymmetry,  $p = -i\hbar \frac{d^2}{dx^2}$  was linear momentum (bosonic

momentum),  $x$  was bosonic coordinate, and  $\phi(x)$  was bosonic superpotential. Hamiltonian Supersymmetry matrix could be shown as:

$$H_{SS} = \begin{pmatrix} H_+ & 0 \\ 0 & H_- \end{pmatrix} \quad (\text{Eq. 16})$$

where

$$H_- = -\frac{\hbar^2}{2m} \frac{d^2}{dx^2} + \phi^2(x) - \frac{\hbar}{\sqrt{2m}} \frac{d\phi(x)}{dx} \quad (\text{Eq. 17a})$$

$$H_+ = -\frac{\hbar^2}{2m} \frac{d^2}{dx^2} + \phi^2(x) + \frac{\hbar}{\sqrt{2m}} \frac{d\phi(x)}{dx} \quad (\text{Eq. 17b})$$

Eq. (12) caused the results in the generation of degenerated energy  $H_-$  and  $H_+$ , which were SUSY partners of the Fermionic Hamiltonian (descendant) and Bosonic (ascending), both of which were also written as  $H_{SS}$ . The standard Schrödinger equation was stated in the Hamiltonian SUSY as follows

$$H_- = -\frac{\hbar^2}{2m} \frac{d^2}{dx^2} + V_-(x) \quad (\text{Eq. 18a})$$

$$H_+ = -\frac{\hbar^2}{2m} \frac{d^2}{dx^2} + V_+(x) \quad (\text{Eq. 18b})$$

where  $V_-(x)$  and  $V_+(x)$  were called as supersymmetry potential couple,  $\phi(x)$  was superpotential, while  $\phi'(x)$  was the first derivative of  $\phi(x)$ .

Lowering and raising Hamiltonian could be factorized from the equation (18a) and (18b) and respectively were stated as follows:

$$A^+ = -\frac{\hbar}{\sqrt{2m}} \frac{d}{dx} + \phi(x) \quad (\text{Eq. 19a})$$

$$A = \frac{\hbar}{\sqrt{2m}} \frac{d}{dx} + \phi(x) \quad (\text{Eq. 19b})$$

$A^+$  was raising operator and  $A$  was lowering operator (Rodrigues, 2002).

Based on the character of lowering operator ( $A$ ), if ( $A$ ) was operated on the ground state wave function  $\psi_0^{(-)}$ , it will equal to zero (Cooper *et al.*, 1995).

$$A\psi_0^{(-)} = \left( \frac{\hbar}{\sqrt{2m}} \frac{d}{dx} + \phi(x) \right) \psi_0^{(-)} = 0 \quad (\text{Eq. 20})$$

From Eq. (20), then the ground state wave function was determined as

$$\psi_0^{(-)}(x) = N \exp \left[ -\frac{\sqrt{2m}}{\hbar} \int_{-x}^x \phi(x) dx \right] \quad (\text{Eq. 21})$$

with  $N$  was the normalization factor.

### 3. RESULTS AND DISCUSSION:

The radial part of the Schrodinger equation with energy eigenvalue and potential was expressed as

$$-\frac{\hbar^2}{2m_0} \frac{\partial^2 K}{\partial \mu^2} + \frac{\hbar^2}{2m_0} \left[ -\frac{1}{4 \sinh^2 \mu} - \frac{\lambda_2}{\sinh^2 \mu} \right] K + V(\mu)K = \varepsilon' K \quad (\text{Eq. 22})$$

$$\text{with } \varepsilon' = \lambda_1 \frac{\hbar^2}{2m_0} + E.$$

Yukawa potential was used and it's general form was (Yukawa, 1935).

$$V(\rho) = -V_0 \frac{\hbar^2}{2m_0} \left( \frac{e^{-\xi \rho}}{\rho} \right) \quad (\text{Eq. 23})$$

By set  $\xi \rho = \mu$

$$V(\mu) = -V_0 \xi \frac{\hbar^2}{2m_0} \left( \frac{e^{-\mu}}{\mu} \right) \quad (\text{Eq. 24})$$

The following approximation for centrifugal terms was applied (Greene and Aldrich, 1976; Qiang and Dong, 2007; Jia, *et al.*, 2009; Dong, *et al.*, 2013).

$$\frac{1}{\mu^2} \approx 4\xi^2 \frac{e^{-2\xi\mu}}{(1 - e^{-2\xi\mu})^2} \quad (\text{Eq. 25})$$

$$\frac{1}{\mu} \approx \frac{2\xi e^{\mu}}{e^{2\mu} - 1} \quad (\text{Eq. 26})$$

Then Eq. (24) was modified as

$$V(\mu) = -\frac{\hbar^2}{2m_0} V_0 \xi^2 (\coth \mu - 1) \quad (\text{Eq. 27})$$

Eq. (27) was inserted into Eq. (22)

$$-\frac{\hbar^2}{2m_0} \frac{\partial^2 K}{\partial \mu^2} + \frac{\hbar^2}{2m_0} \left[ \frac{v(v-1)}{\sinh^2 \mu} - V_0 \xi^2 \coth \mu + V_0 \xi^2 \right] K = \left( \lambda_1 \frac{\hbar^2}{2m_0} + E \right) K \quad (\text{Eq. 28})$$

$$\text{where } -\frac{1}{4} - \lambda_2 = v(v-1).$$

This was the second-order differential equation of the Schrodinger equation. The shape invariant potential was used, so the hypothetical superpotential function in supersymmetric quantum mechanics was

$$\Phi(\mu) = A \coth \mu + B \quad (\text{Eq. 29})$$

to satisfy the Riccati equation below

$$\Phi^2(\mu) - \frac{\hbar}{\sqrt{2m_0}} \Phi'(\mu) = V_{\text{eff}} - \varepsilon \quad (\text{Eq. 30})$$

$$\left( A^2 + \frac{\hbar}{\sqrt{2m_0}} A \right) \text{csch}^2 \mu + 2AB \coth \mu + A^2 + B^2 = \frac{\hbar^2}{2m_0} (v(v-1) \text{csch}^2 \mu - V_0 \xi^2 \coth \mu + V_0 \xi^2) - \varepsilon \quad (\text{Eq. 31})$$

where  $\varepsilon$  was the lowest energy eigenvalue. Comparing the left and the right side of Eq. (31), the solutions were determined.

$$A = \frac{\hbar}{\sqrt{2m_0}} v \quad (\text{Eq. 32})$$

$$B = -\frac{\hbar}{\sqrt{2m_0}} \frac{V_0 \xi^2}{2v} \quad (\text{Eq. 33})$$

$$\varepsilon = \frac{\hbar^2}{2m_0} \left( V_0 \xi^2 - \frac{(V_0 \xi^2)^2}{4v^2} - v^2 \right) \quad (\text{Eq. 34})$$

With Eq. (29), Eq. (32), Eq. (33), Eq. (18a) and Eq. (18b), the two partner potentials which have an invariant form were constructed as follows:

$$V_-(a_0, \mu) = \frac{\hbar^2}{2m_0} \left( \frac{(v^2 + v) \text{csch}^2 \mu - V_0 \xi^2 \coth \mu}{+\frac{(V_0 \xi^2)^2}{4v^2} + v^2} \right) \quad (\text{Eq. 35})$$

$$V_+(a_0, \mu) = \frac{\hbar^2}{2m_0} \left( \frac{(v^2 - v) \text{csch}^2 \mu - V_0 \xi^2 \coth \mu}{+\frac{(V_0 \xi^2)^2}{4v^2} + v^2} \right) \quad (\text{Eq. 36})$$

Then, a new set of the parameter was defined as  $a_1 = v - 1$  from the old set of parameter  $a_0 = v$ .



$$V_-(a_1, \mu) = \frac{\hbar^2}{2m_0} \left( \frac{(v^2 - v) \operatorname{csch}^2 \mu - V_0 \xi^2 \coth \mu}{+ \frac{(V_0 \xi^2)^2}{4(v-1)^2} + (v-1)^2} \right) \quad (\text{Eq. 37})$$

$$V_+(a_1, \mu) = \frac{\hbar^2}{2m_0} \left( \frac{((v-1)^2 - (v-1)) \operatorname{csch}^2 \mu}{-V_0 \xi^2 \coth \mu + \frac{(V_0 \xi^2)^2}{4(v-1)^2} + (v-1)^2} \right) \quad (\text{Eq. 38})$$

In term of the parameter of the problem, the following relations were obtained:

$$R(a_1) = V_+(a_0, \mu) - V_-(a_1, \mu) = \frac{\hbar^2}{2m_0} \left( \frac{(V_0 \xi^2)^2}{4v^2} - \frac{(V_0 \xi^2)^2}{4(v-1)^2} + v^2 - (v-1)^2 \right) \quad (\text{Eq. 39})$$

$$R(a_2) = V_+(a_1, \mu) - V_-(a_2, \mu) = \frac{\hbar^2}{2m_0} \left( \frac{(V_0 \xi^2)^2}{4(v-1)^2} - \frac{(V_0 \xi^2)^2}{4(v-2)^2} + (v-1)^2 - (v-2)^2 \right) \quad (\text{Eq. 40})$$

The energy eigenvalue was determined as:

$$E_n^{(-)} = \sum_{k=1}^n R(a_k) = \frac{\hbar^2}{2m_0} \left( \frac{(V_0 \xi^2)^2}{4v^2} - \frac{(V_0 \xi^2)^2}{4(v-n)^2} + v^2 - (v-n)^2 \right) \quad (\text{Eq. 41})$$

This gave the energy equation as

$$E_n = E_n^{(-)} + E_0 = \frac{\hbar^2}{2m_0} \left( V_0 \xi^2 - \left( \frac{V_0 \xi^2}{2(v-n)} \right)^2 - (v-n)^2 \right) \quad (\text{Eq. 42})$$

where  $\hbar$  was Planck constant,  $m_0$  was the mass of the particle,  $V_0$  was the potential depth,  $\xi$  was the potential width,  $v$  was the parameter of Yukawa potential, and  $n$  was the quantum number.

From Eq. (42), the energy spectra were determined from the energy eigenvalue with the variation of the quantum number, potential depth, and parameter of Yukawa potential in Table 1.

In Figure 3, when  $v=1$  and  $v=2$  the graph was tended to tilt to the left, while  $v=4$  and  $v=5$  the graph was tended to tilt to the right. It was

symmetrical at the center when  $v=n=3$ . Table 1 and Figure 3 showed that the increasing value of the quantum number ( $n$ ) causing the energy value to increase until it reached the highest value when  $n = v$ . After that, the energy value was decreased for the system in a toroidal coordinate. It also had a symmetric curve and when  $n = v$  it became the axis of symmetry.

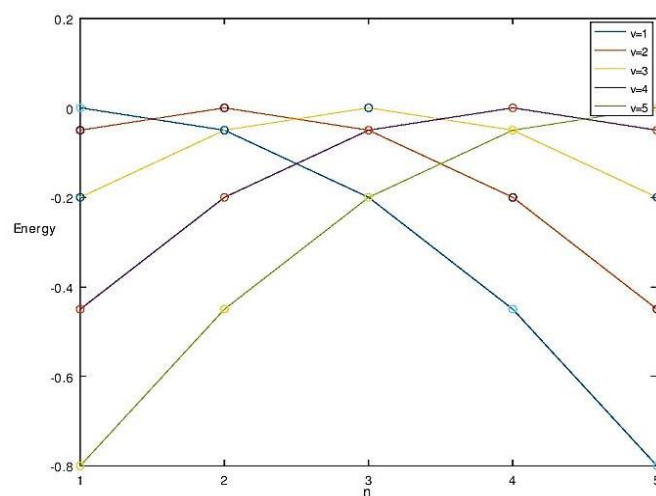


**Figure 3.** Energy spectra of Yukawa potential in toroidal coordinate ( $V_0 = 0$ ,  $\hbar = 1$ ,  $m_0 = 1$ ,  $\xi = 0,01$ )

For the increasing value of the potential parameter  $v$ , the energy both increased and decreased. So, practically the potential parameter did not have a direct impact on the value of the energy.

To obtain the un-normalized wave function, the superpotential was defined again as stated in Eq. (29).

$$\Phi(\mu) = \frac{\hbar}{\sqrt{2m_0}} \left( v \coth \mu - \frac{V_0 \xi^2}{2v} \right) \quad (\text{Eq. 43})$$

The relation of shape invariance in SUSY QM was used and the raising and lowering operators were obtained from Eq. (43).

$$A^\dagger = -\frac{\hbar}{\sqrt{2m_0}} \frac{d}{d\mu} + \frac{\hbar}{\sqrt{2m_0}} \left( v \coth \mu - \frac{V_0 \xi^2}{2v} \right) \quad (\text{Eq. 44})$$

$$A = \frac{\hbar}{\sqrt{2m_0}} \frac{d}{d\mu} + \frac{\hbar}{\sqrt{2m_0}} \left( v \coth \mu - \frac{V_0 \xi^2}{2v} \right) \quad (\text{Eq. 45})$$

So, the ground state wave function  $\Psi_0^{(-)}$  was obtained

$$\left\{ \frac{\hbar}{\sqrt{2m_0}} \frac{d}{d\mu} + \Phi(\mu) \right\} \Psi_0^{(-)} = 0 \quad (\text{Eq. 46})$$

$$\Psi_0^{(-)} = \frac{CV_0 \xi^2 \mu}{2\nu} \sinh^{-\nu} \mu \quad (\text{Eq. 47})$$

The raising operator in Eq. (44) was operated to the ground state wave function  $\Psi_0^{(-)}$  in Eq. (47) and the un-normalized excited wave function was determined.

$$\Psi_1^{(-)}(x; a_0) = \Psi_0^{(-)} \frac{\hbar}{\sqrt{2m_0}} \frac{\nu}{\nu+1} \left( \frac{\sinh \mu}{v \coth \mu - \frac{V_0 \xi^2}{2\nu} - \frac{1}{\mu}} + (v+1) \cosh \mu \right) \quad (\text{Eq. 48})$$

#### 4. CONCLUSIONS:

The analytical solution of the Schrodinger equation using Yukawa potential in the form of hyperbolic function in the toroidal coordinate was obtained. The energy spectra and wave function were solved with the Supersymmetric Quantum Mechanics method (SUSY QM). The energy spectra were reported numerically based on the energy eigenvalue equation. The un-normalized ground state wave function and the excited state wave function was determined by operating the lowering and raising operator.

#### 5. ACKNOWLEDGMENTS:

This research was partly supported by the mandatory research grand of sebelas maret university with contract number 452/un27.21/pn/2020.

#### 6. REFERENCES:

1. Adebimpe, O., Onate, C. A., Salawu, S. O., Abolanriwa, A., and Lukman, A. F. (2019). Eigensolutions, scattering phase shift and thermodynamic properties of Hulthén-Yukawa potential. *Results in Physics*, 14, 102409. doi: 10.1016/j.rinp.2019.102409
2. Andrews, M. (2006). Alternative separation of Laplace's equation in toroidal coordinates and its application to electrostatics. *Journal of electrostatics*, 64(10), 664-672. doi: 10.1.1.205.5658
3. Bednarik, M., and Cervenka, M. (2017). The exact solution of the Schrödinger equation with a polynomially spatially varying mass. *Journal of Mathematical Physics*, 58(7), 072103. doi: 10.1063/1.4993194
4. Cari, C., Suparmi, S., and Saregar, A. (2016). Solution of the Schrödinger Equation for Trigonometric Scarf Plus Poschl-Teller Non-Central Potential Using Supersymmetry Quantum Mechanics. *INDONESIAN JOURNAL OF APPLIED PHYSICS*, 4(01), 1-13. Retrieved from [https://www.researchgate.net/profile/Antomi\\_Saregar2/publication/303036225](https://www.researchgate.net/profile/Antomi_Saregar2/publication/303036225)
5. Cooper, F., Khare, A., and Sukhatme, U. (1995). Supersymmetry and quantum mechanics. *Physics Reports*, 251(5-6), 267-385. doi: 10.1142/4687
6. Suparmi, A., Dianawati, D. A., and Cari, C. (2019). Solution of Klein-Gordon equation for fraction potential with q-deformed of radial momentum using Romanovski polynomial. In *AIP Conference Proceedings* (Vol. 2202, No. 1, p. 020037). AIP Publishing LLC. doi: 10.1063/1.5054568
7. Dong, S., Sun, G. H., and Dong, S. H. (2013). Arbitrary l-wave solutions of the Schrödinger equation for the screen coulomb potential. *International Journal of Modern Physics E*, 22(06), 1350036. doi: 10.1142/S0218301313500365
8. Elviyanti, I. L., Pratiwi, B. N., Suparmi, A., and Cari, C. (2018). The Application of Minimal Length in Klein-Gordon Equation with Hulthen Potential Using Asymptotic Iteration Method. *Advances in Mathematical Physics*, 2018, 9658679. doi: 10.1155/2018/9658679
9. Falkovsky, L. A. (2008). Optical properties of graphene. In *Journal of Physics: conference series* (Vol. 129, No. 1, p. 012004). IOP Publishing. doi: 10.1088/1742-6596/129/1/012004
10. Faniandari, S., Ma'arif, M., Suparmi, A., and Cari, C. (2019, December). Rényi entropy of ground state eigen function of non-relativistic particle in the presence of DRSCO potential and cosmic string framework. In *AIP Conference Proceedings* (Vol. 2202, No. 1, p. 020031). AIP Publishing LLC. doi: 10.1063/1.5141644

11. Golubov, A. A., and Mazin, I. I. (1997). Effect of magnetic and nonmagnetic impurities on highly anisotropic superconductivity. *Physical Review B*, 55(22), 15146. doi: 10.1103/PhysRevB.55.15146
12. Goudarzi, H., and Vahidi, V. (2011). Supersymmetric approach for Eckart potential using the NU method. *Adv. Studies Theor. Phys*, 5(10), 469-476. Retrieved from [https://www.researchgate.net/profile/Hadi\\_Goudarzi2/publication/267386470](https://www.researchgate.net/profile/Hadi_Goudarzi2/publication/267386470)
13. Greene, R. L., and Aldrich, C. (1976). Variational wave functions for a screened Coulomb potential. *Physical Review A*, 14(6), 2363. doi: 10.1103/PhysRevA.14.2363
14. Jia, C. S., Chen, T., and Cui, L. G. (2009). Approximate analytical solutions of the Dirac equation with the generalized Pöschl–Teller potential including the pseudo-centrifugal term. *Physics Letters A*, 373(18-19), 1621-1626. doi: 10.1016/j.physleta.2009.03.006
15. Krisch, J. P., and Glass, E. N. (2003). A space–time in toroidal coordinates. *Journal of Mathematical Physics*, 44(7), 3046-3058. doi: 10.1063/1.1580999
16. Lucht, P. (2016). *The Charged Bowl in Toroidal Coordinates*. Utah, UT: Rimrock Digital Technology.
17. Ma'arif, M., Faniandari, S., Suparmi, A., Cari, C., and Pambudi, N. A. (2019, December). Tsallis entropy of ground state classical cosmic string framework with DRSCO potential. In *AIP Conference Proceedings* (Vol. 2202, No. 1, p. 020032). AIP Publishing LLC. doi: 10.1063/1.5141645
18. Meyur, S., Maji, S., and Debnath, S. (2014). Analytical solution of the Schrödinger equation with spatially varying effective mass for generalised Hylleraas potential. *Advances in High Energy Physics*, 2014, 952597. doi: 10.1155/2014/952597
19. Moon, P., and Spencer, D. E. (1971). *Field Theory Handbook*. Berlin, Germany: Springer.
20. Oliveira, M. D., and Schmidt, A. G. (2019). Exact solutions of Schrödinger and Pauli equations for a charged particle on a sphere and interacting with non-central potentials. *Journal of Mathematical Physics*, 60(3), 032102. doi: 10.1063/1.5079798
21. Onate, C. A., Adebimpe, O., Lukman, A. F., Adama, I. J., Okoro, J. O., and Davids, E. O. (2018). Approximate eigensolutions of the attractive potential via parametric Nikiforov-Uvarov method. *Heliyon*, 4(11), e00977. doi: 10.1016/j.heliyon.2018.e00977
22. Qiang, W. C., and Dong, S. H. (2007). Analytical approximations to the solutions of the Manning–Rosen potential with centrifugal term. *Physics Letters A*, 368(1-2), 13-17. doi: 10.1016/j.physleta.2007.03.057
23. Rodrigues, R. D. L. (2002). *The Quantum Mechanics SUSY Algebra: an Introductory Review*. Cajazeiras, Brazil: Federal University of Campina Grande.
24. Suparmi, A., Cari, C., Handhika, J., Yanuarief, C., and Marini, H. (2012). Approximate Solution of Schrodinger Equation for Modified Poschl-Teller plus Trigonometric Rosen-Morse Non-Central Potentials in Terms of Finite Romanovski Polynomials. *IOSR Journal of Applied Physics (IOSR-JAP)*, 2(2), 43-51. Retrieved from <https://www.researchgate.net/publication/258655314>
25. Suparmi, A., Cari, C., Pratiwi, B. N., and Nugraha, D. A. (2017, March). Construction of solvable potential partner of Generalized Hylleraas potential in one-dimensional Schrodinger system. In *Journal of Physics: Conference Series* (Vol. 820, No. 1, p. 012023). IOP Publishing. Retrieved from <http://iopscience.iop.org/1742-6596/820/1/012023>
26. Suparmi, (2011). *Mekanika Kuantum II*. Surakarta, Indonesia: Jurusan Fisika FMIPA UNS.
27. Witten, E. (1981). Dynamical breaking of supersymmetry. *Nuclear Physics B*, 188(3), 513-554. doi: 10.1016/0550-3213
28. Yukawa, H. (1935). On the interaction of elementary particles. I. *Proceedings of the Physico-Mathematical Society of Japan*. 3rd Series, 17, 48-57. doi: 10.11429/ppmsj1919.17.0\_48

**Table 1.** Energy Spectra of Yukawa Potential in Toroidal Coordinate ( $\hbar = 1$ ,  $m_0 = 1$ , and  $\xi = 0,01eV$  )

| $\nu$ | $V_0$ | $E$         |             |             |             |             |
|-------|-------|-------------|-------------|-------------|-------------|-------------|
|       |       | $n = 1$     | $n = 2$     | $n = 3$     | $n = 4$     | $n = 5$     |
| 1     | 1     | 0,00000050  | -0,00499950 | -0,01999950 | -0,04499950 | -0,07999950 |
|       | 5     | 0,00000250  | -0,00499750 | -0,01999750 | -0,04499750 | -0,07999751 |
|       | 10    | 0,00000500  | -0,00499500 | -0,01999501 | -0,04499501 | -0,07999502 |
| 2     | 1     | -0,00499950 | 0,00000050  | -0,00499950 | -0,01999950 | -0,04499950 |
|       | 5     | -0,00499850 | 0,00000150  | -0,00499850 | -0,01999850 | -0,04499850 |
|       | 10    | -0,00499500 | 0,00000500  | -0,00499500 | -0,01999501 | -0,04499501 |
| 3     | 1     | -0,01999950 | -0,00499950 | 0,00000050  | -0,00499950 | -0,01999950 |
|       | 5     | -0,01999750 | -0,00499750 | 0,00000250  | -0,00499750 | -0,01999750 |
|       | 10    | -0,01999501 | -0,00499500 | 0,00000500  | -0,00499500 | -0,01999501 |

# NOVA SÍNTESE E CARACTERIZAÇÃO DE ESTRUTURAS MACROMOLECULARES

## NEW MACROMOLECULAR STRUCTURES SYNTHESIS AND CHARACTERIZATION

JABBAR, Adel Ismael<sup>\*1</sup>, RAWI, Rehab Ayal<sup>2</sup>, ABDULHAMEED, Jasim Mohammed<sup>3</sup>

<sup>1,2,3</sup>Ministry of Education, Al-Anbar, Iraq

<sup>\*</sup> Corresponding author

e-mail: [adilwaleed@yahoo.com](mailto:adilwaleed@yahoo.com)

Received 19 February 2020; received in revised form 10 April 2020; accepted 11 May 2020

### RESUMO

Os cristais líquidos são únicos em suas propriedades e usos e têm um papel essencial na área de aplicações tecnológicas como elétrica, ótica, *display*, mapa de temperatura e materiais de comutação. Este estudo teve como objetivo sintetizar derivados de hexaetnilbenzeno a partir de 1,3,5-triclorobenzeno benzeno como núcleo central substituído por três anéis aromáticos e três braços de 2-cloro-4,6-bis ((3,7-dimetiloct-6-en-1-il) oxi) -1,3,5-triazina. Essas moléculas são formadas pela ligação covalente de três braços simetricamente a um núcleo central que podem ser ligados ao núcleo central através de ligantes flexíveis, semiflexíveis ou rígidos. A substituição ocorre na periferia acetilênica no anel central do benzeno e foi obtida com eficiência pelo acoplamento Sonogashira. Os compostos de seis braços baseados no núcleo do benzeno foram misturados com a razão complementar 1:1 do ácido 4-dodeciloxibenzóico, que já possuía propriedades de cristais líquidos para aumentar a possibilidade de formação destes resultando em um sal orgânico. Os sais orgânicos obtidos foram investigados quanto ao seu comportamento em cristal líquido por microscopia óptica de polarização (POM) e calorimetria de varredura diferencial (DSC). Todos os compostos intermediários e finais foram confirmados por técnicas espectroscópicas (1H RMN, 13C RMN e espectrometria de massa).

**Palavras-chave:** *Triazina, Cristais líquidos, Ligação de hidrogênio, Síntese e Caracterização.*

### ABSTRACT

Liquid crystals are unique in their properties and use and has an essential role in the area of technological applications such as electrical, optical, displays, temperature maps, and switching materials. This study aimed to synthesize hexaethynylbenzene derivatives starting from 1,3,5-trichlorobenzene benzene as a central core substituted with three aromatic ring and three armed of 2-chloro-4,6-bis((3,7-dimethyloct-6-en-1-yl) oxy)-1,3,5-triazine. These molecules are formed by the covalent linking of three arms symmetrically to a central core which may be attached to the central core through flexible, semi-flexible or rigid linkers. The substitution occurred at the acetylenic periphery on the central benzene ring and was achieved efficiently by Sonogashira coupling. The six-armed compounds based on the benzene core was mixed with the complementary 4-dodecyloxybenzoic acid 1:1 ratio, which already possessed liquid crystal property to increase the formation of these resulting in an organic salt. The obtained organic salts were investigated for their liquid crystal behaviour by polarizing optical microscopy (POM) and differential scanning calorimetry (DSC). All the intermediate and final compounds were confirmed by spectroscopic techniques (1H NMR, 13C NMR, and mass spectrometry).

**Keywords:** *Triazine, Liquid crystals, Hydrogen bonding, Synthesis and Characterization.*

### 1. INTRODUCTION:

Liquid crystal displays (LCDs) are omnipresent in the modern world, representing probably the most prevalent, developed, and profitable technology of thermotropic liquid crystals (Bremer, 2013; Kato, 2018). This application is based on their sensitivity to external electric and magnetic fields, when molecules align fast and at low voltages. This property was the basis for their use in other exciting applications,

especially as sensors. Because of their fluid nature at a specific temperature, liquid crystals (LCs) are very easy to process in thin films, along with maintaining optical properties characteristic to crystalline materials, as the ability to rotate the polarized light plane (birefringence) (Scutaru, 2018).

The chemistry of triazine has gained much increased in the last few decades, due to their applications in organic synthesis and liquid crystal properties (Akkurt *et al.*, 2019). Hexa-

ethynylbenzene derivatives are interested molecular as liquid crystals (Praefcke, 1991; Al-Jumaili, 2020), nonlinear optical material (Kondo, 1995), core structures for dendritic (Kayser, 1999), light-harvesting materials (Mongin, 2000), and building blocks for two-dimensional carbon networks (Kehoe, 2000; Wan, 2000).

Substituted hexa-ethynylbenzenes, in which the ethynyl ends possess different functional groups, are attractive because it would be possible to change the above properties by modifying the substitution pattern of the terminal groups (Sonoda, 2001). The more frequently utilized nucleophilic substitution reactions have been mostly limited to amines and alcohols so far, providing selective substitution at the price of decreased cycloaddition ability due to the electron-donating nature of the new substituent (Boger, 1998; Sakya, 1997; Novák, 2003).

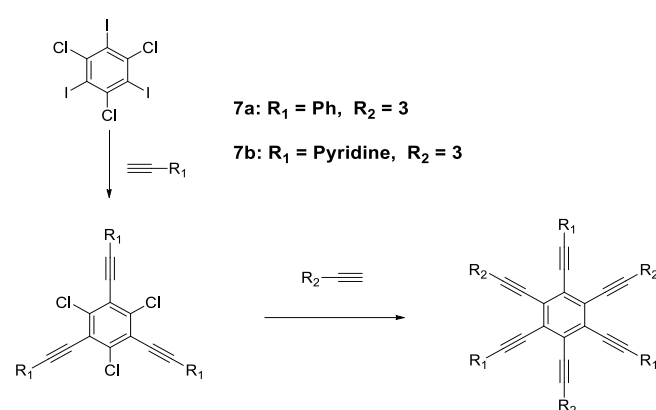
Organic  $\pi$ -conjugated systems, small molecules (Chow, 2014) and polymers, (Tan, 2020) are of great interest for sensing, optical and electronic applications (Usta, 2014). The group of discotic liquid crystals (DLC) offers the additional feature of self-organization, often as a columnar arrangement resulting in anisotropic properties, e.g. one-dimensional charge transport in the liquid-crystalline phase (Kaller, 2012).

Typical DLCs consist of electron-rich polycyclic aromatic units, e.g., triphenylene or hexabenzocoronene, (Kumar, 2005), whereas DLCs with an electron-deficient core are rather scarce (Kestemont, 2001).  $\pi$ -conjugated N-heterocyclic molecules with peripheral aliphatic chains can easily be functionalized to present highly ordered columnar mesomorphism, which results in exciting properties like one-dimensional (1D) high charge carrier mobilities regarding scientific and technological aspects (Gsänger, 2010; Sergeyev, 2007; Demus, 2011).

In the present study on the construction of extended  $\pi$ -electronic systems, it was performed the design and synthesis of new hexaethynylbenzene derivatives starting from 1,3,5-trichlorobenzene benzene as a central core substituted with three aromatic ring and three armed of 2-chloro-4,6-bis((3,7-dimethyloct-6-en-1-yl) oxy)-1,3,5-triazine. These molecules are formed by the covalent linking of three arms symmetrically to a central core (scheme 1). These arms may be linked to the central core through flexible or semi-flexible or rigid linkers. When the central core connecting to the linkers and three rigid arms, shape persistent star-shaped mesogens are obtained (Lehmann, M. 2009).

These molecules lack the shape anisotropy of discotic required to exhibit mesophases. Still, their ability to form mesophases is supported by the nanophase segregation of chemically or physically different molecular subunits and their tendency to fill the space efficiently in bulk (Pradhan, 2016). The advantage of six-armed design with concerning to discotic is the synthetic flexibility of the liquid crystal behaviour (Bisoyi, 2010).

Therefore, this study aimed to synthesize hexaethynylbenzene derivatives starting from 1,3,5-trichlorobenzene benzene as a central core substituted with three aromatic ring and three armed of 2-chloro-4,6-bis((3,7-dimethyloct-6-en-1-yl) oxy)-1,3,5-triazine.



**Scheme 1.** Synthesis route of six arms compounds.

## 2. MATERIALS AND METHODS:

### 2.1. Chemical and Reagents

Cyanuric chloride, dodecan-1-ol, ethynylbenzene, 1,3,5-trichlorobenzene, 2-iodothiophene, 2-ethynylpyridine, ethynyltrimethylsilane, copper iodide, potassium carbonate, tetrakis(triphenylphosphine)palladium and triethylamine. The solvents were used dry (THF, Dioxane) were obtained from distilling over phosphorous pentoxide (merck).

### 2.2. Measurement

Purity of the compounds was checked by TLC on silica gel 60 F<sub>254</sub> (Merck). Synthesized compounds are characterized by <sup>1</sup>H NMR and <sup>13</sup>C NMR spectra using CDCl<sub>3</sub> as a solvent with TMS as an internal standard. IR spectra were recorded in KBr on a Shimadzu FTIR 8400S spectrophotometer. Mass spectra were recorded on a GCMS-QP 1000 mass spectrometer.

### 2.3. 2-chloro-4,6-bis((3,7-dimethyloct-6-en-1-yl)oxy)-1,3,5-triazine (2)

2,4,6-trichloro-1,3,5-triazine (**1**) (0.29g, 1.6 mmol), 3,7-dimethyloct-6-en-1-ol (0.5 g, 3.2 mmol) and  $K_2CO_3$  (0.45 g, 3.2 mmol) were dissolved in 10 mL of THF under argon atmosphere and stirred at 50°C overnight (Scheme 2). The solution was poured into a mixture of ethyl acetate (10 mL) and water (10 mL). The organic layer after separation dried with sodium sulfate. Under vacuum, the solvent was evaporated and the crude product purified by column chromatography with hexane/ethyl acetate (2.5% EtOAc) as an eluent to give white powder with yield (0.25 g, 41%).  $^1H$  NMR (500 MHz,  $CDCl_3$ ) (5.14 (dd,  $J=7.1, 1.3$  Hz, 2H), 4.5 (m, 4H,  $OCH_2$ ), 2.09 (m, 4H,  $CH_2$ ), 1.9 (m, 6H,  $CH_3$ ), 1.8 (m, 6H,  $CH_2$ ), 1.6-1.3 (m, 10H,  $CH_2$ ), 1.07-0.95 (m, 6H,  $CH_3$ ),  $^{13}C$  NMR (126 MHz,  $CDCl_3$ ) (172, 171, 131.5, 124, 69, 36.8, 35, 29, 25.7, 25.3, 19.2, 17.6). HRMS=  $M^{+}_{calcd}$  for  $C_{23}H_{38}ClN_3O_2$  = 424.27.  $(M+H)^{+}_{found}$  = 424.27 and  $(M+NH_4)^{+}_{found}$  = 441.311 (441.311 - 18 = 423.3).

### 2.4. 2,4-bis((3,7-dimethyloct-6-en-1-yl)oxy)-6((trimethylsilyl)ethynyl)-1,3,5-triazine (3)

2-chloro-4,6-bis((3,7-dimethyloct-6-en-1-yl)oxy)-1,3,5-triazine (**2**) (1.2 g, 2.5 mmol), ethynyltrimethylsilane (0.29 g, 2.96 mmol),  $K_2CO_3$  (0.4 g, 2.96 mmol),  $Pd(PPh_3)_4$  (0.28 g, 0.24 mmol) and CuI (0.09 g, 0.49 mmol), were dissolved in 10 mL of THF under argon atmosphere then refluxed for 6 hr. (Scheme 2). The solution was poured into a mixture of ethyl acetate (20 mL) and water (20 mL). The organic layer after separation dried with sodium sulfate. The solvent was removed under vacuum to give brown oily material with yield (1.1 g, 81%). HRMS=  $M^{+}_{calcd}$  for  $C_{28}H_{47}N_3O_2Si$  = 485.34.  $(M+H)^{+}_{found}$  = 486.33 and  $(M+Na)^{+}_{found}$  = 508.32 (508.32 - 23 = 485.32).

### 2.5. 1,3,5-trichloro-2,4,6-triiodobenzene (5).

Periodic acid (1.5 g, 6.55 mmol) was added slowly to 25 mL of concentrated sulfuric acid and stirred for one hour then Potassium iodide (3.25 g, 20 mmol) was added to the mixture slowly at 0°C, after the reaction reached room temperature, 1,3,5-trichlorobenzene (**7**) (0.39 g, 2.2 mmol) was added (Scheme 3). The solution was poured into a mixture of ethyl acetate (25 mL) and water (25 mL). The organic layer after separation dried with sodium sulfate. The solvent was removed under vacuum to give solid materials with a yield (0.75 g, 62%), MP. 280°C. HRMS=  $M^{+}_{calcd}$  for  $C_3Cl_3I_3$  = 557.62.  $(M+H)^{+}_{found}$  = 558.6 and  $(M+Na)^{+2}_{found}$  = 582.6.

### 2.6. ((2,4,6-trichlorobenzene-1,3,5-triyl) tris(ethyne-2,1-diyl)) tribenzene (6a)

1,3,5-trichloro-2,4,6-triiodobenzene (**5**) (0.5 g, 0.89 mmol), ethynylbenzene (0.27 g, 2.68 mmol),  $Pd(PPh_3)_4$  (0.01 g, 0.09 mmol), CuI (0.03 g, 0.18 mmol) and  $Et_3N$  (0.28 g, 2.86 mmol) were dissolved in 10 mL of dioxane under argon atmosphere then stirred at 75 °C for 6 hr. (Scheme 3). The solution was poured into a mixture of ethyl acetate (10 mL) and water (10 mL). The organic layer after separation dried with sodium sulfate. Under vacuum the solvent was evaporated and the crude product purified by column chromatography with hexane/ethyl acetate (5% EtOAc) as an eluent to give white powder with yield (0.35 g, 81%), MP. 140-145 °C.  $^1H$  NMR (500 MHz,  $CDCl_3$ ) (7.6 (m, 6H, Ar-H), 7.4 (m, 9H, Ar-H).  $^{13}C$  NMR (126 MHz,  $CDCl_3$ ) (142, 132.5, 129.2, 128.5, 121.8, 81.6, 74). HRMS=  $M^{+}_{calcd}$  for  $C_{30}H_{15}Cl_3$  = 481.80.  $(M+H)^{+}_{found}$  = 483.02, and  $(M+Na)^{+}_{found}$  = 505.0219.

### 2.7. 2,2',2''-((2,4,6-trichlorobenzene-1,3,5-triyl) tris(ethyne-2,1-diyl)) tripyridine (6b)

1,3,5-trichloro-2,4,6-triiodobenzene (**5**) (0.43 g, 0.76 mmol), 2-ethynylpyridine (0.24 g, 2.29 mmol),  $Pd(PPh_3)_4$  (0.09 g, 0.07 mmol), CuI (0.03 g, 0.15 mmol),  $Et_3N$  (0.24 g, 2.44 mmol) were dissolved in 10 mL of dioxane under argon atmosphere then stirred at 75°C for 6 hr. (Scheme 3). The solution was poured into a mixture of ethyl acetate (10 mL) and water (10 mL). The organic layer after separation dried with sodium sulfate. Under vacuum, the solvent was evaporated and the crude product purified by column chromatography with hexane/ethyl acetate (3% EtOAc) as an eluent to give white powder with yield (0.29 g, 78%), MP. 195-200 °C.  $^1H$  NMR (500 MHz,  $CDCl_3$ ) (7.45 (m, 3H), 7.42 (m, 6H), 7.3 (m, 3H).  $^{13}C$  NMR (500 MHz,  $CDCl_3$ ) (145.6, 140.8, 134, 133.8, 129.6, 128.69, 128.6, 100.4, 97.9). HRMS=  $M^{+}_{calcd}$  for  $C_{27}H_{12}Cl_3N_3$  = 483.02.  $(2M^{+})_{found}$  = 968.0178.

### 2.8. 6,6',6''-((2,4,6-tris(phenylethynyl)benzene-1,3,5-triyl) tris(ethyne-2,1-diyl)) tris(2,4-bis((3,7-dimethyloct-6-en-1-yl)oxy)-1,3,5-triazine) (7a).

((2,4,6-trichlorobenzene-1,3,5-triyl)tris(ethyne 2,1-diyl))tribenzene (**6a**) (0.15 g, 0.31 mmol), 2,4-bis((3,7-dimethyloct-6-en-1-yl)oxy)-6((trimethylsilyl)ethynyl)-1,3,5-triazine (**3**) (0.48 g, 0.99 mmol),  $Pd(PPh_3)_4$  (0.03 g, 0.03 mmol), CuI (0.01 g, 0.06 mmol) and  $K_2CO_3$  (0.15 g, 1.08 mmol), were dissolved in 10 mL of dioxane under argon atmosphere then stirred at

80 °C for 16 hours (Scheme 3). The solution was poured into a mixture of ethyl acetate (10 mL) and water (10 mL). The organic layer after separation dried with sodium sulfate. Under vacuum the solvent was evaporated and the crude product purified by column chromatography with hexane/ethyl acetate (2.5% EtOAc) as an eluent to give oily light brown material with yield (0.37 g, 74%). <sup>1</sup>H NMR (7.36 (m, 9H, Ar-H), 7.2 (m, 6H, Ar-H), 4.8 (s, 6H), 4.2 (t, 12H, OCH<sub>2</sub>), 1.9 (m, 12H, CH<sub>2</sub>), 1.74 (m, 18H, CH<sub>3</sub>), 1.5-1.3 (m, 12H, CH<sub>2</sub>), 1.1-0.88 (m, 36H, CH<sub>2</sub>), 0.7 (m, 18H, CH<sub>3</sub>). <sup>13</sup>C NMR (126 MHz, CDCl<sub>3</sub>) (172.5, 170.9, 133, 131.8, 129.7, 128.9, 125.1, 125.08, 122.3, 88.5, 86.45, 82, 74.4, 66.8, 42.8, 42.5, 37.7, 37.5, 36.4, 36.3, 30.22, 29.9, 29.4, 26.2, 25.9, 20.02, 19.9, 18.3, 13.7, 13.5, 13.25, 13.23). FT-IR (2969, 2919, 2853, 1748, 1566, 1525, 1495, 1460, 1431, 1410, 1303) cm<sup>-1</sup>. HRMS = M<sup>+</sup><sub>calcd</sub> for C<sub>105</sub>H<sub>129</sub>N<sub>9</sub>O<sub>6</sub> = 1612.01. (M+3H)<sup>+</sup><sub>found</sub> = 538.34 and (M+3Na)<sup>+</sup><sub>found</sub> = 560.67.

## 2.9. 6,6',6''-((2,4,6-tris(pyridin-2-ylethynyl) benzene-1,3,5-triyl) tris(ethyne-2,1-diyl)) tris(2,4-bis((3,7-dimethyloct-6-en-1-yl) oxy)-1,3,5-triazine) (7b).

2,2',2''-((2,4,6-trichlorobenzene-1,3,5-triyl)tris(ethyne-2,1-diyl))tripyrindine (**6b**) (0.12 g, 0.25 mmol), Pd(PPh<sub>3</sub>)<sub>4</sub> (0.03 g, 0.02 mmol), 2,4-bis((3,7-dimethyloct-6-en-1-yl)oxy)-6-((trimethylsilyl)ethynyl)-1,3,5-triazine (**3**) (0.36 g, 0.74 mmol), CuI (0.01 g, 0.04 mmol) and K<sub>2</sub>CO<sub>3</sub> (0.12 g, 0.86 mmol), were dissolve in in 10 mL of dioxane under argon atmosphere then stirred at 80 °C for 16 hours. (Scheme 3). The solution was poured into a mixture of ethyl acetate (10 mL) and water (10 mL). The organic layer after separation dried with sodium sulfate. Under vacuum, the solvent was evaporated and the crude product purified by column chromatography with hexane/ethyl acetate (2.5% EtOAc) as an eluent to give light brown with yield (0.25 g, 62%). <sup>1</sup>H NMR (500 MHz, CDCl<sub>3</sub>) (7.58 (m, 3H, Ar-H), 7.4 (m, 3H, Ar-H), 7.22 (m, 6H, Ar-H), 4.9 (s, 6H), 4.23 (t, 12H, OCH<sub>2</sub>), 1.84 (m, 18H, CH<sub>2</sub>), 1.66 (m, 18H, CH<sub>3</sub>), 1.5- 1.3 (m, 12H, CH<sub>2</sub>), 1.25 – 0.86 (m, 36H, CH<sub>2</sub>), 0.78 (m, 18H, CH<sub>3</sub>). <sup>13</sup>C NMR (171.7, 171.2, 142.5, 137.5, 136.2, 132.05, 131.14, 127.9, 124.7, 123.6, 121.9, 99.5, 99.3, 82, 67, 41.3, 41.1, 37.2, 35.9, 31.9, 29.6, 29.4, 25.7, 25.4, 22.62, 19.5, 17.6, 14.12, 13.5, 13.19). FT-IR (2966, 2925, 2853, 1732, 1566, 1521, 1501, 1458, 1430, 1411, 1374) cm<sup>-1</sup>. HRMS: M<sup>+</sup><sub>calcd</sub> for C<sub>102</sub>H<sub>126</sub>N<sub>12</sub>O<sub>6</sub> = 1616. (M+3Na)<sup>+</sup><sub>found</sub> = 561.98.

## 2.10. 4-(dodecyloxy) benzoic acid (4-DBA) (8)

4-hydroxy benzoic acid (8.2 mmol), 1-bromododecane (5.5 ml, 23 mmol, 2.8 eq) and KOH (1.3 g, 23 mmol, 2.8 eq) were dissolve in (25 ml) of ethanol and reflux for two days (Scheme 4). The mixture was hydrolysis by adding 10% aqueous KOH (12 ml) and refluxed overnight. After cooling down, the reaction mixture was acidified with HCl (6 M), the precipitate filtered, washed with water and recrystallized from ethanol to obtain the pure product 4-dodecyloxybenzoic acid white solid material with yield (4.55 g, 91 %). <sup>1</sup>H NMR (500 MHz, CDCl<sub>3</sub>) (δ 8.10 (d, 2H), 6.98 (d, 2H), 4.07 (t, 2H), 1.84 (m, 2H), 1.48 (m, 2H), 1.37-1.28 (m, 16H), 0.91 (t, 3H). FT-IR (2914, 2848, 2559, 1670, 1604) cm<sup>-1</sup>.

## 2.11. Synthesis of Organic Salts 9(a,b)

4-DBA mesogenic unit (**8**) reacted with **7(a-b)** in 10 mL of dry THF with one to one ratio (Scheme 4). The resulting solution was sonicated for 15 min until observing a transparent solution. Then, the solvent was removed in vacuum.

**The organic salt (9a).** <sup>1</sup>H NMR (500 MHz, CDCl<sub>3</sub>) (7.92 (d, 2H), 7.4 (d, 6H, Ar-H), 7.24 (m, 9H, Ar-H), 6.8 (d, 2H, Ar-H), 4.97 (s, 6H), 4.2 (t, 12H, OCH<sub>2</sub>), 3.8 (t, 2H, OCH<sub>2</sub>), 1.78 (t, 18H, CH<sub>3</sub>), 1.6-1.3 (m, 24H, CH<sub>2</sub>), 1.1- 0.9 (m, 60H, CH<sub>2</sub>), 0.78 (m, 18H, CH<sub>3</sub>). <sup>13</sup>C NMR (171.7, 170, 165, 163, 132.5, 132.3, 131.3, 131.2, 129, 128, 124, 121.7, 121.3, 114.18, 81.5, 73.8, 68, 66, 42, 41.2, 37.3, 35.6, 32.4, 30.2, 31, 29.9, 29.8, 29.5, 28.8, 26.3, 25.8, 23.3, 22, 19.8, 18.1, 17, 14.6, 12). FT-IR (2916, 2846, 1674, 1603, 1522, 1503, 1459, 1425, 1362, 1335). HRMS= M<sup>+</sup><sub>calcd</sub> for C<sub>124</sub>H<sub>159</sub>N<sub>9</sub>O<sub>9</sub> = 1918.23. (M + 3K)<sup>+</sup><sub>found</sub> = 678.7.

**The organic salt (9b).** <sup>1</sup>H NMR (500 MHz, CDCl<sub>3</sub>) (7.9 (d, 2H, Ar-H), 7.58 (m, 6H), 7.4 (m, 3H), 7.22 (m, 3H), 6.75 (d, 2H, Ar-H), 4.9 (s, 6H), 4.2 (t, 12H, OCH<sub>2</sub>), 3.75 (t, 2H, OCH<sub>2</sub>), 1.78 (t, 18H, CH<sub>3</sub>), 1.6-1.3 (m, 24H, CH<sub>2</sub>), 1.1- 0.9 (m, 60H, CH<sub>2</sub>), 0.78 (m, 18H, CH<sub>3</sub>). FT-IR (2923, 2852, 1736, 1567, 1521, 1501, 1458, 1413). HRMS = M<sup>+</sup><sub>calcd</sub> for C<sub>121</sub>H<sub>156</sub>N<sub>12</sub>O<sub>9</sub> = 1921.21. (M+3K)<sup>+</sup><sub>found</sub> = 680.36 and 679.7.

## 3. RESULTS AND DISCUSSION:

In this study, six-armed compounds based on benzene ring as a central core was synthesized via sonogashira reaction. 1,3,5-trichlorobenzene and 2,4,6-trichloro-1,3,5-triazine were the starting material. The intermediate compound 2-chloro-4,6-bis((3,7-dimethyloct-6-en-1-yl) oxy)-1,3,5-



triazine was obtained by sequential nucleophilic substitution of chlorine atoms in cyanuric chloride and used further in the synthesis of six armed structures as described in (Scheme 2 - 4). The obtained compounds were confirmed by spectroscopic analysis and the organic salts were investigated by polarized optical microscope (POM) and differential scanning calorimetry (DSC).

The formation of ionic interaction between the six-armed  $\pi$ -conjugated system and the mesogenic carboxyl group was mainly studied by FT-IR. The carboxylic peak corresponding to 4-DBA at  $1670\text{ cm}^{-1}$  shifted to  $1566\text{ cm}^{-1}$  in both organic salt (**9a**, **9b**). Whereas, the stretching vibration of the C=C bond in both organic salt appears at  $1675\text{ cm}^{-1}$  and  $1635\text{ cm}^{-1}$  (Figure 1). Besides, peaks at  $2900$  and  $2800\text{ cm}^{-1}$  belonging to hydrogen stretching (Türkçü, 2016).

Also, NMR spectroscopy confirmed the formation of organic salt (**9a**, **9b**). The signals belong to the aromatic protons of alkoxy benzoate unit in both compounds shift to (7.8, 6.7) ppm and (7.9, 6.75) ppm respectively as compared with the signals of pure 4-DBA at (8.05, 6.95) ppm, due to increase in electron density of aromatic ring. Similarly, the signals of oxymethylene protons of 4-DBA in ion complex shift to higher field 3.8 ppm and 3.75 ppm as compared with the signals of pure 4-DBA at 4.05 ppm (Figure 2). Additionally, the singlets of aromatic ring protons in organic salt (**9a**, **9b**) didn't show any shifting due to their electronic environment did not change. These changes in chemical shift related to the difference in electron density after the interaction.

However, the  $^{13}\text{C}$  NMR spectra show that the carbonyl carbon of 4-DBA shifted from 171.6 to 165.12 ppm, similarity the aromatic carbon next to alkoxy group of 4-DBA shift slightly from 163.69 to 163.6 ppm. These change in chemical shift due to decrease of electron density after the ionic interaction (Figure 3). Additionally, the peaks which belong to triazine ring didn't show any shifting.

Additionally, the mass spectrometry of organic salt (**9a**) confirmed the molecular structure by the presence of  $(M+3K)^{+3}$  at 678.70 peaks, which correspond to  $\text{C}_{124}\text{H}_{159}\text{N}_9\text{O}_9$ , similarity the molecular structure of organic salt (**9b**) confirmed by the presence of  $(M+3K)^{+3}$  peaks at 680.36 and 680.03, which correspond to  $\text{C}_{121}\text{H}_{156}\text{N}_{12}\text{O}_9$ , (Figure 4).

Compound 4-DBA, which has a terminal chain, and already shows liquid crystalline, so to obtain liquid crystalline material for our synthesized compounds, the equimolar mixture between six-

armed  $\pi$ -conjugated system and 4-DBA was obtained through ionic interaction. Concerning to 4-DBA, upon heating showed three peaks corresponding to Cr-SmC-N-Iso transitions. On cooling from isotropic phase, the same behavior of reverse transitions was observed. In addition to this, a calorimetric peak corresponding to Cr-Cr transition at  $65.86^\circ\text{C}$  was detected in cooling DSC thermogram (Kumar, 2010; Pisupati, 2000).

The equimolar mixtures of the organic salt (**9a**, **9b**) based on the benzene core were investigated by using an optical polarizing microscope (PM) and differential scanning calorimeter (DSC). The compounds (**9a**, **9b**) show one endotherm corresponds to crystal to the isotropic (Iso) transition in heating DSC thermogram. The organic salts (**9a**, **9b**) show no liquid crystal behavior by an optical polarizing microscope (PM) observation.

The organic salt (**9a**, **9b**) exhibit a phase transition sequence of Cr-Col-Iso, which is in agreement with two endotherms in DSC heating curves. Compound (**9a**) on cooling from the isotropic liquid, exhibited one peak in phase transition with the dendritic growing texture was observed between  $(64-18)^\circ\text{C}$ , whereas compound (**9b**) phase transition with the growing dendritic texture was observed between  $(71-20)^\circ\text{C}$ , (Figure 5). Both organic salts with multi-side chains, the differential scanning calorimetry, and optical polarized microscope showed no liquid crystal behavior.

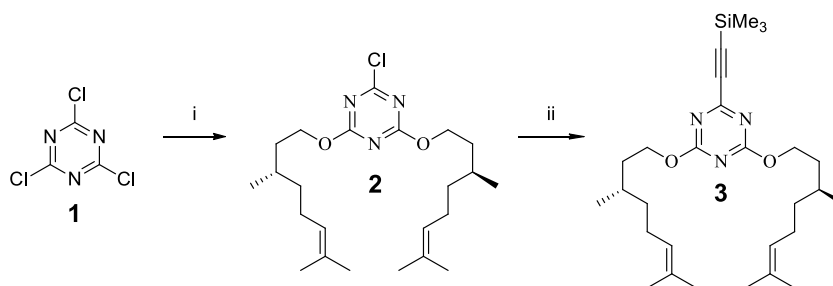
#### 4. CONCLUSIONS:

New six arms macromolecular structures was efficiently prepared which composed of 1,3,5-trichlorobenzene central core, three armed of 2-Ethynylpyridine (2-Ethynylbenzene), and three armed of 1,3,5-triazine rings carrying dodecyloxy chains which are positioned at the peripheries of the central core by acetylenic bridges. The six-armed compounds was non liquid crystal therefore the compounds were mixed with 4-dodecyloxy benzoic acid to obtain organic salt. The organic salts, which made between the  $\pi$ -conjugated system and 4-dodecyloxy benzoic acid were investigated for their liquid crystal properties by optical polarizing microscope (POM) and differential scanning calorimetry (DSC), it's found no liquid crystalline behaviours even after ionic interaction through hydrogen bonding. All the synthesized compounds were confirmed by spectroscopic analyses ( $^{13}\text{C}$  NMR,  $^1\text{H}$  NMR, FT-IR, and HRMS).

## 5. REFERENCES:

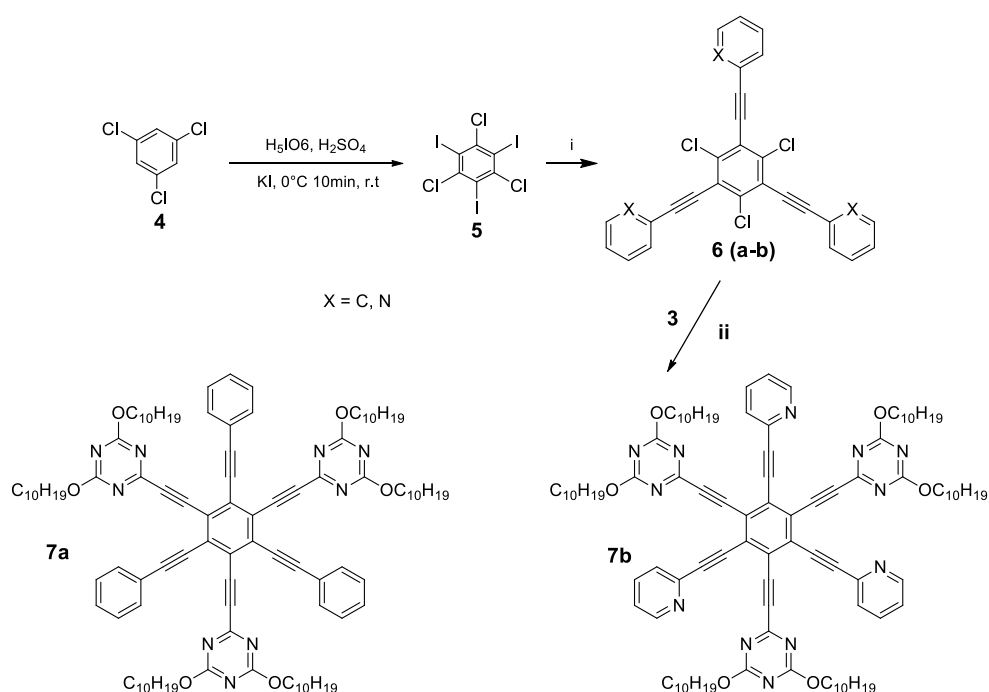
- Bremer M, Kirsch P, Klasen-Memmer M, Tarumi K. (2013). The TV in your pocket: Development of liquid-crystal materials for the new millennium. *Angewandte Chemie* (International Ed. in English). 52(34):8880-8896. DOI: 10.1002/anie.201300903
- Kato T, Uchida J, Ichikawa T, Sakamoto T. (2018). Functional liquid crystals towards the next generation of materials. *Angewandte Chemie* (International Ed. in English). 57(16):4355-4371. DOI: 10.1002/anie.201711163
- Scutaru, D., Carlescu, I., Bulai, E. R., Ciobanu, C. I., Lisa, G., and Hurdac, N. (2018). Bent-Core Liquid Crystals: Structures and Mesomorphic Properties. *Liquid Crystals-Self-Organized Soft Functional Materials For Advanced Applications*.
- Akkurt, N., Al-Jumaili, M. H. A., ERAN, B. B., Ocak, H., and Torun, L. (2019). Acetylene-bridged triazine  $\pi$ -conjugated structures: synthesis and liquid crystalline properties. *Turkish Journal of Chemistry*, 43(5), 1436-1444.
- Praefcke, K., Kohne, B., Gündogan, B., Singer, D., Demus, D., Diele, S., ... and Bakowsky, U. (1991). News on nematic-biaxial liquid crystals. *Molecular Crystals and Liquid Crystals*, 198(1), 393-405.
- Al-Jumaili, M. H., Hamed, A. S., Akkurt, N., and Torun, L. (2020) Six-armed Structures Based on Benzene Ring, Synthesis and Characterization Via Sonogashira Coupling. *Indonesian Journal of Chemistry*.
- Kondo, K., Yasuda, S., Sakaguchi, T., and Miya, M. (1995). The third-order optical non-linearity of the phenylethynyl-substituted benzene system. *Journal of the Chemical Society, Chemical Communications*, (1), 55-56.
- Kayser, B., Altman, J., and Beck, W. (1999). Benzene-Bridged Hexaalkynylphenylalanines and First-Generation Dendrimers Thereof. *Chemistry-A European Journal*, 5(2), 754-758.
- Mongin, O., Hoyler, N., and Gossauer, A. (2000). Synthesis and Light-Harvesting Properties of Naphthyrins. *European Journal of Organic Chemistry*, 2000(7), 1193-1197.
- Kehoe, J. M., Kiley, J. H., English, J. J., Johnson, C. A., Petersen, R. C., and Haley, M. M. (2000). Carbon networks based on dehydrobenzoannulenes. 3. synthesis of graphyne substructures. *Organic letters*, 2(7), 969-972.
- Wan, W. B., Brand, S. C., Pak, J. J., and Haley, M. M. (2000). Synthesis of expanded graphdiyne substructures. *Chemistry-A European Journal*, 6(11), 2044-2052.
- Sonoda, M., Inaba, A., Itahashi, K., and Tobe, Y. (2001). Synthesis of differentially substituted hexaethynylbenzenes based on tandem Sonogashira and Negishi cross-coupling reactions. *Organic letters*, 3(15), 2419-2421.
- Boger, D. L., Schaum, R. P., and Garbaccio, R. M. (1998). Regioselective Inverse Electron Demand Diels-Alder Reactions of N-Acyl 6-Amino-3-(methylthio)-1, 2, 4, 5-tetrazines. *The Journal of organic chemistry*, 63(18), 6329-6337.
- Sakya, S. M., Groskopf, K. K., and Boger, D. L. (1997). Preparation and inverse electron demand Diels-Alder reactions of 3-methoxy-6-methylthio-1, 2, 4, 5-tetrazine. *Tetrahedron letters*, 38(22), 3805-3808.
- Novák, Z., and Kotschy, A. (2003). First cross-coupling reactions on tetrazines. *Organic letters*, 5(19), 3495-3497.
- Chow, T. J. (Ed.). (2014). *Organic structures design: applications in optical and electronic devices*. CRC Press.
- Tan, Z. Y., Wu, K. X., Huang, L. S., Wu, R. S., Du, Z. Y., and Xu, D. Z. (2020). Iron-catalyzed cross-dehydrogenative coupling of indolin-2-ones with active methylenes for direct carbon-carbon double bond formation. *Green Chemistry*.
- Usta, H., Sheets, W. C., Denti, M., Generali, G., Capelli, R., Lu, S., ... and Facchetti, A. (2014). Perfluoroalkyl-functionalized thiazole-thiophene oligomers as n-channel semiconductors in organic field-effect and light-emitting transistors. *Chemistry of Materials*, 26(22), 6542-6556.
- Kaller, M., Beardsworth, S. J., Staffeld, P., Tussetschlager, S., Gießelmann, F., and Laschat, S. (2012). Increased mesophase range in liquid crystalline crown ethers via lower molecular symmetry. *Liquid Crystals*, 39(5), 607-618.
- Kumar, S. (2005). Triphenylene-based discotic liquid crystal dimers, oligomers and polymers. *Liquid crystals*, 32(9), 1089-1113.

21. Kestemont, G., De Halleux, V., Lehmann, M., Ivanov, D. A., Watson, M., and Geerts, Y. H. (2001). Discotic mesogens with potential electron carrier properties. *Chemical communications*, (20), 2074-2075.
22. Gsänger, M., Oh, J. H., Könnemann, M., Höffken, H. W., Krause, A. M., Bao, Z., and Würthner, F. (2010). A crystal-engineered hydrogen-bonded octachloroperylene diimide with a twisted core: an n-channel organic semiconductor. *Angewandte Chemie International Edition*, 49(4), 740-743.
23. Sergeyev, S., Pisula, W., and Geerts, Y. H. (2007). Discotic liquid crystals: a new generation of organic semiconductors. *Chemical Society Reviews*, 36(12), 1902-1929.
24. Demus, D., Goodby, J. W., Gray, G. W., Spiess, H. W., and Vill, V. (Eds.). (2011). *Handbook of liquid crystals, volume 2A: low molecular weight liquid crystals I: calamitic liquid crystals*. John Wiley and Sons.
25. Lehmann, M. (2009). Star Mesogens (Hekates)—Tailor-Made Molecules for Programming Supramolecular Functionality. *Chemistry—A European Journal*, 15(15), 3638-3651.
26. Pradhan, B., Pathak, S. K., Gupta, R. K., Gupta, M., Pal, S. K., and Achalkumar, A. S. (2016). Star-shaped fluorescent liquid crystals derived from s-triazine and 1, 3, 4-oxadiazole moieties. *Journal of Materials Chemistry C*, 4(25), 6117-6130.
27. Bisoyi, H. K., and Kumar, S. (2010). Discotic nematic liquid crystals: science and technology. *Chemical Society Reviews*, 39(1), 264-285.
28. Kumar, C. R. S., Jha, A., and Sastry, S. S. (2010). Induced crystal G phase of liquid crystalline amide through inter molecular hydrogen bonding. *Journal of non-crystalline solids*, 356(6-8), 334-339.
29. Pisupati, S., Kumar, P. A., and Pisupati, V. G. K. M. (2000). Induced crystal G phase through intermolecular hydrogen bonding II. Influence of alkyl chain length of n-alkyl p-hydroxybenzoates on thermal and phase behaviour. *Liquid Crystals*, 27(5), 665-669.
30. Türkçü, H. N., Ocağ, H., Gürbüz, M. U., Çakar, F., Bilgin-Eran, B., and Tülü, M. (2016). A study of dendritic ionic liquid crystals: Using (S)-4-citronellyloxybenzoic acid and polypropylene imine dendrimers. *Journal of Molecular Liquids*, 216, 209-215.



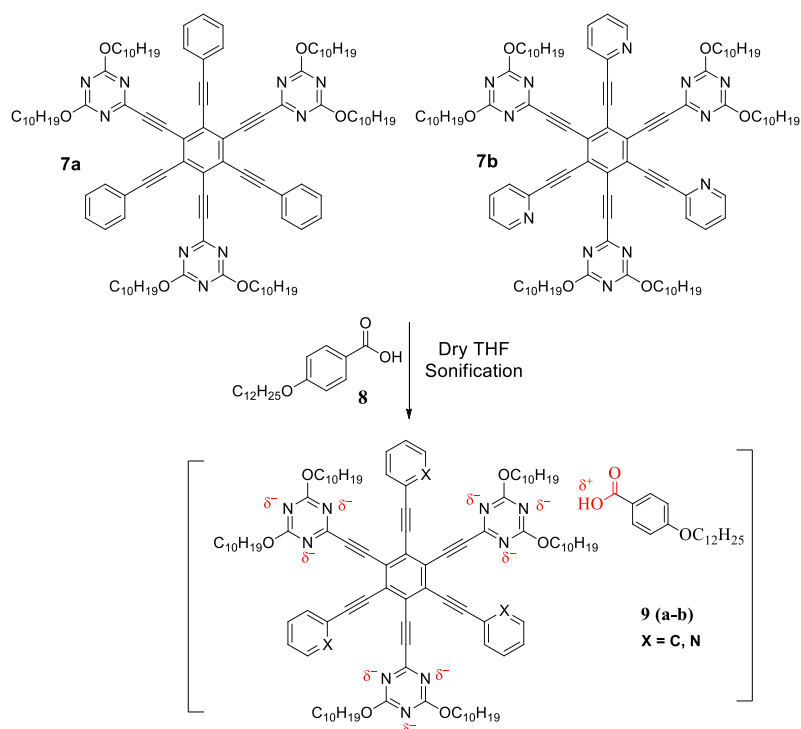
**Scheme 2.** Synthesis of intermediate compound

**Reaction and conditions:** i) 3,7-dimethyloct-6-en-1-ol (2 eq),  $K_2CO_3$ , 0-50°C, 6hr, THF, ii) Trimethylsilyl acetylene,  $K_2CO_3$ , Pd ( $PPh_3$ )<sub>4</sub>, CuI, THF, Reflux.



**Scheme 3.** Synthesis of six-armed compounds

**Reaction and condition:** i) 2-Ethynylpyridine (2-Ethynylbenzene), Pd( $PPh_3$ )<sub>4</sub> (0.02), CuI (0.04),  $Et_3N$  (3.2 eq), Dioxane, 75 °C, 6 hr. ii) Pd( $PPh_3$ )<sub>4</sub>, CuI,  $K_2CO_3$ , Dioxane, 80°C, 16 hr.



**Scheme 4:** Synthesis procedure of organic salt (**9a**, **9b**).

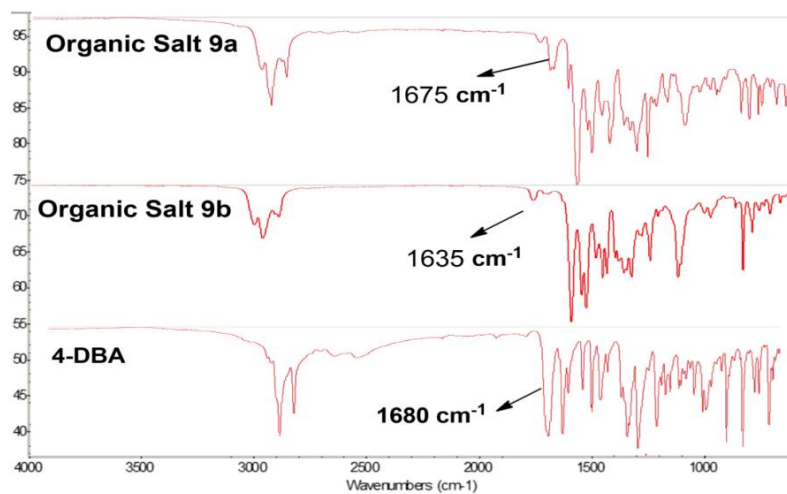


**Figure 1.** FT-IR spectra of organic salts (**9a**, **9b**) and benzoic acid (**4-DBA**).

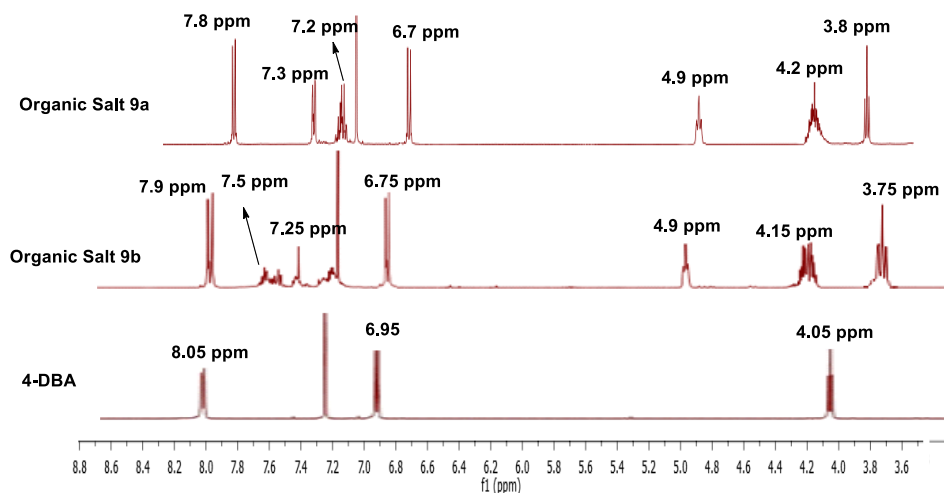


**Figure 2.** The comparison of  $^1\text{H}$  NMR spectra (in  $\text{CDCl}_3$ ) of organic salts (9a, 9b) and benzoic acid (4-DBA).

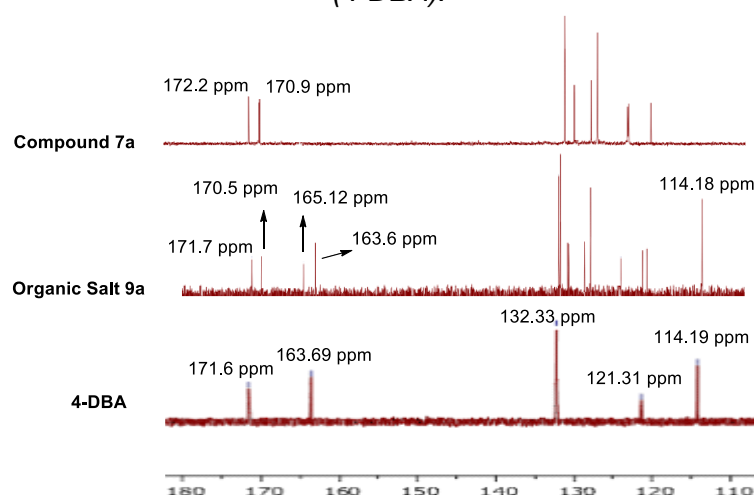


**Figure 3.**  $^{13}\text{C}$  NMR spectra (in  $\text{CDCl}_3$ ) of compound (7a), organic salt (9a) and benzoic acid (4-DBA).

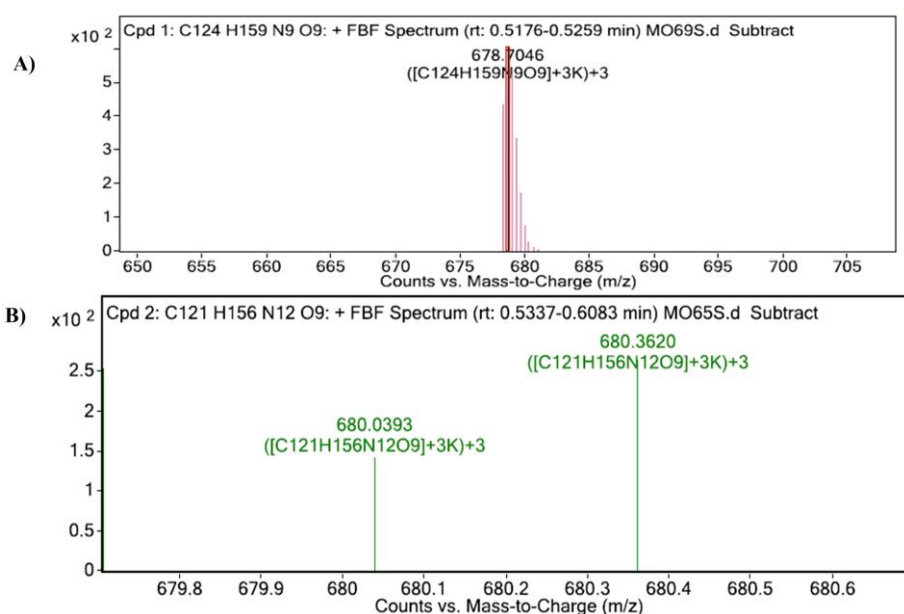


**Figure 4.** HRMS result of organic salt (9a, 9b).

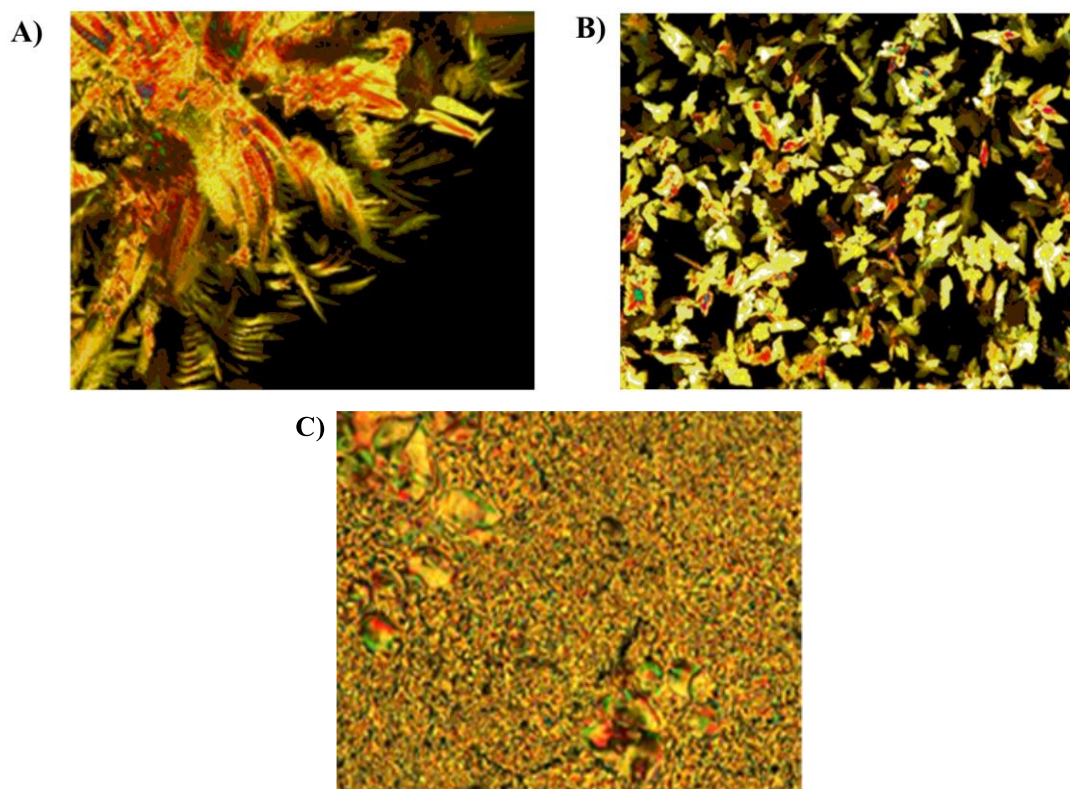


**Figure 5.** Optical textures of organic salt (9a (left), 9b (right)) as observed between crossed polarizers in an ordinary glassplates. C) A typical texture of smectic C mesophase of compound 4-DBA.

**Table 1.** Mesophases and phase transition temperatures as observed on heating ( $H \rightarrow$ ) and cooling ( $\leftarrow C$ ) and corresponding transition enthalpies of organic salts (9a, 9b) and 4-DBA

| Comp.              | T/°C [ $\Delta H$ kJ/mol]  |
|--------------------|--|
| 4-DBA <sup>b</sup> | $H \rightarrow$ : Cr 99.98 [39.01] SmC 132.43 [2.39] N 138.42 [2.05] Iso                                       |
| OS (9a)            | $H \rightarrow$ : Cr 52 [170.46], Col 81.53 [22.4] Iso<br>Cr 16.30 [142.59] Col 69 [11.2] Iso : $\leftarrow C$ |
| OS (9b)            | $H \rightarrow$ : Cr 25.2 [190.46], Col 78.4 [19.4] Iso<br>Cr 18.2 [182.73] Col 64 [13.2] Iso : $\leftarrow C$ |

<sup>a</sup>Perkin-Elmer DSC-6; enthalpy values in italics in brackets taken from the 1<sup>st</sup> heating and cooling scans at a rate of 10 °C min<sup>-1</sup>; Abbreviations: Cr = crystalline, SmC= tilted smectic phase, N= nematic phase; Col= columnar mesophase, Iso = isotropic liquid phase.

## USANDO O APRENDIZADO BASEADO EM PROBLEMAS PARA MELHORAR AS HABILIDADES CRÍTICAS DOS ESTUDANTES PARA LIDAR COM INFORMAÇÕES ENGANOSAS EM QUÍMICA

## USING PROBLEM-BASED LEARNING TO IMPROVE STUDENTS' CRITICAL THINKING SKILLS TO DEAL HOAX INFORMATION IN CHEMISTRY

FADIAWATI, Noor<sup>1</sup>; DIAWATI, Chansyanah<sup>2</sup>; SYAMSURI, M. Mahfudz Fauzi<sup>3\*</sup><sup>1,2,3</sup>University of Lampung, Faculty of Teacher Training and Education, Department of Chemical Education, Lampung, Indonesia

\* Corresponding author

e-mail: mahfudz.085279907995@fkip.unila.ac.id

Received 16 April 2020; received in revised form 05 May 2020; accepted 14 June 2020

## RESUMO

O pensamento crítico é a capacidade de pensar racional e reflexivamente sobre o que deve ser feito ou acreditado. Essa habilidade permite tomar decisões lógicas, com base nas informações obtidas e processadas de acordo com a habilidade. O desenvolvimento de habilidades de pensamento crítico na aprendizagem é importante porque permite que os alunos lidem efetivamente com problemas sociais, científicos e práticos. Portanto, esta pesquisa teve como objetivo descrever a efetividade da aprendizagem baseada em problemas para melhorar as habilidades de pensamento crítico dos alunos para lidar com informações fraudulentas em química. Esta pesquisa foi realizada utilizando um grupo controle e outro experimental. Os dados foram coletados de 60 alunos do 11º ano do ensino médio da província de Lampung, na Indonésia, e analisados pelo SPSS versão 23.0. A efetividade da aprendizagem baseada em problemas foi mensurada com base no ganho *n*. O valor de ganho *n* das classes experimental e controle foi de 0,709 (alto) e 0,332 (médio), respectivamente. Os resultados indicaram que a aprendizagem baseada em problemas facilitou e é eficaz para melhorar as habilidades de pensamento crítico dos alunos.

**Palavras-chave:** *habilidades de pensamento crítico; informações fraudulentas; aprendizagem baseada em problemas; aprendizagem prática*

## ABSTRACT

Critical thinking is the ability to think rationally and reflectively about what must be done or believed. This skill allows one to make logical decisions based on information obtained and processed according to ability. The development of critical thinking skills in learning is essential because they enable students to deal effectively with social, scientific, and practical problems. Therefore, this research aimed to describe the effectivity of problem-based learning to improve students' critical thinking skills to deal with hoax information in chemistry. This research was carried out through the control and experimental groups. Data were collected from 60 the 11<sup>th</sup>-grade students of the State High School in Lampung Province, Indonesia, and analyzed by using SPSS version 23.0. The effectivity of problem-based learning was measured based on the *n*-gain. The *n*-gain value of experimental and control classes was 0.709 (high) and 0.322 (medium), respectively. The results indicated that problem-based learning has facilitated and effective to improve students' critical thinking skills.

**Keywords:** *critical thinking skills; hoax information; problem-based learning; hands-on learning*



## 1. INTRODUCTION:

The world is now in the era of the industrial revolution of 4.0. In this era, there was a rapid development of science and technology, both censorship, interconnection, and data analysis, thus bringing up ideas to be integrated into various fields of industry. Due to the fast development of science and technology, the problems faced are increasingly numerous and complex. On the other hand, the 4.0 industrial revolution will affect not only the industry, but also the labor market (Van den Bergh *et al.*, 2006; Lowden *et al.*, 2011; Danczak, Thompson, and Overton, 2020). Workforce needs have been transformed from routine work to shift to non-routine work (Trilling and Fadel, 2009). Because of this, a problem solver is needed to overcome them.

As a problem solver, knowledge alone is not enough to deal with increasingly complex problems in the current disruptive era. The contemporary job market demands the production of someone who can work in a disruptive and ill-defined environment, face non-routine and abstract work processes, make decisions, take responsibility, and work in teams (Van den Bergh *et al.*, 2006; Baygin *et al.*, 2016; Diawati *et al.*, 2017; Diawati *et al.*, 2018; Fadiawati, Diawati, and Syamsuri, 2019). This ability is related to skills demanded in the 21st century, one of which is critical thinking skills (CTS).

Critical thinking (CT) is rational and reflective thinking with an emphasis on making decisions about what to believe and do (Norris and Ennis, 1989). Based on the Delphi Report, CT is self-regulation in deciding which has goals that produce interpretations, analyzes, evaluations and inferences as well as concrete, conceptual explanations, as well as having methods, criteria or contextual considerations on which these decisions are based (Facione, 1990; Dwyer, Hogan, and Stewart, 2014; Stephenson and Sadler-McKnight, 2016).

The development of CTS has been the main focus of several researchers (Halpern, 2014; Moore, 2015; Butler and Halpern, 2020; Danczak, Thompson, and Overton, 2020). CTS is important because they enable students "to deal effectively with social, scientific, and practical problems" (Shakirova, 2007). Some cognitive psychology researchers report that CTS could be developed within a variety of discipline areas to make knowledge retrieval easier. McMillan (1987) argued that standalone and integrated courses were equally successful in developing CTS. On the other hand, Ennis (1990) accepted that CTS

also could be effectively improved with or without discipline-specific areas. Davies (2013) agreed that CTS is a fundamental skill at the basis of all disciplines of knowledge. CTS can be a need to accommodate the discipline-specific needs in higher education. CTS could be transferred to situations encountered in daily life (Butler and Halpern, 2020); one of them is about hoax information circulating through social networks.

Facebook, Youtube, WhatsApp, dan Instagram are social networks that are widely accessed by internet users. Among social networks, Facebook users number 2.414 billion, while Youtube with 2 billion active users, WhatsApp users number 1.6 billion, and Instagram with 1 billion active users (Clement, 2020). Fellow social networks users share a variety of news broadcasts dan information. Other users can quickly see both.

However, not only real news and information but also fake and mislead (hoax) news and information shared. Hoax information was made based on individual opinions that cannot be accounted for, and they shared in a chain through social networks. Related to circulating hoax information, CTS is needed in media literacy. Some learning models which suggested to developing CTS in chemistry are problem-based (Kek and Huijser, 2011; Martyn *et al.*, 2014), open-ended practical (Klein and Carney, 2014), and inquiry (Gupta *et al.*, 2015).

In this article, it is described the results of developed CTS dealing with hoax information by using problem-based learning (PBL). Fogarty (1997) defines PBL as a learning model that deals with real-life or real-world problems that are ill-structured, open-ended, and ambiguous. In these learning, students are faced with hoax information problems related to some food and drinks circulating through social networks. For example, hoax information received by the public is related to noodles and carbonated water. Based on information flowing, noodles and carbonated water are considered poisonous and dangerous. This is because if noodles with iodine drop, they will turn purple. On the other hand, carbonated water contains high levels of acid so that it can dissolve bones and teeth.

This corresponds with the outbreak of hoax information in Indonesia has become a national problem. The survey results of the Indonesian Telematics Society (2019) that a variety of hoax information that is often accepted by the public. Some of them are issues about health by 40.70%, issues about food and drinks by 30.00%, and

issues about science and technology by 20.00%. As a result of the circulation of the hoax information, the community became restless and was overtaken by excessive fear (Zuria and Suyanto, 2018). On the other hand, noodles and carbonated water producers suffer losses due to competition and trademark pollution (Apriyani, Fadiawati, and Syamsuri, 2017).

Furthermore, based on the hoax information in circulation, students look for information from reliable sources, conduct investigations, and use their knowledge and to be analyzed and confirm whether the information can be trusted or not. Therefore, this research aimed to describe the effectivity of PBL to improve students' CTS to deal with hoax information in chemistry.

## 2. MATERIALS AND METHODS:

This research is a quasi-experimental and carried out in the State High School in Lampung Province, Indonesia, by using nonequivalent control-group design (Creswell and Creswell, 2017). The population of this research is the 11<sup>th</sup>-grade students totaling 200 students. By using purposive sampling obtained 60 students, and every one declares to agree to participate in this research. Furthermore, students are grouped into experimental and control classes. Purposive sampling is done with consideration to obtain samples with the same or relatively similar characteristics based on prior information of a population (Fraenkel, Wallen, and Hyun, 2011).

Before the intervention, both the experimental and control classes were given pretest Norris-Ennis's CTS in the form of open-ended questions (Appendix 1). Next is the intervention stage by applying PBL in the experimental class and conventional learning in the control class.

Learning begins by orienting students to the hoax information problems. In the organized students' phase, students are asked to gather information related to the problem. Furthermore, students make investigation design and apply it to confirm whether or not the hoax information is being faced. Data obtained are then presented. In the last phase, students will be asked and answered on the work between groups to bring up various opinions or ideas. The learning process is guided by student worksheets to match the PBL syntax. During the learning process, student performance is also assessed. At the end of the learning, both classes were given a post-test Norris-Ennis's CTS in the form of open-ended

questions.

Statistical testing with SPSS version 23.0 was carried out on the results of the pretest through normality (One Sample Kolmogorov-Smirnov's Test), homogeneity of variance (Levene's Test), and independent sample t test. Increasing the score of each class (n-gain) also statistically tested through normality and One Way ANOVA. The n-gain categorized as high, medium, or low (Hake, 1998).

## 3. RESULTS AND DISCUSSION:

### 3.1. Results

Average scores of the pretest and post-test students' CTS were presented in Figure 1. Table 1 informed the results of the statistical analysis of the pretest score where the significance value (sig. > 0.05) indicates that average scores of the pretest come from populations that were normally distributed and have homogeneous variances. Based on the significance value (sig. > 0.05) on the independent sample t-test results obtained information that there was no difference between average scores of the pretest in the two classes.

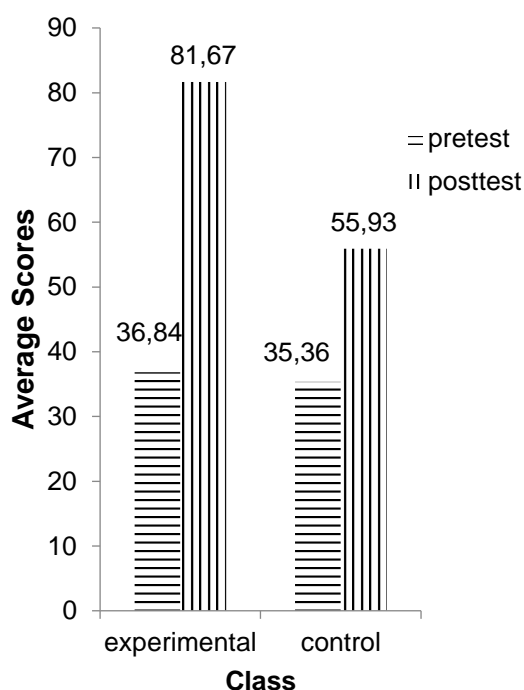


**Figure 1.** The average scores of pretest and post-test students' CTS.

The average n-gain of the experimental and control classes was presented in Figure 2.

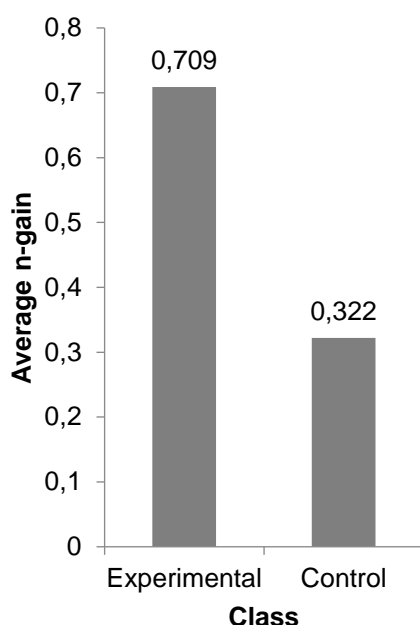


**Figure 2.** The average n-gain students' CTS.

Based on Table 2, normality test results for n-gain indicate that the significance value obtained (sig.) was greater than 0.05. This indicates that the average n-gain of CTS comes from a normally distributed population. One Way ANOVA test results show the significance value obtained was less than 0.05. Thus it could be said that there is a difference between the average n-gain of CTS between the experimental and control classes. Based on the significance value (sig. <0.05) on the independent sample t-test results obtained information that n-gain average of the experimental class was higher than the control class.

### 3.2. Discussion

The above description informs that the PBL model was effective in improving students' CTS compared to conventional learning. Students' CTS were trained at each stage of problem-based learning guided by student worksheets.

#### 3.2.1 Phase 1, Student Orientation to the Problems

At this phase, students were faced with a problem related to hoax information circulating in the community packaged into the discourse. The discourse contains information that instant noodles contain poisons that harm the body. If noodles with iodine drop, they will turn purple. In a different discourse also informed that carbonated water contains acids that can clean the toilet and iron rust. When taken by mouth, the acid content is illustrated will mix and react with gastric acid in

the stomach. This makes people who used to consume both noodles and carbonated water uneasy. Regarding their information and understanding of discourse were presented in Figures 3 and 4 (the authentic source was available in Appendix 2). Based on this, this phase trains students' CTS.

**Q: What information do you know based on the discourse above?**

A: 1) Instant noodles contain free radicals which are proven by changes in color when dipped in iodine solution  
2) Instant noodles are dangerous because they are made from chemicals

**Q: What information do you not know based on the discourse above?**

A: The content of instant noodles

**Figure 3.** Students' understanding of the discourse of the danger of noodles.

**Q: What information do you know based on the discourse above?**

A: 1) Carbonated water are dangerous to consume because they contain acids that can clean iron rust and toilets  
2) Carbonated water added to glasses filled with clear liquid turn into chocolate foam, it is possible the same thing happens in our stomach

**Q: What information do you not know based on the discourse above?**

A: The content of carbonated water

**Figure 4.** Students' understanding of the discourse of the danger of carbonated water.

After students understand the problem critically, students were asked to formulate the main questions critically. Based on discourse, students should first consider the truth of the information. In the 1<sup>st</sup> worksheet, several students wrote question statements that do not fit the content of the discourse. A similar thing happened in the 2<sup>nd</sup> worksheet. Some students were not confident and were doubtful about the formulation of the questions they asked. The following were some of the questions written by students in Figures 5 and 6 (the authentic source was available in Appendix 2).

In learning, the formulation of the main questions raised was not appropriate to the problems listed in the discourse. Related to this, the teacher guided the students to determine the

main question of the air following late to the content of the discourse. Based on the direction was given by the teacher, students improved the statement of question formulation in the 1<sup>st</sup> and 2<sup>nd</sup> worksheets, as shown in Figure 7 and Figure 8 (the authentic source was available in Appendix 2).

#### Question Statement

- 1) Why instant noodles are still being sold in the market?
- 2) Why did the instant noodles dip in iodine solution turn purple?

**Figure 5.** Question statement in the 1<sup>st</sup> worksheet is not appropriate to the content.

#### Question Statement

- 1) Why carbonated water are still being sold in the market?
- 2) Why carbonated water can be used to clean toilets?

**Figure 6.** Question statement in the 2<sup>nd</sup> worksheet is not appropriate to the content.

#### Question Statement

- 1) Is it true that instant noodles are dangerous if consumed?
- 2) What are the ingredients of instant noodles?
- 3) Why do instant noodles turn purple when dipped in an iodine solution?
- 4) What chemicals are contained in instant noodles?
- 5) Do instant noodles contain free radicals?

**Figure 7.** Question statement in the 1<sup>st</sup> worksheet, which has been fixed.

#### Question Statement

- 1) Is it true that carbonated water are harmful to the body?
- 2) Is it true that information that carbonated drinks can be used to clean toilets?
- 3) What are the compositions contained in carbonated water?
- 4) Why carbonated drinks can clean iron rust?
- 5) What acid compounds are contained in carbonated water?

**Figure 8.** Question statement in the 2<sup>nd</sup> worksheet, which has been fixed.

Based on the improvement of the question

statement raised information obtained that students could critically determine the problems that exist in the discourse. Besides, students were increasingly skilled in making questions related to discourse.

In this study, the skills to understand the problems given critically could be said to increase. An increase in skills to understand the problem critically was also supported by student activities in learning. Students were frequently seen asking questions and giving their opinions. Therefore, PBL could increase information literacy, one of which was identifying issues or problems faced (Chu, Tse, and Chow, 2011).

### 3.2.2 Phase 2, Organize Students

To answer the questions that have been asked, students were asked to gather information from various sources relevant to the discourse. In its completion, students were guided by an assignment sheet. There were two activities, namely defining the problem and organizing learning tasks related to discourse, as well as gathering appropriate information so that they can submit hypotheses. Students in groups were given three days to define the problem and collect information along with the source. The same thing was done in the 2<sup>nd</sup> worksheet.

By teacher's guide, students answered the formulation of questions by finding and gathering information related to the problem, including: (1) the content contained in instant noodles and beverage drinks; (2) information about the color changes that occur in instant noodles after dipped in a solution of iodine and pH in carbonated drinks; (3) information about any food ingredients that have a content that is not much different from instant noodles or drinks or solutions that have a pH not much different from carbonated drinks. Through these activities, students were expected to be able to sort out relevant and trusted information in solving problems carefully. Accordingly, this phase trains the skills to gather relevant information. The results of the assignments were presented in Figures 9 and 10 (the authentic source was available in Appendix 2).

During these activities, students were asked to report the results of the task to the teacher periodically. The teacher evaluated the assignment and given direction when there was less relevant information, and the source was not credible. For this advice, students made improvements and obtain information on the 1<sup>st</sup> worksheet, among others: (1) the content

contained in instant noodles, (2) the content contained in the iodine, (3) carbohydrate testing, and (4) the cause of the occurrence discoloration of instant noodles after dipping the solution of iodine. On the other hand, information obtained in the 2<sup>nd</sup> worksheet includes: (1) the content contained in carbonated water, (2) the acidity of carbonated water, (3) buffering solutions in the blood, and (4) metal corrosion.

#### Assignment Sheet

**Q: Find information from various sources regarding the content of instant noodles!**

A: content of instant noodles: carbohydrates, fats, proteins, cholesterol, sodium, vitamins, calcium, iron

**Q: Find information from various sources regarding the color change in iodine-dripped instant noodles!**

A: discoloration of instant noodles that are dropped with iodine indicates carbohydrate content

**Q: Find information from various sources about some food ingredients that have the same content as instant noodles!**

A: rice, bread, corn, potatoes

**Figure 9.** Information obtained by students related to instant noodles.

#### Assignment Sheet

**Q: Find information from various sources regarding the composition of Cola!**

A: content of cola: carbonated water, sugar, caramel coloring, phosphoric acid, caffeine, citric acid

**Q: Find information on the pH of carbonated water!**

A: Carbonated water has a pH = 3

**Q: Find information on types of drinks or solutions whose pH is the same as carbonated water!**

A: lime juice, vinegar, tamarin juice, lemon juice

**Figure 10.** Information obtained by students related to carbonated water.

Based on observations, at first, students still found it difficult to sort out credible and

relevant information, especially if it was connected with chemical material. Most of the students' answers contain general things and not following the learning objectives, as well as information questions about food in the form of macromolecules that are absorbed by the nutritional content, students answer "protein and carbohydrate" without knowing that there are still many nutrients that are absorbed by the body. This might be due to a lack of understanding of problems and questions and accustomed to taking information from web blog sources, news, or literature whose clarity has not been proven.

To overcome this, a discussion was held for 25 minutes, in turn, eight groups consulted about students' answers with the teacher, so that information was obtained following problem-solving. In consultation activities, the teacher directed students' answers to solutions related to chemical materials, and the answers obtained were the nutrient content absorbed by the body, including "glucose, amino acids, vitamins and minerals, and water." To convince students, then the teacher invited students to conduct a literature study on other people's research related to the nutrient content absorbed by the body. This activity could indirectly train students' CTS, especially on indicators considering the credibility of the source.

CTS could be done by figuring out what to believe or what to do and doing it reflectively and reasonably (Ennis, 1990). Therefore, to obtain reliable information, students must conduct investigative activities to obtain appropriate conclusions so that meaningful construction of knowledge does not occur.

#### 3.2.3 Phase 3, Individual and Group Research Guide

In the 1<sup>st</sup> worksheet, an experiment was carried out on a carbohydrate test on several foods with a solution of iodine. Investigation activities require students to be actively involved and train students in their opinions to get explanations and problem-solving. Something that is not much different was done in the 2<sup>nd</sup> worksheet regarding the removal of rust on iron with a solution or drink that has the same pH or almost the same as carbonated water.

Before investigation activities were carried out through experimental activities, students were required to make experimental designs. The intended experimental design includes: (1) identifying variables; (2) controlling variables; (3) compile experimental procedures; (4) identifying

tools and materials used; and (5) design an observation table (Fadiawati and Syamsuri, 2016; 2018). The experimental design was then consulted with the teacher. Based on the direction given by the teacher, students improved the design of the experiment.

Furthermore, students conducted experiments based on the results of experimental designs. In the 1<sup>st</sup> worksheet, students were asked to compare colors in instant noodles before and after dipping in iodine solution. In the 2<sup>nd</sup> worksheet, students were directed and guided to conduct experiments, ranging from measuring the volume of each solution as much as 10 mL, match by using universal indicators, comparing the amount of rust on nails that have been immersed in each solution for 10 minutes. Investigative activities through practicum make the learning process of students more meaningful (Hodson, 1990; Garnett, Garnett and Hacking, 1995; Hofstein and Lunetta, 2004; Hofstein and Mamlok-Naaman, 2007; Abrahams and Millar, 2008).

Faced this situation, students were required to be critical and careful in observing each process and the results obtained during the experiment to be able to conclude precisely and reasonably. On the other hand, through this activity students will get used to working together in groups so that it will foster a disciplined, honest, and thorough attitude in conducting learning activities and group discussions. Diawati *et al.* (2018) suggest that when students are assigned to work on worksheets and undertake learning activities and group discussions, students practice working together between group members to discuss the tasks contained in worksheets. Through this group discussion, students exchange opinions, assess the views of friends regarding problems correctly.

### **3.2.4 Phase 4, Develop and Present the Work**

After conducting an investigation and experiment, students were then asked to develop and present their work in the form of observations during the experiment which are then submitted to the teacher. Furthermore, students wrote the experimental data, answered questions that were challenging related to the experimental data to be able to develop ideas or ideas by linking the results obtained during the experiment with various information that they have obtained from various sources, and reported the solution obtained as a work.

In the initial phases of developing and presenting the results of an experiment, students have not been very active in discussions to

analyze the results of experiments and draw conclusions. To overcome this, the teacher provided guidance and checks the work of students in each group if there are difficulties. At the next meeting, it was seen that students were increasingly actively discussing and even asking critical questions to the teacher. Students' inference skills have improved.

In this condition, when students were assigned to work on a worksheet with their study groups, students practiced being able to work together between group members to discuss the tasks contained in worksheets. Through discussion activities, students exchanged opinions, assess the opinions of friends, or reject or accept the opinions of friends so that they are expected to be able to give the right conclusions. Thus, student activities in doing assignments, working together, and discussing supported the improvement of students' CTS.

Syamsuri and Fadiawati (2019) revealed that inference means identifying and obtaining the elements needed to draw acceptable conclusions. Inference skills can be trained in the stage of developing and presenting work. At this stage students also do information processing to find the linkage of one information with other information, so students can conclude the linkages of that information.

### **3.2.5 Phase 5, Analyze and Evaluate the Problem-Solving Process**

In the last phase, student learning outcomes were evaluated in terms of the material learned and ask each group to communicate their work. In this way, students will be asked and answered on the work between groups to bring up various opinions, or ideas, such as the use of used plastic cups instead of chemical cups. Thus they will be understood the problem more deeply and can be developed ideas more broadly.

Through PBL, students were trained to be able to formulate the main questions. Students were also required to gather the information needed to confirm the truth of information circulating based on discourse. In searching for information, students were trained to choose sources that are relevant and credible, so that the information they get could be trusted, and then students can make inferences (Syamsuri and Fadiawati, 2019). Through investigation activities, students could determine what actions should be taken to confirm the truth of information circulating based on discourse. In presenting the work, could bring up various ideas. Students were also able to

communicate their work to others. With this learning phase, students' CTS could certainly be trained (Dehkordi and Saeed, 2008; Fadiawati, Diawati, and Syamsuri, 2019; Hung and Amida, 2020).

#### 4. CONCLUSIONS:

By using PBL to deal with the circulating hoax information, students look for information from reliable and credible sources, conduct investigations, and use their knowledge and to be analyzed and confirm whether the information can be trusted or not. Additionally, the n-gain value of the experimental class in high categorized, while the n-gain value of the control class in medium categorized. Therefore, it could be said that PBL applied in this research has facilitated and effective in improving students' CTS.

#### 5. REFERENCES:

1. Abrahams, I., and Millar, R. (2008). Does practical work really work? A study of the effectiveness of practical work as a teaching and learning method in school science. *International Journal of Science Education*, 30(14), 1945-1969.
2. Apriyani, T.D., Fadiawati, N., and Syamsuri, M.M.F. (2019). The Effectiveness of Problem-Based Learning on the Hoax Informations to Improve Students' Critical Thinking Skills (Related to Some Foods and Beverages). *International Journal of Chemistry Education Research*, 3(1), 15-22.
3. Baygin, M., Yetis, H., Karakose, M., and Akin, E. (2016, September). An effect analysis of industry 4.0 to higher education. In *2016 15th international conference on information technology based higher education and training (ITHET)* (pp. 1-4). IEEE.
4. Butler, H.A., and Halpern, D.F. (2020). Critical Thinking Impacts Our Everyday Lives. *Critical Thinking in Psychology*, 152.
5. Chu, S.K.W., Tse, S.K., and Chow, K. (2011). Using collaborative teaching and inquiry project-based learning to help primary school students develop information literacy and information skills. *Library and Information Science Research*, 33(2), 132-143.
6. Clement, J. (2020). Global social networks ranked by number of users 2020, Retrived from <https://www.statista.com/statistics/272014/global-social-networks-ranked-by-number-of-users/>, accessed March 28<sup>th</sup>.
7. Creswell, J.W., and Creswell, J.D. (2017). *Research design: Qualitative, quantitative, and mixed methods approaches*. Sage publications.
8. Danczak, S.M., Thompson, C.D., and Overton, T.L. (2020). Development and validation of an instrument to measure undergraduate chemistry students' critical thinking skills. *Chemistry Education Research and Practice*, 21(1), 62-78.
9. Davies, M. (2013). Critical thinking and the disciplines reconsidered. *Higher Education Research and Development*, 32(4), 529-544.
10. Dehkordi, A.H and Saeed, M.H. (2008). The effects of problem-based learning and lecturing on the development of Iranian nursing students' critical thinking. *Pak J Med Sci*, 24(5).
11. Diawati, C., Liliarsari, Setiabudi, A., and Buchari. (2017, May). Students' construction of a simple steam distillation apparatus and development of creative thinking skills: A project-based learning. In *AIP Conference Proceedings* (Vol. 1848, No. 1, p. 030002). AIP Publishing LLC.
12. Diawati, C., Liliarsari, Setiabudi, A. and Buchari. (2018). Using Project-Based Learning to Design, Build, and Test Student-Made Photometer by Measuring the Unknown Concentration of Colored Substances. *Journal of Chemical Education*, 95(3), 468-475.
13. Dwyer, C.P., Hogan, M. J., and Stewart, I. (2014). An integrated critical thinking framework for the 21st century. *Thinking Skills and Creativity*, 12, 43-52.
14. Ennis, R.H. (1990). The extent to which critical thinking is subject-specific: Further clarification. *Educational researcher*, 19(4), 13-16.
15. Facione, P. (1990). *Critical thinking: A statement of expert consensus for purposes of educational assessment and instruction* (The Delphi Report).
16. Fadiawati, N., Diawati, C., and Syamsuri, M.M.F. (2019). Constructing a simple distillation apparatus from used goods by using project-based learning, *Periodico Tchê Química*, 32(2), 207-213.
17. Fadiawati, N. and Syamsuri, M.M.F. (2016).

- Merancang Pembelajaran Kimia di Sekolah. Berbasis Hasil Riset Pengembangan. Yogyakarta: Media Akademi.
18. Fadiawati, N. and Syamsuri, M.M.F. (2018). Perancangan Pembelajaran Kimia. Yogyakarta: Graha Ilmu.
  19. Fogarty, R. (1997). *Problem-based learning and other curriculum models for the multiple intelligences classroom*. South Clearbrook Drive, Arlington Heights: IRI/Skylight Training and Publishing, Inc.
  20. Fraenkel, J. R., Wallen, N. E., and Hyun, H. H. (2011). *How to design and evaluate research in education*. New York: McGraw-Hill Humanities/Social Sciences/Languages.
  21. Garnett, P.J., Garnett, P.J., and Hackling, M.W. (1995). Refocusing the chemistry lab: A case for laboratory-based investigations. *Australian Science Teachers Journal*, 41(2), 26-32.
  22. Gupta, T., Burke, K.A., Mehta, A., and Greenbowe, T.J. (2015). Impact of guided-inquiry-based instruction with a writing and reflection emphasis on chemistry students' critical thinking abilities. *Journal of Chemical Education*, 92(1), 32-38.
  23. Halpern, D.F. (2014). *Critical thinking across the curriculum: A brief edition of thought and knowledge*. Routledge.
  24. Hake, R.R. (1998). Interactive-engagement versus traditional methods: A six-thousand-student survey of mechanics test data for introductory physics courses. *American journal of Physics*, 66(1), 64-74.
  25. Hodson, D. (1990). A critical look at practical work in school science. *School Science Review*, 71(256), 33-40.
  26. Hofstein, A., and Lunetta, V.N. (2004). The laboratory in science education: Foundations for the twenty-first century. *Science education*, 88(1), 28-54.
  27. Hofstein, A., and Mamlok-Naaman, R. (2007). The laboratory in science education: the state of the art. *Chemistry education research and practice*, 8(2), 105-107.
  28. Hung, W., and Amida, A. (2020). Problem-Based Learning in College Science. In *Active Learning in College Science* (pp. 325-339). Springer, Cham.
  29. Indonesian Telematics Society. (2019). *Results of the 2019 National HOAX Outbreak Survey*. Retrived from <https://mastel.id/hasil-survey-wabah-hoax-nasional-2019/> accessed Mei 28<sup>th</sup>.
  30. Kek, M.Y.C.A., and Huijser, H. (2011). The power of problem-based learning in developing critical thinking skills: preparing students for tomorrow's digital futures in today's classrooms. *Higher Education Research and Development*, 30(3), 329-341.
  31. Klein, G.C., and Carney, J.M. (2014). Comprehensive approach to the development of communication and critical thinking: Bookend courses for third-and fourth-year chemistry majors. *Journal of Chemical Education*, 91(10), 1649-1654.
  32. Lowden, K., Hall, S., Elliot, D., and Lewin, J. (2011). *Employers' perceptions of the employability skills of new graduates*. London: Edge Foundation.
  33. Martyn, J., Terwijn, R., Kek, M.Y., and Huijser, H. (2014). Exploring the relationships between teaching, approaches to learning and critical thinking in a problem-based learning foundation nursing course. *Nurse education today*, 34(5), 829-835.
  34. McMillan, J.H. (1987). Enhancing college students' critical thinking: A review of studies. *Research in higher education*, 26(1), 3-29.
  35. Moore, T. (2015). Knowledge, disciplinary and the teaching of critical thinking. *The Routledge International Handbook of Research on Teaching Thinking*, 243-253.
  36. Norris, S.P., and Ennis, R.H. (1989). *Evaluating Critical Thinking*. The Practitioners' Guide to Teaching Thinking Series. Critical Thinking Press and Software, Box 448, Pacific Grove.
  37. Shakirova, D.M. (2007). Technology for the shaping of college students' and upper-grade students' critical thinking. *Russian Education and Society*, 49(9), 42-52.
  38. Stephenson, N.S., and Sadler-McKnight, N. P. (2016). Developing critical thinking skills using the science writing heuristic in the chemistry laboratory. *Chemistry Education Research and Practice*, 17(1), 72-79.
  39. Syamsuri, M.M.F. and Fadiawati, N. (2019). Revealing pre-service chemistry teachers' conceptions of hydrogen atomic orbitals using open-ended tests: a case study in indonesia. *Periódico Tchê Química*, 16(32), 250-256.
  40. Trilling, B., and Fadel, C. (2009). *21st century*



skills: *Learning for life in our times*. John Wiley and Sons.

41. Van den Bergh, V., Mortelmans, D., Spooren, P., Van Petegem, P., Gijbels, D., and Vanthournout, G. (2006). New assessment modes within project-based education-the stakeholders. *Studies in educational evaluation*, 32(4), 345-368.
42. Zuria, F.S., and Suyanto, T. (2018). Kajian keterampilan intelektual mahasiswa UNESA dalam mengenali berita hoax di media sosial. *Kajian Moral dan Kewarganegaraan*, 6(2): 565-580.

**Table 1.** Statistical testing result of average score of the pretest

|                           | Experimental Class | Control Class |
|---------------------------|--------------------|---------------|
| Normality test            |                    |               |
| Kologorov-Smirnov Z       | 0.125              | 0.155         |
| Significance value        | 0.200              | 0.063         |
| Homogeneity test          |                    |               |
| F value                   | 1.059              |               |
| Significance value        | 0.308              |               |
| Independent sample t-test |                    |               |
| t value                   | -0.255             |               |
| Significance value        | 0.800              |               |

**Table 2.** Statistical testing result of average n-gain

|                           | Experimental Class | Control Class |
|---------------------------|--------------------|---------------|
| Normality test            |                    |               |
| Kologorov-Smirnov Z       | 0.138              | 0.104         |
| Significance value        | 0.147              | 0.200         |
| One way ANOVA test        |                    |               |
| F value                   | 114.636            |               |
| Significance value        | 0.000              |               |
| Independent sample t-test |                    |               |
| t value                   | 10.707             |               |
| Significance value        | 0.000              |               |

## APPENDIX 1

### Pretest Questions

#### DISCOURSE 1

Read the following discourse to answer the questions below!

Have you ever seen a viral video on Youtube (<https://www.youtube.com/watch?V=dUGndfBS5Fk>) about an experiment of instant noodles with iodine drop? What will happen after a few minutes? It turns out that instant noodles immediately change color to purple.



The following information is obtained from Facebook (<https://www.facebook.com/91201988700/posts/temanstaukah-kalian-kalau-mie-instan-mandung-radikal-bebas-yang-sangat-berbah/10153784538233701/>) In the news was informed that instant noodles contain free radicals which are very dangerous for the body. This is proven by dipping instant noodles in the iodine solution. The result is a color change in instant noodles to purple. The change in color indicates that instant noodles contain negative toxins derived from chemicals.

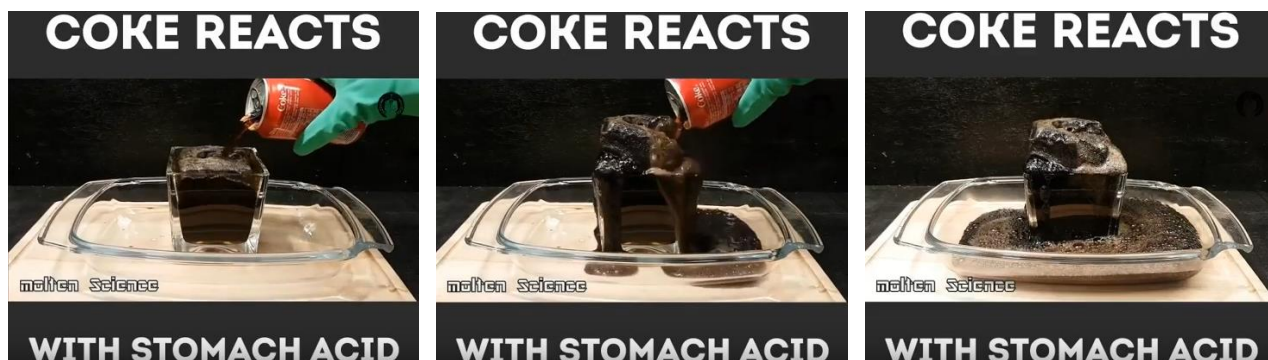
Based on this discourse, answer the following questions!

1. **CTS indicator: understanding the problems critically.**  
Do you believe the information in the discourse above? Explain with reasons!
2. **CTS indicator: making the questions.**  
Ask questions related to the discourse above, regarding:
  - a. main question
  - b. questions besides the main questions
3. **CTS indicator: collecting and considering the pieces of information.**  
What information do you need to answer the questions you ask

#### DISCOURSE 2

Read the following discourse to answer the questions below!

Coke Cola is a carbonated drink that tastes good when thirsty. Almost all people like this drink. But lately, there has been information circulating on social media such as Youtube, Whatsapp, Facebook, Twitter, and Instagram that illustrates the dangers of carbonated drinks when mixed with stomach acid. On social media Youtube (<https://www.youtube.com/watch?v=ISGJkA1T8fY>), a video is displayed when a colorless liquid in a glass container is added with carbonated drinks. When the two are mixed, it turns out to react to form a blackish-brown froth which over time looks solid. The uploader of the video illustrates the same thing would happen if carbonated drinks in the stomach were mixed with gastric acid.



There are also other videos on social media Youtube (<https://www.youtube.com/watch?v=Zj1MXEZ-90M>) that shows the use of carbonated drinks as a toilet cleaner. On social media Youtube ([https://www.youtube.com/watch?v=KYcVJt6\\_cSQ](https://www.youtube.com/watch?v=KYcVJt6_cSQ)) also shows videos related to the use of carbonated drinks to clean iron rust. The use of carbonated beverages as a toilet cleaner and iron rust is associated with the acid content in the drink.



The videos then spread sequentially through Whatsapp, Facebook, Twitter, and Instagram. The distribution of the videos is accompanied by information that illustrates the dangers of carbonated drinks. As a result, many people assume that carbonated cola drinks are very dangerous for the body because they are made from hazardous chemicals.

Based on this discourse, answer the following questions!

4. **CTS indicator: understanding the problems critically.**  
Do you believe the information in the discourse above? Explain with reasons!
5. **CTS indicator: making the questions.**  
Ask questions related to the discourse above, regarding:
  - a. main question
  - b. questions besides the main questions
6. **CTS indicator: collecting and considering the pieces of information.**  
What information do you need to answer the questions you ask

## APPENDIX 2

The authentic source of Figures 3 to 10

### Need to know

1. Informasi apa yang kalian ketahui dari wacana di atas?  
1 mie instan mengandung radikal bebas yang dibuktikan dengan mencelupkan mie kedalam air merah berbedin  
2 mie instan berbahaya karena dibuat dari bahan kimia
2. Informasi apa yang tidak kalian ketahui dari wacana di atas?  
Kandungan mie instan, Benarkah mie instan berbahaya?

Source for Figure 3

### Need to know

1. Informasi apa yang kalian ketahui dari wacana di atas?  
1 minuman berkarbonasi berbahaya dikonsumsi karena mengandung asam yang dapat membersihkan kaku, karat besi  
2 minuman berkarbonasi yang ditambahkan kedalam gelas berisi cairan tak berwarna akan membentuk buih coklat. Hal yg sama terjadi pada labung kita minuman berkarbonasi terbuat dr bahan kimia
2. Informasi apa yang tidak kalian ketahui dari wacana di atas?  
Bahan / kandungan minuman berkarbonasi  
Apakah beritanya sudah benar?  
Bagaimana bisa minuman tersebut membersihkan kaku?

Source for Figure 4

### Pertanyaan

1. Mengapa mie instan masih saja dijual dipasaran?
2. Mengapa mie instan yang dicelupkan kedalam larutan obat merah beriodin berubah menjadi ungu kehitaman?

Source for Figure 5

Setelah kamu membaca dan memahami wacana diatas, ajukanlah pertanyaan mengenai hal yang belum kalian mengerti!

### Pertanyaan

1. Mengapa minuman berkarbonasi masih saja dijual dipasaran?
2. Mengapa minuman berkarbonasi dapat digunakan untuk membersihkan kloset?

Source for Figure 6

### Pertanyaan

1. Apakah benar mie instan berbahaya jika dikonsumsi?
2. Apasaja kandungan komposisi dari mie instan?
3. Mengapa mie instan berubah menjadi berwarna ungu?
4. Bahan kimia apa yang terkandung dalam mie instan?
5. Apakah mie instan mengandung radikal bebas?

Source for Figure 7

### Pertanyaan

1. Apakah minuman berkarbonasi benar berbahaya bagi tubuh manusia?
2. Apakah benar informasi minuman berkarbonasi dapat membersihkan kilet?
3. Apasaja komposisi yang terkandung pada minuman berkarbonasi?
4. Mengapa minuman berkarbonasi dapat membersihkan karat besi?
5. kandungan Asam apa yang terdapat dalam minuman berkarbonasi?

Source for Figure 8

### Lembar Penugasan

1. Carilah informasi dari berbagai sumber mengenai kandungan mie instan !

Kandungan gizi pada mie instan yaitu karbohidrat, lemak, protein, kolesterol, sodium, vitamin A, kalium, zat besi.

2. Carilah informasi dari berbagai sumber mengenai perubahan warna pada mie instan yang diberi larutan obat merah beriodin!

Adanya perubahan warna pada mie instan yang diberi larutan obat merah beriodin menunjukkan adanya kandungan karbohidrat.

3. Carilah informasi dari berbagai sumber mengenai beberapa bahan makanan yang memiliki kandungan yang sama!

- Nasi
- Ruri
- Jengkol
- Kentang

Source for Figure 9

### Lembar Penugasan

Carilah informasi mengenai komposisi dari minuman bersoda jenis *cola* dari berbagai sumber!

Air karbonasi, gula, pewarna karamel,  
Asam fosfat, kafein, asam sitrat,

2. Carilah informasi mengenai pH minuman bersoda!

$\text{pH} = 3$

3. Carilah informasi minuman atau larutan yang memiliki pH sama dengan pH minuman bersoda! Minimal 3 jenis minuman!

- Air Jeruk Nipis
- Asam Cuka
- Air Asam Jawa
- Air lemon

Source for Figure 10

# ANÁLISE DE FÁCIES E ARQUITETURA DE SEQUÊNCIA ESTRATIGRÁFICA EM UMA BACIA DE ARCO TRASEIRO NO IRÃ CENTRAL: UM ESTUDO DE CASO DO MIOCENO INICIAL DA FORMAÇÃO QOM

## FACIES ANALYSIS AND STRATIGRAPHIC SEQUENCE ARCHITECTURE IN A BACK-ARC BASIN IN CENTRAL IRAN: A CASE STUDY FROM THE EARLY MIOCENE OF THE QOM FORMATION

آنالیز رخساره‌ای و چارچوب چین‌نگاری سکانسی سازند قم با سن اوایل میوسن در حوضه پشت کمانی واقع در ایران مرکزی

HASSANZADEH, Sara<sup>1\*</sup>; ADABI, Mohammad Hossein<sup>2</sup>; KOHANSAL GHADIMVAND, Nader<sup>1</sup>; JALALI, Mahmood<sup>3</sup>; ARIAN, Mohammad Ali<sup>4</sup>.

<sup>1,4</sup> Islamic Azad University, North Tehran Branch, Faculty of Science, Department of Geology, Tehran, Iran

<sup>2</sup> Shahid Beheshti University, Faculty of Earth Science, Department of Sedimentary basins and Petroleum, Tehran, Iran

<sup>3</sup> National Iranian Oil Company, Exploration Directorate, Tehran, Iran

\* Corresponding author  
e-mail: m-adabi@sbu.ac.ir

Received 22 February 2020; received in revised form 11 May 2020; accepted 14 June 2020

### RESUMO

Os depósitos marinhos da Formação Qom, que é um importante reservatório de gás no Irã Central com a idade do Oligoceno Inicial ao Mioceno Inicial, são estudados para determinar fácies, paleoambiente sedimentar e seqüências deposicionais. A litologia primária é o calcário, que é acompanhado por um conglomerado, marga arenosa, marga e calcário arenoso. Com base no conteúdo siliciclástico, na análise textural e nos constituintes bióticos, dez fácies foram identificadas. Essas fácies pertencem a cinco locais deposicionais, incluindo delta, enseada de maré, lagoa, cardume e mar aberto. De acordo com a ausência de recifes de barreira contínuos e grandes, variação vertical gradual das fácies do ambiente de transição (delta) para o mar aberto raso, a ausência de grãos oncoídes, pisóides e agregados que estão principalmente presentes em ambientes com prateleiras de carbonato com aros, a ausência de calciturbiditos e estruturas de queda e deslizamento, a Formação Qom foi depositada em uma rampa homoclinal (rampa interna, média e externa). Estudos de campo e arquitetura de variação vertical de fácies no âmbito de sistemas deposicionais levaram ao reconhecimento de duas seqüências deposicionais de 3ª ordem no tempo do Mioceno Primitivo (Aquitânico). Fácies sedimentares na Formação Qom que ocorreram principalmente no meio da rampa revelam um padrão de empilhamento principalmente agregado nas seqüências deposicionais. A arquitetura estratigráfica das seqüências do Mioceno Primitivo da Formação Qom, com base em gráficos de correlação, é semelhante às seqüências regionais da placa da Arábia e da bacia de Zagros.

**Palavras-chave:** *Facies, Paleoambiente sedimentar, Estratigrafia de seqüências, Aquitânico, Formação Qom*

### ABSTRACT

Marine deposits of the Qom Formation, which is an important gas reservoir in Central Iran with the age of Early Oligocene to Early Miocene, is studied to determine facies, sedimentary paleoenvironment, and depositional sequences. The primary lithology is limestone, which is accompanied by a conglomerate, sandy marl, marl, and sandy limestone. Based on siliciclastic content, textural analysis, and the biotic constituents, ten facies have been identified. These facies belong to five depositional settings, including delta, a tidal inlet, lagoon, shoal, and open marine. According to the absence of continuous and large barrier reefs, gradual vertical variation in facies from the transitional environment (delta) to shallow open marine, the absence of oncoid, pisoid and aggregate grains that are mostly present in rimmed carbonate shelf environments, the absence of calciturbidites and slump and slide structures, the Qom Formation has been deposited in a homoclinal ramp setting (inner, middle and outer ramp). Field studies and vertical facies variation architecture in the framework of depositional system tracts led to the recognition of two 3rd order depositional sequences in the Early Miocene (Aquitanian) time. Sedimentary

facies in the Qom Formation that mainly occurred in the middle ramp setting reveal a mostly aggradational stacking pattern in depositional sequences. The Early Miocene sequences stratigraphic architecture of the Qom Formation based on correlation charts are similar to the regional sequences of the Arabian plate and Zagros basin.

**Keywords:** *Facies, Sedimentary paleoenvironment, Sequence stratigraphy, Aquitanian, Qom Formation*

## چکیده

نهشته‌های دریایی سازند قم به سن اوایل الیگوسن تا اوایل میوسن که یک مخزن گازی بزرگ در ایران مرکزی را تشکیل می‌دهد به منظور تعیین رخساره‌ها، محیط رسوبی دیرینه و چینه‌نگاری سکانشی مورد مطالعه قرار گرفت است. سنگ‌شناسی اصلی در این رخنمون‌ها شامل سنگ آهک است که با لایه‌هایی از کنگلومرا، مارن، مارن ماسه‌ای و سنگ آهک ماسه‌ای همراه است. در منطقه مورد مطالعه بر اساس میزان مواد تخریبی ورودی به حوضه، آنالیز بافت رسوبی و محتوای فسیلی ده رخساره شناسایی گردید. این رخساره‌ها در پنج جایگاه نهشته‌ای شامل دلتا، تاییدال اینلت، لاگون، شول و دریای باز نهشته شده‌اند. شواهدی نظیر عدم حضور ریف‌های سدی بزرگ و فاقد تداوم جانبی، تغییرات تدریجی رخساره‌ها در جهت قائم از محیط انتقالی (دلتا) تا دریای باز، عدم حضور دانه‌های آنکوئیدی، پیژوئیدی و دانه‌های اگرگاتی که خاص شلف‌های کربناته بوده و با به ندرت در رمپ‌ها یافت می‌شوند و در نهایت عدم مشاهده کلسی‌توربیدایت‌ها و ساختارهای ریزشی و لغزشی، تاییدی بر نهشت سازند قم در منطقه مورد مطالعه در یک پلاتفرم رمپ هموکلینال از رمپ داخلی تا رمپ میانی و خارجی است. مطالعات صحرایی به همراه نحوه تغییرات رخساره‌ها در چارچوب سیستم تراکت‌های نهشته منجر به شناسایی دو سکانش رسوبی درجه سوم به سن اکتانین در سازند قم گردید. الگوی برانبارش جمعی در سکانش‌های نهشته سازند قم که رخساره‌های رسوبی در آن به طور عمده در محیط رمپ میانی نهشته شده‌اند، غالب است. سکانش‌های نهشته سازند قم به سن اکتانین در برش‌های مورد بررسی دارای مطابقت بالایی با سکانش‌های رسوبی شناسایی شده در حوضه زاگرس و پلیت عربی با سن مشابه است.

**کلیدواژه‌ها:** رخساره، محیط رسوبی دیرینه، چینه‌نگاری سکانشی، اکتانین، سازند قم

## 1. INTRODUCTION:

Tectonic activities cause the on-going volcanism during the Late Eocene in Central Iran. These activities led to a regional unconformity in the base of Oligocene deposits (Stocklin and Setudehnia, 1991). This unconformity is overlain by evaporitic and siliciclastic deposits of the Lower Red Formation formed by Late Eocene and Early Oligocene epirogenic movements in Central Iran. Following these marine deposits of the Qom Formation, which is a crucial gas reservoir in Central Iran, is formed with raising of sea-level and a transgression in the Early Oligocene Sea, which lasts till the Early Miocene (Dozy, 1955). The Qom Formation marl, limestone, and siliciclastic rocks have been overlain and underlain with an unconformity by continental deposits of the Lower Red and Upper Red formations, respectively (Stocklin and Setudehnia, 1991; Reuter *et al.*, 2009). The well-known fractured reservoir of the Asmari Formation is isochronous with the Qom Formation (Motiea, 1993).

No type section has been introduced for the Qom Formation, but a type area has been defined for this formation in the Qom Plain in Central Iran microplate (Aghanabati, 2011). In Central Iran, the Qom Formation is deposited with variation in lithostratigraphy, biozone, and microfacies characteristics. The Qom Formation is Oligocene-Miocene in age, based on larger benthic foraminifera biostratigraphy by Yazdi-Moghaddam (2011).

A stratigraphic sequence correlation

between the Qom Formation succession and its comparison with isochronous formations in adjacent areas can explain the depositional model and transgression of the Tethyan Seaway in Central Iran. Since the Qom Formation is a gas reservoir formed in a back-arc basin, this study can help to understand the characteristics of these deposits in the Middle East.

Biostratigraphy of the Qom Formation in this study has been reported as the Lower Eocene age (Aquitanian) by Maghfoori-Moghaddam and Yasboulaghi (2015). The purpose of this research is to describe the depositional setting of the Qom Formation, sequence stratigraphy, and its correlation with the Oligocene-Miocene Asmari Formation in the Zagros Basin.

## 2. GEOLOGICAL SETTING AND LOCATION OF THE STUDY AREA:

The final collision of the African-Arabian Plate with the Iranian plate, which began in the Mesozoic, formed the microplate of Central Iran (Coleman-Sadd, 1982). The closure of the Neotethys during the Miocene time was the result of the collision of these plates (Harzhauser and Piller 2007, Reuter *et al.*, 2009). This collision has also formed the Sanandaj–Sirjan Basin (a fore-arc basin), Urumieh–Dokhtar magmatic arc (an intra-arc basin), and the Qom Basin (a back-arc basin) as a result of the Zagros oceanic crust (Neotethys) and southwestern Iranian cratonic plate subduction at the north-eastern margin of the Neotethys on the Iranian Plate (Figure 1a). A



volcanic arc system that developed during the Eocene series has separated these basins (Stocklin and Setudehina, 1991). Thus, during the Late Oligocene-Early Miocene, the Qom Formation was deposited in this back-arc basin in the central and northern part of the central Iran microplate (Berberian, 1983). The age, thickness, and lithology of the Qom Formation vary in different sections. These are caused respectively by (1) marine transgression of the Neoethys in the Iranian Plate started from the southeast and continued northwestward gradually, and (2) various positions of the Qom Formation within the Qom back-arc basin (Schuster and Wielandt 1999). Furthermore, the thickness and lithofacies variations seen within the Qom Formation may have controlled regional faults and subsidence and uplift in the Qom basin (Nogol-e-Sadat, 1985).

In this research, two sections have been investigated in the northwestern margin of the back-arc basin of the Qom Basin in Markazi Province. The study sections include Ashtiyan and Kordijan, which are located in north and northeast of Ashtiyan, about 67 km north of Arak City in central Iran (Figure 1b). The Ashtiyan section at the geographic location of 34°32'45"N and 50°01'18"E and the Kordijan section occurred at 34°38'09"N and 50°07'23"E are examined in detail for sedimentological investigation. In these sections, thick to medium and thin-bedded limestone with a few argillaceous limestone beds and marl formed the main lithologies. Some units consist of conglomerate, sandy marl, and sandy limestone that are minor lithologies. In both sections, the Qom Formation is unconformably underlain by the Oligocene Lower Red Formation and overlain by the Miocene Upper Red Formation (Figure 1c and Figure 2).

### 3. MATERIALS AND METHODS:

The complete sections of the Qom Formation in Ashtiyan and Kordijan were measured and sampled in the Ashtiyan area in north of Markazi Province. In the Kordijan section, with a thickness of 94 m, thirty-four samples have been collected. The thickness of the Ashtiyan section is 103 m, and 25 samples have been studied. The classification of the carbonate rocks is based on Dunhan (1962). The siliciclastic rocks follow the nomenclature of Folk (1980). The composition percentage of allochems in sedimentary rocks is based on the Bacelle and Bosellini (1965) visual diagrams. Samples are stained by potassium ferricyanide and alizarin red-s to distinguish carbonate minerals (Dickson, 1965). Facies classification and their

environmental interpretation are based on textural features, fabric, and biota content following Read (1985), Burchette and Wright (1992), Wright and Burchette (1996), and Flugel (2010). The construction of sequence stratigraphy is based on the environmental changes across limiting surfaces, the landward or seaward stepping following Catuneanu (2006), Catuneanu *et al.* (2009), and Catuneanu (2017).

## 4. RESULTS AND DISCUSSION:

### 4.1. Facies Analysis

Ten different carbonate and siliciclastic facies were identified from the Qom Formation in the studied sections. This facies were divided into five facies belts, representing the main depositional paleoenvironments, including delta, tidal inlet, lagoon, shoal, and open marine. The facies have been differentiated based on the sedimentological and paleontological criteria. The general setting is interpreted to be a carbonate ramp system, subdivided into inner, middle, and outer ramp settings following the terminology of Burchette and Wright (1992). Vertical distribution of textures and the identified facies and their relevant paleoenvironment along with sequence stratigraphic architecture of the Qom Formation in the both studied sections are shown in Figure 3.

### 4.2. Deltaic facies (transitional)

#### 4.2.1 F1: Conglomerate

Conglomerate facies at the base of the Qom Formation in both sections have been seen as massive beds. Carbonate cement is predominant between grains in nearly all samples. Particles vary in size from small sand-size to pebble (<64 mm) — silt and tiny sand-size form the matrix. The particles are sandstone, shale, and limestone fragments, which form a poorly to moderate-sorted and mostly subrounded to angular polymictic conglomerate up to 2-5 m thick. This facies has seen heterogeneous mass with reddish in color (Figures 4a and 4b).

Interpretation: The poorly sorted matrix-supported conglomerates which form coarsening-upwards cycles are attributed to the accumulation of clasts in deltaic environments (Martini *et al.*, 2017; Arp *et al.*, 2019). The mostly red color of the matrix shows the oxic condition in time of deposition. Sedimentological characteristics include graded bedding (coarsening upward), the red color of texture, sand to pebble size of particles with angular to semi-rounded clasts, and its

vertical and lateral changes to carbonate facies reveal high-energy water with high bedload in a deltaic environment system. The source of sediments is from nearby highs of Lower Red Formation that surrounded the Qom back-arc basin and have transported to the basin by river channels along with a short distance. The rounding and sorting associated with this conglomerate and the lithology of the conglomerate features will confirm the short distance and the nearby source rock.

#### 4.3. Tidal inlet facies (inner ramp)

##### 4.3.1 F2: *Bioclastic hybrid arenite*

This facies includes bioclastic carbonate up to 20 percent — the bio-clasts consist of echinoid, brachiopod, operculina, and bryozoan. The matrix is made of carbonate mud, which dolomitized in some portions. Monocrystalline and less polycrystalline quartz grains, which are silt to medium sand in size, formed the major detrital particles. This facies consists of a poorly to well sorted with angular to semi-rounded grains (Figures 4c and 4d).

Interpretation: The bioclastic hybrid arenite is a typical facies in mixed carbonate-siliciclastic environments that their framework is made of detrital clasts. The 'arenite' term suggested for rocks consisting of more than 50 percent detrital clasts that accompanied by carbonate clasts (Zuffa, 1985). Deposition of such facies took place in an attached onshore carbonate platform setting with remarkable nearby high topography that transported a large volume of siliciclastic material into the basin (Friedman and Sanders, 1978; Flugel, 2010; Sengupta, 2017). According to sedimentological characteristics such as open marine bioclasts and stratigraphic position adjacent to carbonate shoal, the depositional setting could be tidal inlet that connected the continental area to the ocean and also channels that transported siliciclastic material from delta to the open marine. The large volume of siliciclastic material confirms the deposition of this facies in a short distance to the source rock and as channels connecting the open marine to the shoreline (Flugel, 2010). The channels are maintained by tidal flow; the presence of open marine biota with siliciclastic material confirms this statement.

#### 4.4. Lagoonal facies (inner ramp)

##### 4.4.1 F3: *Bioclast miliolid packstone*

Despite the packstone fabric, the biotic

variations are low, and the constituents include different species of Miliolidae such as *Quinqueloculina* sp., *Pyrgo* sp., *Triloculina* sp., and *Miliola* sp. echinoid, red algae, bryozoan, and bivalve forms the minor features by <10%. Silt size quartz grains are present by 2-5%. This facies shows medium sorting and rounding and only seen in the Kordijan section (Figure 5a).

Interpretation: Miliolid is predominant in a restricted lagoonal environment (Geel, 2000). Recently, most of the porcelaneous benthic foraminifera live in shallow tropical and sub-tropical environments (Lee, 1990; BouDagher-Fadel, 2008; Benedetti and Frezza, 2016). Thus, this facies deposited in a nearly restricted lagoonal setting above the fair-weather wave base (FWWB). The restricted condition can be confirmed by a low distribution of normal marine biota, low variation of foraminifera, and the predominance of porcelaneous foraminifera. The predominance of porcelaneous foraminifera has also revealed waters with high salinity (Read, 1985; Flugel, 2010).

#### 4.5. Bioclastic shoal (inner ramp)

##### 4.5.1 F4: *Bioclast, red algae rudstone/grainstone*

Sparry calcite cement, including blocky and poikilotopic cement, formed the texture. The major biotic constituents are red algal species such as *Lithophyllum* sp. and *Lithothamnium* sp. with 20-30% in abundance and larger than 2 mm in size. Other major biota include echinoid with overgrowth cement, rotalia, bryozoan, and large fragments of bivalves. Gastropod, miliolid, brachiopod spin, and unknown fragments of hyaline benthic foraminifera form the minor biota. Silt, and small and medium-size quartz grains with 5-7% in abundance form the siliciclastic features. All the features in a sparry texture show medium to good sorting and low to medium roundness (Figure 5b).

Interpretation: According to the abundance and large size of the red algae, it seems that these biota have been deposited in the nearest place to their habitat. The best condition for red algae growth is an environment with high nutrition, sufficient oxygen, the wave energy to provide these materials, and a depth of water where appropriate light can penetrate (Bassi, 2005; Halfar and Mutti, 2005). Textural characteristics, including the absence of micrite, sparry cement between the constituent along with specific sorting and rounding, reveal an environment with medium to high wave energy. Thus, based on the biota and sedimentological characteristics, this facies is

deposited in a bioclastic shoal setting above FWFB in the inner ramp.

#### 4.6. Open marine facies (middle ramp)

##### 4.6.1 F5: *Echinoid, bryozoan, red algal packstone/rudstone*

This texture has mainly seen as packstone and occasionally with large size red algae bearing biotic constituents as rudstone. The major biota with 30-40% in abundance are bryozoan (0.5-2 mm in size) and *Lithophyllum* sp. and *Lithothamnium* sp. (both 5 mm to larger than 10 mm in size). Miliolid is present with 3-5% in abundance. The minor biota consists of gastropod, rotalia, brachiopod, and worm tubes. Small to medium sand-size quartz grains are present with 5-10% in abundance. The texture has partly dolomitized or filled by sparry calcite cement (Figure 5c).

Interpretation: high abundance and large size of red algae, partly presence of sparry calcite cement between biota, and the presence of dispersed fragments of benthic foraminifera and rotalia can confirm its proximity to the reef assemblages of the bioclastic carbonate shoal. The predominance of carbonate mud in texture along with oligo-photoc biota such as miliolid, and the predominance of photic dependent biota such as red algal species that is also able to grow and develop in oligo-photoc condition indicating the shallowest open marine facies adjacent to carbonate shoal, with high to medium wave energy (Halfar and Mutti, 2005; Barattolo *et al.*, 2007; Brandano *et al.*, 2009). Thus, this facies based on the presence of photic dependent and independent biota is deposited in waters with normal salinity below FWFB in the middle ramp and adjacent to carbonate shoal.

##### 4.6.2 F6: *Bioclast, nummulitids, operculina wackestone*

The major biotic constituents consist of operculina and nummulites. Echinoid, red algae, brachiopods, bryozoan, and occasionally rotalia form the minor biota in this facies carbonate micrite dolomitized in some parts of the texture. The frequency of quartz grains are 20-30% and vary in size from fine to medium sand (Figure 5d). Interpretation: The predominance of larger benthic foraminifera with a low diameter-thickness (D/T) ratio shows relatively shallow parts of open marine with oligophotic conditions (Geel 2000; Bassi *et al.* 2007). Also, light penetration decrease in the depositional environment reveals by stretched forms of larger benthic foraminifera with low

diameter-thickness (D/T) ratio (Nebelsick *et al.*, 2005; Bassi *et al.* 2007; Khatibi-Mehr and Adabi 2014). Thus, larger benthic foraminifera as the major biota along with echinoid and bryozoan in carbonate mud texture can demonstrate medium to low energy open marine environment between fair-weather wave base (FWFB) and storm wave base (SWB) in the middle ramp (Flügel 2010; Adabi *et al.*, 2016).

##### 4.6.3 F7: *Red algae, bryozoan, brachiopod packstone/rudstone*

The main biotic constituents are brachiopod, bryozoan, and some echinoid fragments. Red algal fragments show low frequency. Rotalia and miliolid forms minor biota. Small to medium sand-size quartz grains with 5-10% in abundance are dispersed within the matrix. Dolomitization occurred in some parts of the micritic matrix (Figure 5e).

Interpretation: Bryozoan assemblages are common in calm and low energy waters of shallow open marine. Although they are photic independent heterotroph organisms and found independently of water depth (Pomar, 2001; Drinia *et al.*, 2009), nonetheless, the presence of red algae as the main biota with high frequency reveals shallow parts of open marine. A high abundance of red algal fragments defines waters with sufficient light and relatively high energy in front of carbonate shoal (Pomar, 2001). In this facies, the biotic constituents suggest calm and low to relatively medium energy waters with normal salinity. The medium sand-size of red algal fragments and their medium roundness can be indicative of much more movement with greater distance (Perrin, 1995; Brandano *et al.*, 2009). Thus, based on all textural and biotic pieces of evidence, this facies was deposited in low energy open marine setting in middle ramp above SWB.

##### 4.6.4 F8: *Echinoid, bryozoan, brachiopod wackestone/floatstone*

This texture reveals as wackestone but in a few samples contain bryozoan and brachiopod, larger than 2 mm and even centimeter in size that are floating in a mud matrix reveal as floatstone. The major biota are echinoid, bryozoan, and brachiopod. Small benthic foraminifera such as miliolid is rarely present. Ostracod and unknown micritized biota (peloid) has also present. The frequency of quartz grains is 1-5%, which varies in size from small to coarse sand (Figure 5f).

Interpretation: Echinoid as the main biota has been deposited in relatively deep waters of

open marine in the middle ramp (Barattolo *et al.*, 2007). All the main biota in these facies including bryozoan and brachiopod are photic independent biota and can deposit in relatively deeper parts of open marine settings. Furthermore, these biota are stenohaline and indicators of waters with normal salinity (Holcová and Zágöršek, 2008; Drinia *et al.*, 2009). The low variety and well-preserved coarse grain biotic features, along with the predominance of carbonate mud suggest a low energy depositional environment. The main biotic constituents such as brachiopod, bryozoan, and echinoid with low biotic abundances suggest lower parts of the middle ramp, adjacent and above SWB with limited water circulation.

#### 4.7. Open marine facies (outer ramp)

##### 4.7.1 F9: Sandy mudstone

This facies mainly consists of carbonate mud deposits. Silt and small sand-size quartz grains are scattered through the matrix with a 10-20% frequency. Glauconite is observed with minor amounts. Unknown shell fragments have also been present. This facies in hand specimen is dark cream to light gray. Pyritization occurred in the matrix (Figure 5g).

Interpretation: During a sea-level rising or subsidence in a sedimentary basin, carbonate deposits are drowned, and deep water limy mud is dominant (Tucker and Wright, 2009). All evidence including the presence of glauconite, pyritization, and dark color of this facies in both microscopically and hand specimen suggest that deposition took place in low energy and anoxic waters of open marine in an outer ramp setting below SWB.

##### 4.7.2 F10: Shaly mudstone

Shaly mudstone facies includes the marl lithology interval of the Qom Formation in the Kordijan section. The rocks showing these facies are microscopically light gray, and in hand specimen is gray. Silt size quartz grains are scattered within the matrix in a minor amount. Shaly mudstone facies are completely homogenous, and no biota or shell fragments have been observed (Figure 5h).

Interpretation: During the sea-level rise, mudstone and shale can be formed in deep waters of open marine settings. The lime and clay that formed the shaly mudstone occur as suspended and will precipitate in a low energy marine environment. Thus, according to their stratigraphic position, which is taking place above open marine

limestone strata, they have deposited in a low energy condition below SWB in an outer ramp setting. This facies belongs to relatively deep waters with no biotic fragments, and due to its distance from land and the source area, there are no siliciclastic materials.

The description and characteristics of the identified sedimentary facies, as well as facies associations and some of their main features recognized within the studied sections, are summarized in Table 1.

#### 4.8. Sedimentary Environment

Due to the specific characteristics of the Qom Basin and its widespread in microplate of Central Iran along with high facies variation, thickness, and back-arc geometry, a distinct sedimentary model for different parts of Iran, is impossible. Based on sedimentological and biological data in surface and subsurface sections, different sedimentary models are suggested for deposition of the Qom Formation by many researchers, e.g. a homoclinal ramp by Reuter *et al.* (2007), Saddighi *et al.* (2012) and Amirshahkarami and Karavan (2015) in Qom Province and Esfahan-Sirjan region. However, a rimmed shelf by Vaziri-Moghaddam and Torabi (2004), and a non-rimmed shelf by Mohamadi *et al.* (2011) have also been proposed.

The factors controlling the rate and type of carbonate production are nutrient, light, temperature, salinity, water depth, and chemistry. These factors, along with geological setting, control the carbonate platform geometry and determine the grain type, grain distribution, and the rate of carbonate factory (Brandano *et al.*, 2009).

Facies analysis based on lithology, sedimentary structures, texture, and biotic and abiotic features from the studied sections of the Qom Formation led to the recognition of ten facies deposited in five subenvironments, including delta, a tidal inlet, lagoon, shoal, and open marine. Palaeoenvironmental reconstruction based on the identified facies suggests a homoclinal carbonate ramp for the Qom Formation in the studied area (Figure 6). This suggestion is supported by some evidence including the absence of continuous and large barrier reefs, gradual variation in facies from delta to shallow open marine, the absence of calciturbidites, and slump and slide structures, and lack of oncoid, pisoid and aggregate grains that are mostly present in rimmed carbonate shelf environments. Burchette and Wright (1992) divided a carbonate ramp into an inner ramp

(above FWWB), middle ramp (between FWWB and SWB), and outer ramp (below SWB). Sedimentary facies in the Qom Formation mainly occurs in the middle ramp setting.

The inner ramp includes delta, tidal flat, lagoon, and shoal facies respectively recognized by occurrence of coarsening upward massive polymictic conglomerate (F1, delta), bioclastic hybrid arenite including high sand and open marine biota (F2, tidal flat), porcelaneous foraminifera in a carbonate mud matrix (F3, lagoon), and abundance of red algae accompanied by open marine biota and siliciclastic sediments in a sparry texture (F4, shoal).

The middle ramp consists of four facies from proximal (adjacent to shoal) to distal (adjacent to SWB) part. The middle ramp in the proximal part is characterized by larger benthic foraminifera (e.g. operculum and nummulitids), and shoal derived bioclasts such as red algae in a packstone and rudstone texture (F5-6). The distal parts of the middle ramp include mainly photic independent heterotroph and stenohaline organisms (such as bryozoan and echinoids) that are indicators of normal salinity waters of open marine (Drinia *et al.*, 2009).

The outer ramp is characterized by sandy and shaly mudstone with pyritization in the matrix that is evidence of relatively deep waters with anoxic condition and small unknown shell fragments and glauconite (F9-10).

#### 4.9. Sequence Stratigraphy

A stratigraphic sequence model defines depositional sequences as genetically related chronostratigraphic units that are representative of a single cycle of relative sea-level rise and fall, bounded by unconformity surfaces (e.g. Posamentier and Vail, 1988; Van Wagoner *et al.*, 1990; Posamentier and James 1993; Catuneanu *et al.*, 2006). Retrogradational, aggradational, and progradational stacking patterns in the framework of a depositional sequence are developed due to eustatic sea-level fluctuations.

The stratigraphic sequence interpretation that is proposed for the Qom Formation is based on age, field description, and the broad paleoenvironmental inferences revealed by facies analysis and stacking patterns of facies (Figure 3). In the carbonate platform of the Qom Formation with predominant of warm climate, which is Early Miocene (Aquitania) in age, the sequence boundaries are characterized by siliciclastic facies

(delta and tidal inlet). The depositional sequences consist of three systems tracts, including lowstand system tract (LST), transgressive system tract (TST), and highstand system tract (HST). Each sequence comprises complex facies of subtidal, including lagoon, shoal, and open marine, which covered by siliciclastic facies. The maximum flooding surface (F9-10) is characterized by water deepening and the maximum transgressive in seawater, which is defined by outer ramp facies association. Vertical facies variations and identified environments connected with relative sea-level changes led to the identification of two third-order depositional sequences in the Qom Formation (Figure 3).

##### 4.9.1 Depositional sequence 1 (DS1)

The depositional sequence 1 with the age of Aquitania is 70.75m and 58.07m thick, respectively, in Kordijan and Ashtian sections. The DS1 is divided into LST, TST, and HST. The delta massive conglomerate beds of F1, which is a transitional environment, formed the basal part of DS1. The enormous conglomerate in both sections is deposited over the sandstone beds of the Oligocene Lower Red Formation (Figure 3). The basal deltaic conglomerate with a coarsening upward sequence has been deposited during the period of falling sea level as an LST. The overlying carbonate rocks with shoal and middle ramp facies association of F4 (shoal), F5, F7, and F8 (all open marine: middle ramp) have been deposited during the period of sea-level rise and are interpreted as transgressive system tract (TST) with retrogradational stacking pattern. The TST is characterized by packstone, grainstone, rudstone, and floatstone textures with normal waters biota such as rotalia, red algae, bryozoan, and Echinoidea. The photic independent of open marine biota reveals a rise in sea level that reaches the maximum, equivalent to the maximum flooding surface (MFS). The sandy and shaly mudstone of the F9 and F10 with glauconite and shell fragments and pyritization in matrix characterize the MFS. The main packstone and rudstone textures of the lagoon (F3), shoal (F4), and open marine (proximal middle ramp facies association: F5-6) with mainly aggradational and a few progradational stacking pattern that overlies the MFS characterize the HST. The upper part of the HST is characterized by bioclast hybrid arenite (F2) in both sections and indicate the tidal inlet environment and a type 2 sequence boundary (SB2).

##### 4.9.2 Depositional sequence 2 (DS2)

The depositional sequence 2 is 23.75m thick in the Kordijan section and 43.92m thick in the Ashtian section with the age of Aquitanian. The DS2 can be subdivided into TST and HST (Figure 3). The carbonate rocks of middle ramp facies association (F5-7) with retrogradational stacking patterns are formed during a period of sea-level rise and are interpreted as transgressive deposits of TST (Figure 3). The facies of TST (F5-7) consist of larger benthic foraminifera such as Nummulitidae and Operculina as well as red algae, brachiopod and bryozoan. Large fragments of bryozoan and brachiopod along with Nummulitidae and broad and flat operculina, larger than 2mm in size with rudstone texture, are terminated in outer ramp facies association (F9-10) with evidence of low energy and anoxic condition of relatively deep waters. These facies indicate a maximum increase in sea-level changes, equivalent to the MFS. The mostly packstone and rudstone textures of shoal and proximal middle ramp facies association with dominant of benthic foraminifera (e.g. rotalia) and red algae are overlain by the MFS. These sediments are interpreted as deposition of the HST with a progradational stacking pattern (Figure 3). The upper part of the HST is characterized by bioclast hybrid arenite (F2: tidal inlet) in the Ashtian section and bioclast, red algae rudstone/grainstone (F4: shoal) in the Kordijan section indicating tidal inlet and shoal environments. The Upper Red Formation of Miocene age overlies the DS2 in both sections. There is a type 1 sequence boundary (SB1) between the Qom Formation and the Upper Red Formation.

#### 4.10. Correlation of Depositional Sequences

Precipitation of carbonate sediments is influenced by subsidence and sedimentation rate that are related to the tectonic evolution of the belts that surrounded the Qom back-arc basin. The Oligocene-Miocene sedimentary rocks of the Qom Formation in microplate of Central Iran have some similarities with the Oligocene-Miocene sedimentary deposits of the Asmari Formation in the Zagros Basin and the equivalent formations in the Arabian Plate. For instance, the biotic constituents are the same, and the sedimentary paleoenvironments are a homoclinal ramp system; however, according to the geological setting these basins have not been connected during the Early Miocene. Sharland *et al.* (2001, 2004) and Simmons *et al.* (2007) in Arabian Plate have defined a set of regional maximum flooding surfaces (MFS). They have used MFS for

subdividing the sedimentary succession of the Arabian Plate into a series of synchronous packages. These packages, which are genetic stratigraphic sequences (Galloway, 1989) took place within a set of Tectonostratigraphic Megasequences (TMS) that subdivide the geological history of the Arabian Plate from Precambrian to the Present. These TMS are defined as the package of sediments lying between the unconformity marking both the onset of Red Sea Rifting and the first continental collision between Arabia and Eurasia and the present-day topographic surface. The Qom Formation with the age of Oligocene–Miocene sits within the latest of the TMS (AP11), which is defined as sedimentary packages that took place between two signs of unconformity (Sharland *et al.*, 2001, 2004). The correlative sequence boundaries between Sharland *et al.* (2001, 2004), Simmons *et al.* (2007) and this study with increasing age are as following (Figure 7):

1. The Ng20 SB is equal to the type 1 SB at the top of DS2.
2. The Ng10 SB is equal to type 1 SB at the base of DS1.

The previous sequence stratigraphic studies on Oligo-Miocene deposits of the Zagros Basin include Ehrenberg *et al.* (2007) and Van Buchem *et al.* (2010). In their studies of the Oligo-Miocene Asmari Formation in Dezful Embayment and Izeh zone located in the southwest of Iran defined seven sequence surfaces that were dated and correlated between several outcrops and sub-surfaces wells. Among these sequence surfaces with the Early Miocene (Aquitanian) age of the Qom Formation three sequence boundaries are correlative with those of Ehrenberg *et al.* (2007) and Van Buchem *et al.* (2010). With increasing age, these surfaces are as following:

1. Bu20 SB and SB VI is equal to the type 1 SB at the top of DS2.
2. Aq20/Bu10 and SB V is equal to the type 2 SB between DS1 and DS2.
3. Aq10 and SB IV is equal to the type 1 SB at the base of DS1.

In this study, three recognized sequence boundaries are well-matched with the sequence boundaries that are proposed by Ehrenberg *et al.* (2007) and Van Buchem *et al.* (2010) (Figure 7).

## 5. CONCLUSIONS:

Based on field observations, textural analysis, and biotic constituents, ten facies have

been identified. The Early Miocene (Aquitania) Qom Formation in the Qom back-arc basin in the microplate of Central Iran has been deposited in a homoclinal ramp setting including delta, a tidal inlet, lagoon, shoal, and open marine subenvironments. The absence of continuous large barrier reefs, pisolite, oncolite, slump structures, and calciturbidites support this suggestion. The Qom Formation in studied sections mainly occurs in an open marine setting. Furthermore, based on sequence stratigraphic studies, two third-order depositional sequences in the Aquitania of the Qom Formation have been recognized. Based on the chronostratigraphic sequence correlation, these depositional sequences have a good correlative architecture with Arabian Plate sedimentary successions and the sequences that have been recognized for the Oligocene-Miocene Asmari Formation in Dezful Embayment and Izeh zone in the southwest of Iran by other researchers.

## 6. REFERENCES:

1. Adabi, M.H., Kakemem, U. and Sadeghi, A. (2016). Sedimentary facies, depositional environment, and sequence stratigraphy of Oligocene–Miocene shallow-water carbonate from the Rig Mountain, Zagros basin (SW Iran). *Carbonates and evaporites*, 31(1), 69-85.
2. Aghanabati, A. (2011). *Geology of Iran: Geological Survey of Iran*, 586p. (In Persian)
3. Amirshahkarami, M. and Karavan, M. (2015). Microfacies models and sequence stratigraphic architecture of the Oligocene–Miocene Qom Formation, south of Qom City, Iran. *Geoscience Frontiers*, 6(4), 593-604.
4. Arp, G., Schultz, S., Karius, V. and Head III, J.W. (2019). Ries impact crater sedimentary conglomerates: Sedimentary particle 'impact pre-processing', transport distances and provenance, and implications for Gale crater conglomerates, Mars. *Icarus*, 321, 531-549.
5. Bacelle, L., and Bosellini, A. (1965). Diagrams for visual estimation of percentage composition in sedimentary rocks [Diagrammi per la stima visiva della composizione percentuale nelle rocce sedimentarie]. *Ann. Univ. Ferrara, NS, sez. IX., Sci. Geol. Paleont.*, 1, 59-62.
6. Barattolo, F., Bassi, D., and Romano, R. (2007). Upper Eocene larger foraminiferal–coralline algal facies from the Klokova Mountain (southern continental Greece). *Facies*, 53(3), 361-375.
7. Bassi, D. (2005). Larger foraminiferal and coralline algal facies in an Upper Eocene storm-influenced, shallow-water carbonate platform (Colli Berici, north-eastern Italy). *Palaeogeogr Palaeoclimatol Palaeoecol*, 226, 17-35.
8. Bassi, D., Hottinger, L., and Nebelsick, J.H. (2007). Larger foraminifera from the Upper Oligocene of the Venetian area, north-east Italy. *Paleontology*, 50(4), 845-868.
9. Benedetti, A., and Frezza, V. (2016). Benthic foraminiferal assemblages from shallow-water environments of northeastern Sardinia (Italy, Mediterranean Sea). *Facies*, 62(2), 14.
10. Berberian, M. (1983). The southern Caspian: a compressional depression floored by a trapped, modified oceanic crust. *Canadian Journal of Earth Sciences*, 20(2), 163-183.
11. BouDagher-Fadel, M.K. (2008). Evolution and Geological Significance of Larger Benthic Foraminifera. *Developments in Palaeontology and Stratigraphy*, 21, Elsevier, 540 p.
12. Brandano, M., Frezza, V., Tomassetti, L., Pedley, M., and Matteucci, R. (2009). Facies analysis and palaeoenvironmental interpretation of the late Oligocene Attard Member (lower Coralline Limestone Formation), Malta. *Sedimentology*, 56(4), 1138-1158.
13. Burchette, T.P., and Wright, V.P. (1992). Carbonate ramp depositional systems. *Sedimentary Geology*, 79(1-4), 3-57.
14. Catuneanu, O. (2006). *Principles of Sequence Stratigraphy*. Elsevier, Amsterdam, 375 p.
15. Catuneanu, O. (2017). Sequence stratigraphy: Guidelines for a standard methodology. In *Stratigraphy and Timescales*, Academic Press, 2, 1-57.
16. Catuneanu, O., Abreu, V., Bhattacharya, J. P., Blum, M. D., Dalrymple, R. W., Eriksson, G., ... Winker, C. (2009). Towards the standardization of sequence stratigraphy. *Earth Science Reviews*, 92, 1-33.

17. Colman-Sadd, S.P. (1982). Two-stage continental collision and plate driving forces. *Tectonophysics*, 90(3-4), 263-282.
18. Dickson, J. A. D. (1966). Carbonate identification and genesis as revealed by staining, *Journal of Sedimentary Research*, 36(2), 491-505.
19. Dozy, J.J. (1955). A Sketch of past Cretaceous volcanism in Central Iran: Leidsche, *Geologische Mededeelingen*, 20, 48-57.
20. Drinia, H., Tsaparas, N., and Antonarakou, A. (2016). Palaeoenvironmental implications recorded by foraminifera and bryozoan faunas from the early late Miocene of Gavdos Island.
21. Dunham, R.J. (1962). Classification of carbonate rocks according to depositional texture. *American Association of Petroleum Geologists Memoir*, 1, 108-121.
22. Ehrenberg, S.N., Pickard, N.A.H., Laursen, G.V., Monibi, S., Mossadegh, Z.K., Svåná, T.A., ... Thirlwall, M.F. (2007). Strontium Isotope Stratigraphy of the Asmari Formation (Oligocene-Lower Miocene), SW Iran. *Journal of Petroleum Geology*, 30(2), 107-128.
23. Flügel, E. (2010). *Microfacies of carbonate rocks: analysis, interpretation, and application*. Springer Science and Business Media.
24. Folk, R.L. (1980) *Petrology of sedimentary rocks*. Hemphill publishing company.
25. Friedman, G.M., and Sanders, J.E. (1978). *Principles of sedimentology*. Wiley.
26. Galloway, W.E. (1989). Genetic stratigraphic sequences in basin analysis II: application to northwest Gulf of Mexico Cenozoic basin. *AAPG Bulletin*, 73(2), 143-154.
27. Geel, T. (2000). Recognition of stratigraphic sequences in carbonate platform and slope deposits: empirical models based on microfacies analysis of Palaeogene deposits in southeastern Spain. *Paleogeography, Palaeoclimatology, Palaeoecology*, 155(3-4), 211-238.
28. Halfar, J. and Mutti, M. (2005). Global dominance of coralline red-algal facies: a response to Miocene oceanographic events. *Geology*, 33(6), 481-484.
29. Harzhauser, M., and Piller, W.E. (2007). Benchmark data of a changing sea—paleogeography, palaeobiogeography, and events in the Central Paratethys during the Miocene. *Paleogeography, Palaeoclimatology, Palaeoecology*, 253(1-2), 8-31.
30. Holcová, K., and Zágöršek, K. (2008). Bryozoa, foraminifera and calcareous nannoplankton as environmental proxies of the “bryozoan event” in the Middle Miocene of the Central Paratethys (Czech Republic). *Paleogeography, Palaeoclimatology, Palaeoecology*, 267(3-4), 216-234.
31. Lee JJ. (1990). Fine structure of the rhodophycean *Porphyridium purpureum* in situ in *Peneroplis pertusus* (Forskal) and *P. acicularis* (Batsch) and in axenic culture. *J Foraminifer Res.* 20, 162-169.
32. Maghfouri Moghaddam, I., and Yasboulaghi, S. (2015). Small Pelecypoda of Qom Formation (Early Miocene) in the west of Ashtian, Central Iran, *Journal of Geoscience*, 24(95), 275-280.
33. Martini, I., Ambrosetti, E., and Sandrelli, F. (2017). The role of sediment supply in large-scale stratigraphic architecture of ancient Gilbert-type deltas (Pliocene Siena-Radicofani Basin, Italy). *Sedimentary Geology*, 350, 23-41.
34. Mehr, M.K., and Adabi, M.H. (2014). Microfacies and geochemical evidence for original aragonite mineralogy of a foraminifera-dominated carbonate ramp system in the late Paleocene to Middle Eocene, Alborz basin, Iran. *Carbonates and Evaporites*, 29(2), 155-175.
35. Moghadam, M.Y. (2011). Early Oligocene larger foraminiferal biostratigraphy of the Qom Formation, south of Uromieh (NW Iran). *Turkish Journal of Earth Sciences*, 20(6), 847-856.
36. Moghaddam, H.V., and Torabi, H. (2004). Biofacies and sequence stratigraphy of the Oligocene succession, Central basin, Iran. *Neues Jahrbuch für Geologie und Paläontologie-Monatshefte*, 321-334.
37. Mohammadi, E., Safari, A., Vaziri-Moghaddam, H., Vaziri, M.R., and Ghaedi, M. (2011). Microfacies analysis and paleoenvironmental interpretation of the Qom Formation, South of the Kashan, Central Iran. *Carbonates and Evaporites*,



- 26(3), 255.
38. Motiei, H. (1993). Stratigraphy of Zagros: Geological Survey of Iran Publication (in Persian). 536 p.
  39. Nebelsick, J.H., Rasser, M.W., and Bassi, D. (2005). Facies dynamics in Eocene to Oligocene circumalpine carbonates. *Facies*, 51(1-4), 197-217.
  40. Nogole-Sadat, M.A.A. (1985). Les zones de Decrochement et les Virgations structurales en Iran: Consequences des resultats de l'analysis structurale de la region de Qom: Geological Survey of Iran.
  41. Perrin, C., Bosence, D., and Rosen, B. (1995). Quantitative approaches to palaeozonation and palaeobathymetry of corals and coralline algae in Cenozoic reefs. Geological Society, London, Special Publications, 83(1), 181-229.
  42. Pomar, L. (2001). Types of carbonate platforms: a genetic approach. *Basin research*, 13(3), 313-334.
  43. Posamentier, H. W., and Vail, R. (1988). Eustatic controls on clastic deposition. II. Sequence and systems tract models. In: Wilgus, C. K., Hastings, B. S., Kendall, C. G. St. C., Posamentier, H. W., Ross, C. A., Van Wagoner, J. C. (Eds.), *Sea-Level Changes – An Integrated Approach*. SEPM Special Publication 42, 125-154.
  44. Posamentier, H.W., and James, D.P. (1993). An overview of sequence-stratigraphic concepts: uses and abuses. In *Sequence stratigraphy and facies associations*, Blackwell Oxford, 18, 3-18.
  45. Read, J.F. (1985). Carbonate platform facies models. *AAPG Bulletin*, 69(1), 1-21.
  46. Reuter, M., Piller, W.E., Harzhauser, M., Mandic, O., Berning, B., Rögl, F., ... Hamedani, A. (2009). The Oligo-Miocene Qom Formation (Iran): evidence for an early Burdigalian restriction of the Tethyan Seaway and closure of its Iranian gateways. *International Journal of Earth Sciences*, 98(3), 627-650.
  47. Schuster, F., and Wielandt, U. (1999). Oligocene and Early Miocene coral faunas from Iran: palaeoecology and palaeobiogeography. *International Journal of Earth Sciences*, 88(3), 571-581.
  48. Seddighi, M., Vaziri-Moghaddam, H., Taheri, A., and Ghabeishavi, A. (2012). Depositional environment and constraining factors on the facies architecture of the Qom Formation, Central Basin, Iran. *Historical Biology*, 24(1), 91-100.
  49. Sengupta, S. (2017). *Introduction to sedimentology*. Routledge.
  50. Sharland, R., Archer, R., Casey, D.M., Davis, R.B., Hall, S.H., Heward, A.P., ... Simmons, M.D. (2001). Arabian plate sequence stratigraphy. *Geo-Arabia*, 2, 1-371.
  51. Sharland, R., Casey, D.M., Davies, R.B., Simmons, M.D., and Sutcliffe, O.E. (2004). Arabian plate sequence stratigraphy-revisions to SP2. *Geo-Arabia*, 9, 199-214.
  52. Simmons, M.D., Sharland, R., Casey, D.M., Davies, R.B., and Sutcliffe, O.E. (2007). Arabian Plate sequence stratigraphy: Potential implications for global chronostratigraphy. *GeoArabia*, 12(4), 101-130.
  53. Stocklin, J., and Setudehnia, A. (1991). *Stratigraphic Lexicon of Iran*. Geological Survey of Iran Publication, 3rd edition, 18, 376 p.
  54. Tucker, M.E., and Wright, V.P. (2009). *Carbonate sedimentology*. John Wiley and Sons.
  55. Van Buchem, F.S.P., Allan, T.L., Laursen, G.V., Lotfpour, M., Moallemi, A., Monibi, S., ... Vincent, B. (2010). Regional stratigraphic architecture and reservoir types of the Oligo-Miocene deposits in the Dezful Embayment (Asmari and Pabdeh Formations) SW Iran. Geological Society, London, Special Publications, 329(1), 219-263.
  56. Van Wagoner, J. C., Mitchum Jr., R. M., Campion, K. M., Rahmanian, V. D. (1990). Siliciclastic sequence stratigraphy in well logs, core, and outcrops: concepts for high-resolution correlation of time and facies. *American Association of Petroleum Geologists Methods in Exploration*, 7, 55 p.
  57. Wright, V.P., and Burchette. (1996). Shallow-water carbonate environments. *Sedimentary environments: processes, facies and stratigraphy*. Blackwell Science, Oxford, 325-394.
  58. Zuffa, G.G. (1985). Optical analyses of arenites: influence of methodology on compositional results. In *Provenance of arenites*, Springer, Dordrecht, 165-189.

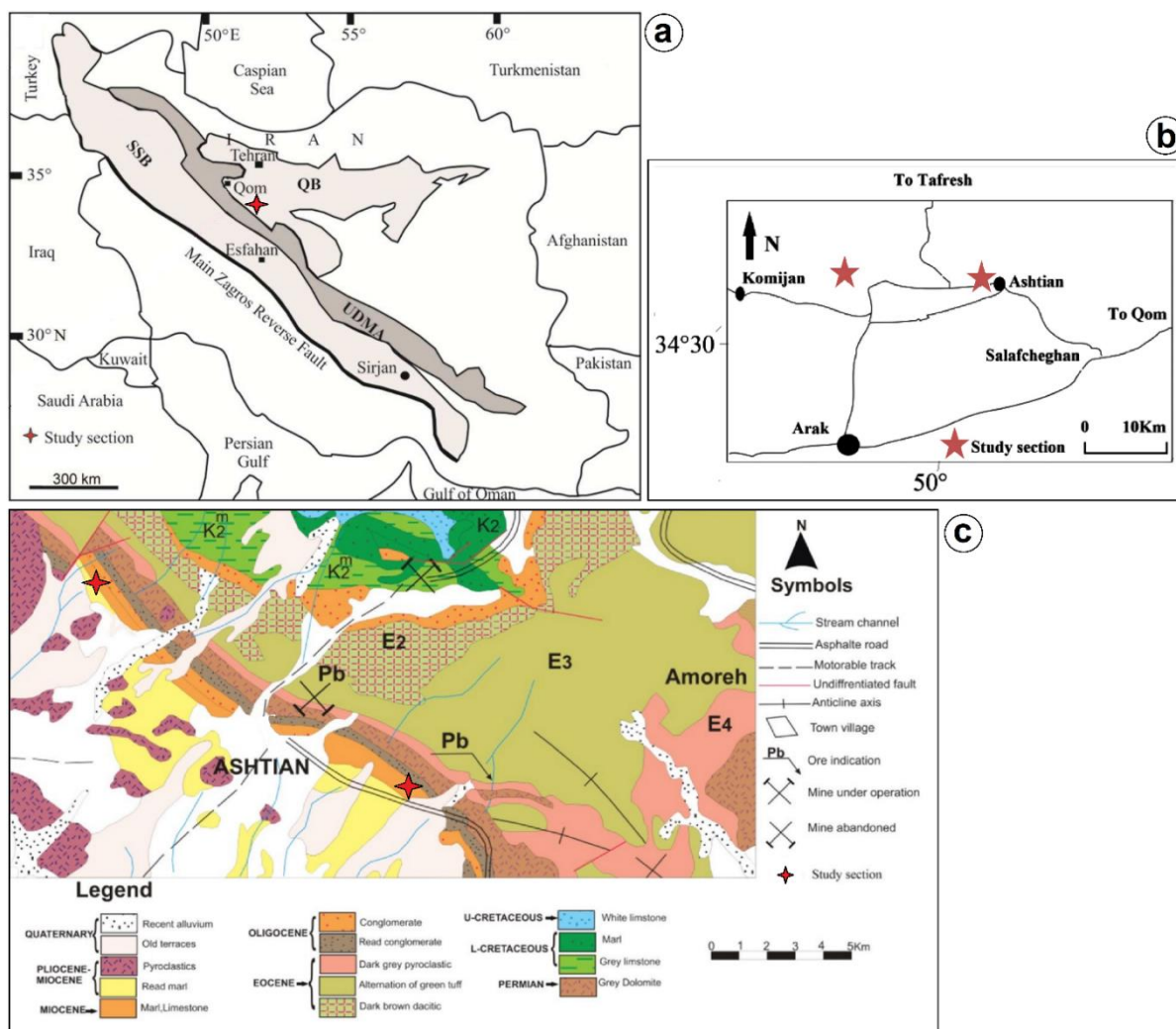


**Figure 1.** Geological setting, location, and geological map of the study area; (a) a general map showing the distribution of the Qom Formation in different basins of Iran including QB or Qom Basin (Back-arc basin), UDMA or Urumieh–Dokhtar Magmatic arc (Intra-arc basin), and SSB or Sanandaj–Sirjan Basin (Fore-arc basin) (adapted from Reuter et al., 2009); (b) Location of the studied area in the Qom back-arc basin; (c) Geological map of the study area, showing the Oligocene–Miocene of the Qom Formation and underlying and overlying formations (adopted from geological survey of Iran).



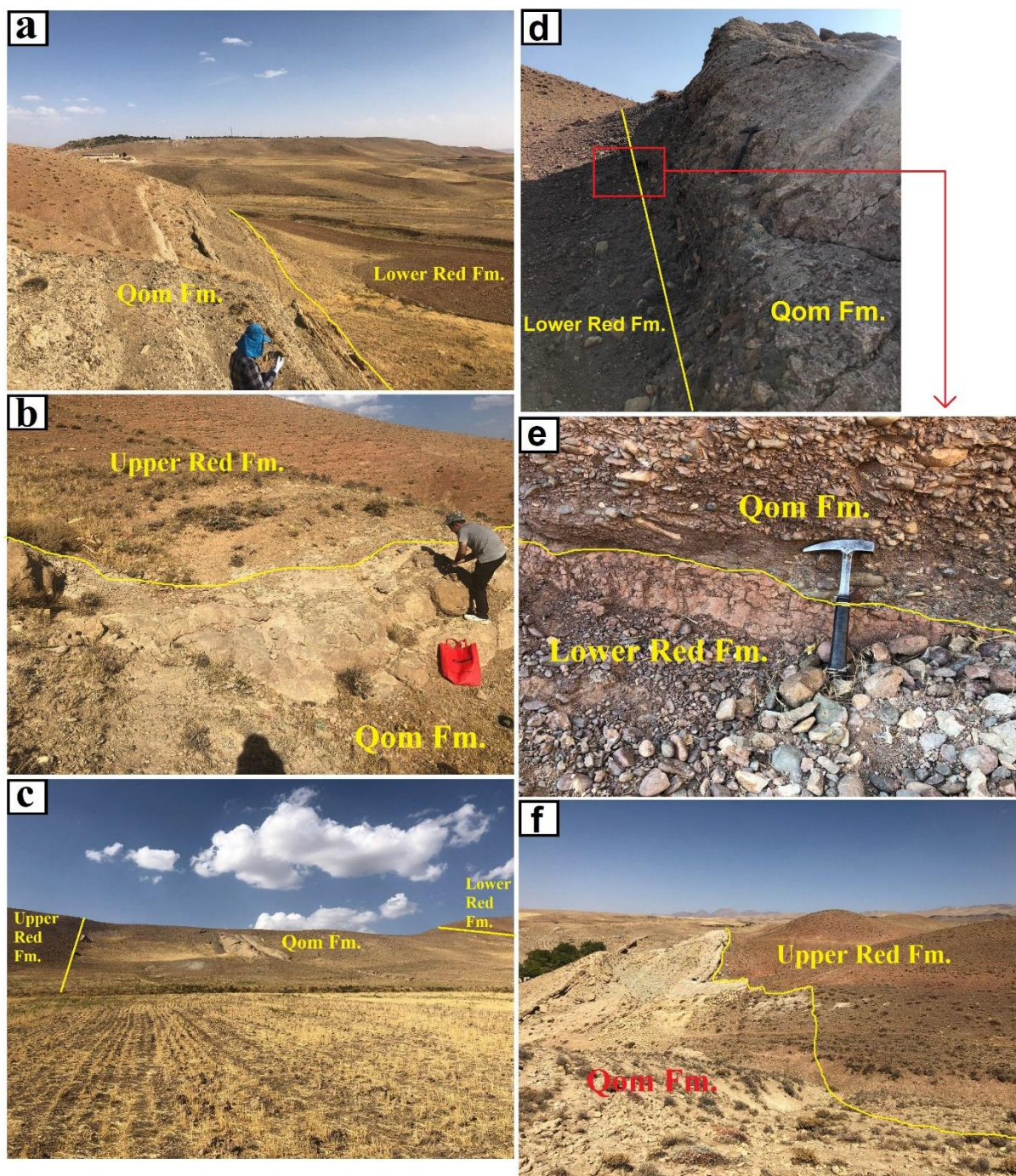


**Figure 2.** A general view of sections. (a), (b) and (c) showing the Qom Formation with underlying Upper Red Formation and overlying Lower Red Formation in Ashtian section; (d) and (e) basal conglomerate of the Qom Formation that overlain Lower Red Formation in Kordijan section; (f) view of the Qom Formation boundary with Upper Red Formation in Kordijan section.



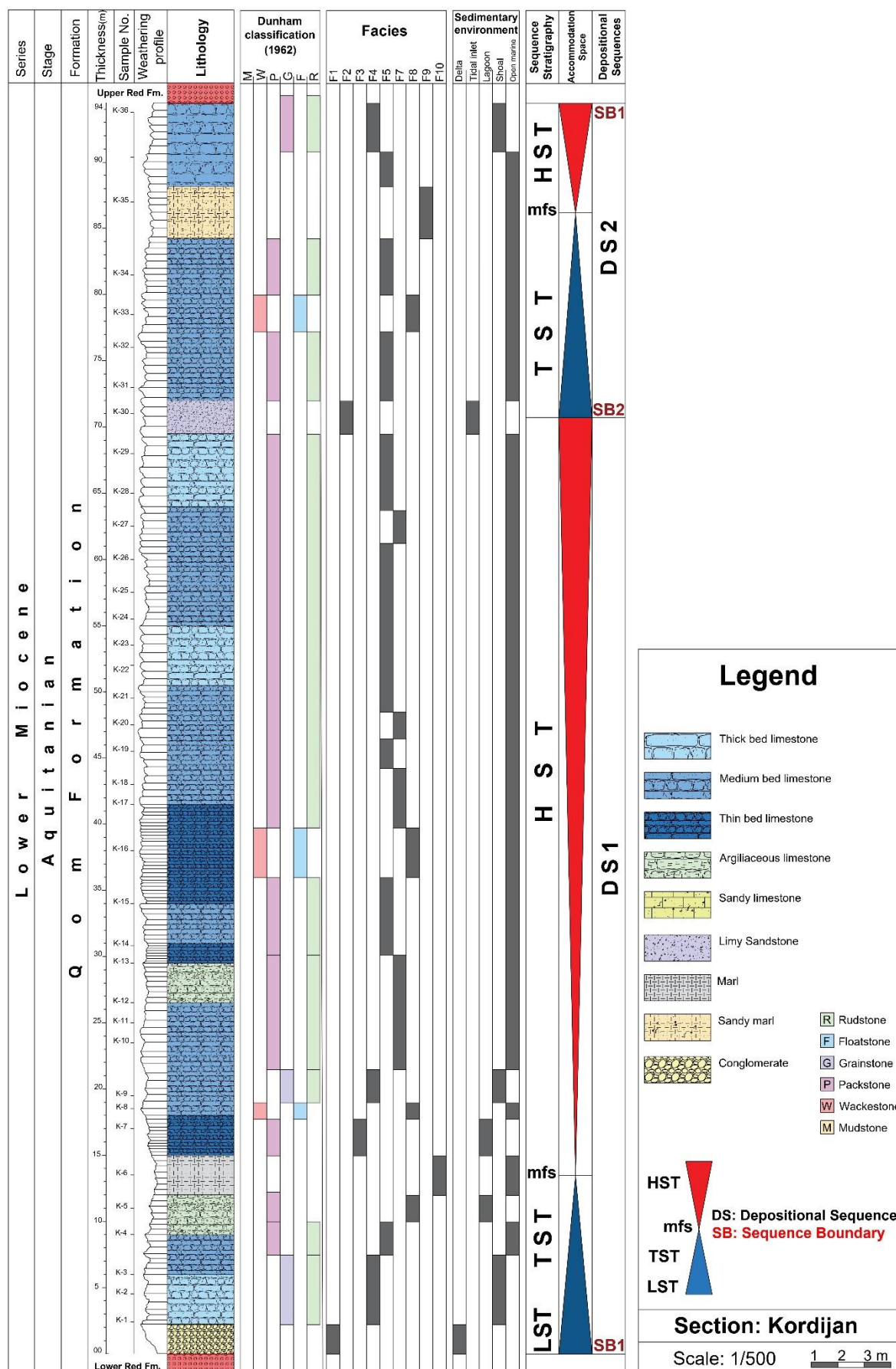


**Figure 3.** Vertical facies distribution showing paleoenvironmental and sequence stratigraphic characteristics of the Qom Formation in studied sections in the Qom Back-arc Basin.

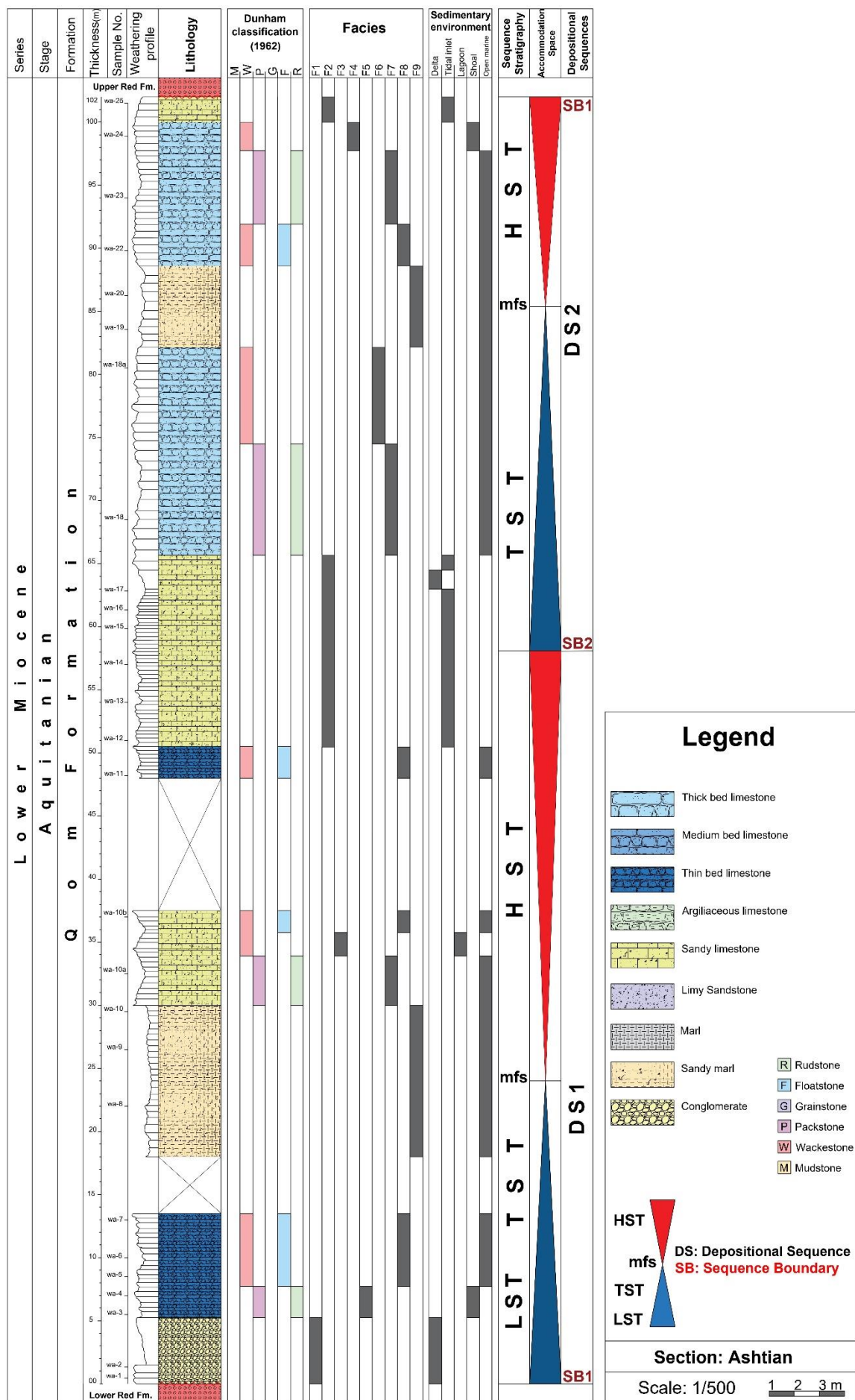
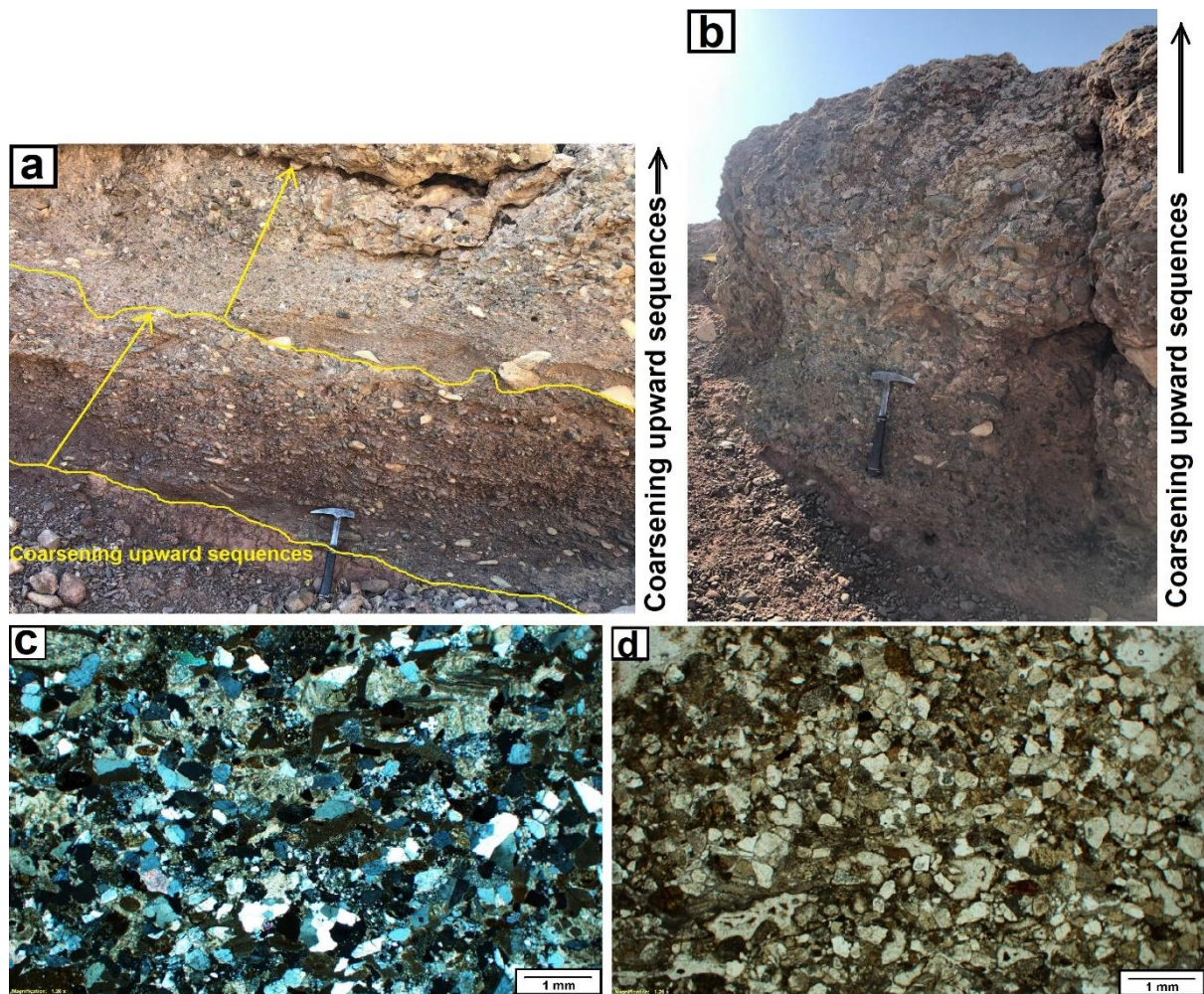


Figure 3. Continue





**Figure 4.** Facies types of the Qom Formation in Ashtian and Kordijan sections. (a) and (b) F1: Conglomerate facies showing coarsening upward sequences (transitional, delta); (c) and (d) F2: Bioclastic hybrid arenite with open marine bioclast features of open marine such as red algae, echinoid, and bryozoan (inner ramp, tidal inlet).



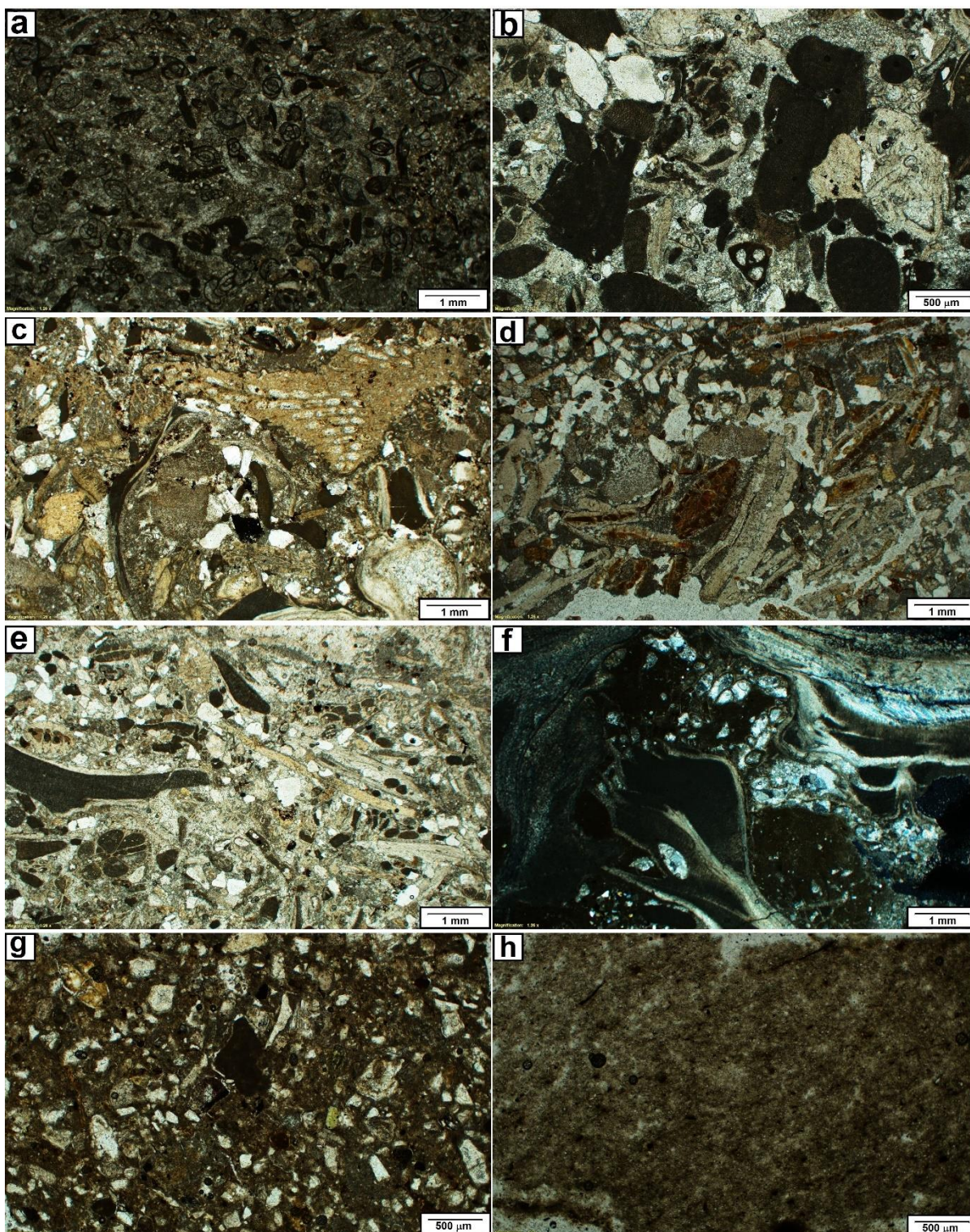


**Figure 5.** Different facies types of the Qom Formation in Ashtian and Kordijan sections. (a) F3: Bioclast miliolid packstone (inner ramp, lagoon); (b) F4: Bioclast, red algae rudstone/grainstone (inner ramp, shoal); (c) F5: Echinoid, bryozoan, red algal packstone/rudstone (middle ramp, open marine below FWB); (d) F6: Bioclast, nummulitids, operculina wackestone (middle ramp, open marine below FWB); (e) F7: Red algae, bryozoan, brachiopod packstone/rudstone (middle ramp, open marine below FWB); (f) F8: Echinoid, bryozoan, brachiopod wackestone/floatstone (middle ramp, open marine below FWB); (g) F9: Sandy mudstone (outer ramp, open marine below SWB); (h) shaly mudstone (outer ramp, open marine below SWB).



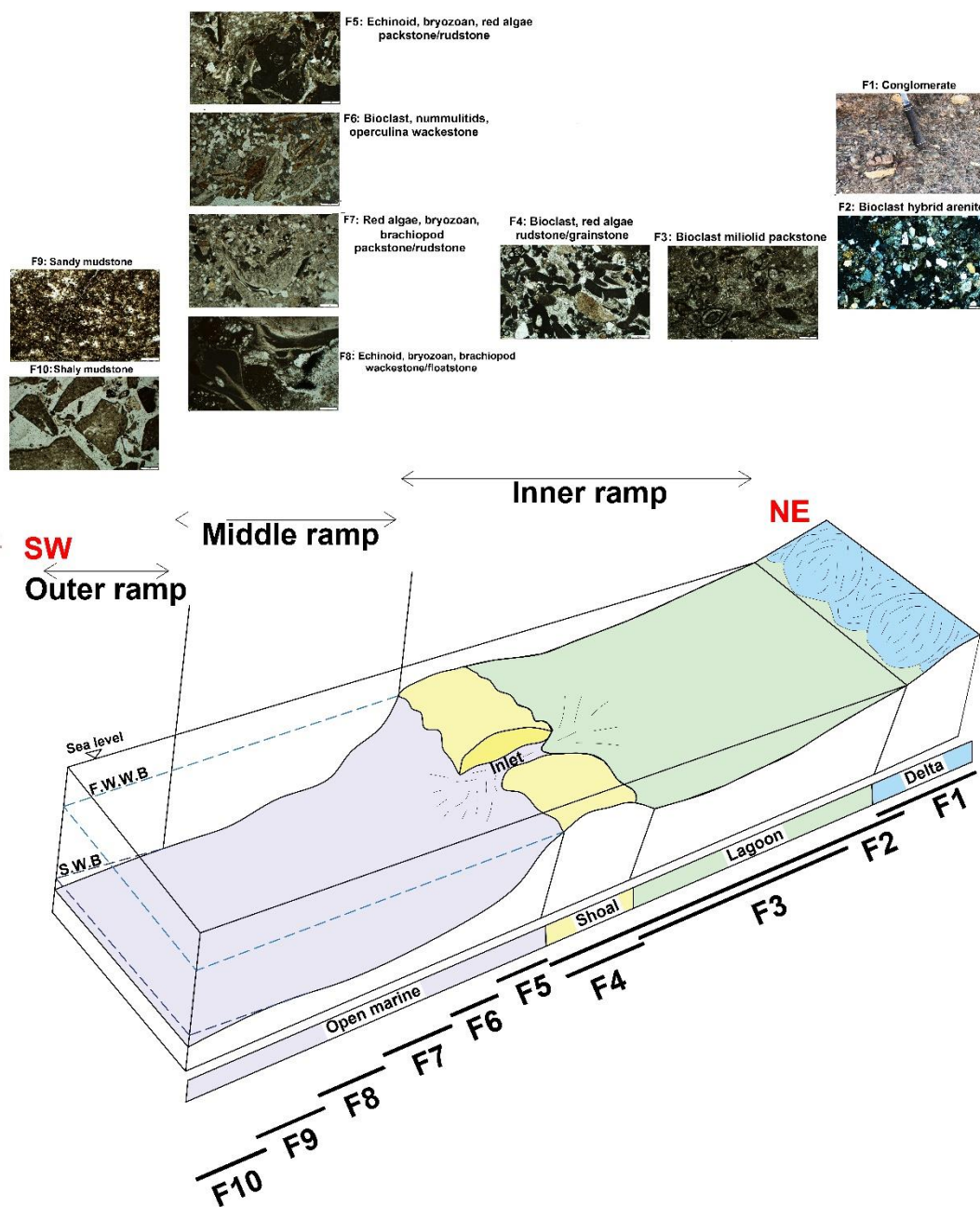
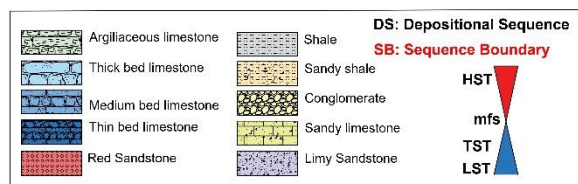


**Figure 6.** Homoclinal carbonate ramp depositional model proposed for the Qom Formation. FWWB (fair-weather wave base), SWB (storm wave base)





| Age          | Epoch         | Stage       | Arabian Plate                                       | Dezful Embayment and Izeh zone (SW Iran) |                         |
|--------------|---------------|-------------|---|--|-------------------------|
|              |               |             | Sharland et al., 2001/2004;<br>Simmons et al., 2007 | Ehrenberg et al., 2007                   | Van Bachem et al., 2010 |
| 20           | Lower Miocene | Burdigalian | 17.5 Ng20   | 18.5 Base Gachsaran                      | 18.5 SB VII             |
|              |               |             | 19.0 Ng20 SB  |  |                         |
|              |               | Aquitanian  | 20.0 Ng10   | 20.2 Bu20 SB                             | 20.2 SB VI              |
|              |               |             | 21.6 Aq20/Bu10 SB                                   | 21.4 SB V                                |                         |
|              |               |             |   |  | 23.0 Ng10 SB            |
|              |               |             | Chattian  | 24.5 Pg50                                | 24.9 Ch30 SB            |
|              |               | 29.0 Pg40   |   | 28.0 Ch20 SB                             | 28.8 SB II              |
|              |               |             |   | 28.9 Ru30/Ch10 SB                        |                         |
|              |               |             |   | 30.0 Ru20 SB                             |                         |
|              |               | Rupelian    | 30.0 Pg30   | 34.0 SB I                                |                         |
| 33.5 Pg30 SB |               |             |   |  |                         |

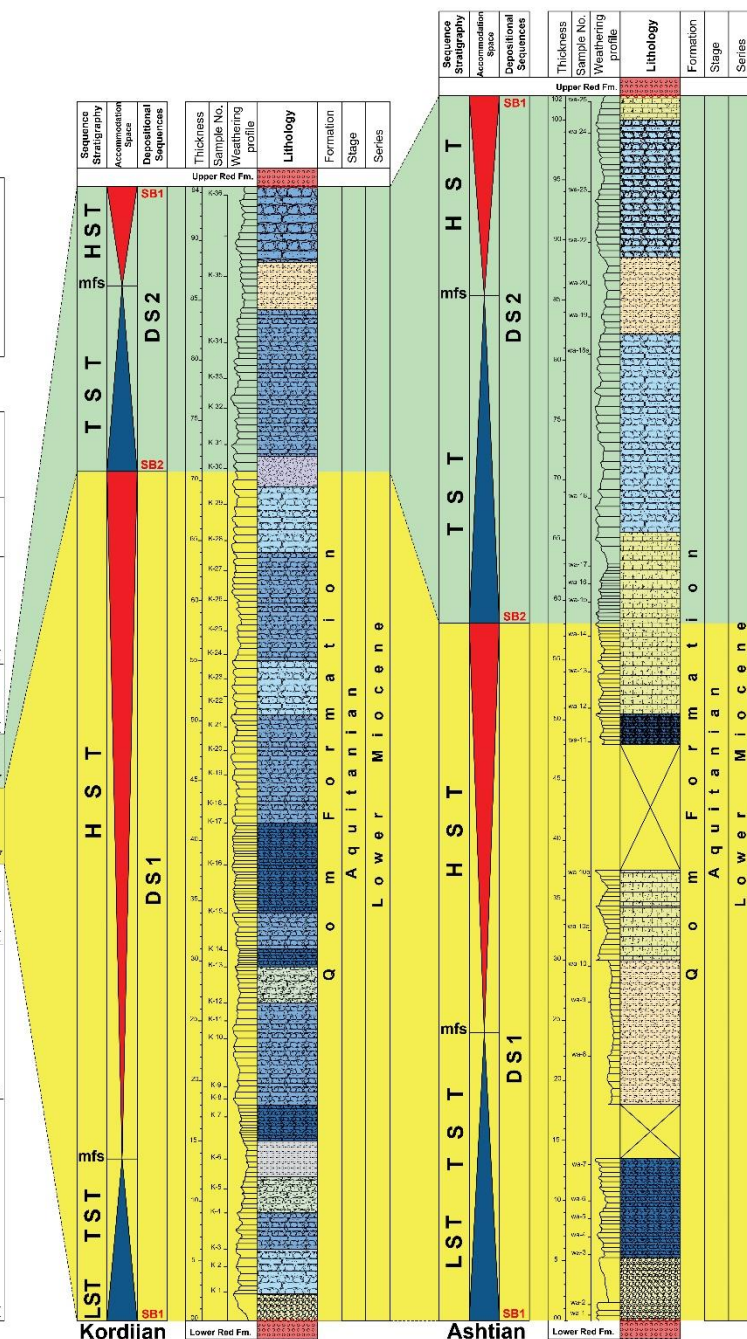


**Figure 7.** Comparison of sequences of the Qom Formation with the Oligocene-Miocene Asmari Formation in Dezful Embayment and Izeh zone in southwest of Iran and Arabian Plate sedimentary successions

**Table 1. Facies type, facies associations and depositional environments of the Qom Formation in the studied sections.**

| Facies code | Facies type   | Lithology  | Facies characteristics   | Grain size  | Sorting          | Energy level   | Flügel (2010) (SMF/RMF) | Depositional environment | Facies association |
|-------------|---|--|--|-------------|------------------|----------------|-------------------------|--------------------------|--------------------|
| F1          | Conglomerate  | Polimictic-conglomerate                          | Massive heterogenous Conglomerate with Silt and very small sand as the matrix that is formed of sandstone, shale and limestone.  | Pebble/sand | Poorly           | High           | -                       | Delta                    | Transitional       |
| F2          | Bioclastic hybrid arenite                               | Limy sandstone                                   | Includes carbonate bio-clasts consists of echinoid, brachiopod, operculina, and bryozoan up to 20 percent. The matrix is made of carbonate mud. Monocrystalline and less polycrystalline quartz grains formed the major detrital clasts. | Sand        | Poorly to medium | High           | -                       | Tidal inlet              |                    |
| F3          | Bioclast miliolid packstone                             | Limestone  | Biotic features variation are low and includes different species of Miliolidae. Echinoid, red algae, bryozoan, and bivalve forms the minor features by <10%.   | Sand/mud    | Poorly to medium | Low            | SMF18/RMF20             | Lagoon                   | Inner ramp         |
| F4          | Bioclast, red algae rudstone/grain stone                | Limestone/sandy limestone                        | The major biotic constituents are red algae, echinoid, Rotalia, bryozoan, and bivalves in a spary texture. Gastropod, miliolid, brachiopod, and fragments of larger benthic foraminifera form the minor biota.                           | Pebble/sand | Medium to good   | High           | SMF13/RMF27             | Shoal                    |                    |
| F5          | Echinoid, bryozoan, red algal packstone/rudstone        | Limestone  | The major biota are bryozoan and <i>Lithophyllum</i> sp. and <i>Lithothamnium</i> sp. Miliolid is present by 3-5% abundance. The minor biota are include gastropod, Rotalia, brachiopod, and worm tubes.                                 | Pebble/sand | Poorly           | Medium to high | SMF18/RMF14             | Open marine (below FWWB) | Middle ramp        |
| F6          | Bioclast, nummulitids, operculina wackestone/floatstone | Limestone  | The main biotic features are include Operculina and Nummulites. Echinoid, red algae, brachiopods, bryozoan, and Rotalia form the minor biota.  | Pebble/sand | Poorly           | Low to medium  | SMF8/RMF13              | Open marine (below FWWB) |                    |
| F7          | Red algae, bryozoan, brachiopod packstone/rudstone      | Limestone/sandy limestone                        | The main biota are brachiopod, bryozoan, and less echinoid fragments. Red algae, Rotalia, and miliolid form the minor biota.   | Pebble/sand | Poorly           | Low to medium  | SMF12 S/RMF8            | Open marine (below FWWB) |                    |
| F8          | Echinoid, bryozoan, brachiopod wackestone/floatstone    | Limestone/sandy limestone/argillaceous limestone | The major biota are echinoid, bryozoan, and brachiopod. Miliolid, ostracod and unknown micritized biota have also seen.  | Pebble/sand | Poorly           | Low            | SMF12 C/RMF7            | Open marine (below FWWB) |                    |
| F9          | Sandy mudstone  | Sandy marl                                       | Mainly formed of carbonate mud with Silt and small sand-size quartz grains and shell fragments. Glauconite is observed and pyritization occurred in the matrix.  | Sand/mud    | -                | Low            | SMF3/RMF2               | Open marine (below SWB)  | Outer ramp         |
| F10         | shaly mudstone  | Marl   | It is completely homogenous and no biota or shell fragments have been observed. Silt size quartz grains are scattered within the matrix.   | Mud         | -                | Low            | -                       | Open marine (below SWB)  |                    |

SMF: standard microfacies type; RMF: ramp microfacies type

### MEDULA ÓSSEA DE OSSOS TUBULARES NO PROCESSO ONCOLÓGICO

### BONE MARROW OF TUBULAR BONES IN THE ONCOLOGICAL PROCESS

### КОСТНЫЙ МОЗГ ТРУБЧАТЫХ КОСТЕЙ ПРИ ОНКОЛОГИЧЕСКОМ ПРОЦЕССЕ

NIKOLAEVA, Liudmila<sup>1\*</sup>.

<sup>1\*</sup>Candidate of medical sciences, assistant of the Department, Krasnoyarsk State Medical University – Russia

\* Corresponding author  
e-mail: [lpnikolaeva@yandex.ru](mailto:lpnikolaeva@yandex.ru)

Received 23 February 2020; received in revised form 11 May 2020; accepted 05 June 2020

## RESUMO

A causa do câncer em pacientes permanece um mistério. Várias teorias e suposições não dão confiança na compreensão do processo de câncer. Até que a etiologia do câncer seja estudada, não poderemos avançar apesar do desenvolvimento de tecnologias farmacêuticas e tratamentos inovadores. Para resolver esse problema, pretende-se usar todos os dados relacionados ao desenvolvimento do câncer, mesmo que eles não tenham um vínculo óbvio com a doença. Mesmo quando uma célula cancerígena aparece e começa a criar seu pool de células cancerígenas alteradas, não sabemos. Os médicos diagnosticam o câncer quando o tumor atinge certos tamanhos e afeta a função do órgão. O número de células cancerígenas aumenta muito rapidamente. Os fatores que aceleram essa reprodução das células cancerígenas são muitos, o que significa que ainda não vemos a verdadeira causa. A célula cancerígena mantém os recursos da célula original em graus variados, da semelhança pronunciada à perda quase completa de propriedades celulares saudáveis. Quanto mais a célula estranha é alterada, mais rápido ela cresce e o prognóstico para o paciente se deteriora. O mais preocupante é que a incidência de câncer está aumentando, o que significa que a causa não foi encontrada. As mortes por câncer continuam altas. Este artigo discute o caso de um paciente com um membro amputado por câncer (câncer de pele do pé). Durante um estudo de 10 anos da medula óssea do fêmur, pela primeira vez, a medula óssea foi obtida do fêmur de um paciente com câncer. As descobertas podem ajudar pesquisadores e médicos a entender melhor o processo do câncer e a encarar o problema de maneira diferente.

**Palavras-chave:** *medula óssea femoral, células-tronco, células-tronco hematopoiéticas, câncer de pele.*

## ABSTRACT

The cause of cancer in patients remains a mystery. Various theories and assumptions do not give confidence in understanding the cancer process. Until the etiology of cancer is studied, we will not be able to move forward despite the development of pharmaceutical technologies and innovative treatments. To solve this problem, it is intended to use all data related to cancer development, even if they have no obvious link to the disease. Even when a cancer cell appears and starts creating its pool of altered cancer cells we don't know. Doctors diagnose cancer, when the tumor reaches certain sizes and disorders the function of the organ. The number of cancer cells increases very quickly. The factors that accelerate this reproduction of cancer cells are many, which means that we still do not see the true cause. The cancer cell retains the features of the original cell to varying degrees from pronounced similarity to almost complete loss of healthy cell properties. The more the foreign cell is altered, the faster it grows and the prognosis for the patient is deteriorated. The most worrying thing is that the incidence of cancer is increasing, which means the cause is not found. Cancer deaths remain high. This article discusses the case of a patient having a limb amputated for cancer (foot skin cancer). During a 10-year study of bone marrow from the femur, for the first time, bone marrow was obtained from the femur of a patient with cancer. The findings could help researchers and doctors better understand the cancer process and look at the problem differently.

**Keywords:** *femoral bone marrow, stem cells, hematopoietic stem cells, skin cancer.*

## АННОТАЦИЯ

Причина возникновения рака у больных остается загадкой. Различные теории и предположения не

дают уверенности в понимании онкологического процесса. До тех пор, пока этиология рака не будет изучена, мы не сможем двигаться вперед, несмотря на развитие фармацевтических технологий и инновационных методов лечения. Для решения этой проблемы предполагается использовать все данные, связанные с развитием рака, даже если они не имеют очевидной связи с болезнью. Даже когда появляется раковая клетка и начинает создавать свой пул измененных раковых клеток, мы этого не знаем. Врачи диагностируют рак, когда опухоль достигает определенных размеров и нарушается функция органа. Количество раковых клеток увеличивается очень быстро. Факторов, ускоряющих такое размножение раковых клеток, очень много, а это значит, что мы до сих пор не видим истинной причины. Раковая клетка сохраняет черты исходной клетки в разной степени - от ярко выраженного сходства до почти полной потери свойств здоровой клетки. Чем больше чужеродная клетка изменяется, тем быстрее она растет и прогноз для пациента ухудшается. Самое тревожное заключается в том, что заболеваемость раком растет, а значит, причина не найдена. Смертность от рака остается высокой. В данной статье рассматривается случай пациента, которому ампутировали конечность по поводу рака (рак кожи стопы). Во время 10-летнего исследования костного мозга из бедренной кости впервые был получен костный мозг из бедренной кости больного раком. Полученные результаты могут помочь исследователям и врачам лучше понять процесс развития рака и взглянуть на проблему по-другому.

**Ключевые слова:** *костный мозг трубчатых костей, стволовые клетки, гемопоэтические стволовые клетки, рак кожи.*

## 1. INTRODUCTION:

Worldwide, the number of cancer patients is increasing. In overwhelming numbers, these are older people, regardless of gender. The importance of determining the cause of cancer and the overall understanding of the pathogenesis of the process is understood by doctors in all countries. But there is no consensus, most hold the hypothesis of immune system disruption, which stops determining cells are necessary for removal (Weaver, *et al.*, 2008).

The assumption of the cause of the cancer process as a result of the incorrect protective work of the immune system does not explain the whole variety of cancer transformations. The cancer process is based on two important details, cell growth, which can be different and loss of differentiation, the degree of which can differ greatly from the healthy cell of this tissue. In recent years, we have studied the cellular mechanisms of cancer development, the discovery of oncogenes and antioncogenes. So far, this is of interest, but will this data make a difference? By influencing the work of anti-oncogenes, the fight against cancer can be improved, but the problem remains problem (Hernández, 2015).

The most important thing is to understand the function and features of the cancer cell, without fine study of this cell there is no point in looking for a drug for treatment. For now, we're still losing cancer in the fight. In surgical practice, they are periodically forced to amputate the lower limb because it is impossible to preserve it (Nikolaeva *et al.*, 2017). High amputations lead to limited social adaptation of patients (Nikolaeva *et al.*, 2015), significantly reduce the life expectancy of

patients as a result of damage to the contralateral limb and the addition of various complications (Sisla *et al.*, 2011).

The lower limb that is removed during a forced amputation is an important bone marrow depot, where about 25% of the patient's total bone marrow is located in the femoral cavity. Currently, it is proved that the restoration of a damaged organ occurs not only due to the activation of organ regional stem cells, but also due to migration to the zone of damage of MMSCs from other organs, and primarily from the bone marrow (Nikolaeva 2015; Bruder *et al.*, 1994; Gu *et al.*, 2008).

The immediate goal of biomedical research in this area is to use innovative cell technologies (Paladino *et al.*, 2008; Weaver *et al.*, 2008; Krause, *et al.*, 2002). Most of the known technologies for taking bone marrow from living individuals for subsequent bone marrow transplantation (Nolan *et al.*, 2010; Zielins *et al.*, 2016; Rothrauff *et al.*, 2013). use of an isolated stem cell concentrate involves the use of invasive trepanobiopsy techniques (Vos *et al.*, 2006; Jamshidi *et al.*, 1971; Lu *et al.*, 2011). For the first time, mesenchymal stem cells were found in the bone marrow (Norgren *et al.*, 2007; Onodera *et al.*, 2010), but all bone marrow studies were conducted on the bone marrow of flat bones – the red bone marrow (sternal puncture or iliac crest (Hernández 2015; Eagle *et al.*, 2018; Wei *et al.*, 2013). Studies of the bone marrow of tubular bones were not performed due to the impossibility of obtaining it in vivo.

This study aimed a quantitative analysis of multipotent mesenchymal stromal (MMSC) and hematopoietic stem cells (HSCs) in bone marrow samples of amputated limbs in a patient with skin

cancer of the limb.

## 2. MATERIALS AND METHODS:

### 2.1. Characteristics of the patient

This case is presented by one patient who had a lower limb amputation after signing informed consent. The indication for amputation was: a trophic ulcer of the limb with signs of malignancy. Obtaining bone marrow samples: The test bone marrow sample was obtained in the operating room immediately after the amputation of the lower limb. Bone marrow was extracted from the lumen of the femur with a Volkmann spoon into a sterile test tube, which was transported to the laboratory.

The bone marrow was subjected to soft homogenization with the addition of a phosphate-salt buffer. The removal of adipose tissue was carried out by 10 minutes of settling the sample, while the fat of the bone marrow rises to the upper layer. Without affecting the upper layer, the lower phase of nucleated bone marrow cells was taken into a new tube and washed twice in a phosphate buffer, followed by centrifugation at 400g for 5 minutes. The cell sediment was resuspended in 300 µl of phosphate buffer, and their number was calculated in the Goryaev chamber. The cell suspension was diluted with a phosphate buffer to a concentration of 107 cells/ml.

### 2.2. Immunophenotyping of HSCs and MMSCs

The study of the HSC and MMSC phenotype was performed by flow cytometry using direct immunofluorescence. We used ready-made monoclonal antibodies from B.D. Biosciences (Becton Dickinson, USA) labeled with FITC (fluorescein isothiocyanate), P.E. or RD1 (phycoerythrin), PC5, 5 (phycoerythrin-cyanin 5.5), PC7 (phycoerythrin-cyanin 7), and APC (allophycocyanin). The cd90-PE/CD45-PC5,5/CD45RA-PC5,5/CD34-PC7/CD38-APC panel was used for phenotyping HSCs. The human MSC Analysis Kit (Becton Dickinson, USA) containing the CD90-FITC/CD45-PE/CD34-PE/CD11b-PE/CD19-PE/HLA-DR-PE/CD105-PC5, 5/CD73-APC panel was used for phenotyping MMSCs. The distribution of antibodies along the fluorescence channels was carried out in accordance with the principles of panel formation for multicolored cytofluorimetric studies (*Kudryavtsev et al., 2015*). Sample preparation was performed using the standard method (*Sutherland et al., 2018*). At least 50,000 cells were analyzed in each sample.

A total of 5 µl of antibodies were added to

a 50 µl bone marrow sample, incubated in the dark for 15 min., 500 µl of BD FACS Solution 1X (Becton Dickinson) lysing solution was added, incubated for 10 min. in the dark, then centrifuged at 1500 rpm for 5 min., the supernatant was drained, the precipitate was washed three times with BD FACS Flow (Becton Dickinson) solution, followed by centrifugation at 1500 rpm for 5 min. 300 µl of BD FACS flow solution was diluted and analyzed using a flow cytometer BD FACSCantoII (Becton Dickinson). For immunophenotyping, HSCs used antibodies to surface antigens of human cells on the recommendation of the manufacturer B.D. Biosciences (Becton Dickinson) PE-Cy7 CD34, PE CD90 and a mixture of negative control antibodies (APC CD38, PerCP-Su5. 5 CD45 and PerCP-Su5. 5 CD45RA). Immunophenotyping of MMSCs was performed using the Human MSC Analysis Kit (Becton Dickinson), which contains conjugated antibodies to MMSC markers (FITC CD90, PerCP-Su5.5 CD105, and APC CD73), and a mixture of negative control antibodies (PE CD45, PE CD34, PE CD11b, PE CD19, and PE HLA-DR).

### 2.3. Characteristics of the used markers

CD11b is non-covalently associated with  $\beta 2$  integrin and is expressed on granulocytes, macrophages, dendritic cells, N.K. cells, and subsets of T and B cells. CD11b It participates in the transfusion of cells such as neutrophils and monocytes, increases the activity of neutrophils, causes granulocyte adhesion, increases the activity of neutrophils (<https://www.biolegend.com/en-us/products/fic-anti-human-cd11b-antibody-8299>).

CD19 is part of the superfamily of immunoglobulins expressed on B cells and follicular dendritic cells. CD19 is involved in the development, activation, and differentiation of B cells. CD34 is a monomeric sialomucin-like type I glycoprophosphoprotein, selectively expressed on most hematopoietic stem/progenitor cells, bone marrow stromal cells, capillary endothelial cells, embryonic fibroblasts, and some nerve tissues. CD34 mediates cell adhesion of lymphocytes by binding to L-selectin and E-selectin ligands.

CD38 is expressed on early hematopoietic progenitors and white blood cells, liver stellate cells, astrocytes, and epithelial cells. CD38 expression can be increased when cells are activated. CD38 catalyzes the production of ADP cyclic ribose. CD38 induces proinflammatory cytokine production and proliferation.

CD90, also known as Thy-1, a member of

the immunoglobulin superfamily, interacts with CD45 during signal transduction during lymphocyte proliferation and differentiation. CD90 is expressed on hematopoietic stem cells, neurons, thymocytes, peripheral T cells, fibroblasts, and stromal cells (Alexa Fluor®). CD45, a panleukocytic marker represented by a single-stranded I-type membrane glycoprotein. CD45 is a signaling molecule that regulates various cellular processes, including cell growth, differentiation, cell cycle, and oncogenic transformation.

CD45RA, a marker of young cells, a variant of the 4-exon compound of CD45 tyrosine phosphatase. The CD45RA isoform is expressed on resting T cells, medullary thymocytes, B cells, and monocytes. CD73 is expressed on mesenchymal stem cells, T and B cells and their derivatives (<https://www.biolegend.com/en-us/products/pe-anti-human-cd73-ecto-5-nucleotidase-antibody-6092>). CD73 performs t-cell costimulation and mediates lymphocyte adhesion to follicular dendritic cells and endothelial cells.

CD105, an integral membrane homodimeric type I protein found on vascular endothelial cells and placental syncytiotrophoblasts. CD105 is not expressed on fibroblasts, but is detected on macrophages and monocytes (<https://www.biolegend.com/en-us/products/pe-anti-human-cd105-antibody-3711>). CD105 expression is increased on activated endothelium in tissues undergoing angiogenesis, such as tumors, or in cases of wound healing or skin inflammation.

HLA-DR, a marker of activated cells, an antigen of the main histocompatibility complex of class II, is expressed on B cells, activated T cells, monocytes/macrophages, dendritic cells, and other non-professional antigen-presenting cells

### 3. RESULTS AND DISCUSSIONS:

It is known that the amount of bone marrow obtained depends on the level of amputation (Nikolaeva, 2015). The level of amputation in this study was determined individually. The volume of extracted bone marrow was determined by the level of amputation (upper, lower, or middle third of the thigh) and was equal from 10 to 100 ml the largest amount of bone marrow (up to 100 ml) was obtained when the limb was amputated at the level of the upper third of the thigh. Bone marrow is a ready-made drug with many important effects (Zielins *et al.*, 2016; Rothrauff and Tuan, 2013). In this case, the patient was amputated at the level

of the middle third of the thigh. The number of cells in the bone marrow depended on the amount of bone marrow obtained and was approximately 500 thousand to 3 million cells per sample.

On average, the content of MMSC and HSC in the bone marrow of amputated limbs is the same, with a small predominance of the number of MMSCs. This patient was diagnosed with skin cancer of the lower leg, MMSCs were completely absent, it was the only bone marrow that did not have mesenchymal stem cells.

Malignant neoplasms have their own stem tumor cells. This is a small subpopulation of the least specialized cancer cells that have the ability to self-renew and give rise to all cell populations present in the original tumor, including initiating neoangiogenesis and growth of the tumor stroma. In all normal organs and tissues, there are stem cells that are responsible for self-renewal-physiological or reparative regeneration, as well as more specialized and Mature cells that perform the main functions of the organ or tissue. The same is true for tumors. That is, the tumor resembles an organ in structure and, of course, should not differ from the General principle of building biological structures.

It should be noted that for a long time, there was a question of how much cancer stem cells are similar to normal stem cells. And which type of stem cells first begins to change in malignant neoplasm. It was assumed that the tumor begins with changes in completely undifferentiated stem cells, giving rise to all other cells capable of almost unlimited self-renewal. Cancer stem cells in leukemia, these important cells-self-replicating beginnings of tumors do not originate from undifferentiated stem cells, but from their offspring-partially committed non-self-renewing progenitor cells (short-lived cells that can give rise to several, but not all, types of blood cells).

The genetic program of fully developed leukemic stem cells is not the same as that of normal stem cells. This is a very important discovery, which is likely to be typical for most other types of tumors because the most important properties of stem cells are resistance to damaging factors and rare division. These properties do not allow stem cells to accumulate the mass of genetic changes that are necessary for the transformation of a normal cell into a cancer cell. But progenitor cells, on the contrary, actively proliferate, but less plastic than stem cells. They are committed, and the ways of their further development are predetermined by gene expression and limited. In the study of the femoral bone marrow, hematopoietic and mesenchymal



stem cells were determined in the resulting bone marrow. Usually, the number of cells did not exceed 3 million. In this patient with skin cancer, the total number of cells was 75 million, which is much higher than the cell content in comparison with other amputations (25 times). In addition to the absence of MMSCs, this patient had a higher hematopoietic stem cell content than other amputations of 0.025%.

The cause of cancer is not yet clear, and this is a big problem. There are many theories, each representing some aspect and revealing the mystery of the curtain of the origin of the disease. But there are also those who contradict each other, and the general answer to the question—where does cancer come from? "not yet. At the present stage, the immune theory prevails, because the immune system is being suppressed, it is the immune system that first begins to fight mutated cells and destroys them in the first stages.

The etiology is based on several factors: there is an influence both external and internal, on genes during cell division and during normal life. As a result, the cells' genetics break down, and they mutate, turning into cancer cells. After that, such tissues begin to divide and grow endlessly, absorbing, and damaging the nearest organs. The so-called oncogenes were found — these are genes that, under certain conditions and external factors, begin to regenerate any cell in the body into a cancer cell. Until this state, these genes are dormant. That is, a gene is that part of the program code in the body that begins to work only at a certain moment and under certain conditions. That is why the risk of getting sick in people whose parents had cancer is higher than in others. But we must remember that all mutated or damaged cells are fought by our immune system, which constantly scans the body for damage and destroys dangerous cells. If the immune system is lowered, the chance of getting sick in this case is greater.

Today, this theory is the main and most common, which is used by almost all oncologists and scientists. Since all other theories are mostly just a risk factor, whether it's viruses or hepatogenic, it has been observed that most oncocytes occur in an acidic environment. In such an environment, the immune system and all nearby tissues of the body are weakened. And if the environment is made alkaline, then everything will be the opposite, and cancer cells will simply not be able to survive in it, and the immune system will be normal. When the environment is acidic, the immune system is greatly reduced, and the body has a favorable environment for the emergence of

cancer cells. Proponents of the immune theory believe that cancer cells constantly occur in the course of life, but the immune system periodically destroys them. With any impact inside the body and during the regeneration process, our cells grow and repair all damage. And the whole process is controlled by the immune system.

But with the constant occurrence of damage and various disorders, mutation may occur, and control may stop. In the laboratory, under any conditions, no doctor or scientist in the world has been able to turn a normal cell into a cancer cell. They were affecting it with both chemical reagents and radiation. No one in the lab was able to initiate metastasis. The DNA of a cancer cell is 70% similar to that of protozoa. Healthy cells cannot turn into cancer, changing by 70%. They can't move around the body and metastasize, forming new tumors.

The basis of the pathogenesis of all neoplasms is the appearance and reproduction of genetically modified tumor cells with special properties in the body. Tumor cells are changed genetically in the sense that they are able to transmit their pathological properties to descendants: when a tumor cell divides, daughter cells are formed, at least some of which retain their tumor properties. This transfer of tumor properties by cells to descendants can occur in an infinite number of generations. In most cases, the division of tumor cells is the main way to grow primary tumor nodes.

Primary nodes of many types of human and animal tumors are clones, i.e., all cells of this node are descendants of one original tumor cell. The tumor tissue also retains specific antigens of the original tissue. Therefore, successful transplantation of tumors to animals of other species (heterotransplantation) is possible only if the recipient's immune responses are weakened or prevented. This can be achieved in several ways:

1. transplanting tumor cells into tissues where immune responses are weakly induced, such as the anterior chamber of the eye or the brain;
2. introducing immunosuppressive drugs to the recipient;
3. using animals with genetic defects in the immune response as recipients.

Against the background of a weakened immune system, human tumors have already been successfully transplanted to animals. The properties of a population of tumor cells can



change during the growth of primary and secondary tumor nodes, as well as during the passivation of the transplanted tumor. These changes seem to be a consequence of the fact that new genetic variants of tumor cells with properties different from those of most cells in the population may appear in the tumor tissue. If these cell variants have any "advantages" over most tumor node cells, then as a result of selection, these cells will accumulate in the tumor tissue.

Persistent irreversible changes in one or more properties of tumor tissues are called tumor progression. The progression of each tumor can be multi-stage: during the development and growth of this tumor, several different variants of tumor cells may consistently prevail in it. Under normal conditions, each subsequent stage of progression increases the difference between the tumor tissue and the original normal tissue. As a result of tumor growth, its individual cells can break off, get into other organs and tissues, and cause the growth of a secondary, daughter tumor there. This process is called metastasis, and the daughter tumor is called metastasis.

Only malignant neoplasms are prone to metastasis. In this case, the structure of metastases usually does not differ from the primary tumor. Very rarely, they have even lower differentiation, and therefore are more malignant. There are three main ways of metastasis: lymphogenic, hematogenic, and implantation.

- a. The lymphogenic pathway of metastasis is the most frequent. Depending on the ratio of metastases to the lymph flow pathway, antegrade and retrograde lymphogenic metastases are isolated.
- b. The hematogenic pathway of metastasis is associated with the entry of tumor cells into the blood capillaries and veins.
- c. The implantation pathway of metastasis is usually associated with the entry of malignant cells into the serous cavity (when all layers of the organ wall germinate) and from there - to neighboring organs. The fate of a malignant cell that has entered the circulatory or lymphatic system, as well as the serous cavity, is not completely predetermined: it can give rise to a daughter tumor, or it can be destroyed by macrophages.

Currently, there are no changes in the clinical and biochemical parameters of blood that are specific for oncological processes. However, recently, tumor markers (O.M.) have become

increasingly important in the diagnosis of malignant tumors. O.M. in most cases are complex proteins with a carbohydrate or lipid component, synthesized in tumor cells in high concentrations. These proteins can be associated with cellular structures and then they are detected in immunohistochemical studies.

A large group of O.M. is secreted by tumor cells and accumulates in the biological fluids of cancer patients. In this case, they can be used for serological diagnostics. The concentration of O.M. (primarily in the blood), to a certain extent, may correlate with the occurrence and dynamics of the malignant process. In recent years, there have been a number of trends in the epidemiological situation of cancer morbidity and mortality: first, there has been an increase in cancer morbidity and mortality in all countries of the world.

For many years, oncological diseases have confidently occupied the 2nd place in the structure of causes of death after cardiovascular pathology. Since there is now a tendency to reduce mortality from the latter, tumors have a clear chance of becoming a leader among the causes of death in the XXI century. Secondly, the increase in the incidence of tumors is registered in all age groups, but the largest number of cancer patients are people older than 50 years. Proto-oncogenes: these are normal cell genes that are usually inactive. Their activation and transformation into oncogenes that encode certain oncoproteins are accompanied by cell proliferation. Normally, this process takes place in embryogenesis, with age-related growth of organs and tissues, and regeneration. Antioncogenes: Genes that have the opposite effect. The most studied antioncogene p53. Pathological activation of oncogenes or suppression of antioncogenes can lead to tumor growth.

#### 4. CONCLUSIONS:

The development of a pathological process of an oncological nature is affected by the state of the bone marrow. Perhaps this is the root cause of the etiological factor. If mesenchymal stem cells are completely absent, it can be assumed that the body's defenses are exhausted. (in this case, the patient died after four weeks). A significant number of hematopoietic stem cells show that the generalization process occurs through these stem cells.

Mesenchymal stem cells (MSCS) are the precursors of a number of human tissues and have a wide range of possible applications in medicine. The uniqueness of MSCS is that when cells are

grown outside the body, they multiply rapidly, but do not differentiate into anything specific until a unique stimulus is applied. The peculiarity of mesenchymal cells is their ability to give rise to many cells such as muscle cells, bone cells, fat cells, and even neurons, and hematopoietic stem cells only all blood cell lines ( <https://www.differencebetween.com/difference-between-mesenchymal-and-hematopoietic-stem-cells/>).

Stem cells are undifferentiated or non-specialized cells present in our bodies. They are able to divide and give the same type of stem cells or differentiate into specialized cells in tissues that have specific functions. These features of stem cells make it possible to apply them in regenerative medicine. These two types of stem cells each perform certain functions. Presumably, hematopoietic stem cells are more differentiated than mesenchymal stem cells. Mesenchymal stem cells are a type of adult stem cells that are multipotent and can differentiate into several different specialized cell types, including cells of neurons, bones, cartilage, muscle, and adipose tissue. These cells are stromal cells or connective tissue cells. Mesenchymal stem cells are small in size with thin processes on the surface.

Pluripotent stem cells are also hematopoietic stem cells, which are especially abundant in the bone marrow of flat bones. Hematopoietic stem cells provide the hematopoietic system with all the necessary cells. Therefore, the process of differentiation of hematopoietic stem cells (hematopoiesis) mainly occurs in the bone marrow. Since hematopoietic stem cells can form any type of blood cell, they are also called blood stem cells. In addition to the bone marrow, there are few hematopoietic stem cells in the peripheral blood and cord blood.

Hematopoietic and mesenchymal stem cells of the bone marrow are multipotent. They can differentiate into different types of specialized cells. They are found in tissues throughout the body. They are also found in cord blood, cord tissue, and placental tissue. Both types of cells are used in the repair and regeneration of damaged tissue. The bone marrow contains both of these types of cells. Mesenchymal stem cells facilitate hematopoiesis.

Mesenchymal stem cells are multipotent stem cells that can differentiate into cells of neurons, bones, cartilage, muscle, and adipose tissue, whereas hematopoietic stem cells are multipotent stem cells that can differentiate into any type of blood cell. The main difference

between mesenchymal and hematopoietic cells is differentiation into different end cells.

Mesenchymal stem cells are now found in many tissues. Hematopoietic stem cells are found in the bone marrow and peripheral blood, especially in cord blood. Both types of cells are of great importance in the treatment of diseases. Mesenchymal stem cells are used in the treatment of diabetes, heart disease, liver disease, stroke injuries, spinal cord injuries, lung cancer, etc., while hematopoietic stem cells are used in the treatment of blood and bone diseases, including blood cancer, autoimmune disorders. And some genetic disorders, etc. So this is also the difference between mesenchymal and hematopoietic stem cells.

Hematopoietic and mesenchymal stem cells ensure the restoration of tissues and organs in case of damage, ensuring the functional state of the body as a whole. Each type of these cells ensures the constancy of the cellular composition of blood and tissues (<https://www.differencebetween.com/difference-between-mesenchymal-and-hematopoietic-stem-cells/>). Mesenchymal stem cells can differentiate into cells of neurons, bones, cartilage, muscle, and adipose tissue, while hematopoietic stem cells can differentiate into blood cells of any type. In addition, mesenchymal stem cells are present in bone marrow. Mesenchymal stem cells have a higher differentiation potential and create a greater variety of cells. In hematopoietic stem cells, it is much lower, they are responsible for the presence

First of all, a hematopoietic cell is a cell that gives rise to all blood cells. Over time, it differentiates and forms certain histogenetic series for white blood cells, red blood cells, and platelets. All these seemingly different cells came from a single cell. The hematopoietic cell is the least immature. The process of its maturation and hematopoiesis begins directly in the red bone marrow under the action of certain components such as macrophages, reticulocytes, cytokines, and growth factors. Stem hematopoietic cells, as well as mesenchymal cells, are used for transplantation, receiving them from the bone marrow and cord blood

By their nature, mesenchymal stem cells (MSCS) and hematopoietic cells share a common ancestor. However, in the process of differentiation, they have taken very different paths histogenesis. Thus, MSCS gives rise to the connective tissue itself, the cells lining the vessels, and other mesenchyma derivatives.

Accordingly, getting it will be the same, but

the application will be different. Violation of the processes of regenerative regeneration of an organ, accompanied by a lack of its function, is characterized by growing and not compensated cell death. This is facilitated by violations of information intercellular interaction, regulated primarily by cells of the immune system, and deep inhibition of migration activity of stem and progenitor cells that provide structural replacement of differentiated dead cells. The bone marrow is the only organ in which two different types of stem cells coexist and interact functionally.

The main functions of bone marrow MSCs are 1. Formation of a hematopoietic microenvironment (GIM). 2. The formation of a stromal microenvironment. 3. Participation in morphogenesis. 4. Self-maintenance and recovery of the MSK pool. 5. Participation in homeostatic reactions of the body and in the processes of regeneration, repair, and adaptation of the mesenchymal cell system in normal and pathological conditions.

Mesenchymal stem cells play an important role in the capture of hematopoietic stem cells by the stroma (extracellular matrix and stromal cells), differentiation of hematopoietic cell precursors into Mature cells under the influence of various secretory factors. It is assumed that the study of mesenchymal stem cells of the bone marrow in various diseases of the hematopoietic system will help to detect the mechanisms of regulation and maintenance of normal hematopoiesis.

Along with the increased interest in mesenchymal stem cells, the vast majority of research is conducted with samples of mesenchymal stem cells from healthy subjects and removed from various areas. On the other hand, the presence of various pathologies of hematopoietic cells, such as leukemia, suggested the presence of possible compensatory adaptive changes in mesenchymal stem cells, which are components of the bone marrow microenvironment, the study of which will lead to a better understanding of the mechanism of the development of blood pathology.

## 5. ETHICS:

Permission was obtained from the Ethics Committee to conduct this study (Protocol No. 56/2014).

## 6. REFERENCES:

1. Nikolaeva, L. P., Cherdantsev, D. V., and Titov, K. S. (2017). The characteristic of bone marrow stem cells of patients with the complicated diabetes. *Russian Journal of Biotherapy*, 16(1), 47–50. <https://doi.org/10.17650/1726-9784-2017-16-1-47-50>
2. Nikolaeva L.P., Cherdantsev DV., Gorbenko AS., Olkhovsky IA. (2015). Amputee bone marrow as a possible source of stem cells. *Basic research*, 6:301. (In Russian)] DOI 10.17513/spno.21082
3. Sislá, B. Manual of laboratory Hematology. Per. from English. M.: Practical medicine; 2011. 352 s. (In Russian)]
4. Nikolaeva, L. P. (2015). Peculiarities of hematopoiesis in the yellow bone marrow of a human. *Modern Problems of Science and Education*, (6). <http://dx.doi.org/10.17513/spno.130-23914>
5. Krivolapov, Yu. A. (2011). Histological examination of trepanobiopsy bone marrow : selected lectures. Saint Petersburg: COSTA.
6. Paladino, L., Sinert, R., Wallace, D., Anderson, T., Yadav, K., and Zehtabchi, S. (2008). The utility of base deficit and arterial lactate in differentiating major from minor injury in trauma patients with normal vital signs. *Resuscitation*, 77(3), 363–368. <https://doi.org/10.1016/j.resuscitation.2008.01.022>
7. Vos, G., Engel, M., Ramsay, G., and van Waardenburg, D. (2006). Point-of-care blood analyzer during the interhospital transport of critically ill children. *European Journal of Emergency Medicine*, 13(5), 304–307. <https://doi.org/10.1097/00063110-200610000-00013>
8. Nolan, J. P., Soar, J., Zideman, D. A., Biarent, D., Bossaert, L. L., Deakin, C., ... Böttiger, B. (2010). European Resuscitation Council Guidelines for Resuscitation 2010 Section 1. Executive summary. *Resuscitation*, 81(10), 1219–1276. <https://doi.org/10.1016/j.resuscitation.2010.08.021>
9. Norgren, L., Hiatt, W. R., Dormandy, J. A., Nehler, M. R., Harris, K. A., and Fowkes, F. G. R. (2007). Inter-Society Consensus for the Management of Peripheral Arterial Disease (TASC II). *Journal of Vascular Surgery*, 45(1), S5–S67. <https://doi.org/10.1016/j.jvs.2006.12.037>

10. Bruder, S. P., Fink, D. J., and Caplan, A. I. (1994). Mesenchymal stem cells in bone development, bone repair, and skeletal regeneration therapy. *Journal of Cellular Biochemistry*, 56(3), 283–294. <https://doi.org/10.1002/jcb.240560303>
11. Gu, Y. Q., Zhang, J., Guo, L. R., Qi, L. X., Zhang, S. W., Xu, J., ... Wang, Z. G. (2008). Transplantation of autologous bone marrow mononuclear cells for patients with lower limb ischemia. *Chinese Medical Journal*, 121(11), 963–967.
12. Weaver, C. V., and Garry, D. J. (2008). Regenerative biology: a historical perspective and modern applications. *Regenerative Medicine*, 3(1), 63–82. <https://doi.org/10.2217/17460751.3.1.63>
13. Krause, J. (2002). Bone marrow overview. In B. Rodak (Eds.). *Hematology: Clinical Procedures and Applications* (pp. 188–195). 2nd ed. Philadelphia: WB Saunders.
14. Jamshidi, K., and Swaim, W. R. (1971). Bone marrow biopsy with unaltered architecture: a new biopsy device. *The Journal of Laboratory and Clinical Medicine*, 77(2), 335–342.
15. Lu, D., Chen, B., Liang, Z., Deng, W., Jiang, Y., Li, S., ... Chen, S. (2011). Comparison of bone marrow mesenchymal stem cells with bone marrow-derived mononuclear cells for treatment of diabetic critical limb ischemia and foot ulcer: A double-blind, randomized, controlled trial. *Diabetes Research and Clinical Practice*, 92(1), 26–36. <https://doi.org/10.1016/j.diabres.2010.12.010>
16. Onodera, R., Teramukai, S., Tanaka, S., Kojima, S., Horie, T., Matoba, S., ... Fukushima, M. (2010). Bone marrow mononuclear cells versus G-CSF-mobilized peripheral blood mononuclear cells for treatment of lower limb ASO: pooled analysis for long-term prognosis. *Bone Marrow Transplantation*, 46(2), 278–284. <https://doi.org/10.1038/bmt.2010.110>
17. Cobellis, G., Silvestroni, A., Lillo, S., Sica, G., Botti, C., Maione, C., ... Sica, V. (2008). Long-term effects of repeated autologous transplantation of bone marrow cells in patients affected by peripheral arterial disease. *Bone Marrow Transplantation*, 42(10), 667–672. <https://doi.org/10.1038/bmt.2008.228>
18. Hernández, P. (2015). Use of bone marrow-derived cells for regenerative medicine in Cuba. *Bone Marrow Transplantation*, 51(1), 134–134. <https://doi.org/10.1038/bmt.2015.200>
19. Eagle, M. J., Man, J., Rooney, P., and Kearney, J. N. (2018). Comparison of bone marrow component removal from processed femoral head bone from living and deceased donors: presence of geodes in living donor bone can prevent maximum removal of marrow components. *Cell and Tissue Banking*, 19(4), 727–732. <https://doi.org/10.1007/s10561-018-9726-x>
20. Wei, H., Shen, G., Deng, X., Lou, D., Sun, B., Wu, H., ... Zhao, J. (2013). The role of IL-6 in bone marrow (BM)-derived mesenchymal stem cells (MSCs) proliferation and chondrogenesis. *Cell and Tissue Banking*, 14(4), 699–706. <https://doi.org/10.1007/s10561-012-9354-9>
21. Zielins, E. R., Ransom, R. C., Leavitt, T. E., Longaker, M. T., and Wan, D. C. (2016). The role of stem cells in limb regeneration. *Organogenesis*, 12(1), 16–27. <https://doi.org/10.1080/15476278.2016.1163463>
22. Rothrauff, B. B., and Tuan, R. S. (2013). Cellular therapy in bone-tendon interface regeneration. *Organogenesis*, 10(1), 13–28. <https://doi.org/10.4161/org.27404>
23. FITC anti-human CD11b Antibody. Retrieved from <https://www.biolegend.com/en-us/products/fits-anti-human-cd11b-antibody-8299>
24. Alexa Fluor® 488 anti-rat CD90/mouse CD90.1 (Thy-1.1) Antibody. Retrieved from <https://www.biolegend.com/en-us/products/alexa-fluor-488-anti-rat-cd90-mouse-cd90-1-thy-1-1-antibody-3126>
25. PE anti-human CD73 (Ecto-5'-nucleotidase) Antibody. Retrieved from <https://www.biolegend.com/en-us/products/pe-anti-human-cd73-ecto-5-nucleotidase-antibody-6092>
26. PE anti-human CD105 Antibody. Retrieved from <https://www.biolegend.com/en-us/products/pe-anti-human-cd105-antibody-3711>
27. Difference Between Mesenchymal and Hematopoietic Stem Cells. Retrieved from <https://www.differencebetween.com/difference-between-mesenchymal-and-hematopoietic-stem-cells>

## PULVERIZAÇÃO POR MAGNETRON DE FILMES FINOS NANOCRISTALINOS DE TiN E PROPRIEDADES DE CORROSÃO

### MAGNETRON SPUTTERED NANOCRYSTALLINE TiN THIN FILMS AND CORROSION PROPERTIES

خصائص التآكل للأغشية الرقيقة النانوية TiN المحضرة بطريقة التريز الماكتروني للتيارات المستمرة

HAMIL, Muslim Idan<sup>1\*</sup>, KHALAF, Mohammed K<sup>2</sup>, AL-SHAKBAN, Mundher<sup>3</sup>

<sup>1,3</sup> Department of Physics, Faculty of Science, University of Misan, Maysan, Iraq.

<sup>2</sup> Center of Applied Physics, Directorate of Materials Research, Ministry of Science and Technology, Baghdad, Iraq.

\* Corresponding author

e-mail: muslim.iddan@uomisan.edu.iq

Received 26 March 2020; received in revised form 01 May 2020; accepted 16 May 2020

## RESUMO

Neste relatório, filmes finos nanocristalinos de TiN foram depositados em substratos de vidro e Ti-6Al-4V utilizando o processo de pulverização por magnetron DC. Os filmes de TiN foram pulverizados usando um alvo de Ti puro (99,9%) com 40W de potência em atmosfera de mistura de gás Ar/N<sub>2</sub>. A estrutura dos filmes de TiN foi caracterizada por difração de raios-X, já que os filmes preparados exibiam uma orientação preferida (200), enquanto o filme recozido a 500 °C mostra os (111), (200) e (311). Filmes de TiN policristalinos, cúbicos e orientados a (111) foram produzidos com temperatura de recozimento de 500 °C. O efeito da temperatura depositada nas morfologias microestruturais dos filmes finos foi estudado por Microscópio Eletrônico de Varredura por Emissão de Campo (FESEM). O tamanho das partículas dos filmes de TiN pulverizados variou de 50 a 70 nm e foi fortemente influenciada pelas temperaturas de recozimento, a morfologia dos filmes depositados antes e após o recozimento apresenta uma aglomeração característica de partículas. A análise de polarização potenciodinâmica dos filmes de TiN confirma a relação inversa entre resistência de polarização e corrente de corrosão. Também foram obtidas as medidas de biocorrosão para filmes de TiN depositados no substrato Ti-6Al-4V em solução de NaCl a 3,5%. Foi observada uma clara melhoria na resistência à corrosão, e em oposição as não tratadas, especialmente para amostras de TiN/Ti-6Al-4V com recozimento térmico (500 °C). A taxa de corrosão foi de 0,1458 mm/ano para a amostra não revestida, enquanto que nas amostras de TiN/Ti-6Al-4V após o recozimento foi de 2,668·10<sup>-4</sup> mm/ano. O potencial médio de corrosão calculado foi 0,117 V. Os resultados confirmaram que as ligas revestidas com tratamento térmico a 500 °C exibiram um melhor comportamento eletroquímico em comparação com as ligas não revestidas e não tratadas termicamente, possivelmente devido ao melhor grau de coesão dos revestimentos.

**Palavras-chave:** Técnica PVD, filmes finos, nitreto de titânio, liga Ti-6Al-4V, biocorrosão.

## ABSTRACT

In this report, TiN nanocrystalline thin films were deposited on glass and Ti-6Al-4V substrates using a DC-magnetron sputtering technique. The TiN films were sputtered using a pure Ti target (99.9%) with 40W of power in Ar/N<sub>2</sub> gas mixture atmosphere. The structure of the TiN films was characterized by X-Ray diffraction, as prepared films exhibited a (200) preferred orientation, while film annealed at 500 °C shows the (111), (200) and (311). Polycrystalline, cubic, (111)-orientated TiN films were produced by annealing temperature of 500 °C. The effect of deposited temperature on the microstructural morphologies of the thin films was studied by Field Emission Scanning Electron Microscope (FESEM). The particle size of the sputtered TiN films ranged from 50 to 70 nm and was strongly influenced by annealing temperatures, the morphology of the films deposited before and after annealing has a characteristic agglomeration of particles. Potentiodynamic polarization analysis of the TiN films confirms the inverse relationship between polarization resistance and corrosion current. The biocorrosion measurements for TiN films deposited on the Ti-6Al-4V substrate in 3.5% NaCl solution have also been obtained. Clear improvement in the corrosion resistance was observed rather than for untreated, especially for thermally annealed (500 °C) TiN/Ti-6Al-4V samples. The corrosion rate was 0.1458 mm/y for the uncoated sample, while 2.685·10<sup>-4</sup> mm/y for TiN/Ti-6Al-4V in samples after annealing. The average corrosion

potential calculated was - 0.117 V. The results confirmed that coated alloys with 500 °C thermally treated exhibited a better electrochemical behavior compare with uncoated and non-thermally treated alloys possibly due to the better cohesion degree of the coatings.

**Keywords:** PVD technique, thin films, titanium nitride, Ti-6Al-4V alloy, biocorrosion.

## المخلص

في هذا البحث، تم إجراء هذه الدراسة من أجل زيادة مقاومة التآكل البيولوجي للأغشية الرقيقة النانوية TiN المرسبة بإحدى طرائق التبخير الفيزيائية (Physical Vapor Deposition). تم ترسيب الأغشية الرقيقة النانوية TiN على ركائز الزجاج وسبيكة Ti-6Al-4V باستخدام تقنية الترديد الماكنتروني للتيارات المستمرة. حيث تم ترديد الأغشية الرقيقة باستخدام هدف من التيتانيوم النقي (Ti) بقوة 40 W تحت خليط من غاز الأركون والنيتروجين Ar/N<sub>2</sub>. شخص التركيب البلوري للأغشية الرقيقة TiN باستخدام تقنية حيود الأشعة السينية X-Ray. حيث أظهرت الأغشية الرقيقة المطلية على الزجاج اتجاهها (200)، بينما بعد التلدين وعند درجة حرارة 500 درجة مئوية أظهرت مزيج من الاتجاهات (111)، (200) و (310). نستنتج من ذلك أن الغشاء الرقيق TiN ذات اتجاه (111)، مكعبي و Polycrystalline. بعد ذلك، تم دراسة تأثير الحرارة على التركيب النانوي للغشاء الرقيق المشخص باستخدام المجهر الإلكتروني الماسح (FE-SEM)، وبفعل المعالجة الحرارية، ازداد الحجم الحبيبي للأغشية الرقيقة من 50 إلى 70 نانومتر مع زيادة تكتل الحبيبات النانوية للغشاء الرقيق. لقياسات التآكل البيولوجي، تم غمر السبيكة Ti-6Al-4V المطلية بالغشاء الرقيق TiN في محلول كلوريد الصوديوم وبنسبة ( 3.5% NaCl)، إذ تم حساب التآكل البيولوجي لهذا السبائك المطلية وغير المطلية من خلال Potentiodynamic Polarization. لوحظ أن مقاومة التآكل للغشاء الرقيق المملن ازدادت بشكل واضح، بالإضافة إلى أن معدل التآكل للسبيكة النقية (غير المطلية)  $0.1458 \text{ mm/y}$  إلى  $2.685 \times 10^{-4} \text{ mm/y}$ ، بينما معدل التآكل للسبيكة المطلية والمملنة انخفض إلى  $2.685 \times 10^{-4} \text{ mm/y}$ . أظهرت النتائج أن المعالجة الحرارية حسنت من صفات السبيكة المطلية والمعالجة حرارياً عند درجة حرارة 500 درجة مئوية وأيضاً أظهرت هذه السبائك سلوكاً كهروكيميائياً أفضل بالمقارنة مع السبائك غير المطلية وغير المملنة ربما بسبب درجة التماسك الأفضل للطلاء.

**الكلمات المفتاحية:** تقنية الترسيب التبخير الفيزيائية، الأغشية الرقيقة، نيتريد التيتانيوم، سبيكة Ti-6Al-4V، التآكل البيولوجي

## 1. INTRODUCTION:

Titanium nitride has shown its potential application in various industries including an anti-corrosive coating or a hard coating on cutting tools because of its important properties such as corrosion resistance and high hardness (Borah, Pal, Bailung, and Chutia, 2008; Fenker, Balzer, Kappl, and Banakh, 2005). TiN thin films have been prepared using several methods such as electrodeposition (Ma, Jiang, and Xia, 2017), dynamic mixing (Takano, Isobe, Sasaki, and Baba, 1989), hollow cathode discharge ion plating (Chou, Yu, and Huang, 2001), and pulsed laser deposition (Xu, Du, Sugioka, Toyoda, and Jyumonji, 1998). However, DC-magnetron sputtering was mostly used to deposit TiN thin films, and this method presents a high ionization rate (> 40 %) which make it a good technique to obtain dense coatings (Kouznetsov, Macak, Schneider, Helmersson, and Petrov, 1999; Manouchehri, AlShiaa, Mehrparparvar, Hamil, and Moradian, 2016; Paulitsch, Mayrhofer, Münz, and Schenkel, 2008; Paulitsch, Schenkel, Zufraß, Mayrhofer, and Münz, 2010), as well as good mechanical properties, increase the adhesion between the film and the ceramics and/or metals substrates (Schönjahn *et al.*, 2000). The deposition of TiN using magnetron sputtering has significant specific advantages such as low levels of impurities and easy control of the deposition rate. This method enables the production of thin films in various morphology and crystallographic structures (Kelly and Arnell, 2000; Khalaf,

Hassan, Khudiar, and Salman, 2020).

The use of Ti and TiN films as protective coatings is rapidly growing so that it is important to know their corrosion properties. Also, Ti compounds and its alloys such as Ti-6Al-4V and TiN, in particular, are being increasingly used as biomaterials (Manso-Silvan, Martínez-Duart, Ogueta, García-Ruiz, and Pérez-Rigueiro, 2002), they also have excellent properties, e.g., biocompatibility, corrosion resistance, low density, mechanical strength, and relatively low cost. These properties make titanium and its alloys a potential dental implant material. Among these features, the corrosion resistance is of great importance, not only because it determines the device's service life, but also because of the harmfulness of the corrosion processes taking place in the living organism (Veiga, Davim, and Loureiro, 2012).

This paper reports data for TiN thin films grown on glass and Ti-6Al-4V substrates by using DC magnetron-sputtering deposition. The corrosion behavior was investigated by measuring the polarization curve (Tafel). We focus on the annealing temperature in controlling the structural and corrosion properties of the TiN films produced.

## 2. MATERIALS AND METHODS:

### 2.1. Experimental

TiN thin films were deposited on glass,

and Ti6Al4V substrates by D.C were sputtering. The glass substrates were cleaned ultrasonically by ethanol and deionized water for 15 min before sputtering and then loaded to the substrate holder of the sputtering machine. Corning # 7059 glasses (30 × 40 × 1.2 mm<sup>3</sup>) were used, while the Ti-6Al-4V samples were cut to 20 mm × 20 mm diameter then grinded by 500 microns SiC grinding paper. The substrates were cleaned by using ultrasonic twice in ethanol 96% (Sigma Aldrich, England), then by distilled water for 15 min and allowed to dry in discaiter at room temperature for 24 h (Hamil, Siyah, and Khalaf, 2020). The sputtering target was a pure Ti disc (99.99%, 2 inches, and diameter 5 mm thick). The base pressure was 1·10<sup>-5</sup> Torr, and the sputtering was carried out in Ar:N<sub>2</sub> (90:10) atmosphere. Before starting the deposition, the target was pre-sputtering for 15 min with a shutter located between the target and substrate. During all depositions, the target to substrate distance and sputtering power were adjusted at 60 mm and 40 W, respectively. The pressure of the sputtering chamber was pumped down to 5·10<sup>-3</sup> Torr before deposition. Then nitrogen gas was introduced into the chamber, and the required pressure was set. After that, argon gas was introduced until the preset pressure was reached.

When the preset total pressure was reached, the nitrogen was shut off, and the target was preset in an argon atmosphere for around 10 min to avoid the target's surface oxide layer. After presputtering, the nitrogen gas was again introduced into the chamber with a flow rate ratio of Ar(90)/N<sub>2</sub>(10), and the sputtering process starts. The sputtering conditions are listed in Table 1.

The structural properties of TiN films were obtained by the X-ray diffraction (Philips Geiger using CuKα ( $\lambda = 1.54 \text{ \AA}$ ). The FE-SEM (TESCAN MIRA3) was used to observe the morphology of the films. The corrosion process was determined using ASTM G1-03/ASTM G102, and the corrosion behavior was investigated by measuring the polarization curve (Tafel).

### 3. RESULTS AND DISCUSSION:

#### 3.1 X-Ray diffraction

Figure 2 shows X-ray diffraction patterns of the samples before and after heat treatment at 500 °C for 2 h. The low intensity of the X-ray diffraction peaks, as well as its large widths, clearly indicates that the deposited films are not fully crystalline and that a large fraction of the

films are still amorphous and are in agreement with previous studies (Vasu, Krishna, and Padmanabhan, 2011). As-deposited Titanium nitride films deposited before thermal annealing shows a single crystalline peak corresponding to a plane (200) at  $2\theta = 36.86^\circ$  for comparison (JCPDS file number 77-1893) (Vasu *et al.*, 2011). The Bragg angle of the plane (200) had shifted to another angle. Close examination of the XRD pattern of the thermally annealed films deposited at 500°C with deposition time 2 h revealed that the tetragonal TiN phase had appeared more clearly with planes (111) and (311) (Chawla, Jayaganthan, and Chandra, 2008; Fenker *et al.*, 2005). At 500 °C thermally annealed thin films, the intensity of the Bragg reflections had increased in comparison with the as deposited thin films, at higher annealing temperatures, thermal energy enhances the mobility of the active sites, and this leads to grain growth (Kavitha, Kannan, Reddy, and Rajashabala, 2016), which is evidence for improved crystallinity.

The XRD pattern of the deposited film shows a weak peak at  $37^\circ$ , which can be related to the (111) crystallographic orientations of TiN with a face-centered cubic (FCC) structure (JCPDS card number 02-1159) (Kavitha *et al.*, 2016). It is known that the FCC structure of TiN may form when nitrogen atoms occupy all the octahedral sites of titanium with hexagonal close-packed (HCP) or body-centered cubic (BCC) structures. This transformation in titanium structure from HCP and BCC to FCC occurs due to the accommodation of nitrogen atoms with a small size in the interstitial sites of Ti with the larger size. The absence of a titanium peak in the XRD pattern demonstrates the absence of Ti atoms in the structure of the films and completes the nitride formation process. The competition between the surface energy, the strain energy, and the stopping energy of different lattice planes of a film affect the preferred orientation and lowest total energy of the film (Pelleg, Zevin, Lungu, and Croitoru, 1991; Zhao *et al.*, 1997). In the case of TiN film, the direction of the lowest energy is (111) direction. Annealing, the film did not influence the preferred orientation but increased the intensity of the peak. By increasing the annealing temperatures to 500 °C, TiN (111), peak intensity is increased. Thermal energy produced by annealing leads to the enhancement of mobility of active sites. The increase of mobility can be attributed to grain growth and the reduction of defects during the annealing treatment (Wang *et al.*, 2013).



### 3.2 Surface morphology of the TiN layers

Typical FESEM images of TiN films deposited on glass substrates under different deposition currents, before and after annealing at 400 and 500 °C, are shown in figure 3 (a – f). The amorphous particles and nonuniform clumps were observed before heat treatment. The agglomeration of the particles resulted in the formation of clusters. The FESEM micrograph of as-deposited TiN revealed that the average particle size of TiN is in the range of (25 nm). It is found that the TiN crystallite size has been increased after annealing, where the average particle size of TiN coated at 400, and 500 °C increased to 50 nm to 70 nm, respectively. The increase in annealing temperature (i.e., The crystallinity of the film increases), provides extra energy to the adatoms and results in increasing order of the microstructure and particle size. However, the excessive supply of annealing temperature may cause a degradation of the preferred orientation, and the film will suffer from the bombardment of highly energized particles, resulting in internal defects of the film (Chen, McEwen, Zaveri, Karpagavalli, and Zhou, 2012).

### 3.3 Corrosion measurements

Various electrochemical techniques have been applied to study the behavior of corrosion, for example, potentiodynamic polarization (Tafel analysis). Tafel analysis is a well-established electrochemical technique, and the current is recorded when the open-circuit potential is imposed on a metal sample. The corrosion rate calculated from combined Equation 1 and 2 (Chen *et al.*, 2012; Hamil *et al.*, 2020), polarization resistance ( $R_p$ ) has an inverse relationship with corrosion current.

$$I_{corr} = \frac{\beta_a \beta_c}{2.3 R_p (\beta_a + \beta_c)} \quad (\text{Eq. 1})$$

Where,  $\beta_a$  = anodic Tafel slope,  $\beta_c$  = cathodic Tafel slope.

$$\text{Corrosion Rate (C.R)} = \frac{I_{corr} \times K \times EW}{d \times A} \quad (\text{Eq. 2})$$

K= constant that define the units of the corrosion rate =  $3.272 \cdot 10^{-3}$  mm/( $\mu\text{A}$  year), EW= equivalent weight (g/equivalent) = 11.768 g/eq., d = density ( $\text{g/cm}^3$ ) =  $4.420 \text{ g/cm}^3$ , A = sample area ( $\text{cm}^2$ ) =  $0.151 \text{ cm}^2$ .

The polarization curve (Tafel) diagram for TiN coated on Ti6Al4V alloy were presented in figure (4). When the Ti6Al4V alloy was immersed in simulated biological 3.5% NaCl solution (Bodunrin, Chown, van der Merwe, and Alaneme, 2018; Bodunrin, Chown, van der Merwe, and Alaneme, 2019; Dai, Zhang, Zhang, Chen, and Wu, 2016), the average corrosion potential is (-0.117) V. The corrosion potential shifted to the cathode side for samples coated with TiN before, and after annealing, the potential values were -0.0547 and -0.048 V, respectively. Moreover, the corrosion current  $I_{corr}$  was obtained from the polarization curves by extrapolation of the anodic and the cathodic branches of the polarization curve to the corrosion potential. The corrosion current of TiN films before and after annealing were  $4.6323 \cdot 10^{-8}$  and  $4.6541 \cdot 10^{-9}$  A/ $\text{cm}^2$ , respectively. Also, the corrosion rate of coated samples was lower compared with Ti-6Al-4V alloy, and this was expected because the reduction in corrosion rate means the reduction in weight loss from sample material. The weight loss (W) was calculated from Equation 3 (Hamil *et al.*, 2020), Table (2).

$$W = \text{Corr. Rate} \frac{mm}{y} \times \rho \times 3.17 \times 10^{-9} \quad (\text{Eq. 3})$$

Also, open-circuit potential (OCP) is the other typical technique to study the corrosion. Figure (5) shows the variation of OCP with immersion time for TiN coated Ti-6Al-4V alloy in 3.5 NaCl% solution at 25 °C. The initial OCP for uncoated Ti-6Al-4V was -0.772 V, the potential gradually increased to be -0.512 and 0.067 V for the samples TiN coated before and after thermal annealing.

In general, the coated samples show a positive shift in corrosion potential value and decreasing in both corrosion current and corrosion rate values in comparison with the bare substrate. Moreover, a positive shift in corrosion potential value and decreasing in both corrosion current and corrosion rate values with thermal annealing are observed. These results can be ascribed to the formation of a passive layer.

## 4. CONCLUSIONS:

TiN films were prepared by DC-magnetron sputtering technique, film annealed at 500 °C exhibited cubic phase TiN. It has been observed that the particle sizes and corrosion properties were strongly influenced by temperature

annealing, where the average particle size increased to 50 and 70 nm for the films heated at 400 and 500 °C. The corrosion rate of TiN film deposited on Ti-6Al-4V substrate decreased, where it was 0.1458 mm/year for uncoated sample while being  $2.685 \cdot 10^{-4}$  mm/year TiN for the sample annealed at 500 °C, this sample also presents the polarization resistance ( $R_p$ ) of 3247 KΩ/cm<sup>2</sup>, while it was 1.719 KΩ/cm<sup>2</sup> for the uncoated sample.

## 6. REFERENCES:

1. Bodunrin, M. O., Chown, L. H., van der Merwe, J. W., and Alaneme, K. K. (2018). Corrosion behavior of Ti-Al-xV-yFe experimental alloys in 3.5 wt% NaCl and 3.5 M H<sub>2</sub>SO<sub>4</sub>. *Materials and Corrosion*, 69(6), 770-780.
2. Bodunrin, M. O., Chown, L. H., van der Merwe, J. W., and Alaneme, K. K. (2019). Corrosion behaviour of low-cost Ti<sub>4.5</sub> Al-x V-y Fe alloys in sodium chloride and sulphuric acid solutions. *Corrosion Engineering, Science and Technology*, 54(8), 637-648.
3. Borah, S. M., Pal, A. R., Bailung, H., and Chutia, J. (2008). Optimization of plasma parameters for high rate deposition of titanium nitride films as protective coating on bell-metal by reactive sputtering in cylindrical magnetron device. *Applied Surface Science*, 254(18), 5760-5765.
4. Chawla, V., Jayaganthan, R., and Chandra, R. (2008). Structural characterizations of magnetron sputtered nanocrystalline TiN thin films. *Materials characterization*, 59(8), 1015-1020.
5. Chen, Q., McEwen, G. D., Zaveri, N., Karpagavalli, R., and Zhou, A. (2012). Corrosion resistance of Ti-6Al-4V with nanostructured TiO<sub>2</sub> coatings *Emerging Nanotechnologies in Dentistry* (pp. 165-179): Elsevier.
6. Chou, W.-J., Yu, G.-P., and Huang, J.-H. (2001). Deposition of TiN thin films on Si (100) by HCD ion plating. *Surface and Coatings Technology*, 140(3), 206-214.
7. Dai, N., Zhang, L.-C., Zhang, J., Chen, Q., and Wu, M. (2016). Corrosion behavior of selective laser melted Ti-6Al-4 V alloy in NaCl solution. *Corrosion Science*, 102, 484-489.
8. Fenker, M., Balzer, M., Kappl, H., and Banakh, O. (2005). Some properties of (Ti, Mg) N thin films deposited by reactive dc magnetron sputtering. *Surface and Coatings Technology*, 200(1-4), 227-231.
9. Hamil, M. I., Siyah, M. A., and Khalaf, M. K. (2020). Electrophoretic deposition of Thin film TiO<sub>2</sub> on Ti<sub>6</sub>Al<sub>4</sub>V alloy surface for biomedical applications. *Egyptian Journal of Chemistry*.
10. Kavitha, A., Kannan, R., Reddy, P. S., and Rajashabala, S. (2016). The effect of annealing on the structural, optical and electrical properties of Titanium Nitride (TiN) thin films prepared by DC magnetron sputtering with supported discharge. *Journal of Materials Science: Materials in Electronics*, 27(10), 10427-10434.
11. Kelly, P. J., and Arnell, R. D. (2000). Magnetron sputtering: a review of recent developments and applications. *Vacuum*, 56(3), 159-172.
12. Khalaf, M. K., Hassan, N., Khudiar, A., and Salman, I. (2020). Photoconductivities of Nanocrystalline Vanadium Pentoxide Thin Film Grown by Plasma RF Magnetron Sputtering at Different Conditions of Deposition. *Physics of the Solid State*, 62(1), 74-82.
13. Kouznetsov, V., Macak, K., Schneider, J. M., Helmersson, U., and Petrov, I. (1999). A novel pulsed magnetron sputter technique utilizing very high target power densities. *Surface and Coatings Technology*, 122(2-3), 290-293.
14. Ma, C., Jiang, M., and Xia, F. (2017). Preparation and characterization of Ni-TiN thin films electrodeposited with nickel baths of different TiN nanoparticle concentration. *Surface Review and Letters*, 24(05), 1750063.
15. Manouchehri, I., AlShiaa, S. A. O., Mehrparparvar, D., Hamil, M. I., and Moradian, R. (2016). Optical properties of zinc doped NiO thin films deposited by RF magnetron sputtering. *Optik*, 127(20), 9400-9406.
16. Manso-Silvan, M., Martínez-Duart, J., Ogueta, S., García-Ruiz, P., and Pérez-Rigueiro, J. (2002). Development of human mesenchymal stem cells on DC sputtered titanium nitride thin films.

17. Paulitsch, J., Mayrhofer, P. H., Münz, W.-D., and Schenkel, M. (2008). Structure and mechanical properties of CrN/TiN multilayer coatings prepared by a combined HIPIMS/UBMS deposition technique. *Thin Solid Films*, 517(3), 1239-1244.
18. Paulitsch, J., Schenkel, M., Zufraß, T., Mayrhofer, P. H., and Münz, W.-D. (2010). Structure and properties of high power impulse magnetron sputtering and DC magnetron sputtering CrN and TiN films deposited in an industrial scale unit. *Thin Solid Films*, 518(19), 5558-5564.
19. Pelleg, J., Zevin, L., Lungo, S., and Croitoru, N. (1991). Reactive-sputter-deposited TiN films on glass substrates. *Thin Solid Films*, 197(1-2), 117-128.
20. Schönjahn, C., Donohue, L., Lewis, D., Münz, W.-D., Twesten, R., and Petrov, I. (2000). Enhanced adhesion through local epitaxy of transition-metal nitride coatings on ferritic steel promoted by metal ion etching in a combined cathodic arc/unbalanced magnetron deposition system. *Journal of Vacuum Science and Technology A: Vacuum, Surfaces, and Films*, 18(4), 1718-1723.
21. Takano, I., Isobe, S., Sasaki, T., and Baba, Y. (1989). Preparation of TiN thin films by the dynamic mixing method using an N<sub>2</sub><sup>+</sup> ion beam of 1 keV. *Thin Solid Films*, 171(2), 263-270.
22. Vasu, K., Krishna, M. G., and Padmanabhan, K. (2011). Substrate-temperature dependent structure and composition variations in RF magnetron sputtered titanium nitride thin films. *Applied Surface Science*, 257(7), 3069-3074.
23. Veiga, C., Davim, J., and Loureiro, A. (2012). Properties and applications of titanium alloys: a brief review. *Rev. Adv. Mater. Sci*, 32(2), 133-148.
24. Wang, F., Wu, M., Wang, Y., Yu, Y., Wu, X., and Zhuge, L. (2013). Influence of thickness and annealing temperature on the electrical, optical and structural properties of AZO thin films. *Vacuum*, 89, 127-131.
25. Xu, S., Du, L., Sugioka, K., Toyoda, K., and Jyumonji, M. (1998). Preferred growth of epitaxial TiN thin film on silicon substrate by pulsed laser deposition. *Journal of materials science*, 33(7), 1777-1782.
26. Zhao, J., Wang, X., Chen, Z. Y., Yang, S., Shi, T., and Liu, X. (1997). Overall energy model for preferred growth of TiN films during filtered arc deposition. *Journal of Physics D: Applied Physics*, 30(1), 5.



**Figure 1.** The main experimental set-up used in this work.

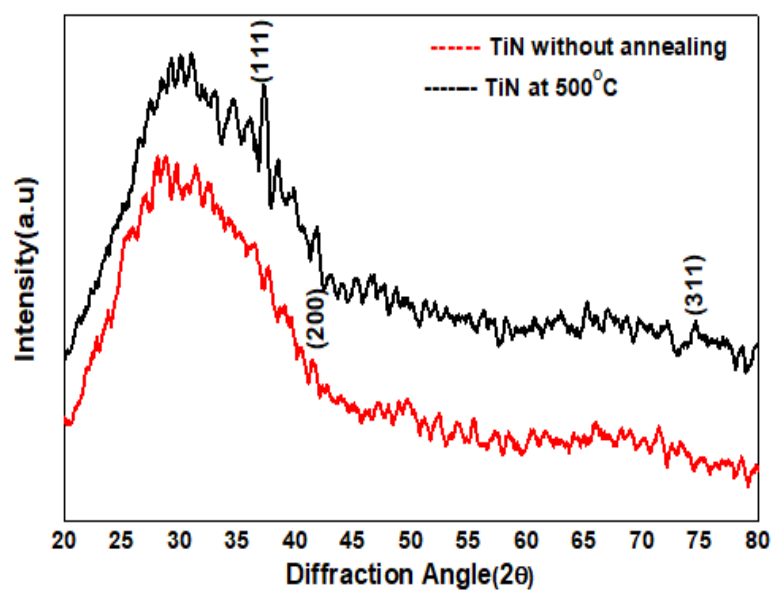


**Figure 2.** The X-ray diffraction of TiN films deposited on a glass substrate.

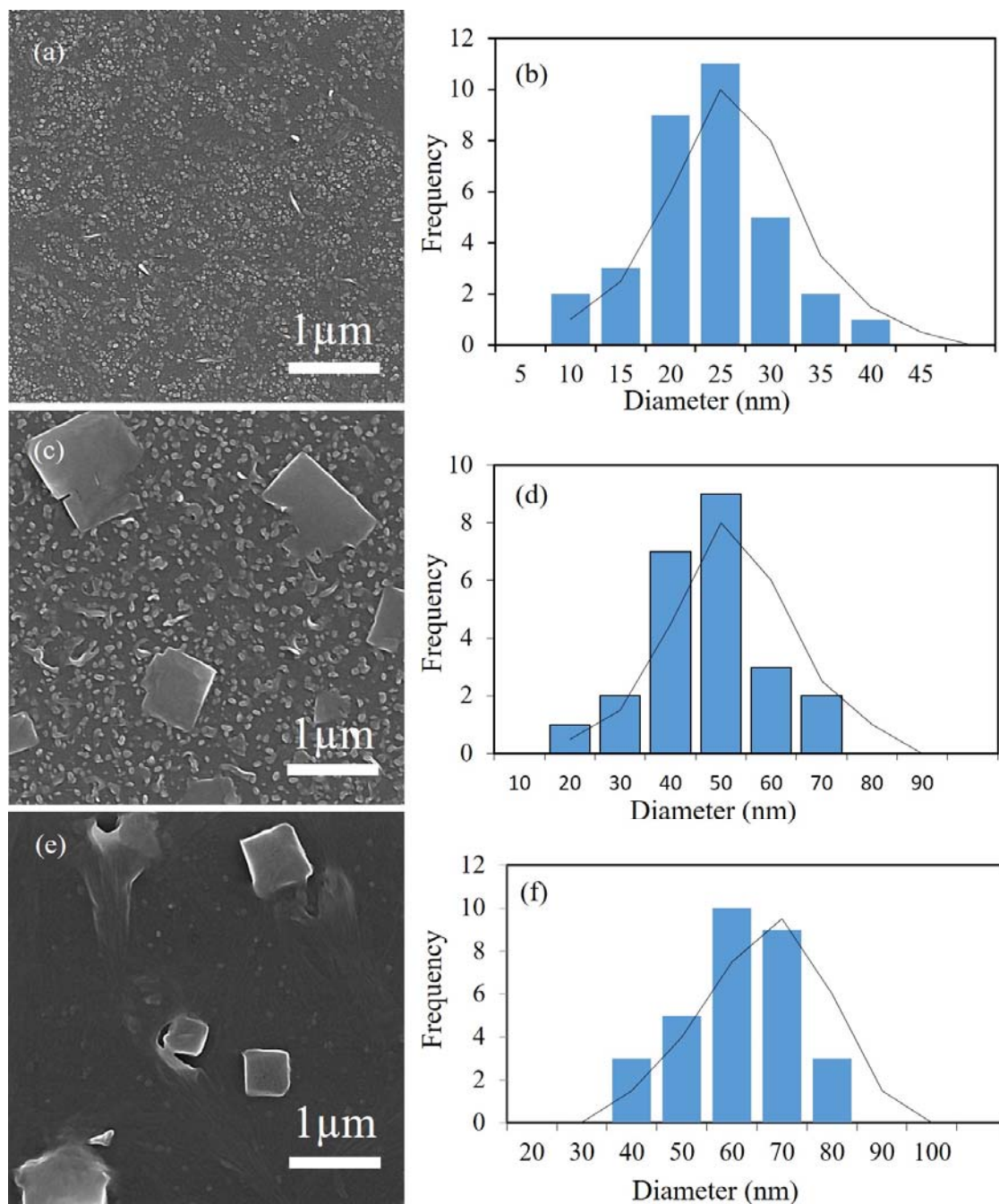


**Figure 3.** (a-b) FESEM image and histogram of TiN film before annealing, (c-d) FESEM image and histogram of TiN film coated at 400 °C, (e-f) FESEM image and histogram of TiN film coated at 500 °C. TiN films deposited on glass substrates by D.C sputtering method.

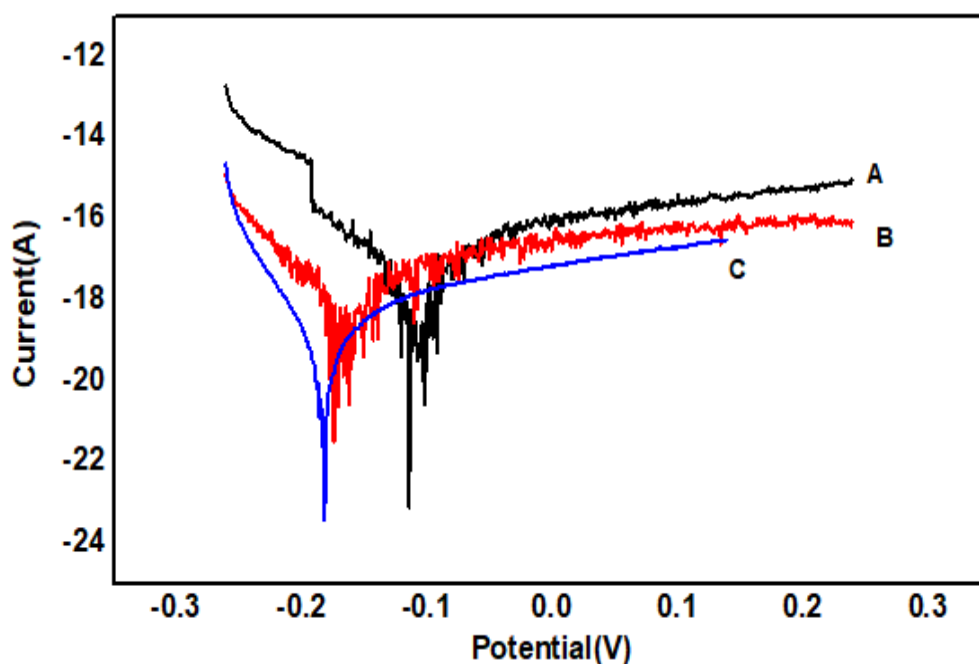


**Figure 4.** Polarization curves (Tafel) for TiN films deposited on Ti-6Al-4V alloy by D.C sputtering at 40 W for 2 hours. (A)Ti-6Al-4V alloy, (B) TiN coated Ti-6Al-4V alloy (C)TiN coated Ti-6Al-4V alloy with thermal annealing.

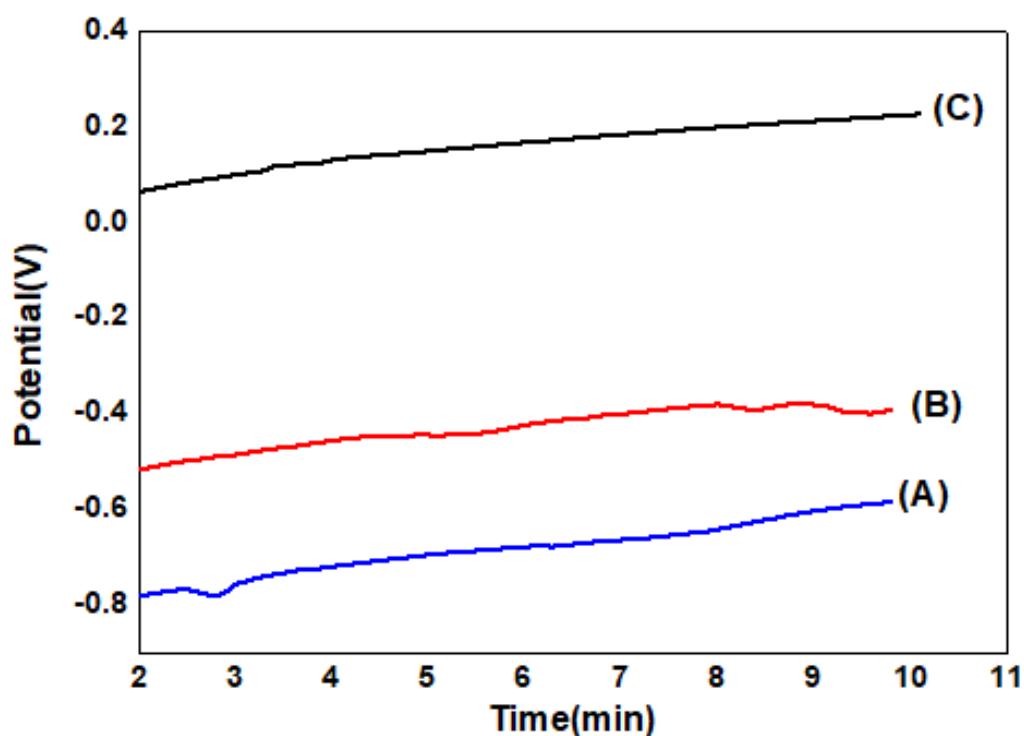


**Figure 5.** Open-circuit potential variation with time curve of TiN coated on Ti-6Al-4V alloy by D.C sputtering 40 W for 2 hours. (A)Ti-6Al-4V alloy, (B) TiN coated Ti-6Al-4V alloy (C) TiN coated Ti-6Al-4V alloy with thermal annealing.

**Table 1.** Reactive DC sputtering conditions for depositing TiN thin films

| Parameters                               | Values            |
|--|-------------------|
| Total pressure (Torr)                    | $5 \cdot 10^{-3}$ |
| Sputtering power (Watt)                  | 40                |
| The target to substrate distance (mm)    | 60                |
| Substrates                               | glass, Ti6AL4V    |
| Gases mixture ratio (Ar:N <sub>2</sub> ) | (90:10)           |
| Deposition time (hour)                   | 2                 |
| Substrate temperature                    | 373K              |

**Table 2.** Corrosion characteristics of Ti-6Al-4V samples coated with TiN.

| Item   | $I_{corr}$ .<br>Amp/cm <sup>2</sup> | $\beta_a$<br>(vol) | $\beta_c$<br>(vol) | Corrosion<br>potential<br>(vol) | Corr.Rate<br>(mm/y)   | Rp<br>KΩ/cm <sup>2</sup> | Weight loss<br>(mg.cm <sup>-2</sup> .s <sup>-1</sup> ) |
|--|-------------------------------------|--------------------|--------------------|---------------------------------|-----------------------|--------------------------|--|
| Ti6Al4V alloy                                      | $2.528 \cdot 10^{-7}$               | 0.097              | 0.587              | -0.117                          | 0.145                 | 1.719                    | $2.043 \cdot 10^{-9}$                                  |
| TiN coated Ti-6Al-4V alloy                         | $4.632 \cdot 10^{-8}$               | 0.069              | 0.569              | -0.054                          | $2.667 \cdot 10^{-3}$ | 580                      | $3.738 \cdot 10^{-11}$                                 |
| TiN coated Ti-6Al-4V alloy with thermal annealing. | $4.654 \cdot 10^{-9}$               | 0.049              | 0.119              | -0.048                          | $2.685 \cdot 10^{-4}$ | 3247                     | $3.763 \cdot 10^{-12}$                                 |



## POLIMORFISMO DO GENE *DGAT1* E SUAS RELAÇÕES COM RENDIMENTO DO LEITE DE GADO E SUA COMPOSIÇÃO QUÍMICA

### *DGAT1* GENE POLYMORPHISM AND ITS RELATIONSHIPS WITH CATTLE MILK YIELD AND CHEMICAL COMPOSITION

### تعدد المظاهر الوراثية لجين *DGAT1* وعلاقتها بإنتاج الحليب ومكوناته الكيميائية في الماشية

FARAJ, Salah H.<sup>1\*</sup>; AYIED, Asaad Y.<sup>2</sup>; SEGER, D. K.<sup>3</sup>

<sup>1</sup>Department of Biology, College of Science, University of Misan, Maysan, Iraq.

<sup>2</sup>Department of Animal Production, College of Agriculture, University of Basrah, Iraq.

<sup>3</sup>Department of Animal Production, College of Agriculture, University of Sumer, Iraq.

\* Corresponding author

e-mail: salah81ss@uomisan.edu.iq

Received 20 March 2020; received in revised form 02 May 2020; accepted 19 May 2020

## RESUMO

Vários polimorfismos em diferentes locos gênicos afetam características de produção, como rendimento e composição do leite. O presente estudo teve como objetivo determinar a frequência alélica e genotípica do gene *DGAT1* e avaliar as associações entre variantes genéticas do *DGAT1* e produção de leite e sua composição química de bovinos iraquianos locais. Amostras de sangue de 100 vacas foram obtidas para isolamento do DNA. O iniciador usado neste estudo amplificou fragmentos de 411-pb no exon 8 do gene *DGAT1*. Métodos de sequenciamento de DNA foram aplicados para detectar polimorfismo de nucleotídeo único do gene *DGAT1* em 100 vacas. As sequências nucleotídicas do exon 8 do gene *DGAT1* foram registradas para bovinos iraquianos locais no Centro Nacional de Informações de Biotecnologia (NCBI), Banco de Dados de DNA do Japão (DDBJ) e Arquivo Europeu de Nucleotídeos (ENA) sob os seguintes números de acesso (LC492073 e LC492074). Os resultados mostraram a presença de dois sítios polimórficos, levando à construção de 2 haplótipos diferentes na vaca. A diversidade de haplótipos foi de 0,536, enquanto a diversidade de nucleotídeos foi de 0,0031. Foram detectados dois locais de polimorfismo de nucleotídeo único (SNP) do gene *DGAT1*, a saber A10433G (A / G) e A10434C (A / C). O resultado dessa mutação altera a substituição da lisina por alanina na posição 232 (mutação A232K) da sequência de aminoácidos. O software genético V. 2020.0.4 foi utilizado para detectar genótipos do gene *DGAT1*, pois o alinhamento da sequência mostrou a presença de três genótipos. As frequências genotípicas de KK, KA e AA foram de 0,40, 0,30 e 0,30, respectivamente. As frequências dos alelos K e A foram de 0,60 e 0,40, respectivamente. O genótipo KK foi significativamente ( $P < 0,05$ ) associado ao maior rendimento de gordura. Portanto, o gene *DGAT1* poderia servir como um marcador genético para a seleção do rendimento de gordura em vacas.

**Palavras-chave:** Gene *DGAT1*, gado iraquiano local, produção de leite, polimorfismo de nucleotídeo único.

## ABSTRACT

Several polymorphisms in different gene loci have been noted to affect production traits such as milk yield and milk composition. The present study aimed to determine the allelic and genotypic frequency of the *DGAT1* gene and evaluate the associations between *DGAT1* genetic variants and milk yield and its chemical composition of local Iraqi cattle. Blood samples from 100 cows were obtained for DNA isolation. The primer used in this study amplified 411-bp fragments at exon 8 of the *DGAT1* gene. DNA sequencing methods were applied to detect single nucleotide polymorphism of the *DGAT1* gene in 100 cows. The nucleotide sequences of exon 8 of the *DGAT1* gene were registered for local Iraqi cattle in the National Center for Biotechnology Information (NCBI), DNA Data Bank of Japan (DDBJ), and the European Nucleotide Archive (ENA) under the following accession numbers (LC492073 and LC492074). The results showed the presence of two polymorphic sites leading to the construction of 2 different haplotypes in the cow. Haplotype diversity was 0.536, while nucleotide diversity was 0.0031. Two single-nucleotide polymorphism (SNP) loci of the *DGAT1* gene were detected, namely A10433G (A/G) and A10434C (A/C). The resulting of this mutation changes lysine to alanine substitution at position 232 (A232K mutation) of amino acid sequence. Geneious software V. 2020.0.4 was used to detect genotypes of the *DGAT1*

gene, as the sequence alignment showed the presence of three genotypes. The genotypic frequencies of KK, KA, and AA were 0.40, 0.30, and 0.30, respectively. Frequencies of K and A alleles were 0.60 and 0.40, respectively. The KK genotype was significantly ( $P < 0.05$ ) associated with higher fat yield. Therefore, the DGAT1 gene could serve as a genetic marker for the selection of fat yield in cows.

**Keywords:** DGAT1 gene, local Iraqi cattle, Milk yield, single-nucleotide polymorphism.

## الخلاصة

العديد من التشكلات الوراثية في عدة مواقع جينية تم ملاحظة تأثيراتها في الصفات الانتاجية مثل انتاج الحليب ومكوناته. تهدف الدراسة الحالية قياس التباين الوراثي وتحديد تكرار الاليلات والتركييب الوراثية لجين DGAT1 وعلاقتها بأنتاج الحليب ومكوناته الكيميائية في الماشية المحلية العراقية. تم الحصول على عينات الدم من 100 بقرة لغرض استخلاص الحامض النووي منقوص الاوكسجين. البادئات المستخدمة في هذه الدراسة لتضخيم قطعة بطول 411 زوج قاعدي في الاكسون الثامن من جين DGAT1. استعملت تقنية تتابعات الحامض النووي منقوص الاوكسجين لغرض تحديد التشكلات الوراثية للنوكليوتيدات المنفردة. تم تسجيل تسلسل النوكليوتيدات exon 8 من جين DGAT1 للماشية المحلية العراقية في المركز الوطني لمعلومات التكنولوجيا الحيوية (NCBI) وبنك بيانات الحامض النووي الياباني (DDBJ) وأرشيف النوكليوتيد الأوروبي (ENA) تحت أرقام الانضمام التالية (LC492073 و LC492074). أظهرت النتائج وجود نمطين فرديين (H) نتج عنهما تشككين وراثيين (NH) في الالبغار المدروسة. كانت قيمة تنوع النمط الفردي 0.536 بينما كانت قيمة تنوع النوكليوتيدات 0.0031. تم تحديد تشككين وراثيين للنوكليوتيدات المنفردة (SNP) في جين DGAT1 هما A10433G و A10434C نتج عنها تغير الحامض الاميني اللابسين الى الحامض الاميني الالنين في الموقع 232 (A232K) من تسلسل الاحماض الامينية. استخدم برنامج Geneious (V. 2020.0.4) للكشف عن التراكيب الوراثية في الجين المدروس، إذ أظهرت محاذاة التتابعات عن وجود ثلاثة تراكيب وراثية. بلغ تكرار التراكيب الوراثية KK و KA و AA 0.40 و 0.30 و 0.30 على التوالي اما تكرار الاليلات K و A كانت 0.60 و 0.40 على التوالي. أظهر التركيب الوراثي KK فرق معنوي ( $P < 0.05$ ) بزيادة نسبة الدهن مقارنة بالتراكيب الوراثية الاخرى لذلك يمكن استخدام هذا الجين كواسم وراثي لعلاقته بدهن الحليب في الالبغار.

**الكلمات المفتاحية:** جين DGAT1، الالبغار المحلية العراقية، انتاج الحليب، التشكلات الوراثية للنوكليوتيدة المنفردة.

## 1. INTRODUCTION:

Iraqi local cattle are scattered on most areas and differ in appearance from each other and are believed to be due mostly to the origins of Indian cows (Zebu) where they have similar characteristics of the species (*Bos Indicus*), which occupy the hot areas, it differs from European cattle belonging to the *Bos Taurus* (Paulson and Thompson, 2015). Among these, Jenoubi is found in the southern, more humid part of Iraq. Alshawi *et al.*, (2019) showed that a significant level of genetic diversity in indigenous Iraqi cattle in line with their history and genome-wide analysis releases the genes that play an important role in immunity (parasitic, bacterial disease) and other environmental adaptive traits (heat tolerance).

The synthesis of milk components has to be increased to improve the efficiency of milk production. This may be carried out by way of combining genetic enhancements and true management, which include improving the availability of the vital nutrients that the udder uses to produce milk. After advances in molecular biology, it became clear that DNA transcription in a laboratory and identifying the form of the genome that made up it became a compelling manner to persuade the phenotypic systems of individuals. In addition to transcription, many post-translation events could significantly affect the phenotype, along with protein phosphorylation constitutes a primary one (Osorio *et al.*, 2016).

The amount of milk, milk fat, and proteins are important traits in the dairy cattle breeding. Milk production depends on the ability of the mammary gland to metabolize fat. Milk fat consists of approximately 98% triglycerides, and the acyl-CoA: diacylglycerol acyltransferase 1 (DGAT1) enzyme has an essential function in milk fat synthesis because it catalyzes the final step in the formation of triglycerides (Lu, *et al.*, 2015). Evidence has pointed to the role of DGAT1 enzyme on milk yield and composition (Cole *et al.*, 2011).

The Diacylglycerol Acyltransferase-1 (DGAT1) gene is one of the functional candidate genes affecting milk composition traits (Juhlin *et al.*, 2012). The cattle DGAT1 gene is located on chromosome 14 and contains 17 exons ((Lešková *et al.*, 2013). The dinucleotide change (AA/GC) at positions 10433 and 10434 (rs AJ318490.1) in exon 8 leads to a non-conservative substitution of Lysine by Alanine at position 232 and has been shown to affect milk yield strongly and milk composition in Italian Holsteins (Bobbo, *et al.*, 2018), White Fulani and Borgou cattle breeds (Houaga *et al.*, 2017) and Holstein, Simmental and Brown Swiss cattle breeds in Croatia (Dokso *et al.*, 2015). In a study, demonstrated that the lysine variant, which represents the "wild type" and is defined by K allele, is characterized by a higher velocity rate in producing triacylglycerols than the A allele (alanine variant) and thus increasing the fat content in animal milk (Grisart *et al.*, 2004). In animals with KK genotype, DGAT1 activity of KK

genotype was reported to be five times higher than AK and AA individuals (Lacorte *et al.*, 2006)

This study aimed to provide an overview of the association between DGAT1 polymorphisms and milk yield and its chemical composition of local Iraqi cattle.

## 2. MATERIALS AND METHODS:

The present study was undertaken in the Genetic Engineering Laboratory, Department of Animal Production, College of Agriculture, University of Basrah, Iraq.

### 2.1. Animals and genomic DNA isolation

The study included the use of 100 Iraqi local cattle. Farmers own the animals used in this study. Before sampling, the objectives of the study were explained to them in their local languages so that they could make an informed decision regarding giving consent to sample their animals. Government veterinary, animal welfare, and health regulations were observed during sampling of the populations analyzed here. The procedures involving animal sample collection also followed the recommendation of directive 2010/63/EU. Collection of blood samples was permitted by the Iraqi Ministry of Agriculture.

The blood samples (5ml/cow) from the jugular vein were collected and immediately transported to the laboratory in a cool box containing ice and stored at  $-20^{\circ}\text{C}$  until further analysis. A 50 ml tubes were used to collect milk samples and sent to the physiology laboratory (College of Agriculture, University of Babylon) for the analysis of milk components by Funke Gerber, Germany.

Genomic DNA was extracted from the whole blood using gSYNC™ DNA Extraction Kit manufactured by the Taiwanese Geneaid company. The DNA concentration was determined using Nanodrop Thermo scientific spectrophotometer (260/280) and then diluted to the final working concentration of a 50 ng/ $\mu\text{l}$ . A fragment (411bp) of the DGAT1 gene in cattle by using the primer F: 5'-GCACCATCCTCTTCTCAAG-3' and R: 5'-GGAAGCGCTTTCGGATG-3' (Kaupe *et al.*, 2004). The PCR amplifications were conducted in a 50  $\mu\text{l}$  volume containing 6  $\mu\text{l}$  genomic DNA, 25  $\mu\text{l}$  of Master Mix, 2  $\mu\text{l}$  each primer, 15  $\mu\text{l}$  free water. The amplification conditions included one cycle of denaturation at  $94^{\circ}\text{C}$  for 2 min and 35 cycles for 30 min, 30 sec of annealing at  $59^{\circ}\text{C}$ , and extension at  $72^{\circ}\text{C}$  for 45 sec, as well as the final extension at

$72^{\circ}\text{C}$  for 10 min. The PCR results were extracted using apparatus at 2% agarose gel with the visualized by contact with ultraviolet light. The PCR product was sequenced by Yang ling Tianrun aoka biotechnology company.

### 2.2. Data analysis

The sequencing results of the DGAT1 gene were compared with accession No. MF351623 at the NCBI by BioEdit 7.0 software (Hall, 1999). Haplotype diversity (HD) and nucleotide diversity ( $\pi$ ) were analyzed using DnaSP V5. 10 software (Librado and Rozas, 2009). The Geneious prime (version 2020.0.4) program was used to detect genotypes.

### 2.3. Statistical analysis

The Completely Randomized Design (CRD) was used to analyze the production data studied within the SPSS (2016) Statistical program Version 24. Least Significant Test within the program was performed to compare different means.

## 3. RESULTS AND DISCUSSION:

The nucleotide sequences of exon 8 of the DGAT1 gene were registered for Iraqi local cattle in the National Center for Biotechnology Information (NCBI), DNA Data Bank of Japan (DDBJ), and the European Nucleotide Archive (ENA) under the following accession numbers (LC492073 and LC492074).

### 3.1. Genetic Diversity

The results of the genetic diversity of the DGAT1 gene showed that their total number of sequences (N) was 100, and the number of haplotypes (H) was 2 haplotypes resulting in 2 genetic polymorphisms (NH). The values of haplotype diversity (HD) and nucleotide diversity ( $\pi$ ) were 0.536 and 0.0031, respectively (Table 1).

The results in Figure 1 and Table 2 showed the analysis of nucleotides and protein of exon 8. They recorded two SNPs; adenine (A) to guanine (G) and adenine (A) to cytosine (C) in position 10433 and 10434, respectively. Thus, the amino acids changed to A232K.

The sequencing analysis of the DGAT1 gene at exon 8 revealed three genotypes namely, KK, KA and AA in this fragment (Figure 2). The genotypic frequencies are shown in Table 3 (0.40, 0.30 and 0.30 respectively). Two different alleles K and A were identified. All alleles were present in

the studied animals but at different frequencies (0.60 and 0.40, respectively).

In this study, the higher frequency of the K allele (lysine variant, 0.60) at the DGAT1 locus was in line with reported frequencies in Kenya (Houaga *et al.*, 2017) alleles were 0.91 and 0.77 in White Fulani and Borgou breeds respectively, Croatia (Dokso *et al.*, 2015), New Zealand (Spelman *et al.*, 2002) and Greece (Oikonomou *et al.*, 2009), with values of 0.77, 0.60 and 0.62, respectively. But slightly different from other regions in German (Kaupe *et al.*, 2007), UK (Banos *et al.*, 2008), Polish (Nowacka-Woszek *et al.*, 2008) and France (Vanbergue *et al.*, 2016) Holsteins showed very similarly K allele frequency, ranging from 0.53 to 0.55. The differences in DGAT1 gene allele frequencies in different countries and regions may be due to differences in inbreeding and selection programs.

### 3.2. DGAT1 Polymorphisms and Milk Chemical Content

The present study supports the hypothesis that genotypes located within the DGAT1 gene may be associated with milk production traits in dairy cattle. The results were consistent with work in dairy cattle showing that the allele responsible for lysine (K) is usually associated with increased milk fat (Table 4). As in the following studies in Denmark (Bovenhuis *et al.*, 2015), Croatia (Dokso *et al.*, 2015) and Kenya (Houaga *et al.*, 2017). However, the effect of diallelic DGAT1 on milk production traits also can be partly explained by the presence of multiple alleles in the locus of DGAT1 or other mutations in genes closely related (Kühn *et al.*, 2004). The K allele is associated with a high-fat yield in milk (Argov-Argaman *et al.*, 2013), the A allele is associated with high milk yield (Marchitelli *et al.*, 2013). Previous studies on *Bos Taurus* and *Bos indicus* had determined the K allele index as a wild type and inferred that the replacement of A allele had occurred after the separation of the *Bos Taurus* and *Bos indicus* lineages (Kaupe *et al.*, 2007). It was well documented that DGAT1 encoded an enzyme play a major role in the synthesis of triglycerides (Ali, 2015). Triglycerides are the major components of fat are formed by binding of diacylglycerol to long-chain fatty acyl-CoAs. These reactions controlled by some enzymes, one of them encoded by the DGAT1 gene (Klimov, *et al.*, 2018). After these findings, DGAT1 was recommended as a functional candidate gene for milk production traits (Houaga *et al.*, 2018).

## 4. CONCLUSIONS:

A significant association between the KK genotype of the DGAT1 gene with higher fat yield in Iraqi local cattle was detected. These results implied that the DGAT1 gene could be great candidate genes or linked to significant genes that affect milk production traits in cattle.

## 5. REFERENCES:

1. Ali, S. A. M. (2015). Molecular and phenotypic characterization of Sudanese Dairy cattle (Kenana and Butana). Ph.D. Thesis, College of Graduate Studies-Sudan University of Science and Technology.
2. Alshawhi, A.; Essa, A.; Al-Bayatti, S.; Hanotte, O. (2019). Genome Analysis Reveals Genetic Admixture and Signature of Selection for Productivity and Environmental Traits in Iraqi Cattle. *Frontiers in Genetics*, 10, 1-16. <https://doi.org/10.3389/fgene.2019.00609>
3. Argov-Argaman, N.; Mida, K.; Cohen, B. C.; Visker, M.; Hetingga, K. (2013). Milk fat content and DGAT1 genotype determine lipid composition of the milk fat globule membrane. *PLoS ONE*, 8(7), 1-8.
4. Banos, G.; Woolliams, J. A.; Woodward, B. W.; Forbes, A. B.; Coffey, M. P. (2008). Impact of single nucleotide polymorphisms in leptin, leptin receptor, growth hormone receptor and diacylglycerol acyltransferase (DGAT1) gene loci on milk production, feed, and body energy traits of UK dairy cows. *J. Dairy Sci.*, 91, 3190-3200.
5. Bobbo, T.; Tiezzi, F.; Penasa, M.; De Marchi, M.; Cassandro, M. (2018). Short communication: Association analysis of diacylglycerol acyltransferase (DGAT1) mutation on chromosome 14 for milk yield and composition traits, somatic cell score, and coagulation properties in Holstein bulls. *Journal of Dairy Science*, 101(9), 8087-8091. <https://doi.org/10.3168/jds.2018-14533>
6. Bovenhuis, H.; Visker, M. H. P. W.; van Valenberg, H. J. F.; Buitenhuis, A. J.; van Arendonk, J. A. M. (2015). Effects of the DGAT1 polymorphism on test-day milk production traits throughout lactation. *Journal of Dairy Science*, 98(9), 6572-6582.
7. Cole, J. B.; Wiggans, G. R.; Ma, L.; Sonstegard, T. S.; Jr, T. J. L.; Crooker, B. A.; Van Tassell, C. P.; Yang, J.; Wang, S.; Matukumalli, L. K.; Da, Y. (2011). Genome-

- wide association analysis of thirty one production, health, reproduction and body conformation traits in contemporary U.S. Holstein cows. *BMC Genomics*, 12,1-17.
8. Dokso, A.; Ivanković, A.; Zečević, E.; Brka, M. (2015). Effect of DGAT1 gene variants on milk quantity and quality. *Mljekarstvo*, 65(4), 238-242.
  9. Grisart, B.; Farnir, F.; Karim, L.; Cambisano, N.; Kim, J. J.; Kvasz, A.; Mni, M.; Simon, P.; Frere, J.; Coppieters, W.; Georges, M. (2004). Genetic and functional confirmation of the causality of the DGAT1 K232A quantitative trait nucleotide in affecting milk yield and composition. *Proceedings of the National Academy of Sciences of the United States of America*, 101(8), 2398-2403. <https://doi.org/10.1073/pnas.0308518100>
  10. Hall, T. (1999). BioEdit: a user-friendly biological sequence alignment editor and analysis program for Windows 95/98/NT. In *Nucleic Acids Symposium Series*, 41, 95-98.
  11. Houaga, I.; Muigai, A. W. T.; Kyallo, M.; Githae, D.; Youssao, I. A. K.; Stomeo, F. (2017). Effect of breed and Diacylglycerol acyltransferase 1 gene polymorphism on milk production traits in Beninese White Fulani and Borgou cows. *Global Journal of Animal Breeding and Genetics*, 5(5), 403-412.
  12. Houaga, I.; Muigai, A. W. T.; Ng'ang'a, F. M.; Ibeagha-Awemu, E. M.; Kyallo, M.; Youssao, I. A. K.; Stomeo, F. (2018). Milk fatty acid variability and association with polymorphisms in SCD1 and DGAT1 genes in White Fulani and Borgou cattle breeds. *Molecular Biology Reports*, 45(6), 1849-1862.
  13. Juhlin, J.; Fikse, W. F.; Pickova, J.; Lundén, A. (2012). Association of DGAT1 genotype, fatty acid composition, and concentration of copper in milk with spontaneous oxidized flavor. *Journal of Dairy Science*, 95(8), 4610-4617. <https://doi.org/10.3168/jds.2011-4915>
  14. Kaupe, B.; Brandt, H.; Prinzenberg, E. M.; Erhardt, G. (2007). Joint analysis of the influence of CYP11B1 and DGAT1 genetic variation on milk production, somatic cell score, conformation, reproduction, and productive lifespan in German Holstein cattle. *Journal of Animal Science*, 85(1), 11-21.
  15. Kaupe, B.; Winter, A.; Fries, R.; Erhardt, G. (2004). DGAT1 polymorphism in *Bos indicus* and *Bos taurus* cattle breeds. *Journal of Dairy Research*, 71(2), 182-187.
  16. Klimov, E.; Arkhipova, A.; Kovalchuk, S. (2018). Frequencies of Genotypes and Alleles of the K232A Substitution in the DGAT1 Gene in Four Cattle Breeds of Russian Selection. *Annual Research and Review in Biology*, 29(6),1-4.
  17. Kühn, C.; Thaller, G.; Winter, A.; Bininda-Emonds, O. R. P.; Kaupe, B.; Erhardt, G.; Bennewitz, J.; Schwerin, M.; Fries, R. (2004). Evidence for multiple alleles at the DGAT1 locus better explains a quantitative trait locus with major effect on milk fat content in cattle. *Genetics*, 167(4), 1873-1881.
  18. Lacorte, G. A.; Machado, M. A.; Martinez, M. L.; Campos, A. L.; Maciel, R. P.; Verneque, R. S.; Teodoro, R. L.; Peixoto, M. G.; Carvalho, M. R.; Fonseca, C. G. (2006). DGAT1 K232A polymorphism in Brazilian cattle breeds. *Genetics and Molecular Research*, 5(3), 475-482.
  19. Lešková, L.; Bauer, M.; Chrenek, P.; Lacková, Z.; Soročinová, J.; Petrovič, V.; Kováč, G. (2013). Detection of DGAT1 gene polymorphism and its effect on selected biochemical indicators in dairy cows after calving. *ACTA Vet. BRNO*, 82, 265-269.
  20. Librado, P.; Rozas, J. (2009). DnaSP v5: A software for comprehensive analysis of DNA polymorphism data. *Bioinformatics*, 25(11), 1451-1452.
  21. Lu, J.; Boeren, S.; van Hooijdonk, T.; Vervoort, J.; Hettinga, K. (2015). Effect of the DGAT1 K232A genotype of dairy cows on the milk metabolome and proteome. *Journal of Dairy Science*, 98(5), 3460-3469.
  22. Marchitelli, C.; Contarini, G.; De Matteis, G.; Crisà, A.; Pariset, L.; Scatà, M. C.; Catillo, G.; Napolitano, F.; Moili, B. (2013). Milk fatty acid variability: Effect of some candidate genes involved in lipid synthesis. *Journal of Dairy Research*, 80(2), 165-173.
  23. Nowacka-Woszek, J.; Noskowiak, A.; Strabel, T.; Jankowski, T.; Świtoński, M. (2008). An effect of the DGAT1 gene polymorphism on breeding value of Polish Holstein-Friesian sires. *Animal Science Papers and Reports*, 26(1), 17-23.
  24. Oikonomou, G.; Angelopoulou, K.; Arsenos, G.; Zygyiannis, D.; Banos, G. (2009). The effects of polymorphisms in the DGAT1, leptin and growth hormone receptor gene loci on body energy, blood metabolic and reproductive traits of Holstein cows. *Animal Genetics*, 40(1), 10-17.

25. Osorio, J. S.; Lohakare, J.; Bionaz, M. (2016). Biosynthesis of milk fat, protein, and lactose: Roles of transcriptional and posttranscriptional regulation. *Physiological Genomics*, 48(4), 231-256.
26. Paulson, E. K.; Thompson, W. M. (2015). Review of small-bowel obstruction: The diagnosis and when to worry. *Radiology*, 275(2), 332-342.
27. Spelman, R. J.; Ford, C. A.; McElhinney, P.; Gregory, G. C.; Snell, R. G. (2002). Characterization of the DGAT1 gene in the New Zealand dairy population. *Journal of Dairy Science*, 85(12), 3514-3517.
28. Vanbergue, E.; Peyraud, J. L.; Guinard-Flament, J.; Charton, C.; Barbey, S.; Lefebvre, R., ... Hurtaud, C. (2016). Effects of DGAT1 K232A polymorphism and milking frequency on milk composition and spontaneous lipolysis in dairy cows. *Journal of Dairy Science*, 99(7), 5739-5749.

**Table 1.** Genetic Diversity of Iraqi Local Cattle Breed in the sample study

| Gene  | Number of Sequences (N) | Haplotype Number (H) | Number of Polymorphisms (NH) | Haplotype Diversity (HD) | Nucleotide Diversity ( $\pi$ ) |
|-------|-------------------------|----------------------|------------------------------|--------------------------|--------------------------------|
| DGAT1 | 100                     | 2                    | 2                            | 0.536                    | 0.0031                         |

**Table 2.** Type of amino acid change in the DGAT1 gene in Iraqi local cattle.

| Location of mutation | Nucleotide change | Amino acid change | Type of mutation |
|----------------------|-------------------|-------------------|------------------|
| 232                  | AAG>GCG           | Ala > Lys         | Transition       |

Ala: Alanine, Lys: Lysine

**Table 3.** Genotype and Allele frequency of the DGAT1 gene in the sample study.

| Breed              | Number of animals | Genotype | Frequency | Allele | frequency | H.W.E ( $\chi^2$ -value) |
|--------------------|-------------------|----------|-----------|--------|-----------|--------------------------|
| Iraqi local cattle | 40                | KK       | 0.40      | K      | 0.6       | 0.02                     |
|                    | 30                | KA       | 0.30      | A      | 0.4       |                          |
|                    | 30                | AA       | 0.30      |        |           |                          |

**Table 4.** Association of DGAT1 K232A polymorphisms on milk composition in Iraqi local cattle.

| Genotype | Fat (%) | Protein (%) | Lactose (%) | SNF (%) |
|----------|---------|-------------|-------------|---------|
| KK       | 4.35*   | 3.00        | 4.31        | 7.68    |
| KA       | 3.59    | 3.25        | 4.37        | 7.81    |
| AA       | 3.50    | 3.08        | 3.89        | 7.96    |
| Total    | 3.86    | 3.10        | 4.20        | 7.80    |

\*Significant at (P>0.05)

|          |       |   |       |
|----------|-------|---|-------|
| MF351623 | 10274 | ACCTCTGGTGCCGAGAGCGCAGGGCTGGGGCCAAGGCCAAGGCTGGTGAGGGCTGCCTCG  | 10333 |
| LC492074 | 1     | ACCTCTGGTGCCGAGAGCGCAGGGCTGGGGCCAAGGCCAAGGCTGGTGAGGGCTGCCTCG  | 60    |
| MF351623 | 10334 | GGCTGGGGCCACTGGGCTGCCACTTGCCCTCGGGACCGGCAGGGGCTCGGCTCACCCCCGA | 10393 |
| LC492074 | 61    | GGCTGGGGCCACTGGGCTGCCACTTGCCCTCGGGACCGGCAGGGGCTCGGCTCACCCCCGA | 120   |
| MF351623 | 10394 | CCCGCCCCCTGCCGCTTGCTCGTAGCTTTGGCAGGTAAGAAAGGCCAACGGGGGAGCTGCC | 10453 |
| LC492074 | 121   | CCCGCCCCCTGCCGCTTGCTCGTAGCTTTGGCAGGTAAGCGGCCAACGGGGGAGCTGCC   | 180   |
| MF351623 | 10454 | CAGCGCACCGTGAGCTACCCGACAACCTGACCTACCGCGGTGAGGATCCTGCCGGGGGC   | 10513 |
| LC492074 | 181   | CAGCGCACCGTGAGCTACCCGACAACCTGACCTACCGCGGTGAGGATCCTGCCGGGGGC   | 240   |
| MF351623 | 10514 | TGGGGGACTGCCCCGGCGGCCTGGCCTGCTAGCCCCGCCCTCCCTTCCAGATCTCTACTA  | 10573 |
| LC492074 | 241   | TGGGGGACTGCCCCGGCGGCCTGGCCTGCTAGCCCCGCCCTCCCTTCCAGATCTCTACTA  | 300   |
| MF351623 | 10574 | CTTCCTCTTCGCCCCACCCGTGTGCTACGAGCTCAACTTCCCCCGCTCCCCCGCATCC    | 10632 |
| LC492074 | 301   | CTTCCTCTTCGCCCCACCCGTGTGCTACGAGCTCAACTTCCCCCGCTCCCCCGCATCC    | 359   |

**Figure 1.** Sequencing of DGAT1 gene in Iraqi Local Cattle in gene bank (LC492074) vs. reference Sequencing (MF351623).

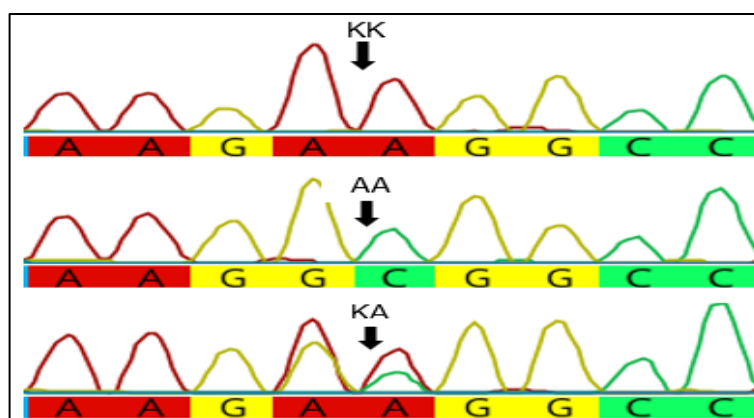


**Figure 2.** The sequencing of genotypes namely, KK, KA and AA in exon 8 of the DGAT1 gene of Iraqi local cattle



## EXTRATO DE SEMENTES DE ABÓBORA COMO INIBIDOR DE CORROSÃO DE LIGA DE AÇO LEVE EM SOLUÇÃO ÁCIDA

### THE EXTRACT OF PUMPKIN SEEDS AS A CORROSION INHIBITOR OF MILD STEEL ALLOY IN ACIDIC SOLUTION

JASIM, Ekhlas Qanber<sup>1</sup>; ALASADI, Erfan A.<sup>1</sup>; MOHAMMAD-ALI, Munther Abduljaleel<sup>1\*</sup>

<sup>1</sup> Pharmaceutical Chemistry Department, College of Pharmacy, University of Basrah, Basrah, Iraq

\* Corresponding author

e-mail: munther.ali@uobasrah.edu.iq

Received 05 March 2020; received in revised form 25 March 2020; accepted 06 April 2020

## RESUMO

O problema da corrosão nas fábricas e instalações vitais continua sendo um dos obstáculos mais importantes que atrasam o progresso da produção e o aumento de sua quantidade. Para resolver o problema de corrosão, muitos inibidores inorgânicos e orgânicos têm sido usados. Recentemente, foram utilizados inibidores feitos de extratos vegetais, mais baratos e ambientalmente amigáveis. A inibição do extrato de sementes de abóbora na liga de aço leve à corrosão no meio ácido foi investigada por espectroscopia da impedância eletroquímica, técnica eletroquímica e método de perda de massa com solução aquosa estática ambiental. O efeito das concentrações de inibidores (10-50 mg/L) e o tempo de imersão (1 a 5 h) foram estudados na eficiência da inibição ( $\eta\%$ ) do extrato em aço leve (AL) imerso em uma solução de HCl 0,5 M. Todas as técnicas mostraram resultados muito bons nos valores do coeficiente de inibição. O percentual ótimo de  $\eta$  estava na faixa de 71 a 76%, dependendo do método utilizado. O tempo ideal foi de 5 horas. Os resultados das curvas de Tafel mostraram uma visão clara do comportamento do extrato, que atua como inibidor do tipo misto. Além disso, o teste de microscopia de força atômica foi aplicado para o estudo da morfologia da superfície da liga. Pelo exposto, o extrato de plantas de abóbora pode ser de grande benefício na inibição da corrosão na indústria.

**Palavras-chave:** AFM, Corrosão, Impedância eletroquímica, Polarização potenciodinâmica, Sementes de abóbora.

## ABSTRACT

The problem of corrosion in factories and vital installations remains one of the most important obstacles that delay the progress of production and the increasing of its quantity. To solve the problem of corrosion, many inorganic and organic inhibitors have been used. Recently, inhibitors made from plant extracts, cheaper and environmentally friendly, were used. The inhibition of pumpkin seed extract on the corrosion mild steel alloy in the acidic medium was investigated using spectroscopy of the electrochemical impedance, Electrochemical technique and mass losing method with a static environmental aqueous acidic solution. Effect of inhibitor concentrations (10-50 mg/L) and immersion time (1–5 h) was studied on the inhibition efficiency ( $\eta\%$ ) of the extract on Mild Steel (MS) immersed in a 0.5 M HCl solution. All techniques showed very good matching results in the inhibition coefficient values. The optimum  $\eta\%$  was in the range 71-76% depending on the method used. The optimum time was 5 hours. Tafel curves results showed a clear view of the extract behavior, which acts as a mixed-type inhibitor. Furthermore, the atomic force microscopy test was applied for studying surface morphology of alloy. From the foregoing, the pumpkin plant extract can be of great benefit in inhibiting corrosion in the industry.

**Keywords:** AFM, Corrosion, Electrochemical impedance, Potentiodynamic polarization, Pumpkin seed.

## 1. INTRODUCTION:

The acidic solutions may be used to remove the rust effect in different parts of the industrial processes. For example, diluted hydrochloric acid is used as broadly the pickling of steel alloys in oil and water pipes. Therefore,

different types of inhibitors, which may be organic, inorganic, and natural extracts are widely used to reduce or control the dissolutions of metal (Karthiga *et al.*, 2015; Kliškić *et al.*, 2000).

The organic and inorganic inhibitors had very good anticorrosive activity, but they are toxic to both humans and the environment. These

inhibitors may cause chronic or acute diseases because of damage in tissues of different organ systems or disturbing the vital function of metabolism or enzymic systems. In addition to these hazardous effects, this type of inhibitors is very costly and forced companies to spend millions on them that made the researchers instead of these synthetic inhibitors by naturally ones. Furthermore, this type of inhibitors are environmentally friendly, available sources, and cheap cost (El-Etre, 1998; Zhang *et al.*, 2015).

Up till now, many plant extracts have been investigated for their corrosion inhibitors behavior using acidic media on the mild steel. For example, *Murraya koenigii* (Yadav *et al.*, 2015; Sharmila *et al.*, 2010), *Terminalia chebula* (Patel *et al.*, 2009), *Carica papaya* (Kasuga *et al.*, 2018; Nwigwe *et al.*, 2019), *Nypa fruticans wurmb* (Orubite and Oforka, 2004; Michael and Olubunmi, 2014), *Emblia officianilis* (D'souza and Chattree, 2015; Saratha and Vasudha, 2010), and many other (El-Etre *et al.*, 2003). These studies including the effect of seed, leave or other parts extracts of plants as corrosion inhibitors on the mild steel in various concentrations of acidic media.

The inhibition behavior of *Murraya koenigii* (curry) leaves extract on the corrosion resistance of mild steel (MS) in nitric acid medium has been studied by gravimetric (or weight loss) measurements and scanning electron microscopy (Quraishi *et al.*, 2010). The inhibiting action of the fruit extract of *Terminalia chebula* (TC) on mild steel corrosion in 1 M HCl solution was studied using gravimetric, potentiodynamic polarization, and electrochemical impedance spectroscopy (EIS) techniques. Other plant extracts have been investigated for their corrosion inhibitors behavior using acidic media on mild steel (Oguzie *et al.*, 2014). Many other studies, including the effect of seed, leave or other parts extracts of plants as corrosion inhibitors on the mild steel in various concentrations of acidic media (El-Etre, 2006; Zucchi and Omar, 1985).

The purpose of this research was to study the pumpkin seed extract as a corrosion inhibitor for mild steel (MS) alloy in acidic solution using electrochemical impedance, polarization of the potentiodynamic technique and mass losing method along with the surface morphology study of alloy using Atomic Force Microscopy (AFM).

## 2. MATERIALS AND METHODS:

### 2.1. Preparation of seed extract

Pumpkin seed that collected from the market of Basrah Old City was left to dry and ground to a fine powder. Twelve grams of this plant powder were mixed with D.W. (1000 mL) and subjected to reflux for about three hours. The resulting solution was passed through fine filter paper, and the clear solution was reduced to obtain 1 gram of extracted solid material of the original volume. The resulting new volume was utilized to test the corrosive inhibitor behavior by preparing different concentrations of aqueous solutions 10, 20, 30, 40, and 50 mg/L.

The coupons of mild steel (N80) was used to study the corrosion properties on a supplied from South Oil Company in Basrah that have the composition (wt.%): 0.80% Mn, 0.3% C, 0.22% Cu, 0.07% Ni, 0.05% P, 0.041%S and Fe is the remainder. The coupon was cleaned by smooth emery papers with grade

The coupons were rinsed with D.W. and subjected to degreasing by acetone and left to dry at room temperature, then kept in a desiccator until use. The concentrated HCl was used to prepare the solution of 0.5 M HCl by dilution with D.W. All the experiments were performed and repeated in the static solution.

### 2.2. Mass losing method

The experiments of mass loss were carried out on the mild steel alloy with a coupon dimensions (2.5 cm length) × (2.0 cm width) × (0.025 cm height) in a static solution of 0.5 M HCl with and without plant aqueous extract with diverse concentrations. The mass of each coupon was recorded by a digital sensitive balance with four decimal digital values and then immersed in 100 mL of acid solution with duration times 1 to 5 h at the temperature 25°C.

After every immersing time, the coupon was washed with distilled water, and the weighed again so as to calculate the efficiency of inhibition ( $\eta_{WL}$ ) and the rate of corrosion ( $R_{corr}$ ). For each run, all solutions were freshly prepared, and the temperature of the tested solution was controlled by a thermostatic auxiliary tool to give an accurate value.

Equation (1) used to calculate the corrosion rate ( $R_{corr}$ ) of mild steel (Batah *et al.*, 2017):

$$R_{corr} = \frac{\Delta W * K}{A * D * T} \quad (\text{Eq. 1})$$

$\Delta W$ = mass losing of alloy (g),  $K$ = constant value ( $5.34 \times 10^5$ ),  $A$ = coupon area ( $\text{cm}^2$ ),  $D$ = density of alloy ( $\text{g}/\text{cm}^3$ ) and  $T$ = exposed time (h).

Equations (2) and (3) used to obtain the inhibition efficiency  $\eta_{WL}(\%)$  and the degree of surface coverage  $\theta_{WL}$ , respectively (Fouda *et al.*, 2017):

$$\eta_{WL}(\%) = \frac{W_o - W_i}{W_o} * 100 \quad (\text{Eq. 2})$$

$$\theta_{WL} = \frac{W_o - W_i}{W_o} \quad (\text{Eq. 3})$$

where,  $W_o$  and  $W_i$  ( $\text{mg dm}^{-2}$ ) mass of the coupon after the dipping in acidic solution without or with extracted inhibitor.

### 2.3. Electrochemical measurements

The assays were performed at room temperature using three-electrode electrochemical cells containing a carbon steel working electrode with a  $1 \text{ cm}^2$  surface area, a platinum auxiliary electrode, and a saturated calomel electrode (Reference electrode). The instrument used to obtain the curve of Tafel depends on the automatic changing in the potential electrode within the range from a positive value of 250 mV to the negative value of 250 mV assistant by scan rate of 0.5 mV per second of open circuit potential to investigate the inhibitory effect of the plant extract on the alloy of mild steel corrosion. The corrosion current densities ( $i$ ) were utilized to draw the linear relationship of the Tafel segment. Then finally, the equation (4) used to calculate the inhibition efficiency  $\eta_{pol}(\%)$  from the obtained values of current densities ( $i$ ) (El Aoufir *et al.*, 2017; Abdul-Nabi and Jasim, 2014):

$$\eta_{pol}(\%) = \frac{i - i_o}{i} \times 100 \quad (\text{Eq. 4})$$

where  $i$  and  $i_o$  are the uninhibited and inhibited corrosion current densities, respectively.

### 2.4. Impedance measurements

The impedance tests were investigated by AC signals of amplitude (10 mV) using the frequency spectrum range 100 kHz - 0.01 Hz. The values of charge transfer resistance (CTR) were obtained by Nyquist plots through the measurement of semi-circles diameter. The inhibition efficiency  $\eta_{EIC}(\%)$  of the inhibitor was

calculated from the values of CTR using equation (5) (Yang *et al.*, 2018):

$$\eta_{EIC}(\%) = \frac{R'_{ct} - R_{ct}^o}{R'_{ct}} \times 100 \quad (\text{Eq. 5})$$

where  $R_{ct}^o$  and  $R'_{ct}$  represent the resistance of charge-transfer (RC-T) in the without and in with the diverse concentration of inhibitor.

The values of impedance from the plot were used to obtain the magnitudes of double-layer capacitance ( $C_{dl}$ ) by using the equation (6) (Lgaz *et al.*, 2017):

$$|Z| = \frac{1}{2\pi f C_{dl}} \quad (\text{Eq. 6})$$

## 2.5. Atomic Force Microscopy (AFM)

Atomic Force Microscopy (AFM) model CentaurU HR (Russia) was utilized in Physics and Energetic Faculty, Udmurtia, The Federal Republic of Russia. The alloy of mild steel that used as sections with the dimensions of (length 2.5 cm x width 2.5 cm and height 0.4cm) were subjected to dipping in the specific acidic solution using different concentrations of pumpkin seed extract (10, 20, 30, 40 and 50 mg/L) as corrosive inhibitors at 25°C for 24 h. After this periodic time, the coupons were take out, washed with D.W., left to dry, and then used for AFM tests.

## 3. RESULTS AND DISCUSSION:

### 3.1. Mass losing measurements

Table 1 and Figure 1 represent the output data of the study for the corrosion process of mild steel alloy in the acidic solution of 0.5 M using different amounts of pumpkin seed extract at 25°C. The equations (1), (2) and (3) were used to calculate the corrosion rate ( $R_{corr}$ ), the efficiency of inhibition ( $\eta_{WL}(\%)$ ) and the coverage of surface ( $\theta$ ) values, respectively.

Table 1 and Figure 2 show the effect of concentration of plant extract on the inhibition efficiency, and the results indicate that by increasing the concentration the  $\eta_{WL}(\%)$  increases to reach the best effect of inhibitor at the concentration of 50 mg/L (Lgaz. *Et al.*, 2018). On the other hand, there is decreasing in the corrosion rate with increasing concentration, which gives a significant indication of the effect of the inhibitor on the corrosion process.

### 3.2. Tafel Polarization Measurements

The output data of the polarization measurements are listed in Table 2 for the corrosion of M-steel test in the 0.5 M acidic solution without and with different concentrations of pumpkin seed extract at the temperature of 25 °C. Figure 3 and Table 2 indicate that increasing the concentrations of pumpkin seed gives a significant decrease in reactions of H<sub>2</sub> reduction (cathodic process) and metal dissolution (anodic process). According to these results, the inhibitor gave the mechanisms of mixed type (Babic-Samardzija *et al.*, 2005; Jasim *et al.*, 2017).

The values of  $\eta_{pol}(\%)$  and  $\theta$  from pumpkin seed tests were calculated using Equation 4. Table 2 shows the determined values of  $I_{corr}$ ,  $E_{corr}$ , Tafel slopes ( $\beta_a$  and  $\beta_c$ ) and  $\eta_{pol}(\%)$ . The data indicated that there is an inversing effect between  $I_{corr}$  and the concentrations of pumpkin seed. The values of  $\beta_a$  and  $\beta_c$  remained almost unchanged with the addition of pumpkin seed concentrations, which gave a clear view that the adsorbed inhibitor decreases  $E_{corr}$  without affecting the reaction mechanism.

### 3.3. EIS measurements

EIS technique at OCP in a wide frequency range was used to study the capacitance at metal/electrolyte interface, which related to corrosion processes on the surface of mild steel coupons using the extract of pumpkin seed. Figure 4 shows Nyquist diagram for mild steel alloy dipped in 0.5M HCl solution at 25 °C using a series of concentrations of the extract as an inhibitor and without inhibitor at the certain open circuit potential.

From Figure 4, it's clear that there is increasing in the semi-circle diameter with inhibitor concentration rising. This result referred to the fact about an increase in corrosion resistance of the material. The optimum concentration of the extract was 50 mg/L, which gave  $R_p$  of 2100 reflected inhibition coefficient percentage of 76.19% as compared with the closed values calculated from Tafel and weight loss methods 74.41% and 71.93, respectively.

The opposite frequency values  $f_{max}$  can be used to calculate the magnitudes of electrochemical double-layer capacitance ( $C_{dl}$ ) by utilizing equation (7) (Migahed *et al.*, 2016):

$$C_{dl} = \frac{1}{2 \pi f_{max} R_{ct}} \quad (\text{Eq.7})$$

Where  $f_{max}$  is the opposite frequency when the imaginary component was maximum.

Table 3 referred to the EIS data which showed that the magnitudes of  $\eta_{EIC}(\%)$  and  $R_{ct}$  is proportional to the concentration of inhibitor, whereas the  $C_{dl}$  values are proportional reversibly.

These results may be referred to the lowering of dielectric constant which effect on the rising in the thickness of the adsorbed electric double layer, which referred to the action of the inhibitor molecules as a thin layer to isolate the alloy from acidic solution by mix adsorption mechanism (Jasim *et al.*, 2015).

### 3.4. Morphology analysis by AFM

Figures 5-*i*, 5-*ii*, and 5-*iii* show the images of AFM for clear metal (control), the surface that subjected to corrosion by acidic medium (0.5M HCl) using or not the inhibitor extract. The pictures of the AFM gave a clear view of the smooth surface of the metal by using pumpkin seed extract concentrations inhibitor in 0.5M HCl. Table 4 gives the results of the AFM study represented by the values of  $R_a$  and  $R_q$ . The value of RMS, which equal to 55.2 nm, referred to the smoothing of the metal surface due to the adsorption of plant extract, which prevents the corrosion process as compared with the RMS value in the absence of inhibitor (120nm) (Elmsellem *et al.*, 2014).

## 4. CONCLUSIONS:

The pumpkin seed aqueous extract can be used to inhibit the corrosion of MS in the static acidic medium at 25°C. The optimum concentration of plant extract should be determined and utilized to give perfect protection efficiency. Using of plant extract in the industry as corrosion inhibitor enhances the green chemistry and environment friendly. The pumpkin seed extract gave good corrosion inhibitor efficiency with closed values using different methods. Morphology analysis referred to the excellent inhibitory behavior of the plant extract.

## 5. REFERENCES:

1. Abdul-Nabi A.S., Jasim E.Q. Synthesis, Characterization and Study of Some Tetrazole Compounds as New Corrosion Inhibitors for C-steel in 0.5 M HCl Solution. *International Journal of Engineering Research*. 2014, 3, 613-617.

2. Babic-Samardzija K., Lupu C., Hackerman N., Barron A.R. Inhibitive properties, adsorption and surface study of butyn-1-ol and pentyn-1-ol alcohols as corrosion inhibitors for iron in HCl. *Journal of Materials Chemistry*. 2005, 15, 1908-1916.
3. Batah A., Anejjar A., Bammou L., Belkhaouda M., Salghi R., Bazzi L. Carbon Steel Corrosion Inhibition by Rind and Leaves Extracts of Grapefruit in 1.0 M Hydrochloric Acid. *Journal of Materials and Environmental Science*. 2017, 8, 3070-3080.
4. D'souza R., Chattree A. Emblica Officinalis Leaves Extract as Corrosion Inhibitor, *Chemical Science Transactions*, 2015, 4(3), 865-870.
5. El Aoufir Y., El Bakri Y., Lgaz H., Zarrouk A., Salghi R., Warad I., Ramli Y., Guenbour A., Essassi E.M., Oudda H. Understanding the adsorption of benzimidazole derivative as corrosion inhibitor for carbon steel in 1 M HCl: experimental and theoretical studies. *Journal of Materials and Environmental Science*. 2017, 8, 3290-3302.
6. El-Etre A.Y. Inhibition of aluminum corrosion using Opuntia extract. *Corrosion science*. 2003, 45, 2485-2495.
7. El-Etre AY. Khillah extract as inhibitor for acid corrosion of SX 316 steel. *Applied Surface Science*. 2006, 252, 8521-8525.
8. El-Etre, A.Y. Natural honey as corrosion inhibitor for metals and alloys. I. Copper in neutral aqueous solution. *Corrosion Science*. 1998, 40, 1845-1850.
9. Elmsellem H., Aouniti A., Khoutoul M., Chetouani A., Hammouti B., Benchat N., Touzani R., Elazzouzi M. Theoretical approach to the corrosion inhibition efficiency of some pyrimidine derivatives using DFT method of mild steel in HCl solution. *Journal of Chemical and Pharmaceutical Research*. 2014, 6, 1216-1224.
10. Fouda A.S., Abd El-Maksoud S.A., Mostafa H.M. Tilia Leaves as Eco-Friendly Corrosion Extract for MS in Aqueous Solutions, *Journal of Applied Chemistry*. 2017, 6, 190-203.
11. Jasim E., M-Ali M.A., Hussain R. Synthesis and Characterization of Some Thiadiazole Compounds as New Corrosion Inhibitors for Mild Steel in Cooling Water, *Asian Journal of Chemistry*. 2017, 29, 2361-2365.
12. Jasim E.Q., Mohammed-Ali M.A., Hussain A.A. Investigation of Salvadora persica Roots Extract as Corrosion Inhibitor for Mild Steel in 1 M HCl and in Cooling Water. *Chemistry and Materials Research*. 2015, 7, 147-158.
13. Karthiga, N., Rajendran, S., Prabhakar, P., Rathish, R.J. Corrosion inhibition by plant extracts-An overview. *International Journal of Nano Corrosion Science and Engineering*, 2015, 2, 31-49.
14. Kasuga B., Park E., Machunda R.L. Inhibition of Aluminium Corrosion Using Carica papaya Leaves Extract in Sulphuric Acid, *Journal of Minerals and Materials Characterization and Engineering*, 2018,06, 1-14
15. Kliškić, M., Radošević, J., Gudić, S., Katalinić, V. Aqueous extract of Rosmarinus officinalis L. as inhibitor of Al-Mg alloy corrosion in chloride solution. *Journal of applied electrochemistry*. 2000 30, 823-830.
16. Lgaz H., Bhat K.S., Salghi R., Jodeh S., Algarra M., Hammouti B., Ali I.H., Essamri A. Insights into corrosion inhibition behavior of three chalcone derivatives for mild steel in hydrochloric acid solution. *Journal of Molecular Liquids*. 2017, 238, 71-83.
17. Lgaz H., Salghi R., Ali I.H. Corrosion Inhibition Behavior of 9-Hydroxyrisperidone as a Green Corrosion Inhibitor for Mild Steel in Hydrochloric Acid: Electrochemical, DFT and MD Simulations Studies, *International Journal of Electrochemical Science*. 2018, 13, 250-264.
18. Michael N.C., Olubunmi J.A. The corrosion inhibition of mild steel in sulphuric acid solution by flavonoid (catechin) separated from Nypa fruticans Wurmb leaves extract, *Science Journal of Chemistry*, 2014, 2, 27-32.
19. Migahed M.A., Negm N.A., Shaban M.M., Ali T.A., Fadda A.A. Synthesis, characterization, surface and biological activity of diquaternary cationic surfactants containing ester linkage. *Journal of Surfactants and Detergents*. 2016 19, 119-128.

20. Nwigwe S.U., Umunakwe R., Mbam S.O., Yibowei M., Okon K., Kalu-Uka G. The inhibition of Carica papaya leaves extract on the corrosion of cold worked and annealed mild steel in HCl and NaOH solutions using a weight loss technique, *Engineering and Applied Science Research*, 2019, 46, 114-119.
21. Oguzie E.E., Chidiebere M.A., Oguzie K.L., Adindu C.B., Momoh-Yahaya H. Biomass Extracts for Materials Protection: Corrosion Inhibition of Mild Steel in Acidic Media by Terminalia chebula Extracts, *Chemical Engineering Communications*. 2014, 201, 790–803.
22. Orubite K.O., Oforka N.C. Inhibition of the corrosion of mild steel in hydrochloric acid solutions by the extracts of leaves of Nypa fruticans Wurmb, *Materials Letters*, 2004, 58, 1768–1772.
23. Patel N.S., Jauhari S., Mehta G.N. Inhibitor for the Corrosion of Mild Steel in H<sub>2</sub>SO<sub>4</sub>, *South African Journal of Chemistry*, 2009, 62, 200–204
24. Quraishi M.A., Singha A., Singha V.K., Yadav D.K., Singh A.K. Green approach to corrosion inhibition of mild steel in hydrochloric acid and sulphuric acid solutions by the extract of Murraya koenigii leaves, *Materials Chemistry and Physics*, 2010, 122, 114–122
25. Saratha R., Vasudha V.G. Emblica Officinalis (Indian Gooseberry) Leaves Extract as Corrosion Inhibitor for Mild Steel in 1N HCl Medium, *E-Journal of Chemistry*, 2010, 7(3), 677-684.
26. Sharmila A., Prema A.A., Sahayaraj P.A. Influence of Murraya koenigii (curry leaves) extract on the corrosion inhibition of carbon steel in HCL solution, *Rasayan Journal of Chemistry*, 2010, 3, 74-81
27. Yadav K., Gupta A., Selvam N., Ramachandran M. Murraya koenigii as Green corrosion inhibitor for mild steel in nitric acid medium, *Indian Journal of Chemical Technology*, 2018, 25, 94-100.
28. Yang Z.N., Liu Y.W., Chen Y. Linseed oil based amide as corrosion inhibitor for mild steel in hydrochloric acid. *International Journal of Electrochemical Science*. 2018, 13, 514-529.
29. Zhang B., He C., Wang C., Sun P., Li F., Lin Y. Synergistic corrosion inhibition of environment-friendly inhibitors on the corrosion of carbon steel in soft water, *Corrosion Science*, 2015, 94, 6-20.
30. Zucchi F., Omar I.H. Plant extracts as corrosion inhibitors of mild steel in HCl solutions. *Surface Technology*. 1985, 24, 391-399.

**Table 1.** Effect of pumpkin seed extract on Dissolution Mild steel in 0.5M HCl

| Concentration (mg/L) | $\Delta W$ (g) | Time (h) | $R_{corr}$ | $\eta_{WL}(\%)$ | $\theta$ |
|----------------------|----------------|----------|------------|-----------------|----------|
| 0                    | 0.0028         | 1        | 66.63      |                 |          |
|                      | 0.0062         | 2        | 73.77      |                 |          |
|                      | 0.0098         | 3        | 77.73      |                 |          |
|                      | 0.0134         | 4        | 79.72      |                 |          |
|                      | 0.0171         | 5        | 81.38      |                 |          |
| 10                   | 0.0026         | 1        | 50.76      | 7.14            | 0.0714   |
|                      | 0.0041         | 2        | 40.02      | 33.87           | 0.3387   |
|                      | 0.0062         | 3        | 40.35      | 36.73           | 0.3673   |
|                      | 0.0080         | 4        | 39.05      | 40.30           | 0.4030   |
|                      | 0.0091         | 5        | 35.53      | 46.78           | 0.4678   |
| 20                   | 0.0023         | 1        | 44.90      | 17.86           | 0.1786   |
|                      | 0.0039         | 2        | 38.07      | 37.10           | 0.3710   |
|                      | 0.0055         | 3        | 35.79      | 43.88           | 0.4388   |
|                      | 0.0072         | 4        | 35.14      | 46.27           | 0.4627   |
|                      | 0.0088         | 5        | 34.36      | 48.54           | 0.4854   |
| 30                   | 0.0019         | 1        | 45.21      | 32.14           | 0.3214   |
|                      | 0.0033         | 2        | 39.26      | 46.77           | 0.4677   |
|                      | 0.0045         | 3        | 35.69      | 54.08           | 0.5408   |
|                      | 0.0056         | 4        | 33.31      | 58.21           | 0.5821   |
|                      | 0.0071         | 5        | 33.79      | 58.48           | 0.5848   |
| 40                   | 0.0019         | 1        | 45.21      | 32.14           | 0.3214   |
|                      | 0.0030         | 2        | 35.69      | 51.61           | 0.5161   |
|                      | 0.0041         | 3        | 32.52      | 58.16           | 0.5816   |
|                      | 0.0050         | 4        | 29.74      | 62.69           | 0.6269   |
|                      | 0.0057         | 5        | 27.13      | 66.67           | 0.6667   |
| 50                   | 0.0016         | 1        | 38.07      | 42.86           | 0.4286   |
|                      | 0.0028         | 2        | 33.31      | 54.84           | 0.5484   |
|                      | 0.0039         | 3        | 30.93      | 60.20           | 0.6020   |
|                      | 0.0046         | 4        | 27.36      | 65.67           | 0.6567   |
|                      | 0.0048         | 5        | 22.84      | 71.93           | 0.7193   |



**Table 2.** The galvanostatic polarization results for mild steel

| Concentration of Inhibitor (mg/L) | $I_{corr}$<br>$\mu\text{A}/\text{cm}^2$ | $E_{corr}$<br>mVolt | $\beta_c$<br>mV/dm | $\beta_a$<br>mV/dm | $\eta_{pol}(\%)$ |
|-----------------------------------|---|---------------------|--------------------|--------------------|------------------|
| Blank                             | 570                                     | -221.2              | -113.1             | 95.2               |                  |
| 10                                | 334.46                                  | -335.2              | -103.1             | 87                 | 41.32            |
| 20                                | 263.97                                  | -334.5              | -96.5              | 72.3               | 53.68            |
| 30                                | 209.18                                  | -332.4              | -95.2              | 86.1               | 63.30            |
| 40                                | 184.61                                  | -331.2              | -138.9             | 75.5               | 67.61            |
| 50                                | 145.83                                  | -328.4              | -140               | 70.7               | 74.41            |

**Table 3.** EIS parameters for MS in the various concentrations pumpkin in 0.5M HCl

| Concentration (mg/L) | $R_p$ | $C_{dl}$ | $\eta_{EIC}(\%)$ |
|----------------------|-------|----------|------------------|
| 0                    | 249   | 639.50   |                  |
| 10                   | 500   | 318.47   | 50.20            |
| 20                   | 666   | 239.09   | 62.61            |
| 30                   | 750   | 212.31   | 66.80            |
| 40                   | 1000  | 159.23   | 75.10            |
| 50                   | 2100  | 75.83    | 76.19            |

**Table 4.** The morphology data by AFM

| Sample                                    | Average (Ra)<br>Roughness (nm) | RMS (Rq)<br>Roughness (nm) |
|---|--------------------------------|----------------------------|
| Clear mild (Control)                      | 10.4                           | 13.9                       |
| Mild steel immersed in 0.5M HCl           | 94                             | 120                        |
| Mild steel immersed in 0.5M HCl + pumpkin | 43                             | 55.2                       |

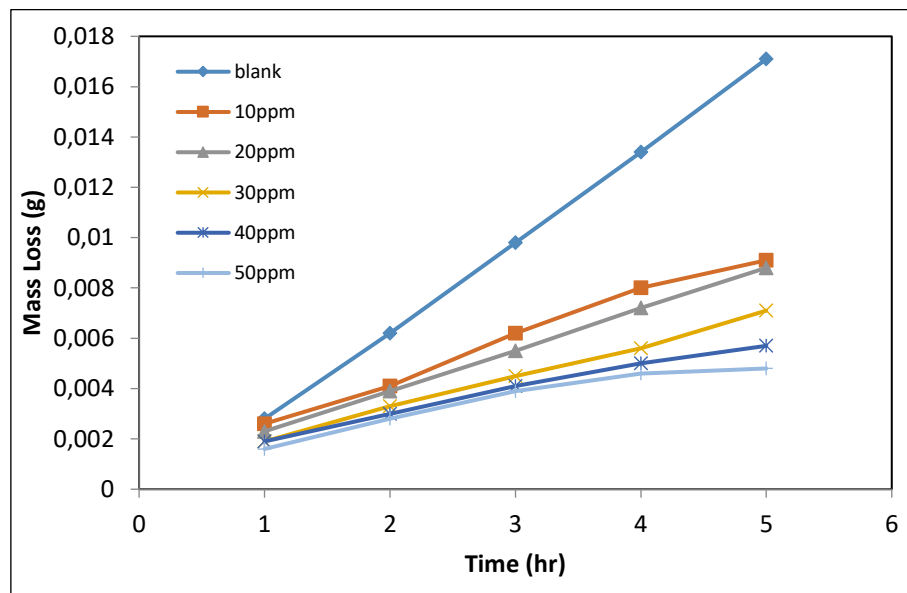


**Figure 1.** Relationship between mass loss (g) of mild steel and time (hr) in 0.5M HCl using pumpkin extracts

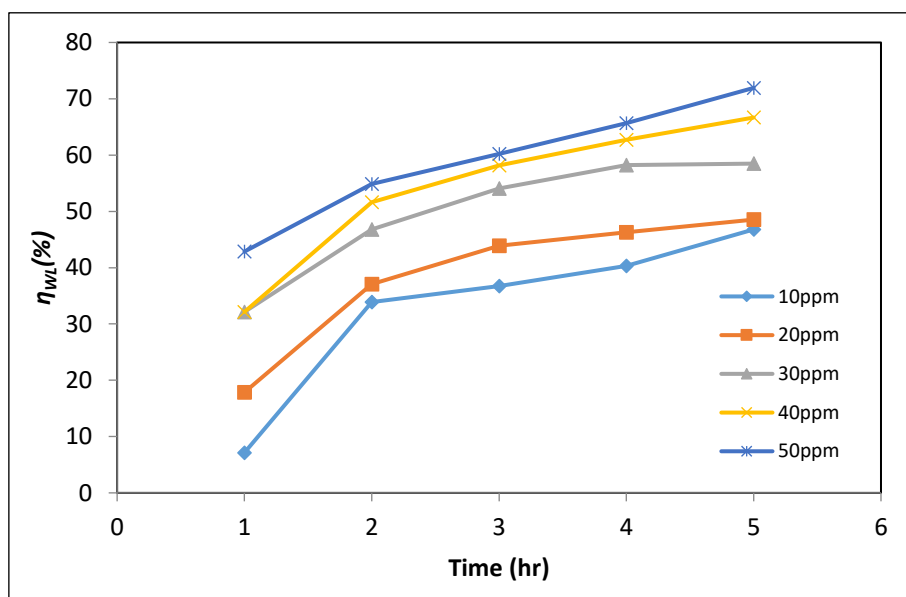


**Figure 2.** Relationship between inhibition efficiency and time (hr) of mild steel in 0.5M HCl using pumpkin extracts

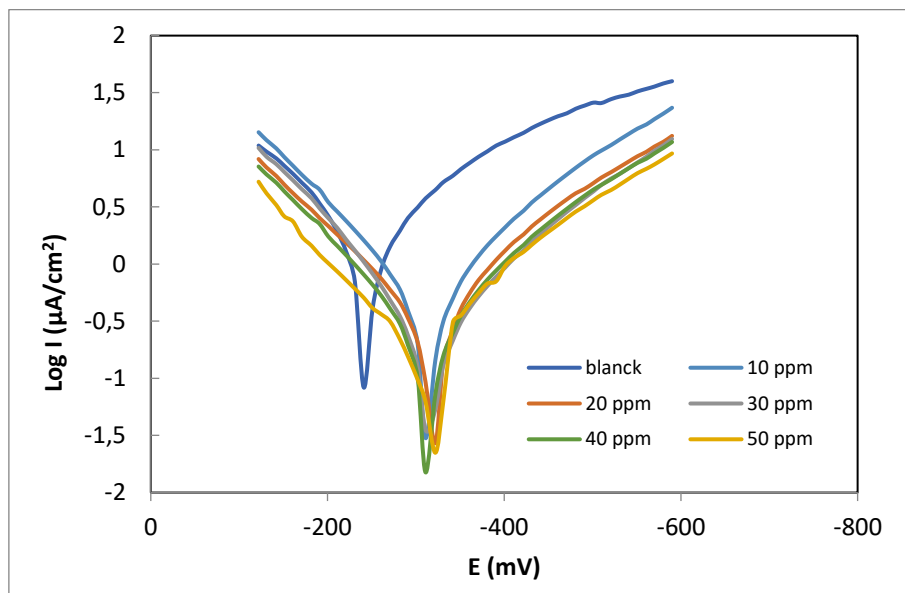


**Figure 3.** Tafel curves of mild steel in 0.5 M HCl solution in the absence and presence of different concentrations of pumpkin inhibitor at 25°C

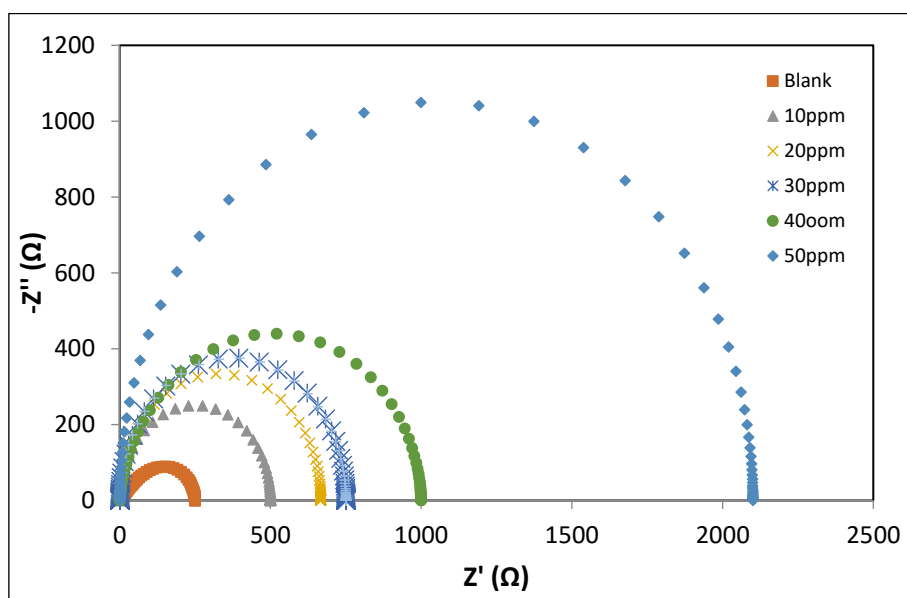


**Figure 4.** Nyquist plots of mild steel in 0.5 M HCl with various concentrations of pumpkin seeds extracted at 25 °C

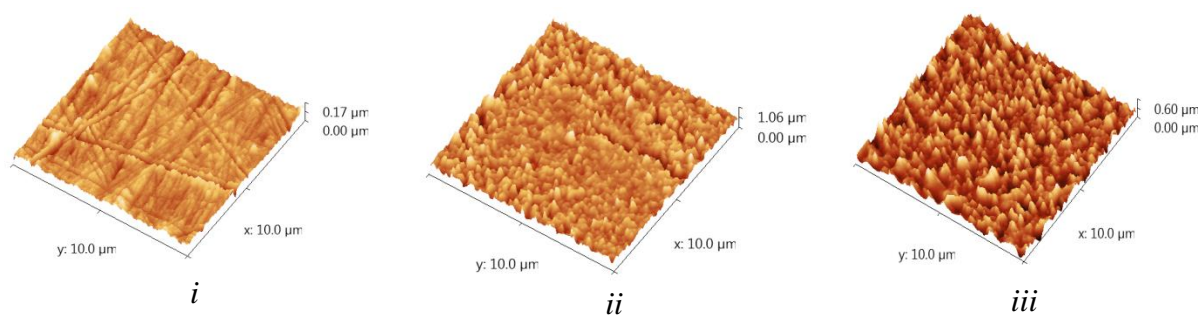


**Figure 5.** The images of AFM of MS, *i*=Control, *ii*=immersed in 0.5M solution of HCl and *iii*=immersed in 0.5M solution of HCl + pumpkin seed extract

**ALTERAÇÕES NOS PARÂMETROS FÍSICO-QUÍMICOS DOS SOLOS CASTANHOS DO CAZAQUISTÃO OCIDENTAL SOB A INFLUÊNCIA DAS TECNOLOGIAS DE PASTAGEM****CHANGES IN THE PHYSICOCHEMICAL PARAMETERS OF CHESTNUT SOILS IN WESTERN KAZAKHSTAN UNDER THE INFLUENCE OF THE GRAZING TECHNOLOGIES****ИЗМЕНЕНИЕ ФИЗИКО-ХИМИЧЕСКИХ ПОКАЗАТЕЛЕЙ КАШТАНОВЫХ ТИПОВ ПОЧВ ЗАПАДНОГО КАЗАХСТАНА ПОД ВЛИЯНИЕМ ТЕХНОЛОГИЙ ВЫПАСА**

NASIYEV, Beybit<sup>1</sup>; BEKKALIYEV, Askhat<sup>1</sup>; ZHANATALAPOV, Nurbolat<sup>1</sup>; SHIBAIKIN, Vladimir<sup>2</sup>; YELESHEV, Rakhimzhan<sup>3</sup>

<sup>1</sup> Zhangir khan West Kazakhstan Agrarian - Technical University, Kazakhstan

<sup>2</sup> Saratov State Vavilov Agrarian University, Russia

<sup>3</sup> Kazakh National Agrarian University, Kazakhstan

*\* Corresponding author  
e-mail: beybit.nasiyev@bk.ru*

Received 20 April 2020; received in revised form 18 May 2020; accepted 25 May 2020

**RESUMO**

O gerenciamento dos recursos de pastagem do Cazaquistão Ocidental é complicado devido à deterioração dos parâmetros físico-químicos dos solos, manifestando degradação e alcalinização como resultado de pastoreio intensivo. A pesquisa teve como objetivo estudar a tecnologia de pastejo de gado para preservar os parâmetros físico-químicos dos solos e aumentar a eficiência do uso de pastagens. A avaliação e análise estatística dos indicadores físico-químicos dos solos foram realizadas com métodos padronizados durante o período de 2018 a 2019, o que permitiu identificar a melhor tecnologia de pastejo. Os resultados da pesquisa mostraram que, sob a influência de pastoreio intensivo, os parâmetros físico-químicos pioraram, foi detectada uma diminuição nas reservas de húmus em 10,88-12,35%, o solo degradado até o terceiro grau e tornou-se alcalino como resultado do aumento da permutabilidade. sódio a 1,65 cmol (equiv.)/kg. A tecnologia de pastejo moderado afeta positivamente os parâmetros físico-químicos dos solos dos ecossistemas de pastagem. Os solos castanhos das pastagens, onde foi aplicada tecnologia moderada de pastejo, permaneceram resistentes à degradação e salinização. Com essa tecnologia, o húmus do solo foi preservado de forma confiável no nível de 1,15-2,50%, o fósforo móvel estava dentro da faixa ideal de 0,87-1,60 mg/100g. Concluiu-se que é importante usar a tecnologia de pastoreio moderado para melhorar o manejo dos recursos das pastagens, que é a novidade científica da pesquisa.

**Palavras-chave:** *solo castanho, índices, degradação, pastoreio, tecnologias.*

**ABSTRACT**

Managing pasture resources of Western Kazakhstan is complicated due to the deterioration of the physicochemical parameters of soils, manifesting degradation, and alkalinization as a result of intensive grazing. The research has been aimed at studying the technology of cattle grazing for preserving the physicochemical parameters of soils and increasing the efficiency of pasture use. The assessment and statistical analysis of physicochemical indicators of soils were carried out with standard methods during 2018 – 2019, which allowed identifying the most optimal grazing technology. The results of the research showed that under the influence of intensive grazing, physicochemical parameters worsened, a decrease in the humus reserves by 10.88-12.35% was detected, soil degraded to the third degree, and became alkaline as a result of the increase in exchangeable sodium to 1.65 cmol (equiv.)/kg. The technology of moderate cattle grazing favorably affects the physicochemical parameters of the soils of pasture ecosystems. The chestnut soils of the pastures, where moderate grazing technology was applied, remained resistant to degradation and salinization. With this technology, the soil humus was reliably preserved at the level of 1.15-2.50%, mobile phosphorus was within the optimal range of 0.87-1.60 mg/100g. It has been concluded that it is important to use the technology of moderate cattle grazing to improve the management of pasture resources, which is the scientific novelty of the research.

**Keywords:** *chestnut soil, indices, degradation, grazing, technologies.*

## ABSTRACT

Процесс управления пастбищными ресурсами Западного Казахстана усложняется из-за ухудшения физико-химических показателей почв с проявлением процессов деградации и солонцевания в результате интенсивного выпаса скота. Целью исследований является изучение технологии выпаса с.х. животных для сохранения физико-химических показателей почв и повышения эффективности использования пастбищ. Применение стандартных методов оценки и статистического анализа физико-химических показателей почв проводилось с 2018 по 2019 годы, что позволило выделить наиболее оптимальную технологию выпаса. Результаты исследований показали, что под воздействием интенсивного выпаса ухудшаются физико-химические показатели, выявлено снижения запаса гумуса на 10,88-12,35%, в результате увеличения обменного натрия до 1,65 смol(equiv.)/kg почва деградировалась до 3 степени и перешла в категорию солонцеватой. Умеренная технология выпаса с.х. животных благоприятно действует на физико-химические показатели почв пастбищных экосистем. Каштановые почвы пастбищ, где применялись умеренная технология выпаса сохраняли устойчивость к деградации и осолонцеванию. При такой технологии гумус почвы достоверно сохранился на уровне 1,15-2,50%, подвижный фосфор находился в оптимальных пределах 0,87-1,60 мг/100г. В этой работе был сделан вывод, что важно использовать умеренную технологию выпаса с.х. животных для повышения эффективности управления пастбищными ресурсами, в чем заключается и научная новизна исследований.

**Keywords:** *Каштановые почвы, показатели, деградация, выпас скота, технологии.*

## 1. INTRODUCTION:

The global growth of the population (the world's population in 2050 is expected to be about 9.2 billion people), the global climate changes and their adverse effects on the agriculture, the depletion of natural resources, which is of great importance for the development of the world's agriculture, food safety, and new ethical requirements for the producers are the future challenges associated with sustainable management of natural resources, and investments in food production and agriculture (Kučera *et al.*, 2020).

Grasslands, which constitute a significant part of the global ecosystem, occupy 37 % of the Earth's land area and contribute significantly to the food security, providing the largest part of energy and proteins required by ruminant animals for the production of meat and milk. It is believed that proper pasture management and improvement of the state of degraded pastures can play a fundamental role in mitigating the effect of greenhouse gas emissions, especially concerning carbon accumulation and absorption (Conant *et al.*, 2011; O'Mara, 2012; Nordborg and Röö, 2016).

Multiple scientific studies and developments of agricultural and biological scientific institutions show that in order to maintain the pastures' capability of constant seed and vegetative regeneration and reproduction of the required level of feed resources, they are to be

used within the environmental imperative. The first environmental commandment for the rational use of the pastures is the compliance with the principle of matching their natural capacity with the number of grazing animals. Multiyear scientific studies performed in the second half of the 20th century by the scientists from various countries show that, without harm to the subsequent productivity of the pastures, it is possible to withdraw 25 – 75 % of the aboveground plant mass in various natural zones. In the arid conditions of Russia and Central Asia, 60 – 75 % of the annual plants' growth may be withdrawn (Shamsutdinov, 2012; Nasiyev *et al.*, 2015; Gayevskaya and Krasnopolin, 2016; Nasiyev, 2016; Baytkanov, 2017).

One of the essential levers for restoring and preserving the pastures' biodiversity is grazing management and ecological optimization of the grazing load, which would also improve the productivity of the pastures and ensure environmental sustainability and economic efficiency (Costas *et al.*, 2015).

Among the agrotechnical methods of increasing the pastures' productivity, providing rest from grazing for medium- and highly-degraded pastures is of paramount importance. Even one year's rest will allow pastures to significantly restore their sparse grass cover (Loris *et al.*, 2019).

Studies of the scientists from the USA and China have shown reduced productivity and deteriorated state of vegetation in the heavy grazing conditions (Raiymbekov *et al.*, 2017; Kubenkulov *et al.*,

2019). For improving the state and the rational use of pastures, monitoring the current state of pasture soil resources is the priority task.

## 2. MATERIALS AND METHODS:

### 2.1 Study area

The research was conducted during 2018 and 2019 years at the initiative of the Ministry of Agriculture in the territories of three zones of Western Kazakhstan with different types of chestnut soils for detecting changes in the physicochemical parameters of the soil cover under the influence of different technologies of cattle grazing, and efficient managing pasture resources.

*Zone 1* was the dry-steppe zone with the following coordinates of the reference plot and the pastures: reference plot —  $49^{\circ}01'N$ ;  $018^{\circ}27'103''E$ , moderate grazing pastures —  $50^{\circ}57'N$ ;  $050^{\circ}46'390''E$ , weak grazing pastures —  $50^{\circ}57'N$ ;  $050^{\circ}48'049''E$ , and intensive grazing pastures —  $50^{\circ}59'N$ ;  $E050^{\circ}47'223''E$ .

*Zone 2* was the arid steppe zone with the following coordinates of the reference plot and the pastures: reference plot —  $50^{\circ}21'N$ ;  $051^{\circ}00'073''E$ , moderate grazing pastures —  $50^{\circ}19'N$ ;  $050^{\circ}58'091''E$ , weak grazing pastures —  $50^{\circ}19'N$ ;  $050^{\circ}57'064''E$ , and intensive grazing pastures —  $50^{\circ}20'N$ ;  $E050^{\circ}53'225''E$ .

*Zone 3* was the semi-desert zone with the following coordinates of the reference plot and the pastures: reference plot —  $49^{\circ}05'N$ ;  $049^{\circ}08'101''E$ , moderate grazing pastures —  $49^{\circ}08'N$ ;  $048^{\circ}42'751''E$ , weak grazing pastures —  $49^{\circ}09'N$ ;  $E048^{\circ}42'452''E$ , and intensive grazing pastures —  $49^{\circ}08'N$ ;  $048^{\circ}41'017''E$ .

*Soil sampling.* To determine the effect of grazing on these indicators, soil samples were taken at three farms with moderately, weakly, and intensively used pastures located in three zones of Western Kazakhstan with dark chestnut (Haplic, Luvic), chestnut (Luvic Kastanozems) and Light chestnut soils (Calcic Kastanozems) from the 0 – 10 cm, 10 – 20 cm, and 20 – 30 cm layers. To identify the changes in the soil parameters through comparison, soil samples were taken from the reference plots (without grazing) from the 0 – 10 cm, 10 – 20 cm, and 20 – 30 cm layers in each zone. The experiment was repeated four times.

### 2.2 Physicochemical soil analysis

The changes in the physicochemical parameters of pastures were detected both in the

field and in the laboratory environment with the use of modern generally adopted methods.

Soil density was determined in the field environment using cylinder bores by N.A. Kachinsky. In the field, samples were taken from the soil horizon with a cylinder bore with a volume of about 500 cm<sup>3</sup>. At the same time, soil samples were collected in weighing bottles to determine moisture. In the laboratory, the soil was dried at 105°C to constant weight. Knowing the mass of the weighing bottle with dried soil and the mass of the empty weighing bottle, the mass of air-dry soil was found. Then, dividing the mass of dry soil by its volume (ring volume), the density of the soil was established.

The structural state of the soil was assessed by aggregate analysis using the dry sieving method. According to the results of the aggregate analysis, the structural coefficient (Cstr) was calculated, which was understood as the ratio of the number of aggregates from 0.25 to 10 mm (in%) to the total content of aggregates less than 0.25 and more than 10 mm (in%). The more Cstr was, the better the structure of the soil was. A scale developed by S.I. Dolgov and P.U. Bakhtin was used to assess the structural state of soils (Gabdulov *et al.*, 2018).

In the laboratory environment, the soil content of humus, mobile phosphorus, and exchangeable sodium was determined by the analysis of soil samples.

The content of humus in the soil was determined by the method of I.V. Tyurin based on the oxidation of soil organic matter by chromic acid until the release of carbon dioxide. A solution of K<sub>2</sub>Cr<sub>2</sub>O<sub>7</sub> in sulfuric acid was used as an oxidizing agent.

Mobile phosphorus compounds were determined by the photometric method of I. Machigin based on the extraction of mobile phosphorus and potassium compounds from the soil with ammonium carbonate solution at a concentration of 10 g/dm<sup>3</sup> with soil to solution ratio of 1:20 and the subsequent determination of phosphorus in the form of a phosphorus-molybdenum blue complex on photoelectric colorimeter and of potassium on a flame photometer (Gabdulov *et al.*, 2018).

The content of exchangeable sodium in the soil was established by the photometric method by extracting exchangeable and soluble sodium with ammonium acetate solution at a concentration of 1 mol/dm<sup>3</sup> with soil sample mass to solution volume ratio of 1:20 and the subsequent



determination of sodium in the extract using a flame photometer. At the same time, soluble sodium in the aqueous extract was determined, and the difference in sodium was calculated. According to the content of the exchangeable sodium in the cation exchange capacity, the degree of soil alkalinization was established.

The degree of soil cover degradation was established by the physical criteria for land assessment approved by the Ministry of Agriculture of the Republic of Kazakhstan (Order No.185 of the Minister of Agriculture of the Republic of Kazakhstan, 2017).

**Statistical analysis.** The results of the studies were statistically processed following the method of the analysis of variance (Dospekhov, 2015) in the Statistica 6.0 application. Two individual samples were analyzed nonparametrically using the Mann-Whitney U-test, and statistical diagrams were made).

### 3. RESULTS AND DISCUSSION:

**Agrochemical parameters of the pastures.**  
**The dynamics of decreasing the humus content.** Studying the content and humus reserves in the pastures of Western Kazakhstan is a prerequisite for assessing their fertility and for addressing the issues of the rational use of pasture ecosystems. In the studies, the content and humus reserves depended on the technology of farm animals' grazing on the pastures. With that, more dynamic changes in the humus content occurred on the pastures with the arid climate of the third semi-desert zone with light chestnut soils. In the pastures with moderate grazing conditions in this zone, the humus content in the 0 – 30 cm soil layer reduced by 0.15 %, compared to the reference. The humus reserves were 44.16 t/ha, which was less by 7.19 %, compared to the reference. The humus content in the pastures with weak grazing conditions on light chestnut soils was 1.25 % with the humus reserves of 46.50 t/ha.

In the territory of the third semi-desert zone, the lowest humus content was found in the pastures with intensive grazing conditions. With the humus content of 0.83 %, the humus reserves in the 0 – 30 cm soil layer were 34.36 t/ha. Compared to the reference, the reduction of the humus reserves amounted to 27.78 %. In terms of the humus reserves, the soil in this plot degraded to the second degree. Since grazing has a significant effect on some ecosystem services (e.g., retention of nutrients, water storage, reduction of pollution), reduction of these

parameters may result in decreased soil fertility and, consequently, land degradation (Mamontov *et al.*, 2012). According to the hypotheses of the authors, a strong change in the content and reserves of humus in the pastures of the third semi-desert zone was the result of excessive loads from farm animals' grazing on the background of the arid climate (Nasiyev *et al.*, 2015).

On dark chestnut and chestnut soils of the pastures in zones 1 and 2 with the technology of weak and moderate grazing, compared to the soil in the reference plots, the humus content reduced insignificantly (from 0.11 to 0.22 %), and the humus reserves in the 0 – 30 cm soil layer amounted to 4.59 – 6.67 %. With a certain degree of conditionality, it may be assumed that the humus in the soil in these zones was as though "preserved" under the influence of grazing, accompanied by the reduced ingress of the live and dead plant materials into the soil. It should be noted that oxidation of the organic matter in the soil does not occur in the pastures, i.e., the phenomena resulting in the dehumification of the arable land due to its annual plowing do not manifest themselves; hummus is not consumed there, and formation of plants biomass changes its species composition and productivity under the influence of failure (Tesla, 2016; Nasiyev and Bekkaliyev, 2019).

In the case of intensive grazing, the content of humus in chestnut and light chestnut soils reduced by 0.35 - 0.42 %, while the humus reserves reduced by 10.88 - 12.35 %. With that, in terms of humus reserves, the soil degraded to the first degree.

The results of the statistical analysis confirmed the dependence of the humus content on the intensity of the pasture use. The intensity of the changes in the humus content was determined by the type of soil and had a negative tendency. This tendency was described by a linear regression equation. The most significant reduction in the percentage of humus with an increase in the grazing intensity was observed in light chestnut soils of the third semi-desert zone (Figure 1).

The changes in the humus reserves also occurred according to the linear function in all types of soil. Regression analysis showed that the highest rate of humus reserves reduction depended on the type of soil and had a linear tendency. The most intensive reduction of humus content in the soil with increasing the intensity of pasture use was observed on the light chestnut

soils of the third semi-arid zone.

*The content of mobile phosphorus and exchangeable sodium.* In chestnut soils, one of the limiting elements of soil fertility is the content of phosphorus (Barbara *et al.*, 2016). In this regard, it is important to maintain the content of mobile phosphorus in chestnut soils in agricultural use. According to the results of the studies, the grazing of farm animals insignificantly changed the content of mobile phosphorus in chestnut soils of the three zones of Western Kazakhstan. In the zone of dark chestnut soils, the reduction of mobile phosphorus content ranged from 0.23 to 0.59 mg/100 g of soil, compared to the reference. In chestnut soils of the pastures in the second zone, the changes in the content of mobile phosphorus from the reference were 0.43 - 0.69 mg/100 g of soil. In the third zone in the light chestnut soils, the content of mobile phosphorus reduced from 0.10 to 0.41 mg/100 g of soil, compared to the reference (Table 1).

The U-test showed the effect of the grazing technology on the response of the effective index of mobile phosphorus content. In the column with the *p-value* in the table, the significance of the effective index (F) response to the technology by the soil zones takes the *p-value* < 0.05. The exception is the technology of moderate grazing for the third zone. Based on this indicator, a conclusion may be drawn that all technologies in the first, second, and third zones have a significant effect on the content of mobile phosphorus.

The quantitative expression of this effect is determined by the difference between the median for the corresponding technology and the technology without grazing.

On dark chestnut soils of the first zone, the difference between the median values of phosphorus in the case of the technology of weak grazing, compared to that without grazing, was 0.24 mg/100 g, in the case of the technology of moderate grazing, the difference was 0.41 mg/100 g, and in the case of the technology of intensive grazing — 0.61 mg/100 g.

For chestnut soils in the second zone, the difference between the median values of the content of mobile phosphorus in the case of the technology without grazing and that of weak grazing was 0.45 mg/100 g, in the case of the technology without grazing and that of moderate grazing — 0.61 mg/100 g, and in the case of the technology without grazing and that of intensive grazing — 0.69 mg/100 g.

For light chestnut soils in the third zone, the response to the grazing technologies was the

following: weak grazing — 0.1 mg/100 g and intensive grazing — 0.41 mg/100 g, respectively. By the significance level of the *p-value*, the technology of moderate grazing in this sample did not cause a significant response to the quantitative indicator of mobile phosphorus content (F, mg/100 g).

Thus, it was found that the content of mobile phosphorus increased with increasing the intensity of grazing in all types of soil, except for the moderate grazing technology in the third zone of light chestnut soils.

In turn, the deterioration of the physicochemical properties resulted in the increased content of metabolic sodium in the soil, which was an indicator of salinity and increased soil salinization (Nasiev, 2016). In chestnut soils of pastures of the second zone, the content of exchangeable sodium, depending on the grazing technology, increased from 0.08 to 0.32 cmol (equiv.)/kg, compared to the reference. In the soils of the pastures, the content of exchangeable sodium ranged from 4.98 to 5.92 % of the amount of exchange bases, which corresponded to the degree of weak alkalinity. In light chestnut soils in the third zone, with the sum of exchange bases of 15.10 – 15.65 cmol (equiv.)/kg, the content of exchangeable sodium was 1.41 – 1.65 cmol (equiv.)/kg, or 9.33 – 10.54 % of the cationic exchange. By the content of exchangeable sodium, the soil in the pastures with weak and moderate grazing was weakly alkaline, and the soil with intensive grazing was medium alkaline.

In dark chestnut soils, the content of exchangeable sodium, depending on the grazing technology, amounted to 0.36 – 0.61 cmol (equiv.)/kg, or 1.71 – 2.77 % of the total amount of exchangeable bases. By the content of exchangeable sodium, dark chestnut soils in the first pasture zone were non-alkaline (Table 2).

The U-test showed the effect of the grazing technology on the response of the effective index of exchangeable sodium content. In the column with the *p-value* in the table, the significance of the effective index response to the technology by the soil zones takes the *p-value* < 0.05. Therefore, all technologies in the first, the second, and the third zones had a significant effect on the content of exchangeable sodium. The technology in this sample caused a significant response to the quantitative indicator of exchangeable sodium content.

The quantitative expression of this effect was determined by the difference between the median for the corresponding technology and the

technology without grazing.

In terms of the grazing technology on the dark-chestnut soils in the first zone, the difference between the median value of the exchange of sodium in the case of the technology of weak grazing and without grazing was 0.09 cmol (equiv.)/kg, in the case of the technology of moderate grazing and without grazing — 0.29 cmol (equiv.)/kg, and in the case of the technology of intensive grazing and without grazing — 0.33 cmol (equiv.)/kg.

For chestnut soils in the second zone, the difference between the median value for the technology without grazing and weak grazing was 0.09 cmol (equiv.)/kg, for the technology without grazing and that of moderate grazing — 0.29 cmol (equiv.)/kg, and for the technology without grazing and that of intensive grazing — 0.33 cmol (equiv.)/kg.

For light chestnut soils in the third zone, the responses to the grazing technologies were the following: weak grazing — 0.10 cmol (equiv.)/kg, moderate grazing — 0.19 cmol (equiv.)/kg, and intensive grazing — 0.34 cmol (equiv.)/kg.

The tests confirmed the presence of a statistical regularity of increasing the content of exchangeable sodium in all types of soil with increasing the intensity of grazing.

*Agrophysical indicators.* Soil density and structural coefficient are the most important indicators of its fertility. They do not provide the required nutrients to plants, but they can influence their growth and development. Therefore, the knowledge of the soil physical characteristics and the ability to adjust them are required for extended reproduction of soil fertility (Nasiyev, 2014; Blanco *et al.*, 2016; Tesla, 2016).

Assessment of the density and the structural coefficient of chestnut soils in Western Kazakhstan by the main indicators, depending on the grazing technology, showed their sensitivity to trampling. The agrophysical properties of chestnut soils depended on their types and grazing technology. However, with the reduction of loads by the use of weak and moderate grazing technologies, the physical properties of the pastures varied considerably compared to the virgin areas, which could be explained mainly by grass restoration processes in pastures and, therefore, by solid soil phase properties and soil structure stability. Therefore, in the case of weak and moderate grazing, the deterioration of the physicochemical properties of the pasture ecosystems occurred less rapidly than in the case

of intensive grazing (Angassa, 2014; Tesla, 2016).

The analysis of the dynamics of the structural-and-aggregate composition of dark chestnut, chestnut, and light chestnut soils showed certain deterioration in the soil structure under the influence of prolonged pasture use and the pronounced tendency to the restoration that had been observed during the observation period.

Despite the certain deterioration of the structure under the influence of grazing, the soil in the pasture areas with weak and moderate grazing conditions showed good content of agronomically valuable aggregates and structure due to the restoration of vegetation. For instance, on dark chestnut soils with moderate and weak grazing, the soil structure was 63.83 – 71.20 %, with a structural coefficient of 1.80 – 2.48.

On chestnut soils in the case of weak grazing, the soil structure was 65.57 % with the structural coefficient of 2.73, while in the case of moderate grazing, the structure was 65.57 % with the structural coefficient of 1.92.

In the case of moderate grazing, the soil structure of the pastures with light chestnut soils (67.50 %), compared to the structural properties of the soil of the reference plot (75.03 %), reduced by 7.53 %. The structural coefficient of the soil in this pasture plot was 2.10.

In the case of moderate grazing, the structural coefficient of the pastures on light chestnut soils was 1.88, while the soil structure was 64.41 %, which was 10.62 % less than in the reference. In all the soil and climatic zones on the pastures with weak and moderate grazing, the state of the soil structure was "good".

Intensive grazing can change the soil structure (Řeháček *et al.*, 2017). In all the types of chestnut soils with strong grazing, the soil structure reduced to 53.06 – 60.57 % with the structural coefficient of 1.22 – 1.50; the soil structure and the structural coefficient corresponded to "satisfactory" (Table 3).

The U-test showed the effect of the grazing technology on the response of the effective index of agronomically valuable structural aggregates. In the column with the p-value in Table 3, the meaning of the response of the content of agronomically valuable structural aggregates to soil-zone technologies takes a p-value < 0.05. The exception is the technology of weak grazing for the second zone. Based on this indicator, it may be concluded that all the technologies in the first, the second, and the third zones have a significant effect on the content of the agronomically valuable

structural aggregates. The quantitative expression of this effect is determined by the difference between the corresponding technology median and non-grazing technology.

On dark chestnut soils of the first zone, the difference between the median values of structural aggregates in the case of the technology of weak grazing, compared to that without grazing, was 5.6 %, compared to that of moderate grazing — 12.95 %, and compared to that of intensive grazing — 16.89 %.

For chestnut soils in the second zone, the difference between the median values for the technology without grazing and that of moderate grazing was 10.46 %, for the technology without grazing and that of intensive grazing — 21.2 %. The technology of weak grazing in this sample did not cause a significant response in the quantitative indicator of the content of the agronomically valuable structural aggregates.

For light chestnut soils in the third zone, the response to the grazing technologies was the following: weak grazing — 7.53 %, medium grazing — 10.13 %, and intensive grazing — 21.97 %.

Based on the obtained results, it may be concluded that there is a statistical regularity of decreasing the content of agronomically valuable structural aggregates with increasing the grazing intensity for all types of soil, except for the technology of weak grazing in the second zone of chestnut soils.

Another fundamental property of the soil is its density. In contrast to the soil structure, which is a well-known regulator of the physical conditions in it, and has only an indirect effect on plants, the density of the soil directly influences the processes of their life activity (Khadka *et al.*, 2019).

Without knowing the soil density, it is impossible to perform quantitative soil assessment. Therefore, the data about the density of the soil layers and horizons necessarily accompany a full description of the soil profile (Wojciechowski *et al.*, 2020).

Overgrazing may lead to soil degradation and loss of the fertile topsoil, especially in the case of little rainfall and significant evaporation (Khadka *et al.*, 2019). It was confirmed by the results of the research studies. In the third semi-arid zone with an arid climate, the soil in the pastures with intensive grazing in terms of the density degraded to the third degree, the soil density in the 0 – 30 cm soil layer was 1.38 g/cm<sup>3</sup>, or the level of light chestnut soils density under the influence of

grazing was 13.11 %. Such high soil compaction creates anaerobic-like conditions in the root layer and changes the structure of the soil horizons (Tesla, 2016; Lobanov *et al.*, 2020).

The destructive effect of intensive grazing on physical properties, especially on soil density, was reported by many researchers (Nasiyev, 2014; Angassa, 2014; Blanco *et al.*, 2016).

On light chestnut soils in the third zone, the soil density in the reference plot in the 0 – 30 cm horizon was 1.22 g/cm<sup>3</sup>. When grazing was organized following the technology of weak grazing, the density changes in the 0 – 30 cm soil layer were insignificant (1.24 g/cm<sup>3</sup> or soil compaction by 0.02 g/cm<sup>3</sup>). In the case of moderate grazing, slight soil compaction from 1.22 to 1.28 g/cm<sup>3</sup>, or by 4.91 %, was also observed.

The studies also revealed compaction of chestnut and dark chestnut soils in the first and the second zones upon the increased load on the pastures. For instance, in the first dry steppe zone of dark-chestnut soils with intensive grazing, the soil was compacted, compared to the density of the reference plot, by 5.38% (from 1.30 to 1.37 g/cm<sup>3</sup>). In the second zone of arid steppes on chestnut soils, in the case of intensive grazing, the soil density increased from 1.23 g/cm<sup>3</sup> (reference) to 1.30 g/cm<sup>3</sup>, or by 5.69 %. The soil of these zones in the case of intensive grazing degraded to the first degree.

The variation of physical conditions is one of the factors for preserving and maintaining the biodiversity, which is important ecological component of any ecosystem, including the soil one. Assessment of the parameters of linear regression allowed concluding that light chestnut soils had the greatest tendency toward compaction under the influence of grazing. The growth rate in the case of changing the technology was 0.052 g/cm<sup>3</sup>. The degree of degradation was the third one. In this regard, the study was very relevant (Figure 2).

#### 4. CONCLUSIONS:

1. The deterioration of physicochemical indicators, soil degradation, and salinization processes are the most common and significant complications in the management of pasture ecosystems in Western Kazakhstan, requiring for the right decisions due to their environmental impact, as well as reduction of the production rate of safe livestock products.

2. Physicochemical indicators affect the soil quality, which leads to deterioration of the ecological situation in agrocenoses and the

productivity and state of vegetation of pasture ecosystems.

3. Technology of moderate cattle grazing is necessary to solve the problems of qualitative and efficient use of pastures.

4. The main principle of moderate grazing technology implies the use of 65-75% of plants in the grazing season, which, resulting from the vital activity of plants, contributes to the improvement of the physicochemical parameters of soils. This hypothesis is confirmed by the data of standard assessment methods and statistical analysis of physicochemical parameters of chestnut soil types of pasture ecosystems in the territories of three zones of Western Kazakhstan.

5. The idea and research data serve as a prerequisite for the development of conservation measures for the efficient use of pasture ecosystems outside Kazakhstan, in countries and regions with similar pasture management systems.

## 5. ACKNOWLEDGMENTS:

The work was carried out in the Zhangir khan West Kazakhstan Agrarian-Technology University within the framework of program-targeted financing of the Ministry of Agriculture of the Republic of Kazakhstan on the topic BR 06249365 "Creating highly productive pasture lands in the context of North and West Kazakhstan region and the sustainable use thereof".

## 6. REFERENCES:

1. Angassa, A. (2014). Effects of grazing intensity and bush encroachment on herbaceous specie and rangeland condition in southern Ethiopia. *Land Degradation and Development*, 25,438–451.
2. Barbara, F.; Krzysztof, P.; Elżbieta, J. B.; Tomasz, M. G. (2016). Sheep and Horse Grazing in a Large-Scale Protection Area and its Positive Impact on Chemical and Biological Soil Properties. *Polish Journal of Soil Science*, 49(2), 111-123.
3. Baytkanov, K. A. (2017). Experience in the development and use of salt in the dry steppe and semi-desert zone. *Fodder base of livestock breeding. Moscow*, 53-56.
4. Blanco, A.; Salazar, M. J.; Cid, C. V.; Pereyra, C.; Cavaglieri, L. R.; Becerra, A. G.; Pignata, L. V.; Rodriguez, J. H. (2016). Multidisciplinary study of chemical and biological factors related to Pb accumulation in sorghum crops grown in contaminated soils and their toxicological implications. *Journal of Geochemical Exploration*, 166, 18-26.
5. Conant, R. T.; Paustian, K.; Elliott, E. T. (2011). Grassland management and conversion into grassland: Effects on soil carbon. *Ecological Applications*, 11(2), 343-355.
6. Costas, K.; Vassilis, D.; Mina, K.; Kate, K.; Penny, V.; Luca, S. (2015). Exploring Long-Term Impact of Grazing Management on Land Degradation in the Socio-Ecological System of Asteroussia Mountains. Greece. *Land*, 4, 541-559.
7. Dospekhov, B. A. (2015). *Methods of Field Experimentation. Moscow*, 72-90.
8. Gabdulov, M. A.; Vyurkov, V. V.; Archipkin, V. G.; Turganbayev, T. A.; Rakhimgaliyeva, S. J.; Kushenbekova, A. K.; Baymukanov, E. N. (2018). *Methods of field and laboratory research. Uralsk: WKATU Zhangir Khan*, 41.
9. Gayevskaya, L. S.; Krasnopolin, E. S. (2016). Changes in the vegetative cover of sheep pastures of the Clay desert and the foothill desert of Central Asia. *Botanical Journal*, 7, 156-168.
10. Khadka, D.; Lamichhane, S.; Bhandana, P.; Timilsina, A. P.; Ansari, A. R.; Joshi, K. S. (2019). Soil analysis gis-based fertility assessment and mapping of agricultural research station. *Pakribas, Dhankuta, Nepal. Polish Journal of soil science*, LII/1, 23-42.
11. Kubenkulov, K.; Naushabaev, A.; Abdirahymov, N.; Rustemov, B.; Bazarbaev, S. (2019). Particularities of Forming Desert Pastures Near Settlements of Southern Balkhash (Kazakhstan). *Journal of Ecological Engineering*, 20(8), 129–134.
12. Kučera, J.; Podhrázská, J.; Karásek, P.; Papaj, V. (2020). The Effect of Windbreak Parameters on the Wind Erosion Risk Assessment in Agricultural Landscape. *Journal of Ecological Engineering*, 21(2), 150–156.
13. Lobanov, G. V.; Avramenko, M. V.; Protasova, A. P.; Drozdov, N. N. (2020). Seasonal and long-term changes of vegetation index of arable lands of Bryansk region (Central Russia): regularities and dynamics factors. *Periodico Tchê Química*, 34(17), 745-753.
14. Loris, T.; Jianshuang, Wu.; Roberta, M.; Mauro, P.; Paolo, T. (2019). Estimating soil degradation in montane grasslands of

- North-eastern Italian Alps. *Heliyon*, 5(6), 18-25.
15. Nasiyev, B. N. (2016). The study of the processes, degradation factors and the selection of crops for the restoration of bioresources capacity of the grassland and of semi-desert zones. *Research Journal of Pharmaceutical, Biological and Chemical Sciences*, 7, 2637-2646.
  16. Nasiyev, B. N.; Bekkaliyev, A. K. (2019). The Impact of Pasturing Technology on the Current State of Pastures. *Annals of Agri-Bio Research*, 24(2), 246-254.
  17. Nasiyev, B. N.; Tulegenova, D.; Zhanatalapov, N.; Shamsutdinov, Z. Sh. (2015). Studying the impact of grazing of the current state of grassland in the semi-desert zone. *Biosciences biotechnology research Asia*, 12, 1735-1742.
  18. Nasiyev, B. N. (2014). Innovative techniques in production of fodder protein in adaptive crop science of west Kazakhstan. *Life Science Journal*, 11(3s), 150-153.
  19. Nordborg, M.; Röö, E. (2016). Holistic management. A critical review of Allan Savory's grazing method. *SLU: Swedish University of Agricultural Sciences and Chalmers*, 5-15.
  20. O'Mara, F. P. (2012). The role of grasslands in food security and climate change. *Annals of Botany*, 110(6), 1263-1270.
  21. Order No.185 of the Minister of Agriculture of the Republic of Kazakhstan. (April 27, 2017). On approval of the Measuring method to combat the degradation and desertification of pastures, including arid areas. Retrieved from: [https://tengrinews.kz/zakon/pravitelstvo\\_respublikkazakhstan\\_premier\\_ministr\\_rk/selskoe\\_hozyaystvo/id-V1700015128/](https://tengrinews.kz/zakon/pravitelstvo_respublikkazakhstan_premier_ministr_rk/selskoe_hozyaystvo/id-V1700015128/)
  22. Raiymbekov, B. A.; Orazbayev, S. A.; Seitkarimov, A.; Yancheva, Hr. G. (2017). Promising species of artemisia in the desert zone of Southern Kazakhstan. *Ecology, Environment and Conservation*, 23(2), 1195-1201.
  23. Řeháček, D.; Khel, T.; Kugera, J.; Vopravill, J.; Petera, M. (2017). Effect of Windbreaks on Wind Speed Reduction and Soil Protection against Wind Erosion, *Soil and Water Res*, 12(2), 128-135.
  24. Shamsutdinov, Z. Sh. (2012). Long-term pasture agrophytocenosis in the arid zone of Uzbekistan. *FAN UzR*, 6, 45-57.
  25. Tesla, A. B. (2016). Structure of common black soils in High Volga region under natural pastures. *Vestnik OGU*, 1, 310-312.
  26. Wojciechowski, T.; Mazur, A.; Przybylak, A.; Piechowiak, J. (2020). Effect of Unitary Soil Tillage Energy on Soil Aggregate Structure and Erosion Vulnerability. *Journal of Ecological Engineering*, 21(3), 180-185.

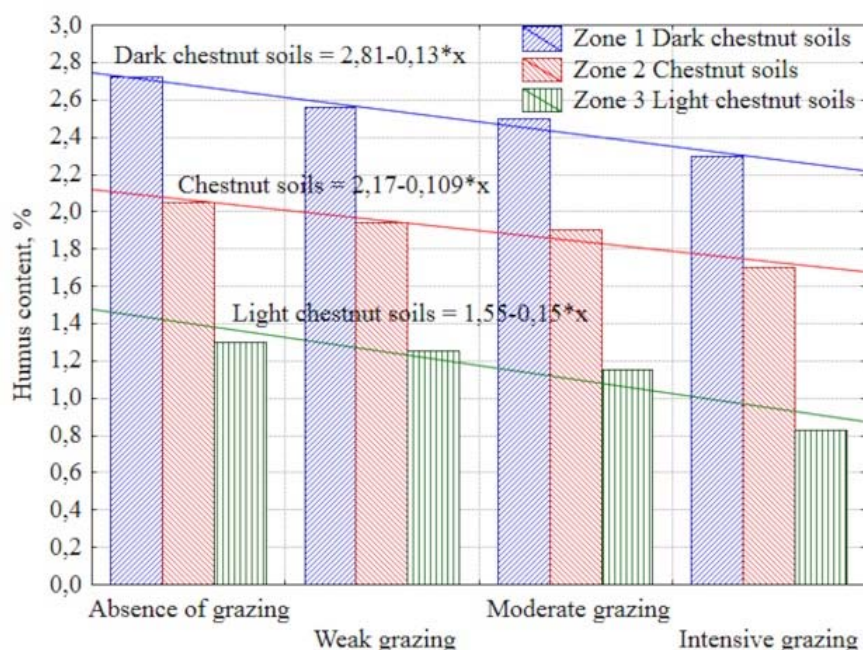


**Figure 1.** The humus content in chestnut soils in the pastures of Western Kazakhstan, depending on the grazing technology

**Table 1.** The content of mobile phosphorus in chestnut soils of the pastures in Western Kazakhstan, depending on the grazing technology, in the 0 – 30 cm soil layer, mg/100 g

| Grazing technology | Zone 1<br>Dark chestnut soils | Zone 2<br>Chestnut soils | Zone 3<br>Light chestnut soils |
|--------------------|-------------------------------|--------------------------|--------------------------------|
| No grazing         | 2.00 ± 0.047                  | 1.54 ± 0.023             | 1.05 ± 0.008                   |
| Weak grazing       | 1.77 ± 0.016                  | 1.11 ± 0.015             | 0.95 ± 0.009                   |
| Moderate grazing   | 1.60 ± 0.018                  | 0.94 ± 0.009             | 0.87 ± 0.093                   |
| Intensive grazing  | 1.41 ± 0.030                  | 0.85 ± 0.007             | 0.64 ± 0.004                   |

**Table 2.** Exchange sodium content in the 0 – 30 cm soil layer of chestnut soils in the pastures of Western Kazakhstan, depending on the grazing technology, cmol (equiv.)/kg

| Grazing technology | Zone 1<br>Dark chestnut soils | Zone 2<br>Chestnut soils | Zone 3<br>Light chestnut soils |
|--------------------|-------------------------------|--------------------------|--------------------------------|
| No grazing         | 0.29 ± 0.011                  | 0.92 ± 0,014             | 1.30 ± 0.010                   |
| Weak grazing       | 0.36 ± 0.005                  | 1.00 ± 0,015             | 1.41 ± 0.004                   |
| Moderate grazing   | 0.57 ± 0.007                  | 1.20 ± 0.013             | 1.50 ± 0.015                   |
| Intensive grazing  | 0.61 ± 0.015                  | 1.24 ± 0.012             | 1.65 ± 0.015                   |

**Table 3.** The content of agronomically valuable structural aggregates and the structural coefficient of chestnut soils in the pastures of Western Kazakhstan, depending on the grazing technology in the 0 – 30 cm soil layer, %

| Grazing technology | Zone 1<br>Dark chestnut soils | Zone 2<br>Chestnut soils | Zone 3<br>Light chestnut soils |
|--------------------|-------------------------------|--------------------------|--------------------------------|
| No grazing         | 77.10 ± 1.30                  | 76.00 ± 1.09             | 75.03 ± 0.43                   |
| Weak grazing       | 71.20 ± 0.21                  | 71.89 ± 1.05             | 67.50 ± 0.72                   |
| Moderate grazing   | 63.83 ± 0.24                  | 65.57 ± 0.42             | 64.91 ± 1.10                   |
| Intensive grazing  | 60.57 ± 0.89                  | 54.82 ± 0.50             | 53.06 ± 1.31                   |



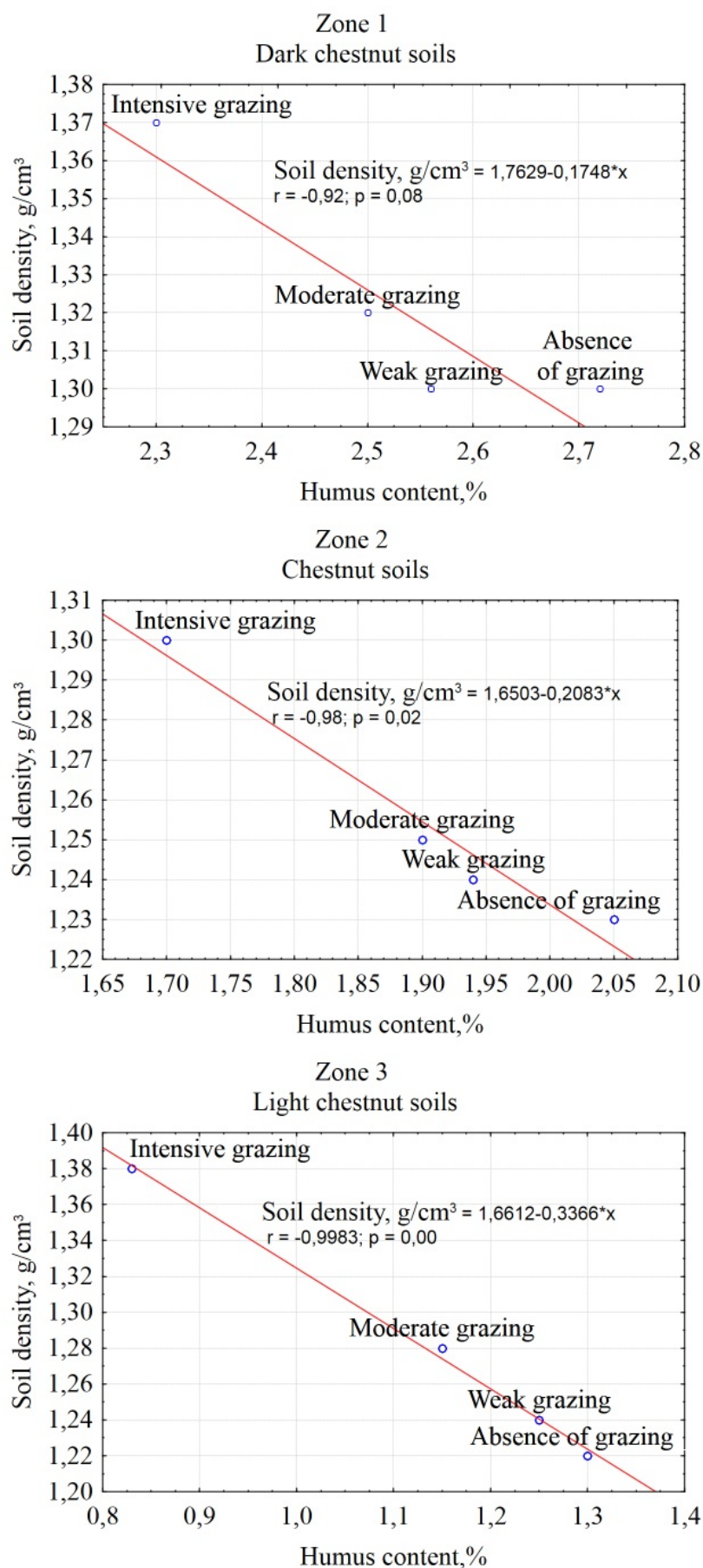


**Figure 2.** The density of chestnut soil types in the pastures of Western Kazakhstan, depending on the grazing technology, in the 0 – 30 cm soil layer



## MODELAGEM MOLECULAR, MEDIDAS CONDUTIMÉTRICAS E ESPECTROS UV-VIS DO ÁCIDO ASCÓRBICO PARA FORMAÇÃO DE SISTEMAS QUÍMICOS COMPLEXOS.

## MOLECULAR MODELING, CONDUCTIVE MEASUREMENTS, AND UV-VIS SPECTERS OF ASCORBIC ACID FOR FORMATION OF COMPLEX CHEMICAL SYSTEMS.

LIMA, Sarah Giovanna Montenegro<sup>1</sup>; CRUZ, Thiago Jackson Torres<sup>2</sup>; PEREIRA, Francisco Claudece<sup>2</sup>; SILVA, Ademir Oliveira da<sup>2</sup>; LIMA, Francisco José Santos<sup>2\*</sup>.

<sup>1</sup> Universidade Federal do Rio Grande do Norte, Faculdade de Farmácia

<sup>2</sup> Universidade Federal do Rio Grande do Norte, Instituto de Química

\* Autor correspondente  
e-mail: limafjs@yahoo.com

Received 17 April 2020; received in revised form 22 May 2020; accepted 10 June 2020

### RESUMO

O ácido ascórbico, geralmente conhecido como vitamina C, é um ácido fraco e antioxidante natural que exerce funções biológicas importantes na participação da formação do colágeno e na absorção de ferro pelo organismo. O objetivo desse trabalho foi verificar, através da modelagem molecular, cargas parciais e avaliação de parâmetros de reatividade PRM que o mesmo apresenta densidades eletrônicas favoráveis em posições estereoquimicamente localizadas para a formação de sais metálicos associados a pretensos sistemas complexos. Suas propriedades eletrolíticas mostraram um comportamento do tipo 1:1 em solução aquosa milimolar recém-preparada. Isto é concordante com os valores de pH,  $K_{a1}$  e  $K_{a2}$  respectivamente, avaliados para uma situação de equilíbrio através do programa RAÍZES 1.0, desenvolvido pelos autores. A decomposição térmica se inicia em torno de 180 - 190 °C, e segue até atingir a temperatura de 570,3 °C, na qual um pequeno percentual experimental de resíduo foi associado a presença de carbono reduzido. O espectro de absorção na região do infravermelho identificou as principais transições atribuídas a C=O, C-O, C=C, OH presentes em seus grupos funcionais. O espectro de absorção UV-Vis mostrou uma banda intensa que ocorre entre 207 – 312 nm, com pico de absorção máxima,  $A_{m\acute{a}x} = 3,6123$  em 249 e 250 nm. Esta banda se apresenta na região onde ocorrem as transições  $n \rightarrow \pi^*$ ,  $n \rightarrow \sigma^*$  e  $\pi \rightarrow \pi^*$  associada aos grupos cromóforos. A força do oscilador  $f$  é comparável aquelas apresentadas por grupos cromóforos que têm transições moleculares intensas, em que alguns tipos de moléculas são usadas como corantes e outras análogas utilizadas como sensibilizadoras em fotocélulas solares ou dispositivos emissores de radiação eletromagnética.

**Palavras-chave:** Ácido ascórbico, parâmetros de reatividade, força do oscilador, programa RAÍZES.

### ABSTRACT

Ascorbic acid, commonly known as vitamin C, is a weak acid and natural antioxidant that plays essential biological roles in the participation of collagen formation and the absorption of iron by the body. The objective of this work was to verify, through molecular modeling, partial loads and evaluation of PRM reactivity parameters, that it presents favorable electronic densities in stereochemically located positions, for the formation of metallic salts, associated with supposed complex systems. Its electrolytic properties showed a type 1: 1 behavior in freshly prepared aqueous millimolar solution. This is in agreement with the values of pH,  $K_{a1}$  and  $K_{a2}$  respectively, evaluated for an equilibrium situation through the program RAÍZES 1.0, developed by the authors. Thermal decomposition starts around 180-190°C and continues until reaching a temperature of 570.3 °C, in which a small experimental percentage of waste has been associated with the presence of reduced carbon. The absorption spectrum in the infrared region identified the main transitions attributed to C = O, C = C, OH, present in their functional groups. The UV-Vis absorption spectrum showed an intense band that occurs between 207 - 312 nm, with maximum absorption peak,  $A_{max} = 3,6123$  at 249, and 250 nm. This band presents itself in the region where the  $n \rightarrow \pi^*$ ,  $n \rightarrow \sigma^*$  e  $\pi \rightarrow \pi^*$  transitions occur associated with the chromophore groups. The strength of the oscillator is comparable to those presented by chromophore groups that have intense molecular transitions, in which some types of molecules are used as dyes and other analogs used as sensitizers in solar photocells or devices emitting electromagnetic radiation.

**Keywords:** Ascorbic acid, reactivity parameters, oscillator strength, RAÍZES program.

## 1. INTRODUÇÃO:

O ácido ascórbico ( $C_6H_8O_6$ ), denominado comumente de vitamina C, é um ácido fraco e antioxidante natural que exerce funções biológicas importantes na participação da formação do colágeno e na absorção de ferro pelo organismo (ARRIGONI and TULLIO, 2002; LYKKESFELDT and TVEDEN-NYBORG 2019). Além disso, sua ação antioxidante atribui capacidade de aumentar o tempo de conservação dos alimentos (BAUERNEFEIND and PINKERT, 1970). Foi observado neste trabalho que o mesmo apresenta densidades eletrônicas favoráveis para a formação de sais metálicos, precursores de pretensos sistemas complexos, atribuindo a esta substância outras aplicações também relevantes na ciência. Em sua estrutura há 4 grupos  $-OH$ , um oxigênio ligado internamente a um grupo de cinco átomos de carbono, e outro oxigênio periférico mais externo com uma dupla ligação, apresentando assim boa solubilidade em água, devido à formação de ligações de H. Possui ponto de fusão em torno de 190-192 °C, donde a partir daí se decompõe por aquecimento. Na presença da luz, oxigênio, em solução aquosa e sensibilizadores, sofre oxidação aos ácidos desidroascórbico e dicetogulônico, onde este último não apresenta mais nenhuma atividade do composto (TAVARES *et al.*, 2003; ZENG, 2005). Possui dois hidrogênios ionizáveis com  $pK_{a1} = 4,17$  e  $pK_{a2} = 11,2$  (BOBBIO and BOBBIO, 1995), porém tem-se observado na literatura, compostos de ascorbato monovalentes de sódio, lítio, magnésio e cálcio (KOZIOL *et al.*, 1992).

O ácido ascórbico forma também complexos com íons metálicos do tipo MA e MHA (M = metal, A = ascorbato, HA ácido ascórbico), dependendo do pH do meio, mas esses complexos são relativamente instáveis (FORNARO and COICHEV, 1997). Dados da literatura têm sugerido que para complexos formados com uma variedade de cátions divalentes como  $Ca^{2+}$ ,  $VO^{2+}$ ,  $Mn^{2+}$ ,  $Zn^{2+}$  e  $Cd^{2+}$ , o ácido ascórbico atua como ligante monodentado. Estudos de RMN de  $C^{13}$  levaram à conclusão de que para os íons metálicos  $Co^{2+}$ ,  $Fe^{2+}$  e  $Mn^{2+}$ , em pH 8,5, os complexos ascorbato-íon metálico são formados por quelação através dos átomos O5 e O6 na modelagem molecular realizada para este trabalho mostrada na Figura 1A para o ácido ascórbico e pelos átomos O-2 e O-3 na perspectiva proposta por KOZIOL e colaboradores (KOZIOL *et al.*, 1992), para o ânion ascorbato mostrado na Figura 1B. Estudos similares com  $Ni^{2+}$  em presença de ácido

ascórbico mostraram que o ascorbato também está ligado ao íon metálico pelos oxigênios, e a exemplo destes tem-se o Ferro(III)-ácido ascórbico e o cis-1,2-diaminociclohexano-platina(II)/ácido ascórbico, sendo que para este último, a Pt se coordena pelo O2 e C5 na modelagem molecular (Figura 1A) e pelos átomos O-5 e pelo C-2 na estrutura do íon (Figura 1B), segundo a literatura (FORNARO and COICHEV, 1997). Outros complexos envolvendo a Pt também corroboram a complexação através da Pt-C e Pt-O (YUGE *et al.*, 2002). A Figura 02 A, mostra a modelagem molecular para o ácido ascórbico, nuvem de potencial coulômbico, distância de ligação, ângulos de ligação e cargas parciais e a Figura 02 B, ilustra a comparação de algumas propriedades da modelagem do ácido ascórbico e do íon ascorbato segundo o programa WebLab (WEBLAB, 1998).

Poucos trabalhos foram encontrados na literatura sobre a determinação das estruturas de complexos estáveis em solução entre o ascorbato e íons metálicos. No entanto, muitos estudos comprovam a formação de complexos como espécies intermediárias durante as reações de oxidação do ácido ascórbico por íons metálicos (FORNARO and COICHEV, 1997).

O objetivo desse trabalho foi contribuir com informações adicionais desta espécie na formação de sistemas complexos, abordando propriedades estruturais, parâmetros de reatividade, estabilidade térmica, eletrônicas e espectrais do ácido ascórbico e o íon ascorbato livre e em solução.

## 2. DESENVOLVIMENTO:

A modelagem molecular foi realizada através do programa WebLab ViewerPro para os estudos preliminares de parâmetros de reatividade moleculares PRM's, seguindo metodologia proposta pela literatura (GEORGE, 1971; CHANDRA, 1981; WEBLAB, 1998; LIMA *et al.*, 2007, 2019; COSTA *et al.*, 2015). Os valores de cargas parciais foram obtidos através do programa WebLab-Viewer Pro© (WEBLAB, 1998) e os parâmetros de reatividade PRM calculados através da equação 01.

$$\Re = \frac{\int qid\tau}{\sum |\int qid\tau|} \quad (\text{Eq.01})$$

A Figura 2A e Tabela 1 mostram a modelagem, alguns parâmetros estruturais, ângulos e distâncias de ligação, cargas parciais e

os parâmetros de reatividades moleculares PRM's, calculados para o ácido ascórbico. A Figura 2B mostra a comparação de algumas propriedades da modelagem entre o ácido ascórbico e o íon ascorbato, pelo uso do programa WebLab (WEBLAB, 1998).

Nas práticas experimentais, foi utilizado o ácido ascórbico PA comercial de marca CRQ pureza 99,0 % para obter as medidas de pH e estudos do equilíbrio, medidas das condutividades molares, análise térmica, caracterização dos espectros infravermelhos e estudos dos espectros uv-vis do estado sólido e das soluções respectivamente.

Medidas de pH foram realizadas em diferentes concentrações em um pHmetro TECNOPON mPA-210 de precisão  $\pm 0,005$ , em temperatura ambiente de  $25 \pm 1$  °C. Também foi usado o programa RAÍZES 1.0 em linguagem QBASIC, elaborado com o propósito de avaliar o equilíbrio, e calcular as concentrações de  $H^+$  e valores de pH, para verificar a concordância teórico-experimental dos resultados deste trabalho (LIMA *et al.*, 2017, 2019; PERRIN, 1974; PRICHARD, 2003; VALCÁRCEL, 2000; VOGEL'S 1996). A Tabela 02 mostram os cálculos para  $[H^+]$  e pH teóricos em solução aquosa obtidos pelo programa RAÍZES 1.0 e as medidas de pH experimentais.

A condutividade foi medida através de um condutímetro MS-TECNPON mCa-150, com precisão  $\pm 0,001 \mu S cm^{-1}$ . O propósito de uso desta técnica é avaliar a condutância das amostras preparadas e observar o tipo de eletrólito da espécie molecular, com a expectativa de correlacionar com a condutividade repassada aos seus produtos derivados e a sua capacidade como íon livre coordenante (ANDJELKOVIÆ *et al.*, 2001; CHANDRAMOHAN and CHANDRALEKA, 2014; COSTA, *et al.*, 2013; GEARY, 1971; MELO *et al.*, 2009; SCHOLZ, 2010; SOUSA *et al.*, 2018; WANG, 2000). Os valores de condutividade molar foram calculados a partir da equação 02

$$\Lambda_M = (k_{sol} - k_{solv}) \cdot 10^3 / M \quad (Eq\ 02),$$

conforme suportado pela literatura pesquisada (COSTA, *et al.*, 2013; GEARY, 1971; GUTTMAN, 1976; LIMA, *et al.*, 2016).

A Tabela 3 mostra os dados e condições das soluções avaliadas, a condutividade  $k$  e a condutividade molar  $\Lambda_M$ .

A análise térmica foi realizada através de um equipamento TA Instruments, modelo SDTQ600. Os ensaios foram realizados em

cadinho de platina sob atmosfera de ar sintético com vazão do gás de purga 100 mL/min e razão de aquecimento de 10 °C/min iniciando em temperatura ambiente de 24 °C até 900 °C, com massa de amostra de 10,3 mg. A Figura 3 ilustra as curvas TG e DTG do ácido ascórbico e a Tabela 4 ilustra uma proposta para a decomposição térmica (ANDJELKOVIÆ *et al.*, 2001; CHANDRAMOHAN and CHANDRALEKA, 2014; OLIVEIRA *et al.*, 2011; SEIF *et al.*, 2020).

O espectro de absorção na região do infravermelho foi registrado em um espectrofotômetro com transformada de Fourier, modelo IR Affinity-1 da Shimadzu, utilizando amostras sólidas em pastilhas de KBr e as transições foram atribuídas para os grupos funcionais mais importantes (BUENO, 1980; HUHEY, 1983; COTTON, F. A. and WILKINSON, 1988; NAKAMOTO, 1978; SILVEIRA, 2018; SÓCRATES, 1980; THOMPSON, 1979). A Figura 4 mostra o espectro obtido e a Tabela 5 contém as atribuições experimentais.

Espectros uv-vis foram registrados em solução aquosa pelo uso de um equipamento UV-VIS SHIMADZU 1650 PC no intervalo de 190 – 900 nm, com precisão de absorbância de  $\pm 0,002$  e comprimento de onda  $\pm 0,1$  nm. As medidas foram obtidas em temperatura ambiente de  $25 \pm 1$  °C. A Figura 05 ilustra transições generalizadas entre estados eletrônicos moleculares, atribuições de transições, e o espectro uv-vis do HAsc  $5,00 \times 10^{-4}$  mol/L em solução aquosa completo 190 – 1000 nm e da área de interesse 190 – 350 nm. Na Tabela 06 estão os parâmetros espectrais uv-vis para o espectro obtido do HAsc.

A Tabela 6 contém os cálculos obtidos a partir dos dados espectrais. Foram utilizados os métodos citados na literatura para o cálculo da área sob a curva do espectro de absorção e a força do oscilador  $f$  (DRAGO, 1965; FIGGIS, 1966; LIMA *et al.*, 2014, 2018),

$$\text{Drago: } f = 4,6 \times 10^{-9} \cdot \int \epsilon_{(\sigma)} d\sigma \quad (Eq.03)$$

$$\text{Figgs: } f = 4,32 \times 10^{-9} \cdot \int \epsilon_{(\sigma)} d\sigma \quad (Eq\ 04)$$

Na qual a integral  $\int \epsilon_{(\sigma)} d\sigma$  corresponde a área sob a curva de absorção, e neste trabalho foi obtida pela aproximação da gaussiana através da avaliação da meia-banda,

$$\epsilon_{\text{máx}} \cdot (1/\lambda_1 - 1/\lambda_2) \quad (Eq.05)$$

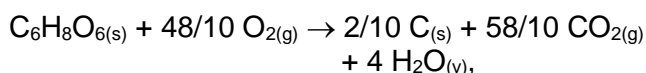
### 3. RESULTADOS E DISCUSSÕES:

Através da modelagem molecular foi possível avaliar que o ascorbato possui

parâmetros de reatividade compatíveis e densidades eletrônicas favoráveis, localizadas em grupos de átomos doadores de elétrons, imprescindíveis para a formação de sistemas complexos, podendo se comportar como um versátil agente quelante na química de coordenação, como já observado em alguns compostos (KOZIOL, *et al.*, 1992; YUGE, *et al.*, 2002). As cargas parciais situadas nos átomos de maiores relevâncias se encontram no O1 (-0,3935), O2 (-0,3875) e O6 (-0,3597), (Figuras 1A, 2A, 2B e Tabela 01) podendo, inclusive ocorrer situações em que átomos de carbono formam ligações com algum centro metálico de natureza ácido mole, a exemplo da Pt no complexo cis-1,2-diaminociclohexano-platina(II)/ácido ascórbico, que se coordena pelo O(5) e pelo C(2) na estrutura do íon ascorbato da Figura 01 II e na modelagem molecular na Figura 01 I, pelo O2 (-0,3875) e C5 (+0,1738) segundo a literatura (FORNARO and COICHEV, 1997; YUGE, *et al.*, 2002). Acredita-se que a ligação entre O-Pt-C neste complexo, que ocorre através de densidades negativas e positivas, se dá por um mecanismo de transferência de elétrons (de densidade eletrônica), na qual a Pt recebe em alguma magnitude densidade eletrônica pelo átomo de oxigênio e doa, também parcialmente, densidade eletrônica para o átomo de carbono, em um tipo de retrodoação envolvendo orbitais  $\sigma$  e  $\pi$ .

As medidas de condutância realizadas indicam que o comportamento eletrolítico empírico da amostra é do tipo 1:1 em solução aquosa milimolar recém-preparada, o que é totalmente concordante com os valores de pH,  $K_{a1}$  e  $K_{a2}$  respectivamente, mesmo possuindo 4 grupos -OH e dois hidrogênios ionizáveis conforme mostrado na Figura 1 e Tabelas 2 e 3.

Observou-se que na análise térmica do ácido ascórbico, a decomposição se inicia em torno de 180 - 190 °C, sendo concordante com a literatura (REDA, 2011) e segue até atingir a temperatura de 570,3 °C, na qual o percentual experimental do resíduo, que foi associado a presença de carbono reduzido, atingiu 1,3615 % da amostra inicial. Em comparação com o calculado teoricamente de 1,364 %, verifica-se que está em boa concordância com o que foi proposto estequiometricamente para a decomposição completa da amostra, conforme a reação:



mostrado na Figura 3 e Tabela 4.

O espectro de absorção na região do infravermelho mostra as bandas principais proporcionadas pelos grupos funcionais da molécula, tais como: estiramentos C=O da lactona (1760  $\text{cm}^{-1}$ ), C-O (1109, 1110, 1134, 1195  $\text{cm}^{-1}$ ), C=C (1668  $\text{cm}^{-1}$ ), e bandas OH (3217, 3309, 3404, 3533  $\text{cm}^{-1}$ ) segundo a literatura (SILVEIRA, 2018; SOUZA *et al.*, 2015; UNARELOGLU, *et al.*, 2002). A Figura 04 e Tabela 5 mostram as atribuições especificadas. Estas transições serão de grande valia na constatação de evidências de formação de ligações químicas em sistemas complexos (BUENO, 1980; COTTON, F. A. and WILKINSON, 1988; HUHEY, 1983; NAKAMOTO, 1978; SILVEIRA, 2018; SÓCRATES, 1980; SOUZA *et al.*, 2015; THOMPSON, 1979; UNARELOGLU, *et al.*, 2002).

O espectro de absorção UV-Vis do HAsc em solução aquosa  $5 \times 10^{-4}$  mol/L recém-preparada, mostrou uma banda intensa que ocorre entre 207 - 312 nm, com pico de absorção máxima,  $A_{\text{máx}} = 3,6123$ , em 249 e 250 nm. Esta banda se apresenta na região onde ocorrem as transições  $n \rightarrow \pi^*$ ,  $n \rightarrow \sigma^*$  e  $\pi \rightarrow \pi^*$  (ASSIS, 2013; ATKINS, 1991; PAVIA, 2010; SKOOG, 2002), associada aos cromóforos C=C-C=O (220-315 nm), C=O (150-250 nm) e C=C (200-700 nm), também presentes em moléculas similares. A Figura 05 ilustra o mecanismo de absorção de fótons, atribuições de transições e o espectro UV-Vis para a solução aquosa do ácido ascórbico. A Tabela 06 contém os parâmetros espectrais calculados, conforme a literatura (LIMA *et al.*, 2014).

#### 4. CONCLUSÕES:

Através da modelagem molecular foi possível avaliar que o íon ascorbato possui parâmetros de reatividade compatíveis e densidades eletrônicas favoráveis, localizadas em grupos de átomos doadores de elétrons, para a formação de sistemas complexos, podendo se comportar como um versátil agente quelante na química de coordenação. As cargas parciais de densidade negativa de maiores relevâncias estão situadas nos átomos O1 (-0,3935), O2 (-0,3875) e O6 (-0,3597), (ver modelagem na Figura 1 I e Tabela 1). Ainda assim, a possibilidade de interações com moléculas de água, através de ligações de hidrogênio, favorece a uma grande solubilidade em água e podem inviabilizar algumas dessas possibilidades de ligações com cátions metálicos, dependendo do meio

reacional, além de ser possível, dependendo da reatividade do cátion metálico, reações que formem outros derivados como subprodutos oriundos de sucessivas etapas de oxidação do ácido ascórbico e do ascorbato.

O comportamento eletrolítico empírico do ácido ascórbico é do tipo 1:1 em solução aquosa milimolar (CHANDRAMOHAN and CHANDRALEKA, 2014; GEARY, 1971; GUTTMAN, 1976), o que é totalmente concordante com os valores de pH,  $K_{a1}$  e  $K_{a2}$  calculados e experimentalmente confirmados, mesmo possuindo 4 grupos -OH e dois hidrogênios ionizáveis.

Observou-se que na análise térmica do ácido ascórbico, ao atingir a temperatura de 570,3 °C o percentual de carbono residual experimental chegou a 1,3615 %, que em comparação ao teórico, está de acordo com o estabelecido estequiometricamente.

O espectro na região do IV do ácido ascórbico mostra as bandas principais proporcionadas pelos grupos funcionais da molécula, tais como os estiramentos C=O lactona (1760  $\text{cm}^{-1}$ ), C=C (1668  $\text{cm}^{-1}$ ), C-O (1109, 1110, 1134, 1195  $\text{cm}^{-1}$ ), O-H (3217, 3309, 3404, 3533  $\text{cm}^{-1}$ ), segundo a literatura (SILVEIRA, 2018; SOUZA *et al.*, 2015; UNARELOGLU, *et al.*, 2002), característicos para atribuições de formação de ligações envolvendo estes grupos em particular (BUENO, 1980; NAKAMOTO, 1978; SÓCRATES, 1980).

Os espectros UV-Vis revelaram uma banda de absorção entre 207-312 nm, com um pico em 249 nm de  $\epsilon_{\text{máx}} = 7,225 \times 10^3 \text{ L mol}^{-1} \text{ cm}^{-1}$ , atribuída às transições moleculares  $n \rightarrow \sigma^*$ ;  $\pi \rightarrow \pi^*$  e  $n \rightarrow \pi^*$ , referente a presença dos cromóforos C=O, C=C e O=C-C=C presentes na molécula. A força do oscilador  $f$  é comparável, aquelas apresentadas por grupos cromóforos em transições moleculares, em que alguns tipos de moléculas usadas como corantes e outras análogas usadas como sensibilizadoras de fotocélulas solares, apresentam valores da ordem de  $10^{-1} - 1$ , o que reforça a potencialidade de aplicação destes sistemas em dispositivos bombeadores de elétrons em sistemas químicos complexos (COTTON and WILKINSON, 1988; HUHEY, 1983; SHRIVER *et al.*, 1994; THOMPSON, 1979), e emissores de radiação e/ou de elétrons.

## 5. AGRADECIMENTOS:

Os autores agradecem ao IQ da UFRN,

pelo registro das curvas de análise térmica TG e DTG, e pelos espectros na região do Infravermelho e Uv-Visível. Também agradecem ao aluno de IC do IQ-UFRN Lucas da Silva Araújo pelas contribuições pontuais neste trabalho.

## 6. REFERÊNCIAS:

1. Andjelkoviæ, K., Sumar, M. and Ivanoviæ-Burmazoviæ. I., (2001) - Thermal Analysis In Structural Characterization Of Hydrazone Ligands And Their Complexes - *Journal of Thermal Analysis and Calorimetry*, Vol. 66, 759-778.
2. Arrigoni, O. and Tullio, M. C., (2002) – Acid Ascorbic: Much More Than Just An Antioxidant – *Bochimica and Biophysica Acta*, 1569, 1-9.
3. Assis, O. B. G., (2013) - A Asa da Borboleta e a Nanotecnologia: Cor Estrutural - *Rev. Bras. Ensino Fís.*, 35(2), 2301(1)-2301(9), São Paulo, SP.
4. Atkins, P. W., (1991) – *Quanta* (2a ed.) Oxford University Press, New York
5. Bauernfeind. J. C. and Pinkert, D. M., (1970) - Food Processing With Added Ascorbic Acid. - *Adv Food Res.*, 18, 219 - 315.
6. Bobbio, F. O.; Bobbio, P. A., (1995) - *Introdução a Química de Alimentos*, (2.ed.) Ed., Varela, p223, São Paulo, SP.
7. Bueno, W. A., (1980) - *Manual de Espectroscopia Vibracional* – Mc Graw-Hill, São Paulo.
8. Chandra, A. K., (1981) – *Introductory Quantum Chemistry* (2ª ed.), TATA McGraw-Hill, Publ. Co. LTD., New Delhi
9. Chandraleka, S. and Chandramohan, G., (2014) - Synthesis, Characterization and Thermal Analysis of the Copper(II) Complexes With 2,2'bipyrididyl and 1-10-Phenanthroline - *African Journal of Pure and Applied Chemistry*. Vol. 8 (10), 162-175.
10. Costa., L. H. M.; Lima, F. J. S.; e Silva, A. O., (2013) – Síntese, Complexometria, Análise Térmica e Condutância Molar dos Cloretos de Lantânio, Neodímio e Érbio Hidratados - *Periódico Tchê Química*, 10(19), 38-45.

11. Costa, L. H., Lima, F. J. S., Silva, A. O., (2015) - Estudo Térmico e Estereoquímico do Acetato de Uranilo Dihidratado, *Periódico Tchêquímica*, 12(23), 66-73.
12. Cotton, F. A. and Wilkinson, F. R. S., (1988) - *Advanced Inorganic chemistry. A comprehensive text.*, (5a ed.), Wiley-Interscience Publication, New York, NY.
13. Denari, G. B.; Cavaleiro, E. T. G., (2012) - *Princípios e Aplicações de Análises Térmicas*. Universidade de São Paulo, Instituto de Química de São Carlos.
14. Drago, R. S., (1965) - *Physical Methods in Inorganic Chemistry* - Van Nostrand Reinhold Company, printed Holland.
15. Figgis, B. N., (1966) - *Introduction to Ligands Fields* - Interscience Publishers, New York, NY.
16. Fornaro, A. and Coichev, N., (1998) - Ácido L-ascórbico: Reações de Complexação e de Óxido-Redução com alguns Íons Metálicos de Transição, *Química Nova*, 21(5), 642-650.
17. Geary, W. J., (1971) - The Use Of Conductivity Measurements In Organic Solvents For The Characterization Of Coordination Compounds - *Coord. Chem. Rev.*, 7, 81-122.
18. George, D. V., (1972) - *Principles Quantum Chemistry*, Pergamon Press Inc., Maxwell House, Fairview Park, Elmsford, NY.
19. Guttman, V., (1976) - Empirical Parameters for Donor and Acceptor Properties of Solvents - *Eletochim. Acta.*, 21, 661-70.
20. Huhey, J. E., (1983) - *Inorganic Chemistry, Principles of Structure and Reactivity* (3a ed.), Ch.16, 795-820, Harper International SI Ed., New York, NY.
21. Koziol, A. E.; Stepniak, K. And Lisz, T., (1992) - The Crystal Structure of Lithium L-Ascorbate Dihydrate - *Carbohydrate Research*, 226, 43-48.
22. Lima, F. J. S.; Melo, R. M.; Silva, A. O. E Braga, C. C. M., (2007) - Parâmetros de Reatividade Molecular - *Periódico Tchêquímica*, 4(7), 7-15.
23. Lima, F. J. S. Costa, L. H. M E Silva, A. O., (2014) - Estudos Espectroquímicos do Íon  $\text{UO}_2^{2+}$  Coordenado no Acetato de Uranila - *Periódico Tchêquímica*, 11(22), 33-46.
24. Lima, F. J. S, Costa, L. H. M., Azevedo, D. M., Silva, A. O., E Claudece, F. P., (2016) - Parâmetros de Reatividade Molecular e a Correlação Com a Condutividade Molar da Quinolina-N-Óxido, Nicotinamida-N-Óxido e a 2,2-Dithiobispiridina-N-Óxido, *Periódico Tchêquímica*, 13(26), 88-96.
25. Lima, S. G. M., Lima, F. J. S., Pereira, F. C. E Cruz, T. J. T., (2017) - Modelagem Molecular, Medidas Condutimétricas e Espectros Uv-Vis do Ácido Ascórbico Para Formação de Sistemas Químicos Complexos - *Trabalho apresentado na CIENTEC – XXIII SEMANA DE CIÊNCIA, TECNOLOGIA E CULTURA*, de 25 a 27 de outubro em Natal - RN.
26. Lima, F. J. S., Costa, L. H. M. Da, Silva, A. O. Da, Pereira, F. C., (2018) - Espectroscopia de Absorção Molecular na Região do Uv-Vis Para os Ligantes Quinolina-N-Óxido, Nicotinamida-N-Óxido e 2,2-Dithiobispiridina-N-Óxido - *Periódico Tchêquímica*, 15(29), 164-170.
27. Lima, F. J. S.; Silva, J. L. C. Da, E Silva, A. O. Da, (2019) - Modelagem Molecular e Avaliação das Propriedades Térmicas, Condutimétricas e Espectrais do Ácido Maleico para Aplicação em Sistemas Químicos Promissores - *Periódico Tchê Química*, 16(31), 937-943.
28. Lykkesfeldt, J. and Tveden-Nyborg, P., (2019) - The Pharmacokinetics of Vitamin C - *Nutrients*, 11, 2412 (1-20).
29. Melo, R. M.; Lima, F. J. S.; Silva, A. O., E Braga, C. C. M., (2009) - Síntese e Caracterização dos Maleatos Hidratados de Lantânio, Neodímio e Érbio - *Periódico Tchê Química*, 6(11), 31-42.
30. Nakamoto, K. (1978) - *Infrared and Raman Spectra of Inorganic and Coordination Compounds*, (3rd ed.), Copyright John Wiley & Sons, Ltd. All rights reserved, John Wiley, New York, NY.
31. Oliveira, M. A., Yoshida, M. I., e Gomes, E. C. L., (2011) - Análise Térmica Aplicada a Fármacos e Formulações Farmacêuticas na Indústria Farmacêutica - *Quim. Nova*, Vol. 34, No. 7, 1224-1230.

32. Pavia, D. L.; Lampman, G. M.; Kriz, G. G.; Vyvyan, J. R., (2010) – *Introdução a Espectroscopia*, CENGAGE Learning, São Paulo, SP.
33. Perrin, D. D., (1974) - *In Buffers for pH and Metal Ion Control*, Chapman and Hall, New York.
34. Prichard, E. R. S. C., (2003) - *Measurement of pH* - Editora, Cambridge, USA.
35. Reda S. Y., (2011) - Evaluation of Antioxidants Stability by Thermal Analysis and its Protective Effect in Heated Edible Vegetable Oil - *Cienc. Tecnol. Aliment., Campinas*, 31(2): 475-480, abr.-jun.
36. Scholz, F., (2010) - *Eletroanalytical Methods, Guide to Experiments and Applications* - Springer, Germany.
37. Seif, H., Tahereh, G., Seif, S., Ghoreishia, S. M., Salavati-Niasarib, M., (2020) - A Review on Current Trends in Thermal Analysis and Hyphenated Techniques in the Investigation of Physical, Mechanical and Chemical Properties of Nanomaterials – Journal Pre-proof To appear in: *Journal of Analytical and Applied Pyrolysis*, © 2020 Published by Elsevier., 1-68.
38. Silveira, T. R., (2018) - Observação Via Espectroscopia Infravermelho do Efeito Oxirredutor do Ácido Ascórbico Nas Espécies Reativas da Prolina Induzidas por Prótons (H<sup>+</sup>) e Elétrons - *Tese de Doutorado*, apresentada ao Instituto de Física da Universidade Federal da Bahia
39. Silverstein, R. M.; Webster, F. X.; Kiemle, D. J., (2007) - *Identificação Espectrométrica de Compostos Orgânicos*. (7 ed.), LTC Rio de Janeiro, RJ.
40. Shriver, D. F. Atkins, P. W., Langford, C. H. (1994) – *Inorganic Chemistry* (2<sup>nd</sup> ed.), Oxford University Press, Oxford, Melbourne, Tokyo.
41. Skoog, D. A., Holler, F. J., Nieman, T. A., (2002) - *Princípios de Análise Instrumental* - Bookman, Porto Alegre, RS.
42. Sócrates, G., (1980) - *Infrared Characteristic Group Frequencies* – John Wiley & Sons, printed in Great Britain.
43. Sousa, A. G., Chagas, F. W. M., Gois, L. C., Silva, J. G., (2018) - Determinação Condutométrica e Potenciométrica de Ácido Acetilsalicílico em Aspirina: Uma Sugestão de Prática para a Análise Instrumental - *Revista Virtual de Química*, Rvq Vol. 10 N° 3, 502-517.
44. Souza, C. A. G. De; Siqueira, S. M. C.; Amorim, A. F. V. De; Morais, S. M. De, Gomes, T. G. R. N.; Cunha, A. P., E Ricardo, N. M. P. S., (2015) - Encapsulação do Ácido L-ascórbico no Biopolímero Natural Galactomanana por Spray drying: Preparação, Caracterização e Atividade Antioxidante - *Quim. Nova*, Vol. 38, No. 7, 877-883.
45. Tavares, J. T. q, Santos, C. M. G., Teixeira, L. J., Santana, R. S., e Portugal, A. M., (2003) - Estabilidade do Ácido Ascórbico em Polpa de Acerola Submetida a Diferentes Tratamentos Magistra, v. 15, n. 2, jul./dez. Cruz das Almas – BA.
46. Thompson, L. C., (1979) - *Complexes - Handbook on the Physics and Chemistry of Rare Earths*, V.3, Ch. 25, 209-97.
47. Unareloglu, C., Zumreloglu-Karan, B., Mert, Y., (2002) – Zinc Ascorbate: A Combined Experimental and Computational Study for Structure Elucidation – *Journal Of Molecular Structure* 605, 227 – 233.
48. Valcárcel, M., (2000) - *Principles of Analytical Chemistry*, Springer, Germany.
49. Vogel's., (1996) - *Qualitative Inorganic Analysis* (7<sup>a</sup> ed.), Pearson Education Limited, Singapore.
50. Yuge, H And Miyamoto, T. K., (2002) - Steric Influence on Platinum(II) Ascorbate Complexes, *Inorganica Chimica Acta*, 329, 66–70.
51. Wang, J., (2000) - *Analytical Electrochemistry*, (2<sup>a</sup> ed.), John Wiley, USA.
52. Weblab ViewerPro, (1998) - *Copyright ©, Molecular Simulations, Inc., Web Lab and ViewerPro are trademarks of Molecular Simulation Inc.*
53. Zeng, W., Martinuzzi, F. and MacGregor, A., (2005) - Development and application of a novel UV method for the analysis of ascorbic acid - *Journal of Pharmaceutical and Biomedical Analysis* 36, 1107–1111.



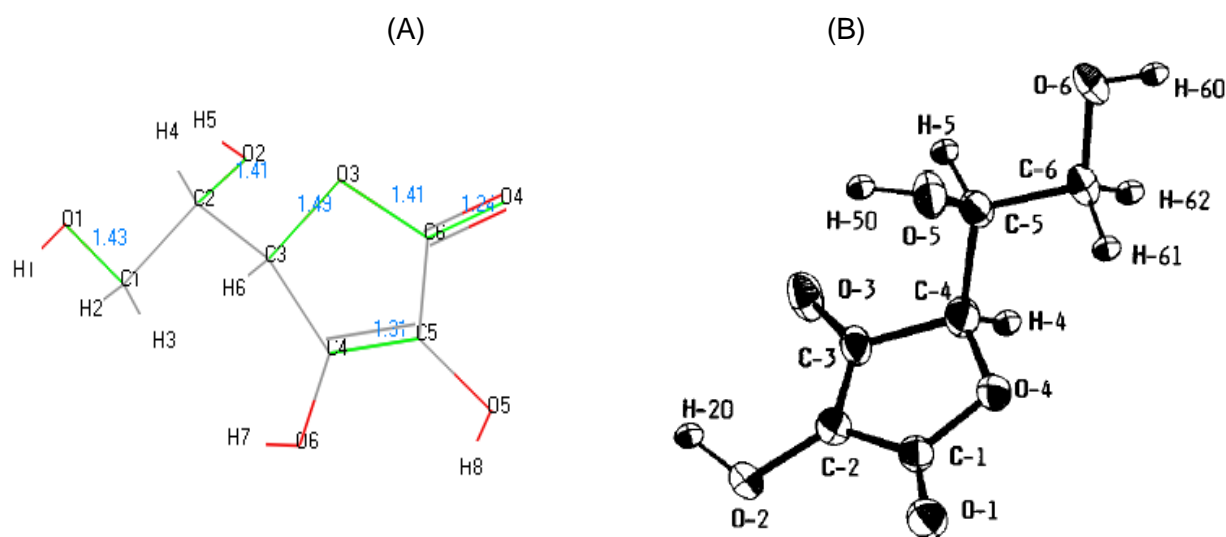


**Figura 1.** (A) Modelagem molecular do ácido ascórbico deste trabalho e (B) perspectiva do ânion ascorbato segundo a literatura (KOZIOL et al., 1992).

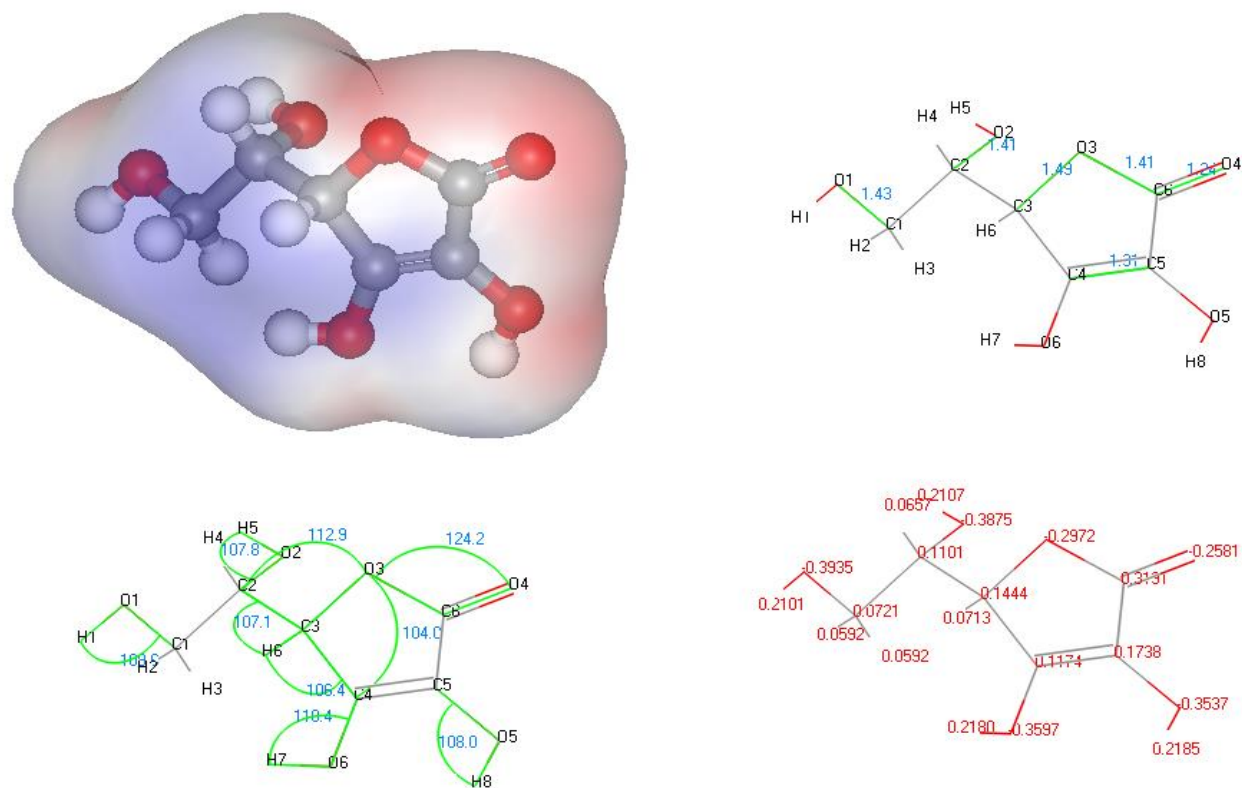


**Figura 2.** (A) Modelagem molecular para o ácido ascórbico, nuvem de potencial coulômbico, distância de ligação, ângulos de ligação e cargas parciais.

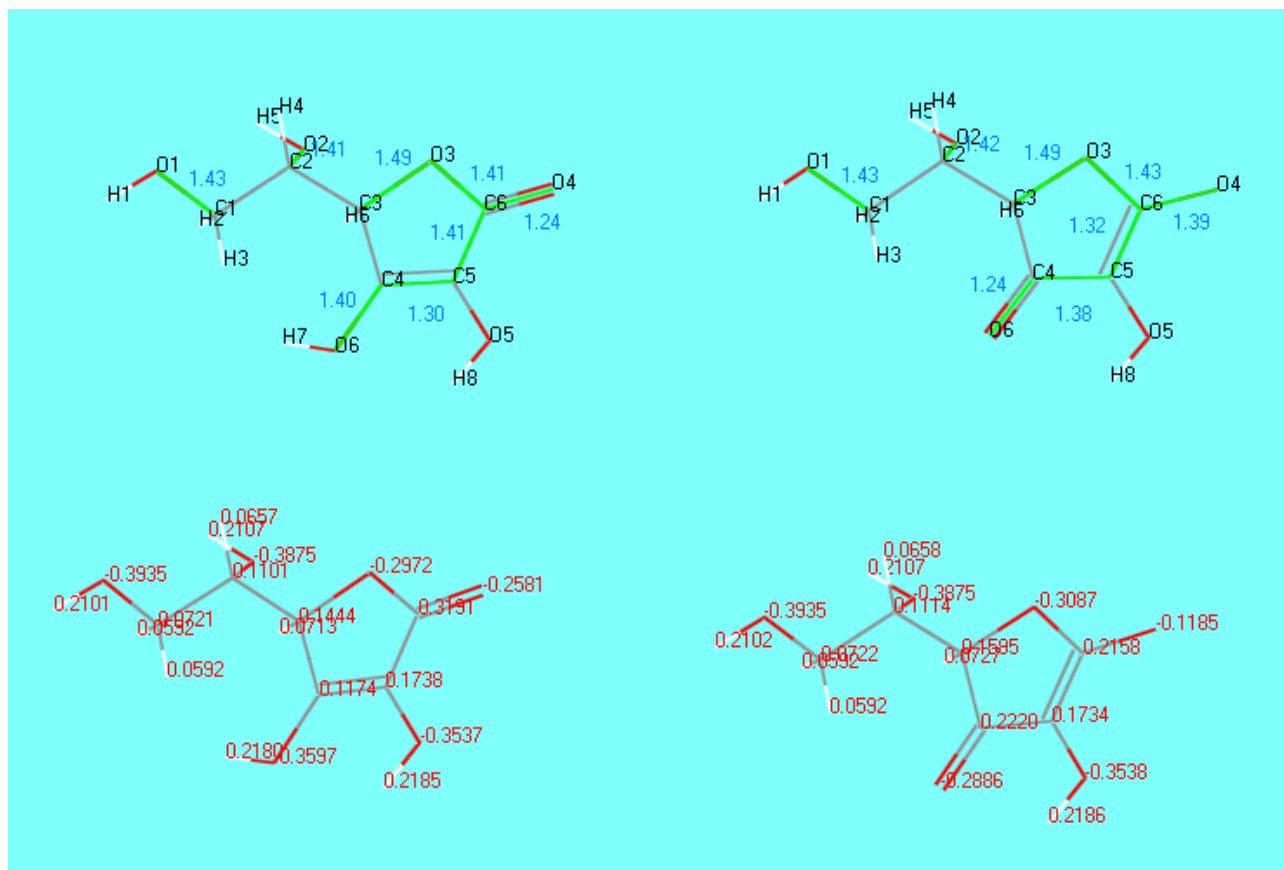


**Figura 2.** (B) Comparação de algumas propriedades da modelagem do ácido ascórbico e do íon ascorbato.

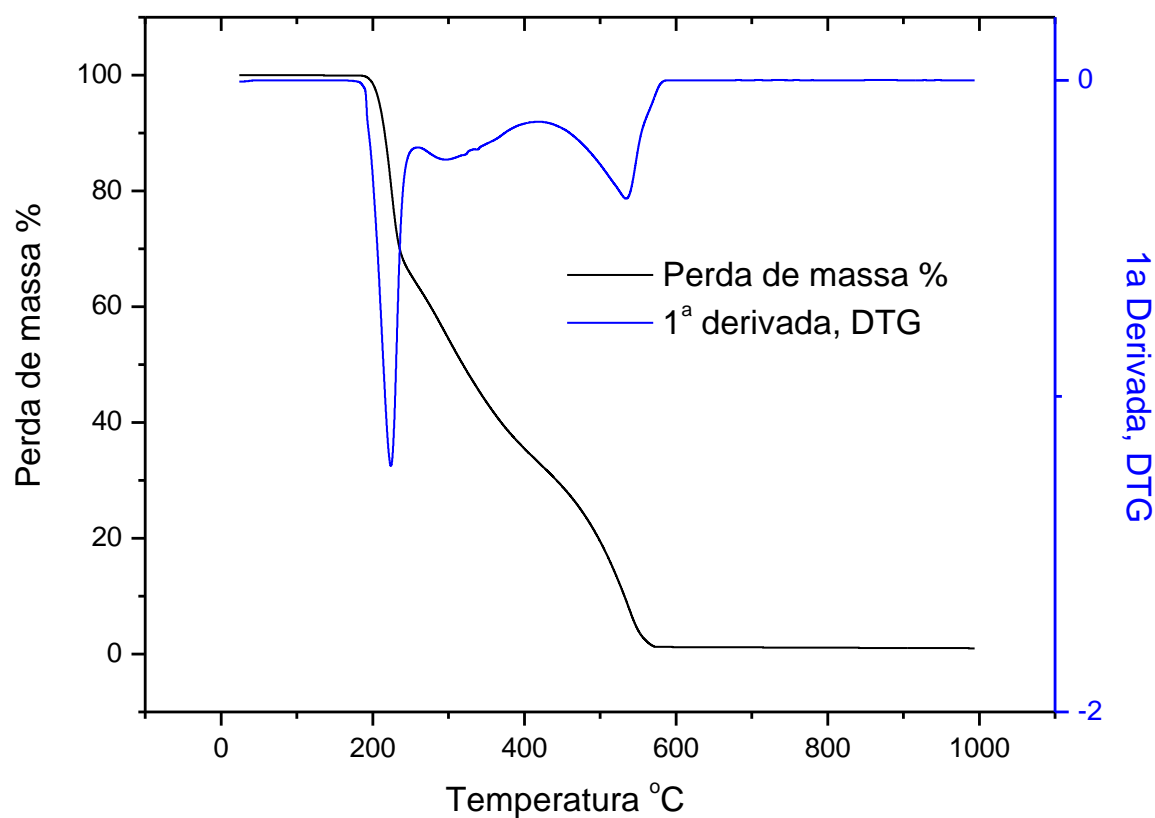


**Figura 3.** Curvas TG e DTG do ácido ascórbico.

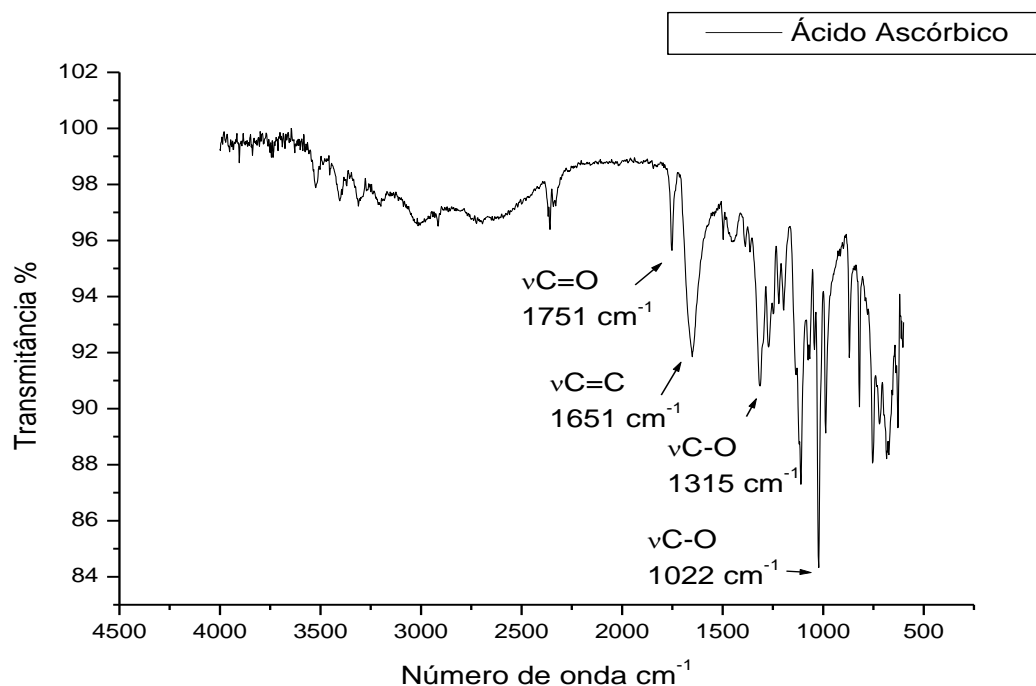


**Figura 4.** Espectro de absorção na região do infravermelho para o ácido ascórbico sólido em KBr.

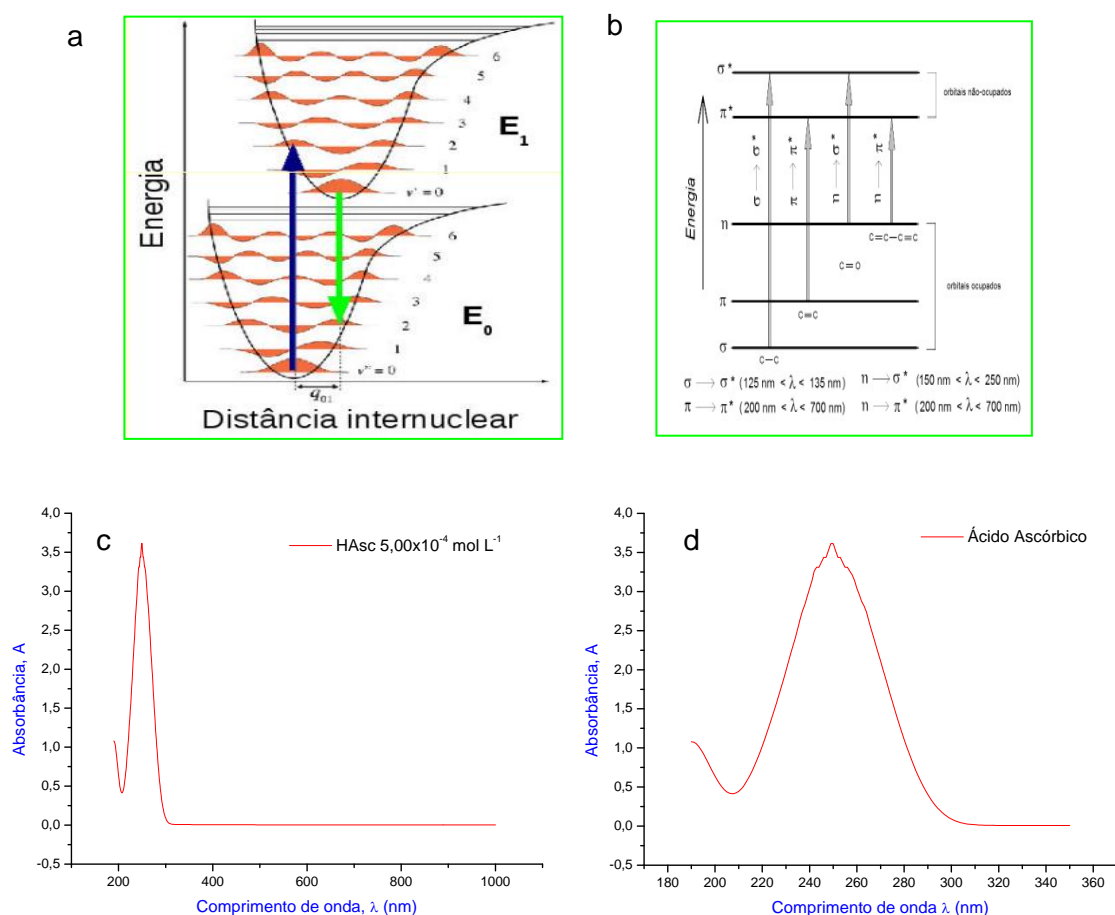


**Figura 5.** (A) Transição entre estados eletrônicos em moléculas, (B) atribuições de transições em compostos moleculares, (C) espectro uv-vis do HAsc  $5,00 \times 10^{-4} \text{ mol/L}$  em solução aquosa completo 190 – 1000 nm e (D) da área de interesse 190 – 350 nm.

**Tabela 1.** Cargas parciais e PRM para o ácido ascórbico

| Cargas Parciais |                              |                              |                       | PRM    |                              |                              |                                   |
|-----------------|------------------------------|------------------------------|-----------------------|--------|------------------------------|------------------------------|-----------------------------------|
|                 | Ácido Ascórbico <sup>1</sup> | Ânion Ascorbato <sup>2</sup> | $\Delta^*$            |        | Ácido Ascórbico <sup>1</sup> | Ânion Ascorbato <sup>2</sup> | $\Delta^*$                        |
| Átomos          | $\delta^-$                   | $\delta^+$                   | $\delta_2 - \delta_1$ | Átomos | $\mathfrak{R}$               | $\mathfrak{R}$               | $\mathfrak{R}_2 - \mathfrak{R}_1$ |
| O1              | -0,3935                      | -0,3935                      | 0                     | O1     | -0,1920                      | -0,2126                      | -0,0206                           |
| H1              | 0,2101                       | 0,2102                       | 0,0001                | H1     | 0,1025                       | 0,1135                       | 0,0110                            |
| C1              | 0,0721                       | 0,0722                       | 0,0001                | C1     | 0,0352                       | 0,0390                       | 0,0038                            |
| H2              | 0,0592                       | 0,0592                       | 0                     | H2     | 0,0289                       | 0,0320                       | 0,0031                            |
| H3              | 0,0592                       | 0,0592                       | 0                     | H3     | 0,0289                       | 0,0320                       | 0,0031                            |
| C2              | 0,1101                       | 0,1114                       | 0,0013                | C2     | 0,0537                       | 0,0602                       | 0,0065                            |
| H4              | 0,0657                       | 0,0658                       | 0,0001                | H4     | 0,0321                       | 0,0356                       | 0,0035                            |
| O2              | -0,3875                      | -0,3875                      | 0                     | O2     | -0,1890                      | -0,2094                      | -0,0204                           |
| H5              | 0,2107                       | 0,2107                       | 0                     | H5     | 0,1028                       | 0,1139                       | 0,0111                            |
| C3              | 0,1444                       | 0,1595                       | 0,0151                | C3     | 0,0704                       | 0,0862                       | 0,0158                            |
| H6              | 0,0713                       | 0,0727                       | 0,0014                | H6     | 0,0348                       | 0,0393                       | 0,0045                            |
| C4              | 0,1174                       | 0,2220                       | 0,1046                | C4     | 0,0573                       | 0,1200                       | 0,0627                            |
| O6              | -0,3597                      | -0,2886                      | 0,0711                | O6     | -0,1755                      | -0,1560                      | 0,0195                            |
| H7              | 0,2180                       | 0                            | -0,2180               | H7     | 0,1064                       | 0                            | -0,1064                           |
| C5              | 0,1738                       | 0,1734                       | -0,0004               | C5     | 0,0848                       | 0,0937                       | 0,0089                            |
| O5              | -0,3537                      | -0,3538                      | -0,0001               | O5     | -0,1726                      | -0,1912                      | -0,0186                           |
| H8              | 0,2185                       | 0,2186                       | 0,0001                | H8     | 0,1066                       | 0,1181                       | 0,0115                            |
| C6              | 0,3191                       | 0,2158                       | -0,1033               | C6     | 0,1557                       | 0,1166                       | -0,0391                           |
| O4              | -0,2581                      | -0,1185                      | 0,1396                | O4     | -0,1259                      | -0,0640                      | 0,0619                            |
| O3              | -0,2972                      | -0,3087                      | -0,0115               | O3     | -0,1441                      | -0,1668                      | -0,0227                           |

(\*) Valores de  $\Delta$  interpretados para cada átomo como:

$\delta_2 - \delta_1$ ;  $\Delta < 0$  aumento relativo de densidade de carga negativa e  $\Delta > 0$  aumento relativo de densidade de carga positiva.

$\mathfrak{R}_2 - \mathfrak{R}_1$ ;  $\Delta < 0$  aumento relativo de parâmetro de carga negativa e  $\Delta > 0$  aumento relativo de parâmetro de carga positiva.

Obs. Os valores de  $\Delta$  não devem ser interpretados como valores absolutos, mas como valores relativos para comparação superficial de resultados.

**Tabela 2.** Cálculos para  $[H^+]$  e pH em solução aquosa ( $pH_{\text{água}} = 6,80$ ), usando o programa “RAIZES”, para o ácido ascórbico de  $Ka_1 = 6,76 \times 10^{-5}$  em temperatura ambiente de  $25 \pm 1$  °C.

|                  | $M_o$ (Mol L <sup>-1</sup> ) | $[H^+]_{\text{teor}}$ (Mol L <sup>-1</sup> ) | pH <sub>teor</sub> | pH <sub>exp</sub> / ( $\Delta$ ) |
|------------------|------------------------------|--|--------------------|----------------------------------|
| H <sub>2</sub> O | 55,5                         | $1,00 \times 10^{-7}$                        | 7,00               | 6,80 / (0,20)                    |
| HAsc             | 0,1                          | $2,57 \times 10^{-3}$                        | 2,59               | 2,53 / (0,06)                    |
|                  | 0,01                         | $7,89 \times 10^{-4}$                        | 3,10               | 3,05 / (0,05)                    |
|                  | 0,001                        | $2,28 \times 10^{-4}$                        | 3,64               | 3,51 / (0,13)                    |

**Tabela 3.** Valores de concentração, condutividades e condutância molar para as soluções de ácido ascórbico.

| Composto         | Temperatura (°C) | Concentração M (Mol L <sup>-1</sup> ) | Condutividade $k \times 10^{-6}$ S cm <sup>-1</sup> | Condutividade Molar $\Lambda_M$ S cm <sup>2</sup> mol <sup>-1</sup> |
|------------------|------------------|---------------------------------------|---|---|
| H <sub>2</sub> O | 25,1             | 55,5                                  | 2,21  | $3,98 \times 10^{-5}$   |
| HAsc             | 25,0             | $1,00 \times 10^{-3}$                 | 119,1   | 116,89  |
| HAsc             | 25,0             | $1,00 \times 10^{-2}$                 | 562,0   | 55,98   |
| HAsc             | 25,3             | $1,00 \times 10^{-1}$                 | 1582  | 15,80   |

**Tabela 4.** Proposta de decomposição térmica do ácido ascórbico, a qual foi verificada uma pequena quantidade de carbono residual.

| Ácido<br>ascórbico<br>(g/mol)                            |   | Oxigênio<br>(g/mol)              |   | Carbono<br>residual<br>(g/mol) |   | Gás<br>carbônico<br>(g/mol)       |   | Água<br>(g/mol)                            |
|--|---|----------------------------------|---|--------------------------------|---|-----------------------------------|---|--|
| C <sub>6</sub> H <sub>8</sub> O <sub>6(s)</sub><br>176,1 | + | 48/10 O <sub>2(g)</sub><br>153,6 | → | 2/10 C <sub>(s)</sub><br>2,402 | + | 58/10 CO <sub>2(g)</sub><br>255,3 | + | 4 H <sub>2</sub> O <sub>(v)</sub><br>72,08 |
| Carbono residual teórico (%)                             |   |                                  |   | 1,364                          |   |                                   |   |  |
| Carbono residual experimental (%)                        |   |                                  |   | 1,3615                         |   |                                   |   |  |
| Temperatura final da TG (°C)                             |   |                                  |   | 570,3                          |   |                                   |   |  |
| Massa do reagente (g/mol)                                |   |                                  |   | Massa do produto (g/mol)       |   |                                   |   |  |
| 329,7  |   |                                  |   | 329,7                          |   |                                   |   |  |

**Tabela 5.** Atribuição de transições para os grupos funcionais presentes no espectro infravermelho do ácido ascórbico.

|                  | Região de absorção<br>(SIVERSTEIN, 2007) | Região de absorção<br>(SOUZA <i>et al.</i> , 2015) | Região de absorção<br>Atribuições deste<br>trabalho | Modos     |
|------------------|--|--|---|-----------|
| O-H              | 2700 – 3800                              | 3533, 3404, 3309, 3217                             | 3524, 3404, 3311 3213                               | $\nu$ O-H |
| C=O<br>ác carbox | 1600 – 1850<br>1680 - 1690               | 1760<br>-  | 1751<br>1670 ombro                                  | $\nu$ C=O |
| C=C              | 1500 - 1900                              | 1668   | 1651  | $\nu$ C=C |
| C-O<br>ác carbox | 1250-1300<br>800 – 1300                  | -<br>1024  | 1315<br>1109, 1110, 1134, 1195<br>1022, 1024        | $\nu$ C-O |

**Tabela 6.** Parâmetros espectrais uv-vis para a solução aquosa  $5 \times 10^{-4}$  M do HAsc

| Transição<br>nm<br>mecanismo  | $\epsilon_{\text{máx}}$<br>$\text{L mol}^{-1} \text{cm}^{-1}$<br>$\times 10^3$ | $\int A_{(\sigma)} d\sigma$<br>$\sigma$<br>$\text{cm}^{-1}$ | $\int \epsilon_{(\sigma)} d\sigma$<br>$\text{L mol}^{-1} \text{cm}^{-2}$<br>$\times 10^7$ | $f = 4,6 \times 10^{-9} \int \epsilon_{(\sigma)} d\sigma$<br>$f_{\text{Drago}}$ | $f = 4,32 \times 10^{-9} \int \epsilon_{(\sigma)} d\sigma$<br>$f_{\text{Figgs}}$ |
|---|--|---|---|---|--|
| 207 – 312<br>$n \rightarrow \sigma^*$<br>$\pi \rightarrow \pi^*$<br>$n \rightarrow \pi^*$ | 7,225  | 26116   | 5,223   | 0,2403  | 0,2256   |

**IMPLEMENTAÇÃO DO MODELO DE APRENDIZAGEM BASEADO EM PROBLEMAS PARA AUMENTAR A AUTO-CONFIANÇA E COMPREENSÃO DE ESTUDANTES DE GRADUAÇÃO ACERCA DO CONCEITO DE ELETROQUÍMICA NA EDUCAÇÃO QUÍMICA****IMPLEMENTATION OF PROBLEM-BASED LEARNING MODEL TO INCREASE SELF-CONFIDENCE AND UNDERGRADUATE STUDENTS UNDERSTANDING OF THE ELECTROCHEMISTRY CONCEPT IN CHEMICAL EDUCATION**

RUDIBYANI, Ratu Betta

Universitas Lampung, FKIP Department, Lampung, Indonesia.

\* Corresponding author

e-mail: ratu.betta.r@gmail.com

Received 24 March 2020; received in revised form 02 May 2020; accepted 22 May 2020

**RESUMO**

A química é uma das disciplinas científicas consideradas difíceis para a compreensão dos seus conceitos microscópicos e macroscópicos por parte dos alunos. Os estudantes também afirmam que esta disciplina é tediosa e complicada. Eles são incapazes de conectar o que é mostrado na estrutura visual ao processo e fenômeno. No contexto da automotivação dos estudantes universitários, há mais chances de expandir a estimulação da aprendizagem. Este estudo teve como objetivo melhorar a autoconfiança e o domínio de conceitos dos estudantes de ensino de química usando a aprendizagem baseada em problemas. Foi utilizado o método quase-experimental com o design do grupo de controle pré-teste-pós-teste não equivalente. A população incluiu todos os alunos da aula de eletroquímica da Universidade Lampung em 2019. A técnica de amostragem proposital empregada dividiu a amostra em dois grupos. O primeiro grupo foi chamado Classe A e foi considerado como a classe experimental - usando aprendizado baseado em problemas -. O segundo grupo, Classe B, foi considerado como a classe de controle - usando o modelo convencional em que o professor aplicava o método de fala na entrega dos materiais durante a aula -. A autoconfiança e o domínio de conceitos da classe A têm um valor n-Gain maior que a classe B e o resultado do tamanho do efeito é que a classe B tem um efeito maior que a classe A. Com base no resultado, pode-se concluir que a aprendizagem baseada em problemas tem um grande influência na melhoria da autoconfiança e do domínio de conceitos sobre o tema eletroquímico.

**Palavras-chave:** *aprendizagem baseada em problemas, autoconfiança, domínio de conceitos e eletroquímica*

**ABSTRACT**

Chemistry is one of the scientific disciplines considered difficult for students to understand its microscopic and macroscopic concepts. Students also claim that this discipline is tedious and complicated. They are unable to connect what is shown in the visual structure to the process and phenomenon. In the context of self-motivation among university students, there is a higher chance of expanding the stimulation of learning. This study aimed to improve self-confidence and the mastery of concepts of chemistry teaching students using problem-based learning. The quasi-experimental method was used with the design of the non-equivalent pre-test-post-test control group. The population included all students in the electrochemistry class at Lampung University in 2019. The purposeful sampling technique employed divided the sample into two groups. The first group was called Class A and was considered as the experimental class - using problem-based learning -. The second group, Class B, was recognized as the control class - using the conventional model in which the teacher applied the speech method in the delivery of materials during the class -. Class A's self-confidence and mastery of concepts have a higher n-Gain value than class B, and the result of the effect size is that class B has a more significant effect than class A. Based on the outcome, one can conclude that problem-based learning has a significant influence on improving self-confidence and mastery of concepts on the electrochemical theme.

**Keywords:** problem-based learning, self-confidence, concept mastering, and electrochemistry.



## 1. INTRODUCTION:

Either teachers or lecturers must develop their competence in teaching. Chemistry lesson needs experiences (Toshio, 2015; Ezazi and Nourian, 2016). A study has shown that students have difficulty experienced in solving a problem relating to the ability to visualize the structure and the processes that happened at a minimal level and relating between the phenomenons in chemistry at another level (Sunyono and Sudjarwo, 2018). Chemistry commonly refers to failure, boring, and the reluctance of most students (Nurhadi, 2004; Ayyildiz, and Tarhan, 2018). The condition can cause students hard to catch up with the materials given (Keller, 2016). The factor that causes the problems in chemistry is namely models, methods, and strategies that are not precisely used or not optimum used and the chemistry lesson itself.

Chemistry is a branch of science that involves either microscopic or macroscopic concepts, which cause students hard to understand and reluctant to continue their studies in chemistry (Sirhan, 2007). The ability to understand the idea must be improved moreover. (Sunyono and Meristin, 2018) shown that chemistry lesson must be guided to increase the student multi-representation both verbally and visually in order their ability to associate the chemistry phenomenon can be improved. Commonly students experience difficulty understanding the concept are namely misconception, incapable of interpreting information to relate to the chemistry topic given (Michaliskova and Proksa, 2018). More explained explicitly by (Tamani *et al.*, 2015) that senior high school students do not have ideas and contact related to the thermodynamics concept.

The understanding of students' learning can help the teacher to manage strategies in teaching. A correct learning model applying is needed to solve the problems. Other researchers used problem-based learning (PBL) to solve chemistry problems are (Maysara, 2016; Ayyildiz, and Tarhan, 2017; Acar-sesen and Tarhan, 2013). The Basic concept of PBL model is to provide the basic concepts, instructions, references, or links and skills needed in the learning where the teacher becomes facilitator (Leou, Abder, Riordan, and Zoller, 2006; Yazar Soyadı, 2015). This is intended so that students enter the learning atmosphere more quickly and get an accurate 'map' of the direction and purpose of learning (Pratiwi, Cari, Aminah, and Affandy, 2019; Rani, 2018; Rudibayani, 2018). Furthermore, this is needed to

ensure students get the primary key learning material, so there is no possibility of being missed by students as can happen if students learn independently. The concepts given need not be detailed, preferably in the form of outlines so that students can develop them independently in-depth (Nagarajan and Overton, 2019; Pratiwi *et al.*, 2019). Problem-based learning is recently used widely and improved because this model has an underlying assumption that the students can solve the problems in their daily life so that the students have learned (Marra *et al.*, 2014).

The problem-based learning model is a learning model that presents contextual problems that stimulate students to learn. In classes that apply problem-based learning, students work in teams to solve real-world problems (Isaksen and Lauer, 1998; Madhuri, Kantamreddi, and Prakash Goteti, 2012; Raiyn and Tilchin, 2015). In this model, the students will be faced with the daily problems that relate to the topic given to activate the prior knowledge, and then the experience will be brought in collaboration in a small group to discuss the problem given (Affandy, Aminah, and Supriyanto, 2019; Pratiwi *et al.*, 2019; Raiyn and Tilchin, 2015).

Schmidt *et al.*, (2011) shown something to be concerned about the problem given, it must: 1) Authentic 2) Adapted from prior knowledge 3) involve the students in discussion 4) guided to learning issues identification 5) stimulate self-directed learning (SDL) and 6) attractive. The effect of applying PBL with the pre-test/post-test method in learning compared to the conventional method in engineering students can increase the achievement (Yadev *et al.*, 2011).

In the PBL, the teacher gives the instructions then the student constructs their knowledge independently based on the guidance from the teacher. A teacher is a good facilitator in involving the students in collaboration, discussion, communication, and training their logic and critical thinking. The teacher that applied PBL helps the students to develop their ability that needed in daily life activities are namely cooperative, analysis, communicative, researching, synthesis, and problem solving (Abanikannda, 2016).

With PBL meaningful learning will occur. Students who learn to solve a problem will apply the knowledge they have or try to find out the knowledge needed (Isaksen and Lauer, 1998; Yazar Soyadı, 2015). Learning can be more meaningful and can be expanded when students are dealing with situations where the concept is applied (Isaksen and Lauer, 1998; Rosidin,

Maskur, Kadaritna, and Saputra, 2019). Besides the cognitive aspect, namely the ability to mastering the concept, the affective aspect also needs to be concerned in chemistry learning. One of the characters is self-confidence. Self-confidence is the positive attitude of an individual in developing good values for both the environment and themselves. (Schmude, Serow, and Tobias, 2011). There is no study related to problem-based learning model and self-confidence in chemistry learning at school. The students in their studies need confidence.

Self-confidence can improve the achievement of the student academically in the cognitive test (Kleitman and Stankov, 2005). A class that has a diversity of student input will give pressure on their self-development. Moreover, self-confidence can be influenced by gender, just like showed in the study of Federicova *et al*, (2018). Self-efficacy became a part of the self-esteem of a person. Around 46.82% of Mulawarman students showed self-efficacy to pass organic chemistry (Erika, 2017). The data of the Program for International Student Assessment (PISA) has shown that self- efficacy of the student affects their achievement both in academics and their attitude. To practice and improve the self-confidence of the students, the specific learning model is needed (Erika, 2017).

The proposed problem statement in this study is that "How does the application of PBL model improve the self-confidence and concept mastery of the student?"

Therefore, this study aimed to evaluate the effect of applying PBL model to the self-confidence and the concept mastery of the student in electrochemistry material at the university level.

## 2. MATERIALS AND METHODS:

The research method is quasi-experimental with a non-equivalent pretest-posttest control group design (Fraenkel, 2012; Sugiyono, 2013) to compare the PBL model and the conventional model. The design is shown in Table 1.

**Table 1.** Research design (Fraenkel, 2012; Sugiyono, 2013)

| Class        | Treatment      |   |                |
|--------------|----------------|---|----------------|
| Experimental | O <sub>1</sub> | X | O <sub>2</sub> |
| Control      | O <sub>1</sub> | - | O <sub>2</sub> |

Note: O<sub>1</sub> is pre-test; X is the PBL model, and O<sub>2</sub> is the post-test.

The participants who took part in the research consisted of 50 students in total for both classes (experiment and control class). Regarding the gender, it covers 30 female and 20 male students by age ranging from 20 to 21 years old. They sat in the first semester from the running academic year of 2019/ 2020 in their university calendar. There was no special exclusion or inclusion applied as the sample intended supposed to be diverse from age, gender, and character background. They had declared their agreement about to involve in the data collection from their responses to be used for scientific purposes without any term and conditions apply. They were two classes taken covering class A as the experimental that used a problem-based learning model and class B as the control group that used the conventional model. The random sampling was used as a sampling technique. The dependent variable in this research is the PBL model; the independent variable is self-confidence and concept mastery, while the control variable is the electrochemistry topic.

The type of data in this research was test result data of pre-test and post-test on concept mastery and self- confidence, the questionnaires of self-confidence, and also observation result of teaching-learning activity as the primary data. This research was used instruments to collect the data. Tools used in this research were pre-test and post-test questions about concept mastery that consist of 5 essay questions and 10 on questionnaires about self-confidence that comprised of 15 statements as described in Appendix 1 and 2. Besides that, there was an assignment paper, namely an observation sheet of PBL activity.

The validity and reliability of the instrument were analyzed with SPSS v.22 for windows software. The question validity was determined by comparing the r-table value (the fixed score of data showing the effectiveness) with the r-calculate value (the gained score data processing to see the significance) spreading by the range scale score is 1-100. The criteria are if the rtable < rcalculate then the question is valid. Cronbach's Alpha determined the reliability with the requirements of reliability degree (Arikunto, 2013; Istiyono, Mardapi, and Suparno, 2014; Mardapi, 2012).

The next is to know that the result applies to the population so that the t-test was conducted. Before it, the normality and homogeneity test was done to the pre-test and post-test results and the value of n-gain using SPSS v.22 for windows software. The normality test was determined by

the value of significance (Sig). In the Shapiro-Walk column. In contrast, the homogeneity test was established by the value of sig. in the Test of Homogeneity of Variance Column.

### 3. RESULTS AND DISCUSSION:

#### 3.1. Validity and Reliability

The result of the self-confidence instrument test is shown in Table 2 and Table 3 for the mastery concept. Based on Tables 2 and 3, all questions are valid. The result calculation of the instrument reliability test showed based on the value of Cronbach's Alpha is 0.904 for mastery concept and 0.958 for self-confidence, which means the instrument test has high criteria of reliability, so the test was stated valid and reliable.

#### 3.2. The result of Pre-test and Post-test

The average of pre-test and post-test value of mastery concept of the student is shown in Figure 1. Based on Figure 1, the average pre-test value of the control class is 47.29, and the experimental class is 35.00. While for the average post-test value of the control class is 71.97 and the experimental class is 80.45. It showed that the value of the experimental class was more significant than the control class.

The averages value of self-confidence can be seen in Figure 2. As shown in Figure 2, the average initial value of the control class is 63.45, and the experimental class is 63.14, while after treatment, the value of the control class is 73.31 and the experimental class is 83.88. It showed that the value of self-confidence in the experimental class is greater than the control class.

Then the result of the n-gain value of concept mastery and self-confidence was observed. All the data processing result were generated for all aspects by considering the n-Gain value for the self-confidence form initial and final ability. The n-Gain value for concept mastery was generated from pre-test and post-test that was tested to the experimental class using PBL model and the control class using conventional one.

The result of the data processing result was shown in Figure 3. Based on Figure 3, the average n-gain value of self-confidence in the experimental class is 0.53 with the "medium" criteria, and the control class is 0.26 with "low" criteria. While the average n-gain value of concept mastery in the experimental class is 0.71 with "high" criteria, and the control class is 0.29 with

"low" criteria. It showed that the average n-gain value in the experimental class has greater than the control class. The difference of n-gain caused by the treatment, the PBL model in the experimental class and the conventional model in the control class.

#### 3.3. The result of normality and homogeneity test

Based on the normality test of self-confidence n-gain value in the experimental class known that the significant value is 0.311 is greater than 0.05 so can be concluded that the hypothesis where PBL contributed positively to the students understanding on chemistry concept was accepted or the data comes from the normally distributed population. Then, the significant value for self-confidence n-gain of the control class was 0.069 has greater than 0.05, so it means the hypothesis H0 was accepted or H1 was rejected, or the data comes from the normally distributed population. The normality test of concept mastery n-gain value in the experimental class has a significant value 0.754, while for the control class is 0.379, both of them were greater than 0.05, so the hypothesis H0 was accepted or H1 was rejected, or the data comes from the normally distributed population.

The sig obtained the homogeneity test of self-confidence n-gain value is 0.080, and for the concept, mastery is 0.271. The result showed that significant value is higher than 0.05 it means H0 was accepted or the variance of the population was homogenous.

#### 3.4. The result of Independent Sample T-Test

The result of two average difference tests for self-confidence showed in Table 4, while the concept mastery aspect showed in Table 5.

**Table 4.** Independent sample t-test self-confidence test value

| Class        | The average value of n-Gain | p sig (2-tiled) |
|--------------|-----------------------------|-----------------|
| Experimental | 0.53                        | 0.000           |
| Control      | 0.26                        |                 |

Both the result was showed that the sig 2-tailed value is  $0.000 < 0.05$ ; it means that H0 was rejected, and H1 was accepted, or the average of n-gain in both aspects was higher in the experimental class with the PBL model than the control class with the conventional model. Hermawati stated that the concept of mastery of learning would be better if there were optimum

students' involvement in the learning process (Hermawati, 2012). Fuaidah (2017) showed the contextual approach-based worksheet could improve the self-confidence of the student in mathematics learning.

**Table 5.** Independent sample t-test value

| Class        | The average value of n- | p sig (2-tiled) |
|--------------|-------------------------|-----------------|
| Experimental | 0.71                    | 0,000           |
| Control      | 0.31                    |                 |

### 3.5. The calculation result of Effect Size

After the t-test of pre-test and post-test in both aspects self-confidence and concept mastery, then the value of tcalculate was used to calculate the effect size. The result of self-confidence showed in Table 6 and the concept mastery showed in Table 7.

**Table 6.** Self-confidence Effect size Value

| Class        | T <sub>count</sub> | Effect size | Criteria |
|--------------|--------------------|-------------|----------|
| Experimental | -17.31             | 0.81        | Large    |
| Control      | -10.73             | 0.63        | Medium   |

**Table 7.** Concept mastery Effect size Value

| Class        | T <sub>count</sub> | Efeect size | Criteria |
|--------------|--------------------|-------------|----------|
| Experimental | -21.634            | 0.87        | Large    |
| Control      | -10.189            | 0.60        | Medium   |

### 3.5. Implementation of the PBL model

The result in the experimental class showed in following Table 8.

**Table 8.** Implementation of the PBL model

| Meeting | %     | The average | Criteria  |
|---------|-------|-------------|-----------|
| 1       | 75.00 | 85.87       | Very high |
| 2       | 89.58 |             |           |
| 3       | 93.05 |             |           |

According to Table 8, the average value of the PBL model implementation in the experimental class increased from the first meeting to the third meeting, and it has "very high" criteria. These criteria showed that the learning activity ran well. The aspect that assigned in the implementation occupied the learning enthusiasm, student activity,

team-work, and the last was the result.

The analysis result of the PBL model implementation with very high achievement showed that the student improved in the experimental class. The improvement of student's activity in the experimental class showed that learning activity ran effectively. This result in line with Warsita's statement that a learning activity will run effectively if the student involved actively in organizing and founding the information. (Warsita, 2008). Wulandari (2011) stated the one of learning model that can solve the problem is the PBL model.

Students who learn to solve a problem will apply the knowledge they have or try to find out the experience needed (Adolphus, Alamina, Aderonmu, Education, and State, 2013; Bacong and S, 2015; Hake, 1998). In this situation, students integrate knowledge and skills simultaneously and apply them in relevant contexts. Learning can be more meaningful and can be expanded when students are dealing with cases where the concept is used. The facilitator presents the scenario or problem, and in the group, students carry out various activities (Lsaksen and Lauer, 1998; Wenno, 2010). First, brainstorming is carried out through all group members expressing opinions, ideas, and responses to scenarios freely, so that various alternative viewpoints can emerge. Each group member has the same right in giving and conveying ideas in discussions and documenting their own views in the working paper.

Also, each group must look for terms that are less well known in the scenario and try to discuss their intentions and their meanings. If there are students who know the meaning, immediately explain it to other friends. If there is a part that cannot be solved in the group, it is written in the group problem. Furthermore, if there is a part that cannot be solved in the group, it is written as an issue in the group's problem. Second, to make alternative selections to choose more focused opinions. Third, determine and carry out the division of tasks in groups to find references to solve the issues that were obtained. The facilitator validates the choices students make. At the end of the step, students are expected to have a clear picture of what they know, what they don't know, and what knowledge is needed to bridge it (Adolphus *et al.*, 2013; Retno, Sunarno, and Marzuki, 2019). To ensure each student follows this step, defining the problem is done by following the instructions.

The PBL model is a learning model that

collaborate in problem-solving and founding the concept independently. This model is sufficient to improve creative thinking skills because the student was given the freedom to state their ideas from the inside of themselves and the environment that supports their learning activities (Tan, 2009).

Abanikannda (2016) stated that problem-based learning became a practical pedagogic approach insight of affective and pedagogic changes. Especially in the medical, architecture, and engineering fields for more than forty years.

Uce (2016) stated that in science learning, the PBL model helps the students to improve their ability in learning science procedures are namely observation, measurement, communicating, prediction, determining variables, suggesting a hypothesis, planning, experiment, and many other.

Hermawati stated that the concept mastery would be better if the students were getting involved in the learning activity processes. (Hermawati, 2012).

#### 4. CONCLUSIONS:

It can be concluded that the applying of the PBL model has a significant effect on improving the self-confidence and concept mastery of the student in the electrochemistry topic. Problem Based Learning (PBL) is a learning model that encourages to be more active and maximize the ability of self-confidence to get solutions to problems in the real world. By implementing the PBL model, students can become more competent in solving and taking answers to a problem. Also, this method designs issues that motivate them to gain valuable knowledge so that they have their learning strategy and the ability to participate in discussion groups. The learning process uses a systemic approach to solving problems or challenges needed in everyday life. It has shown by the "very high" average percentage of the PBL implementation. The average n-Gain value of self-confidence is "medium" and "high" for concept mastery and also the value of size effect that categorized as "huge."

#### 5. REFERENCES:

1. Abanikannda, M.O. (2016). Influence Of Problem-Based Learning In Chemistry On Academic Achievement Of High School Students In Osun state, Nigeria. *International Journal of Education, Learning and Development* Vol.4, No.3: pp.55-63
2. Astriani, N., Edy, S., and Edi, S. (2017). The Effect of Problem Based Learning on Students' Mathematical Problem Solving Ability. *International Journal of Advance Research and Innovative Ideas in Education*, 3(1): 3441-3446.
3. Ayyildiz, Y., and Tarhan, L. (2018). Problem-based learning in teaching chemistry: enthalpy changes in systems. *Research in Science and Technological Education*, 36(1): 35-54.
4. Adolphus, T., Alamina, J., Aderonmu, T., Education, T., and State, R. (2013). *The Effects of Collaborative Learning on Problem Solving Abilities among Senior Secondary School Physics Students in Simple Harmonic Motion*. 4(25), 95–101.
5. Affandy, H., Aminah, N. S., and Supriyanto, A. (2019). The correlation of character education with critical thinking skills as an important attribute to success in the 21<sup>st</sup> century. *Journal of Physics: Conference Series*, 1153(1). <https://doi.org/10.1088/1742-6596/1153/1/012132>
6. Bacong, H., and S, S. (2015). Profil Kreativitas Mahasiswa Berdasarkan Gaya Berpikirnya dalam Memecahkan Masalah Fisika di Universitas Negeri Makassar. *Indonesian Journal of Applied Physics*, 5(01), 1. <https://doi.org/10.13057/ijap.v5i01.250>
7. Bénabou, R., and Tirole, J. (2002). Self-confidence and personal motivation. *The Quarterly Journal of Economics*, 117(3): 871-915.
8. Dincer, S. (2015). Effect of Computer Assisted Learning on Student Achievement in Turkey: a Meta-Analysis. *Journal of Turkish Science Education*, 12(1): 99-118.
9. Erika, F. (2017). Student's self-efficacy in organic chemistry learning: *Proceeding of chemistry conference*, vol. 2.
10. Ezazi, M, Nourian, M. (2016). A Study Of Chemistry Teaching Method, Experimental Analysis, by Student-Teachers in Internship Lesson. *Journal of Science Research in Science*. S(2). 495-504.
11. Federicova, M, Pertold, F, Smith, ML. (2018). Children Left Behind: Self-Confidence of Pupils in Competitive Environments. *Education in Economics*. 26:2,145-160.
12. Fraenkel, J. R., Wallen, N. E., dan H. H. Hyun, (2012). *How to design and evaluate research in education 8th edition*. McGraw-Hill, A

Business Unit Of The McGraw-Hill Companies, Inc., 1221 Avenue of The Americas, New York, NY 10020.

13. Fuaidah, W.I. (2017). Pengaruh Pendekatan Kontekstual Terhadap Kemampuan Pemahaman Konsep Matematis dan *Self-confidence* Siswa. (skripsi). Universitas Lampung. Bandar Lampung.
14. Habibah Elias., Rahil Mahyuddin., Nooreen Noordin., Maria Chong Abdullah. (2009). Self-Efficacy Beliefs of At-Risk Students in Malaysian Secondary Schools. *The International Journal of Learning*, 16: 201-210
15. Hake, R. R. (2002). Relationship of individual Student Normalized Learning Gains in Mathematics with Gender, High School, Physics, and Pre Test Scores in Mathematics and Spatial Visualization. Physics Education Research Conference. Cited from <http://www.physics.indiana.edu/~hake/PERC2002h-Hake.pdf>. Accessed on October 6, 2017.
16. Hake, R. R. (1998). Interactive-engagement versus traditional methods: A six-thousand-student survey of mechanics test data for introductory physics courses. *American Journal of Physics*, 66(1), 64–74. <https://doi.org/10.1119/1.18809>
17. Isaksen, S. G., and Lauer, K. J. (1998). *The Relationship Between Cognitive Style and Individual Psychological Climate: Reflections On a Previous Study*. New York: Creative Problem Solving Group.
18. Istiyono, E., Mardapi, D., and Suparno. (2014). Pengembangan Tes Kemampuan Berpikir Tingkat Tinggi (PysTHOTS) Peserta Didik SMA. *Jurnal Penelitian Dan Evaluasi Pendidikan*, 18(1), 1–12.
19. Jahjouh, Y. M. A. (2014). The Effectiveness of Blended E-Learning Forum in Planning for Science Instruction. *Journal of Turkish Science Education*, 11(4): 3-16.
20. Keller, J. M. (2016). Motivation, learning, and technology: Applying the ARCS-V motivation model. *Participatory Educational Research*, 3(2), 1-15.
21. Kleitman, S., Stankov, L. (2005). Self-Confidence and Meta Cognitive Processes. *Зборник Института за педагошка истраживања. Година XXXVII • Број 1 • Јун*.
22. Leou, M., Abder, P., Riordan, M., and Zoller, U. (2006). Using “HOCS-centered learning” as a pathway to promote science teachers’ metacognitive development. *Research in Science Education*, 36(1–2), 69–84. <https://doi.org/10.1007/s11165-005-3916-9>
23. Madhuri, G. V., Kantamreddi, V. S. S. N., and Prakash Goteti, L. N. S. (2012). Promoting higher order thinking skills using inquiry-based learning. *European Journal of Engineering Education*, 37(2), 117–123. <https://doi.org/10.1080/03043797.2012.661701>
24. Mardapi, D. (2012). *Pengukuran, Penilaian, dan Evaluasi Pendidikan*. Yogyakarta: Nuha Litera.
25. Marra, R.M, Jonassen, D.H, Palmer, B, Luft, S. (2014). Why Problem-Based Learning Works: Theoretical Foundations. *Journal of Excellence in College Teaching*. 25(3and4).221-238.
26. Maysara. The Effectiveness Of Problem Based Learning (Pbl) Model On Students’ Learning Outcomes At Class Xi Ipa 2 Of Senior High School 5 South Konawe On The Subject Of Colloid System. *International Journal of Education and Research*. Vol 4.
27. Nagarajan, S., and Overton, T. (2019). Promoting Systems Thinking Using Project-And Problem-Based Learning. *Journal of Chemical Education*. <https://doi.org/10.1021/acs.jchemed.9b00358>
28. Pratiwi, S. N., Cari, C., Aminah, N. S., and Affandy, H. (2019). Problem-Based Learning with Argumentation Skills to Improve Students’ Concept Understanding. *Journal of Physics: Conference Series*, 1155(1). <https://doi.org/10.1088/1742-6596/1155/1/012065>
29. Raiyn, J., and Tilchin, O. (2015). Higher-Order Thinking Development through Adaptive Problem-based Learning. *Journal of Education and Training Studies*, 3(4).
30. Rani, P. E. W. (2018). Efektivitas Problem Based Learning untuk Meningkatkan Keterampilan Berpikir Orisinil Siswa pada Materi Asam Basa. *Jurnal Pendidikan Dan Pembelajaran Kimia*, 7(2).
31. Retno, N. H. D., Sunarno, W., and Marzuki, A. (2019). Influence of physics problem-solving ability through the project based learning towards vocational high school students’ learning outcomes. *Journal of Physics: Conference Series*, 1307, 012009. <https://doi.org/10.1088/1742->

32. Rosidin, U., Maskur, R., Kadaritna, N., and Saputra, A. (2019). Attitude towards technology for pre-service science teachers in Indonesia: An exploratory factor analysis. *Periodico Tchê Química*, 16(33), 854–864.
33. Rudibyani, R. B. (2018). Improving Students' Creative Thinking Ability Through Problem Based Learning Models on Stoichiometric Materials. *Journal of Physics Conference Series*.
34. Sugiyono. (2013). *Metode Penelitian Kuantitatif dan R and D*. Bandung: Alfabeta.
35. Schmidt, G.H, Rotgans, J.I, Yew, E.H.J. 2011. *The Process of Problem-Based Learning: What Works and Why*. Medical Education. 45: 792-806.
36. Schmude, M. A. R. T. I. N., Serow, P. E. N. E. L. O. P. E., and Tobias, S. T. E. P. H. E. N. (2011). Improving self-confidence and abilities: A problem-based learning approach for beginning mathematics teachers. *Mathematics: Traditions and [new] practices*, 676-684.
37. Sirhan, G.(2007). Learning Difficulties in Chemistry: An Overview. *Journal of Turkish Science Education*. Vol 4.Issues 2.2-20.
38. Suhendri, H. (2012). *Pengaruh Kecerdasan Matematis-Logis, Rasa Percaya Diri, dan Kemandirian Belajar Terhadap Hasil Belajar Matematika*. Prosiding Seminar Nasional Matematika dan Pendidikan Matematika UNY. Suherman, E. 2003. *Evaluasi Pembelajaran Matematika*. JICA UPI: Bandung.
39. Sunyono, Yuanita, L.and Muslimin, I. (2015). Supporting Students in Learning with Multiple Representation to Improve Student Mental Models on Atomic Structure Concepts. *Science Education International*, 26 (2), 104-125
40. Tamani, S, Jamali, SE, Dihaj, N, Radid, M. (2015). Chemical Thermodynamic Concept Mastering by Chemistry Students. *Procedia-Social and Behavioral Science*. 197. 281-285.
41. Toshio, H. (2015). A Strategy for High School Chemistry Teaching: The Basic and Fundamental Content. *Chemical Education Journal*. Vol. 17 No 17-205.
42. Uce, M., and Ismail A. (2016). Problem-Based Learning Method: Secondary Education 10<sup>th</sup> Grade Chemistry Course Mixture Topic. *Journal of Education and Training Studies*. Vol. 4. No. 16: page. 31.
43. Wenno, I. H. (2010). Berbasis Problem Solving Method. *Jurnal Cakrawala Pendidikan*, (2), 176–188.
44. Yazar Soyadı, B. B. (2015). Creative and Critical Thinking Skills in Problem-based Learning Environments. *Journal of Gifted Education and Creativity*, 2(2), 71–71. <https://doi.org/10.18200/jgedc.2015214253>
45. Yadav, A., Subedi, D. Lundeberg, M.A.,andBunting, C.(2011).Problem-based learning: Influence on students learning in an electrical engineering course. *Journal of Engineering Education*, 100(2), 253-280.

**Table 2.** The result of self-confidence instrument validity test

| Questions on Self- Confidence | r <sub>count</sub> | r <sub>table</sub> | Criteria |
|-------------------------------|--------------------|--------------------|----------|
| 1                             | 0.448              | 0.554              | Valid    |
| 2                             | 0.426              | 0.565              | Valid    |
| 3                             | 0.420              | 0.562              | Valid    |
| 4                             | 0.501              | 0.555              | Valid    |
| 5                             | 0.410              | 0.588              | Valid    |
| 6                             | 0.447              | 0.555              | Valid    |
| 7                             | 0.510              | 0.543              | Valid    |
| 8                             | 0.448              | 0.554              | Valid    |
| 9                             | 0.438              | 0.557              | Valid    |
| 10                            | 0.410              | 0.574              | Valid    |

**Table 3.** Results of Concept Mastery instrument validity test

| Questions on Concept mastery | r <sub>count</sub> | r <sub>table</sub> | Note  |
|------------------------------|--------------------|--------------------|-------|
| 1                            | 0.793              | 0.444              | Valid |
| 2                            | 0.696              | 0.444              | Valid |
| 3                            | 0.785              | 0.444              | Valid |
| 4                            | 0.696              | 0.444              | Valid |
| 5                            | 0.660              | 0.444              | Valid |

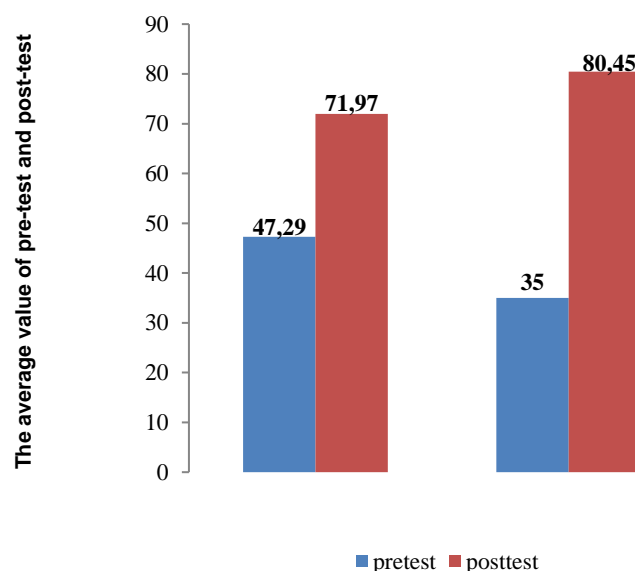


**Figure 1.** The average of the absolute value of pre-test and post-test on concept mastery



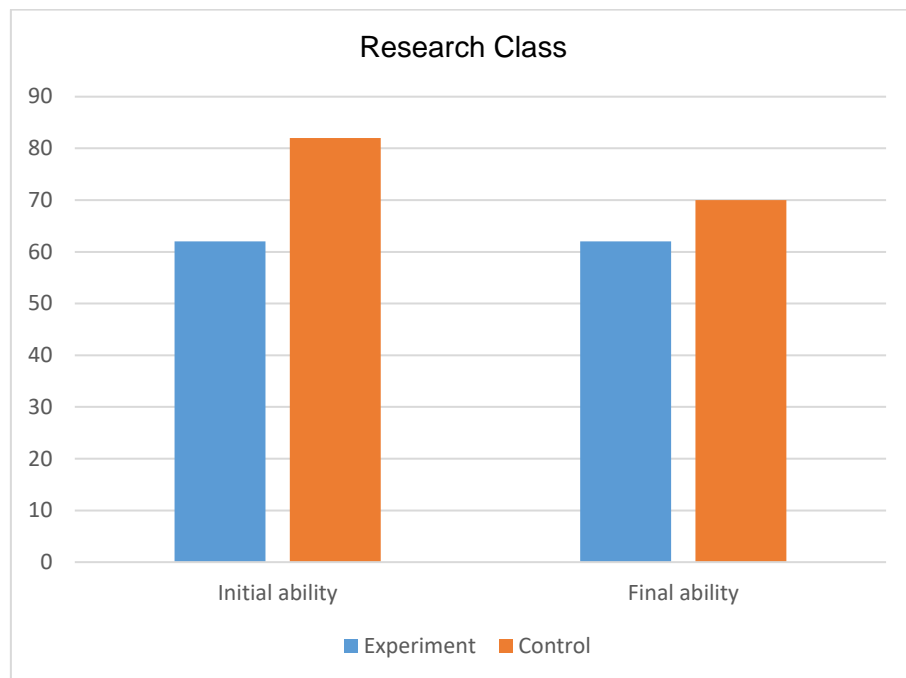


**Figure 2.** The average of the absolute value of self-confidence

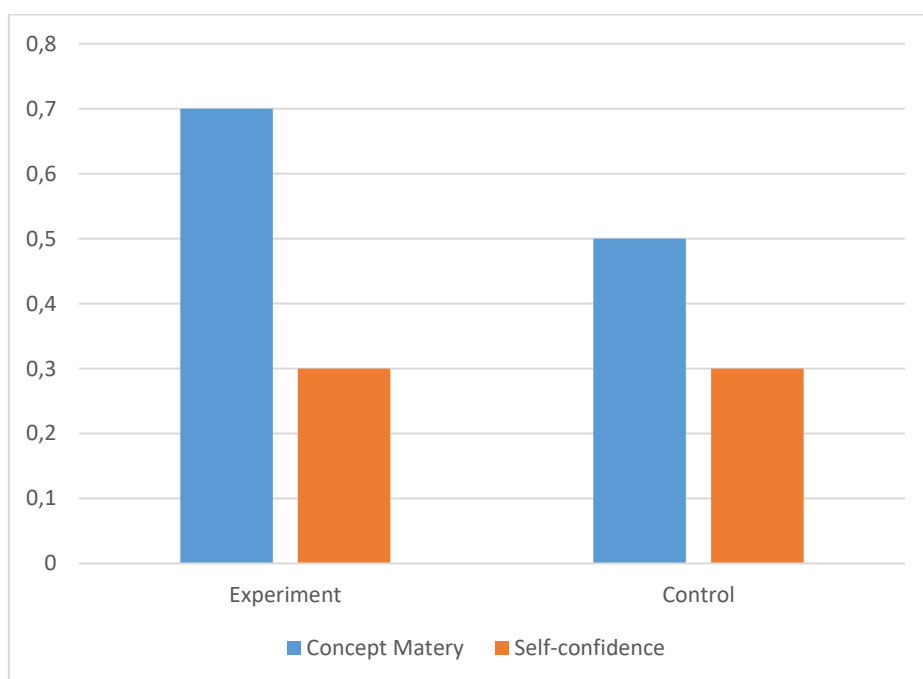


**Figure 3.** The average of the absolute n-Gain value for self-confidence and concept mastery

**Appendix 1.** The Students' Questionnaire on Self-Confidence

| No | Questions  | Never | Sometimes | Often | Always |
|----|--|-------|-----------|-------|--------|
| 1  | When I see a new problem on the chemistry course, I can use what I have learned to solve the problem |       |           |       |        |
| 2  | I can see what I can know to design and build something mechanical that works                        |       |           |       |        |
| 3  | In laboratory activities, I can use what I have learned to design a solution                         |       |           |       |        |
| 4  | I can effectively lead a learn to design and build a hands-on project                                |       |           |       |        |
| 5  | I know where I can find the information that I need to solve severe problems                         |       |           |       |        |
| 6  | I can use what I have learned to teach myself how to construct a chemistry formulation               |       |           |       |        |
| 7  | I can explain chemistry or related science to my friends to help them understand                     |       |           |       |        |
| 8  | I can understand the basic concepts of chemistry easily  |       |           |       |        |
| 9  | I can get good grades in chemistry   |       |           |       |        |
| 10 | I can get good grades in laboratory practice   |       |           |       |        |

**Appendix 2.** The Students' Test on Concept Mastery

| No | Concept Mastery Indicator   | Correct Answers<br>(n =100) (%) | Correct Reasons<br>(n =100) (%) |
|----|---|---------------------------------|---------------------------------|
| 1  | Understanding the principles of chemistry quantities measurement direct and indirectly, carefully, thoroughly, and objectively. |                                 |                                 |
| 2  | Understanding the natural phenomena and their regularities in chemical reactions.   |                                 |                                 |
| 3  | Understanding the concept of reactions and oxidations and its changing concerning the laws of chemical equation.                |                                 |                                 |
| 4  | Analyzing concepts and principles of chemical reactions in various problem solving and technology products                      |                                 |                                 |
| 5  | Understanding concepts and principles of chemical reactions and its application in various problem solving                      |                                 |                                 |

## ESTIMATIVA DOS FATORES QUE AFETAM O CRESCIMENTO DE ALGAS NO LAGO DE UM EL-NAAJ USANDO TÉCNICAS DE SENSORIAMENTO REMOTO

### ESTIMATION THE FACTORS AFFECTING ON GROWTH OF ALGAE IN UM EL-NAAJ LAKE BY USING REMOTE SENSING TECHNIQUES

تقدير العوامل المؤثرة على نمو الطحالب في بحيرة أم النعاج باستخدام تقنيات الاستشعار عن بعد

AL NAQEEB, Neran A.<sup>1,3\*</sup>; MASHEE, Fouad K.<sup>2</sup>; AL HASSANY, Jinan S.<sup>1</sup>;

<sup>1</sup>Biology Department, College of Science for Women, University of Baghdad, Baghdad, Iraq

<sup>2</sup>Remote Sensing Unit, College of Science, University of Baghdad, Baghdad, Iraq

<sup>3</sup>Department of Biology, College of Science, University of Misan, Maysan, Iraq

\* Correspondence author

e-mail: neranecology@uomisan.edu.iq

Received 24 April 2020; received in revised form 15 May 2020; accepted 22 May 2020

## RESUMO

As algas epífitas aderentes às plantas aquáticas são um elo essencial na composição da cadeia alimentar de qualquer ecossistema. As algas epífitas atuam como produtoras primárias da cadeia alimentar no ecossistema aquático e como alimento natural para o zooplâncton herbívoro e peixes. Este estudo teve como objetivo detectar a presença de colônias de algas através de sensoriamento remoto e analisar fatores que afetam o crescimento de algas por meio de levantamento de campo e interpretação visual de imagens de satélite no lago Um El-Naaaj. As amostras foram coletadas em seis locais no lago Um El-Naaaj no período de novembro de 2018 a junho de 2019. As amostras de algas foram coletadas de partes submersas de plantas aquáticas emergentes (macrófitas aquáticas *Phragmites australis*) e armazenadas em sacos plásticos com pouca água do ambiente e soluções para a preservação no campo e no laboratório. Amostras de água foram coletadas para estudar os fatores nutricionais que influenciam o crescimento das algas, incluindo a concentração de fosfato, nitrato e sílica (dióxido de silício). Os resultados mostraram que os valores de fósforo total apresentaram aumento de 1,0, 0,9 e 0,8 mg/L, em janeiro, nos locais 2, 5 e 6, respectivamente. O valor mais alto do nitrato foi de 11,2 mg/L, em dezembro, no local 5, enquanto os menores valores de concentração foram em novembro (2,2 mg/L no local 6, e 3,7 mg/L no local 4). Além disso, a menor concentração de silicato foi de 0,4 mg/L, em novembro, no local 2, ao passo que a maior foi 2,4 mg/L, em junho de 2019, no local 6. Com base nos achados, é possível concluir que, durante o inverno, o nível da água aumentou devido às chuvas. Por esse motivo, as concentrações de nutrientes foram baixas durante o último período. Além disso, com o uso de mapas e técnicas de sensoriamento remoto, é possível determinar os valores esperados em torno da localização da estação como leituras preditivas futuras que compensam a dificuldade de alcançar essas áreas.

**Palavras-chave:** Concentração de  $\text{NO}_3$ ,  $\text{PO}_4$  e  $\text{SiO}_2$ , Algas Nutrientes, Técnicas de Sensoriamento Remoto, Pântanos Um El-Naaaj, Qualidade da Água.

## ABSTRACT

Epiphytic algae adherent to aquatic plants are an essential link in the composition of the food chain of any ecosystem. Epiphytic algae act as primary producers of the food chain in the aquatic ecosystem and as natural food for herbivorous zooplankton and fish. This study aimed to detect the presence of algae colonies through remote sensing and to analyze factors that affect the growth of algae through field survey and visual interpretation of satellite images in Lake Um El-Naaaj. Samples were collected from six locations on Lake Um El-Naaaj from November 2018 to June 2019. The algae samples were collected from submerged parts of emerging aquatic plants (aquatic macrophytes *Phragmites australis*) and stored in plastic bags with little ambient water and solutions for preservation in the field and the laboratory. Water samples were collected to study the nutritional factors that influence the growth of algae, including the concentration of Phosphate, Nitrate, and Silica (silicon dioxide). The results showed that the values of total phosphorus increased by 1.0, 0.9, and 0.8 mg/L, in January, in places 2, 5, and 6, respectively. The highest nitrate value was 11.2 mg/L in December at site 5, while the lowest concentration values were in November (2.2 mg/L at site 6 and 3.7 mg/L at site 4). Besides, the lowest

silicate concentration was 0.4 mg/L in November at site 2, while the highest was 2.4 mg/L in June 2019 at site 6. Based on the findings, it is possible to conclude that, during the winter, the water level increased due to the rain. For this reason, nutrient concentrations were low during the last period. Also, with the use of maps and remote sensing techniques, it is possible to determine the expected values around the station's location as future predictive readings that compensate for the difficulty of reaching these areas.

**Keywords:**  $NO_3$ ,  $PO_4$ , and  $SiO_2$  concentration, Nutrient Algae, Remote Sensing Techniques, Um El-Naaj Marshes, Water Quality.

## المخلص

تعتبر الطحالب الملتصقة بالنباتات المائية حلقة مهمة في تكوين السلسلة الغذائية لأي نظام بيئي. تمثل الطحالب الملتصقة بالنباتات كمنتج رئيسي للسلسلة الغذائية في النظام البيئي المائي وكغذاء طبيعي للعوالق الحيوانية والأسماك العاشية. هدفت هذه الدراسة للكشف عن وجود مستعمرات الطحالب وتحليل العوامل المؤثرة على نمو الطحالب من خلال المسح الميداني والتفسير المرئي لصور الأقمار الصناعية في بحيرة أم النعاج. تم جمع العينات من ستة مواقع في بحيرة أم النعاج من شهر تشرين الثاني 2018 إلى شهر حزيران 2019. جُمعت عينات الطحالب من الأجزاء الغاطسة للنباتات المائية من نبات الطحالب المائية الناشئة (القيصوب الاسترالي). جُمعت عينات النباتات في أكياس بلاستيكية مع القليل من الماء البيئي واستخدمت محاليل للمحافظة على الطحالب في الحقل والمختبر. تم جمع عينات المياه لدراسة العوامل الغذائية المؤثرة على نمو الطحالب منها تركيز الفوسفات والنترات والسيليكا (ثاني أكسيد السيليكون). أوضحت النتائج أن قيم الفوسفور الكلي أظهرت ارتفاع (1.0، 0.9، و 0.8) ملغم في شهر كانون الثاني في المواقع 2، 5، و 6 على التوالي. أعلى قيمة للنترات كانت تركيز 11.2 ملغم في شهر كانون الأول في الموقع 5، وأدنى قيمة نترات تركيز 2.2 ملغم في شهر تشرين الثاني في موقع 6 و 3.7 ملغم في الموقع 4. كما أن أدنى قيمة للسيليكا كانت 0.4 ملغم في شهر تشرين الثاني في موقع 2 وأعلى تركيز 2.4 ملغم في شهر حزيران من 2019 في الموقع 6. بناء على النتائج يمكن استنتاج ارتفاع مستوى الماء خلال فصل الشتاء بسبب الأمطار، لهذا السبب كانت تراكيز المغذيات منخفضة خلال الفترة الأخيرة، كما أن استخدام خرائط تقنيات الاستشعار عن بعد للتنبؤ بالقيم المتوقعة المحيطة بموقع المحطة كقرارات تنبؤية مستقبلية تُعوض عن صعوبة الوصول إلى هذه المناطق.

**الكلمات المفتاحية:** تركيز النترات، والفوسفات، السيليكا، مغذيات الطحالب، الاستشعار عن بعد، هور ام النعاج، نوعية المياه.

## 1. INTRODUCTION:

Epiphytic algae are found attached on surfaces of plants like mosses, other algae, and higher plants. Benthic algae require enough light for growth and suitable sites for connecting like submerged aquatic plants and emergent aquatic plants that found at the edge of the water body (Edward and David, 2010). Epiphytic algae play a vital role in the freshwater ecosystems because they are sources of primary production and an excellent nutrition source for the zooplankton (herbivores and for fish) (Graham *et al.*, 2009). Furthermore, they participate in sediment stabilization and regulation of the nutrients cycle (AL-Hassany and Hindi, 2016; AL Naqeeb *et al.*, 2020).

Epiphytic algae move the energy from the sediment to the water column (Salman *et al.*, 2013) and play a crucial function in the photosynthesis process transforming inorganic materials into organic ones. Also, it recycles nutrients and contributes to oxygen production via photosynthesis (Pouličková *et al.*, 2008). Phosphorus is a major ingredient that all organisms need, including algae, to build up nucleic acids (RNA and DNA), energy materials (ATP and ADP), and plasma membranes (Jarvis, 2000).

The importance of total phosphorus is due to the possibility of being used by aquatic organisms as a source of Phosphate after

conversion to inorganic phosphorus by the group of enzymes (Phosphatase), and dissolved total phosphorus is a determining factor for the growth of algae (McDowell and Sharpley, 2001).

Phosphorus often shows low concentrations in natural Waters. Algae are characterized by their ability to use the optimum concentration of phosphorus available for absorption and storage at concentrations beyond their need and more than what is found in the médium. This is called Luxury Uptake. Mixing from rain helps to release Phosphate from sediment, a source of water-soluble Phosphate. Nitrogen is a major component of algal growth and has an important role in cell division and some metabolic activities such as the building of fatty acids and proteins in algal cells (Boney, 1975). Fatty acids are the main source of Nitrogen in water, and its presence is associated with organic matter in water because it is a determinant of primary productivity in some environment (Ault *et al.*, 2000).

Silicon dioxide,  $SiO_2$ , also known as Silica, is a major nutrient for the growth of diatoms in particular to build their structures (Reynolds, 1984). It is noted that the rate of dissolution of Silica has an essential role in regulating the pH as it acts as buffer solution Buffering Solution, and most natural water contains the element of Silica abundantly and available to diatoms in the basal water than acidic water (Wen and Chen, 2000; Hassan *et al.*, 2012). To study the growth of algae

and its effect on nutrients in the water surface.

A remote sensing program has been used. This progress has helped to achieve the accuracy in obtaining information from orthophoto imagery (aircraft, aerial photo, and satellite); it has become a basic science used to solve many issues related to land, atmosphere, surface phenomena and natural conditions without contact with any variances, through the amount of collection information provided and manipulation with digitization by high technology (Lillesand *et al.*, 2015; Hadi, and Mashee, 2017).

Sensing provides a unique method for obtaining land surface temperature (LST) information at the regional and global scale since most of the energy detected by the sensor in this spectral region is directly emitted by the land surface (Mashi, 2018).

The definitions interpolation process technique is making assumption areas that are closing to one another, which are corresponding to alike than those nearest apart, which led to clear predict values for any unmeasured regions, which influence those farther away. The inverse distance weighting (IDW) technique uses the values measured in observation stations to predict the expected values surrounding the station location as future predictive readings that compensate for the difficulty of reaching remote areas (Mitchel, 2005; Al Ramahi and Al Bahadly, 2017).

This study aimed to detect the presence of algae colonies that are environmentally friendly and community and analyze factors affecting algal traits through field survey and visual interpretation of satellite images and the use of statistical methods and theories.

## 2. MATERIALS AND METHODS:

### 2.1. Study area

The study area in Maysan Province that in the south of Iraq located in Universal Transverse Mercator (UTM) is in wright top 618607.7, 3632754.577 meter, and 770955.209, 3449601.505 meter in the left top. The Huwaizah marshes are located within the governorate of Maysan to the east of the Tigris River. The Huwaizah is bordered to the east and southeast by transnational area with Iran; to the south and southwest by the Basrah Governorates administer active boundary. The Huwaizah marshes represent the northeast corner of the property, with a total surface area of 90,691ha of primarily freshwater marsh.

The Huwaizah is the first national site that declared a Ramsar site for wetlands of international importance (Hassan *et al.*, 2012; Garstecki and Amr, 2011). Um El-Naaj lake, it is one of the most massive open water bodies partially dried during the marshes drying process in 1990. It is located in the northwest part of the Hawizeh marsh in Universal Transverse Mercator (UTM) is in wright top 5294772.863, 3523084.449 meter, and 5308522.835, 3511666.143 meter in left bottom, covering an area of between 140 and 200 km<sup>2</sup> (Garstecki and Amr, 2011). Six sites were selected in Hor Al Huweiza Um El-Naaj lake identified by Ground Positioning System (GPS), (Table 1 and Figure 1).

The algae samples were collected from the submersible aquatic macrophyte plant (*Phragmites australis*) in plastic bags with little of the environment water. Formalin 4% was used for the preservation of algae in the field. Lugol's solution was also used to keep the original characteristics of the samples. Lugol was prepared by dissolving 20 g of Potassium Iodide in 200 ml of distilled water. After, 10 g of Iodine crystals were added; then, glacial acetic acid was added to the mixture, and this solution was preserved in a dark bottle and used by a proportion of 1% (1mL of the solution to every 100 mL of the sample that contains algae) (Prescott, 1964).

### 2.2. Epiphytic Algae Colony

Epiphytic algae attached to plants or to artificial surfaces contribute to taking the phytonutrients present from the water column in the growing season, as they have a role in removing 80% of ammonium, 15% of nitrates and 70% of the adequate soluble phosphorus entering the water surface within 15 days of exposure to these plant nutrients as these high removal rates increase the growth of adherent Epiphytic algae and then use it to treat water-rich in plant nutrients.

The rate of taking phosphorous by adherent Epiphytic algae ranges from 1-3 mg phosphorous/m<sup>2</sup> of wetland area per week, so many of these algae are essential consumers of phosphorus from the water column. Therefore algae is vital evidence of the availability of plant nutrients and pollution as well as being a candidate for materials Water suspended solid (Morgan and Kitting, 1984; Cronk and Mitsch, 1994; Dere *et al.*, 2002).

Given the great environmental importance of algae, as it is an important factor in determining the nutritional level of any ecosystem, this has led to the researchers' interest in studying it

qualitatively and quantitatively (Figure 2).

### 2.3. Total Nitrogen ( $\mu\text{g/L}$ )

The total Nitrogen in the sample was converted to Nitrate in the digestion method with potassium persulphate. According to Rice *et al.*, 2012; Salman *et al.*, 2017, 25 mL of the sample were put in an autoclave  $121^{\circ}\text{C}$  for 30 minutes after the addition of 0.3 g of potassium persulphate; then, it was cooled to the room temperature and pH regulated with NaOH and HCl solution to reach 7 - 9; later, the volume was completed to 100 mL with  $\text{NH}_4\text{Cl}$ -EDTA concentrate solution. After that, the sample passed through the Cadmium column, and the given sample gathered after neglecting the first 25 mL. The first reagent Sulphanilamide has been added, and the sample was put in the darkness for 4 - 6 minutes. The second reagent, naphthyl ethylenediamine-dihydrochloride, has been added, and, finally, after 10 - 12 minutes, the absorption has been measured by the spectrophotometer on wavy length 543 nanometers.

### 2.4. Total Phosphate ( $\text{mg/L}$ )

The total Phosphate was measured by the method of absorption (Rice *et al.*, 2012; Parsons *et al.*, 1984). A total of 100 mL of the sample was put in the autoclave  $121^{\circ}\text{C}$  after the addition of 5 mL of sulphuric acid 1N and 0.7 g of potassium persulphate. Then, it was cooled to the room temperature and treated with 10 mL of the reduced solution composed of ascorbic acid, antimony potassium tartrate, ammonium molybdate, and diluted sulphuric acid. The color was changed to blue. Finally, the absorption was measured by the spectrophotometer on 885-nanometer wavy length.

### 2.5. Reactive Silicate (Silicon Dioxide $\text{SiO}_2$ , $\mu\text{g/L}$ )

The reactive silicate was measured according to the method described by Rice *et al.*, 2012; Salman *et al.*, 2017; and Parsons *et al.*, 1984. A total of 25 mL of the sample was taken. Another 10 mL of ammonium molybdate was added. Then, the flask was shaken. After 10 minutes, 15 mL of the reduced solution (sulfide, oxalic acid, and sulphuric acid) was added. The sample was then left 2-3 hours until the blue color stabilizes. Finally, the absorption was measured by the spectrophotometer on the 810-nanometer wavy length.

## 2.6. Remote Sensing (RS) Processing

Data of remote sensing techniques used in this study included three Imaginary, three periods of time, Landsat-8 OLI images Shaped and rectangular dimensions path: 167 km and row: 38 km. These data were acquired on the 22<sup>nd</sup> November 2018, 24<sup>th</sup> December 2018, and 20<sup>th</sup> January 2019. These periods matched with the timing of fieldwork data collection. The images were downloaded from the United States Geological Survey (USGS, 2017; Al-Ramahi, 2020).

The Landsat images were first converted to Top-of-Atmosphere (TOA) radiance using radiometric calibration coefficients in the metadata file. ArcGIS 10.5 is the digital image processing software used to process the Landsat 8 IMAGES. Twenty-six ground control points (GCPs) were selected from the images and rectified to the UTM (Universal Transverse Mercator). World Geodetic System 1984 (WGS 84) projection using coordinates obtained from Global Positioning System (GPS), (20). For the spatial interpolation of the geometric correction, the image's original digital numbers (DNs) were preserved by subsequently using a Bilinear resampling method. After geometric correction, the images were atmospherically corrected. The atmosphere may potentially affect image by absorbing, scattering, and refracting light.

## 3. RESULTS AND DISCUSSION:

### 3.1. Analysis of Factors Affecting Algal Trait ( $\text{NO}_3$ , $\text{PO}_4$ , $\text{SiO}_2$ )

The samples were analyzed in the laboratory and extracted the values of ( $\text{NO}_3$ ,  $\text{PO}_4$ ,  $\text{SiO}_2$ ). The data was tabulated to explain it in Geographic Information Systems (GIS) programs, which is the best application program to simulate spatial data with remote sensing techniques, and through Landsat 8 satellite imagery.

### 3.2. Spatial Analysis

The spatial analysis of these samples and the simulation of the study area maps were made, aiming to know the effect of these factors on the water quality and algae present in this region. Moreover, it was intended to know the unknown areas in which it is difficult to obtain data (the prediction process). Through these six stations, data is not sufficient to cover the study area. Through the application of theories and statistical

methods used in geographic information systems (GIS) (Al Ramahi, and Al Bahadly, 2020), it was possible to know and cover the study area of Um El-Naaj lake in Al-Hweizeh marsh (Table 2).

### 3.3. Factors Affecting ( $\text{PO}_4$ ) Analysis

Phosphorus is an important nutrient, representing an intermediate component of energy metabolism (Schulze *et al.*, 2005). Phosphorus is found in many forms and may be present in the soluble or pigmented form. The pigmented way is found mainly in algae and aquatic plants (Smith, 2004). The dissolved form is found in various forms such as Orthophosphate, Polyphosphate, and the Orthophosphate may be rapidly represented by living organisms, in natural water (Wetzel and Likens, 2013). The concentration of total phosphorus raised 1.0, 0.9, and 0.8 mg/L, in January, at sites 2, 5, and 6, respectively (Table 2). The lowest concentration was found in November and December on all sites. The results of phosphorus concentrations showed a significant increase that may be a result of high water levels or rainfall that washed off phosphorus compounds from soil to the river when washing agricultural land fertilized with phosphate fertilizers (Sims and Sharpley, 2005). The high concentration of Phosphate leads to the dense growth of algae, which in turn reduces light transmittance and dissolved oxygen concentrations, resulting in slow decomposition of organic matter and nutrient recycling (McDowell and Sharpley, 2001; Adamus, 2001). On the other hand, low concentrations may be explained by the consumption of Phosphate by algae and aquatic plants (Kassim and Al-Saadi 1995) (Figures 3 and 4).

### 3.4. Factors Affecting ( $\text{NO}_3$ ) Analysis

The Nitrate is the predominant form of inorganic Nitrogen in the aquatic environment (Smith, 2004), and the variation in nitrogen compounds is due to increased human activity in agriculture and industry and the resulting residues of a container on nitrogen compounds (Johnson, 2004). The results showed that the lowest nitrate concentrations were 2.2 mg/L in November at site 6, and 3.7 mg/L in the same month, but site 5. In December, the highest concentration was 11.2 mg/L (Table 2).

The high concentration of nitrates is due to the washing of the land adjacent to the river and the erosion of the soil containing nitrogen compounds from the animal residues (Al-Nimma, 1982). The decrease in Nitrate may be due to its

consumption of revival, which is the primary source of plants in general and algae in particular (Saad and Antoine 1978) (Figure 5).

### 3.5. Factors Affecting ( $\text{SiO}_2$ ) Analysis

Silicates are widely found in Iraqi waters, and they are of great importance for diatoms as they are needed for the building of their siliceous skeletons (Goldman and Horne, 1983). Its concentration ranges from 1-10 mg.L<sup>-1</sup> in natural water. The concentration of Silica between 0.5-0.8 mg.L<sup>-1</sup> is determinant for the growth of diatoms (Reid, 1961). It plays a vital role in increasing the number of diatoms and the length of their survival (Chatterjee, 2014). High concentrations of silicate characterize Iraq waters. This is due to the geological nature of land in which Tigris and Euphrates Rivers flow. The results showed the lowest concentration of silicate was 0.4 mg/L, in November, at site 2; The highest concentration was 2.4 mg/L in June 2019 at site 6, and there were no significant spatial differences among the study sites. In general, the active silicate concentrations in the studied area exceeded the need for phytoplankton. This phenomenon is known in Iraqi waters, which have high concentrations of active silicates. The concentrations of silicates obtained are not consistent with the study of (AL-Saeedy, 2014; AL-Hassany and Hindi, 2016), shown in Figure 6.

## 4. CONCLUSIONS:

The samples were analyzed in the laboratory and extracted the values of  $\text{NO}_3$ ,  $\text{PO}_4$ ,  $\text{SiO}_2$ . The data was tabulated to analyze in Geographic Information Systems (GIS) programs. The nutrient values ranged from 0.01 - 1 mg/L for  $\text{PO}_4$ ; 2.2 - 11.2 mg/L for  $\text{NO}_3$ ; and 0.4 - 2.44 mg/L for  $\text{SiO}_2$ . Also, it can be concluded that, during the winter, the water level was increased due to rainfall; that is, the nutrients concentrations were low during the last period.

The Sample concentrations were useful in determining the acceptable water quality, which helped in the presence of a great diversity of some species in the marshes (Um El-Naaj lake). By using remote sensing techniques, maps were produced to predict the expected values surrounding the station's location as future predictive readings that compensate for the difficulty in reaching these areas.

## 5. REFERENCES:

1. Edward, G. B., and David, C. S. (2010).

- Freshwater algae identification and use as bioindicators. A John Wiley and Sons, Ltd, 101.
2. Graham, L. E., Graham, J. M., and Wilcox, L. W. (2009). *Algae*. Benjamin-Cummings Publishing Company, pp: 616.
  3. AL-Hassany, J. S., and Hindi, M. T. (2016). A Study of Epiphytic and Epipelagic Algae in Al-Dora Site/Tigris River in Baghdad Province-Iraq. *Baghdad Science Journal*, 13(4), 721-733.
  4. Salman, J.M., Jawad, H.J., Nassar, A.J., Hassan, F.M. (2013) A Study of Phytoplankton Communities and Related Environmental Factors in Euphrates River ( between Two Cities: Al-Musayyab and Hindiya), Iraq. *Journal of Environmental protection*, 4(10):1071–9.
  5. Poulíčková, A., Hašler, P., Lysáková, M., and Spears, B. (2008). The ecology of freshwater epipelagic algae: an update. *Phycologia*, 47(5), 437-450.
  6. Jarvis, P. J. (2000). *Ecological principles and environmental issues*. Pearson Education, Padstow, Cornwall, 361 pp.
  7. McDowell, R. W., and Sharpley, A. N. (2001). Approximating phosphorus release from soils to surface runoff and subsurface drainage. *Journal of environmental quality*, 30(2), 508-520.
  8. Boney, A. D. (1975). *Phytoplankton*. Camelot Press. Ltd. Southampton. 116 pp
  9. Ault, T., Velzeboer, R., and Zammit, R. (2000). Influence of nutrient availability on phytoplankton growth and community structure in the Port Adelaide River, Australia:[2pt] bioassay assessment of potential nutrient limitation. *Hydrobiologia*, 429(1-3), 89-103.
  10. Reynolds, C. S. (1984). *The ecology of freshwater phytoplankton*. Cambridge University Press, Cambridge, pp: 384.
  11. Wen, Z. Y., and Chen, F. (2000). Heterotrophic production of eicosapentaenoic acid by the diatom *Nitzschia laevis*: effects of silicate and glucose. *Journal of Industrial Microbiology and Biotechnology*, 25(4), 218-224.
  12. Hassan, F. M., Hadi, R. A., Kassim, T. I., and Al-Hassany, J. S. (2012). Systematic study of epiphytic algal after restoration of Al-Hawizah marshes, southern of Iraq. *Int. J. of Aquatic Science*, 3(1), 37-57.
  13. Lillesand, T., Kiefer, R. W., and Chipman, J. (2015). *Remote sensing and image interpretation*. John Wiley and Sons.
  14. Al Ramahi, F. K. M., and Al Bahadly, Z. K. I. (2017). Estimation of Suaeda aegyptiaca Plant distribution regions at Iraq using RS and GIS Applications. *Iraqi Journal of Science*, 58(2A), 767-777.
  15. Mashi, F.K. (2018) Monitoring AL-Hammar Marsh Topography and Climatic Applied Satellite Modis Imagery, *Indian Journal of Natural Sciences*: 8 (47); 13704-13714.
  16. Mitchel, A. (2005). The ESRI Guide to GIS analysis, Volume 2: Spatial measurements and statistics. *ESRI Guide to GIS analysis*.
  17. Mashee, F.K., and Hadi, G.S. (2017). Study the Wet Region in Anbar Province by Use Remote Sensing (RS) and Geographic Information System (GIS) Techniques. *Iraqi Journal of Science*, 58(3A), 1333-1344.
  18. Garstecki, T., and Amr, Z. (2011). Biodiversity and ecosystem management in the Iraqi Marshlands—screening study on potential World Heritage Nomination. *Amman, Jordan: IUCN*.
  19. Rice, E. W., Baird, R. B., Eaton, A. D., and Clesceri, L. S. (2012). Standard methods for the examination of water and wastewater. *American Public Health Association: Washington, DC, USA*, 10.
  20. Salman, J. M., Hassan, F. M., and Baiee, M. A. (2017). Practical methods in environmental and pollution laboratory. *Environmental Research and Studies center, University of Babylon* 144p.
  21. Parsons, T. R., Maita, Y., and Lalli, C. M. (1984). A manual of chemical and biological methods for seawater analysis. *Oxford: Pergamon*, 1, 173.
  22. Al Ramahi, F. K. M., and Al Bahadly, Z. K. I. (2020). The Spatial Analysis for Bassia eriophora (Schr.) Asch. Plant Distributed in all IRAQ by Using RS and GIS Techniques. *Baghdad Science Journal*, 17(1), 126-135.
  23. USGS (United States Geological Survey), (2017). Landsat—A Global Land-Imaging Mission.[Online] Available at: <http://remotesensing.usgs.gov>.
  24. Al-Ramahi, F. K. M. (2020). Spatial Analysis Of Radon Gas Concentration Distributed At



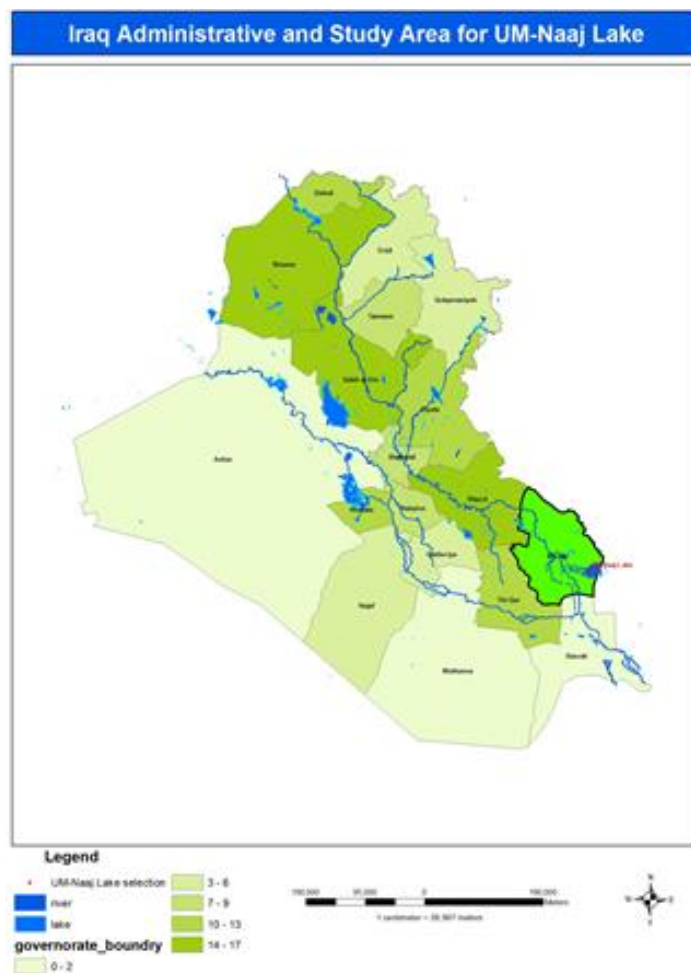
- Baghdad City Using Remote Sensing And Geographic Information System Techniques. *Iraqi Journal Of Agricultural Sciences*, 51(Special).21-32.
25. Schulze, E. D., Beck, E., and Müller-Hohenstein, K. (2005). *Plant Ecology*– Springer Berlin.
  26. Smith, R. (2004). Current methods in aquatic science. *University of Waterloo, Canada*.
  27. Wetzel, R. G., and Likens, G. E. (2013). *Limnological analyses*. Springer Science and Business Media.
  28. Sims, J. T., and Sharpley, A. N. (2005). *Phosphorus: agriculture and the environment*. American Society of Agronomy.
  29. Adamus, P. R. (2001). Indicators for monitoring biological integrity of inland, freshwater wetlands: A survey of North American technical literature (1990-2000).
  30. Kassim, T. I., and Al-Saadi, H. A. (1995). Seasonal variation of epiphytic algae in a marsh area [Southern Iraq]. *Acta hydrobiologica*, 3(37).
  31. Johnson, C.B. (2004). Capacity of Freshwater Marsh to Process Nutrients in Directed Mississippi River water Ms. Thesis , Louisiana state University and Agricultural and Mechanical College in the Department of Agronomy and Environmental Management, pp: 85.
  32. Al-Nimma, B. A. B. (1982). A study on the limnology of the Tigris and Euphrates rivers. *Sc. This University of Salahaddin Erbil, Iraq*.
  33. Saad, M. A., and Antoine, S. E. (1978). Limnological studies on the River Tigris, Iraq. II. Seasonal variations of nutrients. *Internationale Revue der gesamten Hydrobiologie und Hydrographie*, 63(5), 705-719.
  34. Goldman, C. R., and Horne, A. J. (1983). *Limnology*. McGraw-Hill.
  35. Reid, G.K. (1961). *Ecology of Inland Waters and Eusteries*. Van Nostrand Rein hold Publishing. New York, 375 pp.
  36. Chatterjee, A. (2014). Role of benthic microalgae in a coastal zone: biomass, productivity and biodiversity (Doctoral dissertation).
  37. AL-Saeedy, R. N. Q. (2014). *An Ecological study of epiphytic algae on Aquatic Macrophytes in Tigris River within Baghdad city/Iraq* (Doctoral dissertation, M. Sc. Thesis. College of Science for Women, University of Baghdad. pp: 165).
  38. AL Naqeeb, N. A., Al Hassany, J.S., and Mashi, F. K. (2020). Assessment of the water quality of Um El-Naaj Marshes by Diatoms. *Eco. Env. and Cons.* 26 (1), 405-410.
  39. Prescott, G. W. (1964). How to know the freshwater algae. *How to know the freshwater algae*. Michigan State Univ., East Lansing, pp.272.

**Table 1.** The station Location Names and global coordinate system ( $\lambda$ ,  $\varphi$ ) converted to Universal Transverse Mercator (UTM) coordinate ( $x$ ,  $y$ ).

| Stations (ST) | Stations Name (E) | Latitude Degree ( $\lambda$ ) | Longitude Degree ( $\varphi$ ) | x-axis coordinate (UTM) | y-axis coordinate (UTM) |
|---------------|-------------------|-------------------------------|--------------------------------|-------------------------|-------------------------|
| 1             | Um bzazen         | 31.617211                     | 47.603245                      | 746945                  | 3500950                 |
| 2             | AboAthba 1        | 31.644485                     | 47.636462                      | 750024                  | 3504050                 |
| 3             | AboAthba 2        | 31.634116                     | 47.636401                      | 750046                  | 3502900                 |
| 4             | Alkhabta          | 31.617198                     | 47.570533                      | 743841                  | 3500870                 |
| 5             | Aboliefia 1       | 31.611951                     | 47.670161                      | 753309                  | 3500520                 |
| 6             | Aboliefia 2       | 31.586911                     | 47.673059                      | 753652                  | 3497750                 |

**Table 2.** The concentration of  $\text{NO}_3$ ,  $\text{PO}_4$ , and  $\text{SiO}_2$  according to the station and month of analysis.

| Station | November                          |                      |                                    | December                          |                      |                                    | January                           |                      |                                    |
|---------|-----------------------------------|----------------------|------------------------------------|-----------------------------------|----------------------|------------------------------------|-----------------------------------|----------------------|------------------------------------|
|         | $\text{NO}_3$ ( $\mu\text{g/L}$ ) | $\text{PO}_4$ (mg/L) | $\text{SiO}_2$ ( $\mu\text{g/L}$ ) | $\text{NO}_3$ ( $\mu\text{g/L}$ ) | $\text{PO}_4$ (mg/L) | $\text{SiO}_2$ ( $\mu\text{g/L}$ ) | $\text{NO}_3$ ( $\mu\text{g/L}$ ) | $\text{PO}_4$ (mg/L) | $\text{SiO}_2$ ( $\mu\text{g/L}$ ) |
| St1     | 4                                 | 0.035                | 0.666                              | 4.23                              | 0.048                | 0.666                              | 3.33                              | 0.432                | 1.67                               |
| St2     | 5.12                              | 0.069                | 0.45                               | 6.21                              | 0.79                 | 0.475                              | 4.97                              | 0.839                | 1.01                               |
| St3     | 6.5                               | 0.051                | 0.625                              | 6.62                              | 0.067                | 0.725                              | 4.88                              | 0.72                 | 0.68                               |
| St4     | 3.72                              | 0.032                | 0.642                              | 4.29                              | 0.011                | 0.681                              | 3.77                              | 0.627                | 0.98                               |
| St5     | 5.32                              | 0.014                | 0.663                              | 11.2                              | 0.121                | 0.71                               | 7.2                               | 0.917                | 1.5                                |
| St6     | 2.2                               | 0.012                | 0.567                              | 8.72                              | 0.181                | 0.7                                | 8.31                              | 1.02                 | 2.44                               |



(a)



(b)

(c)



(d)

**Figure 1.** (a) represents Iraq Administrator; (b) the satellite Landsat imagery; (c) Study Area Site in Maysan city; and (d) Observation station name in study area Um El-Naaj lake including the six stations. Note: The study was conducted during three months, from November 2018- January 2019.



**Figure 2.** Types of Epiphytic algae affixed to aquatic plants in one of the station sites, which contribute to the ecosystem and a major nutrient.

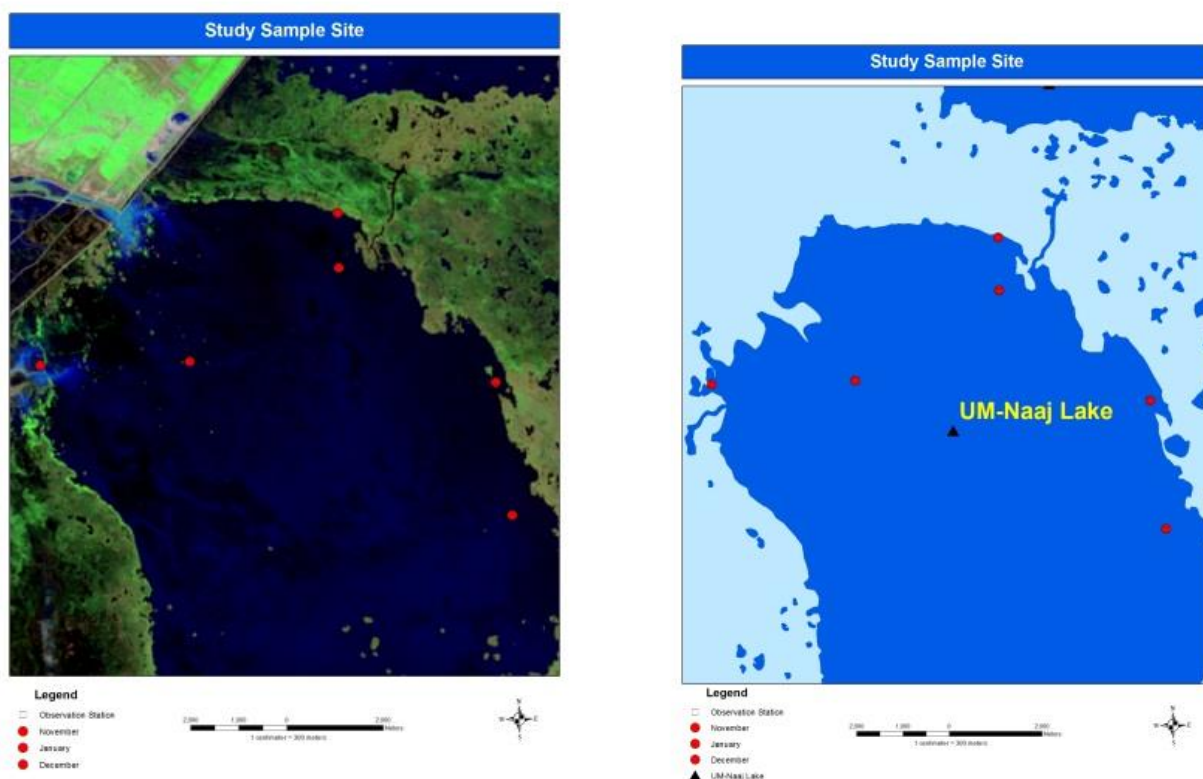


**Figure 3.** Study Area. The satellite Landsat imagery 8 is representing composite bands (4, 3, 2); The form shapefile (polygon) simulated study area as Um El-Naaj lake Station site.



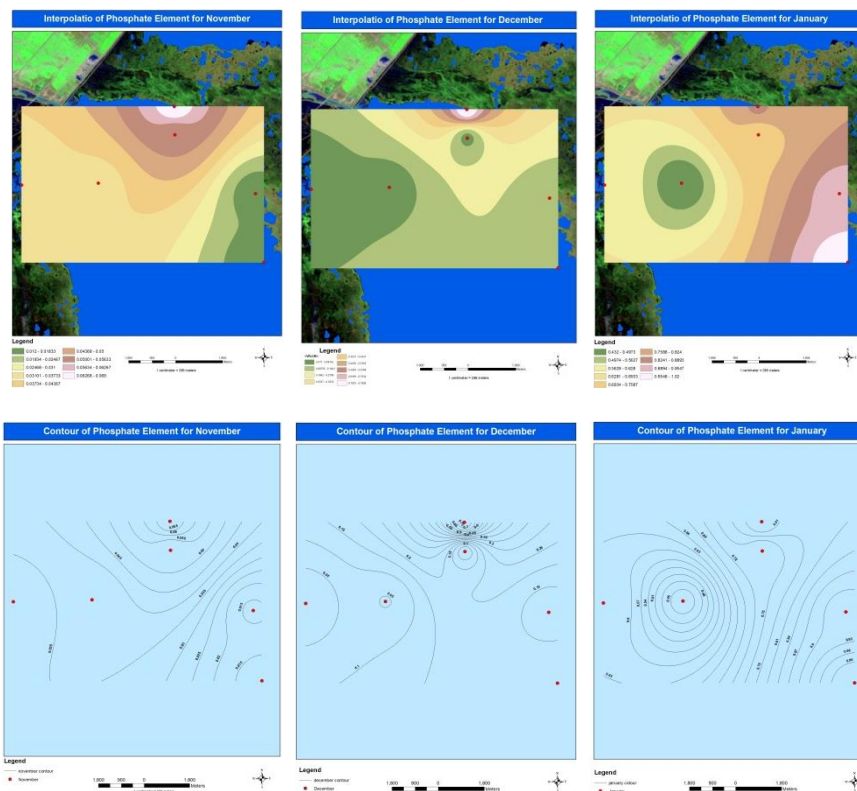


**Figure 4.** Factors Affecting Phosphorus ( $\text{PO}_4$ ) Analysis, applied Interpolation and contour line techniques for all six observation stations in November, December, and January and remarked the  $\text{PO}_4$  values.

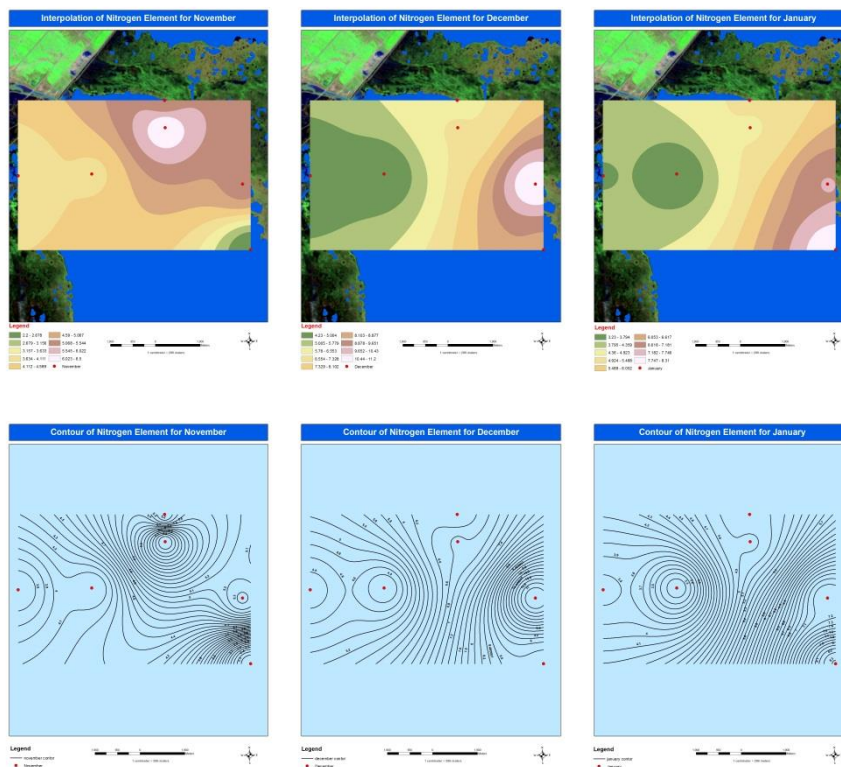


**Figure 5.** Factors Affecting Nitrate ( $\text{NO}_3$ ) Analysis, applied Interpolation and contour line techniques for all six observation stations in November, December, and January and remarked the  $\text{NO}_3$  values.

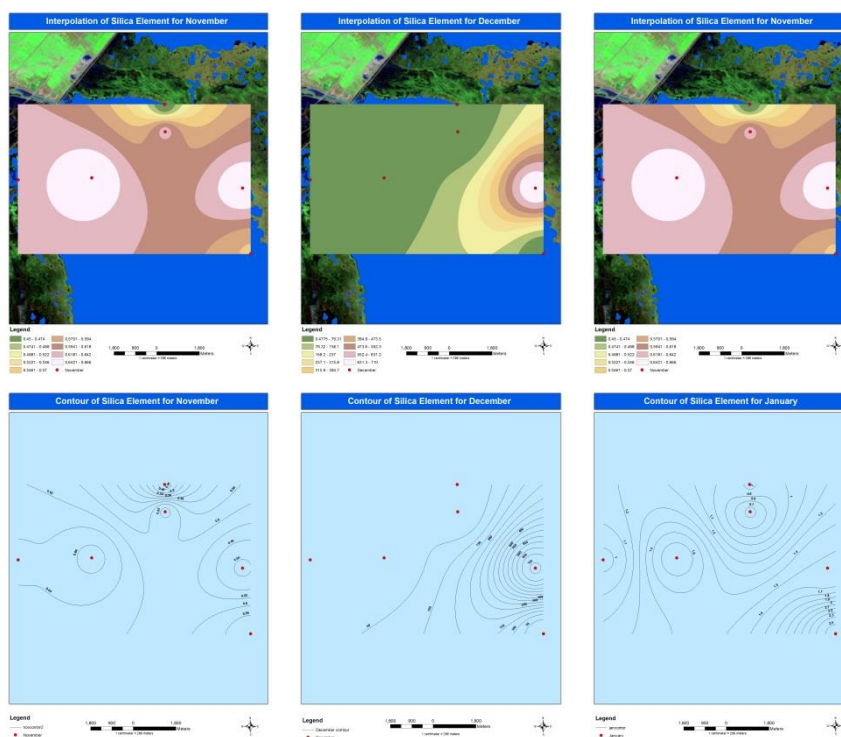


**Figure 6.** Factors Affecting Silica (SiO<sub>2</sub>) Analysis, applied Interpolation and contour line techniques for all six observation stations in November, December, and January and remarked the Si values.

**ESTUDOS EXPERIMENTAIS DO GRÃO DE CEVADA DE BAISHESHEK PROCESSADO PELA MISTURA DE ÍON-OZÔNIO****EXPERIMENTAL STUDIES OF THE BAISHESHEK BARLEY GRAIN PROCESSED BY THE ION-OZONE MIXTURE****ЭКСПЕРИМЕНТАЛЬНЫЕ ИССЛЕДОВАНИЯ ЗЕРНА ЯЧМЕНЯ «БАЙШЕШЕК», ОБРАБОТАННОГО ИОН-ОЗОННОЙ СМЕСЬЮ**

IZTAYEV, Auyelbek<sup>1</sup>; BAIBATYROV Torebek<sup>2</sup>; MUKASHEVA Tarbiye<sup>3</sup>; MULDABEKOVA, Bayan<sup>4</sup>; YAKIYAYEVA, Madina<sup>5\*</sup>;

<sup>1,4,5</sup> Almaty Technological University, Department of Technology of bread and processing industries, 100 Tole Bi st., zip code 050012, Almaty – Kazakhstan

<sup>3</sup> Kostanai Engineering and Economic University named after M. Dulatov, Faculty of Engineering and Technology, 59 Chernyshevsky str., zip code 110000, Kostanay – Kazakhstan

<sup>2</sup> Zhangir Khan West Kazakhstan agrarian-technical University, Department of Food Processing Technologies, 51 Zhangir Khan str., zip code 090009, Uralsk – Kazakhstan

\* Correspondence author  
e-mail: yamadina88@mail.ru

Received 09 March 2020; received in revised form 11 May 2020; accepted 23 May 2020

**RESUMO**

O artigo apresenta os resultados de um estudo experimental do grão de cevada da cultivar Baisheshek tratado com uma mistura de íon-ozônio. O objetivo deste estudo foi desenvolver uma tecnologia inovadora para o processamento de cevada com uma mistura íon-ozônio, a fim de aumentar seus parâmetros tecnológicos, produtividade, qualidade e segurança de grãos. O Cazaquistão aumentou drasticamente a exportação de cevada e todos os agrônomos, produtores e criadores estão migrando ativamente para o desenvolvimento dessa cultura, enquanto aumentam a produção, a produtividade, melhoram a qualidade do produto, reduzem suas perdas e garantem a segurança do armazenamento, que é uma tarefa urgente. Os microrganismos desempenham um papel importante durante o armazenamento, estes penetram nos produtos agrícolas de várias maneiras e, se caírem em condições desfavoráveis de armazenamento após a colheita, os produtos agrícolas se deterioram rapidamente, substâncias nocivas se acumulam - toxinas, fungos e outros, o que reduz o valor da mercadoria. Para resolver esses problemas, foram realizados estudos experimentais em cevada da cultivar Baisheshek, tratada com uma mistura de íon-ozônio com e sem o uso de pressão excessiva (cavitação). O delineamento fatorial completo calculado das experiências dos 2<sup>3</sup> (8 experimentos) e 2<sup>4</sup> (16 experimentos) possibilitou a obtenção de equações de regressão descrevendo a alteração nas propriedades semente, físicos bioquímicos e fisiológicas da cevada de Baisheshek. A solução de um modelo abrangente de otimização de programação para diferentes indicadores de cevada permitiu estabelecer ótimos modos de processamento tecnológico e níveis alcançáveis de qualidades tecnológicas de grãos. O efeito da tecnologia proposta para o tratamento de íons ozônio e cavitação íon ozônio foi a mistura do íon ozônio, que produz a desodorização, desinfecção de grãos, de acordo com processos físicos e químicos, aumenta o valor biológico, acelera os processos de metabolismo de grãos. Os estudos realizados para melhorar a germinação, viabilidade e força de crescimento mostram uma imagem bastante clara em termos de seu valor final. Observações fenológicas mostraram que os efeitos do tratamento com cavitação íon ozônio e cavidade íon ozônio são desencadeados após 25 a 30 dias. Verificou-se que a maior tendência à superioridade é observada no tratamento da cavitação íon ozônio, seguido pelo íon ozônio, e a amostra de controle está significativamente atrás.

**Palavras-chave:** cevada, variedade, de tratamento, de íon-ozônio, cavitação.

**ABSTRACT**

The article presents the results of an experimental study of Baisheshek barley grain treated with an ion-

ozone mixture. This study aims to develop an innovative technology for processing barley with an ion-ozone mixture in order to increase their technological parameters, yield, quality, and grain safety. Kazakhstan has sharply increased the export of barley, and all agronomists, producers, and breeders are actively moving to the cultivation of this crop, while increasing production, productivity, improving product quality, reducing their losses and ensuring storage safety are an urgent task. Microorganisms play an important role during storage, they fall into crop production in a variety of ways, and if they fall into unfavorable storage conditions after harvesting, crop production quickly deteriorates, harmful substances such as toxins, mold, and others accumulate in it, which reduces the commodity value. To solve these problems, experimental studies were conducted on barley of the Baisheshek cultivar treated with an ion-ozone mixture with and without using excess pressure (cavitation). The calculated full-factorial design of experiments of the 2<sup>3</sup> (8 experiments) and 2<sup>4</sup> (16 experiments) degrees made it possible to obtain regression equations describing the change in the seed, physico-biochemical, and physiological properties of barley of the Baisheshek variety. The solution of a comprehensive model for optimizing programming for different barley indices made it possible to establish optimal technological processing modes and achievable levels of technological qualities of grain. The effect of the proposed technology for ion-ozone and ion-ozone cavitation treatment is the ion-ozone mixture, which produces deodorization, disinfection of grain, following chemical-physical processes, increases biological value, accelerates the processes of grain metabolism. Studies conducted to improve germination, viability, and growth strength show a reasonably clear picture in terms of their ultimate value. Phenological observations showed that the effects of ion-ozone and ion-ozone cavitation treatment is triggered after 25-30 days. It was found that the greatest tendency for superiority is observed with ion-ozone cavitation treatment, followed by ion-ozone, and the control sample is significantly behind.

**Keywords:** *barley, variety, treatment, ion-ozone, cavitation.*

## АННОТАЦИЯ

В статье приведены результаты экспериментальных исследований зерна ячменя «Байшешек», обработанного ион-озонной смесью. Целью данного исследования является разработка инновационной технологии обработки ячменя с ион-озонной смесью с целью повышения их технологических показателей, урожайности, качества и обеспечения безопасности зерна. Казахстан резко нарастил экспорт ячменя и все агрономы, производители и селекционеры активно переходят к выращиванию этой культуры, при этом увеличение производства, урожайности, повышения качества продукции, сокращение их потерь и обеспечение безопасности при хранении являются актуальной задачей. При хранении большую роль играют микроорганизмы, в растениеводческую продукцию они попадают разнообразными путями и если они попадают после уборки урожая в неблагоприятные условия хранения, то растениеводческая продукция быстро портится, в ней накапливаются вредные вещества – токсины, плесень и другие, что снижает товарную ценность. Для решения данных проблем были проведены опытно-экспериментальные исследования ячменя сорта «Байшешек», обработанного ион-озонной смесью с и без использования избыточного давления (кавитация). Рассчитанные полнофакторные планирования экспериментов 2<sup>3</sup> (8 опытов) и 2<sup>4</sup> (16 опытов) степени позволили получить уравнения регрессии, описывающие изменение семенных, физико-биохимических и физиологических свойств ячменя сорта «Байшешек». Решение комплексной модели оптимизации программирования по разным показателям ячменя позволило установить оптимальные технологические режимы обработки и достижимые уровни технологических качеств зерна. Эффектом предлагаемой технологии по ион-озонной и ион-озон-кавитационной обработке является ион-озонная смесь, которая производит дезодорацию, дезинфекцию зерна, в соответствии с квантовофизическими процессами, повышает биологическую ценность, ускоряет процессы метаболизма зерна. Проведенные исследования, направленные на повышения всхожести, жизнеспособности и силы роста показывают достаточно четкую картину в смысле их окончательной ценности. Фенологические наблюдения показали, что эффекты от ион-озонной и ион-озонной кавитационной обработки срабатывает через 25-30 дней. Были установлены, что наибольшая тенденция превосходства наблюдается при ион-озонной кавитационной обработке, затем следует ион-озонная, а контрольный образец существенно отстает.

**Ключевые слова:** *ячмень, сорт, обработка, ион-озон, кавитация.*

## 1. INTRODUCTION

Carriers of electricity in liquids are called ions: cations (positive ions, that are atomic ions) and anions (negative ions, that are molecular ions). Studying the effect on animals and

vegetation of animals only atomic and only molecular ions obtained artificially immediately revealed a remarkable difference in the biological effect of ions: molecular air ions turned out to be a biologically beneficial factor, atomic air ions most often had an adverse or even harmful effect



on the body. After it was firmly established in many experiments that molecular ions have a beneficial effect on the viability of animals and plants, increasing their growth and weight, protecting against several diseases, contributing to the conservation and proceeding from some theoretical facts, it was found that the carrier of negative charges polarity in atmospheric air is the oxygen of this air (Maemerov *et al.*, 2006; Urazaliev, 2012; Sagitov *et al.*, 2012).

Grains infected with pathogenic microorganisms are often the cause of mass human diseases and the death of birds and animals, and products prepared from them quickly deteriorate, harmful substances (toxins) accumulate, which reduces nutritional value. Of particular danger are mold fungi, which cause the accumulation of toxins in the finished product. The most dangerous is the complex toxin is aflatoxin, which affects both individual organs and entire body systems. Thus, microorganisms not only lead to the development of infection, but also to toxicosis, which causes great harm to humans, animals, and birds – inhibits growth and development, with severe bactericidal pollution lead to death (Naleev, 1993; Malin, 2005; Tikhonov *et al.*, 2006; Voblikov *et al.*, 2001).

The solution to this problem is ozone technology. The practical application of ozone technology was carried out in the research laboratory of food and processing industries of the Almaty Technological University, which allows cleaning grain, disinfection, increasing yields up to 20%, acquiring good sowing qualities with hereditary transmission to their offspring (Kokhmetova *et al.*, 2014; Maemerov, 2004).

In post-harvest processing, get refined crop products, improve the baking qualities of wheat. By combining the electrical circuits of the ionizer and ozonator installation, an ion-ozonator installation is developed that neutralizes all harmful synthesized impurities. As a result, a pure ion-ozone mixture without harmful side impurities is obtained. The oxides of nitrogen and carbon, together with other harmful impurities and radiation during the synthesis of the ion-ozone mixture in the ion-ozonator installation, are neutralized.

The technology of ion-ozone cavitation treatment of seeds of sowing grain materials is environmentally safe and does not use chemicals and types of radiation harmful to humans, animals, and the environment.

The use of a cavitation installation before sowing almost destroys insect pests, eliminates

the need for pesticides, eliminates plant diseases, activates plant growth forces and eliminates the lack of nitrogen and water in plant leaves, which will significantly reduce chemical and soil pollution pesticides and reduce the use of mineral fertilizers (Erkmen, 2001; Akulichev, 1978; Pirsol, 1975; Ivanov, 1980; Maemerov *et al.*, 2011).

Structural and functional changes in the membrane formations of cells and intracellular organelles, which in our understanding are targets of ion-ozone cavitation, are the basis for increasing the biological value of the processed seed and food grains and obtaining the effect.

As a result of this interaction, a physicochemical basis is created for changing metabolic processes associated with proton and electron transfers in cell membranes. On this basis, successive nonspecific reactions of the cell and the organism as a whole arise. Differences exist only in the biophysical subtleties of the interaction of ion-ozone cavitation and biological tissues (Sereev, 2014; Baymagambetova *et al.*, 2014; Kim *et al.*, 2003).

The technical solution to the problem is achieved by the simultaneous processing of the moistened grain with an ion-ozone mixture in the cavitation zone with an overpressure of 2.0-6.0 at in the moistened grain processing tank with a grain processing exposure of 5.0 to 20.0 minutes, with an ozone concentration of 2.0 to 6.0 mg/m<sup>3</sup>, molecular ions from 1000 to 5000 m<sup>3</sup>. After the processing time has elapsed in the tank for ion-ozone processing of moistened grain, a sharp discharge of excess pressure to atmospheric pressure occurs (Iztaev *et al.*, 2013; Iztaev *et al.*, 2018c).

Ion-ozone treatment of moistened grain in the cavitation field is carried out at an ozone concentration of 2 mg/m<sup>3</sup> to 6 mg/m<sup>3</sup> and from 1000 units/cm<sup>3</sup> to 50,000 units/cm<sup>3</sup> of molecular oxygen ions, depending on:

- increase the biological value (2,0–10,0 mg/m<sup>3</sup>);
- destruction of harmful microorganisms and grain pests, grain disinfection, and rodent disinfection (20,0–80,0 mg/m<sup>3</sup>) (Iztaev *et al.*, 2018a).

At the post-harvest stage, to obtain purified grain mass from pests improved the technological qualities of grain crops. From year to year, environmental requirements are violated, and in this regard, special attention is being paid to the food safety of foodstuffs consumed by the

population. In meeting the requirements of environmental friendliness and safety of the production of products from seed preparation, in the processes of cultivation, harvesting, transportation, primary processing at grain enterprises, storage, and further processing, the production of flour, cereals, animal feed, bread, pasta, flour and confectionery products and other food products first of all pay attention to the original quality of crops used for this chain (Urazaliev *et al.*, 2010; Knapp *et al.*, 1974).

In this regard, special experimental studies have been carried out to identify the environmental friendliness and food safety of ion-ozone and ion-ozone cavitation technology, processing by electro-ion-charged particles of the air-flow during the cultivation of grain crops.

To improve the seed, yield and technological qualities of grain during short-term and long-term storage, ion-ozone flow processing of grain products in a stream of electrically charged particles is effective, which makes it possible to use the potential of biological and environmental resources.

In order to increase the efficiency of the use of crop products, scientists of the Almaty Technological University have developed various electrophysical methods for processing, storage, and processing of crop products: ion-ozone, ion-ozone cavitation processing of crop products, which contribute to improving the quality and preservation of grain.

The controlled effect on the biological environment of the ion-ozone mixture using ion-ozone cavitation allows for intensive bubbling of biological products of crop production with activation and stimulation, as well as inhibiting viruses, bacteria, spore formations with a delay in the flow of physiological and physicochemical processes in them, with suppression their infectious activity (Tursunbayeva *et al.*, 2019; Iztayev *et al.*, 2018b; Yakiyayeva *et al.*, 2016).

## 2. MATERIALS AND METHODS

The object of the study is the pre-sowing ion-ozone, ion-ozone cavitation treatment of the pre-sowing material, as well as the treatment of sprouts of crop products in the field in the zone of charged particles of molecular and atomic ions. As an object of research, plots of Baisheshek barley varieties were prepared for the treatment of green plants in the full earing phase.

The following regulatory documents were used in this work: GOST 10845-98. Grain and products of its processing. Method for the determination of starch; GOST 10846-91. Grain and products of its processing. Method for determination of protein; GOST 12041-82. Seeds of crops. Method for determination of moisture content; GOST 12042-80 Seeds of crops. Methods for determining the mass of 1000 seeds; GOST 10968-88. Grain. Methods for determining germination energy and germination capacity; ST RK GOST R 51411-2006 Grain and products of its processing. Method for the determination of ash.

Such indicators as the energy of germination and germinability belong to seed characteristics. As seed germinability, there is understood the quantity of normally germinated seeds in the test, taken for the analysis, evaluated as a percentage. The energy of the germination of seeds characterizes an aggregate of the appearance of normal germinants for the term fixed for each culture.

The seeds are couched in the germinators or Petri dishes, placed in the thermostat with a specified temperature condition. As a ground litter (bed), use quartz sand or filter paper. Quartz sand for decontamination has to be well washed and calcined, and filter paper must be sterilized in an exsiccator at a temperature of 130°C within 1 hour. The ground litter is damped before the seed sprouting: quartz sand - to 60% of the full moisture and filter paper and gauze - completely, allowing draining of excess water.

If the seeds are couched on filter paper, then they are arranged in rows at a distance of not less than 0,5-1,5 cm from each other over the ground litter, which is placed on the bottom of the germinator in 2-3 layers. The germinators are closed by the glass plates and are placed in the thermostat. On each of them, there is stuck down a label with the indication of the sample number and test, date of seed laying, and dates of determination of germinability and energy of germination. The majority of grain crops and leguminous plants are couched at a constant temperature of 20 °C. It is necessary to check constantly moistening of the ground litter, without allowing its drying.

The sprouted seeds are counted in two terms: in 3-5 days for determination of the energy of germination and in 7-10 days for determination of germinability. Both indicators are expressed as a percentage of the sprouted seeds to their total in the test. Sprouted seeds are considered those

at which the rootlets or one main rootlet have a length not less than the length of a seed, and a sprout is not less than half of the length of the seed. Average values of germinability and energy of germination of seeds are considered reliable if deviations are expressed in all four tests within  $\pm 2\%$  at average germinability from 98 to 100%;  $\pm 3\%$  – at 95-97,9%,  $\pm 4\%$  – at 90-94, 9% and  $\pm 5\%$  – at 85-89,9%. Otherwise, average values are fixed by the three tests if deviations in them don't exceed admissibly; or the analysis is repeated again if admissible values have only two tests (Odjo *et al.*, 2018; Morales-de la Peña *et al.*, 2019; Naumenko *et al.*, 2018; Singh *et al.*, 2015).

In experimental studies, two methods of processing crops were studied:

- ion-ozone treatment of cereals;
- ion-ozone cavitation treatment of cereals.

Carriers of electricity in liquids are called ions: cations (positive ions, that are atomic ions) and anions (negative ions, that are molecular ions). Ions of air allowed to solve a number of mysteries of atmospheric electricity (thunderstorms, lightnings, electrical conductivity of gases, and others).

Molecular ions differ from atomic ions in greater mobility, greater diffusion coefficient, "greater ionizing force". It has been established that molecular ions arise in the air due to oxygen molecules, and atomic ions due to nitrogen and carbon dioxide molecules.

By combining the electrical circuits of the ionizer and ozonator installation, an ion-ozonator installation has been developed that neutralizes all harmful synthesized impurities, as a result, a pure ion-ozone mixture is obtained without harmful impurities. Oxides of nitrogen and carbon, together with other harmful impurities and radiation during the synthesis of the ion-ozone mixture in the ion-ozonator installation, are neutralized.

When the corresponding voltage of the electric current is applied to the electrodes of the ion-ozonizer, an ion-ozone mixture is formed, in accordance with Figure 1, namely, in the ozone generator, the primary processes of ozone formation from air proceed depending on the amount of applied energy. In accordance with the energy potential, the electrons in the ionization volume in the electric field of the ozone generator accelerate, ionizing the gas, creating an avalanche of new electrons. In this case, the emission of

electrons from the cathode to the anode is formed by positive ions, subsequently rushing towards the cathode, also ionizing neutral atoms and molecules, forming negative ions. Upon collision with the cathode, ions knock electrons out of it, which, falling into the volume, again cause ionization.

Excitation of an oxygen molecule occurs at an electron energy of 6.1 eV and all free electrons are captured by oxygen molecules, as a result of electron energy of 12.2 eV, molecular ions are formed and, with an increase in energy within 19.2 eV, dissociation occurs in oxygen and with the participation of the atom and molecular ions, when the molecule is excited, ozone formation occurs (Figure 2).

Along with this, oxygen, molecular and atomic ions, nitrogen and carbon oxides, atomic oxygen, atomic ozone, and others are formed. With the appropriate energy, the formation of ions, electrons, and molecules is associated with their collision with other particles (electrons, atoms, ions). In this case, the formation of positive ions and free electrons from atoms or molecules with an appropriate degree of ionization accompany the origin of impact ionization. The probability of the occurrence of impact ionization is characterized by an effective ionization cross-section and depends on the kind of ionizable and bombarding particles, depending on the kinetic energy with a certain minimum (threshold) value. This minimum value is probably equal to zero, and, with an increase in energy above the threshold, it first rapidly increases, reaches a maximum, and then, with corresponding energy potentials, decreases (Iztayev *et al.*, 2018d; Kalinina *et al.*, 2016).

The energy that needs to be reported to an atom (molecule) for its ionization is called the ionization energy. If the energy transferred to ionized particles in collisions is large enough, then under certain conditions, a particle can ionize in collisions. In this case, only part of the energy necessary for ionization is transferred to it, and first, the atoms (molecules) in the primary collisions are transferred to the excited state, after which shock ionization occurs, and it is enough to tell the missing energy (equal to the difference between the ionization energy and the excitation energy), multistage ionization occurs. It is possible if collisions occur so often that the particle in the interval between two collisions does not have time to lose the energy received in the first of them. And also, in the same cases when the particle has metastable states, and with

the ability to conserve the excitation energy relatively long, multiple ionization occurs.

The processes associated with impact, multistage, and multiple ionization play an important role in the synthesis of ozone, which occurs in a strong electric field of an ion-ozonator generator. As a result, in such a field, the electrons in the conduction band acquire kinetic energy greater than the bandgap, and electrons are knocked out of the valence band of the molecules with the transformation of the energy of other molecules. At a certain critical field strength, impact, multistage, and multiple ionization leads to a sharp increase in current density, to an increase in ozone concentration, and in the absence of regulation of the energy potential, with repeated ionization, the electrical breakdown is possible.

The ability to transform the energy of nitrogen and carbon into an increase in ozone concentration shows that with an increase in the voltage of the electric current in the ozone generator from 0.5 to 3.0 kV, the rate of ozone formation is higher than after impact ionization. The intensity of ozone formation increases, apparently due to the transformation of the energy of nitrogen and carbon, since the degree of oxygen ionization is 13.618 eV, nitrogen - 14.53 eV, and the degree of carbon ionization - 11.26 eV. When the corresponding energy is supplied during the ionization period, the nitrogen and carbon atoms are able to attract electrons. Namely, the nitrogen atom attracts one electron into the outer orbit, the carbon atom two electrons. As a result, six electrons are obtained in the outer orbit of the nitrogen and carbon atoms, which corresponds to the number of oxygen electrons. Nitrogen and carbon atoms, transforming into oxygen, contribute to the synthesis of ozone.

At the same time, an ion generator having an electric charge of negative polarity produces molecular ions and attracts atomic ions, nitrogen, and carbon oxides having an electric charge of positive polarity, knocking out oxygen not only from the ozone synthesized by it but also from the environment. The synthesized ozone, oxygen, molecular ions, having a negative polarity, slip through an ozone generator having a negative polarity of the electric current and, interacting with each other, form oxygen, and then ozone. Molecular ions, combining with a neutral atom, form a stable molecular ion, and with further connection with the electron 9, form a heavy molecular ion 10.

Positive ion 11 and other positively charged particles from the environment rush to the ion generator, where they are neutralized. Further, ozone enters into a chemical reaction with biological substances or, as an unstable gas, decomposes into oxygen, which subsequently forms other compounds. With a positive polarity of the ion generator 6, we obtain the components of the positive sign ion-ozone technology, that is, atomic ozone, atomic oxygen and atomic ions, nitrogen and carbon oxides harmful to all living things.

Ion-ozone cavitation occurs as a result of a local critical increase in excess pressure above 4 at and a sharp release of excess pressure to the atmospheric environment during product processing. And they can also occur either with an increase in its velocity or with the creation of a sharp drop in excess pressure during the half-cycle of rarefaction (acoustic ion-ozone cavitation), there are other reasons for the effect. Moving with the flow to a region with a higher overpressure or during the half-compression period, the cavitation bubble filled with the ion-ozone mixture slams, emitting a shock wave with an ozone explosion, which facilitates the interaction of the ion-ozone mixture with the processed product. At the same time, bubbling, instant destruction of microorganisms, pests of products of biological origin, on the basis of quantum-physical processes in comparison with similar technologies occurs intensively, the biological value of the product increases more, resistance to external irritants is acquired, and the time of the positive effect of ion-ozone interaction on the processed product is reduced.

Usually, this is achieved due to a critical overpressure of 4 at or more with a sharp release of excess pressure to atmospheric pressure, the design of hydroturbines, or by passing an ion-ozone mixture through a ring-shaped opening that has a narrow inlet and a significantly larger outlet: a forced decrease in pressure leads to ion-ozone cavitation since the ion-ozone mixture tends to the side of a larger volume (with increasing pressure, ozone acquires potential energy to explode). This method can be controlled by devices that control the size of the inlet, which allows you to adjust the process in various environments. The outer side of the mixing valves, along which the ion-ozone-cavitation bubbles move in the opposite direction to cause implosion (internal explosion), is subjected to tremendous pressure and is often made of heavy-duty or rigid materials, for example, stainless steel, stellite. This device is

called the ion-ozone cavitation installation (Kalinina *et al.*, 2018; Zhakatayeva *et al.*, 2020; Zapevalov *et al.*, 2015).

Grain processing was carried out on an experimental ion-ozone cavitation installation, consisting of an ion-ozonator generator 1 and a cavitation capacity 2 (Figure 3).

During ion-ozone treatment, crops are loaded into an ion-ozone cavitation unit pre-filled with an ion-ozone mixture with an ozone concentration of 0.5 mg/dm<sup>3</sup> to 4 mg/dm<sup>3</sup> (or from 0.5·10<sup>-3</sup> to 4·10<sup>-3</sup> mg/cm<sup>3</sup>) and molecular ions ranging from 500 to 60,000 units/cm<sup>3</sup>. In this case, the ratio of ion concentration (units/cm<sup>3</sup>) to ozone concentration (mg/cm<sup>3</sup>)  $C_{i/o}$  is (1-15)·10<sup>-6</sup> units/mg, that is 1-15 million units/mg. Then for 10 to 20 minutes produce ion-ozone ventilation of crops.

In the case of ion-ozone cavitation treatment of grain after ventilation, the cavitation installation is hermetically closed, and the ion-ozone mixture is pumped into the tank until an overpressure of 2 to 4 at is created, after which the overpressure is sharply discharged, while the ozone tends to explode. In this case, a sharp discharge of excess pressure and the power of an ozone explosion adds up. During the explosion, cavitation processes occur, in which the pores of the treated cultures increase, the ion-ozone mixture penetrates more efficiently. At the same time, ozone destroys harmful impurities, and harmful insects, molecular oxygen ions based on quantum-physical processes increase the biological value of the product.

The following factors were selected as factors affecting the properties and quality indicators of the treated crops:

- ratio of ion concentration (units/cm<sup>3</sup>) to ozone concentration (mg/cm<sup>3</sup>)  $C_{i/o}$ , units/mg;
- overpressure (for cavitation treatment)  $P$ , at;
- sample moisture before processing  $w$ , %;
- processing time  $t_1$ , min.

In the experiments for all the studied crops, the following quality indicators were determined:

- $y_1$  – germination energy, %;
- $y_2$  – germination in 5 days, %;
- $y_3$  – germination in 7 days, %;
- $y_4$  – humidity after processing, %;
- $y_5$  – nature, g/l;
- $y_6$  – grain density, g/cm<sup>3</sup>;

- $y_7$  – weight of 1000 grains, g;
- $y_8$  – protein, %;
- $y_9$  – starch, %;
- $y_{10}$  – greenery index, ml.

The same quality indicators were also determined for control (untreated) grain samples.

To optimize the processing regimes of grain crops, the following indicators were selected as target functions:

- for seed properties – germination energy ( $y_1$ );
- for physical properties – density ( $y_6$ );
- for biochemical properties – protein ( $y_8$ );

The rest of the above grain quality indicators were considered as limitations.

### 3. RESULTS AND DISCUSSION

Given the relatively large number of factors, in order to reduce the number of experiments and obtain reliable results in the studies, methods for planning multi-factor experiments were used, in particular, the use of plans for full factor experiments (FFE) of the FFE-2<sup>3</sup> type (for ion-ozone treatment) and FFE-2<sup>4</sup> (for ion-ozone cavitation treatment).

Based on the least-squares studies of the developed algorithms and sequential regression analysis programs (Ostapchuk *et al.*, 1992; Ostapchuk, 2007), regression equations were obtained that adequately (according to the Fisher's Criterion) describe the dependences of the above quality indicators of processed crops, respectively, on conditions and modes of their ion-ozone (IO) and ion-ozone cavitation treatment (IOC).

The concentration of ozone in the ion-ozone mixture is from 2.0 to 6.0 g/m<sup>3</sup>, molecular ions from 1000 to 50,000 units/cm<sup>3</sup>. Exposure time from 5 to 20 min, which is determined to a greater extent by the quality and infection of the grain.

The optimal regimes of ion-ozone processing of seed and food grains identified during experimental studies are of practical value, which made it possible to develop, with a refinement in the engineering calculation of the plant parameters, and to create a laboratory-controlled ion-ozone mixture for processing seed

and food grains.

Quality indicators of control (unprocessed) cereal crops are given in Tables 1. The matrices for planning experiments with the experimental conditions and the results of determining the quality indicators of the treated crops are given in Tables 2 and 3.

here:

$C_{i/o}$  – ratio of ion concentration (units/cm<sup>3</sup>) to ozone concentration (mg/cm<sup>3</sup>), units/mg;  
 $P$  – overpressure (for cavitation treatment), at;  
 $w$  – sample moisture before processing, %;  
 $t_1$  – processing time, min.  
 $y_1$  – germination energy, %;  
 $y_2$  – germination in 5 days, %;  
 $y_3$  – germination in 7 days, %;  
 $y_4$  – humidity after processing, %;  
 $y_5$  – nature, g/l;  
 $y_6$  – grain density, g/cm<sup>3</sup>;  
 $y_7$  – weight of 1000 grains, g;  
 $y_8$  – protein, %;  
 $y_9$  – starch, %;  
 $y_{10}$  – greenery index, ml.

The regression equations obtained based on processing the results of the experiments are given below in the corresponding mathematical models used in optimizing the processing regimes of the cultures studied. All the equations obtained adequately describe the experimental data.

From the data in Tables 1 to 3, it can be seen that during processing, the preparation of seeds of barley of the Baisheshek variety requires bioenergetic activation due to ion-ozone and ion-ozone cavitation treatment. As a result, the germ cells of these cultures pass from the deceased to an active state, and the seed germination energy is manifested rapidly.

With ion-ozone and ion-ozone cavitation treatment of seeds of grain crops, the energy of germination and germination of seeds is significantly increased. It accelerates their germination, increases the productivity of agricultural plants, and the technological quality of food products by 25-30 %. After ion-ozone cavitation treatment of barley seeds, the biological and nutritional value of processed grain seeds increases more intensively due to increased accumulation of proteins, sugars, organic acids, vitamins, and macronutrients in them.

Ion-ozone treatment of the dry and wet state of seeds of grain crops helps to maintain

stability during the storage of barley varieties without increasing acidity and respiratory rate. Ion-ozone cavitation treatment of the dry and wet state of grain seeds allows creating more favorable conditions for the storage of barley varieties compared to ion-ozone treatment.

Data processing and calculations were carried out using the algorithm developed by the Odessa National Academy of Food Technologies and the sequential regression analysis program PLAN. The program first gives the values of all the regression coefficients and their confidence intervals (errors), then checks the significance of the regression coefficients and, after removing all the insignificant coefficients, the remaining significant coefficients and their confidence errors are printed.

Mathematical models of ion-ozone seed treatment of grain crops are shown in table 4.

here:

$y_{ger}$  – germination, %;  
 $x_2$  – overpressure, at;  
 $s_y, s_{ag}$  – Root mean square deviation;  
 $F_r, F_{cr}$  – Fisher's Criterion;  
 $t_{cr}$  – Student Criterion.

Restrictions on the range of variation in the regime parameters of ion-ozone treatment of all the investigated cereal crops were as follows:

$$1 \text{ mln. unit/mg} \leq C_{i/o} \leq 15 \text{ mln. unit/mg}$$

$$13 \% \leq w \leq 20 \%; 10 \text{ min} \leq t_1 \leq 20 \text{ min}$$

The mathematical model for optimizing the modes of ion-ozone treatment of barley of the variety Baisheshek has this form:

*Seed properties:*

– objective function:

$$80 \leq y_1 = 132,50 - 2,50 \cdot w - 2,32 \cdot t + 0,129 \cdot w \cdot t, \% \leq 100 \rightarrow \max \text{ (Eq. 1)}$$

– restrictions on quality indicators:

$$85 \leq y_2 = 119,89 + 1,61 \cdot w, \% \leq 100 \text{ (Eq. 2)}$$

$$85 \leq y_3 = 117,57 - 1,43 \cdot w, \% \leq 100 \text{ (Eq. 3)}$$

*Physical properties:*

– objective function

$$1,0 \leq y_6 = 1,105, \text{ g/cm}^3 \leq 1,2 \rightarrow \max \text{ (Eq. 4)}$$

– restrictions on quality indicators:

$$12,0 \leq y_4 = 4,47 + 0,634 \cdot w, \% \leq 22,0 \text{ (Eq. 5)}$$

$$600 \leq y_5 = (62,86) \cdot 10 \text{ g/l} \leq 650 \text{ (Eq. 6)}$$

$$45,0 \leq y_7 = 16,55 + 1,59 \cdot C_{i/o} + 2,23 \cdot w - 0,0867 \cdot C_{i/o} \cdot w, \text{ g} \leq 65,0 \text{ (Eq. 7)}$$

#### *Biochemical properties:*

– objective function

$$5,5 \leq y_8 = 12,04 - 0,174 \cdot w, \% \leq 10,0 \rightarrow \max; \text{ (Eq. 8)}$$

– restrictions on quality indicators:

$$56,0 \leq y_9 = 62,67, \% \leq 75,0 \text{ (Eq. 9)}$$

$$28,0 \leq y_{10} = 33,01, \% \leq 35,0 \text{ (Eq. 10)}$$

here:

$C_{i/o}$  – ratio of ion concentration (units/cm<sup>3</sup>) to ozone concentration (mg/cm<sup>3</sup>), units/mg;  
 $P$  – overpressure (for cavitation treatment), ati;  
 $w$  – sample moisture before processing, %;  
 $t_1$  – processing time, min.  
 $y_1$  – germination energy, %;  
 $y_2$  – germination in 5 days, %;  
 $y_3$  – germination in 7 days, %;  
 $y_4$  – humidity after processing, %;  
 $y_5$  – nature, g/l;  
 $y_6$  – grain density, g/cm<sup>3</sup>;  
 $y_7$  – weight of 1000 grains, g;  
 $y_8$  – protein, %.  
 $y_9$  – starch, %;  
 $y_{10}$  – greenery index, ml.

The nature of the dependence of the energy of barley germination Baisheshek on the factors  $w$  and  $t$  is shown in Figure 4. The remaining dependencies of objective functions on the investigated factors, as follows from mathematical models, do not need graphical representation.

Using ion-ozone processing (IO), mathematical models were obtained for optimizing the technological regimes and quality indicators of barley of the Baisheshek variety. The results are shown in Table 5.

here:

$C_{i/o}$  – ratio of ion concentration (units/cm<sup>3</sup>) to ozone concentration (mg/cm<sup>3</sup>), units/mg;  
 $w$  – sample moisture before processing, %;

$t_1$  – processing time, min.

$y_1$  – germination energy, %;

$y_2$  – germination in 5 days, %;

$y_3$  – germination in 7 days, %;

$y_4$  – humidity after processing, %;

$y_5$  – nature, g/l;

$y_6$  – grain density, g/cm<sup>3</sup>;

$y_7$  – weight of 1000 grains, g;

$y_8$  – protein, %.

$y_9$  – starch, %;

$y_{10}$  – greenery index, ml.

The data in Table 5 indicates that there is no need for the nature of the dependence of the germination energy of Baisheshek barley on the factors  $w$  and  $t$  and the rest of the dependence of the objective functions on the factors studied.

Restrictions on the range of variation in the regime parameters of ion-ozone cavitation treatment of all the investigated cereal crops were as follows:

$$1 \text{ mln. unit./mg} \leq C_{i/o} \leq 15 \text{ mln. unit./mg}$$

$$1 \text{ ati} \leq P \leq 4 \text{ ati}$$

$$13 \% \leq w \leq 20 \%$$

$$10 \text{ min} \leq t \leq 20 \text{ min}$$

Taking into account the acceptable ranges of changes in the investigated factors ( $C_{i/o}$ ,  $P$ ,  $w$ , and  $t$ ), mathematical models for optimization of ion-ozone cavitation processing of grain are presented below.

The mathematical model for optimizing the modes of ion-ozone cavitation processing of barley of the variety Baisheshek has this form:

#### *Seed properties:*

– objective function

$$84 \leq y_1 = 113,95 - 0,929 \cdot w - 0,275 \cdot t, \% \leq 100 \rightarrow \max \text{ (Eq. 11)}$$

– restrictions on quality indicators:

$$86 \leq y_2 = 113,48 - 0,893 \cdot w - 0,200 \cdot t, \% \leq 100 \text{ (Eq. 12)}$$

$$88 \leq y_3 = 98,25 + 0,769 \cdot t - 0,0557 \cdot w \cdot t, \% \leq 100 \text{ (Eq. 13)}$$

#### *Physical properties:*

– objective function

$$1,0 \leq y_6 = 1,11, \text{ g/cm}^3 \leq 1,14 \rightarrow \max \text{ (Eq. 14)}$$

– restrictions on quality indicators:

$$12,0 \leq y_4 = 4,14 + 0,660 \cdot w, \% \leq 18,0 \text{ (Eq. 15)}$$

$$600 \leq y_5 = 627,3, \text{ g/l} \leq 650 \text{ (Eq. 16)}$$

$$47,0 \leq y_7 = 35,68 + 1,05 \cdot w, \text{ g} \leq 62,0 \text{ (Eq. 17)}$$

#### *Biochemical properties:*

– objective function

$$7,0 \leq y_8 = 11,59 - 0,167 \cdot w, \% \leq 11,0 \rightarrow \max \text{ (Eq. 18)}$$

– restrictions on quality indicators:

$$55,0 \leq y_9 = 62,49, \% \leq 67,0 \text{ (Eq. 19)}$$

$$28 \leq y_{10} = 33,78 - 0,121 \cdot C_{i/o} + 0,127 \cdot t + 0,0434 \cdot C_{i/o} \cdot P - 0,0321 \cdot P \cdot t, \% \leq 38 \text{ (Eq. 20)}$$

From the mathematical models, it can be seen that all the objective functions of barley have a simple character - the germination energy depends only on two factors (grain moisture and processing time), the density of barley grain does not change statistically (constant), and the mass fraction of the starch depends only on the moisture content of the grain. Therefore, the graphical dependence is presented only for the germination energy (Figure 5). It is seen that it inversely decreases with increasing barley moisture and the duration of its treatment.

The optimal modes and quality indicators of the grain of barley Baisheshek after ion-ozone cavitation treatment are shown in table 6.

here:

$C_{i/o}$  – ratio of ion concentration (units/cm<sup>3</sup>) to ozone concentration (mg/cm<sup>3</sup>), units/mg;  
 $P$  – overpressure (for cavitation treatment), at;  
 $w$  – sample moisture before processing, %;  
 $t_1$  – processing time, min.  
 $y_1$  – germination energy, %;  
 $y_2$  – germination in 5 days, %;  
 $y_3$  – germination in 7 days, %;  
 $y_4$  – humidity after processing, %;  
 $y_5$  – nature, g/l;  
 $y_6$  – grain density, g/cm<sup>3</sup>;  
 $y_7$  – weight of 1000 grains, g;  
 $y_8$  – protein, %;  
 $y_9$  – starch, %;

$y_{10}$  – greenery index, ml.

Table 6 indicates that in order to improve the seed and biochemical properties of Baisheshek barley, ion-ozone cavitation treatment should be carried out at  $C_{i/o} = 1$  million units/mg,  $P = 1$  at,  $W = 13\%$  and  $t = 10$  min. With the same values of  $C_{i/o}$ ,  $P$ ,  $t$ , physical properties will also improve, but grain processing should be carried out at grain moisture of 20 %.

To compare the quality of control (unprocessed) samples of the studied cultures and the optimal parameters obtained after their ion-ozone (IO) and ion-ozone cavitation (IOC) treatment.

Summary of the optimal indicators of the quality of barley after ion-ozone and ion-ozone cavitation treatment in comparison with control (unprocessed) samples are shown in Table 7.

here:

$y_1$  – germination energy, %;  
 $y_2$  – germination in 5 days, %;  
 $y_3$  – germination in 7 days, %;  
 $y_4$  – humidity after processing, %;  
 $y_5$  – nature, g/l;  
 $y_6$  – grain density, g/cm<sup>3</sup>;  
 $y_7$  – weight of 1000 grains, g;  
 $y_8$  – protein, %;  
 $y_9$  – starch, %;  
 $y_{10}$  – greenery index, ml.

Analysis of these tables showed that the optimum regimes of ion-ozone and ion-ozone cavitation treatment to improve the considered seed, physical, biochemical properties and the state of preservation of grain is the same, in the moisture content of the grain – optimal results were obtained when processing wet grain (20%). For seed, physical, biochemical, and state of preservation, the best results were obtained when processing dry grain (13%).

The full-factor planning of experiments of 2<sup>3</sup> and 2<sup>4</sup> degrees made it possible to obtain regression equations describing the change in the seed, physico-biochemical and physiological properties of grain crops from the influencing factors of ion-ozone and ion-ozone cavitation processing of grain and to identify priority grain indicators for constructing a linear and non-linear programming model with the indication of target and restrictive functions.

Integrated programming optimization models for individual varieties of grain crops made it possible to establish optimal



technological processing modes (IO and IOC) and increase achievable levels of seed, physico-biochemical, flour, baking, physiological properties, and their technological qualities for the intended purpose.

Thus, mathematical models have been calculated and developed that describe changes in the seed and technological properties of grain seeds during ion-ozone and ion-ozone cavitation preparation of grain seeds, which subsequently allow optimizing processing conditions. As a result, regression models were obtained based on  $2^3$  and  $2^4$  full-factor experts for the Baisheshek barley variety.

Photographs were taken of growing Baisheshek barley under experimental conditions. When growing crops, the treatment with electrically charged air particles was carried out in two versions: open and closed in the form of greenhouses during treatment with air ions with a duration of 25 minutes, and the results are shown in Figures 6-8.

The physical and biochemical studies aimed at increasing germination, vitality, and growth strength show a reasonably clear picture in terms of their final value. Phenological observations have shown that the effects of ion-ozone and ion-ozone cavitation treatment are triggered after 25-30 days, where the greatest tendency of the superiority of ion-ozone cavitation treatment is observed, ion-ozone follows, and the control, of course, significantly lags.

#### 4. CONCLUSIONS

Determining the strength of seed growth provides higher objectivity in assessing seeds by their ability to germinate and form seedlings. Along with a high growth force, seeds during germination formed seedlings with four and five roots and seedlings with three roots predominated in those variants.

Studies of changes in the seed properties and technological qualities of grain crops using ion-ozone (IO) and ion-ozone cavitation (IOC) processing of cereals into full-factor experiments  $2^3$  (8 experiments) and  $2^4$  (16 experiments) allowed to create the basis for the development of regression models to describe the change indicators of seed properties and technological qualities and in the future for the rational organization of equipment and technology of IO and IOC processing.

Ion-ozone treatment of seeds for sowing barley varieties and further cultivation with the treatment of plants with a stream of electrically charged air particles generally increase their yield, seed, and technological properties. The obtained data of these properties during ion-ozone treatment are much better compared to the traditional version, while there is an improvement in physical and biochemical parameters, and the seeds become more stable during storage, providing an increase in their safety.

The obtained results of the above properties during ion-ozone cavitation treatment (IOC) become better compared to traditional and ion-ozone treatment (IO). Moreover, indicators characterizing the studied properties of grain varieties in terms of their physical and biochemical properties and state of conservation have high potentials for their effective use in the production of grain products and meeting the requirements for preparing export batches of grain crops.

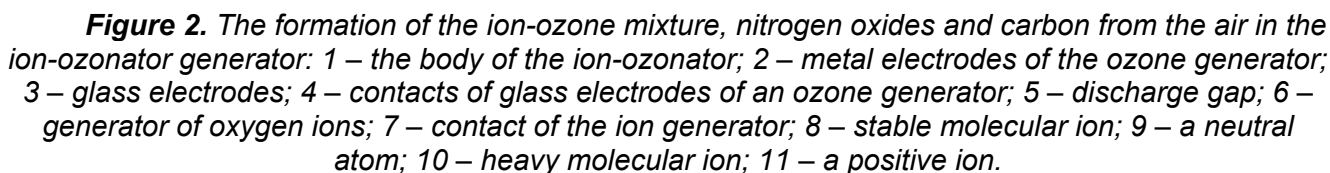
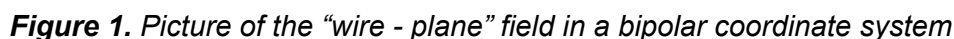
The developed mathematical models describe changes in the seed and technological properties of grain seeds during ion-ozone and ion-ozone cavitation preparation of barley seeds, and they can be used to optimize processing conditions.

#### 5. REFERENCES

1. Akulichev, V. A. (1978). *Cavitation in cryogenic and boiling liquids*. Moscow: Science, 280.
2. Baymagambetova, K. K., Nurpeisov, I. A., Gass, O. S., Sereda, G. A., Chudinov, V. A., Bekenova, L. V., and Bishimbaeva, N. K. (2014). *Ecological test of wheat precocious lines obtained by biotechnology methods*. Plant biology and biotechnology international conference. Almaty, 93.
3. Erkmen, O. (2001). Uses of Ozone to Improve the Safety and Quality of Foods. *J. Gida Teknolojisi*, 5 (3), 58–64.
4. GOST 10845-98. (2001). Grain and products of its processing. Method for the determination of starch. M.: *IPK Standards Publishing House*, 1-4.
5. GOST 10846-91. (2009). Grain and products of its processing. Method for determination of protein. M.: *Standartinform*, 1-8.

6. GOST 12041-82. (2011). Seeds of crops. Method for determination of moisture content. *M.: Standartinform*, 109-114.
7. GOST 12042-80. (2011). Seeds of crops. Methods for determining the mass of 1000 seeds. *M.: Standartinform*, 116-118.
8. GOST 10968-88. (2009). Grain. Methods for determining germination energy and germination capacity. *M.: Standartinform*, 1-3.
9. Iztaev, A. I., Kulajanov, T. K., Maemerov, M. M., Assangalieva, J. R. (2013). *Elektromagnetik ion-ozone grain processing*. Materials of International scientific and practical working Conference Pakistan Engineering Council at National University of Sciences Technology: 5-th World Engineering Congress (WEC-2013), Islamabad, 31.
10. Iztaev, A., Kulazhanov, T., Yakiyayeva, M., Maemerov, M., Iztaev, B., and Mamayeva, L. (2018a). The Efficiency of Ionocavitation Processing and Storage in the Nitrogen Medium of Oilseeds. *Journal of Advanced Research in Dynamical and Control Systems*, 10 (7), 2032–2040.
11. Iztayev, A., Urazaliev, R., Yakiyayeva, M., Maemerov, M., Shaimerdenova, D., Iztayev, B., Toxanbayeva, B., and Dauletkeldi, Ye. (2018b). The investigation of the impact of dynamic deterioration of ozone on grass growth and the consequence of ion-ozone cavitation treatment. *Journal of Advanced Research in Dynamical and Control Systems*, 10(13), 663-671.
12. Iztayev, A., Yakiyayeva, M., Maemerov, M., Iztayev, B., Urazaliev, R., Dauletkeldi, Y., Shaimerdenova, D., and Toxanbayeva, B. (2018c). Regress models of ion-ozone treatment without and with cavitation, describing changes of indicators for grain crops quality. *Acta Technica CSAV (Ceskoslovensk Akademie Ved)*, 63(1B), 1-8.
13. Iztayev, A., Yakiyayeva, M., Kulazhanov, T., Kizatova, M., Maemerov, M., Stankevych, G., Toxanbayeva, B., and Chakanova, Zh. (2018d). Controlling the implemented mathematical models of ion-ozone cavitation treatment for long-term storage of grain legume crops. *Journal of Advanced Research in Dynamical and Control Systems*, 10(13), 672-680.
14. Ivanov, A. N. (1980). *Hydrodynamics of developed cavitation currents-55*. Leningrad: Shipbuilding, 237.
15. Kalinina, I. V., and Fatkullin, R. I. (2016). Application of the effects of ultrasonic cavitation effects as a factor in the intensification of the extraction of functional ingredients. *Vestnik SUSU. Series "Food and Biotechnology"*, 4(1), 64–70.
16. Kalinina, I., Naumenko, N., and Fatkullin, R. (2018). *Perspectives of Using of Ultrasonic Cavitation in Water Treatment Technology for the Food Productions*. IOP Conference Series: Earth and Environmental Science, 272, 1–9.
17. Kim, J. G., Yousef, A. E., Khadre, M. A. (2003). Ozone and its Current and Future Application in the Food Industry. *J. Advances in Food and Nutrition Research*, 45, 167–218.
18. Knapp, R., Daily, J., and Hammit, F. (1974). *Cavitation*. Moscow: World, 678.
19. Kokhmetova, A., Sapakhova, Z., Yessimbekova, M., Yeleshev, R., and Morgounov, A. (2014). Principles and methods of selection of grain crops at the present stage. *J. Vestnik of Agricultural Science of Kazakhstan, Almaty*, 1, 3-19.
20. Maemerov, M. M. (2004). *Increase in the role of ozone as an environmentally friendly method for treating plant raw materials*. Materials of International Conference Strategy for the development of food and light industry, Almaty, 59–60.
21. Maemerov, M. M., Kulazhanov, K. S., and Iztaev, A. I. (2006). *Ion-ozone technology – the way to prosperity and well-being*. Materials of International Conference dedicated to the 70th anniversary of the National Engineering Academy of the Republic of Kazakhstan. J. Light and food industry, Almaty, 175-177.
22. Maemerov, M. M., Iztaev A. I., Kulazhanov, T. K., and Iskakova, G. K. (2011). *Scientific bases of ion-ozone technology of grain processing and products of its processing*. Almaty: LEM, 258.
23. Malin, N. I. (2005). *Grain storage technology*. Moscow: Kolos, 280.
24. Morales-de la Peña, M., Welte-Chanes, J., and Martín-Belloso, O. (2019). Novel technologies to improve food safety and quality. *Current Opinion in Food Science*, 30, 1–7.
25. Naleev, O. N. (1993). *Grain storage technology*. Almaty: RIK, 212.
26. Naumenko, N. V., Potoroko, I. Yu., Kretova, Yu. I., Kalinina, I. V., Paimulina, A. V., and Caturov, A. V. (2018). On the issue of intensification of the process of grain

- germination. *Far Eastern Agrarian Bulletin*, 4 (48), 109–115.
27. Odjo, S., Bera, F., Beckers, Y., Foucart, G., and Malumbad, P. (2018). Influence of variety, harvesting date and drying temperature on the composition and the in vitro digestibility of corn grain. *Journal of Cereal Science*, 79, 218–225.
  28. Ostapchuk, M. V. (2007). *Mathematical modeling on the computer*. Odessa: Druk, 313.
  29. Ostapchuk, N. V., Kaminsky, V. D., Stankevich, G. N., and Chuchuy, V. P. (1992). *Mathematical modeling of food production processes*. Kiev: Vishcha shola, 175.
  30. Pirsol, I. (1975). *Cavitation*. Moscow: Mir, 96.
  31. Sagitov, A. O., Dixanbaeva, F. T., and Asangalieva, J. R. (2012). *Environmental safety of the grain reserves protection system from pests*. Materials of V World International Congress of Engineering Technologies – Wcet-2012 "Science and technology is a step into the future", Almaty, 206-207.
  32. Sereev, I. (2014). Effect of spring biomass removal on expression of agronomic traits of winter wheat. *World Applied Sciences Journal*, 30 (3), 322-329.
  33. Singh, A. K, Rehal, J., Kaur, A., and Jyot, G. (2015). Enhancement of attributes of cereals by germination and fermentation: a review. *Critical Reviews in Food Science and Nutrition*, 55 (11), 1575–1589.
  34. ST RK GOST R 51411-2006. (2007). Grain and products of its processing. Method for the determination of ash. *Nur-Sultan: KazInSt*, 1-6.
  35. Tikhonov, N. I., and Belyakov, A. M. (2006). *Grain storage*. Volgograd: VolGU, 108.
  36. Tursunbayeva, Sh. A., Iztayev, A., Magomedov, M., Yakiyayeva, M. A., and Muldabekova, B. Zh. (2019). Study of the quality of low-class wheat and bread obtained by the accelerated test method. *J. Periodico Tchê Química*, 16(33), 809-822.
  37. Urazaliev, R. A. (2012). *State, problems, mechanisms of development of innovative innovation in selection and seed farming of agricultural crops*. Cultures. Materials of International Conference State and Prospects of Seed Growing in Agricultural Crops. Cultures in Kazakhstan, Almaty, 10-24.
  38. Urazaliev, R. A., Absattarova, A. S., Roder, M. S., Kenjebaeva, S., and Morgounov, A. I. (2010). *Allelic diversity at XGWM261 locus in Kazakhstan bread wheat varieties*. Materials of 20-th International Triticeae Mapping Initiative, 2-nd Wheat Genomics in China conference. Beijing, 180.
  39. Voblikov, E. M., Bukhancov, V. A., Maratov, B. K., and Prokopec, A. S. (2001). *Post-harvest processing and storage of grain*. Rostov-na-Donu: MarT, 229.
  40. Yakiyayeva, M., Iztaev, A., Kizatova, M., Maemerov, M., Iztaeva, A., Feydengold, V., Tarabaev, B., and Chakanova, Zh. (2016). Influence of ionic, ozone ion-ozone cavitation treatment on safety of the leguminous plants and oil-bearing crops at the storage. *Journal of Engineering and Applied Sciences*, 11(6), 1229-1234.
  41. Zapevalov, M.V., Kovalenko, N.V., and Petrova, G.V. (2015). Post-harvest grain processing. *News of the Orenburg State Agrarian University*, 3 (53), 80-83.
  42. Zhakatayeva, A., Iztayev, A., Muldabekova, B., Yakiyayeva, M., and Hrivna, L. (2020). Scientific security assessment of safety risk of raw sugar products. *J. Periodico Tchê Química*, 17(34), 352-368.



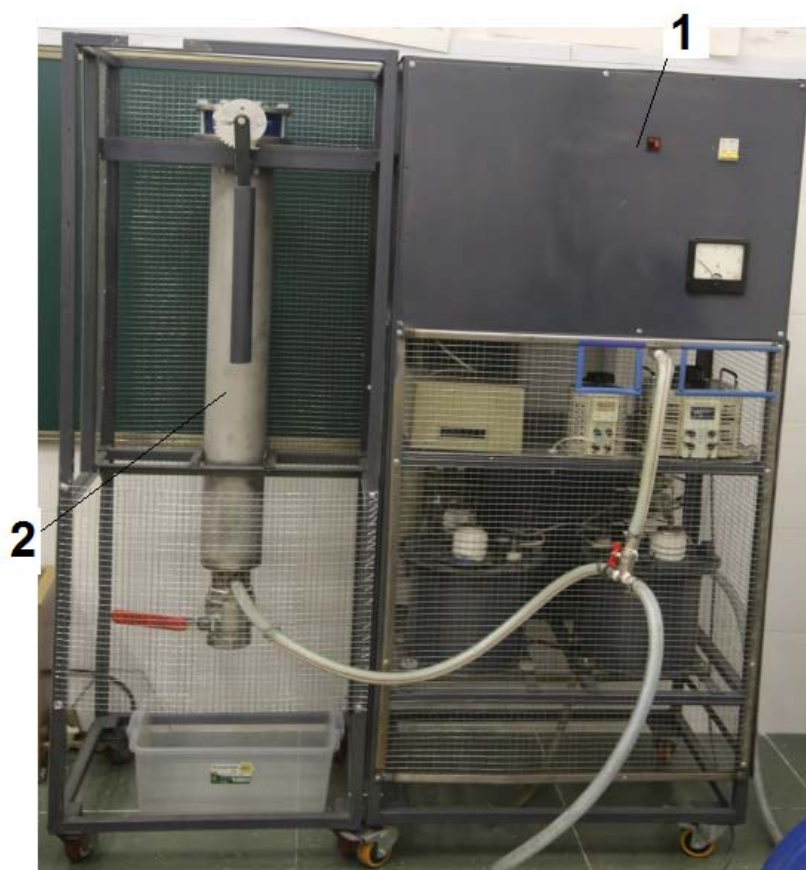


**Figure 3.** Ion-ozone cavitation installation: 1 – ion-ozone generator; 2 – cavitation capacity

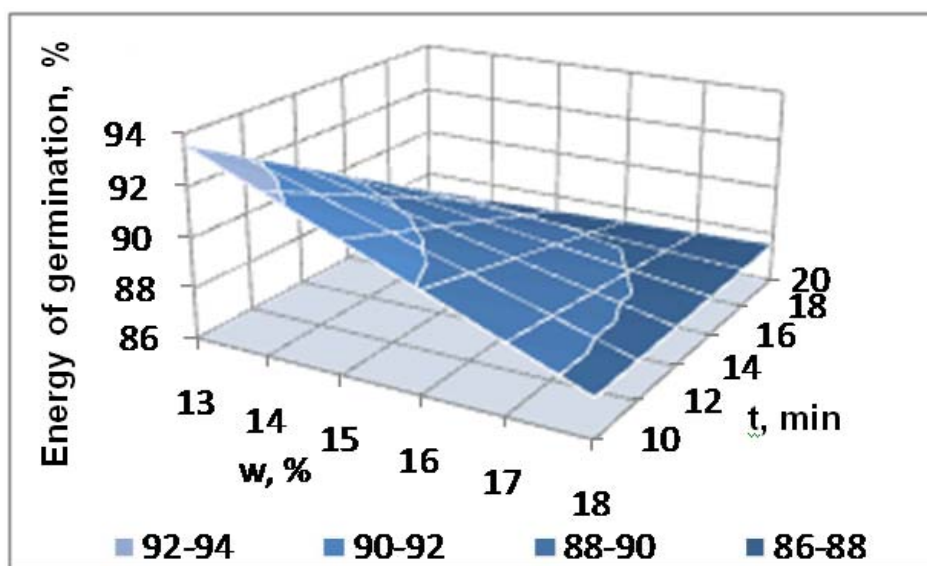


**Figure 4.** Surfaces of the response of the dependence of the energy of barley germination "Baisheshek" treated with ion-ozone streams on the factors  $w$  and  $t$

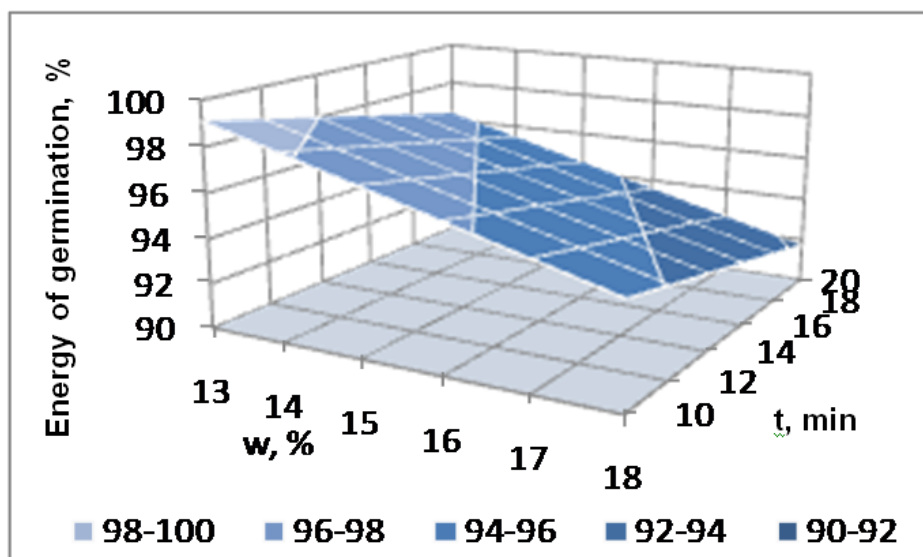


**Figure 5.** Surfaces of the response of the dependence of the energy of barley germination *Baisheshek* treated with ion-ozone cavitation streams on the factors *w* and *t*



**Figure 6.** Barley *Baisheshek* – a control sample





**Figure 7.** Barley Baisheshek processed by ion-ozone flows



**Figure 8.** Barley Baisheshek processed by ion-ozone cavitation

**Table 1.** Quality indicators of control (unprocessed) samples of barley Baisheshek

| Seed properties                |                          |                         | Technological properties |                |                   |                          |                             |                |                     |
|--------------------------------|--------------------------|-------------------------|--------------------------|----------------|-------------------|--------------------------|-----------------------------|----------------|---------------------|
| Germination energy in 3 days,% | Germination in 5 days, % | Germination in 7 days,% | Physical                 |                |                   |                          | Biochemical                 |                |                     |
|                                |                          |                         | humidity, %              | Nature, g / l  | Density , g / cm³ | Weight of 1000 grains, g | Mass fraction of protein, % | Starch, %      | Greener y Index, ml |
| Function Indicators            |                          |                         |                          |                |                   |                          |                             |                |                     |
| y <sub>1</sub>                 | y <sub>2</sub>           | y <sub>3</sub>          | y <sub>4</sub>           | y <sub>5</sub> | y <sub>6</sub>    | y <sub>7</sub>           | y <sub>8</sub>              | y <sub>9</sub> | y <sub>10</sub>     |
| 97                             | 98                       | 100                     | 12.66                    | 642            | 1.12              | 49                       | 9.59                        | 65.03          | 32.12               |

**Table 2.** Conditions and results of full-factorial experiments of FFE-2<sup>3</sup> on the ion-ozone treatment of barley Baisheshek

| Experiment Numbers | Ratio of ion concentrations to ozone, million units/mg | humidity before processing, % | Processing time, min | Seed properties                |                          |                         | Technological properties     |                |                              |                          |                             |                |                    |  |
|--------------------|--|-------------------------------|----------------------|--------------------------------|--------------------------|-------------------------|------------------------------|----------------|------------------------------|--------------------------|-----------------------------|----------------|--------------------|--|
|                    |  |                               |                      | Germination energy in 3 days,% | Germination in 5 days, % | Germination in 7 days,% | Physical                     |                |                              |                          | Biochemical                 |                |                    |  |
|                    |  |                               |                      |                                |                          |                         | humidity after processing, % | Nature, g / l  | Density, g / cm <sup>3</sup> | Weight of 1000 grains, g | Mass fraction of protein, % | Starch, %      | Greenery Index, ml |  |
|                    | Experimental conditions                                |                               |                      | Quality indicators             |                          |                         |                              |                |                              |                          |                             |                |                    |  |
|                    | C <sub>i/o</sub> , mln. units/mg                       | w, %                          | t, min               | y <sub>1</sub>                 | y <sub>2</sub>           | y <sub>3</sub>          | y <sub>4</sub>               | y <sub>5</sub> | y <sub>6</sub>               | y <sub>7</sub>           | y <sub>8</sub>              | y <sub>9</sub> | y <sub>10</sub>    |  |
| 1                  | 15   | 20                            | 20                   | 89                             | 89                       | 90                      | 16,68                        | 627            | 1,11                         | 60                       | 8,88                        | 61,34          | 32,24              |  |
| 2                  | 1  | 20                            | 20                   | 86                             | 88                       | 89                      | 17,32                        | 622            | 1,12                         | 62                       | 8,15                        | 61,05          | 32,54              |  |
| 3                  | 15   | 20                            | 20                   | 85                             | 99                       | 99                      | 12,75                        | 634            | 1,11                         | 52                       | 9,82                        | 63,96          | 33,48              |  |
| 4                  | 1  | 20                            | 20                   | 89                             | 99                       | 99                      | 12,72                        | 638            | 1,09                         | 46                       | 9,60                        | 64,24          | 33,27              |  |
| 5                  | 15   | 13                            | 20                   | 84                             | 87                       | 88                      | 17,11                        | 621            | 1,09                         | 58                       | 8,42                        | 60,98          | 32,74              |  |
| 6                  | 1  | 13                            | 20                   | 86                             | 87                       | 89                      | 17,47                        | 614            | 1,11                         | 60                       | 8,78                        | 61,34          | 33,15              |  |
| 7                  | 15   | 13                            | 20                   | 95                             | 99                       | 99                      | 12,72                        | 638            | 1,12                         | 53                       | 9,83                        | 64,29          | 32,63              |  |
| 8                  | 1  | 13                            | 20                   | 92                             | 99                       | 99                      | 12,64                        | 635            | 1,09                         | 46                       | 9,85                        | 64,19          | 34,03              |  |



**Table 3.** Conditions and results of full-factorial experiments of FFE-2<sup>4</sup> on the ion-ozone cavitation processing of barley Baisheshek

| Experiment Numbers                | Ratio of ion concentrations to ozone, million units/mg | Overpressure (cavitation), ati | humidity before processing, % | Processing time, min | Seed properties                |                          |                         | Technological properties     |                |                  |                          |                             |                 |                    |
|-----------------------------------|--|--------------------------------|-------------------------------|----------------------|--------------------------------|--------------------------|-------------------------|------------------------------|----------------|------------------|--------------------------|-----------------------------|-----------------|--------------------|
|                                   |  |                                |                               |                      |                                |                          |                         | Physical                     |                |                  |                          | Biochemical                 |                 |                    |
|                                   |  |                                |                               |                      | Germination energy in 3 days,% | Germination in 5 days, % | Germination in 7 days,% | humidity after processing, % | Nature, g / l  | Density, g / cm³ | Weight of 1000 grains, g | Mass fraction of protein, % | Starch, %       | Greenery Index, ml |
|                                   | Experimental conditions                                |                                |                               |                      | Quality indicators             |                          |                         |                              |                |                  |                          |                             |                 |                    |
| C <sub>i/o</sub> , mln. units /mg | P, ati   | w, %                           | t, min                        | y <sub>1</sub>       | y <sub>2</sub>                 | y <sub>3</sub>           | y <sub>4</sub>          | y <sub>5</sub>               | y <sub>6</sub> | y <sub>7</sub>   | y <sub>8</sub>           | y <sub>9</sub>              | y <sub>10</sub> |                    |
| 1                                 | 15   | 4                              | 20                            | 20                   | 92                             | 93                       | 93                      | 17,57                        | 615            | 1,11             | 57                       | 8,10                        | 61,19           | 35,42              |
| 2                                 | 1  | 4                              | 20                            | 20                   | 88                             | 92                       | 92                      | 17,04                        | 625            | 1,11             | 60                       | 7,75                        | 60,37           | 33,10              |
| 3                                 | 15   | 1                              | 20                            | 20                   | 85                             | 87                       | 89                      | 17,44                        | 615            | 1,11             | 56                       | 8,03                        | 61,15           | 33,53              |
| 4                                 | 1  | 1                              | 20                            | 20                   | 90                             | 91                       | 92                      | 17,27                        | 622            | 1,11             | 61                       | 8,77                        | 61,19           | 36,96              |
| 5                                 | 15   | 4                              | 13                            | 20                   | 98                             | 98                       | 99                      | 12,64                        | 635            | 1,11             | 49                       | 9,41                        | 64,15           | 34,45              |
| 6                                 | 1  | 4                              | 13                            | 20                   | 96                             | 98                       | 98                      | 12,48                        | 639            | 1,11             | 50                       | 9,00                        | 64,55           | 33,28              |
| 7                                 | 15   | 1                              | 13                            | 20                   | 98                             | 99                       | 99                      | 12,75                        | 632            | 1,11             | 48                       | 9,26                        | 63,83           | 35,89              |
| 8                                 | 1  | 1                              | 13                            | 20                   | 98                             | 100                      | 100                     | 12,72                        | 639            | 1,11             | 48                       | 9,58                        | 63,85           | 34,28              |
| 9                                 | 15   | 4                              | 20                            | 10                   | 91                             | 91                       | 91                      | 17,51                        | 618            | 1,11             | 60                       | 8,26                        | 60,64           | 35,76              |
| 10                                | 1  | 4                              | 20                            | 10                   | 94                             | 95                       | 95                      | 17,18                        | 616            | 1,12             | 54                       | 8,55                        | 61,56           | 34,76              |
| 11                                | 15   | 1                              | 20                            | 10                   | 97                             | 98                       | 98                      | 17,43                        | 621            | 1,11             | 53                       | 8,33                        | 60,83           | 33,27              |
| 12                                | 1  | 1                              | 20                            | 10                   | 93                             | 94                       | 94                      | 17,22                        | 622            | 1,12             | 53                       | 8,19                        | 61,18           | 34,51              |
| 13                                | 15   | 4                              | 13                            | 10                   | 96                             | 97                       | 97                      | 12,8                         | 634            | 1,11             | 49                       | 9,19                        | 63,74           | 32,52              |
| 14                                | 1  | 4                              | 13                            | 10                   | 98                             | 100                      | 100                     | 12,77                        | 637            | 1,11             | 50                       | 9,70                        | 63,85           | 34,58              |
| 15                                | 15   | 1                              | 13                            | 10                   | 98                             | 99                       | 99                      | 12,77                        | 631            | 1,11             | 50                       | 9,59                        | 64,27           | 33,49              |
| 16                                | 1  | 1                              | 13                            | 10                   | 100                            | 100                      | 100                     | 12,78                        | 636            | 1,09             | 51                       | 9,62                        | 63,57           | 34,29              |

**Table 4.** Calculation of the least-squares regression coefficients according to the linear plan taking into account inter-factor interactions, germination in 7 days – 2<sup>3</sup>

| Name              | Type of equation (Optimization)     | Numeric characteristics |                             |                                     |                                       |
|-------------------|-------------------------------------|-------------------------|-----------------------------|-------------------------------------|---------------------------------------|
|                   |                                     | Average value           | Root mean square deviation  | Fisher's Criterion – F <sub>r</sub> | Student's Criterion – t <sub>cr</sub> |
| Barley Baisheshek | $Y_{ger}=117,5714-1,4285 \cdot x_2$ | 94                      | sy = 1.2500<br>sag = 0.5774 | Fr= 4.69<br>Fcr=5.14                | 4.304                                 |

**Table 5.** Optimal regimes and quality indicators of Baisheshek barley grain after ion-ozone treatment

| Properties<br>(purpose) of<br>grain | Processing modes               |         |           | The objective<br>function    | Quality indicators<br>(limitations)                                     |
|-------------------------------------|--------------------------------|---------|-----------|------------------------------|---|
|                                     | $C_{i/o}$ ,<br>mln<br>units/mg | w,<br>% | t,<br>min |                              |   |
| Seed                                | 1                              | 13      | 10        | $y_1 = 93,57 \%$             | $y_2 = 98,96 \%$ ; $y_3 = 98,98 \%$                                     |
| Physical                            | 1                              | 20      | 10        | $y_6 = 1,105 \text{ g/cm}^3$ | $y_4 = 17,15 \%$ ; $y_5 = 629 \text{ g/l}$ ;<br>$y_7 = 61,01 \text{ g}$ |
| Biochemical                         | 1                              | 13      | 10        | $y_8 = 9,78 \%$              | $y_9 = 62,67 \%$ ; $y_{10} = 33,01 \text{ ml}$                          |

**Table 6.** Optimal regimes and quality indicators of Baisheshek barley grain after ion-ozone cavitation treatment

| Properties<br>(purpose)<br>of grain | Processing modes               |           |         |           | The objective<br>function   | Quality indicators<br>(limitations)  |
|-------------------------------------|--------------------------------|-----------|---------|-----------|-----------------------------|--|
|                                     | $C_{i/o}$ ,<br>mln<br>units/mg | P,<br>ati | w,<br>% | t,<br>min |                             |  |
| Seed                                | 1                              | 1         | 13      | 10        | $y_1 = 84,12 \%$            | $y_2 = 99,87 \%$ ;<br>$y_3 = 98,70 \%$                                     |
| Physical                            | 1                              | 1         | 20      | 10        | $y_6 = 1,11 \text{ g/cm}^3$ | $y_4 = 17,34 \%$ ;<br>$y_5 = 627 \text{ g/l}$ ;<br>$y_7 = 56,68 \text{ g}$ |
| Biochemical                         | 1                              | 1         | 13      | 10        | $y_8 = 9,42 \%$             | $y_9 = 62,49 \%$ ;<br>$y_{10} = 34,65 \%$                                  |

**Table 7.** Summary of the optimal indicators of the quality of barley Baisheshek after ion-ozone and ion-ozone cavitation treatment in comparison with control (unprocessed) samples

| Indicators           | Ion-ozone treatment |         | Ion-ozone cavitation treatment |         |
|----------------------|---------------------|---------|--------------------------------|---------|
|                      | Optimum             | Control | Optimum                        | Control |
| $y_1, \%$            | 93,57               | 97      | 84,12                          | 97      |
| $y_2, \%$            | 98,96               | 98      | 99,87                          | 98      |
| $y_3, \%$            | 98,98               | 100     | 98,70                          | 100     |
| $y_4, \%$            | 17,15               | —       | 17,34                          | —       |
| $y_5, \text{g/l}$    | 629                 | 614     | 627                            | 614     |
| $y_6, \text{g/cm}^3$ | 1,105               | 1,11    | 1,11                           | 1,11    |
| $y_7, \text{g}$      | 61,01               | 52      | 56,68                          | 52      |
| $y_8, \%$            | 9,78                | 5,57    | 9,42                           | 5,57    |
| $y_9, \%$            | 62,67               | 57,87   | 62,49                          | 57,87   |
| $y_{10}, \text{ml}$  | 33,01               | 29,81   | 34,65                          | 29,81   |

**COMPOSIÇÃO, PROPRIEDADES E USO DE RECURSOS SECUNDÁRIOS COMO FERTILIZANTES ORGÂNICOS DE SOLOS****COMPOSITION, PROPERTIES, AND USE OF SECONDARY RESOURCES AS ORGANIC SOIL FERTILIZERS****СОСТАВ, СВОЙСТВА И ИСПОЛЬЗОВАНИЕ ВТОРИЧНЫХ РЕСУРСОВ В КАЧЕСТВЕ ОРГАНИЧЕСКИХ УДОБРЕНИЙ ПОЧВЫ**

ASYLBAEV, Ilgiz \*; NIGMATZYANOV, Almas; KHABIROV, Ilgiz; SERGEEV, Vladislav; KURMASHEVA, Nadezhda

Federal State Budgetary Educational Establishment of Higher Education "Bashkir State Agrarian University",  
Department of Soil Science, Agricultural Chemistry, and Precision Farming. Russian Federation.

*\* Correspondence author*

*e-mail: ilgizasylbayev@yahoo.com*

Received 26 March 2020; received in revised form 18 May 2020; accepted 25 May 2020

**RESUMO**

O artigo discute as reservas de matérias-primas secundárias, fertilizantes orgânicos locais e ameliorantes (turfa, sapropel, fosfogesso, fosforitos, carvões de linhito, zeólitos, gipsita, calcário) na República do Bascortostão. O efeito do fosfogesso e do esterco de aves na fertilidade do solo e no rendimento da batata é estudado. O uso de gesso para melhorar o solo tem sido estudado e utilizado na agricultura e na restauração ambiental há muitos anos. A maior parte da literatura publicada é dedicada à influência do uso de gesso nas propriedades do solo e não no rendimento. O artigo apresenta os resultados de um experimento de campo sobre o uso de fosfogesso juntamente com resíduos de aves, com documentação detalhada de alterações na composição de microelementos dos solos, modo de precipitação e rendimento total após a fertilização. Os resultados do trabalho fornecido serão úteis na determinação das normas de aplicação de gesso; há também recomendações para pesquisas futuras sobre o uso de gesso para a melhoria do solo. A melhoria do rendimento pode ser o resultado de um efeito aditivo ou sinérgico; portanto, é altamente recomendável uma meta-análise de experimentos de gesso para melhorar as recomendações para o uso de gesso em vários ambientes. As taxas ideais de aplicação de matérias-primas secundárias são encontradas. O conteúdo do húmus do solo melhora e o rendimento da batata aumenta de 13,9 para 75,7 C/ha quando o fosfogesso é aplicado separadamente e em combinação com o esterco de aves. Existe o valor nutricional do esterco de aves, com os principais elementos como nitrogênio, fósforo e potássio. O fosfogesso é caracterizado com alto teor de estrôncio (14691 mg/kg) e elementos de terras raras (cério - 1358 mg/kg, praseodímio - 123,9 mg/kg, neodímio - 418,5 mg/kg, samário - 77,5 mg/kg, európio - 19,9 mg/kg, gadolínio - 58,9 mg/kg, térbio - 6,91 mg/kg e disprósio - 25 mg/kg). O conteúdo das formas totais de elementos no fosfogesso foi determinado por espectrometria de massa por plasma acoplado indutivamente (ICP-MS) usando um espectrômetro de massa VG Plasma Quad e Elan-6100.

**Palavras-chave:** *fertilizante; Agricultura orgânica; fosfogesso; estrume de aves; produtividade.*

**ABSTRACT**

The paper discusses reserves of secondary raw materials, local organic fertilizers, and ameliorants (peat, sapropel, phosphogypsum, phosphorites, lignite coals, zeolites, gypsum, limestone) in the Republic of Bashkortostan. The effect of phosphogypsum and poultry manure on soil fertility and potato yields is studied. The use of gypsum to improve soil has been studied and used in agriculture and environmental restoration for many years. Most of the published literature is devoted to the influence of the use of gypsum on soil properties and not on yield. The paper presents the results of a field experiment on the use of phosphogypsum together with poultry waste, with detailed documentation of changes in the microelement composition of soils, the mode of precipitation, and the total yield after fertilizing. The results of the given work will be useful in determining gypsum application norms; there are also recommendations for future research on the use of gypsum for soil improvement. The yield improvement may be the result of an additive or synergistic effect; therefore, a meta-analysis of gypsum experiments is strongly recommended to improve recommendations for the use of gypsum in various environments. The optimal application rates of secondary raw materials are found. The soil humus

content improves, and potato yield increases from 13.9 to 75.7 C/ha when phosphogypsum is applied separately and in combination with poultry litter. There is the nutritional value of the poultry manure, with the main elements as nitrogen, phosphorus, and potassium. Phosphogypsum is characterized with high content of strontium (14691 mg/kg) and rare earth elements (cerium – 1358 mg/kg, praseodymium – 123.9 mg/kg, neodymium – 418.5 mg/kg, samarium – 77.5 mg/kg, europium – 19.9 mg/kg, gadolinium – 58.9 mg/kg, terbium – 6.91 mg/kg and dysprosium – 25 mg/kg). The content of total element forms in phosphogypsum was determined by inductively coupled plasma mass spectrometry (IPC-MS) using a VG Plasma Quad and Elan-6100 mass spectrometer.

**Keywords:** *fertilizer; organic agriculture; phosphogypsum; poultry manure; productivity.*

## АННОТАЦИЯ

В статье рассматриваются запасы вторичного сырья, местных органических удобрений и мелиорантов (торф, сапропель, фосфогипс, фосфориты, лигнитные угли, цеолиты, гипс, известняк) в Республике Башкортостан. Изучено влияние фосфогипса и птичьего помета на плодородие почвы и урожайность картофеля. Использование гипса для улучшения почвы изучалось и использовалось в сельском хозяйстве и восстановлении окружающей среды в течение многих лет. Большая часть опубликованной литературы посвящена влиянию использования гипса на свойства почвы, а не на урожайность. Мы предлагаем результаты полевого эксперимента по использованию фосфогипса вместе с отходами птицеводства с результатами изменения микроэлементного состава почв, количества осадков и урожая после внесения удобрений. Результаты нашей работы будут полезны при определении норм применения гипса и использованию гипса для улучшения почвы. Повышение урожайности в наших исследованиях может быть результатом аддитивного или синергетического эффекта, поэтому перед применением фосфогипса в различных средах рекомендуется предварительный его метаанализ. Найдены оптимальные нормы внесения вторичного сырья. Содержание гумуса в почве улучшается, а урожай картофеля увеличивается с 13,9 до 75,7 ц / га при применении фосфогипса отдельно и в сочетании с птичьим пометом. Существует питательная ценность птичьего помета с основными элементами, такими как азот, фосфор и калий. Фосфогипс характеризуется высоким содержанием стронция (14691 мг/кг) и редкоземельных элементов (церия - 1358 мг/кг, празеодима - 123,9 мг / кг, неодима - 418,5 мг/кг, самария - 77,5 мг/кг, европия - 19,9 мг/кг, гадолиний - 58,9 мг/кг, тербий - 6,91 мг/кг и диспрозий - 25 мг/кг). Общее содержание элементов в фосфогипсе было определено с помощью масс-спектрометрии с индукционной плазмой используя спектрометры VG Plasma Quad и Elan-6100.

**Ключевые слова:** *удобрение; органическое земледелие; фосфогипс; птичий помет; урожайность.*

## 1. INTRODUCTION

Soil is a living substance with a sanitary ecological function being one of the most important (Dobrovolsky and Grishina, 1985). The soil can process a large amount of foreign materials and convert them into humus substances useful to restore fertility. The soil systems are more adapted to process organic substances of animal and plant origin (droppings of wild birds, animals) into stable organomineral humus compounds due to their enzymatic mechanisms developed during the evolution (Nasir *et al.*, 2019; Szajdak and Simakina, 2008). However, this does not work the same for mineral fertilizers (Kiryushin, 2012; Willer and Kilcher, 2011).

The distinctive features of current farming systems are the prevention of soil degradation and the reduction of the risk of environmental violations in the production of agricultural products (Gabassova *et al.*, 2017; Khamaletdinov *et al.*, 2018; Surekha *et al.*, 2013). Improved

environmental performance of agriculture requires bringing it in line with the laws of fertility, addressing the issues of biodiversity conservation, adaptation to agroecological conditions, optimizing the ratio of natural and agricultural lands, creating an optimal infrastructure of agricultural landscapes taking into account energy and mass transfer (Kiryushin, 2012; Willer and Kilcher, 2011). It has now become evident that natural, biological technologies are the alternative to the chemical load on agriculture (Gelashvili *et al.*, 2002). Biotechnology uses the ability of microorganisms, worms, cell cultures, tissues, their constituent parts to synthesize compounds important for humans (Gukalov, 2009). At the same time, the soil accumulates carbon, nitrogen, potassium, phosphorus, and microelements, getting better regime and structure and less effect of toxic substances (Kiryushin, 2012, 2015). Biotechnologies can restore soil fertility as well as its productivity as a result of lower pesticide load, higher plant resistance to adverse environmental

conditions (Khaibullin *et al.*, 2018; Sokolov, 1975).

Organic farming is a system that uses organic sources to feed crops and biological sources to control pests and diseases. Biofertilizers are also essential components of organic farming. They stimulate plant growth, biological restoration of the soil and its natural fertility, protect against drought, and some plant diseases. Composting can play an essential role in solid waste management programs and can significantly reduce the amount of wastes in a landfill. Moreover, it saves resources and reduces soil pollution (Pathak, 2011; Surekha *et al.*, 2013).

The growing interest in more significant organic farming and agricultural production is due to the constant increase in prices for agrochemicals and energy sources, low utilization of mineral fertilizers by plants, significant soil nutrient losses, decreased product quality with intensive use of mineral fertilizers and pesticides. The total number of farms introducing biological methods of agriculture is growing by about 8,9% per year. Their area has grown from 15.8 million hectares to 37.2 million hectares worldwide over the past decade (Paull, 2011; Wai, 2007; Willer and Kilcher, 2011).

The soil can process significant amounts of foreign material into stable organomineral humus compounds to restore and improve the fertility of leached Chernozem and increase the productivity of cultivated crops. The need to develop effective methods of soil fertility recovery to create optimal conditions and increase the agricultural biocenoses productivity underlies the importance of this direction.

The goal of this work is to assess the efficiency in using secondary resources (wastes of the poultry industry and the production of mineral fertilizers) as the primary sources of organic substances and nutrients entering the soil.

## 2. MATERIAL AND METHODS

### 2.1. Experimental site

The experimental work was carried out by stationary field and laboratory-analytical methods. Stationary field studies were conducted on leached Chernozem (*Luvic Chernozems*) in the southern forest-steppe zone during the plantation of the Nevsky potato variety in 2015-2017.

Mainly, it was the experimental field of the Educational and scientific center of the Bashkir State Agrarian University, Russia. The sections of the field experiment had a width of 4–5, a length of 8–9 m, and a slope of 1–3°. A topographic survey (scale 1:100) in the international coordinate system (WGS) -84) and the Baltic elevation system with an interval between the contours of 0.1 m was performed to obtain more fundamental characteristics of the plots. The plots were leveled, equipped with sewage and water intake, bordered around the perimeter and separated from each other by earthen walls; On the arable land, plowing of slabs to a depth of 20 cm was practiced; the original vegetation cover of the deposit consisted of purple alfalfa (*Medicago sativa*) and meadow and weed plants: reeds (*Anthemisarvensis*), milk thistle (*Sonchus arvensis*), common wormwood (*Artemisia absinthium* L.) and field bindweed (*Convolvulus arven* L.). The soil was suitable for weakly leached and weakly weathered clay-clay-illuvial arable chernozem (*Luvic Chernozem* (*Clayic, Aric, Pachic*)). It was characterized by medium-deep humus horizons (AU + AU<sub>b</sub> 60 cm), average humus content, and slightly acid reaction. The aggregate state and porosity of the plow layer were evaluated as ideal; The water-resistance of the soil structure was high. The total amount of irrigation water was determined using rain gauges (5 sensors) installed around the periphery of the studied areas.

### 2.2. Sampling

The water permeability of the soil was determined by the cylindrical method (Vadiunina & Korchagina, 1986). Soil samples for determining the structural-aggregate composition and density were taken in layers of 0–10 and 10–20 cm in four repetitions. Samples were taken before, and after irrigation, soil moisture in the upper layer between irrigation was 15–20%, air temperature 20–25 °C; wind speed did not exceed 2 m/s.

### 2.3. Fertilizer application

After moldboard plowing and secondary tillage (harrowing), two plots of 0,1 hectares each were selected. The experiment scheme included a traditional farming system and variants to improve soil fertility: 1- control (without application); 2- Phosphogypsum, 5 t/ha; 3- Phosphogypsum, 10 t/ha; 4- Phosphogypsum, 20 t/ha; 5- poultry manure, 40 t/ha; 6-

Phosphogypsum+poultry manure, 1:10 ratio of 1:10, dose 40 t/ha.

#### 2.4. Laboratory analytical methods

Soil samples were selected based on the upper genetic horizons of the soil profile, laboratory and analytical studies were carried out using methods accepted in soil science. The total humus was determined by the method of I. V. Tyurin, soil moisture, and macronutrients (nitrogen, phosphorus, potassium) were detected according to the available guidelines for agrochemical indicators (Arinushkina, 1970; Vadiunina and Korchagina, 1986).

The content of total element forms in phosphogypsum was determined by mass spectrometry with inductively coupled plasma-ICP-MS on a VG Plasma Quad and Elan-6100 mass spectrometer under standard change conditions using imported reference samples in the laboratory of the Federal State Unitary Enterprise "All-Russian Research Institute of mineral raw materials named after N. M. Fedorovsky". The measurement error at the level of units and hundredths is no more than 15%. The device was calibrated with standard solutions containing a set of appropriate elements. The element concentration was based on the following: the analyzed solution was sprayed, the flow of argon brings it into a high-temperature plasma, where most of the atoms are ionized. Some of the ions formed in the plasma fall into a vacuum chamber, where they were accelerated and focused using ion lenses. Then the ion beam enters the inhomogeneous electromagnetic field of the quadrupole, where ions are spatially separated by weight. When scanning the electromagnetic field of the quadrupole, ions of a certain weight fell sequentially on the ion detector and were registered using electrical measuring devices. The received signals were proportional to the content of certain ions in the plasma, were processed using a computer system, and the analyses results were printed out.

Statistical processing of experimental data was performed using Microsoft Office Excel 2007 and SNEDECOR V. 5.80 software.

### 3. RESULTS AND DISCUSSION

Due to the sharp disparity in prices for agricultural products, and material costs for its production, the use of mineral fertilizers is sharply limited at present. There is much concern about

the reproduction of soil fertility. Having conducted an analytical analysis of the possible economically and environmentally beneficial ways to reproduce soil fertility, we figured it to be possible to use the available resources, which the Republic of Bashkortostan possesses.

Stocks of the secondary material resources, local organic fertilizers, and ameliorants are huge, but they are not used to the full (Khabirov, 2015). Some of them are practically not used (Table 1).

The Meleuz plant of mineral fertilizers has 11 million tons of phosphogypsum, which is practically not used. Phosphogypsum stacks occupy a large area and are a danger to the local ecological situation, although phosphogypsum is a valuable multi-component fertilizer. It is not actually applied to the soils of the Republic of Bashkortostan since there are no enough recommendations for its use. Poultry farms of the Republic of Bashkortostan collect hundreds of thousands of tons of poultry manure every year. For example, in storage facilities of the Poultry Production unit named after M. Gafuri, there about 500 thousand tons of high-quality turkey manure. We have taken the first steps to develop complex multi-component organic and mineral fertilizers based on phosphogypsum, and turkey manure, since the sources of raw materials are close to each other.

At the site where raw poultry manure of the M. Gafuri Poultry Production unit is stored, there is an unpleasant stinking smell. The manure mass contains much weed seeds, eggs and larvae of worms and flies, and a lot of microorganisms. Long-distance transportation of manure is not economically justified and requires a lot of equipment, labor, and money. However, waste is usually concentrated in small areas, which exacerbates its negative effect. As a result, the components of ecosystems located in the zone of large poultry farms are significantly transformed (Kiryushin, 2012; Gabassova *et al.*, 2017).

Manure processing can be a reasonable solution to this situation. In particular, high-temperature drying turns manure into a decontaminated, highly concentrated fast-acting organic fertilizer with favorable physical properties, devoid of smell, and germinating weed seeds. The value and nutritional properties of dry manure will be determined by the chemical composition of the raw materials taken for processing (the original raw manure) and the drying technology. However, before

recommending the final product (dry manure) for use as a fertilizer, it is necessary to determine its potential fertilizing properties and assess its safety for environmental components.

The nutritional value of manure, like any other fertilizer, is determined by the content of the main elements of plant nutrition as nitrogen, phosphorus, and potassium (Table 2).

The nitrogen content in the manure taken for processing is low. One ton of this organic fertilizer can introduce just 6.3 kg of nitrogen into the soil. It is due to both the high moisture content of the source material and the relatively low concentration of the element per dry substance. As a rule, the nitrogen content is reduced during the drying process for its ammonia form that rapidly evaporates under thermal action.

Poultry manure is evenly applied to the fallow once per crop rotation with further placement to accelerate the transformation process.

Such important plant nutrition elements as calcium, phosphorus, and sulfur make phosphogypsum an attractive fertilizer (Davari *et al.*, 2002). Currently, the average level of the nutritive efficiency of this industrial waste is no more than 2.0 %, although in previous years it was about 2.5 million tons/year (over 10% of the current output) In agricultural production phosphogypsum can be used for the following purposes:

- for improving physical soil properties;
- for the optimization of plant nutrition with calcium, sulfur, silicon, phosphorus and trace elements;
- for soil reclamation (Tayibi *et al.*, 2009).

For Chernozem soils, the use of phosphogypsum is even more in demand, since the content of phosphorus is one of the main limiting factors.

According to literature data, recommended doses of phosphogypsum vary from 2 to 35 t / ha depending on the type of soil, crops to be grown, method and type (continuous or selective) of application and fertilizers to be used (Kotova *et al.*, 2002)

The analysis of phosphogypsum (waste from the Meleuz mineral plant) shows a high content of strontium (14691 mg/kg) and rare earth elements (cerium-1358 mg/kg, praseodymium – 123.9 mg/kg, neodymium – 418.5 mg/kg, samarium – 77.5 mg/kg, europium

– 19.9 mg/kg, gadolinium – 58.9 mg/kg, terbium-6.91 mg/kg and dysprosium 25 mg/kg), which is not typical for soils and rocks of the southern Urals. The content of oxides in phosphogypsum is shown in Table 3.

Taking into account the chemical composition of phosphogypsum, its direct and indirect influence on soil fertility, the following experimental scheme was developed:

- control
- phosphogypsum, 5 t / ha;
- phosphogypsum, 10 t / ha;
- phosphogypsum, 20 t / ha;
- poultry manure, 40 t / ha;
- phosphogypsum+poultry manure, 1:10 (40 t/ha)

Based on the current situation, a sharp decrease in the content of organic matter in the soil, the paper presents the content of humus.

When conducting experimental research, there were changes in the humus state of the soil. When applying pure phosphogypsum, there was no significant effect on the content of humus in the soil. However, when applying it together with poultry manure, there was an increase in the humus content by 0.34%. Maximum values of 7.02-7.10 % were observed when applying pure poultry manure at a dose of 40 t / ha (Table 4).

Potatoes of the Nevsky variety were grown on the experimental plots for three years. In the first year of studies, the maximum increase (307C/ha) was observed in the variants with 40 T/ha of introduced poultry manure. The use of phosphogypsum in pure form also increased from 22.2 to 91.7 C/ha with higher rates of application (Table 5). There was a higher yield at 137 C/ha in the variant with applied manure and phosphogypsum compared to the control one. As scientists claim (Baibekov *et al.*, 2012; Belyuchenko and Muravyov, 2009), at the phosphogypsum application rate of 5 t/ha, 100-130 kg of P<sub>2</sub>O<sub>5</sub> in digestible form can enter the soil. It covers the costs of agriculture significantly for phosphogypsum transportation and introduction.

The second year of research (2016) was dry, and the soil moisture content was 140 mm. It affected the yield of potatoes. The yield development by variants remained in the same sequence as the first year of research (Zinkovskaya, 2010). It is established that the phosphogypsum application at the rate of 2-4



C/ha can meet the needs of agricultural plants in nutrients and increase crop yields.

In 2017, the largest increase was observed on the variants with pure poultry manure and in a mixture with phosphogypsum, 75.7, and 63.2, respectively. The aftereffect of phosphogypsum provided a significant increase in all years of research. The application of a higher rate of phosphogypsum resulted in lower potato yield. A negative impact on the growth and development of plants led to potato inhibition. There were no toxic metals and nitrates in potato tubers in examining.

The current scientific papers provide similar ways to improve the agrochemical qualities of the soil, neutralize the reaction of the soil solution medium (Pavani and Shanmugam, 2019). Alternatively, to suppress the intake of heavy metal salts in plants (Sattar *et al.*, 2019).

However, an approach comparable to ours, involving the simultaneous synergistic use of phosphate gypsum with poultry waste, is relatively rare (Xue *et al.*, 2020).

Also, more often the mechanism of the positive effect on the crop is not appropriately discussed, and it is difficult to translate the improvement of individual soil qualities in connection with the improvement of the yield, despite the obviousness of this connection, the fact is that it is difficult to accurately determine the positive effects of the use of gypsum, which are responsible for the increase in yield because in the soil there are often many simultaneous physical and chemical changes. Improving yields may result from the additive or synergistic effect of each of these potential changes. Besides, these potential changes, no matter how different they may seem, also differ depending on the crop, soil type, and precipitation regime (Zoca and Penn, 2017).

Taking into account the chemical composition of phosphogypsum, research variants with different application rates, climatic conditions for three years provide reliable data on their impact on crop yields.

The problem of heavy metals in soils is relevant for agriculture, scientists Santos *et al.* (2006), Davari *et al.* (2012), Alloway (1990), and Mineev (1990) point out the possible accumulation of toxic metals in the soil as a result of the phosphogypsum application. Nevertheless, the authors found no significant changes in the natural levels of heavy metals if ameliorant is introduced at recommended rates directly after

the phosphogypsum application as well as in long biogeosystem sequences. Moreover, it was shown in the work of Sattar *et al.* (2019) that the use of gypsum together with poultry waste could contribute to the reduction of heavy metals in agricultural products, even at high levels of heavy metal charging of the original soils (before the application of gypsum and poultry waste).

In addition, the essential role of phosphogypsum as a fertilizer is that it has other macro and microelements in its composition. When applied to the soil in small rates, it does not have a harmful effect and, therefore, can serve as a mineral supplement (Bauer *et al.*, 2019). Another component of the fertilizer offered by the authors is poultry waste, having been widely used as a fertilizer, the subject of many papers for a long time (Szogi *et al.*, 2019). Thus, the first results of studies have shown the phosphogypsum efficiency applied both separately and in a mixture with poultry manure.

#### 4. CONCLUSIONS

The application of phosphogypsum and poultry droppings in pure form and a mixture is characterized by environmental safety. There is a high potential fertilizing value and expediency of applying secondary resources as organic fertilizers. When applied to the soil in all ratios and rates, phosphogypsum and poultry manure improve the humus state, significantly increase the yield of potatoes from 13.9 to 75.7 C/ha. Meanwhile, potatoes do not contain toxic elements and nitrates exceeding the MPC values.

#### REFERENCES

1. Alloway, B. J. Y. (1990). *Heavy metals in Soils*. New York: Wiley and Sons.
2. Arinushkina, E. V. (1970). *Guide to chemical analysis of soils*. Moscow: Moscow State University Publ.
3. Baibekov, R. F.; Shilnikov, I. A.; Akanova, N. I.; Dobrydnev, E. P.; Loktionov, M. Yu.; Sheujen, A. Kh.; Kizinyok, C. B. (2012). *Scientific and practical recommendations for using phosphogypsum neutralized as a chemical ameliorant and sulfur fertilizer*. Moscow: VNIIA Publ.
4. Bauer, P. J.; Szogi, A. A.; Shumaker, P. D. (2019). Fertilizer efficacy of poultry litter ash blended with lime or gypsum as fillers. *Environments*, 6, 50.

5. Belyuchenko, I. S.; Muravyov, E. I. (2009). Influence of industrial and agricultural wastes on physical and chemical properties of soils. *Ecological Bulletin of Northern Caucasus*, 5, 84.
6. Vadiunina, A. F.; Korchagina, Z. A. (1986). Methods to study physical properties of the soil. Moscow: Agropromizdat Publ.
7. Davari, M.; Sharma, S. N.; Mirzakhani, M. (2012). The effect of combinations of organic materials and biofertilisers on productivity, grain quality, nutrient uptake and economics in organic farming of wheat. *Journal of Organic Systems*, 7(2), 26-35
8. Dobrovolsky, G. V.; Grishina, L. A. (1985). *Conservation of soil*. Moscow: Moscow State University Publ.
9. Gabassova, I. M.; Suleymanov, A. R.; Garipov, T. T.; Sidorova, L. V.; Sayfullin, I. Yu.; Suleymanov, A. R. (2017). Assessment of slope soil suitability for irrigation in the Northern forest-steppe of Bashkortostan. *Agrarian Russia*, 5, 2-7
10. Gelashvili, D. B.; Basurov, V. A.; Efimova, N. I. (2002). Ecological and economic analysis of environmental hazards of enterprises in the agro-industrial complex. Ecological and economic bases to develop agrobiogeocenoses. *Nizhnii Novgorod*, 1, 31-35.
11. Gukalov, V. V. (2009). Influence of phosphogypsum on winter wheat growth and productivity. In *The I All-Russian scientific conference. Issues on recultivation of household, industrial, and agricultural waste* (pp. 32-34). Krasnodar: Kuban State Agrarian University Publ.
12. Khabirov, I. K. (2015) The challenge of maintaining and improving soil fertility in the Republic of Bashkortostan. *Parliament proceedings, State Assembly Kurultai of the Republic of Bashkortostan*, 60-63.
13. Khaibullin, M. M.; Kirillova, G. B.; Yusupova, G. M.; Kagirow, E. S.; Ismagilov, R. Z.; Rakhimov, R. R.; Bagautdinov, F. Y. (2018). Influence of percentage fertilizer systems on change of agrochemical properties of the arable layer of leach Chernozem and on the crops productivity of crop rotation. *Journal of Engineering and Applied Sciences*, 13(S8), 6527-6532.
14. Khamaletdinov, R. R.; Gabitov, I. I.; Mudarisov, S. G.; Khasanov, E. R.; Negovora, A. V.; Martynov, V. M.; Shirokov, D. Y. (2018). Improvement in engineering design of machines for biological crop treatment with microbial products. *Journal of Engineering and Applied Sciences*, 13(S8), 6500-6504.
15. Kiryushin, V. I. (2012). Problem of agriculture ecologization in Russia (Belgorod model). *Achievements of Science and Technology in Agriculture*, 12, 3-9.
16. Kiryushin, V. I. (2015). Developing knowledge on landscape functions with reference to better landscape management. *Bulletin of the Soil Institute named after V.V. Dokuchaev*, 80, 16-25.
17. Kotova, L. G.; Pomazkina, L. V.; Repina, O. V.; Prokofiev, A. Yu. (2002). The effect of gray forest soil pollution with fluoride on the productivity and mineral nutrition of spring wheat. *Agrokhimiya (Agrochemistry)*, 12, 31-36.
18. Mineev, V. G (1990). *Chemization of agriculture and the natural sphere*. Moscow: Agropromizdat Publ.
19. Nasir, B.; Rosmini, R.; Lasmini, S. A.; Wahyudi, I.; Edy, N. (2019). Combined application of mulches and organic fertilizers enhance shallot production in dryland. *Agronomy Research*, 17(1), 165-167.
20. Pathak, R. K. (2011). Homa jaivik Krishi: A ray of hope for sustainable horticulture MARDI's initiatives. In *National symposium cum brainstorming workshop on organic agriculture, CSKHPKV, Palampur, India held on April* (pp. 19-20).
21. Paull, J. (2011). The uptake of organic agriculture: A decade of worldwide development. *Journal of Social and Development Sciences*, 2(3), 111-120.
22. Pavani, K.; Shanmugam, P. M. (2019). Maximization of rice yield in sodic soil through combined application of gypsum and organic amendments. *Research on Crops*, 20(4), 676-684.
23. Santos, A. J. G.; Mazzilli, B. P.; Fávaro, D. I. T.; Silva, P. S. C. (2006). Partitioning of radionuclides and trace elements in phosphogypsum and its source materials based on sequential extraction methods. *Journal of Environmental Radioactivity*, 87(1), 52-61.
24. Sattar, H.; Anwar-ul-Haq, M.; Ahmad, H. R.; Jaskani, M. J. (2019). Immobilization of chromium by poultry manure and gypsum in soil and reducing its uptake by spinach grown with textile effluent irrigation. *Pakistan Journal of Agricultural Sciences*, 56(4), 791.
25. Sokolov, A. V. (1975). *Agrochemical methods of soil research*. Moscow: Nauka

- Publ.
26. Surekha, K.; Rao, K. V.; Shobha Rani, N.; Latha, P. C.; Kumar, R. M. (2013). Evaluation of organic and conventional rice production systems for their productivity, profitability, grain quality and soil health. *Agrotechnology*, 11, 1-6.
  27. Szajdak, G. S. L.; Simakina, I. (2008). Changes in the structure of nitrogen-containing compounds of peat-, sapropel-, and brown coal-based organic fertilizers. *Agronomy Research*, 6(1), 149-160.
  28. Szogi, A. A.; Shumaker, P. D.; Ro, K. S.; Sigua, G. C. (2019). Nitrogen mineralization in a sandy soil amended with treated low-phosphorus broiler litter. *Environments*, 6(8), 96.
  29. Tayibi, H.; Choura, M.; Lopez, F. A.; Alguacil, F. J.; Lopez Delgado, A. (2009). Environmental impact and management of phosphogypsum. *Journal of Environmental Management*, 90, 2377-2386.
  30. Wai, K. O. (2007). Organic Asia. *The Organic Standard*, 71(3), 3-6.
  31. Willer, H.; Kilcher, L. (2011). *The world of organic agriculture: statistics and emerging trends 2011*: Bonn: International Federation of Organic Agriculture Movements (IFOAM). Frick, Switzerland: Research Institute of Organic Agriculture (FiBL).
  32. Xue, S.; Ke, W.; Zhu, F.; Ye, Y.; Liu, Z.; Fan, J.; Hartley, W. (2020). Effect of phosphogypsum and poultry manure on aggregate-associated alkaline characteristics in bauxite residue. *Journal of Environmental Management*, 256, 109981.
  33. Zinkovskaya, T. S. (2010). *Recultivation problems of household, industrial, and agricultural waste*. Krasnodar.
  34. Zoca, S. M.; Penn, C. (2017). An important tool with no instruction manual: a review of gypsum use in agriculture. In *Advances in Agronomy* (Vol. 144, pp. 1-44). Academic Press.

**Table 1.** Raw material resources of local fertilizers and ameliorants in the Republic of Bashkortostan

| Natural raw materials   | Effect on physical and physico-chemical properties of soils  | Application efficiency depending on the type of degradation | Reserves in the Republic of Bashkortostan, mln. t |
|---|--|---|---|
| Peat  | Higher moisture capacity, porosity, absorption capacity, humus content, lower acidity              | Physical (erosion), depletion, pollution, pyrogenesis       | 134.3   |
| Phosphogypsum, phosphorites, including phosphates (peat vivianite, vivianite) | Higher phosphorus content, moisture capacity, absorption capacity, nitrogen content, microelements | Physical (erosion), depletion                               | 15.5  |
| Lignite coals   | Higher moisture and absorption capacity, adsorbing ability   | Pollution, salination                                       | 257.5   |
| Sapropel  | Higher content of humus, nitrogen, phosphorus, microelements, adsorbing ability, lower acidity     | Physical (erosion), depletion, salination                   | no data   |
| Zeolites  | Higher moisture content, absorption capacity, adsorbing ability                                    | Pollution, salination, drying                               | no data   |
| Gypsum  | Exchange sodium is replaced by calcium, and alkalinity is weakened                                 | Alkalinization  | 84.1  |
| Limestone   | Neutralized acidity  | Acidification, depletion                                    | 59.5  |

**Table 2.** *Characteristics of the nutritional value of poultry manure*

| Manure type                               | Humidity, % | Content, % per crude substance |          |          |
|---|-------------|--------------------------------|----------|----------|
|   |             | N                              | P2O5     | K2O      |
| Manure before drying                      | 75          | 0.54                           | 0.85     | 0.79     |
| Requirements for dry manure               | 14          | 4.03                           | 3.78     | 2.00     |
| The average composition of the dry manure | no > 15     | no < 2.0                       | no < 2.0 | no < 0.8 |

**Table 3.** *Chemical composition of phosphogypsum*

| Element                | Content mg/kg | Element                   | Content mg/kg |
|------------------------|---------------|---------------------------|---------------|
| Calcium oxide (CaO)    | 30.9          | Sodium oxide (Na2O)       | 0.049         |
| Iron oxide (Fe2O3)     | 0.091         | The potassium oxide (K2O) | 0.043         |
| Titanium oxide (TiO2)  | 0.079         | Magnesium oxide (MgO)     | 0.011         |
| Aluminum oxide (Al2O3) | 0.047         |                           |               |

**Table 4.** *Changes in the content of total humus in Chernozemic soil (black soil with high humus content)*

| Name of experiments                             | Humus, % |      |      |         |
|---|----------|------|------|---------|
|   | 2015     | 2016 | 2017 | average |
| Control   | 6.64     | 6.61 | 6.60 | 6.61    |
| Phosphogypsum, 5 t/ha                           | 6.65     | 6.66 | 6.64 | 6.65    |
| Phosphogypsum, 10 t/ha                          | 6.81     | 6.82 | 6.72 | 6.78    |
| Phosphogypsum, 20 t/ha                          | 6.85     | 6.81 | 6.76 | 6.81    |
| Poultry manure, 40 t/ha                         | 7.08     | 7.10 | 7.02 | 7.07    |
| Phosphogypsum + poultry litter, 1: 10 (40 t/ha) | 6.97     | 7.02 | 6.94 | 6.98    |

**Table 5. *Potato yield***

| Experiment<br>Variants                             | 2015  |          | 2016  |          | 2017  |          |
|--|-------|----------|-------|----------|-------|----------|
|  | Yield | Increase | Yield | Increase | Yield | Increase |
|  | C/ha  |          |       |          |       |          |
| Control  | 113.0 | -        | 98.9  | -        | 74.3  | -        |
| Phosphogypsum, 5 t/ha                              | 135.2 | 22.2     | 100.4 | 1.5      | 88.9  | 14.6     |
| Phosphogypsum, 10 t/ha                             | 140.3 | 27.3     | 102.2 | 3.3      | 91.0  | 16.7     |
| Phosphogypsum, 20 t/ha                             | 210.1 | 97.1     | 100.9 | 2.0      | 88.2  | 13.9     |
| Poultry manure, 40 t/ha                            | 420   | 307      | 150   | 51.1     | 150   | 75.7     |
| Phosphogypsum + poultry<br>litter, 1: 10 (40 t/ha) | 250.0 | 137      | 132.5 | 33.6     | 137.5 | 63.2     |

**MODELAGEM E PROVA DE SOLUÇÕES DE PROJETO PARA A RECONSTRUÇÃO DA ESTAÇÃO DE TRATAMENTO DE ÓLEO E ÁGUA****MODELING AND PROVING OF DESIGN SOLUTIONS FOR THE RECONSTRUCTION OF TREATMENT FACILITY OF OIL AND WATER****МОДЕЛИРОВАНИЕ И ОБОСНОВАНИЕ ПРОЕКТНЫХ РЕШЕНИЙ ПРИ РЕКОНСТРУКЦИИ ПЛОЩАДНОГО ОБЪЕКТА ПОДГОТОВКИ НЕФТИ И СТОЧНОЙ ВОДЫ**

LEKOMTSEV, Alexander Viktorovich<sup>1\*</sup>; ILIUSHIN, Pavel Yurjevich<sup>2</sup>; KOROBV, Grigory Yurievich<sup>3</sup>

<sup>1,2</sup> Perm National Research Polytechnic University, Perm, Russian Federation

<sup>3</sup> St. Petersburg Mining University, St. Petersburg, Russian Federation

\* Correspondence author  
e-mail: alex.lekومتsev@mail.ru

Received 13 May 2020; received in revised form 21 May 2020; accepted 11 June 2020

**RESUMO**

O problema de preparar produtos de petróleo de alta qualidade é que produz água para reutilização e injeção no reservatório em condições de capacidade limitada das instalações. Essa é uma questão relevante no setor de petróleo e gás. Assim, o objetivo desta pesquisa foi desenvolver uma abordagem para a justificativa das decisões de projeto durante a reconstrução da Unidade Preliminar de Descarga de Água. O artigo considera a questão da modelagem de soluções de projeto para a reconstrução da unidade preliminar de descarga de água (região de Perm) com uma unidade móvel. As principais tarefas industriais são reduzir o corte de água do produto e o volume de bombeamento de lastro na Unidade de Preparação de Óleo (OPU) para fornecer a qualidade da água de fundo para injeção na formação atendendo aos requisitos da norma industrial. A instalação móvel é um desenvolvimento inovador e possui todo o equipamento necessário para recriar o processo de produção da preparação de produtos de poço em uma escala de aproximadamente 1: 100. Os resultados da simulação do processo de produção do poço mostraram que pode ser alcançado 1% com aquecimento a 30°C na injeção dos desmulsificadores SNPH-4880, STH-9. O método complicado mostrou uma dependência funcional e estável dos indicadores de temperatura e qualidade do processo na presença de um desmulsificador. Durante os testes de bancada foram encontrados valores de indicadores tecnológicos que proporcionaram a redução do volume de bombeamento de lastro em uma média de 5-6%. Estudos de amostras de água da saída da unidade móvel mostraram os melhores resultados ao testar o STH-9. Os resultados obtidos são de grande importância prática, e o método e o equipamento móvel especial proposto no artigo podem ser usados em qualquer planta de produção de tratamento de óleo.

**Palavras-chave:** refino de petróleo, refino de águas profundas, produção de poços, instalação móvel, emulsão de água e óleo.

**ABSTRACT**

The problem with preparing high-quality petroleum products is that it produces water for reuse and injection into the reservoir under conditions of limited facility capacity. This is a relevant issue in the oil and gas sector. Thus, the objective of this research was to develop an approach to justify project decisions during the reconstruction of the Preliminary Water Discharge Unit. The article considers the issue of modeling design solutions for the restoration of the preliminary water discharge unit (Perm region) with a mobile unit. The main industrial tasks are to reduce the water cut of the product and the volume of ballast pumping in the Oil Preparation Unit (OPU) to provide the quality of the background water for injection in the formation meeting the requirements of the industrial standard. The mobile installation is an innovative development and has all the necessary equipment to recreate the production process of the preparation of well products on a scale of approximately 1: 100. The results of the simulation of the well production process showed that it could be achieved 1 % with heating at 30°C in the injection of demulsifiers SNPH-4880, STH-9. The complicated method showed a functional and stable dependence on the temperature and quality indicators of the process in the presence of a demulsifier.

During bench tests, values of technical indicators were found that reduced the volume of ballast pumping by an average of 5-6%. Studies of water samples from the outlet of the mobile unit showed the best results when testing the STH-9. The results obtained are of great practical importance, and the method and the special mobile equipment proposed in the article can be used in any oil treatment production plant.

**Keywords:** *oil refining, refining of bottom water, well production, mobile installation, water-oil emulsion*

## АННОТАЦИЯ

Проблема подготовки высокого качества нефтепродуктов заключается в том, что в процессе образуется попутно добываемой вода для повторной использования и закачки в пласт в условиях ограниченных производственных мощностях. Это актуальная проблема в нефтегазовой области. Таким образом, цель этого исследования состояла в том, чтобы разработать подход для обоснования проектных решений по реконструкции установки предварительного сброса воды. В статье рассматривается вопрос моделирования проектных решений для восстановления работы установки предварительного сброса воды (Пермский край) с использованием мобильной установки. Основными производственными задачами являются снижение обводненности подготовленной продукции, уменьшение объема балластных перекачек на установке подготовки нефти (УПН), а также доведение качества подтоварной воды для закачки в пласт до требований отраслевого стандарта. Мобильная установка является инновационной разработкой и обладает всеми необходимым оборудованием для воссоздания производственного технологического процесса подготовки скважинной продукции в масштабе примерно 1:100. Результаты моделирования процесса подготовки скважинной продукции показали, что возможно достичь обводненность 1% при нагреве до 30°C в присутствии деэмульгаторов СНПХ-4880, СТХ-9. Комплексный метод на показал устойчивую функциональную зависимость температуры процесса и показателей качества в присутствии деэмульгатора. В ходе стендовых испытаний установлены диапазоны технологических показателей, при которых снизился объем балластных перекачек, в среднем, на 5-6%. Исследования проб воды по выходу из мобильной установки показали наилучшие результаты при испытании СТХ-9. Полученные результаты имеют важное практическое значение, а предложенные в статье метод и специальное мобильное оборудование может быть использовано на любой производственной установке подготовки нефти.

**Ключевые слова:** *подготовка нефти, подготовка подтоварной воды, скважинная продукция, мобильная установка, водонефтяная эмульсия*

## 1. INTRODUCTION:

To refine oil and wastewater, there is a regular need for technologies and technical means to be used and to improve the quality of the final product up to the relevant standards, regulated by the state authorities and regulatory documentation of oil and gas companies. There is no detected strictly defined combination of methods and technologies in industry practice to bring the quality of products to the commercial standards or standards of a company within the terms of physical and chemical properties diversity and variable composition of the crude oil (Kokal, 2002). Therefore, there is a need for oil and gas companies to test the most appropriate and effective methods regarding the refining of oil and wastewater per each area facility. This question becomes particularly relevant as the current time technology of refining at the area facility in the short term will not be sufficient, which will require operational changes in the technological process (Kokal, Wingrove, 2000). Any change of procedure of the area facility requires a significant investment (time, administrative, finance) and,

ultimately, might be technologically and economically feasible (Marquez-Silva, 1997). The results of laboratory modeling of the process regarding the refining are often turned to be estimated due to researching within the conditions to be different from the real (Tronov, 1977).

Increasing interest is received by mini- and micro-installations, the use of which is aimed at solving a specific problem within an industrial facility (Lekomtsev, Ilyushin, *et al.*, 2018). Laboratory studies performed on model samples, when well production has complex compositions and properties, become uninformative (Ilyushin, Usenkov *et al.*, 2017). The results of the studies often do not correlate with the actual situation in production (Tretyakov, Mazein, *et al.*, 2017). The current trend in the refining of downhole products is minimizing the size of the equipment with an increase in their level of manufacturability (Bahadori, 2014), as well as the transition from laboratory research to field tests (Li, Wengerter, *et al.*, 2016). This opinion proves the need to create a site (testing ground) for testing modern scientific methods and technologies and adapting

theoretical studies to the existing practice (Lekomtsev, Ilyushin, 2016). The way out is the creation of mobile units (The Canadian Association of Petroleum Producers, 2014).

A disadvantage of the known studies is the lack of a systematic approach and the corresponding technology for carrying out bench (field) testing of techniques for improving the quality of the preparation of tank oil and water for injection into the reservoir. Based on the Scientific-educational Centre for Geology and the Development of Oil and Gas Fields of the Perm National Research Polytechnic University, there is a unit created allowing to simulate different technological modes onto the current facility of refining without affecting the primary process (Tretyakov, Usenkov, *et al.*, 2016).

The principle of the unit is the destruction of Water-Oil Emulsion (WOE) by traditional and new technologies that are available at industrial facilities (Rzayev, Rasulov, 2013). Modern ideas about the stability of water-oil emulsions are concentrated in the theory of Deryagin-Landau-Fairway-Overbek (DLFO theory) (Deryagin, 1986). According to the method, the formation of structural-mechanical protective layers at the interphase boundaries is decisive importance in ensuring the stability of a WOE (Salager, 1990). Resistant layers can resist deformation and destruction and can "heal" defects arising from the contact of particles of the dispersed phase (the wedging effect of the Rebinder). Three stages determine the staging of the process of destruction of a WOE. For each stage, it is used technologies that are characterized by different efficiency and manufacturability (Zhang, 2010). The main ones are the use of chemical reagents, coalescing nozzles, magnetic, electric, and acoustic impact (Wallau, Schlawitschek *et al.*, 2016), heating (Schubert, Brandner, 2001), centrifugation and sedimentation with specific equipment and materials (Wang, 2016).

The developed unit has all the necessary equipment to recreate the production process of refining well products on a scale of approximately 1: 100. Due to this, in real-time, it is possible to assess the current and future possibilities of the refining facility when changing volume and composition crude oil production. It has the potential to allow to predict the product quality for several years ahead in the future.

The main practical value of the unit is the approbation of projects for the modernization of industrial plants and the rationale for investment costs for the purchase of equipment and the

construction of additional facilities. The article considers the issue of assessing design solutions for the reconstruction of a Preliminary Water Discharging Unit (PWDU) using a developed mobile unit in the Perm region (Russia). The aim of technological reconstruction of the area facility was the bringing of oil quality to the conformity of group 3 under Russian Government Standard requirements (GOST 51858-2002) regarding the content of water to reduce ballast pumpings up to Oil Preparing Unit (OPU) and to improve the quality of produced water (SSP – 15 mg/L; oil products – 15 mg/L).

The target of field treatment of crude oil is to reduce the resistance of WOE, to their disintegration, and to degrade the SSP and oil ratio within the wastewater (Tumanyan, 2000). To disintegrate the WOE, the most important aspect is the process of Armoured Shells (AS) removing of Emulsified Water Droplets (EWDs) and the separation of oil and water into separate phases (Nebogina, 2010). WOE stability is a critical factor regarding the disintegration of oil and water mixture and characterizes the ability not to be exfoliated for oil and water within a time specified. The factors greatly influence a drop AS stability (kinetic and aggregative) within the emulsion as following: coagulation and fragmentation of drops within a turbulent flow; disperse composition; physical and chemical properties of natural emulsifiers forming armored shells; the double emulsion layer presence on EWDs; the temperature of miscible liquids (oil and water); specific consumption of demulsifier; the pH of the reservoir water emulsified (Sakhabutdinov, Kosmacheva *et al.*, 2007). Also, one of the methods of water refining is electrocoagulation. Electrocoagulation is a progressive technological direction for getting rid of water from polluting substances by cleaning it in an electrolyzer with soluble electrodes. When an aqueous solution is found under the influence of a constant electric field, coarse impurities are destroyed, colloidal contaminants are aggregated, which stimulates the process of phase separation and water purification. The method of electrocoagulation of water shows excellent results in the refining of industrial water from finely dispersed organic monomers and polymers, emulsions, and refined products. It is useful in ridding water solutions of excess phosphates and chromates (Tetreault, 2003).

The purpose of this work was to develop an approach to the justification of design decisions during the reconstruction of the Preliminary Water Discharging Unit and select the necessary



equipment to reduce the water content of products refined. Also, it is aimed to decrease the number of ballast pumpings onto OPU, as well as bringing the quality of the produced water to be injected into the formation up to the requirements of Industrial Standard (IS-39-225-88).

During the research and pilot tests, the following tasks were solved:

- the confirmation of the technological scheme of the facility;
- the determination of temperature mode of refining;
- the selection of reagent-demulsifier from the number of recommended ones due to the results of laboratory tests.

## 2. MATERIALS AND METHODS:

### 2.1. The description of the mobile unit

The mobile well production preparing unit (MU) provides a core technology for oil refining (regarding the Russian government standard GOST 51858-2002): demulsification (dehydration), desalting, purification from mechanical impurities, oil stabilization (hot separation). According to this standard, oil is divided into three groups depending on the value of this parameter. Refining of wastewater used for flooding oil fields (regarding the Industrial Standard IS 39-225-88) – removal of oil products and Solid Suspended Particles (SSP). Due to mobility, the unit allows executing the refining of oil and water onto the well cluster sites with their low capacity of the product pumped without capital construction and arrangement of the area facility (Figures 1a and 1b). The mobile well production preparing unit technical characteristics are represented in Table 1. The PWDU existing and technological design schemes are shown in Figures 2a and 2b.

Under the technological project scheme of refining, the products shall come into the BE-2 container, which is used as a two/three-phase separator with its possibility of separating and discharging of formation water. From BE-2, the liquid separated from the gas under the pressure of 0.2-0.25 MPa is supplied to the pump intake of inner pumping P-1,2, which pumps the pressure up to 0.45 MPa, and feed the fluid into the heating block, consisting of two heaters H-1,2, which provides the liquid heating up to 40-45 °C. The heated flow past the heaters is fed to the OG-1 oil sumps, 2, where the thermochemical process of

oil dehydrating at a pressure of 0.3 MPa is performed. The dehydrated oil with its water content of up to 3 % is supplied into the BE-3 buffer tank. From BE-3 via the pump of oil external transporting through the oil metering unit, it is periodically pumped out onto the OPU. The gas separated in the process is sent to the gas turbine unit and is used as an energy source for heating the incoming raw materials. The content of sulfur-containing volatile compounds is low; therefore, associated petroleum gas is used without preliminary treatment.

Under the current scheme, the mobile unit was connected prior to the BE-2 serving as a buffer-degasser (E-1 in the MU). The modeling of piping the heaters was implemented by the heating system consisting of a heat exchanger, the H-4 pump, and the E-4 tank with the heaters. The E-5 horizontal type unit was consistent with the oil-settling tanks OG-1, 2. The products from the E-5 output were supplied into the drainage system. Within the field activities onto the mobile well production preparing unit prior to the maintenance, the demulsifier was brought into. To keep the experiment pure, the feeding of the demulsifier at the facility was not executed.

The properties of oil feeding into the PWDU are represented in table 2. Crude oil has an average viscosity, high gas factor, and is highly asphaltenic (Vyatkin, Kochnev, *et al.*, 2017).

### 2.2. The calibration and testing of the mobile unit

The calibration of the mobile unit prior conducting the simulation was to define the operating parameters (flow, pressure, temperature) under which the quality parameters (water content within the oil, chlorinated salts, mechanical impurities) of the mobile well production preparing unit output product and the refining facility were corresponding. The mobile unit performed the calibration mode past a series of experiments with regard to compliance of well products time spent within technological devices while ensuring the performance indicators as following (Table 3).

The water content at the outfeed of the bench (MU) and field installations is equal to 2%. The indicators of formation water quality have their differences, and the SSP content past the stand is above the field data, the oil content in water is lower than within the field facility. This fact indicates the high velocity of water discharging and capturing a more significant number of solid particles within the flow. The consumption rate at the time of the recording mode exceeded the

estimated per 53%. The increased content of oil products in the water at the outfeed from the production facility in comparison with the bench data is associated with the process temperature, which at the time of the experiment differed per 3 °C.

When increasing the flow rate of oil up to 0.76 m<sup>3</sup>/h (corresponds to 88 m<sup>3</sup>/h at the PWDU), the water content is risen sharply at the outfeed up to 18%, and the water quality worsens: SSP – 76 mg/l; oil products – 159 mg/L. Thus, the mobile well production preparing unit calculated mode fully describes the technological process of the PWDU.

### 2.3. The experimental-industrial testing

The modeling of advanced technological scheme past establishing a calibration mode of operation was performed under the rates calculated below.

The consumption of oil within the mobile well production preparing unit when testing is selected based on the equil time of treatment into operating volumes of OG-1, 2 at the PWDU and the E-5 tank installed on Mobile Unit:

$$Q_{MWPPU} = Q_{PWDU} \frac{\frac{L_{liq\ E-1}}{d_{E-1}} V_{E-5}}{V_{OG-1\ perf} + V_{OG-2\ perf}} = 0.22 \frac{m^3}{h} \quad (\text{Eq. 1})$$

Where  $V_{nom\ E-1}$  – the E-5 nominal volume – 1.6 m<sup>3</sup>;  $L_{liq\ E-1}$  – the liquid level – 740 mm;  $d_{E-1}$  – the E-5 diameter – 800 mm;  $V_{OG-1\ perf}$ ,  $V_{OG-2\ perf}$  – the operating volumes of OG-1, 2 – 100 m<sup>3</sup>,  $Q_{PWDU}$  – the pumping of oil from PWDU – 720 m<sup>3</sup>/day or 30 m<sup>3</sup>/h; daily water injection under the PWDU – 200-220 m<sup>3</sup>/day 8.3-9.2 m<sup>3</sup>/h; the ratio of oil pumping out/water pumping out – 27.8-30.6%.

To ensure the time of degassing of products input into the Mobile Unit, corresponding to a PWDU, the working volume of the E-1 should be:

$$V_{E-1} = V_{BE-2\ nom} \frac{L_{liq}}{L_{nom}} \frac{Q_{MU}}{Q_{PWDU}} = 0.82 m^3 \quad (\text{Eq. 2})$$

Where  $L_{liq}$  – the fluid level within the BE-2 – 1.9 m,  $L_{nom}$  – the nominal level within the BE-2 – 3.4 m. The fluid level in E-1 will be:

$$L_{liq\ E-1} = L_{nom\ E-1} \frac{V_{E-1}}{V_{nom\ E-1}} = 0.94 m \quad (\text{Eq. 3})$$

The consumption of water within the mobile well production preparing unit is regulated regarding the interface level in the E-5 at around

280-350 mm and, on average,  $Q_{MU(v)} = 0,076 m^3/h$ , which is 30% of the pumping volume of oil.

When conducting the field tests, the technological standards met the calculated values accordingly. Before the pilot tests on a mobile unit for model samples of emulsions, demulsifiers were selected. The most effective were brand demulsifier SNPH-4880, SNH-4114, STH-9 with the consumption of 70 g/ton. Demulsifiers showed the highest rate of emulsion separation; therefore, they were selected for field tests. Within the modeling process, it was succeeded to heat the products up to 30 °C in connection with the frequency of fluid intake because of the presence of the cork of the pumping mode till the PWDU and high velocity of the liquid phase flowing under images.

### 3. RESULTS AND DISCUSSION:

The results of the process modelling on refining of well production show that under the existing volumes of crude oil feeding, the refined oil pumping to the OPU and time and sediment term, it was enabled to reduce the water content u to 1% when heated to 30 °C in the presence of demulsifiers SNPH-4880, STH-9 (Figures 3 and 4).

The quality of oil refining onto the PWDU under the current scheme is not regulated and the water content at the outfeed of the installation varies from 2 to 10%. The proportion of the fluid fed at the OPU is 8.6%. The reducing and maintaining the water content up to 3% will decrease the daily volume of ballast pumping more than 40 m<sup>3</sup>.

The studies of water samples at the mobile well production preparing unit output have shown their best results within the testing of the STH-9. It is clear from Figures 3 and 4 that the synergistic effect of heating and chemical reagent supplying is decreased under the process temperature increasing. This is due to the high emulsion stability and the strength of armored shells of small droplets within the dispersed phase, requiring higher energy to perform its disintegrating (Zlobin, 2015). Besides, the size of the particles remaining in suspension under the flow temperature increased is not involved in the process of sedimentation and put away with water flow. The limitations on the effectiveness of thermo-chemical and gravitational processes of water refining are estimated at up to 45 °C for the given conditions (Figures 3 and 4). The bench tests, together with the results of sewage samples analysis, represent stable, functional dependence

of the process temperature and the quality parameters under the action of the demulsifier. They are ensuring the temperature of the refining process up to 37-40 °C evidences the fulfillment of the industrial standard requirements regarding the SSP and oil content within produced water.

In this field research, the similarity method is used to study the effect of destruction WOE and application study results to the real industry (Yemelyanov et al., 2019). This section discusses the technique of modeling crude oil refining with a developed mobile unit.

#### 4. CONCLUSIONS:

Thus, within the course of bench tests regarding the modeling of the refining process at the pilot mobile unit, the effectiveness of the PWDU designed technological scheme has been approved. According to the results of the studies conducted, it is possible to conclude the following:

1. The new product developed – mobile well production preparing unit – is industrially applicable and has shown its high convergence of scalable technology.
2. The proposed approach regarding the transition from the laboratory modelling to the field testing within a facility real conditions allows to increase the reliability of the results obtained and to justify the design decisions.
3. The ranges of technological parameters onto an area facility are set, under which it is possible to reduce the volume of ballast pumping an average of 5-6%.

The dependence of the wastewater quality indicators is set, based on the design scheme of an area facility depending on the process temperature and the demulsifier brand. The calculated boundaries per the heating temperature of the well production in the range of 37-40 °C to meet the requirements for commercial water quality up to the requirements of industry standards have been defined.

#### 5. ACKNOWLEDGMENTS:

The article was prepared on the basis of research conducted with financial support from the Russian Ministry of Education and Science within the framework of the Federal Target Program "Research and Development in Priority Directions for the Development of the Russian Science and Technology Complex for 2014–2020" (Unique project identifier RFMEFI62120X0038.)

#### 6. REFERENCES:

1. Bahadori A., Hazardous Area Classification in Petroleum and Chemical Plants. A Guide to Mitigating Risk, 2014.
2. Deryagin B.V. The Theory of Stability of Colloids and Thin Films. Moscow: Science, 1986, 368 p.
3. Ilyushin P.Yu., Usenkov A.V., Tretyakov O.V., Lekomtsev A.V., Mazein I.I., Khasanov R.F., Gorbushin A.V., Durbazhev A.Y., (2016). Unit for pretreatment of production fluid: pat. 2616466 Russian Federation no. 2016114262; appl. 12.04.16; publ. 17.04.17. Bull. no. 11.
4. Kokal S. Crude oil emulsions: A state-of-art review, SPE Paper 77497, 2002 SPE Annual Technical Conference and Exhibition, San Antonio, TX, USA, September 29-October 2.
5. Kokal S., Wingrove M., (2000). Emulsion Separation Index: From Laboratory to Field Case Studies. Presented at the SPE Annual Technical Conference and Exhibition, Dallas, Texas, 1-4 October. SPE-63165-MS. <http://dx.doi.org/10.2118/63165-MS>.
6. Lekomtsev A.V., Ilyushin P. Yu., Martyshev D.A., (2018). Experience of introduction of intensification device on the mobile plant for preparation of oil well product. Chemical and Petroleum Engineering, Volume 54, Issue 3–4: 213-218. <https://doi.org/10.1007/s10556-018-0465-4>
7. Lekomtsev A.V., Ilyushin P.Yu., Shishkin D.A., (2016). Cluster technology of preparation and injection of produced water into the reservoir using a pipe phase divider. Exposition Oil & Gas 7: 85-88.
8. Li Y.a, Wengerter M.b, Gerken I.a, Nieder H.c, Scholl S.b, Brandner J.J.a. Development of an efficient emulsification process using miniaturized process engineering equipment. Chemical Engineering Research and Design. Volume 108, 1 April 2016, Pages 23-29
9. Marquez-Silva R.L., Key S., Marino J. et al., (1997). Chemical Dehydration: Correlations between Crude Oil, Associated Water and Demulsifier Characteristics, in Real Systems.

- Presented at the International Symposium on Oilfield Chemistry, Houston, Texas, 18-21 February. SPE-37271-MS. <https://doi.org/10.2118/37271-MS>.
10. Nebogina N. A., Prozorova, I. V., Savinykh, Yu. V., Yudina, N. V. (2010). The influence of natural surfactants on the stabilization of oil-water emulsions. *Petroleum Chemistry*, vol. 50, 2: 158-163.
  11. Rzaev V. G., Rasulov S. R., Abasova I. A., Ragimova S. N., (2013). The Modelling of Nanotechnological Processes of Formation and Disintegration of Oil Emulsions. *The Equipment and Technologies for Oil and Gas Industry* 5: 54-58.
  12. Sakhabutdinov R. Z., Kosmacheva T. F., Gubaydulin F. R., Tatyana O. S., (2007). The Causes of Water-Oil Emulsions Stability Increasing. *Oil Industry* 1: 74-77.
  13. Salager J.L. The Fundamental Basis for the Action of a Chemical Dehydrant: Influence of Physical and Chemical Formulation on the Stability of an Emulsion. *Intl. Chemical Engineering* 30 (1): 103.1990.
  14. Schubert K., Brandner J., Fichtner M., Linder G., Schygulla U., Wenka A. Microstructure devices for applications in thermal and chemical process engineering. *Microscale Thermophysical Engineering*, 5 (1) (2001), pp. 17-39
  15. Small, Portable Oil & Gas Production Facilities: Recommended Solutions for Design and Operation. SAFETY GUIDE, The Canadian Association of Petroleum Producers (CAPP), July 2014.
  16. Tetreault, A. Electrocoagulation Process for Wastewater Treatment. Sydney NSW: 1-29. 2003.
  17. Tretyakov O. V., Mazein I. I., Usenkov A. V., Lekomtsev, V. A., Ilyushin, P. Yu., (2017). The Development and Implementation of a Mobile Unit for Preparation of Well Products. *Oil & Gas Exhibition* 2: 80-82.
  18. Tretyakov O.V, Usenkov A.V, Lekomtsev A.V, Ilyushin P.Yu., Galkin S.V., (2016). Results of pilot tests of mobile unit for well production treatment. *Oil Industry* 12: 131-135.
  19. Tronov V.P., 1977. Oil treatment. Moscow: Science.
  20. Tumanyan B. P., (2000). The Scientific and Applied Aspects of the Theory of Petroleum Disperse Systems. – M.: Technology.
  21. Vyatkin K.A., Kochnev A.A., Lekomtsev A.V., (2017). Evaluation of oil viscosity expansion and property investigation of oil-water emulsion in Perm region. *Exposition Oil & Gas* 2: 89-93.
  22. Wallau W., Schlawitschek C., Arellano-Garcia H. Electric Field Driven Separation of Oil-Water Mixtures: Model Development and Experimental Verification. *Industrial and Engineering Chemistry Research*. Volume 55, Issue 16, 27 April 2016, Pages 4585-4598
  23. Wang Z. Rapid and efficient separation of oil from oil-in water emulsions using a janus cotton fabric. *Industrial and Engineering Chemistry Research*. Volume 55, Issue 16, 27 April 2016, Pages 4585-4598.
  24. Yemelyanov, V. A., Yemelyanova, N. Y., Nedelkin, A. A., Glebov, N. B., & Tyapkin, D. A. (2019). Information system to determine the transported liquid iron weight. Paper presented at the Proceedings of the 2019 IEEE Conference of Russian Young Researchers in Electrical and Electronic Engineering, EIConRus 2019, 377-380. doi:10.1109/EIConRus.2019.8656693
  25. Zhang L.-M. Desing, experiment and practical application of high voltage electrostatic coalesce. *Gaodianya Jishu*. High Voltage Engineering. Volume 36, Issue 7, July 2010, Pages 1797-1802.
  26. Zlobin A. A., (2015). The Experimental Studies of the Processes of Aggregation and Self-Assembly of Nanoparticles within the Oil Disperse Systems. *The Bulletin of Perm National Research Polytechnic University. Geology. Oil and Gas Treatment*, 2015, V. 14, No. 15: 57-72.

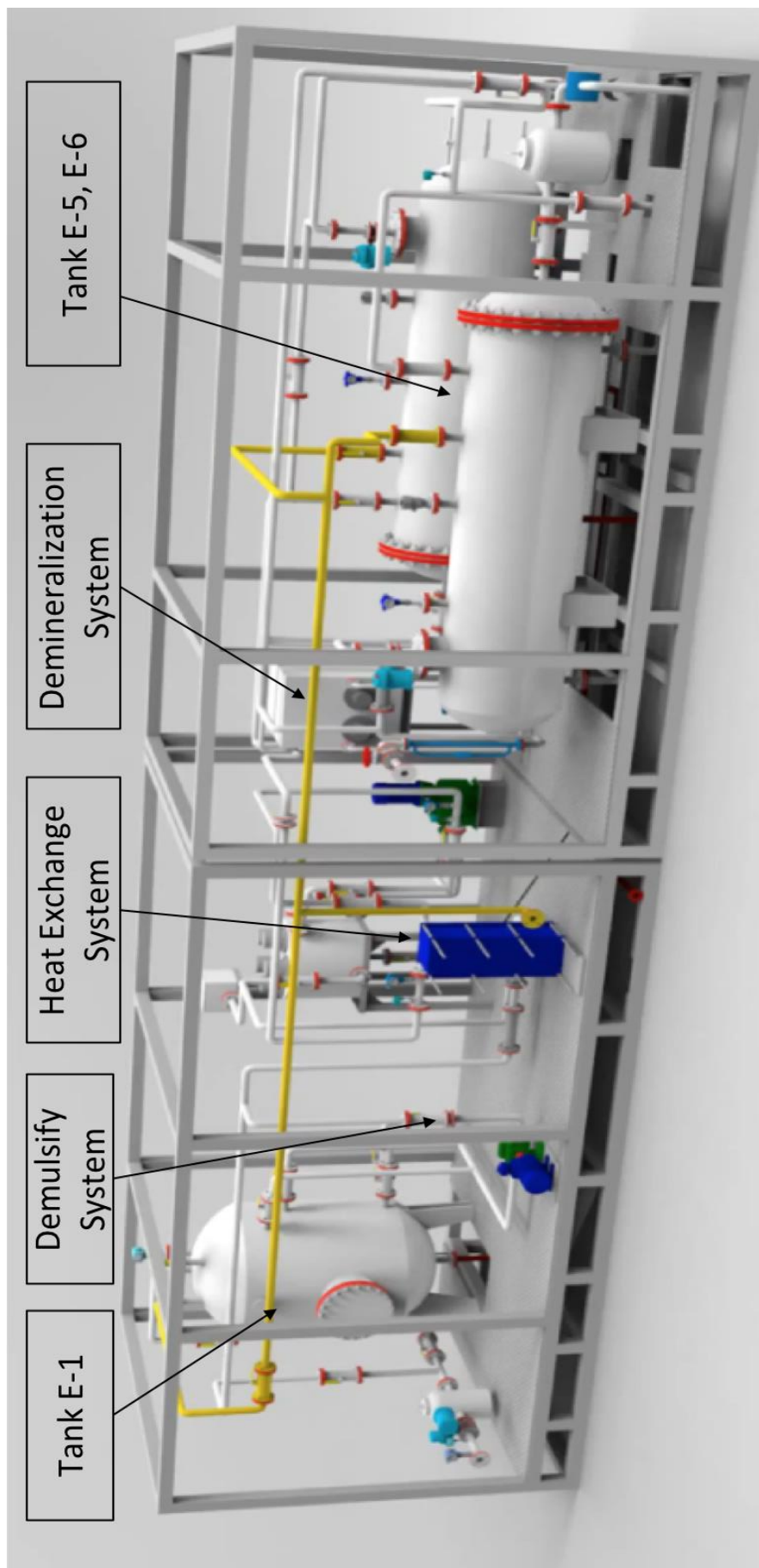


**Figure 1a.** View of Mobile Unit - Inside view



**Figure 1b.** View of Mobile Unit - Outside view

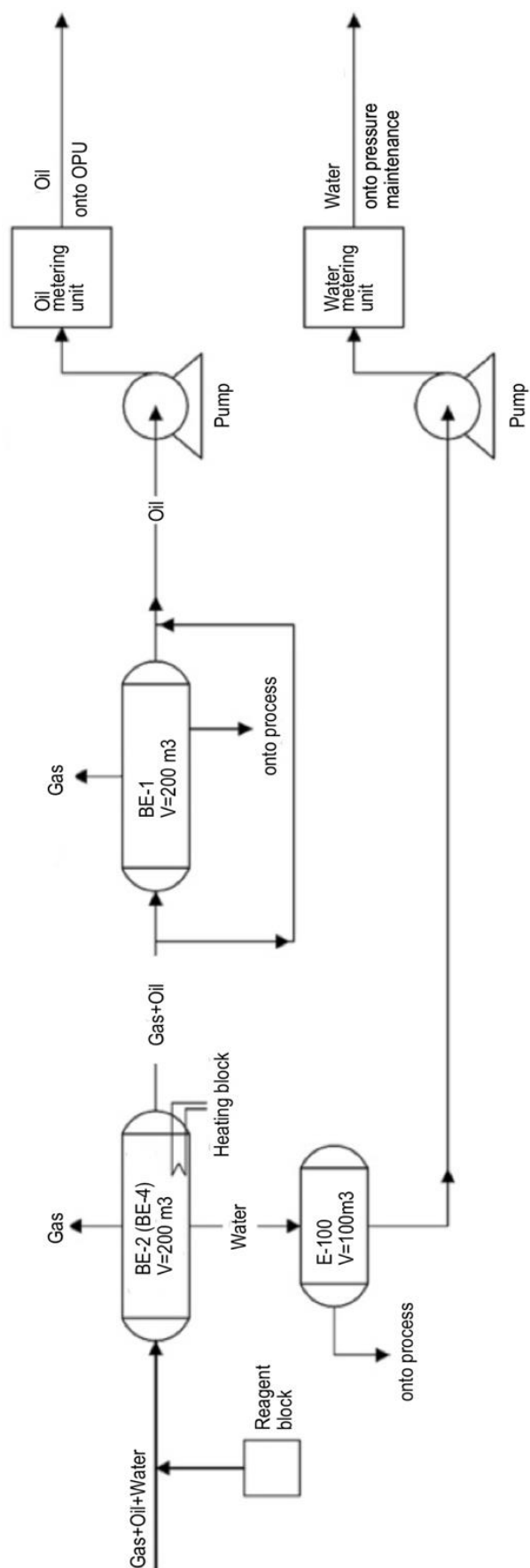


**Figure 2a.** The Technological Scheme - Acting





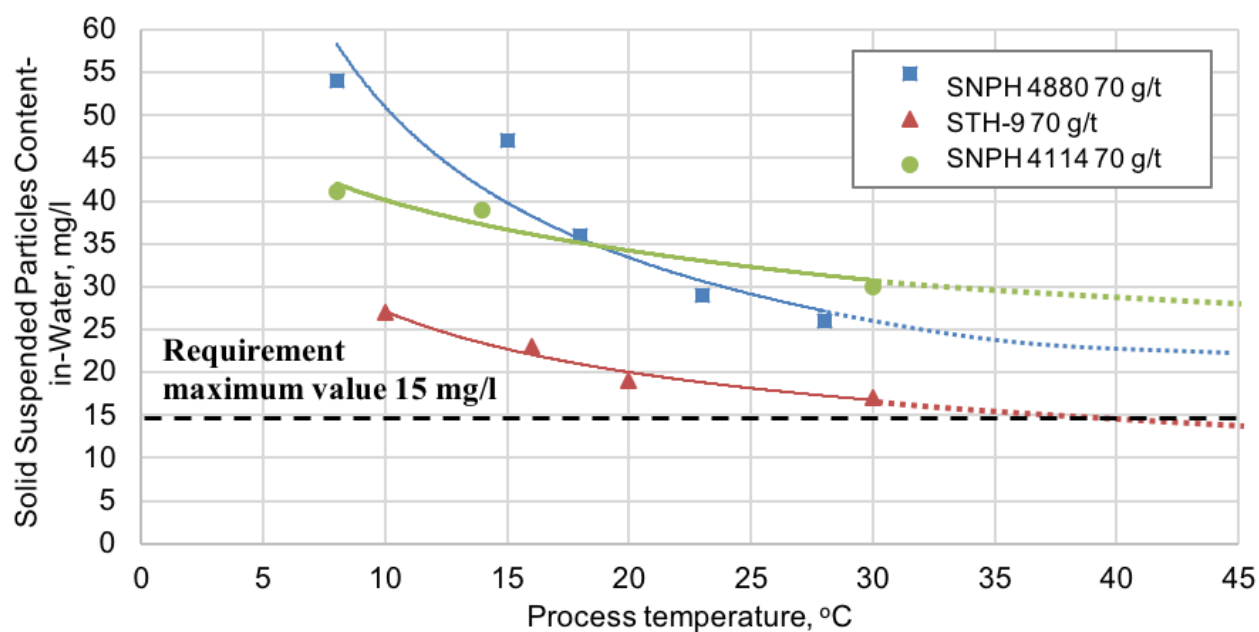


**Figure 3.** The results of wastewater testing on the solid suspended particles content under the testing of demulsifiers.

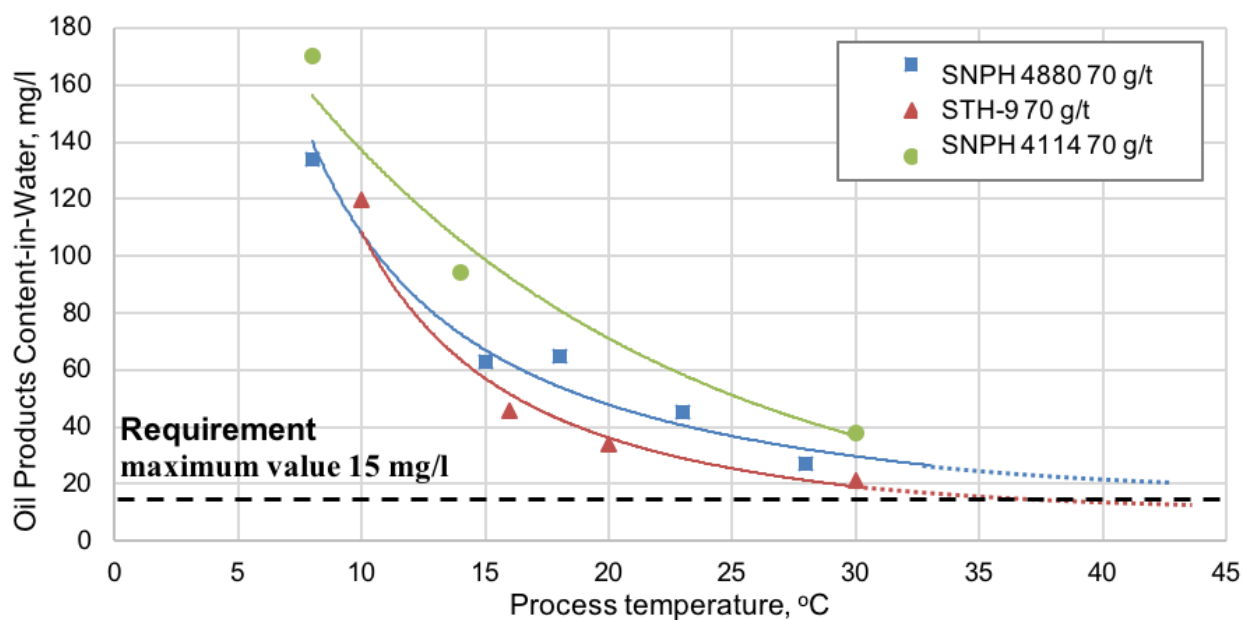


**Figure 4.** The results of wastewater testing on the oil products content under the testing of demulsifiers

**Table 1.** *The MU Technical Characteristics*

| Name                                 | Units             | Value       |
|--------------------------------------|-------------------|-------------|
| The unit productivity                | m <sup>3</sup> /h | 0.1...2     |
| The pressure in the connection point | MPa               | 0.015...1.0 |
| The temperature of fluid pumped      | °C                | +5...+70    |
| The water content                    | %                 | 1...99      |
| The power consumption                | kW                | 80          |
| The unit overall dimensions          | mm                |             |
| length                               |                   | 12000       |
| width                                |                   | 3000        |
| height                               |                   | 3300        |
| Net weight                           | kg                | 13000       |

**Table 2.** *The Properties of Oil*

| Parameters                                 | Value |
|--|-------|
| Degassed Oil Density, kg/m <sup>3</sup>    | 901   |
| Oil Viscosity within the Reservoirs, MPa·s | 18.96 |
| Content, % wt.                             |       |
| Paraffin                                   | 6.84  |
| Resins and Asphaltenes                     | 19.04 |
| Sulfur                                     | 2.2   |
| Gas Content, m <sup>3</sup> /t             | 43    |
| Saturation Pressure, MPa                   | 11.48 |

**Table 3.** *The Calibration Mode of Production Refining onto Mobile Unit and Industrial Unit*

| The Norm of the Technological Mode                 | Mobile Unit | Industrial Unit |
|--|-------------|-----------------|
| Volume of Fluid under Dehydration, m <sup>3</sup>  | 0.676       | 78              |
| Refining Period, h                                 | 2.6         |                 |
| Temperature, °C                                    | 13          | 10              |
| Pressure, kgs/cm <sup>2</sup>                      | 1.2         | 1.2             |
| Liquid Consumption Rate, m <sup>3</sup> /h         | 0.26        | 30              |
| Consumption (Discharge) of Water m <sup>3</sup> /h | 0.116       | 9.2             |
| Ratio of Pumping Oil/Pumping Water, %              | 44.6        | 30.6            |
| <b>Analytical Control</b>                          |             |                 |
| Water Content (in oil), %                          | 2           | 2               |
| The Content of SSP (in water), mg/l                | 51          | 21              |
| Oil Products Content (in water), mg/l              | 24.6        | 59              |

## ANÁLISE DE FATORES EXPLORATÓRIOS DO INTERESSE DE CARREIRA DE CIÊNCIA, TECNOLOGIA, ENGENHARIA E MATEMÁTICA PARA FUTUROS PROFESSORES DE MATEMÁTICA E CIÊNCIA: UM CASO DA UNIVERSIDADE DE LAMPUNG, INDONÉSIA

### EXPLORATORY FACTOR ANALYSIS OF SCIENCE, TECHNOLOGY, ENGINEERING AND MATHEMATICS CAREER INTEREST FOR PRE-SERVICE MATH AND SCIENCE TEACHERS: A CASE OF LAMPUNG UNIVERSITY, INDONESIA

SUNYONO, Sunyono<sup>1</sup>; TANIA, Lisa<sup>2\*</sup>; SAPUTRA, Andrian<sup>3</sup>

<sup>1,2,3</sup> Department of Chemical Education, University of Lampung, Indonesia.

\* Corresponding author

e-mail: lisa.tania@fkip.unila.ac.id

Received 13 March 2020; received in revised form 17 May 2020; accepted 28 May 2020

## RESUMO

A abordagem de aprendizado CTEM (Ciência, Tecnologia, Engenharia e Matemática) integra quatro disciplinas, a saber, ciência, tecnologia, engenharia e matemática na resolução de problemas da vida cotidiana e no fornecimento de muitas experiências de aprendizado aos alunos. Este estudo teve como objetivo analisar o interesse profissional no campo de CTEM para futuros professores indonésios de Matemática e Ciências Naturais (MIPA), estudando os padrões de relacionamento entre fatores, níveis de preferência e quais fatores o influenciam. A amostra da pesquisa foi de 300 futuros professores do MIPA na Faculdade de Formação e Educação de Professores da Universidade de Lampung. Este trabalho envolveu várias etapas como (1) adaptação e transliteração dos instrumentos de interesses de carreira STEM com base em fontes da literatura, (2) análise da validade do conteúdo com base no julgamento de especialistas, (3) disseminação de ferramentas para amostras de pesquisa e (4) avaliação de resultados de pesquisa, avaliação bivariada correlações e o nível de preferência de interesse. Os dados obtidos foram analisados estatisticamente utilizando técnicas de análise fatorial exploratória e confirmatória, análise de confiabilidade e variância e correlação produto-momento de Pearson. Os resultados da pesquisa mostraram que as informações referentes aos itens do questionário foram agrupadas em quatro fatores: atitude na carreira de engenharia, atitude na carreira em matemática, atitude na carreira em ciências e atitude na carreira em tecnologia com fatores de carga que variando de 0,575 a 0,848. Todos esses fatores foram capazes de explicar a atitude profissional da CTEM na soma de 62,43%. A atitude profissional em ciências e matemática é a preferência dominante para os futuros alunos de professores de Matemática e Ciências Naturais terem uma carreira no futuro. Além disso, os instrumentos utilizados são válidos e confiáveis para serem usados para analisar as atitudes profissionais de CTEM nos candidatos a professores de Matemática e Ciências Naturais.

**Palavras-chave:** *Interesses de carreira CTEM, candidatos a professores do MIPA, Universidade de Lampung.*

## ABSTRACT

STEM (Science, Technology, Engineering, and Math) learning approach integrates four disciplines, namely science, technology, engineering, and mathematics, in solving everyday life problems and giving many learning experiences to students. This study aimed to analyze career interest in the field of STEM for prospective Indonesian Mathematics and Natural Sciences (MIPA) teachers, studying the patterns of relationships between factors, preference levels, and what factors influence it. The research sample was 300 prospective MIPA teachers at the Faculty of Teacher Training and Education, Lampung University. This work involved several stages as (1) adapting and transliterating STEM career interests instruments based on literature sources, (2) analyzing content validity based on expert judgment, (3) spreading tools to research samples and (4) evaluating research data results, assessing bivariate correlations, and the level of interest preference. The data obtained were analyzed statistically using exploratory and confirmatory factor analysis techniques, reliability and variance analysis, and Pearson product-moment correlation. The research results showed information regarding the items in the questionnaire were grouped into four factors, namely engineering career attitude, mathematics career attitude, science career attitude, technology career attitude with loading factors ranging from 0.575 to 0.848. All these factors were able to explain the career attitude of STEM to the sum of 62.43%. The science and mathematics career attitude is the dominant preference for prospective students of Mathematics and Natural Sciences teachers to have a career in the future. Furthermore, the instruments used are valid and reliable to be used to analyze

**Keywords:** *STEM career interests, MIPA teacher candidates, Lampung University.*

## 1. INTRODUCTION:

STEM education is a learning approach that integrates four disciplines, namely science, technology, engineering, and mathematics, to solve problems in everyday life (Lin *et al.*, 2015; Jurdak, 2016; Shahali *et al.*, 2016; Tsai *et al.*, 2017; Gullen, 2018; Thibaut *et al.*, 2018; Chai, 2019). The learning curricula in several developed countries starting from elementary school to tertiary level nowadays have adopted the STEM approach because it is believed that this approach can provide a lot of learning experiences to students (Stohlmann, 2011; Pinnel, 2013; Barrak and Assal, 2018; Garner *et al.*, 2018; Roberts *et al.*, 2018; Bennett and Saunders, 2019; Morris *et al.*, 2019; Tytler *et al.*, 2019; Wu *et al.*, 2019). The continued application of the STEM approach in the learning process is believed to be able to shape and strengthen student character as a problem solver who is better, independent, innovative, inventive, creative, logical thinker, critical, and technology literate (Wells, 2019; Ibáñez, and Delgado-Kloos, 2018; Morrison, 2006). Moreover, STEM education positively impacts students' attitudes and interests in school (Bragow, Gragow and Smith, 1995), motivates students to learn (Guthrie, Wigfield and Von Secker, 2000) and improves student learning achievement (Hurley, 2001). Compared to teaching four disciplines as separate and discrete subjects, STEM integrates these disciplines into a cohesive paradigm based learning based on real-world applications (Hom, 2014).

Recently, the demand for a workforce well educated in science, technology, engineering, and math (STEM) is growing to stimulate economic growth and enhance innovation. The positive impact of the STEM approach to the learning process should be able to influence and enlarge the interest of students who will graduate vocational schools or students who will graduate from undergraduate to continue their education and/or have a career in the STEM field. However, many countries in the world face difficulties in carrying out the task of recruiting more people into science, the technology industry, engineering, and mathematics (STEM) (Hill *et al.* 2010; Regisford, 2012). The government, observers, and education practitioners want the STEM education curriculum to be able to internalize STEM values in student life to encourage increased student interest in a

career in the field of STEM after graduating from college. Especially as prospective MIPA teachers, it is hoped that they will have careers in the STEM field after graduation.

Several studies have examined STEM career interests at various levels of education ranging from elementary (Kim *et al.*, 2015; Campbell *et al.*, 2017; Peterson, 2018; Toma and Greca, 2018), intermediate (Aeschlimann, Herzog and Makarova, 2016; Kier *et al.*, 2014; Sadler, 2014; Robnett, and Leaper, 2013), and higher education levels (Beier *et al.*, 2019; Moakler and Kim, 2014). Knowledge about STEM career interests of teacher candidates can help researchers, teachers, government, and other education stakeholders to map their career tendency and create innovative learning strategies.

This study aimed to analyze the STEM career interest of prospective math and science teacher at Lampung University.

## 2. MATERIALS AND METHODS:

### 2.1. Research Sample

This study used a traditional survey method involving 300 students (269 female and 31 male) in which all participants agreed to spontaneously participate in this study once there is no official document demanded by the University to this kind of study. Participants were active students of Mathematics and Natural Sciences (physics, chemistry, biology) Education in the Department of Mathematics and Natural Sciences, Lampung University. The survey research design is a procedure in quantitative research in which the researcher surveys the sample to describe the attitudes, opinions, behavior, or characteristics of the population (Creswell, 2012).

### 2.2. Instrument

The instrument (survey) was adapted from the STEM Career Interest Survey (STEM-CIS) instrument developed by Kier *et al.* (2014). The instrument was adapted and transliterated into Indonesian, making it easier for research subjects to understand each item in the instrument. The instrument was then converted into a *google form* to make it easier for students to access, easy to

collect data, and paperless.

This 5-point Likert scale questionnaire consists of four dimensions or variables, namely career interests in the fields of science, mathematics, technology, and engineering, where each size includes eleven items. The full detail of the questionnaire is presented in Appendix 1.

### 2.3. Data Collection Technique and Analysis

The data collection technique is a conventional survey technique through the distribution of a questionnaire instrument to each sample. The students are asked to access the Google form website page, fill in questions in the form of a 5-Likert scale, and submit the results of their answers online.

Subsequently, the construct validity of the instrument used was determined for the data obtained using the exploratory factor analysis technique (EFA) using SPSS software version 23. Exploratory factor analysis (EFA) was carried out to uncover factor structures and correlation patterns between the observed variables (questionnaire items) and latent variables, which were considered as hidden variables representing these items.

Before further EFAs are carried out, it must first be tested against a group of data obtained, whether it is suitable for analysis by EFA. This can be done by observing the value of the Kaiser-Meyer-Olkin (KMO) sampling adequacy test and the Bartlett sphericity test. The Kaiser-Meyer-Olkin (KMO) test is a measure of how well the data fit for Factor Analysis. This test measures the adequacy of the sample for each variable in the model and the complete model. Statistics is a measure of the proportion of variance between variables that might be general variance. The lower the balance, the more your data fits in with Factor Analysis.

Meanwhile, the Bartlett sphericity test is used to compare the obtained correlation matrix (in this case, the Pearson correlation matrix) with the identity matrix. In other words, the Bartlett test checks whether there is redundancy between variables, which can be summarized by several factors. The Bartlett test is also able to identify unrelated variables and is therefore not suitable for structural detection. Small values (less than 0.05) of the significance level indicate that factor analysis might yield useful information with the data used.

The validation criteria in the EFA analysis are based on Stevens (2002), where items retained in the instrument must have a loading

factor more than 0.40, so items with a loading factor less than 0.40 will automatically be eliminated in the analysis of each item in the instrument. The principle of extraction of the main components with orthogonal rotation was used to estimate the number of possible factors while contributing to the construct validity in the developed instrument.

The reliability test for each dimension in the instrument is based on Cronbach's alpha coefficient calculation. Furthermore, determining the level of preference of STEM career interest (according to their perceptions) is conducted by determining the mean and standard deviation for each dimension and comparing them to the grand mean scores. The correlation of each dimension of STEM career interest is conducted by using the Pearson product-moment analysis.

### 3. RESULTS AND DISCUSSION:

The KMO and Bartlett chi-square test values obtained were 0.937 and 11872.889 ( $p < 0.05$ ), as shown in Table 1. These values indicate that the research data are suitable for use in the EFA analysis and are expected to provide useful interpretation.

After finding out that the research data obtained was ideal for EFA analysis, an investigation was carried out on the value of extraction communalities. Communalities shows the amount of variance in each variable that is considered. Initial communalities are estimates of variation in each variable recorded by all components or factors. For central component extraction, this is always equal to 1.0 for correlation analysis. Meanwhile, Extraction communalities are estimates of the variance in each variable that is taken into account by the component. Communalities have high enough extraction values ranging from 0.611 to 0.787, which shows that the components extracted represent the variables well (Table 2)

The researcher makes a limitation that items that can be accepted to represent latent factors are items that have a loading factor of more than 0.40, according to Stevens (2002) criteria. Stevens (2002) suggested that retained questions in the questionnaire must have a loading factor of more than 0.40. This has implications for the removal of items that have a loading factor of less than 0.40. The principle of extracting major components with orthogonal rotation was used in this study to estimate the number of possible factors while contributing to the construct validity in the scientific attitude instruments

developed. From the results of the EFA analysis, it was found that the items clustered into four main factors, with loading factors ranging from 0.575 to 0.848. Meanwhile, eight items were excluded from the EFA analysis due to factor loading values below 0.40. Furthermore, each factor can be declared reliable based on Cronbach's alpha complete information is 0.980, which indicates that the factors in the instrument have a high level of internal consistency to evaluate the attitude of prospective MIPA teachers for a career in the STEM field (Table 3).

### 3.1. Attitude level towards STEM careers

The STEM career attitude level analysis was conducted by comparing the mean values obtained for each latent factor against the grand mean, according to Suprpto (2016). A mean value more significant than the dignified way is seen as a dominant tendency for STEM careers in prospective MIPA teacher candidates. From the data in Table 4, information is obtained that science and mathematics have a mean value more significant than the grand mean. These results indicate that science and mathematics are the dominant tendencies of the attitude of prospective MIPA teacher students compared to technology and engineering.

### 3.2. Correlation between factors

Correlation analysis between factors was conducted by taking into account the Pearson product-moment correlation coefficient. From the results of the correlation analysis, information is obtained that all factors correlate significantly with a 99% confidence level (Table 5)

A factor analysis technique was used to identify structural factors of the attitude of the prospective MIPA teacher students to have a career in STEM. In general, the instruments have high validity and reliability for measuring the positions of prospective MIPA teacher students to pursue careers in the STEM field. The STEM career attitude instrument consists of 36 statement items in which these items can explain 62.437% of STEM career attitudes with a breakdown of 17.320%; 15.842%; 15.105%; and 14.171% for careers in science, mathematics, technology, and engineering. The results of this study also provided information that the attitude of the prospective MIPA teacher students for a career in the STEM field can be classified into four main factors, namely:

- a. Science career attitude (factor 1) consisting of 9 items ( $\alpha = 0.917$ ;  $s^2 = 7.320\%$ ); explore the

position of prospective MIPA teacher students to pursue careers in the field of science such as science assignments and study at school, interest in working in the sciences, and seriousness in science courses.

- b. Mathematics career attitude (factor 2) consisting of 9 items ( $\alpha = 0.927$ ;  $s^2 = 15.842\%$ ); explore the attitudes of prospective MIPA teacher students to pursue careers in the field of mathematics such as mathematics assignments and learning in school, interest in working in mathematics, and seriousness in mathematics courses.
- c. Technological career attitude (factor 3) consisting of 9 items ( $\alpha = 0.911$ ;  $s^2 = 15.105\%$ ); explore the perspectives of prospective MIPA teacher students to pursue careers in technology such as assignments and technology learning at school, interest in working in technology, and seriousness in technology courses.
- d. Engineering career attitude (factor 4) consisting of 9 items ( $\alpha = 0.936$ ;  $s^2 = 14.171\%$ ); explore the perspectives of prospective MIPA teacher students to pursue careers in engineering such as assignments and learning about engineering at school, interest in working in engineering, and seriousness in engineering courses.

Out of the four STEM career attitudes, the majority of MIPA teacher candidates prefer a career in the fields of mathematics and science over technology and engineering. This is indicated based on the mean value of the career of science and mathematics is higher than the value of the grand mean compared to technology and engineering. This certainly can be understood based on the specialization curriculum pursued by prospective MIPA teacher students, where most of the courses are dominated by science and mathematics. At the same time, classes that contain technological and engineering content will certainly not be too dominant. The results of the Pearson product-moment correlation analysis illustrate that each factor or dimension of STEM career attitudes correlates with each other significantly with a 99% confidence level. This result can be understood because STEM attitudes are indeed associated with each other, like the results of research from Suprpto (2016). Hence it does not rule out that STEM career attitudes will also influence each other.

The results of this study are consistent with previous studies that found that there is a positive impact of the STEM approach to the learning

process, which affects and increases the interest of students of vocational schools or undergraduate program students to continuing education and/or have a career in the field of STEM (Business Europe, 2011; Healy *et al.*, 2011). Besides, other studies have found that STEM education can have a direct impact on learning, both in schools and in universities. STEM education encourages the formation and strengthening of the character of students to be able to solve problems, be independent, thinkers, and, most importantly, be literate in technological literacy (Wells, 2019; Morrison, 2006). Thus, the results of this study are expected to have a positive impact on making changes to the curriculum in the department of mathematics and natural science education in fostering career spirit and motivation in STEM students.

#### 4. CONCLUSIONS:

Exploratory and reliability analysis revealed that the instrument used in this study had high internal consistency and was able to explain more than half of the overall STEM attitudes of MIPA teacher candidates. This indicates that the instrument is appropriate to be used for analyzing students' career interests in the STEM field and reasonably pleasant to explain the students' tendency to have a STEM career after graduating from college.

Moreover, the second aim of this study was to investigate which preference is more dominant among the four STEM fields. Mean, and grand mean comparison analysis revealed that science and mathematics career attitudes become the prevailing preference for the future career of prospective MIPA teachers. This indicates that working in the fields of science and mathematics is more desirable than technology and engineering;

The last, Pearson product-moment analysis confirmed that all factors significantly correlate with each other. It means that efforts to improve one dimension of STEM career attitudes will directly impact on improving career attitudes in different dimensions, and vice versa.

#### 5. REFERENCES:

1. Aeschlimann, B., Herzog, W., and Makarova, E. (2016). How to foster students' motivation in mathematics and science classes and promote students' STEM career choice. A study in Swiss high schools. *International Journal of Educational Research*, 79, 31-41.
2. Barak, M., and Assal, M. (2018). Robotics and STEM learning: Students' achievements in assignments according to the P3 Task Taxonomy—practice, problem solving, and projects. *International Journal of Technology and Design Education*, 28(1), 121-144.
3. Beier, M. E., Kim, M. H., Saterbak, A., Leautaud, V., Bishnoi, S., and Gilberto, J. M. (2019). The effect of authentic project-based learning on attitudes and career aspirations in STEM. *Journal of Research in Science Teaching*, 56(1), 3-23.
4. Bennett, J. A., and Saunders, C. P. (2019). A Virtual Tour of the Cell: Impact of Virtual Reality on Student Learning and Engagement in the STEM Classroom. *Journal of microbiology and biology education*, 20(2).
5. Business Europe. (2011). Plugging the skills gap: the clock is ticking - Science, technology, engineering, mathematics (STEM). 1-16, Retrieved from <https://www.busesseurope.eu/sites/buseur/files/media/imported/2011-00855-E.pdf>.
6. Campbell, C., Speldewinde, C., Howitt, C., and MacDonald, A. (2017). Early childhood STEM: Pedagogy and practices. In *27th EECERA Conference*.
7. Chai, C. S. (2019). Teacher professional development for science, technology, engineering and mathematics (STEM) education: A review from the perspectives of technological pedagogical content (TPACK). *The Asia-Pacific Education Researcher*, 28(1), 5-13.
8. Garner, P. W., Gabitova, N., Gupta, A., and Wood, T. (2018). Innovations in science education: infusing social emotional principles into early STEM learning. *Cultural Studies of Science Education*, 13(4), 889-903.
9. Gulen, S. (2018). Determination of the Effect of STEM-Integrated Argumentation Based Science Learning Approach in Solving Daily Life Problems. *World Journal on Educational Technology: Current Issues*, 10(4), 95-114.
10. Healy, J., Mavromaras, K., and Zhu, R. (2012). Consultant report: Securing Australia's future STEM: Country comparisons. *Australian Council of*

11. Jurdak, M. (2016). STEM Education as a Context for Real-World Problem Solving. In *Learning and Teaching Real World Problem Solving in School Mathematics* (pp. 151-163). Springer, Cham.
12. Kier, M. W., Blanchard, M. R., Osborne, J. W., and Albert, J. L. (2014). The development of the STEM career interest survey (STEM-CIS). *Research in Science Education*, 44(3), 461-481.
13. Kim, C., Kim, D., Yuan, J., Hill, R. B., Doshi, P., and Thai, C. N. (2015). Robotics to promote elementary education pre-service teachers' STEM engagement, learning, and teaching. *Computers and Education*, 91, 14-31.
14. Lin, K. Y., Yu, K. C., Hsiao, H. S., Chu, Y. H., Chang, Y. S., and Chien, Y. H. (2015). Design of an assessment system for collaborative problem solving in STEM education. *Journal of Computers in Education*, 2(3), 301-322.
15. Moakler Jr, M. W., and Kim, M. M. (2014). College major choice in STEM: Revisiting confidence and demographic factors. *The Career Development Quarterly*, 62(2), 128-142.
16. Morris, J., Slater, E., Fitzgerald, M. T., Lummis, G. W., and van Etten, E. (2019). Using local rural knowledge to enhance STEM learning for gifted and talented students in Australia. *Research in Science Education*, 1-19.
17. Peterson, B. M. (2018). *Applying Curriculum Treatments to Improve STEM Attitudes and Promote STEM Career Interest in Fifth Graders* (Doctoral dissertation, Virginia Tech).
18. Pinnell, M., Rowley, J., Preiss, S., Blust, R. P., Beach, R., and Franco, S. (2013). Bridging the gap between engineering design and PK-12 curriculum development through the use the STEM education quality framework. *Journal of STEM Education*, 14(4).
19. Roberts, T., Jackson, C., Mohr-Schroeder, M. J., Bush, S. B., Maiorca, C., Cavalcanti, M., ... and Cremeans, C. (2018). Students' perceptions of STEM learning after participating in a summer informal learning experience. *International journal of STEM education*, 5(1), 1-14.
20. Robnett, R. D., and Leaper, C. (2013). Friendship groups, personal motivation, and gender in relation to high school students' STEM career interest. *Journal of Research on Adolescence*, 23(4), 652-664.
21. Sadler, P. M., Sonnert, G., Hazari, Z., and Tai, R. (2014). The Role of Advanced High School Coursework in Increasing STEM Career Interest. *Science Educator*, 23(1), 1-13.
22. Shahali, E. H. M., Halim, L., Rasul, M. S., Osman, K., and Zulkifeli, M. A. (2016). STEM learning through engineering design: Impact on middle secondary students' interest towards STEM. *EURASIA Journal of Mathematics, Science and Technology Education*, 13(5), 1189-1211.
23. Stohlmann, M., Moore, T. J., McClelland, J., and Roehrig, G. H. (2011). Impressions of a middle grades STEM integration program. *Middle School Journal*, 43(1), 32-40.
24. Toma, R. B., and Greca, I. M. (2018). The effect of integrative STEM instruction on elementary students' attitudes toward science. *Eurasia Journal of Mathematics, Science and Technology Education*, 14(4), 1383-1395.
25. Tsai, H. Y., Chung, C. C., and Lou, S. J. (2017). Construction and development of iSTEM learning model. *Eurasia Journal of Mathematics, Science and Technology Education*, 14(1), 15-32.
26. Tytler, R., Prain, V., and Hobbs, L. (2019). Rethinking disciplinary links in interdisciplinary STEM learning: A temporal model. *Research in Science Education*, 1-19.
27. Wu, B., Hu, Y., and Wang, M. (2019). Scaffolding design thinking in online STEM preservice teacher training. *British Journal of Educational Technology*, 50(5), 2271-2287.



## **APPENDIX 1**

### **STEM Career Interest Survey (STEM-CIS)**

#### **Science (S)**

- S1 I am able to get a good grade in my science class.
- S2 I am able to complete my science homework.
- S3 I plan to use science in my future career.
- S4 I will work hard in my science classes.
- S5 If I do well in science classes, it will help me in my future career.
- S6 My parents would like it if I choose a science career.
- S7 I am interested in careers that use science.
- S8 I like my science class.
- S9 I have a role model in a science career.
- S10 I would feel comfortable talking to people who work in science careers.
- S11 I know of someone in my family who uses science in their career.

#### **Mathematics (M)**

- M1 I am able to get a good grade in my math class.
- M2 I am able to complete my math homework.
- M3 I plan to use mathematics in my future career.
- M4 I will work hard in my mathematics classes.
- M5 If I do well in mathematics classes, it will help me in my future career.
- M6 My parents would like it if I choose a mathematics career.
- M7 I am interested in careers that use mathematics.
- M8 I like my mathematics class.
- M9 I have a role model in a mathematics career.
- M10 I would feel comfortable talking to people who work in mathematics careers.
- M11 I know someone in my family who uses mathematics in their career.

#### **Technology (T)**

- T1 I am able to do well in activities that involve technology.
- T2 I am able to learn new technologies.
- T3 I plan to use technology in my future career.
- T4 I will learn about new technologies that will help me with school.
- T5 If I learn a lot about technology, I will be able to do lots of different types of careers.

- T6 My parents would like it if I choose a technology career.  
 T7 I like to use technology for class work.  
 T8 I am interested in careers that use technology.  
 T9 I have a role model who uses technology in their career.  
 T10 I would feel comfortable talking to people who work in technology careers.  
 T11 I know of someone in my family who uses technology in their career.

### Engineering (E)

- E1 I am able to do well in activities that involve engineering.  
 E2 I am able to complete activities that involve engineering.  
 E3 I plan to use engineering in my future career.  
 E4 I will work hard on activities at school that involve engineering.  
 E5 If I learn a lot about engineering, I will be able to do lots of different types of careers.  
 E6 My parents would like it if I choose an engineering career.  
 E7 I am interested in careers that involve engineering.  
 E8 I like activities that involve engineering.  
 E9 I have a role model in an engineering career.  
 E10 I would feel comfortable talking to people who are engineers.  
 E11 I know of someone in my family who is an engineer.

**Table 1.** KMO and Bartlett's Test

|   |                    |           |
|---|--------------------|-----------|
| <b>Kaiser-Meyer-Olkin Measure of Sampling Adequacy.</b> |                    | .937      |
| <b>Bartlett's Test of Sphericity</b>                    | Approx. Chi-Square | 11872.898 |
|   | Df                 | 630       |
|   | Sig.               | .000      |

Notes: Df and Sig. are degree of freedom and significance, respectively

**Table 2.** Communalities

| Item      | Initial | Extraction |
|-----------|---------|------------|
| <b>S1</b> | 1.000   | .708       |
| <b>S2</b> | 1.000   | .713       |
| <b>S3</b> | 1.000   | .666       |
| <b>S4</b> | 1.000   | .678       |
| <b>S5</b> | 1.000   | .687       |
| <b>S6</b> | 1.000   | .709       |
| <b>S7</b> | 1.000   | .721       |

|   |       |      |
|---|-------|------|
| <b>S8</b>   | 1.000 | .709 |
| <b>S10</b>  | 1.000 | .668 |
| <b>M1</b>   | 1.000 | .750 |
| <b>M2</b>   | 1.000 | .769 |
| <b>M3</b>   | 1.000 | .749 |
| <b>M4</b>   | 1.000 | .736 |
| <b>M5</b>   | 1.000 | .699 |
| <b>M6</b>   | 1.000 | .699 |
| <b>M7</b>   | 1.000 | .789 |
| <b>M8</b>   | 1.000 | .728 |
| <b>M10</b>  | 1.000 | .695 |
| <b>T1</b>   | 1.000 | .623 |
| <b>T2</b>   | 1.000 | .724 |
| <b>T3</b>   | 1.000 | .662 |
| <b>T4</b>   | 1.000 | .661 |
| <b>T5</b>   | 1.000 | .706 |
| <b>T6</b>   | 1.000 | .683 |
| <b>T7</b>   | 1.000 | .594 |
| <b>T8</b>   | 1.000 | .616 |
| <b>T10</b>  | 1.000 | .611 |
| <b>E1</b>   | 1.000 | .750 |
| <b>E2</b>   | 1.000 | .737 |
| <b>E3</b>   | 1.000 | .735 |
| <b>E4</b>   | 1.000 | .724 |
| <b>E5</b>   | 1.000 | .684 |
| <b>E6</b>   | 1.000 | .634 |
| <b>E7</b>   | 1.000 | .772 |
| <b>E8</b>   | 1.000 | .787 |
| <b>E10</b>  | 1.000 | .666 |
| <b>Extraction Method: Principal Component Analysis.</b> |       |      |

**Table 3.** Loading factor and variance for each factors and items

| Item | Factor 1<br>( $\alpha = 0.917$ ; $s^2 = 17.320\%$ ) | Factor 2<br>( $\alpha = 0.927$ ; $s^2 = 15.842\%$ ) | Factor 3<br>( $\alpha = 0.911$ ; $s^2 = 15.105\%$ ) | Factor 4<br>( $\alpha = 0.936$ ; $s^2 = 14.171\%$ ) |
|------|---|---|---|---|
| E8   | .848  |   |   |   |
| E7   | .833  |   |   |   |
| E3   | .782  |   |   |   |
| E1   | .741  |   |   |   |
| E2   | .738  |   |   |   |
| E10  | .738  |   |   |   |
| E6   | .734  |   |   |   |
| E4   | .704  |   |   |   |
| E5   | .655  |   |   |   |
| M7   |   | .855  |   |   |
| M3   |   | .841  |   |   |
| M8   |   | .824  |   |   |
| M1   |   | .751  |   |   |
| M2   |   | .716  |   |   |
| M4   |   | .714  |   |   |
| M6   |   | .713  |   |   |
| M10  |   | .710  |   |   |
| M5   |   | .670  |   |   |
| S7   |   |   | .781  |   |
| S8   |   |   | .767  |   |
| S3   |   |   | .757  |   |
| S5   |   |   | .732  |   |
| S6   |   |   | .721  |   |
| S10  |   |   | .713  |   |
| S4   |   |   | .696  |   |
| S2   |   |   | .613  |   |
| S1   |   |   | .573  |   |
| T6   |   |   |   | .717  |
| T4   |   |   |   | .711  |
| T2   |   |   |   | .702  |
| T5   |   |   |   | .699  |
| T8   |   |   |   | .695  |
| T3   |   |   |   | .671  |
| T1   |   |   |   | .658  |
| T7   |   |   |   | .654  |
| T10  |   |   |   | .585  |

Notes: Factor 1, Factor 2, Factor 3, and Factor 4 are Science career attitude, Mathematics career attitude, Technology career attitude, and Engineering career attitude, respectively

**Table 4.** Degree of STEM career interest

|             | Mean  | Std. Deviation | Rank*          |
|-------------|-------|----------------|----------------|
| Science     | 3.849 | .642           | 2              |
| Math        | 3.853 | .604           | 1              |
| Technology  | 3.813 | .609           | 3 <sup>#</sup> |
| Engineering | 3.768 | .593           | 4 <sup>#</sup> |

\*Grandmean = 3.821; <sup>#</sup>nilai mean < grandmean

**Table 5.** Interrelationship between factors STEM career interest

|             | Science | Math   | Technology | Engineering |
|-------------|---------|--------|------------|-------------|
| Science     | 1       | .965** | .960**     | .877**      |
| Math        |         | 1      | .978**     | .947**      |
| Technology  |         |        | 1          | .956**      |
| Engineering |         |        |            | 1           |

\*\* . Correlation is significant at the 0.01 level (2-tailed).

# **AVALIAÇÃO ANTRÓPICA NO LITORAL PARANAENSE ATRAVÉS DA DETERMINAÇÃO DA CONCENTRAÇÃO DO ÍON FOSFATO EM RECURSOS HÍDRICOS**

## **ANTHROPIC EVALUATION IN THE PARANÁ COAST THROUGH THE ION PHOSPHATE CONCENTRATION DETERMINATION IN WATER RESOURCES**

SILVA, Ednilson Barros<sup>1</sup>; ROCHA<sup>2\*</sup>, José Roberto Caetano da

<sup>1,2</sup>Universidade Estadual do Paraná - Campus de Paranaguá, Colegiado de Ciências Biológicas

\* Autor correspondente

e-mail: jose.rocha@unespar.edu.br

Received 28 April 2020; received in revised form 10 May 2020; accepted 28 May 2020

### **RESUMO**

O aumento da poluição nos recursos hídricos é proveniente praticamente de todas as atividades humanas, sejam elas domésticas, comerciais ou industriais. O meio ambiente não tem capacidade de absorver todos os poluentes, pois cada uma dessas atividades econômicas gera poluentes característicos que apresentam determinadas implicações ambientais e afetam diretamente na qualidade de qualquer recurso hídrico. O crescimento populacional é outro fator que leva ao aumento de geração de resíduos, dos quais se podem destacar os esgotos domésticos, ricos em nutrientes e, quando depositados irregularmente, causam desequilíbrio no corpo hídrico. O presente estudo tem como objetivo identificar a concentração do elemento fósforo na forma do íon fosfato nos recursos hídricos do litoral do Paraná. Para quantificar esse elemento, foi utilizado o método espectrofotométrico do azul de molibdênio. Avaliaram-se amostras de dez pontos de águas continentais da região litorânea que sofrem maior ou menor influência antrópica. Foram realizados ensaios no período de agosto de 2017 a maio 2019. Na metodologia analítica, foram utilizadas soluções de molibdato de amônio, ácido ascórbico, ácido nítrico e glicerina. Quando essas soluções são misturadas em amostras ou soluções padrão que contenham o elemento fósforo, há a formação do complexo azul de molibdênio. Foram realizadas cinco repetições em cada uma das amostras para que, no final, fosse obtido o valor médio das medidas. Observou-se que as concentrações de fósforo através do íon fosfato apresentaram resultados acima de 0,150 mg. L<sup>-1</sup>, valor máximo deste macronutriente em amostras de água preconizado pela legislação, exceto pelo resultado obtido no ponto 8 no mês de novembro, cuja concentração foi de 0,08 mg. L<sup>-1</sup>. Os resultados mostraram, portanto que há poluição nas águas continentais amostradas. Por consequência, é possível destacar que a alta concentração de íon fosfato nas amostras é oriunda da ação humana, principalmente naqueles rios que estão mais próximos a contingentes urbanos.

**Palavras-chave:** *Fósforo, Azul de Molibdênio, Macronutriente, Poluição da Água.*

### **ABSTRACT**

The increase in pollution in water resources comes from practically all human activities, whether domestic, commercial, or industrial. The environment cannot absorb all pollutants, as each of these economic activities generates specific pollutants, which have certain environmental implications and directly affect the quality of any water resource. Population growth is another factor that leads to an increase in the generation of waste, of which domestic sewage, rich in nutrients and, when deposited irregularly, causes an imbalance in the water body that can be highlighted. This study aimed to identify the concentration of the phosphorus element in the form of the phosphate ion in the water resources of the coast of Paraná. To quantify this element, the spectrophotometric method of molybdenum blue was used. Samples from ten points of continental waters in the coastal region were evaluated, which suffer a greater or lesser anthropic influence. Tests were carried out from August 2017 to May 2019. In the analytical methodology, solutions of ammonium molybdate, ascorbic acid, nitric acid, and glycerin were used. When these solutions are mixed in samples or standard solutions that contain the element phosphorus, there is the formation of the blue molybdenum complex. Five repetitions were performed in each of the samples so that, in the end, the average value of the measurements was obtained. It was observed that the phosphorus concentrations through the phosphate ion showed results above 0.150 mg L<sup>-1</sup>, the maximum value of this macronutrient in water samples, recommended by the legislation, except for the result obtained in point 8 in November, whose concentration was 0.08 mg L<sup>-1</sup>. The results showed, therefore, that there is pollution in the sampled continental waters. As a consequence, it is possible to highlight that the high concentration of phosphate ion in the samples comes from human action, especially in those rivers that are closer to urban contingents.

## 1. INTRODUÇÃO:

O aumento significativo da poluição nos recursos hídricos é proveniente praticamente de todas as atividades humanas, sejam elas domésticas, comerciais ou industriais (Costa e Rocha, 2017). O meio ambiente não tem capacidade de absorver todos os poluentes, pois cada uma dessas atividades econômicas gera poluentes característicos que apresentam determinadas implicações ambientais e afetam diretamente na qualidade de qualquer recurso hídrico (Pereira, 2004).

O crescimento populacional leva ao aumento de geração de resíduos, dos quais se podem destacar os esgotos domésticos, ricos em fósforo e nitrogênio e, quando depositados irregularmente, causam desequilíbrio no corpo hídrico (Cordeiro, Motyl, Rocha, 2019). O rio Itiberê é um dos rios do litoral paranaense com maior quantidade de despejo de esgoto *in natura* produzido na cidade de Paranaguá (Godoy, 2013).

No município de Paranaguá está localizado o maior porto graneleiro do hemisfério sul. O Porto de Paranaguá é o principal porto brasileiro em movimentação de grãos sólidos como soja, milho e fertilizantes (França, Moraes, Rocha, 2017). Desta forma, esse porto é um dos maiores corredores de importação e exportação desses produtos do agronegócio. Já a fase final do transporte desses produtos ocorre pela malha rodoviária e pela malha ferroviária local, regional e inter-regiões brasileiras. O transporte rodoviário é um dos principais responsáveis por inúmeros impactos ambientais no município de Paranaguá, provocando ações antrópicas que agredem o meio ambiente, afetam a economia e refletem na sociedade de forma negativa, mas também positiva (Mariano, 2013).

O Porto de Paranaguá conta com um sistema de logística reversa, ou seja, os caminhões e trens que chegam carregados com farelos ou grãos para a exportação retornam carregados com adubos ou fertilizantes para as regiões produtoras dos grãos (Silva, Souza, Rocha, 2018). Em ambos os casos, parte da produção se perde ao longo da linha de trem ou no acostamento da Rodovia BR-277, sendo consumida pelas aves ou roedores locais, ou sofrem decomposição natural. Decompostos ou não esses resíduos são transportados pelas águas das chuvas para os recursos hídricos da

região. Outro fator preponderante é a perda contínua de fertilizantes durante o processo arcaico de carga e descarga no Porto de Paranaguá. Quantidades significativas de fertilizantes caem na Baía de Paranaguá, sendo que os mesmos, após sua solubilização, são transportados para o interior do continente pelo processo de marés (Staszczak e Rocha, 2018).

A principal consequência dos impactos antrópicos nos ecossistemas aquáticos é a ocorrência acelerada de processos eutrofizantes (Smaha e Gobbi, 2003) que causam enriquecimento artificial desses ecossistemas pelo aumento das concentrações de nutrientes na água, principalmente compostos nitrogenados e fosfatados (Cassol *et al.*, 2012; Brasil, 2014). Este processo destaca-se pela interferência na qualidade da água para abastecimento da população local, morte de peixes e organismos de determinado ambiente, trazendo assim grande desafio de manejo e gerenciamento dos recursos hídricos (Pantano, *et al.*, 2016).

O uso de fertilizantes no Brasil é um dos fatores que mais se destaca devido ao país ser um dos maiores produtores mundiais de alimentos e agronegócio, sendo um dos maiores segmentos da economia brasileira que utiliza grandes concentrações dos mesmos, devido ao solo brasileiro ser pobre em fósforo (P), potássio (K) e Nitrogênio (N) (Molin *et al.*, 2009; Frazão *et al.*, 2014). Nota-se também que o agronegócio é responsável por 42% das receitas nacionais de exportações (Cunha e Rocha, 2015). Somente o porto de Paranaguá recebeu de janeiro a outubro 8,4 bilhões de toneladas de fertilizantes por via marítima (Silva e Fernandes, 2018).

Observando alguns trabalhos que avaliaram a contaminação antrópica da região litorânea Paranaense que corresponde às cidades de Antonina, Guaraqueçaba, Guaratuba, Matinhos, Morretes, Paranaguá e Pontal do Paraná (Cunha e Rocha, 2015), percebe-se que a concentração em solos (Reis, Cavallet, Rocha, 2014), em recursos hídricos (Reis *et al.*, 2015) e em sedimentos (Cazati, 2010) estão muito acima daqueles preconizados para esses recursos ambientais. Na Resolução nº 357/2005 do Conselho Nacional do Meio Ambiente (CONAMA) para ambientes lóticos, a concentração máxima do elemento fósforo é de 0,150 mg. L<sup>-1</sup>.

O fósforo tem função essencial para vários organismos vivos, como plantas e animais, além

de desempenhar um papel fundamental na produtividade primária dos organismos. Atualmente desempenha um papel importante nas atividades econômicas, principalmente na gestão da produção agrícola, usado como fertilizante (Pantano *et al.*, 2016). Não esquecendo que esses elementos estão entre os principais nutrientes que limitam a produtividade primária de grãos na agricultura, sendo assim a disponibilidade dos mesmos também influencia a variedade e abundância dos organismos aquáticos (Marguti, Ferreira Filho, Piveli, 2008). A emissão antrópica de nutrientes (N e P), para muitos ecossistemas aquáticos, vem superando de forma quantitativa as emissões naturais (Molisani *et al.*, 2013).

A metodologia considerada oficial para a determinação do elemento fósforo na forma fosfato é a espectrofotométrica com a formação do complexo azul de molibdênio (Kronka *et al.* 1997; Masini, 2008). Por meio dessa metodologia foi possível determinar a concentração desse elemento no litoral Paranaense, bem como monitorar os valores obtidos durante o estudo.

Portanto, o objetivo deste estudo foi avaliar e monitorar a concentração do elemento fósforo nos recursos hídricos da região litorânea Paranaense devido à importância estratégica econômica local dos diferentes rios avaliados (Silva; Souza; Rocha, 2018), bem como verificar se os mesmos estão de acordo com a resolução Nº 357/2005 estipulado pelo CONAMA.

## 2. MATERIAIS E MÉTODOS:

O macronutriente fósforo foi determinado espectrofotometricamente, na forma de fosfato, em amostras provenientes de rios, sendo que as amostragens foram realizadas trimestralmente pelo período de dois anos. Os ensaios nas amostras reais foram realizados após determinar a curva padrão das soluções padrões de fosfato no equipamento calibrado em comprimento de onda 660 nm.

### 2.1. Área de estudo e pontos de amostragem

Foram retiradas amostras de dez pontos geográficos das cidades litorâneas Paranaenses de Paranaguá e Pontal do Paraná (Tabela 1). Na Figura 1 é possível observar esses mesmos pontos, representados ao longo das Rodovias BR-277, PR-508 e PR-407, no mapa das cidades de Paranaguá e Pontal do Paraná. As coletas foram realizadas em agosto e novembro de 2017, fevereiro, maio, agosto, novembro de 2018,

fevereiro e maio de 2019. A prioridade foi a amostragem de pontos próximos ao Porto de Paranaguá e, posteriormente, foram avaliados recursos hídricos que sofrem forte influência das marés e todas as análises de cada etapa foram realizadas no mesmo dia da coleta.

Essas amostras foram transportadas para o Laboratório de Avaliação dos Impactos Ambientais (LAVIMA) da Região de Paranaguá da UNESPAR, *Campus* de Paranaguá, onde foram realizados ensaios para quantificar o elemento fósforo na forma do íon fosfato, segundo metodologia considerada padrão (Rice *et al.*, 2012).

### 2.1.1 Metodologia analítica

O elemento químico fósforo disponível foi determinado por espectrofotometria, na forma do íon fosfato, utilizando espectrofotômetro U2M Quimis. Após a mistura das amostras ou das soluções padrões com soluções reativas A (molibdato de amônio e ácido nítrico) e B (ácido ascórbico e glicerina), ocorreu à formação da coloração do azul de molibdênio (Masini, 2008). Em seguida realizaram-se todas as medidas dos valores de absorbância em 660nm, incluindo a calibração do equipamento e também obtenção do branco.

Todos os ensaios analíticos foram realizados com cinco repetições, para que dessa forma os possíveis erros, que comumente ocorrem em um processo analítico, fossem minimizados.

Utilizaram-se os valores médios de absorbância obtidos nos ensaios de cada uma das soluções padrão para traçar a equação padrão (Figura 2). Posteriormente, os cálculos foram realizados utilizando a equação padrão para obter os valores da concentração de  $P-PO_4^{3-}$  em cada um dos ensaios realizados nas dez amostras reais, bem como os resultados da média e desvio padrão das mesmas.

## 3. RESULTADOS E DISCUSSÃO:

Com os resultados obtidos em cada período amostral, produziu-se o gráfico dos valores de absorbância em função das concentrações de cada uma das soluções padrão de onde se obteve a equação padrão.

Na Figura 3 é possível observar o gráfico produzido com os resultados obtidos nos ensaios padrão do sexto período de amostragem. As equações lineares da reta produzidas em cada um



dos oitos períodos amostrais estão disponíveis na Tabela 2, sendo que com essas equações foi possível determinar a concentração de fósforo na forma de fosfato, em cada uma das amostras retiradas nos diferentes períodos e pontos amostrais.

Durante o monitoramento da concentração de fosfato, em todos os pontos amostrais da primeira fase (Figura 4), percebeu-se que a quase totalidade deles está muito acima do parâmetro máximo estabelecido pela Resolução Nº 357/2005 CONAMA. Verificou-se, nos mesmos, que as concentrações de fósforo apresentaram resultados acima de  $0,150 \text{ mg L}^{-1}$ , ou seja, quase 60 vezes superior ao parâmetro estipulado. O único valor abaixo da norma foi encontrado no Riacho localizado no Km 1 da Rodovia Matinhos, provavelmente devido ao processo de diluição que ocorre no período de chuvas, além desse local não sofrer processo significativo das marés.

Ao longo dessa segunda fase do projeto, percebeu-se que a concentração de fosfato, em todos os pontos amostrais e em todos os períodos amostrados estavam muito acima do parâmetro máximo estabelecido pela Resolução Nº 357/2005 CONAMA, que é de  $0,150 \text{ mg L}^{-1}$ . Verificou-se que esses valores são, no mínimo, seis vezes maiores que o valor estipulado pelo CONAMA e até quase sessenta vezes superior ao mesmo valor (Figura 5). Percebeu-se, ainda que a influência desses altos valores esteja relacionada com o processo de maré (Staszczak e Rocha, 2018), bem como pelo descarte inadequado de resíduos domésticos, comerciais e industriais da região litorânea (SILVA *et al.*, 2012). Todos esses fatores impactam de forma negativa na contaminação ambiental da região.

O fósforo em concentrações adequadas é importantíssimo em diferentes funções biológicas entre elas a fotossíntese, o metabolismo de açúcares, o armazenamento e a transferência de energia através do ATP, na divisão celular, no alargamento das células e na transferência da informação genética (Oliveira *et al.*, 2013).

Por outro lado, quando esse elemento se apresenta em excesso no ambiente, pode provocar diversos impactos negativos, com especial referência à qualidade das águas. Quando aumenta a concentração de nutrientes (fosfatos, principalmente) em rios e lagos, pode causar eutrofização, podendo ser visível em alguns pontos dos rios (Santos e Araújo, 2010). O aumento na concentração de fosfato chegou até nos pontos mais distantes do centro da cidade. Este fato, como já informado, está diretamente

relacionado tanto ao processo de influência das marés, como da proximidade dos mesmos com as rodovias responsáveis pelo excessivo fluxo de caminhões que transportam grãos e fertilizantes até o Porto (Souza *et al.*, 2019). Ao longo do percurso ocorre derramamento destes produtos, devido à baixa qualidade da rede de transporte, que vai acumulando-se na lateral da via, sendo levado pelo processo das chuvas para os rios próximos (Lopes *et al.*, 2019).

Avaliando pontualmente, foi observado que os pontos mais afetados pelo impacto antrópico foram os pontos amostrais 2, 3, 8 em agosto de 2019, e 8 e 9, em fevereiro de 2019.

É possível destacar que somente o ponto 9, em novembro de 2017, apresentou concentração abaixo do permitido pela resolução CONAMA.

Segundo Reis *et al.* (2015), as concentrações do elemento fósforo na sua forma mais estável, fosfato, já apresentavam valores acima do estipulado pelo CONAMA Nº 357/2005 nos rios Guaraguaçu e São Joãozinho, confirmando que estas águas continentais possuíam e continuam com altas concentrações do elemento fósforo. Mesmo o rio São Joãozinho, que é considerado um dos rios mais afastados e de difícil acesso.

Os valores de concentração de fósforo encontrados nos rios Itiberê, Rio da Vila, Rio Pery e Rio Guaraguaçu, são similares àqueles encontrados por Cunha *et al.* (2015), Souza *et al.* (2019) e também por Lopes *et al.* (2019). Esses locais sofrem fortes ações antrópicas, recebendo grande quantidade de esgoto sem tratamento. Aterro sanitário dos municípios de Pontal do Paraná e Matinhos que é localizado às margens do Rio Pery, sendo na verdade um “Lixão a Céu Aberto” como definido pelo Ministério Público do Paraná (2018). Além do gerenciamento arcaico do Porto de Paranaguá e a movimentação de fertilizantes pela malha ferroviária e rodoviária local.

#### 4. CONCLUSÕES:

Na maioria dos pontos amostrais, os valores das concentrações do elemento fósforo estiveram muito acima de  $0,150 \text{ mg L}^{-1}$ , parâmetro máximo da resolução Nº 357/2005 do CONAMA, principalmente quando se observam os valores encontrados no rio Itiberê, ponto mais próximo do Porto de Paranaguá. No entanto, o Riacho localizado no Km 1 da Rodovia Matinhos, provavelmente devido ao processo de diluição

que acontece no período de chuvas, além desse local não sofrer processo significativo das marés, foi o único local que apresentou valor abaixo daquele preconizado pela Resolução CONAMA, no mês de novembro/17.

Mediante os dados expostos, faz-se necessária a fomentação de trabalho nas diferentes áreas de conhecimentos, visando estabelecer diferentes meios para recuperação dos rios, evitando assim, o desequilíbrio no ecossistema.

Os valores elevados da concentração do íon fosfato estão relacionados com a ação humana, devido aos rios estarem próximos de regiões urbanas onde, na maioria das vezes, a rede de esgoto é depositada diretamente nos mesmos sem o devido tratamento.

Por fim, o fator preponderante da poluição elevada observada está relacionado com o gerenciamento arcaico do Porto de Paranaguá, onde os fertilizantes são retirados mecanicamente e não por sucção como nos portos mais modernos. Um sistema moderno por sucção evitaria a perda de fertilizantes que são solubilizados nas águas da Baía de Paranaguá e transportados, pelo efeito da maré, nos rios para regiões mais interiores do continente.

## 5. AGRADECIMENTOS:

A Fundação Araucária pela concessão de bolsa de estudo. A PRPPG da UNESPAR concessão de equipamentos necessários para a realização das atividades.

## 6. REFERÊNCIAS:

1. Brasil, (2014) Ministério da Saúde. Fundação Nacional de Saúde. Manual de controle da qualidade da água para técnicos que trabalham em ETAS / Ministério da Saúde, Fundação Nacional de Saúde. – Brasília: FUNASA, 19.
2. Cassol, P.C., Costa, A.C. & Ciprandi, O.; Pandolfo, C. M; Ernani, P. R. (2012) Disponibilidade de Macronutrientes e Rendimento em Latossolo Fertilizado com Dejetos Suíno. *Revista Brasileira de Ciência do Solo*, 36(6), 1911-1923.
3. Cazati, C.A. (2010) Fracionamento do Fósforo em Sedimentos Superficiais do Complexo Estuarino de Paranaguá. Dissertação de Mestrado, UFPR: Centro de Estudos do Mar, Pontal do Paraná, PR, 95.
4. CONAMA. (2005) Resolução CONAMA nº 357, de 17 de março de 2005- Dispõe sobre a classificação dos corpos de água e diretrizes ambientais para o seu enquadramento, bem como estabelece as condições e padrões de lançamento de efluentes, e dá outras providências. Diário Oficial da União de 18/03/2005, Executivo.
5. Cordeiro, T.S., Motyl, T. & Rocha, J.R.C. (2019) Avaliação dos nutrientes presentes nas águas do Rio São Joãozinho, PR. *Analytica*, 17(99) 16-24.
6. Costa, C.C. & Rocha, J.R.C. (2017) Percepção do processo de educação ambiental e da produção de resíduos sólidos por alunos do ensino fundamental. *Periódico Tchê Química*, 14(28), 56-65.
7. Cunha, E.J.N.S. & Rocha, J.R.C. (2015) Avaliação da Concentração de Íon Fosfato em Recursos Hídricos de Algumas Cidades do Litoral Paranaense. *Periódico Tchê Química*. 12(23), 34-38.
8. França, H.T.S., Moraes, S.R. & Rocha, J. R.C. (2017) Característica físico-química das águas do Rio da Vila em Paranaguá, PR. *Espacios*, 38(8), 21.
9. Frazão, J.J., Silva, A.R., Silva, V.L., Oliveira, V.A. & Corrêa, R.S. (2014) Fertilizantes nitrogenados de eficiência aumentada e ureia na cultura de milho. *Revista Brasileira de Engenharia Agrícola e Ambiental*, 18(12), 1262-1267.
10. Godoy, V.A. (2013) Estudo dos mecanismos de transporte de sódio, fosfato e amônio em colunas indeformadas de material inconsolidado residual de arenitos da Formação Adamantina, Dissertação (Mestrado), Escola de Engenharia de São Carlos, Universidade de São Paulo, 255.
11. Kronka, E.A.M., Reis, B.F., Vieira, J.A., Blanco, T. & Gervásio, A.P.G. (1997) Multicomutação e Amostragem Binária em Análise Química em Fluxo. Determinação Espectrofotométrica de Ortofosfato em Águas Naturais. *Química Nova*, 20(4), 372-376.
12. Lopes, E.A.O., Carvalho, K.H., Gomes, S.H. & Rocha, J.R.C. (2019) Evaluation of Physical-Chemical Parameters of Water Resources Quality from Paranaguá City, PR. *IOSR Journal of Applied Chemistry*. 12(8), 12-18.

13. Marguti, A. L., Ferreira Filho, S. S. & Piveli, R. P. (2008) Otimização de Processos Físico-Químicos da Remoção de Fósforo de Esgotos Sanitários por Processos de Precipitação Química com Cloreto Férrico. *Engenharia Sanitária e Ambiental*, 13(4), 395-404.
14. Mariano, T.W. (2013) Diagnóstico dos impactos diretos e indiretos do transporte da soja na gestão ambiental urbana e portuária do município de Paranaguá. Monografia. UFPR: Setor litoral, Matinhos, PR, 67.
15. Masini, J.C. (2008) Demonstrando os Fundamentos, Potencialidades e Limitações da Análise por Injeção Sequencial. *Química Nova*, 31(3), 704-708.
16. MPPR (2018) <http://www.mppr.mp.br/2018/08/20748,11/No-Litoral-do-estado-MPPR-ajuiza-acao-civil-publica-para-regularizar-destinacao-de-residuos-solidos-em-Pontal-do-Parana-e-Matinhos.html> acessado em 29/04/2020 as 17h50.
17. Molin, J.P., Machado T.M., Magalhães, R.P. & Faulin, G.D.C. (2009) Segregação de fertilizantes aplicados a lanço. *Engenharia Agrícola*, 29(4), 614-622.
18. Oliveira, F. T., Mendonça, V., Hafle, O. M., Moreira, J. N., Maracajá, P. B., Augusto, J. & Lopes, J. D. A. (2013) Fontes orgânicas e doses de fosfato natural na produção de porta-enxertos de goiabeira. *Agropecuária Científica no Semi-Árido*. 9(1), 36-42.
19. Pantano, G., Grosseli, G.M., Mozeto, A.A. & Fadini, P. S. (2016) Sustentabilidade no uso do fósforo: uma questão de segurança hídrica e alimentar. *Química Nova*, 39(6), 732-740.
20. Pereira, R.S. (2004) Identificação e Caracterização das Fontes de Poluição em Sistemas Hídricos. *Revista Eletrônica de Recursos Hídricos. IPH – UFRGS*, 1(1), 20-36.
21. Reis, C.S., Cavallet, L.E. & Rocha, J.R.C. (2014) Macronutrientes em Águas de Irrigação em uma Propriedade de Produção Orgânica em Paranaguá, PR. *Periódico Tchê Química*, 11(22), 85-91.
22. Reis, C.S., França, H.T.S., Motyl, T., Cordeiro, T.S. & Rocha, J.R.C. (2015) Avaliação da Atividade Antrópica no Rio Guaraguaçu (Pontal do Paraná, PR). *Engenharia Sanitária e Ambiental*, 20(3), 389-394.
23. Rice, E.W., Baird, R.B., Eaton, A.D. & Clesceri, L.S. (ed.) (2012) Standard Methods for the Examination of Water and Wastewater. 22nd Edition. Washington: American Public Health Association.
24. Santos, A.F. & Araújo, S.C.M. (2010) Fertilizantes fosfatados como tema gerador de conhecimento químico. *Periódico Tchê Química*, 7(14), 57-66.
25. Silva, L.A., Fernandes, N.M. A (2018) Cadeia Produtiva de Adubos e Fertilizantes. In: Anais do II Encontro Científico de Gestão Portuária: Redes de Empresas e Cadeias Produtivas. Anais, Santos (SP) FATECRL.
26. Silva, A.C.C., Souza, G.L.G. & Rocha, J.R.C. (2018) Avaliação espectrofotométrica das concentrações do íon nitrato nos recursos hídricos de Paranaguá e Pontal do Paraná. *Periódico Tchê Química*, 15(30), 201-208.
27. Silva, W.T.L., Novaes, A. P., Kuroki, V., Martelli, L.F.A. & Junior, L.M. (2012) Avaliação Físico-Química de Efluente Gerado em Biodigestor Anaeróbico para Fins de Avaliação de Eficiência e Aplicação de Fertilizante Agrícola. *Química Nova*. 35(1), 35-40.
28. Smaha, N. & Gobbi, M. F. (2003) Implementação de um Modelo para Simular a Eutrofização do Reservatório Passaúna - Curitiba – PR. *Revista Brasileira de Recursos Hídricos*. 8(3), 59-69.
29. Souza, G.L.C., Silva, A.C.C., Carvalho, K.H. & Rocha, J.R.C. (2019) Physical-Chemical Parameters Evaluation of Pery River Waters in Pontal do Paraná, PR. *IOSR Journal of Environmental Science, Toxicology and Food Technology*, 13(6), 69-78.
30. Staszczak, I. & Rocha, J.R.C. (2018) Avaliação da Influência das Marés nos Parâmetros Físico-químicos Presentes nas Águas do Rio Guaraguaçu, PR, *Periódico Tchê Química*. 15(30), 177-184.

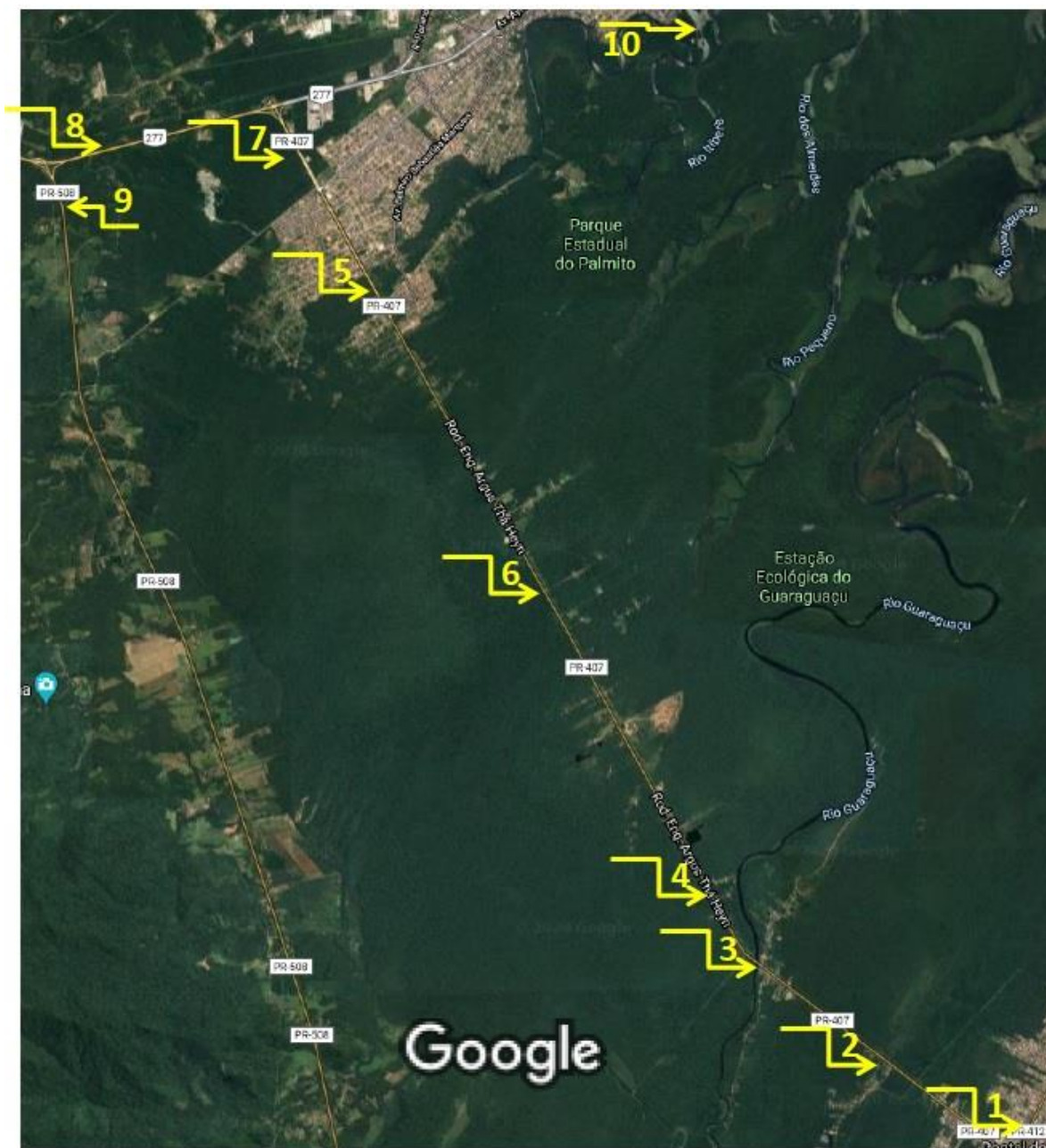


**Figura 1.** Localização no mapa parcial das cidades de Paranaguá e Pontal do Paraná dos dez pontos amostrais dos rios onde foram retiradas amostras para avaliar a concentração de fósforo na forma do íon fosfato. Fonte: Adaptação do autor do Google Maps.

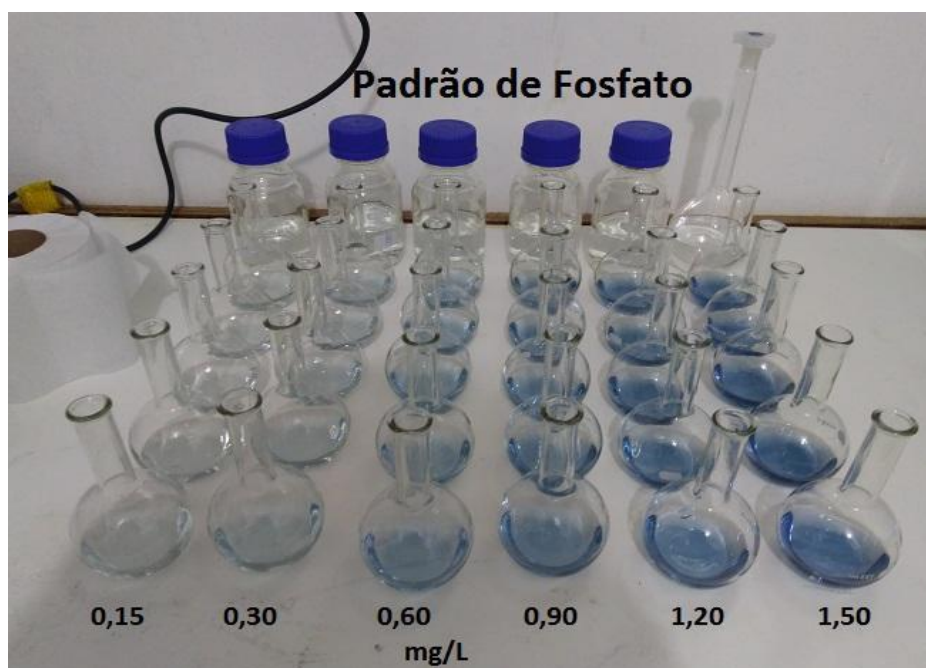


**Figura 2.** Imagem das soluções padrão de fosfato (0,15; 0,30; 0,60; 0,90; 1,20; 1,50 mg L<sup>-1</sup>) após a adição das soluções reagentes A e B com a formação da coloração azul de molibdênio.

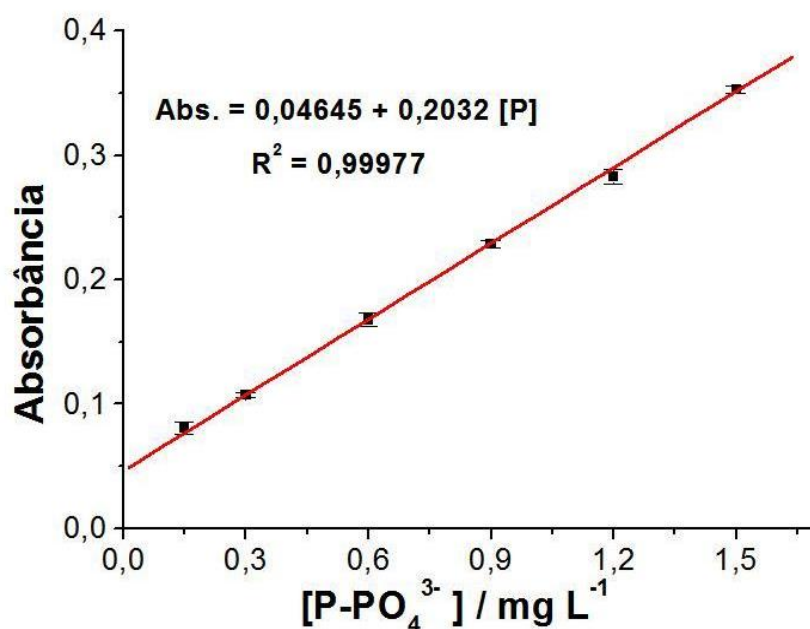


**Figura 3.** Representação gráfica da obtenção da equação padrão de fosfato após a análise linear dos valores de absorbância em função das concentrações das soluções padrões de fósforo na forma de fosfato (0,15; 0,30; 0,60; 0,90; 1,20; 1,50 mg L<sup>-1</sup>) obtida no sexto período amostral (novembro/18).



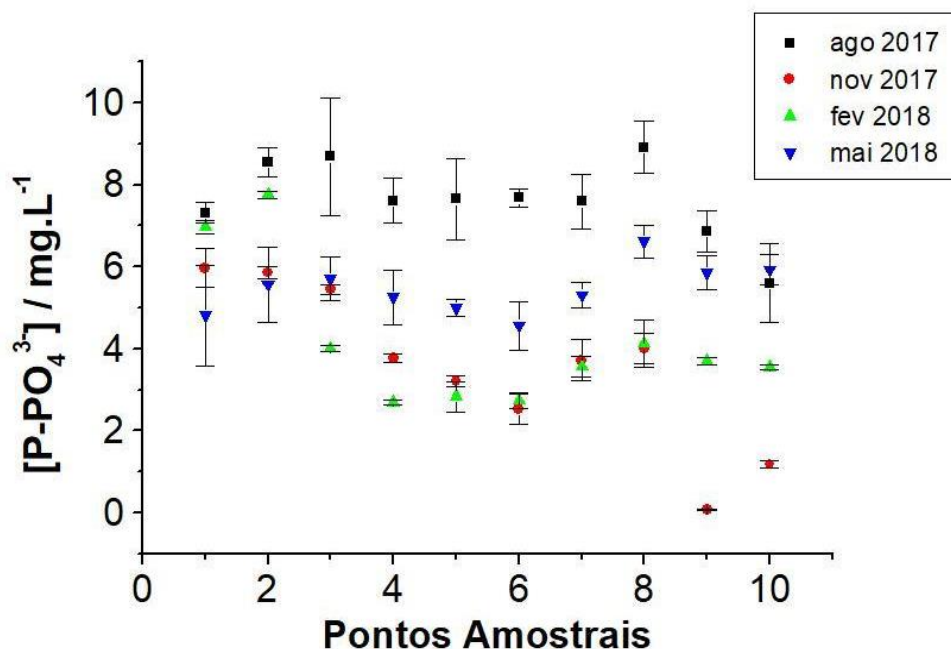


**Figura 4.** Representação gráfica das concentrações de fósforo, na forma de fosfato e desvio padrão das amostras naturais nos meses de agosto/17, novembro/17, fevereiro/18 e maio/18.

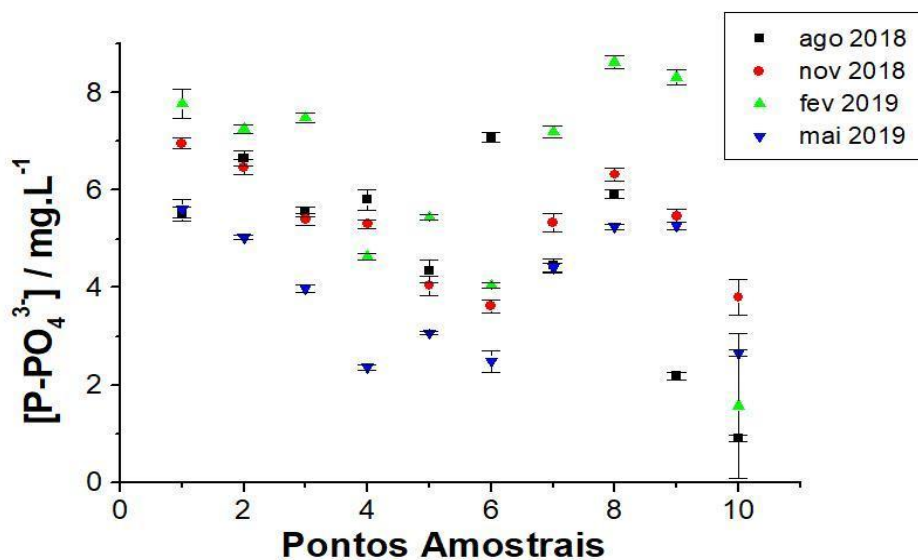


**Figura 5.** Representação gráfica das concentrações de fósforo, na forma de fosfato e desvio padrão das amostras naturais nos meses de agosto/18, novembro/18, fevereiro/19 e maio/19.

**Tabela 1.** Localização e coordenadas geográficas dos pontos amostrais dos rios do litoral paranaense. Fonte: o autor.

| Ponto | Localização                          | Coordenadas                  |
|-------|--------------------------------------|------------------------------|
| 1     | Rio Balneário - Praia de Leste       | 25°69'75.14"S; 48°47'53.59"O |
| 2     | Rio Pery                             | 25°68'76.04"S; 48°49'03.03"O |
| 3     | Rio Guaraguaçu                       | 25°67'19.96"S; 48°51'28.52"O |
| 4     | Rio São Joãozinho                    | 25°66'49.41"S; 48°51'85.81"O |
| 5     | Rio da Vila                          | 25°58'52.67"S; 48°56'78.08"O |
| 6     | Riacho no Km 7 da Rodovia das Praias | 25°56'67.60"S; 48°57'86.10"O |
| 7     | Riacho no Km 1 da Rodovia das Praias | 25°61'56.41"S; 48°54'85.93"O |
| 8     | Rio Vermelho                         | 25°56'66.16"S; 48°60'79.43"O |
| 9     | Riacho no Km 1 da Rodovia Matinhos   | 25°57'21.87"S; 48°61'35.08"O |
| 10    | Rio Itiberê próximo ao DETRAN        | 25°54'24.29"S; 48°52'46.96"O |

**Tabela 2.** Equações lineares da reta obtidas através dos valores de absorbância das soluções padrão versus suas concentrações de fósforo na forma de fosfato (0,15; 0,30; 0,60; 0,90; 1,20 e 1,50 mg L<sup>-1</sup>). Fonte: o autor.

| Amostragem   | Equação Linear da Reta                                     | Coefficiente de Determinação (R <sup>2</sup> ) |
|--------------|--|--|
| agosto/17    | Abs = 0,02858 + 0,25229 [P-PO <sub>4</sub> <sup>3-</sup> ] | 0,99577  |
| novembro/17  | Abs = 0,07690 + 0,20071 [P-PO <sub>4</sub> <sup>3-</sup> ] | 0,99938  |
| fevereiro/18 | Abs = 0,03970 + 0,24657 [P-PO <sub>4</sub> <sup>3-</sup> ] | 0,99428  |
| maio/18      | Abs = 0,04457 + 0,16949 [P-PO <sub>4</sub> <sup>3-</sup> ] | 0,99136  |
| agosto/18    | Abs = 0,05281 + 0,22115 [P-PO <sub>4</sub> <sup>3-</sup> ] | 0,99590  |
| novembro/18  | Abs = 0,04645 + 0,20320 [P-PO <sub>4</sub> <sup>3-</sup> ] | 0,99977  |
| fevereiro/19 | Abs = 0,04818 + 0,11193 [P-PO <sub>4</sub> <sup>3-</sup> ] | 0,99590  |
| maio/19      | Abs = 0,05297 + 0,18546 [P-PO <sub>4</sub> <sup>3-</sup> ] | 0,99936  |

Abs. = valor de absorbância de cada uma das amostras reais.

## MÉTODOS ESPECTROSCÓPICOS PARA A DETERMINAÇÃO DE GEOTITA EM CAULINITA

## SPECTROSCOPIC METHODS TO DETERMINATION OF GEOTHITE IN KAOLINITE

DE SOUZA, Marcelo Kehl<sup>1</sup>; KLUNK, Marcos Antônio<sup>2\*</sup>; XAVIER, Soyane Juceli Siqueira<sup>1</sup>; DAS, Mohuli<sup>3</sup>; DASGUPTA, Sudipta<sup>3</sup>

<sup>1</sup> Department of Geology, University of Vale do Rio dos Sinos, Av. Unisinos 950, São Leopoldo, RS, Brazil

<sup>2</sup> Department of Mechanical Engineering, University of Vale do Rio dos Sinos, São Leopoldo, RS, Brazil

<sup>3</sup> Department of Earth Sciences, Indian Institute of Technology Bombay (IIT Bombay), Powai, India

\* Autor correspondente

e-mail: marcosak@edu.unisinos.br

Received 01 April 2020; received in revised form 27 May 2020; accepted 29 May 2020

## RESUMO

Um dos principais contaminante da caulinita, o ferro, impacta diretamente na qualidade em seu valor comercial. O monitoramento espectroscópico, medido a profundidade da absorção da caulinita, é comparado com a literatura a fim de identificar possíveis contaminantes. A ocorrência da caulinita se deve à formação de minerais primários após a liberação parcial de cátions e silício. Este argilo-mineral tem uma forma simples, com imperfeições cristalográficas variáveis, especialmente na presença de ferro, que substituem o alumínio na cadeia mineral, causando várias desorganizações estruturais. A extração de minerais industriais combinada com estudos geológicos, permite o desenvolvimento de novas fontes de energia, como minerais argilosos, em particular caulinita. Dependendo da origem das caulinitas, a presença de óxidos de ferro em sua estrutura,  $\text{Fe}_2\text{O}_3$  e  $\text{FeO}(\text{OH})$  são comuns. Ao comparar os resultados da espectroscopia (fluorescência de raio-X, difração de raio-X; RAMAN) e no imageamento através do MEV-EDS, foi possível identificar a caulinita, com maior coeficiente de determinação, quando a proporção de caulinita atinge 60% ou mais na mistura. A caulinita pode ser identificada e quantificada com alta correlação na mistura a partir da absorção da amostra. Assim, o método possui grande potencial para auxiliar na quantificação e, conseqüentemente, na discriminação da qualidade da caulinita.

**Palavras-chave:** Goetita, Argilo-minerais; Espectroscopia.

## ABSTRACT

One of the main contaminants of kaolinite, the iron, directly impacts quality in its commercial value. The spectroscopic monitoring, measured the depth of absorption of kaolinite, is compared with the literature in order to identify possible contaminants. The occurrence of kaolinite is due to the formation of primary minerals after the partial release of cations and silicon. This clay-mineral has a simple shape, with variable crystallographic imperfections, especially in the presence of iron, which replaces aluminum in the mineral chain, causing various structural disorganizations. The extraction of industrial minerals combined with geological studies, allows the development of new sources of energy, such as clay minerals, in particular kaolinite. Depending on the origin of the kaolinites, the presence of iron oxides in its structure,  $\text{Fe}_2\text{O}_3$  and  $\text{FeO}(\text{OH})$ , are common. By comparing the results of spectroscopy (X-ray fluorescence, X-ray diffraction, RAMAN) and imaging using SEM-EDS, it was possible to identify kaolinite, with a higher determination coefficient, when the proportion of kaolinite reaches 60% or more in the mix. Kaolinite can be identified and quantified with a high correlation in the mixture from the sample absorption. Thus, the method has great potential to assist in quantifying and, consequently, in discriminating the quality of kaolinite.

**Keywords:** Goethite; Clay Minerals; Spectroscopy.



## 1. INTRODUCTION

Brazil's extractive economy is mainly focused on supplying the metalworking industry (Schrecker *et al.*, 2018; Giacomini *et al.*, 2017; Paulino, 2014). About 85% by volume are of metallic minerals extracted in the country, and the other 15% are non-metallic (Macedo *et al.*, 2003; De Souza *et al.*, 2019). The extraction of industrial minerals combined with geological studies allows the development of new energy sources such as clay-minerals, in particular, kaolinite (Sruthi and Reddy, 2017). A large volume of reserves and production allows the development of the ceramic sector. Kaolinite prices are influenced by the availability of reserves, geographic location (transport), and aggregate technology for processing and treatment (Pardo *et al.*, 2018; Illera *et al.*, 2015). Clay minerals are hydrated aluminum silicates made up of layers of  $\text{SiO}_2$  tetrahedrons and  $\text{Al}_2\text{O}_3$  octahedrons, which are intercalated in proportions: 1: 1 (kaolinite) and 2: 1 (montmorillonite) (Klunk *et al.*, 2019a). These minerals are part of the group defined as hydrated silicates, essentially made up of aluminum, in addition to iron, magnesium, and other impurities (Klunk *et al.*, 2019b).

Clay minerals are widely used in the industry. The use of these minerals as raw material results from the quality of the material produced. Kaolinites can present different degrees of purity and crystallinity due to cationic exchanges, with contaminants such as quartz and iron oxides (Klunk *et al.*, 2019c). Thus, the identification of the minerals present in the clays, as well as their physical-chemical characterization, are critical points in determining and understanding the behavior of the materials for the quality control of the final product (Ruosso *et al.*, 2019; Klunk *et al.*, 2019d; Klunk *et al.*, 2020a). Depending on the origin of the kaolinites, structural defects can occur due to the presence of iron oxides in its structure, being hematite ( $\text{Fe}_2\text{O}_3$ ), and goethite ( $\text{FeO}(\text{OH})$ ) - predominantly, the most common (Klunk *et al.*, 2020b). These compounds can be predicted through geochemical modeling using speciation of the elements (Klunk *et al.*, 2015; Klunk *et al.*, 2019e,f,g).

Thus, it is necessary to evaluate the potential of these materials for applications in the traditional ceramic industry. The goethite concentration is directly related to the depositional system. The availability of water promotes the concentration of humic acids, favoring the

formation of  $\text{FeO}(\text{OH})$  (Klunk *et al.*, 2012). Usually, Fe oxides have a high specific surface, resulting in high anion adsorption power, contributing to the kaolinite ion exchange capacity. However, few studies relate the influence of goethite with kaolinite, mainly on the effect on mineralogy (Fraga *et al.*, 2014).

Therefore, the objectives of this study are to relate the contents of goethite in kaolinite under different mixtures and to follow the evolution of the system through the techniques of XRF, XRD, Scanning Electron Microscopy (SEM) images allied to Spectrometer Energy Dispersive X-ray (EDS and RAMAN). The basic structural unit of iron oxides is associated with the octahedral arrangement, in which each iron atom is surrounded by six oxygen and hydroxyls, so the oxides are differentiated by the type of octahedral arrangement. In this way, it is possible to identify the occurrence of goethite in kaolinite by the manifestation of functional groups related to iron.

## 2. MATERIALS AND METHODS

### 2.1. Sistema de Mistura

The mixtures were performed with kaolinite:goethite, powered (mean diameter < 62  $\mu\text{m}$ ), with a weight proportion of 90:10 % with increments of 10 % in goethite until the proportion of 10:90 %, respectively.

### 2.2. Characterization of the Materials

#### 2.2.1. X-Ray Fluorescence Spectroscopy

The chemical composition of the solid, liquid and gaseous materials can be easily determined by the X-Ray Fluorescence Spectroscopy (XRF), which allows the identification and quantification of chemical elements from almost the entire periodic table (Klunk *et al.*, 2015; Klunk *et al.*, 2018). When a sample is irradiated with primary X-Rays, the electron of the innermost layer of the atom is ejected, causing a void. The excited atom returns to the ground state through a series of electronic transitions. This electronic transition process emits characteristic fluorescent X-Rays. Such a phenomenon is known as X-Ray fluorescence (Elaiopoulos *et al.*, 2010).

Therefore, each element emits characteristic radiation (energy and wavelength defined) that are detected and used for qualitative analysis. The quantitative information of the elements present in the sample is directly related to the intensity of the radiation emitted (Elaiopoulos *et al.*, 2010).

The X-Ray fluorescence technique can be divided into dispersive wavelength (sequential or simultaneous), dispersive, and special energy categories (synchrotron radiation source, total reflection, and particle induction). The dispersive energy fluorescence (EDXRF) technique has a lower resolution than the wavelength dispersion technique (WDXRF), but it is also widely used for rapid and exploratory analysis (Somerset, 2004).

X-Ray Fluorescence by wavelength dispersion (WDXRF) using the fundamental parameters (FP) method provides semi-quantitative and multi-elemental analyzes, as well as being non-destructive and fast. This method relates the theoretical fluorescence intensity of the chemical elements by means of samples of known chemical composition and the measured fluorescent intensity, thus, being able to determine the unknown chemical composition (Caetano *et al.*, 2015a). The XRF technique is not very sensitive for the detection of light elements due to induced Auger emission that reduces the intensity of XRF in the sample (Caetano *et al.*, 2015b).

### 2.2.2. X-Ray Diffraction

The X-Ray Diffraction (XRD) technique has wide application in the field of material characterization due to the information it provides on the mineralogical composition, the arrangement of the atoms and the study of details of the lattice structures in crystalline of the various materials (Caetano *et al.*, 2015c; Cataluña *et al.*, 2018). To identification of the compounds present in kaolinite and Goethite, DRX is an indispensable tool because this type of material has several compounds in crystalline form. X-rays are generated both by the deceleration of the electrons in a metal target and by the excitation of the electrons of the target atoms. An electron bombarded copper target is considered a good target for producing a strong line to CuK $\alpha$  (Caetano *et al.*, 2018; Cataluña *et al.*, 2017).

The phenomenon of diffraction occurs because X-Rays are scattered around the ordered environment of a crystal, causing interference between X-Ray waves. Constructive and

destructive interferences form patterns capable of providing information regarding the characteristics of the compounds present in a sample. Diffraction occurs when the wavelength of radiation is comparable to the characteristic spacings within the object that causes diffraction. Therefore, in order to obtain diffraction patterns of layers of atoms, it is necessary to use radiation having a wavelength comparable to the spacing of the layers, which is the case with X-Rays (Zhang *et al.*, 2018; Suzzoni *et al.*, 2018). The main diffraction methods are: i) Laue Method, which is used for the determination of crystal orientation in solid-state physics experiments; ii) Method of rotating crystal used for the determination of the configuration of enzymes, determination of the form of molecules, among other applications; and iii) Powder Method for Sprayed Samples (Pietzsch *et al.*, 2015; De Aza *et al.*, 2014).

In the diffraction technique by the powder method, a monochromatic X-Ray beam is directed to a sprayed sample, spread on a support, and the diffraction intensity is measured when a detector is moved at different angles. The pattern obtained is characteristic of the material in the sample and can be identified by comparison with standards base of data from ICDD (Joint Committee on Powder Diffraction Standards - JCPDS) da International Union of Crystallography (Cora *et al.*, 2014; Yan *et al.*, 2017).

Thus, XRD by the powder method provides a fingerprint of the sample. It can also be used to identify the size and type of the unit cell by measuring the spacing of the lines in the diffraction pattern (Miranda-Trevino and Coles, 2003).

The central equation for analyzing the results in a powder diffraction experiment is the Bragg equation ( $2d \sin \theta = \lambda$ ); were,  $\theta$  are the angles at which constructive interference occurs with the spacing  $d$  of the layers of atoms in the samples for X-rays of wavelength  $\lambda$  (Atkins e Jones, 2001). X-rays are reflected by the crystal only if the angle of incidence satisfies the condition established by Bragg's Law (Castrillo *et al.*, 2015; Zulfiqar *et al.*, 2015).

### 2.2.3. Scanning Electron Microscopy and Spectrometer Energy Dispersive X-ray

The morphology of materials can be studied by obtaining images through the Scanning Electron Microscopy (SEM) and Spectrometer Energy Dispersive X-ray (EDS) analysis, which provides micrographs at higher resolutions than

those provided by light microscopy, which is limited by diffraction effects of the order of magnitude of the wavelength of the light (Klunk *et al.*, 2019e; Rong *et al.*, 2008; Shahwan *et al.*, 2005; Frost *et al.*, 2002; Gupta *et al.*, 2011).

In a scanning electron microscope, the surface of a solid sample is swept with an electron beam. Samples that conduct electricity are easier to study because the free electron flow minimizes the charge accumulation and the possibility of thermal degradation of the sample. A number of techniques were developed to obtain electron microscopy images of non-conducting samples. The most common procedure involves coating the surface with a thin metallic film.

#### 2.2.4. Raman Spectroscopy

Raman spectroscopy is a spectroscopic technique used to observe vibrational, rotational, and other low-frequency modes in a system (Frost *et al.*, 1997; Klopogge, 2017). This technique is commonly used in chemistry to provide a structural fingerprint by which molecules can be identified (Khanna, 1981; Thibau *et al.*, 1978; De Faria *et al.*, 2007; Clark and Curri, 1998; Oh *et al.*, 1998).

### 3. RESULTS AND DISCUSSION

#### 3.1. Chemical Composition

The chemical composition of Kaolinite and Goethite with its respective mixtures was determined by XRF found in Figure 1. The present compounds are derived from the inorganic fraction in both Kaolinite and Goethite, and therefore, the results are presented in the form of oxides. According to Figure 1, there were large variations between the contents of the main components (kaolinite 100% and goethite 100%) of the different mixtures.

The content of the principal compounds forming the kaolinite structure are  $\text{SiO}_2$  and  $\text{Al}_2\text{O}_3$ , and for goethite is  $\text{Fe}_2\text{O}_3$  (in the form of oxide as read from the XRF equipment). For the kaolinite, the  $\text{SiO}_2$  content varied from 52.80% (100% Kaolinite) to 6.58% (represented by the mixture of G90% + K10%) and the  $\text{Al}_2\text{O}_3$  content ranged from 38.90% (100% Kaolinite) to 3.71 % (represented by the mixture of G90% + K10%).

Thus, for the compounds forming the

goethite structure, the amount of  $\text{Fe}_2\text{O}_3$  varied from 5.97% in the mixture of G 10% + K 90% to 84.42 in the mixture of G 90% + K 10%. Figure 1 shows all fractions of a mixture of kaolinite and goethite.

#### 3.2. Mineralogical Composition

The technique of XRD allowed the identification of the crystalline phase's present kaolinite and goethite. Figure 2 shows the diffractograms of the samples of Kaolinite and Goethite (pattern and in the study), respectively.

The XRD pattern of the kaolinite sample is shown in Figure 2a. The spectrum of the kaolinite sample contains all the major peaks referring to (Joint Committee on Powder Diffraction Standards) JCPDS, database file (PDF-01-089-6538), thus indicating the formation of  $\text{Al}_2\text{Si}_2\text{O}_5(\text{OH})_4$ . The main (hkl) indices of kaolinite like (001) and (002) are indicated in the pattern. The peaks are slightly broad, indicating a smaller crystal size (Phoebe and Medard 1991; Jehan *et al.*, 1970).

The XRD pattern of the goethite samples is shown in Figure 2b. The spectrum of the goethite sample contains all the major peaks referring to (Joint Committee on Powder Diffraction Standards) JCPDS, database file (PDF-17-0536), thus indicating the formation of  $\alpha\text{-FeOOH}$ . The main (hkl) indices of goethite like (020), (110), (120), (130), (111), (121), (140) and (221) are indicated in the pattern. The peaks are slightly broad, indicating a smaller crystal size (Ghosh *et al.*, 2012).

The results of the XRD analysis indicate that in the samples of kaolinite (A) pattern and in the study, we showed the absence of goethite. Therefore, in the samples of goethite (B) pattern and in the study, we find the same behavior of absence of compounds of another nature, thus without traces of kaolinite.

The difference in relative intensity of the diffraction peaks found in the kaolinite and goethite pattern when compared to Kaolinite and Goethite in the study may indicate different proportions of the phases found, as may be the result of sample preparation in the X-ray diffraction tests. The discrepancies between the amounts of the compounds found in the different samples can be attributed to the different geological conditions in the formation of kaolinite and goethite in the study.

### 3.3. Morphology

The technique of Scanning Electron Microscopy (SEM) images allied to Spectrometer Energy Dispersive X-ray (EDS) analysis were used in this present work for the study of morphology. The objective is to complement the other characterization techniques in the evaluation of the shape of the particles and composition present in the samples. Figure 3 shows us the micrographics' of Kaolinite and Goethite in the study.

In Fig. 4 are the micrographies of the mixture of 50% kaolinite + 50% Goethite (A) with their respective EDS (B and C). At point 051 and 052 (Fig. 4A) the Spectrometer Energy Dispersive X-ray show particularity in the diffractogram. Characteristic of each mineral phase in the blend. Kaolinite is represented in EDS-051 and Goethite in EDS-052.

### 3.4. Raman Spectroscopy

The Raman spectroscopic analysis identified the phase of goethite (fig. 5). Raman bands occurring at 299, 400, 484, 550, and 674  $\text{cm}^{-1}$  were assigned to the Fe-OH symmetric bend; Fe-O-Fe/-OH symmetric stretching; Fe-OH asymmetric stretching and Fe-O symmetric stretching, respectively (Dunnwald and Otto 1989; Kieser et al., 1983; Boucherit et al., 1991). As the amount of kaolinite increases in the mixture, the RAMAN spectrum reveals a decrease in Goethite band.

## 4. CONCLUSIONS

With the results obtained from techniques used allowed the following conclusions to be drawn:

- XRD identified crystalline phases of Kaolinite and Goethite;
- XRF showed the compounds present and derived from the mixture fraction in both Kaolinite and Goethite;
- SEM-EDS showed the grain morphology in the Kaolinite mixture 50% + Goethite 50% with the respective compositions);
- RAMAN (reveals a decrease of Goethite peaks as the percentage of Kaolinite increases in the

mixture) made it possible to characterize Kaolinite and Goethite in a mixing system.

We show in this research the potential of spectroscopy in the identification and quantification of mineral kaolinite in mixtures with mineral Fe. We conclude that kaolinite can be identified and quantified with a high correlation in the mix from the depth of the main diagnostic absorption feature with little sample preparation. Thus, the method has great potential to assist in quantification and, consequently, in the discrimination of kaolinite quality.

With little or no sample preparation, the spectroscopy can be used in obtaining many important information of mineralogy. The spectroscopy is a non-expensive, fast, and non-evasive, or little evasive methodology that offers great potential for the identification and qualification of minerals and mix.

## 5. ACKNOWLEDGMENTS

This project was financially supported by the projects Modelagem Digital de Afloramentos utilizando GPU (MCT/FINEP - Pré-Sal Cooperativos ICT - Empresas 03/2010 - Contract 01.23.4567.89) and FINEP-PROINFRA (Contract: 01.13.0302.00). MKS thanks PROSUP/CAPES for the financial support of the Ph.D. scholarship. MRV thanks the Brazilian Council for Scientific and Technological Development (CNPq) for the research grant (Process 309399/2014-9).

## 6. REFERENCES

1. Schrecker, T., Birn, A.-E., Aguilera, M. How extractive industries affect health: Political economy underpinnings and pathways. *Health & Place*, **2018**, 52, 135–147.
2. Giacomini, A. M., Garcia, J. B., Zonatti, W. F., Silva-Santos, M. C., Laktim, M. C., Baruque-Ramos, J. Brazilian silk production: economic and sustainability aspects. *Procedia Engineering*, **2017**, 200, 89–95.
3. Paulino, E. T. The agricultural, environmental and socio-political repercussions of Brazil's land governance system. *Land Use Policy*, **2014**, 36, 134–144.
4. Macedo, A. B., de Almeida Mello Freire, D. J., Akimoto, H. Environmental management in the Brazilian non-metallic small-scale mining sector. *Journal of*

- Cleaner Production*, **2003**, 11(2), 197–206.
5. De Souza, C. A. R., Souza, A. M., Souza, F. M., da Veiga, C. P., da Silva, W. V. The importance of principal components in studying mineral prices using vector autoregressive models: Evidence from the Brazilian economy. *Resources Policy*, **2019**, 62, 9–21.
  6. Sruthi, P. L., Reddy P, H. P. Characterization of kaolinitic clays subjected to alkali contamination. *Applied Clay Science*, **2017**, 146, 535–547.
  7. Pardo, F., Jordan, M. M., Montero, M. A. Ceramic behaviour of clays in Central Chile. *Applied Clay Science*, **2018**, 157, 158–164.
  8. Illera, L. C., Illera, C. C., Contreras, K. A. Raw material for the ceramic industry in Norte de Santander. III. Assessment of the technological properties when the residue test of deep abrasion is added. *Boletín de La Sociedad Española de Cerámica y Vidrio*, **2015**, 54(2), 77–83.
  9. Klunk, M.A., Shah, Z., Wander, P.R. Use of Montmorillonite Clay for Adsorption Malachite Green Dye. *Periódico Tchê Química*, **2019a**, 16(32), 279-286.
  10. Klunk, M.A., Dasgupta, S., Nunes, B.V.G., Wander, P.R. Synthesis of Sodalite Zeolite to Treatment of Textile Effluents. *Periódico Tchê Química*, **2019b**, 16(31), 778-783.
  11. Klunk, M. A., Dasgupta, S., Das, M., Wander, P. R., Shah, Z., Adsorption Study of Crystal Violet and Malachite Green Dyes in Zeolitic Material. *Periódico Tchê Química*, **2019c**, 16(33), 70-81.
  12. Ruoso, F. S., Bittencourt, L. C., Sudati, L. U., Klunk, M. A., Caetano, N. R. New Parameters for the Forest Biomass Waste Ecofirewood Manufacturing Process Optimization. *Periódico Tchê Química*, **2019**, 16(32), 560-571.
  13. Klunk, M. A., Dasgupta, S., Das, M., Cunha, M. G., Wander, P. R. Synthesis of Sodalite Zeolite and Adsorption Study of Crystal Violet Dye. *ECS Journal of Solid State Science and Technology*, **2019d**, 8(10), N144–N150.
  14. Klunk, M. A., Das, M., Dasgupta, S., Impiombato, A. N., Caetano, N. C., Wander, P. R., Moraes, C. A. M. Comparative study using different external sources of aluminum on the zeolites synthesis from rice husk ash. *Materials Research Express*, **2020a**, 7, 015023.
  15. Klunk, M. A., Schröpfer, S. B., Dasgupta, S., Das, M., Caetano, N. R., Impiombato, A. N., Wander, P. R., Moraes, C. A. M. (2020B). Synthesis and characterization of mordenite zeolite from metakaolin and rice husk ash as a source of aluminium and silicon. *Chemical Papers*, **2020b**, 74, 2481-2489.
  16. Klunk, M. A., Damiani, L. H., Feller, G., Rey, M. F., Conceição, R. V., Abel, M., De Ros, L. F. Geochemical modeling of diagenetic reactions in Snorre Field reservoir sandstones: a comparative study of computer codes. *Brazilian Journal of Geology*, **2015**, 45, 29-40.
  17. Klunk, M. A., Dasgupta, S., Schropfer, S. B., Nunes, B. V. G., Wander, P. R. Comparative Study of Geochemical Speciation Modeling Using GEODELING Software. *Periódico Tchê Química*, **2019e**, 16(31), 816-822.
  18. Klunk, M. A., Dasgupta, S., Das, M., Wander, P. R. Computer Codes of Geochemical Modeling used to Water-Rock Interaction Simple and Complex Systems. *Periódico Tchê Química*, **2019f**, 16(32), 108-118.
  19. Klunk, M. A., Dasgupta, S., Das, M., Wander, P. R., Di Capua, A. Geochemical Speciation and Batch Mode Simulation in the Carbonate Depositional Environments. *Periódico Tchê Química*, **2019g**, 16(33), 736-748.
  20. Klunk, M. A., Oliveira, A., Furtado, G., Knornschild, G. H., Dick, L. F. P. Study of the Corrosion of Buried Steel Grids of Electrical Power Transmission Towers. *ECS Transactions*, **2012**, 43, 23-27.
  21. Fraga, A., Klunk, M. A., Oliveira, A., Furtado, G., Knornschild, G. H., Dick, L.F.P. Soil corrosion of the AISI1020 steel buried near electrical power transmission line towers. *Materials Research*, **2014**, 17, 1637-1643, 2014.
  22. Klunk, M. A., Damiani, L. H., Feller, G., Rey, M. F., Conceição, R. V., Abel, M., De Ros, L. F. Geochemical modeling of diagenetic reactions in Snorre Field reservoir sandstones: a comparative study of computer codes. *Brazilian Journal of Geology*, **2015**, 45, 29-40.
  23. Klunk, M. A., Dasgupta, S., Conceição, R. V. Computerized geochemical modeling of burial diagenesis of the Eocene turbidite reservoir elements: Urucutuca Formation, Espírito Santo Basin, southeastern Brazil passive margin. *Journal of Palaeogeography*, **2018**, 7, 12-26.
  24. Elaiopoulos, K., Perraki, T., Grigoropoulou,

- E. Monitoring the effect of hydrothermal treatments on the structure of a natural zeolite through a combined XRD, FTIR, XRF, SEM and N<sub>2</sub>-porosimetry analysis. *Microporous and Mesoporous Materials*, **2010**, 134(1-3), 29–43.
25. Somerset, V. The use of X-ray fluorescence (XRF) analysis in predicting the alkaline hydrothermal conversion of fly ash precipitates into zeolites. *Talanta*, **2004**, 64(1), 109–114.
  26. Caetano, N. R., Cataluña, R., Vielmo, H. A. Analysis of the Effect on the Mechanical Injection Engine Using Doped Diesel Fuel by Ethanol and Bio-Oil. *International Review of Mechanical Engineering*, **2015a**, 9(2), 124–128.
  27. Caetano, N. R., Soares, D., Nunes, R. P., Pereira, F. M., Schneider, P. S., Vielmo, H. A., van der Laan, F. T. A comparison of experimental results of soot production in laminar premixed flames. *Open Engineering*, **2015b**, 5, 213–219.
  28. Caetano, N. R., Stapasolla, T. Z., Peng, F. B., Schneider, P. S., Pereira, F. M., Vielmo, H. A. Diffusion Flame Stability of Low Calorific Fuels. *Defect Diffusion Forum*, **2015c**, 362, 29–37.
  29. Cataluña, R., Shah, Z., Venturi, V., Caetano, N. R., Da Silva, B. P., Azevedo C. M. N., Da Silva, R., Suarez, P. A. Z., Oliveira, L. P. Production process of di-amyl ether and its use as an additive in the formulation of aviation fuels. *Fuel*, **2018**, 228, 226–233.
  30. Caetano, N. R., Venturini, M. S., Centeno, F. R., Lemmertz, C. K., Kyprianidis, K. G. Assessment of mathematical models for prediction of thermal radiation heat loss from laminar and turbulent jet non-premixed flames. *Thermal Science and Engineering Progress*, **2018**, 7, 241–247.
  31. Cataluña, R., Shah, Z., Pelisson, L., Caetano, N. R., Da Silva, R., Azevedo, C. Biodiesel Glycerides from the Soybean Ethylic Route Incomplete Conversion on the Diesel Engines Combustion Process. *Journal of the Brazilian Chemical Society*, **2017**, 28(12), 2447–2454.
  32. Zhang, Q., Yan, Z., Ouyang, J., Zhang, Y., Yang, H., Chen, D. Chemically modified kaolinite nanolayers for the removal of organic pollutants. *Applied Clay Science*, **2018**, 157, 283–290.
  33. Suzzoni, A., Barre, L., Kohler, E., Levitz, P., Michot, L. J., M'Hamdi, J.. Interactions between kaolinite clay and AOT. *Colloids and Surfaces A: Physicochemical and Engineering Aspects*, **2018**, 556, 309–315.
  34. Pietzsch, A., Nisar, J., Jämstorp, E., Gråsjö, J., Århammar, C., Ahuja, R., Rubensson, J.-E. Kaolinite: Defect defined material properties – A soft X-ray and first principles study of the band gap. *Journal of Electron Spectroscopy and Related Phenomena*, **2015**, 202, 11–15.
  35. De Aza, A. H., Turrillas, X., Rodriguez, M. A., Duran, T., Pena, P. Time-resolved powder neutron diffraction study of the phase transformation sequence of kaolinite to mullite. *Journal of the European Ceramic Society*, **2014**, 34(5), 1409–1421.
  36. Cora, I., Dódon, I., Pekker, P. Electron crystallographic study of a kaolinite single crystal. *Applied Clay Science*, **2014**, 90, 6–10.
  37. Yan, K., Guo, Y., Fang, L., Cui, L., Cheng, F., Li, T. Decomposition and phase transformation mechanism of kaolinite calcined with sodium carbonate. *Applied Clay Science*, **2017**, 147, 90–96.
  38. Miranda-Trevino, J. C., Coles, C. A. Kaolinite properties, structure and influence of metal retention on pH. *Applied Clay Science*, **2003**, 23(1-4), 133–139.
  39. Franco, F. The influence of ultrasound on the thermal behaviour of a well ordered kaolinite. *Thermochimica Acta*, **2003**, 404(1-2), 71–79.
  40. Atkins, P.; Jones, L. Princípios de Química – questionando a vida moderna e o meio ambiente. Porto Alegre: Bookman, **2001**.
  41. Castrillo, P. D., Olmos, D., & González-Benito, J. Kinetic study of the intercalation process of dimethylsulfoxide in kaolinite. *International Journal of Mineral Processing*, **2015**, 144, 70–74.
  42. Zulfiqar, S., Sarwar, M. I., Rasheed, N., & Yavuz, C. T. Influence of interlayer functionalization of kaolinite on property profile of copolymer nanocomposites. *Applied Clay Science*, **2015**, 112-113, 25–31.
  43. Klunk, M. A., Shah, Z., Caetano, N. R., Conceição, R. V., Wander, P. R., Dasgupta, S., Das, M. CO<sub>2</sub> sequestration by magnesite mineralization through interaction between Mg-brine and CO<sub>2</sub> : integrated laboratory experiments and computerized geochemical modelling. *International Journal of Environmental Studies*, **2019e**, 1-18.
  44. Rong, X., Huang, Q., He, X., Chen, H., Cai,

- P., Liang, W. Interaction of *Pseudomonas putida* with kaolinite and montmorillonite: A combination study by equilibrium adsorption, ITC, SEM and FTIR. *Colloids and Surfaces B: Biointerfaces*, **2008**, 64(1), 49–55.
45. Shahwan, T., Zünbül, B., Tunusoğlu, Ö., Eroğlu, A. E. AAS, XRPD, SEM/EDS, and FTIR characterization of Zn<sup>2+</sup> retention by calcite, calcite–kaolinite, and calcite–clinoptilolite minerals. *Journal of Colloid and Interface Science*, **2005**, 286(2), 471–478.
  46. Frost, R. L., Van Der Gaast, S. J., Zbik, M., Klopogge, J. T., Paroz, G. N. Birdwood kaolinite: a highly ordered kaolinite that is difficult to intercalate—an XRD, SEM and Raman spectroscopic study. *Applied Clay Science*, **2002**, 20(4-5), 177–187.
  47. Gupta, V., Hampton, M. A., Stokes, J. R., Nguyen, A. V., Miller, J. D. Particle interactions in kaolinite suspensions and corresponding aggregate structures. *Journal of Colloid and Interface Science*, **2011**, 359(1), 95–103.
  48. Frost, R. L., Thu Ha, T., & Kristof, J. FT-Raman spectroscopy of the lattice region of kaolinite and its intercalates. *Vibrational Spectroscopy*, **1997**, 13(2), 175–186.
  49. Klopogge, J. T. Raman and Infrared Spectroscopies of Intercalated Kaolinite Groups Minerals. *Infrared and Raman Spectroscopies of Clay Minerals*, **2017**, 343–410.
  50. Khanna, R. K. Raman-spectroscopy of oligomeric SiO<sub>2</sub> species isolated in solid methane. *Journal of Chemical Physics*, **1981**, 74 (4), 2108.
  51. Thibau, R. J., Brown, C. W., Heidersbach, R. H. Raman spectra of possible corrosion products of iron. *Applied Spectroscopy*, **1978**, 32, 532–535.
  52. De Faria, D. L. A., Lopes, F. N. Heated goethite and natural hematite: Can Raman spectroscopy be used to differentiate them? *Vibrational Spectroscopy*, **2007**, 45(2), 117–121.
  53. Clark, R. J. H., Curri, M. L. The identification by Raman microscopy and X-ray diffraction of iron-oxide pigments and of the red pigments found on Italian pottery fragments. *Journal of Molecular Structure*, **1998**, 440, 105–111.
  54. Oh, S. J., Cook, D. C., Townsend, H. E. Characterization of iron oxides commonly formed as corrosion products on steel. *Hyperfine Interactions*, **1998**, 112, 59–65.
  55. Phoebe, H., Medard, T. A method combining SWIR and XRD for the identification of clay minerals; I, Interstratified kaolinite/smectite clays: Program and Abstracts - 28<sup>th</sup> Annual Clay Minerals Conference, Clay Minerals Society, **1991**, 28, 69.
  56. Jehan, K., Qaiser, M. A., Khan, A. H. Quantitative estimation of kaolinite in clays by differential thermal analysis. *Pakistan Journal of Scientific and Industrial Research*, **1970**, 13(1-2), 169-173.
  57. Ghosh, M. K., Poinern, G. E. J., Issa, T. B., Singh, P. Arsenic adsorption on goethite nanoparticles produced through hydrazine sulfate assisted synthesis method. *Korean Journal of Chemical Engineering*, **2012**, 29(1), 95-102.
  58. Dunnwald, J., Otto, A. An investigation of phase transitions in rust layers using raman spectroscopy. *Corrosion Science*, **1989**, 29(9), 1167-1176.
  59. Kieser, J. T., Brown, C. W., Heidersbach, R. H. Characterization of the passive film formed on weathering steels. *Corrosion Science*, **1983**, 23(3), 251-259.
  60. Boucherit, N., Hugot-Le, Goff, A., Joiret, S. Raman studies of corrosion films grown on Fe and Fe-6Mo in pitting conditions. *Corrosion Science*, **1991**, 32(5-6), 497-507.

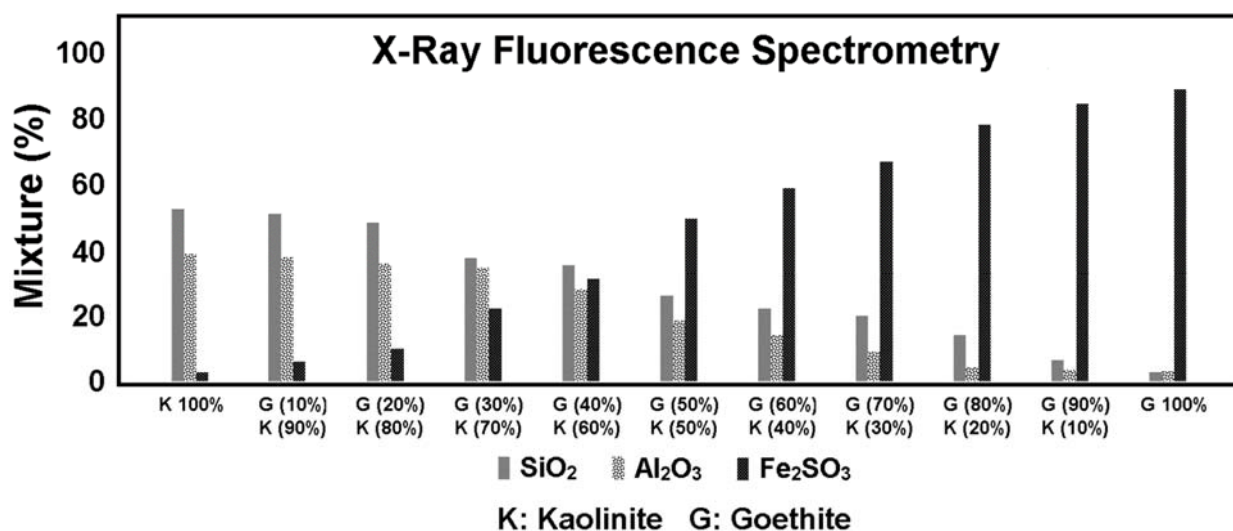


**Figure 1.** XRF of kaolinite (K) and goethite (G) with mixture respective.

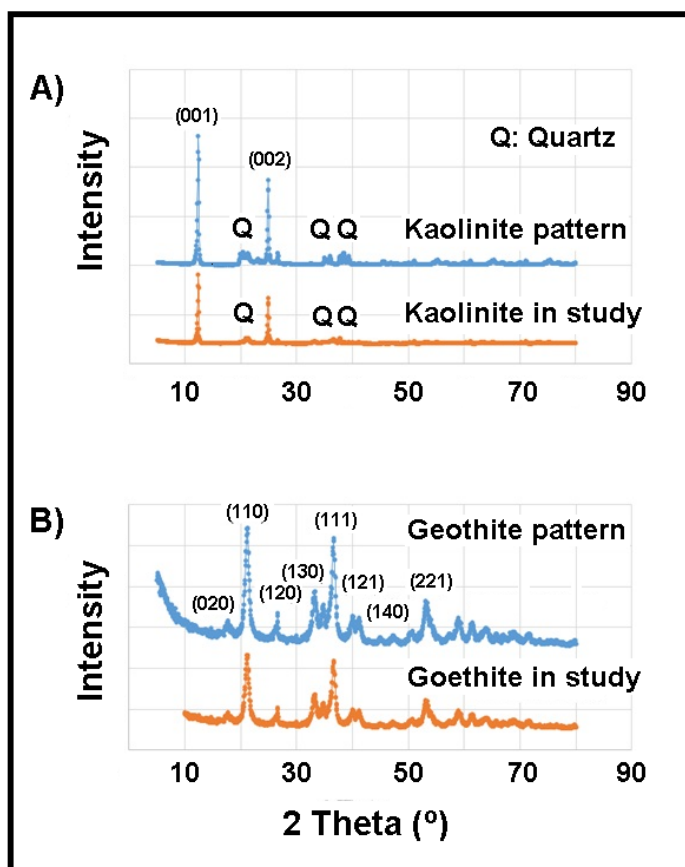


**Figure 2.** XRD of kaolinite (a) and goethite (b).



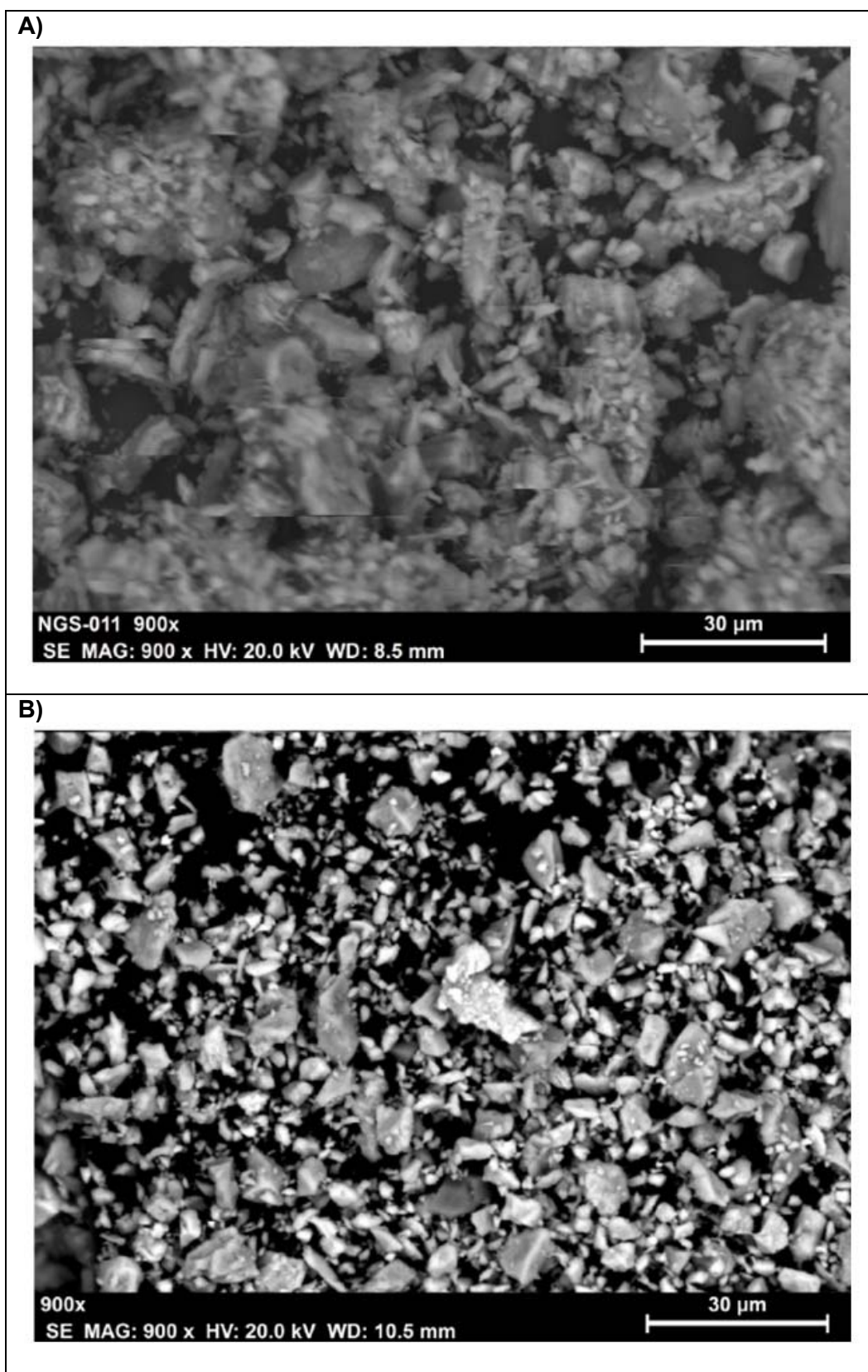
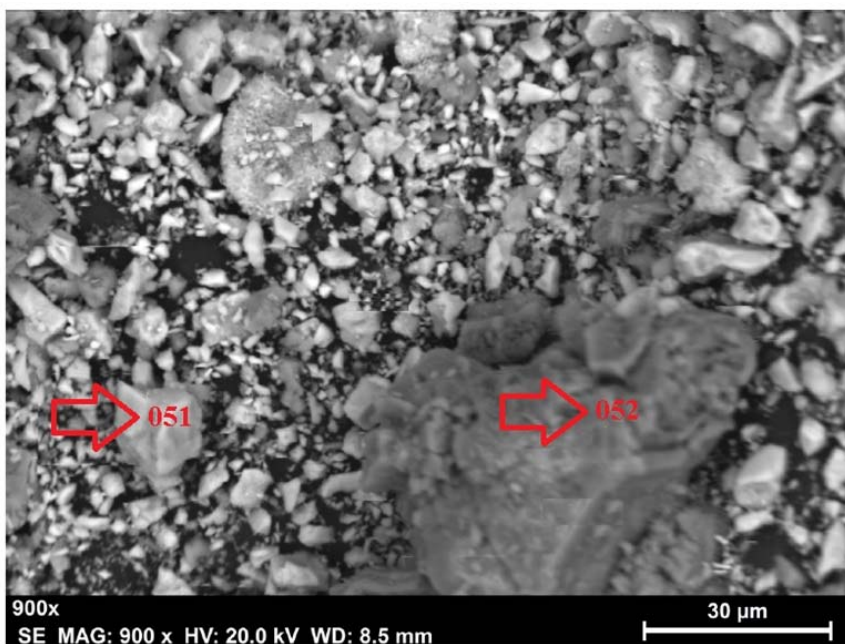
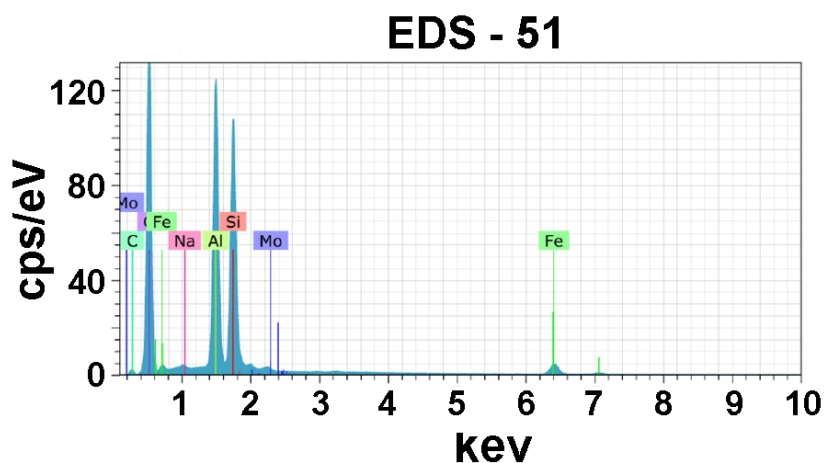


**Figure 3.** SEM of kaolinite *in study* (A), goethite *in study* (B).

A)



B)



C)

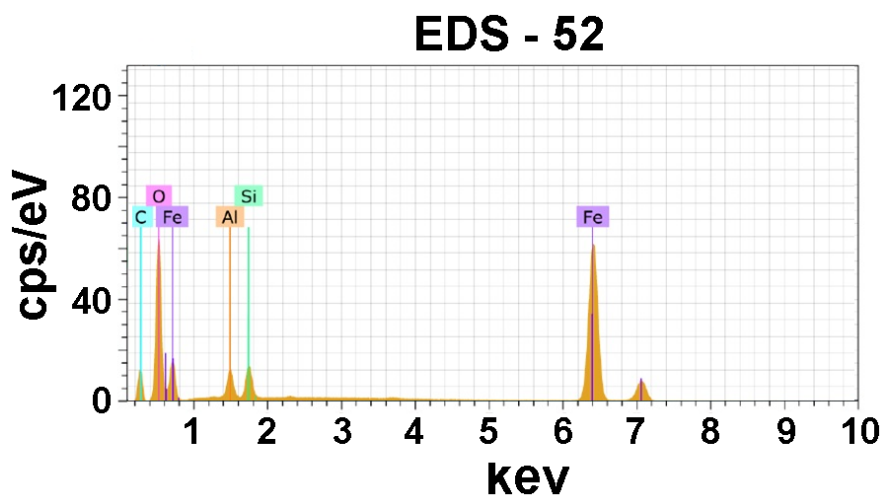


**Figure 4.** SEM of the mixture 50% kaolinite + 50% goethite (A) in study with yours EDS (B and C).

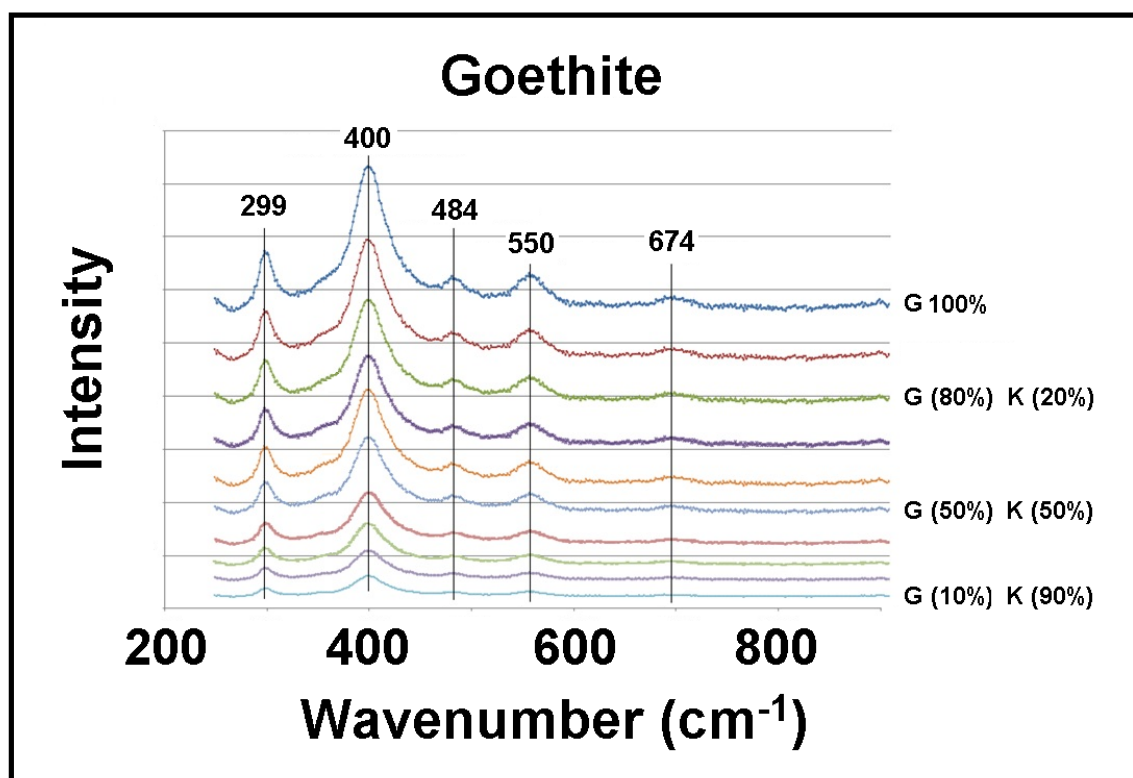


**Figure 5.** Raman spectroscopic of goethite in the study (100%) plus a mixture of the kaolinite.

POLUIÇÃO POR METAIS PESADOS EM CAMPOS DE TRIGO (SOLO E FOLHAS)  
AMOSTRADOS NAS PROVÍNCIAS DE BASRAH E MAYSAN

HEAVY METALS POLLUTION OF WHEAT FIELDS (SOIL AND LEAVES) SAMPLED  
FROM BASRAH AND MAYSAN PROVINCES

التلوث بالمعادن الثقيلة في حقول الحنطة ( عينات تربة و اوراق ) في محافظتي البصرة وميسان

MADHI, Qusai Hattab<sup>1\*</sup>; ABASS, Mohammed Hamza<sup>1</sup>; MATROOD, Abdulnabi Abdul Ameer<sup>1</sup>

<sup>1</sup>Plant Protection Department, College of Agriculture, University of Basrah, Basrah, Iraq

\* Correspondence author

e-mail: Qusaihattab82@yahoo.com

Received 20 April 2020; received in revised form 28 May 2020; accepted 01 June 2020

## RESUMO

Este estudo foi realizado para estimar o nível de alguns metais pesados, principalmente chumbo (Pb), cádmio (Cd), cromo (Cr) e cobalto (Co) no solo e nas folhas de trigo de algumas lavouras de trigo na província de Basra e Maysan; as áreas de amostragem foram Al-Qurna, Al-Madinah, Al-Amara, Kumit, Ali Al-Sharqi e Ali Al-Gharbi. A análise foi realizada utilizando um espectrofotômetro atômico de chama. Os resultados indicaram um aumento nas concentrações dos metais pesados mencionados acima em todas as áreas examinadas; Verificou-se que os níveis em solos agrícolas excediam os limites internacionalmente permitidos, de acordo com as normas da UE-2000; os níveis mais altos de poluição foram observados no local de Al-Qurna, com diferenças significativas em relação a outros locais, para as concentrações disponíveis e totais de metais pesados no solo. Indicando a disponibilidade dos metais, de acordo com as concentrações disponíveis no solo analisado, foi o seguinte: chumbo (21,32) > cobalto (14,63) > cromo (11,06) > cádmio (1,15) em mg/kg de solo. Além disso, os resultados mostraram que o maior teor de chumbo nas folhas de trigo foi examinado nos campos de Qurna (0,175 mg/kg), seguido por Amara com uma concentração de 0,136 mg/kg. A menor concentração de chumbo foi observada nas folhas de trigo nos campos de Kumit (0,007 mg/kg). Em relação à concentração de Cd nas folhas de trigo, o nível mais alto foi observado em Al-Qurna, com diferença significativa em relação aos demais campos, atingindo 0,009 mg/kg. A menor concentração Cd registrada em Ali Al-Gharbi, que atingiu 0,002 mg/kg. Os resultados da correlação entre a concentração disponível de elementos de metais pesados e as características do solo revelaram uma correlação significativa entre o pH do solo e as concentrações disponíveis de chumbo, cádmio e cromo, enquanto não foi observada correlação com o cobalto e uma correlação significativa entre a CE do solo e o chumbo, e uma correlação negativa altamente significativa com o cobalto. Os resultados provaram os altos níveis de poluição em todas as áreas examinadas nas províncias de Basra e Maysan.

**Palavras-chave:** Metais pesados, poluição, Iraque, textura do solo, planta de trigo.

## ABSTRACT

This study was conducted to estimate the level of some heavy metals, mainly Lead (Pb), cadmium (Cd), chromium (Cr) and cobalt (Co) in the soil and wheat leaves of some wheat fields in Basra and Maysan province; the sampling areas were Al-Qurna, Al-Madinah, Al-Amara, Kumit, Ali Al-Sharqi, and Ali Al-Gharbi. It was performed the analysis using the Flame Atomic Spectrophotometer. The results indicated an increase in the concentrations of above mentioned these heavy metals in all examined areas; the levels in agricultural soils were found to be exceeding the internationally permissible limits according to EU-2000 standards, the highest levels of pollution were observed at Al- Qurna site with significant differences than other sites for both available and total HMs concentrations in soils. Indicating that the arrangement of the metals according to their available concentrations in the analyzed soil was as follows: lead (21.32) > cobalt (14.63) > chromium (11.06) > cadmium (1.15) as mg/Kg of soil. Additionally, results showed that the highest lead content in the wheat leaves was examined in the Qurna fields (0.175 mg/kg), followed by Amara with a concentration of 0.136 mg/kg. The lowest concentration of lead was observed in wheat leaves in the Kumit fields (0.007 mg/kg). In terms of Cd concentration in wheat leaves, the highest level was observed in Al-Qurna, with a significant difference from other fields, reaching 0.009 mg/kg. The lowest concentration of this HM was recorded in Ali Al-Gharbi, which

reached 0.002 mg/kg. The results of the correlation between the available concentration of heavy metals elements and soil characteristics revealed a significant correlation between the soil pH and lead, cadmium, and chromium available concentrations, whereas no correlation with cobalt and a significant correlation between soil EC and lead was observed and a highly significant negative correlation with the cobalt. Results proved the high levels of pollution in all examined areas in Basra and Maysan provinces.

**Keywords:** Heavy metals, pollution, Iraq, soil texture, wheat plant.

## الملخص

أجريت هذه الدراسة لتقدير مستوى بعض المعادن الثقيلة وهي الرصاص، الكاديوم، الكروم والكوبلت في تربة وأوراق بعض حقول الحنطة في محافظتي البصرة و ميسان. وكانت مناطق أخذ العينات هي القرنة والمدينة والعمارة وكميت وعلي الشرقي وعلي الغربي. تم إجراء التحليل باستخدام جهاز مطياف الامتصاص الذري. أظهرت النتائج زيادة في تراكيز هذه المعادن الثقيلة في جميع المناطق التي تم فحصها. تبين أن مستويات التربة الزراعية تجاوزت الحدود المسموح بها دولياً وفقاً لمعايير الاتحاد الأوروبي لعام 2000 ، وقد لوحظت أعلى مستويات التلوث في موقع القرنة مع وجود فروقات معنوية عن المواقع الأخرى لكل من تراكيز المعادن الثقيلة الكلية في التربة والتراكيز الجاهزة وكذلك محتوى أوراق الحنطة من المعادن الثقيلة. أوضحت النتائج أن ترتيب المعادن حسب التراكيز الجاهزة في التربة هو كالتالي: الرصاص (21.32) < كوبالت (14.63) < كروم (11.06) < كاديوم (1.15). بالإضافة إلى ذلك ، أظهرت النتائج أنه تم فحص أعلى محتوى من الرصاص في أوراق القمح في حقول القرنة (0.175 ملغم / كغم) تليها العمارة بتركيز (0.136 ملغم / كغم). ولوحظ أقل تركيز للرصاص في أوراق الحنطة في حقول كميت (0.007 ملغم / كغم). أما تركيز Cd في أوراق الحنطة فقد لوحظ أعلى مستوى في القرنة مع وجود فرق معنوي عن الحقول الأخرى حيث بلغ 0.009 ملغم / كغم. وسجل أقل تركيز لهذا المركب في علي الغربي والذي بلغ (0.002 ملغم / كغم). أظهرت نتائج الارتباط بين التركيز الجاهز للعناصر الثقيلة وخصائص التربة وجود علاقة معنوية بين الرقم الهيدروجيني للتربة والرصاص والكاديوم والكروم الجاهز في حين لم يلاحظ أي ارتباط بالكوبلت ، ووجد ارتباط بين ملوحة التربة والرصاص وارتباط سالب مع الكوبلت. أثبتت النتائج ارتفاع مستويات التلوث في جميع المناطق التي تم فحصها في محافظتي البصرة وميسان.

**الكلمات المفتاحية:** المعادن الثقيلة، التلوث، العراق، نسجة التربة، نبات الحنطة.

## 1. INTRODUCTION

Wheat is one of the main staple foods for feeding human populations throughout the world. Wheat crop *Triticum aestivum* L. is considered as one of the most important and economic crops in the world; and has a substantial role in food reserve all over the world, including Iraq. Their nutritious significance as a source of carbohydrates is remarkably increased during the last decades, and about 4.5 billion people of the third world are consuming wheat on a daily bases (Pathak and Shrivastova 2015; Verma and Khah, 2016). Nowadays, this crop is cultivated in more than seventy different countries worldwide, with approximately 920,096 acres of cultivated areas with around 3,052,939 million tons of harvested grains (FAO, 2017). Iraq, among these countries with wheat production 2974 thousand tons, as well as an area of 4,215,906 acres (Central Agency for Statistics and Information Technology, 2017).

Wheat plant is hugely influenced by several biotic and abiotic factors, causing a significant reduction in their production; among these abiotic factors; environmental pollution is raised as one of the most problematic stressors, and the direct impact of environmental pollution on human health has generated an increase of global concern. Heavy metals are among the most dangerous pollutants, and the seriousness of these pollutants is due to their toxicity and

tends to accumulate in the soil and tissues of living organisms as well as their degradable behavior (Dalman *et al.*, 2006; Akbarzade, 2015; Baghvand *et al.*, 2010). Heavy metals are defined as metals or semi-metals whose density is more than (5 g/cm<sup>3</sup>) (Sussiu *et al.*, 2008). Heavy metals occur naturally, but they also enter into the ecosystem throughout at different concentrations of the anthropogenic activity (You *et al.*, 2015). Heavy metals, among them, are necessary for living organisms but at low concentrations and are toxic at high concentrations such as iron, zinc, chromium, and copper, while lead, cadmium, and mercury are considered as unnecessary elements that have no vital role yet and are toxic at any concentration (McGrath *et al.*, 2001)

Soil is the main storehouse of heavy metals that are emitted to the environment, and that soil pollution, especially agricultural ones, has raised the interest of specialists in this field, not only because of the accumulation of these minerals in the soil but because of the transfer of these toxic metals to crops that grow in polluted soils leading to their entry into the food leading to a significant effect on human health; in addition to plant growth and development (Huand *et al.*, 2007). Soil heavy metals are transported and accumulated in plant tissues that are consumed by humans, leading a severe accumulation in fatty tissue and cause nerve damage and influence on the endocrine system, immunity, and



natural cellular metabolism and other processes (Waisberg *et al.*, 2003; Wang, 2013).

Plants are one of the most sensitive types of organisms that capable of concentrating high levels of heavy metals because they are immobile and their ability to accumulate minerals by absorbing them from the soil or through precipitation into the atmosphere (Zurayk *et al.*, 2001). Plant responses to heavy metals are varied according to the plant species, heavy metals, and their concentrations or forms, the responses appear on plants through their morphology to the biochemical level, such as increasing or decreasing the level of some compounds and molecules in cells or in physiological and biological processes and anatomical composition of the plant, and their effect may reach the level of genetic stability (Shahid *et al.*, 2014). The heavy metals toxicity to plants may be attributed to the enzyme inhibition by binding their sulfhydryl groups (Choudhry and Panda, 2004), it reduces the relative content of water and transpiration by affecting the water balance (Krantev *et al.*, 2006), and increasing the permeability of the plasma membrane. Inhibition of photosynthesis pigments such as chlorophyll-a, b, and carotenoids, and increases reactive oxygen species (ROS) are other plant responses to heavy metals accumulation (Abass *et al.*, 2016); lipid peroxidation is one of the most common responses to heavy metals accumulation on plant cell level (Zouri *et al.*, 2016).

Among the toxic heavy metals, the most dangerous ones are lead, cadmium, chromium, and cobalt, many local studies have indicated the high levels of pollution of heavy metals in Iraqi soil and their transcendence to the internationally accepted limits (Abass *et al.*, 2015; Al-Jabary *et al.*, 2016). The internationally permitted rate according to the standard indicators of lead in agricultural soils is 100 mg/kg of soil and cadmium 3 mg/kg soil. It was found that the rate of accumulation of lead in the different soils of Basra exceeded the international limits, some of which reached 270 mg/kg, and cadmium at a rate of 9 mg/kg of soil (Abass *et al.*, 2015; Abass *et al.*, 2017), indicated that there is a variation in the accumulation rate of lead, cadmium, chromium and nickel elements in different regions of Maysan Governorate, some of which are across the internationally permissible level (Tawfiq and Ghazi, 2017). The aims of the present work were to determine the heavy metals pollution in different wheat fields soil and plant parts in Basra and Maysan governorates.

## 2. MATERIALS AND METHODS

The study was conducted at the laboratory of the Plant Protection Department/ from the College of Agriculture of the Basra University of Basrah.

### 2.1 Description of sampling sites

Maysan province is located in the southeastern part of Iraq, and it is confined between two latitudes (15-31° - 45-32) in the north and between longitude (30 - 46° - 30 - 47°) in the east, and it is bordered in the south by Basra province, while it is bordered in the east and northeast by Iran.

Basrah Governorate is located in southern Iraq and is bordered by Iran, Kuwait, and Saudi Arabia. It is located at 30.53 degrees north latitude, 47.79 degrees east longitude, and 3 meters above sea level. Maysan Governorate is located along with the Basrah Governorate to the north. Six different regions in Basra and Maysan were selected to collect soil samples and leaves of wheat plants. The study sites were: Al-Qurna and Al-Madinah in Basrah province, Al-Amara, Ali Gharbi, Ali Al-Sharqi, and Kumait in Maysan province.

### 2.2 Samples collection

Five fields were selected from each site, marked in Figure 1, and compound soil samples were taken at a depth of 30 cm from each site. Samples of wheat were collected at the age of two months and brought to the laboratory.

### 2.3 Samples preparation

The soil samples were air-dried, mixed, and homogenized well, then passed through a plastic sieve with a diameter of 2 mm, after that the following characteristics were estimated:

#### 2.3.1 Soil texture

The Pipette method was used in Miller and Miller (1987), after extracting the proportions of the three soil segments of sand, silt, and clay - the soil texture triangle is used to determine the soil texture.

#### 2.3.2 Organic matter

It was weighed 1 gram of soil in a glass beaker of 500 ml capacity and add 10 ml of potassium dichromate solution N1, add

concentrated sulfuric acid, move the beaker well to mix the suspension, leave for 30 minutes, add 200 ml of distilled water, add 10 ml of concentrated phosphorous acid. Leave the mixture to cool, add 10 drops of Di-phenyl amine guide, add a magnetic bar and put the beaker on a magnetic stirring device, titrate the ferrous sulfate solution and ammonium sulfate 0.5 M until the color changes from blue to purple to green, bring two blanks containing all the solutions except the soil. The proportion of organic matter is calculated according to the formulas mentioned in (Schulte, 1995).

### **2.3.3 Cation exchange capacity (CEC)**

Weigh 4 g anaerobically dry soil in a 40 mL centrifuge tube, add 1 mL of sodium acetate solution (ternate water molecules) N1, shake the tube for five minutes, remove the plug from the tube and place the tube in the centrifuge 3,000 r / min until it becomes floating liquid is clear, the clear liquid is completely filtered and then cast. Repeat the process four times with 33 mL of sodium acetate solution (triple water molecules) N1. Each time the floating liquid is filtered, then add 33 mL of 95% ethyl alcohol, clog the tube and shake for 5 minutes, lift the plug and place the tube in the centrifuge until The floating liquid becomes clear. Wash the sample with ethyl alcohol (95%) three times, each time the floating liquid is filtered so that the clear conductivity of the clear liquid after the third wash is less than 400  $\mu\text{S}/\text{cm}$ . Replace the chopped sodium from the sample by adding 33 mL of ammonium acetate solution N1 three times each time shaking for 5 minutes. We measure the soil extract and spectrum readings by flame spectroscopy at a wavelength of 767 nm. Calculate the sodium (Na) concentration according to the calibration curve. (Polemio and Rhoades, 1977).

### **2.3.4 Soil Ph**

From dry soils it weighed 50 g in a 100 mL glass Baker, then add 50 mL of distilled water, then mix the suspension and leave it for 3 minutes and move the suspension every 10 minutes, after an hour we move the suspension and then place the combined electrode (German model PH 7110) in the suspension with a depth of about 3 cm. The reading was taken after 30 seconds (McLean 1982).

### **2.3.5 Soil salinity**

Prepare a suspension (1: 1) (soil: water), then filter the suspension using a vacuum

filtration system, put filter paper type Whatman No.42 and in a Buchner funnel, then transfer the filtrate to a 5 mL beaker, then record electrical conductivity using (Italian-made Milwaukee-SM302) (Richards, 1954).

### **2.3.6 Percentage of major nutrients N.P.K**

Ion ( $\text{NH}_4$ ) was estimated by extracting with potassium chloride solution (2N) and using  $\text{MgO}$ , and measuring it using the microceldal device. The nitrate ion was estimated by reducing it via the Devarda alloy, then by using the microceldal device according to a method according to the Brenner (1965) method described in Black (1965). Phosphorous was extracted using  $\text{NaHCO}_3$ , then with ammonium molybdate and ascorbic acid. It was estimated by the spectrophotometer at a wavelength of 882 nm Page *et al.* (1982). Potassium was extracted with ammonium acetate solution (1N) and then measured with Flame- photometer (Black, 1965).

### **2.4 Determination of heavy metals in soil samples and wheat leaves**

Determination of the total and available concentrations of lead metal (Pb), cadmium (Cd), chromium (Cr) and cobalt (Co) in the soil was performed using the Flame Atomic Spectrophotometer (Perkin Elmer AAS analysis 300, USA) according to the following extraction methods:

#### **2.4.1 Extraction of the total concentrations of heavy metals in the soil**

Extraction was done according to the method described in Davidson (2013) by acid digestion procedure, 1 g of dried soil was crushed in a Teflon Beaker heat-resistant plastic baker and moisten with water, then 10 mL of  $\text{HNO}_3$  was added, the mixture was then heated at  $75^\circ\text{C}$ , and left to evaporate until the volume remains 2 mL, then add a mixture of  $\text{HNO}_3$  (25 mL) and 5 mL  $\text{HClO}_4$  (70%) and 1 mL of Hydrofluoric acid (HF) gradually and carefully and heated the mixture (without boiling) until the appearance of brown fume, then add 1 mL of hydrofluoric acid (1:1) (volume:volume), Half an hour after the appearance of brown fume, then heated for a period of 10 minutes, then diluted with distilled water to 100 mL.

#### **2.4.2 Extraction of the available concentrations of heavy metals in the soil**

Extraction solution consisting of: (0.005 mol/L of DTPA, diethylenetriaminepentaacetic acid, 0.01 mol/L of calcium chloride  $\text{CaCl}_2$  and 0.1 mol/L of TEA Triethanolamine), was used to extract the available concentrations of heavy metals in soils; 30 ml of the extraction solution was added to 15 g of dry soil in a glass jar, then shaken well for two hours with a mechanical shaker, then filtered through Whatman No. 4 filter paper, and diluted to 100 ml with distilled water.

#### **2.4.3 Extraction of heavy metals in the wheat leaves**

Heavy minerals were extracted from the wheat plant leaves using the method of wet acid digesting according to the protocol described in Jones (1984). Briefly, by adding 5 ml of nitric acid (70%) and 1.5 ml of hydrochloric acid (60%) to 0.5 g of a sampled leaves, then heated until brown fume disappeared, 5 ml of dilute hydrochloric acid (1:1) was added, and the mixture was diluted to 25 ml with distilled water.

#### **2.5 Permissible limits for heavy metals**

The permissible standard limits for the total soil concentration of heavy metals were adopted from the European Union (2006) to compare the results, and the permissible levels are Lead (Pb) 100 mg/kg, Cadmium (Cd) 3 mg/kg, Chromium (Cr) 100 mg/kg and Cobalt (Co) 50 mg/kg.

#### **2.6 Statistical analysis**

The experiment was designed using Complete Randomization Design (C.R.D), and the Least Significant Difference (L.S.D) test was used to compare the averages at the 0.05 probability level. The Statistical Package for Social Science (SPSS) version (21) was applied data analysis, and the results represented an average of three replicates per treatment.

### **3. RESULTS AND DISCUSSION:**

#### **3.1 Soil properties:**

The results of Table (1) showed the soil properties for the study sites that were chosen to assess the levels of pollution of heavy metals in some fields of Basra and Maysan provinces. The results showed that the pH values were close between the study sites, and their values ranged

between 7.2 and 8.1. Al-Qurnah fields recorded the highest electrical conductivity value of 16.76 dS/m and the lowest value in Ali Al-Gharbi fields, which was 7.50 ds /m. The results of the organic matter percentage for the study sites showed that the Al-Qurna site recorded the highest percentage by 1.80% and with a significant difference from other examined sites. As for the Cation exchange capacity ions, Al-Madinah recorded the highest value, which was 34.71 Ctmol/kg, and the lowest value was in a Kumit site of 13.49 cm/kg, and the results showed that the highest value of nitrogen content element was seen in Ali Al- Sharqi fields by 113.17%, and there are no statistically significant differences between the values of phosphorous for all examined sites. As for the potassium component, Ali Al- Sharqi fields recorded the highest percentage, 121.2%, significant differences than other sites.

Table (2) showed the results of soil texture of the study sites, it was found that the Al-Qurna, Medina, and Al-Amara fields were silt soils, while the soil textures of Ali Al-Sharqia was clay soils, and Ali Al- Gharbi fields were clay sand soils.

#### **3.2 The total concentration of heavy metals in the soil**

The results of Table (3) showed the total concentrations of lead, cadmium, chromium, and cobalt minerals in the soil of several fields in Basra and Maysan provinces, the highest concentrations of these metals were examined in the soil of Al-Qurna fields, and reached 319.93, 10.79, 130.29 and 50.56 mg/kg, respectively, while the lowest concentrations of lead appeared in the soil of Ali Al-Gharbi fields, as it reached 159.98 mg/kg without a significant difference from the fields of Ali Al-Sharqi and Kumit, and a significant difference from the soil of the fields of the rest of the sites.

The lowest concentration of cadmium was reported in the soil of Ali Al-Sharqi fields, as it reached 3.03 mg/kg and without a significant difference from the areas of Kumit and Ali Al-Gharbi. While the chromium, the soil fields of Kumit and Ali Al-Gharbi recorded the lowest concentration 10, 88, 90 and 89 mg/kg respectively, and cobalt element was found to be the lowest total concentration in the soil of Kumait fields, as it reached 25.39 mg/kg, without significant differences were recorded between Ali Al-Gharbi and Ali Al-Sharqi.



To assess the level of pollution of heavy metals in the soil of some fields in Basra and Maysan governorates, the total concentrations of the examined metals were compared with the permissible limits for the total concentration of heavy metals in the soil according to the European Union standard 2006, it was noted that the concentration of lead, cadmium and chromium metals exceeded the permissible limit which was 100 mg/kg for lead, 3 mg/kg for cadmium and 100 mg/kg for chromium and that cobalt concentrations were within the permissible limit of 50 mg/kg with an exception for the soil of Al-Qurna fields, as it reached 50.56 mg/kg.

### 3.3 Available concentrations of heavy metals in the soil

The results of Table (4) showed the available concentrations of heavy metals lead, cadmium, chromium, and cobalt in the soils of some wheat fields of Basra and Maysan provinces, and the results indicated that the highest concentration of lead was examined in the soil of the Al-Qurna fields as it reached 37.32 mg/kg with a significant difference from the rest of the fields, while the lowest concentration was examined in the soil of Ali Al-Gharbi field (13.58 mg/kg). The highest available concentration of cadmium was found in Al-Qurna fields, and reached 1.89 mg/kg, while the lowest concentration was reported in the fields of Kumit, as it reached 0.83 mg/kg with a significant difference than those observed in other fields. The results indicated that the soil of Al-Qurna fields had the highest concentration of Cr with an average of 22.50 mg/kg, while the soil of Ali Al-Sharqi fields had the lowest concentration, as it reached 6.16 mg/kg. The cobalt was found to be high in the fields of the Al-Amarah fields 18.37 mg/kg and without a significant difference from the soil of the fields of Ali Al -Sharqi region that recorded a concentration of 16.52 mg/Kg.

The concentration of HMs, according to their availability, was as follows: Lead (21.32) > Cobalt (14.63) > Chromium (11.06) > Cadmium (1.15). As for the arrangement of the regions according to their pollution with heavy elements, they were as follows:

Lead: Al-Qurna > Al-Amara > Al-Madinah > Ali Al-Sharqi > Kumit > Ali Al-Gharbi, cadmium: Al-Qurna > Al-Amara > Al-Madinah > Ali Al-Sharqi > Ali Al-Gharbi > Kumit

Cobalt: Al- Amara < Ali Al-Sharqi > Kumit > Ali Al-Gharbi > Al-Qurna > Al-Madinah

Chromium: Al-Qurna > Ali Al- Gharbi > Al-Amara > Kumit > Al -Madinah > Ali Al-Sharqi.

Abass *et al.* (2015) showed that the concentrations of heavy elements, Lead, Cadmium, Cobalt, and Chromium exceeded the internationally permitted limits, as the concentrations of these elements were 115.00, 2.80, 10.25 and 60.50 mg/kg respectively. Al-Jabary *et al.* (2016) stated that the concentrations of lead, cadmium, cobalt, and chromium increased and exceeded the internationally permitted limits and were recorded 196.73, 6.27, 35.9 and 107.93 mg/kg, respectively. Khan *et al.* (2016) indicated that the cadmium and chromium exceeded the internationally permissible limits as it reached 0.58 mg/ kg and 50 mg/ kg, respectively. A study conducted by Al-Moussawi and Mustafa (2016) on the soil of Al-Qurna and Al-Madinah revealed the variation in the level of cadmium and lead concentrations in the soil of the study sites, which exceeded the internationally allowed limit.

### 3.4 Heavy metals content in wheat leaves

The results of Table (5) showed the content of heavy metals in the wheat leaves in some areas of Basra and Maysan governorates. The highest lead concentration was 0.175 mg/kg, which examined in the Qurna fields, followed by Amara with a concentration of 0.136 mg/kg. The lowest concentration of lead was observed in wheat leaves in the Kumit fields (0.007 mg/kg). The highest concentration of Cd was recorded in wheat leaves in Al-Qurna, with a significant difference from other fields, reaching 0.009 mg/kg. The lowest concentration of this HM was recorded in Ali Al Gharbi, which reached 0.002 mg/kg.

Kearallah *et al.* (2016), indicated that the average heavy metals of lead for the dry and rainy seasons ranges between 33.4 -35.42 mg/kg, and cadmium ranges between 3.23 -3.60 mg/kg. In a study conducted by Abu -Shanab *et al.*, (2007) on sixty-one plant species in soils contaminated with heavy elements, the content of plants from heavy elements varies, as the concentration of lead was found between 1- 508 mg/kg and cadmium 0.2-6 mg/kg.

### 3.5 Correlation between the total concentration of heavy metals and soil properties

The results of Table (6) showed the correlation coefficient analysis between the soil

characteristics and total concentration of heavy metals, a highly significant negative correlation was seen between HMs content and soil pH, as well as a significant correlation between lead and cadmium with EC. There was no significant association between heavy metals and other soil characteristics.

The results of Table (7) analyzing the correlation between the available concentration of heavy elements and soil characteristics, a significant correlation between the soil pH and lead, cadmium, and chromium available concentrations, whereas no correlation with cobalt and a significant correlation between soil EC and lead was observed and a highly significant negative correlation with the cobalt. No correlation was observed between OM and CEC with available concentrations of heavy metals, with an exception for the cobalt, which recorded a highly significant negative correlation, and no association was observed between heavy metals and major nutrients NPK.

Several studies showed the importance of soil properties and HMs availability. Vishun *et al.* (2007) concluded that the cadmium extracted from clay, sand, and calcareous soils was 8.92, 5.13, and 7.17 mg/kg soil, respectively, and that the amount of cadmium ready increased as the soil content of clay increased.

Zueng (2009) mentioned that the amount of cadmium extracted from the soil is determined by the value of the soil pH as it increases with the increase in the value of soil pH. CEPA(1994) found that high levels of organic matter encouraged the formation of cadmium complexes with organic matter in the soil. The behavior of chromium compounds in the soil is determined by the degree of soil interaction, the soil content of clay, organic matter, oxidation, and reduction effort (Kabata - Pendias and Pendias, 1992). Monday and Michael (2004) concluded that the amount of lead extracted was 98, 198, and 127 mg/kg soil in Spain with pH 7.3, 7.4, and 7.3, respectively, and different content of sand, silt, clay, and organic matter. Additionally; El khatib *et al.* (1990) found that the amount of availability of lead was determined by the quantity and quality of clay minerals, as the amount of lead in clay soil was greater than sandy soils, and this was due to the positive ion exchange capacity of the clay.

#### 4. CONCLUSIONS:

Results revealed that the concentrations of lead, cadmium, cobalt, and chromium elements had been exceeded the internationally permitted limits, and the high concentration of lead and cadmium elements in wheat leaves indicated the soil pollution with these two elements. A difference was observed in the association between heavy elements and chemical soil properties, indicating the effect of some of these properties on the readiness of heavy elements and some traits that do not affect the readiness of heavy elements in the soil.

#### 5. ACKNOWLEDGMENTS:

The authors thank Dr. Rashad Adel for the facilities in carrying out chemical analyzes. Thanks to Professor Dr. Khairallah Al-Jabri for his help in chemical and statistical analysis. Also thanked Dr. Mohamed Husain Manati, Mr. Faraj Abdul hae Alag, Mohamse Hamdan Aldaraji, and Mr. Abass Husain Minshad for the help in taking samples.

#### 6. REFERENCES:

1. Abass, M. H., Hassan, Z. K., and Al-Jabary, K. M. A. (2015). Assessment of heavy metals pollution in soil and date palm (*Phoenix dactylifera* L.) leaves sampled from Basra/Iraq governorate. AES Bioflux, 7(1): 52-59.
2. Abass, M. H., Neama, J. D., and Al-Jabary, K. M. A. (2016). Biochemical responses to cadmium and lead stresses in date palm (*Phoenix dactylifera* L.) plants. AAB Bioflux 8(3):92-110.
3. Abass, M. H., Al-Utbi, S. D., and Al-Samir, I. A. H. (2017). Genotoxicity assessment of high concentrations of 2,4-D, NAA, and Dicamba on date palm callus (*Phoenix dactylifera* L.) using protein profile and RAPD markers. J. Gene. Eng. Biotechnol. 15: 287–295.
4. Abou-Shanab, R. A., Ghazlan, H. A., Ghanem, K. M., and Moawad, H. A. (2007). Heavy Metals in Soils and Plants from Various Metal- Contaminated Sites in Egypt. *Terrestrial and Aquatic Environmental Toxicology*. 1(1), 7-12
5. Al-Jabary, K. M. A., Neama, J. D., and Abass, M. H. (2016). Seasonal variation of heavy metals pollution in soil and date palm *Phoenix dactylifera* L. leaves at Basra governorate /Iraq. IJSRES; 4(6): 186-195.

6. Al-Moussawi, N., and Mustafa, S. W. (2016). Geographical Distribution of the Concentrations of Oil Contaminants in Soils of Qurna and Medina District. *Journal of Basra Studies*.11-22.
7. Al-Saffar, N. M. (2016). Estimation of Some heavy elements (Pb, Cd, Ni, and Co) in chemical and organic fertilizers and their effect on the environment and consumer safety. *Journal of the college of basic education*. Volume 22, Issue 95. (in the Arabic language).
8. Akbarzadeh, A., Jamshidi, S., and Vakhshouri, M. (2015). Nutrient uptake rate and removal efficiency of *Vetiveria zizanioides* in contaminated waters. *Pollution*, 1(1), 1-8.
9. Black, C. A. (1965). *Methods of soil analysis*. Amer. Soc. Of Agron. Inc. USA.
10. Bremner, J.M. (1965). Inorganic forms of nitrogen in C.A. Black. 1965. *Methods of soil analysis*. Amer. Soc. Of Agron. Inc. USA.
11. Baghvand, A., Nasrabadi, T., Nabi, B. G. R., Vosoogh, A., Karbassi, A. R., Mehrdadi, N.(2010).Groundwater quality degradation of an aquifer in Iran central desert. *Desalination*, 260 (1-3), 264-275.
12. CEPA(CanadianEnvironmental Protection Act) (1994).Priority Substances List Assessment Report: Cadmium and its Compounds. Environment Canada and Health Canada.
13. Choudhury, S., and Panda, S.K. (2004). Role of salicylic acid in regulating cadmium-induced oxidative stress in *Oryza sativa* L. roots. *Bulg. J. Plant Physiol.* 30(3-4), 95-110.
14. Central Agency for Statistics and Information Technology (2017). Annual report of wheat production. Ministry of Planning and Development Cooperation. The Republic of Iraq. (in the Arabic language).
15. Dalman, O., Demirak A., and Balci, A. (2006). Determination of heavy metals (Cd, Pb) and trace element (Cu, Zn) in sediments and fish of the Southeastern Aegean Sea (Turkey) by atomic absorption spectrometry. *Food Chem.* 95: 157-162.
16. El-Khatib, E. A., G. M. Elshebing, and Balba, A. M. (1990). Lead Sorption Calcareous Soil. *Environ Pollution* 69:269-276.
17. European Union (2006). Commission regulator (EC) No.1881/2006 of 19th December 2006 setting maximum levels of certain contaminants in foodstuffs. *Off. J. Eur. Union L.*, 364: 4-24.
18. Jones, J. B. (1984). Plants. In: Williams S. (ed.). *Official Methods of Analysis of the Association of Official Analytical Chemists*. Arlington, Virginia 22209, USA. pp 38–64.
19. Huang, S. S., Liao, Q. L., Hua, M., Wu, X. M., Bi, K.S., Yan, C. Y., Chen, B. and Zhang, X. Y. (2007). Survey of heavy metal pollution and assessment of agricultural soil in Yangzhong district, Jiangsu Province, China. *Chemosphere*. 67: 2148–2155.
20. Kabata-Pendias, A., and Pendias, H. (1992). *Trace elements in soils and plants*, second., Crc Press, Inc., Boca Raton, Florida. 365 pp.
21. Krantev, A., Yordanova, R., and Popova, L. (2006).Salicylic acid decreases Cd toxicity in maize plants. *Gen. Appl. Plant Physiol, Special Issue.*, pp. 45-52.
22. McLean, E. O. (1982). Soil pH and lime requirement. In: Page A. L. (Ed.). *Methods of soil analysis. Part 2 - Agronomy*. Am. Soc. Agron. Madison, 1 Miller, W.P., and
23. Miller, W. P., and Miller, D. M. (1987). A micro-pipette method for soil mechanical analysis, *Commun. Soil Sci. Plant Anal.* 18 (1): 1-15.
24. McGrath, S. P., Zhao, F. J., and Lombi, E. (2001). Plant and rhizosphere process involved in phytoremediation of metal-contaminated soils. *Plant and Soil.*, 232: 207-214.
25. Polemio, M., and Rhoades, J.D. (1977). Determining cation exchange capacity: A new procedure for calcareous and gypsiferous soils. *Soil Sci. Soc. Am. J.* 41:524-528.
26. Page, A. L., Miller, R. H., and Kenney, D. R. (1982). *Methods of Soil Analysis. Part 2,2nd ed.* ASA. Inc. Madison, Wisconsin, U.S.A.
27. Pathak, V., and Shrivastav, S.(2015). Biochemical studies on wheat (*Triticum aestivum* L.) *J. Pharmacognosy and phytochemistry*, 4(3):171.
28. Richards, L. A. (1954). *Diagnosis and Improvement of Saline and Alkali Soils*. U. S. Department of Agriculture Handbook No. 60 Washington D. C. USA. 160 pp.
29. Schulte, E. E. (1995). Recommended soil organic matter tests. In: Sims J.T. and Wolf A. M. (Eds.). *Recommended Soil*

- Testing Procedures for Northeastern United. Agricultural Experiment Station, University of Delaware, Newark, DL. pp: 52–60.
30. Shahid, M., Pourrut, B., Dumat, C., Nadeem, M., Aslam, M., and Pinelli E. (2014). Heavy metal-induced reactive oxygen species: phytotoxicity and physicochemical changes in plants. In: Whitacre D.M. (ed). Reviews of Environmental Contamination and Toxicology Vol. 232, Springer sciences+ Business Media, pp.1-44.
  31. Shahid, M., Pourrut, B., Dumat, C., Nadeem, M., Aslam, M., and Pinelli E. (2014). Heavy metal-induced reactive oxygen species: phytotoxicity and physicochemical changes in plants. In: Whitacre D.M. (ed). Reviews of Environmental Contamination and Toxicology Vol. 232, Springer sciences+ Business Media, pp.1-44.
  32. Tawfiq, L. N. M. and Ghazi, F.F. (2017). Heavy Metals Pollution in Soil and Its Influence in the South of Iraq. International Journal of Discrete Mathematics. 2(3): 59-63.
  33. You, M., Huang, Y., Lu J., and Li, C. (2015). Environmental implications of heavy metals in soil from Huainan, China. Anal. Lett. 48: 1802-1814.
  34. Vishnu, P., Sabeha, K., Ouk, I., Rene, V., and Tony, H. (2007). Immobilization of heavy metals in soil using natural and waste materials for vegetation establishment on contaminated sites. Soil and Sediment Contamination. 16: 233-251.
  35. Verma, R. C., and Khah, M. A. (2016). Assessment of Gamma Rays Induced Cytotoxicity in Common wheat (*Triticum aestivum* L.) Cytologia, 81(1):41-45.
  36. Waisberg, M., Joseph, P., Hale, B., Beyersmann, D.(2003). Molecular and cellular mechanisms of cadmium carcinogenesis. Toxicology 192(2–3), 95–117.
  37. Wang, W.X. (2013). Dietary toxicity of metals in aquatic animals: recent studies and perspectives. Chin. Sci. Bull. 58(2), 203–213.
  38. Zurayk, R., Sukkariah, B., and Baalbaki, R. (2001). Common hydrophytes as bioindicators of Nickel, Chromium and Cadmium Pollution. Water Air Soil Pollut. 127(1): 373-388.
  39. Zueng-Sanychen(2009).Relationship between heavy metal concentrations in the soil of Taiwan and uptake by Crops. Aust. Jour. Soil Res.18-61-73.
  40. Zouari, M., Elloumia, N., Ben Ahmeda, C., Delmaild, D., Ben Rouinab, B., Ben Abdallaha, F. and Labroussec, V. (2016). Exogenous proline enhances growth, mineral uptake, antioxidant defense, and reduces cadmium-induced oxidative damage in young date palm (*Phoenix dactylifera* L.). Ecologic. Engin. 86: 202–209.



**Figure 1.** Sampling map in different regions at Basra and Maysan provinces.

**Table 1.** Soil properties of investigated sites.

| Sites        | EC    | PH     | CEC     | OM     | N%       | P%     | K%       |
|--------------|-------|--------|---------|--------|----------|--------|----------|
| Al-Qurna     | 16.76 | 7.2667 | 24.4867 | 1.8033 | 74.0000  | 0.0437 | 89.4667  |
| Al-Madinah   | 14.52 | 7.5333 | 34.7167 | 1.7500 | 63.3333  | 0.0720 | 72.9133  |
| Al-Amarah    | 12.53 | 7.6667 | 18.2167 | 0.9167 | 113.1700 | 0.0883 | 99.4767  |
| Kumit        | 9.60  | 8.1333 | 13.4900 | 0.6733 | 58.8000  | 0.0943 | 71.4200  |
| Al-Al Sharqi | 8.4   | 7.7000 | 24.5533 | 0.8367 | 57.3933  | 0.1057 | 121.1967 |
| AliAl Gharbi | 7.50  | 7.5000 | 29.1700 | 0.7733 | 108.1000 | 0.0947 | 70.8333  |
| L.S.D        | 0.856 | 0.30   | 0.122   | 0.086  | 5.189    | 0.128  | 9.678    |

**Table 2.** Particle size distribution of studied soils.

| Sites         | Soil texture | Sand % | Clay % | Silt % |
|---------------|--------------|--------|--------|--------|
| Al-Qurna      | silt         | 3      | 32     | 65     |
| Al-Madinah    | silt         | 6      | 24     | 70     |
| Al-Amarah     | silt         | 7      | 32     | 61     |
| Kumit         | silt         | 13     | 25     | 61     |
| Ali Al Sharqi | clay         | 1      | 58     | 41     |
| Ali Al Gharbi | Clay sand    | 25     | -      | 24     |

**Table 3.** the total concentrations of heavy metals (*mg/kg*) in the soils of the study sites.

| Sites         | lead   | Cadmium | Cobalt | Chromium |
|---------------|--------|---------|--------|----------|
| Al-Qurna      | 319.93 | 10.79   | 50.56  | 130.29   |
| Al-Madinah    | 219.99 | 5.29    | 33.13  | 85.27    |
| Al-Amarah     | 259.05 | 5.88    | 42.26  | 119.32   |
| Kumit         | 153.74 | 3.15    | 25.39  | 89.90    |
| Ali Al Sharqi | 162.20 | 3.03    | 35.82  | 88.10    |
| Ali Al Gharbi | 159.98 | 3.16    | 35.97  | 96.53    |
| L.S.D         | 11.60  | 0.20    | 5.83   | 10.27    |

**Table 4.** The available concentration of heavy metals (*mg/kg*) in the soils of the study sites.

| Sites         | lead  | Cadmium | Cobalt | Chromium |
|---------------|-------|---------|--------|----------|
| Al-Qurna      | 37.32 | 1.89    | 13.14  | 22.50    |
| Al-Madinah    | 20.23 | 1.04    | 8.69   | 8.29     |
| Al-Amarah     | 24.13 | 1.31    | 18.37  | 9.53b    |
| Kumit         | 15.95 | 0.83    | 15.54  | 8.58     |
| Ali Al Sharqi | 16.72 | 1.01    | 16.52  | 6.16     |
| Ali Al Gharbi | 13.58 | 0.85    | 15.48  | 11.31    |
| L.S.D         | 2.38  | 0.17    | 3.24   | 6.31     |

**Table 5.** heavy metals content (mg/kg) in wheat leaves in the study sites.

| sites         | Lead  | Cadmium |
|---------------|-------|---------|
| Al-Qurna      | 0.175 | 0.009   |
| Al-Madinah    | 0.118 | 0.007   |
| Al-Amarah     | 0.136 | 0.007   |
| Kumit         | 0.007 | 0.006   |
| Ali Al Sharqi | 0.017 | 0.002   |
| Ali Al Gharbi | 0.021 | 0.002   |
| L.S.D         | 0.06  | 0.001   |

**Table 6.** Analysis of correlation between the total concentration of heavy metals and soil characteristics of study sites.

| Metal | PH        | EC     | OM     | CEC    | N     | P      | K     |
|-------|-----------|--------|--------|--------|-------|--------|-------|
| Pb    | 0.633**-  | 0.573* | 0.380  | 0.071  | 0.198 | 0.372- | 0.114 |
| Cd    | 0.644**-  | 0.580* | 0.336  | 0.084  | 0.061 | 0.328- | 0.038 |
| Cr    | -0.6.33** | 0.094  | 0.110- | 0.237- | 0.449 | 0.155- | 0.159 |
| Co    | 0.785**-  | 0.277  | 0.155  | 0.148  | 0.361 | 0.104- | 0.334 |

\* significant    \*\* high significant

**Table7.** Analysis of correlation between the available concentration of heavy metals and soil characteristics of study sites.

| Metal | PH      | EC       | OM       | CEC      | N     | P      | K      |
|-------|---------|----------|----------|----------|-------|--------|--------|
| Pb    | 0.563*- | 0.503*   | 0.267    | 0.019-   | 0.011 | 0.291- | 0.159  |
| Cd    | 0.587*- | 0.431    | 0.199    | 0.003-   | 0.075 | 0.230- | 0.251  |
| Cr    | 0.527*- | 0.306    | 0.044    | 0.037    | 0.122 | 0.275- | 0.123- |
| Co    | 0.354   | 0.811**- | 0.777**- | 0.637**- | 0.386 | 0.212  | 0.430  |

\* significant    \*\* high significant



# COMPOSTOS ORGÂNICOS SINTESIZADOS UTILIZADOS COMO ESTIMULANTES DE CRESCIMENTO PARA PLANTAS LENHOSAS

## SYNTHESIZED ORGANIC COMPOUNDS AS GROWTH STIMULATORS FOR WOODY PLANTS

### СИНТЕЗИРОВАННЫЕ ОРГАНИЧЕСКИЕ СОЕДИНЕНИЯ КАК СТИМУЛЯТОРЫ РОСТА ДЛЯ ДРЕВЕСНЫХ РАСТЕНИЙ

VOSTRIKOVA, Tatiana V.<sup>1\*</sup>; KALAEV, Vladislav N.<sup>2</sup>; MEDVEDEVA, Svetlana M.<sup>3</sup>; NOVICHIKHINA, Nadezhda P.<sup>4</sup>; SHIKHALIEV, Khidmet S.<sup>5</sup>

<sup>1,2</sup> Voronezh State University, Botanical Garden, Russian Federation.

<sup>3,4,5</sup> Voronezh State University, Department of Organic Chemistry, Russian Federation.

\* Correspondence author  
e-mail: tanyavostic@rambler.ru

Received 17 December 2019; received in revised form 01 June 2020; accepted 03 June 2020

## RESUMO

Estudou-se o efeito de compostos orgânicos sintetizados de 6-hidroxi-2,2,4-trimetil-1,2-di-hidroquinolina, seus derivados e análogos hidrogenados sobre a altura de mudas de plantas lenhosas ornamentais. A altura das mudas como parâmetro morfométrico foi medida sete meses após o início do experimento. O tratamento pré-semeadura de *Rhododendron ledebourii* e *Rhododendron smirnowii*, com os compostos estudados, demonstrou que a di-hidro e a tetra-hidroquinolina com concentração de 0,1% foram os mais eficientes. As dihidroquinolinas nas concentrações de 0,05 e 0,1% demonstraram ter o efeito mais forte. As dihidroquinolinas para plantas lenhosas perenes são mais eficazes, depois as tetrahidroquinolinas. Os compostos químicos sintetizados mais eficientes para o *rododendro* contêm substituto de benzoílo. Para *Rh. ledebourii* e *Rh. smirnowii* os mais eficazes são os mesmos compostos químicos sintetizados: 6-hidroxi-2,2,4-trimetil-1,2,3,4-tetra-hidroquinolina, 6-hidroxi-2,2,4-trimetil-1,2-di-hidroquinolina e 1-benzoil-6-hidroxi-2,2,4-trimetil-1,2-di-hidroquinolina com concentrações de 0,01, 0,05 e 0,1%. Estes compostos, quando aplicados com o tratamento de *Rh. ledebourii* e *Rh. smirnowii* antes da sementeira, resultam em um aumento na altura das mudas em 3,6-89,3% e 14,3-57,1%, respectivamente. O efeito de compostos químicos sintetizados de 6-hidroxi-2,2,4-trimetil-1,2-di-hidroquinolina e seu análogo hidrogenado em plantas lenhosas do mesmo gênero não é específico da espécie. Sugere-se o uso de compostos de 6-hidroxi-2,2,4-trimetil-1,2-di-hidroquinolina, seus derivados e análogos hidrogenados como estimuladores do crescimento do rododendro. Os compostos da série quinolina foram testados quanto à genotoxicidade pelo método citológico no objeto modelo (*Betula pendula*) e reconhecidos como ambientalmente amigáveis. As respostas citogenéticas para *Betula pendula* e *Rhododendron* são idênticas; portanto, os compostos positivos influenciam as células de *Betula pendula* devido ao aumento da atividade metabólica, o mesmo ocorre com o *rododendro*. Portanto, compostos orgânicos sintetizados podem ser recomendados como estimuladores de crescimento eficazes.

**Palavras-chave:** estimuladores de crescimento, compostos orgânicos sintetizados, plantas lenhosas.

## ABSTRACT

The effect of synthesized organic compounds of 6-hydroxy-2,2,4-trimethyl-1,2-dihydroquinoline, its derivatives, and hydrogenated analogs on the height of seedlings of ornamental woody plants was studied. The height of seedlings as a morphometric parameter was measured 7 months after the start of the experiment. The pre-sowing seed treatment of *Rhododendron ledebourii* and *Rhododendron smirnowii*, with the studied compounds, demonstrated that dihydro- and tetrahydroquinoline with the concentration of 0.1% proved to be the most efficient. Dihydroquinolines at concentrations of 0.05 and 0.1% proved to have the strongest effect. Dihydroquinolines for perennial woody plants are more effective, then tetrahydroquinolines. The most efficient synthesized chemical compounds for *Rhododendron* contain benzoyl substitute. For *Rh. ledebourii* and *Rh. smirnowii* the most effective are the same synthesized chemical compounds: 6-hydroxy-2,2,4-trimethyl-1,2,3,4-tetrahydroquinoline, 6-hydroxy-2,2,4-trimethyl-1,2-dihydroquinoline, and 1-benzoyl-6-hydroxy-2,2,4-trimethyl-1,2-



dihydroquinoline with concentrations of 0.01, 0.05, and 0.1%. These compounds, when applied with the pre-sowing seed treatment of *Rh. ledebourii* and *Rh. smirnowii*, result in an increase in the height of the seedlings by 3.6-89.3% and 14.3-57.1%, respectively. The effect of synthesized chemical compounds of 6-hydroxy-2,2,4-trimethyl-1,2-dihydroquinoline and its hydrogenated analog on woody plants of the same genus is not species-specific. It is suggested using the compounds of 6-hydroxy-2,2,4-trimethyl-1,2-dihydroquinoline, its derivatives, and hydrogenated analogs as growth stimulators for *Rhododendron*. The compounds of the quinoline series were tested for genotoxicity by the cytological method in the model object (*Betula pendula*) and recognized as environmentally friendly. The cytogenetic responses for *Betula pendula* and *Rhododendron* are identical, so positive compounds influence for *Betula pendula* cells because of increased metabolic activity means the same for *Rhododendron*. Therefore, synthesized organic compounds can be recommended as effective growth stimulators.

**Keywords:** *growth stimulators, synthesized organic compounds, woody plants.*

## АННОТАЦИЯ

Исследовано влияние синтезированных органических соединений 6-гидрокси-2,2,4-триметил-1,2-дигидрохинолина, его производных и гидрированных аналогов на высоту проростков декоративных древесных растений. Высота сеянцев как морфометрический параметр измерялась через 7 месяцев после начала эксперимента. Предпосевная обработка семян *Rhododendron ledebourii* и *Rhododendron smirnowii* изученными соединениями показала, что дигидро- и тетрагидрохинолин с концентрацией 0,1% оказались наиболее эффективными. Дигидрохинолины в концентрациях 0,05 и 0,1% оказались наиболее сильными. Дигидрохинолины для многолетних древесных растений более эффективны, чем тетрагидрохинолины. Наиболее эффективные синтезированные химические соединения для рододендрона содержат бензоильный заменитель. Для *Rh. ledebourii* и *Rh. smirnowii* наиболее эффективными являются одни и те же синтезированные химические соединения: 6-гидрокси-2,2,4-триметил-1,2,3,4-тетрагидрохинолин, 6-гидрокси-2,2,4-триметил-1,2-дигидрохинолин и 1-бензоил-6-гидрокси-2,2,4-триметил-1,2-дигидрохинолин с концентрациями 0,01, 0,05 и 0,1%. Эти соединения, когда применяются при предпосевной обработке семян *Rh. ledebourii* и *Rh. smirnowii*, приводят к увеличению высоты сеянцев на 3,6-89,3% и 14,3-57,1% соответственно. Влияние синтезированных химических соединений 6-гидрокси-2,2,4-триметил-1,2-дигидрохинолина и его гидрированного аналога на древесные растения одного и того же рода не является видоспецифичным. Предлагается использовать соединения 6-гидрокси-2,2,4-триметил-1,2-дигидрохинолина, его производных и их гидрированных аналогов в качестве стимуляторов роста рододендрона. Соединения серии хинолинов были проверены на генотоксичность цитологическим методом на модельном объекте (*Betula pendula*) и признаны экологически чистыми. Цитогенетические ответы для *Betula pendula* и *Rhododendron* идентичны, поэтому положительное влияние соединений на клетки *Betula pendula* из-за повышенной метаболической активности означает то же самое для *Rhododendron*. Поэтому синтезированные органические соединения могут быть рекомендованы в качестве эффективных стимуляторов роста.

**Ключевые слова:** *стимуляторы роста, синтезированные органические соединения, древесные растения*

## 1. INTRODUCTION

The biological effect of quinolinic compounds (Abdel-Gawad *et al.*, 2005; Shuijiang *et al.*, 2005; Williamson, Ward 2005; Denmark, Venkatraman, 2006; Shikhaliev *et al.*, 2014; Ghoneim, Assy, 2015), such as dihydro- and tetrahydroquinoline, on seed germination and the root growth of the stem cuttings of woody plants, is currently being studied (Shmyreva, 2000; Butorina *et al.*, 2002; Baranova, 2013a). Environmentally friendly quinolinic compounds (Dorey *et al.*, 2000; Butorina *et al.*, 2002; Abdel-Gawad *et al.*, 2005; El-Gazzar *et al.*, 2009; Baranova, 2013a) are widely used to produce planting material, which is then planted in

anthropogenically polluted areas (Moiseeva *et al.*, 2012a; Kalaev *et al.*, 2013). It was demonstrated that depending on their concentrations, and quinolinic compounds have a different effect on seed germination and the height of the seedlings of the woody plants of *Rhododendron* L genus (Moiseeva *et al.*, 201a; Kalaev *et al.*, 2013). This means that the same quinolinic compounds at different concentrations may either stimulate or inhibit the biological processes (Dlugosz, Dus, 1996; Gavrilov *et al.*, 1988; Litvinov, 1998; Dorey *et al.*, 2000; El-Sayed *et al.*, 2002a,b, 2004; Saudi *et al.*, 2003; Brown *et al.*, 2004; van Straten *et al.*, 2005; Takahashi *et al.*, 2006, 2007; Le *et al.*, 2007; Balalaie *et al.*, 2008; Trivedi *et al.*, 2008; Fotie *et al.*, 2010). Thus, 1,2-dihydroquinoline-6-oles and

their ester derivatives were biologically (antitrypanosomally) active at micromolar concentrations (Fotie *et al.*, 2010). It was also determined, that 6-oxy-2,2,4-trimethyl-1,2-dihydroquinoline and 6-oxy-2,2,4-trimethyl-1,2-tetrahydroquinoline at concentrations of 100, 50, 25, 12.5, and 6.25  $\mu\text{g ml}^{-1}$  demonstrate bactericidal and bacteriostatic activity against laboratory *M. tuberculosis* H37 Rv indicator (the sample was provided by the museum of the local TB dispensary) and are thus highly effective antituberculous compounds (Litvinov *et al.*, 2009). In terms of percentages, the following concentrations are effective: 0.01, 0.005, 0.0025, 0.00125, and 0.000625%. It is, therefore, interesting to study the effect of 6-hydroxy-2,2,4-trimethyl-1,2-dihydroquinoline, 6-hydroxy-2,2,4-trimethyl-1,2,3,4-tetrahydroquinoline, and their derivatives on woody plants with concentrations between 0.01–0.1%. Due to its importance as substructures in a wide range of natural and designed products, still, great efforts continue to be directed to the development of new quinoline-based structures (Li *et al.*, 1985; Mohammed *et al.*, 1992; Jain *et al.*, 1994; Croisy-Delcey *et al.*, 2000; Abadi, Brun, 2003; Shujang *et al.*, 2005; Elkholy, Morsy, 2006; Marjani *et al.*, 2011; Mosalam *et al.*, 2011a,b; Azizian *et al.*, 2014; Ghoneim, Assy, 2015; Manahelohe *et al.*, 2015a,b).

In all the existing studies, the effect of quinolinic compounds on the growth of the sprouts of woody plants was assessed on the 20th day of the experiment (Moiseeva *et al.*, 2012a, Kalaev *et al.*, 2013). However, the effect of synthesized chemical quinolinic compounds in the later stages of woody plant development (7 months after the start of the experiment) has not been studied yet. It is therefore of great importance to conduct a longitudinal study and measure the height of ornamental woody plants over longer time intervals (e.g., 7 months after the application of the growth regulator) in order to determine whether the growth stimulating effect lasts or deteriorates over time. It should be noted that the effect of the same factor may be species-specific for different plants, which makes it significantly more difficult to determine the optimal concentrations of the compounds. Seed progeny, sprouts, and even adult plants may react differently to the stimulators, which are, in fact, stress factors of various intensity.

Highly decorative species of *Rhododendron* genus have also become more popular lately (Baranova *et al.*, 2018; Burmenko *et al.*, 2018a,b). They are planted in urban and residential areas, and their propagation requires additional

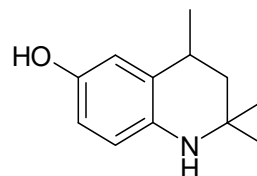
stimulators of growth and seed germination.

Therefore, the aim of our research was to study the effect of synthesized organic compounds of 6-hydroxy-2,2,4-trimethyl-1,2-dihydroquinoline, its derivatives, and hydrogenated analogs on the height of seedlings, when used for pre-sowing seed treatment of the following ornamental woody plants – *Rhododendron ledebourii* and *Rhododendron smirnowii*.

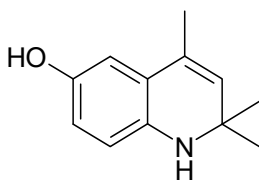
## 2. MATERIALS AND METHODS

In this study, it was used the following ornamental plants: woody plants *Rhododendron ledebourii* Pojark. And *Rhododendron smirnowii* Trautv. *Rhododendron ledebourii* is a perennial plant endemic for Altai and Mongolia. *Rhododendron smirnowii* is native to the forests and mountains of Caucasus, Adjara, and Turkey. *Rhododendron ledebourii* is a semi-evergreen shrub, and *Rhododendron smirnowii*, an evergreen shrub. In a controlled environment, both species grow up to 2-meter height and are highly decorative (Alexandrova, 2003). The long history of studying these species at the B.M. Kozo-Polyansky Botanical Garden of Voronezh State University has demonstrated that *Rhododendron ledebourii* is a winter-hardy, drought-resistant, and fruit-bearing shrub (Moiseeva *et al.*, 2012b; Baranova 2013b). *Rhododendron smirnowii* is also quite winter-hardy, though less drought-resistant. It also grows slower than *Rhododendron ledebourii* (Alexandrova, 2003; Vostrikova, 2011).

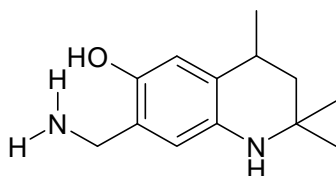
The research was conducted at the B.M. Kozo-Polyansky Botanical Garden of Voronezh State University in 2017. The study focused on the following organic compounds synthesized at the Department of Organic Chemistry of Voronezh State University:



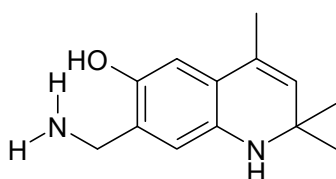
6-hydroxy-2,2,4-trimethyl-1,2,3,4-tetrahydroquinoline (stimulator 1),



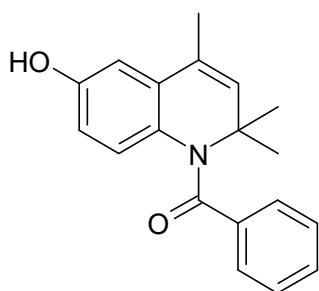
6-hydroxy-2,2,4-trimethyl-1,2-dihydroquinoline (stimulator 2),



7-[(dimethylamino)methyl]-6-hydroxy-2,2,4-trimethyl-1,2,3,4-tetrahydroquinoline (stimulator 3),



7-[(dimethylamino)methyl]-6-hydroxy-2,2,4-trimethyl-1,2-dihydroquinoline (stimulator 4), and



1-benzoyl-6-hydroxy-2,2,4-trimethyl-1,2-dihydroquinoline (stimulator 5), and the way they influence the height of the seedlings of *Rh. ledebourii* and *Rh. smirnowii*.

The stimulator 1 (6-hydroxy-2,2,4-trimethyl-1,2,3,4-tetrahydroquinoline) and stimulator 2 (6-hydroxy-2,2,4-trimethyl-1,2-dihydroquinoline) were synthesized from commercially available 6-ethoxy-2,2,4-trimethyl-1,2-dihydroquinoline (ethoxychine) by the known method (Ivanov *et al.*, 1979). By aminomethylation of stimulators 1 and 2 with bis(dimethylamino)methane resulted in stimulator 3 (7-[(dimethylamino)methyl]-6-hydroxy-2,2,4-trimethyl-1,2,3,4-tetrahydroquinoline) and stimulator 4 (7-[(dimethylamino)methyl]-6-hydroxy-2,2,4-trimethyl-1,2-dihydroquinoline), respectively. The stimulator 5 (1-benzoyl-6-hydroxy-2,2,4-trimethyl-1,2-dihydroquinoline) was obtained as a result of successive reactions of acylation of stimulator 2 an excess of benzoyl chloride and subsequent alkaline hydrolysis of the

resulting diacyl-derivative.

Prior to the sprouting process, the seeds of *Rh. ledebourii*, *Rh. smirnowii* were soaked in water solutions of the above-listed compounds with concentrations of 0.01%, 0.05%, and 0.1% for 18 hours. The control group consisted of the same type of seeds soaked in a tap water solution of a commonly used growth stimulator, Epibrassinolide (commercial fraction *Epin Extra* produced by NNPP NEST M, Russia), with the concentration of 0.05% (in accordance with the instruction). In the case of each of the studied concentrations of the acids, as well as the control group, the experiment was conducted three times using a set of 100 seeds. After soaking, the rhododendron seeds were placed in Petri dishes containing blotting paper and germinated in the laboratory conditions at a constant temperature of 22 °C. On the 21st day, the sprouts were planted in containers filled with high-moor peat and then kept in a greenhouse. The height of the seedlings of *Rhododendron* was measured with a ruler, 7 months after the start of the experiment. Sprouts are formed during the early stage of plant ontogenesis, which starts after the germination stage, i.e., when the seed coat develops, and finishes when the first leaf of the hypocotyledonous stem (the shoot rising from the plumule) develops (Korovkin, 2007). After the first true leaves appear, young plants are considered seedlings (Korovkin, 2007). The results were statistically processed using the STADIA software package. The procedures of data grouping and processing were described by A. P. Kulaichev (2006). The mean values were compared using Student's t-test. The variances were compared using the F-test.

### 3. RESULTS AND DISCUSSION:

The results of the treatment of seeds with the chemical compounds on the height of *Rh. ledebourii* seedlings 7 months after the start of the experiment are given in Table 1 and in Figure 1. It demonstrates that 6-hydroxy-2,2,4-trimethyl-1,2-dihydroquinoline (stimulator 2) appears to have strong stimulating effect with any of the studied concentrations: 0.01, 0.05, and 0.1% (differences with the control group are reliable,  $p < 0.001$ ). Dihydroquinolines (stimulators 4 and 5) and their substitutes 7-[(dimethylamino)methyl]- and especially 1-benzoyl- proved to have the stimulating effect at any of the studied concentrations (Table 3). 6-hydroxy-2,2,4-trimethyl-1,2,3,4-tetrahydroquinoline (stimulator 1)

and 7-[(dimethylamino)methyl]-6-hydroxy-2,2,4-trimethyl-1,2,3,4-tetrahydroquinoline (stimulator 3) appeared to be less active. 7 months after the start of the experiment, the height of *Rh. ledebourii* seedlings increased by 17.9–89.3% (Table 3).

For *Rh. smirnowii*, 7 months after the seed treatment with the studied chemical compounds, the concentration of 0.1% proved to be the most effective (Table 2, Fig. 2) and increased the plants' height of 57.1–14.3% (Table 4).

The effect of certain quinolines on seed germination and the size of seedlings of *Rh. Ledebouriionon*, the 20th day of the experiment was investigated earlier. It was demonstrated that 2,2,4-trimethyl-1,2,3,4-tetrahydroquinoline and 2,2,4-trimethyl-1,2-dihydroquinoline (with a concentration of 0.1%) have a stimulating effect on both the seed germination and the height of the sprouts of *Rhododendron ledebourii* (Moiseeva *et al.*, 2012a; Kalaev *et al.*, 2013).

Besides *Rh. ledebourii*, 6-hydroxy-2,2,4-trimethyl-1,2-dihydroquinoline also had the strongest stimulating effect on *Rh. smirnowii* (Table 2). 7 months after the start of the experiment, the height of *Rh. smirnowii* seedlings increased by 21.4–57.1% (Table 4). 6-Hydroxy-2,2,4-trimethyl-1,2,3,4-tetrahydroquinoline was less effective, with the increase in the height of the seedlings (as compared to the control group) being 14.3–28.6% (Table 2, 4). 1-Benzoyl-6-hydroxy-2,2,4-trimethyl-1,2-dihydroquinoline at concentrations of 0.05 and 0.1% (Tables 2, 4) also demonstrated a stimulating effect.

Thus, dihydroquinolines appear to have the strongest stimulating effect, with benzoyl boosting the effect of the stimulator, while tetrahydroquinolines are less active. Previous studies have determined that the detected antitrypanosomal activity of 1,2-dihydroquinoline-6-oles and their ester derivatives at micromolar concentrations are higher in the compounds containing benzene substitutes for the nitrogen atom (Fotie *et al.*, 2010). However, the latter have different cytotoxicity. 1-benzyl-6-hydroxy-2,2,4-trimethyl-1,2-dihydroquinoline acetate (I) (1-benzyl--6-hydroxy-1,2-dihydro-2,2,4-trimethylquinolin-6-yl acetate) was the most effective and had low cytotoxicity. Its activity involves the formation of the precursor 1-benzyl-6-hydroxy-2,2,4-trimethyl-1,2-dihydroquinoline (1-benzyl--6-hydroxy-1,2-dihydro-2,2,4-trimethylquinolin) (II) (Fotie *et al.*, 2010), which is the structural analogue of 1-benzoyl-6-hydroxy-2,2,4-trimethyl-1,2-dihydroquinoline (1-benzyl--6-hydroxy-1,2-dihydro-2,2,4-trimethylquinolin)

(stimulator 5) we used in our study (Fig. 3) (Fotie *et al.*, 2010).

For the plants of *Rhododendron* L. genus, the strongest stimulating effect was demonstrated by all the studied compounds with a concentration of 0.1%.

For *Rh. ledebourii* and *Rh. smirnowii* the most effective are the same synthesized chemical compounds: 6-hydroxy-2,2,4-trimethyl-1,2,3,4-tetrahydroquinoline, 6-hydroxy-2,2,4-trimethyl-1,2-dihydroquinoline, and 1-benzoyl-6-hydroxy-2,2,4-trimethyl-1,2-dihydroquinoline with concentrations of 0.01, 0.05, and 0.1%.

#### 4. CONCLUSIONS:

For the studied species of *Rhododendron* genus, the compounds of 6-hydroxy-2,2,4-trimethyl-1,2-dihydroquinoline, its derivatives, and hydrogenated analogs with the concentration of 0.1% proved to be the most efficient. Dihydroquinolines with concentrations of 0.05 and 0.1% appear to have the strongest stimulating effect on perennial woody plants, with benzoyl boosting the effect of the stimulator, while tetrahydroquinolines are less active. The effect of synthesized chemical compounds of 6-hydroxy-2,2,4-trimethyl-1,2-dihydroquinoline and its hydrogenated analog on woody plants of the same genus is not species specific. These compounds, when applied with the pre-sowing seed treatment of *Rh. ledebourii*, *Rh. smirnowii* result in an increase in the height of the seedlings by 3.6–89.3%, 14.3–57.1%, respectively. Thus it is suggested using the compounds of 6-hydroxy-2,2,4-trimethyl-1,2-dihydroquinoline, its derivatives, and hydrogenated analogs as growth stimulators for ornamental woody plants. The compounds of the quinoline series were tested for genotoxicity by the cytological method in the model object (*Betula pendula*) and recognized as environmentally friendly (Butorina *et al.*, 2002). The cytogenetic responses for *Betula pendula* and *Rhododendron* are identical, so positive compounds influence for *Betula pendula* cells because of increasing of metabolic activity means the same for *Rhododendron* (Baranova *et al.*, 2018; Burmenko *et al.*, 2018a,b). Therefore, synthesized organic compounds can be recommended as effective growth stimulators.

#### 5. ACKNOWLEDGMENTS:

The study received financial support from the Ministry of Science and Higher

## 6. REFERENCES:

1. Abdel-Gawad, S. M., El-Gagy, M. S. A., Heiba, H. I., Aly, H. M., Ghorab, M. M. Synthesis and radiation stability of some new biologically active hydroquinoline and pyrimido[4,5-b]quinoline derivatives. *J. Chin. Chem. Soc.*, **2005**, 52, 1227–1236.
2. Abadi, A. H., Brun, R. Synthesis and evaluation of novel 7-trifluoromethyl-4-(4-substituted anilino) quinolines as antiparasitic and antineoplastic agents *Arzneimforsch. Drug. Res.*, **2003**, 53, 655–663.
3. Alexandrova, M. S. Rhododendrons. Moscow: ZAO Fiton+, **2003**.
4. Azizian, J., Delbari A. S., One-Pot, K. Y. Three-Component Synthesis of Pyrimido[4,5-b]quinoline-tetraone Derivatives in Water. *Synthetic Commun.*, 2014, 44 (22), 3277–3286. DOI: 10.1080/00397911.2011.626139
5. Balalaie, S., Abdolmohammadi, S., Bijanzadeh, H. R. Amani, A. M. Diammonium hydrogen phosphate as a versatile and efficient catalyst for the one-pot synthesis of pyrano [2,3-d] pyrimidinone derivatives in aqueous media. *Mol. Diversity*, **2008**, 12, 85–91.
6. Baranova, T. V. Accelerated production of plants resistant to urban conditions. *Ecology and Industry of Russia*, **2013a**, 4, 65–67.
7. Baranova, T. V. Phenological characteristics of species of the genus Rhododendron L. in the Central Black Soil. *Bulletin of Krasnoyarsk State Agrarian University*, **2013b**, 4, 74–79.
8. Baranova, T. V., Kalendar, R. N., Kalaev, V. N., Sorokopudov, V. N., Burmenko, Yu. V., Relationship between cytogenetic characteristics and molecular-genetic differences in species of the genus Rhododendron L. when introduced. *Agricultural Biology*, **2018**, 53(3), 511–520. doi: 10.15389/agrobiol
9. Brown, C. W., Liu, S., Klucik, J., Berlin, K. D., Brennan, P. J., Kaur, D., Benbrook, D. M. Novel heteroarotinoids as potential antagonists of Mycobacterium bovis BCG. *Journal of Medicinal Chemistry*, **2004**, 47 (4), 1008–1017.
10. Burmenko, Yu. V., Baranova, T. V., Kalaev, V. N. Comparative Study of Cytogenetic Response of Silver Birch and Rhododendron Ledebourii Seeds to Urban Pollution in Voronezh. *Russian Journal of Forest Science*, **2018a**, 1, 65–73. doi: 10.7868/S0024114818010060
11. Burmenko, Yu. V., Baranova, T. V., Kalaev, V. N., Sorokopudov, V. N. Cytogenetic polymorphism of seed progeny of introduced plants on the example of Rhododendron ledebourii Pojark. *Turczaninowia*, **2018b**, 21 (1), 164–173. doi: 10.14258/turczaninowia.21.1.16
12. Butorina, A. K. Vostrikova, T. V., Shmyreva, J. V., Belchinskaya, L. I., Kondaurava, V. A. The effect of chemical stimulants on germination and cytogenetic indicators of seedlings of birch seeds hanging. *Forestry*, **2002**, 5, 33–35.
13. Croisy-Delcey, M., Corois, A., Carrez, D., Huel, C., Chiaroni, A., Ducrot, P., Bisagni, E., Jin, L., Leclercq, G. Bioorg, Diphenyl quinolines and isoquinolines: synthesis and primary biological evaluation. *Med. Chem.*, **2000**, 8(ii), 2629–2641.
14. Denmark, S., Venkatraman, S. On the mechanism of the Skraup-Doebner-Von Miller quinoline synthesis. *J. Org. Chem.*, **2006**, 71, 1668–1676.
15. Dlugosz, A., Dus, D. F. Synthesis and anticancer properties of pyrimido(4,5-b)quinolines. *Chem Inf Abstr.*, **1996**, 51, 367–374.
16. Dorey, G., Lockhart, B., Lestage, P., Casara, P. New quinolinic derivatives as centrally active antioxidants. *Bioorg. Med. Chem. Lett.*, **2000**, 10, 935–939.
17. Elkholy, Y. M., Morsy, M. A. Facile Synthesis of 5, 6, 7, 8-Tetrahydropyrimido [4, 5-b]- quinoline Derivatives. *Molecules*, **2006**, 11, 890–903.
18. El-Gazzar, A. B. A., Hafez, H. N., Nawwar, G. A. M. New acyclic nucleosides analogues as potential analgesic, anti-inflammatory, anti-oxidant and anti-microbial derived from pyrimido[4,5-b]quinolines. *Eur. J. Medic. Chem.*, **2009**, 44(4), 1427–1436.
19. El-Sayed, O. A., Al-Bassam, B. A., Hussein, M. E. Synthesis of some novel quinoline-3-carboxylic acids and pyrimidoquinoline derivatives as potential

- antimicrobial agents. *Archiv Pharmazie*, **2002a**, 335, 403-410.
20. El-Sayed, O. A., El-Bieh, F. M., El-Aqeel, S. I., Al-Bassam, B. A., Hussein, M. E. Novel 4-aminopyrimido[4,5-b]quinoline derivatives as potential antimicrobial agents. *Bollettino Chimico Farmaceutico*, **2002b**, 141, 461-465.
  21. El-Sayed, O. A., Al-Turki, T. M., Al-Daffiri, H. M., Al-Bassam, B. A., Hussein, M. E. Tetrazolo[1,5-a] quinoline derivatives as anti-inflammatory and antimicrobial agents. *Bollettino Chimico Farmaceutico*, **2004**, 143, 227-238.
  22. Fotie, J., Kaiser, M., Delfrín, D. A., Manley, J., Reid, C. S., Paris, J.-M., Wenzler, T., Maes, L., Mahasen, K. V., Li, C., Werbovetz, K. A. Antitrypanosomal Activity of 1,2-Dihydroquinolin-6-ols and Their Ester Derivatives. *Journal of Medicinal Chemistry*, **2010**, 53, 966-982. DOI: 10.1021/jm900723w
  23. Gavrilov, M. Y., Mardanova, L. G., Kolla, V. E., Konshin, M. E. Synthesis, antiinflammatory and analgesic activities of 2-arylamino-5,6,7,8-tetrahydroquinoline-3-carboxamides. *Pharmaceut. Chem. J.*, **1988**, 22, 554-556.
  24. Ghoneim, A. A., Assy, M. G. Synthesis of Some New Hydroquinoline and Pyrimido[4,5-b] Quinoline Derivatives. *Current Research in Chemistry*, **2015**, 7(1), 14-20. DOI: 10.3923/crc.2015.14.20)
  25. Goldmann, S., Stoltefuss, J. 1,4-Dihydropyridines: Effects of chirality and conformation on the calcium antagonist and calcium agonist activities. *Angewandte Chemie Int. Edn. English*, 1991, 30, 1559-1578.
  26. Ivanov, Yu. A., Zaichenko, N. L., Rykov, S. V., Grinberg, O. Ya., Dubinskii, A. A., Pirozhkov, S. D., Rozantsev, E. G., Pokrovskaya, I. E., Shapiro, A. B. The synthesis of hydroxy, acyloxy, oxo, N-oxides oxo and morpholino derivatives of hydrogenated quinolines and the study of their radical analogs by EPR. *Bulletin of the Academy of Sciences of the USSR. Division of chemical science*, **1979**, 28(8), 1661-1668.
  27. Jain, R., Jain, S., Gupta, R. C., Anand, N., Dutta, G. P., Puri, S. K. Synthesis of amino acid derivatives of 8-[(4-amino-1-methylbutyl)amino]-6-methoxy-4-substituted quinolines as potential antimalarial agents. *Indian J. Chem.*, **1994**, 33B, 251-254.
  28. Kalaev, V. N., Moiseeva, E. V., Baranova, T. V., Medvedeva, S. M., Shikhaliev, H. S., Voronin, A. A. Growth stimulants for species of the genus *Rhododendron* L.: Patent 2490892 Russian Federation. 2012112006/13, declared 29. 03.12, published 27. 08.13, 24.
  29. Korovkin, O. A. Anatomy and morphology of higher plants: a dictionary of terms. Moscow: Drofa, **2007**.
  30. Kulaichev, A. P. Methods and tools for integrated data analysis. Moscow: FORUM: INFA-M, **2006**.
  31. Le, T. C., Berlin, K. D., Benson, S. D., Eastman, M. A., Bell-Eunice, G., Nelson, A. C., Benbrook, D. M. Heteroarotinoids with Anti-Cancer Activity Against Ovarian Cancer Cells. *The Open Medicinal Chemistry Journal*, 2007, 1, 11-23. Li, F., Wang, L., Li, Y., Feng, X. Synthesis of active acrylic esters of 8-Hydroxyquinoline and immobilization of proteins with their polymers. *Chin. J. Polym. Sci*, **1985**, 17(1), 75-79.
  32. Litvinov, V.P., Partially hydrogenated pyridinechalcogenones. *Russ. Chem. Bull.*, **1998**, 47, 2053-2073.
  33. Litvinov, V. I., Makarova, M. V., Ryzhov, A. M., Ivanov, Yu. A., Frolov, A. Yu., Osinin, V. V., Pereverzentsev, V. M. The use of 6-hydroxyl-trimethyl-1,2,3,4-tetrahydroquinoline or 6-hydroxyl-2,2,4-trimethyl-1,2-dihydroquinoline as an anti-tuberculosis substance: Russian Federation. 2008133238/15, declared 14.08.08, published 20.11.09, 32.
  34. Marjani, A. P., Khalafy, J., Ebrahimlo, A. M. R. Facile Synthesis of Some New Pyrimidoquinolines. *Synthetic Commun*, **2011**, 41(16), 2475-2482. DOI: 10.1080/00397911.2010.505701
  35. Manakheloh, G. M., Shikhaliev, H. S., Potapov, A. Yu. Synthesis of 1H-1,2-dithiol-1-thiones and thioamides containing hydroquinoline group. *Eur. Chem. Bull.*, **2015a**, 4(7), 350-355.
  36. Manakheloh, G. M., Shikhaliev, H. S., Potapov, A. Yu. Synthesis of thiocarboxamides containing a hydroquinoline fragment. *Bulletin of the Voronezh State University, Series: Chemistry Biology Pharmacy*, **2015b**, 2, 23-28.

37. Mohammed, A., Abdel-Hamid, N., Maher, F., Farghaly, A. Synthesis and antibacterial activity of certain quinoline derivatives A. *Czech Chem Commun*, **1992**, 57(7), 1547–1552.
38. Moiseeva, E. V., Baranova, T. V., Kalaev, V. N., Kuznetsov, B. I., Shcherbakov, G. S., Voronin, A. A., Potapov, A. Yu., Shikhaliev, H. S. The effect of compounds of the quinoline series on the germination and growth processes of Ledebour's rhododendron (*Rhododendron Ledebourii* Pojark.). *Basic Research*, **2012a**, 5 (1), 172–176.
39. Moiseeva, E. V., Baranova, T. V., Voronin, A. A., Kuznetsov, B. I. A collection of representatives of the genus rhododendron (*Rhododendron* L.) in the botanical garden B.M. Kozo-Polyansky Voronezh State University. *Ecosystems, their optimization and protection*, **2012b**, 7, 39–44.
40. Mosalam, M. A., El Hamouly, S. H., Mahmoud, A. A., Khalil, A. Binary copolymerizations of 8-methacryloxy-quinoline with methyl methacrylate, methyl acrylate, styrene and acrylonitrile. *Journal of Polymer Research*, **2011a**, 18(6), 2141–2150. DOI:10.1007/s10965-011-9624-4
41. Mosalam, M. A., El Hamouly, S. H., Mahmoud, A. A., Khalil, A. Thermal Behavior of 8-methacryloxy-quinoline-Acrylonitrile Copolymers. *International Journal of Chemistry*, **2011b**, 3(2), 14-22. DOI: 10.5539 / ijc.v3n2p14
42. Saudi, M. N. S., Rostom, S. A., Fahmy, H. T. Y., El-Ashmawy I. Synthesis of 2-(4Biphenyl)quinoline-4-carboxylate and Carboxamide Analogues. *Article in ChemInform*, **2003**, 34(39).doi:10.1002 / chin.200339123
43. Shikhaliev, H. S., Selemenev, V. F., Medvedeva, S. M., Ponomareva, L. F., Kopteva, N. I. Mass-spectrometric analysis of 1-acyl-2,2,5-trimethyl-4,4-dichlorocyclopropane [c] quinolines. *Sorption and chromatographic processes*, **2014**, 14 (2), 332–337.
44. Shmyreva, J. V. 2, 2, 4-Trimethylhydroquinolins. Voronezh: VSU, **2000**.
45. Shuijiang, T. U., Fang, F., Tuanjie, L., Songlei, Z., Xiaojing, Z. An efficient one-pot synthesis of novel pyrimidoquinoline derivative under microwave irradiation without catalyst. *J. Heterocycl. Chem.*, **2005**, 42, 707-710.
46. van Straten, N., van Berkel, T., Demont, D., Karstens, W., Merckx, R., Oosterom, J., Schulz, J., van Someren, R., Timmers, C., van Zandvoort, P. Identification of substituted 6-amino-4-phenyltetrahydroquinoline derivatives: potent antagonists for the folliclestimulating hormone receptor. *J. Med. Chem.*, **2005**, 48, 1697–1700.
47. Takahashi, H., Bekkali, Y., Capolino, A., Gilmore, T., Goldrick, S., Nelson, R., Terenzio, D., Wang, J., Zuvela-Jelaska, L., Proudfoot, J., Nabozny, G., Thomson, D. Discovery and SAR study of novel dihydroquinoline containing glucocorticoid receptor ligands. *Bioorg. Med. Chem. Lett.*, **2006**, 16, 1549–1552.
48. Takahashi, H., Bekkali, Y., Capolino, A., Gilmore, T., Goldrick, S., Kaplita, P., Liu, L., Nelson, R., Terenzio, D., Wang, J., Zuvela-Jelaska, L., Proudfoot, J., Nabozny, G., Thomson, D. Discovery and SAR study of novel dihydroquinoline containing glucocorticoid receptor antagonists. *Bioorg. Med. Chem. Lett.*, **2007**, 17, 5091–5095.
49. Trivedi, A., Dodiya, D., Surani, J., Jarsania, S., Mathukiya, H., Ravat N., Shah, V. Facile one-pot synthesis and antimycobacterial evaluation of pyrazolo[3,4 d]pyrimidines. *Archiv Pharmazie*, **2008**, 341, 435-439.
50. Vostrikova, T. V. Ecological and biological features of rhododendrons during introduction in the conditions of the Central Chernozem region. *Bulletin of Krasnoyarsk State Agrarian University*, **2011**, 4, 27–30.
51. Williamson, N., Ward, D. The preparation and some chemistry of 2,2-dimethyl-1,2-dihydroquinolines. *Tetrahedron*, **2005**, 61, 155–165.

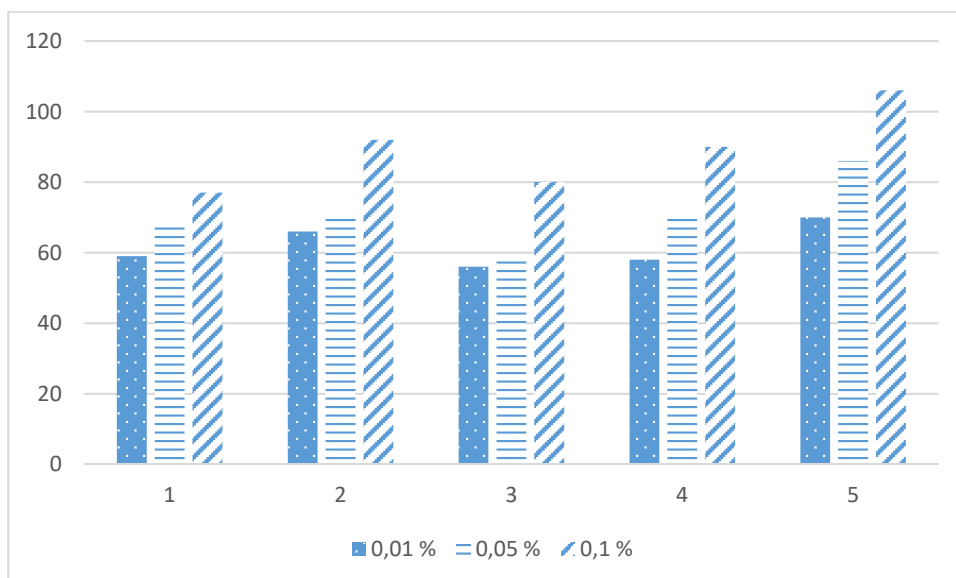


**Figure 1.** Comparative height (in mm) of *Rh. ledebourii* seedlings 7 months after the start of the experiment for the compounds 1-5.

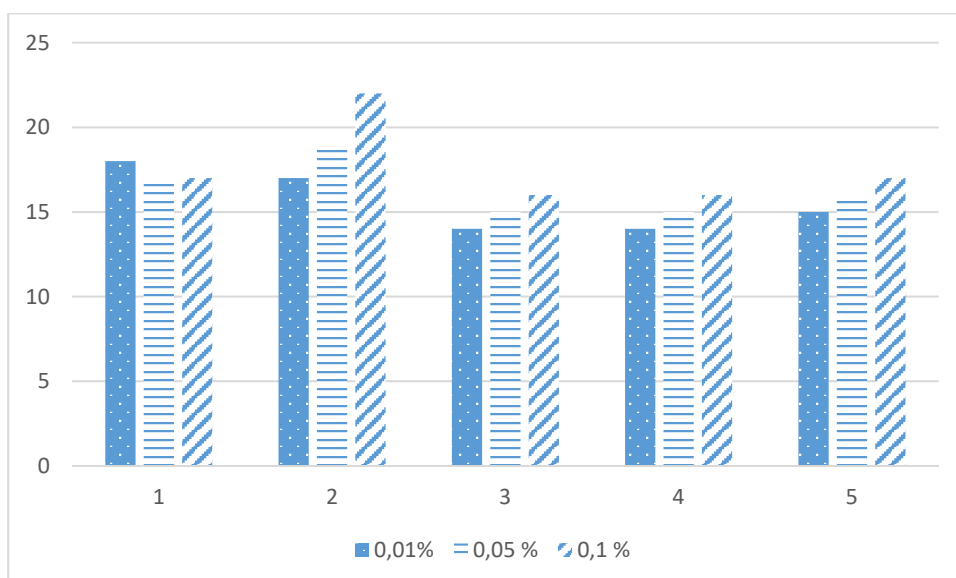


**Figure 2.** Comparative height (in mm) of *Rh. smirnowii* seedlings 7 months after the start of the experiment for the compounds 1-5



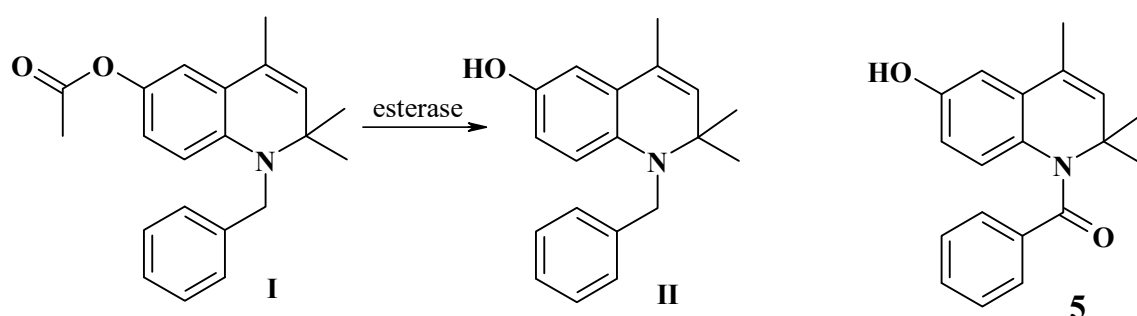


**Figure 3.** Chemical formulae of the compounds used in the experiment

**I** : 1-benzyl-6-hydroxy-2,2,4-trimethyl-1,2-dihydroquinoline acetate

**II** : 1-benzyl-6-hydroxy-2,2,4-trimethyl-1,2-dihydroquinoline

**5** : 1-benzoyl-6-hydroxy-2,2,4-trimethyl-1,2-dihydroquinoline

**Table 1.** The height (in cm) of *Rh. ledebourii* seedlings 7 months after the start of the experiment

| Concen-<br>tration | Control<br>group, % | Epin<br>group, % | Extra | Stimulator 1            | Stimulator 2            | Stimulator 3            | Stimulator 4             | Stimulator 5             |
|--------------------|---------------------|------------------|-------|-------------------------|-------------------------|-------------------------|--------------------------|--------------------------|
| 0.01%              |                     |                  |       | 5.9±0.2** <sup>1</sup>  | 6.6±0.1*** <sup>3</sup> | 5.6±0.2                 | 5.8±0.2*                 | 7.0±0.2*** <sup>3</sup>  |
| 0.05%              | 5.6±0,2             | 5.7±0,2          |       | 6.8±0.2*** <sup>3</sup> | 7.0±0.2*** <sup>3</sup> | 5.8±0.2*                | 7.1±0.2 *** <sup>3</sup> | 8.6±0.3*** <sup>3</sup>  |
| 0.1%               |                     |                  |       | 7.7±0.2*** <sup>3</sup> | 9.2±0.2*** <sup>3</sup> | 8.0±0.2*** <sup>3</sup> | 9.0±0.2*** <sup>3</sup>  | 10.6±0.3*** <sup>3</sup> |

Note for Table 1-2:

\* – differences with the control group are reliable ( $p < 0.05$ )

\* – differences with the control group are reliable ( $p < 0.01$ )

\* – differences with the control group are reliable ( $p < 0.001$ )

<sup>1</sup> - differences with the Epin Extra group are reliable ( $p < 0.05$ );

<sup>2</sup> - differences with the Epin Extra group are reliable ( $p < 0.01$ );

<sup>3</sup> - differences with the Epin Extra group are reliable ( $p < 0.01$ );

6-hydroxy-2,2,4-trimethyl-1,2,3,4-tetrahydroquinoline (stimulator 1),

6-hydroxy-2,2,4-trimethyl-1,2-dihydroquinoline (stimulator 2),

7-[(dimethylamino)methyl]-6-hydroxy-2,2,4-trimethyl-1,2,3,4-tetrahydroquinoline (stimulator 3),

7-[(dimethylamino)methyl]-6-hydroxy-2,2,4-trimethyl-1,2-dihydroquinoline (stimulator 4),

1-benzoyl-6-hydroxy-2,2,4-trimethyl-1,2-dihydroquinoline (stimulator 5).

**Table 2.** The height (in cm) of *Rh. smirnowii* seedlings 7 months after the start of the experiment

| Concentration | Control group, % | Epin Extra group, % | Stimulator 1          | Stimulator 2           | Stimulator 3 | Stimulator 4 | Stimulator 5 |
|---------------|------------------|---------------------|-----------------------|------------------------|--------------|--------------|--------------|
| 0.01%         |                  |                     | 1.8±0.1* <sup>1</sup> | 1.7±0.1* <sup>1</sup>  | 1.4±0.1      | 1.4±0.1      | 1.5±0.1      |
| 0.05%         | 1.4±0.2          | 1.4±0.2             | 1.7±0.1* <sup>1</sup> | 1.9±0.2** <sup>2</sup> | 1.5±0.1      | 1.5±0.1      | 1.6±0.1*     |
| 0.1%          |                  |                     | 1.7±0.1 <sup>1</sup>  | 2.2±0.2** <sup>2</sup> | 1.6±0.1*     | 1.6±0.1*     | 1.7±0.1*     |

**Table 3.** The height (in cm) of *Rh. ledebourii* seedlings 7 months after the start of the experiment

| Concentration | Epin, % | Stimulator 1 | Stimulator 2 | Stimulator 3 | Stimulator 4 | Stimulator 5 |
|---------------|---------|--------------|--------------|--------------|--------------|--------------|
| 0.01%         |         | 28.6         | 21.4         | —            | —            | —            |
| 0.05%         | —       | 21.4         | 35.7         | —            | —            | 14.3         |
| 0.1%          |         | 21.4         | 57.1         | 14.3         | 14.3         | 21.4         |

**Table 4.** The increase (in %) in the height of *Rh. smirnowii* seedlings 7 months after the start of the experiment

| Concentration | Epin, % | Stimulator 1 | Stimulator 2 | Stimulator 3 | Stimulator 4 | Stimulator 5 |
|---------------|---------|--------------|--------------|--------------|--------------|--------------|
| 0.01%         |         | 28.6         | 21.4         | —            | —            | —            |
| 0.05%         | —       | 21.4         | 35.7         | —            | —            | 14.3         |
| 0.1%          |         | 21.4         | 57.1         | 14.3         | 14.3         | 21.4         |

EFEITO DA ILUMINAÇÃO NO CRESCIMENTO E COMPORTAMENTO DO  
BARRIGUDINHO, *POECILIA RETICULATA*

EFFECT OF ILLUMINATION ON GROWTH AND BEHAVIOUR OF GUPPY, *POECILIA  
RETICULATA*

ВЛИЯНИЕ ОСВЕЩЕННОСТИ НА РОСТ И ПОВЕДЕНИЕ ГУППИ, *POECILIA  
RETICULATA*

RUCHIN, Alexander B.

<sup>1</sup> Joint Directorate of Mordovia State Nature Reserve and Smolny National Park, Saransk, Russia.

\* Autor correspondente

e-mail: [ruchin.alexander@gmail.com](mailto:ruchin.alexander@gmail.com)

Received 01 April 2020; received in revised form 10 May 2020; accepted 03 June 2020

## RESUMO

O barrigudinho, *Poecilia reticulata*, é um modelo para muitos estudos ictiológicos. Foi estudado o efeito da luz no crescimento juvenil da *Poecilia reticulata*. Estudos foram realizados em aquários de vinte litros. Para experimentos sobre a escolha arbitrária da intensidade da luz (comportamento da transmissão da luz), foram utilizados aquários radiantes de vidro orgânico medindo 150x15x15 cm, divididos com semi-divisórias transparentes em dez compartimentos de comunicação. A taxa de crescimento específica foi determinada após as experiências. A taxa de crescimento eleva-se com o aumento do nível de luz. A taxa de crescimento é mínima em 0 lx em todas as séries de experimentos. Foi demonstrado que o aumento mais acentuado na taxa de crescimento específico dos barrigudinhos ocorreu quando a iluminação mudou de 0 para 200 lx. Um aumento adicional na intensidade da iluminação praticamente não afetou o crescimento dos barrigudinhos. Além disso, o comportamento juvenil dos barrigudinhos foi estudado em bandejas especiais com luz diferente de 3200 a 5900 lx. A atividade motora dos barrigudinhos aumenta em 30% em condições de gradiente de luz. A frequência (25 s) e a duração dos barrigudinhos (28,3 s) são as mais altas do compartimento, com 4700 lx. A zona de luz preferencial se expande se os jovens estiverem passando fome. À medida que o período de fome aumentava, os barrigudinhos começaram a nadar com frequência quase igual e a permanecer em diferentes zonas de luz. Assim, condições de alta luminosidade estimulam o comportamento de busca e a atividade dos barrigudinhos. Para criar barrigudinhos em condições de produção, é necessária alta iluminação.

**Palavras-Chave:** Luz, Iluminação, *Poecilia Reticulate*, Crescimento, Comportamento.

## ABSTRACT

The guppy, *Poecilia reticulata*, is a model for many ichthyological studies. The effect of light on juvenile growth has been studied on the *Poecilia reticulata*. Studies have been conducted in twenty-liter aquariums. For experiments on the fish arbitrary choice of light intensity (light transmission behavior), it was used radiant pans of organic glass 150 x 15 x 15 cm divided by transparent semi-partitions into ten communicating compartments. The specific growth rate has been determined after the experiments. It increases with the light level increasing. The growth rate is minimal at 0 lx in all series of experiments. It was shown that the sharpest increase in the specific growth rate of guppies occurred when the illumination changed from 0 to 200 lx. A further increase in the intensity of illumination practically did not affect the growth of guppies. Also, the guppy juvenile behavior has been studied in special trays at different light from 3200 to 5900 lx. The motor activity of guppies increases by 30% in light-gradient conditions. The frequency (25 sec) and length of guppies stay (28.3 sec) are the highest in the compartment with 4700 lx. The preferential light zone expands if the juveniles are starving. As the period of starvation increased, guppies began to swim almost equally often and linger in different light zones. Thus, high light conditions stimulate the search behavior and activity of guppies. To grow guppies in production conditions, high illumination is necessary.

**Keywords:** Light, Illumination, *Poecilia Reticulate*, Growth, Behaviour.

## АННОТАЦИЯ

Гуппи (*Poecilia reticulata*) является модельным объектом многих ихтиологических исследований. На этом объекте изучали как воздействует освещенность на рост мальков. Исследования проводили в 20-литровых аквариумах. Для экспериментов по произвольному выбору рыбой интенсивности света (светогradientного поведения) мы использовали прозрачные лотки из органического стекла 150\*15\*15 см, разделенные прозрачными полуперегородками на десять сообщающихся отсеков. После экспериментов определяли скорость роста. Скорость роста повышалась при увеличении уровня освещенности. При 0 лк скорость роста была минимальной во всех сериях экспериментов. Было показано, что наиболее резкое возрастание удельной скорости роста мальков гуппи происходило при изменении освещенности от 0 до 200 лк. Дальнейшее увеличение интенсивности освещения практически не оказало воздействие на рост гуппи. Также исследовали поведение мальков гуппи в специальных лотках при различной освещенности от 3200 до 5900 лк. Двигательная активность гуппи в светогradientных условиях возрастала на 30%. Частота и длительность пребывания гуппи были наивысшими в отсеке с освещенностью 4700 лк 25 и 28.3 с, соответственно. У голодных особей преферентная зона освещенности расширялась. По мере увеличения периода голодания особи гуппи начинали практически одинаково часто заплывать и задерживаться в различных по освещенности зонах. Таким образом, высокая освещенность стимулирует поисковое поведение и активность гуппи. Для выращивания гуппи в производственных условиях необходима высокая освещенность.

**Ключевые слова:** Свет, Освещенность, *Poecilia reticulata*, Рост, Поведение.

## 1. INTRODUCTION

The *Poecilia reticulata*, popular aquarium fish, is a traditional subject of laboratory studies. Guppies live in freshwater both in mountain rivers and in muddy warm water) and in the saltish waters of Venezuela, Guyana, Trinidad, Barbados, Martinique as well as in some parts of northern Brazil (Echevarría and González, 2018). According to Ahmed et al. (1985), it has been found to establish itself in both fresh and polluted waters. In particular, it is used to conduct ethological studies (Fraser and Gilliam, 1987; Abrahams and Dill, 1989; Morrell et al., 2008), to study color and light perception (Smith et al., 2002; Sakai et al., 2016) as well as reproductive behavior (Reeve et al., 2014) and parasitological studies (Gotanda et al., 2013).

Light creates the necessary existence conditions, makes it possible to orient oneself in the environment for many aquatic organism species (Konstantinov et al., 2000; Ruchin et al., 2005; Ruchin, 2007, Ruchin, 2020). Illumination is an important environmental factor that affects different aspects of aquatic animals' existence. Specific environmental conditions have a positive effect on fish and amphibians (Boeuf and Le Bail, 1999). For example, growth of *Epinephelus coioides* yearlings improves with 320-1150 lx illumination (Wang et al., 2013), growth of juvenile *Megalobrama amblycephala* improves with 400 lx (Tian et al., 2015), growth of *Acipenser baerii* juveniles improves with 30-800 lx (Ruchin, 2008), growth of *Salmo salar* juveniles improves with 21-650 lx illumination (Handeland et al., 2013).

According to Toledo et al. (2002), Bădiliță et al. (2010), Ruchin (2016), Ruchin (2018), the embryonic development of fish and amphibians needs specific illumination parameters. Russian biologists such as Ruchin (2000), Ruchin (2004), Kuznetsov, and Ruchin (2001) proved that the larval development of several amphibian species accelerates with illumination above 1000 lx. Inhibition of growth, development, and survival of many species of aquatic vertebrate animals is observed outside of this illumination. Our research is aimed to study the light effect on the guppy growth and behavior.

## 2. MATERIALS AND METHODS

The experiments were conducted in 20 L aquariums. Fluorescent lamps emitted illumination. The intensity of illumination was measured with the U-116 lux meter. In the darkness (0 lx), aquariums were closed with an opaque cover. In each series of experiments, we used one female juvenile. Every time we placed 10–20 juveniles and weighed them at the beginning and the end of the experiment with an accuracy of 0.01 mg (Figure 1). We fed them continuously with zooplankton, and *Artemia* decapsulated eggs. The duration of the experiments ranged from 10 to 20 days. Experiments were repeated from five to nine times. Growth parameters were calculated as follows (Eq. 1):

$$\text{SGR } (\% \text{ day}^{-1}) = \frac{\ln W_f - \ln W_i}{t} \times 100 \quad (\text{Eq. 1})$$

where SGR is the *Specific Growth Rate*.

For experiments on the fish arbitrary choice of light intensity (light transmission behavior), we used radiant pans of organic glass 150 x 15 x 15 cm divided by transparent semi-partitions into ten communicating compartments (Ruchin, 2019). There was emitted a light gradient from 3200 lx at the beginning of the tray to 5900 lx at its end. The illumination in the control corresponded to the average value of the illumination in the experimental tray (4550 lx). We conducted observations in the morning at a temperature of 24 °C. We placed there three or four immature females weighing 9–12 g. We were watching one fish for 10–20 minutes a day. The experiments were repeated ten times. We also conducted research on well-fed and starving individuals. We investigated the options: 1 – well-fed, 2, 3, and 4, respectively, 0.5, 2, and 24 hours after the food's withdrawal.

Based on statistical data, we calculated the average duration of a single fish stay in a particular compartment ( $\tau$ , sec), the swims' number in each compartment ( $n$ ), and the total time of fish stay in each compartment ( $\sum \tau$ , min). All values were reduced to one hour (Ruchin, 2001a). The swimming distance from the beginning of the movement to the turn in the opposite direction was called "single-vector" and was designated as  $S_v$ . We calculated the duration of the continuous single-vector displacement ( $\tau_v$ ) because the motion in the gradient is discrete. Moreover, we noted the total number of single-vector displacements ( $N$ ). Knowing their average length ( $S_v$ ), we calculated the total path traversed by fish per hour as well as calculated the speed of movements ( $S_v/\tau_v$ ), the total time of movements, and the total time of fish delays in the compartments. According to Konstantinov and Zdanovich (1993) and Ruchin (2019), the use of these indicators makes it possible to characterize the fish behavior in gradient conditions more differentiated.

Data between treatments and sampling times were compared by analysis of variance (ANOVA). The data were statistically processed using a standard method with Student's Test.

### 3. RESULTS AND DISCUSSION

Figure 2 shows that the growth rate of guppy juveniles gradually increases with the light increase. Earlier, Ruchin (2001b) obtained similar results in experiments on carp larvae. As we can

see, the specific growth rate of guppy juveniles appeared when the illumination changes from 0 to 200 lx. A further increase in the intensity of illumination had practically no effect on the growth. In some experiments, the maximal increments were noted with 4500 lx and 11500 lx. There was no significant difference between them. In other experiments, in the absence of light (0 lx), the increments were minimal. The survival rate in all experiments was 100%, and we did not register the death.

Analysis of the fish behavior in the light gradient field showed that the juveniles stayed principally in areas with a certain light level. However, they often swam for short periods in compartments with different light values (Table 1).

The frequency (25 s) and duration (28.3 s) of guppy's stay were highest in the compartment with illumination 4700 lx. Table 1 shows that juveniles moved without a definite pattern in the control with balancing illumination, but they lingered in the last compartments. In other words, the "edge" effect appeared in the control. This effect was not registered with light gradient conditions. Individuals began to swim almost equally often and lingered in zones with different illumination as the starvation period increased. For example, the duration of one-time stay of starvation (0.5 hours) individuals with an illumination 4100–5300 lx was 35.3–21.2 s. Two hours after the food absence, the preferential zone expanded to 3800–5600 lx ( $t = 25.0$ –36.3 s), and after 24 hours of fasting, the juveniles stayed almost the same time in all compartments.

Table 2 shows that the motor activity of juvenile guppies in light-gradient conditions was higher in control by 30%. If the number of vector displacements did not differ, in the light gradient, the average displacement distance and the total path were higher by 15% and 18% than the corresponding values in the control with uniform illumination. Consequently, the total time of movement in the experiment exceeded this value with balancing illumination.

Thus, fish motor activity increased due to the increase in the range of movement and swimming speed in a gradient field. Juvenile behavior analysis in the gradient field of the factor shows that the preferential zones vary depending on the period of lack of food. The zone of the preferendum is shifted towards higher illumination values.

It was found that the growth of juveniles was characterized by an optimal range of illumination. Referring to the researches of Trippel

and Neil (2003), Suzer *et al.* (2006), Ruchin (2008), it was concluded that bottom dwellers needed lower luminance values and pelagic fish, including guppies, needed higher luminance (Ruchin, 2001b; Pereira-Davison and Callan, 2018; Jirsa *et al.*, 2009; Wang *et al.*, 2013). The sharply negative effect of zero light on growth (0 lx) was common to all of these fish species.

Many researchers studied fish behavior in various light conditions. Winslade (1974) proved that the juvenile *Ammodytes marinus* possessed positive phototaxis as well as *Cyprinus carpio* and *Carassius auratus* (Ruchin, 2001a) and the atherin *Leuresthes tenuis* (Reynolds *et al.*, 1977). Meanwhile, Britz and Pienaar (1992) revealed that *Clarias gariepinus* had negative phototaxis. Confer *et al.* (1978), Macy *et al.* (1998), Ryer and Olla (1999) showed that light intensity could influence prey selection and consumption rates. According to Keyler *et al.* (2015), food consumption increases with the light intensity. It means that planktonophagous foraging for food (plankton) is oriented toward illumination. Consequently, differences in illumination stimulate guppies to search for food and increase the juvenile activity. Guppy belongs to planktophagous, so its individuals searching for food focus on the light. Although White *et al.* (2005), did not reveal any peculiarities in food consumption. Jain and Sahai (1994), White *et al.* (2005), Barki *et al.* (2013) also indicated a positive phototaxis of different ages guppies.

#### 4. CONCLUSIONS

The obtained results confirm that the appropriate light intensity is needed for guppies growing. The growth of this juvenile species improves with very high values of illumination in a wide range of illumination from 1500 lx to 11500 lx. However, to save energy resources, the authors recommend lighting up 2000-2500 lx for juveniles growing.

#### 5. REFERENCES

1. Echevarría, G; González N. (2018). Fish taxonomic and functional diversity in mesohabitats of the River Kakada, Caura National Park, Venezuela. *Nature Conservation Research*, 3(2), 21–39. DOI:10.24189/ncr.2018.048
2. Ahmed, T. U; Rabbani, M. K. R; Meher-e-Khuda. (1985). Observation of the larvivorous efficiency of *Poecilia reticulata* (Cyprinodontiformes: Cyprinodontidae). *Bangladesh Journal of Zoology*, 13, 7–12.
3. Fraser, D. F; Gilliam, J. F. (1987). Feeding under predation hazard: response of the guppy and Hart's rivulus from sites with contrasting predation hazard. *Behavioral Ecology and Sociobiology*, 21, 203–209.
4. Abrahams, M. V; Dill, L. M. (1989). A determination of the energetic equivalence of the risk of predation. *Ecology*, 70(4), 999–1007.
5. Morrell, L. J; Croft, D. P; Dyer, J. R. G; Chapman, B. B; Kelley, J. L; Laland, K. N; Krause, J. (2008). Association patterns and foraging behaviour in natural and artificial guppy shoals. *Animal Behaviour*, 76, 855–864.
6. Smith, E. J; Partridge, J. C; Parsons, K. N; White, E. M; Cuthill, I. C; Bennett, A. T. D; Church, S. C. (2002). Ultraviolet vision and mate choice in the guppy (*Poecilia reticulata*). *Behavioral Ecology*, 13(1), 11–19.
7. Sakai, Y; Ohtsuki, H; Kasagi, S; Kawamura, S; Kawata, M. (2016). Effects of light environment during growth on the expression of cone opsin genes and behavioral spectral sensitivities in guppies (*Poecilia reticulata*). *BMC Evolutionary Biology*, 16, 106–115. DOI:10.1186/s12862-016-0679-z
8. Reeve, A. J; Ojanguren, A. F; Deacon, A. E; Shimadzu, H; Ramnarine, I. W; Magurran, A. E. (2014). Interplay of temperature and light influences wild guppy (*Poecilia reticulata*) daily reproductive activity. *Biological Journal of the Linnean Society*, 111, 511–520.
9. Gotanda, K. M; Delaire, L. C; Raeymaekers, J. A. M; Perez-Jvostov, F; Dargent, F; Bentzen, P; Scott, M. E; Fussmann, G. F; Hendry, A. P. (2013). Adding parasites to the guppy-predation story: insights from field surveys. *Oecologia*, 172, 155–166. DOI:10.1007/s00442-012-2485-7
10. Konstantinov, A. S; Vechkanov, V. S; Kuznetsov, V. A; Ruchin, A. B. (2000). Oscillation of abiotic environment are required optimal growth and development of a frog *Rana temporaria* L. *Doklady Akademii Nauk*, 371(4), 559–562.
11. Ruchin, A. B; Vechkanov, V. S; Kuznetsov, V. A. (2005). Influence of photoperiod on growth and intensity of feeding of fry of some fish species. *Hydrobiological Journal*, 41(2), 103–109.

- DOI:10.1615/HydrobJ.v41.i2.80
12. Ruchin, A. B. (2007). Effect of Photoperiod on growth, physiological and hematological indices of juvenile Siberian sturgeon *Acipenser baerii*. *Biology Bulletin*, 34(6), 583–589.  
DOI:10.1134/S1062359007060088
  13. Ruchin, A. B. (2020). Environmental colour impact on the life of lower aquatic vertebrates: development, growth, physiological and biochemical processes. *Reviews in Aquaculture*, 12(1), 310–327.  
DOI:10.1111/raq.12319
  14. Boeuf, G; Le Bail, P-Y. (1999). Does light have an influence on fish growth? *Aquaculture*, 177(1–4), 129–152.  
DOI:10.1016/S0044-8486(99)00074-5
  15. Wang, T; Cheng, Y; Liu, Z; Yan, S; Long, X. (2013). Effects of light intensity on growth, immune response, plasma cortisol and fatty acid composition of juvenile *Epinephelus coioides* reared in artificial seawater. *Aquaculture*, 414–415, 135–139.  
DOI:10.1016/j.aquaculture.2013.08.004
  16. Tian, H. Y; Zhang, D. D; Xu, C; Wang, F; Liu, W. B. (2015). Effects of light intensity on growth, immune responses, antioxidant capability and disease resistance of juvenile blunt snout bream *Megalobrama amblycephala*. *Fish & Shellfish Immunology*, 47(2), 674–680.  
DOI:10.1016/j.fsi.2015.08.022
  17. Ruchin, A. B. (2008). The effects of permanent and variable illumination on the growth, physiological and hematological parameters of the Siberian sturgeon (*Acipenser baerii*) juveniles. *Zoologicheskii Zhurnal*, 87(8), 964–972.
  18. Handeland, S. O; Imsland, A. K; Ebbesson, L. O. E; Nilsen, T. O; Hosfeld, C. D; Baeverfjord, G; Espmark, A; Rosten, T; Skilbrei, O. T; Hansen, T; Gunnarsson, G. S; Breck, O; Stefansson, S. O. (2013). Low light intensity can reduce Atlantic salmon smolt quality. *Aquaculture*, 384–387, 19–24.  
DOI:10.1016/j.aquaculture.2012.12.016
  19. Toledo, J. D; Caberoy, N. B; Quinitio, G. F; Choresca, C. H; Nakagawa, H. (2002). Effects of salinity, aeration, and light intensity on oil globule absorption, feeding incidence, growth, and survival of early-stage grouper *Epinephelus coioides* larvae. *Fisheries Science*, 68, 478–483.
  20. Bădiliță, M; Ardelean, A; Bănățean-Dunea, I; Brudiu, I; Rada, O; Crețescu, I. (2010). Study regarding the light influences on embryo development in carp (*Cyprinus carpio*). *Research Journal of Agricultural Science*, 42(2), 197–200.
  21. Ruchin, A. B. (2016). Effect of light on the development of the hard roe of *Acipenser baerii* Brandt, 1869. *Indian Journal of Science and Technology*, 9(29), 89110.  
DOI:10.17485/ijst/2016/v9i29/89110
  22. Ruchin, A. B. (2018). The effects of illumination on the early development of amphibians (Amphibia: Anura and Caudata). *Periódico Tchê Química*, 15(30), 152–159.
  23. Ruchin, A. B. (2000). The effect of light oscillations on the growth of fish juveniles and the brown frog (*Rana temporaria*). *Zoologicheskii Zhurnal*, 79(11), 1331–1336.
  24. Ruchin, A. B. (2004). Effects of temperature and illumination on growth and development of brown frog larvae (*Rana temporaria*). *Zoologicheskii Zhurnal*, 83(12), 1463–1467.
  25. Kuznetsov, V. A; Ruchin, A. B. (2001). Effect of pH and illumination oscillations on growth rate and development of *Rana ridibunda* larvae. *Zoologicheskii Zhurnal*, 80(10), 1246–1251.
  26. Ruchin, A. B. (2019). Effect of illumination on growth and behavior of two carp fish species (*Carassius gibelio* and *C. carassius*). *Periódico Tchê Química*, 32, 8–17.
  27. Ruchin, A. B. (2001a). Some peculiarities of the fish young growth under light-gradient conditions. *Journal Evolutionary Biochemistry and Physiology*, 37(3), 233–234.  
DOI:10.1023/A:1012635827380
  28. Konstantinov, A. S; Zdanovich, VV. (1993). Some characteristics of the behavior of juvenile fishes in thermogradient field. *Moscow University Biological Sciences Bulletin*, 1, 32–38.
  29. Ruchin, A. B. (2001b). Some specific features of growth and energetic in young carp (*Cyprinus carpio*) under various illumination. *Zoologicheskii Zhurnal*, 80, 433–437.
  30. Trippel, E. A; Neil, S. R. E. (2003). Effects of photoperiod and light intensity on growth and activity of juvenile haddock (*Melanogrammus aeglefinus*). *Aquaculture*, 217, 633–645.
  31. Suzer, C; Saka, Ş; Firat, K. (2006). Effects of illumination on early life development

- and digestive enzyme activities in common pandora *Pagellus erythrinus* L. larvae. *Aquaculture*, 260, 86–93.
32. Pereira-Davison, E; Callan, C. K. (2018). Effects of photoperiod, light intensity, turbidity, and prey density on feed incidence and survival in first feeding yellow tang (*Zebrasoma flavescens*) (Bennett). *Aquaculture Research*, 49(2), 890–899. DOI:10.1111/are.13535
  33. Jirsa, D; Drawbridge, M; Stuart, K. (2009). The Effects of tank color and light intensity on growth, survival, and stress tolerance of white seabass, *Atractoscion nobilis*, larvae. *Journal of the World Aquaculture Society*, 40(5), 702–709. DOI:10.1111/j.1749-7345.2009.00290.x
  34. Winslade, P. (1974). Behavioural studies on the lesser sandeel *Ammodytes marinus* (Raitt). 2. The effect of light intensity on activity. *Journal of Fish Biology*, 6(5), 577–586.
  35. Reynolds, W; Thomson, D; Casterlin, M. (1977). Responses of young California grunion, *Leuresthes tenuis*, to gradients of temperature and light. *Copeia*, 1, 144–149.
  36. Britz, P. J; Pienaar, A. G. (1992). Laboratory experiments on the effect of light and cover on the behaviour and growth of African catfish, *Clarias gariepinus* (Pisces; Clariidae). *Journal of Zoology*, 227(1), 43–62.
  37. Confer, J. L; Howick, G. L; Corzette, M. H; Kramer, S. L; Fitzgibbon, S; Landesberg, R. (1978). Visual predation by planktivores. *Oikos*, 1978, 31, 27–37.
  38. Macy, W. K; Sutherland, S. J; Durbin, E. G. (1998). Effects of zooplankton size, concentration, and light intensity on the feeding behavior of Atlantic mackerel *Scomber scombrus*. *Marine Ecology Progress Series*, 172, 89–100.
  39. Ryer, C. H; Olla, B. L. (1999). Light-induced changes in the prey consumption and behavior of two juvenile planktivorous fish. *Marine Ecology Progress Series*, 181, 41–51.
  40. Keyler, T. D; Hrabik, T. R; Austin, C. L; Gorman, O. T; Mensinger, A. F. (2015). Foraging mechanisms of siscowet lake trout (*Salvelinus namaycush* siscowet) on pelagic prey. *Journal of Great Lakes Research*, 41(4), 1162–1171. DOI:10.1016/j.jglr.2015.09.016
  41. White, E. M; Church, S. C; Willoughby, L. J; Hudson, S. J; Partridge, J. C. (2005). Spectral irradiance and foraging efficiency in the guppy, *Poecilia reticulata*. *Animal Behaviour*, 69, 519–527. DOI:10.1016/j.anbehav.2004.05.011
  42. Jain, V. K; Sahai, S. (1994). Phototactic response of some fishes. *Environment and Ecology*, 12, 123–127.
  43. Barki, A; Zion, B; Shapira, L; Karplusa, I. (2013). The effects of illumination and daily number of collections on fry yields in guppy breeding tanks. *Aquacultural Engineering*, 57, 108–113. DOI:10.1016/j.aquaeng.2013.09.001



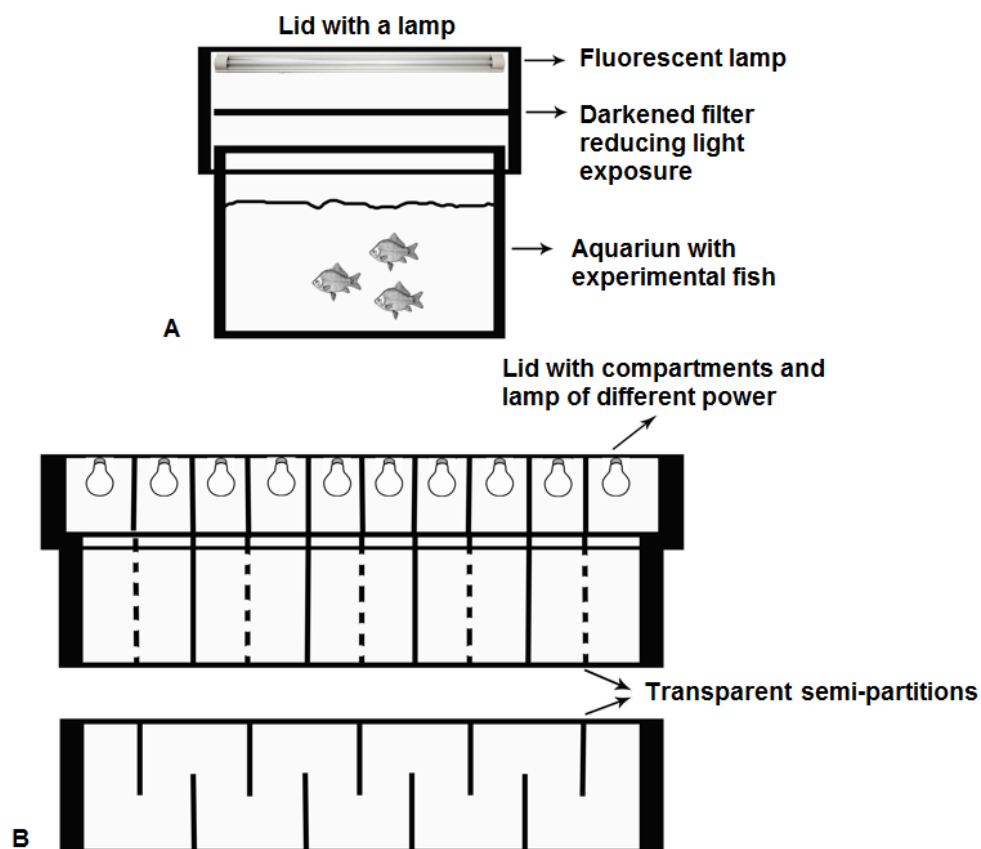


**Figure 1.** The scheme of the experiments: A – the first experiment (there is an aquarium with experimental fish, covered with a lid with a lamp that creates a certain illumination); B – the second experience (Side view and top view; it was described in the text).

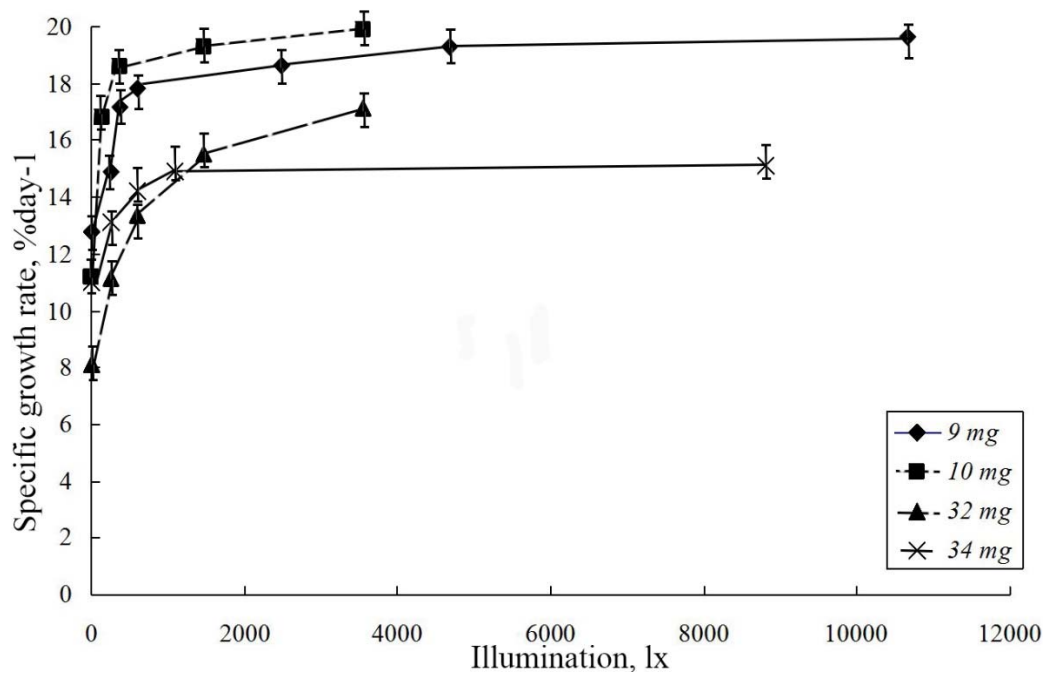


**Figure 2.** Specific growth rate of guppy juveniles with different initial mass at different illumination (in the legend, the figure shows the initial mass of fish before the experiments).

**Table 1.** The frequency of occurrence and the duration of stay of guppy juveniles in various light zones.

| Control          |    |              |              | Experiment       |    |              |              |
|------------------|----|--------------|--------------|------------------|----|--------------|--------------|
| Illumination, lx | n  | $\tau$ , sec | $\Sigma\tau$ | Illumination, lx | n  | $\tau$ , sec | $\Sigma\tau$ |
| 4550             | 13 | 103.8        | 22.5         | 3200             | 5  | 4.8          | 0.4          |
| 4550             | 25 | 10.3         | 4.3          | 3500             | 18 | 9.3          | 2.8          |
| 4550             | 21 | 8.0          | 2.8          | 3800             | 18 | 10.0         | 3.0          |
| 4550             | 18 | 18.7         | 5.6          | 4100             | 13 | 21.2         | 4.6          |
| 4550             | 17 | 20.8         | 5.9          | 4400             | 18 | 24.3         | 7.3          |
| 4550             | 16 | 10.5         | 2.8          | 4700             | 25 | 28.3         | 11.8         |
| 4550             | 14 | 15.0         | 3.5          | 5000             | 23 | 27.6         | 10.6         |
| 4550             | 6  | 21.0         | 2.1          | 5300             | 23 | 27.6         | 10.6         |
| 4550             | 6  | 27.0         | 2.7          | 5600             | 17 | 26.8         | 7.6          |
| 4550             | 4  | 117.0        | 7.8          | 5900             | 5  | 15.6         | 1.3          |

n – the number of swims in the zone per hour;  $\tau$  – the average duration of a one-time stay in the zone, sec;  $\Sigma\tau$  – the total duration of stay in the zone per hour.

**Table 2.** Indicators of the motor activity of young fish in light-gradient conditions (experiment) and under uniform illumination (control) \*

| Parameter   | Experiment | Control |
|---|------------|---------|
| The number of vector displacements (N)                    | 72         | 70      |
| Average distance vector displacement, cm ( $S_v$ )        | 34.0       | 29.6    |
| Total path, m ( $\Sigma S_v \cdot N$ )                    | 24.5       | 20.7    |
| Average duration of vector displacement, sec ( $\tau_v$ ) | 15.4       | 11.8    |
| Travel speed, cm / s ( $S_v / \tau_v$ )                   | 2.2        | 2.5     |
| Total travel time, min                                    | 18.5       | 13.8    |
| Total time of delays in the compartments, min             | 41.5       | 46.2    |

\* - All values were equalized to one hour.

# MONITORAMENTO DA COMPOSIÇÃO QUÍMICA DO RIO IORI

## MONITORING OF THE CHEMICAL COMPOSITION OF IORI RIVER

მდინარე იორის ქიმიური შედგენილობის მონიტორინგი

KUPATADZE, KETEVAN\*

Ilia State University, Faculty of Life science and Medicine, Georgia.

\* Corresponding author

e-mail: ketevan\_kupatadze@iliauni.edu.ge

Received 19 March 2020; received in revised form 20 May 2020; accepted 04 June 2020

### RESUMO

O artigo examina a poluição química do rio Iori, um dos rios mais importantes da Geórgia. Além da Geórgia, este rio é presente no Azerbaijão. O estudo desse rio é crucial, pois a LLC *United Water Supply Company* da Georgia organiza o abastecimento de água das grandes cidades e vilas da Geórgia através da água do Iori. Além disso, a população de duas grandes aldeias usa independentemente a água do rio para várias atividades domésticas: lavagem (lavanderia, produtos, louças), fornecimento de água para animais e irrigação. Não sendo utilizada diretamente como água potável. A água do rio Iori foi monitorada em duas seções: vila Sasadilo e vila Sartichala. No total, foram coletadas 24 amostras ao longo dos anos de 2018 e 2019. Alguma parte da pesquisa foi realizada no local através do instrumento HI83399-02 | Multiparâmetro para água e esgoto (com COD) Fotômetro e medidor de pH. Esses estudos incluíram pH, DBO e a temperatura foi medida diretamente durante a amostragem. O mesmo dispositivo foi usado para medir concentrações aproximadas de metais pesados. Na etapa seguinte do estudo, foi realizada uma pesquisa entre os habitantes para identificar seus conhecimentos sobre questões de limpeza e segurança ambiental. Como resultado do estudo, foi recomendado para a população abster-se ou restringir o uso de água do rio não tratada diretamente nas domesticidades. Os resultados da pesquisa mostraram que a população tem menos informações sobre a probabilidade de reter metais pesados no corpo e desenvolver doenças tumorais.

**Palavras-chave:** *Poluição da água, Contaminantes, Bacia hidrográfica, Produtos químicos tóxicos, pesquisa de habitantes.*

### ABSTRACT

The article examines the chemical pollution of the Iori River, one of the most important rivers in Georgia. In addition to Georgia, this river is found in Azerbaijan. The study of this river is crucial as LLC *United Water Supply Company* of Georgia organizes the water supply of big cities and villages of Georgia through Iori water. Furthermore, the population of two big villages independently uses the river water for various household activities: washing (laundry, products, dishware), livestock watering, and irrigation. They do not use it as drinking water. The water of the Iori River was monitored in two sections: village Sasadilo and village Sartichala. In total, 24 samples were taken over the course of 2018 and 2019 years. Some part of the research was conducted on the site through HI83399-02 | Water & Wastewater Multiparameter (with COD) Photometer and pH meter device. These studies included pH, BOD, and the temperature was measured directly during sampling. The same device was used for measuring approximate concentrations of heavy metals. At the next stage of the study, an inhabitants survey was conducted to identify their knowledge of environmental cleanliness and safety concerns. As a result of the study, our recommendation to the population is to refrain or restrict the use of untreated river water directly in domesticities. The results of the survey showed that the population has less information about the likelihood of getting heavy metals in the body and developing tumor diseases.

**Keywords:** *Water pollution, Contaminants, River basin, Toxic chemicals, inhabitants survey.*

## რეზიუმე

სტატიაში შესწავლილია საქართველოს ერთ-ერთი მნიშვნელოვანი მდინარის იორის ქიმიური დაბინძურების მონიტორინგი. ეს მდინარე საქართველოს გარდა აზერბაიჯანში გვხვდება. მისი კვლევა მნიშვნელოვანია, რადგან იორიდან შპს საქართველოს გაერთიანებული წყალმომარაგების კომპანია, ორგანიზებას უკეთებს დიდი ქალაქებისა და სოფლების მოსახლეობის წყალმომარაგებას. გარდა ამისა, ორი დიდი სოფლის მოსახლეობა დამოუკიდებლად იყენებს მდინარის წყალს სხვადასხვა საოჯახო საქმიანობისთვის: რეცხვისთვის (სარეცხი, პროდუქტი, ჭურჭელი), საქონლის დასარწყულებლად და მოსარწყავად. სასმელ წყლად არ იყენებენ. მდ. იორის წყალზე დაკვირვებას ვაწარმოებდით 2 კვეთზე: ს. სასადილო და ს. სართიჭალა. სულ აღებული იქნა 24 სინჯი, 2018 და 2019 წლის განმავლობაში. კვლევის ნაწილი შესრულდა ადგილზე HI83399-02 | წყლის და ჩამდინარე წყლების მულტიპარამეტრული ფოტომეტრული საზომი აპარატით და pH საზომით. ეს კვლევები იყო pH, ჟანგბადის ბიოლოგიური მოხმარება, ტემპერატურა უშუალოდ სინჯების აღების დროს გაიზომა. ამავე აპარატით გაიზომა მძიმე მეტალების სავარაუდო კონცენტრაციები. კვლევის შემდეგ ეტაპზე ჩატარდა მოსახლეობის გამოკითხვა, რომლის მიზანიც იყო გამოვლენილიყო მათი ცოდნა გარემოს სისუფთავის და სახფრთხეების შესახებ. კვლევის შედეგად, მოსახლეობისადმი ჩვენი რეკომენდაციაა, რომ გაწმენდის გარეშე თავი შეიკავონ ან შეზღუდონ მდინარის წყლის გამოყენება უშუალოდ ოჯახის საქმეებში. გამოკითხვის შედეგებმა აჩვენეს, რომ მოსახლეობას ნაკლები ინფორმაცია აქვს მძიმე მეტალების ორგანიზმში მოხვედრასა და სიმსივნური დაავადებების წარმოქმნის ალბათობის შესახებ.

**საკვანძო სიტყვები:** წყლის დაბინძურება, დამაბინძურებლები, მდინარის აუზი, მომწამლავი აგენტები, მაცხოვრებელთა გამოკითხვა.

## 1. INTRODUCTION:

Recent developments have made it clear that human health, the stability of the country, and the stability of the world may be threatened by various epidemics. The cleanliness of water resources is of particular importance in terms of the spread of various poisonous contaminants. Even if a disease-causing agent is transmitted by airborne droplets, frequent hand washing is recommended according to the recommendations issued by the World Health Organization, 2017. Moreover, for this, clean water is needed (Matthew, Freeman, 2017; Sharma, Bhattacharya, 2017; Daughton, 2004).

Added to this is the growing shortage of freshwater on the planet. Increased demand for global water threatens biodiversity and water supply for food production, other vital human needs. Water scarcity already exists in many regions of the world, with more than one million people left without drinking water (Lomsadze, Makharadze, 2016; Sammons, Maceina, 2009; Danyer, Arda, 2018). Also, 90% of infectious diseases in developing countries are transmitted by water, because in some cases, contaminated water is used for drinking and washing. Sometimes the problem is that people do not have complete information about the dangers of polluted water and they use it.

Consequently, the cleanliness and monitoring of the country's surface waters, i.e., rivers and lakes, take on enormous importance. Especially if the river water is used by inhabitants (Kupatadze, Kiziloz, 2019; Kupatadze, 2018; Abhijit, Ranju, 2012).

Georgia is rich in rivers and lakes, the water of which is used by the population to drink, prepare food, wash products, do housework, and irrigate. See the list of the main rivers of Georgia in Table 1.

This time, the purpose of our research was to study the chemical composition and the degree of water pollution in the Iori River.

Currently, LLC United Water Supply Company of Georgia (<http://water.gov.ge/eng/>) operates all over the area of Alazani and Iori, organizing water supply for large cities and villages.

Surface and underground waters are used for water supply. However, their quantity is not enough for the population today. Therefore, in near-by medium-sized villages, water obtained directly from the river, the so-called Rural Water, though not for drinking, is used for all the rest needs. It is used for washing dishes, fruits, vegetables, and other food products, as well as for irrigation.

For this very reason, monitoring of the degree of pollution is essential.

**Iori** (Fig.1) is the river flowing in Georgia and Azerbaijani. It originates on the southern slope of the Caucasus, near the peak Borbalo, at an altitude of 2600 m above sea level. In the upstream, it flows into the gorge, in the middle, it crosses the Samgori Cave, ultimately joining the Mingachevir reservoir. In the past, Iori used to join the Alazani River on the right side. It is fed from snow and rain waters. Iori has South-East direction. In the beginning, Iori Valley has the shape of a narrow and deep mountain valley, then it passes into Tianeti Valley, with two tributaries flowing into it, ending in the Zion Valley, where the Sioni Reservoir is located. Iori River divides Iori Plateau into two parts: Iori-Alazani and Iori-Mtkvari. On the left bank of the Iori River, humus-sulfate, and saline soils are widespread (Pistric, Klaus, 1989; William, David, 1971).

There is a regulating Sioni Reservoir constructed on the Iori River. Tbilisi Reservoir or "Tbilisi Sea" was formed by Iori water. Dali Mountain Reservoir is constructed in the downstream of the Iori River, with a water volume of 140.0 km<sup>3</sup>. More than 90 thousand hectares are irrigated by the Iori River on the Iori plateau. Several irrigation systems have been built on the river, central of which are the upper and lower water mains.



**Figure 1.** Iori river

## 2. MATERIALS AND METHODS:

The water of the Iori River was monitored at 2 sections: village Sasadilo and village Sartichala. In total, 24 samples were taken over the course of 2018 and 2019 years. Some part of the research was conducted on the site through HI83399-02 Water & Wastewater Multiparameter (with COD) Photometer and pH meter device. These studies included pH, BOD, and the temperature was measured directly during

sampling. The same device with special analytical reagents (HI-93746-03, HR-HI-93709-01HR, HI-93721-01, HI-93731-01, HI-93737-03) was used for measuring approximate concentrations of heavy metals (Pb, Mn, Fe, Zn, Cu).

It is very convenient to use the above-mentioned equipment to do the analysis directly from the source of research material (directly from the river in our case). This photometer features an innovative optical system that uses LEDs, narrow band interference filters, focusing lens, and both a silicon photodetector for absorbance measurement and a reference detector to maintain a consistent light source ensures accurate and repeatable photometric readings every time. Selecting the pH measurement mode allows for the photometer to be used as a professional pH meter with many features, including temperature compensated measurements, automatic two-point calibration.

Analysis for defining the ammonium nitrogen were also performed with HI83399-02 | Water & Wastewater Multiparameter using appropriate reagents. Analysis of total alkalinity and acidity, cations, and anions were performed in the laboratory of Ilia State University. Their protocols are based on the methodology of analytical chemistry, mainly on qualitative (colorimetric) and quantitative analysis (titrimetric).

Alkalinity is a measure of a river's "buffering capacity" or its ability to neutralize acids. Alkaline compounds in the water, such as bicarbonates, carbonates, and hydroxides, remove H<sup>+</sup> ions and lower the acidity of the water (which means increased pH). This is usually done by combining with the H<sup>+</sup> ions to make new compounds. Without this acid-neutralizing capacity, any acid added to a river would cause an immediate change in the pH. Measuring alkalinity is important to determine a river's ability to neutralize acidic pollution (as measured by pH) from rainfall or snowmelt. It's one of the best measures of the sensitivity of the river to acid inputs. Alkalinity comes from rocks and soils, salts, certain plant activities, and certain industrial wastewater discharges. The result is reported as milligrams per liter (mg/l) of calcium carbonate.

Acidity is the quantitative expression of water's capacity to neutralize a strong base to a designated pH and an indicator of how corrosive water is. Acidity can be caused by weak organic acids, such as acetic and tannic acids, and strong mineral acids, including sulfuric and hydrochloric acids; however, the most common source of acidity in unpolluted water is carbon dioxide in the

form of carbonic acid. Standard Methods for the Examination of Water and Wastewater (Standard Methods) recommends titration with sodium hydroxide to an endpoint pH of 3.7 to determine mineral acidity. Titrate to pH 8.3 to determine total acidity (Bhatia, 2013; Lopes, 2017; VanLoon, 2011; Sutton, 2008; Rawn, 2004).

In general, the existence of an ecologically educated population is vital (Lui, 2009; Cross, 2007; Henjum, Barikkmo, 2010). Therefore, in parallel with sampling and analysis, we conducted the inhabitant survey. See the questions in Table 2.

### 3. RESULTS AND DISCUSSION:

In general, the oxygen content in the samples taken was satisfactory. BOD varied within 0.64 – 1.83 mg/l. The nitrogen content of ammonium ranged from 0.016 to 1.672 mg N/l and exceeded the maximum allowable value in five samples. Its average annual concentration was 0.348 mg N/l. The maximum value of 1.672 mg N/l (4.3 maximum allowable concentration (MAC) was observed in January 2019). Mineralization ranged from 203.34–429.65 mg/l. The maximum value 429.65 mg/l was registered in Sartichala. The maximum concentrations of iron and manganese in just one sample exceeded the allowable value. Iron levels ranged from 0.0455 to 4.1684 mg/l. Its average annual concentration amounted to 0.8106 mg/l (2.1 MAC). The maximum value 4.1684 mg/l (13.9 MAC) was registered in September of 2019 by village Sartichala.

It should also be noted that iron (II) compounds are mainly found in groundwater. They are found in water as a result of iron-containing rocks washed out by acids. These acids may be carbonic dioxide or humic acid.

Iron (III) compounds are present in surface waters, however, not in large quantities. They are formed by hydrolysis of salts. Iron ions in water are mainly composed of complexes formed with humic acid, and such water is slightly brown if the content of iron ions exceeds 0.3 mg/l, the water tastes of iron.

The manganese content ranged from 0.0032–0.5974 mg/l. Its average annual concentration amounted 0.1057 mg/l (1.1 MAC). The maximum value of 0.5974 mg / l (6.0 MAC) was observed in September 2019. Concentrations of nitrite and nitrate nitrogen, phosphates, sulfates, chlorides, lead zinc, and copper did not exceed the maximum allowable concentrations.

A total of 12 samples were taken from the lori River, in Sartichala village (Table 3). The oxygen content was satisfactory. BOD varied within 0.64–1.83 mg/l. The nitrogen content of ammonium ranged from 0.047 to 1.672 mg N/l. Its average annual concentration reached 0.445 mg N/l (1.1 MAC). The maximum value of 1.672 mg N/l (4.3 MAC) was observed in January. Mineralization ranged from 231.01–429.65 mg/l. The maximum value was 429.65 mg/l in May. Iron content ranged from 0.0901–4.1684 mg/l. Its average annual concentration was 1.4976 mg/l (5.0 MAC). The maximum value of 4.1684 mg/l (14 MAC) was observed in September. The manganese content ranged from 0.0086–0.5974 mg/l. Its average annual concentration was 0.2068 mg/l (2.1 MAC). The maximum value of 0.5974 mg/l (6.0 MAC) was observed in September. Concentrations of nitrite and nitrate nitrogen, phosphates, sulfates, chlorides, lead, zinc, and copper did not exceed the maximum allowable concentrations.

In total, 12 samples were taken from the lori River in Sasadilo village (Table 4). The oxygen content was satisfactory. BOD varied within 0.72–1.51 mg/l. The nitrogen content of ammonium ranged from 0.016 to 0.505 mg N/l. Its average annual concentration was 0.250 mg N/l. The maximum value of 0.505 mg N / l (1.3 MAC) was observed in March, and it exceeded the limit only once. Mineralization ranged within 203.34–332.32 mg/l. The maximum value was 332.32 mg / l in May. Concentrations of nitrite and nitrate nitrogen, phosphates, sulfates, chlorides, iron, lead, zinc, copper, and manganese did not exceed the maximum allowable concentrations.

As can be seen from the data, heavy metals are present in the water, albeit within the permissible norm.

According to the study (Kiziloz, 2018; Kupatadze, Kiziloz, 2019), the possible impact of heavy metals on human health can be calculated by using equation (1).

$$ADIW_{ing} = C \times IR \times EF \times ED / BW \times AT \quad (Eq.1)$$

Where,  $ADIW_{ing}$  is the average daily intake of heavy metals ingested from water (mg/kg-day),  $C$  is the heavy metal concentration in water (µg/L).  $IR$  is the daily intake of water, approx. 2l/day.  $ED$  is the exposure duration, approx. 80 years.  $EF$  is the exposure frequency, 365 days/year.  $AT$  is the period over which the dose is averaged,  $365 \times 80 = 29.200$  days.  $BW$  is the bodyweight of the exposed individual (75kg approx.).

At the same time, by Equation 2, e.g., "Hazard quotient" (HQ) can also be calculated.

$$HQ=ADI/RfD \quad (Eq.2)$$

Were, ADI is the value obtained from the previous equation. RfD is chronic reference dose values are generally calculated.

For the studied water samples, the values calculated through Equation 1 and 2 are given in Tables 5 and 6.

**Table 5.** ADIW and HQ values for some hazardous metals in lori water Sasadilo

| Ions of heavy metals | ADIWing |       | HQ     |        |
|----------------------|---------|-------|--------|--------|
|                      | 2018    | 2019  | 2018   | 2019   |
| Pb                   | 34.66   | 57.1  | 3.46   | 5.71   |
| Mn                   | 15.024  | 15.93 | 0.3004 | 0.3186 |
| Fe                   | 107.8   | 111.1 | 539    | 555.7  |
| Zn                   | 26.66   | 27.2  | 26.66  | 27.2   |
| Cu                   | 320     | 293   | 3.2    | 2.93   |

**Table 6.** ADIW and HQ values for some hazardous metals in lori water Sartichala

| Ions of heavy metals | ADIWing |       | HQ     |        |
|----------------------|---------|-------|--------|--------|
|                      | 2018    | 2019  | 2018   | 2019   |
| Pb                   | 34,6    | 74.6  | 3.46   | 7.46   |
| Mn                   | 14.17   | 15.93 | 0.2834 | 0.3186 |
| Fe                   | 107.7   | 111,1 | 538    | 555.7  |
| Zn                   | 26.66   | 27.2  | 26.66  | 27.2   |
| Cu                   | 293     | 373   | 2.93   | 3.73   |

### Inhabitant survey

At the second stage of the study, we conducted the inhabitant survey, wondering what they knew about water intake rules and clean water, what information they had about water-borne diseases, or the likelihood of causing such an incurable disease as a malignant tumor. According to the Statistics Office of Georgia, 8731 cases were registered in Georgia in 2018 and 10402 new cases - in 2019.

The results of the survey were included in

Table 7.

The survey clearly showed that the population of Sasadilo and Sartichala villages have little idea that the use of water contaminated by heavy metals, even for irrigation or washing, is linked to the development of malignant tumors.

They are more or less aware of the importance of drinking water and the daily norm of water intake. Only 20% know that water containing chlorine ions cannot be boiled twice. That is, if the water is boiled once to make tea or other hot beverages, the residual water should not be boiled again, because chlorine ions form carcinogen with chromium, which is likely to be present in water, and may trigger cancer in the body over the years.

If the water contains chlorine or the chlorine is used for water disinfection, can it still be boiled for hot drinks after boiling.

### 4. CONCLUSIONS:

Thus, the chemical composition of the water of lori River was monitored in two villages.

The study showed that the main contaminants are: ammonium nitrogen, heavy metals. They do not go far beyond the standard. However, according to the values obtained through the relevant formula, the use of such untreated water in household activities is not recommended.

Also, the overall acidity, alkalinity, and mineralization range within the expected conditions.

Our recommendation to the population is: not to drink water (so-called rural water) entering the yards directly from the river without filtration.

The inhabitants survey showed that the population still needs a lot of educational work to make each of them environmentally educated.

### 5. REFERENCES:

1. Matthew, C., Freeman, J. & Gloria, D. (2017). The impact of sanitation on infectious disease and nutritional status: A systematic review and meta-analysis. *International Journal of Hygiene and Environmental Health*, 6, 928-949.
2. Sharma, S. & Bhattacharya, A. (2017).



- Drinking water contamination and treatment techniques. *Appl Water Science*, 7, 1043–1067.
3. Daughton, Ch. (2004). Review of hazardous agents. *Environmental Impact Assessment Review*, 7, 711-732.
  4. Lomsadze, Z., Makharadze, K. & Pirtskhalava, K. (2016). The ecological problems of rivers of Georgia (the Caspian sea basin). *Annals of Agrarian Science*, 3, 110-119.
  5. Sammons, M. & Maceina, M. (2009). Effects of river flows on growth of redbreast sunfish *Lepomis auritus* (Centrarchidae) in Georgia rivers. *Fish Biology*, 7, 1580-1593.
  6. Danyer, E., Ufuk, E. & Dede, A. (2018). Stranding records of *Mediterranean monk seal* *Monachus monachus* (Hermann, 1779) on the Aegean and Mediterranean Sea coasts of Turkey between 2012 and 2018. *Journal of the black sea Mediterranean Environment*, 2, 128-139.
  7. Kupatadze, K. & Kiziloz, B. (2019). Researching some of the parameters of Kura ("Mtkvari") river in two neighboring countries- Georgia and Turkey, in terms of environmental chemistry. *Periódico Tchê Química*, 31, 450-457.  
<http://www.deboni.he.com.br/Periodico31.pdf>
  8. Kupatadze, K. (2018). Study of Alazani river and surface water composition in some villages of Kakheti region of Georgia. *Southern Brazilian Journal of Chemistry*, 26, 26-33.  
<http://www.deboni.he.com.br/sbjchem/jornal/2018.pdf>
  9. Abhijit, M. & Ranju, C. (2012). General concentrations of some heavy metals in rivers. *Environmental Monitoring, and Assessment*, 23, 4-12.
  10. Pistrick, K. (1989). Collecting plant-genetic resources in the Georgian SSR, 1988 (Kachetia). *Vegetos*, 37, 177-192.
  11. William, A. & David, E. (1971). A History of the Georgian people in the nineteenth century. *Routledge & Kegan Paul*.
  12. Bhatia, S. (2013). "Environmental Chemistry". *CBS Publishers and Distributors Pvt. Ltd.*
  13. Lopes, V. (2017). Water purification, *Journal Tchê Química*. 27:139-146.
  14. VanLoon, G. (2011). "Environmental Chemistry-a global perspective", *Oxford Group*.
  15. Sutton, R. (2008 ). "Chemistry for the Life Sciences", *Taylor&Francis Group*.
  16. Rawn, J. (2004). "General Chemistry", *Wm. C. Brown Publishers, Oxford, England*.
  17. Liu, H. (2009). Study of Epidemiological health. *J. of Public Health*, 31, 32–38.
  18. Cross, F. (2007). Contemporary health physics and solutions. *Health Physics*, 2, 23-34.
  19. Henjum, S. (2010). Endemic goiter and excessive iodine in drinking water. *Public Health Nutrition*, 9, 1472-1477.
  20. Kupatadze, K. & Kiziloz, B. (2016). Natural treatment systems from the point of didactics. *Periódico Tchê Química*, , 24, 69-74.  
<http://www.deboni.he.com.br/Periodico26.pdf>
  21. Kiziloz, B. (2018). Investigation of some hazardous agents and trace elements in drinking water of Kocaeli region. *Periódico Tchê Química*, 26, 44-49.



**Table 1.** River of Georgia

| Rivers        | Length of river, km  | Space of water collecting basin, km |
|---------------|--|-------------------------------------|
| Alazani       | 366/362 (The total length of river/ length on Georgian territory)  | 1180                                |
| Mtkvari       | 1515/351 (The total length of river/ length on Georgian territory) | 188000                              |
| Iori          | 320  | 4650                                |
| Ktsia-Khrami  | 205/201 (The total length of river/ length on Georgian territory)  | 8340                                |
| Algeti        | 118  | 763                                 |
| DidiLiakhvi   | 98   | 2440                                |
| Ksani         | 84   | 885                                 |
| Faravani      | 74   | 2350                                |
| Aragvi        | 66   | 2740                                |
| Mashavera     | 66   | 1300                                |
| PataraLiakhvi | 63   | 513                                 |
| tethami       | 51   | 404                                 |

**Table 2.** Survey questions

| Questions  |
|--|
| Do you think water is important for health?  |
| How much water should we get during a day  |
| If the water contains chlorine or is disinfected with chlorine, can it still be boiled for hot drinks after boiling? |
| What's the connection is between heavy metals in water and the probability of getting cancer?                        |

**Table 3.** The Results from Sartichala village

| Sartichala                            | Unit | Stan dard | 2018   |        | 2019   |        |
|---------------------------------------|------|-----------|--------|--------|--------|--------|
|                                       |      |           | Max    | Min    | Max    | Min    |
| BOD                                   |      |           | 1.930  | 0.78   | 1.730  | 0.69   |
| pH                                    | -    | 6-9       | 6.2    | 7.4    | 7.1    | 6.32   |
| mineralizati on                       | Mg/l |           | 429.65 | 231.01 | 412.00 | 215.9  |
| Fe                                    | mg/L | 0.2       | 4.0423 | 0.0455 | 4.1684 | 0.0901 |
| Mn                                    | µg/L | 50        | 0.5314 | 0.0042 | 0.5974 | 0.0086 |
| Ammonia Nitrogen (NH <sub>3</sub> -N) | mg/L | 0.2       | 1.672  | 0.047  | 1.668  | 0.045  |
| Cu                                    | mg/L | 100       | 11     | 1,7    | 14     | 1.567  |
| Zn                                    | mg/L | 1         | 1      | 0.01   | 1,02   | 0,07   |
| Pb                                    | µg/L | 10        | 1.3    | 0.43   | 2.8    | 1.04   |
| Alkalinity                            | mg/L | <200      | 3,46   | 2,31   | 3,05   | 1,86   |
| Acidity                               | mg/L | <300      | 0,5    | 0,32   | 0,73   | 0,22   |
| Cl                                    | mg/L | 250       | 3.0    | 5.7    | 3.8    | 11.9   |

**Table 4.** The Results from Sasadilo village

| Sasadilo                              | Unit | Standart | 2018   |        | 2019   |        |
|---------------------------------------|------|----------|--------|--------|--------|--------|
|                                       |      |          | Max    | Min    | Max    | Min    |
| BOD                                   |      |          | 1.830  | 0.64   | 1.810  | 0.58   |
| pH                                    | -    | 6-9      | 6-9    | 7.8    | 7.9    | 6.1    |
| mineralization                        | Mg/l |          | 332.32 | 203.34 | 342.01 | 198.1  |
|                                       |      |          |        |        |        |        |
|                                       |      |          |        |        |        |        |
| Ammonia Nitrogen (NH <sub>3</sub> -N) | mg/L | 0.2      | 1.672  | 0.047  | 1.668  | 0.045  |
| Fe                                    | mg/L | 0.2      | 4.0423 | 0.0455 | 4.1684 | 0.0338 |
| Mn                                    | µg/L | 50       | 0.5634 | 0.0032 | 0.5974 | 0.123  |
| Cu                                    | mg/L | 100      | 12     | 0      | 11     | 0.5974 |
| Zn                                    | mg/L | 1        | 1      | 0.01   | 1      | 0,01   |
| Pb                                    | mg/L | 10       | 2.3    | 0.5    | 2      | 0.34   |
| Alkalinity                            | mg/L | <200     | 3,85   | 2,01   | 3,5    | 1,97   |
| Acidity                               | mg/L | <300     | 0,7    | 0,54   | 0,67   | 0,53   |
| Cl                                    | mg/L | 250      | 5.0    | 4.0    | 23.8   | 15.9   |

**Table 7.** The survey results

| Questions  | Answers                 |                |                       |
|--|-------------------------|----------------|-----------------------|
|  | yes                     | No             | No idea               |
| In your opinion water is important for the health?   | 96%                     | 2%             | 2%                    |
| If the water contains chlorine or disinfected with chlorine, can it still be boiled for the second time after boiling? | 20%                     | 80%            | ---                   |
|  | <b>2 liter</b>          | <b>1 liter</b> | <b>It's up to you</b> |
| How much water should we drink during the day  | 89%                     | 5%             | 4%                    |
|  | <b>Can cause cancer</b> | No lincage     | No idea               |
| What is the connection between heavy metals in water and the likelihood of cancer                                      | 25%                     | 35%            | 30 %                  |

**IMPLEMENTAÇÃO DA PROTOTIPAGEM RÁPIDA NA RESOLUÇÃO DE PROBLEMAS APLICADOS NA PRODUÇÃO****INTRODUCTION OF RAPID PROTOTYPING IN SOLVING APPLIED PROBLEMS IN PRODUCTION****ВНЕДРЕНИЕ БЫСТРОГО ПРОТОТИПИРОВАНИЯ ПРИ РЕШЕНИИ ПРИКЛАДНЫХ ЗАДАЧ НА ПРОИЗВОДСТВЕ**

BRYKIN, Veniamin A.<sup>1\*</sup>; VOROSHILIN, Anton P.<sup>2</sup>; RIPETSKIY, Andrey V.<sup>3</sup>; UHOV, Petr A.<sup>4</sup>;

<sup>1</sup> Moscow Aviation Institute (National Research University), Institute of General Engineering Training, Research Department NIO-9, 4 Volokolamskoe shosse, zip code 125993, Moscow – Russian Federation

<sup>2,4</sup> Moscow Aviation Institute (National Research University), Institute No. 12 “Aerospace Science-Based Technologies and Production”, Department of Testing Technology and Operation, 4 Volokolamskoe shosse, zip code 125993, Moscow – Russian Federation

<sup>3</sup> Moscow Aviation Institute (National Research University), Department of Engineering Graphics, 4 Volokolamskoe shosse, zip code 125993, Moscow – Russian Federation

\* Correspondence author  
e-mail: benbrykin@gmail.com

Received 02 March 2020; received in revised form 22 May 2020; accepted 04 July 2020

**RESUMO**

Todas as linhas e máquinas transportadoras devem funcionar sem problemas durante a produção para lançamento dos produtos oportuno. Existem peças e componentes, cuja falha leva à falha de toda a transportadora. É o tempo de entrega e as perdas financeiras devido ao tempo de inatividade do equipamento que tornam relevante o problema de reprodução rápida da peça para substituir a original. Neste artigo, consideramos o processo de criação de uma peça de teste usando a tecnologia de fusão seletiva a laser (SLS). Nesse caso, a eficiência econômica da produção de produtos depende diretamente da solução eficaz e correta dos problemas de preparação tecnológica da produção aditiva. A amostra impressa foi testada em contato direto com o meio aquoso por 500 horas. Os testes de fadiga foram realizados utilizando 40% de pó primário e 60% de pó secundário. Para a avaliação quantitativa das propriedades do material com uma dada geometria, foi realizada uma série de testes de ruptura dos produtos da peça. Para identificar a melhor proporção de resistência, elasticidade e custo de fabricação, nos testes foram apresentadas as amostras com diferentes porcentagens de pó. Observou-se que o custo de fabricação de peças, ferramentas e acessórios de reposição usando a impressão 3D depende de muitos fatores. Os principais fatores de influência foram a geometria dos produtos, que determina seu volume, bem como a densidade de sua disposição na câmara. A experiência acumulada e a análise dos critérios nos permitiram oferecer várias opções de layout que podem levar ao máximo efeito econômico.

**Palavras-chave:** *engenharia reversa, retentor, digitalização 3D, layout automático.*

**ABSTRACT**

All conveyor lines and machines should work smoothly in order to ensure a well-timed production during production. There are parts and nodes, the failure of which leads to the failure of the entire conveyor. It is the delivery time and financial losses due to equipment downtime that make the problem of quick reproduction of the relevant part to replace the original one. In this work, the process of creating a test piece using selective laser fusion (SLS) technology was considered. In this case, the economic efficiency of the fabrication of products depends directly on the effective and correct solution to the problems of technological preparation of additive production. The printed model was tested in direct contact with water for 500 hours. Fatigue tests were performed using 40% primary and 60% secondary powder ratios. To quantify the properties of the material for given geometry, a series of tensile testing of products was carried out. To identify the best ratio of strength, elasticity, and manufacturing cost for testing, samples were offered with different percentages of powder. It was noted that the cost of manufacturing spare parts, tools, and accessories (SPA) using 3D printing depends on many

factors. The product geometry determines their volume, and the density of their arrangement in the chamber was recognized as a crucial impact factor. The accumulated experience and analysis of the criteria allowed us to offer several layout options that can lead to a maximum economic effect.

**Keywords:** *reverse engineering, fixator, 3D scanning, automatic layout.*

## АННОТАЦИЯ

Все конвейерные линии и станки должны работать бесперебойно во время производства для обеспечения своевременного выпуска продукции. Существуют детали и узлы, поломка которых приводит к выходу из строя всего конвейера. Именно сроки поставки и финансовые потери из-за простоя оборудования делают актуальным вопрос быстрого воспроизводства детали для замены оригинальной. В данной работе рассмотрен процесс создания тестовой заготовки по технологии выборочного лазерного сплавления (SLS). В данном случае экономическая эффективность производства изделий зависит напрямую от эффективного и корректного решения задач технологической подготовки аддитивного производства. Напечатанный образец тестировался в непосредственном контакте с водной средой в течении 500 часов. Испытания на усталость проводились с использованием 40% первичного и 60% вторичного соотношения порошка. Для количественной оценки свойств материала при заданной геометрии был проведен ряд испытаний изделий-заготовок на разрыв. Для выявления наилучшего соотношения по прочности, эластичности и стоимости изготовления на испытания были представлены образцы с разным процентным соотношением порошка. Было отмечено, что стоимость изготовления запасных частей, инструментов и принадлежностей (ЗИП) с помощью 3D-печати зависит от множества факторов. Ключевыми факторами влияния были признаны геометрия изделий, определяющая их объем, а также плотность компоновки их в камере. Нарботанный опыт и анализ критериев позволил предложить несколько вариантов компоновок, которые способны привести к максимальному экономическому эффекту.

**Ключевые слова:** *реверс-инжиниринг, фиксатор, 3D сканирование, автоматическая компоновка.*

## 1. INTRODUCTION

Many works have been devoted to the development and modeling of complex composite structures from anisotropic materials (Babaytsev *et al.*, 2017; Koshoridze *et al.*, 2017; Babaytsev, and Zotov, 2019; Babaytsev *et al.*, 2019). Mainly, one of the options for obtaining such structures is 3D printing (Nazarov, 2011; Boytsov *et al.*, 2011; Atzeni and Salmi, 2012; Mellor *et al.*, 2014; Bepalov *et al.*, 2019; Kuzovkin and Suvorov, 2014; Piller *et al.*, 2015; Anamova *et al.*, 2016; Ripetskiy *et al.*, 2016; Babaytsev *et al.*, 2017; Rabinskiy *et al.*, 2017; Ripetskiy *et al.*, 2018; Kuprikov *et al.*, 2019). The area of use of such products is too vast. For example, to ensure the timely manufacture of products, the operation of all conveyor lines and machines should run smoothly. Failure per under such conditions may not be dangerous, provided that spare parts, tools, and accessories are available (SPA) (Bhutani *et al.*, 2017; Böckin and Tillman, 2019; Kolotyryn *et al.*, 2019; Westerweel *et al.*, 2019; Pellens *et al.*, 2020). However, there are parts and components, the failure of which leads to failure of the entire conveyor (Boboc *et al.*, 2019; Zhang, 2019). In the conditions of reality of Russian industrial enterprises to supply spare parts (including ones

of foreign manufacture) is difficult and to predict when the break occurs is not always possible. Therefore, with a slight breakdown, the entire production line can stop (Zhang and Chang, 2011; Yumashev *et al.*, 2019; Bulavin *et al.*, 2018).

Using the example of individual elements of the conveyor, it can be considered the reverse engineering cycle, timing of reproduction, and economic effect compared with the original part. The fixator (Figure 1) is a part of the conveyor for moving workpieces. This part is a knowingly weak link of the machine and most frequently fails. At the same time, it is impossible to predict how long the original part will last. The reason for this includes several factors:

1. The part works in constant contact with workpieces, due to which there is wear at the points of contact.
2. The occurrence of a defective workpiece can ruin the part and damage it.
3. Failure of automatic workpiece feed mode and also disables the part.
4. This part is knowingly weak link to prevent a chain reaction of breakdowns on the conveyor – when the fixator fails, and the workpieces are not transferred further along the

line.

The cost of the original part “fixator” is over 800 units, and the delivery time takes about 1.5 weeks. It is delivery times and financial losses due to equipment downtime that make the issue of quick reproduction of parts relevant for replacing the original ones (Song and Zhang, 2016; Alekseev *et al.*, 2019; Sobczak-Kupiec *et al.*, 2012; Sobczak-Kupiec *et al.*, 2018). The cycle, including 3D scanning, 3D printing using SLS technology, processing, and delivery, takes from 2 to 4 days (Georgios Tsoutsos *et al.*, 2017; Kim, 2019; Tashi *et al.*, 2019; Skvortsov *et al.*, 2012). Depending on the volume and arrangement of the chamber parts and the proportions of the powder used, the benefit can be 50 to 60%. Going through reverse engineering, revision, and printing cycle is becoming preferable for enterprises than waiting for the original spare part (Revilla-León *et al.*, 2018; Sevryukova *et al.*, 2012; Revilla-León *et al.*, 2019; Koltunov *et al.*, 2018; Revilla-León *et al.*, 2020).

## 2. MATERIALS AND METHODS

In this article, the process of creating a test piece using selective laser fusion (SLS) technology was considered. In this case, the economic efficiency of manufacturing the products depends directly on the effective and correct solution to the problems of technological preparation of additive production. The most powerful influence on the result is exerted by the task of the technical layout of products in the construction chamber — the search for a layout solution.

To obtain high-quality electronic models for real products, three-dimensional scanning equipment was used – the FARO Arm EDGE coordinate measurement machine (CMM) and the Kreon ZEPHYR KZ25 laser nozzle. The working area of the CMM is 1800 mm, which is sufficient to obtain electronic models of any spare parts and elements of the conveyor belt line. The Kreon ZEPHYR KZ25 non-contact laser scanner has the technical characteristics presented in Table 1. The use of such mobile CMMs and easily removable nozzles (non-contact laser scanners) calls for their use in close proximity to the production site, which helps to quickly obtain the desired product. The electronic models obtained from the measurement results were put into production.

The arrangement of products is made according to some limiting criteria (Ripetskiy *et al.*, 2016). The experience obtained during the work

with the installation of selective laser sintering EOSINT P 395, allowed to highlight the most important of them:

- the indent from walls of the build chamber to the nearest part should be at least 15 mm;
- the distance between any two points on the surface of two different parts should not exceed 6 mm;
- in order to maintain the homogeneous structure and, as a result, the same strength characteristics, all products, in the beginning, should be oriented identically with respect to the growing direction (vectors perpendicular to the layers of future products should be collinear).

The key parameters that affect cost of the product at the stage of assembly are:

- layout height;
- layout density, determined from the volume of parts placed at the beginning of a given height;
- time spent on choosing the optimal layout solution;

It is important to note that an attempt to increase density of layout and neglect the criteria reduces the reliability of the launch and can lead to spoilage of products, and even to failure of the installation of SLS-printing (Willmann, 2019). Figure 2 displays a horizontal arrangement of the components in manual mode, this layout has height of construction 32 mm and can accommodate 18 parts. The horizontal arrangement allows us to use less material along the height of chamber, but the percentage of unused material is quite high. To calculate the cost of printing, it is should be considered the following indicators:

- assembly height – 26.63 mm;
- placement density – 14.22%;
- use of platform volume – 0.61%;
- volume of parts – 437.834 cm<sup>3</sup>;
- number of parts – 18 pcs.

To achieve the optimal value, it is necessary to increase the number of parts, while reducing the density of placement, taking into account the layout criteria listed above. Subject to the above parameters, taking into account the manual arrangement of parts in chamber, the probability of operator error is high, while the time cost is significantly increased. The best solution

would be to use automatic layout. Figure 3 illustrates realization of automatic layout of fixators in vertical arrangement. In a vertical arrangement, more material is used along height of the chamber, while the number of parts has increased by more than 3 times.

Key indicators for layout variant No. 2 will be as follows:

- assembly height – 90.05 mm;
- density of placement – 16.41%;
- use of platform volume – 2.31%;
- volume of parts – 1605. 389 cm<sup>3</sup>;
- number of parts – 66 pcs.

Another important technological limitation is the requirements of SLS-print to the part geometry and resolution of EOSINT P 395. One example is the impossibility of accurately producing functional holes whose axes are perpendicular to the growing direction. Thus, for example, the product fixing the conveyor belt (Figure 4) has a simple geometry in terms of topology, but it takes up quite a lot of space in the construction chamber when placed taking into account the above technological limitations.

Subject to all technological requirements, the density remains small, and the number of parts does not exceed 23 pieces. Figure 5 shows a possible dense arrangement for the parts.

Key indicators for layout of variant No. 3 will be as follows:

- assembly height – 41.27 mm;
- placement density – 10.74%;
- use of platform volume – 0.71%;
- volume of parts – 512.401 cm<sup>3</sup>;
- number of parts – 23 pcs.

Further analysis will demonstrate that this arrangement will not be cost-effective for the introduction of printed fixative products as spare parts for conveyor belts.

The products were made of PA2200 polyamide powder as the most affordable for the selected technology (SLS), as well as having excellent strength and chemical resistance specifications. Technical specifications of this powder are presented in Table 2.

### 3. RESULTS AND DISCUSSION:

SLS technology allows using unprocessed powder material repeatedly. The percentage of

primary and secondary material affects both product properties and pricing. Thus, for example, the cost of a holder when printing exclusively on secondary powder is 100 units. This increases the flexibility of the product, which affects the operation quality. In order to find the optimal proportion in terms of cost in this case, it is necessary to make products with different proportions of the primary and secondary powder in various operating modes. According to the results, changes to the material's geometry (e.g. increasing the wall thickness with a ratio of "0/100") or increasing the amount of primary material to the detriment of the product's cost are needed.

Since the printed part has a porous structure, it is necessary to take into account the hygroscopicity of the product and its effect on operational characteristics. Figure 6 demonstrates the change in mass compared to the original part before and after testing. The weight of the printed holder before the test was 23.23 g. The printed sample was tested in direct contact with the aqueous medium for 500 hours, while the weight increased to 24.08 g. for sample No. 1 and to 24.31 gr. for sample No. 2. The clearance between the clamps has increased from 0 to 1 mm. Fatigue tests were performed using 40% primary and 60% secondary powder ratios. The functional characteristics of the holder remained in the normal range (Mustafin, 2006; Mustafin and Volkov, 1984).

At the moment, the samples with a different material ratio undergo strength and fatigue tests (Table 3). To quantify the properties of the material for the given geometry, a series of tensile testing of blanks were performed. To identify the best ratio of strength, elasticity, and manufacturing cost, samples with different percentages of powder were offered for testing. So, samples 1.1, 1.2, 1.3, 1.4, 1.5, 1.6, 1.7 have a ratio of 40 % of the primary powder and 60% of the secondary, while samples 1.6 and 1.7 were already tested under production conditions for 2.5 months of continuous operation (Mellor *et al.*, 2014). Samples 1.8 and 1.9 were made entirely of secondary powder, and in the graphs below, it can be seen that these samples are the most elastic. Tensile tests were performed at a speed of 25 mm/min. Figure 7 presents graphs demonstrating the maximum load of the test samples.

The graph shows that the samples, printed with the use of 3D printing, can stand high maximal loads. Products 9 and 10 printed with a 100% ratio of secondary powder have greater elasticity and did not collapse during testing. Static tests were

also carried out at the same time, the task of which was to determine the boundary conditions, after which the sample would lose its elasticity and cease to take its original shape. Table 4 shows the result of static tests of the holding part for 3 months. The highlighted test holder is marked by red, the blue stands for the original holder (Figure 8) (Anamova *et al.*, 2016; Umbetov *et al.*, 2016a; Umbetov *et al.*, 2016b; Rabinskiy *et al.*, 2017). Comparison of the geometries of the original and used holders showed an increase in the gap between the arcs by 5 mm; in this state, the holder is still able to fulfill its main function of holding the workpieces, but such a part must be replaced (Rabinskiy *et al.*, 2017). Problems prototyping are regarded in (Nazarov, 2011; Kalinsky *et al.*, 2019; Boytsov *et al.*, 2011; Atzeni and Salmi, 2012; Kuzovkin and Suvorov, 2014; Piller *et al.*, 2015).

#### 4. CONCLUSIONS:

This work mentions that the cost of manufacturing spare parts using 3D printing depends on many factors. The geometry of the products, which determines their volume, as well as density of their arrangement in the chamber, were recognized as key factors of influence. The same factors become criteria for the economic efficiency of using SLS technology to solve applied production problems.

Several technological parameters and criteria were analyzed that limit the technical engineer in creating effective layouts. The accumulated experience and analysis of the criteria allowed us to suggest several layout options that can lead to a maximum economic effect. Another critical factor is the improvement in the time of delivery of the finished product to the production line. Analysis of specific production line (Nizhnelomovsky enterprise of the United Penza Plant) demonstrated that timely production of spare parts by 3D printing could reduce delivery time by an average of 2 days.

Therefore, the use of SLS printing for the production of individual elements of the conveyor line can reduce delivery times by an average of 2 times, and for individual products - by 2.5-3 times. The cost of a single product decreases by an average of 37.5 %, and for individual products, it is 1/3 of the cost of the original spare part. This effect was proved on example of specific products and can partially be transferred to other applications for quickly creating spare parts in production conditions. The issue of expanded use of SLS printing, as well as other rapid prototyping tools, is part of the task of further research on the

subject.

In addition to the above-mentioned positive effects of the introduction of 3D printing, it is necessary to take into account the series and uniqueness of products, and it is important to understand at which stage it can be switched to other production technologies. Further tasks in this direction are to determine the criteria and requirements for the geometry of products, as well as to create a mathematical apparatus that could let us confidently determine the production technology of specific products to achieve the maximum economic effect. Presently, work in this direction is also proceeding.

#### 5. ACKNOWLEDGMENTS:

The work was carried out with the financial support of the state project of the Ministry of Education and Science on the topic "Theoretical and experimental research in production and processing of advanced metal and composite materials based on aluminum and titanium alloys" FSFF-2020-0017.

#### 6. REFERENCES:

1. Alekseev, A.N., Alekseev, S.A., Zabashta, Y.F., Hnatiuk, K.I., Dinzhos, R.V., Lazarenko, M.M., Grabovskii, Y.E., and Bulavin, L.A. (2019). Two-dimensional ordered crystal structure formed by chain molecules in the pores of solid matrix. *Springer Proceedings in Physics*, 221, 387-395.
2. Anamova, R.R., Zelenov, S.V., Kuprikov, M.U., and Ripetskiy, A.V. (2016). Multiprocessing and correction algorithm of 3D-models for additive manufacturing. *IOP Conference Series: Materials Science and Engineering*, 140(1), Article 012003.
3. Atzeni, E., and Salmi, A. (2012). Economics of additive manufacturing for end-usable metal parts. *The International Journal of Advanced Manufacturing Technology*, 62(9-12), 1147-1155.
4. Babaytsev, A., Dobryanskiy, V. and Solyaev, Y. (2019). Optimization of thermal protection panels subjected to intense heating and mechanical loading. *Lobachevskii Journal of Mathematics*. 40(7), 887-895. DOI: 10.1134/S1995080219070059
5. Babaytsev, A.V., and Zotov, A.A. (2019). Designing and calculation of extruded sections of an inhomogeneous composition. *Russian Metallurgy (Metally)*. 2019(13), 1452-

1455, DOI: 10.1134/S0036029519130020

6. Babaytsev, A.V., Martirosov, M.I., Rabinskiy, L.N., and Solyaev, Y.O. (2017). Effect of thin polymer coatings on the mechanical properties of steel plates. *Russian Metallurgy (Metally)*, 2017(13), 1170-1175. DOI: 10.1134/S003602951713002XF
7. Babaytsev, A.V., Prokofiev, M.V., and Rabinskiy, L.N. (2017). Mechanical properties and microstructure of stainless steel manufactured by selective laser sintering. *International Journal of Nanomechanics Science and Technology*, 8(4), 359-366. DOI: 10.1615/NanoSciTechnolIntJ.v8.i4.60
8. Bespalov, Y.G., Vysotska, O., Porvan, A., Linnyk, E., Stasenko, V.A., Doroshenko, G.D., Omiotek, Z., and Amirgaliyev, Y. (2019). Information system for recognition of biological objects in the RGB spectrum range. Information Technology in Medical Diagnostics II - Proceedings of the International Scientific Internet Conference on Computer Graphics and Image Processing and 48th International Scientific and Practical Conference on Application of Lasers in Medicine and Biology, 2018. doi: 10.1201/9780429057618-13.
9. Bhutani, A., Goettel, B., Thelemann, T., and Zwick, T. (2017). CPW-to-SL transition in LTCC technology. *Electronics Letters*, 53(9), 609-611.
10. Boboc, A., Trimble, P., Jones, G., Fessey, J., Cramp, S., and Studholme, W. (2019). JET FIR Interferometer laser operation and interlock system upgrade to an open automation system. *Fusion Engineering and Design*, 146(A), 835-838.
11. Böckin, D., and Tillman, A.-M. (2019). Environmental assessment of additive manufacturing in the automotive industry. *Journal of Cleaner Production*, 226, 977-987.
12. Boytsov, B.V., Kuprikov, M.Yu., and Maslov, Yu.V. (2011). Improving the quality of production preparation using rapid prototyping technologies. *Transactions of MAI*, 49, Article 6.
13. Bulavin, L.A., Alekseev, O.M., Zabashta, Y., and Lazarenko, M.M. (2018). Phase equilibrium, thermodynamic limit, and melting temperature in nanocrystals. *Ukrainian Journal of Physics*, 63(11), 1036-1040.
14. Georgios Tsoutsos, N., Gamil, H., and Maniatakos, M. (2017). Secure 3D printing: reconstructing and validating solid geometries using toolpath reverse engineering. In *Proceedings of the 3rd ACM workshop on cyber-physical system security (CPSS '17)* (pp. 15–20). New York City, New York: Association for Computing Machinery. DOI: <https://doi.org/10.1145/3055186.3055198>
15. Kalinsky, O.I., Kruzhkova, G.V., Aleksakhin, A.V., and Molchanov, G.A. (2019). Selection of the optimal strategy for the supply of raw materials based on game theory. *Smart Innovation, Systems and Technologies*, 139, 577-583.
16. Kim, H.-J. (2019). 3D printing characteristics of automotive hub using 3d scanner and reverse engineering. *The Korean Society of Manufacturing Process Engineers*, 18(10), 104-109.
17. Kolotyryn, K.P., Bogatyrev, S.A., Savon, D.Y., and Aleksakhin, A.V. (2019). Use of resource-saving technologies in fabrication and restoration of steel bushing-type components via hot plastic deformation. *CIS Iron and Steel Review*, 18, 38-41.
18. Koltunov, I.I., Panfilov, A.V., Poselsky, I.A., Chubukov, N.N., Krechetov, I.V., and Skvortsov, A.A. (2018). Geometric visualization of the problem of medical diagnostics biometric data of the biosensor platform. *Journal of Mechanical Engineering Research and Development*, 41(4), 37-39.
19. Koshoridze, S.I., Levin, Y.K., and Rabinskiy, L.N. (2017). Investigation of Deposits in Channels of Panels of a Heat-Transfer Agent. *Russian Metallurgy (Metally)*, 2017(13), 1194-1201. DOI: 10.1134/S0036029517130092
20. Kuprikov, M.Y., Rabinskiy, L.N., and Kuprikov, N.M. (2019). Business objective for the life cycle of aircraft. *INCAS Bulletin*, 11, 153-162.
21. Kuzovkin, A.V., and Suvorov, A.P. (2014). Development of technology for manufacturing shaped tools based on rapid prototyping. *Bulletin of the Voronezh State Technical University*, 10(1). Retrieved from <https://cyberleninka.ru/article/n/razrabotka-tehnologii-izgotovleniya-fasonnogo-instrumenta-na-osnove-bystrogo-prototipirovaniya>.
22. Mellor, S., Hao, L., and Zhang, D. (2014). Additive manufacturing: A framework for implementation. *International Journal of Production Economics*, 149, 194-201.



23. Mustafin, A. (2006). Two mutually loss-coupled lasers featuring astable multivibrator. *Physica D: Nonlinear Phenomena*, 218(2), 167-176.
24. Mustafin, A.T., and Volkov, E.I. (1984). The role of lipid and antioxidant exchanges in cell division synchronization (mathematical model). *Biological Cybernetics*, 49(3), 149-154.
25. Nazarov, A.P. (2011). Prospects for rapid prototyping by selective laser sintering/melting. *Vestnik MGTU Stankin*, 4, 46-51.
26. Pellens, J., Lombaert, G., and Michiels, M. (2020). Topology optimization of support structure layout in metal-based additive manufacturing accounting for thermal deformations. *Structural and Multidisciplinary Optimization*. Retrieved from <https://link.springer.com/article/10.1007/s00158-020-02512-8>.
27. Piller, F.T., Weller, C., and Kleer, R. (2015). Business models with additive manufacturing – opportunities and challenges from the perspective of economics and management. In *Advances in Production Technology* (pp. 39-48). Cham, Switzerland: Springer.
28. Rabinskiy, L.N., Ripetskiy, A.V., Zelenov, S.V., and Kuznetsova, E.L. (2017). Analysis and monitoring methods of technological preparation of the additive production. *Journal of Industrial Pollution Control*, 33(1), 1178-1183.
29. Revilla-León, M., Ceballos, L., Martínez-Klemm, I., and Özcan, M. (2018). Discrepancy of complete-arch titanium frameworks manufactured using selective laser melting and electron beam melting additive manufacturing technologies. *Journal of Prosthetic Dentistry*, 120(6), 942-947.
30. Revilla-León, M., Meyer, M.J., and Özcan, M. (2019). Metal additive manufacturing technologies: literature review of current status and prosthodontic applications. *International Journal of Computerized Dentistry*, 22(1), 55–67.
31. Revilla-León, M., Meyer, M.J., Zandinejad, A., and Özcan, M. (2020). Additive manufacturing technologies for processing zirconia in dental applications. *International Journal of Computerized Dentistry*, 23(1), 27-37.
32. Ripetskiy, A., Zelenov, S., and Kuznetsova, E. (2018). Current issues of developing methodology and software solutions used in different phases of modelling additive production processes. *Key Engineering Materials*, 771, 97–102.
33. Ripetskiy, A.V., Zelenov, S.V., Vucinic, D., Rabinskiy, L.N., and Kuznetsova, E.L. (2016). Automatic errors correction method based of the layer-by-layer product representation which parallel algorithms are developed for multiprocessor computer hardware. *International Journal of Pure and Applied Mathematics*, 111(2), 343-355. DOI: 10.12732/ijpam.v111i2.17
34. Sevryukova, M.M., Piryatinski, Y.P., Vasylyuk, S.V., Yashchuk, V.M., Viniychuk, O.O., Gerasov, A.O., Slominskii, Y.L., and Kachkovsky, O.D. (2012). Cyanine-like and polyenic relaxation paths of merocyanine derivatives of malonodinitrile in the excited state detecting by low temperature time-resolved fluorescence. *Ukrainian Journal of Physics*, 57(8), 812-823.
35. Skvortsov, A.A., Orlov, A.M., and Zuev, S.M. (2012). Diagnostics of degradation processes in the metal-semiconductor system. *Russian Microelectronics*, 41(1), 31-40.
36. Sobczak-Kupiec, A., Malina, D., Piątkowski, M., Krupa-Zuczek, K., Wzorek, Z., and Tyliczszak, B. (2012). Physicochemical and biological properties of hydrogel/gelatin/hydroxyapatite PAA/G/HAp/AgNPs composites modified with silver nanoparticles. *Journal of Nanoscience and Nanotechnology*, 12(12), 9302-9311.
37. Sobczak-Kupiec, A., Pluta, K., Drabczyk, A., Włoś, M., and Tyliczszak, B. (2018). Synthesis and characterization of ceramic – polymer composites containing bioactive synthetic hydroxyapatite for biomedical applications. *Ceramics International*, 44(12), 13630-13638.
38. Song, J.-Sh.J., and Zhang, Y. (2016). Stock or Print? Impact of 3D printing on spare parts logistics. Retrieved from <https://ssrn.com/abstract=2884459>.
39. Tashi, Ullah, A.S., and Kubo, A. (2019). Geometric Modeling and 3D Printing Using Recursively Generated Point Cloud. *Applied Mathematics and Computation*, 24, Article 83.
40. Umbetov, A.U., Umbetova, M.Z., Abildayev, G.M., Baizakova, S.S., Zhamalova, S.A., Konussova, A.B., and Dosmagulova, K.K. (2016a). Transformation and interference of the laser radiation in composite crystal optical systems. *ARPJ Journal of Engineering and*

41. Umbetov, A.U., Zhumabaeva, S.B., Zhakenova, A., Sadykova, B.S., Tulegenova, A.K., Aubakirova, A.A., and Dzhaketova, S.Z. (2016b). Calculation of the laser beam path through the anisotropic crystalline lens. *Mathematics Education*, 11(7), 2025-2046.
42. Westerweel, B., Song, J.-Sh.J., and Basten, R.J.I. (2019). 3D Printing of Spare Parts Via IP License Contracts. Retrieved from <https://ssrn.com/abstract=3372268>.
43. Willmann, R. (2019, February). *Product design with integrated holistic validation of economics of metal-based 3D-printing by the help of a recommender system*. Paper presented at the 2019 IEEE International Conference on Industrial Technology (ICIT), Melbourne, Australia.
44. Yumashev, A., Semenycheva, I., Rakhadilov, B., and Tsymbal, A. (2019). Development of biocompatible coatings for dental implants based on transition metal nitrides. *Journal of Global Pharma Technology*, 11(5), 22-28.
45. Zhang, Ch.L.Y. (2019). Fusion zone characterization of resistance spot welded maraging steels via selective laser melting. *Journal of Materials Processing Technology*, 273, Article 116253.
46. Zhang, H.F., and Chang, W.H. (2011). Rapid manufacturing technique of casting mould based on the SLS. *Advanced Materials Research*, 291–294, 2970–2973.

**Table 1.** Kreon ZEPHYR KZ25 Laser Scanner Specifications

|                                  |                             |
|----------------------------------|-----------------------------|
| Data collection speed            | 34 fps, up to 30,000 dots/s |
| Number of laser lines per second | 60                          |
| Accuracy, mm                     | ±0.015                      |
| Sensor resolution                | 0.005                       |
| Linear resolution                | 0.03                        |
| Laser type                       | Signal modulation diode     |
| Laser class                      | II                          |
| Wave length, nm                  | 675                         |
| Maximum power, mW                | 3.7                         |

**Table 2.** Mechanical properties of polyamide PA2200

| Mechanical properties                               | Value | Unit              | Test Standart   |
|---|-------|-------------------|-----------------|
| Izod Impact notched (23°C)                          | 4.4   | kJ/m <sup>2</sup> | ISO 180/1A      |
| Shore D hardness (15s)                              | 75    | -                 | ISO 868         |
| Tensile Modulus (X Direction)                       | 1650  | MPa               | ISO 527-1/-2    |
| Tensile Modulus (Y Direction)                       | 1650  | MPa               | ISO 527-1/-2    |
| Tensile Modulus (Z Direction)                       | 1650  | MPa               | ISO 527-1/-2    |
| Tensile Strength (X Direction)                      | 48    | MPa               | ISO 527-1/-2    |
| Tensile Strength (Y Direction)                      | 48    | MPa               | ISO 527-1/-2    |
| Tensile Strength (Z Direction)                      | 42    | MPa               | ISO 527-1/-2    |
| Strain at break (X Direction)                       | 18    | %                 | ISO 527-1/-2    |
| Strain at break (Y Direction)                       | 18    | %                 | ISO 527-1/-2    |
| Strain at break (Z Direction)                       | 4     | %                 | ISO 527-1/-2    |
| Charpy impact strength (+23°C, X Direction)         | 53    | kJ/m <sup>2</sup> | ISO 179/1eU     |
| Charpy notched impact strength (+23°C, X Direction) | 4.8   | kJ/m <sup>2</sup> | ISO 179/1eA     |
| Flexural Modulus (23°C, X Direction)                | 1500  | MPa               | ISO 178         |
| Melting temperature (20°C/min)                      | 176   | °C                | ISO 11357-1/-3  |
| Vicat softening temperature (50°C/h 50N)            | 163   | °C                | ISO 306         |
| Density (lasersintered)                             | 930   | kg/m <sup>3</sup> | EOS GmbH Method |

**Table 3.** The economic effect from the introduction of 3D printing for the production of spare parts

| Product type              | Delivery time |              | Cost, USD    |                    |                    |
|---------------------------|---------------|--------------|--------------|--------------------|--------------------|
|                           | Original      | 3 D printing | Original     | 3 D printing 40/60 | 3 D printing 0/100 |
| Fixator type 1            | from 2 days   | 3-4 days     | from \$ 12.3 | \$ 3.3             | \$ 1.5             |
| Fixator type 2            | from 2 days   | 3-4 days     | from \$ 13.9 | \$ 3.5             | \$ 1.7             |
| Fixator Parametric Model  | from 2 days   | 3-4 days     | n / a        | \$ 3.5             | \$ 1.5             |
| Holder bracket for blanks | 1.5 weeks     | 3-4 days     | from \$ 6.2  | \$ 4.5             | n / a              |

**Table 4.** *The test results*

| Sample label     | Maximum load [kN] | Ultimate strain [%] | Note  |
|------------------|-------------------|---------------------|---|
| 1.0              | 0.2               | 34.433              | Test speed 25 mm / min. Original                      |
| 1.1              | 0.36              | 55.37               | Test speed 25 mm / min. Polyamide.                    |
| 1.2              | 0.35              | 54.62               | Test speed 25 mm / min. Polyamide.                    |
| 1.3              | 0.37              | 57.599              | Test speed 25 mm / min. Polyamide.                    |
| 1.4              | 0.29              | 53.741              | Test speed 25 mm / min. Polyamide.                    |
| 1.5              | 0.34              | 53.599              | Test speed 25 mm / min. Polyamide.                    |
| 1.6              | 0.31              | 55.391              | Test speed 25 mm / min. Polyamide (was in operation). |
| 1.7              | 0.33              | 54.745              | Test speed 25 mm / min. Polyamide (was in operation). |
| 1.8              | 0.47              | 69.266              | Test speed 25 mm / min. Polyamide (secondary powder). |
| 1.9              | 0.39              | 65.683              | Test speed 25 mm / min. Polyamide (secondary powder). |
| 2.10             | 0.65              | 70.037              | Test speed 25 mm / min. Original.                     |
| Minimum          | 0.2               | 34.433              |   |
| Maximum          | 0.65              | 70.037              |   |
| The average      | 0.37              | 56.77               |   |
| Stand. reject    | 0.11              | 9.71                |   |
| Coef. variations | 31%               | 17%                 |   |

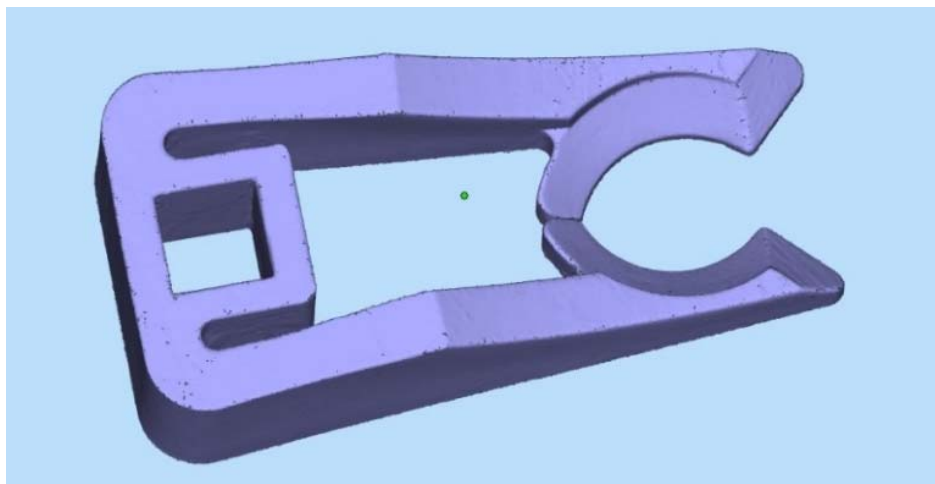


**Figure 1.** 3D model of the workpiece fixator (Type 1)

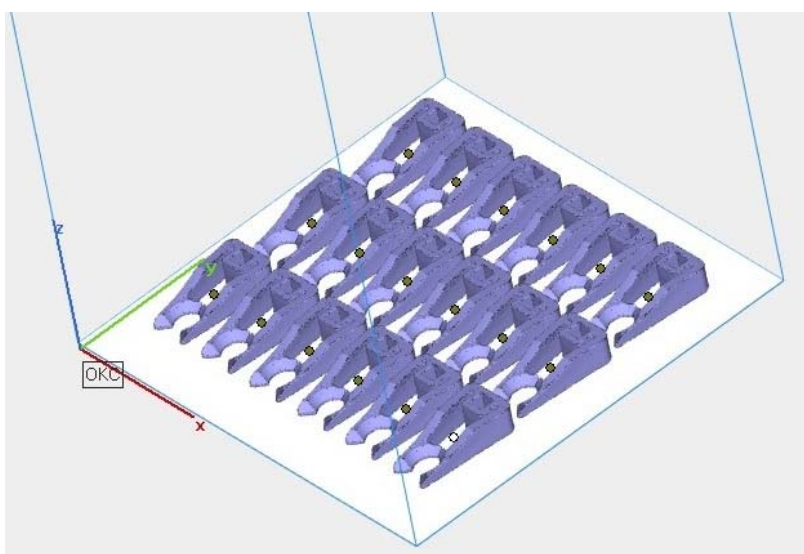


**Figure 2.** The horizontal arrangement of 3D models of fixators (type 1) in a virtual

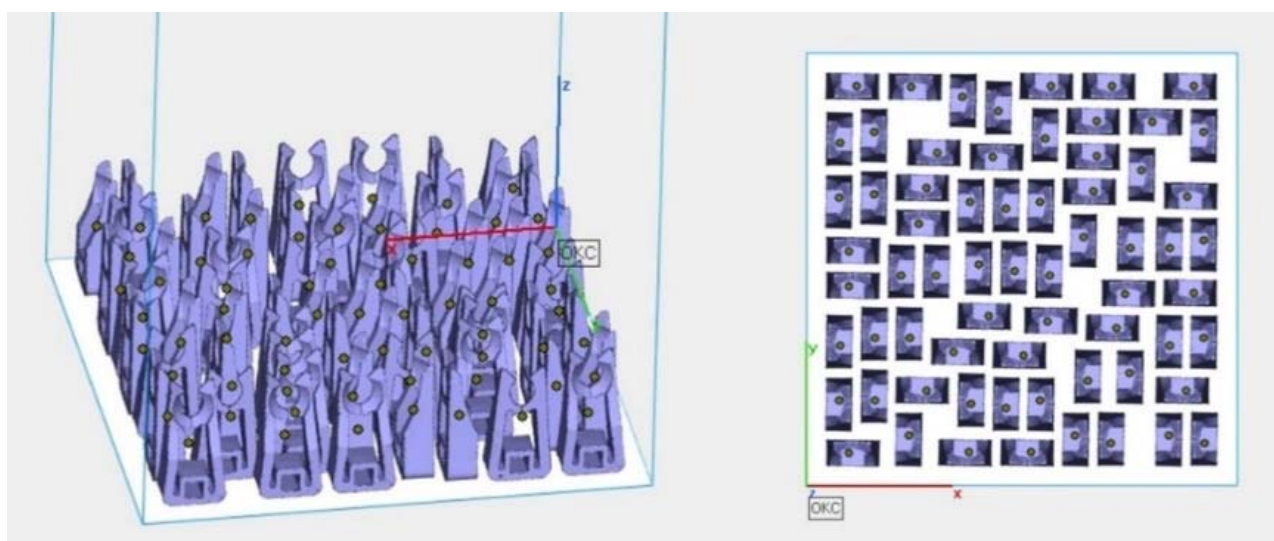


**Figure 3.** Variant of automatic arrangement of products in chamber (vertical arrangement)



**Figure 4.** Conveyor belt bracket

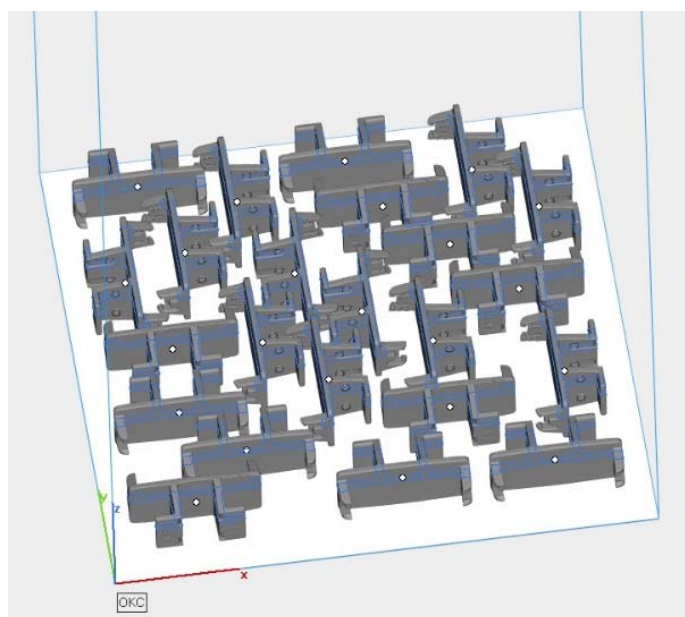


**Figure 5.** The layout of bracket conveyor belt bracket in a virtual camera

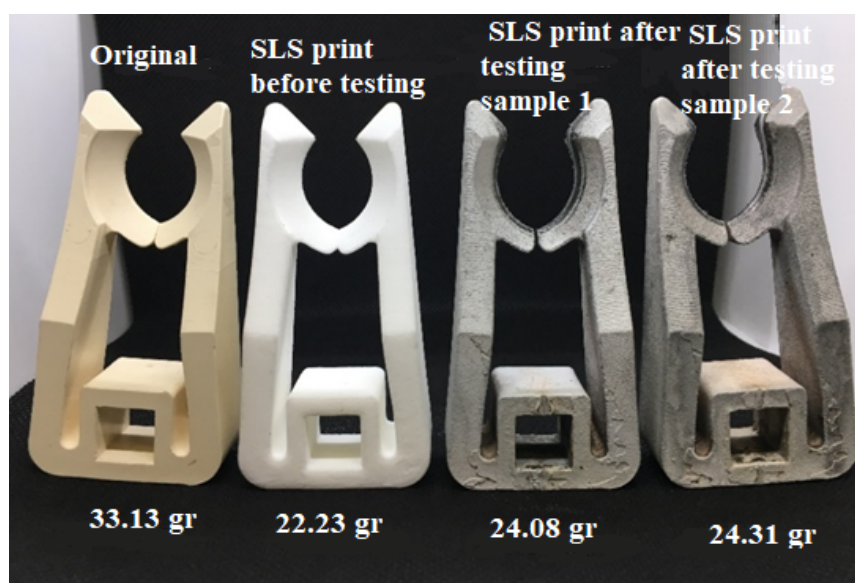


**Figure 6.** Change in the mass of the fixator before and after the tests

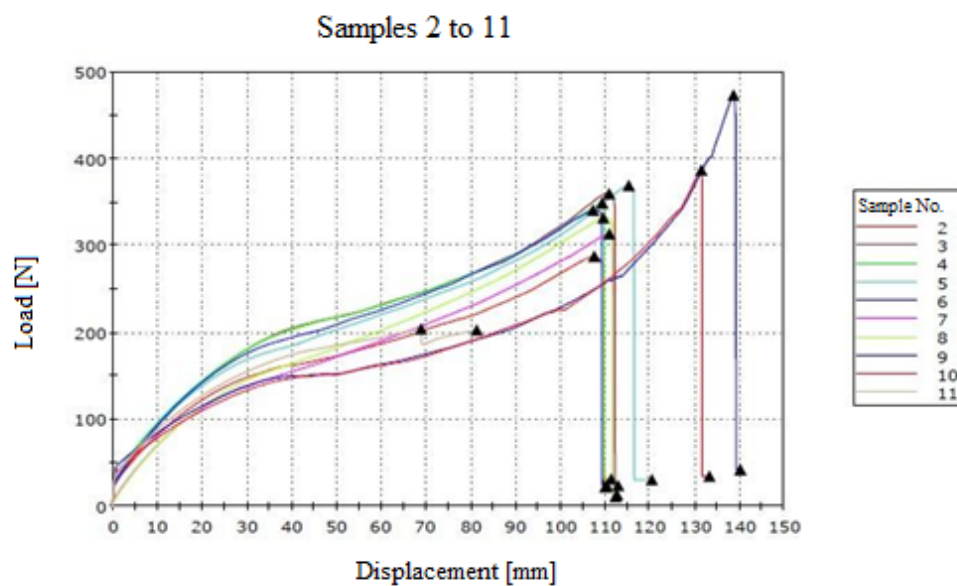


**Figure 7.** Graph of changes in sample loads

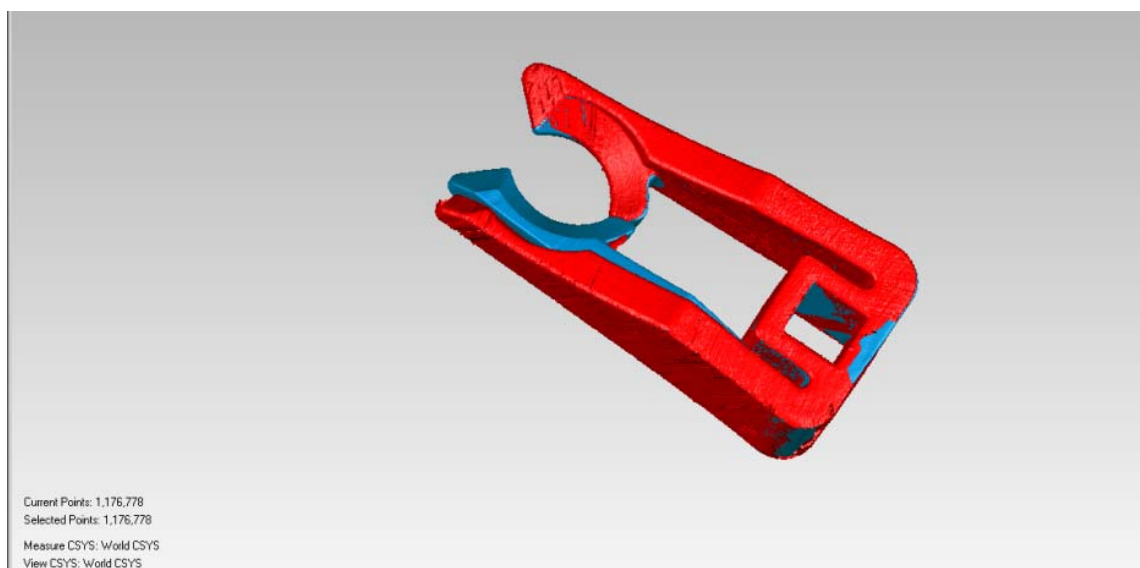


**Figure 8.** Change in holder geometry before and after tests



USO DE EXTRATO DE CEBOLA SELVAGEM ECOLÓGICA (*URGINEA MARITIMA*) COMO INIBIDOR DE CORROSÃO PARA AÇO CARBONO EM ÁCIDO CLORÍDRICOTHE USE OF ECO-FRIENDLY WILD ONION EXTRACT (*URGINEA MARITIMA*) AS CORROSION INHIBITOR FOR CARBON STEEL IN HYDROCHLORIC ACIDWafa K. Essa<sup>1</sup>; Najlaa K. ISSA<sup>2\*</sup>; Walaa H. Abdulqader<sup>3</sup>; Ibtesam M. Kamal<sup>4</sup><sup>1,2,3</sup> University of Duhok, College of Science, Chemistry Department. Iraq.<sup>4</sup> Soran University, Faculty of Engineering, Chemical Engineering Department. Iraq.

\* Corresponding author  
e-mail: najlaa.issa@uod.ac

Received 15 May 2020; received in revised form 30 May 2020; accepted 20 June 2020

## RESUMO

Embora vários compostos sintéticos tenham uma boa ação como anticorrosivo, eles não são baratos e são tóxicos para o meio ambiente e para os seres humanos. No entanto, no aço carbono (aço-C) existe uma preocupação vital que é o sério problema de corrosão devido à exposição a ambientes de acidez agressiva, ou seja, descalcificação, soluções de acidez de poços de petróleo e decapagem. Portanto, este estudo teve como objetivo avaliar o efeito de inibição do extrato de cebola selvagem (WO) como um inibidor ecológico no comportamento da corrosão do aço-C em HCl 0,5 M através da abordagem convencional de perda de peso. Várias concentrações (0%, 0,5%, 1%, 1,5%, 2% e 2,5%) de inibidor em vários períodos de imersão (2, 4 e 8 h) e em diferentes temperaturas (25 °C, 35 °C e 45 °C) foram investigados quanto à inibição da corrosão do aço-C em meios corrosivos. Na presença e ausência do inibidor, a taxa de corrosão (CR) foi investigada como afetada pela temperatura. A concentração do inibidor e a temperatura controlaram a eficiência da inibição (%E) do inibidor. Na existência de extrato de cebola selvagem, a eficiência ideal de inibição para o aço-C foi de 98,95%, 88,99% e 86,79% nas concentrações de inibidor de 2,5% nas temperaturas anteriores, respectivamente. Observou-se que a adsorção era espontânea e física, conforme comprovado pelo valor de adsorção da energia livre de  $\Delta G^{\circ}_{ads}$  (13,5 kJ/mol), além de também ser isotérmica de adsorção de Langmuir. Os dados de cobertura da superfície  $\theta$  e da densidade de corrente de corrosão  $I_{corr}$  confirmaram o resultado anterior em que a inibição ocorre devido à adsorção da natureza física dos componentes do aditivo na superfície do aço-C.

**Palavras-chave:** Cebola selvagem; Aço-C; Inibição de corrosão; Inibição termodinâmica.

## ABSTRACT

Even though various synthetic compounds have a well action as anticorrosive, they are not cheap and are toxic to both environment and humans. Nevertheless, in C-steel, there is a vital concern, which is serious corrosion issues happen through exposure to environments of aggressive acidity i.e., descaling, oil well solutions of acidity, and pickling. Hence, this study aimed to evaluate the inhibition effect of wild onion (WO) extract as an eco-friendly inhibitor on the behavior of corrosion for C-steel in 0.5 M HCl through the conventional weight loss approach. Various concentrations (0%, 0.5%, 1%, 1.5%, 2%, and 2.5%) of inhibitor in various times of immersion (2, 4, and 8 h) and at different temperatures (25°C, 35°C and 45°C) were investigated for their C-steel corrosion inhibition in corrosive media. In the presence and absence of the inhibitor, the corrosion rate (CR) was investigated as affected by temperature. The concentration of the inhibitor and temperature-controlled the inhibition efficiency %E of the inhibitor. At the existence of wild onion extract, the ideal efficiency of inhibition for C-steel was 98.95%, 88.99%, and 86.79% at 2.5% inhibitor concentrations at the preceding temperatures, respectively. It was noticed that adsorption was spontaneous and physical as proved through adsorption value of free energy  $\Delta G^{\circ}_{ads}$  (-13.5 kJ/mol) and also fitted Langmuir adsorption isotherm. The surface coverage  $\theta$  and corrosion current density  $I_{corr}$  data confirmed the previous result where inhibition is due to the adsorption of physical nature for the components of the additive on the C-steel surface.

**Keywords:** Wild onion; C-steel; Corrosion inhibition; Inhibition thermodynamic.



## 1. INTRODUCTION:

In various kinds of industrial applications, carbon steel (C-steel) has a significant role due to its availability and low price (El-Lateef *et al.*, 2016). Nevertheless, in C-steel, there is a vital concern, which is serious corrosion issue happens through exposure to environments of aggressive acidity, i.e., descaling, oil well solutions of acidity, and pickling (Banerjee *et al.*, 2014). The temperature effect is of theoretical and practical significance on chemical reactions. As of most reactions, with elevated temperature, the corrosion rate of steel and Fe increases, particularly at medium where H evolution along with corrosion is accompanied, i.e., through steel corrosion in acidic solution (Hamdy and El-Gendy, 2013). As one of the most vital and significant strategies, inhibitors of corrosion have been practiced for C-steel anti-corrosion, especially in acidic solution, to prevent metal dissolution and acid consumption (Khadom *et al.*, 2009). Although various synthetic compounds have a great action as anticorrosive, they are not cheap and are toxic to both environment and humans (Garai *et al.*, 2012). Toxicity might show manifestation either through compound synthesis or through applications, which makes researchers concentrate on using substances occurring naturally to obtain inhibitors that are non-hazardous and cheap (Ahmed and Quraishi, 2013). The compound to behave as an inhibitor for corrosion, requirements should be available; as far as the behavior of chemical and its structure, an inorganic compound readily oxidizes the metal by forming on the surface a passive layer. Also, an organic molecule should possess inhibitor characters to behave as a corrosion inhibitor; the double bonds, molecules with a large structure and an active group or center, etc. These characters render these molecules cover a considerable area surface of the metal (film) with firm attachment. Plants considered as inhibitor source of many ones, which is clean and cheap (Fouda *et al.*, 2014). Plants extracts (i.e., seeds, leaves, flowers, and fruits) possess various active compounds with the ability of corrosion inhibition in aggressive media had been considered in recent studies (Khadom *et al.*, 2018; Mobin *et al.*, 2018; Haldhar *et al.*, 2018; Banu *et al.*, 2018). In this regard, different

investigators are concentrating on the growth of friendly environmentally inhibitors of corrosion, i.e., natural products, *Spirulina platensis* (Gopiraman *et al.*, 2012), *Brugmansia suaveolens* (Kamal, *et al.*, 2012), green eucalyptus leaves (Dehghani *et al.*, 2016), *Acalypha torta* (Krishnegowda *et al.*, 2013), *Luffa aegyptiaca* (Jyothi and Ravichandran, 2014), watermelon rind (Odewunmi *et al.*, 2015), *Ligularia fischeri* (Prabakaran *et al.*, 2018), *Lansea coromandelica* (Muthukrishnan *et al.*, 2017), *Tilia cordata* (Fouda *et al.*, 2017), sweet melon peels (Saeed *et al.*, 2019), *Griffonia simplicifolia* (Ituen *et al.*, 2017), *Dillenia Pentagyna* fruits (ManjunathHegde *et al.*, 2019), *Pongamia pinnata* (HouariaDerfouf *et al.*, 2019). The existence of organic plant compounds, i.e., carbohydrates, flavonoids, alkaloids, saponins, and phenols, make them well source inhibitors of corrosion. These phytochemicals possess various functional groups like hydroxyl, carbonyl, and amino (Sakunthala *et al.*, 2019). Thus, these plants behave as well as inhibitor sources of corrosion that should not be neglected.

Wild onion (WO) plant (*Urginea maritima*), a medicinal plant from the area of Mediterranean, belongs to the family Liliaceae. WO grows naturally in the wild, explicitly cultivated (Deb and Dasgupta, 1987). The parts of medicinal importance are the bulbs which harvested, transversely sliced, and grounded for being ready to used (Gentry *et al.*, 1987). Genus of *Urginea* is traditionally used in medicine because of its antiepileptic, cardiotoxic, diuretic, anti-asthmatic, and dermatological characteristics (El-Seedi *et al.*, 2013).

The purpose of this study was to investigate the corrosion inhibition ability of WO extract for C-steel in a 0.5 M HCl solution using weight loss measurements.

## 2. MATERIALS AND METHODS:

### 2.1. Preparation of specimens

The coupons of C-steel (5 x 2.6 x 0.3 cm) with the composition of % V, 0.21 wt., 0.34 wt. % C, 0.51 wt. % P, , 0.035 wt. % Cr, 0.44 wt. % Mn, 0.017 wt. % Al, 0.054 wt. % Mo and Fe (balance), were applied in this paper (Figure 1). The coupon surface polished by emery paper of grit from 400 to 600 grades prepares sequentially to the polished surface. After polishing, the coupons

were washed with tap water then by distilled water and dried with clean tissue with hot air and finally in desiccators to get coupons moisture-free before storage and use.



**Figure 1.** Coupons of C-steel.

## 2.2. Wild onion (WO) extraction

WO plant was collected from lawns of Duhok governorate, Kurdistan Region of Iraq (Figure 2). The bulbs were washed and cut into small pieces and then dried under shadow at ambient temperature then ground into a fine powder. For the extraction procedure, 10 g of WO powder was weighed and mixed with 100 ml of (90% methanol) in a conical flask. The mixture was extracted during stirring for 24h at room temperature. The resultant mixture was filtered carefully, and the methanol evaporated by drying in an oven at 45°C for 2h. A yellow-brown sticky residue of dried WO extract was obtained. The dried extract was stored in a refrigerator for further use.



**Figure 2.** Wild onion plant (*Urginea maritima*).  
Courtesy: Jarjes et al.,(2016).

## 2.3. Preparation of corrosive solution

The electrolyte corrosive was 0.5 M HCl solution that was prepared from HCl (37%) analytical grade and distilled water. The inhibited solutions were prepared by adding WO extract to 0.5 M HCl prepared freshly at different concentrations (0.5%,

1%, 1.5%, 2%, and 2.5%).

## 2.4. Loss of weight measurements

Through measurement of weight losing, each coupon specimen was weighted carefully and then immersed in the 0.5 M HCl solution with various dried extract concentrations of WO (0%, 0.5%, 1%, 1.5%, 2%, and 2.5%) at (25, 35 and 45°C), respectively. After (2, 4 and 8hr) immersion in the solution, the specimens were taken out and washed in tap water for removal all products of corrosion on the surface of the metal, washed another time with distilled water (DW), dried by clean tissue and hot air, and then weighed after they have been kept in desiccators for 3h. The same procedure was repeated for each temperature.

From the weight loss data, the CR was calculated by applying Eq. (1) (Tredder, 1984).

$$CR \text{ (mpy)} = \frac{534 W}{D A T} \quad (1)$$

Where:

CR (mpy): is the corrosion rate in mills per year.

W: is weight loss (mg).

D: density (g/cm<sup>3</sup>).

A: area of the C-steel coupon (in<sup>2</sup>).

T: time exposure (h).

By applying Eq. (2), the efficiency of inhibition (%E) was calculated (Danielson, 1982).

$$\%E = \frac{CR_o - CR_i}{CR_o} \times 100 \quad (2)$$

Where:

CR<sub>o</sub> and CR<sub>i</sub>: are the CRs in the presence and absence of various inhibitor concentrations, respectively.

By applying Eq. (3), the coverage of the surface (θ) was calculated (Damaskin, 1971).

$$\theta = 1 - \frac{CR_i}{CR_o} \quad (3)$$

### 3. RESULTS AND DISCUSSION:

#### 3.1 Measurements of weight-losing and temperature effect

CR variation, inhibition efficiency %E and coverage of surface  $\theta$  were evaluated through measurement of C-steel weight losing of in the media of corrosives with different concentrations of (WO) extract, and different temperatures are shown in the Tables 1, 2 and 3 and Figures 3, 4, 5, 6, 7 and 8. Results proved that the CR was declined as the inhibitor concentration elevated; i.e., in the solution of blank acidic, after 2h, the CR of C-steel was 41.45 (mpy), which decreased to 9.56 (mpy) with the addition of 0.5% of (WO) extract at 25°C. In the presence of 2% inhibitor, CR of C-steel was approximately 10 times lower compared to blank solution where the foregoing trials were proved. As the temperature increased, CR increased significantly from 41.45 (mpy) to 109.63 (mpy) and then to 185.7 (mpy) with an increase in temperature at the above, respectively, in blank acidic solution. Nevertheless, the effectiveness at each temperature for inhibitor extract was assumed from the significant CR decrease.

Inhibition efficiency (%E) values and surface coverage  $\theta$  elevated by elevating the concentration of inhibitor because of the inhibitor adsorption on the C-steel surface which occurred and formed a layer of protective coverage on surface of the C-steel (Moore, 1994).

Maximum inhibition efficiency %E of about 98.95% was reached in 2.5% of inhibitor concentration at 25°C and after 8hr. By increasing temperature, the efficiency of inhibition %E declined; i.e. efficiency inhibition %E was decreased from 98.95% to 88.99% and then to 86.79% when temperature elevated to 35°C and to 45°C, respectively from 25°C at 2.5% of the inhibitor concentration. The CR in current density units  $I_{corr}$  can be related to the weight loss by Eq. (4) (Moore, 1994)

$$I_{corr}(\text{mA}/\text{cm}^2) = \frac{2 \cdot 1000 \cdot W \cdot F}{A_w \cdot T \cdot A} \quad (4)$$

Where:

$I_{corr}$  = corrosion current density (mA/Cm<sup>2</sup>).

F = Faraday constant, 96500 coulombs.

$A_w$  = Atomic weight of Fe, 55.9.

T = Exposure time (sec.).

A = Specimen external surface area (Cm<sup>2</sup>).

W = corrosion weight losing (mg.).

Table 4 shows the variation of the corrosion current density  $I_{corr}$  values for the C-steel in HCl solution of 0.5 M with different temperatures, immersion times, and inhibitor concentrations. By concentration elevating, the density of current corrosion  $I_{corr}$  decreased, and the efficiency of WO extract inhibition increased. This might occur because of the adsorption of various inhibitor compounds on the surface of C-steel. Thus, WO extract addition decreased both the partial reaction rate through declining the dissolution of anodic and lowering down the H reaction evolution and blocks C-steel attack in the acid media (Solmaz *et al.*, 2008). Table 4 shows that the values of  $I_{corr}$  were elevated with elevating temperature from 25°C to 45°C; this is due to the temperature increase, which led to the desorption of protective layer on the surface of C-steel increase (Ramesh, 2003; Shaker, 1986; Adam, 1986).

#### 3.2. Immersion time effect

Determination of the inhibitor stability adsorption on the C-steel surface by losing weight measurement was performed with different inhibitor concentrations at different immersion times (2, 4, and 8h) and various temperatures (25°C, 35°C and 45°C). Figures 9, 10, and 11 show that as the immersion time increased, inhibition efficiency %E increased at 25°C. In comparison, at 35°C and 45°C a decrease was found in the inhibitor efficiency %E as the immersion time increased. The recent results may be due to the desorption of inhibitor on the surface of C-steel when the temperature rose. Maximum inhibition efficiency %E was lower at 45°C than at 35°C and 25°C. Based on the available literature, when temperature increased, it caused a decrease in the efficiency of inhibition. This might be attributed to the desorption of inhibitor constituents from the surface of the metal. In this situation, the adsorption is basically because of the interaction of electrostatic that declined at high temperatures. This proved that the

process of adsorption is a physisorption type (Sakunthala, 2013; Karthik and Sundaravadivelu, 2017).

### 3.3. Adsorption isotherm

The isotherms of adsorption are mathematical expressions that provide data about the reciprocal effect of the metal surface and adsorbing species at a fixed temperature. Generally, in acid corrosion, it is presumed that act of inhibitors by an adsorption process on the surface of the metal. The adsorption behavior is dependent on the amount of coverage surface  $\theta$ , were obtained by weight loss studies. An isotherm of adsorption provides the relation between the interface coverage with the species that adsorbed and the species concentration in solution. To examine the isotherm of adsorption, a graphic relation between the concentration inhibitor  $C_{inh}$  and  $C_{inh}/\theta$  at various temperatures was graphed and showed in Figure 12. In this figure, straight lines can be seen, and the correlation values of coefficient  $R^2$  were nearly equal to one pointing this system followed Langmuir isotherm of adsorption Eq. (5) at different temperatures. The above result indicated as well that inhibitor of mono-layer should be adsorbed to the surface of C-steel without any interaction among the molecules that adsorbed (Hamdy and El-Gendy, 2013; Faustin *et al.*, 2015).

$$\frac{C_{inh}}{\theta} = \frac{1}{K_{ads}} + C_{inh} \quad (5)$$

Where:

$C_{inh}$ : the concentration of inhibitor

$\theta$ : average degree of coverage on the surface metal

$K_{ads}$ : adsorption process constant equilibrium.

The inhibitor's equilibrium adsorption constants ( $K_{ads}$ ) were calculated by the linear equations intercept  $C_{inh}/\theta$  versus  $C_{inh}$  [8]. To compute the free energy standard of adsorption, value of  $K_{ads}$  was used ( $\Delta G^\circ_{ads}$ ) value based on the following (Bentiss *et al.*, 2009):

$$\Delta G^\circ_{ads} = -2.303 RT \log (55.5 K_{ads}) \quad (6)$$

The value of 55.5 was the

concentration of water in solution expressed in mol/L. The adsorption constants  $K_{ads}$  and free energy of standard adsorption  $\Delta G^\circ_{ads}$  values at different temperatures were grouped in Table (5).

Generally, the values of  $\Delta G^\circ_{ads}$  up to  $-20$  kJ/mol are accepted, adsorption kinds were considered as physisorption; acts of inhibition were attributed to the interaction of electrostatic between charged metal and the charged molecules, whereas values smaller than  $-40$  kJ/mol or around were observed as chemisorption. This is because of sharing the charge or a transfer to the surface of metal from the molecules of the inhibitor to form covalent bonding (Yurt *et al.*, 2005).

At the present investigation, the negative sign of  $\Delta G^\circ_{ads}$  proved that the inhibitor adsorption was spontaneous. The computed adsorption values of free energy  $\Delta G^\circ_{ads}$  at different temperatures were around of  $-13.5$  kJ/mol that assists the physical mechanism of adsorption (Adejoro *et al.*, 2015; Ali *et al.*, 2017).

### 4. CONCLUSIONS:

The CR declined as the concentration of inhibitor elevated and the efficiency of inhibition %E raised with elevating the inhibitor of concentration but decreased with temperature raising. The decline in the efficiency of inhibition with elevating temperature was suggestive of mechanism for physical adsorption (physisorption). It might be due to solubility increase in the products of protective film precipitated on the C-steel surface, which may otherwise inhibit the process of corrosion. The overall results of the current work revealed that the eco-friendly wild onion extracts is a promising corrosion behavior of C-steel in acidic media.

### 5. REFERENCES:

1. Abd El-Lateef, H., Abo-Riya, M. & Tantawy, A. (2016). Empirical and quantum chemical studies on the corrosion inhibition performance of some novel synthesized cationic gemini surfactants on C-steel pipelines in acid pickling processes. *Corros. Sci.* 108, 94-110.
2. Mourya, P., Banerjee, S., & Singh M. (2014). Corrosion inhibition of mild steel in acidic solution by *Tagetes erecta* (Marigold flower) extract as a green inhibitor. *Corros. Sci.* 85, 352-363.

3. Hamdy, A., Nour, S. & El-Gendy, h. (2013). Thermodynamic, adsorption and electrochemical studies for corrosion inhibition of C-steel by henna extract in acid media. *Egyptian J. of Petroleum*. 22, 17-25.
4. Khadom, A., [Yaro, I., Al Taie, A. & Kadum, H]. Electrochemical, Activations and Adsorption Studies for the Corrosion Inhibition of Low C-steel in Acidic. (2009). *Media. Portugaliae Electrochimica Acta*. 27, 699-712.
5. Garai, S., [Garai, P., Jaisankar, J., Singh, A., Elango, A. (2012). Comprehensive study on crude methanolic extract of *Artemisia pallens* (Asteraceae) and its active components effective corrosion inhibitors of mild steel in acid solution. *Corros. Sci.* 60, 193-204.
6. Ahmed, I. & Quraishi, M. (2009). Bis (benzimidazol-2-yl) disulphide: An efficient water soluble inhibitor for corrosion of mild steel in acid media. *Corros. Sci.* 51, 2006-2013.
7. Fouda, A., [Safaa, H., Etaiw, W.]. (2014). Punica Plant extract as Green Corrosion inhibitor for C-steel in Hydrochloric Acid Solutions. *Int. J. Electrochem. Sci.* 9, 4866 – 4883.
8. Khadom, A., Abd, A., & Ahmed, N. (2018). *Xanthium strumarium* leaves extracts as a friendly corrosion inhibitor of low C-steel in hydrochloric acid: kinetics and mathematical studies. *South Afr. J. Chem. Eng.* 25, 13–21.
9. Mobin, M., Basik, M., & Aslam, J. (2018). *Boswelli aserrata* gum as highly efficient and sustainable corrosion inhibitor for low C-steel in 1 M HCl solution: Experimental and DFT studies. *J. Mol. Liq.* 263, 174–186.
10. Haldhar, R. [Prasad, D., Saxena, A., & Singh, P.]. (2018). *Valeriana wallichii* root extract as a green & sustainable corrosion inhibitor for mild steel in acidic environments: experimental and theoretical study. *Mater. Chem. Front.* 2, 1225–1237.
11. Banu, M., Joany, R., & Rajendran, S. (2018). Green approach to corrosion inhibition of mild steel in acid media by aqueous extract of *Pedaliu murex* L. leaves. *Der PharmaChemica*. 10, 21–28.
12. Gopiraman, M., Sakunthala P., & Kesavan, D. (2012). An investigation of mild C-steel corrosion inhibition in hydrochloric acid media by environment friendly green inhibitors. *J. Coatings Tech. Res.* 9, 15–26.
13. Kamal, C., Sethuraman, M. (2012) *Spirulina platensis* novel green inhibitor for acid corrosion of mild steel. *Arabian J. Chem.* 5, 155–161.
14. Dehghani, A., Ghasem, B. & Ramezanzadeh, B. (2019). Green *Eucalyptus* leaf extract: A potent source of bio-active corrosion inhibitors for mild steel. *Bioelectrochemistry*. 130, 107339.
15. Krishnegowda, P., Venkatesha V. & Krishnegowda, P. (2013). *Acalyphatorta* leaf extract as green corrosion inhibitor for mild steel in hydrochloric acid solution. *Ind. Eng. Chem. Res.* 52, 722–728.
16. Jyothi, S., Ravichandran, J. (2014). *Luffaa egyptiaca* leaves extract as corrosion inhibitor for mild steel in hydrochloric acid medium. *J. Adh. Sci. Tech.* 28, 2347–2363.
17. Odewunmi, N., Umoren, S. & Gasem, Z. (2015). Utilization of watermelon rind extract as a green corrosion inhibitor for mild steel in acidic media. *J. Ind. Eng. Chem.* 21, 239–247.
18. Prabakaran, M., Kim, S. & Kalaiselvi, K. (2016). Highly efficient *Ligulari afischeri* green extract for the protection against corrosion of mild steel in acidic media: electrochemical and spectroscopic investigations. *J. Taiwan Inst. Chem. Eng.* 59, 553–562.
19. Muthukrishnan, P., Jeyaprabha, B. & Prakash, P. (2017). Adsorption and corrosion inhibiting behavior of *Lanneacoro mandelica* leaf extract on mild steel corrosion. *Arabian J. Chem.* 10, 2343–2354.
20. Fouda, A., Abousalem, A. & El-ewady, G. (2017). Mitigation of corrosion of C-steel in acidic solutions using an aqueous extract of *Tiliacordata* as green corrosion inhibitor. *Int. J. Ind. Chem.* 8, 61–73.
21. Mohammed Tariq Saeed, Muhammad Saleem, SoofiaUsmani, Izhar Ahmed Malik, Faisal Ahmad Al-Shammari, KashifMairajDeen. Corrosion inhibitions of mild steel in 1 M HCl by sweet melon peel extract. *J. of King Saud Univ. Sci.* 31, (2019): 1344-1351.
22. Ituen E., Akaranta O., James A., et al. Green and sustainable local biomaterials for oil field chemicals: *Griffonias implicifolia* extract as steel corrosion inhibitor in hydrochloric acid. *Sust. Mater. Technol.* 11, (2017):12–18.
23. Manjunath, & Nayak, S. (2019). Aqueous extract of *Dillenia pentagyna* fruit as green inhibitor for mild steel corrosion in 0.5 M

- hydrochloric acid solution. *J. Mater. Environ. Sci.* 10, 22-31.
24. Houaria, D. [Yahia, H., Lahcen, L., Wan Jeffrey, B. & Magaji L.].(2019). Corrosion inhibition activity of C-steel in 1.0 M hydrochloric acid media using Hammada scoparia extract: gravimetric and electrochemical study. *J. Adhesion Science and Technology*, 33, 808-838.
  25. Sakunthala, P., Vivekananthan, S. & Gopiraman, S. (2013). Spectroscopic investigations of physicochemical interactions on mild steel in an acidic media by environmentally friendly green inhibitors. *J. Surf. Deter.* 16, 251–263.
  26. Deb, D. & Dasgupta, S. (1987). On the identity of three species of *Urginea* (Liliaceae). *J. Boulay Nat. Hist. Sci.* 84, 409–412.
  27. Gentry, H., Verbiscar, A., & Banigan, T. (1987). Red squill (*Urginea maritima*, Liliaceae). *Econ. Bot.* 41, 267–282.
  28. Hesham, R., [El-Seedi, R., Burman, A., Zaki, T., Loutfy, B., Joachim, G. & G"oransson U. (2013). The traditional medical uses and cytotoxic activities of sixty-one Egyptian plants: Discovery of an active cardiac glycoside from *Urginea maritime*. *J. Ethenopharmacol.* 13, 746-757.
  29. Jarjes, Z., Mahmood A., Sallo, A., Ibrahim H. (2016). Identification of some Chemical Constituents and Antibacterial Activity of *Urginea maritima* (L.) Extracts from Kurdistan Region, Bozan area, Alqosh. *ZANCO J. of Pure and Appl. Sci.* 28 (6); 211-232.
  30. Tredder, R. (1984). *Corrosion Basics; an Introduction*, L.S. Van Delinder, ed. (Houston, TX: NACE,).
  31. Danielson, M. (1982). *Electrochemical Techniques in Corrosion Science and Engineering*. *J. Corro.*, (NACE), 11, 570.
  32. Damaski, B. (1971). "Adsorption of Organic Compounds on Electrodes", Plenum Press, New York, NY.
  33. Glasstone, S. & Lewis, D. (1960). "Elements of Physical Chemistry", 2nd Ed., MacMillan Co. Ltd.
  34. Moore, J. (1994). "Corrosion of Metals", a textbook of chemical metallurgy, (Butterworth–Heinemann) Ltd.
  35. Solmaz, R., Kardas, G., & Culha, M. (2008). Investigation of adsorption and inhibitive effect of 2-mercaptothiazoline on corrosion of mild steel in hydrochloric acid media. *Electrochim Acta.* 53, 5941–5952.
  36. Ramesh, S., Rajeswari, S. & Maruthamuthu, S. (2003). *Materials Letters*, 57.
  37. Shaker, N. (1986). M.Sc. Thesis, Tech. Univ. Baghdad, Iraq.
  38. Adam, G. (1986). "Industrial Chemistry", Mosul Univ. Press, Iraq.
  39. Sakunthala, P., Vivekananthan S., & Gopiraman, M. (2013). Spectroscopic investigations of physicochemical interactions on mild steel in an acidic media by environmentally friendly green inhibitors. *J. Surf. Deter.* 16, 251–263.
  40. Karthik, G., Sundaravadivelu, M. (2017). Experimental and theoretical studies of anti-ulcer drugs with benzimidazole rings as corrosion inhibitor for copper in 1 M nitric acid media. *J. Adh. Sci. Tech.* 31, 530–551.
  41. Hamdy, A. & El-Gendy, N. (2013). Thermodynamic, adsorption and electrochemical studies for corrosion inhibition of C-steel by henna extract in acid media. *Egypt. J. Pet.* 22, 17–25.
  42. Faustin, M. [Maciuk, A., Salvin, P., Roos, C. & Lebrini, M. (2015). Corrosion inhibition of C38 steel by alkaloids extract of *Geissospermum mume* in 1 M hydrochloric acid: Electrochemical and phytochemical studies. *Corros. Sci.* 92, 287–300,
  43. Bentiss, F., [Lebrini, M., Vezin, H., Chai, F., Traisnel, M. & Lagrené, M.]. (2009). Enhanced corrosion resistance of carbon steel in normal sulfuric acid medium by some macrocyclic polyether compounds containing a 1,3,4-thiadiazole moiety: AC impedance and computational studies. *Corros. Sci.* 51, 2165–2173.
  44. Yurt, A. [Bereket, G., Kivrak, A., Balaban, A. & Erk, B.]. (2005). Effect of Schiff bases containing pyridyl group as corrosion inhibitors for low C-steel in 0.1 M HCl. *J. Appl. Electrochem*, 35, 1025–1032.
  45. Adejoro, I., Ojo, F. & Obafemi, S. (2015). Corrosion Inhibition potentials of Ampicillin for mild steel in hydrochloric acid solution. *J. Taibah Univ. Sci.* 9, 169-202.
  46. Ali, A., Fali, S., Yousif, N. (2017). Modeling and Optimization of Structural Steel Corrosion Inhibition using Barely Grass Extract as Green



**Table 1.** CR, the efficiency of inhibition %E and coverage surface  $\Theta$  of C-steel in corrosive media at 25°C at different immersion times.

| Conc.<br>(w/v %) | 25 °C    |       |          |       |      |          |       |       |          |
|------------------|----------|-------|----------|-------|------|----------|-------|-------|----------|
|                  | Time (h) |       |          |       |      |          |       |       |          |
|                  | 2        |       |          | 4     |      |          | 6     |       |          |
|                  | CR       | %E    | $\Theta$ | CR    | %E   | $\Theta$ | CR    | %E    | $\Theta$ |
| 0                | 41.45    |       |          | 68.68 |      |          | 94.31 |       |          |
| 0.5              | 9.65     | 76.72 | 0.77     | 8.94  | 87   | 0.87     | 7.01  | 92.57 | 0.92     |
| 1                | 8.41     | 79.71 | 0.8      | 6.01  | 91.2 | 0.912    | 5.57  | 94.09 | 0.94     |
| 1.5              | 6.3      | 84.8  | 0.85     | 4.93  | 92.8 | 0.928    | 3.51  | 96.28 | 0.96     |
| 2                | 4.58     | 88.95 | 0.89     | 2.91  | 95.8 | 0.958    | 2.11  | 97.76 | 0.97     |
| 2.5              | 3.01     | 92.74 | 0.93     | 2.09  | 97   | 0.97     | 0.99  | 98.95 | 0.98     |

**Table 2.** CR, the efficiency of inhibition %E and coverage surface  $\Theta$  of C-steel in corrosive media at 35°C at different immersion times.

| Conc.<br>(w/v %) | 35 °C    |      |          |       |       |          |       |       |          |
|------------------|----------|------|----------|-------|-------|----------|-------|-------|----------|
|                  | Time (h) |      |          |       |       |          |       |       |          |
|                  | 2        |      |          | 4     |       |          | 6     |       |          |
|                  | CR       | %E   | $\Theta$ | CR    | %E    | $\Theta$ | CR    | %E    | $\Theta$ |
| 0                | 109.63   |      |          | 146.8 |       |          | 196.3 |       |          |
| 0.5              | 27.94    | 74.5 | 0.75     | 45.03 | 69.32 | 0.69     | 67.74 | 66    | 0.66     |
| 1                | 19.99    | 81.8 | 0.81     | 35.6  | 75.74 | 0.75     | 52.08 | 73.46 | 0.73     |
| 1.5              | 13.42    | 87.8 | 0.87     | 32.2  | 78.06 | 0.78     | 45.8  | 78.7  | 0.78     |
| 2                | 8.92     | 91.9 | 0.92     | 22.06 | 84.97 | 0.84     | 36.1  | 81.6  | 0.81     |
| 2.5              | 5.87     | 94.6 | 0.94     | 12.04 | 91.79 | 0.91     | 21.6  | 88.99 | 0.88     |

**Table 3.** CR, the efficiency of inhibition %E and coverage surface  $\Theta$  of C-steel in corrosive media at 45°C at different immersion times.

| Conc.<br>(w/v %) | 45 °C    |       |          |       |       |          |       |       |          |
|------------------|----------|-------|----------|-------|-------|----------|-------|-------|----------|
|                  | Time (h) |       |          |       |       |          |       |       |          |
|                  | 2        |       |          | 4     |       |          | 6     |       |          |
|                  | CR       | %E    | $\Theta$ | CR    | %E    | $\Theta$ | CR    | %E    | $\Theta$ |
| 0                | 185.7    |       |          | 196.9 |       |          | 204.6 |       |          |
| 0.5              | 78.24    | 51.48 | 0.51     | 92.83 | 52.85 | 0.52     | 95.85 | 53.15 | 0.53     |
| 1                | 57.78    | 68.23 | 0.68     | 70.71 | 64.08 | 0.64     | 79.7  | 69.84 | 0.69     |
| 1.5              | 32.04    | 82.38 | 0.82     | 47.62 | 75.81 | 0.75     | 51.2  | 74.97 | 0.74     |
| 2                | 19.56    | 89.24 | 0.89     | 27.5  | 86.03 | 0.86     | 36.4  | 82.2  | 0.82     |
| 2.5              | 17.92    | 90.14 | 0.901    | 21.01 | 89.32 | 0.89     | 27.01 | 86.79 | 0.86     |

**Table 4.** Corrosion current densities ( $\text{mA}/\text{cm}^2$ ) at different immersion times, different temperatures, and different inhibitor concentrations of C-steel in the corrosive media.

| Conc.<br>(w/v %) | 25°C               |                    |                    | 35°C               |                    |                    | 45°C               |                    |                    |
|------------------|--------------------|--------------------|--------------------|--------------------|--------------------|--------------------|--------------------|--------------------|--------------------|
|                  | 2h                 |                    |                    | 4h                 |                    |                    | 6h                 |                    |                    |
|                  | I <sub>corr.</sub> | I <sub>corr.</sub> | I <sub>corr.</sub> | I <sub>corr.</sub> | I <sub>corr.</sub> | I <sub>corr.</sub> | I <sub>corr.</sub> | I <sub>corr.</sub> | I <sub>corr.</sub> |
| 0                | 90.64              | 150.2              | 206.2              | 239.73             | 321.01             | 429.25             | 406.09             | 430.56             | 447.4              |
| 0.5              | 21.1               | 19.56              | 15.33              | 61.11              | 98.48              | 148.14             | 171.09             | 203                | 209.27             |
| 1                | 18.4               | 13.14              | 12.2               | 43.73              | 77.86              | 113.89             | 126.36             | 154.63             | 174.28             |
| 1.5              | 13.79              | 10.78              | 7.68               | 29.35              | 70.41              | 100.15             | 70.07              | 104.15             | 111.97             |
| 2                | 10.02              | 6.37               | 4.62               | 19.52              | 48.24              | 78.94              | 42.77              | 60.13              | 79.61              |
| 2.5              | 6.59               | 4.58               | 2.18               | 12.85              | 26.33              | 47.25              | 39.19              | 45.95              | 59.06              |

Note: I<sub>corr</sub> = corrosion current density ( $\text{mA}/\text{Cm}^2$ )

**Table 5.** Thermodynamic parameters obtained from Langmuir adsorption isotherm.

| Temperature | R <sup>2</sup> | K <sub>ads</sub> | $\Delta G^\circ_{\text{ads}}$ |
|-------------|----------------|------------------|-------------------------------|
| 25 °C       | 0.996          | 5.025            | -13.9                         |
| 35 °C       | 0.998          | 4.651            | -14.2                         |
| 45 °C       | 0.994          | 2.227            | -12.7                         |



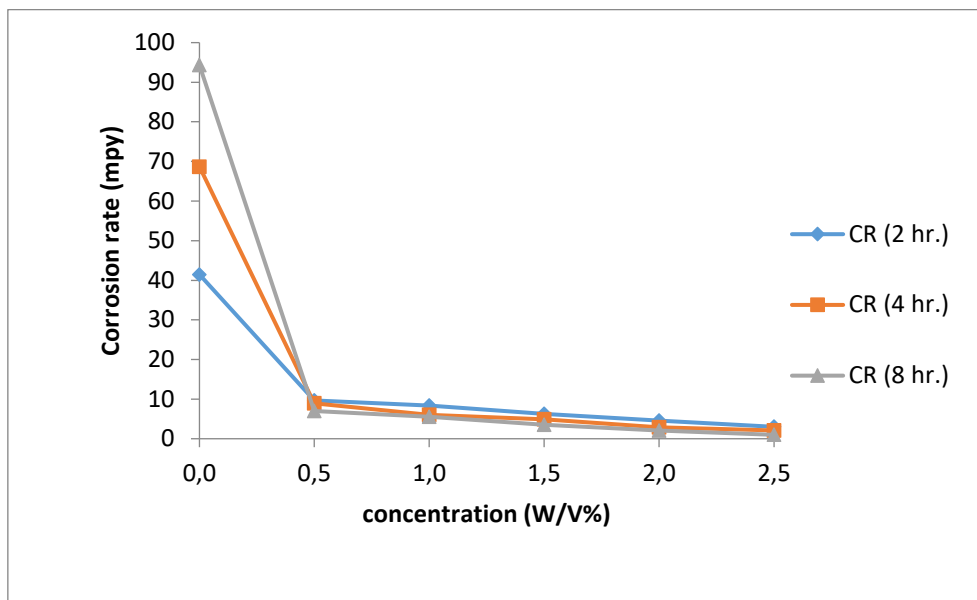


**Figure 3.** Variation of CR with various concentrations of (WO) extract for C-steel coupons in 0.5 M HCl solution at (25°C).

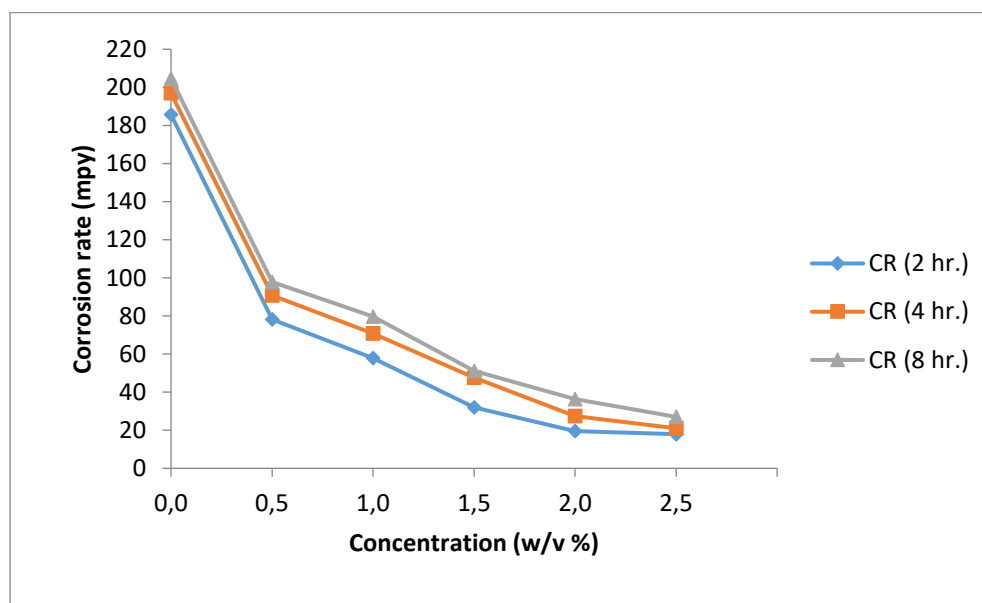


**Figure 4.** Variation of CR with various concentrations of (WO) extract for C-steel coupons in 0.5 M HCl solution at (35°C).

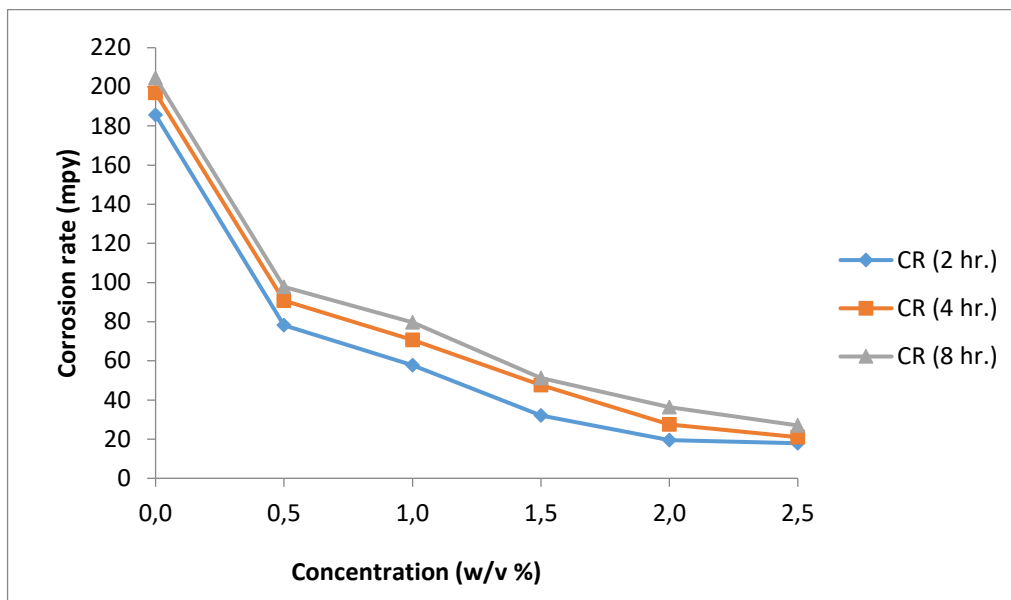


**Figure 5.** Variation of CR with various concentrations of (WO) extract for C-steel coupons in 0.5 M HCl solution at (45°C).

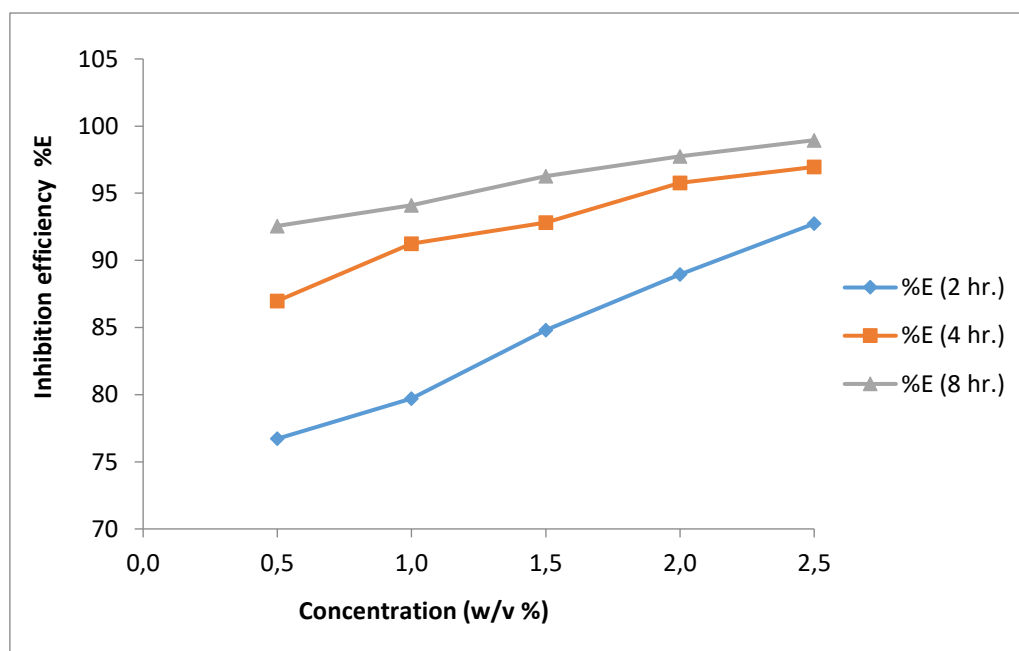


**Figure 6.** Variation of inhibition efficiency %E with various concentrations of (WO) extract for C-steel coupons in 0.5 M HCl solution at (25°C).

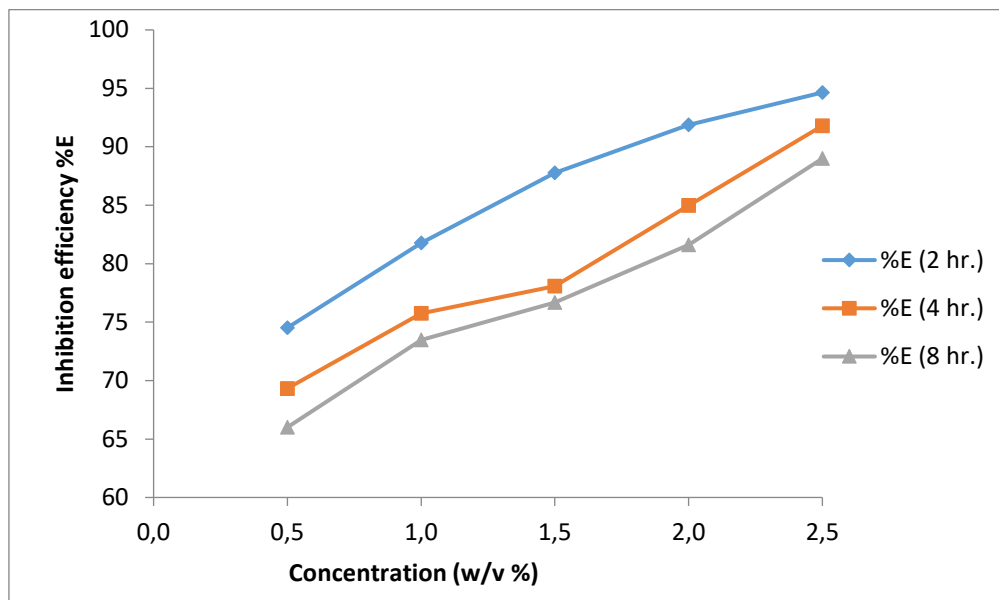


**Figure 7.** Variation of inhibition efficiency %E with various concentrations of (WO) extract for C-steel coupons in 0.5 M HCl solution at (35°C).

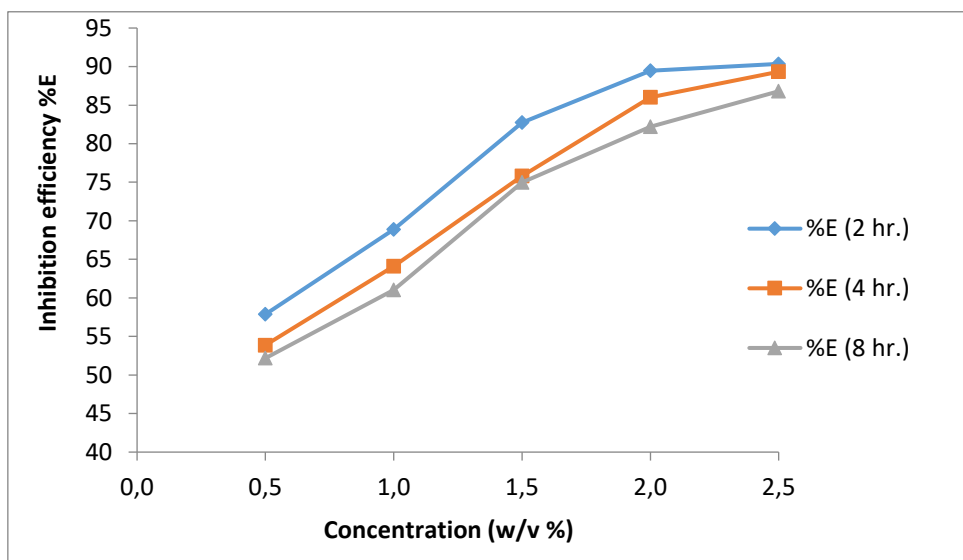


**Figure 8.** Variation of inhibition efficiency %E with various concentrations of (WO) extract for C-steel coupons in 0.5 M HCl solution at (45°C).

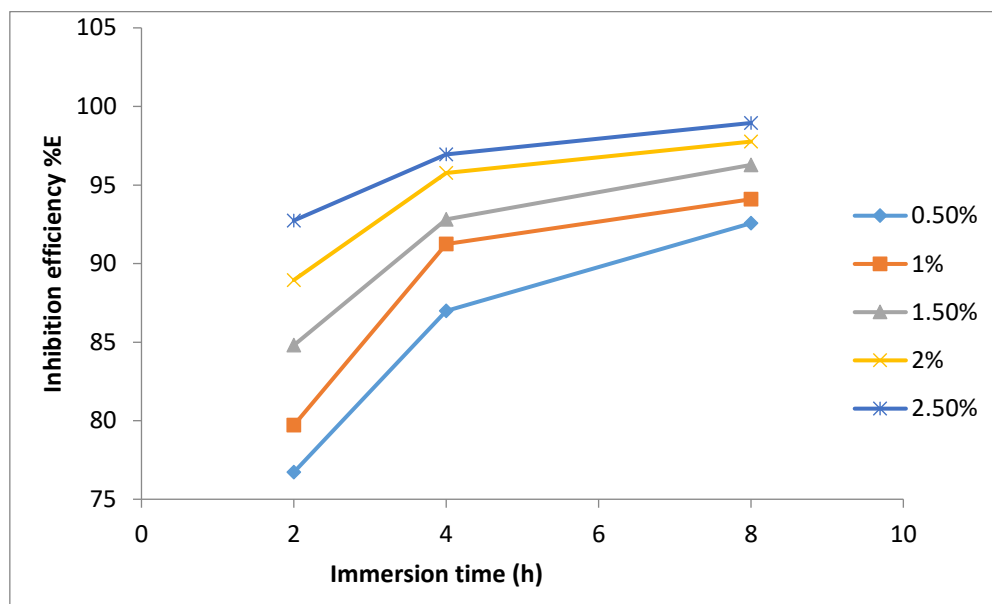


**Figure 9:** Variation efficiency of inhibition %E with various times of immersion for C-steel coupons in solution of 0.5 M HCl in the presence and absence of various (WO) extract concentrations of at (25°C).

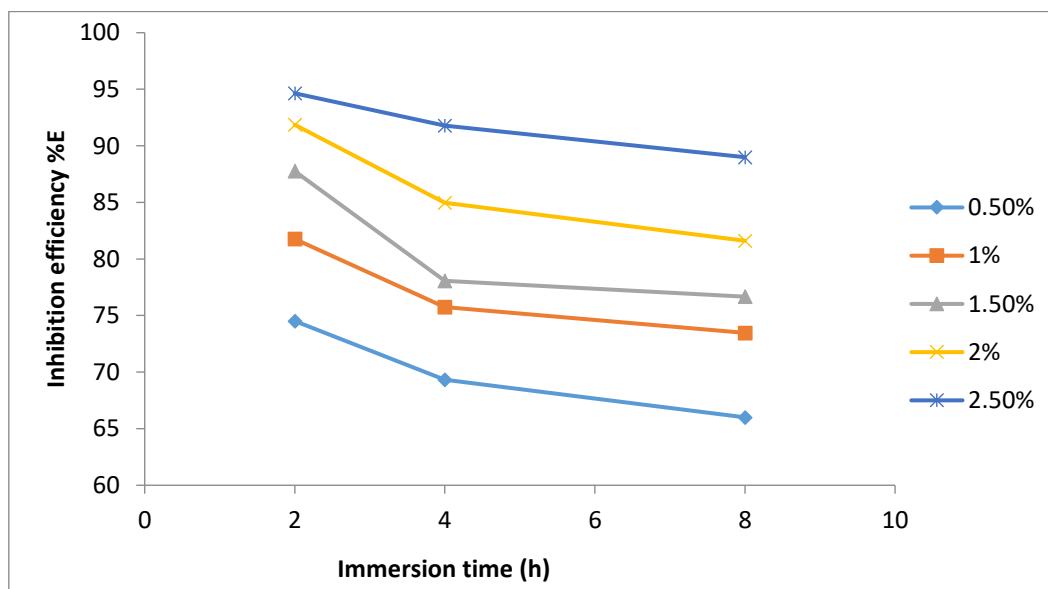


**Figure 10:** Variation efficiency of inhibition %E with various times of immersion for C-steel coupons in solution of 0.5 M HCl in the presence and absence of various (WO) extract concentrations of at (35 °C).

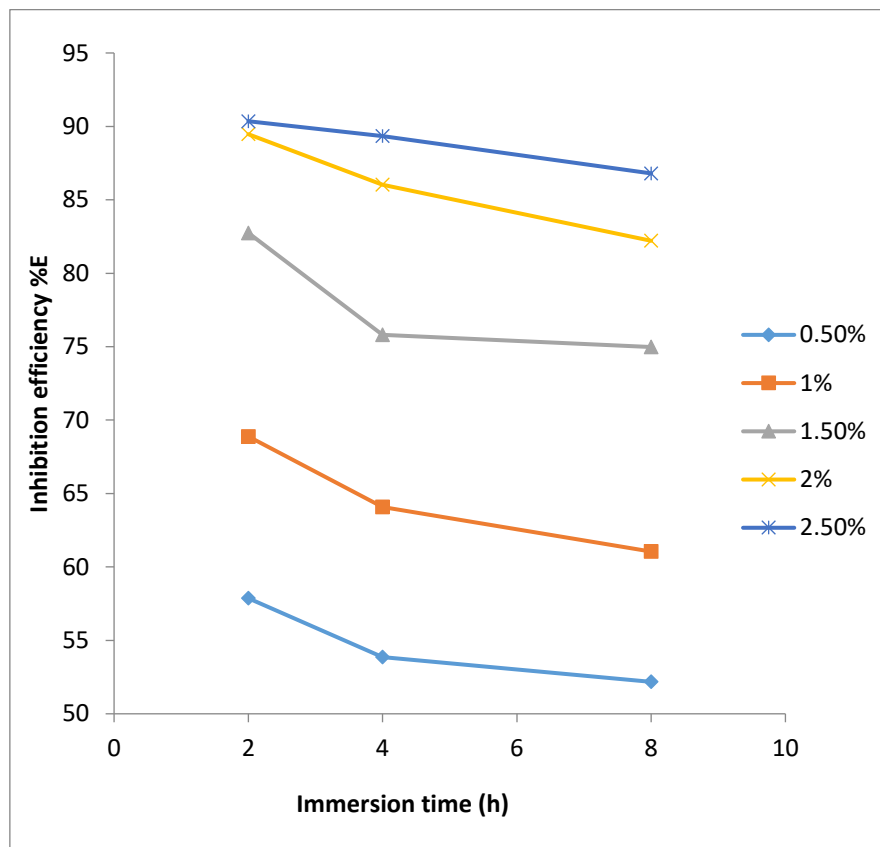


**Figure 11.** Variation efficiency of inhibition %E with various times of immersion for C-steel coupons in solution of 0.5 M HCl in the presence and absence of various (WO) extract concentrations of at (45°C).

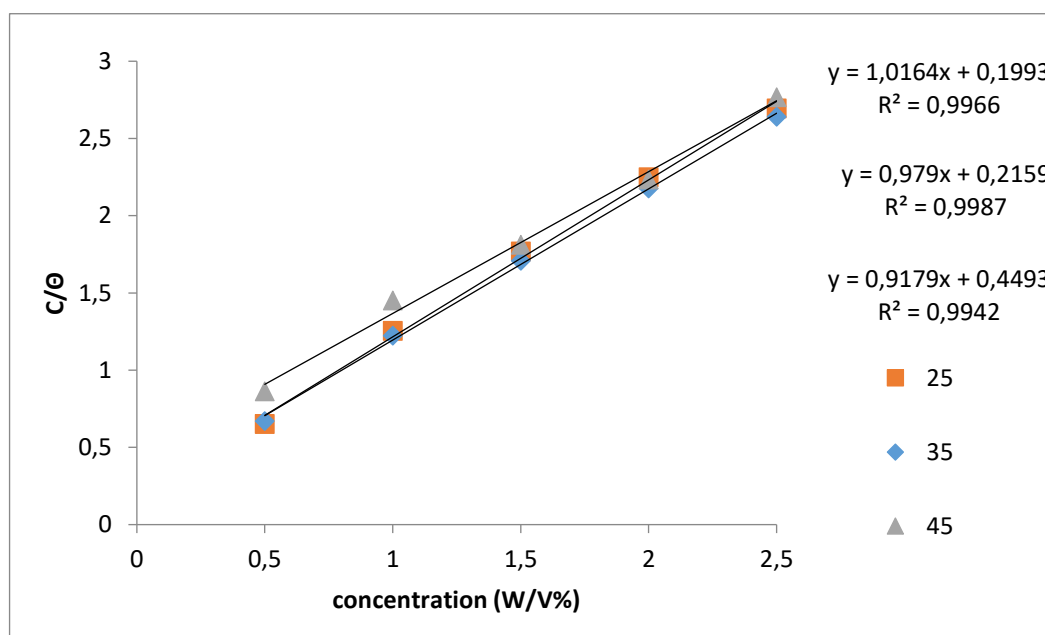


**Figure 12.** Langmuir of isotherm adsorption model of (WO) extract on the surface of C-steel at (25°C ,35°C and 45°C).

**ANÁLISE DA EFICÁCIA DA IMUNOTERAPIA USANDO UM COMPLEXO AUTOLÓGICO DE IMUNOPEPTÍDEOS NO TRATAMENTO CIRÚRGICO DA PERIODONTITE****ANALYSIS OF THE EFFECTIVENESS OF IMMUNOTHERAPY USING AN AUTOLOGOUS COMPLEX OF IMMUNOPEPTIDES IN THE SURGICAL TREATMENT OF PERIODONTITIS****АНАЛИЗ ЭФФЕКТИВНОСТИ ПРИМЕНЕНИЯ ИММУНОТЕРАПИИ С ИСПОЛЬЗОВАНИЕМ АУТОЛОГИЧНОГО КОМПЛЕКСА ИММУНОПЕПТИДОВ ПРИ ХИРУРГИЧЕСКОМ ЛЕЧЕНИИ ПАРОДОНТИТА**

SEVBITOV, Andrei\*; DAVIDYANTS, Alla; BALYKIN, Roman; TIMOSHIN, Anton;  
KUZNETSOVA, Mariya

Department of Propaedeutic of Dental Diseases  
of I. M. Sechenov First Moscow State Medical University (Sechenov University)

\* Correspondence author  
e-mail: avsevbitov@mail.ru

Received 21 March 2020; received in revised form 26 May 2020; accepted 04 July 2020

**RESUMO**

A doença periodontal na população adulta é um dos problemas mais urgentes da odontologia em todo o mundo. Graças à introdução de modernas tecnologias na prática, foi possível identificar os principais mecanismos de desenvolvimento desta doença nos níveis molecular e genético. A interação de patógenos periodontais com fatores imunes da proteção antimicrobiana do corpo é a base da inflamação do tecido periodontal e leva ainda à destruição do osso alveolar. As células epiteliais da mucosa gengival desempenham um papel crucial contra bactérias patogênicas periodontais. Os fatores de imunidade inata desempenham um papel não apenas na proteção antimicrobiana, mas também apóiam as condições necessárias para a cura e regeneração dos tecidos periodontais. Portanto, várias abordagens terapêuticas que afetam os fatores de imunidade inata são consideradas efetivas e promissoras. O exame clínico e a determinação dos fatores de imunidade inata foram realizados em 115 pacientes. Indivíduos saudáveis compunham um grupo de 30 pessoas. Pacientes com periodontite crônica generalizada com diferentes graus de gravidade eram 85 pessoas. Cada paciente foi submetido à ortopantomografia no ortofantomógrafo Orthophosis XG-DS/Ceph (SIRONA Dental System GmbH, Alemanha) para avaliar o estado do tecido ósseo dos maxilares (o grau de destruição da camada cortical, o grau de reabsorção do interalveolar). Radiografias intraorais direcionadas foram usadas para avaliar o estado do tecido ósseo e a qualidade do tratamento cirúrgico. Os métodos imunológicos de pesquisa foram realizados em várias etapas. Os achados deste artigo afirmam que o uso de imunopeptídeos complexos autólogos no tratamento cirúrgico da periodontite reduz o tempo de obtenção de um efeito terapêutico 2 vezes, resultando no alívio rápido dos sintomas de inflamação e na aceleração dos processos reparativos.

**Palavras-chave:** *imunidade, periodontite, imunopeptídeos, retalhos, tecido ósseo.*

**ABSTRACT**

Periodontal disease in the adult population is one of the most pressing problems of dentistry around the world. Thanks to the introduction of modern technologies in practice, it was possible to identify the main mechanisms of the development of this disease at the molecular and genetic level. The interaction of periodontal pathogens with immune factors of antimicrobial protection of the body is the basis of periodontal tissue inflammation and further leads to the destruction of the alveolar bone. Epithelial cells of the gum mucosa play a crucial role against periodontal pathogenic bacteria. Factors of innate immunity play a role not only in antimicrobial protection, but they also support the conditions necessary for the healing and regeneration of periodontal tissues. Therefore, various therapeutic approaches that affect the factors of innate immunity are considered as effective and promising. Clinical examination and determination of factors of innate immunity were performed in 115 patients. Healthy individuals made up a group of 30 people. Patients with chronic generalized periodontitis with varying degrees of severity were 85 people. Each patient underwent orthopantomography on the orthopantomograph Orthophosis XG DS/Ceph (SIRONA Dental System GmbH, Germany) in order to assess the state of the bone tissue of the jaws (the degree of destruction of the cortical layer, the degree of resorption of the

interalveolar partitions). Targeted intraoral radiographs were used to assess the state of bone tissue and the quality of surgical treatment. Immunological methods of research were carried out in several stages. The findings of this article make the claim that the use of autologous complex immunopeptides in the surgical treatment of periodontitis reduces the time of achieving a therapeutic effect 2 times, resulting in the rapid relief of the symptoms of inflammation and acceleration of reparative processes.

**Keywords:** *immunity, periodontitis, immunopeptides, patchwork, bone tissue.*

## АННОТАЦИЯ

Заболевания пародонта среди взрослого населения представляют одну из актуальных проблем стоматологии во всем мире. Благодаря внедрению в практику современных технологий, удалось выявить основные механизмы развития данного заболевания на молекулярно-генетическом уровне. Взаимодействие пародонтопатогенов с иммунными факторами противомикробной защиты организма лежит в основе воспаления тканей пародонта и в дальнейшем приводит к деструкции альвеолярной кости. Эпителиальные клетки слизистой оболочки десны играют решающую роль в отношении пародонтопатогенных бактерий. Факторы врожденного иммунитета играют роль не только в противомикробной защите, они также поддерживают условия, необходимые для заживления и регенерации тканей пародонта. Поэтому различные лечебные подходы, влияющие на факторы врождённого иммунитета, рассматриваются как эффективные и перспективные. Клиническое обследование и определение факторов врождённого иммунитета было проведено у 115 пациентов. Здоровые лица составили группу из 30-и человек. Пациенты с хроническим генерализованным пародонтитом с разной степенью тяжести составили 85 человек. Каждому пациенту проводили ортопантомографию на ортопантомографе Orthophosis XG DS/Ceph (SIRONA Dental System GmbH, Германия) с целью оценки состояния костной ткани челюстей (степень деструкции кортикального слоя, степень резорбции межальвеолярных перегородок). С целью оценки состояния костной ткани и качества хирургического лечения использовали прицельные внутриротовые рентгенограммы. Иммунологические методы исследования проводили в несколько этапов. Результаты исследования данной статьи позволяют сделать утверждение, что применение аутологичного комплекса иммунопептидов при хирургическом лечении пародонтита сокращает сроки достижения лечебного эффекта в 2 раза, что выражается в быстром снятии симптомов воспаления и ускорении репаративных процессов.

**Ключевые слова:** *иммунитет, пародонтит, иммунопептиды, лоскутные операции, костная ткань.*

## 1. INTRODUCTION

Periodontal diseases in the adult population are one of the most pressing problems of dentistry in the world. Thanks to the introduction of modern technologies in practice, it was possible to identify the main mechanisms of development of this disease at the molecular genetic level [Balykin, 2016; Zorina *et al.*, 2016, 2017; Mamedov *et al.*, 2019; Utyuzh *et al.*, 2019].

Epithelial cells of the gingival mucosa together with humoral and cellular factors of saliva and gingival fluid from the first line of protection of the body from infection and play a crucial role against periodontal pathogenic bacteria [Platonova *et al.*, 2018; Sevbitov *et al.*, 2018; Mitin *et al.*, 2019; Sevbitov *et al.*, 2020; Timoshin *et al.*, 2018, 2019]. The epithelium of the gingival mucosa expresses Toll-like receptors (TLR) that recognize the lipopolysaccharides of anaerobic bacteria and contribute to the production of proinflammatory cytokines, chemokines, and other mediators that regulate inflammation [Sevbitov *et al.*, 2019, 2020;

Bostanci *et al.*, 2012; Kolodkina *et al.*, 2018; Kuznetsova *et al.*, 2018]. Along with cytokines, the epithelium of the gingival mucosa produces antimicrobial peptides  $\beta$ -defensins (hBD), which have a wide range of antimicrobial activity, causing the death of microorganisms due to violation of the integrity of their membranes [Belibasakis *et al.*, 2015; Cochran, 2008; Cortés-Vieyra *et al.*, 2016; Turgaeva *et al.*, 2020].

Factors of innate immunity play a role not only in antimicrobial protection, but they also support the conditions necessary for healing and regeneration of periodontal tissues. Therefore, various therapeutic approaches that affect the factors of innate immunity are considered as effective and promising [Ding *et al.*, 2014; Dommisch *et al.*, 2015; Garlet *et al.*, 2010; Giannobile *et al.*, 2015; Groeger *et al.*, 2015; Voloshina *et al.*, 2018 ].

At the present stage of periodontitis, treatment attempts are being made to restore all periodontal structures simultaneously, and methods of tissue

engineering and directed tissue regeneration are actively implemented [Hans *et al.*, 2011; Katz *et al.*, 1989; Mudda *et al.*, 2011; Sevbitov *et al.*, 2018, 2019, 2020].

One of the ways to stimulate reparative tissue regeneration is the possibility of influencing cell proliferation and differentiation by a composition of cytokines and growth factors synthesized by autologous cells of the immune system [Reddi, 2001; Shuai *et al.*, 2018; Shue *et al.*, 2012; Song *et al.*, 2016; Enina *et al.*, 2019; Ergesheva *et al.*, 2018; Mironov *et al.*, 2020].

The purpose of our study: to evaluate the effectiveness of immunotherapy using an autologous complex of immunopeptides in the surgical treatment of periodontitis.

## 2. MATERIALS AND METHODS

Clinical examination and determination of factors of innate immunity were carried out in 115 patients. Healthy individuals made up a group of 30 people. Patients with chronic generalized periodontitis with varying degrees of severity were 85 people. With a mild degree - 25 patients, with an average - 40 patients, with a severe-20 patients. Patients with moderate periodontitis (40 people) received conservative treatment, and 1 month after it, surgical treatment was performed in the form of flap operations. The monitoring of long-term results after surgical treatment was carried out within 1, 3, and 6 months.

The gender distribution of patients was as follows: 73 women and 42 men. The age of the surveyed was from 35 to 65 years. The median age was 52 years (Table 1).

**Table 1.** Age distribution of patients

| Groups surveyed        | Age of persons examined (years) |       |       |       |
|------------------------|---------------------------------|-------|-------|-------|
|                        | n                               | 35-45 | 46-55 | 56-65 |
| Healthy faces          | 30                              | 12    | 9     | 9     |
| ChP (complex) patients | 85                              | 22    | 40    | 23    |
| Total                  | 115                             | 34    | 49    | 32    |

The group of people surveyed was

dominated by women, and they were 1.7 times more than men (Table 2).

During the examination of patients, General clinical methods were used (survey, examination, determination of clinical indices), x-ray methods, and filling out medical documentation (Appendix 1).

**Table 2.** Gender distribution of patients

| Groups surveyed        | n   | Men | Women |
|------------------------|-----|-----|-------|
| Healthy faces          | 30  | 12  | 18    |
| ChP (complex) patients | 85  | 30  | 55    |
| Total                  | 115 | 42  | 73    |

Each patient underwent orthopantomography using an orthopantomograph Orthophosis XG DS/Ceph (SIRONA Dental System GmbH, Germany) to assess the condition of the jaw bone (the degree of destruction of the cortical layer, the degree of resorption of the interalveolar septa). In order to assess the state of bone tissue and the quality of surgical treatment, targeted intraoral radiographs were used.

Immunological research methods were carried out in several stages (Figure 6). The first stage involved determining factors of innate immunity in healthy individuals (30 patients) and patients with ChP (complex) with varying degrees of severity (85 patients) before treatment.

At the second stage, in patients with moderate ChP (complex) (40 patients), the factors of innate immunity were determined before and after conservative treatment before they underwent surgical treatment.

The third, fourth, and fifth stages included determining factors of innate immunity in patients with moderate ChP (complex) after surgical treatment within 1, 3, and 6 months.

To determine the expression of the TLR4 and hBD-3 gene in the gum epithelium, a scrape was obtained in the area of the attached gum using disposable sterile probes, which placed an Eppendorf test tube for 2-3 seconds with 0.5 ml of saline solution and frozen at a temperature of -20 °C until the time of the study (Figure. 1). Biological material was collected before treatment, after conservative treatment, before flap operations,



and then 1, 3, and 6 months after surgical treatment.

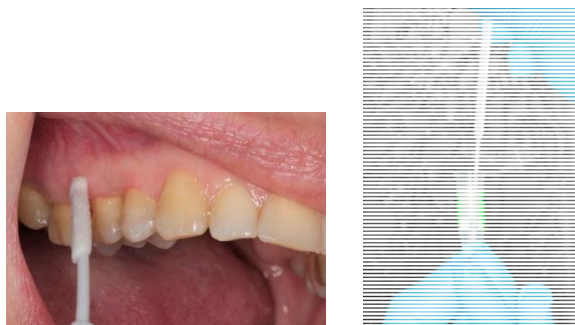


**Figure 1.** Material intake in the area of the gingival margin during periodontitis (a) and placing the biological material in an Eppendorf tube (b)

Of the samples has been isolated RNA using a kit of reagents "Ampli PRIME RIBO-Sorb" To determine the level of expression of the studied genes, cDNA was obtained using a reverse transcription reaction. At the next stage of the study, a real-time polymerase chain reaction (PCR-RV) was performed on the DT-96 device with the resulting reaction OT cDNA. The reaction was performed using "A set of reagents for PCR-RV in the presence of the intercalating dye SYBR Green I".

To determine cytokines, the contents of periodontal pockets (PC) were collected using sterile paper strips made of filter paper, measuring 0.3 by 0.5 mm, for 30 seconds, then placed in an Eppendorf tube with 100 microl of saline solution and frozen at a temperature of -20 °C until the study was completed (Figure. 2).



**Figure 2.** Gingival fluid intake from a pocket for cytokine detection

The study of the cytokine spectrum in the gingival fluid included determining the level of cytokines - interleukin-6 (IL-6) and transforming growth factor - TGF $\beta$ 1. We used commercial sets of TGF $\beta$ 1 "eBioscience" (USA) for setting the solid-

phase enzyme immunoassay (ELISA) according to the recommended methods. This immunological method for determining various compounds in biological fluids is based on the antigen-antibody reaction [Harrington, L. *et al.*, 2005].

Complex treatment consisted of successive stages and included the following measures: pre-treatment stage (thorough professional, hygienic treatment of the oral cavity), conservative treatment (local antibacterial therapy), surgical treatment (conducting flap operations using the Widman-Neumann method). In total, flap operations were performed in 40 patients with moderate ChP (complex) in the area of 165 teeth. Dynamic follow-up was performed 1-3-6 months after surgical treatment.

On the eve of the flap operations, patients were collected 10 ml of venous blood and immediately transported to the laboratory to obtain an autologous complex of immunopeptides (AKI). Then, according to the technology developed at the Department of Immunology, 5-7 ml of AKI containing cytokines and antimicrobial peptides (TNF $\alpha$ , TGF-1,  $\alpha$ -defensin-HNP1-3) were obtained from leukocyte cultures of patients. In parallel, AKI was obtained from white blood cell cultures of 30 healthy donors.

The course of the operation was as follows: under infiltration anesthesia Sol. Ultracaini 2%-5.0 exfoliated the Muco-periosteal flap, removed dental deposits, granulations, polished the bone edge with a drill, de-epithelization of the gingival edge, the wound surface was irrigated with AKI solution from a syringe in an amount of 1.0-1.5 ml.

The bone defect was filled with osteoplastic material, which was also impregnated with AKI, then sutured in each interdental space.

### 3. RESULTS AND DISCUSSION:

In the postoperative period after flap surgery, patients of the main group with the use of AKI on the 1st day showed no pain symptom, and the mucous membrane was pink. On day 2-3, there was no inflammatory reaction (edema, hyperemia), the interdental papillae were in the epithelization stage, and the sutures were preserved. By day 6-7, there was complete epithelization of the mucosa. The gums were tightly attached to the necks of the teeth, had a pink color, and there was a need to remove the sutures, they were removed completely. Without this method of treatment in the comparison group,

all processes of healing and complete epithelization of the mucosa took place on the 9th-10th day. The removal of stitches was on 13-14 days.

**Table 3.** Clinical indicators of the effectiveness of the use of an autologous complex of immunopeptides in the surgical treatment of periodontitis

| Signs  | Without AKI   | Local AKI     |
|--|---------------|---------------|
|  | n=20          | n=20          |
| 1. Disappearance of signs of inflammation (edema, hyperemia) | 7,0±0,3 day.  | 3,0±0,1 day.* |
| 2. Removal of stitches full                                  | 13,0±1,0 day. | 7,0±0,1 day.* |
| 3. Complete tissue repair                                    | 14,0±1,0 day. | 7,0±1,0 day.* |

\* - reliability of differences in indicators compared to the control,  $p < 0,01$ .

For 12 months. after flap operations (period of observation), patients in the main group and in the comparison group were noted: the absence of inflammatory phenomena, the absence of dental pockets, compaction of the gingival margin, and the lack of tooth mobility.

After 12 months. on the x-ray in the area of the operated teeth, the bone density was determined, and the cortical plate was clearly expressed in both groups compared. There were no differences in bone x-rays in these groups (Figure 4,5).



**Figure 4.** Radiograph of patient A. before surgical treatment in the field of teeth 15.16.17. and 45.46.47. and after surgical treatment with AKI in the field of teeth 15.16.17. (a) after 1 year and 45.46.47. after 1.5 years (b)

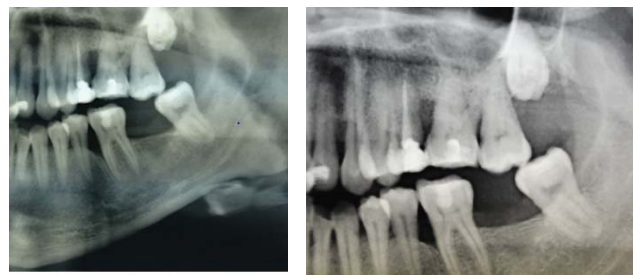


**Figure 5.** Radiograph of patient L. before surgical treatment without the use of AKI in the field of teeth 25.26.27. and 34.35.36. (a) and 6th (b) after surgical treatment without AKI in the field of teeth 25.26.27. after 1 year and 34.35.36. after 1.5 years

Thus, after surgical treatment with the use of AKI, pain relief was observed more pronounced in terms of time, the disappearance of inflammatory phenomena (edema, hyperemia), and the onset of epithelization of the wound. All these phenomena occurred 2-3 times faster than in the comparison group. Treatment with AKI was easily tolerated by patients. It allowed limiting the treatment of the wound with antiseptics and taking antibiotics after surgical treatment. Suppuration or other complications were not observed in any case.

The advantages of surgical treatment with the use of AKI can be attributed to its harmlessness in respect of the hepatitis b virus and HIV.

X-ray analysis was performed to determine the density of bone tissue in the area of the operated teeth, as well as the clear severity of the cortical plate in both groups compared. There were no differences in bone radiographs in these groups.

#### 4. CONCLUSIONS:

In patients with ChP (complex), the expression of the TLR4 gene in the gum epithelial cells was increased by 12 times compared to healthy individuals. In severe ChP (complex), the TLR4 gene expression level was highest, 5 times higher than in mild and 3 times higher than in average. The expression of the hBD-3 gene in the gum epithelium in patients with ChP (complex) is increased by 5 times compared to healthy individuals. In mild ChP (complex), the expression of the hBD-3 gene in the gum epithelial cells exceeded the indicators in moderate and severe cases by 2 times. The use of an autologous complex of immunopeptides in the surgical treatment of periodontitis reduced the time to achieve the therapeutic effect by 2 times, which was expressed in the rapid removal of symptoms

of inflammation and acceleration of reparative processes.

## 5. ETHICS APPROVAL:

The study conforms to strobe guidelines. all procedures performed in studies involving human participants were in accordance with the ethical standards of the Sechenov University ethics committee and with the 1964 Helsinki declaration and its later amendments. All human subjects' rights have been protected by the Sechenov University ethics committee, and written informed consent was obtained from all subjects who participated in the study.

## 6. ACKNOWLEDGMENTS:

This work was done at Sechenov University with supported by the "Russian Academic Excellence Project 5-100".

## 7. REFERENCES:

1. Balykin, R. (2016). The importance of innate immunity factors in the development of inflammatory and destructive periodontal lesions. *Dentistry*, 3, 64-65.
2. Zorina, O., Gankovskaya, L., Balykin, R., and Ivanyushko T. (2016). Expression of TLR4 and HBD-3 genes in mucosal epithelial cells in the surgical treatment of periodontitis. *Dentistry*, 4, 13-15.
3. Zorina, O., Gankovskaya, L., Balykin R. (2016). The study of autologous immunopeptides in the surgical treatment of periodontitis. *Dentistry*, 6, 30-31.
4. Zorina, O., Gankovskaya, L., Balykin R., and Svitich O. (2017). The positive effect of the use of autologous immunopeptides in the surgical treatment of inflammatory and destructive periodontal lesions. *Russian Dental Journal*, 1, 4-7.
5. Zorina, O., Gankovskaya, L., Balykin, R., and Svitich, O. (2017). Molecular mechanisms of the pathogenesis of periodontitis. *Dentistry for everyone*, 3, 41-45.
6. Platonova, V., Sevbitov, A., Shakaryants, A., and Dorofeev, A. (2018). Experimental and clinical justification for the treatment of patients with odontogenic phlegmon of the maxillofacial region using dalargin in the complex therapy. *Clinical laboratory diagnostics*, 63(5), 293-296.
7. Sevbitov, A., Borisov, V., Davidyants, A., Timoshin, A., Ershov, K., Enina, Yu., and Pustokhina, I. (2018). Prevention of injuries of the maxillofacial area in contact sports using sports caps. *Indo American Journal of Pharmaceutical Sciences*, 5(11), 12322-12325.
8. Sevbitov, A., Kuznetsova, M., Dorofeev, A., Borisov, V., Davidyants, A., Mironov, S., Timoshin, A., Paperno, A., and Limonjan V. (2020). *Introduction to cariology and periodontology*, 120.
9. Bostanci, N., Belibasakis, G. (2012) Porphyromonas gingivalis: an invasive and evasive opportunistic oral pathogen. *FEMS Microbiology Letters*, 333(1), 1–9.
10. Kuznetsova, M., Nevдах, A., Platonova, V., Sevbitov, A., and Dorofeev, A. (2018). Evaluation of effectiveness of a preparation on the basis of phytoecdysteroids for treatment of traumatic injuries of oral mucosa in orthodontic patients. *International Journal of Green Pharmacy*, 12(S1), 297-300.
11. Belibasakis, G., Kast, J., Thurnheer, T., and Akdis, C. (2015). The expression of gingival epithelial junctions in response to subgingival biofilms. *Virulence*, 6(7), 704-9.
12. Cochran, D. (2008). Inflammation and bone loss in periodontal disease. *Journal of Periodontology*, 79(8), 1569–1576.
13. Cortés-Vieyra, R., Rosales, C., Uribe-Querol, E. (2016). Neutrophil Functions in Periodontal Homeostasis. *J Immunol Res*, 13961-06.
14. Ding, P., Jin, L. (2014). The role of lipopolysaccharide-binding protein in innate immunity: a revisit and its relevance to oral/periodontal health. *J Periodontal Res*, 49, 1-9.

15. Dommisch, H., Jepsen, S. (2015). Diverse functions of defensins and other antimicrobial peptides in periodontal tissues. *Periodontol 2000*, 69(1), 96-110.
16. Garlet, G. (2010). Destructive and protective roles of cytokines in periodontitis: a re-appraisal from host defense and tissue destruction viewpoints. *Journal of Dental Research*, 9(12), 1349–1363.
17. Giannobile, W., McClain, P. (2015). Enhancing Periodontal Health Through. *Regenerative Approaches Journal of Periodontology*, 86(2), S1-S3.
18. Groeger, S., Meyle, J. (2015). Epithelial barrier and oral bacterial infection. *Periodontol 2000*, 69(1), 46-67.
19. Hans, M., Hans, V. (2011). Toll-like receptors and their dual role in periodontitis: a review. *Journal of Oral Science*. 53(3), 263–271.
20. Katz, J. (1989). Goulschins. The interleukin concept and the periodontal diseases. *Medical Hypotheses*, 29, 251-254.
21. Mudda, J., Bajaj, M. (2011). Stem cell therapy: A challenge to periodontist. *Indian J Dent Res*, 22, 132-139.
22. Reddi, A. (2001). Bone morphogenetic proteins: from basic science to clinical applications. *J. Bone Joint Surg. Am.* 83(1), S1-S6.
23. Shuai, Y., Ma, Y., Guo, T., and Zhang, L. (2018). Dental Stem Cells and Tooth Regeneration. *Adv Exp Med Biol*, 27, 382-8.
24. Shue, L., Yufeng, Z., Mony, U. (2012). Biomaterials for periodontal regeneration: a review of ceramics and polymers. *Biomater*, 2(4), 271-7.
25. Song, B., Zhang, Y., Chen, L., and Zhou, T. (2016). The role of Toll-like receptors in periodontitis. *Oral Dis*, 29, 487-499.
26. Mamedov, A., Morozova, N., Yumashev, A., Dybov, A., and Nikolenko, D. (2019). Criteria for provisional restorations used in preparation for comprehensive orthodontic and orthopedic rehabilitation. *Periodico Tchê Química*, 16(32), 647-655.
27. Utyuzh, A., Nikolenko, D., Yumashev, A., Volchkova, I., and Samusenkov, V. (2019). Adhesion of periodontal pathogens to materials used for long-term temporary crowns. *Periodico Tchê Química*, 16(33), 60-69.
28. Sevbitov, A., Persin, L., Slabkobskaia, A., and Pankratova, N. (1999). The morphological status of the maxillo-dental system in children living in an area contaminated by radionuclides as a result of the accident at the chernobyl atomic electric power station. [Morfologicheskoe sostoyaniye zuchelivshchikh v raione, zagriaznennom radionuklidami v rezul'tate avarii na ChAES.] *Stomatologiya*, 78(6), 41-42.
29. Sevbitov, A., Kuznetsova, M., Dorofeev, A., Borisov, V., Mironov, S., and Iusupova, I. (2020). Dental anomalies in people living in radionuclide-contaminated regions. *Journal of Environmental Radioactivity*, 216, 106190
30. Timoshin, A., Sevbitov, A., Drobot, G., Yumashev, A., and Timoshina, M. (2018). Use of bioresorbable plates on the basis of collagen and digestase for treatment of diseases of oral mucosa (review of clinical cases). *International Journal of Green Pharmacy*, 12(1), 290-296.
31. Sevbitov, A., Davidyants, A., Kuznetsova, M., Dorofeev, A., and Mironov, S. (2019). Analysis of electronic microscopy results based on combining the infiltration method with different restoration technologies and in vitro investigation of enamel focal demineralization treatment at the defect stage. *Periodico Tchê Química*, 16(33), 53-59.
32. Sevbitov, A., Brago, A., Enina, Y., Dorofeev, A., and Mironov, S. (2018). Experience in the application of hybrid

ceramic restorations in the cervical region. *Asian Journal of Pharmaceutics*, 12(3), S1106-S1109.

33. Sevbitov, A., Dorofeev, A., Davidiants, A., Ershov, K., and Timoshin, A. (2018). Assessment of pain perception of elderly patients with different levels of dentophobia during surgical dental appointment. *Asian Journal of Pharmaceutics*, 12(3), S1012-S1016

34. Sevbitov, A., Dorofeev, A., Kuznetsova, M., Timoshin, A., and Ershov, K. (2019). Comparative characteristics of the crystallogram of the oral fluid in patients who use heroin and methadone. *Periodico Tchê Química*, 16(33), 94-101.

35. Sevbitov, A., Timoshin, A., Dorofeev, A., Davidyants, A., Ershov, K., and Kuznetsova, M. (2020). Comparative characteristics of the state of hard dental tissues in drug-dependent patients who use heroin, and methadone as replacement therapy. *Periodico Tchê Química*, 17(34), 135-146.

36. Sevbitov, A., Ergesheva, E., Sirak, S., Enina, Yu., Mallkov, S., and Kuznetsova, M. (2020). Clinical and laboratory analysis of the efficiency of hirudotherapy in complex treatment of endodontal diseases. *Journal of Global Pharma Technology*, 12(1), 253-260.

37. Mironov, S., Emelina, E., Troitskii, V., Yablokova, N., and Kuznetsov, I. (2020). The Impact of Smoking, Including Hookah, on the Human Body. *Journal of Global Pharma Technology*, 12(1), 211-217.

38. Enina, Yu., Sevbitov, A., Dorofeev, A., and Pustokhina, I. (2019). Experimental substantiation of the choice of the restoration method in the cervical area of teeth with abfraction defects. *International Journal of Mechanical Engineering and Technology*, 10(5), 41-47.

39. Sevbitov, A., Mitin, N., Kuznetsova, M., Dorofeev, A., and Ershov, K. (2020). A new modification of the dental prosthesis in the postoperative restoration of chewing function *Opcion*, 36(S26), 864-875.

40. Sevbitov, A., Zhadko, S., Dorofeev, A.,

Ershov, K., Enina, Yu., and Pustokhina, I. (2020). Rationale for the preservation of vital pulp in the use of fixed dentures in the experiment. *Opcion*, 36(S26), 953-968.

41. Sevbitov, A., Danshina, S., Platonova, V., Usatova, G., Borisov, V., and Kuznetsova, M. (2020). Icon as a method of choice for injectable treatment of initial caries in patients with fibrodysplasia ossificans progressive: a clinical case. *Journal of Global Pharma Technology*, 12(2), 270-274.

42. Sevbitov, A., Ershov, K., Dorofeev, A., Borisov, V., Mironov, S., and Enina, Yu. (2020). Analysis of the quality of life of elderly patients with removable orthopedic constructions during rehabilitation. *Prensa Medica Argentina*, 106( 4). 226.

43. Turgaeva, A., Kashirskaya, L., Zurnadzhyants, Yu., Latysheva, O., Pustokhina, I., and Sevbitov, A. (2020). Assessment of the financial security of insurance companies in the organization of internal control. *Entrepreneurship and Sustainability Issues*, 7(3), 2243-2254.

44. Sevbitov, A., Emelina, G., Kuznetsova, M., Dorofeev, A., and Emelina, E. (2019). A study of the prevalence of non-carious dental lesions related to production factors in residents of the city of penza. *Georgian Medical News*, 295, 42-47.

45. Timoshin, A., Sevbitov, A., Ergesheva, E., Mironov, S., Kozhemov, S., Pustokhina, I., and Danshina, S. (2019). Experience in the use of collagen phytoplates in the treatment of gingivitis. *Opcion*, 35(21), 582-598.

46. Sevbitov, A., Enina, Yu., Dorofeev, A., Kamenskov, P., Kozhemov, S., and Nikonova, A. (2019). Study of the impact of various abrasive factors on the microrelief of the surface of hybrid ceramic orthopedic structures. *Opcion*, 35(S24), 598-611.

47. Sevbitov, A., Zhadko, S., Ershov, K., Borisov, V., and Mironov, S. (2019). Rationale for the use of therapeutic and prophylactic complex to prevent intolerance to acrylates in patients with hyperfunction of the thyroid glands. *Periodico Tchê Química*, 16(33), 266-276.

48. Voloshina, I., Borisov, V., Sevbitov, A., Davidiants, A., Mironov, S., Kuznetsova, M., and Ergesheva, E. (2018). Distinctive features of microcrystallization of mixed saliva in children with different levels of activity of carious process. *Asian Journal of Pharmaceutics*, 12(3), S1017-S1020.

49. Ergesheva, E., Davidiants, A., Dorofeev, A., Sevbitova, M., and Timoshina, M. (2018). Evaluation of effectiveness of an alternative method in complex treatment of diseases of endodont. *Asian Journal of Pharmaceutics*, 12(3), S933-S936.

50. Kolodkina, V., Arutyunov, A., Sirak, S., Andriutsa, N., and Tsymbalov, O. (2018). Cytological characteristics of oral cavity tissues of experimental animals when using photo polymeric material. *Medical News of North Caucasus*, 13(4), 637-641.

51. Harrington, L., Hatton, R., Mangan, P., Murphy, K., and Weaver, C. (2005). Interleukin 17-producing CD4<sup>+</sup> effector T cells develop via a lineage distinct from the T helper type 1 and 2 lineages. *Nature Immunology*, 6(11), 1123-1132

Appendix 1. Oral Health Impact Profile (OHIP-14) (Slade G.D., Spencer A.J., 1994)

| Question   | Very often | Rarely | Usually | Almost never | Never |
|--|------------|--------|---------|--------------|-------|
|  | 5          | 4      | 3       | 2            | 1     |
| 1. Have you had trouble pronouncing any words because of problems with your teeth, mouth or dentures?              |            |        |         |              |       |
| 2. Have you felt that your sense of taste has worsened because of problems with your teeth, mouth or dentures?     |            |        |         |              |       |
| 3. Have you had painful aching in your mouth?  |            |        |         |              |       |
| 4. Have you found it uncomfortable to eat any foods because of problems with your teeth, mouth or dentures?        |            |        |         |              |       |
| 5. Have you been self conscious because of your teeth, mouth or dentures?  |            |        |         |              |       |
| 6. Have you felt tense because of problems with your teeth, mouth or dentures?                                     |            |        |         |              |       |
| 7. Has your diet been unsatisfactory because of problems with your teeth, mouth or dentures?                       |            |        |         |              |       |
| 8. Have you had to interrupt meals because of problems with your teeth, mouth or dentures?                         |            |        |         |              |       |
| 9. Have you found it difficult to relax because of problems with your teeth, mouth or dentures?                    |            |        |         |              |       |
| 10. Have you been a bit embarrassed because of problems with your teeth, mouth or dentures?                        |            |        |         |              |       |
| 11. Have you been a bit irritable with other people because of problems with your teeth, mouth or dentures?        |            |        |         |              |       |
| 12. Have you had difficulty doing your usual jobs because of problems with your teeth, mouth or dentures?          |            |        |         |              |       |
| 13. Have you felt that life in general was less satisfying because of problems with your teeth, mouth or dentures? |            |        |         |              |       |
| 14. Have you been totally unable to function because of problems with your teeth, mouth or dentures?               |            |        |         |              |       |



**RESULTADOS DO ESTUDO PARA O TREINAMENTO METODOLÓGICO DE PROFESSORES DE MATEMÁTICA EM CONDIÇÕES DE INOVAÇÃO****STUDY RESULTS FOR METHODOLOGICAL TRAINING OF TEACHERS OF MATHEMATICS IN CONDITIONS OF INNOVATION****РЕЗУЛЬТАТЫ ИССЛЕДОВАНИЯ МЕТОДОЛОГИЧЕСКОЙ ПОДГОТОВКИ УЧИТЕЛЕЙ МАТЕМАТИКИ В УСЛОВИЯХ ИННОВАЦИЙ**

GAVRILOVA, Yekaterina N.<sup>1</sup>; SEITOVA, Sabyrkul M.<sup>2</sup>; KOZHASHEVA, Gulnar O.<sup>3</sup>; ALDABERGENOVA, Aigul O.<sup>4</sup>; KYDYRBAEVA, Galiya T.<sup>5</sup>;

<sup>1,2,3,4,5</sup> Zhetysay State University named after I. Zhansugurov, Department of Mathematics and Computer Science, 187a Zhansugurova Str., zip code 040009, Taldykorgan – Republic of Kazakhstan

\* Correspondence author  
e-mail: [ketrin\\_301290@mail.ru](mailto:ketrin_301290@mail.ru)

Received 06 March 2020; received in revised form 05 June 2020; accepted 25 June 2020

**RESUMO**

O estágio contemporâneo da reforma educacional exige muito da formação de professores e do domínio das mais recentes técnicas e tecnologias de ensino. Em todo o mundo, busca-se novos sistemas educacionais mais democráticos, diversificados e eficazes do ponto de vista dos interesses do indivíduo e da sociedade. Isso requer, por um lado, maneiras novas e mais eficientes de organizar o processo educacional na universidade, em particular, revisando a estrutura e o conteúdo da formação metodológica dos estudantes. Por outro lado, o próprio conceito de “atividade pedagógica profissional de um professor” está passando por certas mudanças. Este estudo teve como objetivo identificar com que eficácia o treinamento metodológico de futuros professores de matemática aumentará com base na introdução de técnicas e métodos de ensino inovadores e como a metodologia de ensino de disciplinas matemáticas nas condições de inovação poderá ser aprimorada. Duzentos e treze pessoas participaram do trabalho experimental, incluindo professores de matemática e estudantes em período integral, estudantes de graduação, doutorado e jovens professores da universidade. Os resultados do experimento determinante tornaram-se a base para a revisão dos propósitos da formação metodológica e profissional de futuros professores de matemática e possibilitaram concluir sobre a necessidade de aperfeiçoar o suporte metodológico do sistema para o ensino de disciplinas matemáticas no ensino superior. Por isso, a formação de um professor de matemática deve torná-lo um matemático experiente, como uma pessoa com uma alta cultura pedagógica e geral, que, ensinando, educaria a geração mais jovem no espírito da modernidade. Pode-se supor que o conteúdo dos cursos de uma universidade pedagógica em disciplinas matemáticas deve, por exemplo, em um nível acadêmico moderno, abranger os assuntos que o professor comunica na escola.

**Palavras-chave:** *ensino de disciplinas matemáticas, processo educacional, programação neurolinguística.*

**ABSTRACT**

The contemporary stage of education reform puts high demands on teacher training and on mastering the newest teaching techniques and technologies. All over the globe, there is a search for new education systems that are more democratic, diversified and effective from the standpoint of the interests of the individual and society. This requires, on the one hand, new, more efficient ways of organizing the educational process at the university, in particular, reviewing the structure and content of the methodological training of students. On the other hand, the very concept of “professional pedagogical activity of a teacher” is currently undergoing certain changes. This study aimed to identify how effectively will the methodological training of future mathematics teachers increase based on the introduction of innovative techniques and teaching methods and how the methodology of teaching mathematical disciplines in the conditions of innovation may be improved. Two hundred thirteen people took part in the experimental work, including teachers of mathematics and full-time students, undergraduates, doctoral students, as well as young teachers of the university. The results of the ascertaining experiment became the basis for revising the purposes of the methodological and professional training of future mathematics teachers and made it possible to conclude on the necessity of improvement of the system-methodological support for teaching mathematical disciplines in higher education. Because of this, the training of a mathematics teacher should form them as a knowledgeable mathematician, as a person with a high pedagogical and general culture, who, by



teaching, would educate the younger generation in the spirit of modernity. It can be assumed that the content of courses in a pedagogical university in mathematical disciplines should, for instance, at a modern academic level, cover those matters that the teacher communicates at school.

**Keywords:** *teaching mathematical disciplines, educational process, neurolinguistics programming.*

## АННОТАЦИЯ

Современный этап модернизации образования предъявляет повышенные требования к профессиональной подготовке преподавателей и освоению ими новейших методик и технологий обучения. Во всем мире идет поиск новых систем образования, более демократичных, диверсифицированных и результативных с позиции интересов личности и общества. Это требует, с одной стороны, новых, более эффективных путей организации учебно-воспитательного процесса в вузе, в частности, пересмотра структуры и содержания методической подготовки студентов. С другой стороны, само понятие «профессиональная педагогическая деятельность преподавателя» подвергается в настоящее время определенным изменениям. Цель данного исследования заключается в определении эффективности совершенствования методической подготовки будущих учителей математики при внедрении инновационных техник и методов обучения, а также улучшении методологии преподавания математических дисциплин в условиях инноваций. В экспериментальной работе приняли участие двести тринадцать человек, в том числе учителя математики и студенты дневного отделения, магистранты, докторанты, а также молодые преподаватели университета. Результаты констатирующего эксперимента стали основой для пересмотра целей методической и профессиональной подготовки будущих учителей математики и позволили сделать вывод о необходимости совершенствования системно-методического обеспечения преподавания математических дисциплин в высшей школе. Учитывая это, подготовка должна сформировать учителя математики как грамотного преподавателя, человека с высокой педагогической и общей культурой, который способен воспитать молодое поколение в духе современности. Содержание курсов в педагогическом университете по математическим дисциплинам на современном академическом уровне должно охватывать те вопросы, с которыми преподаватель сталкивается в школе.

**Ключевые слова:** *преподавание математических дисциплин, учебный процесс, нейролингвистическое программирование.*

## 1. INTRODUCTION:

It is assumed that students who are now finishing a pedagogical university at the age of 22-23 years will, on average, work as teachers for 40-45 years. In this time, new fields will emerge in mathematical science that currently does not exist; school teaching will change in many ways, it will include such problems of mathematics that our students may not yet be studying (Arkhangelsky, 1980; Avramidis and Norwich, 2002; Frade et al., 2013; Stockero, 2013; Van Zoest et al., 2016; Stockero et al., 2017; Bayanov et al., 2019). Therefore, future mathematics teachers have to be taught not only those branches of mathematics that are currently important but also those regarding which there is reason to believe they will develop shortly or will become the basis of future branches of science. In other words, this means that the thinking of students must be developed in such a way that later they can learn new sections of mathematics that they may need to teach in the future at school, even if they do not study them at the moment (Miguel and Mendes, 2010; Mendes, 2013; Mendes and Silva, 2018).

The main trends characteristic and

necessary for the preparation of future mathematics teachers as future specialists (Kravets, 2011; Cohen, 2011; Schejbal, 2012; Stockero and Van Zoest, 2013; Leatham et al., 2015; Seitova et al., 2016; Seitova et al., 2018):

- from a “knowing person”, armed with a system of knowledge, skills, to “a person prepared for life”, that is, a person capable of active and creative thinking, and acting, self-developing intellectually, morally and physically;

- from the concept of “Education for life” to understanding the need for education through life, the psychological readiness for further education and retraining, including the willingness to take them at face value, and not as a life catastrophe, should be formed in the course of modern professional education;

- development of initiative; initiative can guarantee success in life, a person’s mobility, readiness to solve various kinds of problems, the action must not only be maintained but also purposefully, consistently formed;

- from knowledge to competencies; the knowledge-centric model of education doesn’t

satisfy the real needs of the development of society and the individual; it is necessary to involve students as future specialists in the process of hard and diverse work in teaching, acquiring the skills necessary to study the material, it is important to promote cooperation.

Against the backdrop of significant social changes since the early nineties, the education system in many countries of the world is undergoing reform (Pligin, 1997; Breitigam and Karakozov, 2004; Vilensky et al., 2004; Dalinger, 2014; Maslova, 2015; Anamova et al., 2019; Natolochnaya et al., 2020). The need for reforms is caused, in particular, by the fact that in higher education, for example, in Russia, as shown by the results of A.A. Verbitsky (Verbitsky, 1991), V.I. Kagan (Kagan and Chebyshev, 2000), Yu.T. Tatura (Tatur, 2000), O.V. Dolzhenko, V.L. Shatunovsky (Dolzhenko and Shatunovsky, 1990) and others, in some areas there was a significant gap between the global needs of society and the results of education; between the objective requirements of time and the general insufficient level of education; between professional orientation and the need of the individual to satisfy a variety of cognitive interests; between modern methodological approaches to advanced sciences and the archaic style of teaching (Abdudlina, 1976; Babansky, 1982; Yansufina, 2003; Peterson and Leatham, 2009; Bray, 2011; Herbst and Chazan, 2012; Mendes, 2012; Rauner, 2013; Uglev and Ustinov, 2014; Bartell et al., 2015; Lee and Cross Francis, 2018).

I.A. Kolesnikova gives a slightly different interpretation of the issue, analyzing innovation as a form of manifestation of a new quality of pedagogical reality, as a way of future development in pedagogy, thereby outlining the philosophical and teaching foundations for the development of teaching innovation as a scientific and practical field (Kolesnikova, 1999; National Council...2014; Lineback, 2015; Van Zoest et al., 2017).

The works of foreign authors cover certain theoretical and practical aspects of innovative processes as change processes in the educational system, based on various pedagogical innovations. The studies of American and English educators (H. Barnett, J. Bassett, D. Hamilton, N. Gros, M. Miles, R. Eden and others) analyze the management of innovative processes, the organization of changes in education, the conditions necessary for "activity" of innovations, planning of innovations, ways of regulation of pedagogical innovations.

The socio-psychological aspects of the distribution of innovations are well-developed. In essence, a typology of participants in innovation processes, their attitude to innovations, readiness to accept new ideas, reasons for the emergence and ways to overcome psychological barriers, factors for the development of innovative activity (K. Angelowski, E. Rogers, L.A. Korostyleva, O.S. Sovetova, A.M. Khon, M.V. Croz, L.M. Podlesnaya). The matters of managing innovative processes in education are considered in sufficient detail (A.P. Volchkova, O.G. Khomeriki, V.P. Kvasha, N.V. Konoplina, G.A. Krasyn, A.M. Voronin, V.F. But, etc.).

The purpose of the study is to test ways of implementing system-methodological support for innovation in the teaching of mathematical disciplines at the university with an experiment.

The general research question of this study was as follows: how effectively will the methodological training of future mathematics teachers increase based on the introduction of innovative techniques and teaching methods. How may the methodology of teaching mathematical disciplines in the conditions of innovation be improved?

## 2. MATERIALS AND METHODS:

In the course of the study, there were conducted an analysis of scientific and educational literature on the topic of research, a generalization of empirical material, modeling, questioning, testing, methodology with the choice of tasks, observation, recording the results of training and formation, a teaching experiment.

This study describes and analyses the experimental work on the implementation of the methodology for the formation of the readiness of future mathematics teachers to organize innovation in teaching mathematical disciplines at the university. In this case, the experimental work acts as the research method, which allows to scientifically substantiate, prove the idea that the implementation of the developed methodology provides an increase in the level of formation of the readiness of future mathematics teachers to organize innovation. The goals, the content of the stages, the results of the pedagogical experiment are revealed. The purpose of the experimental work was to test the hypothesis of the study. As a constructive basis for its design and implementation, the developed methodology for implementing the innovative orientation in the teaching of mathematical disciplines at the university was adopted following modern

requirements for the training of future specialists.

Two hundred thirteen people took part in the experimental work, including teachers of mathematics and full-time students, undergraduates, doctoral students, as well as young teachers of the university. Innovative work is represented by ascertaining, searching, and educational experiments.

The ascertaining experiment, wherein 120 people took part, was carried out in two stages. The first stage of the ascertaining experiment was carried out through a survey to identify among teachers of mathematics (70 people) their attitude to work in conditions of innovation, whether the development of changes is necessary for the advancement of the educational system, and whether specialists possess the required level of competence for the development of innovative works. Analysis of the results of the survey showed that only less than 50% of the tested teachers were able to positively answer the questions in the amount of 60% and above. The data obtained indicate a low assessment of the attitude towards the process of introducing innovations into the educational process. Moreover, it hints at a low level of formation of the necessary infrastructure for the development and implementation of changes. The second stage of the ascertaining experiment was to identify the levels of creation of the ability to introduce innovative approaches upon teaching mathematical disciplines for students (50 people) of the Faculty of Natural Sciences, specialty "Mathematics" before studying the subjects of methodological training (2nd year) and after (3rd year). Since in the 3rd year, students begin to explore disciplines of a methodological nature and further embark on pedagogical practice.

During the searching experiment, where full-time students and undergraduates took part (93 students), individual innovative teaching methods were tested, effective teaching methods were identified, the research hypothesis was clarified. The educational experiment was organized and conducted in vivo in the educational process of studying "Methods of Teaching Mathematics" by third-year students (47 people) of the Faculty of Natural Sciences of Zhetysu State University named after I. Zhansugurov (Kazakhstan, Taldykorgan).

The objectives of the educational experiment: 1) to identify the pedagogical conditions of the system-methodological support of the innovation in the teaching of mathematical disciplines at the university; 2) to prove the

efficiency of the developed methodology for the application of innovative technologies in the preparation of future mathematics teachers (on the example of the discipline "Methods of teaching mathematics"). Proof of the efficiency of the developed methodology for teaching future mathematics teachers to work in an innovative environment requires a description of diagnostic measures to determine the level of formation of the corresponding skill.

All procedures performed in studies involving human participants were following the ethical standards of the institutional and national research committee and with the 1964 Helsinki declaration and its later amendments or comparable ethical standards. Informed consent was obtained from all individual participants included in the study.

### 3. RESULTS AND DISCUSSION:

As a diagnostic tool, a test consisting of 4 parts was developed, each of which corresponds to one of the indicators. In the first part of the test, students' knowledge in the field of mathematical training was assessed, in the second – their ability to solve typical problems in this area, and in the third and fourth – knowledge and skills that form the basis of the methodological unit of the formed ability. The maturity of each of the indicators was assessed on a 10-point scale. The indicator was considered mature if the student scored 9 or 10 points in the diagnostic event. The test results are presented in Table 1.

It was found that with increasing value  $h_0$ , the amplitude of displacements increases against the direction of the axis  $Ox$ , and the amplitude of displacements in the direction of the axis  $Ox$  decreases. With increasing value  $h_0$ , the maximum and average values of thermoelastic stress  $\sigma$  decreases.

Thus, it was established that only by changing the value  $h_0$ , (and not  $T_{amb0}$ ), i.e., by changing the environmental properties of the surrounding cross-sectional area where heat transfer occurs, the thermally stressed state of the rod under investigation can be changed. For data measured in an ordinal scale, it is advisable to use the homogeneity criterion 2. Objective: to determine the accuracy of coincidences and differences for a pair of experimental data measured in an ordinal scale using the uniformity criterion 2.

A description of the 2nd year group is a

point vector on an ordinal scale with  $L = 5$  different points (levels):  $n1 = (n1, \dots, n1L)$ , 30. A description of the 3rd year group is a point vector:  $n2 = (n2, \dots, n2L)$ , 20. At a significance level of  $\alpha = 0.05$ , using the uniformity criterion 2, check the null hypothesis  $H_0$ : differences in the distribution of students of groups of 2nd year and 3rd year by the maturity level of their methodological training in the conditions of innovation.

The empirical value of the criterion  $\chi^2_{ex} = 4.78346$ , the critical value  $\chi^2_{cr} = 9.46$ . As a result, a statistical conclusion is obtained. Since  $\chi^2_{ex} < \chi^2_{cr}$  the null hypothesis  $H_0$  is not rejected, the descriptions of the compared samples coincide at the significance level  $\alpha = 0.05$ . This means that the experimental results do not confirm the effect of the applied method with a confidence coefficient of 95%. Thus, it is necessary to increase the efficiency of teaching future mathematics teachers to advance innovation in the teaching process by implementing the author's methodology of applying innovative technologies in the learning process.

Students from the control and experimental groups were tested to determine the initial level of maturity of the ability to work in conditions of innovation. Implementation of the developed methodology took place upon studying the sections "Methods and forms of teaching mathematics" and "Psychological and pedagogical foundations of teaching mathematics". The following diagnostic measures were performed: 1) academic conferences and independent work, which were performed to assess the maturity of the indicators  $p1$  and  $p2$ , respectively; 2) questions of express-testing (from 0 to 2 points for each), which were developed with so as to assess the maturity of the indicator  $p3$ ; 3) individual work and homework, which was evaluated up to 4 points (0.2 for each), which were offered to students for assessment of the maturity of the indicator  $p4$ .

The indicator was considered formed if, according to the results of all diagnostic measures aimed at its evaluation, the student scored more than 7 points (from 8 to 10 inclusive). The results of the experiment are presented in Table 2. Paired comparisons shall be done. First, accuracy of coincidences and differences for a pair of experimental data shall be measured on an ordinal scale using the homogeneity criterion 2. At this significance level, the null hypothesis  $H_0: X1 = X2$  about the homogeneity of the two samples is checked. The algorithm is as follows:

1. For the two compared samples, the value

2 and the empirical value of the  $\chi^2$  criterion is calculated using the (Equation 1).

2. Further, this value is compared with a critical value (Equation 2), where  $\alpha$  – significance level,  $\chi^2_{(v,q)}$  – quantile of the Pearson distribution at level  $q$  with the number of degrees of freedom  $v$ .

As a result, a statistical conclusion is obtained. If  $\chi^2 > \chi^2_{cr}$ , then the null hypothesis is rejected, the descriptions of the compared samples vary at the significance level  $\alpha$ . If  $\chi^2 \leq \chi^2_{cr}$ , then the null hypothesis is not rejected; the descriptions of the compared samples coincide at the significance level  $\alpha$ . The statistical significance of the compared samples is verified at the significance level  $\alpha = 0.05$ . Then the critical value  $\chi^2_{cr} = \chi^2_{(4,0.95)} = 9.46$ .

Comparison of the experimental group before the start of the experiment with the experimental group after the end of the experiment. According to the original Table 2, to calculate the empirical value of the criterion according to the Equation (1) an auxiliary Table 3 shall be made.

Next, the empirical and critical values of the criterion (Equation 3) are compared. Since  $\chi^2 > \chi^2_{cr}$ , the null hypothesis is rejected, the descriptions of the compared samples differ at the significance level  $\alpha = 0.05$ . Comparison of the experimental group before the start of the experiment with the control group before the start of the experiment. According to data from the initial Table 2, to calculate the empirical value of the criterion according to the equation (1) an auxiliary Table 4 shall be created.

Then, the empirical and critical values of the criterion (Equation 4) should be compared. Since  $\chi^2 \leq \chi^2_{cr}$ , the null hypothesis is not rejected, the descriptions of the compared samples differ at the significance level  $\alpha = 0.05$ . Comparison of the experimental group before the start of the experiment with the control group after the end of the experiment. According to the data of the initial Table 2, to calculate the empirical value of the criterion according to the equation (Equation 1) an auxiliary Table 5 is created.

Further, the empirical and critical values of the criterion (Equation 5) are compared. Since  $\chi^2 \leq \chi^2_{cr}$ , the null hypothesis is not rejected, the descriptions of the compared samples differ at the significance level  $\alpha = 0.05$ . Comparison of the experimental group after the experiment with the control group before the experiment. According to the data from the initial Table 2, to calculate the empirical value of the criterion according to the

(Equation 1), an auxiliary Table 6 is created.

Next, the empirical and critical values of the criterion (Equation 6) are compared. Since  $\chi^2 > \chi^2_{cr}$ , the null hypothesis is rejected, the descriptions of the compared samples differ at the significance level  $\alpha = 0.05$ . Comparison of the experimental group after the end of the experiment with the control group after the end of the experiment. According to data from the initial Table 2, to calculate the empirical value of the criterion according to the Equation 1, an auxiliary Table 7 is created.

Then, the empirical and critical values of the criterion (Equation 7) are compared. Since  $\chi^2 > \chi^2_{cr}$ , the null hypothesis is rejected, the descriptions of the compared samples differ at the significance level  $\alpha = 0.05$ . Comparison of the control group before the start of the experiment with the control group after the end of the experiment. According to the data from the initial Table 2, to calculate the empirical value of the criterion according to the equation (Equation 1), an auxiliary Table 8 is created.

Further, the empirical and critical values of the criterion (Equation 8) are compared. Since  $\chi^2 \leq \chi^2_{cr}$ , the null hypothesis is not rejected, the descriptions of the compared samples differ at the significance level  $\alpha = 0.05$ . The results of paired comparisons are presented in Table 9. The critical value  $\chi^2_{cr} = 9.46$ . General results of the statistical analysis of paired comparisons are created. Sample descriptions coincide with a significance level of 5% for the following pairs of samples:

- “Experimental group before the start of the experiment” and “control group before the start of the experiment”;
- “Experimental group before the start of the experiment” and “control group after the end of the experiment”;
- “Control group before the start of the experiment” and “control group after the end of the experiment”;

Significant differences were identified for the following pairs of samples (95% confidence):

- “Experimental group before the start of the experiment” and “experimental group after the end of the experiment”;
- “Experimental group after the end of the experiment” and “control group before the start of the experiment”;
- “Experimental group after the end of the experiment” and “control group after the end of the

experiment”;

An analysis of the results shows that there are no significant differences at the beginning of the experiment between the experimental and control groups; however, at the end of the experiment, the results obtained in the experimental and control groups differ significantly. This is explained by the implementation of the methodology for the innovative technologies in the experimental group and the improvement of future mathematics teachers' methodological training.

#### 4. CONCLUSIONS:

Pilot testing is represented by the ascertaining, searching, and educational experiments. In the course of an ascertaining investigation (2016-2017), a survey was conducted among teachers of mathematics, undergraduates and doctoral students of the specialty "Mathematics," including young university teachers. The results of the ascertaining experiment became the basis for revising the purposes of the methodological and professional training of future mathematics teachers and made it possible to conclude on the necessity of improvement of the system-methodological support for teaching mathematical disciplines in higher education.

The training of a mathematics teacher should form them as a knowledgeable mathematician, as a person with a high pedagogical and general culture, who, by teaching, would educate the younger generation in the spirit of modernity. It can be assumed that the content of courses in a pedagogical university in mathematical disciplines should:

- 1) at a modern academic level, cover those matters that the teacher communicates at school;
- 2) provide for students' breadth of knowledge in mathematics, familiarize them with advanced mathematics and its problems as much as possible. Therefore, courses in higher mathematics should shed light on those fundamental issues of modern mathematics, which currently serve as its basis and determine its face. This will provide for a certain fundamental level of mathematical culture for a future mathematics teacher;
- 3) contain sufficiently rich applications of higher mathematics to science and technology. In the process of teaching, this will allow the future teacher of mathematics to provide the students with an idea of life application of the concepts and

processes that will be studied in the elements of higher mathematics at school;

4) teach to think mathematically, that is, to be able to solve mathematical problems and be able, in the simplest cases, to form various problems arising in other sciences in the language of mathematics;

5) ensure the educational nature of training, that is, the development of a common culture and the formation of the student's worldview and personality.

The tasks of the searching experiment (2016-2018) were solved in the course of teaching students: to construct the content of academic disciplines and find the main means of learning; identify indicators of development and develop diagnostic material.

In the course of the educational experiment (2018-2019), providing for the experimental training of students in the natural conditions of the educational process, was proven the efficiency of the proposed methodology for teaching future mathematics teachers in conditions of innovation.

Improving the methodological training of future specialists requires the introduction of a special course "Methodological support for the preparation of future mathematics teachers in an innovative orientation" in the program of training students of the "Mathematics" educational program, where scientific (educational) materials helping to form professional qualities and improve the methodological training of future specialists will be considered.

## 5. REFERENCES:

1. Abdudlina, O.A. (1976). The problem of pedagogical skills in the theory and practice of higher pedagogical education. *Soviet Pedagogy*, 1, 75-84.
2. Anamova, R.R., Bykov, L.V., and Kozorez, D.A. (2019). Aircraft industry staff retraining as a part of vocational education in the Russian Federation. *TEM Journal*, 8(3), 978-983.
3. Arkhangelsky, S.I. (1980). *The educational process in higher education, its regular principles and methods*. Moscow, Russian Federation: Vysshaya shkola.
4. Avramidis, E., and Norwich, B. (2002). Teachers' attitudes towards integration/inclusion: A review of the literature. *European Journal of Special Needs Education*, 17(2), 129-147.
5. Babansky, Yu.K. (1982). *Optimization of the educational process: methodological foundations*. Moscow, Russian Federation: Prosveshcheniye.
6. Bartell, T.G., Bieda, K.N., Putnam, R.T., Bradfield, K., and Dominguez, H. (Eds.). (2015). *Proceedings of the 37th annual meeting of the North American Chapter of the International Group for the Psychology of Mathematics Education*. East Lansing, MI: Michigan State University.
7. Bayanov, D.I., Novitskaya, L.Y., Panina, S.A., Paznikova, Z.I., Martynenko, E.V., Ilkevich, K.B., Karpenko, V.L., and Allalyev, R.M. (2019). Digital technology: Risks or benefits in student training? *Journal of Environmental Treatment Techniques*, 7(4), 659-663.
8. Bray, W. S. (2011). A collective case study of the influence of teachers' beliefs and knowledge on error-handling practices during class discussion of mathematics. *Journal for Research in Mathematics Education*, 42(1), 2-38.
9. Breitigam, E.K., and Karakozov, S.D. (2004). The integrity of the system of basic concepts in the study of mathematics at school and university. *World of Science, Culture, Education*, 3, 190-194.
10. Cohen, D.K. (2011). *Teaching and its predicaments*. Cambridge, MA: Harvard University Press.
11. Dalinger, V.A. (2014). The main directions of improving the training of a mathematics teacher in pedagogical universities. *International Journal of Experimental Education*, 5, 70-72.
12. Dolzhenko, O.V., and Shatunovsky, V.L. (1990). *Modern methods and technology of training in a technical university*. Moscow, Russian Federation: Vysshaya shkola.
13. Frade, C., Acioly-Régner, and Jun, L. (2013). Beyond deficit models of learning mathematics: Socio-cultural directions for change and research. In M.A. Clements, A.J. Bishop, C. Keitel, J. Kilpatrick, and F.K.S. Leung (Eds.), *Third International Handbook of Mathematics Education* (pp. 101-144). New York, NY: Springer.
14. Herbst, P., and Chazan, D. (2012). On the instructional triangle and sources of justification for actions in mathematics teaching. *ZDM Mathematics Education*, 44(5),

15. Kagan, V., and Chebyshev, N. (2000). Higher school of the XXI century: quality problem. *Higher Education in Russia*, 1, 19-26.
16. Kolesnikova, I.A. (1999). *Pedagogical reality in the mirror of inter-paradigmatic reflection*. St. Petersburg. Russian Federation: SPbGUPM.
17. Kravets, O. (2011). The modern pedagogical technologies analysis of automated individualization training. *Psychology, Sociology, Pedagogic* 4, 14–17.
18. Leatham, K. R., Peterson, B. E., Stockero, S. L., and Van Zoest, L. R. (2015). Conceptualizing mathematically significant pedagogical opportunities to build on student thinking. *Journal for Research in Mathematics Education*, 46, 88-124.
19. Lee, M. Y., and Cross Francis, D. (2018). Investigating the relationships among elementary teachers' perceptions of the use of students' thinking, their professional noticing skills, and their teaching practices. *Journal of Mathematical Behavior*, 51, 118–128.
20. Lineback, J.E. (2015). The redirection: An indicator of how teachers respond to student thinking. *Journal of the Learning Sciences*, 24, 419–460
21. Maslova, O.A. (2015). *Methods of teaching future mathematics teachers to work with the structure of mathematical statements*. (Unpublished thesis of the candidate of pedagogical sciences). Volgograd, Russian Federation.
22. Mendes, I.A. (2012). *Research as a principle of teaching and learning Mathematics*. Paper presented at the Department of Educational Practices and Curriculum of the Federal University of Rio Grande do Norte, Natal, Brazil.
23. Mendes, I.A. (2013). The research as a principle for the teaching and learning of mathematics. *International Journal for Research in Mathematics Education*, 3, 40-59.
24. Mendes, I.A., and Silva, C.A.F. (2018). Problematisation and research as a method of teaching mathematics. *International Electronic Journal of Mathematics Education*, 13(2), 41-55. <https://doi.org/10.12973/iejme/2694>
25. Miguel, A., and Mendes, I.A. (2010). Mobilizing histories in mathematics teacher education: memories, social practices, and discursive games. *ZDM Mathematics Education*, 42, 381-392. <https://doi.org/10.1007/s11858-010-0255-8>
26. National Council of Teachers of Mathematics. (2014). Principles to actions: Ensuring mathematical success for all. Reston, VA: National Council of Teachers of Mathematics. Retrieved from [https://www.nctm.org/uploadedFiles/Standards\\_and\\_Positions/PtAExecutiveSummary.pdf](https://www.nctm.org/uploadedFiles/Standards_and_Positions/PtAExecutiveSummary.pdf)
27. Natolochnaya, O.V., Svechnikov, V.A., Posokhova, L.A., and Allalyev, R.M. (2020). The history of the public education system in Vilna governorate (the second half of the 19th and early 20th centuries). Part 3. *European Journal of Contemporary Education*, 9(1), 248-254.
28. Peterson, B.E., and Leatham, K.R. (2009). Learning to use students' mathematical thinking to orchestrate a class discussion. In L. Knott (Ed.), *The role of mathematics discourse in producing leaders of discourse* (pp. 99–128). Charlotte, NC: Information Age.
29. Pligin, A.A. (1997). *Organizational and pedagogical foundations of personality-oriented education in modern conditions*. Moscow, Russian Federation: Nauka.
30. Rauner, F. (2013). *Measuring professional competence*. COMET. Dordrecht, Netherlands: Springer.
31. Schejbal, D. (2012). In search a new paradigm of higher education. *Innovative Higher Education*, 37, 373–386.
32. Seitova, S., Smagulov, Y., Gavrilova, Y., Zhiyembayev, Z., and Zhanatbekova, N. (2018). Studying mathematical subjects to students as an independent work. *Astra Salvensis*. 6(1), 617-630.
33. Seitova, S.M., Kozhasheva, G.O., Gavrilova, Y., Tasbolatova, R., Okpebaeva, G.S., Kydyrbaeva, G.T., and Abdykarimova, A.Z. (2016). Peculiarities of using neuro-linguistic programming techniques in teaching. *Mathematics Education*, 11(5), 1135-1149.
34. Stockero, S.L. (2013). *The effects of framing on mathematics student teacher noticing*. Paper presented at the 35th annual meeting of the North American chapter of the international group for the psychology of mathematics education. Chicago, IL: University of Illinois at Chicago.

35. Stockero, S.L., and Van Zoest, L.R. (2013). Characterizing pivotal teaching moments in beginning mathematics teachers' practice. *Journal of Mathematics Teacher Educators*, 16, 125-147.
36. Stockero, S.L., Van Zoest, L.R., Peterson, B.E., Leatham, K.R., and Rougee, A.O.T. (2017). *Teachers responses to a common set of high potential instances of student mathematical thinking*. Paper presented at the 39th annual meeting of the North American chapter of the international group for the psychology of mathematics education, Hoosier Association of Mathematics Teacher Educators, Indianapolis, IN.
37. Tatur, Yu. (2000). Educational programs: traditions and innovation. *Higher Education in Russia*, 4, 12-16.
38. Uglev, V.A., and Ustinov, V.A. (2014). The new competencies development level expertise method within intelligent automated educational systems. *Advances in Intelligent Systems and Computing*, 293, 157-164.
39. Van Zoest, L.R., Peterson, B.E., Leatham, K.R., and Stockero, S.L. (2016). *Conceptualizing the teaching practice of building on student mathematical thinking*. Paper presented at the 38th annual meeting of the North American chapter of the international group for the psychology of mathematics education, University of Arizona, Tucson.
40. Van Zoest, L.R., Stockero, S.L., Leatham, K.R., Peterson, B.E., Atanga, N.A., and Ochieng, M.A. (2017). Attributes of instances of student mathematical thinking that are worth building on in whole-class discussion. *Mathematical Thinking and Learning*, 19, 33-54.
41. Verbitsky, A.A. (1991). *Active learning in higher education: a contextual approach*. Moscow, Russian Federation: Vysshaya shkola.
42. Vilensky, V.Ya. Obratsov, P.I., and Uman, A.I. (2004). *Technology vocationally-oriented education in higher education*. Moscow, Russian Federation: Pedagogicheskoye obshchestvo Rossii.
43. Yansufina, Z.I. (2003). *Improving the methodological preparation of a future mathematics teacher in a teacher training university based on innovative approaches to learning*. (Unpublished thesis of the candidate of pedagogical sciences). Tobolsk, Russian Federation.



$$\chi^2 = \frac{1}{N_1 N_2} \sum_{j=1}^L \frac{(N_2 n_{1j} - N_1 n_{2j})^2}{n_{1j} + n_{2j}}. \quad (\text{Eq. 1})$$

$$\chi_{cr}^2 = \chi_{(L-1, 1-\alpha)}^2, \quad (\text{Eq. 2})$$

$$\chi^2 = \frac{1}{25 \times 25} (8601.19 + 625 + 625 + 3125 + 8750) = 34.8 > \chi_{cr}^2 \quad (\text{Eq. 3})$$

$$\chi^2 = \frac{1}{25 \times 22} (449.161 + 142.231 + 625 + 625 + 625) = 4.48 < \chi_{cr}^2 \quad (\text{Eq. 4})$$

$$\chi^2 = \frac{1}{25 \times 22} (973.241 + 330.286 + 1250 + 625 + 625) = 6.92 < \chi_{cr}^2. \quad (\text{Eq. 5})$$

$$\chi^2 = \frac{1}{25 \times 22} (4681.14 + 1188.1 + 4.5 + 1204.17 + 5339.27) = 22.6 > \chi_{cr}^2 \quad (\text{Eq. 6})$$

$$\chi^2 = \frac{1}{25 \times 22} (3536.33 + 1632.36 + 261.333 + 1204.17 + 5339.27) = 21.8 > \chi_{cr}^2. \quad (\text{Eq. 7})$$

$$\chi^2 = \frac{1}{22 \times 22} (8 + 32.266 + 161.333 + 0 + 0) = 0.582 < \chi_{cr}^2. \quad (\text{Eq. 8})$$

**Table 1.** Results of the second ascertaining experiment

| Skill maturity levels | 2 year      | 3 year     |
|-----------------------|-------------|------------|
| Zero                  | 4 (12.5%)   | 5 (19.57%) |
| First                 | 15 (51.79%) | 9 (43.48%) |
| Second                | 8 (30.36%)  | 3 (21.74%) |
| Third                 | 2 (3.571%)  | 2 (13.04%) |
| Fourth                | 1 (1.779%)  | 1 (2.17%)  |
| $\Sigma$              | 30 (100%)   | 20 (100%)  |

**Table 2.** Data obtained during the educational experiment

| Skill maturity level | Experimental group, number of people   |                                      | Control group, number of people        |                                      |
|----------------------|--|--------------------------------------|--|--------------------------------------|
|                      | Start of experiment (n <sub>1j</sub> ) | End of experiment (n <sub>2j</sub> ) | Start of experiment (n <sub>3j</sub> ) | End of experiment (n <sub>4j</sub> ) |
| Zero                 | 19 (76%)                               | 2 (8 %)                              | 12 (54.5%)                             | 10 (45.5 %)                          |
| First                | 6 (24 %)                               | 3 (12%)                              | 7 (31.8%)                              | 8 (36.4 %)                           |
| Second               | 0 (0 %)                                | 1 (4 %)                              | 1 (4.55 %)                             | 2 (9.09 %)                           |
| Third                | 0 (0 %)                                | 5 (20 %)                             | 1 (4.55 %)                             | 1 (4.55 %)                           |
| Fourth               | 0 (0 %)                                | 14 (56%)                             | 1 (4.55 %)                             | 1 (4.55 %)                           |
| $\Sigma$             | 25 (100%)                              | 25 (100%)                            | 22 (100%)                              | 22 (100%)                            |

**Table 3.** Comparison of the experimental group before the start of the experiment with the experimental group after the end of the experiment

| J | $n_{1j}$ | $n_{2j}$ | $N_2n_{1j}$ | $N_1n_{2j}$ | $(N_2n_{1j} - N_1n_{2j})^2$ | $n_{1j} + n_{2j}$ | $\frac{(N_2n_{1j} - N_1n_{2j})^2}{n_{1j} + n_{2j}}$ |
|---|----------|----------|-------------|-------------|-----------------------------|-------------------|---|
| 1 | 19 (76%) | 2 (8%)   | 475         | 50          | 180.625                     | 21                | 8,601.19  |
| 2 | 6 (24%)  | 3 (12%)  | 150         | 75          | 5.625                       | 9                 | 625   |
| 3 | 0 (0%)   | 1 (4%)   | 0           | 25          | 6.25                        | 1                 | 625   |
| 4 | 0 (0%)   | 5 (20%)  | 0           | 125         | 15.625                      | 5                 | 3125  |
| 5 | 0 (0%)   | 14 (56%) | 0           | 350         | 122.500                     | 14                | 8750  |

**Table 4.** Comparison of the experimental group before the start of the experiment with the control group before the start of the experiment

| j | $n_{1j}$ | $n_{2j}$   | $N_2n_{1j}$ | $N_1n_{2j}$ | $(N_2n_{1j} - N_1n_{2j})^2$ | $n_{1j} + n_{2j}$ | $\frac{(N_2n_{1j} - N_1n_{2j})^2}{n_{1j} + n_{2j}}$ |
|---|----------|------------|-------------|-------------|-----------------------------|-------------------|---|
| 1 | 19 (76%) | 12 (54.5%) | 418         | 300         | 13924                       | 31                | 449.161   |
| 2 | 6 (24%)  | 7 (31.8%)  | 132         | 175         | 1849                        | 13                | 142.231   |
| 3 | 0 (0%)   | 1 (4.55%)  | 0           | 25          | 625                         | 1                 | 625   |
| 4 | 0 (0%)   | 1 (4.55%)  | 0           | 25          | 625                         | 1                 | 625   |
| 5 | 0 (0%)   | 1 (4.55%)  | 0           | 25          | 625                         | 1                 | 625   |

**Table 5.** Comparison of the experimental group before the start of the experiment with the control group after the end of the experiment

| j | $n_{1j}$ | $n_{2j}$   | $N_2n_{1j}$ | $N_1n_{2j}$ | $(N_2n_{1j} - N_1n_{2j})^2$ | $n_{1j} + n_{2j}$ | $\frac{(N_2n_{1j} - N_1n_{2j})^2}{n_{1j} + n_{2j}}$ |
|---|----------|------------|-------------|-------------|-----------------------------|-------------------|---|
| 1 | 19 (76%) | 10 (45.5%) | 418         | 250         | 28.224                      | 29                | 973.241   |
| 2 | 6 (24%)  | 8 (36.4%)  | 132         | 200         | 4.624                       | 14                | 330.286   |
| 3 | 0 (0%)   | 2 (9.09%)  | 0           | 25          | 2.500                       | 2                 | 1.250   |
| 4 | 0 (0%)   | 1 (4.55%)  | 0           | 25          | 625                         | 1                 | 625   |
| 5 | 0 (0%)   | 1 (4.55%)  | 0           | 25          | 625                         | 1                 | 625   |

**Table 6.** Comparison of the experimental group after the experiment with the control group before the experiment

| j | $n_{1j}$ | $n_{2j}$   | $N_2n_{1j}$ | $N_1n_{2j}$ | $(N_2n_{1j} - N_1n_{2j})^2$ | $n_{1j} + n_{2j}$ | $\frac{(N_2n_{1j} - N_1n_{2j})^2}{n_{1j} + n_{2j}}$ |
|---|----------|------------|-------------|-------------|-----------------------------|-------------------|---|
| 1 | 2 (8%)   | 12 (54.5%) | 44          | 300         | 65.536                      | 14                | 4.681.14  |
| 2 | 3 (12%)  | 7 (31.8%)  | 66          | 175         | 11.881                      | 10                | 1.188.1   |
| 3 | 1 (4%)   | 1 (4.55%)  | 22          | 25          | 9                           | 2                 | 4.5   |
| 4 | 5 (20%)  | 1 (4.55%)  | 110         | 25          | 7.225                       | 6                 | 1.204.17  |
| 5 | 14 (56%) | 1 (4.55%)  | 308         | 25          | 80.089                      | 15                | 5.339.27  |

**Table 7.** Comparison of the experimental group after the end of the experiment with the control group after the end of the experiment

| j | $n_{1j}$ | $n_{2j}$   | $N_2n_{1j}$ | $N_1n_{2j}$ | $(N_2n_{1j} - N_1n_{2j})^2$ | $n_{1j} + n_{2j}$ | $\frac{(N_2n_{1j} - N_1n_{2j})^2}{n_{1j} + n_{2j}}$ |
|---|----------|------------|-------------|-------------|-----------------------------|-------------------|---|
| 1 | 2 (8%)   | 12 (54.5%) | 44          | 250         | 42436                       | 12                | 3536.33   |
| 2 | 3 (12%)  | 7 (31.8%)  | 66          | 200         | 17956                       | 11                | 1632.36   |
| 3 | 1 (4%)   | 1 (4.55%)  | 22          | 50          | 784                         | 3                 | 261.333   |
| 4 | 5 (20%)  | 1 (4.55%)  | 110         | 25          | 7225                        | 6                 | 1204.17   |
| 5 | 14 (56%) | 1 (4.55%)  | 308         | 25          | 80089                       | 15                | 5339.27   |

**Table 8.** Comparison of the control group before the start of the experiment with the control group after the end of the experiment

| j | $n_{1j}$   | $n_{2j}$   | $N_2n_{1j}$ | $N_1n_{2j}$ | $(N_2n_{1j} - N_1n_{2j})^2$ | $n_{1j} + n_{2j}$ | $\frac{(N_2n_{1j} - N_1n_{2j})^2}{n_{1j} + n_{2j}}$ |
|---|------------|------------|-------------|-------------|-----------------------------|-------------------|---|
| 1 | 12 (54.5%) | 10 (45.5%) | 264         | 220         | 1936                        | 22                | 88  |
| 2 | 7 (31.8%)  | 8 (36.4%)  | 154         | 176         | 484                         | 15                | 32.266  |
| 3 | 1 (4.55%)  | 2 (0.09%)  | 22          | 44          | 484                         | 3                 | 161.333   |
| 4 | 1 (4.55%)  | 1 (4.55%)  | 22          | 22          | 0                           | 2                 | 0   |
| 5 | 1 (4.55%)  | 1 (4.55%)  | 22          | 22          | 0                           | 2                 | 0   |

**Table 9.** Paired comparison results

|  | Experimental group before the experiment                              | Experimental group after the end of the experiment                | Control group before the experiment                                    | Control group after the experiment                                     |
|--|---|---|--|--|
| Experimental group before the experiment           | 0   | $34.8 > \chi_{cr}^2$<br>differences are statistically significant | $4.48 < \chi_{cr}^2$<br>differences are not statistically significant  | $6.92 < \chi_{cr}^2$<br>differences are not statistically significant  |
| Experimental group after the end of the experiment | $34.8 > \chi_{cr}^2$<br>differences are statistically significant     | 0   | $22.6 > \chi_{cr}^2$<br>differences are statistically significant      | $21.8 > \chi_{cr}^2$<br>differences are statistically significant      |
| Control group before the experiment                | $4.48 < \chi_{cr}^2$<br>differences are not statistically significant | $22.6 > \chi_{cr}^2$<br>differences are statistically significant | 0  | $0.582 < \chi_{cr}^2$<br>differences are not statistically significant |
| Control group after the experiment                 | $6.92 < \chi_{cr}^2$<br>differences are not statistically significant | $21.8 > \chi_{cr}^2$<br>differences are statistically significant | $0.582 < \chi_{cr}^2$<br>differences are not statistically significant | 0  |

**INTEGRAÇÃO DE PROJETO ROBÓTICO NO PROCESSO DE APRENDIZAGEM NA ESCOLA****INTEGRATION OF ROBOTICS DESIGN INTO THE LEARNING PROCESS AT SCHOOL****ИНТЕГРАЦИЯ ЭЛЕМЕНТОВ МОДЕЛИРОВАНИЯ РОБОТОТЕХНИКИ В ПРОЦЕСС ШКОЛЬНОГО ОБУЧЕНИЯ**

KOZHAGUL, Aidos<sup>1\*</sup>; BIDAIBEKOV, Yessen<sup>2</sup>; BOSTANOV, Bektas<sup>3</sup>; PAK, Nikolay<sup>4</sup>; KOZHAGULOVA, Zhanar<sup>5</sup>;

<sup>1,2,3</sup> Abay Kazakh National Pedagogical University, Department of Informatics and Informatization of Education, Almaty – Republic of Kazakhstan

<sup>4</sup> Krasnoyarsk State Pedagogical University named after V.P. Astafiev, Department of Informatics and Information Technologies in Education, Krasnoyarsk – Russian Federation

<sup>5</sup> Abay Kazakh National Pedagogical University, Department of Chemistry, Almaty – Republic of Kazakhstan

*\* Correspondence author  
e-mail: aidoskozhagul@gmail.com*

Received 05 March 2020; received in revised form 05 June 2020; accepted 27 June 2020

**RESUMO**

A aplicação dos métodos de ensino ao processo de aprendizagem na escola é determinada pelo fato de que cada professor ou desenvolvedor de currículo deseja que seus conceitos de ensino e a formação de princípios educacionais sejam implementados no ambiente educacional da maneira mais eficaz. Tais formas de interação são determinadas pelo fato de que cada professor procura integrar os elementos práticos da área disciplinar no processo educacional, tanto como estruturas metodológicas quanto como as formas complexas formalizadas de didática. O objetivo deste estudo foi identificar esse aspecto do problema pedagógico. A análise dos conhecimentos e habilidades anteriores mostra que o treinamento dos estudantes de classes seniores na área dos métodos de projetos de elementos de robótica tem um potencial significativo para a formação efetiva de competências de disciplinas. Os resultados obtidos no experimento pedagógico como um todo confirmaram a hipótese da pesquisa pedagógica: se aplicarmos o sistema especial de condições, formas e métodos didáticos para desenvolver as habilidades de design dos estudantes de classes seniores para projetar robótica e resolver os problemas e tarefas práticas, com base na construção e estudo da sequência de submodelos, isso aumentará a eficiência do ensino de design de robótica, formação de ideias sobre a natureza de modelo do conhecimento e desenvolvimento de suas habilidades cognitivas e criativas. Os resultados obtidos mostram que o curso de treinamento “Design de robótica como método de resolução de problemas aplicados” para estudantes ajuda a aumentar o nível de habilidades na área de tecnologia robótica dos estudantes de classes seniores no cada critério específico, o que confirma a justificativa pedagógica da introdução de condições didáticas identificadas e teoricamente justificadas para o desenvolvimento de habilidades de design de robótica em estudantes de classes seniores.

**Palavras-chave:** *educação, escola, modelagem, robótica, tecnologia, profissão.*

**ABSTRACT**

The application of teaching methods to the learning process at school is defined by the fact that every teacher or curriculum developer strives to ensure that his or her concepts of teaching and formation of the educational principles are implemented in the educational environment most effectively. Such forms of interaction cause the fact that every teacher strives to integrate the practical elements of the subject area into the learning process both as the exact structures and as the formalized complicated forms of didactics. This study aimed the revealing of this aspect of the pedagogical problem. The analysis of the previous knowledge and abilities shows that teaching the methods for the design of the robotics' elements to the senior school students has a significant potential for the active form of the subject competencies. The obtained results of the teaching experiment have generally proved the hypothesis of pedagogical research. If to apply a unique system of didactic conditions, forms and development methods of the senior school students' robotics design skills to robotic design and solution of

tasks and practical assignments based on the construction and research of the sequence of sub-models, then it will contribute to the increase in the effectiveness of the robotic design teaching, the formation of the students' ideas of the model nature of cognition, and the development of their cognitive and creative abilities. The obtained results show that teaching course 'Robotics Design as a Method for Solution of Application Tasks' to students contributes to the increase in the level of the senior school students' robotics design skills by each particular criteria, which proves the pedagogical rationale of introducing the revealed and theoretically substantiated didactic conditions for the development of the senior school students' robotics design skills.

**Keywords:** *education, school, design, robotics, technology, profession.*

## АННОТАЦИЯ

Применение методов обучения к процессу обучения в школе определяется тем фактом, что каждый учитель или разработчик учебной программы стремится к тому, чтобы его или ее концепции преподавания и формирования образовательных принципов были реализованы в образовательной среде наиболее эффективным образом. Такие формы взаимодействия обуславливают тот факт, что каждый преподаватель стремится интегрировать практические элементы предметной области в учебный процесс как в качестве методических структур, так и в виде формализованных сложных форм дидактики. Целью данного исследования было выявление данного аспекта педагогической проблемы. Анализ предыдущих знаний и умений показывает, что обучение методам проектирования элементов робототехники ученикам старших классов имеет значительный потенциал для эффективного формирования предметных компетенций. Полученные результаты педагогического эксперимента в целом подтвердили гипотезу педагогического исследования: если применить специальную систему дидактических условий, форм и методов развития навыков конструирования учащихся старших классов для робототехнического проектирования и решения задач и практических заданий, основываясь на построении и исследовании последовательности подмоделей, это будет способствовать повышению эффективности обучения робототехническому проектированию, формированию у учащихся представлений о модельной природе познания и развитию их когнитивных и творческих способностей. Полученные результаты показывают, что учебный курс «Дизайн робототехники как метод решения прикладных задач» для студентов способствует повышению уровня навыков робототехники старшеклассников по каждому конкретному критерию, что подтверждает педагогическое обоснование внедрения выявленных и теоретически обоснованных дидактических условий развития у студентов старших классов навыков конструирования робототехники.

**Ключевые слова:** *образование, школа, моделирование, робототехника, технология, профессия.*

## 1. INTRODUCTION:

To find the indicators of the level of senior school students' robotics design skills, it is going to consider the particular skills that are the components of the competence (Kyei-Blankson, 2014; Ali *et al.*, 2018; Anamova *et al.*, 2019; Wu *et al.*, 2018; Tuna & Ahmetoğlu, 2019; Harada, 2020). By the capability of the senior school students in the robotics design, it means the personal competence combining the knowledge and skills, providing an opportunity to set a task in a particular way:

- to choose the design objects and to find the interconnections between the components of the research process;

- to translate the developed concepts into the language of formulas and signs, to understand the algorithms and mathematical methods for the computation of the characteristics of a robotics model;

- to interpret the obtained data, and to

formulate the particular conclusions (Scherer & Beckmann, 2014).

In the context of the study, the structure of the robotics design competence is presented as an aggregate of three interconnected components: theoretical, practical, and personal (Danesi, 2016; Molchanova *et al.*, 2018; Caballero-Gonzalez *et al.*, 2019).

To define the indicators and the levels of the robotics design skills among the senior school students, the process of a senior school student's personal development was investigated (Miller *et al.*, 1995; Damaševičius *et al.*, 2018; Karpenko *et al.*, 2019). In this period of personal development, the primary type of individual activity is learning. In the senior adolescent age, learning is a specific kind of events, where the subject affected by specific external factors and results of his/her activities: acquires the social experience; knowledge; forms the opinions and the view of the world in general which results in the change of his/her behavior; psychic processes; personal traits (Turuntaev, 2018). The successfulness of

acquiring the learning skills, including the robotics design activities, depends on the level of the student's preparedness, so it was chosen the approach concluded in the transition from one level of differentiation to another as the base for the definition of the indicators of the skills' level – a more complicated approach that differs from the previous one (Nilsson & Pareto, 2010; Chekanova & Gazizov, 2019; Gerosa *et al.*, 2019; Bayanov *et al.*, 2019; Marengo *et al.*, 2019; Sarsar & Çakır, 2020).

To develop the program of active development of the robotics design skills among the senior school students at the study of natural mathematical disciplines, it is necessary to define the main indicators, criteria, and levels of these skills (Fessakis *et al.*, 2018; Stepanov, 2019; Haiguang *et al.*, 2020; Yudin *et al.*, 2020). In the context of our study, the development of a school student as an integral process was analyzed, which may be considered only concerning a particular system because it is the result of the action of its elements (Ko *et al.*, 2012; Rativa, 2018; Habib, 2020). If set the objective to study the development process of a particular component, this process should be presented in the form of a system, having divided it into the components and highlighting the environment (Dmitrieva *et al.*, 2018; Kvesko *et al.*, 2018; Kim & Kim, 2020). There is a gradual transition from one level to another, particularly:

- the sophistication of the structural elements causing the refinement of the structure itself;
- the creation of a perfect arrangement of the relationships between the structural elements;
- simultaneous improvement of the fundamental aspects and the structure itself.

## 2. LITERATURE REVIEW:

In the learning process at school, at any level, deal with the concepts, statements, and supplements of a theoretical nature (Daskolia *et al.*, 2018; Loureiro *et al.*, 2019). The digestion of knowledge connected with the robotics design is narrowed to the assimilation of a particular system of concepts, statements, and proofs (Yacsar, 2004). But the purpose of learning is concluded not only in the digestion of the theoretical knowledge, but also in the transfer of skills how to apply this knowledge not only in the metabolism of particular proofs, but also in the formation of the ability to reason, prove, and solve practical tasks (Pohjolainen *et al.*, 2018; Ponce *et al.*, 2019).

The analysis of the previous knowledge and abilities shows that teaching the methods for the design of the robotics' elements to the senior school students has a significant potential for active formation of the subject competencies (Barnes *et al.*, 2017). The intentional development of the senior school students' robotics design skills while solving the application tasks requires a mainly organized learning process and its provision with the methods (Ruth, 2018).

According to the results of the conducted research, it should be revealed the directions for the increase in the effectiveness of the education aimed at the development of the senior school students' robotics design skills in the learning process of the natural mathematical disciplines formed in the didactic conditions (Ramalho & Crato, 2012). Based on the theoretical analysis of the role and place of the method for the robotics design in the modern science, it may be stated that particularly this method and its methodology take one of the leading positions in the system of modern science, being a new universal component of the methodology in any science (Pohjolainen *et al.*, 2018). The main didactic principle is to ensure the compliance of the education to the current level of science. So teaching the basics of the method for the robotics design becomes highly relevant because learning the elements of this method implies not just the digestion of particular rules and ways of action, but the development of a specific form of thinking (Campos, 2013).

The entire process of development of natural science is the process of development of the model knowledge about the objects and processes (Sevinc & Lesh, 2018; Daniela and Lytras, 2019). Particularly during the acquisition of the natural disciplines, the models was created and equipped, learn their properties, and foresee the processes in a wide range of possible conditions (Larson, 2013; Stehling *et al.*, 2016; Eteokleous, 2019; Yang, 2019; Muñoz *et al.*, 2020). The particular means of solving the application tasks is the process of 'solving' the model. In this regard, teaching the robotics design to the students, on the one hand, qualitatively changes the particular approach towards the solution of the tasks, and on the other hand – develops the new type of thinking (Scherer & Beckmann, 2014; Guderian, 2017; Fonseca Ferreira *et al.*, 2018; Jäggle *et al.*, 2018; Oudeyer, 2019; Strutynska, 2019).

### 3. MATERIALS AND METHODS:

To reveal the similarities and differences in the characteristics of the experimental and control groups, the following hypotheses was formulated: the hypothesis of the absence of differences (null hypothesis) and the hypothesis of the significance of differences (alternative hypothesis). To choose the hypothesis (null or alternative), the statistical criteria are applied. Particularly, to measure the data by the order scale, it is reasonable to apply the Pearson's  $\chi^2$  (chi-square) criterion of homogeneity. The empirical value of the statistical criterion  $\chi^2_{emp}$  is calculated (Melis, 2005; Soliman, 2019).

To assess the effectiveness of the traditional (mediated) method and the one was suggested for the development of the knowledge and skills of the robotics design, the indicators of the increment in the initial level of the students' knowledge and expertise was used. At such an approach, the suggested didactic model is considered more productive, more increase in the level of experience, skills, and general intellectual development have been achieved as a result of its application. The correctness of the effectiveness assessment of implemented didactic model significantly depends on the extent of the correctness of the level of skills and knowledge as well as the positive changes among the students of the cognitive sphere. To quantitatively assess the set level, the notion of the information-sense element of the text (ISET), which is based on the structural properties of the educational information, was used. The level every student's knowledge and skills before and after the evaluation of the systematic system for the formation of the robotics design skills was assessed employing coefficient (Equation 1) where  $S$  is the general number of the earlier digested ISET,  $S_i$  – general number of ISET, which were digested and revealed by the  $i$ -student before the beginning of the experiment and after the formation stage.

The average value of the increment in the students' knowledge and skills taught by means of a corresponding methodical system is defined by the following equation (2). Where  $n$  is the number of students in the group,  $K_{1i}$  and  $K_{2i}$  are the similar values of the coefficients of the  $i$ -student's skills and knowledge revealed during the final and initial assessment, respectively.

The structure of our methods for effectiveness assessment of the methodical systems for the formation of the robotics design skills (suggested and traditional indirect ones)

consists of the following components:

1) the definition of the initial level of knowledge and skills and the mathematical development of each student of the experimental and control group;

2) the definition of the final level of the abovementioned parameters of each student in the experimental and control groups (after the teaching experiment);

3) the revealing of the absolute increment in the level of knowledge and skills, the fixation of the positive tendencies in the development of the cognitive sphere of each student of the experimental and control groups;

4) the computation of the average values of the initial and final levels of the knowledge and skills;

5) the computation of the average values of the absolute increment in the level of knowledge and skills, the fixation of the positive tendencies in the general and intellectual development;

6) the revealing of the relative increment in the level of knowledge and skills for the students of each group.

7) mathematical processing of the obtained results (comparison of the values of relative increments in the levels of knowledge and skills, as well as positive tendencies in the development of the cognitive sphere among the students of the experimental and control groups).

### 4. RESULTS AND DISCUSSION:

The changes in the level of the skills and knowledge of students are reflected in Table 1 and Table 2. The coefficients of the level of the robotics design skills were defined according to the equation (1). Where  $S_i$  is the number of digested elements of the knowledge for  $i$ -student,  $S$  is the general number of the knowledge elements containing in the suggested control work. The average coefficient is calculated according to the following equation (3). The average value of the increment in the level of knowledge and skills among the students of each group is computed according to the equation (2). Where  $K_{1i}$  is the coefficient of the level of the robotics design skills defined for  $i$ -student during the final control, while  $K_{2i}$  – during the initial control, respectively (Table 3), the effectiveness assessment of the teaching stage of the experiment may be presented as a diagram in Figure 1.

Let's calculate the scores in the control and



experimental groups. The average rating in the experimental group is  $x_1=77$ , in control one –  $x_2=63$ . The value of dispersions: in the experimental group –  $\sigma_1^2=14.318$ , in the control group –  $\sigma_2^2=16.667$ . The null hypothesis is formulated at the proposition that the deviation of the average values is accidental, i.e., equation (4). The alternative theory suggests that the teaching methods in the experimental group are more productive, i.e., equation (5).

At such a formulation of the alternative hypothesis, the one-sided control of the null hypothesis through the student's t-test is conducted. The statistical characteristic of the control of the null hypothesis is the normalized deviation of the average values (Equation 6), which is subject to the distribution of the student's probabilities with the number of freedom degrees  $k=n_1+n_2-2=206$ . The assessment of the average dispersion out of the group ones is equal to

$$\sigma^2 = \frac{\sum_{i=1}^m \sigma_i^2 n_i}{n_1 + n_2 - 2} = 16,138, \text{ then } t = 25.24.$$

The critical value of the one-sided student's t-test at the level of significance  $\alpha=0.05$  and  $k=206$  is equal to  $t_{0.95}(206)=1.97$ , which is less than the actual one. So, the null hypothesis is rejected. With the 0.95 probability, one may state that the methods applied in the experimental group are more effective. The coefficient of the effectiveness of the suggested methods, in this case, is defined according to the following equation 7. Where  $K_e$  is the coefficient value of the level of the E students' robotics design knowledge and skills according to the results of the final assessment, while C is the coefficient value for the control group. So, the result of the teaching stage of the experiment is the effective coefficient of our robotics design methodical teaching system for students, which is equally as follows  $\eta = \frac{0,488}{0,355} = 1,37$ .

The fact that the obtained values of coefficient  $\eta$  are equal to  $\eta>1$  shows the relative effectiveness of our systematic teaching system. In the process of the element-by-element analysis conducted by the program, the requirements that should satisfy the digestion of the students' knowledge and skills were defined. These requirements imply the knowledge of the essential attributes of the robotics design notions, and their connection and correlation with the other ones.

To test the effectiveness of the developed

educational model of teaching robotics design in the process of the experimental research, it should be defined the following criteria:

- 1) the changes in the emotional Motivation of the students towards learning robotics design;
- 2) the level of the robotics design skills among the students;
- 3) the effect of the suggested didactic model on the level of knowledge of the adjacent disciplines, such as mathematics, economics, and physics. Let's consider each criterion in detail.

Criterion 1: The change in the emotional Motivation of the students while learning robotics design. Parameter: The students' emotional Motivation. Testing method: Surveying students on their emotional Motivation before and after the experiment. Hypothesis: Teaching our developed educational model to the students will improve the emotional Motivation of the students from the experimental group, which will evidence the growth of their interest and the positive inner Motivation to the robotics design. Mann-Whitney U test. The experiment, according to the first criterion, was performed in three stages:

- 1) the development of the survey form for the definition of the emotional state of the students;
- 2) the research of the absence of the differences between the E and C groups before the experiment;
- 3) the research of the emotional state of the students of the E and C groups after the experiment.

Below is the description of each stage. Stage 1: The development of the survey form to define the students' emotional Motivation. The didactic model of teaching the robotics design method to the senior school students, which contains the motivational component of the learning process was developed, including as follows:

- the theoretical material reflecting the specificity of the application of the robotics design method in the learning process of the students;
- the application tasks by the natural science disciplines;
- the practical creative tasks, including the project works.

As a result, the creation of the positive inner Motivation for learning the robotics design method, and the growth of the interest in solving

the application tasks was expected. In order to investigate the effect of the motivational component on the students during the optional course learning, the survey form to define the students' emotional state based on the analysis of the psychodiagnostic methods for the social-psychological research was developed.

Stage 2: The research of the differences between the E and C groups before the experiment. Therefore, it is necessary to compare the average parameters of the emotional disposition of the students from the E and C groups towards learning the proprietary methodology in the form of a didactic model of the optional course 'Robotics Design as a Method for Solution of Application Tasks'. Let  $O_1$  and  $O_2$  be the survey of the students from the experimental group and from the control group respectively regarding their emotional state before the experiment. By applying the Mann–Whitney U test, let us test the equality  $O_1=O_2$  (by the example of the E and C groups of the 11<sup>th</sup> graders).

The number of students in the E group is 16 ( $n_1=16$ ), while in C – 19 ( $n_2=19$ ). Scores (minimum 3, maximum 12), set by the students of both groups to the experiment are shown in Table 4. According to the data of the table, let us find the average score separately for the E and C groups and denote them as  $X_{exp}$  and  $X_{cont}$  respectively.

Based on the average indicators  $X_{exp}=6.44$  and  $X_{cont}=6.47$ , it should be supposed that the emotional states in both groups are almost the same. In order to test this supposition, let us suggest two hypotheses:

1.  $H_0$  – differences between  $X_{exp}$  and  $X_{cont}$  are accidental (or they absent). So, our groups are similar.

2.  $H_1$  – differences between  $X_{exp}$  and  $X_{cont}$  are reliable and significant. They may be caused by a greater range of the individual indicators' values, and then it is necessary to measure either the control or the experimental group.

The testing order of the suggested hypotheses is as follows:

1. The data of both groups are united into a new table in the order of increasing indicators.

2. Each value of the obtained sequence receives its rank. If there are several similar numbers in the sequence, then the rule of the connected ranks is applied.

3. The sum of ranks ( $\sum R$ ) separately for the experimental ( $\sum R_{exp}$ ) and control groups ( $\sum R_{cont}$ ) was found (Table 5). It was found that

$\sum R_{exp} = 286,5$ . The U-test value according to the following equation 8 was calculated. Where  $n_1$  is the number of students in the experimental group;  $n_2$  is the number of students in the control group;  $n_{Rmax}$  – the number of students in the group with a larger sum of ranks;  $R_{max}$  – maximum rank-sum.

4. Using table 'Critical Values of the U-Test ( $p = 0.05$ )', the critical value of the U-test for  $n_1=16$ ;  $n_2=19$ :  $U_{crit}=92$  was found.

If  $U > U_{crit}$ , then  $H_0$  hypothesis is accepted. If  $U < U_{crit}$ , then  $H_1$  hypothesis is accepted. In our case,  $U=146.5$ . So,  $146.5 > 92$ . Therefore,  $H_0$  hypothesis is accepted: the differences between our groups are insignificant.

Stage 3: The research of the emotional Motivation of the students from the E and C groups after the experiment. Based on our supposition, the emotional state of the students from the experimental group should raise, which evidences the growth of their interest in the solution of the application tasks, and the formation of the positive inner motivation to the robotics design.

Let  $O^*_1$  and  $O^*_2$  be the survey of the students from the experimental and the control group respectively regarding their emotional state after the experiment. After the conduction of the teaching experiment, it is necessary to compare the average indicators of the emotional state of the students from the E and C groups in order to test that  $O^*_1 \neq O^*_2$ —the scores set by the students of both groups after the experiment are presented in Table 6.

After the experiment, the average score of the students' emotional state in the experimental group grew up to 7.88 scores ( $X^*_{exp}=7.88$ ), while in the control group, it became equal to 6.37 ( $X^*_{cont}=6.37$ ). If to base on the average indicators, then one may suppose that the positive emotional state in the experimental group grew from  $X^*_{exp}=6.44$  (before the experiment) to  $X^*_{exp}=7.88$  (after the experiment) not accidentally, but thanks to the learning process based on our methods. To test this hypothesis, let us suggest two following hypotheses:

1.  $H_0$  – differences between  $X^*_{exp}$  and  $X^*_{cont}$  are accidental. The experiment failed.

2.  $H_1$  – differences between  $X^*_{exp}$  and  $X^*_{cont}$  are reliable, significant. So, the emotional state in the experimental group grew thanks to the work of the teacher based on our methods.

The data of both groups are united into a

new table (see Table 7) in the order of increasing indicators. Each value of the obtained sequence received its rank. The sum of the ranks separately for the E and C groups was found. It was found that  $\sum R_{exp}^* = 371$ . According to the formula, the  $\sum R_{cont}^* = 257$

value  $U=69$  was calculated. And so,  $U < U_{crit}$  ( $69 < 92$ ), therefore the hypothesis  $H_1$  is accepted: the emotional state in the experimental group has increased thanks to the teacher's work based on our methods. The experiment is successful.

Criterion 2: The level of the students' robotics design skills. Parameter: The level of the E and C group students' robotics design skills. Testing method: The comparison of the final test results in the E and C groups. Hypothesis: The level of the students' robotics design skills (students' academic performance) increases thanks to their teachers' work based on our methods—Statistical Criterion: Student's t-test.

At the end of the academic year, the 11<sup>th</sup> graders of the E and C groups were offered to perform a final test. The results of the 11<sup>th</sup> graders' performed test are presented in Table 8. So, according to the results of the final test of the E students compared with the C group, one may make the following conclusions:

- 1) there are no 1 and 2 scores;
- 2) the number of students received from 3 to 5 scores decreased;
- 3) the number of students received from 6 to 10 scores increased.

The results of the E and C group students' final test are reflected in the form of a diagram in Figure 2. It should be combined the obtained results in accordance with the levels of the 11<sup>th</sup> graders' skills and present them in Table 9. Thus, in the E group compared with the C one:

- 1) the number of students with a low level of skills decreased by 18.6 %;
- 2) the number of students with a moderate level of skills decreased by 9.2 %;
- 3) the number of students with a sufficient level of skills increased by 25.7 %;
- 4) the number of students with a high level of skills increased by 2.1 %;
- 5) the qualitative parameter of the academic performance increased from 17.2 % to 45%.

The dynamics are reflected as a diagram in Figure 3. After the experiment, the average score

of the 11<sup>th</sup> graders' algebra academic performance increased from  $X_{exp}=4.9$  to  $X_{exp}^*=6.3$ , while the parameter of the C group remained unchanged ( $X_{cont}=4.8$ ;  $X_{cont}^*=4.8$ ). So, one may suppose that the academic performance of the 11<sup>th</sup> graders in the experimental groups grew not accidentally but thanks to their teachers' work based on our methods. To test this supposition, let us suggest two hypotheses:

1.  $H_0$  – differences between  $X_{exp}^*$  and  $X_{cont}^*$  are accidental. Experiment failed.

2.  $H_1$  – differences between  $X_{exp}^*$  and  $X_{cont}^*$  are reliable, significant. The algebra academic performance of the 11<sup>th</sup> graders in the experimental groups increased thanks to their teachers' work based on our methods.

The hypotheses will be tested through the student's t-test for independent samples. The testing procedure of the suggested hypotheses is as follows:

–  $\sigma_{exp}$  and  $\sigma_{cont}$  was calculated according to the following equation (9);

– the m value separately for the E and C groups was calculated according to the following formula equation (10);

– the value of the student's t-test was found according to the following equation (11);

– the number of degrees of freedom, which depends on the number of students in both samples (Equation 12) was found. In our case:  $n_1=n_2=435$ . Therefore,  $v=435+435-2= 868$ .

– using table 'Borders of the Student's T-Test Values', the level of statistical significance. If  $t_{emp} \geq t_{tabl}$  was defined, then hypothesis  $H_1$ ; if  $t_{emp} < t_{tabl}$  was accepted, then  $H_0$  was accepted.

The obtained data of the 10<sup>th</sup> graders' groups after the experiment are presented in Table 10. At the level of statistical significance  $p=0.001$ ,  $t_{emp} \geq t_{tabl}$  was ssen, i.e.  $13.49 > 1.96$ . So, hypothesis  $H_1$  was accepted: the experiment is successful. The acceptance of the alternative hypothesis provides the grounds to state that the experimental profession-oriented method of development of the robotics design skills among the 11<sup>th</sup> graders is more effective than the traditional one. At the end of the academic year, the 11<sup>th</sup> graders of the E and C group were offered to perform a final test. The results of the 11<sup>th</sup> graders' performed test are presented in Table 11. So, according to the results of the final test of the E students compared with the C group, one may make the following conclusions:

1) the number of students received from 2 to 5 scores decreased;

2) the number of students received from 6 to 10 scores increased;

3) more than half of the students received from 6 to 7 scores.

The results of the E and C group students' final test are reflected in the form of a diagram in Figure 4. It should be combined with the obtained results per the levels of the 11<sup>th</sup> graders' skills and present them in Table 12. Thus, in the E group compared with the C one:

1) the number of students with a low level of skills decreased by 10.2%;

2) the number of students with a moderate level of skills decreased by 18.1%;

3) the number of students with a sufficient level of skills increased by 24.9%;

4) the number of students with a high level of skills increased by 3.4%;

5) the qualitative parameter of the academic performance and increased from 17% to 45.3%.

The dynamics are reflected as a diagram in Figure 5. After the experiment, the average score of the E 11<sup>th</sup> graders' academic performance increased from  $X_{exp}=4.7$  to  $X_{exp}^*=5.9$ , while in the C group, the parameter remained almost unchanged ( $X_{cont}=4.9$ ;  $X_{cont}^*=4.8$ ). So, one may suppose that the 11<sup>th</sup> graders' academic performance in the experimental groups increased not accidentally but thanks to their teachers' work based on our methods. To test this supposition, let us suggest two hypotheses:

1.  $H_0$  – differences between  $X_{exp}^*$  and  $X_{cont}^*$  are accidental. Experiment failed.

2.  $H_1$  – differences between  $X_{exp}^*$  and  $X_{cont}^*$  are reliable, significant. The algebra academic performance of the 11<sup>th</sup> graders in the experimental groups increased thanks to their teachers' work based on our methods.

The hypotheses will be tested the same as the previous calculations through the student's t-test for independent samples. The obtained data of the students' groups after the experiment are presented in Table 13. At the level of statistical significance  $p = 0.001$ ,  $t_{emp} \geq t_{tabl}$  was seen, i.e.  $9.48 > 1.96$ . So, hypothesis  $H_1$  is accepted: the experiment is successful. The acceptance of the alternative hypothesis provides the grounds to state that the experimental profession-oriented method of development of the robotics design

skills among the students is more effective than the traditional one.

Criterion 3: The effect of the suggested didactic model on the level of knowledge in the adjacent disciplines, particularly: mathematics, economics, and physics. Parameter: The achievement by the E and C group students of the sufficient and high levels of the robotics design skills at the solution of the application tasks. Testing Method:

– the comparison of the final test results in the E and C group by the sufficient and high levels;

– the comparison of the E and C group students taking part in the creative tasks and defense of their own projects.

Hypothesis: teaching our methods to the students contribute to the increase in the sufficient and high levels of their robotics design skills, which shows the development of their interdisciplinary qualities in robotics design. High level of development of the students' interdisciplinary qualities is proved by their capability of solving more complicated application tasks, i.e. the achievement by them of sufficient and high levels of academic performance. The results of the conducted experiment by the second criterion showed as follows:

1) for the 10<sup>th</sup> graders:

– the number of the E students with the sufficient level of skills increased by 112 people (by 25.7 %) compared with the C ones;

– the number of E students with high level of skills increased by 9 people (by 2.1 %) compared with C.

2) for the 11<sup>th</sup> graders:

– the number of the E students with a sufficient level of skills increased by 108 people (by 24.9 %) compared with the C ones;

– the number of the E students with high level of skills increased by 15 people (by 3.4%) compared with the C ones.

## 5. CONCLUSIONS:

Teaching robotics design to students based on proposed didactic model has contributed to the increase in the number of students taking part in the creative tasks and defense of their projects in the E group compared with the C one by 121 people and 123 people respectively for the 10<sup>th</sup> and 11<sup>th</sup> graders. Thus, the hypothesis of the experiment by the third criterion has been

confirmed.

Accordingly, the obtained results of the teaching experiment have generally proved the hypothesis of the pedagogical research: if to apply a special system of didactic conditions, forms and development methods of the senior school students' robotics design skills to robotic design and solution of tasks and practical assignments based on the construction and research of the sequence of sub-models, then it will contribute to the increase in the effectiveness of the robotic design teaching, the formation of the students' ideas of the model nature of cognition, and the development of their cognitive and creative abilities.

The obtained results show that teaching course 'Robotics Design as a Method for Solution of Application Tasks' to students contributes to the increase in the level of the senior school students' robotics design skills by each particular criteria. This proves the pedagogical rationale of introducing the revealed and theoretically substantiated didactic conditions for the development of the senior school students' robotics design skills.

## 6. REFERENCES:

1. Ali, M.A.M., Al-Youif, Sh., Mohammed, M.N., Al-Sanjary, O.I., Abdullah, M.I. (2018, December). *Design and implement sumobot for classroom teaching*. Paper presented at the IEEE Conference on Systems, Process and Control (ICSPC), Melaka, Malaysia.
2. Anamova, R.R., Bykov, L.V., & Kozorez, D.A. (2019). Aircraft industry staff retraining as a part of vocational education in the Russian Federation. *TEM Journal*, 8(3), 978-983.
3. Barnes, D., Wilkerson, T., & Stephan, M. (2017). Contributing to the development of grand challenges in maths education. In G. Kaiser (Ed.), *Mathematical education: Materials of the 13th international congress* (pp. 703-704). Cham, Switzerland: Springer International Publishing.
4. Bayanov, D.I., Novitskaya, L.Y., Panina, S.A., Paznikova, Z.I., Martynenko, E.V., Ilkevich, K.B., Karpenko, V.L., & Allalyev, R.M. (2019). Digital technology: Risks or benefits in student training? *Journal of Environmental Treatment Techniques*, 7(4), 659-663.
5. Caballero-Gonzalez, Y.-A., Garcia Valcarcel Munoz-Repiso, A., Garcia-Holgado, A. (2019). Learning computational thinking and social skills development in young children through problem solving with educational robotics. In: *Technological ecosystems for enhancing multicultural: Proceedings of the seventh international conference*. New York, USA: Association for Computing Machinery.
6. Campos, I.S. (2013). Cognitive processes and math performance: A study with children at third grade of basic education. *European Journal of Psychology of Education*, 28(2), 421-36. <https://doi.org/10.1007/s10212-012-0121-x>.
7. Chekanova, L.A., & Gazizov, T.T. (2019). Modern methods of educational robotics analysis. *Pedagogical Review*, 6, 79-83.
8. Damaševičius, R., Maskeliūnas, R., & Blažauskas, T. (2018). Faster pedagogical framework for steam education based on educational robotics. *International Journal of Engineering & Technology*, 7(2.28), 138-142.
9. Danesi, M. (2016). Math education and learning. In *learning and teaching mathematics in the global village: Math education in the digital age* (pp. 1-36). Cham, Switzerland: Springer International Publishing. [https://doi.org/10.1007/978-3-319-32280-3\\_1](https://doi.org/10.1007/978-3-319-32280-3_1).
10. Daniela, L., & Lytras, M.D. (2019). Educational robotics for inclusive education. *Technology, Knowledge and Learning*, 24, 219-225.
11. Daskolia, M., Kynigos, C., & Kolovou, A. (2018). Addressing creativity in the collaborative design of digital books for environmental and math education. In T.A. Mikropoulos (Ed.), *Research on E-learning and ICT in education: Technological, pedagogical and instructional perspectives* (pp. 69-86). Cham, Switzerland: Springer International Publishing. [https://doi.org/10.1007/978-3-319-95059-4\\_4](https://doi.org/10.1007/978-3-319-95059-4_4).
12. Dmitrieva, T., German, E., Khvatova, T. (2018). Digital technologies and higher education in Russia: new tools of development. *SHS Web of Conferences*, 44, Article number 00029.
13. Eteokleous, N. (2019). Employing educational robotics for the development of problem-based learning skills. In D.B.A.

- Mehdi Khosrow-Pour (Ed.), *Advanced methodologies and technologies in modern education delivery* (pp. 333-344). Hershey, Pennsylvania: IGI Global.
14. Fessakis, G., Karta, P., & Kozas, K. (2018). The math trail as a learning activity model for m-learning enhanced realistic mathematics education: A case study in primary education. In M.E. Auer, D. Guralnick, & I. Simonics (Eds.), *Teaching and learning in a digital world* (pp. 323-332). Cham, Switzerland: Springer International Publishing.
  15. Fonseca Ferreira, N.M., Moita, F., Santos, V.D.N., Ferreira, J., Cândido Santos, J., Santos, F., & Silva, M. (2018). Education with robots inspired in biological systems. In W. Lepuschitz, M. Merdan, G. Koppensteiner, R. Balogh, & D. Obdržálek (Eds.), *Robotics in education* (pp. 149-161). Berlin, Germany: Springer.
  16. Gerosa, A., Koleszar, V., Gómez-Sena, L., Tejera, G., & Carboni, A. (2019, October-November). *Educational robotics and computational thinking development in preschool*. Paper presented at the 2019 XIV Latin American Conference on Learning Technologies (LACLO), San Jose Del Cabo, Mexico.
  17. Guderian, D. (2017). Mathematics in contemporary art and design as a tool for math-education in school. In G. Kaiser (Ed.), *Mathematical education: Materials of the 13th international congress* (pp. 663-664). Cham, Switzerland: Springer International Publishing.
  18. Habib, M.K. (2020). *Revolutionizing education in the age of AI and machine learning*. Hershey, Pennsylvania: IGI Global. <http://doi:10.4018/978-1-5225-7793-5.ch005>
  19. Haiguang, F., Shichong, W., Shushu, X., & Xianli, W. (2020). Research on human-computer cooperative teaching supported by artificial intelligence robot assistant. In N. Pinkwart, & S. Liu (Eds.), *Artificial intelligence supported educational technologies. Advances in analytics for learning and teaching* (pp. 45-58). Cham, Switzerland: Springer International Publishing.
  20. Harada, K. (2020). Robotic Manipulation Research. *Impact*, 2020(2), 15-17.
  21. Jäggle, G., Vincze, M., Weiss, A., Koppensteiner, G., Lepuschitz, W., & Merdan, M. (2018). iBridge – participative cross-generational approach with educational robotics. In W. Lepuschitz, M. Merdan, G. Koppensteiner, R. Balogh, & D. Obdržálek (Eds.), *Robotics in education* (pp. 149-161). Berlin, Germany: Springer.
  22. Karpenko, O.M., Lukyanova, A.V., Bugai, V.V., & Shchedrova, I.A. (2019). Individualization of learning: An investigation on educational technologies. *Journal of History Culture and Art Research*, 8(3), 134-147.
  23. Kim, J., & Kim, J. (2020). Development and application of art based STEAM education program using educational robot. In *Robotic systems: concepts, methodologies, tools, and applications* (pp. 1675-1687). Hershey, Pennsylvania: IGI Global. <http://doi:10.4018/978-1-7998-1754-3.ch080>
  24. Ko, Y., An, J., & Park, N. (2012). Development of computer, math, art convergence education lesson plans based on smart grid technology. In T.-H. Kim (Ed.), *Computer applications for security, control and system engineering* (109-114). Berlin, Heidelberg, Germany: Springer Berlin Heidelberg.
  25. Kvesko, S.B., Kvesko, N.G., Korniyenko, A.A., & Kabanova, N.N. (2018). Educational robotics as an Innovative teaching practice using technology: minimization of risks. *IOP Conference Series: Materials Science and Engineering*, 363, Article number 012004.
  26. Kyei-Blankson, L. (2014). Training math and science teacher-researchers in a collaborative research environment: implications for math and science education. *International Journal of Science and Mathematics Education*, 12(5), 1047-1065. <https://doi.org/10.1007/s10763-013-9444-6>.
  27. Larson, C. (2013). Modeling perspectives in math education research. In R. Lesh, P.L. Galbraith, Ch.R. Haines, & A. Hurford (Eds.), *Modeling students' mathematical modeling competencies: ICTMA 13* (pp. 61-71). Dordrecht, Netherlands: Springer Netherlands. [https://doi.org/10.1007/978-94-007-6271-8\\_5](https://doi.org/10.1007/978-94-007-6271-8_5).
  28. Loureiro, M.J., Moreira, F.T., & Senos, S. (2019). Introduction to computational thinking with Mi-Go: A friendly robot. In L. Oliveira, & A.L. Melro (Ed.), *Open and social*

- learning in impact communities and smart territories* (pp. 110-137). Hershey, Pennsylvania: IGI Global.
29. Marengo, R., Fontes Ferreira, B., Reis Cabral, M., & Rodrigues Magalhães, R. (2019). Training teachers in robotics for science and technology dissemination: A Brazilian case study. *Theoretical and Applied Engineering*, 3(2), 11-18.
  30. Melis, E. (2005). Why proof planning for maths education and how? In D. Hutter, & W. Stephan (Eds.), *Mechanizing mathematical reasoning: Essays in honor of J.H. Siekmann on the occasion of his 60th birthday* (pp. 364–378). Berlin, Heidelberg, Germany: Springer Berlin Heidelberg. [https://doi.org/10.1007/978-3-540-32254-2\\_21](https://doi.org/10.1007/978-3-540-32254-2_21).
  31. Miller, A.D., Hall, S.W. & Heward, W.L. (1995). Effects of sequential 1-minute time trials with and without inter-trial feedback and self-correction on general and special education students' fluency with math facts. *Journal of Behavioral Education*, 5(3), 319–345. <https://doi.org/10.1007/BF02110318>.
  32. Molchanova, V.S., Artemova, S.F., & Balaniuk, L.L. (2018). Teaching singing in the Russian empire educational institutions: Importance and results. *European Journal of Contemporary Education*, 7(1), 220-225.
  33. Muñoz, L., Villarreal, V., Morales, I., Gonzalez, J., Nielsen, M. (2020). Developing an interactive environment through the teaching of mathematics with small robots. *Sensors*, 20, Article number 1935.
  34. Nilsson, A., & Pareto, L. (2010). The complexity of integrating technology enhanced learning in special math education – a case study. In M. Wolper (Ed.), *Sustaining TEL: From innovation to learning and practice* (pp. 638–643). Berlin, Heidelberg, Germany: Springer Berlin Heidelberg.
  35. Oudeyer, P.-Y. (2019). Developmental autonomous learning: AI, cognitive sciences and educational technology. Retrieved from <https://dl.acm.org/doi/10.1145/3308532.3337710>.
  36. Pohjolainen, S., Myllykoski, T., Mercat, Ch., & Sosnovsky, S. (2018). *Modern mathematics education for engineering curricula in Europe: A comparative analysis of EU, Russia, Georgia and Armenia*. Cham, Switzerland: Springer International Publishing. [https://doi.org/10.1007/978-3-319-71416-5\\_7](https://doi.org/10.1007/978-3-319-71416-5_7).
  37. Ponce, P., Molina, A., & Caudana, E.O.L. (2019). Improving education in developing countries using robotic platforms. *International Journal on Interactive Design and Manufacturing*, 13, 1401–1422. <https://doi.org/10.1007/s12008-019-00576-5>
  38. Ramalho, R., & Crato, N. (2012). Balancing math popularization with public debate: A mathematical society's continued efforts to raise the public awareness of mathematics and for youth mathematical education. In E. Behrends, N. Crato, & J. Francisco Rodrigues (Eds.), *Raising public awareness of mathematics*. Berlin, Heidelberg: Springer Berlin Heidelberg, 57–66. [https://doi.org/10.1007/978-3-642-25710-0\\_6](https://doi.org/10.1007/978-3-642-25710-0_6).
  39. Rativa, A.S. (2018). How can we teach educational robotics to foster 21st learning skills through PBL, Arduino and S4A? In W. Lopuschitz, M. Merdan, G. Koppensteiner, R. Balogh, & D. Obdržálek (Eds.), *Robotics in education* (pp. 149-161). Berlin, Germany: Springer.
  40. Ruth, R.G. (2018). Building bridges between the math education and the engineering education communities: A dialogue through modelling and simulation. In G. Kaiser (Ed.), *Invited Lectures from the 13th international congress on mathematical education* (pp. 501–519). Cham, Switzerland: Springer International Publishing.
  41. Sarsar, F., & Çakır, Ö.A. (2020). Designing a training platform for higher education engineering instructors in the Digital Era. In Ş. Serdar Asan & E. Işıklı, (Ed.), *Engineering education trends in the Digital Era* (pp. 53-69). Hershey, Pennsylvania: IGI Global. <http://doi:10.4018/978-1-7998-2562-3.ch003>
  42. Scherer, R., & Beckmann, J.F. (2014). The acquisition of problem solving competence: Evidence from 41 countries that math and science education matters. *Large-scale Assessments in Education*, 2(1), Article number 10. <https://doi.org/10.1186/s40536-014-0010-7>.
  43. Sevinc, S., & Lesh, R. (2018). Training mathematics teachers for realistic math problems: A case of modeling-based



- teacher education courses. *ZDM*, 50(1), 301–314. <https://doi.org/10.1007/s11858-017-0898-9>.
44. Soliman, S.A. (2019). Efficiency of an educational robotic computer-mediated training program for developing students' creative thinking skills: An experimental study. *Arab World English Journal (AWEJ), Special Issue*, Article number 5.
  45. Stehling, V., Schuster, K., Richert, A., & Jeschke, S. (2016). Access all Areas: Designing a hands-on robotics course for visually impaired high school students. In S. Frerich (Eds.), *Engineering Education 4.0* (pp. 753-759). Cham, Switzerland: Springer International Publishing.
  46. Stepanov, A.A. (2019). Improvement of the Russian system of staff training in the conditions of robotic technology development. *Science Journal of Volgograd State University. Global Economic System*, 21(1), 83-91.
  47. Strutyńska, O. (2019). The use of robotics and 3D technologies in the stem education development. *Electronic Scientific Professional Journal "Open Educational Environment of Modern University"*, 7, 96-109.
  48. Tuna, A., & Ahmetoğlu, E. (2019). Use of humanoid robots for students with intellectual disabilities. In L.W. Bailey (Ed.), *Educational technology and the new world of persistent learning* (pp. 208-228). Hershey, Pennsylvania: IGI Global. <http://doi:10.4018/978-1-5225-6361-7.ch011>
  49. Turuntaev, I.S. (2018). EdLeTS: Towards smartness in math education. In V.L. Uskov, J.P. Bakken, R.J. Howlett, & L.C. Jain (Eds.), *Smart universities: concepts, systems, and technologies* (pp. 225–261). Cham, Switzerland: Springer International Publishing. [https://doi.org/10.1007/978-3-319-59454-5\\_8](https://doi.org/10.1007/978-3-319-59454-5_8).
  50. Wu, P.-J., Chiu, F.-Y., Mayerová, K., & Kubincová, Z. (2018, April). *Educational robotics at primary school: comparison of two research studies*. Paper presented at the 17th International Conference on Information Technology Based Higher Education and Training (ITHET), Olhao, Portugal.
  51. Yacsar, O. (2004). Computational math, science, and technology: A new pedagogical approach to math and science education. In A. Laganá (Ed.), *Computational science and its applications – ICCSA 2004* (pp. 807–816). Berlin, Heidelberg, Germany: Springer Berlin Heidelberg.
  52. Yang, F.-Ch.O. (2019, July). *The design of AR-based virtual educational robotics learning system*. Paper presented at the 8th International Congress on Advanced Applied Informatics (IIAI-AAI), Toyama, Japan.
  53. Yudin, A., Vlasov, A., Salmina, M., & Shalashova, M. (2020). Evolution of educational robotics in supplementary education of children. In M. Merdan, W. Lepuschitz, G. Koppensteiner, R. Balogh, & D. Obdržálek (Eds.), *Robotics in education. RiE 2019. Advances in intelligent systems and computing* (pp. 346-343). Cham, Switzerland: Springer International Publishing.



$$K_i = \frac{S_i}{S} \quad (\text{Eq. 1})$$

$$\Delta \bar{K} = \frac{\sum_{i=1}^n (K_{1i} - K_{2i})}{n} \quad (\text{Eq. 2})$$

$$\bar{K} = \frac{\sum_{i=1}^n K_i}{n} \quad (\text{Eq. 3})$$

$$H_0: x_1 = x_2 \quad (\text{Eq. 4})$$

$$H_1: x_1 > x_2 \quad (\text{Eq. 5})$$

$$t = \frac{x_1 - x_2}{\sqrt{\sigma^2 \left( \frac{1}{n_1} + \frac{1}{n_2} \right)}} \quad (\text{Eq. 6})$$

$$\eta = \frac{K_e}{K_k} \quad (\text{Eq. 7})$$

$$U = n_1 \times n_2 + \frac{n_{R_{\max}} \times (n_{R_{\max}} + 1)}{2} - R_{\max} \quad (\text{Eq. 8})$$

$$\sigma^2 = \frac{\sum_{i=1}^n (X_i - X^*)^2}{n - 1} \quad (\text{Eq. 9})$$

$$m = \frac{\sigma}{\sqrt{n}} \quad (\text{Eq. 10})$$

$$t = \frac{X_{\text{exp}}^* - X_{\text{cont}}^*}{\sqrt{m_{\text{exp}}^2 + m_{\text{cont}}^2}} \quad (\text{Eq. 11})$$

$$v = n_1 + n_2 - 2. \quad (\text{Eq. 12})$$

**Table 1.** Dynamics of Changes in the Level of the Skills and Knowledge of the Students regarding the Robotics Design during the Teaching Experiment

| Kind of Assessment | $\bar{K}$ |       | $\Delta \bar{K}$ |       | $\Delta \bar{K} / \bar{K}$ |       |
|--------------------|-----------|-------|------------------|-------|----------------------------|-------|
|                    | E         | C     | E                | C     | E                          | C     |
| Initial            | 0.372     | 0.352 | 0.027            | 0.001 | 0.073                      | 0.003 |
| Intermediate       | 0.440     | 0.353 | 0.039            | 0.001 | 0.089                      | 0.003 |
| Final              | 0.488     | 0.355 | 0.048            | 0.002 | 0.098                      | 0.006 |

**Table 2.** Average Value of the Measured Levels of the Knowledge and Skills regarding Robotics Design during the Teaching Experiment

| Measured Parameters        | Groups |       |
|----------------------------|--------|-------|
|                            | E      | C     |
| $\bar{K}$                  | 0.345  | 0.351 |
| $\Delta \bar{K}$           | 0.143  | 0.004 |
| $\Delta \bar{K} / \bar{K}$ | 0.414  | 0.011 |

**Table 3.** Results of the Teaching Stage of the Experiment (based on the Results of the Initial and Final Assessments) by the example of the School Students

| Kind of Assessment | Number of Students            |     |                                |             |
|--------------------|-------------------------------|-----|--------------------------------|-------------|
|                    | performed the assessment work |     | coped with the assessment work |             |
|                    | E                             | C   | E                              | C           |
| Initial            | 103                           | 108 | 36 (34.5 %)                    | 36 (34.1 %) |
| Final              | 102                           | 103 | 87 (85.7 %)                    | 66 (64.3 %) |

**Table 4.** Emotional Motivation of the 11<sup>th</sup> Graders before the Experiment

| $n_1$ and $n_2$ | Scores E | Scores C | $n_1$ and $n_2$ | Scores E | Scores C | $n_1$ and $n_2$ | Scores E | Scores C |
|-----------------|----------|----------|-----------------|----------|----------|-----------------|----------|----------|
| 1               | 6        | 10       | 8               | 5        | 6        | 15              | 5        | 5        |
| 2               | 9        | 6        | 9               | 5        | 7        | 16              | 8        | 7        |
| 3               | 7        | 3        | 10              | 3        | 5        | 17              |          | 7        |
| 4               | 8        | 4        | 11              | 5        | 6        | 18              |          | 9        |
| 5               | 6        | 8        | 12              | 5        | 6        | 19              |          | 8        |
| 6               | 6        | 7        | 13              | 7        | 8        |                 |          |          |
| 7               | 9        | 6        | 14              | 9        | 5        |                 |          |          |

**Table 5.** Ordered Table of the Experimental Data

| No. | Group | Emotional state | Rank | No. | Group | Emotional state | Rank | No. | Group | Emotional state | Rank |
|-----|-------|-----------------|------|-----|-------|-----------------|------|-----|-------|-----------------|------|
| 1   | E     | 3               | 1.5  | 13  | E     | 6               | 15.5 | 25  | C     | 7               | 22.5 |
| 2   | C     | 3               | 1.5  | 14  | E     | 6               | 15.5 | 26  | E     | 8               | 28   |
| 3   | C     | 4               | 3    | 15  | C     | 6               | 15.5 | 27  | E     | 8               | 28   |
| 4   | E     | 5               | 8    | 16  | C     | 6               | 15.5 | 28  | C     | 8               | 28   |
| 5   | E     | 5               | 8    | 17  | C     | 6               | 15.5 | 29  | C     | 8               | 28   |
| 6   | E     | 5               | 8    | 18  | C     | 6               | 15.5 | 30  | C     | 8               | 28   |
| 7   | E     | 5               | 8    | 19  | C     | 6               | 15.5 | 31  | E     | 9               | 32.5 |
| 8   | E     | 5               | 8    | 20  | E     | 7               | 22.5 | 32  | E     | 9               | 32.5 |
| 9   | C     | 5               | 8    | 21  | E     | 7               | 22.5 | 33  | C     | 9               | 32.5 |
| 10  | C     | 5               | 8    | 22  | C     | 7               | 22.5 | 34  | C     | 9               | 32.5 |
| 11  | C     | 5               | 8    | 23  | C     | 7               | 22.5 | 35  | C     | 10              | 35   |
| 12  | E     | 6               | 15.5 | 24  | C     | 7               | 22.5 |     |       |                 |      |

**Table 6.** Emotional Motivation of the 11<sup>th</sup> graders after the Experiment

| n <sub>1</sub> and n <sub>2</sub> | Scores E | Scores C | n <sub>1</sub> and n <sub>2</sub> | Scores E | Scores C | n <sub>1</sub> and n <sub>2</sub> | Scores E | Scores C |
|-----------------------------------|----------|----------|-----------------------------------|----------|----------|-----------------------------------|----------|----------|
| 1                                 | 8        | 10       | 8                                 | 6        | 5        | 15                                | 8        | 6        |
| 2                                 | 10       | 7        | 9                                 | 7        | 6        | 16                                | 10       | 6        |
| 3                                 | 8        | 4        | 10                                | 6        | 6        | 17                                |          | 6        |
| 4                                 | 9        | 4        | 11                                | 8        | 6        | 18                                |          | 9        |
| 5                                 | 6        | 7        | 12                                | 7        | 6        | 19                                |          | 9        |
| 6                                 | 7        | 6        | 13                                | 7        | 7        |                                   |          |          |
| 7                                 | 10       | 6        | 14                                | 9        | 5        |                                   |          |          |

**Table 7.** Ordered Table of the Data after the Experiment

| No. | Group | Emotional state | Rank | No. | Group | Emotional state | Rank | No. | Group | Emotional state | Rank |
|-----|-------|-----------------|------|-----|-------|-----------------|------|-----|-------|-----------------|------|
| 1   | C     | 4               | 1.5  | 13  | C     | 6               | 10.5 | 25  | E     | 8               | 25   |
| 2   | C     | 4               | 1.5  | 14  | E     | 6               | 10.5 | 26  | E     | 8               | 25   |
| 3   | C     | 5               | 3.5  | 15  | E     | 6               | 10.5 | 27  | E     | 8               | 25   |
| 4   | C     | 5               | 3.5  | 16  | E     | 6               | 10.5 | 28  | E     | 9               | 29.5 |
| 5   | C     | 6               | 10.5 | 17  | E     | 7               | 20   | 29  | E     | 9               | 29.5 |
| 6   | C     | 6               | 10.5 | 18  | E     | 7               | 20   | 30  | C     | 9               | 29.5 |
| 7   | C     | 6               | 10.5 | 19  | E     | 7               | 20   | 31  | C     | 9               | 29.5 |
| 8   | C     | 6               | 10.5 | 20  | E     | 7               | 20   | 32  | E     | 10              | 33.5 |
| 9   | C     | 6               | 10.5 | 21  | C     | 7               | 20   | 33  | E     | 10              | 33.5 |
| 10  | C     | 6               | 10.5 | 22  | C     | 7               | 20   | 34  | E     | 10              | 33.5 |
| 11  | C     | 6               | 10.5 | 23  | C     | 7               | 20   | 35  | C     | 10              | 33.5 |
| 12  | C     | 6               | 10.5 | 24  | E     | 8               | 25   |     |       |                 |      |

**Table 8.** Results of the 10<sup>th</sup> Graders' Final Test after the experiment

| Scores | E                  |                        | C                  |                        |
|--------|--------------------|------------------------|--------------------|------------------------|
|        | Number of students | Number of students (%) | Number of students | Number of students (%) |
| 1      | 0                  | 0.0                    | 2                  | 0.5                    |
| 2      | 0                  | 0.0                    | 15                 | 3.4                    |
| 3      | 20                 | 4.6                    | 84                 | 19.3                   |
| 4      | 36                 | 8.3                    | 143                | 32.9                   |
| 5      | 57                 | 13.1                   | 67                 | 15.4                   |
| 6      | 126                | 29.0                   | 49                 | 11.3                   |
| 7      | 117                | 26.9                   | 36                 | 8.3                    |
| 8      | 45                 | 10.3                   | 25                 | 5.7                    |
| 9      | 21                 | 4.8                    | 10                 | 2.3                    |
| 10     | 13                 | 3.0                    | 4                  | 0.9                    |
| 11     | 0                  | 0.0                    | 0                  | 0.0                    |
| 12     | 0                  | 0.0                    | 0                  | 0.0                    |
| Total  | 435                | 100                    | 435                | 100                    |

**Table 9.** Distribution of the 10<sup>th</sup> Graders by the Level of Skills after the experiment

| Group | Number of students | Levels of the students' skills |                         |                           |                       |
|-------|--------------------|--------------------------------|-------------------------|---------------------------|-----------------------|
|       |                    | Low (1 – 3 scores)             | Moderate (4 – 6 scores) | Sufficient (7 – 9 scores) | High (10 – 12 scores) |
| E     | 435                | 20                             | 219                     | 183                       | 13                    |
|       |                    | 4.6 %                          | 50.4 %                  | 42.0 %                    | 3.0 %                 |
| C     | 435                | 101                            | 259                     | 71                        | 4                     |
|       |                    | 23.2 %                         | 59.6 %                  | 16.3 %                    | 0.9 %                 |

**Table 10.** Data of the 10<sup>th</sup> Graders after the experiment

| Data of E               |                    |  |                               |                  |                  | Data of C      |                    |  |                               |                  |                  |
|-------------------------|--------------------|--|-------------------------------|------------------|------------------|----------------|--------------------|--|-------------------------------|------------------|------------------|
| X <sub>i</sub>          | Number of students | (X <sub>i</sub> -X <sub>exp</sub> ) <sup>2</sup> | σ <sup>2</sup> <sub>exp</sub> | σ <sub>exp</sub> | m <sub>exp</sub> | X <sub>i</sub> | Number of students | (X <sub>i</sub> -X <sub>exp</sub> ) <sup>2</sup> | σ <sup>2</sup> <sub>exp</sub> | σ <sub>exp</sub> | m <sub>exp</sub> |
| 1                       | –                  | –  | 2.38                          | 1.54             | 0.074            | 1              | 2                  | 14.44  | 2.99                          | 1.73             | 0.083            |
| 2                       | –                  | –  |                               |                  |                  | 2              | 15                 | 7.84   |                               |                  |                  |
| 3                       | 20                 | 10.89  |                               |                  |                  | 3              | 84                 | 3.24   |                               |                  |                  |
| 4                       | 36                 | 5.29   |                               |                  |                  | 4              | 143                | 0.64   |                               |                  |                  |
| 5                       | 57                 | 1.69   |                               |                  |                  | 5              | 67                 | 0.04   |                               |                  |                  |
| 6                       | 126                | 0.09   |                               |                  |                  | 6              | 49                 | 1.44   |                               |                  |                  |
| 7                       | 117                | 0.49   |                               |                  |                  | 7              | 36                 | 4.84   |                               |                  |                  |
| 8                       | 45                 | 2.89   |                               |                  |                  | 8              | 25                 | 10.24  |                               |                  |                  |
| 9                       | 21                 | 7.29   |                               |                  |                  | 9              | 10                 | 17.64  |                               |                  |                  |
| 10                      | 13                 | 13.69  |                               |                  |                  | 10             | 4                  | 27.04  |                               |                  |                  |
| 11                      | –                  | –  | 11                            | –                | –                |                |                    |  |                               |                  |                  |
| 12                      | –                  | –  | 12                            | –                | –                |                |                    |  |                               |                  |                  |
| t <sub>emp</sub> ≈13.49 |                    |  |                               |                  |                  |                |                    |  |                               |                  |                  |

**Table 11.** Results of the 10<sup>th</sup> Graders' Final Test after the experiment

| Scores | E                  |      | C                  |      |
|--------|--------------------|------|--------------------|------|
|        | Number of students | %    | Number of students | %    |
| 1      | 0                  | 0.0  | 3                  | 0.7  |
| 2      | 8                  | 1.8  | 19                 | 4.4  |
| 3      | 30                 | 6.9  | 60                 | 13.8 |
| 4      | 34                 | 7.8  | 148                | 34.0 |
| 5      | 35                 | 8.1  | 81                 | 18.6 |
| 6      | 131                | 30.1 | 50                 | 11.5 |
| 7      | 130                | 29.9 | 37                 | 8.5  |
| 8      | 29                 | 6.7  | 26                 | 6.0  |
| 9      | 20                 | 4.6  | 8                  | 1.8  |
| 10     | 18                 | 4.1  | 3                  | 0.7  |
| 11     | 0                  | 0.0  | 0                  | 0.0  |
| 12     | 0                  | 0.0  | 0                  | 0.0  |
| Total  | 435                | 100  | 435                | 100  |

**Table 12.** Distribution of the 11<sup>th</sup> Graders by the Level of Skills after the experiment

| Group | Number of students | Levels of the Students' Skills |                         |                           |                       |
|-------|--------------------|--------------------------------|-------------------------|---------------------------|-----------------------|
|       |                    | Low (1 – 3 scores)             | Moderate (4 – 6 scores) | Sufficient (7 – 9 scores) | High (10 – 12 scores) |
| E     | 435                | 38                             | 200                     | 179                       | 18                    |
|       |                    | 8.7 %                          | 46.0 %                  | 41.2 %                    | 4.1 %                 |
| C     | 435                | 82                             | 279                     | 71                        | 3                     |
|       |                    | 18.9 %                         | 64.1 %                  | 16.3 %                    | 0.7 %                 |

**Table 13.** Data of the 11<sup>th</sup> Graders after the experiment

| Data E                 |                    |                     |                  |                |           | Data C |                    |                     |                  |                |           |
|------------------------|--------------------|---------------------|------------------|----------------|-----------|--------|--------------------|---------------------|------------------|----------------|-----------|
| $X_i$                  | Number of students | $(X_i - X_{exp})^2$ | $\sigma^2_{exp}$ | $\sigma_{exp}$ | $m_{exp}$ | $X_i$  | Number of students | $(X_i - X_{exp})^2$ | $\sigma^2_{exp}$ | $\sigma_{exp}$ | $m_{exp}$ |
| 1                      | –                  | –                   | 3.01             | 1.73           | 0.083     | 1      | 3                  | 14.44               | 2.82             | 1.68           | 0.081     |
| 2                      | 8                  | 15.21               |                  |                |           | 2      | 19                 | 7.84                |                  |                |           |
| 3                      | 30                 | 8.41                |                  |                |           | 3      | 60                 | 3.24                |                  |                |           |
| 4                      | 34                 | 3.61                |                  |                |           | 4      | 148                | 0.64                |                  |                |           |
| 5                      | 35                 | 0.81                |                  |                |           | 5      | 81                 | 0.04                |                  |                |           |
| 6                      | 131                | 0.01                |                  |                |           | 6      | 50                 | 1.44                |                  |                |           |
| 7                      | 130                | 2.21                |                  |                |           | 7      | 37                 | 4.84                |                  |                |           |
| 8                      | 29                 | 4.41                |                  |                |           | 8      | 26                 | 10.24               |                  |                |           |
| 9                      | 20                 | 9.61                |                  |                |           | 9      | 8                  | 17.64               |                  |                |           |
| 10                     | 18                 | 16.81               |                  |                |           | 10     | 3                  | 27.04               |                  |                |           |
| 11                     | –                  | –                   | 11               |                |           | –      | –                  |                     |                  |                |           |
| 12                     | –                  | –                   | 12               |                |           | –      | –                  |                     |                  |                |           |
| t <sub>emp</sub> ≈9.48 |                    |                     |                  |                |           |        |                    |                     |                  |                |           |

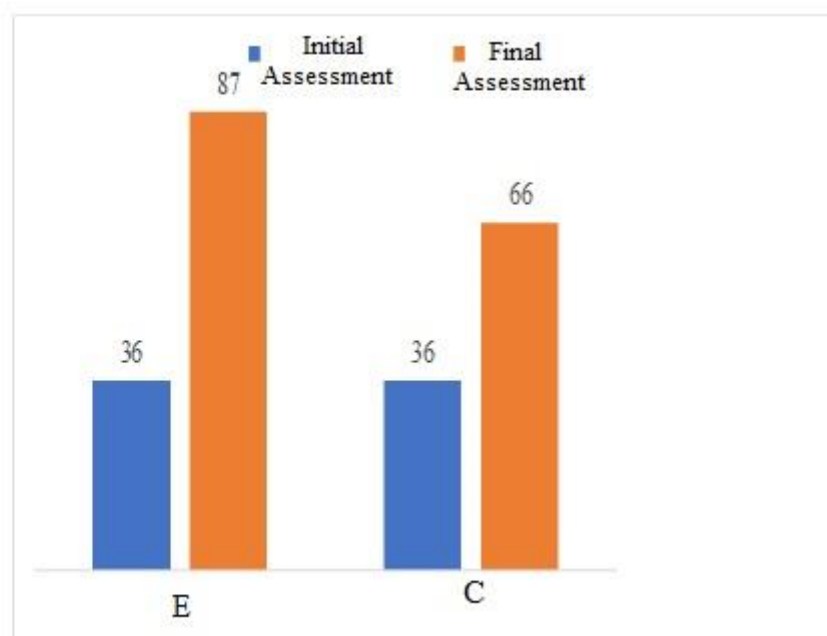


**Figure 1.** Effectiveness Assessment of the Teaching Stage of the Experiment

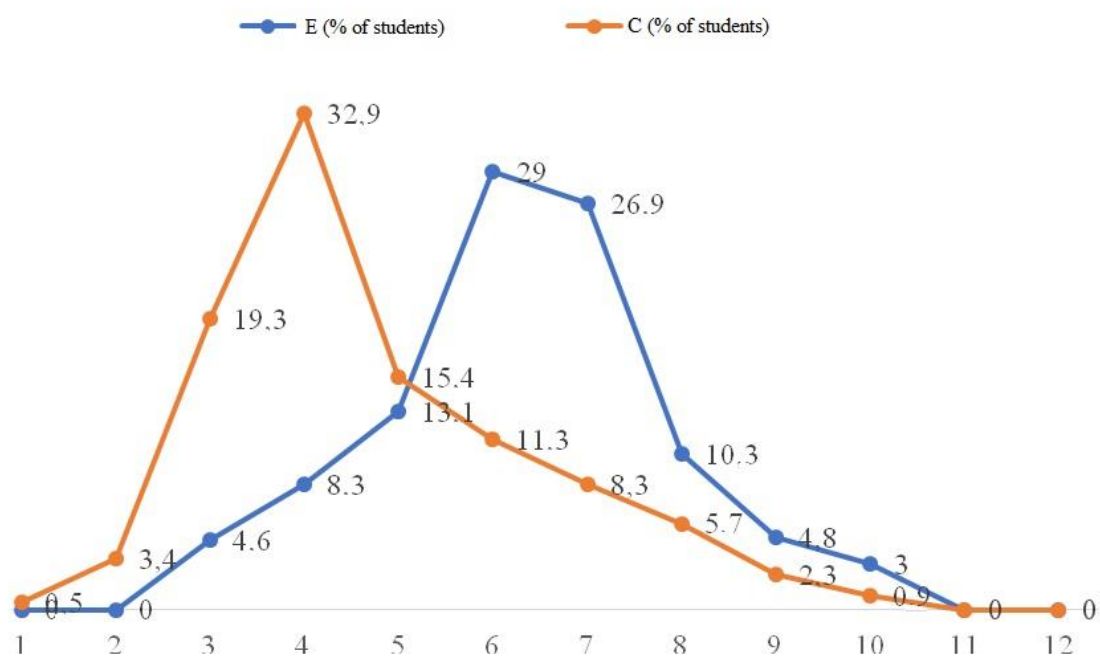


**Figure 2.** Comparative Analysis of the E and C Group 10<sup>th</sup> Graders' Final Test Results



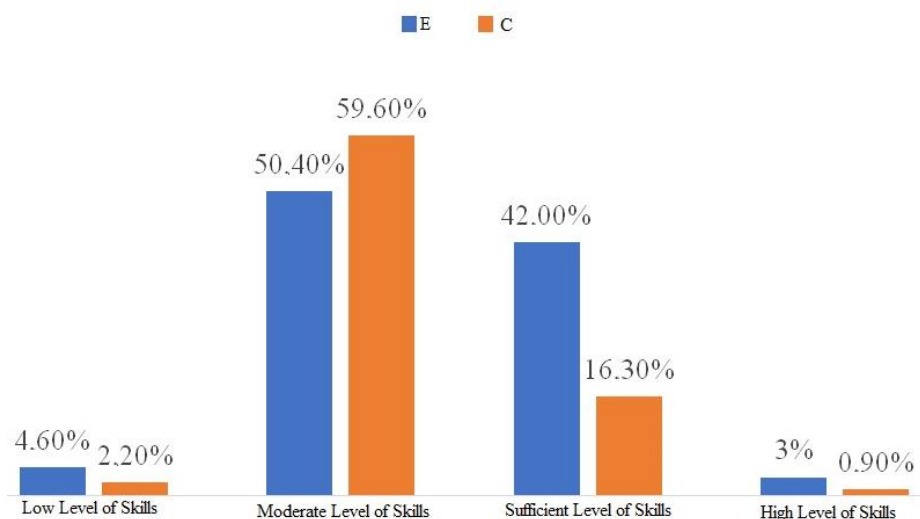


**Figure 3.** Comparative Analysis of the Level of the Robotics Design Skills among the 10<sup>th</sup> graders

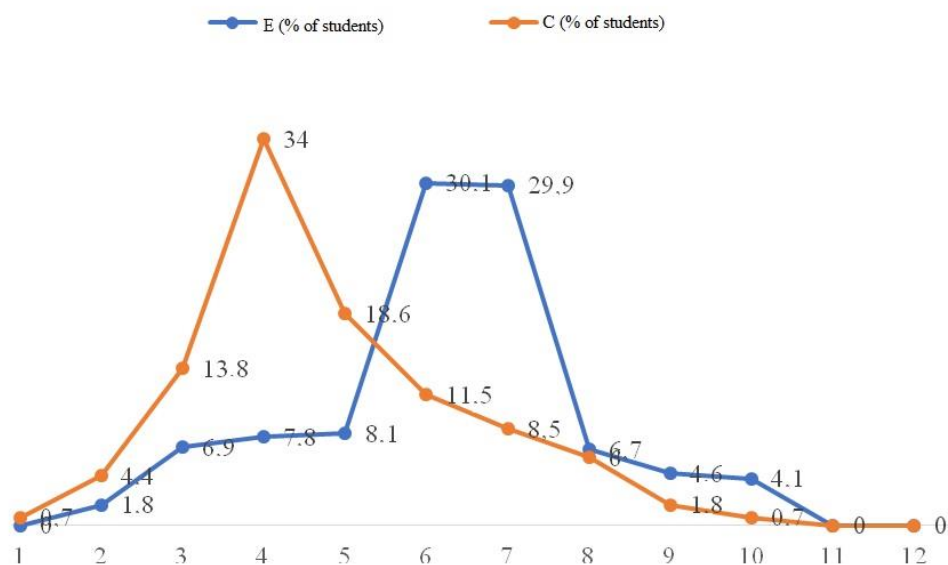


**Figure 4.** Comparative Analysis of the E and C Group Students' Final Test Results

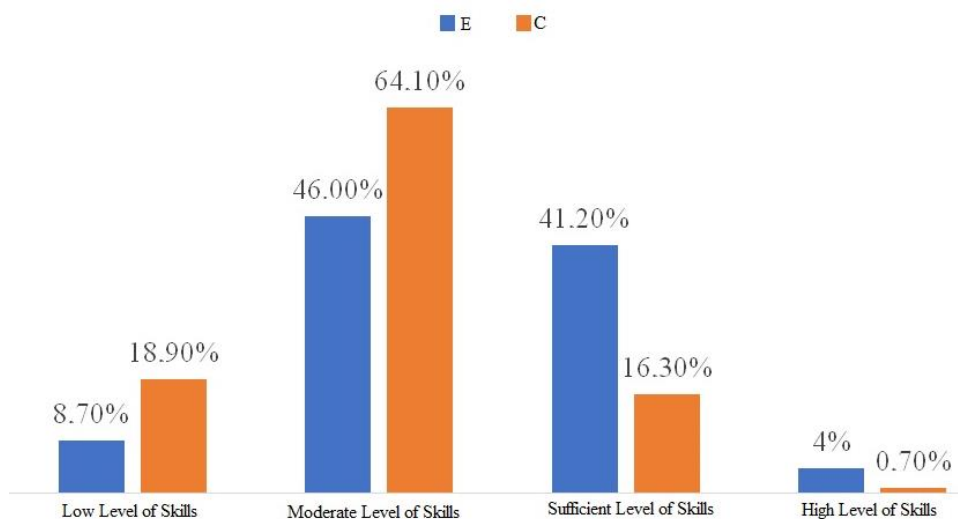


**Figure 5.** Comparative Analysis of the Level of the Skills among the Students after the Experiment

## MÉTODOS PARA ENDURECIMENTO E MELHORIA DAS CARACTERÍSTICAS DE FADIGA DE AMOSTRAS DE LIGAS DE NÍQUEL CROMO-FERRO E TITÂNIO

## METHODS FOR HARDENING AND IMPROVEMENT OF FATIGUE CHARACTERISTICS OF TITANIUM AND IRON-CHROMIUM NICKEL ALLOY SAMPLES

## МЕТОДЫ ПОВЫШЕНИЯ ПРОЧНОСТИ И УСТАЛОСТНЫХ ХАРАКТЕРИСТИК ОБРАЗЦОВ, ИЗГОТОВЛЕННЫХ ИЗ СПЛАВОВ ТИТАНА И ЖЕЛЕЗОХРОМОНИКЕЛЕВЫХ СПЛАВОВ

SKVORTSOV, Arkadiy A.<sup>1\*</sup>; GNATYUK, Evgeniya O.<sup>2</sup>; RYBAKOVA, Margarita R.<sup>3</sup>; BURUKIN, Ivan V.<sup>4</sup>;

<sup>1,3,4</sup> Moscow Polytechnic University; Department of Dynamics, Strength of Machines and Resistance of Materials; Moscow – Russian Federation

<sup>2</sup> JC “United Engine Corporation”; Department of Materials Science; Moscow – Russian Federation

\* Corresponding author

e-mail: SkvortsovAA2009@yandex.ru

Received 13 November 2019; received in revised form 29 April 2020; accepted 05 June 2020

### RESUMO

Este trabalho descreve o procedimento para determinar tensões residuais na superfície usando o método mecânico e quatro métodos de endurecimento de amostras. A urgência do problema declarado no artigo se deve ao fato de que as tensões de tração superficial que surgem na fabricação de peças altamente carregadas podem reduzir significativamente as características mecânicas, de recursos e de fadiga dos produtos. O objetivo do estudo foi endurecer amostras de ligas de titânio e ferro-cromo-níquel para melhorar suas características de resistência, fadiga, recursos e determinar tensões residuais por remoção camada por camada das camadas estudadas por ataque eletroquímico. A determinação das tensões residuais da superfície foi realizada mecanicamente, utilizando um complexo de medição e cálculo durante a gravação contínua do metal a partir da superfície de teste da amostra, o que possibilitou medir as tensões residuais em diferentes profundidades e determinar a energia do estado de estresse da superfície. As tensões residuais foram calculadas a partir da deformação da parte restante da amostra com uma mudança na profundidade das camadas estudadas. O endurecimento das amostras foi realizado de quatro maneiras, a saber: endurecimento por ultrassom; cura por ultrassom + Rosler (processamento de vibração); Rosler (processamento de vibração) + cura por ultrassom; Rosler (processamento de vibração) + endurecimento por ultrassom. Os resultados do estudo mostraram que a superfície dos produtos é uma área mais fraca que a interna. Após a têmpera, surgem tensões compressivas na superfície de todas as amostras de ligas de titânio e ferro-cromo-níquel. O caso preferido de endurecimento é o segundo (endurecimento ultrassônico + endurecimento centrífugo). A presença de tensões compressivas residuais nas camadas externas dos produtos aumenta seu limite de fadiga em  $\pm 20\%$ . Os resultados do trabalho podem ser usados para fabricar produtos com altas características mecânicas, de recursos e de fadiga.

**Palavras-chave:** *tensões residuais, ultrassom, deformação, resistência, macro estresses.*

### ABSTRACT

This work describes the procedure for determining residual surface stresses using the mechanical method and four methods of hardening samples. The urgency of the problem stated in the article is due to the fact that surface tensile stresses arising in the manufacture of highly loaded parts can significantly reduce the mechanical, resource and fatigue characteristics of products. The aim of the study was to harden samples of titanium and iron-chromium-nickel alloys to improve their strength, fatigue and resource characteristics and determine residual stresses by layer-by-layer removal of the studied layers by electrochemical etching. The determination of surface residual stresses was carried out mechanically using a measuring and calculation complex during continuous etching of the metal from the test surface of the sample, which made it possible to measure the residual stresses at different depths and determine the energy of the surface stress state. Residual stresses were calculated from the deformation of the remaining part of the sample with a change in the depth of the studied layers. The hardening of the samples was carried out in four ways, namely: ultrasonic hardening; ultrasonic curing + Rosler (vibration

processing); Rosler (vibration processing) + ultrasonic curing; Rosler (vibration processing) + ultrasonic hardening. The results of the study showed that the surface of the products is a weaker area than the inside. After quenching, surface compressive stresses arise for all samples of titanium and iron-chromium-nickel alloys. The preferred case of hardening is the second (ultrasonic hardening + centrifugal hardening). The presence of residual compressive stresses in the outer layers of the products increases their fatigue limit by  $\approx 20\%$ . The results of the work can be used to manufacture products with high mechanical, resource and fatigue characteristics.

**Keywords:** *residual stresses, ultrasound, deformation, strength, macrostresses.*

## АННОТАЦИЯ

В данной работе описана процедура определения остаточных поверхностных напряжений с использованием механического метода и четырех способов упрочнения образцов. Актуальность заявленной в статье проблемы обусловлена тем, что поверхностные растягивающие напряжения, возникающие при изготовлении высоконагруженных деталей, могут существенно снизить механические, ресурсные и усталостные характеристики изделий. Целью исследования является закалка образцов из титановых и железо-хромоникелевых сплавов для улучшения их прочностных, усталостных и ресурсных характеристик и определения остаточных напряжений путем послойного снятия исследуемых слоев методом электрохимического травления. Определение поверхностных остаточных напряжений проводилось механическим методом с использованием измерительно-расчетного комплекса при непрерывном травлении металла с исследуемой поверхности образца, что позволило измерить остаточные напряжения на разных глубинах залегания и определить энергию напряженного состояния поверхности. Остаточные напряжения рассчитывались по деформации оставшейся части образца с изменением глубины залегания исследуемых слоев. Упрочнение образцов было проведено четырьмя способами, а именно: ультразвуковое упрочнение; ультразвуковое отверждение + рослер (виброобработка); Рослер (виброобработка) + ультразвуковое отверждение; Рослер (виброобработка) + ультразвуковое упрочнение. Результаты исследования показали, что поверхность изделий является более слабой областью, чем внутренняя часть. После закалки возникают поверхностные сжимающие напряжения для всех образцов из титана и железо-хромоникелевых сплавов. Предпочтительным случаем упрочнения является второй (ультразвуковое упрочнение + центробежное упрочнение). Наличие остаточных сжимающих напряжений во внешних слоях изделий увеличивает предел их усталости на  $\approx 20\%$ . Результаты работы могут быть использованы для изготовления изделий с высокими механическими, ресурсными и усталостными характеристиками.

**Ключевые слова:** *остаточные напряжения, ультразвук, деформация, прочность, макронапряжения.*

## 1. INTRODUCTION:

When producing high-loaded details, one of the problems is the presence of surface tensile stresses (Gnyusov *et al.*, 2017; Hou *et al.*, 2018). They can substantially reduce the mechanical, resource, and fatigue characteristics of products (Wojtaszek *et al.*, 2016; Sakhvadze *et al.*, 2017; Pei & Duan, 2017; Huang *et al.*, 2018). The residual stresses exist in products in the absence of external actions. Three types of stresses are distinguished: macro stresses, micro stresses, and elastic stresses (Birger, 1963; Colegrove *et al.*, 2013; Hamad & Hassan, 2018; Astapov *et al.*, 2019a; Astapov *et al.*, 2019b; Cui *et al.*, 2020; Su *et al.*, 2020).

The main methods to determine residual stresses are mechanical and x-ray methods (Liu *et al.*, 2019; Sunder, 2016; Mohanty & Muduli, 2020). The mechanical process is most widely spread because it uses the same concepts of stresses and deformations of elastic body mechanics as those used when calculating the strength, rigidity,

and stability of details. The mechanical method of determination of residual stresses is based on cutting a sample from detail and subsequent layer-by-layer removal of the layers under investigation using electrochemical etching (Antolovich & Armstrong, 2014; Mustafin, 2006; Samarin *et al.*, 2019; Makarenko & Kuznetsova, 2019; Ding *et al.*, 2015).

The object of the work was to harden samples made of titanium and iron-chromium-nickel alloys for improvement of their strength, fatigue, and resource characteristics and determination of residual stresses by layer-by-layer removal of the studied layers using electrochemical etching.

## 2. MATERIALS AND METHODS:

The determination of residual surface stresses was made by the mechanical method using a measuring-calculating complex at the continuous etching of metal from the sample surface under investigation (Figure 1). Such a

plant measures residual stresses at different occurrence depths and determines the energy of surface stressed state, as well as makes it possible to optimize and control the stability of technological processes (Figure 2).

An experiment began by cutting a sample of standard sizes 50×4×2 mm (Figure 3). Then the sample was fastened into a holder (investigated face down); the holder and surface that was not subjected to etching were coated with paraffin. A steel ball was fastened in paraffin at the sample upper surface where deformation was measured (for contact with an inductive transducer). Then the holder with the sample was suspended to a carriage of the gage post, and the steel ball was brought to the inductive transducer to the point of maximal contacting. After this, the carriage was put into the electrolyte, and the etching process began. The balance became disturbed, causing the sample to deform. The residual stresses  $\sigma$  were calculated from the deformation of the remaining part of the sample, with changing occurrence depth of the layers studied (Birger, 1963; Gnatyuk, 2017; Lu *et al.*, 2018; Madzivhandila *et al.*, 2019).

### 3. RESULTS AND DISCUSSION:

#### 3.1. Determination of residual stresses

Let us consider the determination of axial residual stresses in a prismatic rod. We assume that, except for small areas at the ends of the rod, the residual stresses are constant along its length. To determine the residual stresses, we will sequentially remove the ABCD layers of materials (Figure 4) located in the zone of constant (along the length) stresses. The end sections are not removed; they are placed in the grips of the device.

The residual stresses  $\sigma$  in the surface layers of the initial detail were determined as a sum of stresses relaxed because of sample cutting from the detail ( $\sigma_d$ ) and a nonlinear component ( $\sigma_{n.l.}$ ) due to removal of layers from the sample surface (Equation 1). Depending on the sample thickness and value of mechanical stresses in the layers under investigation, layers separation from the detail may lead to its bending  $F_b$  and (or) change of its length  $\varepsilon_b$ . In this case, the variation of the initial stresses may be calculated as a linear component from their occurrence depth (Equation 2). Here  $E$  is the material modulus of elasticity;  $F_b$  is the bending because of sample cutting from the detail;  $K_0$  and  $K_1$  are the coefficients representing both form and sizes of the sample;  $K_{amp}$  is the

deformation amplification coefficient at different ways of fastening the sample and transducer in the process of cutting;  $\varepsilon_b$  is sample's relative extension at cutting.

Let us determine the residual stresses  $\sigma_{n.l.}$  acting in the rod at a distance  $a$  from the upper face of the rod (Figure 4). As a result of the removal of a layer of material with a thickness  $a$ , the remaining part of the rod is deformed under the action of stresses along the planes AB and DC.

Let stresses  $\sigma_{n.l.}(a)$  act at a distance  $\xi$  from the upper face. The bending moment  $M$  from stresses on the face AB relative to the middle of the rod height (point O) is (Equation 3), where  $b$  is the width of the rod. If the rod is bent by the concentrated moments  $M$  at the end, then the deflection is (Equation 4), where  $l$ ,  $h$  is the length and thickness of the rod, respectively,  $J$  is the moment of inertia of the cross-section (Equation 5). Neglecting the influence of axial forces on bending and taking into account (Equation 4) and (Equation 5), we find (Equation 6). Transferring the value  $(h-a)^3$  to the left side of the equality and differentiating the integral over the upper limit  $a$ , we obtain (Equation 7). From (Equation 7) at  $a = 0$  we obtain the formula for determining the residual stresses in the outer layer (Equation 8). After differentiating equality (Equation 7) with respect to  $a$ , we have (Equation 9). Integrating both sides of this equality, we obtain (Equation 10).

Given the relation (Equation 8), we can obtain the equation (Equation 11). The residual stresses varying with occurrence depth of the removing layers were calculated from the expression that takes into account not only the measured deformation for each current depth but also those residual deformations that relaxed due to the removal of the previous layers. The residual stresses component that varies with etching depth was calculated for prismatic samples in real time scale (Equation 11). Here  $L_{et}$  is the etched layer length;  $H$  is the sample thickness;  $F$  is the current value of sample deformation;  $\frac{dF}{da}$  is deformation variation with occurrence depth of the layers under investigation;  $a_i$  is the current depth of removed layers;  $\xi$  is the total current deformation.

When determining the residual stresses, the balance of forces over the sample thickness is violated because of etching of the layers studied that are in the stress state, and the sample bends. The stresses in the layer under investigation are calculated from that bending (deformation). In this

case, the balance of forces is restored, and partial relaxation of stress state occurs on the opposite side of the sample, in accordance with the bending moment (Sangid, 2013; Ahmad *et al.*, 2018; Aguilera-Correa *et al.*, 2019). Due to the specially chosen etching conditions, an exact calculation of the depth of etched layers is done from the amount of passed electric current according to Faraday's law (Equation 12).

Here  $a$  is the etched layer depth;  $t$  is the etching time;  $I$  is current in the etching series;  $\alpha$  is the effective electrochemical equivalent;  $\rho$  is the sample material density;  $B$  is the sample width. Shown in Figures 5 and 6 are the samples of titanium and iron-chromium-nickel alloys after etching. Figures 7 and 8 present the diagrams of surface residual stresses distribution in the samples of titanium (Li *et al.*, 2016; Kumar *et al.*, 2017; Kim *et al.*, 2013) and iron-chromium-nickel alloys (Jiang & Zhao, 2012; Debroy *et al.*, 2018). One can see that surface tensile stresses are present on samples of both types. The presence of such stresses (from 50 MPa and more) considerably reduces vibration and fatigue strength of the product (Malaki & Ding, 2015; Zhu *et al.*, 2017; Lin *et al.*, 2018; Wang *et al.*, 2020).

To solve the above problem, hardening of samples was performed in four ways: 1 – ultrasonic hardening; 2 – ultrasonic hardening + Rosler (vibratory finishing); 3 – Rosler (vibratory finishing) + ultrasonic hardening; 4 – Rosler (vibratory finishing) + ultrasonic hardening (He *et al.*, 2018; Sangid, 2013). In all four cases, the parameters of ultrasonic hardening remained unchanged: amplitude of 100  $\mu\text{m}$  and rated frequency of 20 kHz.

### 3.2. Centrifugal Hardening (Rosler)

Centrifugal treatment (Figure 9) is a high-performance method for finishing and hardening parts. The method of volumetric centrifugal treatment consists in the fact that the granular processing medium with the details is rotationally driven around the vertical axis so that it takes on the shape of a torus in which particles move along spiral paths. The machined parts are loaded into the working chamber and moved together with the working environment. Hardening is carried out due to the relative movement and interaction of the granular medium and the parts wetted by a liquid continuously supplied to the working chamber.

### 3.3. Ultrasonic hardening

The strain hardening of the surface layer of samples during ultrasonic hardening (Figure 10) is

carried out due to the kinetic energy of steel balls randomly moving in a spatially limited volume. The surface treatment takes place in the “cloud” of the working medium (balls) simultaneously from two sides. This type of treatment causes an increase in hardness of the surface layer by 18% and an increase in surface compressive stresses to 1000 MPa. The depth of the riveted layer is 20-25  $\mu\text{m}$ . Structural changes in the surface zones of the part cause an increase in the durability of products up to 1.5 times at cyclic stresses of 1650-2600 MPa. After hardening of samples in four ways, residual surface stresses were measured, and the diagrams of their distribution were obtained (Furuya, 2013; Kim *et al.*, 2016; Cai *et al.*, 2017; Zhan *et al.*, 2018; Su *et al.*, 2018; Klimenko *et al.*, 2018; Qiao *et al.*, 2019; Zhang *et al.*, 2020). The results of the measurements are presented in Figures 11 and 12.

One can see from figures that after hardening, there are surface compressive stresses for all samples made of titanium and iron-chromium-nickel alloys. The preferred case of hardening is the second (ultrasonic hardening + centrifugal hardening). In this case, the maximum compressive residual stresses reach 550 MPa at a depth of 50  $\mu\text{m}$ . The presence of residual compressive stresses in the outer layers of products increases their fatigue limit by  $\approx 20\%$ .

## 4. CONCLUSIONS:

The results of the investigations showed that the surface of products studied is a “weaker” area than the interior. Therefore, any process that leads to appearance and increase of surface compressive stresses will be positive for material operation. After quenching, surface compressive stresses arise for all samples of titanium and iron-chromium-nickel alloys. The preferred case of hardening is the second (ultrasonic hardening + centrifugal hardening). The presence of residual compressive stresses in the outer layers of the products increases their fatigue limit by  $\approx 20\%$ . The results of the work can be used to manufacture products with high mechanical, resource and fatigue characteristics.

## 5. ACKNOWLEDGMENTS:

This study is conducted with financial support from the Ministry of Education and Science of the Russian Federation (project No. FZRR-2020-0023/code 0699-2020-0023).

## 6. REFERENCES:

1. Aguilera-Correa, J.-J., Auñón, Á., Boiza-Sánchez, M., Mahillo-Fernández, I., Mediero, A., Eguibar-Blázquez, D., Conde, A., Arenas, M.-Á., de-Damborenea, J.-J., Cordero-Ampuero, J., & Esteban, J. (2019). Urine aluminum concentration as a possible implant biomarker of pseudomonas aeruginosa infection using a fluorine- and phosphorus-doped Ti-6Al-4V alloy with osseointegration capacity. *ACS Omega*, 4(7), 11815-11823
2. Ahmad, B., van der Veen, S. O., Fitzpatrick, M. E., & Guo, H. (2018). Measurement and modelling of residual stress in wire-feed additively manufactured titanium. *Materials Science and Technology*, 34(18), 2250-2259. <https://doi.org/10.1080/02670836.2018.1528747>
3. Antolovich, S. D., & Armstrong, R. W. (2014). Plastic strain localization in metals: Origins and consequences. *Progress in Materials Science*, 59(1), 1-160. <https://doi.org/10.1016/j.pmatsci.2013.06.001>
4. Astapov, A.N., Kuznetsova, E.L., & Rabinskiy, L.N. (2019b). Operating capacity of anti-oxidizing coating in hypersonic flows of air plasma. *Surface Review and Letters*, 26(2), Article number 1850145.
5. Astapov, A.N., Lifanov, I.P., & Rabinskiy, L.N. (2019a). Perspective heat-resistant coating for protection of C/SiC composites in air plasma hypersonic flow. *High Temperature*, 57(5), 744-752.
6. Birger, I. A. (1963). *Residual stresses*. Moscow: Russian Federation: Mashgiz.
7. Cai, Z.B., Pang, X.J., Cui, X.F., Wen, X., Liu, Z., Dong, M.L., Li, Y., & Jin, G. (2017). In situ laser synthesis of high entropy alloy coating on Ti-6Al-4V alloy: Characterization of microstructure and properties. *Materials Science Forum*, 898, 643-650. <https://doi.org/10.4028/www.scientific.net/msf.898.643>
8. Colegrove, P. A., Coules, H. E., Fairman, J., & Martina, F. (2013). Microstructure and residual stress improvement in wire and arc additively manufactured parts through high-pressure rolling. *Journal of Materials Processing Technology*, 213(10), 1782-1791. <https://doi.org/10.1016/j.jmatprotec.2013.04.012>
9. Cui, F., Wang, G., Yu, D., Gan, X., Tian, Q., & Guo, X. (2020). Towards "zero waste" extraction of nickel from scrap nickel-based superalloy using magnesium. *Journal of Cleaner Production*, 262, article number 121275.
10. Debroy, T., Wei, H. L., Zuback, J. S., Elmer, J. W., Beese, A. M., & Zhang, W. (2018). Additive manufacturing of metallic components – Process, structure and properties. *Progress in Materials Science*, 92, 112-224. <https://doi.org/10.1016/j.pmatsci.2017.10.001>
11. Ding, D., Pan, Z., Cuiuri, D., & Li, H. (2015). Wire-feed additive manufacturing of metal components: technologies, developments and future interests. *International Journal of Advanced Manufacturing Technology*, 81(1-4), 465-481. <https://doi.org/10.1007/s00170-015-7077-3>
12. Furuya, Y. (2013). Visualization of internal small fatigue crack growth. *Materials Letters*, 112, 139-141. <https://doi.org/10.1016/j.matlet.2013.09.015>
13. Gnatyuk, E.O. (2017). Statement of the experiment for the limiting state of samples from materials VT8 and IP718VD under biharmonic loading. In *Proceedings of the MIKMUS* (pp. 465-467). Moscow, Russian Federation: MIKMUS.
14. Gnyusov, S.F., Rotshtein, V.P., Mayer, A.E., Astafurova, E.G., Rostov, V.V., Gunin, A.V., & Maier, G.G. (2017). Comparative study of shock-wave hardening and substructure evolution of 304L and Hadfield steels irradiated with a nanosecond relativistic high-current electron beam. *Journal of Alloys and Compounds*, 714, 232-244.
15. Hamad, D., & Hassan, B. (2018). Evaluation of salivary nickel, chromium and iron ions in patients treated with fixed orthodontic appliances in vivo study. *Erbil Dental Journal (EDJ)*, 1(2), 109-116. <https://doi.org/10.15218/edj.2018.15>
16. He, Y., Xiao, G., Li, W., & Huang, Y. (2018). Residual stress of a titanium alloy after belt grinding and its impact on the fatigue life. *Materials*, 11(11), article number 2218. <https://doi.org/10.3390/ma11112218>

17. Hou, X., Liu, Z., Wang, B., Lv, W., Liang, X., & Hua, Y. (2018). Stress-strain curves and modified material constitutive model for Ti-6Al-4V over the wide ranges of strain rate and temperature. *Materials*, 11, article number 938.
18. Huang, S., Zhu, Y., Guo, W., Peng, P., & Diao, X. (2018). Effects of laser shock processing on impact toughness of Ti-17 titanium alloy. *High Temperature Materials and Processes*, 37(4), 325-332. doi: <https://doi.org/10.1515/htmp-2016-0106>
19. Jiang, J., & Zhao, M. (2012). Influence of residual stress on stress concentration factor for high strength steel welded joints. *Journal of Constructional Steel Research*, 72, 20-28. <https://doi.org/10.1016/j.jcsr.2011.09.007>
20. Kim, J.-C., Cheong, S.-K., & Noguchi, H. (2013). Residual stress relaxation and low- and high- cycle fatigue behavior of shot-peened medium – carbon steel. *International Journal of Fatigue*, 56, 114-122. <https://doi.org/10.1016/j.ijfatigue.2013.07.001>
21. Kim, M.J., Yadav, P., & Lee, D.B. (2016). Isothermal and cyclic oxidation of Ti-6Al-4V alloy. *Defect and Diffusion Forum*, 369, 99–103. <https://doi.org/10.4028/www.scientific.net/df.369.99>
22. Klimenko, D., Ozerov, M., Suresh, S., Stepanov, N., Tikhonovsky, M.A., Salishchev, G., & Zharebtsov, S. (2018). Microstructure Evolution and Properties of Ti-6Al-4V Alloy Doped with Fe and Mo during Deformation at 800°C. *Defect and Diffusion Forum*, 385, 144-149.
23. Kumar, S., Chattopadhyay, K., & Singh, V. (2017). Effect of ultrasonic shot peening on LCF behavior of the Ti-6Al-4V alloy. *Journal of Alloys and Compounds*, 724, 187-197. <https://doi.org/10.1016/j.jallcom.2017.07.014>
24. Li, P., Warner, D. H., Fatemi, A., & Phan, N. (2016). Critical assessment of the fatigue performance of additively manufactured Ti-6Al-4V and perspective for future research. *International Journal of Fatigue*, 85, 130-143. <https://doi.org/10.1016/j.ijfatigue.2015.12.003>
25. Lin, D.G., Park, J.M., Kang, T.G., Chung, S.T., Kwon, Y.S., & Park, S.J. (2018). Powder injection molding of Ti-6Al-4V alloy for defect-free high performance titanium parts with low carbon/oxygen contents. *Key Engineering Materials*, 770, 189–194. <https://doi.org/10.4028/www.scientific.net/kem.770.189>
26. Liu, C., Liu, D., Zhang, X., Ma, A., Ao, N., & Xu, X. (2019). Improving fatigue performance of Ti-6Al-4V alloy via ultrasonic surface rolling process. *Journal of Materials Science and technology*, 35(8), 1555-1562. <https://doi.org/10.1016/j.jmst.2019.03.036>
27. Lu, J., Yang, Z., Li, Y., Huang, J., Zhao, X., & Yuan, Y. (2018). Effect of alloying chemistry on fireside corrosion behavior of Ni-Fe-based superalloy for ultra-supercritical boiler applications. *Oxidation of Metals*, 89, 609–621. <https://doi.org/10.1007/s11085-017-9804-7>
28. Madzivhandila, T., Bhero, S., & Varachia, F. (2019). The influence of titanium addition on wettability of high-chromium white cast iron-matrix composites. *Journal of Composite Materials*, 53(11), 1567–1576. <https://doi.org/10.1177/0021998318804616>
29. Makarenko, A.V., & Kuznetsova, E.L. (2019). Energy-efficient actuator for the control system of promising vehicles. *Russian Engineering Research*, 39(9), 776-779.
30. Malaki, M., & Ding, Y. (2015). A review of ultrasonic peening treatment. *Materials and Design*, 87, 1072-1086. <https://doi.org/10.1016/j.matdes.2015.08.102>
31. Mohanty, J., & Muduli, R.C. (2020). Preparation of Fe-Ni Alloy Containing Low Cr and Ti from Red Mud Through Molten Salt Electrolysis. *Journal of The Institution of Engineers (India): Series C*, 101, 401-406.
32. Mustafin, A. (2006). Two mutually loss-coupled lasers featuring a stable multivibrator. *Physica D: Nonlinear Phenomena*, 218(2), 167-176.
33. Pei, Y., & Duan, Ch. (2017). Study on stress-wave propagation and residual stress distribution of Ti-17 titanium alloy by laser shock peening. *Journal of Applied Physics*, 122, article number 193102.
34. Qiao, Y., Xu, D., Wang, S., Ma, Y., Chen, J., Wang, Y., & Zhou, H. (2019). Corrosion and tensile behaviors of Ti-4Al-2V-1Mo-1Fe and Ti-6Al-4V titanium alloys. *Metals*, 9, 1213.

35. Sakhvadze, G.Z., Pugachev, M.S. & Kikvidze, O.G. (2017). Two-sided laser shock processing. *Russian Engineering Research*, 37, 40-45. <https://doi.org/10.3103/S1068798X17010191>
36. Samarin, I.V., Strogonov, A.Y., & Butuzov, S.Y. (2019). Evaluation model of integrated safety of fuel and energy complex facilities. *International Journal of Engineering and Advanced Technology*, 8(5), 2162-2167.
37. Sangid, M.D. (2013). The physics of fatigue crack initiation. *International Journal of Fatigue*, 57, 58-72. <https://doi.org/10.1016/j.ijfatigue.2012.10.009>
38. Su, B., Wang, H., Cao, Y., Pei, X. & Hua, G. (2020). Local deformation and macro distortion of TC4 titanium alloy during laser shock processing. *The International Journal of Advanced Manufacturing Technology*, 106, 5421-5428. <https://doi.org/10.1007/s00170-020-05058-7>
39. Su, B., Zhang, Y., Sun, G., & Ni, Z. (2018). Prediction of micro indentation depth of titanium alloy during laser shock processing. *Japanese Journal of Applied Physics*, 57(12), article number 122703. <https://doi.org/10.7567/JJAP.57.122703>
40. Sunder, R. (2016). Why and how residual stress affects metal fatigue. *Springer Proceeding in Physics*, 175, 489-504. [https://doi.org/10.1007/978-3-319-26324-3\\_34](https://doi.org/10.1007/978-3-319-26324-3_34)
41. Wang, T., Qiao, W., Wang, Sh., Li, Zh., Wang, H. & Lei, J. (2020). Ti-6Al-4V alloy fabricated by laser direct deposition: Dynamic mechanical properties, constitutive model, and numerical simulation. *Surface Review and Letters*. Retrieved from <https://www.worldscientific.com/doi/pdf/10.1142/S0218625X19501919>
42. Wojtaszek, M., Sleboda, T., & Korpala, G. (2016). Hot processing of cast and PM Ti-6Al-4V alloy. *Archives of Metallurgy and Materials*, 61(2B), 1115-1120.
43. Zhan, Y., Zhang, E., Ge, Y., & Liu, C. (2018). Residual stress in laser welding of titanium alloy based on ultrasonic laser technology. *Applied Sciences*, 8(10), article number 1997. <https://doi.org/10.3390/app8101997>
44. Zhang, S.L., Yu, Y.C., Chen, W.Y., Qiu, M.K., & Liu, W L. (2020). Microstructure of Ti-based alloys after rapid solidification. *Materials Science Forum*, 993, 313–320. <https://doi.org/10.4028/www.scientific.net/msf.993.313>
45. Zhu, S.-P., Yue, P., Yu, Z.-Y., & Wang, Q. (2017). A combined high and low cycle fatigue model for life prediction of turbine blades. *Materials*, 10(7), article number 698. <https://doi.org/10.3390/ma10070698>



$$\sigma = \sigma_d + \sigma_{n.l.} \quad (\text{Eq. 1})$$

$$\sigma_d = E \left\{ \left( \frac{K_1}{K_{amp}} \right) \cdot F_b - K_0 \cdot \varepsilon_b \right\} n \quad (\text{Eq. 2})$$

$$M = \int_0^a \sigma_{n.l.}(\xi) \left( \frac{1}{2}(h-a) - \xi \right) b d\xi \quad (\text{Eq. 3})$$

$$f = \frac{Ml^2}{8EJ} \quad (\text{Eq. 4})$$

$$J = \frac{b(h-a)^3}{12} \quad (\text{Eq. 5})$$

$$F(a) = \frac{3l^2}{2E(h-a)^3} \cdot \int_0^a \sigma_{n.l.}(\xi) \left[ \frac{1}{2}(h+a) - \xi \right] b d\xi \quad (\text{Eq. 6})$$

$$(h-a)^2 \frac{dF}{da}(a) - 3(h-a)^2 F(a) = \frac{3l^2}{2E} \left[ \frac{1}{2} \int_0^a \sigma_{n.l.}(\xi) d\xi + \frac{1}{2} \sigma_{n.l.}(a)(h-a) \right] \quad (\text{Eq. 7})$$

$$\sigma_{n.l.}(0) = \frac{4Eh^2}{3l^2} \frac{dF}{da}(0) \quad (\text{Eq. 8})$$

$$(h-a)^2 \frac{d^2 F(a)}{da^2} - 6(h-a) \frac{dF(a)}{da} + 6F(a) = \frac{3l^2}{4E} \frac{d\sigma_{n.l.}(a)}{da} \quad (\text{Eq. 9})$$

$$(h-a)^2 \frac{dF(a)}{da} - 4(h-a)F(a) + 2 \int_0^a F(\xi) d\xi - h^2 \frac{dF(0)}{da} = \frac{3l^2}{4E} [\sigma_{n.l.}(a) - \sigma_{n.l.}(0)] \quad (\text{Eq. 10})$$

$$\sigma_{n.l.} = \left( \frac{4E}{3L_{et}^2 K_{amp}} \right) \cdot \left[ (H-a_i)^2 \cdot \left( \frac{dF}{da} \right) - 4(H-a_i)F_{a_i} + 2 \int_0^{a_i} F(\xi) d\xi \right] \quad (\text{Eq. 11})$$

$$a = \frac{\alpha \cdot t \cdot \int_0^t I dt}{\rho \cdot L_{et} \cdot B} \quad (\text{Eq. 12})$$

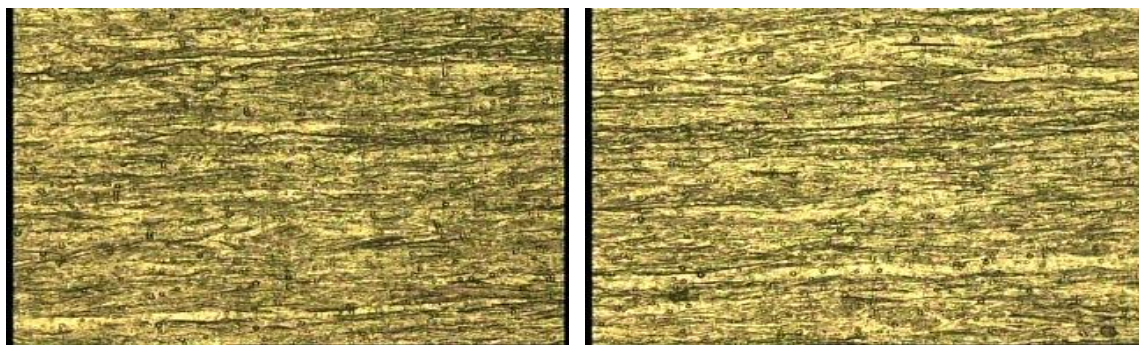


**Figure 1.** Photo of the surface of titanium samples after machining (magnification 100×)

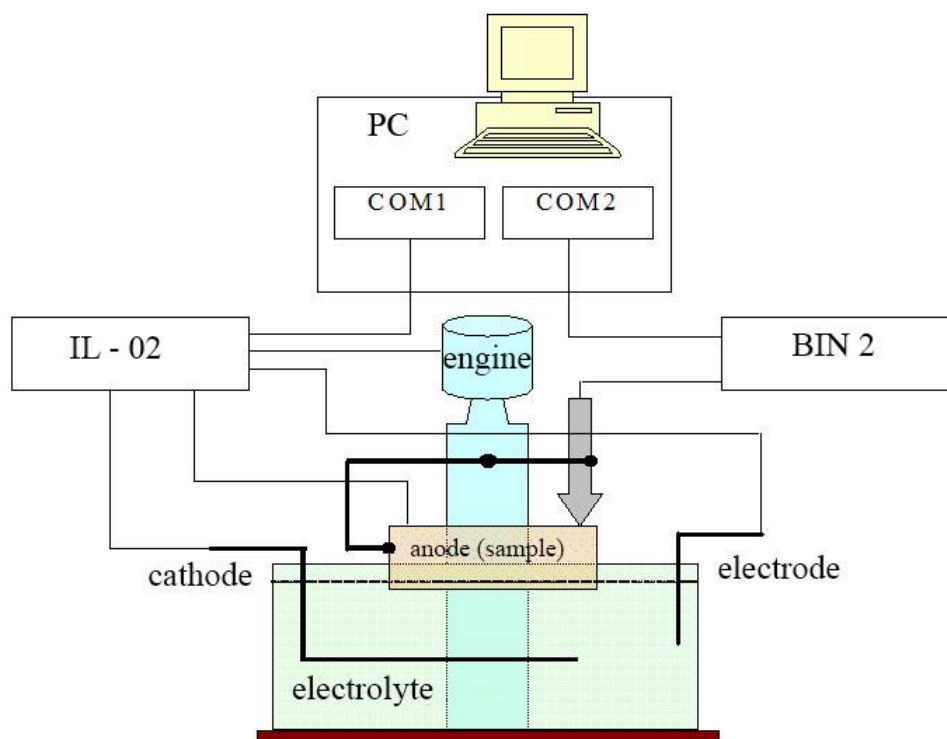


**Figure 2.** Installation diagram: the electric current source IL-02 delivers electric current to a bath with electrolyte; BIN 2 measures sample deformation

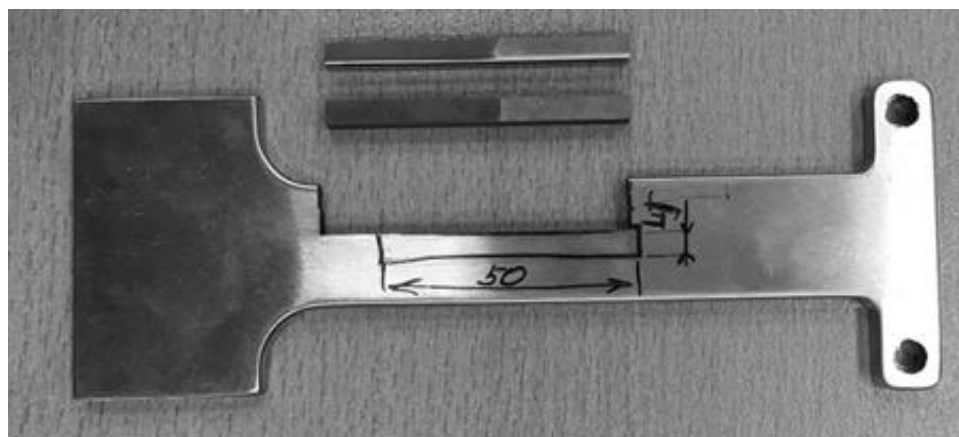


**Figure 3.** The scheme of cutting samples for determining residual stresses

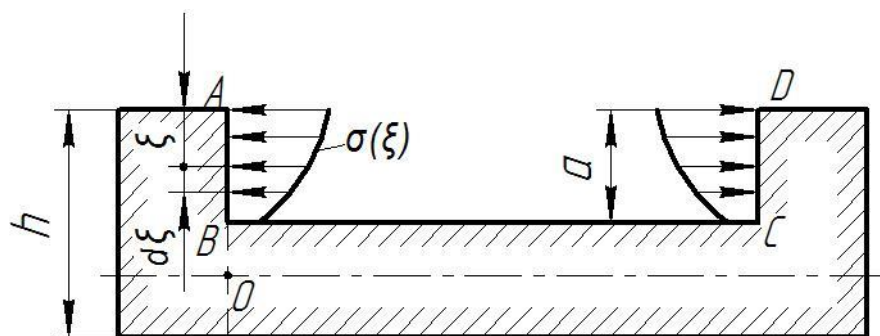


**Figure 4.** The geometry of the rod when etching layers and emerging mechanical stresses



**Figure 5.** Sample of the titanium alloy after etching



**Figure 6.** Sample of the iron-chromium-nickel alloy after etching

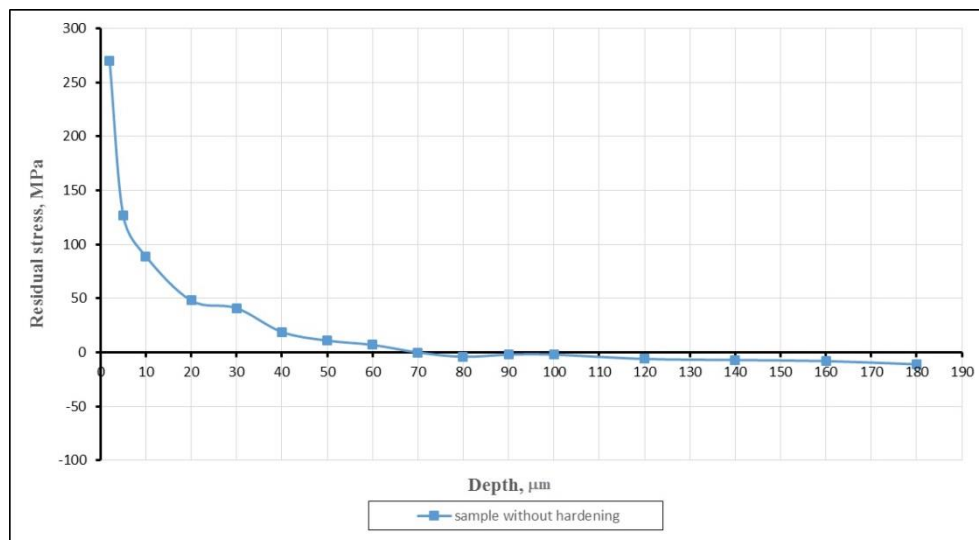


**Figure 7.** Diagram of residual stresses distribution in a sample of titanium alloy before hardening

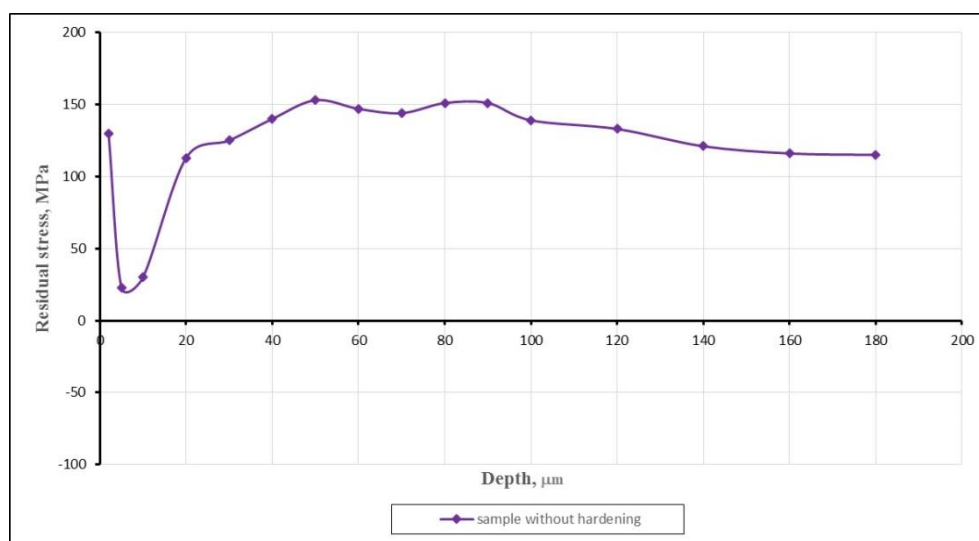


**Figure 8.** Diagram of residual stresses distribution in a sample of iron-chromium-nickel alloy before hardening



**Figure 9.** Installation for centrifugal hardening treatment (Rosler)

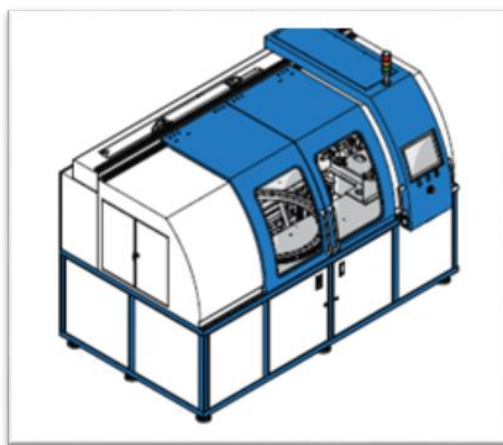


**Figure 10.** Installation for ultrasonic hardening

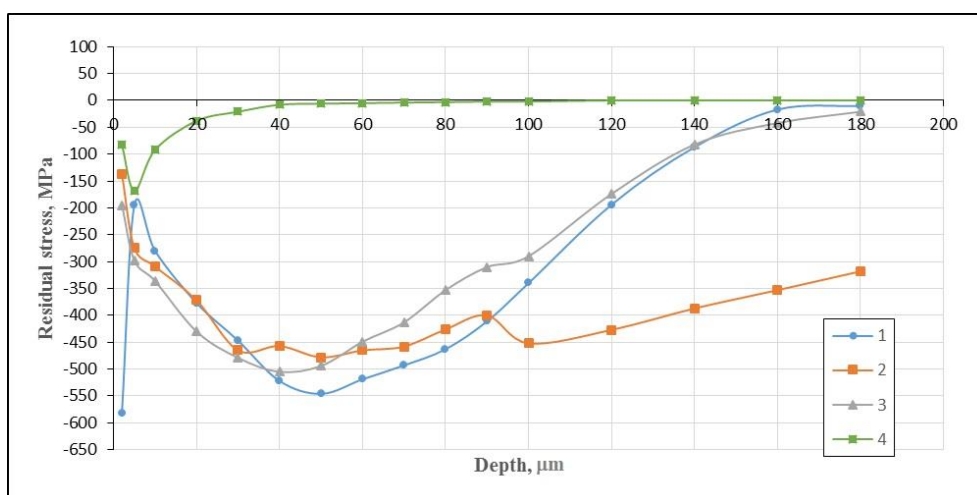


**Figure 11.** Diagram of residual stresses distribution in samples of titanium alloy after hardening

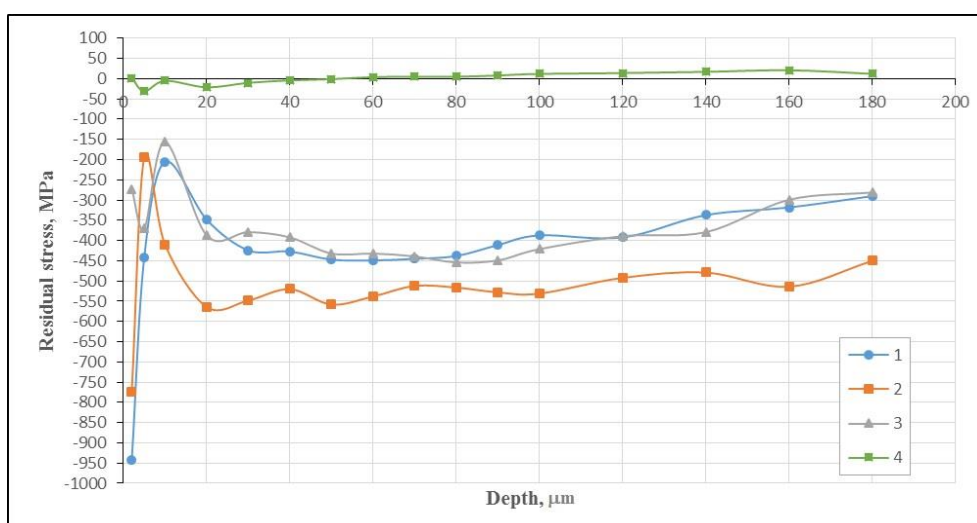


**Figure 12.** Diagram of residual stresses distribution in samples of iron-chromium-nickel alloy after hardening



ESTUDO DA CINÉTICA DA DEGRADAÇÃO TÉRMICA DE COMPÓSITOS DE NANOPARTÍCULAS NÃO-SATURADAS DE POLIÉSTER E POLIÉSTER / SILICA POR TÉCNICAS DE ANÁLISE TGA E DSC

STUDY OF THE KINETICS OF THERMAL DEGRADATION OF UNSATURATED POLYESTER AND POLYESTER/ SILICA NANOPARTICLES COMPOSITES BY TGA AND DSC ANALYSIS TECHNIQUES

دراسة حركيات التحلل الحراري للبوليستر غير المشبع و متراكبات البوليستر / جسيمات السيليكا النانوية بواسطة تقنيات تحليل TGA و DSC

FARHAN, Ahmed Jadah<sup>1\*</sup>

<sup>1</sup>Department of Physics, College of Science, University of Wasit, Wasit, Iraq

\* Correspondence author  
e-mail: aalomairi@uowasit.edu.iq

Received 02 May 2020; received in revised form 28 May 2020; accepted 05 June 2020

## RESUMO

Compósitos são materiais multifásicos que possuem propriedades superiores de engenharia; a combinação de suas fases constituintes atinge essas propriedades. Os compósitos poliméricos reforçados por nanopartículas (NPCs) são novos tipos de compósitos que atraíram muita atenção recentemente e emergiram rapidamente como uma atividade de pesquisa multidisciplinar cujos resultados poderiam ampliar as aplicações dos polímeros em benefício de muitas indústrias diferentes. O objetivo da pesquisa é analisar o efeito da adição de diferentes porcentagens (10, 20 e 30%) de nanopartículas de sílica ao poliéster insaturado (UPE) e identificar a cinética de estabilidade térmica e decomposição para elas. Nesta pesquisa, os nanocompósitos foram preparados a partir de poliéster insaturado (UPE) misturado com diferentes porcentagens (10, 20 e 30%) de nanopartículas de sílica. As curvas de análise gravimétrica térmica (TGA) e calorimetria diferencial de varredura (DSC) foram obtidas a partir da degradação térmica calculada usando o Coats-Redfern. Os parâmetros cinéticos e termodinâmicos foram estudados para todas as amostras, apresentando um excelente coeficiente de correlação linear próximo à unidade usando o Minitab 16. Trabalho experimental mostrou que a degradação de compósitos obtidos a partir da análise termogravimétrica foi mais lenta que a UPE pura. A melhoria da estabilidade térmica foi atribuída ao teor de sílica. Além disso, o resultado mostrou que a decomposição sob o ambiente oxidativo para a UPE pura era muito mais rápida que o ambiente inerte.

**Palavras-chave:** *Decomposição térmica, Análise gravimétrica térmica, Poliéster insaturado aumentado, Nanopartículas de sílica.*

## ABSTRACT

Composites are multi-phase materials that have superior engineering properties; the combination of their constituent phases achieves these properties. Nanoparticle-reinforced polymeric composites (NPCs) are new types of composites that have attracted a lot of attention recently and rapidly emerging as a multidisciplinary research activity whose results could widen the applications of polymers to the benefit of many different industries. The aim of research to analyze the effect of adding different percentages (10, 20, and 30%) of silica nanoparticles into unsaturated polyester (UPE) and identification of the thermal stability and decomposition kinetics for them. In this research, the nanocomposites were prepared from unsaturated polyester (UPE) mixed with different percentages (10, 20, and 30%) of silica nanoparticles. Thermal gravimetric analysis (TGA) and differential scanning calorimetry (DSC) curves were obtained from the thermal degradation computed by using the Coats-Redfern. The kinetic and thermodynamic parameters were studied for all specimens were presented an excellent linear correlation coefficient close to unity using Minitab 16. Experimental work was showed that the degradation of composites obtained from the thermal gravimetric analysis was slower than the pure UPE. The enhancement of thermal stability was attributed to silica content. Also, the result showed that the decomposition under the oxidative environment for the pure UPE was much faster than the inert environment.

**Keywords:** *Thermal decomposition, Thermal gravimetric analysis, Unsaturated polyester risen, Silica nanoparticles.*

المترابكات هي مواد متعددة الأطوار لها خصائص هندسية فائقة؛ يتم تحقيق هذه الخصائص من خلال الجمع بين تلك الأطوار المكونة لها. المترابكات البوليمرية المدعمة بالجسيمات النانوية (NPCs) هي أنواع جديدة من المترابكات جذبت الكثير من الاهتمام مؤخرًا وسرعان ما ظهرت كمنشآت بحثية متعددة التخصصات يمكن أن تؤدي نتائجها إلى توسيع تطبيقات البوليمرات لصالح العديد من الصناعات المختلفة. يهدف البحث إلى تحليل تأثير إضافة نسب مختلفة (20 و 30%) من الجسيمات النانوية للسيليكا إلى البوليستر غير المشبع وتحديد الثبات الحراري وحركية التحلل لهما. في هذا البحث، تم تحضير المترابكات النانوية من البوليستر غير المشبع (UPE) الممزوج مع نسب مئوية مختلفة (10 و 20 و 30%) من جسيمات السيليكا النانوية. تم الحصول على منحنيات كل من التحلل الوزني الحراري (TGA) والمسح الحراري التفاضلي (DSC) من التحلل الحراري المحسوب باستخدام تقنية Coats-Redfern. تمت دراسة المعلمات الحركية والديناميكية الحرارية لجميع العينات وتم تمثيل معامل ارتباط خطي ممتاز قريب من الوحدة باستخدام Minitab 16. وأظهر العمل التجريبي أن تحلل المترابكات التي تم الحصول عليها من التحلل الوزني الحراري كان أبطأ من البوليستر غير المشبع النقي. يعزى تعزيز الاستقرار الحراري إلى محتوى السيليكا. أيضًا، أظهرت النتائج أن التحلل للبوليستر غير المشبع النقي تحت البيئة المؤكسدة كان أسرع بكثير منه في البيئة الخاملة.

**الكلمات المفتاحية:** التحلل الحراري، التحلل الوزني الحراري، راتنج البوليستر غير المشبع، جسيمات السيليكا النانوية.

## 1. INTRODUCTION:

Poly condensation polymers considered very practical in several usages due to their price and easily fabricated, suitable mechanical property, and higher corrosion property (Atta *et al.*, 2005). It is widely employed mainly in the area of coating, electrical application, fabrication parts of automotive, and construction fields (Selly and Mark, 1988; Kramer, 1992; Giovanilton *et al.*, 2009).

Thermal analysis is a technique used to measure a physical property of a substance and/or its reaction product as a function of temperature. Differential scanning calorimetry (DSC) is a technique used to study the thermal transition of a polymer. A sum of essential physical changes in a polymer takes place when a polymer is heated, which can be measured via DSC. These involve the glass transition temperature (Tg), melting temperature (Tm), crystallization temperature (Tc), and degradation or decomposition temperature (TD). Also, chemical changes due to polymerization and degradation reactions and other reactions affecting the specimen can be estimated (Charles and Seymour, 2008; Pearce *et al.*, 1982).

Kinetic parameter and thermodynamic prosperities and thermal stability determined by utilizing thermal gravimetric analysis (TGA) and differential scanning calorimetry (DSC) which gives a very clear idea about the structure of the polymers and the behaviour of various composites under severe heat (Budrugeac *et al.*, 1996; Budrugeac, 1995).

Oxidative and thermal decomposition of polymers and composite usually occurs at higher temperature by the elimination of molecules along the polymer chain followed by random scission of the backbone chain; however, these changes produce more volatiles, gases and eventually all

the polymer convert to high molecules of polynuclear ring so-called chars (Regnier and Mortaigne, 1995; Bansal *et al.*, 1989; Gibson and Hume, 1995; Arie *et al.*, 1998). However, polyester decomposition occurs in two stages, in the first stage, the degradation of the backbone of the main chain occurs by ester change and hydrogen elimination and finally converts to volatiles, gases, and char because of its strong hydrogen bond prevent it from melting in the second stage (Mouritz and Gibson, 2007; Tagle *et al.*, 1992; Pielichowski and Hamerton, 1998).

There are numerous numbers of previous studies related to the kinetics of decomposition have been studied by many researchers, however, they concentrated on constant decomposition rate, activation energy and thermodynamic properties of different polymers and its different composite and they showed the enhancement in thermal stability of composites by using different inclusions for example:

Al-Bayaty and Farhan, (2015) studied unsaturated polyester resin (UPE) mixing with different weight percent 2, 4, and 6% of toner carbon nanopowder (TCNP) to prepare polyester composite. Non-isothermal decomposition kinetics of UPE and UPE/TCNP composites was carried out by utilizing thermogravimetric analysis (TGA). Kinetic parameters were determined for all specimens that were satisfactorily presenting good correlation with a linear correlation coefficient close to the unit using the SPSS package and were in a good agreement with published data. The experimental results show the decomposition of UPE/TCNP composites obtained from the thermal gravimetric analysis is faster comparing with those UPE specimens. This enhancement is attributed to the iron content in TCNP.

Thamer *et al.*, (2019) studied, the thermal analysis methods reported for the characterization

of epoxy/ Hexagonal Boron Nitride Nanoparticles (BNNPs) nanocomposites were conducted using Thermogravimetric Analysis (TGA), Differential Thermal Analysis (DTA) and Differential Scanning Calorimetry (DSC). Non-isothermal kinetics decomposition of epoxy and epoxy/BNNPs nanocomposites were carried out by utilizing Thermogravimetric Analysis (TGA). TGA and DTG curves obtained from the decomposition were analyzed using the Coats-Redfern method. Kinetic parameters were determined for all specimens that show a good correlation with the linear correlation coefficient, where Coats and Redfern's procedure was the best to result in reasonable estimates of the kinetic parameters.

Ferreira *et al.*, (2006) Novel aluminized E-glass fiber reinforced unsaturated polyester composites, formulated initially for enhanced thermal and electrical shielding properties, were evaluated in terms of their thermal performance. The thermal degradation of these specimens was analyzed using a thermogravimetric analyzer (TGA). All samples were decomposed under dry nitrogen (N<sub>2</sub>) at a flow rate of 40 ml/min to yield gases and solid char. Aluminized E-glass composites were compared alongside the unmetalled E-glass and unreinforced composite. The significant weight loss occurred between 200 and 400°C. The unreinforced polyester had a maximum weight loss, 1.25%/°C, happening at 360°C. For the aluminized and unmetalled E-glass composites, the maximum rate of weight loss was 0.34 and 0.55%/°C, respectively. Experimental results show the degradation of the aluminized E-glass composites obtained from TGA tests is higher compared to those of unmetalled E-glass fiber and unreinforced polyester composite. This improvement is correlated to the aluminum coating.

The aim of this current study was, therefore, to fabricate nanocomposite samples using the silica content (10, 20, 30) wt% with the unsaturated polyester resin to improve thermal stability and thermal decomposition of thermoset polyester using by Coats-Redfern method.

## 2. MATERIALS AND METHODS:

### 2.1. Composite fabrication

The materials employed to fabricate the nanocomposites are unsaturated polyester resin (UPE) as a matrix. It is a liquid with moderate viscosity, which can be cured to the solid-state by adding (Methyle EthyleKeton Peroxide, MEKP) as a hardener. At the same time, cobalt octoate acts

as a catalyst to accelerate the solidification process. The percentage of the hardener to the resin is (2%) while it is (0.5%) for the accelerator. Desirable physical properties, easily handled, quickly cured, and stable dimensions after solidification. The features of unsaturated polyester resin are given in (Table 1). Hardener: is a chemical material, which is added to thermosetting resin for the purpose of causing curing or hardening. The terms hardener and curing agent are used interchangeably. Note that these can differ from catalysts, promoters, and accelerators. Curing: To change the physical properties of the material (usually from a liquid to a solid) by chemical reaction, by the action of heat and catalysts, alone or in combination, with or without pressure. Accelerator: A chemical used to speed up a response or cure.

The term accelerator is often used interchangeably with the term promoter (Charles, 1975). Silica nanoparticles with a particle size of 100 nm were used as commercial fillers. The chemical composition of nano-silica is given in (Table 2). Atomic force microscopy (AFM) was used (CSPM scanning probe microscope) to measure the average particle size of nano-silica. The particle size distribution is shown in (Figure 1).

Samples of the polymer and nanocomposites at different Silica content (10, 20, and 30 %) are fabricated by cast molding. All content mixed thoroughly before casting, then the samples left at ambient temperature for 24 hr, and then cured, the specimens were left for 2 hr in an oven at temperature 60°C.

### 2.2. Kinetic theory

The Coats-Redfern method is a multi-heating rate application of the Coats-Redfern equation (Kim and Sea, 2005; Sperling, 2005) has been applied to study the kinetics of the decomposition of the polymer and its composite.

$$\ln \{[-\ln (1-\alpha)/T^2]\} = \ln(AoR/\beta Ea) \{1-(2R T / Ea)\} - (Ea/R T) \quad (\text{Eq. 1})$$

Where

$\alpha$  = The extent of the reaction

$\beta$  = The constant heating rate

$Ao$  = The frequency factor

$R$  = The universal gas constant

$T$  = The decomposition temperature

$Ea$  = The activation energy

By plotting  $\ln\{-\ln(1-\alpha)/T^2\}$  against  $1/T$



for each heating, rate gives a family of straight lines of slope  $-E/R$  Frequency factor directly determined from Y-axis intercept by substituting values of activation energies:

$$\text{Intercept} = \ln(AoR / \beta Ea) \{1 - (2RT / Ea)\} \quad (\text{Eq.2})$$

### 3. RESULTS AND DISCUSSION:

#### 3.1. Thermogravimetric analysis

TGA and DSC is a crucial tool to study the kinetics of thermal decomposition and to describe the way were the polymer degrades and to determine the melting point and glass transition temperature and to explore the thermodynamics of thermal and to demonstrate the stability. Thermal decomposition carried out at a constant heating rate of 10 °C/min in an inert atmosphere between 35-650°C.

Figure 2 shows TGA and DSC profiles for pure polyester resin under oxidative agent; it can be seen the polymer start in losing its weight initially about 6 wt% at a temperature between 190 and 300°C then start losing significant weight 60.9 wt% between 300 and 430°C. However, this represents the first stage degradation, while the second stage starts 405°C till 462°C with a weight loss of 9.97 wt%, then the char starts to gasify. From the DSC profile observed two peaks which represent exothermic decomposition, the first small peak at 407.3°C, which represents the backbone scission followed with a prominent peak at 478.9°C, which represents the gasification of char. Figure 3 shows the profiles of pure polyester under inert conditions were initial lose weight starts 237°C till 310°C with weight lose 5.5 wt% followed by the first stage with weight lost 73.2 wt% between temperature range 310°C to 437°C and the second stage lose 18.8 wt% which ends at 641.8°C, the DSC profile also showed two peaks first at 415°C and the second one at 435°C. Table 3 shows the mass loss of polyester pure and with various weight percent of Silica content. However, there is a difference in the activation energy of oxidative and nonoxidative agents. In oxidative, the activation energy is much lower than nonoxidative, as shown in (Table 4). This is because oxygen enhances the decomposition, consequently reducing activation energies of decay.

The effect of addition Silica filler at different percentages are shown in Figure 4, (Figure 5) and (Figure 6). However, it can be seen the thermal stability increases with increasing Silica content (Figure 6) differs completely than (Figure 2) and

(Figure 3) especially at the initial stage which start 327°C with initial mass loss of composite 5.5 wt% followed with first stage decomposition which ends at 443°C with mass loss 72.5 wt%, while the stage mass loss is 12.49 wt% which is considered much lower comparing with pure polyester (Figure 3). DSC profile showed two peaks; the first appeared at 399°C, while the second at 508.2°C which is considered much higher comparing with (Figure 3), this is because of increased thermal stability.

#### 3.2. The kinetic parameters

There are several methods to determine the kinetic parameters of the degradation process. However, the kinetic parameters were found by applying the Coats-Redfern method, as shown in Figure 7, a typical plot of  $\ln(-\ln(1-\alpha)/T^2)$  against  $(1/T)$  for oxidative thermal decomposition pure unsaturated polyester, for the first-order reaction. The method applied for pure unsaturated polyester, and its composites at different Silica content is shown in (Figure 8).

The thermodynamic properties were estimated by the following equations (3,4, and 5) (Straszko *et al.*, 2000; Silva *et al.*, 2004):

$$\Delta H = E - R T_{\text{peak}} \quad (\text{Eq. 3})$$

$$\Delta S = R [ \ln(h Ao/kbT_{\text{peak}}) - 1 ] \quad (\text{Eq. 4})$$

$$\Delta G = \Delta H - T_{\text{peak}} \Delta S \quad (\text{Eq. 5})$$

Where  $\Delta H$  is activation enthalpy,  $\Delta S$  is activation entropy,  $\Delta G$  is activation free energy of decomposition,  $T_{\text{peak}}$  is maximum peak temperature,  $h$  is Plank constant, and  $kb$  is Boltzmann constant. Table 5 shows the thermodynamics property of pure unsaturated polyester and its composites, according to the Coats-Redfern method used in determining kinetic data.

Figure 9 shows there is a linear relationship between activation energy,  $Ea$ , and Entropy,  $\Delta S$  with accuracy  $R^2=99.3\%$  (Turmanova *et al.*, 2008; Vlaev *et al.*, 2004). Table 5 shows that the activation energy increases with increasing entropy, and the positive values of internal energy mean the degradation process is not spontaneous (Al-Mulla, 2012).

### 4. CONCLUSIONS:

The thermal degradation of a silica-reinforced unsaturated polyester composite has

been successfully studied and experimentally compared to unreinforced polyester. UPE and UPE/silica were degraded in two stages, and almost 94% of the original mass was decomposed into volatiles and char. The activation energy of the nanocomposite materials was found to be higher than that of pure UPE in the oxidation environment by approximately 51.07% at 30%wt silica, and 19.12% higher than the pure UPE in the inert environment at 30%wt silica. Also, the entropy of the silica nanocomposites was higher than the pure UPE in oxidation and inert environment. DSC profiles of the silica nanocomposites showed there was a shift of decomposition peaks towards the right side because of enhancement of thermal stability for composite attributed to silica content as compared with pure UPE in oxidation and inert environment.

## 5. REFERENCES:

1. Al-Bayaty, S. A. and Farhan, A. J. (2015). Thermal decomposition kinetics unsaturated polyester and unsaturated polyester reinforcement by toner carbon nano powder (TCNP) composites. *Int. J. Appl. Innovation Eng. Manag* 4. 139-146.
2. Al-Mulla, A. (2012). Enthalpy-entropy compensation in polyester degradation reactions. *International Journal of Chemical Engineering*. 1-8.
3. Ariei, T., Shoji I., Hideaki N., and Nobuyuki F. (1998). A kinetic study of the thermal decomposition of polyesters by controlled-rate thermogravimetry. *Thermochimica acta* 319, no. 1-2. 139-149.
4. Atta, A. M., Elnagdy, S. I., Abdel-Raouf M. E., Elsaeed S. M., and Abdel-Azim A. (2005). Compressive properties and curing behaviour of unsaturated polyester resins in the presence of vinyl ester resins derived from recycled poly (ethylene terephthalate). *Journal of Polymer Research* 12, no. 5, 373-383.
5. Bansal, R. K., Jagjiwan M., and Prakash S. (1989). Thermal stability and degradation studies of polyester resins. *Journal of applied polymer science* 37, no. 7. 1901-1908.
6. Budrugaec P. (1995). Accelerated thermal ageing of nitrile-butadiene rubber under air pressure. *Polymer Degradation and Stability* 47, no. 1. 129-132.
7. Budrugaec, P., Segal, E., Stere, E., and Petre, A. L. (1996). Thermal degradation of a styrenatedunsaturated polyester resin. *Journal of thermal analysis* 46, no. 5. 1313-1324.
8. Charles, A. (1975). *Handbook of plastics and elastomers*. McGraw-Hill.
9. Charles, E. C., and Seymour, J., (2008) "Polymer Chemistry", Seventh Edition by Taylor & Francis Group, LLC.
10. Ferreira, J. M., Errajhi, O. A. Z., and Richardson, M. O. W. (2006). Thermogravimetric analysis of aluminised E-glass fibre reinforced unsaturated polyester composites. *Polymer testing* 25, no. 8. 1091-1094.
11. Gibson, A. G., and Hume, J. (1995). Fire performance of composite panels for large marine structures. *Plastics, Rubber & Composites Processing and Appl.* 3, no. 23. 175-183.
12. Giovanilton F. S., Fernando, L. C. Caio Glauco S.(2009). Influence of the particle size in kinetic of pyrolysis of unsaturated polyester, 20<sup>th</sup> *International Congress of Mechanical Engineering*, November 15-20, Gramado, RS, Brazil.
13. Kim, H. T., Sea C. O. (2005). Kinetics of thermal degradation of waste polypropylene and high-density polyethylene. *Journal of Industrial and Engineering Chemistry* 11, no. 5. 648-656.
14. Kramer H. (1992). Unsaturated Polyester Resin, *Ullmanns Encyclopedia of Industrial Chemistry*, Weinheim A21, 217.
15. Mouritz, A. P., and Gibson A. G. (2007). *Fire properties of polymer composite materials*. Vol. 143. Springer Science & Business Media.
16. Pearce, E. M. Wright, C. E. Bordoloi, B. K. (1982) Laboratory Experiments in Polymer Synthesis and Characterization, the Pennsylvania State University, University Park, PA,.
17. Pielichowski, K., Hamerton, I. (1998). TGA/FTIR studies on the thermal stability of poly (vinyl chloride) blends with a novel colourant stabilizer: 3-(2, 4-dichlorophenylazo)-9-(2,3 epoxypropane)carbazole. *Polymer* 39, no. 1. 241-244.

18. Regnier, N., Mortaigne, B. (1995). Analysis by pyrolysis/gas chromatography/mass spectrometry of glass fibre/vinylester thermal degradation products." *Polymer degradation and stability* 49, no. 3 419-428.
19. Selly J. Mark, H. F. (1988). *Eyclopedia of Polymer Science and Engineering*. New York; Willey, Vol.12, PP. (256-290).
20. Silva, S., Conceição, M. Souza, A., Shiva P., Silva, M., Fernandes, V., Araújo, A. Sinfrônio, F. (2004). Thermal analysis of the powder and the bran of algaroba. *Journal of thermal analysis and calorimetry* 75, no. 2. 411-417.
21. Sperling, L. H. (2005). *Introduction to physical polymer science*. John Wiley & Sons.
22. Straszko, J., Olszak-Humienik, M. Możejko, J. (2000). Study of the mechanism and kinetic parameters of the thermal decomposition of cobalt sulphate hexahydrate. *Journal of thermal analysis and calorimetry* 59, no. 3. 935-942.
23. Tagle, L., Hand, F. Diaz, L. (1992). Thermogravimetric analysis of polyesters derived from terephthalic, tetrachloroterephthalic and related diacids with bisphenol A. *Thermochimica Acta* 200. 281-291.
24. Thamer, A. Yusr H. A., Jubier, N. J. (2019). TGA, DSC, DTG Properties of Epoxy Polymer Nanocomposites by Adding Hexagonal Boron Nitride Nanoparticles. *Journal of Engineering and Applied Sciences* 14, no. 4. 567-574.
25. Turmanova, S., Genieva, S. D., Dimitrova, A. S. Vlaev, L. T. (2008). Non-isothermal degradation kinetics of filled with rice husk ash polypropene composites. *Express Polymer Letters* 2, no. 2. 133-146.
26. Vlaev, L. T., Markovska, I. G. Lyubchev, L. A. (2004). Kinetics compensation effect at thermal degradation of rice husk. *Oxidation Communications* 27, no. 2. 444-452.

**Table 1.** Typical properties of unsaturated polyester resin.

| Property                      | Unsaturated Polyester (UPE) |
|-------------------------------|-----------------------------|
| Density (gm/cm <sup>3</sup> ) | 1.05-1.4                    |
| Tensile strength (MPa)        | 45-103                      |
| Tensile modulus (GPa)         | 1.3-4.5                     |
| Cure shrinkage %              | 5-12                        |
| T <sub>g</sub> (K)            | 340                         |

**Table 2.** Chemical composition for the silica nanoparticles

| material | Components %     |                                |                                |       |      |                   |                  |       |                                |                   |
|----------|------------------|--------------------------------|--------------------------------|-------|------|-------------------|------------------|-------|--------------------------------|-------------------|
|          | SiO <sub>2</sub> | Al <sub>2</sub> O <sub>3</sub> | Fe <sub>2</sub> O <sub>3</sub> | CaO   | MgO  | Na <sub>2</sub> O | K <sub>2</sub> O | MnO   | Pb <sub>2</sub> O <sub>3</sub> | Cu <sub>2</sub> O |
| Silica   | 0.96             | 0.14                           | 2.16                           | 53.67 | 0.84 | 0.006             | 0.006            | 0.019 | 0.013                          | 0.005             |

**Table 3.** The mass loss during decomposition for unsaturated polyester and its composite.

| The samples     | environment | loss first stage | loss second stage | Total mass loss |
|-----------------|-------------|------------------|-------------------|-----------------|
| UPE pure        | oxidative   | 430.2C°, 60.92%  | 642.6C°, 9.97%    | 70.89%          |
| UPE pure        | inert       | 437.2C°, 73.26%  | 641.8C°, 10.86%   | 84.12%          |
| UPE +10% Silica | inert       | 438.2C°, 80.73%  | 643.9C°, 11.34%   | 92.07%          |
| UPE +20% Silica | inert       | 435.9C°, 82.74%  | 643.7C°, 15.05%   | 97.79%          |
| UPE +30% Silica | inert       | 443.8C°, 72.51%  | 643.2C°, 12.49%   | 85.00%          |

**Table 4.** Kinetics data of non-isothermal degradation of UPE and its composites according to Coats-Redfern method

| The samples     | Environment | Peak Temperature, T <sub>p</sub> (K) | Activation Energy, E <sub>a</sub> (kJ/mol) | Reaction rate constant, A <sub>0</sub> (S <sup>-1</sup> ) | R <sup>2</sup> |
|-----------------|-------------|--------------------------------------|--|---|----------------|
| UPE pure        | Oxidative   | 652                                  | 78.0680                                    | 0.3164 x10 <sup>4</sup>                                   | 99.1%          |
| UPE pure        | Inert       | 660                                  | 99.0030                                    | 22.260 x10 <sup>4</sup>                                   | 99.7%          |
| UPE +10% Silica | Inert       | 665                                  | 100.358                                    | 31.708 x10 <sup>4</sup>                                   | 99.6%          |
| UPE +20% Silica | Inert       | 656                                  | 111.382                                    | 308.222 x10 <sup>4</sup>                                  | 98.7%          |
| UPE +30% Silica | Inert       | 661                                  | 117.934                                    | 835.108 x10 <sup>4</sup>                                  | 99.6%          |

**Table 5.** Thermodynamics property of UPE/Silica composites

| The samples    | Environment | T <sub>peak</sub> ,(K) | ΔH,KJ/mol | -ΔS, J/mol | ΔG, kJ/mol |
|----------------|-------------|------------------------|-----------|------------|------------|
| USP Pure       | Oxidative   | 652                    | 72.647    | 192.721    | 198.301    |
| USP Pure       | Inert       | 660                    | 93.515    | 157.459    | 197.438    |
| USP+10% Silica | Inert       | 665                    | 94.829    | 154.758    | 197.743    |
| USP+20% Silica | Inert       | 656                    | 105.928   | 135.559    | 194.854    |
| USP+30% Silica | Inert       | 661                    | 112.438   | 127.334    | 113.496    |

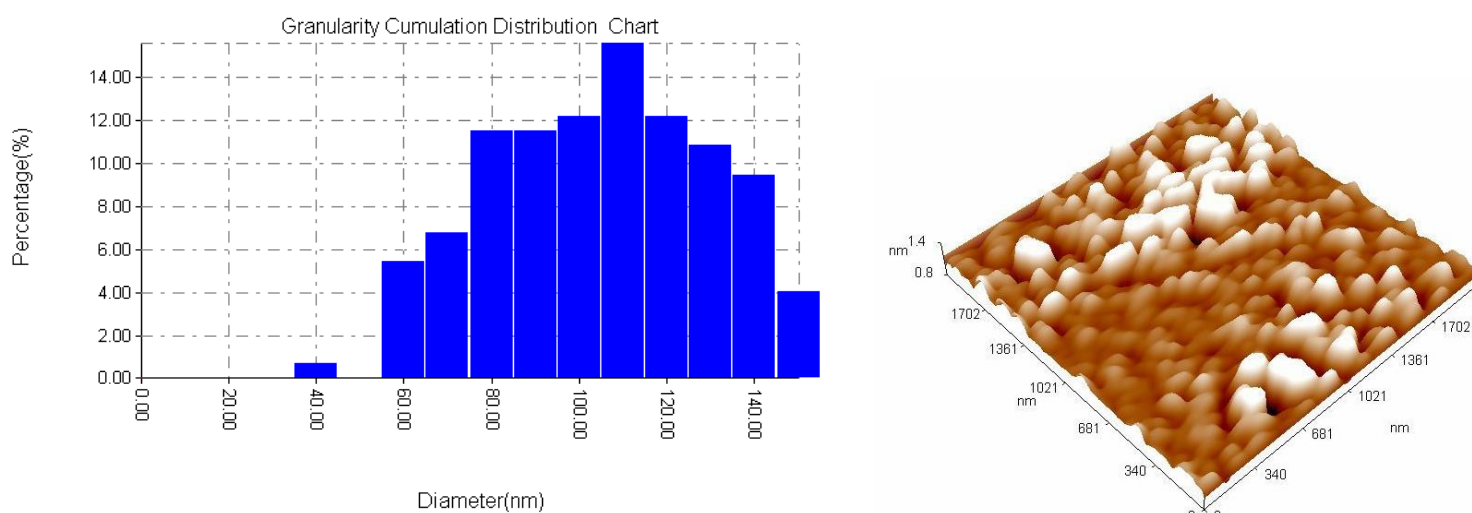


**Figure 1.** AFM of silica nanoparticles

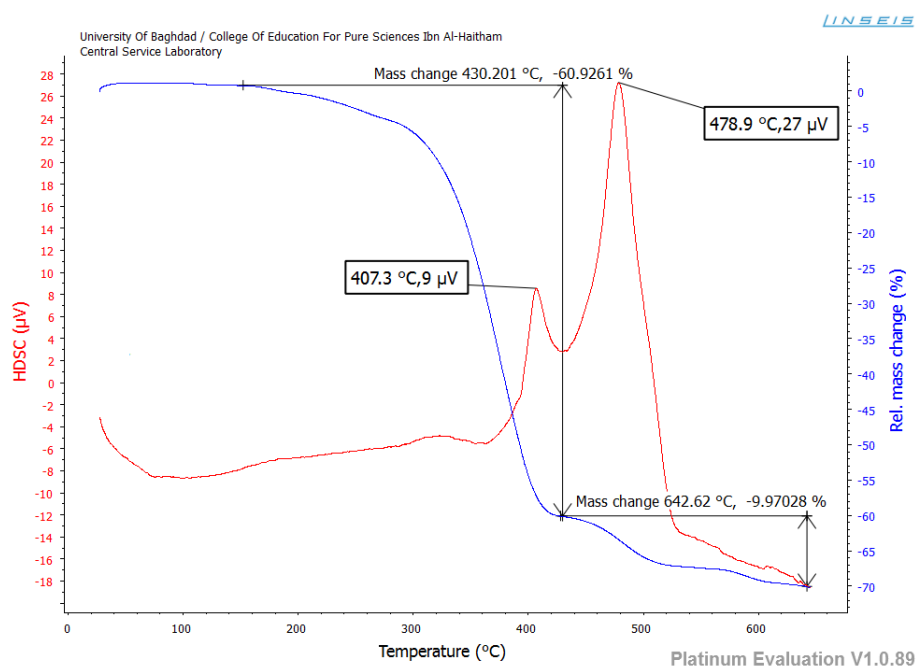


**Figure 2.** TGA and DSC curve for pure polymer under oxidative environment.

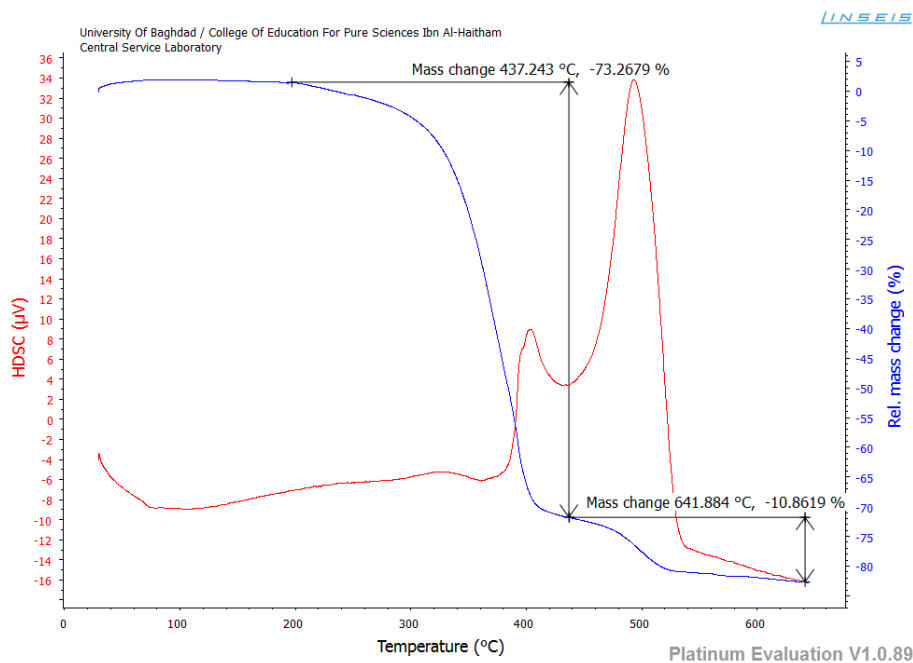


**Figure 3.** TGA and DSC curve for pure polymer under an inert environment

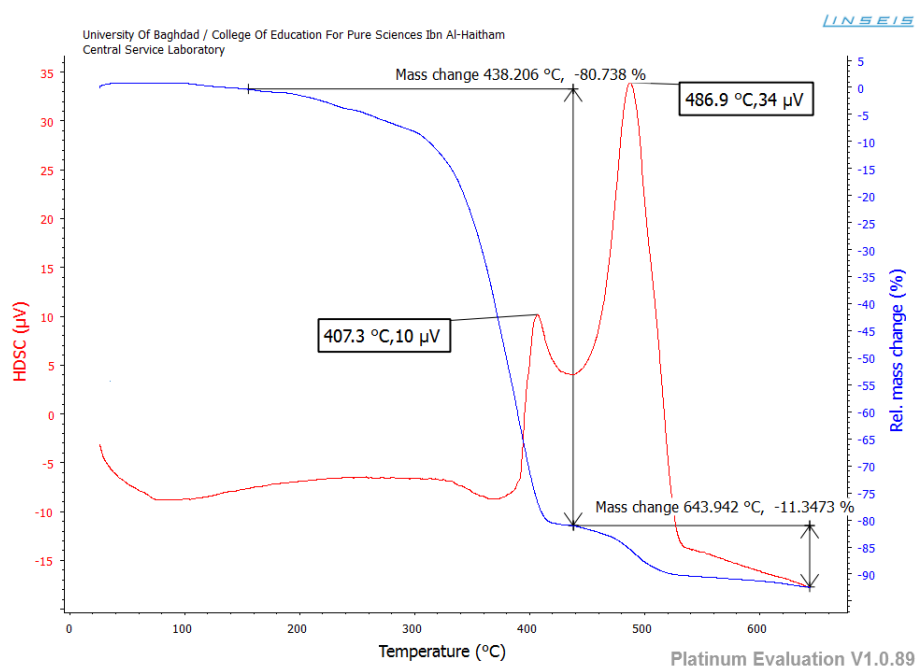


**Figure 4.** TGA and DSC curve for unsaturated polyester/Silica 10 wt%

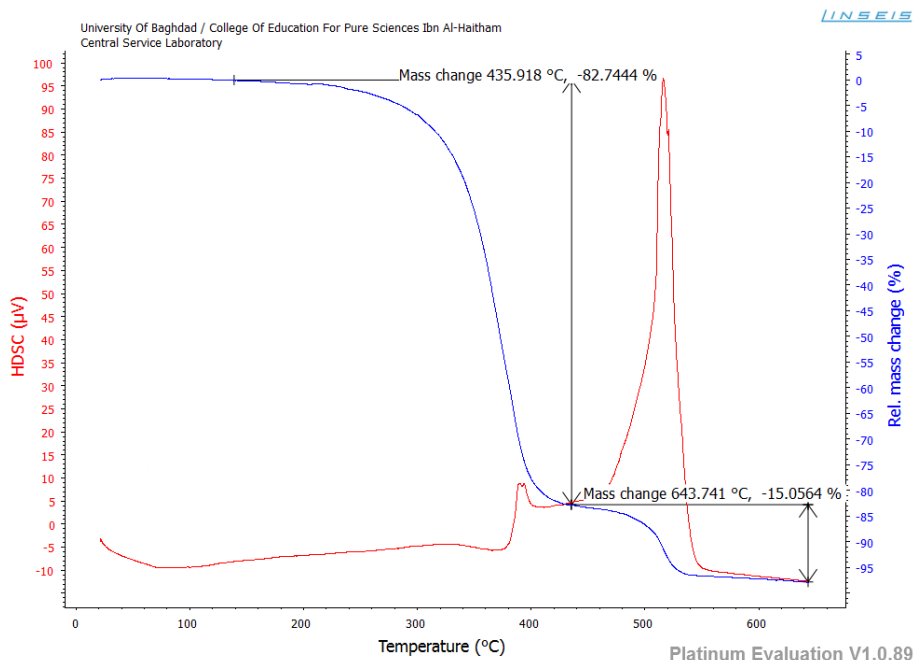


**Figure 5.** TGA and DSC curve for unsaturated polyester/Silica 20 wt%.

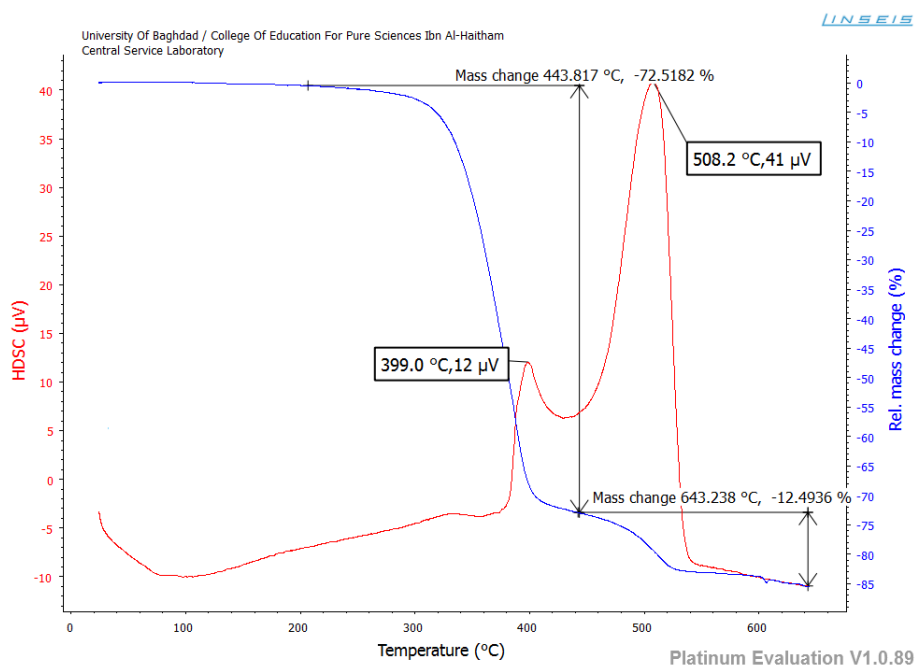


**Figure 6.** TGA and DSC curve for unsaturated polyester/Silica 30 wt%.

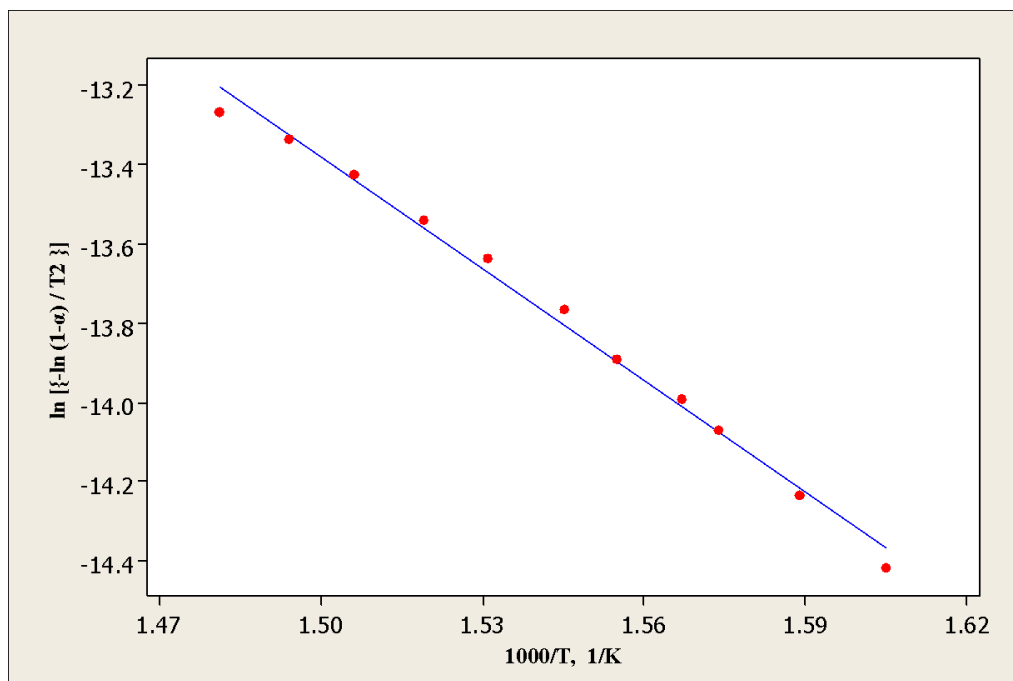


**Figure 7.** A plot of oxidative thermal decomposition utilizing Coats-Redfern method

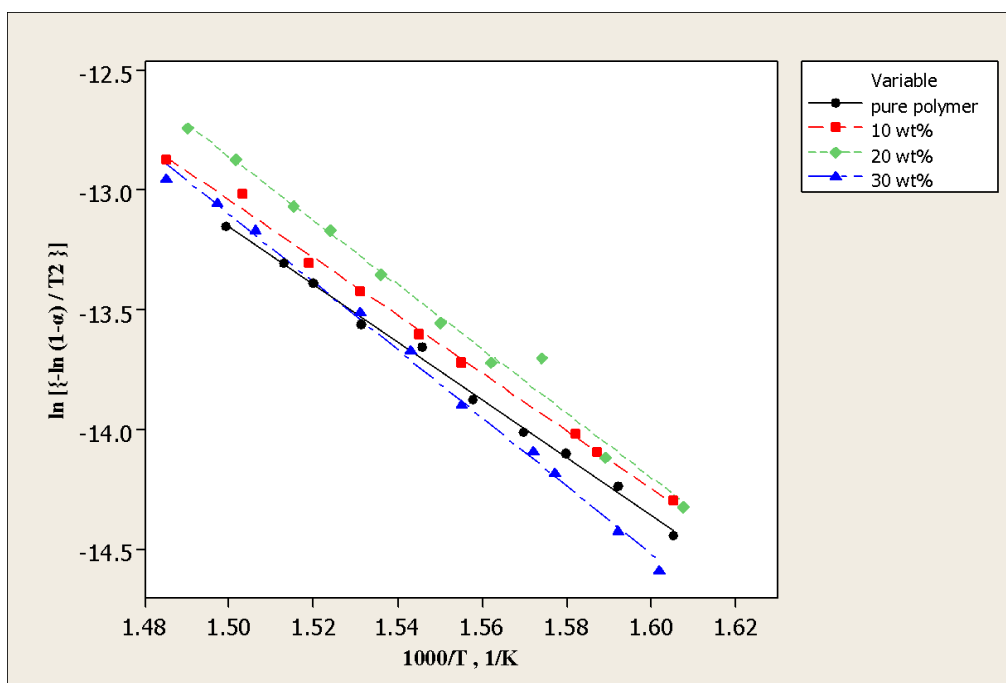


**Figure 8.** A plot of non oxidative thermal decomposition utilizing Coats-Redfern method



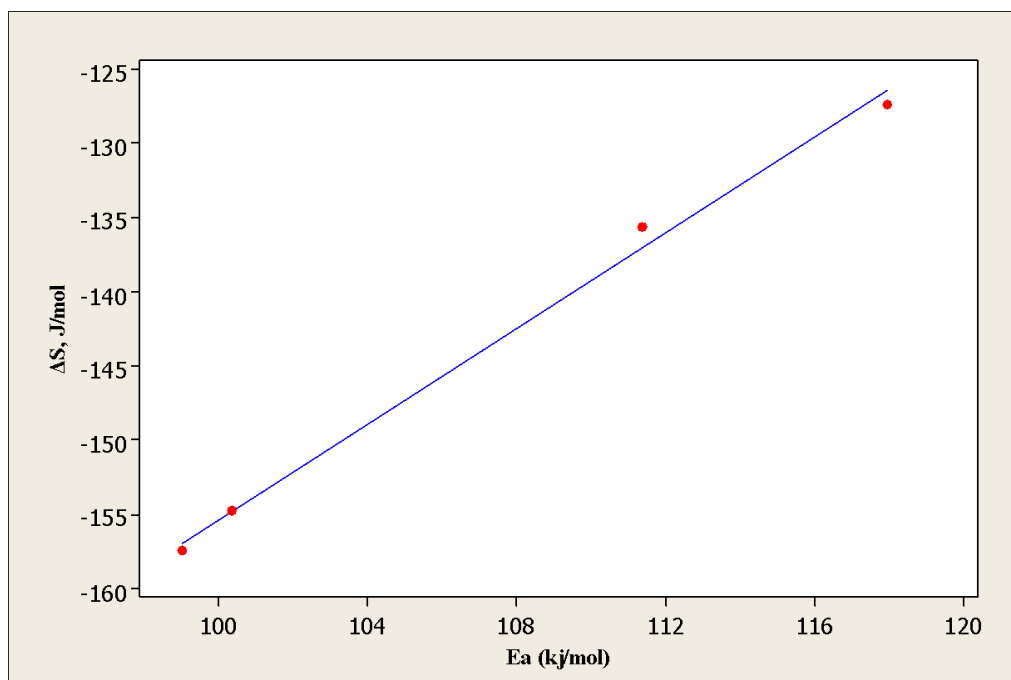


**Figure 9.** Plot of Entropy against Activation energy for thermal decomposition of UPE and its composite

CINÉTICA E MECANISMO DE OXIDAÇÃO DO TETRA-HIDROFURANO PELA CLORAMINA-T EM MEIOS ACIDICOS

KINETICS AND MECHANISM OF TETRAHYDROFURAN OXIDATION BY CHLORAMINE-T IN ACIDIC MEDIA

حركية وميكانيكية أكسدة تيترا-هيدروفيوران بواسطة الكلورامين-T في المحيط الحامضي

SAEED, Noor Hazim Mohammed<sup>1\*</sup>; ABBAS, Ahmed Majed<sup>2</sup>

<sup>1</sup> Department of Chemistry, College of Education for Pure Science, University of Mosul, Mosul, Iraq.

<sup>2</sup> Department of Chemistry, College of Science, University of Misan, Maysan, Iraq

\* Correspondence author

e-mail: noorsaeed@uomosul.edu.iq

Received 07 March 2020; received in revised form 20 May 2020; accepted 06 June 2020

RESUMO

A cinética da oxidação do tetra-hidrofurano pelo N-cloro-p-tolueno sulfonamida de sódio no meio de ácido clorídrico foi estudada neste trabalho a temperatura de 308 K. A taxa de reação mostra uma dependência de primeira ordem em [CAT] e uma dependência em ordem fracionária, cada uma em [THF] e [H<sup>+</sup>]. A lei da taxa derivativa, adequada para resultados experimentais, é a Equação 24. A constante da taxa de primeira ordem foi avaliada a partir da relação entre o gráfico de Log [CAT] e o tempo. A variação da força iônica pela adição de perclorato de sódio (NaClO<sub>4</sub>) e íon cloreto no meio não mostrou efeito significativo na reação. A taxa de reação aumentou com constante dielétrica decrescente (D), enquanto a adição de p-toluenosulfonamida retarda a taxa de reação. A reação de oxidação do tetra-hidrofurano foi estudada a uma temperatura diferente. Foram estimadas as constantes de equilíbrio para a formação de ácido hipocloroso, ácido hipocloroso protonado e o complexo ácido hipocloroso protonado-THF e sua constante de decomposição. Além disso, a taxa constante para a lenta (etapa de determinação da taxa) e o parâmetro de ativação foram calculados. Um mecanismo adequado para a reação de oxidação do tetra-hidrofurano foi proposto com base no achado experimental. O mecanismo inclui a reação de espécies ativas (H<sub>2</sub>OCl) do agente oxidante com o tetra-hidrofurano em uma etapa rápida para dar o complexo (X). Este complexo será então transformado em complexo (X̄) em passo lento e depois em γ-butirolactona em outro passo rápido.

**Palavras-chave:** THF; Cinética; Oxidação; Mecanismo; Cloramina-T; Meio Ácido.

ABSTRACT

The kinetics of tetrahydrofuran oxidation by sodium N-chloro-p-toluene sulfonamide in the hydrochloric acid medium was studied in this work at 308 K. The reaction rate shows a first-order dependence on [CAT] and fractional-order dependence each on [THF] and [H<sup>+</sup>]. The derivative rate law, which suitable for experimental results, is Equation 24. The first-order rate constant has been evaluated from the relationship of the plot of Log [CAT] versus Time. The variation of the ionic strength by the addition of sodium perchlorate (NaClO<sub>4</sub>) and chloride ion on the medium showed no significant effect on the reaction. The reaction rate raised with decreasing dielectric constant (D), while the addition of p-toluene sulfonamide retards the rate of reaction. The oxidation reaction of tetrahydrofuran have been studied at a different temperature, The equilibrium constants for the formation of hypochlorous acid, protonated hydrochlorous acid and protonated hydrochlorous acid-THF complex and its decomposition constant have been estimated. Also, the rate constant for the slow (rate-determining step) and the activation parameter have been calculated. A suitable mechanism for the oxidation reaction of tetrahydrofuran was proposed based on the experimental finding. The mechanism includes the reaction of active species (H<sub>2</sub>OCl) of the oxidizing agent with the tetrahydrofuran in a fast step to give the complex(X). This complex will then transformed into complex (X̄) in slow step then to γ-butyrolactone in another fast step.

**Keywords:** THF; Kinetics; Oxidation; Mechanism; Chloramine-T; Acidic Medium.

المخلص

تمت دراسة حركية أكسدة رباعي هيدروفيوران بواسطة N-chloro-p-toluene sulfonamide في وسط حامض الهيدروكلوريك وعند درجة حرارة 308 كلفن. بينت النتائج أن معدل سرعة التفاعل يعتمد على تركيز الكلورامين-T (الرتبة الأولى) ويعتمد على تركيز كل من تيترا هيدروفيوران وأيون

الهيدروجين (الرتبة كسرية)، وأن قانون سرعة التفاعل المشتق والذي يتلائم مع النتائج العملية موضح في المعادلة (24). تم حساب ثابت سرعة لتفاعل الرتبة الأولى من رسم العلاقة بين لوغاريتم [CAT] مقابل الزمن ووجد أن تغير الشدة الأيونية بإضافة بيركلورات الصوديوم ( $\text{NaClO}_4$ ) واختلاف أيون الكلوريد ليس له أي تأثير على ثابت سرعة التفاعل، بينما يرتفع معدل سرعة التفاعل مع تناقص ثابت العزل الكهربائي (D) وعند إضافة ناتج التفاعل  $\text{p-toluene sulfonamide}$  يؤدي ذلك إلى نقصان معدل سرعة التفاعل. تمت دراسة حركية أكسدة تيترا هيدروفيوران في درجات حرارية مختلفة وتم تقدير ثوابت التوازن لتكوين حامض الهيكلوروس، حامض الهيدروكلوريك البروتوني، معقد حامض الهيدروكلوريك البروتوني - THF وثابت تحلله وحساب ثابت سرعة تفاعل الخطوة البطيئة والمعاملات الترموديناميكية، وأخيراً اقترحت ميكانيكية ملائمة للتفاعل اعتماداً على النتائج العملية والتي تتضمن تفاعل الجزء الفعال ( $\text{H}_2\text{OCl}$ ) من المادة المؤكسدة [CAT] مع تيترا هيدروفيوران بسرعة ليعطي المعقد (X) والذي يتحول ببطء إلى المعقد (X) والذي يعطي بدوره  $\gamma$ -بيوتيرولاكتون بخطوات سريعة أخرى لاحقة.

الكلمات المفتاحية: THF، حركية، أكسدة، ميكانيكية، كلورامين-T، وسط حامضي.

## 1. INTRODUCTION

The chemistry of sodium N-chloro-p-toluenesulfonamide ( $\text{p-CH}_3\text{-C}_6\text{H}_4\text{SO}_2\text{-NClNa}\cdot 3\text{H}_2\text{O}$ ), well known as Chloramine-T (CAT or  $\text{RNCINa}$ ), is a member of the aromatic sulphonyl haloamines. It is expected to behave as an oxidation agent in acidic and alkaline media and delivers a two-electron change in the reaction medium to form (p-TSA;  $\text{RNH}_2$ ) and ( $\text{NaCl}$ ). The oxidation potential of CAT/ $\text{RNH}_2$  modify with the pH of the medium and increase with reducing the pH of the medium (Campbell and Johnson, 1978; Banerji *et al.*, 1987). Different reaction species were recorded depending on the medium acidity (pH), such as N-Chloro-p-Toluenesulfonamide,  $\text{RNHCl}$ , Dichloramine-T,  $\text{RNCl}_2$ ,  $\text{HOCl}$ ,  $\text{H}_2\text{OCl}$  and  $\text{RNH}_2\text{Cl}$  in acid medium,  $\text{OCl}$  and  $\text{RNCl}$  in alkaline medium. Chloramine-T has been vastly utilized as a volumetric reagent in the direct and indirect determination of several compounds (Kotthoff and Belcher, 1957; Jennings and Crit, 1974; Berka and Zvka, 1965).

Limited kinetic studies of these reactions are reported, such as oxidation of cyanide, thiocyanate, hexacyanoferrate, sulfoxide,  $\alpha$ -hydroxy acid, primary and secondary alcohol, phenols, catecholamines, aldehyde, ketones, aldoses, formic acid, ether and substituted of amino acid (Mahadevappa and Gowda, 1979; Ahmed *et al.*, 1980; Mushran and Agrawal, 1971; Mahadevappa *et al.*, 1979; Mushran and Agrawal, 1971; Naidu *et al.*, 1988; Natarajan and Thiagarajan, 1975; Balasubramanian and Thiagarajan, 1975; Jagadeesh and Vaz, 2005; Agrawal and Mushran, 1973; Sanehi and Mushran, 1973; Agrawal and Mushran, 1972; Hassan and Al-Joraycee, 1989; Hassan and Saeed, 2012; Saeed, 2011). In addition, chlorination reactions of aniline, toluene, furan-2-carboxylic acid, and acetanilide have also been studied (Ramanujam and Trieff, 1977; Radhakrishnamurti *et al.*, 1982; Hassan and AL-Hatim, 1995; Hassan and Noor, 2010).

Tetrahydrofuran (THF) is usually utilized

as a reaction medium and also as a chemical reactant. So it is interesting to explore the oxidation kinetics of the THF by CAT in the acidic medium as a solvent as well as, the oxidation of THF was studied by several oxidizing agents like chromium trioxide, lead tetraacetate, ruthenium tetroxide to the corresponding  $\gamma$ -butyrolactone (Lee, 1969; Metsger and Bittner, 2000; Che *et al.*, 1991).

Little attention has been paid to the mechanism oxidation of these reactions. Also, these reactions are free of side reaction and usually give quantitative yields of pure product.

Also, the oxidation of THF by CAT has not been reported in the literature. Therefore, it is the benefit of studying the oxidation of THF by Chloramine-T in acidic medium.

## 2. MATERIALS AND METHODS

### 2.1. Materials

Tetrahydrofuran (Fluka<sup>TM</sup>) of spectra grade (99.5%) used as received. Chloramines-T was purified by the method of Morris *et al.* (1948). CAT aqueous solution was standardized by the iodometric method. All other chemicals of analytical grade. The ionic strength was kept at high constant values utilizing concentrated  $\text{NaClO}_4$  solution.

### 2.2. Kinetic measurements

In glass stoppered Pyrex<sup>TM</sup> tubs, the reaction was carried out beneath pseudo-first-order conditions by keeping with [CAT] in low compare with [THF], which kept in high concentration. In a typical kinetic experiment appropriate of THF, hydrochloric acid, methanol, sodium perchlorate, and water, which was placed in a thermostated – water bath for about 30 min at 308 K. The reaction was initiated by rapidly adding the desired amount of CAT solution to the mixture. CAT solution followed by drawing samples (5 mL)

at different periods to the irrigating solution (2 M sulfuric acid, 5% KI, and water) in the volumetric flask. The absorption of the free iodine at 353 nm was recorded using the C-Cell spectrophotometer. Finally, the pseudo-first-order rate constant  $k$  was obtained from the slope of the straight line of  $\text{Log} [\text{CAT}]$  versus time.

### 2.3. Stoichiometry

Reaction solutions, including different proportions of CAT and THF, were equilibrated at 308 K in the existence of (0.2 M) for one day. Appreciation of the unreacted of chloramine-T showed that one mole of the (THF) expended two moles of (Chloramine-T), the suggested reaction can be seen in Equation 1.

The reaction product p-TSA was identified by chromatography, utilizing benzyl alcohol saturated with water with 0.5% vanillin in one percentage of HCl solution in ethanol as a spray reagent ( $R_f = 0.905$ ). The oxidation product of THF is  $\gamma$ -butyrolactone was identified by infrared spectroscopy and characterized by reaction with hydrazine hydrate to form hydrazide derivative (Saleh and Ayoub, 2014). Pure  $\gamma$ -butyrolactone has a boiling point of 205 °C.

## 3. RESULTS AND DISCUSSION

### 3.1. Results

The kinetics of tetrahydrofuran oxidation by chloramine-T was inspected in different initial concentrations of reaction acid media.

#### 3.1.1. Reactant Concentration Effect

At a high concentration of the reactant with a fixed acid concentration, plots of  $\text{Log}[\text{CAT}]$  or  $\text{Log}[\text{CAT}]_0/[\text{CAT}]_t$  with time were linear ( $r > 0.9975$ ) pointing first – order reliance of  $[\text{CAT}]$  rate. Table 1 included the rate constants of pseudo-first-orderer. The values of  $k$  raise with reactant concentration. Plots of  $\text{Log } k$  with  $\text{Log} [\text{THF}]_0$  is linear ( $r = 0.99$ ) with a slope of (0.42). Figure 1 illustrated the reactant concentration in fractional-order.

#### 3.1.2. Hydrogen ion Concentration Effect

The rate constant of reaction increased with increasing the concentration of hydrogen ion. The rate constant of fractional-order was obtained from the straight-line slope ( $r = 0.9939$ ) of  $\text{log } k^{-1}$  versus  $\text{log}[\text{H}^+]$ , which dependence on hydrogen

ion concentration. No detectable reaction observed between THF and CAT under varying conditions at 308 to 335 K in sulfuric acid rang (0.2-0.5 M) and perchloric acid medium in the range (0.2-0.6 M). The amount of unreacted CAT remained unchanged after 3 hours of the reaction mixture, which contained 0.01 M CAT, 1.4 M THF, and  $\mu = 0.125$  M.

#### 3.1.3. The chloride ion, ionic strength, and p-TSA concentration-effect

Extension of chloride ion from (NaCl) (0.25–0.45 M) at constant  $[\text{H}^+]$  has no effect on the rate (Table 2). At a different concentration of the ionic strength (0.125–0.625 M of  $[\text{NaClO}_4]$ , no significant effect was seen on the rate (Table 2). Extension of the reaction product of p-toluene sulfonamide (0.025–0.125 M) to the reaction mixture retards the reaction rate significantly. The plot of  $\text{Log } k$  versus  $\text{Log} [\text{p-TSA}]$  was linear ( $r = 0.9963$ ) with a slope of nearly inverse unity (Table 2).

#### 3.1.4. The solvent compositions effect

At different compositions of aqueous methanol, the reaction rate has been studied. The rate of the reaction raises with an increase a methanol content (Table 2). Linear plots ( $r = 0.9948$ ) with a positive slope of  $\text{log } k_1$  versus  $1/D$  was seen (where D is the dielectric constant of the medium) (Jouyban *et al.*, 2004). The negligible effect of methanol oxidation was seen in the control experiments with methanol (Table 3).

#### 3.1.5. Temperature effect

At different temperatures (298 K – 318 K), the reaction has been studied. The pseudo-first-order rate constants and the activation parameters of oxidation of THF by CAT are given in Table 4.

### 3.2 Discussion

The dependence of rate on acidity (Table 1) could be a consequence of protonation of either chloramine-T or tetrahydrofuran. The oxonium ions formed by protonation of THF would not readily undergo an electrophilic attack, and hence extensive protonation of the ether would decrease the rate of reaction. However, the enhancement of rate by  $\text{H}^+$  ion indicates that the unprotonated ether is the reacting species, and consequently, the decrease in substrate concentration through the formation of oxonium ions can be neglected.

Chloramine-T behaves like a strong electrolyte, in aqueous solution and dissociates as Equation 2 (Bishop and Jennings, 1958).

In an acid medium, mono Chloramine-T (RNHCl). N-Chloro-p-Toluenesulfonamide has been formed, when the anion contracts a proton (Equation 3).

Due to the disproportionation of free acid, it has given rise to p-toluenesulfonamide ( $\dot{R}NH_2$ ) and Dichloramine-T ( $\dot{R}NCl_2$ ) (Equation 4).

Hypochlorous acid HOCl has been formed from the free acid hydrolyze and Dichloramine-T (Equations 5 and 6). Hypochlorous acid produced can be ionized as Equation 7. Protonation of the free acid in pH < 3 has also been reported Abdulsalam *et al.* (2018), to give (Equation 8). The protonated monochloramine-T ( $RN^+H_2Cl$ ) hydrolyzed to give protonated hydrochlorous acid and  $\dot{R}NH_2$  as Equation 9. In acid solution, free chlorine ( $Cl_2$ ) has been found in the existence of chloride ion as Equations 10 and 11.

The possible reactive species in acidified CAT solution are  $\dot{R}NHCl$ ,  $\dot{R}NCl_2$ , HOCl,  $Cl_2$ , and probably ( $H_2OCl$  and  $\dot{R}N^+H_2Cl$ ) as a result of  $k_a$  values of chlorine which equal to  $4.66 \times 10^{-4}$ . A variation of experimental conditions will often favor one reactive species rather than others. No significant effect on the rate constant was seen when varying ionic strength adds to the reaction mixture by the addition of a concentrated solution of ( $NaClO_4$ ). The reaction rate enhances significantly by decrease the dielectric constants of the medium (by adding methanol). For all aspects mentioned above, the reaction proposed takes place between a neutral molecule and a positive ion. In the opinion of this, either  $H_2O^+Cl$  or  $RN^+H_2Cl$  are likely to be the important probable reactive species. Since the reaction rate shows an enhancement by  $H^+$  ion and retardation by the addition of reaction product p-TSA (Table 2),  $RN^+H_2Cl$  can be excluded as the oxidizing species. Under the supposition,  $H_2O^+Cl$  is the reactive species.

The reaction mechanism can be proposed in schemes 1 and 2. The reaction intermediates X and  $\bar{X}$  involved in schemes 1, 2, and 3 are oxo – chloro derivative of the substrate. Rao *et al.* (1970) have reported the formation of such oxo-halo derivative during the oxidation of THF by sodium bromate. If  $[CAT]_t$  is the overall efficient concentration of CAT, as Equations 12, 13, 14 and 15. Reparation for  $[HOCl]$  and  $[H_2O^+Cl]$  from Equations 14 and 15 respectively in to Equation 13 one obtains Equation 16.

Then substitute for  $[H_2O^+Cl]$  from Equation 15 into equation 14 it is obtained Equation 17. Substituting for  $[H_2O^+Cl]$ ,  $[\dot{R}NHCl]$  and  $[HOCl]$  from Equations 15–17 respectively in to Equation 12 and solution of  $[X]$ , it is obtained Equation 18 (from the slow step of scheme 1).  $[\dot{R}NH_2]$  is negligible compared with other terms in the denominator, then Equation 19 becomes Equation 20. Since the rate =  $k_1[CAT]_t$ , Equation 20 can be converted into Equations 21, 22 and 23. The constant  $k_4$ ,  $K_2$  and  $K_3$  were computed from these equations while the equilibrium constant  $K_1$  can be evaluated using scheme 2 derived law.

The concentration of the total effective of CAT is  $[CAT]_t = [\dot{R}NHCl] + [H_2O^+Cl] + [X]$  and the reaction rate of the slow step =  $k_8[X]$ . Substitute  $[\dot{R}NHCl]$  and  $[H_2O^+Cl]$  obtained from step (i) and (ii) leads to rate law Equation 24. By negligee, the term  $[\dot{R}NH_2]$ , the rate =  $k_1[CAT]$ , Equation 24 can be transformed into Equations 25 and 26. Equations 18 and 24 indicate first-order reliance of  $[CAT]_t$  rate, and fractional-order reliance of each  $[H^+]$  and  $[S]$  rate. Comparing the constants in both schemes 1 and 2, we get that  $k_4 = k_8$ ,  $K_3 = K_7$  and  $K_1K_2 = K_6$ , So Equations 25 and 26 can be written as Equations 27 and 28.

According to Equations 22 and 23, Figure 1 and Figure 2 show the plots of  $1/k_1$  versus  $1/[S]$  ( $r = 0.9949$ ) and  $1/[H^+]$  ( $r = 0.9939$ ) respectively were linear. Form the intercept of  $1/k_1$  versus  $1/[S]$ . The value of  $k_4$  was obtained as  $1.4 \times 10^{-3} \text{ sec}^{-1}$ . Substituted this value in the value of intercept of the plot of  $1/k_1$  versus  $1/[H^+]$  (Equation 23)  $K_3$  was obtained as (7.1). The value of  $k_4$  and  $K_3$  were substituted in the slope of plot  $1/k_1$  versus  $1/[H^+]$ .  $K_2$  value was obtained as (0.546). Then, substitute the value of  $K_4$  and  $K_3$  in the slope of the plot  $1/k_1$  versus  $1/[S]$  (Equation 26). The value of  $K_6/K_1$  was obtained as 0.43, and the value of  $k_1$  is obtained as (0.765) (were  $K_1 = \dot{K}_1/[H_2O] = (1.38 \times 10^2)$ ). Finally, the constants  $K_1$ ,  $K_2$ ,  $K_3$ , and  $k_4$  were utilized to calculate the rate constant under different conditions using Equations 21 and 28, respectively. The calculated rate constants were listed in (Table 5). As can be seen, there is an excellent agreement between the rate values indicating the correctness of the suggested scheme and the derived rate laws. Since the reaction preset a fractional-order relay on  $[S]$ , Michaelis–Menten kinetics was used to calculating the rate constant  $k_4$  from the slop step. The activation parameters reaction rates were calculated by the use of Arrhenius plots of  $\log k_1$  with  $1/T$  (Table 4).

Scheme 3 shows the THF oxidation by CAT, The intermediate of complex (X)

establishment by the electrophilic. The attack of protonated hydrochlorous acid  $\text{H}_2\text{O}^+\text{Cl}$  on the oxygen of the THF gives oxo-chloro derivative of THF ( $\text{X}^-$ ). Elimination of  $\text{H}^+$  and then hydrolysis with the elimination of  $\text{H}^+$   $\text{Cl}^-$  to give  $\alpha$ -THF alcohol. The last will then interact with the second active  $\text{H}_2\text{O}^+\text{Cl}$  molecule in the fast step to give the product  $\gamma$  – butyrolactone.

The derived rate law and the suggested mechanism are confirmed by the following experimental finding. The solvent composition has been changed in different methanol content in the methanol-water mixture. The effect of the solvent on bimolecular reaction has been discussed by Geng and Wei (2007), Laidler and Landskroener (1956), and Amis (1955). Also, this topic and other theories have been illustrated by Entelis and tiger (1976). Equation 29 has been developed for the limiting case of the head-on approach of an ion to the dipolar molecule.

A linear relationship between  $\log k_1$  and  $1/D$  was suggested for the addition Equation 29 with a positive slope for the relationship of negative ion and dipole or between two dipoles. Further, the rate constant of the first order slightly rose with increasing the initial concentration of Chloramine-T (Table 1). This reaction deactivation may result from the formation of small amounts of  $\text{NaClO}_4$  inside reaction, as Equations 30 and 31.

Finally, the suggested mechanism was supported by activation energy and parameter values. The high positive value of enthalpy  $\Delta H^\ddagger$  and activation free energy  $\Delta G^\ddagger$  refer to the slight solvation of the transition state while the negative values of entropy  $\Delta S^\ddagger$  propose the figuration of the activated complex with some reduction in the freedom molecule's degree.

#### 4. CONCLUSIONS

THF is an inert solvent, and it can be easily oxidized under certain conditions. The kinetics of the THF oxidation process is carried out by the formation of  $\text{HOCl}$  in the hydrochloric acid medium at 308 K.  $\text{HOCl}$  has acquired the hydrogen ion to form  $\text{H}_2\text{OCl}$ , which interacts with THF to gives the intermediate compound which in turn gives the final product ( $\gamma$ -butyrolactone). The reaction rate was first-order dependence on  $[\text{CAT}]$ , fractional-order dependence each on  $[\text{THF}]$  and  $[\text{H}^+]$ . No significant effect of the medium ionic strength was seen on the reaction. The inverse relationship was seen between the reaction rate and the dielectric constant ( $D$ ). The equilibrium constants have been suggested for the formation of hypochlorous acid,

protonated hydrochlorous acid, and protonated hydrochlorous acid-THF complex. The reaction mechanism was proposed and found consistent with the observed kinetics.

#### 5. ACKNOWLEDGMENTS

The authors are thankful to the Department of Chemistry, College of Education for Pure Sciences, the University of Mosul for funding and supplying laboratory facilities.

#### 6. REFERENCES

1. Campbell, M. M; Johnson, G. (1978). Chloramine T and related N-halogeno-N-metallo reagents. *Chemical Reviews*, 78(1), 65–79.
2. Banerji, K. K; Jayaram, B; Mahadevappa, D. S. (1987). Mechanistic Aspects of Oxidations by N-Metallo-N-haloarylsulfonamides. *Journal of scientific and industrial research*, 46(2), 65-76.
3. Kotthoff, M; Belcher, R. (1957). Volumetric analysis, Vol. III-titration methods: Oxidation-reduction reactions. *Interscience Publishers, Inc.*, New York, 714 p.
4. Jennings, V. J; Crit C. R. C. (1974). *Reviews in Analytical Chemistry*, 407 p.
5. Berka, A; Vulterin, J; Zýka, J. (2013). Newer Redox Titrants: International Series of Monographs in Analytical Chemistry, 22, 37-45.
6. Mahadevappa, D. S; Gowda, B. T. (1979). Kinetics of oxidation of potassium cyanide by chloramine-T, 484 p.
7. Ahmed, M. S; Gowda, B. T; Mahadevappa, D. S. (1980). Kinetics and Mechanism of Oxidation of Thiocyanate Ion in Metal Salts and Complexes by Chloramine-T in Perchloric Acid Medium. *Indian Journal of Chemistry*, 19A, 650–652.
8. Mushran, S. P; Agrawal, M. C. (1971). Kinetics of the oxidation of hexacyanoferrate (II) by Chloramine-T. *Journal of Physical Chemistry*, 75(6), 838–841.
9. Mahadevappa, D. S; Jadhav, M. B; Naidu, H. M. K. (1979). Kinetics and mechanism of oxidation of dimethyl sulfoxide by chloramine-T in aqueous solution. *International Journal of Chemical Kinetics*, 11(3), 261–273.

10. Naidu, H. M. K; Katgeri, S. N; Mahadevappa, D. S. (1988). Kinetics and Mechanism of Oxidation of Unsaturated Alcohols by Chloramine-T in Sulphuric Acid Medium. *Indian Journal of Chemistry*, 27A, 880–882.
11. Natarajan, M. M; Thiagarajan, V. (1975). Kinetics of oxidation of secondary alcohols by chloramine T. *Journal of the Chemical Society, Perkin Transactions 2*, (14), 1590–1594.
12. Balasubramanian, V; Thiagarajan, V. (1975). Chlorination of substituted phenols with chloramine T. A kinetic study. *International Journal of Chemical Kinetics*, 7(4), 605–623.
13. Jagadeesh, R. V; Vaz, N. (2005). Oxidation of some catecholamines by sodium N-chloro-p-toluenesulfonamide in acid medium: A kinetic and mechanistic approach. *Central European Journal of Chemistry*, 3(2), 326–346.
14. Agrawal, M. C; Mushran, S. P. (1973). Mechanism of oxidation of aldoses by chloramine T. *Journal of the Chemical Society, Perkin Transactions 2*, (6), 762–765.
15. Agrawal, M. C; Mushran, S. P. (1972). Mechanism of Oxidation of some Aliphatic Aldehydes by Chloramine-T. *Zeitschrift für Naturforschung B*, 27(4), 401–404.
16. Sanehi A. K; Mushran S. P. J. (1973) *Indian Chemical Society*, 50,197.
17. Hassan, Y. I; Al-Joraycee, L. A. (1989). Kinetic and oxidation of formic acid with chloramine-T in hydrochloric acid medium. *Education and Science*, 9, 73.
18. Hassan, Y. I; Saeed, N. H. M. (2012). Kinetics and Mechanism of Oxidation of Diethyl Ether by Chloramine-T in Acidic Medium. *Journal of Chemistry*, 9(2), 642–649.
19. Saeed, N. H. (2011). Kinetics and Mechanism of Chlorination of N-Acetyl glycine by Chloramine-T in Acidic Medium. *Journal of Education and Science*, 24(53), 41–50.
20. Ramanujam, V. S; Trieff, N. M. (1977). Kinetic and mechanistic studies of reactions of aniline and substituted anilines with chloramine T. *Journal of the Chemical Society, Perkin Transactions 2*, (10), 1275–1280.
21. Radhakrishnamurti, P. S; Pati, S. C; Dev, B. R. (1982). Kinetics and mechanism of chlorination of toluene and some substituted toluenes by chloramine-T. *International Journal of Chemical Kinetics*, 14(11), 1267–1279.
22. Hassan, Y. I; AL-Hatim A. A. (1995). Kinetics and mechanism of chlorination of furan-2 carboxylic acid by chloramine-T in acidic medium. *Mu'tah Journal of Research Studies*, 15(5), 19.
23. Hassan, Y. I; Saeed, N. H. (2010). Kinetic study of chlorination of p-methoxyacetanilide by chloramine-T in hydrochloric acid medium. *Oriental Journal of Chemistry*, 26(2), 415.
24. Lee, D. G. (1969). Oxidation Techniques and Application in organic synthesis "Vol.I Edited by Augustine, R. L; Dekker, M. 1, 54–65.
25. Metsger, L; Bittner, S. (2000). Autocatalytic oxidation of ethers with sodium bromate. *Tetrahedron*, 56(13), 1905–1910.
26. Che, C. M; Tang, W. T; Wong, K. Y; Li, C. K. (1991). Kinetics of oxidation of aromatic hydrocarbons and tetrahydrofuran by trans-dioxoruthenium (VI) complexes. *Journal of the Chemical Society, Dalton Transactions*, (12), 3277–3280.
27. Morris, J. C; Salazar, J. A; Wineman, M. A. (1948). Equilibrium Studies on N-Chloro Compounds. I. The Ionization Constant of N-Chloro-p-toluenesulfonamide. *Journal of the American Chemical Society*, 70(6), 2036–2041.
28. Saleh, M. Y; Ayoub, A. I. (2014). Synthesis of new derivatives of 2-chloro-3-formyl-1, 8-naphthyridine. *European Journal of Chemistry*, 5(3), 475–480.
29. Jouyban, A; Soltanpour, S; Chan, H. K. (2004). A simple relationship between dielectric constant of mixed solvents with solvent composition and temperature. *International Journal of pharmaceuticals*, 269(2), 353–360.
30. Bishop, E; Jennings, V. J. (1958). Titrimetric analysis with chloramine-T—I: The status of chloramine-T as a titrimetric reagent. *Talanta*, 8(10), 197–212.
31. Abdulsalam, F. O; Reddy, P. K; Iyengar, (2018). Spectrophotometric Study Oxidation of Amlodipine Besylate by Chloramine-T in Acidic Buffer pH (4.3) Medium. *Der Pharma Chemica*, 10(2), 70–76.
32. Rao, V. R. S; Venkappayya, D; Aravamudan, G. (1970). Stability characteristics of aqueous chloramine-T solutions. *Talanta*, 17(8), 770–772.
33. Geng, W; Yu, S; Wei, G. (2007). Treatment of charge singularities in implicit solvent

- models. *The Journal of chemical physics*, 127(11), 114106.
34. Laidler, K. J; Landskroener, P. A. (1956). The influence of the solvent on reaction rates. *Transactions of the Faraday Society*, 52, 200–210.
35. Amis, E. S. (1955). Rates mechanisms and solvent. *Analytical Chemistry*, 27(11), 1672–1678.
36. Entellic S. G; Tiger. R. P. (1976). Reaction Kinetics in the liquid phase. Wiley, New York, 362 p.

## Equations



where  $\text{R} = \text{CH}_3 \cdot \text{C}_6\text{H}_4\text{SO}^{2-}$



$$K_a = 2.82 \times 10^{-5} \text{ at } 298 \text{ K}$$



$$K_d = 6.10 \times 10^{-2} \text{ at } 298 \text{ K}$$



$$K_h = 8.00 \times 10^{-7} \text{ at } 298 \text{ K}$$



$$K_h = 4.88 \times 10^{-8} \text{ at } 298 \text{ K}$$



$$K_i = 3.30 \times 10^{-8} \text{ at } 298 \text{ K}$$



$$K_p = 1.03 \times 10^2 \text{ at } 298 \text{ K}$$







$$K = 2.15 \times 10^3 \text{ at } 298 \text{ K}$$

$$[\text{CAT}]_t = [\dot{\text{R}}\text{NHCl}] + [\text{HOCl}] + [\text{H}_2\text{O}^+\text{Cl}] + [\text{X}] \quad (\text{Eq. 12})$$

$$\text{From step (i) } K_1 = \frac{[\dot{\text{R}}\text{NH}_2][\text{HOCl}]}{[\dot{\text{R}}\text{NHCl}][\text{H}_2\text{O}]}$$

$$\text{or } [\dot{\text{R}}\text{NHCl}] = \frac{[\dot{\text{R}}\text{NH}_2][\text{HOCl}]}{K_1[\text{H}_2\text{O}]} = \frac{[\dot{\text{R}}\text{NH}_2][\text{HOCl}]}{\dot{K}_1} \quad (\text{Eq. 13})$$

$$\text{where } \dot{K}_1 = K_1[\text{H}_2\text{O}]$$

$$\text{From step (ii) } K_2 = \frac{[\text{H}_2\text{O}^+\text{Cl}]}{[\text{HOCl}][\text{H}^+]}$$

$$\text{or } [\text{HOCl}] = \frac{[\text{H}_2\text{O}^+\text{Cl}]}{K_2[\text{H}^+]} \quad (\text{Eq. 14})$$

$$\text{From step (iii) } K_3 = \frac{[\text{X}]}{[\text{H}_2\text{O}^+\text{Cl}][\text{S}]}$$

$$\text{or } [\text{H}_2\text{O}^+\text{Cl}] = \frac{[\text{X}]}{K_3[\text{S}]} \quad (\text{Eq. 15})$$

$$[\dot{\text{R}}\text{NHCl}] = \frac{[\dot{\text{R}}\text{NH}_2][\text{X}]}{\dot{K}_1 K_2 K_3 [\text{H}^+][\text{S}]} \quad (\text{Eq. 16})$$

$$[\text{HOCl}] = \frac{[\text{X}]}{K_2 K_3 [\text{H}^+][\text{S}]} \quad (\text{Eq. 17})$$

$$[\text{CAT}]_t = \frac{[\dot{\text{R}}\text{NH}_2][\text{X}]}{\dot{K}_1 K_2 K_3 [\text{H}^+][\text{S}]} + \frac{[\text{X}]}{K_2 K_3 [\text{H}^+][\text{S}]} + \frac{[\text{X}]}{K_3 [\text{S}]} + [\text{X}]$$

$$[\text{CAT}]_t = [\text{X}] \left\{ \frac{[\dot{\text{R}}\text{NH}_2]}{\dot{K}_1 K_2 K_3 [\text{H}^+][\text{S}]} + \frac{1}{K_2 K_3 [\text{H}^+][\text{S}]} + \frac{1}{K_3 [\text{S}]} + 1 \right\}$$

$$[\text{X}] = \frac{\dot{K}_1 K_2 K_3 [\text{CAT}]_t [\text{H}^+][\text{S}]}{[\dot{\text{R}}\text{NH}_2] + \dot{K}_1 + \dot{K}_1 K_2 [\text{H}^+] + K_1 K_2 K_3 [\text{H}^+][\text{S}]}$$

$$\text{rate} = - \frac{d[\text{CAT}]_t}{dt} = k_4 [\text{X}] \quad (\text{Eq. 18})$$

$$\text{rate} = \frac{k_4 K_1 K_2 K_3 [\text{CAT}]_t [\text{H}][\text{S}]}{[\dot{\text{R}}\text{NH}_2] + \dot{K}_1 + \dot{K}_1 K_2 [\text{H}^+] + \dot{K}_1 K_2 K_3 [\text{H}^+][\text{S}]} \quad (\text{Eq. 19})$$

$$\text{rate} = \frac{K_2 K_3 k_4 [\text{CAT}]_t [\text{H}][\text{S}]}{1 + K_2 [\text{H}^+] + K_2 K_3 [\text{H}^+][\text{S}]} \quad (\text{Eq. 20})$$

$$\dot{K}_1 = \frac{K_2 K_3 k_4 [\text{H}][\text{S}]}{1 + K_2 [\text{H}^+] + K_2 K_3 [\text{H}][\text{S}]} \quad (\text{Eq. 21})$$

$$\frac{1}{\dot{K}_1} = \frac{1}{K_3 k_4 [\text{S}]} \left( \frac{1}{K_2 [\text{H}^+]} + 1 \right) + \frac{1}{k_4} \quad (\text{Eq. 22})$$

$$\frac{1}{\dot{K}_1} = \frac{1}{K_2 K_3 k_4 [\text{H}^+][\text{S}]} + \frac{1}{K_3 k_4 [\text{S}]} + \frac{1}{k_4} \quad (\text{Eq. 23})$$

$$\text{rate} = \frac{K_6 K_7 k_8 [\text{CAT}]_t [\text{H}^+][\text{S}]}{[\dot{\text{R}}\text{NH}_2] + K_6 [\text{H}^+] + K_6 K_7 [\text{H}^+][\text{S}]} \quad (\text{Eq. 24})$$

$$\frac{1}{\dot{K}_1} = \frac{1}{K_7 k_8 [\text{S}]} \left\{ \frac{1}{K_6 [\text{H}^+]} + 1 \right\} + \frac{1}{k_8} \quad (\text{Eq. 25})$$

$$\frac{1}{\dot{K}_1} = \frac{1}{K_6 K_7 k_8 [\text{H}^+][\text{S}]} + \frac{1}{K_7 k_8 [\text{S}]} + \frac{1}{k_8} \quad (\text{Eq. 26})$$

$$\frac{1}{\dot{K}_1} = \frac{1}{K_3 k_4 [\text{S}]} \left\{ \frac{1}{\frac{K_6}{K_1} [\text{H}^+]} + 1 \right\} + \frac{1}{k_4} \quad (\text{Eq. 27})$$

$$\frac{1}{\dot{K}_1} = \frac{\dot{K}_1}{K_6 K_3 k_4 [\text{H}^+][\text{S}]} + \frac{1}{K_3 k_4 [\text{S}]} + \frac{1}{k_4} \quad (\text{Eq. 28})$$

$$\ln k_D = \ln k_\infty + \frac{Ze\mu_0}{DKTr^2} \quad (\text{Eq. 29})$$

where,

$K_\infty$  = rate constant of dielectric constant

$Ze$  = charge on ion

$\mu_0$  = permanent moment of the dipole

$r$  = radius of the ion

$K$  = Boltzmann constant

$T$  = absolute temperature



### Scheme 1



### Scheme 2



### Scheme 3

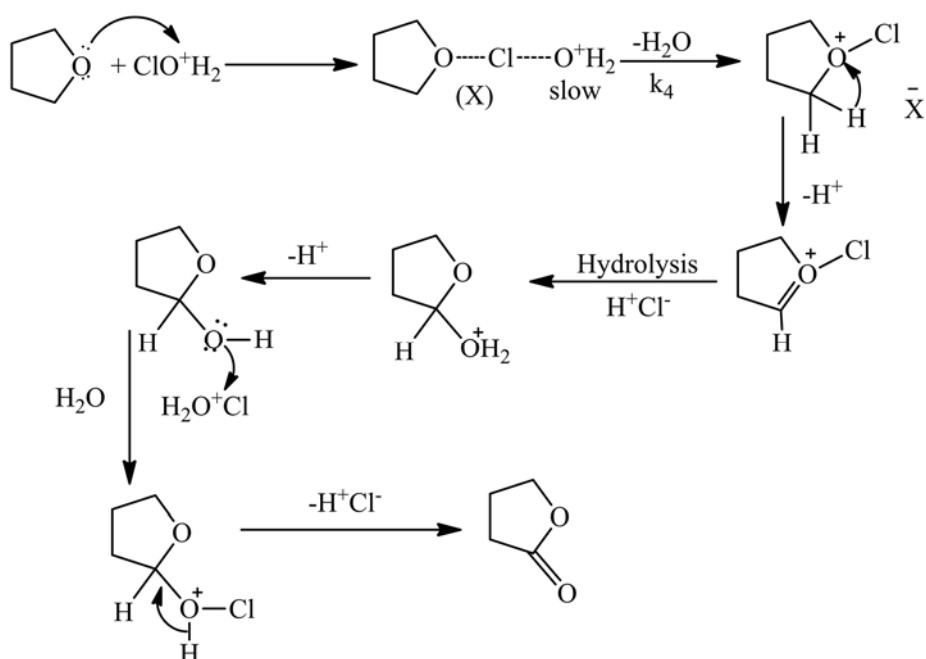


**Table 1:** Effect of different reactant, Chloramine-T, and hydrogen ion concentration on the rate constant at 308K,  $\mu = 0.125$  M.

| $10^2[\text{CAT}]$ M | [THF] M | $[\text{H}^+]$ M | $10^4 k_1$ Sec <sup>-1</sup> | $10^4 k_1 / [\text{H}^+ \text{ or } \text{S}]^n$ |
|----------------------|---------|------------------|------------------------------|--|
| 1.00                 | 1.40    | 0.20             | 6.410                        | --   |
| 1.25                 | 1.40    | 0.20             | 5.140                        | --   |
| 1.50                 | 1.40    | 0.20             | 4.180                        | --   |
| 1.75                 | 1.40    | 0.20             | 3.610                        | --   |
| 2.00                 | 1.40    | 0.20             | 3.000                        | --   |
| 1.00                 | 1.40    | 0.20             | 6.410                        | 5.570  |
| 1.00                 | 2.11    | 0.20             | 7.800                        | 5.560  |
| 1.00                 | 2.80    | 0.20             | 8.910                        | 5.620  |
| 1.00                 | 3.50    | 0.20             | 9.520                        | 5.620  |
| 1.00                 | 4.20    | 0.20             | 10.00                        | 5.500  |
| 1.00                 | 1.40    | 0.10             | 4.980                        | 15.75  |
| 1.00                 | 1.40    | 0.15             | 6.000                        | 15.50  |
| 1.00                 | 1.40    | 0.20             | 6.410                        | 14.83  |
| 1.00                 | 1.40    | 0.25             | 7.640                        | 15.30  |
| 1.00                 | 1.40    | 0.30             | 8.330                        | 15.21  |

(n) was obtained from the slope of  $\log k_1$  with  $\log [\text{H}]$  or  $[\text{THF}]$ , and the unit of  $k_1$  is  $\text{L}^n \cdot \text{mol}^{-n} \cdot \text{sec}^{-1}$ .

**Table 2:** Effect of different chloride ion, ionic strength and p-TSA concentration on the rate constant at 308 K;  $[\text{CAT}]_0 = 0.001$  M;  $[\text{THF}]_0 = 1.4$  M;  $[\text{H}^+] = 0.2$  M;  $\mu = 0.125$  M.

| $[\text{Cl}^-]_t$ M | $10^4 k_1$ Sec <sup>-1</sup> | $[\text{NaClO}_4]$ M | $10^4 k_1$ Sec <sup>-1</sup> | [p-TSA] M | $10^4 k_1$ Sec <sup>-1</sup> |
|---------------------|------------------------------|----------------------|------------------------------|-----------|------------------------------|
| 0.25                | 6.63                         | 0.125                | 6.41                         | 0.025     | 5.18                         |
| 0.30                | 6.53                         | 0.250                | 6.46                         | 0.050     | 2.57                         |
| 0.35                | 6.64                         | 0.375                | 6.50                         | 0.075     | 1.32                         |
| 0.40                | 6.83                         | 0.500                | 6.45                         | 0.100     | 1.27                         |
| 0.45                | 6.53                         | 0.625                | 6.45                         | 0.125     | 1.08                         |

**Table 3:** Effect of different dielectric constant (D) on the rate constant at 308 K;  $[\text{CAT}] = 0.001$  M;  $[\text{THF}] = 1.4$  M;  $[\text{H}^+] = 0.2$  M and  $\mu = 0.125$  M.

| %CH <sub>3</sub> OH | D     | $10^4 k_1$ |
|---------------------|-------|------------|
| 0.00                | 74.93 | 6.41       |
| 10.0                | 70.64 | 6.83       |
| 20.0                | 65.81 | 7.22       |
| 30.0                | 61.12 | 7.67       |
| 40.0                | 58.44 | 8.94       |

**Table 4:** Effect of different temperature on the rate constant,  $[\text{CAT}] = 0.001$  M,  $[\text{THF}] = 1.4$  M,  $[\text{H}^+] = 0.2$  M and  $\mu = 0.125$  M.

| Temperature K                   | 298  | 303  | 308  | 313  | 318  |
|---------------------------------|------|------|------|------|------|
| $10^4 k_1$ (sec <sup>-1</sup> ) | 4.34 | 5.30 | 6.41 | 7.72 | 9.21 |

$E_a = 29.80$  KJ/mole

$\log A = 6.8684$

$\Delta H^\ddagger = 27.11 \pm 0.07$  KJ/mole

$\Delta G^\ddagger = 94.4 \pm 2.18$  KJ/mole

$\Delta S^\ddagger = 21.8 \pm 0.04$  KJ/mole

**Table 5:** The rate constant of the observed and the calculated first-order rate in different concentrations of [THF] and [H<sup>+</sup>] at 308 K [CAT] = 0.00 1M,  $\mu$  = 0.125 M.

| [THF]<br>M | [H <sup>+</sup> ]<br>M | $10^4 k$<br>Sec <sup>-1</sup> | $10^4 k_1/[H^+ \text{ or } S]^n$ | $10^4 k_{\text{cal}}$<br>Sec <sup>-1</sup> | $10^4 k_{\text{cal}}/[h^+ \text{ or } S]^n$ |
|------------|------------------------|-------------------------------|----------------------------------|--|---|
| 1.4        | 0.20                   | 6.410                         | 5.560                            | 6.88                                       | 5.90  |
| 2.1        | 0.20                   | 7.800                         | 5.560                            | 8.28                                       | 5.98  |
| 2.8        | 0.20                   | 8.910                         | 5.650                            | 9.18                                       | 5.91  |
| 3.5        | 0.20                   | 9.520                         | 5.630                            | 9.85                                       | 5.64  |
| 4.2        | 0.20                   | 10.02                         | 5.480                            | 10.36                                      | 5.66  |
| 1.4        | 0.10                   | 4.980                         | 15.80                            | 4.73                                       | 14.44                                       |
| 1.4        | 0.15                   | 6.000                         | 15.50                            | 5.98                                       | 15.13                                       |
| 1.4        | 0.20                   | 6.410                         | 14.85                            | 6.89                                       | 14.95                                       |
| 1.4        | 0.25                   | 7.640                         | 15.30                            | 7.58                                       | 15.20                                       |
| 1.4        | 0.30                   | 8.330                         | 15.20                            | 8.20                                       | 15.00                                       |

(n) was obtained from the slope of the plot  $\log k_1$  with  $\log [H \text{ or } THF]$ , and  $k^a$  is the unit of  $L^n \cdot \text{mol}^{-n} \cdot \text{sec}^{-1}$ .

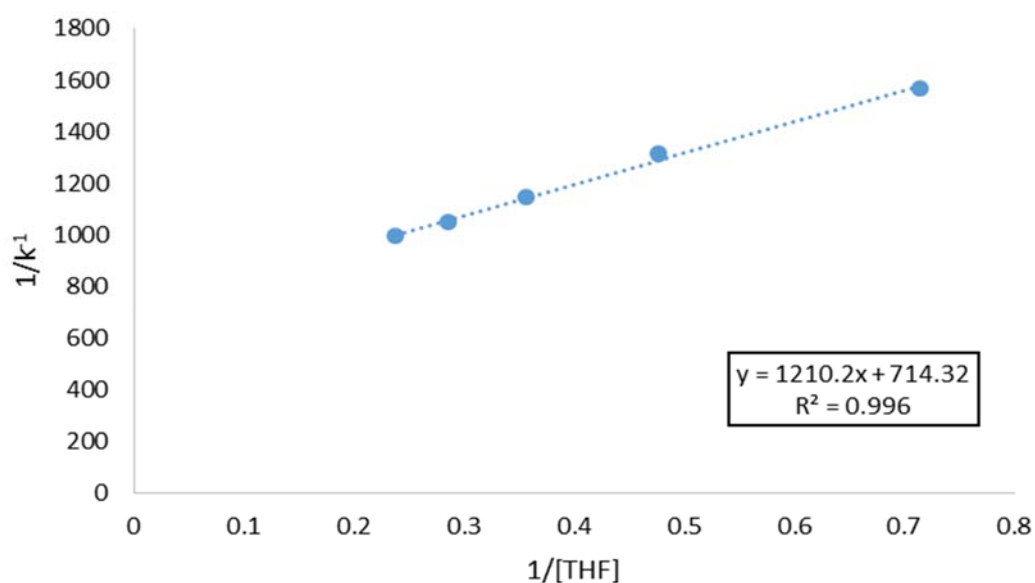


**Figure 1:** Plot of  $1/k_1$  versus  $1/[THF]$ ; [CAT] = 0.0015 M; [H] = 0.2 M;  $\mu$  = 0.125 M; Temperature = 308 K.

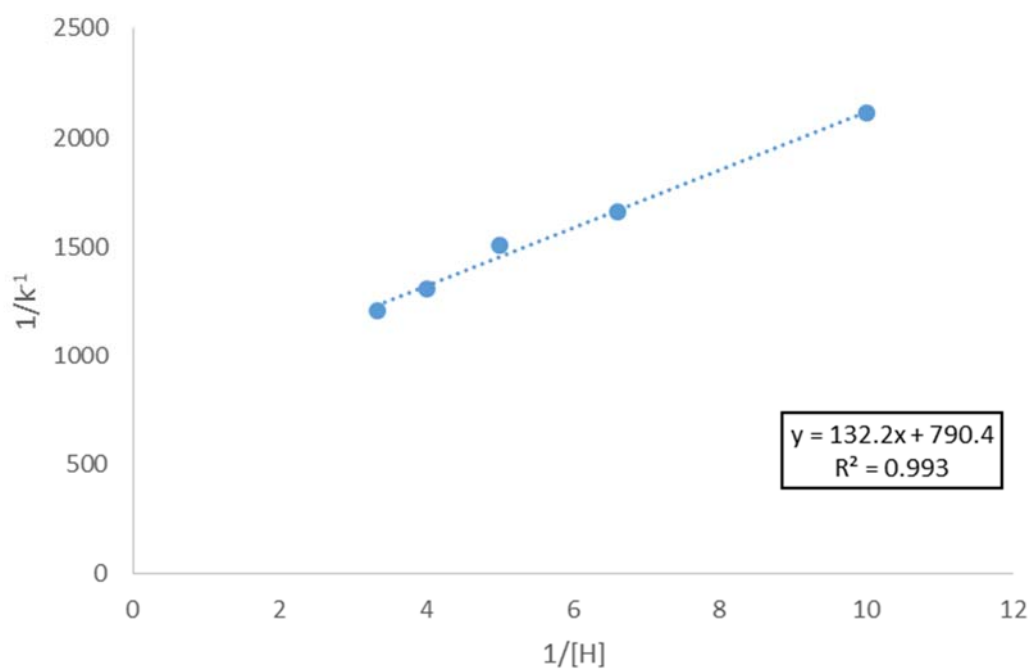


**Figure 2:** Plot of  $1/k_1$  versus  $1/[H]$ ;  $[CAT] = 0.0015\text{ M}$ ;  $[THF] = 1.4\text{ M}$ ;  $\mu = 0.125\text{ M}$ ; Temperature = 308 K.

## ESPECIFICAÇÕES BIOINDICATIVAS, ECOLÓGICAS E ANALÍTICAS DE FLUXOS MENORES SOB A INFLUÊNCIA DE OBJETOS ARTIFICIAIS PERIGOSOS

## BIOINDICATIVE, ECOLOGICAL AND ANALYTICAL SPECIFICATIONS OF MINOR STREAMS UNDER THE INFLUENCE OF HAZARDOUS MAN-MADE OBJECTS

ANISHCHENKO, Lidia<sup>1</sup>; MOSKALENKO, Igor<sup>2\*</sup>; AVRAMENKO, Marina<sup>3</sup>; VOROCHAY, Yuliya<sup>4</sup>; PLAKHOTIN, Aleksey<sup>5</sup>.

<sup>1,2,3,4,5</sup> I.G. Petrovsky Bryansk State University, Department of Geography, Ecology and Land Management. Russian Federation.

\* Correspondence author  
e-mail: moskalenko.hebapsu@bk.ru

Received 26 February 2020; received in revised form 27 May 2020; accepted 09 June 2020

### RESUMO

Os corpos hídricos são os meios mais vulneráveis em termos de impacto causado pelo homem e a coleta de informações de monitoramento sobre o estado da biota e o regime hidroquímico é obrigatória de acordo com as recomendações da Convenção-Quadro da Água. O artigo trata dos arranjos necessários para o monitoramento e análise integrados de bancos de dados analíticos hidrobiológicos e ambientais para fins de prognóstico e remediação em pontos de observação da água afetados por objetos tecnogênicos quimicamente perigosos produzidos pelo homem (armas químicas). O objetivo deste artigo foi apresentar dados de monitoramento hidrobiológico e hidroquímico de rios na área de objetos perigosos fabricados pelo homem (armas químicas), conforme recomendado pela Convenção-Quadro da Água, para uma descrição comparativa das reações da biota aquática europeia aos efeitos do estresse. Foi validado o uso de índices hidrobiológicos e de diversidade biológica para registrar o impacto antropogênico na água. Os recursos dos dados analíticos ambientais para análise adicional da dinâmica das especificações de monitoramento foram identificados. Os parâmetros de escala do monitoramento hidrobiológico com o cálculo da diversidade  $\alpha$ , índice de Shannon e índice de saprobidade devem ser baseados em um exame completo da vegetação e flora aquáticas e semi-aquáticas. A análise do impacto antropogênico de um objeto artificial quimicamente perigoso na região de Bryansk (Federação Russa) em ecossistemas aquáticos por um longo período de tempo usando o método de bioindicação (que consiste na avaliação da diversidade de espécies, cálculo do índice de Shannon e índice de saprobidade da água) revelou que o componente tecnogênico do impacto dos pontos de referência nos cursos de água é mínimo.

**Palavras-chave:** *Monitoramento ambiental integrado, Armas químicas perigosas, Avaliação de impacto, Ions biogênicos, Indicadores hidrobiológicos.*

### ABSTRACT

Water bodies are the most vulnerable mean in terms of human-made impact, and the collection of monitoring information on the state of biota and the hydrochemical regime is mandatory per the recommendations of the Water Framework Convention. The paper deals with the necessary arrangements for integrated monitoring and analysis of hydrobiological and environmental analytical databases for prognostic and remediation purposes at water observation points affected by human-made chemically hazardous technogenic object (chemical weapons). The purpose of this paper was to present data of hydrobiological and hydrochemical monitoring of rivers in the area of hazardous human-made objects (chemical weapons) as recommended by the Water Framework Convention for a comparative description of the reactions of European aquatic biota to stress effects. The use of hydrobiological indices and indices of biological diversity to record the anthropogenic impact on water has been validated. The features of environmental analytical data for additional analysis of monitoring specifications dynamics have been identified. The scale parameters of hydrobiological monitoring with the calculation of  $\alpha$ -diversity, Shannon index, saprobity index should be based on a complete examination of aquatic and semi-aquatic vegetation and flora. The analysis of the anthropogenic impact of a chemically hazardous human-made object in the Bryansk region (Russian Federation) on aquatic ecosystems over a long period of time using bioindication method (which consists in the assessment of species diversity, calculation of the Shannon index and water saprobity index) revealed that the technogenic component of the impact of reference points on watercourses is minimal.

## 1. INTRODUCTION:

The safety of the population in the operation of hazardous technogenic facilities in the Russian Federation and worldwide is a priority task, the solution of which depends on the planning and implementation of integrated environmental monitoring studies, including those conducted at water bodies (Anischenko, 2013; Ashikhmina, 2002, p. 442). A chemically hazardous technogenic object (chemical weapons storage and disposal facility) was in operation for a long time on the territory of the Bryansk region, which is the old-developed region of the Russian Federation.

Water bodies are the most vulnerable objects in terms of human-made impact. Thus, the collection of monitoring information on the state of biota and the hydrochemical regime is mandatory following the recommendations of the Water Framework Convention and is relevant in European countries (Alrumman *et al.*, 2016; European Parliament and Council of the European Union, 2000; Ruiz Jimenez *et al.*, 2011).

When analyzing databases on the current and prospective state of any water bodies, it is necessary to take into account additional environmental factors determining the state of aquatic and semi-aquatic communities, and first of all, the ions of biogenic elements. The presence of ions of biogenic elements, quickly migrating in water, accelerates the development of plant biomass, and also proves to be a limiting and toxic condition for their development (Adesuyi *et al.*, 2015; Mursaleen *et al.*, 2018).

When the facilities make the environmental impact for storage and disposal of chemical weapons, the phosphate ion is recognized as the marker ion for any habitat. Therefore, the detection of an excess amount of this ion in the environment indicates the need for additional monitoring of security systems at the enterprise. Exceeding the maximum permissible concentrations of phosphate ions can be diagnosed in waters based on biomass growth and by increased biodiversity, for example, of pleistophytic communities. A close relationship has been established between such biological indicators as  $\alpha$ -diversity, Shannon index, saprobity index with the concentration of ammonium cation and nitrate ions; dominant biomass and saprobity index are associated with the concentration of phosphate ions (Barinova *et*

*al.*, 2016; Chappuis *et al.*, 2014; Glibert, 2014; Mikulyuk *et al.*, 2011).

In the process of a long-term assessment of any hazardous human-made objects in terms of habitat components, experience in landscapes of the Non-Black Earth Area of the Russian Federation will be in demand, as it is aimed not only at identifying the state of natural ecosystems, but also at revealing the processes of their degradation, providing control of long-term effects (accumulation and transformation in environmental components) of toxic substances and products of their destruction. Bioindicative indicators of aquatic macrophyte communities of small watercourses under the anthropogenic pressure will complement large-scale global hydrobiological studies (Barinova, 2017a; Ostroumov, 2010; Saloua *et al.*, 2017).

The purpose of this paper was to present data of hydrobiological and hydrochemical monitoring of rivers in the area of hazardous man-made objects as recommended by the Water Framework Convention for a comparative description of the reactions of European aquatic biota to stress effects.

## 2. MATERIALS AND METHODS:

Large-scale monitoring of the environment with an integrated focus and analysis of the results was carried out on the premises of this facility at 121 reference points from 2005 to 2016 (Anischenko, 2013; Rybalsky *et al.*, 2007, p. 1144). After the completion of the production cycle, the database of surveys, including those at 5 water reference points, is in demand to optimize observations, assessment, forecast, as well as to arrange remediation measures that are actively deployed on the territory of a chemically hazardous object. The studies of watercourses in the area of a dangerous technogenic object in the Russian Federation were carried out in 2011-2016.

A map of the location of observation points and the location of rivers in the Pochep district of the Bryansk region is shown in Figure 1.

Ecological, production and indication works were carried out based on route survey, on floristic and production analysis of aquatic and semi-aquatic river plants in rivers, as well as on describing the flora of aquatic and semi-aquatic plants; the species was determined taking into



account generally accepted determinants (Karpov and Savostin, 2003, p. 243; Pechenyuk, 2004, p. 129). The nomenclature of species of vascular plants is indicated by the work of S.K. Cherepanov (1995, p. 992).

The aquatic vegetation was surveyed at the reference points of the chemical weapons disposal facility (object 1204) Russian Federation, this vegetation being subject to a powerful anthropogenic impact. The results obtained during the monitoring were to be used for the rehabilitation of water bodies and watercourses.

In the course of the study of aquatic biota, such methods were employed as route, geobotanical methods (according to the recommendations of J. Braun-Blanquet International School (Braun-Blanquet, 1964, p. 865), hydrobiological methods (product definition, calculation of biodiversity indices), statistical methods, the descriptions of which are shown below. To determine the abundance of aquatic plants and the overgrowing of objects, methods of ecological profiling were used on the transects located along-shore and across the entire size of the water body (Karpov and Savostin, 2003; Ramensky, 1909).

The distribution schemes of plant communities were compiled on the basis of maps of the survey area, according to V.G. Papchenkov (Papchenkov, 2003). When geobotanical descriptions are made on the ground, the boundaries of water cenoses were distinguished according to their physiognomic and ecological principles. The sizes of test plots for cenoses descriptions are from 1 to 4 m<sup>2</sup> or within the natural boundaries of communities (Mirkin, 1997). The obtained characteristics of aquatic macrophyte communities were compared to the data of researchers conducted in Europe and Asia (Barinova, 2017b; Chappuis *et al.*, 2012, 2011; Parsons *et al.*, 2011). The names of syntaxons correspond to the code of phytosociological nomenclature, made under the approach of J. Braun-Blanquet (Braun-Blanquet, 1964; Weber *et al.*, 2000).

To measure the biomass on trial plots, from 2 to 4 angle sites of 0.25 m<sup>2</sup> each were laid, the net primary output of hydrophytes was calculated taking into account hydrobiological methods (Mirkin, 1997; Papchenkov, 2003). Floristic diversity is estimated as the number of species on the site of a standard size, as well as the average number of species in the syntaxon coenoflora (Karpov and Savostin, 2003; Shitikov *et al.*, 2003). The uniformity of species is determined using

Simpson and Shannon indices, which were calculated according to standard formulae, with the definition of some statistical characteristics (Lakin, 1990, p. 352; Magarran, 1992, p. 184; Shannon and Weaver, 1998, p. 117; Shitikov *et al.*, 2003, p. 463). The basic ions of biogenic elements were determined by generally accepted standards and were compared with sanitary and hygienic standards (Ministry of Health of the Russian Federation, 2003).

Stationary observation sites are selected following the state environmental monitoring sampling system since information is needed on the background ecological conditions (of air, water, soil). Stationary sites are located according to the following principle: the boundary of the zone of protective measures, ½ of the radius of the zone of protective measures.

The description of plant communities based on the reference points of a chemically dangerous human-made object is presented below.

At point 110, the Costa River, there are communities of *Lemno-Spirodeletum polyrhizae* W. Koch 1954 em. Müll. Et Görs. 1960. Communities are spread in the form of small spots along the backwaters of the river from the depth of 0.2 to 0.7 m. The soil is slightly silty. The total projective cover is 50%.

The coenoses of the association *Lemnetum trisulcae* Kelh. Ex Knapp et Stoffers 1962 with the Far East *Lemna trisulca* are found in the impounded river stretches having a depth of up to 0.7 m. They endure only a weak current and are formed when the illumination is at least 50% of the total. The projective cover is up to 80%. The area of distribution is up to 3-5 m<sup>2</sup>.

Communities of association *Lemno-Hydrocharitetum morsus-ranae* Oberd. 1957, are confined to shallow areas, and described along the banks of the backwaters (mainly up to a depth of 0.6 m), on the stream openings. The total projective cover is from 65%.

The association *Potamogetonetum natantis* Soó 1927, is distributed on silty substrates at a depth of 0.8-1.3 m. *Potamogeton natans* forms the basis of phytocenoses with a projective coating of 75%. Communities are located at a distance of 3-5 meters from the water rim and often have an elongated oval shape. Association *Polygonetum natantis* Soó 1927, these associations are confined to habitats with sandy soils. The distribution depths of phytocenoses are up to 0.95 m. Communities do not form extensive

vegetation, they are encountered in separate «inclusions» along the bank. They are formed when the illumination is from 50 to 100%. The total projective cover of plants is low: from 30 to 65%.

Semi-aquatic communities are mainly formed by the following association communities. The communities of association *Typhetum latifoliae* Nowiński 1930 are common in the riverside strip under study, they are composed of high-grass helophyte - broad-leaved cattail. Plants form small spots, grow to a depth of 0.5 m with silt soils. The total projective cover is up to 90%. The communities of association *Phragmitetum australis* Savnič 1926, are formed along the river banks, and often form a solid «wall» of plants. Semi-aquatic communities grow on medium silty soils, the total projective cover of species is 98%.

Communities of the association *Sagittario sagittifoliae-Sparganietum emersi* Tüxen 1953, are two-tiered, and are composed only of gelophytic species growing on heavily silty soils under conditions of significant lighting of up to 90-100%.

Communities of the association *Rorippo-Phalaridetum arundinaceae* Kopecký 1961, are two-tiered with a total projective cover of up to 100%. They are formed on silty soils, and on the coast – on heavy clay loam.

At point 142 - the Semchanka River there are communities of the association *Lemno-Spirodeletum polyrhizae* W. Koch 1954 em. Müll. Et Görs. 1960, which are distributed throughout the profile of the study area to a depth of 0.4 m with slightly silty soil. The total projective cover is 40%. The communities of Ass. *Elodeetum canadensis* Egler 1933, are distributed in small spots in shallow waters at shallow depths of up to 0.35 m, on silty soils.

Phytocenoses of ass. *Lemno-Sagittarietum natantis* Taran et Tyurin 2005, LW: *Sagittaria sagittifolia*, *Lemna minor*, were registered in areas with sandy-silt soil, and with illumination from 60 to 90%. The total projective cover is from 30 to 65%.

The semi-aquatic communities dominating in the coastal strip are listed below: *Rorippo-Phalaridetum arundinaceae* Kopecký 1961, *Phragmitetum australis* Savnič 1926, *Butometum umbellati* Philippi 1973 which are formed in the shallow waters of the explored river habitats; they are single-tier, monodominant communities, sometimes with a small mixture of floating manna grass. The total projective cover is up to 65%.

Communities of Ass. *Oenanthera aquatica-Rorippetum amphibiae* Lohmeyer 1950, are widely distributed in riverside shallow waters to a depth of 0.3 m in well-lit habitats with silty soils.

In conditions of point 78 - in the Horn River - communities of associations *Lemno-Spirodeletum polyrhizae* W. Koch 1954 em. Müll. Et Görs. 1960, *Lemno-Hydrocharitetum morsuranae* Oberd. 1957, *Potamogetonetum natantis* Soó 1927 are formed.

Communities of Ass. *Ceratophylletum demersi* (Soó 1928) Egler 1933, are registered in the shallow places of the river backwater. Water depths are insignificant - mostly up to 0.5 m. The soil has substantial silt deposit. Association communities occupy the entire water column to the very bottom.

The association *Potamogetonetum lucentis* Huek 1931, the total projective cover of plants in the community is from 60 to 95%. These communities are described in the river to a depth of 1.5 m. The soil in the reservoir is the most diverse: from sandy to heavily silty. Communities evolve when illuminated from 60 to 100%.

The semi-aquatic communities are few in terms of the composition of the cenoses participating in the establishment of vegetation: ass. *Typhetum latifoliae* Nowiński 1930, *Oenanthera aquatica-Rorippetum amphibiae* Lohmeyer 1950, *Sagittario sagittifoliae-Sparganietum emersi* Tüxen 1953.

Association *Equisetetum fluvialitis* Nowiński 1930, is formed on silty soils, in the backwaters of the river to a depth of 0.3 m with a single-tier structure. The total projective cover is small - 45%.

### 3. RESULTS AND DISCUSSION:

The survey of macrophytes, as well as semi-aquatic plants in the biomonitoring system, is a recommended direction for collecting data for the monitoring base, since these objects are highly informative, they are distributed as background ones in aquatic habitats, and have high accumulative capacities (Barinova, 2017a, 2017b; Bolpagni et al., 2012; Bornette and Puijalon, 2011).

Monitoring indicators of the status of water macrophytes and saprobity indices, which form the basis of hydrobiological monitoring in any water objects, are presented for aquatic and semi-aquatic communities during the period of active

observations and active production cycle at the chemical weapons disposal facility.

Hydrobiological indices are determined as indicators of biological diversity in reference points (Table 1, Table 2).

The analysis of the reference points obtained as a result of water biomonitoring using the bioindication method indicates a favorable state of the environment, corresponding to its background state.

The species diversity of macrophytes and semi-aquatic vegetation is high, the Shannon index is significant. The species composition is represented by typically river species of 6 ecological groups. The human-made impact on the watercourse is minimal. The studies of saprobity showed the absence of oxygen starvation, significant overgrowth of the river; the water is clear. The quality of water and the condition of the water body, assessed according to the biomass and dominants productivity, is favorable and characteristic of natural hydrocenoses. The research results did not reveal the impact of a man-made object on the water flow of reference points.

Saprobity indices are shown in Table 3.

The studies of saprobity showed the absence of oxygen starvation, significant overgrowth of the river; the water is clear. The quality of water and the condition of the water body, assessed according to the biomass and dominants productivity, is favorable and characteristic of natural hydrocenoses. The research results did not reveal the impact of a human-made object on the water flow of reference points.

The saprobity indices calculated when conducting monitoring studies in other years using aquatic macrophytes are shown in Table 4.

The studies of saprobity showed the absence of oxygen starvation, significant overgrowth of the river; the water is clear. The quality of water and the condition of the water body, assessed according to the biomass and dominants productivity, is favorable and characteristic of natural hydrocenoses. The research results did not reveal the impact of a man-made object on the water flow of reference points.

To add the data to the database and have their reliable processing, the biomonitoring indicators in the reference points of a chemically hazardous human-made object were supplemented with ecoanalytic signs of water,

obtained following the provisions of the GOST R (Russian National Standard) system.

The dependence of the biological indicators of macrophyte communities on the hydrochemical parameters of water ( $C(NH_4^+)$ ,  $C(NO_3^-)$ ,  $C(PO_4^{3-})$ , mg/l) is represented by the following parameters (Table 5).

The results of statistical analysis of the Shannon index dependence on the content of ammonium ions, which was calculated for macrophyte communities, revealed a significant interrelation of the two values. Still, the most substantial is the effect of the increased concentration of ammonium-containing compounds on the increase in  $\alpha$ -diversity (Figure 2). The dominants biomass does not correlate with the concentration of the ions under consideration.

A linear dependence between the content of nitrate ions and the calculated Shannon index has not been revealed. However, an increase in the concentration of nitrate ions causes a regular increase in  $\alpha$ -diversity (Figure 3) and indicators of saprobity index (the equations are given in Table 6)

A high correlation dependence was revealed between the phosphate content in the points under study and the dominant biomass; the dependence of the calculated saprobity index on the concentration of phosphorus-containing compounds is also high (Figure 4).

Thus, a close relationship between biological indicators:  $\alpha$ -diversity, Shannon index, saprobity index was revealed for the concentration of ammonium cation and nitrate ions, the dominant biomass, and saprobity index are related to the concentration of phosphate ions.

The bioindication method, widely used for the diagnostic assessment of aquatic ecosystems, showed the possibility of its use in terms of the recommendations of the Water Framework Directive of the European Union for small European watercourses. In the monitoring area of a chemical hazardous technogenic object of the Russian Federation, semi-aquatic and aquatic vegetation is represented by two classes of 4 orders, 5 unions and 12 associations, which is determined by the latitudinal gradient and Central European conditions for the development of communities. The number of vegetation species that constitute the community remained unchanged for all years of research (from 63 to 74 species), typically river macrophytes dominate, the change of ecological groups is not registered,

the indicators of  $\alpha$ -diversity indicate a considerable diversity of community species. Indicators of the Shannon index for communities testify to the background state of the waters, the absence of the stressful influence of a man-made object, and are similar to the results obtained by other authors (Bornette and Puijalon, 2011; Chappuis *et al.*, 2011; Moore *et al.*, 2012). Geobotanical and ecological characteristics of aquatic macrophyte communities, which were taken into account for hydrobiomonitoring works of semi-aquatic communities are similar to data obtained in the course of European studies.

A slight change in plant production (biomass) was recorded within the statistical significance of differences due to the dynamics of climatic factors affecting the plants production. The Overgrowing of backwaters of small rivers is small, as the flow factor determines the development of a particular biomass of macrophytes and semi-aquatic plants. Consequently, it is recommended to employ ecological and biological indicators and their change for small rivers under the stressful impact of man-made objects during long-term monitoring work: changes in the spatial and species composition of communities, species diversity and ecological groups of species indicate the direct and indirect effects on river waters (Mikulyuk *et al.*, 2011; Steffen *et al.*, 2014).

According to the index of ecological quality of water bodies, recommended by the Water Framework Convention, the biological elements of the rivers of the Non-Black Earth Region of the Russian Federation show a "good" state of the waters.

The ecological state of waters at the reference points of a dangerous man-made object is also determined by hydrochemical indicators, primarily biogenic ions, oxygen availability, saprobity, which indirectly determines the oxygen regime; as well as by hydrophysical indicators: water consumption, continuity of the water flow and others (Ali *et al.*, 2014; Guggenmos *et al.*, 2011).

Long-term observations of the river water saprobity have shown the absence of oxygen starvation, the preservation of significant water flow. A change in the saprobity index from 2.1 to 2.7 (beta-mesosaprobic zone) corresponds to the European indicators and is typical of natural cenoses (Bolpagni *et al.*, 2012; Bornette and Puijalon, 2011; Chappuis *et al.*, 2012, 2011; Ramavandi and Farjadfard, 2014). Thus, hydrobiological and hydrochemical parameters

are interrelated, and aquatic biota directly determines the chemical parameters of the watercourses under study, which has been proven by many studies (Guggenmos *et al.*, 2011).

Technologically determined methods for controlling discharges into water bodies of the area under study have proven high efficiency: the concentrations of biogenic ions in flowing waters correspond to the most stringent indicators of the Russian rationing. The significant connection between the concentration of ammonium-containing compounds, nitrate ions and the increase in the  $\alpha$ -diversity of vegetation is understandable since aquatic species most successfully absorb nitrogen compounds in this form (Ali *et al.*, 2014).

Phosphate ions that serve as markers for dangerous technogenic objects for the disposal of chemical compounds are the limiting indicators for the development of all aquatic biota according to the empirical rule of J. Liebig. The presence of phosphates in river waters determines the growth of biomass (production) and determines the estimated index of saprobity of monitoring objects (Ali *et al.*, 2014; Guggenmos *et al.*, 2011). According to the recommendations of the Water Framework Convention, in determining the environmental quality of water bodies, it is mandatory to take into account hydromorphological parameters, including bottom sediments, determined by phosphoric compounds. Measuring and controlling water ions of biogenic elements are significant for hydrochemical studies (Barinova, 2017a, 2017b; Bolpagni *et al.*, 2012; Ostroumov, 2010). When the excess concentration of biogenic ions in water is revealed, it is possible to recommend the use of macrophyte biomass for ion sorption and phytoremediation of water bodies (Naghipour *et al.*, 2016; Ramavandi and Farjadfard, 2014; Ruiz Jimenez *et al.*, 2011).

#### 4. CONCLUSIONS:

The analysis of the anthropogenic impact on aquatic ecosystems of a chemically hazardous man-made object in the Bryansk region (Russian Federation) using the method of bioindication (which consists in the assessment of species diversity, calculation of the Shannon index and water saprobity index) revealed that the technogenic component of the impact on watercourses is minimal, the state of water bodies corresponds to natural hydrocenoses, the water is clean.

In the monitoring area of a chemical hazardous technogenic object of the Russian Federation, semi-aquatic and aquatic vegetation is represented by two classes of 4 orders, 5 unions and 12 associations, which is determined by the latitudinal gradient and Central European conditions for the development of communities. Indicators of the Shannon index for communities testify to the background state of the waters, the absence of the stressful influence of a man-made object. It is recommended to employ ecological and biological indicators and their change for small rivers under stressful impact of man-made objects during long-term monitoring work: changes in the spatial and species composition of communities, species diversity and ecological groups of species indicate the direct and indirect effects on river waters. Long-term observations of the river water saprobity have shown the absence of oxygen starvation, the preservation of significant water flow. A change in the saprobity index from 2.1 to 2.7 (beta-mesosaprobic zone) corresponds to the European indicators and is typical of natural cenoses.

Thus, the proposed indicators for the organization of hydrobiological monitoring of hazardous man-made objects and their effect on water stand is most preferable. When analyzing the databases on the current and prospective state of any water bodies, it is necessary to take into account additional environmental factors determining the state of aquatic and semi-aquatic communities: first of all, ions of biogenic elements. The presence of these easily migrating ions in water accelerates the development of plant biomass, and also turns out to be a limiting and toxic condition for their development.

When facilities cause the environmental impact for the storage and disposal of chemical weapons, the phosphate ion is recognized as the marker ion in any habitat. Therefore, the detection of an excess amount of this ion in the environment indicates the need for additional monitoring of security systems in the enterprise. Exceeding the maximum permissible concentrations of phosphate ions can be diagnosed in the waters both by biomass growth and by increasing biodiversity, for example, of pleistophytic communities.

## 5. COMPLIANCE WITH ETHICAL STANDARDS:

This article does not contain any studies involving human participants or animals performed by any of the authors.

## 6. FUNDING:

No funding was received.

## 7. CONFLICT OF INTEREST:

The authors report no conflict of interest.

## 8. REFERENCES:

1. Adesuyi, A.A., Nnodu, V.C., Njoku, K.L. & Jolaoso, A. (2015). Nitrate and Phosphate Pollution in Surface Water of Nwaja Creek, Port Harcourt, Niger Delta, Nigeria. *International Journal of Geology, Agriculture and Environmental Sciences*, 3(5), 14-20.
2. Anischenko, L.N. (2013). Biomonitoring block in the eco-analytical control of chemically hazardous man-made systems (as exemplified by the chemical weapons disposal facility, 1204, Bryansk Region). *Theoretical and applied ecology*, 3, 40-46.
3. Ashikhmina, T.Ya. (2002). Comprehensive environmental monitoring of facilities for the storage and destruction of chemical weapons: theory, methodology, practice: Dis. ... doc tech. sciences (p. 442). Kirov.
4. Barinova, S. (2017). On the Classification of Water Quality from an Ecological Point of View. *Int J Environ Sci Nat Res.*, 2 (2), 555581. DOI: 10.19080/IJESNR.2017.02.555581.08
5. Barinova, S. (2017). Essential and Practical Bioindication Methods and Systems for the Water Quality Assessment. *Int J Environ Sci Nat Res.*, 2(3), 555588. DOI: 10.19080/IJESNR.2017.02.555588
6. Barinova, S., Khuram, I. Asadullah, Ahmad, N. Jan, S. et al. (2016). How water quality in the Kabul River, Pakistan, can be determined with algal bio-indication. *Advance Studies in Biology*, 8(4), 151-171.
7. Bolpagni, R., Fanelli, G., Oggioni, A. & Testi A. (2012). Macrophyte indicators of environmental quality of rivers in Italy at local, regional and geographical scales. *Aquatic Plants and Plant Diseases*, 147-171.
8. Bornette, G. & Puijalon, S. (2011). Response of aquatic plants to abiotic factors: a review. *Aquatic Sciences*, 73, 1–14.

9. Braun-Blanquet, J. (1964). *Pflanzensoziologie. Grundzuge der Vegetationskunde*. 3Aufl. (p. 865). Wien-New York: Springer-Verlag.
10. Chappuis, E., Ballesteros, E. & Gacia, E. (2011). Aquatic macrophytes and vegetation in the Mediterranean area of Catalonia: patterns across an altitudinal gradient. *Phytocoenologia*, 41(1), 35–44.
11. Chappuis, E. Ballesteros, E. & Gacia, E. (2012). Distribution and richness of aquatic plants across Europe and Mediterranean countries: patterns, environmental driving factors and comparison with total plant richness. *Journal of Vegetation Science*, 23, 985–997.
12. Chappuis, E., Gacia E. & Ballesteros E. (2014). Environmental factors explaining the distribution and diversity of vascular aquatic macrophytes in a highly heterogeneous Mediterranean region. *Aquatic Botany*, 113, 72–82.
13. Cherepanov, S.K. (1995). Vascular plants of Russia and neighboring countries (within the former USSR) (p. 992). SPb: World and Family (Mir I Semya).
14. Directive 2000/60/EC of the European Parliament and of the Council of 23 October 2000 establishing a framework for Community action in the field of water policy OJ L 327. (2000, December 22). (p. 1–73).
15. Elham, M.A., Shabaan-Dessouki, S. A., Abdel Rahman, I. S., Ahlam & Shenawy S. El. (2014). Characterization of Chemical Water Quality in the Nile River, Egypt. *Int. J. Pure App. Biosci.* 2 (3), 35-53
16. Glibert, P. M. (2014). Harmful Algal Blooms in Asia: an insidious and escalating water pollution phenomenon with effects on ecological and human health. *ASIANetwork Exchange: A Journal for Asian Studies in the Liberal Arts*, 21, 52-68.
17. GN 2.1.5.1315-03. The maximum permissible concentrations (MPC) of chemicals in water bodies of drinking, household, cultural and social water use facilities (with amendments of August 30, 2016), 78. (2003, April 30). Neftyanik Printing House.
18. Guggenmos, M.R., Daughney, C.J., Jackson, B.M. & Morgenstern, U. (2011). Regional-scale identification of groundwater-surface water interaction using hydrochemistry and multivariate statistical methods, Wairarapa Valley, New Zealand. *Hydrology and Earth System Sciences*, 15(11), 3383 – 3398.
19. Karpov, Yu.A. & Savostin A.P. (2003). *Methods of sampling and sample preparation* (p.243). Moscow: BINOM. Laboratory of Knowledge.
20. Lakin, G.F. (1990). *Biometrics* (p. 352). Moscow: Vysshaya Shkola.
21. Magarran, E. (1992). *Biological diversity and its measurement* (p. 184). Moscow: Mir.
22. Mikulyuk, A., Sharma, S., Van Egeren, S., Erdmann, E., Nault, M.E. & Hauxwell J. (2011). The relative role of environmental spatial and land-use patterns in explaining aquatic macrophyte community composition. *Canadian Journal of Fisheries and Aquatic Sciences* 68, 1778–1789.
23. Mirkin, B.M. (1997). Classification of vegetation: current state and a look into the past. *Bull. MOIP Department of biology*, 102(3), 5-13.
24. Moore, M.J.C., Langrehr, H.A. & Angradi, T.R. (2012). A submerged macrophyte index of condition for upper Mississippi River. *Ecological indicator*, 13, 19-205.
25. Mursaleen, Shah, S.Z., Ali, L., Ahmad, N., Khuram, I. & Barinova, S. (2018). Bioindication of water quality by algal communities in the Mardan River, Pakistan. *International Journal of Biology and Chemistry*, 11 (1), 65–81.
26. Naghipour, D., Taghavi, K., Jaafari, J., Mahdavi, Y., Ghanbari Ghoskiali, M., Ameri, R. Jamshidi, A. & Hossein Mahvi, A. (2016). Statistical modeling and optimization of the phosphorus biosorption by modified Lemna minor from aqueous solution using response surface methodology (RSM). *Desalin Water Treat*, 57, 19431–19442.
27. Ostroumov, S.A. (2010). Biocontrol of water quality: Multifunctional role of biota in water self-purification. *Russian Journal of General Chemistry*, 80(13), 2754–2761.
28. Papchenkov, VG. (2003). Macrophyte production of waters and methods for studying it. *Hydrobotany: Methodology, methods: Materials of the Hydrobotany*

- School* (pp. 137-145). Rybinsk: Rybinsk Press House.
29. Parsons, J.K., Marx, G.E. & Divens, M. (2011). A study of Eurasian watermilfoil, macroinvertebrates and fish in a Washington lake. *J Aquat Plant Manage*, 49, 71-82.
  30. Pechenyuk, Ye. V. (2004). *Atlas of higher aquatic and semi-aquatic plants* (p. 129). Voronezh: Voronezh State University.
  31. Rahou, B.S., Lahsen, A.Ch., Soumaya, H. & Mellal, B. (2017). Evaluation of Biological Water Quality by Biological Macrophytic Index in River: Application on the Watershed of Beht River. *European Scientific Journal*, 13(27), 217- 224.
  32. Ramavandi, B. & Farjadfard, S. (2014). Removal of chemical oxygen demand from textile wastewater using a natural coagulant, *Korean J. Chem. Eng.*, 31(1), 81–87.
  33. Ramensky, L. G. (1909). Water and riverside vegetation. Program for botanic and geographical research. St. Petersburg, 1, 1-34.
  34. Ruiz, C.G., Martinez, M. T. & Camacho, A. (2011). A Review: macrophytes in the Assessment of Spanish Lakes Ecological Status Under the Water Framework Directive (WFD). *Ambientalia*, 1–25.
  35. Rybalsky N.G., Samotesova E.D., Mityukova A.G. (Ed.). (2007). *Natural resources and the environment of the Bryansk region* (p. 1144). Moscow: NIA: Priroda.
  36. Shannon, C.E. & Weaver, W. (1963). *The mathematical theory of communication* (p. 117) Urbana: Illinois Univ. Press.
  37. Shitikov, V.K., Rosenberg, G.S. & Zinchenko, T.D. (2003). *Quantitative hydroecology: methods of system identification* (p. 463). Tolyatti: Publishing house of the Samara Scientific Center of the Russian Academy of Sciences.
  38. Steffen, K., Leuschner C., Müller U., Wiegler G., & Becker, T. (2014). Relationships between macrophyte vegetation and physical and chemical conditions in northwest German running waters. *Aquatic Botany*, 113, 46–55.
  39. Sulaiman, A., Alrumman, Attalla F., El-kott, Sherif M. A. & Keshk S. (2016). Water Pollution: Source & Treatment. *American Journal of Environmental Engineering*, 6(3), 88-98.
  40. Weber, H.E., Moravec, J. & Theourillat, D.-P. (2000). International Code of Phytosociological nomenclature. 3<sup>rd</sup> additional. *Journal of Vegetation Science*, 11(5), 739-768.

**Table 1.** The main indicators of water macrophytes in test sites of reference points

| Points | Data  | Prior data (2011) | Data (2013)        | Data (2015)      | Conclusions  |
|--------|---|-------------------|--------------------|------------------|--|
| 78     | Number of species of macrophytes and semi-aquatic plants ( $\alpha$ -diversity) / species diversity index | 74 / 1.28         | 74 / 1.28          | 74 / 1.28        | The species composition of macrophytes and semi-aquatic species has not changed.   |
|        | Dominants biomass (kg/m <sup>2</sup> of dry matter)   | 2.3               | 2.3                | 2.9              | The biomass of three dominants has increased. The biomass is considerable, which testifies to background conditions of aquatic environments. |
|        | Primary production of dominants (tons)  | 0.023 per year    | 0.023 per year     | 0.031 per year   | The production has increased.  |
|        | The degree of weediness of the area under study % / class   | 9 % / 1st class   | 9 % / 1st class    | 11 % / 1st class | The weediness of the riverside sections is insignificant, indicating a good flow of water.   |
| 142    | Number of species of macrophytes and semi-aquatic plants ( $\alpha$ -diversity) / species diversity index | 65 / 1.04         | 65 / 1.04          | 65 / 1.04        | The species composition of macrophytes and semi-aquatic species has not changed.   |
|        | Dominants biomass (kg/m <sup>2</sup> of dry matter)   | 2.8               | 2.9                | 3.5              | The biomass of three dominants has increased. The biomass is considerable, which testifies to background conditions of aquatic environments. |
|        | Primary production of dominants (tons)  | 0.036 per year    | 0.032 per year     | 0.039 per year   | The production has increased.  |
|        | The degree of weediness of the area under study % / class   | 9.8 % / 1st class | 10.2 % / 1st class | 11 % / 1st class | The weediness of the riverside sections is insignificant, indicating a good flow of water.   |
| 110    | Number of species of macrophytes and semi-aquatic plants ( $\alpha$ -diversity) / species diversity index | 63 / 1.06         | 63 / 1.06          | 63 / 1.06        | The species composition of macrophytes and semi-aquatic species has not changed.   |
|        | Dominants biomass (kg/m <sup>2</sup> of dry matter)   | 2.1               | 2.25               | 3.5              | The biomass of three dominants has increased. The biomass is considerable, which testifies to background conditions of aquatic environments. |
|        | Primary production of dominants (tons)  | 0.019 per year    | 0.019 per year     | 0.024 per year   | The production has increased.  |
|        | The degree of weediness of the area under study % / class   | 8.3 % / 1st class | 8 % / 1st class    | 11 % / 1st class | The weediness of the riverside sections is insignificant, indicating a good flow of water.   |



**Table 2.** The main indicators of water macrophytes in test sites of reference points

| Points | Data  | Data (2012)        | Data (2015)      | Data (2016)        | Conclusions  |
|--------|---|--------------------|------------------|--------------------|--|
| 78     | Number of species of macrophytes and semi-aquatic plants ( $\alpha$ -diversity) / species diversity index | 74 /1.28           | 74 /1.28         | 73 /1.28           | The species composition of macrophytes and semi-aquatic species has decreased (insignificantly).   |
|        | Dominants biomass (kg/m <sup>2</sup> of dry matter)   | 2.3                | 2.9              | 2.7                | The biomass of three dominants has increased. The biomass is considerable, which testifies to background conditions of aquatic environments. |
|        | Primary production of dominants (tons)  | 0.023 per year     | 0.031 per year   | 0.027 per year     | The production has increased.  |
|        | The degree of weediness of the area under study % / class   | 9 % / 1st class    | 11 % / 1st class | 9,0 % / 1st class  | The weediness of the riverside sections is insignificant, indicating a good flow of water.   |
| 142    | Number of species of macrophytes and semi-aquatic plants ( $\alpha$ -diversity) / species diversity index | 65 /1.04           | 65 /1.04         | 65 /1.04           | The species composition of macrophytes and semi-aquatic species has not changed.   |
|        | Dominants biomass (kg/m <sup>2</sup> of dry matter)   | 2.9                | 3.5              | 3.9                | The biomass of three dominants has increased. The biomass is considerable, which testifies to background conditions of aquatic environments. |
|        | Primary production of dominants (tons)  | 0.032 per year     | 0.039 per year   | 0.032 per year     | The production has decreased.  |
|        | The degree of weediness of the area under study % / class   | 10.2 % / 1st class | 11 % / 1st class | 10.2 % / 1st class | The weediness of the riverside sections is insignificant, indicating a good flow of water.   |
| 110    | Number of species of macrophytes and semi-aquatic plants ( $\alpha$ -diversity) / species diversity index | 63 /1.06           | 63 /1.06         | 63 /1.06           | The species composition of semi-aquatic species has not changed.   |
|        | Dominants biomass (kg/m <sup>2</sup> of dry matter)   | 2.25               | 3.5              | 3.5                | The biomass of three dominants has increased. The biomass is considerable, which testifies to background conditions of aquatic environments. |
|        | Primary production of dominants (tons)  | 0.019 per year     | 0.024 per year   | 0.024 per year     | The production has not changed.  |
|        | The degree of weediness of the area under study %/class   | 8 % / 1st class    | 11 % / 1st class | 11 % / 1st class   | The weediness of the riverside sections is insignificant, indicating a good flow of water.   |

**Table 3.** The state of waters on test sites of reference points according to the saprobity index using macrophytes

| Points | Data (2011)                | Data (2013)                | Data (2015)                | Conclusions   |
|--------|----------------------------|----------------------------|----------------------------|---|
| 78     | 2.3 beta-mesosaprobic zone | 2.5 beta-mesosaprobic zone | 2.4 beta-mesosaprobic zone | Saprobity has not changed, the saprobity index indicates the medium decomposition of organic matter, and the background state of water. |
| 142    | 2.7 beta-mesosaprobic zone | 2.7 beta-mesosaprobic zone | 2.5 beta-mesosaprobic zone | Saprobity has decreased, the saprobity index indicates the medium decomposition of organic matter and the background state of water.    |
| 110    | 2.1 beta-mesosaprobic zone | 1.9 beta-mesosaprobic zone | 2.2 beta-mesosaprobic zone | Saprobity has increased, the saprobity index indicates the medium decomposition of organic matter and the background state of water.    |

**Table 4.** The state of waters on test sites of reference points according to the saprobity index using macrophytes

| Points | Data (2012)                | Data (2015)                | Data (2016)                | Conclusions   |
|--------|----------------------------|----------------------------|----------------------------|---|
| 78     | 2.5 beta-mesosaprobic zone | 2.4 beta-mesosaprobic zone | 2.4 beta-mesosaprobic zone | Saprobity has not changed, the saprobity index indicates the medium decomposition of organic matter, and the background state of water.       |
| 142    | 2.7 beta-mesosaprobic zone | 2.5 beta-mesosaprobic zone | 2.7 beta-mesosaprobic zone | Saprobity has slightly increased, the saprobity index indicates the medium decomposition of organic matter and the background state of water. |
| 110    | 1.9 beta-mesosaprobic zone | 2.2 beta-mesosaprobic zone | 2.0 beta-mesosaprobic zone | Saprobity has decreased, the saprobity index indicates the medium decomposition of organic matter and the background state of water.          |

**Table 5.** Dependence of biological indicators of macrophyte communities on hydrochemical water parameters ( $C\ NH_4^+$ ) in reference observation points of a chemically dangerous man-made object

| Reference points (r.p.) / indicators     | $C\ NH_4^+$ | Shannon index   | $\alpha$ -diversity | Dominants biomass (kg/m <sup>2</sup> of dry matter) | Saprobity index |
|--|-------------|-----------------|---------------------|---|-----------------|
| r.p. 78                                  | 0.46        | 1.28            | 74                  | 2.45  | 2.43            |
| r.p. 110                                 | 0.33        | 1.06            | 63                  | 2.52  | 2.02            |
| r.p. 142                                 | 0.41        | 1.04            | 65                  | 3.03  | 2.65            |
| Correlation index (r)                    |             | <b>0.7444*</b>  | <b>0.8849</b>       | 0.02167565  | <b>0.7369</b>   |
| Correlation and regression equation      |             | y=1.5116x+0.522 | y=79.07x+35.705     | -   | y=3.593x+0.9295 |
| Reliable approximation (R <sup>2</sup> ) |             | <b>0.5541</b>   | <b>0.783</b>        | -   | <b>0.543</b>    |

**Table 6.** Dependence of biological indicators of macrophyte communities on hydrochemical water parameters ( $C(NO_3^-)$ ) in reference observation points of a chemically dangerous man-made object

| Reference points (r.p.) / indicators     | $C NO_3^-$ | Shannon index      | $\alpha$ -diversity | Dominants biomass (kg/m <sup>2</sup> of dry matter) | Saprobity index    |
|--|------------|--------------------|---------------------|---|--------------------|
| r.p. 78                                  | 3.9        | 1.28               | 74                  | 2.45  | 2.43               |
| r. p. 110                                | 1.93       | 1.06               | 63                  | 2.52  | 2.02               |
| r.p.142                                  | 3.4        | 1.04               | 65                  | 3.03  | 2.65               |
| Correlation index (r)                    |            | 0.64043199         | <b>0.8086*</b>      | 0.16543099  | <b>0.8266</b>      |
| Correlation and regression equation      |            | y=0.0833x + 0.8704 | y=4.6267x + 53.099  | -   | y=0.2581x + 1.5726 |
| Reliable approximation (R <sup>2</sup> ) |            | 0.4102             | <b>0.6538</b>       | -   | <b>0.6832</b>      |

**Table 7.** Dependence of biological indicators of macrophyte communities on hydrochemical water parameters ( $PO_4^{3-}$ ) in reference observation points of a chemically dangerous man-made object

| Reference points (r.p.) / indicators     | $PO_4^{3-}$ | Shannon index   | $\alpha$ -diversity | Dominants biomass (kg/m <sup>2</sup> of dry matter) | Saprobity index    |
|--|-------------|-----------------|---------------------|---|--------------------|
| r.p. 78                                  | 0.33        | 1.28            | 74                  | 2.45  | 2.43               |
| r. p. 110                                | 0.25        | 1.06            | 63                  | 2.52  | 2.02               |
| r.p.142                                  | 0.8         | 1.04            | 65                  | 3.03  | 2.65               |
| Correlation index (r)                    |             | <b>-0.4473*</b> | <b>-0.2154</b>      | <b>0.9699</b>                                       | <b>0.8467</b>      |
| Correlation and regression equation      |             | -               | -                   | y=1.0334x + 2.1913                                  | y=0.2581x + 1.5726 |
| Reliable approximation (R <sup>2</sup> ) |             | -               | -                   | <b>0.9408</b>                                       | <b>0.6832</b>      |

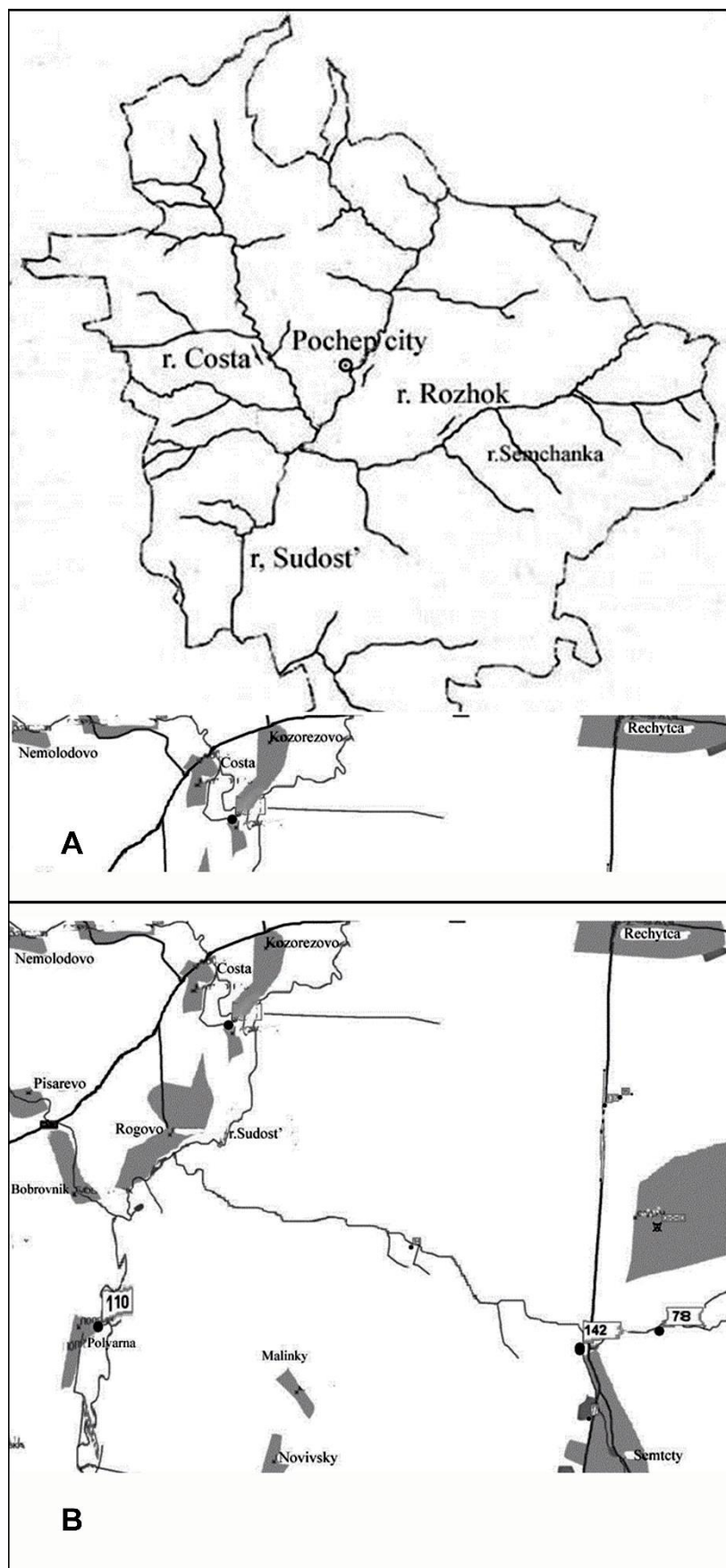


**Figure 1.** The map of the rivers of the Pochep district of the Bryansk region (Russian Federation) (A) and the position of observation points (B)

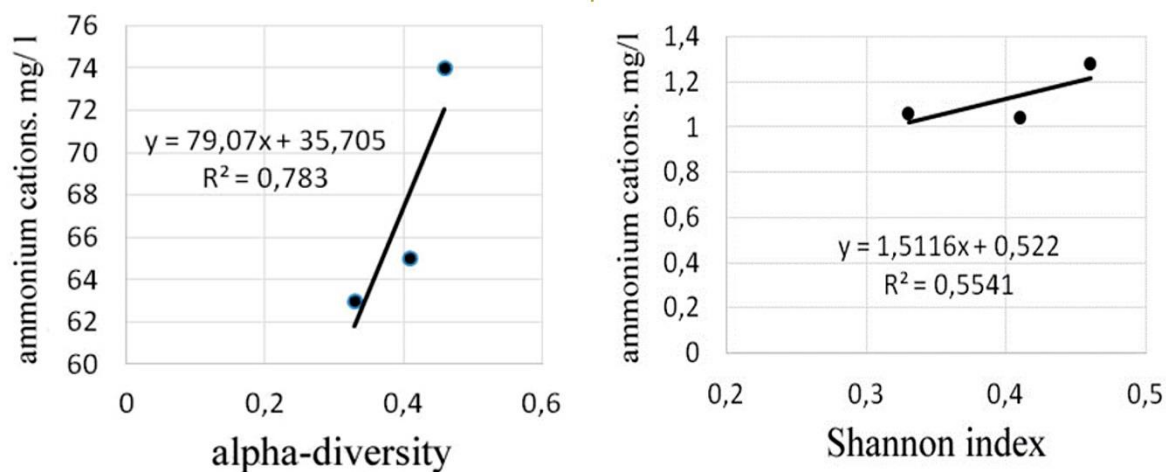


**Figure 2.** Dependence of biological indicators of macrophyte communities on the concentration of ammonium ions ( $\text{NH}_4^+$ )

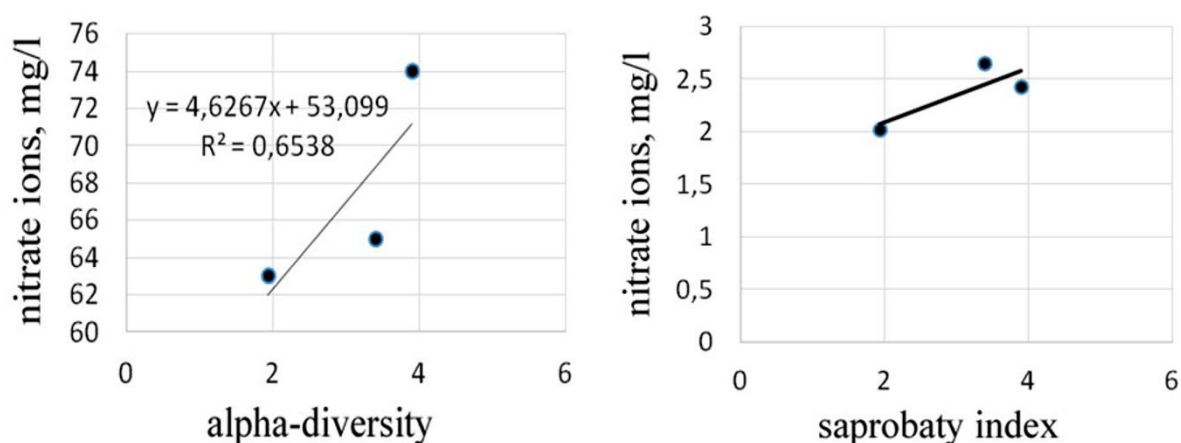


**Figure 3.** Dependence of biological indicators of macrophyte communities on nitrate ions ( $\text{NO}_3^-$ ) concentration

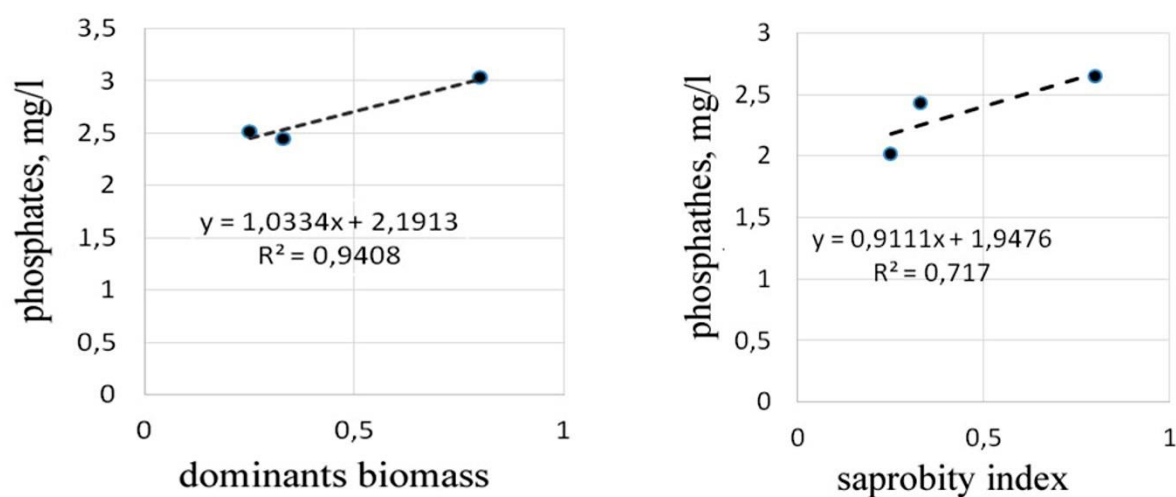


**Figure 4.** Dependence of biological indicators of macrophyte communities on phosphate ions ( $\text{PO}_4^{3-}$ ) concentration

**TESTE DE CONHECIMENTO DE CONCEITOS DE VETORES ELEMENTARES ENTRE ESTUDANTES DO PRIMEIRO SEMESTRE DE BACHARELADO EM ENGENHARIA E DE TECNOLOGIA****TEST OF KNOWLEDGE OF ELEMENTARY VECTORS CONCEPTS AMONG FIRST-SEMESTER BACHELOR OF ENGINEERING AND TECHNOLOGY STUDENTS**

ALAM, Ashraf\*

University of Delhi, Department of Education. India.

\* Corresponding author  
e-mail: ashraf\_alam@live.com

Received 30 January 2020; received in revised form 29 May 2020; accepted 08 June 2020

**RESUMO**

A física, como disciplina acadêmica, possui uma linguagem matemática própria e os vetores são seu constituinte indispensável, mesmo no estágio pré-obrigatório. O objetivo desse estudo foi obter um entendimento claro e profundo sobre a percepção da cognição dos alunos sobre as facetas dos vetores que formam a base da mecânica newtoniana. Este estudo fornece não apenas o conhecimento fundamental sobre a cognição de construções fundamentais de vetores entre os alunos, mas também ajuda a melhorar as pedagogias existentes e, eventualmente, levando ao discernimento dos alunos. O autor desenvolveu um Teste de Conhecimento de Conceitos de Vetor Elementar (TKEVC) que foi entregue aos estudantes de engenharia do primeiro semestre que estavam iniciando o curso obrigatório de física de engenharia durante a 1ª semana de aula, antes de qualquer instrução sobre vetores. O TKEVC foi administrado em uma amostra de 476 alunos provenientes de 7 faculdades e universidades de engenharia diferentes da Índia. O resultado obtido com este teste enuncia que apenas 37% dos alunos matriculados no curso de física de engenharia possuem amplo conhecimento de vetores para avançar com tópicos de física, especificamente mecânica, enquanto quase 67% dos estudantes ingressam no curso sem uma compreensão completa dos princípios dos vetores em qualquer aspecto. Essas descobertas têm implicações fortes para as aulas de matemática e física. O pesquisador discutiu as perguntas feitas aos alunos e suas respostas, enfatizando os erros conceituais e metodológicos que eles cometeram. Os resultados têm fortes implicações no ensino de matemática e física de engenharia, no desenvolvimento profissional de professores e na preparação de equipes de professores para instituições de engenharia.

**Palavras-chave:** *Aprendizagem, Educação matemática, Adição de vetor, Direção de vetor, Magnitude de vetor.*

**ABSTRACT**

Physics, as an academic discipline, has its mathematical language, and vectors are its indispensable constituent, even at the pre-mandatory stage. This study aimed to obtain a clear and deep understanding of the perception of students' cognition about the facets of the vectors that form the basis of Newtonian mechanics. This study not only provides fundamental knowledge about the cognition of theoretical vector constructs among students, but also helps to improve existing pedagogies and, eventually, leading to students' discernment. The author developed a Test of Knowledge of Elementary Vector Concepts (TKEVC) that was delivered to engineering students in the first semester who were starting the required engineering physics course during the 1st week of class, before any instruction on vectors. TKEVC was administered to a sample of 476 students from 7 different engineering colleges and universities in India. The result obtained with this test states that only 37% of students enrolled in the engineering physics course have extensive knowledge of vectors to advance physics topics, specifically mechanics, while almost 67% of students enter the course without a complete understanding of the vector principles in any aspect. These findings have substantial implications for math and physics classes. The researcher discussed the questions asked to the students and their answers, emphasizing the conceptual and methodological errors they made. The results have substantial implications for the teaching of engineering mathematics and physics, the professional development of teachers, and the preparation of teams of teachers for engineering institutions.

**Keywords:** *Learning, Mathematics Education, Vector Addition, Vector Direction, Vector Magnitude.*

## 1. INTRODUCTION:

Physics, as an academic discipline, has a mathematical language of its own, and vectors are its indispensable constituent, even at the introductory stage. The elemental conception of Newtonian mechanics is a *force* – a vector. Constraining the motion to one dimension, as is common at the commencing levels of physics education, cannot avoid the reality that the forces are by and large vectors in a plane. They must be added, by way of the rules of vector addition, to ascertain the net force along the axis of motion. Similarly, any treatment and discourse of electric forces or fields, beyond the exclusively descriptive “like charges repel”, must connect with the superposition of vectors (Deventer, 2008).

There has been extensive study, with astronomically large literature, of learners' preconceived ideas and their incorrect excogitation of the concepts of motion and force. Pupil asperities with the superposition of forces and with drawing and making sense of free-body diagrams are long-familiar. Despite anything to the contrary, a good deal of research has riveted on exclusively one-dimensional illustrations where the vector facets of and of kinematic quantities are not instantly apparent. While it is assuredly a fact that learners confront an immediate obstacle with the basic concepts of force, it may well be that a lack of ability to argue accurately, about conceptions of vectors, portray an important, yet less studied, barrier (Barniol & Zavala, 2010, 2012).

The excessively used *Force Concept Inventory* of (Hestenes, Wells, & Swackhamer, 1992) does dig somewhat into learners' instinctive knowing about how two forces combine. Their results suggest that learners oftentimes utilize non-vectorial reasoning. A common delusion is the “dominance principle”, by or through which, the larger of the two forces “wins out” and establishes the motion. Educatees, even after continued exposure to Newtonian mechanics, will, if asked to verbalize their reasoning, often prove such explanations as “Force A overcomes Force B” (J. Aguirre & Erickson, 1984).

The (Hestenes & Wells, 1992)'s *Mechanics Baseline Test* looks in more astuteness at the directional panoramas of the kinematic vectors and the superposition of force vectors. Some of the lowest accounted scores were fathered by those Baseline questions (particularly questions 5, 7, and 19), necessitating the discernment of vector properties (Flores, Kanim, & Kautz, 2004).

(J. M. Aguirre, 1988) looked into the opinions formed beforehand by high-school leaners regarding vector kinematics in projectile motion. He ascertained a large number of faulty preconceived notions, especially concerning the function and implication of the elements of the velocity vector. Perhaps this is not unexpected. After all, vectors are kind of abstract quantities demanding non-intuitive ideas. These results do, be that as it may, indicate that physics didactics needs to set out by giving denotative rumination to pupil conversance with and learning of vectors (Flores-García, Alfaro-Avena, Dena-Ornelas, & González-Quezada, 2008).

Just how much understanding about vectors and their properties do learners who start out the course bring with them into *engineering physics* class? Do all, or most, enter with a working knowledge of vectors? Anecdotal evidence, from casual conversations, indicates that most college-level physics instructors go forward with the hypothesis that pupils have acquired knowledge about vectors somewhere else and simply require a recapitulation to get them up to speed. Is such a premise reasonable and justified?

To find this out, the researcher has developed a *Test of Knowledge of Elementary Vector Concepts* and gave it to the first semester students who are beginning the *engineering physics* course. These were given to students from 7 different engineering colleges and universities of India. The test is reproduced here for other researchers to use if they wish. The elemental judgment reached out from this test enunciates that only a meager 37% of the educatees enrolled for the engineering physics course have ample cognition of vectors to go ahead with physics topics, specifically mechanics, while almost 67% of the students enter with no utile understanding of the principles of vectors in any respect. These findings have strong implications for both mathematics as well as physics instruction. The method used in this study is “*tests of open-ended problems*”.

With a strong and careful design, this study demonstrates a rather dramatic difference, in the generic mathematical context. While on some level, the findings may not come as a surprise to mathematics and physics teachers, it eventually conjure up several questions that are pretty crucial to the pedagogy of vector education: If a learner answers a problem correctly in the *ijk* format, can we still say that she may not have a good command over addition and subtraction of vectors? What do we actually have in mind when

we say we expect from learners to cognize the underpinnings of addition and subtraction of vectors?

If a learner performs haplessly in the arrow format of vectors, with it, can we conclude their pitiful understanding of the fundamental physics, or can we call it the antiquity of the abstractionism that entrammels proper use of vector conceptions? In the teaching of vectors, by and large, the educators teach arrow format to the learners before the *ijk* format—but can we call it truly befitting? Can there be a more spontaneous order, i.e., can the introduction of *ijk* format before arrow format turn out to be a better idea vis-à-vis student's learning? Should there be a definitive pedagogical goal for the learners to efficiently and effectively formulate or explicate fundamental operations of vectors in both arrow and *ijk* formats, or is making students learn only one format good enough?

While few of the queries above distinctly command empirical investigations, which are to be exceedingly focused, the other interrogatives call for judgment that has to be highly professional, and community discussions can be apprised better with such probes. Consequently, to gain insight into responses to all of these queries, the researcher starts by reporting the results and analysis of the test, engineered to transcribe through empirical observations and effectively portray learners' achievement in the cognition of elementary vector operations in mathematical situations in both *ijk* as well as arrow formats.

Researcher's instructional experience with teaching of vectors has led him to conclude that the inadequate cognition exhibited by the learners with regards to ideas inherent in vector algebra presented in graph form demonstrates a peculiarly unmanageable obstruction to their triumph in becoming proficient in concepts inherently belonging to the discipline of physics. Vector ideas and their graphical and geometrical explanations imbue the totality of the curriculum of engineering physics course. Regardless of most learners' earlier encounter to the constructs that are fundamental to vectors, in their classes on maths or in physics which the learned in senior-secondary school (as has been pointed out in various researches), and the excessive stress educators have directed towards those vector constructs in their curriculum transaction, learners' relentless discombobulation about cardinal notions of vectors has befuddled their pedagogical endeavors.

The researcher, therefore, resolved to conduct an organized and directed examination of engineering students' cognition of fundamental conceptions of the addition of vectors, calculation of its magnitude, and determination of its direction during the first few weeks of their *engineering physics* course.

A study by (Randall D Knight, 1995) is reasonably related to this study, and his work colligates an amalgamation of questions from both arrow and *ijk*-format. Non-familiarity with *ijk* notation was showcased by nearly half of the participants. Constructs and calculation on vector algebra dwell at the core of the curriculum on engineering physics, implicit in almost all the themes covered up during compulsory courses at the higher level of engineering education.

As (Randall D Knight, 1995) has accentuated, the vectorial existence of forces, kinematical quantities, and fields commands that learners shall possess a handy and clear cognition of fundamental constructs about vector algebra if they wish to succeed in dominating even the most fundamental level of engineering physics. Knight has made a more or less disguised reference to the astounding inadequacy of documented investigations with regards to learners' cognition of constructs integral to vectors, and his "*Vector Knowledge Test*" allowed for a priceless primary quick look into the assessment of the knowledge of vectors among learners registered for the course on engineering physics, before the commencement of the course.

The current study focusses on dissecting learners' achievement on a test on vectors where the test has no direct bearing to the discipline of physics. The significant issue in this research is that the questions appearing in the test have focalized on the assessment of learners' cognition of the most basic constructs consociated to working with the vectors, like, for example, components and magnitude of vectors. Are there certain vital and even more all-encompassing facets of vectors in general and vector operations in particular that are inadequately expressed and staged, or even curbed, by the representation of vectors in the arrow format? Is it so that the arrow format complements the *ijk* format or contrarily inhibits learner cognition and functioning? This study focusses on gaining an in-depth, clear and deep understanding about the perception of learners' cognition, marked by careful evaluation and judgment on those facets of vectors, which form the base for Newtonian mechanics. Still, here it is done in generic math format by looking into learners' solutions to problems in both arrow



as well as *ijk* formats. This study provides not only the crucial background knowledge about cognition of fundamental vector constructs among learners but also helps to ameliorate the existing pedagogies and eventually to lead to learners' discernment.

## 2. MOTIVATION:

Concepts in introductory physics, mostly covered in an engineering physics course, taught at the undergraduate level in the engineering colleges, are represented by vectors. Consequently, a comprehensive cognition of such physics constructs requires learners to have an effective hold over fundamental vector constructs. Certain specific issues that need special attention include the need for the development of a comprehensive and complete classification of the most frequently occurring errors that students of engineering colleges make. At the same time, they learn about concepts on vector in an engineering physics course, and this, as a consequence, concerns the availableness of MCQ type measurement instruments for testing learners' vector cognition.

Studies done previously on cognition of vector constructs among learners can be agglomerated into three groups: (1) those that didn't use concepts of physics (Barniol & Zavala, 2010, 2012; Deventer, 2008; Flores, Kanim, & Kautz, 2004; Hawkins, Thompson, & Wittmann, 2009; Hawkins, Thompson, Wittmann, Sayre, & Frank, 2010; Hinrichs, 2010; Randall D Knight, 1995; Nguyen & Meltzer, 2003; Wang & Sayre, 2010; Zavala & Barniol, 2010, 2013), (2) those that used concepts of physics (J. Aguirre & Erickson, 1984; J. M. Aguirre, 1988; J. M. Aguirre & Rankin, 1989; Barniol & Zavala, 2010; Barniol, Zavala, & Hinojosa, 2013; Deventer, 2008; Flores *et al.*, 2004; Wang & Sayre, 2010; Zavala & Barniol, 2013), and (3) those that used the mix of both (Barniol & Zavala, 2010; Deventer, 2008; Shaffer & McDermott, 2005; Wang & Sayre, 2010; Zavala & Barniol, 2013). Studies belonging to the first group (Barniol & Zavala, 2009, 2010, 2012; Deventer, 2008; Flores *et al.*, 2004; Hawkins *et al.*, 2009; Hawkins *et al.*, 2010; Hinrichs, 2010; Randall D Knight, 1995; Nguyen & Meltzer, 2003; Wang & Sayre, 2010; Zavala & Barniol, 2010, 2013) have a direct bearing to our inquiry, for they have analyzed learners' cognition of concepts of vectors in problems that had no context to physics.

Six pieces of research from this aggregation (Deventer, 2008; Flores *et al.*, 2004;

Randall D Knight, 1995; Nguyen & Meltzer, 2003; Wang & Sayre, 2010) identified some frequently occurring errors that students from engineering colleges make while they are learning vector constructs. The methods which they used in their investigations were either interviews from individuals or exercising open-ended tests or both.

Researches have done previously (J. M. Aguirre, 1988; J. M. Aguirre & Rankin, 1989; Barniol *et al.*, 2013; Bollen, van Kampen, Baily, Kelly, & De Cock, 2017; Flores-García, Alfaro-Avena, Dena-Ornelas, & González-Quezada, 2008; Flores *et al.*, 2004; Kanim, 1999) and researcher's didactic exposure depicts that the capability of comprehension of prominent themes in the calculus-based physics curriculum at the introductory level demands a firm grip over the fundamentals of vectors.

As being fully aware or cognizant of the essentiality and the requisiteness of laying the groundwork for vector noesis, (Randall D Knight, 1995) and (Nguyen & Meltzer, 2003) engineered tests to appraise the vector cognition, before the vector concept is taught to the engineering graduates in the calculus-based introductory physics course. Both the researches mentioned above established that out of all the learners enrolled for the course on introductory physics, almost 50% of them lacked the requisite understanding about vectors, even though 86% of them affirmed strongly of their familiarity with vectors, right from senior-secondary school (Randall D Knight, 1995).

With regards to learners' previous experience with vectors in senior-secondary schools, research by (Wutchana & Emarat, 2011) brought out that around 32% of students from senior-secondary schools can give right answers to problems on vector addition after they have been taught vectors in the class. In certain educational institutes of higher learning, the math requirement for the fundamental course in physics is Calculus I, and in some institutions, Calculus II is also a requirement, both of which lack treatment on vectors. The course which comes later on in the STEM (science, technology, engineering, and mathematics) course of study is Calculus III, which has time apportionment of approximately 3 weeks (reasonably close to four hours every week) for extended communication on basics of applications of vectors.

For the first time after the completion of school, engineering educatees are given exposure of vectors, in their course on

mechanics, and they are given a maximum of 1 week (average of 2 hours and 30 minutes) on this very pertinent area of study. There have been made numerous attempts to address the issue as mentioned above, and to this front, many research studies have been conducted for the improvement of learners' cognition of vectors in a physics context. A course of study was formulated by (Shaffer & McDermott, 2005) with the idea that was based entirely on research findings and as a consequence they bring forth these two works: "*Tutorials in Introductory Physics*" and "*Physics by Inquiry*" to meliorate learners' cognition of the concepts of kinematics, viewed in terms of vectors.

Flores *et al.*, 2004 and Barniol *et al.*, 2013, researched on implementation of instructional alterations to raise learners' capability to give reasonable justifications with regards to vectors that typify kinematic quantities and forces. Colligated researches (Bollen *et al.*, 2017; Kanim, 1999) also comprises deliberations applicability of vectors to varied themes, including that of electrostatics, electric circuits, and Gauss' law. But then, specific efforts have been made in the improvement of learners' cognition of vectors alone. (Mikula & Heckler, 2013) enquired certain vector problems with varied angular compositions by introducing pedagogy that made use of computers for practicing vector problems (Mikula & Heckler, 2013).

The research by (Flores-García *et al.*, 2008) concludes that learners' inconvenience in cognizing physics constructs is engendered by a sheer deficiency of skills and comprehension with regards to math, specifically vectors. A majority of learners face difficulty with addition and subtraction of vector even when there is no context to physics in the problem. Learners confront complemental asperities in drawing associations with the conceptual framework when certain contexts on the discipline of physics is added to it (Barniol & Zavala, 2014; Barniol *et al.*, 2013; Deventer, 2008).

An excessively limited number of studies have looked into the learner's cognition of subtraction and addition of vectors in the mathematical and/or fundamental physics constructs; the problems asked students in most of the cases employed vector arrow representation (Heckler & Scaife, 2015). (Heckler & Scaife, 2015) researched the learners' cognition of subtraction and addition of vectors in both arrow and algebraic notation (making use of unit vectors).

Quite a lot of investigators have transcribed an array of learner asperities with vector calculations in physical and mathematical environments (Barniol & Zavala, 2010, 2014; Deventer, 2008; Flores *et al.*, 2004; Hawkins *et al.*, 2009; Nguyen & Meltzer, 2003; Shaffer & McDermott, 2005). Nevertheless, in almost all of these researches, only the representations of vectors in their arrow form were reckoned. Although it is common knowledge that arrow representation of vectors is beyond doubt didactically, viscerally, conceptually, and technically effectual and efficacious, yet significant preconceptions are associated with it among the learners. Thus its small range and scope impede its viability in mathematical or logical computations in its capability and competence to individuate few significant attributes of vector algebra and in its acquirement of the representation of vector quantities (e.g., in 3 dimensions or above).

Comparisons could be drawn between the arrow representation and the algebraic representation with their respective attendant advantages and disadvantages making use of vectors in their unit form  $(\hat{i}, \hat{j}, \hat{k})$  in algebraic representation, which is frequently employed in didactics, specifically in the calculus-based introductory physics courses. While investigating learner cognition of vectors in the arrow format, (Nguyen & Meltzer, 2003) ascertained that only about 60%–70% of students with calculus background and 20%–40% of students with algebra background were able to accurately draw the vector sum presented in arrow format on a 2D grid, and only between 60% and 80% of all learners managed to precisely solve problems that asked to determine the direction and magnitude comparison problems related to arrow vectors on a grid.

Vectors represented by (Flores *et al.*, 2004) in arrow format with given lengths and angles found that while calculating the vector sum for determining the net force, a meager 50% of the learners with calculus background managed to solve those problems. One other observation from the study was that only a very few learners could manage to solve those problems that were qualitative and involved finding the difference of vectors in a physical setting (e.g., in acceleration) where the vectors were in arrow format. (Shaffer & McDermott, 2005) also ascertained from his research that many learners were facing handicap with the subtraction of vector in which the vectors were expressed in arrow format on a grid with single dimensions, and learners did slightly better

(65% correct) in mathematics context in comparison to the physical setting of acceleration (where 45% came up with a correct solution).

Contrarily, (Deventer, 2008) determined that learners performed good in the physics (where 50% of the students correctly solved the problem) in comparison to the situation in mathematics (where 20% students found the correct answer) for subtraction in one dimension, reason being learners were inclined towards usage of physics setting to incur the right directions. (Barniol & Zavala, 2010) also established that learners' solution to test problems, where they were to draw the resultant vectors on a grid as arrows, can be marginally sensitive to the problems' context. The solutions given by learners to the problems on addition of vectors can also be reasonably sensitive to the vector's placement of those that are showcased as arrows, such as tail to tip, tail to tail, or separated (Barniol & Zavala, 2010; Hawkins *et al.*, 2009), although no such effectuates were determined when the arrows were placed on a grid (Hawkins *et al.*, 2009).

### 3. REVIEW OF LITERATURE:

Investigation on learners' vector cognition depicts that learners pretty frequently lack the mental faculty required for vector addition, which can eventually lead to learner deterrents (Deventer, 2008; Flores *et al.*, 2004; Randall D Knight, 1995; Nguyen & Meltzer, 2003; Shaffer & McDermott, 2005). Investigators on the usage of varied visual representations of graphical vector addition problems have depicted substantial altercations in learners' method of solving the tasks on vectors. There are many mannerisms for asking learners to perform vector addition or subtraction, graphically. Learners often make use of varied methodologies for vector addition (Deventer, 2008). Head-to-tail and components are the only methodologies described in the fundamental textbooks used for this course (Randall Dewey Knight, 2008).

An extensive body of literature could be found on learners' cognition on the *mechanics* theme (McDermott & Redish, 1999). Mainly, learners' problems with the relationship between velocity and acceleration have been observed in a variety of researches (Trowbridge & McDermott, 1981). Learners' understanding of the relationship between force and motion has also been extensively researched and transcribed (Clement, 1982; Halloun & Hestenes, 1985; Viennot, 1979). Even though the context in most of the cases here

is one-dimensional motion, few are on vector nature of acceleration as well. (Reif & Allen, 1992) inquired from learners enrolled in the fundamental course on physics and to physics faculty members to describe the direction of acceleration for the motion of objects along various paths.

They ascertained that both students (novices) and faculties (experts) found it challenging to answer qualitative questions about the vector nature of acceleration. Even though the answers that they gave to the problems were mostly right, an initial tendency was observed by the experts in the research to make inappropriate arguments and justifications on taking force as the basis rather than justifying solutions to the problems solely on the grounds of kinematics.

Shaffer (1993), in his research, found that only 6 out of a total of 48 graduate students managed to showcase the approximate direction of acceleration for all positions and the most frequently occurring errors committed were the inclusion of either only the radial or only the tangential components of the acceleration. (Randall D Knight, 1995) in his research found that only about 33% of the students "have sufficient vector knowledge to proceed with mechanics." (Nguyen & Meltzer, 2003) in their research concluded that just over 25% of the students finishing a calculus-based mechanics course and close to 50% completing the algebra-based course could somehow manage to add vectors in two dimensions.

In the inquiry of learner cognition of vectors in electrostatics, (Kanim, 1999) ascertained that most of the learners faced immaculate trouble in thinking coherently and logically about the net electric forces and fields from collections of point sources. That additional inconveniences are brought in when attempting to give a rational justification about the field and force vectors from continuous charge distributions. It has been deduced from nationally administered tests that problems that involve force or acceleration as vector quantities are not easy for most of the learners. For instance, on the Mechanics Baseline Test (Hestenes & Wells, 1992), one problem asks learners to draw a comparison between the magnitudes of four force vectors, acting on an object that is moving at a constant speed.

Another problem demands learners to determine the direction of acceleration for a block when it is at the lowest point on a curved ramp. Learners showcased poor performance on these problems after the standard instruction. About

thirty-six percent managed to solve the problem on force correctly, and a meager eighteen percent solved the problem on acceleration accurately. Contrarily, the Force Concept Inventory (Hestenes *et al.*, 1992) does not test for the cognition of vectors: On the revision of the test, the only question that required an understanding of vectors was removed from it. The aforementioned probes accentuate the essentiality of conceptual cognition of vectors for learners to immerse themselves in engineering physics course efficaciously.

(Kanim, 1999) researched learners' cognition of constructs of a vector in the context of electrical forces and fields. (J. M. Aguirre, 1988) and (J. M. Aguirre & Rankin, 1989) examined learners' conception concerning vector kinematics, their inquiry was cantered around the interrelationships among acceleration, velocity, and force instead of vectors properties intrinsically. (Ortiz, 2002) researched on pupil's inconvenience in cognizing fundamental vector operations commonly made use of in the beginning of physics courses.

## 4. MATERIALS AND METHODS:

### 4.1. Construction and goal of the “test of knowledge of elementary vector concepts”

The goal of the *Test of Knowledge of Elementary Vector Concepts* is neither to judge whether the learners are eloquent in vector mathematics nor that they can effectively utilize vectors in a refined way. Instead, it is to see if they have the minimalistic knowledge and skill required to work with vectors that could eventually make it possible for them to go forward with the study of qualitative and quantitative Newtonian mechanics. The *Test of Knowledge of Elementary Vector Concepts*, reproduced as an appendix to this article, is thus excogitated to assess pupils' knowledge of the most basic level of vector properties and operations. It probes a learners' ability to:

1. Identify and make appropriate use of the components of a vector,
2. Determine the vector's magnitude and direction,
3. Ascertain vector sum using graphs, and
4. Find the sum of two vectors using components.

These are essential skills for success in basic

Newtonian mechanics. Also, the test looks, for completeness, at student ability with the more advanced capabilities of vector multiplication.

The test has two levels. It first asks students if they are familiar with a given vector topic. Those answering in affirmative are the asked one or more fundamental problems. The problems assess whether or not the student's self-rating is correct. There are a total of ten *questions* and ten *problems*. To minimize guessing, students are instructed to leave blank any issues they think they do not know how to work. The second question, asking students if they have studied vectors previously, instructs those answering “NO” to skip the rest of the test. This test structure, with the accompanying instructions, allows students to be classified as:

1. Having no previous experience with a particular topic (if they answer “NO” and leave the problem blank),
2. Having previous experience but having no working knowledge (if they answer “YES” but work the problem wrong), or
3. Having previous experience and working knowledge (if they answer “YES” and work the problem correctly).

The *Test of Knowledge of Elementary Vector Concepts* was given to all the first semester students (N = 476) enrolled in mid-July 2019 where they have a compulsory *engineering physics* course. Approvals were obtained from 11 local ethics committees. To shield the identity of the participants as well as of the engineering institutions, pseudonyms were rendered to them. Samples were drawn from seven engineering colleges and universities in India. It was during the 1<sup>st</sup> week of class, before any instruction about vectors, the test was administered. The students in the class were predominantly computer engineering majors, with sizable admixture of biotechnology, mechanical, electrical, civil, and architecture students.

All the students had cleared JEE Mains (some even had cleared JEE Advanced). Altogether, the students were above average in comparison to students taking up *engineering physics* classes at other engineering colleges and universities of India. Their performance on the *Test of Knowledge of Elementary Vector Concepts* is expected to be typical of engineering students beginning their course at most of the top-ranked engineering colleges and universities of the country.

## 5. RESULTS AND DISCUSSION:

Answer to the first question revealed that 91% of the students were taking the course for the first time while 9% (41 students) were repeating the course. It will be useful to break out the responses for this subgroup to see what light it sheds on why they did not succeed in passing the course previously.

Answer to question two establishes that 96%, i.e., 456 students beginning the *engineering physics* course have studied vectors before. This includes, of course, 100% of the students who were repeating the course as well as 87% of the new students. Their previous exposure to vectors was roughly evenly divided between math courses and prior physics courses, with a large fraction having seen vectors in both places. The response to this question seems to confirm the common assumption that these are not entirely new ideas for most students.

Table 1 presents the complete results of the *Test of Knowledge of Elementary Vector Concepts*. Responses as percentages are shown for three groups:

- i. Students new to the course *and* who have studied vectors before ( $N_1=415$ )
- ii. Students repeating the *engineering physics* course ( $N_2=41$ )
- iii. All the students present in all the classes from 7 institutions who took part in the study ( $N_3=476$ )

Group I examines to what extent students who have studied vectors before can recall and use that knowledge. Group II provides information as to whether a lack of specific skills, in this case, vector mathematics, is a factor for students who fail to complete the course.

"Questions" and "Problems" from the test are indicated in the left column as "Q" or "P". Since students were instructed to leave those questions blank, which they were not able to answer, rather than to guess, "blank" answers are tabulated separately from "wrong" answers. Here "wrong" means that the student provided an incorrect answer. The primary comparison to make with the Table 1 data is between the percentage of students answering "Yes, I know that," and the rate who correctly worked a fundamental problem testing their knowledge of that concept. Except for Problems 2, 5, and 6, the percentage of learners giving the accurate solution to the problems is

invariably less (often much less) than the percentage asserting that they possessed such knowledge.

Ideally, students answering "Yes" to a self-assessment question would then proceed to attempt the subsequent problem or problems while those answering "No" would leave it blank. In this case, the percentage of blank responses to the problem would equal the percentage responding "No" to the question. Sometimes, though, a student would answer "No" to the question and then proceed to attempt the problem anyway – occasionally getting the answer correct! However, the number of students who knew more than they thought was significantly fewer than the number who knew less than they thought.

Question 3 asks students to define a vector in their own words. Any answer mentioning *magnitude* and *direction*, or something equivalent (e.g., "length" rather than "magnitude"), was counted as correct. Answers that said at least something relevant to vectors were counted as partially correct. By far, the most common partially correct response equated vectors with specific physical quantities (e.g., "A vector is a force"). Even with very generous scoring, only 44% of the class provides an adequate definition, while 29% either left it blank or provided an answer having no connection at all to vectors. It is worth noting that many of the responses counted as fully correct seemed to view vectors as something used only in physics rather than as mathematical objects.

Questions 4 and 5 and Problems 1 and 2 are concerned with vector components. Two common errors of problem 1 were to omit the minus sign or to include the unit vector  $\hat{j}$  (i.e.,  $-\frac{21}{22\pi}\hat{j}$ ) as part of the answer. The following error, curiously, was widespread among students repeating the course. Students making these errors fail to realize that the component of a vector is simply a scalar number, possibly signed. In Problem 2, answers are given as "(1, 3, 2)" were accepted, since this is how students often learn about vectors in math classes, but the reasonably common response of " $x + 3y + 2z$ " was not accepted as correct.

Question 6, together with Problems 3 and 4 asks whether students can express a vector in direction and magnitude terms. The percentage of learners who found the magnitude correctly was significantly more than the percentage of learners who found the directions accurately, and these are shown in Table I as "Magnitude OK." Even though 3-4-5 triangles were used, symbolic

answers were accepted since not all students had scientific calculators.

Problem 5, on graphical vector addition, had more wrong attempts than any other problem from P1 through P10. The most common incorrect response, by far, was to draw a vector from the tip of  $\vec{E}$  to the tip of  $\vec{F}$ . Pupils were found making use of the bisector method if they arranged the vectors tail-to-tail and drew the resulting vector between them. Educatees who made use of the bisector method, in particular, showed carelessness with regards to the magnitude of the resultant vector. The success rate of Problem 6, algebraic vector addition, was significantly higher. One possible explanation is suggested by looking at those students who answered Problem 2, when asked to write a vector in a component form, as (1, 3, 2). This group did significantly better than the sample average on Problems 2 and 6, dealing with components, but relatively poor than the sample average on Problem 5, i.e., graphical addition. While the number in this group (N=24) is too small to draw definite conclusions, their responses indicate that some fraction of the learners have learned about vectors exclusively as pairs of numbers, devoid of any geometric content. Together, Problems 1 through 6 covers the basic vector properties and operational need for Newtonian mechanics. The average score for these six problems are shown at the bottom of Table 1. The sample average is only 36% correct responses. The final two questions and four problems are concerned with vector multiplication. These were for informational purposes since vector multiplication is not a prerequisite to a general understanding of mechanics. As anticipated, only a small fraction of students reported reasonable competence with vector multiplication, and even fewer (< 10%) could work a simple problem.

### 5.1. Educational implications

The findings from the *Test of Knowledge of Elementary Vector Concepts* are presented in Table 2. This table showcases the various abilities of students to use vectors (in approximate percentage) drawn from the first semester of engineering courses which have taken up *engineering physics* course. Taken as a whole, the *Test of Knowledge of Elementary Vector Concepts* suggests that roughly 20% of the class is sufficiently skilled with vectors, read the texts of the problem and solve typical problems without further practice. While this group still needs to acquire specific knowledge, such as finding vector directions, they can likely learn these skills with

minimal instruction since their knowledge base is good. Roughly 12% of the students can work on the path of vectors as well. This means that this 12 % of students, i.e., a total of only 57 students out of 476 students enrolled for the course, are ready in the most real sense for the course, and the rest are not. Only these 12% of the entire sample have awareness about vector properties and are very much likely to incorporate vectors into their “working knowledge” of mathematics without additional instruction and practice.

This table presents the approximative percentage of learners who have taken an engineering physics course in their 1<sup>st</sup> semester of engineering program against the skill sets indicated. This leaves a full 88% of the students enrolled for this course in their engineering programs with no utile noesis of vectors in any respect. This does not, in and of itself, invalidate the assumption that most students have seen vectors in previous classes. Question 2 indicates that 96% of students had, indeed, “studied” vectors at some prior time. Further, high percentages of students gave affirmative self-assessments that they “knew” most of these basic ideas. The results of the *Test of Knowledge of Elementary Vector Concepts*, however, indicate otherwise. Since, as noted, the sample students enrolled for this course are relatively typical of a charitable institution, it is expected that similar results would be found at most other top engineering colleges and universities.

The responses of those students repeating the course, after withdrawing or failing on a prior try, are especially interesting. Their knowledge, after a full semester of college-level engineering physics, is only slightly better than that of new students who indicated a previous study of vectors. Only 43% of this group could correctly add two vectors graphically, although 86% thought they knew how, and only 45% gave a satisfactory definition of a vector. Combining force vectors, whether for free-body diagrams or for conceptual reasoning, is an essential skill for success in Newtonian mechanics. Although cause and effect are difficult to disentangle, the results suggest that a major reason for the failure of these students was their lack of understanding of vectors.

Like many other aspects of elementary physics, vectors seem “obvious” to those of us who have used them for many years. They are by no means evident to students, as these results show. Since the previous study, for most, has produced little usable knowledge, it is unlikely that a few quick sketches on the board, with

expressions of “This is how you do it,” will suffice as instruction. From the earliest stages, understanding vectors are essential for progress in physics, so it behooves those who belong to the physics education community to think about how better to incorporate vectors into introductory physics.

It is tempting to think that the physics education community can let the mathematics department do this for them. Unfortunately, standard calculus texts do not treat vectors until shortly before multivariate calculus is introduced. At Indian universities and colleges, students do not see vectors in their “Engineering Mathematics” course until near the end of the first year. Providing learners with the necessary instruction is a task physics teachers themselves will have to take.

Arons & Holbrow, 1990, have discussed student difficulties with learning about vectors noting that “Many students would benefit from more exercises and drill in graphical handling of vectors than are usually available in texts”. That extended, on-going practice is needed seems apparent from the shallow scores of students who had studied vectors before but retained little. Spending one day on the standard vector chapter, found in mostly all texts, followed by one homework assignment is probably not sufficient for most students. There exists a variety of options for dealing with this problem. For example:

1. Instructors should make *explicit* mention of vector properties for several weeks as they proceed through projectile motion, forces, free-body diagrams, and so on. Don't assume that students understand after one day; much reinforcement will be necessary.
2. Additional homework problems on vectors should be assigned for several weeks. Students need to keep practicing vector math and reasoning *after* they get feedback from their first vector homework.
3. A laboratory period early in the course could be devoted to a vector tutorial. Students would receive a hand-out containing a variety of problems on which to practice and then would get immediate feedback from their instructor. Working with groups would encourage discussion and active participation. This could be followed, the following week, with a force

table or similar experiment in which students measure and add non-collinear forces.

4. Basic practice with vector math could be provided via computer-aided instruction. An endless variety of problems could be provided, with hints when needed and immediate feedback. Since such practice deals only with the mechanics of vector manipulation, it would need to be supplemented with a more general discussion of what vectors are and how they are recognized and used in physics.

## 6. CONCLUSIONS:

Irrespective of the method(s) put to use, pupils who take up the *engineering physics* course, need at the very beginning an explicit instruction, leaving nothing to opinions formed beforehand by the educators about their educatees, in and practice with the application of vectors. A bulk of learners join the course with no working knowledge of vectors. These students are not likely to be successful with the basic principles of Newtonian mechanics, such as the superposition of forces until their ability to reason with the use of vectors has been established. The researcher hopes that an investigation of students' cognition of vectors to the general understanding of mechanics can render direction or helpful suggestions toward the designing of course modifications that will eventually beef up learners' perspective of physics as a logically ordered branch of knowledge, instead of the aggregation of discrete facts, where the vector is mere a part. There is a need for heightening learners' instinctual application of vectors in answering varied questions in the physics context. Nonetheless, researchers here also accentuate that improving learners' cognition of vectors continues to be a significant challenge.

## 7. FUTURE RESEARCH:

Although many tests with their unique emphasis that integrate the recommendations, implications, and suggestions of investigators engaged in study of physics education (Beichner, 1994; Ding, Chabay, Sherwood, & Beichner, 2006; Paula V Engelhardt, 2009) have been developed (Aslanides & Savage, 2013; Beichner, 1994; Paula Vetter Engelhardt & Beichner, 2004; Hestenes *et al.*, 1992; Maloney, O'Kuma, Hieggelke, & Van Heuvelen, 2001; McKagan, Perkins, & Wieman, 2010; Singh & Rosengrant, 2003; Thornton & Sokoloff, 1998; Tongchai,

Sharma, Johnston, Arayathanitkul, & Soankwan, 2009; Wuttirom, Sharma, Johnston, Chitaree, & Soankwan, 2009), one that assessed learners' cognition of concepts on vector algebra holistically is yet to be developed and consequently there arise the need for a large-scale longitudinal study at the level involving multiple universities from several countries that would dissect learners' cognition of concepts inherently enshrined in vectors, after finishing their introductory physics courses, is a pressing requirement.

## 8. CONFLICT OF INTEREST:

The author reported no potential conflict of interest in conducting this research.

## 9. REFERENCES:

1. Aguirre, J., & Erickson, G. (1984). Students' conceptions about the vector characteristics of three physics concepts. *Journal of research in Science Teaching*, 21(5), 439-457.
2. Aguirre, J. M. (1988). Student preconceptions about vector kinematics. *The physics teacher*, 26(4), 212-216.
3. Aguirre, J. M., & Rankin, G. (1989). College students' conceptions about vector kinematics. *Physics Education*, 24(5), 290.
4. Arons, A. B., & Holbrow, C. (1990). A guide to introductory physics teaching. *Physics Today*, 43, 67.
5. Aslanides, J., & Savage, C. M. (2013). Relativity concept inventory: Development, analysis, and results. *Physical review special Topics-Physics education research*, 9(1), 010118.
6. Barniol, P., & Zavala, G. (2009). *Investigation of students' preconceptions and difficulties with the vector direction concept at a Mexican university*. Paper presented at the AIP Conference Proceedings.
7. Barniol, P., & Zavala, G. (2010). *Vector addition: Effect of the context and position of the vectors*. Paper presented at the Aip conference proceedings.
8. Barniol, P., & Zavala, G. (2012). *Students' difficulties with unit vectors and scalar multiplication of a vector*. Paper presented at the AIP Conference Proceedings.
9. Barniol, P., & Zavala, G. (2014). Force, velocity, and work: The effects of different contexts on students' understanding of vector concepts using isomorphic problems. *Physical review special Topics-Physics education research*, 10(2), 020115.
10. Barniol, P., Zavala, G., & Hinojosa, C. (2013). *Students' difficulties in interpreting the torque vector in a physical situation*. Paper presented at the AIP Conference Proceedings.
11. Beichner, R. J. (1994). Testing student interpretation of kinematics graphs. *American Journal of Physics*, 62(8), 750-762.
12. Bollen, L., van Kampen, P., Baily, C., Kelly, M., & De Cock, M. (2017). Student difficulties regarding symbolic and graphical representations of vector fields. *Physical Review Physics Education Research*, 13(2), 020109.
13. Clement, J. (1982). Students' preconceptions in introductory mechanics. *American Journal of Physics*, 50(1), 66-71.
14. Deventer, J. V. (2008). Comparing student performance on isomorphic math and physics vector representations.
15. Ding, L., Chabay, R., Sherwood, B., & Beichner, R. (2006). Evaluating an electricity and magnetism assessment tool: Brief electricity and magnetism assessment. *Physical review special Topics-Physics education research*, 2(1), 010105.
16. Engelhardt, P. V. (2009). An introduction to classical test theory as applied to conceptual multiple-choice tests. *Getting Started in PER*, 2(1).
17. Engelhardt, P. V., & Beichner, R. J. (2004). Students' understanding of direct current resistive electrical circuits. *American Journal of Physics*, 72(1), 98-115.
18. Flores-García, S., Alfaro-Avena, L., Dena-Ornelas, O., & González-Quezada, M. (2008). Students' understanding of vectors in the context of forces. *Revista mexicana de física E*, 54(1), 7-14.



19. Flores, S., Kanim, S. E., & Kautz, C. H. (2004). Student use of vectors in introductory mechanics. *American Journal of Physics*, 72(4), 460-468.
20. Halloun, I. A., & Hestenes, D. (1985). Common sense concepts about motion. *American Journal of Physics*, 53(11), 1056-1065.
21. Hawkins, J. M., Thompson, J. R., & Wittmann, M. C. (2009). *Students Consistency of Graphical Vector Addition Method on 2-D Vector Addition Tasks*. Paper presented at the AIP Conference Proceedings.
22. Hawkins, J. M., Thompson, J. R., Wittmann, M. C., Sayre, E. C., & Frank, B. W. (2010). *Students' responses to different representations of a vector addition question*. Paper presented at the AIP Conference Proceedings.
23. Heckler, A. F., & Scaife, T. M. (2015). Adding and subtracting vectors: The problem with the arrow representation. *Physical review special Topics-Physics education research*, 11(1), 010101.
24. Hestenes, D., & Wells, M. (1992). A mechanics baseline test. *The physics teacher*, 30(3), 159-166.
25. Hestenes, D., Wells, M., & Swackhamer, G. (1992). Force concept inventory. *The physics teacher*, 30(3), 141-158.
26. Hinrichs, B. E. (2010). *Writing Position Vectors in 3-d Space: A Student Difficulty With Spherical Unit Vectors in Intermediate E&M*. Paper presented at the AIP Conference Proceedings.
27. Kanim, S. (1999). An investigation of student difficulties in qualitative and quantitative problem solving: Examples from electric circuits and electrostatics. *Unpublished doctoral dissertation, University of Washington, Washington, US*.
28. Knight, R. D. (1995). The vector knowledge of beginning physics students. *The physics teacher*, 33(2), 74-77.
29. Knight, R. D. (2008). *Instructor guide [to accompany] Physics for scientists and engineers: a strategic approach*. Pearson/Addison Wesley.
30. Maloney, D. P., O'Kuma, T. L., Hieggelke, C. J., & Van Heuvelen, A. (2001). Surveying students' conceptual knowledge of electricity and magnetism. *American Journal of Physics*, 69(S1), S12-S23.
31. McDermott, L. C., & Redish, E. F. (1999). Resource letter: PER-1: Physics education research. *American Journal of Physics*, 67(9), 755-767.
32. McKagan, S., Perkins, K., & Wieman, C. (2010). Design and validation of the quantum mechanics conceptual survey. *Physical review special Topics-Physics education research*, 6(2), 020121.
33. Mikula, B. D., & Heckler, A. F. (2013). Student Difficulties With Trigonometric Vector Components Persist in Multiple Student Populations. *2013 PERC Proceedings*, 253-256.
34. Nguyen, N.-L., & Meltzer, D. E. (2003). Initial understanding of vector concepts among students in introductory physics courses. *American Journal of Physics*, 71(6), 630-638.
35. Ortiz, L. (2002). *Identifying student reasoning difficulties with the mathematical formalism of rotational mechanics*. Paper presented at the APS Four Corners Section Meeting Abstracts.
36. Reif, F., & Allen, S. (1992). Cognition for interpreting scientific concepts: A study of acceleration. *Cognition and Instruction*, 9(1), 1-44.
37. Shaffer, P. S., & McDermott, L. C. (2005). A research-based approach to improving student understanding of the vector nature of kinematical concepts. *American Journal of Physics*, 73(10), 921-931.
38. Singh, C., & Rosengrant, D. (2003). Multiple-choice test of energy and momentum concepts. *American Journal of Physics*, 71(6), 607-617.
39. Thornton, R. K., & Sokoloff, D. R. (1998). Assessing student learning of Newton's laws: The force and motion conceptual evaluation and the evaluation of active learning laboratory and lecture curricula. *American Journal of Physics*, 66(4), 338-352.
40. Tongchai, A., Sharma, M. D., Johnston, I. D., Arayathanitkul, K., & Soankwan, C.

- (2009). Developing, evaluating and demonstrating the use of a conceptual survey in mechanical waves. *International Journal of Science Education*, 31(18), 2437-2457.
41. Trowbridge, D. E., & McDermott, L. C. (1981). Investigation of student understanding of the concept of acceleration in one dimension. *American Journal of Physics*, 49(3), 242-253.
  42. Viennot, L. (1979). Spontaneous reasoning in elementary dynamics. *European Journal of Science Education*, 1(2), 205-221.
  43. Wang, T., & Sayre, E. C. (2010). *Maximum Likelihood Estimation (MLE) of students' understanding of vector subtraction*. Paper presented at the AIP Conference Proceedings.
  44. Wutchana, U., & Emarat, N. (2011). Students' understanding of graphical vector addition in one and two dimensions. *Eurasian Journal of Physics and Chemistry Education*, 3(2), 102-111.
  45. Wutiprom, S., Sharma, M. D., Johnston, I. D., Chitaree, R., & Soankwan, C. (2009). Development and use of a conceptual survey in introductory quantum physics. *International Journal of Science Education*, 31(5), 631-654.
  46. Zavala, G., & Barniol, P. (2010). *Students' understanding of the concepts of vector components and vector products*. Paper presented at the AIP Conference Proceedings.
  47. Zavala, G., & Barniol, P. (2013). *Students' understanding of dot product as a projection in no-context, work and electric flux problems*. Paper presented at the AIP conference proceedings.

## APPENDIX: TEST OF KNOWLEDGE OF ELEMENTARY VECTOR CONCEPTS

Question 1: Is this the first time you are taking this course, i.e., a course on *engineering physics*?

\_\_\_\_\_ Yes.

\_\_\_\_\_ No, I am repeating the course.

Question 2: Have you studied vectors before?

\_\_\_\_\_ No. STOP! Do not answer any more questions on this test.

\_\_\_\_\_ Yes. It was in:

Senior Secondary School Math \_\_\_\_\_

Senior Secondary School Physics \_\_\_\_\_

College Maths \_\_\_\_\_

College Physics \_\_\_\_\_

Question 3: Define Vector.

Question 4: Do you know how to write a vector in terms of its components?

\_\_\_\_\_ Yes.

\_\_\_\_\_ No.

Question 5: Are you familiar with the unit vectors  $\hat{i}$ ,  $\hat{j}$ , and  $\hat{k}$ ?

\_\_\_\_\_ Yes.

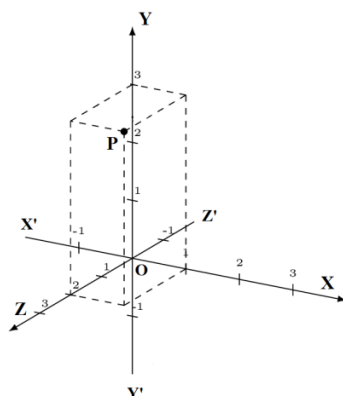
\_\_\_\_\_ No.

**Instructions:** For the problems that follow, answer only those that you can. If you don't know how to solve the problem, leave a blank. Don't make wild guesses.

Problem 1: What is the y-component of the vector:

$$\vec{A} = -\frac{3}{\pi} \frac{(\hat{i} + 7\hat{j} - 9\hat{k})}{22} ?$$

Problem 2: Write the vector  $\overrightarrow{OP}$ , from the adjacent figure, in component form.

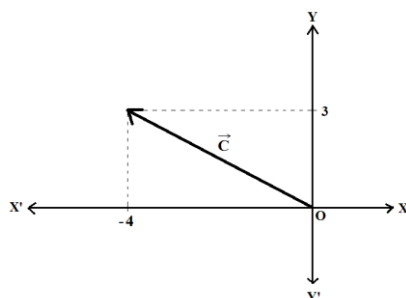


Question 6: Do you know how to express a vector as a magnitude and angle?

\_\_\_\_\_ Yes.

\_\_\_\_\_ No.

Problem 3: Write the vector  $\vec{C}$ , shown in the figure, as a magnitude and an angle.



Problem 4: What is the magnitude and angle of the vector :

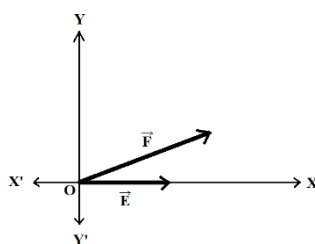
$$\vec{R} = -\frac{3}{4}\hat{i} - \frac{\pi j}{\frac{9}{8}} ?$$

Question 7: Do you know how to add two vectors graphically?

\_\_\_\_\_ Yes.

\_\_\_\_\_ No.

Problem 5: Working directly on this figure, add vectors  $\vec{E}$  and  $\vec{F}$  graphically.



Question 8: Do you know how to add two vectors algebraically?

\_\_\_\_\_ Yes.

\_\_\_\_\_ No.

Problem 6: Given  $\vec{P} = -\frac{3\pi}{29}\hat{i} + \frac{8}{91}\hat{j}$  and  $\vec{Q} = \frac{-34\hat{i} - \frac{5}{3}\hat{j} - 33\pi\hat{k}}{\pi/6}$ ,

what is the sum  $\vec{P} + \vec{Q}$  ?

Question 9: Do you know how to evaluate the “dot product” (or “scalar product”) of two vectors?

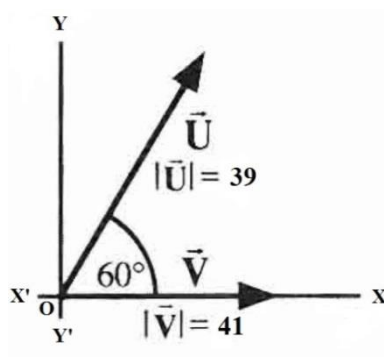
\_\_\_\_\_ Yes.

\_\_\_\_\_ No.

Problem 7: Given  $\vec{P} = -\frac{3\pi}{29}\hat{i} + \frac{8}{91}\hat{j}$  and  $\vec{Q} = \frac{-34\hat{i} - \frac{5}{3}\hat{j} - 33\pi\hat{k}}{\pi/6}$ ,

what is the dot product  $\vec{P} \cdot \vec{Q}$  ?

Problem 8: What is the dot product  $\vec{U} \cdot \vec{V}$  of the vectors  $\vec{U}$  and  $\vec{V}$  shown here?

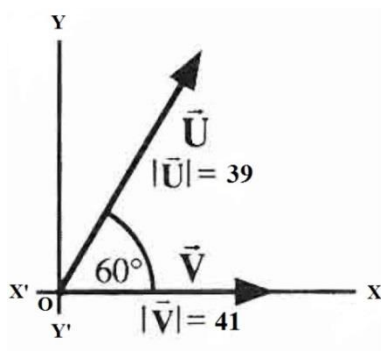


Question 10: Do you know how to evaluate the “cross product” of two vectors?

\_\_\_\_\_ Yes.

\_\_\_\_\_ No.

Problem 9: What is the cross product  $\vec{U} \times \vec{V}$  for the two vectors shown here?



Problem 10: Given  $\vec{U} = -\frac{3\pi}{29}\hat{i} + \frac{8}{91}\hat{j} + 19\hat{k}$  and  $\vec{V} = \frac{-34\hat{i} - \frac{5}{3}\hat{j} - 33\pi\hat{k}}{\pi/6}$ ,

what is the cross product  $\vec{U} \times \vec{V}$  ?

**Table 1.** Results (in percentage) of the test to gauge the knowledge of elementary vector concepts

| Item | Response           | New Students (who have studied vectors before)<br>N <sub>1</sub> =415 | Repeating Students<br>N <sub>2</sub> =41 | Total students<br>N=476 |
|------|--------------------|---|--|-------------------------|
| Q1   | Yes                | 100   | 0  | 91                      |
| Q2   | Yes                | 100   | 100                                      | 96                      |
| Q3   | Correct            | 46  | 45                                       | 44                      |
|      | Partially Correct  | 28  | 31                                       | 27                      |
|      | Wrong              | 17  | 19                                       | 16                      |
|      | Blank              | 9   | 5  | 13                      |
| Q4   | Yes                | 81  | 83                                       | 78                      |
| Q5   | Yes                | 79  | 91                                       | 77                      |
| P1   | Correct            | 38  | 41                                       | 36                      |
|      | Wrong Sign         | 21  | 13                                       | 12                      |
|      | Included $\hat{j}$ | 25  | 43                                       | 31                      |
|      | Completely wrong   | 14  | 2  | 20                      |
|      | Blank              | 2   | 1  | 1                       |
| P2   | Correct            | 71  | 83                                       | 76                      |
|      | Wrong              | 15  | 14                                       | 14                      |
|      | Blank              | 14  | 3  | 10                      |
| Q6   | Yes                | 55  | 79                                       | 54                      |
| P3   | Correct            | 17  | 24                                       | 16                      |
|      | Magnitude OK       | 21  | 37                                       | 21                      |
|      | Completely wrong   | 9   | 4  | 8                       |
|      | Blank              | 53  | 35                                       | 55                      |
| P4   | Correct            | 9   | 19                                       | 9                       |
|      | Magnitude OK       | 18  | 35                                       | 18                      |
|      | Completely wrong   | 4   | 8  | 4                       |
|      | Blank              | 69  | 38                                       | 69                      |
| Q7   | Yes                | 78  | 86                                       | 67                      |

|                         |         |    |    |    |
|-------------------------|---------|----|----|----|
| P5                      | Correct | 43 | 43 | 37 |
|                         | Wrong   | 35 | 48 | 34 |
|                         | Blank   | 22 | 9  | 29 |
| Q8                      | Yes     | 78 | 93 | 76 |
| P6                      | Correct | 49 | 73 | 46 |
|                         | Wrong   | 18 | 15 | 17 |
|                         | Blank   | 33 | 12 | 37 |
| Q9                      | Yes     | 77 | 97 | 78 |
| P7                      | Correct | 11 | 6  | 9  |
|                         | Wrong   | 15 | 27 | 14 |
|                         | Blank   | 74 | 67 | 77 |
| P8                      | Correct | 4  | 6  | 4  |
|                         | Wrong   | 6  | 7  | 5  |
|                         | Blank   | 90 | 87 | 91 |
| Q10                     | Yes     | 77 | 97 | 78 |
| P9                      | Correct | 3  | 2  | 3  |
|                         | Wrong   | 5  | 2  | 4  |
|                         | Blank   | 92 | 96 | 93 |
| P10                     | Correct | 0  | 2  | 1  |
|                         | Wrong   | 4  | 3  | 3  |
|                         | Blank   | 96 | 95 | 96 |
| P1 - P6 average correct |         | 38 | 47 | 36 |

**Table 2.** Learner knowledge of elementary vector concepts

| Item | Student's abilities                                 | Percentage (%) |
|------|---|----------------|
| i.   | Have some idea what a vector is                     | 71             |
| ii.  | Can recognize and use vector components efficiently | 56             |
| iii. | Can find vector magnitudes correctly                | 20             |
| iv.  | Can find vector directions                          | 12             |
| v.   | Can effectively add vectors                         | 41             |
| vi.  | Can evaluate dot products                           | 6              |
| vii. | Can evaluate cross products                         | 3              |

## O EFEITO DA OSTEOTOMIA SEGMENTAR ISOLADA DO QUEIXO (SCO) NO ESPAÇO DAS VIAS AÉREAS FARÍNGEAS

### THE EFFECT OF ISOLATED SEGMENTAL CHIN OSTEOTOMY (SCO) ON THE PHARYNGEAL AIRWAY SPACE

DAKHNO, Larysa<sup>1\*</sup>; LOGVYNENKO, Iryna<sup>2</sup>;

<sup>1</sup> Central Laboratory Diagnosis of the Head, D. Oral & Maxillofacial Pathology and Radiology - Ukraine

<sup>2</sup> Bogomolets National Medical University, Department of Oral and Maxillofacial Surgery – Ukraine

*\* Corresponding author*

*e-mail: larysadakhno1212@gmail.com*

Received 07 April 2020; received in revised form 29 May 2020; accepted 12 June 2020

#### RESUMO

O queixo afeta a estética facial e a harmonia entre as vistas frontal e lateral, sendo uma das estruturas anatômicas mais importantes do terço inferior da face. O objetivo da osteotomia do queixo é a harmonização do perfil facial, equilibrando o tamanho e a forma do terço inferior da face. Assume-se que a cirurgia isolada de genioplastia melhorará o espaço das vias aéreas faríngeas (PAS), promovendo alterações musculares, especificamente puxando o osso hióide para frente e descomprimindo a região da hipofaringe. Dois pacientes sem síndrome da apneia obstrutiva do sono (SAOS) foram submetidos à osteotomia isolada do queixo para fins estéticos. O movimento para frente do queixo pelo ponto Pg foi de 7 mm em um caso e 11 mm no outro. Eles foram avaliados por tomografia computadorizada de feixe cônico no pré e pós-operatório. O espaço das vias aéreas superiores foi subdividido em espaços retropalatais e retroglossais. Depois disso, o espaço das vias aéreas superiores foi analisado através dos seguintes critérios: 1) superfícies tridimensionais, de alta altitude e seção transversal; 2) alterações transversais e anteroposteriores do diâmetro. A genioplastia segmentar isolada foi utilizada após um planejamento virtual preciso e resultou em um aumento do espaço das vias aéreas faríngeas apenas em um caso. Houve correlação relevante entre a alteração vertical e horizontal do queixo e a hipofaringe. Houve uma média de um aumento de 1,6 vezes no volume total do espaço aéreo superior. O espaço retroglossal foi aumentado em 1,5 vezes. Em outro caso, não houve correlação relevante entre a alteração vertical e horizontal do queixo e a PAS. A osteotomia segmentar isolada do queixo fornece um resultado estético previsível na correção de diferentes deformidades anteriores da mandíbula e pode resultar em aumento do volume e alteração morfológica das vias aéreas. Mais estudos devem ser feitos para avaliar o efeito da genioplastia segmentar isolada no espaço das vias aéreas faríngeas.

**Palavras-chave:** Cirurgia de genioplastia, osteotomia segmentar do queixo, deformidade facial, espaço das vias aéreas faríngeas (PAS), síndrome da apneia obstrutiva do sono (SAOS) .

#### ABSTRACT

The chin affects facial esthetics and the harmony between frontal and lateral views and is one of the most important anatomic structures of the lower third of the face. Chin osteotomy is aimed at ensuring the harmonization of the facial profile by balancing the size and form of the lower third of the face. It is assumed that the isolated genioplasty surgery will improve the pharyngeal airway space (PAS) by promoting muscle changes, specifically by pulling forward the hyoid bone and decompressing the hypopharynx region. Two patients without obstructive sleep apnea syndrome (OSAS) underwent isolated chin osteotomy for esthetic purposes. Forward movement of the chin by the Pg point was 7 mm in one case and 11 mm in another case. They were evaluated by preoperative and postoperative cone-beam computed tomography scans. The upper airway space was subdivided into retropalatal and retroglossal spaces. After this, the upper airway space was analyzed through the following criteria: 1) three-dimensional, high-altitude, cross-sectional surfaces; 2) transverse and anteroposterior diameter changes. Isolated segmental genioplasty was used after precise virtual planning and resulted in the PAS increase only in one case. There was a relevant correlation between the vertical and horizontal chin change and the hypopharynx. There was an average of a 1.6-fold increase in the total volume of the upper airway space. The retroglossal space was increased 1.5-fold. In another case, there was no relevant correlation between the vertical and horizontal chin change and the PAS. Isolated segmental chin osteotomy provides predictable esthetic results in the correction of different mandible anterior deformities and may contribute to an increased volume and a morphologic airway change. Further studies should be conducted to



evaluate the effect of isolated segmental genioplasty on the pharyngeal airway space.

**Keywords:** Genioplasty surgery, segmental chin osteotomy, facial deformity, pharyngeal airway space (PAS), obstructive sleep apnea syndrome (OSAS).

## 1. INTRODUCTION:

The chin is one of the most important units of facial structures responsible for common facial appearance and esthetics. Chin osteotomy is an orthognathic surgical procedure that is usually performed in addition to bilateral sagittal split osteotomy of the mandible and sometimes as an isolated surgical procedure (Haggerty and Laughlin, 2015; Santagata *et al.*, 2015; Kawamata *et al.*, 2000). The aim of chin osteotomy is the harmonization of the facial profile by balancing the size and form of the lower third of the face.

Cone-beam computed tomography (CBCT) with a 3-dimensional cephalometric and airway analysis is routinely used as an important and necessary tool for analyzing the skeletal and dental relationships, as well as identifying and quantifying the site of obstruction (Chen *et al.*, 2007; Hwang *et al.*, 2010; Eggensperger *et al.*, 2005).

As it is known, the upper airway volume is directly dependent on the size and relative positions of the maxillofacial skeletal structures and on the dental arches, both relative to one another and the cranial base (Tan *et al.*, 2017; Guven *et al.*, 2005; Pae *et al.*, 2008). Thus, the average rate of the minimum cross-sectional area of the upper airway is 149.3 mm<sup>2</sup> in normal adults. However, the upper airway size of under 52 mm<sup>2</sup> in adults is associated with sleep apnea (Bhattacharyya *et al.*, 2000; Schendel *et al.*, 2012; Al-Moraissi *et al.*, 2015; Choi *et al.*, 2014).

An increase in the airway size associated with maxillomandibular advancement surgery and orthognathic surgery is well studied (Zucconi *et al.*, 1999; Schendel *et al.*, 2011; Abramson *et al.*, 2011; Fairburn *et al.*, 2007; Brown *et al.*, 2013; Pirklbauer *et al.*, 2011; Boyd *et al.*, 2013; Zucconi *et al.*, 1999). However, 3-dimensional morphologic, volumetric, height, cross-sectional surface areas and diameter changes of the pharyngeal airway space (PAS) after isolated segmental chin osteotomy (SCO) are not well understood.

Therefore, this study aimed to prove the assumption that the isolated genioplasty surgery will improve the pharyngeal airway space by promoting muscle changes, specifically by pulling

forward the hyoid bone and decompressing the hypopharynx region.

## 2. MATERIALS AND METHODS:

Two patients without obstructive sleep apnea syndrome (OSAS) underwent isolated segmental chin osteotomy to improve facial esthetics (Logvynenko and Dakhno, 2018). Informed consent in which all benefits, risks, alternatives, and limitations to the technique are considered was obtained before the operations. All methods were performed following the relevant guidelines and regulations of our hospital. The effect of this surgery on the increase of the pharyngeal airway space was studied based on these cases. The hypothesis of the present study was the statement that the advancements of the chin segment – including the mental spines and the genioglossus muscle – will cause a significant increase in the pharyngeal airway volume.

Both patients were evaluated based on preoperative and postoperative CBCT scans, which were done by using the Gendex CB-500 by iCat scanner (Imaging Sciences International, Hatfield, PA) with a low-dose protocol. The procedure was done in Natural Head Position (NHP) while the patients were seated.

The DICOM data were then 3D reconstructed and analyzed using the SIMPLANT O&O software (Materialise N.V., Belgium). The analysis of the upper airway changes was performed by comparing preoperative and postoperative images. The upper airway space was identified and measured from the level of the posterior nasal spine to the lower edge of the hyoid bone (Figure 1).

According to the demands of the study, the upper airway space was subdivided into (1) the retropalatal space (covering the area from the level of the posterior nasal spine at one point and continuing to the lower edge of the soft palate at another point), and (2) the retroglottal space (covering the area from the lower edge of the soft palate and continuing to the hyoid bone, as depicted in Figure 2).

The upper airway was analyzed for a volumetric, cross-sectional surface area, as well as transverse and anteroposterior size changes.

The next step was virtual surgical planning: interactive chin cutting and bony segment repositioning to optimize esthetic results (Figure 3, 4).

The initial 3D model and the surgical simulation 3D model of the skull were printed. An intraoperative positioning surgical guide was designed using Mimics software by Materialise NV. and printed using a 3D printer (Objet30 OrthoDesk jets, Stratasys Ltd. Nasdaq: SSYS) according to the 3D plan of segmental chin osteotomy for proper positioning of the fragments.

In the first case, the patient requested chin augmentation. She had had a bad experience with a silicone implant because of the asymmetric positioning and contouring of the implant margins, which is why it had been removed. So her expectations from chin osteotomy were high, and thorough 3D planning was required. Two pieces' segmental chin osteotomy was planned with the forward movement up to 6,66 mm and the rotation of the fragments providing more V-shape form of the chin and control of the contour of the mandible (Figure 5).

After the 3D project was approved by the patient, the 3D model of the skull was printed, and the surgical guide was designed and printed to help accurately transfer treatment plans to the operating room and to position the fragments properly. Titanium plates were curved and adapted to the fixation fragments on the 3D model.

The second case was represented by the patient with retrusive facial appearance, lip incompetence, and increased lower third of the face. As the patient rejected bimaxillary orthognathic surgery, genioplasty was proposed as an alternative plan (Figure 6).

To improve the facial profile, it was necessary to move Gn forward up to 11 mm and upward up to 5 mm. In reality, such movement is impossible if planned as sliding osteotomy for this patient, because the chin bone fragment will lose any contact with the mandible. Moreover, hanging it by plates has a lot of risks – resorption, loss of stability, steps of the contour of the mandible. That is why a decision was made in favor of segmental chin osteotomy. The combination of forward and upward movements with counterclockwise rotation in the sagittal plane, the divergence of the fragments, and the control of the contour of the mandible give us the possibility to achieve a favorable Gn position and

a fine V-shape form of the chin. The patient was presented with the visualization of the complexity of achieving the desired result.

In the operating room, under general anesthesia, osteotomies were done by piezotome. Minimal bone loss and precise cutting were admitted. In all cases, the attached lingual periosteum on all bone fragments was retained to preserve blood supply. The SCO procedure preserves the attachment of the anterior belly of the digastric muscle. SCO capturing the genial tubercle and the genioglossal muscle was precisely performed, and then the bone parts of the chin were fixed to the surgical guide by screws. After all bone parts were accurately positioned, they were fixed with rigid plates and screws to one another. The final bone gaps were filled by cortical bone particles of xenogenous origin.

Postoperative CBCT scans, 3D cephalometry, and upper airway analyses were re-performed postoperatively in 6 months and 2 years (Figure 7).

CBCT scans were done in Natural Head Position (NHP) on the same Gendex CB-500 by iCat scanner by the same operator while the patient was seated. This type of examination shows the form and size of airways only when the patient is awake and seated steadily upright. One should note that when the patient is asleep and/or lying on the back airways, the soft tissues are more relaxed and can narrow the airways and obstruct the airflow.

The next step was to analyze the DICOM data by using the SIMPLANT O&O software (Materialise N.V., Belgium). Then the upper airway changes were evaluated by comparing preoperative and postoperative scans.

### 3. RESULTS AND DISCUSSION:

This study involved two patients without obstructive sleep apnea syndrome who underwent isolated segmental chin osteotomy. Isolated segmental genioplasty was used after precise virtual planning and resulted in an increased pharyngeal airway space only in one case. The chin segment was moved 11.77 mm in the first case and 8.54 mm in the second (Figures 8 and 9). There were no major complications.

In the first case, the volume of the upper airway increased significantly by 59.5% as a result of chin advancement. The retroglossal volume increased more than the retropalatal volume. The area of the smallest airway (choke

point) before surgery was 84.6 mm<sup>2</sup>, and after surgery – 202,1 mm<sup>2</sup>. Correction to the norm of the airway is confirmed by obvious changes in the PAS shape from a funnel to a tube-like one, as shown in the figures. A closer examination of the surface-area slices reveals that the anteroposterior dimension increased more than the transverse dimension in terms of millimetric changes (Figure 10).

The hyoid bone, a predictor of airway obstruction, changed and moved more superiorly and closer to the mandible. The hyoid to mandibular plane measurement decreased after surgery, indicating an elevation of the hyoid.

In the second case, the upper airway space increased only by 3.5 % in the total volume (Figure 11), which is considered not a clinically significant change. This result might be associated with a different level of osteotomy of the lingual cortical plate of the chin, and fewer muscle attachments were moved forward with the chin fragment (Figure 12). However, more clinical cases are required to be certain about this. All measures are compacted in Tables 1-3.

Obstructive sleep apnea syndrome is a condition having many factors. Its diagnostics and the way of medical treatment have to be personalized and individually differentiated. The multidisciplinary management is also essential. The specific diagnosis and the plan of treatment is usually formed after both comprehensive medical plus dental history analysis and scrupulous mediocal examination being held analysis and examination. Adjunctive diagnostic studies such as CBCT imaging for airway analysis, fiberoptic nasopharyngoscopy, polysomnography, and 3-dimensional cephalometrics are included in the workup. Obstructive sleep apnea is correlated with an upper airway anatomic obstruction. The correction of this anatomic obstruction by surgery is an effective way of treatment. Therefore, it has to be definitive medical decision due to the medical indications and has to be considered as appropriate for patients with mild, moderate, or severe OSAS (Pirklbauer *et al.*, 2011).

As it is known, maxillomandibular advancement surgery with a combination of forward and upward movements with counterclockwise rotation in the sagittal plane plays an important role in OSAS correction. Thus, in a recent study, Boyd *et al.* stated that maxillomandibular advancement should be the surgical option of choice for patients with moderate or greater OSAS (Boyd *et al.*, 2013).

Today, the widespread use of CBCT scans and the development of automated airway analysis systems allow the surgeon to have more refinement in surgical planning since the exact sites and the extent of the obstruction can be better visualized. Thus, surgery can be tailored for each patient. The upper airway can be divided into three anatomic sections for evaluation and treatment.

The first level is the nose. Each internal nose deformation immediately affects the airflow. Deformities or collapses of the alar cartilage will cause airflow reduction at the external nasal valve. Septal deviations or septal spur can obstruct the nose and cause airflow turbulence. The enlargement of turbinates may also cause nasal obstructions and reduce the airflow, so surgical reduction might be indicated. A narrow nasal floor may (anatomically) affect adversely the airflow of the nose. Since the nasal floor is the hard palate, maxillary constriction and crossbites must be considered as causative factors. For such children patients, rapid palatal expanders can be applied. For adult patients, surgically assisted rapid palatal expansion is a choice. It should also be noted that maxilla restriction will affect the tongue position and cause a decrease in the pharyngeal airway space.

The second level includes the retropalatal area and the lateral pharyngeal walls. In the adolescent age, the most widespread reason for airway obstruction is lymphoid hyperplasia with the enlargement of the adenoids and tonsils. This is reported to be the cause of airway obstruction 60% of the time and provokes mouth breathing (Zucconi *et al.*, 1999). The obstruction removal by applying appropriate surgery methods is the most effective solution. However, tonsillectomy and/or adenoidectomy alone do not resolve the obstruction for 27% of these patients. Micrognathia, retrusive maxilla, open bite and/or crossbite, and a Class III malocclusion will also result in the decreased retropalatal airway space. Airway problems can also be observed after cleft palate surgery. Adult people having a long palate may suffer from snoring and progressive thickening of the palatal tissues compounding the airway obstruction.

The third level includes the retroglossal area and the tongue. The retroglossal area is mostly influenced by the position of the mandible and the tongue. Mandibular retrognathia may lead to the base of the tongue to the position posteriorly during sleep and obstruct the airflow. Mandibular retrusion can also cause obstructions

at the palatal level. These deformities can be evaluated with CBCT scans and 3-dimensional cephalometric and 3-dimensional airway analyses.

The tongue, mandible, and hyoid system are functionally composed of two bony components, the hyoid and mandible, and one muscle component, the tongue. The tongue, mandible, and hyoid system are functionally arranged as follows: the genioglossus originates from the apophysis geni superior, and the geniohyoid muscle – from the inferior point (the intrinsic tongue muscle the first and the latter that inserts distally on the hyoid bone). There are also some insertions of the mylohyoid and pharyngeal constrictor muscles supplied additionally by the pterygomandibular ligament (located in the mandible's inner part).

There are insertions of several muscles on the body of the hyoid, originated either from the tongue or the mandible likely to the geniohyoid and mylohyoid muscles, as well as the sternohyoid, sternothyroid, thyrohyoid, and omohyoid ones. There is the insertion of the hyoglossus on the hyoid horns, the pharyngeal constrictor muscles, the stylohyoid, as well as the tendinous pulley of the digastric muscle. There is also the longitudinal superior muscle insertion took place, the longitudinal inferior muscle, and the stylohyoid ligament on the distal part of the horns. Two longitudinal muscles are the internal tongue muscles.

In this regard, seven pairs of these muscles hold the hyoid bone in place and cause it to move when needed. Two of them pull the hyoid bone upward and forward. One pulls it upward and backward. One pulls it upward, and three – downward. Therefore, it was suggested that the forward movement of the chin would cause changes in the hyoid bone position and, as a result, lead to an increase in the PAS volume.

The normal morphology, volume, choke point, and growth pattern of the upper airway were described by Schendel *et al.* (2011). The authors studied 1,300 normal subjects from 6 to 65 years of age and found out that the usual choke point was in the retroglossal space.

Other researchers showed a significant increase in both lateral and anteroposterior airway dimensions with maxillomandibular advancement (Abramson *et al.*, 2011; Fairburn *et al.*, 2007). They concluded that the changes were secondary to the enlargement of the entire velopharynx by elevating the tissues and increasing the tension on the suprahyoid and

velopharyngeal muscles. Based on Pouseille's law, as the radius increases and the height decreases, the resistance decreases. Therefore, an increase in the surface area due to an increase in the anteroposterior and transverse dimensions combined with a decrease in the total airway height results in a total decrease in airway resistance. Airway resistance was most likely also decreased because of the increased airway volume and the decreased airway height, but this required further investigation.

In the first case of segmental chin osteotomy, the most outstanding discovery is probably the increase in the anteroposterior airway dimension that is always less than the transverse airway dimension in cases with maxillomandibular advancement surgery (Schendel *et al.*, 2012; Brown *et al.*, 2013).

Knowledge about the preoperative smallest cross-sectional area (choke-point size) and its position allows surgery to be more precisely planned. For example, a small retroglossal cross-sectional area can be entirely corrected by chin advancement, if it is sufficiently large and the plane of osteotomy is performed high enough.

The CBCT study accounts for the airway shape and size only when the patient is awake, static, and in the upright, seated position. When the patient is in the supine position and asleep, the tissues relax further and can obstruct the airflow. Thus, it is understandable that any measurements of the airway will be worse during normal sleeping in the supine position when the muscles are relaxed.

Furthermore, the study was limited by two cases, presenting two different (controversial) results. This is why more work needs to be done in this area to allow precise planning based on the expected airway changes when chin surgery is used.

## 5. CONCLUSIONS:

Isolated segmental chin osteotomy provides predictable esthetic results in the correction of different mandible anterior deformities. The present study evaluated two patients without OSAS by a 3-dimensional analysis; therefore, clinical correlations in the increase between the PAS and OSAS parameters (apnea-hypopnea index, body mass index, oxygen saturation, etc.) are not possible.

Currently, the protocol of orthodontic examination includes CBCT data used to

diagnose skeletal and dental deformations, which are also ideal for detecting the anatomic obstruction of the upper airway space. CBCT images are an important and required instrument for revealing the area of the decreased airway space and for quantitative evaluation of its volume on different levels, as well as for diagnosing skeletal and dental deformations using a 3D-cephalometric analysis.

Bimaxillary surgery with forward movement and counterclockwise rotation in the sagittal plane is performed on patients with obstructive sleep apnea syndrome to increase the upper airway space. However, this surgery is technically complicated and requires a long rehabilitation time for the patient. Moreover, it significantly changes the appearance of the patient with big (more than 5 mm) forward movements.

In this regard, the use of less traumatic surgery, which can affect the retroglossal area and the tongue position to increase the upper airways, seems more promising in the context of achieving positive dynamics in addressing such medical issues. The study proved that segmental chin osteotomy could increase the pharyngeal airway space, which is associated with the forward movement of the mental area of the mandible and hyoid bone and the tongue muscles following. Such surgery can be an effective way of treatment with a high success rate for patients with an anatomic obstruction of the upper airway, who cannot withstand bimaxillary orthognathic surgery but still want improvements.

The study is limited by two cases with different effects. That is why further examination is needed to test the hypothesis that an increase in the hypopharyngeal region, associated with genioplasty, is clinically effective for OSAS.

## 6. REFERENCES:

1. Haggerty Ch.J., Laughlin R.M. (2015). *Operative Atlas of Oral and Maxillofacial Surgery*. Hoboken.
2. Bhattacharyya N., Blake S.P., Fried M.P. (2000). Assessment of the airway in obstructive sleep apnea syndrome with 3-dimensional airway computed tomography. *Otolaryngol Head Neck Surg*, 123 (4):444-9.
3. Schendel S.A., Jacobson R., Khalessi S. (2012). Airway growth and development: a computerized 3-dimensional analysis. *J Oral Maxillofac Surg.*, 70:2174-83.
4. Zucconi M., Caprioglio A., Calori G., Ferini-Strambi L., Oldani A., Castronovo C. (1999). Craniofacial modifications in children with habitual snoring and obstructive sleep apnoea: a case-control study. *Eur Respir J.*, 13:411-7.
5. Schendel S., Powell N., Jacobson R. (2011). Maxillary, mandibular, and chin advancement: treatment planning based on airway anatomy in obstructive sleep apnea. *J Oral Maxillofac Surg.*, 69:663-76.
6. Abramson Z., Susarla S.M., Lawler M., Bouchard C., Troulis M., Kaban L.B. (2011). Three-dimensional computed tomographic airway analysis of patients with obstructive sleep apnea treated by maxillomandibular advancement. *J Oral Maxillofac Surg.*, 69:677-86.
7. Fairburn S.C., Waite P.D., Vilos G., Harding S.M., Bernreuter, W., Cure, J. (2007). Three-dimensional changes in upper airways of patients with obstructive sleep apnea following maxillomandibular advancement. *J Oral Maxillofac Surg.*, 65:6-12.
8. Brown E.C., Shakoon C., McKenzie D.K., Butler J.E., Gandevia S.C., Bilston L.E. (2013). Tongue and Lateral Upper Airway Movement with Mandibular Advancement. *Sleep.*, 36:397-404.
9. Pirklbauer K., Russmueller G., Stiebellehner L., Nell C., Sinko K., Millesi G. (2011). Maxillomandibular advancement for treatment of obstructive sleep apnea syndrome: a systematic review. *J Oral Maxillofac Surg.*, 69:65-76.
10. Boyd S.B., Walters A.S., Song Y., Wang L. (2013). Comparative effectiveness of maxillomandibular advancement and uvulopalatopharyngoplasty for the treatment of moderate to severe obstructive sleep apnea. *J Oral Maxillofac Surg.* 71:743-51.
11. Logvynenko I., Dakhno L. (2018). Segmental chin osteotomy (SCO): from virtual planning to realization with surgical positioning guide to be published in: *Oral and maxillofacial surgery cases J.*, 4(3):97-107.

12. Santagata M., Tozzi U., Lamart E., Tartaro G. (2015). Effect of Orthognathic Surgery on the Posterior Airway Space in Patients Affected by Skeletal Class III Malocclusion. *Journal of maxillofacial and oral surgery*, 14(3):682-6.
13. Kawamata A., Fujishita M., Arijii Y., Arijii E. (2000). Three-dimensional computed tomographic evaluation of morphologic airway changes after mandibular setback osteotomy for prognathism. *Oral Surg Oral Med Oral Pathol Oral Radiol Endod.*, 89:278-87.
14. Al-Moraissi E., Al-Magaleh S.M., Iskandar R.A., Al-hendi E.A. (2015). Impact on the pharyngeal airway space of different orthognathic procedures for the prognathic mandible. *International Journal of Oral and Maxillofacial Surgery*, 44(9).
15. Choi S.-K., Yoon J.-E., Ch J.-W., Kim J.-W., Kim S.-J., Kim M.-R. (2014). Changes of the Airway Space and the Position of Hyoid Bone after Mandibular Set Back Surgery Using Bilateral Sagittal Split Ramus Osteotomy Technique. *Maxillofacial plastic and reconstructive surgery*, 36: 185-91.
16. Tan S.K., Leung W.K., Tang A.T.H., Zwahlen R.A (2017). How does mandibular advancement with or without maxillary procedures affect pharyngeal airways? An overview of systematic reviews. *Plos One*, 12(7):e0181146.
17. Guven O., Saraçoglu U. (2005). Changes in pharyngeal airway space and hyoid bone positions after body ostectomies and sagittal split ramus osteotomies. *J Cranio Surg.*, 16(1):23-30.
18. Pae E.K., Quas C., Quas J., Garret N. (2008). Can facial type be used to predict changes in hyoid bone position with age? A perspective based on longitudinal data. *Am J Orthod Dentofacial Orthop.*, 134(6):792-7.
19. Chen F., Terada K., Hua Y., Saito I. (2007). Effects of bimaxillary surgery and mandibular setback surgery on pharyngeal airway measurements in patients with Class III skeletal deformities. *Am J Orthod Dentofacial Orthop.*, 131:372-7.
20. Hwang S., Chung C.J., Choi Y.J., Huh J.K., Kim, K.H. (2010). Changes of hyoid, tongue and pharyngeal airway after mandibular setback surgery by intraoral vertical ramus osteotomy. *Angle Orthod.*, 80:302-8.
21. Eggensperger N., Smolka W., Iizuka T. (2005). Long-term changes of hyoid bone position and pharyngeal airway size following mandibular setback by sagittal split ramus osteotomy. *J Craniomaxillofac Surg.*, 33:111-7.

**Table 1.** RPV (cc3) data

| Patient | Chinadvancement (mm) | Change in UAV (%) | RPV (cc3)   |              |
|---------|----------------------|-------------------|-------------|--------------|
|         |                      |                   | Pre-surgery | Post-surgery |
| 1       | 11.77                | 59,5              | 9.42        | 13.53        |
| 2       | 8.54                 | 3.5               | 9.38        | 10.03        |

**Table 2.** RGV (%) data

| Patient | Change in RPV (%) | RGV (cc3)   |              | Change in RGV (%) |
|---------|-------------------|-------------|--------------|-------------------|
|         |                   | Pre-surgery | Post-surgery |                   |
| 1       | 44                | 5,53        | 10.27        | 86                |
| 2       | 7                 | 8.89        | 8.85         | -0.5              |

**Table 3.** Postoperative smallest RG area data

| Patient | Preoperative smallest RG area (mm <sup>2</sup> ) | Postoperative smallest RG area (mm <sup>2</sup> ) |
|---------|--|---|
| 1       | 84.6   | 202.1   |
| 2       | 144.72   | 146.15  |

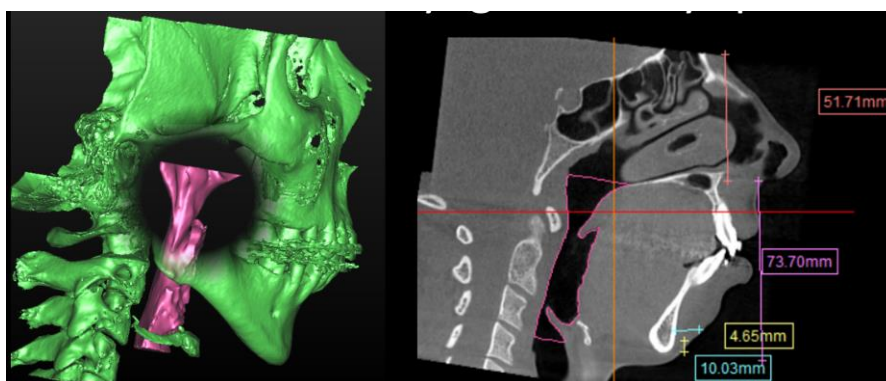


**Figure 1.** Upper airway analysis from the level of the posterior nasal spine to the lower edge of the hyoid bone in the lateral view before SCO surgery



**Figure 2.** Preoperative lateral view of the retropalatal space



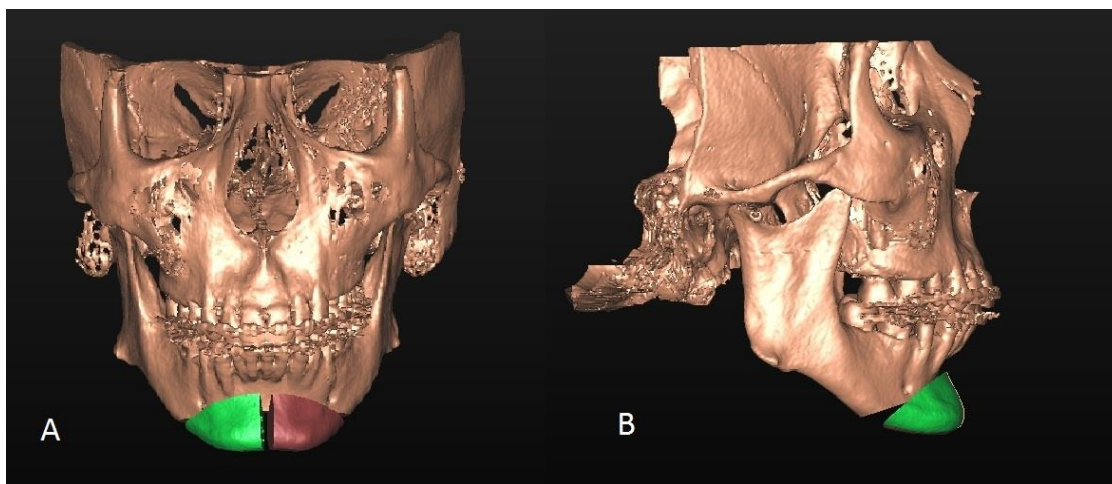


**Figure 3.** SCO 3D planning prepared for augmentation genioplasty: (A) frontal view, (B) lateral view

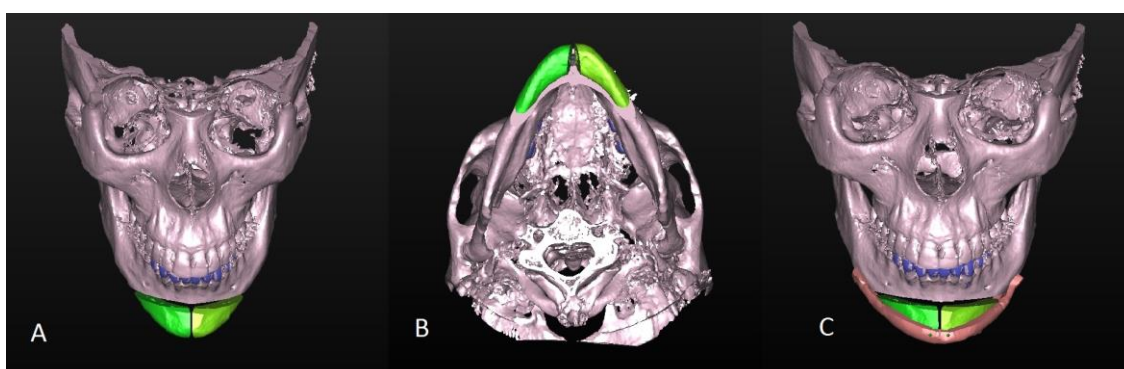


**Figure 4.** SCO 3D planning: (A) frontal view, (B) bottom view, and (C) surgical positioning guide designed for augmentation genioplasty (frontal view)



**Figure 5.** First case – (A) preoperative lateral view showing the irregular contour of the mandible, sagging of soft tissues of the cheek and neck; (B) 3 months postoperative lateral view showing the balance of soft and hard tissues, the clear contour of the mandible, and the submandibular-neck angle



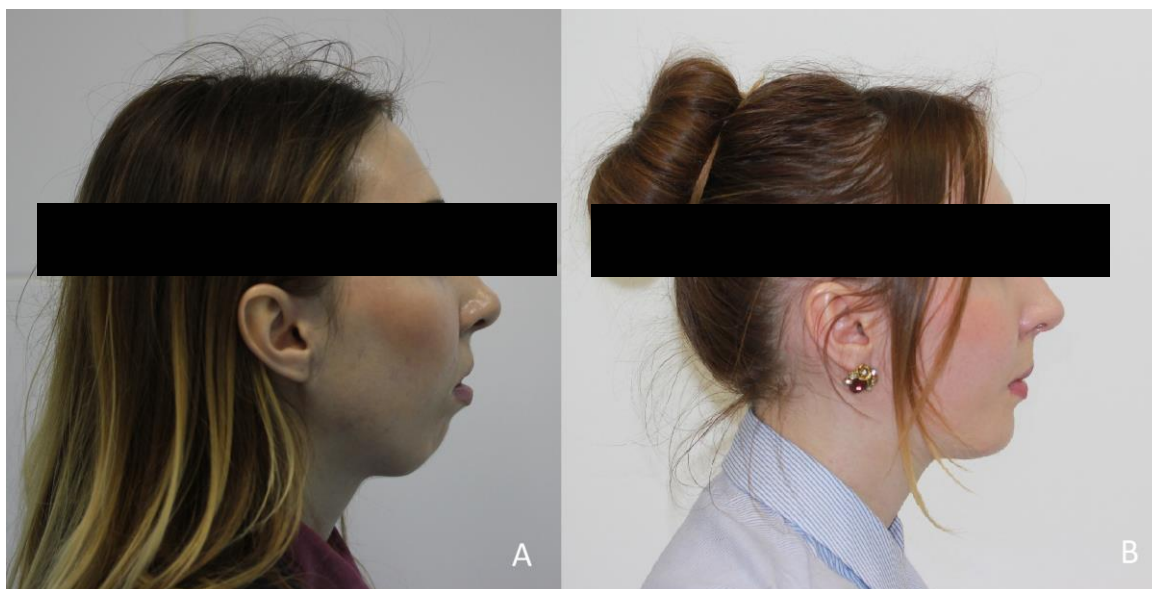


**Figure 6.** Second case – (A) preoperative lateral view showing the poor contour of the mandible and chin, horizontal chin deficiency, short mandible body, increased lower third height of the face, and incompetency of lip closure; (B) 3 months postoperative lateral view showing significant improvement of the balance of soft and hard tissues, the clear contour of the mandible, the submandibular-neck angle, and the passive adequate lip closure

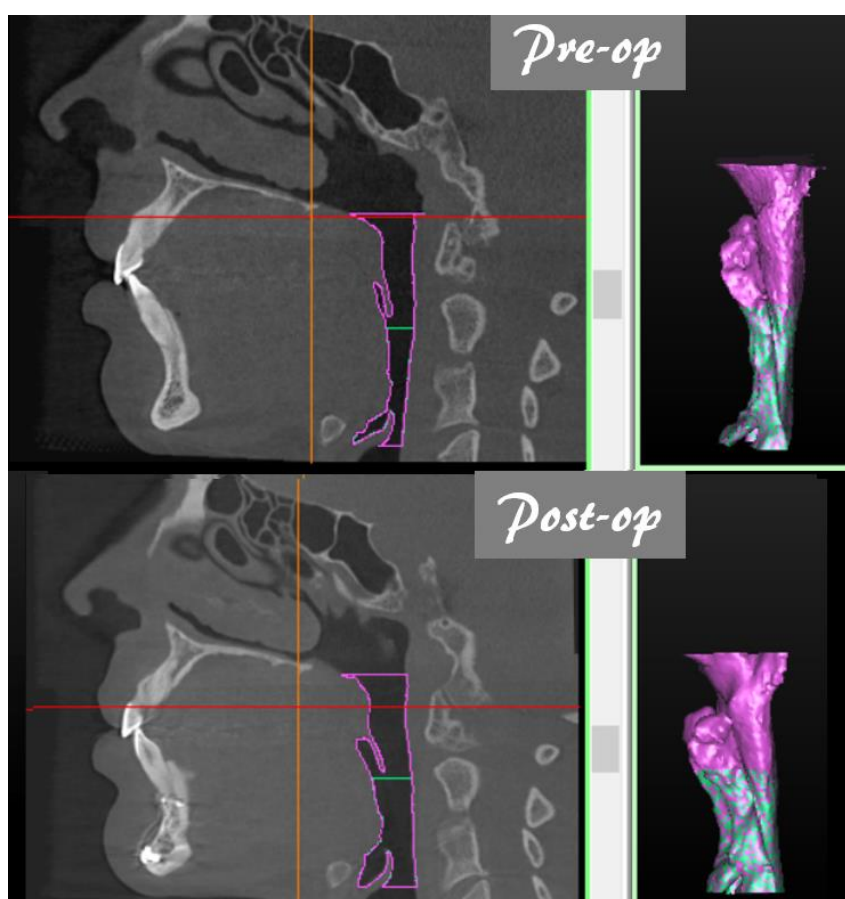


**Figure 7.** Airway comparison analysis in the lateral view before surgery operation (pre-op) and after SCO (post-op), showing a considerable airway increase

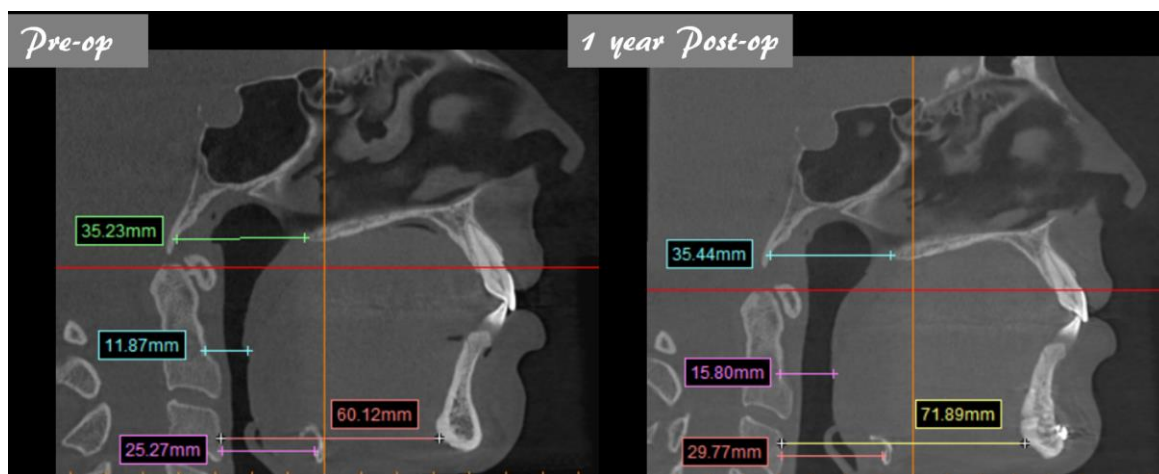


**Figure 8.** Preoperative and postoperative lateral views and measures of the first case-patient showing the advancement after genioplasty

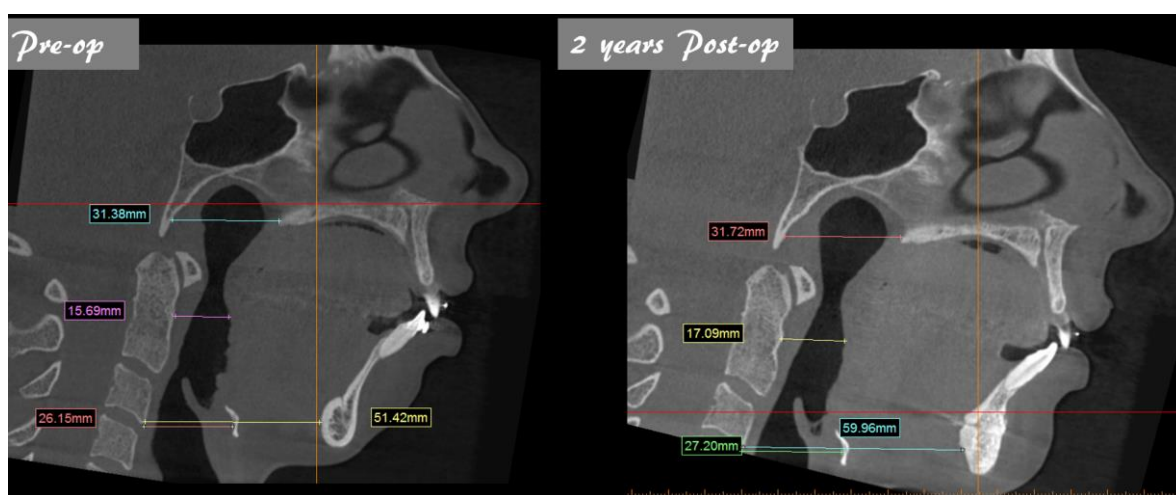


**Figure 9.** Preoperative and postoperative lateral views and measures of the second case-patient showing SCO results

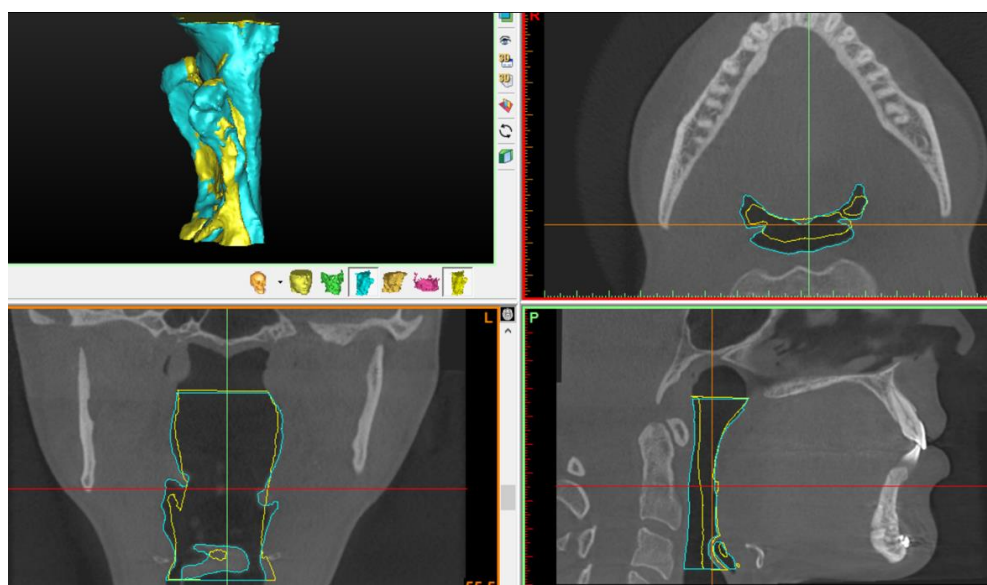


**Figure 10.** Preoperative and postoperative superimposition and changes in the anteroposterior and transverse dimensions of the upper airway in the first clinical case. Yellow outline – preoperative; blue – 1 year postoperative

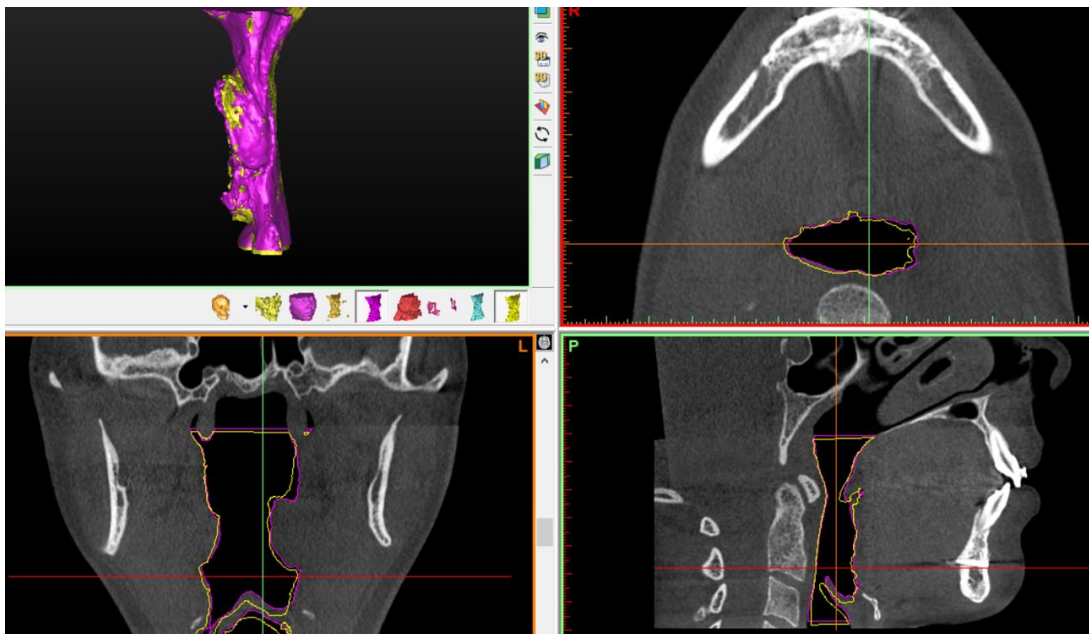


**Figure 11.** Preoperative and postoperative superimposition and changes in the anteroposterior and transverse dimensions of the upper airway in the second clinical case. Yellow outline – preoperative; pink – 1 year postoperative

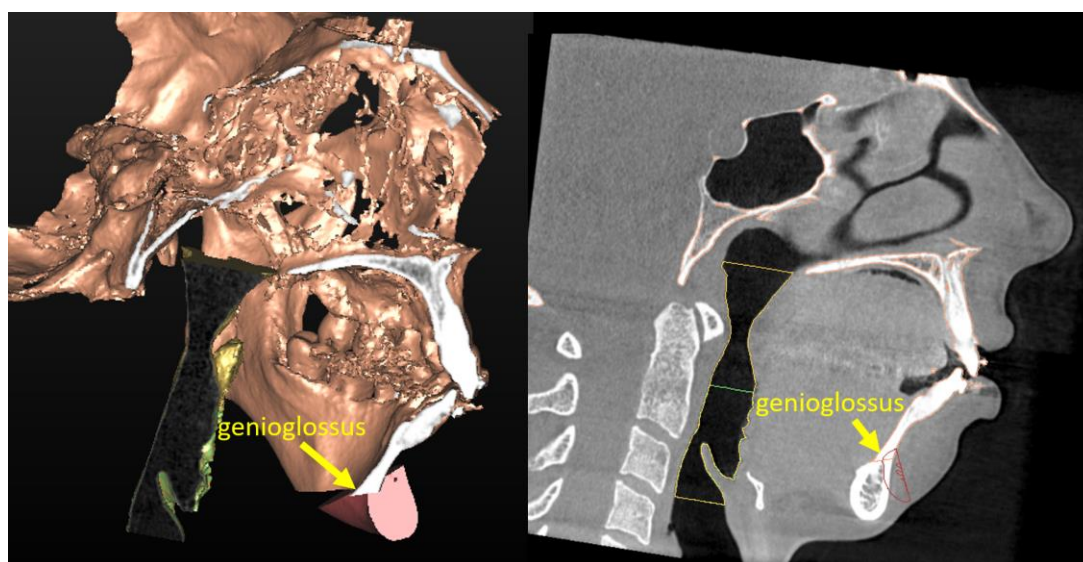


**Figure 12.** Lateral view of the osteotomy level of the chin lower than the apophysis geni superior. The yellow arrow is the origin of the genioglossus muscle in the second case



## AVALIAÇÃO DE TRATAMENTO DE EFLUENTE TÊXTIL POR ELETROFLOCULAÇÃO COM MONITORAMENTO E CONTROLE AUTOMÁTICO CONSIDERANDO ESTUDO DE VIABILIDADE DE USO DE GERAÇÃO FOTOVOLTAICA

## EVALUATION OF TREATMENT OF TEXTILE EFFLUENT BY ELECTROFLOCCULATION WITH MONITORING AND AUTOMATIC CONTROL CONSIDERING A FEASIBILITY STUDY OF THE USE OF PHOTOVOLTAIC GENERATION

COMINOTE, Marina<sup>1\*</sup>; SILVA, Gabriel Libardi<sup>2</sup>; HERINGER, Netalianne Mitchell Fagundes<sup>3</sup>; GAZEL, Façal<sup>4</sup>; OLIVEIRA, Renato César de Souza<sup>5</sup>

<sup>1,2,3,4,5</sup> Instituto Federal do Espírito Santo, *Campus Linhares*

\* *Autor correspondente*  
e-mail: mcominote@ifes.edu.br

Received 03 April 2020; received in revised form 02 June 2020; accepted 24 June 2020

### RESUMO

A eletrofloculação é uma técnica de tratamento de efluente líquido que tem sido largamente usada devido à sua simplicidade de operação e aplicação em diversos tipos de efluentes. O objetivo do trabalho foi avaliar a eficiência do tratamento por eletrofloculação com monitoramento e controle automático de um efluente de indústria têxtil, considerando ainda um estudo de viabilidade de uso de geração fotovoltaica. Os ensaios de eletrofloculação foram realizados com efluente bruto, em reator de batelada com eletrodos de alumínio, e com cuba de vidro. Utilizou-se um sistema eletrônico, constituído de sensores e um microcontrolador, para controlar a corrente e monitorar as variáveis de tensão, temperatura e tempo, processando os dados e enviando-os a um computador. O volume tratado a cada ensaio foi de 3 litros e submetidos às correntes de 1 e 2A, retirando alíquotas em 5, 10, 15 min. Os parâmetros analisados foram: pH, condutividade, turbidez, Demanda Química de Oxigênio e varredura de absorbância na faixa de 200 a 800 nm. As amostras apresentaram na região do visível uma banda com a máxima absorbância em 670nm, assim optou-se por avaliar o sistema nesse comprimento de onda. Os resultados dos ensaios de eletrofloculação mostraram que a melhor remoção de turbidez, DQO e absorbância em 670nm ocorreram nas condições de 2A/10min, com eficiência média acima de 70%. A partir do projeto elaborado de energia fotovoltaica para o sistema de tratamento, foi constatado que a melhor estratégia é conectar o sistema fotovoltaico à rede de energia elétrica. Por meio de simulação financeira foi possível identificar grande economia de energia que compensam os custos com a instalação do sistema fotovoltaico. Pode-se concluir, portanto, que o sistema tem eficiência no tratamento de efluente têxtil e que a demanda de energia elétrica consegue ser atendida por energia fotovoltaica, permitindo que o projeto seja sustentável.

**Palavras-chave:** *resíduo líquido, processo eletroquímico, eficiência, energia fotovoltaica.*

### ABSTRACT

Electroflocculation is a technique for liquid effluent treatment that has been widely used due to simplicity in operation and to the possibility of application in different types of effluents. This study aimed to evaluate the electroflocculation treatment efficiency, monitoring and controlling an effluent automatically from the textile industry, also considering a feasibility study to photovoltaic generation application. The electroflocculation tests were performed with raw effluent, in a batch reactor containing aluminum electrodes and glass vat. Sensors and a microcontroller make up the electronic system, which monitors and controls voltage, temperature, and time variables and also processes and sends the data to the computer. The tests consist of applying 1 and 2A current in a 3 liters volume taking aliquots in 5, 10, 15 min. The parameters analyzed were: pH, conductivity, turbidity, Chemical Oxygen Demand, and absorbance sweep in 200 to 800 nm range. The samples presented in the visible region a band with the maximum absorbance at 670nm; thus, it was decided to evaluate the system at this wavelength. The results of the electroflocculation tests showed that the best removal of turbidity, COD, and absorbance at 670nm occurred in the conditions of 2A / 10min, with average efficiency above 70%. A photovoltaic system was projected to meeting the demand for the energy electroflocculation system, whose analysis found that the best strategy is connecting the photovoltaic system to the electric power grid. Through financial simulation, It was identified as a significant energy-saving which offsets costs related to system installation. In conclusion, the system developed is efficient in textile effluent treatment and that the photovoltaic

system meets the demand for energy from the electroflocculation system, ensuring project sustainability.

**Keywords:** *liquid waste, electrochemical process, efficiency, photovoltaic energy.*

## 1. INTRODUÇÃO:

A poluição das águas superficiais e subterrâneas por efluentes líquidos provoca graves mudanças nas características físicas, químicas e biológicas as quais interferem na qualidade da água e praticamente impossibilitando o seu uso pelo ser humano (Crini e Lichtfouse, 2019).

A legislação ambiental, através das Resoluções CONAMA nº 357/2005 e nº 430/2011, dispõe que os efluentes de qualquer fonte poluidora somente poderão ser lançados diretamente nos corpos d'água após o devido tratamento e desde que obedeçam às condições padrões. Diante dessas exigências as empresas e indústrias buscam a implementação de sistemas de tratamento de efluentes. O sistema ideal para a empresa ou indústria é a integração do processo que gera o efluente com um processo que promova a recirculação ou reúso da água. Para que isso seja viável é necessário um processo de tratamento de efluente líquido de alta eficiência e baixo custo (Crini e Lichtfouse, 2019).

Diante dos inúmeros processos de tratamento de efluentes líquidos, a eletrofloculação (ou eletrocoagulação) é uma técnica que tem sido largamente estudada (Sen *et al.*, 2019; Babu *et al.*, 2019) devido à sua simplicidade de operação e aplicação em diversos tipos de efluentes tais como: têxtil (Núñez *et al.*, 2019; Tomassoni *et al.*, 2019), indústria de processamento de coco (Crespilho *et al.*, 2004; Jose *et al.*, 2019), laticínio (Dallago *et al.*, 2012; Tchamango *et al.*, 2020), lavanderia industrial (Orssatto *et al.*, 2016; Nugroho *et al.*, 2020), água pluvial (Zhang *et al.*, 2012; Carvalho *et al.*, 2019), reciclagem de papel (Katal e Pahlavanzadeh, 2011; Izadi *et al.*, 2018), doméstico (Kurt *et al.*, 2008; Bracher *et al.*, 2019), refinaria de óleos vegetais (Preethi *et al.*, 2020; Swati *et al.*, 2020), metais tóxicos (Koby et al., 2017; Krystynik *et al.*, 2019).

Esta técnica de tratamento faz uso de corrente elétrica para a geração de agentes coagulantes/floculantes em reações de oxidação. Os metais mais utilizados nos eletrodos de sacrifício são o ferro (Fe) e o alumínio (Al) devido a eficácia no processo de floculação e ao seu baixo custo (Sen *et al.*, 2019). Entretanto, a

eficiência do sistema pode alterar entre os eletrodos de ferro (Fe) e alumínio (Al) (Sher *et al.*, 2019; Aygun *et al.*, 2019; Papadopoulos *et al.*, 2019).

Para garantir a eficiência do sistema de eletrofloculação no processo de remoção dos contaminantes do efluente, é fundamental monitorar e controlar: a corrente elétrica aplicada, a distância entre os eletrodos, a agitação, o tempo de eletrólise, a condutividade do efluente, o pH inicial do efluente e a temperatura (Hashim *et al.*, 2019; Bracher *et al.*, 2019; Nidheesh *et al.*, 2020).

O consumo de energia elétrica, que se faz necessário na operação do sistema de tratamento por eletrofloculação, é uma das principais desvantagens ao defrontá-lo com sistemas convencionais, pois a mesma pode ser cara em certos lugares (Mollah *et al.*, 2001). Normalmente o consumo de energia contribui acima de 50% do gasto unitário (Mao *et al.*, 2008).

Dentre várias fontes de energia a energia solar fotovoltaica se destaca por ter a capacidade de se instalar em qualquer lugar, gerando eletricidade no mesmo local de utilização, por ter baixa necessidade de manutenção e por ser autossuficiente e renovável (Sampaio e González 2017). Estudos realizados por Pavón-Silva *et al.* (2018) e Khemila *et al.* (2018), em que ambos trabalharam com efluentes sintéticos (produzidos com corantes distintos), com eletrodos de alumínio, com reator de eletrofloculação de fluxo contínuo e com módulos fotovoltaicos conectados diretamente ao reator, obtiveram respectivamente uma eficiência de remoção dos corantes de 70% e 95%, demonstrando que é possível utilizar essa fonte de energia. Entretanto Pavón-Silva *et al.* (2018), salienta que além da eficiência de remoção de poluentes no efluente é importante também levar em consideração os custos de implementação dessa fonte de energia.

Diante do exposto e frente a escassez dos recursos naturais e contaminação dos recursos hídricos este trabalho visou montar e avaliar em escala laboratorial um sistema de tratamento para efluente líquido gerado por empresa têxtil, utilizando a técnica de eletrofloculação com monitoramento e controle

automático, considerando ainda um estudo de viabilidade econômica de uso de geração de energia fotovoltaica.

## 2. MATERIAIS E MÉTODOS:

Com base na tipologia do efluente proposto para os ensaios de tratamento por eletrofloculação optou-se pelo efluente bruto de uma empresa localizada no município de Linhares/ES, na qual apresenta atividade de lavanderia (descoloração) e tingimento. Esse processo industrial gera grande volume de efluente e com enorme diversidade e complexidade de compostos orgânicos e inorgânicos tóxicos em emulsão, os quais se destacam os corantes (Kumar e Saravanan, 2017; Hossini *et al.*, 2017; Samanta *et al.*, 2019).

As amostras foram coletadas na caixa de entrada da estação de tratamento de efluentes da empresa nos dias 26/04/18, 14/06/18, 12/04/19, 10/05/19 e 31/05/19. A caracterização do efluente foi realizada no laboratório de química do Ifes *campus* Linhares por meio dos seguintes parâmetros: pH, condutividade, turbidez, demanda química de oxigênio (DQO). As análises foram realizadas seguindo metodologias propostas pelo "Standart Methods for the Examination of Water and Wasterwater" (Rice *et al.*, 2012).

### 2.1. Reator de bancada

O reator de batelada foi construído com eletrodos de alumínio constituído por 8 lâminas com dimensões de 19 cm de comprimento, 3 cm de largura, e 1 mm de espessura (Figura 1). A cuba foi construída em vidro com as seguintes dimensões: 20 cm de altura, 20 cm de comprimento e 10 cm de largura.

O reator foi alimentado por uma fonte de corrente contínua regulável, ou seja, que viabilize o ajuste dos valores da intensidade da corrente a ser aplicada no efluente.

Durante o processo de eletrofloculação é necessário que a corrente elétrica permaneça constante. Ocorre que no início do processo a resistência do meio aquoso (eletrólito) é maior, assim se faz necessário aplicar uma tensão mais alta para um dado valor de corrente. Com o decorrer da reação de oxidação são liberados íons de alumínio ( $Al^{3+}$ ) aumentando a condutividade e consequentemente diminuindo a resistência elétrica apresentada pelo eletrólito, sendo assim, o valor de tensão para manter a corrente constante deve ser menor.

Desta forma, foi necessário monitorar a tensão e ainda a temperatura a fim de realizar as análises necessárias. O sistema eletrônico utilizado para fazer o monitoramento e controle dos ensaios de eletrofloculação foi composto por um microcontrolador Atmega328P presente na plataforma Arduino Nano, sendo o responsável pela atuação, leitura e envio de informações do reator para o computador através de uma interface USB.

Para ler e armazenar os valores da tensão aplicada aos eletrodos, foi necessário realizar um condicionamento de dados, por meio de um circuito divisor de tensão resistivo, e um filtro com uso de capacitor.

A leitura da temperatura foi realizada por meio do sensor DS18B20 que possui uma faixa de medição de  $-55^{\circ}C$  a  $125^{\circ}C$ , exatidão de  $0.5^{\circ}C$ . A comunicação entre sensor e microcontrolador foi realizada através das bibliotecas "Dallas Temperature e OneWire".

As informações coletadas e tratadas pelo microcontrolador foram enviadas a um computador portátil por meio de uma comunicação serial com a porta USB. O software PLX-DAQ foi utilizado em conjunto com um software de edição de planilhas para receber, armazenar e exibir todas as variáveis do processo em uma planilha (Figura 2).

A Figura 3 apresenta o sistema eletrônico montado.

### 2.2. Ensaios de eletrofloculação

Os ensaios foram realizados com as amostras coletadas nos dias 12/04/19, 10/05/19 e 31/05/19. O volume do efluente a cada ensaio foi de 3 litros e manteve sob constante agitação (300 rpm), com auxílio de agitador magnético. Essas amostras foram submetidas a correntes de 1 e 2A, recolhendo alíquotas de 100ml nos tempos de 5, 10 e 15 minutos. Para a remoção das alíquotas adotou-se o seguinte procedimento: desligar a agitação, esperar 2 minutos para o material flotar ou sedimentar, e com auxílio de uma pipeta posicionada no centro da cuba retirar o volume de 100ml.

As alíquotas foram filtradas à vácuo com papel de filtro qualitativo que retém partículas maiores que  $19\mu m$  (marca: J. Prolab). Esse procedimento foi adotado para evitar possíveis variações nos resultados relativos aos diferentes tempos de flotação ou sedimentação das partículas de cada amostra. Posteriormente foram executados os ensaios dos parâmetros:

pH, turbidez, demanda química de oxigênio (DQO) e varredura de absorvância na faixa de 200 a 800 nm em espectrofotômetro Agilent-Cary60/UV-Vis.

### 2.3. Energia fotovoltaica

Analisando a literatura e outros trabalhos que utilizam a energia fotovoltaica de forma a prover o fornecimento de energia a sistemas de eletrofloculação, foram levantadas três possíveis maneiras de trabalhar com o sistema fotovoltaico: I) sistema *off-grid* com armazenamento de energia em baterias (Vieira e Cavalcante, 2018; de Lima *et al.*, 2019); II) sistema *off-grid* conectado ao sistema de eletrofloculação sem meios de armazenamento (de Lima *et al.*, 2019; Rahmani *et al.*, 2017; Balabel *et al.*, 2014); III) sistema *grid-tie* (conectado à rede elétrica de forma híbrida ao fornecimento de energia da concessionária) (Akikur *et al.*, 2013) utilizando a compensação de crédito de energia conforme resolução (ANEEL, 2012).

A primeira opção foi desconsiderada por estar em desacordo com a proposta de sustentabilidade ambiental do trabalho. A utilização de baterias aumenta o custo do sistema e seu descarte gera resíduos poluentes. As outras duas formas descritas foram analisadas para avaliar a melhor proposta. Foi realizado um projeto para atendimento da unidade consumidora considerando apenas o consumo de energia demandado pelo sistema de eletrofloculação, com o intuito de comparar financeiramente o custo de implementação do sistema e o tempo de retorno do investimento.

## 3. RESULTADOS E DISCUSSÃO:

### 3.1. Características físico-químicas do efluente bruto.

Na Tabela 1 encontram-se os resultados de caracterização das amostras de efluente bruto coletadas em dias e anos distintos. Verifica-se que os valores de pH do efluente bruto apresentaram próximo de neutro, com exceção da amostra 5 que apresentou caráter ácido (pH = 4,1). Para esse tipo de efluente já foram encontrados na literatura valores de pH da faixa ácida (Pizato *et al.*, 2016), próximo da neutra (Afanga *et al.*, 2020; Bener *et al.*, 2019; Núñez *et al.*, 2019; Nidheesh *et al.*, 2020) até a alcalina (Cerqueira *et al.*, 2009; Soltani *et al.*, 2019).

O efluente bruto apresentou valores de DQO (173 a 410 mgO<sub>2</sub>/L) próximos aos

resultados encontrados por Afanga *et al.* (2020), Bener *et al.* (2019), Soltani *et al.* (2019) e Núñez *et al.* (2019), e baixo comparando com os teores encontrados por Cerqueira *et al.* (2009), 1.179 a 2.553 mgO<sub>2</sub>/L, por Nidheesh *et al.* (2020) 1.727 mgO<sub>2</sub>/L, e por Pizato *et al.* (2016), 659 mgO<sub>2</sub>/L.

As amostras do efluente de estudo apresentaram valores de turbidez (62,8 a 249 NTU) superior aos identificados por outros trabalhos: Cerqueira *et al.* (2009), 8,0 a 75,3 NTU; Pizato *et al.* (2016), 37 NTU; Bener *et al.* (2019), 15 a 35 NTU; Núñez *et al.* (2019), 12,5 NTU.

A condutividade do efluente de estudo apresentou resultado elevado (52 a 121 mS/cm) comparando com efluentes de mesma tipologia caracterizados por Cerqueira *et al.* (2009), Pizato *et al.* (2016), Afanga *et al.* (2020), Bener *et al.* (2019) e Núñez *et al.* (2019) que foram respectivamente 4,61; 0,80; 2,5; 8,96 e 0,67 mS/cm. Para sistema de tratamento por eletrofloculação esse resultado se torna vantajoso, pois diminui a resistividade do meio demandando menor tensão para manter a corrente.

### 3.2. Avaliação da eficiência do sistema de tratamento

Os resultados dos ensaios de eletrofloculação para a amostra 3 (Tabelas 2 e 3), mostram que a melhor remoção de turbidez e DQO ocorreram nas condições de 2A/10min. com eficiência de 87% e 80% respectivamente. Verifica-se também para a amostra 4, nas mesmas condições (2A/10min.), um comportamento semelhante com remoção de turbidez de 93%, e DQO de 81%. Essa mesma eficiência foi encontrada por Cerqueira *et al.* (2009), turbidez 98% e DQO 87%, entretanto as condições de ensaio foram diferentes, tais como: ajuste de pH inicial do efluente bruto para o valor próximo de 7; formato dos eletrodos de alumínio; corrente 15A; tempo de eletrofloculação de 30min.

Todavia a amostra 5 apresentou comportamento diferente, pois ocorreu melhor remoção de turbidez em 1A/5min de 91%, e a DQO apresentou uma redução máxima de 57% em 2A/10min, valor esse bem inferior comparado com as outras amostras. Sabe-se que o pH inicial do efluente a ser tratado por eletrofloculação influencia significativamente na eficiência do processo (Cerqueira *et al.*, 2009; Tchamango *et al.*, 2020; Nidheesh *et al.*, 2020; Bener *et al.*, 2019). O valor do pH inicial (4,1)

dessa amostra foi o que possivelmente corroborou para a queda da remoção de DQO, esse comportamento também foi constatado por Vepsäläinen e Sillanpää (2020) e por Nidheesh *et al.* (2020), usando eletrodos de alumínio.

Verifica-se que o pH do efluente no decorrer dos ensaios (Tabela 2) aumenta gradualmente até valores na faixa de neutro. Esse sistema de tratamento tem a grande vantagem de manter ou tornar o efluente com pH neutro por meio das reações que ocorrem no catodo, redução do hidrogênio, e no anodo, oxidação do alumínio seguida de hidrólise.

As varreduras espectrais das 3 amostras de efluente bruto filtrado (Figura 4) apresentaram na região do visível uma banda com a máxima absorvância em 670nm. Esse pico de absorvância próximo a esse comprimento de onda também foi constatado por Pizato *et al.* (2016) e Afanga *et al.* (2020) num efluente de mesma tipologia. Assim optou-se por calcular o percentual de remoção ou verificar a eficiência dos ensaios por meio da absorvância nesse comprimento de onda.

A remoção da absorvância em 670nm foi muito rápida, pois logo nos primeiros 5min de ensaio constata-se uma remoção de 74 a 97% na menor amperagem (Tabelas 2 e 3). Assim pode-se considerar que o sistema tem uma ótima eficiência na remoção de substâncias que absorvem nesse comprimento de onda.

A varredura espectral de todos os ensaios realizados com a amostra 3 (Figura 5) mostra que também há decaimento da absorvância em toda a faixa do visível e em parte do ultravioleta. O mesmo comportamento foi observado com as amostras 4 e 5.

Foi possível verificar visualmente a remoção de sólidos em suspensão e a cor das amostras do efluente (Figuras 6 e 7) durante os ensaios. Constata-se também que em ambos os ensaios das amostras 3 e 4 em 2A/15min o sistema encontra-se saturado do agente floculante, pois há uma espessa camada de espuma branca, o que provocou possivelmente o aumento da turbidez e da DQO (Tabela 2).

Durante os ensaios de eletrofloculação a temperatura do efluente foi monitorada e manteve-se entre 25 a 27°C, assim averigua-se que nos ensaios esse parâmetro não variou de forma significativa.

### 3.3. Viabilidade de uso de energia fotovoltaica

Com os resultados da porcentagem média de remoção das amostras 3, 4 e 5 dos parâmetros DQO, turbidez e absorvância em 670nm contidos na Figura 8, verifica-se que a melhor condição do ensaio de eletrofloculação foi com 2A no tempo de 10min.

Nesta condição, foi possível identificar que o maior consumo de energia aconteceu quando o valor de tensão era de 5,38V com 0,6Wh/l (Tabela 2).

De acordo com Kobya *et al.* (2006) o consumo de energia em um reator batelada pode ser calculado utilizando-se a equação 1 adaptada:

$$E = \frac{V \cdot i \cdot t}{1000 \cdot v} \quad (\text{Eq. 1})$$

Onde:

E: energia em KWh

V: tensão elétrica aplicada ao processo em Volts (V).

i: corrente elétrica aplicada em amperes (A).

T: tempo de aplicação da corrente ou tempo de processo (h).

v: volume tratado em m<sup>3</sup>.

Conhecendo o valor de consumo médio mensal encontrado pela equação, para um sistema *grid-tie* (conectado à rede elétrica), o projeto foi realizado considerando inclinação dos módulos em 19° Norte e dados de irradiação solar diária média mensal do local com a base de dados do SunData (Brito, 2008). Uma análise de viabilidade econômica foi levantada considerando os principais critérios abordados na literatura (Lopez, 2012; Türkay e Telli, 2011) Bazilian *et al.*, 2013; de Almeida *et al.*, 2017) como custo de instalação, previsão de geração, tempo de retorno do investimento e economia total no final da vida útil do sistema implantado.

Foi prevista a instalação de 13 módulos Canadian Solar CS6U-320P. Os módulos estariam conectados em série a um inversor Fronius Primo 5.0-1 possibilitando a conexão na rede. A Tabela 4 apresenta a irradiação solar média mensal da região considerada e a Figura 9 apresenta a previsão de geração com o consumo médio considerado do sistema. Com estimativa de preço baseado no mercado, considerando



equipamentos e instalação, o custo médio de instalação do sistema é aproximadamente R\$25.940.

A fim de avaliar financeiramente a viabilidade da utilização deste sistema, considerando a unidade consumidora do grupo A, com geração de energia e abatimento em crédito no horário fora ponta, a simulação foi realizada observando as relevâncias de algumas variáveis como incidência de impostos, previsão de aumento do Kwh ao ano e valor de tarifa baseado na regulamentação da distribuidora onde se encontra a indústria (EDP, 2019). A Figura 10 apresenta o resultado da simulação. Considerando a vida útil do sistema em 25 anos, a economia total simulada ao final da vida útil do sistema é de R\$88.716,00.

Para um sistema *off-grid* (sem bateria), seria necessário a construção de um conversor eletrônico que permitisse a regulação do ponto de operação elétrico do sistema. Considerando o número de módulos utilizados no projeto anterior (sistema *grid-tie*) e a previsão de geração mostrada na Figura 9, é possível identificar que durante os meses de abril a agosto o sistema fotovoltaico geraria menos energia do que seria consumido pelo sistema de eletrofloculação. Contudo se o sistema for *grid-tie* (conectado à rede elétrica), isso não seria um problema, pois a energia excedente nos meses de alta geração compensaria os meses de baixa geração (a energia seria convertida em créditos).

Assim, em um sistema *off grid* (sem bateria), é necessário projetar levando em consideração o pior mês de geração (junho), desse modo o número de módulos deverá aumentar para 17. A previsão de geração é retratada na Figura 11.

Em uma pesquisa de mercado é possível identificar que mesmo sem a utilização do inversor, o preço do sistema sem conexão à rede passa a não compensar pelo fato da geração ser superdimensionada para atender aos meses de menor radiação solar na região. Neste caso o projeto mais indicado é o sistema *grid-tie* (conectado à rede elétrica) que atende à demanda de energia do sistema de eletrofloculação de maneira eficiente.

#### 4. CONCLUSÕES:

A técnica de eletrofloculação com eletrodos de alumínio mostrou-se ter grande eficiência na remoção de substâncias que absorvem a luz na faixa espectral do visível

independente das características iniciais do efluente bruto têxtil. As remoções de turbidez e Demanda Química de Oxigênio (DQO) também foram eficientes, entretanto tiveram variações significativas principalmente em função do pH inicial do efluente.

As condições dos ensaios de eletrofloculação que levaram a melhor eficiência de tratamento do efluente de estudo foram quando se manteve a corrente em 2A e tempo de processo 10 min.

Em relação ao consumo de energia, as simulações financeiras, baseadas no projeto de um sistema fotovoltaico, apontam que o sistema do tipo *grid-tie* (conectado à rede elétrica) é a melhor forma de atender à demanda de energia do sistema de eletrofloculação. Apesar dos custos de instalação do sistema fotovoltaico, a longo prazo, existe não apenas um retorno do investimento, mas também economia financeira, além de garantir a sustentabilidade da proposta.

#### 5. REFERÊNCIAS:

1. ANEEL (2012, 17 de abril). *Resolução normativa nº 482*. Retrieved from <http://www2.aneel.gov.br/cedoc/ren2012482.pdf>.
2. Akikur, R. K., Saidur, R., Ping, H. W., & Ullah, K. R. (2013). Comparative study of stand-alone and hybrid solar energy systems suitable for off-grid rural electrification: A review. *Renewable and Sustainable Energy Reviews*, 27(C), 738-752.
3. Aygun, A., Nas, B., & Sevimli, M. F. (2019). Treatment of reactive dyebath wastewater by electrocoagulation process: Optimization and cost-estimation. *Korean Journal of Chemical Engineering*, 36(9), 1441-1449.
4. Balabel, A., Zaky, M. S., & Sakr, I. (2014). Optimum operating conditions for alkaline water electrolysis coupled with solar PV energy system. *Arabian Journal for Science and Engineering*, 39(5), 4211-4220.
5. Bazilian, M., Onyeji, I., Liebreich, M., MacGill, I., Chase, J., Shah, J., ... & Zhengrong, S. (2013). Re-considering the economics of photovoltaic power. *Renewable Energy*, 53, 329-338.
6. Bener, S., Bulca, Ö., Palas, B., Tekin, G., Atalay, S., & Ersöz, G. (2019).

- Electrocoagulation process for the treatment of real textile wastewater: effect of operative conditions on the organic carbon removal and kinetic study. *Process Safety and Environmental Protection*, 129, 47-54.
7. Bracher, G. H., Carissimi, E., Wolff, D. B., Graepin, C., & Hubner, A. P. (2020). Optimization of an electrocoagulation-flotation system for domestic wastewater treatment and reuse. *Environmental Technology*, 1-11.
  8. Brito, S. D. S. (2008). Centro de referência para energia solar e eólica. *CRESESB Informe-Rio de Janeiro*, 12(13), 3.
  9. Carvalho, E. H. D. S., Cuba, R. M. F., de Carvalho, R. V., & Marra, E. G. (2019). Application of eletrocoagulation/flotation process for rainwater reuse. *Periódico Tchê Química*, 16(31), 89-94.
  10. Cerqueira, A., Russo, C., & Marques, M. R. C. (2009). Electroflocculation for textile wastewater treatment. *Brazilian Journal of Chemical Engineering*, 26(4), 659-668.
  11. CONAMA (2005, 17 de março). *Resolução n° 357*. Retrieved from <http://www2.mma.gov.br/port/conama/legiabre.cfm?codlegi=459>.
  12. CONAMA (2011, 13 de maio). *Resolução n° 430*. Retrieved from <http://www2.mma.gov.br/port/conama/legiabre.cfm?codlegi=646>.
  13. Crespilho, F. N., Santana, C. G., & Rezende, M. O. O. (2004). Tratamento de efluente da indústria de processamento de coco utilizando eletroflotação. *Química Nova*, 27(3), 387-392.
  14. Crini, G., & Lichtfouse, E. (2019). Advantages and disadvantages of techniques used for wastewater treatment. *Environmental Chemistry Letters*, 17(1), 145-155.
  15. Dallago, R., Di Luccio, M., Kühn, M., Krebs, J., Do Nascimento, M. S., Benazzi, T., ... & Mores, R. (2012). Eletrofloculação Aplicada ao Tratamento de Efluente de Laticínio. *PERSPECTIVA, Erechim*, 36(135), 101-111.
  16. Darvishi Cheshmeh Soltani, R., Jorfi, S., Alavi, S., Astereki, P., & Momeni, F. (2020). Electrocoagulation of textile wastewater in the presence of electro-synthesized magnetite nanoparticles: simultaneous peroxi-and ultrasonic-electrocoagulation. *Separation Science and Technology*, 55(5), 945-954.
  17. de Almeida, R. R. G., Brito, N. S. D., Medeiros, M. V. B., Simões, M. C. S., & de Oliveira, S. A. (2017). Proposição de uma metodologia para análise de viabilidade econômica de uma usina fotovoltaica. *Rev Principia*, 1(34), 84-92.
  18. de Lima, G. G. C., de Lima, C. A. P., Costa, R. B., de Medeiros, K. M., & Vieira, F. F. (2019). Eletrofloculação alimentada via energia solar fotovoltaica para o tratamento de águas eutrofizadas. *Congresso Brasileiro de Engenharia Sanitária. 30º Congresso ABES 2019*, II(406), 1-6.
  19. Hashim, K. S., Kot, P., Zubaidi, S. L., Alwash, R., Al Khaddar, R., Shaw, A., ... & Aljefery, M. H. (2020). Energy efficient electrocoagulation using baffle-plates electrodes for efficient Escherichia coli removal from wastewater. *Journal of Water Process Engineering*, 33, 101079.
  20. Hossini, H., Darvishi Cheshmeh Soltani, R., Safari, M., Maleki, A., Rezaee, R., & Ghanbari, R. (2017). The application of a natural chitosan/bone char composite in adsorbing textile dyes from water. *Chemical Engineering Communications*, 204(9), 1082-1093.
  21. EDP (2019, 06 de agosto). Tarifas - clientes atendidos em Baixa Tensão (Grupo B). *Resolução Homologatória: n°2.589*. Retrieved from <https://www.edp.com.br/distribuicao-es/saiba-mais/informativos/tabela-de-fornecimento-de-baixa-tensao>.
  22. Izadi, A., Hosseini, M., Darzi, G. N., Bidhendi, G. N., & Shariati, F. P. (2018). Treatment of paper-recycling wastewater by electrocoagulation using aluminum and iron electrodes. *Journal of Environmental Health Science and Engineering*, 16(2), 257-264.
  23. Jose, S., Mishra, L., Debnath, S., Pal, S., Munda, P. K., & Basu, G. (2019). Improvement of water quality of remnant from chemical retting of coconut fibre through electrocoagulation and activated carbon treatment. *Journal of cleaner production*, 210, 630-637.
  24. Katal, R., & Pahlavanzadeh, H. (2011).

- Influence of different combinations of aluminum and iron electrode on electrocoagulation efficiency: *Application to the treatment of paper mill wastewater. Desalination*, 265(1-3), 199-205.
25. Khemila, B., Merzouk, B., Chouder, A., Zidelkhir, R., Leclerc, J. P., & Lapicque, F. (2018). Removal of a textile dye using photovoltaic electrocoagulation. *Sustainable Chemistry and Pharmacy*, 7, 27-35.
  26. Kobya, M., Demirbas, E., Can, O. T., & Bayramoglu, M. (2006). Treatment of levafix orange textile dye solution by electrocoagulation. *Journal of hazardous materials*, 132(2-3), 183-188.
  27. Kobya, M., Demirbas, E., Ozyonar, F. U. A. T., Sirtbas, G., & Gengec, E. R. H. A. N. (2017). Treatments of alkaline non-cyanide, alkaline cyanide and acidic zinc electroplating wastewaters by electrocoagulation. *Process Safety and Environmental Protection*, 105, 373-385.
  28. Krystynik, P., Masin, P., Krusinova, Z., & Kluson, P. (2019). Application of electrocoagulation for removal of toxic metals from industrial effluents. *International Journal of Environmental Science and Technology*, 16(8), 4167-4172.
  29. Kumar, P. S., & Saravanan, A. (2017). Sustainable wastewater treatments in textile sector. In *Sustainable fibres and textiles. Woodhead Publishing*, 323-346.
  30. Kurt, U.; Gonullu, M.T.; Ilhan, F.; Varinca, K. (2008) Treatment of domestic wastewater by electrocoagulation in a cell with Fe-Fe electrodes. *Environmental Engineering Science*, 25(2), 153-161.
  31. Lopez, R. A. (2012). *Energia solar para produção de eletricidade*. São Paulo: Artliber.
  32. Mao, X., Hong, S., Zhu, H., Lin, H., Wei, L., & Gan, F. (2008). Alternating pulse current in electrocoagulation for wastewater treatment to prevent the passivation of al electrode. *Journal of Wuhan University of Technology-Mater. Sci. Ed.*, 23(2), 239-241.
  33. Mollah, M. Y. A., Schennach, R., Parga, J. R., & Cocke, D. L. (2001). Electrocoagulation (EC)—science and applications. *Journal of hazardous materials*, 84(1), 29-41.
  34. Nidheesh, P. V., Kumar, A., Babu, D. S., Scaria, J., & Kumar, M. S. (2020). Treatment of mixed industrial wastewater by electrocoagulation and indirect electrochemical oxidation. *Chemosphere*, 126437.
  35. Nugroho, F. A., Sani, M. M., Apriyanti, F., & Aryanti, P. T. P. (2020). The Influence of Applied Current Strength and Electrode Configuration in Laundry Wastewater Treatment by Electrocoagulation. In *Journal of Physics: Conference Series*, 1477, 052018.
  36. Núñez, J., Yeber, M., Cisternas, N., Thibaut, R., Medina, P., & Carrasco, C. (2019). Application of electrocoagulation for the efficient pollutants removal to reuse the treated wastewater in the dyeing process of the textile industry. *Journal of hazardous materials*, 371, 705-711.
  37. Orssatto, F., Ewerling, A., do Amaral Domingues, M. D., Eduardo, E. Y. N. G., & Tavaré, M. H. F. (2016). Tratamento de efluente de uma lavanderia industrial por meio da eletrofloculação: Uma opção para o reúso. *Revista ESPACIOS*, 37 (11), 07.
  38. Papadopoulos, K. P., Argyriou, R., Economou, C. N., Charalampous, N., Dailianis, S., Tatoulis, T. I., ... & Vayenas, D. V. (2019). Treatment of printing ink wastewater using electrocoagulation. *Journal of environmental management*, 237, 442-448.
  39. Pavón-Silva, T. B., Romero-Tehuiztil, H., Munguia del Río, G., & Huacuz-Villamar, J. (2018). Photovoltaic energy-assisted electrocoagulation of a synthetic textile effluent. *International Journal of Photoenergy*, 2018.
  40. Pizato, E., Lopes, A. C., Rocha, R. D. C., Barbosa, A. D. M., & Cunha, M. A. A. D. (2017). Caracterização de efluente têxtil e avaliação da capacidade de remoção de cor utilizando o fungo *Lasioidiplodia theobromae* MMPI. *Engenharia Sanitaria e Ambiental*, 22(5), 1027-1035.]
  41. Preethi, V., Ramesh, S. T., Gandhimathi, R., & Nidheesh, P. V. (2020). Optimization of batch electrocoagulation process using Box-Behnken experimental design for the treatment of crude vegetable oil refinery

- wastewater. *Journal of Dispersion Science and Technology*, 41(4), 592-599.
42. Rahmani, A., Zerrouki, D., Djafer, L., & Ayrat, A. (2017). Hydrogen recovery from the photovoltaic electroflocculation-flotation process for harvesting *Chlorella pyrenoidosa* microalgae. *International Journal of Hydrogen Energy*, 42(31), 19591-19596.
  43. Rice, E.W., Baird, R.B., Eaton, A.D., (2012). *Standard methods for the examination of water and wastewater* (22nd ed.). Washington, U.S.A: American Public Health Association, American Water Works Association and Water Environment Federation.
  44. Samanta, K. K., Pandit, P., Samanta, P., & Basak, S. (2019). Water consumption in textile processing and sustainable approaches for its conservation. In *Water in textiles and fashion*. Woodhead Publishing, 41-59.
  45. Sampaio, P. G. V., & González, M. O. A. (2017). Photovoltaic solar energy: Conceptual framework. *Renewable and Sustainable Energy Reviews*, 74, 590-601.
  46. Sen, S., Prajapatib, A. K., Bannatwalac, A., & Pala, D. (2019). Electrocoagulation treatment of industrial wastewater including textile dyeing effluent—a review. *DESALINATION AND WATER TREATMENT*, 161, 21-34.
  47. Sher, F., Hanif, K., Iqbal, S. Z., & Imran, M. (2020). Implications of advanced wastewater treatment: Electrocoagulation and electroflocculation of effluent discharged from a wastewater treatment plant. *Journal of Water Process Engineering*, 33, 101101.
  48. Swati, S., Ahmet, A., & Halis, S. (2020). Electrochemical treatment of sunflower oil refinery wastewater and optimization of the parameters using response surface methodology. *Chemosphere*, 126511.
  49. Syam Babu, D., Anantha Singh, T. S., Nidheesh, P. V., & Suresh Kumar, M. (2019). Industrial wastewater treatment by electrocoagulation process. *Separation Science and Technology*, 1-33.
  50. Tchamango, S. R., Wandji Ngayo, K., Belibi Belibi, P. D., Nkouam, F., & Ngassoum, M. B. (2020). Treatment of a dairy effluent by classical electrocoagulation and indirect electrocoagulation with aluminum electrodes. *Separation Science and Technology*, 1-12.
  51. Tomassoni, F., Giroletti, C. L., Dalari, B. L. S. K., Nagel-Hassemmer, M. E., Recio, M. Á. L., & Lapolli, F. R. (2019). Otimização da eletrocoagulação aplicada em efluente têxtil. *A Revista DAE é classificada pelo QUALI/CAPEs e está adicionada/indexada nas seguintes bases*, 67, 89-102.
  52. Türkay, B. E., & Telli, A. Y. (2011). Economic analysis of standalone and grid connected hybrid energy systems. *Renewable energy*, 36(7), 1931-1943.
  53. Vieira, S. P., & Cavalcanti, L. A. P. (2018). Construção de protótipo de eletrofloculação em fluxo contínuo alimentado por energia solar fotovoltaica para purificação de efluentes. *Revista Brasileira de Gestão Ambiental e Sustentabilidade*, 5(9), 181-190.
  54. Zhang, G., Gong, S., Wu, F., Yang, S., & Liu, L. (2012). Study on optimum parameter for turbidity removal in rainwater collection by electro-coagulation in northwest region. *Journal of Water Resources and Water Engineering*, (1), 10.

**Tabela 1.** Características físico-químicas do efluente bruto

| Amostra | Data da coleta | pH  | Turbidez (NTU) | Condutividade (mS/cm) | DQO* (mgO <sub>2</sub> /L) |
|---------|----------------|-----|----------------|-----------------------|----------------------------|
| 1       | 26/04/18       | 6,7 | 69,9           | 98                    | 347                        |
| 2       | 14/06/18       | 6,7 | 249            | 52                    | 410                        |
| 3       | 12/04/19       | 6,8 | 62,8           | 104                   | 292                        |
| 4       | 10/05/19       | 7,0 | 106            | 94                    | 226                        |
| 5       | 31/05/19       | 4,1 | 70,1           | 121                   | 187                        |

\* Média aritmética simples de triplicata.

**Tabela 2.** Resultados das análises das amostras filtradas, antes e após os ensaios de Eletrofloculação.

| Amostra | Corrente (A) | Tempo (min) | Turbidez (NTU) | DQO* (mgO <sub>2</sub> /L) | Absorbância** (670nm) | pH  | Tensão Média (V) |
|---------|--------------|-------------|----------------|----------------------------|-----------------------|-----|------------------|
| 3       | -            | 0           | 38,9           | 182                        | 0,1593                | 6,5 | -                |
|         | 1            | 5           | 13,5           | 147                        | 0,0410                | 7,6 | 3,55             |
|         |              | 10          | 5,49           | 141                        | 0,0082                | 7,6 | 3,55             |
|         |              | 15          | 4,21           | 102                        | 0,0054                | 7,6 | 3,61             |
|         | 2            | 5           | 6,60           | 85                         | 0,0125                | 7,5 | 5,64             |
|         |              | 10          | 5,03           | 36                         | 0,0070                | 7,8 | 5,38             |
|         |              | 15          | 5,39           | 104                        | 0,0122                | 8,0 | 5,00             |
| 4       | -            | 0           | 45,3           | 131                        | 0,1540                | 7,0 | -                |
|         | 1            | 5           | 11,0           | 126                        | 0,0272                | 7,1 | 2,09             |
|         |              | 10          | 9,80           | < 25                       | 0,0108                | 7,3 | 2,00             |
|         |              | 15          | 7,08           | 97                         | 0,0061                | 7,3 | 2,06             |
|         | 2            | 5           | 8,58           | 71                         | 0,0101                | 7,4 | 2,97             |
|         |              | 10          | 3,36           | < 25                       | 0,0032                | 7,8 | 2,83             |
|         |              | 15          | 4,98           | 45                         | 0,0071                | 8,6 | 2,89             |
| 5       | -            | 0           | 28,0           | 177                        | 0,0799                | 3,7 | -                |
|         | 1            | 5           | 2,57           | 146                        | 0,0042                | 4,0 | 0,24             |
|         |              | 10          | 7,14           | 79                         | 0,0008                | 4,5 | 0,45             |
|         |              | 15          | 5,38           | 94                         | 0,0006                | 5,6 | 0,66             |
|         | 2            | 5           | 9,09           | 119                        | 0,0021                | 4,5 | 0,62             |
|         |              | 10          | 8,56           | 76                         | 0,0084                | 5,7 | 1,23             |
|         |              | 15          | 13,2           | 152                        | 0,0182                | 6,2 | 1,84             |

\* Média aritmética simples de triplicata;

\*\* Valor da absorbância da amostra menos a absorbância da água destilada.

**Tabela 3.** Porcentagem de remoção dos parâmetros físico-químicos nos ensaios de Eletrofloculação.

| Amostra | Corrente (A) | Tempo (min) | Porcentagem de remoção (%) |     |                     |
|---------|--------------|-------------|----------------------------|-----|---------------------|
|         |              |             | Turbidez                   | DQO | Absorbância (670nm) |
| 3       | 1            | 5           | 65                         | 19  | 74                  |
|         |              | 10          | 86                         | 23  | 95                  |
|         |              | 15          | 89                         | 44  | 97                  |
|         | 2            | 5           | 83                         | 53  | 92                  |
|         |              | 10          | 87                         | 80  | 96                  |
|         |              | 15          | 86                         | 43  | 92                  |
| 4       | 1            | 5           | 76                         | 4   | 82                  |
|         |              | 10          | 78                         | 81  | 93                  |
|         |              | 15          | 84                         | 26  | 96                  |
|         | 2            | 5           | 81                         | 46  | 93                  |
|         |              | 10          | 93                         | 81  | 98                  |
|         |              | 15          | 89                         | 66  | 95                  |
| 5       | 1            | 5           | 91                         | 18  | 95                  |
|         |              | 10          | 75                         | 55  | 99                  |
|         |              | 15          | 81                         | 47  | 99                  |
|         | 2            | 5           | 68                         | 33  | 97                  |
|         |              | 10          | 69                         | 57  | 89                  |
|         |              | 15          | 53                         | 14  | 77                  |

**Tabela 4.** Dados de irradiação solar média mensal da região e previsão de geração mensal.

| Irradiação solar diária média mensal [kWh/m2.dia] |        |        |        |        |        |        |        |        |        |        |        |             |
|---|--------|--------|--------|--------|--------|--------|--------|--------|--------|--------|--------|-------------|
| Jan   | Fev    | Mar    | Abr    | Mai    | Jun    | Jul    | Ago    | Set    | Out    | Nov    | Dez    | Média anual |
| 6,12  | 6,1    | 5,28   | 4,46   | 3,87   | 3,54   | 3,63   | 4,27   | 4,78   | 4,93   | 4,99   | 5,91   | 4,82        |
| Previsão de geração média mensal [kWh]            |        |        |        |        |        |        |        |        |        |        |        |             |
| Jan   | Fev    | Mar    | Abr    | Mai    | Jun    | Jul    | Ago    | Set    | Out    | Nov    | Dez    | Total anual |
| 630,12  | 628,06 | 543,63 | 459,20 | 398,46 | 364,48 | 373,74 | 439,64 | 492,15 | 507,59 | 513,77 | 608,49 | 5.959,32    |

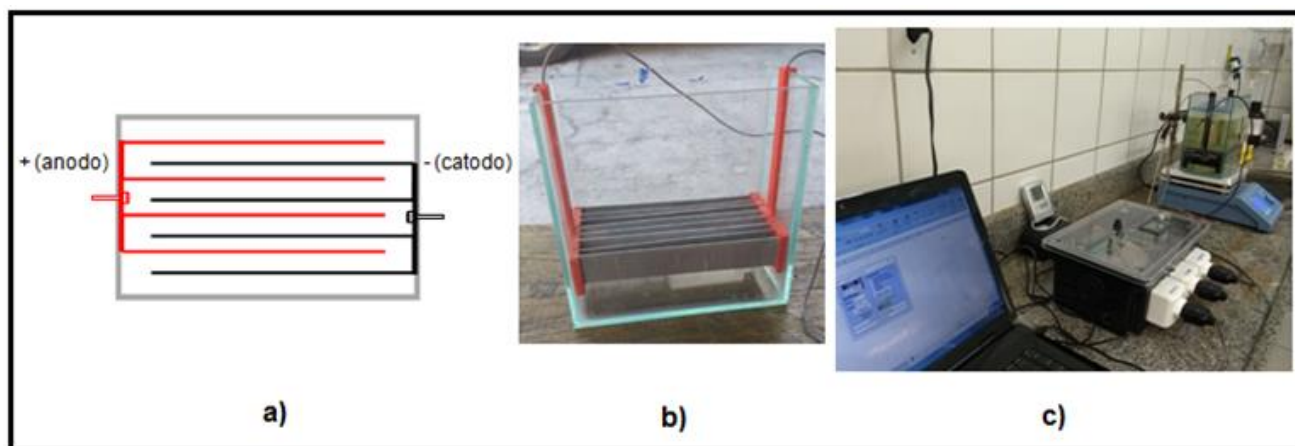


**Figura 1.** (a) Desenho do formato do eletrodo, vista de cima; (b) posição do eletrodo na cuba; (c) conjunto da unidade do reator de eletrofloculação de bancada.

| Hora     | Tensao | Temperatura |
|----------|--------|-------------|
| 10:53:59 | 3,06   | 25,4        |
| 10:54:01 | 3,01   | 25,3        |
| 10:54:03 | 2,92   | 25,3        |
| 10:54:05 | 2,92   | 25,4        |
| 10:54:08 | 2,92   | 25,5        |
| 10:54:10 | 2,92   | 25,3        |
| 10:54:12 | 2,88   | 25,3        |
| 10:54:14 | 2,88   | 25,5        |
|          |        |             |
|          |        |             |
|          |        |             |
|          |        |             |
|          |        |             |
|          |        |             |
|          |        |             |
|          |        |             |
|          |        |             |
|          |        |             |

PLX-DAQ for Excel "Version 2" by Net^Devil

### Settings

Port:

Baud:

☒ Reset on Connect

☒ Use 1st Worksheet at the time of "Connect"
 ☐ Use active Worksheet at the time of "Connect"

### Control

☐ Download Data  
☐ Clear Stored Data  
☐ User1  
☐ User2

### Controller Messages:

PLX-DAQ Status

**Figura 2:** Software de aquisição e armazenamento.

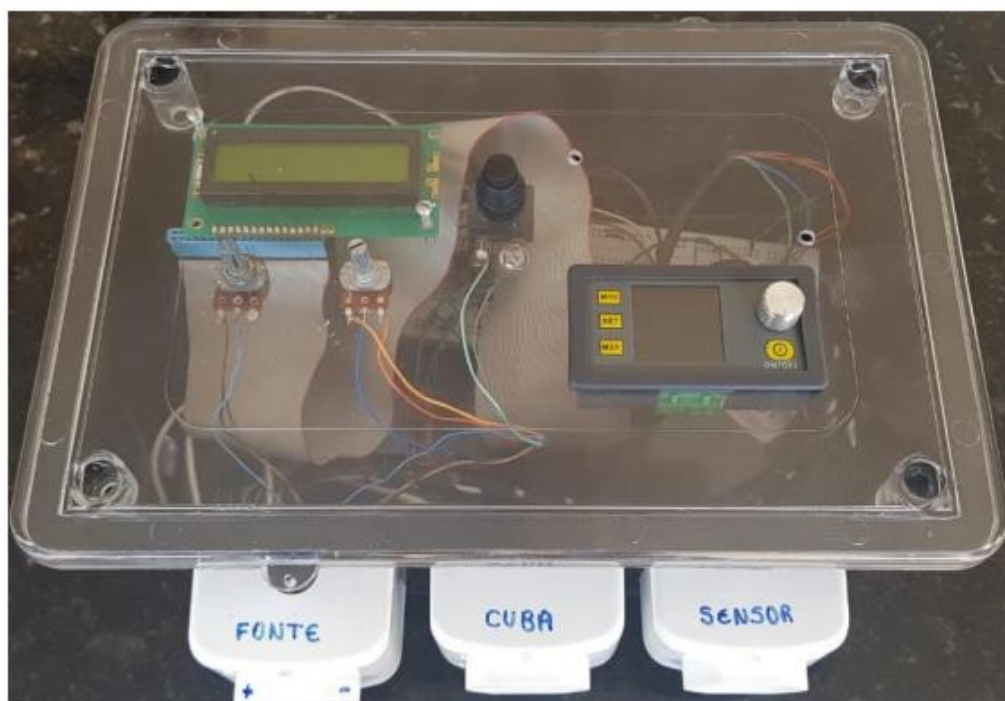


**Figura 3:** Sistema eletrônico.

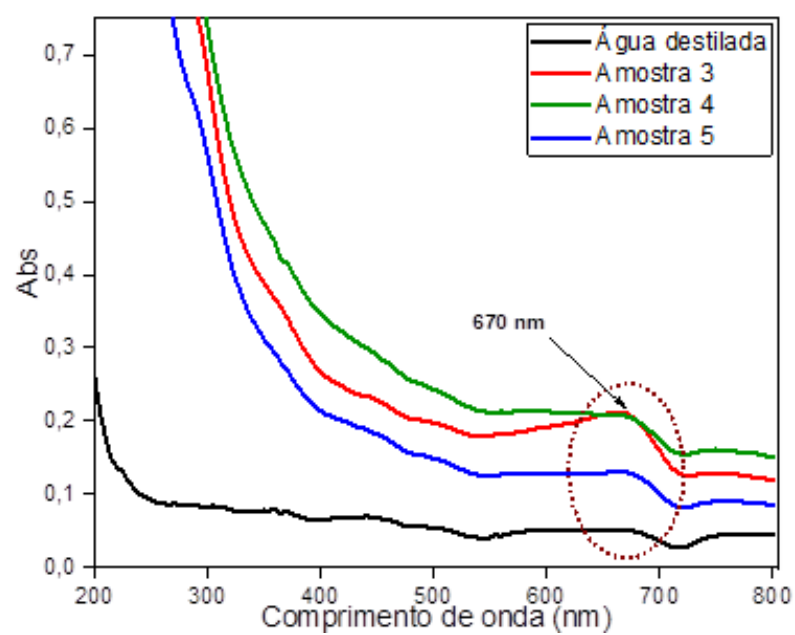


**Figura 4.** Varredura espectral das amostras filtradas antes dos ensaios de eletrofloculação.



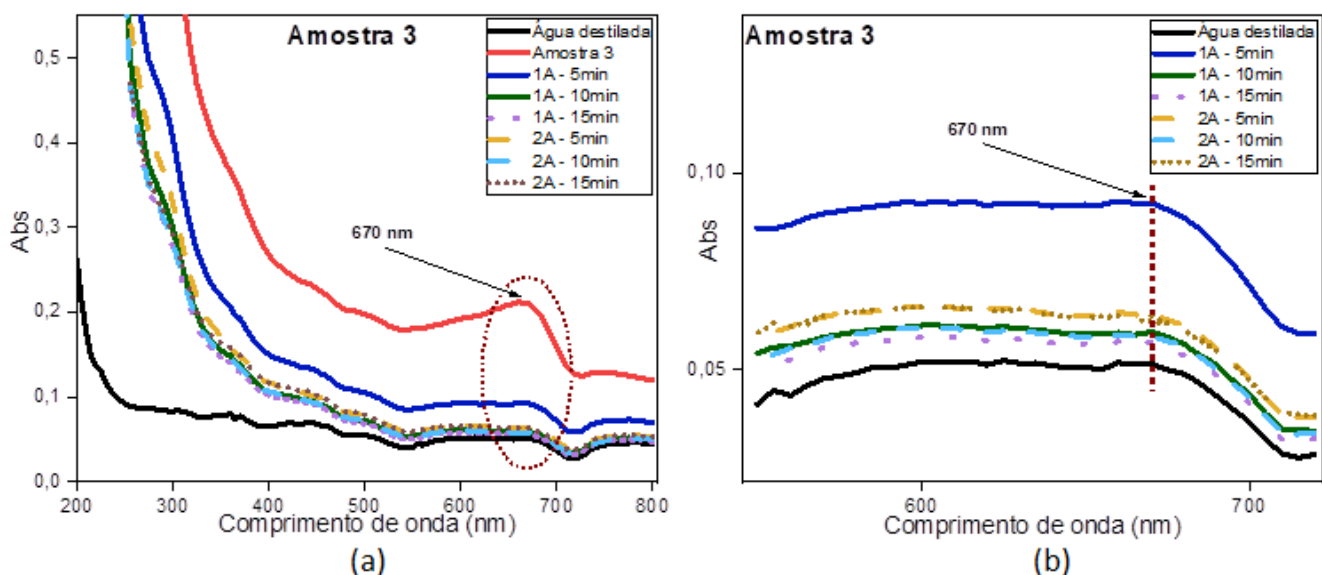


**Figura 5.** Varredura espectral da amostra 3 após todos os ensaios de eletrofloculação: (a) em toda faixa UV e Vis (200 a 800nm); (b) ampliação da região do visível de maior absorbância.

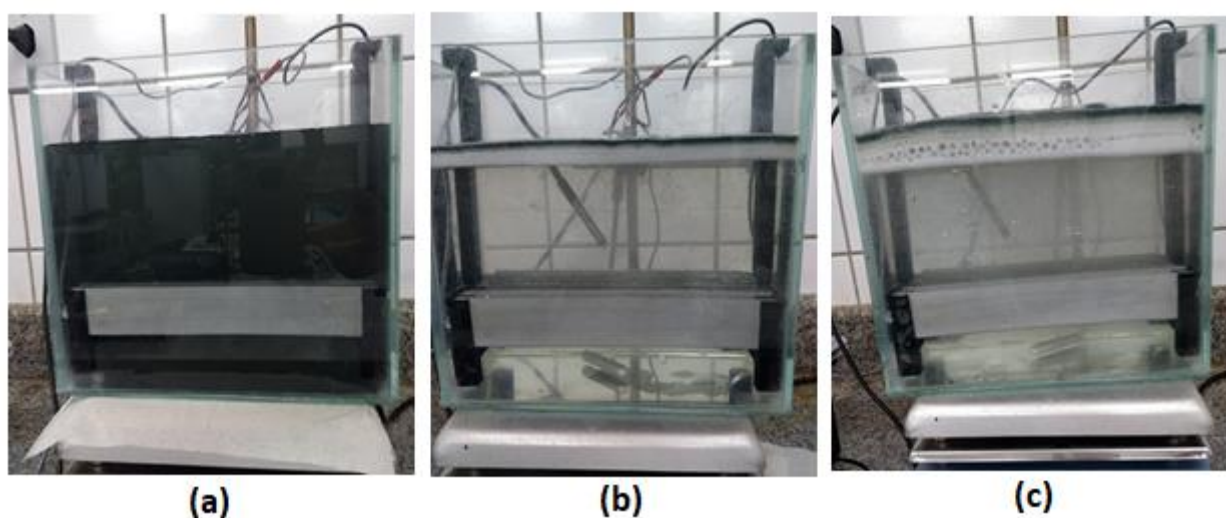


**Figura 6.** Ensaios de Eletrofloculação (EF) amostra 3: (a) efluente bruto; (b) 1A/15 min.; (c) 2A/15min.

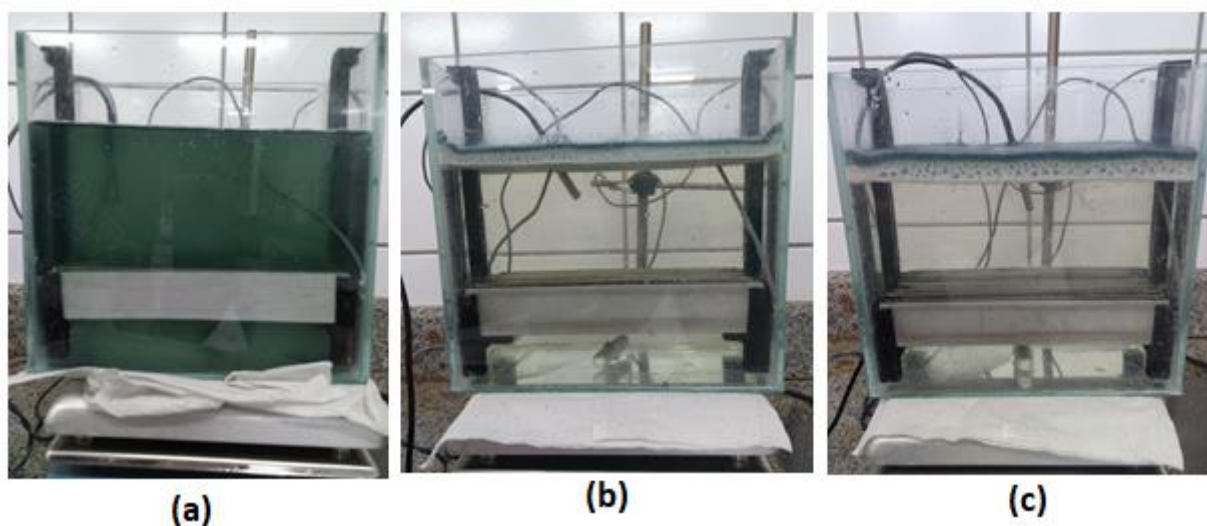


**Figura 7.** Ensaios de Eletrofloculação (EF) amostra 4: (a) efluente bruto; (b) 1A/15 min.; (c) 2A/15min.

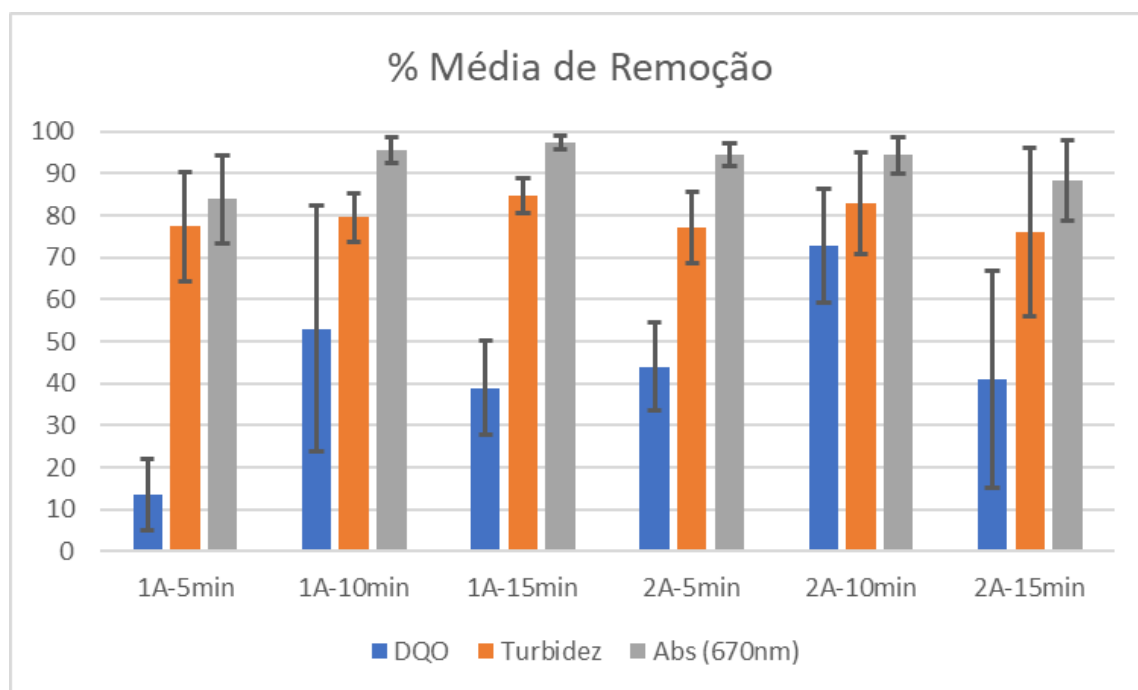


**Figura 8.** Porcentagem média (das amostras 3, 4 e 5) de remoção dos parâmetros DQO, Turbidez e Absorbância em 670nm, com seus respectivos desvios padrões.

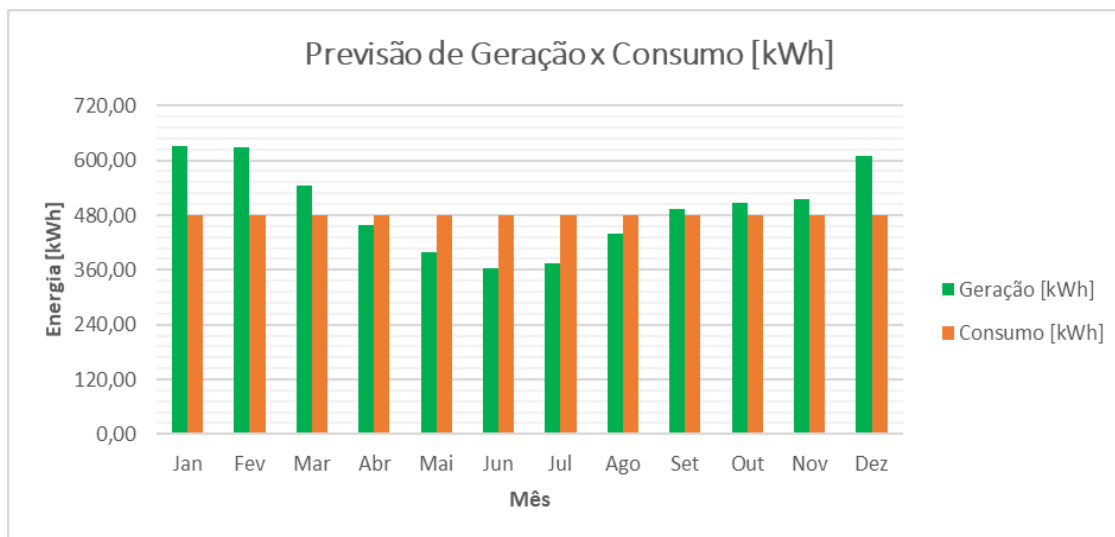


**Figura 9.** Previsão de geração e consumo médio de energia do sistema grid-tie projetado

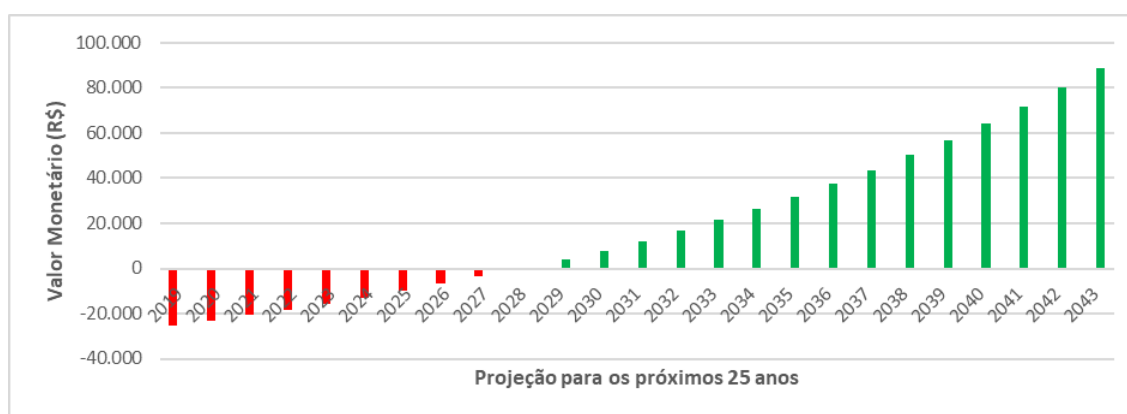


**Figura 10.** Simulação financeira do sistema grid-tie projetado

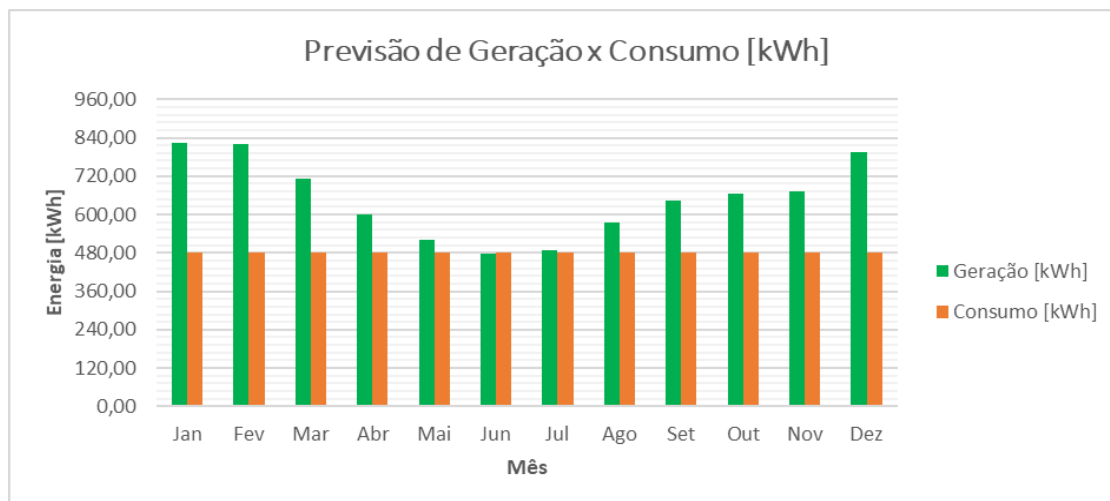


**Figura 11.** Previsão de geração e consumo médio de energia do sistema off- grid sem bateria projetado

## A RECONSTRUÇÃO DO CONHECIMENTO CIENTÍFICO SOBRE A BIOATIVIDADE DE BAJAKAH KALALAWIT (*UNCARIA GAMBIR ROXB*) COMO ETNOMEDICINA

### THE RECONSTRUCTION OF SCIENTIFIC KNOWLEDGE ABOUT BAJAKAH KALALAWIT (*UNCARIA GAMBIR ROXB*) BIOACTIVITY AS ETHNOMEDICINE

UNNES, Sudarmin<sup>1\*</sup>; SUMARNI, Woro<sup>2</sup>; DILIAROSTA, Skunda<sup>3</sup>; RAMADANTY, Isabela<sup>4</sup>

<sup>1,2</sup>Chemistry Department, Faculty of Mathematics and Natural Science, Universitas Negeri Semarang, Indonesia

<sup>3</sup>Science Education Programs, Faculty of Mathematics and Natural Science, Universitas Negeri Padang, Indonesia

<sup>4</sup>Chemistry Student, Faculty of Mathematics and Natural Science, Universitas Negeri Semarang, Indonesia

\* Correspondence author  
e-mail: sudarmin@mail.unnes.ac.id

Received 29 April 2020; received in revised form 27 May 2020; accepted 11 June 2020

#### RESUMO

A Indonésia tem mais de 25.000-30.000 espécies de plantas. A floresta tropical da Indonésia é uma fonte enorme de compostos metabólicos secundários benéficos para a saúde e a vida. Um dos tesouros é Bajakah Kalalawit (*Uncaria gambir roxb*), uma planta endêmica de Bornéu que se acredita hereditariamente curar tumores e cânceres. Esta pesquisa pertence a um estudo educacional que reconstruiu o conhecimento científico sobre as bioatividades de Bajakah por compostos de metabólitos secundários como etnomedicina e teve como objetivo restabelecer a pesquisa científica sobre bioatividades de Bajakah para medicamentos contra câncer e tumores. A madeira e a raiz de Bajakah Kalalawit da Floresta Nacional de Conservação, Samarinda, Indonésia, foram tomadas como amostra. O pó da raiz e da madeira foi isolado e extraído para seus compostos de metabólitos secundários usando água, etanol + água e etanol + hexano como solventes. Os isolados resultantes foram testados quanto à fitoquímica, estrutura e bioatividade em relação a *Bacillus subtilis* e *Escherichia coli* (*E. Colli*). Os resultados foram apoiados por testes de estrutura com a espectroscopia FTIR que mostrou a aparência de captação de grupos funcionais para hidroxila, carbonila e aromática que correspondiam às moléculas secundárias de metabólitos. A análise dos dados obtidos concluiu que a raiz de Bajakah e o extrato de madeira contêm a atividade inibitória de células e tumores cancerígenos, pois contêm compostos de metabólitos secundários, incluindo terpenos, fenóis, alcalóides e flavonóides. Os compostos de metabólitos secundários dos isolados de Bajakah foram capazes de inibir a atividade de *Bacillus subtilis* e *Escherichia coli* (*E. Colli*).

**Palavras-chave:** Reconstrução, Bajakah (*Uncaria Gambir Roxb*), Planta Tropical, Conhecimento científico

#### ABSTRACT

Indonesia has more than 25.000-30.000 plant species. The Indonesia tropical forest is a huge source for secondary metabolite compounds that are beneficial for health and life. One of the treasures is Bajakah (*Uncaria gambir roxb*), a plant endemic to Borneo that has been hereditarily believed to cure tumors and cancers. This research belongs to an educational study that reconstructed scientific knowledge about secondary metabolite compounds' bioactivities of Bajakah as ethnomedicine and aimed at reestablishing scientific research on bioactivities of Bajakah for cancer and tumor medication. The wood and root of Bajakah Kalalawit of the National Conservation Forest, Samarinda, Indonesia, were taken as the sample. The root and wood powder was isolated and extracted for their secondary metabolite compounds using water, ethanol + water, and ethanol + hexane as the solvents. The resulted isolates were tested for the phytochemical, structure, and bioactivity towards *Bacillus subtilis* and *Escherichia coli* (*E. Colli*). The results were supported by structure tests with FTIR spectroscopy, which showed the appearance of uptake of functional groups for hydroxyl, carbonyl, and aromatics that corresponded to secondary metabolite molecules. The analysis of the obtained data concluded that the Bajakah root and the wood extract contain the inhibitory activity of cancer cells and tumors because they contain compounds of secondary metabolites, including terpenes, phenols, alkaloids, and flavonoids. The secondary metabolite compounds from the Bajakah isolates were able to inhibit the activity of *Bacillus subtilis* and *Escherichia coli* (*E. Colli*).

**Keywords:** Reconstruction, Bajakah (*Uncaria Gambir Roxb*), Tropical Plant, Scientific Knowledge.

## 1. INTRODUCTION:

Indonesia has more than 25.000-30.000 plant species, 17.000 islands/isles, 50 types of ecosystem, and 300-700 ethnics (Kartawinata, 2010). The ethnic diversity of Indonesia has resulted in sundry cultures, traditions, and local wisdom. One of the local wisdom is the use of surrounding diversity as a medication of various diseases (Amir *et al.*, 2017). Locals made use of local plants to maintain their health and are known as medicinal plants. The knowledge of medicinal plants is generally passed on orally so that knowledge is only limited to a group of people and is known as indigenous science (Kandowangko *et al.*, 2018; Aziz *et al.*, 2018). This knowledge is vulnerable to degradation due to cultural acculturation and modernization (Mikako & Hirokazu, 2020). Thus, it needs to be conserved (Daval, 2009).

A study revealed that more than 80% of secondary metabolite compounds found in local plants are used as the first compound source to common medicines in the pharmaceutical industry (Fabricant & Farnsworth, 2001). Currently, research on local herbs as the traditional medication is a hot topic, particularly in ethnobotanical, ethnomedicine, and ethnopharmacology field (Kandowangko *et al.*, 2018; Evrizal *et al.*, 2013; Silalahi & Nisyawati, 2018; Lense, 2012).

Research about secondary metabolite compounds and their bioactivation to a particular disease is essential to carry out. Indonesia's tropical forest is a huge source for secondary metabolite compounds that are beneficial for health and life (Silalahi *et al.*, 2015). One of the treasures is Bajakah (*Uncaria gambir roxb*), a plant endemic to Borneo that has been hereditarily believed to cure tumors, cancers; maintain stamina, and stop bleeding (Moris, 2020).

The utilization of Bajakah (*Uncaria gambir roxb*) by the Inland Dayak Tribe should be discussed in the context of ethnomedicine. Etymologically, the word 'ethnomedicine' means the connectivity of ethnicity and medicine as Local Knowledge. Scientifically, ethnomedicine is said to be a perception and conception of local people, and Local Knowledge in understanding health, or, research about the medical system of traditional ethnic (Bhasin, 2007). An ethnomedicine study is done to understand health from society's point of view to be reconstructed into scientific knowledge (Walujo, 2011; Walujo, Ethnopharmacology:

Knowledge Saintification for the Development of the Drug and Pharmaceutical Chemical Industry in Indonesia, 2013).

Ethnomedicine, reviewed from the scientific field, is a part of anthropology that discusses medicinal plants, their ethnobotanics, and marketing (Lee *et al.*, 2008). Moreover, it also talks about the bioactivities of the secondary metabolite compounds, morphological characters, and scientific explanations (Andrade-Cetto & Heinrich, 2011; Toksoy *et al.*, 2010). Some medicines that derive from local knowledge include the quinine which is adapted from the knowledge of Incas who had long used *Chinchona* as a cure for malaria. There is also reserpine from *Rauwolfia serpentina* that has been utilized by the Indian community to reduce blood pressure. These medicines are some of the proofs of ethnomedicine development in recent years. Mostly, ethnomedicine focuses on finding new secondary metabolite compounds that are beneficial for modern medicine production to heal fatal diseases like tumors and cancers.

Public knowledge is correct at a certain level, but people should also be educated about a scientific explanation of a medicinal plant and how to protect the plant, which belongs to Indonesia's natural wealth (Hisa *et al.*, 2018). The conservation knowledge of medicinal plants has been owned by the Marori tribe in Masur Merauke National Park and Karimunjawa society (Sudarmin *et al.*, 2017; Supriyadi & Sudarmin, 2020). This research intends to follow the prior study, which provides explanations to the society about the medicinal plants. Frankly, this study is the development of the preceding research as it uses ethnoscience, ethnomedicine, and strengthened by laboratory-based scientific work in explaining people's indigenous science. Similar research was also done in Vietnam by (Hoang *et al.*, 2008), Turkey (Akbulut & Bayramoglu, 2013), Pakistan (Aziz *et al.*, 2018), China (Lee *et al.*, 2008), Cameroon (Mikako & Hirokazu, 2020), while here in Indonesia (Hisa *et al.*, 2018; Hariyadi & Ticktin, 2010; Kandowangko *et al.*, 2018; Lense, 2012; Silalahi, 2014; Silalahi *et al.*, 2015; Silalahi & Nisyawati, 2018; Supriyadi & Sudarmin, 2020; Septriyanto *et al.*, 2018) are researchers who are interested in benefitting local herbs as treatments.

Stood on the above description, inquiry-based findings related to the medicinal plant's advantage must be informed. The process of scientific explanation of public knowledge through scientific work-based inquiry in the laboratory is

known as the process of reconstructing scientific knowledge (Sudarmin *et al.*, 2019; Sumarni *et al.*, 2016; Sumarni & Sudarmin, 2019). This research is important because public knowledge about traditional medicine and local knowledge has not been widely explained scientifically (Sumarni, 2019). Previously, students of a High School in Palangkaraya experimented on mice induced by tumor and cancer cell growth substances. They used Bajakah (*Uncaria gambir roxb*) extract as a medication for the mice and were succeeded in saving the mice's life. This result turns out to be the basis of this research in examining the ability of Bajakah (*Uncaria gambir roxb*) like cancer and tumor medication, and the secondary metabolite compounds contained in it.

This research belongs to an educational study that reconstructed scientific knowledge about secondary metabolite compounds' bioactivities of Bajakah as ethnomedicine and aimed at reconstructing scientific research on bioactivities of Bajakah for cancer and tumor medication.

## 2. MATERIALS AND METHODS:

### 2.1. Ethnomedicine Data Retrieval

The interviewee of this study was a 37 years-old native man who resides near the National Conservation Forest, Samarinda in which Bajakah comes from. He is also one of the many residents there who has used Bajakah to cure cancer and tumors for his relatives or neighbors. At present, he is cultivating and selling Bajakah wood and root to various regions through online sales. The research team obtained ethnomedical information about Bajakah and pictures from him.

This research belongs to an ethnomedicine study in which the data were gathered from a face to face interview (Akbulut & Bayramoglu, 2013). Referring to (Reyes-García *et al.*, 2006) and Praptiwi's procedure (Praptiwi, 2004), the focus of this research include: (1) the local name of Bajakah (*Uncaria gambir roxb*); (2) characteristics of plants; (3) how plants are used as medicines; (4) ways to mix the fruit extract; (5) additive ingredients for the fruit extract; (6) its medical components; (7) ways of community conservation; and (8) seedling pattern. The data of organoleptic secondary metabolite test, phytochemical test, structure test, and antibacterial test were carried out a scientific inquiry at the Chemistry and Microbiology Laboratory at UNNES (Universitas Negeri Semarang). The inquiry activities included isolation and identification of phytochemicals and

secondary metabolite structures of Bajakah (*Uncaria gambir roxb*) wood and root. The procedure of isolation and identification refers to the Organic Chemistry practicum manual prepared by UNNES Bioorganic Lecturer Team (Supartono *et al.*, 2016), which is explained as follows.

### 2.2. The Isolation of Bajakah (*Uncaria gambir roxb*) Wood and Root from Borneo Island

The first step was the making of bajakah wood and root powder. The dried wood and root were cut into pieces and put in a blender at the UNNES Chemistry Laboratory to make a fine powder. The fine powder obtained was weighed (25 grams) then extracted by maceration procedure in an Erlenmeyer Glass (Merck brand) Volume 200 mL using 100 mL water solvent or 100 mL ethanol solvent. The solvent replacement was done every 24 hours and then filtered with filter paper. All macerates were collected and put into a rotary evaporator at 100°C. Furthermore, the remaining filtrate was evaporated using a vaporizer cup in a water bath until a thick, stable isolate extract was obtained. As for other wood and root powder, the isolation

Other than the isolation and extraction, a Soxhlet process was performed to the powder sample using 50 mL of ethanol + 50 mL of n-hexane (pa) and 50 mL of ethanol + 50 mL of benzene (pa) for approximately 48 hours. At this point, the ethanol and benzene mixture solvent has isolated all secondary metabolite components of the powder. Then the solvent obtained from the Soxhlet process was filtered with filter paper. All the extractant was put into a rotary evaporator at 100°C, and the obtained extractant as Bajakah (*Uncaria gambir roxb*) isolate was ready for Phytochemical testing, structure test with FTIR; and bioactivity testing of *Bacillus subtilis* and *Escherichia coli* bacteria.

In addition to the use of ethanol and benzene, a mixture of ethanol and hexane (pa) was also employed. The process of Soxhlet process was the same for both samples from the root and wood powder, which was carried out, referring to Supartono *et al.* (2016).

### 2.3. Procedure for Phytochemical Test of the Secondary Metabolite Compounds

This step of the research was the phytochemical test and bioactivity test of Bajakah extract against *Bacillus subtilis* (positive gram bacteria) and *Escherichia coli* (negative gram bacteria). The research results were then



compared to prior studies and expert judgment about Bajakah (*Uncaria gambir roxb*), to produce an established reconstruction of scientific knowledge.

The procedure of the phytochemical test included several stages. Firstly, alkaloids identification using Mayer and Dragendorf reagents. The extract, as a result of isolation using methanol solvent, is shaken. If a deposition/white mist or an orange-red precipitate is formed after the Dragendof reagent is added, it means that the Bajakah extract (*Uncaria gambir roxb*) contains Alkaloids. Secondly, steroids and terpenoids identification using Liberman Buchard. If a red or purplish-red mist is formed, then Bajakah isolate contains terpenoids, and if a green or bluish-green mist is formed, Bajakah isolate restrains steroids. Third, the flavonoids test by putting a few drops of Bajakah isolate water fraction into a test tube, then adding Mg metal powder and a few drops of concentrated HCl. If it turns into pink to red (except for isoflavones), then the isolate carries Flavonoids. Fourth, phenolics identification by adding several drops of water fraction of Bajakah isolate (*Uncaria gambir roxb*) into a test tube, then putting in some drops of  $\text{FeCl}_3$ . If it turns into blue or purplish-blue, the isolate is declared phenolics-positive. Last, saponin identification by putting 1 mL of Bajakah isolate water fraction into a test tube then shaken for 1-2 minutes. If temporal foam (which lasts for about 5 minutes) is built, then the isolate is saponin-positive.

#### 2.4. Secondary Metabolite Structure Test with Elmer 100 FT-IR Perki Spectroscopy

In assisting the results of scientific knowledge reconstruction, a molecular structure test of Bajakah's secondary metabolite structures was carried out using the Perkin Elmer 100 FT-IR (Fourier Transform Infra-Red) spectroscopy. FT-IR is a tool employed to analyze chemical compounds. The infrared spectra of a compound can provide a picture and molecular structure of the compound. In this research, the test was carried out by following (Srinovaz, 2014) procedure.

In strengthening the findings of the phytochemical test and explaining scientifically about the secondary metabolites' type of functional group, the structural analysis of the functional group type was done using the Perkin Elmer Inc 10 FTIR spectroscopy (Figure 2a). A total of 1 mL of the sample (Figure 2b) of secondary metabolites as the result of Bajakah wood and root soxhletation with ethanol-hexane was prepared. Before analyzing the type of

functional group, a temperature reconditioning and FTIR tool examination was carried out. Temperature recondition was done by pressing the power button and set to 25°C. After the tool was set up, the next step is to examine the spectra data scan by clicking the background icon, filling in the sample name by writing 'Bajakah root sample-1', and set the wavenumber between 750-3700  $\text{cm}^{-1}$ . A total of 1  $\mu\text{L}$  of the root sample was injected into the holder sample; then, the scan icon was clicked. After about 8 minutes, a spectrum scan appeared.

The obtained data were then compared to those saved in the reference section by clicking 'setup' on the toolbar, chose 'compare references' → 'compare.' In a few minutes, the comparison spectra scan appeared. To sort the most similar references, the researchers clicked 'libraries' and 'search.' After a while, some references for the spectra scan popped out for the researcher to analyze carefully. Once the desired references have been found, then the researchers closed and saved them.

#### 2.5. Antibacterial Bioactivity Test

The test procedure modified what has been done by (Septiani *et al.*, 2017; Alen *et al.*, 2009). The preparation stage included bacterial rejuvenation, bacterial suspension making, paper disc making (6 mm in diameter), preparation of negative and positive control, and concentration series making of 300, 400, and 500 mg/mL. The antibacterial activity test used was the Disc Diffusion method (Kirby-Bauer Test). The suspension of bacteria test, as much as 20  $\mu\text{L}$ , was placed in the Petri then rubbed with sterile cotton on the test media (Gardjito *et al.*, 2007). This procedure was repeated twice. The paper disc was placed above the media, which included 50  $\mu\text{g}$  of Ciprofloxacin as the positive control, 20% of DMSO as the negative control, and 300, 400, and 500 mg/mL of ethanol extract from Bajakah (*Uncaria gambir roxb*) isolate. The media were then incubated at 37°C for 24 hours, then the inhibition zone diameter was measured with a caliper expressed in millimeters.

#### 2.6. Data Analysis

The research data obtained through interviews with a source person in the research site were analyzed. The questions raised to the interviewee were the local name, the characteristics of the plant, the benefits of the extract, and how to use it as cancer and tumor medication. the resource person, Moris (37 years



old) is a native of the community residing near the national tropical forest, Samarinda, Indonesia. The data taken from the interview were then reconstructed based on Hempel (2014). To strengthen the reconstruction, a series of experiments were conducted in the Chemistry Laboratory of Universitas Negeri Semarang (UNNES) for the isolation process, phytochemical tests, structure tests, and bioactivity tests of the extracts against *Bacillus subtilis* and *Escherichia coli*. The conclusion was drawn up based on the experiment results.

### 3. RESULTS AND DISCUSSION:

#### 3.1. The Results of Scientific Knowledge Reconstruction

Figure 1 presents the pictures of Bajakah wood and Bajakah tea taken by Moris in the research location. Moreover, the data and information obtained from the interview are shown in Table 1. Departing from the interviewee's answers regarding the local name and characteristics, the researchers did a literature study to seek for the suitability of the data with the scientific records and found that the Bajakah mentioned by the interviewee belongs to Bajakah kalalawit (*Uncaria gambir roxb*). Its leaves vary from yellow, brown, and white, while its small flower is purple, pink, and white.

The species contains phenol, antibacterial agent, and high catechins to prevent heart disease, obesity, and help the formation of collagen (Medical Team Universitas Lambung Mangkurat, 2017). The polyphenols are found in the leaves, yet the type and content are mainly affected by the leaf's age. Gardjito *et al.* (2007) revealed that Bajakah (*Uncaria gambir roxb*) leaves were found in compounds belonging to the phenolic group. The bioactivity of the compounds is presented in Table 2.

The results of interviews, as presented in Table 1, reveals that the community consumes Bajakah by brewing/boiling the dried leaves, bark, or root and drinks it as tea. This process, in the context of scientific knowledge, is called as the maceration process. The tea was observed to have reddish to yellow in color, which indicates the existence of secondary metabolite compounds. Moreover, in the context of scientific knowledge related to chemistry solution, the secondary metabolite compounds are solute while water is the solvent (Supartono *et al.*, 2016). Another way to consume Bajakah is revealed by Ujung (2017) who found that there are two other species of

Bajakah found in Borneo that are also believed to cure cancer, they are Bajakah Tampala (*Spatholobus Littoralis Hassk*) and Bajakah Lamei which grows in the tropical forest. Its stem stores much edible water and this water is commonly consumed as medication to cure various diseases.

The phytochemical test results of Bajakah (*Uncaria gambir roxb*) wood and root extract carried out in this research are presented in Table 3. Table 3 indicates that the secondary metabolite compounds found in this research are similar to those found in the prior study done in Universitas Lambung Mangkurat. These compounds result in bioactivity towards cancer and tumor cells that serve as an antibacterial agent and could stop bleeding. Nevertheless, the Ministry of Health of the Republic of Indonesia (2018) stated that Bajakah (*Uncaria gambir roxb*) as cancer, tumor, or other medication needs further research. On the other hand, Bajakah tea has empirically proven to hinder cancer cells by releasing hydroxyl compounds to bond the cancer cell so that the cell growth obstructs. For that reason, this study strengthens the phytochemical test for Bajakah isolates extracted using an organic solvent.

The results of the structure test with the FTIR Spectra Tool (Figure 3) showed the absorption of the main functional groups of secondary metabolite compounds contained in Bajakah wood and root extracts, namely hydrosol, carbonyl, aromatic, and methyl. The FT-IR spectra strengthen the presence of -OH (hydroxyl) and a carbonyl group. The presence of C-O bonds reinforces the -OH group, while the presence of methyl and methylene is shown by 100-1120 cm<sup>-1</sup>. The results test indicated compatibility with the phytochemical test results of secondary metabolite compounds of bark and root extract (Medical Team of Universitas Lambung Mangkurat, 2017).

This research only shows the concordance of the research findings with the results by the medical team of Lambung Mangkurat University (2017) and has not shown the molecular structure of the secondary metabolite compounds. This follows the aim of the research, which is to explain why Bajakah extract is a potential cancer drug. This question has been answered by the finding of phenolics, terpenoids, and saponins. The analysis results showed that these metabolites can inhibit cancer cells since active groups such as hydroxyl groups (-OH) weaken cancer cells with different patterns of mechanisms (Panda, A, and Gunawan, YE, 2018, Maulidie, M *et al.*, 2019 ). This is in line with Maulina *et al.* (2019), indicating that the phytochemical test for the rough extract of Bajakah

root dissolved in ethanol results in the same type of secondary metabolite compounds found in this research.

Furthermore, to determine the chemical structure and specific types for each secondary metabolite, it is necessary to purify and separate Bajakah extract isolates, followed by further structural analysis tests which include Ultra Violet Visible (UV-Vis) spectroscopy, Nuclear Magnetic Resonance (NMR) spectroscopy, and Carbon Core Magnetic Resonance Spectroscopy (13C-NMR). This research has not done these tests yet.

### 3.2 The Bioactivity of Secondary Metabolite Compounds with *Bacillus subtilis* and *Escherichia coli*

The antibacterial test toward Bajakah (*Uncaria gambir roxb*) isolates employed *Bacillus subtilis* (positive gram) and *Escherichia Coli* (negative gram). The test results are displayed in Figure 4 and Table 4. Based on this experiment, the inhibition test was performed, and the results are presented in Table 4. Table 4 informs that the bioactivity test results found that Bajakah (*Uncaria gambir roxb*) root isolate dissolved in water has a stronger inhibition zone than the isolate dissolved in ethanol or n-hexane, both for *Bacillus subtilis* and *Escherichia coli*. In other words, this study has granted a scientific explanation that Bajakah wood and root contain saponins as the antibacterial agent (Medical Team of Universitas Lambung Mangkurat, 2017). This is different from what was found by Gardjito *et al.* (2007) that the extract of polyphenols and catechins from *Uncaria gambir roxb* does not show as an antibacterial agent for *Escherichia coli*, but has antibacterial properties against *Staphylococcus aureus*.

## 4. CONCLUSIONS:

1. Bajakah root and wood extract contain the inhibitory activity of cancer cells and tumors as they contain secondary metabolite compounds including terpenes, phenols, alkaloids, and flavonoids;
2. The results were supported by structure tests with Perken Elmer Inc.10 FTIR spectroscopy, which showed the appearance of functional groups for hydroxyl (-OH), Carbonil (-C = O), which were bound to the structure of secondary metabolites. When cancer occurs, the oxidation process happens in Deoxyribonucleic acid (DNA), and the secondary metabolites found in Bajakah have the ability to act as antioxidants to

protect DNA and inactivate the growth of cancer cells.

3. The secondary metabolite compounds from Bajakah isolates were able to inhibit the activity of *Bacillus subtilis* and *Escherichia coli* (*E.Coli*), yet the isolates embattle *E.Coli* stronger than *B. Subtili*.

This reconstruction is in line with what has been stated in the previous results about Bajakah's bioactivities. In other words, this research confirms prior research claims about the benefits of Bajakah (*Uncaria gambir roxb*) as ethnomedicine. It is expected that this study could be a reference for stakeholders to make use of Bajakah (*Uncaria gambir roxb*) as an alternative for cancer and tumor medication.

## 5. ACKNOWLEDGMENTS:

Thank you to the Ministry of Research and Technology of Indonesia for the funding through the Higher Education Primary Research scheme year 2020-2022.

## 6. REFERENCES:

1. Akbulut, S., & Bayramoglu, M. (2013). The Trade and Use of Some Medical and Aromatic Herbs in Turkey. *Ethno Med*, 7(2) , 67-77 .
2. Alen, Y., Guslianti, E., & Suharti, N. (2009). Isolation and Activity Assay of Secondary Metabolites of *Aspergillus niger* in-Habiting in Termite's Queen Nest *Macrotermes gilvus* Hagen., on Enriched Media. *Indonesian Journal of Pharmaceutical Science and Technology (IJPST)*, 6(1) , 1-10.
3. Amir, H., Murcitra, B. A., & Kassim, M. (2017). The Potential Use Of *Phaleria Macrocarpa* Leaves Extract As An Alternative Drug For Breast Cancer Among Women Living In Poverty. *Asian Journal For Poverty Studies* 3(2) , 138 - 145.
4. Andrade-Cetto, A., & Heinrich, M. (2011). From The Field into The Lab: Useful Approaches to Selecting Species Based on Local Knowledge. *Front. Pharmacol* , 2, 1-5.
5. Aziz, M. A., Khan, A., Adnan, M., & Ullah, H. (2018). Traditional uses of medicinal plants used by Indigenous communities for veterinary practices at Bajaur Agency,

- Pakistan. *J Ethnobiol Ethnomed.* 14 (11). , 1-18.
6. Bhasin, V. (2007). Medical Anthropology: A Review. *Ethno.Med.* , 1 (1), 1-20.
  7. Daval, N. (2009). *Conservation and Cultivation of Ethnomedicinal Plants in Jharkhand.* in: Trivedi, P.C.(Ed). Jaipur India: Aavishkar Publishers.
  8. Evrizal, R., Setyaningrum, E., Ardian, Wibawa, A., & Aprilani, D. (2013). *Seminar Nasional FMIPA* (pp. 279-286). Lampung: Universitas Lampung.
  9. Fabricant, D., & Farnsworth, N. (2001). The Value of Plant Used Medicine for Drug Discovery. *Environ Health Perspect.* , 109 (1), 69-75.
  10. Gardjito, M., Sudarmadji, S., & Rahayu, K. (2007). Kandungan Fenolik Ekstrak Daun Gambir (*Uncaria gambir* Roxb) dan Aktivitas Antibakterinya. *Agritech*, 27(2) .
  11. Hariyadi, B., & Ticktin, T. (2010). Uras: Medicinal and Ritual Plants of Serampas, Jambi Indonesia. *Ethnobotany Research and Application* , 10, 133-150.
  12. Hempel, C. (2014). *Scientific Explanation, Stanford Encyclopedia Philosophy* .
  13. Hisa, L., Mahuze, A., & Arka, I. (2018). *Etnobotani: Pengetahuan Lokal suku Marori di Taman Nasional Masur Merauke.* Merauke: Balai Taman Nasional Wasur Merauke.
  14. Hoang, V., Bas, P., & Keßler, P. (2008). Traditional Medicine Plant in Ben En National Park, Vietnam. . *Blumea* , 53, 569-601.
  15. Kandowangko, N., Latief, M., & Yusuf, R. (2018). Short Communication: Inventory of traditional medicinal plants and their uses from Atinggola, North Gorontalo District, Gorontalo Province, Indonesia. *Biodiversitas*, 19(6) , 2294-2301.
  16. Kartawinata, K. (2010). Dua Abad Mengungkap Kekayaan Flora dan Ekosistem Indonesia. *LIPi*, (pp. 1-38).
  17. Lee, S., Xiao, C., & Pei, S. (2008). Ethnobotanical survey of medicinal plants at periodic markets of Honghe Prefecture in Yunnan Province, SW China. *J Ethnopharmacol.* , 117, 362-377.
  18. Lense, O. (2012). The wild plants used as traditional medicines by indigenous people of Manokwari, West Papua . *Biodiversitas* 13 (2) , 98-106.
  19. Maulina, S., Pratiwi, D. R., & Erwin. (2019). Phytochemical screening and bioactivity of root extract of *Uncaria nervosa* Elmer (BAJAKAH). *Jurnal Atomik* , 4(2) , 100-102.
  20. Medical Team of Universitas Lambungmangkurat. (2017). *Komponen Metabolit Sekunder Bajakah.* UNiversitas Lambung Mangkurat, Banjarmasin.
  21. Mikako, T., & Hirokazu, Y. (2020). Unreflective Promotion Of The Non-Timber Forest Product Trade Undermines The Quality Of Life Of The Baka: Implications Of The Irvingia Gabonensis Kernel Trade In Southeast Cameroon. *African Study Monographs, Suppl.* 60 , 85–98.
  22. Moris. (2020). *Tanaman Bajakah dan Manfaatnya Bagi Kesehatan.* Narasumber Pemilik dan Penjual Bajakah Kalimantan.
  23. Panda, A., & Gunawan, Y. (2018). Linking Zoopharmacognocny with Ethnomedication, An Evidence Base from Sebangau National Park, Central Kalimantan Indonesia. *Journal of Tropical Life Science*, 8(3) , 323-329.
  24. Praptiwi. (2004). *Pedoman pengumpulan data keanekaragaman tumbuhan.* Puslit Biolog iLIPI.
  25. Reyes-García, V., Vadez, V., Tanner, S., McDade, T., Huanca, T., & Leonard, W. (2006). Evaluating indices of traditional ecological knowledge: a methodological contribution. *J Ethnobiol Ethnomed.* 2(21) , 1-9.
  26. Saputera, M., Marpaung, T., & Ayuchecaria, N. (2019). Konsenytrasi Hambat Minimum (KHM) Kadar Ekstrak Etanol Batang Bajakah Tampala (*Apatholobus littoralis* Hassk) terhadap bakteri *Escherichia coli* melalui metode sumuran. *Jurnal Ilmiah Manuntung*, 5(2) , 167-173.
  27. Septriyanto, Rosye, S., Tanjung, H. R., Maury, H., & Meiyanto, E. (2018). Cytotoxic Activity and Phytochemical Analysis of *Breynia cernua* from Papua. *Indonesian Journal of Pharmaceutical Science and Technology* , 1 (1), 31-36.
  28. Silalahi, M. (2014). *Tumbuhan etnomedisin padaetnis Batak Sumatera Utara dan perspektif konservasinya.*

- Universitas Indonesia. Jakarta: FMIPA Universitas Indonesia.
29. Silalahi, M., Supriatna, J., Walujo, E., & Nisyawati. (2015). Local knowledge of medicinal plants in sub-ethnic Batak Simalungun of North Sumatra, Indonesia. *Biodiversitas* 16 (1), 44-54.
  30. Silalahi, M.; Nisyawati, N. (2018). An ethnobotanical study of traditional steam-bathing by the Batak people of North Sumatra, Indonesia. *Pacific Conservation Biology*, 1-18.
  31. Srinovaz. (2014). *Cara Menggunakan FTIR*.
  32. Sudarmin; Sumarni, W; Sumarti, S.S. (2019). *Model Pembelajaran Kimia Organik Bahan Alam Terintegrasi Etnosains Untuk Membumikan Karakter Konservasi Mahasiswa*. Universitas Negeri Semarang. Semarang: Universitas Negeri Semarang.
  33. Sudarmin; Zaenuri; Sumarni, W. (2017). *Pengembangan Model Pembelajaran Sains Berbasis Kearifan Lokal Mahasiswa*. Universitas Negeri Semarang. Semarang: Universitas Negeri Semarang.
  34. Sumarni, W. (2019). The scientification of jamu: A study of Indonesian's traditional medicine. *J. Phys.Conf. Ser* 1321 032057, 1-7.
  35. Sumarni, W., & Sudarmin. (2019). *Eksplorasi dan rekonstruksi pengetahuan asli masyarakat Jawa sebagai pendukung pembelajaran kimia berpendekatan STEM terintegrasi etnosains*. Semarang: LPPM UNNES.
  36. Sumarni, W., Sudarmin, Wiyanto, & Supartono. (2016). The Reconstruction of Society Indigenous Science into Scientific Science in the Production Process of Palm Sugar. *Journal of Turkish Science Education* 13(4), 281-292. doi: 10.12973/tused.
  37. Supartono, Kusuma, E., & Sudarmin. (2016). *Experiment of Organic Chemistry 2*. Universitas Negeri Semarang, Semarang.
  38. Supriyadi, & Sudarmin. (2020). *Pengembangan Bahan Ajar IPA Kontekstual Papua Terintegrasi Pendekatan Etnosains dan STEM Berbasis Indigenous Science Suku Malind*. Penelitian Kerjasama Perguruan Tinggi (PKPT), Universitas Musamus, Merauke.
  39. Toksoy, D., Bayramoglu, M., & Hacisalihoglu, S. (2010). *Journal of Enviromental Biology*, 31 (5), 623-628.
  40. Uyung, A. (2017). *Ternyata, Bajakah Bukan Nama Tanaman*. Retrieved March 1, 2020, from <https://health.detik.com>
  41. Walujo, E.B. (2013). *Etnofarmakologi : Saintifikasi Pengetahuan Untuk Pengembangan Industri Kimia Obat dan Farmasi di Indonesia*.

**Table 1. The Interview Results**

| No  | Question   | Answer   |
|-----|--|--|
| 1.  | What does Dayak Tribe call it?   | Bajakah, it means roots in Dayak language. Literature results found that the Latin name for Bajakah is <i>Uncaria gambir roxb.</i>   |
| 2.. | What are the characteristics of Bajakah?   | Vines are growing from the trunk of the tree and twisting to other trees. The tree diameter can reach 10 cm. The color of the trunk is brown, the surface of the bark is rough and dry. It secretes clear water when cut. The surface of the leaves is delicate, and the branches grow parallel right and left.  |
| 3.  | Before going viral, what are the advantages of the plant believed by the locals? | Bajakah has been used as a medicine for generations by the Dayak tribe since the nomadic life. Mostly, they consumed it to increase stamina when clearing forest land into fields.   |
| 4.  | Which part of the tree is mostly utilized?                                       | The main part is wood, but the leaves and roots are also used.   |
| 5.  | What are the steps of extracting Bajakah traditionally?                          | Separate wood with its bark, wash and rinse with running water. Cut into small pieces having 4-5 cm in length and dry it under the sunlight. Then boiled the dried wood in 1 liter of water up to reaching the remaining half (0.5 liters). The water could be consumed 3 times a day.<br><br>The wood could also be processed into powder by finely grounding the dried wood. The Bajakah powder can be consumed by brewing a teaspoon of powder with a glass of hot water. |
| 6.  | Do the locals conserve the plant?  | They only take big Bajakah tree having > 4 cm in diameter.   |
| 7.  | What do you know about Bajakah's chemical contents and their benefits?           | I am aware of the research results done by scientists in Universitas Lambung Mangkurat that there are 40 substances advantageous for health, mainly for killing cancer/tumor cells.  |

**Table 2. The Bioactivity of Secondary Metabolite Compounds Found in Bajakah or *Uncaria gambir roxb* (The Medical School of Lambung Mangkurat, 2017)**

| No | Secondary Metabolite Compound | Bioactivity and Benefit for Health   |
|----|-------------------------------|--|
| 1. | Saponins                      | Antibacterial, lower cholesterol levels, fight cancer cells, prevent tumors, increase body immune  |
| 2. | Alkaloids                     | Relieve pain and stop bleeding   |
| 3. | Steroids                      | Accelerate wound healing, and maintain stamina   |
| 4. | Terpenoids                    | Antiseptic, anti-microbial, overcome the menstrual disorder, relieve inflammation, malaria and diabetes medication                       |
| 5. | Flavonoids                    | Antioxidant, treat allergies, infections, and arthritis, restore damaged cells due to free-radical, maximalize the benefits of vitamin C |
| 6. | Tanin                         | Antioxidant, diarrhea medication, the antibacterial, antidote  |
| 7. | Phenolics                     | Antioxidant, prevent heart disorders, prevent cancer cell growth, prevent diabetes   |

**Table 3.** The Phytochemical Test Results of Bajakah (*Uncaria gambir roxb*) Wood and Root Extract (Sudarmin et al., 2020)

| No. | Sample | Isolation and Extraction Process               | Characteristics of Substances (Organoleptic) | Positive phytochemical and metabolite results  |
|-----|--------|--|--|--|
| 1.  | Root   | Soxhletation with an ethanol solvent           | Yellowish orange liquid                      | Alkaloids, terpenoids, flavonoids,             |
|     |        | Soxhletation with ethanol and n-hexane solvent | Brownish orange liquid                       | Terpenoids                                     |
|     |        | Maceration with water solvent                  | Colorless liquid                             | Alkaloids, flavonoids, phenolics, and saponins |
| 2   | Wood   | Soxhletation with an ethanol solvent           | Yellow liquid                                | Terpenoids                                     |
|     |        | Soxhletation with ethanol and n-hexane solvent | Light brown or creme liquid                  | Unidentified                                   |
|     |        | Soxhletation with ethanol and benzene solvent  | Light brown or creme liquid                  | Alkaloids, terpenoids, phenolics, and saponins |

**Table 4.** Antibacterial Bioactivity Test Results of Bajakah (*Uncaria gambir roxb*) extract (Sudarmin et al, 2020)

| No | Sample | Solvent              | Bacterial Inhibition  |
|----|--------|----------------------|---|
| 1. | Root   | Water (Maceration)   | The inhibition zone to <i>B. Subtili</i> is 12.25 mm and 61.25 mm to <i>E. Coli</i> |
|    |        | Ethanol (Extraction) | The inhibition zone to <i>B. Subtili</i> is 0.00 mm and 55.00 mm to <i>E. Coli</i>  |
|    |        | Benzene (Extraction) | The inhibition zone to <i>B. Subtili</i> is 7.25 mm and 7.725 mm to <i>E. Coli</i>  |
| 2. | Wood   | Water (Maceration)   | The inhibition zone to <i>B. Subtili</i> is 70.50 mm and 10.25 mm to <i>E. Coli</i> |
|    |        | Ethanol (Extraction) | The inhibition zone to <i>B. Subtili</i> is 66.00 mm and 8.25 mm to <i>E. Coli</i>  |
|    |        | Benzene (Extraction) | The inhibition zone to <i>B. Subtili</i> is 79.50 mm and 7.75 mm to <i>E. Coli</i>  |

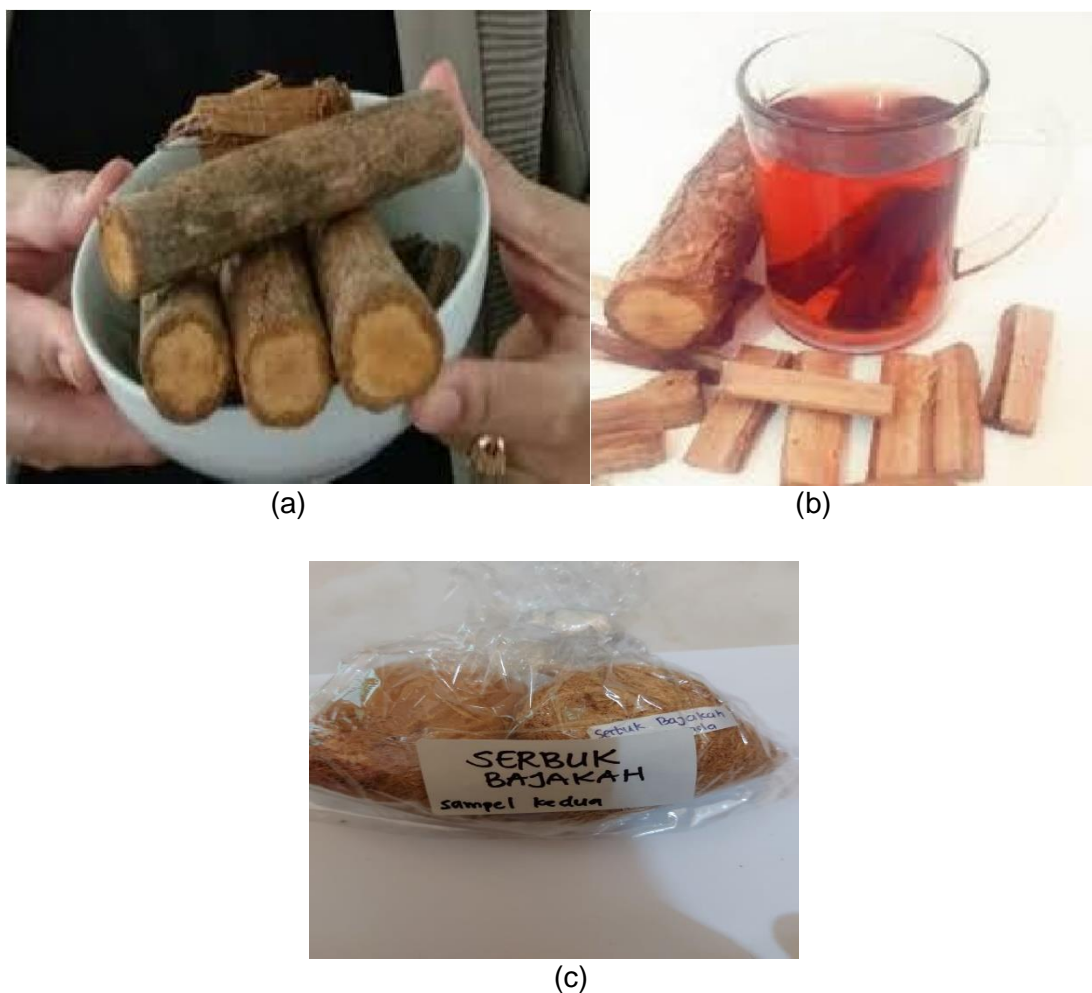


**Figure 1.** (a) Bajakah Wood, (b) Bajakah Tea, (c) Bajakah Powder. (Source: Sudarmin et al., 2020)

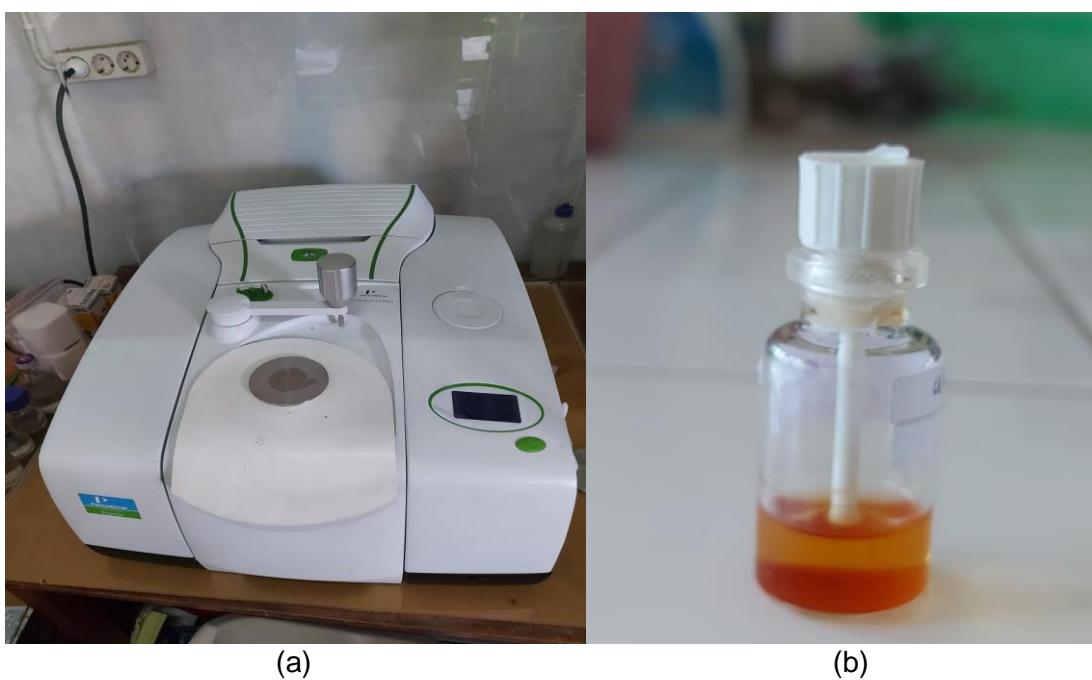
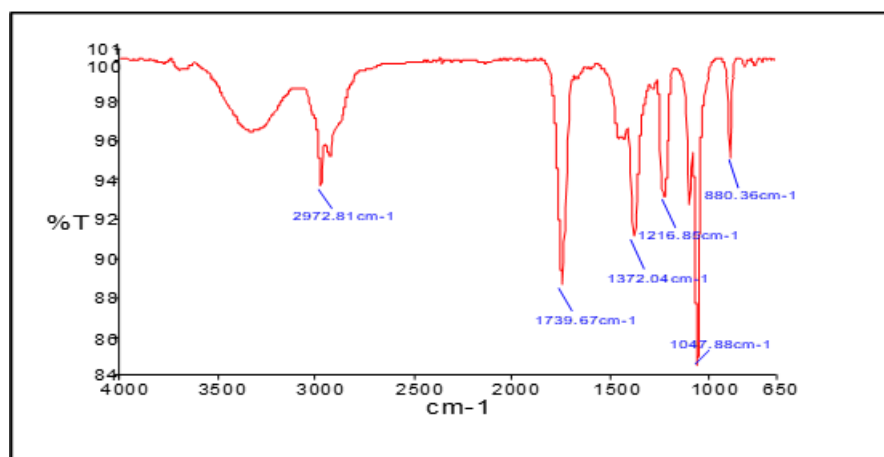
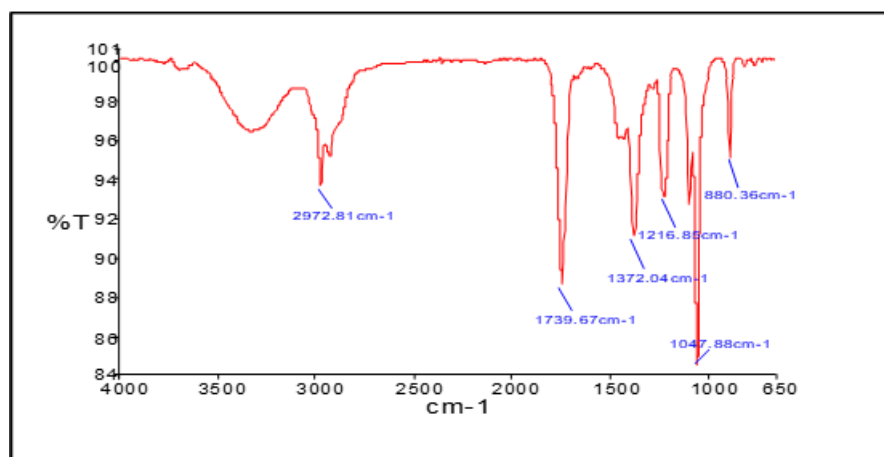


**Figure 2.** (a) Spectroscopic Tool 100 FTIR produced by Perkin Elmer Inc.; (b) Sample of Bajakah Isolate.



(a)



(b)

**Figure 3.** FTIR Spectra for Bajakah (*Uncaria gambir roxb*) Wood (a) and Root (b) Isolates in the mixer of Ethanol and n-Hexane Solvents.

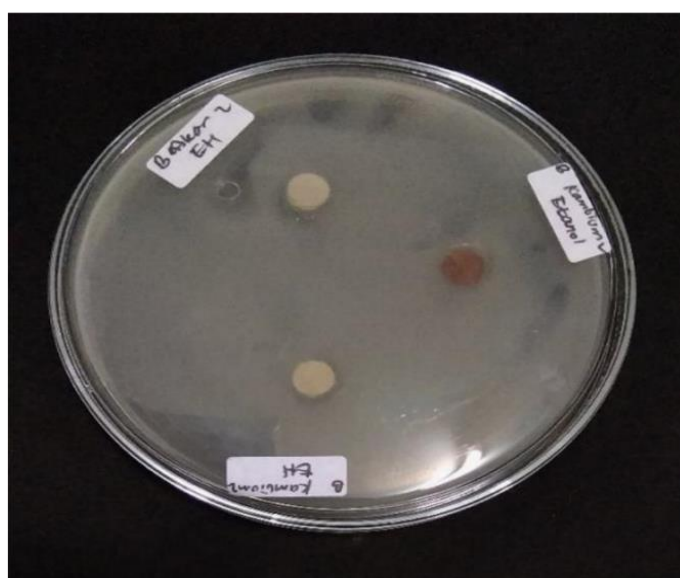


**Figure 4.** Antibacterial Bioactivity Test Results of Bajakah Extract from Borneo Island (Sudarmin et al., 2020).



# UM NOVO MÉTODO ANALÍTICO PARA RESOLVER A EQUAÇÃO DE TELEGRAFIA LINEAR E NÃO-LINEAR

## A NOVEL ANALYTIC METHOD FOR SOLVING LINEAR AND NON-LINEAR TELEGRAPH EQUATION

Al-JABERI, Ahmed K.<sup>1</sup>, HAMEED, Ehsan M.<sup>2</sup>, Abdul-WAHAB, Mohammed S.<sup>3</sup>

<sup>1,3</sup> Department of Mathematics, College of Education for Pure Sciences, University of Basrah, Basrah, Iraq.

<sup>2</sup> Department of Mathematics, College of Computer Science and Mathematics, University of Thi-Qar, Thi-Qar, Iraq.

\* Corresponding author

e-mail: [ahmed.shanan@uobasrah.edu.iq](mailto:ahmed.shanan@uobasrah.edu.iq)

Received 18 May 2020; received in revised form 29 May 2020; accepted 12 June 2020

### RESUMO

A modelagem de muitos fenômenos em vários campos, como matemática, física, química, engenharia, biologia e astronomia, é feita pelas equações diferenciais parciais não lineares (PDE). A equação do telégrafo hiperbólico é uma delas, onde descreve as vibrações de estruturas (por exemplo, edifícios, vigas e máquinas) e é a base para equações fundamentais da física atômica. Existem vários métodos analíticos e numéricos para resolver a equação do telégrafo. Uma solução analítica considera enquadrar o problema de uma forma bem compreendida e calcular a resolução exata. Também ajuda a entender as respostas para o problema em termos de precisão e convergência. Esses métodos analíticos têm limitações com precisão e convergência. Portanto, um novo método analítico aproximado é proposto para lidar com restrições neste artigo. Este método usa as séries de Taylors em sua derivação. O método proposto foi usado para resolver a equação hiperbólica de segunda ordem (equação Telegraph) com a condição inicial. Três exemplos foram apresentados para verificar a eficácia, precisão e convergência do método. As soluções do método proposto também foram comparadas com as obtidas pelo método de decomposição adomiana (ADM) e pelo método de análise de homotopia (HAM). A técnica é fácil de implementar e produz resultados precisos. Em particular, esses resultados mostram que o método proposto é eficiente e melhor que os outros métodos em termos de precisão e convergência

**Palavras-chave:** *Equação do Telégrafo Hiperbólico, Série de Taylor, Solução Analítica, Precisão, Operador Não Linear.*

### ABSTRACT

The modeling of many phenomena in various fields such as mathematics, physics, chemistry, engineering, biology, and astronomy is done by the nonlinear partial differential equations (PDE). The hyperbolic telegraph equation is one of them, where it describes the vibrations of structures (e.g., buildings, beams, and machines) and are the basis for fundamental equations of atomic physics. There are several analytical and numerical methods are used to solve the telegraph equation. An analytical solution considers framing the problem in a well-understood form and calculating the exact resolution. It also helps to understand the answers to the problem in terms of accuracy and convergence. These analytic methods have limitations with accuracy and convergence. Therefore, a novel analytic approximate method is proposed to deal with constraints in this paper. This method uses the Taylors' series in its derivation. The proposed method has used for solving the second-order, hyperbolic equation (Telegraph equation) with the initial condition. Three examples have presented to check the effectiveness, accuracy, and convergence of the method. The solutions of the proposed method also compared with those obtained by the Adomian decomposition method (ADM), and the Homotopy analysis method (HAM). The technique is easy to implement and produces accurate results. In particular, these results display that the proposed method is efficient and better than the other methods in terms of accuracy and convergence.

**Keywords:** *Hyperbolic Telegraph Equation, Taylors' Series, Analytical Solution, Accuracy, Non-Linear Operator.*

## 1. INTRODUCTION:

Telegraph's equation is one of the most investigated problems in over four centuries. Generally, it uses to model the vibrations of structures (e.g., buildings, beams, and machines) and are the basis for fundamental equations of atomic physics (Kolesov and Rozov 2000) and (Alonso, Mawhin, and Ortega 1999).

Linear hyperbolic telegraph equation with constant coefficients forms a blend between wave propagation and diffusion by inserting a term that accounts for impacts of finite velocity to the standard heat or mass transport equation (El-Azab and El-Gamel 2007). In general, the hyperbolic telegraph equation is used in signal analysis for transmission and propagation of electrical signals (A. C. Metaxas 1983) and also has applications in other fields (see (Roussy and Pearce 1998) and the references therein).

Recently, several numerical methods have been developed to solve hyperbolic partial differential equations (PDEs), such as alternating direction implicit Method (Mohanty, Jain, and Arora 2002), Chebyshev tau method (Saadatmandi and Dehghan 2010), Interpolating Scaling Functions Method (Lakestani and Saray 2010), Radial Basis Functions method (De Su, Jiang, and Jiang 2013), collocation points and approximating the solution using thin-plate splines radial basis function method (Dehghan and Shokri 2008), the modified cubic B-Spline differential quadrature method (Singh 2016), a collocation method (Bhatia 2014), reproducing kernel method (Mustafa Inc 2013), finite difference method (Mohanty, Jain, and George 1996), and (Gao and Chi 2007), finite volume method (Sheng and Zhang 2018), Galerkin method (Liu and Gu 2004), improved element-free Galerkin method (Zhang, Deng, and Liew 2014), and differential quadrature method (Mittal and Jiwari 2009).

These techniques consider a necessitate as computational resources to solve some problems that appear in other sciences such as in image processing. Still, these techniques perhaps complicated and require a high computational cost, which means they consume time and effort to obtain accurate solutions for different nonlinear PDEs. Furthermore, applying these techniques may be needed for transforming. Thus, they do not avoid linearization, discretization, or any realistic assumption to providing an efficient solution. Therefore, it is considered positive points for analytical methods to find the most efficient and high accurate approximate and exact solutions for the linear and nonlinear differential equations.

There are many used methods to find the exact solution, such as ( $G'/G$ ) expansion method (Naher, Hasibun 2012), sine-cosine method (Yusufoğlu and Bekir 2006), homogeneous balance method (Eslami, Fathi Vajargah, and Mirzazadeh 2014), etc. Also, there are other types of analytical techniques that combine between exact and approximate methods called semi-analytical methods. For instance, Adomian decomposition method (ADM), (Adomian 1994) and (Biazar and Ebrahimi 2007), the extended of ADM (Al-Badrani et al. 2016), Differential transform method (DTM) (Zhou 1986), Variational Iteration Method (VIM) (Biazar, Ebrahimi, and Ayati 2008), Reduced differential transform method (Mukesh K. Awasthi, R. K. Chaurasia 2013) and (Srivastava, Awasthi, and Chaurasia 2014), Daftardar-Gejji-Jafaris (DGJ) method (Sari, Gunay, and Gurarslan 2014), Reimann method (ZAVALANI 2009), Sumudu method (Ayad Ghazi Naser Al-Shammari, Wurood R. Abd AL-Hussein 2018), the modified simple equation method (Taghizadeh et al. 2012), Chebyshev Cardinal functions are used for solution of the second-order one-dimensional telegraph Equation (Dehghan and Lakestani 2009), Wavefront solutions of a nonlinear telegraph equation (Gilding and Kersner 2013), Homotopy analysis method (HAM) (Raftari and Yildirim 2012), Homotopy analysis Sumudu transform method (Rathore et al. 2012) and (Jaradat et al. 2018), and Laplace transform method (LDM) (Jaradat et al. 2018).

One of these methods which has received much concern is the Adomian decomposition method (ADM) (Biazar and Ebrahimi 2007). The ADM has been employed to solve various linear and nonlinear models. The ADM yields a rapidly convergent series solution with much less computational work (Abbaoui and Cherruault 1995). The ADM is unlike the traditional numerical methods, where ADM is used extensively to solve nonlinear differential equations because it works based on calculation Adomian polynomials for non-linear terms (El-Sayed and Kaya 2004) and (Inc 2007).

While, the analytical solutions of differential transform method (DTM) (Zhou 1986), are as a polynomial form which is different from the traditional higher-order Taylor series method because the Taylor series method needs huge computational for large orders. So, the DTM uses a different procedure to obtain an analytic Taylor series solution of the PDE (Abazari and Borhanifar 2010) and (Saeideh Hesam 2011).

On the other hand, many complicated problems in different applied sciences have been

successfully solved by the homotopy analysis method (HAM) (Liao 1992), (Kheiri, H. 2011), (Usman et al. 2013) and (Arafa, Rida, and Mohamed 2011). Homotopy perturbation method (HPM) (Raftari and Yildirim 2012), as well has been handled successfully to solve many linear and non-linear PDEs (Roul 2010).

Whereas, the variational iteration method (VIM) (He 1997), can be applied to solve all types of linear or nonlinear differential equations, constant or variable coefficients with homogeneous or inhomogeneous (Yulita Molliq et al. 2009) because it effectively used to solve these nonlinear equations with a good convergent to the exact solutions.

All of these analytical methods are active and strong in finding solutions of linear and non-linear PDEs. Generally, the basic idea of these methods through writing the PDEs in the form of operators after that the inverse operator of time (or space) is taken to calculate the solutions on the interval of the solution domain. In the last years, these analytical methods have been enhanced and modified and to overcome the difficulties encountered in the numerical methods such as finding the exact solution, round off errors, low accuracy, and weak convergence by many researchers. Furthermore, these analytical methods introduced efficiency and high accuracy in finding the analytical exact and approximate solutions for the linear and nonlinear PDEs, which made a good impression of these analytical methods. Therefore, we proposed a new analytical approximate method for solving linear and non-linear telegraph equations.

This study aimed to find approximate analytical solutions to the linear and nonlinear telegraph equation with initial conditions and boundary conditions by using a novel analytical technique, which is considered as extending and developing to that in (wiwatwanich, 2016). This technique is based on the Taylor series, which is efficient to solve nonlinear equations. Also, the survey reveals that no attempt has ever been made to study the current model by using this technique. These reasons stimulated and employed us to solve the linear and intricate nonlinear problems such as the one-dimensional telegraph equation. Several test problems are given, and their results are compared with the solutions obtained by ADM (Biazar and Ebrahimi 2007), and HAM (Raftari and Yildirim 2012) to confirm the excellent accuracy and small absolute errors of the proposed technique.

## 2. MATERIALS AND METHODS:

In this work, it was studied the second-order one-dimensional telegraph equation:

$$\frac{\partial^2 w}{\partial t^2} + 2\alpha \frac{\partial w}{\partial t} + \beta^2 w = \frac{\partial^2 w}{\partial x^2} + h(x, t) + g(w), \quad (1)$$

where  $w = w(x, t)$ ,  $\alpha$ ,  $\beta$  are real constants,  $x$  is distance and  $t$  is time, with initial and boundary conditions

$$w(x, 0) = h_0(x), \quad \frac{\partial w}{\partial t}(x, 0) = h_1(x), \quad (2)$$

$$w(0, t) = g_0(t), \quad w(1, t) = g_1(t), \quad t \geq 0 \quad (3)$$

If  $g(w) = 0$ , then equation (1) called a linear hyperbolic telegraph equation in a double conductor, the equation (2.1) is satisfied in both the electric voltage and current. For  $\alpha > 0$ ,  $\beta = 0$  it represents a damped wave equation, and  $\alpha > \beta > 0$ , which is called a telegraph equation.

### 2.1. Generating an analytical approach

In this section, the basic ideas for constructing a novel analytical approach will be discussed. Let us consider the initial value problems:

$$w_{tt}(x, t) = G(w_t, w, w_x, w_{xx}, \dots), \quad (4)$$

with initial condition

$$w(x, 0) = h_0(x), \quad w_t(x, 0) = h_1(x). \quad (5)$$

By using the integral for the two sides of equation (4) from 0 to  $t$ , we get

$$w_t(x, t) - w_t(x, 0) = \int_0^t F[w] dt,$$

$$w_t(x, t) - h_1(x) = \int_0^t F[w] dt.$$

Then,

$$w_t(x, t) = h_1(x) + \int_0^t F[w] dt, \quad (6)$$

where  $G[w] = G(w_t, w, w_x, w_{xx}, \dots)$ .

Then, when the integral of two sides of equation (6) is used from 0 to  $t$ , we obtain

$$w(x, t) - w(x, 0) = h_1(x)t + \iint_0^t G[w] dt dt,$$

$$w(x, t) - h_0(x) = h_1(x)t + \iint_0^t G[w] dt dt.$$

Thus,

$$w(x, t) = h_0(x) + h_1(x)t + \iint_0^t G[w] dt dt. \quad (7)$$

The Taylor series is extended for  $G[w]$  about  $t = 0$ , which is

$$G[w] = G[w_0] + G'[w_0]t + G''[w_0]\frac{t^2}{2!} + G'''[w_0]\frac{t^3}{3!} + \dots + G^{(n)}[w_0]\frac{t^n}{n!} + \dots \quad (8)$$

Substituting equation (8) by equation (7), we get

$$\begin{aligned} w(x, t) &= h_0(x) + h_1(x)t + G[w_0]\frac{t^2}{2!} + G'[w_0]\frac{t^3}{3!} + \\ &G''[w_0]\frac{t^4}{4!} + \dots + G^{(n-2)}[w_0]\frac{t^n}{n!} + \dots, \\ &= a_0 + a_1t + a_2\frac{t^2}{2!} + a_3\frac{t^3}{3!} + \dots + a_n\frac{t^n}{n!} + \dots, \end{aligned} \quad (9)$$

where

$$a_0 = h_0(x),$$

$$a_1 = h_1(x),$$

$$a_2 = G[w_0],$$

$$a_3 = G'[w_0],$$

$$a_n = G^{(n-2)}[w_0].$$

where  $n$  is the highest derivative of  $u$ . The formal of Equation (9) is expand Taylor's series for  $w$  about  $t = 0$ . This means

$$a_0 = w(x, 0),$$

$$a_1 = \frac{\partial}{\partial t} w(x, 0),$$

$$a_2 = \frac{\partial^2}{\partial t^2} w(x, 0),$$

$$a_3 = \frac{\partial^3}{\partial t^3} w(x, 0),$$

$$a_n = \frac{\partial^n}{\partial t^n} w(x, 0).$$

### 2.1.1 Test Problems

**Example 1.** Solve the following linear telegraph equation (Lakestani and Saray 2010):

$$\begin{aligned} \frac{\partial^2 w(x, t)}{\partial t^2} + 2\alpha \frac{\partial w(x, t)}{\partial t} + \beta^2 w(x, t) &= \frac{\partial^2 w(x, t)}{\partial x^2} + \\ (3 - 4\alpha + \beta^2)e^{-2t} \sinh(x), \\ \frac{\partial^2 w(x, t)}{\partial t^2} &= -2 \\ &\alpha \frac{\partial w(x, t)}{\partial t} - \beta^2 w(x, t) + \frac{\partial^2 w(x, t)}{\partial x^2} \\ &+ (3 - 4\alpha + \beta^2)e^{-2t} \sinh(x). \end{aligned} \quad (10)$$

**Solution:**

By the following equation (4), we can note after rewrite equation (10):

$$\begin{aligned} F[w] &= -2\alpha \frac{\partial w(x, t)}{\partial t} - \beta^2 w(x, t) + \frac{\partial^2 w(x, t)}{\partial x^2} + \\ (3 - 4\alpha + \beta^2)e^{-2t} \sinh(x), \\ a_0 &= h_0(x) = \sinh(x), \end{aligned}$$

$$a_1 = h_1(x) = -2 \sinh(x),$$

$$\begin{aligned} a_2 &= G[w_0] = -2\alpha \frac{\partial w(x, 0)}{\partial t} - \beta^2 w(x, 0) + \\ &\frac{\partial^2 w(x, 0)}{\partial x^2} + (3 - 4\alpha + \beta^2)e^{-2(0)} \sinh(x) \\ &= -2\alpha a_1 - \beta^2 a_0 + (a_0)_{xx} + \\ &(3 - 4\alpha + \beta^2)e^{-2(0)} \sinh(x) \\ &= 4\alpha \sinh(x) - \beta^2 \sinh(x) + \\ &\sinh(x) + (3 - 4\alpha + \beta^2) \sinh(x) \\ &= (4\alpha - \beta^2) \sinh(x) + \sinh(x) + \\ &3 \sinh(x) + (-4\alpha + \beta^2) \sinh(x) \\ &= 4 \sinh(x) \end{aligned}$$

$$\begin{aligned} G'[w] &= -2\alpha \frac{\partial^2 w(x, t)}{\partial t^2} - \beta^2 \frac{\partial w(x, t)}{\partial t} + \frac{\partial^3 w(x, t)}{\partial t \partial x^2} - \\ &2(3 - 4\alpha + \beta^2)e^{-2t} \sinh(x) \\ a_3 &= G'[w_0] = -2\alpha \frac{\partial^2 w(x, 0)}{\partial t^2} - \beta^2 \frac{\partial w(x, 0)}{\partial t} + \\ &\frac{\partial^3 w(x, 0)}{\partial t \partial x^2} - 2(3 - 4\alpha + \beta^2)e^{-2(0)} \sinh(x) \\ &= -2\alpha a_2 - \beta^2 a_1 + (a_1)_{xx} - \\ &2(3 - 4\alpha + \beta^2) \sinh(x) \\ &= -8\alpha \sinh(x) + 2\beta^2 \sinh(x) - \\ &2 \sinh(x) - 2(3 - 4\alpha + \beta^2) \sinh(x) \end{aligned}$$

$$\begin{aligned}
&= (-8 \alpha + 2\beta^2) \sinh(x) - \\
&2 \sinh(x) - 6 \sinh(x) + (8 \alpha - 2\beta^2) \sinh(x) \\
&= -8 \sinh(x).
\end{aligned}$$

Now by using equation (9),

$$\begin{aligned}
w(x, t) &= a_0 + a_1 t + a_2 \frac{t^2}{2!} + a_3 \frac{t^3}{3!} + \dots + a_n \frac{t^n}{n!} + \dots \\
&= \sinh(x) - 2 \sinh(x) t + 4 \sinh(x) \frac{t^2}{2!} - \\
&8 \sinh(x) \frac{t^3}{3!} + \dots \\
&= \sinh(x) (1 - (2t) + \frac{(2t)^2}{2!} - \frac{(2t)^3}{3!} + \dots) \\
&= \sinh(x) e^{-2t}.
\end{aligned}$$

Therefore, the graph of exact, analytical solutions, and absolute errors of example 1 for  $t = 1$  are given in Figure 1. Table 1 shows the absolute error using the proposed technique, ADM, and HAM of example 1 with  $t = 1, k = 0.001$  and different values of  $\alpha = 10$ , and  $\beta = 5$ .

When the value of  $n$  increases, the approximate solution gradually approaches the exact solution and the absolute error will decrease. Also, the values of  $\alpha$  and  $\beta$  do not affect the solution.

**Example 2.** Solve the following linear telegraph equation (Lakestani and Saray 2010):

$$\begin{aligned}
\frac{\partial^2 w(x, t)}{\partial t^2} + 2 \alpha \frac{\partial w(x, t)}{\partial t} + \beta^2 w(x, t) &= \frac{\partial^2 w(x, t)}{\partial x^2} - 2 \alpha \sin(t) \sin(x) + \beta^2 \cos(t) \sin(x), \\
\frac{\partial^2 w(x, t)}{\partial t^2} &= -2 \alpha \frac{\partial w(x, t)}{\partial t} - \beta^2 w(x, t) + \frac{\partial^2 w(x, t)}{\partial x^2} - 2 \alpha \sin(t) \sin(x) + \beta^2 \cos(t) \sin(x) \quad (11)
\end{aligned}$$

**Solution:** By the following equation (4), we can note after rewrite equation (11):

$$\begin{aligned}
G[w] &= -2 \alpha \frac{\partial w(x, t)}{\partial t} - \beta^2 w(x, t) + \frac{\partial^2 w(x, t)}{\partial x^2} - 2 \alpha \sin(t) \sin(x) + \beta^2 \cos(t) \sin(x), \\
a_0 &= h_0(x) = \sin(x),
\end{aligned}$$

$$a_1 = h_1(x) = 0,$$

$$\begin{aligned}
a_2 &= G[w_0] = -2 \alpha \frac{\partial w(x, 0)}{\partial t} - \beta^2 w(x, 0) + \\
&\frac{\partial^2 w(x, 0)}{\partial x^2} - 2 \alpha \sin(0) \sin(x) + \beta^2 \cos(0) \sin(x)
\end{aligned}$$

$$= -2 \alpha a_1 - \beta^2 a_0 + (a_0)_{xx} +$$

$$\begin{aligned}
&\beta^2 \sin(x) \\
&= -2 \alpha (0) - \beta^2 \sin(x) + (\sin(x))_{xx} + \\
&\beta^2 \sin(x)
\end{aligned}$$

$$= -\sin(x),$$

$$G'[w] = -2 \alpha \frac{\partial^2 w(x, t)}{\partial t^2} - \beta^2 \frac{\partial w(x, t)}{\partial t} + \frac{\partial^3 w(x, t)}{\partial t \partial x^2} - 2 \alpha \cos(t) \sin(x) - \beta^2 \sin(t) \sin(x),$$

$$\begin{aligned}
a_3 &= G'[w_0] = -2 \alpha \frac{\partial^2 w(x, 0)}{\partial t^2} - \beta^2 \frac{\partial w(x, 0)}{\partial t} + \\
&\frac{\partial^3 w(x, 0)}{\partial t \partial x^2} - 2 \alpha \cos(0) \sin(x) - \\
&\beta^2 \sin(0) \sin(x) \\
&= -2 \alpha a_2 - \beta^2 a_1 + (a_1)_{xx} - 2 \alpha \sin(x)
\end{aligned}$$

$$\begin{aligned}
&= 2 \alpha \sin(x) - \beta^2 (0) + (0)_{xx} - 2 \alpha \sin(x) \\
&= 0,
\end{aligned}$$

$$G''[w] = -2 \alpha \frac{\partial^3 w(x, t)}{\partial t^3} - \beta^2 \frac{\partial^2 w(x, t)}{\partial t^2} + \frac{\partial^4 w(x, t)}{\partial t^2 \partial x^2} + 2 \alpha \sin(t) \sin(x) - \beta^2 \cos(t) \sin(x),$$

$$\begin{aligned}
a_4 &= G''[w_0] = -2 \alpha \frac{\partial^3 w(x, 0)}{\partial t^3} - \beta^2 \frac{\partial^2 w(x, 0)}{\partial t^2} + \\
&\frac{\partial^4 w(x, 0)}{\partial t^2 \partial x^2} + 2 \alpha \sin(0) \sin(x) - \beta^2 \cos(0) \sin(x) \\
&= -2 \alpha a_3 - \beta^2 a_2 + (a_2)_{xx} - \\
&\beta^2 \sin(x) \\
&= -2 \alpha (0) + \beta^2 \sin(x) + \sin(x) - \\
&\beta^2 \sin(x) \\
&= \sin(x),
\end{aligned}$$

Now, by using the equation (9),

$$\begin{aligned}
w(x, t) &= a_0 + a_1 t + a_2 \frac{t^2}{2!} + a_3 \frac{t^3}{3!} + \dots + a_n \frac{t^n}{n!} + \dots \\
&= \sin(x) + (0)t + (-\sin(x)) \frac{t^2}{2!} + (0) \frac{t^3}{3!} + \\
&(\sin(x)) \frac{t^4}{4!} + \dots \\
&= \sin(x) - \sin(x) \frac{t^2}{2!} + \sin(x) \frac{t^4}{4!} + \dots \\
&= \sin(x) (1 - \frac{t^2}{2!} + \frac{t^4}{4!} + \dots) \\
&= \sin(x) \cos(t).
\end{aligned}$$

Therefore, the graph of exact, analytical solutions, and absolute errors of example 2 for  $t = 1$  are given in Figure 2. Table 2 shows the absolute error using the proposed technique, ADM, and HAM of example 2 with  $t = 1, k = 0.001$  and different values of  $\alpha = 10$ , and  $\beta = 5$ .

When the value of  $n$  increases, the approximate solution gradually approaches the exact solution and the absolute error will decrease. Also, the values of  $\alpha$  and  $\beta$  do not affect the solutions.

**Example 3.** Solve the following nonlinear telegraph equation (Bhatia 2014):

$$\begin{aligned}\frac{\partial^2 w(x,t)}{\partial t^2} + \frac{\partial w(x,t)}{\partial t} &= \frac{\partial^2 w(x,t)}{\partial x^2} - 2 \sin(w(x,t)) - \\ &\pi^2 e^{-t} \cos(\pi x) + 2 \sin(e^{-t}(1 - \cos(\pi x))), \\ \frac{\partial^2 w(x,t)}{\partial t^2} &= -\frac{\partial w(x,t)}{\partial t} + \frac{\partial^2 w(x,t)}{\partial x^2} - 2 \sin(w(x,t)) - \\ &\pi^2 e^{-t} \cos(\pi x) + 2 \sin(e^{-t}(1 - \cos(\pi x))).\end{aligned}\quad (12)$$

**Solution:** By the following equation (4), we can note after rewrite equation (12):

$$\begin{aligned}G[w] &= -\frac{\partial w(x,t)}{\partial t} + \frac{\partial^2 w(x,t)}{\partial x^2} - 2 \sin(w(x,t)) - \\ &\pi^2 e^{-t} \cos(\pi x) + 2 \sin(e^{-t}(1 - \cos(\pi x))), \\ a_0 &= h_0(x) = 1 - \cos(\pi x),\end{aligned}$$

$$a_1 = h_1(x) = -1 + \cos(\pi x),$$

$$\begin{aligned}a_2 &= G[w_0] = -\frac{\partial w(x,0)}{\partial t} + \frac{\partial^2 w(x,0)}{\partial x^2} - \\ &2 \sin(w(x,0)) - \pi^2 e^{-(0)} \cos(\pi x) + \\ &2 \sin(e^{-(0)}(1 - \cos(\pi x))) \\ &= -a_1 + (a_0)_{xx} - 2 \sin(a_0) - \\ &\pi^2 \cos(\pi x) + 2 \sin((1 - \cos(\pi x))) \\ &= 1 - \cos(\pi x) + \pi^2 \cos(\pi x) - \\ &2 \sin(1 - \cos(\pi x)) - \pi^2 \cos(\pi x) + \\ &2 \sin((1 - \cos(\pi x))) \\ &= 1 - \cos(\pi x),\end{aligned}$$

$$\begin{aligned}G'[w] &= -\frac{\partial^2 w(x,t)}{\partial t^2} + \frac{\partial^3 w(x,t)}{\partial t \partial x^2} - \\ &2 \cos(w(x,t)) \frac{\partial w(x,t)}{\partial t} + \pi^2 e^{-t} \cos(\pi x) + \\ &2 \cos(e^{-t}(1 - \cos(\pi x))) e^{-t}(-1 + \cos(\pi x)),\end{aligned}$$

$$\begin{aligned}a_3 &= G'[w_0] = -\frac{\partial^2 w(x,0)}{\partial t^2} + \frac{\partial^3 w(x,0)}{\partial t \partial x^2} - \\ &2 \cos(w(x,0)) \frac{\partial w(x,0)}{\partial t} + \pi^2 e^{-(0)} \cos(\pi x) + \\ &2 \cos(e^{-(0)}(1 - \cos(\pi x))) e^{-(0)}(-1 + \cos(\pi x)) \\ &= -a_2 + (a_1)_{xx} - 2 \cos(a_0)a_1 + \\ &\pi^2 \cos(\pi x) \\ &\quad + 2 \cos((1 - \cos(\pi x)))(-1 +\end{aligned}$$

$$\begin{aligned}\cos(\pi x)) \\ &= -1 + \cos(\pi x) - \pi^2 \cos(\pi x) - \\ &2 \cos(1 - \cos(\pi x))(-1 + \cos(\pi x)) \\ &\quad + \pi^2 \cos(\pi x) + 2 \cos((1 - \cos(\pi x)))(-1 + \cos(\pi x)) \\ &= -1 + \cos(\pi x),\end{aligned}$$

Now, by using the equation (9),

$$\begin{aligned}w(x,t) &= a_0 + a_1 t + a_2 \frac{t^2}{2!} + a_3 \frac{t^3}{3!} + \dots + a_n \frac{t^n}{n!} + \dots \\ &= (1 - \cos(\pi x)) - (1 - \cos(\pi x))t + \\ &(1 - \cos(\pi x)) \frac{t^2}{2!} - (1 - \cos(\pi x)) \frac{t^3}{3!} + \dots \\ &= (1 - \cos(\pi x))(1 - t + \frac{t^2}{2!} - \frac{t^3}{3!} + \dots) \\ &= (1 - \cos(\pi x))e^{-t}.\end{aligned}$$

Then, the graph of exact, analytical solutions, and absolute errors of example 3 for  $t = 1$  are given in Figure 3. Table 3 shows the absolute error using the proposed technique, ADM, and HAM of example 3 with  $t = 1, k = 0.001$ . When the value of  $n$  increases, the approximate solution gradually approaches the exact solution and the absolute error will decrease.

### 3. RESULTS AND DISCUSSION:

Three test problems are introduced for confirming the validity of the novel proposed technique, which used to find the solutions of linear and nonlinear one-dimensional telegraph equations. Figures (1-3) showed that the exact solution, analytical solution, and absolute errors at  $t = 1, k = 0.001$ . Also, the analytical solutions obtained by a proposed technique have been compared with the solutions obtained by ADM (Biazar and Ebrahimi 2007), and HAM (Raftari and Yildirim 2012) in three test examples, which are given in Tables (1-3). We then found that the analytical solutions obtained by a proposed technique are more identical to the exact solutions than those obtained using ADM and HAM of linear and nonlinear one-dimensional telegraph equation. Therefore, it can be seen that the absolute errors of the proposed technique are smaller than ADM and HAM, which are shown in Tables (1-3). More precisely, the measurement of absolute errors for these examples guarantees the ability of the proposed technique and its accuracy in finding the analytical solutions of linear and

nonlinear one-dimensional telegraph equation. Moreover, according to the computations that are introduced in the figures and tables, we can say that, the analytical technique is an effective and good technique to find the solutions of linear and nonlinear one-dimensional telegraph equations compared to the ADM, and HAM.

### 3.1. Convergence analysis

Consider the PDE (1.1) in the following form:

$$w(x, t) = G(w(x, t)), \quad (1)$$

where  $G$  is a nonlinear operator. The solution that obtained by the presented technique is equivalent to the following sequence:

$$S_n = \sum_{i=0}^n w_i = \sum_{i=0}^n \delta_i \frac{(\Delta t)^i}{(i)!}. \quad (2)$$

**Theorem 3.1** (Convergence of linear and nonlinear telegraph equation)

Let  $G$  be an operator from a Hilbert space  $H$  into  $H$  and  $w$  be the exact solution of equation (3.1). The approximate solution  $\sum_{i=0}^{\infty} w_i = \sum_{i=0}^{\infty} \delta_i \frac{(\Delta t)^i}{(i)!}$  is converged to exact solution  $w$ , when  $\exists 0 \leq \delta < 1$ ,  $\|w_{i+1}\| \leq \delta \|w_i\| \forall i \in \mathbb{N} \cup \{0\}$ .

**Proof:** We want to prove that  $\{S_n\}_{n=0}^{\infty}$  is a converged Cauchy sequence,

$$\|S_{n+1} - S_n\| = \|w_{n+1}\| \leq \delta \|w_n\| \leq \delta^2 \|w_{n-1}\| \leq \dots \leq \delta^n \|w_1\| \leq \delta^{n+1} \|w_0\|. \quad (3)$$

Now for  $n, m \in \mathbb{N}, n \geq m$  we get

$$\begin{aligned} \|S_n - S_m\| &= \|(S_n - S_{n-1}) + (S_{n-1} - S_{n-2}) + \dots + (S_{m+1} - S_m)\| \\ &\leq \|S_n - S_{n-1}\| + \|S_{n-1} - S_{n-2}\| + \dots + \|S_{m+1} - S_m\| \\ &\leq \delta^n \|w_0\| + \delta^{n-1} \|w_0\| + \dots + \delta^{m+1} \|w_0\| \\ &\leq (\delta^{m+1} + \delta^{m+2} + \dots + \delta^n) \|w_0\| = \\ &\delta^{m+1} \frac{1 - \delta^{n-m}}{1 - \delta} \|w_0\|. \quad (4) \end{aligned}$$

Hence,  $\lim_{n, m \rightarrow \infty} \|S_n - S_m\| = 0$ , i. e.,  $\{S_n\}_{n=0}^{\infty}$  is a Cauchy sequence in the Hilbert space  $H$ .

Thus, there exist  $S \in H$  such that  $\lim_{n \rightarrow \infty} S_n = S$ , where  $S = w$ .

**Definition 3.2** For every  $n \in \mathbb{N} \cup \{0\}$ , we define

$$\delta_n = \begin{cases} \frac{\|w_{n+1}\|}{\|w_n\|}, & \|w_n\| \neq 0 \\ 0, & \text{otherwise.} \end{cases} \quad (5)$$

**Corollary 3.3** From Theorem 3.1,

$$\sum_{i=0}^{\infty} w_i = \sum_{i=0}^{\infty} \delta_i \frac{(\Delta t)^i}{(i)!},$$

is converged to exact solution  $w$  when  $0 \leq \delta_i < 1$ ,  $i = 0, 1, 2, \dots$

To illustrate the convergence of analytical approximate solutions for the three examples, it was applied Corollary 3.3 as follows.

In the first example where  $(x, t) \in (0, 1)^2$ ,

$$\delta_1 = \frac{\|w_2\|}{\|w_1\|} = 0.7745966694 < 1,$$

$$\delta_2 = \frac{\|w_3\|}{\|w_2\|} = 0.5634361702 < 1,$$

$$\delta_3 = \frac{\|w_4\|}{\|w_3\|} = 0.4409585516 < 1.$$

In the second example where  $(x, t) \in (0, 1)^2$ ,

$$\delta_1 = \frac{\|w_2\|}{\|w_1\|} = 0.06211299938 < 1,$$

$$\delta_2 = \frac{\|w_3\|}{\|w_2\|} = 0.02773500981 < 1,$$

$$\delta_3 = \frac{\|w_4\|}{\|w_3\|} = 0.01561561843 < 1.$$

In the third example where  $x \in (0, 2)$  and  $t \in (0, 1)$ ,

$$\delta_1 = \frac{\|w_2\|}{\|w_1\|} = 0.3872983346 < 1,$$

$$\delta_2 = \frac{\|w_3\|}{\|w_2\|} = 0.2817180849 < 1,$$

$$\delta_3 = \frac{\|w_4\|}{\|w_3\|} = 0.2204792759 < 1.$$

Therefore, the convergence of analytical solutions is valid. Finally, the theoretical proofs for the analysis of convergence coincide with the computation results presented in the above figures and tables.

#### 4. CONCLUSIONS:

The proposed technique is an efficient methodology with good accuracy and convergence and a powerful tool to find approximate analytic solutions for the linear and nonlinear problems. The tests confirm the validity of a novel technique to handle current linear and nonlinear PDEs. In the future, this research can be extended to the investigation by applying this technique for more complicated problems such as systems of nonlinear PDEs.

#### 5. REFERENCES:

1. A. C. Metaxas, Roger J. Meredith. 1983. "Industrial Microwave Heating - A. C. Metaxas, Roger J. Meredith - Google Books." : No. 4. IET.
2. Abazari, Reza, and A. Borhanifar. 2010. "Numerical Study of the Solution of the Burgers and Coupled Burgers Equations by a Differential Transformation Method." *Computers and Mathematics with Applications* 59(8): 2711–22.
3. Abbaoui, K., and Y. Cherruault. 1995. "New Ideas for Proving Convergence of Decomposition Methods." *Computers and Mathematics with Applications* 29(7): 103–8.
4. Adomian, G. 1994. "Solving Frontier Problems of Physics: The Decomposition Method, With a Preface by Yves Cherruault. Fundamental Theories of Physics." *Kluwer Academic Publishers Group, Dordrecht*, 1.
5. Al-Badrani, Hind et al. 2016. "Numerical Solution for Nonlinear Telegraph Equation by Modified Adomian Decomposition Method." *Nonlinear Analysis and Differential Equations* 4(5): 243–57.
6. Alonso, Jose Miguel, Jean Mawhin, and Rafael Ortega. 1999. 78 J. Math. Pures Appl *BOUNDED SOLUTIONS OF SECOND ORDER SEMILINEAR EVOLUTION EQUATIONS AND APPLICATIONS TO THE TELEGRAPH EQUATION \**.
7. Arafa, A.A.M., S.Z. Rida, and H. Mohamed. 2011. "Homotopy Analysis Method for Solving Biological Population Model." *Communications in Theoretical Physics* 56(5): 797.
8. Ayad Ghazi Naser Al-Shammari, Wurood R. Abd AL-Hussein, and Mohammed G. S. AL-Safi. 2018. "A New Approximate Solution for the Telegraph Equation of Space-Fractional Order Derivative by Using Sumudu Method." *Iraqi Journal of Science, Baghdad University*. Volume. 59, Issue. 3A , (1301-1311).
9. Bhatia, R. C. Mittal and Rachna. 2014. "A Collocation Method for Numerical Solution of Hyperbolic Telegraph Equation with Neumann Boundary Conditions." *International Journal of Computational Mathematics*: Volume 2014, ID 526814.
10. Biazar, J, and H Ebrahimi. 2007. 2 *International Mathematical Forum An Approximation to the Solution of Telegraph Equation by Adomian Decomposition Method*.
11. Biazar, J, H Ebrahimi, and Z Ayati. 2008. "An Approximation to the Solution of Telegraph Equation by Variational Iteration Method."
12. Dehghan, Mehdi, and Mehرداد Lakestani. 2009. "The Use of Chebyshev Cardinal Functions for Solution of the Second-Order One-Dimensional Telegraph Equation." *Numerical Methods for Partial Differential Equations* 25(4): 931–38.
13. Dehghan, Mehdi, and Ali Shokri. 2008. "A Numerical Method for Solving the Hyperbolic Telegraph Equation." *Numerical Methods for Partial Differential Equations* 24(4): 1080–93.
14. El-Azab, M. S., and Mohamed El-Gamel. 2007. "A Numerical Algorithm for the Solution of Telegraph Equations." *Applied Mathematics and Computation* 190(1): 757–64.
15. El-Sayed, Salah M., and Doğan Kaya. 2004. "On the Numerical Solution of the System of Two-Dimensional Burgers' Equations by the Decomposition Method." *Applied Mathematics and Computation* 158(1): 101–9.
16. Eslami, M., B. Fathi Vajargah, and M. Mirzazadeh. 2014. "Exact Solutions of Modified Zakharov-Kuznetsov Equation by the Homogeneous Balance Method." *Ain Shams Engineering Journal* 5(1): 221–25.



17. Gao, Feng, and Chunmei Chi. 2007. "Unconditionally Stable Difference Schemes for a One-Space-Dimensional Linear Hyperbolic Equation." *Applied Mathematics and Computation* 187(2): 1272–76.
18. Gilding, B. H., and R. Kersner. 2013. "Wavefront Solutions of a Nonlinear Telegraph Equation." *Journal of Differential Equations* 254(2): 599–636.
19. He, Jihuan. 1997. "A New Approach to Nonlinear Partial Differential Equations." *Communications in Nonlinear Science and Numerical Simulation* 2(4): 230–35.
20. Inc, Mustafa. 2007. "Exact Solutions with Solitary Patterns for the Zakharov-Kuznetsov Equations with Fully Nonlinear Dispersion." *Chaos, Solitons and Fractals* 33(5): 1783–90.
21. Jaradat, Emad K., Read S. Hijawi, Belal R. Alasassfeh, and Omar K. Jaradat. 2018. "Solution for the Nonlinear Telegraph Equation with Two Space Variables."
22. Kheiri, H., and A. Jabbari. 2011. "homotopy analysis and homotopy pade methods for two-dimensional coupled burgers'equations." *Iranian Journal of Mathematical Sciences and Informatics*. Vol. 6, No. 1 (2011), pp 23-31
23. Kolesov, Andrei Yu, and Nikolai Kh Rozov. 2000. "Parametric Excitation of High-Mode Oscillations for a Non-Linear Telegraph Equation." *Sbornik: Mathematics* 191(8): 1147–69.
24. Lakestani, Mehrdad, and Behzad Nemati Saray. 2010. "Numerical Solution of Telegraph Equation Using Interpolating Scaling Functions." *Computers and Mathematics with Applications* 60(7): 1964–72.
25. Liao, S.J. 1992. Thesis, Shanghai Jiao Tong University *The Proposed Homotopy Analysis Technique for the Solution of Nonlinear Problems (Doctoral Dissertation, Ph. D.*
26. Liu, G. R., and Y. T. Gu. 2004. "Boundary Meshfree Methods Based on the Boundary Point Interpolation Methods." In *Engineering Analysis with Boundary Elements*, Elsevier, 475–87.
27. Mittal, R. C., and Ram Jiware. 2009. "Differential Quadrature Method for Two-Dimensional Burgers' Equations." *International Journal of Computational Methods in Engineering Science and Mechanics* 10(6): 450–59.
28. Mohanty, R. K., M. K. Jain, and Urvashi Arora. 2002. "An Unconditionally Stable ADI Method for the Linear Hyperbolic Equation in Three Space Dimensions." *International Journal of Computer Mathematics* 79(1): 133–42.
29. Mohanty, R.K., M.K. Jain, and Kochurani George. 1996. "On the Use of High Order Difference Methods for the System of One Space Second Order Nonlinear Hyperbolic Equations with Variable Coefficients." *Journal of Computational and Applied Mathematics* 72(2): 421–31.
30. Mukesh K. Awasthi, R. K. Chaurasia, and M. Tamsir. 2013. "The Telegraph Equation and Its Solution by Reduced Differential Transform Method." *Modelling and Simulation in Engineering: Volume 2013*, ID 746351.
31. Mustafa Inc, Ali Akgül. 2013. "Numerical Solutions of the Second-Order One-Dimensional Telegraph Equation Based on Reproducing Kernel Hilbert Space Method." *Abstract and Applied Analysis: Volume 2013*, ID 768963.
32. Naher, Hasibun, and Farah Aini Abdullah. 2012. ""The Improved \$(G'/G)\$ \$-Expansion Method for the (2+ 1)-Dimensional Modified Zakharov-Kuznetsov Equation."." *Journal of Applied Mathematics*.
33. Raftari, Behrouz, and Ahmet Yildirim. 2012. "Analytical Solution of Second-Order Hyperbolic Telegraph Equation by Variational Iteration and Homotopy Perturbation Methods." *Results in Mathematics* 61(1–2): 13–28.
34. Rathore, Sushila, Devendra Kumar, Jagdev Singh, and Sumit Gupta. 2012. 4 Int. J. Industrial Mathematics *Homotopy Analysis Sumudu Transform Method for Nonlinear Equations*.
35. Roul, Pradip. 2010. "Application of Homotopy Perturbation Method to Biological Population Model." *Applications and Applied Mathematics: An International Journal* 05(2): 1369–78.
36. Roussy, G., and J. A. Pearce. 1998. "Foundations and Industrial Applications of Microwaves and Radio Frequency Fields. Physical and Chemical Processes." In *OPTIM 1998 - Proceedings of the 6th*

- International Conference on Optimization of Electrical and Electronic Equipments*, Institute of Electrical and Electronics Engineers Inc., 115–16.
37. Saadatmandi, Abbas, and Mehdi Dehghan. 2010. "Numerical Solution of Hyperbolic Telegraph Equation Using the Chebyshev Tau Method." *Numerical Methods for Partial Differential Equations* 26(1): 239–52.
  38. Saeideh Hesam, Alireza Nazemi and Ahmad Haghbin. 2011. "Analytical Solution for the Zakharov-Kuznetsov Equations by Differential Transform Method." *World Academy of Science, Engineering and Technology* 51.
  39. Sari, Murat, Abdurrahim Gunay, and Gurhan Gurarslan. 2014. 17 online) *International Journal of Nonlinear Science A Solution to the Telegraph Equation by Using DGJ Method*.
  40. Sheng, Ying, and Tie Zhang. 2018. "The Finite Volume Method for Two-Dimensional Burgers' Equation." *Personal and Ubiquitous Computing* 22(5–6): 1133–39.
  41. Singh, Brajesh Kumar. 2016. "A Novel Approach for Numeric Study of 2D Biological Population Model" ed. Vladimir Evgenyevich Fedorov. *Cogent Mathematics* 3(1).
  42. Srivastava, Vineet K, Mukesh K Awasthi, and R K Chaurasia. 2014. "Reduced Differential Transform Method to Solve Two and Three Dimensional Second Order Hyperbolic Telegraph Equations." *Journal of king saud university - engineering sciences*.
  43. De Su, Ling, Zi Wu Jiang, and Tong Song Jiang. 2013. "Numerical Solution for a Kind of Nonlinear Telegraph Equations Using Radial Basis Functions." In *Communications in Computer and Information Science*, Springer Verlag, 140–49.
  44. Taghizadeh, N., M. Mirzazadeh, A. Samiei Paghaleh, and J. Vahidi. 2012. "Exact Solutions of Nonlinear Evolution Equations by Using the Modified Simple Equation Method." *Ain Shams Engineering Journal* 3(3): 321–25.
  45. Usman, Muhammad et al. 2013. "Homotopy Analysis Method for Zakharov-Kuznetsov (ZK) Equation with Fully Nonlinear Dispersion." *Scientific Research and Essays* 7(23): 1065–72.
  46. Wiwatwanich, araya. 2016. *a novel technique for solving nonlinear differential equations*. faculty of science burapha university.
  47. Yulita Molliq, R., M. S.M. Noorani, I. Hashim, and R. R. Ahmad. 2009. "Approximate Solutions of Fractional Zakharov-Kuznetsov Equations by VIM." *Journal of Computational and Applied Mathematics* 233(2): 103–8.
  48. Yusufoglu, E., and A. Bekir. 2006. "Solitons and Periodic Solutions of Coupled Nonlinear Evolution Equations by Using the Sine-Cosine Method." *International Journal of Computer Mathematics* 83(12): 915–24.
  49. Zavalani, gentian. 2009. "Numerical and Analytical Solution of Telegraph Equation." *academia.edu*.
  50. Zhang, L. W., Y. J. Deng, and K. M. Liew. 2014. "An Improved Element-Free Galerkin Method for Numerical Modeling of the Biological Population Problems." *Engineering Analysis with Boundary Elements* 40: 181–88.
  51. Zhou, J. K. ". 1986. "Differential Transformation and Its Applications for Electrical Circuits." : 1279-1289.

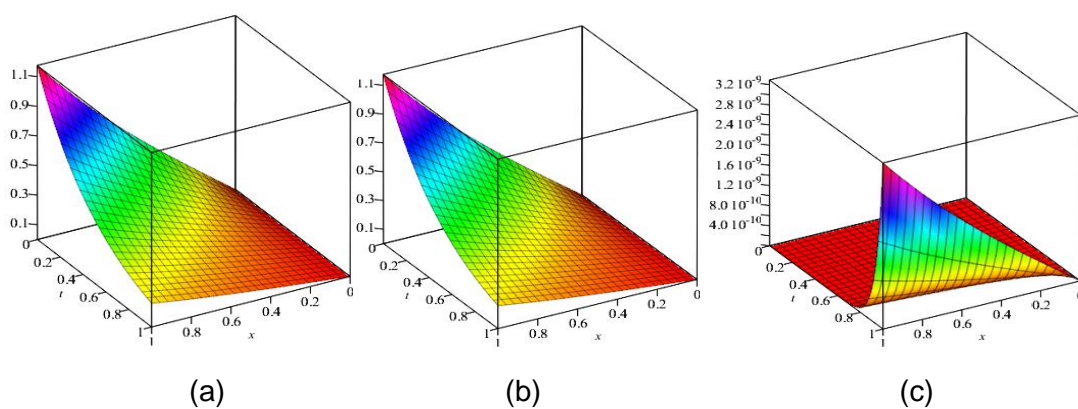


**Figure 1.** (a) Exact solution, (b) Approximate solution, (c) Absolute errors for example 1 when  $t=1$ .

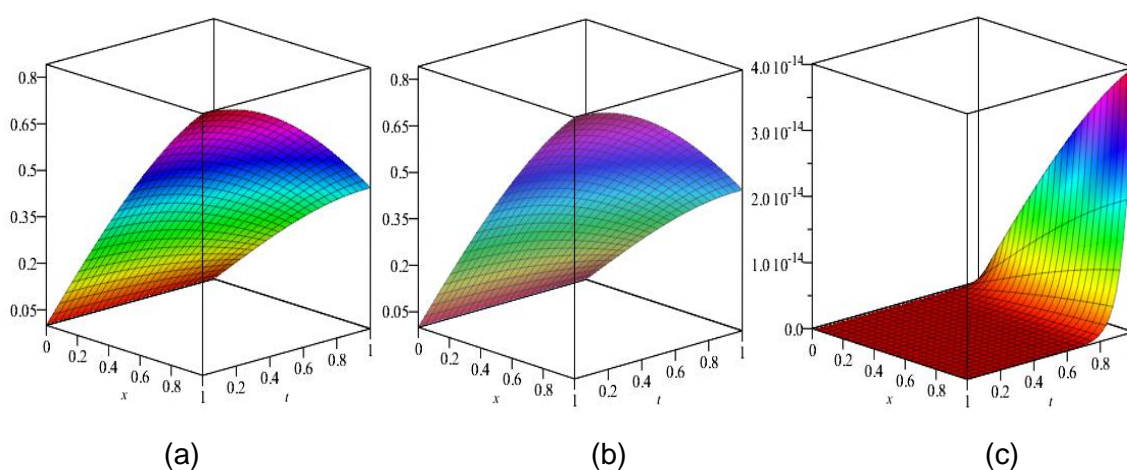


**Figure 2.** (a) Exact solution, (b) Approximate solution, (c) Absolute errors for example 2 when  $t=1$ .

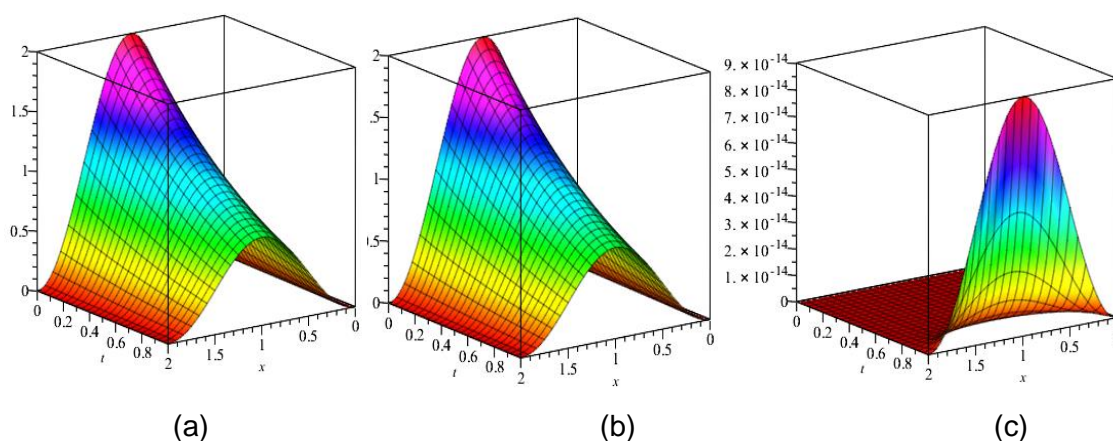


**Figure 3.** (a) Exact solution, (b) Approximate solution, (c) Absolute errors for example 3 when  $t=1$ .

**Table 1.** Comparison of absolute errors among different methods and present method, for example, 1 with  $t = 1$ ,  $k = 0.001$ ,  $\alpha = 10$ ,  $\beta = 5$ .

| Method          | x   | n=10     | n=11     | n=12     | n=13     | n=14     | n=15     |
|-----------------|-----|----------|----------|----------|----------|----------|----------|
| Proposed method | 0.1 | 8.84E-06 | 1.49E-06 | 2.32E-07 | 3.34E-08 | 4.48E-09 | 5.64E-10 |
| ADE method      |     | 2.44E-05 | 2.87E-04 | 3.24E-06 | 4.42E-06 | 2.71E-06 | 2.16E-08 |
| HAM method      |     | 1.54E-05 | 3.51E-05 | 1.92E-05 | 2.90E-05 | 3.84E-07 | 6.47E-07 |
| Proposed method | 0.3 | 1.80E-05 | 3.04E-06 | 4.72E-07 | 6.81E-08 | 9.14E-09 | 1.15E-09 |
| ADE method      |     | 2.23E-05 | 6.14E-05 | 6.11E-05 | 4.76E-06 | 7.66E-08 | 2.16E-06 |
| HAM method      |     | 3.54E-04 | 4.27E-04 | 1.53E-03 | 5.33E-07 | 3.27E-07 | 3.83E-08 |
| Proposed method | 0.5 | 2.80E-05 | 4.71E-06 | 7.32E-07 | 1.05E-07 | 1.42E-08 | 1.78E-09 |
| ADE method      |     | 5.11E-04 | 6.03E-04 | 6.03E-06 | 3.88E-06 | 6.56E-05 | 4.11E-05 |
| HAM method      |     | 3.03E-04 | 3.62E-04 | 4.16E-05 | 7.36E-04 | 2.45E-06 | 2.74E-07 |
| Proposed method | 0.7 | 3.91E-05 | 6.57E-06 | 1.02E-06 | 1.47E-07 | 1.98E-08 | 2.49E-09 |
| ADE method      |     | 6.54E-04 | 2.82E-05 | 7.15E-03 | 4.11E-05 | 5.78E-07 | 4.33E-06 |
| HAM method      |     | 4.76E-03 | 5.67E-05 | 5.44E-04 | 7.54E-04 | 2.14E-05 | 2.54E-08 |
| Proposed method | 0.9 | 5.16E-05 | 8.70E-06 | 1.35E-06 | 1.95E-07 | 2.62E-08 | 3.29E-09 |
| ADE method      |     | 6.23E-04 | 4.65E-03 | 7.73E-04 | 5.22E-05 | 6.25E-07 | 6.15E-07 |
| HAM method      |     | 3.90E-03 | 3.32E-04 | 4.51E-05 | 3.12E-06 | 5.32E-06 | 3.41E-06 |

**Table 2.** Comparison of absolute errors among different methods and present method for example 2 with  $t = 1$ ,  $k = 0.001$ ,  $\alpha = 10$ ,  $\beta = 5$ .

| Method          | x   | n=10     | n=11     | n=12     | n=13     | n=14     | n=15     |
|-----------------|-----|----------|----------|----------|----------|----------|----------|
| Proposed method | 0.1 | 4.12E-10 | 4.12E-10 | 2.27E-12 | 2.27E-12 | 9.46E-15 | 9.46E-15 |
| ADE method      |     | 3.54E-09 | 2.23E-08 | 4.01E-09 | 4.90E-10 | 7.21E-12 | 6.87E-11 |
| HAM method      |     | 2.04E-07 | 3.64E-07 | 3.66E-10 | 2.11E-11 | 5.99E-11 | 7.33E-09 |
| Proposed method | 0.3 | 8.09E-10 | 8.09E-10 | 4.45E-12 | 4.45E-12 | 1.86E-14 | 1.86E-14 |
| ADE method      |     | 6.64E-08 | 5.33E-07 | 3.49E-10 | 1.13E-10 | 2.18E-11 | 4.21E-11 |
| HAM method      |     | 6.72E-08 | 6.97E-09 | 2.19E-10 | 2.91E-11 | 3.02E-10 | 2.99E-12 |
| Proposed method | 0.5 | 1.17E-09 | 1.17E-09 | 6.45E-12 | 6.45E-12 | 2.69E-14 | 2.69E-14 |
| ADE method      |     | 3.06E-05 | 3.91E-07 | 5.03E-10 | 4.51E-11 | 6.91E-10 | 3.42E-10 |
| HAM method      |     | 3.77E-07 | 5.64E-06 | 3.16E-10 | 4.18E-10 | 3.02E-11 | 7.11E-11 |
| Proposed method | 0.7 | 1.49E-09 | 1.49E-09 | 8.19E-12 | 8.19E-12 | 3.42E-14 | 3.42E-14 |
| ADE method      |     | 3.33E-06 | 5.55E-06 | 6.67E-10 | 5.61E-08 | 3.91E-11 | 7.98E-10 |
| HAM method      |     | 6.54E-06 | 3.96E-06 | 4.88E-09 | 7.98E-10 | 6.22E-10 | 3.90E-12 |
| Proposed method | 0.9 | 1.75E-09 | 1.75E-09 | 9.61E-12 | 9.61E-12 | 4.01E-14 | 4.01E-14 |
| ADE method      |     | 6.32E-06 | 4.36E-06 | 7.21E-09 | 8.19E-10 | 2.18E-10 | 2.66E-11 |
| HAM method      |     | 3.55E-06 | 3.28E-06 | 5.27E-10 | 6.03E-09 | 2.80E-09 | 4.18E-10 |

**Table 3.** Comparison of absolute errors among different methods and present method for example 3 when  $t = 1$ ,  $k = 0.001$ .

| Method          | x   | n=10     | n=11     | n=12     | n=13     | n=14     | n=15     |
|-----------------|-----|----------|----------|----------|----------|----------|----------|
| Proposed method | 0.1 | 1.13E-09 | 9.48E-11 | 7.33E-12 | 5.26E-13 | 3.52E-14 | 2.21E-15 |
| ADE method      |     | 2.04E-07 | 3.47E-10 | 4.02E-10 | 7.04E-11 | 4.41E-10 | 1.49E-12 |
| HAM method      |     | 2.44E-08 | 5.97E-09 | 3.83E-09 | 6.48E-10 | 3.28E-11 | 4.47E-10 |
| Proposed method | 0.3 | 9.53E-09 | 7.99E-10 | 6.18E-11 | 4.43E-12 | 2.97E-13 | 1.86E-14 |
| ADE method      |     | 2.42E-07 | 1.72E-08 | 5.24E-08 | 3.04E-10 | 2.72E-11 | 3.16E-10 |
| HAM method      |     | 3.07E-06 | 7.92E-07 | 2.47E-09 | 2.82E-09 | 6.21E-10 | 2.45E-12 |
| Proposed method | 0.5 | 2.31E-08 | 1.94E-09 | 1.50E-10 | 1.08E-11 | 7.20E-13 | 4.51E-14 |
| ADE method      |     | 5.11E-05 | 3.64E-07 | 6.12E-07 | 4.63E-10 | 2.57E-09 | 6.77E-08 |
| HAM method      |     | 4.37E-06 | 5.23E-06 | 4.69E-08 | 6.99E-08 | 6.02E-09 | 4.92E-09 |
| Proposed method | 0.7 | 3.67E-08 | 3.08E-09 | 2.38E-10 | 1.71E-11 | 1.14E-12 | 7.17E-14 |
| ADE method      |     | 8.20E-06 | 7.87E-06 | 7.74E-06 | 3.42E-09 | 2.11E-09 | 7.52E-11 |
| HAM method      |     | 4.65E-05 | 4.43E-07 | 4.04E-08 | 5.11E-08 | 7.06E-10 | 3.82E-10 |
| Proposed method | 0.9 | 4.51E-08 | 3.78E-09 | 2.92E-10 | 2.10E-11 | 1.40E-12 | 8.81E-14 |
| ADE method      |     | 4.06E-07 | 3.87E-07 | 4.21E-08 | 4.01E-06 | 3.93E-09 | 3.01E-10 |
| HAM method      |     | 6.27E-06 | 5.90E-07 | 5.64E-09 | 1.23E-09 | 6.73E-07 | 4.25E-08 |

**DEPENDÊNCIA DOS MECANISMOS DE DESTRUIÇÃO “GLARE” DA EXTENSÃO DE AMOSTRAS EM TESTES DE FLEXÃO DE TRÊS PONTOS****DEPENDENCE OF GLARE DESTRUCTION MECHANISMS ON THE ELONGATION OF SAMPLES IN TESTS TO THREE-POINT FLEXURAL****ЗАВИСИМОСТЬ МЕХАНИЗМОВ РАЗРУШЕНИЯ GLARE ОТ УДЛИНЕНИЯ ОБРАЗЦОВ В ИСПЫТАНИЯХ НА ТРЕХТОЧЕЧНЫЙ ИЗГИБ**SHA, Minggong<sup>1\*</sup>; PROKUDIN, Oleg A.<sup>2\*</sup>; SOLYAEV, Yury O.<sup>3,4</sup>; VAKHNEEV, Sergey N.<sup>5</sup><sup>1</sup> Northwestern Polytechnical University (NPU), School of Civil Aviation, 127 West Youyi Road, zip code 710072, Beilin District, Xi'an Shaanxi – People's Republic of China<sup>2,3</sup> Moscow Aviation Institute (National Research University), Institute of General Engineering Training, 4 Volokolamskoe highway, zip code 125993, Moscow – Russian Federation<sup>4</sup> Institute of Applied Mechanics of Russian Academy of Sciences, 7 Leningradsky Ave., zip code 125040, Moscow – Russian Federation<sup>5</sup> Moscow Aviation Institute (National Research University), Department of Engineering Graphics, 4 Volokolamskoe highway, zip code 125993, Moscow – Russian Federation

\* Corresponding author  
e-mail: 695792773@qq.com

Received 15 April 2020; received in revised form 10 June 2020; accepted 16 June 2020

**RESUMO**

Os testes de flexão são uma das maneiras eficazes de determinar experimentalmente os módulos de elasticidade e cisalhamento. Uma tarefa importante na implementação dos materiais compósitos em estruturas aeroespaciais é o desenvolvimento de métodos para determinar as características físico-mecânicas dos materiais. O artigo apresenta os resultados de testes de flexão de três pontos de amostras do material compósito metal-polímero GLARE. Foram estudadas as amostras constituídas por 17 camadas para as quais a dureza aparente entre camadas foi determinada de acordo com os resultados dos testes de flexão de três pontos. Foi estabelecido que, para as amostras estudadas, mecanismos de cisalhamento entre camadas são realizados quando a relação entre comprimento e espessura é menor que 10. A destruição está localizada na zona da camada central, que atende aos requisitos dos padrões de teste de feixe curto. No entanto, esses testes de GLARE são sempre acompanhados pela ocorrência de deformações plásticas significativas associadas à presença de camadas de alumínio na estrutura do material. Com o alongamento de amostras acima de 10, realiza-se um mecanismo de destruição, no qual ocorrem a separação de camadas e perda de estabilidade das camadas externas no lado comprimido da amostra. Quando o alongamento das amostras é menor que 4, nas amostras realiza-se o mecanismo de destruição de acordo com o tipo de indentação com grandes deformações não lineares. De acordo com os resultados do teste, foi determinada a dependência dos mecanismos de destruição realizados no alongamento das amostras.

**Palavras-chave:** GLARE, flexão de três pontos, feixe curto, mecanismos de destruição, dureza entre camadas.

**ABSTRACT**

Tests on bending are one of the effective ways to experimentally determine the elasticity and shear moduli. An important task in the implementation of composite materials in aerospace structures is the development of methods for determining the physical and mechanical characteristics of materials. The paper presents of tests for three-point bending of samples of metal-polymer composite material "GLASS-REinforced" Fibre Metal Laminate (GLARE) are presented. Examined samples, consisting of 17 layers, for which apparent interlayer strength of the results of tests on three-point bending was established by the method of "short beam". It was established that for the studied samples, interlayer shear mechanisms were realized at the ratio of dimensions of length to thickness of at least 10. Localization of fracture occurs in the area of the central layer,

which corresponds to the requirements of standards for conducting tests of the method of short beams. Nonetheless, such GLARE tests are always accompanied by the occurrence of significant plastic deformations associated with the presence of aluminum layers in the structure of the material. With the elongation of samples of more than 10, a fracture mechanism is realized in them, during which delamination and loss of stability of the outer layers on the compressed side of the sample occur. When the elongation of samples of less than 4 is implemented in samples takes place, the mechanism of destruction of indentation type with large nonlinear deformations. According to the test results, the dependence of the realised fracture mechanisms on the elongation of the samples is determined.

**Keywords:** *GLARE, three-point bending, short beam, fracture mechanisms, interlayer strength.*

## АННОТАЦИЯ

Испытания на изгиб являются одним из эффективных способов экспериментального определения модулей упругости и сдвига. Важной задачей при внедрении композиционных материалов в авиакосмических конструкциях является разработка методов определения физико-механических характеристик материалов. В работе представлены результаты испытаний на трехточечный изгиб образцов металлополимерного композиционного материала GLARE. Исследованы образцы, состоящие из 17 слоев, для которых определена кажущая межслоевая прочность по результатам испытаний на трехточечный изгиб. Установлено, что для исследованных образцов реализуется механизмы межслоевого сдвига при соотношении размеров длины к толщине менее 10. Локализация разрушения происходит в зоне центрального слоя, что соответствует требованиям стандартов на проведение испытаний по методу короткой балки. Однако, такие испытания GLARE всегда сопровождаются возникновением значительных пластических деформаций, связанных с присутствием алюминиевых слоев в структуре материала. При удлинении образцов более 10 в них реализуется механизм разрушения, при котором происходит отслоение и потеря устойчивости внешних слоев на сжатой стороне образца. При удлинении образцов менее 4 в образцах реализуется механизм разрушения по типу индентирования с большими нелинейными деформациями. По результатам испытаний определена зависимость реализующихся механизмов разрушения от удлинения образцов.

**Ключевые слова:** *GLARE, трехточечный изгиб, короткая балка, механизмы разрушения, межслоевая прочность.*

## 1. INTRODUCTION:

Composite metal-polymer materials of GLARE type are promising structural materials for use in the construction of aviation vehicles (Kablov *et al.*, 2016; Podzhivotov *et al.*, 2016; Antipov *et al.*, 2018; Serebrennikova *et al.*, 2016; Topchiy *et al.*, 2019). These composite materials are laminated panels, formed by alternating thin layers of fiberglass and aluminum alloys. By comparison with metals, GLARE has increased specific strength, long-term durability, fire resistance. Examination of dependency on mechanical properties of GLARE from the parameters of the reinforcement is an important task, the solution of which is necessary for conducting the strength calculations and optimal design structures. One of the important characteristics determining the structural properties of GLARE, as well as other composite materials, is the interlayer strength.

Testing samples in three-point bending by the method of "short beam" (ASTM D2344...; Babaytsev *et al.*, 2017; GOST R 57745-2017...

2018) is one of the simplest methods for determining the interlayer strength of composite material (Vasiliev and Morozov, 2018). This method is widely used at research and development of composite structures since it does not require the use of complex experimental equipment and strain measurement. At the same time, the interlayer strength is an important parameter from the point of view of design, so it is used when formulating criteria for the strength of composite materials (Jones, 2014; Dmitriev *et al.*, 2011; Vasiliev and Morozov, 2018), and, in particular, when assessing the strength of the structures of GLARE. The occurrence of interlaminar cracks can lead to a reduction in carrier capacity element designs and, subsequently, to their degradation, e.g., by the mechanism of local loss resistance (Remmers and De Borst, 2011; Alekseev *et al.*, 2019; Kachanov, 2012; Sevryukova *et al.*, 2012; Lapidus and Abramov, 2018).

Though, such a simple method as a test to three-point bending contains certain deficiencies associated, in the first place, with the fact that

when these tests in samples are implemented in a complex stress state, there arise not only the tensions of the interlayer shift but also tensile/compressive stress, leading to errors in determining characteristics of material (Vasiliev and Morozov, 2018). The complexity that arises when testing samples for interlayer shear, in addition to the indicated errors associated with the inhomogeneous stress state of the samples, also lies in the fact that interlayer strength determined in the tests is not a material constant, but depends on the distance between supports. This problem is known and for ordinary composite materials (Wisnom, 1991; Xie, and Adams, 1995; Li *et al.*, 1999; Ossipyan *et al.*, 2004; Privalko *et al.*, 2005; Abali *et al.*, 2013) and for metal-polymer composites (Hinz *et al.*, 2005; Hinz *et al.*, 2009; Polilov and Tatus, 2012; Lin *et al.*, 2018; Li *et al.*, 2018; Jakubczak *et al.*, 2018; Lin *et al.*, 2019), and it is explained by the decrease of tangential stresses for working short samples (by the standards relative elongation of the samples should be 6 – 11), in comparison with the classical models of beams, which assume a constant value of the shear force and, accordingly, constant values of shear stresses (accurate to the sign) along the length of the sample. Therefore, the use of the usual ratio for estimating the shear stresses acting in a beam using the Equation 1 (ASTM D2344...) leads to an increase in the seeming interlayer strength of the material. Moreover, the effect of the length of sample on the results of tests of the interlayer strength is explained by 1) concentration of stress near the poles, for the exclusion of which special tooling is applied (Podzhivotov *et al.*, 2016; Antipov *et al.*, 2018;) 2) a statistical dependence of durability on sizes of the sample (Wisnom, 1991), 3) the occurrence of interlayer cracks outside of the neutral axis of the sample (Li *et al.*, 1999) and 4) specific dependence of the interlayer strength on parameters of mechanics of fracture (Polilov and Tatus, 2012).

In recent years there was a large amount of work, in which ways of finding the interlayer strength of metal-polymer composites were examined, according to the method of "short beam" (Lin *et al.*, 2018; Hinz *et al.*, 2005; Lin *et al.*, 2019; Hinz *et al.*, 2009; Li *et al.*, 2018; Jakubczak *et al.*, 2018; Polilov and Tatus, 2012). In GLARE, the destruction of the interlayer shear can occur both at the boundary of the contact metal and within the composite layers. In the first case, in fact, according to the results of tests defined by adhesive strength of the contact metal/composite with shear, and in the second – interlayer strength inside the composite layer. Consequently, in tests,

it is possible to determine only the characteristic that is of less value. An additional feature, which arises when testing GLARE samples by "short beam" method, is the plasticity of aluminum layers, which leads to a substantially nonlinear diagram of load-displacement, which, however, is not a hindrance to use estimates of tangential stresses in classical Equation 1, which is valid for any type of material, both elastic and plastic (Vladimirov, 2016; Antipov *et al.*, 2017). Thus, the main object of studies using GLARE is determining the degree of the error, which is realized when using the method of "short beams" by relation to more accurate, but, and more labor-intensive methods of testing. In particular, in this study, the effect of dimensions (elongation) of samples on the fracture mechanisms realized in the GLARE tests was examined.

## 2. MATERIALS AND METHODS:

For test samples with GLARE structure, 9/8 with unidirectional circuit reinforcing composite layers were made (Figure 1, Figure 2 a). The thickness of the samples was 5.5 mm, the width was 7 mm, and the length was 20-170 mm. The thicknesses of layers of fiberglass and aluminum alloy were ~ 0.32 mm. As a substitute for fiberglass, basalt fiber can be used in the manufacture of the test sample. According to its mechanical characteristics, continuous basalt fiber occupies an intermediate position between fiberglass and carbon fibers at a relatively low price. This makes this product extremely attractive for consumers for whom there are restrictions on the entry price, but at the same time, high mechanical properties are important. Selection of said structure samples is due, firstly, to the available equipment and diameter poles in the test machine, which does not allow testing too short samples and using 17 – layered GLARE, with thickness 5.5 mm, enables testing of samples of length 25-55 mm (i.e., there is an extension of 5-10, which corresponds to standard requirements) on existing supports.

Secondly, the selection of unidirectional structure of reinforcement allows to reduce the likelihood of formation of the bundles within the composite layers and, therefore, allows to evaluate the interlayer strength of the contact aluminum/composite. Using any other reinforcement schemes would lead to primary delamination at the most weakened internal boundaries between the layers of fiberglass with different directions of reinforcement. With this in process operation, it was assumed that the initial interlayer strength of the composite layers is



known, or can be determined by standard methods.

The third factor influencing the selection of the scheme of reinforcement in samples is the need to localize interlaminar cracks on boundaries by maximally closely spaced to the neutral axis of the sample. It is important to note that multilayer cracks in GLARE, even if they pass through the center of the sample, always turn out to be shifted by half the thickness of the metal layer located on the neutral line. Thus, the use of samples of large thickness allows to reduce the relative displacement of cracks from the neutral axis, and, therefore, to reduce the calculation errors of the standard Equation 1, which gives accurate values only in case of the central location of an interlayer crack (Equation 2).

Where  $P$  is the effective load,  $b$ ,  $h$  are the width and thickness of the sample.

Tests were carried out on the set Instron 5969 (Figure 2b) with lower supports of 5 mm diameter and a top support diameter of 10 mm. The test speed was 1 mm/min. Tests stopped at the decrease of the load more than 50% of the maximum. The test results were processed on the basis of Equation 1 in accordance with which the apparent (conditional) interlayer strength was determined.

Three-point bending tests were conducted in accordance with ASTM D2344. In the test the specimens were placed symmetrically on the supports and loaded by the loading nose of testing machine at the center. Deflections in the center of specimens for the prescribed loading level were registered in the tests. Corresponding load-deflection curves were plotted and used for the evaluation of the load-bearing capacity and interlaminar shear strength of specimens with different length.

### 3. RESULTS AND DISCUSSION:

According to the test results, it was established that the interlayer shift could be realized in samples with elongation of not more than eight and not less than 4.5. A typical mechanism of destruction can be well observed in the course of the test on lateral ends of all the samples (Figure 3a), but after removing the load, interlayer cracks were well distinguishable only in samples with elongation over 6 (Figure 3b). For samples with elongation of more than 10, the fracture mechanism changed. For such samples, detachment and loss of stability of the metal layer were realized in the compressed area of the sample near the support (Figure 4). For a very

short sample with elongation, less than 4 took place wrinkling of the samples, i.e., took place the failure mechanism with large transverse strains – "indentation" (Figure 5).

The characteristic diagrams of load-displacement for GLARE samples are presented in Figure 6. We can see that the given sample at a load above 1000 N chart becomes nonlinear, which can be explained by appearance plastic deformations in the layers of aluminum. With the destruction and start of an interlayer crack, a sharp drop in load occurs, which can be explained by a decrease in bending stiffness of the sample (Xie and Adams, 1995).

The dependence of breaking load on the distance between the supports obtained in the tests is presented in Figure 7. These points indicate the experimental data and the lines show theoretical approximation by the relations given below. Firstly, it follows from the obtained results that the bearing capacity of the sample decreases with increasing distance between the supports, which qualitatively corresponds to classical solutions from the theory of resistance of materials. In particular, reduction of the breaking load may be attributed to the assumption that there is a certain critical value of compressive stress, leading to detachment of the upper metal layer (as in Figure 4). The level of stress in this layer due to its small thickness can be considered as constant, and it can be found by classical beam theory. Hence, at the time of destruction, there is the Equation 3.

From this follows the estimate for maximum load (Equation 4). Where all values are known, except for critical stresses, the value of which was selected to describe the available experimental data  $\bar{\sigma} = 1020 \text{ MPa}$ . The recorded estimate (Equation 4) is qualitative and approximate, though, it shows that the maximum load in the three-point bend is inversely proportional to the elongation of the sample Equation 5 for elongations greater than 10, and this dependence is confirmed by experiment. For smaller values of elongation, this law does not work, and the dependence becomes different – the mechanism of destruction is changed to interlayer shift at the center of the sample (Figure 3). The implementation of such a mechanism is an objective of the tests. Nonetheless, it can be seen from Figure 7 that the maximum load during the interlayer shear is also dependent on the distance between the supports. This effect is known for composite materials (as it was noted above), but it is involved in contradiction with the classical solution of theory resistance materials with a

three-point bending shearing force constant on the right and left of the applied load and, consequently, are tangent strains change in an analogous manner along the length of the sample and are not dependent on this length. Apparently, in the experiment, this was not observed.

To describe the resulting dependence and for the evaluation of true interlayer strength, it is proposed to use a modified solution of the problem of three-point bending, which may be obtained in the framework model beams, built under gradient theory of elasticity (Babaytsev *and* Zotov, 2019; Lurie *and* Solyaev, 2018; Lurie *et al.*, 2018; Berezovskii *et al.*, 2015). This dependence is determined by the following relationship (Equation 6). Where –  $\tau_0$  is true interlayer strength, and the parameter  $d$  is the scale parameter of the problem, it has the dimension of length and, generally speaking, its value should be correlated with the diameter of bearings, which are used in the tests, in particular for very thin supports ( $d \sim 0$ ) is the solution (Equation 6) goes to the classical solution (Equation 2). To describe the experimental data, values of the indicated solution parameters (Equation 5) were selected, and they amounted to:

– True interlayer strength  $\tau_0 = 60.4$  MPa,

– Scale parameter –  $d = 2.7$  mm (that is, approximately, the radius of the lower supports in the area where the destruction takes place).

The obtained dependence is presented in Figure 7 by a solid line. It can be seen that in case of the small extension of samples and with the mechanism of destruction of interlayer shear, the solution (Equation 6) better describes the experimental data in comparison with the solution (Equation 4), as well as, obviously, and by comparison with classic solution, which requires independence of carrier load from a distance between the supports during the interlayer shear. The load corresponding to the constant (true) interlayer strength of 60.4 MPa is presented by the horizontal dashed line in Figure 7. The dependence of the apparent interlayer strength on the distance between the supports can be found via a combination of Equation 2 and Equation 6 in the following form (Equation 7).

This dependence is presented in Figure 8 (solid line). The points on this figure represent the experimental data obtained by processing the results of the tests (Figure 7) with the use of Equation 2. The horizontal dotted line is the calculated true interlayer strength. The deviation of relation (Equation 7) from the experiment for the shortest samples may be caused by the change in

the mechanism of their destruction. As it was said, large transverse inelastic deformations occur in such samples upon destruction.

The results of tests of GLARE samples of various elongations for three-point bending were demonstrated.

#### 4. CONCLUSIONS:

In the work, the “short beam” method was analyzed in order to determine the elasticity characteristics of composite materials, which allow to implement a program for determining the complex of elasticity characteristics of composite materials necessary for structural analysis according to the technical theory, and can be used in the development and improvement of standards. In these tests, the samples with a large number of layers and with unidirectional reinforcement schemes were used, which allowed reducing the experimental error when using standard equipment. According to the test results, the dependence of the realized fracture mechanisms on the elongation of the samples was established.

Obtained estimation of interlayer strength for GLARE  $\sim 60$  MPa, which corresponds to a typical level of interlayer strength of polymer composite materials, but in the tests, destruction took place on the border of the contact metal and composite layers, which allows us to state that the found value of interlayer strength is the characteristic of metal/composite contact, as it is realized in GLARE.

#### 5. ACKNOWLEDGMENTS:

This work was supported by the grant of the Russian Science Foundation (project No. 17-79-20105) in Moscow Aviation Institute.

#### 6. REFERENCES:

1. Abali, F., Pora, A., *and* Shivakumar, K. (2003). Modified short beam shear test for measurement of interlaminar shear strength of composites. *Journal of Composite Materials*. Retrieved from <https://journals.sagepub.com/doi/10.1177/0021998303037005053>
2. Alekseev, A. N., Alekseev, S. A., Zabashta, Y. F., Hnatiuk, K. I., Dinzhos, R. V., Lazarenko, M. M., Grabovskii, Y. E., *and* Bulavin, L. A. (2019). Two-dimensional ordered crystal structure formed by chain molecules in the pores of solid matrix.

*Springer Proceedings in Physics*, 221, 387-395.

3. Antipov, V.V., Dobryansky, V.N., Korolenko, V.A., Lurie, S.A., Serebrennikova, N.Yu., and Solyaev, Yu.O. (2018). Evaluation of the effective mechanical characteristics of laminated aluminoglass plastic under uniaxial tension. *Bulletin of the Moscow Aviation Institute*, 25(2), 221-229.
4. Antipov, VV, Serebrennikova, N.Yu., Shestov, VV, Sidelnikov, VV (2017). Layered hybrid materials based on sheets of aluminum-lithium alloys. *Aviation Materials and Technologies*, S, 212-224.
5. ASTM D2344 – Short-beam strength testing of polymer matrix composite materials (interlaminar shear). Retrieved from <https://www.testresources.net/applications/standards/astm/astm-d2344-short-beam-testing-of-polymer-matrix-composite-materials/>
6. Babaytsev, A.V., and Zotov, A.A. (2019). Designing, and Calculation of Extruded Sections of an Inhomogeneous Composition. *Russian Metallurgy (Metally)*, 2019(13), 1452-1455. DOI: 10.1134/S0036029519130020
7. Babaytsev, A.V., Martirosov, M.I., Rabinskiy, L.N., and Solyaev, Y.O. (2017). Effect of Thin Polymer Coatings on the Mechanical Properties of Steel Plates. *Russian Metallurgy (Metally)*, 13, 1170-1175. DOI: 10.1134/S003602951713002XF
8. Berezovskii V.V., Solyaev Y.O., and Lur'e S.A. (2015). Mechanical properties of a metallic composite material based on an aluminum alloy reinforced by dispersed silicon carbide particles. *Russian Metallurgy (Metally)*, 10, 790-794. DOI: 10.1134/S0036029515100055
9. Dmitriev, A.I., Skvortsov, A.A., Koplak, O.V., Morgunov, R.B., and Proskuryakov, I.I. (2011). Influence of the regime of plastic deformation on the magnetic properties of single-crystal silicon Cz-Si. *Physics of the Solid State*, 53(8), 1547-1553.
10. GOST R 57745-2017 Polymer composites. Determination of the ultimate strength in the interlayer shear of laminates using the short-beam method. (2018). Retrieved from <http://docs.cntd.ru/document/1200156917>
11. Hinz, S., Heidemann, J., and Schulte, K. (2005). Damage evaluation of GLARE®4B under interlaminar shear loading at different temperature conditions. *Advanced Composites Letters*, 14(2), 47-55.
12. Hinz, S., Omoori, T., Hojo, M., and Schulte, K. (2009). Damage characterization of fiber metal laminates under interlaminar shear load. *Composites Part A: Applied Science and Manufacturing*, 40(6-7), 925-931. DOI: 10.1016/j.compositesa.2009.04.020.
13. Jakubczak, P., Bienias, J., and Surowska, B. (2018). Interlaminar shear strength of fiber metal laminates after thermal cycles. *Composite Structures*, 206, 876-887. DOI: 10.1016/j.compstruct.2018.09.001.
14. Jones, R.M. (2014). *Mechanics of composite materials*. Boca Raton: CRC Press.
15. Kablov, E.N., Antipov, V.V., and Klochkova, Yu.Yu. (2016). Aluminium-lithium alloys of new generation and aluminum fiberglass laminates on their basis. *Tsvetnye Metally*, 8(884), 86-91. DOI: 10.17580/tsm.2016.08.13.
16. Kachanov, L. (2012). *Delamination buckling of composite materials (Vol. 14)*. Berlin: Springer Science and Business Media.
17. Lapidus, A., and Abramov, I. (2018). Implementing large-scale construction projects through application of the systematic and integrated method. *IOP Conference Series: Materials Science and Engineering*, 365(6), 062002.
18. Li, H., Xu, Y., Hua, X., Liu, C., and Tao, J. (2018). Bending failure mechanism and flexural properties of GLARE laminates with different stacking sequences. *Composite Structures*, 187, 354-363. DOI: 10.1016/j.compstruct.2017.12.068.
19. Li, M., Matsuyama, R., and Sakai, M. (1999). Interlaminar shear strength of C/C-composites: the dependence on test methods. *Carbon*, 37(11), 1749-1757. DOI: 10.1016/S0008-6223(99)00049-4.
20. Lin, Y., Huang, Y., Huang, T., Liao, B., Zhang, D., and Li, C. (2019). Characterization of progressive damage behavior and failure mechanisms of carbon fiber reinforced aluminum laminates under three-point bending. *Thin-Walled Structures*, 135, 494-506. DOI: 10.1016/j.tws.2018.12.002.
21. Lin, Y., Liu, C., Li, H., Jin, K., and Tao, J. (2018). Interlaminar failure behavior of GLARE laminates under double beam five-

- point-bending load. *Composite Structures*, 201, 79-85. DOI: 10.1016/j.compstruct.2018.06.037.
22. Lurie, S., and Solyaev, Y. (2018). Revisiting bending theories of elastic gradient beams. *International Journal of Engineering Science*, 126, 1-21.
  23. Lurie, S.A., Lomakin, E.V., Rabinsky, L.N., and Solyaev Yu.O. (2018). A semi-inverse solution to the problem of pure beam bending in the gradient theory of elasticity: the absence of scale effects. *Reports of the Academy of Sciences*, 479(4), 390-394.
  24. Ossipyan, Yu.A., Morgunov, R.B., Baskakov, A.A., Orlov, A.M., Skvortsov, A.A., Inkina, E.N., and Tanimoto, Y. (2004). Magneto resonant hardening of silicon single crystals. *JETP Letters*, 79(3), 126-130.
  25. Podzhivotov, N.Yu., Kablov, E.N., Antipov, V.V., Erasov, V.S., Serebrennikova, N.Yu., Abdullin, M.R., and Limonin, M.V. 2016. Layered metal-polymer materials in aircraft structural elements. *Promising Materials*, 10, 5-19.
  26. Polilov, A.N., and Tatus, N.A. (2012). Energy criteria for the separation of polymer fiber composites (PCM). *Bulletin of Perm National Research Polytechnic University. Mechanics*, 3, 176-203.
  27. Privalko, V.P., Dinzhos, R.V. and Privalko, E.G. (2005). Enthalpy relaxation in the cooling/heating cycles of polypropylene/organosilica nanocomposites: I: Non-isothermal crystallization. *Thermochimica Acta*, 432(1), 76-82.
  28. Remmers, J.J.C., and De Borst, R. (2001). Delamination buckling of fiber-metal laminates. *Composites Science and Technology*, 61(15), 2207-2213.
  29. Serebrennikova, N.Yu., Antipov, V.V., Senatorova, O.G., Erasov, V.S., and Kashirin, V.V. (2016). Hybrid laminated materials based on lithium aluminum alloys as applied to aircraft wing panels. *Aviation Materials and Technology*, 3(42), 3-8. DOI: 10.18577/2071-9140-2016-0-3-3-8.
  30. Sevryukova, M.M., Piryatinski, Y.P., Vasylyuk, S.V., Yashchuk, V.M., Viniychuk, O.O., Gerasov, A.O., Slominskii, Y.L., and Kachkovsky, O.D. (2012). Cyanine-like and polyenic relaxation paths of merocyanine derivatives of malonodinitrile in the excited state detecting by low temperature time-resolved fluorescence. *Ukrainian Journal of Physics*, 57(8), 812-823.
  31. Topchiiy, D.V., Bolotova, A.S., Zelentsov, A.A., Vorobev, A.S., and Atamanenko, A.V. (2019). Technical rationing of the construction technology of reinforced concrete floor slabs using non-removable empitness-liners. *International Journal of Civil Engineering and Technology*, 10(2), 2160-2166.
  32. Vasiliev, V.V., and Morozov, E.V. (2018). *Advanced mechanics of composite materials and structures*. Saunders: Elsevier.
  33. Vladimirov, A.P. (2016). Speckle metrology of dynamic macro- and microprocesses in deformable media. *Optical Engineering*, 55(12)1-10. DOI: 10.1117/1.OE.55.12.121727.
  34. Wisnom, M.R. (1991). The effect of specimen size on the bending strength of unidirectional carbon fiber-epoxy. *Composite Structures*, 18(1), 47-63. DOI: 10.1016/0263-8223(91)90013-O.
  35. Xie, M., and Adams, D.F. (1995). Study of three- and four-point shear testing of unidirectional composite materials. *Composites*, 26(9), 653-659. DOI: 10.1016/0010-4361(95)98914-7.

$$\bar{\tau} = \frac{3P}{4bh} \quad (\text{Eq. 1})$$

$$\bar{\tau} = \frac{3P}{4bh} \quad (\text{Eq. 2})$$

$$\frac{3LP_{\max}}{2bh^2} = \bar{\sigma} \quad (\text{Eq. 3})$$

$$P_{\max} = \bar{\sigma} \frac{2bh^2}{3L} \quad (\text{Eq. 4})$$

$$P_{\max} \sim (L/h)^{-1} \quad (\text{Eq. 5})$$

$$P_{\max} = \frac{4}{3}bh \frac{\tau_0}{1 - 1/\text{ch}(L/(4d))} \quad (\text{Eq. 6})$$

$$\bar{\tau} = \frac{\tau_0}{1 - 1/\text{ch}(L/(4d))} \quad (\text{Eq. 7})$$

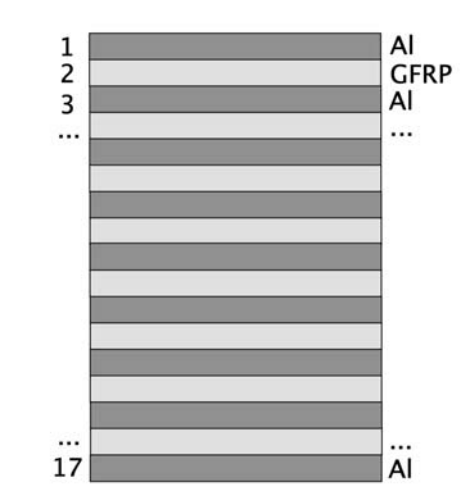


**Figure 1.** Structure of 17-layer GLARE laminate

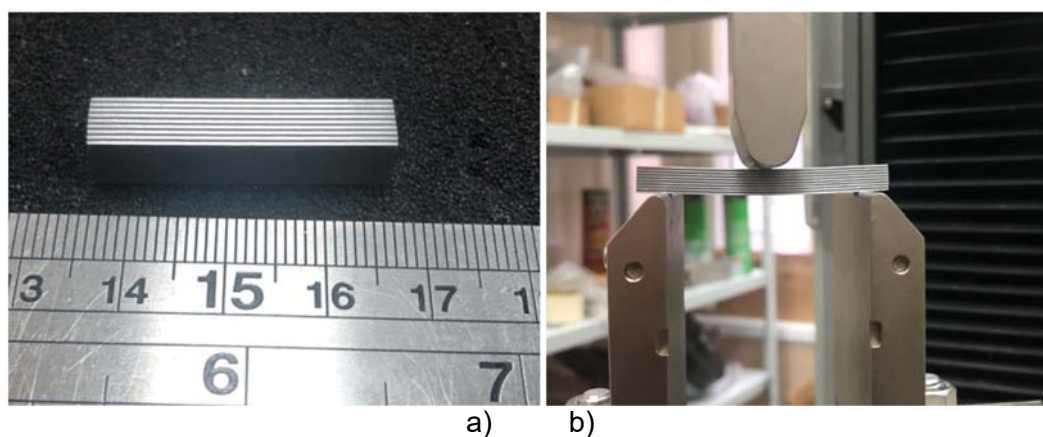
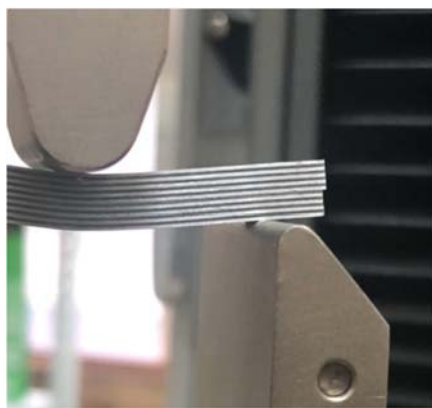
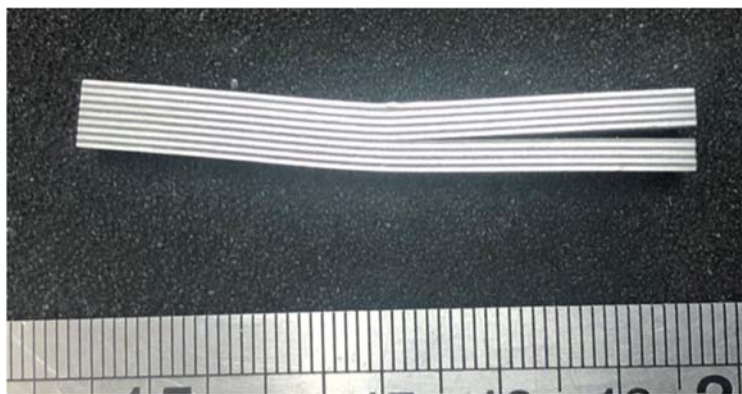


**Figure 2.** Samples of 17-layer GLARE (a) for tests on the three-point bending (b)



a)



b)

**Figure 3.** The interlayer shifts in samples of GLARE, a: displacement of layers in the end zone of the sample, b: sample after conducting the test.

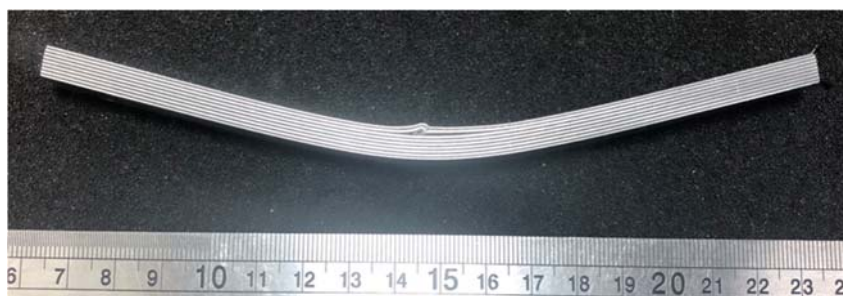


**Figure 4.** Destruction of samples of large elongation ( $> 8$ )

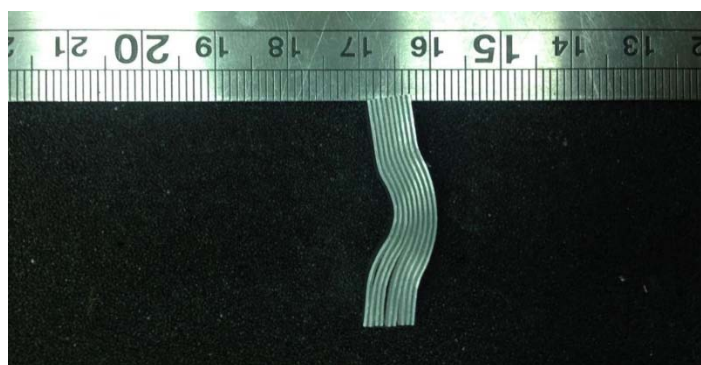


**Figure 5.** The nature of fracture and permanent deformations in samples of small elongation ( $< 4.5$ )

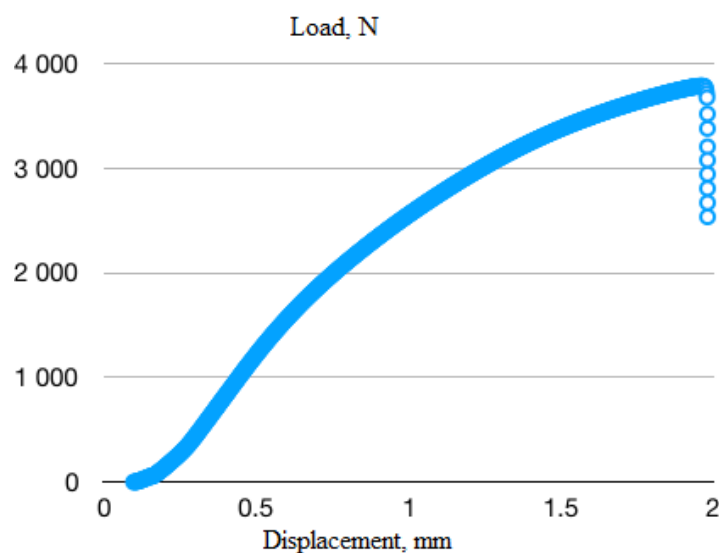


**Figure 6.** Load-displacement diagram, obtained when testing GLARE sample on the three-point flexural

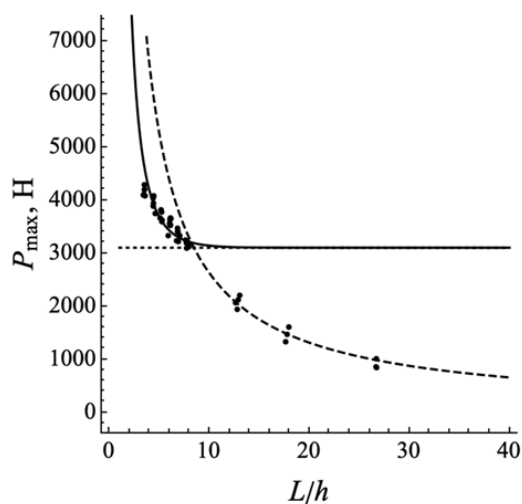


**Figure 7.** The dependence of the breaking load during bending on the relative distance between the supports, normalized to the thickness of the sample.

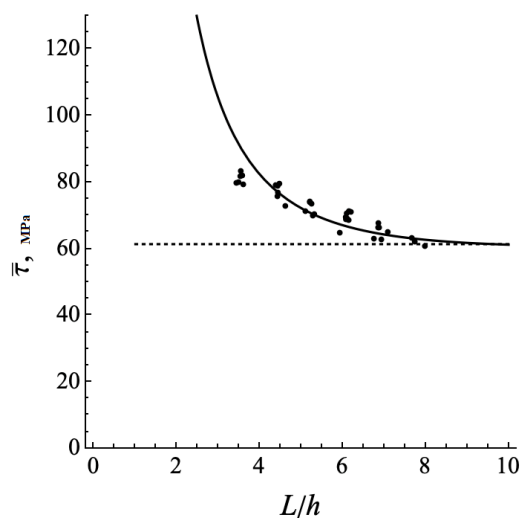


**Figure 8.** The dependence of the apparent interlayer strength on the relative distance between supports in the tests using the short-beam method. The points are experiment data, and the solid line is data from formula (5).



**PRECURSORES POLIMÉRICOS PARA A CRIAÇÃO DE UMA CÂMARA DE DESCARGA DE GÁS DO MOTOR DE FOGUETE ELÉTRICO****POLYMER PRECURSORS FOR CREATING GAS DISCHARGE CHAMBER FOR ELECTRIC ROCKET ENGINE****ПОЛИМЕРНЫЕ ПРЕКУРСОРЫ ДЛЯ СОЗДАНИЯ ГАЗОРАЗРЯДНОЙ КАМЕРЫ ЭЛЕКТРИЧЕСКОГО РАКЕТНОГО ДВИГАТЕЛЯ**

NIGMATZYANOV, Vladislav V.<sup>1\*</sup>; POGODIN, Veniamin A.<sup>2</sup>; RABINSKIY, Lev N.<sup>3</sup>; SITNIKOV, Sergey A.<sup>4</sup>; ZIN HEIN, Thant<sup>5</sup>;

<sup>1</sup> Moscow Aviation Institute (National Research University), Research Institute of Applied Mechanics and Electrodynamics, 4 Volokolamskoe highway, zip code 125993, Moscow – Russian Federation

<sup>2, 3, 4</sup> Moscow Aviation Institute (National Research University), Department of Perspective Materials and Technologies of Aerospace Designation, 4 Volokolamskoe highway, zip code 125993, Moscow – Russian Federation

<sup>5</sup> Defence Services Technological Academy (DSTA), Marine Electrical System and Electronics – Myannar Navy, Mandalay-Lashio highway, Pyin Oo Lwin, Mandalay Division, Myanmar

*\* Corresponding author  
e-mail: nigmatzyanov@mail.ru*

Received 29 April 2020; received in revised form 09 June 2020; accepted 16 June 2020

**RESUMO**

Motores de foguete elétricos são amplamente utilizados em tecnologia espacial. Além disso, atualmente, os motores de propulsão elétricos também são usados como motores de propulsão principais para voos no espaço interplanetário. Nas naves espaciais modernas, os seguintes tipos dos motores de propulsão elétricos são usados principalmente: motores de plasma estacionários e motores de íons com grades. Ao usar esses motores como motores de propulsão principais, é importante aumentar a potência total para obter a tração necessária e o impulso específico. Com o aumento da potência total, o volume da câmara de descarga aumenta, o que leva a dificuldades tecnológicas na fabricação de câmaras de descarga a partir de materiais cerâmicos. Portanto, a tarefa de encontrar alternativas aos materiais cerâmicos é relevante e necessária no desenvolvimento de motores de íons de alta frequência. O artigo discute a criação de um material compósito à base de materiais de tecido de quartzo e um aglutinante de silício orgânico como precursor preenchido com nitreto de silício para a fabricação de uma câmara de descarga de gás do motor de íons de alta frequência. Por análise termogravimétrica, selecionamos um aglutinante termo-reativo que atende aos requisitos de resistência à vibração e permeabilidade eletromagnética da câmara de descarga de gás na faixa de megahertz. Com base nesse aglutinante, preenchido com pó de nitreto de silício, reforçado com material de tecido de quartzo, foi feita a câmara de descarga de gás. O produto resultante foi testado como parte do motor de propulsão elétrico de laboratório com um diâmetro de 100 mm e uma potência de 200W.

**Palavras-chave:** *cerâmica, resinas de silício orgânico, materiais compósitos, motores de foguetes elétricos, câmara de descarga de gás.*

**ABSTRACT**

Electric rocket engines are widely used in space technology. Furthermore, at present, electric propulsion engines are also used as mid-flight engines for flights in interplanetary space. On modern spacecraft, the following types of electric propulsion are mostly used: SPT and grid ion thruster. When using these engines as sustainers, it is important is to increase the total power for obtaining the required thrust and specific impulse. With an increase in total power, the volume of the discharge chamber increases, which leads to technological difficulties in the manufacture of discharge chambers from ceramic materials. Thus, the task of finding alternative ceramic materials is relevant and necessary in the development of high-frequency ion thrusters. The article discusses the issues of creating a composite material based on woven quartz materials and organosilicon binder as a precursor



filled with silicon nitride for the manufacture of gas discharge chamber (GDC) of high-frequency ion thruster (RFIT). By thermos-gravimetric analysis, a thermosetting binder, which meets the requirements of vibration resistance and electromagnetic permeability of GDC in the megahertz range, was selected. Based on the binder filled with silicon nitride powder, reinforced by quartz woven fabrics, manufactured GDC. The resulting product was tested as part of the laboratory electric propulsion device with a diameter of 100 mm and power of 200W.

**Keywords:** *ceramics, organosilicon resins, composite materials, electric rocket engines, gas discharge chamber.*

## АННОТАЦИЯ

Электрические ракетные двигатели нашли широкое применение в космической технике. Также в настоящее время, ЭРД применяются и как маршевые двигатели для полетов в межпланетном пространстве. На современных космических аппаратах в основном используются следующие типы ЭРД: СПД и сеточные ионные двигатели. При использовании данных двигателей в качестве маршевых, важным является увеличение суммарной мощности для получения необходимой тяги и удельного импульса. При увеличении суммарной мощности объем разрядной камеры увеличивается, что приводит к технологическим трудностям при изготовлении разрядных камер из керамических материалов. Поэтому задача поиска альтернативных керамическим материалам является актуальной и необходимой при разработке высокочастотных ионных двигателей. В работе обсуждаются вопросы по созданию композиционного материала на основе тканых кварцевых материалов и кремнийорганического связующего в качестве прекурсора наполненного нитридом кремния, для изготовления газоразрядной камеры (ГРК) высокочастотного ионного двигателя (ВЧИД). Путем термогравиметрического анализа подобрали термореактивное связующее, отвечающее требованиям вибростойкости и электромагнитной проницаемости ГРК в мегагерцовом диапазоне. На основе данного связующего, наполненного порошком нитрида кремния, армированного кварцевым тканым материалом, изготовили ГРК. Полученное изделие прошло испытания в составе лабораторного ЭРД диаметром 100 мм, мощностью 200Вт.

**Ключевые слова:** *керамика, кремнийорганические смолы, композиционные материалы, электроракетные двигатели, газоразрядная камера.*

## 1. INTRODUCTION:

Electric rocket engines are extensively used in space technology. These types of engines, the main principle of which is ionization and acceleration of working substance, are used to stabilize and correct the position of spacecraft in orbit (Antropov *et al.*, 2002; Gorshkov *et al.*, 2008; Khartov *et al.*, 2013; Loeb, 2015; Orlov *et al.*, 2001; Rabinsky *et al.*, 2016a; Sitnikov, 2017). Also, at present, the electric propulsion engines are used as mid-flight engines for flights in interplanetary space.

On modern spacecraft, the following types of electric propulsion are mainly used: SPT and grid ion engines. The principles of their work and the design of these types are different. The acceleration and ionization of the working fluid in the SPT is carried out in the discharge channel, while the processes of ionization and acceleration are separated in grid ion thruster. Separation of the processes of ionization and acceleration makes it possible to obtain a specific impulse of up to 50,000 s, which exceeds the maximum specific impulse of SPT (about 20,000 s).

One of the types of grid ion thrusters is RFIT. The principle of operation of this engine is

based on ionization by the electromagnetic field of the working fluid (xenon) in the discharge chamber of the engine. The acceleration of ions occurs in the ion-optical system. The schematic diagram of the engine is presented in Figure 1.

For this kind of engine, the electromagnetic properties of the material of the walls of the discharge chamber are important. Presently, alumina-based ceramics are used as the material, and silicon nitride-based ceramics are also used in laboratory samples. These ceramic materials provide required radio transparency at frequencies from 500 kHz to 2 MHz and higher. The diameter of present experimental chambers reaches 500 mm, with wall thicknesses up to 8 mm (Lurie *et al.*, 2011; Formalev *et al.*, 2015; Pogodin *et al.*, 2016; Poliakov *et al.*, 2016; Ripetsky *et al.*, 2016; Rabinsky *et al.*, 2016b; Skvortsov and Karizin, 2012; Pogodin *et al.*, 2019). It is worth noting that when using ceramic materials, the question arises about their strength qualities, especially at the stage of launching a spacecraft into operational orbit.

It is also worth mentioning that when using these engines as marching, it is important to increase the total power to obtain the necessary

thrust and specific impulse. With an increase in the total power, the volume of the discharge chamber increases, which leads to technological difficulties in the manufacture of discharge chambers from ceramic materials. All this, together, makes the task of finding alternatives to ceramic materials appropriate and necessary in the development of high-frequency ion engines.

Earlier, GDC was obtained based on polymethylphenylsiloxane rubber modified with terminal vinyl groups and filled with silicon nitride by molding. The main drawback of the material used was its low heat resistance, limited by the temperature of 370°C at a residual pressure of 10-5 Pa. Taking into account the requirements for heat resistance, the binder was advanced by using MQ resins and stabilising the main polymer chain. Hence, it was possible to increase the heat resistance of the GDC material to 410°C. As a result of the tests, and it was found that with a diameter of GDC 100 mm, the material of the chamber fully met all the requirements for nodes RFIT. Nonetheless, an increase in specific capacities during optimization of RFIT design leads to the appearance of local sections of short-term heating of the gas distribution system to a value of 450°C and higher. As a result, there was a need to create a radio transparent, vibration-resistant material for GDC with increased (up to 600 °C ) heat resistance.

To accomplish this task, the authors revised the concept of composite material for the manufacture of gas distribution systems for promising RFIT (Golushko and Semisalov, 2015; Pintossi *et al.*, 2019). Despite the high resistance of silicones to heat, among other polymers, it is limited by temperatures of the order of 400-420 °C. Organic-silicon polymers in the composition of GRC, compensated for vibration loads at low temperatures, due to the low glass transition temperature. Stiff requirements for heat resistance to the binder forced to continue the search for an alternative material from the class of organic-silicon polymers operating at temperatures up to 800 °C . With complete loss of elasticity, some organosilicon polymers (for example, thermostable net siloxanes (Voronkov *et al.*, 1976; Sevryukova *et al.*, 2012; Andrianov and Sokolov, 1995) allow the GDC material to retain its electrical insulating properties, dielectric constant, and low dielectric loss tangent at temperatures up to 800 °C and higher. The densely reticulated structure of polyorganosiloxanes is characterized by low mass loss after pyrolysis of the binder and high yield of ceramo-forming residue. Therefore, composite materials based on them are characterized by high

heat resistance and can withstand repeated heating in an oxidizing environment up to 550 ... 600 °C. Composite materials based on them can work up to 1000 °C. For cross-linked polymers, the main proportion falls on the main polymer chain, represented by silicon and oxygen atoms. Correspondingly, the proportion of organic framing can be less than 20% of the mass.

The most optimal compound is methylphenylcyclospiroxiloxane (Figure 2). A distinctive feature of this oligomer is the curing mechanism by the polycondensation reaction without the release of low molecular weight substances. The use of this product is difficult due to the complexity of its synthesis by heterocondensation of silicon tetrachloride and methyl phenylsilandiol in the presence of pyridine (Andrianov *et al.*, 1978; Tkachev *et al.*, 2018).

An alternative way to obtain methylphenylcyclospiroxiloxane is the cohydrolysis of tetramethoxysilane and methylphenyl dimethoxysilane (Efremova *et al.*, 2014). Though, as a result, a low molecular weight product is formed with terminal methoxyl groups, and, as is typical for the polycondensation reaction, further molecular weight growth is difficult due to the loss of reactivity of terminal functional groups. If dysfunctional methylphenyldimethoxysilane is replaced by trifunctional vinyltrimethoxysilane, the molecular weight will increase while preserving solubility according to the critical point and Flory gelation (Florry, 1953). To increase the conversion rate by functional groups is desirable to use a polycondensation catalyst when curing the composition. Similar results were given in (Antufev *et al.*, 2019; Alekseev *et al.*, 2019; Nikitin *et al.*, 2019a; Rabinskiy and Tushavina, 2019; Umbetov *et al.*, 2017; Nikitin *et al.*, 2019b).

Since cross-linked polyorganosiloxanes, thermostable materials, are not characterized by good elastic deformation, reinforcement with woven materials is used to maintain vibration stability. According to the principle, the similar is combined with the similar, the most suitable are quartz fibers, which are characterized by a low value of the coefficient of thermal expansion, high dielectric properties and heat resistance up to 1200 °C.

## 2. MATERIALS AND METHODS:

The starting polymer was obtained by partial cohydrolysis of tetramethoxysilane methyltrimethoxysilane, vinyltrimethoxysilane, and γ-

aminopropyltrimethoxysilane, the finished product was 22-25% solution in acetonitrile, with medium viscosity molecular weight of 2700-3500 g/mol. As a reinforcing filler, quartz fabric material of TS-8/3-K brand, manufactured by NPO Fiberglass, was used (Fouquet *et al.*, 2015; Herbert *et al.*, 2009).

Silicon nitride for the filling was obtained in the SHS process by nitriding silicon powder, and the material was characterized by a specific surface of 10 m<sup>2</sup>/g. The fibrous structure of the  $\alpha$  and  $\beta$  phases of silicon nitride crystals. Crystal size  $D_{50} = 5 \mu\text{m}$ .

The pre-preg was prepared by mixing a colloidal solution of the raw polymer and silicon nitride powder; the proportion of silicon nitride was 60 wt%, relative to the binder and subsequent impregnation of silica fiber" (Dimitrakellis and Gogolides, 2018; Mansour *et al.*, 2019). The composite material was solidified at 200 °C and residual pressure of 1–3 mm Hg., tetrabutoxy titanium was used as a curing catalyst, the curing process was carried out for 2 hours. The final processing of the composite GDC material was carried out at 800°C in argon (Andrianov and Sokolov, 1995). The pyrolysis process was carried out in argon by heating to 800 degrees. Celsius at a speed of 10 degrees per minute.

The structural transformations occurring during heating of materials were studied by synchronous thermal analysis using the STA 449 F3 Jupiter device from NETZSCH (Germany) (Figure 3) in differential scanning calorimetry (DSC) mode together with thermogravimetric analysis (TGA) mode.

The samples were heated to 900°C in open crucibles from Al<sub>2</sub>O<sub>3</sub> with a volume of 0.085 ml at linearly increasing furnace temperature at a rate of 10°C/min. The crucibles were placed in cylindrical recesses of the upper part of the DSC/TG sensor made of Pt-Rh alloy. The argon flow rate through the measuring cell (sample and standard) during the experiment remained constant at 50 ml/min. A vacant crucible was used as a standard. The sample and reference temperatures were measured using built-in S-type thermocouples made of Pt-Rh alloys. The temperature measurement accuracy was  $\pm 0.3$  °C. The sample weight change was recorded with precision of 1  $\mu\text{g}$ . The isothermal balance drift over the entire temperature range was not greater than 10  $\mu\text{g/h}$ . Data collection and calculations, as well as device operation control, were made using the NETZSCH Proteus Software (Germany) software operating under the MS-Windows system.

Operational tests of prototypes of RFIT gas

distribution system with a diameter of 100 mm were carried out on a 0.4 m<sup>3</sup> vacuum test bench (Figure 4). The pumping system of the stand provided a dynamic vacuum of 10 –3 Pa at xenon flow rates of up to 0.65 mg/s.

### 3. RESULTS AND DISCUSSION:

The pyrolysis process was accompanied by the thermolysis of methyl, vinyl, substituents at silicon atom. As a result of pyrolysis, amorphous silicon oxide was formed. The yield of pyrolysis residue was about 80%. Losses of mass up to 400°C can be associated with the condensation of terminal methoxyl groups, with the release of methanol. In this area, the molecular weight increased slightly. The loss of mass above 400°C was due to the initiation of the process of thermal degradation of framing of the main polymer chain, primarily aminopropyl and vinyl substituents at silicon atom. Hence, processes that proceed up to 400°C can be associated with the progress of reaction along with unreached functional groups, the telomerization reaction, the intramolecular rearrangement of macromolecules, and removal of low boiling substances. Figure 5 displays graphs of DTA polymer filled with Si<sub>3</sub>N<sub>4</sub> 60% by weight in argon.

The heat resistance of the obtained composite material filled with Si<sub>3</sub>N<sub>4</sub> 60 wt% was somewhat higher. As can be seen from the diagram in Figure 6, a slight drift of the mass loss curve on the isotherm at 800°C is observed, which is associated with the hydrolysis of the filler, silicon nitride, and the release of ammonia, which was experimentally established. During the hydrolysis of silicon nitride, an amorphous oxynitride phase forms, which reacts with the pyrolysis residue of polymer binder (Figure 7).

Despite the loss of flexibility inherent in elastomers, the tested material did not significantly affect the performance of GDC. The introduction of quartz fibers made it possible to increase the vibration resistance of the obtained chamber by 50% compared to the ceramic counterpart.

The resulting composite material is characterized by the following properties:

- Shore hardness –85 to 90 (scale D);
- density –1.65 to 1.67 g / cm<sup>3</sup>;
- stress rupture at elongation for fibers – based on tissue 1000 kgf;
- tensile strength for fibers – Warp and weft 550 kgf;
- volumetric shrinkage after curing: 3 to 4%;

- the temperature coefficient of linear expansion:  $1.0$  to  $1 \cdot 10^{-3} \text{K}^{-1}$ ;
- electrical strength:  $15$  to  $20 \text{ kV / mm}$ ;
- dielectric loss tangent:  $0.2 \%$  to  $0.02 \%$ .

#### 4. CONCLUSIONS:

In the outline of the work carried out, the vacuum temperature stability of densely cross-linked polyorganosilaxane obtained by the cohydrolysis of tetramethoxysilane, vinyltrimethoxysilane,  $\gamma$ -aminopropyltrimethoxysilane was studied to create a polymer-ceramic composite. The resulting material, combined with the filling of quartz fibers and silicon nitride, ensured the required electrophysical and operational characteristics for RFIT (radio transparency, manufacturability, vibration resistance and other).

It was demonstrated that the studied material is characterized by high heat resistance. Silicon nitride obtained by SHS is characterized by a small fraction of free nitrogen, which is replaced by a hydroxyl group during hydrolysis. Therefore, during heating, the formation of a mixed oxynitride phase can be observed due to the interaction of silicon nitride and amorphous silicon oxide.

#### 5. ACKNOWLEDGMENTS:

This work was supported by the grant of the Russian Foundation for Basic Research in Moscow Aviation Institute, project No. 18-29-18083/18.

#### 6. REFERENCES:

1. Alekseev, A. N., Alekseev, S. A., Zabashta, Y. F., Hnatiuk, K. I., Dinzhos, R. V., Lazarenko, M. M., Grabovskii, Y. E., and Bulavin, L. A. (2019). Two-dimensional ordered crystal structure formed by chain molecules in the pores of solid matrix. *Springer Proceedings in Physics*, 221, 387-395.
2. Andrianov, K. A., and Sokolov, N. N. (1995). The chemistry of the formation of organopolysiloxanes. *DAN USSR*, 101(1), 81-84.
3. Andrianov, K. A., Zachernyuk, A. B., and Solomatin, G. V. (1978). *Patent SU 603 645 A1. Organopolyspirocyclosiloxanes and method for their preparation*. Moscow: Organization of the Order of Lenin Institute of Organoelement Compounds of the USSR Academy of Sciences.
4. Antropov, N. N., Dyakonov, G. A., Pokryshkin, A. I., Popov, G. A., Kazeev, M. N., and Hodnenko, V. P. (2002). Pulse plasma engines in spacecraft control systems. *Applied Physics*, 2002, 1. Retrieved from <http://applphys.orion-ir.ru/appl-02/02-1/02-1-5r.htm>.
5. Antufev, B. A., Egorova, O. V., and Rabinskiy, L. N. (2019). Dynamics of a cylindrical shell with a collapsing elastic base under the action of a pressure wave. *INCAS Bulletin*, 11, 17-24.
6. Dimitrakellis, P., and Gogolides, E. (2018). Hydrophobic and superhydrophobic surfaces fabricated using atmospheric pressure cold plasma technology. *Advances in Colloid and Interface Science*, 254, 1-21.
7. Efremova, N. V., Ivanov, P. V., and Majorova, N. G. (2014). *Patent RU 2507217 C1. The method of obtaining polyelementorganospirocyclosiloxanes*. Moscow: Limited Liability Company "Research and Production Firm" MIX "(LLC" NPF "MIX")
8. Florry, P.J. (1953). *Principles of Polymer Chemistry*. New York: Cornell University Press.
9. Formalev, V. F., Kuznetsova, E. L., and Rabinskiy, L. N. (2015). Localization of thermal disturbances in nonlinear anisotropic media with absorption. *High Temperature*, 53(4), 548-553.
10. Fouquet, T., Mertz, G., Delmée, M., Fetzer, L., and Becker, C. (2015). Thermal analysis goes with mass spectrometry to evaluate the molecular weight of a fluorinated plasma polymer. *Plasma Processes and Polymers*, 12(9), 980-990.
11. Golushko, S. K., and Semisalov, B. V. (2015). Numerical modeling of deformation of anisogrid structures using high-precision schemes without saturation. *Mathematical Modeling and Numerical Methods*, 2(6), 23-45.
12. Gorshkov, A. S., Muravyov, V. A., and Shagayda, A. A. (2008). *Hall and ion plasma engines for spacecraft*. Moscow: Mechanical Engineering.
13. Herbert, P. A. F., O'Neill, L., and Jaroszyńska-Wolińska, J. (2009). Soft Plasma Polymerization of Gas State

- Precursors from an Atmospheric Pressure Corona Plasma Discharge. *Chemistry of Materials*, 21(19), 4401–4407.
14. Khartov, S. A., Balashov, V. V., Sitnikov, S. A. (2013). The choice of structural materials for high-frequency ion engines. *Proceedings of the Moscow Aviation Institute*, 63. Retrieved from <http://trudymai.ru>.
  15. Loeb, H. W. (2015). A realistic concept of a manned Mars mission with nuclear-electric propulsion. *Acta Astronautica*, 116, 299-306
  16. Lurie, S. A., Belov, P. A., Rabinsky, L. N., and Zhavoronok, S. I. (2011). *Large-scale effects in the mechanics of continuous media. materials with microstructure and nanostructure*. Moscow: MAI-Print Publishing House (Moscow).
  17. Mansour, A., Poncin-Epaillard, F., and Debarnot, D. (2019). Affinity and distribution of silver nanoparticles within plasma polymer matrices. *Journal of Materials Science*, 54(19), 12972-12987.
  18. Nikitin, P. V., Rabinskiy, L. N., and Tushavina, O. V. (2019a). Features of heat transfer in dissociated air supersonic flows. *Asia Life Sciences*, 2, 645-655.
  19. Nikitin, P. V., Tushavina, O. V., and Shkuratenko, A. A. (2019b). Calculation of heat transfer on the catalytically active surface of high-speed aircraft. *INCAS Bulletin*, 11(SI), 191-201.
  20. Orlov, A. M., Skvortsov, A. A., and Gonchar, L. I. (2001). Magnetically stimulated variation of dislocation mobility in plastically deformed n-silicon. *Physics of the Solid State*, 43(7), 1252-1256.
  21. Pintossi, D., Saakes, M., Borneman, Z., and Nijmeijer, K. (2019). Electrochemical impedance spectroscopy of a reverse electrodialysis stack: A new approach to monitoring fouling and cleaning. *Journal of Power Sources*, 444, Article number 227302.
  22. Pogodin, V. A., Rabinsky, L. N., and Sitnikov, S. A. (2019). Technological aspects of 3D-printing of parts of a gas-discharge chamber of an electric rocket engine. *STIN*, 4, 20-21.
  23. Pogodin, V. A., Sitnikov, S. A., and Solyaev, Yu. O. (2016). The study of porous ceramics based on silicon nitride obtained using three-dimensional printing technology. *New Refractories*, 11, 33-37.
  24. Poliakov, P. O., Soliayev, Y. O., and Sitnikov, S. A. (2016). Numerical modeling of residual thermal stresses in Si<sub>3</sub>N<sub>4</sub> based high-porous fibrous ceramics. *International Journal of Pure and Applied Mathematics*, 111(2), 319-330.
  25. Rabinskiy, L. N., and Tushavina, O. V. (2019). Problems of land reclamation and heat protection of biological objects against contamination by the aviation and rocket launch site. *Journal of Environmental Management and Tourism*, 10(5), 967-973.
  26. Rabinsky, L. N., Sitnikov, S. A., and Khartov, S. A. (2016a). Creation of working prototypes of ceramic gas-discharge chambers of high-frequency ion engines resistant to ion-plasma spraying by the method of layer-by-layer modeling. In *Abstracts of the V international scientific seminar "Dynamic deformation and contact interaction of thin-walled structures when exposed to fields of various physical nature"* (pp. 159-160). Moscow: Publishing House "TR-Print" LLC.
  27. Rabinsky, L. N., Sitnikov, S. A., and Solyaev, Yu. O. (2016b). Comparative assessment and choice of a solution to the problem of developing a technology for the manufacture of samples and structural elements from composite nitride-silicon ceramics. In *Materials of the XXII International Symposium "Dynamic and Technological Problems of Mechanics of Structures and Continuous Media" named after A.G. Gorshkov* (pp. 108-109). Moscow: Publishing House "TR-print" LLC.
  28. Ripetsky, A., Sitnikov, S., and Rabinskiy, L. (2016). Fabrication of porous silicon nitride ceramics using binder jetting technology. *IOP Conference Series: Materials Science and Engineering*, 1-6. Retrieved from <http://iopscience.iop.org/article/10.1088/1757-899X/140/1/012023/pdf>.
  29. Sevryukova, M. M., Piryatinski, Y. P., Vasylyuk, S. V., Yashchuk, V. M., Viniychuk, O. O., Gerasov, A. O., Slominskii, Y. L., and Kachkovsky, O. D. (2012). Cyanine-like and polyenic relaxation paths of merocyanine derivatives of malonodinitrile in the excited state detecting by low temperature time-resolved fluorescence. *Ukrainian Journal of Physics*, 57(8), 812-823.
  30. Sitnikov, S. A. (2017). *Development of ion erosion-resistant materials based on silicon nitride for discharge chambers of electric*

rocket engines: thesis of the candidate of technical sciences. Moscow: Moscow Aviation Institute (National Research University).

31. Skvortsov, A. A., and Karizin, A. V. (2012). Magnetoplasticity and diffusion in silicon single crystals. *Journal of Experimental and Theoretical Physics*, 114(1), 85-88.
32. Tkachev, S. Y., Alekseev, O. M., Lazarenko, M. M., Lazarenko, M. V., Kovalov, K. M., Bokhvan, S. I., Grabovskii, Y. E., and Hoshlyk, N. V. (2018). Topological solitons in branched aliphatic molecules. *Molecular Crystals and Liquid Crystals*, 665(1), 166-180.
33. Umbetov, A., Kozhahmet, M., Sabitbekova, G., Amirov, M., Hamit, A., Alieva, G., Karimova, D., and Uspanova, V. (2017). Interference of coherent radiation in a crystalline two-component lens. *Far East Journal of Electronics and Communications*, 17(5), 923-939.
34. Voronkov, M. G., Mileshekevich, V. P., and Yuzhelevsky, Yu. A. (1976). *Siloxane bond*. Novosibirsk: Nauka.

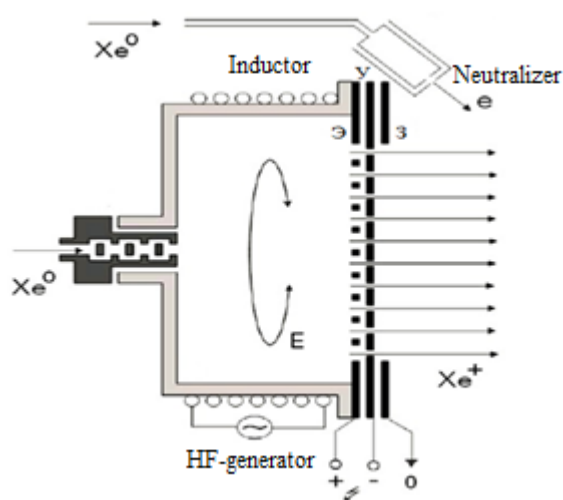


**Figure 1.** Schematic diagram of RFIT operation

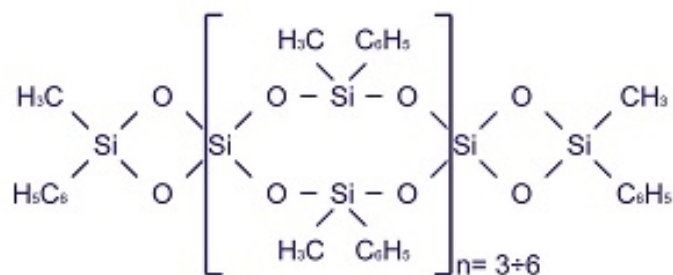


**Figure 2.** Methylphenylcyclospirosiloxane



**Figure 3.** STA 449 F3 Jupiter device from NETZSCH (Germany)



**Figure 4.** The prototype GDC mounted on RFIT layout (left) and general view of the vacuum test bench for RFIT (right)

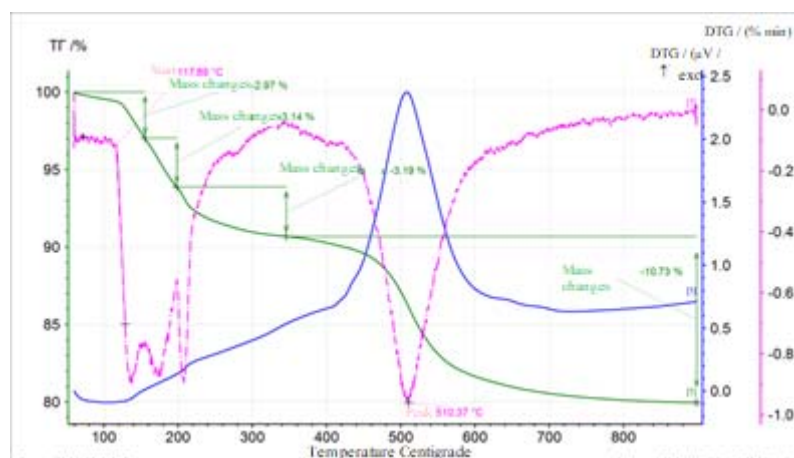


**Figure 5.** Dependence of mass loss on temperature during DTA of the product of partial hydrolysis of  $\text{Si}(\text{OMe})_4$ ,  $\text{MeSi}(\text{OMe})_3$ ,  $\text{ViSi}(\text{OMe})_3\text{NH}_2\text{PrSi}(\text{OMe})$  in air



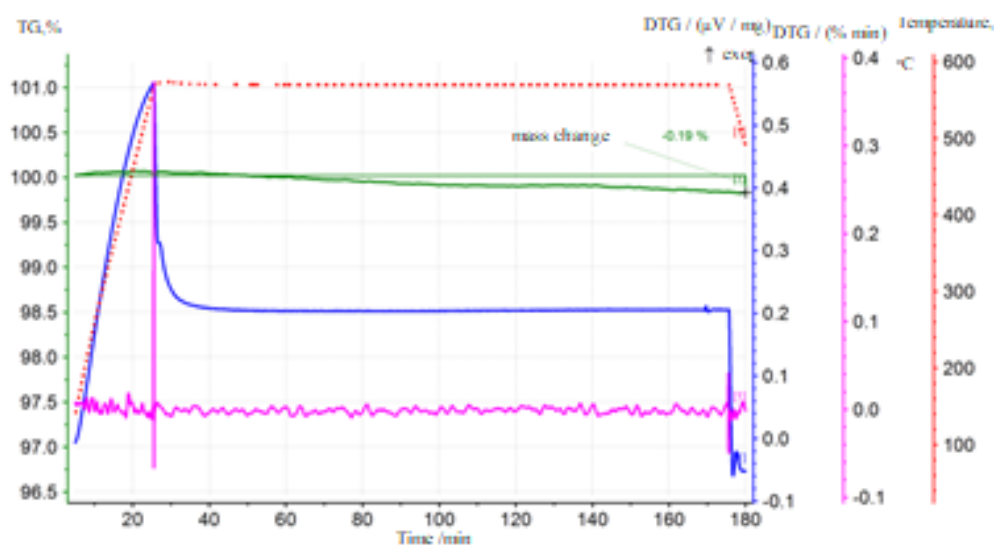


**Figure 6.** Dependence of mass loss on the temperature of GDC material in the air

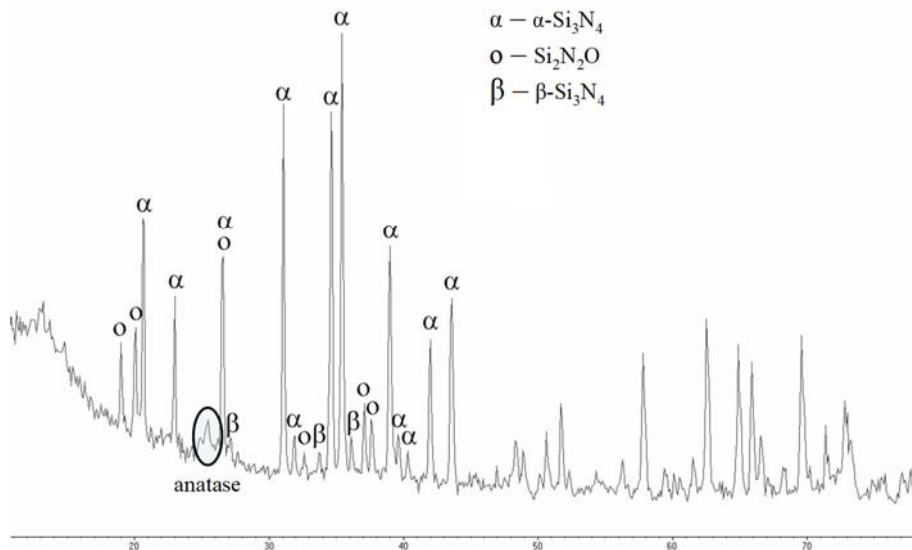


**Figure 7.** Radiograph of a sample of GDC material



## PREPARAÇÃO DE UM NOVO COMPOSTO AZO (HAZM) UTILIZADO PARA DETERMINAÇÃO ESPECTROFOTOMÉTRICA ANALÍTICA DE GLICOSE NO SANGUE E NA SALIVA

### PREPARATION OF A NEW AZO COMPOUND (HAZM) USED FOR ANALYTICAL SPECTROPHOTOMETRIC DETERMINATION OF GLUCOSE IN BLOOD AND SALIVA

تحضير مركب آزو جديد (حازم) يستعمل للتقدير التحليلي للجلوكوز في الدم واللحاح

HALBOOS, Mohanad Hazim<sup>1\*</sup>; HUSSEIN, Bayan Jabr<sup>2</sup>; SAYHOOD, Aayad Ammar<sup>3</sup>

<sup>1</sup> University of Kufa, Faculty of Science, Department of Ecology. Iraq.

<sup>2</sup> University of Kufa, Faculty of Dentistry, Department of Oral Histology. Iraq.

<sup>3</sup> University of Kufa, Faculty of Dentistry, Department of Basic Sciences. Iraq.

\* Corresponding author

e-mail: muhaned.halbus@uokufa.edu.iq

Received 26 May 2020; received in revised form 12 June 2020; accepted 16 June 2020

#### RESUMO

Como os recursos de saúde são limitados, condições de baixa renda exigem desenvolvimento tecnológico acessível. O projeto e a análise são um método colorimétrico de baixo custo para monitoramento diagnóstico diabético não invasivo por detecção de glicose da saliva e do sangue discutido, onde um novo composto (HAZM) foi preparado por meio de uma reação 4-aminoantipirina com 1-fenil-2-metil-5-pirazolon; este composto sintético foi analisado pelas técnicas de FTIR, <sup>1</sup>HNMR e <sup>13</sup>CNMR. As amostras foram processadas e analisadas utilizando o equipamento de produção usando a reação das enzimas glicose oxidase (GO) e peroxidase (PO) com (HAZM); dê ao método a capacidade de calcular o nível de glicose em menos de 15 segundos com precisão. A inclinação da curva de calibração é igual a 0,0026,  $\epsilon = 468,26$  e sensível a Sandel é igual a 0,384 mg/dL, para quantificar as concentrações salivares de glicose e o sangue (5-500 mg / dL) a 423 nm. Atingir um limite de detecção de 0,421 mg/dL, onde 5 % CV a (n = 3). Porque os testes HAZM foram realizados de acordo com um método de kit, que reflete os valores médios do kit (101,35  $\pm$  3,647 mg/dL) e os resultados do HAZM (104,41  $\pm$  4,951 mg / dL) com viés positivo de 3,1 mg / dL no sangue. Comparando os níveis médios de kit e glicose HAZM na saliva, 99,48  $\pm$  1,26 e 100,97  $\pm$  2,38 mg/dL, respectivamente, mostram viés positivo de 1,5 mg/dL para o processo do kit. Os resultados do uso desse método para medir glicose em amostras de sangue e saliva indicam que ele é eficaz, pois oferece resultados precisos e baratos, em comparação com outras técnicas comerciais.

**Palavras-chave:** *Composto Azo, Espectrofotométrico, Glicose, Sangue e Saliva.*

#### ABSTRACT

Because health resources are limited, low-income conditions demand affordable technological development. The design and analysis is a low-cost colorimetric method for non-invasive diabetic diagnostic monitoring by glucose detection of the saliva and blood discussed, where a new compound (HAZM) was prepared through a reaction 4-aminoantipyrine with 1-phenyl-2-methyl-5-pyrazolon; FTIR, <sup>1</sup>HNMR, and <sup>13</sup>CNMR diagnosed for this synthetic compound. Samples have been processed and analyzed using the production equipment using glucose oxidase (GO) and peroxidase (PO) enzymes reaction with (HAZM); give the method the ability to calculate glucose level in less than 15 seconds accurately. The slope of the calibration curve is equal to 0.0026,  $\epsilon = 468.26$ , and Sandel sensitive equals 0.384 mg/dL, to quantify the glucose salivary concentrations and blood (5-500 mg/dL) at 423 nm. Achieve a detection limit of 0.421 mg/dL where 5 % CV to (n = 3). Because HAZM tests performed according to a kit method, which reflects the mean kit values (101.35  $\pm$  3.647 mg/dL) and the results of HAZM (104.41  $\pm$  4.951 mg/dL) with 3.1 mg/dL positive bias in blood. Comparing the mean kit and HAZM glucose levels in saliva, 99.48  $\pm$  1.26, and 100.97  $\pm$  2.38 mg/dL, respectively, shows 1.5 mg/dL positive bias for the kit process. Results from the use of this method for measuring glucose in blood and saliva samples indicate that it is effective, as it offers accurate, and its cheap results compared to other

**Keywords:** Azo compound, Spectrophotometric, Glucose, Blood and Saliva.

## الخلاصة

لأن الموارد الصحية محدودة ، تتطلب الظروف منخفضة الدخل تطوراً تكنولوجياً ميسور التكلفة. التصميم والتحليل هو طريقة قياس الألوان منخفضة التكلفة لرصد تشخيص السكري عن طريق الكشف عن الجلوكوز في اللعاب والدم الذي تمت مناقشته ، حيث تم تحضير مركب جديد (حازم) من خلال تفاعل 4-امينو انتي بايرين مع 2-1-فينيل ميثيل 5 بيرازولون. تم تشخيص هذا المركب الاصطناعي بواسطة FTIR و  $^1\text{H}$ NMR و  $^{13}\text{C}$ NMR. تمت معالجة العينات وتحليلها باستخدام معدات الإنتاج باستخدام تفاعل إنزيمات الجلوكوز أوكسيداز (GO) وإنزيم البيروكسيداز (PO) مع (HAZM) ؛ امنح الطريقة القدرة على حساب مستوى الجلوكوز في أقل من 15 ثانية بدقة. يساوي انحدار منحنى المعايرة  $0.0026$  ،  $\epsilon = 468.26$  ، وحساسية ساندل تساوي  $0.384$  مجم / ديسيلتر ، لتحديد تركيزات الجلوكوز اللعابية والدم ( $500\text{--}5$  مجم / ديسيلتر) عند  $423$  نانومتر. تحقيق حد كشف  $0.421$  مجم / ديسيلتر حيث تكون  $5\%$  من السيرة الذاتية على ( $n = 3$ ). لأن اختبارات (حازم) تم إجراؤها وفقاً لطريقة عدة ، والتي تعكس متوسط قيم المجموعة ( $101.35 \pm 3.647$  مجم / ديسيلتر) ونتائج (حازم) ( $104.41 \pm 4.951$ ) مع  $3.1$  ملجم / ديسيلتر تحيز إيجابي في الدم. بمقارنة متوسط المجموعة ومستويات الجلوكوز (حازم) في اللعاب ،  $1.26 \pm 99.48$  ، و  $2.38 \pm 100.97$  مجم / ديسيلتر ، على التوالي ، يظهر انحياز إيجابي  $1.5$  مجم / ديسيلتر لعملية المجموعة. تشير نتائج استخدام هذه الطريقة لقياس الجلوكوز في عينات الدم واللعاب إلى أنها فعالة ، لأنها تقدم نتائج دقيقة ورخيصة مقارنة بالتقنيات التجارية الأخرى.

**الكلمات المفتاحية:** مركب آزو ، طريقة طيفية ، الجلوكوز ، الدم واللعاب.

## 1. INTRODUCTION:

Diabetes was the leading cause of impairment and death due to higher blood glucose (Deshpande, Harris-Hayes, and Schootman, 2008). The accepted standard level of the blood glucose range is 87.88 to 123.78 mg/dL (Owens, Dada, Cyrus, Adedoyin, and Adunlin, 2020). Blood glucose control levels are essential in the prevention of severe chronic disease complications (Mian, Hermayer, and Jenkins, 2019). In general, coupling enzymatic reactions in glucose oxidase (GO) and peroxidase (PO) because of the advantages of variables such as substrate specificity, reaction rate, pH, products inhibition, quality, and cost of enzymes have been taken into account amongst the various detection techniques (Bankar, Bule, Singhal, and Ananthanarayan, 2009). Glucose coupling enzymatisation begins with GO oxidation, producing by-products of  $\text{H}_2\text{O}_2$  where used by PO to oxidize the aromatic organic component by electron donor substrate (EDS) (Galant, Kaufman, and Wilson, 2015). It is possible to estimate glucose levels in the blood or saliva by changing the absorbance intensity of the unique interaction with the responsible enzymes by varying the response speed according to each concentration (Villamena, 2017); such as Trinder's method (Abrera, Sützl, and Haltrich, 2020). Azo compounds may interact with the PO enzyme to indicate that the blood sugar level is measured (Sarkar *et al.*, 2020).

In this research, a new chemical azo compound, (Z)-1,5-dimethyl-4-((1-methyl-3-oxo-2-phenyl-2,3-dihydro-1H-pyrazol-4-yl)diazinyl)-2-phenyl-1,2-dihydro-3H-pyrazol-3-one, which is

called (HAZM) acronym, it was prepared in a direct synthesis process, through which the concentration of glucose in blood and saliva samples was measured for several volunteers in addition to a number of patients with diabetes and a number of healthy people, depending on enzymatic reactions and a spectral technique that can be relied upon in clinical laboratories in hospitals or routine tests for people with diabetes as they are fast and inexpensive.

## 2. MATERIALS AND METHODS:

All the chemicals used in this research were highly pure. A number of spectral devices were used, such as FTIR Shimadzu measurements model 8400 Series,  $^1\text{H}$ NMR spectra BRUKER AV 400,  $^{13}\text{C}$ NMR spectra BRUKER AV 100, and Shimadzu UV-Vis Spectrophotometer Shimadzu UV-1650Pc.

### 2.1. Preparation of azo compound (HAZM):

2.0325 g from 4-aminoantipyrine (0.01 mol) was diazotized by dissolving it in 50 mL of ethanol; then, 5ml of HCl [5M] was added. The temperature was kept between 0 to 5 °C. It was slowly added a 1% solution  $\text{NaNO}_2$ , and then it was left resting for one hour (Sayhood and Mohammed, 2015a, 2015b). Later, an alkaline well-cooled solution of (1.7420 g) 1-phenyl-2-methyl-5-pyrazolon (0.01 mol) was slowly added to the diazonium salt. The mixture formed a precipitated, and it was washed with a 0.5:1 (ethanol: water) to it was recrystallized and dried after that Scheme 1 demonstrates the synthesis of (Z)-1,5-dimethyl-4-((1-methyl-3-oxo-2-phenyl-2,3-dihydro-1H-pyrazol-4-yl)diazinyl)-2-phenyl-

1,2-dihydro-3H-pyrazol-3-one (HAZM); this synthetic compound was analyzed using FTIR,  $^1\text{H}$ NMR, and  $^{13}\text{C}$ NMR, where these techniques were essential for the exact chemical structure of the synthesis compound to be decided (Balci, 2005; Karabacak *et al.*, 2014).

## 2.2. FTIR measurement:

The FTIR spectra were recorded in the region (4000-400)  $\text{cm}^{-1}$  by used 0.1 g of (HAZM), which mixed with 0.1 g KBr and ground together to form a transparent disk about 1 cm in diameter and 1 mm thick after pressing the mixture.

## 2.3. $^1\text{H}$ NMR and $^{13}\text{C}$ -NMR measurement:

10 mg of (HAZM) dissolved in pure deuterated DMSO as a solvent and tetramethylsilane as an internal standard to the analysis of  $^1\text{H}$ NMR and  $^{13}\text{C}$ -NMR spectra.

## 2.4. Preparation of (HAZM) solution with enzymes:

The preparation of the mixture was accompanied by freshly-prepared enzyme solutions. In the phosphate buffer, 0.01 M (2 mL, pH 7.6) of GO (0.25 mg) and PO (0.5 mg) were separately prepared and kept at 4 °C during experimental procedures. (2 mg) of HAZM was dissolved into ethanol with (5 mL, pH 7.6) of 0.01 M phosphate buffer. The solutions have been degaussed as well as the stability of solution changes has been monitored throughout three days with UV / VIS spectroscopy. No change was observed in the HAZM solution absorption spectrum at 423 nm (Figure 1) due to auto-oxidation or precipitation (Banham *et al.*, 2015; Najafi, 2017).

## 2.5. Preparing blood serum and saliva samples:

For the establishing of the methodologies, the Al-Najaf Center for Diabetes and Endocrine obtained both saliva and blood test. The Sample was taken under a fasting state from the volunteers. Two volunteer groups aged 18-61 years, with 94 diabetics and 22 non-diabetics. Whole blood (5 mL) has been drawn into the non-anti-coagulant vacuum tube. To facilitate coagulation, it remained still for 20 minutes. The serum was suctioned, then maintained at 4 °C after the centrifugation (10 min at 25000 cycles). Collected saliva samples 2 mL of the whole unstimulated saliva has been used to assess the salivary glucose level. The samples were then centrifuged (3 min at 25000 cycles), and glucose tests were performed on the resulting supernatant. In order to determine the connection

between blood glucose and the salivary concentration, the Center carried out simultaneous blood sampling for every volunteer.

## Ethical Consent

*"Verbal consent was taken from all participants after explaining the aims, methods, sources of funding, any possible conflicts of interest, institutional affiliations of the researcher, the anticipated benefits and potential risks of the study and the discomfort it may entail."* (Schroter, Plowman, Hutchings, and Gonzalez, 2006)

## 2.6. Determination of glucose:

In order to establish the HAZM method, a commercial Glucose Assay Kit was used to examine test samples in which a (1 mL) solution kit was added to ten  $\mu\text{L}$  of serum tests. The mixture was 20-minute incubated at 25 °C, and it is measured at 516 nm. The concentration of glucose was determined from the typical vendor curve.

In the HAZM method, a test solution consisting of phosphate buffer (0.01 mM) containing GO (0.025 pM), PO (0.05 pM), and HAZM (0.02 mM), where the final volume was (2 mL), was applied to the blood sample serum (20  $\mu\text{L}$ ). After 15 seconds, the optical density change was registered at 423 nm. The concentration of glucose was determined from the resulting calibration curve (Figure 2). In order to determine the HAZM method for evaluating the level of salivary glucose, in the testing solution, 10 $\mu\text{L}$  of a resulting supernatant has been used after drawing 0.5 mL of freshly saliva and centrifugation; and measure at 423 nm.

# 3. RESULTS AND DISCUSSION:

## 3.1. Explanation of the process:

Actual blood glucose monitoring systems are based on photometric or electrochemical techniques (Pu *et al.*, 2016). Direct glucose oxidation by GO was used to produce electrochemical sensors for personal optical measuring instruments (Zhang *et al.*, 2019). The replicability of tests, in addition to the sensitivity of electrochemical sensors to specific significant interventions, nevertheless decreases as the system time of life (Aljafery, Sayhood, Abdulridha, and Yousif, 2018). Unlike electrochemical electrode construction, it is simpler and cheaper to create photometric instruments (Al-Shirifi, Dikran, and Halboos,

2018; Halboos, Ammar Sayhood, and Ala'a Hussein, 2019). Even so, the precision of these instruments depends both on the overall performance of the technique and on the technical specifications (Hwang *et al.*, 2017).

Trinder method for measuring glucose in the blood is the first procedure based on the use of  $\text{H}_2\text{O}_2$  (GO by-product) in clinical laboratories. Still, it has not been developed by researchers to benefit from them in measuring glucose in the miniaturized personal colorimeters (Kengne, Erasmus, Levitt, and Matsha, 2017).

The spectrum of the HAZM method showed one peak at 423 nm Figure 1. HAZM's reaction to varying quantities of PO with a constant  $\text{H}_2\text{O}_2$  concentration has linear. For the tests, 2 mL of PO 5 nM was chosen, HAZM response was also linear to different amounts of  $\text{H}_2\text{O}_2$ . Consequently, PO oxidation of HAZM was coupled with GO (2.5 nM) glucose oxidation. The oxidation response of the HAZM procedure to various glucose levels was linear of 5-500 mg/dL glucose; this result is considered good if compared to previous studies (Bruen, Delaney, Florea, and Diamond, 2017; Dominguez, Orozco, Chávez, and Márquez-Lucero, 2017).

### 3.2. FTIR Analysis

Spectroscopy of the synthetic compound (HAZM) was performed using FTIR, where the analysis showed a number of peaks as shown in (Figure 3) having a wide band of  $3485\text{ cm}^{-1}$  (s) attributable for the stretching, vibration of O-H,  $\nu\text{C-H}$  aromatic at  $3157\text{ cm}^{-1}$  (m). Carbonyl group  $\nu(\text{C=O})$  stretching frequency at  $1674\text{ cm}^{-1}$  (s). Likewise the frequency at  $1537\text{ cm}^{-1}$  (w) and  $1491\text{ cm}^{-1}$  (m) corresponding to  $\nu(\text{N=N})$ .

### 3.3. $^1\text{H}$ NMR and $^{13}\text{C}$ -NMR Analysis

The following signals are shown in the deuterated DMSO solution with the tetra methylsaline internal standard:  $^1\text{H}$ NMR (Figure 4) and  $^{13}\text{C}$ -NMR (Figure 5) of the prepared azo compound (HAZM). The  $^1\text{H}$ -NMR (HAZM) spectrum has a multiplied spectrum of  $\delta$  (7.57-7.33) ppm (s, 12H, Ar) due to phenyl groups, -N-CH=(4-Aminoantipyrin) due to  $\delta$  (3.4) ppm (s, H) and =C-CH<sub>3</sub> due to  $\delta$  (2.6) ppm, -N-CH= (1-phenyl-2-methyl-5-pyrazolone) due to a multiple  $\delta$  (3.1) ppm (s, H) and =C-CH<sub>3</sub> due to  $\delta$  (2.5) ppm. The signals in  $^{13}\text{C}$ -NMR show (HAZM) were: (138-126) ppm (12C, Ar-C); 151 ppm (C=O); 31.9 ppm (C-CH<sub>3</sub>) (1-phenyl-2-methyl-5-pyrazolone) 39 ppm (N-CH<sub>3</sub>); 34.8 ppm (C-CH<sub>3</sub>) (4-aminoantipyrine), 40.3 ppm (N-CH<sub>3</sub>) 143 ppm (-C-N=N-C-).

### 3.4. Glucose measurements in blood:

The glucose levels of 116 serum samples were examined by kit and HAZM system in order to verify the relevant HAZM process. A review of results from Pearson showed a strong association ( $r > 0.95$ ) between kit and HAZM tests. The experimental (t-test) of levels of sugar blood there in samples tested using HAZM and kits approaches did not show a significant distinction between these results ( $P > 0.05$ ). Because HAZM tests were performed according to a kit method, more favorable mistakes were reported, which reflect the mean kit values ( $101.35 \pm 3.647\text{ mg/dL}$ ) and the results of HAZM ( $104.41 \pm 4.951\text{ mg/dL}$ ) with 3.1 mg/dL positive bias. This is expected to be caused by delayed glycolysis (Moutasim and Thomas, 2020).

### 3.5. Glucose measurements in saliva:

Early identification and prevention of many diseases were assisted by salivary diagnosis (Lee, Garon, and Wong, 2009). The reliance on HAZM for non-invasive control of the salivary glucose concentration has been evaluated based on the promising potential saliva application areas in personal dentistry (Olczak *et al.*, 2019), and much more crucially, the limit of detection for the HAZM method ( $0.421\text{ mg/dL}$ ). In this study, both kit and HAZM methods evaluated non-stimulated whole saliva of diabetic and non-diabetic samples. The speedy samples obtained to limit the effects of possible interference substances, particularly  $\text{C}_2\text{H}_4\text{OHCOOH}$ , where can has a significant effect in saliva pH (Kubáň, Dvořák, and Kubáň, 2019). Analysis of the data of the HAZM and the kit data for salivary glucose concentration indicated insignificant results differences ( $P > 0.05$ ). The results of diabetic and non-diabetic individuals' salivary glucose concentration were also correlated with corresponding fasting glucose level values. Comparing the mean kit and HAZM glucose levels,  $99.48 \pm 1.26$  and  $100.97 \pm 2.38\text{ mg/dL}$  respectively, show 1.5 mg/dL positive bias for kit process.

#### Conflict of Interest:

*"The authors declare that they have no conflict of interest."*

## 4. CONCLUSIONS:

The current method for blood sugar calculation and salivary samples using coupled enzyme GO and PO was based primarily on the

spectrophotometric characteristics of HAZM. It is stable and accurately calculates the glucose levels in less than 15 seconds. Taking into consideration that only the first stage in the combined enzyme assay quantification of blood glucose has also been modified in the HAZM method. It will be possible to develop this method in the near future to make it one of the techniques that are characterized by ease of dealing with it.

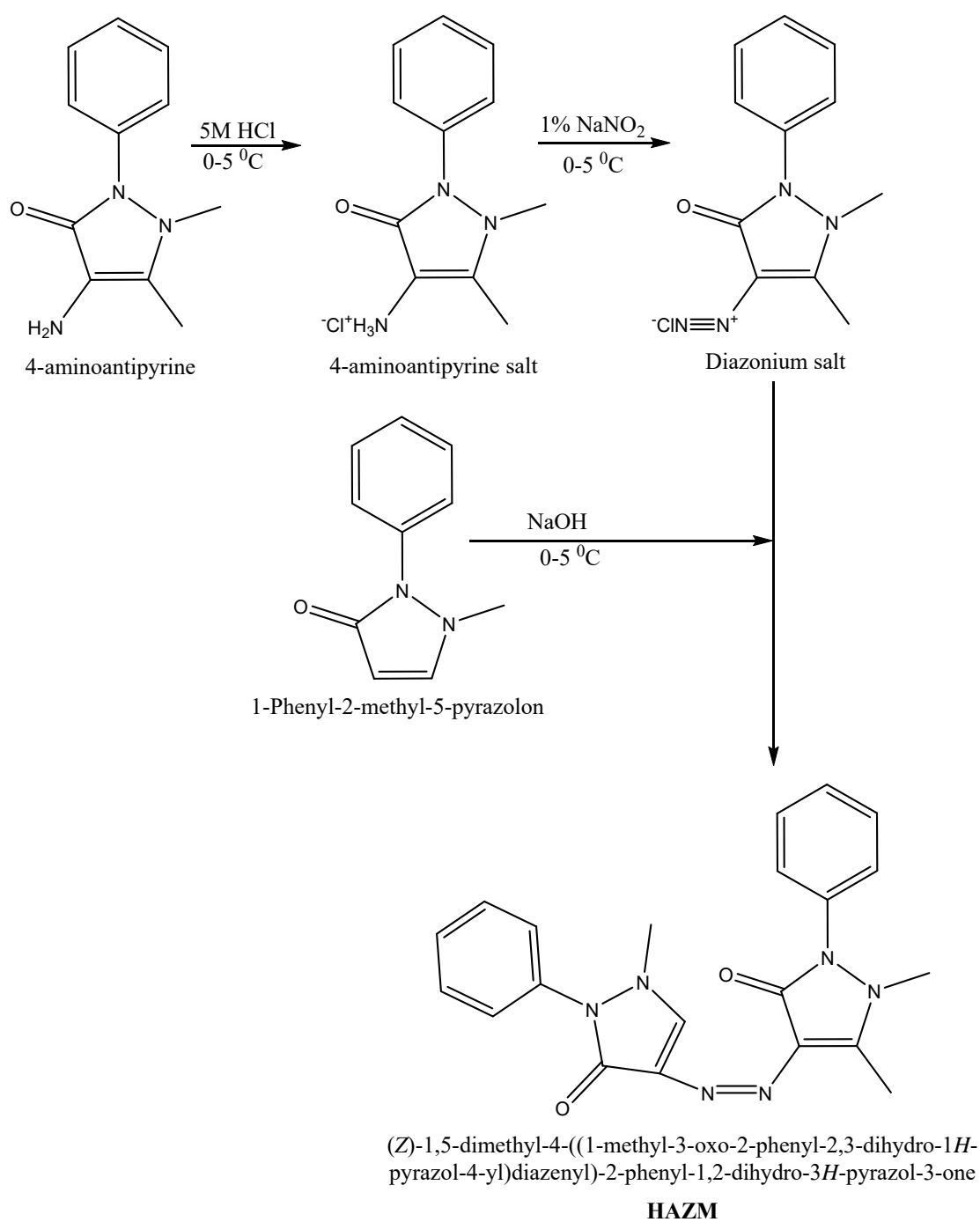
## 5. ACKNOWLEDGMENTS:

The authors thank and gratefully appreciate the staff of the Al-Najaf Center for Diabetes and Endocrine for their facilities to accomplish this research.

## 6. REFERENCES:

1. Abrera, A. T., Sützl, L., and Haltrich, D. (2020). Pyranose oxidase: A versatile sugar oxidoreductase for bioelectrochemical applications. *Bioelectrochemistry*, 132, 107409. <https://doi.org/10.1016/j.bioelechem.2019.107409>
2. Al-Shirifi, A. N. M., Dikran, S. B., and Halboos, M. H. N. (2018). Application of central composite design method to oxidative coupling spectrophotometric determination of metoclopramide hydrochloride in pure form and pharmaceutical preparations. *Journal of Global Pharma Technology*, 10(5), 143–152.
3. Aljafery, A. M. A., Sayhood, A., Abdulridha, W. M., and Yousif, A. M. (2018). Evaluation the tensile strength of cold-cured acrylic resin denture base material by adding silver nanoparticles. *Indian Journal of Public Health Research and Development*, 9(10), 917–922. <https://doi.org/10.5958/0976-5506.2018.01258.5>
4. Balci, M. (2005). *Basic 1H- and 13C-NMR Spectroscopy*. Elsevier. <https://doi.org/10.1016/B978-0-444-51811-8.X5000-1>
5. Banham, D., Ye, S., Knights, S., Stewart, S. M., Wilson, M., and Garzon, F. (2015). UV-visible spectroscopy method for screening the chemical stability of potential antioxidants for proton exchange membrane fuel cells. *Journal of Power Sources*, 281, 238–242. <https://doi.org/10.1016/j.jpowsour.2015.02.002>
6. Bankar, S. B., Bule, M. V., Singhal, R. S., and Ananthanarayan, L. (2009). Glucose oxidase - An overview. *Biotechnology Advances*, 27(4), 489–501. <https://doi.org/10.1016/j.biotechadv.2009.04.003>
7. Bruen, D., Delaney, C., Florea, L., and Diamond, D. (2017). Glucose sensing for diabetes monitoring: Recent developments. *Sensors*, 17(1866), 1–21. <https://doi.org/10.3390/s17081866>
8. Deshpande, A. D., Harris-Hayes, M., and Schootman, M. (2008). Epidemiology of Diabetes and Diabetes-Related Complications. *Physical Therapy*, 88(11), 1254–1264. <https://doi.org/10.2522/ptj.20080020>
9. Dominguez, R. B., Orozco, M. A., Chávez, G., and Márquez-Lucero, A. (2017). The Evaluation of a Low-Cost Colorimeter for Glucose Detection in Salivary Samples. *Sensors*, 17(2495), 1–11. <https://doi.org/10.3390/s17112495>
10. Galant, A. L., Kaufman, R. C., and Wilson, J. D. (2015). Glucose: Detection and analysis. *Food Chemistry*, 188, 149–160. <https://doi.org/10.1016/j.foodchem.2015.04.071>
11. Halboos, M. H., Ammar Sayhood, A., and Ala'a Hussein, T. (2019). Determination celioprolol hydrochloride drug by used zero, first, second and third order derivative and peak area spectrophotometry method in its pure form and in pharmaceutical tablets. *Journal of Physics: Conference Series*, 1294, 52035. <https://doi.org/10.1088/1742-6596/1294/5/052035>
12. Hwang, J. H., Kim, H., Cho, S., Bellemans, T., Lee, W. Do, Choi, K., ... Joh, C. H. (2017). An examination of the accuracy of an activity-based travel simulation against smartcard and navigation device data. *Travel Behaviour and Society*, 7, 34–42. <https://doi.org/10.1016/j.tbs.2017.01.001>
13. Karabacak, M., Kose, E., Atac, A., Sas, E. B., Asiri, A. M., and Kurt, M. (2014). Experimental (FT-IR, FT-Raman, UV-Vis, 1H and 13C NMR) and computational (density functional theory) studies on 3-bromophenylboronic acid. *Journal of Molecular Structure*, 1076, 358–372. <https://doi.org/10.1016/j.molstruc.2014.07.058>
14. Kengne, A. P., Erasmus, R. T., Levitt, N.

- S., and Matsha, T. E. (2017). Alternative indices of glucose homeostasis as biochemical diagnostic tests for abnormal glucose tolerance in an African setting. *Primary Care Diabetes*, 11(2), 119–131. <https://doi.org/10.1016/j.pcd.2017.01.004>
15. Kubáň, P., Dvořák, M., and Kubáň, P. (2019). Capillary electrophoresis of small ions and molecules in less conventional human body fluid samples: A review. *Analytica Chimica Acta*, 1075, 1–26. <https://doi.org/10.1016/j.aca.2019.05.004>
  16. Lee, J. M., Garon, E., and Wong, D. T. (2009). Salivary diagnostics. *Orthodontics and Craniofacial Research*, 12(3), 206–211. <https://doi.org/10.1111/j.1601-6343.2009.01454.x>
  17. Mian, Z., Hermayer, K. L., and Jenkins, A. (2019). Continuous Glucose Monitoring: Review of an Innovation in Diabetes Management. *American Journal of the Medical Sciences*, 358(5), 332–339. <https://doi.org/10.1016/j.amjms.2019.07.003>
  18. Moutasim, K. A., and Thomas, G. J. (2020). Salivary gland tumours: update on molecular diagnostics. *Diagnostic Histopathology*, 26(4), 159–164. <https://doi.org/10.1016/j.mpdhp.2020.01.002>
  19. Najafi, A. (2017). An investigation on dispersion and stability of water-soluble fullereneol (C60OH) in water via UV–Visible spectroscopy. *Chemical Physics Letters*, 669, 115–118. <https://doi.org/10.1016/j.cplett.2016.12.030>
  20. Olczak, M., Poniatowski, Ł. A., Niderla-Bielińska, J., Kwiatkowska, M., Chutorański, D., Tarka, S., and Wierzbobrowicz, T. (2019). Concentration of microtubule associated protein tau (MAPT) in urine and saliva as a potential biomarker of traumatic brain injury in relationship with blood–brain barrier disruption in postmortem examination. *Forensic Science International*, 301, 28–36. <https://doi.org/10.1016/j.forsciint.2019.05.010>
  21. Owens, F. S., Dada, O., Cyrus, J. W., Adedoyin, O. O., and Adunlin, G. (2020). The effects of *Moringa oleifera* on blood glucose levels: A scoping review of the literature. *Complementary Therapies in Medicine*, 50, 102362. <https://doi.org/10.1016/j.ctim.2020.102362>
  22. Pu, Z., Wang, R., Wu, J., Yu, H., Xu, K., and Li, D. (2016). A flexible electrochemical glucose sensor with composite nanostructured surface of the working electrode. *Sensors and Actuators, B: Chemical*, 230, 801–809. <https://doi.org/10.1016/j.snb.2016.02.115>
  23. Sarkar, S., Banerjee, A., Chakraborty, N., Soren, K., Chakraborty, P., and Bandopadhyay, R. (2020). Structural-functional analyses of textile dye degrading azoreductase, laccase and peroxidase: A comparative in silico study. *Electronic Journal of Biotechnology*, 43, 48–54. <https://doi.org/10.1016/j.ejbt.2019.12.004>
  24. Sayhood, A. A., and Mohammed, H. J. (2015a). Synthesis of new azo reagent for determination of Pd(II), Ag(I) and applied to enhance the properties of silver nano particles. *International Journal of Chemical Sciences*, 13(3), 1123–1136.
  25. Sayhood, A. A., and Mohammed, H. J. (2015b). Synthesis of novel azo reagents derived from 4-aminoantipyrine and their applications of enhancement of silver nano particles. *Der Pharma Chemica*, 7(8), 50–58.
  26. Schroter, S., Plowman, R., Hutchings, A., and Gonzalez, A. (2006). Reporting ethics committee approval and patient consent by study design in five general medical journals. *Journal of Medical Ethics*, 32(12), 718–723. <https://doi.org/10.1136/jme.2005.015115>
  27. Villamena, F. A. (2017). UV–Vis Absorption and Chemiluminescence Techniques. In *Reactive Species Detection in Biology* (pp. 203–251). Elsevier. <https://doi.org/10.1016/b978-0-12-420017-3.00006-2>
  28. Zhang, D., Chen, X., Ma, W., Yang, T., Li, D., Dai, B., and Zhang, Y. (2019). Direct electrochemistry of glucose oxidase based on one step electrodeposition of reduced graphene oxide incorporating polymerized L-lysine and its application in glucose sensing. *Materials Science and Engineering C*, 104, 109880. <https://doi.org/10.1016/j.msec.2019.109880>



**Scheme 1.** Steps to synthesize the compound (HAZM)

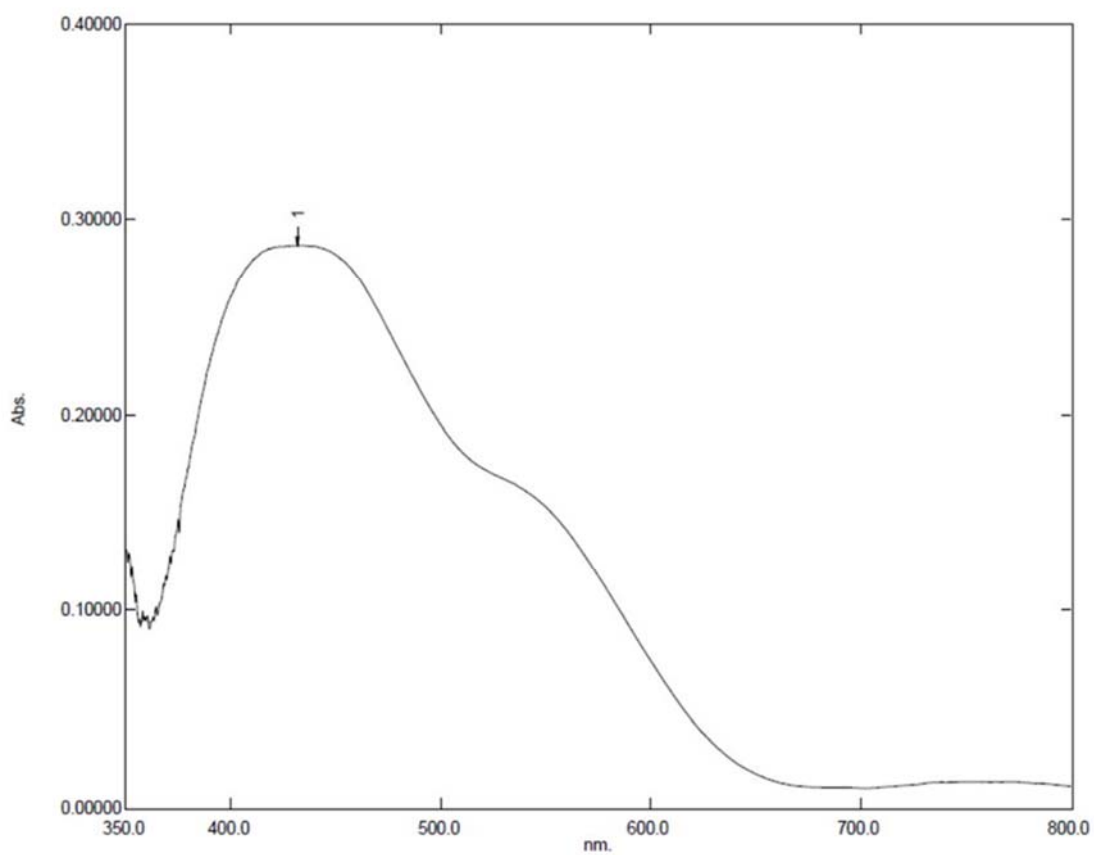


**Figure 1.** Absorption spectra of HAZM method at 423 nm

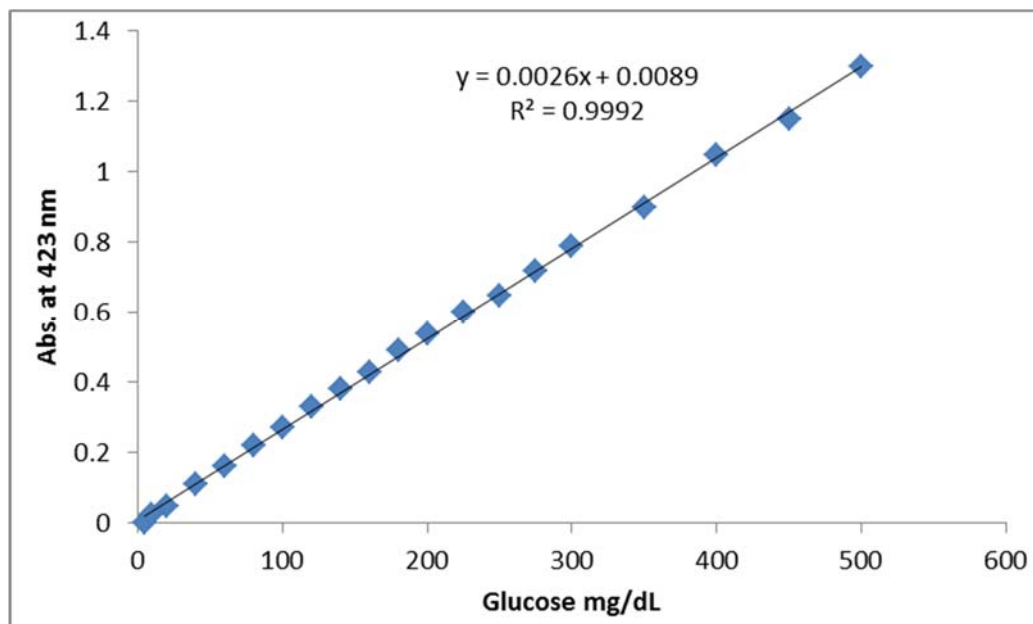


**Figure 2.** Calibration curve of HAZM method at 423 nm



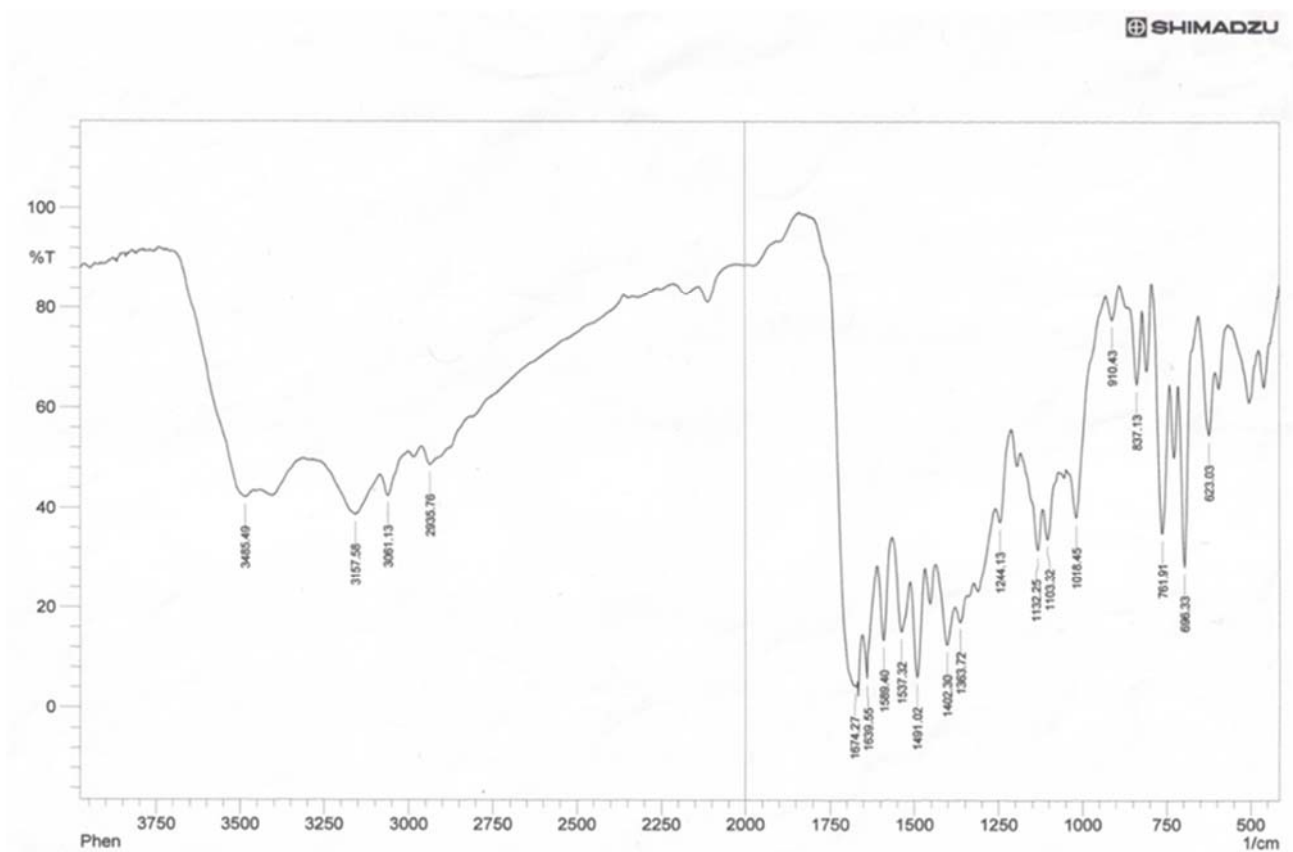


**Figure 3.** FTIR spectra of HAZM compound

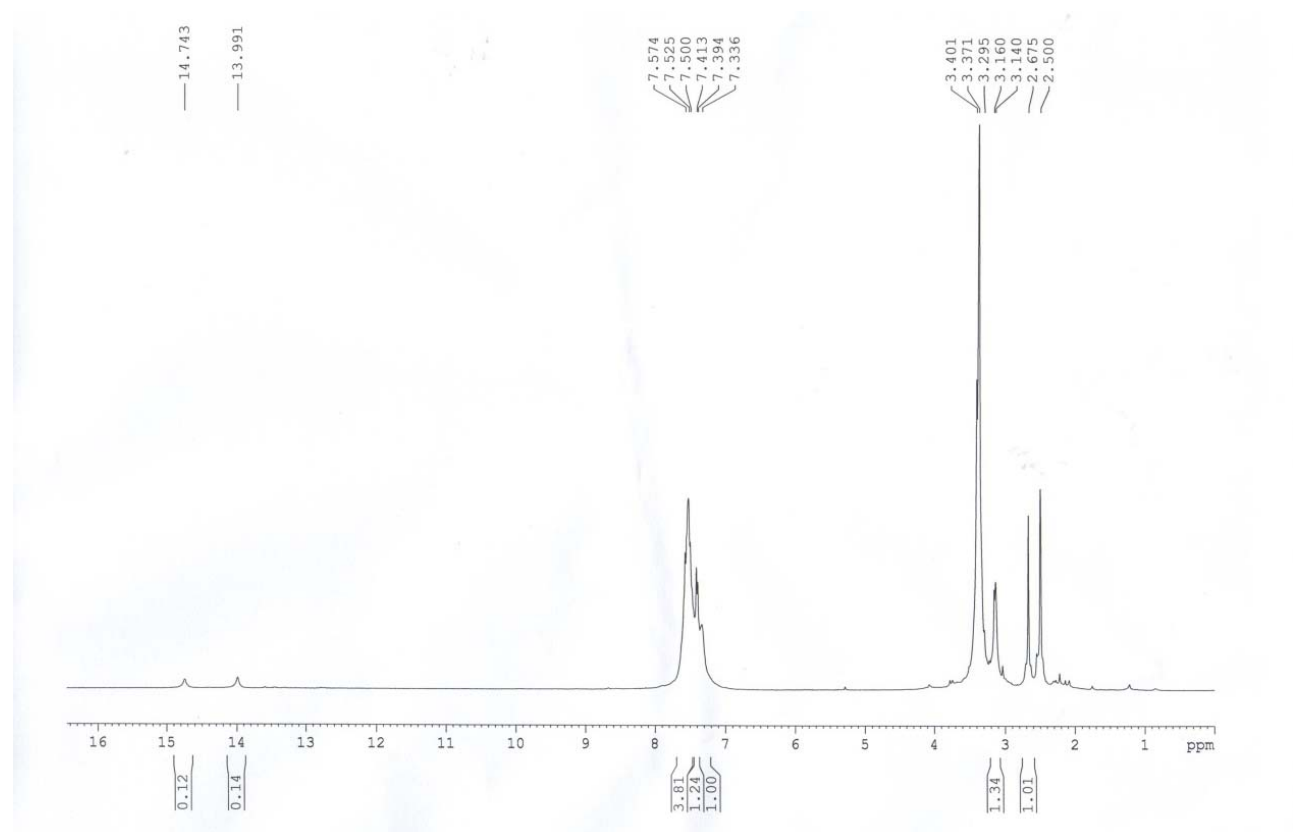


**Figure 4.** <sup>1</sup>H NMR spectra of HAZM compound

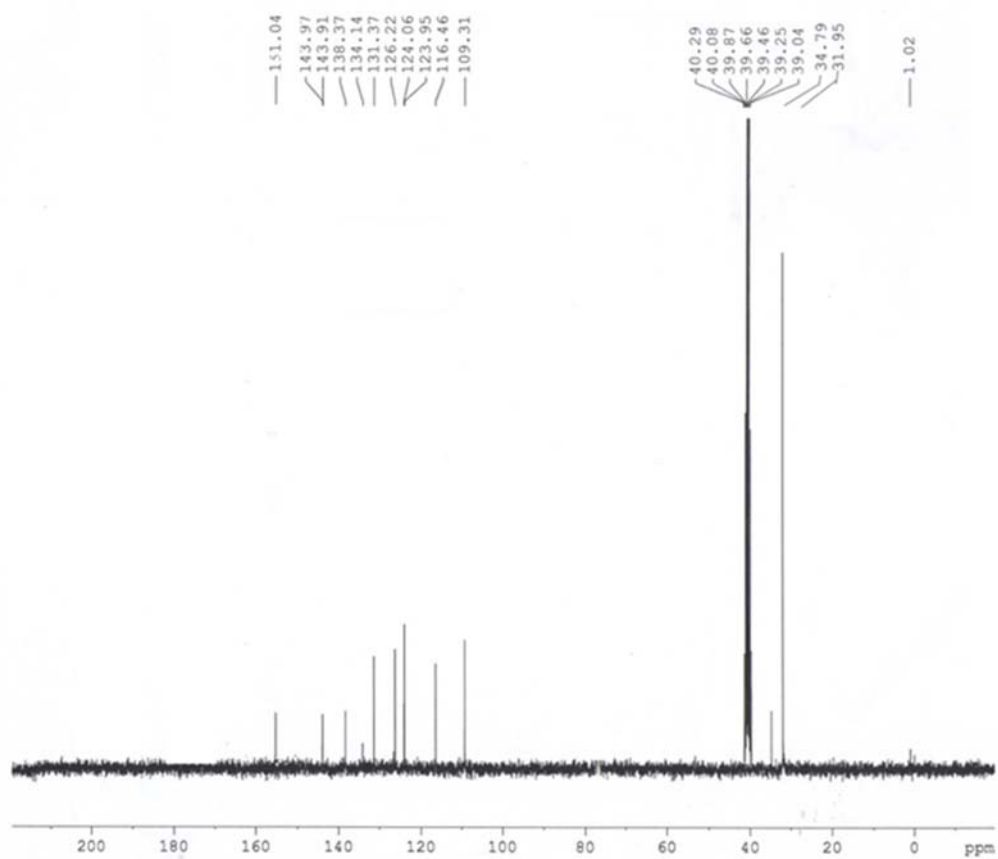


**Figure 5.**  $^{13}\text{C}$ NMR spectra of HAZM compound

## SENSORES ELETROQUÍMICOS À BASE DE FILME POLI (L-FENIL ALANINA) EM MWCNT PARA DETERMINAÇÃO DE TPS

## ELECTROCHEMICAL SENSORS BASED ON POLY (L-PHENYL ALANINE) FILM ON MWCNT FOR DETERMINATION OF TPS

EMAN A. M. Al-Jawadi <sup>1\*</sup>; MOHAMMED I. Majeed <sup>2</sup>

<sup>1</sup> Department of Biophysics, College of Science, University of Mosul, Mosul, Iraq.

<sup>2</sup> Department of Biology, College of Science, University of Mustansiriyah, Baghdad, Iraq

\* Corresponding author

e-mail: e\_abd2012@yahoo.com

Received 2 May 2020; received in revised form 10 June 2020; accepted 15 June 2020

### RESUMO

Neste estudo, a voltametria cíclica (CV) é apresentada com uma técnica eletroquímica sensível para a avaliação do medicamento anticâncer Toposar (TPS). O eletrodo foi formado na superfície de um eletrodo de carbono vítreo modificado com MWCNT usando um revestimento de L-fenil alanina para se tornar o novo eletrodo em uma fórmula (PPA-MWCNT/GCE). O PPA foi polimerizado em pH 8,0, o que mostrou vantagens avançadas para o estudo e estimativa do tratamento por eletroanálise por TPS. Um grupo de fatores no eletrodo de carbono vítreo vazio foi estudado para aprimorar o trabalho do eletrodo no estudo do TPS, incluindo esses fatores (influência do pH, curva de calibração, estabilidade do eletrodo, taxa de varredura, potencial de deposição, etapa de voltagem, equilíbrio) tempo, tempo de deposição). Como resultado do desenvolvimento do eletrodo, a estabilidade do eletrodo preparado foi observada com a camada de PPA com a morfologia da camada pela análise SEM, mostrando a morfologia de PPA/GCE e MWCNTs/PPA/GCE por SEM, respectivamente. A largura do filme PPA na resposta TPS tem maior sensibilidade na superfície de MWCNTs/PPA/GCE em comparação com GCE, e reversibilidade redox aumentada com número de 8 ciclos, o CV de 5,0 nM TPS no GCE com taxas de varredura entre 50 e 400 mV·s<sup>-1</sup>. Essa reação foi prevista para um mecanismo irrevogável de eletrodo. Uma comparação foi feita entre os CVs do TPS nos MWCNTs e o eletrodo modificado pelo PPA com o GCE desencapado a pH 7,0 com uma taxa de varredura de 100 mV·s<sup>-1</sup>, a corrente de oxidação é 11,18 vezes maior que a comparável no GCE desencapado.

**Palavras-chave:** *Toposar, poli L-fenil alanina, voltametria cíclica, Sensor, MWCNT*

### ABSTRACT

In this study, cyclic voltammetry (CV) is presented with a sensitive electrochemical technique for the assessment of the anti-cancer medicine Toposar (TPS). The electrode was formed on the surface of a modified glassy carbon electrode with MWCNT using a coating of L-phenyl alanine to become the new electrode in a formula (PPA-MWCNT / GCE). PPA was polymerized at pH 8.0, which showed advanced advantages for the study and estimation of TPS electroanalysis treatment. A group of factors on the bare glassy carbon electrode were studied to enhance the electrode 's work to study TPS, including these factors (Influence of pH, calibration curve, the stability of the electrode, scan rate, deposition potential, voltage step, equilibration time, deposition time). As a result of the electrode development, the stability of the prepared electrode was observed with the PPA layer with the Morphology of the layer by the SEM analysis showing the morphology of PPA/GCE and MWCNTs/PPA/GCE by SEM, respectively. The PPA film width on TPS response has higher sensitivity on the surface of MWCNTs/PPA/GCE compared to GCE and increased redox reversibility with 8 cycles number. The CV of 5.0 nM TPS on GCE with scanning rates of between 50 and 400 mV·s<sup>-1</sup> This reaction was predicted for an irrevocable electrode mechanism. A comparison was made between the TPS CVs on the MWCNTs, and the PPA modified electrode with the bare GCE at pH 7.0 with a scan rate of 100 mV·s<sup>-1</sup>, the oxidation current is 11.18 times higher than the comparable one on the bare GCE.

**Keywords:** *Toposar, poly L-phenyl alanine, cyclic voltammetry, Sensor, MWCNT.*

## 1. INTRODUCTION:

Toposar (TPS), as a chemotherapy drug, is used for the treatment of testicular cancer, lymphomas, and small cell lung cancer (Toffoli *et al.*, 2004; Sissolak *et al.*, 2010). TPS acts by harming the DNA of the cancer cells. Topoisomerase inhibition, as well as apoptosis, causes DNA damage (Osherooff., 1989; Kovacic and Osuna., 2000).

Podophyllotoxin (PTOX) has been suggested as an anti-cancer drug for the therapy of tumor cells through blocking the tubulin polymerization, which induces the detention of cell cycle at mitosis, and stops cancer cell growth. PTOX products, including TPS, have been proposed for venereal wart and cancer therapies. One of the significant issues with this naturally extracted-plant derivative is its reservoirs (Ardalani *et al.*, 2017).

During electropolymerization, the thickness of polymer film is controlled by the number of cycles. Deposited films on surface electrodes by electropolymerization provide good homogeneity to the electrode surface. Based on the literature review, electrochemical detection of TPS, using a poly (L-phenylalanine) glassy carbon of modified electrode (PPA/GCE), has never been investigated previously. Amino acids have different functional groups, acting as the building blocks of protein structures, and allowing the adsorption mechanism to occur on electrocatalytic surfaces.

The condensation reaction of amino acids occurs when the C-terminus of one comes in proximity of the N-terminus of the other. Initially, oxygen and hydrogen atoms from the associated group of carboxyl and then hydrogen atom from the NH group of amino form a molecule of water (Andrea *et al.*, 2011).

Amino acid adsorption is essential for protein interaction with surfaces (Khan *et al.*, 1996). Generally, the electrochemical determination of medicines, using a poly L-phenylalanine (PPA) film (PPA/GCE) by electrochemical techniques, is a very selective and sensitive method. Voltammetric methods are appropriate for assessing the redox characteristics of functional medicine (Ozkan, 2012; Wang, 1998; Uslu, 2010; Dogan *et al.*, 2011).

Techniques that are applied to examine the medicine communications with DNA are as follows: UV-Visible spectrophotometry (Marky *et al.*, 1983), fluorescence spectroscopy (Jenkins *et*

*al.*, 1998; Song *et al.*, 2006), constant wavelength synchronous fluorescence spectroscopy (CW-SFS) (Garbett *et al.*, 2007), circular dichroism (Garbett *et al.*, 2007; Pasternack., 2003), spectroscopy of Raman resonance (Manfait *et al.*, 1982) and Fourier transform infrared spectroscopy (Nafisi *et al.*, 2013).

## 2. MATERIALS AND METHODS:

The devices, materials, and arrangement of Poly (L-phenylalanine) on GCE used in this work, are described in the following paragraphs:

### 2.1. Instrumentation

Voltammetric measurements were done by 797 VA (Computrace Metrohm, Switzerland). A standard three-electrode complex comprised a working electrode, which is modified, a reference electrode, Ag/AgCl with saturated KCl, a bare GCE, and a wire of platinum as an auxiliary, used in all electrochemical tests. All tests were conducted at a temperature of  $25.0 \pm 0.5$  °C. The pH meter (digital HANNA, Portugal) was used to measure the pH (Mohammed *et al.*, 2019).

### 2.2. Reagents

TPS and the required dosage of pharmaceutical form were acquired by Koçak Farma Inc. (Istanbul, Turkey). L-phenylalanine used in this study was of analytical grade, acquired from Fluka. The supporting electrolytes used here were as follows: Phosphate, Tris-HCl, and Britton Robinson buffers. All solutions were kept in the dark and utilized on a day to prevent decay. All chemicals and reagents were of analytical grade (Fluka, BDH), applied as received with no further purification. Double distilled water (DDW) was utilized during the experimental study.

### 2.3. Arrangement of Poly (L-phenylalanine) Altered GCE on multi-walled carbon nanotubes (MWCNTs)

Before the electrochemical alteration, the GCE was cleaned with a slurry of alumina of 0.3 and 0.05  $\mu\text{m}$  pore size, to a mirror-like surface, then it was rinsed with DDW. Afterward, the GCE was treated consecutively with 1:1 nitric acid: absolute ethanol, and distilled water in an ultrasonic bath for 5 min, respectively. For the electropolymerization of the L-phenylalanine on the MWCNTs/GCE, after cleaning, the GCE was deposited in 0.01 M phenylalanine solution (0.2 M

PBS, pH 8.0), formerly degassed with high purity nitrogen for 5 min. The electrode was subjected to cyclic scanning between -1.5 and 2.5 V, with a scan rate of 80 mV.s<sup>-1</sup>, using 8 cycles. A polymer of blue color on the GCE surface was formed and washed with reagent water type IV (ASTM D1193) (Daniel *et al.*, 1982); the electropolymerization mechanism is represented in Figure 1

### 3. RESULTS AND DISCUSSION:

#### 3.1.1. Voltammetric study of Toposar

The redox mechanism of TPS, a medicine for anti-cancer treatment, was investigated as a further application for bio-detection in 0.2 M PBS at pH 7, by cyclic voltammetry (CV) sweeps from -1.5 to +2.0 V, with a scan rate of 100 mV.s<sup>-1</sup>, until stable voltammograms were acquired, as presented in Figure 2. The oxidation potential was performed at 0.42 V versus Ag/AgCl/sat. KCl, following the instrument default conditions.

#### 3.1.2. Voltammetric study of Toposar

To optimize the conditions for measurement by CV technique, a cyclic voltammogram of 3.0 nM TPS in PBS at pH 7.0, studied previously (Bozal *et al.*, 2013), used as a supporting electrolyte. Table 1 shows all the parameters optimized for the measurement of TPS.

#### 3.1.3. Voltammetric study of Toposar

The influence of pH of the solution on the feedback of 3.0·10<sup>-9</sup> M TPS was tested in the pH, ranging from 4.0 to 9.0 in PBS, by CV at a scan rate of 100 mV.s<sup>-1</sup> (Figure 3-a). As pH was increasing, the peak potential switched to more negative values, at pH 9.0, and turned out unmeasurable. The linear correlation between oxidation potential and pH can be presented as Equation 1.

$$E_{pa} = -58.3 \text{ pH} + 845.8 \quad (\text{Eq. 1})$$

Where  $E_{pa}$  is expressed in mV, with  $r = 0.997$ .

The pH of the solution significantly influenced the oxidation current. The PBS at pH 7.0 was selected for the assessment of TPS with the highest peak current (Figure 3-b).

#### 3.1.4. The calibration curve of the TPS

The relation between concentrations of TPS and oxidation current was examined in serial experiments with different concentrations of TPS in PBS at pH 7.0 (Figure 4). The experiment was performed under optimal conditions, as illustrated in Table 1.

#### 3.1.5. Stability of TPS

The TPS stability was measured in 0.3 nM of TPS, in PBS at pH 7.0, by simulating measurements on the electrode and preparing a periodic assessment of readings for the same cell, as shown in Figure 5.

#### 3.2.1. Electropolymerization of PPA

The PPA film thickness is managed by the number of cycles of voltammetric scans throughout the electrochemical alteration of a GCE surface, as shown in Figure 6 in PBS at pH 8.0.

#### 3.2.2. Morphology characterized by SEM of PPA/GCE & MWCNTs/PPA/GCE

Figure-7 (a-c) and Figure-7 (d-f) show the morphology of PPA/GCE and MWCNTs/PPA/GCE by SEM, respectively.

#### 3.3.1. Impact of the PPA film width on the response of TPS

The diameter of the PPA film on the electrode surface was investigated by CV, concerning the electrochemical response of TPS. The peak currents of TPS were much depended on the thickness of the PPA film. Reduction and oxidation current peak augmented with the thickness elevation of the PPA film. At the same time, the reduction and oxidation potential were negatively and positively shifted, respectively, showing the redox reversibility of TPS was weakened with the thickness elevation of PPA. TPS has higher sensitivity and better redox reversibility; therefore, 8- cycle was chosen to control the PPA film thickness.

#### 3.3.2. The influence of pH on the polymerization of PA

The effect of pH on oxidation currents of PPA on GCE was examined. Figure 8-a shows that by increasing pH, the reduction potential shifted negatively. The increasing pH for PPA was negatively shifted for the potential related to the

current ( $I_{pa}/\mu A$ ), as shown for L-phenylalanine at pH 8.0 (Figure. 8). Therefore, pH 8.0 was selected as an optimal condition for L-phenylalanine.

### 3.3.3. Effect of pH on PPA for detection of TPS

The impact of the pH of PBS on the reaction of TPS was examined by CV. The TPS was well-behaved in PBS, as pH increased, the anodic peak potential became negative, and a good linear correlation was found in the graph of  $E_{pa}$  vs. pH in PBS, with pH ranging from 5.0 to 9.0. Equation 2 is the linear regression equation.

$$E_{pa} V = 0.5631 - 0.422 \text{ pH} \quad (\text{Eq. 2})$$

With an  $R^2 = 0.9712$ , as shown in Figure 9.

### 3.3.4. Electrochemical Oxidation of TPS at the PPA Modified Electrode

TPS oxidation potential and current can be determined on bare GCE; oxidation current is more significant than the comparable one, on the naked GCE. This demonstrated that the catalytic response happened between the PPA altered electrode and TPS. The catalytic response simplifies the relocation of an electron between the modified electrode and hydroquinone (TPS). Therefore the redox potential of TPS turned out to be simpler. PPA itself is electroinactive in the potential range from -1.5 to 2.0V (Figure10-a). Because of the high porosity of the PPA, the entire exterior area of the GC electrode is much bigger than that of bare GCE. Therefore, oxidation current elevates more clearly, more detailed in Figure10-b.

### 3.3.5. Impact of Scan Rate

The impact of the scan rate on oxidation current and the oxidation potential of TPS was examined. For this study, we documented the CV of  $5.0 \cdot 10^{-9}$  M TPS on GCE with scan rates, ranging from 50 to 400  $\text{mV} \cdot \text{s}^{-1}$  (Figure 11-a). By elevation of the scan rates, the peak potential ( $E_{pa}$ ) for the oxidation of TPS was increased. This reaction was predicted for an irrevocable electrode mechanism. The linear graph of  $I_{pa}$  as a function of  $u^{1/2}$  (Figure 11-b) demonstrates that the oxidation of TPS on the GCE was diffusion-managed. For TPS, the graph of the logarithm of the scan rate as a function of the logarithm of peak current was linear with a slope of 0.91; this amount is near the theoretical value of 1.0, which demonstrates that a standard reaction is a diffusion-managed electrode mechanism (Figure. 11-c). Equation 3 can be presented as

$$\text{Log } I_{pa} (\mu A) = 0.918 \text{ log } u (\text{s})^{-1} + 0.7696 \quad (\text{Eq. 3})$$

With a  $R^2 = 0.9506$ .

### 3.3.6. Electrochemical Oxidation of TPS at the MWCNTs-PPA Modified Electrode

A comparison was made between the CVs of TPS on MWCNTs, PPA modified electrode with that of bare GCE. The CVs on bare GCE is demonstrated in Figure 12-curve a, and on MWCNTs PPA modified electrode in Figure 12 - curve b at pH 7.0 with the scan rates of 100  $\text{mV} \cdot \text{s}^{-1}$ . The oxidation current is 11.18-fold larger than the comparable one on the bare GCE.

## 4. CONCLUSIONS:

In this work, a novel approach was presented for the creation of a new voltammetric sensor of TPS depended on MWCNTs PPA coating. Excellent sensitivity, high selectivity, and fast electron transfer were acquired for the oxidation of TPS on the PPA modified electrode. The current GC altered electrode (PPA/GCE) demonstrated a distinguished selectivity, antifouling characteristics, and sensitivity, as well as can isolate oxidation peaks for TPS, which are identical on the naked electrode. Chemically modified electrode, MWCNTs PPA is a promising sensor and has the potential to be used for drug assessment.

## 6. REFERENCES:

1. Andrea S., José M. O., Rodes A., Juan M. (2011). Adsorption of Glycine on Au(hkl) and Gold Thin Film Electrodes: An in Situ Spectroelectrochemical Study. *J. Phys. Chem.*, 115: 16439-16450.
2. Ardalani H., Avan A., Ghayour-Mobarhan, M. (2017). Podophyllotoxin: a novel potential natural anti-cancer agent. *Avicenna J. Phytomed.*, 7: 285-294.
3. ASTM D1193-06(2018), Standard Specification for Reagent Water, ASTM International, West Conshohocken, PA, 2018. DOI: 10.1520/D1193-06R18
4. Bi S., Qiao C., Song D., Tian Y., Gao D., Sun Y., Zhang H. (2006) Study of interactions of flavonoids with DNA using acridine orange as a fluorescence probe. *Sensors Actuators B Chem*, 119(1):199–208.

5. Bozal-Palabiyik B., Burcu D, Uslu B., Alp C., Ozkan, S. A.(2013). Sensitive voltammetric assay of etoposide using modified glassy carbon electrode with a dispersion of multi-walled carbon nanotube. *Journal of Solid State Electrochemistry*, 17: 2815-2822.
6. Daniel R. T., Toth, K., Durst R. D., Wilson G. S. (2001). Electrochemical Biosensors: Recommended Definitions and Classification. *Biosensors & Bioelectronics*, 16 (s 1–2):121–131
7. Dogan-Topal K. D., Ozkan SA., Uslu B.(2011) Anodic behaviour of fulvestrant and its voltammetric determination in pharmaceuticals and human serum on highly boron-doped diamond electrode using differential pulse adsorptive stripping voltammetry. *J Appl Electrochem.*, 41:1253-1260.
8. G. Sissolak, D. Sissolak, Jacobs P. (2010) Human immunodeficiency and Hodgkin lymphoma. *Transfus Apher Sci.* ,42: 131-139.
9. Garbett N. C., Ragazzon P. A., Chaires J. B. (2007) Circular dichroism to determine binding mode and affinity of ligand–DNA interactions. *Nat Protoc.*, 2: 3166-3172.
10. Jenkins T. C. (1997) Optical Absorbance and Fluorescence Techniques for Measuring DNA-drug Interactions. *Methods Mol Biol*, 90:195-218
11. Khan M. A., Williams R. L., Williams D. F. (1996) In-vitro corrosion and wear of titanium alloys in the biological environment *Biomaterials*, 17: 2117-2126.
12. Kovacic P., Osuna J. A. (2000) Mechanisms of Anti-Cancer Agents: Emphasis on Oxidative Stress and Electron Transfer. *Jr. Curr Pharm Des.*, 6: 277-309.
13. Manfait M., Alix A. J., Jeannesson P., Jardillier J. C., Theophanides T. (1982) Interaction of adriamycin with DNA as studied by resonance Raman spectroscopy. *Nucleic Acids Res.*, 10: 3803-3816.
14. Marky L. A., Snyder J. G., Remeta D. P., Breslauer K. J.(1983) Thermodynamics of drug-DNA Interactions. *J Biomol Struct Dyn.*, 1: 487-507.
15. Mohammed I, Al-jawadi E., (2019) Electrochemical Biosensor Hemoglobin Immobilization Determination of the Breast Cancer Drug (Adriamycin). *Raf. J. Sci.*, 28(2):152-163
16. Nafisi F. G. K. S., Azizi E., Zebarjad N., Tajmir-Riahi H.-A. (2007). Interaction of zanamivir with DNA and RNA: Models for drug–DNA and drug–RNA bindings *J. Mol. Struct.* ,830(1-3): 182–187.
17. Osheroff N. (1989) *Effect of antineoplastic agents on the DNA cleavage/religation reaction of eukaryotic topoisomerase II: inhibition of DNA religation by etoposide.* *Biochemistry*, 28: 6157-6160.
18. Ozkan. SA, (2012) *Electroanalytical methods in pharmaceutical analysis and their validation*, HNB Publishing, New York, 1st ed.
19. Pasternack R. F., (2003) circular dichroism and the interactions of water-soluble porphyrins with DNA. *Chirality*, 15: 329-332.
20. Toffoli G., Corona G., Basso B., Boiocchi M. (2004) Pharmacokinetic optimisation of treatment with oral etoposide. *Clin Pharmacokinet.* ,43: 441-466.
21. Uslu B., Canbaz D. (2010) Anodic voltammetry of zolmitriptan at boron-doped diamond electrode and its analytical applications *DiePharm.*, 65: 245-250.
22. Wang J. (1998) *Electroanalytical techniques in clinical chemistry and laboratory medicine*. VCH, New York.

**Table 1.** Optimized conditions for 3.0 nM TPS in PBS at pH 7.0 resulting in a peak resolution with higher current

| Optimum Condition        | Values |
|--------------------------|--------|
| Scan rate (V/s)          | 0.1    |
| Deposition potential (V) | 0.7    |
| End Potential (V)        | 2.0    |
| Start Potential (V)      | -1.5   |
| Voltage step (V)         | 0.008  |
| Equilibration time (s)   | 10     |
| Deposition time (s)      | 5      |

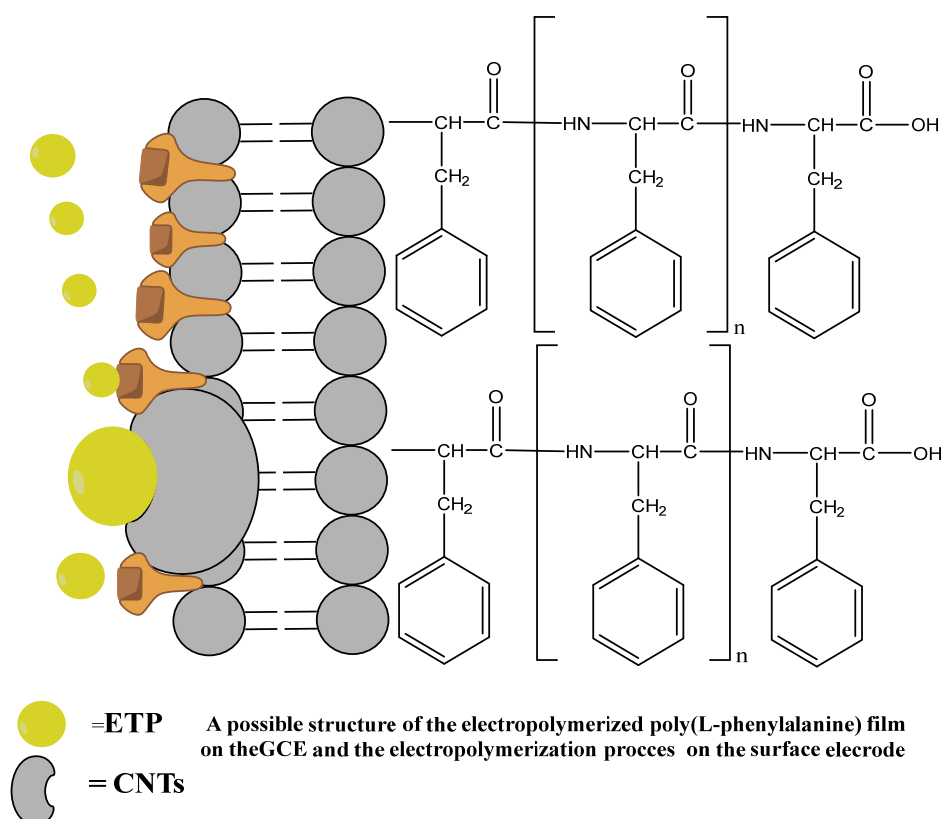


**Figure 1.** The proposed process of the electropolymerization of L-phenylalanine



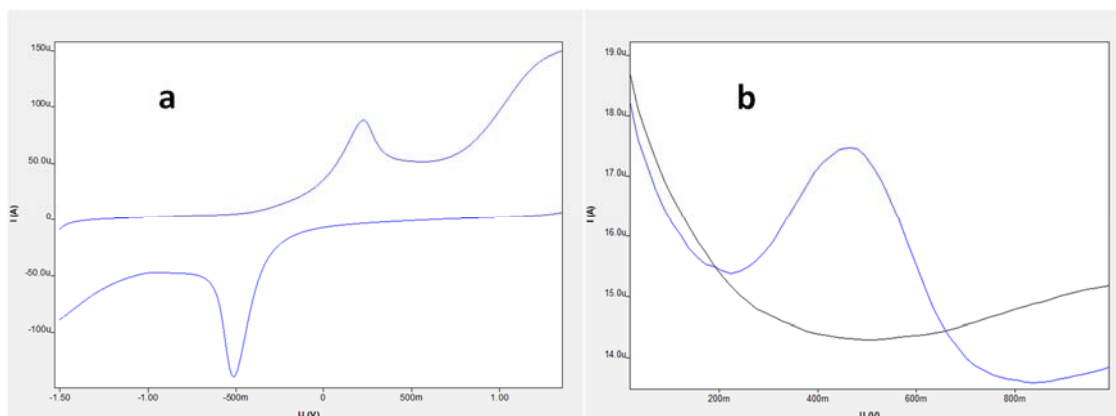


**Figure 2.** a) The cyclic voltammetry of TPS in PBS at pH 7.0 with a scan rate of  $100 \text{ mV} \cdot \text{s}^{-1}$ , b) The square wave voltammetry of TPS in PBS at pH 7.0

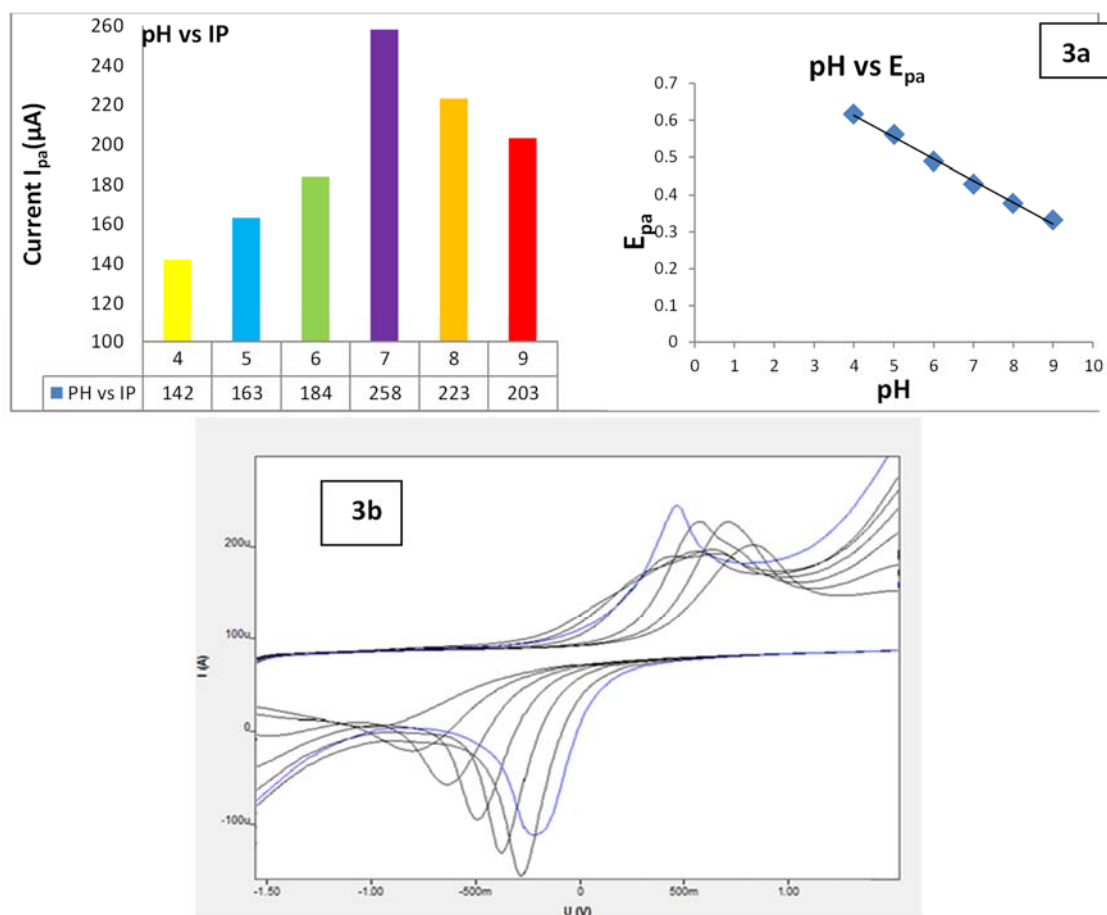


**Figure 3.** a) The influence of pH on TPS peak currents and peak potentials, TPS concentration of  $3.0 \cdot 10^{-9} \text{ M}$ , b) The cyclic voltammogram of TPS in PBS (pH 4.0-9.0)

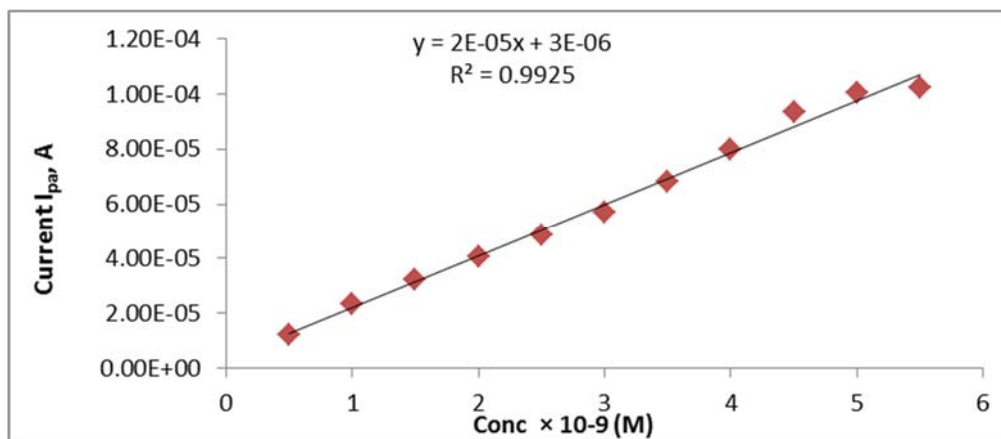


**Figure 4.** The relationship between concentrations of TPS and oxidation current

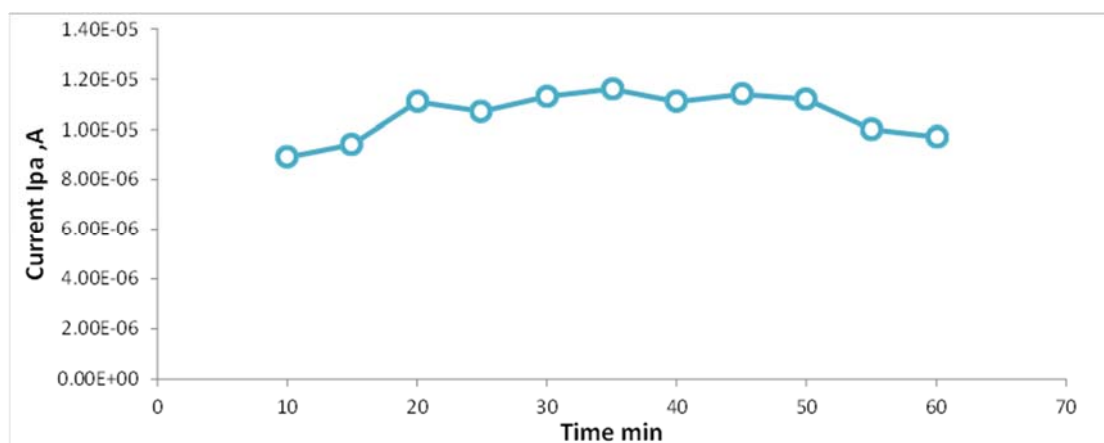


**Figure 5.** The stability of TPS / GCE

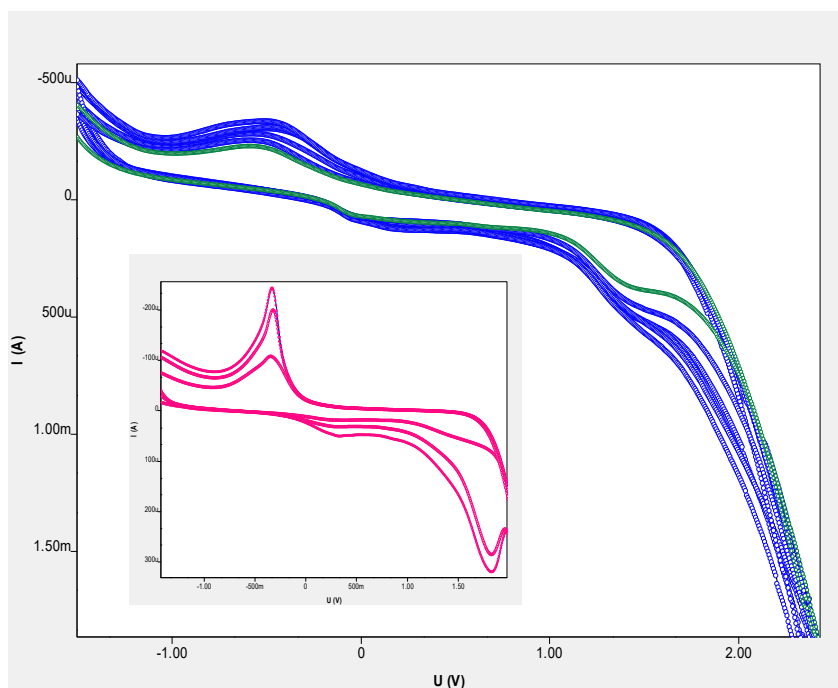


**Figure 6.** The cyclic voltammograms for electropolymerization of L-phenylalanine on a GCE

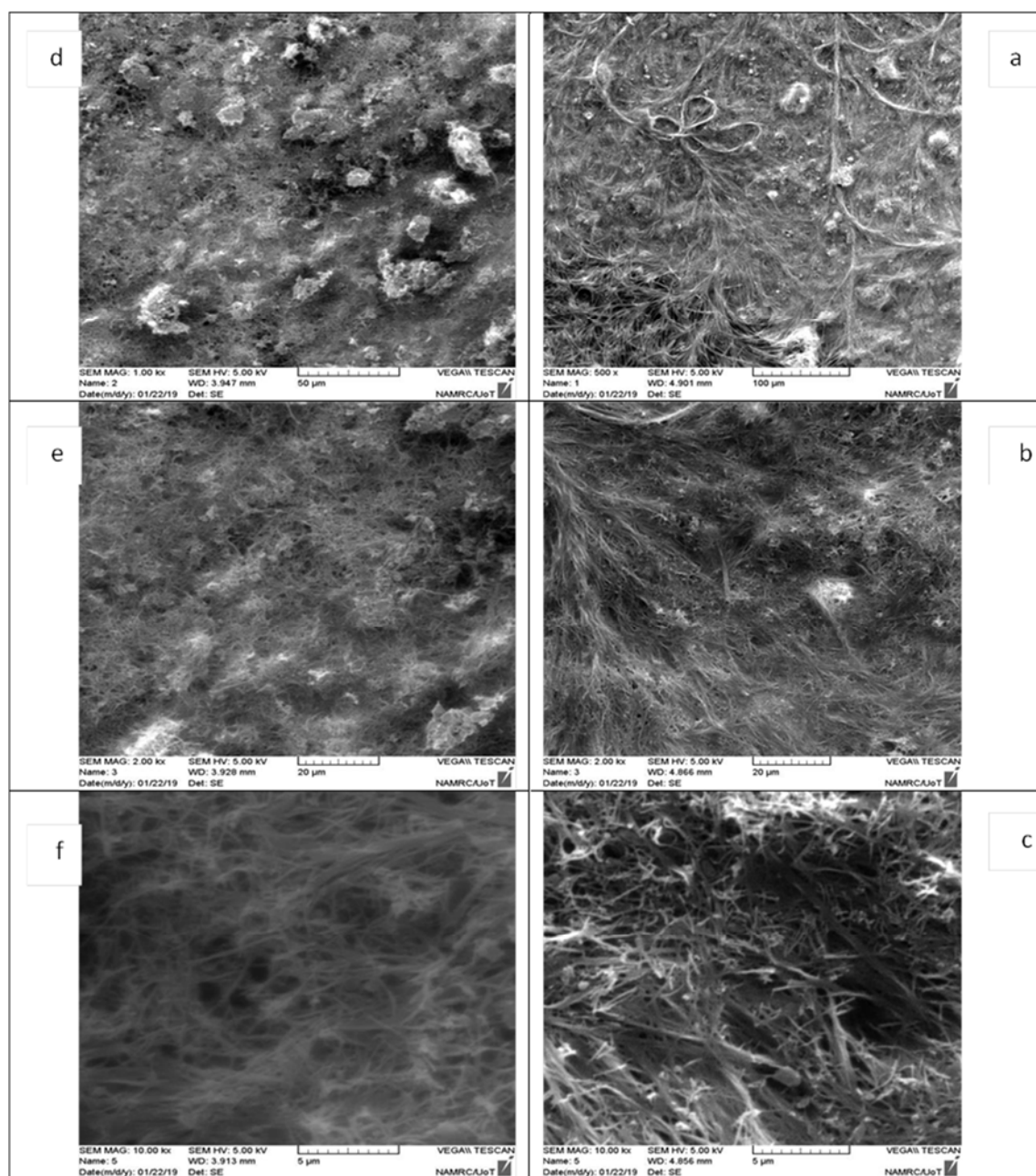


**Figure 7.** The morphology of PPA/GCE&MWCNTs/PPA/GCE characterized by SEM

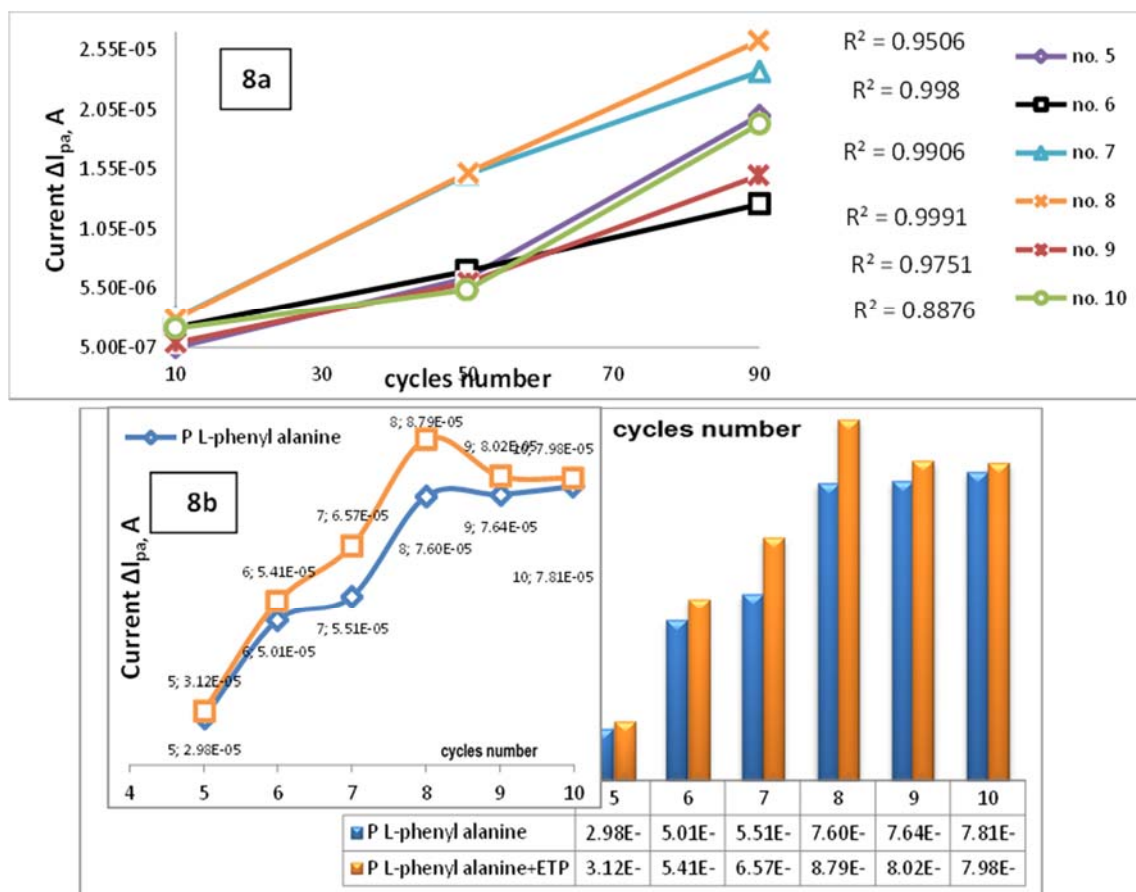


**Figure 8.** a) The correlation between cycle number and the oxidation current of PPA under the effect of concentration (Calibration Curve), b) The correlation between cycle number and the oxidation current of PPA on GCE (blue color), and oxidation current of TPS on PPA/GCE (orange color)

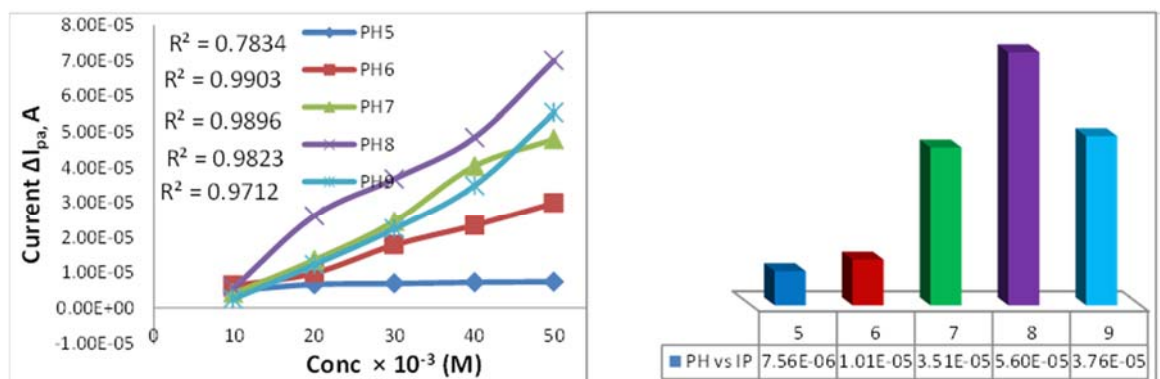


**Figure 9.** The relation between  $I_{pa}/\mu A$  vs. pH

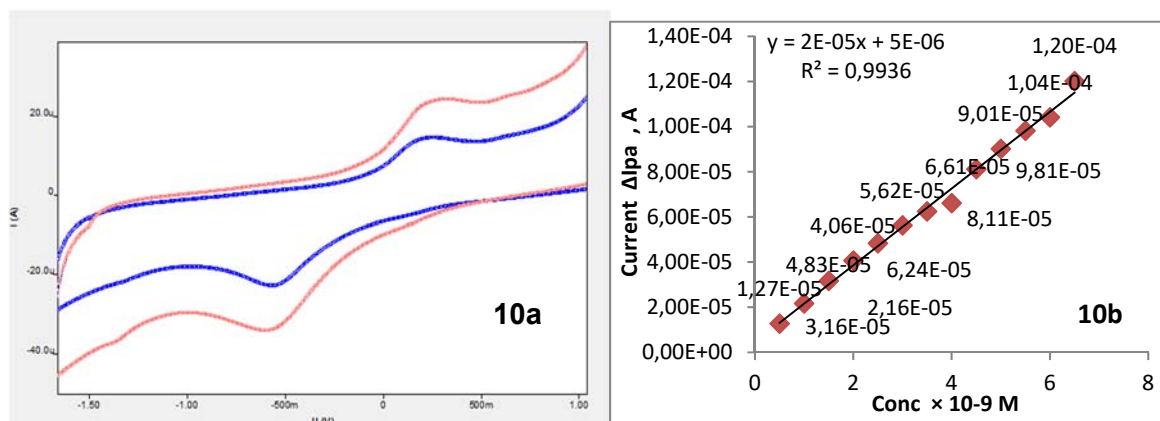


**Figure 10.** a) The Cyclic voltammograms of TPS on bare GCE (a) and PPA modified electrode (b) with 0.2 M PBS (pH 7.0); scan rate of 100 mV s<sup>-1</sup>, b) A plot of concentration of TPS and the oxidation current on PPA/GCE

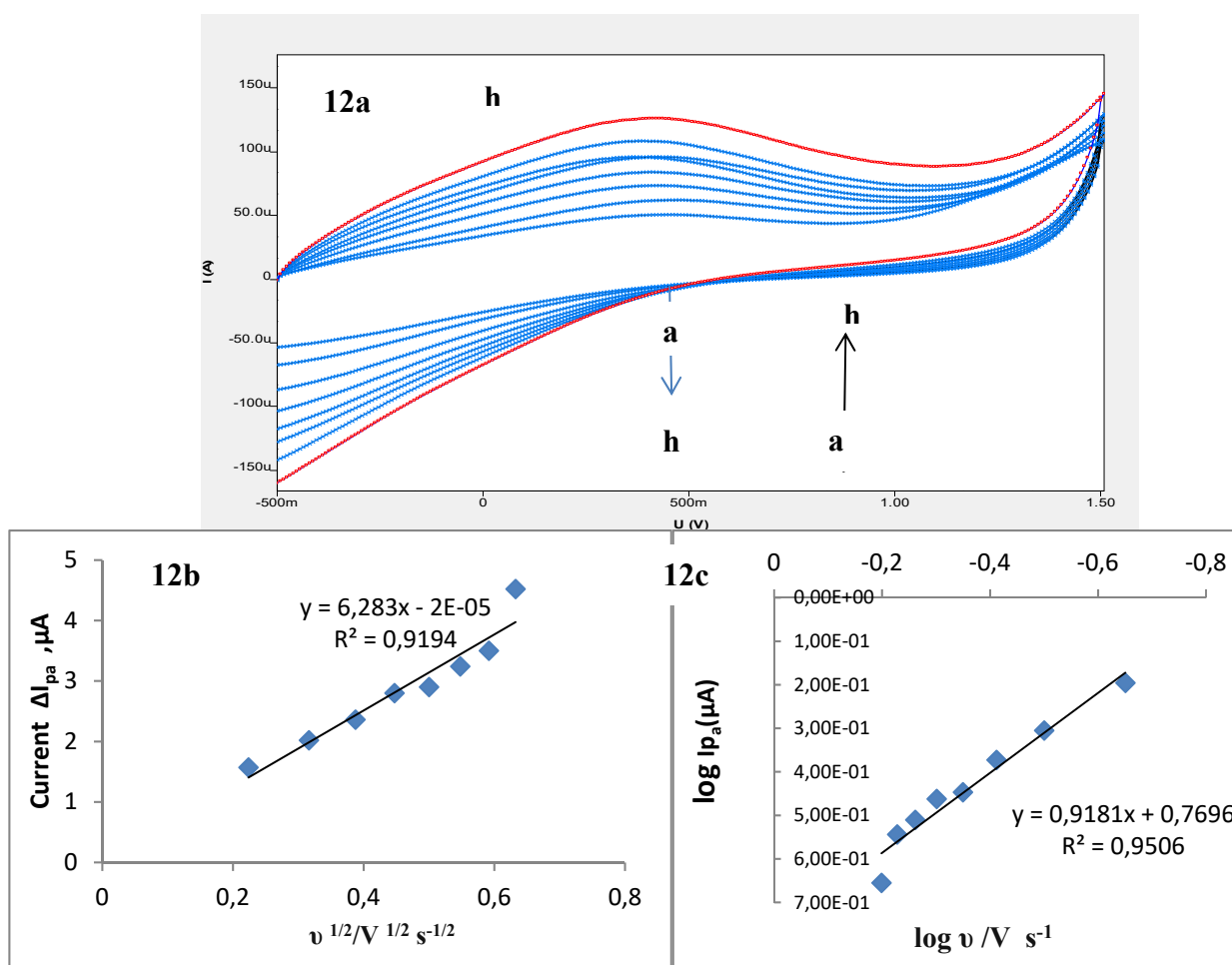


**Figure 11.** a) The cyclic voltammograms for the oxidation of TPS on a GCE at scan rates of (a) 0.05; (b) 0.1; (c) 0.15; (d) 0.2; (e) 0.25; (f) 0.3; (g) 0.35; (h) 0.4 V s<sup>-1</sup>, b) The oxidation currents is correlated with the square root of scan rates, c) Logarithm of oxidation current is correlated with the logarithm of scan rates

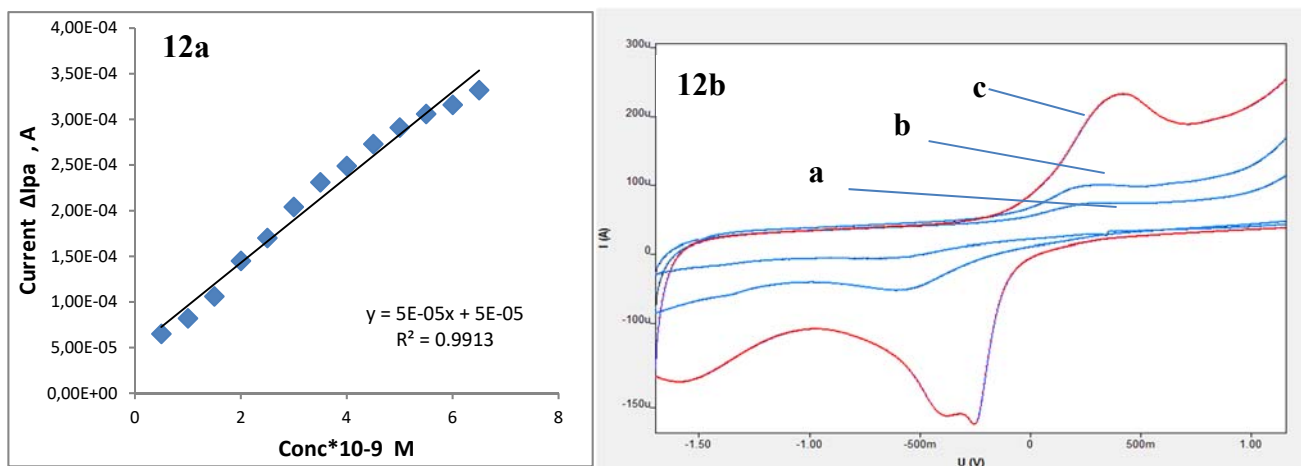


**Figure 12.** a) A plot of oxidation current peak of TPS as a function of the concentration of the TPS on MWCNTs-PPA/GC modified electrode, b) The cyclic voltammograms of TPS on (a) bare GCE (b) PPA modified electrode, (c) and MWCNTs PPA modified electrode with 0.2 M PBS (pH 7.0); scan rate of 100 mV·s<sup>-1</sup>

**MODELAGEM DE PROCESSOS DE DESENVOLVIMENTO DE FISSURAS EM ELEMENTOS COMPOSITOS BASEADOS NOS MODELOS “VIRTUAL CRACK CLOSURE TECHNIQUE” E “COHEZIVE ZONE MODE”****MODELLING OF CRACK DEVELOPMENT PROCESSES IN COMPOSITE ELEMENTS BASED ON VIRTUAL CRACK CLOSURE TECHNIQUE AND COHESIVE ZONE MODEL****МОДЕЛИРОВАНИЕ ПРОЦЕССОВ РАЗВИТИЯ ТРЕЩИН В КОМПОЗИТНЫХ ЭЛЕМЕНТАХ НА ОСНОВЕ МОДЕЛЕЙ VIRTUAL CRACK CLOSURE TECHNIQUE И COHESIVE ZONE MODEL**

LI, Yulong<sup>1\*</sup>; DOBRYANSKIY, Vasilii N.<sup>2</sup>; OREKHOV, Alexander A.<sup>3</sup>;

<sup>1</sup> Northwestern Polytechnical University (NPU), School of Civil Aviation, 127 West Youyi Road, zip code 710072, Beilin District, Xi'an Shaanxi – People's Republic of China

<sup>2</sup> Moscow Aviation Institute (National Research University), Institute of General Engineering Training, 4 Volokolamskoe highway, zip code 125993, Moscow – Russian Federation

<sup>3</sup> Moscow Aviation Institute (National Research University), Institute of General Engineering Education, 4 Volokolamskoe highway, zip code 125993, Moscow – Russian Federation

\* Correspondence author  
e-mail: liyulong@nwpu.edu.cn

Received 15 April 2020; received in revised form 01 July 2020; accepted 15 July 2020

**RESUMO**

Os compósitos de fibra baseados em matrizes poliméricas são um componente essencial na criação da técnica robusta. Devido aos vários fatores, o design da engenharia aeroespacial deve consistir em materiais de alta durabilidade, resistência ao calor e ter outras propriedades qualitativas. Os problemas associados à destruição de compósitos de fibras foram relevantes em todas as etapas do desenvolvimento da tecnologia. A variedade de fibras de reforço e ligantes de polímero, bem como esquemas de reforço, permite controlar direccionalmente a resistência, rigidez, nível de temperatura operacional e outras propriedades dos materiais compósitos poliméricos. Este artigo discute o método de determinação experimental das propriedades mecânicas de materiais compósitos poliméricos à base de fibra de carbono, incluindo a determinação da tenacidade às fissuras entre camadas sob carga sob condições de rasgo, usando o método Direct Bonded Copper (DCB) e a tenacidade às fissuras sob condições de cisalhamento transversal usando o método End-notched flexural test (ENF) e resistência entre camadas. São apresentados os resultados dos testes de amostras de materiais compósitos poliméricos com reforço de carbono com diferentes densidades de superfície. Foi estabelecido que tais características como resistência entre camadas e resistência às fissuras são os parâmetros importantes e determinantes da durabilidade. Foi determinado que o esgotamento da durabilidade de camadas individuais do compósito nem sempre afeta o estado atual de tensão de toda a estrutura e às vezes é difícil de detectar experimentalmente, mas pode afetar significativamente o comportamento adicional do objeto em estudo, desde que a zona de fissura progrida. Foi estabelecida a resistência entre as camadas das amostras com valores experimentais variados. Os dados experimentais foram utilizados para identificar os parâmetros dos modelos de Crack Closure Technique (VVCT) e Cohezive Zone Model (CZM) utilizados para descrever o desenvolvimento de fissuras nos compósitos considerados.

**Palavras-chave:** fibra de carbono, parâmetros de resistência as fissuras, tenacidade às fissuras, resistência entre camadas, polímero.

**ABSTRACT**

Fiber composites based on polymer matrices are promising structural materials that meet high requirements for strength, reliability, durability, and hardness. Therefore, composite materials are widely used as structural materials for aerospace products. The problems associated with the destruction of fiber composites



were relevant at all stages of technology development. A variety of reinforcing fibers and polymer binders, as well as reinforcement schemes, allow directional control of strength, stiffness, level of working temperatures and other properties of polymer composite materials. This article discusses a methodology for experimental determination of the mechanical properties of carbon-based fiber-reinforced polymer composite materials, including the determination of the interlayer fracture toughness under loading under separation conditions using the double-cantilever beam method (DCB) and the fracture toughness under transverse shear conditions using the ENF (End-Notched Flexure) method and interlayer strength. The test results of samples of polymer composite materials with a carbon reinforcing filler with different surface densities are presented. The experimental data were used to identify the parameters of the VCCT (Virtual Crack Closure Technique) and CZM (Cohesive Zone Model) closure models used to describe the development of cracks in the composites under consideration. It was found that the parameters determining the strength of layered composites are such characteristics as interlayer strength and crack resistance. It was found that the decrease in the strength of individual layers of the composite does not always affect the current stress state of the entire structure, which is often difficult to detect experimentally, but can significantly affect the further behavior of the object under study provided that the crack develops further.

**Keywords:** *carbon fiber, crack resistance parameters, fracture toughness, interlayer strength, polymer.*

## АННОТАЦИЯ

Волокнистые композиты на основе полимерных матриц являются перспективными конструкционными материалами, отвечающими высоким требованиям к прочности, надежности, долговечности, твердости. Поэтому композиционные материалы нашли широкое применение в качестве конструкционных материалов для изделий аэрокосмической отрасли. Проблемы, связанные с разрушением волокнистых композитов, были актуальны на всех этапах развития технологии. Разнообразие армирующих волокон и полимерных связующих, а также схемы армирования позволяют направленно контролировать прочность, жесткость, уровень рабочих температур и другие свойства полимерных композиционных материалов. В данной статье рассмотрена методика экспериментального определения механических свойств волокнистых полимерных композиционных материалов на основе углеродных волокон, включающая определение межслоевой вязкости разрушения при нагружении в условиях отрыва по методу двухконсольной балки (DCB – Double Cantilever Beam), вязкости разрушения в условиях поперечного сдвига по методу ENF (End-Notched Flexure) и межслоевой прочности. Приведены результаты испытаний образцов полимерных композиционных материалов с углеродным армирующим наполнителем с различной поверхностной плотностью. Результаты экспериментальных данных использованы для идентификации параметров моделей закрытия виртуальной трещины VCCT (Virtual Crack Closure Technique) и когезионной зоны CZM (Cohesive Zone Model), использованных для описания развития трещин в рассматриваемых композитах. Установлено, что определяющими прочностью слоистых композитов параметрами являются такие характеристики как межслоевая прочность и трещиностойкость. Было установлено, что снижение прочности отдельных слоев композита не всегда влияет на текущее напряженное состояние всей конструкции, что зачастую трудно обнаружить экспериментально, но может существенно повлиять на дальнейшее поведение исследуемого объекта при условии дальнейшего развития трещины.

**Ключевые слова:** *углеродное волокно, параметры трещиностойкости, вязкость разрушения, межслойная прочность, полимер.*

## 1. INTRODUCTION

To create modern aerospace technology, materials with high strength, hardness, heat resistance, corrosion resistance, other characteristics and combinations of these properties are required. Fibre composites based on polymer matrices are promising structural materials since they have good specific characteristics of strength and stiffness. These materials are nowadays increasingly being used as part of aviation, space, transport, and other structures (Babaytsev and Zotov, 2019). This is

due to the requirements for weight efficiency of products, to satisfy which it is necessary to use materials with high levels of specific properties (Naghypour *et al.*, 2011; Krayushkina *et al.*, 2016; Landry and La Plante, 2012). The use of composite materials in the aviation industry significantly reduces the material consumption of structures, increases the material utilisation rate up to 90%, reduces the number of equipment, and dramatically reduces the complexity of manufacturing structures by several times reducing the quantity of parts included in them.

Nonetheless, there are many problems



specific to layered composite materials, which limit their scope (Babaytsev and Zotov, 2019). One of the main issues that arise in the design of structures made of polymer composite materials is ensuring strength under the conditions of prolonged stress and in the conditions of damage development. Notably, essential and determining strength parameters are such characteristics as interlayer strength and fracture toughness (Belnoue *et al.*, 2016; Orlov *et al.*, 2003; Nelson and O'Toole, 2019; Kyanishbayev *et al.*, 2016; Zhang *et al.*, 2019; Krayushkina *et al.*, 2019). For a more accurate assessment of strength and resource characteristics of the material, sophisticated tests are required, including tests targeted at determining the parameters of crack resistance.

To evaluate the stress-strain state of multilayered structures, we can use the final parameter of fracture mechanics can be used – the intensity of energy release –  $G$ . To find this value, the Virtual Crack Closure Technique (VCCT) method is frequently used (Liu and Islam, 2013; Krueger, 2013; Senthil *et al.*, 2013). At the same time, the use of interface elements based on CZM (Cohesive Zone Model) model (Chandra *et al.*, 2002; Skvortsov *et al.*, 2014; Cornec *et al.*, 2003; De Borst, 2003; Yang and Cox, 2005; Xie and Waas, 2006; Harper and Hallet, 2010) makes it possible to study the nucleation and development of stratification without specifying the initial defect and rearrangement of finite element mesh during its propagation. The inclusion of temperature effects was considered in (Formalev *et al.*, 2018; Bulychev and Kuznetsova, 2019; Makarenko and Kuznetsova, 2019; Hnatiuk *et al.*, 2019; Formalev and Kolesnik, 2019; Formalev *et al.*, 2019).

Therefore, resistance to interlayer fracture is a necessary condition for ensuring the solidity and operability of layered composite materials during the operation. Moreover, theoretical and experimental study of crack resistance parameters is an urgent problem of modern composite materials mechanics.

## 2. MATERIALS AND METHODS

The authors examined carbon-polymer composite materials with different surface densities for laying reinforcing filler: 400 g/m<sup>2</sup>, 600 g/m<sup>2</sup>, 800 g/m<sup>2</sup>. Reinforcing filler brand Torey T800, matrix - Poly (bisphenol-A-co-epichlorohydrin) Liquid Epoxy resin (Biphend A type) The characteristics of the materials are presented in Table 1.

To study the interlayer strength, tests were performed on three-point bending samples. Tests were done according to ASTM D2344. The study of interlayer fracture toughness (fracture toughness) under loading for tear conditions under the DCB method was studied according to ASTM D 5528 on rectangular samples with preliminary delamination in the middle plane at one end (ASTM D5528, 2013). This artificial defect initiated further stratification (Chung and Blaser, 1980; Kwatra *et al.*, 2009). White paint and a scale were applied to the side face of each sample, which is required to identify the crack. The load on the sample was transmitted through hinges. Three batches of samples were tested, 10-15 pieces each. Samples were 125 mm long, 25.1 mm wide, and 3.3 – 4.5 mm thick (depending on the batch) (Figure 1).

The fracture toughness under shear conditions was determined pursuant to the ENF method according to ASTM D 7075, as in the experiments described above, on rectangular samples, at one end of which a non-adhesive insert was inserted in the middle plane during production. Three batches were tested, each containing 10 to 15 samples. The simulation of experiments on ASTM D 5528 (ASTM D5528, 2013) and ASTM D 7905 (ASTM D7905, 2013) was done using software packages Simulia ABAQUS and Ansys. The methods used were the VCCT (Virtual Crack Closure Technique) and CZM (Cohesive Zone Model). The samples were modelled as deformable three-dimensional bodies consisting of two parts of equal thickness.

The virtual crack technique (VCCT) uses the principles of linear mechanics of elastic fracture and, therefore, is suitable for tasks in which brittle crack propagation occurs along predetermined surfaces. The VCCT technique is based on the assumption that the strain energy released when a crack increases by a certain amount is the same as the energy needed to close a crack by the same value. A “surface-to-surface” contact was fixed between the two halves. The bundle formation zone was modeled using the VCCT element. To simulate tests according to ASTM D 7905, the procedure described above was also applied, except the boundary conditions (ASTM D7905, 2013). Here the sample was tested for three-point bending.

Tests on the separation and simulations using the CZM models. The Cohesive Zone Model (CZM) is based on the assumption that the ability to transfer stress between two separated faces when they are separated from each other is not

entirely lost, but instead becomes a progressive event, determined by a gradual deterioration in the rigidity of the interlayer surface. A strong point of the CZM method: a model using the CZM predicts the beginning and describes the delamination process without having to accept the assumption that there is a small supposed crack. Weak points: the need for data that can only be obtained from a complex set of experiments, as well as high sensitivity to input parameters, required fine mesh. The simulation of the experiment was carried out in a flat setting. The sample was modelled, consisting of two parts of identical thickness.

### 3. RESULTS AND DISCUSSION:

According to tests, it was established that the interlayer strength of the samples was 37 MPa (400 g/m<sup>2</sup>), 35 MPa (600 g/m<sup>2</sup>), 57 MPa (800 g/m<sup>2</sup>) with a variation of experimental values not more than 10%. The test results of ASTM D 5528 for determining the fracture toughness under shear conditions are shown in Figure 2 and Table 2 (ASTM D5528, 2013). Test results of ASTM D 7905 to determine fracture toughness in terms of the separation are presented in Figure 2b and Tables 3, and 4 (ASTM D7905, 2013). The calculation, according to ASTM, was done by several methods: Modified Beam Theory (MBT) Method, Compliance Calibration (CC) Method, Modified Compliance Calibration (MCC) Method.

Simulation of experiments implemented according to the methods of VCCT and CZM provides a good comparison with the experiment, but only from the beginning of the growth of the separation. It was not possible to predict further stratification growth using the applied techniques. For example, a result of the calculation by the model CZM rendered the following dependency (Figure 3).

The model of the cohesive zone is susceptible to input parameters. For solution within the framework of this model, it is essential to know the crack resistance parameters, which can only be learned from the experiment on individual samples by specific methods. This model also requires a fine mesh and thorough adjustment of the solver.

### 4. CONCLUSIONS:

As part of the research, an experimental and theoretical study of mechanical properties of composite materials reinforced with carbon filler

was carried out. A feature of the deformation of spatial structures made of composite materials is the possibility of the occurrence of not only cracks due to rupture of fibres and matrix material, but also the formation of delamination zones during deformation. As a result, a technique was developed for doing CRFP tests aimed at studying the interlayer strength, determining the specific work of stratification in conditions of the GIC separation using the DCB method, and under transverse shear conditions GIIC using the ENF method. An experimental base was developed; practical recommendations were arranged for further research. Samples of carbon fibre with different densities of reinforcing filler were tested.

As a result of experimental tests, it was found that the interlayer strength of the samples is 37 MPa (400 g/m<sup>2</sup>), 35 MPa (600 g/m<sup>2</sup>), 57 MPa (800 g/m<sup>2</sup>) with a variation of experimental values of not more than 10%. The experimental data were compared with models of processes of appearance and development of cracks in the finite element complexes ABAQUS and Ansys based on VCCT models, cohesive elements. Using the VCCT model, it was possible to obtain only the critical load of the start of the first crack, further stratification using this model could not be modelled, the results obtained did not correlate with experimental data at all.

The cohesion area model is susceptible to input parameters. To solve within the framework of this model, it is necessary to know the crack resistance parameters, which can only be learned from experiments on individual samples by specific methods. This model also requires a fine mesh and thorough adjustment of the solver. Within the framework of this model, it was possible to track the appearance of the first crack, and also to trace further development of the crack within the first three growth stages with an acceptable error.

### 5. ACKNOWLEDGMENTS:

This work was supported by the grant of the Russian Science Foundation (project No. 17-79-20105) in Moscow Aviation Institute.

### 6. REFERENCES:

1. ASTM D5528. (2013). Retrieved from <https://www.astm.org/Standards/D5528>
2. ASTM D7905. (2013). Retrieved from <https://www.astm.org/Standards/D790-RUS.htm>

3. Babaytsev, A.V., and Zotov, A.A. (2019). Designing and calculation of extruded sections of an inhomogeneous composition. *Russian Metallurgy (Metally)*, 2019(13), 1452-1455. DOI: 10.1134/S0036029519130020.
4. Belnoue, J.P.-H., Giannis, S., Dawson, M., Hallett, S.R. (2016) Cohesive/adhesive failure interaction in ductile adhesive joints Part II: Quasi-static and fatigue analysis of double lap-joint specimens subjected to through-thickness compressive loading. *International Journal of Adhesion and Adhesives*, 68, 369-378.
5. Bulychev, N.A., and Kuznetsova, E.L. (2019). Ultrasonic application of nanostructured coatings on metals. *Russian Engineering Research*, 39(9), 809-812.
6. Chandra, N., Scheider, I., and Ghomen, K.H. (2002). Some issues in the application of cohesive zone models for metal-ceramic interfaces. *International Journal of Solids and Structures*, 39(11), 2827-2855.
7. Chung, J.Y., and Blaser, D.A. (1980). Transfer function method of measuring induct acoustic properties. I. Theory. *Journal of acoustical society of America*, 68(3), 907-913. DOI: 10.1121/1.384778
8. Cornec, A., Scheider, I., and Schwalbe, K.H. (2003). On the practical application of the cohesive model. *Engineering Fracture Mechanics*, 70, 1963-1987.
9. De Borst, R. (2003). Numerical aspects of cohesive zone models. *Engineering Fracture Mechanics*, 70, 1743-1757.
10. Formalev, V.F., and Kolesnik, S.A. (2019). On thermal solitons during wave heat transfer in restricted areas. *High Temperature*, 57(4), 498-502.
11. Formalev, V.F., Kolesnik, S.A., and Kuznetsova, E.L. (2019). Effect of components of the thermal conductivity tensor of heat-protection material on the value of heat fluxes from the gas-dynamic boundary layer. *High Temperature*, 57(1), 58-62.
12. Formalev, V.F., Kolesnik, S.A., and Selin, I.A. (2018). Local non-equilibrium heat transfer in an anisotropic half-space affected by a non-steady state point heat source. *Herald of the Bauman Moscow State Technical University, Series Natural Sciences*, 80(5), 99-111.
13. Harper, P.W., and Hallet, S.R. (2010). A fatigue degradation law cohesive interface element – Development and application to composite materials. *International Journal of Fatigue*, 32(11), 1774-1787.
14. Hnatiuk, K.I., Dinzhos, R.V., Simeonov, M.S., Alekseev, A.N., Alekseev, S.A., Sirko, V.V., Zabashta, Yu.F., Koseva, N.S., and Lazarenko, M.M. (2019). Melting of 1-octadecene inside the pores of open-morphology silica gel: thermodynamic model and experimental studies. *Journal of Thermal Analysis and Calorimetry*. DOI: 10.1007/s10973-019-09133-4. Retrieved from <https://link.springer.com/article/10.1007/s10973-019-09133-4>
15. Krayushkina, K., Khymeryk, T., and Bieliatynskiy, A. (2019). Basalt fiber concrete as a new construction material for roads and airfields. *IOP Conference Series: Materials Science and Engineering*, 708, Article number 012088.
16. Krayushkina, K., Prentkovskis, O., Bieliatynskiy, A., Giginishvili, J., Skrypchenko, A., Laurinavičius, A., Gopalakrishnan, K., and Tretjakovas, J. (2016). Perspectives on using basalt fiber filaments in the construction and rehabilitation of highway pavements and airport runways. *Baltic Journal of Road and Bridge Engineering*, 11(1), 77-83.
17. Krueger, R. (2013). The virtual crack closure technique: history, approach, and applications. *Applied Mechanics Reviews*, 57(1-2), 109-143.
18. Kwatra, N., Su, J., Gretarsson, J.T., and Fedkiw, R. (2009). A method for avoiding the acoustic time step restriction in compressible flow. *Journal of Computational Physics*, 228, 11, 4146-4161.
19. Kyanishbayev, S.B., Umbetov, A.U., Duisebekova, A.E., Umbetova, M.Z., Schongalova, K.S., Akhatova, Z.E., Azhibekova, P.S., and Sokabayeva, A.S. (2016). Interference of spherical laser radiation in a crystalline compound lens. *International Journal of Environmental and Science Education*, 11(18), 11593-11610.

20. Landry, B., and La Plante, G. (2012). Modeling delamination growth in composites under fatigue loadings of varying amplitudes. *Composites Part*, 43(2), 533–541.
21. Liu, P.F., and Islam, M.M. (2013). A nonlinear cohesive model for mixed-mode delamination of composite laminates. *Composite Structure*, 106, 47-56.
22. Makarenko, A.V., and Kuznetsova, E.L. (2019). Energy-efficient actuator for the control system of promising vehicles. *Russian Engineering Research*, 39(9), 776-779.
23. Naghipour, P., Bartch, M., and Vonggenreiter, H. (2011). Simulation and experimental validation of mixed mode delamination in multidirectional CF/PEEK laminates under fatigue loading. *International Journal of Solids and Structures*, 48, 1070–1081.
24. Nelson, S.M., and O'Toole, B.J. (2018) Computational analysis of blast loaded composite cylinders. *International Journal of Impact Engineering*, 119, 26-39.
25. Orlov, A.M., Skvortsov, A.A., and Litvinenko, O.V. (2003). Bending vibrations of semiconductor wafers with local heat sources. *Technical Physics*, 48(6), 736-741.
26. Senthil, K., Arockiarajan, A., Palaninathan, R., Santhosh, B., and Usha, K.M. (2013). Defects in composite structures: Its effects and prediction methods – A comprehensive review. *Composite Structure*, 106, 139-149.
27. Skvortsov, A.A., Kalenkov, S.G., and Koryachko, M.V. (2014). Phase transformations in metallization systems under conditions of nonstationary thermal action. *Technical Physics Letters*, 40(9), 787-790.
28. Xie, D., and Waas, A.M. (2006). Discrete cohesive zone model for mixed-mode fracture using finite element analysis. *Engineering Fracture Mechanics*, 73, 1783-1796.
29. Yang, Q.D., and Cox, B.N. (2005). Cohesive models for damage evaluation in laminated composites. *International Journal of Fracture*, 133, 107-137.
30. Zhang, W., Jiang, W., Yu, Y., Zhou, F., Luo, Y., and Song, M. (2019) Fatigue crack simulation of the 316L brazed joint using the virtual crack closure technique. *International Journal of Pressure Vessels and Piping*, 173, 20-25.

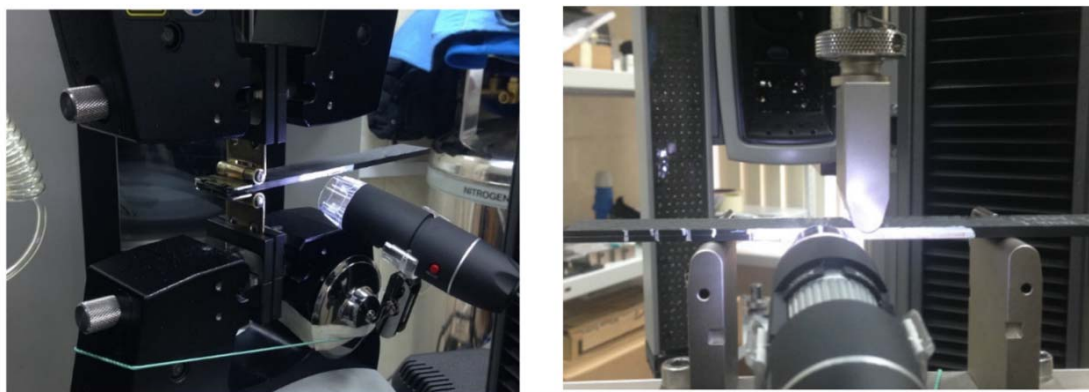
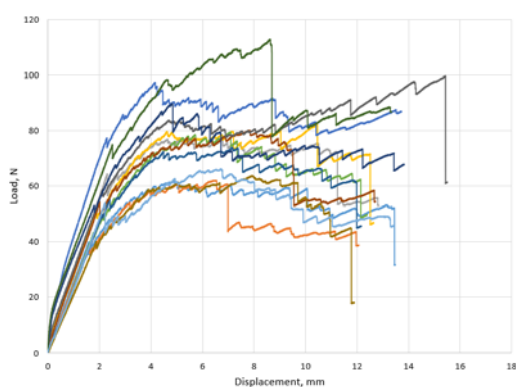
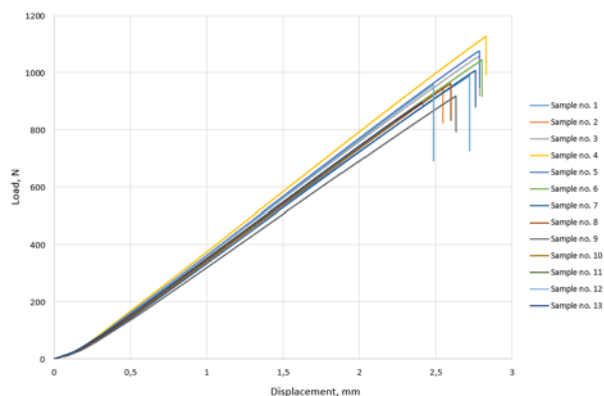


**Figure 1.** The test process according to ASTM D5528 (2013) and ASTM D7905 (2013)



a



b

**Figure 2.** a: Test results for determining fracture toughness under the separation conditions (example for samples of  $600 \text{ g/m}^2$ ), b: Test results for determining of fracture toughness under conditions of shear (example for samples of  $800 \text{ g/m}^2$ )

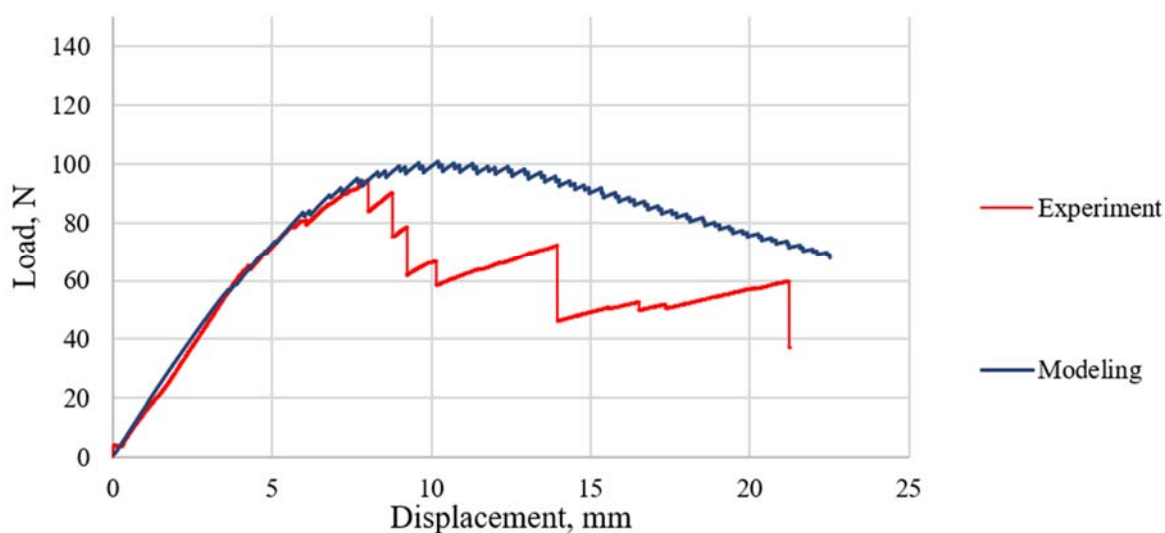


**Figure 3.** Simulations of the delamination process by CZM method

**Table 1.** Mechanical properties of the materials used

| Sample Type          | $E_1$<br>[ kgf / mm <sup>2</sup> ] | $E_2$<br>[ kgf / mm <sup>2</sup> ] | $E_3$<br>[ kgf / mm <sup>2</sup> ] | $G_{12, 13, 23}$ [ kgf / mm <sup>2</sup> ] |     |
|----------------------|------------------------------------|------------------------------------|------------------------------------|--|-----|
| 400 g/m <sup>2</sup> | 6500                               | 6500                               | 800                                | 0.3  | 450 |
| 600 g/m <sup>2</sup> | 7130                               | 7130                               | 800                                | 0.3  | 450 |
| 800 g/m <sup>2</sup> | 7105                               | 7105                               | 800                                | 0.3  | 450 |

**Table 3.** The results of tests for determining fracture toughness in conditions of the separation

| Sample                       | MBT [ kgf / mm ] | MBT corrected [ kgf / mm ] | SS [ kgf / mm ] | MCC [ kgf / mm ] | Min [ kgf / mm ] | Load [ kgf ] |
|------------------------------|------------------|----------------------------|-----------------|------------------|------------------|--------------|
| <b>400 g/m<sup>2</sup></b>   |                  |                            |                 |                  |                  |              |
| Min                          | 0.072            | 0.053                      | 0.053           | 0.054            | 0.053            | 7.411        |
| Max                          | 0.112            | 0.088                      | 0.086           | 0.090            | 0.086            | 11.597       |
| Middle                       | 0.088            | 0.066                      | 0.065           | 0.068            | 0.064            | 9.003        |
| The coefficient of variation | 16.01 %          | 16.37 %                    | 15.59 %         | 15.35 %          | 15.95 %          | 15.80 %      |
| Standard deviation           | 0.014            | 0.011                      | 0.010           | 0.010            | 0.010            | 1.422        |
| <b>600 g/m<sup>2</sup></b>   |                  |                            |                 |                  |                  |              |
| Min                          | 0.050            | 0.048                      | 0.048           | 0.051            | 0.048            | 5.065        |
| Max                          | 0.090            | 0.085                      | 0.086           | 0.147            | 0.085            | 7.073        |
| Middle                       | 0.073            | 0.065                      | 0.067           | 0.077            | 0.065            | 6.144        |
| The coefficient of variation | 15.48 %          | 18.76 %                    | 16.29 %         | 31.09 %          | 18.71 %          | 10.10 %      |
| Standard deviation           | 0.011            | 0.012                      | 0.011           | 0.024            | 0.012            | 0.621        |
| <b>800 g/m<sup>2</sup></b>   |                  |                            |                 |                  |                  |              |
| Min                          | 0.034            | 0.032                      | 0.029           | 0.029            | 0.029            | 5.303        |
| Max                          | 0.069            | 0.062                      | 0.051           | 0.052            | 0.051            | 9.779        |
| Middle                       | 0.052            | 0.048                      | 0.041           | 0.042            | 0.041            | 7.223        |
| The coefficient of variation | 20.88 %          | 19.60 %                    | 17.44 %         | 16.14 %          | 17.44 %          | 18.78 %      |
| Standard deviation           | 0.011            | 0.009                      | 0.007           | 0.007            | 0.007            | 1.356        |

**Table 4.** Test results for determining fracture toughness under shear conditions

| Sample label                 | G <sub>2</sub> C [ kgf / mm ] | G <sub>2</sub> C* [ kgf / mm ] | P [ kgf ] | P* [ kgf ] |
|------------------------------|-------------------------------|--------------------------------|-----------|------------|
| <b>400 g/m<sup>2</sup></b>   |                               |                                |           |            |
| Min                          | 0.06                          | 0.053                          | 58,953    | 69,998     |
| Max                          | 0.085                         | 0.135                          | 71,523    | 111,926    |
| Middle                       | 0.074                         | 0.090                          | 65,865    | 80,143     |
| The coefficient of variation | 10.90 %                       | 27.11 %                        | 6.63 %    | 14.93 %    |
| Standard deviation           | 0.008                         | 0.024                          | 4,369     | 11,964     |
| <b>600 g/m<sup>2</sup></b>   |                               |                                |           |            |
| Min                          | 0.090                         | 0.127                          | 48,743    | 57,810     |
| Max                          | 0.137                         | 0.203                          | 56,515    | 69,632     |
| Middle                       | 0.109                         | 0.161                          | 52,890    | 66,096     |
| The coefficient of variation | 9.94 %                        | 13.75 %                        | 4.93 %    | 5.29 %     |
| Standard deviation           | 0.011                         | 0.022                          | 2,606     | 3,497      |
| <b>800 g/m<sup>2</sup></b>   |                               |                                |           |            |
| Min                          | 0.06                          | 0.044                          | 73,423    | 73,423     |
| Max                          | 0.169                         | 0.1                            | 114,840   | 103,041    |
| Middle                       | 0.115                         | 0.073                          | 96,491    | 86,913     |
| The coefficient of variation | 23.05 %                       | 22.19 %                        | 12.16 %   | 9.88 %     |
| Standard deviation           | 0.027                         | 0.016                          | 11,730    | 8,585      |

## DEFINIÇÃO DE DEFORMAÇÕES NA ESTRUTURA COMPOSTA DE GRADE SOB A AÇÃO DE CARGAS COMPRESSIVAS

## DETERMINATION OF DEFORMATION IN MESH COMPOSITE STRUCTURE UNDER THE ACTION OF COMPRESSIVE LOADS

## ОПРЕДЕЛЕНИЕ ДЕФОРМАЦИИ В СЕТЧАТОЙ КОМПОЗИТНОЙ КОНСТРУКЦИИ ПРИ ДЕЙСТВИИ СЖИМАЮЩИХ НАГРУЗОК

OREKHOV, Alexander A.<sup>1\*</sup>; UTKIN, Yuri A.<sup>2</sup>; PRONINA, Polina F.<sup>3</sup>;

<sup>1</sup> Moscow Aviation Institute (National Research University), Institute of General Engineering Education, 4 Volokolamskoe highway, zip code 125993, Moscow – Russian Federation

<sup>2</sup> Moscow Aviation Institute (National Research University), Department of Engineering Graphics, 4 Volokolamskoe highway, zip code 125993, Moscow – Russian Federation

<sup>3</sup> Moscow Aviation Institute (National Research University), Institute of Aerospace, Department of Managing Exploitation of Space-Rocket Systems, 4 Volokolamskoe highway, zip code 125993, Moscow – Russian Federation

\* Corresponding author  
e-mail: [lsk.orekhov@gmail.com](mailto:lsk.orekhov@gmail.com)

Received 16 March 2020; received in revised form 29 May 2020; accepted 15 July 2020

### RESUMO

Uma das tecnologias inovadoras importantes é a criação de estruturas de grande porte que funcionam por um longo período no espaço e atendem a restrições rigorosas das características gerais de massa. Entre essas estruturas, em primeiro lugar, está a seção de treliças de suporte de carga. Este artigo apresenta os resultados de estudos experimentais de compressão das seções de treliças de suporte de carga na estrutura de grade. Recentemente, os invólucros cilíndricos de grade compostos são usados como carcaças de naves espaciais. O invólucro de grade é uma estrutura de suporte à qual os instrumentos e mecanismos da espaçonave estão conectados. A seção de treliça de suporte é feita do material compósito de polímero da estrutura de grade usando fibras de carbono. O objetivo dos testes é confirmar a possibilidade de criar uma estrutura de grade leve usando um material compósito de polímero reforçado com fibra de carbono. Para atingir esse objetivo, os autores definiram as seguintes tarefas: escolher o preenchimento de carbono de materiais compósitos de polímeros (MCP); escolher os ligantes de MCP, determinar o grau de reforço de fibra de carbono; escolher o número e trajetórias de orientação das nervuras em espiral, o número de nervuras anulares e o tamanho das nervuras individuais. Para teste, foi desenvolvida a "Instalação para teste da treliça de suporte". Como resultado da pesquisa, são obtidos os indicadores calculados para garantir a capacidade de carga e a rigidez sob a aplicação de carga compressiva axial. Simultaneamente com a determinação da capacidade de carga, as características de deformação da estrutura são determinadas duas vezes para confirmar sua repetibilidade, bem como a natureza linear da dependência de deformações axiais e radiais como resultado da carga aplicada.

**Palavras-chave:** *tetronamotka, fibra de carbono, treliça de suporte, nave espacial, lançador de foguetes.*

### ABSTRACT

One of the significant innovative technologies is the creation of large-sized structures that work for a long time in space and meet stringent restrictions on overall mass characteristics. Among these structures, in the first place, is the section of bearing truss (BT). This article presents the results of experimental studies of sectors of load-bearing trusses of mesh design for compression. Recently, composite mesh cylindrical shells are used as spacecraft housings. The mesh shell is a supporting structure to which the instruments and mechanisms of the spacecraft are attached. The truss section is made of cross-linked polymer composite material with carbon fibers. The objective of the tests is to confirm the possibility of creating a lightweight mesh construction using a carbon fiber reinforced polymer composite material. To achieve this goal, the authors were assigned the following tasks: selection of carbon filler of polymer composite materials (PCM); selection of PCM binder; determination of the



degree of carbon fiber reinforcement; choice of the number and orientation paths of spiral ribs, number of ring ribs and the sizes of individual ribs. As a result of the research, the calculated indicators for ensuring the bearing capacity and stiffness under the application of axial compressive load were obtained. At the same time, with the determination of bearing capacity, the deformation characteristics of the structure were twice determined in order to confirm their repeatability, as well as linear nature of the dependence of axial and radial deformations as a result of the applied load.

**Keywords:** *tetra-winder, carbon fiber, bearing truss, spacecraft, rocket launcher.*

## АННОТАЦИЯ

Одной из важных инновационных технологий является создание крупногабаритных конструкций, длительное время работающих в условиях космического пространства и отвечающих жестким ограничениям по габаритно-массовым характеристикам. К числу таких конструкций, в первую очередь, относится секция несущих ферм (НФ). В данной статье приведены результаты экспериментальных исследований секций несущих ферм сетчатой конструкции на сжатие. В последнее время композитные сетчатые цилиндрические оболочки находят применение в качестве корпусов космических аппаратов. Сетчатая оболочка является несущей конструкцией, к которой присоединяются приборы и механизмы космического аппарата. Секция несущей фермы изготовлена из полимерного композиционного материала сетчатой конструкции с использованием углеродных волокон. Целью испытаний является подтверждение возможности создания облегченной сетчатой конструкции с использованием полимерного композиционного материала, армированного углеродным волокном. Для достижения поставленной цели перед авторами были поставлены такие задачи: выбор углеродного наполнителя полимерных композиционных материалов (ПКМ); выбор связующего ПКМ, определение степени армирования углепластика; выбор количества и траекторий ориентации спиральных ребер, количества кольцевых ребер и размеров индивидуальных ребер. Для проведения испытаний была разработана «Установка для испытаний несущей фермы». В результате исследований получены расчетные показатели по обеспечению несущей способности и жесткости в условиях приложения осевой сжимающей нагрузки. Одновременно с определением несущей способности дважды определяются деформационные характеристики конструкции с целью подтверждения их повторяемости, а также линейного характера зависимости осевых и радиальных деформаций в результате действия приложенной нагрузки.

**Ключевые слова:** *тетрамотка, углеродное волокно, несущая ферма, космический аппарат, ракетный носитель.*

## 1. INTRODUCTION:

One of the essential innovative technologies is the creation of large-sized structures that work for a long time in space and meet stringent restrictions on overall mass characteristics. Among these structures, in the first place, is the section of bearing truss (BT). For the production of a section truss of structural carbon fiber, the technology of tetra-winding can be effectively used, which allows one to obtain cylindrical compartments that withstand intense compressive loads. This design has high bending stiffness and compressive strength in combination with reduced weight (Berezovskii *et al.*, 2015; Babaytsev *et al.*, 2017a; Varsavas and Kaynak, 2018).

To increase rigidity, BT design provides reinforcing axial stringers (longitudinal ribs) in four planes along four ribs, as well as ending flanges made in a single technological winding cycle together with mesh shell. These problems

were considered in detail in (Antufev *et al.*, 2019a; Antufev *et al.*, 2019d; Antufev *et al.*, 2019c; Bodryshev *et al.*, 2019; Zhavoronok *et al.*, 2019; Rabinskiy and Tushavina, 2019; Dmitriev *et al.*, 2011).

The section of bearing truss (BT) is one of the structures that have been operating for a long time in outer space conditions and meet stringent restrictions on overall mass characteristics. Power elements of the design of spacecraft stages, interstage compartments, propulsion systems, space tug support frames, spacecraft, and space platforms are traditionally made in the form of frame-tubular shells from various alloys (aluminum, titanium), as well as stainless steel (Babaytsev *et al.*, 2017a; Babaytsev *et al.*, 2017b; Antufev *et al.*, 2019a; Antufev *et al.*, 2019b; Babaytsev and Zotov, 2019; Sevryukova *et al.*, 2012). In recent years, both in foreign and domestic practice, non-metallic composite materials reinforced with glass, organic, or carbon fibers have become increasingly used to reduce



the mass characteristics of structures for space constructions (Berezovskii *et al.*, 2015; Kyanishbayev *et al.*, 2016; Suprun *et al.*, 2018; Babaytsev *et al.*, 2017a; Babaytsev *et al.*, 2017b; Koshoridze *et al.*, 2017; Babaytsev and Zotov, 2019; Babaytsev *et al.*, 2019). Some examples are the following:

- mesh shells of transition compartments made of organoplastic having unidirectional reinforcement with the technology of continuous winding of the thread on forming tooling;

- conical adapters and cylindrical power truss of spacecraft and space platforms in the form of wire-mesh shells made of carbon fiber reinforced with high-strength carbon fiber.

As practice demonstrates, the use of composites provides a more than twofold decrease in the characteristics of the load-bearing elements of power frames and trusses in comparison with metal structures with the same levels of bearing capacity, rigidity, and stability of shells. Production capabilities make it possible to create large enough products with a diameter of more than 2 meters and a length of more than 6 meters with the appropriate refinement of the process and technological equipment (Golushko and Semisalov, 2015; Pintossi *et al.*, 2019).

## 2. MATERIALS AND METHODS:

As applied to the section of bearing truss (BT) of spacecraft, the smallest weight characteristics can be realized using PCM reinforced with both aramid and carbon fibers, however, taking into account rather high levels of radiation exposure, requirements for a long-term stay of the product in open space and higher stiffness characteristics, preference ought to be given to carbon fiber structures (Umbetov *et al.*, 2016; Mustafin, 2006).

Polymer composite materials are understood as multicomponent materials consisting of a plastic base (matrix), which is reinforced with fillers that have high strength and rigidity. The properties of the new material quantitatively and qualitatively differ from the properties of each of its components. By changing the composition of the matrix and the filler, their ratio, the orientation of the filler, a wide range of materials with the desired set of properties is obtained. The use of polymer composite materials can reduce the mass of the structure while maintaining or improving its mechanical features.

The use of PCMs based on glass, polymer,

carbon, and ceramic fibers is currently directly related to progress in rocket science, aviation, automotive, shipbuilding, mechanical engineering, construction (Tokiwa *et al.*, 2009; Farhadinia, 2014). The properties of PCMs depend on the choice of the initial components and their ratio, the interaction between them, the method and technological conditions for manufacturing the product (pressure, temperature, time), additional processing of the product, and a number of other factors. The determining factor in creating a PCM is the interaction and mutual influence of components at the fiber-matrix interface (binder). The higher the required properties of the PCM created for structural use, the more complex the set of requirements must be maintained when choosing the source components (Gattringer *et al.*, 2019; Mishra *et al.*, 2019; Hao *et al.*, 2019). The final characteristics of carbon-epoxy composites are strongly influenced by the chemical structure of the epoxy resin, its properties, and curing conditions. Improving the adhesive characteristics is achieved by creating a covalent chemical bond at the interface as a result of surface treatment of the fibers and modification of the composition of the binder (Alosime, 2019; Kumar, 2019). The mesh structure consists of two symmetrical systems of spiral ribs and a system of ring ribs. Spiral ribs are located at angles to the generatrix of the cylinder. The annular ribs pass through the midpoints of the segments of the spiral ribs located between the points of their intersection.

In this case, the most relevant development objectives are:

- selection of carbon filler of PCM (fiber) that meets the optimal set of requirements for physic-mechanical characteristics and provides the possibility of its application in continuous winding technologies (except for breaks at a tension of the thread and kinks both in the manufacture of elements of large curvature and in the movement of thread (wisp) in the layout and saturation systems of the binder;

- selection of PCM binder that provides uniform impregnation of carbon tow and sufficient adhesion to the formed unidirectional matrix;

- determination of the degree of carbon fiber reinforcement, which is responsible for compressive strength of unidirectional PCM (in the direction of calculations and carbon tow) at least 0.5 GPa and tensile strength at least 0.9 GPa;

- to optimize the rigidity and strength of PCM while minimizing the mass of the mesh shell – choice of the number and orientation paths of

spiral ribs, number of ring ribs and the sizes of individual ribs (width, height – for the implementation of automated manufacturing in a single technological cycle – it is advisable to keep the ribs dimensions constant over the entire mesh surface).

To test the BT at this stage of the study, the axial compressive force was adopted as the main load acting on the shell: the calculated value of which corresponds to the bearing capacity of 14 tf. Total dimensions of the BT section are – diameter 1200 mm, length 3800 mm. To increase rigidity, the design provides reinforcing axial stringers (longitudinal ribs) in four planes of four ribs, as well as end flanges (Skvortsov *et al.*, 2012; Tkachev *et al.*, 2018; Baymuratov *et al.*, 2018).

The mesh elements have the following geometric dimensions:

- rib height – 15 mm,
- the thickness of the spiral ribs is 3 mm,
- the thickness of the annular ribs – 3 mm,
- the thickness of the longitudinal ribs – 4.2 mm
- the angle of orientation of the spiral ribs relative to the generatrix – 29 degrees.

BT has two end frames. The frames intersecting the ribs of the mesh structure are made of carbon fiber. Based on the accepted structural parameters and geometric dimensions, the design of the BT section was done. A general view of BT is presented in Figure 1.

To test the design of BT for mechanical strength (axial compression), "Installation for testing the load-bearing truss" was developed and manufactured. The test bench layout is displayed in Figure 2. The structure of the stand includes base floor plate 1; lower mounting plate with a restrictive ring to prevent radial displacement of the model from the axis and its alignment 2; the upper base and mounting plate with a restrictive ring to prevent radial displacement of the model from the axis and its alignment 3; power exciter (manual hydraulic jack) 4; force meter (strain gauge force sensor) 5; set of centering sleeves 6; technological support for mounting 7; string type displacement sensors, potentiometric – 8 (four vertical through 900 (Dat1-Dat4) and one horizontal in diameter (Dat5). Sensors Dat1 and Dat2 are nearby, as are Dat3, Dat 4.

The model was loaded according to the step diagram with a step of ~ 20 kN and exposure at each step of ~ 100 seconds to the total compressive force of ~ 138 kN (14 tf). Continuously recorded magnitude of the

deformation of BT in the axial and radial directions and accompanied by visual monitoring of the state of the structure. At the maximum value of the applied compressive force with a hold time of 10 minutes.

### 3. RESULTS AND DISCUSSION:

Two tests of the BT section with the identical loading mode were carried out. The second test was carried out in order to confirm the absence of the phenomenon of micro-tears and cracks caused by the cyclic regime of load changes. The reduction in length and increase in diameter in cross-section in the middle of the height of the truss model is shown in Figure 2 and Tables 1, 2.

The design of the transition compartment constitutes the core system that remains unchanged after exposure to loads. The farm is manufactured by continuously winding a tow with a binder based on phenolic resins. Production of transition compartments started involving carbon composite materials to reduce mass characteristics while maintaining the strength and rigidity of the structures. The use of such materials provides a more than twofold decrease in mass characteristics compared to metal structures while maintaining the rigidity and strength of structural elements.

Figure 3 and Figure 4 present the first readings of recording devices during a time period. The stepwise nature of loading can be seen. During the initial period of time, a linear increase in readings of the string displacement sensors is observed at practically constant load. This mode corresponds to the movement of the plate 7 up to its contact with the counter plane of the end flange and the formation of the snug fit of both plates of the stand to the corresponding flanges of the model. At some point in time, the force sensor begins to register an increase in corresponding value, and at the same time, the nature of the sensor's readings changes to a gentler one. Based on the tests, was obtained a dependency on indications of sensors (external load) on time. (Figure 3). Figure 4 presents a compression diagram (the dependence of truss movements and an increase in diameter depending on the applied forces).

### 4. CONCLUSIONS:

1. Through the measurement range, the model of the BT section retained its integrity and stability, and there were no violations of continuity

of the polymer composite material, cracks, or delamination.

2. The nature of the deformation of the BT prototype when applying axial force is close to linear, which indicates the absence of irreversible fracture processes in the polymer composite material and development of only elastic stresses without accumulation of damage. The elastic nature of displacements is also confirmed by the similarity of displacement curves in the load-unloading modes of the model (there are no residual deformations within the measurement accuracy).

3. The relative value of axial strain was ~ 0.1%. There was good convergence of the measurement results with the strength calculation data, and the errors did not exceed 6%.

4. The registered small levels of structural displacements under the action of compressive load and their satisfactory reproducibility, including at significant forces of 14 tf, lets us consider the possibility of modernizing the design scheme of the model of BT section to provide an additional reduction in its mass.

Particularly, it is advisable to optimize the size and number of axial ribs (stringers). Likewise, in further work, it is advisable to clarify the possible variation in properties of the polymer composite material implemented in the design of the model using the suggested manufacturing technology.

BT tests have demonstrated that at a given axial load of 14 tf, the product retains its bearing capacity and stability at the levels of relative deformations of no more than 0.1%, which corresponds to the results of strength calculations for given properties of the material. Deformations of the product are noticed in the elastic region without significant changes. The deformation characteristics of the model remain stable and vary linearly depending on the applied load.

## 5. ACKNOWLEDGMENTS:

The work was carried out with the financial support of the state project of the Ministry of Education and Science project code "Modern technologies of experimental and digital modeling and optimization of spacecraft systems parameters", project code FSFF-2020-0016.

## 6. REFERENCES:

1. Alosime, E.M. (2019). A review on Copoly(ether-ester) elastomers: degradation and stabilization. *Journal of Polymer Research*, 26, Article number: 293
2. Antufev, B.A., Egorova, O.V., and Rabinskiy, L.N. (2019a). Quasi-static stability of a ribbed shell interacting with moving load. *INCAS Bulletin*, 11, 33-39.
3. Antufev, B.A., Egorova, O.V., and Rabinskiy, L.N. (2019b). Dynamics of a cylindrical shell with a collapsing elastic base under the action of a pressure wave. *INCAS Bulletin*, 11, 17-24.
4. Antufev, B.A., Kuznetsova, E.L., Rabinskiy, L.N., and Tushavina, O.V. (2019c). Complex stressed deformed state of a cylindrical shell with a dynamically destructive internal elastic base under the action of temperature fields of various physical nature. *Asia Life Sciences*, 2, 775-782.
5. Antufev, B.A., Kuznetsova, E.L., Rabinskiy, L.N., and Tushavina, O.V. (2019d). Investigation of a complex stress-strain state of a cylindrical shell with a dynamically collapsing internal elastic base under the influence of temperature fields of various physical nature. *Asia Life Sciences*, 2, 689-696.
6. Babaytsev, A., Dobryanskiy, V., and Solyaev, Y. (2019). Optimization of Thermal Protection Panels Subjected to Intense Heating and Mechanical Loading. *Lobachevskii Journal of Mathematics*, 40(7), 887-895. DOI: 10.1134/S1995080219070059
7. Babaytsev, A.V., and Zotov, A.A. (2019). Designing and Calculation of Extruded Sections of an Inhomogeneous Composition. *Russian Metallurgy (Metally)*, 2019(13), 1452-1455. DOI: 10.1134/S0036029519130020
8. Babaytsev, A.V., Martirosov, M.I., Rabinskiy, L.N., and Solyaev, Y.O. (2017a). Effect of Thin Polymer Coatings on the Mechanical Properties of Steel Plates. *Russian Metallurgy (Metally)*, 2017(13), 1170-1175. DOI: 10.1134/S003602951713002XF
9. Babaytsev, A.V., Prokofiev, M.V., and Rabinskiy, L.N. (2017b). Mechanical properties and microstructure of stainless steel manufactured by selective laser sintering. *International Journal of Nanomechanics Science and Technology*, 8(4), 359-366. DOI: 10.1615/NanoSciTechnolIntJ.v8.i4.60

10. Baymuratov, B.H., Tashpulatov, S.S., Akbarov, R.D., Ilhamova, M., Yusuphodjaeva, G.A., Uzakov, U.T., and Yusuphodjaeva, N.A. (2018). Development of special fabrics protecting from electromagnetic radiation. *IOP Conference Series: Materials Science and Engineering*, 459(1), Article number 012031.
11. Berezovskii, V.V., Solyaev, Y.O., Lur'e, S.A., and Babaitsev, A.V. (2015). Mechanical properties of a metallic composite material based on an aluminum alloy reinforced by dispersed silicon carbide particles. *Russian Metallurgy (Metally)*, 2015(10), 790-794. DOI: 10.1134/S0036029515100055
12. Bodryshev, V.V., Nartova, L.G., and Rabinskiy, L.N. (2019). Digital interpretation of gas dynamics problems as a means of optimizing fundamental general engineering education. *Asia Life Sciences*, 2, 759-774.
13. Dmitriev, A.I., Skvortsov, A.A., Koplak, O.V., Morgunov, R.B., and Proskuryakov, I.I. (2011). Influence of the regime of plastic deformation on the magnetic properties of single-crystal silicon Cz-Si. *Physics of the Solid State*, 53(8), 1547-1553.
14. Farhadinia, M. (2014). Analysis investigation of composite lattice conical shell as satellite carrier adapter for aerospace applications. *International Journal of Advances in Applied Mathematics and Mechanics*, 1, 40-51.
15. Gattringer, C., Mandl, M., and Törek, P. (2019). New density of states approaches to finite density lattice QCD. *Physical Review D*, 100(11), Article number 114517
16. Golushko, S.K., and Semisalov, B.V. (2015). Numerical modeling of deformation of anisogrid structures using high-precision schemes without saturation. *Mathematical Modeling and Numerical Methods*, 2(6), 23-45.
17. Hao, S., Wu, Z., Li, F., and Zhang, C. (2019). Numerical and experimental investigations on the band-gap characteristics of metamaterial multi-span beams. *Physics Letters, Section A: General, Atomic and Solid State Physics*, 383(36), Article number 126029.
18. Koshoridze, S.I., Levin, Y.K., Rabinskiy, L.N., and Babaytsev, A.V. (2017). Investigation of Deposits in Channels of Panels of a Heat-Transfer Agent. *Russian Metallurgy (Metally)*, 13, 1194-1201. DOI: 10.1134/S0036029517130092
19. Kumar, C.V. (2019). Kandasubramanian, B. Advances in Ablative Composites of Carbon Based Materials: A Review. *Industrial and Engineering Chemistry Research*, 58, 22663-22701
20. Kyanishbayev, S.B., Umbetov, A.U., Duisebekova, A.E., Umbetova, M.Z., Schongalova, K.S., Akhatova, Z.E., Azhibekova, P.S., and Sokabayeva, A.S. (2016). Interference of spherical laser radiation in a crystalline compound lens. *International Journal of Environmental and Science Education*, 11(18), 11593-11610.
21. Mishra, A., Shetti, N.P., Basu, S., Raghava Reddy, K., and Aminabhavi, T.M. (2019). Carbon Cloth-based Hybrid Materials as Flexible Electrochemical Supercapacitors. *ChemElectroChem*, 6(23), 5771-5786
22. Mustafin, A. (2006). Two mutually loss-coupled lasers featuring a stable multivibrator. *Physica D: Nonlinear Phenomena*, 218(2), 167-176.
23. Pintossi, D., Saakes, M., Borneman, Z., and Nijmeijer, K. (2019). Electrochemical impedance spectroscopy of a reverse electrodialysis stack: A new approach to monitoring fouling and cleaning. *Journal of Power Sources*, 444, Article number 227302
24. Rabinskiy, L.N., and Tushavina, O.V. (2019). Investigation of an elastic curvilinear cylindrical shell in the shape of a parabolic cylinder, taking into account thermal effects during laser sintering. *Asia Life Sciences*, 2, 977-991.
25. Sevryukova, M.M., Piryatinski, Y.P., Vasylyuk, S.V., Yashchuk, V.M., Viniychuk, O.O., Gerasov, A.O., Slominskii, Y.L., and Kachkovsky, O.D. (2012). Cyanine-like and polyenic relaxation paths of merocyanine derivatives of malonodinitrile in the excited state detecting by low temperature time-resolved fluorescence. *Ukrainian Journal of Physics*, 57(8), 812-823.
26. Skvortsov, A.A., Orlov, A.M., and Zuev, S.M. (2012). Diagnostics of degradation processes in the metal-semiconductor system. *Russian Microelectronics*, 41(1), 31-40.
27. Suprun, A.D., Vasylyuk, S.V., and Yashchuk, V.N. (2018). The possible mechanisms of conductivity in polyene-like polymers and types of conductivity in

maximally feeble external fields. *Springer Proceedings in Physics*, 210, 89-102.

28. Tkachev, S.Y., Alekseev, O.M., Lazarenko, M.M., Lazarenko, M.V., Kovalov, K.M., Bokhvan, S.I., Grabovskii, Y.E., and Hoshylyk, N.V. (2018). Topological solitons in branched aliphatic molecules. *Molecular Crystals and Liquid Crystals*, 665(1), 166-180.
29. Tokiwa, Y., Calabia, B., Ugwu, C., and Aiba, S. (2009) Biodegradability of plastics. *International Journal of Molecular Sciences*, 10(9), 3722–3742
30. Umbetov, A.U., Uzakova, B.Z., Abdrakhmanova, M.T., Tulegenova, A.K., Aubakirova, A.A., and Dzhaketova, S.Z. (2016). Laser measuring apparatus based on using bifocal lenses. *Mathematics Education*, 11(6), 1945-1959.
31. Varsavas, S.D., and Kaynak, C. (2018). Effects of glass fiber reinforcement and thermoplastic elastomer blending on the mechanical performance of polylactide. *Compos Commun*, 8, 24–30
32. Zhavoronok, S.I., Kurbatov, A.S., Orekhov, A.A., and Rabinskii, L.N. (2019). Stability of Panels of a Thermoelastic Shell Heated at the Edge by a Mobile Point Source. *Russian Engineering Research*, 9(9), 793-796.



**Figure 1.** Image of the mesh structure

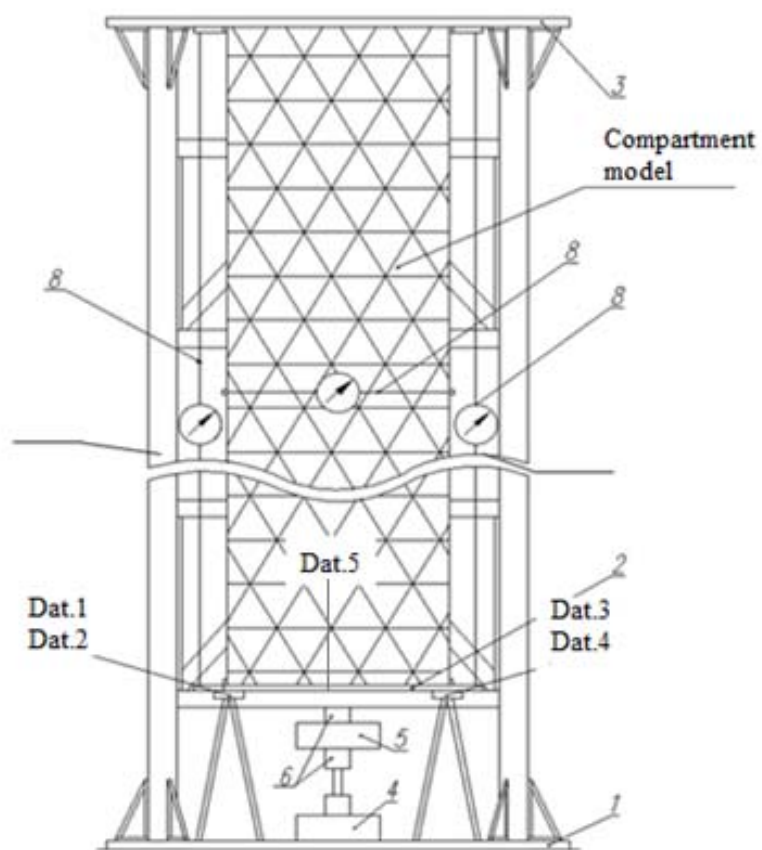


**Figure 2.** Scheme of the test stand



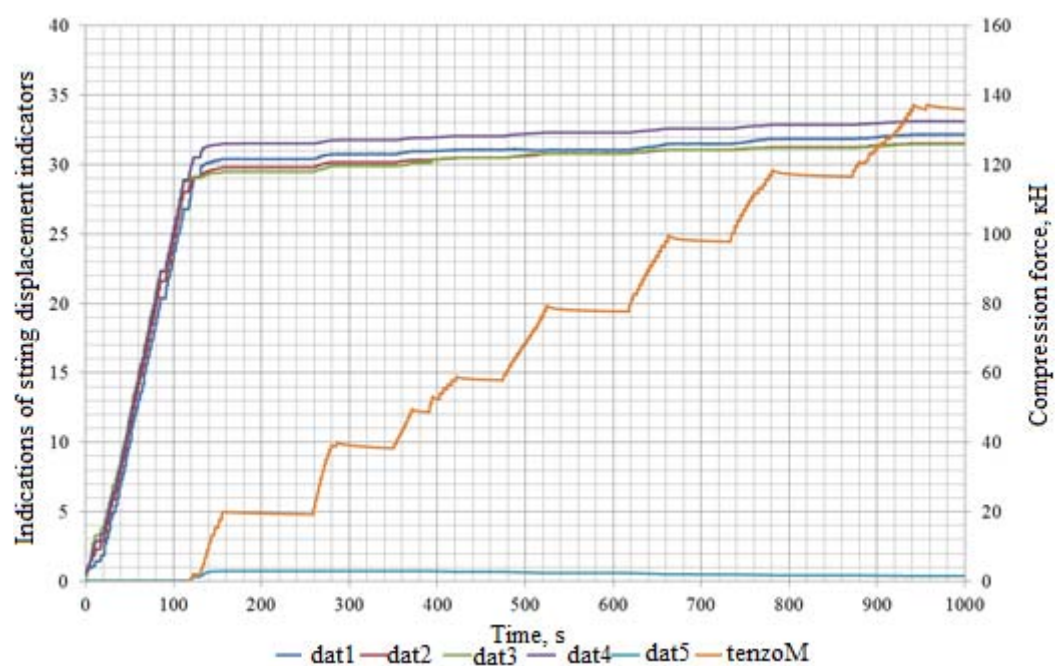


**Figure 3.** The dependence of displacements and compressive forces on time

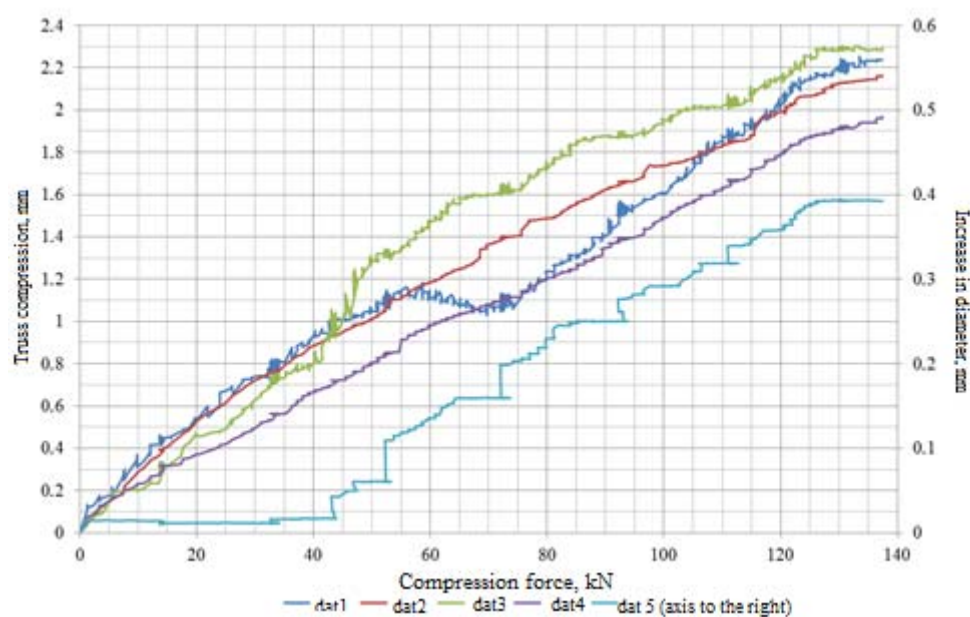


**Figure 4.** The compression Chart

**Table 1.** Average values of deformation characteristics. Test 1

| Compressive load, kN | Truss compression * $\Delta l$ , mm | Diameter increase $\Delta D$ , mm |
|----------------------|-------------------------------------|-----------------------------------|
| 20                   | 0.45                                | 0.00                              |
| 40                   | 0.80                                | 0.00                              |
| 60                   | 1.20                                | 0.15                              |
| 80                   | 1.45                                | 0.23                              |
| 100                  | 1.52                                | 0.30                              |
| 120                  | 2.00                                | 0.35                              |
| 138                  | 2.10                                | 0.39                              |

**Table 2.** Average values of deformation characteristics. Test 2

| Compressive load, kN | Truss compression * $\Delta l$ , mm | Diameter increase $\Delta D$ , mm |
|----------------------|-------------------------------------|-----------------------------------|
| 20                   | 0.45                                | 0.00                              |
| 40                   | 0.80                                | 0.00                              |
| 60                   | 1.05                                | 0.10                              |
| 80                   | 1.35                                | 0.20                              |
| 200                  | 1.70                                | 0.23                              |
| 120                  | 2.0                                 | 0.30                              |
| 138                  | 2.20                                | 0.32                              |



**ESTUDO COMPARATIVO DA PREVALÊNCIA DA REATIVIDADE DE IGE A ALÉRGENOS RECOMBINANTES****COMPARATIVE STUDY OF THE PREVALENCE OF IGE REACTIVITY TO RECOMBINANT ALLERGENS ON THE BACKGROUND OF ALLERGEN-SPECIFIC IMMUNOTHERAPY****СРАВНИТЕЛЬНОЕ ИЗУЧЕНИЕ РАСПРОСТРАНЕННОСТИ IGE РЕАКТИВНОСТИ К РЕКОМБИНАНТНЫМ АЛЛЕРГЕНАМ**SALTABAYEVA, Ulbossyn Sh.<sup>1</sup>; MORENKO, Marina A.<sup>2</sup>; ROZENSON, Rafail I.<sup>3</sup>;<sup>1</sup>Astana Medical University, Faculty of Nursing, 49 a Beybitshilik Str., zip code 010000, Nur-Sultan – Republic of Kazakhstan<sup>2,3</sup>Astana Medical University, Department of Children's Diseases No. 1, 49 a Beybitshilik Str., zip code 010000, Nur-Sultan – Republic of Kazakhstan

\* Correspondence author

e-mail: s.ulbosyn@mail.ru

Received 12 April 2020; received in revised form 10 June 2020; accepted 14 June 2020

**RESUMO**

As doenças alérgicas são um dos problemas mais prementes da medicina prática. Segundo estatísticas da Organização Mundial da Saúde, cerca de 40% da população mundial sofre de alergias. Atualmente, o diagnóstico de alergia molecular (AM) é o método mais útil para selecionar os pacientes para prescrever imunoterapia com o objetivo de tratar alergias (imunoterapia com alérgenos), determinar a reatividade cruzada e a gravidade da reação associada a vários alérgenos. O diagnóstico de alergia molecular tem vantagens no diagnóstico de pacientes com sintomas alérgicos – asma, febre do feno, eczema, urticária, sintomas gastrointestinais, síndrome alérgica oral ou anafilaxia. Baseia-se na escolha pelo médico de alérgenos individuais ou no uso de microchips e oferece uma grande quantidade de informações relacionadas ao perfil de IgE de pacientes sensíveis a alérgenos. O método mais eficaz de tratamento de doenças alérgicas é a imunoterapia com alérgenos, que afeta todas as partes patogênicas do processo alérgico e tem um longo efeito preventivo após a conclusão dos cursos de tratamento. O objetivo do artigo é estudar a prevalência de reatividade de IgE a importantes alérgenos recombinantes no contexto de tipos de imunoterapia com alérgenos. Durante o trabalho, os pacientes foram examinados pelo método de diagnóstico molecular alérgico. O artigo apresenta os resultados do estudo comparativo da presença de IgE específica no soro de pacientes com sensibilidade confirmada aos principais alérgenos recombinantes: absinto Art vI, Art v3, Phleum Phl p1, Phl p5 e bétula Bet v1 por um período de três anos. Os dados obtidos confirmam a alta eficácia da imunoterapia com alérgenos e seu efeito positivo na diminuição da sensibilidade em pacientes com febre do feno em comparação com os resultados do grupo de imunoterapia parenteral.

**Palavras-chave:** febre do feno, diagnóstico de alergia molecular, principais alérgenos recombinantes, imunoterapia com alérgenos.

**ABSTRACT**

Allergic diseases are one of the most urgent problems of practical medicine. According to statistics of the World Health Organization, about 40% of the world's population suffers from allergies. Molecular allergy diagnostics (MA) is currently the most useful patient selection method for prescribing allergen-specific immunotherapy (ASIT), determining cross-reactivity, and the severity of the reaction associated with various allergens. Molecular allergic diagnosis has advantages for the diagnosis of patients with allergic symptoms – asthma, pollinosis, eczema, hives, gastrointestinal symptoms, oral allergic syndrome, or anaphylaxis. It is based on the choice of individual allergens by a doctor or the use of microarrays and offers a large amount of information related to the IgE profile of sensitized patients. The most effective method of treatment for allergic diseases is allergen-specific immunotherapy, which affects all pathogenetic links of the allergic process and has a long-term preventive effect after the completion of treatment courses. The aim of the article is to study the prevalence of IgE

reactivity to major recombinant allergens on the background of the types of allergen-specific immunotherapy. In the course of the work, patients were examined by allergic molecular diagnostics. The article shows the results of a comparative study of the presence of specific IgE in the serum of patients with confirmed sensitization to major recombinant allergens: wormwood Art vI, Art v3, timothy Phl p1, Phl p5 and birch Bet v1 for a three-year period. The data obtained confirm the high efficiency of sublingual immunotherapy (SLIT) and its positive effect on the reduction of sensitization in patients with pollinosis compared with the results of the parenteral immunotherapy group (sublingual immunotherapy).

**Keywords:** *pollinosis, molecular allergodiagnosics, major recombinant allergens, allergen-specific immunotherapy.*

## АННОТАЦИЯ

Аллергические заболевания на сегодняшний день являются одной из наиболее актуальных проблем практической медицины. Согласно статистическим данным Всемирной организации здравоохранения, аллергией страдают около 40% населения нашей планеты. На сегодняшний день молекулярная аллергодиагностика (МА) является наиболее полезным методом отбора пациентов для назначения аллерген-специфической иммунотерапии (АСИТ), определения перекрестной реактивности и тяжести реакции, ассоциированной с различными аллергенами. Полисенситизированные пациенты с неясными симптомами, типом сенситизации, или у кого нет ответа на лечение, могут быть диагностированы в стандартной лаборатории при доступности в ней МА. Молекулярная аллергодиагностика обладает преимуществами для диагностики пациентов с аллергическими симптомами – астмой, поллинозом, экземой, крапивницей, желудочно-кишечными симптомами, оральным аллергическим синдромом или анафилаксией. Определение истинной сенситизации так же важно, как и выявление вторичной сенситизации под действием перекрестно реагирующих аллергенов. Молекулярная аллергодиагностика, основанная на выборе врачом отдельных аллергенов или использовании микроматриц, предлагает большой объем информации, относящейся к IgE-профилю сенситизированных пациентов. Наиболее эффективным методом лечения при аллергических заболеваниях является аллерген-специфическая иммунотерапия, воздействующая на все патогенетические звенья аллергического процесса и обладающая длительным профилактическим эффектом после завершения лечебных курсов. Целью исследования явилось изучение наличия специфических IgE в сыворотке крови пациентов с подтвержденной сенситизацией к рекомбинантным мажорным аллергенам на фоне аллерген-специфической иммунотерапии. В статье изображены результаты сравнительного изучения наличия специфических IgE в сыворотке крови пациентов с подтвержденной сенситизацией к рекомбинантным мажорным аллергенам: полыни Art vI, Art v3, тимopheевки Phl p1, Phl p5 и березы Bet v1 в течение трехлетнего периода. Полученные данные подтверждают высокую эффективность сублингвальной аллерген-специфической иммунотерапии (СЛИТ) и ее положительное влияние на снижение сенситизации у больных поллинозом в сравнении с результатами группы парентеральной аллерген-специфической иммунотерапии (ПИТ).

**Ключевые слова:** *поллиноз, молекулярная аллергодиагностика, рекомбинантные мажорные аллергены, аллерген-специфическая иммунотерапия.*

## 1. INTRODUCTION

Allergic diseases are one of the most urgent problems of practical medicine. This is due to the high prevalence and the continuous increase in the number of diseases, as well as the increase in severe clinical manifestations, which often cause a deterioration in the quality of life and disability of patients (Canonica *et al.*, 2013a; Perkin and Genuneit, 2017; Brozek and Cuello-Garcia, 2016; Namazova-Baranova, 2011; Morenko, 2010). According to statistics of the World Health Organization, about 40% of the world's population suffers from allergies. The first place are respiratory allergies, about 12-45% of them, specifically pollinosis (Ilyina and Pavlova,

2016; Bousquet *et al.*, 2016; FitzGerald *et al.*, 2014; Papadopoulos *et al.*, 2012).

A feature of allergic diseases in the Republic of Kazakhstan is that the main allergenic plants are wormwood and other weeds, the intensity of sensitization is about one million times greater than that observed in Central Europe and the European part of the Russian Federation (Kurbacheva *et al.*, 2013; Maslova, 2012; Calderon *et al.*, 2011; Gorbash *et al.*, 2015; Zhumambayeva *et al.*, 2014). The main reason of the increase in the incidence of pollen and the prevalence of its medium and heavy forms is the leadership of symptomatic pharmacotherapy over pathogenetic allergen-specific immunotherapy

(ASIT) The most effective method of treatment for allergic diseases is allergen-specific immunotherapy, which affects all pathogenetic links of the allergic process and has a long-term preventive effect after the completion of treatment courses (Saltabaeva and Morenko, 2015; Durham, 2006; Canonica *et al.*, 2014; Zhuravleva *et al.*, 2019; Valovirta, and Berstad, 2011). If parenteral methods developed in 1911 have already received general acceptance worldwide, then oral methods for decades have been discredited by using untreated vaccines. Such vaccines have not been depolymerized and depigmented (Calderon *et al.*, 2012; Abdrakhmanova *et al.*, 2019).

Only in the last two decades, these methods began to be widely used first in European countries, later in North and Central America, and in the last years methods are already used in Kazakhstan. A comparative study of the efficacy of oral and parenteral allergen-specific immunotherapy (ASIT) has not been adequately studied, mainly in European countries (Cheryl *et al.*, 2013, Douladiris, 2013; Kudabayeva *et al.*, 2014; Kudabayeva *et al.*, 2017; Valenta *et al.*, 2014). In our republic, similar results of the study were not previously published. The region of Northern Kazakhstan, where the capital Nur-Sultan is located, is characterized by heterogeneous climatic conditions due to the long extent, heterogeneous surface structure, and characteristic landscapes. The specificity of pollination in Nur-Sultan is special in relation to a relatively short summer, where there are shifts in time of flowering of trees, weeds, and meadow grasses, which complicates the establishment of true sensitization to certain allergens. Nur-Sultan is located in a spacious steppe and is exposed to a wind rose, with a strong pollen direction from the southern regions and the influence of several different pollen sources of allergens at the same time, which lead to cross-allergy (The climate of Astana, 2019). To determine the true sensitization in cross-reactions in polysensitized patients when traditional diagnostic tests and case history data are insufficient to determine significant allergens for the correct selection of therapy, prognosis, and effectiveness, molecular allergy diagnostics with recombinant allergens is used (Becker *et al.*, 2016; Canonica *et al.*, 2013b; Ramilyeva *et al.*, 2019; Burkitbaiev *et al.*, 2017; Fooke-Achterrath *et al.*, 2012; Spergel, 2010; Valenta *et al.*, 2011).

The aim of the article is to study the prevalence of IgE reactivity to major recombinant allergens on the background of the types of allergen-specific immunotherapy.

## 2. MATERIALS AND METHODS

Molecular allergy diagnostics (MA) is currently the most useful patient selection method for prescribing allergen-specific immunotherapy (ASIT), determining cross-reactivity, and the severity of the reaction associated with various allergens. Polysensitized patients with unclear symptoms, type of sensitization, or who have no response to treatment can be diagnosed in a standard laboratory with the availability of MA in it. Molecular allergic diagnosis has advantages for the diagnosis of patients with allergic symptoms – asthma, pollinosis, eczema, hives, gastrointestinal symptoms, oral allergic syndrome, or anaphylaxis. Determining true sensitization is just as important as identifying secondary sensitization by cross-reacting allergens. Molecular allergy diagnosis, based on the choice of individual allergens by a doctor or the use of microarrays, offers a large amount of information related to the IgE profile of sensitized patients (Valenta *et al.*, 1991; Smiyan *et al.*, 2015; Cromwell *et al.*, 2011; Jutel *et al.*, 2005; Saltabaeva and Morenko, 2017).

The study focuses on the presence of specific IgE in the serum of patients with confirmed sensitization (by Molecular allergy diagnostics) to pollen from wormwood to recombinant major recombinant allergens: wormwood Art vI, Art v3, timothy Phl p1, Phl p5 and birch Bet v1 for a three-year period (Tables 1, 2, and 3). Surveys were carried out in the medical and health center “Umit” (Nur-Sultan, Republic of Kazakhstan). The study involved 228 patients with varying degrees of severity of hay fever, among whom were children from 5 to 18 years old and an adult population (113 patients were males, 115 were females). The average age was  $23.5 \pm 0.9$  years, and the minimum age was 5 five years, t, the maximum was 60 years. The studied respondents were randomized into two groups: group 1 included 126 (55.3%) patients who took sublingual immunotherapy (SLIT) (Durham, 2006), group 2 included 102 (44.7%) patients who received parenteral immunotherapy (PIT) (Kurbacheva *et al.*, 2013).

In the course of the work, 153 (67.1%) patients from the 1st group (SLIT) 95 (75.4%), from the 2nd group (PIT) 58 (56.9%) patients with pollinosis were examined by allergic molecular diagnostics and having positive skin scratch tests for native allergens with polysensitivity to mixes of weeds, meadow grasses, and trees (Douladiris, 2013).

Non-parametric methods of research,

Wilcoxon criterion, Mann-Whitney criterion, Friedman criterion, mean value, standard deviation, median, 25th, and 75th percentile were used to evaluate the parameters (Saltabayeva *et al.*, 2016a; Saltabayeva *et al.*, 2016b).

### 3. RESULTS AND DISCUSSION:

The enzyme immunosorbent assay using major recombinant allergens Art vI, Art v3, Phl p1, Phl p5, and Bet v1 was diagnosed with sensitization to these allergens as follows: Art v 1 – in 26 (17.0%), Art v3 – in 9 (5.9%), Art v1-Art v3 – in 73 (47.7%), Art v1.3-Bet v1 – in 20 (13.1%), Art v1.3-Phl p1.5 – in 16 (10.5%), Art v1,3-Bet v1-Phl p1.5 – in 9 (5.9%) (Figure 1).

Among inhaled pollen allergens, the highest degree of sensitization was determined to Art v1-Art v3. After a course of specific immunotherapy, the total number of patients with significant sIgE decreased 1.4 times. The results obtained correlate with known scientific data. In a number of works (Kulis, 2011; Radauer *et al.*, 2010) a high level of sensitization to recombinant wormwood allergens is noted in various populations of the European part of Russia, Kyrgyzstan, including wormwood, which coincides with our data and confirms the presence of a large number of IgE epitopes in Art v1-Art v3 to weed pollen allergens.

At the same time, antibodies to the main allergen of the monopole Art v1-Art v3 are found in 73 (47.7%) patients with seasonal allergic rhinitis. The identification of high levels of Art V1-Art v3 major antibodies in patients was important for developing criteria for the selection of therapy and evaluating the effectiveness of ASIT. Most scientific sources confirm this data, which describes nine different allergens isolated from wormwood pollen (*Artemisia vulgaris*), including two major allergens (Art vI and Art v3), which are often responsible for cross-allergy (Eigenmann, 1998). The complete structure of all known wormwood allergens has recently been deciphered (Guideline on the clinical development..., 2008). The main native wormwood allergen Art vI is a highly glycosylated glycoprotein with a molecular weight of 24 to 28 kDa, has an unusual tertiary structure and the end portion of the molecule, the so-called “head and tail”, which explains its extraordinary biochemical properties (Incorvaia and Fuiano, 2013).

Different groups studied, sensitization to allergens from Art vI wormwood, Art v3, Timothy Phl p1, Phl p5, and Bet v1 birch had a similar distribution of the trait in most patients; no

statistically significant difference was found between these groups ( $p = 0.501$ ). The greatest sensitization was also detected in both groups to the major recombinant allergens of the wormwood Art vI-Art v3.

Also, when evaluating the results obtained by serological examination of patients' blood, we identified a statistically significant difference between the relative concentrations of major recombinant allergens of wormwood, ambrosia, timothy, and birch  $p < 0.001$  before and after sublingual immunotherapy. The distribution of signs was different from normal.

In the studied patients of group 1 (SLIT), the frequency of positive sensitization results to various recombinant major allergens Art vI, Art v3, Phl p1, Phl p5 and Bet v1 changed as follows: Art v 1 – from 17 (17.9%) to 11 (11.2%), Art v3 – from 6 (6.3%) to 4 (3.9%), Art v1-Art v 3 – from 43 (45.3%) to 27 (28.3%), Art v1,3-Bet v1 – from 13 (13.7%) to 8 (8.6%), Art v 1,3-Phl p1.5 – from 11 (11.6%) to 7 (7.2 %), Art v1,3-Bet v1-Phl p1.5 – from 5 (5.3%) to 3 (3.3%) (Figure 2).

For a comparative study of the immunological efficacy of SLIT and PIT, we studied the concentrations of major recombinant allergens before each course of ASIT. In patients of group 1, the level of specific IgE antibodies to the allergens of Art v1 wormwood to SLIT (Me, 25–75%) was 27.1 (11.2–35.8) Ku/l and corresponded to (Me, 25–75%) 3, 4 (3.1–3.9) class, after the 1st course SLIT (Me, 25–75%) was 23.6 (9.8–31.1) Ku/l and corresponded (Me, 25–75%) 3.4 (3.1–3.9) class, after the 2nd course SLIT (Me, 25–75%) was 18.1 (7.5–23.9) Ku/l and corresponded to (Me, 25–75%) 3.4 (3.1–3.9) class, after the 3rd course SLIT (Me, 25–75%) was 17.4 (7.2–22.9) Ku/l, corresponding to (Me, 25–75%) 3.4 (3.1–3.9) class. When evaluating the effectiveness of SLIT in patients with pollinosis for three courses, the concentration of Art v1 in serum was statistically significantly reduced 1.6 times (Friedman test:  $\chi^2 = 72.2$ ;  $p < 0.001$ ) (Figure 3).

The level of specific IgE antibodies to wormwood Art v3 allergens to SLIT (Me, 25–75%) was 8.0 (0.4–14.0) ku/l and corresponded to (Me, 25–75%) 1.3 (1, 1–3.9) class, after the 1st course SLIT (Me, 25–75%) was 7.3 (0.4–12.7) ku/l, corresponding to (Me, 25–75%) 1.3 (1.1–3.9) class, after the 2nd course SLIT (Me, 25–75%) was 5.6 (0.3–9.8) ku/l, corresponding to (Me, 25–75%) 1.3 (1.1–3.9) class, after the 3rd course SLIT (Me, 25–75%) was 5.4 (0.3–9.3) ku/l and corresponded (Me, 25–75%) 1.3 (1.1–3.9) class. Thus, the concentration of Art v3 in serum was statistically

significantly reduced by 1.5 times (Friedman test:  $x^2 = 64.1$ ;  $p < 0.001$ ).

The level of specific IgE antibodies to meadow grass allergens Phl p1 to SLIT (Me, 25-75%) was 1.0 (0.0-1.5) ku/l, corresponding to (Me, 25-75%) 0, 2 (0, 1-2.9) class, after the 1st course SLIT (Me, 25-75%) was 0, 9 (0.0-1.2) ku/l and corresponded to (Me, 25-75%) 0, 2 (0.1-2.9) class, after the 2nd course SLIT (Me, 25-75%) was 0.7 (0.0-1.0) ku/l, corresponding to (Me, 25-75%) 0.2 (0.1-2.9) class, after the 3rd course SLIT (Me, 25-75%) was 0, 6 (0.0-0.9) ku/l and corresponded to (Me, 25-75%) 0, 2 (0.1-2.9) class. Thus, the concentration of Phl p1 in serum was statistically significantly reduced 1.6 times (Friedman test:  $x^2 = 42.4$ ;  $p < 0.001$ ) (Figure 4).

The level of specific IgE antibodies to meadow grass allergens Phl p5 to SLIT (Me, 25-75%) was 0, 2 (0.0-1.1) ku/l and corresponded to (Me, 25-75%) 0.2 (0.1-2.9) class, after the 1st course SLIT (Me, 25-75%) was 0.15 (0.0-0.8) ku/l, corresponding to (Me, 25-75%) 0, 2 (0.1-2.9) class, after the 2nd course SLIT (Me, 25-75%) was 0.11 (0.0-0.7) ku/l, corresponding to (Me, 25-75%) 0.2 (0.1-2.9) class, after the 3rd course SLIT (Me, 25-75%) was 0.10 (0.0-0.6) ku/l and corresponded to (Me, 25-75%) 0, 1 (0.1-1.9) class. That is, the concentration of Phl p 5 in serum was statistically significantly reduced by 1.5 times (Friedman test:  $x^2 = 36.0$ ;  $p < 0.001$ ).

The level of specific IgE antibodies to Bet v1 birch allergens to SLIT (Me, 25-75%) was 1.4 (0.2-2.1) ku/l and corresponded to (Me, 25-75%) 0, 2 (0, 1-2.9) class, after the 1st course SLIT (Me, 25-75%) was 1, 2 (0.0-1.9) ku/l, corresponding to (Me, 25-75%) 0, 2 (0.1-2.9) class, after the 2nd course SLIT (Me, 25-75%) was 0, 9 (0.0-1.2) ku/l and corresponded to (Me, 25-75%) 0, 2 (0.1-2.9) class, after the 3rd course SLIT (Me, 25-75%) was 0.8 (0.0-0.9) ku/l, corresponding to (Me, 25-75%) 0.2 (0.1-2.9) class, the concentration of Bet v1 in serum significantly decreased 1.5 times (Friedman test:  $x^2 = 56.1$ ;  $p < 0.001$ ).

After SLIT, in patients of group 1, the content of serum specific IgE antibodies to wormwood allergens Art v1 significantly decreased (Wilcoxon matched pairs test:  $z = 8.3$ ;  $p < 0.001$ ), to Art v3 (Wilcoxon matched pairs test:  $z = 7.5$ ;  $p < 0.001$ ), to meadow grass allergens Phl p1 (Wilcoxon matched pairs test:  $z = 4.1$ ;  $p < 0.001$ ), to Phl p5 (Wilcoxon matched pairs test:  $z = 3.4$ ;  $p < 0.05$ ), to Bet v1 birch allergens (Wilcoxon matched pairs test:  $z = 4.5$ ;  $p < 0.001$ ). In the study, the content of recombinant major allergens in the serum of patients with polysensitization showed

their statistically significant decrease after SLIT ( $p < 0.001$ ).

As in group 1 and group 2, when evaluating the results obtained by a serological method for examining patients' blood, a statistically significant difference was found between the relative concentrations of recombinant allergens of wormwood, timothy and birch ( $p < 0.001$ ) before and after the ICU, but which was less SLIT. The distribution of signs was also distinguishable from normal. Therefore, non-parametric research methods were used to evaluate the parameters.

In patients of group 2 (PIT), the frequency of positive sensitization results to various recombinant major allergens Art v1, Art v3, Amb a1, Phl p1, Phl p5 and Bet v1 changed as follows: Art v1 – from 9 (15.5%) to 7 (11.9%), Art v3 – from 3 (5.2%) to 2 (4.0%), Art v1-Art v3 – from 30 (51.7%) to 23 (39.8%), Art v1,3-Bet v1 – from 7 (12.1%) to 5 (9.3%), Art v1,3-Phl p1.5 – from 5 (8.6%) to 4 (6.6%), Art v1,3-Bet v1-Phl p1.5 – from 4 (6.9%) to 3 (5.3%) (Figure 5).

In the group of patients who received parenteral immunotherapy, the level of specific IgE antibodies to wormwood Art v1 allergens to PIT (Me, 25-75%) was 32.5 (13.4-42.9) Ku/l and corresponded to (Me, 25-75%) 3.4 (3.1-3.9) class, after the 1st course PIT (Me, 25-75%) was 29.5 (12.2-39.0) Ku/l, corresponding to (Me, 25-75%) 3.4 (3.1-3.9) class, after the 2nd course PIT (Me, 25-75%) was 24.6 (10.2-32.5) Ku/l, corresponding to (Me, 25-75%) 3.4 (3.1-3.9) class, after the 3rd course of PIT (Me, 25-75%) was 23.6 (9.8-31, 2) Ku/l and corresponded to (Me, 25-75%) 3.4 (3.1-3.9) class. When evaluating the effectiveness of PIT in patients with pollinosis during three courses, the concentration of Art v1 in serum significantly decreased 1.4 times (Friedman test:  $x^2 = 64.2$ ;  $p < 0.001$ ).

The level of specific IgE antibodies to wormwood Art v3 allergens before PIT (Me, 25-75%) was 8.8 (0.3-15.4) Ku/l and corresponded to (Me, 25-75%) 3.4 (3, 1-3.9) class, after the 1st course PIT (Me, 25-75%) was 8.7 (0.3-15.3) Ku/l, corresponding to (Me, 25-75%) 1, 3 (1.1-3.9) class, after the 2nd course of PIT (Me, 25-75%) was 7.2 (0.2-12.7) Ku/l and corresponded (Me, 25-75%) 0.3 (0.1-3.9) class, after the 3rd course of PIT (Me, 25-75%) was 6.8 (0.2-11.9) Ku/l, corresponding to (Me, 25-75%) 0.3 (0.1-3.9) class, the concentration of Art v3 in serum was statistically significantly reduced 1.3 times (Friedman test:  $x^2 = 48.6$ ;  $p < 0.001$ ).

The level of specific IgE antibodies to meadow grass allergens Phl p1 to PIT (Me, 25-

75%) was 1.5 (0.0-2.2) Ku/l and corresponded to (Me, 25-75%) 0.2 (0.1-2.9) class, after the 1st course PIT (Me, 25-75%) was 1.2 (0.0-1.8) Ku/l, corresponding to (Me, 25-75%) 0.2 (0.1-2.9) class, after the 2nd course of PIT (Me, 25-75%) was 0.04 (0.0-0.6) Ku/l and corresponded (Me, 25-75%) 3, 0, 1 (0.1-1.9) class, after the 3rd course SLIT (Me, 25-75%) was 1.1 (0.0-1.6) Ku/l Corresponding to (Me, 25-75%) 0, 2 (0.1-2.9) class, the concentration of Phl p1 in serum significantly decreased 1.3 times (Friedman test:  $\chi^2 = 29.6$ ;  $p < 0.001$ ).

The level of specific IgE antibodies to meadow grass allergens Phl p5 to PIT (Me, 25-75%) was 0.17 (0.0- 1.0) Ku/l and corresponded to (Me, 25-75%) 0.2 (0.1-2.9) class, after the 1st course of PIT (Me, 25-75%) was 0.15 (0.0-0.9) Ku/l, corresponding to (Me, 25-75%) 0.2 (0.1-2.9) class, after the 2nd course SLIT (Me, 25-75%) was 0.14 (0.0-0.6) Ku/l, corresponding to (Me, 25 - 75%) 0.1 (0.08-1.9) class, after the 3rd course PIT (Me, 25-75%) was 0.14 (0.0-0.5) Ku/l and corresponded to (Me, 25-75%) 0, 1 (0.1-1.9) class. Thus, the concentration of Phl p5 in serum was statistically significantly reduced by 1.2 times (Friedman test:  $\chi^2 = 54.0$ ;  $p < 0.001$ ).

The level of specific IgE antibodies to Bet v1 birch allergens before PIT (Me, 25-75%) was 2.3 (0.0-2.9) Ku/l and corresponded to (Me, 25-75%) 0.2 (0, 1-2.9) class, after the 1st course of PIT (Me, 25-75%) was 2.1 (0.0-2.7) Ku/l, corresponding to (Me, 25-75%) 0, 2 (0.1-2.9) class, after the 2nd course PIT (Me, 25-75%) was 1.8 (0.0-2.1) Ku/l, corresponding to (Me, 25- 75%) 0.2 (0.1-2.9) class, after the 3rd course of PIT (Me, 25-75%) was 1.7 (0.0-1.9) Ku/l and corresponded to (Me, 25-75%) 0.2 (0.1-2.9) class. The serum Bet v1 concentration was statistically significantly reduced 1.5 times (Friedman test:  $\chi^2 = 56.1$ ;  $p < 0.001$ ). After PIT, the content of serum specific IgE antibodies to Art v1 wormwood allergens (Wilcoxon matched-pairs test:  $z = 8.4$ ;  $p < 0.001$ ) and Art v3 (Wilcoxon matched-pairs test:  $z = 7.6$ ;  $p < 0.001$ ), to meadow grass allergens Phl p1 (Wilcoxon matched-pairs test:  $z = 5.1$ ;  $p < 0.01$ ), to Phl p5 (Wilcoxon matched-pairs test:  $z = 3.8$ ;  $p < 0.05$ ), to birch allergens Bet v1 (Wilcoxon matched-pairs test:  $z = 5.4$ ;  $p < 0.001$ ).

As it is known, a significant clinical task in allergology for polysensitization and cross-allergy is to make an accurate diagnosis. For diagnostic accuracy and optimization of therapy, in particular immunotherapy, the development of recombinant allergens was an important step in medicine (Nelson, 2016; Pauli *et al.*, 2008; Ferreira, 1996; Valenta *et al.*, 2010).

Scientists of the Research Institute of Molecular Biology V.A. Engelhard, O. Smoldovskaya, G. Feyzkhanova, and their co-authors (2016) were studied in a multicenter comparative study of patients with hypersensitivity to birch pollen and cat dander using biological microchips, as well as skin scarification samples. As a result of the work, it was established that the diagnostic accuracy with the use of recombinant allergens was higher compared to skin test samples (Smoldovskaya *et al.*, 2016). An important conclusion and our study show that among all inhaled allergens, the highest rate relates to wormwood, which significantly decreased after the courses ASIT. Similar data were obtained in domestic surveys in epidemiological studies, where the main cause of seasonal allergy in Kazakhstan was pollen of weeds (Saltabayeva *et al.*, 2017).

Therefore, further study of allergic anamnesis and skin scarification tests with other allergens that have common allergenic properties, including an assessment of pollen, timothy and birch pollen reactivity, is needed to study cross-section properties with recombinant allergens, which is necessary to determine a more accurate profile of specific IgE reactivity to recombinant allergens in patients living in the north of Kazakhstan. Continuing research to determine whether the recombinant allergens match the spectrum of allergen-specific antibodies detected in this population will facilitate the use of recombinant allergens for diagnosing, monitoring, and selecting the right treatment with specific immunotherapy for patients with pollinosis in our region with multiple pollen influences.

#### 4. CONCLUSIONS:

Upon completion of the three courses of PIT, a statistically significant ( $p < 0.001$ ) decrease in the concentration of major recombinant allergens in the blood serum was detected, but which was relatively inferior to the SLIT group. The data obtained confirm the high efficiency of SLIT and its positive effect on the reduction of sensitization in patients with pollinosis compared with the results of the parenteral immunotherapy group.

Thus, the presence of a positive response from patients to major allergens of pollen from Art v1 wormwood, Art v3, Timothy Phl p1, Phl p5 and Bet v1 birch with cross allergy decreased after three courses of immunotherapy in group 1 (SLIT) 1.5 times and in group 2 (PIT) 1.3 times.

Analysis of the effects of ASIT in patients

with positive *in vitro* results on major recombinant allergens showed that after a three-year course of ASIT in two groups, a decrease in serum concentration of major recombinant allergens was observed, but more significant results were obtained in the group of patients who took the sublingual type of immunotherapy compared with the parenteral immunotherapy group ( $p < 0.001$ ).

## 5. ETHICAL APPROVAL

All procedures performed in studies involving human participants were in accordance with the ethical standards of the institutional and national research committee and with the 1964 Helsinki declaration and its later amendments or comparable ethical standards. Informed consent was obtained from all individual participants included in the study.

## 6. REFERENCES:

1. Abdrakhmanova, S.A., Zhanzakova, Z.Z., Turganbekova, A.A., and Saduakas, Z.K. (2019). Assessment of hematopoietic stem cell molecular engraftment based on STR analysis. *Cellular Therapy and Transplantation*, 8(3), 26-27.
2. Becker, S., Schleiderer, T., Kramer, M.F., and Haack, M. (2016). Real-life study for the diagnosis of house dust mite allergy – the value of recombinant allergen-based IgE serology. *International Archives of Allergy and Immunology*, 170, 132-137.
3. Bousquet, J., Canonica, G.W., and Valenta, R. (2016). Care pathways implementing emerging technologies for predictive medicine in rhinitis and asthma across the life cycle. *Clinical and Translational Allergy*, 6, 1-47.
4. Brozek, J.L., and Cuello-Garcia, C.A. (2016). World Allergy Organization-mcmaster university guidelines for allergic disease prevention (GLAD-P): Prebiotics. *World Allergy Organization Journal*, 1(3), 466-476.
5. Burkitbaiev, J.K., Abdrakhmanova, S.A., Savchuk, T.N., and Zhiburt, E.B. (2017). The implementation of NAT-screening of infections in blood donors of the Republic of Kazakhstan. *Klinicheskaya Laboratornaya Diagnostika*, 3, 154-156.
6. Calderon, M.A., Penagos, M., Sheikh, A., and Canonica, G.W. (2011). Sublingual immunotherapy for allergic conjunctivitis: cochrane systematic review and meta-analysis. *Clinical and Experimental Allergy*, 7, 1263–1272.
7. Calderon, M.A., van Wijk, R.G., Eichler, I., and Kopp, M.V. (2012). Perspectives on allergen-specific immunotherapy in childhood: an EAACI position statement. *Pediatric Allergy and Immunology*, 23(4), 300-306.
8. Canonica, G.W., Ansotegui, I.J., and Pawankar, R. (2013a). A WAO – ARIA – GA<sup>2</sup>LEN consensus document on molecular-based allergy diagnostics. *World Allergy Organization Journal*, 6(1), 1-17.
9. Canonica, G.W., Bousquet, J., Cox, L., and Pawankar, R. (2014). Sublingual immunotherapy. *World Allergy Organization Journal*, 7(1), 1-6.
10. Canonica, G.W., Pawankar, R., and Holgate, S.T. (2013b). *WAO WHITE BOOK on allergy*. Milwaukee, Wisconsin: World Allergy Organization.
11. Cheryl, S., Hankin, C.S., Cox, L., and Bronstone, A. (2013). Allergy immunotherapy: reduced health care costs in adults and children with allergic rhinitis. *Journal of Allergy and Clinical Immunology*, 131(4), 1084-1091.
12. Cromwell, O., Häfner, D., and Nandy, A. (2011). Recombinant allergens for specific immunotherapy, *Journal of Allergy and Clinical Immunology*, 127, 865-872.
13. Douladiris, N. (2013). A molecular diagnostic algorithm to guide pollen immunotherapy in southern Europe: towards component-resolved management of allergic diseases. *International Archives of Allergy and Immunology*, 162, 163-172.
14. Durham, S.R. (2006). Sublingual immunotherapy with once-daily grass allergen tablets: a randomized controlled trial in seasonal allergic Rhinoconjunctivitis. *Journal of Allergy and Clinical Immunology*, 117(4), 802-809.
15. Eigenmann, P.A. (1998). Prevalence of IgE-mediated food allergy among children with atopic dermatitis. *Pediatrics*, 101(3), 8-79.
16. Ferreira, F. (1996). Dissection of immunoglobulin E and T lymphocyte reactivity of isoforms of the major birch pollen allergen Bet v 1: potential use of hypoallergenic isoforms for immunotherapy. *Journal of Experimental Medicine*, 183, 599–609.
17. FitzGerald, J.M., Bateman, E.D., Boulet, L.-Ph., Cruz, A.A., Haahtela, T., Levy, M.L.,



- O'Byrne, P., Paggiaro, P., Pedesen, S.E., Soto-Quiroz, M., Reddel, H.K., and Wong, G.W. (2014). *Global strategy for asthma management and prevention*. Retrieved from <https://ginasthma.org/wp-content/uploads/2019/01/2014-GINA.pdf>.
18. Fooke-Achterrath, M., Rubina, A.Y., Feizkhanova, G.U., and Filippova, M.A. (2012). Multiplex assay of allergen-specific and total immunoglobulins of E and G classes in the biochip format. *Archives of Biochemistry and Biophysics*, 447, 289-293.
  19. Gorbas, V.A., Smiyan, O.I., and Kurhanska, V.O. (2015). Changes in the colon microflora of school-age children with bronchial asthma. *New Armenian Medical Journal*, 9(3), 45-47.
  20. Guideline on the clinical development of products for specific immunotherapy for the treatment of allergic diseases. (2008). Retrieved from [http://www.ema.europa.eu/docs/en\\_GB/document\\_library/Scientific\\_guideline/2009/09/WC500003605.pdf](http://www.ema.europa.eu/docs/en_GB/document_library/Scientific_guideline/2009/09/WC500003605.pdf).
  21. Ilyina, N.I., and Pavlova, K.S. (2016). Modern aspects of solving urgent problems of allergology in Russia. *Remedium*, 1-2, 28-30.
  22. Incorvaia, C., and Fuiano, N. (2013). Seeking allergy when it hides: which are the best fitting tests? *World Allergy Organization Journal*, 6(1), 1-11.
  23. Jutel, M., Jaeger, L., and Suck, R. (2005). Allergen-specific immunotherapy with recombinant grass pollen allergens. *Journal of Allergy and Clinical Immunology*, 116, 608-613.
  24. Kudabayeva, K., Batyrova, G., Bazargaliyev, Y., Agzamova, R., and Nuftieva, A. (2017). Microelement status in children with enlarged thyroid gland in West Kazakhstan region. *Georgian Medical News*, 263, 64-71.
  25. Kudabayeva, K.I., Bazargaliyev, Y.S., Batenobna, K., and Agzamova, R.T. (2014). Peculiarities of chronic gastritis in diabetes mellitus type 2. *European Journal of Physical and Health Education*, 6, 1-5.
  26. Kulis, M. (2011). Pioneering immunotherapy for food allergy: clinical outcomes and modulation of the immune response. *Immunologic Research*, 49(3), 216-226.
  27. Kurbacheva, O.M., Pavlova, K.S., and Kozulina, I.E. (2013). Allergen-specific immunotherapy: history, methods and new possibilities. *Medical Council*, 3-2, 10-19.
  28. Maslova, L.V. (2012). Epidemiological aspects of allergic rhinitis in the Republic of Belarus. *Ars Medica*, 11, 61-66.
  29. Morenko, M.A. (2010). *Clinical and pharmacological rationale for the inclusion of glycyrrhizic acid preparations in the pharmacotherapy system of bronchial asthma in children*: (Unpublished thesis of the doctor of medical sciences). Astana: Medical University, Astana, Kazakhstan.
  30. Namazova-Baranova, L.S. (2011). *Allergy in children: from theory to practice. Series "Modern Pediatrics"*. Moscow, Russian Federation: Union of Pediatricians of Russia.
  31. Nelson, H.S. (2016). Allergen immunotherapy now and in the future. *Allergy and Asthma Proceedings*, 37(4), 268-272.
  32. Papadopoulos, N.G., Hatzler, L., and Hofmaier, S. (2012). Allergic airway diseases in childhood – marching from epidemiology to novel concepts of prevention. *Pediatric Allergy and Immunology: Official Publication of the European Society of Pediatric Allergy and Immunology*, 23(7), 616-622.
  33. Pauli, G., Larsen, T.H., Rak, S., and Valenta, R. (2008). Efficacy of recombinant birch pollen vaccine for the treatment of birch-allergic rhinoconjunctivitis. *Journal of Allergy and Clinical Immunology*, 122, 951-960.
  34. Perkin, M.R., and Genuneit, J. (2017). Overview of systematic reviews in allergy epidemiology. *Allergy*, 149(1), 32-37.
  35. Radauer, C., Bublin, M., Wagner, S., Mari, A., and Breiteneder, H. (2010). Allergens are distributed into few protein families and possess a restricted number of biochemical functions. *Journal of Allergy and Clinical Immunology*, 121, 847-852.
  36. Ramilyeva, I.R., Burkitbaev, Zh.K., Abdrakhmanova, S.A., Turganbekova, A.A., Baimukasheva, D.K., and Zhiburt, E.B. (2019). Distribution pattern for HLA specificities in the patients with acute myeloid leukemia. *Medical Immunology (Russia)*, 21(5), 965-972.
  37. Saltabaeva, U.Sh., and Morenko, M.A. (2015). *Comparative effectiveness of types of allergen-specific immunotherapy in pollinosis*. (pp. 17-18). Paper presented at the IX International scientific conference of the Eurasian Scientific Association "Prospects for



- the modernization of modern science ENO, Moscow, Russian Federation.
38. Saltabayeveva, U.Sh., and Morenko, M.A. (2017). *Allergen-specific immunotherapy for pollinosis*. Paper presented at the XVIIth International Scientific Congress "Asthma and Allergies". Almaty, Republic of Kazakhstan.
  39. Saltabayeva, U., Morenko, M., Garib, V., and Rozenson, R. (2016a). Comparative assessment of the effectiveness of the allergenspecific immunotherapy types with pollinosis. *The European Academy of Allergy and Clinical Immunology Annual Congress*, 7, 2691-2697.
  40. Saltabayeva, U., Morenko, M., Garib, V., Rozenson, R., Ispayeva, Z., Gatauova, M., Zulus, L., Karaulov, A., Gastager, F., and Valenta, R. (2016b). *Superior economic efficacy of allergen molecule-based diagnosis for prescription of immunotherapy in an area with multiple pollen exposure: a real life study*. (p. 51). Paper presented at the Annual Meeting of the OEGAI Innsbruck, Austria.
  41. Saltabayeva, U., Morenko, M., Garib, V., Rozenson, R., Ispayeva, Zh., Gatauova, M., Zulus, L., Karaulov, A., Gastager, F., and Valenta, R. (2017). Greater real-life diagnostic efficacy of allergen molecule-based diagnosis for prescription of immunotherapy in an area with multiple pollen exposure. *International Archives of Allergy and Immunology*, 173(2), 93–98.
  42. Smiyan, O.I., Plakhuta, V.A., Bunda, T.P., and Popov, S.V. (2015). Dynamics of cytokines in infants with acute obstructive bronchitis and thymomegalia. *Likars'ka sprava / Ministerstvo okhorony zdorov'ia Ukraïny*, 1-2, 81-85.
  43. Smoldovskaya, O., Feyzkhanova, G., Arefieva, A., Voloshin, S., Ivashkina, O., Reznikov, Y., and Rubina, A. (2016). Allergen extracts and recombinant proteins: comparison of efficiency of in vitro allergy diagnostics using multiplex assay on a biological microchip. *Allergy Asthma and Clinical Immunology*, 12(9), 12-17.
  44. Spergel, J.M. (2010). From atopic dermatitis to asthma: the atopic march. *Annals of Allergy, Asthma and Immunology*, 30, 269–280.
  45. The climate of Astana. (2019). Retrieved from <https://www.weatherbase.com/weather/weather-summary.php3?s=351881&cityname=Astana,+Kazakhstan>.
  46. Valenta, R., Breiteneder, H., Petternburger K., and Breitenbach, M. (1991). Homology of the major birch-pollen allergen, Bet v I, with the major pollen allergens of alder, hazel, and hornbeam at the nucleic acid level as determined by cross-hybridization. *Journal of Allergy and Clinical Immunology*, 87, 677-682.
  47. Valenta, R., Cabauatan, C., and Niespodziana, K. (2014). Induction of allergen-specific blocking IgG using patch delivered recombinant Bet v 1 in guinea pigs. *Clinical and Translational Allergy*, 4(2), 6-8.
  48. Valenta, R., Lidholm, J., and Ferreira, F. (2010). From allergen genes to allergy vaccines. *Annual Review of Immunology*, 28, 211-241.
  49. Valenta, R., Linhart, B., and Niederberger, V. (2011). Recombinant allergens for allergen-specific immunotherapy: 10 years anniversary of immunotherapy with recombinant allergens. *Allergy*, 66, 775–783.
  50. Valovirta, E., and Berstad, A.K. (2011). Design and recruitment for the GAP trial, investigating the preventive effect on asthma development of an SQ-standardized grass allergy immunotherapy tablet in children with grass pollen-induced allergic rhinoconjunctivitis. *Clinical Therapeutics*, 7, 1537-1546.
  51. Zhumambayeva, S., Rozenson R., Tawfik, A., Awadalla, N.J., and Zhumambayeva, R. (2014). Date of birth and hay fever risk in children and adolescents of Kazakhstan. *International Journal of Pediatric Otorhinolaryngology*, 78(2), 214-217.
  52. Zhuravleva, L.A., Zykova, S.S., Talismanov, V.S., and Karmanova, O.G. (2019). Antioxidant and anti-radical effects of quercetin and rutin: Methyl linoleate model. *International Journal of Pharmaceutical Research*, 11(4), 168-175.

**Table 1.** Frequency of joint positive results in vitro testing of patients for major recombinant allergens

| Recombinant major allergens                 | Total patient | Number of patients with significant sIgE (> 0.35 kE/l), (p<0.01) |       | % of the total number of patients (p <0.01) |       |
|---|---------------|--|-------|---|-------|
|   |               | before   | after | before                                      | after |
| Art v 1                                     | 153           | 26   | 17    | 17.0  | 11.1  |
| Art v 3                                     | 153           | 9  | 5     | 5.9   | 3.3   |
| Art v 1 – Art v 3                           | 153           | 73   | 47    | 47.7  | 30.7  |
| Art v1 – Art v3 – Bet v1                    | 153           | 20   | 13    | 13.1  | 8.5   |
| Art v1 – Art v3 – Phl p1 – Phl p5           | 153           | 16   | 11    | 10.5  | 7.2   |
| Art v1 – Art v3 – Bet v 1 – Phl p1 – Phl p5 | 153           | 9  | 7     | 5.9   | 4.6   |
| Total                                       | 153           | 153  | 100   | 100.0                                       | 65.4  |

**Table 2.** Frequency of joint positive results in vitro testing of patients of group 1 (SLIT) for recombinant allergens

| Recombinant major allergens                 | Total patient | Number of patients with significant sIgE (> 0.35 kE/l), (p<0.01) |       | % of the total number of patients (p <0.01) |       |
|---|---------------|--|-------|---|-------|
|   |               | before   | after | before                                      | after |
| Art v 1                                     | 95            | 17   | 10    | 17.9  | 10.5  |
| Art v 3                                     | 95            | 6  | 3     | 6.3   | 3.2   |
| Art v 1 – Art v 3                           | 95            | 43   | 26    | 45.3  | 27.4  |
| Art v1 – Art v3 – Bet v1                    | 95            | 13   | 8     | 13.7  | 8.4   |
| Art v1 – Art v3 – Phl p1 – Phl p5           | 95            | 11   | 8     | 11.6  | 8.4   |
| Art v1 – Art v3 – Bet v 1 – Phl p1 – Phl p5 | 95            | 5  | 4     | 5.3   | 4.2   |
| Total                                       | 95            | 95   | 59    | 100.0                                       | 62.1  |

**Table 3.** Frequency of joint positive results in vitro testing of patients of group 2 (PIT) for recombinant allergens

| Recombinant major allergens                 | Total patient | Number of patients with significant sIgE (> 0.35 kE/l), (p<0.01) |       | % of the total number of patients (p <0.01) |       |
|---|---------------|--|-------|---|-------|
|   |               | before   | after | before                                      | after |
| Art v 1                                     | 58            | 9  | 7     | 15.5  | 12.1  |
| Art v 3                                     | 58            | 3  | 2     | 5.2   | 3.4   |
| Art v 1 – Art v 3                           | 58            | 30   | 22    | 51.7  | 37.9  |
| Art v1 – Art v3 – Bet v1                    | 58            | 7  | 5     | 12.1  | 8.6   |
| Art v1 – Art v3 – Phl p1 – Phl p5           | 58            | 5  | 3     | 8.6   | 5.2   |
| Art v1 – Art v3 – Bet v 1 – Phl p1 – Phl p5 | 58            | 4  | 3     | 6.9   | 5.2   |
| Total                                       | 58            | 58   | 42    | 100.0                                       | 72.4  |

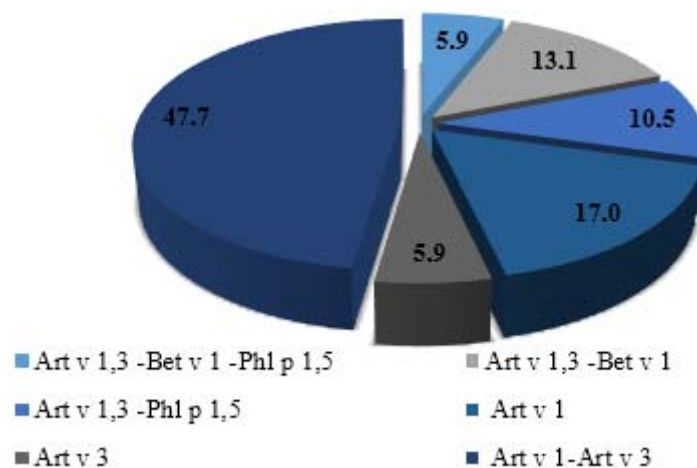


**Figure 1.** The degree of sensitization to various recombinant allergens Art v1, Art v3, Amb a1, Phlp p1, Phl 5 and Bet v1

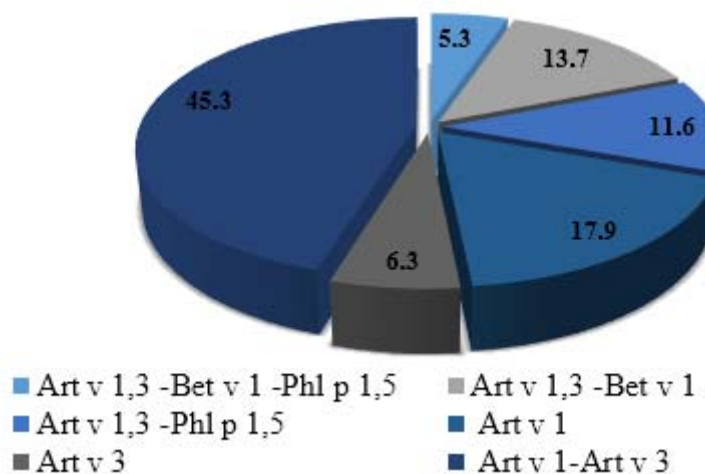


**Figure 2.** The degree of sensitization of group 1 (SLIT) to various recombinant major allergens Art v1, Art v3, Phl p1, Phl 5 and Bet v1

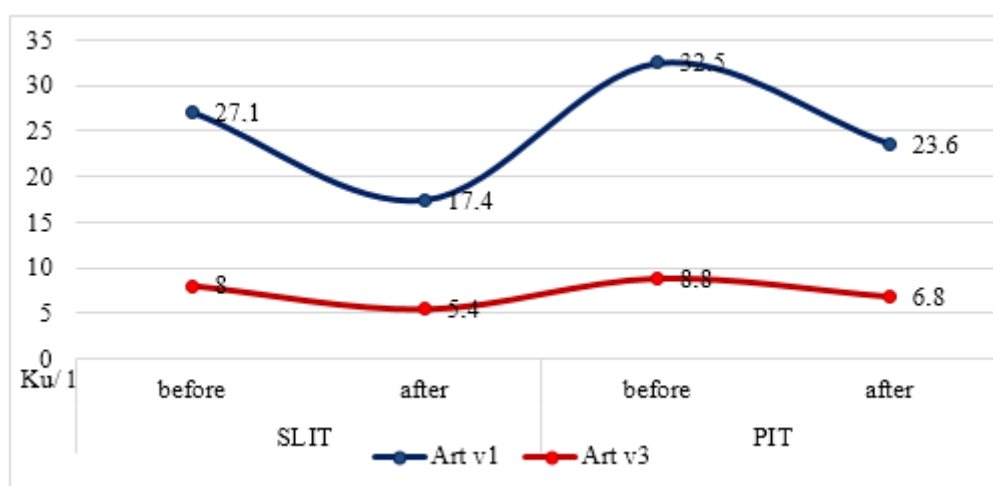


**Figure 3.** Comparative evaluation of recombinant major allergens Art v1, Art v3 against the background of SLIT and PIT

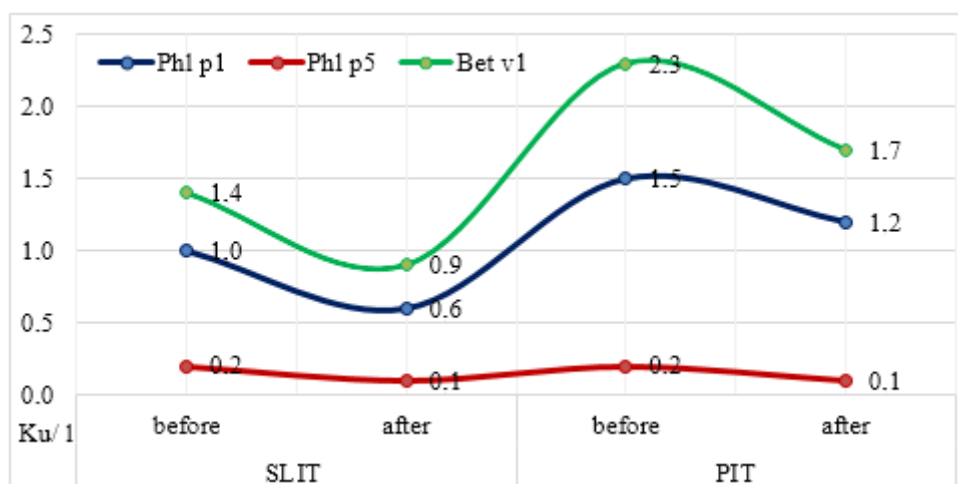


**Figure 4.** Comparative evaluation of recombinant major allergens Phl p1, Phl 5, Bet v1 on the background of SLIT and PIT

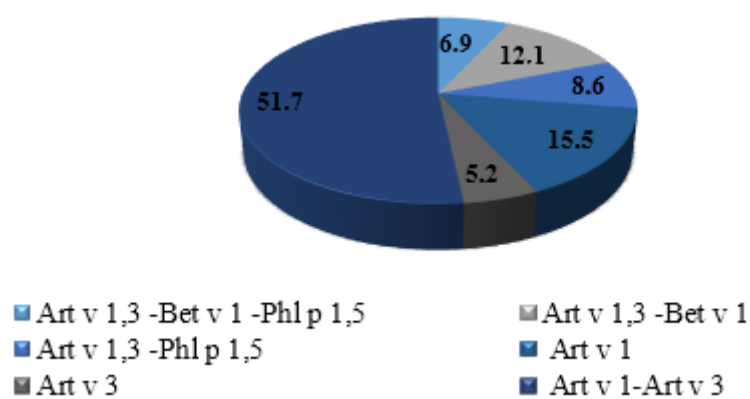


**Figure 5.** The degree of sensitization of patients of group 2 (PIT) to various recombinant major allergens

## PADRÃO DE PRODUÇÃO DE CÁPSULAS DE *ESCHERICHIA COLI* UROPATOGÊNICAS DE PACIENTES COM INFECÇÃO DO TRATO URINÁRIO EM HOSPITAIS DE KIRKUK

### CAPSULE PRODUCTION PATTERN OF UROPATHOGENIC *ESCHERICHIA COLI* OF URINARY TRACT INFECTION PATIENTS IN KIRKUK HOSPITALS

نمط إنتاج الكبسول لبكتيريا الإشريكية القولونية البولية من مرضى التهاب المسالك البولية في مستشفيات كركوك

UMRAN, May Ali Hussien<sup>1</sup>; AL-KHATEEB, Sumaya Najim<sup>2\*</sup>

<sup>1</sup> Alzahrawi Surgical Hospital, Maysan Health Directorate, Ministry of Health, Iraq.

<sup>2</sup> Faculty of Medicine, University of Kufa, Najaf, Iraq.

\* Correspondence author

e-mail: sumayanajim30@gmail.com

Received 16 May 2020; received in revised form 22 May 2020; accepted 17 June 2020

## RESUMO

A bactéria *Escherichia coli* é um dos melhores organismos de vida livre estudados em profundidade. É uma espécie surpreendentemente diversificada, já que algumas cepas de *E. coli* vivem no intestino de animais como comensais inofensivos, enquanto outros genótipos distintos, como uma *E. coli* enteropatogênica ou enterohemorrágica, por exemplo, causam morbidade e morte marcadas como patógenos intestinais humanos. Este estudo teve como objetivo desenvolver e validar um ensaio de PCR para uma região gênica conhecida e suspeita de fator de virulência (*kpsMT*) de *E. coli* uropatogênica para determinar a distribuição do gene e seu papel no desenvolvimento de doenças clínicas do sistema urinário. Um total de 25 amostras de urina foram coletadas de pacientes com infecção do trato urinário (ITU) dos hospitais Azadi e Kirkuk, na cidade de Kirkuk, Iraque. Foram coletadas amostras de ambos os sexos e idades diferentes de pacientes com suspeita de infecção do trato urinário de acordo com as manifestações clínicas e sintomas diagnosticados pelo médico examinador. As amostras foram cultivadas e as amostras positivas foram submetidas ao teste IMViC para identificar as bactérias *E. coli* e, posteriormente, identificadas usando o sistema compacto Vitek 2. Entre 25 amostras, 24 (96%) apresentaram resultados positivos para o crescimento cultural bacteriano. Dessas, 17 (68%) foram identificadas como *Escherichia coli*. Do total de 17 isolados, 14 tinham infecção no trato urinário leve e 3 tinham urosepsia. O gene *kpsMT* estava presente em 14 isolados (82,3%), incluindo 11 (78,5%) isolados de infecção no trato urinário leve e 3 (100%) isolados de pacientes com urosepsia. Concluiu-se que *Escherichia coli* é a mais prevalente em amostras de infecção no trato urinário na urina. Devido à abundância do gene *kpsMT* na *Escherichia coli* uropatogênica (UPEC), esse gene desempenha um papel importante no desenvolvimento de ITU se não for tratado corretamente e rapidamente; casos leves de ITU podem se transformar em urosepsia.

**Palavras-chave:** *Escherichia coli*, uropatogênico, IMViC, Capsule, gene *kpsMT*.

## ABSTRACT

The bacterium *Escherichia coli* is one of the best free-living organisms studied in depth. It is a surprisingly diverse species, since some strains of *E. coli* live in the intestine of animals as harmless commensals, while other distinct genotypes, such as an enteropathogenic or enterohemorrhagic *E. coli*, for example, cause morbidity and death marked as human intestinal pathogens. The purpose of this study was to develop and validate a PCR assay for a known and suspected uropathogenic *E. coli* virulence factor (*kpsMT*) gene region to determine the distribution of the gene and its role in the development of clinical diseases of the urinary system. A total of 25 urine samples were collected from patients with urinary tract infection (UTI) at Azadi and Kirkuk hospitals in the city of Kirkuk, Iraq. Samples of both genders and different ages were collected from patients with suspected urinary tract infection according to the clinical manifestations and symptoms diagnosed by the examining physician. The samples were cultured and positive samples were subjected to the IMViC test to identify *E. coli* bacteria and subsequently identified using the Vitek 2 compact system. Among 25 samples, 24 (96%) showed positive results for bacterial cultural growth. Of these, 17 (68%) were identified as *Escherichia coli*. Of the total of 17 isolates, 14 from patients with mild urinary tract infection, and 3 from patients with Urosepsis. The *kpsMT* gene was present in 14 isolates (82.3%), including 11 (78.5%) isolates from patients with mild urinary tract infection, and 3 (100%) isolates from patients with Urosepsis. It was concluded that *Escherichia coli* is the most prevalent

in urine tract infection samples. Due to the abundance of the *kpsMT* gene in uropathogenic *Escherichia coli* (UPEC), this gene plays an important role in developing UTI if it is not treated correctly and quickly; mild cases of UTI can turn into Urosepsis.

**Keywords:** *Escherichia coli*, Uropathogenic, IMViC, Capsule, *kpsMT* gene.

## المخلص

بكتيريا الإشريكية القولونية هي واحدة من أفضل الكائنات الحية التي تمت دراستها بعمق. هذه الأنواع تكون متغيرة فيما بينها بشكل مثير للدهشة، حيث أن بعض سلالات الإشريكية القولونية تعيش في الأمعاء كعلاقة تبادل منفعة، بينما الانماط الجينية الأخرى، مثل الإشريكية القولونية الممرضة المعوية أو الإشريكية القولونية النزفية، على سبيل المثال، تسبب الأمراض والوفيات والذي يشار إليها بمسببات الأمراض المعوية البشرية. الغرض من هذه الدراسة هو لتطور وتحقق اختبار تفاعل البوليميراز المتسلسل لمنطقة معلومة ومشتبهة لجين عامل الضراوة *kpsMT* لتحديد معرفة توزيع هذا الجين ودوره في تطوير الأمراض السريرية للجهاز البولي. تم جمع 25 عينة بول من مرضى يعانون من عدوى المسالك البولية في مستشفيات آزادي وكركوك في مدينة كركوك، العراق. تم جمع عينات من كلا الجنسين ومن أعمار مختلفة من المرضى الذين يشتبه في إصابتهم بالتهاب المسالك البولية وفقاً للمظاهر والأعراض السريرية التي تم تشخيصها من قبل الطبيب الفاحص. تم زرع العينات والعينات الوجيهة للنمو أجري لها اختبار IMViC لتحديد بكتيريا الإشريكية القولونية ومن ثم شُخصت باستخدام نظام Vitek 2 compact system. من بين 25 عينة، أظهرت 24 عينة (96%) نتائج إيجابية للنمو البكتيري، حيث تم تحديد 17 (68%) منها على أنها بكتيريا الإشريكية القولونية. في هذه الدراسة، من أصل 17 عينة كان 14 من المصابين بالتهاب مجرى البول البسيط و 3 من المصابين بآنتان المسالك البولية، كان الجين *kpsMT* موجوداً في 14 عينة (82.3%) بما في ذلك 11 (78.5%) من المصابين بالتهاب مجرى البول البسيط و 3 (100%) من مرضى آنتان المسالك البولية. خلُصت هذه الدراسة إلى أن الإشريكية القولونية هي الأكثر انتشاراً في عينات المسالك البولية. بسبب وفرة الجين *kpsMT* في سلالات بكتيريا الإشريكية القولونية البولية (UPEC) حيث يلعب دوراً مهماً في تطوير التهاب المسالك البولية إذا لم يتم التعامل معها بشكل صحيح وسريع، فقد تتطور الحالات البسيطة من التهاب المسالك البولية إلى آنتان المسالك البولية.

**الكلمات المفتاحية:** الإشريكية القولونية، مسببة لأمراض الجهاز البولي، IMViC، الكبسول، جين *kpsMT*.

## 1. INTRODUCTION:

The bacterium *Escherichia coli* is one of the best free-living organisms studied in depth. It's a surprisingly diverse species as well since some *E. coli* strains live in animal intestines as harmless commensals, whilst other distinct genotypes, including enteropathogenic, enterohemorrhagic, enteroinvasive, enterotoxigenic and enteroaggregative *E. coli* causes marked morbidity and death as human intestinal pathogens. Extraintestinal *E. coli* are another diverse category of life-threatening pathogenic bacteria. This latter group of pathogens includes separate clonal groups responsible for sepsis of neonatal meningitis and infections of the urinary tract. The uropathogenic group accounts for 70–90% of the 7 million cases of acute cystitis and 250,000 cases of pyelonephritis reported in the United States annually (Hooton and Stamm, 1997).

The extraintestinal *E. coli* differs from diarrheal pathogens because when they enter the urinary tract, bloodstream, or cerebrospinal fluid, they can act as either harmless human intestinal inhabitants or serious pathogens (Welch *et al.*, 2002). Within each of these broad groups are sets of strains known as pathotypes that share common virulence factors and elicit similar pathogenic outcomes (Marrs *et al.*, 2005). Several pathotypes of diarrheagenic *E. coli* give rise to gastroenteritis, but rarely cause disease outside of the intestinal tract. ExPEC, on the other hand, has

maintained the ability to exist in the intestine without consequence but can spread and colonize different host niches, including the blood, central nervous system, and urinary tract, leading to disease (Wiles *et al.*, 2008). Urosepsis refers to severe infection of the urinary tract and/or the male genital tract (e.g., prostate) with features consistent with systemic inflammatory response syndrome (Kalra and Raizada, 2006).

The severity of disease conditions that are associated with UTI depends on multiple UPEC VFs and host susceptibility. A wide range of VFs genes such as adhesins (*fim*, *sfa*, *afal*, *iha*, *papC*, *tsh*, and *papGI*, -II, and also -III), iron acquisition systems (*irp2*, and *iuc*, *iroN*), protectins (*kpsMT*, and *iss*, *ompT*), and genes encoding for toxins (*astA*, *cnf1*, *hlyA*, *usp*, *set*, *vat*, and *cva/cvi*) are involved in the pathogenicity conditions of UPEC (Abe *et al.*, 2008; Chiou *et al.*, 2010). Pathogenic bacteria produce a thick, mucus-like layer of polysaccharide, called capsule coat antigenic proteins on the bacterial surface, otherwise, induce an immune response and lead to the destruction of the bacteria. Polysaccharides capsules are water-soluble, usually acidic, thermo-stable, and have molecular weights on the order of 100–2000 kDa, linear and consist of regularly repeating subunits of one to six monosaccharides. There is massive structural diversity; nearly two hundred different polysaccharides are produced by *E. coli* alone (Yun *et al.*, 2014). The gene *kpsMT* encodes for the K antigen capsule, which Enables UPEC to

evade the host's innate immune defenses (e.g., the complement system) (Justice *et al.*, 2006).

This study aimed to develop and validate a PCR assay for a known and suspected uropathogenic *E. coli* virulence factor (*kpsMT*) gene region to determine the distribution of the gene and its role in the development of clinical diseases of the urinary system.

## 2. MATERIALS AND METHODS:

### 2.1. Sample collections and strain identification assay

A total of 25 midstream urine samples were collected from hospitalized UTI patients of different ages and gender from local hospitals in Kirkuk / Iraq. Permission to conduct this study was issued by the Health institutional, and the collection of samples of individuals was carried out by under public health technician supervision. All participants have agreed to participate in this study, which was conducted from September 2019 to December 2019. All 25 specimens have been cultured on Blood agar, MacConkey agar, and Eosin methylene blue agar. The preparation of biochemical tests to confirm differentiation of *E. coli* from other lactose fermenters among Enterobacteriaceae was done by the following: IMViC test include: indole positive, methyl red positive, negative in the Voges-Proskauer, and, Simmons citrate also urease production, (MacFaddin, 2002). The results of biochemical tests for the final identification of *E. coli* were based on growth morphology on EMB agar and Vitek 2 compact system.

### 2.2. Primer design

The primers used to amplify *kpsMT* gene were designed using (Pick Primers) tool in the National Center for Biotechnology Information (NCBI) website and were manufactured by the Alpha company (Canada). The primers information is described in Table 1.

### 2.3. Extraction of Deoxyribonucleic acid

Bacterial chromosomal DNA of *E. coli* isolates was extracted by Geneaid™ DNA Isolation Kit based on the manufacturer's instructions. The Deoxyribonucleic acid has been evaluated by a nanodrop system that tuned to 260/280nm. Then the DNA was preserved at temperature (-20°C) till further use.

### 2.4. Polymerase chain reaction analysis

The PCR assay was performed to detect the Virulence gene (Table 1), were primer *kpsMT* gene that encodes for capsule in *Escherichia coli* based on specified primers. The virulence gene was screened by PCR technique. For the detection this gene; The Chromosomal DNA extracted from all isolates were subjected to primers by monoplex PCR. The mixture of PCR for each primer with final volume 20 µl/reaction and The protocol used depends on Master Mix(AccuPower® PCR PreMix (Bioneer, Korea) instructions. Each monoplex PCR reaction mixture consisted of 2µl Forward Primer (10 picomole), 2µl Reverse Primer (10 picomole), 9µl De-ionized water, and 7µl the DNA of the isolates were added into the AccuPower® Taq PCR PreMix tubes that contain (Taq DNA polymerase, dNTPs, KCl, MgCl<sub>2</sub>, and buffer). All PCR components were assembled in PCR tube and mixed by micro-centrifuge at 50 rcf (850 rpm) for 10 second. The PCR reactions began with a 94°C Denaturation for 5 minutes and were terminated with 72°C extension for 3 minutes and a 4°C hold and The Condition for other steps for this primer consisted of 25 cycles of a denaturation at 94°C for 2 min annealing at 65°C for 1 min then extension at 72°C for 2 min in the thermal cycler based on the primer design designated T<sub>m</sub> and some modifications for optimization (Qadir *et al.*, 2018).

### 2.5. PCR product analysis

PCR product has been examined via Electrophoresis instrument in a 0.9% agarose gel substance with the use of TBE buffer, which stained by Ethidium Bromide. The product was visualized and documented under ultra-violet trans-illuminator (Mishra *et al.*, 2010).

## 3. RESULTS AND DISCUSSION:

Characterization of *E. coli* strains is essential for both epidemiological and clinical implications. Pathogenic behavior is predicted both by repertoire of the virulence factor and by phylogenetic background (Duriez *et al.*, 2001; Picard *et al.*, 1999). Urinary tract infection can, in time, develop into a real threat, capable of expanding to renal failure. Enhanced knowledge of the virulence characteristics of the causative organism allows the clinician to predict the evolution of infection within the host. In the current study, From 25 urine samples, 18 (72%) were from female, and 7 (28%) from male, 17 (68%) isolates of *E. coli*, 4 (16%) isolates *Klebsiella pneumonia*,

3 (12%) isolates *Proteus mirabilis* and one sample (4%) showed no growth, the profile of the causative agents are listed in Table 2. Among *E. coli* causing infection, out of 17 isolates, 12 (70.5%) were taken from female patients, and 5 (29.4%) were from male patients, and this rate was close to the results of (Qadir *et al.*, 2018) in Wasit/Iraq and (Aljebory and Mohammad, 2019) in Kirkuk/Iraq as they showed that *E. coli* was the most predominant cause of UTI and that females were more susceptible to it than male. Moreover, the female to male ratio concerning Mild-UTI/Urosepsis is described in Table 3.

Recently, several different prevalence rates of UPEC strains related to UTIs have been described in different countries (Derakhshandeh *et al.*, 2015), (Mohajeri *et al.*, 2014), (Lee *et al.*, 2013). The capsule-encoding gene, *kpsMT*, is commonly prevalent in UPEC strains associated with pyelonephritis than in strains associated with other UTIs (Sussman, 1997). In the current study, the gene *kpsMT* was investigated due to its role in evading the immune system, hence causing severe conditions of UTI. The study finding of this gene have shown that 14 (82.3%) isolates were carrying *kpsMT* gene including 11 (78.5%) isolates from Mild-UTI, and 3 (100%) isolates from Urosepsis patients which leads to the assumption that even the (Mild-UTI) patients are susceptible to severe UTI conditions or Urosepsis if not managed in a short period. A demonstration of the assay is shown in Figure 1. The distribution of *kpsMT* gene in relation to Mild-UTI/Urosepsis is shown in Table 4.

Fever, flank pain, dysuria, frequency, urgency, and suprapubic pain has been the observed clinical symptoms of our study and can be compared with the Bent's report (Bent *et al.*, 2002). Several studies have had an approaching result to this study; there was a report of *kpsMT* gene's existence to be (84.4%) among Uropathogenic *E. coli* isolates revealed by (Yun *et al.*, 2014), similar results were shown by (Aljebory and Mohammad, 2019) in Kirkuk/Iraq as they found that (76.4%) of the isolates were carrying *kpsMT* gene, (Qadir *et al.*, 2018) in Wasit/Iraq and (Yamamoto, 2007) in Japan had close results to this study. However, the results of researches done by (Alqasim *et al.*, 2020) and (Johnson and Stell, 2000) did not match with this study as they revealed (51.7%) and (63%) respectively. However, these strains need to be sequenced by 16S rRNA or RAPD-typing for further studies as recommended by Salih and Shafeek, 2019; Banoon *et al.*, 2019; Aldujaili and Banoon, 2020).

## 4. CONCLUSIONS:

*Escherichia coli* are the most prevalent among UTI urine samples. Due to the abundance of the gene *kpsMT* in UPEC, there is a role of this gene in developing UTI. For the same reasons above, mild UTI cases can develop into Urosepsis if not treated accordantly and quickly.

## 5. ACKNOWLEDGMENTS:

I would like to show my appreciation to Karwan Azeez Mohammed Shaexany at Kirkuk University, College of Science, Department of Biology for collecting the samples and designing the PCR primers, due to his support, this research was doable.

## 6. REFERENCES:

1. Abe, C. M., Salvador, F. A., Falsetti, I. N., Vieira, M. A., Blanco, J., Blanco, J. E., Machado, A. M.O., Elias, W.P., Hernandez, R.T., and Gomes, T. A. (2008). Uropathogenic *Escherichia coli* (UPEC) strains may carry virulence properties of diarrhoeagenic *E. coli*. *FEMS Immunology & Medical Microbiology*, 52(3), 397-406.
2. Aldujaili, N H and Banoon, S. R.(2020) Antibacterial Characterization of Titanium Nanoparticles Nanosynthesized by *Streptococcus Thermophilus*. *Periódico Tchê Química*. 17(34):311-320.
3. Aljebory, I. S., and Mohammad, K. A. (2019) Molecular Detection of Some Virulence Genes of *Escherichia coli* Isolated from UTI Patients in Kirkuk City, Iraq. *Journal of Global Pharma Technology*, 11(03) (Suppl.), 349-355.
4. Alqasim, A., Jaffal, A. A., and Alyousef, A. A. (2020). Prevalence and molecular characteristics of sequence type 131 clone among clinical uropathogenic *Escherichia coli* isolates in Riyadh, Saudi Arabia. *Saudi Journal of Biological Sciences*, 27(1), 296-302.
5. Banoon, S. R., Kadhim, Z. K., Aziz, Z. S., and EWadh, R. M. (2019). Using Random Amplified Polymorphic DNA (RAPD) Fingerprinting Technique to Analyze Genetic Variation in *Staphylococcus Aureus* Isolated from Different Sources in Babylon Province Hospitals. *Indian Journal of Public Health Research & Development*, 10(9), 1300-1305.



6. Bent, S., Nallamotheu, B. K., Simel, D. L., Fihn, S. D., and Saint, S. (2002). Does this woman have an acute uncomplicated urinary tract infection?. *Jama*, 287(20), 2701-2710.
7. Chiou, Y. Y., Chen, M. J., Chiu, N. T., Lin, C. Y., and Tseng, C. C. (2010). Bacterial virulence factors are associated with occurrence of acute pyelonephritis but not renal scarring. *The Journal of urology*, 184(5), 2098-2102.
8. Derakhshandeh, A., Firouzi, R., Motamedifar, M., Motamedi Boroojeni, A., Bahadori, M., Arabshahi, S., Novinrooz, A. and Heidari, S. (2015). Distribution of virulence genes and multiple drug-resistant patterns amongst different phylogenetic groups of uropathogenic *Escherichia coli* isolated from patients with urinary tract infection. *Letters in applied microbiology*, 60(2), 148-154.
9. Duriez, P., Clermont, O., Bonacorsi, S., Bingen, E., Chaventre, A., Elion, J., Picard, B. and Denamur, E. (2001) Commensal *Escherichia coli* isolates are phylogenetically distributed among geographically distinct human populations. *Microbiology*, 147(6), 1671-1676.
10. Hooton, T. M., and Stamm, W. E. (1997). Diagnosis and treatment of uncomplicated urinary tract infection. *Infectious Disease Clinics*, 11(3), 551-581.
11. Johnson, J. R., and Stell, A. L. (2000). Extended virulence genotypes of *Escherichia coli* strains from patients with urosepsis in relation to phylogeny and host compromise. *The Journal of infectious diseases*, 181(1), 261-272.
12. Justice, S. S., Hunstad, D. A., Seed, P. C., and Hultgren, S. J. (2006). Filamentation by *Escherichia coli* subverts innate defenses during urinary tract infection. *Proceedings of the National Academy of Sciences*, 103(52), 19884-19889.
13. Kalra, O. P., and Raizada, A. (2006). Management issues in urinary tract infections. *J Gen Med*, 18, 16-22.
14. Lee, D. S., Choe, H. S., Lee, S. J., Bae, W. J., Cho, H. J., Yoon, B. I., Cho, Y.H., Han, C. H., Jang, H., Park, S.B., Cho, W.J., and Lee, S.J.(2013). Antimicrobial susceptibility pattern and epidemiology of female urinary tract infections in South Korea, 2010-2011. *Antimicrobial agents and chemotherapy*, 57(11), 5384-5393.
15. MacFaddin, J. F. (2000). Biochemical Tests for Identification of Medical Bacteria, Williams and Wilkins. *Philadelphia, PA*, 113.
16. Marrs, C. F., Zhang, L., and Foxman, B. (2005). *Escherichia coli* mediated urinary tract infections: are there distinct uropathogenic *E. coli* (UPEC) pathotypes?. *FEMS microbiology letters*, 252(2), 183-190.
17. Mishra, V., Nag, V. L., Tandon, R., and Awasthi, S. (2010). Response Surface Methodology-Based Optimisation of Agarose Gel Electrophoresis for Screening and Electrophoretotyping of Rotavirus. *Applied biochemistry and biotechnology*, 160(8), 2322-2331.
18. Mohajeri, P., Khademi, H., Ebrahimi, R., Farahani, A., and Rezaei, M. (2014). Frequency distribution of virulence factors in uropathogenic *Escherichia coli* isolated from Kermanshah in 2011-2012. *International Journal of Applied and Basic Medical Research*, 4(2), 111.
19. Picard, B., Garcia, J.S., Gouriou, S., Duriez, P., Brahimi, N., Bingen, E., Elion, J. and Denamur, E. (1999) The link between phylogeny and virulence in *Escherichia coli* extraintestinal infection. *Infection and immunity*, 67(2), 546-553.
20. Qadir, H. A. H., Abdulla, A. B. A. S., and Abduljabbar, H. N. (2018). Molecular Study of Virulence Factors of *Escherichia coli* Isolated from Patient with urinary tract infection in Wasit Province.
21. Salih, T. S., and Shafeek, R. R. (2019). In silico Detection of Acquired Antimicrobial Resistance Genes in 110 Complete Genome Sequences of *Acinetobacter baumannii*. *Jordan Journal of Biological Sciences*, 12(5).
22. Sussman, M. (1997). *Escherichia coli* and human disease. *Escherichia coli Mechanisms of virulence*, 3-48.
23. Welch, R. A., Burland, V., Plunkett, G. I. I., Redford, P., Roesch, P., Rasko, D., Buckles, E. L., Liou, S. R., Boutin, A., Hackett, J., Stroud, D., Mayhew, G. F., Rose, D. J., Zhou, S., Schwartz, D. C., Perna, N. T., Mobley, H. L. T.,

- Donnenberg, M. S., and Blattner, F. R. (2002). Extensive mosaic structure revealed by the complete genome sequence of uropathogenic *Escherichia coli*. *Proceedings of the National Academy of Sciences*, 99(26), 17020-17024.
24. Wiles, T. J., Kulesus, R. R., and Mulvey, M. A. (2008). Origins and virulence mechanisms of uropathogenic *Escherichia coli*. *Experimental and molecular pathology*, 85(1), 11-19.
25. Yamamoto, S. (2007). Molecular epidemiology of uropathogenic *Escherichia coli*. *Journal of infection and Chemotherapy*, 13(2), 68-73.
26. Yun, K. W., Kim, H. Y., Park, H. K., Kim, W., & Lim, I. S. (2014). Virulence factors of uropathogenic *Escherichia coli* of urinary tract infections and asymptomatic bacteriuria in children. *Journal of Microbiology, Immunology and Infection*, 47(6), 455-461.

**Table 1.** Primers information

|                            | Primer sequence (5'→3') | Template strand | Length | Primer coordinates |      | Tm    | GC%   | GenBank accession number |
|----------------------------|-------------------------|-----------------|--------|--------------------|------|-------|-------|--------------------------|
|                            |                         |                 |        | Start              | Stop |       |       |                          |
| <b>Forward</b>             | GTGTCCCAGCCCAGGTTTTTA   | Plus            | 21     | 3659               | 3679 | 60.48 | 52.38 | AF007777.1               |
| <b>Reverse</b>             | CATCACGTAACAAGATGCCCA   | Minus           | 21     | 4860               | 4840 | 58.64 | 47.62 |                          |
| <b>Product length (bp)</b> |                         | 1202            |        |                    |      |       |       |                          |

**Table 2.** The profile of the causative agentes

| Samples       | Total   | <i>E. coli</i> (%) | <i>Klebsiella pneumonia</i> (%) | <i>Proteus mirabilis</i> (%) | no growth (%) |
|---------------|---------|--------------------|---------------------------------|------------------------------|---------------|
| <b>Total</b>  | 25      | 17 (68)            | 4 (16)                          | 3 (12)                       | 1 (4)         |
| <b>Male</b>   | 7 (28)  | 5 (20)             | 2(8)                            | 0(0)                         | 0(0)          |
| <b>Female</b> | 18 (72) | 12 (48)            | 2(8)                            | 3(12)                        | 1(4)          |

**Table 3.** Female to Male ratio in relation to Mild-UTI/Urosepsis caused by *E. coli*

| Cases     | Total (n=17) | Female (n=12) | Male (n=5) |
|-----------|--------------|---------------|------------|
| Mild-UTI  | 14           | 10            | 4          |
| Urosepsis | 3            | 2             | 1          |

**Table 4.** Distribution of *kpsMT* gene in relation to Mild-UTI/Urosepsis

| Cases     | Total n=17 | <i>kpsMT</i> Positive n=14 (%) |
|-----------|------------|--------------------------------|
| Mild-UTI  | 14         | 11 (78.5)                      |
| Urosepsis | 3          | 3 (100)                        |

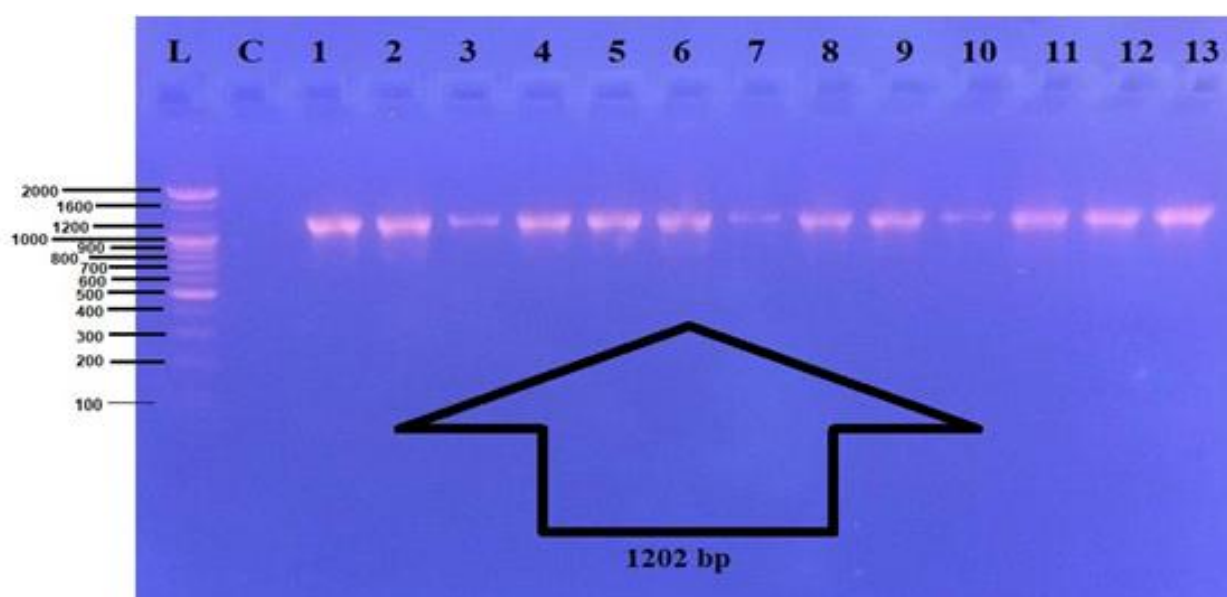


**Figure 1.** Electrophoresis of agarose Gel for products of PCR for the inspection of *kpsMT* gene (1202bp) in 0.9% agarose at 70 volt for 60 minutes, stained via ethidium bromide, L: 100-2000bp Ladder, Lane C: negative control, lanes (1 to 13): Positive for *kpsMT* gene (1202bp).

## EXTRAÇÃO DE PONTO DE NÉVOA ECO-AMIGÁVEL ACOPLADA COM UM MÉTODO ESPECTROFOTOMÉTRICO PARA A DETERMINAÇÃO DO HIDROCLORETO RANITIDINA EM AMOSTRAS FARMACÊUTICAS

### ECO-FRIENDLY CLOUD POINT EXTRACTION COUPLED WITH A SPECTROPHOTOMETRIC METHOD FOR THE DETERMINATION OF RANITIDINE HYDROCHLORIDE IN PHARMACEUTICAL SAMPLES

الاستخلاص بنقطة الغيمة مع طريقة طيفية لتقدير الرانيتيدين هيدروكلوريد في النماذج الصيدلانية

SHAHEED, Ihsan Mahdi <sup>1\*</sup>; HATAM, Raghad Saad<sup>2</sup>; KUDHAIR, Ahmed F.<sup>3</sup>, and MOHAMMED, Noor Jamal<sup>4</sup>

<sup>1,3</sup> University of Kerbala, Faculty of Science, Department of Chemistry, Kerbala. Iraq.

<sup>2</sup> University of Kerbala, Faculty of Science, Department of biology, Kerbala. Iraq.

<sup>4</sup> University of Baghdad, Faculty of Science for Women, Department of Chemistry, Baghdad, Iraq.

\* Correspondence author

e-mail: ihsan.aldahan@uokerbala.edu.iq

Received 07 March 2020; received in revised form 20 May 2020; accepted 18 June 2020

## RESUMO

O método simples, rápido, econômico e ambientalmente amigável foi desenvolvido para a determinação espectrofotométrica do cloridrato de ranitidina (R-HCl) em amostras farmacêuticas após extração pelo método do ponto de névoa. O método baseado na redução de Fe(III) pelo cloridrato de ranitidina em Fe(II), que posteriormente reagiu com o ferricianeto para formar produtos coloridos em (pH 4,0), o surfactante Triton X-114 foi usado como um extrator do cloridrato de ranitidina. A linearidade da curva de calibração foi mantida a partir de concentrações entre 0,5-60,0 µg/mL na absorção máxima de 693 nm. Fatores necessários para condições de reação, incluindo pH, FeCl<sub>3</sub> e K<sub>3</sub>[Fe(CN)<sub>6</sub>], volume de surfactante, temperatura, tempo e ordem de adição foram investigados. A análise de regressão indica que o coeficiente de correlação foi de 0,9998 e a capacidade de absorção molar foi de 0,46·10<sup>4</sup> L/mol.cm. Os limites de detecção e quantificação foram de 0,475 e 1,567 µg/mL, respectivamente. O limite de confiança do declive e o limite de confiança do intercepto a 95% foram 0,0147 ± 0,00015 e 0,0642 ± 0,01033. A sensibilidade de Sandell também foi calculada e foi encontrado 0,0680 µg/cm<sup>2</sup>. O fator de pré-concentração foi de 50,0%. Os estudos de validação para três concentrações diferentes (5,0, 10,0 e 30,0) µg/mL de cloridrato de ranitidina deram desvios padrão relativos entre 0,142-0,728 e a porcentagem de recuperações variou de 98,780 ± 0,719 – 99,840 ± 0,142. O método proposto foi aplicado com sucesso para a determinação do cloridrato de ranitidina em alguns de seus produtos farmacêuticos, com recuperação entre 99,108–99,808 e RSD% entre 0,012– 0,031. Os resultados obtidos com o método proposto o tornam adequado para uso na determinação do cloridrato de ranitidina em sua forma de dosagem a granel e em comprimidos.

**Palavras-chave:** *Ponto de névoa; Ranitidina; Espectrofotometria.*

## ABSTRACT

The simple, rapid, economical, and environmentally friendly method was developed for spectrophotometric determination of ranitidine hydrochloride (R-HCl) in pharmaceutical samples after extraction by the cloud point method. The method based on the reduction of Fe(III) by ranitidine hydrochloride to Fe(II), which subsequently reacted with ferricyanide to form colored products at (pH 4.0), then Triton X-114 surfactant was used as an extractant for ranitidine hydrochloride. The linearity of the calibration curve was maintained from concentrations between 0.5–60.0 µg/mL at the maximum absorption 693 nm. Factors required for reaction conditions including pH, FeCl<sub>3</sub>, and K<sub>3</sub>[Fe(CN)<sub>6</sub>] concentration, the volume of surfactant, temperature, time, and order of addition were investigated. Regression analysis indicates that the correlation coefficient was 0.9998 and the molar absorptivity was 0.46·10<sup>4</sup> L/mol.cm. Detection and quantification limits were 0.475 and 1.567 µg/mL, respectively. The confidence limit of slope and the confidence limit of the intercept at 95% were 0.0147 ± 0.00015

and  $0.0642 \pm 0.01033$ . Sandell's sensitivity was also calculated and it was found  $0.0680 \mu\text{g}/\text{cm}^2$ . The preconcentration factor was 50.0%. Validation studies for three different concentrations (5.0, 10.0 and 30.0)  $\mu\text{g}/\text{mL}$  of ranitidine hydrochloride gave relative standard deviations between 0.142–0.728 and the percentage recoveries ranged from  $98.780 \pm 0.719$  –  $99.840 \pm 0.142$ . The proposed method was successfully applied for the determination of ranitidine hydrochloride in some of its pharmaceutical products with recovery between 99.108–99.808 and RSD% between 0.012– 0.031. The results obtained from the proposed method make it suitable to use in the determination of ranitidine hydrochloride in its bulk and tablet dosage form.

**Keywords:** Cloud point; Ranitidine; Spectrophotometry.

## المخلص

تم تطوير طريقة بسيطة، سريعة، اقتصادية وصديقة للبيئة لتقدير الرانيتيد هيدروكلورايد في الأقراص الدوائية بعد استخلاصه بطريقة نقطة الغيمة. الطريقة تعتمد على اختزال الحديد الثلاثي بواسطة الرانيتيد هيدروكلورايد إلى الحديد الثنائي والذي بدوره يتفاعل مع فروسانييد الحديد لتكوين ناتج ملون عند دالته حامضية 4 بعدها استخدم تريتون X-114 لاستخلاص الرانيتيد هيدروكلورايد. الخطية لمنحنى المعايرة تم الحصول عليها عند تراكيز تراوحت بين 0.5 و 60.0 مايكروكروم /مل عند امتصاصية عظمى 693 نانومتر. تم اختيار العوامل المطلوبة لظروف التفاعل بما في ذلك الدالته الحامضية، تركيز  $\text{FeCl}_3$  و  $\text{K}_3[\text{Fe}(\text{CN})_6]$ ، حجم مخفض الشد السطحي، درجة الحرارة، الوقت وتسلسل الإضافات. يشير تحليل الانحدار إلى أن معامل الخطية 0.9998 والامتصاص المولاري  $0.46 \times 10^4$  لتر /مول. سم. حد الكشف وحد الكشف الكمي كانت 0.0147 و  $0.0642 \pm 0.01033$  و 0.475 و 1.567 مايكروكروم / مل على التوالي. حد الثقة للميل والقطع عند حدود ثقة 95% كانت  $0.0147 \pm 0.00015$  و  $0.0642 \pm 0.01033$  على التوالي. تم أيضاً دراسة حساسية ساندل وقد وجد أنها تساوي 0.0680 مايكروكروم /سم<sup>2</sup>. عامل التركيز المسبق كان 50.0%. الدراسة التقييمية لثلاث تراكيز من الرانيتيد هيدروكلورايد (5.0، 10.0 و 30.0) مايكروكروم /مل أعطت انحراف قياسي نسبي منوي يتراوح بين (0.142 و 0.728) والاستيعابية المئوية بين  $98.780 \pm 0.719$  -  $99.840 \pm 0.142$ . الطريقة المقترحة يجعل منها طريقة مناسبة لاستخدامها في تقدير الرانيتيد هيدروكلورايد في المستحضرات الصيدلانية.

الكلمات الرئيسية: غيمة. رانيتيد. قياس الطيف الضوئي.

## 1. INTRODUCTION

Ranitidine hydrochloride (R-HCl) has the chemical name, according IUPAC ((E)-1-N'-[2-[[5-[(dimethylamino)methyl]furan-2-yl]methylsulfany]ethyl]-1-N-methyl-2-nitroethene-1,1-diamine hydrochloride and the trade name is Zantac. The structure of ranitidine with the formula ( $\text{C}_{13}\text{H}_{22}\text{N}_4\text{O}_3\text{S} \cdot \text{HCl}$ ) explained in Figure 1 (Keith, 2000).

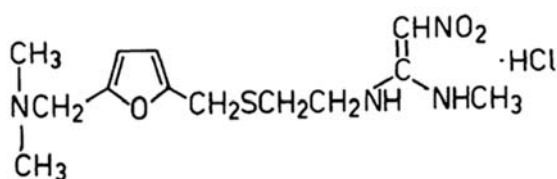


**Figure 1.** Structure of ranitidine hydrochloride.

R-HCl is classified under the medication that has the ability to act as histamine  $\text{H}_2$ -blocker on parietal cells in a stomach leading to decrease secretion of acid by these cells. Generally, ranitidine used to duodenal ulcer treatment and also in the management of the hypersecretory condition. R-HCl, in many cases, used in the treatment of gastro esophageal reflux and peptic ulcer diseases (Zhang *et al.*, 2015; Narayana *et al.*, 2010; Darwish *et al.*, 2008).

R-HCl has the ability to coordinate with the transition metals and also to form ion-pair

complexes with dyes in the acidic medium due to the presence of amine group and thioether sulphur in its structure (Kiszkziel *et al.*, 2015; El-Yazbi *et al.*, 2003; Pérez-Ruiz *et al.*, 2001).

In brief, CPE (*cloud point extraction*) at optimized temperature (above the cloud point temperature) cloudy aqueous solutions contain non-ionic surfactant will have formed lowering the solubility of surfactant in water, thereby formation of two phases, aqueous poor phase and a small volume of organic-rich phase. The analyte will be partitioning between these two phases related to its hydrophobicity (Bai *et al.*, 2001; Takagai and Hinze, 2009; Hinze and Pramauro, 1993; Stalikas, 2002; Delgado *et al.*, 2004).

In CPE, phase separation was maintained due to the formation of the micellar phase by using appropriate surfactant under optimized conditions. These micelles will aggregate at the CMC (*critical micelles concentration*), which is the minimum concentration of surfactant. CPE was considered environmentally friendly due to the use of a small amount of solvent and non-volatile surfactant and non-toxic. In addition to that in CPE the analyte can be determined and the matrix can be removed in one step (Jia *et al.*, 2008).

Many analytical methods were reported for determination of R-HCl, some of these methods include spectrophotometry, flow injection, voltammetry, potentiometry, conductometric, HPLC, Redox reaction, ESI-LC-MS/MS and TLC

(Baqir *et al.*, 2014; Moldovan and Aboul-Enein, 2012; Basavaiah and Nagegowda, 2004; Elbashir and Merghani, 2018; Issa *et al.*, 2005; Frag *et al.*, 2011; Ahamed *et al.*, 2006; Vicentini *et al.*, 2016; Tang *et al.*, 2007; Merghani and Elbashir, 2018; Bindewald *et al.*, 2018; Sharma *et al.*, 2011; Alamgir *et al.*, 2017; Kantariya *et al.*, 2013; Amin *et al.*, 2003; Bellorio *et al.*, 2013).

The present study aimed to develop a new, economic, friendly, and rapid cloud point extraction coupled with a spectrophotometric method for extraction and determination of ranitidine hydrochloride from pharmaceutical preparations.

## 2. MATERIALS AND METHODS

### 2.1. Reagent and materials

The standard of ranitidine hydrochloride (99.0%) supplied from Merck was prepared by dissolving 0.01 g in distilled water, then complete the volume to 100 mL in a volumetric flask. Triton X-114 (99.9%) purchased from Sigma-Aldrich company was prepared by diluting 10 mL in distilled water with gently heating at 30 °C for complete dissolving, then complete the volume to the mark with 100 mL distilled water in a volumetric flask.

Ferric chloride (99.9%) obtained from the BDH company was prepared by dissolving 0.0162 g in 1 mL concentrated HCl and then made up to 100 mL volumetric flask with distilled water.

Sodium hydroxide (99.0%) supplied from BDH company was prepared by dissolving 0.4 g in distilled water and complete to the mark in 100 mL volumetric flask with distilled water. Potassium ferricyanide (99.0%) provided from Sigma-Aldrich was prepared by dissolving 0.0329 g in distilled water and complete to the mark in 100 mL volumetric flask with distilled water.

HCl supplied from BDH was prepared by diluting 0.877 mL in distilled water and complete to the mark in 100 mL distilled water in a volumetric flask.

### 2.2. Apparatus

In SHIMADZU double-beam spectrophotometer (UV-1800) was used for absorbance measurements, pH-meter, (HANNA™) for pH measurement, shaking water bath (JULABO™) was used for temperature control throughout carrying the experiments of cloud point extraction.

### 2.3. Sample preparation

Ten tablets of each different product that contain 150 mg of R-HCl were grinded and mixed well to obtain bulky homogenous powders from each product. Weight equivalent to 0.01 g of pure R-HCl has been taken and dissolved in distilled water, then filtered and transferred to 100 mL volumetric flask and complete the volume to the mark to prepare 100 µg/mL. From these stock solutions of different products dilute solutions were prepared for applying the proposed method (Basavaiah and Nagegowda, 2004).

### 2.4. General procedure for cloud point extraction

Different volumes of standard solutions were added in 10 mL centrifugal screw tubes ranging from 0.05–6.0 mL of 100 µg/mL which corresponding to 0.5–60.0 µg/mL of ranitidine-HCl. Giving sequence, 0.8 mL of  $8.0 \cdot 10^{-3}$  M  $\text{FeCl}_3$  solution were added for each tube followed by addition of 0.6 mL of  $6.0 \cdot 10^{-5}$  M  $\text{K}_3\text{Fe}(\text{CN})_6$  solution and adjusted the pH of solutions (pH 4.0) by using 0.1 M NaOH and/or 0.1 M HCl.

For cloudy solutions, 0.7 mL of Triton X-114 was added to the final solution and completed to the mark with 10 mL distilled water, then incubated for 20 min in water bath at 50 °C, then cooled. The aqueous layer was removed by microsyringe, and the organic-rich phase was diluted with 0.5 mL ethanol. The absorbance of each solution was measured at  $\lambda_{\text{max}}$  693 nm against a blank solution (Khammas and Ahmad, 2016).

## 3. RESULTS AND DISCUSSION

### 3.1. Absorption spectra

R-HCl (50 µg/mL),  $\text{FeCl}_3$  ( $1.0 \cdot 10^{-3}$  M),  $\text{K}_3[\text{Fe}(\text{CN})_6]$  ( $1.0 \cdot 10^{-3}$  M) solutions and the colored complex were scanned in the UV-Vis from 190–1100 nm against the blanks for spectral study. It was found that ranitidine R-HCl,  $\text{FeCl}_3$ ,  $\text{K}_3[\text{Fe}(\text{CN})_6]$  and Triton X-114 gave maximum absorption at 308 nm, 290 nm, 303 nm, and 224 nm respectively. While the colored solution for R-HCl after addition of  $\text{FeCl}_3$  and  $\text{K}_3[\text{Fe}(\text{CN})_6]$  in the presence of Triton X-114 gave maximum absorption at 693 nm. This absorption for the colored product was adopted for further optimization in Figure 2.

### 3.2. Optimization of experimental conditions

Cloud point extraction affected by a various factor that can improve the extraction thereby the efficiency of the proposed method, for those such parameters like pH, incubation time, the temperature of equilibrium, Triton X-114 volume,  $\text{FeCl}_3$ , and  $\text{K}_3[\text{Fe}(\text{CN})_6]$  concentrations were investigated by the classical optimization. Triton X-114 selected due to its low cloud point temperature (22 to 23 °C) and low critical micelles concentration (~0.2 mM) (Santaladchaiyakit, and Srijaranai, 2012).

#### 3.2.1. Effect of pH

Extraction efficiency was widely affected by pH value, thereby affecting the absorbance of organic rich-phase. Thus, pH of the solution was study in the range of 2.0–10.0 at 50 °C for 20 min at R-HCl within concentration of 50  $\mu\text{g/mL}$ . All other parameters kept constant as in the described procedure. From the results in Figure 3, was chosen pH 4.0 due to the highest response.

Change in the pH generally affects the ionization form of the analyte leading to change water solubility and the extractability of analyte. pH adjustment should be optimized to ensure that the neutral molecular form of the drug was present before the CPE step also. The pH value affects the partitioning of analyte in the CPE. It was clearly explained in Figure 3 that in pH 4.0 had the highest response, and afterthought, this point the pH decreases. Thus, pH 4.0 was selected for optimization.

#### 3.2.2. Effect of ferric chloride concentration

Fe (III) salt like  $\text{FeCl}_3$  can be used as oxidant agent for the determination of some compound to form oxidizing colored product. Fe (II) was used as a reduced form of Fe(III), for that the concentration of  $\text{FeCl}_3$  on the formation of the colored product complex was investigated by adding the different volume of  $1.0 \times 10^{-3}$  M  $\text{FeCl}_3$  solution ranged from (0.1–1.0) mL at pH 4 and keeping the other condition constant (Figure 4). R-HCl reduce Fe (III) and forming Fe (II) which is subsequently reacted with  $\text{K}_3[\text{Fe}(\text{CN})_6]$  to form the blue product which measured at 693 nm. From Figure 4, the highest absorption was maintained when the concentration of  $\text{FeCl}_3$  was  $8.0 \times 10^{-5}$  M (0.8 mL of  $1.0 \cdot 10^{-3}$  M in 10 mL final aqueous solution). So this concentration was chosen for further optimization.

#### 3.2.3. Effect of potassium ferricyanide

Some of the oxidizing agents have an important effect on the coupling reaction between ligand and the metal. To this reason, effect of potassium ferricyanide was tested by the addition of various volumes of  $\text{K}_3[\text{Fe}(\text{CN})_6]$  ranged from (0.1–1.0) mL (Figure 5).

The maximum signal obtained was at volume 0.6 mL, which is related to the concentration of  $1.0 \times 10^{-5}$  M  $\text{K}_3[\text{Fe}(\text{CN})_6]$  in 10 mL final solution, for that this concentration was adopted for optimization.

#### 3.2.4. Effect of surfactant amount

The efficiency of extraction in CPE highly depended on the concentration of surfactant which is also affected the preconcentration factor, Thus, different volume of surfactant ranged from (0.1–2.0) mL of 10% Triton X-114 was tested. We can see the results in Figure 6.

The optimized volume of the surfactant was 0.7 mL, as explained in Figure 6. Below this point, it was difficult to separate the surfactant rich phase due to the small volume of rich phase relative to the total volume of solution. The other hand, above this point the volume of surfactant led to a decrease in the preconcentration factor and to interfere with the back-extraction.

Generally, the volume of surfactant added to the sample solution in CPE was low due to the high viscosity of surfactant ( $\eta \sim 20$  cP) and low CMC for Triton X-114 (0.20–0.35 mM) (Sirimanne *et al.*, 1998).

However, the efficiency of extraction was strongly affected by the amount of surfactant used. Maximum extraction efficiency maintained when the ratio of volume of rich phase to that of aqueous phase ( $V_s/V_a$ ) is minimum leading to improve the preconcentration factor (Khammas and Mubdir, 2014).

#### 3.2.5. Effect of temperature and time

Cloud point extraction is a type of equilibrium extraction. The optimal extraction efficiency was obtained once the equilibrium temperature and incubation time were established. The two factors were studied in the range of 20.0–80.0 °C and 5.0–70.0 min, respectively, as shown in Figures 7 and 8.

According to the results (Figures 7 and 8), maximum absorption was achieved at a

temperature 50 °C, and at time 20 min for that, these two factors were recommended for the CPE procedure.

### 3.2.6. Effect of order addition

Several experiments have been tried for the purpose of testing the order of reactants addition. According to the highest absorption maintained number 1 was chosen for the CPE procedure. This can be explained due to the reduction of  $\text{Fe}^{+3}$  to  $\text{Fe}^{+2}$  ion by R-HCl, then reacted with ferricyanide to produce a Prussian blue color product. These experiments sorted in Table 1.

### 3.2.7. Calibration curve

Under optimization conditions, linearity was achieved at a concentration between (0.5–60.0)  $\mu\text{g/mL}$ . The calibration curve was maintained by plotting absorption versus concentrations of R-HCl at  $\lambda_{\text{max}} = 693 \text{ nm}$  (Figure 9). The analysis of data obtained from the calibration curve, as illustrated in Table 2.

## 3.3. Method Validation

### 3.3.1. Accuracy and precision

Accuracy and precision regarded as the most requirements for testing the method reliability and quality of the results obtained. For that accuracy was studied in term of percentage recovery by subjected three different concentrations within the calibration curve (5.0, 10.0 and 30.0  $\mu\text{g/mL}$ ) to CPE procedure. Precision also studied in terms of repeatability for five times. All results of accuracy and precision were illustrated in Table 3. The results indicated that the proposed method has a good precise, and small systematic error, which can be useful for analysis the of R-HCl in pharmaceutical preparations.

## 3.4. Application

Two products contain R-HCl (Reptidine 150 mg and Ranimac 150 mg) were chosen from a local pharmacy for application study. Ten tables of each product were weighted, grind and mix well to form bulky homogenous powders. Then 0.1 g of pure R-HCl from each product was dissolved in distilled water and complete the volume to the mark in 100 mL volumetric flask to prepare 1000

$\mu\text{g/mL}$ . From these two solutions 50  $\mu\text{g/mL}$  was prepared for the application study for the proposed method.

## 4. CONCLUSIONS

A newly developed method was preceded by a combination of cloud point extraction (CPE) and spectrophotometry to determine ranitidine-HCl in the pharmaceutical dosage form. This method could be a good alternative for the liquid-liquid extraction (LLE), method which consumes a large volume of solutions and also more useful than solid-phase extraction (SPE) due to the high cost of SPE columns.

The developed CPE–spectrophotometry method was economical, rapid, and simple, due to the analytical parameters obtained (percentage recovery of extraction, LOD, LOQ, and RSD%), it can be used for monitoring R-HCl in pharmaceutical preparations.

## 5. ACKNOWLEDGMENTS

The authors were very grateful for the support provided from the colleagues in the departments of Chemistry and biology – College of science.

## 6. REFERENCES

1. Keith, G. (2000). In; Remington, J. P; Gennaro, A. R. The Science and Practice of Pharmacy, 20<sup>th</sup> ed., Lippincott Williams and Wilkins, USA, 2100 p.
2. Zhang, W; Zhu, D; Fan, H; Liu, X; Wan, Q; Wu, X; Liu, P; Tang, J. Z. (2015). Simultaneous extraction and purification of alkaloids from *Sophora flavescens* Ait. by microwave-assisted aqueous two-phase extraction with ethanol/ammonia sulfate system. *Separation and Purification Technology*, 141, 113–123.
3. Narayana, B; Ashwini, K; Shetty, D. N; Veena, K. (2010). Spectrophotometric determination of ranitidine hydrochloride based on the reaction with p-dimethylaminobenzaldehyde. *Eurasian Journal of Analytical Chemistry*, 5, 63–72.
4. Darwish, I. A; Hussein, S. A; Mahmoud, A. M; Hassan, A. I. (2008).



- Spectrophotometric determination of H<sub>2</sub>-receptor antagonists via their oxidation with cerium (IV). *Spectrochimica Acta Part A: Molecular and Biomolecular Spectroscopy*, 69, 33–40.
5. Kiszkiel, I; Starczewska, B; Lesniewska, B; Póznia, P. (2015). Extraction of ranitidine and nizatidine with using imidazolium ionic liquids prior spectrophotometric and chromatographic detection. *Journal of Pharmaceutical and Biomedical Analysis*, 106, 85–91.
  6. EL-yazbi, F; Gazy, A. A; Mahgoub, H; EL-Sayed, M; Youssef, R. M. (2001). Spectrophotometric and titrimetric determination of nizatidine in capsules. *Journal of Pharmaceutical and Biomedical Analysis*, 31, 1027–1034.
  7. Perez-ruiz, T; Martı́nez-Lozano, C; Tomás, V; Sanz, A; Sahuquillo, E. (2001). Flow-injection extraction-spectrophotometric method for the determination of ranitidine in pharmaceutical preparations. *Journal of Pharmaceutical and Biomedical Analysis*, 26, 609–615.
  8. Bai, D; Li, J; Chen, S; Chen, B.-H. (2001). A novel cloud-point extraction process for preconcentrating selected polycyclic aromatic hydrocarbons in aqueous solution. *Environmental Science and Technology*, 35, 3936–3940.
  9. Takagai, Y; Hinze, W. L. (2009). Cloud Point Extraction with Surfactant Derivatization as an Enrichment Step Prior to Gas Chromatographic or Gas Chromatography- Mass Spectrometric Analysis. *Analytical Chemistry*, 81, 7113–7122.
  10. Hinze, W. L; Pramauro, E. (1993). A critical review of surfactant-mediated phase separations (cloud-point extractions): theory and applications. *Critical Reviews in Analytical Chemistry*, 24, 133–177.
  11. Stalikas, C. D. (2002). Micelle-mediated extraction as a tool for separation and preconcentration in metal analysis. *TrAC Trends in Analytical Chemistry*, 21, 343–355.
  12. Delgado, B; Pino, V; Ayala, J. H; González, V; Afonso, A. M. (2004). Nonionic surfactant mixtures: a new cloud-point extraction approach for the determination of PAHs in seawater using HPLC with fluorimetric detection. *Analytica Chimica Acta*, 518, 165–172.
  13. Jia, G; Lv, C; Zhu, W; Qiu, J; Wang, X; Zhou, Z. (2008). Applicability of cloud point extraction coupled with microwave-assisted back-extraction to the determination of organophosphorous pesticides in human urine by gas chromatography with flame photometry detection. *Journal of Hazardous Materials*, 159(2-3), 300–305.
  14. Baqir, S. J; ALshirifi, A. N; Alsayegh, A. M. (2014). New spectrophotometric determination of Ranitidine Hydrochloride in different pharmaceutical samples. *Iraqi National Journal of Chemistry*, 56, 357–366.
  15. Moldovan, Z; Aboul-Enein, H. Y. (2012). Spectrophotometric method for ranitidine determination in drugs using Rhodamine B. *Journal of the Chilean Chemical Society*, 57, 1422–1427.
  16. Basavaiah, K; Nagegowda, P. (2004). Determination of ranitidine hydrochloride in pharmaceutical preparations by titrimetry and visible spectrophotometry using bromate and acid dyes. *Il Farmaco*, 59, 147–153.
  17. Elbashir, A. A; Merghani, S. M. (2018). Spectrophotometric determination of ranitidine hydrochloride (RNH) in pharmaceutical formulation using 9-fluorenylmethyl chloroformate (Fmoc-Cl). *Asian Journal of Pharmaceutical Research and Development*, 6, 7–14.
  18. Issa, Y. M; Badawy, S. S; Mutair, A. A. (2005). Ion-selective electrodes for potentiometric determination of ranitidine hydrochloride, applying batch and flow injection analysis techniques. *Analytical Sciences*, 21, 1443–1448.
  19. Frag, E. Y; Mohamed, A. M; Mohamed, G. G; Alrahmony, E. E. (2011). Construction and performance characterization of ion selective electrodes for potentiometric determination of ranitidine hydrochloride in pharmaceutical preparations and biological fluids. *International Journal of Electrochemistry*, 6, 3508–3524.
  20. Ahamed, A. M. K; Khaleel, A. I; Amine, S. T. (2006). Determination of ranitidine-HCl in pharmaceutical formulations by kinetic spectrophotometric and flow injection-activated chemiluminescence methods. *Iraqi National Journal of Chemistry*, 534–550.
  21. Vicentini, F. C; Janegitz, B. C; Bonifácio, V. G; Fatibello-Filho, O; Marcolino-Júnior, L. H. (2016). Novel flow injection

- spectrophotometric determination of ranitidine in pharmaceuticals. *Canadian Journal of Chemistry*, 94, 604-607.
22. Tang, Y. H; Wang, N. N; Xiong, X. Y; Xiong, F. M; Sun, S. J. (2007). A new sensitive flow-injection chemiluminescence method for the determination of H<sub>2</sub>-receptor antagonists. Luminescence. *The journal of Biological and Chemical Luminescence*, 22, 343-348.
  23. Merghani, S; Elbashir, A. (2018). Development of chemically modified electrode using cucurbit (6) uril to detect ranitidine hydrochloride in pharmaceutical formulation by voltammetry. *Journal of Analytical & Pharmaceutical Research*, 7, 634-639.
  24. Bindewald, E. H; Da Rosa-Sobrinho, J. C; Bergamini, M. F; Marcolino-Júnio, L. H. (2018). Simple, fast and inexpensive method for determination of ranitidine hydrochloride based on conductometric measurements. *Eclética Química*, 43, 37-43.
  25. Sharma, N; Singh, R; Reddy, P. S; Malleswara Reddy, A. (2011). A validated stability-indicating liquid-chromatographic method for ranitidine hydrochloride in liquid oral dosage form. *Scientia Pharmaceutica*, 79, 309-322.
  26. Alamgir, M; Khuawar, M; Memon, S; Hayat, A; Zounr, R. (2017). HPLC Determination of Metformin, Famotidine and Ranitidine by Derivatization with Benzoin from Drugs and Biological Samples. *Pharmaceutica Analytica Acta*, 8, 2-7.
  27. Kantariya, B; Agola, A; Roshani, H; Ghetia, U; Shivam, S. (2013). Development and validation of a RP-HPLC method for the simultaneous estimation of ranitidine hydrochloride and dicyclomine hydrochloride in tablet dosage forms. *International Journal for Pharmaceutical Research Scholars*, 258-267.
  28. Amin, A; Ahmed, I; Dessouki, H; Gouda, E. (2003). Utility of oxidation-reduction reaction for the determination of ranitidine hydrochloride in pure form, in dosage forms and in the presence of its oxidative degradates. *Spectrochimica Acta Part A: Molecular and Biomolecular Spectroscopy*, 59, 695-703.
  29. Bellorio, K. B; Alves, M. I. R; Antoniosi Filho, N. R. (2013). Determination of ranitidine in human plasma by SPE and ESI-LC-MS/MS for use in bioequivalence studies. *ISRN Chromatography*, 2-7.
  30. Khammas, Z. A; Ahmad, S. S. (2016). Cloud point extraction of carbendazim pesticide in foods and environmental matrices prior to visible spectrophotometric determination. *Science*, 4, 30-41.
  31. Santaladchaiyakit, Y; Srijaranai, S. (2012). A simplified ultrasound-assisted cloud-point extraction method coupled with high performance liquid chromatography for residue analysis of benzimidazole anthelmintics in water and milk samples. *Analytical Methods*, 4, 3864-3873.
  32. Sirimanne, S. R; Patterson, D. G; Ma, L; Justice, J. B. (1998). Application of Cloud-Point Extraction/Reversed-Phase High Performance Liquid Chromatography: A Preliminary Study of the Extraction and Quantification of Vitamins A and E in Human Serum and Whole Blood. *Journal of Chromatography B: Biomedical Sciences and Applications*, 716 (1-2), 129-137.
  33. Khammas, ZA-A; Mubdir N.S. (2014). An eco-friendly method for extraction and determination of ciprofloxacin in blood serum and pharmaceuticals. *Science Journal of Analytical Chemistry*, 2(5), 47-54.

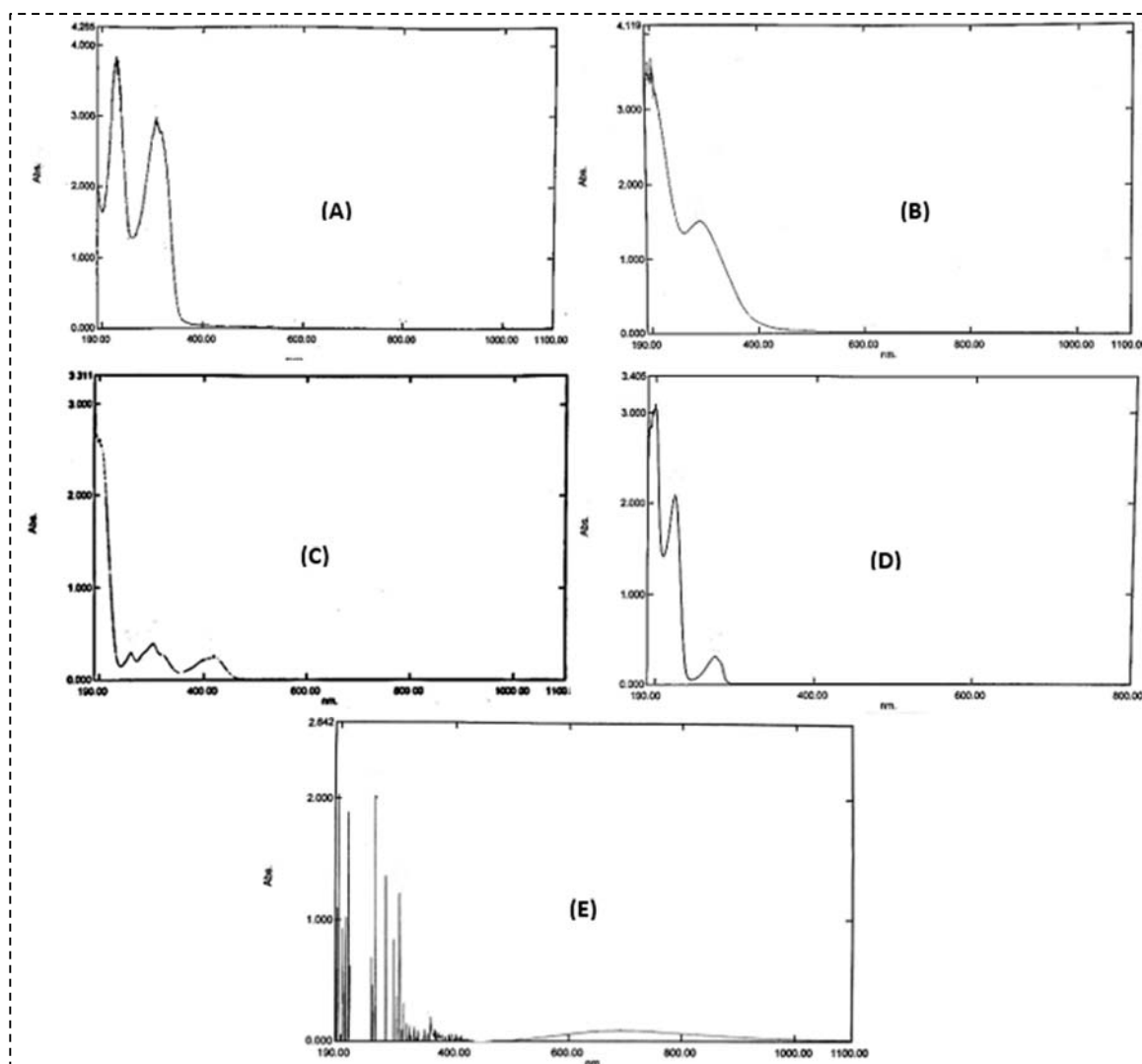


**Figure 2.** Absorption spectra of  $R-HCl$  (A),  $K_3[Fe(CN)_6]$  (B),  $FeCl_3$  (C), Triton X-114 (D) and colored product complex (E).

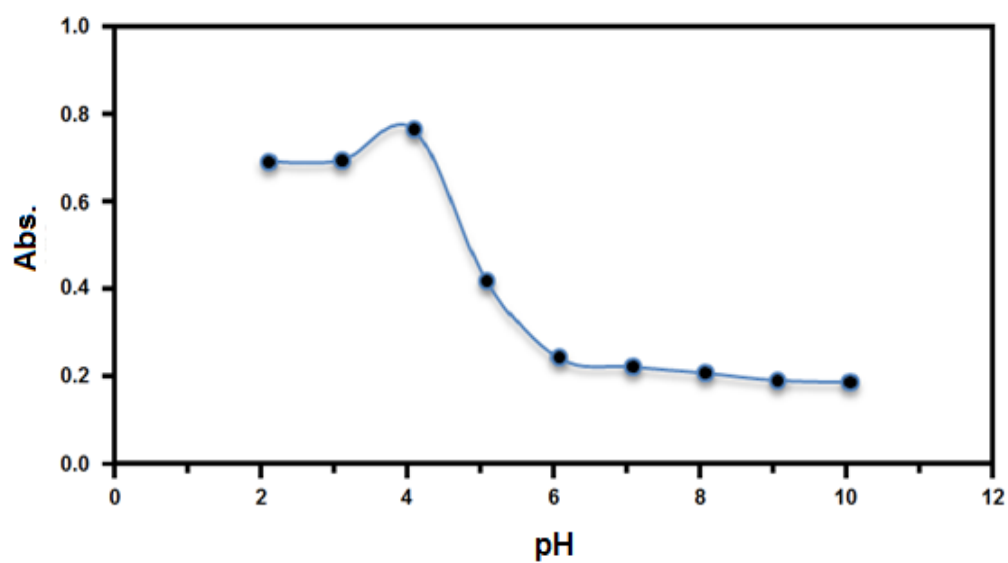


**Figure 3.** Effect of pH on the absorption of  $R-HCl-(Fe^{+2})$  complex.

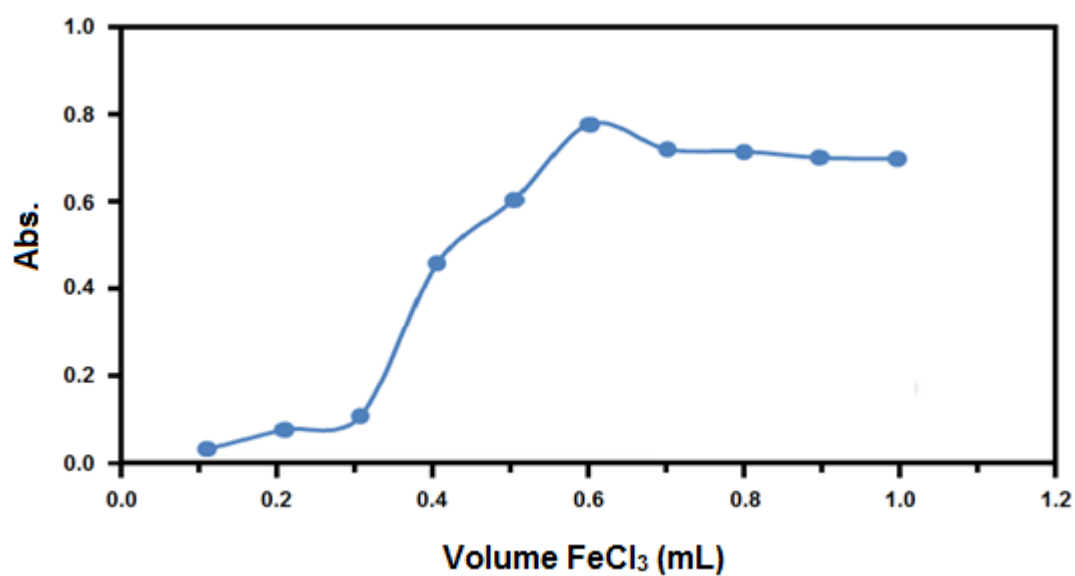


**Figure 4.** Effect of  $\text{FeCl}_3$  concentration on the absorption of  $\text{R-HCl}-(\text{Fe}^{+2})$  complex.

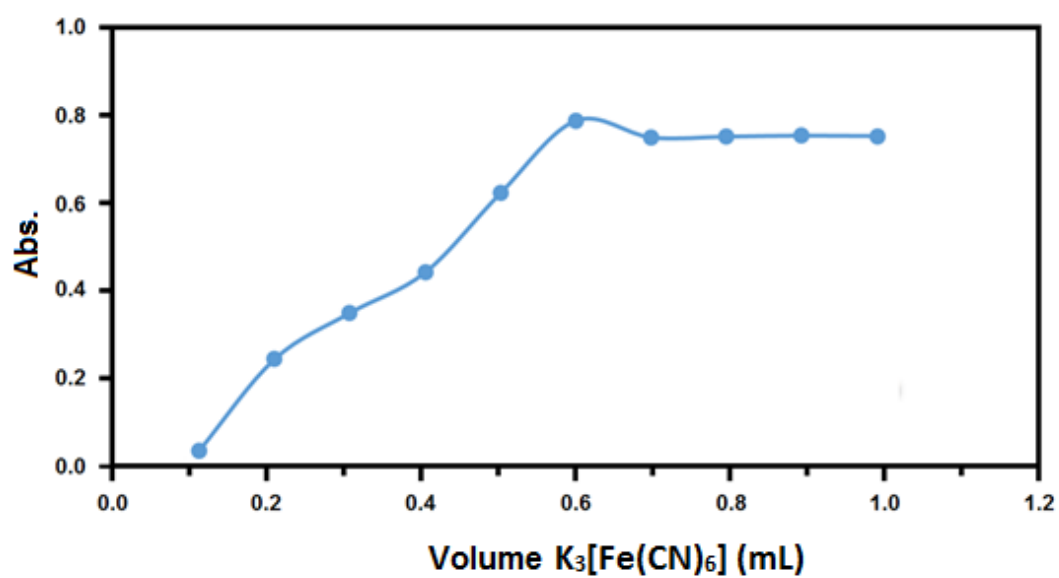


**Figure 5.** Effect of potassium ferricyanide on the absorption of  $\text{R-HCl}-(\text{Fe}^{+2})$  complex.

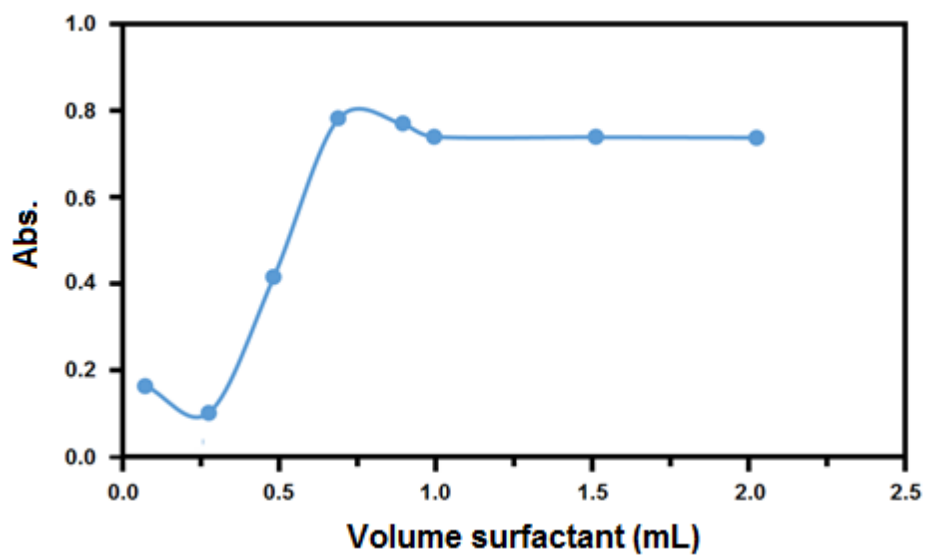


**Figure 6.** Effect of surfactant volume on the absorbance of  $R\text{-HCl}-(\text{Fe}^{+2})$  complex.

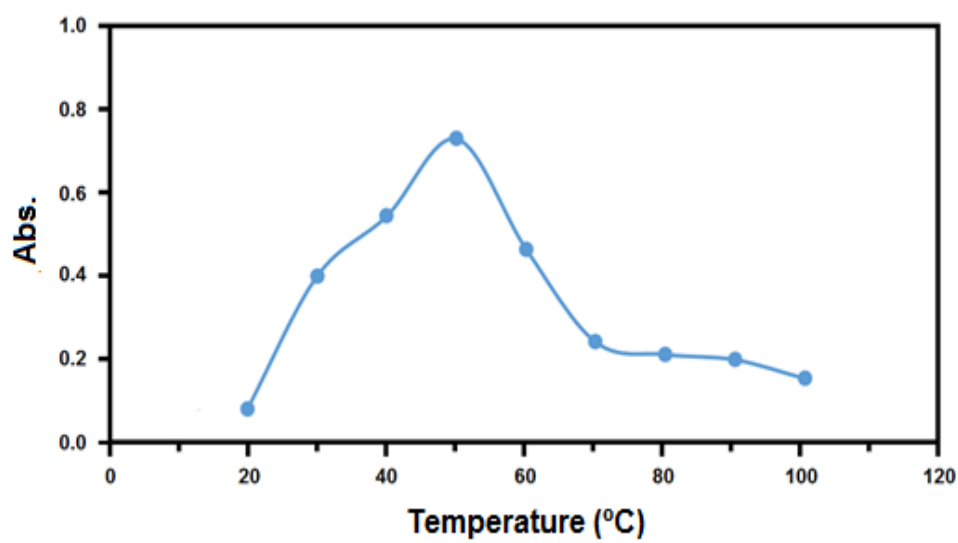


**Figure 7.** Effect of temperature on the absorption of  $R\text{-HCl}-(\text{Fe}^{+2})$  complex.

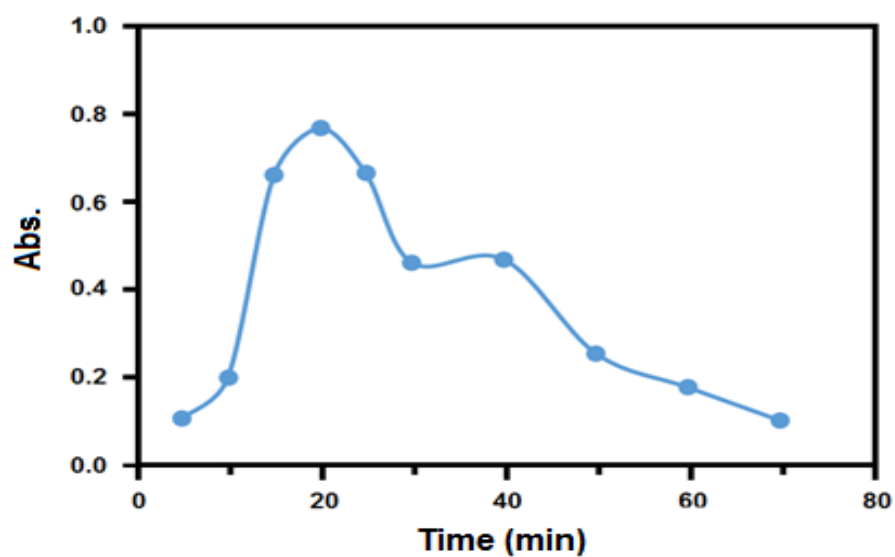


**Figure 8.** Effect of time on the absorption of R-HCl –( $\text{Fe}^{+2}$ ) complex.

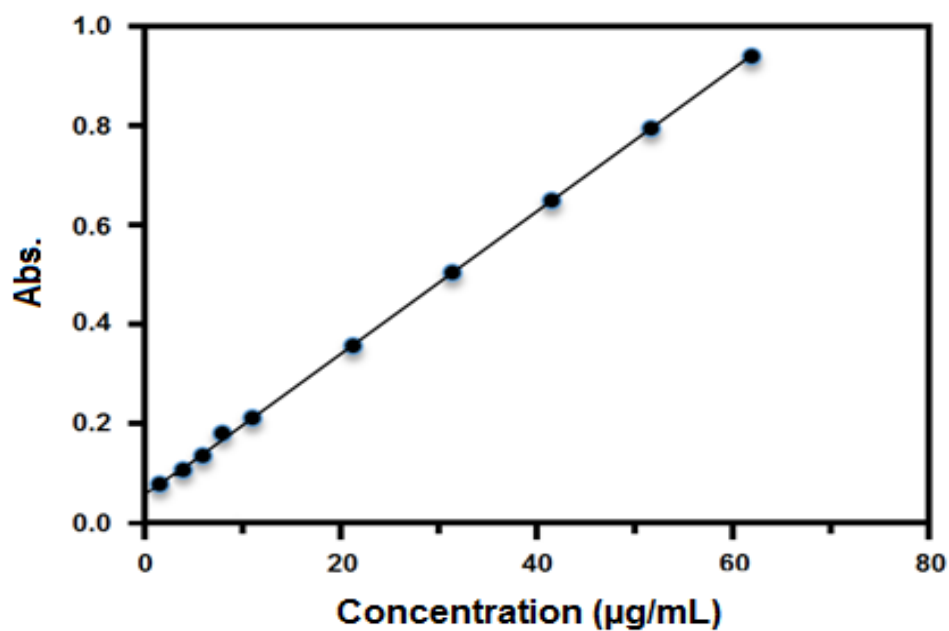


**Figure 9.** Calibration curve of the Ranitidine hydrochloride complex.

**Table 1.** Effect of order addition of reactants.

| No. | Addition  | Abs.  |
|-----|---|-------|
| 1   | R-HCl + FeCl <sub>3</sub> + K <sub>3</sub> [Fe(CN) <sub>6</sub> ] + Buffer (4) + Triton X-114 | 0.775 |
| 2   | R-HCl + K <sub>3</sub> [Fe(CN) <sub>6</sub> ] + FeCl <sub>3</sub> + Buffer (4) + Triton X-114 | 0.698 |
| 3   | R-HCl + Buffer (4) + FeCl <sub>3</sub> + K <sub>3</sub> [Fe(CN) <sub>6</sub> ] + Triton X-114 | 0.595 |

**Table 2.** Data Analysis for Ranitidine-HCl determination.

| Parameter   | Data Analysis          |
|---|------------------------|
| $\lambda_{\max}$ (nm)                               | 693                    |
| Regression equation                                 | $y = 0.0147x + 0.0642$ |
| Standard deviation of regression line ( $S_{y/x}$ ) | 0.0045                 |
| Correlation coefficient (r)                         | 0.9998                 |
| C.L for the slope ( $b \pm ts_b$ ) at 95%           | $0.0147 \pm 0.00015$   |
| C.L for the intercept ( $a \pm ts_a$ ) at 95%       | $0.0642 \pm 0.01033$   |
| Linearity range ( $\mu\text{g/mL}$ )                | 0.5–60.0               |
| Limit of detection ( $\mu\text{g/mL}$ )             | 0.475                  |
| Limit of quantification ( $\mu\text{g/mL}$ )        | 1.567                  |
| Sandell's sensitivity ( $\mu\text{g/cm}^2$ )        | 0.0680                 |
| Molar absorptivity ( $\text{L/mol.cm}$ )            | $0.46 \times 10^4$     |
| Preconcentration factor*                            | 50.0%                  |

\*Preconcentration factor was the ratio of the original volume of sample to that of extracted volume or rich surfactant-phase

**Table 3.** Accuracy and precision for the determination of Ranitidine-HCl.

| Amount of R-HCl ( $\mu\text{g/mL}$ ) |  | Recovery%<br>(mean $\pm$ SD) | RSD%<br>(n=5) | $E_{\text{rel}}\%$ |
|--------------------------------------|--|------------------------------|---------------|--------------------|
| Taken                                | Found<br>at 95% C.L<br>$\left(\bar{x} \pm t \frac{s}{\sqrt{n}}\right)$ |                              |               |                    |
| 5.0                                  | $4.966 \pm 0.014$  | $99.320 \pm 0.228$           | 0.230         | 0.680              |
| 10.0                                 | $9.878 \pm 0.089$  | $98.780 \pm 0.719$           | 0.728         | 1.220              |
| 30.0                                 | $29.952 \pm 0.053$   | $99.840 \pm 0.142$           | 0.142         | 0.160              |

**Table 4.** Application of the proposed method for the determination of Ranitidine-HCl.

| Name of product | Amount of R-HCl ( $\mu\text{g/mL}$ ) |  | Recovery%<br>(mean $\pm$ SD) | RSD%<br>(n=5) | $E_{\text{rel}}\%$ |
|-----------------|--------------------------------------|--|------------------------------|---------------|--------------------|
|                 | Taken                                | Found<br>at 95% C.L<br>$\left(\bar{x} \pm t \frac{s}{\sqrt{n}}\right)$ |                              |               |                    |
| Reptidine       | 50                                   | $49.904 \pm 0.0068$  | $99.808 \pm 0.012$           | 0.012         | 0.192              |
| Ranimac         | 50                                   | $49.554 \pm 0.0183$  | $99.108 \pm 0.310$           | 0.031         | 0.892              |

**CRIAÇÃO DO MODELO MATEMÁTICO DE COMPUTADOR DO PROCESSO BIOTECNOLÓGICO DO PROCESSAMENTO DE MATÉRIAS-PRIMAS****CREATION OF A COMPUTER-ASSISTED MATHEMATICAL MODEL FOR THE RAW MATERIALS BIOLOGICAL PROCESSING****СОЗДАНИЕ КОМПЬЮТЕРНОЙ МАТЕМАТИЧЕСКОЙ МОДЕЛИ БИОТЕХНОЛОГИЧЕСКОГО ПРОЦЕССА ОБРАБОТКИ СЫРЬЯ**

TLEBAYEV, Manat B.<sup>1\*</sup>; BIIBOSUNOV, Bolotbek I.<sup>2</sup>; TASZHUREKOVA, Zhazira K.<sup>3</sup>;  
BAIZHARIKOVA, Marina A.<sup>4</sup>; AITBAYEVA, Zamira K.<sup>5</sup>;

<sup>1,3</sup> M.Kh. Dulaty Taraz State University, Department of Applied Informatics and Programming, 60 Tole Bi Str., zip code 010000, Taraz – Republic of Kazakhstan

<sup>2,4,5</sup> I. Arabaev Kyrgyz State University, Department of Applied Informatics, 51A Razzakov Str., zip code 720026, Bishkek – Kyrgyz Republic

\* Correspondence author  
e-mail: tlebaev\_mb@mail.ru

Received 12 March 2020; received in revised form 30 May 2020; accepted 19 June

**RESUMO**

2020

No processo de digestão anaeróbica, a alternância de substâncias líquidas e sólidas na composição do substrato faz com que as bactérias se adaptem às condições variáveis, o que reduz significativamente a emissão de biogás e a concentração de metano, bem como aumenta o tempo de presença do substrato no biorreator. A solução para esse problema ao usar a destruição de cavitação pode não apenas minimizar a heterogeneidade da temperatura, mas também resolver o problema da mesma carga na biocenose e na superfície de contato máxima das bactérias durante a digestão anaeróbica no biorreator. As pesquisas realizadas mostraram que a composição e quantidade de biogás não são constantes e dependem do tipo de substrato que está sendo processado e da tecnologia de produção de biogás. Para estabilizar a composição do biogás resultante e torná-lo em uma fonte de energia alternativa independente e de alta qualidade, é possível usar a destruição da membrana ou a moagem de matérias-primas orgânicas. O consumo de energia, o tempo de fermentação e a concentração de metano na produção final de biogás dependem do tratamento primário. No presente artigo, propõe-se um modelo matemático do processo de moagem, dispersão e homogeneização de resíduos de fazendas leiteiras e de engorda, que permite determinar e otimizar seus parâmetros operacionais, bem como promover a digestão anaeróbica eficaz do substrato no biorreator. Para determinar o modelo matemático do processo biotecnológico de processamento de matérias-primas com parâmetros teóricos ou experimentais conhecidos, foram utilizados os métodos numéricos, que são uma das poderosas ferramentas matemáticas para solucionar o problema. Os resultados dos parâmetros operacionais dos processos estudados foram obtidos no ambiente Mathcad e testados no pacote de software de controle e monitoramento automatizado SCADATraceMode 6.10.1.

**Palavras-chave:** usina de biogás, destruição de cavitação, regressão hiperbólica.

**ABSTRACT**

During anaerobic fermentation, the alternation of liquid and solid substances in the substrate makes the bacteria adapt to changing conditions, which significantly reduces the biogas yield, reduces the methane concentration in it, and increases the retention time of the substrate in the bioreactor. The solution to this problem when using cavitation destruction can not only minimize temperature nonuniformity but also solve the problem of the same load on the biocenosis and maximum contact surface of bacteria during anaerobic fermentation in the bioreactor. Studies have shown that the composition and quantity of biogas are not constant and depend on the type of substrate being processed and the biogas production technology. To stabilize the composition of the resulting biogas and bring it to a high-quality, independent alternative energy source, it is possible using membrane destruction or crushing of organic raw materials. The energy consumption, fermentation time, and methane concentration in the final biogas output depend on the primary treatment. This work proposes a



mathematical model of the process of crushing, dispersing, and blending waste from dairy and fattening farms, which allows to determine and optimize its operating parameters, as well as to promote effective anaerobic fermentation of the substrate in the bioreactor. To determine the mathematical model for the raw materials biological processing with known theoretical or experimental parameters, numerical methods were used, which are one of the powerful mathematical tools for solving the problem. The results of the operational parameters of the studied processes were obtained using the Mathcad environment and tested in the SCADA Trace Mode 6.10.1 automated process control and monitoring software package.

**Keywords:** *biogas unit, cavitation destruction, hyperbolic regression.*

## АННОТАЦИЯ

В процессе анаэробного сбраживания чередование жидких и твердых веществ в составе субстрата заставляют бактерии приспосабливаться к меняющимся условиям, что значительно сокращает выход биогаза, снижают концентрацию метана в нем и увеличивает срок пребывания субстрата в биореакторе. Решение данной проблемы при применении кавитационной деструкции позволяет не только свести к минимуму температурную неоднородность, но и решить вопрос одинаковой нагрузки на биоценоз и максимальную поверхность контакта бактерий во время анаэробного сбраживания в биореакторе. Проведенные исследования показали, что состав и количество биогаза не являются постоянными и зависят от вида перерабатываемого субстрата и технологии производства биогаза. Для стабилизации состава получаемого биогаза и доведение его до качественного, самостоятельного альтернативного источника энергии возможно при использовании мембранной деструкции или измельчении органического сырья. От первичной обработки зависят энергозатраты, время брожения и концентрация метана в конечном выходе биогаза. В статье предложена математическая модель процесса измельчения, диспергации и гомогенизации отходов молочно-товарных и откормочных ферм, позволяющая определить и оптимизировать его режимные параметры, а также способствовать эффективному анаэробному сбраживанию субстрата в биореакторе. Для определения математической модели процесса биотехнологического процесса обработки сырья при известных теоретических или экспериментальных параметрах использовали численные методы, которые являются одним из мощных математических средств решения задачи. Результаты режимных параметров исследуемых процессов были получены с использованием среды Mathcad и протестированы в программном комплексе автоматизированного управления и контроля за технологическими процессами SCADATraceMode 6.10.1.

**Ключевые слова:** *биогазовая установка, кавитационная деструкция, гиперболическая регрессия.*

## 1. INTRODUCTION

There are works of domestic and foreign scientists, as well as specialists in the field of intensification of anaerobic fermentation of cattle excrement in biogas units, their degree of automation, and control: S. D. Durdybaev, Yu. N. Sidyganov, V. Baader, B. Eder, E.S. Pankshava, V. P. Druzianova, V. I. Marchenko, E. Hashimoto, A. G. Kudryashova, L. I. Ruzhinskaya, I. A. Trakhunova, E. K. Vachagina, V. A. Ivanov (Akhnazarova and Kafarov, 1985; Druzyanova, 2008; Eder and Schulz, 2011; Kudryashova, 2011; Ivanov and Gasparyan, 2013; Ruzhinskaya and Fomenkova, 2014; Tlebayev *et al.*, 2017; Butova *et al.*, 2018). These authors noted that during anaerobic fermentation, the alternation of liquid and solid substances in the substrate makes the bacteria adapt to changing conditions, which significantly reduces the biogas yield, reduces the methane concentration in it, and increases the retention time of the substrate in the bioreactor

(Biogas manual..., 2010; Dong *et al.*, 2018; Kusuma *et al.*, 2019).

In animal waste, there are various solid particles, such as sand, clay, *et al.*, which cause the formation of sediment, while light materials like straw and others rise to the surface of the bioreactor and form a crust, which leads to a decrease in gas formation (Koller *et al.*, 2017; Zagorulko *et al.*, 2018; Sokolova *et al.*, 2018; Isakov *et al.*, 2019; Kudrin *et al.*, 2019; Popov *et al.*, 2019). Therefore, plant residues (straw, scraps and others) must be crushed before loading into the reactor, and it is necessary to strive for the absence of solids in the raw materials (Sidyganov *et al.*, 2008; Golubtsova, 2017). To eliminate the problem, Figure 1 presents a developed primary treatment system for cavitation destruction of cattle excrement and anaerobic fermentation in a psychrophilic (are extremophilic organisms that are capable of growth and reproduction in low temperatures) mode (Dotsenko *et al.*, 2017; Kulbjakina and Dolotovskij, 2018; Chandra *et al.*,

2019).

The main goal of the raw materials processing unit mathematical modeling is to determine the optimal conditions for the process, to control it on the basis of a mathematical model, and transfer the results to a real object in the Birlik-Tuimekent SEC.

Liquid raw materials (cattle manure) 2 weighing 600 liters, humidity 80-85% enters tank 1, where it mixes with water at room temperature, in a ratio of 1:1, to a moisture content of 92%. From the tank 1, the raw material enters through the pipe 3, with the help of the pump 4, into the spiral separator 5, where large particles of the raw material are crushed. Next, the pre-crushed biomass enters the tank 6. Entering the macerator 9, solid particles are crushed, and heavy impurities are simultaneously separated. Further, the gerotor type pump 10 breaks the long fibrous inclusions present in the biomass, pumping the substrate into the dispersing agent 11, which exposes the composition of the substrate to destruction and creates a homogeneous mixture. While the biomass is in the tank 6, an automatic mixer 7 periodically mixes it. During crushing of the biomass in the tank 6, biogas enriched in CO<sub>2</sub> is released and removed through the pipe 13. When the required size of crushing is reached, the lower valve 12 is closed, and the upper valve 12 is opened, where the crushed substrate pumped into the bioreactor of the second stage of the biogas unit.

The biogas unit (BGU) effectiveness is greatly influenced by the preliminary preparation of the initial substrate. The smaller the particle sizes of the organic feedstock components, the greater their specific surface area and, accordingly, the fermentation processes occur more intensively. When analyzing literary sources, as articles by I. V. Meshcheryakov, "Development and research of a multistage hydro-percussion and cavitation device for fine crushing of complex ores" and A.T. Zhumagazhinov, N.K. Algazinov "Methods of intensification of the anaerobic fermentation processes" (Meshcheryakov, 2014; Kiss et al., 2015; Vachagina and Karaeva, 2009; Zhumagazhinov and Algazinov, 2014; Trakhunova, 2014), a table of the relationship between the destruction efficiency and performance was compiled (Table 1).

## 2. MATERIALS AND METHODS

To determine the mathematical model for the raw materials biological processing with known theoretical or experimental parameters, numerical

methods were used, which are one of the powerful mathematical tools for solving the problem.

To find the Equation 4, the approximation method was used in the work. Approximation allows us to study the numerical characteristics and qualitative properties of an object, reducing the problem to the study of simpler or more convenient objects (for example, characteristics of which are easily calculated or whose properties are already known).

To find the function in work, the approximation approach was used. At the initial stage, it was compiled a table of auxiliary quantities (Table 2).

To verify the found function was used, a computer experiment method implemented through the Scada Trace Mode automated process control and monitoring system. At the same time, to implement the full software package, all possible programming methods were used—namely, the creation of modules in different programming languages of the International Electrotechnical Commission 6-1131/3 standard. Firstly, as the fundamental programming languages of this standard, the Tehno Structured Text (a high-level programming language similar to Pascal) and the Tehno Instruction List (the simplest mnemonic instruction language that looks like assembly), as well as the Tehno Function Block Diagram visual languages (is a diagram consisting of a set of functional blocks interconnected via inputs and outputs), Techno Sequential Function Chart (a tool for structuring complex algorithms), Techno Ladder Diagram (ladder logic diagrams).

## 3. RESULTS AND DISCUSSION:

In domestic and foreign practices are increasingly being used energy supply systems for agricultural enterprises using an alternative energy source - biogas. Biogas is formed as a result of anaerobic fermentation of organic substances when waste is processed, and highly effective biofertilizers are obtained. It also solves the environmental and agrobiological problems of agricultural enterprises. For the production of biogas, bioreactors are widely used. In most countries of the world, biogas technologies have become the standard for the processing of biowaste in order to obtain additional raw materials and energy resources. The need to increase the energy efficiency of a biogas plant is due to the large energy consumption for the technological needs of the equipment. According to the classification presented in the article, the main

instruments in the technological scheme of the processing of organic raw materials are a mixing tank, a macerator, a gerotor pump, a cavitation destructor, which largely determines the effectiveness of the technology as a whole. A promising measure to increase the energy efficiency of methane fermentation technology is the availability of primary processing of raw materials.

The data from Table 1 point that after the 6th cycle, the values of the change in the size of the initial particles are minimal, less than 10 microns; it was considered the 6th cycle to be inappropriate.

It was calculated the a and b coefficients for the hyperbolic regression equation (Equation 1). According to the well-known equations (Equations 2-3) (Akhnazarova and Kafarov, 1985). In sum, the desired regression equation has the form (Equation 4). Where x is the number of passes, and y is the particle size of the crushed mixture after the x-th pass.

Let's analyze the graph of the regression equation using the Mathcad program (Figure 2). In this connection, the index of correlation (Equation 5). And the determination index:  $R^2 = 0.9725^2 \approx 0.9457$ . Analyzing the graph, it could be concluded that equation (4) describes the crushing process only up to  $x \leq 4$  or before crushing at 14 microns. With large crushing, the error of approximation increases, and the data becomes incorrect.

To find the function that describes the crushing process after about 14 microns, the Trendline function in Excel was used (Figure 3). The average error of approximation (Equation 6). Moreover, the average approximation error is 17.89%, which indicates a good "fit" of the obtained function to the parameters under study. It was simulated this function in Mathcad (Figure 4).

Further, the organic raw materials processing (crushing) can be described by the system of equations (Equation 7). This equation describes the grinding process, where x is the number of passes of the processing of organic raw materials, f(x) is the size of the particles of the crushed mixture after the x pass, while the first equation is applicable for large grinding, and the second describes the grinding process after about 14 microns.

Find the intersection point of the graphs to determine the conditions of the system (Figure 5). Figure 5 shows that the graphs intersect at  $x =$

3.7282,  $y = 18.184$ . Rounding off the values to integers, a system of equations with limitations was obtained (Equation 8).

To display the general equation of the processing of the raw materials through the preferred parameters (processing time and loading volume), the equation for the processing time was derived, so the number of cycles necessary to complete in one pass is defined as (Equation 9). Where  $V_{vol}$  is the volume of loaded raw material (l), the parameter  $V_{pip}$  is the total volume of the system pipes ( $V_{vol}=4.69$ ).

Processing time in one pass is calculated as (Equation 10). Where  $T_u$  is the total execution time of one cycle ( $T_{cycl}=9.61$ ). Further, the total runtime of the processing of the raw materials can be represented in the form (Equations 11-12).

Using the static parameters of the system was obtained (Equations 13-14). It was substituted the obtained value of X into the system of equations, general expression (Equation 15). For a given system (Equation 16), having simplified was obtained (Equation 17).

The time required to crush a given value (micron) can be calculated by a function in a general form (Equation 18). For a given system for organic raw materials processing (Equation 19), where V is the volume of the loaded raw material (l), L is the desired output size (microns),  $T_{o6}$  which is the required time to complete the process (sec).

For finer crushing, you should use the second function of the system, in general, the function of finding the processing time will have a form (Equation 20). Where:  $V_{vol}$  is the volume of loaded raw material (l);  $T_{cycl}$  – the total execution time of one cycle ( $T_u=9.61$ ); L is the desired output size (microns);  $V_{pip}$  – the volume of the pipe system;  $T_{o6}$  – the required time to complete the process (sec).

Substituting the parameter values was obtained (Equation 21). Thus, the system of equations for finding the processing time in a general form can be represented as (Equation 22) for the studied processing system as (Equation 23). It was constructed the resulting system of equations in Mathcad (Figure 6).

The increase in the degree of decomposition is proportional to the increase in the active surface of the organic substance involved in the process of methane formation and has a substantially nonlinear character, which

makes it possible to use this effect to intensify gas escape in biogas technologies.

The use of cavitation destructors can significantly reduce the time of raw materials pretreatment, due to the effect of the destruction of the membrane of raw materials particles. Cavitation destructor allows us to use the destructive effect of cavitation to give the feedstock a homogeneous mass. Under the influence of directed and controlled cavitation in the biological raw materials, complex bonds of the fibers of organic substances at the molecular level (lignin, cellulose) are breaking. As a consequence of this process, the dispersion of biological raw materials is significantly increased, and its particles are reduced in size to 0.1 - 8 microns. Thus, it becomes easier for all bacterial strains involved in the biogas formation at all its stages to decompose biogenic materials, because their homogeneous structure is destroyed and, accordingly, the area covered by bacteria of biological raw materials increases. (Obolensky and Kravynov, 2012). All these factors contribute to improving energy efficiency and reducing equipment wearing.

Of course, even the most complex models are not yet able to describe all the existing relationships, reflect the whole variety of behavior of complex agrobiological systems in various situations. However, the obtained equations are able to describe the process of crushing dispersion and homogenization of the substrate for an optimal control system, the regime of periodic loading of a new portion of raw materials, and the temperature regime of the fermentation in the capacity of the psychrophilic regime, while saving energy (Yudaev *et al.*, 2019; Barisa *et al.*, 2020).

To analyze the resulting mathematical model, a computer experiment was conducted in the Scada Trace Mode. Trace Mode consists of an instrumental system and a set of executive modules (runtimes). Using the Trace Mode executive modules, the project of the automated control system is launched for execution in real-time at the workplace by dispatcher or operator. If we need to organize communication between Trace Mode and Arduino, we can use the modbus-rtu protocol and connect the converter to RS – 485 or RS-232.

An automated system for controlling the technological processes of organic raw material recycling is a form divided into four logical zones (Figure 7):

1. A graphical representation of the raw materials processing unit structural elements.

2. Parameters and schedule for raw materials crushing.

3. Calculation of indicators for heating raw materials at a psychrophilic mode.

4. Calculation of the CO<sub>2</sub> concentration at the outlet.

As a reference plan for the experiment, a matrix of initial and final parameter values will be created (Zhumagazhinov and Algazinov, 2014). To identify the relationship between the particle size at the outlet and the concentration of biogas, it was assumed that (Table 3):

- the volume of loaded raw materials;
- the volume of the pipes of the raw materials processing unit;
- the initial temperature of raw materials;
- the desired temperature of the raw material, there are constant values, and only the desired particle size at the outlet changes.

Thus, when entering the initial parameters, the system calculates the outlet parameters (Figure 8). Similarly, all other experiments will be conducted. After conducting the experiments, the data obtained was analyzed (Table 4).

As can be seen from the graph (Figure 9), with a decrease in particles, methane yield (CH<sub>4</sub>) increases, and the percentage of carbon dioxide (CO<sub>2</sub>) decreases. However, it can be seen that after particle crushing by less than 10 microns, the methane increase is insignificant, but the processing time of the raw materials increases and, consequently, the financial costs and equipment wear increase (Figure 10).

Thus, particles of a fraction of 10 µm will be the main ones for biogas production and will have a high level of flotation; smaller particles make a small contribution to the formation of methane and are prone to precipitation. This confirms the previously obtained assumption, based on the values of Table 1, about the inappropriateness of processing raw materials of more than 10 microns.

In a production environment, in addition to the main set of factors studied using a computer experiment, process indicators are influenced by many factors that are difficult or impossible to control. This leads to the fact that the optimal conditions found through a computer experiment are often not reproduced in industry. In this regard, it is necessary to periodically conduct an experiment directly at an industrial facility to refine and control the initial parameters.

The mathematical modeling of the process of animal waste crushing using cavitation destruction consists of three interrelated stages:

- compilation of a mathematical description of the raw materials processing unit;

- the choice of a solution method of the system of equations of mathematical description and its implementation in the form of a modeling program;

- establishing conformity (adequacy) of the raw materials processing unit model of pilot industrial biogas technology at the facility in the Birlik – Tuimekent SEC;

- at the stage of compiling the mathematical description, the main factors and parameters in the raw materials processing unit are identified, and then the relationships between them are established. Further, for each selected parameter and factor, a system of equations reflecting its functioning and the equations of connection between them was wrote;

- at the stage of choosing a solution method and developing a modeling program. The system of nonlinear equations was solved in the Mathcad environment, which was distinguished by the speed of obtaining and accuracy of the solution and its implementation first in the form of a solution algorithm, and then in the form of a program suitable for computer calculation;

- at the stage of testing the mathematical model, a computer experiment was conducted in the TRACE MODE tool system;

- the raw materials processing unit model built on the basis of physical concepts qualitatively and quantitatively describes the properties of the simulated process and is adequate to the real object in the Birlik – Tuimekent SEC;

- at the stage of checking the adequacy of the mathematical model for the real process, the results of measurements at the Birlik – Tuimekent SEC were compared with the calculation results obtained from the mathematical model and mathematical modeling.

In this article:

1. The physical and chemical foundations of the process of biogas production during anaerobic solid waste fermentation were considered;

2. The component parts of the organic raw materials processing unit were examined;

3. Literary sources were analyzed using numerical methods of data processing, and a

mathematical model was obtained for the process of organic raw materials primary procession.

4. A visual model of the biomass grinding process was built;

5. The parameters of heating the substrate to the parameters of the psychrophilic temperature regime were considered;

6. The equation for determining the percentage of biogas concentration was calculated;

7. The optimal time of biomass processing to the required size was calculated with the modified parameters of the modernized system;

8. An automated process control system was developed based on the received data;

9. A computer experiment was conducted to identify the optimal working parameters of the biogas plant.

#### 4. CONCLUSIONS:

The greening of all production processes today is quite relevant. Therefore, in the article, a computer-assisted mathematical model for the raw materials biological processing was created. To analyse the resulting mathematical model, a computer experiment was conducted in the Scada Trace Mode system.

It was established that particles of the 10  $\mu\text{m}$  fraction will be key for biogas production, since they have a high level of flotation, smaller particles make a small contribution to the formation of methane and are prone to precipitation.

It has been demonstrated that the use of cavitation destruction can significantly reduce the volume of natural organic raw materials and destroy intercellular membranes, thereby use plant fibers most efficiently, significantly increase the speed and depth of extraction of raw materials, as well as its subsequent period of fermentation. And the use of modern automation systems for production processes, such as ScadaTraceMode and others, allows us to save time and technological resources, to avoid equipment deterioration during the experiment.

#### 5. REFERENCES:

1. Akhnazarova, S. L., and Kafarov, V. V. (1985). *Methods of optimizing an experiment in chemical technology*. Moscow, Russian Federation: Vysshayashkola.
2. Barisa, A., Kirsanovs, V., and Safronova, A.

- (2020). Future transport policy designs for biomethane promotion: A system dynamics model. *Journal of Environmental Management*, 269, article number 110842.
3. Biogas manual. From receipt to use. (2010). Retrieved from <https://mediathek.fnr.de/media/downloadable/files/samples/h/a/handreichungbiogasru2012.pdf>.
  4. Butova, S. N., Salnikova, V. A., Ivanova, L. A., Schegoleva, I. D., and Churmasova, L. A. (2018). Studying the properties of oils from secondary raw materials. *International Journal of Engineering and Technology(UAE)*, 7(2), 297-300.
  5. Chandra, S., Stanford, D., Fletcher, E., and Walker, L. A. (2019). Raw materials production and manufacturing process control strategies. In R. Sasisekharan, S.L. Lee, A. Rosenberg, and L.A. Walker (Eds.), *The science and regulations of naturally derived complex drugs* (pp. 175-190). Cham, Switzerland: Springer International Publishing.
  6. Dong, X. T., Chen, W., Li, J. Q., and Zhang, S. (2018). Research on biogas fermentation raw materials. *E3S Web of Conferences*, 53, article number 01030.
  7. Dotsenko, A. S., Rozhkova, A. M., Gusakov, A. V., and Sinitsyn, A. P. (2017). Improving the efficiency of the bioconversion of plant raw materials with mutant cellulases of *Penicillium verruculosum*. *Catalysis in Industry*, 9(1), 71-76.
  8. Druzyanova, V. P. (2008). Resource-saving technology for utilization of uncontrolled waste in the conditions of the Republic of Sakha (Yakutia). *Agrarian Bulletin of the Urals*, 1(43), 63-64.
  9. Eder, B., and Schulz, H. (2011). *Biogas plants*. Kyiv, Ukraine: Sorg Biogas.
  10. Golubtsova, J. (2017). Assessing quality of fruit raw material for developing a method of its identification in food products. *Journal of Pharmaceutical Sciences and Research*, 9(5), 504-512.
  11. Iskakov, R. M., Iskakova, A. M., Issenov, S., Beisebekova, D. M., and Khaimuldinova, A. K. (2019). Technology of multistage sterilization of raw materials with the production of feed meal of high biological value. *Journal of Pure and Applied Microbiology*, 13(1), 307-312.
  12. Ivanov, V. A., and Gasparyan, G. R. (2013). Mathematical modeling of cavitation during debarking of timber in the aquatic environment. *Systems. Methods Technology. Mathematical Modeling*, 3(19), 171-178.
  13. Kiss, A.A., Grievink, J., and Rito-Palomares, M. (2015). A systems engineering perspective on process integration in industrial biotechnology. *Journal of Chemical Technology and Biotechnology*, 90(3), 349-355.
  14. Koller, M., Maršálek, L., de Sousa Dias, M. M., and Braunegg, G. (2017). Producing microbial polyhydroxyalkanoate (PHA) biopolyesters in a sustainable manner. *New Biotechnology*, 37, 24-38.
  15. Kudrin, M. R., Krasnova, O. A., Koshchaev, A. G., Koshchaeva, O. V., Ulimbashe, M. B., Konik, N.V., and Shabunin, S.V. (2019). Biological processing of renewable raw materials resources with regard to the environmental and technological criteria. *Journal of Ecological Engineering*, 20(11), 58-66.
  16. Kudryashova, A. G. (2011). *Substantiation and development of means for increasing the energy efficiency of the three-stage digester*. Izhevsk, Russian Federation: Izhevsk State Agricultural Academy.
  17. Kulbjakina, A. V., and Dolotovskij, I. V. (2018). Methodological aspects of fuel performance system analysis at raw hydrocarbon processing plants. *Journal of Physics: Conference Series*, 944(1), article number 012068.
  18. Kusuma, I. M., Syafrudin, and Yulianto, B. (2019). Utilization of fish waste processing as compost raw material in Tambak Lorok Market. *E3S Web of Conferences*, 125, article number 07004.
  19. Meshcheryakov, I.V. (2014). *Development and research of a multistage hydropercussion-cavitation device for fine grinding of hard-to-concentrate ores*. Krasnoyarsk, Russian Federation: Siberian State Industrial University.
  20. Popov, V. P., Dudorov, V. E., Sidorenko, G. A., Akhmediyeva, Z. R., Tsyraeva, E. A., and Sagitov, R. F. (2019). Economic assessment of the need for processing of raw materials of animal origin. *IOP Conference Series: Materials Science and Engineering*, 560(1), article number 012199.

21. Ruzhinskaya, L. I., and Fomenkova, A. A. (2014). Mathematical modeling of the processes of anaerobic digestion of an organic substrate. Overview. *ScienceRise*, 4/2(4), 63-69.
22. Sidyganov, Yu. N., Shamshurov, D. N., and Kostromin, D. V. (2008). Anaerobic waste processing for biogas production. *Mechanization and Electrification of Agriculture*, 6, 42-43.
23. Sokolova, I., Skobtsova, K., Naumova, L., Slizhov, J., Selyanina, S., and Orlov, A. (2018). Spectral, luminescent, and photochemical properties of humic acids with different genesis of organic raw materials. *IOP Conference Series: Earth and Environmental Science*, 201(1), article number 012022.
24. Tlebayev, M. B., Tazhiyeva, R. N., Doumcharieva, Z. E., Aitbayeva, Z. K., and Baijarikova, M. A. (2017). Mathematical research of the accelerated three-stage process of substrate fermentation in bioreactors. *Journal of Pharmaceutical Sciences and Research*, 9(4), 392-400.
25. Trakhunova, I. A. (2014). *Improving the efficiency of anaerobic processing of organic waste in a digester with hydraulic stirring based on a numerical experiment*. Kazan, Russian Federation: Kazan Scientific Center of the Russian Academy of Sciences.
26. Vachagina, E. K., and Karaeva, Yu. V. (2009). A mathematical model of the motion of a two-phase gas-liquid medium in a cylindrical fermenter of a biogas plant. *Alternative Energy and Ecology*, 10, 79-84.
27. Vedenev, A. G., and Vedeneva, T. A. (2006). *PF "Fluid" Biogas technologies in the Kyrgyz Republic*. Bishkek, Kyrgyz Republic: Euro Printing House.
28. Yudaev, I., Stepanchuk, G., Kaun, O., Ukraitsev, M., and Ponamareva, N. (2019). Small-sized irradiation structures for intensive year-round cultivation of green vegetable crops. *IOP Conference Series: Earth and Environmental Science*, 403(1), 012084.
29. Zagorulko, A., Zahorulko, A., Kasabova, K., Chervonyi, V., Omelchenko, O., Sabadash, S., Zahorko, N., and Peniov, O. (2018). Universal multifunctional device for heat and mass exchange processes during organic raw material processing. *Eastern-European Journal of Enterprise Technologies*, 6(1-96), 47-54.
30. Zhumagazhinov, A. T., and Algazinov, N. K. (2014). Methods of intensification of the processes of anaerobic digestion. *Bulletin of the Innovative Eurasian University*, 1, 34-37.

$$y = a + \frac{b}{x} \quad (\text{Eq. 1})$$

$$b = \frac{n \sum \frac{y_i}{x_i} - \sum \frac{1}{x_i} \sum y_i}{n \sum \frac{1}{x_i^2} - \left( \sum \frac{1}{x_i} \right)^2} = \frac{6 \cdot 234.721 - 2.45 \cdot 295.71}{6 \cdot 1.49138889 - 2.45^2} \approx 232.1369 \quad (\text{Eq. 2})$$

$$a = \frac{1}{n} \sum y_i - \frac{b}{n} \sum \frac{1}{x_i} = \frac{1}{6} \cdot 295.71 - \frac{232.1369}{6} \cdot 2.45 \approx -45.5042 \quad (\text{Eq. 3})$$

$$y = -45.5042 + \frac{232.1369}{x} \quad (\text{Eq. 4})$$

$$R = \sqrt{1 - \frac{\sum (y_i - \bar{y}_i)^2}{\sum (y_i - \bar{y}_i)^2}} = \sqrt{1 - \frac{1519.4042}{27976.6806}} \approx 0.9725 \quad (\text{Eq. 5})$$

$$\bar{A} = \frac{1}{n} \sum \left| \frac{y_i - \bar{y}_i}{y_i} \right| \cdot 100\% = \frac{4.033}{6} \cdot 100\% \approx 67.2172\% \quad (\text{Eq. 6})$$

$$\begin{cases} f(x) = -45.5042 + \frac{232.1369}{x} \\ f(x) = 161.11x^{-1.705} \end{cases} \quad (\text{Eq. 7})$$

$$\begin{cases} f(x) = -45.5042 + \frac{232.1369}{x}, x < 4 (f(x) \geq 18) \\ f(x) = 161.11x^{-1.705}, x > 3 (f(x) < 18) \end{cases} \quad (\text{Eq. 8})$$

$$N = \frac{V_{vol}}{V_{pip}} \quad (\text{Eq. 9})$$

$$T_{vol} = N \cdot T_{cycl} \quad (\text{Eq. 10})$$

$$T_{cycl} = \frac{V_{vol}}{V_{pip}} \cdot T_{cycl} \cdot x \quad (\text{Eq. 11})$$

$$X = \frac{T_{vol} \cdot V_{pip}}{V_{vol} \cdot T_{cycl}} \quad (\text{Eq. 12})$$

$$T_{vol} = \frac{V_{vol}}{4.69} \cdot 9.61 \cdot x = 2.049 \cdot V \cdot x \quad (\text{Eq. 13})$$

$$= \frac{T_{vol}}{2.049 \cdot V} = 0.49 \cdot \frac{T_{vol}}{V_{vol}} \quad (\text{Eq. 14})$$

$$\begin{cases} f(x) = -45.5042 + \frac{232.1369 \cdot V_{vol} \cdot T_{cycl}}{V_{pip} \cdot T_{vol}}, x \leq 4 (x \geq 18 \text{ microns}) \\ f(x) = 161.11 \cdot \left( \frac{V_{pip} \cdot T_{vol}}{V_{vol} \cdot T_{cycl}} \right), x > 4 (x < 18 \text{ microns}) \end{cases} \quad (\text{Eq. 15})$$

$$\begin{cases} f(x) = -45.5042 + \frac{232.1369 \cdot V}{0.49 \cdot T_{vol}}, x \leq 4 (x \geq 18 \text{ microns}) \\ f(x) = 161.11 \cdot \left( \frac{2.04 \cdot V_{vol}}{T_{vol}} \right), x > 4 (x < 18 \text{ microns}) \end{cases} \quad (\text{Eq. 16})$$

$$\begin{cases} f(x) = -45.5042 + 475 \cdot \frac{V}{T_{vol}}, x \leq 4 (x \geq 18 \text{ microns}) \\ f(x) = 543 \cdot \left( \frac{V_{vol}}{T_{vol}} \right)^{1.705}, x > 4 (x < 18 \text{ microns}) \end{cases} \quad (\text{Eq. 17})$$

$$T_{vol} = \frac{233.1369 \cdot V_{vol} \cdot T_{cycl}}{L + 45.5042} \quad (\text{Eq. 18})$$

$$T_{vol} = \frac{475 \cdot V}{L + 45.5042} \quad (\text{Eq. 19})$$

$$T_{vol} = \left( \frac{161.11 \cdot V_{vol}^{-1.705} \cdot T_{cycl}^{1.705}}{L \cdot V_{pip}^{1.705}} \right)^{0.59} \quad (\text{Eq. 20})$$

$$T_{vol} = \left( \frac{543.67 \cdot V_{vol}^{-1.705}}{L} \right)^{0.59} \quad (\text{Eq. 21})$$

$$\begin{cases} T_{vol} = \frac{233.1369 \cdot V_{vol} \cdot T_{cycl}}{L + 45.5042}, x \leq 4 (x \geq 18 \text{ microns}) \\ T_{vol} = \left( \frac{161.11 \cdot V_{vol}^{1.705} \cdot T_{cycl}^{1.705}}{L \cdot V_{pip}^{1.705}} \right)^{0.59}, x > 4 (x < 18 \text{ microns}) \end{cases} \quad (\text{Eq. 22})$$



$$\left\{ \begin{array}{l} T_{vol} = \frac{475 \cdot V}{L + 45.5042}, x \leq 4 (x \geq 18 \text{ microns}) \\ T_{vol} = \left( \frac{543.67 \cdot V_{vol}^{1.705} \cdot T_{cycl}^{1.705}}{L} \right)^{0.59}, x > 4 (x < 18 \text{ microns}) \end{array} \right. \quad (\text{Eq. 23})$$

**Table 1.** The relationship between destruction efficiency and performance

| Cycle No. | I (destruction efficiency) | D(destruction size) micron | Q(dispersing agent performance) m <sup>3</sup> /h |
|-----------|----------------------------|----------------------------|---|
| 1         | -                          | 200                        | 8.547   |
| 2         | 4.74                       | 42.19                      | 9.048   |
| 3         | 2.17                       | 19.44                      | 9.426   |
| 4         | 1.47                       | 13.22                      | 10.148  |
| 5         | 1.21                       | 10.93                      | 11.687  |
| 6         | 1.1                        | 9.93                       | 12.348  |

**Table 2.** Auxiliary quantities

| I               | $x_i$ | $y_i$  | $\frac{1}{x_i}$ | $\frac{1}{x_{2i}}$ | $\frac{y_i}{x_i}$ |
|-----------------|-------|--------|-----------------|--------------------|-------------------|
| 1               | 1     | 200    | 1               | 1                  | 200               |
| 2               | 2     | 42.19  | 0.5             | 0.25               | 21.095            |
| 3               | 3     | 19.44  | 0.33333333      | 0.11111111         | 6.48              |
| 4               | 4     | 13.22  | 0.25            | 0.0625             | 3.305             |
| 5               | 5     | 10.93  | 0.2             | 0.04               | 2.186             |
| 6               | 6     | 9.93   | 0.16666667      | 0.02777778         | 1.655             |
| $\Sigma \Sigma$ | 21    | 295.71 | 2.45            | 1.49138889         | 234.721           |

**Table 3.** The matrix of initial values of the experiment

| Parameter  | Experiment number N |      |     |     |     |     |     |     |
|--|---------------------|------|-----|-----|-----|-----|-----|-----|
|  | 1                   | 2    | 3   | 4   | 5   | 6   | 7   | 8   |
| volume of loaded raw materials                               | 600                 | 600  | 600 | 600 | 600 | 600 | 600 | 600 |
| desired particle size at the outlet                          | 2000                | 1000 | 200 | 100 | 50  | 20  | 10  | 5   |
| the volume of the pipes of the raw materials processing unit | 5                   | 5    | 5   | 5   | 5   | 5   | 5   | 5   |
| heating element power  | 50                  | 50   | 50  | 50  | 50  | 50  | 50  | 50  |
| initial temperature of raw materials                         | 10                  | 10   | 10  | 10  | 10  | 10  | 10  | 10  |
| desired temperature of the raw material                      | 25                  | 25   | 25  | 25  | 25  | 25  | 25  | 25  |

**Table 4.** The dependence of the selected parameters

| Parameter                           | Experiment number N |        |       |      |       |       |       |       |
|-------------------------------------|---------------------|--------|-------|------|-------|-------|-------|-------|
|                                     | 1                   | 2      | 3     | 4    | 5     | 6     | 7     | 8     |
| desired particle size at the outlet | 2000                | 1000   | 200   | 100  | 50    | 20    | 10    | 5     |
| time of raw materials crushing      | 10 min              | 21 min | 1.31  | 2.33 | 3.54  | 5.42  | 6.43  | 7.23  |
| methane content                     | 22.92               | 32.92  | 53.36 | 61.1 | 68.26 | 76.91 | 82.17 | 84.43 |
| carbon dioxide content              | 77.07               | 67.07  | 46.63 | 38.9 | 31.74 | 23.08 | 17.10 | 15.57 |

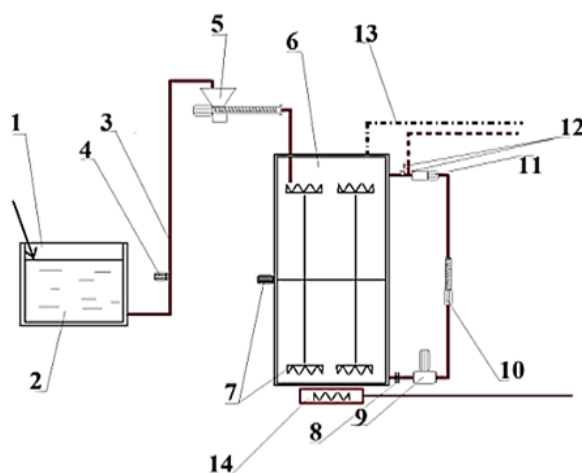


**Figure 1.** Processing line of nodes for cavitation destruction of animal waste and anaerobic fermentation in a psychrophilic mode: 1 – a tank for mixing cattle manure with water; 2 – liquid manure; 3 – 57 mm pipe; 4 – pump for transferring liquid manure into the inducer; 5 – spiral separator; 6 – facility for temporary storage, crushing and fermentation of biomass; 7 – automatic mixer; 8 – coupling; 9 – macerator; 10 – gerotor type pump; 11 – dispersing agent; 12 – valves that regulate the direction of the substrate; 13 – biogas outlet pipe; 14 – boiler for heating the tank (6)

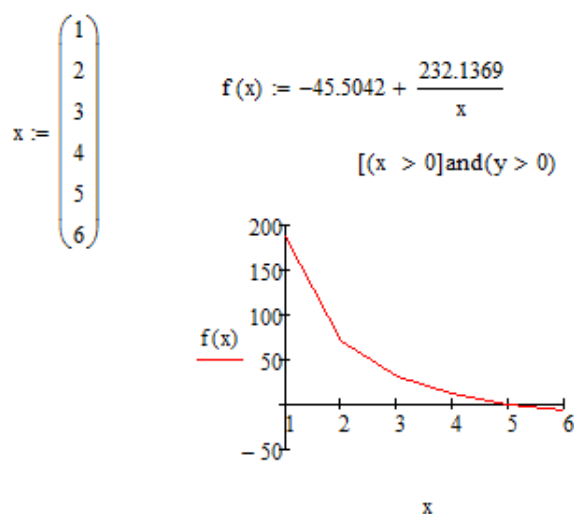


**Figure 2.** The graph of the regression equation

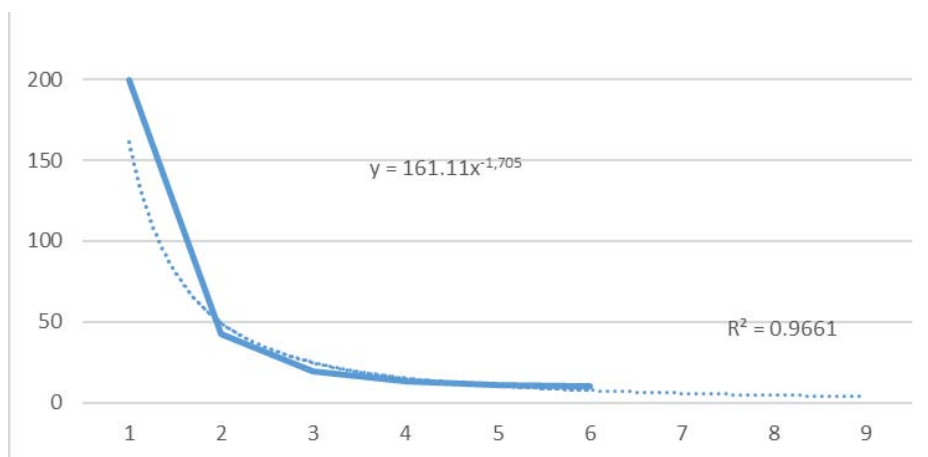


**Figure 3.** The Trendline function

$$f(x) := 161.11 \cdot x^{-1.705}$$

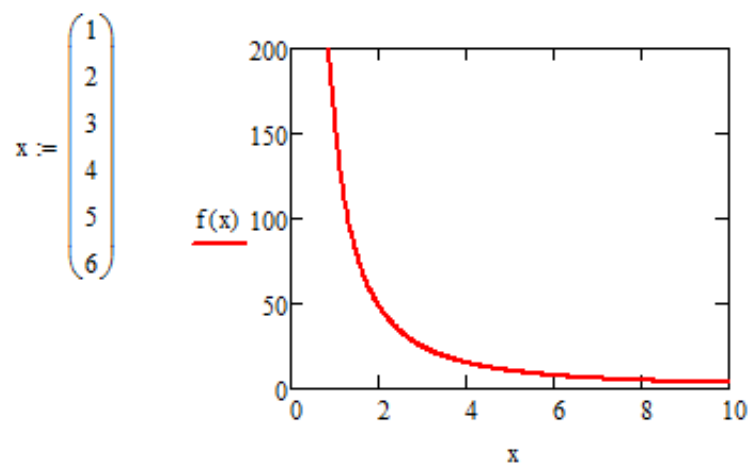


**Figure 4.** Power function implementation in Mathcad

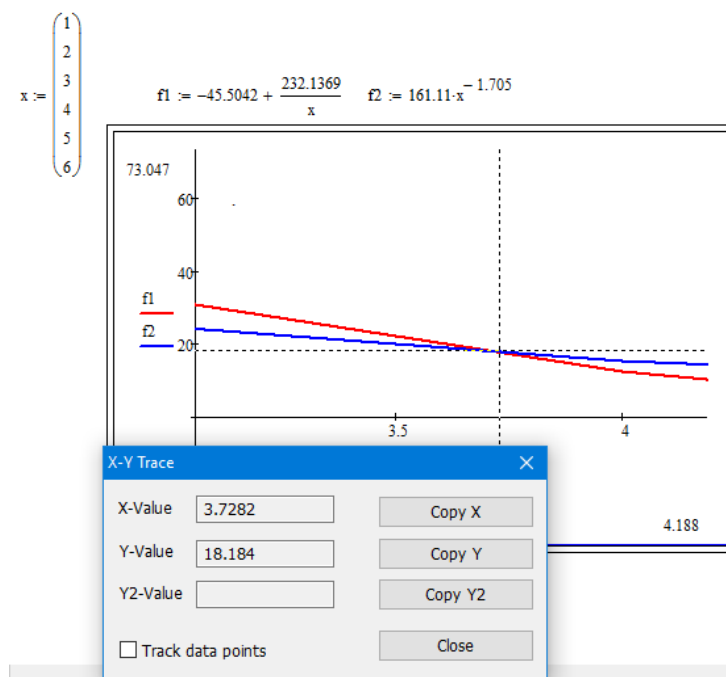


**Figure 5.** Definitions of system limitations

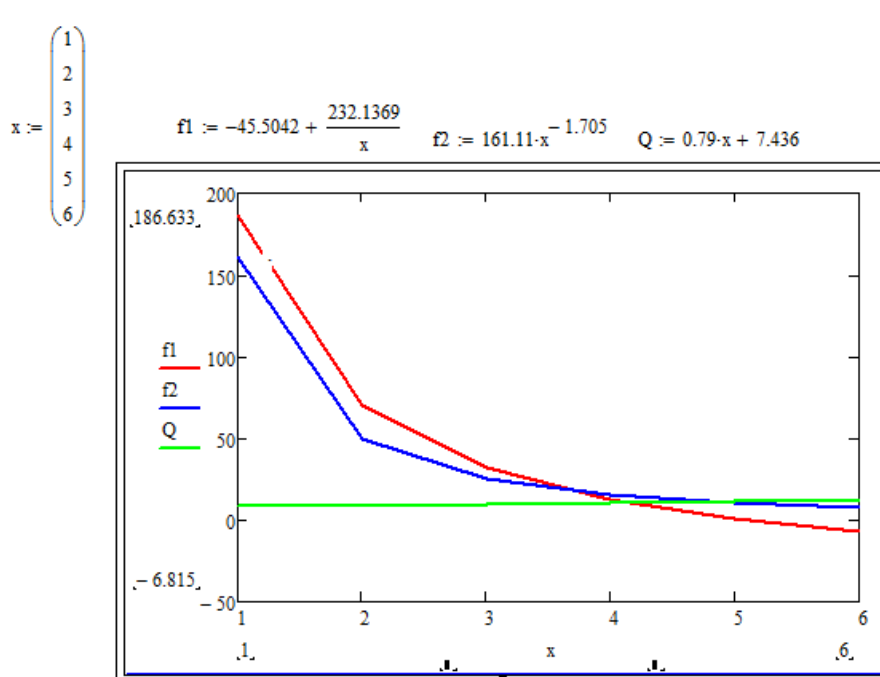
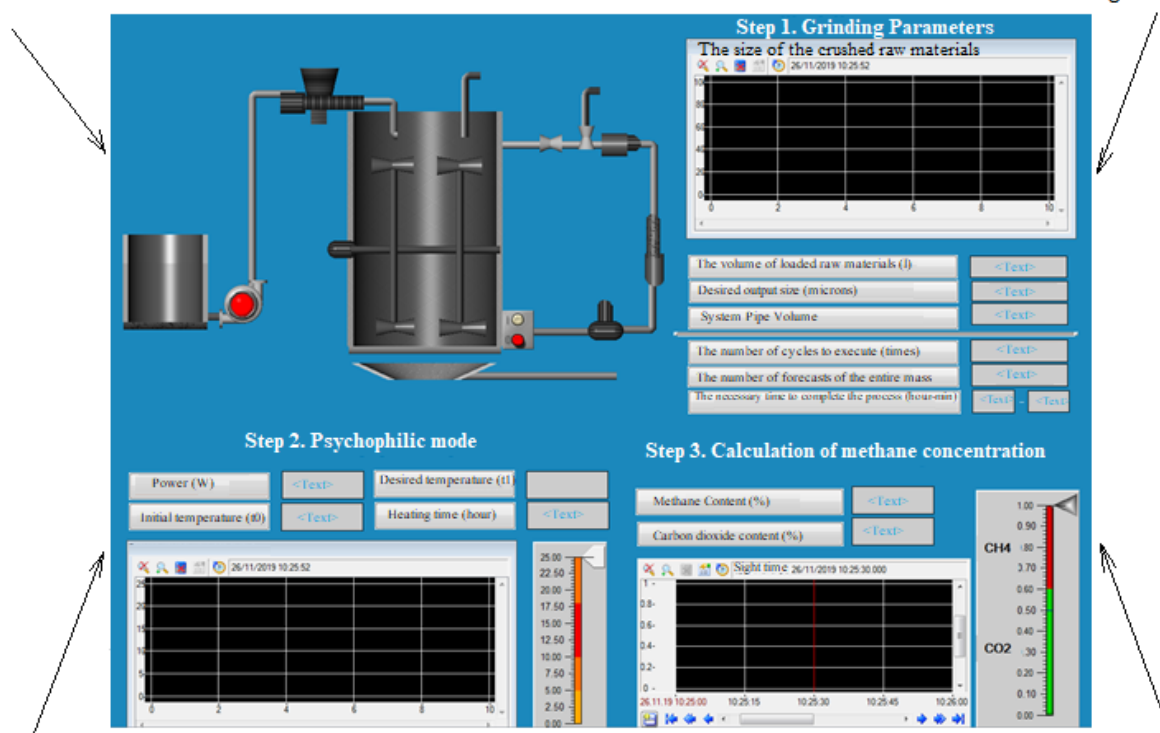


**Figure 6.** The system of equations

A graphical representation of the raw materials processing unit structural elements.

Parameters and schedule for raw materials crushing.



Calculation of indicators for heating raw materials at a psychophilic mode.

Calculation of the CO<sub>2</sub> concentration at the outlet.

**Figure 7.** Four logical zones of an automated system for managing technological processes of organic raw materials recycling. Source: Vedenev and Vedeneva (2006)

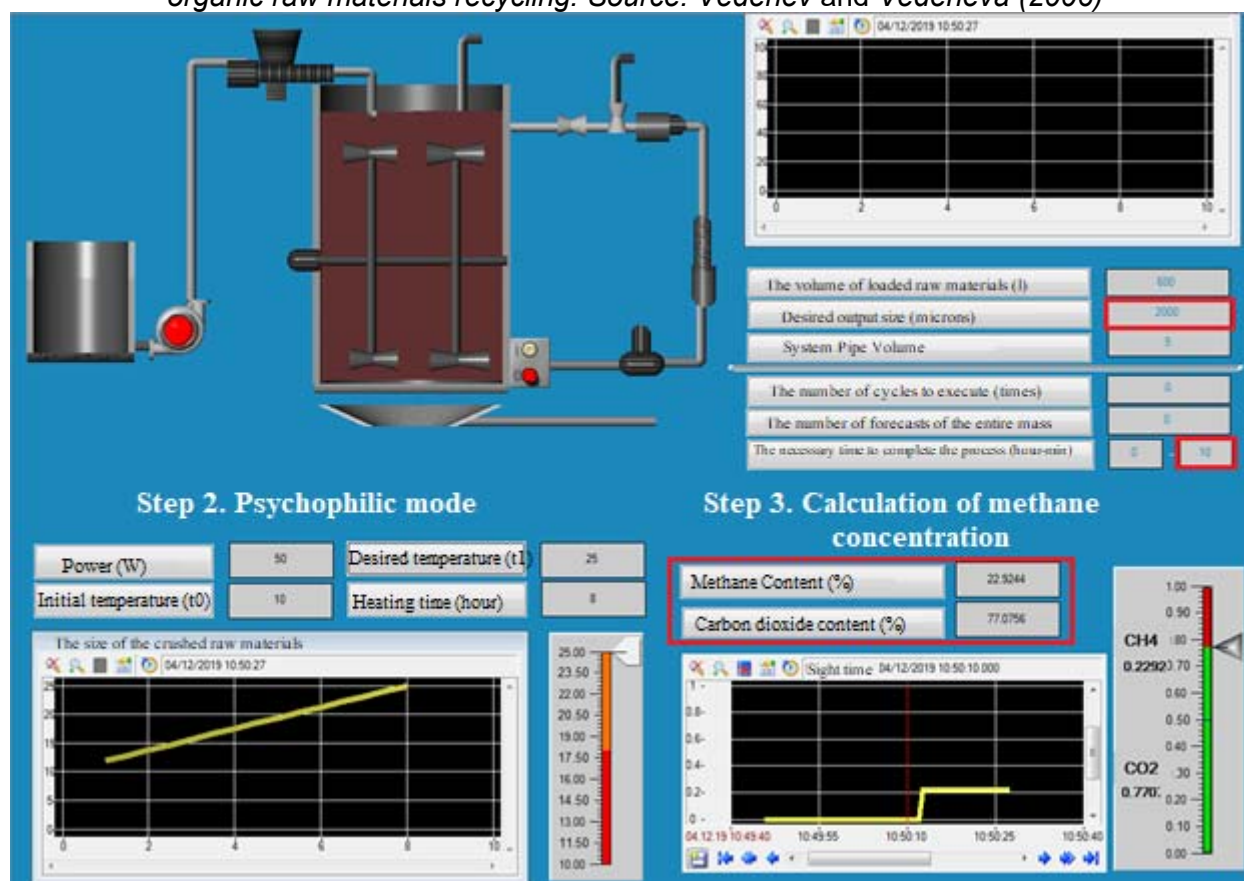


**Figure 8.** The calculation of the outlet parameters

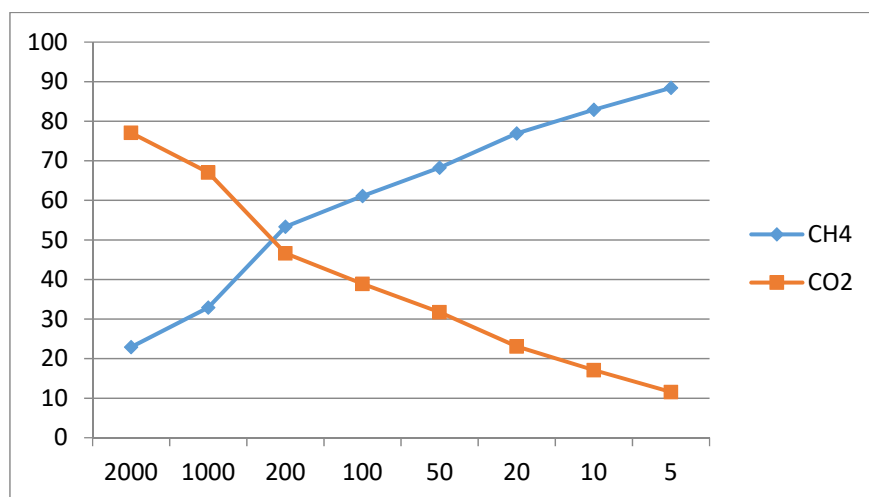


**Figure 9.** The relationship between particle size and biogas concentration

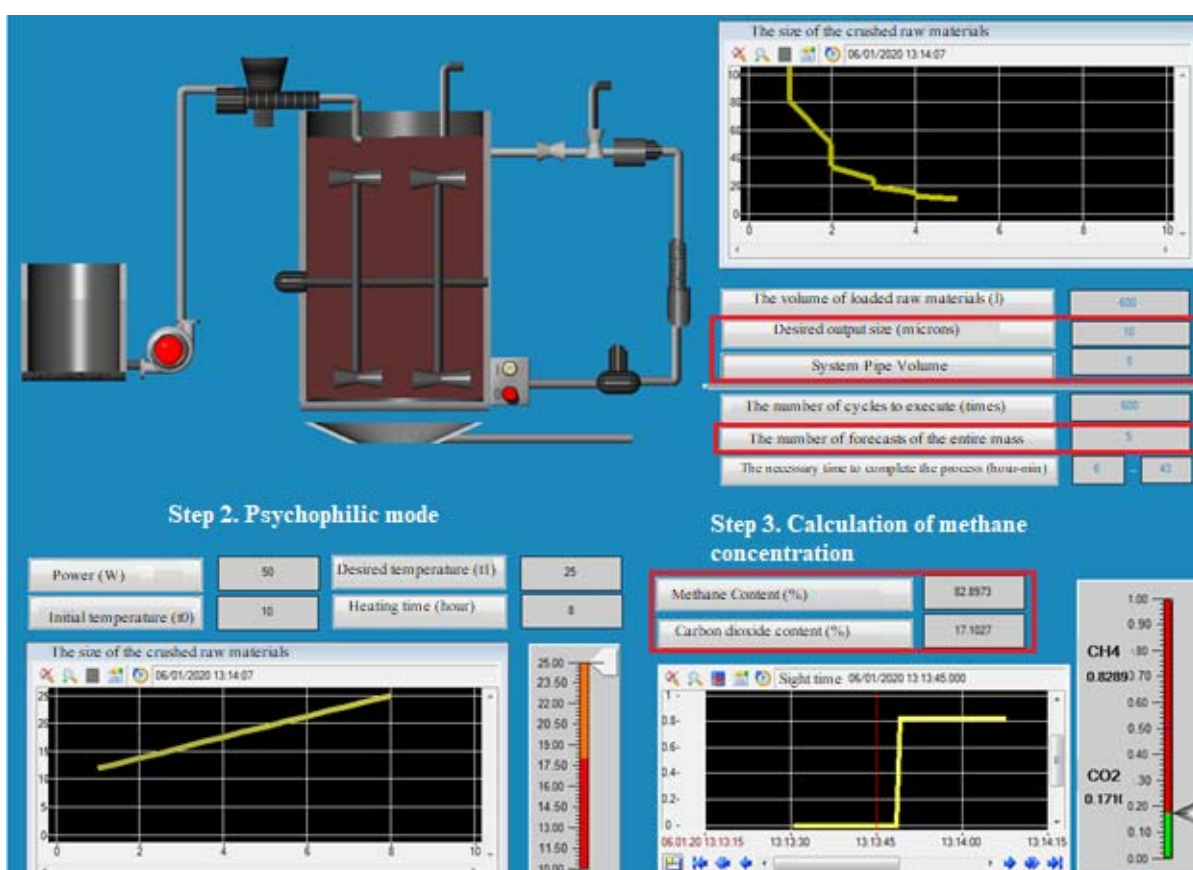


**Figure 10.** The process of particles crushing by less than 10 microns

**ESTUDO DA INFLUÊNCIA DE INCLUSÕES ESFÉRICAS EM CARACTERÍSTICAS MECÂNICAS****STUDY OF THE INFLUENCE OF SPHERICAL INCLUSIONS ON MECHANICAL CHARACTERISTICS****ИССЛЕДОВАНИЕ ВЛИЯНИЯ СФЕРИЧЕСКИХ ВКЛЮЧЕНИЙ НА МЕХАНИЧЕСКИЕ ХАРАКТЕРИСТИКИ**

BABAYTSEV, Arseniy V.<sup>1\*</sup>; KYAW, Ye Ko<sup>2</sup>; VAKHNEEV, Sergey N.<sup>3</sup>; ZIN HEIN, Thant<sup>4</sup>;

<sup>1,3</sup> Moscow Aviation Institute (National Research University), Department of Engineering Graphics, 4 Volokolamskoe Highway, zip code 125993, Moscow – Russian Federation

<sup>2</sup> Defense Services Technological Academy (DSTA), Department of Mathematics, Mandalay-Lashio Highway, Mandalay Division, Pyin Oo Lwin – Myanmar

<sup>4</sup> Defense Services Technological Academy (DSTA), Marine Electrical System and Electronics, Mandalay-Lashio Highway, Pyin Oo Lwin, Mandalay Division – Myanmar

\* Correspondence author  
e-mail: Ar77eny@gmail.com

Received 12 June 2020; received in revised form 30 November 2020; accepted 14 December 2020

**RESUMO**

A relevância do artigo deve-se ao crescimento estável da indústria de compósitos. Devido às suas altas características físicas e mecânicas, os materiais compósitos (MC) desempenham um papel vital em muitas áreas da tecnologia, como indústria aeroespacial, aviação, indústria automotiva, engenharia e instrumentação e a indústria médica. Ao criar os materiais com as características mecânicas e térmicas necessárias, são frequentemente usados vários aditivos e enchimentos que afetam a resistência e a elasticidade das amostras obtidas. Neste artigo, estudamos o efeito de inclusões esféricas em resina epóxi nas propriedades mecânicas do material. Uma estrutura composta de resina epóxi ED-20 com inclusões na forma de partículas esféricas de vidro PBS-50 foi considerada. O tamanho característico das partículas foi de cerca de 50 µm. No âmbito deste estudo, foram produzidos lotes de amostras com o volume característico de inclusões de 5%, 10%, 15% e 20%. Cada lote consistia em 6 amostras do mesmo tipo. Para verificar a distribuição do volume de partículas e estudar as inclusões, a microestrutura da seção delgada da amostra e o pó foram estudadas separadamente. Usando métodos de modelagem do processo, as amostras foram submetidas ao teste de flexão de três pontos. Com base nos resultados de testes mecânicos, foram obtidos o módulo de elasticidade, a resistência à tração e as deformações finais. Como parte do estudo dos materiais, foram realizados os cálculos numéricos usando o software Digimat (MSC Software) para modelar a estrutura e obter propriedades efetivas do material. Também foram realizados os cálculos de tensões usando o método dos elementos finitos em Ansys Workbench. O cálculo foi realizado para o conteúdo volumétrico de inclusões da ordem de 5%, 10%, 15% e 20% e na ausência de inclusões. Os resultados numéricos obtidos foram comparados com o estudo experimental. Com base nos cálculos numéricos, foi obtida a dependência da porcentagem de inclusões na resistência à tração e no módulo de elasticidade.

**Palavras-chave:** material compósito, inclusão esférica, teste de flexão, proporção de volume, propriedades mecânicas.

**ABSTRACT**

The relevance of the article is due to the stable growth of the composite industry. Due to its high physical and mechanical characteristics, composite materials (CM) play a vital role in many areas of technology, such as aerospace, aviation, automotive, engineering and instrumentation, and the medical industry. When creating materials with the required mechanical and thermal characteristics, various additives and fillers are often used that affect the strength and elasticity of the samples obtained. In this paper, we study the influence of spherical inclusions in epoxy on the mechanical properties of the material. A composite structure of ED-20 epoxy with

inclusions in the form of spherical particles of PBS-50 glass was considered. The characteristic particle size was about 50  $\mu\text{m}$ . Within the framework of this study, batches of samples with a specific volumetric inclusion content of 5%, 10%, 15%, and 20% were produced. Each batch consisted of 6 samples of the same type. To check the distribution of particle volume and inclusion studies, the microstructure of the thin section of the sample and separately the powder were studied. Using methods of modeling the process, the samples were tested for 3-point bending. Based on the results of mechanical tests, the elastic module, strength limit, and ultimate strains were obtained. As part of the study of materials, numerical calculations were performed using Digimat software (MSC Software) to model the structure and obtain effective material properties, as well as strength analysis using the finite element method in Ansys Workbench. The calculation was carried out for the volumetric content of inclusions of 5%, 10%, 15%, and 20% order and in the absence of inclusions. The obtained numerical results were compared with an experimental study. Based on the numerical calculations, the dependence of the percentage of inclusions on the strength limit and elastic module was obtained.

**Keywords:** *composite material, spherical inclusion, bend test, volume fraction, mechanical characteristics.*

## АННОТАЦИЯ

Актуальность статьи обусловлена стабильным ростом композитной промышленности. Благодаря высоким физико-механическим характеристикам, композитные материалы (КМ) играют жизненно важную роль во многих областях техники, таких как аэрокосмическая, авиационная техника, автомобильная промышленность, машиностроение и приборостроение, медицинская отрасли. При создании материалов с требуемыми механическими и тепловыми характеристиками часто используются различные добавки и наполнители, влияющие на прочность и упругость полученных образцов. В данной работе исследуется влияние сферических включений в эпоксидной смоле на механические свойства материала. Рассматривалась композитная структура из эпоксидной смолы ЭД-20 с добавленными в нее включениями в виде сферических частиц стекла ПБС-50. Характерный размер частиц составлял порядка 50 мкм. В рамках данного исследования изготавливались партии образцов с характерным объемным содержанием включений равным 5%, 10%, 15% и 20%. Каждая партия состояла из 6 однотипных образцов. Для проверки распределения частиц по объему и исследования включения проводились исследования микроструктуры шлифа образца и отдельно порошка. Используя методы моделирования процесса, образцы испытывались на 3х точечный изгиб. По результатам механических испытаний были получены модуль упругости, предел прочности и предельные деформации. В рамках исследования материалов проводились численные расчеты с использованием программного обеспечения Digimat (MSC Software) для моделирования структуры и получения эффективных свойств материала, а также, проводился прочностной расчет с использованием метода конечных элементов в среде Ansys Workbench. Расчет проводился для объемного содержания включений порядка 5%, 10%, 15% и 20% и при отсутствии включений. Полученные численные результаты сравнивались с экспериментальным исследованием. На основании проведенных численных расчетов была получена зависимость процентного содержания включений от предела прочности и модуля упругости.

**Ключевые слова:** *композиционный материал, сферическое включение, испытание на изгиб, объемная доля, механические свойства.*

## 1. INTRODUCTION

The production and use of composite materials (CM) is growing steadily every year. Currently, CMs play a vital role in many areas of technology, such as aerospace, aeronautical engineering, automotive industry, mechanical engineering, and instrumentation, the medical industry and more (Yushkova *et al.*, 2010; Dmitriev *et al.*, 2011; Shershak, 2019; Yu Timkina *et al.*, 2019). The reasons for this rapid growth of the composite industry are low density of products, high physical and mechanical characteristics, resistance to corrosion and aggressive environments, as well as the ability to create

materials with the required mechanical and thermal characteristics (Lakes *et al.*, 2002; Orlov *et al.*, 2001; Jae-soon, 2012). One of the options for obtaining the necessary properties of materials is the use of various additives, for example, the addition of inclusions in the polymer matrix (Trofimov *et al.*, 2017; Wang *et al.*, 2019; Prentkovskis *et al.*, 2012).

The matrix (binding agent) is the most important element of the composite and determines the nature of the change in its properties when exposed to various factors (temperature, chemical resistance, electrical and other properties). A deeper understanding of the



interaction of inclusions and matrix, as well as the influence of the volumetric content of the included particles on the physical and mechanical characteristics, has emerged with the development of nanotechnologies. That is why the study of the mechanical characteristics of CM samples with various fillers and additives is an extremely urgent task (Tagliavia *et al.*, 2010; Tkachev *et al.*, 2018; Xinfeng *et al.*, 2018; Umbetov *et al.*, 2016). At the moment, there are many studies describing the use of inclusions to improve the physical and mechanical characteristics of composites (Odegard *et al.*, 2005; Sanchez-Soto *et al.*, 2007; Vettegren *et al.*, 2007; Song, 2009; Hurang *et al.*, 2010; Markus *et al.*, 2013; Seighalani *et al.*, 2015; Babaytsev *et al.*, 2017; Kenzhaev, 2019; Ryapukhin *et al.*, 2019; Formalev *et al.*, 2019; Jeyaprakash and Devaraju, 2020). However, the addition of particles is nonlinear and depends on many factors, such as the structure of the material from which the inclusions are made, the shape and size of the particles, as well as the volume fraction of inclusions (Markus *et al.*, 2013; Hnatiuk *et al.*, 2019; Jeyaprakash and Devaraju, 2019).

The aim of this work is to prepare and study the mechanical characteristics of glass dispersed and epoxy-filled composites. In this work, we consider the composite structure of the ED-20 epoxy, into which glass particles with a characteristic size of about 50  $\mu\text{m}$  are added. In this paper, five different batches of samples are presented, depending on the volume fraction of inclusions. Each batch consisted of 6 samples of the same type. To check the distribution of particle volume and inclusion studies, the microstructure of the thin section of the sample and separately the powder was studied. Moreover, to study the influence of inclusions (spheres) on the mechanical characteristics of CMs, tests were carried out on samples with three-point bending. As part of the study, a numerical calculation was performed using Digimat MSC Software and Ansys Workbench (Odegard *et al.*, 2005; Lakes *et al.*, 2002; Hurang *et al.*, 2010; Yushkova *et al.*, 2010; Jae-soon, 2012; Xinfeng *et al.*, 2018; Shershak, 2019).

## 2. MATERIALS AND METHODS

In the study, samples of epoxy with inclusions and pure epoxy were studied. An ED-20 epoxy was used as a matrix, and PBS-50 glass spheres with a characteristic sphere size of about 50  $\mu\text{m}$  were used as inclusions. The volumetric content of inclusions was 5%, 10%, 15% and 20%. The material for the samples in this study was

epoxy composites filled with spherical glass particles with a characteristic size of about 50  $\mu\text{m}$ . The particle-filled polymer composites used in the experiments are batches of samples consisting of five types of volume fraction of the filler: 0%, 5%, 10%, 15%, and 20%. A diagram of the process of manufacturing samples is given in Figure 1. In the framework of this study, samples with a rectangular cross-section of 10 mm x 4 mm and a length of 80 mm were used. Quality control – visual inspection, mixing lasted for 25 minutes, vacuum with degassing was used, cooling took place within 3 hours.

To do this, a plate was made, and then samples were cut from it. For each batch of samples, six samples of the same type were produced. Photos of the studied samples are presented in Figure 2. To check the distribution of inclusions by volume, their percentage, as well as confirm the size of the inclusions, we studied the microstructure of the thin section of the sample and separately the powder. The results of microscopy are presented in Figure 3.

To determine the effect of inclusions on the mechanical characteristics of CM, bend tests were performed. The tests were carried out according to standard test procedures on an Instron 5969 universal testing machine with Bluehill software. For each tested batch, a stress-strain curve was constructed (Figure 4). As can be seen from the test results, the presence of inclusion significantly affects the CM mechanical characteristics.

## 3. RESULTS AND DISCUSSION:

For a more detailed study of the structure under study, a numerical calculation was performed. For this purpose, using the Digimat MF software, a structure with the exact use of matrix and inclusion properties, as well as the distribution of inclusions by volume, were preliminarily modeled. All materials were considered as isotropic linearly elastic materials for spherical inclusion and an epoxy polymer matrix and were presented in Table 1.

For each variant of the volumetric content of inclusions, a calculation and determination of the stress-strain curve of the structure under study were carried out. A representative elementary volume with a volume fraction of inclusions is shown in Figure 5. In a representative fragment, it was assumed that the contact between the particles and the matrix is perfect, there is no slip. The result obtained in the process of this calculation for each case under consideration is presented in Figure 6.

After obtaining the characteristics of the CM, a sample was created similar to the experimental sample in ANSYS Workbench. A three-point bending test process was simulated, where the boundary conditions for a rectangular plate were taken from the condition of free bearing on supports. Of course, the elemental model consisted of 16.469 nodes and 3.200 elements, with an element size of ~ 1 mm (Figure 7a). An example of a strain-stress state of the epoxy plate without inclusion is shown in the figure (Figure 7b).

Thus, based on the numerical calculations, the dependence of the percentage of inclusions on the strength limit and elastic module was obtained. The numerical results obtained are in good agreement with experimental results, which makes it possible to select such a volumetric content of inclusions in order to obtain the necessary physical and mechanical characteristics of the CM. However, in such CMs with a sufficiently large number of inclusions, these particles become stress concentrates and significantly reduce the strength limit and ultimate strains.

The tests performed showed a significant effect of the presence of inclusions of more than 15% on the strength limit and ultimate strain. As part of this study, a numerical analysis of the tested structure was performed using Digimat and Ansys. The results of numerical simulation are in good agreement with the experimental results until the inclusion is equal to 10%. In addition, with an increase in the volumetric content of inclusions, the divergence of the numerical and experimental results begins. This is most likely due to the condition of contact between the inclusions and the matrix and with possible internal defects.

#### 4. CONCLUSIONS:

The mechanical characteristics of glass dispersed and epoxy-filled composites, samples with various inclusions were manufactured. Microscopy and mechanical testing of samples were carried out. Structural studies confirmed the size of the inclusions and their distribution over the sample volume. Based on the results of mechanical tests, the elastic module, strength limit, and ultimate strains were obtained. The tests performed showed a significant influence of the presence of inclusions of more than 15% on the strength limit and ultimate strain. The results of numerical modeling are in good agreement with the experimental results, and with an increase in the volumetric content of inclusions, the divergence of the numerical and experimental

results begins. This is due to the condition of contact between the inclusions and the matrix and with possible internal defects, and therefore requires additional research and more accurate modeling.

#### 5. ACKNOWLEDGMENTS:

The work was carried out with the financial support of the state project of the Ministry of Education and Science on the subject "Theoretical and experimental research in the field of production and processing of promising metal and composite materials based on aluminum and titanium alloys", project code FSFF-2020-0017.

#### 6. REFERENCES:

1. Babaytsev, A. V., Prokofiev, M. V., and Rabinskiy, L. N. (2017). Mechanical properties and microstructure of stainless steel manufactured by selective laser sintering. *International Journal of Nanomechanics Science and Technology*, 8(4), 359-366.
2. Dmitriev, A. I., Skvortsov, A. A., Koplak, O. V., Morgunov, R. B., and Proskuryakov, I. I. (2011). Influence of the regime of plastic deformation on the magnetic properties of single-crystal silicon Cz-Si. *Physics of the Solid State*, 53(8), 1547-1553.
3. Formalev, V.F., Kolesnik, S.A., and Kuznetsova, E.L. (2019). Effect of Components of the Thermal Conductivity Tensor of Heat-Protection Material on the Value of Heat Fluxes from the Gasdynamic Boundary Layer. *High Temperature*, 57(1), 58-62.
4. Hnatiuk, K. I., Dinzhos, R. V. Simeonov, M. S., Alekseev, A. N., Alekseev, S. A., Sirko, V. V., Zabashta, Yu. F., Koseva, N. S., and Lazarenko, M. M. (2019). Melting of 1-octadecene inside the pores of open-morphology silica gel: thermodynamic model and experimental studies. *Journal of Thermal Analysis and Calorimetry*. DOI: 10.1007/s10973-019-09133-4. <https://link.springer.com/article/10.1007/s10973-019-09133-4>
5. Hurang, H., Landon, O., and Ayo, A. (2010). Characterizing and Modeling Mechanical Properties of Nanocomposites. *Journal of Minerals and Materials Characterization and Engineering*, 9(4), 275-319.
6. Jae-soon, J. (2012). *Particle size effect on mechanical and thermal properties of SiO<sub>2</sub>*

*particulate polymer composites*. Newark, New Jersey: University of Delaware.

7. Jeyaparakash, P., and Devaraju, A. (2020). Prediction of effective elastic modulus for glass microspheres loaded polymer composites. *Materials Today: Proceedings*, 22(3), 492-498. <https://doi.org/10.1016/j.matpr.2019.08.064>.
8. Kenzhaev, D. R. (2019). Properties of polymer-composite materials modified with copper (II) oxalate nanoparticles. *Universum: Chemistry and biology. Electronic Science Journal*, 6(60). Retrieved from <http://7universum.com/ru/nature/archive/item/7442>.
9. Lakes, R. S., Kose, S., and Bahia, H. (2002). Analysis of high volume fraction irregular particulate damping composites. *Journal of Engineering Materials and Technology*, 124, 174-178.
10. Markus, K. U., Tadaharu, A., Kouzo, O., Higuchi, M., and Major, Z. (2013). Mechanical properties of nano-silica particulate-reinforced epoxy composites considered in terms of crosslinking effect in matrix resins. *Journal of Material Science*, 48, 5148-5156. DOI: 10.1007/s10853-013-7300-2.
11. Odegard, G. M., Clancy, T. C., and Gates, T. S. (2005). Modeling of the mechanical properties of nanoparticle/polymer composites. *Polymer*, 46, 553-62.
12. Orlov, A. M., Skvortsov, A. A., and Gonchar, L. I. (2001). Magnetically stimulated variation of dislocation mobility in plastically deformed n-silicon. *Physics of the Solid State*, 43(7), 1252-1256.
13. Prentkovskis, O., Tretjakovas, J., Švedas, A., Bieliatynskiy, A., Daniūnas, A., and Krayushkina, K. (2012). The analysis of the deformation state of the double-wave guardrail mounted on bridges and viaducts of the motor roads in Lithuania and Ukraine. *Journal of Civil Engineering and Management*, 18(5), 761-771.
14. Ryapukhin, A. V., Kabakov, V. V., and Zaripov, R. N. (2019). Risk management of multimodular multi-agent system for creating science-intensive high-tech products. *Espacios*, 40 (34). Retrieved from <https://revistaespacios.com/a19v40n34/a19v40n34p19.pdf>.
15. Sanchez-Soto, M. P., Lacorte, P. T., Bricen, K., and Carrasco, F. (2007). Study and mechanical characterization of glass bead filled tri-functional epoxy composites. *Composites Science and Technology*, 67, 1974-1985.
16. Seighalani, A. M., Mertiny, H., and Mertiny, P. (2015). Composite polymer with random distribution of spherical particles. *Canadian International Conference on Composite Materials*. Retrieved from [https://www.researchgate.net/publication/281601689\\_COMPOSITE\\_POLYMER\\_WITH\\_RANDOM\\_DISTRIBUTION\\_OF\\_SPHERICAL\\_PARTICLES](https://www.researchgate.net/publication/281601689_COMPOSITE_POLYMER_WITH_RANDOM_DISTRIBUTION_OF_SPHERICAL_PARTICLES).
17. Shershak, P. V. (2019). Features of national standardization of test methods for polymer composite materials. *Proceedings of VIAM*, 2(74), 77-88.
18. Song, M. (2009). Effects of volume fraction of SiC particles on mechanical properties of SiC/Al composites. *Transactions of Nonferrous Metals Society of China*, 19(6), 1400-1404.
19. Tagliavia, G., Porfiri, M., and Gupta, N. (2010). Analysis of flexural properties of hollow-particle filled composites. *Composites: Part B: Engineering*, 41(1), 86-93. <https://doi.org/10.1016/j.compositesb.2009.03.004>.
20. Tkachev, S. Y., Alekseev, O. M., Lazarenko, M. M., Lazarenko, M. V., Kovalov, K. M., Bokhvan, S. I., Grabovskii, Y. E., and Hoshlyk, N. V. (2018). Topological solitons in branched aliphatic molecules. *Molecular Crystals and Liquid Crystals*, 665(1), 166-180.
21. Trofimov, A. N., Simonov-Emelyanov, I. D., and Pleshkov, L. V. (2017). Controlling the softening temperature of epoxy oligomers and their mixtures. *Polymer Science, Series D* 10, 119-122. <https://doi.org/10.1134/S1995421217020228>
22. Umbetov, A. U., Umbetova, M. Z., Abildayev, G. M., Baizakova, S. S., Zhamalova, S. A., Konussova, A. B., and Dosmagulova, K. K. (2016). Transformation and interference of the laser radiation in composite crystal optical systems. *ARPJ Journal of Engineering and Applied Sciences*, 11(19), 11561-11573.
23. Vettegren, V. I., Bashkarev, A. Ya., and Suslov, M. A. (2007). The effect of the shape of the filler particles on the strength of the polymer composite. *Journal of Technical Physics*, 77(6), 135-138.
24. Wang, J., Yan, P., Dong, L., and Atluri, S.N.

(2019). Eshelby tensors and overall properties of nano-composites considering both interface stretching and bending effects. *Computational Physics*. Retrieved from <https://arxiv.org/abs/1907.00591>.

25. Xinfeng, W., Bo, T., Jinhong, Y., Xiao, C., Chongyin, Zh., and Yonggen, L. (2018). Preparation and Investigation of Epoxy Syntactic Foam (Epoxy. Graphite Reinforced Hollow Epoxy Macro sphere. Hollow Glass Microsphere Composite). *Fibers and Polymers*, 19(1), 170-187.
26. Yu Timkina, S., Stepanchuk, O. V., and

Bieliatynskiy, A. A. (2019). The design of the length of the route transport stops' landing pad on streets of the city. *IOP Conference Series: Materials Science and Engineering*, 708, Article number 012032.

27. Yushkova, N. A., Bastrakov, V. M., and Zabrodin, A. G. (2010). The study of the properties of the matrix for polymer composite materials. *Bulletin of the Samara Scientific Center of the Russian Academy of Sciences*, 4(3), 702-705.

**Table 1.** Physical and mechanical characteristics of materials

| Characteristics            | Unit of measurement | ED-20 epoxy | PBS-50 glass spheres |
|----------------------------|---------------------|-------------|----------------------|
| Young's of elasticity, $E$ | hPa                 | 4.9         | 7.0                  |
| Poisson number, $\nu$      | -                   | 0.3         | 0.2                  |
| Density, $\rho$            | kg/m <sup>3</sup>   | 1.25        | 2200                 |
| Heat conductivity factor   | W/m.K               | 0.92        | 1.15                 |
| Bulk modulus               | hPa                 | 4.08        | 3.88                 |
| Shear coefficient          | hPa                 | 1.88        | 2.91                 |

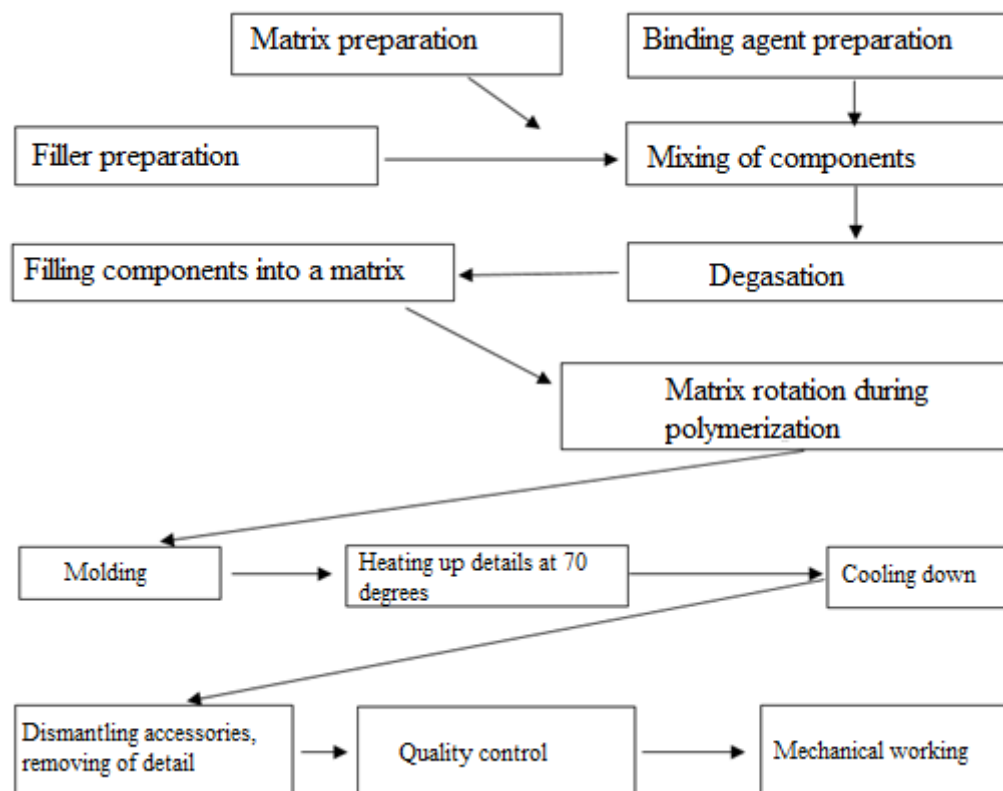


**Figure 1.** The technological scheme of manufacturing a composite

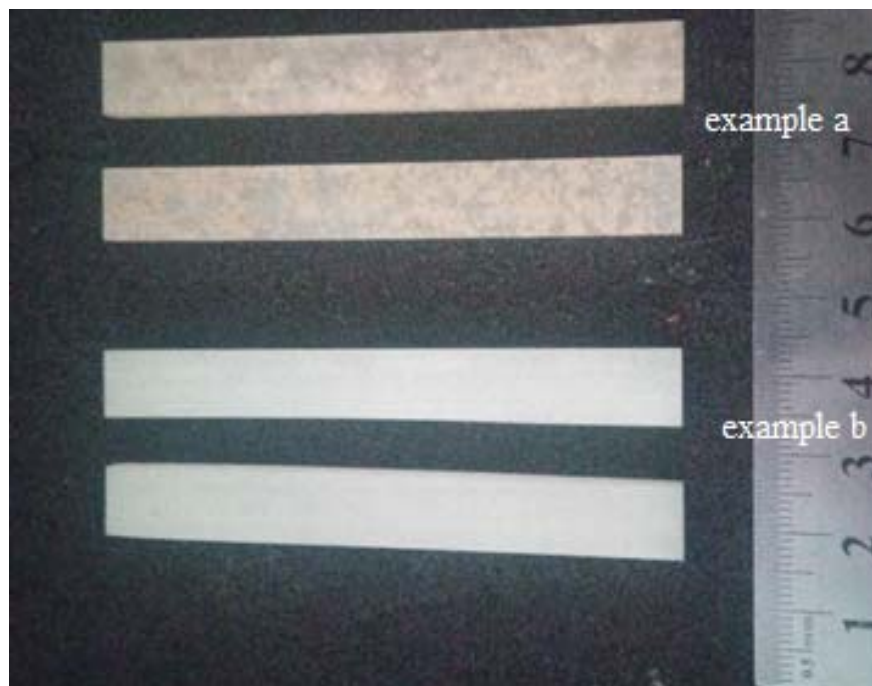


**Figure 2.** Photographs of test samples from each batch (top-down sample from a batch with inclusions of 15%, 10%, 5%, and pure epoxy)

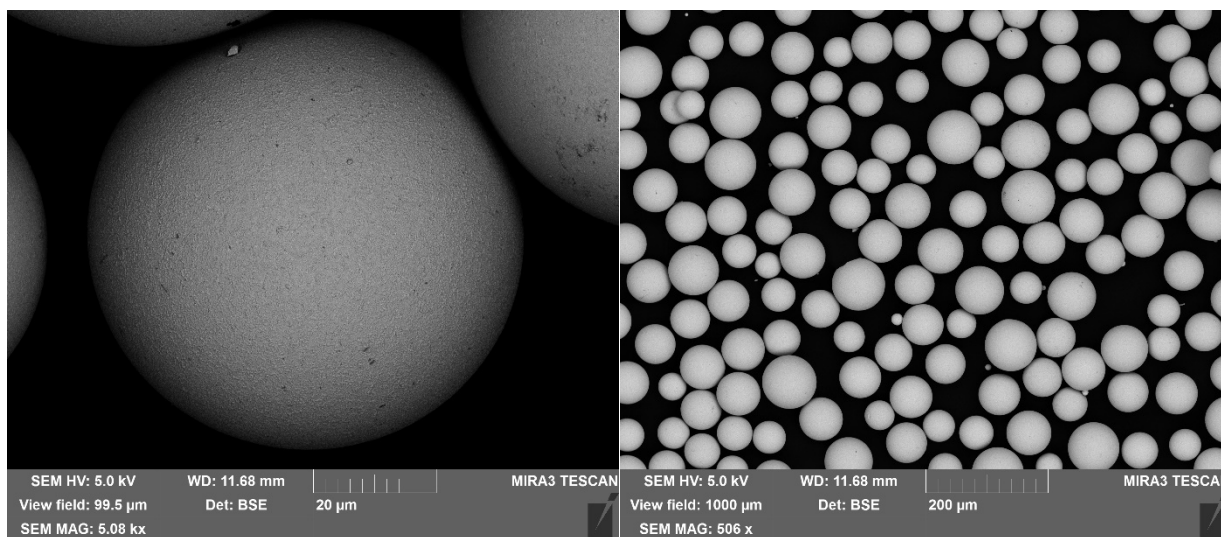


**Figure 3.** Microscopy results

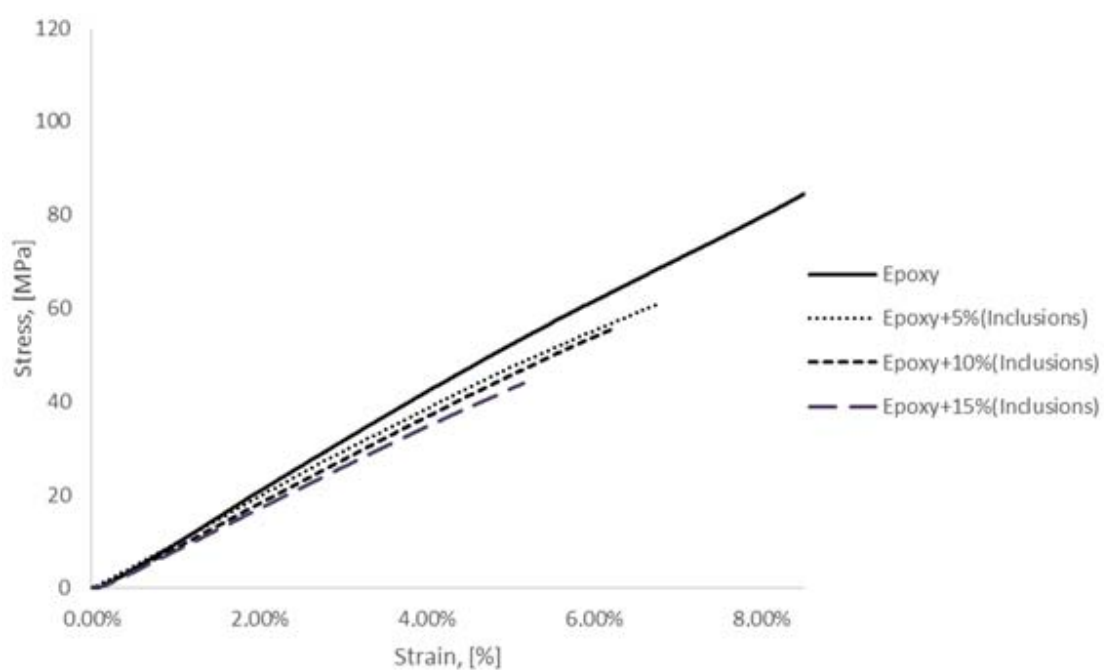


**Figure 4.** Graph of stress-strain curves

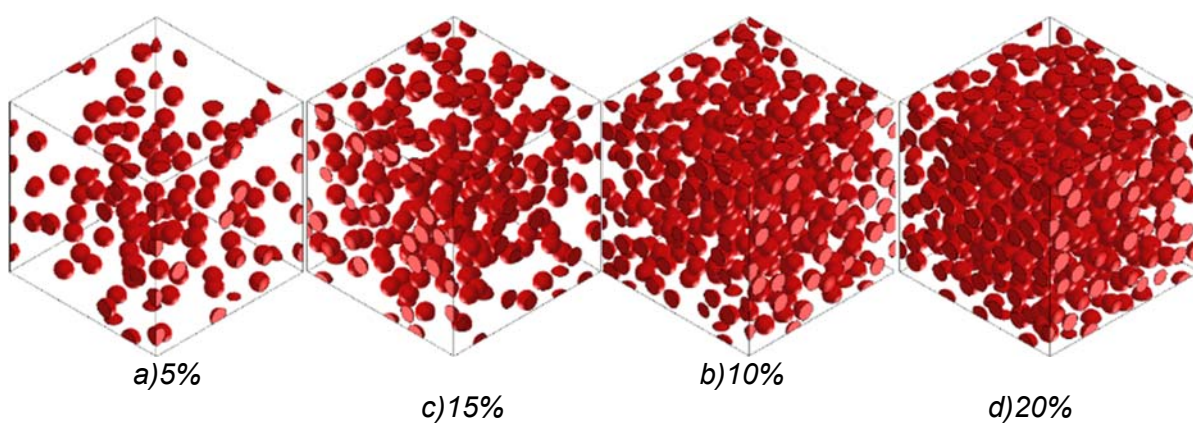


**Figure 5.** Representative elementary volume with a volume fraction of inclusions



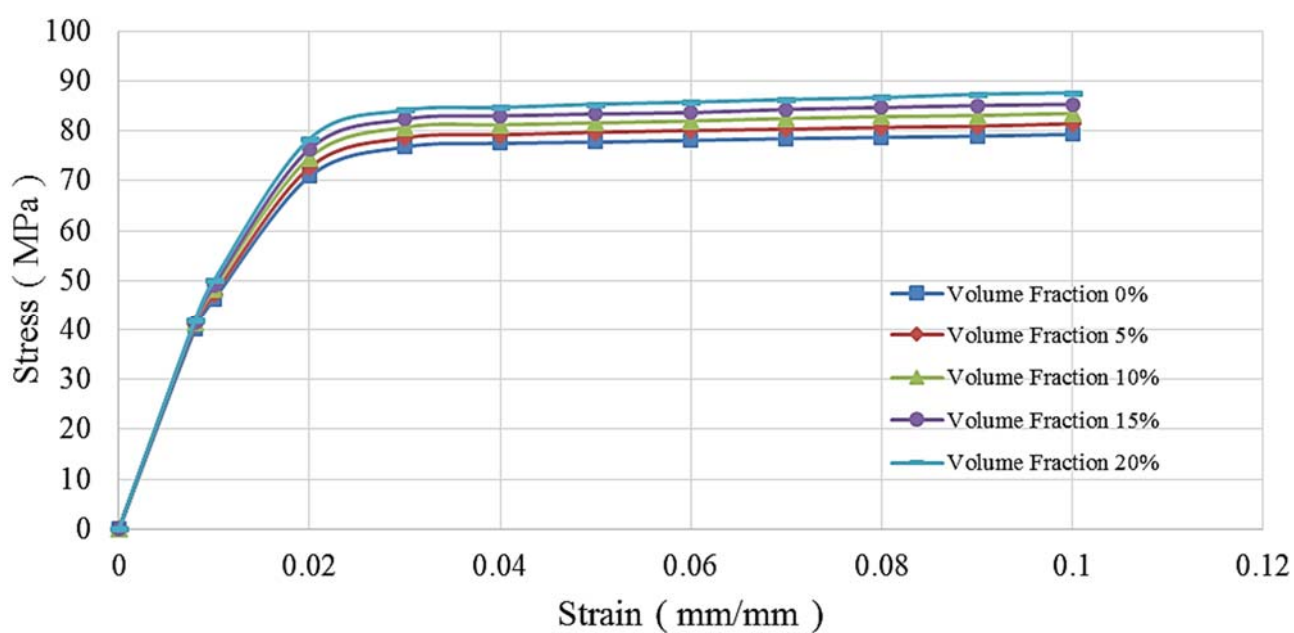


**Figure 6.** Linear stress – strains with the different volume fraction of inclusion obtained using Digimat MF software

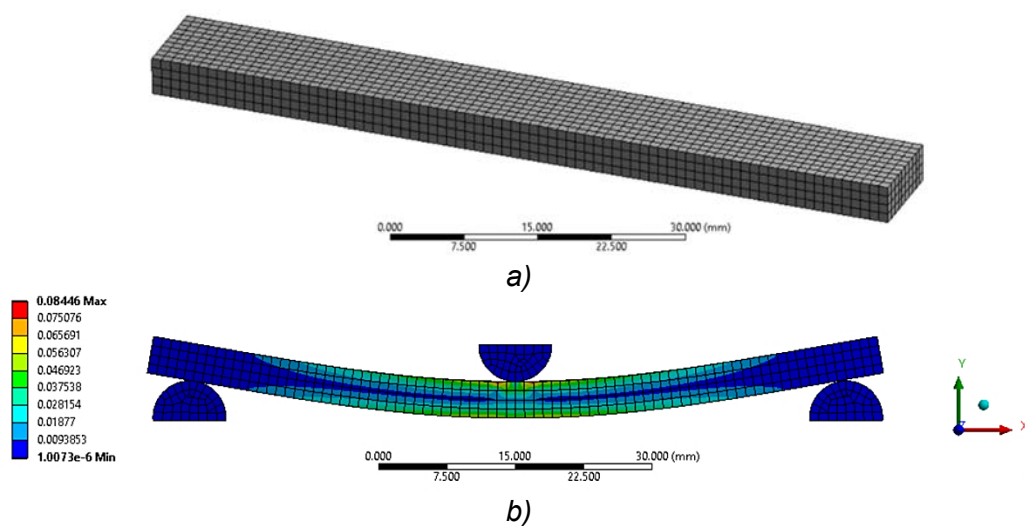


**Figure 7.** Stress-strain state of a finite element model when modeling a bending test

**PROJETO DE ENSAIO EXPERIMENTAL DE TECNOLOGIA DE INUNDAÇÃO DE  
POLÍMEROS EM DEPÓSITOS DO CAZAQUISTÃO OCIDENTAL****EXPERIMENTAL SUPPORT OF FIELD TRIAL ON THE POLYMER FLOODING  
TECHNOLOGY SUBSTANTIATION IN THE OIL FIELD OF WESTERN KAZAKHSTAN****ПРОЕКТ ОПЫТНО-ПРОМЫСЛОВОГО ИСПЫТАНИЯ ТЕХНОЛОГИИ ПОЛИМЕРНОГО  
ЗАВОДНЕНИЯ НА МЕСТОРОЖДЕНИЯХ ЗАПАДНОГО КАЗАХСТАНА**

MOLDABAYEVA, Gulnaz<sup>1\*</sup>; SULEIMENOVA, Raikhan<sup>2</sup>; KARIMOVA, Akmaral<sup>3</sup>; AKHMETOV,  
Nurken<sup>4</sup>; MARDANOVA, Lyailya<sup>5</sup>;

<sup>1,2</sup> Satbayev University, Department of Petroleum Engineering, 22a Satpaev Str., zip code 050013, Almaty –  
Republic of Kazakhstan

<sup>3,4</sup> Atyrau University of Oil and Gas, Department of Oil and Gas, 45a Baimukhanov Str., zip code 060027, Atyrau  
– Republic of Kazakhstan

<sup>5</sup> Atyrau University of Oil and Gas, Department of Physics and Mathematics Disciplines, 45a Baimukhanov Str.,  
zip code 060027, Atyrau – Republic of Kazakhstan

*\* Correspondence author  
e-mail: moldabayeva@gmail.com*

Received 01 May 2020; received in revised form 23 May 2020; accepted 19 June 2020

**RESUMO**

Um dos métodos químicos de impacto no reservatório para melhorar a eficiência do processo de desenvolvimento de campos de petróleo é inundação de polímeros. Este artigo descreve um estudo de viabilidade da eficácia da aplicação da tecnologia de inundação de polímeros no campo no Cazaquistão Ocidental. Este campo é caracterizado por alta viscosidade do óleo do reservatório, corte de água e heterogeneidade dinâmica do reservatório. A experiência mundial na aplicação de inundações de polímeros em campos análogos mostra alta eficiência tecnológica. São apresentados os resultados da análise da experiência da aplicação da tecnologia em campos análogos, estudos físico-químicos de polímeros, estudos de filtração em tubos cheios de areia, modelagem hidrodinâmica de inundações de polímeros e a relação custo-benefício esperada da introdução da tecnologia, aplicada às condições do campo de Karazhanbas com alta viscosidade do óleo de reservatório. A análise baseada na experiência de aplicação de inundações de polímeros em campos de petróleo de alta viscosidade, estudos de laboratório e cálculos estimados da produção esperada no modelo geológico e hidrodinâmico do setor mostra a diminuição no corte de água, o aumento na produção de petróleo e na recuperação atual e final de óleo.

**Palavras-chave:** *estudos de filtração, modelagem hidrodinâmica, eficiência técnica e econômica, inundação de polímeros, ensaio de campo.*

**ABSTRACT**

One of the chemical methods of stimulating the reservoir to increase the efficiency of the oil field development process is polymer flooding. This article conducted a feasibility study of the effectiveness of the application of polymer flooding technology in one field in Western Kazakhstan. This field is characterized by high viscosity of reservoir oil, water cut, and dynamic heterogeneity of the reservoir. World experience in the application of polymer flooding in analogous fields shows high technological efficiency. Presented results of the analysis of the experience of applying technology in analogous fields, physicochemical studies of polymers, filtration studies on bulk models, hydrodynamic modeling of polymer flooding and the expected cost-effectiveness of introducing the technology, as applied to the conditions of the Karazhanbas oil field with high viscosity of reservoir oil. The analysis based on the experience of applying polymer flooding in high-viscosity oil fields, laboratory studies and estimated calculations of the expected production in the sector geological and hydrodynamic model shows a decrease in water cut, an increase in oil production, and an increase in current and final oil recovery.



**Keywords:** *filtration studies, hydrodynamic modeling, technical and economic efficiency, polymer flooding (PF), field trial (FT).*

## АННОТАЦИЯ

Одним из химических методов воздействия на пласт для повышения эффективности процесса разработки нефтяных месторождений является полимерное заводнение пластов. В данной статье проведено технико-экономическая оценка эффективности применения технологии полимерного заводнения на одной месторождения Западного Казахстана. Данное месторождение характеризуется высокой вязкостью пластовой нефти, обводненностью и динамической неоднородностью пласта. Мировой опыт применения полимерного заводнения на месторождениях аналогах показывает высокую технологическую эффективность. Приведены результаты анализа опыта применения технологии на месторождениях аналогах, физико-химических исследований полимеров, фильтрационных исследований на насыпных моделях, гидродинамического моделирования процесса полимерного заводнения и ожидаемой экономической эффективности внедрения технологии, применительно к условиям месторождения Каражанбас с высокой вязкостью пластовой нефти. Проведенный анализ на основе опыта применения полимерного заводнения на месторождениях высоковязкой нефти, проведенных лабораторных исследований, оценочных расчетов ожидаемой добычи на секторной геолого-гидродинамической модели, показывает снижение обводненности, увеличение добычи нефти, прироста текущей и конечной нефтеотдачи.

**Ключевые слова:** *фильтрационные исследования, гидродинамическое моделирование, технико-экономическая эффективность, полимерное заводнение (ПЗ), опытно-промысловое испытание (ОПИ).*

## 1. INTRODUCTION

Traditional methods for increasing oil recovery in high-viscosity and heavy oil fields are aimed at reducing its viscosity and increasing mobility by injecting the heat into the reservoir. In some cases, thermal methods do not give a good result, for example, for thin-layered or deep-seated formations. Currently, the chemical methods of stimulation are the most commonly used to increase the efficiency of oil field development.

It was previously believed that polymer flooding was limited to use only in fields with light oil or with medium viscous oil, and thermal oil recovery methods were strictly applied in fields characterized by high viscosity oil (Babaytsev *et al.*, 2017; Kuznetsova and Rabinskiy, 2019; Formalev *et al.*, 2017; Gendler *et al.*, 2019). However, recently in world practice, this provision is no longer observed in connection with the successful use of polymer flooding for high-viscosity oil, where thermal methods do not seem feasible (Radyuk *et al.*, 2019; Samarin *et al.*, 2019). With the accumulation of new knowledge about the process, the development of new polymer compositions, and the reassessment of the rationality of polymer flooding parameters, this technology becomes economically viable when oil is extracted from reservoirs with a viscosity exceeding 100 mPa·s (Buzinov and Umrikhin,

1984).

This article presents the results of an analysis of the experience of applying technology in analogous fields, physicochemical studies of polymers, filtration studies on bulk models, hydrodynamic modeling of polymer flooding and the expected cost-effectiveness of introducing the technology, as applied to the conditions of the Karazhanbas field with high viscosity of reservoir oil. The results of experimental studies and hydrodynamic modeling of the polymer flooding process shows high technical and economic efficiency and gives the basis for field trial (Delamaide *et al.*, 2015; Orlov *et al.*, 2001; Lazarenko *et al.*, 2019; Formalev *et al.*, 2019; Bulychev, 2019; Sultanbekov *et al.*, 2020).

The experience of using analogs at deposits, to compare the results of the technology implementation at analogs deposits, the main technological parameters were summarized in Table 1 (Moe Soe Let *et al.*, 2012; Delamaide *et al.*, 2013). In this article, according to the author, we present the most striking example of the application of polymer flooding technology in a field with high viscosity of reservoir oil. The Pelican Lake field is similar to the Karazhanbas field in geological and physical parameters and is located 250 km north of Edmonton, Alberta, Canada. Development began in 1980. The field covers an area of 177.000 hectares and is part of the significantly larger "Wabasca" oil field. Geological

reserves are estimated at 6.4 billion barrels, and oil recovery factor is in the range of 5-10% (Delamaide *et al.*, 2013).

The dissolved gas is used as the development mode. However, the initial reservoir pressure is low, and very little dissolved gas is contained in the oil. Also, due to the high viscosity of the oil, the first vertical wells drilled in 1980-1981 were unprofitable with a flow rate below 30 barrels per day, characterized by an intensive drop to 10 barrels per day. The use of thermal methods could not improve oil recovery due to heat loss in such small thickness deposits. The introduction of horizontal well drilling yielded slightly better results in oil production by increasing coverage over the area.

## 2. MATERIALS AND METHODS

Despite the high oil viscosity, the conditions and characteristics of the field were ideal for polymer flooding: low formation temperatures, low water salinity, lack of active water (aquifer), and high permeability values (Wei *et al.*, 2007; Manichand *et al.*, 2010; Xiaodong and Jian, 2013). The first polymer flooding test was launched in 1996 in a cell with one injection well and two responsive production wells. This FT was unsuccessful due to the failure to achieve the planned viscosity (100-200 mPa\*s) (Akulshin, 2000). In addition, aquifer water in this area contained a large amount of  $\text{Fe}^{2+}$ . In this regard, preliminary aeration of the solution was started with the aim of changing  $\text{Fe}^{2+}$  in  $\text{Fe}(\text{OH})_3$ . Despite this, the injection decreased significantly due to the clogging of the incorrectly installed filter by iron particles, and the FT was stopped due to a change of management and incorrect conduct of the FT (Azga and Settari, 1982; Orlov *et al.*, 2003; Wassmuth *et al.*, 2007; Delamaide, 2014; Sheng *et al.*, 2015; Sultanbekov and Nazarova, 2019).

The second FT was launched in May 2005 with a planned initial solution viscosity of 20 mPa\*s, followed by a decrease to 13 mPa\*s. After analyzing the results of the first FT and laboratory studies, it was found that there is no need for high values of the viscosity of the polymer solution to improve the mobility coefficient. In order to avoid colmatization, it was also decided to reduce the molecular weight of the polymer to  $12.5 \times 10^6$  Daltons. A cell of 5 horizontal wells with a horizontal stem of 1.400 m and a borehole distance of 175 m was selected as the FT site. The response of production wells to injection was observed in February, April, and September 2006 for each of the three wells. In the first well, oil

production increased from 18 bbl/day to 232 bbl/day, from 9 bbl/day to 364 bbl/day in the central well, and from 16 bbl/day to 139 bbl/day in the last well (Figure 1).

The main indicator of the success of applying the PF is the relatively low rate of water cut growth for all three wells compared to the adjacent plot of water flow with normal flooding (Figure 2) (Amelin *et al.*, 1978; Amelin and Subbotina, 1986; Barashkin and Samarin, 2005). The cumulative injection is 0.3 d. pore volume (PV), the final predicted oil recovery factor reaches 25%. Based on the results of the successful conduct of the FT, it was decided to expand the impact area and start the PF in new areas.

A FT was also conducted at Pelican Lake to determine the effectiveness of the PF from the very beginning of development instead of the usual waterflooding and the regime of dissolved gas and to determine the variability of the effect of the PF with even more highly viscous oil. According to the results, it was found that the efficiency of oil production and improved oil recovery as a whole increase. The use of oil and gas at the present time indicates that the efficiency becomes lower compared to an increase in the viscosity of the oil, but nevertheless, the oil recovery becomes higher compared to a traditional refinery.

Based on the results of the successful conduct of several field trials at the Pelican Lake field, the effectiveness of PF was also proven for oil with a viscosity of up to 10,000 cPs. However, the effectiveness of PF in areas with an oil viscosity from 1000 cPs to 2000 cPs remains better and is characterized by a low rate of increase in water cut (Bagrintseva, 1982; Amelin *et al.*, 1991; Amelin *et al.*, 1994). With increasing viscosity, this effect decreases, but in the end, a significant increase in oil recovery is still achieved. In the case when the PF is used as the primary method of oil recovery from the very beginning of development, the effectiveness of the PF reaches its maximum value and is accompanied by a long and stable selection of oil.

To align the injectivity profile and regulate the waterflooding process, was used a technology with polymer systems based on a water-soluble AN-132 brand of acrylamide. Area of use, collector type is terrigenous – porous. Productive zone of the well occurring in the chalk deposits. They are represented by sandstones and argillaceous sandstones, characterized by alternating formations with medium and high porosity and permeability. The artificial bottom hole is 1330 m,

the current bottom hole is 1291.5 m. The accumulated injection is 4 056 344 m<sup>3</sup> of water.

### 3. RESULTS AND DISCUSSION:

#### 3.1. Site-Specific Conditions of the Karazhanbas Deposit

The effectiveness of polymer flooding technology is largely determined by the properties of the reagents used. The selection of reagents should be carried out, taking into account the individual characteristics and development status of a particular field (Balakin *et al.*, 1998). Associative polymers are one of the promising types of polymers for highly viscous deposits. These polymers have in their structure hydrophilic and hydrophobic units of macromolecules and consist of a long hydrophilic chain with a small number of hydrophobic groups located along with the main chain or at its ends (Barenblatt *et al.*, 1984; Barenblatt *et al.*, 1992).

Associative polymers have a high thickening ability in waters of various salinity, and this fact is an advantage of associative polymers over hydrolyzed polyacrylamides. Another advantage of associative polymers is their higher resistance to mechanical degradation due to the more rigid structure of macromolecules (Figure 3).

The authors propose to test the technology of polymer flooding with a combination of straightening of the injectivity profile deep in the reservoir. To do this, you need to choose two types of polymer, one for displacement (PF), the other conformance control (CC). When selecting a polymer for the conditions of a particular field, one should take into account: physico-chemical properties of produced and injected water; reservoir temperature; permeability and porosity of the formation; pore size; reservoir heterogeneity; mineralogical composition of reservoir rocks (Barenblatt *et al.*, 1960; Buzinov and Umrikhin, 1984; Bourdais and Algoa, 1984; Bourdais *et al.*, 1984; Basniev *et al.*, 1993).

For flooding at the Karazhanbas field, its own produced water is used (Table 2), the studied water according to the Sulin type is referred to as calcium chloride, with a total salinity of 26 g/l (at a density of 1.018 g/cm<sup>3</sup>), with a predominant content of chloride ions (15.7 g/l), pH of water at the neutral level – 7.1 units. The reservoir temperature of the Karazhanbas deposit in the zones of water injection does not exceed 30°C. The temperature regime of the reservoir is favorable for polymer flooding.

#### 3.2. Application of Polymer Flooding Technology

Permeability, porosity, the pore size of the collector are interrelated factors, and their magnitude influences the choice of molecular weight and polymer size (Bourdais *et al.*, 1983). The molecular size of the polymer decreases with increasing salinity of the water while increasing the restriction on permeability. The molecular size of the polymer is selected according to the existing size range of the pore channels. Existing types of polymers for PNP have a limit on the permeability of at least 50 mD and injectivity of at least 50 m<sup>3</sup>/day (Vakhitov *et al.*, 1980; Victorin, 1988). The permeability of the productive horizons of the field (against core, well logging, well test) vary widely from units to several thousand mD. In the areas of water injection, the injectivity is an average of 50 m<sup>3</sup>/day with restriction by the nozzle and can potentially take more than 200 m<sup>3</sup>/day and higher. Existing ranges of permeability and injection well regimes are favorable for polymer flooding (Vlasov *et al.*, 1997; Vlasov *et al.*, 1998; Volkov *et al.*, 1998).

To assess the effectiveness of polymer flooding in this work, we tested two types of polymer: 1) for oil displacement (PF) – AR-RV-1 with a molecular weight of 7.39 million Daltons; 2) for conformance control (CC) – AR-RV-2 with a molecular weight of 15.15 million Daltons. The experiments used real formation water purified from oil products, solids, and iron ions (Table 2). The dynamic viscosity of the solutions was measured on an Anton-Paar automatic high-precision viscometer in the ranges of shear rates of 0-100 s<sup>-1</sup> and temperature of 40°C. Measurement of the rheological properties of each sample was repeated twice and averaged under the condition of the minimal discrepancy; in the opposite case, the measurement was repeated. All samples of the polymer solution were prepared under atmospheric conditions. The results of physico-chemical analyzes and rheological studies are presented in Tables 3-5 and in Figure 4. As follows from the presented tables and figures, associative polymers have high thickening ability, good filterability, excellent solubility, and high resistance to aging under reservoir conditions of the Karazhanbas field.

In this work, a series of filtration studies were carried out to assess the effectiveness of filtration in the low-permeable part of the reservoir, the blocking coefficient of the high-permeable part of the reservoir, and to replace the residual oil after flooding. Bulk models with layered heterogeneous permeability, which are typical for the

Karazhanbas field, were used as a reservoir model. Model size: 4.5x4.5x30cm, permeability by layers: 100/500/1200 mD, thickness by layers: 0.75/3.15/0.6 cm (Figure 5). The viscosity of the model reservoir oil was 881.7 cps, a combination of oil and diesel was used as model oil, the temperature was 28°C. Figures 6-7 and Tables 6-10 show the results of the studies. As follows from the presented table and figure data, these experiments confirm the positive ability of the polymer solution to be filterable in the rock. This can be seen by the pressure gradient of the injection and its stabilization through 7-10 pore volumes of pumping the solution.

The results of filtration studies are presented in Tables 8-10 and Figure 7. As follows from the presented figures and tables, the optimal concentration of AR-RV-1 polymer in water was 2000 mg/l, and the optimal rim size was 0.3 units. Pore volume (PV), the optimal concentration of the CC rim, is 0.1 PV at a concentration of 3000 mg/l of AR-RV-2 polymer. With this design of injection, the maximum increase in the displacement coefficient is reached and amounts to 19.07%.

The thickness of an effective oil-saturated formation is not less than 10 m; weighted average permeability over the thickness of the reservoir is more than 200 mD; formation temperature – not more than 70°C; bedding – more than three layers; the coefficient of variation by bedding is less than 0.5; weighted average current oil saturation – more than 0.45; absence of a gas cap; absence of underlying water; absence or low degree of fracture.

Based on the selection criteria, a site with four conjugate elements of a 7-point waterflooding system was selected. The calculation of development indicators was carried out on the model of non-volatile oil (Black oil model). The prediction of polymer flooding was carried out on the “Polymer flooding” module, with setting the parameters of adsorption on the rock, polymer viscosity, mechanical destruction, resistance coefficient according to the results of laboratory studies of this work.

The forecast of the main technological development indicators was carried out in two ways:

- 1) The basic option is to continue flooding to 12/31/2034, while the injectivity and production rates of the wells remain constant and equal to the levels of December 2018.

- 2) Polymer flooding – from 01/01/2019 to 03/18/2020 injection of a polymer solution AR-

RV-2 with a concentration of 3.000 mg/l (viscosity 561.44 cPz), from 03/19/2020 to 10/24/2023 injection of a polymer solution with a concentration of 2.000 mg/l (viscosity 39.56 cPs), from 10.25.2023 to 12.31.2034 water injection.

In the basic option, by December 31, 2035, cumulative oil production will amount to 514.862 thousand tons, oil recovery factor 26.4%. In the case of polymer flooding, by December 31, 2035, cumulative oil production will amount to 724.2 thousand tons, an oil recovery factor of 37.1%. The increase in oil recovery due to polymer flooding will amount to 10.8%, additional oil production – 209.338 thousand tons. The dynamics of the development indicators for the base case and polymer flooding option are presented in Figure 8.

#### 4. CONCLUSIONS:

The polymer solution AR-RV-2 shows excellent blocking ability of highly permeable channels, on average, when pumping from 0.2 to 0.6 units. The pore volume blocking coefficient is more than 99%. Filtration studies on oil displacement were carried out in three stages:

1. Tests to add oil with a polymer solution of various concentrations after pumping two pore volumes of water in order to determine the optimal ratio of the mobility of displaced and displacing phases and optimizing the concentration (viscosity) of the polymer rim.

2. At the same concentration of the polymer solution according to step 1, after pumping two pore volumes of water, pumping the polymer solution with different volumes of the rim, in order to optimize the rim volume.

3. Modification of the design of rims with the complex effect of PF and CC – pumping of different variants of the rim and polymer concentration (CC) during polymer exposure taking into account stage 1 and 2.

The optimal concentration of AR-RV-1 polymer in water made up 2000 mg/L; the optimal rim size was 0.3 units. Pore volume (PV), the optimal concentration of the runway rim is 0.1 PV at a concentration of 3000 mg/l of AR-RV-2 polymer. With this design of injection, the maximum increase in the displacement coefficient is reached and amounts to 19.07%.

To select a site for the field trial of polymer flooding (PF FT), a two-stage screening of the field was performed according to a number of geological, physical, and technological criteria.

During the first stage, an analysis was made of the current state of development of the field by objects in order to determine the site, and then, during a detailed analysis of the site, waterflooding elements were selected for the water treatment.

The analysis based on the experience of applying polymer flooding in high-viscosity oil fields, laboratory studies and estimated calculations of the expected production in the sector geological and hydrodynamic model shows a decrease in water cut, an increase in oil production, and an increase in current and final oil recovery. An economic analysis, taking into account the existing market situation, shows that the payback index is 4.8 units, and the payback period is 5 years. This direction for increasing oil recovery is promising and requires further testing at the Karazhanbas field.

## 5. ACKNOWLEDGMENTS:

The authors would like to thank the Ministry of Education of the Republic of Kazakhstan (MOERK), SATBAYEV UNIVERSITY Almaty, Kazakhstan, to support this study through a research management grant. Competition for grant funding for scientific and technical projects for 2018-2020, AR 05130483 "Scientific and technical foundations for reducing the viscosity of Kazakhstani oils, providing a significant increase in oil recovery".

## 6. REFERENCES:

1. Akulshin, A. L. (2000). Investigation of oil displacement from a fractured-pore formation using the POLICAR polymer. *Oil Industry*, 1, 36-38.
2. Amelin, I. D., and Subbotina, E. V. (1986). Features of the development of oil deposits with carbonate reservoirs. *VNIIOENG. Overview information. Series "Oilfield business"*, 8(115), 46.
3. Amelin, I. D., Andriasov, R. S., Gimatudinov, Sh. K., Korotaev, Yu. P., Levykin, E. V., and Lutoshkin, G. S. (1978). *Operation and technology for the development of oil and gas fields*. Moscow, Russian Federation: Nedra.
4. Amelin, I. D., Davydov, A. V., and Lebedinets, N. P. (1991). *Analysis of the development of oil deposits in fractured reservoirs*. Moscow, Russian Federation: CMEA.
5. Amelin, I. D., Surguchev, M. L., and Davydov, A. V. (1994). *The forecast for the development of oil deposits at a late stage*. Moscow, Russian Federation: Nedra.
6. Azga, X., and Settari, E. (1982). *Mathematical modeling of reservoir systems*. Moscow, Russian Federation: Nedra.
7. Babaytsev, A. V., Martirosov, M. I., Rabinskiy, L. N., and Solyaev, Y. O. (2017). Effect of thin polymer coatings on the mechanical properties of steel plates. *Russian Metallurgy (Metally)*, 2017(13), 1170-1175. DOI: 10.1134/S003602951713002X.
8. Bagrintseva, K. I. (1982). *Fractured sedimentary rocks*. Moscow, Russian Federation: Nedra.
9. Balakin, V. V., Vlasov, S. A., and Fomin, A. V. (1998). Modeling polymer flooding of a layered heterogeneous formation. *Oil Industry*, 1, 47-48.
10. Barashkin, R. L., and Samarin, I. V. (2005). Computer system of simulating operating duty of a gaslifting well. Presented at *11th International Scientific and Practical Conference of Students, Postgraduates and Young Scientists; "Modern Techniques and Technologies"*, MTT 2005 – Proceedings. Tomsk, 21-27 March. Tomsk: IEEE.
11. Barenblatt, G. I., Entov, V. M., and Ryzhik, V. M. (1984). *The movement of liquids and gases in natural strata*. Moscow, Russian Federation: Nedra.
12. Barenblatt, G. I., Entov, V. M., and Ryzhik, V. M. (1992). *The theory of non-stationary filtration of liquid and gas*. Moscow Russian Federation: Nedra.
13. Barenblatt, G. I., Yellow, Yu. P., and Kochina, I. N. (1960). On the basic concepts of the theory of filtration of homogeneous liquids in fractured rocks. *Applied Mathematics and Mechanics*, 24(1), 852-864.
14. Basniev, K. S., Kochina, I. K., and Maksimov, V. M. (1993). *Underground hydromechanics*. Moscow, Russian Federation: Nedra.
15. Bourdais, D., and Algoa, A. (1984). An advanced method for interpreting hydrodynamic studies of wells. *Oil, Gas, and Petrochemicals Abroad*, 9, 5-10.
16. Bourdais, D., Algoa, A., Eub, J. A., and Pirar, I. M. (1984). Analysis of hydrodynamic studies of wells completed on fractured formations using reference curves. *Oil, Gas, and Petrochemicals Abroad*, 4, 20-25.
17. Bourdais, D., Witt, T. M., Douglas, A. A., and Pirard, I. M. (1983). A new method of

reference curves for the study of wells. *Oil, Gas, and Petrochemicals Abroad*, 5, 32-37.

18. Bulychiev, N. A. (2019). On the hydrogen production during the discharge in a two-phase vapor-liquid flow. *Bulletin of the Lebedev Physics Institute*, 46(7), 219-221.
19. Buzinov, S. N., and Umrikhin, I. D. (1984). *Study of oil and gas wells and reservoirs*. Moscow, Russian Federation: Nedra.
20. Delamaide, E. (2014). *Polymer flooding of heavy oil – from screening to full-field extension*. Richardson, Texas: Society of Petroleum Engineers DOI: 10.2118/171105-MS.
21. Delamaide, E., Tabary, R., Renard, G., and Dwyer, P. (2015). *Field-scale polymer flooding of heavy oil: the pelican lake story*. Paper presented at the 21st World Petroleum Congress, Moscow, Russian Federation.
22. Delamaide, E., Zaitoun, A., Renard, G., and Tabary, R. (2013). Pelican lake Field: First successful application of polymer flooding in heavy oil reservoir. Retrieved from <https://www.eor-alliance.com/pelican-lake-field-first-successful-application-of-polymer-flooding-in-a-heavy-oil-reservoir/>.
23. Formalev, V. F., Kolesnik, S. A., and Kuznetsova, E. L. (2017). Time-dependent heat transfer in a plate with anisotropy of general form under the action of pulsed heat sources. *High Temperature*, 55(5), 761-766.
24. Formalev, V. F., Kolesnik, S. A., and Kuznetsova, E. L. (2019). Effect of components of the thermal conductivity tensor of heat-protection material on the value of heat fluxes from the gasdynamic boundary layer. *High Temperature*, 57(1), 58-62.
25. Gendler, S. G., Gridina, E. B., and Egorova, N. A. (2019). Calculation of the volume of air for ventilation of mining workings when operating self-propelled diesel equipment. *Naukovyi Visnyk Natsionalnoho Hirnychoho Universytetu*, 2019(6), 107-111.
26. Kuznetsova, E. L., and Rabinskiy, L. N. (2019). Heat transfer in nonlinear anisotropic growing bodies based on analytical solution. *Asia Life Sciences*, 2, 837-846.
27. Lazarenko, M. M., Alekseev, A. N., Alekseev, S. A., Zabashta, Yu. F., Grabovskii, Yu. E., Hnatiuk, K.I. Dinzhos, R. V., Simeonov, M. S., Kolesnichenko, V.G., Ushcatse, M. V., and Bulavin, L. A. (2019). Nanocrystallite–liquid phase transition in porous matrices with chemically functionalized surfaces. *Physical Chemistry Chemical Physics*, 21, 24674-24683.
28. Manichand, R., Mogollon, J. L., Bergwijn, S., Graanoogst, F., and Ramdajal, R. (2010). *Preliminary assessment of Tambaredjo heavy oilfield polymer flooding pilot test*. Richardson, Texas: Society of Petroleum Engineers. DOI: 10.2118/138728-MS.
29. Moe Soe Let, K. P., Manichand, R. N., and Seright, R. S. (2012). *Polymer flooding a 500-cp oil*. Tulsa, Oklahoma: Society of Petroleum Engineers.
30. Orlov, A. M., Skvortsov, A. A., and Gonchar, L. I. (2001). Magnetically stimulated variation of dislocation mobility in plastically deformed n-silicon. *Physics of the Solid State*, 43(7), 1252-1256.
31. Orlov, A. M., Skvortsov, A. A., and Litvinenko, O. V. (2003). Bending vibrations of semiconductor wafers with local heat sources. *Technical Physics*, 48(6), 736-741.
32. Radyuk, A. G., Gorbatyuk, S. M., Tarasov, Y. S., Titlyanov, A. E., and Aleksakhin, A. V. (2019). Improvements to mixing of natural gas and hot-air blast in the air tuyeres of blast furnaces with thermal insulation of the blast duct. *Metallurgist*, 63(5-6), 433-440.
33. Samarin, I. V., Strogonov, A. Y., and Butuzov, S. Y. (2019). Evaluation model of integrated safety of fuel and energy complex facilities. *International Journal of Engineering and Advanced Technology*, 8(5), 2162-2167.
34. Sheng, J. J., Leonhardt, B., and Azri, N. (2015). Status of polymer-flooding technology. *Journal of Canadian Petroleum Technology*, 54(02), 116-126. DOI: 10.2118/174541-PA
35. Sultanbekov, R. R., and Nazarova, M. N. (2019). Determination of compatibility of petroleum products when mixed in tanks. Presented at *6th Scientific Conference*, Tyumen, 25-29 March. Tyumen: European Association of Geoscientists and Engineers.
36. Sultanbekov, R. R., Terekhin, R. D., and Nazarova, M. N. (2020). Effect of temperature fields and bottom sediments of oil products on the stress-strain state of the design of a vertical steel tank. *Journal of Physics: Conference Series*, 1431(1), 012055.
37. Vakhitov, G. G., Oganjanyants, V. G., and Polishchuk, A. M. (1980). An experimental study of the effect of polymer additives in water on the relative permeability of porous

media. *Bulletin of the USSR Academy of Sciences, MZHG*, 4, 163-167.

38. Victorin, V. D. (1988). *The effect of carbonate reservoir features on the efficiency of oil field development*. Moscow, Russian Federation: Nedra.
39. Vlasov, S. A., Dyakonov, V. A., Fomin, A. V., and Khavkin, A.-Ya. (1997). Calculations of the influence of permeability of heterogeneity of the Pokamasovskoye field on phase permeability and oil recovery. *Oil Industry*, 8, 41-42.
40. Vlasov, S. A., Krasnopevtseva, K. V., and Kagan, Ya. M. (1998). New perspectives of polymer flooding in Russia. *Oil Industry*, 5, 46-49.
41. Volkov, Yu. A., Konyukhov, V. M., Kosterin, A. V., and Chekalin, A.N. (1998). *On the displacement of oil in stratified inhomogeneous formations by rims of thickeners. KN. Priority methods of increasing oil recovery and the role of super technologies*. Kazan, Russian Federation: Novoe znanie.
42. Wassmuth, F.R., Green, K., Hodgins, L., and Turta, A.T. (2007). *Polymer Flood technology for heavy oil recovery*. Paper presented at the Canadian International Petroleum Conference, Calgary, Canada.
43. Wei, Zh., Jian, Zh., Ming, H., Wentao, X., Guozhi, F., Wei, J., Fujie, S., Shouwei, Zh., Yongjun, G., and Zhongbin, Ye. (2007). *Application of hydrophobically associating water-soluble polymer for polymer flooding in China offshore heavy oilfield*. Paper presented at the International Petroleum Technology Conference, Dubai, U.A.E.
44. Xiaodong, K., and Jian, Zh. (2013). *Offshore heavy oil polymer flooding test in JZW area*. Paper presented at the SPE Heavy Oil Conference, Calgary, Canada.

**Table 1.** Technological parameters of the most famous works on the use of PF

| <b>Deposit occurrence</b> | <b>Country</b> | <b>PF status</b> | <b>Depth, m</b> | <b>Bed temp., °C</b> | <b>Effective depth, m</b> | <b>Porosity coef. , %</b> | <b>Permeability coef. , mD</b> | <b>Initial pressure, bar</b> | <b>Density, API</b> | <b>Keservoir oil viscosity, cPs</b> | <b>Injected amount, PV</b> |
|---------------------------|----------------|------------------|-----------------|----------------------|---------------------------|---------------------------|--------------------------------|------------------------------|---------------------|-------------------------------------|----------------------------|
| Pelican lake              | Canada         | All deposits     | 300-450         | 12-17                | 1-9                       | 28-32                     | 300-5000                       | 18-26                        | 12-14               | 800-10000                           | >0.35                      |
| Marmul                    | Oman           | All deposits     | 900             | 46                   | 20                        | 25-30                     | 100-2000                       | 80                           | 22                  |                                     | 0.63                       |
| Bodo                      | Canada         | FT               | 770             | 25                   | 3.2                       | 27-33                     | 1000                           | 68                           | 14                  | 400                                 |                            |
| Suffied Caen              | Canada         | FT               | 950             | 21                   | 2-9                       | 26.5                      | 500-2000                       | 104.4                        | 17                  | 70-100                              |                            |
| El Corcobo                | Argentina      | FT               | 650             | 38                   | 0.5-18                    | 27-33                     | 500-4000                       | 32.4                         | 18                  | 160-300                             |                            |
| SZ36-1, Bohai bay         | China          | FT               | 1300-           | 65                   | 61.5                      | 28-35                     | 2600                           | 143                          | 11.4-19             | 13-380                              | >0.067                     |
| JZW, Bohai bay            | China          | FT               | 1700            | 57                   | 20                        | 22-36                     | 10-5000                        |                              | 17-22               | 10-30                               | >0.18                      |
| Diademina                 | Argentina      | Ext. FT          | 1020            | 50                   | 4-12                      | 30                        | 10-5000                        |                              | 20                  | 100                                 | 0.8                        |
| Karazhanbas               | Kazakhstan     | Project          | 300-400         | 26                   | 8-20                      | 33                        | 510-1500                       | 38-48                        | 19                  | 378-541                             | 0.4                        |



**Table 1.** The results of physico-chemical analysis of wastewater for pressure maintenance method

| Index   | Results      |
|---|--------------|
| pH medium   | 7.1          |
| Density, g/cm <sup>3</sup>  | 1.018        |
| Calcium content (Ca <sup>2+</sup> ), mg / dm <sup>3</sup>                                 | 1 202.4      |
| Magnium content (Mg <sup>2+</sup> ), mg/dm <sup>3</sup>                                   | 608.0        |
| The amount of potassium and sodium (K <sup>+</sup> +Na <sup>+</sup> ), mg/dm <sup>3</sup> | 7 894.8      |
| Chloride content (Cl <sup>-</sup> ), mg/dm <sup>3</sup>                                   | 15 714.6     |
| Sulfate content (SO <sub>4</sub> <sup>2-</sup> ), mg/dm <sup>3</sup>                      | Not detected |
| Hydrocarbon content (HCO <sub>3</sub> <sup>-3</sup> ), mg/dm <sup>3</sup>                 | 561.2        |
| Mineralization, mg/dm <sup>3</sup>  | 26 008.0     |
| Sulin type  | Cl-Ca        |
| Total water hardness, mg-Equiv/l  | 110.0        |
| Total iron content(Fe <sup>2+</sup> , Fe <sup>3+</sup> ), mg/dm <sup>3</sup>              | 50.4         |

**Table 2.** Physico-chemical analysis of polymers AR-RV-1, AR-RV-2

| Parameter                            | AR-RV-1 |           | AR-RV-2 |           |
|--------------------------------------|---------|-----------|---------|-----------|
|                                      | Fact    | Valuation | Fact    | Valuation |
| Molecular weight, mil. Daltons       | 7.39    | -         | 15.15   | -         |
| The content of the main substance, % | 92.51   | >90       | 90.31   | >90       |
| Degree of hydrolysis, %              | 20.6    | 15-25     | 16.96   | 15-25     |
| Intrinsic viscosity, dl/g            | 12.6    | 10-30     | 22.3    | 10-25     |
| Insoluble residue, %                 | 0.88    | <1        | 0.31    | <1        |
| Filterability, ea                    | 0.6     | <=1.5     | 1.04    | <=1.5     |
| Dissolution time, hr                 | 3       | 3         | 3       | 3         |
| Compliance with the requirements     | Match   |           | Match   |           |

**Table 3.** Viscosity of polymers at various concentrations

| Polymer concentration, ppm | Dynamic viscosity at 7,34c-1, cPs |              |
|----------------------------|-----------------------------------|--------------|
|                            | AR-RV-2 (CC)                      | AR-RV-1 (PF) |
| 1000                       | 27.5                              | 13.3         |
| 2000                       | 242.6                             | 47.0         |
| 3000                       | 540.6                             | 70.0         |
| 5000                       | 1162.0                            | 199.8        |

**Table 4.** The results of determining the resistance to the aging of polymers within 15 days

| Polymer      | Resistance to aging, % |        |         |
|--------------|------------------------|--------|---------|
|              | 0 days                 | 7 days | 14 days |
| AR-RV-1 (PF) | 100%                   | 99%    | 93%     |
| AR-RV-2 (CC) | 100%                   | 97%    | 97%     |

**Table 6.** The results of the injection test of the polymer solution AR-RV-1 on the core

| Polymer concentration, mg/l | Permeability, mD |           | Porosity, % | Polymer viscosity, cPs |      | Injection stabilization pressure, mPa | Coefficient, U. |                     |
|-----------------------------|------------------|-----------|-------------|------------------------|------|---------------------------------------|-----------------|---------------------|
|                             | for gas          | for water |             | in                     | out  |                                       | resistance      | residual resistance |
| 2000                        | 200              | 29        | 16.2        | 47                     | 34.5 | 2.07                                  | 213.32          | 31.53               |
| 2000                        | 200              | 31        | 16.12       | 47                     | 33.1 | 1.35                                  | 150.53          | 27.88               |

**Table 5.** Studies on the blocking ability of the polymer solution AR-RV-2

| Sample permeability, mD | Pore volume pumped, unit fraction | Injection pressure, mPa | Permeability after, mD | Blocking coefficient, % |
|-------------------------|-----------------------------------|-------------------------|------------------------|-------------------------|
| 370.2                   | 0.2                               | 0.379                   | 3.5                    | 99.05                   |
| 352.9                   | 0.4                               | 0.79                    | 1.8                    | 99.49                   |
| 419.2                   | 0.6                               | 1.06                    | 2                      | 99.52                   |

**Table 6.** Results of filtration studies of the 1st stage

| Concentration, mg/l | Viscosity, cPs | No. spec. | Water permeability, mD | Porosity, % | Oil saturation % | Displacement ratio, % |       |        |
|---------------------|----------------|-----------|------------------------|-------------|------------------|-----------------------|-------|--------|
|                     |                |           |                        |             |                  | before                | after | growth |
| 0                   | 1              | 6         | 213                    | 15,46       | 59.77            | 26.79                 | 30.19 | 3.4    |
| 1000                | 12             | 7         | 209                    | 14,54       | 60.1             | 28                    | 37.8  | 9.8    |
| 1500                | 23             | 2         | 205                    | 14,76       | 60.36            | 27.65                 | 40.98 | 13.33  |
| 2000                | 35             | 3         | 218                    | 14,57       | 60.8             | 27.71                 | 43.94 | 16.23  |
| 2500                | 48             | 1         | 212                    | 15          | 60.4             | 27.25                 | 44.15 | 16.9   |
| 3000                | 64             | 5         | 201                    | 14,22       | 59.81            | 27.76                 | 45.1  | 17.34  |

**Table 7. Results of filtration studies of the 2nd stage**

| Polymer rim size, PV | No. sp. | Water permeability, mD | Porosity, % | Oil saturation % | Displacement ratio, % |       |        |
|----------------------|---------|------------------------|-------------|------------------|-----------------------|-------|--------|
|                      |         |                        |             |                  | before                | after | growth |
| 0                    | 6       | 213                    | 15.46       | 59.77            | 26.79                 | 30.19 | 3.4    |
| 0.1                  | 8       | 198                    | 14.7        | 59.86            | 27.6                  | 35.2  | 7.6    |
| 0.2                  | 9       | 197                    | 14.13       | 59.78            | 27.29                 | 49.49 | 13.2   |
| 0.3                  | 3       | 218                    | 14.57       | 60.8             | 27.71                 | 43.94 | 16.23  |
| 0.4                  | 16      | 206                    | 14.76       | 60.2             | 26.92                 | 44.32 | 17.4   |
| 0.5                  | 4       | 203                    | 14.34       | 60.36            | 27.06                 | 45.64 | 18.58  |

**Table 8. Results of filtration studies of the 3rd stage**

| AR-RV-2 CC + AR-RV-1 PF       | Visco-sity, cPs | No. spec. | Water permeability, mD | Poro-sity, % | Oil saturation % | Displacement ratio, % |       |        |
|-------------------------------|-----------------|-----------|------------------------|--------------|------------------|-----------------------|-------|--------|
|                               |                 |           |                        |              |                  | before                | after | growth |
| 0 PV+0.3PV2000 mg/l           | -/35            | 3         | 208                    | 14.57        | 60.8             | 27.71                 | 43.94 | 16.23  |
| 0.05PV2000mg/l +0.3pv2000mg/l | 173/35          | 14        | 210                    | 14.15        | 59.86            | 27.77                 | 44.66 | 16.89  |
| 0.1PV2000mg/l+0.3PV2000mg/l   | 173/35          | 10        | 203                    | 14.39        | 60.43            | 27.2                  | 45    | 17.8   |
| 0.05PV3000mg/l +0.3pv2000mg/l | 505/35          | 15        | 193                    | 14.44        | 60.02            | 27.2                  | 45.6  | 18.4   |
| 0.1PV3000mg/l +0.3PV2000mg/l  | 505/35          | 30        | 209                    | 16.11        | 60.44            | 27.04                 | 46.11 | 19.07  |

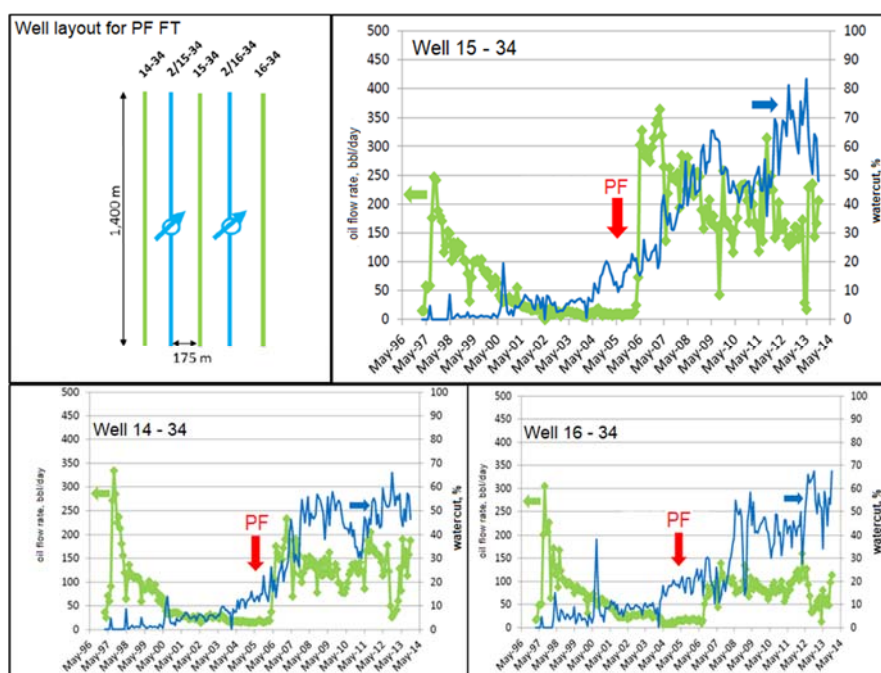


**Figure 1. Scheme of the implementation of the FT (a) and production dynamics by wells: (b) – well 15-34; (c) – well 14-34; (d) – well 16-34**

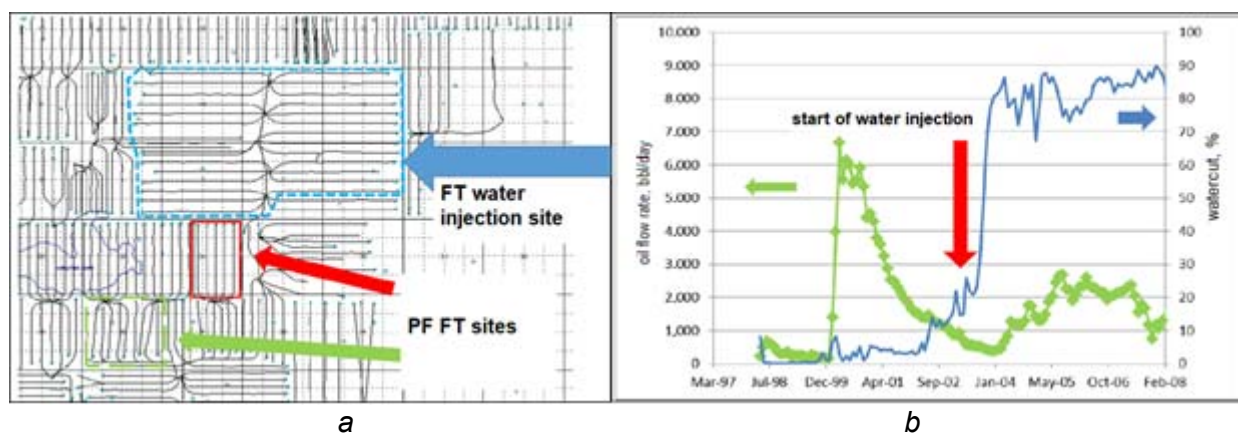


**Figure 2.** Scheme for the implementation of the water supply injection (a) and production dynamics in the area (b)

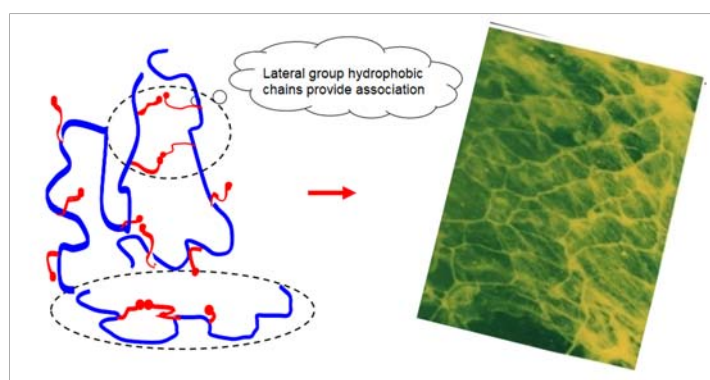


**Figure 3.** The molecular structure of associative polymers

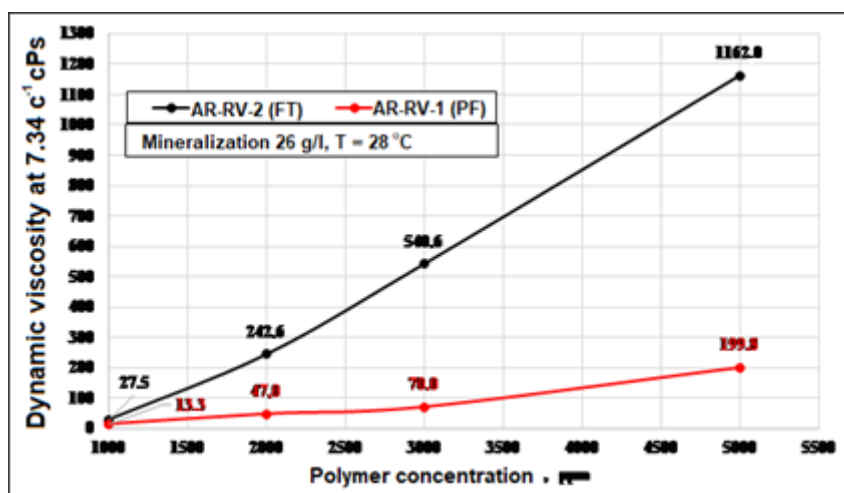


**Figure 4.** Comparison of the viscosity characteristics of polymers AR-RV-1, AR-RV-2

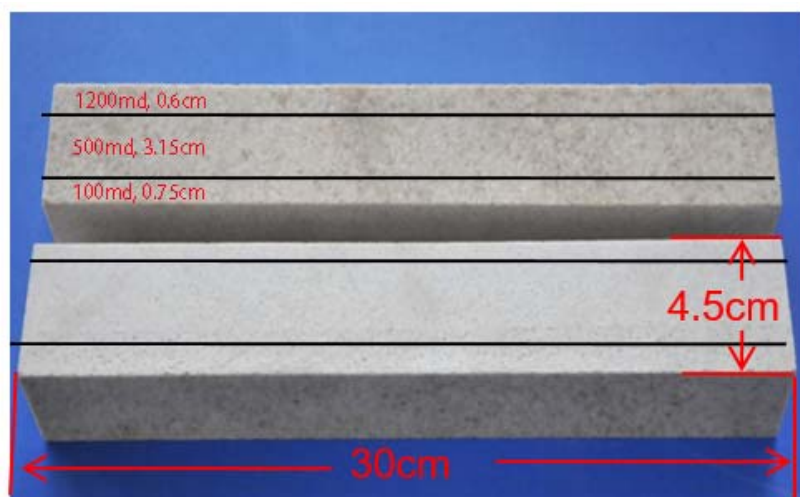


**Figure 5.** Three-layer artificial heterogeneous reservoir model of the Karazhanbas field

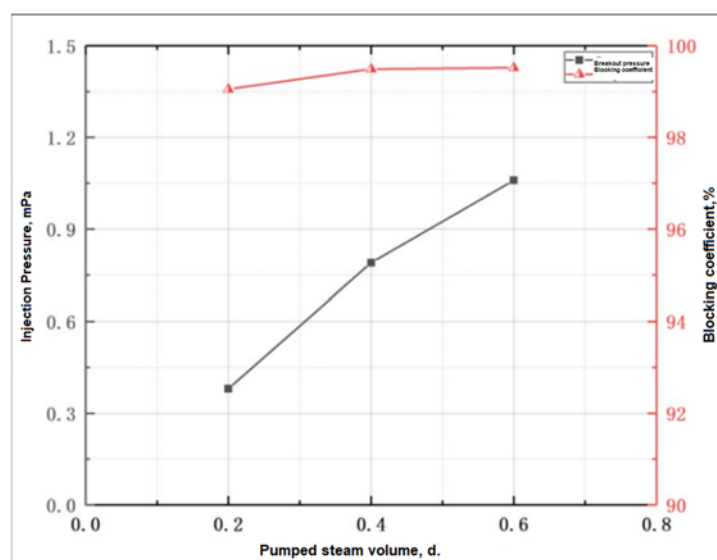


**Figure 6.** Studies on the blocking ability of polymer solution AR-RV-2

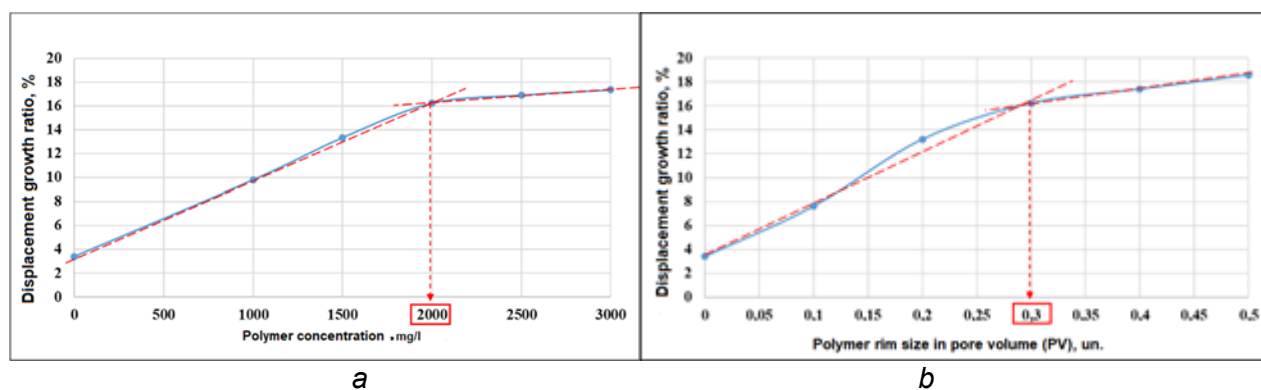


**Figure 7.** The results of filtration studies of the 1st (a) and 2nd (b) stage

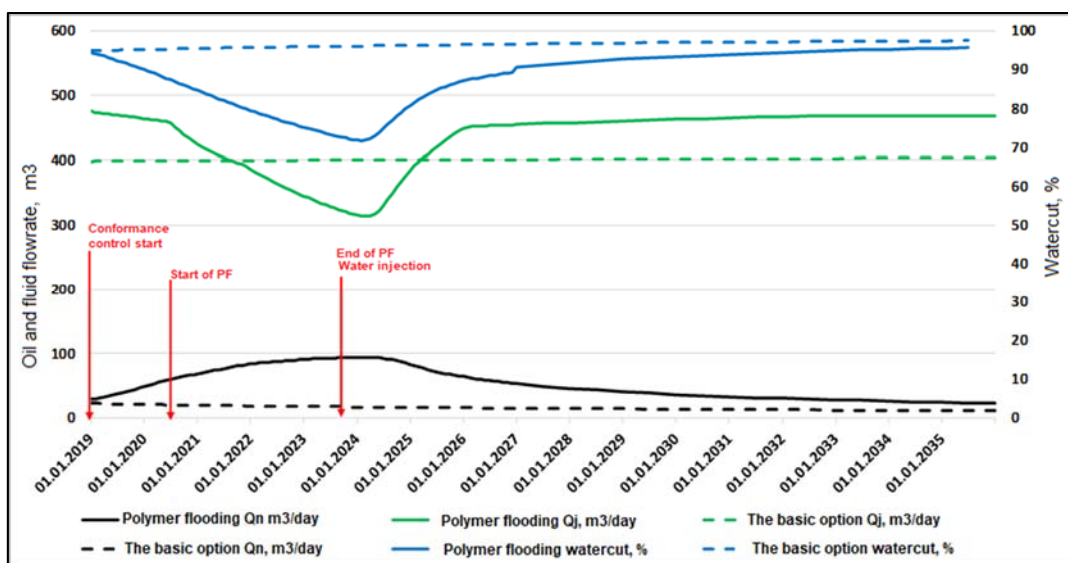


**Figure 8.** Oil production dynamics according to base and polymer flooding options

DETECÇÃO DA ATIVIDADE DE NANOPARTÍCULAS DE PRATA, *PSEUDOMONAS FLUORESCENS* E *BACILLUS CIRCULANS* NA INIBIÇÃO DO CRESCIMENTO DE *ASPERGILLUS NIGER* ISOLADO A PARTIR DE FRUTAS ALARGADASDETECTING THE ACTIVITY OF SILVER NANOPARTICLES, *PSEUDOMONAS FLUORESCENS* AND *BACILLUS CIRCULANS* ON INHIBITION OF *ASPERGILLUS NIGER* GROWTH ISOLATED FROM MOLDY ORANGE FRUITS

الكشف عن فعالية الجسيمات النانوية للفضة، الزانفة المتألقة و عصوية سيركيولانز على تثبيط نمو الرشاشية السوداء المعزول من ثمار البرتقال المتعفن

HASSAN, Baydaa Abood<sup>1</sup>; LAWI, Zahraa Kamil Kadhimi<sup>1</sup>; Banoon, Shaima Rabee<sup>2\*</sup>

<sup>1</sup> Department of Biology, Faculty of Science, University of Kufa, Najaf, Iraq.

<sup>2</sup> Department of Biology, College of Science, University of Misan, Maysan, Iraq.

\* Correspondence author

e-mail: shimarb@uomisan.edu.iq

Received 12 March 2020; received in revised form 26 May 2020; accepted 19 July 2020

## RESUMO

O acondicionamento e armazenamento inadequados das laranjas (*Citrus sinensis*) pode resultar na deterioração e crescimento de microrganismos, incluindo *Aspergillus* spp. estes fungos são onipresentes e crescem em frutos após a colheita. Certas espécies de *Aspergillus* produzem toxinas que podem afetar a saúde de seres humanos e animais. O presente estudo teve como objetivo isolar *Aspergillus niger* de laranjas mofadas, testar sua capacidade de produzir aflatoxina pelo método Saito e Machida e avaliar sua toxicidade de alguns parâmetros bioquímicos em ratos brancos machos. Além disso, a eficiência da inibição de nanopartículas de prata (AgNPs), *Pseudomonas fluorescens* e *Bacillus circulans* foi avaliada contra isolados de *A. niger*. O resultado da triagem de todos os nove isolados pelo método Saito e Machida demonstrou a capacidade de um isolado produzir aflatoxinas em grandes quantidades. O filtrado desse isolado mostrou um aumento no nível de enzimas GPT e GOT (24,2 U/ml e 18,3 U/ml), respectivamente, em comparação com o isolado de aflatoxinas não produtoras e o controle (16,6 e 12,2 U/ml) e (8,5 e 8,2 U/ml), respectivamente. O nível de glicose foi aumentado para (130,2 mg/dl) nos ratos tratados com o filtrado do isolado produtor de aflatoxinas em comparação com (95 mg/dl) e (86,4 mg/dl) tratados com o filtrado do isolado não produtor e o controle respectivamente. Além disso, o nível de LDL-colesterol foi reduzido para 120,2 mg/dl e 101 mg/dl com o produtor de filtrado e os isolados de aflatoxinas não produtoras, respectivamente, em comparação com 144,3 mg/dl para o controle. Os AgNPs mostraram um efeito inibitório contra o crescimento de *A. niger*, com a maior zona de inibição de 28,38 mm a uma concentração de 100 µl. Por outro lado, *Pseudomonas fluorescens* e *Bacillus circulans* também mostraram uma excelente taxa de inibição (100%) na concentração de 2 g/L do filtrado do fungo. Esses resultados expuseram que os AgNPs são capazes de inibir *A. niger* e, consequentemente, os AgNPs podem ser usados como um candidato antifúngico.

**Palavras-chave:** *Citrus sinensis*, *Aspergillus niger*, Parâmetros bioquímicos, In vitro, Nanopartículas de prata.

## ABSTRACT

The improper packaging and storage of oranges (*Citrus sinensis*) may result in decay it and growth of microorganisms, including *Aspergillus* spp. these fungi are omnipresent and growing on post-harvest fruits. Certain species of *Aspergillus* produce toxins that can affect humans and animals health. This study aimed to isolate *Aspergillus niger* from moldy oranges, test its ability to produce aflatoxin using the Saito and Machida method, and evaluation of their toxicity of some biochemical parameters in white rat males. Moreover, the inhibition efficiency of silver nanoparticles (AgNPs), *Pseudomonas fluorescens*, and *Bacillus circulans* were assessed against *A. niger* isolates. The outcome of screening all nine isolates by the Saito and Machida method has shown the capability of one isolate to produce aflatoxins in large amounts. The filtrate of this isolate showed an increase in the level of GPT and GOT enzymes (24.2 U/ml and 18.3 U/ml) respectively, compared to the



non-producing aflatoxins isolate and the control (16.6 and 12.2 U/ml) and (8.5 and 8.2 U/ml) respectively. Glucose level was increased to (130.2 mg/dl) in the rats treated with the filtrate of aflatoxins producer isolate compared to (95 mg/dl) and (86.4 mg/dl) treated with the filtrate of the non-producer isolate and the control respectively. Additionally, the LDL-cholesterol level was reduced to 120.2 mg/dl, and 101 mg/dl with the filtrate producer and the non-producer aflatoxins isolates respectively compared to 144.3 mg/dl for the control. AgNPs have shown an inhibitory effect against *A. niger* growth with the largest inhibition zone of 28.38 mm at a concentration of 100µl was recorded. On the other hand, *Pseudomonas fluorescens* and *Bacillus circulans* have also shown an excellent inhibition rate (100%) at the concentration of 2 g/L of the fungus filtrate. These results exposed that AgNPs are able to inhibit *A. niger*, and consequently, AgNPs can be used as an antifungal candidate.

**Keywords:** *Citrus sinensis*, *Aspergillus niger*, Biochemical parameters, In vitro, Silver nanoparticles.

## المخلص

التغليب والتخزين غير المناسبين للبرتقال (*Citrus sinensis*) قد يؤدي الى تحلله ونمو الكائنات الحية الدقيقة بما في ذلك نوع الرشاشيات هذه الفطريات منتشرة في كل مكان وتنمو على فاكهة ما بعد الحصاد. تنتج بعض انواع الرشاشيات السموم التي يمكن أن تؤثر على صحة الإنسان والحيوان. تهدف هذه الدراسة إلى عزل فطريات الرشاشية السوداء من البرتقال المتعفن، اختبار قدرتها على إنتاج الأفلاتوكسين باستخدام طريقة Saito و Machida، وتقييم سميتها لبعض المعايير الكيموحيوية في ذكور الجرذان البيضاء. علاوة على ذلك، تم تقييم كفاءة تثبيط الجسيمات النانوية للفضة، بكتيريا الزائفة المتألقة و عصوية سيركيولانز ضد عزلات فطر الرشاشية السوداء. أظهرت نتائج مسح جميع العزلات التسعة بطريقة Saito و Machida قدرة عزلة واحدة على إنتاج الأفلاتوكسين بكميات كبيرة. أظهر راشح هذه العزلة زيادة في مستوى إنزيمات GOT و GPT (24.2 وحدة/مل و 18.3 وحدة/مل) على التوالي، مقارنة بالعزلة غير المنتجة للأفلاتوكسين ومعامل الضبط (16.6 و 12.2 وحدة/مل) و (8.5 و 8.2 وحدة/مل) على التوالي. مستوى الجلوكوز ازداد إلى (130.2 مجم/ديسيلتر) في الجرذان المعاملة براشح العزلة المنتجة الأفلاتوكسين مقارنة بـ (95 مجم/ديسيلتر) و (86.4 مجم/ديسيلتر) المعاملة براشح العزلة غير المنتجة والمجموعة الضابطة على التوالي. بالإضافة إلى ذلك، أنخفض مستوى الكوليسترول الضار إلى 120.2 مجم/ديسيلتر و 101 مجم/ديسيلتر المعاملة مع راشح العزلات المنتجة وغير المنتجة للأفلاتوكسين على التوالي مقارنة بـ 144.3 مجم/ديسيلتر للمجموعة الضابطة. أظهرت الجسيمات النانوية للفضة تأثير مثبط ضد نمو فطر الرشاشية السوداء مع أكبر منطقة تثبيط 28.38 ملم بتركيز 100 ميكرو لتر. من ناحية أخرى، أظهرت أيضا كل من بكتيريا الزائفة المتألقة وعصوية سيركيولانز معدل تثبيط ممتاز (100 %) عند تركيز 2 جم/لتر من راشح الفطر. كشفت هذه النتائج أن الجسيمات النانوية للفضة قادرة على تثبيط فطر الرشاشية السوداء وبالتالي يمكن ترشيحها لاستخدامها كمضاد للفطريات.

**الكلمات المفتاحية:** البرتقال، فطر الرشاشية السوداء، المعايير الكيموحيوية، خارج الجسم، جسيمات الفضة النانوية.

## 1. INTRODUCTION

Orange (*Citrus sinensis*) is a type of citrus fruit that belongs to the family Rutaceae. It is one of the winter fruits with an excellent source of vitamin C, in addition to some other vitamins such as B1, B2, B3, B5, B6, A, and E. Furthermore, many other essential nutrients are found in orange, for example, the essential potassium, calcium, iron, zinc, and phosphorus (Butu and Rodino, 2019). Orange is very rich in natural antioxidants, and phenolic compounds, being an important source of flavanones, particularly hesperidin and naringenin. In addition to the hydroxycinnamic acids, orange has a high content of carotenoids, which is an important dietary source of vitamin A carotenoids ( $\beta$ -carotene,  $\alpha$ -carotene, and  $\beta$ -cryptoxanthin) and antioxidant carotenoids ( $\beta$ -carotene,  $\beta$ -cryptoxanthin, zeaxanthin, and lutein) and numerous volatile organic compounds producing orange aroma, including aldehydes, esters, terpenes, alcohols, and ketones (Perez-Cacho and Rouseff, 2008; Galaverna and Dall'Asta, 2014; Aschoff et al., 2015; Tamokou et al., 2017; Capurso et al., 2018). Orange peel is plentiful in flavonoids, including methylated derivatives such

as PMFs, which exhibited strong anti-inflammatory effects at both gene expression and enzyme activity levels (Yu et al., 2004; Sandhy et al., 2011; Manthey et al., 1999).

Previous studies have shown that 20% of processed fruits and vegetables are lost due to spoilage (Mailafia et al., 2017). Oranges withstand at room temperature for long enough but can last up to three weeks if kept in the refrigerator (Butu and Rodino, 2019).

The improper handling, packaging, warehousing, and transportation may result in decomposition and growth of microorganisms. The decay becomes activated because of changes in the physiological state of the fruits, as the pH level becomes lower, in addition to any other reasons, for instance, the high moisture content and the high nutrient composition which both assist in making the fruits very susceptible to attack by pathogenic fungi, which at the end causing rot, and may also make the fruits unfit for consumption by producing mycotoxins (Moss, 2002; Jay, 2003). Common air molds such as *Penicillium* and *Aspergillus* species may enter into the tissues and causing loss during packaging. The extensive production of spores by these pathogens allows it to maintain its



presence wherever fruits were handled, including field, packinghouse, equipment, storage rooms, transit containers, and market place (Ismail and Zhang, 2004).

*Aspergillus niger* is a parasitic fungus that penetrates the tissues of citrus fruits through micro-wounds and bruises. *Aspergillus* rot has a black mold on the fruits, and even adjacent fruits are infected as the spores contaminate the whole lot. High temperatures (the most favorable temperature is 25–40 °C) and high relative humidity support these organisms to develop. *Aspergillus niger* causes rapid decay and spreads at 30–35 °C very quickly. *Aspergillus* does not get below 15 °C, and in that respect is no increase at all under refrigerated conditions. The fungus is very sensitive to temperature. Interestingly, acid lime fruit stored at 30–35 °C develops very high rates of decay and sporulation when infected, while fruits from the same lot stored under cooled conditions (8–10 °C) is free of decay. *Aspergillus niger* is increasingly widespread in Indian citrus fruits (Milind, 2008).

Nanoparticles are one of the materials that reflect an excessive interest due to their properties that make them an excellent candidate for numerous castigations such as medicine, biology, bioengineering, and much more. Silver, copper, gold, magnesium, titanium has been used as nanoparticles against different species of microbes. However, the silver nanoparticles are presently interesting, and the attention to this metal is increased to be used in many uses, including antifungal agents (Gong *et al.*, 2007; Ahmad *et al.*, 2006; Aldujaili and Banoon, 2020).

Silver nanoparticles (AgNPs) are metal structures at the nanoscale and the most important choice for solving various medical problems due to their biocompatible chemical structure, inertness, oxidation resistance, and the broad spectrum of antimicrobial activity against a diverse range of bacteria and fungi. Additionally, silver nanoparticles have very little chance of developing microbial strains resistant to drugs (Mallmann *et al.*, 2015). Silver nanoparticles, therefore, have synthesized as potential antimicrobial material against fungi and bacteria to treat many of the infectious diseases caused by human pathogens and to eliminate the multidrug resistance problems (Prabhu and Poulouse, 2012; Salem *et al.*, 2015; Gudikandula *et al.*, 2017).

This study aimed to isolate *A. niger* from fruits of moldy oranges, test there ability to produce aflatoxins using the Saito and Machida

method, and evaluation the toxicity of *A. niger* on some biochemical parameters in white rat males and assessment the inhibition efficiency of silver nanoparticles, *Pseudomonas fluorescens* and *Bacillus circulans* against *A. niger* isolate that produced the aflatoxins.

## 2. MATERIALS AND METHODS

### 2.1 Bacterial model species used in this study:

*Pseudomonas fluorescens* and *Bacillus circulans* were used in this study. Both strains were identified and confirmed by applying the biochemical tests and using the VITEK-2 compact system using GP and BCL cards, respectively (Garrrity *et al.*, 2004).

### 2.2 *Aspergillus niger* isolated from decayed orange fruits

*Aspergillus niger* was isolated from moldy orange fruits which were surface disinfected with 4% sodium hypochlorite for 2 min, the surface of disinfected fruits were plated on sterilized Petri dishes contained Potato Dextrose Agar (PDA) which was prepared according to (Mackie 1996). The plates were incubated at 28 °C for seven days. The identification of *Aspergillus niger* isolates was based on cell and colony morphology characteristics according to the method described by (Klich 2002; Samuel *et al.*, 2015). At the final stage of the incubation period, the percent of the appearance of fungus was calculated by Equation no.1.

### 2.3 Detection of the capacity of *Aspergillus niger* isolates to produce aflatoxins

Nine isolates of *A. niger* were obtained from a total of 15 fungal samples. The ability of these isolates to produce the aflatoxins was tested according to (Saito and Machida, 1999) on Coconut Extract Agar (CEA) medium and ammonia solution at a concentration of 20%. The plates were incubated at 28 °C for 7-14 days. The CEA medium was prepared according to (Alvarez-Barrea *et al.*, 1982).

### 2.4 The effect of the *A. niger* Filtrate on white rat males

#### 2.4.1 Preparation of Fungal Filtrate

Three flasks (500 ml) were prepared, and 250 ml from liquid yeast extract medium was

added to each flask. After the sterilization and cooling of the medium, two discs of *A. niger* isolate that produced the aflatoxins were added into the first flask, two discs of *A. niger* isolate that does not produce the aflatoxins were added into the second flask. The third flask that does not contain any fungi isolates was used as a control treatment. All three flasks were incubated at  $25 \pm 2$  °C for three weeks. After the incubation period, the components of the fungus (fungus and spores) were separated using turmeric papers (Whatman NO. 4) with the Buchner suppression. The fungal filtrate for both isolates were then collected and used in the dosages of animals (Al-Janabi, and Al-gumaili, 2009).

#### 2.4.2 Preparation of Laboratory animals

In this experiment, 15 white male rats (10 weeks of age, average weight: 200 g) were tested. They were obtained from the University of Kufa, Najaf City, Iraq. The rats were acclimatized for three weeks and housed in polyethylene boxes with bedding of wood shavings. They were maintained under standard conditions, which included a temperature of approximately 22-24 °C with a regular 12h light/12h dark cycle. All rats were given standard rodent pellet food and water. These rats were separated into three groups. Each group includes five rats:

Group A: 5 rats were orally injected with *A. niger* filtrate produced the aflatoxins and in a dose of (1 ml/ 100 g /day) per body weight.

Group B: 5 rats were orally injected with *A. niger* filtrate non-produced the aflatoxins at the same concentration and method mentioned in group A.

Group C: 5 rats were treated with filtrate of the third flask that does not contain any fungi isolates, and the same concentration and method mentioned in group A, treated as a control.

The dosage was taken every 48 hours by oral gavage (Waynforth and Flecknall, 1980), after three weeks of the experiment, the animals were left for three days, the animals were anesthetized and sacrificed.

#### 2.5 Biochemical parameters

The biochemical parameters, including the determination of the GOT and GPT levels, determination of glucose level in serum, and estimate the level of cholesterol in the blood, were carried out according to the manufacturer's instructions (Linear Chemical, Spain).

## 2. 6 Preparation of Silver Nanoparticles

Silver nanoparticles powder (Shanghai Ximeng New Materials Technology co., Ltd, China) Type 2, Purity > 99.95%, with particle size (50nm) was used, The aqueous solution of silver nanoparticles was prepared by dissolving 20 mg of AgNPs in 100 ml of deionized water. The resulted solution was stirred well by the sonication process to obtain a homogeneous solution and to avoid the accumulation of the nanoparticles. This mixture was then autoclaved at 15 psi pressure, 121 °C for 5 minutes. The solution was yellowish, the serial dilution concentrations of silver nanoparticles were required in this study prepared 25, 50, 75, and 100 (µl) (Mohanty *et al.*, 2012).

#### 2.6 Antifungal activity of the silver nanoparticles

The procedure described by (Alananbeh *et al.*, 2017) was followed here with some modification; by preparation of the PDA medium. The PDA was sterilized in the autoclave and poured into 6 Petri dishes. The dishes were then inoculated with *A. niger* isolate, which produced the aflatoxin. The fungicidal activity of the silver nanoparticles was determined using the agar well diffusion assay method. All the dishes were incubated at  $25 \pm 2$  °C for five days, and the plates were examined for evidence of zone of inhibition, which appeared as a clear area around the wells, the diameter of such zones of inhibition was measured using a meter ruler.

#### 2. 7 Antifungal activity for the bacteria used in this study

The PDA was prepared and distributed in three flasks at 250 ml per flask. The growth medium was autoclaved for 15 min, after cooling the flasks, the bacterial concentrations (1, 2) g/L were added. The contents of each flask were poured into six dishes, and all dishes were incubated at  $25 \pm 2$  °C from 5 to 7 days (Leben *et al.*, 1987). The dishes were vaccinated with *A. niger* isolate produced the aflatoxins, but the content of the third flask used without bacteria as control. The dishes were then incubated at  $25 \pm 2$  °C for a week. The percentage inhibition of growth of the fungus was calculated using Equation 2 (Kra *et al.*, 2009). In Equation no. 2, A, and B are the average diameter of fungal growth on the control medium with and without bacteria, respectively.

## 2.8 Statistical Analysis

The obtained data were statistically analyzed using the software SPSS Version 6. Treatment averages were compared at the  $p \leq 0.05$  level of probability using LSD (Norris, 1999).

## 3. RESULTS AND DISCUSSION

### 3.1 Isolation of Fungi from the orange fruits

Nine isolates were obtained from *A. niger* with an occurrence of 60%. Also, five isolates of *A. flavus* were obtained with 33.33%, while one isolate from *Rhizopus stolonifer* was obtained with 6.66% (Figure 1). These results are close to the results reported by (Reuther, 1967), who confirmed the ability of *A. niger*, *A. flavus*, and *Rhizopus* to infect orange and apple fruits after harvesting. *A. niger* has the highest frequency since it is considered as one of the widespread fungi in different soils, and it can tolerate drought and a wide range of wet tension (Hillocks and Waller, 1997). Also, *A. niger* spores have been found to withstand at high temperatures (up to 50 °C) (Gabler *et al.*, 2004). The present study agreed with (Mailafia *et al.*, 2017), the authors found that *Aspergillus niger* had the highest occurrence in pineapple, watermelon, oranges, pawpaw, and tomatoes with a frequency of 38%. The percentage of *Rhizopus* as the lowest agree with (Muhammad *et al.*, 2018) found the *Rhizopus* spp (20%), according to other fungi that isolated from sweet orange.

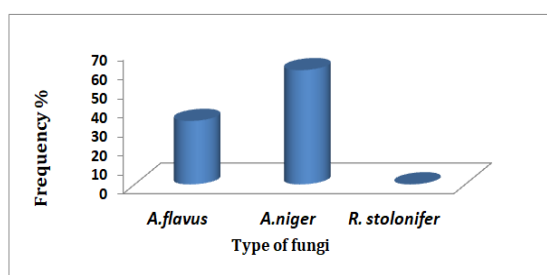


**Figure 1.** The frequency rate of isolated fungi from orange fruits

### 3.2 Detection of the ability of *A. niger* isolates to produce aflatoxins

The results of the chemical detection using the coconut medium and ammonia have shown that some of the *A. niger* isolates were able to produce aflatoxins (Table 1). It was noticed that the isolate no. 2 produced large

quantities of aflatoxins while isolates no.5 and no. 8 produced small quantities of aflatoxins, other isolates were negative for aflatoxin production. The difference in the ability of the isolates to produce aflatoxins, as mentioned by (Saito and Machida, 1999), depends on the degree of red color, the dark red indicates its ability to produce larger quantities of aflatoxins, and this result agrees with (Scott and Trucksess, 1997) who confirmed the ability of *Aspergillus niger*, *Aspergillus ruber*, *Aspergillus wentii*, and *Aspergillus ostianus* to produce aflatoxins but in lower quantities of *Aspergillus flavus*. Also (Hasan, 2000) reported that some of the *A.niger* isolates that were isolated from apple fruits could produce aflatoxins. A study by (Akinola *et al.*, 2019) reported that twenty-three isolates from *Aspergillus* were positive for aflatoxin production. Some *A. niger* strains have been reported to produce potent mycotoxins called ochratoxins, which can be harmful to humans and animals (Mailafia *et al.*, 2017).

**Table 1.** *Aspergillus niger* isolates producing and non-producing the aflatoxins

| No. of <i>niger</i> isolates | A. Quantities Aflatoxins | The ability of aflatoxins production |
|------------------------------|--------------------------|--------------------------------------|
| An1                          | -                        | -                                    |
| An2                          | Large                    | ++                                   |
| An3                          | -                        | -                                    |
| An4                          | -                        | -                                    |
| An5                          | Small                    | +                                    |
| An6                          | -                        | -                                    |
| An7                          | -                        | -                                    |
| An8                          | Small                    | +                                    |
| An9                          | -                        | -                                    |

An2: *A.niger* isolate that produced aflatoxins in large amount, and it used in this study

An6: *A.niger* isolate that non-producing of aflatoxins, and it used in this study

### 3.3 The toxic effects of the *A. niger* Filtrate on white rat males

#### 3.3.1 Effect on GPT and GOT enzymes

Figures (2 and 3) show the effect of two isolates of *A. niger* on GPT and GOT enzymes. The *A. niger* isolate that produced the aflatoxins increased the activity of the GPT and GOT to 24.2 U/ml and 18.3 U/ml, respectively. In

contrast, the *A. niger* isolate that non-produced the aflatoxins increased the activity of two enzymes to 16.6 U/ml and 12.2 U/ml, respectively, compared to the control treatment of 8.5 and 8.2 U/ml.

The increase in the activity of enzymes in the serum of treated animals can be explained by the fungal filtrate that may have an effect on the liver cells containing these enzymes, which leads to releasing the enzymes to the blood. This mechanism can also affect other organs such as kidneys and membranes of the endoplasmic network, resulting in disruption of the bio-transport system in the body (Meerdink, 2004). This study agrees with (Al- Janabi and Al-gumaili, 2009), who showed that the isolate of *A. flavus*, which produces aflatoxins, significantly increased the level of GPT and GOT to 22.3 and 14.4 U/ml compared to the control treatment of 8.3 and 8.2 U/ml respectively.

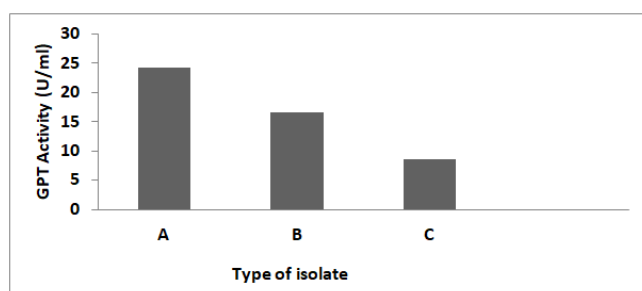


**Figure 2.** Effect of *A. niger* isolates on GPT, A: aflatoxins production isolate B: aflatoxins non-production isolate C: control

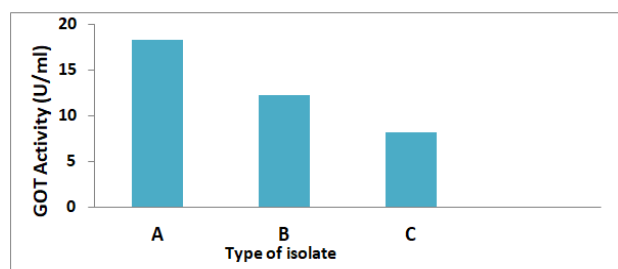


**Figure 3.** Effect of *A. niger* isolates on GOT, A: aflatoxins production isolate B: aflatoxins non-production isolate C: control

### 3.3.2 Effect on Glucose and cholesterol level

The Table (2) shows the results of the effect of the fungal filtrate of *A. niger* isolate on the glucose level, which had caused an increase in the glucose level to (130.2 mg/dl) in the animals that treated with the *A. niger* isolate which producing the aflatoxins and to (95 mg/dl) with the non-producing isolate compared to the

control which was 86.4 mg/dl.

Mechanisms of increasing of the concentration of glucose during aflatoxicosis are not well understood, but this may be due to hormone alteration or stress condition that occurs during aflatoxicosis, which is known to raise blood sugar by altering insulin action. Hyperglycemia in the presence of cirrhosis and some other liver disease may be greater in degree and more prolonged (Yeung and Wang, 1974). The reason of the high sugar level may be due to the metabolic products of the *A. niger* that is normally interfered with the metabolic pathway of glucose and influences the enzymes responsible for regulating the amount of sugar in the blood, including insulin, this is indicated by (WHO, 2003; Sacks *et al.*, 2002). A study by (Mor *et al.*, 2017) reported that Ochratoxin A from *Aspergillus* leads to decreases in insulin levels and increases in blood glucagon and glucose levels. This phenomenon, due to the Ochratoxin A, cause pancreatic damage on the Langerhans islet cells and predispose rats to diabetic Mellitus.

The blood glucose decrease during the course of aflatoxicosis, then after 30 days of treatment, blood glucose levels slowly increased, as indicated by decreasing the concentration of glycogen in the liver, kidney, and heart, which may result from the reducing tissue glucose intake (Busby and Wogan, 1981; Kolhe, 2016).

For the LDL cholesterol, the filtrate of *A. niger* isolate that produced aflatoxins reduced the cholesterol level to 120.2 mg/dl while the non-productive isolate reduced to 101 mg/dl compared to the control with a cholesterol level of 144.3 mg/dl. Hussein and Brasel (2001); Pusztahelyi *et al.* (2015), noted that fungal secondary metabolic products contain compounds that have a high affinity for the mitochondrial membrane causing a rapid crash and also inhibit the protein transport chain, this inhibition may lead to a reducing in the production of energy that required to synthesize cholesterol. Also, Javed *et al.* (2014) found that seven indigenously of *Aspergillus* strains were able to produce cholesterol-lowering drug lovastatin, and the *Aspergillus terreus* strain showed maximum production, the optimized lovastatin was extracted from fermented broth and orally administered to rats. It was concluded that fermented lovastatin effectively lowers the cholesterol level of rats, while Rashid *et al.* (2013) found that the highest lovastatin production was produced by *Aspergillus niger* SAR strain.

**Table 2.** Effect of *A. niger* isolates that produced and non-produced of aflatoxins in the level of sugar and cholesterol in white male rats

| Type of treatment                                       | Blood sugar level (mg/dl) | Blood cholesterol level (mg/dl) |
|---|---------------------------|---------------------------------|
| <i>A. niger</i> isolate that produced of aflatoxins     | 130.2                     | 120.2                           |
| <i>A. niger</i> isolate that not produced of aflatoxins | 95                        | 101                             |
| control   | 86.4                      | 144.3                           |
| L.S.D(0.05)   | 0.34                      | 0.16                            |

Note: Each number represents three replicates.

### 3.4 The efficiency of silver nanoparticles in the inhibition of *A.niger* radial growth

The results indicated that the silver nanoparticles were able to inhibit *A. niger* growth. The diameters of the inhibition zone (11.51, 16.28, 23.71, 28.38 mm) at concentrations 25, 50, 75, and 100 (µl), respectively, as shown in Figure 4. Previous studies described the effective applications of silver nanoparticles as an inhibitory agent at different concentrations against fungi such as *Alternaria alternate*, *Fusarium*, *Aspergillus* species, *Trichophyton mentagrophytes*, and *Candida* sp. (Gao *et al.*, 2012; Noorbakhsh *et al.*, 2011; Bocate *et al.*, 2019). Also, a study by (Alananbeh *et al.*, 2017) found that the gradual reduction in growth was clear in both *Aspergillus* species as the silver nanoparticles concentrations were increased, where *A. terreus* had higher reduction compared to *A. niger*. The silver nanoparticles are possible to be used as antifungal substances. The AgNPs mode of action has several explanations. Metal depletion is one of the AgNP's modes of action that forms irregularly shaped pits in the outer membrane and changes membrane permeability caused by the progressive release of molecules and membrane proteins from lipopolysaccharides (Amro *et al.*, 2000). Ag-generated free radicals have been documented using the Ag nanoparticles Electron Spin Resonance (ESR). Ag nanoparticles' antimicrobial function has to do with the creation of free radicals and subsequent free radical-induced damage to the membrane (Danilczuk *et al.*, 2006). Toxicity is concentration-

and size-dependent. Moreover, the effectiveness of AgNPs against microbes depends on their shapes and sizes (Panáček *et al.*, 2009). In this study, 50nm was the diameter of the AgNPs, yet it inhibited the *Aspergillus niger*. This could be explained by the fact that larger particles of AgNPs can persist longer and could serve as continuous Ag ions source Dobias and Bernier-Latmani (2013), and this agrees with Alananbeh *et al.* (2017).

### 3.5 The efficacy of *Pseudomonas fluorescens* in inhibition of the radial growth of *A. niger*

The results showed the ability of the *P. fluorescens* to inhibit the growth of *A.niger* isolate that produced aflatoxins with inhibition rate attained 100% at 2 g/L, as shown in figure (5). These results are consistent with many studies such as (Hassan, 2012), the inhibitory capacity of *P. fluorescens* to their ability to produce multiple types of antibiotics including Oligomycine, Oomycine, Phenazine-1-carboxylic acid (PCA), Pyoluterin (Plt) and Pymolnitrin (Pln) that the most important antibiotics produced by *P. fluorescens* in contrast with *Fusarium graminearum* and *Fusarium moniliforme* (Pal *et al.*, 2001). Also, a study conducted by (Mathre *et al.*, 2003), it was reported that *P. fluorescens* was capable of producing 2,4-Diacetylphloroglucinol 2,4-DPG), which inhibits the growth of many fungi-causing diseases.

### 3.6 The efficacy of *Bacillus circulans* with different concentrations in inhibition of the radial growth of *A.niger*

*Bacillus circulans* proved highly effective in inhibiting the growth of *A. niger* isolate that producing aflatoxins with an inhibition rate attained 100% at 2 g/L, as shown in Figure 6. The effect of *B. circulans* may occur due to the mechanisms that bacteria possess against pathogenic fungi, including *A. niger*. These mechanisms include the production of antifungal compounds, many of these compounds, such as A Zwittermicin, Kanosamine, and Bacillomycin. These compounds affect fungal cell components, such as enzymes and proteins (McSpadden Gardener, 2004).

*Bacillus* species can also produce some enzymes that analyze cellular walls of fungus such as chitinase, which dissolves the substance of chitin, the base component of the cellular walls of fungus (Peraica *et al.*, 1999). Also (Idriss *et al.*, 2002) demonstrated the ability of some species of *Bacillus* to produce the phytase that broken of

Phytic acid in the cell walls of many fungi.

#### 4. CONCLUSIONS

The outcomes of the present study found that one isolate of *A.f A. niger* was able to produce aflatoxins by using the Saito and Machida method.

The isolate of *A. niger* that was producing aflatoxins, which effect on GPT and GOT enzymes that cause increased the level of the two enzymes compared to the isolate of *A. niger* that non-producing aflatoxins and the control treatment.

The results exposed that the silver nanoparticles were able to inhibit *A.niger* isolates growth at concentrations of 25, 50, 75, and 100 (µl). AgNPs can be used as antifungal substances. They considered as less harmful and cost-efficient than other methods for preparing the Nanoparticles.

The results also showed the efficacy of *Pseudomonas fluorescens*, and *Bacillus circulans* in the inhibition of the *A. niger* isolates growth when they used in the concentration of 2 g/L.

#### 5. ACKNOWLEDGMENTS:

Authors thank the Department of Biology, Faculty of Science, University of Kufa, and the University of Misan for providing the facilities to conduct this study.

#### 6. REFERENCES:

1. Ahmad, Z., Pandey, R., Sharma, S., and Khuller, G. K. (2006). Alginate nanoparticles as antituberculosis drug carriers: formulation development, pharmacokinetics, and therapeutic potential. *Indian journal of chest diseases and allied sciences*, 48(3), 171.
2. Akinola, S. A., Ateba, C. N., and Mwanza, M. (2019). Polyphasic Assessment of Aflatoxin Production Potential in Selected *Aspergilli*. *Toxins*, 11(12), 692.
3. Al- Janabi, B. A. H., and Al-gumaili S. A. (2009). A study of Toxic effects of *Aspergillus flavus* on some Biochemical Parameters of female Albino Rats and capacity of Biological control on these effects. *Al-Kufa University Journal for Biology*, 2, 1.
4. Alananbeh, K. M., Al-Refaei, W. J., and Al-Qodah, Z. (2017). Antifungal effect of silver nanoparticles on selected fungi isolated from raw and wastewater. *Indian Journal of Pharmaceutical Sciences*, 79(4), 559-567.
5. Aldujaili, N. H., and Banoon, S. R. (2020). Antibacterial Characterization of Titanium Nanoparticles Nanosynthesized by *Streptococcus Thermophilus*. *Periódico Tchê Química* 17(34): 311-320.
6. Alvarez-Barrea, V., Pearson, A. M., Price, J. F., Gray, J. I., and Aust, S. D. (1982). Some factors influencing aflatoxin production in fermented sausages. *Journal of Food Science*, 47(6), 1773-1775.
7. Amro, N. A., Kotra, L. P., Wadu-Mesthrige, K., Bulychiev, A., Mobashery, S., and Liu, G. Y. (2000). High-resolution atomic force microscopy studies of the *Escherichia coli* outer membrane: structural basis for permeability. *Langmuir*, 16(6), 2789-2796.
8. Aschoff, J. K., Kaufmann, S., Kalkan, O., Neidhart, S., Carle, R., and Schweiggert, R. M. (2015). In vitro bioaccessibility of carotenoids, flavonoids, and vitamin C from differently processed oranges and orange juices [*Citrus sinensis* (L.) Osbeck]. *Journal of agricultural and food chemistry*, 63(2), 578-587.
9. Bocate, K. P., Reis, G. F., de Souza, P. C., Junior, A. G. O., Durán, N., Nakazato, G., Nakazato, G., Furlaneto, M. C., Almeida, R. S., and Panagio, L. A. (2019). Antifungal activity of silver nanoparticles and simvastatin against toxigenic species of *Aspergillus*. *International journal of food microbiology*, 291, 79-86.
10. Brown, B. A. (1976). *Hematology: Principles and Procedures*. 2nd, Lea & Febiger. *Philadelphia, PA*.
11. Busby Jr, W. F., and Wogan, G. N. (1981). Trichothecenes. Mycotoxins and N-Nitroso compounds: environmental risks, 2, 29-41.
12. Butu, M., and Rodino, S. (2019). Fruit and Vegetable-Based Beverages—Nutritional Properties and Health Benefits. In *Natural Beverages* (pp. 303-338). Academic Press.
13. Capurso, A., Crepaldi, G., and Capurso, C. (2018). *Benefits of the Mediterranean Diet in the Elderly Patient*. Springer International Publishing.
14. Danilczuk, M., Lund, A., Sadlo, J., Yamada, H., and Michalik, J. (2006).

- Conduction electron spin resonance of small silver particles. *Spectrochimica Acta Part A: Molecular and Biomolecular Spectroscopy*, 63(1), 189-191.
15. Dobias, J., and Bernier-Latmani, R. (2013). Silver release from silver nanoparticles in natural waters. *Environmental science & technology*, 47(9), 4140-4146.
  16. Gabler, F. M., Mansour, M. F., Smilanick, J. L., and Mackey, B. E. (2004). Survival of spores of *Rhizopus stolonifer*, *Aspergillus niger*, *Botrytis cinerea*, and *Alternaria alternata* after exposure to ethanol solutions at various temperatures. *Journal of applied microbiology*, 96(6), 1354-1360.
  17. Galaverna, G., and Dall'Asta, C. (2014). Production processes of orange juice and effects on antioxidant components. In *Processing and Impact on Antioxidants in Beverages* (pp. 203-214). Academic Press.
  18. Gao, C., Xu, Y., and Xu, C. (2012). In vitro Activity of nano-silver against Ocular Pathogenic Fungi. *Life Sci J*, 9(4), 750-753.
  19. Garrity, G. M., Bell, J. A., and Lilburn, T. G. (2004). Taxonomic outline of the prokaryotes. *Bergey's manual of systematic bacteriology*. Springer, New York, Berlin, Heidelberg.
  20. Gong, P., Li, H., He, X., Wang, K., Hu, J., Tan, W., Zhang, S. and Yang, X. (2007). Preparation and antibacterial activity of Fe<sub>3</sub>O<sub>4</sub>@Ag nanoparticles. *Nanotechnology*, 18(28), 285604.
  21. Gudikandula, K., Vadapally, P., and Charya, M. S. (2017). Biogenic synthesis of silver nanoparticles from white-rot fungi: Their characterization and antibacterial studies. *OpenNano*, 2, 64-78.
  22. Hasan, H. A. H. (2000). Patulin and aflatoxin in brown rot lesion of apple fruits and their regulation. *World Journal of Microbiology and Biotechnology*, 16(7), 607-612.
  23. Hassan, B. A. (2012). Physiological study of *A.niger* and *Penicillium* fungi that isolation from seed of *Arachis hypogaeae* & evaluation of the efficiency the *Pseudomonas flourecens* bacteria in inhibition the radial growth from the two fungi. *Al-Kufa University Journal for Biology*, 4 (1): 65-78.
  24. Hillocks, R. J., and Waller, J. M. (1997). *Soilborne diseases of tropical crops* (No. BOOK). CABI.
  25. Hussein, H. S., and Brasel, J. M. (2001). Toxicity, metabolism, and impact of mycotoxins on humans and animals. *Toxicology*, 167(2), 101-134.
  26. Idriss, E. E., Makarewicz, O., Farouk, A., Rosner, K., Greiner, R., Bochow, H., Richter, T., and Borris, R. (2002). Extracellular phytase activity of *Bacillus amyloliquefaciens* FZB45 contributes to its plant growth promoting effect. *Microbiology*, 148(7), 2097-2109.
  27. Ismail, M., and Zhang, J. (2004). Post-harvest citrus diseases and their control. *Outlooks on Pest Management*, 15(1), 29.
  28. Javed, S., A Bukhari, S., Zovia, I., and Meraj, M. (2014). Screening of indigenously isolated fungi for lovastatin production and its in vivo evaluation. *Current pharmaceutical biotechnology*, 15(4), 422-427.
  29. Jay, J. M. (2003). Microbial spoilage of food. *Modern food microbiology*. (4th ed.). Chapman and Hall Incorporated. New York. pp. 187-195.
  30. Klich, M. A. (2002). Identification of common *Aspergillus* species, CBS, Utrecht. *The Netherlands*, 116.
  31. Kolhe, A. S. (2016) Mycoflora and Biochemical Alterations During Chronic Aflatoxicosis in Domestic Rabbits. Lulu.com.
  32. Kra, K. D., Diallo, H. A., and Kouadio, Y. J. (2009). Antifungal activities of the extract *Chromolaena odorata* (L.) King & Robins *Fusarium oxysporum* two isolates (EF Sm.) Responsible for lethal yellowing leaves of banana trees. *Journal of Applied Biosciences*, 24, 1488-1496.
  33. Leben, S. D., Wadi, J. A., and Easton, G. D. (1987). Effects of *Pseudomonas fluorescens* on potato plant growth and control of *Verticillium dahliae*. *Phytopathology*, 77(11), 1592-1395.
  34. Mackie, T. J. (1996). *Mackie & McCartney practical medical microbiology*. Harcourt Health Sciences.
  35. Mailafia, S., God'spower Richard Okoh, H. O., Olabode, K., and Osanupin, R. (2017). Isolation and identification of fungi associated with spoilt fruits vended in Gwagwalada market, Abuja, Nigeria. *Veterinary world*, 10(4), 393.
  36. Mallmann, E. J. J., Cunha, F. A., Castro,



- B. N., Maciel, A. M., Menezes, E. A., and Fecine, P. B. A. (2015). Antifungal activity of silver nanoparticles obtained by green synthesis. *Revista do Instituto de Medicina Tropical de São Paulo*, 57(2), 165-167.
37. Manthey, J. A., Grohmann, K., Montanari, A., Ash, K., and Manthey, C. L. (1999). Polymethoxylated flavones derived from citrus suppress tumor necrosis factor- $\alpha$  expression by human monocytes. *Journal of Natural Products*, 62(3), 441-444.
  38. Mathre, D. E., Johnston, R. H., and Grey, W. E. (2003). Diagnosis of common root rot of wheat and barley. *Plant Health Progress*, 4(1), 11.
  39. McSpadden Gardener, B. B. (2004). Ecology of *Bacillus* and *Paenibacillus* spp. in agricultural systems. *Phytopathology*, 94(11), 1252-1258.
  40. Meerdink, G. L. (2004). Aflatoxins. *Clinical veterinary toxicology*. St. Louis: Mosby, 231-235.
  41. Milind, S. L. (2008). Citrus fruit: biology, technology, and evaluation. *London WC1X 8RR, UK: Elsevier*, 1-4.
  42. Mohanty, S., Mishra, S., Jena, P., Jacob, B., Sarkar, B., and Sonawane, A. (2012). An investigation on the antibacterial, cytotoxic, and antibiofilm efficacy of starch-stabilized silver nanoparticles. *Nanomedicine: Nanotechnology, Biology and Medicine*, 8(6), 916-924.
  43. Mor, F., Sengul, O., Topsakal, S., Kilic, M. A., and Ozmen, O. (2017) Diabetogenic Effects of Ochratoxin A in Female Rats. *Toxins* 9 ( 4): 144.
  44. Moss, M. O. (2002). Mycotoxin review-1. aspergillus and penicillium. *Mycologist*, 16(3), 116-119.
  45. Muhammad, A. S., Mohammed, I. U., Ameh, M., Bello, I., Haliru, B. S., Bagudo, H. A., and Sanda, A. S. (2018). Isolation and identification of fungi associated with the spoilage of sweet orange *Citrus sinensis* L and banana *Musa sapientum* L in Sokoto Metropolis. *Journal of Applied Biotechnology & Bioengineering*, 5(5).
  46. Noorbakhsh, F., Rezaie, S., and Shahverdi, A. R. (2011). Antifungal effects of silver nanoparticle alone and with combination of antifungal drug on dermatophyte pathogen *Trichophyton rubrum*. In *International conference on bioscience, biochemistry, and bioinformatics* (Vol. 5, pp. 364-7).
  47. Norusis, M. J. (1990). *SPSS/PC and Statistics 4.0 for the IBM PC/XT/AT and PS/2* (No. 005.3/N822).
  48. Pal, K. K., Tilak, K. V. B. R., Saxena, A. K., Dey, R., and Singh, C. S. (2001). Suppression of maize root diseases caused by *Macrophomina phaseolina*, *Fusarium moniliforme*, and *Fusarium graminearum* by plant growth promoting rhizobacteria. *Microbiological research*, 156(3), 209-223.
  49. Panáček, A., Kolář, M., Večeřová, R., Pucek, R., Soukupova, J., Kryštof, V., Hamal, P., Zbořil, R. and Kvítek, L. (2009). Antifungal activity of silver nanoparticles against *Candida* spp. *Biomaterials*, 30(31), 6333-6340.
  50. Peraica, M., Radić, B., Lucić, A., and Pavlović, M. (1999). Toxic effects of mycotoxins in humans. *Bulletin of the World Health Organization*, 77(9), 754-766.
  51. Perez-Cacho, P. R., and Rouseff, R. (2008). Processing and storage effects on orange juice aroma: a review. *Journal of agricultural and food chemistry*, 56(21), 9785-9796.
  52. Prabhu, S., and Poulouse, E. K. (2012). Silver nanoparticles: mechanism of antimicrobial action, synthesis, medical applications, and toxicity effects. *International nano letters*, 2(1), 32.
  53. Pusztahelyi, T., Holb, I. J., and Pócsi, I. (2015). Secondary metabolites in fungus-plant interactions. *Frontiers in plant science*, 6, 573.
  54. Rashid, S. A., Ibrahim, D., Nyoman, I., and Aryantha, P. (2013). Effect of Cultural Conditions on Lovastatin Production by *Aspergillus niger* SAR I Using Combination of Rice Bran and Brown Rice as Substrate. *International Journal of Applied Biology and Pharmaceutical Technology* 4(2):150-156.
  55. Reuther, W. (1967). *The citrus industry: crop protection, post-harvest technology, and early history of citrus research in California* (Vol. 3326). UCANR Publications.
  56. Sacks, D. B., Bruns, D. E., Goldstein, D. E., Maclaren, N. K., McDonald, J. M., and Parrott, M. (2002). Guidelines and recommendations for laboratory analysis in the diagnosis and management of diabetes mellitus. *Clinical chemistry*, 48(3), 436-472.
  57. Saito, M., and Machida, S. (1999). A rapid



- identification method for aflatoxin-producing strains of *Aspergillus flavus* and *A. parasiticus* by ammonia vapor. *Mycoscience*, 40(2), 205-208.
58. Salem, W., Leitner, D. R., Zingl, F. G., Schratter, G., Prassl, R., Goessler, W., Reidl, J. and Schild, S. (2015). Antibacterial activity of silver and zinc nanoparticles against *Vibrio cholerae* and enterotoxigenic *Escherichia coli*. *International Journal of Medical Microbiology*, 305(1), 85-95.
  59. Samuel, O., Ifeanyi, O., and Ugochukwu, O. (2015). Filamentous fungi associated with the spoilage of post-harvest sweet orange fruits (*Citrus sinensis*) sold in Awka major markets, Nigeria. *Bioeng. Biosci*, 3(3), 44-49.
  60. Sandhy, S.S., Kumar, S., Vinod, K.R., and Banji, D., Kumar, K. (2011). Plants as Potent Anti Diabetic and Wound Healing Agents-A Review. *Hygeia J. D. Med.*; 3(1): 11-19.
  61. Scott, P. M., and Trucksess, M. W. (1997). Application of immunoaffinity columns to mycotoxin analysis. *Journal of AOAC International*, 80(5), 941-950.
  62. Tamokou, J. D. D., Mbaveng, A. T., and Kuate, V. (2017). Antimicrobial activities of African medicinal spices and vegetables. In *Medicinal spices and vegetables from Africa* (pp. 207-237). Academic Press.
  63. Waynforth, H. B., and Flecknell, P. A. (1980). Experimental and surgical technique in the rat (Vol. 127). London: Academic press.
  64. World Health Organization. (2003). Laboratory diagnosis and monitoring of diabetes mellitus.
  65. Yeung, R. T., and Wang, C. C. (1974). A study of carbohydrate metabolism in postnecrotic cirrhosis of liver. *Gut*, 15(11), 907-912.
  66. Yu, H., Robert, R. T., and Ho, C. T. (2004). Anti-inflammatory activity of polymethoxyflavones in sweet orange (*Citrus sinensis*) peel and metabolites study of nobiletin. In *Abstracts Of Papers Of The American Chemical Society* (Vol. 227, pp. U31-U31). 1155 16TH ST, NW, WASHINGTON, DC 20036 USA: AMER CHEMICAL SOC.

$$\text{The percentage of appearance} = \frac{\text{number of samples in which the fungus appeared}}{\text{The total number of samples}} \times 100 \quad (\text{Eq. 1})$$

$$\text{percentage inhibition} = \frac{(A-B)}{A} \times 100 \quad (\text{Eq. 2})$$

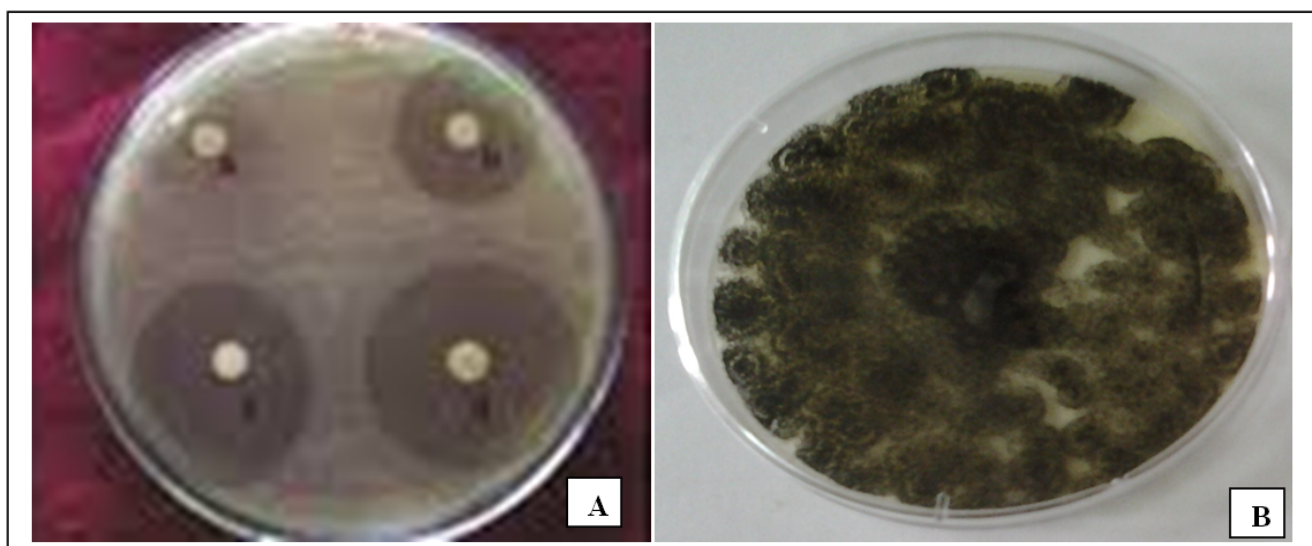


**Figure 4.** The capacity of silver nanoparticles in inhibition of the radial growth of *A. niger*: A. Effect of different concentrations of silver nanoparticles B. The control treatment.

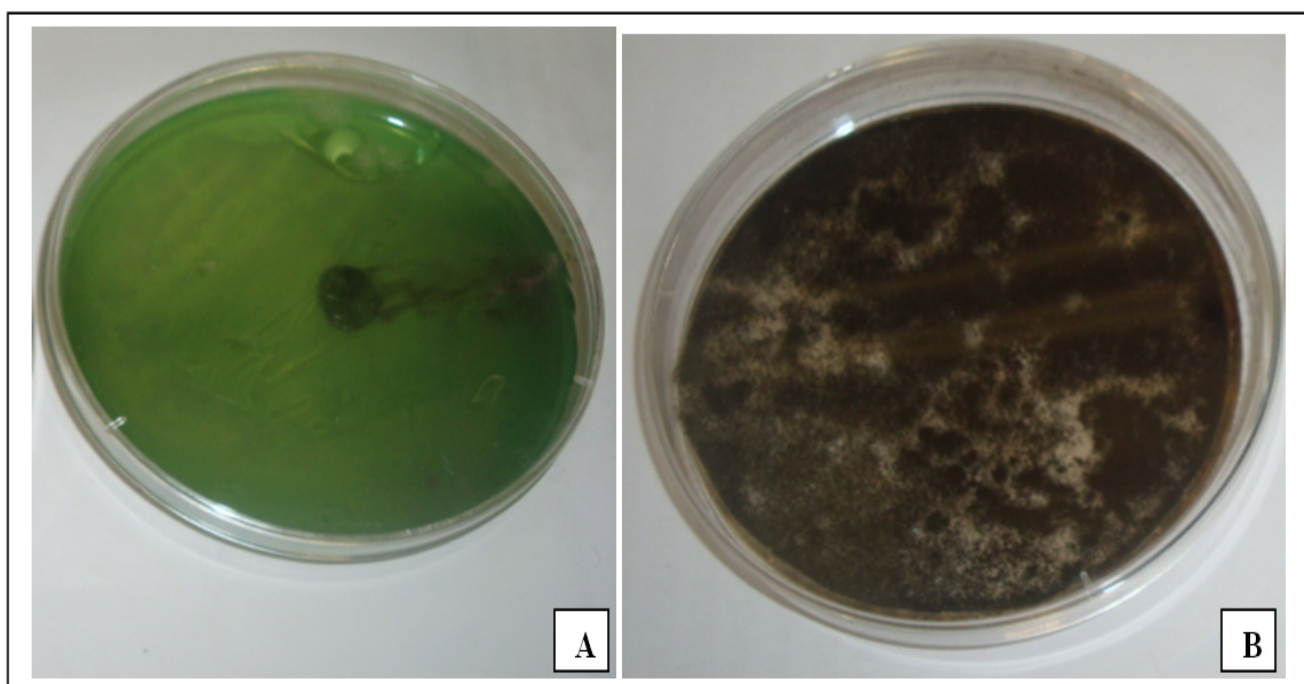


**Figure 5.** The efficacy of *P. fluorescens* in inhibition of the radial growth of *A. niger* isolate that producing aflatoxins, A: The *P. fluorescens* treatment in the concentration of 2g/L, B: The control treatment.

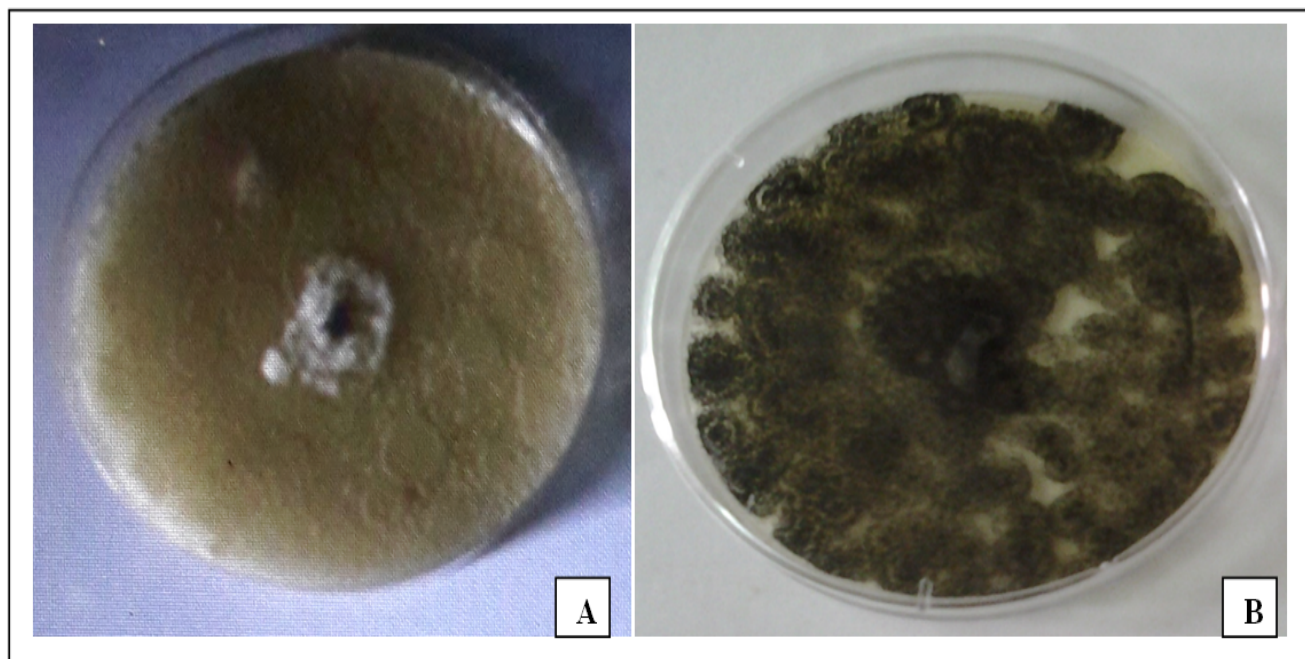


**Figure 6.** The efficacy of *B. circulans* in inhibition of the radial growth of *A. niger* isolate that producing aflatoxins, A: The *B. circulans* treatment in the concentration of 2g/L, B: The control treatment.

# LUMINESCÊNCIA DE A-WILLEMITE NA OXIDAÇÃO CATALÍTICA DE MONÓXIDO DE CARBONO

## LUMINESCENCE OF A-WILLEMITE IN THE CATALYTIC OXIDATION OF CARBON MONOXIDE

### ЛЮМИНЕСЦЕНЦИЯ А-ВИЛЛЕМИТА ПРИ КАТАЛИТИЧЕСКОМ ОКИСЛЕНИИ МОНООКСИДА УГЛЕРОДА

SHIGALUGOV, Stanislav H.<sup>1\*</sup>; TYURIN, Yuriy I.<sup>2</sup>; DUBROV, Dmitriy V.<sup>3</sup>; BOROVITSKAYA, Anna O.<sup>4</sup>; DERIABINA, Larissa B.<sup>5</sup>;

<sup>1,3,4,5</sup> Norilsk State Industrial Institute, Department of Physical and Mathematical Disciplines, 7 50 let Oktyabrya Str., zip code 663310, Norilsk – Russian Federation

<sup>2</sup> National Research Tomsk Polytechnic University, Department of Experimental Physics, 30 Lenin Ave., zip code 634050, Tomsk – Russian Federation

\* Correspondence author

e-mail: fizika@norvuz.ru

Received 21 April 2020; received in revised form 06 May 2020; accepted 19 June 2020

## RESUMO

A interação de partículas neutras de gás de energias térmicas (moléculas e átomos) com a superfície do sólido é acompanhada por radiação nas partes visível e infravermelha do espectro. Nesse caso, a superfície do sólido atua como um catalisador para as reações de recombinação de partículas de gás. Neste contexto, é interessante a possibilidade de excitar a luminescência durante a oxidação catalítica do monóxido de carbono diretamente pela forma atômica de oxigênio pré-adsorvido na superfície do sólido. Os métodos cinéticos e espectrais foram utilizados para estudar a luminescência resultante da oxidação catalítica do monóxido de carbono pela forma atômica de oxigênio pré-adsorvido na superfície do sólido – uma amostra de  $\alpha$ -willemite  $\text{Zn}_2\text{SiO}_4:\text{Mn}^{2+}$ . As principais etapas dos mecanismos de recombinação entre as partículas dos adsorbatos são estabelecidas. As transições eletrônicas em complexos de adsorção e no íon ativador foram identificadas. Durante o processo de entrada, a temperatura da amostra foi mantida pelo sistema de controle eletrônico de alta velocidade constante da corrente do aquecedor. Isso ajudou a evitar os efeitos térmicos colaterais. As principais etapas dos mecanismos de recombinação entre as partículas dos adsorbatos são estabelecidas. As transições eletrônicas em complexos de adsorção e no íon ativador foram identificadas. Verificou-se que a excitação da luminescência ocorre em duas etapas principais, um pouco deslocadas no tempo. O mecanismo de duas etapas da oxidação catalítica do monóxido de carbono na superfície da  $\alpha$ -willemite pelo oxigênio atômico pré-adsorvido permite descrever consistentemente a luminescência observada neste caso. Este tipo de luminescência tem a perspectiva no estudo dos mecanismos de oxidação catalítica do monóxido de carbono.

**Palavras-chave:** cristalofósforo,  $\alpha$ -willemite, monóxido de carbono, cinética de luminescência, espectro de luminescência.

## ABSTRACT

The interaction of neutral gas particles of thermal energies (molecules and atoms) with the surface of a solid is accompanied by radiation in the visible and I.R. parts of the spectrum. In this case, the surface of a solid body acts as a catalyst for the recombination reactions of gas particles. In this connection, the possibility of exciting luminescence during the catalytic oxidation of carbon monoxide directly by the atomic form of oxygen pre-adsorbed on the surface of a solid is of interest. Kinetic and spectral methods were used to study the luminescence arising from the catalytic oxidation of carbon monoxide by the atomic form of oxygen pre-adsorbed on the surface of a solid – a sample of  $\alpha$ -willemite  $\text{Zn}_2\text{SiO}_4:\text{Mn}^{2+}$ . The main stages in the mechanisms of recombination between adsorbate particles are established. Electronic transitions in adsorption complexes and the activator ion have been identified. During the filling process, the sample temperature was maintained by a constant high-speed electronic control system of the heater current. This made it possible to avoid thermal

side effects. The main stages in the mechanisms of recombination between adsorbate particles are established. Electronic transitions in adsorption complexes and the activator ion have been identified. It was found that luminescence excitation proceeds in two main stages, somewhat time-shifted. The two-stage mechanism for the catalytic oxidation of carbon monoxide on the surface of  $\alpha$ -willemite with pre-adsorbed atomic oxygen allows a consistent description of the luminescence observed in this case. This type of luminescence has the prospect of using for studying the mechanisms of catalytic oxidation of carbon monoxide.

**Keywords:** *crystallophosphorus,  $\alpha$ -willemite, carbon monoxide, luminescence kinetics, luminescence spectrum.*

## АННОТАЦИЯ

Взаимодействие нейтральных газовых частиц тепловых энергий (молекул и атомов) с поверхностью твердого тела сопровождается излучением в видимой и инфракрасной частях спектра. При этом поверхность твердого тела выступает в роли катализатора реакций рекомбинации газовых частиц. В связи с этим вызывает интерес возможность возбуждения люминесценции при каталитическом окислении монооксида углерода непосредственно атомарной формой кислорода, преадсорбированной на поверхности твердого тела. Кинетическими и спектральными методами исследована люминесценция, возникающая при каталитическом окислении монооксида углерода атомарной формой кислорода, преадсорбированной на поверхности твердого тела – образца  $\alpha$ -виллемита  $\text{Zn}_2\text{SiO}_4\text{:Mn}^{2+}$ . Установлены основные стадии в механизмах рекомбинации между частицами адсорбатов. Идентифицированы электронные переходы в адсорбционных комплексах и в ионе активатора. В процессе напуска температура образца поддерживалась постоянной быстродействующей электронной системой регулирования тока нагревателя. Это позволило избежать побочных тепловых эффектов. Установлены основные стадии в механизмах рекомбинации между частицами адсорбатов. Идентифицированы электронные переходы в адсорбционных комплексах и в ионе активатора. Было обнаружено, что возбуждение люминесценции происходит в два основных этапа, несколько смещенных во времени. Двухстадийный механизм каталитического окисления оксида углерода на поверхности  $\alpha$ -виллемита предварительно адсорбированным атомарным кислородом позволяет последовательно описать люминесценцию, наблюдаемую в этом случае. Этот тип люминесценции имеет перспективу использования для изучения механизмов каталитического окисления оксида углерода.

**Ключевые слова:** *кристаллофосфор,  $\alpha$ -виллемит, оксид углерода, кинетика люминесценции, спектр люминесценции.*

## 1. INTRODUCTION

The interaction of neutral gas particles of thermal energies (molecules and atoms) with the surface of a solid is accompanied by radiation in the visible and I.R. parts of the spectrum (Rufov *et al.*, 1966; Volkenstein *et al.*, 1976; Arnold and Coleman, 1988; Formalev *et al.*, 2019; Radyuk *et al.*, 2019). In this case, the surface of a solid body acts as a catalyst for the recombination reactions of gas particles. Claydel and his coworkers introduced the concept of cathodoluminescence (Breysse *et al.*, 1978) to denote the glow of a solid during a catalytic process on its surface. In particular, in (Breysse *et al.*, 1978; Lurie *et al.*, 2017), it is a question of chemiluminescence arising during the (Equation 1) catalytic process on the  $\text{ThO}_2$  surface activated by rare-earth ions  $\text{Pr}^{3+}$ ,  $\text{Eu}^{3+}$ ,  $\text{Dy}^{3+}$  and  $\text{Gd}^{3+}$ . The interpretation of this type of luminescence is given in the model of the energy bands of a solid with allowance for the local levels induced on the surface by the adsorbate (Achatz *et al.*, 2011). Radiative transitions are supposed from the  $\text{O}^-$  level formed

by the dissociative charged form of molecular oxygen adsorption to the  $\text{CO}^+$  level in the band gap and from the conduction band to the activator level.

In this connection, the possibility of exciting luminescence during the catalytic oxidation of carbon monoxide directly by the atomic form of oxygen pre-adsorbed on the surface of a solid and, thereby, obtaining more detailed information on the mechanism of catalytic oxidation of carbon monoxide is of interest (Kharisov and Kharissova, 2019). As an adsorbent,  $\alpha$ -willemite  $\text{Zn}_{1.98}\text{Mn}_{0.02}\text{SiO}_4$  was selected (sample FGI-520-1 of crystallophosphorus  $\text{Zn}_2\text{SiO}_4\text{:Mn}^{2+}$ , synthesized at the State Institute of Applied Chemistry, Russian Federation). Due to the high luminescence efficiency during cathodic and photoexcitation, chemical and thermal stability, this crystallophosphorus is widely used in optoelectronic technology and lighting devices (Juanjuan *et al.*, 2015; Ni *et al.*, 2018). The morphology, phase composition, and structure of the crystal lattice have been well studied for



$\text{Zn}_2\text{SiO}_4\text{:Mn}^{2+}$ , and the main electronic transitions in spectral laws have been determined (Palumbo and Brown, 1970; Stevels and Vink, 1974; Dove *et al.*, 1981; Hess and Krautz, 1981; Rivera-Enríquez *et al.*, 1981; Formalev *et al.*, 2018; Skvortsov *et al.*, 2014). In addition,  $\text{Zn}_2\text{SiO}_4\text{:Mn}^{2+}$  demonstrates a clear ability for radical recombination luminescence upon excitation by atomic gases (Rufov *et al.*, 1966; Barashkin and Samarin, 2005). All this leads to the choice of  $\alpha$ -willemite as a sample for studying this type of luminescence in order to facilitate the interpretation of the kinetic and spectroscopic results of the experiment (Sarrigani and Amiri, 2019; Koshoridze *et al.*, 2017).

## 2. MATERIALS AND METHODS

The experiments were performed on a special high-vacuum installation, whose main components are given in (Shigalugov *et al.*, 2019). A dynamic vacuum of  $10^{-8}$  Torr in the sample chamber was maintained by two magnetic discharge pumps NMD-04-1 and NMD-016-1 (with a total pumping rate of 550 l/s). High purity gases were used: oxygen puriss. spec. (99.998%) and carbon monoxide CO puriss. (99.9%). The luminescence intensity was recorded using photoelectric devices: a photomultiplier (FEM-84-3), the signal from which was fed through a preamplifier (C7319 HAMAMATSU) to a computer recording module (ML-840 PowerLab 4/20 ADInstruments), or (at low light fluxes) to a photosensor module (H7468-01 HAMAMATSU) docked with an IBM PC (Zhou *et al.*, 2015). Luminescence spectra in the region of 350-1150 nm with a resolution of 1.5 nm were recorded by a scanning CCD array spectrograph (QE 65000 OCEAN OPTICS), also controlled by P.C. The temperature of a finely dispersed sample deposited from an alcohol suspension in the form of a thin layer ( $h \leq 100 \mu\text{m}$ ) on a heater substrate could be kept constant with an accuracy of  $\leq 1\%$  or quickly ( $< 10$  s) be changed using an electronic controller with the heater current (Delodovici *et al.*, 2017). Atomic oxygen with a flux density of up to  $j_{\text{O}} = 10^{14} \text{ cm}^{-2}\text{s}^{-1}$  was obtained by  $\text{O}_2$  thermolysis according to the procedure (Brennan, 1967) on a current-heated rhodium (Rh) ribbon measuring  $0.015 \times 1 \times 20$  mm.

A stream of CO molecules with a density of up to  $j_{\text{CO}} \sim 2 \cdot 10^{20} \text{ cm}^{-2}\text{s}^{-1}$  could be introduced into a sample of  $\text{Zn}_2\text{SiO}_4\text{:Mn}^{2+}$  pre-purified by long-time ( $\sim 2$  hours) high-temperature ( $T \sim 700$  K) heating in high vacuum ( $\sim 10^{-8}$  Torr).

Free O atoms obtained by dissociation of  $\text{O}_2$  on a ribbon (Rh) heated to 1800 K were previously adsorbed on the surface of  $\text{Zn}_2\text{SiO}_4\text{:Mn}^{2+}$  for 15 minutes from a mixture of  $\text{O}_2 + \text{O}$  at an oxygen pressure of 0.02 Torr for 13 minutes at a sample temperature constant for all experiments (400 K and 2 minutes) when setting the operating temperature (379 K, 400 K, 550 K) (Achatz *et al.*, 2010; Lemmerer, 2020). Then the reaction volume with the sample was pumped out for 10 minutes to a vacuum of  $3 \cdot 10^{-4}$  Torr and, further, a stream of CO was rapidly let in to a pressure of 0.5 Torr. The effect of triboluminescence, in this case, as shown by control experiments with nitrogen and inert gases, was negligible (Shang, 2017; Hsu *et al.*, 2017). During the filling process, the temperature of the sample was maintained by a constant high-speed electronic control system of the heater current. This made it possible to avoid side thermal effects (thermostimulated luminescence due to heat generation in the processes of adsorption and recombination, quenching of luminescence due to sample cooling during gas inlet, etc.) (Tanaka *et al.*, 2018; Bulychev, 2019; Bonacchi *et al.*, 2011; Hasobe, 2020). The flow of CO molecules onto the sample was supplied using a vacuum gate for a time  $\Delta t < 1$  s to 90% of 0.5 Torr and then remained unchanged during continuous pumping (curves 6 and 3 in Figure 1 and Figure 2).

## 3. RESULTS AND DISCUSSION:

Figure 1 shows the luminescence kinetics in the activator ( $\text{Mn}^{2+}$  ion) emission band  $\lambda_{\text{max}} = 527$  nm of the surface of  $\alpha$ -willemite  $\text{Zn}_{1.98}\text{Mn}_{0.02}\text{SiO}_4$  with pre-adsorbed O atoms that occurs when the stream of CO molecules is poured (Figure 1).

At the initial moment, the luminescence has the form of an adsorb luminescent (A.L.) flash (curves 1-5) (Accetta *et al.*, 2011; Sánchez-Carnerero *et al.*, 2015). At "low" sample temperatures ( $T = 300$  K, 370 K, curves 1, 2), after the flare, the luminescence monotonically decreases according to the law characteristic of AL (Grankin *et al.*, 1981), in this case, the Eley-Rideal shock recombination process (Equation 2).

In Equation 2, L is the symbol of the adsorption center on the surface;  $h\nu$  is the symbol of the emitted quantum of light. The luminescence decay kinetics is well described by the dependences of the form (Equation 3) at  $T = 300$  K (curve 1) (Equation 4) at  $T = 370$  K (curve

2). Here  $I$  is the luminescence intensity (relative units),  $t$  is time (seconds) (Babin *et al.*, 2015). At sample temperatures above 400 K, the second maximum begins to appear on the kinetic curve of luminescence decay, which is so pronounced at  $T = 625$  K that it significantly exceeds the initial flash of luminosity and light sum (Figure 1, curve 5). Further luminescence decay after the second maximum occurs by law (Equation 5) at  $T = 625$  K (Figure 1, curve 5) (which is characteristic of the second-order recombination process according to the Langmuir–Hinshelwood mechanism) (Zhu *et al.*, 2011; Kuznetsova and Rabinskiy, 2019). The second stage is possible only in the presence of adsorbed O-L atoms on the surface. Indeed, when CO is poured onto the same  $\text{Zn}_2\text{SiO}_4:\text{Mn}^{2+}$  sample, whose surface is filled only with molecular oxygen  $\text{O}_2\text{-L}$ , such luminescence curves with two maxima are not observed, and the intensity is almost two orders of magnitude lower than in the previous case (Figure 2).

In the opinion of the authors, the complex nature of the kinetic luminescence curves (Figure 1) may be due to the almost simultaneous occurrence of two types (stages) of the recombination process (Fahlman, 2018).

1. The stage of shock recombination (which is responsible for the initial flash) occurs non-activation. This is evidenced by the practical independence of the flash value on the sample temperature. The excitation of luminescence at this stage is most likely associated with the formation of electronically excited carbon dioxide molecules  $\text{CO}_2^e$  on the surface of solids (Bui and Dowell, 2020).

The formation of  $\text{CO}_2^e$  upon heterophasic oxidation of CO followed by radiative relaxation, is well known (Pravilov and Smirnova, 1981; Persson and Avouris, 1983). Figure 3 shows the dependence of the OC-O bond energy on the configuration coordinate (Pravilov and Smirnova, 1981). When the reagents come closer along the coordinate, the carbon dioxide molecule can enter the electronically excited states of  $\text{CO}_2^e$  ( $^3\text{B}_2$ ,  $^1\text{B}_2$ ).

It was shown in (Persson and Avouris, 1983) that even on the surface of metals, CO and  $\text{CO}_2$  retain their individuality, in particular, the local structure of electronic terms remains almost unchanged (Pham *et al.*, 2016; Gupta, 2018). On the surface of crystallophosphorus (semiconductors, dielectrics) having a much lower density of electronic states, the formation of electronically excited states along the adiabatic

interaction path of (Equation 6) is much more likely (Figure 3). A further adsorbed electron-excited  $\text{CO}_2^e\text{-L}$  molecule can radiatively relax to the ground state (Liu *et al.*, 2016). Luminescence in the blue and near-UV regions can be observed, slightly shifted to the short-wavelength region concerning homogeneous chemiluminescence with  $\lambda_{\text{max}} \sim 430$  nm (Pravilov and Smirnova, 1981). On the surface of the crystallophosphorus-insulator, non-radiative energy transfer becomes possible from  $\text{CO}_2^e(^3\text{B}_2)$  to the luminescence center ( $\text{Mn}^{2+}$  in our case) with the conservation of the total spin in the system (Equation 7) (Shigalugov *et al.*, 2000).

Since in the spectrum of this type of  $\text{Zn}_2\text{SiO}_4:\text{Mn}^{2+}$  luminescence (Figure 4) there is no (Equation 8) band with  $\sim 430$  nm, it can be assumed that the transfer of electron excitation energy from the  $\text{CO}_2^e(^3\text{B}_2)\text{-L}$  state to the surface and near-surface luminescence centers occurs at a rate significantly exceeding that of radiative relaxation ( $10^5\text{--}10^7$  s $^{-1}$ ) in the (Equation 9) donor.

2. The second stage (with activation), responsible for the high-temperature maximum on the kinetic curve  $I(t)$  (Figure 1, curves 3, 4 and 5), cannot be satisfactorily explained, like the source (Breysse *et al.*, 1978), only by surface recombination of adsorbed carbon monoxide molecules and oxygen atoms of the type (Equation 10).

This leads to a contradictory interpretation (process without and with activation) of different sections of the kinetic curves in Figure 1. The interpretation of this stage as the result of surface recombination of O-L atoms stimulated by the formed adsorption layer is most adequate (Liu and Qiu, 2015; Kumar and Srivastava, 2018). This layer consists, in this case, mainly of  $\text{CO}_2\text{-L}$  molecules, due to the intense oxidation of CO molecules flying from the gas phase (Dhbaibi *et al.*, 2018). As accumulation on the surface of  $\text{CO}_2\text{-L}$ , at an elevated sample temperature ( $T > 400$  K), the process of recombination of pre-adsorbed O-L atoms in the layer of  $\text{CO}_2\text{-L}$  begins (Equation 11).

An increase in temperature is necessary here to accelerate the surface diffusion of O-L atoms with the participation of  $\text{CO}_2\text{-L}$ . This model corresponds to the quadratic in  $t$  of the regions of acceleration and decay of luminescence (Tsuchiya *et al.*, 2019; Hasobe, 2020). This is consistent with experience (second maxima in curves 4 and 5 of Figure 1). The band gap (about 6 eV) of the  $\text{Zn}_2\text{SiO}_4:\text{Mn}^{2+}$  sample significantly

exceeds the binding energy (5.18 eV) in the O<sub>2</sub> molecule (Chang *et al.*, 1999). The (O-O) bond has a small anharmonicity (12.2 cm<sup>-1</sup>) and a small value of the vibrational quantum ( $\eta\omega_o < 0.2$  eV). For these conditions, the adiabatic mechanism of luminescence excitation at this stage is most probable (Styrov *et al.*, 1989). The resulting adsorption complexes in the neutral (O-L + O-L) and charged (O-L + O<sup>-</sup>-L) forms can adiabatically enter electronically excited states  $A^3\Sigma_u^+$ ,  $c^1\Sigma_u^-$  for the neutral form O<sub>2</sub><sup>e</sup>-L and  $^4\Sigma_u^-$ ,  $^2\Pi_u$ ,  $^2\Sigma_u^-$  for the charged form (O<sub>2</sub><sup>-</sup>)<sup>e</sup>-L (Rosen, 1970).

An effective non-radiative dipole transition with simultaneous energy transfer to luminescence centers located in the surface and near-surface regions is likely from the  $^2\Pi_u$  term (Crassous, 2020; Tadashi, 2020). For example, the relaxation of an (O<sub>2</sub><sup>-</sup>)<sup>e</sup>-L molecular ion to the ground state  $X^2\Pi_g^1$  from the  $^4\Sigma_u^-$ ,  $^2\Pi_u$ ,  $^2\Sigma_u^-$  states can occur in conjunction with the (Equation 12) transitions in the Mn<sup>2+</sup> ion in Zn<sub>2</sub>SiO<sub>4</sub>:Mn<sup>2+</sup> with the total spin remaining in the system. It is also possible to transfer energy to the centers of the activator and from neutral electronically excited (O<sub>2</sub>)<sup>e</sup>-L molecules (for example, upon transitions from (Equation 13) in the (O<sub>2</sub>)<sup>e</sup>-L molecule and (Equation 12) in the Mn<sup>2+</sup> ion.

#### 4. CONCLUSIONS:

Based on the experimental study carried out by spectral and kinetic methods, it was found that when a stream of carbon monoxide molecules is injected onto the surface of a solid – Zn<sub>2</sub>SiO<sub>4</sub>:Mn<sup>2+</sup> crystallophosphorus with pre-adsorbed atomic oxygen, a luminescent glow appears in the characteristic activator emission band of the Mn<sup>2+</sup> ion with a maximum near 527 nm, having a complex temporal nature. It was found that luminescence excitation proceeds in two main stages, somewhat time-shifted.

The first stage, which is responsible for the initial flare, proceeds non-activation according to the law characteristic of the shock recombination process. In this case, recombination of carbon monoxide molecules flying from the gas phase with oxygen atoms previously adsorbed on the surface of α-willemite appears according to the Eley–Rideal mechanism. In this case, the elementary mechanism of luminescence excitation includes the formation on the surface as a result of recombination of electronically excited carbon dioxide molecules, followed by non-radiative

transfer of excess energy to the Mn<sup>2+</sup> luminescence centers.

The second stage has a pronounced activation character and begins to manifest itself only at temperatures above 400 K. The kinetics of the decay of luminescence at this stage obeys the law characteristic of the second-order recombination reaction. In this case, the luminescence excitation model in the acts of surface recombination of pre-adsorbed oxygen atoms according to the Langmuir–Hinshelwood mechanism stimulated by the formed adsorption layer of carbon dioxide molecules is most adequate to experiment. The excitation micromechanism of this model involves the formation on the surface of α-willemite of electronically excited molecular ions and neutral oxygen molecules from adiabatically recombining oxygen atoms in charged and neutral forms. Further, effective non-radiative dipole transitions in oxygen ions and molecules with simultaneous energy transfer to the Mn<sup>2+</sup> luminescence centers located in the surface and near-surface regions while maintaining the full spin in the system become possible.

The proposed two-stage mechanism for the catalytic oxidation of carbon monoxide on the surface of α-willemite with pre-adsorbed atomic oxygen allows a consistent description of the luminescence observed in this case. This type of luminescence has the prospect of using for studying the mechanisms of catalytic oxidation of carbon monoxide, since using very sensitive informative optical methods allows revealing the details of the interaction of carbon monoxide with a crystalline catalyst containing atomic forms of oxygen in the surface layer, establishing the main stages of heterogeneous chemical reactions and studying patterns of atomic-molecular and electronic processes occurring on the surface.

#### 5. REFERENCES:

1. Accetta, A., Corradini, R., and Marchelli, R. (2011). Enantioselective sensing by luminescence. In L. Prodi, M. Montalti, and N. Zaccheroni (Eds.), *Luminescence Applied in Sensor Science* (pp. 175-216). Berlin, Germany: Springer. doi:10.1007/978-3-642-19420-7
2. Achatz, D. E., Meier, R. J., Fischer, L. H., and Wolfbeis, O. S. (2010). Luminescent sensing of oxygen using a quenchable probe and upconverting nanoparticles. *Angewandte*



*Chemie International Edition*, 50(1), 260-263.  
doi:10.1002/anie.201004902

3. Achatz, D. E., Reham, A., and Wolfbeis, O. S. (2011). Luminescent chemical sensing, biosensing, and screening using upconverting nanoparticles. In L. Prodi, M. Montalti, and N. Zaccheroni (Eds.), *Luminescence Applied in Sensor Science* (pp. 29-50). Berlin, Germany: Springer. doi:10.1007/128\_2010\_98
4. Arnold, G. S., and Coleman, D. J. (1988). Surface mediated radical recombination luminescence: O+NO+Ni. *Journal of Chemical Physics*, 88(11), 7147-7156.
5. Babin, V., Chernenko, K., Lipińska, L., Mihokova, E., Nikl, M., Schulman, L.S., Shalapska, T., Suchocki, A., Zazubovich, S., Zhydachevskii, Ya. (2015). Luminescence and excited state dynamics of Bi<sup>3+</sup> centers in Y<sub>2</sub>O<sub>3</sub>. *Journal of Luminescence*, 167, 268-277. doi:10.1016/j.jlumin.2015.06.029
6. Barashkin, R. L., and Samarin, I. V. (2005). Computer system of simulating operating duty of a gaslifting well. In *11th International Scientific and Practical Conference of Students, Postgraduates and Young Scientists; "Modern Techniques and Technologies", MTT 2005 – Proceedings*. Retrived from <https://ieeexplore.ieee.org/document/4493238>
7. Bonacchi, S., Genovese, D., Juris, R., Montalti, M., Prodi, L., and Rampazzo, E. (2011). Luminescent chemosensors based on silica nanoparticles. In L. Prodi, M. Montalti, and N. Zaccheroni (Eds.), *Luminescence Applied in Sensor Science* (pp. 93-138). Berlin, Germany: Springer. doi:10.1007/978-3-642-19420-7
8. Brennan, D. (1967). Atomization of diatomic molecules on metals. In *Catalysis. Physical and Chemistry of Heterogeneous Catalysis* (pp. 288-317). Moscow, Russian Federation: Mir.
9. Breyse, M., Claydel, B., Faure, L., and Guenin, M. (1978). Chemiluminescence induced by catalysis. *Reviews of Chemical Intermediates*, 2, 75-103.
10. Bui, M., and Dowell, N.M. (2020). *Carbon capture and storage*. Cambridge, United Kingdom: Royal Society of Chemistry.
11. Bulychev, N. A. (2019). On the hydrogen production during the discharge in a two-phase vapor-liquid flow. *Bulletin of the Lebedev Physics Institute*, 46(7), 219-221.
12. Chang, H., Park, H. D., Sohn, K. S., and Lee, J.D. (1999). Electronic Structure of Zn<sub>2</sub>SiO<sub>4</sub> and Zn<sub>2</sub>SiO<sub>4</sub>: Mn. *Journal of the Korean Physical Society*, 34, 545–548.
13. Crassous, J. (2020). Circularly polarized luminescence in Helicene and Helicenoid derivatives. In *Circularly Polarized Luminescence of Isolated Small Organic Molecules* (pp. 53-97). Retrived from <https://www.springer.com/gp/book/9789811523083>. doi:10.1007/978-981-15-2309-0
14. Delodovici, F., Manini, N., Wittman, R.S., Choi, D.S., Fahim, M.A., and Burchfield, L.A. (2017). Protomene: A new carbon allotrope. *Carbon*, 126, 574-579. doi:10.1016/j.carbon.2017.10.069
15. Dhbaibi, K., Favereau, L., Srebro, M., Jean, M., Vanthuyne, N., Zinna, F., Jamoussi, B., Di Bari, L., Autschbach, J., and Crassous, J. (2018). Exciton coupling in diketopyrrolopyrrole-helicene derivatives leads to red and near-infrared circularly polarized luminescence. *Chemical Science*, 9, 535-778. doi:10.1039/C7SC04312K
16. Dove, D. B., Takamori, T., Chang, I. F., Thioulouse, P., Mendez, E.E., and Giess, E.A. (1981). Influence of electron trap on the phosphorescence of Zinc silicate mn phosphors. *Journal of Luminescence*, 24, 317–320.
17. Fahlman, B. D. (2018). *Materials chemistry*. Retrived from <https://link.springer.com/book/10.1007/978-94-007-0693-4>
18. Formalev, V. F., Kolesnik, S. A., and Kuznetsova, E. L. (2018). Wave heat transfer in the orthotropic half-space under the action of a nonstationary point source of thermal energy. *High Temperature*, 56(5), 727-731.
19. Formalev, V. F., Kolesnik, S. A., and Kuznetsova, E. L. (2019). Effect of components of the thermal conductivity tensor of heat-protection material on the value of heat fluxes from the gasdynamic boundary layer. *High Temperature*, 57(1), 58-62.
20. Grankin, V. P., Nikolaev, I. A., Styrov, V. V., and Tyurin, Yu. I. (1981).

- Adsorboluminescence of crystals in molecular oxygen beams. *Theoretical and Experimental Chemistry*, 17(6), 757–773.
21. Gupta, T. (2018). *Carbon The Black, the Gray and the Transparent Authors*. Berlin, Germany: Springer International Publishing. doi:10.1007/978-3-319-66405-7
  22. Hasobe, T. (2020). Structural control of fluorescent helicates for improved circularly polarized luminescence properties. In T. Mori (Ed.), *Circularly polarized luminescence of isolated small organic molecules* (pp. 99–116). Singapore, Singapore: Springer Nature. doi:10.1007/978-981-15-2309-0
  23. Hess, H., and Krautz, E. (1981). Photoluminescence and photoconductivity of undoped and doped zinc silicate. *Journal of Luminescence*, 24, 321–324.
  24. Hsu, C.-P., Hejazi, Z., Armagan, E., Zhao, S., Schmid, M., Zhang, H., Guo, H., Weidenbacher, L., Rossi, R.M., Koebel, M.M., Boesel, L.F., and Toncelli, C. (2017). Carbon dots and fluorescein: The ideal FRET pair for the fabrication of a precise and fully reversible ammonia sensor. *Sensors and Actuators B: Chemical*, 253, 714–722. doi:10.1016/j.snb.2017.07.001
  25. Juanjuan, P., Teoh, C. L., Zeng X., Samanta A., Wang, L., Xu, W., Su, D., Yuan, L., Liu, X., and Chang, Y.-T. (2015). Development of a highly selective, sensitive, and fast response upconversion luminescent platform for hydrogen sulfide detection. *Advanced Functional Materials*, 26(2), 191–199. doi:10.1002/adfm.201503715
  26. Kharisov, B. I., and Kharissova, O. V. (2019). General data on carbon allotropes. In *Carbon allotropes: Metal-complex chemistry, properties and applications* (pp. 1–8). Cham, Switzerland: Springer.
  27. Koshoridze, S. I., Levin, Y. K., Rabinskiy, L. N., and Babaytsev, A. V. (2017). Investigation of deposits in channels of panels of a heat-transfer agent. *Russian Metallurgy (Metally)*, 2017(13), 1194–1201.
  28. Kumar, N., and Srivastava, V.C. (2018). Simple synthesis of large graphene oxide sheets via electrochemical method coupled with oxidation process. *ACS Omega*, 3(8), 10233–10242. doi:10.1021/acsomega.8b01283
  29. Kuznetsova, E. L., and Rabinskiy, L. N. (2019). Heat transfer in nonlinear anisotropic growing bodies based on analytical solution. *Asia Life Sciences*, 2, 837–846.
  30. Lemmerer, M. (2020). *Chemoselective nucleophilic  $\alpha$ -amination of amides*. Wiesbaden, Germany: Springer Fachmedien Wiesbaden. doi:10.1007/978-3-658-30020-3
  31. Liu, X., and Qiu, J. (2015). Recent advances in energy transfer in bulk and nanoscale luminescent materials: from spectroscopy to applications. *Chemical Society Reviews*, 44(23), 8714–8746. doi:10.1039/C5CS00067J
  32. Liu, Y., Cerezo, J., Mazzeo, G., Lin, N., Zhao, X., Longhi, G., Abbate, S. and Santoro, F. (2016). Vibronic coupling explains the different shape of electronic circular dichroism and of circularly polarized luminescence spectra of hexahelicenes. *Journal of Chemical Theory and Computation*, 12, 2799–2819.
  33. Lurie, S. A., Solyaev, Y. O., Lizunova, D. V., Rabinskiy, L. N., Bouznik, V. M., and Menshykov, O. (2017). Influence of mean distance between fibers on the effective gas thermal conductivity in highly porous fibrous materials. *International Journal of Heat and Mass Transfer*, 109, 511–519.
  34. Ni, F., Zhu, Z., Tong, X., Xie, M., Zhao, Q., Zhong, C., Zou, Y., and Yang, C. (2018). Organic emitter integrating aggregation-induced delayed fluorescence and room-temperature phosphorescence characteristics, and its application in time-resolved luminescence imaging. *Chemical Science*, 9, 6150–6155. doi:10.1039/C8SC01485J 1970.
  35. Palumbo, D. T., and Brown, J. J. (1970). Electronic States of Mn<sup>2+</sup>-Activated Phosphors. *Journal of the Electrochemical Society*, 117, 1184–118.
  36. Persson, B. N., and Avouris, Ph. (1983). On the nature and decay electronically exited states at metal surfaces. *Journal of Chemical Physics*, 79(10), 5156–5162.
  37. Pham, T. N., Ono, S., and Ohno, K. (2016). Ab initio molecular dynamics simulation study of successive hydrogenation reactions of carbon monoxide producing methanol. *Journal of Chemical Physics*, 144, article number 144309. doi:10.1063/1.4945628

38. Pravilov, A. M., and Smirnova, L. G. (1981). Chemiluminescence processes in the  $O(3P) + CO + M$  system. Isolation of the heterogeneous component of reactions involving impurities. *Kinetic and Catalysis*, 22(3), 559-563.
39. Radyuk, A. G., Gorbatyuk, S. M., Tarasov, Y. S., Titlyanov, A. E., and Aleksakhin, A. V. (2019). Improvements to mixing of natural gas and hot-air blast in the air tuyeres of blast furnaces with thermal insulation of the blast duct. *Metallurgist*, 63(5-6), 433-440.
40. Rivera-Enríquez, C. E., Fernandez-Osorio, A., and Chavez-Fernandez, J. (1981). Luminescence properties of a- and b-  $Zn_2SiO_4:Mn$  nanoparticles prepared by a co precipitation method. *Journal of Alloys and Compounds*, 688, 775—782.
41. Rosen, B. (Ed). (1970). *Spectroscopic data relative to diatomic molecules*. Oxford, United Kingdom: Pergamon Press.
42. Rufov, Yu. N., Kadushin, A. A., and Roginsky S. Z. (1966). The emergence of luminescence during the adsorption of vapors and gases on solids. *Doklady AN SSSR*, 171(4), 905-906.
43. Sánchez-Carnerero, E. M., Agarrabeitia, A. R., Moreno, F., Maroto, B. L., Muller, G., Ortiz, M. J., and de la Moya, S. (2015). Circularly polarized luminescence from simple organic molecules. *Chemistry Europe*, 21(39), 13488-13500. doi:10.1002/chem.201501178
44. Sarrigani, G. V., and Amiri, I. S. (2019). Willemite-based glass ceramic doped by different percentage of erbium oxide and sintered in temperature of 500-1100C. In *Physical and optical properties* (pp.65-66). Cham, Switzerland: Springer. doi:10.1007/978-3-030-10644-7
45. Shang, R. (2017). *New carbon-carbon coupling reactions based on decarboxylation and iron-catalyzed C-H activation*. Singapore, Singapore: Springer. doi:10.1007/978-981-10-3193-9
46. Shigalugov, S. H., Tyurin, Y. I., Borovitskaya, A. O., and Dubrov D. V. (2019). Experimental installation phosphors luminescence excitation, stimulation and extinguishing by atomic and molecular beams. *Periodico Tchê Química*, 16 (31), 809-815.
47. Shigalugov, S. Kh., Tyurin, Yu. I., Styrov, V. V., and Tolmacheva, N. D. (2000). Heterogeneous chemiluminescence of crystallophosphorus catalysts in a  $CO + O$  mixture. *Kinetics and Catalysis*, 41(4), 566-592.
48. Skvortsov, A. A., Kalenkov, S. G., and Koryachko, M. V. (2014). Phase transformations in metallization systems under conditions of nonstationary thermal action. *Technical Physics Letters*, 40(9), 787-790.
49. Stevels, A. L. N., and Vink, A. T. (1974). Fine Structure in the low temperature luminescence of  $Zn_2SiO_4:Mn$  and  $Mg_4Ta_2O_9:Mn$ . *Journal of Luminescence*, 8, 443-451.
50. Styrov, V. V., Tyurin, Yu. I., and Shigalugov, S. X. (1989). Luminescence of crystalline phosphors in atomic oxygen, P. Excitation mechanisms. *Kinetics and Catalysis*, 30(2), 389—395.
51. Tadashi, M. (2020). Frontiers of circularly polarized luminescence chemistry of isolated small organic molecules. In M. Tadashi (Ed.), *Circularly polarized luminescence of isolated small organic molecules* (pp. 1-10). Singapore, Singapore: Springer.
52. Tanaka, H., Inoue, Y. and Mori, T. (2018). Circularly polarized luminescence and circular dichroism in small organic molecules: correlation between excitation and emission dissymmetry factors. *ChemPhotoChem*, 2, 386-402.
53. Tsuchiya, Y., Ikesue, K., Nakanotani, H., and Adachi, C. (2019). Photostable and highly emissive glassy organic dots exhibiting thermally activated delayed fluorescence. *Chemical Communications*, 55, 5215-5218. doi:10.1039/C9CC01420A
54. Volkenstein, F. F., Gorban, A. N., and Sokolov, V. A. (1976). *Radical recombination luminescence of semiconductors*. Moscow, Russian Federation: Nauka.
55. Zhou, J., Liu, Q., Feng, W., Sun, Y., and Li, F. (2015). Upconversion luminescent materials: Advances and applications. *Chemical Reviews*, 115(1), 395-465.
56. Zhu, S., Fischer, T., Wan, W., Descalzo, A. B., and Rurack, K. (2011). Luminescence amplification strategies integrated with microparticle and nanoparticle platforms. In

L. Prodi, M. Montalti, and N. Zaccheroni (Eds.), *Luminescence applied in sensor science* (pp. 51-91). Berlin, Germany: Springer.

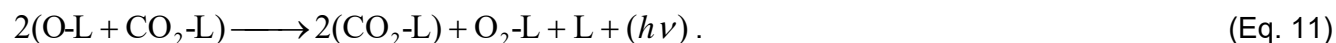
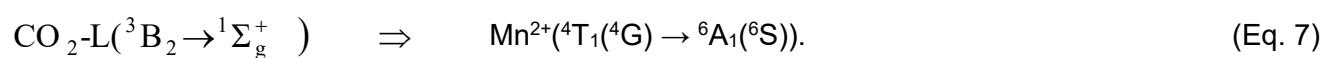
$$\text{CO} + 1/2\text{O}_2 \rightarrow \text{CO}_2 \quad (\text{Eq. 1})$$

$$\text{CO} + \text{O-L} \rightarrow \text{CO}_2\text{-L} + (h\nu). \quad (\text{Eq. 2})$$

$$I(t) = \frac{35}{t}(1 - e^{-1.2t}), \quad (\text{Eq. 3})$$

$$I(t) = \frac{123}{t}(e^{-0.02t} - e^{-0.473t}) \quad (\text{Eq. 4})$$

$$I(t) = 3 \cdot 10^3 / (1 + 1.1t)^2 \quad (\text{Eq. 5})$$



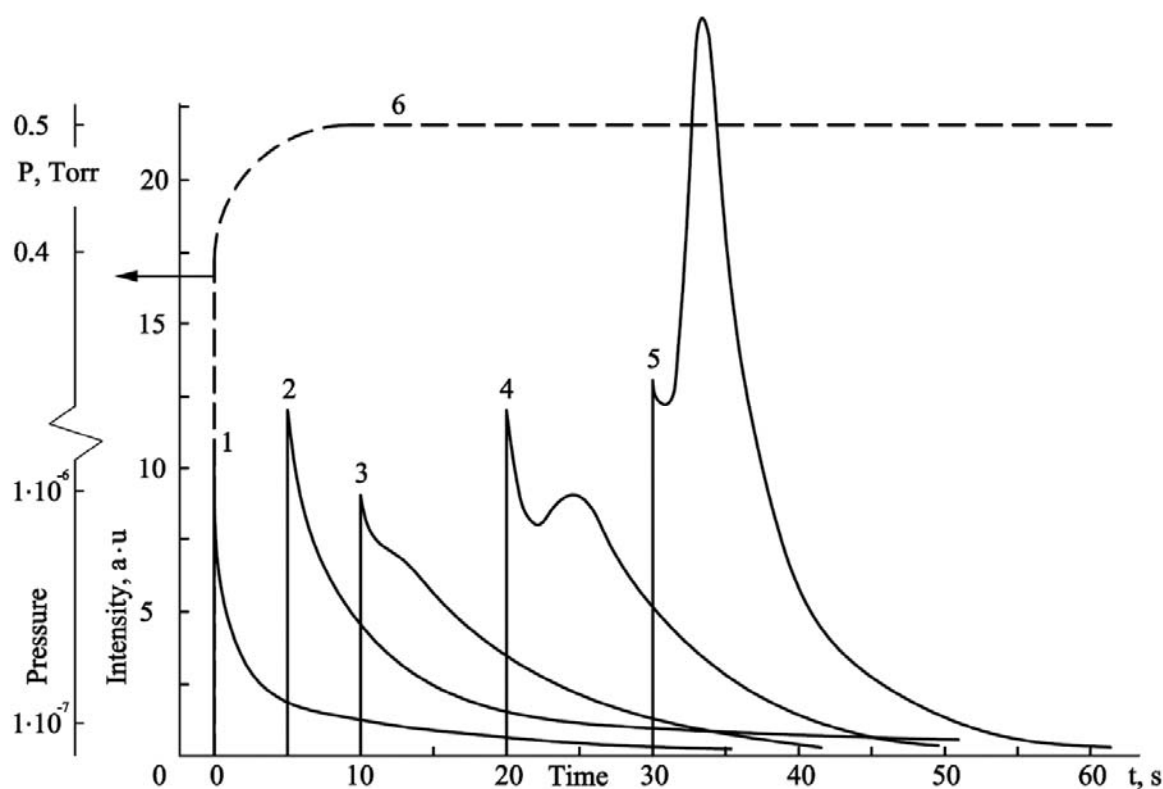


**Figure 1.** Luminescence flashes of  $\alpha$ -willemite ( $\lambda_{\max} = 527 \text{ nm}$ ) upon admission of a flow of CO molecules ( $j_{\text{CO}} = 1.9 \cdot 10^{20} \text{ cm}^{-2} \cdot \text{s}^{-1}$ ) onto the surface of  $\text{Zn}_2\text{SiO}_4\text{:Mn}^{2+}$  with pre-adsorbed O-L atoms. Sample temperature 300 K (1), 370 K (2), 400 K (3), 550 K (4) ad 625 K (5). O atoms obtained thermolytically (by dissociation of  $\text{O}_2$  on an Rh tape) were preliminarily adsorbed by  $\alpha$ -willemite for 15 minutes at  $p_{\text{O}+\text{O}_2} = 0.02 \text{ Torr}$  and  $T = 295 \text{ K}$ ; 6 – kinetics of establishing the pressure of CO in the chamber. Source: the author

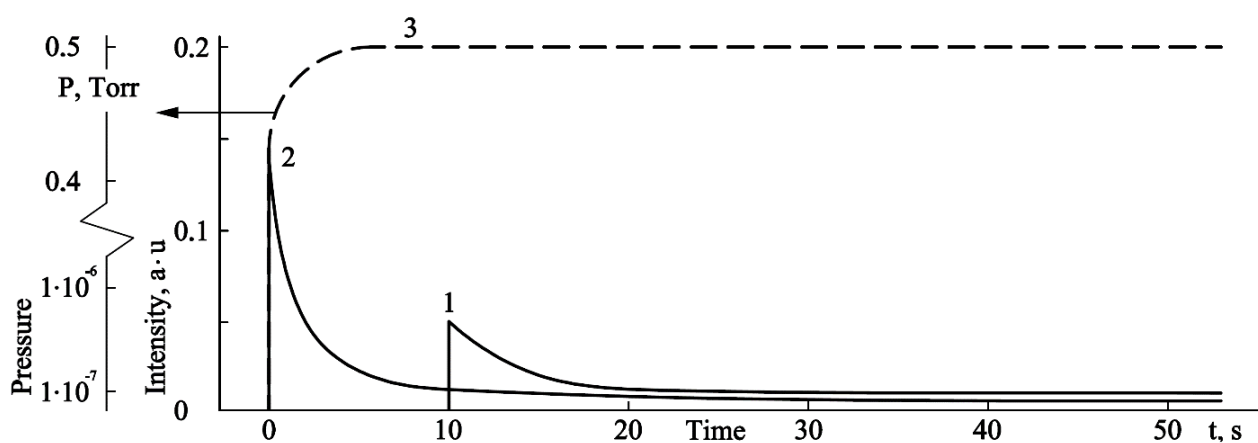


**Figure 2.** Luminescence flashes of  $\alpha$ -willemite ( $\lambda_{\max} = 527 \text{ nm}$ ) upon the inlet of a flow of CO molecules ( $j_{\text{CO}} = 1.9 \cdot 10^{20} \text{ cm}^{-2} \cdot \text{s}^{-1}$ ) onto the surface of  $\text{Zn}_2\text{SiO}_4\text{:Mn}^{2+}$  pre-filled with  $\text{O}_2\text{-L}$  molecules (pre-adsorption of  $\text{O}_2$  15 minutes at  $p_{\text{O}_2} = 0.02 \text{ Torr}$  and  $T = 295 \text{ K}$ ). Sample temperature 400 K (1) and 550 K (2); 3- kinetics of establishing the pressure of CO in the chamber. Source: the author

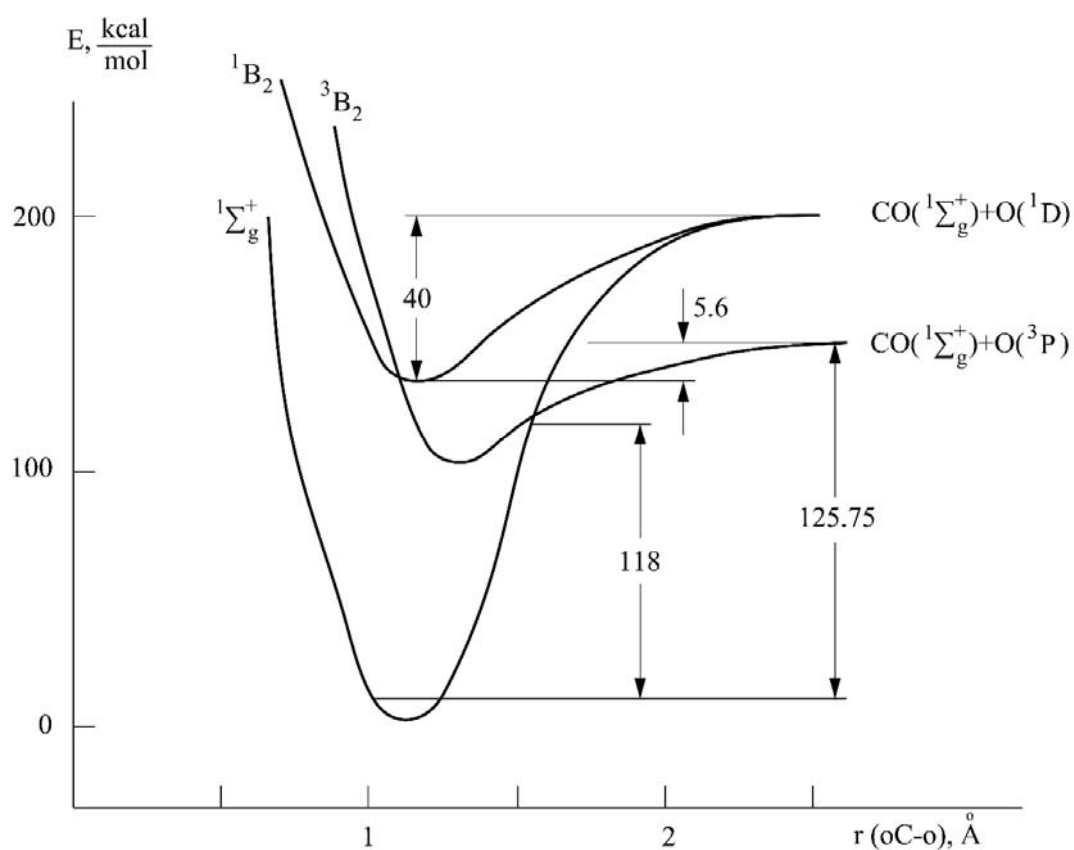


**Figure 3.** The dependence of the binding energy (OC-O) on the configuration coordinate  $r$ . Source: according to Pravilov and Smirnova (1981)

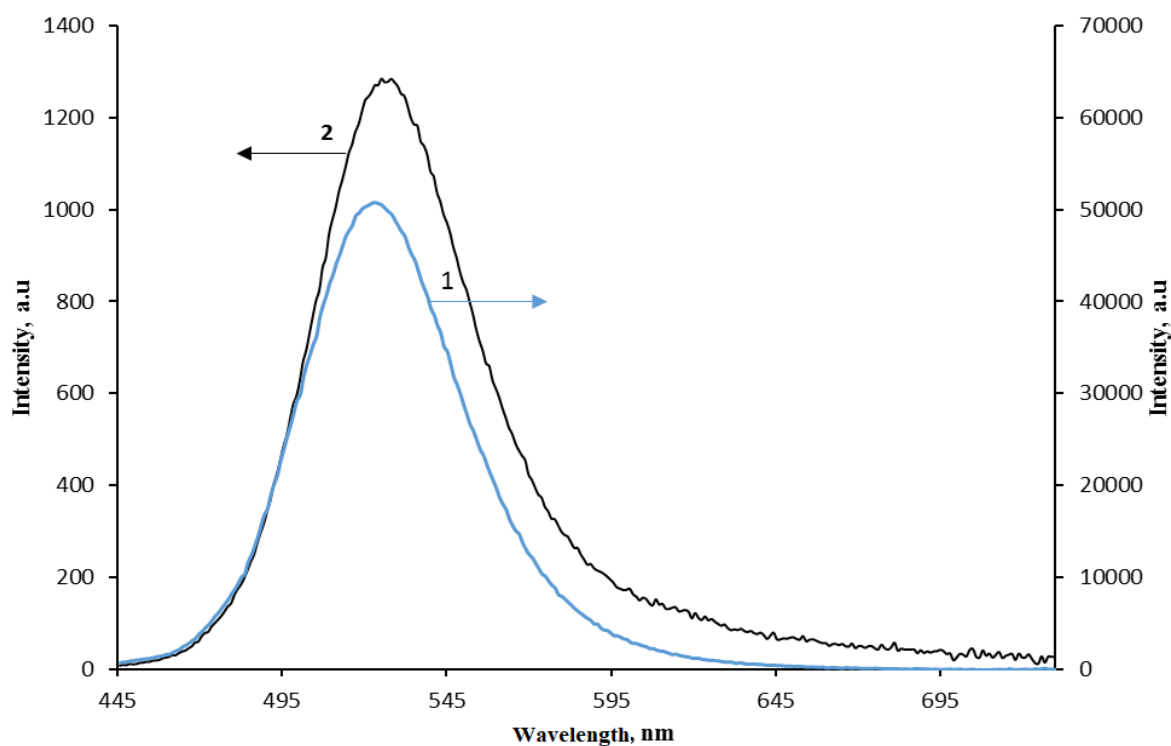


**Figure 4.** The spectrum of photoluminescence (1) and chemiluminescence (2) of  $\alpha$ -willemite  $\text{Zn}_{1.98}\text{Mn}_{0.02}\text{SiO}_4$  at  $T = 625$  K. Source: the author

**PROPRIEDADES FÍSICO-MECÂNICAS E TERMOFÍSICAS DE COMPOSITOS POLÍMEROS À BASE DE POLIPROPILENO SECUNDÁRIO PREENCHIDOS DE CASCA DE ARROZ****PHYSICAL AND MECHANICAL AND THERMOPHYSICAL PROPERTIES OF POLYMER COMPOSITES BASED ON RECYCLED POLYPROPYLENE FILLED WITH RICE HUSK****ФИЗИКО-МЕХАНИЧЕСКИЕ И ТЕПЛОФИЗИЧЕСКИЕ СВОЙСТВА ПОЛИМЕРНЫХ КОМПОЗИТОВ НА ОСНОВЕ ВТОРИЧНОГО ПОЛИПРОПИЛЕНА, НАПОЛНЕННОГО РИСОВОЙ ШЕЛУХОЙ**

SADRITDINOV, Aynur R.<sup>1\*</sup>; KHUSNULLIN, Aygiz G.<sup>2</sup>; PSYANCHIN, Artur A.<sup>3</sup>; ZAKHAROVA, Elena M.<sup>4</sup>; ZAKHAROV, Vadim P.<sup>5</sup>;

<sup>1,2,3,5</sup> Bashkir State University, Department of Macromolecular Compounds and General Chemical Technology, 32 Zaki Validi Str., zip code 450076, Ufa – Russian Federation.

<sup>4</sup>Ufa Federal Research Centre of the Russian Academy of Sciences, Department of Macromolecular Compounds, 71 Oktyabrya Ave., zip code 450054, Ufa – Russian Federation.

\* Correspondence author  
e-mail: aynur.sadritdinov@mail.ru

Received 02 May 2020; received in revised form 06 June 2020; accepted 18 June 2020

**RESUMO**

A relevância do estudo se deve à deterioração da situação ambiental no mundo associada ao aumento da quantidade de resíduos plásticos, o que determina a viabilidade de desenvolvimento dos métodos para os envolver na reciclagem e produção futura de produtos plásticos. Este artigo tem como objetivo estudar os padrões de alterações nas propriedades físico-mecânicas e termofísicas de compósitos poliméricos à base de polipropileno secundário preenchido com casca de arroz na ausência de compatibilizadores. A principal abordagem para o estudo deste problema é a determinação do módulo de elasticidade na ruptura e flexão, resistência à tração na ruptura, deformação na ruptura e flexão, temperatura de flexão sob carga e temperatura de amolecimento Vicat, resistência de impacto de Charpy e Izod, parâmetros termofísicos dos compósitos poliméricos, o que possibilita considerar de forma abrangente as propriedades de compósitos biodegradáveis à base de polipropileno secundário na presença de casca de arroz. O artigo mostra que, com o aumento no teor de casca de arroz no compósito polimérico à base de polipropileno secundário, ocorre o aumento no módulo de elasticidade durante a ruptura e flexão. O enchimento de polipropileno com casca de arroz reduz um pouco a resistência à tração e reduz significativamente a elasticidade do polímero. O polipropileno secundário possui uma resistência ao impacto de Charpy superior à viscosidade de Izod. O enchimento do polímero com casca de arroz leva a diminuição da resistência ao impacto, de acordo com Charpy e com Izod. Além disso, com o conteúdo de carga superior a 5 partes de massa esses dois indicadores são quase idênticos. Nesse caso, há um ligeiro aumento na temperatura do início da decomposição térmica dos compósitos, o que determina sua estabilidade térmica durante o processamento. Foi revelado que compósitos poliméricos contendo 2-10 partes de massa de casca de arroz são caracterizados por um grau aumentado de cristalinidade da fase polimérica. Os materiais do artigo são de valor prático para o processamento de polímeros termoplásticos secundários, bem como para a criação de compósitos poliméricos biodegradáveis.

**Palavras-chave:** *força, elasticidade, resistência ao calor, termogravimetria, calorimetria diferencial de varredura.*

**ABSTRACT**

The relevance of the study is due to the deterioration of the environmental situation in the world associated with an increase of plastic waste, which determines the feasibility of developing methods for their involvement in recycling for the production of plastic products. Thereby, this article is aimed at studying the patterns of changes in the physical and mechanical and thermophysical properties of polymer composites based on recycled polypropylene filled with rice husk in the absence of compatibilizers. The leading approach to



the study of this problem is the determination of the modulus of elasticity in flexure, tensile strength at break, strain-to-failure, and bending strain, bending temperature under load and Vicat softening temperature, Charpy V-notch impact energy and Izod impact strength, as well as the thermophysical parameters of polymer composites. The article shows that with an increase in the content of rice husk in a polymer composite based on recycled polypropylene, an increase in the modulus of elasticity in flexure occurs. Filling polypropylene with rice husk slightly reduces the tensile strength and significantly reduces the elasticity of the polymer. Recycled polypropylene has a higher Charpy V-notch impact energy than Izod impact strength. Filling the polymer with rice husk leads to a decrease in impact strength according to both Charpy and Izod, and with a compound content of more than 5 phr, both of these indicators are almost identical. In this case, there is a slight increase in the onset temperature of the composites, which determines their thermal stability during processing. It was revealed that polymer composites containing 2-10 mass parts of rice husk are characterized by an increased degree of crystallinity of the polymer phase. The materials of the article are of practical value for the processing of recycled thermoplastic polymers, as well as the creation of biodegradable polymer composites.

**Keywords:** *failure resistance, elasticity, heat-distortion temperature, thermogravimetric analysis, differential scanning calorimetry.*

## АННОТАЦИЯ

Актуальность исследования обусловлена ухудшением экологической ситуации в мире, связанной с ростом количества пластиковых отходов, что определяет целесообразность разработки способов их вовлечения в повторную переработку с целью производства пластмассовых изделий. В этой связи большие перспективы связаны с разработкой биоразлагаемых композитов, одним из направлений, создания которых является наполнение синтетических полимеров компонентами растительного происхождения. В связи с этим, данная статья направлена на изучение закономерностей изменения физико-механических и теплофизических свойств полимерных композитов на основе вторичного полипропилена, наполненного рисовой шелухой в отсутствии совместителей. Ведущим подходом к исследованию данной проблемы является определение модуля упругости при разрыве и изгибе, прочности при разрыве, деформации при разрыве и изгибе, температуры изгиба под нагрузкой и температуры размягчения по Вика, ударной вязкости по Шарпи и Изоду, теплофизических параметров полимерных композитов (температура начала разложения, тепловые эффекты плавления и кристаллизации), что позволяет комплексно рассмотреть свойства биоразлагаемых композитов на основе вторичного полипропилена в присутствии рисовой шелухи. В статье показано, что с увеличением содержания рисовой шелухи в полимерном композите на основе вторичного полипропилена происходит увеличение модуля упругости при разрыве и изгибе. Наполнение полипропилена рисовой шелухой незначительно снижает прочность при разрыве и существенно уменьшает эластичность полимера. Вторичный полипропилен имеет более высокое значение ударной вязкости по Шарпи по сравнению с вязкостью по Изоду. Наполнение полимера рисовой шелухой приводит к снижению ударной вязкости как по Шарпи, так и по Изоду, причем при содержании наполнителя более 5 м.ч. оба этих показатели практически совпадают. Наполненные рисовой шелухой полимерные композиты обладают большей теплостойкостью. При этом наблюдается небольшое повышение температуры начала термического разложения композитов, что определяет их термическую устойчивость в процессе переработки. Выявлено, что полимерные композиты, содержащие 2-10 массовые части рисовой шелухи, характеризуются повышенной степенью кристалличности полимерной фазы. Материалы статьи представляют практическую ценность для переработки вторичных термопластичных полимеров, а также создания биоразлагаемых полимерных композитов.

**Ключевые слова:** *прочность, эластичность, теплостойкость, термогравиметрия, дифференциальная сканирующая калориметрия.*

## 1. INTRODUCTION

Currently, there is not a single application area where materials based on synthetic polymers are not used. Along with their obvious advantage over other materials related to the possibility of obtaining products with a wide range of operational properties, some practically decompose under the influence of environmental factors when released into nature. With the

increase in the production and consumption of synthetic polymers, the urgency of the problem of extracting these materials from waste and developing methods for their recycling increases. One of the most effective ways to solve this problem is to create polymer composites, the polymer matrix of which is recycled thermoplastic polymers in the presence of fillers, giving the material the required performance properties.

To date, a significant number of studies are devoted to the development of polymer composites based on thermoplastic polymers in the presence of vegetable compounds, which makes the material biodegradable (Yonghui *et al.*, 2015; Väisänen *et al.*, 2017; Yang, 2017; Erdogan and Huner, 2018; Orlov *et al.*, 2003; Krechetov *et al.*, 2018; Dipen *et al.*, 2019; Formalev *et al.*, 2018; Tarrés *et al.*, 2019). The use of a thermoplastic polymer makes it possible to repeatedly process such material by traditional methods (extrusion, injection molding), and a vegetable compound provides a reduction in the cost and weight of finished products, imparting the required performance characteristics and environmental friendliness of plastic products (Kasakova *et al.*, 2018; Usenbekov *et al.*, 2014).

One of the promising vegetable compounds for creating polymer composites based on thermoplastic polymers is rice husk (Arjmandi *et al.*, 2015; Chen *et al.*, 2016; Kenechi *et al.*, 2016; Arjmandi *et al.*, 2017; Dasa *et al.*, 2019). Prospects for the use of rice husk to obtain polymer composites are due to its low water absorption (Chen *et al.*, 2016; Lomakin *et al.*, 2018) and increased thermal stability (Hidalgo-Salazar and Salinas, 2019) due to the high content of silicon oxide in the compound (Cardona-Urbe *et al.*, 2018). Due to the thermodynamic incompatibility of rice husks and polymer matrices, various compatibilizers are traditionally used to create polymer composites with the required physical and mechanical properties (Arjmandi *et al.*, 2015; Majeed *et al.*, 2017; Formalev *et al.*, 2016; Lomakin *et al.*, 2017; Raghu *et al.*, 2018; Orji and McDonald, 2020), which increases the cost of finished plastic products. The purpose of this work was to study the patterns of change in the physical and mechanical and thermophysical properties of polymer composites based on recycled polypropylene filled with rice husk in the absence of compatibilizers.

## 2. MATERIALS AND METHODS

Recycled polypropylene was used in the work as a polymeric matrix in the form of crushed material from substandard plastic products produced by injection molding. Rice husk was used to fill the recycled polypropylene (composition: cellulose 40-45%, lignin 20-25%, hemicellulose 15-17%, mineral substances 18-22%) with a particle diameter of not more than 0.4 mm. The ratio of parts by mass (phr) of the compound was calculated on 100 mass parts of the polymer (Binoj *et al.*, 2016; Danilova-Tretiak

*et al.*, 2017). The test samples were obtained by injection molding on a Babyplast 6/10P injection-molding machine at a temperature in the zones of 225 °C, 235 °C, 220 °C, an injection pressure of 65 bar, an injection speed of 30%, and a clamping force of 35 bar. The temperature of the supply of cooling water to the mold was 12 °C, and the dwelling time was 10 s.

The physical and mechanical properties of the test samples at the break and cross breaking were determined according to GOST 11262-2017 and GOST 4648-2014, respectively, on a Shimadzu AGS-X universal testing machine at a temperature of 23 °C, a moving, gripping speed of 1 mm/min when determining the module of elasticity and 5 mm/min when determining other characteristics (GOST 11262-2017; GOST 4648-2014). Uniaxial tensile mechanical tests were performed on prototypes with dimensions according to GOST 11262-2017 (type 5). The tests were carried out on a universal testing machine AGS-X10kN (Shimadzu, Japan) at a temperature of 23±2 °C and a moving capture speed of 1 mm/min to determine the modulus of elasticity (GOST 9550-81) and a speed of 5 mm/min to determine other characteristics. Mechanical tests for static bending were performed on samples with sizes recommended according to GOST 4648-2014. The tests were carried out on a universal testing machine AGS-X10kN (Shimadzu, Japan) at a temperature of 23±2 °C and a traverse speed of 1 mm/min to determine the modulus of elasticity (GOST 9550-81) and a speed of 5 mm/min to determine other characteristics. Charpy V-notch impact energy and Izod impact strength (notched and unnotched) were determined according to GOST 4647-2015 and GOST 19019-2017, respectively, on a GT-7045-HMH pendulum (GOST 4647-2015; GOST 19019-2017). The Charpy impact toughness (with notch and without notch) was determined according to GOST 4647-2015 on the pendulum testing machine GT-7045-HMH (Taiwan, Gotech Testing Machines). The summary of test method in which a sample lying on two supports is subjected to a pendulum impact at a constant speed (when struck "flat" or "with edge"), the impact line being located in the middle between the supports and directly opposite the notch of the notched prototypes. The impact is applied to the surface of the prototype opposite the notch.

The Izod impact toughness of prototypes (with and without notches) was determined according to GOST 19109-2017 on the GT-7045-HMH pendulum testing machine (Taiwan,

Gotech Testing Machines). The summary of test method consists in destruction of the cantilevered sample by the impact of the pendulum at a certain distance from the fixing point, in the case of a notched sample, from the midline of the notch. The bending temperature under load (1.8 MPa) and the Vicat softening temperature (50 N) were determined according to GOST 32657-2014 and GOST 15088-2014, respectively, on an HV-3000-P3 device. Bending temperature under load. The prototype is subjected to three-point bending under the action of a constant load from the side of the main (preferably) or lateral plane of the prototype to obtain bending stress. The temperature is raised at a uniform speed and its value is measured at which a standard deflection occurs, corresponding to the established increase in stress during bending.

The softening temperature of thermoplastics according to Vicat. The summary of the method is to determine the temperature at which a standard indenter with a flat bottom surface under the influence of load penetrates into the test prototype, heated at a constant speed, to a depth of 1 mm. Indenter is located perpendicularly to the surface of the prototype (GOST 32657-2014; GOST 15088-2014).

The methods of thermogravimetric analysis (TGA) and differential scanning calorimetry were used (DSC) in order to analyze the thermophysical parameters of polymer composites. Studies of polymer samples were carried out under the following conditions: TGA – temperature range 25-600 °C, dynamic mode – the heating rate of 5 deg/min, medium – air, TGA-DSC device; DSC – temperature range – 40-200 °C, dynamic mode – heating/cooling rate of 10 deg/min, medium – air, DSC-1 device. These methods allow to determine the following thermophysical indicators:  $T_c$  is the onset temperature;  $T_1$ ,  $T_5$  is the temperature corresponding to a decrease in the mass of the sample by 1 and 5%, respectively;  $T_{max}$  is the temperature corresponding to the maximum rate of mass loss at TGA;  $T_{ml}$ ,  $T_{cr}$  is the melting and crystallization temperature;  $\Delta H_{ml}$ ,  $\Delta H_{cr}$  is the thermal effect of melting and crystallization.

### 3. RESULTS AND DISCUSSION:

The results showed that the modulus of elasticity both at the break and cross breaking increases as the content of the vegetable compound in the polymer composite increases (Table 1). The modulus of elasticity at the break

for a recycled polypropylene filled with rice husk in a volume of 30 phr increases by 1.36 times, and the modulus of elasticity in flexure – by 1.47 times in comparison with the initial polymer. In light of the fact that the modulus of elasticity correlates with the ability of a polymer sample to deform elastically under the influence of an external load, the filling of polypropylene with rice husks determines the possibility of obtaining more rigid plastic products (Das *et al.*, 2018; Rutkowska *et al.*, 2018).

It should be noted that plastic products made from polymer composites in the presence of a vegetable compound are more resistant to elastic deflections. This is confirmed by minor changes in the breaking elongation for polymers with varying degrees of filling of rice husk (Table 1). Filling recycled polypropylene with even a small amount of rice husk leads to a significant decrease in the tensile elasticity of the material. Addition 2 phr of rice husk reduces the strain at break from 588% for recycled polypropylene without compound to 26% for the composite (Table 1).

A further increase in the content of rice husk successively reduces the breaking elongation to 5% for a composite with 30 phr of the compound (Saigal and Pochanard, 2019; Stolin *et al.*, 2020). Compared to recycled polypropylene, a polymer composite has a lower tensile strength at break. With an increase in the content of rice husk up to 15 phr, the strength decreases almost linearly from 25.5 MPa to 21.3 MPa, and a further two-fold increase in the compound concentration determines a decrease in tensile strength by only 2.3% (Table 1).

Along with a decrease in the cross-breaking strength for filled composites, the resistance of plastics to dynamic impact worsens, which manifests itself in a corresponding change in impact value (Figure 1). Recycled polypropylene has a relatively high Charpy V-notch impact energy (rib impact) of 40.7 kJ/m<sup>2</sup>. The Izod impact strength for this polymer is 26.1 kJ/m<sup>2</sup>. Filling the polymer with rice husk leads to a decrease in impact strength according to both Charpy and Izod, and with a compound content of more than 5 phr, both of these indicators are almost identical (Bisht and Gope, 2015; Sutar *et al.*, 2018). Applying a notch simulating the presence of a mechanical defect in a plastic product significantly reduces the impact strength, according to both Charpy and Izod (Figure 1). For notched specimens, Izod impact strength is higher than Charpy V-notch impact energy for all considered polymer

composites. Compared with recycled polypropylene, an increase in impact value is observed with the addition of 2 phr of rice husks, which can be used to obtain plastic products more resistant to external dynamic effects (Figure 1).

The use of rice husks can increase the heat-distortion temperature of plastic products based on recycled polypropylene (Figure 2). Introduction to the polymer 2 phr of compound leads to a slight decrease in bending temperature under load, the value of which with a further increase in the degree of filling of the composite increases from 57.4 °C for recycled polypropylene to 65.5 °C for a polymeric composition filled with 30 phr of rice husk. The Vicat softening temperature, in this case, rises from 75 °C for polypropylene to 84.6 °C for a composite with 30 phr of rice husk (Figure 2).

Rice husk used as a compound has a low value for the onset temperature  $T_H$ ; a decrease in the mass of the product begins even at temperatures above 26 °C. A noticeable (by ~ 4%) decrease in the mass of the sample upon heating to 100 °C indicates the presence in the rice husk of a sufficiently large number of volatile components (probably moisture or solvent).

A further increase in temperature is accompanied by a gradual decrease in the mass of the product. The decomposition of rice husk on the differential thermal analysis (DTA) curve corresponds to two main temperature ranges (Table 2). At the stage of the temperature range of 170-358 °C with a maximum  $T_{max,1}$  at 288°C, a 55% decrease in product mass is observed. At the stage of the temperature range of 358-470 °C with a maximum  $T_{max,2}$ =403°C, there is a decrease in the mass of the product by 23%, which, apparently, corresponds to the burnup of the resulting coke residue (Table 2).

It should be noted that the temperatures ( $T_{max,1}$  and  $T_{max,2}$ ) on the DTA curve, corresponding to the maximum decomposition rate of rice husk, are shifted to the lower values relative to similar parameters for recycled polypropylene (Table 2). The value of the residue (27.9%) after heating the rice husk to a temperature of 400 °C is noticeably larger compared to the same parameter for recycled polypropylene (Gowda *et al.*, 2018; Mohapatra, 2018). This indicates that the decomposition of rice husk, the main component of which is cellulose, in this temperature range occurs to a lesser extent (with a lower rate), compared with polypropylene. A relatively large amount of

residue (17.2%) after heating the rice husk to 600 °C indicates the presence of thermally stable silicon oxide in the product (Cardona-Urbe *et al.*, 2018; Dorca *et al.*, 2019). Composites based on recycled polypropylene filled with various amounts of rice husk have rather close values of the onset temperature  $T_c$  218-231°C (Table 2). It is noteworthy that the indicated  $T_c$  values are higher than that of rice husks and recycled polypropylene (Table 2).

An increase in the content of the vegetable compound from 2 to 30 phr does not lead to a significant change in the parameter  $T_c$  of the polymer composite, the values of parameters  $T_1$  (242-252 °C) and  $T_5$  (262-267 °C) are also in a rather narrow range (Table 2). It is seen that thermal-oxidative breakdown of polymer composites proceeds in two stages: the main decomposition (by 85-94%) occurs in the temperature range from  $T_c$  to 380-400°C; the temperature range of 400-600 °C corresponds to a decrease in the mass of the sample by ~ 3-7% (Table 2). With an increase in the content of vegetable compound in the polymer composite from 5 to 30%, the maximum temperature on the DTA curve shifts to a lower range:  $T_{max,1}$  from 356 to 327 °C and  $T_{max,2}$  from 421 to 417 °C. The observed changes are due to the influence of rice husk, whose decomposition corresponds to lower temperatures, compared with the decomposition of polypropylene (Gadzama *et al.*, 2020; Ghosh and Dwivedi, 2020). With an increase in the filler content in the compound from 2 to 30 phr the proportion of the product remaining after heating the sample to 400 °C (from 6.5 to 11.4%) and 600 °C (3.2% to 5.9%) increases, and the dependence of the residue on the compound content is linear (Nyior and Mgbeahuru, 2018; Pandey, 2020).

When conducting DSC analysis, it was found that filling the recycled polypropylene with rice husk in the range of 2-30 phr does not lead to a noticeable change in the melting ( $T_{mi}$ =166.2-166.7°C) and crystallization ( $T_{cr}$ =116.2-117.8°C) temperatures of composites whose values are close to the corresponding indicators of recycled polypropylene (Table 3). At the same time, the compound has a significant effect on the enthalpy (thermal effect) of the melting and crystallization of the polymer phase. The introduction of already a small amount (2 phr) of rice husk into the polymer leads to a noticeable (12 J/g) increase in the melting enthalpy of the composite compared to an unfilled polymer, and the crystallization enthalpy also increases, but to a lesser extent (Table 3). It should be noted that

$\Delta H_{ml}$  and  $\Delta H_{cr}$  of composites containing 2-10 phr of rice husk is higher than that of the initial polypropylene. It can be assumed that the compound particles can play the role of crystallization nuclei, which contributes to an increase in the degree of crystallinity of the polymer phase and an increase in the heat of fusion and crystallization. With a further increase in the compound content in the polymer composite, the values of the enthalpy of melting and crystallization naturally decrease. When changing the content of rice husks in the composite from 2 to 30 phr the values of  $\Delta H_{ml}$  and  $\Delta H_{cr}$  decrease, respectively, by 1.47 and 1.36 times (Table 3), which, obviously, is associated with a decrease in the amount of the polymer phase in the composite.

#### 4. CONCLUSIONS:

With an increase in the content of rice husk in a polymer composite based on recycled polypropylene, an increase in the modulus of elasticity in flexure occurs, and plastic products made from polymer composites with the compound are more resistant to flexural deflections. Filling polypropylene with rice husk slightly reduces the tensile strength at break and significantly reduces the elasticity of the polymer. Recycled polypropylene has a higher Charpy V-notch impact energy than Izod impact strength. Filling the polymer with rice husk leads to a decrease in impact strength according to both Charpy and Izod, and with a compound content of more than 5 phr, both of these indicators are almost identical. Applying a notch simulating the presence of a mechanical defect in a plastic product significantly reduces the impact strength, according to both Charpy and Izod.

For notched specimens, Izod impact strength is higher than Charpy V-notch impact energy for all considered polymer composites. Polymer composites filled with rice husks have a greater heat-distortion temperature, characterized by bending temperature under load and Vicat softening temperature. In this case, there is a slight increase in the onset temperature of the composites, which determines their thermal stability during processing. It was revealed that polymer composites containing 2-10 phr of rice husks are characterized by an increased degree of crystallinity of the polymer phase.

Compared with pure polypropylene, rice husk based composites have a higher modulus of elasticity at break and bending. Polymer

composites are more resistant to high temperature, which is manifested in high values of bending temperature under load, Vicat softening and the beginning of decomposition. Filling polypropylene with rice husk leads to a decrease in strength and breaking elongation, decrease of Charpy and Izod impact toughness.

#### 5. ACKNOWLEDGMENTS:

The reported study was funded by RFBR, project number 19-33-90087.

#### 6. REFERENCES:

1. Arjmandi, R., Hassan, A., and Zakaria, Z. (2017). Rice husk and kenaf fiber reinforced polypropylene biocomposites. In M. Jawaid, M. T. Paridah, and N. Saba (Eds.), *Lignocellulosic fibre and biomass-based composite materials* (pp. 77-94). Sawston, United Kingdom: Woodhead Publishing Series in Composites Science and Engineering. doi:10.1016/B978-0-08-100959-8.00005-6.
2. Arjmandi, R., Hassan, A., Majeed, K., and Zakaria, Z. (2015). Rice husk filled polymer composites. *International Journal of Polymer Science*, 2015, 1-32. doi:10.1155/2015/501471.
3. Binoj, J. S., Edwin Raj, R., Daniel, B. S. S. and Saravanakumar, S. S. (2016). Optimization of short Indian Areca fruit husk fiber (*Areca catechu* L.) reinforced polymer composites for maximizing the mechanical property. *International Journal of Polymer Analysis and Characterization*, 21(2), 112-122. doi:10.1080/1023666X.2016.1110765.
4. Bisht, N., and Gope, P. Ch. (2015). Mechanical properties of rice husk flour reinforced epoxy bio-composite. *Journal of Engineering Research and Applications*, 5(6), 123-128.
5. Cardona-Urbe, N., Arenas-Echeverri, C., Betancur, M., Jaramillo, L., and Martínez, J. (2018). Possibilities of rice husk ash to be used as reinforcing filler in polymer sector – a review. *Revista UIS Ingenierías*, 17(1), 127-142. doi:10.18273/revuin.v17n1-2018012.
6. Chen, R. S., Ahmad, S., and Gan, A. (2016). Characterization of rice husk-incorporated recycled thermoplastic blend composites. *BioResources*, 11(4), 8470-8482. doi:10.15376/biores.11.4.8470-8482.

7. Danilova-Tretiak, S. M., Evseeva, L. E., Tanaeva, S. A., and Nikalayeva, K. V. (2017). Thermal behavior of polymer composites based on polyamide. *Polymer Materials and Technologies*, 3(3), 44-49.
8. Das, S., Paul, D., Fahad, M., Rahman, G. and Khan, M. (2018). Effect of fiber loading on the mechanical properties of jute fiber reinforced polypropylene composites. *Advances in Chemical Engineering and Science*, 8, 215-224. doi:10.4236/aces.2018.84015.
9. Dasa, O., Hedenqvist, M. S., Prakash, Ch., and Lin, R. J. T. (2019). Nanoindentation and flammability characterisation of five rice husk biomasses for biocomposites applications. *Composites Part A: Applied Science and Manufacturing*, 125, article number 105566. doi: 10.1016/j.compositesa.2019.105566.
10. Dipen, K. R., Durgesh, D. P., Pradeep, L. M., and Emanoil, L. (2019). Fiber-reinforced polymer composites: manufacturing, properties, and applications. *Polymers*, 11(10), article number 1667. doi: 10.3390/polym11101667.
11. Dorca, Y., Greciano, E. E., Valera, J. S., Gomez, R., and Sanchez, L. (2019). Hierarchy of asymmetry in chiral supramolecular polymers: toward functional, helical supramolecular structures. *Chemistry – A European Journal*, 25, 5848-5864.
12. Erdogan, S., and Huner, U. (2018). Physical and mechanical properties of PP composites based on different types of lignocellulosic fillers. *Journal of Wuhan University. Technology.-Materials. Science. Edition*, 33, 1298-1307. doi:10.1007/s11595-018-1967-9.
13. Formalev, V. F., Kolesnik, S. A., and Kuznetsova, E. L. (2016). Nonstationary heat transfer in anisotropic half-space under the conditions of heat exchange with the environment having a specified temperature. *High Temperature*, 54(6), 824-830.
14. Formalev, V. F., Kolesnik, S. A., and Kuznetsova, E. L. (2018). Wave heat transfer in the orthotropic half-space under the action of a nonstationary point source of thermal energy. *High Temperature*, 56(5), 727-731.
15. Gadzama, S., Sunmonu, O., Isiaku, U., and Danladi, A. (2020). Effects of surface modifications on the mechanical properties of reinforced pineapple leaf fibre polypropylene composites. *Advances in Chemical Engineering and Science*, 10, 24-39. doi:10.4236/aces.2020.101002.
16. Ghosh, A.K., and Dwivedi, M. (2020). Characterization and testing of polymeric composites. In *Processability of polymeric composites* (pp. 229-264). New Delhi, India: Nature India Private Limited.
17. GOST 11262-2017. Plastics. Tensile test method. Retrived from <http://docs.cntd.ru/document/1200158280>
18. GOST 15088-2014. Plastics. Method for determining the softening temperature of thermoplastics according to Vick. Retrived from <http://docs.cntd.ru/document/1200110856>
19. GOST 19019-2017. Boring holders for direct fastening of a prismatic cutter with a pin to turret lathes. Construction and dimensions. Retrived from <http://www.omegametall.ru/Index2/1/4294834/4294834249.htm>
20. GOST 32657-2014. Polymer composites. Test methods. Determination of bending temperature under load. Retrived from <http://docs.cntd.ru/document/1200112320>
21. GOST 4647-2015. Plastics. Charpy impact strength determination method (as amended). Retrived from <http://docs.cntd.ru/document/1200127778>
22. GOST 4648-2014. Plastics. Static bending test method (as amended). Retrived from <http://docs.cntd.ru/document/1200110853>
23. GOST 9550-81. Plastics. Methods for determining the modulus of elasticity in tension, compression and bending. Retrived from <http://docs.cntd.ru/document/gost-9550-81>
24. Gowda, T.G.Y., Sanjay, M. R., Bhat, K. S., Madhu, P., Senthamaraiannan, P., and Yogesha, B. (2018). Polymer matrix-natural fiber composites: an overview. *Cogent Engineering*, 5, article number 1446667.
25. Hidalgo-Salazar, M. A., and Salinas, E. (2019). Mechanical, thermal, viscoelastic performance, and product application of PP-rice husk Colombian biocomposites. *Composites Part B: Engineering*, 176, article number 107135. doi:10.1016/j.compositesb.2019.107135.
26. Kasakova, A. S., Yudaev, I. V., Fedorishchenko, M. G., Mayboroda, S. Y.,

- Ksenz, N. V., and Voronin, S.M. (2018). New approach to study stimulating effect of the pre-sowing barley seeds treatment in the electromagnetic field. *OnLine Journal of Biological Sciences*, 18(2), 197-207.
27. Kenechi, N.-O., Linus, C., and Kayode, A. (2016). Utilization of rice husk as reinforcement in plastic composites fabrication – a review. *American Journal of Materials Synthesis and Processing*, 1(3), 32-36. doi:10.11648/j.ajmsp.20160103.12.
  28. Krechetov, I. V., Skvortsov, A. A., Poselsky, I. A., Paltsev, S. A., Lavrikov, P. S., and Korotkovs, V. (2018). Implementation of automated lines for sorting and recycling household waste as an important goal of environmental protection. *Journal of Environmental Management and Tourism*, 9(8), 1805-1812.
  29. Lomakin, E. V., Lurie, S. A., Belov, P. A., and Rabinskii, L. N. (2017). Modeling of the locally-functional properties of the material damaged by fields of defects. *Doklady Physics*, 62(1), 46-49.
  30. Lomakin, E. V., Lurie, S. A., Rabinskiy, L. N., and Solyaev, Y.O. (2018). Semi-inverse solution of a pure beam bending problem in gradient elasticity theory: the absence of scale effects. *Doklady Physics*, 63(4), 161-164.
  31. Majeed, K., Arjmandi, R., Al-Maadeed, M.A., Hassan, A., Ali, Z., Khan, A.U., Khurram, M.S., Inuwa, I.M., and Khanam, P.N. (2017). Structural properties of rice husk and its polymer matrix composites: An overview. In M. Jawaid, M.T. Paridah, and N. Saba (Eds.), *Lignocellulosic fibre and biomass-based composite materials* (pp. 473-490). Sawston, United Kingdom: Woodhead Publishing Series in Composites Science and Engineering.
  32. Mohapatra, R. (2018). Experimental study on optimization of thermal properties of natural fibre reinforcement polymer composites. *Open Access Library Journal*, 5, 1-15. doi:10.4236/oalib.1104519.
  33. Nyior, G. B., and Mgbeahuru, E. Ch. (2018). Effects of processing methods on mechanical properties of alkali treated bagasse fibre reinforced epoxy composite. *Journal of Minerals and Materials Characterization and Engineering*, 6, 345-355. doi:10.4236/jmmce.2018.63024.
  34. Orji, B., and McDonald, A. G. (2020). Evaluation of the mechanical, thermal, and rheological properties of recycled polyolefins rice-hull composites. *Materials*, 13(3), article number 667. doi:10.3390/ma13030667.
  35. Orlov, A. M., Skvortsov, A. A., and Litvinenko, O. V. (2003). Bending vibrations of semiconductor wafers with local heat sources. *Technical Physics*, 48(6), 736-741.
  36. Pandey, P. (2020). Preparation and characterization of polymer nanocomposites. *Soft Nanoscience Letters*, 10, 1-15. doi:10.4236/snl.2020.101001.
  37. Raghu, N., Kale, A., Chauhan, S., and Aggarwal, P.K. (2018). Rice husk reinforced polypropylene composites: mechanical, morphological, and thermal properties. *Journal of the Indian Academy of Wood Science*, 15(1), 96-104. doi:10.1007/s13196-018-0212-7.
  38. Rutkowska, M., Płotka-Wasyłka, J., Morrison, C., Wieczorek, P.P., Namieśnik, J., and Marć, M. (2018). Application of molecularly imprinted polymers in analytical chiral separations and analysis. *Trends in Analytical Chemistry*, 102, 91-102.
  39. Saigal, A. and Pochanard, P. (2019). The application of a representative volume element (RVE) model for the prediction of rice husk particulate-filled polymer composite properties. *Materials Sciences and Applications*, 10, 78-103. doi:10.4236/msa.2019.101008.
  40. Stolin, A. M., Stel'makh, L. S. and Karpov, S.V. (2020). High-temperature indirect compaction of powder materials with active action of an external friction force. *Journal of Engineering Physics and Thermophysics*, 93, 317-323. doi:10.1007/s10891-020-02123-6.
  41. Sutar, H., Chandra Sahoo, P., Suman Sahu, P., Sahoo, S., Murmu, R., Swain, S. and Mishra, S.Ch. (2018). Mechanical, thermal and crystallization properties of polypropylene (PP) reinforced composites with high density polyethylene (HDPE) as matrix. *Materials Sciences and Applications*, 9, 502-515. doi:10.4236/msa.2018.95035.
  42. Tarrés, Q., Soler, J., Rojas-Sola, J. I., Oliver-Ortega, H., Julián, F., Espinach, F. X., Mutjé, P., and Delgado-Aguilar, M. (2019). Flexural properties and mean intrinsic flexural strength of old newspaper reinforced polypropylene composites. *Polymers*, 11(8),

article number 1244.  
doi:10.3390/polym11081244.

43. Usenbekov, B. N., Kaykeev, D.T., Yhanbirbaev, E. A., Berkimbaj, H., Tynybekov, B. M., Satybaldiyeva, G. K., Baimurzayev, N. B., and Issabayeva, G. S. (2014). Doubled haploid production through culture of anthers in rice. *Indian Journal of Genetics and Plant Breeding*, 74(1), 90-92.
44. Väisänen, T., Das, O., and Tomppo, L. (2017). A review on new bio-based constituents for natural fiber-polymer composites. *Journal of Cleaner Production*, 149, 582-596. doi:10.1016/j.jclepro.2017.02.132.

45. Yang, H. (2017). Thermal and dynamic mechanical thermal analysis of lignocellulosic material-filled polyethylene bio-composites. *Journal of Thermal Analysis and Calorimetry*, 130, 1345-1355. doi:10.1007/s10973-017-6572-1.
46. Yonghui, Z., Mizi, F., Lihui, C., and Jiandong, Z. (2015). Lignocellulosic fibre mediated rubber composites: An overview. *Composites Part B: Engineering*, 76, 180-191. doi:10.1016/j.compositesb.2015.02.028.

**Table 1.** Physical and mechanical properties of polymer composites

| Content of rice husk, phr | Modulus of elasticity at the break, MPa | Tensile strength at break, MPa | Breaking elongation, % | Modulus of elasticity in flexure, MPa | Relative flexural strain, % |
|---------------------------|---|--------------------------------|------------------------|---------------------------------------|-----------------------------|
| 0                         | 1132.1                                  | 25.5                           | 588.4                  | 878.2                                 | 19.1                        |
| 2                         | 1154.2                                  | 24.7                           | 26.4                   | 981.0                                 | 19.2                        |
| 5                         | 1161.1                                  | 23.9                           | 15.6                   | 1019.4                                | 19.9                        |
| 10                        | 1373.5                                  | 22.9                           | 11.6                   | 1104.1                                | 20.4                        |
| 15                        | 1453.9                                  | 21.3                           | 5.6                    | 1228.2                                | 20.1                        |
| 30                        | 1537.5                                  | 20.8                           | 5.2                    | 1288.9                                | 18.8                        |

**Table 2.** The results of the thermogravimetric analysis of polymer composites

| Content of rice husk, phr | T <sub>H</sub> , °C | T <sub>1</sub> , °C | T <sub>5</sub> , °C | Residue, % |          | T <sub>max</sub> , °C |     |
|---------------------------|---------------------|---------------------|---------------------|------------|----------|-----------------------|-----|
|                           |                     |                     |                     | at 400°C   | at 600°C | 1                     | 2   |
| 0                         | 211                 | 243                 | 262                 | 5.4        | 2.4      | 349                   | 443 |
| 2                         | 226                 | 252                 | 267                 | 6.5        | 3.2      | 332                   | 467 |
| 5                         | 218                 | 242                 | 262                 | 6.4        | 2.8      | 356                   | 421 |
| 10                        | 229                 | 250                 | 266                 | 8.5        | 4.3      | 329                   | 445 |
| 15                        | 231                 | 249                 | 266                 | 10.7       | 5.5      | 326                   | 417 |
| 30                        | 231                 | 247                 | 265                 | 11.4       | 5.9      | 327                   | 417 |
| 100                       | 172                 | 193                 | 208                 | 27.9       | 17.2     | 288                   | 403 |

**Table 3.** Parameters of melting and crystallization of polymer composites

| Content of rice husk, phr | T <sub>ml</sub> , °C | ΔH <sub>cr</sub> , J/g | T <sub>cr</sub> , °C | ΔH <sub>cr</sub> , J/g |
|---------------------------|----------------------|------------------------|----------------------|------------------------|
| 0                         | 166.0                | -80.4                  | 118.2                | 102.1                  |
| 2                         | 166.3                | -92.6                  | 117.2                | 104.1                  |
| 5                         | 166.2                | -86.7                  | 116.2                | 103.5                  |
| 10                        | 166.3                | -84.5                  | 116.3                | 100.7                  |
| 15                        | 166.2                | -71.3                  | 117.2                | 86.3                   |
| 30                        | 165.5                | -63.0                  | 117.8                | 76.3                   |



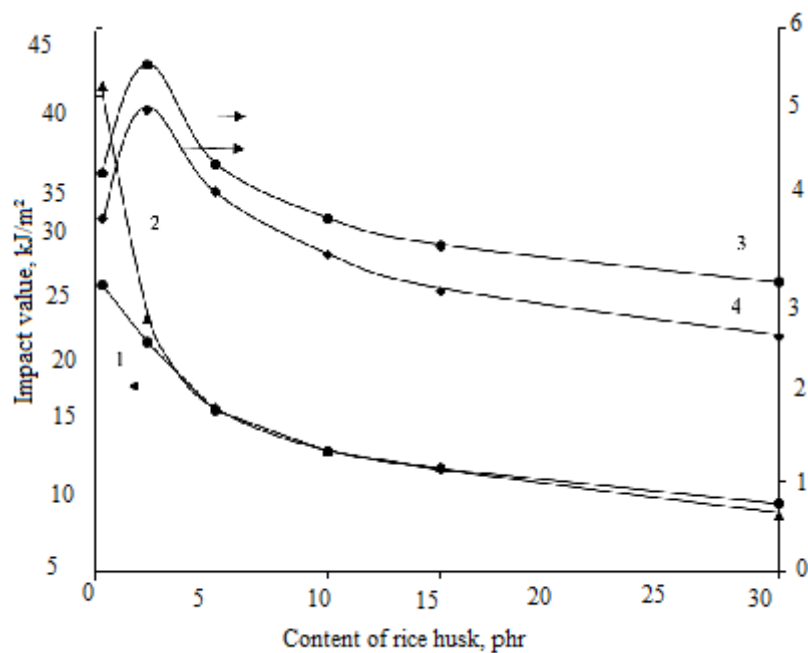


**Figure 1.** Dependence of Izod impact strength (1.3) and Charpy V-notch impact energy (rib impact) (2.4) on the content of rice husk in a polymer composite. Unnotched samples (1.2), notched samples (3.4)

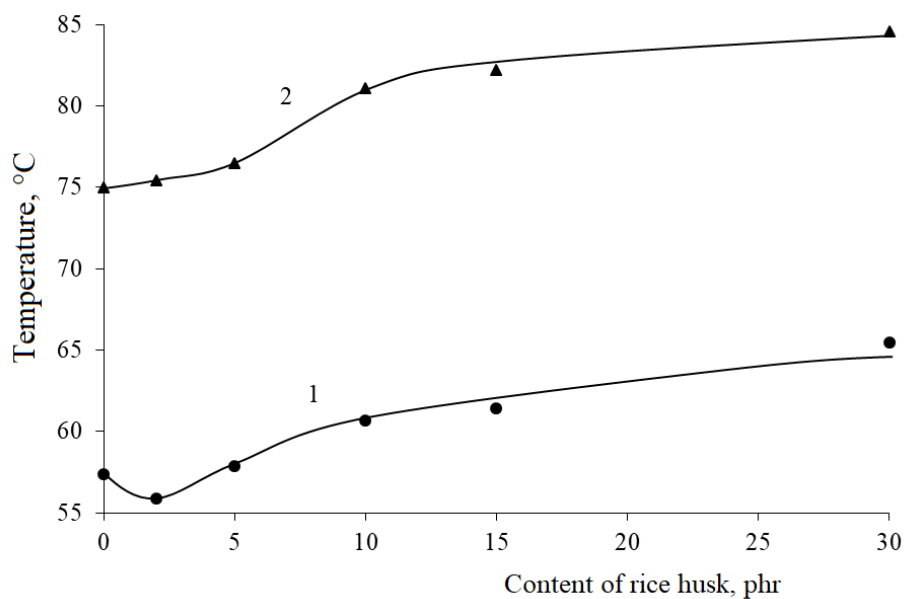


**Figure 2.** Dependence of bending temperature under load (1.8 MPa) (1) and Vicat softening temperature (50 N) (2) on the content of rice husk in a polymer composite

## **CRIAÇÃO E USO DO CONSÓRCIO DE MICROORGANISMOS NA PRODUÇÃO DE CARNES**

### **CREATION AND USE OF MICROORGANISM CONSORTIUM IN MEAT PRODUCTION**

### **СОЗДАНИЕ И ИСПОЛЬЗОВАНИЕ КОНСОРЦИУМА МИКРООРГАНИЗМОВ ПРИ ПРОИЗВОДСТВЕ МЯСНЫХ ПРОДУКТОВ**

GIZATOV, Albert<sup>1\*</sup>; GIZATOVA, Natalia<sup>2</sup>; MIRONOVA, Irina<sup>3</sup>; GAZEYEV, Igor<sup>4</sup>;  
NIGMATYANOV, Azat<sup>5</sup>

<sup>1,2,3</sup> Bashkir State Agrarian University, Department of technology of meat, dairy products, and chemistry.  
Russian Federation

<sup>4</sup> Bashkir State Agrarian University, Faculty of food technologies, Department of life safety, and technological equipment. Russian Federation

<sup>5</sup> Ufa State Petroleum Technological University, Department of special chemical technologies. Russian Federation

\* Corresponding author  
e-mail: albertgizatov@yahoo.com

Received 07 March 2020; received in revised form 22 May 2020; accepted 18 June 2020

## **RESUMO**

O objetivo desta pesquisa é desenvolver produtos funcionais a partir de subprodutos biomodificados de baixa qualidade e resíduos usando consórcios de microrganismos. Para criar condições para uma dieta equilibrada e melhorar a saúde da população, foi proposta a técnica de utilização de métodos biotecnológicos direcionados à atração de recursos não tradicionais. O objetivo do estudo foram subprodutos secundários da carne e resíduos da indústria de processamento de carne. Os produtos cárneos e resíduos foram processados com bactérias lácticas como *Lactobacillus bulgaricus*, *Bifidumbacterium siccum* e *Staphylococcus carnosus*. As bactérias do ácido láctico foram cultivadas passo a passo em diferentes combinações: *Staphylococcus carnosus* e *Lactobacillus bulgaricus*; *Bifidumbacterium siccum* e *Staphylococcus carnosus*; *Lactobacillus bulgaricus* e *Bifidumbacterium siccum*. Mudanças na atividade de crescimento das espécies selecionadas de bactérias lácticas em várias combinações foram realizadas em vários meios nutricionais. Ao cultivar as cepas estudadas em um meio de agar de carne e peptona, sua identificação completa foi realizada. A etapa final foi a análise da qualidade dos objetos reais: carne de cavalo, flank e tecido muscular padrão da carne bovina. A dinâmica das mudanças nos indicadores de propriedades funcionais, tecnológicas e organolépticas da carne provou um efeito positivo do uso de bactérias do ácido láctico. As raças desenvolvidas demonstraram a capacidade de suprimir ativamente a microflora prejudicial nos produtos à base de carne. Além disso, amoleceram a carne secundária para processamento e provaram positivamente melhorar as características organolépticas do produto acabado. O processamento de recursos secundários de subprodutos e resíduos permitirá o uso mais econômico e racional da reserva alimentar mais essencial de carne e derivados, contendo colágeno. A cobertura insuficiente desta questão sobre o uso de uma cepa combinada dessas espécies de microrganismos para a biomodificação de subprodutos secundários contendo colágeno e resíduos na indústria de carne indica a relevância do tópico escolhido.

**Palavras-chave:** biomodificação; biotecnologia; subprodutos e resíduos contendo colágeno, bactérias do ácido láctico.

## **ABSTRACT**

This research purpose is to develop functional products from biomodified low-grade by-products and waste using microorganism consortia. To create conditions for a balanced diet and improve the health of the population, the technique of using biotechnological methods directed at attracting non-traditional resources was proposed. The object of the study was secondary meat by-products and waste from the meat processing industry. The meat products and waste were processed with such lactic-acid bacteria as *Lactobacillus bulgaricus*, *Bifidumbacterium siccum*, and *Staphylococcus carnosus*. Lactic-acid bacteria were cultured step-

by-step in different combinations: *Staphylococcus carnosus* and *Lactobacillus bulgaricus*; *Bifidumbacterium siccum* and *Staphylococcus carnosus*; *Lactobacillus bulgaricus* and *Bifidumbacterium siccum*. Changes in the growth activity of selected species of lactic-acid bacteria in various combinations were carried out in various nutrient media. When growing the studied strains in a medium of meat-and-peptone agar, their complete identification was carried out. The final stage was the analysis of the quality of real objects: horse meat, flank, and standard beef muscle tissue. The dynamics of changes in indicators of functional and technological and organoleptic meat properties proved a positive effect from the use of lactic acid bacteria. Developed races have shown the ability to suppress harmful microflora in meat products actively. Moreover, they softened the secondary meat for processing and positively proved to improve the finished product's organoleptic characteristics. Processing of secondary resources of by-products and waste will allow more economical and rational use of the most essential collagen-containing food reserve of meat and meat products. The insufficient coverage of this issue on the use of a combined strain of these species of microorganisms for the biomodification of secondary collagen-containing by-products and waste in the meat industry indicates the relevance of the chosen topic.

**Keywords:** biomodification; biotechnology; collagen-containing by-products and waste, lactic-acid bacteria.

## АННОТАЦИЯ

Цель исследования - разработка функциональных продуктов из биомодифицированного низкосортного сырья с использованием консорциумов микроорганизмов. Для создания условий для рационального питания и улучшения здоровья населения нами предлагается использовать прием, направленный на привлечение нетрадиционных ресурсов с использованием методов биотехнологии. В качестве объекта исследования служило вторичное мясное сырьё мясоперерабатывающей промышленности: мяса конины, пашины и говяжьей мышечной ткани второго сорта. Объектом исследования выступили *Lactobacillus bulgaricus*, *Bifidumbacterium siccum*, *Staphylococcus carnosus*. Культивация молочнокислых бактерий осуществлялась поэтапно в разных сочетаниях: *Staphylococcus carnosus* и *Lactobacillus bulgaricus*; *Bifidumbacterium siccum* и *Staphylococcus carnosus*; *Lactobacillus bulgaricus* и *Bifidumbacterium siccum*. Активность роста молочнокислых бактерий изучали на различных питательных средах (мясопептонный агар и мясопептонный желатин). Для этого суспензию культур культивировали в стерильных условиях на питательных средах, являющейся оптимальной для их роста. В процессе выращивания исследуемых штаммов на среде с применением мясопептонного агара была проведена полная их идентификация. Для оценки скорости роста тестируемых штаммов использовали специфические питательные среды. На завершающем этапе был проведен анализ качества реальных объектов: мяса конины, пашины и говяжьей мышечной ткани второго сорта по показателям функционально-технологических свойств и был установлен положительный эффект от их применения, поскольку выведенные расы проявили способность активно подавлять вредную микрофлору, развивающуюся в мясных продуктах. Кроме того, переработки вторичных сырьевых ресурсов позволит более экономно и рационально использовать важнейшие пищевой коллагенсодержащий резерв мяса и мясных продуктов. Недостаточная освещенность данного вопроса по применению комбинированного штамма данных видов микроорганизмов для биомодификации вторичного коллагенсодержащее сырьё мясной промышленности свидетельствует об актуальности выбранной темы.

**Ключевые слова:** биомодификация, биотехнология, коллагенсодержащее и вторичное сырьё, молочнокислые бактерии.

## 1. INTRODUCTION:

Currently, it is possible to produce new types of meat by-products and waste for general, special and therapeutic purposes, improve methods of enzymatic processing of meat raw materials in order to improve its functional and technological properties, produce food and feed hydrolysates, synthesize flavorings, dyes, biologically active substances, to synthesize feed proteins, and in the future, proteins for human nutrition based on biotechnology in the meat industry (Antipova, 2001; Antipova *et al.*, 2011; Armuzzi *et al.*, 2001; Audenaert *et al.*, 2010;

Dušková *et al.*, 2016; Wanget *et al.*, 2013).

Products containing consortia of lactic acid and bifidobacteria play an essential role in the nutrition of people, especially children, the elderly, and patients. First of all, the dietary properties of such products are in that they improve metabolism, stimulate the secretion of gastric juice, and stimulate the appetite. Being in food products and making up most of the microflora of the human gastrointestinal tract, taking root in the intestines, they actively suppress putrefactive microflora and lead to inhibition of putrefactive processes and stop the formation of toxic decay products of proteins

entering the human blood. Along with this, microorganisms are active producers of useful substances that are capable of transforming natural or chemically synthesized compounds into substances valuable to humans. Their sources are inexpensive and practically inexhaustible. Many of them must synthesize heterogeneous systems of enzymes that convert proteins. This suggests the effectiveness of their use for biotransformation of protein systems of low-grade meat by-products and waste by microbial fermentation with the selection of specific consortia (Armuzzi *et al.*, 2001; Dušková *et al.*, 2016).

Some American factories use a pure culture of *Pediococcus cerevisiae* to manufacture summer types of sausages such as cervelat and salami. When sugar is added, it promotes the formation of lactic acid and gives the sausages a specific, characteristic flavor. When using this culture, the sausage manufacturing process is reduced to 48 hours while usually it is kept at (7-10) °C for 3-7 days, and then smoked at (27-44) °C for 2 -3 days (Antipova *et al.*, 2016; Gavrilova *et al.*, 2019).

From the point of view of aroma formation, the starting culture of *Moraxella phenylpyruvica*, the Danish Meat Institute's development product, is of interest. This is a psychrophilic culture – an optional anaerobic which allows it to develop in the thickness of the product actively and, as studies have shown, to produce substances that are precursors of aroma. Along with traditional bacteria, such as *Lactobacillus* and *Pediococcus*, American technologists include *Micrococcus* in the starter cultures, which can reduce nitrates to nitrites while improving the taste and color of finished sausages (de Souza Barbosa *et al.*, 2015).

In Italy, strains of *Micrococcus* sp., *Lactobacillus bulgaricus* were tested to study the organoleptic properties of dry sausages as starter cultures. A new bacterial culture, *Lactobacillus pentosus*, was tested in the laboratory of R. Muller (Germany) in the production of dry sausages. Several other cultures were used to compare the technological effect: *Petrostreptococcus parvulus*, *Lactobacillus bulgaricus*, *Pediococcus acidilactici*, and their combination with *Streptococcus carnosus* MIII. In all variants of testing microorganisms, the best results were obtained with *Lactobacillus pentosus*. The effect was expressed in a rapid decrease in pH by obtaining sausages of attractive color, soft-sour taste, and pronounced meat aroma (Cocolin *et al.*, 2009).

In the meat industry, biotechnology is used in raw meat processing with enzyme preparations to soften its stiffness and increase the nutritional value, making it possible to use low-grade raw materials to produce high-quality meat products. Experts consider the enzymatic method of softening meat one of the most effective (de Souza Barbosa *et al.*, 2015; Doulgeraki *et al.*, 2012; Ilina *et al.*, 2017).

The All-Russian Scientific Research Institute of the Meat Industry (VNIIMPom) conducted studies on the use of microbial preparations for the complete separation of meat from bones after deboning and sending the resulting mass to prepare meat pastes, emulsions, hydrolysates (Antipova and Uspenskaj, 2016; Gavrilova *et al.*, 2019). Studies were conducted at the same institute on the use of brewer yeast biomass as polyezyme preparations for the hydrolysis of blood proteins in slaughtered animals, resulting in an increase in the biological efficiency of blood proteins by 10-30%. Hydrolyzed by yeast, blood is recommended to be used as an additive to meat products to give them a good taste.

One of the biotechnology applications to obtain additional protein sources is the use of unicellular bacteria, fungi, yeast, and algae for the enrichment of meat products. As shown by studies conducted by institutes of the Russian Academy of Sciences, the Russian Academy of Medical Sciences (Antipova *et al.*, 2016), VNIIMPom, this method allows getting diet meat products. The Kemerovo Technological Institute of the Food Industry researched the use of cooked sausages in technology to replace soy protein brewing yeast, which is the secondary raw material for brewing (Antipova *et al.*, 2015; Gavrilova *et al.*, 2019). One of the new biotechnology areas in sausage production is the improvement of the taste, color, and aroma of meat products of high-quality flavorings, various flavoring substances of microbial origin (Armuzzi *et al.*, 2001; Cocolin *et al.*, 2009). Another promising area of application of the principles of biotechnology is the fortification of meat products and the solution of issues related to the development of this problem. Scientists of VNIIMP, KemTIIP, and others are enriching foods with vitamins (Antipova *et al.*, 2011; Audenaert *et al.*, 2010). For example, KemTIIP experts in collaboration with scientists of the Institute of Nutrition RAMS developed a technology to enrich meat products with vitamins C, B1, B2, and PP, which allows saving almost half of their activity (Gabitov *et al.*, 2019; Wang *et al.*, 2013). In the

neighboring countries, research is also being carried out to introduce biotechnological processes in the meat industry, which in their direction coincide with the Russian ones. In Belarus, technology has been developed for two bacterial preparations: Acidolact and Lactobact (liquid and dry) used as part of multi-component brine for extrusion of beef products (Bonomo *et al.*, 2008).

In Kazakhstan, the Semipalatinsk Institute of Meat and Dairy Industry created a composition for producing a protein fortifier used in sausage production (de Souza Barbosa *et al.*, 2015; Dušková *et al.*, 2016). In the Almaty branch of the Dzhambul Technological Institute of Light and Food Industries, a biological product of decolorized sedimentary yeast used to enrich sausages was obtained (Gabitov *et al.*, 2018; Konashova *et al.*, 2018).

Much attention is paid to the application of biotechnological techniques in the meat industry in far abroad countries. The directions there are mainly focused on improving the quality of meat products, intensifying production, creating new types of products based on meat balanced in chemical composition, environmentally friendly directed actions, including therapeutic and prophylactic purposes (Buchanan and Gibbons, 1994).

The main areas of application of biotechnology in sausage production are the use of biomass of microorganisms and preparations based on them as a substitute for meat raw materials, a source of vitamins, micro and macro elements for the production of sausages, increased nutritional value, producer of enzymes, amino acids, flavorings, and colorings in order to improve technological processes, create fundamentally new technologies, improve genetic safety, lengthen the shelf life, improve the taste, aroma and other values of product quality; the use of immobilized enzymes, the advantage of which is the possibility of their repeated use, the increased stability, and duration of enzymatic activity, the possibility of use in continuous technological processes, the relatively short exposure time to the substrate, the possibility of creating multi-enzyme systems that are highly effective and, finally, in hygienic safety (Holko *et al.*, 2013; Nesterenko *et al.*, 2018).

In recent years, in Romania, Italy, Bulgaria, Switzerland, and other countries, the use of molds for producing smoked sausages has increased. It was noted that sausages with a dense coating of white or gray mold on the shell

are better than without it. Swedish scientists have developed a method for the production of minced meat with improved properties. According to this method, the meat is treated with a heat-sensitive proteinase (Gizatova *et al.*, 2014). In the UK, it is recommended to use two groups of enzymes in the food industry. The first group includes enzymes of animal and vegetable origin, and the second – enzymes of microbial origin – temporarily used (Ammor and Mayo, 2007). A new direction is being planned in the fermentation of meat. For improving the quality of meat, enzyme preparations (papain) are introduced into the blood of slaughtered animals immediately before slaughter, which significantly improves the meat grade. A mixture of papain and bromelin can be used for salting beef (Casquete *et al.*, 2011; Gizatov and Gizatova, 2015; Nesterenko *et al.*, 2016; Rakhimov *et al.*, 2018).

The problem of obtaining proteins from non-traditional types of raw materials (bacteria, fungi, yeast) to use them in meat products is intensively worked in the USA, Great Britain, Italy (Iliina *et al.*, 2017; Juntunen *et al.*, 2001; Knolet *et al.*, 2001). In the USA, dietary sausages are being produced with the protein product Muco protein, which is made from a filamentous fungus that can double its volume in 2.5 hours (Dušková *et al.*, 2015). In Italy, yeast extract is used in the production of cooked, liveried, semi-smoked, and cooked smoked sausages. In Yugoslavia, studies are being conducted on the use of brewer yeast preparations as substitutes for sodium caseinate and soy isolate in meat products (Argyriet *et al.*, 2015).

For the production of dry sausages in the hot season, foreign enterprises of Germany and Italy use pure culture *Pediococcus cerevisiae* as part of the recipe. According to the technology for the preparation of sausages, a certain amount of sugar is introduced, favorably affecting the formation of a taste and aroma specific to this type of product. The introduction of *Pediococcus cerevisiae* reduces the production time of sausages to 48 hours against 3-7 days required for precipitation and 2-3 days for smoking (Sydykova *et al.*, 2019; Vladimirovna and Borisovich, 2016; Zinina and Rebezov, 2016).

From the point of view of aroma formation, the Danish Meat Institute's development, the *Moraxella phenylpyruvica* culture, is of interest. It is a psychrophilic culture – an optional anaerobic that allows growing exponentially in the thickness of the product and, as studies have shown, producing substances that are precursors of aroma. Along with native bacteria, such as

Lactobacillus and Pediococcus, American technologists include Micrococcus in starter cultures, which can restore nitrates to nitrites, improving the taste and color of finished sausages (Karam *et al.*, 2013). In Italy, when studying sensory properties, strains of *Micrococcus* sp., *Lactobacillus bulgaricus* were used as test starter cultures (Adams and Mitchell, 2002). During the development of uncooked smoked sausages, a new bacterial culture of *Lactobacillus pentosus* was tested in the research laboratory of R. Muller (Germany). Many other cultures were used to compare the effect of the technology: *Petrostreptococcus parvulus*, *Lactobacillus bulgaricus*, *Pediococcus acidilactici*, as well as their combination with *Streptococcus carnosus*. Of all the microorganisms tested, the best results were obtained with *Lactobacillus pentosus*. There was a rapid decrease in pH, which resulted in an attractive color, soft-sour taste, and a pronounced meat aroma of the obtained sausages (Martynov *et al.*, 2018). The aim of this study is to combine the above microorganism strains to soften the secondary collagen-containing by-products and waste of the meat industry.

## 2. MATERIALS AND METHODS:

Meat and meat products are an excellent source for the development of lactic acid bacteria. They get everything they need from meat: sources of carbon, nitrogen, vitamins, and mineral salts. The meat's pH and humidity also contribute to growth (Martynov *et al.*, 2018). The objects of study were: – fresh and frozen beef of the highest, first and second grades according to GOST 779 (Ilin *et al.*, 2017), model minced meat, sausages obtained on its basis with and without biotechnological processing methods; – sturdy and low-grade collagen-containing raw materials of the meat industry (beef flank, beef veins, horse meat). Beef and horsemeat samples for research were taken under GOST R 51447, GOST 9792 (Antipova, 2001; Dušková *et al.*, 2015; Kno *et al.*, 2001) after which they made a combined sample and, denoting the name of the sample, were wrapped in parchment. Processing model minced meat with an ingredient such as salt does not adversely affect the growth of lactic acid bacteria, as most strains can withstand salt concentration. The temperature has a definite effect on the salt tolerance of lactic acid bacteria. At optimal growth of temperatures, they resist a salt concentration of up to 12%. Certain doses of

salt even stimulate growth (Martynov *et al.*, 2018).

An essential parameter of the starter culture quality is the suitability of the product, which should be confirmed in the study. When compiling a consortium of crops, it is necessary to take into account the characteristics of the product being produced, the temperature regime of the product (Bulat *et al.*, 2012; Ivanov *et al.*, 2018; Konashova *et al.*, 2018). The temperature should be maintained at an optimum level without violating the boundaries. The most commonly used thermophilic cultures are *Str. thermophilus*, *lac. bulgaricus*, *Las. lactis*, *Lbm. helveticus* and *Lbm. acidophilus*. In a broader sense, the *Bifidus* group (the *Bifidobacterium* *Atinomyetaceae* family) can be assigned to this group of microorganisms (Bulat *et al.*, 2012).

Like mesophilic organisms, thermophilic biomass culture has antimicrobial properties due to the inhibition of nutrients, low pH, the formation of antibiotics, and other factors that have a deterrent effect. When choosing, a number of requirements were taken into account, including those that are not harmful to the human body, a high growth rate, and, therefore, cell reproduction.

During the experiment, the growth activity of lactic acid bacteria on various nutrient media (meat peptone agar and meat peptone gelatin) was studied in order to select strains with specific properties and create consortia based on them taking into account physiological and biochemical characteristics. The suspension of cultures was cultivated under sterile conditions in a box, introduced into nutrient media in meat peptone agar and meat peptone gelatin, and grown in a thermostat at an optimum temperature of + 28°C for growth.

The next stage of our research was to study the growth of selected strains of lactic acid bacteria on specific nutrient media: gelatin and collagen gels, which were prepared by hydration of gelatin and animal protein with meat broth in a ratio of 1:5. During cultivation, pH, acidity, and mass fraction of protein were determined by the biuret method in a nutrient medium for 8 hours. The macro morphological properties of the consortium of lactic acid bacteria were studied in order to search for optimal combinations and concentrations of lactic acid bacteria in association with each other and their effective influence on the meat systems. The bacteria *Staphylococcus carnosus*, *Lactobacillus bulgaricus*, and *Bifidobacterium siccum* were cultivated on a gelatin gel. When sowing on

gelatin gel, the number of bacteria was taken into account. The number of bacteria was not less than  $1 \cdot 10^7$  CFU/g. Before sowing on gelatin gel, nutrient media were preliminarily prepared, and then lactic acid bacteria were cultured in stages in different combinations: *Staphylococcus carnosus* and *Lactobacillus bulgaricus*; *Bifidumbacterium siccum* and *Staphylococcus carnosus*; *Lactobacillus bulgaricus* and *Bifidumbacterium siccum* in milk to identify the nature of the biological interaction of our crops and their growth rate.

Next, we studied the change in the functional and technological properties (moisture-binding capacity (MBC), water-holding capacity (WHC), fat-holding ability (FHC), yield, emulsion stability (ES) of minced meat from flank and horsemeat upon salting with the addition of a complex of lactic acid bacteria. All changes are functional; technological properties were investigated according to established methods.

Moisture binding ability (MBC) was evaluated by the pressing method. A sample of muscle tissue of  $(0.30 \pm 0.01)$  g was weighed on an analytical balance on a mug of polyethylene with a diameter of 15-20 mm. It was then transferred to an anesthetized filter with a diameter of 9-11 cm, placed on a glass or Plexiglass plate so that the hitch was under a plastic circle. The hinge was covered with a plate of the same size as the bottom. A load of 1 kg was placed on it for 10 minutes. Then the filter with a hitch was freed from the load and the lower plate. A contour of the spot around the compressed meat was outlined with a pencil. The contour of the wet spot appears when the filter paper dries in the air. The area of the spot formed by adsorbed moisture was calculated by the difference between the total area of the spot and the area of the spot formed by the meat. The area of spots formed by compressed meat and adsorbed moisture was measured with a planimeter. It was experimentally established that  $1 \text{ cm}^2$  of the filter's wet spot area corresponds to 8.4 mg of water (Martynov *et al.*, 2018).

For determining the mass fraction of total moisture, a sample of tissue weighing  $(2.00 \pm 0.01)$  g was placed in a paper bag with a filter paper insert and evenly distributed. Then it was placed in a Chizhova apparatus (a high-frequency device), preheated to  $(160^\circ \text{C})$ , and dried for 3-5 minutes. After drying, the bag was cooled and weighed with an accuracy of  $\pm 0.1$  g. The contents of the bag were released, and the bag was weighed. The results were recorded and used in calculating the SCD of muscle tissue

samples.

Determination of water holding capacity (WHC). A sample weighing  $(5.00 \pm 0.01)$  g was uniformly applied with a glass rod on the inner surface of a wide part of the milk butyrometer. The butyrometer was tightly closed with a stopper and placed in a water bath at the boiling point with a narrow part down for 15 minutes. The calculated paths determined the mass of released moisture by the number of divisions on the butyrometer scale (Martynov *et al.*, 2018).

When determining the WHC, the mass of meat remaining in the butyrometer was found with an accuracy of  $\pm 0.0001$  g. The meat was placed in a bottle and dried to a constant mass at a temperature of  $150^\circ \text{C}$  for 1.5 hours. After drying, a weight of  $(2.0000 \pm 0.0002)$  g was placed in a porcelain mortar, where 2.5 g of fine calcined sand and 6 g of  $\alpha$ -monobromonaphthalene were added. The contents of the mortar were thoroughly triturated for 4 minutes and filtered through a folded paper filter. 3-4 drops of the test solution were uniformly applied with a glass rod to the refractometer's lower prism. The prism was closed, fastened with a screw. A beam of light was directed using a mirror onto the refractometer's prism, setting the telescope so that intersecting filaments were clearly visible. The pointer is moved until the boundary between the illuminated and dark parts coincides with the point of intersection of the threads, and the refractive index is counted. At the same time, the refractive index of monobromo-naphthalene was determined. The determinations were repeated several times using average data in the calculation (Konashova *et al.*, 2018).

For determining the stickiness (adhesion), the minced meat sample was uniformly applied on a polished metal plate with a uniform thickness of 3 mm and pressed against the top from the top with a second polished metal plate with a 2 mm protrusion. Thus, an even layer of minced meat with a thickness of 2 mm was created between the plates. A load weighing 1 kg was placed on the upper plate and connected to a dynamometer. By increasing the force applied to the dynamometer, they achieved separation of the upper plate from the stuffing surface. At the time of separation, the dynamometer readings were recorded. The stickiness calculation  $\rho$ , ( $\text{N}/\text{cm}^2$ ) was carried out according to the formula (Martynov *et al.*, 2018).

For determining the yield, samples of model minced meat were prepared similarly to the

determination of BCC. The prepared samples were kept at a temperature from 0 to 4°C. After a predetermined time, the samples were heat-treated in a microwave oven for 15 minutes at a 100 W power, after which they were re-weighed. The control was samples subjected to salting without microbial treatment for 12 hours.

The pH of solutions and meat systems was determined using the potentiometric method on a universal pH-121 ionometer. A portion of each meat sample weighing ( $10.00 \pm 0.02$ ) g was extracted with distilled water in a ratio of 1:10 for 30 min at  $(20 \pm 5)^\circ\text{C}$ , mixed and filtered through a folded paper filter.

The determination of the mass fraction of proteins in muscle tissue was carried out according to the Kjeldahl method. The test samples were ground. 0.2 g of collagen gel was added to a Kjeldahl flask with a capacity of 50 cm<sup>3</sup>. Using a piece of glass, the sample was lowered to the bottom of the flask. 1-2 cm<sup>3</sup> of concentrated sulfuric acid, 1 g of a mixture of copper sulfate, and potassium sulfate as a catalyst were added. The contents of the flask were heated in a fume hood. When the mixture turned brown, the flask was removed from the heat, cooled at room temperature. 2-3 cm<sup>3</sup> of hydrogen peroxide solution with a mass fraction of 30% was added, and heating continued until a colorless mineralate was obtained. The latter is used for the quantitative determination of protein (Ammor and Mayo, 2007; Zinina *et al.*, 2016).

The mineralate was cooled, quantitatively transferred into a volumetric flask with a capacity of 250 cm<sup>3</sup>. The volume was adjusted to the mark with distilled water. The contents were mixed. 5 cm<sup>3</sup> of the obtained mineralizate solution was added to a volumetric flask with a capacity of 100 cm<sup>3</sup>. The volume was re-adjusted to the mark with distilled water. For the color reaction, 1 cm<sup>3</sup> of the re-diluted mineralizate was introduced into the tube, and 5 cm<sup>3</sup> of reagent 1 and 5 cm<sup>3</sup> of reagent 2 were added sequentially. The contents of the tube were mixed. At the same time, a control solution was prepared using a control mineralizate (sample using distilled water). After 30 minutes, the optical density of the solutions was determined on a red color filter photo electro colorimeter. The measurement was carried out in comparison with a control solution. The determination of lactic acid content was carried out by color reaction with para-oxydiphenyl. Sample preparation: 10 cm<sup>3</sup> of trichloroacetic acid solution with a mass fraction of 10% and 2-4 g of minced meat were introduced into the mortar and ground for 10 minutes. The resulting suspension

was transferred into a volumetric flask with a capacity of 50 cm<sup>3</sup>, first using 20 cm<sup>3</sup> of a trichloroacetic acid solution with a mass fraction of 10%, and then a few cubic centimeters of distilled water. The flask was left for 30 min at room temperature, shaking every 10 min, then the volume was adjusted to the mark with distilled water, the flask was closed with a stopper, the contents were well mixed, transferred to centrifuge tubes, centrifuged at a speed of 50 s<sup>-1</sup> for 10-15 min. The centrifuge was poured into a dry flask, 25 cm<sup>3</sup> of a clear liquid was taken, transferred to a volumetric flask with a capacity of 100 cm<sup>3</sup>, and the volume was adjusted to the mark with distilled water. Analysis: For carbohydrates' precipitation, 1 cm<sup>3</sup> of a copper sulfate solution with a mass fraction of 20% was added to 2 cm<sup>3</sup> of the diluted centrifuge. Distilled water was adjusted to 10 cm<sup>3</sup> with water, pipetted with water, or from a burette. 1 g of powdered calcium hydroxide was added, shaken vigorously and left resting for 30 minutes, shaken from time to time, and then centrifuged. The centrifuge was poured into a flask. For the color reaction, 1 cm<sup>3</sup> of the centrifugate was transferred to a flask of about 25x200 mm in size, 1 drop of a solution of copper sulfate was added with a mass fraction of 4%, and placed in ice water. With stirring, 6 cm<sup>3</sup> of concentrated sulfuric acid was added from the micro burette. The tube was placed for 5 minutes in a water bath at the boiling temperature, and then it was cooled in cold water to 20 °C. A vapor solution—oxydiphenyl (0.1 cm<sup>3</sup>) was added to the tube, mixed very carefully, after which the tubes were placed for 30 minutes in a water bath at 30 °C, occasionally slightly shaking. After this period, the tube was placed in a strongly boiling water bath for 90 s, then it was cooled in cold water, and the color intensity was measured using a spectrophotometer. The measurement was carried out at a wavelength of 560 nm. The thickness of the cuvette is 1 cm. A control experiment with reagents was carried out starting from the moment of carbohydrate precipitation. Instead of 2 cm<sup>3</sup> of the centrifugate of our sample, we used 0.3 cm<sup>3</sup> of a solution of trichloroacetic acid and 1.7 cm<sup>3</sup> of distilled water. We built a calibration graph. According to the calibration graph, the concentration of lactic acid in the volume of the solution taken for the color reaction was found (Sarbatova *et al.*, 2018).

Determination of shear forces. To do this, turn on the PM-3 device with the VK toggle switch. The handle leads the arrow of the device to zero, and the holes in the plate of the working body and the shifting clamp are combined. The prepared meat sample is carefully placed in the



formed cylindrical hole, and pressure plates with a knife surface at the end are inserted into the guides to cut off the excess meat and fix the sample. By pressing the “Start” button, the drive of the working body is set in motion, the shifting plate of which produces a slice of the sample. The force required to cut the sample is transmitted to the strain gauge and, through the strain gauge, is fixed in the form of a peak on the tape of the potentiometer (Omarovet *al.*, 2018).

### 3. RESULTS AND DISCUSSION:

In the process of cultivation on meat and peptone agar, we studied morphology and carried out a complete identification of the selected strains of microorganisms. The choice was limited to three species: *Lactobacillus bulgaricus*, *Bifidumbacterinumsiccum*, *Staphylococcus carnosus*. *Lactobacillus bulgaricus* and *Staphylococcus carnosus* were selected because of the fast growth during cultivation on different nutrient media. Bifidobacteria are present in large amounts in the intestinal microflora. Therefore, *Bifidumbacterinumsiccum* was the third type of bacteria to be selected.

When cultivated on meat peptone gelatin, biochemical properties were studied by determining microorganisms' proteolytic activity in thinning the gelatin medium. It was found that *Lactobacillus bulgaricus* and *Staphylococcus carnosus* have greater proteolytic activity since they liquefied gelatin on the 4th day of cultivation. *Bifidumbacterinumsiccum* enzyme systems were less active and thinned dense media only for 6 days at room temperature.

During the cultivation of *Lactobacillus bulgaricus*, the pH of the collagen gel decreased from 6.54 at the beginning of cultivation to 5.8 eight hours later after the beginning of cultivation. The acidity accordingly increased from 35°T to 82°T, which indicates the intensive growth and metabolism of the bacteria *Lactobacillus bulgaricus*.

The growth and development of *Bifidumbacterinumsiccum* were less active: acidity increased from 36°T to 74°T, the mass fraction of protein decreased from 1.51 to 1.09 mg/cm<sup>3</sup>, and the pH from 6.83 to 6.09. After interpreting the obtained data, it can be concluded that the biosynthetic activity of *Bifidumbacterinumsiccum* and *Lactobacillus bulgaricus* is slightly different and has special features.

During the cultivation of *Staphylococcus carnosus*, the pH decreased from 6.61 to 5.9, and the acidity increased from 65.3°T to 98°T. In contrast to other lactic acid bacteria, the proportion of protein increased from 1.5 to 1.62, indicating a lower degree of protein hydrolysis in the presence of *Staphylococcus carnosus*. The data obtained are shown in figures 1, 2, 3.

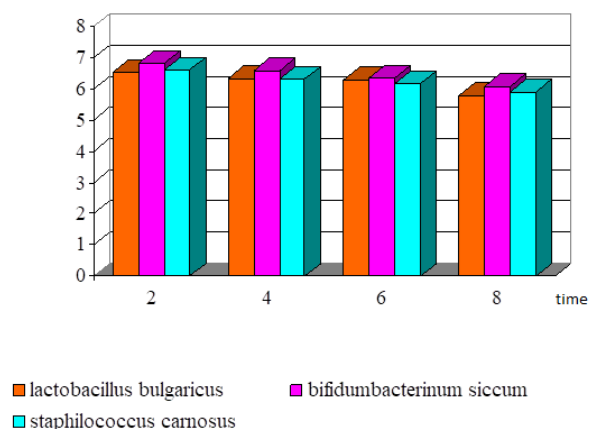


**Figure 1.** pH values during the growth of lactic acid bacteria on collagen gel

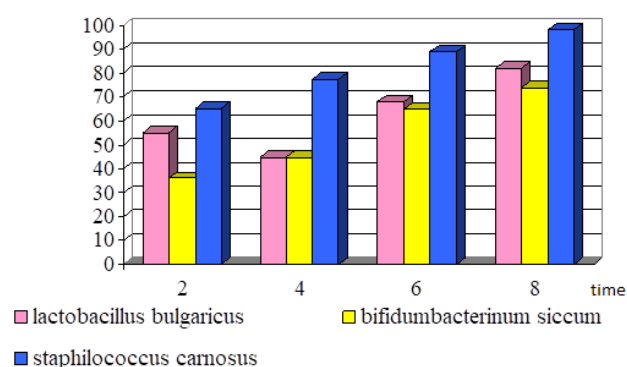


**Figure 2.** Acidity values of the medium during the growth of lactic acid bacteria on collagen gel

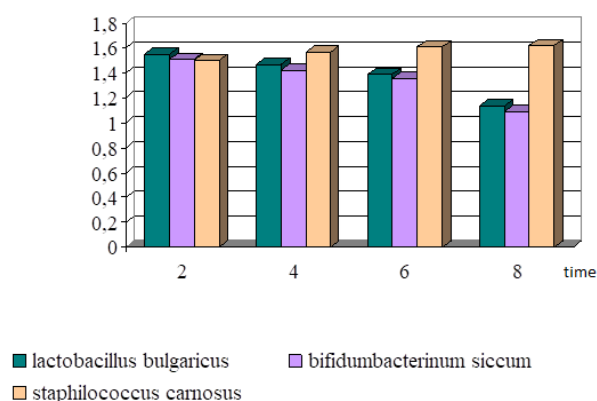


**Figure 3.** Values of the protein fraction of the medium during the growth of lactic acid bacteria on collagen gel

During cultivation on a gelatin gel, the pH and mass fraction of protein was determined by the biuret method, every two hours during the first 10 hours of cultivation. Simultaneously, 2 cm<sup>3</sup> of an alkaline protein extract was taken for analysis and mixed with 15 cm<sup>3</sup> of a biuret solution. A control experiment was prepared similarly.

It was found that over this period, the pH value decreased from 6.19 at the beginning of cultivation to 5.8 at the end of cultivation. There was also a decrease in the proportion of protein from 0.45 mg/cm<sup>3</sup> to 0.26 mg/cm<sup>3</sup>. The control when measuring pH was an extract from the minced meat without adding a consortium of microorganisms.

The minced meat's functional and technological properties, which were obtained, are presented in Figures 4, 5.

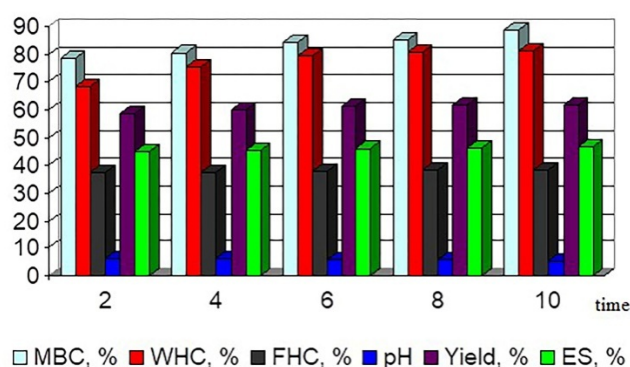


**Figure 4.** Minced flank meat with the addition of lactic acid bacteria complex

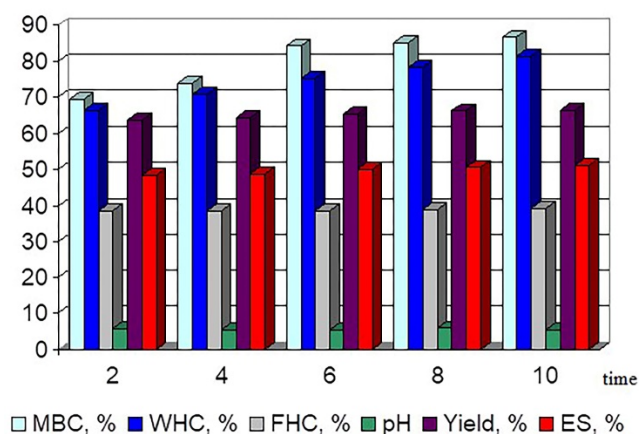


**Figure 5.** Stuffed horse meat with the addition of a complexo-flactic-acid bacteria

The research results indicate a positive symbiosis of the selected strains with the preservation of all biochemical properties. The formed consortium of lactic acid bacteria was used in the processing of real objects: horse meat, flank, and beef muscle tissue of the second grade.

Connective tissue, which is connected with muscle tissue and is organically part of the meat, reduces its nutritional value: the utilization rate in anabolism for connective tissue is three times less than for meat. Besides, it increases its rigidity. Therefore, the quality of meat depends not only on the amount of connective tissue but also on the ratio of elastin and collagen fibers, their structure, and thickness.

Many researchers use one single pure culture as a culture of microorganisms. Some cultures are very rarely used in the consortium. Microorganism cultures are mostly used only as starter cultures to accelerate the production of raw smoked sausages (Adams and Mitchell, 2002; Argyriet al., 2015; Audenaert et al., 2010; Bonomo et al., 2008; Dušková et al., 2016; Gizatov and Gizatova, 2015; Gizatova et al., 2014; Holko et al., 2013). In this regard, the superiority of these studies is precisely the use of microorganism cultures in the form of a consortium and their use in the production of any kind of sausages as not an accelerator, but a softener of low-value meat raw materials. Cocolinet al. (2009), De Souza Barbosa et al. (2015), Juntunen et al. (2001), Dušková et al. (2016) were developing the use of starter cultures as additives to fermentable sausages. Selected starter cultures (SAS) (i.e., *Lactobacillus sakei* 8416, *Lactobacillus sakei* 4413, and *L. sakei* 8426, *L. Plantarum* 7423 and *L. curvatus* 8427) were used as starter cultures in addition to the control

treatment in the production of fermented sausages. SAS cultures had rapid growth, and the randomness of the LAB population prevailed throughout fermentation and maturation. A process of improvement in sensory properties was observed compared to the control sample. Besides the treatment obtained with *L. sakei* 8416, all other SAS cultures prevented lipid oxidation to below 1 mg malondialdehyde/kg.

The number of Micrococcaceae and the redness of the sausages were not affected. The acidification during the fermentation in the treatment is performed with *L. sakei* 8416 and *L. sakei* 4413. The values for *L. sakei* 4413 were the lowest (\* P <0.05), the content of all biogenic amines compared with control, the decrease in tyramine was 13%, tryptamine 55%, cadaverine 60%, and putrescine 72%. Sausages made with SAS cultures of *L. sakei* 4413 and *L. sakei* 8416 had the highest ratings for all sensory properties. The results showed that the SAS culture of *L. sakei* 4413 is the best starting culture for fermented sausages (Andreeva *et al.*, 2018; Omarov *et al.*, 2018). Several researchers are involved in the use of starter crops in sausage production (Adams and Mitchell, 2002; Cocolinet *et al.*, 2009; Doulgeraki *et al.*, 2012; Dušková *et al.*, 2015; Iliina *et al.*, 2017; Juntunen *et al.*, 2001; Knolet *et al.*, 2001). To improve the food safety of Chinese fermented sausages, starter cultures of *Lactobacillus sakei* were added to sausages, and the effects on sausage quality were studied. The results clearly showed that due to *L. sakei* inoculation, lactic acid bacteria quickly dominated. In total, the microflora and growth of foodborne pathogens such as *E. coli* and enterobacteria was completely eradicated in fermentable sausages. The pH of sausages fermented through *L. sakei* significantly decreased from 6.31 to 4.52, while spontaneous fermentation decreased from 6.41 to 5.42. In addition, the nitrite content of sausages fermented by *L. sakei* quickly fell from 100 ppm to 9.6 ppm. Accordingly, spontaneous fermentation, the nitrite content, slowly fell from 100 parts per million to 32.1 ppm. After a sensory evaluation, sausages fermented through *L. sakei* are accepted with pleasure and are in high demand with consumers. *L. sakei* vaccination was beneficial for microbiological quality against the growth of foodborne pathogens and contributed to the depletion of nitrite and improved sensory characteristics (Ivanov *et al.*, 2018).

In the cultivation process on GMK-1 nutrient medium, we studied morphology and carried out a complete identification of the selected

microorganism strains (*Lactobacillus bulgaricus*, *Bifidobacterium sicum*, *Staphylococcus carnosus*).

When identifying, it was noted the differentiating features characteristic of these types of microorganisms:

- for staphylococci, the cells are spherical, gram-positive, motionless, the arrangement of cells in the form of irregular clusters

- bifidobacteria are characterized by straight or branched bacilli, bifurcated Y – or V – forms, club-shaped or lap-shaped, gram-positive, motionless.

- for lactobacilli long and thin to short, straight, or curved gram-positive sticks.

During the microscopic examination of cultures under a light microscope, microphotography of microorganisms' strains at a magnification of 7x90 was carried out. It was also revealed that during cultivation in the consortium of the selected types of bacteria, growth inhibition does not occur, which indicates the synergism of microorganisms in relation to each other.

The number of cells of microorganisms was also calculated. Counting was carried out from the same crops. The number of microorganisms was: *Lactobacillus bulgaricus* 394.0 10<sup>5</sup> CFU/g, *Bifidobacterium sicum* 393.0 10<sup>5</sup> CFU/g, *Staphylococcus carnosus* 396.5 10<sup>5</sup> CFU/g.

When cultivating *Lactobacillus bulgaricus*, the pH of collagen gel decreased by 19% compared to the initial value 24 hours after the beginning of cultivation. The amount of accumulated lactic acid was 27 mg%; the degree of protein hydrolysis was 17% of the initial value. During the cultivation of *Bifidobacterium sicum*, the pH decreased by 14%, the amount of lactic acid was 20 mg%, the degree of hydrolysis of proteins was 13% of the initial value. For *Staphylococcus carnosus*, respectively, these data were pH decreased by 15.8%, the amount of lactic acid 30 mg%, the degree of hydrolysis of proteins 19% to the initial, respectively.

The data obtained indicate that the selected microorganism strains grow on a collagen gel, as evidenced by the accumulation of lactic acid and a decrease in pH, as well as the breakdown of the protein of the collagen connective tissue, which makes the meat stiff. As a result, there is an accumulation of free amino acids and polypeptides. At the same time, the selected bacteria were cultured on a collagen gel in various combinations: 1) *Lactobacillus bulgaricus* + *Bifidobacterium sicum*; 2) *Staphylococcus*

*carnosus* + *Lactobacillus bulgaricus*; 3) *Staphylococcus carnosus* + *Bifidobacterium sicum*. During cultivation, the same values were determined as in the cultivation of each species separately.

The research results showed that the selected microorganism strains grow well on a collagen gel with the intensive accumulation of lactic acid with a decrease in pH, which indicates the absence of antagonism between the selected microorganism strains. In this case, gel proteins are actively cleaved, which is ensured by the presence of a high level of proteolytic activity.

An important factor in the application of the created consortium of microorganisms is the resistance of these types of bacteria to the action of various temperature parameters used in the production of meat products. For conducting the study, a consortium of microorganisms was activated for 12 hours in skim milk under sterile conditions at an optimum microorganism growth temperature of 30 °C in a thermostat. After activation, a consortium was added to ground beef at a temperature of + 4 °C, + 12 °C, + 20 °C, + 40 °C, + 80 °C. The temperature parameters were chosen in accordance with the sausages used in the technology. + 4 °C – temperature for salting and ripening meat, + 12 °C – drying temperature, + 20 °C – smoking temperature, + 40 °C – hot smoking temperature, 80 °C – cooking temperature. The growth of microorganisms was monitored by the dynamics of titratable acidity of ground beef meat for 24 hours. During the study, it was found that at all variants of the selected temperatures, except for a temperature of 80 °C, titratable acidity of ground beef increases, which indicates the development and consortium of microorganisms. At 80 °C, changes in acid formation were practically not observed, which indicates the death of microorganisms.

Assessment of the growth ability and manifestations of the biochemical activity of the created consortium of lactic acid bacteria on real objects to the most significant functional and technological properties of meat systems: moisture-binding, the moisture-holding ability of meat raw materials, its stickiness, especially in sausage technology. It was interesting to study the effect of raw meat's fermentation on the numerical values of these values. In the process of traditional salting, a gradual increase in MBC occurs, which stabilizes over time. A study of the influence of a consortium of microorganisms showed that their use in the salting process leads to insignificant (3-8%) and stable growth of MBC

during salting time for all three types of minced meat. When using a traditional way of salting, the nature of the dependence can be explained by the fact that during the initial stages of hydrolysis, the formation of hydrolysis products of protein molecules occurs due to the proteolytic activity of microorganisms included in the consortium, which leads to an increase in the number of readily available charged groups that can hold water. With deeper hydrolysis, oligopeptides, and free amino acids accumulate, which are not known to be capable of efficiently binding water. The results obtained during salting with the addition of microorganisms are obviously associated with an increased intensity of the action of microorganisms on the connective tissue proteins of minced meat raw materials. Obviously, these results in the accumulation of a large number of readily available charged groups, and lactic acid bacteria assimilate the formed amino acids during the life process. The water-holding capacity (WHC) of raw materials is the most critical indicator for meat products subjected to heat treatment with traditional salting. A sharp increase in WHC in the first hours of salting occurs.

The maximum WHC values are achieved after 2 hours of processing for minced meat from horse meat and muscle tissue of beef, 4 hours – for minced meat from the beef flank, after which the WHC values decrease. When using consortia, a smooth increase in the WHC occurs during the first 4-6 hours, and then a slight decrease in the WHC occurs, and the final values when using a consortium of microorganisms for all types of minced meat are significantly higher than with traditional salting without adding a consortium of microorganisms. Such results indicate the synergistic (mutual reinforcement) action of a consortium of microorganisms and salt in the process of salting.

In scientific studies, Adams and Mitchell (2002), Bonomo *et al.* (2008), Coccolinet *et al.* (2009), it was revealed that after three days of product storage, the number of *thermophilic streptococcus* was  $1.3 \cdot 10^7$  CFU/g. When storing the product, the total number of microorganisms with different microbial contamination of the meat component remained at the same level within seven days,  $1 \cdot 10^2$  CFU/g. According to the results of these studies, three days after development, the number of lactic acid and bifidobacteria cells was  $1 \cdot 10^8$  CFU/g, on the seventh day of storage, it was  $1.4 \cdot 10^6$  CFU/g and remained at that level.

The use of our complex of lactic acid

bacteria both to the flank and to horse meat and beef muscle tissue leads to an increase in the values of functional and technological properties such as MBC, WHC, as well as to a decrease in the pH of the environment, which is important when producing meat and sausage products. It should be recognized that the processing of raw meat with lactic acid and bifidobacteria is effective and economically feasible since salting time is halved during the addition of lactic acid and bifidobacteria. The nature of the action of the consortium of microorganisms allows us to recommend it for use with the goal of softening, improving the quality of raw materials in the technology of a wide range of meat products with different ratios of muscle and connective tissue.

The developed product, enriched with consortiums of microorganisms, will have a positive effect on human health. It will contribute to economically and rationally use the most important food resources. Using selection methods opens up the possibility of obtaining products with valuable characteristics (original taste, aroma, right color consistency). It is assumed that the resulting race can severely suppress the harmful microflora that grows in meat products.

## 5. CONCLUSIONS

The macro morphological and biochemical properties of microorganisms were studied during the research: *Lactobacillus bulgaricus*, *Lactobacillus casei*, *Staphylococcus carnosus*, as well as their synergism on various nutrient media, including collagen gel. The laws of growth and changes in the biochemical properties of strains were established. The selection of strains for creating a consortium was justified. The consortium's influence on the functional and technological properties of the biomodified model minced meat from horse meat, flank, and beef grade II was studied.

The analysis of the obtained results proves that, against the background of a positive symbiosis of the selected strains, it was possible to create a consortium of microorganisms with preserving all biochemical properties. The addition of the studied consortium of wet organisms to both flank and horse meat increased the functional and technological properties such as MBC, WHC, FHC, Yield, ES, as well as to lower the pH of the medium, which is not unimportant in the production of meat and

sausages. The results of these studies, compared with analogs, are in a more advantageous position since the use of the obtained consortium in the production of meat products allows not only accelerating the maturation of minced systems but also makes it possible to use low-value meat raw materials in production by increasing the grade of low-grade raw materials in the fermentation process.

Sausages produced using this technology have functional properties as they are rich in mineral matters (calcium 98.75 mg, sodium 9.07 mg, magnesium 33.85 mg, iron 1.27 mg, respectively) B vitamins 2.8 mg%. The economic effect of the use of a consortium of microorganisms in the technology of sausage production consists of a reduction in terms of salting and replacement of the main raw materials and amounts to 3875.26 rubles per ton of the finished product.

## 5. ACKNOWLEDGMENT:

The authors thank the universities (Bashkir State Agrarian University and Ufa State Petroleum Technological University) for the study's support.

## 6. REFERENCES:

1. Adams, M., and Mitchell, R. (2002). Fermentation and pathogen control: a risk assessment approach. *International Journal of Food Microbiology*, 79(1-2), 75-83.
2. Ammor, M. S., and Mayo, B. (2007). Selection criteria for lactic acid bacteria to be used as functional starter cultures in dry sausage production: An update. *Meat science*, 76(1), 138-146.
3. Andreeva, A. V., Nikolaeva, O. N., Ismagilova, E. R., Tuktarov, V. R., Fazlaev, R. G., Ivanov, A. I., ... and Khakimova, A. Z. (2018). Effect of probiotic preparations on the intestinal microbiome. *Journal of Engineering and Applied Sciences*, 13(S8), 6467-6472.
4. Antipova, L. V. (2001). *Methods used to study meat and meat products*. Moscow: Kolos.
5. Antipova, L. V., and Uspenskaj, M. E. (2016). Bio-modification of plasma protein complex blood of farm animals in preventive technologies and products for special purposes. In *Collection of articles: Modern state and development prospects*

- of dairy farming and agrifood industry. *Proceedings of International Scientific and Practical conference* (pp. 167-171). Omsk State Agrarian University named after P.A. Stolypin. Institute of International Education.
6. Antipova, L. V., Glotova, I. A., Storublevtsev, S. A., Boltyhov, J. V., Vtorushina, I. V., Ilina, N. M., and Galina, J. F. (2011). Realization of biopotential minor collagen raw materials in processing branches of agrarian and industrial complex on the basis of biotechnological methods. In *Biotechnology and the Ecology of Big Cities* (pp. 159-170).
  7. Antipova, L. V., Gorbunkov, M. Y., and Storublevtsev, S. A. (2015). The experience of enzyme preparations application in the processing of animal origin raw materials. *European Journal of Natural History*, 2, 42-43.
  8. Antipova, L. V., Gorbunkov, M. Y., and Storublevtsev, S. A. (2016). New biotechnologies of raw animal materials. In *Collection of articles: Immediate problems of chemistry, biology, and biotechnology. Proceedings of the 10th All-Russian Scientific conference* (pp. 296-297).
  9. Argyri, A. A., Mallouchos, A., Panagou, E. Z., and Nychas, G. J. E. (2015). The dynamics of the HS/SPME–GC/MS as a tool to assess the spoilage of minced beef stored under different packaging and temperature conditions. *International journal of food microbiology*, 193, 51-58.
  10. Armuzzi, A., Cremonini, F., Ojetto, V., Bartolozzi, F., Canducci, F., Candelli, M., ... and Gasbarrini, G. (2001). Effect of Lactobacillus GG supplementation on antibiotic-associated gastrointestinal side effects during Helicobacter pylori eradication therapy: a pilot study. *Digestion*, 63(1), 1-7.
  11. Audenaert, K., D'Haene, K., Messens, K., Ruysen, T., Vandamme, P., and Huys, G. (2010). Diversity of lactic acid bacteria from modified atmosphere packaged sliced cooked meat products at sell-by date assessed by PCR-denaturing gradient gel electrophoresis. *Food Microbiology*, 27(1), 12-18.
  12. Bonomo, M. G., Ricciardi, A., Zotta, T., Parente, E., and Salzano, G. (2008). Molecular and technological characterization of lactic acid bacteria from traditional fermented sausages of Basilicata region (Southern Italy). *Meat Science*, 80(4), 1238-1248.
  13. Buchanan, R. E., and Gibbons, N. E. (1994). *Manual of Determinative Bacteriology*. Bergey's 8 ed. Baltimore: The Williams and Wilkins Company.
  14. Bulat, P. V., Zasuhin, O. N., and Uskov, V. N. (2012). On classification of flow regimes in a channel with sudden expansion. *Thermophysics and Aeromechanics*, 19(2), 233-246.
  15. Casquete, R., Benito, M. J., Martín, A., Ruiz-Moyano, S., Hernández, A., and Córdoba, M. G. (2011). Effect of autochthonous starter cultures in the production of "salchichón", a traditional Iberian dry-fermented sausage, with different ripening processes. *LWT-Food Science and Technology*, 44(7), 1562-1571.
  16. Cocolin, L., Dolci, P., Rantsiou, K., Urso, R., Cantoni, C., and Comi, G. (2009). Lactic acid bacteria ecology of three traditional fermented sausages produced in the North of Italy as determined by molecular methods. *Meat Science*, 82(1), 125-132.
  17. de Souza Barbosa, M., Todorov, S. D., Ivanova, I., Chobert, J. M., Haertlé, T., and de Melo Franco, B. D. G. (2015). Improving safety of salami by application of bacteriocins produced by an autochthonous Lactobacillus curvatus isolate. *Food microbiology*, 46, 254-262.
  18. Doulgeraki, A. I., Ercolini, D., Villani, F., and Nychas, G. J. E. (2012). Spoilage microbiota associated to the storage of raw meat in different conditions. *International journal of food microbiology*, 157(2), 130-141.
  19. Dušková, M., Kameník, J., Lačanin, I., Šedo, O., and Zdráhal, Z. (2016). Lactic acid bacteria in cooked hams—Sources of contamination and chances of survival in the product. *Food Control*, 61, 1-5.
  20. Dušková, M., Kameník, J., Šedo, O., Zdráhal, Z., Saláková, A., Karpíšková, R., and Lačanin, I. (2015). Survival and growth of lactic acid bacteria in hot smoked dry sausages (non-fermented salami) with and without sensory deviations. *Food Control*, 50, 804-808.
  21. Gabitov, I. I., Mudarisov, S. G., Gafurov, I. D., Ableeva, A. M., Negovora, A. V., Davletshin, M. M., ... and Yukhin, G. P. (2018). Evaluation of the efficiency of



- mechanized technological processes of agricultural production. *Journal of Engineering and Applied Sciences*, 13(S10), 8338-8345.
22. Gabitov, I. I., Negovora, A. V., Khasanov, E. R., Galiullin, R. R., Farshatov, M. N., Khamaletdinov, R. R., ... and Razyapov, M. M. (2019). Risk reduction of thermal damages of units in machinery heat preparation for load acceptance. *Journal of Engineering and Applied Sciences*, 14(3), 709-716.
  23. Gavrilova, N., Chernopolskaya, N., Rebezov, M., Moisejkina, D., Dolmatova, I., Mironova, I., ... and Derkho, M. (2019). Advanced biotechnology of specialized fermented milk products. *International Journal of Recent Technology and Engineering*, 8(2), 2718-2722.
  24. Gizatov, A. Y., and Gizatova, N. V. (2015). Biotechnological aspects of bifidobacteria usage to obtain products of animal origin with the desired properties. In *Innovative Processes in AgroIndustrial Complex* (pp. 105-106).
  25. Gizatova, N. V., Gizatov, A. I., and Mironova, I. V. (2014). Reason in selecting microorganism species for collagen containing raw materials. In *Collection of articles: Prospects of innovative development of Agri-Industrial complex. Proceedings of International Scientific and Practical conference within the framework of the 24<sup>th</sup> International Specialized Exhibition "Agrocomplex-2014"* (pp. 19-24).
  26. Holko, I., Hrabě, J., Šalaková, A., and Rada, V. (2013). The substitution of a traditional starter culture in mutton fermented sausages by *Lactobacillus acidophilus* and *Bifidobacterium animalis*. *Meat Science*, 94(3), 275-279.
  27. Ilina, N. M., Kutsova, A. E., Builenko, Iu. S., and Fomina, T. (2017). Application of biotechnological methods in meat production. *Bulletin of the South Ural State University Vestnik. Series of papers: Food Technologies*, 5(3), 21-28.
  28. Ivanov, A. I., Andreeva, A. V., Skovorodin, E. N., Shaimukhametov, M. A., Altynbekov, O. M., Sultangazin, G. M., ... and Nikolaeva, O. N. (2018). Anaerobic microflora impact on pathomorphogenesis of swine dysentery. *Journal of Engineering and Applied Sciences*, 13(S11), 8796-8802.
  29. Juntunen, M., Kirjavainen, P. V., Ouwehand, A. C., Salminen, S. J., and Isolauri, E. (2001). Adherence of probiotic bacteria to human intestinal mucus in healthy infants and during rotavirus infection. *Clinical and Diagnostic Laboratory Immunology*, 8(2), 293-296.
  30. Karam, L., Jama, C., Dhulster, P., and Chihib, N. E. (2013). Study of surface interactions between peptides, materials and bacteria for setting up antimicrobial surfaces and active food packaging. *Journal of Materials and Environmental Science*, 4(5), 798-821.
  31. Knol, J., Poelwijk, E. S., Van der Linde, E. G. M., Wells, J. C. K., Bronstrup, A., Kohlschmidt, N., ... and Fusch, C. (2001). Stimulation of endogenous bifidobacteria in term infants by an infant formula containing prebiotics. *Journal of Pediatric Gastroenterology and Nutrition*, 32, 399.
  32. Konashova, S. I., Sultanova, R. R., Khairtdinov, A. F., Gabdrakhimov, K. M., Konovalov, V. F., Rakhmatullin, Z. Z., ... and Muftakhova, S. I. (2018). Forestry and ecological aspects of the broad-leaved forest formation. *Journal of Engineering and Applied Sciences*, 13(S11), 8789-8795.
  33. Martynov, V. M., Gabitov, I. I., Karimov, K. T., Masalimov, I. K., Permyakov, V. N., Ganeev, I. R., ... and Saitov, B. (2018). Reasoning barley grain drying modes for vacuum-infrared drying machines. *Journal of Engineering and Applied Sciences*, 13(S11), 8803-8811.
  34. Nesterenko, A. A., Keniiz, N. V., Ilina, N. M., and Korshunova, Y. M. (2016). Studying the properties of starter cultures in meat raw materials. In *Collection of articles: Modern problems of fundamental and applied sciences development* (pp. 18-24). Printing house "Maestro".
  35. Nesterenko, A., Koshchaev, A., Keniiz, N., Akopyan, K., Rebezov, M., and Okuskhanova, E. (2018). Biomodification of Meat for Improving Functional-Technological Properties of Minced Meat. *Research Journal of Pharmaceutical Biological and Chemical Sciences*, 9(6), 95-105.
  36. Omarov, R. S., Antipova, L. V., Konieva, O. N., Meshcheryakov, V. A., and Shlykov, S. N. (2018). Biotechnological aspects in the development of functional food products.

37. Rakhimov, Z., Mudarisov, S., Rakhimov, I., Farkhutdinov, I., Mukhametdinov, A., Gareev, R., ... and Tarkhova, L. (2018). Reasoning a construction diagram and parameters of tillers for primary cultivation. *Journal of Engineering and Applied Sciences*, 13(S11), 8812-8818.
38. Sarbatova, N. Y., Frolov, V. Y., Omarov, R. S., Sycheva, O. V., and Antipova, L. V. (2018). Study of biotechnological potential of blood agricultural animals and poultry for the development of new balanced food products. *Research Journal of Pharmaceutical, Biological and Chemical Sciences*, 9(2), 555-562.
39. Sydykova, M., Nurymkhan, G., Gaptar, S., Rebezov, Y. M., Khayrullin, M., Nesterenko, A., and Gazeev, I. (2019). Using of lactic-acid bacteria in the production of sausage products: modern conditions and perspectives. *International Journal of Pharmaceutical Research*, 11(1), 1073-1083.
40. Wang, X. H., Ren, H. Y., Liu, D. Y., Zhu, W. Y., and Wang, W. (2013). Effects of inoculating *Lactobacillus sakei* starter cultures on the microbiological quality and nitrite depletion of Chinese fermented sausages. *Food Control*, 32(2), 591-596.
41. Zinina, O. V., and Rebezov, M. B. (2016). A Biotechnological processing of collagen containing by-products of bovine animals. *Research Journal of Pharmaceutical Biological and Chemical Sciences*, 7(1), 1530-1534.
42. Zinina, O. V., Rebezov, M. B., and Vaiscrobova, E. S. (2016). A microstructure of the modelling systems on the basis of the ferment raw material with a high collagen content. *Pakistan Journal of Nutrition*, 15(3), 249-254.



ANÁLISE RETROSPECTIVA DO CURSO DE CÂNCER DE TIREÓIDE COM  
METÁSTASES NOS PULMÕES APÓS RADIODIOTERAPIA

RETROSPECTIVE ANALYSIS OF THE COURSE OF THYROID CARCINOMA WITH LUNG  
METASTASES AFTER RADIOIODINE THERAPY

РЕТРОСПЕКТИВНИЙ АНАЛІЗ ПЕРЕБІГУ РАКУ ЩИТОВИДНОЇ ЗАЛОЗИ З  
МЕТАСТАЗАМИ В ЛЕГЕНЯХ ПІСЛЯ РАДІОЙОДТЕРАПІЇ

ASTAPIEVA, Olha M.<sup>1\*</sup>; GRUSHKA, Ganna V.<sup>2</sup>; PASKEVYCH, Olga I.<sup>3</sup>; FEDULENKOVA,  
Yuliia Ya.<sup>4</sup>; MAKSIMISHYN, Oleksii V.<sup>5</sup>;

<sup>1,2,3,4,5</sup> Kharkiv National Medical University, Department of Radiology and Radiation Medicine, 4 Nauky Ave.,  
ZIP code 61022, Kharkiv – Ukraine

\* Correspondence author  
e-mail: [astapyeva\\_on@ukr.net](mailto:astapyeva_on@ukr.net)

Received 21 April 2020; received in revised form 11 June 2020; accepted 18 June 2020

## RESUMO

As metástases de tumores malignos são um dos problemas mais agudos da oncologia. Por frequência de lesões entre os órgãos e sistemas do corpo humano, um dos primeiros locais é ocupado pelos pulmões, o que provavelmente está intimamente relacionado às características anatômicas de sua estrutura e fisiologia. No primeiro exame de pacientes com câncer, as metástases pulmonares são encontradas em 6 a 15%, metástases linfogênicas – em 50 a 81%. No carcinoma diferenciado da glândula tireóide (glândula tireóide) muitas vezes se encontram as metástases nos pulmões (até 15% dos casos). Ao mesmo tempo, as taxas de sobrevivência de 5 e 10 anos são de 50 a 92,6% e 42 a 86%, respectivamente. O uso de iodeto de sódio (<sup>131</sup>I) é a base para o tratamento desses pacientes. O objetivo do artigo é estudar a eficácia da terapia com radioiodo em metástases de carcinoma de tireóide nos pulmões. Utilizamos os métodos radiológicos clínicos, laboratoriais para diagnosticar carcinoma de tireóide e metástases pulmonares. De 1986 a 2010, o estudo envolveu 68 pacientes da clínica do S. P. Hryhoriiev Instituto de Radiologia Médica de Academia de Ciências Médicas da Ucrânia. Metástases pulmonares foram encontradas em pacientes com todos os estágios da doença e com diferentes tamanhos de tumor primário da tireóide. Após o tratamento cirúrgico, os pacientes receberam iodeto de sódio (<sup>131</sup>I) em várias doses de radioatividade. O efeito terapêutico completo da radioterapia foi alcançado em 5 pacientes (7,8%) durante o período de tratamento de 3 anos e no período de 5 anos - em 28 (43,8%); estabilização ou efeito parcial foi observado em 24 pacientes (37,8%), progressão da doença em 12 pacientes (17,6%). A mortalidade por progressão da doença foi de 12,5%

**Palavras-chave:** *minimização de energia potencial, método dos elementos finitos, isolamento térmico, temperatura, coeficiente de transferência de calor.*

## ABSTRACT

Metastasis of malignant tumors are one of the most acute problems of oncology. Among the organs and systems of the human body in terms of frequency of damage, one of the first places is occupied by the lungs, which is probably closely related to the anatomical features of their structure and physiology. During the first examination of cancer patients, metastases in the lungs are revealed in 6-15%, lymphogenous metastases are observed in 50-81%. With differentiated thyroid carcinoma (thyroid gland), metastases in the lung are most often detected (up to 15% of cases). At the same time, 5- and 10-year survival rates are 50-92.6% and 42-86%, respectively. The use of <sup>131</sup>I-sodium iodide is central to the treatment of these patients. The purpose of the paper is to study the effectiveness of radioiodine therapy for metastases of thyroid carcinoma in the lung. We used clinical, laboratory, radiological methods for the diagnosis of thyroid carcinoma and pulmonary metastases. From 1986 to 2010, 68 patients from the clinic of the S.P. Hryhoriev Institute of Medical Radiology of the Academy of Medical Sciences of Ukraine were included in the study. Lung metastases were found in patients with all stages of the disease and with diverse sizes of the primary thyroid tumor. After the surgical treatment of patients, <sup>131</sup>I-sodium iodide was used in various doses of radioactivity. The full therapeutic effect of radiotherapy was achieved in 5 patients (7.8%) over a 3-year period of treatment, and a 5-year period – in 28 (43.8%); stabilization or partial

effect was noted in 24 patients (37.8%), disease progression was observed in 12 patients (17.6%). Mortality from disease progression was 12.5%.

**Keywords:** *differentiated thyroid carcinoma, lung metastases, radioiodine therapy.*

## АНОТАЦІЯ

Метастази злоякісних пухлин є однією з найбільш гострих проблем онкології. Серед органів і систем організму людини за частотою ушкоджень одне з перших місць займають легені, що, ймовірно, тісно пов'язано з анатомічними особливостями їх будови і фізіології. При першому обстеженні хворих на рак метастази в легені виявляють у 6-15%, лімфогенні метастази - у 50-81%. При диференційованій карциномі щитовидної залози (щитовидна залоза) найчастіше виявляються метастази в легенях (до 15% випадків). У той же час 5- і 10-річна виживаність становить 50-92.6% і 42-86% відповідно. Використання <sup>131</sup>I-йодиду натрію є основою для лікування цих пацієнтів. Метою статті є вивчення ефективності радіойодтерапії при метастазах карциноми щитовидної залози в легенях. Ми використовували клінічні, лабораторні, рентгенологічні методи діагностики карциноми щитовидної залози і легеневих метастазів. З 1986 по 2010 рік в дослідженні брали участь 68 пацієнтів з клініки Інституту медичної радіології ім. С.П. Григор'єва АМН України. Метастази в легенях були виявлені у пацієнтів з усіма стадіями захворювання і з різними розмірами первинної пухлини щитовидної залози. Після хірургічного лікування пацієнтів застосовували <sup>131</sup>I-йодид натрію в різних дозах радіоактивності. Повний терапевтичний ефект променевої терапії досягнуто у 5 пацієнтів (7,8%) протягом 3-річного періоду лікування, а 5-річного періоду - у 28 (43,8%); стабілізація або частковий ефект відзначено у 24 пацієнтів (37,8%), прогресування захворювання спостерігалось у 12 пацієнтів (17,6%). Смертність від прогресування хвороби становила 12,5%.

**Ключові слова:** *диференційована тироїдна карцинома, легеневі метастази, радіойодтерапія.*

## 1. INTRODUCTION

Metastasis of malignant tumors are one of the pressing issues of clinical oncology. Often, distant metastases are detected in the process of examination of primary patients or at different times after the treatment of malignant neoplasms localized in the lungs. Upon examining lung metastases, 6–30% of patients with tumors of different localization are determined, mainly in kidney, breast, chorionepithelioma, tumors of the testis, and sarcomas, rarely – in tumors of other localizations (Paches and Prop, 1995; Valdina, 2001).

In many patients, the process of metastasis begins long before the detection of the primary tumor and the initial distant micrometastases, which are not always found with the use of modern research methods. In the lungs, approximately 38% of all distant metastases of cancers of different localization are identified (Paches and Prop, 1995; Schlumberger and Pacini, 1999; Valdina, 2001).

Among the organs and systems of the body, lungs occupy an important place in the frequency of metastatic lesions in malignant neoplasms of different locations (Schlumberger, 1998; Valdina, 2001; Drozdovsky *et al.*, 2002; Podolkhova *et al.*, 2006). At the initial examination,

lung metastases (LM) reveal, according to various authors, 6-15% of patients with malignant tumors, and after treatment, in the event of progression of the process, as a rule, the lungs are affected in most cases (Paches and Prop, 1995; Valdina, 2001; Vini and Harmer, 2003; Afanasieva, 2004). LM are spread by the lymph-hematogenous pathway in 50.0–81.8% of cases, rarely by hematogenous (9.4–30.2%) and lymphogenous (4.3–23.5%) pathways (Valdina, 2001; Lin *et al.*, 2004; Bachelot *et al.*, 2005; Dadu and Cabanillas, 2012; Marotta *et al.*, 2013; Chopra *et al.*, 2015; Kudabaeva *et al.*, 2016; Gorbas *et al.*, 2015).

The share of thyroid carcinoma is 0.4–2.0% (Schlumberger *et al.*, 1996; Schlumberger and Pacini, 1999; Afanasyeva, 2006). of all malignant tumors. Over the last decade, the incidence of thyroid carcinoma has notably increased (Paches and Prop, 1995; Vini and Harmer, 2003). Long-term metastases in patients with thyroid carcinoma are observed in 7.1–17.0% of cases (Schlumberger and Pacini, 1999; Tzavara *et al.*, 1999; Blagitko *et al.*, 2003; Garbuzov, 2003; Afanasyeva, 2006; Smiyan *et al.*, 2015).

Lungs are more often the sites of distant metastasis – from 4.4 to 15.0% (Paches, 2000; Kozak *et al.*, 2004). According to the data in the domestic and foreign literature, the 5- and 10-year

survival of patients with differentiated thyroid carcinoma (DTC) with lung metastases after radioiodine therapy (RIT) is 50.0-92.6% and 42-86%, respectively. In the case of combined lesion of the lungs and mediastinal lymph nodes – 88% and 72%, respectively (Valdina, 2001; Drozdovsky *et al.*, 2002; Garbuzov, 2003; Afanasieva, 2004; Kozak *et al.*, 2004; Huang *et al.*, 2012; Schneider and Chen, 2013; Kudabayeva *et al.*, 2017; Burkitbaev *et al.*, 2017). The use of <sup>131</sup>I has a leading role in the treatment of remote metastases of the thyroid gland.

The full effect of treatment was noted in the absence of ultrasound signs of local and regional recurrence in the absence of pathological lesions on the lung radiograph, physiological distribution of the isotope in scintigraphy, and normalization of thyroglobulin level. Incomplete (partial) treatment or stabilization effects were determined if, in the presence of local and regional recurrence, the size of the tumor was reduced, the size of lung metastases decreased or stabilized, and the titration of thyroglobulin decreased. The absence of effect or disease progression was assessed with recurrence of a neck tumor, enlargement of metastatic lesions in the lungs and/or mediastinum, and/or multiple lung metastases. The conventional method of treatment of such patients involves oral administration of empirical activities of radioiodine in several stages with an interval of 6 months and more until complete visualization of the metastatic lesion has disappeared (Afanasyeva, 2006; Podolkhova *et al.*, 2006; Mechev *et al.*, 2010; Nixon *et al.*, 2012; Kim *et al.*, 2014; Song *et al.*, 2015; Burkitbaev *et al.*, 2017) technique of systematic repetition of courses of treatment with a continuous increase of radioiodine activity with each subsequent stage of treatment allows neutralizing the effect of the so-called "stunning", or damping of thyroid tissue. The successive graded increase in therapeutic activity makes it possible to effectively overcome the threshold of increased radioresistance of those groups of thyroid cells that remained intact after the previous stage of the RIT. The sharp reduction in the time of the summation of the total therapeutic activity (for 9 months, but not for the classic 2-3 years) allows maximizing the effect of preserving the radiosensitivity of thyroid cells, which are lost during prolonged courses of radioiodine therapy (Mechev *et al.*, 2010).

The use of <sup>131</sup>I has a leading role in the diagnosis and treatment of remote metastases of the thyroid gland (Paches and Prop, 1995; Tzavara *et al.*, 1999; Valdina, 2001; Drozdovsky *et al.*, 2002; Vini and Harmer, 2003; Afanasyeva,

2006; Podolkhova *et al.*, 2006). The RIT technique is based on the mechanism of active accumulation of <sup>131</sup>I in thyroid tumor cells, which allows achieving a high absorbed dose in focus with minimal radiation load on the surrounding tissues (Drozdovsky *et al.*, 2002; Vini and Harmer, 2003; Kudabaeva *et al.*, 2015; Abdrakhmanova *et al.*, 2019).

The problems of RIT in patients with thyroid carcinoma with distant metastases are defined – the diagnosis and treatment of metastases, devitalization of thyroid tissue after surgical treatment. This reduces the risk of local recurrence and uses thyroglobulin (TG) as a tumor marker (Kisileva *et al.*, 1987; Paches and Prop, 1995; Reiners and Farahati, 1999; Schlumberger and Pacini, 1999; Drozdovsky *et al.*, 2002; Vini and Harmer, 2003; Kozak *et al.*, 2004; Afanasyeva, 2006; Mechev *et al.*, 2010; Drozdovsky and Podolkhova, 2007; Ramilyeva *et al.*, 2019).

To determine the prevalence of thyroid carcinoma, research methods such as computed tomography of the neck and lungs with contrast in the presence of radiolucent and functionally active lung metastases are used; study of thyroglobulin levels and its antibodies (furthermore, for early diagnosis of thyroid carcinoma relapse) (Paches, 2000; Valdina, 2001; Drozdovsky *et al.*, 2002; Afanasieva, 2004; Tkachenko *et al.*, 2005; Afanasyeva, 2006).

According to the treatment protocol, patients with differentiated thyroid carcinoma in the presence of lung metastases undergo several courses of RIT with the aim of the destruction of all metastatic lesions capable of accumulating radioiodine. For adults, radioiodine treatment activities can reach 24 GBq for a single RIT course. Lung metastases can be detected after several courses of treatment: after partial or complete ablation of residual thyroid tissue or lymph node metastases (Valdina, 2001; Paches and Prop, 1995; Podolkhova *et al.*, 2006; Afanasieva, 2004; Kozak *et al.*, 2004; Drozdovsky and Podolkhova, 2007) in adult patients with lung metastases up to 14% of the total number of patients with thyroid carcinoma. To reduce the level of thyroglobulin and ablation of metastases, several courses of RT are necessary (Afanasyeva, 2004; Kozak *et al.*, 2004; Podolkhova *et al.*, 2006; Drozdovsky and Podolkhova, 2007; Mechev *et al.*, 2010). Typically, in practice, therapeutic activity in the treatment of thyroid carcinoma is determined empirically. If distant metastases are detected at the first diagnostic scan, they use the activity of about 6,000 MBq (Kozak *et al.*, 2004). Some authors believe that to achieve the maximum

therapeutic effect, and one can use the highest activities that the patient can tolerate without complications caused by radiation (Reiners and Farahati, 1999; Tzavara *et al.*, 1999; Podolkhova *et al.*, 2006). However, the result of treatment depends on such factors as the histological structure of the tumor, the patient's age, the number and size of lymph node metastases, the size of the residual tissue of the thyroid gland, etc. It was proven, however, that the course of treatment is substantially determined by the magnitude of the first and second activity, the duration of the break between courses of radioiodine (Kisileva *et al.*, 1987; Reiners and Farahati, 1999; Kozak *et al.*, 2004; Mechev *et al.*, 2010; Drozdovsky and Podolkhova, 2007x).

The purpose of the study is to investigate the efficiency of radioiodine therapy of thyroid carcinoma metastases in the lung.

## 2. MATERIALS AND METHODS

The computer database of the clinic provided a retrospective analysis of the clinical data, the nature of the course of thyroid cancer in the process of cancer treatment, and the results of follow-up care for 68 patients with lung metastases after completion of treatment from 1986 to 2018.

Statistical processing used Fisher's exact test using the Biostatistica software package, v. 4.03. The accuracy of the diagnostic test was analyzed by determining the sensitivity and specificity as the operational characteristics of the diagnostic method. The survey included a group of patients, making up 51 women (73.5%) and 17 men (26.5%) aged 16 to 68 years (median age – 50.5 years).

The distribution of patients is presented in Table 1. The histological structure of thyroid carcinoma in 53 cases (77.9%) revealed papillary carcinoma in 9 cases (13.2%) – follicular carcinoma, papillary carcinoma, follicular variant – in 6 patients (8.9%), medullary carcinoma – 7 patients (8.8% of cases). Background benign thyroid pathology was observed in 18 patients (28% of cases). Oncological heredity was found in 14 patients (22.8% of cases).

The patients underwent single or multiple surgeries. The distribution of patients by the nature of the intervention is presented in Table 2.

The duration of treatment ranged from 1 to 26 years. The prevalence of primary tumor, according to the international TNM classification, was found in 51 patients (79.7% of cases). In 13 patients (20.3% of cases), TX was observed. Most

patients – 17 patients (26.6% of cases) had a T2 size tumor; T3 and T4 were found in 13 patients each (20% of cases). Lymph nodes at the time of diagnosis were observed in 42 patients (66% of cases). That is, in 36 cases (56.2% of patients), which is almost half of patients, they received radical surgical treatment. Also, in 23.4% of cases, patients underwent supplementary surgery – a finishing thyroidectomy, which was accompanied by additional anesthesia, which was recognized as a negative factor for the cardiovascular and nervous systems in elderly patients.

According to the stage of the disease, patients were allocated as follows: stage I – in 19 patients (29.7% of cases); II – in 14 (21.9% of cases); III – in 14 (21.9% of cases); stage IV – in 17 patients (26.6% of cases). Pulmonary metastases at the time of diagnosis were detected radiographically in 18 patients (28.7% of cases), the presence of metastatic lung lesions in the latter patients was further discovered upon chest scintigraphy on “residual” activities  $^{131}\text{I}$  after issuing therapeutic activities  $^{131}\text{I}$ , or radiologically. Data on a primary diagnosis of pulmonary metastases are presented in Table 3.

Four weeks before the radiotherapy, hormone therapy was canceled. The level of thyrotropin in the serum of patients before treatment ranged from 18 to 53 mIU/L (the norm is 0.3–4.0). Thyroglobulin titre was elevated in 53 patients (82.8% of cases).

All patients underwent RIT, the activity of radiopharmaceutical agents for one course ranged from 1.110 to 7.030 MBq. Total activity throughout the treatment period was in the range of 11,740–43,586 MBq. Suppressive hormone therapy was renewed after 48-72 hours. By reducing the radiation dose rate to 3  $\mu\text{Sv/h}$  at a distance of 1 meter from the patient, whole-body scintigraphy was performed on “residual” activities on the Ohio-nuclear gamma camera to detect the centers of accumulation of radiopharmaceutical agents. Follow-up RIT courses were conducted in 3-6 months. Treatment continued until the complete absence of foci of radioiodine accumulation, radiological signs of the disease, and normalization of the level of thyroglobulin content in the serum.

The full effect of treatment was determined in the absence of ultrasound signs of local or regional recurrence, in the absence of pathological lesions of the X-ray image, as well as foci of accumulation of radioiodine on whole body scintigrams on “residual” activities of  $^{131}\text{I}$ , normalization of the level of thyroglobulin in

patients' serum.

During the observation period, 8 patients (12.5%) died from localized relapse and distant metastasis of thyroid carcinoma. The studies were performed under the supervision of the local ethics committee for clinical and experimental research at the S.P. Hryhoriev Institute of Medical Radiology of the Academy of Medical Sciences of Ukraine with obtaining patients' consent to use information.

### 3. RESULTS AND DISCUSSION:

The full effect of RIT over the 3-year treatment period was achieved in 5 patients (7.8%), with the total introduced the activity of  $^{131}\text{I}$  varying from 7.030 to 16.720 MBq (number of courses 3-5). This indicates different levels of radiosensitivity of tumor cells, which is confirmed by studies of other authors (Kisileva *et al.*, 1987; Paches and Prop, 1995; Valdina, 2001; Kozak *et al.*, 2004; Afanasieva, 2004; Podolkhova *et al.*, 2006).

Accumulation of radioiodine only at the site of "residual" thyroid tissue was observed in 14 patients (21.9% of cases) with radiographic signs of lung metastases. The total therapeutic activity of radiopharmaceutical agents in these cases ranged from 1,110 to 3,700 MBq.

The accumulation of radiopharmaceutical agents in the "residual" thyroid tissue and lungs was observed in 31 patients (42.2% of cases – that is, a partial therapeutic effect). Radioiodine fixation in the lungs alone was established in 14 cases (21.8%). The accumulation of  $^{131}\text{I}$  in the lymph nodes of the neck and the remains of the thyroid gland – in 3 patients (4.7% of cases), in 1 case – in both the lungs and lymph nodes of the neck. That is, these patients experienced a local and long-term continuation of the disease. Therefore, they required further treatment.

For the 5 years, the full therapeutic effect was achieved in 28 patients (43.8% of cases), which corresponds to the data of some researchers (Kisileva *et al.*, 1987; Reiners and Farahati, 1999; Afanasieva, 2004; Podolkhova *et al.*, 2006; Drozdovsky and Podolkhova, 2007). Stabilization or partial effect of treatment was achieved in 24 patients (35.3% of cases); unfortunately, the progression of the disease (i.e., the occurrence of localized relapse, metastasis in the lymph nodes of the neck) was observed in 12 patients (18.8% of cases). Subsequently, 8 of them (12.5% of cases) died from progression of thyroid carcinoma (according to other authors,

mortality ranged from 4.9% to 20.7%) (Podolkhova, 2006; Afanasyeva, 2006).

Therefore, in 2/3 of the patients, metastatic lesion of regional lymph nodes was observed before the start of treatment with  $^{131}\text{I}$ , which indicated an extra-organ distribution of primary thyroid tumor, which makes it advisable to conduct a more detailed radiological examination of patients at the diagnostic stage (CT of the neck and MRI of the lungs).

A considerable number of non-radical surgical interventions (almost 44%) make it necessary to improve diagnostic methods of verification of thyroid carcinoma (obligatory performance of a fine needle puncture biopsy of focal changes in the thyroid gland, assessment of the degree of vascularization of pathological lesions in the thyroid gland, altered by the size and structure of regional lymph nodes).

To illustrate the above material, below, clinical examples that characterize the features of the course of the thyroid gland at different stages of the established diagnosis are given, the unpredictable continuation of the disease, even in patients with a non-aggressive course of thyroid microcarcinoma is demonstrated.

Example 1. Patient P., born 1965. Diagnosis: papillary thyroid carcinoma pT1N0M0, after complex treatment, lung metastases, stage I, 2nd clinical group. Severe hypothyroidism.

Considers herself sick since June 2008, when she was ill with pleuropneumonia (received anti-inflammatory therapy in the outpatient clinic with), which was complicated by left-sided dry pleuritis. Upon bronchoscopy, no data on bronchial and lung oncopathology were noted. At the same time, ultrasound of the neck incidentally detected a node 1.0 x 0.8 cm in size in the right lobe of the thyroid gland, which resulted in an aspiration puncture biopsy of this neoplasm. Cytologically, data were obtained on the proliferation of the follicular epithelium. Therefore, surgical treatment is recommended. The patient went to the endocrinological clinic in Kharkiv, where she underwent thyroidectomy on June 25, 2008. PGV No. 2141-44 from 02.07.2008: encapsulated papillary microcarcinoma with a diameter of 1 cm. Further treatment of the patient continued at the S.P. Hryhoriev Institute of Medical Radiology of the Academy of Medical Sciences of Ukraine, where after checking the micro preparations, the carcinoma diagnosis was confirmed. As a result, on 14.08.2008, the patient received  $^{131}\text{I}$  treatment at 3.700 MBq for the medical purpose. After completing the

radiometrics, she had a scintigram of a section of the neck and chest at the "residual" activities of  $^{131}\text{I}$ , upon which fixation of radiopharmaceutical agents was observed only in the neck (Figure 1). Subsequently, the patient received suppressive hormone therapy with euthyrox at a dose of 225  $\mu\text{g}$  per day (TSH level was 0.0105-0.08 mIU/L).

The control study of the patient after six months detected a significant increase in serum content of thyroglobulin and antibodies to it against the background of the abolition of hormone therapy (79.4 ng/ml and 326 IU/ml, respectively). The patient underwent X-ray computed tomography of the neck and chest, which revealed the presence of multiple metastases in the parenchyma of the lung (Figure 2). Therefore, on March 26, 2009, the patient received  $^{131}\text{I}$  treatment at 4,000 MBq for medical purposes. Scintigraphy of the neck and thorax area on the "residual"  $^{131}\text{I}$  activities revealed the accumulation of radioiodine in the lung parenchyma, indicating that the patient had functionally active metastases of thyroid carcinoma in the lung (Figure 3).

In November 2009 and June 2010, the patient received regular courses of radioiodine treatment. At the same time, after each course, there was an accumulation of radioiodine in the lung parenchyma. Currently, the patient receives a suppressive dose of euthyrox, is under the supervision of a regional oncologist.

This example demonstrates the unpredictable nature of the course of encapsulated microcarcinoma, and previous "pleuropneumonia" could be the first manifestation of lung metastases (the so-called pneumonic form of thyroid carcinoma metastasis in the lung).

**Example 2. Patient B-ko. Diagnosis:** papillary thyroid cancer pT2N1aMo, metastases in the cervical lymph nodes on the left, after surgical treatment, and radioiodine therapy. Metastases in the lung parenchyma. Stage I, second clinical group. Severe hypothyroidism.

From the anamnesis of the disease, it is known that in 2008, an ultrasound of the neck incidentally detected a node in the left region of the thyroid gland 14 x 8 mm. Cytologically after aspirational needle biopsy of this node, papillary thyroid carcinoma was confirmed. In this connection, on 10.02.2009, thyroidectomy was performed at the S.P. Hryhoriev Institute of Medical Radiology of the Academy of Medical Sciences of Ukraine. PGV No. 1855-72/09 – papillary thyroid carcinoma (pT2N1aMo). According to the planned program of treatment of

this disease, on March 4, 2009, the patient received treatment at 2,923 MBq for therapeutic purposes. Scintigraphy of the residual activities of the  $^{131}\text{I}$  neck and thorax area revealed an outbreak of radiopharmaceutical agents fixation in the thyroid gland projection (Figure 4). To achieve the ablation of residual tissue, a second course of  $^{131}\text{I}$  radioiodine therapy with activity at 1,480 MBq was performed on 16.09.2009.

Upon scintigraphy on "residual" activities of  $^{131}\text{I}$ , the fixation of radiopharmaceutical agents at the typical site and parenchyma of both lungs were noted (Figure 5), i.e., Functionally active metastases of the thyroid gland in lungs were detected. In addition, this was confirmed by significantly increase thyroglobulin levels in the blood (494.2 ng/ml).

A Ct of the chest was performed to clarify the diagnosis and follow the protocol for the study of patients with cancer. In the study of a series of tomograms, only signs of chronic obstructive bronchitis were identified (in this case, negative X-ray metastases of the thyroid carcinoma were observed). Subsequently, the patient underwent suppressive hormone therapy and was recommended long-term radioiodine therapy.

#### 4. CONCLUSIONS:

Thus, radioiodine therapy was effective in 52 (76.5%) patients, which allows continuing the use of radioiodine therapy for the treatment of patients with pulmonary metastases. In 12 people (17.6% of cases), the treatment was ineffective, the spread of metastatic lesions was observed during the entire period, in 4 cases (5.9%), there were metastases in the cervical lymph nodes.

Therefore, the analysis of the obtained data proved a relatively high efficacy of RIT in patients with thyroid carcinoma with metastatic lung injury – 28 patients (13.8% of cases) received a full therapeutic effect after 5 years of treatment, which even corresponds to the data reported in the literature. The obtained results indicate the need for further use of RIT, improvement of treatment methods (e.g., radical surgery with compulsory lymph node dissection), the use of recombinant human thyroid-stimulating hormone to prolong suppressive hormone therapy for the period of RIT, the use of differentiating therapy in the presence of partial or complete radioiodine-resistant "residual" thyroid tissue, metastatic lymph node lesions, lung metastases in patients.

In 5 years of treatment with patients with radioiodine in almost half of cases of metastatic

lung injury achieved full effect in 43.8% of cases, stabilization or partial effect – in 37.5% of cases. Full body scintigraphy for “residual” activities of  $^{131}\text{I}$  after the issuance of therapeutic activities  $^{131}\text{I}$ -sodium-iodide gives definitive information about the prevalence of the tumor process and in 26% of cases allows to detect pulmonary radiographies metastases after surgical treatment.

## 5. REFERENCES:

1. Abdrakhmanova, S. A., Zhanzakova, Z. Z., Turganbekova, A. A., and Saduakas, Z. K. (2019). Assessment of hematopoietic stem cell molecular engraftment based on STR analysis. *Cellular Therapy and Transplantation*, 8(3), 26-27.
2. Afanasieva, N. I. (2004). Treatment of differentiated thyroid carcinoma. *URG*, 12(4), 459-464.
3. Afanasyeva, Z. A. (2006). *Comprehensive diagnosis, treatment and rehabilitation of patients with thyroid carcinoma*: (Unpublished thesis of the Doctor of Medical Sciences). Military-medical Academy, St. Petersburg, Russian Federation.
4. Bachelot, A., Leboulleux, S., and Baudin, E. (2005). Neck recurrence from thyroid carcinoma: serum thyroglobulin and high-dose total body scan are not reliable criteria for cure after radioiodine treatment. *Journal of Clinical Endocrinology and Metabolism*, 62, 376–379.
5. Blagitko, E. M., Tolstykh, G. N., and Dobrov, S. D. (2003). *Difficulties in the diagnosis of thyroid carcinoma*. Paper presented at the 11th scientific symposium by surgical endocrinology “Modern aspects of surgical endocrinology”, St. Petersburg, Russian Federation.
6. Burkitbaev, J. K., Ramileva, I. R., Turganbekovaa, A., Baimukasheva, D. K., Imashpaev, D., and Isaev, T. K. (2017). The character of distribution of HLA specificities in oncological patients. *Klinicheskaya Laboratornaya Diagnostika*, 62(5), 282-285.
7. Burkitbaev, J. K., Abdrakhmanova, S. A., Savchuk, T. N., and Zhiburt, E. B. (2017). The implementation of NAT-screening of infections in blood donors of the Republic of Kazakhstan. *Klinicheskaya Laboratornaya Diagnostika*, 3, 154-156.
8. Chopra, S., Garg, A., and Ballal, S. (2015). Lung metastases from differentiated thyroid carcinoma: prognostic factors related to remission and disease-free survival *Journal of Clinical Endocrinology and Metabolism*, 82, 445–52.
9. Dadu, R., and Cabanillas, M. E. (2012). Optimizing therapy for radioactive iodine-refractory differentiated thyroid cancer: current state of the art and future directions. *Minerva Endocrinologica*, 37, 335–356.
10. Drozdovsky, B. Ya., and Podolkhova, N. V. (2007). The effectiveness of radioiodine therapy in patients with thyroid carcinoma with metastases to the lungs and mediastinum. *Endocrinology Problems*, 5, 22-24.
11. Drozdovsky, B. Ya., Rodichev, A. A., and Garbuzov, P. I. (2002). *On the need for radioiodine therapy in the treatment of differentiated thyroid carcinoma in children and adolescents*. Paper presented at the scientific conference “The role of radiation therapy in the development of organ-preserving treatments for malignant neoplasms”, Moscow, Russian Federation.
12. Garbuzov, P. I. (2003). Algorithms for the diagnosis and treatment of highly differentiated thyroid carcinoma. *Clinical Thyroiditis*, 1(3), 27–31.
13. Gorbash, V. A., Smiyan, O. I., and Kurhanska, V. O. (2015). Changes in the colon microflora of school-age children with bronchial asthma. *New Armenian Medical Journal*, 9(3), 45-47.
14. Huang, I. C., Chou, F. F., and Liu, R. T. (2012). Long-term outcomes of distant metastasis from differentiated thyroid carcinoma. *Journal of Clinical Endocrinology and Metabolism*, 76, 439–47.
15. Kim, T. Y., Kim, W. G., and Kim, W. B. (2014). Current status and future perspectives in differentiated thyroid cancer. *Clinical Endocrinology and Metabolism*, 29, 217–225.
16. Kisileva, E. S., Skorobogatov, N.M., Zvekotkina, L. S., and Voronetskiy, I. B. (1987). Comprehensive treatment of metastases of thyroid carcinoma in the lungs in childhood and adolescence. *Medical Radiology*, 32(3), 7–10.
17. Kozak, O. V., Sukach, T. G., and Trembach, O. M. (2004). The influence of therapeutic activity on the number of courses of radioiodine therapy in metastatic lung lesions in patients with differentiated thyroid carcinoma. *URJ*, 12(3), 305–309.

18. Kudabaeva, K. I., Yermukhanova, L. S., Koshmaganbetova, G. K., Bazargaliev, Y. S., Baspakova, A. M., Kaldybaev, K. K., and Kaldybaeva, A. T. (2015). Estimation of the thyroid gland volume by means of ultrasonography among school children in Aktobe Area, Kazakhstan. *Research Journal of Pharmaceutical, Biological and Chemical Sciences*, 6(2), 87-93.
19. Kudabaeva, Kh.I., Koshmaganbetova, G.K., Bazargaliev, Y.Sh., and Baspakova, A.M. (2016). Assessment of the iodine status in the population in Western Kazakhstan according to data of urinary iodine concentrations. *Gigiena i Sanitariia*, 95(3), 251-254.
20. Kudabayeva, K., Batyrova, G., Bazargaliyev, Y., Agzamova, R., and Nuftieva, A. (2017). Microelement status in children with enlarged thyroid gland in West Kazakhstan region. *Georgian Medical News*, 263, 64-71.
21. Lin, J. D., Chao, T. C., and Chou, S. C. (2004). Papillary thyroid carcinomas with lung metastases. *Clinical Thyroiditis*, 14, 1091-1096.
22. Marotta, V., Ramundo, V., and Camera, L. (2013). Sorafenib in advanced iodine-refractory differentiated thyroid cancer: efficacy, safety, and exploratory analysis of role of serum thyroglobulin and FDG-PET. *Journal of Clinical Endocrinology and Metabolism*, 78, 760-7.
23. Mechev, D. S., Krushynskiy, M. V., and Shcherbina, O. V. (2010). Radionuclide therapy of patients with highly differentiated thyroid carcinoma with multiple lung metastases. *URF*, 18(3), 311-313.
24. Nixon, I. J., Whitcher, M. M., and Palmer, F. L. (2012). The impact of distant metastases at presentation on prognosis in patients with differentiated carcinoma of the thyroid gland. *Clinical Thyroiditis*, 22, 884-889.
25. Paches, A.I. (2000). *Tumours of the head and neck*. Moscow, Russian Federation: Medicine.
26. Paches, A. I., and Prop, R. M. (1995). *Thyroid carcinoma*. Moscow, Russian Federation: Center for the implementation of science and technology.
27. Podolkhova, N. V., Drozdovsky, B. Ya., and Garbuzov, P. I. (2006). Long-term results of radioiodine therapy of patients with thyroid carcinoma with metastases to the lungs and mediastinum. *Siberian Oncology Journal*, 20(4), 46-50.
28. Ramilyeva, I. R., Burkitbaev, Zh. K., Abdrakhmanova, S. A., Turganbekova, A. A., Baimukasheva, D. K., and Zhiburt, E. B. (2019). Distribution pattern for HLA specificities in the patients with acute myeloid leukemia. *Medical Immunology (Russia)*, 21(5), 965-972.
29. Reiners, C., and Farahati, J. (1999). 131I therapy of thyroid carcinoma patients. *The Quarterly Journal of Nuclear Medicine and Molecular Imaging*, 43(4), 324-335.
30. Schlumberger, M., and Pacini, F. (1999). *Thyroid tumours*. Paris, France: Editions Nucleon.
31. Schlumberger, M., Challeton, C., and De Vathaire, F. 1996. Radioactive iodine treatment and external radiotherapy for lung and bone metastases from thyroid carcinoma. *Journal of Nuclear Medicine*, 37, 598-605.
32. Schlumberger, M. J. (1998). Papillary and follicular thyroid carcinoma. *The New England Journal of Medicine*, 338(5), 297-306.
33. Schneider, D. F., and Chen, H. (2013). New developments in the diagnosis and treatment of thyroid cancer. *CA*, 63, 374-94.
34. Smiyan, O. I., Plakhuta, V. A., Bunda, T. P., and Popov, S. V. (2015). Dynamics of cytokines in infants with acute obstructive bronchitis and thymomegalia. *Likars'ka sprava / Ministerstvo okhorony zdorov'ia Ukraïny*, 1-2, 81-85.
35. Song, H. J., Qiu, Z. L., and Shen, C. T. (2015). Pulmonary metastases in differentiated thyroid cancer: efficacy of radioiodine therapy and prognostic factors. *European Journal of Endocrinology*, 173, 399-408.
36. Tkachenko, G. I., Vasilyev, L. Y., and Grushka, G. V. (2005). Protocol of medical care for patients with thyroid carcinoma. *URJ*, 13(3), 488-491.
37. Tzavara, I., Vlassopoulou, B., and Alevizaki, C. (1999). Differentiated thyroid carcinoma: A retrospective analyses of 832 cases Greece. *Clinical Endocrinology*, 50(5), 643-654.
38. Valdina, E.A. (2001). *Thyroid disease*. St. Petersburg, Russian Federation: Piter.
39. Vini, L., and Harmer, C. (2003). Treatment of thyroid carcinoma. Review. *Medicine of the World*, 15(4), 264-275.



**Table 1.** Distribution of patients by sex and age

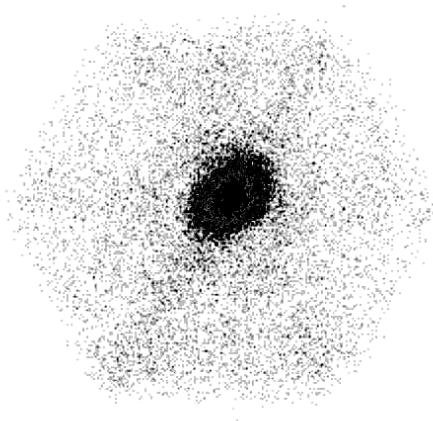
|              | Abs. | %        | Average   | Median | Min  | Max  |
|--------------|------|----------|-----------|--------|------|------|
| All patients | 68   | 100      | 46.3±14.6 | 50.5   | 16.0 | 68.0 |
| Men          | 17   | 26.5±5.6 | 42.4±15.8 | 45.0   | 16.0 | 67.0 |
| Women        | 51   | 73.5±5.6 | 47.7±19.9 | 51.0   | 21.0 | 68.0 |

**Table 2.** Distribution of patients by type of surgery

| Type of surgery                                | Number of patients |      |
|--|--------------------|------|
|  | abs.               | %    |
| Single radical surgery                         | 25                 | 32.8 |
| Non-radical surgery                            | 28                 | 43.8 |
| Non-radical surgery + definitive thyroidectomy | 15                 | 23.4 |
| Total  | 68                 | 100  |

**Table 3.** The presence of remote metastases of the thyroid gland, depending on the size of the primary tumor according to T data

| Metastases | The size of the primary tumor of the thyroid gland by T |      |      |      |      |     |      |      |      |      |
|------------|---|------|------|------|------|-----|------|------|------|------|
|            | T1  |      | T2   |      | T3   |     | T4   |      | Tx   |      |
|            | Abs.  | %    | Abs. | %    | Abs. | %   | Abs. | %    | Abs. | %    |
| M0         | 18  | 28.1 | 17   | 26.6 | -    | -   | 8    | 12.5 | 3    | 4.7  |
| M1         | -   | -    | 4    | -    | 5    | 7.8 | 5    | 7.8  | 8    | 12.5 |
| Total      | 18  | 28.1 | 21   | 26.6 | 5    | 7.8 | 13   | 20.3 | 11   | 17.2 |

**Figure 1.** Scintigram of the neck and chest area in the forward direct projection on "residual"  $^{131}\text{I}$  activity after receiving therapeutic  $^{131}\text{I}$  activity

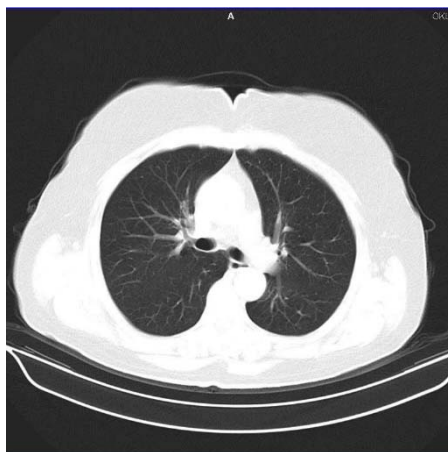


**Figure 2.** *Computed tomography of the chest*

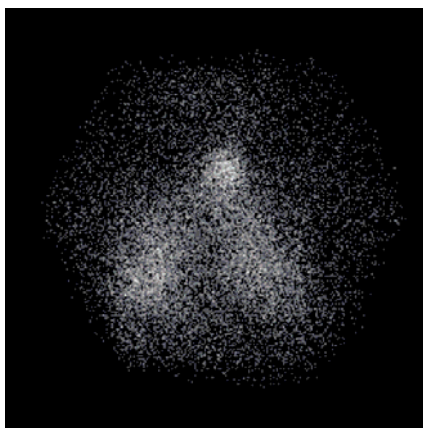


**Figure 3.** *Scintigram of the neck and chest area in the forward direct projection on “residual”  $^{131}\text{I}$  activity after receiving therapeutic  $^{131}\text{I}$  activity*

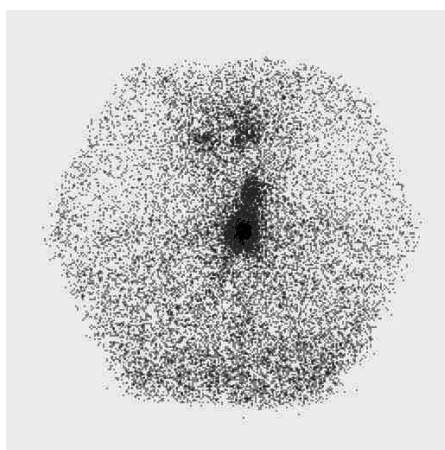


**Figure 4.** *Scintigraphy of the neck and chest area on “residual”  $^{131}\text{I}$  activity after radioiodine treatment activity*

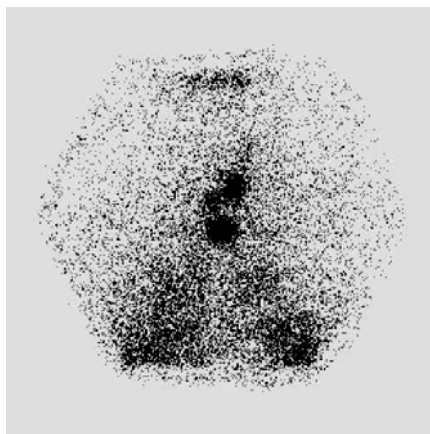


**Figure 5.** Scintigraphy of the neck and chest area on “residual”  $^{131}\text{I}$  activity after radioiodine treatment activity

# DESENVOLVIMENTO DE LASERS DE ALTA INTENSIDADE ULTRACURTOS PARA A FAIXA DE ESPECTROS VISÍVEIS

## DEVELOPMENT OF ULTRA-SHORT HIGH INTENSITY LASERS FOR THE VISIBLE SPECTRA RANGE

ABDULRAHMAN, Hayder J.<sup>1</sup>; MOHAMMED, Suzan B.<sup>2</sup>

<sup>1,2</sup> Department of Basic Medical Sciences, Faculty of Dentistry, Kirkuk University, Kirkuk

\* Corresponding author

e-mail: hyder.baban@uokirkuk.edu.iq

Received 31 May 2020; received in revised form 13 June; accepted 23 June 2020

### RESUMO

Os pulsos de laser ultracurtos são particularmente adequados para o processamento de micro-ferramentas feitas de materiais dielétricos e ultraduros. Os pulsos de laser ultracurtos fornecem uma fabricação precisa e sem contato de materiais sensíveis ao calor, como a faixa de espectros visível. A gama de espectros visíveis possui propriedades únicas, o que a torna um material importante nas indústrias de ferramentas, joias e semicondutores. O processamento da faixa de espectros visíveis por pulsos de laser ultracurtos é complexo, pois a luz visível e o infravermelho próximo geralmente não são absorvidos. No entanto, a intensidade dos pulsos de laser ultracurtos é extremamente alta, de modo que a absorção varia de maneira não linear com a intensidade e, portanto, a luz visível ou no infravermelho próximo pode ser absorvida. A complexidade também resulta de muitas variáveis de processo parcialmente interdependentes, como taxa de repetição, sobreposição de pulso, sobreposição de faixa e velocidade de varredura. Um excelente conhecimento do processo é, portanto, essencial para a produção de micro-ferramentas. Para tornar o processamento a laser acessível a um campo mais amplo do usuário, o operador pode ser suportado por um projeto auxiliado por computador (CAD). O objetivo desta pesquisa foi modelar um laser de alta intensidade ultracurto para a faixa de espectros visível em diferentes ambientes do ângulo de incidência, velocidade de varredura, pulso e sobreposição de faixa. O processo experimental incluiu o processamento a laser pulsado ultracurto da faixa de espectros visíveis e análise de superfície com relação a modificações e ablação a laser ultracurto. Os volumes de ablação foram analisados para pulsos únicos, multipulsos e blocos. Experimentos com sonda em bomba revelaram propriedades ópticas transitórias, como transmissão ou refletividade. Concluiu-se que os pulsos de laser ultravioleta são mais adequados para induzir danos ou modificações nas superfícies visíveis da faixa de espectros. Além disso, comprimentos de onda mais curtos têm outras vantagens, como comprimentos de Rayleigh potencialmente mais longos e tamanhos de ponto menores.

**Palavras-chave:** Gama de espectros, processamento a laser, laser ultracurto, estrutura, comprimento de onda.

### ABSTRACT

Ultra-short laser pulses are particularly suitable for processing micro tools made of ultra-hard and dielectric materials. Ultra-short laser pulses provide a contact-free and precise fabrication of heat-sensitive materials such as visible spectra range. Visible spectra range has unique properties, which makes it an essential material in the tool, jewelry, and semiconductor industries. The processing of visible spectra range by ultra-short laser pulses is complex, as visible and near-infrared light is generally not absorbed. However, the intensity of ultra-short laser pulses is extremely high, so that the absorption scales nonlinearly with the intensity and, thus, visible or near-infrared light can be absorbed. The complexity also results from many partially interdependent process variables, such as the repetition rate, pulse overlap, track overlap, and scan speed. Excellent knowledge of the process is, therefore, essential for the production of micro tools. To make the laser processing accessible to a broader user field, the operator can be supported by a computer-aided design (CAD). The aim of this research was to the modeling of an ultra-short high-intensity laser for the visible spectra range in different environments of the angle of incidence, scanning speed, pulse, and track overlap. The experimental process included ultra-short pulsed laser processing of visible spectra range and surface analysis concerning modifications and ablation of the ultra-short laser. Ablation volumes were analyzed for single pulses, multi-pulses, and pockets. Pump-probe experiments reveal transient optical properties such as transmission or reflectivity. It was concluded that ultraviolet laser pulses are best suited to induce damage or modifications to visible spectra range surfaces. Additionally, shorter wavelengths have further advantages such as potentially longer Rayleigh lengths and smaller spot sizes.

## 1. INTRODUCTION:

Visible spectra range is a remarkable range and due to its unique range best suited as raw material for (cutting) tools. The high intensity of visible spectra range is unmatched by any other material, which makes visible spectra range hard to machine and thus limits the available tooling methods. Indeed, visible spectra fields can cut different visible spectra ranges, but this method involves laser technologies that can avoid significant abrasive wear (Chowdhury, 2015). Wear, and thus this research paper will focus on laser machining. Laser machining not only prevents wear but also exhibits no processing forces and can be applied to any other ultra-hard material (Weinberg, 1979).

Ultra-hard materials can be processed with nanosecond and more extended pulsed lasers, which are inexpensive and robust laser sources. On the other hand, these laser sources exhibit a significant heat affected zone, which is detrimental for heat-sensitive material such as visible spectra range. In the last years, the technology of ultra-short pulsed lasers has emerged in the industrial market with sufficient power and low pulse duration of a few picoseconds (Rethfeld, 2017). These picosecond pulsed lasers can reduce the heat-affected zone and improve the quality and lifespan of the visible spectra range tool. Thus, the ultra-short pulse technology with small focus diameters promotes the miniaturization of tools. Besides tool manufacturing, the laser machining of visible spectra range is also attractive for other applications (Kobayashi, 2018).

Visible spectra range is applied in many different industry branches because of its unique properties such as its high intensity, thermal conductivity, high brilliance, reflectivity, stiffness, chemical inertness, and transparency over a broad spectral range. Notably, the semiconductor, electrical, and jewelry industry process visible spectra range, and due to its properties, visible spectra ranges are often indispensable. In these other industries, ultra-short pulsed lasers can be used to process visible spectra range into the desired shape or improve the surface functionality (Bloembergen, 2016). Overall, there are many good reasons to research and develop the technology of ultra-short pulsed laser processing. But every new technology also has some obstacles that need to be overcome. For instance,

laser technology is accompanied by a large number of process parameters which can be either property of the laser, the material, or the process (Jones, 2019).

The laser properties include parameters such as the wavelength, pulse energy, repetition rate, temporal shape, and duration of the pulse, spatial intensity distribution, beam quality or beam diameter. Furthermore, the beam diameter is a laser parameter that directly affects the properties of the process. On the process side, process parameters are the angle of incidence, scanning speed, pulse, and track overlap, which can be summarized as scanning strategy. In the case of visible spectra range, essential material parameters are the refractive index, band gap energy, electron-phonon coupling parameter, electron relaxation rate, heat capacity, electrical and thermal conductivity, effective mass, molar mass, density, temperature dependent graphitization rate, enthalpy of graphitization, enthalpy of sublimation, sublimation temperature and surface topology. (Tawfik, 2018).

This research is concerned with the evaluation of ultra-short high-intensity lasers for the visible spectra range. A first step is developing a model to describe single pulse ablation and find material-specific parameters. The model should describe changes in the material and the change in the light pulse during propagation (Rosenfeld, 2019). Essential for the light propagation are optical parameters such as the absorption coefficients or penetration depth. Another material parameter is the threshold fluence for single pulse ablation. All these material parameters help to set up a model describing the laser processing.

Further, the single pulse ablation model can also narrow down the parameter range for an efficient process. The single pulse model can also reveal the key process parameters, which give an idea of how a process model can be realized (Stuart, 2016). For industry, the development of a process model is essential because it can be implemented in a laser CAD. Using a CAD, everyone operating a milling machine can be trained to perform a laser machine. This eliminates the need for a laser specialist in ultra-short pulsed laser processing to develop new tools or to operate a laser machine. (Page, 2008)

The aim of this research was to the modeling of an ultra-short high-intensity laser for the visible spectra range in different environments

of the angle of incidence, scanning speed, pulse, and track overlap. This aim is intended to be achieved by accomplishing the following objectives:

1. Investigate the performance and identify the structural deficiencies of the ultra-short high-intensity lasers for the visible spectra range.
2. Determine the contribution of the high intensity of laser on different materials.
3. Assess the performance of high-intensity laser on the visible spectra range.
4. Outline guidelines for designing similar lasers for the visible spectra.
5. Assist in determining strengthening techniques to increase the ultra-short high-intensity lasers for the visible spectra range.

## 2. BACKGROUND:

The literature review includes an analysis of ultra-short high-intensity lasers phenomenon, and, in summary, a single pulse model generates data, which is a keystone to set up a laser process model. In turn, the laser process model is a keystone for developing a CAD for laser processing of ultra-hard materials. (Li, 2012) The development of CAD software is the ultimate goal that this work should tackle by improving the understanding of laser interaction and determining material-specific parameters. The long-term outlook is that an operator has CAD interfaces to produce laser manufactured micro-tools or more general workpieces with sub-micron feature sizes (Jiang, 2015). Figure 1 shows that all three ultra-short lasers substrate represented by blue, dielectric represented by green and AR coating represented by red color. Most ultra-short pulsed laser systems operate at visible or near-infrared regimes, and it seems to be contradicting that large bandgap dielectrics can absorb these low photon energies.

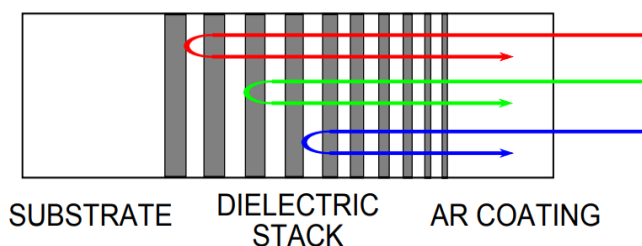


**Figure 1.** All three ultra-short lasers substrate represented by blue, dielectric represented by green and AR coating represented by red color (Jiang, 2015).

The apparent contradiction resolves around the term ultra-short pulsed. Compared to more extended pulsed lasers, ultra-short pulsed lasers stand out due to much higher electric fields (Sanner, 2009). These strong fields induce non-linear effects in the bulk material, causing strong-field excitations. Another widely used term is strong-field ionization, but the electrons are merely excited to the conduction band and are, in fact, not free or unbound carriers as the term ionization suggests. For this reason, conduction electrons are referred to as quasi-free electrons and are therefore physically treated as free electrons. This is justified by introducing an effective electron mass, which is used to simplify the attraction force of the band structure on the electron (Schuricke, 2011).

### 2.1. Free-carrier absorption and collisional excitation in laser processing

The photoexcitation process generates quasi-free electrons in the conduction band. These free charge carriers can absorb further photon energy and gain kinetic energy. Figure 2 shows this free carrier absorption process, which is also called inverse bremsstrahlung. Further, the accelerated electrons can transfer the increased kinetic energy to valence electrons through inelastic collisions. If the transferred energy is larger than the bandgap, the valence electrons are excited to the conduction band. This process is either called collisional or impact excitation and can lead to an avalanche-like increase of free electrons. For this reason, avalanche excitation is the process of inverse bremsstrahlung, followed by collisional excitation. The relative significance of collisional excitation is a topic of ongoing discussions (Sanner, 2009). Figure 3 shows a schematic diagram of electron excitation mechanisms such as strong-field excitation. For pulse durations of a few dozen femtoseconds, the free electrons have no time to acquire enough energy for collisional excitation.

On the other hand, avalanche excitation becomes more dominant for increasing pulse duration and laser intensity. The onset of avalanche excitation also depends on the photon energy and bandgap. It could start for near-infrared pulses between a few picoseconds to several picoseconds pulse durations for silica and sapphire (Itina, 2015).

### 2.2. Multiple pulse mechanism in the laser processing

In this research, so far, the discussion

considered only the interaction of single laser pulses at various pulse durations. From single pulses to several pulses (multiple shots), the interaction becomes more complicated due to an increase of essential variables such as the repetition rate (Mirza, 2016). The repetition rate is the frequency of the consecutive pulse, which has a fixed temporal distance. For single pulses, the total energy of the pulse is given by the number of photons within the pulse. With the number of pulses, the total energy incident on the dielectric increases. The consecutive pulses impinge on a highly exciting material with increased temperature. This temperature increase could have already led to material extrusion. The extruding material can interact with the consecutive pulses. The temperature increase could also lead to material modifications, e.g., phase or morphological changes, affecting absorption. The higher ablation rate for multiple pulses results from the incubation effect, which is observed for ultra-short pulses up to 100 and beyond 100 pulses. Due to incubation, the ablation threshold is reduced in the multiple shot regimes (Cheng, 2017). For instance, (Lenzner, 2019) had shown that in fused silica, multiple laser shots reduce the threshold compared to single pulses. Summing up, the incubation effect alters the optical properties of a dielectric material.

### 2.3. Ultra-short pulsed excitation

As shown in figure 4, just like all dielectric materials, ultra-short laser pulses can induce strong-field excitation. Accordingly, Ultra-short pulsed excitation can be classified as follows:

#### 2.3.1 Modeling ultra-short pulsed excitation

Finite-difference and molecular dynamics models have predicted that the ablation threshold and the heat-affected zone are minimized for ultra-short pulses in visible spectra range. (Lenzner, 2019) The damage and ablation threshold can also be determined by theoretical approaches such as molecular dynamic (MD) simulations. MD simulations describe transient atomic interactions and movements by numerically solving Newton's equations of motion for a system of particles. (Baerbel, 2017) The inter-atomic forces and potential energy are defined by molecular mechanics force fields. In general, MD simulations have been utilized in a broad range of scientific work dealing with Short and ultra-short pulsed laser ablation. The MD simulations are limited to microscopic scales in space and time. Thus, MD is not well suited to simulate several pulses or

realistic sample sizes of several tens of micrometers or even larger. These kinds of simulations are covered, for instance, by macroscopic models based on heat equations or rate equations. (Boerner, 2019)

#### 2.3.2 Damage and ablation threshold from pulsed lasers

Due to a lower threshold, it is more efficient to machine visible spectra range with ultra-short pulsed lasers. Another argument for such lasers is that ultra-short pulsed lasers show a reduction in the heat-affected zone compared to longer pulsed lasers. Minimizing the heating of visible spectra range is essential to avoid the phase transition to graphite, which has no apparent high intensity. Visible spectra range is a metastable phase of carbon, which is stable at ambient temperatures, but the phase transition becomes more probable with rising temperatures (Mingareev, 2019). Different phases are also typical in other dielectric materials, but no other dielectrics have such remarkable thermal properties as carbon. For instance, the thermal conductivity of the visible spectra ranges phase is unmatched by any other naturally occurring material. (Chimier, 2011) Most materials with high thermal conductivity are metals, and heat transport is based on the conducting electrons. Heat transport by electrons is not possible in dielectrics, which explains that these materials are, in general, poor conductors. Besides electron thermal conductivity, heat can also be conducted through phonons. Phonons are so-called quasi-particles and describe the elemental or collective excitation of lattice vibrations in solids. Visible spectra range has strong covalent bonding and low phonon scattering, which explains its high lattice thermal conductivity (Sanner, 2009).

#### 2.3.3 Cost and Complexity of Visible Spectra Range

Besides pulse duration, the second key aspect is the wavelength, where shorter wavelengths are better suited to machine visible spectra range. Figure 5 shows that the visible spectra range of laser represented in wavelength. Especially, ultraviolet light is well suited but has some cons on the handling side. First, laser sources emitting at ultraviolet wavelengths have some inherent dangers concerning active laser media. Second, ultraviolet light can harbor risk for human skin depending on the wavelength. Last, such laser light requires special optics, which are suited for these wavelengths and might degrade. In contrast, standard optics are available for visible and near-infrared wavelengths. By default, the



main wavelength is in the spectrum for many types of ultra-short pulsed lasers. Higher harmonic generation provides shorter wavelengths in the visible and ultraviolet spectral range (Stoian, 2018). Naturally, high harmonic generation increases the cost and complexity of the laser system. Again, degeneration of the optics is an issue for the generation of ultraviolet light. In summary, it is desirable to investigate laser processing of visible spectra ranges with a focus on picosecond pulse durations with different wavelengths. Experimental findings are incomplete without a suited model, but a model is also an incomplete image of the reality. (Brown, 2009).

### 2.3.4 Ultra-Short Laser Excitation

Most models describe laser excitation of dielectrics in the femtosecond or nanosecond regime. (Zhdanovich, 2012) Figure 6 shows that ultra-short laser excitation with energy up to 100 MeV for dielectrics in the femtosecond or nanosecond regime. The most investigated materials are silicon, silica, sapphire or materials with similar band gaps. In contrast, visible spectra range is a more exotic material, which is only used if its unique properties are required (Ashkenasi, 2017) (Samad, 2010). For this research paper, only macroscopic models are considered because only such models can describe processes for realistic sample sizes and longer timescales. Such models use statistical quantities such as the temperature to describe melting, vaporization, sublimation, or ablation of small parts of the sample.

## 3. MATERIALS AND METHODS:

The laser-induced damage threshold (LIDT) of optical components is a critical quality parameter for laser systems and their applications operating at high power levels. Furthermore, the LIDT parameter of a material marks the onset of the well-directed laser machining of this material. The determination of this parameter is described in the ISO standards. (Wang, 2004) The basic idea is to shoot a laser pulse with defined pulse energy on the surface and evaluate the irradiated area with a microscope if the surface has been damaged or not. The onset of damage can be determined by successively increasing the pulse energy. Between single pulses, the sample is moved in the focal plane to shoot each pulse at a different position. This procedure is repeated for each pulse energy several times to get statistical information about the occurrence of damage. The event of

damage can also be determined for multiple pulses. The multiple pulse LIDT applies a fixed number of pulses, which are shot on each surface area evaluated in this study.

### 3.1. Ablation threshold - Depth method

The depth regression method considers the vertical distance between the crater bottom and the initial sample surface as a function of the fluence. This depth method is determining the ablation threshold fluence, and thus the results must differ from the previous (damage threshold) methods. (Pietroy, 2012)

The photomicrographs show the morphology induced by a single laser pulse using the maximum pulse energy of the first picosecond laser. The irradiated surface area is arched upward to build a hump. Raman spectroscopy of the hump reveals bands at  $1250\text{ cm}^{-1}$  and  $1580\text{ cm}^{-1}$ , which corresponds to graphite or instead hybridized carbon. In contrast, the purely visible spectra range surface shows a distinct peak located at  $1333\text{ cm}^{-1}$ , indicating hybridized carbon. Such humps have also been observed in other bandgap material such as silicon and attributed to the expansion of molten material that is re-solidified. In this case, the morphological change must not necessarily depend on a previous melting due to meet stability of the visible spectra range. More precisely, visible spectra range converts to graphite in an exothermic reaction. The conversion rate is insignificant at ambient temperature but increases at elevated temperatures. Graphite has a lower density than the visible spectra range, which differs by a factor of 1.56 and supports the development of the hump. Figure 7 shows the visible spectra range generated by a single laser pulse at high pulse energy.

Consequently, the depth regression method can only be applied to multi-pulse experiments. For a few pulses, the graphite humps have also been observed at lower pulse energies. By increasing the pulse energy, the humps start to disappear. The occurrence of humps also goes for more than 50 pulses. This is one reason why this section focuses on the examination of 100 pulses. Another reason is that 100 pulses are almost in the processing regime and, therefore, an average number, which makes it comparable with other studies.

### 3.2. Design and Contraction Visible Spectra Range

Volume regression is another method to determine the ablation threshold. It is not only the



combination of the diameter and depth method but also comprises more information because it considers the depth of every area element. Therefore, volume regression is the most accurate method, but it takes a longer measuring time to evaluate the volume. (Lyu, 2019) Figure 8 shows the flowchart and design for the measured volumes as a function of the laser fluence. The total volume can also be converted to a volume per pulse by division by 100. Within the low fluence domain, all three wavelengths show a linear dependence between ablated volume and the natural logarithm of the fluence. The threshold fluences are determined by interpolating the fit curve to zero-volume.

The ablation efficiency as a function of the laser fluence for different wavelengths. Comparing those wavelengths, UVA has the highest efficiency closely followed by VIS and NIR. The NIR wavelength has its maximum efficiency at approximately  $10 \text{ J cm}^{-2}$ . The efficiency increases monotonically from the threshold fluence to  $10 \text{ J cm}^{-2}$  and then decreases monotonically for increasing fluences. The efficiency curves of VIS and UVA wavelength show similar behavior but reach their maximum at approximately  $5 \text{ J cm}^{-2}$ . Thus, with shorter wavelengths, higher efficiency at lower fluence can be achieved. The efficiency curve has typical curve progression but needs more values between the zero's to maximum ablation efficiency. This is difficult to achieve with single-pulse experiments because the ablation depth has to be larger than the surface roughness. The ablation depth has already been increased by applying multiple pulses. The heat accumulated has been minimized by choosing a repetition rate of a few Hertz. However, it can be assumed that the first pulses change the surface morphology and improve the absorption of consecutive pulses. The machining, measurement, and evaluation is even more simplified by machining pockets. Pockets are more suited to resolve the low fluence domain but result in a decreased ablation threshold due to incubation. Nonetheless, the next section will investigate a single pulse but with femtosecond pulse durations.

### 3.3. Pump and Probe Experiments in Ultra-Fast Phenomena

Pump and probe experiments can be used to obtain information on ultra-fast phenomena. For example, such experimental setups are used to uncover the dynamics of charge carrier transport in semiconductors, chemical reactions or oscillations, and energy transfer in molecules. (Alexeev, 2015) The general measuring principle

is illustrated in figure 9. A sample is hit by a high intensive pump pulse (red beam), which generates an excitation or modification of the sample. After an adjustable time, delay ( $t = x/c$ ), a probe pulse (green beam) hits the sample. The time delay is controlled by an optical delay line (dark gray rectangle) with varying distance  $x/2$ . The reflection or transmission of the probing pulse is measured as a function of the delay.

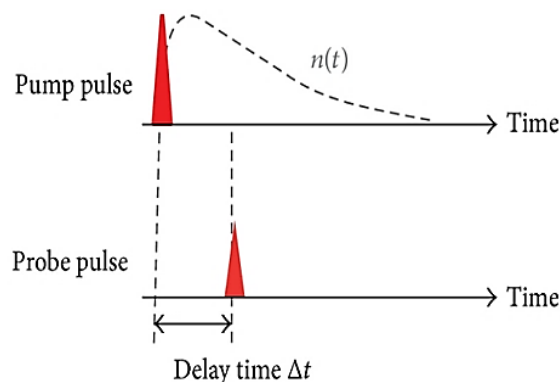


**Figure 9.** Working principle of the pump (upward) and probe (downward) setup. The downward pulse is delayed by extending the beam path by the time  $n(t)$ . The beam splitter in works in both directions: splitting or combining beam paths.

Usually, the probe pulse has a lower intensity and negligible effect on the excited state. By monitoring the probe signal as a function of the time delay, it is possible to map the dynamic response of the sample. This response can reveal information on the decay of the generated excitation or on other processes initiated by the pump pulse. The temporal resolution is fundamentally limited only by the pulse duration of the pump and probe pulses. In conclusion, the pump and probe technique is a versatile tool with a variety of different setups and applications.

In the following, some details will be described to improve the understanding of the measuring results in the subsequent sections. The pump and probe pulses are generated with the help of a pellicle beam splitter. The beam splitter divides the incident laser pulse into a pump (reflected) and probe (transmitted) pulse — the working principle of a beam splitter. Further, the beam splitter can be used not only for splitting but also for joining beam paths.

In general, the pulse energy of the split pulses depends on the properties of the beam splitter and incident beam. The experimental setup uses the pellicle beam splitter, which divides the incident pulse into equal parts. In contrast, a polarizing beam splitter can be used to reflect s-

polarized and transmit p-polarized parts of a pulse. Waveplates and optical density filters are used to adjust the required polarization and pulse energy, respectively. Another pellicle beam splitter can then rejoin the pump and probe beam path.

### 3.4. Transient Reflectivity in Ultra-Short Laser

Using a 90-fs laser, a high temporal resolution of the transient transmission and reflectivity measurement is achieved. The literature results are depicted the transient reflectivity (a) and transient transmission (b). The transient reflectivity is evaluated with respect to electron-phonon relaxation time. The critical melting flounce of the visible spectra range is according. (a), a pump pulse with  $5.9 \text{ J cm}^{-2}$  is impinging the sample at time zero. This excitation causes the reflectivity to jump from its initial value of 0.2 to 0.4. The jump can be explained by an abrupt increase in the electron density due to strong-field excitation. The maximum reflectivity is almost as high as in the graphite sample. The difference could be attributed to the density difference between the liquefied visible spectra range and HOPG. Between 1 PS and 10 PS, the reflectivity is slowly decreasing from 0.4 to 0.1. This decrease requires a closer look and root cause analysis. Reitze *et al.* explain the reduction in reflectivity by a distortion of the surface optical properties. Furthermore, the misuse is attributed to a release of internal pressure and hydrodynamic expansion of the plasma. Figure 10 shows transient reflectivity and transmission as a function of the pump-probe delay.

Alternative hypotheses explain the reflectivity decrease with fundamental changes (e.g., electron density, scattering rate or refractive index), material removal, scattering due to rapid structural damage, or metal-dielectric transition (reconversion). A reconversion from metal to dielectric is unlikely because the transient transmission does not recover. In contrast, the occurrence of the delayed reflectivity decrease is precisely correlated with the appearance of a damage crater in graphite. The presence of the damage crater suggests that material removal can cause decreasing reflectivity. This argument is reinforced by similar observations in silicon, which shows nearly the same reflectivity values and flounce dependence suggesting a common ablative mechanism. Furthermore, it is excluded that structural or electronic equilibration takes 10 PS to 30 ps. Molecular dynamics simulations show that this equilibration is within 1 PS of heating to the melting temperature.

## 4. RESULTS AND DISCUSSION:

This research investigated ultra-short pulsed laser processing of visible spectra range and related materials. The laser-material interaction is studied theoretically by developing an ultra-short pulsed laser model for visible spectra range. A variety of experiments supplements the modeling and theoretical studies. The experimental examination includes surface analysis for modifications, ablation. Ablation volumes are analyzed for single pulses, multi-pulses, and pockets. Also, transient properties such as ultra-fast changes of the reflectivity are investigated. The experimental and theoretical studies exhibit process parameters and process windows, which can be used as an input parameter for developing a CAD system.

### 4.1. Ultra-Short Laser Types

The simulation results of the models are discussed in this section. The simulation results are compared with the literature and experimental findings. The model is used to investigate several topics such as the impact of the pulse duration and wavelength on the ablation rate. Figure 11 shows the different types of ultra-short laser types with shorter penetration depth and a higher excitation level. Increasing the pulse duration decreases the excitation, and the transient change of the penetration depth starts at a later point in time. This starting point can be represented by the first value of the transient penetration depth below 1 m. The change starts between  $t = 1 \text{ PS}$  and  $t = 400 \text{ fs}$ . This transient change starts earlier in the case of the 700 fs pulses due to the earlier rise of the intensity. Noticeably, the final penetration depth is shorter for 400 fs pulse. The reason for the shorter penetration depth is the higher excitation level, which contrasts with the assumption that shorter pulse duration might accelerate the electrons deeper into the bulk. The MRE model does not consider this effect of high acceleration.

### 4.2. Structural Modeling and Analysis of Design

In general, the total energy of a light pulse can be split into an absorbed, reflected, and transmitted part. Thus, the absorptivity, reflectivity, and transmissivity are determined by the relation:

$$A + R + T = 1 \quad (1)$$

The ideal case for laser machining is  $A = 1$  and thus  $R = T = 0$ . The initial reflectivity is approximately 17 % to 18 % depending on the wavelength, as shown in table 6.1, as well as the

material and surface structure. Thus, the highest possible absorptivity is in the order of 83 % if the transmissivity decreases to zero, and the reflectivity does not change. The reflectivity will rather increase than decrease. Nonetheless, at a certain electron density, the reflectivity has shown a dip. The dip might be interesting in the future to gain the last bit of absorption efficiency. The absorption efficiency might be further increased by using temporal shaped pulses or two consecutive pulses. The idea is to excite a certain electron level so that the reflectivity is decreased and then use this window to deposit the energy of the second pulse or second part of the pulse. The feasibility of such an approach could be investigated by simulation. The simulation will show if such a window is stable enough for energy deposition or if it disappears too fast due to the transient character of the optical parameters. The understanding of ultra-short laser excitation is already deepened by investigating the transient absorptivity of a single Gauss-shaped pulse. First, the transient absorptivity is studied for pulse energy, pulse duration, and wavelength.

#### 4.3. Computer-Aided Design for Ultra-Short Laser

The computer-aided design for ultra-short laser supplements the results of the ultra-short laser model discussed in the methodology sections. The computer-aided design for ultra-short laser uses two coupled heat equations to simulate the electron and phonon temperatures. The phonon temperature is used to predict damage and ablation in the visible spectra range. If the phonon temperature exceeds the modification temperature, the visible spectra range transforms to the ultra-short high-intensity laser.

Graphitization is an exothermic process, and the enthalpy of formation of visible spectra range is released. The enthalpy of formation is considered in the lattice specific heat capacity as a module. If required, the module can be activated, and the graphitization occurs at visible spectra range or, preferably a high-intensity range. Evaluation of high-intensity laser with ultra-short wavelength might be further increased by using temporal shaped pulses or two consecutive pulses in three different cases 0%, 4.5%, and 10.5%, as illustrated in figure 12.

#### 4.4. Wavelength analysis

It is well known that the wavelength has a big influence on the absorption of light. Visible spectra range is transparent for a broad spectral

range between ultraviolet and mid-infrared. In the mid-infrared range, it is possible to excite optical phonons, while direct electronic excitation is only possible in visible spectra range for ultraviolet light. The wavelength analysis concentrates on the transparent range where absorption must have a non-linear character. Figure 13 shows the waveform for the ultra-short high-intensity laser changes of the reflectivity are investigated with time.

### 5. CONCLUSIONS:

The transient reflectivity of visible spectra range increases due to the ultra-fast generation of free electrons (Géneaux, 2019). On a picosecond timescale, the reflectivity decreases below the initial value, which is attributed to the hydrodynamic expansion of plasma. More precisely, the plasma expansion decreases the (electron) density. This changes the refractive index and thus the reflectivity. Therefore, the decrease of the reflectivity is not a relaxation mechanism since the transient transmission does not recover. Morphological and topological surface changes are responsible that the reflectivity does not fully recover for long pump-probe delays.

The experimental results suggest that plasma expansion affects the reflectivity. Different methods are discussed to determine the damage and ablation threshold. In the case of damage, the stochastic method gives the most reliable results. This is similar to (Elishakoff, 1990) conclusions in that the worst-case error shown from the stochastic method is always less than the worst-case error shown from any other spectral manner. The damage threshold decreases with the number of pulses due to incubation. (Harold; 1986) postulates that this denotes irreversible accumulation of permanent material change or irreversible accumulation of long-lived states. More precisely, the damage threshold first decreases and then saturates after a few hundred pulses. The saturation value is the threshold flounce for processes. The wavelength study shows that a frequency doubling from infrared to visible decreases the damage threshold by laser factor. This is equivalent to observations of (Yoshida, 2006). Even lower threshold values can be achieved with laser light of the third harmonic.

*Finally*, it is concluded that

- Ultraviolet laser pulses are best suited to induce damage or modifications to visible spectra range surfaces.

- Additionally, shorter wavelengths have further advantages such as potentially longer Rayleigh lengths and smaller spot sizes.
- Alternatively, the diameter method is used to determine the damage threshold or approximate the ablation threshold.

## 6. REFERENCES:

1. Alexeev; I., Heberle; J., Cvecek; K., Nagulin; K. and Schmidt; M. (2015). High Speed Pump-Probe Apparatus for Observation of Transitional Effects in Ultrafast Laser Micromachining Processes. *Micromachines*. 6. 1914-1922. 10.3390/mi6121462.
2. Ashkenasi; D., Stoian; R., and Rosenfeld; A. (2017) Single and multiple ultra-short laser pulse ablation threshold of Al<sub>2</sub>O<sub>3</sub> (corundum) at different etch phases. *Applied Surface Science*, 154-155:40–46.
3. Baerbel; R., Dmitriy; S. I., Martin; E. G. and Sergei I. A. (2017) modelling ultrafast laser ablation, *J. Phys. D: Appl. Phys.* 50; 193001
4. Bloembergen; N. (2016) Laser-induced electric breakdown in solids. *IEEE Journal of Quantum Electronics*, 10(3):375–386.
5. Boerner; P., Hajri; M., Ackerl; N. and Wegener; K. (2019) Experimental and theoretical investigation of ultrashort pulsed laser ablation of diamond, *Journal of Laser Applications*. 31. 10.2351/1.5096088
6. Brown; J., Vishwanath; K., Palmer; G. and Ramanujam, N. (2009). Advances in Quantitative UV-Visible Spectroscopy for Clinical and Pre-clinical Application in Cancer. *Current opinion in biotechnology*. 20. 119-31. 10.1016/j.copbio.2009.02.004.
7. Cheng, Liu; C.-S., Shang; S., Liu; D., Perrie; W., Dearden; G. and Watkins; K. (2017) Optics & Laser Technology A review of ultrafast laser materials micromachining. *Optics and Laser Technology*, 46:88–102.
8. Chimier; B., Utéza; O., Sanner; N., Zeitoun; D., Itina; T., Lassonde; P., Légaré; F., Vidal; F. and Kieffer; j. c. (2011). Damage and ablation thresholds of fused-silica in femtosecond regime. *Phys. Rev. B*. 84. 10.1103/PhysRevB.84.094104.
9. Chowdhury; H., Wu; A. Q., Xu; X. and Weiner; A. M. (2015) Ultra-fast laser absorption and ablation dynamics in wide-band-gap dielectrics. *Applied Physics A*, 81(8):1627– 1632.
10. Elishakoff; I., Lin; Y.K. (1990), *Stochastic Structural Dynamics 2: New Practical Applications* Second International Conference on Stochastic Structural Dynamics, Boca Raton, Florida, USA
11. Généaux; R., Marroux; H., Guggenmos; A. Neumark; D. and Leone, S. (2019). Transient absorption spectroscopy using high harmonic generation: A review of ultrafast X-ray dynamics in molecules and solids. *Philosophical Transactions of the Royal Society of London*. 377. 10.1098/rsta.2017.0463.
12. Harold; E. B., Arthur; H. G. (1986) *Laser Induced Damage in Optical Materials*, Proceedings of a Symposium Sponsored by: National Bureau of Standards, Boulder, Colorado.
13. Itina; T., Rudenko; A., Colombier; J., Shcheblanov; N. (2015) Effect of Laser field on Collision Frequencies and Absorption during Ultra-Short Laser Interactions with Dielectric Materials.
14. Jiang; L. and Tsai; H. L. (2015) Energy transport and material removal in wide band gap materials by a femtosecond laser pulse. *International Journal of Heat and Mass Transfer*, 48(3-4):487–499.
15. Jones; S. C., Braunlich; P., Casper; R. T., Shen; X. A., and Kelly; P. (2019) Recent Progress on Laser-Induced Modifications and Intrinsic Bulk Damage of Wide-Gap Optical Materials. *Optical Engineering*, 28:28–30.
16. Kobayashi; T. (2018). Development of Ultrashort Pulse Lasers for Ultrafast Spectroscopy. *Photonics*. 5. 19. 10.3390/photonics5030019.
17. Lenzner; M., Krüger; J., Kautek; W., and Krausz; F. (2019) Incubation of laser ablation in fused silica with 5-fs pulses. *Applied Physics A: Materials Science and Processing*, 69(4):465–466.
18. Li, Jeremy. (2012) *Applications of Computer-aided Design Technology in Research, Engineering and Industry*. < [https://www.researchgate.net/publication/267925418\\_Applications\\_of\\_Computer-](https://www.researchgate.net/publication/267925418_Applications_of_Computer-)

19. Lyu; S., Liu; Y., Hou; M., Gao; Z., Yang; X. and Gu; M. (2019) Designing and construction of the spectral library for typical pigments used in chinese paintings. ISPRS - International Archives of the Photogrammetry, Remote Sensing and Spatial Information Sciences. XLII-2/W15 703-709. 10.5194/isprs-archives-XLII-2-W15-703-2019
20. Mingareev (2019) ultrafast dynamics of melting and ablation at large laser intensities. Ph.D. research paper, RWTH Aachen.
21. Mirza, Bulgakova; N. M., Tomáščík; J. and Michálek; V. (2016) Ultra short pulse laser ablation of dielectrics: Thresholds, mechanisms, role of breakdown. Nature Publishing Group, 6(39133):1–11.
22. Page, Thorsteinsson; G. and Ha, J. (2008) A Feasibility Study into the Application of CAD/CAM in a Traditional Industry Sector. Design Knowledge: Journal of the Korean Design Knowledge Forum, ISSN: 2005-0623. 8. 131-140. 10.17246/jkdk.2008..8.015.
23. Pietroy; D., Di; M. Y., Moine; B., Baubeau; E. and Audouard; E. (2012). Femtosecond laser volume ablation rate and threshold measurements by differential weighing. Optics Express. 20. 29900-29908. 10.1364/OE.20.029900.
24. Rethfeld; B. (2017) Free-electron generation in laser-irradiated dielectrics. Contributions to Plasma Physics, 47(4-5):360–367.
25. Rosenfeld, Lorenz; M., Stoian; R., and Ashkenasi; D. (2019) Ultra short-laser-pulse damage threshold of transparent materials and the role of incubation. *Applied Physics A: Materials Science and Processing*, 69(7).
26. Samad; R., Courrol; L., Baldochi; S. and Vieira; D. (2010). Ultrashort Laser Pulses Applications. 10.5772/13095.
27. Sanner; N., Utéza; O., Bussiere; B., Coustillier; G., Leray; A., Itina; T. and Zeitoun; D. (2009). Measurement of femtosecond laser-induced damage and ablation thresholds in dielectrics. *Applied Physics A*. 94. 889-897. 10.1007/s00339-009-5077-6.
28. Schuricke; M., Zhu; G., Steinmann; J., Simeonidis; K., Ivanov; I., Kheifets; A., Grum-Grzhimailo; A. and Ullrich; J. (2011) Strong-field ionization of lithium, *Physical Review A*, 83. 10.1103/PHYSREVA.83.023413.
29. Stoian; R., Ashkenasi; D., Rosenfeld; A. and Cadpbell; E. E. B. (2018) Coulomb explosion in ultra-short pulsed laser ablation of Al<sub>2</sub>O<sub>3</sub>. *Physical Review B - Condensed Matter and Materials Physics*, 62(19):13167–13173.
30. Stuart, Feit; M., Herman; S., Rubenchik; A., Shore; B., and Perry; M. (2016) Nanosecond- to-femtosecond laser-induced breakdown in dielectrics. *Physical Review B*, 53(4):1749– 1761.
31. Tawfik; W. (2018) Experimental study on creation of ultrashort pulses using selfphase modulation in hollow-core fiber. *J Mod Appl Phys*; 2(1): 02-03.
32. Wang; Y., Zhao; Y., Weidong; G. and Fan, Z. (2004). Laser-induced damage threshold of the antireflection coatings on quartz and sapphire under different laser modes. *Optical Engineering*. 43. 87-90. 10.1117/1.1631004.
33. Weinberg; Z. A., Rubloff; G. W., and Bassous; E. (1979) Transmission, photoconductivity, and the experimental band gap of thermally grown SiO<sub>2</sub> films. *Physic Rev B*, 19(6):3107– 3117.
34. Yoshida; H., Fujita; H., Nakatsuka; M., Yoshimura; M., Sasaki, T., Kamimura; T. and Yoshida, K. (2006). Dependences of Laser-Induced Bulk Damage Threshold and Crack Patterns in Several Non-linear Crystals on Irradiation Direction. *Japanese Journal of Applied Physics*. 45. 766. 10.1143/JJAP.45.766.
35. Zhdanovich; S., Bloomquist; C., Floß; J., Averbukh; I., Hepburn; J. and Milner; V. (2012). Quantum Resonances in Selective Rotational Excitation of Molecules with a Sequence of Ultrashort Laser Pulses. *Physical Review Letters*. 109. 10.1103/PhysRevLett.109.043003.

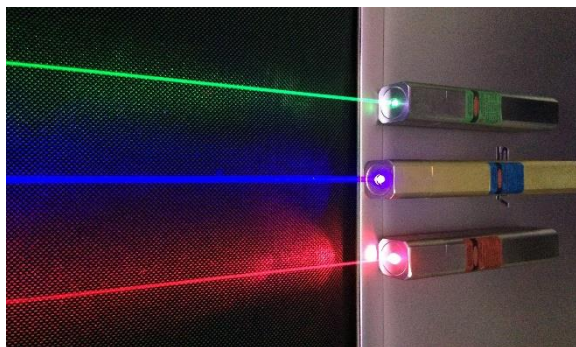


**Figure 2.** The ultra-short high-intensity lasers for the visible spectra range in a vacuum (Sanner, 2009).

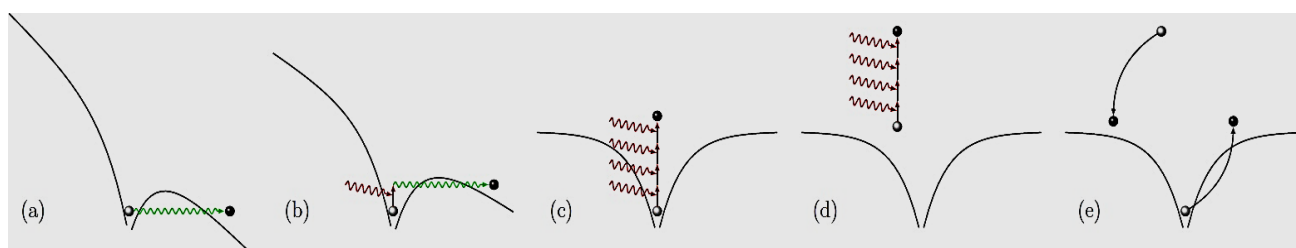


**Figure 3.** Schematic diagram of electron excitation mechanisms such as strong-field excitation (a) - (c), free carrier absorption (d), and collisional excitation (e). The strong-field excitation is subdivided into multiphoton absorption (a), a combination of photon absorption and tunneling (b) And tunneling.

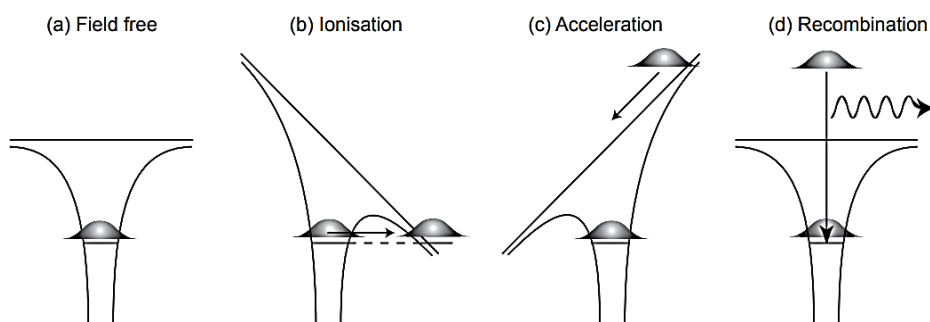


**Figure 4.** High-intensity laser represented by the different models of the field-free state. (a) Field free, (b) Ionization, (c) Acceleration and (d) Recombination

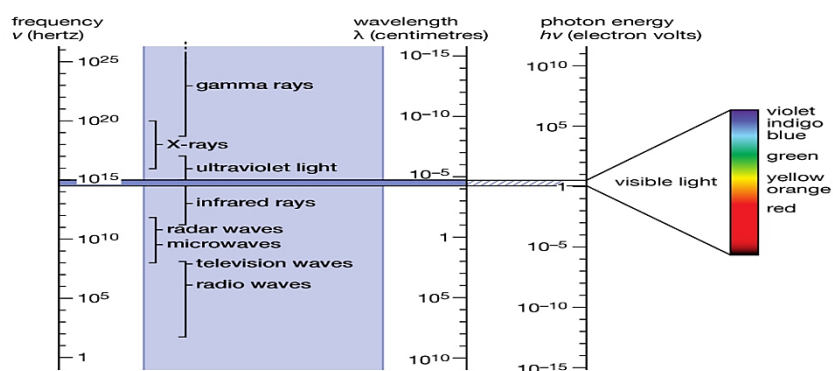


**Figure 5.** The visible spectra range of laser represented in wavelength (Stoian, 2018).

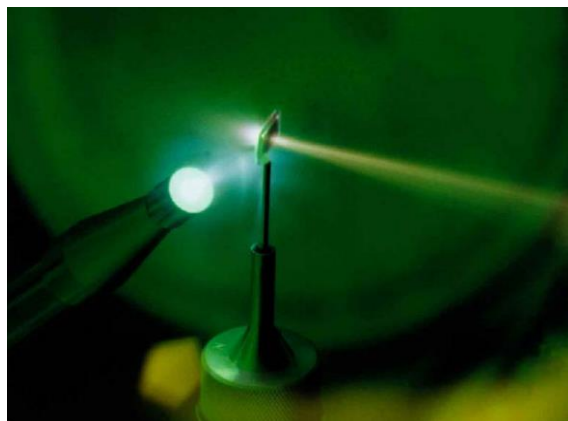


**Figure 6.** Ultra-short laser excitation with energy up to 100 MeV for dielectrics in the femtosecond or nanosecond regime (Samad, 2010).

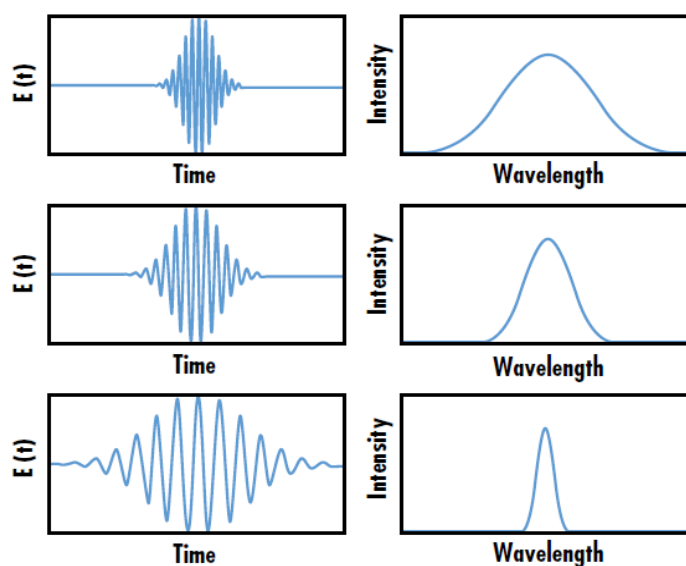


**Figure 7.** Visible spectra range generated by a single laser pulse at a high pulse energy

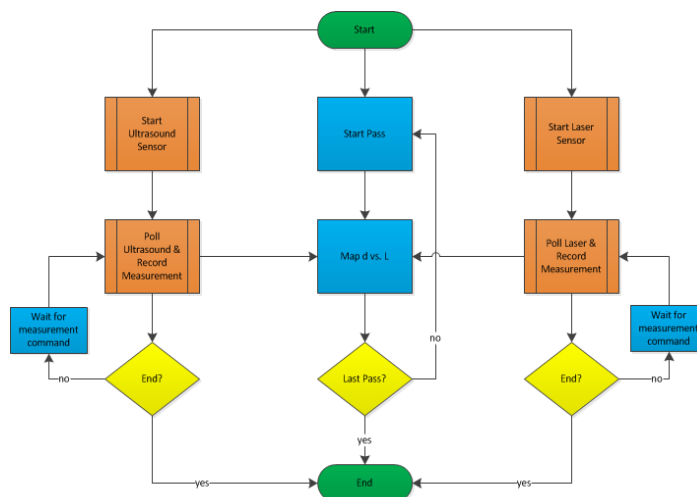


**Figure 8.** The design and flowchart of high-intensity visible spectra range solid curves are fitted. Dotted lines correspond to a logarithmic fit and determine the ablation threshold values.



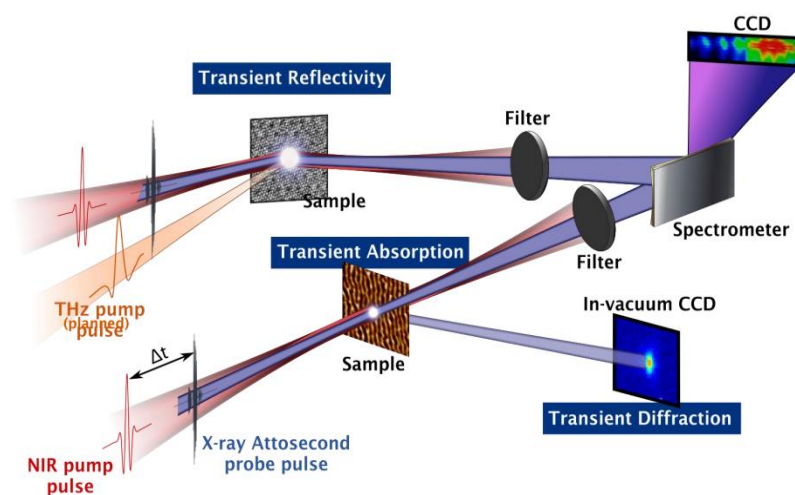


**Figure 10.** Transient reflectivity and transmission as a function of the pump-probe delay.

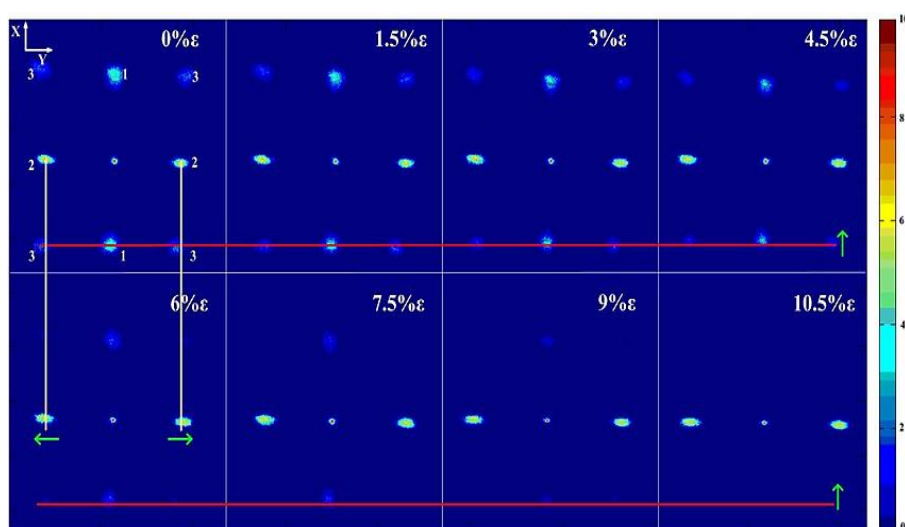


**Figure 11.** The different types of ultra-short laser types with shorter penetration depth and a higher excitation level.



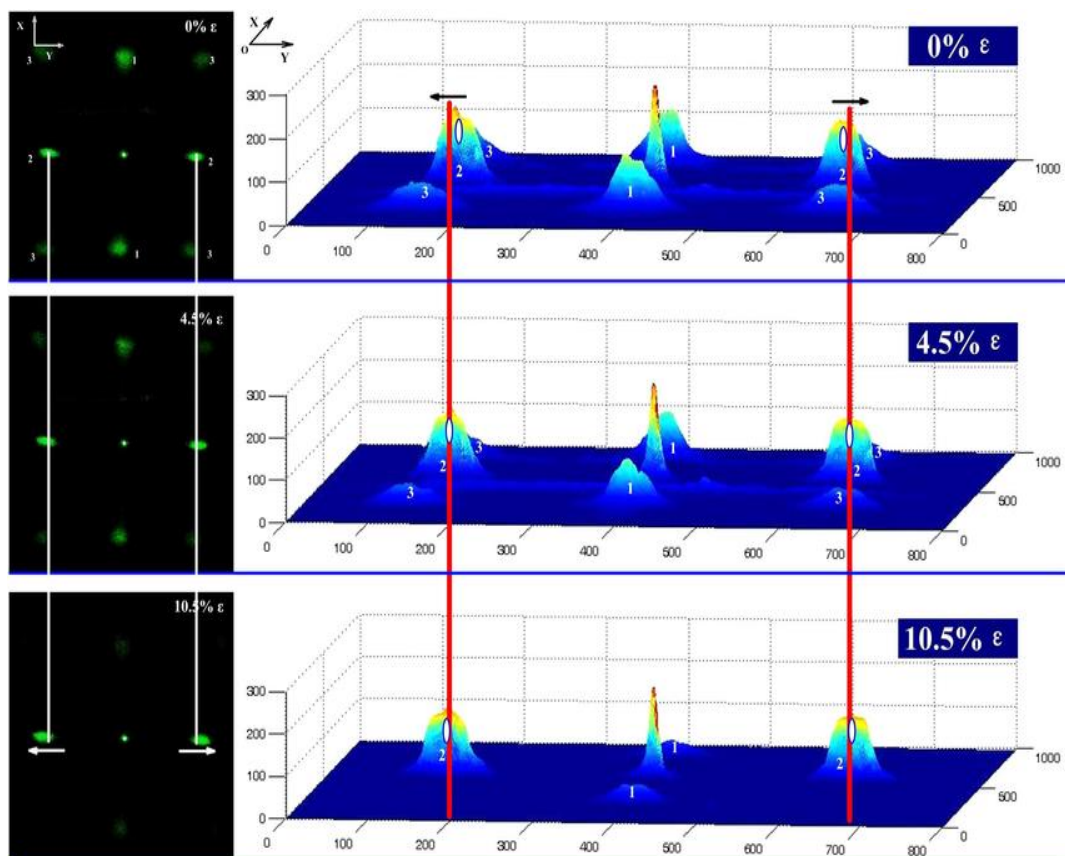


**Figure 12.** Evaluation of high-intensity laser with ultra-short wavelength might be further increased by using temporal shaped pulses or two consecutive pulses in three different cases 0%, 4.5%, and 10.5%.

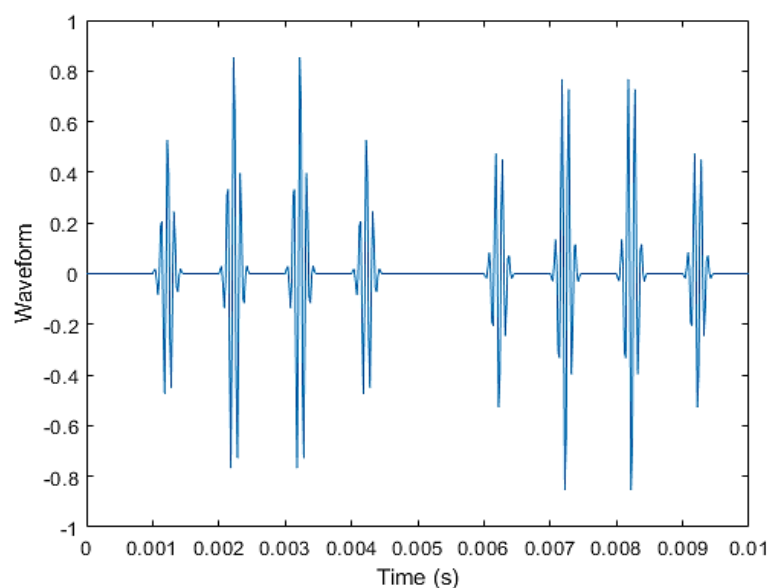


**Figure 13.** The waveform for the ultra-short high-intensity laser changes of the reflectivity investigated with time.

**ESTUDO DA SITUAÇÃO DE RADIAÇÃO EM MOSCOU POR MEIO DA PESQUISA DOS ORGANISMOS ELASTOPLÁSTICOS NO FLUXO DE NÊUTRONS, CONSIDERANDO OS EFEITOS DO CALOR****STUDY OF THE RADIATION SITUATION IN MOSCOW BY INVESTIGATING ELASTOPLASTIC BODIES IN A NEUTRON FLUX TAKING INTO ACCOUNT THERMAL EFFECTS****ИЗУЧЕНИЕ РАДИАЦИОННОЙ ОБСТАНОВКИ В МОСКВЕ ПУТЕМ ИССЛЕДОВАНИЯ УПРУГОПЛАСТИЧЕСКИХ ТЕЛ В НЕЙТРОННОМ ПОТОКЕ С УЧЕТОМ ТЕПЛОВЫХ ЭФФЕКТОВ**

PRONINA, Polina F.<sup>1\*</sup>; TUSHAVINA, Olga V.<sup>2</sup>; STAROVOITOV, Eduard I.<sup>3</sup>;

<sup>1</sup> Moscow Aviation Institute (National Research University), Institute of Aerospace, Department of Managing Exploitation of Space-Rocket Systems, 4 Volokolamskoe Highway, zip code 125993, Moscow – Russian Federation

<sup>2</sup> Moscow Aviation Institute (National Research University), Institute of Aerospace, 4 Volokolamskoe Highway, zip code 125993, Moscow – Russian Federation

<sup>3</sup> Belarusian State University of Transport, Department of Building Mechanics, 34 Kirov Str., zip code 246653, Gomel – Republic of Belarus

\* Correspondence author

e-mail: pronina-p19.94@yandex.ru

Received 21 April 2020; received in revised form 09 June 2020; accepted 19 June 2020

**RESUMO**

Este artigo examina o estudo do nível de radiação de fundo em Moscou e seu impacto no meio ambiente. Para identificar os efeitos radiológicos nas condições de vida, foi realizado um estudo sobre os efeitos dos nêutrons rápidos na infraestrutura e nos objetos biológicos. Foram consideradas as organizações de pesquisa em larga escala que realizam desenvolvimento tecnológico, pesquisa científica e material utilizando materiais nucleares na cidade de Moscou e na região. O sistema de monitoramento de radiação do meio ambiente, cobrindo uma área de mais de 1091 km<sup>2</sup>, foi examinado em detalhes. Uma pesquisa radioecológica realizada nos distritos administrativos Troitskiy e Novo-Moskovskiy foi analisada para identificar e descrever a situação da radiação. A análise da radiação de fundo em Moscou mostra que os valores dos parâmetros controlados da poluição radioativa de objetos ambientais estão dentro das flutuações de longo prazo do fundo tecnogênico da capital. Nesse caso, surgem vários efeitos térmicos, causados pela exposição à radiação de sólidos. O estudo da infraestrutura e dos objetos biológicos é realizado com base na determinação de efeitos, que resultam em mudança das características elásticas e especialmente plásticas das substâncias expostas à irradiação de nêutrons e aos efeitos térmicos. Nesse caso, os principais fatores importantes são o endurecimento por radiação do material (aumento do limite de extensão gradual) e o inchaço induzido por radiação (aumento da deformação volumétrica).

**Palavras-chave:** *monitoramento radioecológico, dose de radiação absorvida, taxa de dose de exposição, atividade volumétrica de equilíbrio equivalente, carga quasistática.*

**ABSTRACT**

This article discusses the study of the background radiation level in Moscow and its impact on the environment. To identify the radiological impact on living conditions, a study of the effects of fast neutrons on infrastructure and biological objects was made. Large-scale research organizations carrying out technological development, scientific and materials research using nuclear materials in the city of Moscow and the region are considered. A system of environment radiation monitoring, covering an area of more than 1091 km<sup>2</sup>, was examined in detail. A radioecological survey conducted in the Troitsky and Novomoskovsky administrative districts was analyzed to identify and describe the radiation situation. An analysis of background radiation in Moscow

shows that the values of the controlled parameters of radioactive pollution of environmental objects are within the long-term fluctuations of the technogenic background of the capital. In this case, various thermal effects arise caused by radiation exposure to solids. The study of infrastructure and biological objects is carried out based on the determination of effects, because of which the elastic and mainly plastic characteristics of substances exposed to neutron irradiation and thermal effects change. Here, the main essential factors are radiation hardening of the material (increase in yield stress) and radiation swelling (increase in volumetric strain).

**Keywords:** *radioecological monitoring, absorbed radiation dose, exposure dose rate, equilibrium equivalent concentration, quasistatic loading.*

## АННОТАЦИЯ

В данной статье рассматривается исследование уровня радиационного фона в Москве и воздействие его на окружающую среду. Для выявления радиологического воздействия на условия жизни было проведено исследование воздействия быстрых нейтронов на инфраструктуру и биологические объекты. Рассмотрены крупномасштабные научно-исследовательские организации, выполняющие технологические разработки, научные и материаловедческие исследования с использованием ядерных материалов в городе Москве и области. Была детально рассмотрена система радиационного мониторинга окружающей среды, занимающая площадь более 1091 км<sup>2</sup>. Радиоэкологическое обследование, проведенное в Троицком и Ново-Московском административных округах, было проанализировано с целью выявления и описания радиационной обстановки. Анализ фоновой радиации в Москве показывает, что значения контролируемых параметров радиоактивного загрязнения объектов окружающей среды находится в пределах многолетних колебаний техногенного фона столицы. При этом возникают различные тепловые эффекты, которые вызываются радиационным облучением твердых тел. Исследование инфраструктуры и биологических объектов проводится на основе определения эффектов, в результате которых изменяются упругие и особенно пластические характеристики веществ, подверженных воздействию нейтронному облучению и тепловому воздействию. Здесь основными важными факторами являются радиационное упрочнение материала (увеличение предела текучести) и радиационное разбухание (увеличение объемной деформации).

**Ключевые слова:** *радиоэкологический мониторинг, поглощённая доза облучения, мощность экспозиционной дозы, эквивалентная равновесная объемная активность, квазистатические нагружения.*

## 1. INTRODUCTION

In recent years, the radiation situation on Earth has undergone significant changes. As a result of numerous ground atomic testings, the radioactivity build-up occurred (Sean Hubar, 2017; Cuttler, 2019; Huang *et al.*, 2020; Inoue *et al.*, 2020). 12.5 tons of fission products were thrown into the biosphere (Pant *et al.*, 2018; Saha *et al.*, 2019; Orlov *et al.*, 2003; Skvortsov *et al.*, 2014; Litvishko *et al.*, 2020; Mietelski and Povinec, 2020). All explosions from atmospheric nuclear tests changed the equilibrium content of tritium by almost 100 times and by 2.6% to equilibrium content of carbon-14, which led to an excess of the natural background radiation by 2% (Aleikin *et al.*, 2019; Pivovarov and Mikhalev, 2004; Chubirko *et al.*, 2019; Tushavina *et al.*, 2019; Yakovlev *et al.*, 2020; Dridi *et al.*, 2020).

The accident at the Chernobyl nuclear power plant led to the release of 15 tons of radioactive substances into the biosphere.

However, the danger of nuclear fuel cycle facilities is not only in the field of accidents and disasters (Rabi *et al.*, 2017; Ali *et al.*, 2018; Renaud *et al.*, 2020). Even without them, about 250 radioactive isotopes fall into the environment as a result of the nuclear facilities operation (Kuznetsov, 2003; Tushavina *et al.*, 2019; Topchy, 2018; Kuznetsov *et al.*, 2019). One of the most acute problems in the world is the problem of radioactive waste (Prister *et al.*, 2018; Umbetov *et al.*, 2016; Yudaev *et al.*, 2019; Carlberg *et al.*, 2019; Taleyarkhan, 2020). In 1994, 554 "lost" or unauthorized dumping sites of ionizing radiation sources in Moscow, St. Petersburg, Bratsk, Volgograd, and hundreds in other territories were identified in Russia. Thus, the highest levels of pollution were found in St. Petersburg (> 40 R/h) and Cherepovets (> 2 R/h) (Zverev, 2010; Okhrimenko *et al.*, 2017; Shugurov and Knyazyuk, 2018; Umbetov *et al.*, 2017; Trotsenko *et al.*, 2019).

On the territory of Moscow, in the course of scrupulous surveys carried out after the Chernobyl events, up to 80 places of unregistered "burial

sites" of used radionuclides were found. In general, over ten years after the accident, up to 600 "mortuaries" of this kind were liquidated (Kuznetsov, 2003; Mikayilova, 2017). Moscow is the only capital of the world where on December 25, 1946, the first reactor on the European continent was launched. The city also has large research organizations that carry out technological developments, scientific and materials research using nuclear materials. This is the Russian Scientific Centre "Kurchatov Institute" since 1943, the State Scientific Center High-Tech Research Institute of Inorganic Materials named after Academician A.A. Bochvar since 1945, ARRICT since 1951. Therefore, our work aimed to examine the city of Moscow to determine the radiation situation, as well as to study the behavior of various bodies and biological objects under the influence of neutron and thermal radiation.

The study of infrastructure and biological objects is carried out based on the determination of effects, as a result of which the elastic and mainly plastic characteristics of substances exposed to neutron irradiation and thermal effects change (Liu and Wu, 2018; Bulavin *et al.*, 2018; Lazarenko *et al.*, 2018; Forkapić *et al.*, 2019; Chao *et al.*, 2020). Here, the main essential factors are radiation hardening of the material (increase in yield stress) and radiation swelling (increase in volumetric strain).

In this work, the radiation exposure to solids, which is accompanied by numerous thermal effects, as a result of which additional volumetric strain  $\theta_1$  arises in them, and elastic and mainly plastic characteristics of the substance change was studied.

## 2. MATERIALS AND METHODS

The system of radioecological monitoring in Moscow covers the entire territory of the city ( $> 1091 \text{ km}^2$ ) and consists of stationary and mobile means of monitoring, the central laboratory complex, and the information-analytical center. Because of the research, a methodology for studying the stress-strain state of elastoplastic bodies and biological objects under cyclic loading in neutron and heat fluxes is proposed. To study the radiation exposure of solid materials, which is accompanied by numerous thermal effects, were chosen isotropic materials based on aluminum and steel. It was believed that neutrons fall with the same average energy and intensity. The temperature field was assumed to be constant. The kinematic and dynamic parameters of elastoplastic bodies in a neutron flux, taking into

account thermal effects, were determined on the basis of the methods of the dynamic theory of elastoplastic bodies (Taleyarkhan, 2020).

Consider an initial homogeneous isotropic body occupying the half-space  $z \geq 0$ . The half-space is affected by the neutron flux and the temperature field (Figure 1). If neutrons with the same average energy and intensity  $\varphi_0$ , neutron/( $\text{m}^2\text{sec}$ ) are incident on the boundary ( $z = 0$ ) parallel to the  $z$ -axis, then the intensity of the neutron flux reaching the plane  $z = \text{const}$  will be Equation 1 (Starovoitov *et al.*, 2009). The temperature field is assumed to be constant and determined by the function  $\Delta T$ . The quantity  $\mu$  in (1) is called the macroscopic cross-section and is of the order of  $1/\text{m}$ . For any chemical element, it is calculated by Equation 2 (Starovoitov *et al.*, 2009), where  $\sigma$  is the cross-section assigned to one core,  $n_0$  is the number of cores per  $1 \text{ cm}^3$ ,  $A_0$  is the Avogadro's number,  $\rho$  is the density,  $A$  is the atomic weight.

As an example, aluminum  $\sigma = 0.21 \cdot 10^{-24} \text{ cm}^2$ ,  $A_0 = 6.022 \cdot 10^{23} \text{ mol}^{-1}$  density  $\rho = 2.7 \text{ g/cm}^3$ ,  $A = 27$  dalton was considered. Substituting these values in Equation 2,  $\mu = 1,26 \text{ m}^{-1}$  was obtained. If  $\varphi_0$  is constant, then by the time  $t$ , a flux will pass through section  $z$  (Equation 3). In a rough approximation, it can be assumed that the change in the volume of a substance is directly proportional to the flux  $I(z)$  and, therefore (Equation 4), where  $B$  is the experimental constant. Value (Equation 5) gives the total neutron flux per unit surface area of the body. In reactors,  $\varphi_0$  is of the order of  $10^{17}$ – $10^{18}$  neutrons/( $\text{m}^2\text{sec}$ ), and  $I_0$  reaches  $10^{23}$ – $10^{27}$  neutrons/( $\text{m}^2\text{sec}$ ), with  $\theta_1$  being of the order of 0.1. Therefore, depending on the energy of neutrons and the irradiated material, the value of  $B$  can be of the order of  $10^{-28}$ – $10^{-24} \text{ m}^2/\text{neutron}$  (Starovoitov *et al.*, 2009).

The dependences of the elasticity modulus, yield stress and ultimate stress limit, and the entire stress-strain diagram on  $I_0$  for various energies were studied experimentally after irradiation of the samples in atomic reactors. For massive bodies with a flat boundary, the number of neutrons passing at a depth  $z$  below this boundary in time  $t$  is determined by Equation 3. Therefore, the yield stress will be variable in thickness  $z$ . On the body surface ( $z = 0$ ), the effect of radiation on the plasticity limit  $\sigma_y$  is quite satisfactorily described by the equation of radiation hardening (Equation 6) (Starovoitov *et al.*, 2009), where  $\sigma_{y0}$  is the plasticity limit of unirradiated material, where the neutron flux value  $I(z)$  is described by Equation

**Erro! Fonte de referência não encontrada.**;  $A, \xi$  are the constants of the material obtained from the experiment.

### 3. RESULTS AND DISCUSSION:

Let's consider the process of effects of external forces and radiation flux on a deformable body within the framework of the theory of small elastoplastic strains. Suppose that at the initial moment, a body in a natural state is immediately affected by external forces  $F_i'$ ,  $R_i'$  at interface displacement  $u_{i0}'$ , and at the same time a neutron flux of  $I_0 = \varphi_0 t$  is incident on its surface. It is assumed that under such an impact, areas of elastic and plastic strains appear in the body. The change in the elastic moduli due to neutron irradiation was neglected. The stresses, strains, and displacements arising in the body are marked with one stroke at the top.

For example, if for aluminum alloy 356,  $A = 1.09$ ;  $m^2/\text{neutron}$  was taken, then satisfaction with known experimental data can be judged by Figure 2. Dark points – experiment, solid line – calculation by equation (6). The corresponding deformation values are denoted by  $\varepsilon_{y0}$ ,  $\varepsilon_y$ .

In the elastic regions of a solid body, Hooke's law is valid, and the well-known relations between the stress deviators and strain deviators  $s'_{ij}$ ,  $\varepsilon'_{ij}$ , and their spherical parts  $\sigma'$ ,  $\varepsilon'$  corrected for additional volumetric strain due to the influence of  $B/I$  neutron irradiation and thermal effects  $\Delta T$  are fulfilled (Equation 7), where  $G$  is the modulus of elasticity in shear,  $K$  is the volumetric strain modulus,  $\alpha$  is the linear expansion coefficient of the material,  $\Delta T$  is the temperature change.

For those areas of the solid body where plastic strains appeared, the connection of deviators in the case of simple loading can be represented as (Equation 8), where  $f'(\varepsilon'_u, I, a'_k)$  is the plasticity function, which depends on the strain intensity  $\varepsilon'_u$ , the magnitude of the neutron flux  $I$  and the approximation parameters  $a'_k$ .

With a sufficiently fast "instantaneous" application of the power load, the hardening effect of radiation will not have time to affect, and the resulting areas of plastic strain will be the same as without the influence of the neutron flux. Under slow active loading, the outer layers of the body will become hardened over time, and the areas of plastic strain in them may turn out to be less or absent altogether, compared with an unirradiated body. In its effect on elastoplastic bodies, radiation

exposure is opposite to thermal, which reduces the yield stress and leads to an increase in plastic strain zones at the same loads (Figure 3).

To relations (Equation 8), differential equations of equilibrium, Cauchy equations, and boundary conditions under the assumption of small deformations was added (Equations 9-10). The comma in the subscript indicates the differentiation operation by the coordinate following it. Changes in the time of external loads and interface displacements occur in such a way that the corresponding loading paths do not belong to the class of substantially complex loads, and radiation hardening and thermal action occur after the forced strain of a solid body.

Let, starting from time  $t_1$ , the influence of the neutron flux ceases ( $\varphi = 0$ ), and the external forces change in such a way that unloading and subsequent alternating loading with bulk  $F_i''$  and surface forces  $R_i''$  (on  $S_\sigma$ ) occur at all points of plastically deformable regions of the body  $V_p'$  at the interface displacement  $u_{i0}''$  (on  $S_u$ ). The level of exposure to the body remains constant and equal to its value before unloading (Equation 11).

The plasticity limit at points of the body depends on the  $z$  coordinate and becomes equal to  $\sigma_y''(I_1(z))$ , that is, it depends on the magnitude of the strain and radiation hardening (Figure 3). Following (Starovoitov *et al.*, 2019), one can determine the kinematic and dynamic parameters of elastoplastic bodies in a neutron flux, taking into account the thermal effects. For this, as an example, the problem of repeated radiation-force bending of a three-layer cantilever beam under the influence of a temperature field was considered.

For the three-layer beam, which is asymmetric in thickness, the hypotheses of a broken normal are accepted: Kirchhoff hypothesis is valid in the base layers, the normal remains straight in the filler, does not change its length, but rotates by some additional angle  $\psi(x)$ . Let the outer base layers of the beam be made of metal and the inner layer (filler) incompressible in thickness – from polymer. The base layers are accepted as elastoplastic, and the filler is nonlinearly elastic. An analytical solution to the corresponding problem of the elasticity theory is given in (Gorshkov *et al.*, 2005). The study of thermal processes in various media is described in (Rabinskii and Tushavina, 2019; Rabinskiy and Tushavina, 2019a; Rabinskiy and Tushavina, 2019b; Starovoitov and Leonenko, 2019; Rabinskiy *et al.*, 2019; Astapov *et al.*, 2019; Antufev *et al.*, 2019; Rabinsky and Kuznetsova, 2019; Makarenko and Kuznetsova, 2019).

Let to the outer surface (Equation 12) of the considered three-layer beam, in addition to the distributed power load,  $p(x), q(x)$  a neutron flux of density  $\varphi_0$  is supplied in the direction opposite to the external normal and the temperature field (Figure 4). To describe the deformation of layer materials in a neutron flux, equations of state of type (Equation 8) was used (Equation 13), where  $f^{(k)}$  is the universal function of nonlinearity at loading from a natural state (Equation 14)  $\omega^{(k)}(\varepsilon_u^{(k)}, I)$  in the base layers, the plasticity function of Ilyushin is used, in the filler – the function of nonlinearity.

In the future, it will be assumed that changes in time of external loads and interface displacements occur in such a way that the corresponding loading paths do not belong to the class of essentially complex loads. Also, the radiation growth in the plasticity limit does not exceed the growth in the strain intensity at the irradiated points of the solid body, which would prevent the formation of plastic strains.

The considered problem of loading from a natural state was solved by the method of linear approximation (Gorshkov *et al.*, 2005). In our case, following relations (Equation 14) (under the influence of a neutron flux and a temperature field), the solution was obtained by the same method. As a result, the desired strains are determined by the following recurrence equations ( $n$  is the approximation number) (Equation 15). Here,  $p_\omega^{(n-1)}, h_\omega^{(n-1)}, q_\omega^{(n-1)}$  additional “external” loads serve as corrections for the plasticity and physical nonlinearity of the materials of the layers under repeated loading and take into account the effect of the neutron flux and temperature. They are taken equal to zero at the first step ( $n = 1$ ), and further calculated by the results of the previous approximation, the fourth-order function  $g^{(n)}(x)$ , coefficients  $\alpha_1, \alpha_2, \alpha_3, \beta^2, \gamma_1, \gamma_2, \gamma_3$ , and linear integral operators  $L_2^{-1}, L_3^{-1}, L_4^{-1}$  are defined in (Gorshkov *et al.*, 2005). Integration constants  $C_1^{(n)}, \dots, C_8^{(n)}$  take into account the effects of neutron and heat fluxes. In the case of a *rigid cantilever termination* of the left end of the rod with a free right, satisfying the boundary conditions, was obtained (Equation 16).

With repeated alternating loading, the recurrent solution for quantities with asterisks will be similar (Equation 16) (Equation 17). Numerical results were obtained for a three-layer beam, the layers of which are made of D16T – fluoroplastic –

D16T. Relative layer thicknesses:  $h_1 = h_2 = 0.03$ ,  $c=0.09$ . The mechanical and radiation parameters of the layer materials included in the equation (16) are given in (Gorshkov *et al.*, 2005; Tushavina *et al.*, 2019). In addition, it was taken:  $B = 10^{-23}$  m<sup>2</sup>/neutron, which ensures a volumetric strain of 3–3.5% in the layers of the considered rod,  $\mu = 1.26$  cm for duralumin, and  $\mu = 3.21$  cm for fluoroplastic.

Figure 5 shows the change in the deflection  $w - a$  along the axis of the three-layer rod under consideration, calculated according to various physical equations of state with cantilever restraint of the left end. Curves with one stroke correspond to loading from the natural state: 1, 2 – elastic and elastoplastic rods without irradiation, 3 – elastoplastic rods at  $\varphi = 10^{18}$  neutron/(m<sup>2</sup>s) and  $\Delta T = 300$  K. With repeated loading, the displacements decrease by 2–3%, both for unirradiated and irradiated rods, which is explained by the cyclic hardening of the material with each change in the sign of the load. On each half-cycle, the conditions of simple loading at small strains are satisfied.

#### 4. CONCLUSIONS:

It is shown that the maximum level of neutron irradiation can cause loosening of the substance, and the heat flux is harmful to biological objects. Calculations show that the impact of the radiation situation slightly affects the stress-strain state of elastoplastic bodies and biological objects. In this case, the action of the temperature field significantly affects the kinematic and static parameters of the objects.

A method for studying the stress-strain state of elastoplastic bodies under cyclic loading of a neutron flux is proposed, which significantly simplifies the solution of a whole class of boundary value problems. The mathematical model presented in the work has restrictions on the maximum level of neutron irradiation, which should not cause loosening of the substance. In this case, on each half-cycle, the conditions of simple loading and deformation must be satisfied.

#### 5. ACKNOWLEDGMENTS:

The work was carried out with the financial support of the state project of the Ministry of Education and Science project code “Modern technologies of experimental and digital modeling and optimization of spacecraft systems parameters”, project code FSFF-2020-0016.

## 6. REFERENCES:

1. Aleikin, V.V., Generalova, V.V., Gromov, A.A., and Kovalenko, O.I. (2019). State primary special standard of the unit of absorbed dose rate of intense photon, electron, and beta radiation for radiation technologies get 2009-2014. *Atmospheric Measurement Techniques*, 62, 587–591. <https://doi.org/10.1007/s11018-019-01664-4>
2. Ali, M.Y.M., Hanafiah, M.M., and Khan, M.F. (2018). Potential factors that impact the radon level and the prediction of ambient dose equivalent rates of indoor microenvironments. *Science of The Total Environment*, 626, 1-10.
3. Antufev, B.A., Egorova, O.V., Medvedskii, A.L., and Rabinskiy, L.N. (2019). Dynamics of shell with destructive heat-protective coating under running load. *INCAS Bulletin*, 11, 7-16. <https://doi.org/10.13111/2066-8201.2019.11.S.2>.
4. Astapov, A.N., Lifanov, I.P., and Rabinskiy, L.N. (2019). Perspective heat-resistant coating for protection of Cf/SiC composites in air plasma hypersonic flow. *High Temperature*, 57(5), 744-752.
5. Bulavin, L.A., Alekseev, O.M., Zabashta, Y., and Lazarenko, M.M. (2018). Phase equilibrium, thermodynamic limit, and melting temperature in nanocrystals. *Ukrainian Journal of Physics*, 63(11), 1036-1040.
6. Carlberg, M., Hedendahl, L., Koppel, T., and Hardell, L. (2019). High ambient radiofrequency radiation in Stockholm city, Sweden. *Oncology Letters*, 17, 1777-1783. <https://doi.org/10.3892/ol.2018.9789>
7. Chao, N., Yang, H., Liu, Y.-K., Xia, H., and Ayodeji, A. (2020). A local method of characteristics for dose assessment. *Radiation Physics and Chemistry*, 173, Article number 108869.
8. Chubirko, M.I., Klepikov, O.V., Kurolap, S.A., Kuzmichev, M.K., and Studenikina, E.M. (2019). Estimation of the equivalent dose rate of gamma radiation in the open territory of the city of Voronezh. *Radiation Hygiene*, 12(4), 66-71. <https://doi.org/10.21514/1998-426X-2019-12-4-66-71>
9. Cuttler, J.M. (2019). Evidence of dose threshold for radiation-induced leukemia: absorbed dose and uncertainty. *Dose-Response*. Retrieved from <https://journals.sagepub.com/doi/10.1177/1559325818820973>.
10. Dridi, W., Daoudi, M., Faraha, K., and Hosni, F. (2020). Monte Carlo validation of dose mapping for the Tunisian Gamma Irradiation Facility using the MCNP6 code. *Radiation Physics and Chemistry*, 173, Article number 108942.
11. Forkapić, S., Lakatoš, R., Čeliković, I., Bikit Schroeder, K., Mrdja, D., Radolić, V., and Samardžić, S. (2019). Proposal and optimization of method for direct determination of the thoron progeny concentrations and thoron equilibrium. *Radiation Physics and Chemistry*, 159, 57-63.
12. Gorshkov, A.G., Starovoitov, E.I., and Yarovaya, A.V. (2005). *Mechanics of layered viscoelastic structural elements*. Moscow, Russian Federation: FIZMATLIT.
13. Huang, J., Wang, Q., Qi, Z., Zhou, S., Zhou, M., and Wang, Z. (2020). Lipidomic profiling for serum biomarkers in mice exposed to ionizing radiation. *Dose-Response*. Retrieved from <https://journals.sagepub.com/doi/10.1177/1559325820914209>.
14. Inoue, K., Sahoo, S.K., Veerasamy, N., Kasahara, Sh. and Fukushima, M. (2020). Distribution patterns of gamma radiation dose rate in the high background radiation area of Odisha, India. *Journal of Radioanalytical and Nuclear Chemistry*, 324, 1423–1434. <https://doi.org/10.1007/s10967-020-07176-8>
15. Kuznetsov, V.K., Sanzharova, N.I., Panov, A.V., and Isamov, N.N. (2019). Radioecological monitoring of agroecosystems in the npp vicinity: Methodology and results of investigations. *Medical Radiology and Radiation Safety*, 4, 25-31.
16. Kuznetsov, V.M. (2003). *Nuclear danger*. Moscow, Russian Federation: Yabloko.
17. Lazarenko, M.M., Alekseev, A.N., Alekseev, S.A., Grabovsky, Y., Lazarenko, M.V., and Hnatiuk, K.I. (2018). Structure and thermal motion of 1-octadecene, confined in the pores of porous silicon. *Molecular Crystals and Liquid Crystals*, 674(1), 19-30.
18. Litvishko, V., Akhmetova, A., Kodasheva, G., Zhussupova, A., Malikova, R., and Kuralova, A. (2020). Formation of ecological education of the population. *E3S Web of Conferences*, 159, 01009.



19. Liu, R., and Wu, H. (2018, August). *Study on Radiation effects of central cities in Beijing-Tianjin-Hebei region*. Paper presented at the International Conference on Construction and Real Estate Management, Charleston, South Carolina.
20. Makarenko, A.V., and Kuznetsova, E.L. (2019). Energy-efficient actuator for the control system of promising vehicles. *Russian Engineering Research*, 39(9), 776-779.
21. Mieltski, J.W., and Povinec, P. (2020). Environmental radioactivity aspects of recent nuclear accidents associated with undeclared nuclear activities and suggestion for new monitoring strategies *Journal of Environmental Radioactivity*, 214–215, Article number 106151.
22. Mikayilova, A.C. (2017). Radioecological monitoring in the Central Zone of Azerbaijan. *Applied Science Reports*, 17(3). Retrieved from <https://ssrn.com/abstract=3200928>.
23. Okhrimenko, S.E., Korenkov, I.P., Miklyaev, P.S., Prokhorov, N.I., Verbova, L.F., Orlov, Yu.V., Petrova, T.B., Lashchyonova, T.N., Akopova, N.A., and Kiselev, S.M. (2017). Ranking of the territory of the city of Moscow for potential radon danger. *Hygiene and Sanitation*, 96(3). Retrieved from <https://www.medlit.ru/journalsview/gigsan/view/journal/en/2017/issue-3/2626-ranking-of-the-territory-of-the-city-of-moscow-for-potential-radon-danger/>.
24. Orlov, A.M., Skvortsov, A.A., and Litvinenko, O.V. (2003). Bending vibrations of semiconductor wafers with local heat sources. *Technical Physics*, 48(6), 736-741.
25. Pant, P., Kandari, T., Prasad, M., Semwal, P. and Ramola, R.C. (2018). Continuous measurement of equilibrium equivalent radon/thoron concentration using time-integrated flow-mode grab sampler. *Acta Geophysica*, 66, 1267–1272. <https://doi.org/10.1007/s11600-018-0163-9>
26. Pivovarov, Yu.P., and Mikhalev, V.P. (2004). *Radiation ecology*. Moscow, Russian Federation: Akademiya.
27. Prister, B.S., Vinogradskaya, V.D., Lev, T.D., Talerko, M.M., Garger, E.K., Onishi, Y., and Tischenko, O.G. (2018). Preventive radioecological assessment of territory for optimization of monitoring and countermeasures after radiation accidents. *Journal of Environmental Radioactivity*, 184–185, 140-151
28. Rabi, R., Oufni, L., and Amrane, M. (2017). Modeling of indoor  $^{222}\text{Rn}$  distribution in ventilated room and resulting radiation doses measured in the respiratory tract. *Journal of Radiation Research and Applied Sciences*, 10(3), 273-282.
29. Rabinskii, L.N., and Tushavina, O.V. (2019). Composite Heat Shields in Intense Energy Fluxes with Diffusion. *Russian Engineering Research*, 39(9), 800-803.
30. Rabinskiy, L.N., and Tushavina, O.V. (2019a). Investigation of an elastic curvilinear cylindrical shell in the shape of a parabolic cylinder, taking into account thermal effects during laser sintering. *Asia Life Sciences*, 2, 977-991.
31. Rabinskiy, L.N., and Tushavina, O.V. (2019b). Problems of land reclamation and heat protection of biological objects against contamination by the aviation and rocket launch site. *Journal of Environmental Management and Tourism*, 10(5), 967-973.
32. Rabinskiy, L.N., Tushavina, O.V., and Formalev, V.F. (2019). Mathematical modeling of heat and mass transfer in shock layer on dimmed bodies at aerodynamic heating of aircraft. *Asia Life Sciences*, 2, 897-911.
33. Rabinsky, L.N., and Kuznetsova, E.L. (2019). Simulation of residual thermal stresses in high-porous fibrous silicon nitride ceramics. *Powder Metallurgy and Metal Ceramics*, 57(11-12), 663-669.
34. Renaud, J., Palmans, H., Sarfehnia, A., and Seuntjens, J. (2020). Absorbed dose calorimetry. *Physics in Medicine and Biology*, 65, Article number 05TR02
35. Saha, P., Uddin, M.H., and Reza, M.T. (2019). A steady-state equilibrium-based carbon dioxide gasification simulation model for hydrothermally carbonized cow manure. *Energy Conversion and Management*, 191(1), 12-22.
36. Sean Hubar, J. (Ed.). (2017). *Fundamentals of oral and maxillofacial radiology*. Hoboken, New Jersey: John Wiley and Sons, Inc.
37. Shugurov, O., and Knyazyuk, A. (2018). Radiation situation in typical mining-processing agglomerations of the Dnepropetrovsk region. *Ecology and Noospherology*, 29(1), 8-12. <https://doi.org/https://doi.org/10.15421/031802>



38. Skvortsov, A.A., Kalenkov, S.G., and Koryachko, M.V. (2014). Phase transformations in metallization systems under conditions of nonstationary thermal action. *Technical Physics Letters*, 40(9), 787-790.
39. Starovoitov, É.I., and Leonenko, D.V. (2019). Effect of heat flow on the stressed state of a three-layer rod. *Journal of Engineering Physics and Thermophysics*, 92(1), 60-72. DOI 10.1007/s10891-019-01907-9.
40. Starovoitov, E.I., Kubenko, V.D., and Tarlakovskii, D.V. (2009). Vibrations of circular sandwich plates connected with an elastic foundation. *Russian Aeronautics*, 52(2), 151-157.
41. Taleyarkhan, R.P. (2020). Monitoring neutron radiation in extreme Gamma/X-Ray Radiation fields. *Sensors*, 20, Article number 640.
42. Topchy, D.V. (2018). Organisational and technological measures for converting industrial areas within existing urban construction environments. *International Journal of Civil Engineering and Technology*, 9(7), 1975-1986.
43. Trotsenko, A.A., Zhuravleva, N.G., Aleksandrova, Ye.Yu., Yerokhova, N.V., and Udalova, O.A. (2019). Recommended practices for radioecological monitoring of the environment. *IOP Conference Series: Earth and Environmental Science*, 315(5). Retrieved from <https://iopscience.iop.org/article/10.1088/1755-1315/315/5/052077/meta>.
44. Tushavina, O.V., Nadezhkina, E.V., Sorokin, A.E., Blinohvatov, A.A., and Zubkova, V.M. (2019). Study of the radiation situation in the city of Moscow. *Ecology of Urban Territories*, 3, 73-76.
45. Umbetov, A., Kozhahmet, M., Sabitbekova, G., Amirov, M., Hamit, A., Alieva, G., Karimova, D., and Uspanova, V. (2017). Interference of coherent radiation in a crystalline two-component lens. *Far East Journal of Electronics and Communications*, 17(5), 923-939.
46. Umbetov, A.U., Umbetova, M.Z., Abildayev, G.M., Baizakova, S.S., Zhamalova, S.A., Konussova, A.B., and Dosmagulova, K.K. (2016). Transformation and interference of the laser radiation in composite crystal optical systems. *ARNP Journal of Engineering and Applied Sciences*, 11(19), 11561-11573.
47. Yakovlev, E.Y., Zyкова, E.N., Zykov, S.B., Malkov, A.V., and Bazhenov, A.V. (2020). Heavy metals and radionuclides distribution and environmental risk assessment in soils of the Severodvinsk industrial district, NW Russia. *Environmental Earth Sciences*, 79, Article number 218. Retrieved from <https://doi.org/10.1007/s12665-020-08967-8>
48. Yudaev, I., Stepanchuk, G., Kaun, O., Ukraitsev, M., and Ponamareva, N. (2019). Small-sized irradiation structures for intensive year-round cultivation of green vegetable crops. *IOP Conference Series: Earth and Environmental Science*, 403(1), 012084.
49. Zverev, V.L. (2010). *Fundamentals of ecology and problems of its development*. Moscow, Russian Federation: Ministry of Natural Resources and Ecology of the Russian Federation.

$$\varphi(z) = \varphi_0 e^{-\mu z} \quad (\text{Eq. 1})$$

$$\mu = \sigma n_0 = \sigma \frac{A_0 \rho}{A}, \quad (\text{Eq. 2})$$

$$I(z) = \varphi_0 t e^{-\mu z}. \quad (\text{Eq. 3})$$

$$\theta_l = BI(z), \quad (\text{Eq. 4})$$

$$l_0 = \varphi_0 t \quad (\text{Eq. 5})$$

$$\sigma_y = \sigma_{y0} \left[ 1 + A \left( 1 - \exp(-\xi I_0) \right)^{1/2} \right], \quad (\text{Eq. 6})$$

$$s'_{ij} = 2G\vartheta'_{ij}, \quad \sigma' = K(3\varepsilon' - BI - \alpha \Delta T), \quad (\text{Eq. 7})$$

$$s'_{ij} = 2G\vartheta'_{ij} f'(\varepsilon'_u, I, a'_k), \quad (\text{Eq. 8})$$

$$2\varepsilon'_{ij} = \mathcal{U}'_{i'j} + \mathcal{U}'_{ij}; \quad \sigma'_{ij} l_j = R'_i \quad (\text{Eq. 9})$$

$$\sigma'_{ij} l_j = R'_i \text{ to } S_\sigma, \mathcal{U}'_i = \mathcal{U}'_{0i} \text{ to } S_u. \quad (\text{Eq. 10})$$

$$l_1 = \varphi t_1. \quad (\text{Eq. 11})$$

$$\mathbf{z} = \mathbf{c} + h_1 \quad (\text{Eq. 12})$$

$$s^{(k)}_x = 2G_k f^{(k)}(\varepsilon^{(k)}_u, I) \vartheta^{(k)}_x, \quad \sigma^{(k)} = K_k \left( 3\varepsilon^{(k)} - B_k I - \alpha_k \Delta T \right), \quad (k=1, 2, 3), \quad (\text{Eq. 13})$$

$$s^{(3)}_{xz} = 2G_3 f^{(3)}(\varepsilon^{(3)}_u, I) \vartheta^{(3)}_{xz},$$

$$f^{(k)}(\varepsilon^{(k)}_u, I) = \begin{cases} 1, \\ 1 - \omega^{(k)}(\varepsilon^{(k)}_u, I), \end{cases} \quad (\text{Eq. 14})$$

$$\varepsilon^{(k)}_u \leq \varepsilon^{(k)}_y(I),$$

$$\varepsilon^{(k)}_u > \varepsilon^{(k)}_y(I);$$

$$\begin{aligned} \psi^{(n)}(x) &= C_2^{(n)} \operatorname{sh}(\beta x) + C_3^{(n)} \operatorname{ch}(\beta x) + \\ &+ \frac{1}{\beta} \left[ \operatorname{sh}(\beta x) \int g^{(n)} \operatorname{ch}(\beta x) dx - \operatorname{ch}(\beta x) \int g^{(n)} \operatorname{sh}(\beta x) dx \right]. \\ u^{(n)}(x) &= \gamma_3 \psi^{(n)} + \frac{1}{\alpha_2} \left[ -a_4 L_2^{-1} \left( p' - p_{\omega}^{(n-1)} \right) + a_7 L_3^{-1} \left( q' - q_{\omega}^{(n-1)} \right) + \frac{a_7}{2} C_1^{(n)} x^2 \right] + C_7^{(n)} x + C_8^{(n)}, \\ w^{(n)}(x) &= \frac{1}{\alpha_2} \left[ \alpha_1 \int \psi^{(n)} dx - a_7 L_3^{-1} \left( p' - p_{\omega}^{(n-1)} \right) + a_1 L_4^{-1} \left( q' - q_{\omega}^{(n-1)} \right) + \right. \\ &\quad \left. + \frac{1}{6} a_1 C_1^{(n)} x^3 \right] + \frac{1}{2} C_4^{(n)} x^2 + C_5^{(n)} x + C_6^{(n)}. \end{aligned} \quad (\text{Eq. 15})$$

$$\begin{aligned}
C_1^{(n)} &= -L_1^{-1}(q' - q_{\omega}^{(n-1)})|_{x=l}, C_3^{(n)} = \frac{1}{\beta} \int g'^{(n)}(x) \operatorname{sh}(\beta x) dx|_{x=0}, \\
C_2^{(n)} &= \frac{1}{\beta} \left[ \frac{\operatorname{ch}(\beta l)}{\operatorname{sh}(\beta l)} \left( \int g'^{(n)} \operatorname{sh}(\beta x) dx|_{x=l} - \int g'^{(n)} \operatorname{sh}(\beta x) dx|_{x=0} \right) - \int g'^{(n)} \operatorname{ch}(\beta x) dx|_{x=l} \right], \\
C_4^{(n)} &= \frac{a_7}{\alpha_2} \left[ L_1^{-1}(p' - p_{\omega}^{(n-1)}) + \sum_{k=1}^3 (B_k I_k + \alpha_k \Delta T) K_k h_k \right]|_{x=l} - \\
&- \frac{a_1}{\alpha_2} \left( L_2^{-1}(q' - q_{\omega}^{(n-1)}) + (B_1 I_1 + \alpha_1 \Delta T) K_1 h_1 \left( c + \frac{h_1}{2} \right) - (B_2 I_2 + \alpha_2 \Delta T) K_2 h_2 \left( c + \frac{h_2}{2} \right) \right)|_{x=l} - \frac{a_1}{\alpha_2} C_1^{(n)} l, \\
C_5^{(n)} &= \frac{a_7}{\alpha_2} L_2^{-1}(p' - p_{\omega}^{(n-1)})|_{x=0} - \frac{a_1}{\alpha_2} L_3^{-1}(q' - q_{\omega}^{(n-1)})|_{x=0}, \\
C_6^{(n)} &= \frac{a_7}{\alpha_2} L_3^{-1}(p' - p_{\omega}^{(n-1)})|_{x=0} - \frac{a_1}{\alpha_2} L_4^{-1}(q' - q_{\omega}^{(n-1)})|_{x=0} - \frac{\alpha_1}{\alpha_2} \int \psi'^{(n)} dx|_{x=0}, \\
C_7^{(n)} &= \frac{a_4}{\alpha_2} \left[ L_1^{-1}(p' - p_{\omega}^{(n-1)})|_{x=l} + \sum_{k=1}^3 (B_k I_k + \alpha_k \Delta T) K_k h_k \right] - \\
&- \frac{a_7}{\alpha_2} \left( L_2^{-1}(q' - q_{\omega}^{(n-1)})|_{x=l} + (B_1 I_1 + \alpha_1 \Delta T) K_1 h_1 \left( c + \frac{h_1}{2} \right) - (B_2 I_2 + \alpha_2 \Delta T) K_2 h_2 \left( c + \frac{h_2}{2} \right) - C_1^{(n)} l \right), \\
C_8^{(n)} &= \frac{a_4}{\alpha_2} L_2^{-1}(p' - p_{\omega}^{(n-1)})|_{x=0} - \frac{a_7}{\alpha_2} L_3^{-1}(q' - q_{\omega}^{(n-1)})|_{x=0}.
\end{aligned} \tag{Eq. 16}$$

$$\begin{aligned}
\psi^{(n)*}(x) &= C_2^{(n)*} \operatorname{sh}(\beta x) + C_3^{(n)*} \operatorname{ch}(\beta x) + \\
&+ \frac{1}{\beta} \left[ \operatorname{sh}(\beta x) \int g^{(n)*} \operatorname{ch}(\beta x) dx - \operatorname{ch}(\beta x) \int g^{(n)*} \operatorname{sh}(\beta x) dx \right]. \\
u^{(n)*}(x) &= \gamma_3 \psi^{(n)*} + \frac{1}{\alpha_2} \left[ -a_4 L_2^{-1}(p^* - p_{\omega}^{(n-1)*}) + a_7 L_3^{-1}(q - q_{\omega}^{(n-1)*}) + \frac{a_7}{2} C_1^{(n)*} x^2 \right] + \\
&+ C_7^{(n)*} x + C_8^{(n)*}, \\
w^{(n)*}(x) &= \frac{1}{\alpha_2} \left[ \alpha_1 \int \psi^{(n)*} dx - a_7 L_3^{-1}(p^* - p_{\omega}^{(n-1)*}) + a_1 L_4^{-1}(q^* - q_{\omega}^{(n-1)*}) + \right. \\
&\left. + \frac{1}{6} a_1 C_1^{(n)*} x^3 \right] + \frac{1}{2} C_4^{(n)*} x^2 + C_5^{(n)*} x + C_6^{(n)*}.
\end{aligned} \tag{Eq. 17}$$

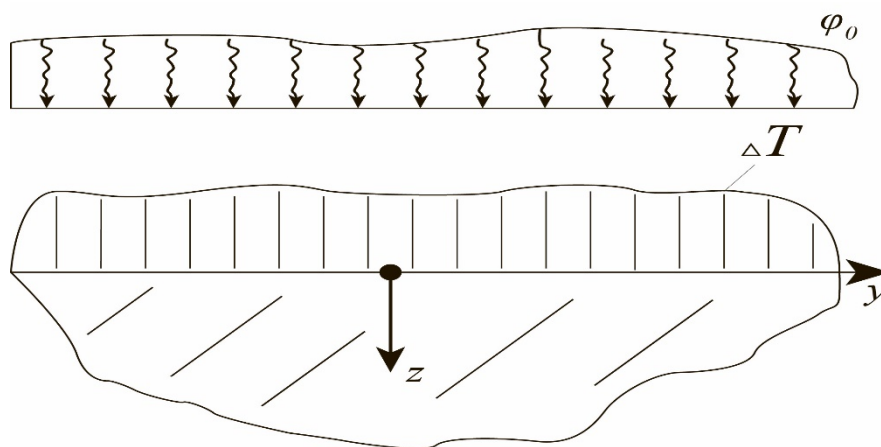


**Figure 1.** Diagram of loading on an isotropic body

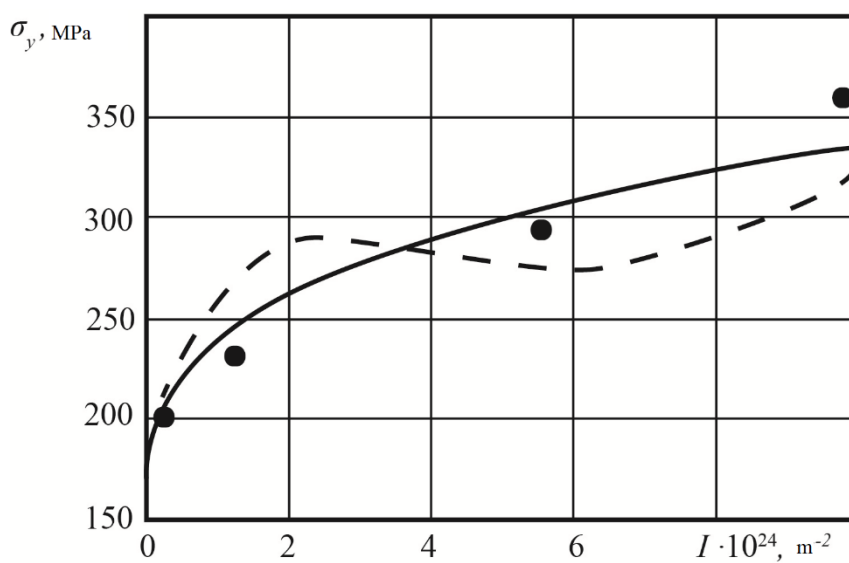


**Figure 2.** The dependence of stress on the neutron flux magnitude

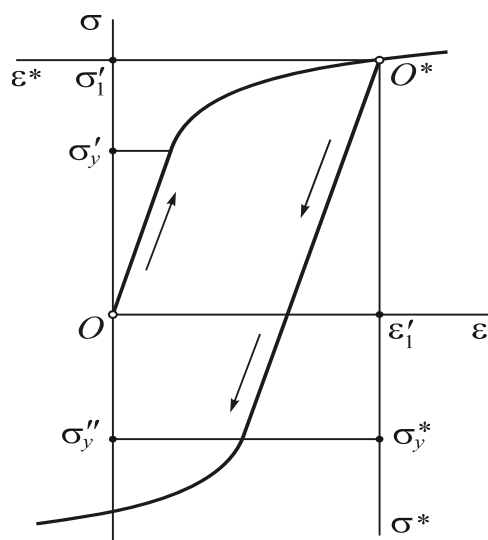


**Figure 3.** The diagram of stress-strain and unloading

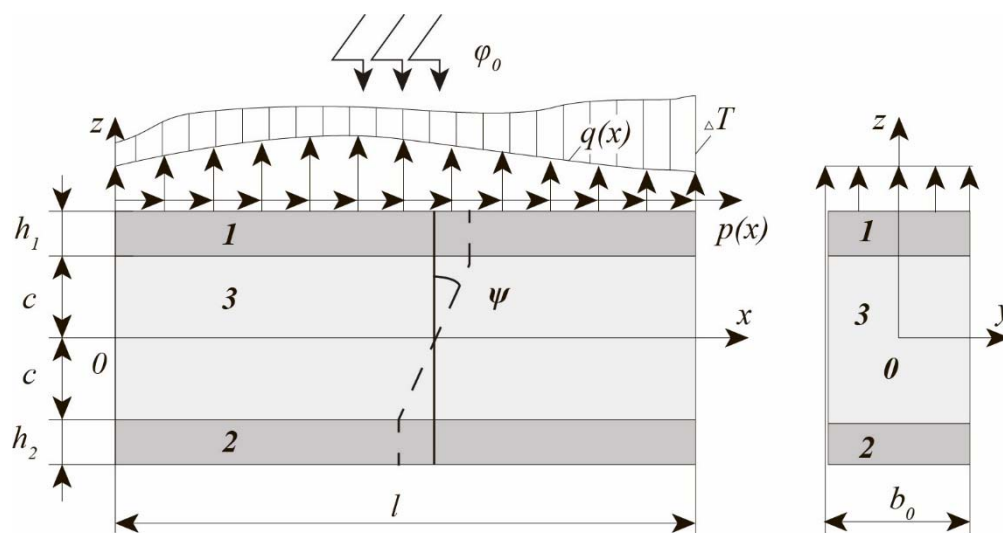


**Figure 4.** The load on the three-layer beam

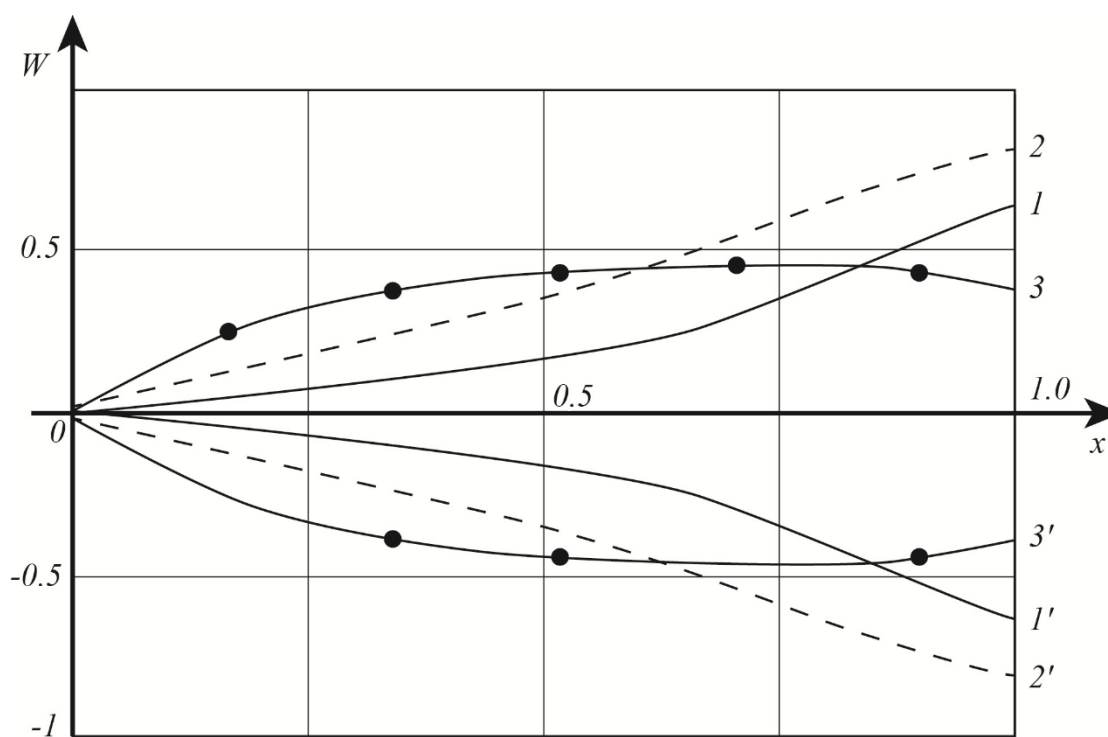


**Figure 5.** The distribution of deflection along the axis of a three-layer rod

## MÉTODO NUMÉRICO PARA DETERMINAR A DEPENDÊNCIA DO ESTADO DE TENSÃO TÉRMICA DA HASTE DA TEMPERATURA DO MEIO AMBIENTE NA PRESENÇA SIMULTÂNEA DE PROCESSOS TÉRMICOS

## A NUMERICAL METHOD FOR DETERMINING THE DEPENDENCE OF THE THERMALLY STRESSED STATE OF A ROD ON AMBIENT TEMPERATURE WITH THE SIMULTANEOUS PRESENCE OF THERMAL PROCESSES

## ЧИСЛЕННЫЙ МЕТОД ОПРЕДЕЛЕНИЯ ЗАВИСИМОСТИ ТЕРМОНАПРЯЖЕННОГО СОСТОЯНИЯ СТЕРЖНЯ ОТ ТЕМПЕРАТУРЫ ОКРУЖАЮЩЕЙ СРЕДЫ ПРИ ОДНОВРЕМЕННОМ НАЛИЧИИ ТЕПЛОВЫХ ПРОЦЕССОВ

MYRZASHEVA, Aigul N.<sup>1</sup>; KENZHEGULOV, Beket<sup>2\*</sup>; SHAZHEDEKEEVA, Nurgul K.<sup>3</sup>; TULEUOVA, Raigul U.<sup>4</sup>;

<sup>1,2,3,4</sup> Atyrau State University named after Kh. Dosmukhamedov, Department of Mathematics and Methods of Teaching Mathematics, 1 Studenchesky Ave., zip code 060011, Atyrau – Republic of Kazakhstan

\* Correspondence author

e-mail: b.kenzhegulov@asu.edu.kz

Received 12 May 2020; received in revised form 06 June 2020; accepted 19 June 2020

### RESUMO

Os métodos existentes para estudar o estado termicamente deformado e tenso de uma haste de comprimento limitado feita de liga especial resistente ao calor não levam em conta a presença simultânea de processos térmicos, como transferência de calor, força axial, isolamento térmico, temperatura local, condições operacionais da haste e o fato, que em larga escala o coeficiente de expansão térmica do material da haste depende de temperatura. Para resolver esses problemas, os autores propõem um novo método numérico para estudar o estado termomecânico de uma haste de comprimento limitado feita da liga resistente ao calor ANV-300. Esta haste é de comprimento limitado e rigidamente comprimida com duas extremidades. A superfície lateral das seções  $(0 \leq x \leq L/3)$  e  $(2L/3 \leq x \leq L)$  o núcleo são isolados termicamente. No local  $(L/3 \leq x \leq 2L/3)$  da haste, é fornecida a temperatura local, que varia em coordenada por uma lei linear. Os estudos foram realizados em diferentes temperaturas ambientes. Os padrões da distribuição do campo de deslocamentos elásticos do componente elástico da deformação são construídos de acordo com a lei de Hooke, com os valores do componente elástico da tensão e levando em consideração a dependência do campo entre o coeficiente de expansão térmica e temperatura. Como resultado do estudo, verificou-se que uma mudança na temperatura da área transversal da extremidade esquerda do ambiente tem um efeito menor no estado de tensão térmica da haste considerada do que o efeito da mudança.

**Palavras-chave:** minimização da energia potencial, método dos elementos finitos, isolamento térmico, temperatura, coeficiente de transferência de calor.

### ABSTRACT

Existing methods for studying the thermally stressed and deformed state of a rod of the limited length from a special heat-resistant alloy do not take into account the simultaneous presence of thermal processes, such as heat exchange, axial force, thermal insulation, local temperature, operating conditions of the rod and the full-scale dependence of the coefficient of thermal expansion of the material of the rod on temperature. To solve such problems, the authors propose a new numerical method for studying the thermomechanical state of a rod of the limited length from the heat-resistant alloy ANV-300. This rod is of a limited length and rigidly clamped at both ends. The lateral surface of sections  $(0 \leq x \leq L/3)$  and  $(2L/3 \leq x \leq L)$  of the rod is thermally insulated. At the site  $(L/3 \leq x \leq 2L/3)$  of the rod, the local temperature is given, which varies in coordinate by a linear law. The studies were carried out at different ambient temperatures. The laws of the distribution field of elastic displacements of the elastic component of deformation are constructed, respectively, according to Hooke's law, the values of the elastic component of stress, taking into account the field dependence between the coefficient of thermal expansion and temperature. As a result of studies, it was found that a change in the temperature of the

surrounding cross-sectional area of the left end of the medium has little effect on the thermally stressed state of the considered rod than the effect of the change.

**Keywords:** *minimization of potential energy, finite element method, thermal insulation, temperature, heat transfer coefficient.*

## АННОТАЦИЯ

Существующие методы исследования термически напряженного и деформированного состояния стержня ограниченной длины из специального жаропрочного сплава не учитывают одновременное наличие тепловых процессов, таких как теплообмен, осевая сила, теплоизоляция, локальная температура, условия эксплуатации стержня и натурная зависимость коэффициента теплового расширения материала стержня от температуры. В статье на основе минимизаций потенциальной энергии упругих деформаций с применением метода квадратичного конечного элемента с тремя узлами разработана математическая модель термонапряженно-деформированного состояния горизонтального стержня из жаропрочного сплава АНВ-300. Данный стержень ограниченной длины и жестко зашпелен с двумя концами. Боковая поверхность участков  $(0 \leq x \leq L/3)$  и  $(2L/3 \leq x \leq L)$  стержня теплоизолированная. На участке  $(L/3 \leq x \leq 2L/3)$  стержня дана локальная температура, меняющаяся по координате линейным законом. Через площадь поперечных сечений обоих концов данного стержня происходит тепловой обмен с окружающими их средами. Закономерности распределения поля упругих смещений упругой составляющей деформации строятся в соответствии с законом Гука, значениями упругой составляющей напряжений с учетом полевой зависимости между коэффициентом теплового расширения и температурой. В результате исследования было установлено, что изменение температуры окружающей площади поперечного сечения левого конца среды оказывает меньшее влияние на термически напряженное состояние рассматриваемого стержня, чем влияние изменения.

**Ключевые слова:** *минимизация потенциальной энергии, метод конечных элементов, теплоизоляция, температура, коэффициент теплообмена.*

## 1. INTRODUCTION

The influence of ambient temperature on the thermally stressed state of a rod of this alloy in the presence of local temperature is carried out, and numerical results of the study are presented. Ambient temperature affects the rod through the cross-section of the left end. The studies were carried out at different ambient temperatures. The laws of the distribution field of elastic displacements of the elastic component of deformation are constructed, respectively, according to Hooke's law, the values of the elastic component of stress, taking into account the field dependence between the coefficient of thermal expansion and temperature. As a result of studies, it was found that a change in the temperature of the surrounding cross-sectional area of the left end of the medium has little effect on the thermally stressed state of the considered rod than the effect of the change. Thus, only by changing the value (and not), i.e., by changing the environmental properties of the surrounding cross-sectional area where heat transfer occurs, the thermally stressed state of the rod under investigation can be changed.

Existing methods for studying the thermally stressed and deformed state of a rod of the limited

length from a special heat-resistant alloy do not take into account the simultaneous presence of thermal processes, such as heat exchange, axial force, thermal insulation, local temperature, operating conditions of the rod and the full-scale dependence of the coefficient of thermal expansion of the material of the rod on temperature (Geng *et al.*, 2018; Kudaykulov *et al.*, 2019; Litvishko *et al.*, 2020; Shen *et al.*, 2019). To solve such problems, the authors propose a new numerical method for studying the thermomechanical state of a rod of the limited length from the heat-resistant alloy ANV-300, which allows one to take into account the dependence between the coefficient of thermal expansion and the field of temperature distribution, operating conditions, and fixing. Chemical composition in % for grade ANV-300: C (max 0.1), Si (max 0.5), Mn (max 0.5), Ni (64.2-70.1), S (max 0.01), P (max 0.015), Cr (14-17), W (7-10), Ti (1.4-2), Al (4.5-5.5), B (max 0.1), Ni – basis. It is used for the manufacture of ingots and cast rods intended for further remelting in the manufacture of shaped castings.

The determining fundamental relations of thermoelasticity of weakly compressible materials are considered in (Mikhlin, 1974; Lee *et al.*, 2017; Pandiyan *et al.*, 2019; Rabinskiy and Tushavina,

2019; Dmitriev *et al.*, 2011; Kolokoltsev *et al.*, 2020). Using a small parameter, an analytical solution to the problem of stretching a rod from a weakly compressible material under nonisothermal conditions is obtained. In (Nozdrev, 1967; Fedotov *et al.*, 2018; Starovoitov *et al.*, 2016; Qiu *et al.*, 2017; Bartels, 2019; Krechetov *et al.*, 2018; Civallek *et al.*, 2020), the basic problems of thermodynamics and their application are described in sufficient detail. Zenkevich (1975) is devoted to the presentation of the finite element method, as one of the most effective methods for the numerical solution of engineering, physical and mathematical problems using computers. In (Timoshenko and Goodyear, 1975; Chen *et al.*, 2017; Park *et al.*, 2019; Hou and Gao, 2020; Santos *et al.*, 2020), a systematic presentation of the theory of elasticity was given, starting with the derivation of the main relations and ending with some solutions obtained in recent years. The plane problem, the problem of torsion and stress concentration, some spatial problems, variational principles, and methods for solving problems are considered in detail.

Based on energy principles in combination with the use of a finite quadratic element with three nodes, a mathematical model, a computational algorithm, and a set of applied programs were developed in (Kudaykulov, 2009; Kudaykulov *et al.*, 2009; Formalev *et al.*, 2019; Formalev and Kolesnik, 2019; Myrzasheva and Shazhdekeyeva, 2015; Myrzasheva *et al.*, 2016; Akhmetov and Kudaykulov, 2017; Myrzasheva *et al.*, 2018; Deepa and Rajendran, 2018; Kuznetsova and Rabinskiy, 2019). With the help of these developments, the problems of determining the thermomechanical and thermo-stress-strain states of a rod of constant cross-section, depending on the presence of local thermal insulation, temperature, heat transfer, and their operating condition, are numerically solved. The mechanical properties of heat-resistant steels and alloys at room and high temperatures, the influence of alloying elements on the structure, and methods of thermal and hot processing of alloys are considered in (Himushin, 1969). Also considered are heat-resistant alloys on iron, nickel, cobalt bases, and several refractory metals and their alloys. The most important methods and techniques of computational mathematics are described in (Demidovich and Maron, 1960; Yano *et al.*, 2018; Leon and Chen (Roger), 2019; Sun *et al.*, 2020).

At present, in our republic and abroad, there are many scientific works devoted to the problem of determining the dependence of the

thermally stressed-deformed state of bar elements of complex construction. Of these works, scientific studies by scientists of our country and neighboring countries can be noted: A.K. Kudaykulov (2009), B.B. Orazbaev (Orazbaev *et al.*, 2017), M.M. Ermekov (2011), V.V. Afanasyeva (Afanasyeva and Lazerson, 1995), V.N. Bakulin (1985), I.A. Birger (1992), G.S. Pisarenko (Pisarenko *et al.*, 1973), A.I. Oleinikov (Korobeinikov *et al.*, 2008), Yu.A. Fedorov (2001), F.F. Himushin (1969) and others, as well as foreign scientists, like O. Zenkevich (1975), F. Krieth (1973), V.F. Nozdrev (1967), L. Segerlind (1979) and others.

## 2. MATERIALS AND METHODS

Consider a rod of limited length  $L, (cm)$  made of the heat-resistant alloy ANV-300. Both ends of the shaft are rigidly pinched. The cross-sectional area of the rod is  $F, (cm^2)$ , which is constant over its entire length. The thermal expansion coefficient of the rod material  $\alpha(T), (1/^\circ K)$  depends on the field temperature distribution. The thermal conductivity coefficient of the rod material is  $K_{xx}, \left(\frac{watt}{cm \cdot ^\circ K}\right)$ , the elastic modulus is  $E, \left(\frac{kG}{cm^2}\right)$ . The elastic modulus of the heat-resistant alloy ANV-300 is temperature independent. Through the cross-sectional areas of the two pinched ends of the rod, heat exchange occurs with their surroundings. For the left end of the rod ( $x = 0$ ), the heat transfer coefficient is denoted by  $h_0, \left(\frac{watt}{cm^2 \cdot ^\circ K}\right)$ , and the ambient temperature by  $T_{amb\ 0}, (^\circ K)$ . Similarly, for the right end ( $x = L$ ) –  $h_L, \left(\frac{watt}{cm^2 \cdot ^\circ K}\right)$  and  $T_{amb\ L}, (^\circ K)$ . Side surfaces, which are  $\frac{1}{3}$  of the length of the rod, i.e.,  $(0 \leq x \leq (L/3))$  and  $((2L/3) \leq x \leq L)$  we consider the core to be thermally insulated. In the area of the rod  $((L/3) \leq x \leq (2L/3))$ , the local temperature is given. It can be constant, varying along the local length of the rod with linear and quadratic laws.

In the presence of heat sources due to thermal expansion and pinching, a stress-strain state appears in the inner sections of the rod. In this case, the components of the deformation and stress will be respectively, elastic  $(\varepsilon_x, \sigma_x)$ , temperature  $(\varepsilon_T, \sigma_T)$  and thermoelastic  $(\varepsilon, \sigma)$ . If the field shows the temperature distribution and



thermal expansion coefficient along the length of the rod, then the expression of the function that characterizes the potential energy of elastic deformations of the considered rod has the following form (Equation 1), where  $V$  is the volume of the rod; Equation 2 is component of elastic deformation; Equation 3 is the field of elastic displacement along the length of the rod; Equation 4 is elastic component of stress; Equation 5 is the law distribution of the coefficient of thermal expansion along the length of the rod;  $E$  – module of elasticity of the core material; Equation 6 is law temperature distribution along the length of the rod.

To construct a mathematical model of the thermal stress state of a heat-resistant alloy rod pinched by two ends, we discretize it by quadratic elements with three nodes. Given that the process under consideration is a steady-state, within each discrete element, the field distribution of temperature, coefficient of thermal expansion and elastic displacement is approximated by a full second-order polynomial passing through three nodal points  $i, j$  and  $k$  (the length of the discrete element is  $\lambda$ , starting point  $i$ , mid- $j$ , and finite- $k$  and  $x_i = 0$ , Equations (7)-(8)). Within each discrete field element, the distribution of these functions is expressed by the following Equations (9)-(11) (Mikhlin, 1974; Nozdrev, 1967; Zenkevich, 1975). Where  $T_i, T_j, T_k$  are the values of  $T(x)$  the nodal points  $i, j, k$ ;  $u_i, u_j, u_k$  are the displacements of the sections along the coordinate, which are the coordinates of the nodes  $i, j, k$ , respectively;  $\alpha_i, \alpha_j, \alpha_k$  are values of  $\alpha(T(x))$  at these nodal points, respectively, in the interval  $x \in (x_i \leq x \leq x_k)$ ;  $\gamma_i(x), \gamma_j(x)$  and  $\gamma_k(x)$  are the form functions for a quadratic element with three nodes, where (Equation 12).

The properties of these forms functions will ensure the continuity of the desired functions during the transition from one element to the next. For this case, the expression of the functional characterizing the potential energy of elastic deformation, in the presence of heat sources for one discrete element, has the following form (Equation 13). Where  $V_i$  is the volume of the discrete quadratic element under consideration with three nodes. Then the potential energy of elastic deformation of the entire rod in the presence of heat sources expressed as Equation 14. Where NDE is the number of discrete elements in the rod (Zenkevich, 1975; Timoshenko and

Goodyear, 1975; Kudaykulov, 2009; Kudaykulov *et al.*, 2009).

Considering each integral in expression (Equation 13) separately and from (Equation 12), finding the expression for partial derivatives  $\frac{\partial \gamma_i}{\partial x}, \frac{\partial \gamma_j}{\partial x}, \frac{\partial \gamma_k}{\partial x}$ , and substituting them in Equation 13, we obtain an integrated expression of the function that characterizes the potential energy of elastic deformation of a discrete element in the presence of a temperature field (Equation 15). Further, minimizing the last functional concerning the nodal values of elastic displacement, we obtain a mathematical model of the thermally stressed state of a discrete element in the form of resolving systems of linear algebraic equations for the movement of element nodes (Equations 16-18).

These equations are obtained for nodes of one discrete element. Since we discretize the considered rod with a set of quadratic elements with three nodes, the expression for the functional of the potential energy of elastic deformation should be written for each element, taking into account the temperature field (Zenkevich, 1975; Myrzasheva and Shazhdekeyeva, 2015). Then, the general expression of potential energy for the considered rod as a whole has the form (Equation 14). The total number of nodes will be equal  $2 \times nn + 1$ . In the general case, the mathematical system of the thermally stressed state of the considered rod pinched by two ends is the following system of linear algebraic  $2 \times nn + 1$  equation (19), where  $i$  is presented in the Equation 20. The displacement values of the two ends of the rod (due to rigid pinching) are equal to  $u_1 = u_{2 \times nn + 1} = 0$ .

Solving system (Equation 19), the nodal values of elastic displacements are determined. The values of the elastic component of the deformation in the first half of the element are determined as Equation 21. Similarly, for the second half of the element, we have (Equation 22). Accordingly, according to Hooke's law, the values of the elastic component of stress are determined as follows (Equation 23). The values of the temperature component of the deformation and stress are determined as follows (Equations 24-25). When  $\varepsilon_x^I; \varepsilon_x^{II}; \varepsilon_T^I; \varepsilon_T^{II}; \sigma_x^I; \sigma_x^{II}; \sigma_T^I; \sigma_T^{II}$  are known, values of thermoelastic strain and stress components are determined (Equations 26-27).

Based on the developed mathematical model, we will carry out a numerical simulation of the thermally stressed state of the considered rod in dependence  $T_{amb}$ , for fixed values of all other

parameters. The core works in the presence of heat transfer, thermal insulation, and temperature. The temperature varies along the local length of the rod by a linear law, i.e., (Equation 28) at  $((L/3) \leq x \leq (2L/3))$ , where (Equation 29). We coordinate the coordinate axis  $Ox$  from left to right (Figure 1). It is required to study the thermal stress state of a rod made of heat-resistant alloy ANV-300 clamped at both ends, depending on, for fixed values of all other parameters. Task. The values of the necessary parameters are as follows:

$$T_{amb\ 0} = T_{amb\ L} = 40\ (^{\circ}K) \cdot a = 40; \quad L = 30\ (cm);$$

$$T = 40x; \text{ Equations (30)-(32) at } 10 \leq x \leq 20\ (cm).$$

We vary the value of the ambient temperature with the cross-sectional area of the left end ( $x = 0$ ) of the rod:  $T_{amb\ 0} = 10\ (^{\circ}K); 20\ (^{\circ}K); 30\ (^{\circ}K); 40\ (^{\circ}K)$ .

As mentioned above, in the presence of the given heat sources and partial thermal insulation, the rod tries to expand. However, due to the pinching of both ends, compressive forces  $R$  appear. In this regard, and due to the inhomogeneous temperature field, an inhomogeneous stress field arises in the inner sections of the rod. Components of the strain will be  $\varepsilon_x, \varepsilon_T, \varepsilon$ , and stresses  $\sigma_x, \sigma_T, \sigma$ . It is required to determine the displacement field (Equation 33), elastic deformations  $\varepsilon_x$ , temperature deformations  $\varepsilon_T$ , thermoelastic deformations  $\varepsilon$ , as well as elastic, temperature, and thermoelastic stresses  $\sigma_x, \sigma_T$  and  $\sigma$ .

To solve this problem, the considered rod is discretized  $n=150$  by quadratic elements with three nodes. Then the length of each element will be  $\Delta l = 0.2\ cm$ . For each discrete element, an expression is written of the functional of the potential energy of elastic deformation, taking into account the presence of a temperature field. Next, summing them overall discrete elements, we find the expression of the corresponding functions for the considered rod as a whole. The total number of equations in the system will be  $2n+1=301$ . Since both ends of the rod are rigidly pinched, then  $u_1 = u_{301} = 0$ . In this regard, the number of equations in the system will be 299. By minimizing the potential energy of elastic deformation, taking into account the presence of a local field of temperature distribution and heat exchanges, we obtain (Equation 19), a system of resolving equations.

Moreover, if the number of discrete elements in the rod is  $n$  (where  $n$  is a positive

integer), then the number of nodes in the rod will be  $2n+1$ . Nevertheless, since both ends of the rod are rigidly clamped, the movement of the extreme nodes will be zero, i.e.  $u_1 = u_{2n+1} = 0$ . Therefore, the minimization of the functional characterizing the potential energy of elastic deformations in the presence of a temperature field is minimized by nodal displacements (Equation 34). Solving the last system, we find the nodal values of displacement. Further, according to (Equations 21-27), the value of the components  $\varepsilon_x, \varepsilon_T, \varepsilon$   $\sigma_x, \sigma_T, \sigma$  in the given sections of the rod are determined. The task (Equation 35) is accepted (Myrzasheva *et al.*, 2016; Akhmetov and Kudaykulov, 2017).

### 3. RESULTS AND DISCUSSION:

To obtain the results of the problem, first it was considered the case when  $T_{amb\ 0} = 10\ (^{\circ}K)$ . In this case, the nodal values of the displacement are given in Table 1. The corresponding field distribution of displacement along the length of the considered rod is shown in Figure 2a). From this Table and the Figure, it can be seen that the sections of the rod that are on the site  $0 < x < 24.85\ (cm)$  move against the direction of the axis  $Ox$ . Moreover, in this direction, the section with the coordinate  $x = 13.2\ (cm)$  moves most. The value of the displacement of this section is  $u_{132} = -0.03066239\ (cm)$ . Cross-section of the rod, which are located on the site  $24.85 < x < L = 30\ (cm)$ , move in the direction of the axis  $Ox$ . In this case, a section whose coordinate is  $x = 27.4\ (cm)$  moves more than other sections. The value of the displacement of this section is  $u_{274} = 0.001973\ (cm)$ . Comparing, we find that  $|u_{132}| > |u_{274}|$ .

The nodal values of the strain components of elastic  $\varepsilon_x$ , temperature  $\varepsilon_T$  and thermoelastic  $\varepsilon$  are respectively given in Tables 2 and 3. The field distribution of these strain components along the length of the considered rod is shown in Figure 3a). From these Tables and the Figure, it can be seen that the behavior of the elastic component of the deformation in the sections  $0 < x \leq 13.15\ (cm)$  and  $27.35 \leq x < L = 30\ (cm)$  of the rod will be compressive. However, in the area  $13.15 < x < 27.35\ (cm)$  of the rod behaves tensile. The other two components of the deformation  $\varepsilon_T$

and  $\mathcal{E}$  along the entire length of the rod will have a compressive character. From Figure 3a), it is also seen that the field distribution of the components of elastic strains  $\varepsilon_x$  and thermoelastic strains  $\mathcal{E}$  will be symmetric concerning a straight line whose equation is  $\varepsilon = 0.0000033 x - 0.0052$ .

Nodal values of the component stresses of elastic  $\sigma_x$ , temperature  $\sigma_T$ , and thermoelastic  $\sigma$  are given in Tables 4 and 5. The corresponding field distribution of these component stresses is given in Figure 4a). From Tables 4 and 5, Figure 4a), it is seen that the behavior of the elastic component of the stress  $\sigma_x$  in the sections  $0 < x \leq 13.15(\text{cm})$  and  $27.35 \leq x < L = 30(\text{cm})$  of the rod will have a compressive character, and in the remaining sections of the rod  $\sigma_x$  behaves tensile. The remaining two components of stress  $\sigma_T$ , and  $\sigma$  along the entire length of the rod will have a compressive character. Also, it can be seen from Figure 4 that the distribution field  $\sigma_x$  and  $\sigma$  along the length of the considered rod will be symmetric for the straight line, the equation of which has the following form  $\sigma = 9.304x - 10326.544$  (Himushin, 1969; Myrzasheva *et al.*, 2018).

In the next step, increase the value  $T_{amb\ 0}$ , we accept  $T_{amb\ 0} = 20 (^{\circ}\text{K})$ . The corresponding displacement distribution field is shown in Figure 2b). From this graph, it can be seen that the cross-sections of the rod located on the coordinate plane section  $0 < x \leq 24.85(\text{cm})$  move against the axis direction  $Ox$ . In this direction, the greatest displacement belongs to the coordinate section  $x = 13.2(\text{cm})$ . The value is the displacement section of this section  $u_{132} = -0.0305186 (\text{cm})$ . The sections of the rod located on the site  $24.85 < x < L = 30(\text{cm})$  move in the direction of the axis  $Ox$ . In this case, the greatest displacement belongs to the point with the coordinate  $x = 27.4(\text{cm})$ , and its largest value is  $u_{274} = 0.001996 (\text{cm})$ . This also shows that  $|u_{132}| > |u_{274}|$ .

The field distribution of the elastic  $\varepsilon_x$ , temperature  $\varepsilon_T$  and thermoelastic  $\mathcal{E}$  deformation components along the length of the considered rod is shown in Figure 3b). From this figure, it is seen that the nature of the components of the deformation  $\varepsilon_T$  and  $\mathcal{E}$  along the entire length of

the rod will be compressive. In contrast, their behavior of elastic deformations  $\varepsilon_x$  in the sections  $0 < x \leq 13.15(\text{cm})$  and  $27.35 \leq x < L = 30(\text{cm})$  the rod will be compressive, and in the remaining sections of the rod  $\varepsilon_x$  behaves in a tensile manner. It can also be seen from this figure that the field distribution of the strain components along the length of the considered rod will be symmetric to the straight line  $\varepsilon = 0.0000033 x - 0.0052$ .

The field of distribution of elastic  $\sigma_x$ , temperature  $\sigma_T$ , and thermoelastic  $\sigma$  components of stress along the length of the considered rod is shown in Figure 4 b). In this case, the behavior of the components of the voltage  $\sigma_T$  and  $\sigma$  along the entire length of the rod will be compressive. In contrast, the nature of the behavior of the elastic component of the stress  $\sigma_x$  will be of a different kind. The elastic component of the stress  $\sigma_x$  is compressive in the sections of the rod  $0 < x \leq 13.15(\text{cm})$  and  $27.35 \leq x < L = 30(\text{cm})$ , and in the remaining sections of the rod  $\sigma_x$  behaves in a tensile character. Figure 4b) also shows that this field, the distribution of the voltage components  $\sigma_x$ , and  $\sigma$  along the length of the considered rod will be symmetrical to the straight line, the equation of which has the following form  $\sigma = 9.1128x - 10337.835$ .

Now consider the case when  $T_{amb\ 0} = 30 (^{\circ}\text{K})$ . The corresponding displacement field along the length of the considered rod is given in Figure 2c). From this graph, the displacement field shows that the sections of the rod located on the coordinate plane plot  $0 < x < 24.75(\text{cm})$  move against the direction of the axis  $Ox$ , the largest displacement in this direction belongs to the point with the coordinate  $x = 13.2(\text{cm})$ . The displacement value of this section is  $u_{132} = -0.03037379 (\text{cm})$ . The sections of the rod located on the site  $24.75 < x < L = 30(\text{cm})$  move in the direction of the axis  $Ox$ , the largest movement in this direction belongs to a point with a coordinate  $x = 27.4(\text{cm})$ , whose value is  $u_{274} = 0.0020191194 (\text{cm})$ . It should also be noted that  $|u_{132}| > |u_{274}|$ .

The corresponding field distribution of the elastic  $\varepsilon_x$ , temperature  $\varepsilon_T$ , and thermoelastic  $\mathcal{E}$  deformation components along the length of the

considered rod is shown in Figure 3 c). From these materials, it can be seen that the behavior of the elastic component of deformation  $\varepsilon_x$  in the sections  $0 < x \leq 13.15(\text{cm})$  and  $27.35 \leq x < L = 30(\text{cm})$  the rod will have a compressive character, and in the remaining sections of the rod  $\varepsilon_x$  behaves tensile. In contrast to elastic deformations  $\varepsilon_x$ , the behavior of the remaining components of the deformation  $\varepsilon_T$  and  $\varepsilon$  along the entire length of the considered rod will have a compressive character. It can also be seen from this figure that the field distribution of the strain components along the length of the considered rod will be symmetric to the straight line  $\varepsilon = 0.0000033x - 0.0052$ .

The corresponding field of distribution of elastic, temperature  $\sigma_x$ ,  $\sigma_T$ , and thermoelastic  $\sigma$  components of stresses is given in Figure 4c). From these results, it is clear that the behavior of the two-component stresses  $\sigma_T$ , and  $\sigma$  along the entire length of the rod will be compressive. In contrast, their elastic component of stress  $\sigma_x$  in the sections  $0 < x \leq 13.15(\text{cm})$  and  $27.35 \leq x < L = 30(\text{cm})$  the rod behaves compressive, and in the rest of it, it has a tensile character. From Figure 4c), it can also be observed that the field of distribution of the component voltages  $\sigma_x$  and  $\sigma$  are symmetric to a straight line, the equation of which has the following form  $\sigma = 8.92x - 10349.218$ . When the value  $T_{amb0} = 40(^{\circ}\text{K})$  is varied, the corresponding field of the distribution of displacement, elastic, temperature, and thermoelastic components of the deformation  $\varepsilon_x$ ,  $\varepsilon_T$  and  $\varepsilon$ ,  $\sigma_x$ ,  $\sigma_T$  and  $\sigma$  stress along the length of the considered rod is given in Figures 2d), 3d), 4d) (Demidovich and Maron, 1960; Kudaykulov *et al.*, 2009).

By analyzing the studies of this problem by values  $T_{amb0} = 10(^{\circ}\text{K})$ ;  $20(^{\circ}\text{K})$ ;  $30(^{\circ}\text{K})$ ;  $40(^{\circ}\text{K})$ , we can construct the following comparative Table 6. These results show that in the case  $T(x) = 40x$  at  $(L/3) \leq x \leq (2L/3)$ , the temperature changes with the surrounding cross-sectional area of the left end of the medium, i.e.  $T_{amb0}$ , minimal effect in comparison with  $h_0$  the thermally stressed state of the investigated rod. Earlier, it was carried out a numerical study of the laws governing the influence of the heat transfer coefficient  $h_0$  on the thermally stressed state of a rod at a temperature that varies linearly, taking into account

$\alpha = \alpha(T(x))$ .  $\alpha = \alpha(T(x))$  – the law is the distribution of the coefficient of thermal expansion along the length of the rod, which expresses the full-scale dependence between the coefficient of thermal expansion and temperature. The rod is also made of heat-resistant alloy ANV-300 and pinched by two ends.

The laws of the fields of distribution of elastic displacements, component deformations, and stresses according to the values of the heat transfer coefficient  $h_0 = 7.5$ ;  $10$ ;  $15$ ;  $30$  ( $\text{watt} / (\text{cm}^2 \cdot ^{\circ}\text{K})$ ) are constructed. Based on the results of these studies, the following comparative table 7 is constructed.

#### 4. CONCLUSIONS:

It was found that with increasing value  $h_0$ , the amplitude of displacements increases against the direction of the axis  $Ox$ , and the amplitude of displacements in the direction of the axis  $Ox$  decreases. With increasing value  $h_0$ , the maximum and average values of thermoelastic stress  $\sigma$  decreases.

Thus, it was established that only by changing the value  $h_0$ , (and not  $T_{amb0}$ ), i.e., by changing the environmental properties of the surrounding cross-sectional area where heat transfer occurs, the thermally stressed state of the rod under investigation can be changed.

#### 5. REFERENCES:

1. Afanasyeva, V.V., and Lazerson, A.G. (1995). Dynamic chaos in two-cavity klystron oscillators with delayed feedback. News of Universities. *Applied Nonlinear Dynamics*, 3, 88-99.
2. Akhmetov, S., and Kudaykulov, A. (2017). On the method of construction of the dependence of the heat extension coefficient on the temperature in heat-resistant alloys. *International Journal of Engineering Research and Science (IJOER)*, 3(8), 20-29.
3. Bakulin, V.N. (1985). *The finite element method for studying the stress-strain state of three-layer cylindrical shells*. Moscow, Russian Federation: TsSTI Information.
4. Bartels, S. (2019). Finite element simulation of nonlinear bending models for thin elastic rods and plates. Retrieved from <https://arxiv.org/abs/1901.09835>.
5. Birger, I.A. (1992). *Rods, plates, shells*.

Moscow, Russian Federation: Fizmatlit.

6. Chen, S.-K., Wan, C.-M., Liu, E.-H., Chu, S.-B., Liang, C.-Y., Yuan, L.-J. and Wan, C.-C. (2017). The microstructure of electrolytically deuterium-loaded palladium rods. *Fusion Technology*, 29(2), 302-305.
7. Civalek, Ö., Uzun, B., Özgür Yaylı, M. and Akgöz, B. (2020). Size-dependent transverse and longitudinal vibrations of embedded carbon and silica carbide nanotubes by nonlocal finite element method. *The European Physical Journal Plus*, 135, Article number 381.
8. Deepa, I.B., and Rajendran, V. (2018). Pure and Cu metal doped WO prepared via co-precipitation method and studies on their structural, morphological, electrochemical and optical properties. *Nano-Structures and Nano-Objects*, 16, 185-192.
9. Demidovich, B.P., and Maron, I.A. (1960). *Fundamentals of computational mathematics*. Moscow, Russian Federation: Nauka.
10. Dmitriev, A.I., Skvortsov, A.A., Koplak, O.V., Morgunov, R.B., and Proskuryakov, I.I. (2011). Influence of the regime of plastic deformation on the magnetic properties of single-crystal silicon Cz-Si. *Physics of the Solid State*, 53(8), 1547-1553.
11. Ermekov, M.M. (2011). *Collection and field preparation of oil and gas: textbook: for organizations of technical and vocational education*. Astana, Republic of Kazakhstan: Tome.
12. Fedorov, Yu.A. (2001). The choice of the design scheme of multilayer rods when calculating the temperature effect. In: B. Rymsza (Ed.), *10 rosyjsko-polskie seminarium "Teoretyczne podstawy budownictwa" Moskwa-Iwanowo* (pp. 215-218). Warszawa, Poland: Oficyna Wydawnicza PW.
13. Fedotov, A.M., Murzakhmetov, A.N., and Dyusembaev, A.E. (2018). Expansion of ideas and processes in social and biological communities. *Eurasian Journal of Mathematical and Computer Applications*, 6(4), 17-28.
14. Formalev, V.F., and Kolesnik, S.A. (2019). Heat transfer in a half-space with transversal anisotropy under the action of a lumped heat source. *Journal of Engineering Physics and Thermophysics*, 92(1), 52-59.
15. Formalev, V.F., Kartashov, É.M., and Kolesnik, S.A. (2019). Simulation of nonequilibrium heat transfer in an anisotropic semispace under the action of a point heat source. *Journal of Engineering Physics and Thermophysics*, 92(6), 1537-1547.
16. Geng, J., Zhang, H., Mutuku, F., and Lee, N.-C. (2018). Novel solder alloy with wide service temperature capability for automotive applications. *International Symposium on Microelectronics*, 2018(1), Article number 000075-000083.
17. Himushin, F.F. (1969). *Heat resistant steels and alloys* (2nd revised and enlarged edition). Moscow, Russian Federation: Metallurgy.
18. Hou, F., and Gao, Ch. (2020). Thermal effects analysis of end-pumped Er: YAG rod and slab by using finite element method. *International Conference on Optical Instruments and Technology: Advanced Laser Technology and Applications*, 11437, Article number 1143709.
19. Kolokoltsev, V.M., Savinov, A.S., Andreev, S.M., and Angold, K.V. (2020). Calculation of a thermal stress state, when heating a steel cylindrical object. *Vestnik of Novosibirsk State Technical University*, 18(1), 37-45.
20. Korobeinikov, S.N., Oleinikov, A.I., Gorev, B.V., and Bormotin, K.S. (2008). Mathematical modeling of creep processes of metal products from materials having different tensile and compression properties. *Computational Methods and Programming: New Computational Technologies*, 9(1), 346-365.
21. Krechetov, I.V., Skvortsov, A.A., Poselsky, I.A., Paltsev, S.A., Lavrikov, P.S., and Korotkov, V. (2018). Implementation of automated lines for sorting and recycling household waste as an important goal of environmental protection. *Journal of Environmental Management and Tourism*, 9(8), 1805-1812.
22. Krieth, F. (1973). *Principles of heat transfer*, 3rd ed. New York City, New York: Futext Educational Publishers.
23. Kudaykulov, A., Arinov, E., Ispulov, N., Qadir, A., and Begaliyeva, K. (2019). *Numerical study of a thermally stressed state of a rod*. Retrieved from <https://www.hindawi.com/journals/amp/2019/8986010/>.
24. Kudaykulov, A.K. (2009). *Mathematical (finite*

element) modeling of applied problems of heat distribution in one-dimensional structural elements. Turkestan, Republic of Kazakhstan: Baiterek.

25. Kudaykulov, A.K., Myrzasheva, A.N., and Kenzhegulov, B.Z. (2009, June 30 – July 4) *Mathematical modeling of thermomechanical processes in pivotal element of the designs made from thermal stable infusible alloys*. Paper presented at the III Congress of the World Mathematical Society of Turkic-speaking Countries, Section No. 8, Mathematical Model, Almaty, Republic of Kazakhstan.
26. Kuznetsova, E.L., and Rabiniski, L.N. (2019). Linearization of radiant heat fluxes in the mathematical modeling of growing bodies by the action of high temperatures in additive manufacturing. *Asia Life Sciences*, 2, 943-954.
27. Lee, T.-H., Ha, H.-Y., Jang, J.H., Kang, J.-Y., Moon, J.J., Park, Y., Lee, C.-H., and Park, S.-J. (2017). Self-twinning in solid-state decomposition. *Acta Materialia*, 123, 197-205.
28. Leon, G., and Chen (Roger), H.-L. (2019). Direct determination of dynamic elastic modulus and poisson's ratio of Timoshenko rods. *Vibration*, 2, 157-173.
29. Litvishko, V., Akhmetova, A., Kodasheva, G., Zhussupova, A., Malikova, R., and Kuralova, A. (2020). Formation of ecological education of the population. *E3S Web of Conferences*, 159, Article number 01009.
30. Mikhlin, S.G. (1974). *Variational-grid approximation*. Moscow Russian Federation: Nauka.
31. Myrzasheva, A.N., and Shazhdekeyeva, N. (2015). A numerical study of the dependence of the rod elongation on the ambient temperature, in the presence of a temperature that varies linearly. *Science and World. International Scientific Journal*, 1(8(24)), 18-21.
32. Myrzasheva, A.N., Shambilova, G.K., and Shazhedekeeva, N.K. (2018). The temperature of the temperature of Bolshan Zhadayd rod termokerneulik kyyiniñ zhylu almasu coefficient keniinen tueldigin sandy q zertteu a zhene mathikalyq modeldeu. *Bulletin of the Karaganda University, Mathematics Series*, 1(89), 84-89.
33. Myrzasheva, A.N., Shazhdekeyeva, N., and Tuleuova, R. (2016). Mathematical modeling of nonlinear thermomechanical processes in rods made of heat-resisting alloys. *International Journal of Pharmacy and Technology*, 8(3), 17722-17732.
34. Nozdrev, V.F. (1967). *The course of thermodynamics*. Moscow, Russian Federation: Mir.
35. Orazbaev, B.B., Kenzhebaeva, T.S., Orazbaeva, K.N., Shzhedekeeva, N.K., and Myrzasheva, A.N. (2017). The study of sulfur processes at the Claus reactor and the development of models for assessing the quality of sulfur produced. *Vestnik of ENU*, 4(119), 155-161.
36. Pandiyan, A., Arunkumar, G., and Premkumar, G. (2019). Design, analysis and topology optimization of a connecting rod for single cylinder 4-stroke petrol engine. *International Journal of Vehicle Structures and Systems*, 11(4), 439-442.
37. Park, T.H., Woo, S.H., Lee, S.J., Sohn, D.M., Chung, C.K., Kim, Y.J., and Sohn, S. (2019). Cross-link is a risk factor for rod fracture at pedicle subtraction osteotomy site: A finite element study. *Journal of Clinical Neuroscience*, 66, 246-250.
38. Pisarenko, G.S., Agaev, V.A. Kvitka, A.L., Popkov, V.G. and Umansky, E.S. (Eds.). (1973). *Resistance of materials*. Kiev, Ukraine: Publishing House "Higher School".
39. Qiu, Y., Young, M.L. and Nie, X. (2017). High strain rate compression of martensitic niti shape memory alloy at different temperatures. *Metallurgical and Materials Transactions A*, 48, 601-608.
40. Rabiniski, L.N., and Tushavina, O.V. (2019). Problems of land reclamation and heat protection of biological objects against contamination by the aviation and rocket launch site. *Journal of Environmental Management and Tourism*, 10(5), 967-973.
41. Santos, S.C., Rodrigues Jr., O., and Campos, L.L. (2020). Synthesis, processing and electron paramagnetic resonance response of YEuOmicro rods. *International Journal of Modern Physics: Conference Series*, 48, Article number 1860112.
42. Segerlind, L. (1979). *Application of the finite element method*. Moscow, Russian Federation: Mir.
43. Shen, Z., Li, H., Liu, X., and Hu, G. (2019). Thermal-structural dynamic analysis of a satellite antenna with the cable-network and

hoop-truss supports. *Advances in Mathematical Physics*, 42(11), 1339-1356.

44. Starovoitov, É.I., Leonenko, D.V., and Tarlakovskii, D.V. (2016). Thermal-force deformation of a physically nonlinear three-layer stepped rod. *Journal of Engineering Physics and Thermophysics*, 89, 1582–1590.
45. Sun, G., Wu, M., Wu, J., and Chen, R. (2020). Experimental study on mechanical properties of 35CrMo-GLG650 steel rods at elevated temperatures. *Journal of Materials in Civil Engineering*, 32(7), 239-247.
46. Timoshenko, S.P., and Goodyear, J. (1975).

*Theory of elasticity*. Moscow, Russian Federation: Nauka.

47. Yano, T., Makoto, H., and Koichi, N. (2018). Effect of interfacial heat transfer on basic flow and instability in a high-Prandtl-number thermocapillary liquid bridge. *International Journal of Heat and Mass Transfer*, 125, 1121-1130.
48. Zenkevich, O. (1975). *Method of finite elements in technology*. Moscow, Russian Federation: Mir.

$$\Pi = \int_V \frac{\sigma_x}{2} \varepsilon_x dV - \int_V \alpha(T(x)) \cdot E \cdot T(x) \cdot \varepsilon_x dV \quad (\text{Eq. 1})$$

$$\varepsilon_x = \frac{\partial u}{\partial x} \quad (\text{Eq. 2})$$

$$u = u(x) \quad (\text{Eq. 3})$$

$$\sigma_x = E \cdot \varepsilon_x \quad (\text{Eq. 4})$$

$$\alpha = \alpha(T(x)) \quad (\text{Eq. 5})$$

$$T = T(x) \quad (\text{Eq. 6})$$

$$x_j = \frac{\lambda}{2} \quad (\text{Eq. 7})$$

$$x_k = \lambda \quad (\text{Eq. 8})$$

$$T(x) = \gamma_i(x) \cdot T_i + \gamma_j(x) \cdot T_j + \gamma_k(x) \cdot T_k, \quad 0 \leq x \leq \lambda, \quad (\text{Eq. 9})$$

$$\alpha(T(x)) = \gamma_i(x) \cdot \alpha_i + \gamma_j(x) \cdot \alpha_j + \gamma_k(x) \cdot \alpha_k, \quad x \in (x_i \leq x \leq x_k) \quad (\text{Eq. 10})$$

$$u(x) = \gamma_i(x) \cdot u_i + \gamma_j(x) \cdot u_j + \gamma_k(x) \cdot u_k \quad (\text{Eq. 11})$$

$$\gamma_i(x) = \frac{\lambda^2 - 3\lambda x + 2x^2}{\lambda^2}; \quad \gamma_j(x) = \frac{4(\lambda x - x^2)}{\lambda^2}; \quad \gamma_k(x) = \frac{2x^2 - \lambda x}{\lambda^2}, \quad 0 \leq x \leq \lambda \quad (\text{Eq. 12})$$

$$\begin{aligned} \Pi_i &= \int_{V_i} \frac{E}{2} \left( \frac{\partial u}{\partial x} \right)^2 dV - \int_{V_i} \alpha(T(x)) \cdot E \cdot T(x) \cdot \left( \frac{\partial u}{\partial x} \right) dV = \\ &= \int_{V_i} \frac{E}{2} \left( \frac{\partial \gamma_i}{\partial x} u_i + \frac{\partial \gamma_j}{\partial x} u_j + \frac{\partial \gamma_k}{\partial x} u_k \right)^2 dV - \int_{V_i} E (\gamma_i \alpha_i + \gamma_j \alpha_j + \gamma_k \alpha_k) (\gamma_i T_i + \gamma_j T_j + \gamma_k T_k) \times \end{aligned}$$

$$\times \left( \frac{\partial \gamma_i}{\partial x} u_i + \frac{\partial \gamma_j}{\partial x} u_j + \frac{\partial \gamma_k}{\partial x} u_k \right) dV \quad (\text{Eq. 13})$$

$$\Pi = \sum_{i=1}^{NDE} \Pi_i \quad (\text{Eq. 14})$$

$$\begin{aligned} \Pi_i = & \frac{EF}{2} \left[ \frac{7}{3\lambda} u_i^2 - \frac{16}{3\lambda} u_i u_j + \frac{2}{3\lambda} u_i u_k + \frac{16}{3\lambda} u_j^2 - \frac{16}{3\lambda} u_j u_k + \frac{7}{3\lambda} u_k^2 \right] - \\ & - EF \left\{ \left[ -\frac{1}{3} \alpha_i T_i - \frac{1}{5} \alpha_i T_j + \frac{1}{30} \alpha_i T_k - \frac{1}{5} \alpha_j T_i - \frac{8}{15} \alpha_j T_j + \frac{1}{15} \alpha_j T_k + \frac{1}{30} \alpha_k T_i + \right. \right. \\ & + \frac{1}{15} \alpha_k T_j + \frac{1}{15} \alpha_k T_k \left. \right] u_i + \left[ \frac{2}{5} \alpha_i T_i + \frac{4}{15} \alpha_i T_j + 0 + \frac{4}{15} \alpha_j T_i + 0 - \frac{4}{15} \alpha_j T_k + 0 - \right. \\ & - \frac{4}{15} \alpha_k T_j - \frac{2}{15} \alpha_k T_k \left. \right] u_j + \left[ -\frac{1}{15} \alpha_i T_i - \frac{1}{15} \alpha_i T_j - \frac{1}{30} \alpha_i T_k - \frac{1}{15} \alpha_j T_i + \frac{8}{15} \alpha_j T_j + \right. \\ & \left. \left. + \frac{1}{5} \alpha_j T_k - \frac{1}{30} \alpha_k T_i + \frac{1}{5} \alpha_k T_j + \frac{1}{3} \alpha_k T_k \right] u_k \right\} \end{aligned} \quad (\text{Eq. 15})$$

$$\begin{aligned} \frac{\partial \Pi}{\partial u_i} = 0; \Rightarrow & \frac{EF}{2} \left[ \frac{14}{3\lambda} u_i - \frac{16}{3\lambda} u_j + \frac{2}{3\lambda} u_k \right] - EF \left[ -\frac{1}{3} \alpha_i T_i - \frac{1}{5} \alpha_i T_j + \frac{1}{30} \alpha_i T_k - \frac{1}{5} \alpha_j T_i - \right. \\ & \left. - \frac{8}{15} \alpha_j T_j + \frac{1}{15} \alpha_j T_k + \frac{1}{30} \alpha_k T_i + \frac{1}{15} \alpha_k T_j + \frac{1}{15} \alpha_k T_k \right] = 0 \end{aligned} \quad (\text{Eq. 16})$$

$$\begin{aligned} \frac{\partial \Pi}{\partial u_j} = 0; \Rightarrow & \frac{EF}{2} \left[ -\frac{16}{3\lambda} u_i + \frac{32}{3\lambda} u_j - \frac{16}{3\lambda} u_k \right] - EF \left[ \frac{2}{5} \alpha_i T_i + \frac{4}{15} \alpha_i T_j + \frac{4}{15} \alpha_j T_i - \frac{4}{15} \alpha_j T_k - \right. \\ & \left. - \frac{4}{15} \alpha_k T_j - \frac{2}{5} \alpha_k T_k \right] = 0 \end{aligned} \quad (\text{Eq. 17})$$

$$\begin{aligned} \frac{\partial \Pi}{\partial u_k} = 0; \Rightarrow & \frac{EF}{2} \left[ \frac{2}{3\lambda} u_i - \frac{16}{3\lambda} u_j + \frac{14}{3\lambda} u_k \right] - EF \left[ -\frac{1}{15} \alpha_i T_i - \frac{1}{15} \alpha_i T_j - \frac{1}{30} \alpha_i T_k - \frac{1}{15} \alpha_j T_i + \right. \\ & \left. + \frac{8}{15} \alpha_j T_j + \frac{1}{5} \alpha_j T_k - \frac{1}{30} \alpha_k T_i + \frac{1}{5} \alpha_k T_j + \frac{1}{3} \alpha_k T_k \right] = 0 \end{aligned} \quad (\text{Eq. 18})$$

$$\frac{\partial \Pi}{\partial u_i} = 0 \quad (\text{Eq. 19})$$

$$i = 2 \div (2 \times nn - 1). \quad (\text{Eq. 20})$$

$$\varepsilon_x^I = \frac{\partial u}{\partial x} \left( x = \frac{x_j - x_i}{2} \right) = \frac{\partial u_i \left( x = \frac{x_j - x_i}{2} \right)}{\partial x} u_i + \frac{\partial u_j \left( x = \frac{x_j - x_i}{2} \right)}{\partial x} u_j + \frac{\partial u_k \left( x = \frac{x_j - x_i}{2} \right)}{\partial x} u_k. \quad (\text{Eq. 21})$$



$$\varepsilon_x^{II} = \frac{\partial u}{\partial x} \left( x = \frac{x_k - x_j}{2} \right) = \frac{\partial u_i \left( x = \frac{x_k - x_j}{2} \right)}{\partial x} u_i + \frac{\partial u_j \left( x = \frac{x_k - x_j}{2} \right)}{\partial x} u_j + \frac{\partial u_k \left( x = \frac{x_k - x_j}{2} \right)}{\partial x} u_k \quad (\text{Eq. 22})$$

$$\sigma_x^I = E \cdot \varepsilon_x^I; \quad \sigma_x^{II} = E \cdot \varepsilon_x^{II} \quad (\text{Eq. 23})$$

$$\varepsilon_T^I = -\alpha \left( x = \frac{x_j - x_i}{2} \right) \cdot T \left( x = \frac{x_j - x_i}{2} \right); \quad \varepsilon_T^{II} = -\alpha \left( x = \frac{x_k - x_j}{2} \right) \cdot T \left( x = \frac{x_k - x_j}{2} \right), \quad (\text{Eq. 24})$$

$$\sigma_T^I = E \cdot \varepsilon_T^I; \quad \sigma_T^{II} = E \cdot \varepsilon_T^{II}. \quad (\text{Eq. 25})$$

$$\varepsilon^I = \varepsilon_x^I + \varepsilon_T^I; \quad \varepsilon^{II} = \varepsilon_x^{II} + \varepsilon_T^{II}. \quad (\text{Eq. 26})$$

$$\sigma^I = \sigma_x^I + \sigma_T^I; \quad \sigma^{II} = \sigma_x^{II} + \sigma_T^{II} \quad (\text{Eq. 27})$$

$$T(x) = ax \quad (\text{Eq. 28})$$

$$a = \text{const} > 0 \quad (\text{Eq. 29})$$

$$K_{xx} = 100 \left( \frac{\text{watt}}{\text{cm} \cdot ^\circ K} \right) \quad (\text{Eq. 30})$$

$$h_L = 10 \left( \frac{\text{watt}}{\text{cm}^2 \cdot ^\circ K} \right) \quad (\text{Eq. 31})$$

$$E = 2 \cdot 10^6 \left( \frac{\text{kG}}{\text{cm}^2} \right) \quad (\text{Eq. 32})$$

$$u = u(x) \quad (\text{Eq. 33})$$

$$\frac{\partial \Pi}{\partial u_i} = 0, \quad i = 2 \div 2n \quad (\text{Eq. 34})$$

$$h_0 = h_L, \left( \frac{\text{watt}}{\text{cm}^2 \cdot ^\circ K} \right) \quad (\text{Eq. 35})$$

**Table 1.** Nodal values of displacement at  $T = 40x$ ;  $T_{amb\ 0} = 10\ (^{\circ}K)$

| Nodal point | $u\ [cm]$    | Nodal point | $u\ [cm]$    | Nodal point | $u\ [cm]$    | Nodal point | $u\ [cm]$    | Nodal point | $u\ [cm]$    |
|-------------|--------------|-------------|--------------|-------------|--------------|-------------|--------------|-------------|--------------|
| 1.          | 0.0000000000 | ...         | ...          | ...         | ...          | ...         | ...          | ...         | ...          |
| 2.          | 0.0003794378 | 131.        | 0.0306567073 | 247.        | 0.0002250534 | 273.        | 0.0019694815 | 299.        | 0.0002668764 |
| 3.          | 0.0007556759 | 132.        | 0.0306623933 | 248.        | 0.0000589692 | 274.        | 0.0019730125 | 300.        | 0.0001377738 |
| ...         | ...          | 133.        | 0.0306563753 | 249.        | 0.0000952486 | 275.        | 0.0019654461 | 301.        | 0.0000000000 |
| ...         | ...          | ...         | ...          | ...         | ...          | ...         | ...          | ...         | ...          |

**Table 2.** Nodal values of  $\varepsilon_x$  at  $T = 40x$ ;  $T_{amb\ 0} = 10\ (^{\circ}K)$

| Nodal point | $\varepsilon_x$ | Nodal point | $\varepsilon_x$ | Nodal point | $\varepsilon_x$ | Nodal point | $\varepsilon_x$ | Nodal point | $\varepsilon_x$ |
|-------------|-----------------|-------------|-----------------|-------------|-----------------|-------------|-----------------|-------------|-----------------|
| 1.          | 0.0037943776    | ...         | ...             | ...         | ...             | ...         | ...             | ...         | ...             |
| 2.          | 0.0037623810    | 130.        | 0.0000646200    | 200.        | 0.0046474371    | 273.        | 0.0000353106    | 298.        | 0.0012852206    |
| 3.          | 0.0037602403    | 131.        | 0.0000568600    | 201.        | 0.0046476582    | 274.        | 0.0000756646    | 299.        | 0.0012910264    |
| ...         | ...             | 132.        | 0.0000601800    | 202.        | 0.0045233648    | 275.        | 0.0000830244    | 300.        | 0.0013777378    |
| ...         | ...             | ...         | ...             | ...         | ...             | ...         | ...             | ...         | ...             |

**Table 3.** Nodal values of  $\varepsilon_H$  at  $T = 40x$ ;  $T_{amb\ 0} = 10\ (^{\circ}K)$

| Nodal points | $\varepsilon$ | Nodal points | $\varepsilon$ | Nodal points | $\varepsilon$ |
|--------------|---------------|--------------|---------------|--------------|---------------|
| 1.           | -0.0065317029 | ...          | ...           | ...          | ...           |
| 2.           | -0.0065317133 | 200.         | -0.0138470109 | 298.         | -0.0087514338 |
| 3.           | -0.0065616728 | 201.         | -0.0138500651 | 299.         | -0.0086701528 |
| ...          | ...           | 202.         | -0.0138500651 | 300.         | -0.0086701528 |
| ...          | ...           | ...          | ...           | ...          | ...           |

**Table 4.** Nodal values of  $\sigma_x$  at  $T = 40x$ ;  $T_{amb\ 0} = 10 (^{\circ}K)$

| Nodal point | $\sigma_x [kG / cm^2]$ | Nodal point | $\sigma_x [kG / cm^2]$ | Nodal point | $\sigma_x [kG / cm^2]$ | Nodal point | $\sigma_x [kG / cm^2]$ | Nodal point | $\sigma_x [kG / cm^2]$ |
|-------------|------------------------|-------------|------------------------|-------------|------------------------|-------------|------------------------|-------------|------------------------|
| 1.          | 7588.7551487           | ...         | ...                    | ...         | ...                    | ...         | ...                    | ...         | ...                    |
| 2.          | 7524.7620767           | 130.        | 129.2400053            | 200.        | 9294.8741280           | 273.        | 70.6212747             | 298.        | 2570.441200            |
| 3.          | 7520.4806567           | 131.        | 113.7200053            | 201.        | 9295.3164533           | 274.        | 151.3291253            | 299.        | 2582.052784            |
| ...         | ...                    | 132.        | 120.3599947            | 202.        | 9046.7295733           | 275.        | 166.0488053            | 300.        | 2755.475664            |
|             |                        | ...         | ...                    | ...         | ...                    | ...         | ...                    |             |                        |

**Table 5.** Nodal values of  $\sigma_{II}$  at  $T = 40x$ ;  $T_{amb\ 0} = 10 (^{\circ}K)$

| Nodal points | $\sigma [kG / cm^2]$ | Nodal points | $\sigma [kG / cm^2]$ | Nodal points | $\sigma [kG / cm^2]$ |
|--------------|----------------------|--------------|----------------------|--------------|----------------------|
| 1.           | -13063.4058686485    | ...          | ...                  | ...          | ...                  |
| 2.           | -13063.4266416485    | 200.         | -27694.0218719856    | 298.         | -17502.8676999818    |
| 3.           | -13123.3456316485    | 201.         | -27700.1301866520    | 299.         | -17340.3055239819    |
| ...          | ...                  | 202.         | -27700.1301866521    | 300.         | -17340.3055239819    |
|              |                      | ...          | ...                  |              |                      |

**Table 6.** Influence of ambient temperature on the stress-strain state of the test rod at different values  $T_{amb0}$

| No. | $T_{amb\ 0} (^{\circ}K)$ | $u_{min}(cm)$ | Coord.of the corres section (cm) | $u_{max}(cm)$ | Coord.of the corres section (cm) | $\sigma_{max} \left( \frac{kG}{cm^2} \right)$ | $\sigma_{midd} \left( \frac{kG}{cm^2} \right)$ | Coord.of the corres section, where $u=0$ (cm) |
|-----|--------------------------|---------------|----------------------------------|---------------|----------------------------------|---|--|---|
| 1   | 10                       | -0.03066      | $x = 13.2$                       | 0.001973      | $x = 27.4$                       | -27700.1                                      | -19675.5                                       | $x = 24.85$                                   |
| 2   | 20                       | -0.03051      | $x = 13.2$                       | 0.001996      | $x = 27.4$                       | -27717.1                                      | -19707.4                                       | $x = 24.85$                                   |
| 3   | 30                       | -0.03037      | $x = 13.2$                       | 0.002019      | $x = 27.4$                       | -27502.9                                      | -19739.5                                       | $x = 24.75$                                   |
| 4   | 40                       | -0.03023      | $x = 13.2$                       | 0.002042      | $x = 27.4$                       | -27751.5                                      | -19771.9                                       | $x = 24.75$                                   |

**Table 7.** The effect of the heat transfer coefficient on the stress-strain state of the investigated rod

| No. | $h_0 \left( \frac{\text{watt}}{\text{cm}^2 \cdot ^\circ\text{K}} \right)$ | $u_{\min} (\text{cm})$ | Coord. of the corres section (cm) | $u_{\max} (\text{cm})$ | Coord. of the corres section (cm) | $\sigma_{\max} \left( \frac{\text{kG}}{\text{cm}^2} \right)$ | $\sigma_{\text{midd}} \left( \frac{\text{kG}}{\text{cm}^2} \right)$ | Coord. of the corres section, where $u=0$ (cm) |
|-----|---|------------------------|-----------------------------------|------------------------|-----------------------------------|--|---|--|
| 1   | 7.5   | -0.02946               | $x = 13.3$                        | 0.00217                | $x = 27.1$                        | -27842.5   | -19942.6  | $x = 24.65$                                    |
| 2   | 10  | -0.03023               | $x = 13.2$                        | 0.00204                | $x = 27.4$                        | -27751.5   | -19771.9  | $x = 24.75$                                    |
| 3   | 15  | -0.03125               | $x = 13.2$                        | 0.001878               | $x = 27.4$                        | -27630.1   | -19544.1  | $x = 24.95$                                    |
| 4   | 30  | -0.0327                | $x = 12.9$                        | 0.001656               | $x = 27.6$                        | -27459.6   | -19224.6  | $x = 25.25$                                    |

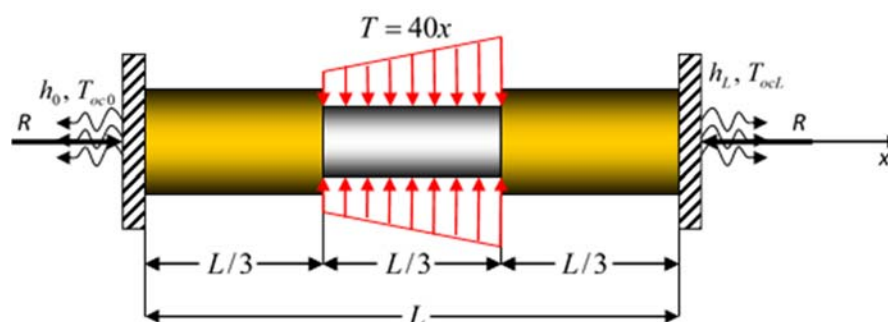


**Figure 1.** The calculation scheme of the problem

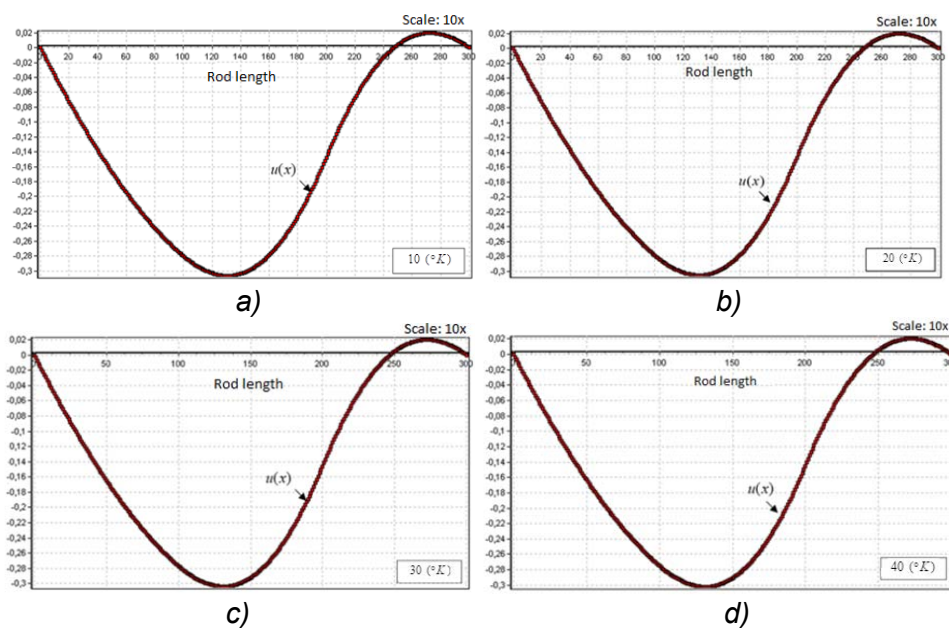


**Figure 2.** Field distribution of elastic displacements along the length of the rod at  $T_{\text{amb } 0} = 10 (^{\circ}\text{K}); 20 (^{\circ}\text{K}); 30 (^{\circ}\text{K}); 40 (^{\circ}\text{K})$

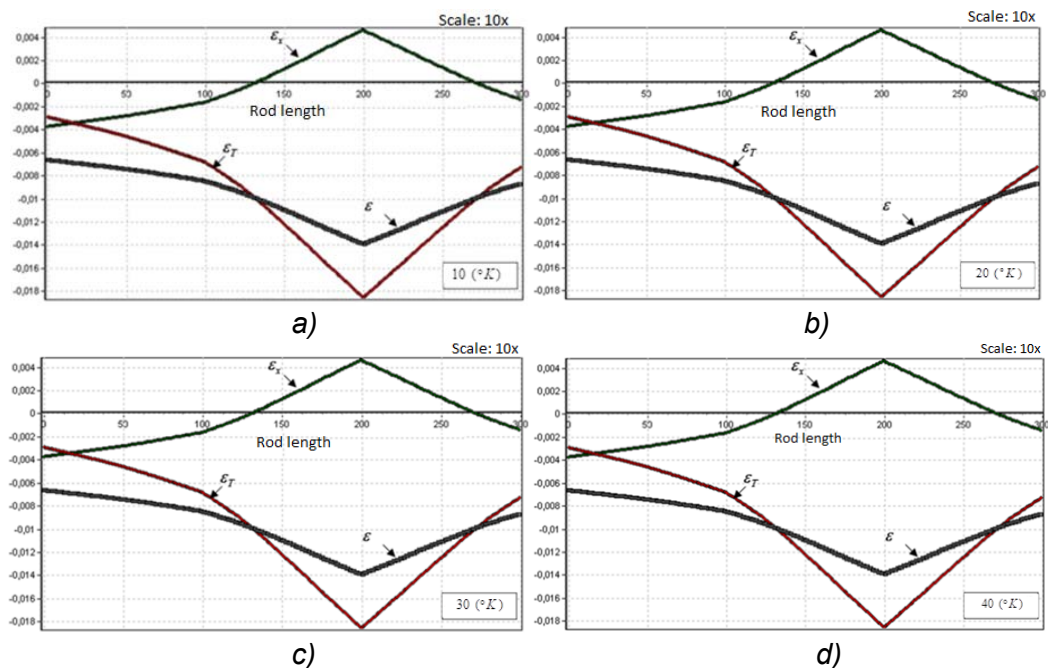


**Figure 3.** Field distribution of deformations along the length of the rod at  
 $T_{amb\ 0} = 10\ (^{\circ}K)$ ;  $20\ (^{\circ}K)$ ;  $30\ (^{\circ}K)$ ;  $40\ (^{\circ}K)$

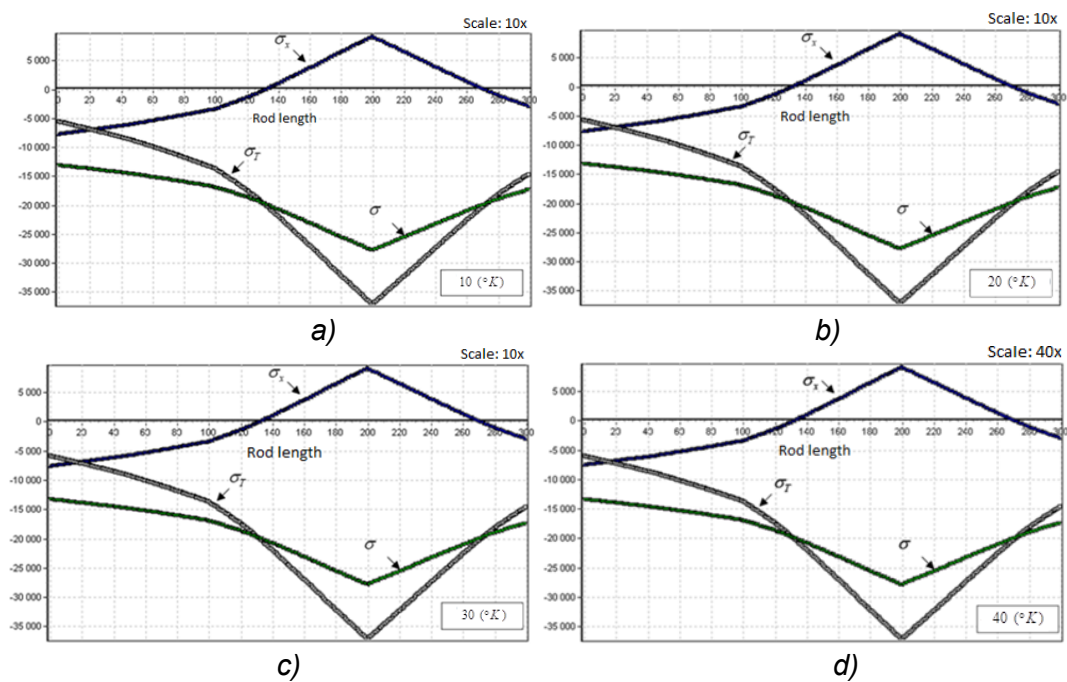


**Figure 4.** Field stress distribution along the length of the rod at  
 $T_{amb\ 0} = 10\ (^{\circ}K)$ ;  $20\ (^{\circ}K)$ ;  $30\ (^{\circ}K)$ ;  $40\ (^{\circ}K)$

USO DE NOVOS COMPOSTOS DA SÉRIE QUINOLINA COMO ESTIMULANTES EFICAZES DOS PROCESSOS DE CRESCIMENTO

USE OF NEW COMPOUNDS OF THE QUINOLINE SERIES AS EFFECTIVE STIMULANTS OF GROWTH PROCESSES

ИСПОЛЬЗОВАНИЕ НОВЫХ СОЕДИНЕНИЙ ХИНОЛИНОВОГО РЯДА КАК ЭФФЕКТИВНЫХ СТИМУЛЯТОРОВ РОСТОВЫХ ПРОЦЕССОВ

VOSTRIKOVA, Tatiana V.<sup>1\*</sup>; KALAEV, Vladislav N.<sup>2</sup>; POTAPOV, Andrey Yu.<sup>3</sup> POTAPOV, MICHAEL A.<sup>4</sup>; SHIKHALIEV, Khidmet S.<sup>5</sup>

<sup>1,2</sup> Voronezh State University, Botanical Garden, Russian Federation.

<sup>3,4,5</sup> Voronezh State University, Department of Organic Chemistry, Russian Federation.

\* Correspondence author

e-mail: tanyavostric@rambler.ru

Received 12 January 2020; received in revised form 20 May 2020; accepted 20 June 2020

RESUMO

Os resultados de um estudo da ação de compostos da fórmula geral: 1-alkyl-2,2,4-trimethyl-6-aminocarbothiopyl-1,2-dihydroquinoline and 1-alkyl-2,2,4-trimethyl-6-aminocarbothiopyl-1,2,3,4-tetrahydroquinoline. Os estimulantes de crescimento mais eficazes dos compostos das séries 1-alkyl-2,2,4-trimethyl-6-aminocarbothiopyl-1,2-dihydroquinoline and 1-alkyl-2,2,4-trimethyl-6-aminocarbothiopyl-1,2,3,4-tetrahydroquinoline para rododendro amarelo (*Rhododendron luteum*) e rododendro Ledebur (*Rhododendron ledebourii*). As mudas de rododendro foram contadas para estudar a germinação em laboratório e plantadas em caixotes em terreno fechado, aos 21 dias após o início do experimento. Foi estabelecido que os produtos químicos sintetizados causam estímulo ao crescimento de espécies do gênero *Rhododendron* em comparação com as preparações comerciais existentes. A eficiência do uso de soluções de compostos das séries 1-alkyl-2,2,4-trimethyl-6-aminocarbothiopyl-1,2-dihydroquinoline and 1-alkyl-2,2,4-trimethyl-6-aminocarbothiopyl-1,2,3,4-tetrahydroquinoline e suas concentrações. É divulgado um método de utilização de compostos desta série como estimulantes do crescimento, que permite aumentar a germinação de espécies do gênero *Rhododendron* de 20 para 50%, aumentar a altura de mudas de *Rhododendron luteum* de 18 para 63% e *Rhododendron ledebourii* de 33 para 183%. As dihydroquinolinas são mais eficazes para espécies do gênero *Rhododendron*. Os compostos contendo um substituinte di-hidro-6-quinolinil estimulam o crescimento dessas plantas. A especificidade da ação dos estimulantes do crescimento é observada. A conveniência de usar compostos da série quinolina para a produção de material de plantio de plantas ornamentais para paisagismo é mostrada. Sugere-se a atividade auxina de compostos da fórmula geral: 1-alkyl-2,2,4-trimethyl-6-aminocarbothiopyl-1,2-dihydroquinoline and 1-alkyl-2,2,4-trimethyl-6-aminocarbothiopyl-1,2,3,4-tetrahydroquinoline. Supõe-se que os compostos das séries 1-alkyl-2,2,4-trimethyl-6-aminocarbothiopyl-1,2-dihydroquinoline and 1-alkyl-2,2,4-trimethyl-6-aminocarbothiopyl-1,2, A 3,4-tetrahydroquinoline pode ter atividade de proteção ao estresse para espécies do gênero *Rhododendron*. Os materiais do artigo são de valor prático para biólogos, ecologistas e cultivadores de plantas.

**Palavras-chave:** *estimuladores de crescimento, processos de crescimento, compostos orgânicos sintetizados, plantas ornamentais.*

ABSTRACT

The results of a study of the action of compounds of the general formula: 1-alkyl-2,2,4-trimethyl-6-aminocarbothiopyl-1,2-dihydroquinoline and 1-alkyl-2,2,4-trimethyl-6-aminocarbothiopyl-1,2,3,4-tetrahydroquinoline are presented. The most effective growth stimulants from compounds of the series 1-alkyl-2,2,4-trimethyl-6-aminocarbothiopyl-1,2-dihydroquinoline and 1-alkyl-2,2,4-trimethyl-6-aminocarbothiopyl-1,2,3,4-tetrahydroquinoline for yellow rhododendron (*Rhododendron luteum*) and Ledebur rhododendron (*Rhododendron ledebourii*) were revealed. *Rhododendron* seedlings were counted to study laboratory germination and planted in crates in closed ground on 21 days after the start of the experiment. It was established that the synthesized chemicals cause stimulation of the growth of species of the genus *Rhododendron* in comparison with existing commercial preparations. The efficiency of using solutions of compounds of the series 1-alkyl-2,2,4-trimethyl-6-

aminocarbothioyl-1,2-dihydroquinoline and 1-alkyl-2,2,4-trimethyl-6-aminocarbothioyl-1,2,3,4-tetrahydroquinoline and their concentrations. A method of using compounds of this series as growth stimulants is disclosed, which allows increasing seed germination of species of the genus *Rhododendron* from 20 to 50%, increasing the height of *Rhododendron luteum* seedlings from 18 to 63%, and *Rhododendron ledebourii* from 33 to 183 %. Dihydroquinolines are most effective for species of the genus *Rhododendron*. Compounds containing a dihydro-6-quinolinyl substituent stimulate the growth of these plants. The specificity of the action of growth stimulants is noted. The expediency of using quinoline series compounds for the production of planting material of ornamental plants for landscaping is shown. It is suggested the auxin activity of compounds of the general formula: 1-alkyl-2,2,4-trimethyl-6-aminocarbothioyl-1,2-dihydroquinoline and 1-alkyl-2,2,4-trimethyl-6-aminocarbothioyl-1,2,3,4-tetrahydroquinoline. It is assumed that compounds of the series 1-alkyl-2,2,4-trimethyl-6-aminocarbothioyl-1,2-dihydroquinoline and 1-alkyl-2,2,4-trimethyl-6-aminocarbothioyl-1,2,3,4-tetrahydroquinoline may have the stress-protective activity for species of the genus *Rhododendron*. The materials of the article are of practical value for biologists, ecologists, plant growers.

**Keywords:** growth stimulators, growth processes, synthesized organic compounds, ornamental plants.

## АННОТАЦИЯ

Представлены результаты исследования действия соединений общей формулы: 1-алкил-2,2,4-триметил-6-аминокарботиоил-1,2-дигидрохинолин и 1-алкил-2,2,4-триметил-6-аминокарботиоил-1,2,3,4-тетрагидрохинолин. Выявлены наиболее эффективные стимуляторы роста из соединений ряда 1-алкил-2,2,4-триметил-6-аминокарботиоил-1,2-дигидрохинолина и 1-алкил-2,2,4-триметил-6-аминокарботиоил-1,2,3,4-тетрагидрохинолина для рододендрона желтого (*Rhododendron luteum*) и рододендрона Ледебера (*Rhododendron ledebourii*). Проростки рододендрона подсчитывали для изучения лабораторной всхожести и высаживали в ящики в закрытом грунте на 21 день после начала эксперимента. Установлено, что синтезированные химические вещества вызывают стимуляцию роста видов рода *Rhododendron* по сравнению с существующими коммерческими препаратами. Эффективность использования растворов соединений ряда 1-алкил-2,2,4-триметил-6-аминокарботиоил-1,2-дигидрохинолина и 1-алкил-2,2,4-триметил-6-аминокарботиоил-1,2,3,4-тетрагидрохинолина и их концентрации. Раскрыт способ использования соединений этой серии в качестве стимуляторов роста, который позволяет увеличить всхожесть семян видов рода *Rhododendron* с 20 до 50%, увеличить высоту сеянцев *Rhododendron luteum* с 18 до 63%, а *Rhododendron ledebourii* с 33 до 183%. Таким образом, дигидрохинолины наиболее эффективны для видов рода *Rhododendron*. Соединения, содержащие дигидро-6-хинолинийный заместитель, стимулируют рост этих растений. Отмечена специфичность действия стимуляторов роста. Показана целесообразность использования соединений серии хинолинов для производства посадочного материала декоративных растений для ландшафтного дизайна. Предполагается ауксиновая активность соединений общей формулы: 1-алкил-2,2,4-триметил-6-аминокарботиоил-1,2-дигидрохинолин и 1-алкил-2,2,4-триметил-6-аминокарботиоил-1,2,3,4-тетрагидрохинолин. Предполагается, что соединения ряда 1-алкил-2,2,4-триметил-6-аминокарботиоил-1,2,3,4-тетрагидрохинолина и 1-алкил-2,2,4-триметил-6-аминокарботиоил-1,2,3,4-тетрагидрохинолин может обладать стресс-защитной активностью для видов рода *Rhododendron*. Материалы статьи представляют практическую ценность для биологов, экологов, растениеводов.

**Ключевые слова:** стимуляторы роста, ростовые процессы, синтезированные органические соединения, декоративные растения

## 1. INTRODUCTION

Maintenance of seed quality is mandatory for the sale of seed as well as for assuring the required plant population and final yields to end-user (Sudhakar *et al.*, 2016). It is possible to increase seed germination and the quality of plants obtained from them using growth regulators (Bashmakov *et al.*, 2012). Seed lots are evaluated based on their germination capabilities and vigor (Sudhakar *et al.*, 2016). In the physiological sense, germination begins with seed water uptake and

ends with the initiation of elongation by the embryonic axis, usually the radicle (Welbaum *et al.*, 1998). However, many tests used to evaluate seed physiological characteristics require time and skilled laboratory, making it a costly process (Neverova, 2004; Vetchinnikova, 2004; Kalaev *et al.*, 2006; Takahashi *et al.*, 2006, 2007; Bukharina, 2011; Gar'kova *et al.*, 2011; Popov *et al.*, 2011; Yakymchuk, 2015; Lapshina *et al.*, 2016; Sudhakar *et al.*, 2016; Baranova, Kalaev, 2017). Models have been developed to predict germination based on thermal time, hydrotime,

and combined hydrothermal time (Welbaum *et al.*, 1998). These population-based models indicate that the timing of germination is closely tied to physiologically determined temperature and water potential thresholds for radicle emergence, which vary among individual seeds in a population (Welbaum *et al.*, 1998). The tests of the germination capability and the height of the seedlings are used in modern research (Fedorova, Shunelko, 2003; Vetchinnikova, 2004; Ivanov, 2011; Lyanguzova, 2011; Moiseeva *et al.*, 2012a,b; Bome *et al.*, 2015; Opalko, Opalko, 2015; Kuzemko, 2016; Fachi *et al.*, 2019).

Currently, an active search is underway for regulators of growth processes among new synthesized organic substances that could have a stronger positive effect compared to existing commercial preparations. Hydroquinoline derivatives with wide biological activity are essential heterocyclic compounds for the synthesis of organic and medical chemistry (Mohammed *et al.*, 1992; Shmyreva, 2000; Abadi, Brun, 2003; Saudi *et al.*, 2003; Abdel-Gawad *et al.*, 2005; Shujiang *et al.*, 2005; Williamson, Ward 2005; Denmark, Venkatraman, 2006; Trivedi *et al.*, 2008; Litvinov, 2009; Mosalam *et al.*, 2011a,b; Azizian *et al.*, 2014; Shikhaliev *et al.*, 2014; Ghoneim, Assy, 2015). It seems relevant to reveal the species-specific reactions of seedlings of herbaceous and woody plants to seed pretreatment with synthesized organic compounds, the effect of aftereffect of seed treatment, and the influence of the substitute base compound.

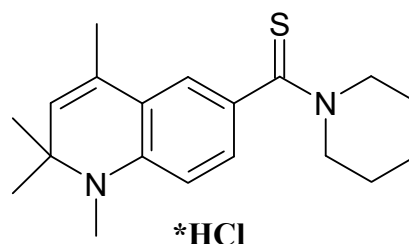
The purpose of the study was to study the effects of the synthesized organic compounds of the series 1-alkyl-2,2,4-trimethyl-6-amino carbothiyl-1,2-dihydroquinoline and 1-alkyl-2,2,4-trimethyl-6-aminocarbothiyl-1,2,3,4-tetrahydroquinoline at growth indicators (by which we meant seed germination and plant height) of *Rhododendron ledebourii* and *Rhododendron luteum*.

## 2. MATERIALS AND METHODS

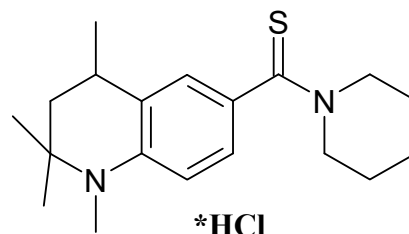
Seeds were treated with compounds synthesized at the Department of Organic Chemistry of the Voronezh State University according to the methods developed by the staff, which are described in the literature (Manahelohe *et al.*, 2015a,b). Below is a general scheme for the synthesis of organic compounds of the series 1-

alkyl-2,2,4-trimethyl-6-aminocarbothiyl-1,2-dihydroquinoline and 1-alkyl-2,2,4-trimethyl-6-aminocarbothiyl-1,2,3,4-tetrahydroquinoline (Fig. 1).

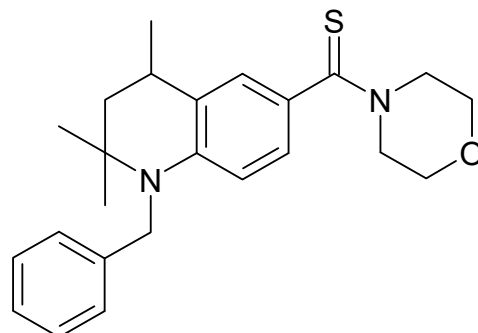
A mixture of the corresponding hydroquinoline carboxaldehyde (1 mmol), amine (1.33 mmol), and elemental sulfur (1.33 mmol) in dimethylformamide (2 ml) was heated under reflux until the completion of the reaction (the control by the thin layer chromatography). After cooling, the reaction mass was poured into 5 ml of ice water with vigorous stirring. The solidified after grinding, and the precipitate was filtered, washed with water, and recrystallized from 75% ethanol. Non-hardening thiocarboxamides were treated with a double excess of hot 2M hydrochloric acid, filtered and recrystallized from ethanol.



1,2,2,4-tetramethyl-6-(1-piperidinylcarbothiyl)-1,2-dihydroquinoline hydrochloride (compound 1);

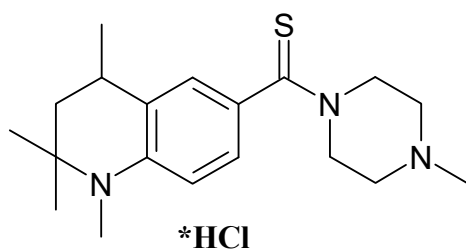


1,2,2,4-tetramethyl-6-(1-piperidinylcarbothiyl)-1,2,3,4-tetrahydroquinoline hydrochloride (compound 2);

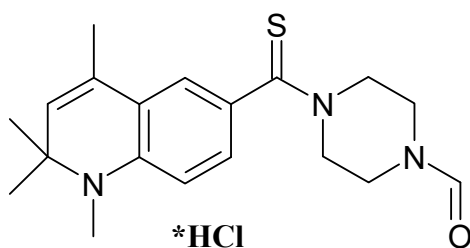


1-benzyl-2,2,4-trimethyl-6-(4-morpholinylcarbothiyl)-1,2,3,4-tetrahydroquinoline (compound 3);





1,2,2,4-tetramethyl-6-[(4-methyl-1-piperazinyl)carbothioyl]-1,2,3,4-tetrahydroquinoline hydrochloride (compound 4);



4-[(1,2,2,4-tetramethyl-1,2-dihydro-6-quinolyl)carbothioyl]-1-piperazinylcarbaldehyde hydrochloride (compound 5).

To identify the biological effects of the synthesized organic compounds, morphometric parameters of perennial woody plants: Ledebour rhododendron (*Rhododendron ledebourii* Pojark.) and yellow rhododendron (*Rhododendron luteum* Sweet.) (Alexandrova, 2003; Baranova *et al.*, 2018; Burmenko *et al.*, 2018a,b).

The seeds of the test plants were kept in aqueous solutions of the above chemical compounds at concentrations of 0.01%, 0.05% and 0.1% for 18 hours. As a traditional stimulator, the commercial preparation Epin-Extra (Russian produced by NNPP NEST M) in a working concentration according to the instructions for use - 0.05%. The control seeds were soaked in tap water. The experiment was carried out in triplicate (100 seeds in each). Seeds were germinated under laboratory conditions at a constant temperature of 22 ° C. The germination of seeds and the determination of the germination was carried out according to GOST 13056.6-97. The laboratory germination of seeds was determined as the ratio of the number of germinated seeds to the total number of seeds and was expressed in%, according to the recommendations (GOST 13056.6-97). *Rhododendron* seedlings were counted to study laboratory germination and planted in crates in closed ground on 21 days after the start of the experiment. The height of the seedlings was measured using a ruler.

Computer statistical processing was performed using the Stadia software package. The procedures for grouping data and their processing were described in the work of A. P. Kulaichev (2006). The seed germination in the control and experimental variants was compared according to the criterion of frequency agreement using Z-statistics. The comparison of mean values was carried out using Student's t-test. The influence of the chemical treatment factor at different concentrations on growth rates was determined using a two-way analysis of variance.

### 3. RESULTS AND DISCUSSION:

The results of the influence of tested chemical compounds on the germination of *Rhododendron* seeds are presented in Table 1-2.

The seed germination of Ledebour rhododendron (*Rhododendron ledebourii*) and yellow rhododendron (*Rhododendron luteum*) increase all tested chemical compounds at the concentration of 0.1%. For *Rh. ledebourii* compound 1 is the most effective and for *Rh. luteum* also compound 5 at concentrations 0.01%, 0.05% and 0.1%. A positive effect (stimulation) is observed when treating the seeds of the *Rhododendron* species with compounds 1, 3-5 in all tested concentrations (0.01%, 0.05%, and 0.1%). The germination of Ledebur rhododendron seeds under the influence of synthesized organic substances at the indicated concentrations (0.01%, 0.05%, and 0.1%) was increased from 24.3 to 54% for yellow rhododendron - from 21.4 to 56.2%.

The height of the seedlings of species of the genus *Rhododendron* grown from seeds treated by synthesized chemical compounds is presented in Tables 3-4. Compounds 1 and 5 at concentrations of 0.01%, 0.05%, and 0.1% is shown the most significant stimulating effect. All tested substances are effective at concentrations of 0.05% and 0.1%. The height of Ledebur rhododendron seedlings under the influence of synthesized organic compounds was risen from 33.3 to 183.3%, for yellow rhododendron - from 18.2 to 63.6%.

The influence of the "chemical compound treatment" and "concentration" factors was evaluated by the results of the analysis of variance, which showed a significant effect on the height of seedlings *Rh. ledebourii* ( $P < 0.05$ ), *Rh. luteum* ( $P < 0.05$ ).

Mild and moderate stress activates the body's defenses. The use of various growth stimulants that can protect the plant and reduce the harmful effects of heavy metals on the body is based on this mechanism. For example, the effect of the synthetic growth regulator of the cytokinin type of action (cytodef) and heavy metal ions:  $\text{Pb}^{2+}$ ,  $\text{Sr}^{2+}$ ,  $\text{Zn}^{2+}$  and  $\text{Ni}^{2+}$  on the rate of generation of superoxide anion radical, the intensity of lipid peroxidation and the content of carotenoids in the leaves of 7-day-old cucumber plants (*Cucumis sativus* L., cultivar Graceful) was studied. The use of a synthetic growth regulator of the cytokinin type of action (cytodef) in some cases reduced the toxicity of heavy metals ( $\text{Pb}^{2+}$ ,  $\text{Sr}^{2+}$ ,  $\text{Zn}^{2+}$ , and  $\text{Ni}^{2+}$ ), which was manifested in partial or complete removal of the negative effect of metals on oxidative processes and an increase in the concentration of antioxidants (carotenoids) (Bashmakov *et al.*, 2012). The use of some biological growth regulators allows one to obtain a crop with a lower content of lead and cadmium ions (Titov *et al.*, 2011).

The results of this work are consistent with earlier studies by R. G. Gafurov and co-workers on carbon N- and O-benzyl-containing compounds that have a bright auxin activity (Gafurov, Makhmutova, 2003, 2005). In this regard, it is assumed that compounds of the series 1-alkyl-2,2,4-trimethyl-6-aminocarbothioyl-1,2-dihydroquinoline and 1-alkyl-2,2,4-trimethyl-6-aminocarbothioyl-1,2,3 may have the stress-protective activity for species of the genus *Rhododendron*.

#### 4. CONCLUSIONS:

Thus, the greatest effect on increasing the germination of seeds of species of the genus *Rhododendron* was produced by the synthesized organic compounds of the 1-alkyl-2,2,4-trimethyl-6-aminocarbothioyl-1,2-dihydroquinoline and 1-alkyl-2,2,4-trimethyl-6-aminocarbothioyl-1,2,3,4-tetrahydroquinoline at a concentration of 0.1%. Dihydroquinolines or compounds containing a dihydro-6-quinoliny substituent are most effective. All of the compounds under consideration show a clear tendency to increase seed germination with increasing concentration. All tested substances exhibit a stimulating effect at the studied concentrations and increase the height of seedlings of species of the genus *Rhododendron* in comparison with the control. Synthesized chemical compounds of the series 1-alkyl-2,2,4-trimethyl-6-aminocarbothioyl-1,2-dihydroquinoline and 1-alkyl-2,2,4-trimethyl-6-aminocarbothioyl-

1,2,3,4-tetrahydroquinoline cause the growth increase of species of the genus *Rhododendron* compared to existing commercial preparations, such as Epin-Extra, and it is advisable to use them as growth stimulators for the production of planting material.

#### 5. ACKNOWLEDGMENTS:

The study received financial support from the Ministry of Science and Higher Education of the Russian Federation within the framework of State Contract with universities regarding scientific research in 2020–2022, project No. FZGU-2020-0044

#### 6. REFERENCES:

1. Abdel-Gawad, S. M., El-Gagy, M. S. A., Heiba, H. I., Aly, H. M., Ghorab, M. M. Synthesis and radiation stability of some new biologically active hydroquinoline and pyrimido[4,5-b]quinoline derivatives. *J. Chin. Chem. Soc.*, **2005**, 52, 1227-1236.
2. Abadi, A. H., Brun, R. Synthesis and evaluation of novel 7-trifluoromethyl-4-(4-substituted anilino) quinolines as antiparasitic and antineoplastic agents *Arzneimforsch. Drug. Res.*, **2003**, 53, 655–663.
3. Alexandrova, M. S. *Rhododendrons*. Moscow: ZAO Fiton+, **2003**.
4. Azizian, J., Delbari A. S., One-Pot, K. Y. Three-Component Synthesis of Pyrimido[4,5-b]quinoline-tetraone Derivatives in Water. *Synthetic Commun*, 2014, 44 (22), 3277-3286. DOI: 10.1080/00397911.2011.626139
5. Baranova, T. V., Kalaev, V. N. Comparative Cytogenetic Analysis of Indigenous and Introduced Species of Woody Plants in Conditions of Anthropogenic Pollution. In: Nourani, C. F., Zaikov, G. E., Weisfeld, L. I., Lisitsyn, E. M., Bekuzarova, S. A. (Eds.); *Heavy Metals and Other Pollutants in the Environment: Biological Aspects*. Oakville: Apple Academic Press Inc., **2017**, 241-254.
6. Baranova, T. V., Kalendar, R. N., Kalaev, V. N., Sorokopudov, V. N., Burmenko, Yu.

- V., Relationship between cytogenetic characteristics and molecular-genetic differences in species of the genus *Rhododendron* L. when introduced. *Agricultural Biology*, **2018**, 53(3), 511-520. DOI: 10.15389/agrobiology
7. Bashmakov, D. I., Pynenkova, N. A., Sazanov, K. A., Lukatkin, A. S. Effect of the synthetic growth regulator Cytodef and heavy metals on oxidative status in cucumber plants. *Russian Journal of Plant Physiology*, **2012**, 59(1), 59-64.
8. Bome, N. A., Weisfeld, L. I., Bekuzarova, S. A., Bome, A. Y. Optimization of the Structurally Functional Changes in the Cultured Phytocoenoses in the Areas with Extreme Edaphic-Climatic Conditions. In: Weisfeld, L. I., Opalko, A. I., Bome, N. A., Bekuzarova, S. A. (Eds.); *Biological Systems, Biodiversity, and Stability of Plant Communities*, Oakville: Apple Academic Press Inc., **2015**, 19-32.
9. Bukharina, I. L. Features of the dynamics of the content of ascorbic acid and tannins in the shoots of woody plants under the conditions of the city of Izhevsk. *Plant Resources*, **2011**, 47(2), 109-117.
10. Burmenko, Yu. V., Baranova, T. V., Kalaev, V. N. Comparative Study of Cytogenetic Response of Silver Birch and *Rhododendron Ledebourii* Seeds to Urban Pollution in Voronezh. *Russian Journal of Forest Science*, **2018a**, 1, 65-73.  
doi: 10.7868/S0024114818010060
11. Burmenko, Yu. V., Baranova, T. V., Kalaev, V. N., Sorokopudov, V. N. Cytogenetic polymorphism of seed progeny of introduced plants on the example of *Rhododendron ledebourii* Pojark. *Turczaninowia*, **2018b**, 21 (1), 164-173.  
doi: 10.14258/turczaninowia.21.1.16
12. Denmark, S., Venkatraman, S. On the mechanism of the Skraup-Doebner-Von Miller quinoline synthesis. *J. Org. Chem.*, **2006**, 71, 1668-1676.
13. Fachi, L. R., Krause, W., Duarte, H., Viana, A. P. Digital image analysis to quantify genetic divergence in passion fruit (*Passiflora edulis*) seeds. *Genetics and Molecular Research*, **2019**, 18(3). DOI: 10.4238 / gmr18331
14. Fedorova, A. I., Shunelko, E. V. Pollution of the surface horizons of the soil of the city of Voronezh with heavy metals. *Vestnik VSU. A series of geography and geoecology*, **2003**, 1, 74-82.
15. Gafurov, R. G., Makhmutova, A. A. A new group of synthetic auxin biomimetics: N- and O-benzyl-containing compounds. *Reports of the Russian Academy of Sciences*, **2003**, 391, 562-565.
16. Gafurov, R. G., Makhmutova, A. A. Growth-regulating activity of N- and O-benzyl-containing compounds - a new group of synthetic analogues of natural auxins. *Applied Biochemistry and Microbiology*, **2005**, 41(2), 245-249.
17. Gar'kova, A. N., Rusyaeva, M. M., Nushtaeva, O. V., Aroslankina, Y. N., Lukatkin, A. S. Treatment with the herbicide granstar induces oxidative stress in cereal leaves. *Russian Journal of Plant Physiology*, **2011**, 58(6), 1074-1081.
18. Ghoneim, A. A., Assy, M. G. Synthesis of Some New Hydroquinoline and Pyrimido[4,5-b] Quinoline Derivatives. *Current Research in Chemistry*, **2015**, 7(1), 14-20. DOI: 10.3923/crc.2015.14.20
19. Ivanov, V. B. Using the roots as test objects for the assessment of biological action of chemical substances. *Russian Journal of Plant Physiology*, **2011**, 58(6), 1082-1089.
20. Kalaev, V. N., Butorina, A. K., Sheluchina, O. Yu. Assessment of anthropogenic pollution in the districts of Stary Oskol based on cytogenetic indicators of seed seedlings of weeping birch. *Ecological genetics*, **2006**, 4(2), 9-23.
21. Kalaev, V. N., Moiseeva, E. V., Baranova, T. V., Medvedeva, S. M., Shikhaliev, H. S., Voronin, A. A. Growth stimulants for species of the genus *Rhododendron* L.: Patent 2490892 Russian Federation. 2012112006/13, declared 29. 03.12, published 27. 08.13, 24.
22. Kulaichev, A. P. Methods and tools for integrated data analysis. Moscow: FORUM: INFA-M, **2006**.
23. Kuzemko, A. A. Influence of Anthropogenic Pressure on Environmental Characteristics of Meadow Habitats in the Forest and Forest- Zones. In: Bekuzarova, S. A., Bome, N. A., Opalko, A. I. (Eds.);

- Temperate Crop Science and Breeding: Ecological and Genetic Studies, Oakville: Apple Academic Press Inc., **2016**, 385-404.
24. Lapshina, L. A., Reunov, A. V., Nagorskaya, V. P. Effects of exogenous H<sub>2</sub>O<sub>2</sub> on the content of endogenous H<sub>2</sub>O<sub>2</sub>, activities of catalase and hydrolases, and cell ultrastructure in tobacco leaves. *Biology Bulletin*, **2016**, 43(5), 419-425.
  25. Lyanguzova, I. V. Effect of industrial air pollution on wild plant seed germination and seedling growth. *Russian Journal of Plant Physiology*, **2011**, 58(60), 991-998.
  26. Litvinov, V. I., Makarova, M. V., Ryzhov, A. M., Ivanov, Yu. A., Frolov, A. Yu., Osinin, V. V., Pereverzentsev, V. M. The use of 6-hydroxyl-trimethyl-1,2,3,4-tetrahydroquinoline or 6-hydroxyl-2,2,4-trimethyl-1,2-dihydroquinoline as an anti-tuberculosis substance: Russian Federation. 2008133238/15, declared 14.08.08, published 20.11.09, 32.
  27. Manakhelohe, G. M., Shikhaliev, H. S., Potapov, A. Yu. Synthesis of 1*H*-1,2-dithiol-1-thiones and thioamides containing hydroquinoline group. *Eur. Chem. Bull.*, **2015a**, 4(7), 350-355.
  28. Manakhelohe, G. M., Shikhaliev, H. S., Potapov, A. Yu. Synthesis of thiocarboxamides containing a hydroquinoline fragment. Bulletin of the Voronezh State University, Series: *Chemistry Biology Pharmacy*, **2015b**, 2, 23-28.
  29. Mohammed, A., Abdel-Hamid, N., Maher, F., Farghaly, A. Synthesis and antibacterial activity of certain quinoline derivatives A. *Czech Chem Commun*, **1992**, 57(7), 1547-1552.
  30. Moiseeva, E. V., Baranova, T. V., Kalaev, V. N., Kuznetsov, B. I., Shcherbakov, G. S., Voronin, A. A., Potapov, A. Yu., Shikhaliev, H. S. The effect of compounds of the quinoline series on the germination and growth processes of Ledebour's rhododendron (*Rhododendron Ledebourii* Pojark.). *Basic Research*, **2012a**, 5 (1), 172-176.
  31. Moiseeva, E. V., Baranova, T. V., Voronin, A. A., Kuznetsov, B. I. A collection of representatives of the genus rhododendron (*Rhododendron* L.) in the botanical garden B.M. Kozo-Polyansky Voronezh State University. *Ecosystems, their optimization, and protection*, **2012b**, 7, 39-44.
  32. Mosalam, M. A., El Hamouly, S. H., Mahmoud, A. A., Khalil, A. Binary copolymerizations of 8-methacryloxy-quinoline with methyl methacrylate, methyl acrylate, styrene, and acrylonitrile. *Journal of Polymer Research*, **2011a**, 18(6), 2141-2150. DOI:10.1007/s10965-011-9624-4
  33. Mosalam, M. A., El Hamouly, S. H., Mahmoud, A. A., Khalil, A. Thermal Behavior of 8-methacryloxy-quinoline-Acrylonitrile Copolymers. *International Journal of Chemistry*, **2011b**, 3(2), 14-22. DOI: 10.5539 / ijc.v3n2p14
  34. Neverova, O. A. Ecological assessment of the state of woody plants and environmental pollution of an industrial city (by the example of Kemerovo): Thesis for the degree of Doctor of Biology: Moscow, **2004**.
  35. Opalko, A. I., Opalko, O. A. Anthropo-Adaptability of Plants as a Basis Component of a New Wave of the "Green Revolution". In: Weisfeld, L. I., Opalko, A. I., Bome, N. A., Bekuzarova, S. A. (Eds.); *Biological Systems, Biodiversity, and Stability of Plant Communities*, Oakville: Apple Academic Press Inc., **2015**, 3-18.
  36. Popov, V. N., Eprintsev, A. T., Maltseva, E. V. Activation of genes encoding mitochondrial proteins involved in alternative and uncoupled respiration of tomato plants treated with low temperature and reactive oxygen species. *Russian Journal of Plant Physiology*, **2011**, 58(5), 914-920.
  37. Saudi, M. N. S., Rostom, S. A., Fahmy, H. T. Y., El-Ashmawy I. Synthesis of 2-(4Biphenyl)quinoline-4-carboxylate and Carboxamide Analogues. *Articlein ChemInform*, **2003**, 34(39).doi:10.1002 / chin.200339123
  38. Shikhaliev, H. S., Selemenev, V. F., Medvedeva, S. M., Ponomareva, L. F., Kopteva, N. I. Mass-spectrometric analysis of 1-acyl-2,2,5-trimethyl-4,4-dichlorocyclopropane [c] quinolines. *Sorption and chromatographic processes*, **2014**, 14 (2), 332-337.

39. Shmyreva, J. V. 2, 2, 4-Trimethylhydroquinolins. Voronezh: VSU, **2000**.
40. Shuijiang, T. U., Fang, F., Tuanjie, L., Songlei, Z., Xiaojing, Z. An efficient one-pot synthesis of novel pyrimidoquinoline derivative under microwave irradiation without catalyst. *J. Heterocycl. Chem.*, **2005**, 42, 707-710.
41. Sudhakar, P., Latha, P., Reddy, P. V. Seed physiological and biochemical traits. In: *Phenotyping Crop Plants for Physiological and Biochemical Traits*, **2016**, 17-24.
42. Takahashi, H., Bekkali, Y., Capolino, A., Gilmore, T., Goldrick, S., Nelson, R., Terenzio, D., Wang, J., Zuvela-Jelaska, L., Proudfoot, J., Nabozny, G., Thomson, D. Discovery and SAR study of novel dihydroquinoline containing glucocorticoid receptor ligands. *Bioorg. Med. Chem. Lett.*, **2006**, 16, 1549-1552.
43. Takahashi, H., Bekkali, Y., Capolino, A., Gilmore, T., Goldrick, S., Kaplita, P., Liu, L., Nelson, R., Terenzio, D., Wang, J., Zuvela-Jelaska, L., Proudfoot, J., Nabozny, G., Thomson, D. Discovery and SAR study of novel dihydroquinoline containing glucocorticoid receptor antagonists. *Bioorg. Med. Chem. Lett.*, **2007**, 17, 5091-5095.
44. Titov, V. N., Smyslov, D. G., Dmitrieva, G. A., Bolotova, O. I. Plant growth regulators as a biological factor in reducing the level of heavy metals in a plant. *Vestnik Ore/GAU*, **2011**, 31(4), 4-6.
45. Trivedi, A., Dodiya, D., Surani, J., Jarsania, S., Mathukiya, H., Ravat N., Shah, V. Facile one-pot synthesis and antimycobacterial evaluation of pyrazolo[3,4 d]pyrimidines. *Archiv Pharmazie*, **2008**, 341, 435-439.
46. Vetchinnikova, L. V. Birch: questions of variability (morphophysiological and biochemical aspects) (Ed.); Titov, A. F., M.: Science, **2004**.
47. Vostrikova, T. V. Ecological and biological features of rhododendrons during introduction in the conditions of the Central Chernozem region. *Bulletin of Krasnoyarsk State Agrarian University*, **2011**, 4, 27-30.
48. Welbaum, G. E., Bradford, K. J., Yim, K.-O. Booth, D. T. Biophysical, physiological and biochemical processes seed germination. *Seed Science Research*, **1998**, 8(02), 161-172.
49. Williamson, N., Ward, D. The preparation and some chemistry of 2,2-dimethyl-1,2-dihydroquinolines. *Tetrahedron*, **2005**, 61, 155-165.
50. Yakymchuk, R. A. Cytogenetic After-Effects of Mutagen Soil Contamination with Emissions of Burshtynska Thermal Power Station. In: Opalko, A. I., Weisfeld, L. I., Bekuzarova, S. A., Bome, N. A., Zaikov, G. E. (Eds.); *Ecological Consequences of Increasing Crop Productivity: Plant Breeding and Biotic Diversity*: New Jersey: Apple Academic Press Inc., **2015**, 217-227.

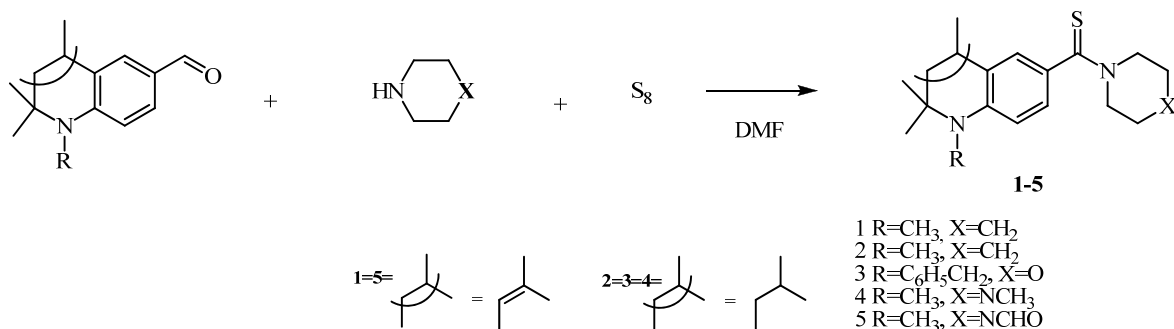


**Figure 1.** The general scheme for the synthesis of 2,2,4-tetramethylhydroquinolin-6-ylcarbothioamides 1-5.

**Table 1.** The seed germination (in%) of *Ledebur rhododendron* treated with synthesized organic compounds

| Concentration | Control group, % | Epin group, % | compound 1 | compound 2 | compound 3 | compound 4 | compound 5 |
|---------------|------------------|---------------|------------|------------|------------|------------|------------|
| 0,01%         | 41.1             | 43.3          | 52.8**2    | 42.2       | 51.1*1     | 52.2**2    | 47.8*1     |
| 0,05%         |                  |               | 58.6**2    | 45.7       | 57.6**2    | 58.9**2    | 53.5*1     |
| 0,1%          |                  |               | 63.3**2    | 55.4*1     | 64.4**2    | 61.7**2    | 58.2**2    |

Note for Table 1-4:

\* – differences with the control group are reliable ( $p < 0.05$ )

\* – differences with the control group are reliable ( $p < 0.01$ )

\* – differences with the control group are reliable ( $p < 0.001$ )

<sup>1</sup> - differences with the Epin group are reliable ( $p < 0.05$ );

<sup>2</sup> - differences with the Epin group are reliable ( $p < 0.01$ );

<sup>3</sup> - differences with the Epin group are reliable ( $p < 0.01$ );

1,2,2,4-tetramethyl-6-(1-piperidinylcarbothioyl)-1,2-dihydroquinoline hydrochloride (compound 1);

1,2,2,4-tetramethyl-6-(1-piperidinylcarbothioyl) -1,2,3,4-tetrahydroquinoline hydrochloride (compound 2);

1-benzyl-2,2,4-trimethyl-6-(4-morpholinylcarbothioyl)-1,2,3,4-tetrahydroquinoline (compound 3);

1,2,2,4-tetramethyl-6-[(4-methyl-1-piperazinyl)carbothioyl]-1,2,3,4-tetrahydroquinoline hydrochloride (compound 4);

4-[(1,2,2,4-tetramethyl-1,2-dihydro-6-quinoliny)carbothioyl]-1-piperazinylcarbaldehyde hydrochloride (compound 5).

**Table 2.** The seed germination (in %) of yellow *rhododendron* treated with synthesized organic compounds

| Concentration | Control group, % | Epin group, % | compound 1 | compound 2 | compound 3 | compound 4 | compound 5 |
|---------------|------------------|---------------|------------|------------|------------|------------|------------|
| 0,01%         | 52.3             | 58.4          | 68.1*1     | 54.2       | 68.6**2    | 57.8       | 72.2**2    |
| 0,05%         |                  |               | 76.5**2    | 58.7*      | 72.4**2    | 63.5*1     | 78.4**2    |
| 0,1%          |                  |               | 80.4**2    | 64.8*1     | 76.3**2    | 68.2**2    | 81.7**2    |

**Table 3.** The height (in cm) of *Rhododendron ledebourii* seedlings 21 days after the start of the experiment

| Con<br>centr<br>ation | Control<br>group, % | Epin<br>group, % | compound<br>1    | compound<br>2    | compound<br>3         | compound<br>4 | compound<br>5    |
|-----------------------|---------------------|------------------|------------------|------------------|-----------------------|---------------|------------------|
| 0.01<br>%             | 0.6±0.02            | 0.7±0.02*        | 1.4±0.04**<br>*3 | 0.8±0.03**       | 0.6±0.02 <sup>1</sup> | 0.7±0.02*     | 1.3±0.03**<br>*3 |
| 0.05<br>%             |                     |                  | 1.5±0.04**<br>*3 | 0.9±0.02**<br>*3 | 0.7±0.02*             | 0.7±0.02*     | 1.3±0.03**<br>*3 |
| 0.1<br>%              |                     |                  | 1.7±0.04**<br>*3 | 0.9±0.03**<br>*3 | 0.9±0.02**<br>*3      | 0.8±0.03**    | 1.4±0.02**<br>*3 |

**Table 4.** The height (in cm) of *Rhododendron luteum* seedlings 21 days after the start of the experiment

| Con<br>centr<br>ation | Control<br>group, % | Epin Extra<br>group, % | compound<br>1    | compound<br>2    | compound<br>3    | compound<br>4    | compound<br>5    |
|-----------------------|---------------------|------------------------|------------------|------------------|------------------|------------------|------------------|
| 0.01<br>%             | 1.1±0.03            | 1.2±0.02*              | 1.6±0.04**<br>*3 | 1.5±0.02**<br>*3 | 1.4±0.02**<br>*3 | 1.3±0.02**<br>1  | 1.6±0.03**<br>*3 |
| 0.05<br>%             |                     |                        | 1.7±0.03**<br>*3 | 1.6±0.02**<br>*3 | 1.5±0.02*        | 1.4±0.02**<br>*2 | 1.6±0.03**<br>*3 |
| 0.1<br>%              |                     |                        | 1.8±0.03**<br>*3 | 1.7±0.03**<br>*3 | 1.6±0.03**<br>*3 | 1.5±0.03**<br>*3 | 1.7±0.04**<br>*3 |

**CRESCIMENTO DE TUBERCULOS DE SEMENTE DE BATATA SEM VÍRUS EM PLANTIO AEROPÔNICO****GROWING OF VIRUS-FREE POTATO SEED TUBERS IN THE AEROPONIC PLANT****ВЫРАЩИВАНИЕ ПОСАДОЧНОГО МАТЕРИАЛА КАРТОФЕЛЯ НА БЕЗВИРУСНОЙ ОСНОВЕ С ИСПОЛЬЗОВАНИЕМ АЭРОПОННОЙ УСТАНОВКИ**

ISMAGILOV, Rafael<sup>1\*</sup>; ASYLBAEV, Ilgiz<sup>2</sup>; URAZBAKHTINA, Nuriya<sup>1</sup>; ANDRIYANOV, Denis<sup>1</sup>; AVSAKHOV, Firdavis<sup>2</sup>

<sup>1</sup> Federal State Budgetary Educational Institution of Higher Education "Bashkir State Agrarian University", Department of Crop Production, Plant Breeding and Biotechnology. Russian Federation

<sup>2</sup> Federal State Budgetary Educational Institution of Higher Education "Bashkir State Agrarian University", Department of Soil Science, Agrochemistry and Precision Agriculture. Russian Federation

\* Corresponding author  
e-mail: [rismagilov@yahoo.com](mailto:rismagilov@yahoo.com)

Received 03 March 2020; received in revised form 20 May 2020; accepted 20 June 2020

**RESUMO**

As batatas como cultura alimentar são de grande importância no mundo. As infecções virais estão entre as principais razões por trás das más propriedades das sementes do material de plantio, baixa qualidade e baixo rendimento da colheita da batata. O uso de sementes sem vírus é uma das formas com alto potencial para aumentar os índices de rendimento e a eficiência do cultivo de batata. A aeropônia é uma área promissora para o cultivo de batatas sem vírus. O estudo teve como objetivo avaliar o potencial e melhorar a tecnologia do cultivo de tubérculos de batata sem doenças usando plantação aeropônica. A tecnologia aeropônica da produção de semente de batata é uma maneira segura e econômica de produzir mini tubérculos. As práticas aeropônicas exigem menos água e energia por unidade de volume de material de sementes em comparação com as práticas convencionais de cultivo. A tecnologia elimina doenças transmitidas pelo solo e danos causados por pragas. Condições artificiais, como iluminação adicional, podem ser facilmente fornecidas em estufa para o cultivo de variedades cultivadas em diferentes regiões. Cálculos econômicos mostraram que a tecnologia aeropônica pode ser praticável na produção de sementes de batata em larga escala.

**Palavras-chave:** *planta aeropônica; mini tubérculos; batatas; material de sementes; produção de sementes.*

**ABSTRACT**

Throughout the world, potatoes, as a food crop, are very important. One of the main reasons for the poor quality of planting material, yield and potatoes themselves are viral infections. The use of virus-free seed material is one of the high-potential ways to increase the yield and efficiency of potato production. Aeroponics is a promising direction in obtaining a virus-protected crop. This study aimed to assess the potential and improve the technology for growing healthy mini-tubers of potatoes using the aeroponic method, which is a safe and economical method. Compared to the usual method of growing crops, aeroponics assumes lower water and energy costs per unit of production, as well as excludes soil diseases of the plant and does not allow damage to the tuber caused by pests. For growing different varieties of crops in different regions, artificial conditions such as additional lighting in greenhouses can be easily provided. In this study, economic calculations have shown that, from a practical point of view, Aeroponics technology may be appropriate for large-scale production of seed potatoes.

**Keywords:** *aeroponic plant; mini-tubers; potatoes; seed material; seed production.*

**АННОТАЦИЯ**

Во всем мире картофель, как продовольственная культура, имеет очень большое значение. Одной из основных причин низкого качества посадочного материала, урожайности и самого картофеля являются



вирусные инфекции. Использование безвирусного семенного материала является одним из высокопотенциальных путей для повышения урожая и эффективности картофелеводства. Аэропоника – это перспективное направление в получении защищенного от вирусов урожая. Данное исследование имело за цель оценить потенциал и усовершенствовать технологию выращивания здоровых мини-клубней картофеля с использованием аэропонного метода, являющегося безопасным и экономичным способом. По сравнению с обычной методикой выращивания сельскохозяйственных культур, аэропоника предполагает более низкие затраты воды и энергии на единицу продукции, а также исключает почвенные заболевания растения и не допускает повреждений клубня, вызванных насекомыми-вредителями. Для выращивания разных сортов сельскохозяйственных культур в различных регионах, такие искусственные условия, как дополнительное освещение в теплицах, могут быть легко обеспечены. В рамках данного исследования, экономические расчеты показали, что, с практической точки зрения, технология аэрооники может быть целесообразной при крупномасштабном производстве семенного картофеля.

**Ключевые слова:** аэропонная установка; миниклубни; картофель; семенной материал; семеноводство.

## 1. INTRODUCTION:

Potato (*Solanum tuberosum*) ranks third in the world among the most important food crops after rice and wheat; 374 million tons of potato tubers are produced in the world. However, potato yields are significantly below the yield potential in most developing countries, mainly due to poor potato seed properties (Tessema and Dagne, 2018). Due to biological characteristics, potatoes are more susceptible to viral and viroid diseases than other crops (Anisimov *et al.*, 2014). Viral diseases are among the major causes of poor potato seed properties and low productivity (Priegnitz *et al.*, 2019). As a result of multi-year reproduction, potatoes tend to accumulate diseases, mainly viral ones. The viral infections, in turn, lead to degeneration in potatoes (Li *et al.*, 2018; Dupuis *et al.*, 2019). The potato aphids and Colorado beetles transmit viruses from diseased to healthy plants, then viruses spread from one generation to another through vegetative reproduction of potatoes (Tessema and Dagne, 2018). Potato yields and storage capacity tend to decrease with each subsequent planting. Global potato losses from viral infections are 90 million tons, and the yield is reduced by 40-50%; tuber losses during storage can reach 15-20% (Adikini *et al.*, 2016; Khelifa, 2019). Such factors as the pathogen type and strain, stability rate of the variety, growing and weather conditions determine potato yield losses. Mild viral diseases reduce the yield by an average of 10-20%; potato yields drop by 70-85% in severe viral diseases. Starch values fall by 0.8-4.6% in diseased tubers compared to healthy tubers. The diseased potato tubers have lower values of crude protein, vitamin C, B<sub>1</sub>, B<sub>2</sub> (Ateş *et al.*, 2019; Inglis *et al.*, 2019; Ogero *et al.*, 2019).

Therefore, the use of the virus-free seed material is one of the high-potential ways for

increasing yield indices and efficiency of potato growing (Anisimov *et al.*, 2014; Mbiri *et al.*, 2015; Wang *et al.*, 2017; Tessema and Dagne, 2018). There are many methods for improving potato seed material (thermotherapy, chemotherapy). Thermotherapy is the treatment of plants, shoots, and tubers with high temperatures (+37 - +42 °C) for pathogen inactivation. Chemotherapy relies on the introduction of Virazole at 20-50 mg/l concentration into the nutrient medium, where apical meristems are grown. The main objective of reproducing the virus-free source material was to achieve the maximum net reproduction with the lowest risk of repeated viral infection and to produce material suitable for planting in the open ground (Anisimov *et al.*, 2009; 2014). Currently, to solve the problem, researchers use new techniques such as clonal propagation of meristem cultures and year-round reproduction of the source material in the closed environment (Lakhari *et al.*, 2018; Singh *et al.*, 2019). These are the main methods of seed material reproduction used in potato seed tuber production: improving seed material through tissue cultures and selecting the most virus-free lines; clonal propagation of micro-plants in the laboratory environment; growing disease-free mini-tubers on the protected ground or in hydroponic modules; selection of healthy source plants and clones in the field based on visual assessment and laboratory testing methods for viral, viroid and bacterial infection (Martirosyan, 2014; Oves *et al.*, 2014 Khutinaev *et al.*, 2016).

Aeroponics is a promising area for growing virus-free potatoes (Mateus-Rodríguez *et al.*, 2012; Sumarni *et al.*, 2013; Rykaczewska, 2016; Abdul *et al.*, 2018; Hajiaghahi Kamrani *et al.*, 2019;). Aeroponics is a type of hydroponics: plants are grown suspended with their roots periodically sprayed with a nutrient-rich solution. The basic principle of the aeroponic plant growing

is atomizing the plant with a mineral-rich nutrient water solution in the closed or semi-closed environment (Martirosyan, 2014; Rykaczewska, 2016b; Wang *et al.*, 2017).

Aeroponics provides opportunities for the selection of seed tubers without interrupting the vegetative growth of potatoes. The sufficient root zone provided full visual monitoring and easy access to the plant root system, careful management of the roots during multiple harvests of mini-tubers. Therefore, the number of seed tubers harvested from one potato plant was several times larger, which increased the net reproduction of high-value potato seed tubers (Mateus-Rodriguez *et al.*, 2013; Basiev *et al.*, 2019; Rykaczewska, 2016b). On average, 805 - 900 mini-tubers could be picked from the area of 1 m<sup>2</sup> (Abdullateef *et al.*, 2012; Rykaczewska, 2016b). Aeroponics allows researchers to develop fully automatic plant growing systems much more straightforward than substrate cultivation systems (Gabitov *et al.*, 2018; 2018b).

So far, this technique is not widespread and has not been adequately studied, especially in Russia. Several countries have recommended aeroponic cultivation as the most effective and convenient practice for growing plants than soil and other soilless techniques. Aeroponics based cultivation of potato seed tubers requires less water and energy (Tessema and Dagne, 2018). Aeroponics is recommended as a modern plant cultivation technique for potato seed production by the International Potato Center (CIP) (Mateus-Rodriguez *et al.*, 2013).

Although the approaches to the issue are generally the same, there is no standard practice on applying aeroponics for growing potato mini-tubers (Oraby *et al.*, 2015; Khaksar *et al.*, 2018; Zhuravleva *et al.*, 2018; Kaur *et al.*, 2019;). In this regard, the study aimed to assess the potential and improve the technology of growing disease-free potato seed tubers using an aeroponic plant.

## 2. MATERIALS AND METHODS:

The study was conducted in the laboratory of potato breeding and seed production at Bashkir State Agrarian University.

The source tubers were taken from visually healthy potato plants without frank disease symptoms. Potato tubers were placed in the thermal chamber, where the temperature was raised daily by 2°C from 25°C to 37°C during the first week. The potato tubers were kept in the thermal chamber for 14 weeks at a relative

humidity of 90%. For reducing the saprophytic microorganism population, the explants were washed with soap solution, rinsed with tap water then with reagent water type IV, and then treated with 70% ethanol solution. 0.1% diacid solution was used as a sterilizing solution. After sterilization, the explants were washed with distilled water.

The explants were appropriately tested for viral, viroid, bacterial diseases. So the material could be used for future grafting during the year, thereby reducing the costs of buying new disease-free material. The study used the Polymerase chain reaction (PCR) to diagnose viral diseases. This method offers high sensitivity as it has the advantage of producing results within 24 hours for some infections.

The cultivated plants were then grown in a nutrient medium (Figure 1).

The modified MS nutrient medium contained mineral salts and growth stimulants. PVP (polyvinylpyrrolidone) (5000-10000 mg/l) was used as an anti-oxidant. The nutrient medium was sterilized in an autoclave at 120 °C and 1 atm for 20 min. Micro-plants were grown at 3 thousand lx (16-hour photoperiod) at 25 °C and 70% of relative humidity. Then the potato micro-plants were placed in the aeroponic plant.

The study used the FTA 60 aeroponic phytotron for growing potato mini-tubers of the Alekseevsky variety (Khamaletdinov *et al.*, 2018). The FTA-60 aeroponic phytotron comprises a tray equipped with an aeroponic system (3); a rack (3); a pump station (1); a hydraulic storage unit (1); a solenoid valve (1); a container for spray solution (1); a digital timer (1); a submerged type pump (1). The phytotron can accommodate 60 plants. The plants were placed on a lightproof cover of the container with a built-in siphon tube, which was periodically one-quarter filled with the nutrient solution. The stem and leaves were above the cover and received lighting while the roots were under the cover. 1/5 of the roots were submerged in the solution, and the rest were suspended in the air between the solution and the cover. The hanging roots were recurrently sprayed with the nutrient solution through the atomizers fixed to the cover.

The study used the LED 101 W lamp under the 4:3 red and blue ratio for vegetative growth and 109 W lamp under the 3:1 ratio for tuber formation.

CFX96 Real-Time PCR Detection System was employed in the Polymerase chain reaction (PCR) method to diagnose potato virus infection.

### 3. RESULTS AND DISCUSSION:

The production of disease-free seed potato tubers consisted of three major stages: microcloning and growing of test-tube plants, cultivation of mini-tubers in the aeroponic phytotron, and planting potato tubers in the greenhouse.

The explant was isolated and introduced into the culture at the first stage. Under sterile conditions, the apical meristem, a culture of actively dividing cells, was isolated from the tip growth region and put in a nutrient medium. Apical meristems of 200-400 microns were isolated by applying micro-cuts to the plants in LAMSYSTEMS laminar flow cabinet under aseptic conditions using a 20x binocular magnifier.

The test tube plants were small (the length was 10 cm, the weight was 3-5 g), so the first three days of cultivation were crucial (Figure 2).

The study showed that the plants needed special care (watering and lighting) in that period. The root zone was kept moistened by periodic spraying of the nutrient solution. For spraying, the study used a high-pressure pump and atomizers. The plant was fixed with a soft clip or in lattice pots at the top of the container. Plants grown in the aeroponics system have a more robust root system than plants grown in the soil medium. The aeration of the roots resulted in quick absorption of nutrients. Thorough spraying of the nutrient solution is crucial in the process. It is necessary to cover all the roots with the solution droplets. The optimal droplet size for a large number of plants was 20-100 microns. This range allows small droplets to saturate the air, maintaining the required humidity level, and large droplets to fall on the plant roots and be absorbed. The solution was sprayed in the following order: at first, the nutrient solution was sprayed for 60 seconds every 15 minutes during the two weeks after planting, and then for 30 seconds every 15 minutes. This scheme eliminated drying out of the root system as the plant absorbed nutrients continuously, and reduced operating costs by saving electricity during the pump idle time.

Lighting and temperature regulation, as well as the composition of the nutrient solution, are essential in the aeroponic cultivation practice. At the initial stage (days 1-10), the lighting period was 24 hours. From day 11, the lighting period was reduced to 18 hours per day. By day 15, the plants gained vegetative weight and had a developed root system of light color. The length of

lighting was gradually reduced by 1 hour per day from day 16 to day 24. By the end of the period, the length of lighting was 10 hours per day. When the lower leaves dried (days 77-80), the light phase was reduced to 6-8 hours per day to stimulate tuber growth; this increased necrosis of the top and stimulated outflow of plastic substances from the top into the tubers.

The optimal temperature for the first three potato growth stages was 22-24/16-18°C day/night (Adikini *et al.*, 2016). The second half of the growing season (stages 4,5) requires decreasing temperature to 18-20°C during the day and to 14-16 °C at night (Adikini *et al.*, 2016). The temperature requirements were met in the study.

'Basaplant' soluble fertilizers served as a basis for the nutrient solution. 'Basaplant 15-10-15 +ME' and 'Basaplant 8-12-24 +ME' soluble fertilizers were used in 0.7:0.3 ratio during the first period of the plant growing. The solution-specific conductance was 0.8-0.9 millisiemens (mSm), the acidity (pH) was 7.7-6.9 from day 1 to day 16. The acidity level gradually decreased to 6.3 by day 14 and 5.7 by day 16. The optimal acidity level (pH 6,9-6,7) was maintained by adding the tap water with a high level of calcium salts and sodium bicarbonate. However, the yellowing of the lower leaves was observed in some plants on day 13; the number of plants with yellowed leaves increased on day 15. Therefore, the concentration of the nutrient solution was increased from day 17 to day 20, and the specific conductance was 1.1 mSm.

Ferrous sulfate was added to the nutrient solution to eliminate iron-induced chlorosis. However, the resultant solution appeared ineffective. Therefore, on day 20, the solution was enriched with NPP compounds such as ammonium nitrate, potassium sulfate, and double superphosphate as well as micro-fertilizers such as hydrogen borate and potassium permanganate. The specific conductance raised to 1.8 mSm, and the level was maintained to day 31.

'Basaplant 8-12-24 +ME' soluble fertilizer was applied from day 32 to day 51. The fertilizer contains little nitrogen (8%), phosphorus (12%), and much potassium (24%). The specific conductance reached 1.8-1.9 mSm, so the solution concentration was decreased by adding water until the specific conductance fell to 1.3-1.4 mSm.

'Basaplant 15-5-30' fertilizer was applied at the next stage (from day 54 to harvesting). The specific conductance was maintained at 1.3-1.4

mSm from day 54 to day 62. Then, the concentration of the nutrient solution was gradually decreased from day 63 to day 74, so the specific conductance fell to 1.1 mSm, from day 75 to day 79 the index fell to 1.0-0.9 mSm. The solution-specific conductance was kept constant (0.7-0.9 mSm) till the end of potato harvesting.

The study demonstrated that concentration indices should be monitored daily and be kept at the optimum level via adding fertilizers or water; the solution acidity should be managed by changing the nutrient solution or adding calcium carbonate or phosphoric acid. The optimum acidity for potato growing should be maintained at 6.8-7.4. The nutrient solution should be replaced at least twice a month.

Harvesting of potato mini-tubers started on day 96. The harvesting was over on day 108.

Thirty-four mini-tubers were picked from one potato plant (Figure 3). The maximum weight of a tuber was 78 g. The yield of the optimum sized tubers (20-30 mm in diameter) was 72.1 percent. Large tubers (more than 30 mm) were 9.3 %, small tubers (15-20 mm) were 11.4%, and smaller tubers (< 15 mm) were 7.2 %.

The yield of the optimum sized mini-tubers was 969 pcs from 1 m<sup>2</sup> of the FTA-60 aeroponic plant. The study analysed the costs for aeroponic production of seed potato mini-tubers, and the analysis showed that the cost of one seed potato minituber was 10 roubles.

Production of seed potato mini-tubers allows it to grow potato mini-tubers free from viral infections. The aeroponics technology optimizes access to air and carbon dioxide for potato growth as opposed to practices involving a substrate medium. The yield of the optimum sized mini-tubers was 969 pcs from 1 m<sup>2</sup> of the FTA-60 aeroponic plant. This figure is slightly higher than indices obtained by some growers *in regular medium* (805-900 mini-tubers per 1 m<sup>2</sup>) (Abdullateef *et al.*, 2012; Mateus-Rodriguez *et al.*, 2013).

Aeroponic production of potato mini-tubers requires systematic monitoring for temperature, humidity, light intensity, nutrients, pH, and mSm indices of the nutrient solution, spraying length, and time. The study used controls to adjust the parameters. Wireless sensors introduced into the aeroponic technology can ensure early detection of the parameter fluctuations. So, the farmer could monitor several parameters without using laboratory instruments (Lakhia *et al.*, 2018).

The optimal temperature for the first three

potato growth stages was 22-24/16-18°C day/night. The second half of the growing season (stages 4,5) requires decreasing temperature to 18-20°C during the day and to 14-16°C at night (Adikini *et al.*, 2016). The temperature parameters are consistent with the findings obtained by other researchers (Oraby *et al.*, 2015). The density of planting in the aeroponic unit is crucial for successful plant growth. In the study, tubers were planted at a density of 40 plants per 1m<sup>2</sup>. The plant density of 60 plants per m<sup>2</sup> showed the most significant results (Abdullateef *et al.*, 2012).

Several researchers have proved that aeroponics-based technology is effective in potato seed production (Mateus-Rodriguez *et al.*, 2013; Martirosyan, 2014; Rykaczewska, 2016b; Tessema and Dagne, 2018). At the same time, some growers point out (Chang *et al.*, 2012; Tican *et al.*, 2017) that the hydroponics technology is also a successful strategy for the production of seed potatoes. The hydroponic system employs a circulating nutrient solution; it has a positive effect on the average weight of mini-tubers per plant. Moreover, aeroponics technology requires a constant power supply and trained maintenance personnel throughout the crop growing season. Unreliable power supply and expensive boiler-based sterilization methods for growing media hinder the successful application of aeroponics technology. Mini-tubers produced in the sand culture hydroponic system were larger than grown based on the conventional aeroponics technology. The initial cost of the hydroponic unit and the cost of the sand hydroponics system per season is lower than that of the conventional aeroponics system. Sand hydroponics can replace the traditional system of quality seed potato production (Mbiri *et al.*, 2015) and general potato growing techniques in crop growing (Rodríguez-Delfín, 2011).

#### 4. CONCLUSIONS:

The aeroponic practice of seed potato production is a safe and economical way to produce mini-tubers. Less water and energy per volume unit of seed material are needed for aeroponic systems compared to the hydroponic growing practice. The aeroponic technology optimizes access to air and carbon dioxide for potato growth as opposed to practices involving a substrate medium. Aeroponics can prevent disease transmission as the diseased plant can be quickly removed. The technology eliminates soil-borne diseases and pest damage. Artificial conditions such as additional lighting can be easily

provided in the greenhouse for cultivating crop varieties grown in different regions.

## 5. REFERENCES

1. Abdul, M., and Zahir, M. (2018). Potato production in Pakistan: challenges and prospective management strategies -a review. *Pakistan journal of botany*, 0(5), 2077-2084.
2. Abdullateef, S., Böhme, M. H., and Pinker, I. (2012). Potato Minituber Production at Different Plant Densities Using an Aeroponic System. *XXVIII international horticultural congress on science and horticulture for people (ihc2010): international symposium on greenhouse 2010 and soilless cultivation*, 927, 429-436.
3. Adikini, S., Mukasa, S. B., Mwanga, R. O., and Gibson, R.W. (2016). Effects of Sweet potato feathery mottle virus and Sweet potato chlorotic stunt virus on the yield of sweetpotato in Uganda. *Journal of Phytopathology*, 164(4), 242-254.
4. Anisimov, B. V., Simakov, E. A., Oves, E. V., Yurlova, S. M., Chugunov, V.S., and Shatilova, O. N. (2014). Effectiveness of various schemes of the sequential technological process of the original potato seed production. Modern potato industry: state and development prospects. *Proceedings of the 6<sup>th</sup> interregional scientific and practical conference* (pp. 97-105). Cheboksary.
5. Anisimov, B. V., Smolegovets, D. V., and Shatilova, O. N. (2009). *Recommendations on in vitro micro-tubers growing technology and their use in the process of original seed production* (pp. 21). Russian Agricultural Academy, VNIKH, Moscow.
6. Ateş, S. Y., İnan, S., Ayyaz, M., Dündar, I., and Yabangülü, D. (2019). Effect Of Thermotherapy In Combination With Meristem Culture For Eliminating Potato Virus Y (PVY) And Potato Virus S (PVS) From Infected Seed Stocks. *Japs, Journal of Animal and Plant Sciences*, 29(2), 549-555.
7. Basiev, S.S., Gerieva, F.T., Alikov, A.A., and Bekmurzov, B.V. (2019). Growing minicubers using an aero-hydroponic method of cultivating potato plants. *Scientific Life*, 14(5 (93)), 595-602.
8. Chang, D.C., Park, C.S., Kim, S.Y., and Lee, Y.B. (2012). Growth and tuberization of hydroponically grown potatoes. *Potato Research*, 55(1), 69-81.
9. Dupuis, B., Bragard, C., and Schumpp, O. (2019). The resistance of Potato Cultivars as a Determinant Factor of Potato virus Y (PVY) Epidemiology. *Potato Research*, 62(2), 123-138.
10. Gabitov, I., Yukhin, G., Martynov, V., Galiullin, R., Kostarev, K., Negovora, A., and Baltikov, D. (2018). Modeling the Power Plant Operation to Optimize the Technological and Design Parameters of the Gas Generator Unit. *Journal of Engineering and Applied Sciences*, 13(S11), 8857-8864.
11. Gabitov, I. I., Mudarisov, S.G., Gafurov, I. D., Ableeva, A. M., Negovora, A. V., Davletshin, M. M., and Yukhin, G. P. (2018b). Evaluation of the Efficiency of Mechanized Technological Processes of Agricultural Production. *Journal of Engineering and Applied Sciences*, 13(S10), 8338-8345.
12. Hajiaghahi Kamrani, M., Rahimi Chegeni, A., and Hosseinniya, H. (2019). Effects of Different Growing Media on Yield and Growth Parameters of Potato Mini-tubers (*solanum Tuberosum* L.). *Communications in Soil Science and Plant Analysis*, 50(15), 1838-1853.
13. Inglis, D. A., Gundersen, B., Beissinger, A., Benedict, C., and Karasev, A. V. (2019). Potato virus Y in Seed Potatoes Sold at Garden Stores in Western Washington: Prevalence and Strain Composition. *American Journal of Potato Research*, 96(3), 235-243.
14. Kaur, R. P., Minhas, J. S., Singh, S., Singh, A. K., and Singh, R. K. (2019). High-density planting of potato (*Solanum tuberosum*) mini-tubers for increased seed productivity. *Indian Journal Of Agricultural Sciences*, 89(6), 989-993.
15. Khaksar, E. V., Romanova, M. S., Leonova, N., and Novikov, O. O. (2018). Virus-free potato production at aero-hydroponic plants at SibNIISH - branch of the Siberian Scientific Center for Scientific and Technical Research of the Russian Academy of Sciences. *Actual problems of potato growing: fundamental and applied aspects. Materials of the All-Russian scientific and practical conference with international participation* (pp. 270-274). Moscow.
16. Khamaletdinov, R., Gabitov, I., Mudarisov, S., Khasanov, E., Negovora, A., Martynov, V., ... and Shirokov, D. (2018). Improvement in engineering design of machines for biological crop treatment with microbial products. *Journal of Engineering and*

- Applied Sciences*, 13(S8), 6500-6504.
17. Khelifa, M. (2019). Detection and quantification of Potato virus Y genomes in single aphid stylets. *Plant Disease*, (ja), 103(9), 2315-2321.
18. Khutinaev, O. S., Anisimov, B. V., Yurlova, S. M., and Meleshin, A. A. (2016). Mini tubers by the method of aero-hydroponics. *Potatoes and vegetables*, 11, 28-30.
19. Lakhia, I.A., Gao, J., Syed, T.N., Chandio, F.A., and Buttar, N.A. (2018). Modern plant cultivation technologies in agriculture under a controlled environment: A review on aeroponics. *Journal of plant interactions*, 13(1), 338-352.
20. Lakhia, I. A., Jianmin, G., Syed, T., Chandio, F., Buttar, N., and Qureshi, W. (2018). Monitoring and Control Systems in Agriculture Using Intelligent Sensor Techniques: A Review of the Aeroponic System. *Journal of Sensors*, 2018, 1-18.
21. Li, J., Chen, H., Li, J., Zhang, Z., Blystad, D.R., and Wang, Q.C. (2018). Growth, microtuber production, and physiological metabolism in virus-free and virus-infected potato in vitro plantlets grown under NaCl-induced salt stress. *European journal of plant pathology*, 152(2), 417-432.
22. Martirosyan, Yu. Ts. (2014). Aeroponic technologies in primary potato seed production - advantages and prospects. Biotechnology methods in potato breeding and seed production. *Proceedings of the international scientific and practical conference. Collection of scientific papers. Series 'Potato production'* (pp 175-179).
23. Mateus-Rodríguez, J., de Haan, S., Andrade-Piedra, J., Maldonado, L., Hareau, G., Barker, I., ... and Pereira, A. (2013). Technical and economic analysis of aeroponics and other systems for potato mini-tuber production in Latin America. *American journal of potato research*, 90(4), 357-368.
24. Mateus-Rodríguez, J., De Haan, S., and Barker, I. (2012). Response of Three Potato Cultivars Grown in a Novel Aeroponics System for Mini-Tuber Seed Production. *2nd International Symposium on Soilless Culture and Hydroponics* (pp. 361-367). Puebla. MEXICO.
25. Mbiri, D., Schulte-Geldermann, E., Otazu, V., Kakuhenzire, R., Demo, P., and Schulz, S. (2015). *An Alternative Technology for Pre-basic Seed Potato Production—Sand Hydroponics* (pp. 249). Potato and Sweetpotato in Africa: Transforming the Value Chains for Food and Nutrition Security.
26. Ogero, K., Kreuze, J., McEwan, M., Luambano, N., Bachwenkizi, H., Garrett, K., and van der Vlugt, R. A. A. (2019). The efficiency of insect-proof net tunnels in reducing virus-related seed degeneration in sweet potato. *Plant Pathology*, 68(8), 1472-1480.
27. Oraby, H., Lachance, A., and Desjardins, Y. (2015). A low nutrient solution temperature and the application of stress treatments increase potato mini-tubers production in an aeroponic system. *American journal of potato research*, 92(3), 387-397.
28. Oves, E. V., Kolesova, O. S., and Fenina, N.A. (2014). In vitro micro-tubers cultivation using container technology. Modern Potato Industry: State and Development Prospects. *Proceedings of the 6th Interregional Scientific and Practical Conference* (pp. 111-115). Cheboksary.
29. Priegnitz, U., Lommen, W. J., van der Vlugt, R. A., and Struik, P. C. (2019). Impact of Positive Selection on Incidence of Different Viruses During Multiple Generations of Potato Seed Tubers in Uganda. *Potato Research*, 62(1), 1-30.
30. Rodríguez-Delfín, A. (2011). Advances of hydroponics in Latin America. In *II International Symposium on Soilless Culture and Hydroponics* (pp 23-32).
31. Rykaczewska, K. (2016). The potato minituber production from microtubers in aeroponic culture. *Plant, Soil, and Environment*, 62(5), 210-214.
32. Rykaczewska, K. (2016b). Field performance of potato mini-tubers produced in aeroponic culture. *Plant, Soil, and Environment*, 62(11), 522-526.
33. Singh, R.K., Buckseth, T., Tiwari, J.K., Sharma, A.K., Singh, V., Kumar, D., and Chakrabarti, S. (2019). Seed potato (*Solanum tuberosum*) production systems in India: A historical outlook. *Indian Journal Of Agricultural Sciences*, 89(4), 578-587.
34. Sumarni, E., Suhardiyo, H., and Seminar, K.B. (2013). Seed Potato Production Using Aeroponics System with Zone Cooling in Wet Tropical Lowlands. *2nd Asia Pacific Symposium on Postharvest Research Education and Extension (APS)*, 1011, 141-145.
35. Tessema, L., and Dagne, Z. (2018). Aeroponics and Sand Hydroponics: Alternative Technologies for Pre-Basic Seed Potato Production in Ethiopia. *Open*



- Agriculture*, 3(1), 444-450.
36. Tican, A., Chiru, N., Cioloca, M., and Bădăraș, C.L. (2017). Obtaining Mini-tubers By Applying Hydroponic Culture. *Romanian Agricultural Research*, 35, 141-146.
  37. Wang, K., He, W., Ai, Y., Hu, J., Xie, K., Tang, M., and Zaag, P.V. (2017). Optimizing seed potato production by aeroponics in China. *Philippine Journal of Crop Science*, 42(1), 69-74.
  38. Zhuravleva, E.V., Kabunin, A.A., and

Kabunina, I.V. (2018). Aspects of the organization of selection and seed production of potatoes in Russia - problems and possible solutions. *Achievements of science and technology of the agro-industrial complex*, 32(10), 5-9.

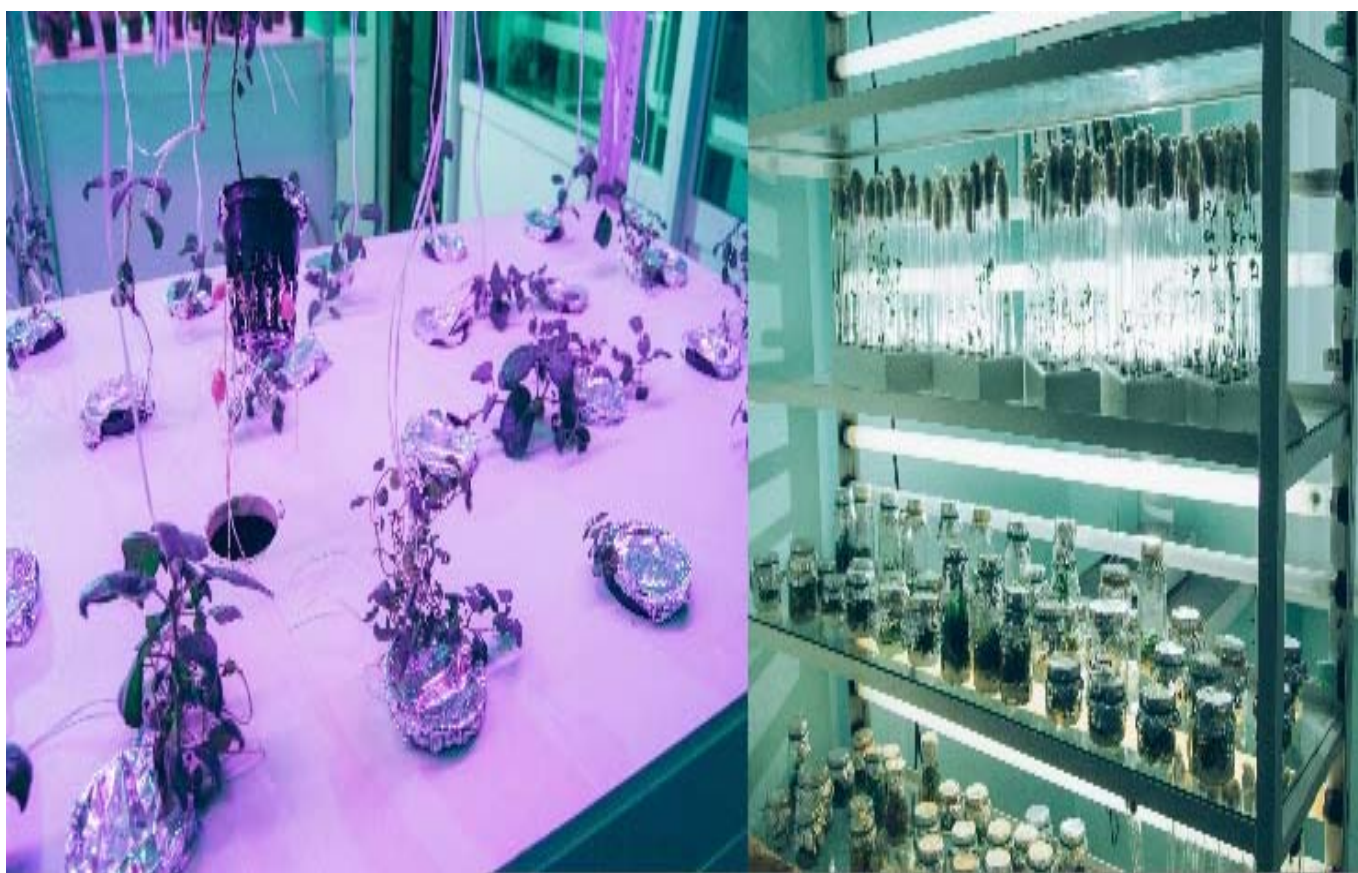


**Figure 1.** Potato growing place



**Figure 2.** Potato samples in test tubes



**Figure 3.** Mini potato tubers grown in the aeroponic plant.



**O USO DE BIOSTIMULANTE PARA AUMENTAR O GANHO DE PESO CORPORAL DE FRANGOS****THE USE OF BIOSTIMULANT FOR INCREASING THE BODY WEIGHT GAIN OF CHICKENS****ВЛИЯНИЕ БИОСТИМУЛЯТОРА НУКЛЕОСТИМ НА ЖИВУЮ МАССУ ЦЫПЛЯТ БРОЙЛЕРОВ**

DOLININ, Ilgiz\*; BAZEKIN, George; SKOVORODIN, Evgeny; SHARIPOV, Almaz; CHUDOV, Ivan

Federal State Budgetary Educational Establishment of Higher Education "Bashkir State Agrarian University",  
Department of morphology, pathology, pharmacy, and non-communicable diseases. Russia.

\* Corresponding author  
e-mail: dolininil@rambler.ru

Received 20 March 2020; received in revised form 16 May; 29 May 2020; accepted 20 June 2020

**RESUMO**

A avicultura ocupa um lugar especial garantindo a demanda do consumidor pelos produtos da indústria, que fornece à população produtos alimentares essenciais, tais como ovos e carne, que contêm micro e macro nutrientes vitais, proteínas, lipídios e vitaminas. Portanto, as questões da alimentação racional e economicamente viável de aves de galinheiro, como galinhas de corte, são tarefas urgentes. Também é essencial encontrar métodos eficazes de aplicação para corrigir a resistência natural e a reatividade imunológica e biológica das aves. O objetivo desta pesquisa é estudar o efeito do estimulante biológico Nucleostim no crescimento e desenvolvimento de galinhas, parâmetros hematológicos e imunológicos do sangue de aves. Na aplicação de Nucleostim, o ganho de peso vivo de frangos aumentou 9,7%. No final do experimento, a habitabilidade dos pintos do grupo experimental tratado com Nucleostim chegou a 88%, comparado com os 72% do grupo de controle. O uso de Nucleostim teve um efeito estimulante no fígado de galinhas, contribuindo para o desenvolvimento do timo no contexto da distrofia geral. Assim, Nucleostim melhora a habitabilidade dos pintinhos e aumenta o ganho de peso corporal. O estimulante biológico Nucleostim como agente adaptógeno, anabólico e imunoestimulador é promissor para encontrar novos medicamentos que melhorem a saúde e a produtividade das aves.

**Palavras-chave:** Galinhas, crescimento e desenvolvimento, habitabilidade, Nucleostim, avicultura, resistência

**ABSTRACT**

Poultry farming holds a special place in ensuring the products that the consumers demand, it provides the population with essential food products, such as eggs and meat, that contain vital micro and macronutrients, proteins, lipids, and vitamins. Therefore, the issues of rational, economically feasible feeding of meat poultry, namely broiler chickens, are an urgent task. It is also essential to find effective methods of their application in order to correct the natural resistance and immune and biological reactivity of birds. The purpose of this research is to study the effect of the biological stimulant-Nucleostim on the growth and development of chickens, hematological, and immunological parameters of the blood of birds. This Biostimulant is a purified bovine spleen extract containing at least 1 mg / ml of low molecular weight peptides (nucleotides and nucleosides) formed as a result of autolysis, using dry whey and diatomite as fillers. On the application of Nucleostim, the gain in live weight of chickens was increased by 9.7%. At the end of the experiment, the livability of the chicks of the experimental group treated with Nucleostim came up to 88%, compared with the 72% of the control group. The use of biostimulant had a stimulating effect on the liver of chickens confirmed by the research results presented in the article, as well as contributed to the development of the thymus in the setting of general dystrophy. Thus, it improved chick livability and increased body weight gain. The biological stimulant-Nucleostim as an adaptogenic, anabolic, and immunostimulatory agent is promising for finding new drugs that improve the health and productivity of poultry.

**Keywords:** Chickens, growth and development, livability, Nucleostim, poultry farming, resistance.

## АННОТАЦИЯ

Птицеводство занимает особое место, так как обеспечивает население необходимыми пищевыми продуктами, такими как яйца и мясо, которые содержат жизненно важные микро- и макроэлементы, белки, липиды и витамины. Поэтому вопросы рационального, экономически целесообразного кормления мяса птицы, а именно цыплят-бройлеров, являются актуальной задачей. Также важно найти эффективные методы их применения для коррекции естественной резистентности и иммунной и биологической реактивности птиц. Целью данного исследования является изучение влияния биологического стимулятора-Нуклеостима на рост и развитие цыплят, гематологические и иммунологические показатели крови птиц. Этот биостимулятор представляет собой очищенный экстракт бычьей селезенки, содержащий не менее 1 мг/мл. низкомолекулярных пептидов (нуклеотидов и нуклеозидов), образованных в результате автолиза, с использованием сухой сыворотки и диатомита в качестве наполнителей. При применении Нуклеостима прирост живой массы цыплят увеличился на 9,7%. В конце эксперимента выживаемость цыплят экспериментальной группы, получавших Нуклеостим, достигла 88% по сравнению с 72% контрольной группы. Применение биостимулятора оказало стимулирующее действие на печень кур, подтвержденное результатами исследований, представленными в статье, а также способствовало развитию вилочковой железы в условиях общей дистрофии. Таким образом, это улучшило жизнеспособность цыплят и увеличило прирост массы тела. Биологический стимулятор Нуклеостим как адаптогенное, анаболическое и иммуностимулирующее средство является перспективным для поиска новых лекарств, улучшающих здоровье и продуктивность домашней птицы.

**Ключевые слова:** цыплята, рост и развитие, живность, нуклеостим, птицеводство, устойчивость.

## 1. INTRODUCTION:

Poultry farming provides the population with essential food products – eggs and meat that contain easily digestible proteins, lipids, trace elements, and vitamins. Therefore, the issues of rational, economically feasible feeding of poultry, namely broilers, appear relevant. Preliminary results of 2019 indicate that the volume of poultry meat production in Russia has grown by 1.3%: from 4.98 million tons in 2018 to 5.045 million tons. Poultry meat farming surpasses all other livestock industries in terms of feed conversion. The production of 1 kg of broiler meat requires 1.5 and 2.5 times less feed than the same amount of pork and beef. In the world ranking of poultry producing countries, Russia is among the top five countries. The main factors of production growth are the implementation of innovative processes and comprehensive modernization of poultry farming within the framework of the national project “Development of agriculture” and the State program for agricultural development (Government of the Russian Federation, 2012; Buyarov and Buyanov, 2015; Fisnin *et al.*, 2017; Buyarov *et al.*, 2018).

World meat production is constantly increasing. In 2016, it was 259.3 million tons, and in 2019 it raised to 301 million tons. The production of meat of all animal species in the world increased sevenfold between 1950 and 2019. The maximum

growth rate for the same period is in line with the production of poultry meat – 11.8-fold. In 2018, in the structure of world production, pork accounted for 37.4% of meat in the slaughter-weight; poultry – for 34.1%; beef – for 22.2% and lamb – for 4.5%. According to the FAO forecast for 2011-2025, the annual increase in meat will be 3.1% for poultry, 2.6% for pork, and 1.3% for beef. The most significant amounts of poultry meat consumption are observed in the UAE, Israel, Hong Kong, the United States, Singapore, and Brazil (Gharahveysi *et al.*, 2020).

Estimates show that following the results of 2019, poultry meat production in the world will come up to 106 million tons. Of these, 20.111 million tons are produced in the United States; 18.517 – in China; 11.500 million tons – in Brazil. The E.U. indicator will reach 12.738 million tons, with an increase of 188 thousand tons over the year. By 2020, Brazil will be among the largest exporters of poultry meat, taking the leading position, followed by the United States, China, the European Union, and Russia.

The viability of broiler chickens is an essential factor in determining the profitability of poultry farming. Chicken embryo tissues contain a high proportion of polyunsaturated fatty acids in the lipid fraction and therefore need antioxidant protection. The antioxidant system of the developing embryo and newly hatched chicken includes antioxidant enzymes, water-soluble

antioxidants, fat-soluble antioxidants, and selenium. Natural antioxidants play a pivotal role in the maternal diet affecting the development of chicken embryos and their viability in their early neonatal life (Gharahveysi *et al.*, 2020).

Upon zootechnical and economic indicators, floor-grown broilers of the cross Ross-308 were more effective than broilers of the cross Hubbard f 15. The profitability of production and sales of meat from Ross-308 cross broilers was higher than that of Hubbard f 15 cross broilers by 1.9% (Buyarov *et al.*, 2018).

The level of metabolic energy in poultry feed is one of the most critical indicators that ensure optimal growth and development of the body (Fisinin, 2013). Various feed additives, fats, and oils are used to optimize the composition of feed for broilers in terms of this indicator. They have the highest caloric content among all types of feedstock, and therefore constitute the main source of energy for poultry (Fisinin *et al.*, 2017). When choosing a food source for feeding broilers, in some cases, it is necessary to take into account not only the level of live weight gain, feed conversion, and carcass quality but also the indicators that characterize the quality of the meat itself.

Boosting the production of eggs and poultry meat is based on a significant increase in the productivity of birds with a simultaneous increase of the poultry stock with a high payment for feed by meat products and a rise in labor productivity (Nozdrin *et al.*, 2018).

However, at present, great importance is attached not only to increase the number of poultry, but also, mainly, to increase their viability, the resistance of the organism, productivity, improving meat qualities, and egg production (Fisinin *et al.*, 2017). The latter depends on the genetic-environmental interaction.

The use of biological stimulants is one of the most promising areas in poultry farming (Dementyev *et al.*, 2018).

Several authors cite data on studies of the nature of autarcesis of birds on increasing live weight and egg production, preserving poultry stock, viability, and its variability as affected by the external and internal environment. Despite this, many aspects of the presented problem remain unexplored, such as improving the quality of meat, reducing the time of poultry rearing, increasing the degree of mineralization of the organic matrix of bone tissue and bone density in the process of growth and development (Buyarov *et al.*, 2012,

2018; Fisinin, 2013; Ahmadiet *al.*, 2018; Jahanian and Ashnagar, 2018; Nozdrin *et al.*, 2018; Rubio *et al.*, 2019).

Despite the available information on the use of biological stimulants, this issue remains relevant. It is also important to find effective methods of their application in order to correct the natural resistance and immune and biological reactivity of birds.

Poultry farming plays a significant role in providing the population with high-quality food. Interest in this industry is constant both in large specialized enterprises and on small farms. At the same time, the species range of captive birds, from ostriches to quails, is expanding, although industrial production of meat and eggs of chickens is more traditional for agriculture (Buyarov *et al.*, 2018). Also, to achieve that technological capacities have been established, conditions for keeping and feeding poultry have been brought about. Low feed consumption, a short period of reproduction, the plasticity of an organism of hens and chicks are the advantages of breeding poultry (Fisinin, 2013).

However, the genetic potential of the birds' organism for meat production is not enough. One of the keys to an extensive increase in poultry production capacity is to find opportunities for the use of biologically-active preparations, i.e., medicinal substances with bioactive properties and a regulating effect on the growth and development of birds, the intensity of exchange processes; enhancing the functional activity of organs and body systems; increasing autarcesis of the organism of birds and at the same time safe for own body and its products to humans and the environment (Julean *et al.*, 2013).

In connection with the above, the research objective was to study the effect of the biological stimulant biostimulator on the growth and development of chickens, hematological, and immunological parameters of the blood of birds.

Biostimulant is a purified bovine spleen extract containing at least 1 mg/ml of low molecular weight peptides (nucleotides and nucleosides) formed as a result of autolysis, using dry whey and diatomite as fillers.

## 2. MATERIAL AND METHODS:

One hundred broiler chickens of the crosses ROSS 308 and Rodonit were used for the research. The conditions for conducting

experiments were identical for the control and experimental groups, and they meet the requirements of "Sanitary rules for the construction, equipment, and maintenance of experimental and biological clinics (vivariums)" No. 1045-73 as well as of GOST (All-Union State Standard) R 53434-2009 "Principles of good practice" corresponding to international GLP standards. The diet of the young birds consisted of a balanced complete feed PC-2 produced by the Bogdanovich feed mill (Table 1). Water was supplied *ad libitum*.

Biopreparation was used in the study – a water-soluble premix for poultry containing natural growth stimulants represented by low molecular weight biologically active peptides–nucleosides and nucleotides. Bioadditive was introduced into the diet of birds in the right concentrations and fed with the feeding stuff according to the instructions for use – broiler chickens: 10 g/kg of feed every other day for ten days. The optimal dose of biopreparation was 10 g/kg of feed. The investigational product mixed with feed was given daily for ten days.

The live weight was determined by individual weighing using laboratory electronic scales AND GF-600. The broiler stock was weighed from the first to the ninth week of research (Figure 1). The chick livability was determined by taking into account the mortality rate.

The development of internal organs was determined by necropsy from the 30<sup>th</sup> to 38<sup>th</sup> days of chickens' life at the Department of morphology, pathology, pharmacy, and non-infectious diseases of Bashkir state agrarian university (Russia) with further evaluation of the weight and size of internal organs.

Anatomical and morphological methods were used to measure the size, weight, and topography of internal organs (Skovorodinet *al.*, 2019). The central organs of the bird's immune system (thymus, spleen, Bursa), heart, and liver were used as research materials. The investigational organs were weighed by analytical laboratory scales AND GF-600.

Based on the data obtained, the relative weight of the organ was calculated.

Modern clinical assessment of general condition, thermometry, assessment of mucous membranes, pulse rate and breathing, assessment of feather cover, hematological (erythrocytes, hemoglobin, color index, leucocytes) and biochemical research

methods (total protein, protein fractions, total bilirubin, AST, ALT) were used in the work.

Hematological studies of whole blood were performed using an automatic hematological analyzer Abacus Junior 5Vet (Diatron Messtechnik GmbH), which determines 22 hematological parameters: leucocytes,  $10^9/l$ , lymphocytes, %, lymphocytes,  $10^9/l$ , monocytes %, monocytes,  $10^9/l$ , neutrophils, %, neutrophils,  $10^9/l$ , eosinophils %, eosinophils,  $10^9/l$ , basophils, %, basophils,  $10^9/l$ , erythrocytes,  $10^{12}/l$ , hemoglobin, g/l, hematocrit, %, mean corpuscular volume, fl, mean contents of hb in er., pg, mean hb conc. in er, g/l, the distribution range of erythrocytes population, %, platelets,  $10^9/l$ , platelet count, %, average platelet volume, fl, distribution range of platelets population, %).

Verification and calibration of the hematological analyzer were carried out within the framework of in-laboratory control with the formulation of studies of standardized whole blood samples with normative and pathological values of indicators issued by Diatron Messtechnik GmbH. Biochemical blood tests were performed using a semi-automatic biochemical blood analyzer StatFax 1904+ (Awareness Technology Inc.,) using standardized reagents Vital Diagnostics Spb.

### Statistical analyses

The obtained data were statistically processed using Microsoft Excel.

### Ethical issues

The experiments are approved by the Commission on Bioethics of Bashkir state agrarian University established to monitor and evaluate the policy of working with laboratory animals, methodological and experimental base for the humane treatment of animals and their rational use, guided by the legislation of the Russian Federation, the provisions of the "European Convention for the protection of vertebrates used for experimental and other scientific purposes", as well as the provisions of the Guide for the Care and Use of Laboratory animals and other rules of international law which regulate the maintenance and use of laboratory (experimental) animals (Protocol No. 18-2020 of January 14, 2020).

## 3. RESULTS AND DISCUSSION:

The immunobiology of the animal organism during fetal development is characterized by certain features. First of all, during this period of ontogenesis, germinal organs are formed and function – the placenta, gall bladder, allantois, and amnion, which perform metabolic and fetus-protecting functions. Protection of the fetus by temporary germinal organs involves maintaining the immunological balance of the mother and the fetus and preventing infection of the latter. The chicken organism is also able to transmit its own antibodies transovarially. Poor supply of the fetus with maternal antibodies in itself implies the autoreproduction of antimicrobial factors by the fetus. The antimicrobial activity of autarcesis plays an important role in the life of chickens.

As known, many biological stimulants have an anabolic effect due to the increased formation of nucleic acids and protein in the liver and muscles. Therefore, the live weight of broiler chickens was one of the main indicators in the study of the properties of biopreparation. The values of the live weight of birds when compared with the norm and control, the average daily gain, as well as the livability of the broiler stock for the entire time of the experiment, were paid attention to (Julean *et al.*, 2013).

The experiment conducted involved adding the biological product Nucleostimat a dose of 10 g/kg of feed into the diet of broiler chickens of the cross ROSS-308 in order to stimulate growth as well as protect them from diseases during rearing.

Day-old chickens were divided into 2 groups. The first group totaling 50 birds was fed standard feed with the addition of vitamins, trace elements, and biopreparation at a dose of 10 g/kg. The second group consisting of 50 chickens, was fed standard feed and served as the control.

It is known that in the postnatal period, the growth of chickens depends on the initial weight of biologically active tissue. The live weight of the cross ROSS 308 chickens was  $40.5 \pm 0.4$  g in the experimental group and  $39.9 \pm 0.3$  g in the control group.

Chickens are markedly affected by an indoor microclimate. Constant temperature (in the first days up to 32°C), light regime, humidity, and air exchange were maintained in the poultry house (Dementyev *et al.*, 2018).

The development of chickens is affected by compound poultry feed (crumb) with the correct calorie-protein ratio and their enrichment with vitamins, trace elements, and antibiotics, which

increases the biological usefulness of the feed (Salem *et al.*, 2018).

It is known that getting weighty chickens in the first week of fattening can affect the degree of increase in body weight in the following weeks (Table 2).

The table shows that during the first week of life, the increase in live weight of chickens fed biopreparation increased by 9.7% compared with the control. After three weeks, chickens treated with bioadditive overweighed the control by 87.4 g, and in 5 weeks, the average live weight of broiler chickens exposed to biopreparation was  $1060.0 \pm 15.0$  g and of control chickens –  $848.5 \pm 15.0$  g. The chickens of the experimental group overweighed the control ones by 211.5 g.

At the end of the study, that is, at the age of 9 weeks, the average live body weight of one chick fed biostimulator was  $2180.0 \pm 50.0$  g, and of the control –  $1850.5 \pm 48.5$  g.

Thus, the chickens exposed to bioadditive overweighed the chickens of the control group by 290.5 g.

At the end of the experiment, the livability of the experimental group of chickens was 88%, and of the control group – 72%.

As a result of the use of bioadditive at a dose of 10 g/kg of feed, there has been an overall survival growth of chickens and an increase in the live weight gain.

The second set of experiments was performed for therapeutic purposes with 36 64-day-old chickens of the cross Rodonit which were rejected due to general dystrophy (failure in growth, weight, development) and divided into three following groups of 12 birds each:

1. Control
2. bioadditive at a dose of 10 g/kg of feed
3. bioadditive at a dose of 5 g/kg of feed.

The chickens were weighed at the age of 64, 74, 84, and 94 days. The data obtained are shown in Table 3.

Analyzing the obtained data, it can be observed that the chickens of the experimental group had a significantly high average daily increase compared to the chickens of the control group. The highest results were observed in the group of chickens fed biopreparation at a dose of 10 g/kg of feed. So, throughout the research, the increase in live weight of chickens in that group was 104.4%, in the group of chickens exposed to biological stimulator at a dose of 5 g/kg of feed –

93.3% compared to chickens in the control group.

The chick livability in the experimental and control groups was similar. In the control group, nine chickens lived through the experiment, and the mortality rate was 20%; in the second group, 11 chickens survived, or 91.6%, and in the third group – 90%.

The impact of bioadditive on the development of internal organs was studied on 30-38 days old chickens. Four groups of 10 birds each were formed. The test stock was fed standard mixed feed. In addition, to feed, the biostimulant under investigation was given daily for ten days. Group 1 – biological stimulator (10 g/kg of feed). Group 2 – biological stimulator (5 g/kg of feed). Group 3 – biological stimulator (15 g/kg of feed). Group 4 – control.

The effect of the biopreparation was evaluated by the condition of the digestive organs (liver, glandular stomach) and the immune system (thymus, Bursa). Special attention was paid to the central immune organs of birds since they all grow rapidly in the first months of life and reach maximum development: the thymus by 3.5-4 months, and the Bursa by 4-4.5 months. Then thymus gradually mummifies upon reaching puberty.

Autopsies were performed from the 30<sup>th</sup> to 38<sup>th</sup> day of the life of chickens at the Department of morphology, pathology, pharmacy, and non-infectious diseases of Bashkir state agrarian university. No pathological changes were found in the organs. The weight and size of internal organs were evaluated. The study data are shown in Table 4.

Table 4 shows that in three experimental groups, the weight of the internal organs of broiler chickens is greater than in the control group. The most significant increase in organs was observed in chickens exposed to bioadditive at a dose of 10 g/kg of feed.

When conducting research for therapeutic purposes on 64-day-old cross Rodonit chickens with clinical signs of general dystrophy, deficiency in live weight, and failure in growth and development were found. According to domestic and foreign sources, there is a correlation between the condition of some internal organs and the overall condition of the body of chickens. So, when the depletion increases, the thymus lobes grow less, and when the feed ration of birds improves, the gland regeneration begins in parallel (Skovorodin *et al.*, 2013).

Studies have shown that throughout the

experiment, the development of the thymus was registered in all groups of chickens. Apparently, this was due to improved feeding during the study period.

The absolute weight of the thymus in the control group of chickens was  $0.8 \pm 0.07$  g, and in chickens fed biopreparation at a dose of 10 g/kg of feed –  $1.006 \pm 0.03$  g which was 0.206 g more.

Thus, the use of biostimulator contributed to the development of the thymus in chickens in the setting of general dystrophy.

The absolute weight of the liver of Rodonit cross chickens that were treated with biopreparation at doses of 10, and 5 g/kg of feed at the age of 64-days was  $12.25 \pm 0.35$  and  $10.85 \pm 0.18$  g, respectively, which was 2.05 and 0.65 g more than the liver weight of the control chickens.

In such a way, bioadditive has a stimulating effect on the liver of chicks of experimental and control groups. At the same time, the relative weight of the organ is less than in control, which implies physiological hepatomegaly.

The blood system is directly involved in specific and non-specific reactions of the body affecting its resistance and reactivity. Blood readily responds to any exposure and serves as an important criterion for the physiological condition of the animal body and the metabolic rate.

The study of morphological and immunological parameters of chicken blood was carried out by many researchers. However, there are splits over the dynamics of blood indicators of young chickens. It was found that they changed depending on the age and physiological state of chickens, which indicated a different intensity of metabolic processes in each period of their life, which was confirmed by our research.

The stimulatory action of various biostimulants on hematopoiesis, and especially on leukopoiesis, has been mentioned by many scientists.

Morphological studies have shown that the use of biostimulator did not have any significant impact on the dynamics of indicators of red and white blood of birds. During the experiment, they were within the physiologically normal state for that age and type of production.

The minimum content of red blood cells and hemoglobin was registered at the age of 30 days (Table 5), which was consistent with the data of domestic and foreign scientists. By the 40<sup>th</sup> day of the life of chickens (in the first set of

experiments), the indicators increased on average by 14.8%. After the treatment with biopreparation, the content of red blood cells in the second experimental group (Nucleostim 10 g/kg of feed) increased by 16% compared to the control.

At the age of 40 days, the difference in the content of red blood cells in the experimental and control groups raised up to 10.5-31.6% and of hemoglobin – to 10.8-24.6% (Table 5).

In the blood of experimental and control groups of chickens, the content of white blood cells was found to be quite high, which was typical for that age. The leukogram of the chickens of experimental and control group showed the ratio of individual white blood cells within the physiological range, but some specific features were observed. For example, the percentage of eosinophils and basophils in the control group was 20% higher than in the experimental group, which indicated a more pronounced sensitization of chickens in that group (by 30 days of age, the chickens were challenged with five different vaccines). At the same time, a slight increase in the number of lymphocytes (by 3-8%) in the blood of chickens of the experimental groups compared to the control indicates the mobilization of the immune system in response to exposure, including the use of the compounds under investigation (Table 6).

An increase in the level of lymphocytes in the blood indicates an enhancement in the specific immunity of birds since these cells are the main executive element in the manifestation of cellular and humoral protection of the body.

It is known that many biological stimulants can increase the phagocytic activity of white blood cells. This increases both the number of phagocytic cells and the number of microbes they absorb (Tang *et al.*, 2007).

To characterize the system of non-specific immunity in birds when exposed to the investigational product bioadditive the functional activity of pseudo-eosinophils, monocytes and platelets of the whole blood of chicks in phagocytic reactions (for phagocytic number and phagocytic index) and the reduction reaction of nitro blue tetrazolium (spontaneous and latex-induced NBT-test) and the level of complement in blood serum have been studied.

The results of the research are shown in Table 7, analyzing which one can see that before the experiment, the phagocytosis indicators and the level of complement in the blood of chickens were within the physiological range. When re-analyzing the blood of animals after the use of the

compounds under investigation, there were significant deviations in the indicators of the experimental groups compared to the control (Table 7).

In groups using biostimulator, there was an increase in the absorption activity of white blood cells, and in the level of complement compared to the control group. The complementary activity of the blood serum of chickens in those groups increased by 24.6 and 25.6% compared to the control group. The average number of latex particles absorbed by a single cell (PHI) was 23% higher than in the control group. The activity index of pseudo-eosinophils in the "spontaneous" test increased by 50% compared to the control, and by 6.7% when induced by latex, respectively. The optimal effect was observed at a dose of 10 g/kg of feed. Reducing the dose to 5 g/kg of feed led to a slight decrease in the functional activity of phagocytes.

Thus, the use of bioadditive had a stimulating effect on the phagocytic activity of pseudo-eosinophils, monocytes, and platelets of the blood of birds and on the complement system – a non-specific factor of humoral immunity. The new biological stimulant Nucleostim is recommended for use in veterinary medicine as an adaptogenic, anabolic, and immunostimulating agent and is promising for finding new drugs that improve the health and productivity of poultry.

Many biological stimulants have an anabolic effect due to the increased formation of nucleic acids and protein in the liver and muscles. Therefore, the live weight of broiler chickens was one of the main indicators in the study of the properties of biopreparation. Attention was drawn to the values of the live weight of birds when compared with the norm and control, the average daily gains as well as the livability of the broiler stock throughout the experiment (Julean *et al.*, 2013; Khaziev *et al.*, 2018; Santos *et al.*, 2019).

The development of chickens is affected by compound poultry feed (crumb) with the correct calorie-protein ratio, their enrichment with vitamins, trace elements, and antibiotics, which increases the biological usefulness of the feed (Sharipova and Khaziev, 2015; Salem *et al.*, 2018).

It is known that getting weighty chickens in the first week of fattening can affect the degree of increase in body weight in subsequent weeks (Buyarov *et al.*, 2018). In the first week of life, the live weight gain of chickens treated with bioadditive increased by 9.7% compared with the control chickens. After three weeks, the chickens exposed to biostimulator overweighed the control

ones by 87.4 g, and after five weeks – by 211.5 g.

At the end of the study, that is, at the age of 9 weeks, the average live body weight of one chick treated with biostimulator was  $2180.0 \pm 50.0$  g and of the control –  $1850.5 \pm 48.5$  g. The chickens exposed to biostimulator outweighed the control chicks by 290.5 g. At the end of the experiment, the livability of the experimental group of chickens was 88%, and of the control group – 72%.

As a result of the use of bioadditive at, a dose of 10 g/kg of feed, there is an increase in the livability of chickens and an increase in their live weight gain. The livability of chickens in the experimental and control groups was similar. In the control group, nine chickens lived through the experiment, and the mortality rate was 20%; in the second group, 11 chickens stayed alive or 91.6%, and in the third group – 90%.

The effect of the biopreparation on internal organs was assessed by the state of the digestive organs (liver, glandular stomach) and the immune system (thymus, Bursa). Special attention was paid to the central organs of immunity in birds since they all grow rapidly in the first months of life and reach maximum development: the thymus by 3.5-4 months and the Bursa by 4-4.5 months. Then the thymus gradually mummifies upon reaching puberty (Nasrin *et al.*, 2012; Skovorodin *et al.*, 2013).

No pathological changes were found in the organs. The weight and size of internal organs were estimated (Tanget *et al.*, 2007; Skovorodin *et al.*, 2019).

When conducting research for therapeutic purposes on 64-day-old Rodonit cross chickens with clinical signs of general dystrophy deficiency in live weight and failure in growth and development were found. According to domestic and foreign sources, there is a correlation between the state of some internal organs and the general state of the body of chickens. Thus, when the depletion increases, the thymus lobes grow less and when the feeding diet of birds improves, the gland regeneration begins in parallel (Aluwong *et al.*, 2013; Skovorodin *et al.*, 2013; Fisinin *et al.*, 2017; Jahanian and Ashnagar, 2018; Rubio *et al.*, 2019).

Studies have shown that throughout the experiment, the development of the thymus was registered in all groups of chickens. Apparently, this was due to improved feeding during the study period. Biostimulant Nucleostim has a stimulating effect on the liver of chicks of experimental and control groups. At the same time, the relative

weight of the organ is less than in control, which indicates physiological hepatomegaly.

The study of morphological and immunological parameters of the blood of broiler chickens was carried out by many researchers. However, there are splits over the dynamics of blood indicators of young chickens. It was found that they changed depending on the age and physiological state of chickens, which pointed to a different intensity of metabolic processes in each period of their life, which was confirmed by our research. The stimulating effect of various biostimulants on hematopoiesis, and especially leukopoiesis, has been noted by many scientists (Julean *et al.*, 2013; Sharipova and Khaziev, 2015; Salem *et al.*, 2018; Khaziev *et al.*, 2020).

Morphological studies have shown that the use of biopreparation did not have a significant impact on the dynamics of indicators of red and white blood of birds. During the experiment, they were within the physiological range for that age and type of productivity. The minimum content of red blood cells and hemoglobin was registered at the age of 30 days, which was consistent with the data of domestic and foreign scientists. After application of biopreparation, the content of red blood cells in the second experimental group (biostimulator 10 g/kg of feed) increased by 16% compared to the control group (Buyarov *et al.*, 2012; Fisinin, 2013; Ahmadi *et al.*, 2018; Buyarov *et al.*, 2018; Jahanian and Ashnagar, 2018; Nozdrin *et al.*, 2018; Rubio *et al.*, 2019).

In the blood of experimental and control groups of chickens, the content of white blood cells was found to be quite high, which was typical for that age. The leukogram of experimental and control groups of chickens showed the ratio of individual white blood cells to fall within the physiological range, but some specific features were observed. An increase in the level of lymphocytes in the blood indicates an increase in the specific immunity of birds since these cells are the main executive element in the manifestation of cellular and humoral protection of the body (Buzala *et al.*, 2017).

Many biological stimulants can increase the phagocytic activity of white blood cells. This increases both the number of phagocytic cells and the number of microbes absorbed by them (Buyarov *et al.*, 2012, 2018; Fisinin, 2013; Ahmadi *et al.*, 2018; Jahanian and Ashnagar, 2018; Nozdrin *et al.*, 2018; Rubio *et al.*, 2019).

To characterize the system of non-specific immunity in birds when exposed to the investigational product Nucleostim, the functional



activity of pseudo-eosinophils, monocytes, and platelets of whole blood of chicks in phagocytic reactions (for phagocyte number and phagocytic index) and the reduction reaction of nitro blue tetrazolium (spontaneous and latex-induced NBT-test) and the level of complement in blood serum were studied (Cuetos *et al.*, 2017; Abdulameer, 2018).

Thus, the use of biopreparation had a stimulating effect on the phagocytic activity of pseudo-eosinophils, monocytes, and platelets of birds' blood and on the complement system – a non-specific factor of humoral immunity. The new biological stimulant Nucleostim is recommended for use in veterinary medicine as an adaptogenic, anabolic, and immunostimulatory agent and is promising for finding new drugs that improve the health and productivity of poultry.

The new biological stimulant is recommended for use in veterinary medicine as an adaptogenic, anabolic, and immunostimulating agent and is promising for finding new drugs that improve the health and productivity of poultry

#### 4. CONCLUSION:

The body weight gain of chickens exposed to bioadditive increases by 9.7%; after three weeks, chickens treated with biopreparation overweighed the control group by 87.4 g, after five weeks – by 211.5 g. The livability of the experimental group of chickens was 88%, and of the control group – 72%. As a result of the use of biopreparation at a dose of 10 g/kg of feed, there is an increase in chick livability and an increase in their live weight gain.

The use of the biostimulant contributed to the development of the thymus in chickens against the background of general dystrophy. It had a stimulating effect on the liver of chicks of the experimental and control groups. At the same time, the relative weight of the organ is less than in control, which indicates physiological hepatomegaly. The use of biostimulator had a stimulating effect on the phagocytic activity of pseudo-eosinophils, monocytes, and platelets in the blood of birds and on the complement system – a non-specific factor of humoral immunity.

#### 5. REFERENCES:

1. Abdulameer, Y. S. (2019). The effects of dietary vitamin C and Citrus Sinensis peel on growth, hematological characteristics, immune competence, and carcass characteristics in broilers exposed to heat stress. *Iraqi Journal of Veterinary Sciences*, 32(2), 253-260.
2. Ahmadi, M., Ahmadian, A., and Seidavi, A. R. (2018). Effect of Different Levels of Nano-selenium on Performance, Blood Parameters, Immunity, and Carcass Characteristics of Broiler Chickens. *Poultry Science Journal*, 6(1), 99-108.
3. Aluwong, T., Kawu, M., Raji, M., Dzenda, T., Govwang, F., Sinkalu, V., and Ayo, J. (2013). Effect of yeast probiotic on growth, antioxidant enzyme activities, and malondialdehyde concentration of broiler chickens. *Antioxidants*, 2(4), 326-339.
4. Buyarov, A. V., Kalabukhov, I. V., and Andreychuk, O. A. (2018). Efficiency of industrial cultivation of broiler chickens of various crosses. *Technology of production and processing of agricultural products and zootechnics*, 2, 15-18.
5. Buyarov, A. V., and Buyanov, V. S. (2015). Priority directions of development of meat poultry farming in Russia. *Bulletin of the Altai state agrarian University*, 6(128), 165-171.
6. Buyarov, V. S., Buyarov, A.V., Kleymenov, I. S., and Shalimova, O. A. (2012) State and prospects of development of meat poultry farming. *Bulletin of the Orel GAU*, 1(34), 49-61.
7. Buzala, M., Stomka, A., Janicki, B., Ponczek, M. B., and Żekanowska, E. (2017). The mechanism of blood coagulation, its disorders and measurement in poultry. *Livestock Science*, 195, 1-8.
8. Cuetos, M. J., Martinez, E. J., Moreno, R., Gonzalez, R., Otero, M., and Gomez, X. (2017). Enhancing anaerobic digestion of poultry blood using activated carbon. *Journal of advanced research*, 8(3), 297-307.
9. Dementyev, E. P., Bazekin, G. V., Tokarev, I. N., Lobodina, G. V., Karimov, F. A., Andreeva, A. V., ... and Bliznetsov, A. V. (2018). The application of physical and biological stimulants in livestock breeding. *Journal of Engineering and Applied Sciences*, 13(S10), 8325-8330.
10. Fisinin, V. I. (2013). Poultry Farming in Russia and the world: state and challenges of the future. *Animal Husbandry of Russia*, 6, 2-4.
11. Fisinin, V. I., Roiter, Ya. S., Roiter, L.M., and Akopyan, A. G. (2017). Reduction of imports

- in poultry farming – the potential for growth of the industry's competitiveness. *Poultry and Poultry Products*, 2, 67-69.
12. Gharahveysi, S., Irani, M., Kenari, T. A., and Mahmud, K. I. (2020). Effects of colour and intensity of artificial light produced by incandescent bulbs on the performance traits, thyroid hormones, and blood metabolites of broiler chickens. *Italian Journal of Animal Science*, 19(1), 1-7.
  13. Government of the Russian Federation (2012). State program for the development of agriculture and regulation of markets for agricultural products, raw materials, and food for 2013-2020. <http://gov.garant.ru/SESSION/PILOT/main.htm>. Accessed 2019-11-18.
  14. Jahanian, R., and Ashnagar, M. (2018). Effects of dietary supplementation of choline and carnitine on growth performance, meat oxidative stability and carcass composition of broiler chickens fed diets with different metabolisable energy levels. *British poultry science*, 59(4), 470-476.
  15. Julean, C., Drinceanu, D., Ștef, L., Simiz, E., and Bura, M. (2013). Effect of mineral supplements on bioproductive performances on mixed breeds avian youth in organic system. *Journal of Food, Agriculture and Environment*, 11(2), 567-570.
  16. Khaziev, D., Galina, S., Gadiev, R., Valitov, F., Gumarova, G., and Galyautdinov, I. (2020). Phytoecdysteroids from serratulacoronata when raising ducklings. *Scientific research in the field of veterinary medicine*, 128, 170-176.
  17. Khaziev, D. D., Gadiev, R. R., and Sharipova, A. F. (2018). Probiotic feed additive vetosporin-active in the composition of the diet of broiler chickens. *Proceedings of the Orenburg state agrarian University*, 6(74), 259-262.
  18. Nasrin, M., Siddiqi, M. N. H., Masum, M. A., and Wares, M. A. (2012). Gross and histological studies of digestive tract of broilers during postnatal growth and development. *Journal of the Bangladesh Agricultural University*, 10(1), 69-77.
  19. Nozdrin, G. A., Rafikova, E. R., Lelyak, A. I., Ledeneva, O. Y., and Novik, Y. V. (2018). New Preparation Based on Duddingtonia Flagrans as an Alternative Trigger for Growth Stimulating Factors in the Organisms of Broilers. *Journal of Pharmaceutical Sciences and Research*, 10(10), 2537-2542.
  20. Rubio, M. S., Laurentiz, A. C., Sobrane, F., Mello, E. S., Filardi, R. S., Silva, M. L. A., and Laurentiz, R. S. (2019). Performance and Serum Biochemical Profile of Broiler Chickens Supplemented with Piper Cubeba Ethanolic Extract. *Brazilian Journal of Poultry Science*, 21(1), eRBCA-2019-0789.
  21. Salem, R., El-Habashi, N., Fadl, S. E., Sakr, O. A., and Elbialy, Z. I. (2018). Effect of probiotic supplement on aflatoxicosis and gene expression in the liver of broiler chicken. *Environmental toxicology and pharmacology*, 60, 118-127.
  22. Santos, R. R., Awati, A., Roubos-van den Hil, P. J., van Kempen, T. A., Tersteeg-Zijderfeld, M. H., Koolmees, P. A., ... and Fink-Gremmels, J. (2019). Effects of a feed additive blend on broilers challenged with heat stress. *Avian Pathology*, 48(6), 582-601.
  23. Sharipova, A. F., and Khaziev, D. D. (2015). Effect of the probiotic additive "Vetosporin-active" on the efficiency of broiler chicken rearing. *Scientific notes of the Kazan state Academy of veterinary medicine*, 221(1), 253-258.
  24. Skovorodin, E., Davletova, V., and Dudbin, O. (2013). Effect of solvimin selen and selemag preparations on the growth and development of Muscovy ducks. *Journal of Veterinary*, 9, 16-20.
  25. Skovorodin, E., Bronnikova, G., Bazekin, G., Dyudbin, O., and Khokhlov, R. (2019). Antioxidant influence on poultry liver morphology and hepatocyte ultrastructure. *Veterinary World*, 12(11), 1716.
  26. Tang, X., Ma, H., Zou, S., and Chen, W. (2007). Effects of dehydroepiandrosterone (DHEA) on hepatic lipid metabolism parameters and lipogenic gene mRNA expression in broiler chickens. *Lipids*, 42(11), 1025.

**Table 1.** PC-2 complete feed composition for broiler chickens produced at the Bogdanovich feed mill (Bogdanovich town, Sverdlovsk region, 64, Stepan Razin street).

| The composition of the feed PC-2 in % |       |
|---------------------------------------|-------|
| Wheat                                 | 43.72 |

|                       |       |
|-----------------------|-------|
| Corn                  | 30.41 |
| Soybean meal          | 11.15 |
| Sunflower cake        | 8,0   |
| Fish flour            | 1.80  |
| Lysine                | 0.45  |
| Feed methionine       | 0.2   |
| Table salt            | 0.24  |
| Monocalcium phosphate | 1.33  |
| Limestone             | 1.61  |
| Premix (P5 - 1)       | 1.00  |

**Table 2.** Effect of the biostimulant Nucleostim on the average daily body weight gain of ROSS 308 cross broiler chickens

| Weeks | Number of chicks in the group | biological stimulator, at a dose of 10g/kg of feed |                       | Control        |                       |
|-------|-------------------------------|--|-----------------------|----------------|-----------------------|
|       |                               | live weight, g                                     | average daily gain, g | live weight, g | average daily gain, g |
| Day   | 50                            | 40.5±0.4   |                       | 39.9±0.3       |                       |
| 1     | 50                            | 135.3±8.5  | 11.9                  | 123.4±8.0      | 10.5                  |
| 2     | 50                            | 379.1±10.0   | 29.5                  | 300.0±12.0     | 19.6                  |
| 3     | 50                            | 520.3±20.0   | 35.2                  | 432.9±15.9     | 22.9                  |
| 4     | 50                            | 830.8±21.0   | 34.5                  | 700.9±20.0     | 25.4                  |
| 5     | 50                            | 1060.0±15.0  | 36.30                 | 848.5±35.0     | 29.5                  |
| 6     | 50                            | 1095.5±17.0  | 70.4                  | 996.2±26.8     | 49.6                  |
| 7     | 50                            | 1290.9±20.0  | 89.3                  | 1040.7±15.8    | 85.3                  |
| 8     | 50                            | 1510.5±30.0  | 55.5                  | 1269.1±19.9    | 38.6                  |
| 9     | 50                            | 2093.0±50.0  | 70.1                  | 1799.5±27.5    | 61.1                  |

**Table 3.** Effect of the Biostimulant Nucleostim on the live weight of Rodonit cross chickens

| Item          | Dose g/kg of feed | Live weight, g | Daily live weight gain, g | Relative gain, % | Gain-norm relation, % |
|---------------|-------------------|----------------|---------------------------|------------------|-----------------------|
| 64 days old   |                   |                |                           |                  |                       |
| Control       | -                 | 420.0±3.08     | -                         | -                | -                     |
| biostimulator | 10.0              | 435.0±4.92     | -                         | -                | -                     |
| biostimulator | 5.0               | 425.0±9.84     | -                         | -                | -                     |
| 74 days old   |                   |                |                           |                  |                       |
| Control       | -                 | 539.0±9.05     | 14.9                      | 24.8             | 62.0                  |
| biostimulator | 10.0              | 629.0±7.99     | 24.3                      | 36.5             | 101.0                 |
| biostimulator | 5.0               | 595.0±7.03     | 21.3                      | 33.3             | 88.5                  |
| 84 days old   |                   |                |                           |                  |                       |
| Control       | -                 | 635.0±13.18    | 12.0                      | 16.4             | 100.0                 |

|               |      |             |      |      |       |
|---------------|------|-------------|------|------|-------|
| biostimulator | 10.0 | 731.0±7.03  | 12.4 | 15.0 | 106.3 |
| biostimulator | 5.0  | 694.0±6.67  | 12.4 | 15.4 | 103.2 |
| 94 days old   |      |             |      |      |       |
| Control       | -    | 666.0±20.58 | 6.2  | 4.8  | 62.0  |
| biostimulator | 10.0 | 784.0±9.24  | 10.6 | 7.0  | 106.0 |
| biostimulator | 5.0  | 738.0±7.98  | 8.8  | 6.2  | 88.0  |

**Table 4.** Effect of the Biostimulant Nucleostim on the development of internal organs of ROSS 308 cross broiler chickens

| Test organs | Weight, g |                               |                              |                                |
|-------------|-----------|-------------------------------|------------------------------|--------------------------------|
|             | Groups    |                               |                              |                                |
|             | Control   | biostimulator 10 g/kg of feed | biostimulator 5 g/kg of feed | biostimulator 15 g /kg of feed |
| Thymus      | 0.8±0.07  | 1.006±0.03                    | 0.84±0.045                   | 0.84±0.02                      |
| Liver       | 10.2±0.16 | 12.25±0.35                    | 10.85±0.18                   | 10.70±0.46                     |
| Stomach     | 2.2±0.19  | 2.68±0.13                     | 2.33±0.03                    | 2.35±0.05                      |

**Table 5.** Effect of Nucleostim on the morphological parameters of chicken blood

| Material under investigation | Dose g/kg | Erythrocytes million/mm <sup>3</sup> | Hemoglobin g % | Color indicator | Leucocytes thousand/mm <sup>3</sup> |
|------------------------------|-----------|--------------------------------------|----------------|-----------------|-------------------------------------|
| age 30 days                  |           |                                      |                |                 |                                     |
| Before experiment            | -         | 1.8±0.08                             | 8.8±0.72       | 1.5±0.15        | 58.4±1.50                           |
| age 40 days                  |           |                                      |                |                 |                                     |
| Control                      | -         | 1.7±0.04                             | 10.3±0.21      | 1.8±0.06        | 56.2±3.65                           |
| biostimulator                | 10.0      | 2.1±0.15                             | 10.4±0.21      | 1.7±0.15        | 58.1±3.43                           |
| biostimulator                | 5.0       | 1.8±0.09                             | 10.3±0.21      | 1.8±0.06        | 58.3±3.22                           |
| Normal                       | -         | 1.5–4                                | 8–12           | 1–3             | 20–40                               |

**Table 6.** Effect of Nucleostim on the percentage of different groups of leucocytes in chicken blood

| Groups            | Dose g/kg | Basophils | Eosinophils | Pseudo eosino-phils | Lymphocytes | Monocytes |
|-------------------|-----------|-----------|-------------|---------------------|-------------|-----------|
| age 30 days       |           |           |             |                     |             |           |
| Before experiment |           | 5.8±0.43  | 7.5±0.43    | 23.3±0.48           | 57.2±4.49   | 5.8±0.23  |
| age 40 days       |           |           |             |                     |             |           |
| Control           | -         | 6.2±0.60  | 7.0±0.64    | 26.6±1.72           | 52.8±1.50   | 5.0±0.43  |
| biostimulator     | 10.0      | 6.0±0.60  | 7.4±0.43    | 25.4±1.72           | 55.0±1.07   | 6.4±0.64  |

|           |     |          |          |           |           |          |
|-----------|-----|----------|----------|-----------|-----------|----------|
| biostimul | 5.0 | 5.0±0.43 | 6.6±0.64 | 26.2±2.58 | 59.0±2.15 | 5.2±0.43 |
| ator      |     |          |          |           |           |          |
| Normal    |     | 2–5      | 2–20     | 15–35     | 40–70     | 2–11     |

**Table 7.** Effect of Nucleostim on the intensity of phagocytosis and the complement level in chicken blood

| Item              |           | Phagocytosis          |                    | NBT-test    |                        | Level of complement |
|-------------------|-----------|-----------------------|--------------------|-------------|------------------------|---------------------|
|                   | Dose g/kg | Phagocytic number, %, | Phagocytic index % | spontaneous | induced                |                     |
| age 30 days       |           |                       |                    |             |                        |                     |
| Before experiment |           | 3.49±0.20             | 0.39±0.01          | 0.18±0.01   | 0.50±0.04              | 34.50±0.30          |
| age 40 days       |           |                       |                    |             |                        |                     |
| Control           |           | 3.3±0.12              | 0.35±0.01          | 0.16±0.02   | 0.45±0.04              | 30.1±1.35           |
| bioadditive 10.0  | 10.0      | 3.9±0.09              | 0.43±0.011         | 0.24±0.01   | 0.48±0.02              | 38.8±0.4            |
| bioadditive 5.0   | 5.0       | 3.7±0.09              | 0.43±0.011         | 0.21±0.01   | 0.47±0.01 <sup>#</sup> | 37.5±0.50           |

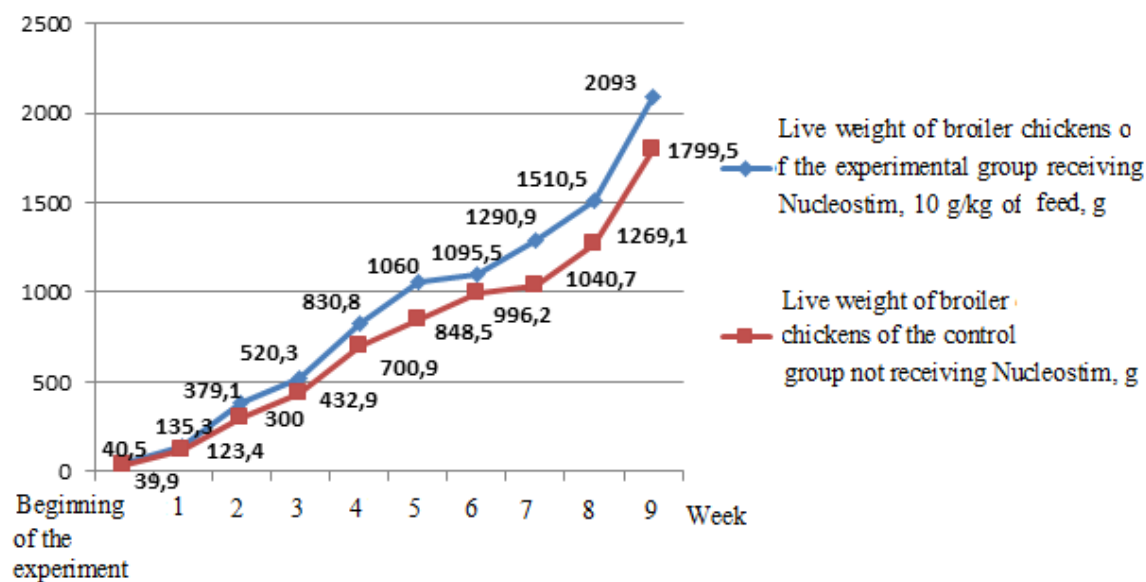


**Figure 1.** Influence of the biostimulant Nucleostim on the live weight of ROSS 308 cross broiler chickens during the period of intensive growth

**INFLUÊNCIA DA PRODUÇÃO DE CITOCINAS, METABOLITOS DE ÓXIDO DE NITROGÊNIO E TROCA DE LÍPIDOS NA FORMAÇÃO DE ESTÁGIOS EXTERNOS DE ENDOMETRIOSE GENITAL NOS PACIENTES EM IDADE REPRODUTIVA****INFLUENCE OF CYTOKINES PRODUCTION, NITROGEN OXIDE METABOLITES AND LIPIDS EXCHANGE ON THE FORMATION OF EXTERNAL GENITAL ENDOMETRIOSIS STAGES IN PATIENTS OF REPRODUCTIVE AGE****ВЛИЯНИЕ ПРОДУКЦИИ ЦИТОКИНОВ, МЕТАБОЛИТОВ ОКСИДА АЗОТА И ОБМЕНА ЛИПИДОВ НА ФОРМИРОВАНИЕ СТАДИЙ НАРУЖНОГО ГЕНИТАЛЬНОГО ЭНДОМЕТРИОЗА У ПАЦИЕНТОК РЕПРОДУКТИВНОГО ВОЗРАСТА**

ERMOLOVA, Natalya Victorovna<sup>\*1</sup>; PETROV, Yuriy Alekseevich<sup>1</sup>;  
LEVKOVICH, Marina Arkadevna<sup>1</sup>; KOLESNIKOVA, Ludmila Valerievna<sup>1</sup>;  
DRUKKER, Nina Aleksandrovna<sup>1</sup>;

Rostov State Medical University, Russian Federation

*\* Correspondence author*  
*e-mail: rniiap.ermolova@gmail.com*

Received 10 April 2020; received in revised form 26 May 2020; accepted 20 June 2020

**RESUMO**

A relevância do estudo se deve à prevalência e aumento da incidência de endometriose, principalmente em pacientes jovens, sua influência na função reprodutiva e a falta de diagnóstico não invasivo confiável da doença e seus estágios. Não existem opiniões unificadas sobre a etiologia e patogênese multifatorial desta doença. Este artigo tem como objetivo revelar os mecanismos de formação de estágios de endometriose com base no estudo do efeito da produção de citocinas, metabólitos de óxido nítrico e metabolismo lipídico. A principal abordagem para estudar esse problema é investigar os níveis sistêmico (soro sanguíneo) e local (líquido peritoneal), sua comparação. Isso permite uma consideração abrangente da patogênese da doença e a determinação do valor dos fatores biologicamente ativos mencionados, dependendo dos estágios da doença. O artigo apresenta novos dados sobre o conteúdo de lipoproteínas de alta e baixa densidade, colesterol, fator de crescimento transformador  $\beta 1$  e fator de necrose tumoral  $\alpha$ , conteúdo de metabólitos de óxido nítrico e sua interpretação clínica é dada de acordo com os estágios da doença. Os materiais do artigo são de valor prático para pesquisadores de endometriose e praticantes de ginecologistas e obstetras.

**Palavras-chave:** *endometriose genital externa, lipoproteínas, óxido nítrico, fator de crescimento transformador beta 1, fator de necrose tumoral alfa.*

**ABSTRACT**

The relevance of the study is due to the prevalence and increase in the incidence of endometriosis, especially in young patients, its influence on reproductive function, and the lack of reliable non-invasive diagnosis of the disease and its stages. There are no unified views on the etiology and multifactorial pathogenesis of this disease. This article is aimed at revealing the mechanisms of the formation of endometriosis stages basing on the study of the effect of cytokines production, nitric oxide metabolites and lipid metabolism. The main approach to study this problem is both to investigate systemic (blood serum) and local (peritoneal fluid) levels, their comparison. This allows comprehensive consideration of the pathogenesis of the disease and determination of the value of the mentioned biologically active factors depending on the stages of the disease. The article presents new data on the content of high- and low-density lipoproteins, cholesterol, transforming growth factor  $\beta 1$  and tumor necrosis factor  $\alpha$ , the content of nitric oxide metabolites

and their clinical interpretation is given according to the stages of the disease. The materials of the article are of practical value for researchers of endometriosis and practicing obstetrician-gynecologists..

**Keywords:** *external genital endometriosis, lipoproteins, nitric oxide, transforming growth factor beta 1, tumor necrosis factor alpha.*

## АННОТАЦИЯ

Актуальность исследования обусловлена распространенностью и ростом заболеваемости эндометриозом, особенно у пациенток молодого возраста, влиянием его на репродуктивную функцию, отсутствием надежной неинвазивной диагностики заболевания и его стадий. Нет единых взглядов на этиологию и многофакторный патогенез этого заболевания. В связи с этим, данная статья направлена на раскрытие механизмов формирования стадий эндометриоза на основании изучения влияния продукции цитокинов, метаболитов оксида азота и обмена липидов. Ведущим подходом к исследованию данной проблемы является исследование как системного (сыворотка крови), так и местного (перитонеальная жидкость) уровней, их сопоставление. Это позволяет комплексно рассмотреть патогенез заболевания и определить значение обозначенных биологически активных факторов в зависимости от стадий заболевания. В статье представлены новые данные по содержанию липопротеинов высокой и низкой плотности, холестерину, трансформирующего фактора роста  $\beta 1$  и фактора некроза опухолей  $\alpha$ , содержанию метаболитов оксида азота и дана их клиническая интерпретация в соответствии со стадиями заболевания. Материалы статьи представляют практическую ценность для исследователей эндометриоза и практикующих врачей акушеров-гинекологов.

**Ключевые слова:** *наружный генитальный эндометриоз, липопротеины, оксид азота, трансформирующий фактор роста бета 1, фактор некроза опухоли альфа.*

## 1. INTRODUCTION

Endometriosis is a chronic, recurring, genetically determined, inflammatory disease. Its main clinical manifestations are persistent pain and infertility. According to morphological and functional properties It is a benign growth outside the uterine cavity tissue similar to the endometrium (Adamyan *et al.*, 2016).

About 2-10% of women of the reproductive age in the population suffer from this disease (Adamyan *et al.*, 2016; Falcone and Lebovic, 2011) and up to 50% of women screened for infertility (Vercellini *et al.*, 2011). Still there are no non-invasive markers of external genital endometriosis (EGE). Scientists discuss the problem of the systematic progression of this disease but no solution is found.

Processes occurring in the peritoneal cavity play an important role in the development of external genital endometriosis in patients of the reproductive age. The amount of peritoneal fluid (PF) is known to be increased in women with endometriosis comparing with healthy women without endometriosis (Sonova *et al.*, 2010). PF in these patients is characterized by a high content of activated macrophages (Berbic *et al.*, 2009) producing cytokines: TNF- $\alpha$  (Sonova *et al.*, 2011), TGF- $\beta 1$  (Ermolova, 2009) stimulating angiogenesis (Wang *et al.*, 2009) and also

contains a large amount of lipoproteins, especially of low density, which generate oxidized lipid components as part of a macrophage inflammatory medium (Anderson Sanches Melo *et al.*, 2010)

The TGF- $\beta 1$ , found in high concentrations in the PF of patients with EGE (Charles *et al.*, 2010), has anti-inflammatory properties and is able to inhibit TNF- $\alpha$ , IL-1 $\beta$  and other cytokines synthesis, inhibit endothelial cell proliferation.

Information on the TNF- $\alpha$  role in the cell is rather contradictory, and often it produces opposite effects on the same cell types (Laschke, 2011). TNF- $\alpha$  activates lipolysis and inhibits lipogenesis.

The development of so-called local aseptic inflammation and immunocompetent cell dysfunction is generally considered as a fact established both in an experimental model of endometriosis in mice and in the abdominal cavity of patients with endometriosis (Schmidt *et al.*, 2015). In endometriosis macrophages are not able to perform their all functions, and an estrogen-dependent chronic inflammation is triggered (Takebayashi *et al.*, 2014). Imbalance in the formation of free radicals makes the basis of the inflammatory process in endometriosis (Darling, 2013).

Nitric oxide plays the role of a universal regulator of many biological functions having both protective and damaging character. Thus, being an important regulator of vascular tone, providing immune responses, neuronal transmission and antioxidant protection, nitric oxide can under certain conditions also act as a free radical, which has a pronounced destructive effect (Babushkina, 2009; . Bryan *et al.*, 2009). Nitric oxide is formed in cells from L-arginine under the action of NO-synthase enzyme (Vanin, 2008). There is a second way of converting L-arginine, by means of arginase, it is hydrolyzed to ornithine and urea, followed by the formation of proline (Babushkina, 2009), which in turn is a source of tissue hardening, and, it is well known, moderate and severe degree of EGE in 100% of cases is accompanied by the development of the adhesive process (Luciano and Adhesion, 2008). In this case, the problem is not only in the clinical manifestations of the adhesive process (pelvic pain, infertility) (Chernukha, 2011), but also in the high recurrence rate after mechanical adhesiolysis during laparoscopy. Arginase and NO-synthase compete with each other for a common substrate - L-arginine. Arginase, an enzyme in the urea synthesis cycle, has a higher activity and exceeds that of NO-synthase (Vanin, 2008).

N. Santanam *et al.* (2002), found the presence of an acidic environment in the PF of women with endometriosis. PF lipoproteins in patients with endometriosis have a greater ability to oxidation compared with blood plasma lipoproteins.

Many scientists search for new non-invasive markers of endometriosis, and biochemical and immunohistochemical indicators already developed are unfortunately not specific (Vodolazkaia, 2012; Gajbhiye *et al.*, 2012). Additional studies are necessary to determine the effectiveness of the early diagnosis of dyslipidemia in order to prevent endometriosis in patients of reproductive age. Of particular interest is the participation of cytokines, metabolites of nitric oxide and lipoproteins in the formation of the stages of the disease, which will allow to personalize the treatment tactics of these patients.

The purpose of the study was to determine clinical significance of lipid and cytokine markers status, nitric oxide metabolites in the formation of disease stages in patients of reproductive age with external genital endometriosis.

## 2. MATERIALS AND METHODS

The study, approved by the Local Ethics Committee of the Research Institute of Obstetrics and Pediatrics at Rostov State Medical University, included 96 patients, 74 were patients with EGE and 22 women without endometriosis (control group) who underwent examination and treatment at the gynecology department of the Research Institute of Rostov State Medical University.

All patients were divided into 3 clinical groups: group I consisted of 28 patients with I-II stages of EGE according to r-AFS classification (1985), group II - 46 patients with stages III-IV of the disease. The III control group consisted of 22 patients without endometriosis.

To achieve the above purpose, the following methods were used: clinical (medical history, examination), laboratory, ultrasound, endoscopic (laparoscopy, hysteroscopy, colposcopy), histological examination of biopsy specimens obtained during laparoscopy.

The following criteria were used to include the patients into the study: Criteria for the inclusion of patients in the study: 1. The patient underwent endoscopic surgery (laparo- and hysteroscopy), confirming EGE with subsequent morphological verification of the diagnosis, in patients without EGE to exclude tubal-peritoneal infertility factor, sterilization. 2. Reproductive age of patients. 3. Complaints of infertility and/or pain. 4. Body mass index 18.5 - 25 kg/m<sup>2</sup>.

The criteria for the exclusion from the study were the puberty and perimenopausal age of the patients, obesity or metabolic syndrome.

The patients were included into the study after obtaining informed consent and were recorded according to the standards of the Ethics Committee of the Russian Federation (protocol No. 46 dated 04/17/2014). Blood, peritoneal fluid of patients obtained by laparoscopy was used in the study.

Analysis of clinical data showed that in all patients menstrual cycle was preserved, its mean duration in group I (EGE stage I-II) was  $28.04 \pm 1.2$  days, in group II (EGE stage III-IV) -  $28.7 \pm 1.4$  days, in group III (control) -  $26.1 \pm 1.3$  days. Early menarche (up to 11 years old) was more common in patients with EGE from group II (60.9%) and group I (52.7%), i.e. in patients with EGE, early menarche was found, unlike patients in the control group. The mean age menstruation beginning was in group I  $10.2 \pm 0.11$  years, in group II -  $11.8 \pm 0.19$  years, in group III -  $13.4 \pm$



0.1 years. Algomenorrhea occurred in 50% of patients with EGE with menarche, in 85.1% of patients with I-II stage of EGE and only in 21.7% of patients with III-IV stage of EGE.

34.9% of patients with EGE complained of progressively increasing pelvic pains, before and during menstruation 54%, dyspareunia 22%, spotting blood excretions before or during menstruation 28%. It should be noted that with minimal forms of the disease, pelvic pain was found only in 4% patients, while in severe forms (stage III-IV of EGE) this symptom was present in more than half (55.2%) of patients which is significantly higher ( $p < 0.05$ ) when conducting intergroup comparisons. Psychoemotional disorders were in 38% in patients with EGE. Progression of the disease leads to increased frequency of symptoms. The severity and intensity of complaints prevailed in the group of patients with III - IV stage of EGE.

40.8% with EGE had primary infertility. In patients with EGE I-II stages it was registered in 68% of cases, which was 1.2 times higher than in the group with EGE III-IV stages, 39.5%. Secondary infertility was in 21.2% with EGE: in the first group of patients it was in 28% of patients and in the second group – in 23.6% of patients.

79.7% of the patients with stage I-II EGE (group I) had in their anamnesis sexually transmitted infections (STIs), and inflammatory diseases of the pelvic organs (PID) in 57.4% of patients, while in group II patients with EGE of the III-IV stage of STIs were found in 78.3%, and PID - in 60.9% of women.

Analysis of the duration of the disease from the onset of clinical manifestations to the 1st hospitalization revealed that this period ranged from 3 months to 6 years.

In 53.9% of patients ultrasound examination showed endometrioid cysts from 4 to 10 cm in size with a fine suspension of both unilateral (4%) and bilateral (95%). Only in 18% of patients with EGE typical endometrioid infiltrates from 2.5 to 3 cm were identified in the area of the uterine isthmus.

Colposcopy revealed background diseases of the cervix in 60.1% of patients with EGE stage I-II, in 76.6% of patients with EGE stage III-IV, while cervical dysplasia was found in 16.9% of in group I patients and in 21.7% group II patients. In the control group of patients, background cervical pathology was found in 30%, and cervical dysplasia in 10% of women.

In all cases surgical treatment was performed by laparoscopic access in the organ-saving volume. The main tasks of laparoscopic treatment were: maximum removal of all endometrioid foci; elimination of the adhesive process; restoration of the normal anatomy of the internal genital organs. Endometriosis prevalence was determined by laparoscopy using the recommendations of the revised classification developed by the American Society for Fertility (r-AFS) (1985). In our study, laparoscopy revealed a high percentage of endometrioid ovarian cysts (53.97%), which may indicate the untimely diagnosis of EGE. Superficial foci of endometriosis in the ovaries were detected in 42.8% of cases. Sacro-uterine ligaments (77.7%) and the rectum-uterine space (69.8%) lesions were most common, while in the vesicoureteral space foci of endometriosis were detected only in 31.7% of cases. On the wide uterus ligament endometriotic lesions were detected less often - 4.7% of cases.

In patients of the first group with EGE stage I-II, adhesions of the I degree were found in 12.8% of patients, of the II degree – in 10.8%, of the III degree – in 2.7%, and of the IV degree – in 2%. In women of the second group, with EGE stage III - IV, adhesions were found in 12%, 16.3%, 17.4%, 16.3% of cases, respectively.

In stage I-II, ovarian lesions were registered in 31% of cases, endometrioid cysts in 4%. Only peritoneum lesion was in 66.2%, combined forms - (peritoneum and ovaries) – in 48.7%. In EGE stages III - IV ovarian lesions in the form of endometrioid cysts were revealed in 94.6% of cases. Damage to the peritoneum was in 40.2% of cases. Combined forms (peritoneum and ovaries) were in 78% of patients.

Hysteroscopy revealed endometrial hyperplastic process in the form of simple hyperplasia without atypical signs was detected in 27% of group I patients and in 35.3% of group II patients, while in the control group this pathology was found only in 5% of women.

EGE was histologically confirmed in all patients of clinical groups I and II. Endometriosis verification was carried out according the degree of the process prevalence and the morphofunctional characteristics of heterotopic foci. The morphological diagnosis was based on the microscopic detection of ectopic endometrioid epithelium in combination with elements of the endometrioid stroma. Macrophages containing hemosiderin were also found in it. Endometrioid heterotopy was microscopically presented by an

accumulation of cellular formations, tubular, branching or cystically dilated. Internally the glands were lined with a cylindrical epithelium, sometimes even with cilia. In heterotopic foci, there were two types their existence – progression and regression. Proliferation of glandular epithelium of varying severity, secretory changes, decidualization of the cytogenic stroma were most common and typical for the progressing EGE foci. Regressing OGE foci without signs of functional activity were characterized by the presence of cystic gland transformation, epithelial atrophy, fibroplastic restructuring and angiomatosis of the cytogenic stroma in 19.6% of all patients, in EGE I-II stages – in 13.5% of patients, III- IV stages - in 24.5% of women. Histological examination of the surgical material revealed endometrial glands in endometrioid heterotopia in 71.7% of cases, 49.6% of patients had it in the proliferation phase, 50.4% of patients – in the secretion phase, and 18.3% in the middle secretion phase – 18.3%, in late - 81.7%. Since laparoscopy was performed in the first phase of the menstrual cycle, the data obtained indicate that in half of cases there was no correlation of the state of endometrioid heterotopy to the uterine cycle.

Angiomatosis was more pronounced (24.5% of cases) in patients with EGE stage III-IV. Moreover, in the stroma surrounding the gland, a mild lymphoid and plasmocytic infiltration was in 11.7% of cases of a focal character. As a percentage, there were no differences in EGE stages. Thus, at stage I-II they made 13.4% and in EGE stage III-IV - 12.5%. Stromal sclerosis was found in 55.7% of EGE patients. Moreover, diffuse sclerosis, which develops at the end of inflammation, or chronic insufficiency of blood supply, was in 50% of cases, while focal sclerosis occurred in 25% of patients. In OGE stage I-II it was revealed in 43.9% of patients, in stage III-IV – in 65.2% of patients. Hyalinosis was found in 33.4% of patients, and it was more pronounced with OGE stage III-IV – 42.9% of patients, versus 21.6% of patients with stage I-II of the disease. Inflammation in the stroma of endometrioid heterotopia in was found in 34.9% of cases in the general group, in OGE stages I-II – in 43.2% of patients, in stages III-IV – in 28.3% of patients. It should be noted that inflammatory changes in endometrioid heterotopies are more pronounced in EGE stage I-II, while sclerosis and tissue hyalinosis as outcomes of this process prevail in patients with EGE stage III-IV.

Serum lipoproteins and EGE were determined using Randox kits (Germany) on

Sapphire-400 biochemistry analyzer (Japan). The endogenous level of nitric oxide in the form of a nitrite anion (NO-) was determined using Griss reagent. Nitroxide synthase (NOS) activity was assessed by the increased nitric oxide production from L-arginine in the presence of NADPH. Growth factors, cytokines, were determined by enzyme-linked immunosorbent assay using “R&D Systems” kits (USA). Statistical data processing was carried out using the Statistica licensed software package (version 5.1, made by Stat Soft). The sample size in the work completely corresponds to the range of obtaining a confidence interval of probability, 0.95, and accuracy of calculation of statistical parameters, 0.05. Results are presented as median and interquartile interval. The significance of differences between the compared parameters was determined by the Mann-Whitney criterion for nonparametric distributions. The results were considered to be statistically significant at  $p < 0.05$ . In correlation analysis of the data, the Pearson criterion was used in the case of a normal distribution of variables and otherwise the Spearman criterion, and the significance level was 0.05.

### 3. RESULTS AND DISCUSSION

The results obtained in patients with stages I-II of EGE are presented in Table 1. It shows that the content of TGF- $\beta$ 1 in the blood serum in these was 1.4 times higher compared to the control group of women ( $p < 0.004$ ).

The study of lipoproteins revealed significant changes in the content of HDL in the blood serum, characterized by their increase of 1.1 times ( $p < 0.013$ ) (Table 1). Nitric oxide (NOx) metabolites content in the blood serum of patients with I-II stages of EGE was 6.9 times higher than in the control group ( $p < 0.041$ ), while NO synthase activity was not change significantly and remained at physiological level.

At stage III-IV of EGE, the content of TNF- $\alpha$  in the blood serum of patients was 1.9 times higher compared with the data of women in the control group ( $p < 0.014$ ).

Significant changes in the content of the studied lipid fractions concerned only HDL both in minimal and severe forms of EGE ( $p < 0.013$  and  $p < 0.06$ , respectively). The content of NOx in the blood serum of patients with III-IV stages of EGE (Table 1) was 13.4 times higher than in the control group ( $p < 0.001$ ).

The study of the lipid spectrum in the PF in patients with stages I-II of EGE showed the increase of free cholesterol 1.43 times content, HDL - 1.73 times and HDL - 1.6 times ( $p < 0.008$ ,  $p < 0.004$ ,  $p < 0.003$ , respectively) (Table 2).

The content of TNF- $\alpha$  in the PF in patients with stages III-IV of EGE was 1.5 times less compared with the control group of women ( $p < 0.050$ ) (Table 2), while the level of TGF- $\beta$ 1 in these patients was 1.7 times higher than the control ( $p < 0.001$ ).

The content of NOx in the PF of patients with III-IV stages of EGE was 3.3 times higher than in patients in the control group ( $p < 0.039$ ) (Table 2). The activity of NO synthase exceeded physiological parameters by almost 1.5 times ( $p < 0.001$ ).

There is no doubt that for the most successful solution of the EGE problem it is necessary to use modern methodological approaches, in particular, a comprehensive study of the molecular basis of the disease development and the relationship of metabolic disorders at the local and systemic levels. Formation of the disease stages is of special interest since it makes the basis for the further management of patients. The proliferation factors of endometrioid heterotopia (cytokines and growth factors) and metabolic (lipid) parameters that affect the activity of enzymes involved in the processes of angiogenesis were studied.

Biologically active polypeptides - growth factors that stimulate or inhibit angiogenesis, and also regulate cellular mitogenic effects play an important role in the regulation of intracellular metabolism. This refers to TGF $\beta$ 1 (Burlev, 2012; Ermolova, 2008; Ermolova, 2009). TGF $\beta$ 1 inhibits proliferation and induces differentiation of most types of cells that have been studied already. As for TGF $\beta$ 1 metabolic features, it inhibits NO synthase activity and activates arginase (Babushkina, 2009). Significance of the systemic level of regulation of metabolic processes that control cell growth (TGF- $\beta$ 1) in the study indicates the presence of compensatory reactions in patients with I-II EGE stages.

It was shown in the experiments that incubation of recruited macrophages with cholesterol causes a significant increase in TGF- $\beta$ 1 (Schwartz, 2009). Cholesterol can directly induce the synthesis and secretion of TGF- $\beta$ 1 in monocytes - macrophages.

Variations in the lipid content of cell membranes can also significantly change the

activity of proteins that are their components (Keelet, 2012). In the presence of inflammatory processes in the body, cholesterol and phospholipids content changes. Cell membranes, mainly the middle phospholipid layer, with intensively occurring processes, serve as a screen to reflect the aggressive effects of the cascade of toxic products. As a result of the changes caused, the structure, membrane functions, balance between radical oxidative processes and the functional antioxidant defense system are disturbed. A large number of low-density lipoproteins (LDL) generate very low-density lipoproteins (VLDL) (oxidized components), which enhance the growth of heterotopia by activating endometrial cell growth factors (Verit, 2013; Melo, 2010).

HDL increase causes paraoxonase-1 (PON-1) increase in the content, which is a part of lipoprotein complex, and, consequently, its activity. Study of the paraoxonase gene polymorphism (Kolesnikova *et al.*, 2012) confirms this proposition, which showed the absence of its differences compared with the parameters in patients of the control group. HDL modification in women with EGE I-II stages at the systemic level is compensatory in nature, aimed at preventing the formation of more "significant" endometrioid heterotopia in the peritoneal cavity.

Increase in nitric oxide production is due to the activation of the nitrite reductase pathway for its synthesis. NO metabolites hyperproduction contributes to the progression of endometrioid heterotopia due to vasodilation of the existing vessels and the formation of new ones by stimulating migration and proliferation of endothelial cells (Sonova *et al.*, 2010). Nitric oxide is also known as a powerful anti-apoptotic compound, high generation of which plays an important role in the synthesis and deposition of collagen, which contributes to the formation of adhesions (Adamyan *et al.*, 2016; Guidice, 2010).

An almost 2-fold increased TNF- $\alpha$  level enhances the induction of phospholipase A2 (FLA2), which is involved in the triggering of the arachidonic acid cascade, resulting in the synthesis of prostaglandins that cause pain syndrome. According to our study, 68.9% of patients with EGE suffered periodic pains before or during menstruation, 8.1% had dyspareunia. 66.0% of patients had dysmenorrhea with menarche, which was significantly higher than in the control group (13.6%). TNF- $\alpha$  acts on proliferating cells by enhancing apoptosis. These patients had an inflammatory process, since TNF- $\alpha$  synthesis is observed in stimulated cells,

suggesting that its high level is the result of infection, which was found in 78.3% (pelvic inflammatory diseases) and in 14.4% (sexually transmitted infections) of patients.

LDL in patients with stages III-IV of the disease at the system level corresponded to control values. This is provided by an increased HDL content, which includes the enzyme paraoxonase, which protects against LDL oxidation. This enzyme promotes the breakdown and elimination of oxidized cholesterol. High levels of HDL cholesterol (hLDPV) in patients with external genital endometriosis at all stages of the disease suppresses inflammation. This situation follows from the previously identified inflammatory process in the pancreas, confirmed by the increased content of proinflammatory cytokines (TNF- $\alpha$  and IL-1 $\beta$ ) in it (Ermolova, 2008). However, it was found that in the inflammatory process, HDLPs change their function to pro-inflammatory due to a decrease in the concentration of the main HDL apolipoprotein - ApoA. It provides reverse transport of cholesterol to the liver and increases the activity of paraoxonase. If the detected high level of HDL in the pancreas increases the anticoagulant properties of red blood cells - on the one hand, and on the other hand, it manifests pro-inflammatory properties on the background of the inflammatory process, which enhances inflammation, then a complex metabolic situation is revealed when it is difficult to determine which HDL function predominates.

In the pancreas of women with I-II stages of EGE, the increased LDL level ( $p < 0.003$ ) was found comparing to the control data, which may be the result of compensatory reactions aimed at increasing the activity of PLA2, LDL structural unit.

A correlation analysis of the actual material was carried out in the experiment. Significant negative correlation between the content of free cholesterol and metabolites of nitric oxide ( $r = -0.8$ ) in the blood serum and between free cholesterol and the activity of NO synthase ( $r = -0.85$ ) is of special interest. The revealed regularity shows that at the systemic level there is a dependence of nitric oxide production and NO-synthase activity on the lipid spectrum, and in particular, on the level of free cholesterol in women with EGE I-II stages.

Changes in TNF- $\alpha$  production suggest that there is a reduced function of this cytokine as an angiogenesis factor (Guidice, 2010) and cell proliferation in the pancreas. TNF- $\alpha$  regulatory

capabilities in the pancreas are determined by its ability to induce apoptosis and produce antibacterial protective effect. In this case they are sharply reduced.

Change of metabolic processes at the systemic level can play a significant role in their disruption at the local level. First, TGF- $\beta$ 1 high level as a factor that reduces proliferation is controlled by the central cerebral structures. However, modification of the molecular relationships of lipid metabolism (HDL) with angiogenic compounds in endothelial cells increases NO generation, causing an increase in heterotopies blood supply. It should be pointed out that a high level of TGF- $\beta$ 1 inhibits NO-synthase, reducing one of the reactions of NO formation, i.e. the development of compensatory processes occurs at the systemic level.

Thus, the metabolic features of the formation of I-II stages of EGE in patients at the systemic level (blood serum) are significantly increased levels of TGF- $\beta$ 1, HDL and nitric oxide metabolites. Besides, significant changes in the content of lipid metabolism products were found in the pancreas (local level). They were characterized by a significant increase in cholesterol, HDL and LDL, which contribute to the formation of oxidative stress in the abdominal cavity.

In EGE stages III – IV a high level of TGF- $\beta$ 1 is a factor in the development of fibrosis, which underlies the adhesive process. According to the data obtained by of N.V. Ermolova (2008), a high level of this growth factor is due to the inflammatory process both at the systemic and local levels.

Nonsteroidal products of the mevalonate lipid exchange pathway perform prenylation of small G-proteins (Rho, Rac), which ensure their integration into membranes and manifestation of functional activity. Modification of molecular bonds of lipid metabolism in endothelial cells increases NO generation, causing an increase in blood supply to endometrioid formations.

In this study, in women with EGE stages III-IV, different lipid fractions were differentiated in connection with the existing metabolic relationship of the mevalonate lipid exchange pathway and the generation of the main vasodilator, nitric oxide. In EGE stages III-IV, an increase in HDL content at the systemic level obviously plays a significant role in the state of lipid metabolism at the local level.

The increased blood supply to endometrioid heterotopia is due to the high content of nitric oxide metabolites in the pancreas of patients with EGE stages III-IV stages. This compound is a powerful vascular growth factor, vasodilator, and apoptosis inhibitor (Guidice, 2010). NOx excess is accompanied by oxidative stress and acts as a mutagenic, carcinogenic, and antiapoptotic factor (Sonova *et al.*, 2010; Adamyan *et al.*, 2016). High NOx generation in the pancreas, is due to the NO-synthase pathway, as evidenced by the high activity of this enzyme. There are few reports on the increased NO-synthase expression in endometrioid heterotopies, which can be explained by the presence of a functionally defective enzyme form or the secondary nature of this process (Kinugasa, 2011; Cayci, 2011; Rogers *et al.*, 2013).

The revealed very high NO generation in the peritoneal fluid can play an important role in the development of hypoxia. Recently, it has been proved that in the case of excessive NO production, its interaction with superoxidion ( $O_2^-$ ) is observed with the formation of peroxynitrite ( $ONOO^-$ ), a powerful oxidizing agent that modifies hemoglobin and changes its affinity for oxygen (Zinchuk, 2006). The latter leads to a decrease in the oxygen-binding properties of blood, and, consequently, to hypoxia, which leads to cellular metabolism disorders during endometriosis foci formation of (Taylor *et al.* 2002; Lee *et al.*, 2009).

Correlation analysis of the studied parameters in the blood serum of patients with EGE stages III-IV showed a close positive relationship between the HDL level and TNF- $\alpha$  content of ( $r = 0.60$ ). In this case, a negative correlation between NO-synthase activity and the TGF- $\beta 1$  level ( $r = -0.33$ ) was found. A significant negative relationship was in the peritoneal fluid between HDL and NO ( $r = -0.75$ ).

There is no doubt that the accompanying inflammatory process, immunological dysregulation, apoptosis inhibition, angiogenesis activation, and oxidative stress in the abdominal cavity are pathogenetic factors contributing to the survival and growth of endometrioid heterotopies (Adamyan, 2016).

Patients from our clinical sample mainly complained of infertility and / or pain, so we tried to find an explanation of their origin within the limits of our studies. We found prevalence of primary infertility regardless of the EGE stage. However, in percentage terms, both primary and

secondary infertility prevailed in patients with EGE stage I-II stage (57.1% and 32.1%, respectively). Apparently, both ovarian factors and the adhesion process in the abdominal cavity, characterized in our conditions by the involvement of the peritoneum of the sub-ovarian fossa and cul-de-sac, which may interfere with fertilization. The decrease in the ovarian reserve was due to the existing formation of endometrioid ovarian cysts from 3 to 10 cm, marked high TGF- $\beta 1$  content, influencing arginase and, subsequently, enhancing the synthesis of proline, the main substrate of the connective tissue. On the other hand, it is not possible ignore in this connection (with TGF $\beta 1$ ) the importance of high nitric oxide generation due to nitrite reductase synthesis in the absence of NO-synthase activity changes, which also contributed to the formation of adhesions. In this metabolic situation, significantly high HDL levels both in blood serum and peritoneal fluid should be taken into consideration, since they contribute to high generation of nitric oxide metabolites and the formation of oxidative stress.

The pain syndrome in our patients was probably due to the significant production of prostaglandins, which, on the one hand, were stimulated by high TNF- $\alpha$  content, which activates phospholipase A2 (a structural unit of LDL). On the other hand, the high generation of nitric oxide metabolites, changing the metabolism of arachidonic acid, acts on cyclooxygenase and thereby stimulates the formation of prostaglandins.

The revealed changes in the relationship of the lipid spectrum, growth factors, and angiogenic compounds are the theoretical basis for additional therapeutic measures aimed at normalizing metabolic processes in OGE.

#### 4. CONCLUSION

In patients with EGE stages I-II a high content of TGF- $\beta 1$ , HDL and nitric oxide metabolites was found in the blood serum (systemic level). Modification of metabolic processes at the systemic level plays a significant role in disrupting them locally (peritoneal cavity). A change in the molecular interactions of lipid metabolism (HDL) and angiogenic compounds in endothelial cells increases nitric oxide generation, which enhances blood supply to heterotopies.

Compensatory processes develop at the system level, in the form of a nitrite reductase pathway for the synthesis of nitric oxide, since a

high level of TGF- $\beta$ 1 inhibits NO-synthase. Adaptive reactions in the peritoneal cavity, contributing to a decrease in proliferation and inflammation, are caused by an increase in free cholesterol, LDL and HDL.

In patients with EGE stages III-IV there is relationship between HDL and TNF- $\alpha$  at the systemic level, which has anti-inflammatory properties. In the pancreas of patients of this group the parameters of TGF- $\beta$ 1, nitric oxide metabolites and NO-synthase are significantly increased, which indicates NO-synthase pathway for the synthesis of nitric oxide.

The change in the relationship of the lipid spectrum, nitric oxide metabolites and cytokines is the theoretical basis for additional therapeutic measures aimed at normalizing metabolic processes in EGE.

## 5. REFERENCES

1. Adamyan, L. V.; Kulakov, V. I.; Andreeva, E.N. Endometriosis Clinical recommendations. Moscow, 2016.
2. Babushkina, A. V. L-arginine from the point of view of evidence-based medicine *Ukr. Honey. Chasis*. **2009**, 74 (XI / XII).
3. Burlev, V.A.; Dubinskaya, E. D.; Ilyasova, N.A.; Burlev, A.V.; Gasparov, A.S. Pro- and anti-inflammatory activity in patients with peritoneal form of endometriosis and adhesions of the pelvic peritoneum. *Problems of reproduction*. **2012**, 4, 6-11.
4. Vanin, A.F.; Adamyan, L.V. Dinitrosol complexes of iron with thiolate ligands as the basis for the development of drugs with different effects. *Problems of reproduction. Spec. Issue, 21st Century Technologies in Gynecology*. **2008**, 86-89.
5. Ermolova, N.V. The pathogenetic role of endothelial factors and sex hormones in the formation of external genital endometriosis. *Russian Bulletin of the Obstetrician-Gynecologist*. **2007**, 8(3), 29-32.
6. Ermolova, N.V.; Pathogenetic mechanisms of the formation of external genital endometriosis and its stages in patients of reproductive age. Ph.D. thesis, Rostov-on-Don, 2009.
7. Zinchuk, V.V. NO as a ligand that determines the oxygen-binding properties of blood. Mater. Int. Symptosis "Active forms of oxygen, nitrogen and chlorine in the regulation of cellular functions in normal and pathological conditions." Grodno 2006, 89-93.
8. Keelet, E.P.; Korneeva, I.E.; Shurshalina, A.V. Infertility of unclear origin: the focus of modern scientific research. *Probl. Reprod*. **2010**, 16(1), 32-35.
9. Kolesnikova, L.V.; Ermolova, N.V.; Linde, V.A.; Shiring, A.V.; Slesareva, K.V.; Tomay, L.R.; Skachkov, N.N. The absence of the negative effect of paraoxanase gene polymorphism in the exchange of lipoproteins with external genital endometriosis. *Journal of Obstetrics and Women's Diseases. Specialist. issue*, **2012**, LXI, 28-29.
10. Sonova, M.M.; Arslanyank, N.; Loginova O.N.; Maksimova Yu.V.; Murdalova Z.Kh.; Shulyak I.Yu. Optimization of the treatment of external genital endometriosis using antioxidant agents. New technologies in the diagnosis and treatment of gynecological diseases. A. S. XXIII International Congress with a course of endoscopy. Moscow. 2010, 163-164.
11. Sonova; M.M.; Didenko, L.F.; Antonova, S.A.; Tikhonova, E.S.; Osipova, A.A.; Arslanyan, K.N. The participation of macrophages in the pathogenesis of genital endometriosis. *Reproduction problems. V International Congress on Reproductive Medicine. Specialist. issue*, **2011**, 152-153.
12. Chernukha, G. E. Endometriosis and chronic pelvic pain: causes and consequences. *Problems of reproduction*. **2011**, 5, 83-89.
13. Schwartz, Ya.Sh.; Khoshchenko, O.M.; Dushkin, M.I.; Feofanova, N.A. The effect of cholesterol and agonists of hormonal nuclear receptors on the production of transforming growth factor  $\beta$  in macrophages. *Bulletin of experimental biology and medicine*. **2009**, 148, 9, 294-297.
14. Anderson Sanches Melo; Julio Cesar Rosa-e-Silva; Ana Carolina Japur de Sa Rosa-e-Silva; Omero Benedicto Poli-Neto; Rui Alberto Ferriani; Carolina Sales Vieira. Unfavorable lipid profile in women with endometriosis. *Fertility and Sterility*. **2010**; 93, 7, 2433-2436.
15. Berbic, M.; Shuike, L.; Markham, R.;

- Tokushige, N.; Zhou, J. Macrophage expression in endometrium of women with and without endometriosis. *Hum Reprod* **2009**; 94: 623-31.
16. Bryan, N.S.; Bian, K.; Murad, F. Discovery of the nitric oxide signaling pathway and targets for drug development. *Frontiers in Bioscience*, **2009**, 14: 1-18.
  17. Cayci, T.; Akgul, E.O.; Kurt, Y.G.; Ceyhan, T.S.; Aydin, I.; Onguru, O.; Yaman, H. The levels of nitric oxide and asymmetric dimethylarginine in the rat endometriosis model. *ObstetGynaecol Res.* **2011**, 37(8), 1041-7.
  18. Charles, O.A. Omwandho; Lutz Konrad; Gulden Halis; Frank Oehmke; Hans-Rudolf Tinneberg. Role of TGF- $\beta$ s in normal human endometrium and endometriosis. *Human Reproduction*, **2010**, 25, 101-109.
  19. Darling, A.M.; Chavarro, J.E.; Malspeis, S.; Harris, H.R.; Missmer S.A. A prospective cohort study of Vitamins B, C, E, and multivitamin intake and endometriosis. *J Endometr.* **2013**, 5(1), 17-26.
  20. Falcone, T., Lebovic, D.I. Clinical management of endometriosis. *Obstet Gynecol.* **2011**, 118(3), 691-705.
  21. Gajbhiye, R.; Sonawani, A.; Khan, S.; Suryawanshi, A.; Kadam, S.; Warty, N.; Raut, V.; Khole, V. Identification and evaluation of new serum markers for early diagnosis of endometriosis. *Human Reproduction.* **2012**, 2 (26), 35-45.
  22. Guidice, L.C. Endometriosis, *N Engl J Med*, **2010**, 362, 2389-2398.
  23. Gupta, S.; Agarwal, A.; Krajcir, N.; Alvarez, J.G. Role of oxidative stress in endometriosis. *Reprod Bio Med Online.* - **2006**, 13(1), 126-134.
  24. Kinugasa, S.; Shinohara, K.; Wakatsuki, A. Increased asymmetric dimethylarginine and enhanced inflammation are associated with impaired vascular reactivity in women with endometriosis. *Atherosclerosis.* **2011**, 219(2), 784-8.
  25. Laschke, M.W.; Giebels, C.; Menger, M.D. Vasculogenesis: a new piece of the endometriosis puzzle. *Hum Reprod Update.* **2011**, 17(5), 628-36.
  26. Lee, B.; Du, H.; Taylor, H.S. Experimental murine endometriosis induces DNA methylation and altered gene expression in eutopic endometrium. *BiolReprod* **2009**, 80, 79-85.
  27. Luciano, D.; Roy, G.; Luciano, A.A. Adhesion reformation after laparoscopic adhesiolysis: where, what type, and in whom they are most likely to recur. *J Minim Inv Gynecol.* **2008**, 15(1), 44-48.
  28. Melo, A.S.; Rosa-e-Silva, J.C.; Poli-neto, O.B.; Ferriani, R.A.; Vieira C.S. Unfavorable lipid profile in women with endometriosis. *Fertil Steril.* **2010**, 93(7), 2433-2436.
  29. Rogers, P.A.; D'Hooghe, T.M.; Fazleabas, A. Defining Future Directions for Endometriosis Research: Workshop Report From the 2011 World Congress of Endometriosis in Montpellier, France. *Reprod Sci.* **2013**, 20(5), 483-499.
  30. Santanam, N.; Murphy, A.A.; Parthasarathy, S. Macrophages, oxidation, and endometriosis. *Ann NY AcadSci* **2002**, 955, 461-467.
  31. Schmidt, N.; Laux-Biehlmann, A.; Boyken, J.; Koch, M.; Dahllof, H.; Zollner, T.M.; J. Nagel. Inflammation and pain in mouse model of retrograde menstruation. *Journal of Endometriosis and Pelvic Pain Disorders* **2015**, 7, 93-94.
  32. Takebayashi, A.; Kimura, F.; Kishi, Y.; Ishida, M.; Takahashi, A. The Association between Endometriosis and Chronic Endometritis. *PLOS ONE.* **2014**, DOI: 10.1371/journal.pone.0088354.
  33. Taylor R.N.; Lebovic, D.I., Mueller, M.D. Angiogenic factors in endometriosis. *Ann. N. Y. Acad. Sci.*, **2002**, 955, 89-100.
  34. Vercellini, P., Grossignani, P.G., Someglia, E. «Waiting for Go dot»: a commonsens approach to the medical treatment of endometriosis. *Hum Reprod* **2011**, 26, 3-13.
  35. Verit, F. F.; Yucek, O. Endometriosis, leiomyoma and adenomeiosis: the risk of gynecologic malignancy. *Asian Pac J Cancer Prev.* **2013**, 14(10), 5589-97.
  36. Vodolazkaia, A.; El-Alamat, Y.; Popovic, D. Panel of plasma biomarkers can predict endometriosis with high sensitivity in patients with ultrasound negative endometriosis. *Hum Reprod.* **2012**, 27(9), 2698-711.

37. Wang, G.; Tokushige, N.; Markham, R.; Fraser, I.S. Rich innervations of deep infiltrating endometriosis. *Hum Reprod* **2009**; 24:827-34.

**Table 1. Parameters Indicators of cell metabolism regulators in patients with EGE (blood serum).**

| Parameter                | EGE stage                   | Control                    | P            |
|--------------------------|-----------------------------|----------------------------|--------------|
| <b>I-II EGE stage</b>    |                             |                            |              |
| TGF- $\beta$ 1 (pg/ml)   | 12936.0<br>[7650.0-28050.0] | 9332.0<br>[4736.0-21100.0] | <b>0.004</b> |
| HDL (mmol/l)             | 1.25<br>[0.77-2.20]         | 1.10<br>[0.56-1.80]        | <b>0.013</b> |
| NOx (mmol/l)             | 16.50<br>[0.80-61.50]       | 2.39<br>[0.10-62.50]       | <b>0.041</b> |
| <b>III-IV EGE stage</b>  |                             |                            |              |
| TNF- $\alpha$<br>(pg/ml) | 15.56<br>[4.70-64.00]       | 8.04<br>[0.40-23.60]       | <b>0.014</b> |
| TGF (mmol/l)             | 1.25<br>[0.91-2.30]         | 1.10<br>[0.56-1.80]        | <b>0.006</b> |
| NOx (mmol/l)             | 32.00<br>[0.48-56.00]       | 2.39<br>[0.10-62.50]       | <b>0.001</b> |

Note: Results are presented as median and interquartile interval.

p - significance of differences compared with the control group.



**Table 2. Parameters of cell metabolism regulators in patients with EGE (peritoneal fluid)**

| Parameter               | EGE stage                  | Control                     | P            |
|-------------------------|----------------------------|-----------------------------|--------------|
| <b>I-II EGE stage</b>   |                            |                             |              |
| Cholesterol (mmol/l)    | 2.0<br>[1.07 –3.09]        | 1.39<br>[1.21 – 1.81]       | <b>0.008</b> |
| HDL (mmol/l)            | 0.78<br>[0.34-1.17]        | 0.45<br>[0.33-0.59]         | <b>0.004</b> |
| LDL (mmol/l)            | 0.77<br>[0.0-1.21]         | 0.48<br>[0.01-0.70]         | <b>0.003</b> |
| <b>III-IV EGE stage</b> |                            |                             |              |
| TNF- $\alpha$ (pg/ml)   | 8.30<br>[0.02-29.86]       | 12.59<br>[4.0-31.20]        | <b>0.050</b> |
| TGF- $1\beta$ (pg/ml)   | 2480.0<br>[1513.60-5720.0] | 1425.40<br>[1011.0-2200.40] | <b>0.001</b> |
| NOx (mcmol/l)           | 24,00<br>[7.52-65.00]      | 7.25<br>[0.14-64.50]        | <b>0.039</b> |
| NO-synthase (mcmol/l)   | 35.00<br>[28.60-67.40]     | 23.00<br>[0.79-57.60]       | <b>0.001</b> |

Note: results are presented as median and interquartile interval.

p - significance of differences compared with the control group.

**ANÁLISE DOS ERROS DE CONEXÃO MATEMÁTICA DOS ALUNOS NA RESOLUÇÃO DE PROBLEMAS DE IDENTIDADE TRIGONOMÉTRICA****ANALYSIS OF STUDENTS' MATHEMATICAL CONNECTION ERRORS IN TRIGONOMETRIC IDENTITY PROBLEM SOLVING**MARDIYANA<sup>1\*</sup>; USODO, Budi <sup>2</sup>; BUDIYONO<sup>3</sup>; JINGGA, Anisa Astra<sup>4</sup>; FAHRUDIN, Dwi<sup>5</sup><sup>1,2,3</sup> Lecturer at Mathematics Education, Universitas Sebelas Maret<sup>4,5</sup> Postgraduate Student at Mathematics Education, Universitas Sebelas Maret

\* Correspondence author

e-mail: mardiyana@staff.uns.ac.id

Received 26 May 2020; received in revised form 18 June 2020; accepted 28 June 2020

**RESUMO**

A identidade trigonométrica é importante no aprendizado de matemática, porque exige que os alunos pensem crítica, lógica, sistematicamente e completamente. A resolução de problemas de identidade trigonométrica exige que os alunos relacionem conhecimento conceitual ou conhecimento processual, que depois é usado em perguntas. Este estudo envolveu alunos da série X do ensino médio, que foram examinados para descobrir os tipos de erros de conexão matemática e as causas dos erros. Antes das entrevistas baseadas em tarefas, 36 estudantes foram inicialmente submetidos a um teste. Com base em várias considerações, sete estudantes (três homens e quatro mulheres) foram selecionados para serem submetidos a uma entrevista baseada em tarefas. Esta pesquisa empregou um método qualitativo de pesquisa com desenho de estudo de caso. Os resultados da pesquisa indicam que os erros na conexão com o conhecimento conceitual são mais comumente o erro de conectar o conceito algébrico. Por outro lado, 86,11% dos estudantes experimentaram erros na conexão com o conhecimento processual. Esse erro ocorreu quando os alunos trabalharam em problemas com identidades trigonométricas que raramente encontravam em exercícios. Erros nas conexões matemáticas da identidade trigonométrica são causados pela falta de compreensão da operação aritmética algébrica, ênfase no conceito e conhecimento estratégico. Isso mostra que os alunos precisam de uma variedade de problemas para poderem dominar várias formas de identidades trigonométricas. O resultado desta pesquisa também reforça o importante papel dos conceitos algébricos como conhecimento prévio no estudo da identidade trigonométrica.

**Palavras-chave:** conexão matemática; erro; conhecimento prévio; processual; conceptual**ABSTRACT**

The trigonometric identity is essential in learning Mathematics because it requires students to think critically, logically, systematically, and thoroughly. Solving trigonometric identity problems requires students to relate conceptual knowledge or procedural knowledge, which then used in questions. This study involved grade X students of senior high school, which were examined to find out the types of mathematical connections errors and causes of the errors. Before task-based interviews were conducted, 36 students were first given a test. Based on several considerations, seven students (three males and four females) were selected to undergo a task-based interview. This research employed a qualitative research method with a case study design. The results of the analysis indicate that the errors in connecting to conceptual knowledge are most commonly the mistake of connecting the algebraic concept. On the other hand, 86.11% of students experienced errors in connecting to procedural knowledge. This error happened when the students worked on problems with trigonometric identities, which they had rarely encountered in exercises. Errors in mathematical connections in trigonometric identity are caused by the lack of understanding of the algebraic arithmetic operation, emphasis on the concept, and strategic knowledge. It shows that students need a variety of problems to be able to master various forms of trigonometric identities. This research's result also reinforces the critical role of algebraic concepts as prior knowledge in studying trigonometric identity.

**Keywords:** mathematical connection; error; prior knowledge; procedural; conceptual

## 1. INTRODUCTION:

Trigonometry is one of the earliest mathematics topics that link algebraic, geometric, and graphical reasoning; it can serve as an essential precursor towards understanding pre-calculus and calculus (Weber, 2005). Trigonometric identities play a significant role when students study geometry and calculus at the next level. The essence of learning trigonometric identity is not only knowing its knowledge but also understanding the discovery or derivation of its properties. The trigonometric identities hone students' ability to think deductively, creatively, and practice the problem-solving skill.

During the process of learning mathematics, students need the ability to relate various mathematical concepts as conveyed in Bruner's connectivity theorem, "in mathematics, each concept relates to other concepts." Therefore, students must be allowed to make mathematical connections to be more successful in learning mathematics. Mathematical connections are explained by Hiebert and Carpenter (1992) as part of structured networks such as spider webs, "The junctures, or nodes, can be thought of as pieces of represented information, and threads between them as the connections or relationships." Hiebert and Carpenter attributed the process of conceptualizing the conceptual knowledge to the corresponding structure, which was then highlighted that knowledge only exists when some insight can be interconnected. Also, conceptual understanding can be formed by increasing the number of connections between these pieces of knowledge.

Mathematical connections relate with the connection between one concept to another, one procedure to another, as well as the relationship between facts and procedures, we can see that mathematical connection are related to the ability to link conceptual knowledge and procedural knowledge. Students need both applications of theoretical and procedural knowledge to solve any problem correctly (Taconis, et al., 2000; Cracolice, et al., 2008). Thus, we can divide the mathematical connection errors into two types, namely errors in connecting to conceptual knowledge and errors in connecting to procedural knowledge (Table 1).

Procedural knowledge is a knowledge that focuses on skills and step-by-step procedures without explicit reference to mathematical ideas (Marchionda, 2006). Meanwhile, conceptual knowledge, according to McCormick (1997), relates to the relationship between various

knowledge, so that when students can identify this relationship, it can be said that they have a conceptual understanding. Surf's research (2012) showed that there is a significant relationship between theoretical knowledge and procedural knowledge in solving problems.

The study aimed to find out the types of students' mathematical connections errors and causes of the errors. Insights provided by this research can serve some useful indications such as an error in connecting to conceptual or procedural knowledge, which was done by students and the one that became our particular concern. Besides, it is expected to be useful as an input for teachers about the importance of making mathematical connections for students so that they can be considered in teachers' plans and learning instruction.

## 2. LITERATURE REVIEW:

Many studies have concerned about misconceptions and making errors (Bush, 2011; Dhlamini & Kibirige, 2014; Sarwadi & Shahrill, 2014; Mohyuddin & Khalil, 2016; Ndemo & Ndemo, 2018; Sudihartinih & Purniati, 2020). A few researchers have also mentioned students' misconceptions and errors in trigonometry, such as Orhun (2015) and Usman & Hussaini (2017). Usman & Hussaini's research is based on Newman Error Hierarchical Model, which differs from this research in terms of research method, which was used. Orhun's research is about the difficulties faced by students in using trigonometry for solving problems in trigonometry. Although Orhun studied the students' ability to develop the existing concept in trigonometry, the focus of his research is the trigonometric ratio. On the other hand, Brown (2006) studied students' understanding of sine and cosine. He found out a framework, called trigonometric connection. Although Brown's research was on trigonometric link, the focus of the study was only on the rules of sine and cosine; therefore, this research focuses on trigonometric identity. The identity of trigonometry is one of the topics that high school students should study. Orhun (2015) found that the students did not develop the concept of trigonometry with certainty.

Various literature (NCTM, 2000; Mousley, 2004; Blum, et al., 2007) have identified two main types of mathematical connections. The first is to recognize and apply mathematics to contexts outside mathematics (the relationship between mathematics, other disciplines, or the real world). The second concerns the interconnections

between ideas in mathematics.

Moreover, students can understand mathematics deeply if they have an understanding of conceptual and procedural knowledge (Wilkins, 2000). Conceptual knowledge focuses on understanding the relationship between mathematical ideas and concepts. Meanwhile, procedural knowledge focuses on symbolism, skills, rules, and algorithms that used step by step in completing mathematical tasks. Students must learn the concepts at once with procedures so that they can see the relationship. In line with Wilkins, the NCTM's Principles and Standards for School Mathematics (2000, p. 35) states that developing fluency in mathematical problem solving requires a balance and connection between conceptual understanding and computational ability. The procedures used by the students while solving mathematical problems show the various levels of students' conceptual understanding (Ghazali & Zakaria, 2011). Meanwhile, the issue of conceptual knowledge is a problem experienced even by undergraduate students and prospective teachers (Arjudin, et al., 2016; Dündar & Gündüz, 2017).

### 3. MATERIALS AND METHODS:

#### 3.1. Research methods and participants

Qualitative research method with case study design was used to investigate the grade X students in a high school located in Kartasura, Indonesia. The reason for choosing this school was because the percentage of national examination results on high school trigonometric from 2013-2017 was lower than another topic. Moreover, the results of interviews with teachers indicated that students have difficulty in studying the identity of trigonometry than other issues. Also, the researchers did not teach in the school; it is to minimize the bias of research, which may occur due to the subjectivity of the researchers with students and school staff.

Researchers have received approval to research the school concerned through a letter of agreement signed by the Assistant Principal of Public Relations and Partnership. Moreover, all participants have agreed to participate in this study. Researchers kept their identity to be confidential.

The qualitative approach was appropriate because the analysis of the learners' responses to the given was used to generate theory (Dhlamini & Kibirige, 2014). The case study method was chosen in the hope that through the study of a

somewhat unique individual, valuable insights would be gained (Fraenkel & Wallen, 2000).

#### 3.2. Data collection

This research used task-based interviews that have been used by researchers in qualitative research in mathematics education to gain knowledge about an individual or group of students' existing and developing mathematical knowledge and problem-solving behaviors (Lerman, 2014). The tasks used in this research consists of three items with various degrees of difficulty. It is intended to identify the mathematical connection errors of upper students and anticipate the possibility that only a few students who can answer the questions. Problems given in this research are as follows:

Problem A (for the first test):

- 1) Prove that  $\sec x - \sec x \sin^2 x = \cos x$  !
- 2) Known:
  - $a \cos x + \tan x = \sec x$  and
  - $-b - \tan x = \sec x$ ,
  - determine the simplest form of a.b !
- 3) Prove that  $\frac{\cos x}{1 + \sin x} = \frac{1 - \sin x}{\cos x}$  !

Problem B (for the interview):

- 1) Prove that  $\csc x - \csc x \cos^2 x = \sin x$  !
- 2) Known:
  - $a \sin x + \csc x = \csc x$  and
  - $-b - \csc x = \csc x$ ,
  - determine the simplest form of a.b !
- 3) Prove that  $\frac{\sin x}{1 + \cos x} = \frac{1 - \cos x}{\sin x}$  !

Question number one is a matter of easy category since it only tests students' ability to relate their knowledge of distributive properties (a matter of pre-condition) and then comparing it to the concept of trigonometric identity. Problem number two is a tricky category because it examines the ability of students to identify the relationship between the first equation and the second equation, which can be operated to produce a trigonometric identity formula. So, this problem requires students' ability to relate the concept of arithmetic algebra and then linking the results obtained to the idea of trigonometric identity. Problem number three is a matter of medium category because it tests the ability of students in doing algebraic manipulation that can generate trigonometric identity form associated with the form of trigonometric identity, which will be proven.

Before task-based interviews are conducted, 36 students were given a test first (see Problem A). Task-based interviews are conducted for students who have different content analysis results (different from other students) and fulfill

almost every indicator, based on these considerations, seven students (three males and four females) were selected to undergo a task-based interview. Task-based interviews are carried out to get valid data about errors in mathematical connections that students do and to get data about the causes of failures. Accurate data regarding the purpose of the failure is obtained by conducting interviews at different times.

During the task-based interview, the researchers gave the test to the students in which the problem of the test was similar to the question presented in the previous test (see problem B). The problem is made similar to avoiding the possibility of students memorize the answers. The data were in the form of statements about things done during the fulfillment of tests, errors in making a mathematical connection, causes of mistakes, and guidance from the researcher.

### 3.3. Data analysis

The study used a content analysis technique that was also used by Luneta (2015) when researching students' misconceptions. In this technique, each question is analyzed according to the content they contain (student errors); in this case, the students' answers are indicative of their ability to interact with trigonometric identity questions. The variables measured are their responses (misconceptions and related errors) to the correct answers. The analysis made inferences to the communication (student's answers) by systematically and objectively identifying specific characteristics of the student's errors in the answers. The unit of analysis was the errors students displayed on each questions. Errors made by subjects are grouped and identified its characteristics. Indicators of the type of mathematical connection errors can be expressed in Table 1.

## 4. RESULTS AND DISCUSSION:

The following is the analysis of the mathematical connection error that students do in working on the problem of trigonometric identity along with its causes. A summary of students' errors on the items is provided in Table 2.

In the transcript, the researcher is referred to as R meanwhile, the seven students interviewed are referred to as S.N.2, S.N.5, S.N.6, S.N.12, S.N.1, S.N.33, and S.N.34 which imply the students' serial number in the class. There is also an abbreviation in the figure such as K.S.17.1. K.S

refers to student errors, 17 refers to the serial number of students in the class, and 1 refers to the error number.

### 4.1. Error in mathematical connection problem number 1

#### 4.1.1 Type A

In question number 1, four students include subject number 33, failed in relating knowledge of algebraic arithmetical operations. During the initial test, the student performed a reduction operation on  $\sec x - \sec x \sin^2 x$ , which resulted in  $\sin^2 x$ . When the student was asked to solve a question for a task-based interview, the student redid the same mistake. It can be seen from the quotation I as follows:

Quote I

**S.N.33:**  $\frac{1}{\sin x} - \frac{1}{\sin x} (1 - \sin^2 x)$  results in  $(1 - \sin^2 x)$  because  $\frac{1}{\sin x} - \frac{1}{\sin x}$  the result is zero.

**R:** Look,  $\frac{1}{\sin x}$  multiplied by  $1 - \sin^2 x$ , right?

**S.N.33:** Yeah ...

**R:** Let this  $a$  (the researcher designated  $\frac{1}{\sin x}$ ) minus  $b$  (the researcher pointed  $1 - \sin^2 x$ ) multiplied by  $a$ , what is the result?

**S.N.33:**  $a - ab$

**R:** So, is it true if you write it as this (designate  $\frac{1}{\sin x} - \frac{1}{\sin x} (1 - \sin^2 x)$ )? Is it true if the result is  $1 - \sin^2 x$ ?

**S.N.33:** No ...

According to quote I, the student thought that  $\frac{1}{\sin x} - \frac{1}{\sin x} (1 - \sin^2 x)$  resulted in  $1 - \sin^2 x$ . It shows that the student failed in relating the concept of algebraic form calculation, which had been learned in junior high school to be applied to this problem. That algebraic form contains fractions, Bush (2011) in his research, showed that students often applied the wrong algorithm when adding, subtracting, multiplying, or dividing fractions. When the researcher simplified the algebraic form, the student was able to answer the researcher's question correctly. So, this error occurred since the student did not understand the concept of algebraic arithmetic operations. Problems regarding understanding algebraic concepts are problems that have attracted the attention of many researchers (House & Telese, 2008; Nathan & Koellner, 2007; Bush, 2011; Pournara, et al., 2016), this suggests that the notion of algebraic concepts are things that are commonly experienced by students. The results of

this research, which focuses on trigonometric identities, also found students who lacked understanding of algebraic concepts; this finding supports the research of Usman & Hussaini (2017) which focused on the manipulation of trigonometrical ratios using formula and the right-angled triangle. They noted that the students' error in solving trigonometrical problems was due to their weaknesses in basic arithmetical operations.

#### 4.1.2 Type B

In question number 1, four students failed in relating their knowledge about distributive properties to change an algebraic form. One of four students who experienced this failure is subject 33, as seen in the following quotation II:

Quote II

**R:** In this " $a - ab$ " form ( $a$  stands for  $\frac{1}{\sin x}$  and  $b$  stands for  $(1 - \sin^2 x)$ ), can you change its shape based on its distributive properties? (Students were asked to change " $a - ab$ " form into " $a(1 - b)$ " form)

**S.N.33:** Yes ..... it becomes  $a - b$ .

**R:** Really? If we apply distributive properties to this form, it will become " $a$ ". Then, what is inside the bracket?

**S.N.33:** Uh, it becomes 1.

**R:** Okay, 1 and then?

**S.N.33:** Minus  $b$ .

The student cannot explore her cognitive ability about distributive properties on  $\frac{1}{\sin x} - \frac{1}{\sin x} (1 - \sin^2 x)$  becomes  $\frac{1}{\sin x} (1 - (1 - \sin^2 x))$  or becomes  $\frac{1}{\sin x} - \frac{1}{\sin x} + \frac{1}{\sin x} \cdot \sin^2 x$ . It indicates that the student has failed to relate her prior knowledge. Gentile & Lalley (2003) revealed that the mastery of prior knowledge was required by students in the study of mathematics, it is an important step in concept development. This happens because the learning process in Mathematics is categorized as a widely related hierarchical learning process (Usman & Hussaini, 2017). If prior knowledge or skills do not exist, the task of learning becomes more difficult, if the prior knowledge has been wrongly understood, the need to learn a new topic results in students for getting previous misconceptions.

Based on quote I, students still encounter difficulties and need guidance from the researcher to apply distributive properties although  $\frac{1}{\sin x} -$

$\frac{1}{\sin x} (1 - \sin^2 x)$  has been simplified its algebraic form into  $a - ab$ . Thus, we can conclude that the cause of these errors is the inability to apply their basic knowledge of distributive properties to new situations. Mulungye, et al. (2016) stated that the distributive property says that  $a(b + c) = ab + ac$ . Therefore, students use this rule in new situations that are not appropriate. The distributive properties of the multiplication toward the sums are memorized in their minds that they intuitively misapplied them to a similar situation.

Students also failed to relate their knowledge about  $1 - \sin^2 x = \cos^2 x$ , which was then applied to question number 1. The four students use similar methods in solving problems. They changed  $\sec x$  to  $\frac{1}{\cos x}$ , during the first test, but all four students made a mistake when changing the form of  $\csc x$  in the second test. The students did not know that another form of  $\csc x$  is  $\frac{1}{\sin x}$  although the researcher had tried to guide them; so, they still cannot answer the question correctly. The fact that they can change  $\sec x$  to  $\frac{1}{\cos x}$ , but cannot change  $\csc x$  to  $\frac{1}{\sin x}$  Indicates that they memorize the similarities that exist in trigonometric identities. Tobias (1993) stated that mathematical anxiety can cause a person to forget. This is consistent with the results of further interviews; the subject number 34 said that he felt depressed and considered the topic confusing, this anxiety caused him to forget the trigonometry identities. Mathematical anxiety is a feeling of tension and anxiety that interferes the manipulation of numbers and solving mathematical problems in various academic situations and everyday life. Some students tend to experience this anxiety in exams. Meanwhile, others are only afraid of mathematical calculations. Wells (1994) identified anxiety as a significant factor that hinders students' reasoning, memory, understanding of general concepts, and respect to Mathematics.

#### 4.2. Error in mathematical connection problem number 2

##### 4.2.1 Type A

As many as 44.4% of students failed to relate their knowledge about the concept of algebraic operation, especially in trigonometric identities. Students concluded that if  $1 - \sin^2 x = \cos^2 x$  then  $1 - \sin x = \cos x$ . The student thought that  $\sqrt{1} = \sqrt{\sin^2 x + \cos^2 x}$  produces  $1 = \sin x + \cos x$ . Students considered that the square root function was linear. Students tend to over-regenerate what has been experienced as



something 'true' (De Bock, Van Dooren, Janssens, & Verschaffel, 2002)

The failure to relate knowledge of algebraic arithmetic operations also occurred when changing the form of  $a \cos x + \tan x = \sec x$  into  $a = -\cos x - \tan x + \sec x$ . This error occurred since the student did not understand the concept of addition, reduction, and multiplication, which are operated together. The researcher found that when the algebraic form was still in a complicated form, the students were not able to cope, but when the algebraic form was already in a simple form, the students were able to overcome it. Researchers found that students can overcome errors in connecting the concept of algebraic operations when researchers simplify the algebraic form. The student was able to answer the question and followed the direction given by the researcher when the researcher simplified the algebraic form and gave direction to him. Thus, the cause of this error was that the students do not understand the concept of algebraic operation. The findings of this research support Norasiah's research (2002) which noted that most average students faced difficulty in performing trigonometrical operations.

#### 4.2.2 Type B

As many as 52.78% of students did not try to associate trigonometric identities with other trigonometric identities. Still, they chose to elaborate trigonometric identity formulas, which lead to more complex counting operations. If the student was able to handle such complexity as student number 26, he would achieve the simplest form. If the student was unable to handle it, he would have difficulty in finding the most straightforward way; it is experienced by subject number 17 (Figure 1).

When the students were asked to work on similar problems and then interviewed about the results of their work, they reused this strategy. It can be seen in the following quotation III

Quote III

**R:** Why did you choose this strategy? Did you elaborate each of these identities?

**S.N.17:** If it was not elaborated, the answer would not be the simplest one ...

**R:** Oohh... like that ... do you know the identity which has something to do with  $\csc x$  and  $\cot x$ ? Something with a quadratic form?

**S.N.17:** Yes ...

**R:** What is it?

**S.N.17:** Cosecant  $x$  is equal to one per sinus  $x$

**R:** No ...something about  $\csc^2 x$ ...

**S.N.17:**  $\csc^2 x = \frac{1}{\sin^2 x}$

**R:** No...cosecant  $x$  is connected with cotangent  $x$ ...

**S.N.17:** I forgot ...

**R:** Do you ever think about this? This is  $\cot x$ , and this is  $\csc x$ ; then, its  $b$  is also there  $\cot x$ ,  $\csc x$  ... then you look for  $a$  itself... $b$  itself which were then sought the relationship between the two?

**S.N.17:** No ...It is hard to think.

Handwritten mathematical work of subject number 17. The work is divided into several sections labeled K.S.17.1, K.S.17.2, K.S.17.3, and K.S.17.4. K.S.17.1 shows the derivation of  $a = \sec x$  from  $a \cos^2 x + \sin x = 1$ . K.S.17.2 shows the derivation of  $b = \frac{1 + \sin x}{-\cos x}$  from  $-b \cos x - \sin x = 1$ . K.S.17.3 shows the calculation of  $a \cdot b = \frac{1 + \sin x}{-\cos^2 x}$ . K.S.17.4 shows the final result  $a \cdot b = \frac{1 + \sin x}{-\cos^2 x}$ .

**Figure 1.** The response of subject number 17

Based on the quotation III, it indicates that the student failed to associate his knowledge about  $\sec^2 x - \tan^2 x = 1$ , which was then applied to the results of multiplication  $a$  and  $b$ . It happened because the student thought that a simple form would be achieved if each trigonometric identity was altered. The selection of such strategy resulted in complicated calculations; in this case, student number 17 was not able to overcome the complexity, which resulted in a miscalculation (see K.S.17.3 in Figure 1). Wright (2014) stated that students need the ability to choose the applicable formula based on the context of the mathematical problems they encounter.

As many as 5.6% of students chose the strategy of eliminating the system of equations, which caused some more complex counting operations. Although the students tried to solve this problem by linking their knowledge of

elimination rules, this strategy is not appropriate. It indicates that the students did not understand the concept that the two equations are not linear equations (error type A). Although the students could change the equations in the form of linear equations, the number of unknown factors was more than the sum of the equations. It caused the system of linear equations not to have a solution. If it had a solution, it would have an infinite number of solutions. Besides, the student also failed to associate the fact that  $\sec^2 x - \tan^2 x$  is equal to 1 (error type B). One of the students using this strategy was student number 6, as seen in the following quotation IV:

Quote IV

**R:** Why did not you try another strategy to solve this problem? Such as determining the value of  $a$  and  $b$  first, then doing the multiplication operation towards  $a$  and  $b$ ?

**S.N.6:** Uumm ...I did not think like that.

**R:** Was it because there were two equations, then you chose to eliminate them?

**S.N.6:** Yes... if there are two equations, I solve it by elimination.

Based on quote IV, it shows that the student eliminated both equations (see K.S.6.1 and K.S.6.2 in Figure 2). The cause was the student's lack of understanding of the concept of the linear equation system. The student assumed that two equations had to be solved by elimination. The choice of such a strategy resulted in more complicated calculations. In this case, subject number 6 was not able to overcome the complexity which occurred (see K.S.6.3 and K.S.6.4 in Figure 2) due to complicated forms, resulting in the student making errors in the calculations.

The figure shows handwritten mathematical work for subject number 6. It includes several boxed sections labeled K.S.6.1, K.S.6.2, K.S.6.3, and K.S.6.4. K.S.6.1 shows two equations:  $a \cos x + \tan x = \sec x$  and  $-b - \tan x = \sec x$ , which are then manipulated. K.S.6.2 shows a similar manipulation. K.S.6.3 and K.S.6.4 show increasingly complex algebraic expressions involving trigonometric functions and fractions, resulting from the elimination process.

**Figure 2.** The response of subject number 6

Based on the results of the analysis on students number 6 and 17, it shows that the

students did not have good ability to relate one trigonometric identity with other trigonometric identities. Based on the interview, all students who made mistakes in number 3 did not know the identity value of the  $\sec^2 x - \tan^2 x$ , even though, based on observations, the teacher has given detailed knowledge about  $\sec^2 x - \tan^2 x = 1$ . However, the teacher did not provide enough emphasis on this identity. The given problem was less varied. It only focused on the relationship of  $\sin^2 x + \cos^2 x = 1$ . In this case, the researcher assumed that the cause of the student's error in relating his knowledge of  $\sec^2 x - \tan^2 x = 1$  to be used in the results of multiplication  $a$  and  $b$  was the lack of emphasis on the concept and lacking of strategic knowledge. This is in accordance with the results of Lopez's (1996) study which focuses on mathematical word problems, he also found that weakness in understanding concepts and lacking of strategic knowledge result in difficulties in problem-solving. Moreover, students who were weak in conceptual understanding were found to lack arithmetic and procedural skills (Narayanan, 2007).

#### 4.3. Error in mathematical connection problem number 3

##### 4.3.1 Type B

Some students failed to relate their knowledge of multiplication to convert  $1 + \cos x$  into  $1 - \cos^2 x$ . Based on the interview result, it shows that the student already knew that he had to use the fact that  $1 - \cos^2 x$  is equal to  $\sin^2 x$  to solve this problem. However, the student could not exploit his cognitive ability to change  $1 + \cos x$  into  $1 - \cos^2 x$ . It indicates that the student failed in relating his knowledge of multiplication with a conjugate pair. The student already knew which identity formula should be utilized after getting directions from the researcher. However, the student did not know how to direct  $1 + \cos x$  to be converted into  $1 - \cos^2 x$ . So, the cause of student's error was less skill in doing the algebraic manipulation.

The error which occurred in problem number 3 is classified as minimal since only seven students who experienced this problem. Moreover, no student experienced error type B on this problem. Based on the observation done by the researcher, the teacher has given practice and provided a discussion on this kind of problem. Besides, some problems with the students' worksheets also honed their ability to solve this kind of problem. If the students are accustomed to solving certain types of problems, they will be able to solve other problems that are similar in types; it



is because the students already understand the way of settlement. A question or a mathematical problem is said to be a problem if the person who faces the challenge feels the gap between where it is and where it should be but do not know how to cross the deficit, this results in difficulties in solving existing problems (Reid & Yang, 2002).

## 5. CONCLUSION:

The results of this study have provided a new description of the error of mathematical connections in solving trigonometric identities. There are two types of mathematical connection errors. The first one is errors in connecting to conceptual knowledge (type A), and the second one is errors in connecting to procedural knowledge (type B). Students most commonly do error type A is the mistake of connecting the algebraic concept. Although the percentage is small, we can see that in-depth conceptual understanding of the linear equation system can cause connection errors in trigonometric identity problem solving.

In the second type (type B), an error occurred most often when the students worked on problems with trigonometric identities, which they had rarely encountered in exercises; 86.11% of students experienced this error. If the given problem contained common trigonometric identities encountered in their daily practice, only 30.56% students experience connection errors, from this fact, we could include that the second type of error was caused by the lack of emphasis on the concept and lack of strategic knowledge. Errors committed by the students in learning trigonometry can be useful for the teachers in evaluating their teaching as well as being able to correct the students' works appropriately.

## 6. LIMITATION AND STUDY FORWARD:

In this paper, we just discussed the error of mathematical connections in solving trigonometric identities. For the next researcher can discuss the topics more widely.

## 7. ACKNOWLEDGEMENTS:

The authors thank to Kartosuro Senior High School for giving research permission. We also thank to Universitas Sebelas Maret Surakarta for budget supporting. The authors are grateful to the reviewers for helpful comments.

## 8. REFERENCES:

1. Arjudin, Sutawidjaja, A., Irawan, E. B. & Sa'dijah, C. (2016). Characterization of Mathematical Connection Errors in Derivative Problem Solving. *IOSR Journal of Research & Method in Education*, 6, 5, 7-12.
2. Blum, W., Galbraith, P. L., Henn, H.-W. & Niss, M. (2007). *Modelling and applications in mathematics education*. New York: Springer US.
3. Brown, A. S. (2006). *The trigonometric connection: students' understanding of sine and cosine*. Prague, PME30, 228.
4. Bush, S. B. (2011). *Analyzing common algebra-related misconceptions and errors of middle school students*, University of Louisville: Unpublished Dissertations.
5. Cracolice, M. S., Deming, J. C. & Ehlert, B. (2008). Concept learning versus problem solving: a cognitive difference. *Journal of Chemical Education*, 85, 6, 873-878.
6. De Bock, D., Van Dooren, W., Janssens, D. & Verschaffel, L. (2002). Improper use of linear reasoning: An in-depth study of the nature and the irresistibility of Secondary School Students' Errors. *Educational Studies in Mathematics*, 50, 3, 311-334.
7. Dhlamini, Z. B. & Kibirige, I. (2014). Grade 9 Learners' Errors And Misconceptions In Addition Of Fractions. *Mediterranean Journal of Social Sciences*, 5, 8, 236-244.
8. Dündar, S. & Gündüz, N. (2017). Justification for the Subject of Congruence and Similarity in the Context of Daily Life and Conceptual Knowledge. *Journal on Mathematics Education*, 8, 1, 35-54.
9. Fraenkel, J. R. & Wallen, N. E. (2000). *How to Design & Evaluate Research in Education*. Boston: McGraw-Hill Companies, Inc.
10. Gentile J. R & Lalley, J. P. (2003). *Standards and Mastery Learning Aligning Teaching and Assessment so All Children can Learn*. Thousand Oaks: Corwin Pres, Inc.
11. Ghazali, N. H. C. & Zakaria, E. (2011). Students' Procedural and Conceptual Understanding of Mathematics. *Australian Journal of Basic and Applied Sciences*, 5, 7, 684-691.
12. Hiebert, J. & Carpenter, T. P. (1992). *Learning and teaching with understanding*.

*Handbook of Research in Teaching and Learning of Mathematics*. Grouws D. W ed. New York: Macmillan.

13. House, J. D. & Telese, J. A. (2008). Relationships between students and instructional factors and algebra achievement of students in United States and Japan: An analysis of TIMSS 2003 data. *Educational Research and Evaluation*, 14, 1, 101-112.
14. Lerman, S. (2014). *Encyclopedia of Mathematics Education*. London: Springer.
15. Lopez, L. (1996). *Helping at-risk students solve mathematical word problems through the use of direct instruction and problem solving strategies*, Orlando: Unpublished Thesis.
16. Luneta, K. (2015). Understanding students' misconceptions: An analysis of final Grade 12 examination questions in geometry. *Pythagoras*, 36, 1, 1-11.
17. Marchionda, H. (2006). *Preservice teacher procedural and conceptual understanding of fractions and the effects of inquiry based learning on this understanding*, Clemson University: Unpublished Doctoral Dissertation.
18. McCormick, R. (1997). Conceptual and Procedural Knowledge. *International Journal of Technology and Design Education* 7, 141-159.
19. Mohyuddin, R. G., & Khalil, U. (2016). *Misconceptions of Students in Learning Mathematics at Primary Level*. Lahore: University of Management and Technology.
20. Mousley, J. (2004). *An Aspect of Mathematical Understanding: The Notion of "Connected Knowing"*. Bergen, International Group for the Psychology of Mathematics Education, 377-384.
21. Mulungye, M., O'Connor, M. & Ndethiu. (2016). Sources of student errors and misconceptions in algebra and effectiveness of classroom practice remediation in Machakos County- Kenya. *Journal of Education and Practice*, 7, 10, 31-33.
22. Narayanan, L. M. (2007). *Analysis of Error in Addition and Subtraction of Fraction among Form 2*, Universiti Malaya: Unpublished Thesis.
23. Nathan, M. J. & Koellner, K. (2007). A Framework for understanding and cultivating the transition from arithmetic to algebraic reasoning. *Mathematical Thinking and Learning*, 9, 3, 179-192.
24. NCTM. (2000). *Principles and Standards for School Mathematics*. Reston, VA: The National Council of Teachers of Mathematics, Inc..
25. Ndemo, O., & Ndemo, Z. (2018). Secondary School Students' Errors and Misconceptions in Learning Algebra. *Journal of Education and Learning (EduLearn)*, 12(4), 690-701. doi:10.11591/edulearn.v12i4.9956
26. Norasiah, A. (2002). *Error type diagnosis in learning simultaneous equation*, s.l.: Unpublished .
27. Orhun, N. (2015). *Students' Mistakes And Misconceptions On Teaching Of Trigonometry*. 1 ed. Eskisehir: Anadolu University.
28. Pournara, C., Hodgen, J., Sanders, Y. & Adler, J. (2016). Learners' errors in secondary algebra: Insights from tracking a cohort from Grade 9 to Grade 11 on a diagnostic algebra test. *Pythagoras*, 37, 1, 1-10.
29. Reid, N. & Yang, M.-J. (2002). The solving of problems in chemistry: the more open-ended problems. *Research in Science and Technological Education*, 2, 1, 83-96.
30. Sarwadi, H., & Shahrill, M. (2014). Understanding Students' Mathematical Errors and Misconceptions: The Case of Year 11 Repeating Students. *Mathematics Education Trends and Research*, 1-10. doi:10.5899/2014/metr-00051
31. Sudihartinih, E., & Purniati, T. (2020). Students' Mistakes and Misconceptions on the Subject of Conics. *International Journal of Education*, 12(2), 92-129. doi:10.17509/ije.v12i2.19130
32. Surif, J., Ibrahim, N. H. & Mokhtar, M. (2012). *Conceptual and Procedural Knowledge in Problem Solving*. s.l., Elsevier, Ltd, 416-425.
33. Taconis, R., Ferguson-Hessler & Broekkamp, H. (2000). Science teaching problem solving: an overview of experimental work. *Journal of Research in Science Teaching*, 38, 4, 442-468.
34. Tambychik, T. & Meerah, T. S. M. (2010). *Students' Difficulties in Mathematics Problem-Solving*. Malacca, Elsevier Ltd,

142-151.

35. Tobias, S. (1993). *Overcoming math anxiety revised and expanded*. New York: Norton.
36. Usman, M. H. & Hussaini, M. M. (2017). Analysis of students' error in learning of trigonometry among Senior Secondary School students in Zaria Metropolis, Nigeria. *IOSR Journal of Mathematics*, 13, 2, 1-4.
37. Weber, K. (2005). Students' understanding of trigonometric functions. *Mathematics Education Research Journal*, 17, 3, 91-112.
38. Wells, D. (1994). Anxiety, insight and appreciation. *Mathematics Teaching*, Volume 147, 8-11.
39. Wilkins, J. (2000). Preparing for the 21<sup>st</sup> century: The status of quantitative literacy in the United States. *School Science and Mathematics*, 100, 8, 405-418.
40. Wright, J. E. (2014). *An investigation of factors affecting student performance in algebraic word problem solutions*, North Carolina: Gardner-Webb University.

**Table 1. Indicators for Types of Mathematical Connection Errors**

| No. | Type of Mathematical Connection Errors                | Indicators  |
|-----|---|---|
| 1   | Errors in connecting to conceptual knowledge (Type A) | Applying the concept of calculation incorrectly<br>Using concepts to prior knowledge inappropriately  |
| 2   | Errors in connecting to procedural knowledge (Type B) | Using improper trigonometric rules or formulas<br>Making a mistake/ unable to do algebraic manipulation<br>Making sign errors in count operations |

**Table 2. Percentage of Students' Failures on Each Item**

| Item |        | Description of errors   | Percentage of students' errors |
|------|--------|---|--------------------------------|
| 1    | Type A | Relating knowledge of algebraic arithmetical operations (eg. $\frac{1}{\sin x} - \frac{1}{\sin x}(1 - \sin^2 x)$ produces $1 - \sin^2 x$ )  | 5.56                           |
|      | Type B | Relating their knowledge that $1 - \sin^2 x$ is equal with $\cos^2 x$   | 13.89                          |
|      |        | Relating distributive properties to change an algebraic form  | 8.33                           |
| 2    | Type A | Relating their knowledge of the algebraic rule (e.g. conclude that $\sqrt{1} = \sqrt{\sin^2 x + \cos^2 x}$ produces $1 = \sin x + \cos x$ ) | 44.44                          |
|      |        | Relating their knowledge of the algebraic rule ( $a \cos x + \tan x = \sec x$ into $a = -\cos x - \tan x + \sec$ )                          | 38.89                          |
|      |        | Relating their knowledge about the concept of linear equation system  | 5.56                           |
|      | Type B | Relating their knowledge that $\sec^2 x - \tan^2 x$ is equal with 1   | 52.78                          |
|      |        | Relating distributive properties to change an algebraic form  | 11.11                          |
| 3    | Type B | Relating their knowledge of multiplication with conjugate pair to change an algebraic form  | 11.11                          |

## APPENDIX

### INTERVIEW GUIDELINES

#### The purpose of the interview

Obtain information about student mathematical connection errors in solving trigonometric identity problems and obtain information about the causes of these difficulties.

#### Interview Conditions

1. The questions adapted to the problem-solving conditions of the students (writing and explanation)
2. If students have difficulty to understand certain questions, the interviewer can provide a guide to simpler questions without reducing the gist of the problem.

#### Interview Implementation

1. Provide trigonometric identity test questions.
2. Ask students to read the test questions carefully. Make sure students understand each question and give students time to work on it.
3. To dig up data regarding errors in connecting to conceptual knowledge (Type A) is done with
  - a. Asking main questions on the subject, for example, "What is the reason you get this final result?"
  - b. Give follow-up questions so that you can explore the information processing done by the subject in detail when using concepts in initial knowledge, for example, "In this section, how do you/ what reasons do you get results like this?"
  - c. Give follow-up questions so that you can explore the information processing carried out by the subject in detail when applying the concept of calculation, for example, "Please pay attention to the calculations in this section, is there a miscalculation?"
4. To dig up data regarding errors in connecting to procedural knowledge (Type B) done with
  - a. Asking main questions on the subject, for example, "How will you solve the problem?"
  - b. Give follow-up questions so that you can explore the information processing done by the subject in detail at the stage of determining trigonometric rules or formulas, for example, "What are the trigonometric identities that you use to solve the problem?"
  - c. Give follow-up questions so that you can explore the mistakes made by the subject in detail, for example, "How do you change this algebraic form into another algebraic form?"
  - d. Give follow-up questions so that you can explore the sign mistake made by the subject in detail, for example, "Is the sign of the operation/operation of your calculation correct?"

# ATIVIDADE ANTIBIÓTICA DE NOVAS ESPÉCIES DE COMPLEXOS DE METAIS DE BASE DE SCHIFF

## ANTIBIOTIC ACTIVITY OF NEW SPECIES OF SCHIFF BASE METAL COMPLEXES

ALI, Safaa Hussein<sup>1\*</sup>; ABD ALREDHA, Hassan Mwazi<sup>2</sup>; ABDULHUSSEIN, Haider Sabah<sup>3</sup>;

<sup>1,3</sup> University of Thi-Qar, College of Veterinary Medicine, Department of Microbiology. Iraq.

<sup>2</sup> Education directory of Thi-Qar, Department of Education, Al-Shatrah. Iraq.

\* Corresponding author  
e-mail: safaa.ali@stu.edu.iq

Received 12 June 2020; received in revised form 30 November 2020; accepted 14 December 2020

### RESUMO

A resistência bacteriana é um crescente desafio enfrentado pelos cientistas de design de medicamentos para encontrar novos medicamentos ou atualizar o antibiótico comumente usados. O objetivo deste estudo foi sintetizar, estruturar e destacar características biológicas de novas espécies de complexos metal-orgânicos  $[(MCl_2)_2L_1]$   $\{M = Ni, Cu, L_1 = N, N'-1, 4\text{-Fenilenobis (metanililideno) bis (etano-1,2-diamina)}\}$  e  $[(NiCl_2)_2L_2]$ . Os ligantes da base de Schiff foram preparados em excelentes campos, adicionando tereftalaldeído a 1,2-etano-diamina ou 1,4-butano-diamina. Três complexos binucleares de metais básicos de Schiff foram sintetizados em uma reação simples de um reator por reação dos sais correspondentes de cloreto de metal ( $NiCl_2$  e  $CuCl_2$ ) com os ligantes da base de Schiff  $\{L_1 = N, N'-(1,4\text{-fenilenobis (metanililideno) bis (1,2-dietilamina)})$  e  $L_2 = N, N'-(1,4\text{-fenilenobis (metanililideno) bis (butano-1,4-diamina)})\}$ . Os complexos de metal base schiff obtidos foram caracterizados analiticamente por um conjunto de técnicas espectroscópicas, tais como espectroscopia FT-IR, espectros de RMN de  $^1H$  e espectros de massa. Os estudos de caracterização de estruturas sugerem que os ligantes da base de Schiff se comportam como ligantes bidentados N para centros de metal de níquel e cobre que são conhecidos por atuarem como ácidos de Lewis. A atividade biológica da base Schiff dos complexos de níquel (II) e cobre (II) foi testada usando o método de diluição em caldo. Os complexos mostraram atividade antibacteriana contra todas as bactérias gram-negativas e gram-positivas (*Enterobacter cloacae* G-, *Citrobacter* G-, *Pseudomonas* G-, *Klebsiella* G-, *Staphylococcus* G + e *Streptococcus* G +) utilizadas nos ensaios. Conclui-se que os complexos de metais básicos de Schiff são um bom candidato ao medicamento antibacteriano devido à sua boa atividade contra cepas gram-negativas e gram-positivas demonstradas no presente estudo, bem como em outros estudos na literatura.

**Palavras-chave:** atividade antibacteriana, organometálica, complexos, síntese, espectroscópica.

### ABSTRACT

Bacterial resistance is a growing challenge facing drug design scientists to find new medications or update commonly used antibiotics. The objective of this study was to synthesize, structure and highlight biological features of new species of metal-organic complexes  $[(MCl_2)_2L_1]$   $\{M = Ni, Cu, L_1 = N, N'-1,4\text{-Phenylenebis(methanylylidene)bis(ethane-1,2-diamine)}\}$  and  $[(NiCl_2)_2L_2]$ . The Schiff base ligands were prepared in an excellent yeilds by adding terephthalaldehyde to 1,2-ethane-diamine or 1,4-butane-diamine. Three binuclear Schiff base metal complexes were synthesized in a simple one-pot reaction by reacting the corresponding metal chloride ( $NiCl_2$  and  $CuCl_2$ ) salts with the Schiff base ligands  $\{L_1 = N, N'-(1,4\text{-phenylenebis(methanylylidene)bis(1,2-diethylamine)})$  and  $L_2 = N, N'-(1,4\text{-phenylenebis(methanylylidene)bis(butane-1,4-diamine)})\}$ . The obtained Schiff base metal complexes were analytically, characterized by a set of spectroscopic techniques such as FT-IR spectroscopy,  $^1H$  NMR spectra, and mass spectra. The structures characterization studies suggest that Schiff base ligands behave as N bidentate ligands for nickel and copper metal centers, which are known to act as Lewis acids. The biological activity of the Schiff base of nickel(II) and copper(II) complexes was tested by using the broth dilution method. The complexes showed antibacterial activity against all gram-negative and gram-positive bacteria (*Enterobacter cloacae* G-, *Citrobacter* G-, *Pseudomonas* G-, *Klebsiella* G-, *Staphylococcus* G+, and *Streptococcus* G+) that used in the trials. It is concluded that Schiff base metal complexes are a good candidate for the antibacterial drug because of its good activity against gram-negative and gram-positive strains demonstrated in the present study, as well as in other studies in the literature.

## 1. INTRODUCTION:

Schiff bases are an essential ligand system in developing coordination chemistry due to their tunable and chelating properties (Radha et al., 2018). Chelating ligands containing O, N, and S donor atoms are well known as having a broad biological activity (Shi et al., 2007). Moreover, this activity can be increased when such ligands are bonded to a metal ion (Chohan et al., 2007; Tsapkov et al., 2008).

Intensive studies have been reported on the biological activity of Schiff bases like antibacterial (Panneerselvam et al., 2009; Rai, and Kumar, 2013), antifungal (Ramesh and Maheswaran, 2003), antitumor (Liu et al., 1992), antiviral (Kumar et al., 2010), anti-HIV (Vicini et al., 20103), herbicides (Holla et al., 2000), insecticides (Alcock et al., 1980) and anti-influenza virus (Zhao et al., 2011). In addition, a wide range of applications have been reported in food and dye industries, analytical chemistry, catalysis, agrochemical, and anti-inflammable and antiradical (Kuddushi et al., 2018). Furthermore, anti-corrosion properties were also investigated (Shaju et al., 2014).

The importance of Schiff bases and their metal complexes was also demonstrated in electrochemical (Neelakantan et al., 2010) and redox catalysis (Vedanayaki et al., 2010; Canpolat, and Kaya, 2004). The role of chlorophyll, hemoglobin, carbonic anhydrase, vitamin B12, xanthine oxidase, and hemocyanin, illustrates the intimate linkage between inorganic chemistry and biology (Singh and Bhatnagar, 2004).

This study aimed to explore the antimicrobial activity of Schiff base metal complexes against six different strains of gram-negative and gram-positive bacteria (*Enterobacter cloacae* G-, *Citrobacter* G-, *Pseudomonas* G-, *Klebsiella* G-, *Staphylococcus* G+, and *Streptococcus* G+).

## 2. MATERIALS AND METHODS:

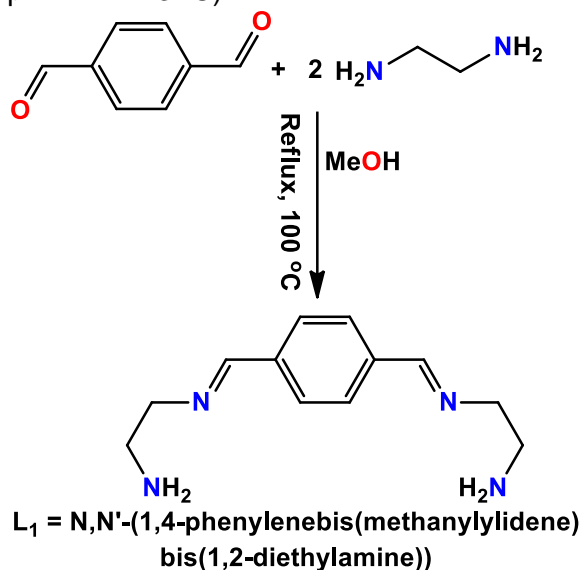
### 2.1. Chemical materials

All chemicals were of analytical reagent grade, purchased from Sigma-Aldrich and used without further purification. FT-IR spectra (KBr

matrix) (4000-200  $\text{cm}^{-1}$ ) were recorded on an FT-IR Spectrometer Model C103 (Shimadzu).  $^1\text{H}$  NMR spectra were obtained on a Varian 400 NMR spectrometer and recorded in DMSO- $d_6$ . Chemical shifts ( $\delta$ ) are expressed in parts per million downfield using tetramethylsilane as an internal reference or by using the residual protonated solvent. Mass spectra of the compounds were recorded on an Agilent Technologies (HP) 5973 Network Mass Selective Detector. NMR and Mass analyses were performed at the Central Instrumental Lab., School of Chemistry, College of Science, University of Tehran, Enghelab St., Tehran, Iran.

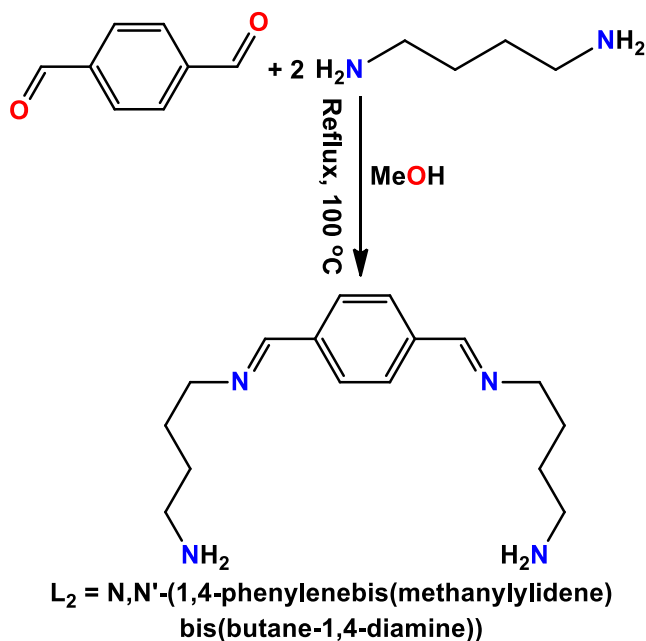
### 2.2. Ligands synthesis

The condensation reaction (Vinita et al., 2013) was employed to synthesize Schiff base ligands  $L_1$  and  $L_2$ . Initially, terephthalaldehyde (0.13 g, 1 mmol) and 1,2-ethane-diamine (0.12 g, 2 mmol) or 1,4-butane-diamine (0.17 g, 2 mmol) were dissolved in 25 mL methanol in a 50-mL round-bottomed flask equipped with a condenser (Equations 1 and 2). The reaction mixture was stimulated by droplets of acetic acid, refluxed, and stirred for 4 h, then cooled, filtered, and dried in a desiccator over anhydrous  $\text{CaCl}_2$  and recrystallized from methanol. Orange powder of  $L_1$  was obtained (Yield = 0.20 g, 80%, m.p. = 265-267  $^\circ\text{C}$ ) or white powder of  $L_2$  (Yield = 0.25 g, 83%, m.p. = 241-243  $^\circ\text{C}$ ).



Equation 1





**Equation 2**

### 2.3. Schiff base metal complexes synthesis

$NiCl_2$  and  $CuCl_2$  salts were reacted with Schiff base  $L_1$  or  $L_2$  to form the following solid complexes  $[(NiCl_2)_2L_1]$ ,  $[(CuCl_2)_2L_1]$  and  $[(NiCl_2)_2L_2]$  (**Scheme 1**). These complexes were prepared by addition of (2 mmol, 0.25 g)  $NiCl_2$  or (2 mmol, 0.26 g)  $CuCl_2$  in about 25 mL of hot ethanol to a solution of (1 mmol, 0.21 g)  $L_1$  or (1 mmol, 0.27 g)  $L_2$  Schiff bases in about 15 mL ethanol with continuous stirring. The reaction mixture was refluxed for 4 h. Colored complexes were filtered, washed with methanol, and dried in a vacuum desiccator (Mishra et al., 2015; Salehi et al., 2016; Nagesh and Mruthyunjayaswamy, 2015).

### 2.4. Biological activity

The antibacterial activity of the chemical compounds  $[(NiCl_2)_2L_1]$  (**1**),  $[(CuCl_2)_2L_1]$  (**2**) and  $[(NiCl_2)_2L_2]$  (**3**) was *in vitro* screened using the disc diffusion method (CLSI, 2010). The strains were treated with compounds **1**, **2**, **3** and a ligand, which were dissolved in DMSO. The biological activity of these compounds was tested against a set of pathogenic gram-negative and gram-positive bacteria, respectively, *Enterobacter cloacae* G-, *Citrobacter* G-, *Pseudomonas* G-, *Klebsiella* G-, *Staphylococcus* G+, and *Streptococcus* G+. Sterilized needles were used to transfer the required microorganisms to the nutrient agar. Amoxicillin and Azithromycin (10 mg mL<sup>-1</sup>) were used as reference drugs, DMSO was used in the measurement as a control. The diffusion was done by placing plates at room

temperature for 1 h and incubated at 37 °C for 24 h. A scale was used to measure the inhibition diameters of the clear zone. Minimum inhibitory concentration (MIC) studies of the prepared Schiff base complexes lead to promising antimicrobial activity. The Microwell dilution technique (CLSI, 2012) was employed to determine the minimum inhibitory effect of the Schiff base, and its metal complexes and Muller-Hinton (Ansari et al., 2011) broth was used as culture media. Complexes (**1-3**) were prepared with 1000 mg mL<sup>-1</sup> and the discs were incubated at 50°C for 30 min to increase solubility.

## 3. RESULTS AND DISCUSSION:

Schiff base metal complexes described above (**Scheme 1**) were synthesized by the direct reaction between the ligands ( $L_1$ ,  $L_2$ ) and ( $NiCl_2$ ,  $CuCl_2$ ) in 1:2 molar ratio in ethanol. All the complexes showed a high level of stability at room temperature (25 °C) while the solubility in some organic solvents was limited, except in DMSO. The solubility difficulties of complexes **1-3** did not allow us to perform single-crystal X-ray diffraction analysis in this study for structure elucidation. Thus, all ligands and their complexes were diagnosed according to the results of a set of accurate analysis.

### 3.1. $[(NiCl_2)_2L_1]$ (**1**)

A metathesis reaction between  $NiCl_2$  and  $L_1$  (**Scheme 1**) led to the formation of complex (**1**) in good yield (0.18 g, 85 %, m.p. 243-245 °C).

### 3.2. $[CuCl_2)_2L_1]$ (**2**)

Similar product (**2**) with an excellent yield (0.19 g, 90 %, m.p. 237-239 °C) was obtained starting from  $CuCl_2$  and  $L_1$ .

### 3.3. $[(NiCl_2)_2L_2]$ (**3**)

The complex **3** was prepared by following the same described route for complexes **1** and **2**, resulting in a moderate product yield (0.17 g, 62 %, m.p. 246-248 °C).

### 3.4. FT-IR spectra

FT-IR spectra analysis of the Schiff base ligands  $L_1$  and  $L_2$  show strong bands, respectively, at 1643 and 1635 cm<sup>-1</sup>, assigned to azomethine  $\nu(C=N)$  group confirming the success of ligand synthesis. The shift toward higher or lower frequencies is a common trend in coordination chemistry due to the association of the metal ions



with the azomethine group with a symmetric ring. The nature of the metal ion and the associated atoms and bonds can shift the frequencies toward higher or lower values. Spectra of compounds **1**, **2** and **3** also showed the disappearance of the band attributed to carbonyl (C=O) group of aldehydes, the starting material, confirming the success of ligand synthesis. Schiff bases metal complexes (**1-3**) were also characterized by the appearance of bands at the region 2939, 3387, and 3302  $\text{cm}^{-1}$  respectively, due to the  $\tilde{\nu}(\text{C-H})$  aromatic vibrations.

#### 3.4.1 $[(\text{NiCl}_2)_2\text{L}_1]$ (**1**)

The following IR bands were observed in **Figure 1** at  $\tilde{\nu}$  equal to: 3541 (w), 2939 (w), 2839 (s), 2110 (m), 1697 (w), 1643 (s), 1550 (w), 1442 (s), 1350 (m), 1296 (s), 1211 (m), 1111 (m), 1049 (w), 1002 (m), 964 (m), 918 (w), 871 (w), 833 (s), 686 (s), 524 (w), 462 (w), 393 (s), 316 (m), 270 (m). In comparison with the spectra of the Schiff bases ligand, the  $\tilde{\nu}(\text{C=N})$  band exhibits an upward shift to 1697  $\text{cm}^{-1}$ , which is in agreement with the azomethine group that coordinated to the metal ion, as previously reported (Das et al., 2014). The strong band that appeared at 1643 was assigned to C=C stretching. Moreover, medium intensity bands that appear at 3541 (w)-2839 (w)  $\text{cm}^{-1}$  assigned to  $\tilde{\nu}\text{NH}_2$  group proved the M-NH<sub>2</sub> coordination (Khan et al., 2016). Furthermore, the appearance of medium intensity bands at the range 678- 316  $\text{cm}^{-1}$  attributed to  $\tilde{\nu}(\text{M-N})$  vibrations is another evidence that confirms the coordination between the ligand and the metal atoms through the azomethine nitrogen atom. The strong and medium two bands appeared at 1442 (s) and 1350 (m) were attributed to CH<sub>2</sub> deformation vibrations (Khan et al., 2017; Bhattacharyya et al., 2015).

#### 3.4.2 $[\text{CuCl}_2)_2\text{L}_1]$ (**2**)

The following IR bands were observed in **Figure 2** at  $\tilde{\nu}$  equal to: 3302 (m), 3232 (m), 3124 (w), 3024 (w), 2916 (m), 2854 (m), 1697 (s), 1635 (s), 1450 (s), 1365 (s), 1280 (s), 1203 (s), 1111 (m), 1010 (s), 972 (m), 840 (s), 678 (m), 532 (s), 432 (s), 362 (w), 339 (w), 277 (m). The compound  $[(\text{CuCl}_2)_2\text{L}_1]$  (**2**) showed two strong bands that shifted upward assigned to the  $\tilde{\nu}(\text{C=N})$  group of the azomethine function, as previously reported (Das et al., 2014). The intense band that appeared at 1635 was assigned to C=C stretching. Comparing with the previously reported complexes (Khan et al., 2016), the bands observed at 3302 (m), and 3024 (w)  $\text{cm}^{-1}$  clearly confirm the M-NH<sub>2</sub> coordination. Methylene (CH<sub>2</sub>)

deformation vibrations are responsible for the two bands appeared at 1450 (s) and 1365 (s). IR spectrum of compound  $[\text{CuCl}_2)_2\text{L}_1]$  can provide further support to confirm the coordination by the presence of bands at the range from 678 (m) to 277 (m)  $\text{cm}^{-1}$ , related to  $\tilde{\nu}(\text{M-N})$  vibrations (Khan et al., 2017; Bhattacharyya et al., 2015).

#### 3.4.3 $[(\text{NiCl}_2)_2\text{L}_2]$ (**3**)

The following IR bands were observed in **Figure 3** at  $\tilde{\nu}$  equal to: 3595 (w), 3387 (w), 3024 (w), 2939 (s), 2839 (s), 2060 (w), 1697 (s), 1635 (s), 1458 (s), 1342 (s), 1296 (s), 1211 (s), 1095 (w), 1049 (w), 1002 (m), 964 (m), 918 (w), 825 (s), 740 (w), 678 (w), 516 (s), 385 (w), 331 (w), 270 (w). The  $\tilde{\nu}(\text{C=N})$  at 1697 (s)  $\text{cm}^{-1}$  for compound  $[(\text{NiCl}_2)_2\text{L}_2]$  (**3**), at higher frequencies compared to the spectrum of the Schiff base ligand confirms the coordination to the metal ion (Das et al., 2014). Aromatic C=C stretching originated the band at 1635. Moreover, the prove of M-NH<sub>2</sub> coordination can simply be highlighted by the appearing of bands at 2939 (s)-2060 (w)  $\text{cm}^{-1}$ , following previously reported complexes (Khan et al., 2016). Two sharp bands appeared at 1458 (s), and 1342 (s) were attributed to (CH<sub>2</sub>) deformation vibrations. Further comparison with reported structures (Khan et al., 2017; Bhattacharyya et al., 2015) proves the M-NH<sub>2</sub> coordination by another clear evidence, which is the appearance of  $\tilde{\nu}(\text{M-N})$  vibrations in the range from 678 (w) to 270 (w)  $\text{cm}^{-1}$ .

#### 3.5. <sup>1</sup>H NMR spectra

<sup>1</sup>H NMR spectra of the complexes (**1** and **2**) were recorded at room temperature in DMSO and interpreted using TMS as an internal reference, while <sup>1</sup>H NMR spectrum could not be obtained for compound (**3**) due to its poor solubility in DMSO. The spectrum of the DMSO as a solvent has been zeroed. The <sup>1</sup>H NMR spectra of compounds (**1**) and (**2**) are given in **Figures 4** and **5**, respectively. The behavior of compounds (**1** and **2**) in solution is an important indicator of the complexation since the characteristic signals of the free ligand have suffered noticeable changes after complexation. <sup>1</sup>H NMR spectra of azomethine group of all complexes show signals shifted to the down field as a result of the coordination between the metal ion and the ligand. This shifting toward downfield is caused by the deshielding of protons as it is well-known; its electron density is reduced after coordination (Silva et al., 2008). The chemical shift detected for the NH<sub>2</sub> group in the ligand was not observed in any of the complexes (**1**) and (**2**).

### 3.5.1 [(NiCl<sub>2</sub>)<sub>2</sub>L<sub>1</sub>] (1)

The <sup>1</sup>H NMR (400 MHz, DMSO, 25°C) peaks are observed at δ/ppm equal to: 8.21 (s, 2H, CH=N-), 8.00-7.49 (m, 4H, Ar), 2.50, 3.33 (8H, CH<sub>2</sub>), 1.09 (d, 4H, NH<sub>2</sub>). The formation of the Ni Schiff base complex [(NiCl<sub>2</sub>)<sub>2</sub>L<sub>1</sub>] was further confirmed by the NMR spectrum. The <sup>1</sup>H NMR spectrum given in **Figure 5** showed multiple small signals in the aromatic region (7.49 - 8.00 ppm) related to the phenyl aromatic protons and the integration of these signals corresponds to the composition of the compound. The spectrum also showed the appearance of two triplets in the region between 2.50 and 3.33 ppm attributed to the methylene groups. Chemical integrations show that the singlet at (8.21 ppm) is related to azomethine.

### 3.5.2 [(CuCl<sub>2</sub>)<sub>2</sub>L<sub>1</sub>] (2)

The <sup>1</sup>H NMR (400 MHz, DMSO, 25°C) peaks are observed at δ/ppm equal to: 10.14 (d, 2H, CH=N-), 8.12-7.80 (m, 4H, Ar), 2.50, 3.40 (8H, CH<sub>2</sub>), 1.21 (t, 4H, NH<sub>2</sub>). The <sup>1</sup>H NMR spectrum of the compound [(CuCl<sub>2</sub>)<sub>2</sub>L<sub>1</sub>] confirmed the formation of the complex. The two signals appearing at 2.50 and 3.40 ppm are attributed to the methylene groups. Also, multiple independent signals are observed around 8.12-7.80 ppm related to aromatic protons of the phenyl group.

## 3.6. Mass spectra

The mass spectra were collected at 70 V cone voltage for all complexes (**1**, **2** and **3**) to reduce the dissociation of ligand. Chemical elements have different isotopes that occurred naturally. Due to isotopic abundance, for some fragments the number of peaks was higher than the calculated. The voltage and the nature of the substitution groups relatively can affect the peak intensity (Keypour et al., 2014). Some water molecules suggested being involved with complexes structures to justify mass spectra results as it is very often in such syntheses to obtain chemical structures with water molecules such as [(NiCl<sub>2</sub>)<sub>2</sub>L<sub>1</sub>].7H<sub>2</sub>O, [(CuCl<sub>2</sub>)<sub>2</sub>L<sub>1</sub>].6H<sub>2</sub>O and [(NiCl<sub>2</sub>)<sub>2</sub>L<sub>2</sub>].3H<sub>2</sub>O due to wet solvents that used in syntheses such as EtOH and MeOH.

### 3.6.1 [(NiCl<sub>2</sub>)<sub>2</sub>L<sub>1</sub>]

In the mass spectrum of the complex [(NiCl<sub>2</sub>)<sub>2</sub>L<sub>1</sub>].7H<sub>2</sub>O, the molecular ion peak (M<sup>+</sup>) was observed at m/z 599.60. The spectrum shows

two other main peaks (577.60 and 551.60) (**Figure 6**), corresponding to the ions of [(NiCl<sub>2</sub>)<sub>2</sub>L<sub>1</sub>].5H<sub>2</sub>O and [(NiCl<sub>2</sub>)<sub>2</sub>L<sub>1</sub>].4H<sub>2</sub>O respectively. Later [(NiCl<sub>2</sub>)<sub>2</sub>L<sub>1</sub>] complex losing NH<sub>4</sub>Cl and NH<sub>3</sub> leaving ions at m/z (calc. 401.96, found 400.20, and calc. 373.92, found 381.30) respectively.

### 3.6.2 [(CuCl<sub>2</sub>)<sub>2</sub>L<sub>1</sub>]

In the mass spectrum of [(CuCl<sub>2</sub>)<sub>2</sub>L<sub>1</sub>] complex, the peak at 594.60 m/z is due to the molecular ion [(CuCl<sub>2</sub>)<sub>2</sub>L<sub>1</sub>].6H<sub>2</sub>O<sup>+</sup>. The peaks at 551.60 m/z is related to [(CuCl<sub>2</sub>)<sub>2</sub>L<sub>1</sub>].4H<sub>2</sub>O fragment. The intensity of these peaks is clear evidence of the stability of these fragments. The mass fragmentation pattern of the Cu(II) complex is depicted in **Figure 7**. The spectrum of [(CuCl<sub>2</sub>)<sub>2</sub>L<sub>1</sub>] complex shows a peak at m/z (calc. 448.91, found 451.50), indicating the loss of NH<sub>3</sub>, 4H<sub>2</sub>O, and Cl. The ion at m/z 451.50 loses CH<sub>3</sub>CH<sub>2</sub>NH<sub>4</sub>Cl, leaving an ion at m/z (calc. 313.97, found 313.30), which further loses two CH<sub>3</sub>CH<sub>3</sub> molecules to leave an ion at m/z (calc. 231.91, found 236.30). Two intense peaks observed at low mass (57.20 and 83.10 m/z) are due to trace of unreacted starting material such as CuCl<sub>2</sub> fragments.

### 3.6.3 [(NiCl<sub>2</sub>)<sub>2</sub>L<sub>2</sub>]

The mass spectrum of [(NiCl<sub>2</sub>)<sub>2</sub>L<sub>2</sub>].3H<sub>2</sub>O complex shows a molecular ion peak at m/z 591.60. Two main peaks, at 577.60 and 551.60 m/z (**Figure 8**) attributed to [(NiCl<sub>2</sub>)<sub>2</sub>L<sub>2</sub>].2H<sub>2</sub>O and [(NiCl<sub>2</sub>)<sub>2</sub>L<sub>2</sub>].H<sub>2</sub>O fragments and their intensity prove the fragments stability. The molecular ion of [(NiCl<sub>2</sub>)<sub>2</sub>L<sub>2</sub>] complex loses NH<sub>4</sub>Cl and Cl leaving an ion at m/z (calc. 460.02, found 466.50), which by its turn, loses NH<sub>3</sub>, Cl, and HCl giving an ion at m/z (calc. 386.08, found 381.50).

## 3.7. Biological activity

The prepared metal complexes (**1**, **2**, **3**) and L<sub>1</sub> ligand were *in vitro* screened for their antibacterial activity by the disc diffusion and microdilution methods, according to the European Committee on Antimicrobial Susceptibility Testing and Clinical and Laboratory Standards Institute guidelines (Ansari et al., 2011). The biological activity of these compounds was tested against a set of human pathogenic gram-negative and gram-positive bacteria, respectively, *Enterobacter cloacae* G-, *Citrobacter* G-, *Pseudomonas* G-, *Klebsiella* G-, *Staphylococcus* G+, and *Streptococcus* G+. The minimum effective concentration of compounds was also

investigated and compared with Amoxicillin and Azithromycin as reference drugs (10 mg mL<sup>-1</sup>) (**Table 1**). At low concentration, approximately, all complexes displayed destruction activity to all tested bacteria. **Table 1** shows the inhibition zone of Gr- bacteria by Schiff base metal complexes and L<sub>1</sub> ligand. Metal complex (**2**) inhibited *Enterobacter cloacae* G- growth significantly in comparison with the ligand L<sub>1</sub> using the same strain. This clearly indicates that the metal complex (**2**) has a destructive effect on bacteria activity. Among the prepared compounds, complexes **1** and **3** were found to be less active than L<sub>1</sub> against *Enterobacter cloacae* G- with MIC (minimum inhibitor concentration) expressed in terms of generated inhibition zones (13 and 14 mm) values, respectively, but showed higher inhibition than the reference drug (**Figure 9**). Moreover, compounds (**1-3**) and L<sub>1</sub> are more effective against *Enterobacter cloacae* G- than the reference drugs.

Inhibition percentages for the compounds (**1-3**) and L<sub>1</sub> presented in **Figure 10** exhibited an excellent effect (inhibition zones of 4, 28, 45, 48 mm) against *Citrobacter* G- compared to other isolated strains and the reference drugs. As seen in **Figure 10** and **Table 1**, inhibition activity increases significantly for the L<sub>1</sub> ligand after coordination with metal ions (Gündüzalp et al., 2016; Parlakgümüş et al., 2016).

Compounds (**1-3**) and L<sub>1</sub> ligand were shown to have promising antimicrobial activity against *Pseudomonas* G-. **Figure 11** and **Table 1** clearly showed a significant increase in the inhibition activity of L<sub>1</sub> Schiff base ligand after coordination to metal ions (Ansari et al., 2011). The anti-*Pseudomonas* G- inhibition activity of L<sub>1</sub> was (0 mm) and became (25, 30, 15 mm) for compounds **1**, **2** and **3**, respectively. Also, in comparison with reference drugs, this experiment clearly proves the significant distraction action of the metal complexes antibiotic *versus* organic antibiotic (Gündüzalp et al., 2012).

As expected *Klebsiella* G- showed a strong resistance to complexes **1-3** and L<sub>1</sub> (**Figure 12**) as it is well-known its resistance to a wide array of antibiotics. Complexes **1-3** and L<sub>1</sub> in addition to the reference drugs did not show any antibacterial activity against *Klebsiella* G- and the inhibition zones were 0 mm for all tested compounds (€Ozbek et al., 2013).

All four tested compounds showed significant activity against the selected gram-positive pathogens (*Staphylococcus* G+, and *Streptococcus* G+), the L<sub>1</sub> ligand activity against

*Staphylococcus* G+ increases significantly after coordinating to metal ions. Complex **3** showed maximum inhibiting activity against the organisms here study. Complex **2** did not show any antibacterial activity against *Streptococcus* G+, which could be related to the experimental condition. The results (**Table 2** and **Figures 13** and **14**) show that the compounds affect more the *Staphylococcus* G+ and less the *Streptococcus* G+ (Muche et al., 2017).

#### 4. CONCLUSIONS:

The prepared complexes showed promising results in the conducted biological tests. Highly air and thermal stable Schiff base metal complexes [(NiCl<sub>2</sub>)<sub>2</sub>L<sub>1</sub>], [(CuCl<sub>2</sub>)<sub>2</sub>L<sub>1</sub>] and [(NiCl<sub>2</sub>)<sub>2</sub>L<sub>2</sub>] with a melting point ranged between (237-248 °C) were synthesized in one step reaction pot by reacting tetradentate ligands (Eqn. 1) with different metal chlorides. Complexes (**1**, **2**, **3**) showed high chemical stability in DMSO for at least 72 h. The compounds were chemically characterized using a set of analytical techniques such as IR, <sup>1</sup>HNMR spectroscopy, and MS spectrometry. The biological properties of the complexes were determined according to the broth microdilution technique by employing a range of gram-negative and positive bacteria strains such as *Enterobacter cloacae* G-, *Citrobacter* G-, *Pseudomonas* G-, *Klebsiella* G-, *Staphylococcus* G+, and *Streptococcus* G+. It was established out that complexes are very effective inhibition activity ranged between (13-50 mm) against gram negative and gram positive pathogens. The comparison results revealed better antibacterial activity of the synthesized complexes than reference drugs (Amoxicillin and Azithromycin). These results encourage further studies of these species to identify the activity of the compound toward new pathogens.

#### 5. ACKNOWLEDGMENTS:

We gratefully acknowledge Thi-Qar University for provided some research facilities. Part of this research was undertaken at the Environmental Centre, Al-Shatrah Technical Institute, Southern Technical University.

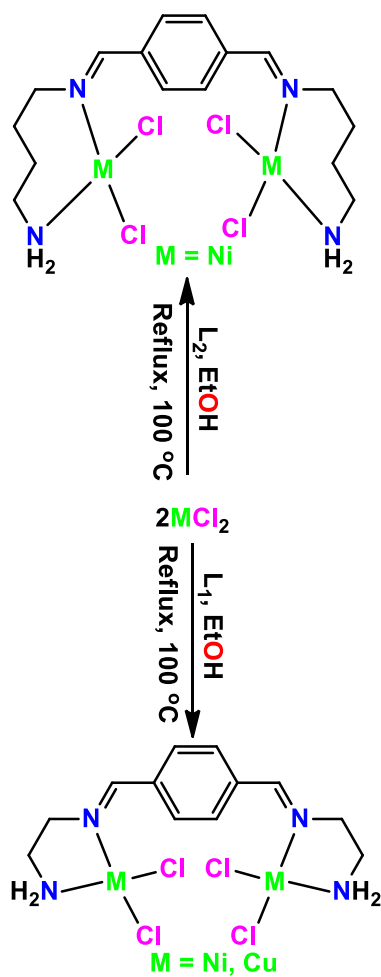
#### 6. REFERENCES:

1. Ansari, M. A., Khan, H. M., Khan, A. A., Malik, A., Sultan, A., Shahid, M., Shujatullah, F., Azam, A., Evaluation of antibacterial activity of silver nanoparticles against MSSA and MSRA on isolates from skin infections,

- Biology and Medicine*. 3(2) (2011) 141-146.  
[http://www.biolmedonline.com/Articles/MAA-SCON-1/Vol3\\_2\\_141-146.pdf](http://www.biolmedonline.com/Articles/MAA-SCON-1/Vol3_2_141-146.pdf)
2. Alcock, N. W., Cook, D. F., McKenzie, E. D., Worthington, J. M., Metal (III) compounds of potentially septadentate  $[N_4O_3]$  ligands. Part II. Crystal and molecular structures of  $[M(C_{27}H_{24}Cl_3N_4O_3) \cdot 3H_2O]$  ( $M = Cr, Mn$ ), *Inorganica Chimica Acta* 38 (1980) 107-112. [https://doi.org/10.1016/S0020-1693\(00\)91943-1](https://doi.org/10.1016/S0020-1693(00)91943-1)
  3. Bhattacharyya, A., Sen, S., Harms, K., Chattopadhyay, S., Formation of three photoluminescent zinc (II) complexes with  $Zn_2O_2$  cores: Examples of bi-dentate bonding modes of potentially tri- and tetra-dentate Schiff bases, *Polyhedron* 88 (2015) 156-163. <https://doi.org/10.1016/j.poly.2014.12.018>
  4. CLSI, Methods for antimicrobial dilution and disk susceptibility of infrequently isolated or fastidious bacteria, approved guideline, 2nd ed., CLSI document M45-A2. Clinical and Laboratory Standards Institute, 950 West Valley Road, Suite 2500, Wayne, Pennsylvania 19087, USA, 2010. [https://clsi.org/media/1450/m45ed3\\_sample.pdf](https://clsi.org/media/1450/m45ed3_sample.pdf)
  5. CLSI, Methods for dilution antimicrobial susceptibility tests for bacteria that grow aerobically, approved standard, 9th ed., CLSI document M07-A9. Clinical and Laboratory Standards Institute, 950 West Valley Road, Suite 2500, Wayne, Pennsylvania 19087, USA, 2012. [https://clsi.org/media/1632/m07a10\\_sample.pdf](https://clsi.org/media/1632/m07a10_sample.pdf)
  6. Canpolat, E., Kaya, M., Studies on mononuclear chelates derived from substituted Schiff-base ligands (part 2): synthesis and characterization of a new 5-bromosalicyliden-p-aminoacetophenoneoxime and its complexes with Co (II), Ni (II), Cu (II) and Zn (II), *Journal of Coordination Chemistry* 57(14) (2004) 1217-1223. <https://doi.org/10.1080/00958970412331285913>
  7. Chohan, Z. H., Arif, M., Sarfraz, M., Metal-based antibacterial and antifungal amino acid derived Schiff bases: their synthesis, characterization and in vitro biological activity, *Applied Organometallic Chemistry* 21(4) (2007) 294-302. <https://doi.org/10.1002/aoc.1200>
  8. Das, M., Chatterjee, S., Harms, K., Mondal, T. K., Chattopadhyay, S., Formation of bis ( $\mu$ -tetrazolato) dinickel (II) complexes with N, N, O-donor Schiff bases via in situ 1, 3-dipolar cyclo-additions: isolation of a novel bi-cyclic trinuclear nickel (II)-sodium (I)-nickel (II) complex, *Dalton Transactions* 43(7) (2014) 2936-2947. <https://doi.org/10.1039/C3DT52796D>
  9. €Ozbek, N., Alyar, S., Alyar, H., Sahin, E., Karacan, N., Synthesis, characterization and antimicrobial evaluation of Cu(II), Ni(II), Pt(II) and Pd(II) sulfonylhydrazone complexes; 2D-QSAR analysis of Ni(II) complexes of sulfonylhydrazone derivatives, *Spectrochimica Acta Part A: Molecular and Biomolecular Spectroscopy* 108 (2013) 123-132. <https://doi.org/10.1016/j.saa.2013.01.005>
  10. Gündüzalp, A. B., €Ozsen, I., Alyar, H., Alyar, S., €Ozbek, N., Biologically active Schiff bases containing thiophene/furan ring and their copper (II) complexes: Synthesis, spectral, nonlinear optical and density functional studies, *Journal of Molecular Structure* 1120 (2016) 259-266. <https://doi.org/10.1016/j.molstruc.2016.05.002>
  11. Gündüzalp, A. B., €Ozbek, N., Karacan, N., Synthesis, characterization, and antibacterial activity of the ligands including thiophene/furan ring systems and their Cu (II), Zn (II) complexes, *Medicinal Chemistry Research* 21(11) (2012) 3435-3444. <https://doi.org/10.1007/s00044-011-9878-8>
  12. Holla, B. S., Rao, B. S., Shridhara, K., Akberali, P. M., Studies on arylfuran derivatives: part XI. Synthesis, characterisation and biological studies on some Mannich bases carrying 2, 4-dichlorophenylfurfural moiety, *Farmaco* 55(5) (2000) 338-344. [https://doi.org/10.1016/S0014-827X\(00\)00033-1](https://doi.org/10.1016/S0014-827X(00)00033-1)
  13. Keypour, H., Zebarjadian, M. H., Rezaeivala, M., Chehreghani, A., Amiri-Rudbari, H., Bruno, G., Synthesis, characterization, crystal structure and antibacterial studies of some new heptadentate manganese (II), cadmium (II) and zinc (II) macrocyclic Schiff base complexes with two 2-pyridylmethyl pendant arms, *Journal of the Iranian Chemical Society* 11(1) (2014) 101-109. <https://doi.org/10.1007/s13738-013-0280-y>

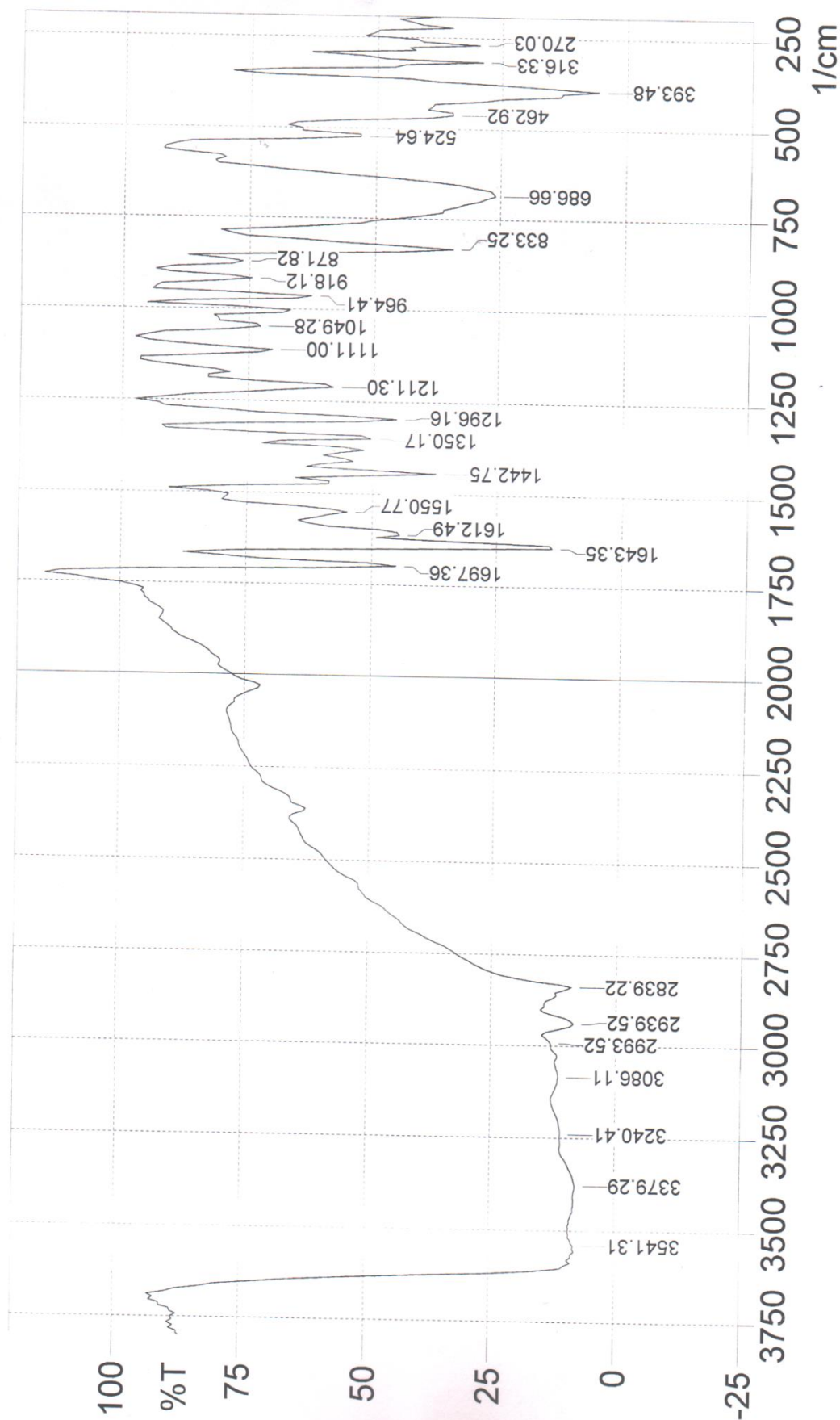
14. Khan, S., Jana, S., Drew, M. G. B., Bauzá, A., Frontera, A., Chattopadhyay, S., A novel method for copper (II) mediated region-selective bromination of aromatic rings under mild conditions, *RSC advances* 6(66) (2016) 61214-61220.  
<https://doi.org/10.1039/C6RA13215D>
15. Khan, S., Masum, A. A., Islam, M. M., Drew, M. G. B., Bauzá, A., Frontera, A., Chattopadhyay, S., Observation of  $\pi$ -hole interactions in the solid state structures of three new copper (II) complexes with a tetradentate N4 donor Schiff base: Exploration of their cytotoxicity against MDA-MB 468 cells, *Polyhedron* 123 (2017) 334-343.  
<https://doi.org/10.1016/j.poly.2016.11.012>
16. Kumar, K. S., Ganguly, S., Veerasamy, R., De Clercq, E., Synthesis, antiviral activity and cytotoxicity evaluation of Schiff bases of some 2-phenyl quinazoline-4 (3H)-ones, *European Journal of Medicinal Chemistry* 45(11) (2010) 5474-5479.  
<https://doi.org/10.1016/j.ejmech.2010.07.058>
17. Kuddushi, M. M. Y., Malek, M. A. H., Patidar, V. L., Synthesis and characterization of schiff base aniline with 5-bromo -2- hydroxyl benzaldehyde and their metal complexes, *International Journal of Recent Scientific Research* 9(4) (2018) 26026-26030.  
<http://dx.doi.org/10.24327/ijrsr.2018.0904.1977>
18. Liu, M. C., Lin, T. C., Sartorelli, A. C., Synthesis and antitumor activity of amino derivatives of pyridine-2-carboxaldehyde thiose micarbazone, *Journal of Medicinal Chemistry* 35(20) (1992) 3672-3677.  
<https://doi.org/10.1021/jm00098a012>
19. Mishra, M., Tiwari, K., Mourya, P., Singh, M. M., Singh, V. P., Synthesis, characterization and corrosion inhibition property of nickel (II) and copper (II) complexes with some acylhydrazine Schiff bases, *Polyhedron* 89 (2015) 29-38.  
<https://doi.org/10.1016/j.poly.2015.01.003>
20. Muche, S., Levacheva, I., Samsonova, O., Biernasiuk, A., Malm, A., Lonsdale, R., Popiolek, Ł., Bakowsky, U., Hołynska, M., Synthesis, structure and stability of a chiral imine-based Schiff-based ligand derived from L-glutamic acid and its [Cu<sub>4</sub>] complex, *Journal of Molecular Structure* 1127 (2017) 231-236.  
<https://doi.org/10.1016/j.molstruc.2016.07.100>
21. Neelakantan, M. A., Esakkiammal, M., Mariappan, S. S., Dharma raja, J., Jeyakumar, T., Synthesis, characterization and biocidal activities of some schiff base metal complexes, *Indian Journal of Pharmaceutical Sciences* 72(2) (2010) 216-222. <https://dx.doi.org/10.4103/0250-474X.65015>
22. Nagesh, G. Y., Mruthyunjayaswamy, B. H. M., Synthesis, characterization and biological relevance of some metal (II) complexes with oxygen, nitrogen and oxygen (ONO) donor Schiff base ligand derived from thiazole and 2-hydroxy-1-naphthaldehyde, *Journal of Molecular Structure* 1085 (2015) 198-206.  
<https://doi.org/10.1016/j.molstruc.2014.12.058>
23. Panneerselvam, P., Rather, B. A., Reddy, D. R. S., Kumar, N. R., Synthesis and antimicrobial screening of some Schiff bases of 3-amino-6, 8-dibromo-2-phenylquinazolin-4 (3H)-ones, *European Journal of Medicinal Chemistry* 44(5) (2009) 2328-2333.  
<https://doi.org/10.1016/j.ejmech.2008.04.010>
24. Parlakgümüş, G., Gündüzalp, A. B., Uzun, D., Özdemir, Özmen, Ü., Özbek, N., Sarı, M., Tunç, T., Carbonic anhydrase inhibitors: Synthesis, characterization and inhibition activities of furan sulfonylhydrazones against carbonic anhydrase I (hCA I), *Journal of Molecular Structure* 1105 (2016) 332-340.  
<https://doi.org/10.1016/j.molstruc.2015.10.054>
25. Rai, B. K., Kumar, A., Synthesis, characterization and biocidal activity of some Schiff base and its metal complexes of Co (II), Cu (II) and Ni (II), *Oriental Journal of Chemistry* 29(3) (2013) 1187-1191.  
<http://dx.doi.org/10.13005/ojc/290349>
26. Ramesh, R., Maheswaran, S., Synthesis, spectra, dioxygen affinity and antifungal activity of Ru (III) Schiff base complexes, *Journal of Inorganic Biochemistry* 96(4) (2003) 457-462.  
[https://doi.org/10.1016/S0162-0134\(03\)00237-X](https://doi.org/10.1016/S0162-0134(03)00237-X)
27. Radha, V.P., Kirubavathy, S. J., Chitra, S., Synthesis, characterization and biological investigations of novel Schiff base ligands containing imidazoline moiety and their Co (II) and Cu (II) complexes, *Journal of Molecular Structure* 1165 (2018) 246-258.  
<https://doi.org/10.1016/j.molstruc.2018.03.109>

28. Shi, L., Ge, H. M., Tan, S. H., Li, H. Q., Song, Y. C., Zhu, H. L., Tan, R. X., Synthesis and antimicrobial activities of Schiff bases derived from 5-chloro-salicylaldehyde, *European Journal of Medicinal Chemistry* 42(4) (2007) 558-564.  
<https://doi.org/10.1016/j.ejmech.2006.11.010>
29. Shaju, K. S., Thomas, K. J., Raphael, V., effect of iodide on the corrosion inhibitive behaviour on carbon steel by an azomethine compound derived from anthracene-9(10 h)-one, *Oriental Journal of Chemistry* 30(2) (2014) 807-813.  
<http://dx.doi.org/10.13005/ojc/300255>
30. Singh, L. P., Bhatnagar, J. M., Copper (II) selective electrochemical sensor based on Schiff Base complexes, *Talanta* 64(2) (2004) 313-319.  
<https://doi.org/10.1016/j.talanta.2004.02.020>
31. Salehi, M., Ghasemi, F., Kubicki, M., Asadi, A., Behzad, M., Ghasemi, M. H., Gholizadeh, A., Synthesis, characterization, structural study and antibacterial activity of the Schiff bases derived from sulfanilamides and related copper (II) complexes, *Inorganica Chimica Acta* 453 (2016) 238-246.  
<https://doi.org/10.1016/j.ica.2016.07.028>
32. Silva, A. M. S., Sousa, R. M. S., Jimeno, M. L., Blanco, F., Alkorta, I., Elguero, J., Experimental measurements and theoretical calculations of the chemical shifts and coupling constants of three azines (benzalazine, acetophenoneazine and cinnamaldazine), *Magnetic Resonance in Chemistry* 46(9) (2008) 859-864.  
<https://doi.org/10.1002/mrc.2272>
33. Tsapkov, V. I., Prisakar, V. I., Buracheeva, S. A., Lazakovich, D. V., Gulya, A. P., Synthesis and antimicrobial activity of sulfazine-containing copper (II) coordination compounds with substituted salicylaldehyde benzoyl hydrazones, *Pharmaceutical Chemistry Journal* 42(9) (2008) 523-526.  
<https://doi.org/10.1007/s11094-009-0173-7>
34. Vicini, P., Geronikaki, A., Incerti, M., Busonera, B., Poni, G., Cabras, C. A., Colla, P. L., Synthesis and biological evaluation of benzo[d]isothiazole, benzothiazole and thiazole Schiff bases, *Bioorganic and Medicinal Chemistry* 11(22) (2003) 4785-4789.  
[https://doi.org/10.1016/S0968-0896\(03\)00493-0](https://doi.org/10.1016/S0968-0896(03)00493-0)
35. Vedanayaki, S., Sandhanamalar, D., Jayaseelan, P., Rajavel, R., Synthesis, structural characterization, thermal and antimicrobial evaluation of binuclear Cu(II), Ni(II) and VO(IV) schiff base complexes, *International Journal of Pharmacy and Technology* 2(4) (2010) 1118-1132.  
<http://www.ijptonline.com/wp-content/uploads/2009/10/1118-1132.pdf>
36. Vinita, G., Sanchita, S., Gupta, Y. K., Synthesis and Antimicrobial Activity of some Salicylaldehyde Schiff bases of 2-aminopyridine, *Research Journal of Chemical Sciences* 3(9) (2013) 26-29.  
<http://www.isca.in/rjcs/Archives/v3/i9/5.ISCA-RJCS-2013-127.php>
37. Zhao, X., Li, C., Zeng, S., Hu, W., Discovery of highly potent agents against influenza A virus, *European Journal of Medicinal Chemistry* 46(1) (2011) 52-57.  
<https://doi.org/10.1016/j.ejmech.2010.10.010>



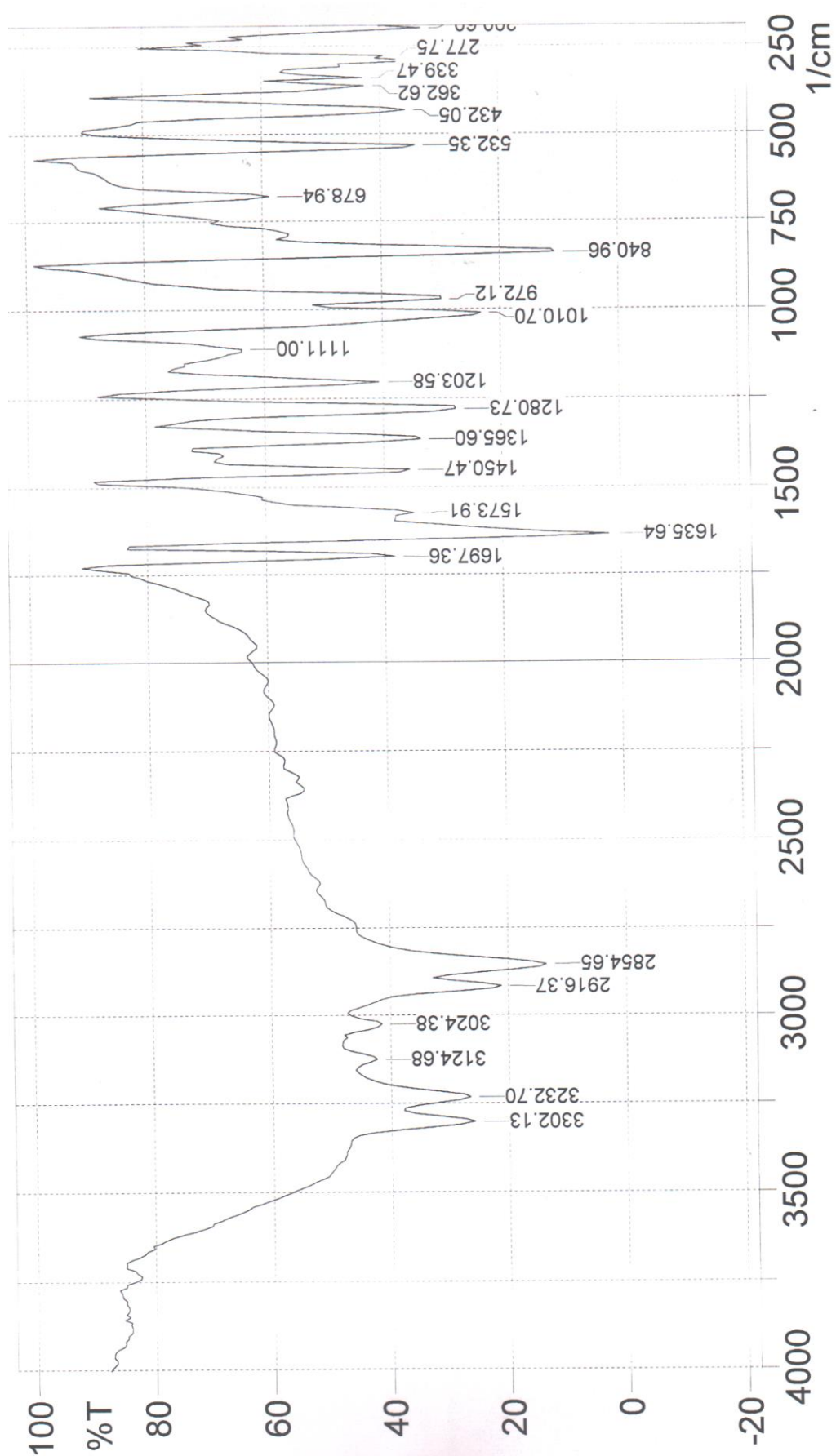
**Scheme 1**



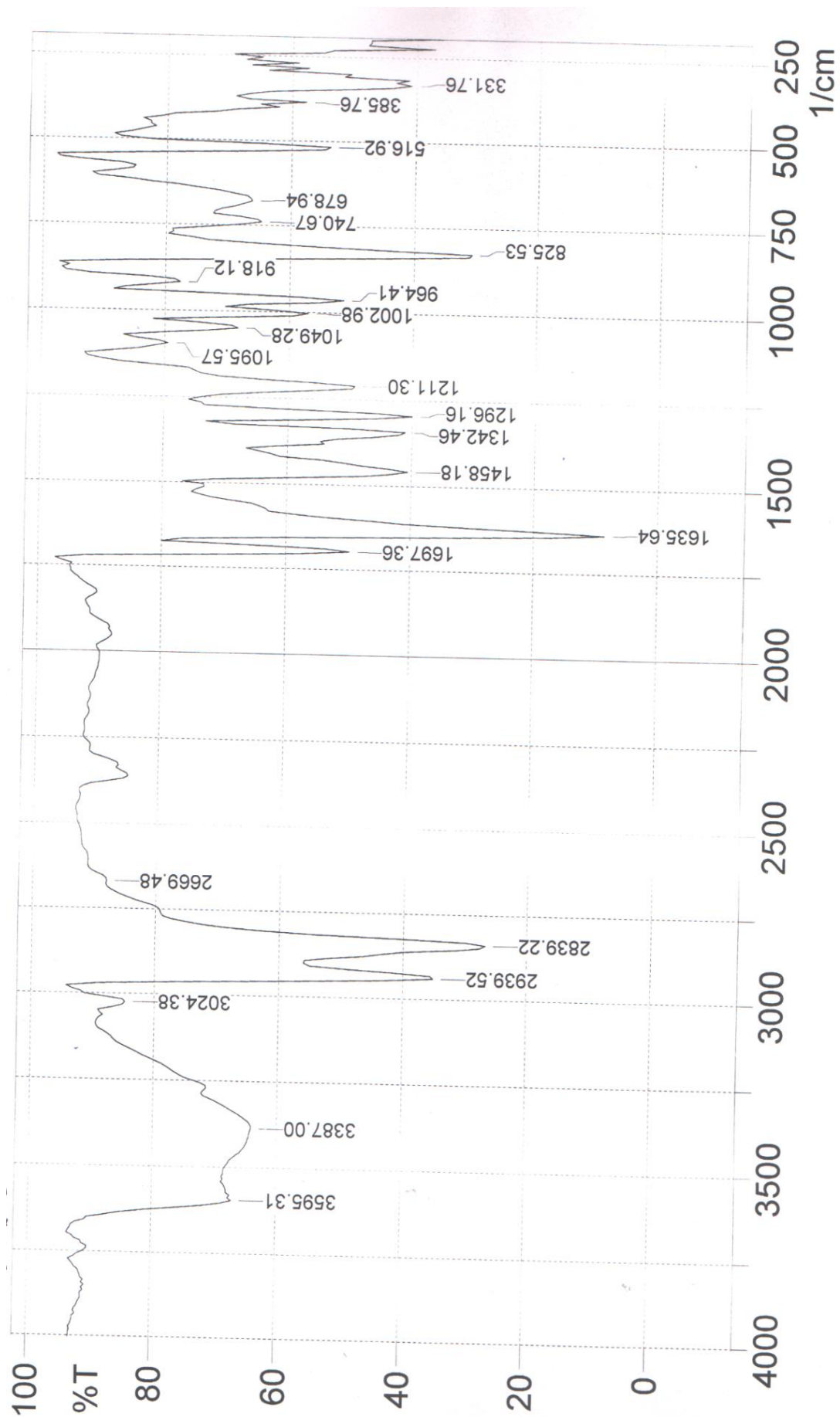


**Figure 1.** FT-IR spectrum of  $[(\text{NiCl}_2)_2\text{L}_1]$  complex.

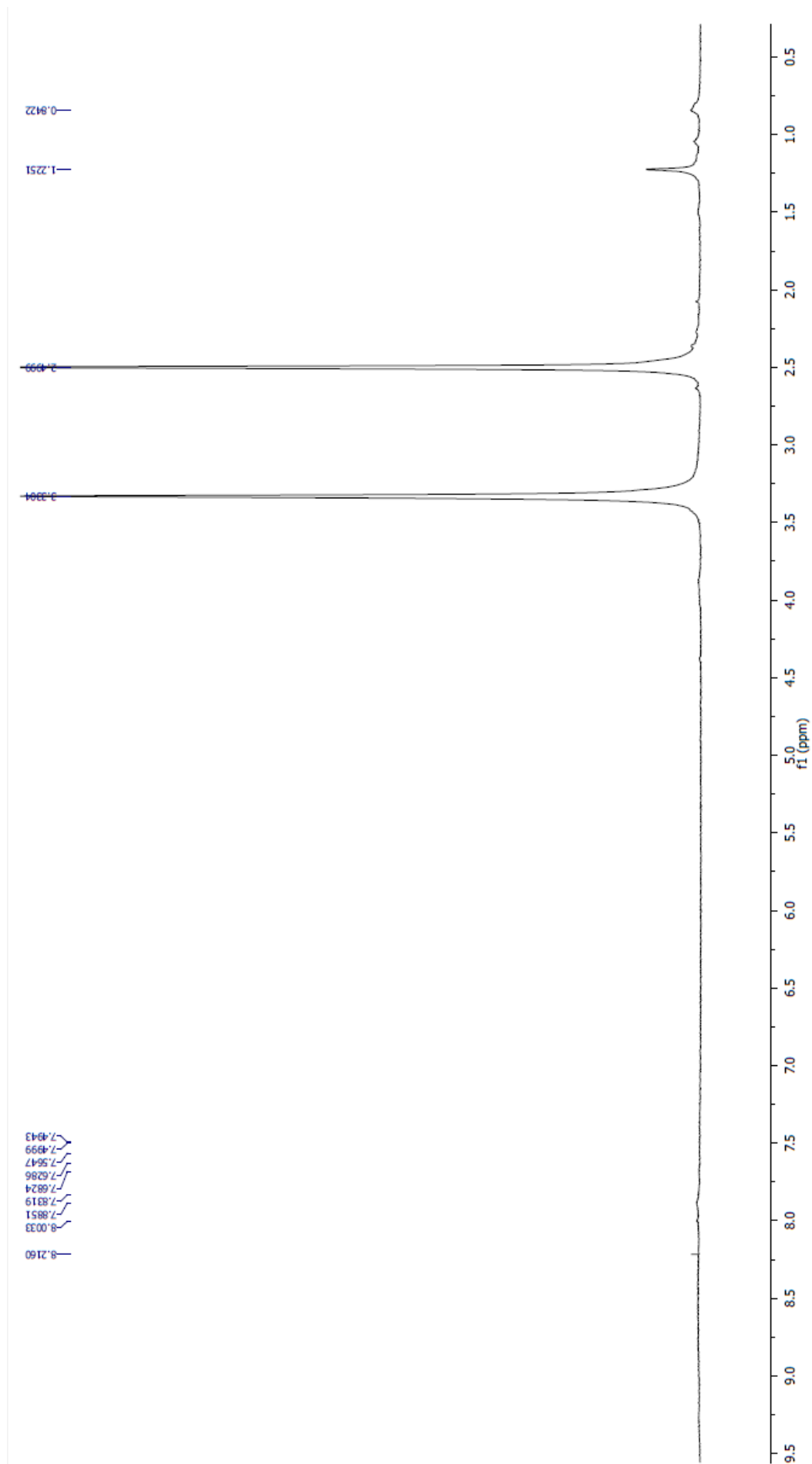




**Figure 2.** FT-IR spectrum of  $[(\text{CuCl}_2)_2\text{L}_1]$  complex.



**Figure 3.** FT-IR spectrum of  $[(\text{NiCl}_2)_2\text{L}_2]$  complex.



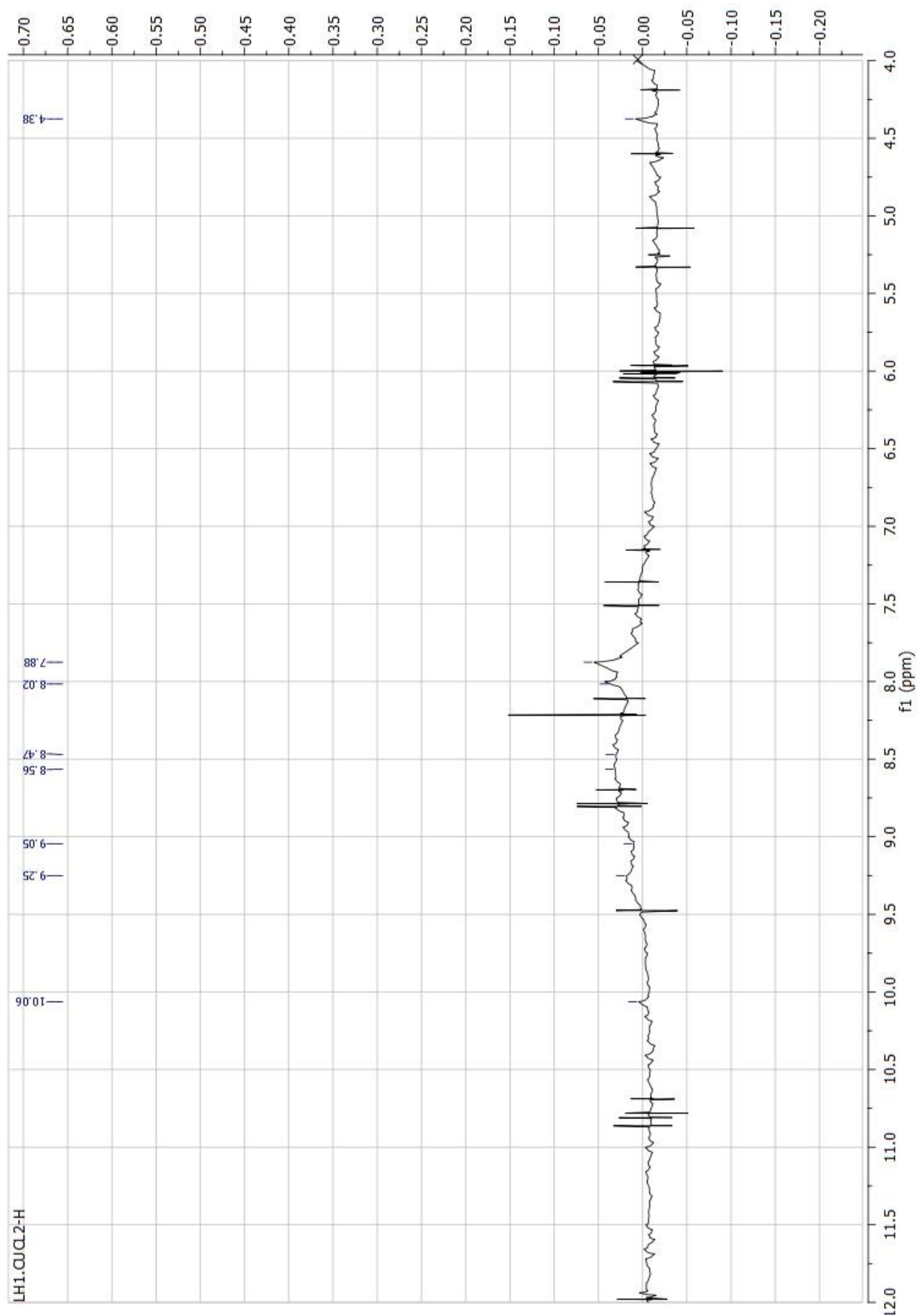


**Figure 4.**  $^1\text{H}$  MNR spectrum of  $[(\text{NiCl}_2)_2\text{L}_1]$  complex.

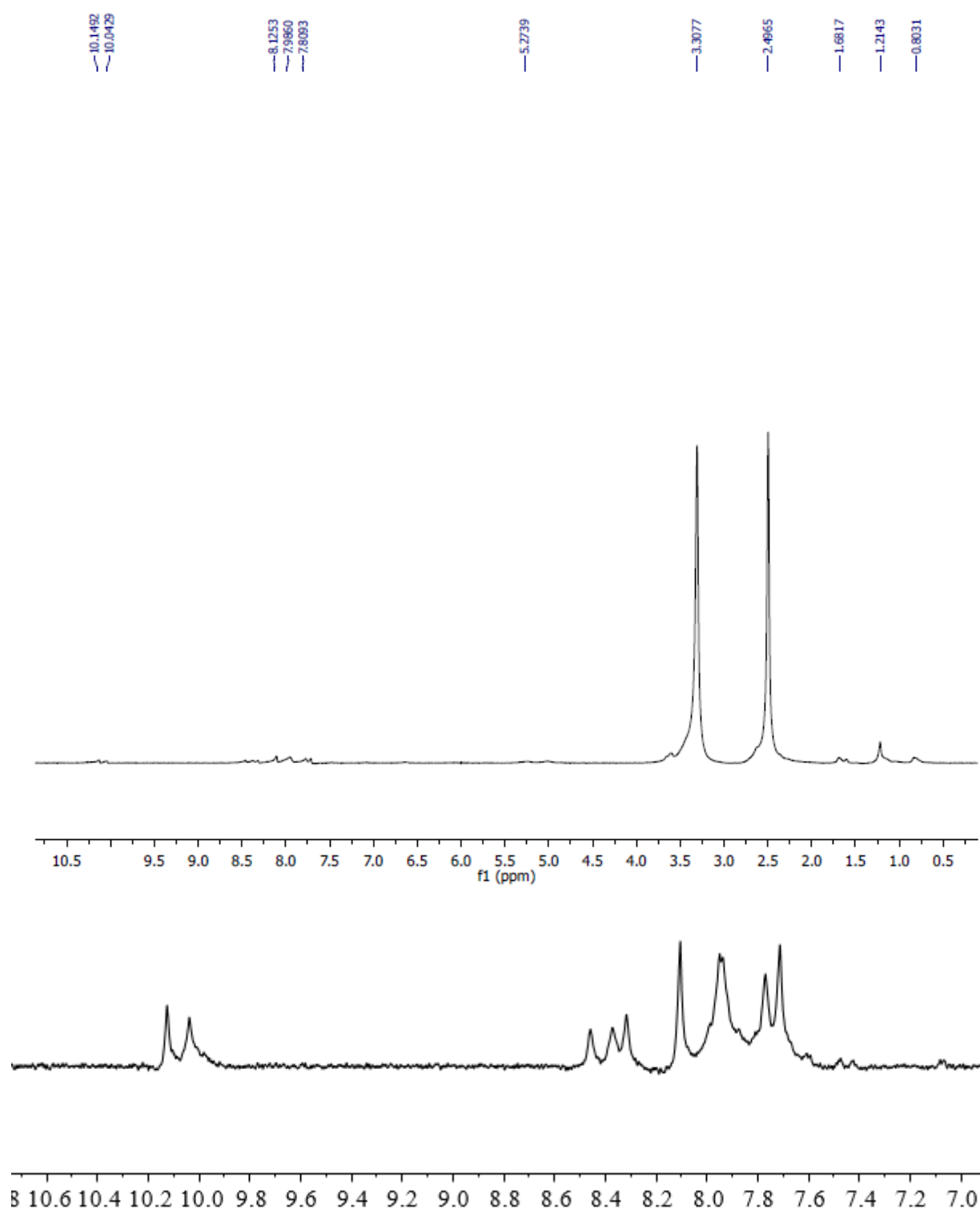


**Figure 5.**  $^1\text{H}$  MNR spectrum of  $[(\text{CuCl}_2)_2\text{L}_1]$  complex.

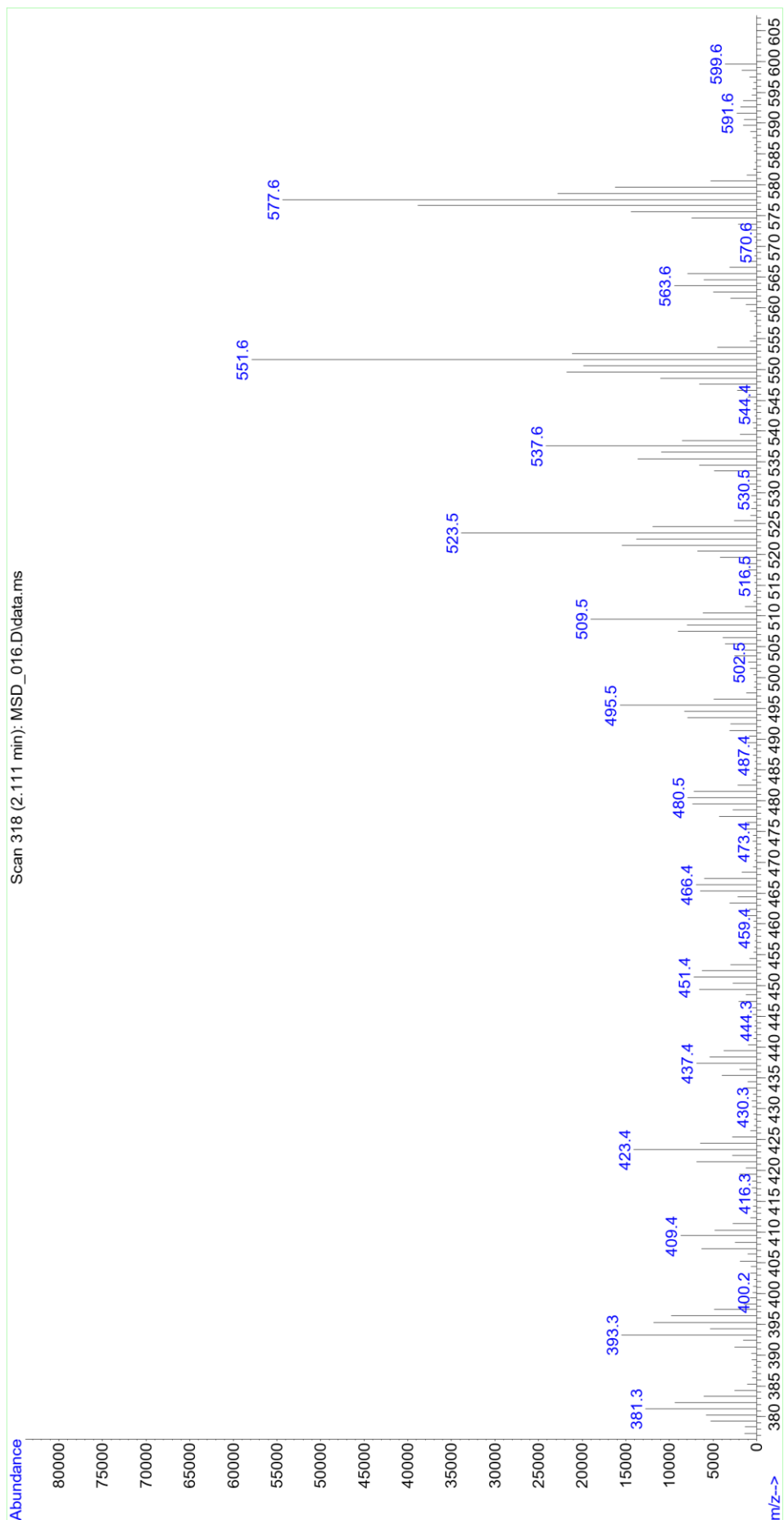


**Figure 6.** Mass spectrum of  $[(\text{NiCl}_2)_2\text{L}_1]$  complex.

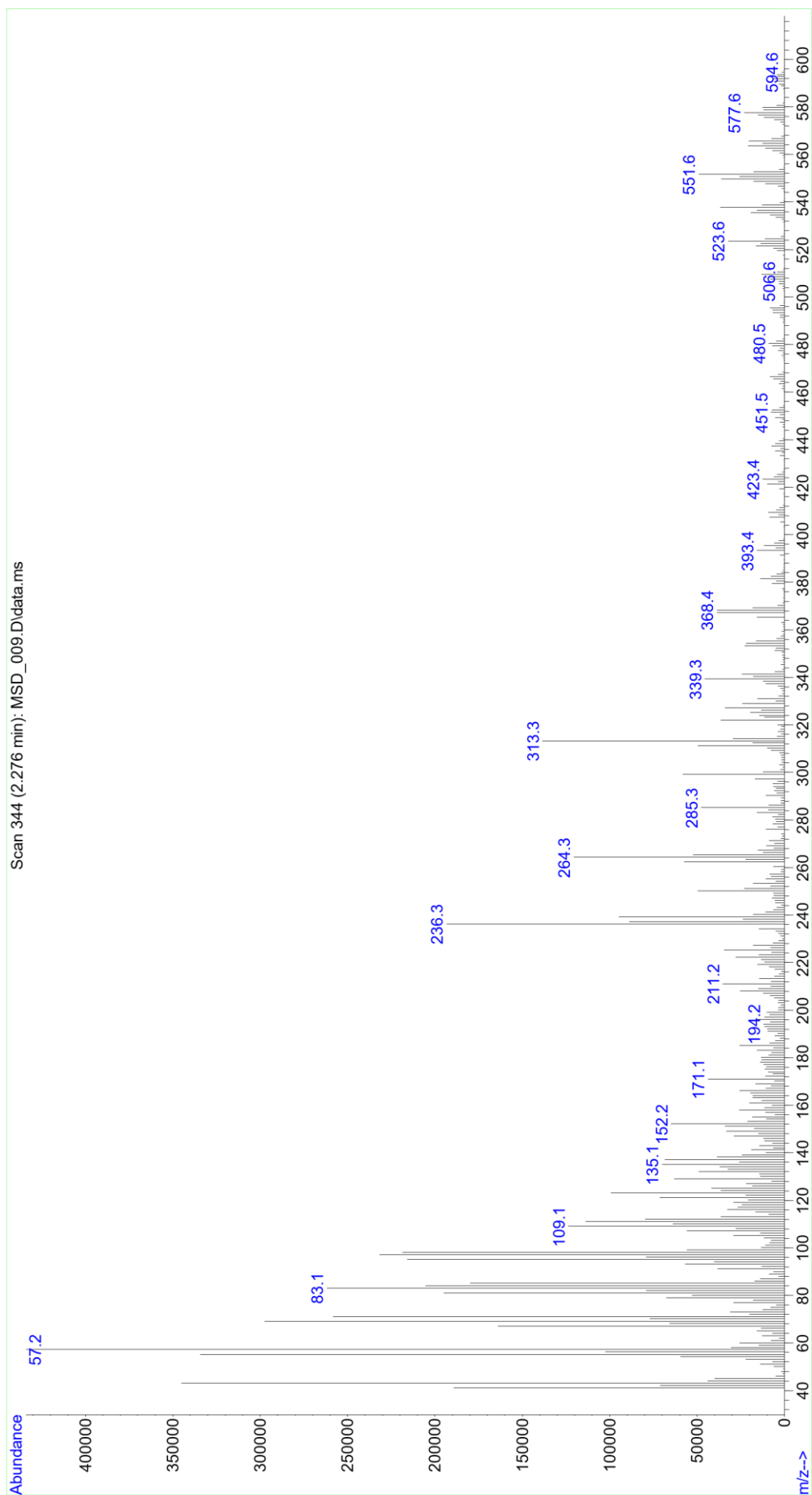


**Figure 7.** Mass spectrum of  $[(\text{CuCl}_2)_2\text{L}_1]$  complex.

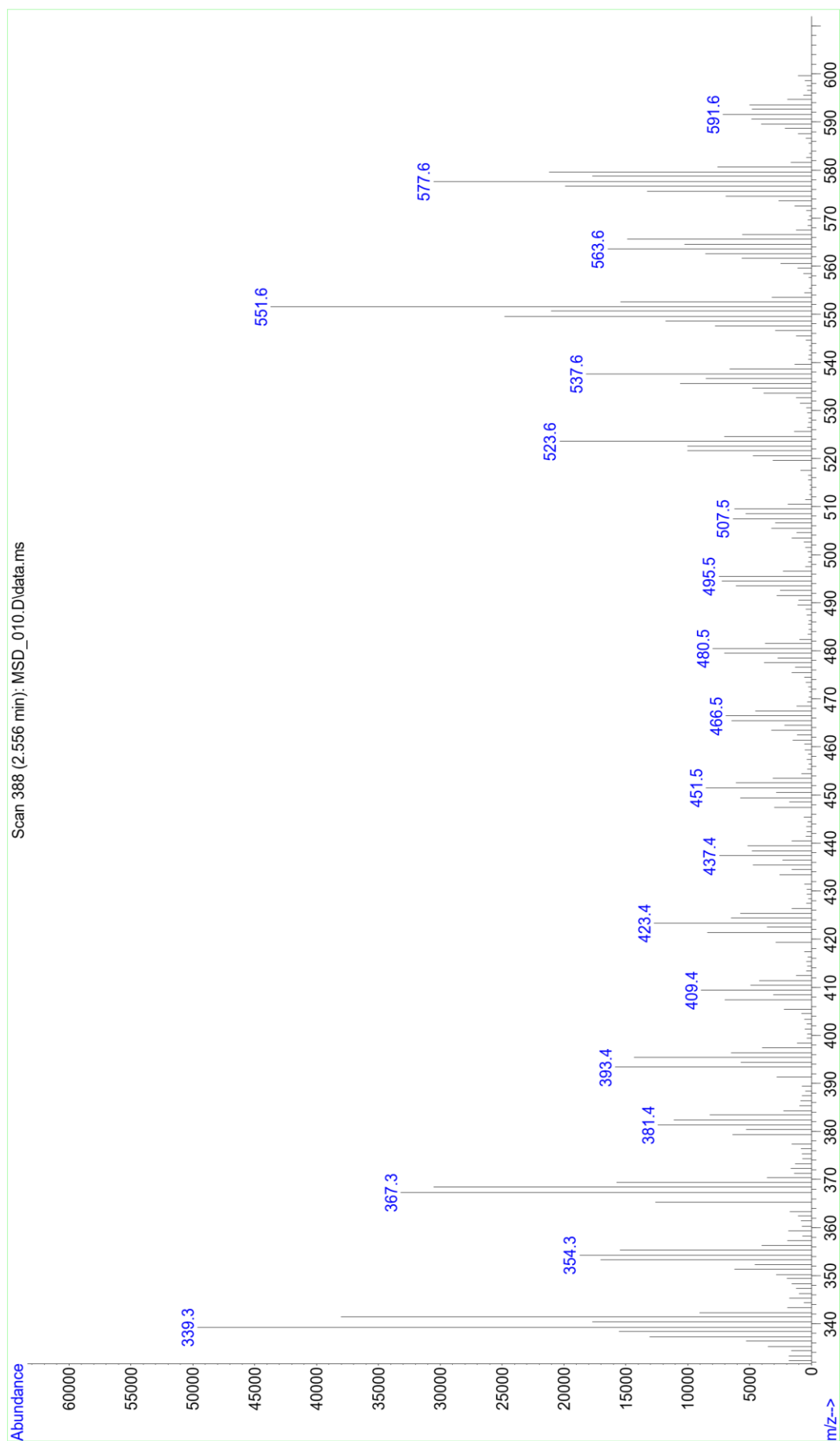


**Figure 8.** Mass spectrum of  $[(\text{NiCl}_2)_2\text{L}_2]$  complex.



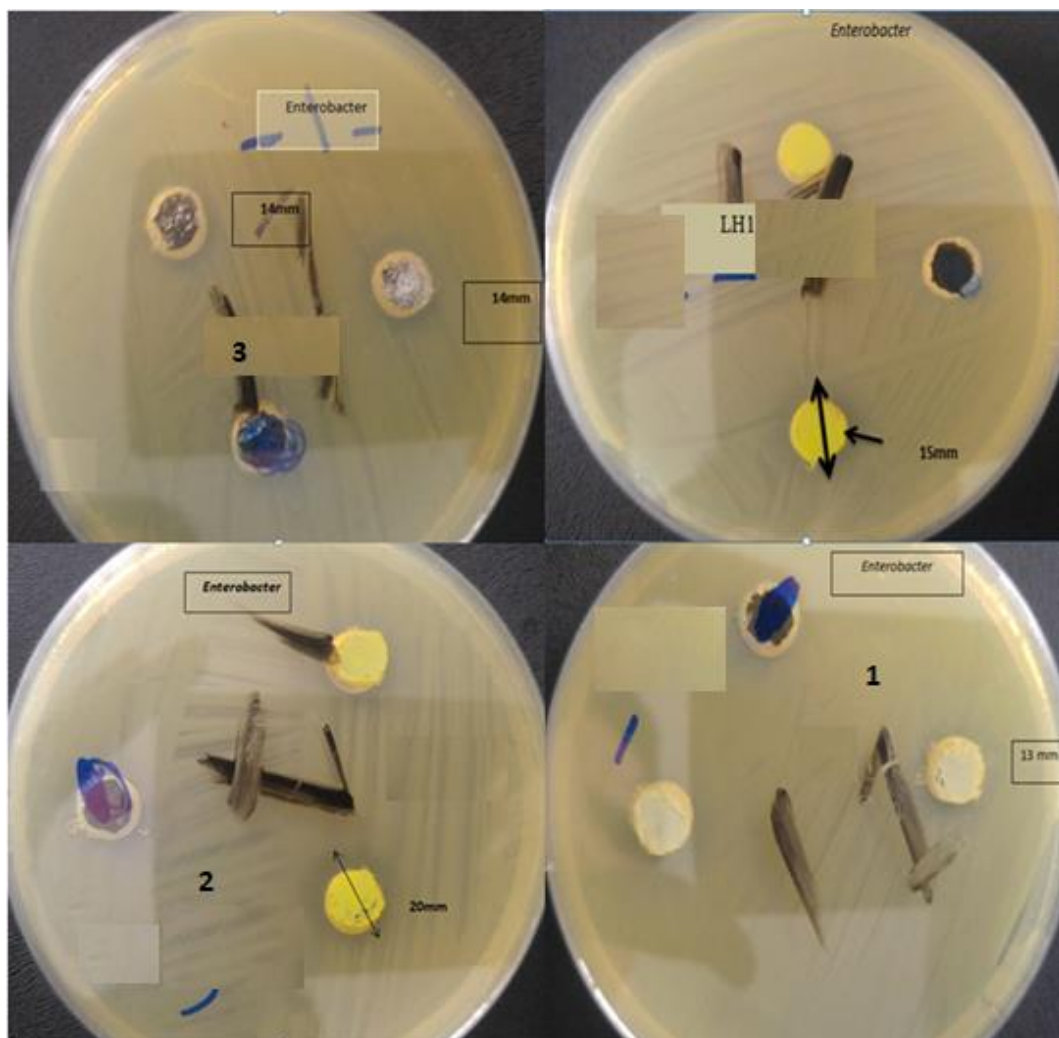


**Figure 9.** Inhibition zones for *Enterobacter* generated by  $L_1$ , **1**, **2** and **3** are 13, 15, 20 and 13 mm.

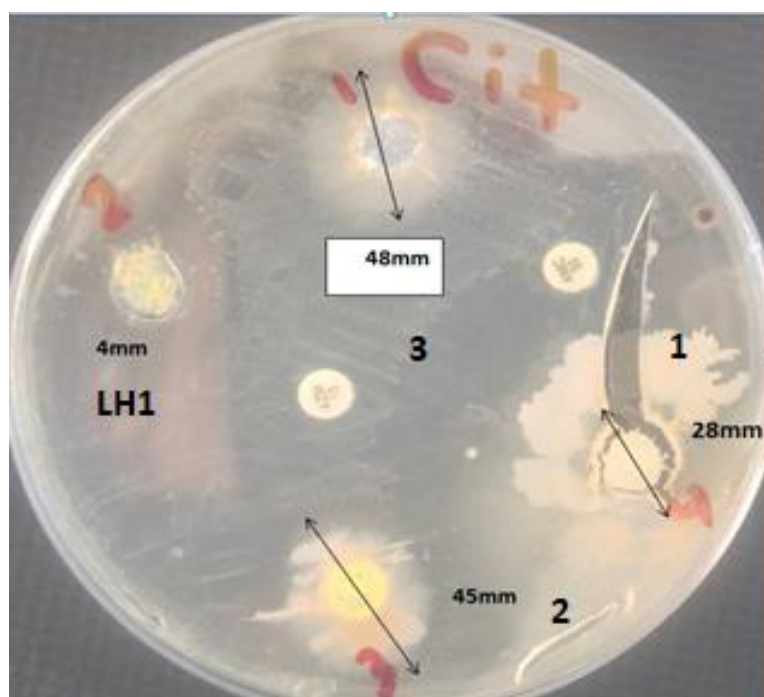


**Figure 10.** Shows inhibition zone of *Citrobacter* by the effects of ( $L_1$ , **1**, **2** and **3**) was (4, 28, 45 and 48 mm) respectively.

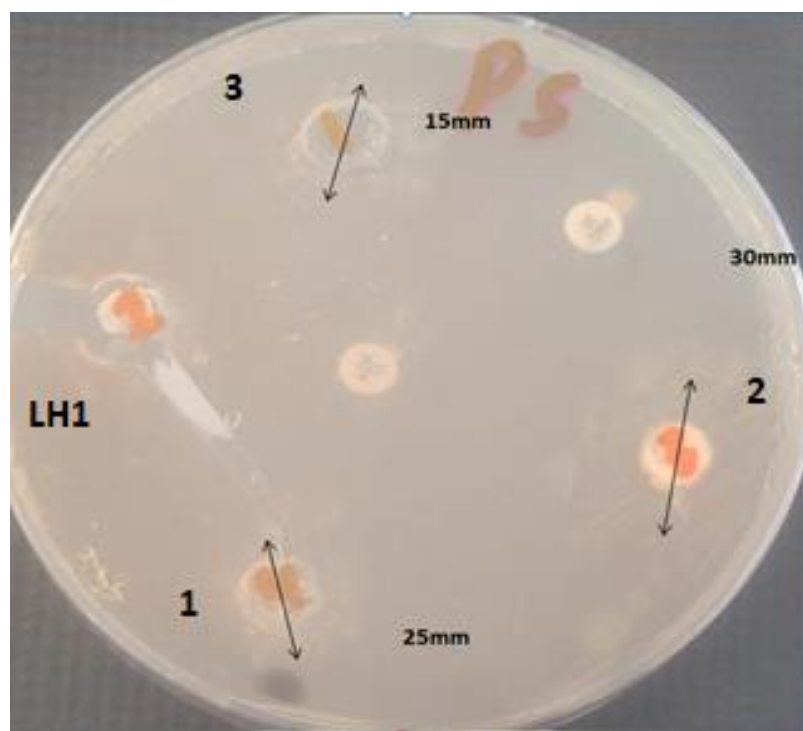


**Figure 11.** Shows inhibition zone of *Pseudomonas* by the effects of ( $L_1$ , 1, 2 and 3) were (0, 25, 30 and 15 mm) respectively.

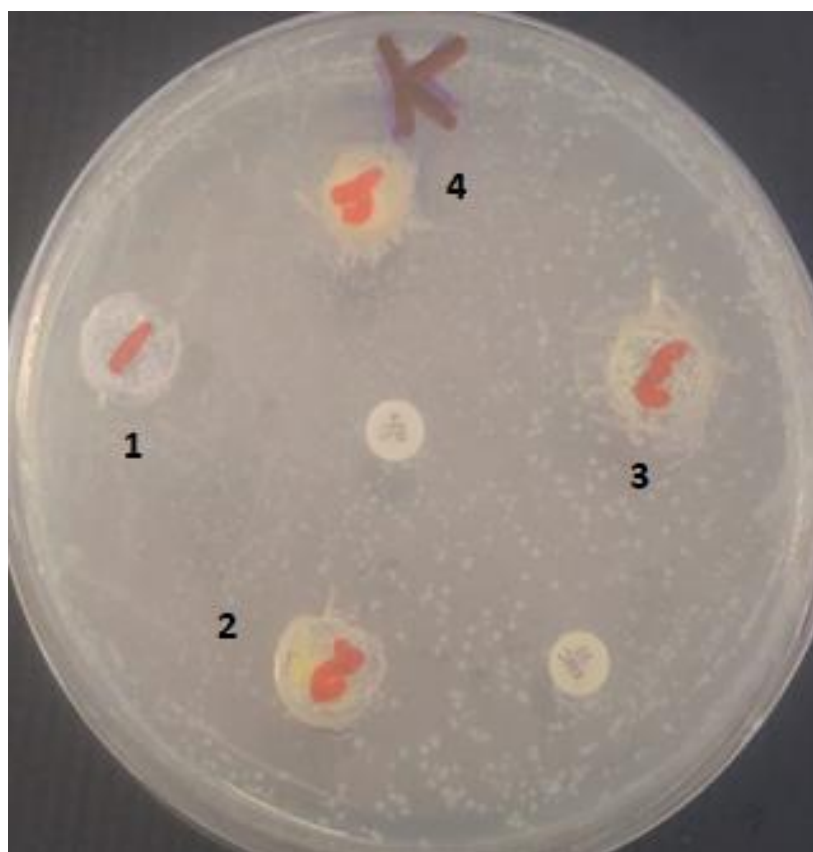


**Figure 12.** Showing inhibition zone of *Klebsiella* by the effects of ( $L_1$ , 1, 2 and 3) was (0, 0, 0 and 0 mm) respectively.

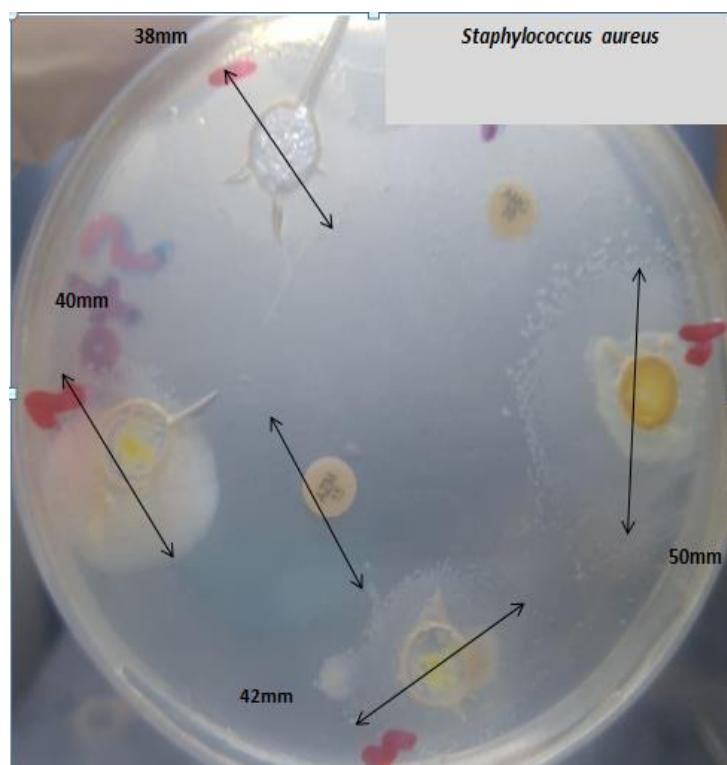


**Figure 13.** Showing inhibition zone of *Staphylococcus* by the effect of ( $L_1$ , **1**, **2** and **3**) were (38 mm, 40 mm, 42 mm and 50 mm).

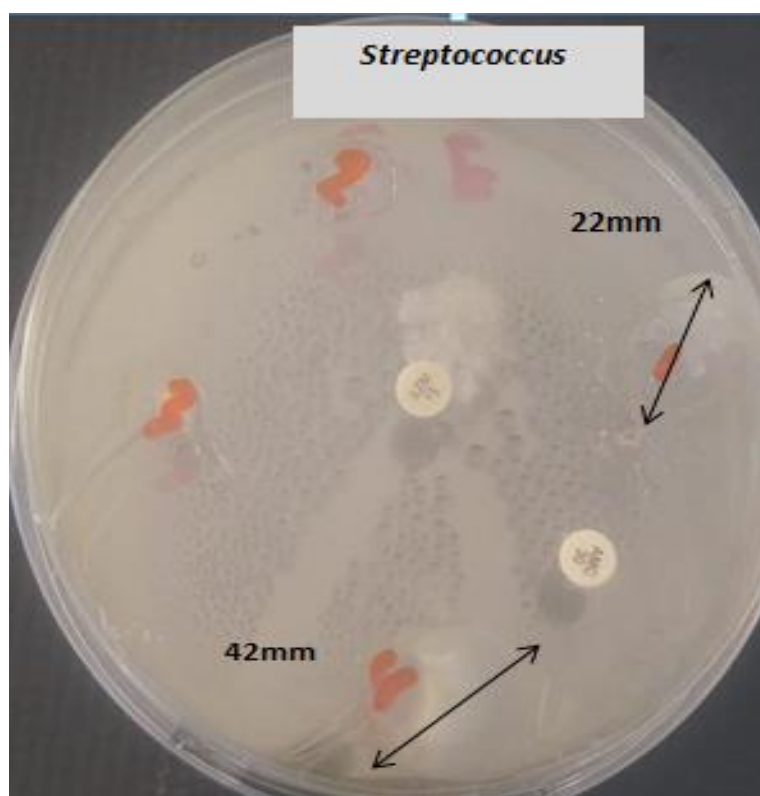


**Figure 14.** Showing inhibition zone of *Streptococcus* by the effect of ( $L_1$ , **1**, **2** and **3**) was (22, 0, 0 and 42mm).

**Table 1.** The effects of chemical compounds (inhibition zone) on Gr-bacteria.

| Test No. | Types of isolates      | Antibiotics |       | Chemical compounds |      |      |      |
|----------|------------------------|-------------|-------|--------------------|------|------|------|
|          |                        | Amc*        | Azm** | L <sub>1</sub>     | 1    | 2    | 3    |
| 1        | <i>Enterobacter</i> G- | 0           | 0     | 15mm               | 13mm | 20mm | 14mm |
| 2        | <i>Citrobacter</i> G-  | 12mm        | 10mm  | 4mm                | 28mm | 45mm | 48mm |
| 3        | <i>Pseudomonas</i> G-  | 0           | 0     | 0mm                | 25mm | 30mm | 15mm |
| 4        | <i>Klebsiella</i> G-   | 0           | 0     | 0mm                | 0mm  | 0mm  | 0mm  |

\* Amc = Amoxicillin \*\*Azm = Azithromycin

**Table 2.** The effects of chemical compounds (zone inhibition) on Gr+ bacteria.

| Test No. | Types of isolates        | Antibiotics |       | Chemical compounds |       |       |       |
|----------|--------------------------|-------------|-------|--------------------|-------|-------|-------|
|          |                          | Amc*        | Azm** | L <sub>1</sub>     | 1     | 2     | 3     |
| 1        | <i>Staphylococcus</i> G+ | 0 mm        | 28 mm | 38 mm              | 40 mm | 42 mm | 50 mm |
| 2        | <i>Streptococcus</i> G+  | 0 mm        | 0 mm  | 0 mm               | 22 mm | 0 mm  | 42 mm |

\* Amc = Amoxicillin \*\*Azm = Azithromycin

**ESTRATÉGIAS DE APRENDIZAGEM BASEADAS EM PROBLEMAS USANDO VÁRIAS REPRESENTAÇÕES E ESTILOS DE APRENDIZAGEM PARA MELHORAR AS COMPREENSÕES CONCEITUAIS DA QUÍMICA****PROBLEM-BASED LEARNING STRATEGIES USING MULTIPLE REPRESENTATIONS AND LEARNING STYLES TO ENHANCE CONCEPTUAL UNDERSTANDINGS OF CHEMISTRY**ARSANI, Ida Ayu Anom<sup>1,2\*</sup>; SETYOSARI, Punaji<sup>2</sup>; KUSWANDI, Dedi<sup>2</sup>; DASNA, I Wayan<sup>3</sup><sup>1</sup> Department of Mechanical Engineering, Politeknik Negeri Bali, Indonesia.<sup>2</sup> Department of Instructional Technology, Faculty of Education, Universitas Negeri Malang, Indonesia<sup>3</sup> Department of Chemistry, Faculty of Mathematics and Science, Universitas Negeri Malang, Indonesia

\* Corresponding author

e-mail: ayuanomarsani@pnb.ac.id

Received 11 May 2020; received in revised form 12 June 2020; accepted 26 June 2020

**RESUMO**

Estudos na área de ensino de química descobriram que as estratégias de aprendizagem baseada em problemas (PBL) melhoram efetivamente a compreensão conceitual dos alunos. No entanto, há informações muito limitadas sobre a eficácia do PBL se ele for aplicado com representação múltipla (RM) para estudantes com diferentes preferências de aprendizado. Este estudo teve como objetivo provar os efeitos das estratégias de aprendizagem baseada em problemas (PBL) usando múltiplas representações (RM) e os estilos de aprendizagem dos alunos no entendimento conceitual em química. Havia duas aulas intactas no Departamento de Engenharia Mecânica do Politécnico do Estado de Bali que foram designadas para serem grupo experimental ( $n = 59$ ) e grupo controle ( $n = 58$ ). O Índice de Estilo de Aprendizagem (ILS) de Felder-Soloman foi aplicado para diferenciar as preferências de aprendizagem dos alunos, enquanto seu entendimento conceitual em química foi avaliado usando um teste após 6 semanas de tratamento. A análise de covariância (ANCOVA) mostra que a compreensão conceitual dos alunos ensinados usando estratégias de PBL com RM foi significativamente melhor do que aqueles ensinados usando apenas estratégias de PBL. Além disso, com base na variação dos estilos de aprendizagem, os alunos com estilo visual tiveram uma melhor compreensão conceitual do que aqueles com estilo verbal, mas a diferença não foi estatisticamente significativa. A ausência de efeito de interação entre estratégias de PBL com RM e estilo de aprendizagem na compreensão conceitual dos alunos sugere que o suporte de múltiplas representações nas estratégias de PBL pode efetivamente aprimorar a compreensão dos conceitos dos alunos em química, independentemente de seu estilo de aprendizagem.

**Palavras-chave:** representações múltiplas, aprendizagem baseada em problemas, estilos de aprendizagem, química

**ABSTRACT**

Studies in the area of chemistry teaching discovered that problem-based learning strategies (PBL) effectively improve students' conceptual understanding. However, there is minimal information about the effectiveness of PBL if it is applied with multiple representations (MR) for the students with different learning preferences. This study aimed to prove the effects of problem-based learning strategies (PBL) using multiple representations (MR) and students' learning styles on the conceptual understanding in chemistry. There were two whole classes in the Mechanical Engineering Department of Bali State Polytechnic that were assigned to be the experimental group ( $n=59$ ) and control group ( $n=58$ ). Felder-Soloman's Index of Learning Style (ILS) was applied to differentiate the students' learning preferences, while their conceptual understanding in chemistry was assessed using a test after 6 weeks of treatment. The analysis of covariance (ANCOVA) shows that the conceptual understanding of students taught using PBL strategies with MR was significantly better than those taught using PBL strategies only. Besides, based on the variation of learning styles, students with a visual style had a better conceptual understanding than those with verbal style, but the difference was not statistically significant. The absence of interaction effect between PBL strategies with MR and learning style on students' conceptual understanding suggests that the support of multiple representations in PBL strategies can effectively

enhance students' understanding of concepts in chemistry regardless of their learning style.

**Keywords:** *multiple representations, problem-based learning, learning styles, chemistry*

---

## 1. INTRODUCTION:

Improving the quality of instruction is challenging for education institutions in Indonesia, especially vocational education, as a polytechnic, to generate human resources who can compete in a global age. Education at the Polytechnic prioritizes the application of practical aspects rather than theory. Chemistry, as one of the courses of theory in the field of mechanical engineering at the Polytechnic, faces challenges in the learning process that was implemented during this time because students who attend the program have a non-linear science field with chemistry. According to the majority of students, chemistry is difficult to understand, even though the application of chemical concepts in the field of mechanical engineering can support its competence in solving problems in the field such as corrosion control, the development of green energy, metal coating and waste treatment. Difficulties in understanding concepts in chemistry are related to student characteristics. Learning about chemistry needs a lot of conceptual understandings for students to be able to solve problems related to the thoughts which they learned. Conceptual understanding is a crucial aspect of instructional because the critical purpose of teaching is to help the student understand concepts in the subject matter as well as to explore a topic deeply (Santrock, 2011).

Complex challenges to understand concepts and to connect between concepts in finding new knowledge, require instructional strategies that are simple and useful for students. Chemistry is a complicated subject but has relevance and an essential role in engineering studies. Solutions to overcome these challenges through innovation in chemical learning include instructional strategies and media with new technologies that are contextual with the subject matter (Llorens-Molina & Pinto, 2014).

An instructional strategy is one or more procedures that are received by the individual to facilitate the learning task. Problem-based learning (PBL) is an instructional strategy that represents a significant change in the educational paradigm and recognized as a more proper way of education in the 21st century (Gwee, 2009). The characteristics of PBL are including, empowering learners to do research, encouraging them to integrate theory and practice and to apply

knowledge and skill to resolve the real problem (Savery, 2006). PBL has two fundamental postulates. First, learning by problem-solving is more useful for the learner to create knowledge that can use in the future. Second, the learner would have problem-solving skills instead of memorizing (Barrows & Tamblyn, 1980). The implementation of the PBL strategy of instructional has a contribution to the development of learner's creative thinking skills. Enhancing individual's creative thinking is one of the high-level thinking skills. This is a crucial point because nowadays, there is a lot of individual needs to think creatively (Ersoy & Başer, 2014).

An important aspect of PBL strategy starts with the problem as the focus of the learning process that can encourage students to find information needed for problem-solving and to learn to integrate and organize data so that later, students can maintain and apply the knowledge while solving problems. PBL strategies involve the use of individual intelligence, human groups, and the environment to solve urgent, relevant, and contextual problems. In PBL strategies, understanding comes from interacting with problem scenarios and the learning environment, helping students to build their knowledge and thinking skills, involvement with problems, and the process of problem inquiry as well as social, collaborative processes (Tan, 2003). PBL strategies are complex real-world problems that motivate students to identify and research concepts and principles (Duch, Groh, & Allen, 2001). PBL is a good learning strategy to improve student academic achievement, to develop social skills, to be active in group discussions, and to become independent learners (Argaw *et al.*, 2017). The PBL strategy has advantages compared to other learning strategies. PBL is very useful for increasing student knowledge, learning the results, and having a positive effect on their learning achievement (Maysaraa, 2016; Wilder, 2014; Yew & Goh, 2016).

Studies in the area of chemistry teaching discovered that PBL effectively improves students' conceptual understanding (Ayyildiz, & Tarhan, 2017; Bilgin, Şenocak, & Sözbilir, 2009; Günter & Alpat, 2016; Overton & Randles, 2015; Taşoğlu & Bakaç, 2014; Valdez & Bungihan, 2019; Yaayin, 2018). PBL offers chances for students to learn in a team, improve presentation skills, learn negotiating skills, and improve research skills as



well as other skills (Mossuto, 2009). PBL enhances group activities, as well as improves students' soft and hard skills (Nurtanto *et al.*, 2018). In the area of vocational education, especially in technical engineering, PBL as an instructional strategy was proven to be effective in accelerating the student's high-level skills in communication and the ability to apply new knowledge and skills corresponding to vocational education (Sada *et al.*, 2015). Besides, PBL strategies would also increase professional awareness and communication skills (Jabarullah & Hussain, 2019). Problem scenario designed in PBL presenting real-world problems which are relevant to their professional field, which will encourage them to involve in the instructional topic and develop their understanding level to achieve the instructional objective.

Achieving the expected learning objectives is not only determined by the instructional strategies applied but also requires the delivery strategies in the representation of a concept. Students need support to integrate new ideas from a visualization with their prior knowledge (Garcia & Elene, 2014). Representation is also something that represents, visualize, and symbolize object and process (Goldin, 2002). Representational competence is a part of conceptual understandings that include the ability to explain a phenomenon and integrate new knowledge gained from various or multiple representations. Representational competence is a part of conceptual understandings that include the ability to explain a phenomenon and integrate new knowledge from multiple representations.

There are three functions of multiple representations. First, to give a presentation contains complementary information or to help to complete the cognitive process. Second, to limit mistake possibilities in interpreting other representations. And third, to help learners building deep situation concepts (Ainsworth, 1999). Multiple representations can encourage the learner to construct ideas genuinely and connect representations. The representations of chemical concepts consist of macroscopic level, sub-microscopic level, and symbolic (Johnstone, 1993). The macroscopic level refers to representation obtained through real experience, and that can see directly. The sub-microscopic level describes an abstract of the chemical phenomenon and explains the structure and process in the particle levels, and that cannot see directly. The symbolic level is a representation to identify entities using qualitative and quantitative symbolic language, such as chemical formulas,

equations, stoichiometry. A representation is concluded as a way to express phenomena, objects, abstract concepts, ideas, processes, and mechanisms. Students can understand the concept of chemistry intact if they can connect representations at the macroscopic, sub-microscopic, and symbolic levels (Gilbert & Treagust, 2009). The success of understanding a concept in learning is not only influenced by the learning strategies and delivery that is applied, but is also influenced by students' learning styles in processing information.

Learning style refers to a group of psychological traits that determine how individuals perceive, interact, and respond emotionally to the learning environment (Heinich *et al.*, 2002). It includes not only the cognitive aspect of learners but also the affective aspect, which makes it a reflection of learners' personality (Litzinger, 2007). Learning styles are closely related to the information design, format, and delivery method used in facilitating students in learning, understanding concepts, and problem-solving abilities. Therefore, it can be differentiated based on learners' sensory preferences. There are four dimensions of learning style, including; perception (sensing-intuitive), input (visual-verbal), processing (active-reflective, and understanding (sequential-global) (Felder & Silverman, 1988). This model is often used to study and identify the learning styles of students in science and engineering education.

Many strategies can be adapted to stimulate students to respond to learning materials based on their learning style preferences. Studies in the area of learning style found that it had a significant effect on chemistry learning achievement and student success and have distribution to improving the understanding concept (Murat, 2013; Olić & Adamov, 2018). Learning styles contribute positively to the improvement in efficiency, the effectiveness of the learning process, and the academic performance of students (Magulod, 2019; Sidiropoulou & Mavroidis, 2019). The learning style emphasized in this study is the verbal-visual dimension because it relates to multiple representations.

Based on the reviews, as mentioned above on PBL strategies, multiple representations, and learning styles, this study aims to investigate the effect of PBL strategies with the support of multiple representations and learning styles on students' conceptual understanding of chemistry.

## 2. MATERIALS AND METHODS:

### 2.1. Research Design

This study used a quasi-experimental research design to examine whether the effect of PBL strategies using multiple representations on students' conceptual understanding depends on their learning style. There were two whole classes in the Mechanical Engineering Department of Bali State Polytechnic that were assigned to be the experimental group ( $n=59$ ) and control group ( $n=58$ ). It was confirmed that all participants agreed to participate in this study. Based on the result of the pre-test, the control group gained a mean total score = 34.913, while the experimental group gained = 34.966. This result indicates that both classes had the same level of conceptual understanding and were eligible for the following experimental procedures. The experimental group was experiencing PBL strategies with multiple representations (MR), while the control group was implemented PBL strategies. Those treatment procedures were last for 6 meetings. Learning style compared in this study emphasizes on two dimensions, namely verbal-visual, acting as a moderator variable. The overall research subjects were male, with the majority were graduated from vocational high schools.

The outline of the research design is illustrated in Figure 1.

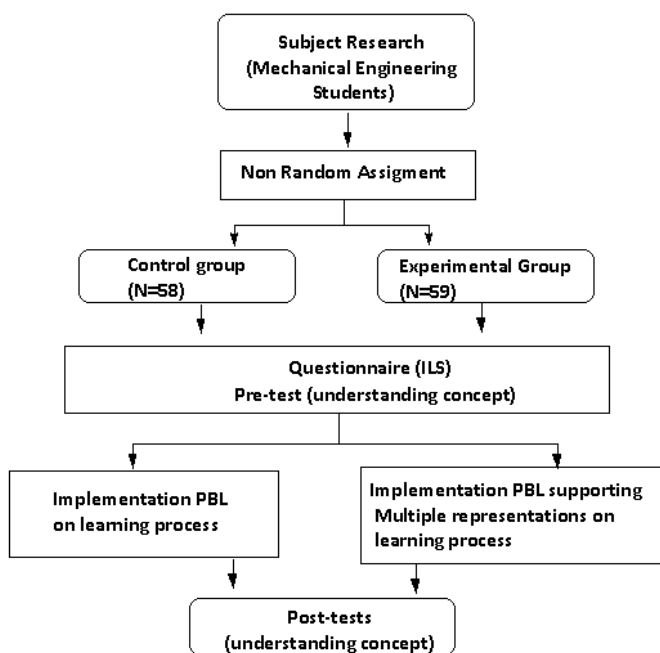


**Figure 1.** Outline of Research Design

### 2.2. Instruments

The instruments used to collect data were tests and questionnaires. The test consists of 25 multiple choice questions related to electrochemical concepts, such as oxidation-reduction reactions in electrochemical cells, the direction of electron movement in cells, cathode-anodes, reduction or oxidation reactions, energy changes, salt bridges, charge and recharge processes on batteries, mechanism of action fuel cell, corrosion process, and metal coating process (Appendix 1). This test has been regularly used to evaluate the students' conceptual understanding of chemistry in the Mechanical Engineering Department.

The questionnaire, consisting of 11 questions, was used to determine the subject's learning style, especially on the verbal-visual dimension. The questionnaire was adopted from the Index of Learning Style (ILS) developed by Felder and Solomon (North Carolina State University, Felder, & Solomon, 2020) (Appendix 2). The internal consistency reliability of the 11 verbal-visual dimension questions of ILS is .76 indicated by Cronbach Alpha coefficient (Litzinger *et al.*, 2007).

### 2.3. Implementation of PBL Strategy

The topic of the chemistry subject given in this research is about electrochemistry. Learning outcomes based on the syllabus of applied chemistry course are students understanding and explaining oxidation-reduction reactions, potential standard cells, Voltaic cells, batteries, corrosion, fuel cells, electrolytic cells, electroplating. They can explain the difference between voltaic cells and electrolytic cells. Worksheets are given to students both in the control group, and the experimental group complimented with problem scenarios based on facts happened in the field, in the daily life and real problem, which related to the given subject matter. The real-life context of an applied aspect of chemistry in the learning scenario helps the students to identify the problem. The problem scenarios given to all groups are the same. The topics were selected from the news that occurs in the field and related to the electrochemical concept, as presented in Table 1.

Implementation of the PBL strategy in research adopted a set of rules (syntax) (Arends, 2012, p. 414). During the PBL implementation process, the instructor acts as a facilitator and motivator, who help the students to develop critical thinking skills, independent learning and build new



knowledge as an effort to find solutions to problems. The detailed implementation of PBL Strategy in both the control group & experimental group is provided in Table 2.

The null hypotheses are formulated as follows:

1. There is no difference in chemistry conceptual understandings between the students in the control group and the experimental group
2. There is no difference in chemistry conceptual understandings between the students verbal and visual learning style
3. There is no interaction effect between PBL strategies and learning styles on chemistry conceptual understanding.

### 3. RESULTS AND DISCUSSION:

#### 3.1 The Result of Learning Style Questionnaire

The results of the distribution of learning style questionnaires to all research subjects showed that most of the research subjects had visual learning styles, as shown in Table 3.

**Table 3.** Students' based on Learning Style

| Groups       | Learning Style |        | Total |
|--------------|----------------|--------|-------|
|              | Verbal         | Visual |       |
| Control      | 13             | 45     | 58    |
| Experimental | 16             | 43     | 59    |

#### 3.2. The Result of Control Group Activity

Strategy activities in the control group, based on the four givens, all information collected to find solutions to the problems identified and also complete the tasks contained in the worksheet. Some Problems were identified by each group, such as reactions that occur in batteries, reduction-oxidation reactions, differences between primary and secondary batteries, the difference between dry batteries and wet batteries, reactions in fuel cells, corrosion occurs in metals, electrolysis cells, and electroplating with chrome metal.

#### 3.3. The Result of Experimental Group Activity

In the experimental group, the activities carried out were almost the same as the control class. Information is collected to find solutions to problems that have been identified, including macroscopic, submicroscopic, and symbolic

aspects, for example, about electroplating mechanisms. Answering the question, the information collected is related to the electrode, the direction of the electron's movement in the coating process, the process of oxidation, and reduction. An Understanding process in chemical reaction requires visualization technology that can integrate into three levels of representation so that it can be presenting simultaneously. Therefore, in the experimental group to solve problems and answer tasks requires electrochemical multimedia modules that are supported by a dynamic visualization of abstract concepts.

#### 3.4. The Effect of PBL Strategies with Multiple Representation and Learning Style on Students' Conceptual Understanding

Table 4 shows the pre-test result and also the post-test results from both of the groups after six meeting treatments. The post-test mean score of the control group is 60.759, and the experimental group is 74.711. In Table 5, the inferential statistical analysis using ANCOVA shows that the significance value of the applied PBL strategies on conceptual understanding in the post-test is 0.000 ( $p < 0.05$ ). It means that the first null hypothesis is rejected. There were significant differences between the learning strategies (PBL) applied toward students' conceptual understanding.

The level of understanding of students' concepts measured by the score gained from the pre-test and post-test. The average scores of pre-test and post-test on electrochemical conceptual knowledge can be seen in Figure 2.

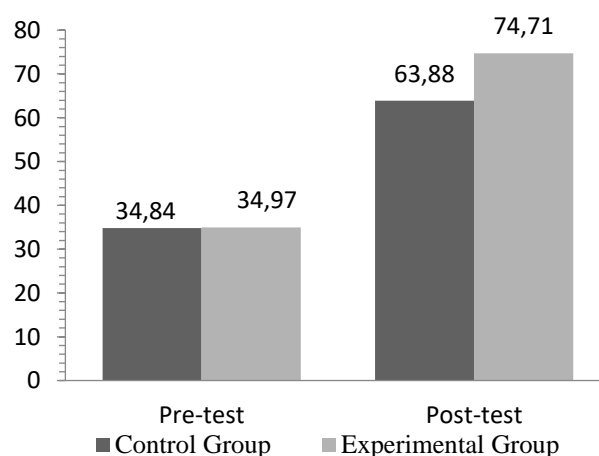


**Figure 2.** The Average Scores of Pre-test and Post-test on Electrochemical Conceptual Understanding

As shown in Table 5, the significance value of the learning style variables on conceptual understanding in the post-test is 0.962 ( $p > 0.05$ ). It means that there is not enough evidence to reject the second null hypothesis. The differences of conceptual understanding between students with verbal and visual learning styles were not significant.

Figure 3 shows the gain comparison of the post-test results on electrochemical conceptual understanding based on instructional strategies applied and students' learning styles aspects. It shows that the discrepancy was only identified between the students taught using PBL and PBL plus multiple representation strategies. There is no meaningful score difference found between students with verbal or visual learning preferences.

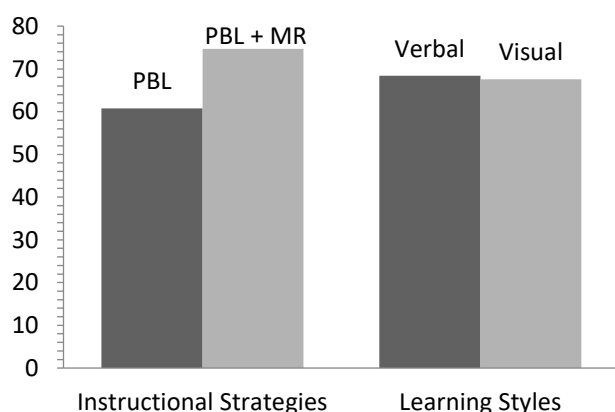


**Figure 3.** The Post-test Results on Electrochemical Conceptual Understanding based on Instructional Strategies and Learning Styles Aspects

To answer the third hypothesis, referring to Table 5, it can be explained that there was no interaction between PBL strategies with MR and learning styles toward conceptual understandings. In other words, support of Multiple Representations in Problem-Based Learning strategies can effectively enhance students' understanding of concepts in chemistry regardless of their learning style.

The implementation of PBL strategies with MR in learning has a positive effect on students' understanding of concepts in chemistry for mechanical engineering students. Presenting concrete facts about the application of chemical concepts in the field of mechanical engineering through the design of the scenarios provided is an attraction for students to learn to understand the concepts being studied. The plot designed is

adapted to real situations that occur in everyday life and has to do with the concept of electrochemical material that can apply to the field of mechanical engineering. The instructor acts as a facilitator, motivator, and directs students who are divided into groups to make a hypothesis of the problem found by the scenario presented. Students in control and experimental groups seemed eager to follow the stages of the PBL implementation process. Fostering the ability to work together between individuals in a group is also an advantage of PBL.

The concept of electrochemistry is a material that is very applicable in the field of mechanical engineering. Having a good understanding of the concepts of chemistry, especially electrochemistry, will be able to support the competencies of students in developing their resources. The experimental group that was given the PBL strategy with the support of multiple representations gave better results to the improvement of understanding of the concept compared to without multiple representations. That is because Chemistry with scientific characters dominated by abstract concepts is very important to be supported by multiple representations in the chemistry learning process to minimize the difficulty of students understanding concepts.

Several research results have proven that multiple representations in chemistry learning have an important role in improving students' understanding of concepts and the quality of chemistry learning (Emine & Yakmaci-Guzel, 2013; Sunyono & Meristin, 2018). They learn science concepts; students need to understand various representations of scientific concepts, be able to translate between different representations, and demonstrate the capacity to construct representations in any form for specific purposes (Cheng & Gilbert, 2009). Understanding the concept of chemistry intact is if it can connect representations at the macroscopic, sub-microscopic, and symbolic levels. The combination of levels of representation (macroscopic, symbolic, and submicroscopic) can develop a deeper and more structured understanding of concepts (Baptista, *et al.*, 2019).

Some applications of chemical concepts in the field of mechanical engineering can significantly support the competence of an engineer in developing his scientific resources. Engineering students are also expected to have an excellent conceptual understanding of basic science, including chemistry. Similar results also to find, the application of PBL in learning basic

science for engineering students can improve conceptual understanding and an effective teaching pedagogy to enhance professional skills for engineering students (Beagon & NíFhloinn, 2018; Sahin, 2010). Multiple representations are essential in the study of chemistry, because learning chemical concepts, not only presented phenomena that can see with the naked eye but also abstract phenomena. For example, the characteristics of metal undergoing corrosion can be seen directly from the change in its color, but the process of the change cannot be seen immediately (sub-microscopic). Sub microscopic representation can use with the help of visualization technology. The experimental group in studying electrochemical concepts with multiple representations has an impact on being able to understand the direction of electron movement in galvanic cells, corrosion processes, batteries, electrolytic cells, and electroplating.

In connection with the findings in answering the second hypothesis, no effect was found between learning styles on conceptual understanding. Based on the results of the questionnaire distribution of learning styles, it is seen that visual learning styles are more dominant than verbal. Still, these results do not contribute to increasing conceptual understanding. This result is supported by several findings from the results of the study (Garner-O'Neale & Harrison, 2013; Kidanemariam, Atagana, & Engida, 2014) concluded that learning styles do not contribute to improving the academic achievement of chemistry students, fundamental understanding concepts and learning outcomes. The same results, that interaction between learning style and academic achievement was not significant and did not affect academic achievement (Sahin, 2010). Learning styles relate to each individual's way of receiving new information. In the context of this study, there are indications that the strategies implemented can accommodate how students obtain new information in improving the understanding of concepts. Although learning styles do not have a direct effect, learning styles possessed by students in learning are essential to consider.

#### 4. CONCLUSIONS:

Based on the findings in this study, it can be concluded that the PBL strategy could enhance the students' understanding of the concept in chemistry. However, PBL strategies that apply with multiple representations show significantly better results compared to those without multiple representations. Besides, students' learning style

does not directly influence the improvement of students' understanding of concepts. So that, the support of Multiple Representations in Project-Based Learning strategies can effectively enhance students' understanding of concepts in chemistry regardless of their learning style.

It is envisaged that this study might contribute to the research in instructional strategies, especially in the area of chemistry teaching, by providing two leading suggestions. First, the chemistry teacher may apply the PBL strategies with MR to improve students' conceptual understanding without worrying about students' input preferences. Second, other researchers should corroborate this study in other contexts and might ensure the effectiveness of PBL with MR by considering the different dimensions of students' learning preferences

#### 5. ACKNOWLEDGMENTS:

This research project was supported by Lembaga Pengelola Dana Pendidikan (LPDP) and Beasiswa Unggulan Dosen Indonesia Dalam Negeri (BUDI-DN) RistekDikti research grant.

#### 6. REFERENCES:

1. Ainsworth, S. (1999). The functions of multiple representations. *Computers & Education*, 33(2-3), 131– 152. doi:10.1016/s0360-1315(99)00029-9
2. Arends, R. I. (2012). *Learning to Teach*. Tenth Edition. New York: McGrawHill Education
3. Argaw, A. S., Haile, B. B., Ayalew, B. T., & Kuma, S. G. (2017). The effect of problem-based learning (PBL) instruction on students' motivation and problem-solving skills of physics. *EURASIA Journal of Mathematics, Science and Technology Education*, 13(3), 857-871. doi:10.12973/eurasia.2017.00647a
4. Ayyildiz, Y., & Tarhan, L. (2017). Problem-based learning in teaching chemistry: enthalpy changes in systems. *Research in Science & Technological Education*, 36(1), 35–54. doi:10.1080/02635143.2017.13668
5. Baptista, M., Martins, I., Conceição, T., & Reis, P. (2019). Multiple representations in the development of the students' cognitive structures about the saponification reaction. *Chemistry Education Research and Practice*. doi:10.1039/c9rp00018f

6. Barrows, H. S., & Tamblyn, R. (1980). Problem-based learning: An approach to medical education. New York: Springer
7. Beagon, Ú., Niall, D., & NíFhloinn, E. (2018). Problem-based learning: student perceptions of its value in developing professional skills for engineering practice. *European Journal of Engineering Education*, 1–16. doi:10.1080/03043797.2018.1536114
8. Bilgin, I., Şenocak, E., & Sözbilir, M. (2009). The effects of problem-based learning instruction on university students' performance of conceptual and quantitative problems in gas concepts. *Eurasia Journal of Mathematics, Science and Technology Education*, 5(2), 153–164. doi:10.12973/ejmste/75267
9. Cheng, M., & Gilbert, J. K. (2009). Towards a better utilization of diagram in research into the use of representative levels in chemical education. In J. K. Gilbert & D. F. Treagust (Eds), *Multiple representations in chemical education*. (pp. 55-73). Dordrecht: Springer
10. Duch, B. J., Groh, S. E., & Allen, D. E. (2001). *The Power of Problem-Based Learning: A Practical "How to" for Teaching Undergraduate*. Virginia: Stylus Publishing
11. Emine, A. & Buket Yakmaci-Guzel. (2013). Use of multiple representations in developing preservice chemistry teachers' understanding of the structure of matter. *International Journal of Environmental & Science Education* 8(1), www.ijese.com/
12. Ersoy, E., & Başer, N. (2014). The effects of problem-based Learning method in Higher Education on creative thinking. *Procedia-Social and Behavioral Sciences*, 116, 3494–3498. doi: 10.1016/j.sbspro.2014.01.790
13. Garner-O'Neale, L. D., & Harrison, S. (2013). An Investigation of the Learning styles and Study Habits of Chemistry Undergraduates in Barbados and their Effect as Predictors of Academic Achievement in Chemical Group Theory. *Journal of Educational and Social Research*. doi:10.5901/jesr.2013.v3n2p107
14. Goldin, G. A. (2002). Representation in mathematical learning and problem solving. In L. D. English (Ed.), *Handbook of international research in mathematics*. Nahwah, New Jersey: Lawrence Erlbaum Associated, Inc.
15. Günter, T & Alpat, S. K., 2016. The effects of problem-based learning (PBL) on the academic achievement of students studying 'Electrochemistry'. *Chemistry Education Research and Practice*. <http://dx.doi.org/10.1039/C6RP00176A>
16. Gwee, M. C.-E. (2009). Problem-Based Learning: A Strategic Learning System Design for The Education of Healthcare Professionals in the 21ST century. *The Kaohsiung Journal of Medical Sciences*, 25(5), 231–239. doi:10.1016/s1607-551x(09)70067-1
17. Heinich, R., Molenda, M., Russell, J. D., & Smaldino, S. E. (2001). *Instructional media and technologies for learning* (7th ed.), Englewood Cliffs, NJ: Prentice Hall
18. Jabarullah, N. H., & Iqbal Hussain, H. (2019). The effectiveness of problem-based learning in technical and vocational education in Malaysia. *Education + Training*. doi:10.1108/et-06-2018-0129
19. Johnstone, A. H. (1993). The development of chemistry teaching: A changing response to changing demand. *Journal of Chemical Education*, 70(9), 701. doi:10.1021/ed070p701
20. Kidanemariam, D. A., Atagana, H.I., & Engida, T. (2014). Do Learning Styles Influence Students' Understanding of Concepts and Academic Performance in Chemistry? *Mediterranean Journal of Social Sciences* Vol 5 No 16. doi:10.5901/mjss.2014.v5n16p256
21. Lawson, A.E., Abraham, M.R., & Renner, I.W., (1989), *A Theory of Instruction: Using the Learning Cycle to Teach Science Concepts and Thinking Skills*. NARST Monograph Number One, Cincinnati, OH: National Association for Research in Science Teaching
22. Liu, Y. & Ginther, D. (1999). Cognitive Styles and Distance Education. *Online Journal of Distance Learning Administration*, 2 (3).
23. Litzinger, T. A., Lee, S. H., Wise, J. C., & Felder, R. M. (2007). A Psychometric Study of the Index of Learning Styles. *Journal of Engineering Education*, 96(4),

- 309–319. doi:10.1002/j.2168-9830.2007.tb00941.x
24. Loyens, S. M. M., Jones, S. H., Mikkers, J., & van Gog, T. (2015). Problem-based learning as a facilitator of conceptual change. *Learning and Instruction*, 38, 34–42. doi:10.1016/j.learninstruc.2015.03.002
  25. Maysaraa. (2016). The Effectiveness Of Problem Based Learning (PBL) Model On Students' Learning Outcomes At Grup XI IPA 2 Of Senior High School 5 South Konawe On The Subject Of Colloid System. *International Journal of Education and Research*, 4(7), 493-504. Retrieved from <https://www.ijern.com/journal/2016/July-2016/39.pdf>
  26. Magulod, G.C., Jr. (2019). Learning styles, study habits and academic performance of Filipino university students in applied science courses: Implications for instruction. *Journal of Technology and Science Education*, 9(2), 184-198. <https://doi.org/10.3926/jotse.504>
  27. Mossuto. M. 2009. Problem-Based Learning: Student Engagement. Learning and Contextualized Problem-Solving. Occasional Paper. National Centre for Vocational Education Research Australia: NCVET
  28. Murat, G. 2013. The Effect of Students' Learning Styles to Their Academic Success. *Creative Education*, Vol. 4(10), 627-632. <http://dx.doi.org/10.4236/ce.2013.410090>
  29. Nurtanto, M., Nurhaji, S., Widjanarko, D., Wijaya, MBR., & Sofyan, H., 2018. Comparison of Scientific Literacy in Engine Tune-up Competencies through Guided Problem-Based Learning and Non Integrated Problem-Based Learning in Vocational Education. *IOP Conf. Series: Journal of Physics: Conf. Series* 1114 (2018) 012038. doi :10.1088/1742-6596/1114/1/012038
  30. Overton, T. L., & Randles, C. A. (2015). Beyond problem-based learning: using dynamic PBL in chemistry. *Chemistry Education Research and Practice*, 16(2), 251–259. doi:10.1039/c4rp00248b
  31. Olić, S. & Adamov, J. 2018. The relationship between learning styles and students' chemistry achievement. *Macedonian Journal of Chemistry and Chemical Engineering*. Vol. 37, No. 1, pp. 79–88 . doi: 10.20450/mjcce.2017.1400
  32. Sada, A. M., Mohd, Z. A., Adnan, A., & Yusri, K. (2016). Prospects of Problem-Based Learning in Building Critical Thinking Skills among Technical College Students in Nigeria. *Mediterranean Journal of Social Sciences*. 7 (3). doi:10.5901/mjss.2016.v7n3p356
  33. Savery, J. R. (2006). Overview of Problem-based Learning: Definitions and Distinctions. *Interdisciplinary Journal of Problem-Based Learning*, 1(1). Available at: <https://doi.org/10.7771/1541-5015.1002>
  34. Sockalingam, N. ,& Schmidt, H. G. (2011). Characteristics of Problems for Problem-Based Learning: The Students' Perspective. *Interdisciplinary Journal of Problem-Based Learning*, 5(1). Available at: <http://dx.doi.org/10.7771/1541-5015.1135>
  35. Santrock, Jhon.W. (2011). *Educational Psychology* (5th Ed.). New York: McGraw-Hill
  36. Sunyono, S. & Meristin, A. (2018). The Effect of Multiple Representation-Based Learning (MRL) to Increase Students' Understanding of Chemical Bonding Concepts. *Jurnal Pendidikan IPA Indonesia*. JPPI 7 (4) (2018) 399-406 DOI: 10.15294/jpii.v7i4.16219
  37. Sahin, M. (2010). The impact of problem-based learning on engineering students' beliefs about physics and conceptual understanding of energy and momentum. *European Journal of Engineering Education*, 35(5), 519–537. doi:10.1080/03043797.2010.487149
  38. Sidiropoulou, Zoi & Ilias Mavroidis. (2019). The Relation Between the Three Dimensions of the Community of Inquiry and the Learning Styles of Students in a Distance Education Programme .*International Journal of Emerging Technologies in Learning (IJET)* 14 (23), <https://doi.org/10.3991/ijet.v14i23.11564> )
  39. Taşoğlu & Bakaç. 2014. The Effect of Problem Based Learning Approach on Conceptual Understanding in Teaching of Magnetism Topics. *Eurasian Journal of Physics and Chemistry Education*, 6 (2): 110-122
  40. Treagust, David F. (2008). The role of

- multiple representations in learning science: enhancing students' conceptual understanding and motivation. In Yew-Jin & Aik-Ling (Eds.). Science Education at The Nexus of Theory & Practice
41. Tan, O. S. (2003). Problem-Based Learning Innovation: Using Problems to Power Learning in the 21st Century: Cengage Learning
  42. Valdez, J., & Bungihan, M. (2019). Problem-based learning approach enhances the problem solving skills in chemistry of high school students. *Journal of Technology and Science Education*, 9(3), 282-294. <https://doi.org/10.3926/jotse.631>
  43. Yaayin, B. (2018). The Effectiveness of Problem-Based Learning Approach to Mole Concept among Students of Tamale College of Education. *Journal of Education and Practice*. Vol.9 (12)
  44. Yew, E. H. J., & Goh, K. (2016). Problem-Based Learning: An Overview of its Process and Impact on Learning. *Health Professions Education*, 2(2), 75–79. doi: 10.1016/j.hpe.2016.01.004
  45. Wilder, S. (2014). Impact of Problem-Based Learning on Academic Achievement in High School: A Systematic Review. *Educational Review*, 67(4), 414-435. doi:10.1080/ 00131911.2014.974511

**Table 1.** *The Content of Problem Scenario in Worksheet*

| Problem Scenario   | Description   | Target Concept  |
|--|---|---|
| The battery energy source never separated from our lives     | Energy changes in batteries, electrodes, types of batteries, charge and discharge processes | Oxidation-reduction reactions, galvanic cell, battery                       |
| Fuel cell breakthrough environmentally friendly vehicles     | Electrodes in fuel cells, energy changes, the formation of water as emission                | Oxidation-reduction reactions, galvanic Cell, Fuel cell                     |
| The phenomenon of the impact of corrosion on metal materials | Corrosion as the cause of the collapse of a bridge. Corrosion prevention methods            | Oxidation-reduction reactions, galvanic cell, Potential standard, corrosion |

|                           |   |   |
|---------------------------|---|---|
| Electroplating technology | The principle of electroplating<br>Electroplating used in to prevent corrosion, and<br>Electrodes | Oxidation-reduction reactions, electrolytic cell, energy change |
|---------------------------|---|---|

**Table 2.** *The Implementation PBL Strategy in Control Group & Experimental Group*

| <b>PBL Steps</b>   | <b>Control Group</b><br>(without Multiple Representations)  | <b>Experimental Group</b><br>(with Multiple Representations)  |
|--|---|---|
| <b>Step 1.</b><br>Orienting students to problems.                              | The instructor explains the PBL strategy process in learning, including the role of students and tutors. The instructor explains the instructional objective of the electrochemical — division of groups, then the distribution of worksheets for each group member.  | The instructor explains the PBL strategy process in learning, including the role of students and tutors. The instructor explains the instructional objectives of the electrochemical subject matter, which include macroscopic, submicroscopic, and symbolic aspects. Students are divided into four groups, and then the worksheet is distributed to each individual.  |
| <b>Step 2.</b><br><i>Organizing learners to learn.</i>                         | Students brainstorm and play an active role in group discussions to identify problems from the four problem scenarios given.  | students brainstorm and play an active role in group discussions to identify problems from the four problem scenarios given   |
| <b>Step 3.</b><br><i>Assisting independent and group investigation.</i>        | Each student in the group must be active in the discussion and work together in investigation to construct new knowledge about galvanic cells, batteries, energy changes in galvanic cells, fuel cells, corrosion and electroplating from various learning sources as a solution to problem-solving and to answer the questions on the worksheet. | Each student in the group must be active in the discussion and work together in the investigation to construct new knowledge, about the concept of galvanic cells, batteries, energy changes, fuel cells, corrosion and electroplating which contains macroscopic, submicroscopic and symbolic aspects. Information collected from various learning sources as a solution in problem-solving and to answer the questions on the worksheet |
| <b>Step 4.</b><br><i>Developing and presenting artefacts and exhibits.</i>     | Each group prepares a report of results based on information collected as a solution in solving problems through presentations and posters.   | Each group prepares a report of results based on information collected as a solution in solving problems through presentations and posters.   |
| <b>Step 5.</b><br><i>Analyzing and evaluating the problem-solving process.</i> | Students reconstruct their thoughts and activities during various phases of the lesson, how they get a clear understanding of the problem situation, and find solutions to solve problems together in groups  | Students reconstruct their thoughts and activities during various phases of the lesson, how they get a clear understanding of the problem situation associated with electrochemical concepts with explanations containing aspects of the macroscopic level, submicroscopic level, and symbolic  |

**Table 4.** Descriptive Statistics Pre-test and Post-test Score

| Groups             | Learning Style | Mean     |           | Std. Deviation |           | N   |
|--------------------|----------------|----------|-----------|----------------|-----------|-----|
|                    |                | Pre-test | Post-test | Pre-test       | Post-test |     |
| Control Group      | Verbal         | 33.692   | 61.077    | 3.859          | 10.828    | 13  |
|                    | Visual         | 35.267   | 60.667    | 7.111          | 10.888    | 45  |
|                    | Total          | 34.913   | 60.759    | 6.527          | 10.781    | 58  |
| Experimental Group | Verbal         | 35.750   | 74.312    | 5.222          | 10.222    | 16  |
|                    | Visual         | 34.674   | 74.860    | 6.432          | 8.757     | 43  |
|                    | Total          | 34.966   | 74.711    | 6.102          | 9.088     | 59  |
| Total              | Verbal         | 34.828   | 68.379    | 4.698          | 12.292    | 29  |
|                    | Visual         | 34.977   | 67.602    | 6.755          | 12.161    | 88  |
|                    | Total          | 34.940   | 67.795    | 6.289          | 12.145    | 117 |

**Table 5.** Results of ANCOVA Test for The Influence between Variables

| Source          | Dependent Variable | Type III Sum of Squares | df  | Mean Square | F        | Sig. |
|-----------------|--------------------|-------------------------|-----|-------------|----------|------|
| Corrected Model | Pre-test           | .592 <sup>a</sup>       | 2   | .296        | .007     | .993 |
|                 | Post-test          | 5694.588 <sup>b</sup>   | 2   | 2847.294    | 28.432   | .000 |
| Intercept       | Pre-test           | 106146.916              | 1   | 106146.916  | 2637.484 | .000 |
|                 | Post-test          | 399503.153              | 1   | 399503.153  | 3989.261 | .000 |
| PBL             | Pre-test           | .103                    | 1   | .103        | .003     | .960 |
|                 | Post-test          | 5681.418                | 1   | 5681.418    | 56.732   | .000 |
| Learning styles | Pre-test           | .512                    | 1   | .512        | .013     | .910 |
|                 | Post-test          | .233                    | 1   | .233        | .002     | .962 |
| Error           | Pre-test           | 4587.989                | 114 | 40.246      |          |      |
|                 | Post-test          | 11416.489               | 114 | 100.145     |          |      |
| Total           | Pre-test           | 147424.000              | 117 |             |          |      |
|                 | post-test          | 554860.000              | 117 |             |          |      |

a. R Squared = .000 (Adjusted R Squared = -.017)

b. R Squared = .333 (Adjusted R Squared = .321)



## APPENDIX 1.

### MULTIPLE CHOICE TESTS

#### UNDERSTANDING OF CONCEPT OF ELECTROCHEMISTRY

Directions:

1. Read each question carefully and circle one the best answer.
2. Allocation of time available to take the test is 60 minutes

Take a look at the Galvanic cell series below. The picture is related to several questions.

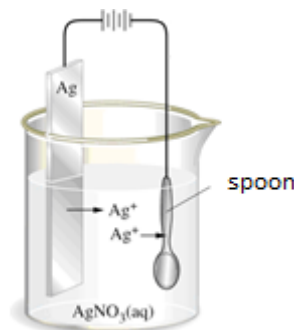


1. When the Galvanic cell is working..
  - a. Chemical energy from reactions in cells converted into electrical energy
  - b. Chemical energy from reactions in cells converted into heat energy
  - c. Electrical energy from reactions in cells converted into chemical energy
  - d. The electrical energy from reactions in cells converted to heat energy
2. Galvanic cells equipped with electrodes. The electrodes are ...
  - a. Semiconductor dipped in an electrolyte solution
  - b. The conductor dipped in an electrolyte solution
  - c. Semiconductor dipped in an acidic or basic solution
  - d. A conductor dipped in an acid or base solution
3. When Galvanic cells work, redox reactions occur ..
  - a. In the electrolyte solution
  - b. On the inside of the electrode
  - c. On the surface of the electrode
  - d. In the electrolyte solution and inside the electrode
4. Read the following statements:
  - i. The anode is a negative pole (-) and where the oxidation reaction takes place
  - ii. The anode is a positive pole (+) and where the oxidation reaction takes place
  - iii. The cathode is the negative pole (-) and the place of the reduction reaction
  - iv. The cathode is the positive pole (+) and where the reduction reaction takes placeThe correct statement is:
  - a. i and iii
  - b. i and iv
  - c. ii and iii

- d. iii
5. Galvanic cells consist of two half cells. Half the cell is:
    - a. Where oxidation and reduction reactions occur in one place
    - b. Where oxidation or reduction reactions take place separately and not at the same time
    - c. Where oxidation or reduction reactions take place separately and at the same time.
    - d. The oxidation or reduction reactions take place separately to form positive and negative ions which dissolve in the electrolyte solution
  6. When the Galvanic cell works:
    - a. The cation from the salt bridge moves to the cathode, while the anion moves to the anode
    - b. The anion from the salt bridge moves to the cathode, while the anion moves to the anode
    - c. Both cations and anions can move to the cathode or anode
    - d. The cations and anions of the salt bridge remain in the salt bridge
  7. The movement of electrons when Galvanic cells work from..
    - a. Anode to the cathode through the salt bridge
    - b. Cathode to the anode through the salt bridge
    - c. The anode to the cathode through the conducting wire.
    - d. Cathode to the anode through the conducting wire
  8. When the Galvanic cell is working..
    - a. Cu reduced to  $\text{Cu}^{2+}$ ; Zn oxidized to  $\text{Zn}^{2+}$
    - b.  $\text{Cu}^{2+}$  oxidized to Cu;  $\text{Zn}^{2+}$  reduced to Zn
    - c.  $\text{Zn}^{2+}$  reduced to Zn; Cu oxidized to  $\text{Cu}^{2+}$
    - d.  $\text{Cu}^{2+}$  reduced to Cu; Zn reduced to  $\text{Zn}^{2+}$
  9. Dry cell batteries are so-called because..
    - a. The used electrolyte is completely dry
    - b. The used electrolyte is a moist paste
    - c. It is using dry electrodes
    - d. None of the above
  10. Which of the following statement is correct..
    - a. The capacity of a cell measured in volts
    - b. Primary cells convert electrical energy into chemical energy
    - c. Galvanizing of ferrous metals can prevent corrosion
    - d. Positive electrodes are called cathodes
  11. Which of the following batteries commonly used at electric power stations?
    - a. Zink-Carbon Battery
    - b. Nickel-Cadmium Battery
    - c. Lead-acid battery
    - d. Lithium battery
  12. Fuel cells used to convert chemical energy into..
    - a. Electricity energy
    - b. Mechanical energy
    - c. Electricity energy
    - d. Potential energy
  13. Choose the wrong statement from the following options..
    - a. Fuel cell emission levels are far below the permitted limit
    - b. Fuel cells have a high level of noise
    - c. Fuel cells have high-efficiency

- d. Fuel cells are modular
14. The change that happened during the process of charging the battery is ..
- Chemical energy becomes heat energy
  - Electrical energy becomes chemical energy
  - Chemical energy becomes electrical energy
  - Chemical energy becomes chemical energy

The picture is related to several questions below



15. What is the energy conversion that occurred in the cell above ....
- Chemical energy becomes heat energy
  - Heat energy becomes electrical energy
  - Electrical energy becomes chemical energy
  - Electrical energy becomes heat energy
16. The occurrence of the electroplating process is marked by..
- Electrons move from the anode to the cathode
  - Electrons move from the cathode to the anode
  - Coating occurs at the anode
  - Anode mass increases
17. In the cell above, what acts as a cathode ..
- Ag
  - Pt
  - Spoon
  - Cu
18. During the reaction in the electrolytic cell ...
- Oxidation occurs at the anode
  - Oxidation occurs at the cathode
  - Reduction occurs at the anode
  - Reduction occurs in the conducting wire
19. Electroplating is an example of the application of electrochemical cells from .....
- Electrolytic cell
  - Galvanic Cells
  - Voltaic Cell
  - Fuel cell
20. The functions of electroplating include, except..
- Aesthetics
  - Harden metal surfaces
  - Protect metal from corrosion
  - Increase corrosion rate

21. In electrolytic cells, chemical reactions take place ....
  - a. Spontaneously
  - b. Not spontaneously
  - c. Back and forth
  - d. Out of circuit
22. The difference between galvanic cells and electrolytic cells is
  - a. Both occur spontaneously
  - b. In a galvanic cell, electrical energy is converted into chemical energy; in electrolytic cells, chemical energy is transformed into electrical energy
  - c. In electrolytic cells, electrical energy is converted into chemical energy on galvanic cells, and chemical energy is transformed into electricity
  - d. Galvanic cells require an external current
23. Factors affecting the rate of corrosion in metals include, except..
  - a. Temperature
  - b. pH
  - c. Concentration
  - d. Bond
24. The battery that is classified as a secondary cell is ...
  - a. Silver oxide battery
  - b. Mercury oxide batteries
  - c. Lead-acid battery
  - d. Zinc-carbon battery
25. The change happened during the process of discharging the battery is...
  - a. Chemical energy becomes heat energy
  - b. Electrical energy becomes chemical energy
  - c. Chemical energy becomes electrical energy
  - d. Chemical energy becomes chemical energy

## APPENDIX 2.

### Visual/Verbal Learning Style Questionnaire

This questionnaire is designed to find out what your learning preferences are; (Verbal/Visual).

Direction:

1. This questionnaire is consisted of 11 questions and should be done in 15 minutes.
  2. Read each of the question carefully and please put a cross (X) on 'a' or 'b' to indicate your answer.
- 
1. When I think about what I did yesterday, I am most likely to get
    - a. picture.
    - b. words.
  2. I prefer to get new information in
    - a. pictures, diagrams, graphs, or maps.
    - b. written directions or verbal information.
  3. In a book with lots of pictures and charts, I am likely to

- a. look over the pictures and charts carefully.
  - b. focus on the written text.
4. I like teachers
- a. who put a lot of diagrams on the board.
  - b. who spend a lot of time explaining.
5. I remember best
- a. what I see.
  - b. what I hear.
6. When I get directions to a new place, I prefer
- a. a map.
  - b. written instructions.
7. When I see a diagram or sketch in class, I am most likely to remember
- a. the picture.
  - b. what the instructor said about it.
8. When someone is showing me data, I prefer
- a. charts or graphs.
  - b. text summarizing the results.
9. When I meet people at a party, I am more likely to remember
- a. what they looked like.
  - b. what they said about themselves
10. For entertainment, I would rather
- a. watch television.
  - b. read a book.
11. I tend to picture places I have been
- a. easily and fairly accurately.
  - b. with difficulty and without much detail.

Adopted from:

North Carolina State University, Felder, R.M., Soloman, B.A. (2020) Index of Learning Styles Questionnaire. *Learning Styles and Index of Learning Styles*. Retrieved from <https://www.webtools.ncsu.edu/learningstyles/>

**A EFICÁCIA DO MODELO DE APRENDIZAGEM EM LABORATÓRIO BASEADO EM ETNOSOCIOECOLOGIA PARA APLICAR A ALFABETIZAÇÃO AMBIENTAL EM PROFESSORES DE BIOLOGIA EM TREINAMENTO****THE EFFECTIVENESS OF INQUIRY LABORATORY-BASED ETHNOSOCIOECOLOGY LEARNING MODEL TO EMPOWER ENVIRONMENTAL LITERACY IN PRESERVICE BIOLOGY TEACHERS**MASHFUFUFAH, Aynin<sup>1\*</sup>; NURKAMTO, Joko<sup>2</sup>; Sajidan<sup>3</sup>; Wiranto<sup>4</sup><sup>1</sup>Doctoral Program of Educational Science, Sebelas Maret University, Surakarta, Central Java, Indonesia<sup>2,3</sup>Teacher Training and Education Faculty, Sebelas Maret University, Surakarta, Central Java, Indonesia<sup>4</sup>Faculty of Math and Science, Sebelas Maret University, Surakarta, Central Java, Indonesia

\* Correspondence author  
e-mail: ayninn@student.uns.ac.id

Received 06 June 2020; received in revised form 20 June 2020; accepted 28 June 2020

**RESUMO**

O ponto principal da alfabetização ambiental é aumentar a preocupação individual com a crise ambiental em ações concretas ou movimentos de cuidado ambiental. Esta pesquisa visa capacitar o conhecimento de professores de biologia da preservação sobre o meio ambiente e seus problemas em contextos ecológicos e sociais e habilidades cognitivas para investigar e planejar soluções para os problemas. O método de pesquisa quantitativa com o design de um grupo pré-teste e pós-teste foi empregado para testar o aumento do conhecimento ambiental após o aprendizado. O efeito estimulante são as habilidades cognitivas para superar problemas ambientais. Os participantes da pesquisa consistiram em 29 professores de biologia em treinamento cursando ciências ambientais no primeiro semestre. O conhecimento ambiental foi medido por meio de um teste de ensaio, enquanto a mensuração das habilidades cognitivas foi realizada por meio de uma rubrica com escala de classificação baseada nos resultados de investigações de problemas ambientais em campo. Verificou-se que o modelo de aprendizagem de etnossocioecologia em laboratório poderia melhorar significativamente o conhecimento ambiental. Além disso, o conhecimento ambiental está positivamente correlacionado com as habilidades cognitivas. Em geral, as habilidades cognitivas aumentam com maior conhecimento ambiental.

**Palavras-chave:** *habilidades cognitivas, conhecimento ambiental, alfabetização ambiental, etnossocioecologia, laboratório de investigação.*

**ABSTRACT**

The main point of environmental literacy is to increase individual concern towards the ecological crisis in concrete action or environmental care movement. This research aims to empower the knowledge of preservice biology teachers about the environment and its problems in environmental, and social contexts and cognitive skills to investigate and plan solutions to the issues. The quantitative research method with the one-group pretest-posttest design was employed to test the increase of environmental knowledge after learning. The nurturant effect is cognitive skills in overcoming environmental problems. The research participants consisted of 29 preservice biology teachers taking the environmental science course in the first semester. Environmental knowledge was measured using an essay test, while the measurement of cognitive skills was performed using a rubric with a rating scale based on the results of investigations of environmental problems in the field. It was found that the inquiry laboratory-based ethnosocioecology learning model could significantly improve environmental knowledge. In addition, environmental knowledge is positively correlated with cognitive skills. In general, cognitive skills increase with higher environmental knowledge.

**Keywords:** *cognitive skills, environmental knowledge, environmental literacy, ethnosocioecology, inquiry laboratory.*

## 1. INTRODUCTION:

Developing countries characterized by high population growth and economic instability encounter various environmental problems. These problems include pollution, deforestation, the decline in natural resources, climate change, and extinction. Declining environmental quality is a result of economic instability. The exploitation of natural resources to increase economic growth is not followed by efforts to rejuvenate the environment (Begon, Harper, & Townsend, 2006; Hanif & Gago-de-Santos, 2017). Indonesia is one of the developing countries with the fourth highest population in the world with Java as the most populous island. Pressure on clean water supply becomes one of the environmental problems found in densely populated areas. The clean water crisis is the impact of the conversion of green land into agricultural land, residential areas, mining, and industry. Flood is no longer a natural phenomenon, but a result of poor land management and spatial planning (Asian Development Bank, 2016).

Considering such conditions, concern for the environment should not only be a tendency towards attitude, but also be manifested in concrete actions (Mishra, Akman, & Mishra, 2014), one of which is to empower students in increasing their knowledge of the environment and applying it to overcome problems that are happening around them (Bodzin, 2016). Environmental education as an agent for formal learning is very effective for students to participate in sustainable development that prioritizes the environmental care aspect (Hoang & Kato, 2016; Varela-Candamio, Novo-Corti, & García-Álvarez, 2018).

One theme in 21<sup>st</sup>-century learning is environmental literacy (Pacific Policy Research Center, 2010) as a response to changes in environmental and socio-economic conditions. These changes stem from pressures due to population growth, urbanization, economic development, increasing inequality, and poverty rate (Delgado-Serrano, Mistry, Matzdorf, & Leclerc, 2017). Environmental literacy can be built through environmental education to gain in-depth knowledge, skills development, and authentic experience about environmental changes around students. More than that, students are expected to become part of a community that actively responds to the environmental crisis through concrete efforts (Coyle, 2005). Environmental education must use a multidisciplinary learning approach in order to produce a broad knowledge

of environmental science and skills to overcome environmental problems. Thus, environmental literacy is the highest goal of environmental education (Bodzin, Klein, & Weaver, 2010).

21<sup>st</sup>-century learning emphasizes mastery of higher-order thinking skills (HOTS) and complex cognitive processes (Greiff, Niepel, & Wüstenberg, 2015; Partnership for 21st Century Skills, 2009). These skills are supported by critical-thinking, problem-solving, communication, and collaboration so that individuals can adapt to various challenges in the globalization era (Saavedra & Opfer, 2012). Critical thinking and problem-solving are part of cognitive skills. Meanwhile, communication, collaboration, and social responsibility belong to interpersonal skills (Koenig, 2011). Creativity as a component of problem-solving skills is obtained when a person develops their thinking from various perspectives and is applied to new conditions (Partnership for 21st Century Skills, 2012).

21<sup>st</sup>-century learning is preferred to integrate approaches based on technology, inventions, problems, and HOTS (Partnership for 21st Century Skills, 2009). Growing technology facilitates students to work both independently and in groups. Technology helps in collecting relevant information, analyzing the relationship between information, constructing new knowledge, and presenting that information clearly from all aspects studied (OECD, 2008). In addition, technology is also used in the assessment of learning (Nikou & Economides, 2017). Students must be accustomed to finding answers to a problem by collecting and assessing the accuracy of the information, organizing information, and concluding (Griffin, McGaw, & Care, 2012; NAAEE, 2015).

Teachers at every level of education must possess in-depth knowledge and relevant experience relating to the environment, both the concept and the problem, before teaching the students (Nagra, 2010). This ability is significantly influenced by experiential learning such as learning that utilizes the natural environment, examines environmental problems, plays an active role in environmental management activities (environmental activists), and teaching practices on environmental education (Torkar, 2014). The important aspects to be considered in environmental education include learning relevant to everyday life, involving various parties such as society, family and role models, allowing students to interact with the social environment, direct experience, freedom to determine learning topics, studying local problems, and encouraging

community movements (Wilson, 2011). Given the importance of environmental education to improve environmental literacy in students, program or curriculum evaluations need to be carried out correctly to determine the progress, difficulties and the level of goal achievement (Spinola, 2015).

Therefore, the study aimed to empower the environmental knowledge and cognitive skills as the variables of the environmental literacy of preservice biology teachers.

## 2. LITERATURE REVIEW:

There are various definitions of environmental literacy and elements that make it up. According to NAAEE (2004), environmental literacy has four main components: (1) curiosity about the condition of the surrounding environment followed up by finding information, testing the truth and building a knowledge; (2) a deep understanding of human interaction with the environment; (3) measures to assess environmental problems and find solutions; and (4) awareness that each individual has a role to better change the environment. The first component consists of special skills, namely asking questions, designing investigations, gathering information, evaluating the truth of information, organizing information, reviewing and conducting simulations, and concluding and delivering explanations. The second component includes an understanding of the earth system, the concept of the environment, humans, and their culture and human interaction with the environment. The third component refers to the skills of analyzing and investigating environmental issues and making decisions. The fourth component includes understanding social values and principles, recognizing the rights and responsibilities as citizens, being confident and responsible for the actions taken (NAAEE, 2015).

According to Hollweg et al. (2011), the component of environmental literacy consists of knowledge, attitudes, competencies, and environmentally-responsible/friendly behaviors. Knowledge includes systems in physics and ecology and environmental issues. Attitude refers to sensitivity, environmental care, the motivation and purpose of taking action to deal with environmental issues. Competence emphasizes the skills and abilities to identify, analyze, create solutions, and evaluate actions to address environmental problems. Environmentally-responsible behavior is manifested in the form of individual or group involvement to overcome problems and prevent the emergence of new

conflicts such as environmental management activities, campaigning for environmental care, and using environmentally-friendly products.

The learning of environmental science is multidisciplinary (Miller & Spoolman, 2010). Students need to learn concepts related to ecology, economics, social, politics, and culture (NAAEE, 2015). The integration of diverse knowledge and scientific disciplines helps students analyze a problem from various perspectives. Not only do students need to master the concepts related to systems and processes that occur in the ecosystem, but they must also critically analyze how economic development, social and cultural changes, and environmental management policies can impact the environment (Kusmawan, O'Toole, Reynolds, & Bourke, 2009). Students need to be accustomed to exploring existing problems in the surrounding environment to grow their concern and awareness of the decline in environmental quality due to human interaction with the environment (Zareie & Navimipour, 2016).

The pilot study shows that the preservice biology teacher in the second semester still has a low or inadequate level of environmental knowledge. There is 63% of a preservice biology teacher who gets a score of less than six from 10 questions. Besides that, there is an inconsistency response, especially about the limitation of private land use and environmental protection of wildlife. Furthermore, the practice of environmental education needs to be improved to grow ecological literacy through the understanding of the environment and its problem and real action to respond to the environmental changes surroundings.

Developing environmental knowledge means increasing environmentally-friendly behavior as it reflects the level of one's environmental knowledge (Zareie & Navimipour, 2016). Educational institutions and the government can collaborate to increase students' knowledge about the environment that refers to the ecological and social context. Through formal efforts, the government mediates the community with academics to collaborate, share information, and conduct research. Thus, various parties contribute to achieving a balance between social and ecological aspects and sustainable development goals. Information and research results are then used as learning content for the development of environmental knowledge, stimuli of changes in environmentally-friendly behaviors, and empowering skills to cope with changing environmental conditions (Krasny, Lundholm, &



Plummer, 2010).

Individuals who care about the environment not only have a deep understanding of environmental problems and issues but also master cognitive skills in addressing environmental problems (Hollweg et al., 2011). Cognitive skills involve students to use their prior knowledge to solve new problems and build new knowledge. Students need to actively explore a problem, apply the knowledge they have learned leading to the discovery of ideas or new problem-solving strategies. Cognitive skills involve the ability to think critically to specify the problem and connect a variety of information and the ability to think creatively to find effective and innovative solutions (Koenig, 2011).

One's action on the environment from the Theory of Reasoned Action perspective is influenced or determined by several factors. The fundamental factors in determining a person's behavior include personal, social, and knowledge background factors. These factors affect one's belief in behaviors and norms that exist in society. A person's trust determines his/her attitude towards a behavior and norm and behavior control. Attitudes, norms, and behavioral control further determine or influence the purpose of an action. Through learning environmental science, students are expected to utilize their prior knowledge of the environment to be transferred into positive attitudes and behaviors towards the environment (Fishbein & Ajzen, 2010).

Applying knowledge to do a set of cognitive skills in problem-solving is an example of experiential learning. Inquiry learning is one example of experiential learning that helps students connect theory with practice. Prior environmental knowledge is enriched through the activities of investigating environmental problems in the field. The prior knowledge and knowledge gained during the investigation are interrelated to test the truth of the previous knowledge. New knowledge that is built through the process of finding information, observing, measuring, and analyzing is utilized as a new stimulus to make decisions in similar new situations. Also, the inquiry method in environmental science learning trains students to reason according to the evidence obtained during the activities of problem identification, gathering facts of the problem, planning problem-solving actions, predictions, making relevant decisions, and linking problems with the specified solutions (Dewey, 1938).

Inquiry laboratory learning is also one example of the application of meaningful learning

theory. Students build new knowledge by organizing the entire prior knowledge with the information being studied (Savin-Baden & Major, 2004). The previously-owned knowledge is adjusted to new conditions or problems in order to produce creative ideas, for example in overcoming the problem of pollution or waste (King, Keohane, & Verba, 1995). Students not only get concepts available in the form of textbooks but also learn to explore information in the field, analyze, organize, and make conclusions about environmental problems and the solutions (Ausubel, 2000).

Environmental science is interdisciplinary. Various disciplines are interconnected, for example in handling fisheries problems. To address these problems, they need to be studied from the aspects of environmental economics, political science, ecology, chemistry, anthropology, and population biology. Explaining the environmental problems at the beginning of the learning is expected to stimulate students' ability to reason from various perspectives and to recall the knowledge or experience they have. Different opinions of the students with heterogeneous academic and communication skills help them in the transfer of knowledge, enriching insight, and cognitive development in social interaction (Vygotsky, 1978). Environmental science learning in study groups encourages students to exchange opinions, consider the advantages and disadvantages of planned solutions, and make decisions based on mutual agreement (Swartz & McGuinness, 2014).

According to the socioecological theory of systems, there is a close relationship between social systems and ecology. Besides living and forming community groups, humans also depend on nature to get ecosystem services (Patten, 2016). This system aims to safeguard and enhance ecological resilience in supporting human survival by continuing to prioritize ecological principles in adaptive ecological management (Mathevet, Thompson, & Folke, 2016). This system is useful for the identification of causal relations between components in ecology and social to produce a mechanism to adapt to changes that occur in both systems (Kappeler, 1999). Local knowledge is one form of adaptive ecological management (Pauli, Abbott, Negrete-Yankelevich, & Andres, 2016).

Knowledge about the environment consists of scientific knowledge and local knowledge. The combination of both kinds of knowledge contributes to reducing the possibility of environmental damage as a result of the use of the environment (Mercer, Dominey-Howes, Kelman, &

Lloyd, 2007; Thornton & Scheer, 2012). Traditional ecological knowledge is obtained from the habit of people interacting with nature directly, including knowledge about living things and natural phenomena, as well as how to manage the environment such as farming, raising livestock, and hunting (Inglis, 1993). Local knowledge arises and develops among the people who have lived in an area for a long period and retained it because it provides benefits for their life and environment. Although local knowledge is not obtained through scientific testing, the truth of the knowledge can be scientifically proven through integrated science learning (Parmin, Sajidan, Ashadi, Sutikno, & Fibriana, 2017).

The use of local knowledge in environmental education can enrich the knowledge of preservice biology teachers related to sustainable environmental management practices. Students are encouraged to participate in overcoming global problems by utilizing local knowledge in their surroundings (Palmer, 2003). Ethnoecology is also called local knowledge, traditional knowledge, or traditional environmental knowledge, which is often used interchangeably. Ethnosocioecology is a set of knowledge and perceptions of local people in environmental management practices to adapt to changes in ecological and social systems.

Integrating local knowledge about the environment in learning has several advantages: (1) it completes and provides reinforcement about science that can generate new thinking and develop problem-solving skills (Evering, 2012); (2) it raises awareness about local knowledge; (3) it facilitates students to develop critical-thinking skills; (4) it fosters cooperation with local communities to create sustainable communities (Dei, 2000).; (5) it strengthens the character education of students (Adilah & Saputra, 2013; Marhayani, 2016); (6) it improves problem-solving skills, scientific investigations and environmental care attitudes (Dewi, Poedjiastoeti, & Prahani, 2017); and (7) it helps students apply and transfer their knowledge to everyday life (Gitari, 2010).

The inquiry laboratory is the fourth level of inquiry after discovery learning, interactive demonstration, and inquiry lessons. Inquiry laboratory has a characteristic that is to demand the independence of students in exploring their knowledge and the locus of control is entirely on students. Students are given the freedom to determine the problems and procedures used in inquiry and problem-solving. Lecturers act as facilitators who provide opportunities for students to conduct investigations and provide support or

assistance only when needed because college students are adult learners who already have the psychological ability to study independently (Flick & Lederman, 2006). The main objective of laboratory inquiry-based learning is to formulate empirical laws based on measurements of variables. The process skills needed in this research include measurement, formulation of empirical laws based on evidence and logic, designing scientific investigations using technology, and calculating (Wenning, 2005; 2010; Wenning, Khan, & Khan, 2011). However, not all students have the same level of process skills in testing or collecting data. Therefore, in this research, students are provided with guiding questions or points that need to be studied as guidance in conducting investigations. Meanwhile, problem-solving planning is entirely determined by students according to their level of critical thinking and creativity.

The inquiry laboratory-based ethnosocioecology learning model consists of observation, manipulation, investigation, generalization, verification, and application stages. The observation stage is the identification of problems in the classroom from the guiding questions raised by students under the topic or theme of learning. Based on the identified problems, students determine one main problem and design a problem investigation procedure (related to the environment) independently at the manipulation stage. The draft includes determining the location of the investigation, compiling a list of questions to gather information directly from the local community related to the topic of the problem, and planning or predicting problem-solving actions. The next stage is the investigation. Students carry out investigation activities in the field according to plan. After obtaining information through interviews and observations, students analyze the problem including the causes and effects supported by the study of relevant theories and determine solutions relevant to the problem. In the generalization stage, students formulate conclusions based on the data analysis. The problems investigated and analyzed are presented in discussions to get various information and responses from other students. This stage is called the verification stage. The application stage is the implementation of the conclusions from the results of the discussion as reinforcement and confirmation of the truth about students' prior knowledge related to environmental problems to solve problems in new situations or answer questions (Figure 1).

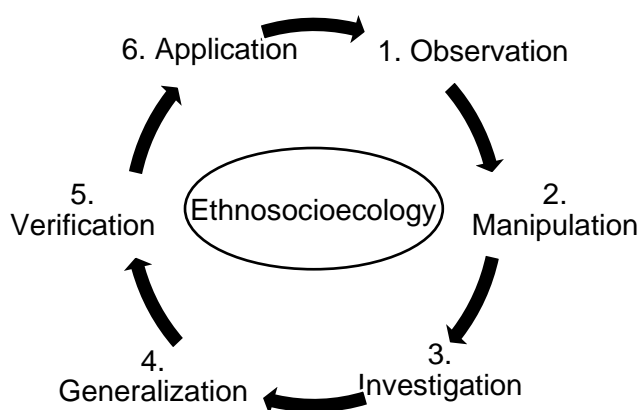


**Figure 1.** *The model of inquiry laboratory-based ethnosocioecology*

In addition to the independence that takes precedence in inquiry laboratory learning, the use of local knowledge content is the basis for students in conducting the stages of inquiry laboratory. Before students determine the environmental problems to be studied, they explore prior knowledge related to local knowledge on the use or management of the environment, components contained in local knowledge (knowledge, practice, and beliefs), how local knowledge arises and is transmitted over generations, and the benefits of applying local knowledge to environmental sustainability. Apart from being used to increase students' knowledge about the environment, local knowledge is also used as a basis for students to develop ideas for solving environmental problems that are further investigated. Thus, students indirectly prove the truth of local knowledge related to its role in environmental preservation.

### 3. MATERIALS AND METHODS:

To test the effect of inquiry laboratory-based ethnosocioecology learning model on the empowerment of environmental literacy, one-group pretest-posttest design was used. Before conduct the study, the researcher submits the research permit that known by the supervisor and approved by the faculty to the head of the biology education study program. The document was forwarded to the practitioner and discuss the form of collaboration between practitioners, students, and researchers along with the study. The sample consisted of 29 preservice biology teachers. As the environmental literacy construct that has been previously defined, which is a set of knowledge about the environment and its problems in ecological and social contexts and cognitive skills in problem-solving, the environmental literacy in this research consists of two variables that are

environmental knowledge (EK) and cognitive skills (CS). This research was conducted in 5 cycles (two meetings of each cycle). In each meeting, there were 29 preservice biology teachers, a practitioner/lecturer, and three observers.

Each meeting lasts for 100 minutes in the classroom. As shown in Figure 1, the syntax of inquiry laboratory-based ethnosocioecology consists of six syntaxes. In each cycle, students investigate one topic of environmental problems and design a solution. The activity of the first meeting in each cycle is observation and manipulation. Environmental problems and local knowledge that have been identified in the classroom are followed up with investigation in the field. Preservice biology teachers do the investigation and generalization syntaxes in the field. The specific problem was investigated and analyzed deeply and designed the solution. The result of field investigation was presented in a paper which consists of problem identification, problem investigation, problem analysis, and solution. Practitioners and biology preservice teachers communicate within a WhatsApp group during field investigation. Students and the lecturer could discuss the difficulties and share the information at the field in the form of pictures or videos, and the lecturer and observer could control the student progress and activity. The second meeting of each cycle is for verification and application syntax. The student reports the field investigation and solution then discuss it with other groups. The observer records the activity of learning such as how the implementation of each syntax, what difficulties, and learning progress.

The materials used in the learning module include (1) introduction to environmental science and ethnosocioecology, (2) environmental principles and ecosystem management models, (3) ethnosocioecology as an example of the application of environmental ethics, (4) components and processes in the ecosphere, and (5) ecosphere problems and the resolution efforts. Investigation topics related to these materials include (1) the problem of green land conversion, (2) environmental management and problems, (3) examples of local knowledge as a form of environmental ethics, (4) carbon cycle disruption, and (5) local environmental problems. These topics encourage students to dig deeper information from various viewpoints, experiences, and public knowledge, and observe environmental conditions directly. Students analyze the data collected with relevant theoretical studies. Based on the facts and study of the theory, students find reinforcement and confirmation of the truth related

to environmental issues that have been the subject of the global discussion. Investigation of local knowledge in the community enables students to think locally and act globally or encourages them to solve global problems by utilizing the local potential around them.

Preservice teachers were given a pretest before learning and posttest after completing learning in each cycle. Pretest and posttest were used to measure students' environmental knowledge. Pretest and posttest were given in the form of description questions that had been tested for validity and reliability. In addition to providing tests, the researcher also assessed students' cognitive skills in solving environmental problems. Cognitive skills were assessed using a rubric with a rating scale. There are 4 indicators of cognitive skills, namely problem identification, problem investigation, problem analysis, and problem-solving. These indicators were assessed through the paper resulted from field investigation. Each indicator was assessed by four rating scales 1 = unclear and irrelevant, 2 = slightly unclear and irrelevant with the problem, 3 = clear but slightly relevant to the problem, 4 = clear and relevant to the problem.

T-test was used to determine differences before and after learning inquiry laboratory-based ethnosocioecology on environmental knowledge. Before conducting the test, the data were tested for normality and homogeneity as prerequisites. To find out whether there is a positive correlation between environmental knowledge and cognitive skills, Pearson's correlation test is performed. Before the data correlation test, the data linearity and normality were tested.

#### 4. RESULTS AND DISCUSSION:

Based on the results of the normality test using the Kolmogorov-Smirnov test, the pretest and posttest data in the five cycles showed normal distribution of data ( $p > 0.05$ ) and based on the homogeneity test using Levene test, the data were homogeneous ( $p > 0.05$ ) (Tables 1 and 2).

The cognitive-skill data in the five cycles also showed normal distribution and had homogeneous variants as well as significant values of more than 0.05 (see Table 3 and 4).

After the prerequisite tests were fulfilled, the data were analyzed using paired t-test to find out whether there are significant differences before and after the application of inquiry laboratory-based ethnosocioecology on students' environmental knowledge. The data from the five

cycles were used in the paired t-test. The analysis showed that there was a significant difference between before and after the treatment ( $p < 0.05$ ) (see Table 5). Thus, the inquiry laboratory-based ethnosocioecology learning model is effective in empowering environmental literacy.

Cognitive skills were measured using an assessment rubric based on the results of investigations of environmental problems and the resolution efforts. The linearity test results from the five cycles showed that the value of deviation from linearity is more than 0.05. This means that environmental knowledge and cognitive skills have a linear relationship. After the prerequisite tests were met, the data were tested using the Pearson correlation. The Pearson correlation test results show a positive correlation coefficient close to 1 with a significance value of less than 0.05 (see Table 6).

This means that environmental knowledge and cognitive skills are positively correlated. In general, higher environmental knowledge will be followed by an increase in cognitive skills. Based on the results of the t-test, it was found that the inquiry laboratory-based ethnosocioecology learning model is effective in increasing environmental knowledge. Higher environmental knowledge will lead to an increase in cognitive skills in solving problems.

In cycle 1, the experimental-class students investigate problems related to the conversion of land use for the batik industry, tourism, shops, housing, and infrastructure. In cycle 2, students study problems regarding environmental management for animal husbandry, tourism, agriculture, and household waste treatment plants. In cycle 3, students investigate examples of local community knowledge in farming, namely the use of straw in growing rice seedlings, crop rotation, polyculture planting systems on private land, and terracing systems. In cycle 4, students conduct interactive simulation activities on carbon cycle disruption and food webs and create a design to overcome these problems. In cycle 5, students study environmental problems that have long been experienced by residents, namely water pollution and waste problems. Students analyze and communicate the results of investigations and design solutions obtained at the second meeting in each cycle.

Various solutions are produced after students analyze the problem. In cycle 1, one of the solutions designed is the use of natural materials from plants such as leaves, flowers, stems or roots, and others as natural batik dyes. The natural batik dyes can reduce water pollution

due to the batik industry with harmful chemical dyes. In connection with the problem of environmental management for cattle farming, namely livestock manure, in cycle 2, students plan a strategy in the form of using animal dung to be made composted and to be made biogas. In cycle 3, relating to examples of local knowledge, students prove the use of straw in increasing soil fertility and moisture applied in the practice of growing rice seeds. Also, students examine the effect of crop rotation and polyculture systems on soil fertility.

In cycle 4, students simulate the carbon cycle for carbon cycle disturbance material. Interactive simulations, instead of investigations in the field, involve students actively in changing certain parameters and observing changes that occur. The data collected are then analyzed to build new knowledge. Through these simulations, students can understand the process of the ongoing carbon cycle, carbon distribution in the ecosphere, and the influence of increased use of fossil fuels and carbon levels on the survival of life on land and water. After analyzing the problem, students create the design of the solution to overcome the carbon cycle problems while still referring to local environmental management practices.

In the simulation of food webs, students practice making predictions of the increase or decrease in the number of producer and consumer populations in an ecosystem. Then, they prove their predictions through simulations and make modifications to the food webs so that each trophic can maintain their survival in the ecosystem. The results of the investigation through simulations are generalized and verified in class discussions. Communicating the results of the simulation also becomes a medium for students to compare the results of their investigations with other study groups.

In cycle 5, they examine the ecosphere problem and its solution. Students study water and garbage pollution problems. Through the activities of problem identification, problem investigation in the field, literature studies, and problem analyses, students can create a water pollution problem-solving plan by utilizing natural materials namely Moringa plant seeds from the surrounding environment combined with a simple screening tool. For the garbage problem, students design solutions by replacing plastic bags with cloth bags that can be used repeatedly, using plastic waste as chairs or tables made up of eco-bricks, and processing cardboard waste into reusable items such as makeup equipment, mini cabinets, tissue

holder, and stationery.

Based on the test results in cycles 1 to 5, there is an increase in the average posttest scores in the experimental class. This shows that the ability of students to analyze and evaluate problems related to environmental management is increasing in each cycle. Besides, there is an increase in the students' ability to solve environmental problems with information obtained during the study group's investigation and discussion. After the paired t-test, it was found that there is a significant difference between the means of the posttest and pretest of environmental knowledge in the experimental class.

Based on the results of the Pearson correlation test, it is known that there is a significant positive correlation between environmental knowledge and cognitive skills. This shows that the high value of environmental knowledge, in general, is followed by the high value of cognitive skills. Thus, the inquiry laboratory-based ethnosocioecology learning model is effective in empowering environmental literacy for the aspects of environmental knowledge and cognitive skills.

Learning activities that examine the problem of land-use conversion, environmental management problems, environmentally-friendly management practices, simulation of material cycle disturbances, and environmental problem resolution help students develop their environmental knowledge (Partanen-Hertell, et al., 1999). Students practice connecting the causes and effects of environmental problems from observation and investigation activities (Erdogan, 2015). Multidisciplinary environmental science encourages students to evaluate the relationship between ecological and social aspects that contribute to the emergence of environmental problems (Steg & Vlek, 2009). Understanding these relationships becomes the basis to apply their knowledge critically in the face of environmental changes that occur (Sorensen et al., 2015). Student-centered learning activities reinforce environmental care (Bissinger & Bogner, 2017).

Studying local knowledge applied by the community such as crop rotation, intercropping system, and using straw in the farming system can foster students' awareness that the practices carried out by local communities need to be preserved. Insights into the benefits of local knowledge encourage students to develop ideas for solving environmental problems that are environmentally friendly that do not lead to new

problems and reduce the environmental damage caused by the existing technological development (Kimmerer, 2012). Learning through direct experience in the field contributes to building knowledge about the environment (Brenner, Hamilton, Drake, & Jordan, 2013; Stevenson et al., 2014).

Students' cognitive skills improve from cycle 1 to 5. The stimuli given in the form of environmental issues encourages students to have group discussions (Savin-Baden & Major, 2004). Students are trained to convey their knowledge, experience, and ideas related to issues that are of concern around them. Investigating environmental problems helps students connect their prior knowledge with information being learned to build new knowledge. Contextual learning contributes to linking theory with practice (Agung, 2015; Reyes-García et al., 2010).

Studying environmental science is not enough to master the concepts of the environment, but it is very important to deepen understanding of environmental issues or problems. An understanding of the environmental conditions around them is expected to lead students to take action. Investigation of environmental problems in the field begins with identifying the problem. Problem identification helps students determine specific problems to be studied further by gathering information in the field. The data obtained are then analyzed to deepen understanding of the cause and effect relationship. The analysis of the problem is then followed up by finding relevant and applicable solutions (Bodzin, Klein, & Weaver, 2010).

The lecturer acts as a facilitator when the students plan and carry out investigation activities. The lecturer actively accommodates students' ideas in preparing investigation plans. When students find it difficult to determine the specific topic to be studied, the lecturer provides an example of his previous experience so that students have a picture and can make decisions. Also, the lecturer provides an immediate response whenever the student needs opinions related to the topic to be further investigated. The lecturer encourages the freedom and independence of students in designing investigation activities while still providing space for discussion. The facilitation used is in the cooperative form (Heron, 1989; 1993).

During the observation and manipulation activities, verbal strategies are applied by the facilitator. The first strategy is giving questions to

train students to express ideas or prior understanding of the issue being discussed. The second is providing support and trust that students can convey their prior knowledge. The third is providing conclusions on the ideas or answers given. The fourth is giving back the questions of the students to be answered or responded by others. It aims to raise students' responsibility to explore their knowledge. In addition, verbal strategies are also carried out during manipulation and investigation. The lecturer suggests alternative ideas when students find it difficult to make decisions and control the progress of study groups in planning and conducting investigation activities (Savin-Baden & Major, 2004).

Study groups with diverse cultural backgrounds and cognitive skills facilitate students in developing their cognitive skills by sharing knowledge and experiences and help them to make adjustments to their environment (Griffin et al., 2012). The same goal to solve environmental problems with the basis of knowledge on local environmental management encourages students to discuss their prior knowledge with one another in class and link the ideas of all group members. Through the process of interactions and dialogs, students can make decisions to take action (Savin-Baden & Major, 2004).

Getting students used to study environmental problems that occur around them and to design solutions-oriented to local knowledge is pivotal in learning environmental science. Students master not only knowledge about the environment, but also skills to solve problems and foster the environment care attitude. Studying environmental problems facilitates students to get used to gathering information related to facts in the field. Based on the information obtained, students learn to develop opinions or determine attitudes towards environmental problems that occur. In addition, students are involved in linking various information about the environment, analyzing the interrelationships of causes and effects of environmental problems, and designing strategies in overcoming environmental problems (Palmer & Neal, 1994).

The integration of traditional or local knowledge in environmental science learning contributes positively (Kimmerer, 2012). First, students can get to know the traditions or habits of environmental management that have been practiced by previous generations. Second, students understand the benefits and importance of applying traditional environmental management practices to the current deteriorating

environmental conditions (Brenner et al., 2013). Third, students gain new knowledge during the process of verifying the truth of local knowledge (Hiwasaki, Luna, Syamsidik, & Shaw, 2014). Fourth, students learn to integrate local and scientific knowledge to design innovative solutions (Makondo & Thomas, 2018; Torri & Laplante, 2009). Fifth, students contribute to preserving local environmental management practices as part of cultural wealth (McCarter & Gavin, 2011). Sixth, students learn to understand the meaning of sustainable living by applying traditional management practices (Dahliani, 2015; Sumane et al., 2017).

## 5. CONCLUSIONS:

Environmental literacy is an urgent demand given the current conditions of the environmental crisis. Environment care and its problems must be instilled in each individual because human is naturally an inseparable part of nature. Growing an attitude of caring for the environment must be done in concrete action. Education as a formal environment, for example, must be able to contribute to the generations that have insight into sustainable development. One strategy is to instill an environmental care attitude through learning. Interdisciplinary learning of environmental science must be able to empower students to be active in studying environmental issues, expressing opinions from a variety of perspectives, analyzing the interrelationships among environmental problems, evaluating the truth of information from various sources, and developing innovative strategies. Inquiry laboratory-based ethnosocioecology learning is one of the strategies to involve the active role of students as independent learners in building new knowledge. New knowledge is obtained by analyzing, linking, organizing prior knowledge with information being learned in the classroom, and the surrounding environment. Students deepen their understanding of environmental issues through investigations in the field, testing the truth of local knowledge, linking the concepts of local knowledge with the conditions of environmental problems, and designing appropriate strategies. Environmental science learning through real experience is not merely memorizing existing concepts. It also allows students to learn to dig up information, to communicate, and interact with peers and the surrounding community, and to argue based on the evidence. Studying the surrounding environmental problems and learning local knowledge practices in managing the

environment, in addition to increasing knowledge about the environment, can also develop the cognitive skills of students in solving problems. Solving environmental problems is one manifestation of the environmental care attitude.

## 6. ACKNOWLEDGMENTS:

Thanks to the BUDI scholarship organized by LPDP. LPDP supports and provides research funding.

## 7. REFERENCES:

1. Adilah, G., & Saputra, S. (2013). Enhancing Local Wisdom Through Local Content of Elementary School in Java, Indonesia. *Global Summit on Education, 2013*(March), 11–12. Kuala Lumpur.
2. Agung, L. (2015). The Development of Local Wisdom-Based Social Science Learning Model with Bengawan Solo as the Learning Source. *American International Journal of Social Science*, 4(4), 51–58.
3. Asian Development Bank. (2016). *Indonesia Country Water Assessment*.
4. Ausubel, D. P. (2000). *The acquisition and retention of knowledge: A cognitive view*. <https://doi.org/10.1017/CBO9781107415324.004>
5. Begon, M., Harper, J. L., & Townsend, C. R. (2006). *Ecology: Individuals, Populations, and Communities*. In *Blackwell science*. <https://doi.org/10.1007/s13398-014-0173-7.2>
6. Bissinger, K., & Bogner, F. X. (2017). Environmental literacy in practice: education on tropical rainforests and climate change. *Environment, Development, and Sustainability*, 1–16. <https://doi.org/10.1007/s10668-017-9978-9>
7. Bodzin, A. M. (2016). Integrating Instructional Technologies in a Local Watershed Investigation With Urban Elementary Learners. *The Journal of Environmental Education*, 39(2), 47–57. <https://doi.org/10.3200/JOEE.39.2.47-58>
8. Bodzin, A. M., Klein, B. S., & Weaver, S. (2010). *The Inclusion of Environmental Education in Science Teacher Education*. London: Springer.

9. Brenner, J. C., Hamilton, J. G., Drake, T., & Jordan, J. (2013). Building local environmental knowledge in undergraduates with experiential wilderness skills and awareness training: The case of environmental sentinels. *Journal of Environmental Studies and Sciences*, 1–12. <https://doi.org/10.1007/s13412-013-0145-9>
10. Coyle, K. (2005). Environmental Literacy in America. In *Environmental Education*. [https://doi.org/10.1641/0006-3568\(2000\)050\[0916:EL\]2.0.CO;2](https://doi.org/10.1641/0006-3568(2000)050[0916:EL]2.0.CO;2)
11. Dahliani, D. (2015). Local wisdom in the built environment in the globalization era. *International Journal of Education and Research*, 3(6), 157–166.
12. Dei, G. J. S. (2000). Rethinking the role of Indigenous knowledge in the academy. *International Journal of Inclusive Education*, 4(2), 111–132. <https://doi.org/10.1080/136031100284849>
13. Delgado-Serrano, M., Mistry, J., Matzdorf, B., & Leclerc, G. (2017). Community-based management of environmental challenges in Latin America. *Ecology and Society*, 22(1), 4. <https://doi.org/10.5751/ES-08924-220104>
14. Dewey, J. (1938). Logic: The Theory of Inquiry. *The Philosophical Review*. <https://doi.org/10.2307/2180803>
15. Dewi, I. N., Poedjiastoeti, S., & Prahani, K. (2017). ELSII learning model based local wisdom to improve students' problem-solving skills and scientific communication. *International Journal of Education and Research*, 5(1), 107–118.
16. Erdogan, M. (2015). The effect of summer environmental education program (SEEP) on elementary school students' environmental literacy. *International Journal of Environmental and Science Education*, 10(2), 165–181. <https://doi.org/10.12973/ijese.2015.238a>
17. Evering, B. (2012). Relationships between knowledge(s): Implications for "knowledge integration." *Journal of Environmental Studies and Sciences*, 2(4), 357–368. <https://doi.org/10.1007/s13412-012-0093-9>
18. Fishbein, M., & Ajzen, I. (2010). *Predicting and Changing Behavior*. <https://doi.org/10.4324/9780203838020>
19. Flick, L. B., & Lederman, N. G. (2006). Scientific Inquiry and Nature of Science: Implication for Teaching, Learning, and Teacher Education. In *Science & Technology Education Library*. <https://doi.org/10.1007/1-4020-2672-2>
20. Gitari, W. (2010). An inquiry into the integration of indigenous knowledge and skills in the Kenyan secondary science curriculum: A case of human health knowledge1. *Canadian Journal of Science, Mathematics and Technology Education*, 3(2), 195–212. <https://doi.org/10.1080/14926150309556560>
21. Greiff, S., Niepel, C., & Wüstenberg, S. (2015). 21st-century skills: International advancements and recent developments. *Thinking Skills and Creativity*, 18, 1–3. <https://doi.org/10.1016/j.tsc.2015.04.007>
22. Griffin, P., McGaw, B., & Care, E. (2012). *Assessment and Teaching of 21st Century Skills*. <https://doi.org/10.1007/978-94-017-9395-7>
23. Hanif, I., & Gago-de-Santos, P. (2017). The importance of population control and macroeconomic stability to reducing environmental degradation: An empirical test of the environmental Kuznets curve for developing countries. *Environmental Development*, 23, 1–9. <https://doi.org/10.1016/j.envdev.2016.12.003>
24. Heron, J. (1989). *The Facilitator's Handbook*. London: Kogan Page.
25. Heron, J. (1993). *Group Facilitation*. London: Kogan Page.
26. Hiwasaki, L., Luna, E., Syamsidik, & Shaw, R. (2014). Process for integrating local and indigenous knowledge with science for hydro-meteorological disaster risk reduction and climate change adaptation in coastal and small island communities. *International Journal of Disaster Risk Reduction*, 10, 15–27. <https://doi.org/10.1016/j.ijdrr.2014.07.007>
27. Hoang, T. T. P., & Kato, T. (2016). Measuring the effect of environmental education for sustainable development at elementary schools: A case study in Da Nang city, Vietnam. *Sustainable Environment Research*, 26(6), 274–286.



- <https://doi.org/10.1016/j.serj.2016.08.005>
28. Hollweg, K. S., Taylor, J. R., Bybee, R. W., Marcinkowski, T. J., McBeth, W. C., & Zoido, P. (2011). *Developing a framework for assessing environmental literacy*. Retrieved from papers3://publication/uuid/94978D29-345A-45B3-80CA-F04DCBC9373B
  29. Inglis, J. T. (1993). *Traditional Ecological Knowledge: Concepts and Cases*. Retrieved from <http://books.google.com/books?hl=en&lr=&id=J2CNS64AFvsC&pgis=1>
  30. Kappeler, P. M. (1999). Primate Socioecology: New Insights from Males. *Natur Wissenschaften*, 85, 18–29.
  31. Kimmerer, R. W. (2012). Searching for synergy: Integrating traditional and scientific ecological knowledge in environmental science education. *Journal of Environmental Studies and Sciences*, 2(4), 317–323. <https://doi.org/10.1007/s13412-012-0091-y>
  32. King, G., Keohane, R. O., & Verba, S. (1995). *Designing Social Inquiry*. New Jersey: Princeton University Press.
  33. Koenig, J. A. (2011). *21<sup>st</sup> Century Skills Summary of a Workshop*. Washington, DC: The National Academic Press.
  34. Krasny, M. E., Lundholm, C., & Plummer, R. (2010). Resilience in social-ecological systems: the roles of learning and education. *Environmental Education Research*, 16, 463–474. <https://doi.org/10.1080/13504622.2010.505416>
  35. Kusmawan, U., O'Toole, J. M., Reynolds, R., & Bourke, S. (2009). Beliefs, attitudes, intentions, and locality: the impact of different teaching approaches on the ecological affinity of Indonesian secondary school students. *International Research in Geographical and Environmental Education*, 18(3), 157–169. <https://doi.org/10.1080/10382040903053927>
  36. Makondo, C. C., & Thomas, D. S. G. (2018). Climate change adaptation: Linking indigenous knowledge with western science for effective adaptation. *Environmental Science and Policy*, 88(January), 83–91. <https://doi.org/10.1016/j.envsci.2018.06.014>
  37. Marhayani, D. A. (2016). Development of Character Education Based on Local Wisdom in Indigenous People Tengahan Sedangagung. *Journal of Education, Teaching and Learning*, 1(2), 66–70.
  38. Mathevet, R., Thompson, J., & Folke, C. (2016). Protected areas and their surrounding territory: social-ecological systems in the context of ecological solidarity. *Ecology Application*, 26, 5–16.
  39. McCarter, J., & Gavin, M. C. (2011). Perceptions of the value of traditional ecological knowledge to formal school curricula: Opportunities and challenges from Malekula Island, Vanuatu. *Journal of Ethnobiology and Ethnomedicine*, 7, 38. <https://doi.org/10.1186/1746-4269-7-38>
  40. Mercer, J., Dominey-Howes, D., Kelman, I., & Lloyd, K. (2007). The potential for combining indigenous and western knowledge in reducing vulnerability to environmental hazards in small island developing states. *Environmental Hazards*, 7, 245–256. <https://doi.org/10.1016/j.envhaz.2006.11.001>
  41. Miller, G. T., & Spoolman, S. E. (2010). *Environmental science*. Belmont: Yolanda Cossio.
  42. Mishra, D., Akman, I., & Mishra, A. (2014). Theory of Reasoned Action application for Green Information Technology acceptance. *Computers In Human Behavior*, 36, 29–40. <https://doi.org/10.1016/j.chb.2014.03.030>
  43. NAAEE. (2004). *Excellence in environmental education: Guidelines for Learning (K-12)*. Washington, DC: NAAEE.
  44. NAAEE. (2015). *Linking environmental literacy and the next generation of science standards: a tool for mapping an integrated curriculum*. Retrieved from <http://www.naaee.net/>
  45. Nagra, V. (2010). Environmental education awareness among school teachers. *Environmentalist*, 30(2), 153–162. <https://doi.org/10.1007/s10669-010-9257-x>
  46. Nikou, S. A., & Economides, A. A. (2017). Computers & Education Mobile-based assessment: Investigating the factors that

- influence behavioral intention to use. *Computers & Education*, 109, 56–73. <https://doi.org/10.1016/j.compedu.2017.02.005>
47. OECD. (2008). 21st Century Learning: Research, Innovation, and Policy. *OECD/CERI International Conference*, 1–13.
  48. Pacific Policy Research Center. (2010). 21st Century Skills for Students and Teachers. In *Research and Evaluation Division*. Honolulu.
  49. Palmer, J. A. (2003). *Environmental education in the 21st Century*. London: Routledge.
  50. Palmer, J., & Neal, P. (1994). *A Handbook of Environmental Education*. <https://doi.org/10.1177/027046769501500439>
  51. Parmin, Sajidan, Ashadi, Sutikno, & Fibriana, F. (2017). Science integrated learning model to enhance the scientific work independence of student-teacher in indigenous knowledge transformation. *Jurnal Pendidikan IPA Indonesia*, 6(2), 365–372. <https://doi.org/10.15294/jpii.v6i2.11276>
  52. Partanen-Hertell M, Harju-Autti P, Kreft-Burman K & Pemberton D. (1999). *Raising environmental awareness in the Baltic Sea area*. Helsinki, The Finnish Environment Institute. The Finnish Environment 327. ISBN 952-11-0528-3.
  53. Partnership for 21st Century Skills. (2009). *P21 Framework Definitions*. Partnership for 21st Century Skills.
  54. Partnership for 21st Century Skills. (2012). *Learning for the 21st Century*. Retrieved from [http://www.p21.org/storage/documents/P21\\_Report.pdf](http://www.p21.org/storage/documents/P21_Report.pdf)
  55. Patten, D. T. (2016). The role of ecological wisdom in managing sustainable interdependent urban and natural ecosystems. *Landscape and Urban Planning*, 155, 3–10. <https://doi.org/10.1016/j.landurbplan.2016.01.013>
  56. Pauli, N., Abbott, L. K., Negrete-Yankelevich, S., & Andres, P. (2016). Farmers' knowledge and use of soil fauna in agriculture : a worldwide review. *Ecology and Society*, 21(3), 19.
  57. Reyes-García, V., Kightley, E., Ruiz-Mallé, I., Fuentes-Peláez, N., Demps, K., Huanca, T., & Martínez-Rodríguez, R. M. (2010). Schooling and local environmental knowledge: Do they complement or substitute each other? *International Journal of Educational Development*, 30, 305–313. <https://doi.org/10.1016/j.ijedudev.2009.11.007>
  58. Saavedra, A. R., & Opfer, V. D. (2012). Learning 21st-century skills requires 21st-century teaching. *Kappanmagazine.Org*, (October), 8–13.
  59. Savin-Baden, M., & Major, C. H. (2004). *Foundations of Problem-based Learning*. New York: Open University Press.
  60. Sorensen, A. E., Jordan, R. C., Shwom, R., Ebert-May, D., Isenhour, C., McCright, A. M., & Robinson, J. M. (2015). Model-based reasoning to foster environmental and socio-scientific literacy in higher education. *Journal of Environmental Studies and Sciences*, 1–8. <https://doi.org/10.1007/s13412-015-0352-7>
  61. Spinola, H. (2015). Environmental literacy comparison between students taught in Eco-schools and ordinary schools in the Madeira Island region of Portugal. *Science Education International*, 26(3), 392–413.
  62. Steg, L., & Vlek, C. (2009). Encouraging pro-environmental behavior: An integrative review and research agenda. *Journal of Environmental Psychology*, 29(3), 309–317. <https://doi.org/10.1016/j.jenvp.2008.10.004>
  63. Stevenson, K. T., Peterson, M. N., Carrier, S. J., Strnad, R. L., Bondell, H. D., Kirby-Hathaway, T., & Moore, S. E. (2014). Role of significant life experiences in building environmental knowledge and behavior among middle school students. *Journal of Environmental Education*, 45(3), 163–177. <https://doi.org/10.1080/00958964.2014.901935>
  64. Sumane, S., Kunda, I., Knickel, K., Strauss, A., Tisenkopfs, T., Rios, I. D. I., ... Ashkenazy, A. (2017). Local and farmers' knowledge matters! How integrating informal and formal knowledge enhances sustainable and resilient agriculture. *Journal of Rural Studies*, 1–10.

- <https://doi.org/10.1016/j.jrurstud.2017.01.020>
65. Swartz, R., & McGuinness, C. (2014). Developing and assessing thinking skills. *The International Baccalaureate Organisation*, (February), 1–100.
  66. Thornton, T. F., & Scheer, A. M. (2012). Collaborative engagement of local and traditional knowledge and science in marine environments: A review. *Ecology and Society*, 17(3), 8. <https://doi.org/10.5751/ES-04714-170308>
  67. Torkar, G. (2014). Learning experiences that produce environmentally active and informed minds. *NJAS - Wageningen Journal of Life Sciences*, 69, 49–55. <https://doi.org/10.1016/j.njas.2014.03.002>
  68. Torri, M. C., & Laplante, J. (2009). Enhancing innovation between scientific and indigenous knowledge: Pioneer NGOs in India. *Journal of Ethnobiology and Ethnomedicine*, 5, 29. <https://doi.org/10.1186/1746-4269-5-29>
  69. Varela-Candamio, L., Novo-Corti, I., & García-Álvarez, M. T. (2018). The importance of environmental education in the determinants of green behavior: A meta-analysis approach. *Journal of Cleaner Production*, 170, 1565–1578. <https://doi.org/10.1016/j.jclepro.2017.09.214>
  70. Vygotsky, L. S. (1978). *Mind in Society: The Development of Higher Psychological Processes*. <https://doi.org/10.1007/978-3-540-92784-6>
  71. Wenning, C. J. (2005). Levels of inquiry: Hierarchies of pedagogical practices and inquiry processes. *Journal of Physics Teacher Education Online*, 2(3), 3–12.
  72. Wenning, C. J. (2010). Level of inquiry: Using inquiry spectrum learning sequences to teach science. *Journal of Physics Teacher Education Online*, 5(4), 11–20.
  73. Wenning, C. J., Khan, M. A., & Khan, A. (2011). Levels of Inquiry Model of Science Teaching: Learning sequences to lesson plans. *Journal of Physics Teacher Education Online*, 6(2), 17–20.
  74. Wilson, C. (2011). Effective approaches to connect children with nature: Principles for effectively engaging children and young people with nature. *Department of Conservation*, 1–17.
  75. Zareie, B., & Navimipour, N. J. (2016). The impact of electronic environmental knowledge on the environmental behaviors of people. *Computers in Human Behavior*, 59, 1–8. <https://doi.org/10.1016/j.chb.2016.01.025>

**Table 1.** Normality Test of Environmental Knowledge for 5 Cycles

| Cycle | Test     | Mean  | Standard Deviation | Sig. |
|-------|----------|-------|--------------------|------|
| 1     | Pretest  | 11.45 | 2.759              | .200 |
|       | Posttest | 22.86 | 2.489              | .200 |
| 2     | Pretest  | 12.79 | 2.513              | .066 |
|       | Posttest | 25.03 | 3.279              | .090 |
| 3     | Pretest  | 11.93 | 2.404              | .200 |
|       | Posttest | 25.79 | 2.366              | .071 |
| 4     | Pretest  | 12.38 | 2.128              | .200 |
|       | Posttest | 26.17 | 2.001              | .190 |
| 5     | Pretest  | 12.14 | 2.386              | .200 |
|       | Posttest | 26.83 | 2.606              | .169 |

Notes:  
Sig.: Significance

**Table 2.** Homogeneity Test of Environmental Knowledge for 5 Cycles

| Cycle | Levene Statistic | Sig. |
|-------|------------------|------|
| 1     | .480             | .491 |
| 2     | .709             | .403 |
| 3     | .004             | .953 |
| 4     | .025             | .876 |
| 5     | 1.401            | .242 |

**Table 3.** Normality Test of Cognitive Skills for 5 Cycles

| Cycle | Mean  | Standard Deviation | Sig. |
|-------|-------|--------------------|------|
| 1     | 10.07 | 1.602              | .051 |
| 2     | 12.14 | 1.846              | .200 |
| 3     | 12.45 | 1.617              | .057 |
| 4     | 12.52 | 1.883              | .200 |
| 5     | 13.34 | 1.696              | .131 |

**Table 4.** Homogeneity Test of Cognitive Skills

| Levene Statistic | Sig. |
|------------------|------|
| .435             | .783 |

**Table 5.** *The Result of T-test*

| Cycle | Test     | Mean  | Standard Deviation | Sig.  |
|-------|----------|-------|--------------------|-------|
| 1     | Posttest | 22,86 | 2,693              | 0,000 |
|       | Pretest  | 11,45 |                    |       |
| 2     | Posttest | 25,03 | 2,214              | 0,000 |
|       | Pretest  | 12,79 |                    |       |
| 3     | Posttest | 25,79 | 2,912              | 0,000 |
|       | Pretest  | 11,93 |                    |       |
| 4     | Posttest | 26,17 | 1,934              | 0,000 |
|       | Pretest  | 12,38 |                    |       |
| 5     | Posttest | 26,83 | 2,020              | 0,000 |
|       | Pretest  | 12,14 |                    |       |

**Table 6.** *The Result of Pearson Correlation test*

| Cycle | Variable | EK      | CS      | Sig.  |
|-------|----------|---------|---------|-------|
| 1     | EK       |         | 0,844** | 0,000 |
|       | CS       | 0,844** |         | 0,000 |
| 2     | EK       |         | 0,937** | 0,000 |
|       | CS       | 0,937** |         | 0,000 |
| 3     | EK       |         | 0,921** | 0,000 |
|       | CS       | 0,921** |         | 0,000 |
| 4     | EK       |         | 0,933** | 0,000 |
|       | CS       | 0,933** |         | 0,000 |
| 5     | EK       |         | 0,959** | 0,000 |
|       | CS       | 0,959** |         | 0,000 |

Notes:  
 EK: Environmental Knowledge  
 CS: Cognitive Skills  
 Sig.: Significance

## APPENDIX

### *Questions to Measure the Environmental Knowledge*

---

#### **Cycle 1**

---

1. Environmental science is multidisciplinary. For example, the problem of decline in fisheries productivity involves collaboration from various science experts to overcome it. Why is that?
  2. Waste that pollutes the mangrove ecosystem area has an impact on increasing coastal abrasion. Besides, the decline in crab and shrimp productivity has a significant effect on the decline in income of the local community. What is the role of environmental science in efforts to improve the economic welfare of coastal communities?
  3. Local people living on the slopes of Mount Lawu reject the plan to use geothermal energy to become a geothermal power plant. What factors underlying the rejection of the use of geothermal energy to be used as a geothermal power plant were assessed from the aspect of ethnosocioecology?
  4. Land areas inhabited by local people have a high level of biodiversity. Why do cultural values play a role in protecting biodiversity?
  5. Economic growth in Indonesia increase in 2018. Gross Domestic Product (GDP) reaches 5.17%, up from 5.07% from the previous year. Java Island still contributed to the growth of gross domestic product by 57.8% (the largest), followed by Sumatra by 23.4%. On the other hand, environmental conditions in Java, especially in densely populated areas, are already alarming. Likewise, the problem of land conversion continues to increase in Java and Sumatra. What is the impact of increasing economic welfare on the environment in Indonesia?
  6. Currently air and water quality in almost all regions of big cities are very poor. Based on the results of the Ministry of Environment research, the air quality index in the DKI Jakarta area is the lowest (53.5) compared to other regions in Indonesia and far below the air quality index national level (87.03). In addition, DKI Jakarta's water quality index was 21.33 and DI Yogyakarta was 20.19. Both are far below the national water quality index which is equal to 58.68. Why is the problem of natural resources not free from population density?
  7. How to use water more efficiently in the middle to upper-income groups in daily life?
  8. What steps need to be taken so that the water supply continues to meet daily needs per person in all social strata?
- 

#### **Cycle 2**

---

1. Java is the island with the largest population of 136.6 million people with a population growth rate of 1.21% per year over the period 2000-2010. Why is a densely populated area such as DKI Jakarta often there is a limited supply of resources?
  2. BNPB showed that the conversion of forest land in Java to agricultural land can cause deviations from the principle of natural resources. Analyze the deviations in the principle of natural resources that occurred in the case.
  3. Ecosystem management is an integrated approach that involves
-

---

social, economic, ecological, and institutional perspectives. Why does ecosystem management need to involve various parties living around the ecosystem, resource users, decision-makers, people's representatives, and taxpayers?

---

4. Decision making of environmental management policies needs to involve various parties. Why are local people as one of the important actors in making decisions about environmental management?

---

5. Production forest management as one of the natural resource management policies involves communities around the forest to be able to apply the forest management paradigm and produce products based on local businesses that can compete and be accepted in the global market. Do you think that the policy meets the principles of environmental science?

---

6. Social forestry management is a natural resource management policy to improve the welfare of life for indigenous and tribal peoples. Does the policy meet the four principles of environmental science? Explain your answer

---

7. What is the action that must be taken by the community and the government if the watershed experiences a water quality crisis and habitat degradation due to land management for agriculture and animal husbandry that is not environmentally friendly?

---

8. In 2001 the local government of Nagekeo, Kupang received a refusal from the local community to build the Lambo reservoir. What is the form of approach that should be used to form good cooperation in environmental management between local communities and the government?

---

### **Cycle 3**

---

1. Why is the understanding of biocentrism considered insufficient as the highest guide in behaving and acting towards the environment as evidenced by the emergence of ecocentrism?

---

2. Kemiren Village in Banyuwangi, East Java has the Sobo River and Gulung River which are to the south and north of the village and never dry throughout the year. Also, there is a spring that is protected and preserved by residents, namely the great-grandfather of Chile. One of the rules imposed is a ban on using source water on certain days and hours and cutting down trees around springs. Why do watersheds need to be managed properly without prioritizing human interests?

---

3. What is the real form or example of anthropocentrism in daily activities that can have an impact on environmental damage (water/land area)?

---

4. Kampung Naga people, Dayak, and Banjar tribes have a tradition of land distribution for residential zones, farming zones, protected zones, and sacred zones. Why do local land divisions and land use arrangements need to be preserved?

---

5. Dayak tribes who live in Kalimantan implement a system of land rest in farming. Meanwhile, the people of West Kutai, East Kalimantan have implemented the Lembo System, which is a mixture of fruit forests and timber. Based on these examples, how can local knowledge apply the principles of environmental ethics?

---

6. The division and arrangement of land is an example of local knowledge of Kampung Naga and Kampung Kuta, which consists of

---

---

clean, sacred, and dirty areas. What is the principle of environmental ethics contained in this knowledge?

---

7. Create a plan to purify the water based on the local knowledge of your home.

---

8. Create a plan to increase the fertility of the land-based on the local knowledge available in your home.

---

#### **Cycle 4**

---

1. The food chain is composed of 4 trophic levels, namely 1-producer trophic level, trophic level 2-consumer 1 (herbivore), trophic level 3-consumer 2 (omnivore), and trophic level 4-consumer 3 (top predator). Why is there a level 2 consumer at the trophic level, omnivorous?

---

2. In a food chain, there is an energy flow from one trophic level to another trophic level. Why the more trophic levels, the less amount of biomass?

---

3. In the period of 2000-2014, Indonesia was recorded as a contributor to the loss of the largest mangrove forest in the world at 4,364 km<sup>2</sup> or around 311 km<sup>2</sup> per year. One of the threats to the decline in mangrove forests is the expansion of brackish water ponds in coastal areas for shrimp and milkfish commodities. How can brackish water ponds business affect the energy flow and material cycle?

---

4. Based on a study conducted by the World Bank, coal extraction has a serious impact on the environment and communities around the mining area. Why does mining disrupt the phosphorus cycle and cause damage to freshwater ecosystems?

---

5. The United States Department of Agriculture explains that globally 1/3 of human food is obtained from plants whose pollination is assisted by bees. In 2008, it was recorded that 36% of bee colonies were lost. The incident was caused by the use of pesticides. How is the impact caused by the decline in bee populations?

---

6. The forest is a habitat for various animals that functions to stabilize local temperatures. Deforestation in Indonesia reaches 1.4 million hectares per year with the remaining 53 million hectares. Under these conditions, what will happen to the hydrological cycle?

---

7. Carbon dioxide emissions from the power generation sector in China, especially by coal-fired power plants, were almost half of the total carbon dioxide emitters. What is your strategy to prevent increased carbon dioxide emissions?

---

8. Phosphorus content in fertilizers can fertilize the soil, but continuous use can cause phosphorus cycle disruption. What strategies can be used in agricultural activities to prevent disturbance in the phosphorus cycle?

---

#### **Cycle 5**

---

1. The damage to coral reefs occurred due to climate change. From March to June 2016, the coral mortality rate reached 30-90% with coverage of NTT, NTB, southern Java, western Sumatra, north Bali, Lombok, Karimun Jawa, and Selayar. How can damage to coral reef ecosystems be fatal to human life and other living things?

---

2. In 2012, land clearing for oil palm plantations covered an area of 276,246 Ha. Riau is a province that has the largest oil palm

---



---

plantations in Indonesia. How can land clearing for plantations affect the decline in the quality of the biotic and abiotic environment?

---

3. Based on scientific studies, there was a decline in food production in Indonesia by 4% over four times the El-Nino period (extreme drought). What is the relationship between global warming and the decline in agricultural productivity?

---

4. The availability of sufficient water will affect productivity, both in the goods and services sector. What is the relationship between decreasing water supply and poverty?

---

5. The Ministry of Environment and Forestry notes that at least 1.1 million hectares or 2% of Indonesia's forests have shrunk every year. What will happen to the biotic, abiotic, and socio-cultural environment if green land is diminishing?

---

6. The population dynamics have a very important influence on ecosystems, including those related to water availability. How can the population affect the fulfillment of clean water needs?

---

7. Make a plan to solve environmental problems due to organic and inorganic waste at the household scale.

---

8. Make a plan to overcome the problem of water pollution in household-scale consumption.

---

## SÍNTESE E PROPRIEDADES DE PROTEÇÃO DOS COMPÓSITOS DE PECTINA / MONTMORILONITA CONTRA A ENTEROCOLITE INDUZIDA POR ASPIRINA

## SYNTHESIS AND PROTECTIVE PROPERTIES OF PECTIN/MONTMORILLONITE COMPOSITES AGAINST ASPIRIN-INDUCED ENTEROCOLITIS

AUYEZKHANOVA, Assemgul S.<sup>1</sup>; TALGATOV Eldar T.<sup>2\*</sup>; AKHMETOVA Sandugash N.<sup>3</sup>; KAPYSHEVA Unzira N.<sup>4</sup>; ZHARMAGAMBETOVA Alima K.<sup>5</sup>

<sup>1,2,3,5</sup> D.V. Sokolskiy Institute of Fuel, Catalysis and Electrochemistry, Department of Catalysis, Laboratory of Organic Catalysis, Almaty, Kazakhstan

<sup>3</sup> Abai Kazakh National Pedagogical University, Almaty, Kazakhstan

<sup>4</sup> Institute of Human and Animal Physiology, Laboratory of Ecological Physiology, Almaty, Kazakhstan

\* Corresponding author  
e-mail: eldar-talgatov@mail.ru

Received 03 June 2020; received in revised form 17 June 2020; accepted 28 June 2020

### RESUMO

O uso prolongado de aspirina para prevenção de eventos cardiovasculares é limitado por seus efeitos adversos gastrointestinais e, portanto, pacientes com alto risco devem receber agentes gastroprotetores. No entanto, os medicamentos gastroprotetores também apresentam alguns efeitos adversos que exigem a busca de alternativas seguras e eficazes. Os compósitos que combinam as propriedades de intumescimento das argilas e a atividade biológica dos polissacarídeos parecem ser candidatos promissores à proteção do trato gastrointestinal. O objetivo deste estudo foi caracterizar compósitos de pectina / montmorilonita e avaliar seu efeito protetor no trato gastrointestinal de ratos em uso de aspirina por um longo período. Uma série de compósitos à base de montmorilonita (MMT) e pectina com baixa esterificação (Pec) foi sintetizada usando o método de adsorção-precipitação. As razões de peso de polissacarídeo para argila foram 1:19, 1: 9 e 1: 4. Os compósitos foram caracterizados por Análise Termogravimétrica (TGA), Espectroscopia no Infravermelho (IR), Microscopia Eletrônica de Varredura (MEV) e Difração de Raios-X (DRX). A pectina foi completamente fixada em MMT e o teor de polissacarídeos nos compósitos foi de aproximadamente 5, 10 e 20% em peso, respectivamente. O deslocamento da banda de absorção do grupo C = O da pectina indicou a interação do polissacarídeo com a argila, confirmando a imobilização efetiva do Pec no MMT. A modificação com pectina alterou a morfologia e a estrutura do MMT devido ao revestimento superficial e à intercalação no espaço entre camadas. Os compósitos incharam em água acidificada (pH = 2,0) e a capacidade de intumescimento foi maior para comparar com o MMT não modificado. A capacidade de sorção dos compósitos Pec / MMT em relação ao ácido acetilsalicílico (ASA) diminuiu de 6,8 para 1,0 mg g<sup>-1</sup> com o aumento do conteúdo de pectina de 5 para 20% em peso. Os compósitos híbridos promoveram proteção do trato gastrointestinal de ratos, aos quais foi administrado ASA com Pec / MMTs por um período de 16 dias. As propriedades protetoras do Pec / MMT foram aprimoradas com o aumento do conteúdo de pectina de 5 a 20% em peso.

**Palavras-chave:** *pectina, MMT, aspirina, doença intestinal, propriedades protetoras.*

### ABSTRACT

Long term use of aspirin for prevention of cardiovascular events is limited by its gastrointestinal adverse effects, and, therefore, patients at high risk should receive gastroprotective agents. However, gastroprotective drugs also have a few adverse effects that require searching for safe and effective alternatives. The composites combining the swelling properties of clays and the biological activity of polysaccharides seem to be promising candidates for gastrointestinal protection. This study aimed to characterize pectin/montmorillonite composites and evaluate their protective effect on the gastrointestinal tract of rats taking aspirin over a long period. A series of composites based on montmorillonite (MMT) and low esterified pectin (Pec) was synthesized using the adsorption-precipitation method. The polysaccharide to clay weight ratios were 1:19, 1:9, and 1:4. The composites were characterized using Thermogravimetric Analysis (TGA), Infrared Spectroscopy (IR), Scanning Electron Microscopy (SEM), and X-Ray Diffraction (XRD). Pectin was completely fixed on MMT, and the polysaccharide content in the composites was approximately 5, 10, and 20 wt%, respectively. The shifting of the absorption band

of the C=O group of the pectin indicated the interaction of the polysaccharide with the clay, confirming effective immobilization of Pec on MMT. Modification with pectin changed the morphology and structure of the MMT due to the surface coating and intercalation into the interlayer space. The composites swelled in acidified water (pH = 2.0), and their swelling ability was higher to compare with unmodified MMT. The sorption capacity of Pec/MMT composites towards acetylsalicylic acid (ASA) was decreased from 6.8 to 1.0 mg g<sup>-1</sup> with increasing of pectin content from 5 to 20 wt%. The hybrid composites promoted the protection of the gastrointestinal tract of rats, which were administered ASA with Pec/MMTs for 16 days. Protective properties of the Pec/MMT have been improved with increasing pectin content from 5 to 20 wt%.

**Keywords:** *pectin, MMT, aspirin, intestinal disease, protective properties.*

## 1. INTRODUCTION:

Acetylsalicylic acid (ASA, aspirin) is now a commonly used drug for the prevention of cerebrovascular and cardiovascular diseases (CVD) (Iijima, 2016; Ali & Sharma, 2018). However, daily aspirin therapy, even at a low dose, can damage the gastrointestinal tract (GI), causing Crohn's disease and ulcerative colitis (Moninuola *et al.*, 2018; Bjarnason *et al.*, 2018). This may lead patients to discontinue therapy, increasing their CVD risk (Lavie *et al.*, 2017). Co-administration of proton pump inhibitors (PPIs) in patients taking aspirin reduces the risk of aspirin-induced upper GI adverse events (Rodriguez *et al.*, 2020). However, PPIs also have adverse effects such as allergic reaction, diarrhea, changed gut microbiome, fundic gland polyp, drug interaction in the gut, etc. (Kinoshita *et al.*, 2018; Fossmark *et al.*, 2019). This requires a search for safe and effective alternatives to PPIs.

The composites combining the properties of clays and polysaccharides seem to be promising candidates for GI protection. The mineral component of such composites (clay) can act as antacid reducing the gastric acidity through adsorption of protons and release of non-toxic ions such as Mg<sup>2+</sup> and Al<sup>3+</sup> (Massaro *et al.*, 2018). The ability of natural clays to adhesion on the gastrointestinal mucosa surface, causing increase barrier thickness, is also of interest (Massaro *et al.*, 2018; Ali *et al.*, 2017). Modification of the layered silicates with polysaccharides can improve their mucoadhesive properties (Sharma *et al.*, 2018). Besides, non-starch polysaccharides provide many benefits for intestinal bowel disease treatment, including tissue healing, anti-oxidation, reduction of toxins adsorption, modulate gut microbiota, etc. (Nie *et al.*, 2017). Of note is that certain gut bacteria ferment the polysaccharides to produce short-chain fatty acids (SCFAs), which maintain the epithelial barrier function and protect against colitis (Zhang *et al.*, 2018). Biocompatible and non-toxic polysaccharide/clay composites are widely used for biomedical applications as drug

delivery systems, tissue engineering scaffolds, wound dressings and detoxifying agents (Wu *et al.*, 2019; Liu *et al.*, 2017). However, such composites have practically not been studied on alleviating ailments caused by the administration of nonsteroidal anti-inflammatory drugs (Dragan & Dinu, 2020; Meirelles & Raffin, 2017).

Long-term co-administration of pectin/montmorillonite intestinal adsorbent with aspirin in rats has previously been shown to possess a positive effect on their blood biochemical parameters (Kapysheva *et al.*, 2019). Therefore, this study aimed to characterize pectin/montmorillonite composites synthesized using a simple adsorption-precipitation method and evaluate their protective effect on the gastrointestinal tract of rats taking aspirin over a long period.

## 2. MATERIALS AND METHODS:

### 2.1. Materials

Montmorillonite (MMT), from the Tagansky deposit (Kazakhstan) produced by Sorbent (Ust-Kamenogorsk, Kazakhstan), and ethanol (96.3%), purchased from Talgar Spirt (Kazakhstan), was used without additional purification. Acetylsalicylic acid, obtained in tablet form from the Borisov Plant of Medical Preparations (Belarus), was separated from the other ingredients using recrystallization with ethanol as the solvent.

### 2.2. Extraction and characterization of pectin

Extraction of the pectin (Pec) from ripe Golden Delicious apple pomace (5 g) was carried out using water acidified with citric acid (pH = 2.0) at 80 °C for 4 hours according to the procedure described in (Devi *et al.*, 2014). The pectin yield (Y<sub>Pec</sub>) was calculated using the following equation (Eq. 1).

$$Y_{Pec}(\%) = \frac{p}{B_i} \times 100 \quad (\text{Eq. 1})$$

Where, p is the amount of extracted pectin (0.38 g), and Bi is the initial amount of apple pomace (5 g).

Characterization of the resulting pectin included determination of equivalent weight (EW), methoxyl content (MeO), total anhydrouronic acid content (AUA), and degree of esterification (DE) (Khamsucharit *et al.*, 2017). Pectin (0.1 g), ethanol (1 mL), sodium chloride (0.2 g) and carbon dioxide-free distilled water (20 mL) were dissolved and titrated against standard 0.01M NaOH until the mixture adjusted to pH 7.5-8.0. The pH values were determined using an ANION-4100 pH meter containing a glass electrode. The volume of NaOH consumed ( $V_1$ , mL) was used for determination of equivalent weight (EW), using the equation (Eq. 2).

$$EW \text{ (g mol}^{-1}\text{)} = \frac{Wt \times 1000}{V_1 \times N} \quad (\text{Eq. 2})$$

Where, Wt is weight of pectin (0.1 g),  $V_1$  is the volume of NaOH consumed for titration (20.6 mL) of free acid groups, and N is normality of NaOH (0.01 M).

The neutral solution was collected after determination of equivalent weight, and 10 mL of sodium hydroxide (0.01 M) was added. The mixed solution was stirred thoroughly and kept at room temperature for 30 min, after which 10 mL of 0.01 M hydrochloric acid was added and titrated against 0.01 M NaOH to the same endpoint as in the previous equivalent weight titration.

Methoxyl content (MeO) was calculated using the following equation (Eq. 3).

$$\text{MeO}(\%) = \frac{V_2 \times N \times 31}{Wt \times 1000} \times 100 \quad (\text{Eq. 3})$$

Where,  $V_2$  is volume of NaOH consumed for titration (9.5 mL) of de-esterified acid groups, Wt is weight of pectin (0.1 g), N is normality of NaOH (0.01 M), and 31 is the molecular weight of the methoxyl group.

Total anhydrouronic acid content (AUA) of pectin was obtained using the equation (Eq. 4).

$$\text{AUA}(\%) = \frac{176 \times 0.01 \times (V_1 + V_2) \times 100}{Wt \times 1000} \quad (\text{Eq. 4})$$

Where, 176 is the molecular weight of 1 unit of the polygalacturonic acid,  $V_1$  (20.6 mL) is the volume of NaOH from equivalent weight determination,  $V_2$  (9.5 mL) is the volume of NaOH

from methoxyl content determination, and Wt is the weight of the sample (0.1 g).

The degree of esterification (DE) of pectin was measured on the basis methoxyl and AUA content and was calculated using the following equation (Eq. 5).

$$\text{DE}(\%) = \frac{176 \times \text{MeO}}{31 \times \text{AUA}} \times 100 \quad (\text{Eq. 5})$$

Where, MeO is methoxyl content (%), AUA is anhydrouronic acid content (%), 176 is the molecular weight of 1 unit of the polygalacturonic acid, and 31 is the molecular weight of the methoxyl group.

### 2.3. Synthesis of Pec/MMT composites

Pec/MMT composites with different pectin content were synthesized as follows. Pectin (0.05, 0.11 and 0.25 g) was dissolved in water (35 mL) at 60 °C and then added to a well-dispersed MMT suspension obtained by the intensive magnetic stirring of 1 g clay in 15 mL of water. Pec:MMT weight ratios were 1:19, 1:9, and 1:4. The mixtures were stirred continuously at ambient temperature for 2 h. Then, the composites were precipitated with ethanol and dried in a weak vacuum at 60°C.

### 2.4. Characterization of Pec/MMT composites

Thermogravimetric analysis (TGA) of samples was carried out in a nitrogen atmosphere at a temperature of 30 to 1000 °C, using a Labsys Evo analyzer from Setaram (France) at a heating rate of 10 °C per minute.

X-ray diffraction (XRD) patterns were obtained on a DRON-4-0.7 diffractometer from Bourevestnik (Russia), with a Co Ka radiation at a wavelength of 0.179 nm. XRD mounts for each sample were prepared by pipetting a small amount of a water-dispersed sample onto an XRD slide and drying in ambient air at room temperature for 3 h. To ensure the comparability of the XRD measurements of the various samples, the XRD mounts were dried at the same temperature and during the same period for all samples, with the XRD measurements taken shortly afterward.

IR spectra were obtained using a Nicolet iS5 from Thermo Scientific (USA), with a resolution of 3  $\text{cm}^{-1}$  in the 4000–350  $\text{cm}^{-1}$  region. Pellets for infrared analysis were obtained by grinding a mixture of 1 mg sample with 100 mg dry KBr, followed by pressing the mixture into a mold.

Morphology and structure of MMT and Pec/MMT composites were studied using a

scanning electron microscope, JEOL JSM-6610 LV (Japan).

## 2.5. Evaluation of sorption properties

The sorption properties of the composites were studied using the following procedure: 10 mL of water were added to 0.1 g of the sorbent and mixed until a homogeneous suspension had been formed. The mixture obtained was thermostated at 36 °C in a water bath. A 10 mL hydrochloric acid solution (0.01 N) was added to 20 mL acetylsalicylic acid solution (0.53 g L<sup>-1</sup>). The resulting ASA solution with a pH of 2.0 was heated to 36 °C and added over a stirred sorbent suspension. Adsorption was carried out for 30 minutes under static conditions. Then an aliquot of the supernatant solution (10 mL) was diluted in 20 mL of ethanol and analyzed using an SF-2000 spectrophotometer (OKB Spectr, Russia), at a 275 nm wavelength (Popova *et al.*, 2016). The amount of ASA adsorbed was determined by change in concentration of supernatant solution before and after sorption.

## 2.6. Histological studies

The protective effect of Pec/MMT composites against aspirin-induced damage to the small intestine was studied in albino Wistar rats (SPF category). The studies were approved by Local Ethical Committee, S Asfendiyarov Kazakh National Medical University, Registrations No 3, and 4. In this study, 50 albino rats (220±10 g) were equally divided into five groups. Oral delivery of acetylsalicylic acid (20 mg) and sorbents (6.3 mg) was performed daily for 16 days. The control group of rats was kept in equivalent laboratory conditions and received the same diet as the experimental animals. Histological studies were carried out on small intestine tissue samples, which were fixed in 10% neutral formaldehyde and routinely processed (Korzhevsky & Gilyarov, 2010). Approximately 5µm thick serial sections were cut and stained with hematoxylin and eosin (H&E). The photos were recorded through an Axiostar plus microscope from Carl Zeiss (Germany).

# 3. RESULTS AND DISCUSSION

## 3.1. Characterization of pectin

The yield of pectin extracted from the ripe Golden Delicious apple pomace was found to be 7.6%, which is consistent with data from prior studies (Perussello *et al.*, 2017). The equivalent weight (EW), methoxyl content (MeO), total anhydrouronic acid content (AUA), and degree of

esterification (DE) of the resulting sample of pectin were found to be 485.4 g mol<sup>-1</sup>, 2.9%, 53.0%, and 31.1%, respectively. These values are comparable with parameters of apple peel pectin (EW = 652.5 g mol<sup>-1</sup>, MeO = 3.7%, AUA = 62.8% and DE = 33.4%), as previously reported (Virk and Sogi, 2004).

## 3.2. Characterization of Pec/MMT composites

Pectin extracted from apple pomace was used for the preparation of Pec/MMT composites. The composites were obtained by adsorption of the polysaccharide onto a clay mineral (Pec:MMT weight ratios were 1:19, 1:9 and 1:4), followed by precipitation of the composites with ethanol, filtration and drying. The treatment with ethanol promotes the aggregation of well-dispersed polymer-inorganic composites and greatly facilitates the filtration process. The filtrate was clear, and visible traces of pectin molecules and MMT particles were not observed.

According to previous results (Talgatov *et al.*, 2019), the mixing of commercial pectin solution and natural montmorillonite suspension led to quantity adsorption of the polysaccharide on clay mineral (more than 90%). Therefore, taking into account the treatment with ethanol, the content of pectin in the Pec/MMT composites may be assumed to be 5, 10 and 20 wt.%.

To confirm this, the composites obtained, with Pec:MMT weight ratios of 1:9 and 1:4, were studied using thermogravimetric analysis (Figure 1).

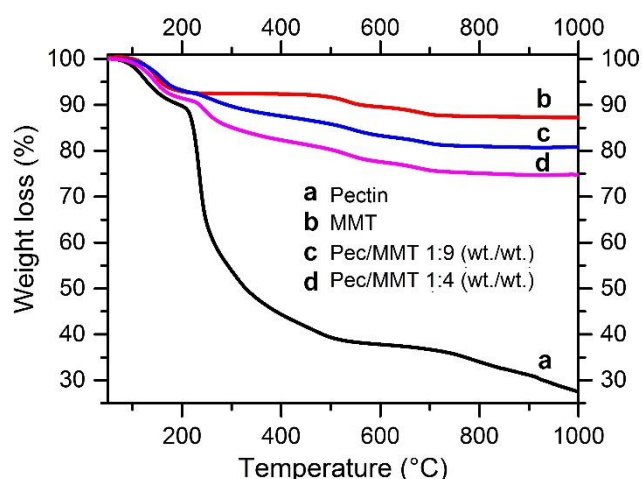


**Figure 1.** TGA of pectin (a), MMT (b) and Pec/MMT composites (c, d)

Figure 1 shows the weight loss curves of MMT, pectin, and Pec/MMT composites, which demonstrate multiphase degradation behaviors.



The thermal degradation of pectin occurred in two stages. Below 200 °C, there is an initial weight loss of 10.3%, which corresponds with the evaporation of bound water in the hydrophilic polymer and the removal of other small molecules (Ahn *et al.*, 2017). The principal weight loss (50.4%) occurs in the range from 200 to 500 °C, corresponding to the decomposition of the polymer. The residual weight of pectin at 500 °C was 39.3%. This result is not far from previously reported values (Ahn *et al.*, 2017; Minhas *et al.*, 2018), where the residual weight of commercial pectin samples was around 32-34% at 500°C. MMT also shows two stages of thermal degradation. The first stage observed below 200 °C, with a weight loss of 7.1%, was related to the evaporation of water molecules adsorbed in pores and between the silicate layers (Alshabanat *et al.*, 2013). The second thermal degradation stage of MMT, observed in the range from 500 to 750 °C, with weight loss 5.1%, can be explained by the elimination of the –OH group from the [AlO<sub>6</sub>] octahedral sheet of MMT (Yi *et al.*, 2017). These dehydration stages are observed for both Pec/MMT samples. The significant difference between the thermogram of the unmodified MMT and that of the Pec/MMT composites is that the organic constituent in the composites decomposes in the range from 200 to 500 °C (Al-Shemmar *et al.*, 2013). The weight loss in this range was found to be 7.4% and 11.2 % for composites with Pec:MMT weight ratios of 1:9 and 1:4, respectively. This suggests that the polymer was fixed entirely on the clay, as pectin lost only 50% of its weight in this temperature range.

The purity of pectin extracted from apple pomace and its interaction with MMT was evaluated using FTIR analysis, and the results are shown in Figure 2.

The spectrum of the pectin extracted (Figure 2a) showed a good match with the spectra of commercial pectin (Kumar & Chauhan, 2010; Luo *et al.*, 2019). The characteristic bands at 3432, 2939, 1749, and 1625 cm<sup>-1</sup> correspond to the stretching vibrations of –OH, –CH, C=O of ester, and C=O of acid groups in the pectin molecule, respectively (Sumathra *et al.*, 2017). The absorbance is lower at 1749 cm<sup>-1</sup> than at 1625 cm<sup>-1</sup>, confirming a low degree of esterification of the pectin. The bands in the wavelength range of 1200-1500 cm<sup>-1</sup> correspond to the stretching and bending vibrations of –C-OH, –C-H and –O-H (Thompson, 2018). The wide band in the area from 950 to 1200 cm<sup>-1</sup> are considered to be the “finger print” region for carbohydrates, because it helps in the identification of major chemical groups (–C-O, C-O-C and C-C) in polysaccharides (Urias-Orona

*et al.*, 2010). The spectrum showed in Figure 2b is typical for MMT (Dankova *et al.*, 2014). The absorption band at 3627 cm<sup>-1</sup> is due to the stretching vibrations of structural OH groups of the MMT. The characteristic bands at 1043, 915, 525 and 471 cm<sup>-1</sup> correspond to the stretching vibrations of Si–O, the bending vibrations of AlAlOH, and the bending vibrations of Al–O–Si and Si–O–Si, respectively. Water in montmorillonite resulted in broadband that peaked at 3429 cm<sup>-1</sup>, corresponding with the H<sub>2</sub>O-stretching vibrations. The shoulder close to 3240 cm<sup>-1</sup> is due to an overtone of the bending vibration of water observed at 1632 cm<sup>-1</sup> (Dankova *et al.*, 2014). The spectrum of the Pec/MMT composite was similar to unmodified MMT (Figure 2c). However, the appearance of bands at 2931, 1745, and 1200-1500 cm<sup>-1</sup> confirmed the presence of pectin. The shifting of the absorption band of the C=O group, compared to the same group in pectin, indicated the interaction of the polysaccharide with montmorillonite. A slight shift of some bands characteristic of Al–O and Si–O was also observed (Table 1).

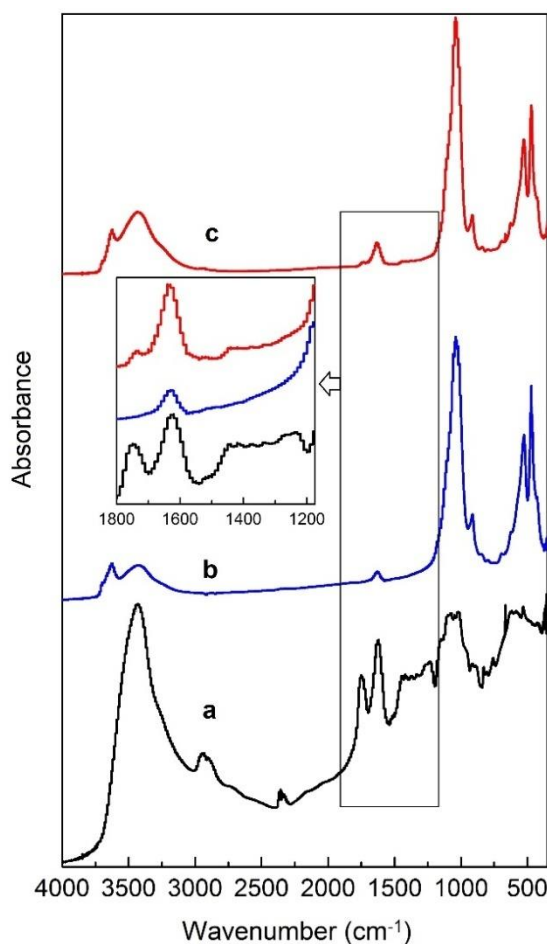


**Figure 2.** IR spectra of pectin (a), MMT (b) and Pec/MMT composite (c)

The anisometric shape of the initial MMT was observed using scanning electron microscopy. A clay mineral consists of microaggregates with poorly traced boundaries (Figure 3a) (Kasprzhitsky *et al.*, 2013). Modification of MMT with pectin leads to a change in surface morphology (Figure 3b). The surface of the composite is more uniform, perhaps, due to the formation of a polymer film.

The results of the XRD study of MMT and Pec/MMT composites are shown in Table 2. The 001 reflection peaks at  $2\theta = 7.0^\circ$ ,  $7.2^\circ$  and  $7.5^\circ$ , corresponding to the basal spacing of calcium ( $d_{001} = 14.6 \text{ \AA}$ ), magnesium ( $d_{001} = 14.3 \text{ \AA}$ ) and sodium ( $d_{001} = 13.6 \text{ \AA}$ ) forms of montmorillonite, were observed in the unmodified MMT (Fedorenko *et al.*, 2010). The appearance of a new 001 reflection peak at  $2\theta = 6.6\text{--}6.7^\circ$  ( $d_{001} = 15.4\text{--}15.6 \text{ \AA}$ ) detected on the XRD patterns of Pec/MMT composites indicates the intercalation of pectin into the interlayer space of layered silicate (Table 2) (Mittal, 2009). The same results have been reported for MMT modified with commercial pectin, where the polysaccharide contributed to changing the surface and structure properties of the clay mineral, due to coating and intercalation, respectively (Talgatov *et al.*, 2016).

### 3.3. Sorption and swelling properties of Pec/MMT composites

Aspirin is rapidly absorbed from the stomach and upper small intestine, reaching maximum drug concentration in plasma through 15–30 minutes after oral administration (Kanani *et al.*, 2015). Therefore, the sorption process was carried out over 30 minutes in an environment simulating the stomach ( $36^\circ\text{C}$  and  $\text{pH} = 2.0$ ) (Lu *et al.*, 2010). The sorption properties of Pec/MMT composites were evaluated using the residual concentration of ASA in the supernatant, and compared with those of unmodified MMT. Results of ASA sorption on MMT and Pec/MMT composites are presented in Table 3.

According to the analysis of the supernatant solution using spectrophotometry, the sorption capacity of MMT increased from  $3.1 \text{ mg g}^{-1}$  after modification with 5 wt.% of pectin. However, further, increase in pectin content to 20 wt.% led to a decrease in the sorption capacity of the hybrid composites to  $1.0 \text{ mg g}^{-1}$ . The capacity of the sorbents towards ASA was correlated with their swelling ability (Figure 4).

Of note is that the Pec/MMT particles demonstrate an excellent dispersibility in neutral medium and swells only in acidified water.

Improving the swelling ability of hybrid composites occurs probably due to the interaction of pectin macromolecules with cations ( $\text{Mg}^{2+}$ ,  $\text{Ca}^{2+}$ ,  $\text{Al}^{3+}$ ) released from clay at low pH (Massaro *et al.*, 2018) and cross-linking of Pec/MMT particles (Gawkowska *et al.*, 2018) with the formation of gel-like structure. This is of interest because polysaccharide hydrogels are considered as an alternative to other gastroprotective drugs (Bor *et al.*, 2019).

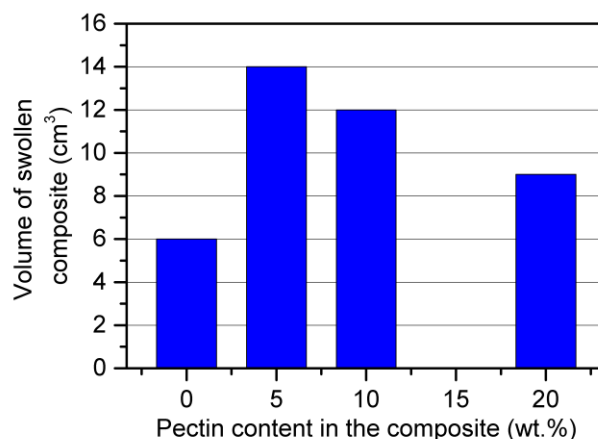


**Figure 4.** Swelling of MMT and Pec/MMT composites in acidified water

### 3.4. Protective properties of Pec/MMT composites

The protective effect of the hybrid composites obtained was evaluated by observing changes in the morphological characteristics of the small intestine of the rats (3 groups), which were administered ASA (20 mg) with Pec/MMT composites (6.3 mg), in comparison with those of control rats and group of rats taking only ASA. A high dose of aspirin ( $90 \text{ mg kg}^{-1} \text{ d}^{-1}$ ) was taken to cause GI adverse events. The results of the histological studies are presented in Figure 5.

The photomicrograph of the small intestine of control rats showed a normal histological structure (Figure 5a). Oral administration of a high dose of ASA to rats for 16 days led to acute small intestinal mucosal injury, corresponding to the development of enterocolitis in test animals (Figure 5b). The mucosal injury scores of groups taking aspirin with Pec/MMT composites (Figure 5c,d,e) were decreased compared with those of rats taking only ASA (Figure 5b). Maximum protective effect demonstrated the composite with a 20 wt.% pectin content. In this case, a normal histological structure of the intestinal mucosa with minor areas of swelling and dystrophy of the parenchyma of the glands was observed (Figure 5e). ASA adsorption on Pec/MMT insufficiently

contributes to the protection of the gastrointestinal tract (Table 3). Therefore, improvement of the protective properties of Pec/MMT composites by increasing the polymer content can be explained by the biological activity of pectin, leading to wound healing (Minzanova *et al.*, 2018). The effect of polymer content on mucoadhesive properties of hybrid composite is also possible (Sharma *et al.*, 2018).

#### 4. CONCLUSIONS:

This paper presents a simple and effective method for the synthesis of Pec/MMT composites with a given biopolymer content. According to data derived from physical and chemical studies, the polysaccharide not only coated the surface of MMT, but was also intercalated into the interlayer space of the natural clay mineral.

The resulting Pec/MMT composites showed insufficient sorption capacity towards ASA molecules (1.0-6.8 mg g<sup>-1</sup>) to protect the gastrointestinal tract. However, regeneration of the small intestine of the experimental rats, which were administered high doses of aspirin along with the composites for 16 days, was observed. Optimal normalization of the morphological parameters of the small intestine was observed in rats treated with the Pec/MMT composite containing 20wt.% pectin. The protective properties of the composites were improved by increasing the pectin content, probably due to the biological activity of the polysaccharide.

It should be noted that the composites swelled in acidified water (pH = 2.0), and their swelling ability was higher to compare with unmodified MMT. This can be caused by the cross-linking of Pec/MMT particles due to the interaction of pectin with cations released from the clay, apparently requiring a separate investigation.

#### 5. ACKNOWLEDGEMENTS:

The study was funded by the Committee of Science of the Ministry of Education and Science of the Republic of Kazakhstan (grants AP05133114 and AP05131542). The authors are grateful to S. Bakhtiyarova and B. Zhaksymov for their assistance.

#### 6. REFERENCES:

1. Iijima, K. (2016). Adverse effects of low-dose aspirin in the gastrointestinal tract. In A. Lanas (Ed.). *NSAIDs and Aspirin* (pp. 143-152). Cham: Springer.
2. Ali, M.; Sharma, A. (2018). Risk of lower gastrointestinal bleeding with low-dose aspirin: To give or not to give? *The National Medical Journal of India*, 31(4), 219-221.
3. Moninuola, O.O.; Milligan, W.; Lochhead, P.; Khalili H. (2018). Systematic review with meta-analysis: association between acetaminophen and nonsteroidal anti-inflammatory drugs (NSAIDs) and risk of Crohn's disease and ulcerative colitis exacerbation. *Alimentary Pharmacology & Therapeutics*, 47, 1428-1439.
4. Bjarnason, I.; Scarpignato, C.; Holmgren, E.; Olszewski, M.; Rainsford, K.D.; Lanas, A. (2018). Mechanisms of damage to the gastrointestinal tract from nonsteroidal anti-inflammatory drugs. *Gastroenterology*, 154, 500-514.
5. Lavie, C.J.; Howden, C.W.; Scheiman, J.; Tursi J. (2017). Upper gastrointestinal toxicity associated with long-term aspirin therapy: Consequences and prevention. *Current Problems in Cardiology*, 42(5), 146-164.
6. Rodriguez, L.A.G.; Lanas, A.; Soriano-Gabarro, M.; Vora, P.; Cea Soriano L. (2020). Effect of proton pump inhibitors on risks of upper and lower gastrointestinal bleeding among users of low-dose aspirin: A population-based observational study. *Journal of Clinical Medicine*, 9(4), 928.
7. Kinoshita, Y.; Ishimura, N.; Ishihara S. (2018). Advantages and disadvantages of long-term proton pump inhibitor use. *Journal of Neurogastroenterology and Motility*, 24(2), 182-196.
8. Fossmark, R.; Martinsen, T.C.; Waldum, H.L. (2019). Adverse effects of proton pump inhibitors – evidence and plausibility. *International Journal of Molecular Sciences*, 20(20), 5203.
9. Massaro, M.; Colletti, C.G.; Lazzara, G.; Riela S. (2018). The use of some clay minerals as natural resources for drug carrier applications. *Journal of Functional Biomaterials*, 9(4), 58.
10. Ali, R.B.; Ounis, A.; Said, D.B.; Dziri, C.; El May, M.V. (2017). Gastroprotective effects of Tunisian green clay on ethanol-induced gastric mucosal lesion in rats. *Applied Clay Science*, 149, 111-117.



11. Sharma, A.; Puri, V.; Kakkar, V.; Singh I. (2018). Formulation and evaluation of silymarin-loaded chitosan-montmorillonite microbeads for the potential treatment of gastric ulcers. *Journal of Functional Biomaterials*, 9(3), 52.
12. Nie, Y.; Lin, Q.; Luo F. (2017). Effects of Non-Starch polysaccharides on inflammatory bowel disease. *International Journal of Molecular Sciences*, 18(7), 1372.
13. Zhang, T.; Yang, Y.; Liang, Y.; Jiao, X.; Zhao C. (2018). Beneficial effect of intestinal fermentation of natural polysaccharides. *Nutrients*, 10(8), 1055.
14. Wu, Y.; Zhang, Y.; Ju, J.; Yan, H.; Huang, X.; Tan, Y. (2019). Advances in halloysite nanotubes-polysaccharide nanocomposite preparation and applications. *Polymers*, 11(6), 987.
15. Liu, X.; Huang, R.; Zhou, X.; Cai, T.; Chen, J.; Shi, X.; Deng, H.; Luo W. (2017). Presence of nano-sized chitosan-layered silicate composites protects against toxicity induced by lead ions. *Carbohydrate Polymers*, 158, 1-10.
16. Dragan, E.S.; Dinu M.V. (2020). Advances in porous chitosan-based composite hydrogels: Synthesis and applications. *Reactive and Functional Polymers*, 146, 104372.
17. Meirelles, L.M.A.; Raffin F.N. (2017). Clay and polymer-based composites applied to drug release: A scientific and technological prospection. *Journal of Pharmacy & Pharmaceutical Sciences*, 20, 115-134.
18. Kapysheva, U.; Bakhtiyarova, S.; Zhaksymov, B.; Talgatov, E. (2019). Effect of pectin/montmorillonite intestinal adsorbents on blood biochemical parameters during chronic treatment with acetylsalicylic acid. *Periodico Tchê Quimica*, 16(33), 920-926.
19. Devi, W.E.; Shukla, R.N.; Bala, K.L.; Kumar, A.; Mishra, A.A.; Yadav, K.C. (2014). Extraction of pectin from citrus fruit peel and its utilization in preparation of jelly. *International Journal of Engineering Research & Technology*, 3(5), 1925-1932.
20. Khamsucharit, P.; Laohaphatanalert, K.; Gavinlertvatana, P.; Sriroth, K.; Sangseethong K. (2017). Characterization of pectin extracted from banana peels of different varieties. *Food Science and Biotechnology*, 27, 623-629.
21. Popova, A.P.; Korneyeva, I.N.; Savchenko, I.A.; Bondarenko, D.Y.; Antonov, I.A.; Komarovskiy, I.V. (2016). Development of method for the determination of acetylsalicylic acid in solutions by spectrophotometry. *International Journal of Applied and Basic Research*, 7(4), 592-596.
22. Korzhevsky, D.E.; Gilyarov, A.V. (2010). *Fundamentals principles of histological technique*. St. Petersburg, Russia: SpetsLit Publishing House.
23. Perussello, C.; Zhang, Z.; Marzochella, A.; Brijesh Kumar, T. (2017). Valorization of apple pomace by extraction of valuable compounds. *Comprehensive Reviews in Food Science and Food Safety*, 16(5), 776-796.
24. Virk, B.S.; Sogi, D.S. (2004). Extraction and characterization of pectin from apple (*Malus Pumila*. Cv Amri) peel waste. *International Journal of Food Properties*, 7(3), 693-703.
25. Talgatov, E.T.; Auyezkhanova, A.S.; Zharmagambetova, A.K.; Kapysheva, U.N.; Bakhtiyarova, S.K.; Zhaksymov, B.I. (2019). Synthesis and bioprotective properties of hybrid montmorillonite-polysaccharide composites. *News of the National Academy of Sciences of the Republic of Kazakhstan. Series chemistry and technology*, 1(433), 57-63.
26. Ahn, S.; Halake, K.; Lee, J. (2017). Antioxidant and ion-induced gelation functions of pectins enabled by polyphenol conjugation. *International Journal of Biological Macromolecules*, 101, 776-782.
27. Minhas, M.U.; Ahmad, M.; Anwar, J.; Khan, S. (2018). Synthesis and characterization of biodegradable hydrogels for oral delivery of 5-Fluorouracil targeted to colon: Screening with preliminary in vivo studies. *Advances in Polymer Technology*, 37(1), 221-229.
28. Alshabanat, M.; Al-Arrash, A.; Mekhamer, W. (2013). Polystyrene/Montmorillonite nanocomposites: Study of the morphology and effects of sonication time on thermal stability. *Journal of Nanomaterials*, 2013, 650725.

29. Yi, D.; Yang, H.; Zhao, M.; Huang, L.; Camino, G.; Frache, A.; Yang, R. (2017). A novel, low surface charge density, anionically modified montmorillonite for polymer nanocomposites. *RSC Advances*, 7, 5980-5988.
30. Al-Shemmar, F.H.J.; Rabah, A.A.; Al-Mulla, E.A.J.; Alrahman, N.O.M.A. (2013). Preparation and characterization of natural rubber latex/modified montmorillonite clay nano-composite. *Research on Chemical Intermediates*, 39, 4293-4301.
31. Kumar, A.; Chauhan, G.S. (2010). Extraction and characterization of pectin from apple pomace and its evaluation as lipase (steapsin) inhibitor. *Carbohydrate Polymers*, 82(2), 454-459.
32. Luo, J.; Xu, Y.; Fan, Y. (2019). Upgrading pectin production from apple pomace by acetic acid extraction. *Applied Biochemistry and Biotechnology*, 187(4), 1300-1311.
33. Sumathra, M.; Govindaraj, D.; Jeyaraj, M.; Arfaj, A.A.; Munusamy, M.A.; Kumar, S.S.; Rajan, M. (2017). Sustainable pectin fascinating hydroxyapatite nanocomposite scaffolds to enhance tissue regeneration. *Sustainable Chemistry and Pharmacy*, 5, 46-53.
34. Thompson, J.M. (2018). *Infrared Spectroscopy*. Singapore: Pan Stanford Publishing.
35. Urias-Orona, V.; Rascon-Chu, A.; Lizardi-Mendoza, J.; Carvajal-Millan, E.; Gardea, A.A.; Ramirez-Wong, B. (2010). A novel pectin material: extraction, characterization and gelling properties. *International Journal of Molecular Sciences*, 11(10), 3686-3695.
36. Dankova, Z.; Mockovciakova, A.; Dolinska, S. (2014). Influence of ultrasound irradiation on cadmium cations adsorption by montmorillonite. *Desalination and Water Treatment*, 52(28-30), 5462-5469.
37. Kasprzhitsky, A.S.; Morozov, A.V.; Lazorenko, G.I.; Talpa, B.V.; Yavna, V.A. (2013). Complex research of the composition and structural characteristics of the rock-forming minerals in Millerovsky bentonite clay. *Engineering Journal of Don*, 3(26), 1-13. Retrieved from <http://www.ivdon.ru/en/magazine/archive/n3y2013/1862>.
38. Fedorenko, G.Y.; Rozhenko, A.N.; Turonok, O.C.; Dyachenko, E.V. (2010). Intrusion nanocomposites with high content of mineral component. *Mineralogical journal (Ukraine)*, 32(4), 34-40.
39. Mittal, V. (2009). Polymer layered silicate nanocomposites: A Review. *Materials*, 2(3), 992-1057.
40. Talgatov, E.T.; Auezkhanova, A.S.; Kapysheva, U.N.; Bakhtiyrova, S.K.; Zharmagambetova, A.K. (2016). Synthesis and detoxifying properties of Pectin-Montmorillonite composite. *Journal of Inorganic and Organometallic Polymers and Materials*, 26, 1387-1391.
41. Kanani, K.; Gatoulis, S.C.; Voelker, M. (2015). Influence of differing analgesic formulations of aspirin on pharmacokinetic parameters. *Pharmaceutics*, 7(3), 188-198.
42. Lu, P.J.; Hsu, P.I.; Chen, C.H.; Hsiao, M.; Chang, W.C.; Tseng, H.H.; Lin, K.H.; Chuah, S.K.; Chen, H.C. (2010). Gastric juice acidity in upper gastrointestinal diseases. *World Journal of Gastroenterology*, 16(43), 5496-5501.
43. Gawkowska, D.; Cybulska, J.; Zdunek, A. (2018). Structure-related gelling of pectins and linking with other natural compounds: A Review. *Polymers*, 10(7), 762.
44. Bor, S.; Kalkan, I.H.; Çelebi, A.; Dinçer, D.; Akyüz, F.; Dettmar, P.; Özen, H. (2019). Alginates: From the ocean to gastroesophageal reflux disease treatment. *Turkish Journal of Gastroenterology*, 30(2), 109-136.
45. Minzanova, S.T.; Mironov, V.F.; Arkhipova, D.M.; Khabibullina, A.V.; Mironova, L.G.; Zakirova, Y.M.; Milyukov, V.A. (2018). Biological activity and pharmacological application of pectic polysaccharides: A Review. *Polymers*, 10(12), 1407.

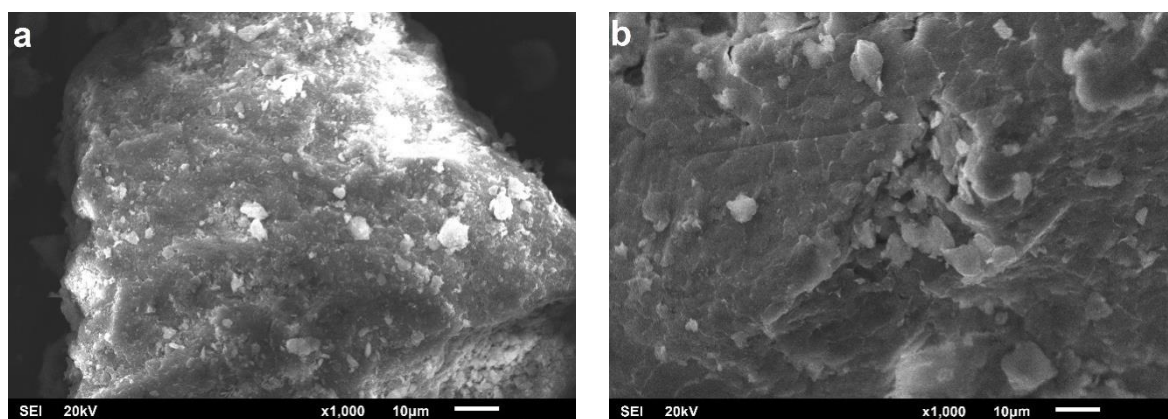


**Figure 3.** SEM images of MMT (a) and 5wt.%Pec/MMT composite (b)

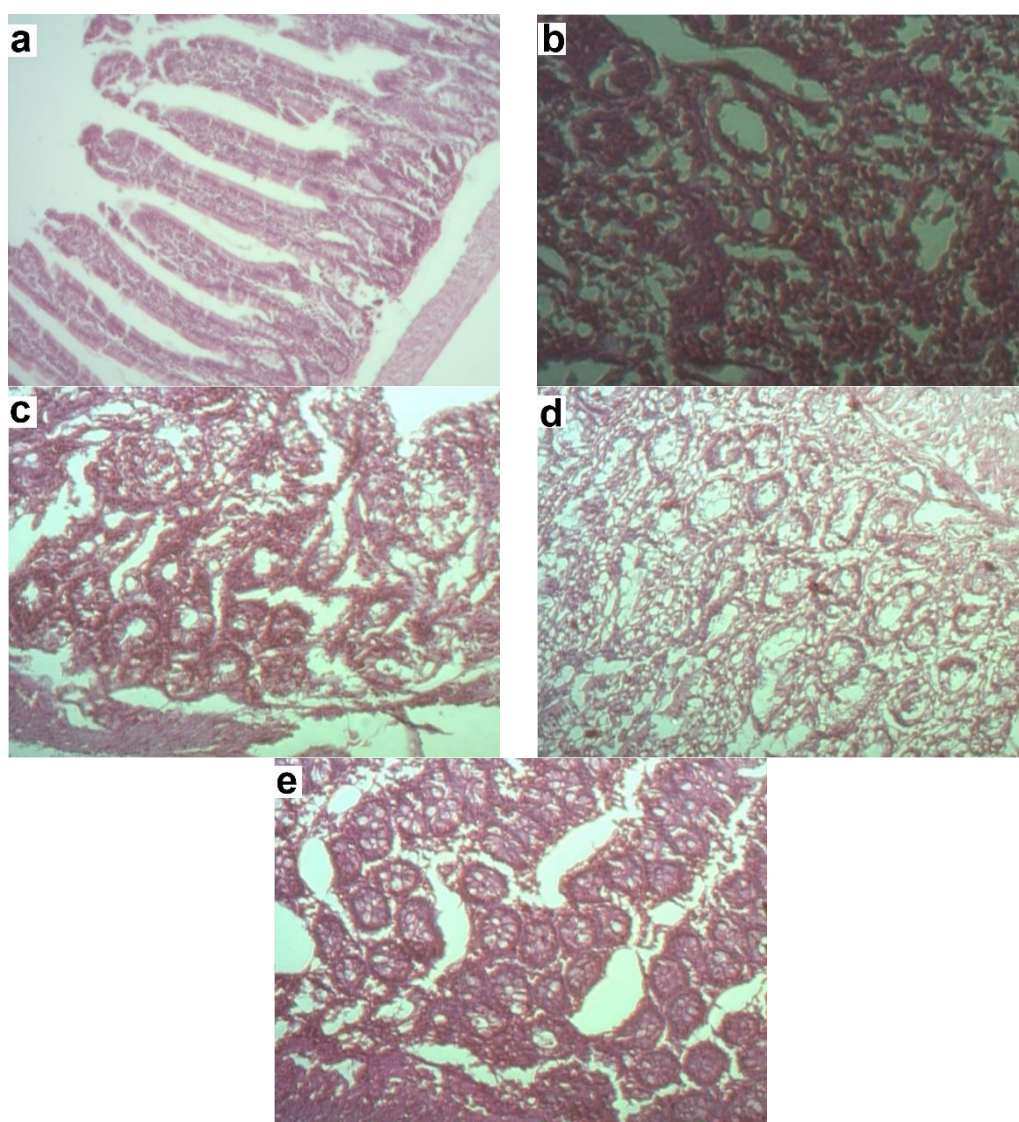


**Figure 5.** The histological structure of the small intestine (H&E 200x) of control rats (a), rats taking only ASA (b), rats taking ASA and treated with 5wt. % Pec/MMT (c), 10%wt. Pec/MMT (d) and 20wt.% Pec/MMT (e) composites

**Table 1.** The results of IR spectroscopy study of pectin, MMT and Pec/MMT composite

| Sample  | $\nu\text{OH}$       | $\nu\text{CH}$ | $\nu(\text{C=O})_{\text{E}}$<br>$\nu\text{COOH}$ | $\delta\text{CH}$<br>$\delta\text{OH}$ | $\nu\text{C-O-C}$<br>$\nu\text{C-C}$<br>$\nu\text{C-O}$ | $\nu\text{Si-O}$<br>$\delta\text{AlAlOH}$<br>$\delta\text{Si-O-Si}$<br>$\delta\text{Al-O-Al}$ |
|---------|----------------------|----------------|--|--|---|---|
| Pectin  | 3432                 | 2939<br>2900   | 1749<br>1625                                     | 1443<br>1330<br>1238                   | 1151<br>1076<br>1018                                    | -   |
| MMT     | 3627<br>3429<br>3242 | -              | -  | -                                      | -   | 1043<br>915<br>525<br>471   |
| Pec/MMT | 3626<br>3430<br>3256 | 2931<br>2853   | 1745   | 1442<br>1329                           | Overlapped<br>by the<br>MMT                             | 1039<br>917<br>527<br>472   |

**Table 2.** The results of XRD study of MMT and Pec/MMT composites

| Peak number           | Position, 2 $\theta$ degree | $d_{001}$ , Å | Peak area, % |
|-----------------------|-----------------------------|---------------|--------------|
| <b>MMT</b>            |                             |               |              |
| 1                     | 7.0                         | 14.6          | 49.3         |
| 2                     | 7.2                         | 14.3          | 36.7         |
| 3                     | 7.5                         | 13.6          | 39.3         |
| <b>5wt.% Pec/MMT</b>  |                             |               |              |
| 1                     | 6.7                         | 15.4          | 100.0        |
| 2                     | 7.2                         | 14.3          | 16.3         |
| 3                     | 7.5                         | 13.6          | 45.0         |
| <b>10wt.% Pec/MMT</b> |                             |               |              |
| 1                     | 6.6                         | 15.6          | 46.5         |
| 2                     | 7.5                         | 13.6          | 46.9         |

**Table 3.** Sorption of ASA on Pec/MMT composites

| Pec content in the composite, wt. % | ASA concentration after sorption, mg L <sup>-1</sup> | Amount of ASA adsorbed, mg | Sorb. capacity, mg g <sup>-1</sup> |
|-------------------------------------|--|----------------------------|------------------------------------|
| 0                                   | 255.7  | 0.31                       | 3.1                                |
| 5                                   | 246.4  | 0.68                       | 6.8                                |
| 10                                  | 246.9  | 0.66                       | 6.6                                |
| 20                                  | 261.0  | 0.10                       | 1.0                                |

**Note.** Process conditions: temperature – 36 °C; pH = 2.0; sorbent loading – 0.1 g; solution volume – 40 mL; initial ASA concentration – 263.5 mg L<sup>-1</sup>; no mixing

DIVERSIDADE MICROBIANA DE SOLOS CONTAMINADOS NOS CAMPOS  
PETRÓLÍFEROS DO CAZAQUISTÃO

MICROBIAL DIVERSITY OF THE CONTAMINATED SOILS IN KAZAKHSTAN OILFIELDS

МИКРОБНОЕ РАЗНООБРАЗИЕ НЕФТЕЗАГРЯЗНЕННЫХ ПОЧВ МЕСТОРОЖДЕНИЙ  
КАЗАХСТАНА

AITKELDIYEVA, Svetlana<sup>1\*</sup>; DAUGALIYEVA, Saule<sup>1</sup>; ALIMBETOVA, Anna<sup>1</sup>; FAIZULINA,  
Elmira<sup>1</sup>; SADANOV, Amankeldi<sup>1</sup>

<sup>1</sup>Research and Production Center for Microbiology and Virology, Kazakhstan.

\* Corresponding author  
e-mail: sa.kz@list.ru

Received 12 April 2020; received in revised form 06 June 2020; accepted 27 June 2020

## ABSTRACT

O petróleo e seus derivados afetam adversamente a biodiversidade dos microorganismos e a função do solo. Em solos contaminados com óleo, desenvolvem-se comunidades bacterianas únicas, adaptadas à poluição. Neste trabalho, a estrutura bacteriana e a diversidade da comunidade microbiana foram estudadas em amostras de solos contaminados com óleo nos depósitos do Cazaquistão usando o sequenciador Illumina MiSeq. Os resultados do estudo mostraram que os representantes dos seguintes filos bacterianos dominaram nas amostras de solo selecionadas: Proteobactérias, predominantes em solos contaminados com óleo (até 48%), Actinobactérias (até 29,33%), Firmicutes (até 25,74%), Bacteroidetes (até 33,28%). Os representantes dos filos de Planctomycetes, Verrucomicrobia, Chloroflexi (0,76% -4,62%) foram encontrados em menor quantidade. Todos os solos não contaminados foram dominados pelas famílias Micrococcaceae, Flexibacteraceae, Sphingomonadaceae, Planococcaceae, Flavobacteriaceae, contaminados pelas famílias Halomonadaceae, Flavobacteriaceae, Alteromonadaceae, Dietziaceae, Pseudomonadaceae, Bacillaceae, Peptomonadaceae, Bacillaceae. No nível de gênero, amostras de solos não contaminados e contaminados também demonstraram diversidade significativa. Os gêneros bacterianos dominantes nas amostras do solo não contaminado foram Hymenobacter, Arthrobacter, Gillisia. Em solos contaminados de três depósitos, os microrganismos dos gêneros Halomonas, Marinobacter, Pseudomonas (principalmente em amostras de solo 2KO), Bellilinea e Mycobacterium (principalmente amostra Md) se espalharam mais amplamente; e uma população muito grande de microrganismos do gênero Halomonas foi encontrada na amostra de solo contaminado da região de Atyrau. Uma comparação da estrutura taxonômica das comunidades microbianas de solos contaminados com óleo indica que a composição da população microbiana muda dependendo do grau de poluição por óleo. Amostras de solos não contaminados foram caracterizadas por maior diversidade bacteriana do que amostras de solos contaminados. Os microrganismos pertencentes aos filos dominantes foram principalmente associados à decomposição de hidrocarbonetos oleosos. A caracterização das comunidades bacterianas que vivem nos solos contaminados e a avaliação de sua capacidade de decompor o óleo podem ser potencialmente um guia para a biorremediação de solos contaminados.

**Keywords:** *metagenômica, solo contaminado com óleo, comunidade microbiana.*

## ABSTRACT

Oil and oil products adversely affect both the biodiversity of the microorganisms and the soil function. In oil-contaminated soils, unique bacterial communities develop that are adapted to pollution. In this work, the bacterial structure and diversity of the microbial community have been studied in samples of oil-contaminated soils in Kazakhstan deposits using the Illumina MiSeq sequencer. The results of the study showed that the representatives of the following bacterial phyla dominated in the selected soil samples: Proteobacteria, prevailing in oil-contaminated soils (up to 48%), Actinobacteria (up to 29.33%), Firmicutes (up to 25.74%), Bacteroidetes (up to 33.28 %). The representatives of Planctomycetes, Verrucomicrobia, Chloroflexi (0.76% -4.62%) phyla were found in smaller amounts. All the uncontaminated soils were dominated by Micrococcaceae, Flexibacteraceae, Sphingomonadaceae, Planococcaceae, Flavobacteriaceae families, contaminated ones – by Halomonadaceae, Flavobacteriaceae, Alteromonadaceae, Dietziaceae, Pseudomonadaceae, Bacillaceae, Xanthomonadaceae, Anaerolinaceae, Mycobacteriaceae and Peptococcaceae families. At the genus level, samples of uncontaminated



and contaminated soils also demonstrated significant diversity. The dominant bacterial genera in the samples of the uncontaminated soil were *Hymenobacter*, *Arthrobacter*, *Gillisia*. In contaminated soils of three deposits the microorganisms of the *Halomonas*, *Marinobacter*, *Pseudomonas* (mostly in 2KO soil sample), *Bellilinea* and *Mycobacterium* (mostly Md sample) genera were spread more widely; and a very large population of the microorganisms of the *Halomonas* genus was found in the contaminated soil sample from the Atyrau region. A comparison of the taxonomic structure of microbial communities of oil-contaminated soils indicates that the composition of the microbial population changes depending on the degree of oil pollution. Samples of uncontaminated background soils were characterized by higher bacterial diversity than samples of contaminated soils. The microorganisms belonging to the dominant phyla were mostly associated with the decomposition of oil hydrocarbons. The characterization of the bacterial communities living in the contaminated soils and the assessment of their ability to decompose oil can potentially be a guide for bioremediation of contaminated soils.

**Keywords:** *metagenomics, oil-contaminated soil, microbial community.*

## АННОТАЦИЯ

Нефть и нефтепродукты отрицательно влияют как на биоразнообразие микроорганизмов, так и на функцию почвы. В нефтезагрязненных почвах развиваются уникальные бактериальные сообщества, адаптированные к загрязнению. В данной работе исследована бактериальная структура и разнообразие микробного сообщества в образцах нефтезагрязненных почв месторождений Казахстана методом секвенирования основанного на технологии Illumina с использованием прибора MiSeq. Результаты исследований показали, что в отобранных образцах почв доминировали представители типов: *Proteobacteria*, преобладающие в загрязненных нефтью почвах (до 48%), *Actinobacteria* (до 29,33%), *Firmicutes* (до 25,74%), *Bacteroidetes* (до 33,28%). В меньшем количестве были обнаружены типы *Planctomycetes*, *Verrucomicrobia*, *Chloroflexi* (0,76%-4,62%). Изучение микробоценоза на уровне семейства и рода показало, что в не загрязненных почвах доминировали семейства *Micrococcaceae*, *Flexibacteraceae*, *Sphingomonadaceae*, *Planococcaceae*, *Flavobacteriaceae*, в загрязненных же почвах - *Halomonadaceae*, *Flavobacteriaceae*, *Alteromonadaceae*, *Dietziaceae*, *Pseudomonadaceae*, *Bacillaceae*, *Xanthomonadaceae*, *Anaerolinaceae*, *Mycobacteriaceae* и *Peptococcaceae*. На уровне рода в образцах незагрязненной и загрязненной почв разнообразие значительно отличалось. Доминантными родами в образцах чистой почвы были представители *Hymenobacter*, *Arthrobacter*, *Gillisia*. В загрязненных почвах трех месторождений более широкое распространение в образце почвы 2КО получили микроорганизмы родов: *Halomonas*, *Marinobacter*, *Pseudomonas*; в образце Md: *Bellilinea*, *Mycobacterium* и в образце At - *Halomonas*. Сравнение таксономической структуры микробных сообществ нефтезагрязненных почв указывает на то, что в зависимости от степени загрязнения нефтью изменяется состав микробной популяции. Более высокое бактериальное разнообразие наблюдалось в незагрязненных фоновых почвах по сравнению с загрязненными образцами. Микроорганизмы, относящиеся к доминирующим типам, связаны в большинстве своем с разложением углеводородов нефти. Характеристика бактериальных сообществ, живущих в загрязненных нефтью почвах, и оценка их способности разлагать нефть могут потенциально служить ориентиром для биоремедиации загрязненных сред.

**Keywords:** *метагеномика, нефтезагрязненная почва, микробное сообщество*

## 1. INTRODUCTION:

Oil is the most valuable raw material, without which modern civilization is impossible. However, the processes of its development, transportation, storage, and processing very often become the sources of environmental contamination and acquire a catastrophic scale. The share of hydrocarbon fuel is 2/3 of the world's energy consumption. The existing demand for oil and oil products annually increases on average by 8 %, and production — by 5.5 % (Diarov *et al.*, 2006). The increasing contamination of the environment with oil and oil products leads to severe disruption in the natural ecosystems, biological balance, and biodiversity. The studies showed that soil properties, such as pH, the

presence of water, air, and nutrients, the redox potential, the presence of organic substances affected the structure of bacterial communities (Wakelin *et al.*, 2008). The abundance and diversity of the microbial communities are indicators of soil quality (Mathew *et al.*, 2012).

Thus, the problem of soil contamination with oil poses a serious environmental threat to the environment and leads to disruption in the ecological balance, to degradation, and even to the desertification of these territories. Emergency oil spills often lead to the formation of technogeneous deserts, where the process of self-healing lasts for 10 – 25 years (Parkhomenko, Soprunova, 2008; Polyanskaya, Zvyagintsev, 2005). The oil biodegradation management should be, first of all, aimed at activating microbial

communities and creating the optimal conditions for their existence. In this regard, studying the microbial complexes in the contaminated soils is of scientific and practical interest.

In Kazakhstan, oil production is concentrated in the Caspian region, in the Atyrau and Mangistau regions, and in the south in the Kyzylorda region. The climate in these regions is sharply continental and arid. The soils are characterized as highly saline gray-brown soils, salt marches, and solonchaks. The development of oilfields leads to contamination of large areas and creates environmental problems that pose a threat to public safety.

Today, in terms of proven oil reserves, Kazakhstan is among the 15 leading countries in the world, with 3% of the world's oil reserves. Oil and gas regions occupy 62% of the country's area and have 172 oilfields, of which more than 80 are under development. More than 90% of oil reserves are concentrated in the 15 largest fields - Kumkol, Tengiz, Kashagan, Karachaganak, Uzen, Zhetybai, Zhanazhol, Kalamkas, Kenkiyak, Karazhanbas, Northern Buzachi, Alibekmola, Central and Eastern Prorva, Kenbai, Korolevskoye. Deposits are located in six of the 14 regions of Kazakhstan. These are Aktobe, Atyrau, West Kazakhstan, Karaganda, Kyzylorda, and Mangystau regions. At the same time, approximately 70% of hydrocarbon reserves are concentrated in the west of Kazakhstan. It should be noted that the Aktas deposit (Mangistau region) and the Zhanatalap deposit (Atyrau region) are not the largest oil and gas deposits.

The Atyrau region possesses the most explored oil reserves. On its territory, more than 75 oilfields with industrial reserves of 930 mln t are discovered. The largest oilfield in the region is Tengiz (initial recoverable reserves are 781.1 mln t). The region ranks first in oil production in the Republic. The Zhanatalap oil and gas deposit was discovered in 1968 and is located in the Isataevsky district of the Atyrau region, 85 km west of Atyrau. The field is located in a very dry, hot, agroclimatic area. The climate is sharply continental, arid, with manifested large annual and daily amplitudes of air temperatures. Low-sulfur oil constitutes 0.12-0.38%, low-paraffin oil – 1.31-1.01%. The operating mode of the reservoir is water driven. Oilfield water contains calcium chloride, has a density of 1,177-1,184 kg/m<sup>3</sup> and mineralization of 277.4-289.2 g/l.

Kumkol is an oil and gas deposit in the Kyzylorda region of Kazakhstan. The total area of the Kumkol field is 23,143 ha. This field referred to

the Turanian oil and gas province and was discovered in February 1984. Kumkol is located 150-170 km north of the city of Kyzylorda. Hydrocarbon deposits are located at a depth of 0.9 - 1.4 km. The initial flow rate of the wells is 20 - 130 t/day. The density of oil is 0.81-0.83 g/cm<sup>3</sup>, the sulfur content is 0.11 - 0.52%, paraffins constitute 10.8-15.5%, asphaltenes content ranges from 0.11-0.92% to 5.7%, resins content – from 4.8% to 19.8%. Recoverable oil reserves at Kumkol field amount to 130 mln t; that of gas – to 15 bln m<sup>3</sup> (Bulekbaev *et al.*, 1996).

In the Mangistau region, over 70 fields have been discovered with recoverable oil reserves of 725 mln t, as well as reserves of condensate equaling to 5.6 mln t. Less than half of the fields are in operation. Most of them are in the late stages of development. The vast majority of residual reserves are classified as hard to recover. The largest deposits are Aktas, Uzen, Zhetybai, Kalamkas, Karazhanbas. The Aktas oil and gas condensate field is located in the Mangistau region, 85 km southeast of Aktau. The oils of productive horizons are heavy (horizons IV, X, XI) and very heavy (horizon III), with a density of 0.87-0.915 g/cm<sup>3</sup>, low content of sulfur (0.2%) and high content of paraffin (20% to 26.14%). The asphaltenes content varies from 2.33 to 5.6%, and silica gel resins content is within the range of 4.54 - 6.8% (Portnov, Petrov, Talerchik, 2015).

The research methods based on microbial cultivation does not provide complete comprehensive knowledge of the microbial community since most microorganisms do not grow on conventional culture media, and researchers deal only with a small fraction of the real soil microbiota (Wolińska, 2019). The widespread use of the molecular methods in studying the ecology of the microorganisms in the contaminated areas provides extraordinary opportunities for new bioremediation strategies. With the introduction of the new-generation sequencing methods in molecular ecology, it has become possible to increase the number of identified types of microorganisms (Ma *et al.*, 2015; Chakraborty *et al.*, 2014).

To comprehensively assess the potential of biodegradation in the contaminated area and the changes in the structure and functional activity of the microbial communities involved in bioremediation, we used the Illumina MiSeq method of high-throughput sequencing. This allowed obtaining a more comprehensive and updated vision of the microbial community in the studied samples.

The present work was aimed at studying the bacterial composition of the contaminated soils in the oilfields of Kazakhstan, compared to the uncontaminated soils, for understanding the dynamics of the bacterial community development using the new generation high-throughput sequencing.

## 2. MATERIALS AND METHODS:

### 2.1. Experimental site

Six soil samples from three regions of Kazakhstan were selected in sterile plastic containers for the analyses according to state standards 17.4.4.02-2017 (GOST 17.4.4.02-2017, 2017). Soil samples were taken sterile layer by layer from the depth of 0-5 and 5-20 cm by the envelope method. Each combined sample consisted of three-point samples weighing from 200 to 250 g of soil each. Samples were taken under aseptic conditions: they were taken with a sterile metal spatula and placed in sterile plastic containers. Then the samples were packed to the cooler bags at 4 °C and immediately delivered to the laboratory.

Two samples were taken from the Atyrau region, the Zhanatalap oilfield: sample **At** — contaminated with oil, sample **PI2** — from the clean area (following the WGS84 system): latitude: 44° 51' 10" N (44.8528), longitude: 65° 30' 33" E (65.5092). Two samples were taken from the Kyzylorda region, the **Kumkol** oilfield: **1KO** — uncontaminated, **2KO** — from the contaminated area (WGS84): latitude: 44° 51' 10" N (44.8528), longitude: 65° 30' 33" E (65.5092). Two samples were taken from the Mangistau region, the Aktas oilfield: **MCI** — uncontaminated, **Md** — from the contaminated area (WGS84): latitude: 43° 39' 0" N (43.65), longitude: 51° 12' 0" E (51.2).

In the area of each oilfield, soil samples were taken at various distances from the oil production zone. Directly from the oilfield, a sample was taken for obtaining soil with a high degree of contamination, and for control (clean, uncontaminated soil, background), a sample was taken from the territory of a settlement 7 km away from oil production. The soil samples were taken from the depth of 20 cm using the method of sampling from five points in three repetitions. One part of the soil was combined in a sterile bag and delivered to the laboratory with a refrigerant for studying the bacterial diversity. The other part was used for determining the oil content. Prior to the analysis, the delivered soil samples had been stored at -20°C. Before the analysis, all samples

had passed through a 2 mm sterile sieve for removing large particles and foreign objects.

### 2.2. Determination of oil content in the soil samples

The quantitative content of oil in the soil was determined by the gravimetric method (Lurie, 1984). For this purpose, 10 g weighed samples of the soil were made. They were put into funnels with filtering paper and poured with chloroform until the extract became colorless. The chloroform oil extract was collected into tared vials and naturally evaporated in a fume hood for 24 hours. The residue was weighed on an Explorer analytical weigher (Ohaus, USA). For each soil sample, three weighed samples were made.

### 2.3. Parameters of the oil from the Kumkol, Zhanatalap, and Aktas oilfields

The specific weight of the oil from the Zhanatalap oilfield was 0.87 g/cm<sup>3</sup>, the density at 20°C was 0.8437 g/cm<sup>3</sup>, the viscosity at 0 °C was 36.4 - Pa · c. The content of paraffin was 1.31 – 1.01 %, of sulfur — 0.12 %, of asphaltenes — 0.02 %, of silica gel resins — 5.62 %, and of sulfate resins — 6 %. The oilfield water was calcium-chloride with a density of 1,177 – 1,184 kg/m<sup>3</sup> and the mineralization of 277.4 – 289.2 g/l. The oil in the productive horizons of the Aktas oilfield was viscous, with a density of 0.87 – 0.91 g/cm<sup>3</sup>; it was low-sulfur (0.2 %), and high-paraffin (20 – 26.14 %). The content of asphaltenes was 2.33 – 5.6 %, and of silica gel resins — 4.54 to 6.8 %. The Kumkol oil was low-viscosity and low-sulfur, relatively light (0.81 – 0.83 g/cm<sup>3</sup>), contained many light fractions, and was distinguished by the absence of harmful impurities. The content of paraffin was 15 %, of sulfur — 0.27 %, of asphaltenes — 5.4 %, and of silica gel resins — 19.2 %. The mineralization of water (calcium chloride) in the horizons was 49.7 – 84 g/l (Nadirov, 1995).

### 2.4. Parameters of the soils in the oilfields

The soils of the Kumkol deposit are characterized as gray-brown desert sandy-clay soils, the soils of Aktas deposit of the Mangystau region are gray-brown solonchak soils, and the soils of Zhanatalap deposit of the Atyrau region are coastal meadow solonchak soils. The amount of humus in the upper soil horizon of Kumkol deposit is 0.9%, of Zhanatalap deposit -1.7%, of Aktas deposit - 1.1%. The soils of all deposits are characterized by a sulfate-chloride type of salinization. The establishment of a taxonomic affiliation (type, subtype, genus) of soils was carried out by the employees of the U.U. Uspanov



Kazakh Research Institute of Soil Science and Agrochemistry in accordance with the methods (Gavrilyuk, 1959) and the regulatory requirements approved for Kazakhstan (Scientific and methodological guidelines for monitoring the land of the Republic of Kazakhstan, 1994). The research was based on the comparative geographical method, which consisted of comparing some soils with others taking into account the conditions of soil formation. A method of obtaining the actual material was field soil studies with subsequent processing and generalization of the results of laboratory chemical analysis of the selected samples.

At the stage of conducting field studies, morphological methods were used (Rozanov, 2004), which ensured the reliability and validity of field soil diagnostics and characteristics of the main morphological properties of soils. The location of the soil section for the characterization of background soils was selected, taking into account the most typical natural conditions. Field soil studies included the laying of soil sections, then their description was made, and soil samples were taken. The location of the soil section for the characterization of background soils was selected, taking into account the most typical natural conditions. The depth of soil sections was determined by the depth of soil formation processes.

The description of the soil section included:

- location and number;
- characteristics of the terrain and underlying rocks;
- the position of the section relative to the macro-, meso- and microrelief;
- the depth of boiling, the form of carbonate emissions;
- characteristics of the soil surface;
- description of genetic horizons.

The selection and description of genetic horizons were carried out according to the following morphological indicators (Gavrilyuk, 1959; Rozanov, 2004):

- horizon thickness;
- color and character of coloring;
- moisturizing;
- structure;
- mechanical composition;
- density;

- porosity;
- allocation of water-soluble salts and other newly formed soil structures;
- the presence and type of inclusions;
- development of the root system of plants;
- the nature of the transition of one horizon to another.

Samples for analysis were taken at the most typical sections characterizing the soil cover of the territory to establish the basic chemical and physicochemical properties of soils. Sampling was carried out over genetic horizons, in a 10-cm layer in their center.

The taxonomic determination of the soil was made on the basis of the description of the soil sections in accordance with the generally accepted classification (Egorov, Ivanova, Friland, 1977) and the systematic list of soils previously developed for the study area (Soils of the Kazakh SSR: Guryev region, 1970; Soils of the Kazakh SSR: Soils of the Kyzylorda region, 1983).

The involvement of regional classifications was due to the fact that they were developed according to the results of extensive systematic soil studies of Kazakhstan; monographs were published for each region, accompanied by soil maps with the 1:300,000 scale where soil diagnostic indicators (morphological and chemical) were determined (Soils of the Kazakh SSR: Guryev region, 1970; Soils of the Kazakh SSR: Soils of the Kyzylorda region, 1983).

To obtain the actual material, field soil studies were carried out with subsequent processing and generalization of the results of laboratory chemical analysis of the selected samples. Organic matter (humus) was determined by the method of Tyurin. The method is based on the oxidation of organic matter by a solution of potassium dichromate in sulfuric acid and the subsequent determination of trivalent chromium equivalent to the content of organic matter. To assess soil salinization, anions ( $\text{CO}_3^{2-}$ ;  $\text{HCO}_3^-$ ;  $\text{Cl}^-$ ;  $\text{SO}_4^{2-}$ ) and cations ( $\text{Ca}^{2+}$ ;  $\text{Mg}^{2+}$ ;  $\text{Na}^+$ ;  $\text{K}^+$ ) of highly soluble salts were determined. The degree of soil salinization was estimated by the total content of highly soluble salts in the water extract of the soil (GOST 26213-91, 1991). It is known that saline soils include soils in which the concentration of highly soluble salts in soil solutions exceeds 5-7 g/l, i.e., soils containing 0.05-1.15% of highly soluble salts depending on their composition.

## 2.5. DNA isolation, amplification, and sequencing on MiSeq Illumina

Two hundred and fifty milligrams of the obtained soil samples were taken for DNA isolation. The general genomic DNA was isolated using a NucleoSpin® Soil kit (Macherey-Nagel GmbH & Co.KG, Duren, Germany), following the manufacturer's guidelines. The DNA concentration was measured on a Qubit® 2.0 fluorimeter using a Qubit™ds DNA HS Assay Kit (Life Technologies, Oregon, USA).

The genetic libraries were prepared for sequencing following the *16S Metagenomic Sequencing Library Preparation* guide (part no. 15044223 rev. A). Each DNA sample was amplified using the KAPA HiFi Hot Star Ready Mix (KAPA Biosystems, Cape Town, South Africa). The PCR amplification was made in Eppendorf Master ProS thermal cycler (Eppendorf AG, Hamburg, Germany). The V3 and V4 regions of the 16Sr RNA gene were amplified using universal bacterial primers with the addition of the Illumina adapters and contained the following sequences of the nucleotide pairs: 5'-TCGTCGGCAGC GTCAGATGTGTATAAGAGACAGCCTACGGG N GGWGCAG-3' for the forward primer, and 5'-GTCTCGTGGGCTCGGAGATGTGTATAAGAGA CAGGACTACHVGGGTATCTAATCC-3' for the reverse primer (Klindworth *et al.*, 2013).

The reaction mixture consisted of 2.5 µl of the DNA template, 5 µl of each primer in the concentration of 1 µM, and 12.5 µl of KAPA HiFi Hot Start Ready Mix in the 2X concentration. The amplification cycles were performed according to the following program: one cycle at 95 °C for three minutes, followed by 25 amplification cycles at 95 °C for 30 seconds, one cycle at 55 °C for 30 seconds, one cycle at 72 °C for 30 seconds, and one cycle at 72 °C for five minutes. The PCR product was purified using an Agencourt AM Pure PCR purification kit (Beckman Coulter Inc. Beverly, Massachusetts, USA). Nextera XT Index primer adapters (Illumina Inc., San Diego, CA, USA) were added to each sample through the amplification in the reaction mixture containing 12.5 µl of KAPA HiFi Hot Start Ready Mix, 5 µl of each index primer, 10 µl of water, and 5 µl of the PCR product. The amplification program included one cycle at 95 °C for three minutes, followed by eight cycles of amplification at 95 °C for 30 seconds, one cycle at 55 °C for 30 seconds, one cycle at 72 °C for 30 seconds, and one cycle at 72 °C for five minutes. The PCR product with added indices was also purified using an Agencourt AM Pure PCR purification kit (Beckman Coulter Inc. Beverly, Massachusetts, USA).

At each stage of preparing the libraries after the amplification, the concentration and the size of the obtained PCR products were determined through their detection in the agarose gel and on Agilent 2100 bioanalyzer (Waldbronn, Germany) using an Agilent DNA 1000 Kit (Agilent Technologies, Waldbronn, Germany). Each sample was diluted to a concentration of 4 nM and combined into a single pool. The pooled libraries were denatured with NaOH and diluted with the hybridization buffer. The pooled libraries were sequenced on Illumina MiSeq device using a 600-cycle MiSeq® Reagent Kit v3 (Illumina Inc., San Diego, CA, USA), following the manufacturer's recommendations.

## 3. RESULTS AND DISCUSSION:

### 3.1. Oil contents in the soil samples

The analysis showed that the oil content in the contaminated soil from the Kumkol oilfield was 7.5 %, from the Zhanatalap oilfield — 7.3 %, and from the Aktas oilfield — 7.8 %.

### 3.2. The 16S rRNA metagenomic analysis of the soils from the oilfields in Kazakhstan

#### 3.2.1. The changes in the composition of the bacterial communities at the phylum level

Microorganisms in the soil play a key role in various biogeochemical processes, and some functionally significant microbial groups can be especially vulnerable to oil spills (Urakawa *et al.*, 2012; Rodriguez *et al.*, 2015). Petroleum hydrocarbons can directly influence the microorganisms, exerting a toxic effect (especially the polyaromatic ones), or changing the physicochemical properties of the soil (reducing the availability of mineral nutrition elements, deteriorating the water and air conditions, deterioration of the nitrogen regime of soils and a decrease in the content of mobile forms of phosphorus) (Voevodina, Rusanov, Vasilchenko, 2015; Liao, Wang, Huang, 2015). As a result of oil ingress, the total population and the structure of the microbial community change. Its composition and the degree of diversity depend both on the type, concentration, and duration of exposure to the pollutant, and on the type of the soil and the state of the microbiocenosis before the ingress of the pollutant (Kirienko, Imranova, 2015; Liao *et al.*, 2015).

The structure of the microbial community was analyzed in three taxonomic categories — the

phyla, the families, and the genus. The structure of bacteriocenosis at the level of phylotypes allowed characterizing the processes in the contaminated samples. As a result of the studies, in considering the taxonomic structure of the soil microbiomes at the three deposits, the dominance of seven bacterial phyla was detected: *Proteobacteria*, *Actinobacteria*, *Bacteroidetes*, *Firmicutes*, *Planctomycetes*, *Verrucomicrobia*, and *Chloroflexi* (Tables 1, 2). All soil samples were dominated by the *Proteobacteria* (21.22 – 44.48 %), *Actinobacteria* (9.66 – 29.33 %), *Bacteroidetes* (3.9 – 33.28 %), and *Firmicutes* (12.44 – 25.79 %) phyla. These are the phylotypes that almost always dominate both in the contaminated and uncontaminated soils (dos Santos *et al.*, 2011). *Proteobacteria* are the largest group of bacteria that play an important role in the cycles of biogenic elements in nature, and are typical dominants in the contaminated soils, especially at the early stages of hydrocarbon degradation. Numerous studies showed that proteobacteria were the dominant group that decomposed PAHs (Winding, Hund-Rinke, Rutgers, 2005; Wu *et al.*, 2016). The greatest number of the microorganisms of this phylogroup was found in the contaminated soil in the Atyrau (At — 44.48 %) and the Kyzylorda regions (2KO — 42.49 %) (Table 2). Their population was two times higher compared to the soils in the Mangistau region. The results were similar to those of other studies, where the *Proteobacteria* were the dominant type decomposing the PAHs found in the contaminated samples (Dörr de Quadros *et al.*, 2016; Yadav *et al.*, 2015).

The representatives of the *Actinobacteria* phylum were the next prevailing group in the analyzed samples. *Actinobacteria* are widely spread in the soil and water contaminated with oil, and can actively decompose diesel oil, n-alkanes, phenols, and PAHs (Zhang, Mortelmaier, Margesin, 2012).

As a rule, the microorganisms belonging to this phylum are well adapted to the environment with limited resources and do not show significant changes due to contamination with xenobiotics. The *Actinobacteria* phyla prevailed in the soil from the Mangistau region (MCI — 29.33 %, and Md — 23.67 %) (Tables 1, 2). According to some researchers, the *Actinobacteria* perform anaerobic degradation of cyclic and aromatic hydrocarbons at the later stages of oil biodegradation (Pineda-Flores *et al.*, 2004). The next group in terms of the population were the microorganisms that were part of two phyla — *Bacteroidetes*, which prevailed in the soil samples from the Kyzylorda region: 1KO

— 14.78 %, 2KO — 12.20 %, and in the sample of the uncontaminated soil PI 2 (Atyrau region) — 33.28 %, and *Firmicutes*, the largest number of which was found in the contaminated soil from the Atyrau region and amounted to 25.79 % (Table 2). The representatives of these two phyla belong to the common component of the soil microorganisms and are present in all types of soils that are resistant to drying; therefore, in arid climatic conditions, they can maintain their population. As a rule, the bacteria in this group have a wide range of physiological adaptations, which allows them to occupy various ecological niches, while multi-enzyme systems ensure the utilization of various substrates as the sources of carbon and energy (Matishov *et al.*, 2013). The largest number of bacteria of the *Chloroflexi* phylum (Md — 19.42 %) was noted in the contaminated soil from the Aktas oilfield in the Mangistau region. In other soil samples, their content was quite low and ranged from 0.68 % to 0.91 %. The representatives of the *Verrucomicrobia* (3.33 % – 3.88 %) and *Planctomycetes* (0.76 % – 4.62 %) phyla were present in the uncontaminated soils from all three oilfields (Table 1). *Verrucomicrobia* are extremely widespread in nature; they amount to 1 – 10 % of the soil microbiota and have an important ecological value, while the *Planctomycetes* phylum plays an important role in the nitrogen cycle, methanogenesis, and methylotrophy (Fuchsman *et al.*, 2012). The content of other representatives of the phyla in the soil samples amounted to small fractions in the range of 0.26 – 1.05 %. The presence of the microorganisms belonging to the *Euryarchaeota* phylum in the soils from the Zhanatalap oilfield and in the contaminated soil from the Aktas oilfield raised interest. Moreover, the highest content was found in the contaminated soil from the Zhanatalap oilfield (5.56 %); besides, the representatives of the *Synergistetes* phylum were found in the contaminated soil from the Aktas oilfield in the Mangistau region (6.06 %). It is known that the representatives of the *Euryarchaeota* phylum are chemoautotrophic unicell organisms that play a significant role in the carbon and nitrogen cycles, and the *Synergistetes* phylum includes the gram-negative anaerobic microorganisms that are found in the soils from the areas of oil production.

### 3.2.2. The changes in the composition of the bacterial communities at the family level

At the family level, a complex community structure was observed (Fig. 1).

The comparison of the diversity of the families in the uncontaminated and contaminated samples from the three deposits showed that the contaminated soil from the Kumkol oilfield in the Kyzylorda region (2KO) was dominated by the *Halomonadaceae* (9.45 %), *Flavobacteriaceae* (8.94 %), *Alteromonadaceae* (5.37 %), *Dietziaceae* (3.59 %), and *Pseudomonadaceae* (5.04 %) families. The soil from the Aktas oilfield in the Mangistau region (Md) was dominated by the *Xanthomonadaceae* (4.90 %), *Anaerolinaceae* (18.85 %), *Mycobacteriaceae* (8.73 %), *Peptococcaceae* (5.27 %), and *Hydrogenophilaceae* (4.30 %) families. In the contaminated soil of the Zhanatalap oilfield in the Atyrau region (At), the *Halomonadaceae* (21.39 %), *Bacillaceae* (12.73 %), *Halobacteriaceae* (5.55 %), and *Alteromonadaceae* (4.15 %) families were identified.

It should be noted that the contaminated soils from all the oilfields differed in the diversity of the families. All the microorganisms belonging to the families named above were active oil destructors. In our opinion, the difference among the families in all the samples of the contaminated soils could be explained by the different fractional composition of the oils at all three oilfields. For example, the oil from the Aktas oilfield in the Mangistau region was heavy, with the density of 0.872 – 0.915 g/cm<sup>3</sup>; the paraffin content in this oil was high (20 – 26.14 %), while the oil from the Zhanatalap and the Kumkol oilfields was slightly viscous, low-sulfur, and relatively light.

All the uncontaminated soils were dominated by the *Micrococcaceae* (3.41 – 8.21 %), *Flexibacteraceae* (3.07 – 7.52 %), *Sphingomonadaceae* (4.75 – 4.82 %), and *Planococcaceae* (3.24 – 9.77 %) families. The last family was not found in the uncontaminated soil from the Kumkol oilfield; however, other families were found in this sample, such as the *Oxalobacteraceae* (3.72 %), *Isosphaeraceae* (3.58 %), and *Chitinophagaceae* (3.01 %) families. The *Halomonadaceae*, *Flavobacteriaceae*, *Rhodobacteraceae*, and *Verrucomicrobiaceae* families were identified in the uncontaminated soil from the Zhanatalap oilfield in the Atyrau region. The diversity of the families was higher in the uncontaminated background soils, both in terms of the qualitative and the quantitative composition. Most representatives of the *Pseudomonadaceae*, *Micrococcaceae*, *Mycobacteriaceae*, *Halomonadaceae*, *Flavobacteriaceae*, *Dietziaceae*, *Pseudomonadaceae*,

*Rhodobacteraceae*, *Verrucomicrobiaceae*, *Bacillaceae*, and other families are directly involved in oil and petroleum hydrocarbons biodegradation. These families include hydrocarbon-oxidizing bacteria, such as *Arthrobacter*, *Pseudomonas*, *Mycobacterium*, *Rhodococcus*, and others, the species of which are active oil destructors in various soil types (Bogan *et al.*, 2003; Nopcharoenkul, Netsakulnee, Pinyakong, 2013).

### 3.2.3. Changes in the composition of the bacterial communities at the genus level

The diversity of the microbial community at the genus level in the soils of all the oilfields revealed a large share of unclassified microorganisms (13.69 % – 26.87 %). According to the data in Figure 2, the dominant bacterial genera in the samples of the uncontaminated soil were *Hymenobacter* (1KO — 3.63 %), *Arthrobacter* (MCL — 6.43 %), and *Gillisia* (P2I — 16.4 %).

In the contaminated soils from all the oilfields, the microorganisms of the *Halomonas* (2KO — 8.11 %), *Marinobacter* (2KO — 5.26 %), *Bellilinea* (Md — 13.69 %), and *Mycobacterium* (Md — 8.73 %) genera were spread more widely, and a very large population of the microorganisms of the *Halomonas* genus (At — 20.32 %) was found in the contaminated soil from the Atyrau region. The increased content of the microorganisms of the *Halomonas* genus (20.32 % and 8.11 %), which dominated in the contaminated soils from the Atyrau and Kyzylorda regions, could be explained by the fact that the soils of these biotopes were salt marshes and solonchaks with a fairly high level of salinity. The representatives of this genus are characterized by growth in the presence of 5 – 25 % of NaCl.

The soils of the Aktas oilfield in the Mangistau region are dominated by the microorganisms of the *Bellilinea* genus (Md — 13.69 %), which belong to the *Chloroflexi* phylum, and by the representatives of the *Mycobacterium* genus (Md — 8.73 %). These microorganisms are relatively resistant to moisture deficiency and are widely spread in dry soils. They have a rich enzymatic apparatus, which allows mineralization of the poorly soluble organic substances, and are actively involved in the decomposition of nitrogen-containing and nitrogen-free organic substances in the soil. According to S. Y. Zhang, mycobacteria can efficiently decompose tetracyclic and pentacyclic aromatic hydrocarbons (Zhang, Wang, Xie, 2012).

The analysis of the microbial composition showed that at the genus level, the diversity in the samples of the uncontaminated and contaminated soils was significantly different. The microbial community was more diverse in the samples of the uncontaminated soil. It should be noted that there were more unclassified microorganisms in the uncontaminated soils compared to the contaminated soils. In considering the dominant genera in the contaminated samples, it is noteworthy that, along with the presence of the *Halomonas*, *Bellilinea*, *Pseudomonas*, *Marinobacter*, and *Mycobacterium* genera, which are active oil destructors in various soil types, representatives of the *Planomicrobium*, *Agromyces*, *Thiobacillus*, and other genera were also found in the samples.

#### 4. DISCUSSION

Currently, there are many studies available on various bacterial communities and the diversity of the soils contaminated with oil at a different time (Yadav *et al.*, 2015; Abed *et al.*, 2014). The abundance and the diversity of the microbial communities are indicators of soil quality (Mathew *et al.*, 2012; García-Orenes *et al.*, 2013). Oil and oil products disrupt the ecological state of the soil cover and deform the structure of the biocenoses. Therefore, restoring the soil microbial communities is important because they are responsible for the physiological and metabolic processes that are of great importance for soil quality (Rutgers *et al.*, 2016). Changing the species composition of some groups of microorganisms reveals a more definite relationship with the degree and the composition of oil pollution. A high degree of oil pollution may cause complete suppression of the growth and development of microorganisms. Upon the ingress of oil and oil products into the soil, microorganisms are involved in the process of their transformation, which should bring the soil system into equilibrium. The changes in the soil microflora may be used for biomonitoring and bioindication of oil pollution (Kolesnikov *et al.*, 2007).

The metagenomic analysis showed that it was mainly formed by the representatives of seven bacterial phyla: *Proteobacteria*, *Actinobacteria*, *Bacteroidetes*, *Firmicutes*, *Planctomycetes*, *Verrucomicrobia*, and *Chloroflexi*, with *Proteobacteria* and *Actinobacteria* dominating in almost all microbiomes. The microorganisms belonging to the listed dominant types are mostly associated with the decomposition of oil hydrocarbons. An important indicator of soil health

is the *Proteobacteria* phylum, the population of which increases markedly in disturbed soils. In analyzing heterogeneous extremal soil habitats, such as desert soils, permafrost, soils contaminated with oil products and other pollutants, these microorganisms, which, most likely, make up the core or the main part of the soil metagenome, may be detected. The absolute champions among such microorganisms are bacteria of the *Pseudomonas* (*Gammaproteobacteria*), *Arthrobacter* (*Actinobacteria*), *Sphingomonas* (*Alphaproteobacteria*), *Bacillus* (*Firmicutes*), *Rhodococcus* (*Actinobacteria*), *Flavobacterium* (*Bacteroidetes*), and some other genera (Chernov, 2016). All of them are common not only in extremal but also in all other types of soils.

Without enough information, it is difficult to comprehensively understand the structural characteristics of the soil bacterial community and the nature of the changes in its diversity. Therefore, the categories of family and genus were also considered in the analysis of the microbocenosis.

An analysis of the data about the diversity of the families in the contaminated soil from all oilfields showed that they were dominated by the *Halomonadaceae*, *Flavobacteriaceae*, *Alteromonadaceae*, *Pseudomonadaceae*, *Xanthomonadaceae*, *Anaerolinaceae*, *Mycobacteriaceae*, *Halomonadaceae*, *Bacillaceae*, *Halobacteriaceae*, and *Alteromonadaceae* families. All uncontaminated soils were dominated by the *Micrococcaceae*, *Flexibacteraceae*, *Sphingomonadaceae*, *Planococcaceae*, *Oxalobacteraceae*, *Isosphaeraceae*, *Chitinophagaceae*, *Halomonadaceae*, *Flavobacteriaceae*, *Rhodobacteraceae*, and *Verrucomicrobiaceae* families.

The above-listed microorganisms are widespread in the environment. Most representatives of the *Pseudomonadaceae*, *Mycobacteriaceae*, *Halomonadaceae*, *Flavobacteriaceae*, *Dietziaceae*, *Pseudomonadaceae*, *Rhodobacteraceae*, *Verrucomicrobiaceae*, *Bacillaceae*, and other families are directly involved in oil and petroleum hydrocarbons biodegradation. These families include hydrocarbon-oxidizing bacteria, such as *Arthrobacter*, *Pseudomonas*, *Mycobacterium*, *Rhodococcus*, and others, the species of which are active oil destructors in various soil types. Most of them are halotolerant.

As noted earlier, studying the

microbocenosis at the genus level showed a huge number of unidentified microorganisms. The comparative analysis showed that in the uncontaminated soils, the microbial community was more diverse than in the contaminated ones. While the contaminated soils were dominated by the bacteria of the *Halomonas*, *Marinobacter*, *Mycobacterium*, *Bellilinea* genera, in the uncontaminated soils from the oilfields, microorganisms of such genera as *Hymenobacter*, *Arthrobacter*, *Gillisia*, *Salinimicrobium*, *Planomicrobium*, *Planococcus*, and *Halomonas* were found. These data correlate with the studies of Lu Gan *et al.* (2018) and Sutton N.B. *et al.* (2013), who found that the presence of oil pollution had a significant effect on the structure and diversity of the bacterial communities, regardless of the type of the soil matrix. Moreover, it was proven that the uncontaminated soil samples were more diverse than the contaminated ones. Other authors, for example, Mu Peng *et al.* (2015) have shown an inverse correlation, when the microbial diversity is higher in the contaminated soils (Peng, Zi, Wang, 2015). Most likely, these kinds of discrepancies in interpreting the diversity of the microbial coenosis depend on many environmental factors (climatic conditions, soil type, temperature, pH, pollutant concentration).

A change in the population of various groups of microorganisms indicated that the soil microbiota was significantly modified upon contamination with oil hydrocarbons, and various groups of microorganisms reacted differently. The population of some of them increased, the population of some of them decreased, and that of the others remained almost constant. At present, it may be taken as the fact that oil pollution causes changes in the functioning of the soil microbiocenosis. The determination of the bacterial structure and the function in the contaminated soil is the basis for further studies aimed at identifying active bacterial strains in bioremediation.

## 5. CONCLUSIONS:

In this work, it was analyzed the bacterial diversity in the contaminated and uncontaminated soil from three oilfields in Kazakhstan, and it was presented that high bacterial diversity is observed in the uncontaminated background soils.

The characterization of the bacterial communities living in the contaminated soils and the assessment of their ability to decompose oil can potentially be a guide for bioremediation of the contaminated soils. Future studies are required for

choosing the bacterial strains that are active in the degradation of various oil fractions, especially PAHs, which may be used for active management of the bioremediation processes.

## 6. FUNDING:

(This study was funded by the Ministry of Education and Science of the Republic of Kazakhstan (Grant no. APO5132128).

## 7. ACKNOWLEDGMENTS:

This study was supported by the Ministry of Education and Science of the Republic of Kazakhstan (Grant no. APO5132128).

## 8. REFERENCES:

1. Abed, R. M., Al-Kindi, S., Al-Kharusi, S. (2014). Diversity of Bacterial Communities along a Petroleum Contamination Gradient in Desert Soils. *Microb. Ecol.*, 69, 95-105.
2. Bogan, B. W., Sullivan, W. R., Kayser, K. J., Derr, K. D., Aldrich, H. C., Paterek, J. R. (2003). *Alkanin diges illinoisensis* gen. nov., sp. nov., an obligately hydrocarbonoclastic, aerobic squalane-degrading bacterium isolated from oilfield soils. *Int. J. Syst. Evol. Microbiol.*, 53, 1389-1395.
3. Bulekbaev, Z. E., Votsalevsky, E. S., Iskuzhiev, B. A., Kamalov, S. M., Korostyshevsky, M. N., Kuandykov, B. M., Kuantaev, N. E., Marchenko, O. N., Matloshinsky, N. G., Nazhmetdinov, A. Sh., Filipiev, G. P., Shabatin, I. V., Shakhbaev, R. S., Shudabaev, K. S. (1996). *Oil and gas deposits of Kazakhstan: guidebook*. Almaty.
4. Chakraborty, A., Das Gupta, C.K., Bhadury, P. (2014). *Application of Molecular Techniques for the Assessment of Microbial Communities in Contaminated Sites*. In *Microbial Biodegradation and Bioremediation*, pp. 85-113.
5. Chernov, T. I. (2016). *Metagenomnyi analiz prokariotnykh soobshchestv profilei pochv evropeiskoi territorii Rossii* [The metagenome analysis of the prokaryotic communities in the soil profiles in the European territory of Russia]: candidate of biological sciences thesis. Moscow: Lomonosov Moscow State University.
6. Diarov, M. D., Kurakov, A. V., Ilyinsky, V. V., Kotelevtsev, S. V., Sadchikov, A. P.

- (2006). *Bioindikatsiya i reabilitatsiya ekosistem pri neftyanykh zagryazneniyakh* [bioindication and rehabilitation of ecosystems after oil pollution]. Moscow: Graphikon.
7. Dörr de Quadros, P., Cerqueira, V. S., Cazarolli, J. C., do Peralba, M. C. R., Camargo, F. A. O., Giongo, A., Bento, F. M. (2016). *Oily sludge stimulates microbial activity and changes microbial structure in a landfarming soil*. *Int. Biodeterior. Biodegrad*, 115, 90-101.
  8. dos Santos, H. F., Cury, J. S., Carmo, F. L., dos Santos, A. L., Tiedje, J., van Elsas, J. D., Soares, R. A., Peixoto, R. S. (2011). Mangrove Bacterial Diversity and the Impact of Oil Contamination Revealed by Pyrosequencing: Bacterial Proxies for Oil Pollution. *PLoS One*, 6(3), e16943.
  9. Egorov, V. V., Ivanova, E. N., Friland, V. M. (1977). Classification and soil diagnostics of the USSR. Moscow: Kolos.
  10. Fuchsman, C. A., Staley, J. T., Oakley, B. B., Kirkpatrick, J. B., Murray, J. W. (2012). Free-living and aggregate associated Planctomycetes in the Black Sea. *FEMS Microbiol. Ecol.*, 80, 402-416.
  11. Gan, L., Wang, J.-P., Wu, Q.-P. (2018). Bacterial Diversity Change in Oil-contaminated Soils in Jiangnan Oilfield via a High-throughput Sequencing Technique. *Biotechnology*, 17, 128-134.
  12. García-Orenes, F., Morugán-Coronado, A., Zornoza, R., Scow, K. (2013). Changes in soil microbial community structure influenced by agricultural management practices in a Mediterranean agroecosystem. *PLoS One*, 8, e80522.
  13. Gavriluk, F. Ya. (1959). Soil survey: guide to field research and soil mapping. Moscow: Dokuchaev Soil Science Institute.
  14. GOST 17.4.4.02-2017. (2017). Interstate standard. Nature protection. Soils. Methods of sampling and preparation for chemical, bacteriological, helminthological analysis.
  15. GOST 26213-91. (1991). State standard of the USSR. Soils. Methods for determination of organic matter.
  16. Kirienko, O. A., Imranova, E. L. (2015). Vliyanie zagryazneniya pochvy nefteproduktami na sostav mikrobnogo soobshchestva [The effect of soil pollution by oil products on the composition of the microbial community]. *Bulletin of Pacific State University*, 3(38), 79-86.
  17. Klindworth, A., Pruesse, E., Schweer, T., Peplies, J., Quast, C., Horn, M., Glöckner, F.O. (2013). Evaluation of general 16S ribosomal RNA gene PCR primers for classical and next-generation sequencing-based diversity studies. *Nucleic Acids Res.*, 41(1).
  18. Kolesnikov, S. I., Kazeev, K. S., Veligonova, N. V., Patrusheva, E. V., Aznauryan, D. K., Valkov, V. F. (2007). Izmenenie kompleksa pochvennykh mikroorganizmov pri zagryaznenii chernozema obyknovennogo neftyu i nefteproduktami [Changes in the complex of soil microorganisms upon contamination of ordinary black soil with oil and oil products]. *Agrochemistry*, 12, 44-48.
  19. Liao, J. Q., Wang, J., Huang, Y. (2015). Bacterial community features are shaped by geographic location, physicochemical properties, and oil contamination of soil in main oilfields of China. *Microb. Ecol.*, 70, 380-389.
  20. Liao, J. Q., Wang, J., Jiang, D. L., Wang, M. C., Huang, Y. (2015). Long-term oil contamination causes similar changes in microbial communities of two distinct soils. *Appl. Microbiol. Biotechnol.*, 99(23), 1029-1031.
  21. Lurie, Y. Y. (1984). *Analiticheskaya khimiya promyshlennykh stochnykh vod* [Analytical chemistry of industrial wastewater]. Moscow: Chemistry.
  22. Ma, Q., Qu, Y., Shen, W., Zhang, Z., Wang, J., Liu, Z., Li, D., Li, H., Zhou, J. (2015). Bacterial community compositions of coking wastewater treatment plants in steel industry revealed by Illumina high-throughput sequencing. *Bioresour. Technol.*, 179, 436-443.
  23. Mathew, R. P., Feng, Y., Githinji, L., Ankumah, R., Balkcom, K. S. (2012). Impact of no-tillage and conventional tillage systems on soil microbial communities. *Applied and Environmental Soil Science*, 2012, 1-10.
  24. Matishov, D. G., Stakheev, V. V., Chirak, E.L., Glushchenko, G. Y. (2013). Metagenomnyi analiz struktury bakterialnogo soobshchestva Azovskogo morya [The metagenomic analysis of the structure of the bacterial community in the Azov Sea]. *Oceanology*, 55(5), 770-775.
  25. Nadirov, N. K. (1995). *Neft i gaz Kazakhstana* [Oil and gas in Kazakhstan]. Almaty: Gylym Publishing House.
  26. Nopcharoenkul, W., Netsakulnee, P.,

- Pinyakong, O. (2013). Diesel oil removal by immobilized *Pseudoxanthomonas* sp. RN402. *Biodegradation*, 24(3), 387-397.
27. Parkhomenko, A. N., Soprunova, O. B. (2008). Vliyanie zagryaznyayushchikh veshchestv neftegazovogo kompleksa na strukturu i chislennost mikrobnikh soobshchestv pochv nizhnego Povolzhya [The influence of the oil and gas industry pollutants on the structure and the population of microbial communities in the soils of the Lower Volga region]. *Environmental protection in the oil and gas industry*, 5, 42-46.
  28. Peng, M., Zi, X., Wang, Q. (2015). Bacterial Community Diversity of Oil-Contaminated Soils Assessed by High Throughput Sequencing of 16S rRNA Genes. *Int J Environ Res Public Health*, 12(10), 12002-12015.
  29. Pineda-Flores, G., Boll-Argüello, G., Lira-Galeana, C., Mesta-Howard, A. M. A. (2004). Microbial consortium isolated from a crude oil sample that uses asphaltene as a carbon and energy source. *Biodegradation*, 15, 145-151.
  30. Polyanskaya, L. M., Zvyagintsev, D. G. (2005). Soderzhanie i struktura mikrobnoi massy, kak pokazatel ekologicheskogo sostoyaniya pochv [The content and the structure of the microbial mass as an indicator of the ecological state of the soils]. *Soil Science*, 6, 705-714.
  31. Portnov, V. S., Petrov, S. N., Talerchik, M.P. (2015). Characterization of oil and gas fields of the Caspian depression. *Modern high technologies*, 1(1), 69-74.
  32. Rodriguez, R. L. M., Overholt, W. A., Hagan, C., Huettel, M., Kostka, J. E., Konstantinidis, K. T. (2015). Microbial community successional patterns in beach sands impacted by the Deepwater horizon oil spill. *ISME J*, 9, 1928-1940.
  33. Rozanov, B.G. (2004). Soil morphology. Moscow: Akademicheskyy proyekt.
  34. Rutgers, M., Wouterse, M., Drost, S.M., Breure, A.M., Mulder, C., Stone, D., Creamer, R.E., Winding, A., Bloem, J. (2016). Monitoring soil bacteria with community-level physiological profiles using Biolog<sup>TM</sup> ECO-plates in the Netherlands and Europe. *Appl. Soil Ecol.*, 97, 23-35.
  35. Scientific and methodological guidelines for monitoring the land of the Republic of Kazakhstan. (1994). Issue of the State Committee of the Republic of Kazakhstan on land relations and land management. Almaty.
  36. Soils of the Kazakh SSR: Guryev region. (1970). Alma-Ata: Nauka.
  37. Soils of the Kazakh SSR: Soils of the Kyzylorda region. (1983). Alma-Ata: Nauka.
  38. Sutton, N. B., Maphosa, F., Morillo, J. A., Al-Soud, W. A., Langenhoff, A. A., Grotenhuis, T., Rijnaarts, H. H. M., Smidt, H. (2013). Impact of long-term diesel contamination on soil microbial community structure. *Appl. Environ. Microbiol.*, 79, 619-630.
  39. Urakawa, H., Garcia, J.C., Barreto, P. D., Molina, G. A., Barreto, J. C. (2012). A sensitive crude oil bioassay indicates that oil spills potentially induce a change of major nitrifying prokaryotes from the archaea to the bacteria. *Environ Pollut.*, 164, 42-45.
  40. Voevodina, T. S., Rusanov, A. M., Vasilchenko, A. V. (2015). Vliyanie nefi na khimicheskie svoystva chernozema obyknovennogo Yuzhnogo Preduralya [The effect of oil on the chemical properties of common black soil of the piedmont of the Southern Urals]. *Bulletin of the OSU*, 10(185), 157-161.
  41. Wakelin, S. A., Macdonald, L. M., Rogers, S. L., Gregg, A. L., Bolger, T. P., Baldock, J. A. (2008). Habitat selective factors influencing the structural composition and functional capacity of microbial communities in agricultural soils. *Soil Biology and Biochemistry*, 40, 803-813.
  42. Winding, A., Hund-Rinke, K., Rutgers, M. (2005). The use of microorganisms in ecological soil classification and assessment concepts. *Ecotoxicol. Environ. Safety*, 62(2), 230-248.
  43. Wolińska, A. (2019). *Metagenomic Achievements in Microbial Diversity Determination in Croplands: A Review*. In *Microbial Diversity in the Genomic Era*. Elsevier, pp. 15-35.
  44. Wu, P., Xiong, X., Xu, Z., Lu, C., Cheng, H., Lyu, X., Zhang, J., He, W., Deng, W., Lyu, Y., Lou, Q., Hong, Y., Fang, H. (2016). Bacterial Communities in the Rhizospheres of Three Mangrove Tree Species from Beilun Estuary, China. *PLoS One*, 11(10), e0164082.
  45. Yadav, T. C., Pal, R. R., Shastri, S., Jadeja, N. B., Kapley, A. (2015). Comparative metagenomics demonstrating a different degradative capacity of activated biomass treating



- hydrocarbon contaminated wastewater. *Bioresour. Technol.*, 188, 24-32.
46. Zhang, D.C., Mortelmaier, C., Margesin, R. (2012). Characterization of the bacterial archaeal diversity in hydrocarbon-contaminated soil. *Science of The Total Environment*, 421-422, 184-196.
47. Zhang, S. Y., Wang, Q. F., Xie, S. G. (2012). Bacterial and archaeal community structures in phenanthrene amended aquifer sediment microcosms under oxic and anoxic conditions. *Int. J. Environ. Res.*, 6(4), 1077-1088.

**Table 1.** Comparative characteristics of the microbial composition of the uncontaminated soils (phyla)

| No. | Phylum                 | Kyzylorda |                 | Mangistau |                 | Atyrau |                 |
|-----|------------------------|-----------|-----------------|-----------|-----------------|--------|-----------------|
|     |                        | 1KO       |                 | MCI       |                 | P2 I   |                 |
|     |                        | %         | Number of Reads | %         | Number of Reads | %      | Number of Reads |
| 1   | <i>Unclassified</i>    | 9.26      | 63.732          | 8.52      | 32.445          | 3.35   | 11.522          |
| 2   | <i>Proteobacteria</i>  | 31.78     | 218.664         | 26.3      | 100.103         | 6.2    | 90.182          |
| 3   | <i>Actinobacteria</i>  | 18.05     | 124.184         | 29.33     | 111.642         | 13.87  | 47.754          |
| 4   | <i>Bacteroidetes</i>   | 14.78     | 101.681         | 10.39     | 39.555          | 33.28  | 114.563         |
| 5   | <i>Firmicutes</i>      | 12.44     | 85.611          | 15.13     | 57.581          | 16.08  | 55.342          |
| 6   | <i>Planctomycetes</i>  | 4.62      | 31.766          | 2.14      | 8.148           | 0.76   | 2.624           |
| 7   | <i>Verrucomicrobia</i> | 3.88      | 26.706          | 3.25      | 12.363          | 3.33   | 11.455          |
| 8   | <i>Chloroflexi</i>     | 0.91      | 6.252           | -         | -               | -      | -               |
| 9   | <i>Tenericutes</i>     | -         | -               | 1.05      | 4.010           | -      | -               |
| 10  | <i>Euryarchaeota</i>   | -         | -               | -         | -               | 1.13   | 3.885           |
| 11  | <i>Synergistetes</i>   | -         | -               | -         | -               | -      | -               |

**Table 2.** Comparative characteristics of the microbial composition of the contaminated soils (phyla)

| No. | Phylum          | Kyzylorda      |                 | Mangistau      |                 | Atyrau         |                 |
|-----|-----------------|----------------|-----------------|----------------|-----------------|----------------|-----------------|
|     |                 | 2KO            |                 | Md             |                 | At             |                 |
|     |                 | (contaminated) |                 | (contaminated) |                 | (contaminated) |                 |
|     |                 | %              | Number of Reads | %              | Number of Reads | %              | Number of Reads |
| 1   | Unclassified    | 5.47           | 13.819          | 8.51           | 14.099          | 6.08           | 3.313           |
| 2   | Proteobacteria  | 42.49          | 107.397         | 21.22          | 35.140          | 44.48          | 178.082         |
| 3   | Actinobacteria  | 20.37          | 51.482          | 23.67          | 39.202          | 9.66           | 38.683          |
| 4   | Bacteroidetes   | 12.20          | 30.841          | 3.9            | 6.458           | 3.99           | 15.963          |
| 5   | Firmicutes      | 13.91          | 35.152          | 14.74          | 24.410          | 25.79          | 103.253         |
| 6   | Planctomycetes  | 1.43           | 3.613           | -              | -               | -              | 3.313           |
| 7   | Verrucomicrobia | 1.29           | 3.250           | -              | -               | -              | -               |
| 8   | Chloroflexi     | 0.85           | 2.143           | 19.42          | 32.157          | 0.84           | 3.382           |
| 9   | Tenericutes     | -              | -               | -              | -               | -              | -               |
| 10  | Euryachaeota    | -              | -               | 1.25           | 2.071           | 5.56           | -               |
| 11  | Synergistetes   | -              | -               | 6.06           | 10.038          | -              | -               |

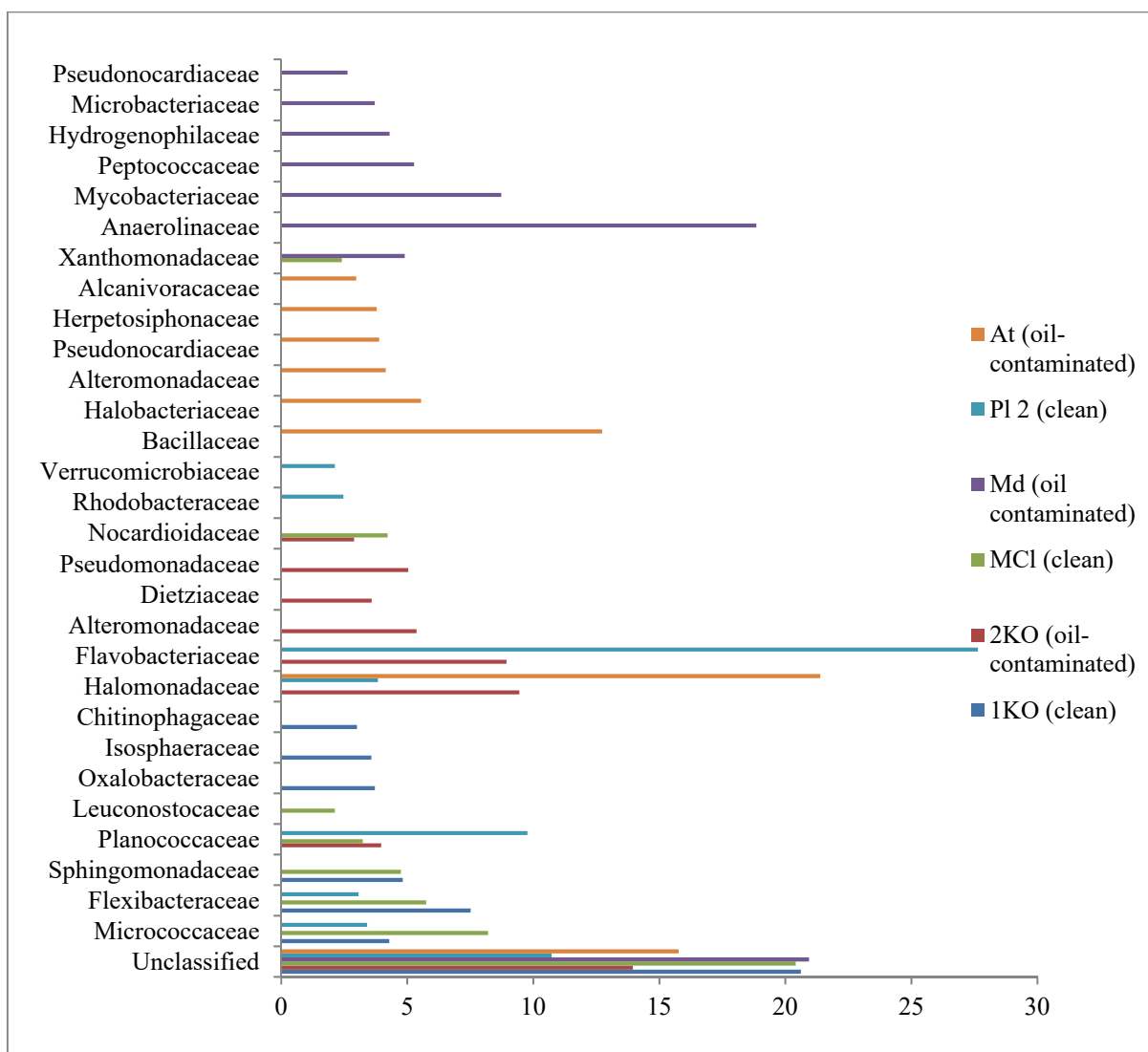


**Figure 1.** Comparison of the relative population (% of the total sequence) of the main bacterial families found in the most dominant bacterial classes in the samples of the contaminated and uncontaminated soil

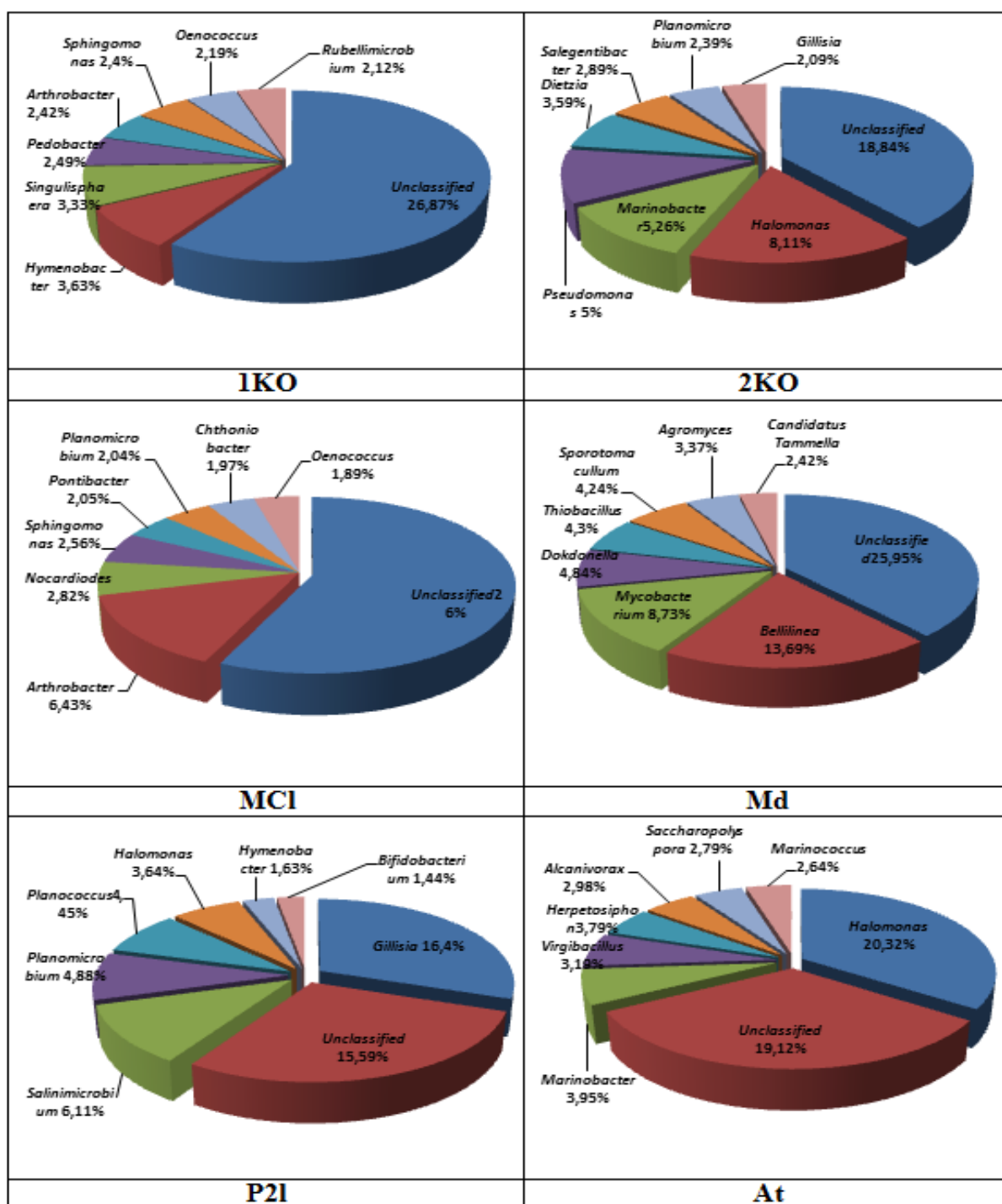


**Figure 2.** The microbial diversity at the genus level. **1KO, MCI, P2L** are samples of the uncontaminated soil; **2KO, Md, At** are samples of the contaminated soil

**USO DE BIOCORRETORES NA ESTIMULAÇÃO DA REGENERAÇÃO  
HEPÁTICA FETAL DE RATOS LESIONADOS MECANICAMENTE****USING OF BIOCORRECTORS IN REGENERATION PACING  
OF MECHANICALLY INJURED RATS' FETAL HEPATIC**

ROMANOVA, Lubov<sup>1\*</sup>; TOLMATCHEVA, Natalia<sup>2</sup>; MASLOVA, Zhanna<sup>3</sup>; KAPITOVA, Irina<sup>4</sup>;  
SHAMITOVA, Elena<sup>5</sup>

<sup>1,2,3,4</sup> I.N. Ulyanov Chuvash State University, Department of Dermatovenereology. Russian Federation.

<sup>5</sup> I.N. Ulyanov Chuvash State University, Department of Pharmacology, Clinical Pharmacology,  
and Biochemistry. Russian Federation.

\* Correspondence author  
e-mail: samung2008@yandex.ru

Received 18 May 2020; received in revised form 05 June 2020; accepted 28 June 2020

**RESUMO**

O artigo é dedicado ao estudo da influência de substâncias biologicamente ativas na regeneração de órgãos internos de mamíferos em estágios iniciais de desenvolvimento. A recuperação completa do órgão após o dano não ocorre. É necessário procurar novas maneiras que revelem os processos que contribuem para a regeneração. O estudo dos processos que ocorrem no corpo antes do nascimento dá a oportunidade de entender os mecanismos do que acontece no período pós-natal nos processos patológicos gerais. Foi estudado o dano mecânico ao fígado em fetos de ratos sob a influência dos biocorretores "Trepel" e "Suvar". Métodos morfológicos, morfométricos, histoquímicos e imuno-histoquímicos foram utilizados para o processamento do material. Os resultados do trabalho indicam que o uso combinado desses biocorretores após o desenvolvimento de um foco de necrose no fígado reduz as manifestações alteradas de hepatócitos, inibe a inflamação reativa ao redor do local da lesão, retarda o recrutamento de fibroblastos para a zona de lesão e inibe a colagenogênese. Ao mesmo tempo, os biocorretores têm um efeito estimulante pronunciado na proliferação de hepatócitos, que, no contexto de atividade enzimática aumentada, se manifesta na forma de ativação da divisão mitótica e poliploidização de hepatócitos. Apesar dos sinais de estimulação regenerativa, como resultado a recuperação completa do fígado no local do tecido morto em ratos experimentais não ocorre; há apenas uma redução de 34,7% no foco da fibrose formada no local do tecido hepático morto, em comparação aos animais de controle.

**Palavras-chave:** *Feto, Hepático, Lesão mecânica, Biocorretores, Hepatócitos.*

**ABSTRACT**

The article is devoted to studying the influence of biologically active substances on the regeneration of internal organs in mammals at the early stages of development. Complete recovery of the organ after damage does not occur. It is necessary to look for new ways that reveal the processes that contribute to regeneration. The study of processes that occur in the body before birth allows understanding the mechanisms of what happens in the postnatal period in general pathological processes. It was studied the mechanical damage to the liver in rat fetuses under the influence of biocorrectors "Trepel" and "Suvar." Morphological, morphometric, histochemical, and immunohistochemical methods were used for processing the material. The results of the work indicate that the combined use of these biocorrectors after the development of a necrosis focus in the liver reduces alternative manifestations of hepatocytes, inhibits reactive inflammation around the injury site, slows down the recruitment of fibroblasts to the injury zone, and inhibits collagen genesis. At the same time, biocorrectors have a pronounced stimulating effect on proliferation of hepatocytes, which, against the background of increased enzymatic activity, manifests itself in the form of mitotic division activation and polyploidization of hepatocytes. Despite the signs of regenerative stimulation, as a result, complete recovery of the liver in the site of the dead tissue in experimental rats does not occur; there is only a 34.7% decrease in the focus of fibrosis formed in the place of dead liver tissue, compared to control animals.

**Keywords:** *Fetus, Hepatic, Mechanical injury, Biocorrectors, Hepatocytes.*

## 1. INTRODUCTION:

Mechanical injury hepatic does not show any regenerative progress neither in late perinatal life (Eltschaninov, 2011), nor after birth (Tournier-Thurneyssen, Feldmann, & Bernuau, 1992). The reason for this is those hepatic hepatocytes belong to highly specialized tissue, unable to regenerate through epimorphosis. Although, nowadays, searching for highly efficient means for the pacing of hepatic regeneration is still in progress, apart from the parallel investigation of stem cells (Wang, Zhao, Fish, Logan, & Nusse, 2015).

From (Sigareva, Gerashev, Svyatash, & Lucanina, 2001; Solopaeva & Solopaev, 1991; Sosina, Molotkov, & Reshedko, 1993) it is known that during long decades many attempts have been made to pace hepatic regeneration after various injuries until complete organ recovery was achieved. Forth is the purpose, to activate hepatocyte division, operating (partial hepatectomy) (Andreev, Ostroushko, Laptiyova, & Glukhov, 2018; Berg et al., 2018; Soltys & Zuevkiy, 2000) and pharmacological methods Grevtsov & Belkina, 2002; Sigareva et al., 2001; Sosina et al., 1993) were used in experimental and clinical conditions.

In present days, for veterinary medicine performance improvement (G. I. Ivanov & Grigoryev, 1998), as well as for treatment of different human diseases (Grevtsov & Belkina, 2002; L. N. Ivanov & Kolotilova, 2005; Kolotilova & Ivanov, 2003; Malov, Ivanov, & Kolotilov, 2018; Malov, Ivanov, Kolotilova, & Karpunina, 2018; Vasiliev, Skrebkov, & Pavlova, 1988), zeolites of Alatyrskoe field, Chuvash Republic of Russian Federation are used. "Trepel" is a natural loses sedimentary rock with a silicon base and rich microelement composition (Malov, 2017).

"Suvar" biocorrector is obtained in the laboratory of I.N. Yulianov Chuvash State University and represents natural terpenoids compound with significant microelement content. Technically it is conifer crude turpentine derivative product (Zazhivikhina, 1998). "Suvar" possesses a stimulating effect on human and animal organisms (Frolov, 2003; Petryankin, & Sherne, 1999; Zazhivikhina, 1998). It is proved that the joint application of "Trepel" and "Suvar" favors the development of various mammal organism functional systems, and has immunostimulating and growth promotion effect (Arkhipova, 2008; Sigareva et al., 2001; Tarasov, 2001).

This study aimed to determine the positive influence of the combined application of "Trepel"

and "Suvar" biocorrectors on rats' fetus hepatic regeneration after mechanical injury.

## 2. MATERIALS AND METHODS:

The experiment included 23 pregnant females of outbred rats 257-310 grams of weight. Rat's fetus at the prenatal stage received a mechanical injury of hepatic. Using the innovator method (Chuvash State University named after I.N. Ulyanov Patent RU 2262135, 2005), pregnant female shave undergone an autopsy of the abdominal cavity, in sterile conditions under deep ether-mask anesthesia on the 17th – 19th day of pregnancy.

Uterus, together with a fetus inside, was taken through the operating wound; afterward, along the upper pole, an incision was made. Then a steel stop needle was used (Chuvash State University named after I.N. Ulyanov Patent RU 2262135, 2005), and firstly, membrane rupture was implemented, and later on, the same procedure was made for a well visible fetus (under visual control), in the right hypochondriac region, in hepatic projection point at the depth 0.4-0.5 cm. As are sultofrupturein the hepatic, there appeared stereotypic damage is with dimensions  $3085.7 \pm 368.3 \mu\text{m}^2$ .

At the end of the rapture procedure, the needle was extracted, and the uterus incision was suture closed. After all, fetuses have systematically undergone the same process; the skin was closed with knot silk suture. At the early stages of observation (1<sup>st</sup> and 3<sup>rd</sup> day after the operation), live fetuses were extracted from the uterus employing cesarian operation; later (5 and more days after the operation), female rats independently delivered viable infant rats, which grew and developed according to age. Infant rats got ether-killed in 1, 2, 3, 4, 5, 7, 9, 11, 15, 20, and 30 days after hepatic mechanical injury operation, in the morning from 7.10 to 9 o'clock.

In total, 112 operated fetuses were taken for experiment. The investigation was conducted in accordance with the order of Ministry of Higher and Secondary Education of the USSR dated 13.11.1984 "On the rules of work using experimental animals" (Interstate Council for Standardization, Metrology, and Certification, 2016), and according to Declaration of Helsinki 1975, revision 2000 "On the rules of work using experimental animals." Stillbirth part among infant rats comprised 3% and was not included in analyzed material. Female rats bore an operation satisfactorily and soon afterward were able to pair and get pregnant again.

Rat females from the moment of operation to goether with regular feed started receiving biocorrectors "Trepel" at a dose of 1.25 g/kg and "Suvar" at a dose of 0.05 g/kg of weight. After birth and along with maturity, infant rats, apart from milk feeding, started having common feed containing biologics.

Control was performed on fetuses of the same age (p-78) similarly operated, but the dietary intake did not include biocorrectors.

Obtained material processing included histological staining with hematoxylin, eosin, and cerasine red, as well as histochemical methods. Tetrazolium method (according to Z. Lloyd) was used to determine SDH (succinate dehydrogenase), NADH (nicotinamide adenine dinucleotide, reduced form) and NADPH (nicotinamide adenine dinucleotide, reduced form). Acid phosphatase was defined through method of simultaneous combination with naphthol phosphates AS and permanent salts of diazonium (according to Z. Lloyd). Alkaline phosphatase was determined by Barston method (Lloyd, Gossrau, & Shibler, 1982).

Quantitative assessment of the enzymatic activity of hepatocytes in dynamics was carried out using photometric measurements, conducted in transmitted light on a "Micromed" microscope with a photomodule FMEL-1 and FEU-79 and an output voltage of the amplifier of 1200 V. In order to obtain a monochromatic light beam in the red region of the spectrum passing through the preparation, an interference filter was used with a maximum light transmission at a wavelength of 620 nm. The light transmission was recorded using a Sch-4300 digital voltmeter, after which, by negative decimal logarithm, the light transmission level was transformed into light absorption, which was expressed in units of optical density. According to the law of Lambert-Bouguer-Baer, the optical density of the preparation is proportional to the amount of stain. In turn, the described method meets the requirements of proportionality of stain concentration and enzyme activity. Optical density is calculated as follows:

$$O.D. = LgUi/100.$$

To detect the DNA content in the nuclei of hepatocytes, the Fölgen reaction was performed (hydrolysis in 5N HCL at 20 degrees for 20 minutes, followed by staining with Schiff's reagent for 1 hour at room temperature). The amount of DNA in the nuclei was determined using a Biolam-70 light microscope with photometry using an FMEL-1 component and an FEU-79A photometer in transmitted light with a blocking filter of maximum light transmission at a wavelength of

570 nm and a supplied voltage of 900 V. The results were subjected to the inverse decimal logarithm according to the formula:

$$A=LgUi/U_0,$$

where A – optical density;

Ui – voltage meter reading on the nucleus;

U<sub>0</sub> - voltmeter readings on unstained areas of the preparation.

Peripheral blood lymphocytes and small lymph nodes lymphocytes served as a diploid standard.

The immunohistochemical method was used to further evaluate the proliferative activity of hepatocytes after a mechanical injury to the hepatic that takes place under the use of biologically-active agents (Kumar & Rudbeck, 2011). For immunohistochemical studies, two commercial monoclonal antibodies by Santa Cruze were used: 1) Ki-67 proliferative activity marker; 2) a marker of apoptosis Bcl-2. Immunohistochemical studies were performed according to a standard protocol. Sections 3 μm thick were applied to high-adhesive glass treated with L-polisine and dried at room temperature for 24 hours. Staining was carried out manually and by hardware using immunohistochemical containers AUTOSTAINER-360 (THERMO, UK) and Leica BOND-MAX (Germany), as well as through Envision imaging systems (DACO Denmark) and NovoLincpolimer (NovoCastr, UK). Nonimmune rabbit and mouse sera, as well as sections of control hepatic tissues, served as a control of the sensitivity and specificity of the reaction. Results of the responses were evaluated by counting the number of stained nuclei per 200 hepatocyte nuclei in six fields of view. Then, the ratio of stained hepatocytes to the total number of hepatocytes was calculated, and the results were expressed as a percentage.

Statistical processing of digital data was carried out according to the particular program "Statistics" with the assistance of the Microsoft office software package (MS Word and MS Excel) on a Pentium 166 MMX computer. Statistical significance was determined by Student's t-test.

### 3. RESULTS AND DISCUSSION:

Histological changes one day after the operation were characterized by a predominance of dystrophic and necrobiotic changes in hepatocytes. Microscopic preparations of the hepatic taken from the site of injury revealed slit damage to the hepatic tissue, in which dead

hepatocytes and erythrocytes were noted. These changes have occurred in both experimental and control animals.

On the 3rd and, especially, the 5th day, a cluster of cells appeared on the periphery of the necrotic focus, represented by macrophages and lymphocytes. In control of infant rats, the intensity of the cellular inflammatory response was more pronounced in comparison with experimental animals, which visually showed a weaker presence of inflammatory cellular elements, macrophages, and lymphocytes around the injury site. On the 7th-9th day, in experimental animals, fibroblasts are fixed among inflammatory cells; fibrous connective tissue is formed 11 days after the operation. In control of infant rats, the appearance of fibroblasts is noted earlier (on the 5th-7th day), and, respectively, the formation of fibrous connective tissue occurs in them earlier - on the 9th day. Thus, among experimental rats, as well as in control, the fibrous connective tissue is found in place of the dead hepatic tissue (Figure 1). However, in experimental animals, it formed later, and the area of the connective tissue scar was 34.7% less than among control rats.

Starting from the first day after operation, hepatocyte proliferation was activated in hepatic of both experimental and control rats (Michalopoulos, 2010). Microscopic preparations revealed all phases of the mitotic cycle, from metaphases to late telophases. The number of mitoses in experimental animals was statistically significantly higher than in control animals ( $p < 0.001$ ). The peak of hepatocyte proliferation in experimental rats was observed in the period from 3 to 11 days; in control animals, the highest number of mitoses was recorded on days 3–7. Mitotic division in experimental pups was observed up to 20 days after the operation. In control, they were absent in the hepatic so far after 11 days, and until the end of the experiment.

Along with mitoses, starting from the 7th day after the operation, the number of binuclear hepatocytes in the hepatic increased; this was the case in animals of both groups, however, compared with the control, in experimental animals, there was a statistically significantly greater number ( $p < 0.001$ ). This trend was observed until the end of the experiment.

An immunohistochemical study confirmed the activation of hepatocyte proliferation: a statistically significant increase in Ki-67 positive nuclei was observed in experimental animals compared to control ones (Figure 2).

Most often, Ki-67 positive nuclei are determined on the 3.5 and 9 days after operation ( $p < 0.001$ ). Almost simultaneously with the activation of hepatocyte proliferation, their hypertrophy and polyploidy increased. From 3 days to 30 days, tetraploid nuclei began to predominate in animals. Moreover, in experimental rats, polyploidy was more pronounced, which manifested itself in the fact that tetraploid cells prevailed over diploid cells, in contrast to the hepatic of control rats. In experimental fetuses, hepatocytes of higher ploidy (8p, 16p, and even 32p) were often fixed, which was absent in control (Table 1).

Hypertrophy of hepatocytes and their nuclei began to increase from the 5th and, especially, from the 7th day, reaching the greatest value on the 20th and 30th days after the operation; in experimental fetuses, it was more pronounced. Restorative processes in the hepatic, especially in experimental rats, took place against the background of an increase in the vital activity of hepatic cells: an increase in the activity of SDH, NADH, NADPH was noted, the number of binucleate hepatocytes went up significantly, which indicates an increase in the protein-synthetic function of hepatic cells (Brodskaya et al., 2010) (Figure 3).

Electron microscopy revealed changes of two types. Hepatocytes with signs of degeneration, manifested by swelling of the mitochondria, focal enlightenment of the matrix, and also a change in the orientation of the cristae up to a decrease in their number in the cells, were observed. There was disorganization of the membranes of the organelles. At the same time, there were cells with changes that indicated the intensity of intracellular hyperplastic processes. This was manifested by hypertrophy and swelling of mitochondria, the convergence of the membranes of the endoplasmic reticulum, hypertrophy, and hyperplasia of ribosomes. These changes could be interpreted as a sign of intracellular regeneration.

Data obtained in the course of this work are generally consistent with the literature references on the morphogenesis of the healing of hepatic injury of various origins and development of regenerative manifestations (Baidyuk, Korshak, Karpov, Kudryavtsev, & Sakuta, 2012). In particular, present research revealed confirmation that healing of hepatic damage always occurs due to regenerative hypertrophy (Eltschaninov, 2011; Tournier-Thurneysen et al., 1992). Increase in the proliferation of hepatocytes was also expected, as it was repeatedly indicated in the



works of various authors (Celton-Morizur & Desdouets, 2010; Eltschaninov & Bolshakova, 2012; Malato et al., 2011; Sakuta, Baidyuk, Zhumagalieva, & Kudryavtsev, 2011; Solopaeva & Solopaev, 1991; Soltys & Zuevkiy, 2000; Yanger et al., 2014).

Also, in this study, the fact of an increasing number of binuclear hepatocytes (Berezovskiy, Yanko, Litovka, & Volovich, 2012; Stupin et al., 1995), and development of hypertrophy and polyploidy of hepatocytes (Soltys and Zuevkiy, 2000) was noted. Proliferation was activated against the background of increased protein-synthetic and enzymatic activity of hepatocytes, also earlier reported (Soltys and Zuevkiy, 2000). Even though all manifestations of a regenerative nature in experimental rats were more intense, complete organ restoration did not take place. Nevertheless, the focus of fibrosis that occurs at the site of dead hepatic tissue in experimental rats was visually much smaller than in control animals, which can be regarded as an encouraging fact, indicating that stimulation of hepatic regeneration is fundamentally possible (Koroy, Yagoda, Gilyazova, & Mukhoramova, 2014).

In previously published works (Juan, Benito, Alvarez, & Fabregat, 1992; Romanova, 2012; Romanova & Malyshev, 2012), an effect on the regeneration of fetal hepatic after a mechanical injury was studied separately for "Trepel" and "Suvar." "Trepel" when introduced into the diet of animals after the operation, is a powerful detoxification agent, which lowered the alternative processes in the hepatic of rat fetuses, suppressed the inflammatory reaction along the periphery of the injury site, and slowed the recruitment of fibroblasts into inflammatory infiltrate.

When only "Suvar" was used in the animal diet, in response to mechanical damage to the hepatic in rat fetuses, hepatocyte proliferation was activated (Romanova, 2012). Thus, "Trepel" and "Suvar", introduced into rat food in isolation, peculiarly influenced the healing morphogenesis but did not lead to a decrease in the size of the connective tissue scar that occurs in the hepatic at the area of dead tissue.

Significant in the study were the results of the combined effect of "Trepel" and "Suvar" biocorrectors on healing of mechanical injury of rat fetuses, which was realized in reducing the area of post-traumatic fibrous connective tissue by 34.7% compared with the control. This follows from the fact that combined action of "Trepel" and "Suvar" biocorrectors led to decrease in the intensity of

alternative manifestations in hepatocytes, reduced inflammatory changes around the injury site, and slowed the recruitment of fibroblasts to the area of injury, which, in turn, reduced the intensity of collagen formation. The described processes proceeded against the background of a revitalization of hepatocyte proliferation, which manifests itself in the form of activation of mitotic division, an increase in the number of binuclear hepatocytes, polyploidy and hypertrophy.

The theoretical significance of the results is that for the first time, data was obtained on the stimulating effect on rat hepatic regeneration using "Trepel" and "Suvar" biocorrectors. This may be a prerequisite for their further study in various pathological processes in mammals, both in the prenatal and postnatal periods. Successful surgical interventions in the organs of the mammals' fetuses, including hepatic (Chuvash State University named after I.N. Ulyanov Patent RU 2262135, 2005), were first performed in Russia; biocorrectors "Trepel" and "Suvar" is a purely Russian development. Literature references search established that abroad there are no works even closely related to this subject. Therefore, this study can attract attention abroad and stimulate further development of the problem.

#### 4. CONCLUSION:

Thus, in experimental animals, the size of the focus of fibrous connective tissue developing at the area of dead hepatic tissue was 34.7% smaller than in infant rats of the control group. The stimulating effect of biocorrectors on organ restoration is explained by their mechanism of action. It has been established that combined use of the "Trepel" and "Suvar" biocorrectors in veterinary medicine is accompanied by hypertrophy of the endocrine glands: adrenal glands (mainly their cortex), thyroid gland (follicular epithelium and follicles themselves), testes. This leads to an increase in production of the corresponding hormones. Female rats receiving biocorrectors as a food supplement feed their newborn rats with milk with a significantly higher hormone content.

The excess content of glucocorticoids in the body of experimental infant rats explains the absence of a pronounced inflammatory reaction around the injury and inhibition of collagen genesis. Iodine-containing thyroid hormones, activating all types of metabolism, sharply increase cellular metabolism, and stimulate the proliferation of hepatocytes. Thus, based on a change in the hormonal background of the

organism of experimental rats, it can be concluded with a high degree of probability that hypertrophied hepatic cells, while slowing down the development of connective tissue, mechanically compress the site of organ damage. Proliferating hepatocytes gradually fill the post-traumatic hepatic defect, as a result of which, along with the connective tissue, it is replaced for a considerable extent by newly formed and hypertrophic hepatocytes. This led to the fact that the size of the focus of fibrosis in experimental infant rats was 34.7% smaller than in control animals.

## 5. REFERENCES:

1. Andreev, A. A., Ostroushko, A. P., Laptiyova, A. Yu., & Glukhov, A. A. (2018). Reparative liver regeneration after segmental resection (literature review). *Postgraduate Bulletin of the Volga Region*, 5–6, 183–190.
2. Arkhipova, M. N. (2008). Stanovleniye i razvitiye funktsional'nykh sistem u borovkov v biogeokhimicheskikh usloviyakh Chuvashskogo Tsentra s naznacheniyem biogennykh soyedineniy [Formation and development of functional systems in boars under biogeochemical conditions of the Chuvash Center with the appointment of nutrients] (PhD thesis). Cheboksary.
3. Baidyuk, E. V., Korshak, O. V., Karpov, A. A., Kudryavtsev, B. N., & Sakuta, G. A. (2012). Cellular mechanisms of regeneration of rats liver after experimental myocardial infarction. *Cytology*, 54(12), 873–882.
4. Berezovskiy, V. A., Yanko, R. V., Litovka, I. G., & Volovich, O. I. (2012). Exogenous melatonin effects of rats liver parenhima Ukrainian morphological almanac. *Ukrainian Morphological Almanac*, 10(4), 178–181.
5. Berg, T., Buggisch, P., Hueppe, D., Mauss, S., Wedemeyer, H., Teuber, G., ... Hinrichsen, H. (2018). Real-Life Experiences with Telaprevir in the Treatment of Chronic Genotype 1 Hepatitis C – The TEPS Study. *Russian Journal of Gastroenterology, Hepatology, Coloproctology*, 28(6), 15–26. <https://doi.org/10.22416/1382-4376-2018-28-6-15-26>
6. Brodskaya, V. Y., Rapoport, S. I., Dubovayac, T. K., Zvezdina, N. D., Fateeva, V. I., & Malchenkov, L. A. (2010). Melatonin Injected into Rat Efficiently Synchronizes the Rhythm of Protein Synthesis in Primary Hepatocyte Cultures Isolated from This Rat. *Ontogeny*, 41, 101–106.
7. Celton-Morizur, S., & Desdouets, C. (2010). Polyploidization of liver cells. *Advances in Experimental Medicine and Biology*, 676, 123–135.
8. Eltschaninov, A. V. (2011). Morfologicheskaya kharakteristika reparativnoy regeneratsii pecheni krysy ploda [Morphological characteristic of reparative regeneration of rat fetal hepatic] (PhD thesis). Moscow.
9. Eltschaninov, A. V., & Bolshakova, G. B. (2012). Proliferation and cell Death of hepatocytes in regenerating rat fetal liver. *Cytology*, 54(4), 313–317.
10. Frolov, A. V. (2003). Fiziologo-biokhimicheskiye i produktivnyye pokazateli pestsov pri vklyuchenii v ratsion preparatov "Suvar", "Yantorosplyus" i "Kombiolaks" [Physiological, biochemical and productive indicators of Arctic foxes when "Suvar", "Yantorosplus" and "Combiolax" are included in the diet] (PhD thesis). Kazan.
11. Grevtsov, A. A., & Belkina, B. L. (2002). O polze tseolitov [About the benefits of zeolites]. *Practitioner: A Practitioner's Journal*, 3–4, 71–72.
12. Interstate Council for Standardization, Metrology and Certification. Guidelines for accommodation and care of animals. Species-specific provisions for laboratory rodents and rabbits. GOST 33216-2014 dated 2016-07-01. , (2016).
13. Ivanov, G. I., & Grigoryev, T. E. (1998). Rezultaty issledovaniy Chuvashskogo otdela NIVI nechernozemnoy zony RF po primeneniyu trepelov pervomayskogo mestorozhdeniya v zhivotnovodstve i veterinarii [Research results of the Chuvash department of the NIVI of the non-chernozem zone of the Russian Federation on the use of Trepel in the Pervomaysky field in livestock and veterinary medicine]. In *Digest of Articles* (pp. 49–54). Cheboksary.

14. Ivanov, L. N., & Kolotilova, M. L. (2005). Eksperimentalnaya terapiya tseolitsoderzhashchim trepelom toksicheskogo gepatita, gastrita i yazvy zheludka [Experimental therapy of zeolite-containing Trepel with toxic hepatitis, gastritis and gastric ulcer]. *Cheboksary*.
15. Juan, C. de, Benito, M., Alvarez, A., & Fabregat, I. (1992). Differential proliferative response of cultured fetal and regenerating hepatocytes to growth factors and hormones. *Experimental Cell Research*, 202(2), 495–500. [https://doi.org/10.1016/0014-4827\(92\)90104-G](https://doi.org/10.1016/0014-4827(92)90104-G)
16. Kolotilova, M. L., & Ivanov, L. N. (2003). *Tseolitsoderzhashchiy trepel v meditsine [Zeolite-containing Trepel in medicine]*. Cheboksary: Publishing House of Chuvash State University named after I.N. Ulyanov.
17. Koroy, P. V., Yagoda, A. V., Gilyazova, G. I., & Mukhoramova, I. S. (2014). Mediators of intercellular interactions and histological signs of chronic viral liver disease. *Russian Journal of Gastroenterology, Hepatology, Coloproctology*, 24(5), 22–28.
18. Kumar, G. L. K., & Rudbeck, L. (Eds.), Frank, L., & Malkov, P. G. (Trans.). (2011). *Education Guide: Immunohistochemical (IHC) Staining Methods* (transl. from English). Moscow.
19. Lloyd, Z., Gossrau, R., & Shibler, T. (1982). *Histochemistry of enzymes, Laboratory methods* (Russian translation). Moscow.
20. Malato, Y., Naqvi, S., Schürmann, N., Ng, R., Wang, B., Zape, J., ... Willenbring, H. (2011). Fate tracing of mature hepatocytes in mouse liver homeostasis and regeneration. *The Journal of Clinical Investigation*, 121(12), 4850–4860. <https://doi.org/10.1172/JCI59261>
21. Malov, I. V. (2017). Ispolzovanie ceolitsoderzhashhego trepela pri lechenii jeksperimental'nogo kariesa [The use of zeolite-containing tripoli in the treatment of experimental caries]. *Nauka i studia*, 2(8), 18–20.
22. Malov, I. V., Ivanov, L. N., & Kolotilov, a M. L. (2018). The influence of zeolite tripoli on biochemical parameters of the gums. *Diary of the Kazan School*, 4(22), 74–78.
23. Malov, I. V., Ivanov, L. N., Kolotilova, M. L., & Karpunina, A. V. (2018). The investigation the on the effectiveness of using zeolite tripoli in order to preventive treatment of experimental caries. *Diary of the Kazan School*, 3(21), 174–177.
24. Michalopoulos, G. K. (2010). Liver regeneration after partial hepatectomy: Critical analysis of mechanistic dilemmas. *The American Journal of Pathology*, 176(1), 2–13. <https://doi.org/10.2353/ajpath.2010.090675>
25. Petryankin, F. P., & Sherne, V. S. (1999). Vliyaniye preparata "Suvar" na reproduktivnyye funktsii svinomatok [Effect of Suvar on the reproductive functions of sows ]. In *Actual Problems of Animal Husbandry and Veterinary Medicine: Material of the Republican Scientific-Industrial Conference* (pp. 226–227). Kazan.
26. Romanova, L. P. (2005). *Chuvash State University named after I.N. Ulyanov Patent RU 2262135*. Retrieved from [https://yandex.ru/patents/doc/RU2262135C1\\_20051010](https://yandex.ru/patents/doc/RU2262135C1_20051010)
27. Romanova, L. P. (2012). Otsenka vliyaniya biogennogo preparata "Suvar" na proliferatsiyu gepatotsitov pri zazhivlenii mekhanicheskoy travmy pecheni v rannem ontogeneze u krys [Evaluation of the influence of the biogenic agent Suvar on the proliferation of hepatocytes during the healing of mechanical liver injury in early ontogenesis in rats]. In *Materials of the Scientific and Educational Conference Dedicated to the 45th Anniversary of Chuvash State University Named after I.N. Ulyanov* (pp. 228–231). Cheboksary.
28. Romanova, L. P., & Malyshev, I. I. (2012). Zazhivleniye mekhanicheskoy travmy pecheni u krys v rannem ontogeneze pri vozdeystvii biogennogo veshchestva "Trepel" [Healing of mechanical hepatic injury in rats in early ontogenesis under the influence of the Trepel nutrient]. In *Materials of the Scientific and Educational Conference dedicated to the 45th anniversary of Chuvash State University named after I.N. Ulyanov* (pp. 232–235). Cheboksary.
29. Sakuta, G. A., Baidyuk, E. V., Zhumagalieva, A. A., & Kudryavtsev, B. N. (2011). Features of liver regeneration of

- the Chinese hamster *Cricetulus griseus*. *Cytology*, 53(11), 868–873.
30. Sigareva, A. N., Gerashev, A. D., Svyatash, G. A., & Lucanina, S. N. (2001). Vliyaniye tseolitov na regeneratsiyu kostnoy tkani v eksperimente [Effect of zeolites on bone tissue regeneration in an experiment]. In *Actual Issues of Veterinary Medicine: Materials of the Scientific-Practical Conference* (pp. 76–77). Novosibirsk: State Agrarian University.
  31. Solopaeva, I. M., & Solopaev, B. P. (1991). Stimulyatsiya regeneratsii patologicheskikh izmeneniy pecheni i khronicheskiy gonadotropin [Stimulation of the regeneration of pathological hepatic changes and chronic gonadotropin]. Novgorod: Publishing House of the UNN.
  32. Soltys, T. V., & Zuevkiy, V. P. (2000). Dvuyadernnyye gepatotsity kak formy vnutrikletочноy regeneratsii pri eksperimentalnom opistorkhoze [Binuclear hepatocytes as a form of intracellular regeneration in experimental opisthorchiasis]. In *Materials of the All-Russian Scientific and Practical Conference* (pp. 204–205). Surgut.
  33. Sosina, T. E., Molotkov, O. V., & Reshedko, V. V. (1993). Vosstanovitelnyye protsessy v pecheni posle yeye mekhanicheskogo povrezhdeniya v usloviyakh primeneniya splenina [Restorative processes in the hepatic after its mechanical damage in the conditions of splenin application]. In *Conference Proceedings, May 20-22, 1993* (pp. 399–400). Smolensk.
  34. Stupin, I. V., Karmanov, P. A., Novokshonov, A. I., Belous, G. G., Krasnyuk, G. K., & Sergeeva, V. S. (1995). Regeneratsiya pecheni posle yeyo rezektsii luchem ionizirovannoy plazmy [Influence of natural zeolites of the Alaty deposit on milk productivity and milk quality]. *Bulletin of Experimental Biology and Medicine*, 4, 431–432.
  35. Tarasov, A. N. (2001). Vliyaniye prirodnykh tseolitov Alatyrskogo mestorozhdeniya na molochnuyu produktivnost i kachestvo moloka [Influence of natural zeolites of the Alaty deposit on milk productivity and milk quality]. In *Newsletter of Chuvash Center for Scientific and Technical Information* (No. 82.082-01). Cheboksary.
  36. Tournier-Thurneysen, I., Feldmann, G., & Bernuau, D. (1992). Cellular analysis of the kinetics of alpha-fetoprotein and nuclear oncogene activation in primary cultures of adult rat hepatocytes stimulated by epidermal growth factor. *Biology of the Cell*, 75(1), 61–68. [https://doi.org/10.1016/0248-4900\(92\)90125-K](https://doi.org/10.1016/0248-4900(92)90125-K)
  37. Vasiliev, Zh. Kh., Skrebkov, G. P., & Pavlova, E. A. (1988). Primeneniye trepela pri lechenii yazvennoy bolezni [The use of Trepel in the treatment of peptic ulcer]. In *Study using siliceous rocks of Chuvashia* (pp. 73–76). Cheboksary.
  38. Wang, B., Zhao, L., Fish, M., Logan, C. Y., & Nusse, R. (2015). Self-renewing diploid Axin2+ cells fuel homeostatic renewal of the liver. *Nature*, 524(7564), 180–185. <https://doi.org/10.1038/nature14863>
  39. Yanger, K., Knigin, D., Zong, Y., Maggs, L., Gu, G., Akiyama, H., ... Stanger, B. Z. (2014). Adult hepatocytes are generated by self-duplication rather than stem cell differentiation. *Cell Stem Cell*, 15(3), 340–349. <https://doi.org/10.1016/j.stem.2014.06.003>
  40. Zazhivikhina, E. I. (1998). Vliyaniye preparata “Suvar” na obmennyye protsessy i produktivnost sviney i ptits [Influence of the agent “Suvar” on metabolic processes and productivity of pigs and birds] (PhD thesis). Kazan.

**Table 1.** Karyometric data on the ploidy of hepatocyte nuclei in infant rats depending on time after operation

| Time after operation, day | Diploid nuclei, % | Tetraploid nuclei, % | Octaploid nuclei, % | 16-ploid nuclei, % | 32-ploid nuclei, % |
|---------------------------|-------------------|----------------------|---------------------|--------------------|--------------------|
| 3                         | 40.6±3.7          | 56.2±6.2             | 1.0±0.6             | 8.4±2.7            | 1.6±0.5            |
| 5                         | 36.4±4.3          | 60.6±5.3             | 2.7±0.9             | 9.1±3.6            | 3.0±1.4            |
| 7                         | 29.1±4.6          | 62.8±7.2             | 6.1±1.4             | 8.5±2.8            | 2.8±0.8            |
| 9                         | 37.2±3.8          | 59.1±6.3             | 2.4±1.2             | 7.0±3.4            | 2.1±0.8            |
| 11                        | 35.4±4.5          | 61.5±7.4             | 2.1±0.8             | 3.3±1.6            | 0.9±0.3            |

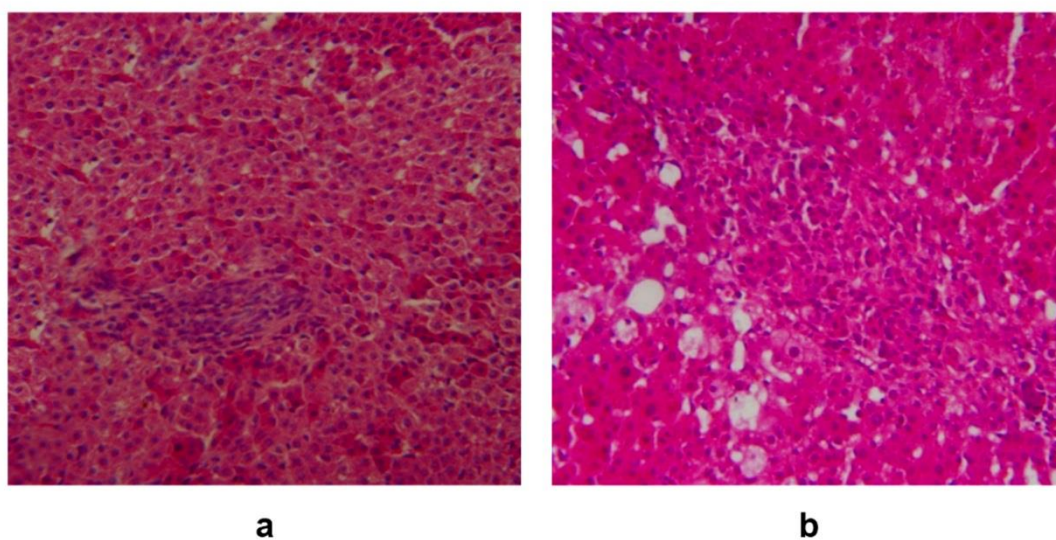


**Figure 1.** Connective tissue portion which appeared in place of injury: a - experiment, b – control. Staining with hematoxylin and eosin x240

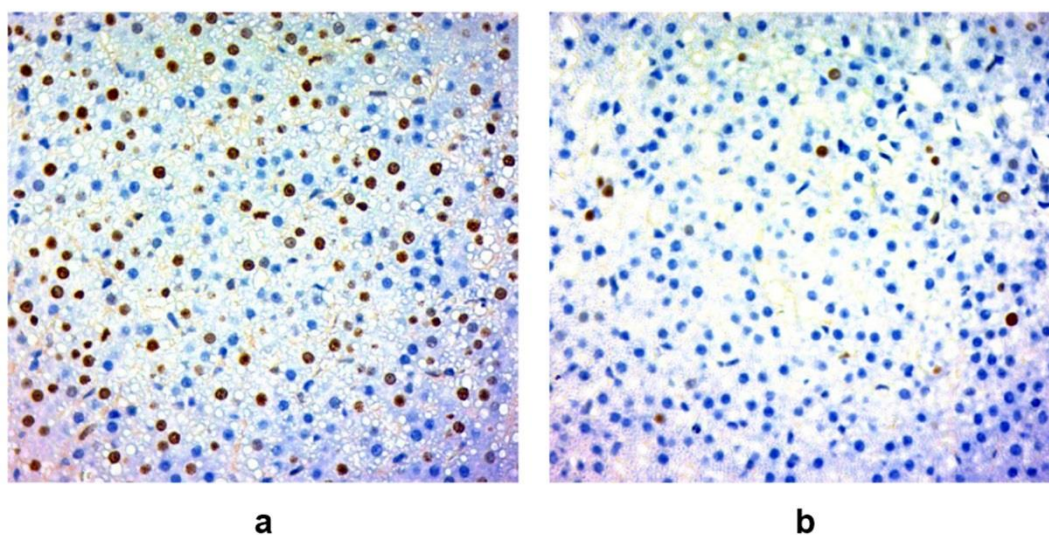


**Figure 2.** Stained with hepatocyte proliferation marker Ki-67 in the experiment (a) and in control (b)



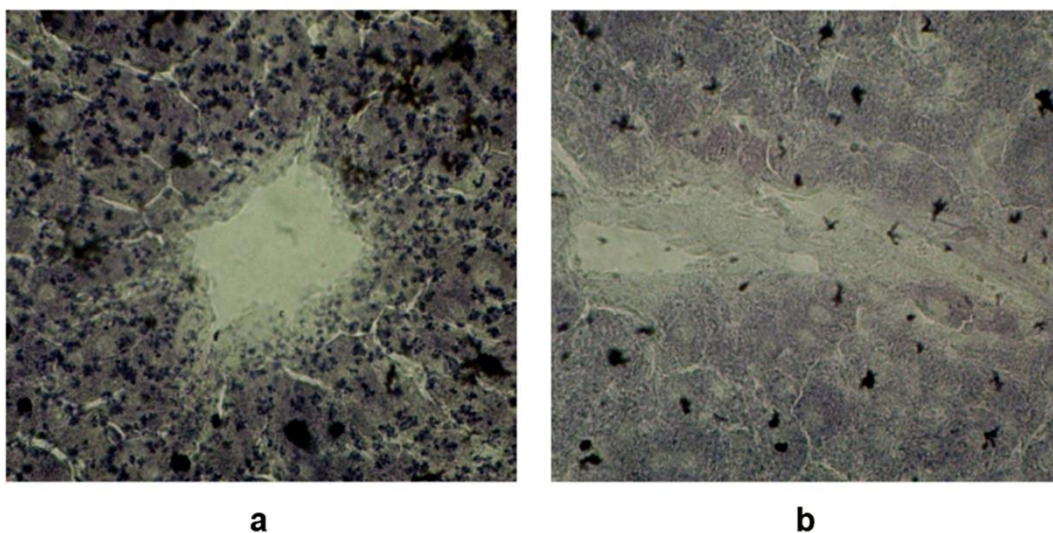


**Figure 3.** *NADH activity in 5 days after operation (a – experiment, b – control), Biolamx 900*

## ESTUDO SOBRE COMPOSIÇÕES DE ÓLEO ESSENCIAL DE SALVIA (*SALVIA NEMOROSA* L.) COLHIDA DO NOROESTE DO IRÃ EM DIFERENTES ESTÁGIOS DE CRESCIMENTO

### STUDY ON ESSENTIAL OIL COMPOSITIONS OF SAGE (*SALVIA NEMOROSA* L.) COLLECTED FROM THE NORTH WEST OF IRAN AT DIFFERENT GROWTH STAGES

#### مطالعه ترکیبات روغن‌های فرار مریم‌گلی (*SALVIA NEMOROSA* L.) جمع‌آوری شده از شمال غرب ایران در مراحل مختلف رشد

GHAFIYEH SANJ, Elham<sup>1</sup>; DILMAGHANI, Kamaladdin<sup>\*2</sup>; CHAPARZADEH, Nader<sup>3</sup>; SAADATMAND, Sara<sup>4</sup>;

<sup>1,4</sup> Department of Biology, Science and Research Branch, Islamic Azad University, Tehran, Iran

<sup>2</sup> Department of Plant Science, Marand Branch, Islamic Azad University, Marand, Iran

<sup>3</sup> Department of Biology, Azarbaijan Shahid Madani University, Tabriz, Iran

\* Corresponding author  
e-mail: dilmaghani.kamal@gmail.com

Received 19 May 2020; received in revised form 17 June 2020; accepted 28 June 2020

### RESUMO

*Salvia nemorosa* L. ou sálvia é uma fonte rica de metabólitos antimicrobianos e antioxidantes. Considerando a importância dessa planta medicinal e da diversidade fitoquímica entre suas populações para o consumo local e os adubos de reprodução, este estudo foi realizado para determinar e comparar a composição de óleo essencial (OE) das plantas sálvia coletadas em quatro regiões do noroeste do Irã, incluindo Ahar, Zonouz, Urmia e Ardabil em dois estágios de crescimento (vegetativo e florido) para finalmente demonstrar os efeitos do crescimento e localização nas características da OE. Os resultados mostraram que o teor de OE das flores nas regiões estudadas foi o mais alto em comparação com as fases vegetativa e florística. A porcentagem e o número de composições voláteis no OE de flores foram as que apresentaram a maior quantidade. Em Zonouz, 87,13% e 12 composições enquanto em Ahar, 80,20% e 19 composições. A menor porcentagem e o número de composições voláteis no OE da flor foi visto em Urmia, 78,56% e 13 composições enquanto em Ardabil, esses números foram 68,61% e 10 composições, respectivamente. O óxido de cariofileno teve o maior teor em todos os óleos essenciais extraídos, sendo o mais alto no estágio de floração das regiões de Zonouz, Ardabil e Urmia, respectivamente. Em Ahar, diferentemente de outras regiões, a maior porcentagem desse composto estava nas folhas da fase vegetativa. Os sesquiterpenos oxigenados aumentaram o teor de OE nas flores das regiões Urmia (46,31%), Zonouz 42,59% e Ardabil (45,60%). Em contraste com outras regiões, para a região de Ahar, a maior quantidade (36,18%) de sesquiterpenos oxigenados foi observada no OE das folhas do estágio de floração. Pode-se concluir que diferentes estágios de crescimento das plantas, época de colheita das plantas, condições ambientais, habitat principal e diferenças nas condições climáticas podem contribuir na concentração, tipo e porcentagem de compostos voláteis no OE da sálvia.

**Palavras-chave:** *Salvia nemorosa*, Metabólitos secundários, Óleos essenciais, Óxido de cariofileno, Sesquiterpenos

### ABSTRACT

*Salvia nemorosa* L. or wood sage is a rich source of antimicrobial and antioxidant metabolites. Considering the importance of this medicinal plant and phytochemical diversity among its populations for local consumption and breeding purposes this study was performed to determine and compare essential oil (EO) compositions of sage plants collected from four regions in the northwest of Iran including Ahar, Zonouz, Urmia, and Ardabil at two growth stages (vegetative and flowering) to finally demonstrate the effects of growth and location on EO features. The results showed the EO content of flowers in the studied regions were the highest in comparison with vegetative and flowering stages leaves. The percentage and the number of volatile compositions in the OE of flowers were those that presented the highest quantity. In Zonouz, 87.13% and 12 compositions while in Ahar, 80.20% and 19 compositions. The lowest percentage and the number of volatile compositions in the OE of flowers was seen in Urmia, 78.56% and 13 compositions while in Ardabil, these numbers were 68.61% and 10 compositions, respectively. Caryophyllene oxide had the highest content in all the extracted essential oils, being the highest in the flowering stage of the regions of Zonouz, Ardabil and Urmia, respectively. In Ahar, differently from other regions, the highest percentage of this compound was in the leaves of the vegetative stage. Oxygenated sesquiterpenes increased the EO content in the flowers of the regions of Urmia (46.31%), Zonouz 42.59% and Ardabil (45.60%). In contrast with other regions, for the region of Ahar, the highest quantity (36.18%) of oxygenated sesquiterpenes was observed in the OE of the leaves of the flowering stage. It can be concluded that different growth stages of plants, harvest time of plants, environmental conditions, main habitat and differences in climatic conditions can contribute to the concentration, type and percentage of volatile compounds in the EO of *Salvia*.

80.20%, and 19 compositions. The lowest percentage and the number of volatile compositions in the OE of the flowers were seen in Urmia, 78.56%, and 13 compositions, while in Ardabil, these numbers were 68.61% and 10 compositions, respectively. Caryophyllene oxide had the highest content in all essential oils extracted, being the highest in the flowering stage leaves of the regions of Zonouz, Ardabil, and Urmia, respectively. In Ahar, unlike other areas, the most significant percentage of this compound was in the leaves of the vegetative stage. The oxygenated sesquiterpenes increased in the EO content of the flowers of the Urmia (46.31%), Ardabil (45.60%) and Zonouz (42.59%) regions. In contrast to other areas, for the Ahar region, the highest amount (36.18%) of oxygenated sesquiterpenes was observed in the EO of the leaves of the flowering stage. It can be concluded that different plant growth stages, plant harvest time, environmental conditions, primary habitat, and differences in climatic conditions can contribute to the concentration, type, and percentage of volatile compounds in the *salvia* EO.

**Keywords:** *Salvia nemorosa*, Secondary metabolites, Essential oils, Caryophyllene oxide, Sesquiterpenes

## چکیده

*Salvia nemorosa* L. یا مریم‌گلی چوبی دارای فعالیت‌های ضد میکروبی، آنتی‌اکسیدانی و منبعی غنی از متابولیت‌های فعال می‌باشند. با در نظر داشتن اهمیت این گیاه دارویی برای مصرف‌کنندگان محلی و اهداف اصلاحی این بررسی در راستای تعیین و مقایسه ترکیبات اسانس در گیاهان مریم‌گلی جمع‌آوری شده در چهار منطقه مختلف شامل زنوز، ارومیه، اردبیل و اهر و در دو مرحله رشد، رویشی و گل‌دهی صورت گرفت تا نهایتاً اثر مرحله رشد و مناطق رشد روی اجزای روغن‌های فرار تعیین گردد. نتایج نشان داد که درصد اسانس سرشاخه‌های گلدار در هر چهار منطقه مورد مطالعه در مقایسه با برگ‌های مراحل رویشی و گل‌دهی از بالاترین میزان برخوردار بودند. بیشترین درصد و تعداد ترکیبات فرار روغن‌های فرار در اندام زایشی مشاهده گردید. با 87.13% و 12 ترکیب در منطقه زنوز، 80/20% و 19 ترکیب در منطقه اهر بالاترین میزان ترکیبات برخوردار بودند. کمترین میزان درصد اسانس با 78.56% و 13 ترکیب در منطقه ارومیه و با 68.61% و 10 ترکیب در منطقه اردبیل مشاهده شد. کاربوفیلین اکساید بالاترین میزان ترکیبات فرار شناسایی شده به ترتیب در اسانس گل‌ها، برگ‌های مراحل رویشی و گل‌دهی در هر چهار منطقه بود. بالاترین درصد کربوفیلین اکساید در برگ مرحله گل‌دهی هر سه منطقه زنوز، اردبیل و ارومیه دیده شد. از سوی دیگر بالاترین درصد این ترکیب در منطقه اهر برخلاف سایر مناطق در برگ مرحله رویشی بود. سسکوئیت‌ترین‌های اکسیژن‌دار در اسانس گل‌های مناطق ارومیه (46.31%)، اردبیل (45.60%) و زنوز (42.59%) افزایش داشتند. در منطقه اهر بر خلاف سایر مناطق، بالاترین میزان سسکوئیت‌ترین‌های اکسیژن‌دار در اسانس برگ مرحله گل‌دهی (36.18%) مشاهده شد. می‌توان این‌گونه نتیجه گرفته که مراحل مختلف رشد گیاه، زمان برداشت گیاه، تاثیر شرایط محیطی، زیستگاه اصلی و اختلاف در شرایط اقلیمی می‌توانند بر نوع و درصد ترکیبات فرار اسانس گیاهان مریم‌گلی تاثیر داشته باشند.

کلمات کلیدی: *Salvia nemorosa*، متابولیت‌های ثانویه، روغن‌های فرار، کاربوفیلین اکسید، سسکوئیت‌ترین‌ها

## 1. INTRODUCTION:

*Salvia* L. is the largest genus of Lamiaceae (tribe Mentheae) with nearly 1000 species (Walker and Sytsma, 2007, Sarac and Ugur, 2007). The genus *Salvia* is derived from the Latin word "Salvare" meaning "to heal" or "to be safe and unharmed," referring to the medicinal properties of the genus (Walker *et al.*, 2004, Giuliani and Maleci Bini, 2008). The members of the genus display a remarkable diversity in growth form, floral morphology, pollination biology, and secondary compounds; they are distributed all around the world (Walker *et al.*, 2004). The genus *Salvia* is represented in Iran by 58 species, 17 of which are endemic (Mozaffarian, 1996, Ipek, 2012).

Many species of *Salvia* are used in traditional medicine throughout the world. In Iranian folk medicine, several *Salvia* species have been used as antiseptic for wounds, as a diuretic, stomach tonic, antifatulent, and constituent, and for the treatment of eye disorders, diarrhea, dyspepsia, fever, rheumatism, excessive

menstruation, common cold, coughing, pertussis, and sinusitis (Naghibi, 2005, Ozkan, 2008, Raal *et al.*, 2007). *Salvia nemorosa* L., commonly known as wood sage, is growing in central Europe and Western Asia (Skala and Wysokinska, 2004).

Leaves of *S. nemorosa* are traditionally used in Turkish folkloric medicine for stop bleeding when applied externally (Takeda *et al.*, 1997; Topcu, 2006). Also, in the Bulgarian traditional medicine, *S. nemorosa* is used mainly for the treatment of stomach ache, diarrhea, hemorrhages, and furuncles (Daskalova, 2004, Farimani *et al.*, 2013). In Russia, *S. nemorosa* is utilized for much the same ailments as *S. officinalis*. Studies have shown that *S. nemorosa* is a rich source of bioactive metabolites (flavonoids and oxygenated sesquiterpenes). Also, *S. nemorosa* exhibited considerable antibacterial, antioxidant, and enzyme inhibitory activities. In conclusion, *S. nemorosa* is a valuable source of natural products and could be used for preparing novel functional foods, cosmetics, and pharmaceutical ingredients (Bahadori, 2017,



Bahadori and Mirzaei, 2015, Wu *et al.*, 2012). In studies conducted by Coisin *et al* (2010) in the volatile oil extracted from *Salvia nemorosa* L. in plant development stage, 22 compounds have been identified. The main chemical compounds belong to monoterpenes group with having antiseptic (bactericide), carminative, antispastic and diuretic properties such as: sabinene (33.93%),  $\beta$ -cariophyllene (19.86%),  $\beta$ -cubebene (11.87%),  $\alpha$ -cariophyllene (6.37%) and other compounds included cariophyllene oxid,  $\gamma$ -terpinene, Limonene,  $\alpha$ -tujone,  $\beta$ -mircene,  $\beta$ -pinene,  $\gamma$ -terpinene, cimol, elixene, terpinolene,  $\beta$ -burbonene, alloaromadendrene oxid (1)  $\gamma$ -cadinene, alloaromadendrene oxid (2)  $\alpha$ -pinene  $\gamma$ -cadinene, pulegone,  $\alpha$ -terpinil-acetate (Coisin *et al*, 2010).

Also, a study on *S. nemorosa* showed that the chemical compositions in leaves and flowers essential oils were sesquiterpenes hydrocarbons, oxygenated sesquiterpenes, and monoterpene hydrocarbons in the highest amount and oxygenated monoterpenes, aliphatic compounds, monoterpene hydrocarbons, sabinene, and limonene were in the lowest amount. In addition, phenolic compounds of *salvia nemorosa* are gallic acid, protocatechuic acid catechin, *p*-hydroxybenzoic acid, caffeic acid, epicatechin, vanillin, *p*-coumaric acid, ferulic acid, sinapic acid, benzoic acid, *O*-coumaric acid, rutin, naringin, hesperidin, rosmarinic acid, trans-cinnamic acid, quercetin, luteolin, kaempferol, apigenin (Bahadori *et al*, 2017).

The aim of this study was to evaluate the composition and comparison of *Salvia nemorosa* essential oils of plants collected plants in four different regions (northwest of Iran) and at two growth stages. This study will allow the realization of two key scientific points in which one is determining the best time of harvest with aromatic properties (quality) or optimal therapeutic properties and the most useful plant origin on its phytochemical compositions. This may help increase the economic efficiency of the production of essential oils and the acquisition of new scientific data on the change in secondary volatile metabolites of sage plants during its phenological cycle that can be utilized by local consumers as well as medicinal plant breeders.

## 2. MATERIALS AND METHODS:

Sage plants (*salvia nemorosa* L.) were collected at two vegetative and flowering stages from four regions in the northwest of Iran including Ahar (75 km from Tabriz to Ahar) (longitude: 38.26

° E' , latitude: 47.04° N and altitude:1391m ) and Zonouz gardens (longitude: 38.26° E' , latitude: 45.46° N and altitude:1550 m) in East Azarbaijan, Urmia, Qasemlu village (longitude: 37.65 ° E', latitude: 47.05° N and altitude:1328m) in western Azarbaijan and Ardabil, Abbasabad village (85 km from khalkhal to Ardabil) (longitude: 38.13° E' , latitude: 48.19° N and altitude:1335 m) in Ardabil province (Figures 1, 2 and Table 3). Plant collection times at the vegetative stage were May 12th to May 26th, 2017, and collection times at the flowering stage were May 19th to June 5th, 2017. After collecting the plants, they were dried at room temperate.

### 2.1. Extraction and analysis of essential oils by GC-MS

After collecting plants at two growth stages (vegetative and flowering) from different regions and after drying them in the shade, essential oils extracted by water distillation using the Clevenger apparatus and then analysis by GC-MS. Therefore, flowers and leaves of plants (vegetative and flowering stages) underwent distillation using Clevenger apparatus for 4 hours. Then, essential oils were kept in the refrigerator at the 4°C and when analyzing they were separated from water and dried over anhydrous sodium sulfate and for identification of essential oils composition was injected to GC-MS (The working conditions were adjusted based on helium as the carrier gas at the rate of 2 mL.min, ionization potential of 70 eV, and mass range of 40-300 u, and column temperature programming was done with the column temperature variation of 60-280 °C at the rate of 3°.min and the injection chamber temperature of 280°C. In each case, after the injection of very small quantities of essential oil (0.1  $\mu$ L), chromatograms were obtained and the mass spectra of various compounds were examined. Then, the spectra were identified and studied. The individual compounds were identified by MS and their identity was confirmed by comparing their retention indices relatives to C8 –C32 n-alkanes and by comparing their mass spectra and retention times with those of authentic samples or with data already available in the NIST library and literature Adams (Adams, 2017).

Identification of GC/MS chromatogram spectra was performed using mass database (Adams, 2017), inhibition index, study of mass spectra of each essential oil component and comparison with standard spectra and the Quatts formula was used to calculate the inhibition index.

### 3. RESULTS AND DISCUSSION:

The results of the composition of sage (*Salvia nemorosa* L.) essential oils in two phenological stages of vegetative and flowering stages showed that in each regions (Ahar, Zonouz, Ardabil and Urmia) separately, essential oils of sage flowers had the highest percentage of components in comprising with essential oils of sage vegetative stage leaves and flowering stage leaves, in which according to Figure 3, the essential oil of *S. nemorosa* flowers had the highest percentage in comparison with the essential oils of vegetative stage leaves and flowering stage leaves in Zonouz, Ahar, Urmia and Ardabil regions so that, the essential oil of sage flowers in Zonouz region had the highest percentage and in Ardabil region showed the lowest percentage. In addition, by comparing the number, type and percentage of identified volatile compound in the essential oil of *S. nemorosa* flowers in every four regions was seen that, the essential oils of flowers of Zounoz region with 12 compounds had the highest of the percentage of essential oils (87.13%) comprising of the essential oils of flowers in other regions while, in the essential oils of flowers of Ardabil region, there were 10 compounds with 68.61% of total oils. In the essential oils of flowers of Ahar region 20 compounds with 80.20% of total oils and in the essential oils of flowers of Urmia region 14 compounds were identified with 78.56% of total oils (Tables 1 and 2; Figure 5 a, b, c, d).

The essential oil of vegetative stage leaves in Urmia and Ahar regions had the lowest percentage and the essential oil of vegetative stage leaves in Ardabil and Zonouz regions increased in comparison with flowering stage leaves (Tables 1 and 2; Figures 3 and 7 a, b, c, d).

Among identified volatile compounds in the essential oils of flowers in Ahar, Zouoz, Urmia and Ardabil regions, respectively, caryophyllene oxide, spathulenol and trans caryophyllene were the main compounds of essential oils. In addition to, compounds such as para cymene, sabinene, terpinen-4-ol, were another main compounds in the essential oils of flowers in Ahar region, para cymene, 1-octen-3-ol were another main compounds in the essential oils of flowers in Urmia region, terpinen-4-ol, camphor and para cymene were another main compounds in the essential oils of flowers in Zounoz region and 1-octen-3-ol was another main compound in the essential oils of flowers in Ardabil region (Table 1 and 2).

In the study of Kashef *et al* (2019) on growth compatibility and medicinal potential of four

*Salvia* species in Semnan climatic conditions, was observed that, in *S. nemorosa* species in seedling stage, caryophyllen (43.91%), caryophyllen oxide (19.65%) and farnesene (12.13%), in meddle of growth seasen, trans-caryophyllen (11.93%), caryophyllen oxide (37.89%) and trans-  $\beta$  farnesene (11.49%) and in the end of growth seasen, trans- caryophyllen (28.94%), caryophyllen (30.13%) and  $\alpha$ - cadinol (5.69%) were the main of composition. In *S. sclarea* and *S. officinalis* plants in seedling stage caryophyllen, caryophyllen oxide, germacrene D, in middle of growth seasen caryophyllen, caryophyllen oxide, trans- $\beta$  farnesene and  $\beta$ - bourdonen, in the end of growth seasen caryophyllen oxide,  $\beta$  farnesene and germacrene D with different percentage were the main of composition (Kashef *et al*, 2019).

In the essential oils of flowering stage leaves in Ahar region 14 volatile compounds with 69.18% of total essential oils, and in Zounoz region only one volatile compound was identified with 8.48% of total essential oils. Also, In the essential oils of flowering stage leaves in the two regions of Urmia and Ardabil, 7 and 4 of volatile compounds, respectively, were identified with almost 58.89% of total oils (Tables 1 and 2; Figure 6 a, b, c, d).

Among the identified volatile compounds in the essential oils of flowering stage leaves in each four studied regions, caryophyllene oxide then Beta- ionone had the highest percentage so that, the highest amount of caryophyllene oxide was seen with 39.40% in the essential oils of flowering stage leaves in Ardabil region and the lowest amount of caryophyllene oxide was seen with 8.48% in the essential oils of flowering stage leaves in Zounoz region. In addition to, 1-octen-3-ol and camphor in the essential oils of *S. nemorosa* L. in Ardabil and Urmia regions and camphor, trans caryophyllene ,1-Octen-3-ol in the essential oil of sages plants in Ahar region were main compound (Table 1 and 2).

Extraction and identification of essential oils volatile compounds showed existence of 10 volatile compounds with 55.54% and 63.89% of total essential oils in vegetative stage leaves of sage collected from Ahar and Ardabil regions. While, essential oil of vegetative stage leaves in Urmia region showed only two volatile compounds with 24.62% of total essential oils. In addition to, essential oils of vegetative stage leaves in Zonouz region showed three volatile compounds with 41.29% of total essential oils. Among identified volatile compounds caryophyllen oxide showed the highest percentage in essential oils of vegetative stage leaves each four regions (Ahar,

Zonouz, Urmia and Ardabil). So that, the highest percentage of caryophyllen oxide was in essential oil of vegetative stage leaves in Ardabil region (31.35%) and the lowest percentage caryophyllen oxide was in essential oils of vegetative stage leaves in Urmia (18.19%). In addition, trans-beta caryophyllen was part of main compound in essential oils of vegetative stage leaves in Ahar, Ardabil and Zonouz regions (Table 1 and 2).

It was reported that existence of compounds such as caryophyllen oxide, beta-caryophyllen, germacrene D and germacrene B were the main compounds of essential oils in *S. nemorosa* and *S. virgata* harvested from Iran (Sefidkon and Mirza, 1999).

By comparing of chemical groups in essential oils of flowers, vegetative stage leaves and flowering stage leaves in all regions (Ahar, Zonouz, Urmia and Ardabil) was observed that oxygenated sesquiterpenes in essential oils were the highest percentage of chemical groups (Figure 4). So that, the highest percentage of oxygenated sesquiterpenes were with 46.31% in essential oils of flowers of sage plants in Urmia region and the lowest percentage of oxygenated sesquiterpenes were seen with 25.60% in essential oils of sage plants in Ahar region (Table 1 and 2, Figure 4).

In essential oils of flowering stage leaves, the highest amount oxygenated sesquiterpenes were with 44.05% in essential oils of sage plants in Ardabil region and the lowest amount this chemical groups were observed with 8.48% in Zonouz region. Also, oxygenated sesquiterpenes showed the highest amount with 37.21% and 34.3%, respectively, in essential oils of vegetative stage leaves in Ardabil and Ahar regions and showed lowest amount with 18.19% in essential oils of vegetative stage leaves in sage plants in Urmia region (Table 1 and 2, Figure 4).

In a study on the composition of essential oils of some wild salvia species growing in Serbia was observed that in the essential oil of *S. nemorosa* flowers, caryophyllen oxide, beta-caryophyllen, sabinene and germacrene D and in the essential oil of *S. glutinosa* flowers, caryophyllen oxide, spathulenol, humulene epoxide were major compositions. In addition, in the essential oils of *S. nemorosa* and *S. glutinosa* plants, sesquiterpenes were the main chemical groups (Chalchat, 2004).

In Yayli *et al* (2010) study on constituents of the essential oil from the flower, leaf and stem of *Salvia viridis* L. grown in Turkey, sesquiterpenes hydrocarbons were the main constituents in organs and the major components in the essential

oils of leaf were  $\beta$ -pinene,  $\beta$ -copaene, trans-muurola-4(14),5-dien which, showed significant difference in the type and percentage of identified compound of *S. nemorosa* essential oil in this study (Yayli *et al.*, 2010).

Comparing the identified compounds in this study with other reports shows the similarities and differences in terms of the type and amount of identified composition. These differences may be due to a variety of reasons, including the time of harvested and the ecological conditions of the sage plants, which can affect the amount and type of compound and it could be due to the collection of *S. nemorosa* plants from different natural environments, which can be said that the results obtained are due to the interaction of genetic factors and the environment (Maskimovic *et al.*, 2007; Figueiredo *et al.*, 2008).

The quantity of active ingredients in medicinal plants is mainly affected by natural variables in the environment. Although the amount of secondary metabolites is under the control of genes, their quantity and accumulation are significantly affected by environmental conditions. Climatic variations and different ecological conditions have caused diversity and richness in medicinal plants throughout Iran (Ebrahimpour *et al.*, 2009, Figueiredo *et al.*, 2008, Russo *et al.*, 2013).

The major habitat conditions in different areas include height, slope direction and percentage, latitude and longitude, temperature, humidity and annual rainfall, soil characteristics, and associated species (Bakhshi *et al.*, 2010, Cheynier *et al.*, 2013, Maksimovic *et al.*, 2007). Considering the growth location of the plant in the environment is one of the main factors of great impact on essential oil and active ingredients. Some reports have expressed associations between the habitat conditions and chemical compounds of plants, manifesting a high correlation between the geographical origin of plants and their active ingredients characteristics between them (Omidbeigi, 2009, Li *et al.*, 2015, Ben farhad, 2009). Furthermore, edaphic and climatic variations and genetic characteristics may have a strong influence on the morphological, agronomic and essential oil chemical characteristics (Mossi *et al.*, 2011, Papageorgiou *et al.*, 2008).

As a result, in this study, different stage of growth of *S. nemorosa* plants, harvest times, different in climatic condition, major habitat and direct relation between ecological and genetic factors have led to differences in the type and

percentage of identified composition in the essential oils of sage plants in Ahar, Ardabil, Zonouz and Urmia regions.

#### 4. CONCLUSIONS:

On the basis of all the analyses, it could be concluded that oxygenated sesquiterpenes were the highest percentage of compounds identified in the essential oils of flowers, vegetative stage leaves, flowering stage leaves in four regions. Also, Sesquiterpene hydrocarbons, oxygenated monoterpenes, and monoterpene hydrocarbons there were in a lower percentage. The main oxygenated sesquiterpene was caryophyllene oxide in essential oils. The most number and the highest rate of the volatile compound identified was seen in essential oils of *S. nemorosa* flowers collected from Zonouz region. It confirms the influence of environmental conditions (harvested time, original habitat and differences in climatic conditions) on the nature of plant chemical composition that has the vital role in plant adaptation and speciation.

#### 5. REFERENCES:

- Adams, R. P. (2017). Identification of Essential oil, components by Gas chromatography/Quadropole Mass spectroscopy. Allured publ. carolstream, LI. 5 online ed.
- Bahadori, M. B.; Asghari, B.; Dinparast, L.; Zengin, G.; Sarikurkcu, C.; Mohammadi, M. A.; Bahador, S. H. (2017). *Salvia nemorosa* L. A novel source of bioactive agents with functional connections. *Food Science and Technology*, 75, 42-50.
- Bahadori, M.B.; Mirzaei, M.; (2015). Cytotoxicity, antioxidant activity, total flavonoid and phenolic contents of *Salvia urmiensis* Bunge and *Salvia hydrangea*. *Research Journal of Pharmacognosy*, 2, pp. 27-32.
- Bakhshi-Khaniki, Gh. R.; Sefidkon, F.; Dehghan, Z. (2010). Effects of site conditions on quantity and quality of oil essential of *Ziziphora clinopodioides* Lam. *Journal of Herbal Drugs*, 1, 11-20.
- Ben farhad, M.; Jordan, M.J.; Chaouech-Hamada, R.; Landoulsi, A.; Sotomayor, J.A. (2009). Variations in essential oils, phenolic compounds and antioxidant activity of Tunisian cultivated *Salvia officinalis* L. *Journal of agricultural and food chemistry*, 57(21), 10349-10356.
- Chalchat, J. C. (2004). Composition of essential oils of some wild salvia species growing in Serbia. *Agriculture Journals*, 16, 476-478.
- Cheyrier, V.; Comte, G.; Davies, K.M.; Iattanzio, V.; Martens, S. (2013). Plant phenolics: recent advances on their biosynthesis, genetics and ecophysiology. *Plant Physiology and Biochemistry*, 72, 1-20.
- Coisin, M.; Padurariu, C.; Raluca Andro, A.; Boz, I.; Magdalena, Z. M.; Burzo, I. (2010). Biochemical and physiological reserarches in *Salvia nemorosa* L. *Analele Stiintifice ale Universitatii*, 56, 31.
- Daskalova, T. (2004). On some specificities of seed formation in *salvia nemorosa* (lamiaceae). *Phytologia Balcanica*, 10, 79-84.
- Ebrahimpour, F.; Eidizadeh, V. (2009). Medicinal plants. Payam Noor University; Tehran. pp. 5- 29.
- Farimani, M. M.; Taheri, S.; Ebrahimi, S. N.; Bahadori, M. B.; khavasi, H. R.; Zimmermann, S. (2012). Hydrangenone, a new isoprenoid with an unprecedented skeleton from salvia hydrangea. *Organic Letters*, 14(1), 166-169.
- Figueiredo, A. C.; Barroso, J. G.; Pedro, L. G.; Scheffer, J.J.C.: (2008). Factors affecting secondary metabolite production in plants: volatile components and essential oils. *Flavour Fragrance Journal*, 23:213–26.
- Giuliani, C.; Maleci Bini, L. (2008). Insight into the structure and chemistry of glandular trichomes of Labiatae, with emphasis on subfamily Lamiioideae. *Plant systematic and Evolution*, 276:199-208.
- Ipek, A.; Gürbüz, B.; Bingöl, M.Ü.; Geven, F.; Akgül, G.; Afshar Pour Rezaeieh, K.; Cosges, B. (2012) Comparison of essential oil components of wild and field grown *Salvia cryptantha* Montbert & Aucher ex Benth, in Turkey. *Turkish Journal of Agriculture and Forestry*, 36668-672.
- Kashefi, B.; Hassani Shariyatpanahi, S. F. H. (2019). Growth Compatibility and Medicinal Potential of Four *Salvia* species in semnan climatic conditions. *Journal of Chemical Health Risks*, 9, 283-292.
- Li, B.; Zhang, C.; Peng, L.; Liang, Z.; Yan, X.; Liu, Y. (2015). Comparision of essential oli composition and phenolic acid content of selected salvia species measured by GC-MS and HPLC method. *Industrial Crops and Products*, 69, 329-334.

17. Maskimovic, M.; Vidic, D.; Milos, M.; Solic, M.E.; Abadzic, S.; Siljak-Yakovlev, S. (2007). effect of the environmental conditions on essential oil profile in two Dinaric salvia species: *S. brachyodon* Vandas and *S. officinalis* L. *Biochemical systematics and Ecology*, 35, 473-47.
18. Mossi, A. J.; Cansian, R. L.; Paroul, N.; Toniazzi, G.; Oliveira, J. V.; Pierozan, M. K.; Pauletti, G.; Rota, L.; Santos, A. C.; Serafini, L. A. (2011). Morphological characterisation and agronomical parameters of different species of *Salvia* sp. (Lamiaceae). *Brazil Journal of Biology*, 71: 21-9.
19. Mozaffarian, V. (1996). A Dictionary of Iranian Plant Names. Farhang Moaser, Tehran, Iran. pp. 542.
20. Naghibi, F.; Mosaddegh, M.; Mohammadi, M.; Ghorbani, A. (2005). *Iranian Journal of Pharmaceutical Research*, 2:63.
21. Omidbeigi, R. (2009). Production and Processing of Medicinal Plants. Tarrahane Nashr, Tehran. pp. 215-220.
22. Ozkan, M. (2008). Glandular and eglandular hairs of salvia recognita Fisch. And Mey. (Lamiaceae) in Turkey. *Bangladesh Journal of Botany*, 37:93-95.
23. Papageorgiou, V.; Gardeli, C.; Mallouchos, A.; papaionannou, M.; Komaitis, M. (2008). variation of the chemical profile and antioxidant behavior of *Rosmarinus officinalis* L. and *Salvia fruticose* Miller grown in Greece. *Journal of Agricultural Food chemistry*, 56, 7254-7264
24. Raal, A.; Orav, A.; Arak, E. (2007). Composition of the essential oil of *Salvia officinalis* L. from various European countries. *Natural Product Research*, 21(5):406-411.
25. Russo, A.; formisano, C.; Rigano, D.; senator, F.; Delfine, S.; Cardine, V.; Rosseli, S.; Buno, M. (2013). Chemical composition and anticancer activity of essential oils of mediterranean sage (*Salvia officinalis*) grown in different environmental conditions. *Food and Chemical Toxicology*, 55:42-47
26. Sarac, N.; Ugur, A. (2007). Antimicrobial activities and usage in folkloric medicine of some Lamiaceae species growing in Mugla, Turkey. *EurAsian Journal of BioScience.*, 1:28-3.
27. Sefidkon, F.; Mirza, M. (1999). Chemical composition of the essential oils of two *Salvia* species from Iran, *Salvia virgata* Jacq. And *Salvia syriaca* L. *Flavour and Fragrance Journal*, 14, 45-46.
28. Skala, E.; Wysokinska, H. (2004). In vitro regeneration of *Salvia nemorosa* L. from shoot tips and leaf explants. *In vitro cellular & developmental biology-Plant*, 40, 596-602.
29. Takeda, Y.; Zhang, H. J.; Matsumoto, T.; Otsuka, H.; Oosio, Y.; Honda, G.; Yesilada, E. (1997). Megastigmane glycosides from *salvia nemorosa*. phytochemistry. *Phytochemistry*, 44, 117-120.
- Topcu, G. (2006). Bioactive triterpenoids from *Salvia* species. *Journal of Natural Products*, 69(3), 482e -487.
30. Walker, J. B.; Sysma, K. J. (2007). Staminal evolution in the genus *Salvia* (Lamiaceae): molecular phylogenetic evidence for multiple origins of the staminal lever. *Annals of Botany*, 100, 375-391.
31. Walker, J. B.; Sysma, K. J.; Treutlein, J.; Wink, M. (2004). *Salvia* (Lamiaceae) is not monophyletic: implications for the systematics, radiation, and ecological specializations of *Salvia* and tribe Mentheae. *American Journal of Botany*, 91, 1115-1125.
32. Wu, Y.B.; Ni, Z.Y.; Shi, Q. W.; Dong, M.; Kiyota, H.; GU, Y.C. (2012). constituents from salvia species and their biological activities. *Chemical reviews*, 112 (11), 5967-6026.
33. Yayli, N.; Cansu, T. B.; Yilmaz, N.; Yasar, A.; Cetin, M.; Yayli, N. (2010). Constituents of the Essential Oil from the Flower, Leaf and Stem of *Salvia viridis* L. Grown in Turkey. *Asian Journal of Chemistry*, 22, 3439-344.

**Table 1.** Comparison of flowers, vegetative stage leaves, flowering stage leaves essential oils of *S.memorosa* collected from Ahar and Ardabil regions

| Components                             | Ahar    |       |                      |       |                       |       | Ardabil |       |                      |       |                       |       |
|--|---------|-------|----------------------|-------|-----------------------|-------|---------|-------|----------------------|-------|-----------------------|-------|
|  | Flowers |       | Flowering stage leaf |       | Vegetative stage leaf |       | Flowers |       | Flowering stage leaf |       | Vegetative stage leaf |       |
|  | KI      | %     | KI                   | %     | KI                    | %     | KI      | %     | KI                   | %     | KI                    | %     |
| Heptane                                | -       | -     | -                    | -     | -                     | -     | 701     | 1.57  | 700                  | 2.58  | -                     | -     |
| $\alpha$ -Thujene                      | 930.1   | 5.02  | -                    | -     | -                     | -     | 929.3   | 1.30  | -                    | -     | -                     | -     |
| $\alpha$ -Pinene                       | 939.9   | 0.52  | -                    | -     | -                     | -     | -       | -     | -                    | -     | -                     | -     |
| 1-Octen-3-ol                           | 967.6   | 4.43  | 968.4                | 5.94  | 965.6                 | 1.13  | 965.2   | 8.57  | 964.3                | 9.10  | 967.2                 | 11.89 |
| Sabinene                               | 975.3   | 5.66  | -                    | -     | -                     | -     | 973.7   | 1.34  | -                    | -     | -                     | -     |
| $\beta$ -pinene                        | 982.7   | 1.04  | -                    | -     | -                     | -     | -       | -     | -                    | -     | -                     | -     |
| Benzene                                | -       | -     | 1020.1               | 1.40  | -                     | -     | 1019.2  | 2.44  | -                    | -     | -                     | -     |
| 1-metri-2                              | -       | -     | -                    | -     | -                     | -     | -       | -     | -                    | -     | -                     | -     |
| 1-methylethyl)                         | 1020.9  | 8.12  | -                    | -     | -                     | -     | -       | -     | -                    | -     | 1019.6                | 0.92  |
| Para-cymene                            | 1056.9  | 3.28  | -                    | -     | -                     | -     | -       | -     | -                    | -     | -                     | -     |
| $\gamma$ -terpinene                    | 1065.4  | 3.21  | -                    | -     | -                     | -     | -       | -     | -                    | -     | -                     | -     |
| Cis-sabinene hydrate                   | 1082.8  | 0.52  | -                    | -     | -                     | -     | -       | -     | -                    | -     | -                     | -     |
| 3,5-heptadien-2-one-6-methyl           | 1087    | 1.27  | -                    | -     | -                     | -     | -       | -     | -                    | -     | -                     | -     |
| $\alpha$ -terpinolene                  | -       | -     | 1090.4               | 1.67  | -                     | -     | -       | -     | -                    | -     | -                     | -     |
| Linalool                               | -       | -     | -                    | -     | -                     | -     | -       | -     | -                    | -     | -                     | -     |
| Trans-sabinene hydrate                 | -       | -     | -                    | -     | -                     | -     | -       | -     | -                    | -     | -                     | -     |
| $\alpha$ -thujone                      | -       | -     | 1098.8               | 1.77  | 1097                  | 0.86  | -       | -     | -                    | -     | -                     | -     |
| $\beta$ -thujone                       | 1109.6  | 1.14  | -                    | -     | -                     | -     | -       | -     | -                    | -     | -                     | -     |
| Camphor                                | 1136.7  | 2.97  | 1138.5               | 4.88  | 1137                  | 3.50  | -       | -     | 1135.8               | 3.16  | 1136.2                | 4.09  |
| Terpinene-4.ol                         | 1176.8  | 7.31  | 1175.9               | 1.44  | 1174                  | 1.14  | 1174.1  | 1.76  | -                    | -     | 1174.1                | 2.07  |
| $\beta$ -cyclocitral                   | -       | -     | 1210.6               | 1.04  | -                     | -     | -       | -     | -                    | -     | -                     | -     |
| Hexadecanoic acid                      | -       | -     | -                    | -     | 1357                  | 4.18  | -       | -     | -                    | -     | -                     | -     |
| Trans- $\beta$ -damasenone             | -       | -     | 1371.4               | 2.22  | -                     | -     | -       | -     | -                    | -     | 1369.6                | 1.02  |
| Cis-caryophyllen                       | -       | -     | -                    | -     | 1417                  | 1.46  | -       | -     | -                    | -     | -                     | -     |
| Geranyl-aceton                         | -       | -     | 1428.8               | 3.73  | 1434                  | 1.82  | -       | -     | -                    | -     | 1425.5                | 1.34  |
| $\beta$ -caryophyllene                 | 1435.3  | 5.93  | 1436.4               | 6.29  | 1434                  | 7.15  | 1433.2  | 6.03  | -                    | -     | 1433.2                | 5.35  |
| Allo-Aromadendrene                     | 1453.8  | 0.59  | 1453.8               | 2.62  | -                     | -     | -       | -     | -                    | -     | -                     | -     |
| $\beta$ -Ionone                        | -       | -     | 1472.8               | 7.32  | 1469                  | 5.95  | 1468.5  | 1.70  | 1468.5               | 4.65  | 1469.5                | 3.28  |
| $\alpha$ -Humulene                     | 1467.4  | 0.52  | -                    | -     | -                     | -     | -       | -     | -                    | -     | -                     | -     |
| Spathulenol                            | 1588.4  | 9.34  | -                    | -     | -                     | -     | 1582.5  | 10.83 | -                    | -     | -                     | -     |
| Caryophyllen oxide                     | 1596.6  | 12.7  | 1597.7               | 25.45 | 1593                  | 28.37 | 1591.9  | 33.07 | 1589.5               | 39.40 | 1593                  | 31.35 |
| Caryophylla 4 (12),8(13)-dien-5-Betaol | -       | -     | 1631.7               | 3.41  | -                     | -     | -       | -     | -                    | -     | 1629.1                | 2.58  |
| Caryophyllenol                         | 1625.7  | 3.47  | -                    | -     | -                     | -     | -       | -     | -                    | -     | -                     | -     |
| Oxygenated sesquiterpene               |         | 25.6  |                      | 36.18 |                       | 34.3  |         | 45.6  |                      | 44.05 |                       | 37.21 |
| Sesquiterpene hydrocarbons             |         | 7.04  |                      | 8191  |                       | 8.61  |         | 6.03  |                      | -     |                       | 5.35  |
| Oxygenated monoterpenes                |         | 17.7  |                      | 16.75 |                       | 7.32  |         | 1.76  |                      | 3.16  |                       | 8.52  |
| Monoterpene hydrocarbons               |         | 24.91 |                      | 1.40  |                       | -     |         | 5.08  |                      | -     |                       | 0.92  |
| Others                                 |         | 4.95  |                      | 5.94  |                       | 5.31  |         | 10.14 |                      | 11.68 |                       | 11.89 |
| All components                         |         | 80.20 |                      | 69.18 |                       | 55.54 |         | 68.61 |                      | 58.89 |                       | 63.89 |

KI: kovats Index on DB-5 in reference to n-alkanes.

**Table 2.** Comparison of flowers, vegetative stage leaves, flowering stage leaves essential oils of *S.memorosa* collected from Urmia and Zonouz regions

| Components                   | Urmia   |       |                      |       |                       |       | Zonouz  |       |                      |       |                       |       |
|------------------------------|---------|-------|----------------------|-------|-----------------------|-------|---------|-------|----------------------|-------|-----------------------|-------|
|                              | Flowers |       | Flowering stage leaf |       | Vegetative stage leaf |       | Flowers |       | Flowering stage leaf |       | Vegetative stage leaf |       |
|                              | KI      | %     | KI                   | %     | KI                    | %     | KI      | %     | KI                   | %     | KI                    | %     |
| Heptane                      | -       | -     | 701                  | 2.47  | -                     | -     | -       | -     | -                    | -     | -                     | -     |
| Thujene                      | 929.3   | 1.58  | -                    | -     | -                     | -     | -       | -     | -                    | -     | -                     | -     |
| 1-octen-3-ol                 | 966.8   | 7.30  | 965.2                | 6.78  | 965.2                 | 6.43  | 966     | 4.64  | -                    | -     | -                     | -     |
| Sabinene                     | 974.1   | 1.63  | -                    | -     | -                     | -     | 973.3   | 2.18  | -                    | -     | -                     | -     |
| Para cymene                  | 1019.2  | 4.48  | -                    | -     | -                     | -     | 1019.2  | 4.74  | -                    | -     | -                     | -     |
| Gamma-terpinene              | 1056.1  | 1.63  | -                    | -     | -                     | -     | 1056.1  | 2.13  | -                    | -     | -                     | -     |
| Cis-sabinene hydrate         | 1063.5  | 1.01  | -                    | -     | -                     | -     | 1063.7  | 2.49  | -                    | -     | -                     | -     |
| Trans sabinene hydrate       | -       | -     | -                    | -     | -                     | -     | 1093.8  | 1.29  | -                    | -     | -                     | -     |
| Camphor                      | 1136.7  | 3.31  | 1136.2               | 4.41  | -                     | -     | 1136.7  | 5.54  | -                    | -     | -                     | -     |
| Terpinen-4-ol                | 1175    | 4.57  | -                    | -     | -                     | -     | 1174.1  | 7.05  | -                    | -     | -                     | -     |
| Neryl-acetone                | 1425.5  | 0.92  | 1425.5               | 2.55  | -                     | -     | -       | -     | -                    | -     | -                     | -     |
| Cis-caryophyllen             | -       | -     | -                    | -     | -                     | -     | 1417.9  | 1.95  | -                    | -     | -                     | -     |
| Trans-β-Damascenen           | -       | -     | -                    | -     | -                     | -     | -       | -     | -                    | -     | 1369.6                | 2.29  |
| Beta-Ionone                  | 1467.9  | 1.59  | 1468.5               | 4.81  | -                     | -     | -       | -     | -                    | -     | 1468.5                | 4.20  |
| Spathulenol                  | 1588.4  | 14.84 | -                    | -     | -                     | -     | 1584.9  | 14.46 | -                    | -     | -                     | -     |
| Caryophyllen oxide           | 1595.4  | 26.41 | 1590.7               | 33.54 | 1590.7                | 18.19 | 1594.2  | 28.13 | 1590.1               | 80.48 | 1589.5                | 26.30 |
| Caryophylla 4(12)8(15)- dien | 1630.01 | 3.47  | 1629.1               | 2.66  | -                     | -     | -       | -     | -                    | -     | -                     | -     |
| Oxygenated sesquiterpenes    |         | 46.31 |                      | 41.01 |                       | 18.19 |         | 42.59 |                      | 8.48  |                       | 30.50 |
| Sesquiterpene hydrocarbons   |         | 5.82  |                      | 2.41  |                       | -     |         | 14.48 |                      | -     |                       | 80.50 |
| Oxygenated monoterpenes      |         | 9.81  |                      | 6.96  |                       | -     |         | 16.34 |                      | -     |                       | 2.29  |
| Monoterpene hydrocarbons     |         | 9.32  |                      | -     |                       | -     |         | 9.05  |                      | -     |                       | -     |
| components                   |         |       |                      |       |                       |       |         |       |                      |       |                       |       |
| Others                       |         | 7.30  |                      | 9.25  |                       | 6.43  |         | 4.64  |                      | -     |                       | -     |
| All components               |         | 78.56 |                      | 59.63 |                       | 24.62 |         | 87.13 |                      | 8.48  |                       | 41.29 |

KI: kovats Index on DB-5 in reference to n-alkanes.

**Table 3:** Geographical characteristics of *S. nemorosa* collection regions

| Collection regions  | Longitude | Latitude | Altitude |
|---|-----------|----------|----------|
| <b>Zonouz<br/>(EastAzarbaijan)</b>                          | 38.26°E'  | 45.46°N  | 1550m    |
| <b>Qasemlu village<br/>urmia<br/>(westernAzarbaijan)</b>    | 37.65°E'  | 47.05°N  | 1328m    |
| <b>Ahar<br/>(East Azarbaijan)</b>                           | 38.26°E'  | 47.04°N  | 1391m    |
| <b>Abbasabad<br/>village Ardabil<br/>(Ardabil province)</b> | 38.13°E'  | 48.19°N  | 1335m    |



**Figure 1.** Map of the collection regions of *s. nemorosa* from the northwest of Iran (Zonouz, Ahar, Ardabil and Urmia)





**Figure 2.** *Salvia nemorosa* L.

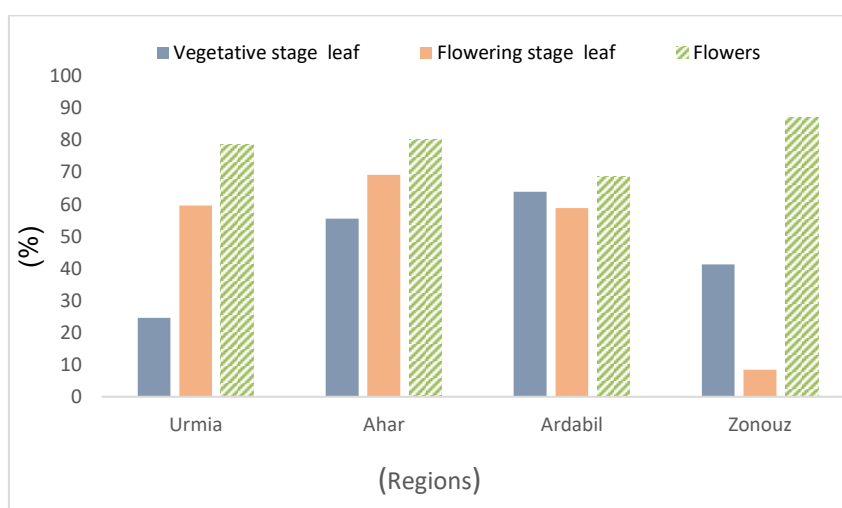


**Figure 3.** Comparison of the amount of essential oil compounds in *S. nemorosa* L. collected from four regions at different stages of growth.

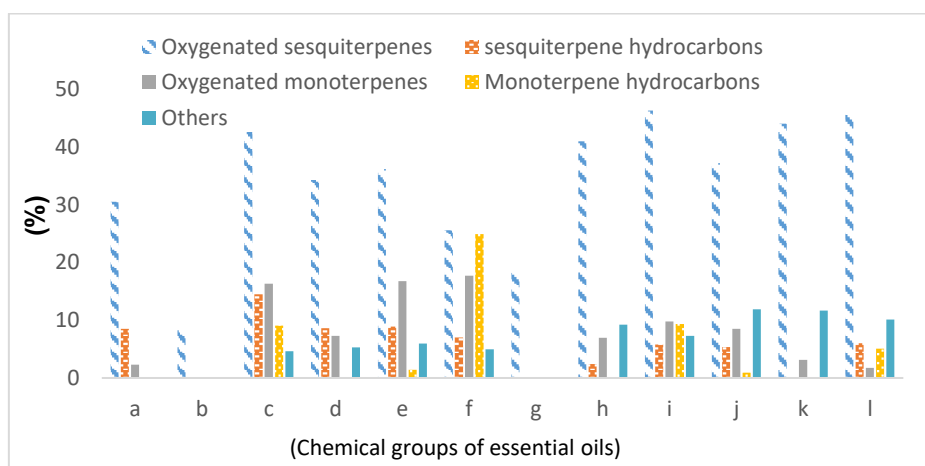
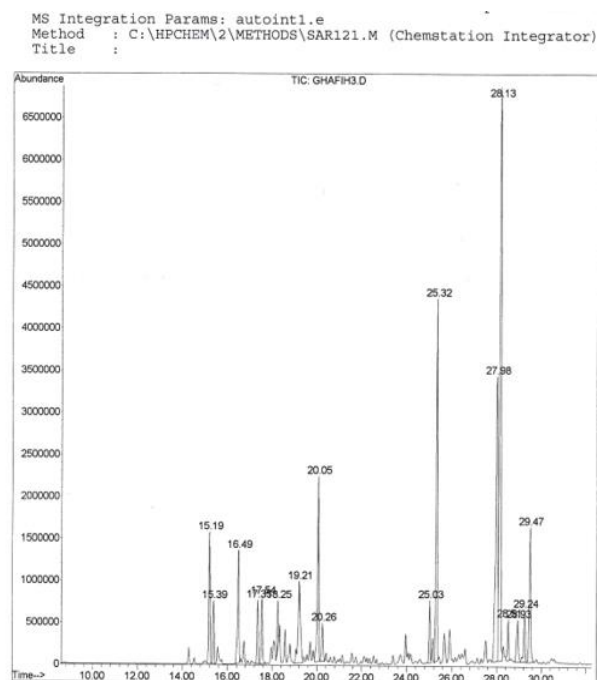
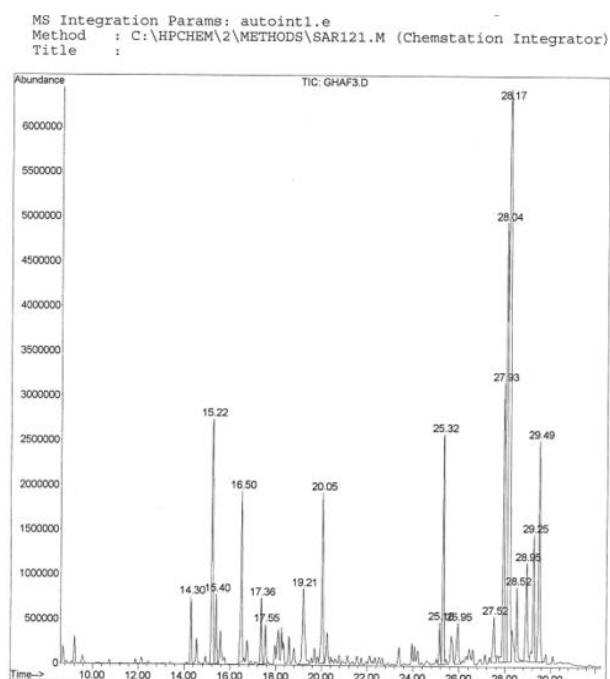


**Figure 4.** Comparison of chemical groups in the essential oil of *S. nemorosa* L. collected from four regions at different stages of growth

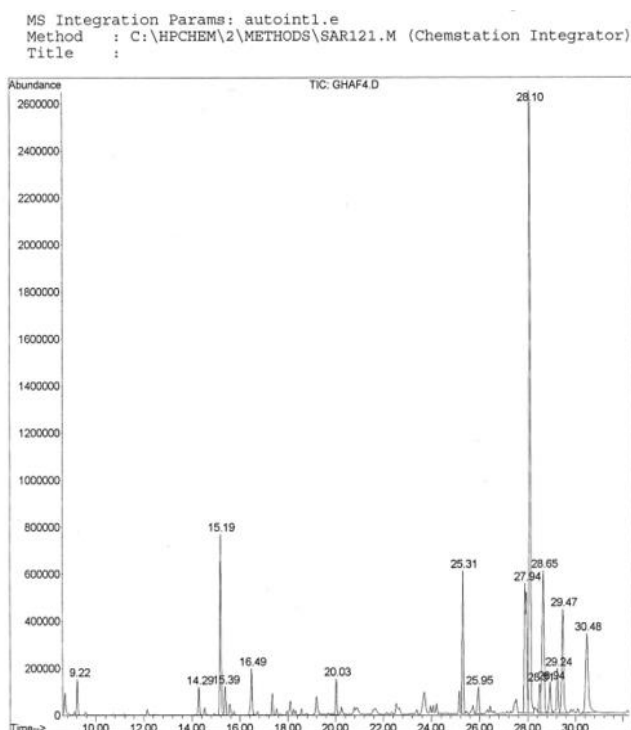
**Note.** a: Zonouz; vegetative stage leaves, b: Zonouz; flowering stage leaves, c: Zonouz; flowers, d: Ahar; vegetative stage leaves, e: Ahar; flowering stage leaves, f: Ahar; flowers, g: Urmia; vegetative stage leaves, h: Urmia; flowering stage leaves, i: Urmia; flowers, j: Ardabil; vegetative stage leaves, k: Ardabil; flowering stage leaves, l: Ardabil; flowers.



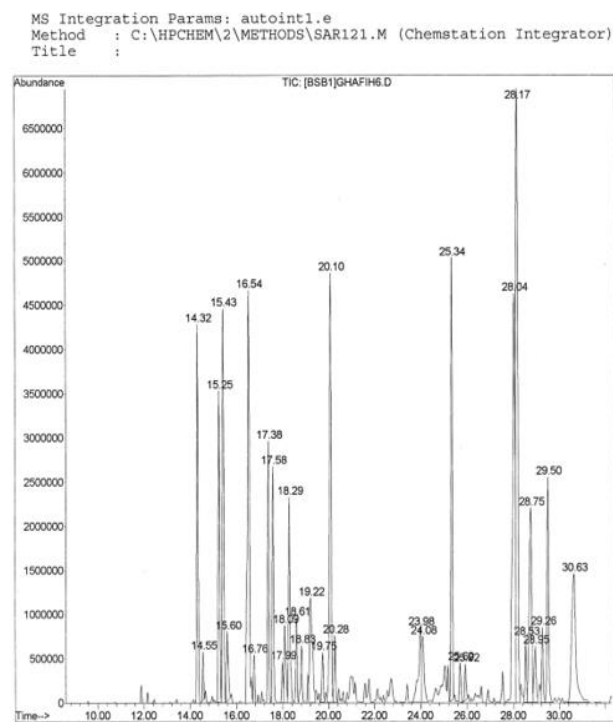
(a)



(b)



(c)



(d)

**Figure 5.** GC-MS chromatogram for essential oil of *Salvia nemorosa* flowers in (a): Zonouz, (b): Urmia, (c): Ardabil and (d): Ahar regions.

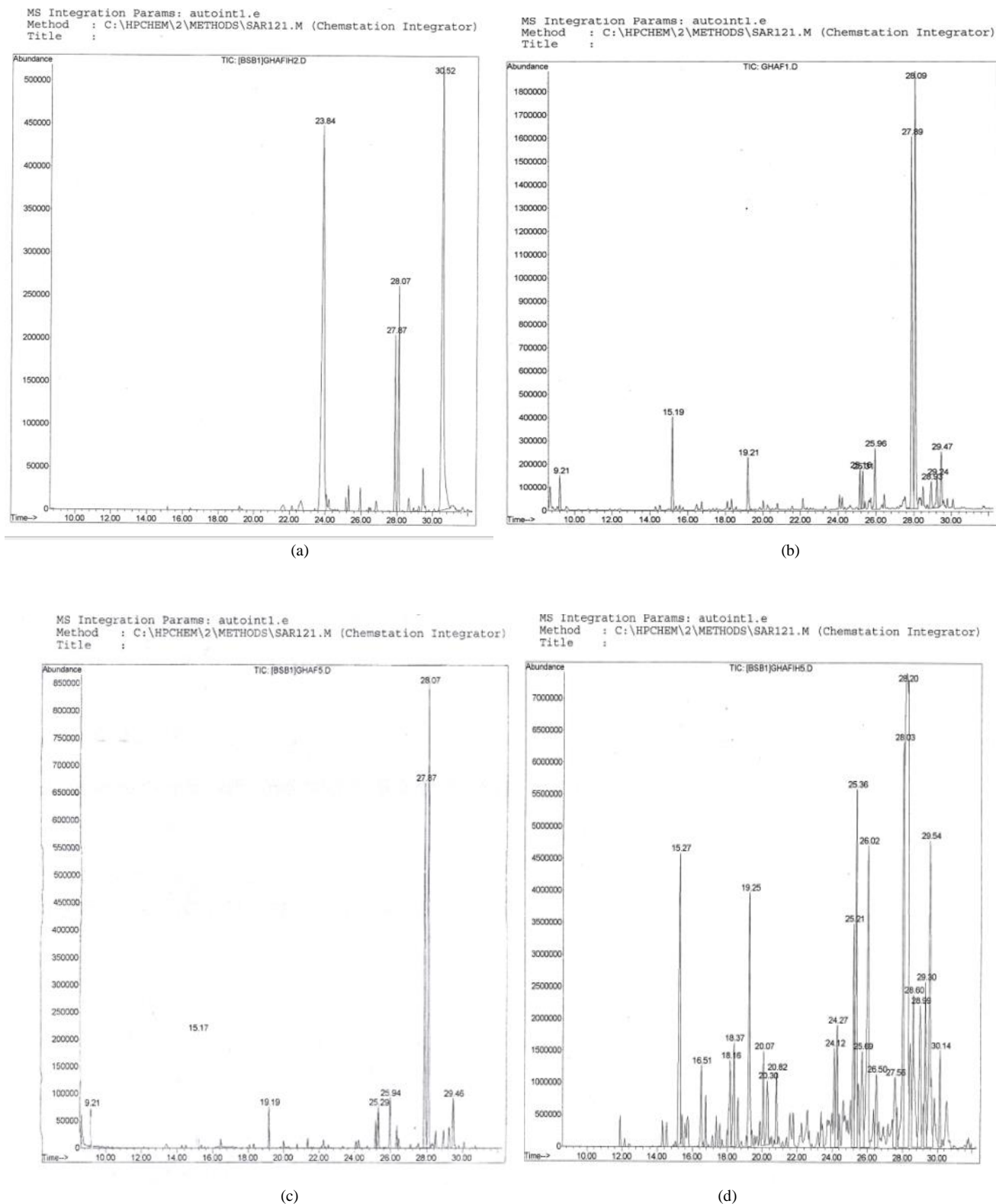
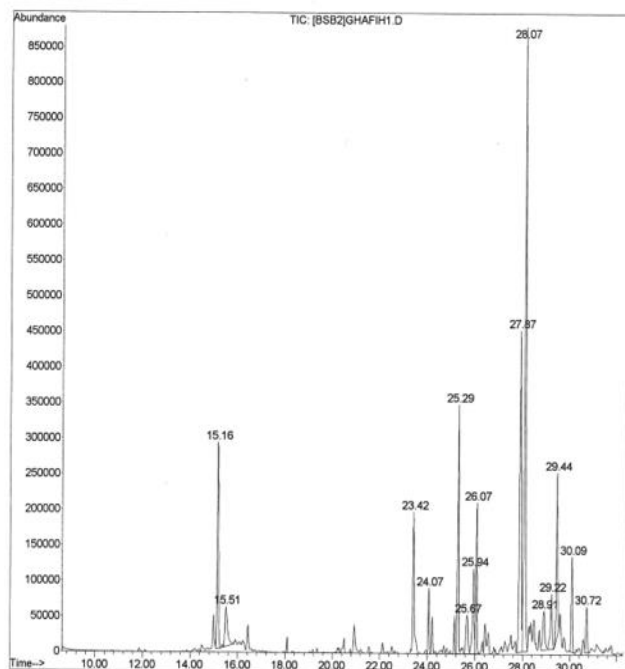


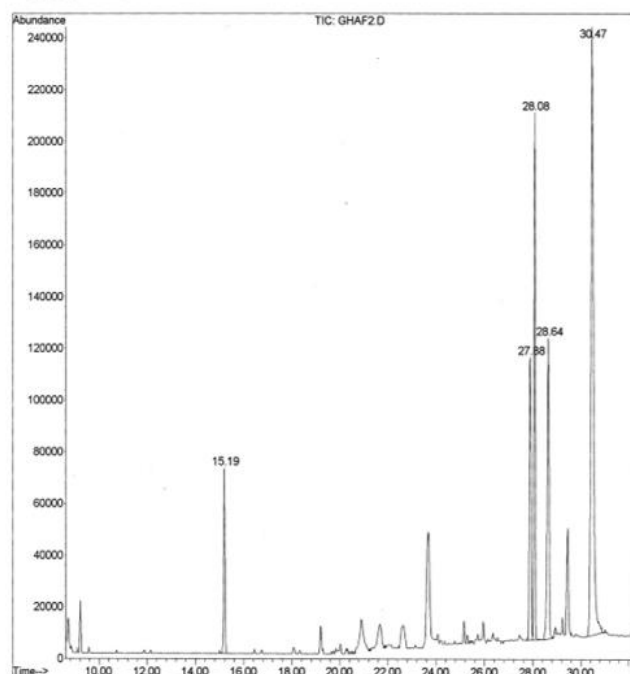
**Figure 6.** GC-MS chromatogram for essential oil of *Salvia nemorosa* flowering stage leaves in (a): Zonouz, (b): Urmia, (c): Ardabil and (d): Ahar regions.

MS Integration Params: autoint1.e  
Method : C:\HPCHEM\2\METHODS\SAR121.M (Chemstation Integrator)  
Title :



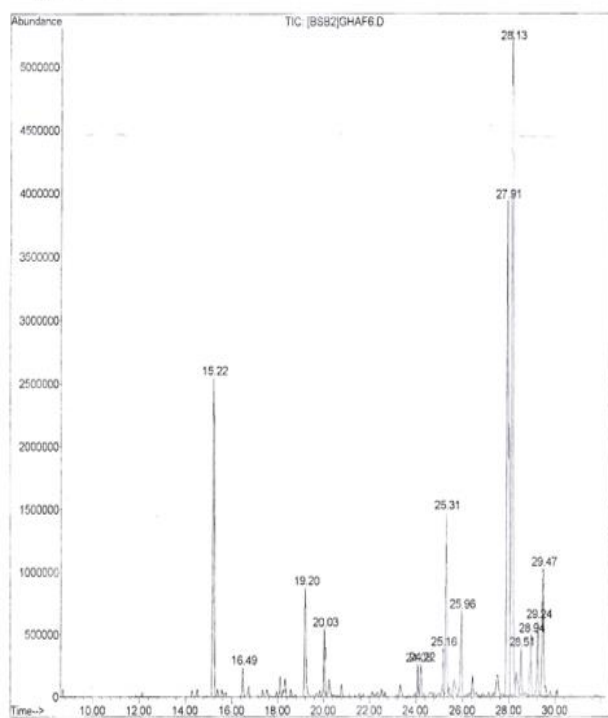
(a)

MS Integration Params: autoint1.e  
Method : C:\HPCHEM\2\METHODS\SAR121.M (Chemstation Integrator)  
Title :



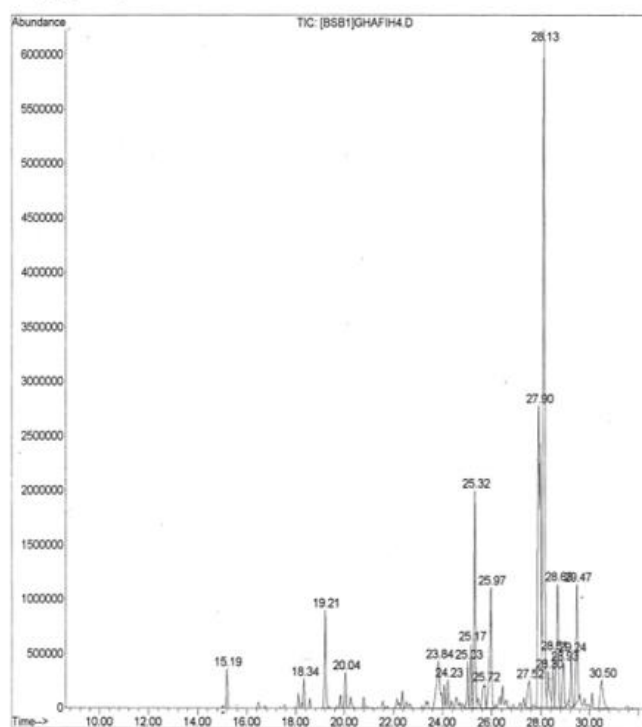
(b)

MS Integration Params: autoint1.e  
Method : C:\HPCHEM\2\METHODS\SAR121.M (Chemstation Integrator)  
Title :



(c)

MS Integration Params: autoint1.e  
Method : C:\HPCHEM\2\METHODS\SAR121.M (Chemstation Integrator)  
Title :



(d)

**Figure 7.** GC-MS chromatogram for the essential oil of *Salvia nemorosa* vegetative stage leaves in (a): Zonouz, (b): Urmia, (c): Ardabil and (d): Ahar regions.

ADSORÇÃO DO HORMÔNIO 17 $\alpha$ -METILTESTOSTERONA EM SOLOSADSORPTION OF HORMONE 17 $\alpha$ -METHYLTESTOSTERONE IN SOILSALBERTON, Matheus Borghezan<sup>1</sup>; LINDINO, Cleber Antonio<sup>2\*</sup>.

<sup>1,2</sup> Universidade Estadual do Oeste do Paraná, Departamento de Química, Laboratório de Estudos em Química Analítica Limpa – LEQAL, Toledo/PR, Brasil.

\* Autor correspondente  
e-mail: lindino99@gmail.com

Received 19 March 2020; received in revised form 19 June 2020; accepted 29 June 2020

## RESUMO

Com o aumento na produção de peixes em sistemas de pisciculturas, principalmente tilápias, o uso do hormônio 17 $\alpha$ -metiltestosterona (MT) como indutor da masculinização de alevinos cresceu conjuntamente. A probabilidade de contaminação de recursos naturais também tende a aumentar e não há legislação brasileira que regulamente o teor deste hormônio em águas. O estudo da interação do hormônio com o solo típico das regiões produtoras é importante para compreender os fatores que influenciam a sua adsorção. Este trabalho utilizou duas amostras de Latossolos Vermelhos Eutroféricos e avaliaram-se as condições de interação do hormônio em processo estático (repouso) e dinâmico (agitação), utilizando-se modelos de isotermas. Os resultados mostraram que o maior teor de matéria orgânica do solo e a maior salinidade do meio aquoso aumentam a adsorção da MT em solo no processo estático. Para o processo dinâmico, o teor de Fe tem influência na maior adsorção em solo. O pH do meio não influencia na adsorção em nenhum dos processos. A adsorção possui características exotérmicas sendo que o equilíbrio de adsorção é atingido em 24 horas e o modelo de Freundlich para a amostra do solo 1 e o modelo de Temkin para a amostra do solo 2 são os que mais se adequam ao processo de adsorção. Segundo parâmetros calculados para a isoterma de Dubinin, tem-se que as adsorções dos solos possuem a tendência de apresentar interações químicas entre adsorvente-adsorvato. Estes resultados mostram a preocupação com a quantidade de hormônio adsorvida em sedimentos em tanques de pisciculturas e sua liberação para o corpo d'água, com possibilidade de contaminação de recursos naturais.

**Palavras-chave:** masculinização, piscicultura, sedimento, isoterma.

## ABSTRACT

With the increase in fish production in fish farming systems, mainly tilapia, the use of the hormone 17 $\alpha$ -methyltestosterone (MT) as an inducer of the masculinization of fry has grown together. The probability of contamination of natural resources also tends to increase, and there is no Brazilian law that regulates the content of this hormone in waters. The study of the interaction of the hormone with the typical soil of the producing regions is essential to understand the factors that influence its adsorption. This work used two samples of Eutropheric Red Oxisols and the conditions of the interaction of the hormone in static (resting), and dynamic (agitation) processes were evaluated, using isothermal models. The results showed that the higher organic matter content of the soil and the higher salinity of the aqueous medium increases the adsorption of MT in the soil in the static process. For the dynamic process, the Fe content influences the higher adsorption in soil. The pH of the medium does not affect the adsorption in any of the processes. The adsorption has exothermic characteristics, and the adsorption equilibrium is reached in 24 hours, and the Freundlich model for the soil 1 sample and the Temkin model for the soil 2 sample is the most suitable for the adsorption process. According to parameters calculated for the Dubinin isotherm, soil adsorption tends to have chemical interactions between adsorbent-adsorbate. These results show concern for the amount of adsorbed hormone sediment in fish farming tanks and their release to the water body, with the possibility of contamination of natural resources.

**Keywords:** Masculinization, fish farming, sediment, isotherm.



## 1. INTRODUÇÃO:

O crescimento populacional humano ocasionou o aumento na produção e consumo de alimentos e, entre eles, o de peixes. A piscicultura vem obtendo destaque no setor do agronegócio e em 2018 registrou a produção nacional de 519,2 mil toneladas, sendo que deste montante, a tilápia (*Oreochromis niloticus*) representou 58,4% do total da despesa brasileira (IBGE, 2019). De acordo com estudo realizado pela Embrapa, a produção de tilápia no Brasil expandiu-se 223% entre 2005 e 2015 (Araújo & Reinol, 2017).

O estado do Paraná vem se destacando cada vez mais na produção nacional de viveiros de peixes e a espécie mais cultivada é a tilápia. No estado paranaense, a produção de pescados tem suma importância nas cidades situadas no Oeste do Estado, nas quais o Valor Bruto da Produção representa 60% do total (Agência de notícias do Paraná, 2019).

Em seu *habitat* natural, a tilápia apresenta-se tanto no sexo feminino quanto no masculino, mas a superpopulação é um problema bastante comum em viveiros. Para contornar isto, técnicas de masculinização dos alevinos são adotadas, obtendo-se melhor desempenho na produção dos pescados (Baldisserotto, 2002). Do ponto de vista econômico, espécies fêmeas gastam muita energia durante a reprodução e com cuidados com a prole; já os machos têm maior peso e maior quantidade de carne, favorecendo o setor produtivo (Oliveira, Santos, Pereira & Lima, 2007).

O processo de masculinização ocorre principalmente por meio da adição do hormônio sintético 17 $\alpha$ -metiltestosterona (MT) à ração administrada aos alevinos, durante os primeiros 30 dias de vida, quando o sexo ainda não está definido (Kubitza, 2009) (Figura 1).

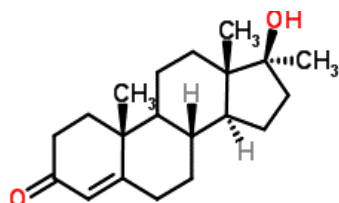


**Figura 1.** Estrutura molecular da 17 $\alpha$ -metiltestosterona. Fonte: ChemSpider (Copyright Royal Society of Chemistry, 2020).

No entanto, o uso intensivo de MT adicionada à ração (60 mg kg<sup>-1</sup>) em pisciculturas ainda suscita preocupações quanto aos riscos para os consumidores e para a saúde ambiental

(Mlalila, Mahika, Kalombo, Swai & Hilonga, 2015). As rotas de contaminação da água envolvem ração não consumida e a eliminação do hormônio não metabolizado (Green & Teichert, 2000). Hormônios esteroides como a MT são rapidamente absorvidos pelos sedimentos devido à sua natureza hidrofóbica e a sua eliminação por meio de processos de biotransformação ou de fotodegradação dependem de vários fatores, como pH, teor de matéria orgânica do meio e salinidade (Green & Teichert, 2000; Kolok & Sellin, 2008; Homklin, Ong & Limpiyakorn, 2011; Ong, Chotisukam & Limpiyakorn, 2012; Young, Latch, Mawhinney, Nguyen, Davis & Borch, 2013; Mlalila, Mahika, Kalombo, Swai & Hilonga, 2015).

Espécies relativamente apolares como a MT presentes nos sedimentos podem ser liberadas para o meio aquoso em reações de equilíbrio químico, ocasionando a contaminação nos tanques e consequente contaminação dos ecossistemas aquáticos, afetando o equilíbrio do *habitat* natural dos organismos ali presentes (Ribeiro, 2001; Baldisserotto, 2002). A legislação brasileira é omissa quanto aos limites máximos permitidos para este hormônio no ambiente (Brasil, 2009; Brasil, 2013).

Os trabalhos disponíveis na literatura científica sobre o processo de adsorção da 17 $\alpha$ -metiltestosterona em sedimentos são escassos e abordam solos e condições que não são típicas do clima tropical (Fitzpatrick & Contreras-Sanchez, 2000; Lee, Strock, Sarmah & Rao, 2003; Kim, Zhiqiang, Baohua & Weillen, 2007 e Ong, Chotisukam & Limpiyakorn, 2012), mostrando a importância de estudos em solos típicos das regiões nas quais se situam as pisciculturas.

Assim, este trabalho estudou o processo termodinâmico e cinético da adsorção do hormônio 17 $\alpha$ -metiltestosterona em solos padronizados por meio de método dinâmico (agitação) e estático (repouso) e a isoterma que melhor descreve o conjunto de dados obtidos.

## 2. MATERIAL E MÉTODOS:

### 2.1. Procedimentos gerais

Todos os reagentes utilizados foram de alto grau de pureza (P.A.). A água utilizada para o preparo de soluções padrões ou diluições de amostras foi destilada e purificada por osmose reversa (ADAMO, resistência da água de 5 M $\Omega$  cm<sup>-1</sup> a 25°C). Duas amostras de solos padronizados secos ao ar, com classificação de

Latossolos Vermelhos Eutroféricos, foram obtidas a partir do laboratório de solos da Cooperativa Central de Pesquisa Agrícola (COODETEC – Cascavel/PR), coletados de 0 a 20 cm de profundidade, cuja caracterização está apresentada na Tabela 1, a partir do laudo do laboratório.

A solução estoque de  $17\alpha$ -metiltestosterona foi preparada a partir da diluição de 0,0302 g do hormônio (DanubioAqua, pureza de  $101,5 \pm 2\%$ ) em 1 mL de etanol (Vetec, 95% v/v). A partir da solução estoque, transferiu-se alíquota de 20  $\mu$ L com micropipeta (Labmate,  $\pm 0,82\%$ ), para balão volumétrico de 50 mL, completando-se o volume com água purificada, com concentração final de  $3,994 \times 10^{-5}$  mol L<sup>-1</sup>. As massas do hormônio e dos solos foram pesadas em balança analítica Shimadzu ( $\pm 0,0001$  g).

As medidas de absorvâncias na região do UV-visível das soluções e dos sobrenadantes foram realizadas em espectrofotômetro Shimadzu 1800 PC com o uso de cubetas de quartzo de caminho ótico de 1,0 cm e varredura nos comprimentos de onda de 200 a 700 nm e resolução de  $\pm 0,1$  nm.

Nos sobrenadantes também se determinou o pH utilizando-se pHmetro de bancada BEL (modelo PHS3BW), calibrado com solução tampão (Buffer) pH  $4,00 \pm 0,02$  e pH  $7,00 \pm 0,02$  (DINAMICA). A condutividade foi medida por meio do condutivímetro MS TECNOPON, com eletrodo de platina (constante de celda de 0,1), calibrado com solução padrão de condutividade  $1412 \mu\text{S cm}^{-1}$  (NEON).

## 2.2. Curva padrão de $17\alpha$ -metiltestosterona

A partir da solução estoque de  $17\alpha$ -metiltestosterona, prepararam-se 13 soluções de 50 mL entre as concentrações de  $2,39 \times 10^{-8}$  mol L<sup>-1</sup> e  $3,994 \times 10^{-5}$  mol L<sup>-1</sup>, obtendo-se a curva analítica que foi utilizada para determinar a concentração de MT a partir das absorvâncias dos sobrenadantes.

## 2.3. Ponto de carga zero (PCZ) dos solos

O valor do Ponto de Carga Zero (PCZ) foi obtido pela mistura de 0,5000 g do solo estudado em 50 mL de solução aquosa de KCl (Vetec, 99-100,5%) na concentração de  $0,5 \text{ mol L}^{-1}$  em valores de pH inicial variando de 3 à 11 as quais foram obtidas com soluções de HCl (Vetec, 37%) ou NaOH (Vetec, 99%) na concentração de  $0,01 \text{ mol L}^{-1}$ . As soluções permaneceram por 24 horas

em contato com os adsorventes sob agitação em mesa agitadora (NewLab), a 110 rpm e 25°C e foram obtidos os valores finais de pH.

## 2.4. Adsorção estática

Transferiu-se 50 mL da solução padrão  $3,994 \times 10^{-5}$  mol L<sup>-1</sup> de MT para proveta de vidro de 100 mL ( $\pm 0,05$ ) contendo 10 cm<sup>3</sup> de volume do solo, tampando-se em seguida e armazenando-se em local protegido da luz. O volume utilizado foi baseado em protocolos de análise de solos (von Raij, 2001). O pH, a condutividade e a absorvância dos sobrenadantes foram determinados semanalmente pelo período de seis semanas. Para o controle utilizou-se água purificada.

A determinação de Fe total no sobrenadante foi realizada empregando a técnica de espectrometria de Fluorescência de Raios X por reflexão total (TXRF) (S2 PICOFOX, Bruker AXS Microanalysis GmbH). Adicionou-se 660  $\mu$ L de amostra em microtubos do tipo Eppendorf com capacidade de 2 mL, nos quais foram adicionados 10  $\mu$ L de solução padrão de Gálio com concentração final na amostra de  $10 \text{ mg L}^{-1}$ . Posteriormente à adição do padrão interno, 5  $\mu$ L das amostras foram pipetados sobre o centro de discos de quartzo. Os discos contendo as amostras foram secos em capela de fluxo laminar à temperatura ambiente. Previamente às análises, os discos de quartzo (30 mm de diâmetro e 3 mm de espessura) foram submetidos a procedimento de limpeza conforme descrito por Espinoza-Quñones, Módenes, de Paula & Palácio (2015).

## 2.5. Determinação do pH em cloreto de cálcio

A partir do protocolo estabelecido por von Raij (2001), transferiu-se 10 cm<sup>3</sup> do solo em recipiente de plástico, adicionando-se 25 mL de solução de cloreto de cálcio ( $\text{CaCl}_2$ )  $0,01 \text{ mol L}^{-1}$ , permanecendo em repouso durante 10 minutos. Em seguida, agitou-se a mistura pelo período de 20 minutos em 110 rpm, usando agitador com movimento circular horizontal, e deixou-se descansar novamente por 10 minutos. Mergulhou-se o eletrodo na suspensão, sem agitar a solução, de modo que a ponta do eletrodo de vidro toque ligeiramente a camada de sedimento e a saída do eletrodo de referência fique submersa. Mediu-se o pH após estabelecido o equilíbrio.

## 2.6. Medida de adsorção com o tempo

As medidas de cinética de adsorção foram realizadas em recipientes plásticos contendo 0,5000 g de cada solo e adicionando-se 50 mL da solução padrão de 17 $\alpha$ -metiltestosterona em pH 5,5 e temperatura de 25,0 °C  $\pm$  0,1 realizadas no intervalo de 1 a 27 horas.

## 2.7. Adsorção dinâmica a 25 °C

Adicionou-se 50 mL da solução padrão 3,994 x 10<sup>-5</sup> mol L<sup>-1</sup> de MT em recipiente plástico contendo 0,5000 g de cada solo estudado e transferiu-se estes para uma mesa agitadora (NewLab) a 110 rpm, controlando-se a temperatura em 25°C  $\pm$  0,1. Após o período de 24 horas de agitação, centrifugou-se as amostras durante 30 minutos a 4000 rpm.

Utilizando as concentrações finais e iniciais, determinou-se a quantidade do hormônio adsorvida por grama de cada material adsorvente ( $q_{eq}$ ), utilizando-se a Equação 1.

$$q_{eq} = \frac{(C_i - C_{eq})}{M} \times V \quad (1)$$

sendo  $C_i$  e  $C_{eq}$  são as concentrações (mg L<sup>-1</sup>) iniciais e finais do hormônio em solução respectivamente,  $V$  é o volume da solução (L) e  $M$  é a massa do adsorvente em solução.

## 2.8. Adsorção dinâmica em diferentes pHs

Em nove recipientes plásticos contendo 0,5000 g de cada solo adicionou-se 50 mL da solução padrão de MT, ajustou-se os pHs de 3 a 11 utilizando-se soluções de NaOH (Vetec, 99%) ou HCl (Vetec, 37%) 0,1 mol L<sup>-1</sup> e, em seguida, transferiu-se as amostras para uma mesa agitadora (NewLab) a 110 rpm controlando a temperatura em 25  $\pm$  0,1°C. Após o período de 24 horas de agitação centrifugou-se as mesmas durante 30 minutos a 4000 rpm.

## 2.9. Estudos de Isoterma de Adsorção

Em recipientes plásticos contendo 0,5000 g de cada solo estudado adicionou-se 50 mL das soluções de MT nas concentrações de 6,0 x 10<sup>-6</sup>, 7,0 x 10<sup>-6</sup>, 8,0 x 10<sup>-6</sup>, 9,0 x 10<sup>-6</sup>, 1,0 x 10<sup>-5</sup>, 2,0 x 10<sup>-5</sup>, 3,0 x 10<sup>-5</sup>, 4,0 x 10<sup>-5</sup> mol L<sup>-1</sup>, corrigindo-se o pH das amostras entre 5,0 e 6,0 com solução de HCl ou solução de NaOH 0,01 mol L<sup>-1</sup>. Transferiu-se estes frascos para uma

mesa agitadora (NewLab) a 110 rpm controlando a temperatura pelo período de 24 horas de agitação (período pré-estabelecido por meio de estudos cinéticos). Este procedimento foi realizado para as temperaturas de 25, 35, 45 e 55°C.

## 3. RESULTADOS E DISCUSSÃO:

A Figura 2 apresenta os espectros característicos do hormônio MT em diferentes concentrações, na região do ultravioleta-visível e a curva analítica obtida.

A curva analítica da 17 $\alpha$ -metiltestosterona (Figura 2) apresenta correlação linear entre absorvância e concentração do hormônio com equação da reta igual a  $Abs = 0,01471 + 21233,63878[MT]$  e  $R^2 = 0,9981$ , entre as concentrações de 5,0 x 10<sup>-6</sup> a 4,0 x 10<sup>-5</sup> mol L<sup>-1</sup>.

A Figura 3 apresenta os resultados das medidas do ponto de carga zero (PCZ). Para o solo 1 o valor ocorre no pH 4,63 e para o solo 2 ocorre no pH 4,71. Já a Figura 4 apresenta a quantidade adsorvida do hormônio em cada solo por agitação e em repouso. Na adsorção em repouso, os resultados mostraram que o  $Q_{eq}$  para o solo 1 foi de 0,0387 mg g<sup>-1</sup>, enquanto para o solo 2 foi de 0,0726 mg g<sup>-1</sup>. Apesar dos baixos valores, o solo 2 adsorveu 87,6% mais a 17 $\alpha$ -metiltestosterona que o solo 1.

O solo 2 apresenta maior teor de matéria orgânica (40,31 g dm<sup>-3</sup>) do que o solo 1 (32,83 g dm<sup>-3</sup>) e, segundo Ong *et al.*, (2012), a sorção do hormônio MT é impactada pelo teor de matéria orgânica nos adsorventes. Quanto maior o teor de matéria orgânica, maior o processo de adsorção da 17 $\alpha$ -metiltestosterona.

O sobrenadante no experimento com o solo 2 tem maior condutividade (2,61 mS cm<sup>-1</sup>) que o do solo 1 (0,03 mS cm<sup>-1</sup>). A salinidade do meio aquoso no qual o hormônio se encontra possui correlação com sua adsorção, já que devido ao efeito *salting-out* há o decaimento na solubilidade aquosa da MT de modo que com o aumento na salinidade da solução, a solubilidade do hormônio diminui, permitindo maior adsorção no sedimento (Ong *et al.*, 2012).

O pH do meio se manteve entre 5,49 e 5,82 (com desvio padrão relativo de 2,3%) no solo 1 e entre 5,83 e 5,90 (com desvio padrão relativo de 0,6%) no solo 2 ao longo das seis semanas de observação. Não há evidência de que o pH possa alterar a adsorção em repouso da MT.



Segundo Kim *et al.*, (2007) e Ong *et al.*, (2012), o pH não possui impacto na sorção da MT. Segundo estes autores, os valores de Kd (coeficiente de distribuição) da isoterma entre os pH 5,6 e 7,5 são similares entre si e estatisticamente não significantes.

O ponto isoelétrico (PI) da 17 $\alpha$ -metiltestosterona é 1,7 (Pubchem, 2005), indicando que em pH maior que este valor a molécula do hormônio MT apresenta carga neutra que favorece a adsorção em um meio mais apolar (com maior teor de matéria orgânica) e que tem menor solubilidade em meios mais salinos, efeito este observado neste trabalho.

Na Figura 5 observa-se que o tempo de equilíbrio pelo método dinâmico foi alcançado em 24 h de contato entre a solução do hormônio e os solos. Acima deste tempo (até 27 horas), a adsorção diminui entre 2,5 a 3,3%. O tempo de 24 h foi utilizado nos estudos posteriores.

Diferentemente dos resultados obtidos no estudo da adsorção estática, no método de adsorção dinâmica há o favorecimento das colisões entre adsorvato (17 $\alpha$ -metiltestosterona) e adsorventes (solos) ocorrendo adsorção mais eficiente, além da área de contato disponível do solo aumentar com a agitação favorecendo a interação mais intensa.

Na adsorção dinâmica, o teor de matéria orgânica e a salinidade do meio influenciam pouco no processo, mas partículas de óxidos de Fe presentes nos solos podem se caracterizar como um adsorvente importante. Hu, Liu, Deng, Chea, Luo, Sun, Yang & Yang (2011) estudaram a adsorção de 17 $\alpha$ -metiltestosterona em nanopartículas de Fe<sub>3</sub>O<sub>4</sub> (tamanho entre 40 e 100 nm) e verificaram que o processo de adsorção segue a isoterma de Langmuir e que o Q<sub>eq</sub> máximo é de 7  $\mu\text{g g}^{-1}$  do adsorvente, indicando que óxidos de Ferro podem adsorver quantidades do hormônio MT. Os óxidos de Ferro são comuns nos Latossolos vermelhos, típicos da região de coletas das amostras. No caso deste estudo, o solo 1 tem o maior teor de Fe total com 42,56 mg dm<sup>-3</sup> em sua composição e o solo 2 tem 32,76 mg dm<sup>-3</sup>. No sobrenadante do solo 1, o Fe total em concentração de 1,126 mg L<sup>-1</sup> e o solo 2 em 0,236 mg L<sup>-1</sup>, valores encontrados por TXRF.

Nos estudos de isotermas de adsorção (Figura 6), verificou-se que a capacidade máxima de adsorção do solo 1 é de 0,3615 mg g<sup>-1</sup> e a do solo 2 é de 0,2304 mg g<sup>-1</sup>.

De acordo com a classificação de Giles, Smith & Huitson (1974), tem-se que a isoterma que melhor descreve o conjunto de dados demonstrados na Figura 5 para todos os solos, é isotérmico do tipo L (Langmuir), que se baseia na movimentação das moléculas adsorvidas sobre a superfície do adsorvente, ocorrendo distribuição uniforme e formando monocamada recobrimdo toda a superfície. Já o subgrupo dos materiais adsorventes apresenta-se diferente, no qual o solo 1 é descrito pelo subgrupo 3, descreve o comportamento da adsorção por uma subida após um ponto de inflexão, enquanto o solo 2 é descrito pelo subgrupo 1, em que esta descreve que os sítios ativos que interage com o adsorvato não atingindo assim uma concentração de equilíbrio. Hu *et al.* (2011) também descreveram a isoterma de Langmuir como o modelo que mais se ajusta ao processo de adsorção da 17 $\alpha$ -metiltestosterona em Fe<sub>3</sub>O<sub>4</sub>.

A adsorção do hormônio em relação aos solos 1 e solo 2 apresentam características exotérmicas, pois nas menores temperaturas em que o sistema foi submetido, a adsorção apresentou-se máxima.

Os modelos matemáticos de Langmuir, Freundlich, Temkin e Dubinin-Radushkevich foram aplicados para ajustar a isoterma experimental. A partir dos parâmetros obtidos para cada isoterma (Tabela 2) constatou-se que o modelo de Freundlich mostrou-se mais adequado para o solo 1 e o modelo de Temkin para o solo 2 de acordo com os valores de R<sup>2</sup> mais próximos de 1.

A isoterma de Freundlich é baseada na distribuição logarítmica de sítios ativos, que consistem em tratamento válido quando não há grande interação entre as moléculas de adsorvato. Este modelo expressa também que a adsorção é realizada em múltiplas camadas. O valor de n > 1 indica que a adsorção ocorre de maneira favorável a este adsorvente (Kalavathy, Kathikeyan, Rajgopal & Miranda, 2005).

A isoterma de Temkin leva em consideração as interações entre adsorvente – adsorvato e a uniformidade da distribuição das energias de ligação (Foo & Hameed, 2010). Este modelo prediz que o calor da adsorção das moléculas na camada tende a decrescer de forma linear e não logarítmica, aumentando a cobertura do adsorvente (Aharoni & Ungarish, 1977).

A Isoterma de Dubinin é utilizada para discernir se o processo de adsorção é de natureza física ou química, sendo que o

parâmetro que descreve este comportamento é o  $E$  (energia de ligação entre adsorvato-adsorvente). O valor de  $E$  de 1 a 8 indica adsorção física e  $E > 8$  indica adsorção química. Este modelo descreve que a vizinhança da superfície do adsorvente é caracterizada por uma série de equipotenciais superficiais tendo o mesmo potencial de sorção. Esta não assume que a superfície está homogênea ou energia potencial constante (Özcan, Özcan, Tunali, Akan & Kiran, 2005; Chen, Yang, Chen, Chen & Chen, 2009).

#### 4. CONCLUSÕES:

Para os Latossolos estudados, verificou-se que estes podem adsorver o hormônio  $17\alpha$ -metiltestosterona, seja em processo estático (repouso) ou dinâmico (agitação). Maiores teores de matéria orgânica no solo e maior salinidade no meio aquoso influenciam a adsorção por método estático, mas não são importantes pelo processo dinâmico, no qual teores de óxidos de Fe tendem a aumentar a adsorção do hormônio. O equilíbrio de adsorção é atingido em 24 horas e o modelo de Freundlich para o solo 1 e o modelo de Temkin para o solo 2 são os que mais se adequam ao processo de adsorção.

A interação entre o hormônio e solos tropicais ainda é pouco explorado e mostrou que este hormônio pode se alocar em sedimentos, permanecer adsorvido e ser liberado lentamente para o corpo d'água, causando a contaminação deste recurso. Este estudo mostra também a necessidade de mais estudos na área da piscicultura no que tange a utilização de  $17\alpha$ -metiltestosterona.

#### 5. AGRADECIMENTOS:

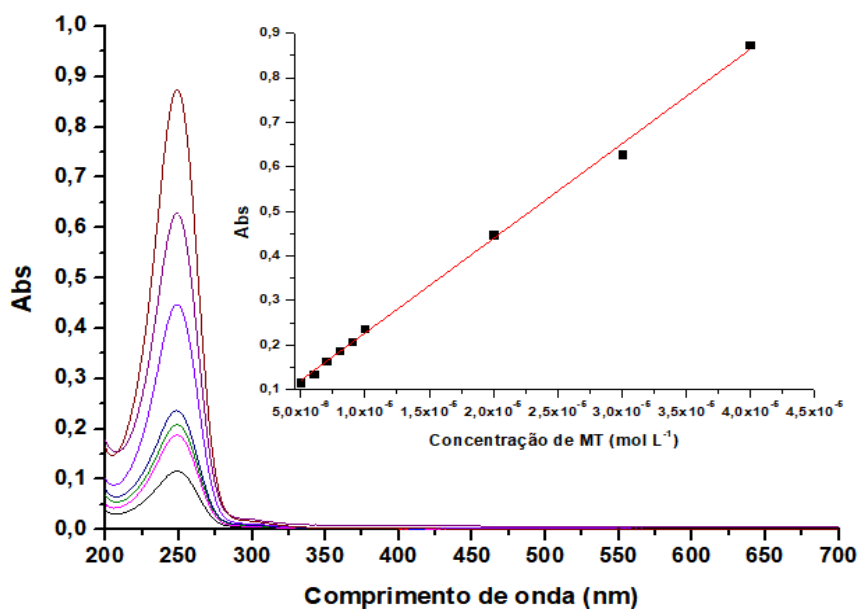
Ao Conselho Nacional de Desenvolvimento Científico e Tecnológico (CNPQ), ao Programa Institucional de Bolsas de Iniciação Científica (PIBIC) e a Fundação Araucária.

#### 6. REFERÊNCIAS:

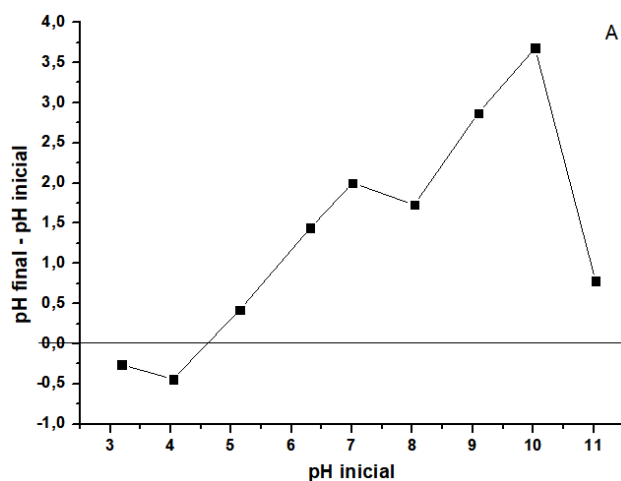
1. Agência de Notícias do Paraná. (2019). Líder na produção de pescados, Paraná prevê crescimento de 20%. Acesso em 03 de abril de 2019. Disponível em: <http://www.aen.pr.gov.br/modules/noticias/article.php?storyid=101686&tit=Lider-na-producao-de-pescados-Parana-preve-crescimento-de-20>.
2. Aharoni, C., & Ungarish, M. (1977). Kinetics of activated chemisorption. *Journal of the Chemical Society, Faraday Transaction*, 73, 456-464.
3. Araújo, C., & Reynol, F. (2017). Produção de tilápia no Brasil cresce 223% em dez anos. Acesso em 03 de abril de 2019. Disponível em: <https://www.embrapa.br/busca-de-noticias/-/noticia/21621836/producao-de-tilapia-no-brasil-cresce-223-em-dez-anos..>
4. van Raij, B. (2001). *Análise química para avaliação da fertilidade de solos tropicais*. Campinas, Brasil: IAC.
5. Baldissotto, B. (2002). *Fisiologia de peixes aplicada à piscicultura*. Santa Maria, Brasil: Editora UFSM.
6. Brasil. Ministério do Meio Ambiente, Conselho Nacional do Meio Ambiente, CONAMA. (2009). Resolução CONAMA nº 413, de 26 de julho de 2009. Dispõe sobre o licenciamento Ambiental da Aquicultura, e dá outras providências.
7. Brasil. Ministério do Meio Ambiente, Conselho Nacional do Meio Ambiente, CONAMA. (2013). Resolução CONAMA nº 459, de 16 de outubro de 2013. Altera a resolução nº 413 de 26 de julho de 2009, e dá outras providências.
8. Chen, A-H., Yang, C-Y., Chen, C-Y., Chen, C., & Chen, C-W. (2009). The chemically crosslinked metal-complexed chitosans for comparative adsorptions of Cu (II), Zn (II), Ni (II) and Pb (II) ions in aqueous medium. *Journal of Hazardous Materials*, 163(2-3), 1068-1075.
9. Espinoza-Quiñones, F.R., Módenes, A.N., De Pauli, A.R., & Palácio, S.M. (2015). Analysis of trace elements in groundwater using ICP-OES and TXRF techniques and its compliance with brazilian protection standards. *Water, Air, Soil Pollut.*, 226(32), 1-12. <https://doi.org/10.1007/s11270-015-2315-8>
10. Fitzpatrick, M. S., & Contreras-Sanchez. (2000). *Fate of methyltestosterone in the pond environment: Detection of MT in soil after treatment with MT food*. Pond Dynamics/Aquaculture CRSP,

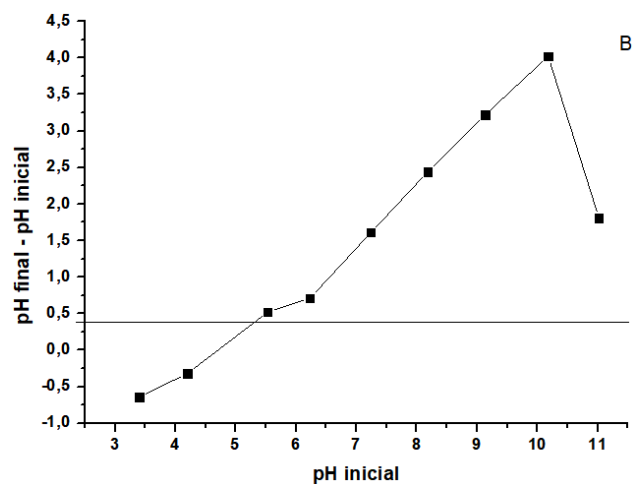
- Seventeenth Annual Technical Report. Corvallis: Oregon State University.
11. Foo, K. Y., & Hameed, B. H. (2010). Insights into the modeling of adsorption isotherm systems. *Chemical Engineering Journal*, 156(1), 2-10. <https://doi.org/10.1016/j.cej.2009.09.013>
  12. Giles, C.H., Smith, D. & Huitson, A. (1974). A general treatment and classification of the solute adsorption isotherm. I. Theoretical. *Journal of Colloid and Interface Science*, 47(3), 755-765.
  13. Green, B. W., & Teichert-Coddington, D. R. (2000). Human Food Safety and Environmental Assessment of the Use of 17 $\alpha$ -Methyltestosterone to Produce Male Tilapia in the United States. *J. World Aquacult. Soc.*, 31(3), 337-357. <https://doi.org/10.1111/j.1749-7345.2000.tb00885.x>
  14. Homklin, S., Ong, S. K., & Limpiyakorn, T. (2011). Biotransformation of 17 $\alpha$ -methyltestosterone in sediment under different electron acceptor conditions. *Chemosphere*, 82(10), 1401-1407.
  15. Hu, X., Liu, B., Deng, Y., Chea, H., Luo, S., Sun, C., Yang, P., & Yang, S. (2011). Adsorption and heterogeneous Fenton degradation of 17 $\alpha$ -methyltestosterone on nano Fe<sub>3</sub>O<sub>4</sub>/MWCNTs in aqueous solution. *Applied Catalysis B: Environmental* 107(3-4), 274-283.
  16. IBGE. Instituto Brasileiro de Geografia e Estatística. Produção da Pecuária Municipal. Rio de Janeiro. 2019, 45. Disponível em: <https://biblioteca.ibge.gov.br/index.php/biblioteca-catalogo?view=detalhes&id=784>. Acesso em 05 mar. 2020.
  17. Kalavathy M.H., Kathikeyan T., Rajgopal, S., & Miranda, L. R. (2005). Kinetic and isotherm studies of Cu (II) adsorption onto H<sub>3</sub>PO<sub>4</sub>-activated rubber wood sawdust. *Journal of Colloid and Interface Science*, 292(2), 354-362.
  18. Kim, I., Zhiqiang, Y., Baohua, X., & Weillin, H. (2007). Sorption of male hormones by soils and sediments. *Environmental Toxicology and Chemistry: An International Journal*, 26(2), 264-270.
  19. Kolok, A. S., & Sellin, M. K. (2008). The Environmental Impact of Growth-Promoting Compounds Employed by the United States Beef Cattle Industry: History, Current Knowledge, and Future Directions. *Rev. Environ. Contam. Toxicol.*, 195, 1-30. [http://doi.org/10.1007/978-0-387-77030-7\\_1](http://doi.org/10.1007/978-0-387-77030-7_1)
  20. Kubitza, F. (2009). O uso de metilttestosterona na masculinização de tilápias um desafio para o MPA. *Panorama da Aquicultura*, 19(116), 14-21.
  21. Lee, L. S. Strock, T. J., Sarmah, A. K., & Rao, P. S. C. (2003). Sorption and dissipation of testosterone, estrogens and their primary transformation products in soils and sediment. *Environmental Science and Technology*, 37(18), 4098-4105.
  22. Mlalila, N., Mahika, C., Kalombo, L., Swai, H., & Hilonga, A. (2015). Human food safety and environmental hazards associated with the use of methyltestosterone and other steroids in production of all-male tilápia. *Environ. Sci. Pollut. Res.*, 22(7), 4922-4931.
  23. Oliveira, E. G., Santos, F. J. S., Pereira, A. M., & Lima, C. B. (2007). *Produção de Tilápia: mercado, espécie, biologia e recreia*. Embrapa. Circular técnica, 45, 1.
  24. Ong, S. K., Chotisukarn, P., & Limpiyakorn, T. (2012). Sorption of 17 $\alpha$ -methyltestosterone onto soils and sediment. *Water, Air, & Soil Pollution*, 223, 3869-3875.
  25. Özcan, A., Özcan, A. S., Tunali, S., Akar, T., & Kiran, I. (2005). Determination of the equilibrium, kinetic and thermodynamic parameters of adsorption of copper (II) ions onto seeds of Capsicum annum. *Journal of Hazardous Materials*, 124,(1-3), 200-208.
  26. Pubchem. (2005). Methyltestosterone. Acesso em 03 de abril de 2019. Disponível em: <https://pubchem.ncbi.nlm.nih.gov/compound/6010#section=Top>
  27. Ribeiro, R. P. (2001). Espécies exóticas. In: Moreira, H. L. M., Vargas, L., Ribiero, R. P., & Zimmermann, S. Fundamentos da Moderna Aquicultura. Canoas: Ulbra.

28. Young, R. B., Latch, D. E., Mawhinney, D. B., Nguyen, T-H., Davis, J. C., & Borch, T. (2013). Direct Photodegradation of Androstenedione and Testosterone in Natural Sunlight: Inhibition by Dissolved Organic Matter and Reduction of Endocrine Disrupting Potential. *Environ. Sci. Technol.*, 47(15), 8416-8424.

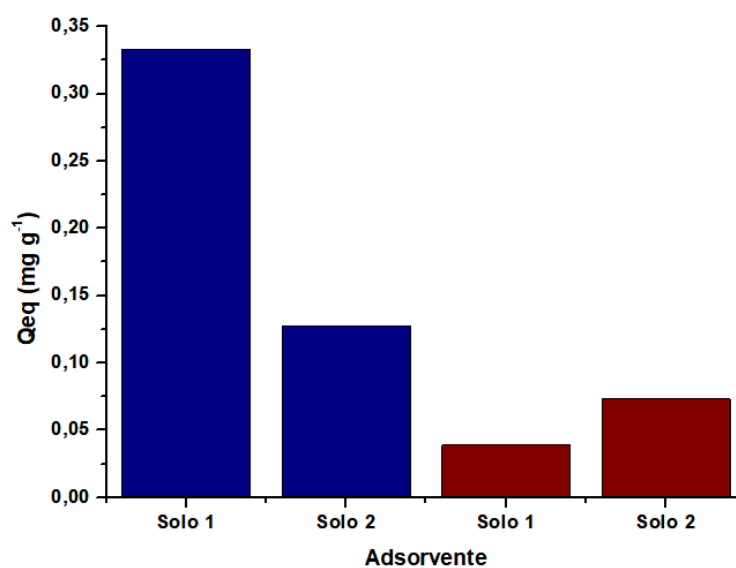


**Figura 2.** Espectros na região do UV-visível para o hormônio 17 $\alpha$ -metiltestosterona em diferentes concentrações em solução aquosa.  $\lambda_{\text{máx.}} = 249 \text{ nm}$ . Insert: Curva analítica do hormônio MT obtida a partir das absorvâncias no comprimento de onda máximo.

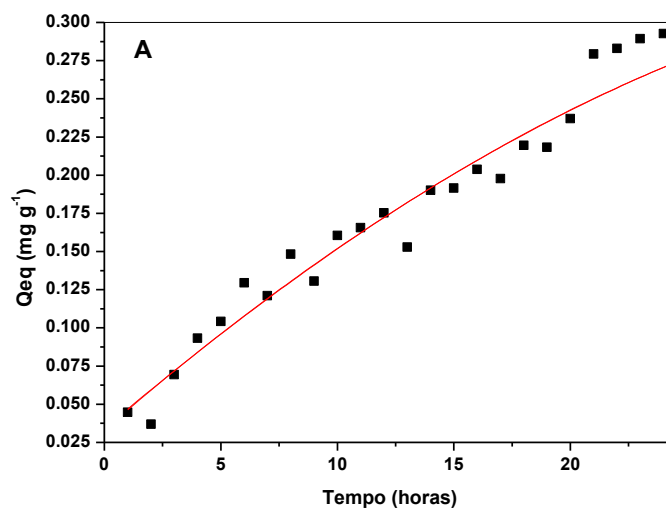




**Figura 3.** Curvas obtidas no estudo do ponto de carga zero (PCZ) para os diferentes solos. A) Solo 1. B) Solo 2.



**Figura 4.** Quantidade máxima de hormônio adsorvido em cada grama do material adsorvente (Qeq) para os solos 1 e 2. (–) Adsorção dinâmica. (–) Adsorção estática.



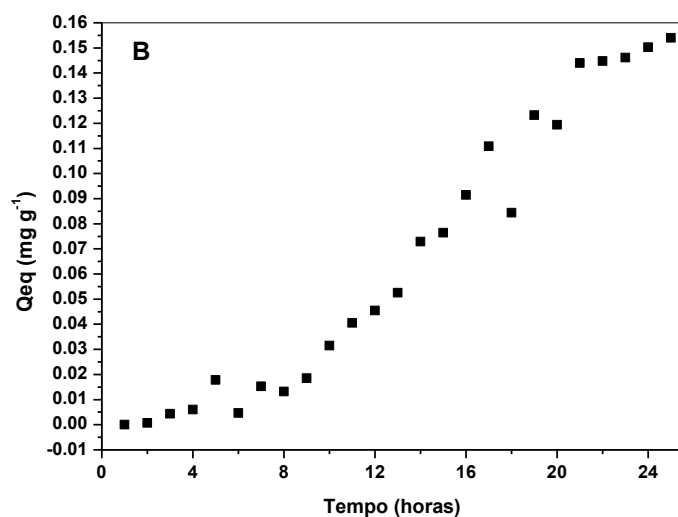


**Figura 5.** Influência do tempo na adsorção de 17 $\alpha$ -metiltestosterona em (A) solo 1; (B) solo 2. Concentração inicial do hormônio:  $3,994 \times 10^{-5} \text{ mol L}^{-1}$ ; 25 °C, pH 5,5.

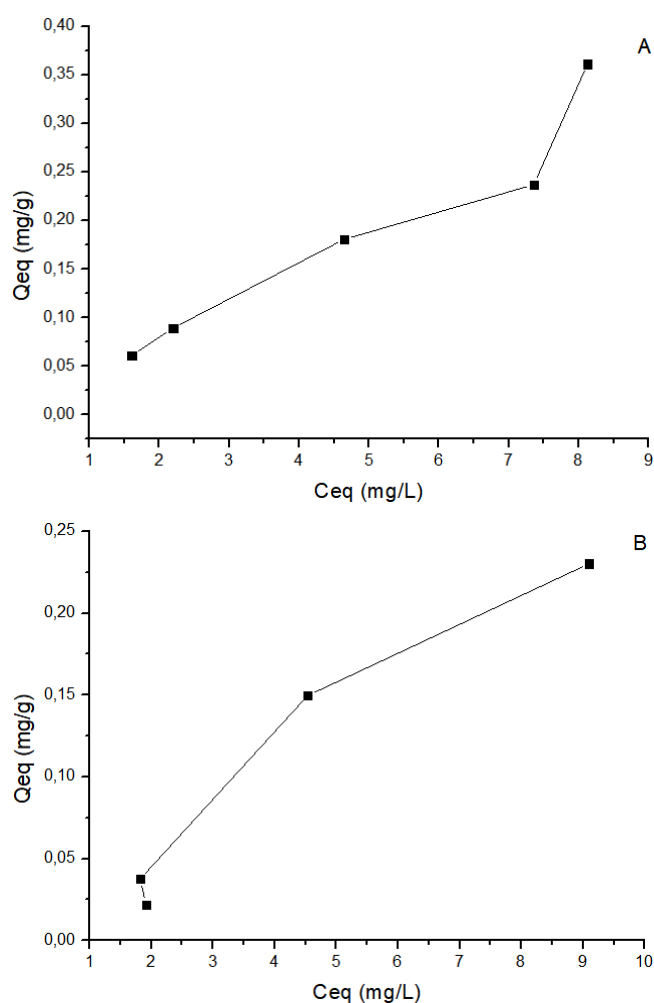


**Figura 6.** Isotermas de adsorção do hormônio em: A) Solo 1. B) Solo 2. Tempo de equilíbrio de 24 h; 25 °C e pH 5,5.

**Tabela 1.** Parâmetros da caracterização dos solos estudados, a partir do Laudo da COODETEC.

| Solo 1                             |  |                  |                             |
|------------------------------------|--|------------------|-----------------------------|
| Macronutrientes                    |  | Micronutrientes  |                             |
| Parâmetro                          | Teor (cmol <sub>c</sub> dm <sup>-3</sup> ) | Parâmetro        | Teor (mg dm <sup>-3</sup> ) |
| K <sup>+</sup>                     | 0,43                                       | Fe total         | 42,56                       |
| Ca <sup>+2</sup>                   | 3,31                                       | Cu <sup>2+</sup> | 7,64                        |
| Mg <sup>+2</sup>                   | 1,38                                       | Zn <sup>2+</sup> | 3,85                        |
| Al <sup>+3</sup>                   | 0,27                                       | Mn total         | 74,02                       |
| H <sup>+</sup> + Al <sup>+3*</sup> | 7,76                                       |                  |                             |
| <b>Parâmetro</b>                   | <b>Teor (mg dm<sup>-3</sup>)</b>           |                  |                             |
| P                                  | 22,18                                      |                  |                             |
| Matéria orgânica (MO)**            | 32,83                                      |                  |                             |
| pH***                              | 4,60                                       |                  |                             |

| Solo 2                             |  |                  |                             |
|------------------------------------|--|------------------|-----------------------------|
| Macronutrientes                    |  | Micronutrientes  |                             |
| Parâmetro                          | Teor (cmol <sub>c</sub> dm <sup>-3</sup> ) | Parâmetro        | Teor (mg dm <sup>-3</sup> ) |
| K <sup>+</sup>                     | 0,46                                       | Fe total         | 32,76                       |
| Ca <sup>+2</sup>                   | 4,89                                       | Cu <sup>2+</sup> | 6,96                        |
| Mg <sup>+2</sup>                   | 2,29                                       | Zn <sup>2+</sup> | 4,07                        |
| Al <sup>+3</sup>                   | ND   | Mn total         | 90,81                       |
| H <sup>+</sup> + Al <sup>+3*</sup> | 5,76                                       |                  |                             |
| <b>Parâmetro</b>                   | <b>Teor (mg dm<sup>-3</sup>)</b>           |                  |                             |
| P                                  | 31,21                                      |                  |                             |
| Matéria orgânica (MO)**            | 40,31                                      |                  |                             |
| pH***                              | 5,20                                       |                  |                             |

\* Tampão SMP. \*\* Fator de correlação de Van Bemmelen (C x 1,724): fonte: Van Raij (2001). \*\*\*em CaCl<sub>2</sub> 0,01 mol L<sup>-1</sup>.

**Tabela 2.** Parâmetros obtidos a partir dos modelos de Langmuir, Freundlich, Temkin e Dubinin.

| Modelos   |   | Solo 1                              | Solo 2          |
|---|---|-------------------------------------|-----------------|
|   |   | $Q_{eq} \text{ (mg g}^{-1}\text{)}$ | 0,361    0,2304 |
| Constante de Langmuir<br>$\frac{C_{eq}}{q_{eq}} = \frac{1}{q_m b} + \frac{C_{eq}}{q_m}$ | $q_m \text{ (mg g}^{-1}\text{)}$            | 1,106                               | 35,752          |
|   | $b \text{ (L mg}^{-1}\text{)}$              | 0,039                               | -2,411          |
|   | $R^2$                                       | -0,319                              | 0,910           |
|   |   |                                     |                 |
| Constante de Freundlich<br>$\log q_{eq} = \log k_f \cdot \frac{1}{n} \cdot \log C_{eq}$ | $K_f \text{ (mg g}^{-1}\text{)}$            | 0,039                               | 0,013           |
|   | $n$   | 1,012                               | 0,724           |
|   | $R^2$                                       | 0,964                               | 0,860           |
|   |   |                                     |                 |
| Temkin<br>$q = B_1 \ln K + B_1 \ln C_{eq}$  | $k_t \text{ (kJ mg}^{-1}\text{)}$           | 0,827                               | 0,684           |
|   | $B_1 \text{ (dm}^3 \text{ mg}^{-1}\text{)}$ | 0,156                               | 0,127           |
|   | $R^2$                                       | 0,834                               | 0,985           |
|   |   |                                     |                 |
| Dubinin (DER)<br>$\ln q_{eq} = \ln q_d - B_d E^2$                                       | $q_d$                                       | 0,288                               | 0,245           |
|   | $B_d$                                       | 0,011                               | 0,019           |
|   | $E \text{ (kJ mol}^{-1}\text{)}$            | 12,219                              | 10,724          |
|   | $R^2$                                       | 0,879                               | 0,891           |

$C_{eq}$  = concentração do adsorvato em equilíbrio,  $q_{eq}$  = quantidade máxima adsorvida por grama do adsorvente,  $b$ = constante de equilíbrio de adsorção,  $q_m$ = quantidade máxima de adsorvato por unidade de massa,  $K_f$  e  $n$ = constante de Freundlich,  $K_t$ = constante de equilíbrio de ligação (corresponde à energia de ligação máxima),  $B_1$ = calor da adsorção,  $B_d$ = constante relacionada à energia livre média de adsorção por mols do adsorvato,  $q_d$ = capacidade da saturação teórica.



**O EFEITO DA ESTRATÉGIA DE APRENDIZAGEM SMART-PBL E DA APRENDIZAGEM ACADÊMICA AUTORREGULADA SOBRE AS HABILIDADES METACOGNITIVAS E DE RESOLUÇÃO DE PROBLEMAS NA APRENDIZAGEM EM QUÍMICA****THE EFFECT OF SMART-PBL LEARNING STRATEGY AND ACADEMIC-SELF REGULATED LEARNING ON METACOGNITIVE & PROBLEM-SOLVING SKILLS IN LEARNING CHEMISTRY**UTAMI, Deka Dyah<sup>1\*</sup>; SETYOSARI, Punaji<sup>2</sup>; KAMDI, Waras<sup>3</sup>; ULFA; Saida<sup>4</sup>; KUSWANDI, Dedi<sup>5</sup><sup>1,2,4,5</sup> Department of Instructional Technology, Faculty of Education, Universitas Negeri Malang, Indonesia<sup>3</sup> Department of Mechanical Engineering, Faculty of Engineering, Universitas Negeri Malang, Indonesia

\* Correspondence author

e-mail: dekadiahutami.10@gmail.com

Received 16 May 2020; received in revised form 17 June 2020; accepted 29 June 2020

**RESUMO**

O aprendizado da química no século XXI deve enfatizar não apenas os resultados da aprendizagem cognitiva, mas também as habilidades metacognitivas e de resolução de problemas. O metacognitivo precisa ser aprimorado para que os alunos possam praticar a organização, o monitoramento e a avaliação do processo de raciocínio na solução de problemas químicos. É necessário desenvolver a solução de problemas para treinar o aluno a tomar decisões e explicações científicas apropriadas ao encontrar problemas químicos. Com base no resultado da observação, as habilidades metacognitivas e de resolução de problemas de professores de ciências em treinamento em Malang, na Indonésia, foram baixas. As habilidades metacognitivas e de resolução de problemas são afetadas pelo aprendizado acadêmico auto-regulado (ASRL) dos alunos. O objetivo deste estudo foi conhecer o efeito da Estratégia Atende à Aprendizagem Baseada em Problemas de Tecnologia de Realidade Aumentada (SMART-PBL) e da aprendizagem acadêmica autorregulamentada (ASRL) na melhoria das habilidades metacognitivas e de resolução de problemas na aprendizagem da química. A SMART-PBL foi modificada pela estratégia de aprendizagem baseada em problemas (PBL) que auxiliou a tecnologia de realidade aumentada como mídia visual. Os sujeitos da pesquisa foram 64 professores de ciências em treinamento divididos em classe controle e experimental, respectivamente de 32 alunos. O método de pesquisa foi o delineamento quasi experimental, com fatorial de projeto de grupo de controle não equivalente 2x2. A classe experimental usou SMART-PBL, enquanto a classe controle PBL. O SMART-PBL teve uma influência significativa nas habilidades metacognitivas e de resolução de problemas em comparação com a estratégia PBL. Além disso, a abordagem SMART-PBL não interagiu com o ASRL para melhorar as habilidades metacognitivas e de resolução de problemas. A implementação do SMART-PBL aprimora não apenas as habilidades metacognitivas e de resolução de problemas, mas também desenvolve habilidades criativas e de pensamento crítico, comunicação e raciocínio científico que aparecem nos alunos durante o aprendizado de química.

**Palavras-chave:** *habilidade metacognitiva, habilidade para resolver problemas, aprendizado baseado em problemas, realidade aumentada, ensino de química.*

**ABSTRACT**

Learning chemistry in the 21st century should emphasize higher-order thinking skills such as metacognitive and problem-solving skills besides cognitive learning outcomes. Metacognitive needs to be improved so students can practice organizing, monitoring, and evaluating their thinking process in solving chemical problems. Problem-solving needs to develop to train students in making the appropriate decision and scientific explanation when encountering chemical issues. Based on observation results, the metacognitive and problem-solving skills of a pre-service science teacher in Malang, Indonesia, were low. Metacognitive and problem-solving skills are affected by academic-self regulated learning (ASRL) by students. This study aimed to know the effect of the Strategy Meets Augmented Reality Technology-using Problem Based Learning (SMART-PBL) and Academic-self regulated learning (ASRL) on improving metacognitive and problem-solving skills in learning chemistry. The SMART-PBL was modified by Problem Based Learning (PBL) strategy, which assisted by Augmented Reality technology as visual media. The research subject was 64 pre-service science teachers divided into control and experimental class, respectively, of 32 students. The research design was Quasi-

Experimental, with Nonequivalent Control Group Design using factorial 2x2. The trial class performed SMART-PBL, which showed a more significant influence on metacognitive and problem-solving skills than the PBL class. The SMART-PBL not interacted with ASRL to improve metacognitive and problem-solving skills. By implementing SMART-PBL improves not only metacognitive and problem-solving skills but also evokes creative and critical thinking, communication, and scientific reasoning skills that appear in students during learning chemistry.

**Keywords:** *metacognitive skill, problem-solving skill, problem-based learning, augmented reality, learning chemistry.*

---

## 1. INTRODUCTION:

Chemistry is a science dimension that tried to explain the occurrence of natural phenomena in the universe scientifically. One of the goals of learning chemistry is building concepts and then using them to solve various natural events in chemistry (Parlan *et al.*, 2018). The idea of chemistry was abstract (Üce and Ceyhan, 2019) and taught in hierarchical manners (Zheng *et al.*, 2017; Armengol and Plaza, 2005). It said to be abstract because it studied real objects which invisible by human vision, for example, the concept of the atom as a constituent of a chemical element. Concepts are arranged in a hierarchy from the basic into the most complex ones consisting of microscopic, symbolic, and macroscopic domains (Jong and Taber, 2007).

Since chemistry concepts were abstract and hierarchy, it considers to be hard to comprehend as a class by students, then the learning process of chemistry has been carried out by teachers with extreme care to prevent misconceptions as were widely reported (Yiin, 2010; Özmen, 2004). So learning activities tend to use a teacher-centered approach. This approach indeed helps students in accelerating in understanding concepts but is not honing their thinking abilities. Whereas higher-order thinking skills such as critical thinking and problem-solving are essential for students in the 21st century (Griffin, Patrick McGraw, 2012).

The most fundamental concept in chemistry was to learn about elements and chemical compounds (Hendry, Robin, 2006; Partington, 1948). This basic concept needs to be master because it studied the atom structure as a constituent of an element, knows the physical and chemical properties, and understands chemical elements' uses before exploring the further complicated concept. When students have mastered the basic concepts, they will find it easier to learn more complex thoughts (Jusniar *et al.*, 2020) to explain the process of occurring natural phenomena caused by the reaction of chemical elements and compounds scientifically.

To explain the process of occurrence of chemical phenomena in daily life, the student needed higher-order thinking skills (HOTS), such as problem-solving skills (Symington, 1977). Developing problem-solving skills required the ability to manage the thinking process, known as the ability to think metacognitive (Jauhangeer, Shuib, and Azizul Hasan, 2018).

Metacognitive is one of the individual thinking skills in managing the process and product of thinking and how to actively monitor and regulate their cognitive processes (Flavell, 1979). Developing metacognitive skills is crucial because it helps identify the level of consciousness, training and tracking this way of thinking, and training on how to solve the problem heuristically (Aurah *et al.*, 2011).

Information about students 'metacognitive knowledge is needed to identify and improve students' thinking patterns in studying chemical material (Parlan, 2019). It supported by research proving that metacognitive skills can help develop problem-solving skills in learning chemistry (Azizah and Nasrudin, 2019). Success in learning chemistry will produce students with analytical thinking skills and scientific attitudes to solve problems scientifically in various situations (Dasna, 2012).

Problem-solving skills also suggested developing in science students while studying chemistry (Stockwell, Stockwell, and Jiang, 2017) due to the fundamental human cognitive processes. The problem occurs when students have no clue how to solve the cases. Problem-solving was a process, consists of systematic observation and critical thinking to find an appropriate solution (Rahman, 2019).

However, based on observations on the research location found several conditions. Besides, low cognitive learning outcomes, apparently new problems were found, metacognitive and problem-solving skills were similar. The level of metacognitive thinking skills was low (51.70%); some students still mistakenly mention the halogen group's chemical elements as noble gas elements. The majority of students

still classify the chemical element of Hydrogen as an alkali metal group. If they had more profound thought about the characteristics of metals, this error would not have occurred. It indicated lower in thinking strategically. This finding supported by a previous study by Ijirana (2018) said that as much as 87% of chemistry educational students had low metacognitive thinking skills.

The level of problem-solving skills was low at (48.07%). Results of interviews with lecturers found that the majority of students still had difficulty explaining scientifically how the reaction of sulfur and other chemical elements can lead to acid rain in industrial and urban areas. This condition was consistent with the findings of Gayon (2003) reported majority high school students have low chemical problem-solving skills. It supported by a similar result by previous studies that science education students have a problem-solving ability that still needs to be improved (Widiasih, 2018).

Based on the results of interviews, students tend to collect assignments lately. It indicates that student's academic self-regulated learning in learning chemistry also found still low. Previous research reported similar findings that only 37% of students used their self-regulated learning ability to predict their performance in general chemistry courses (Miller, 2015).

Based on the explanation above, an effort should be made to develop the ability to think metacognitive and solve problems in pre-service science teachers by improving the quality of the chemistry learning process to provide better learning outcomes.

Previous research published mood for learning chemistry can be built by knowing and linking chemical issues in the history of the invention (Kupatadze, 2018). Improving the quality of learning can be done in several ways, like to empower technology or media in education (Setyosari, 2005). To learn chemistry with complicated and abstract concepts requires media assistance with high abstraction or visualization, such as Augmented Reality technology (AR).

AR was a new technology as well as a field of research sitting at the interface of Virtual Reality (VR), Artificial Intelligence (AI), and Computer Graphics (CG), which the simulated data displayed in a real-world environment. It impacted chemistry for educational purposes and enhanced the illustration of chemical communications (Steven V. Ley, 2016).

The results of a previous study proved that AR could increase interest and motivation to learn chemistry on the learner (Cai, Wang and Chiang, 2014) and help solve chemical problems (Núñez *et al.*, 2008). Besides, the success of AR has widely publicized in improving academic learning outcomes (Efimova, 2012) and chemistry learning outcomes (FS, Irwansyah. Y M, 2018). AR technology cannot be implemented individually in learning. It needed procedural steps in the form of learning strategies (Rosli, 2018). Learners who choose to use a variety of learning strategies tend to earn higher learning outcomes (Simsek, 2010).

(Dewey, 1910) postulated that the thinking process cannot happen suddenly, but can stimulate by presenting a problem, cases, questions, conflict, or confusion about something. Gao *et al.*, (2018) showed his research findings that conceptual understanding and problem-solving skills could improve by implementing learning problem based learning (PBL) strategy. Kamdi (2007) defined PBL as one of the innovative learning models for instructions. PBL famous for using real-world or concrete cases to facilitate learning through a student-centered approach (Salinitri *et al.*, 2015). PBL was modular by Self-Regulated Learning in discovering success. Learners gave responsibility for their learning process and results (Hmelo-Silver, 2004). Academic Self-Regulated Learning (ASRL) affected metacognitive and problem-solving skills. This statement supported by several studies showing the success of self-regulation in solving problems (Ahghar, 2013). The literature states that learners' self-regulation in learning was related to metacognitive skills possessed (Isaacson and Fujita, 2006).

This study implemented the *Strategy Meets Augmented Reality Technology-Using Problem Based Learning* abbreviated as SMART PBL, which integrating Generative and Problem Based Learning (PBL) strategy with Augmented Reality (AR) technology that has successfully developed in the previous study. The difference SMART-PBL from PBL has implemented chemical augmented reality technology as learning media and assignments as a method to explore prior knowledge and build new expertise while solving problems. Modifications added by providing reinforcement of motivation, giving positive perception, constructing knowledge, refining experience, and using knowledge to resolve issues adapted from generative learning theory (Wittrock, 1992).

Several studies have published research about PBL successfully enhanced metacognitive (Pratama, 2018), improved problem-solving skills (Kadir *et al.*, 2016). Generative learning increased problem-solving ability (Wittrock, 1994), increased science comprehension, and self-regulation (Lee, Grabowski and Lim, 2009; Reid and Morrison, 2014).

However, there were no studies yet reported the SMART-PBL learning strategy's success in improving metacognitive thinking and problem-solving skills. Therefore, this study aimed to know the effect of the SMART-PBL learning strategy and academic-self-regulated learning on metacognitive and problem-solving skills in learning chemistry.

## Hypothesis:

This study has six hypotheses:

**H<sub>1</sub>.** There was a significant difference in the metacognitive skill of learners who taught by using the SMART-PBL strategy compared to the PBL strategy.

**H<sub>2</sub>.** There was a significant difference in the metacognitive skill of learners with high ASLR skills and low ASLR skills.

**H<sub>3</sub>.** There was a significant interaction between learning strategies and ASLR's skills to learners' metacognitive skills.

**H<sub>4</sub>.** There was a significant difference in learner's problem-solving skills, which taught using SMART-PBL compared to the PBL strategy.

**H<sub>5</sub>.** There was a significant difference in learner's problem-solving skills with high ASLR skills and low ASLR skills.

**H<sub>6</sub>.** There was a significant interaction between learning strategies and ASLR's skills to learners' problem-solving skills.

## 2. MATERIALS AND METHODS:

### 2.1. Research Design and Samples

This study used a Quasi-experimental design. Following the variables studied, the factorial design used was 2x2 by multivariate analyzes, with Nonequivalent Control Group Design used to play the effect and interaction effect on the dependent variable (Table 1).

The trial class treated using the SMART-PBL strategy with generative assignments, while the control class treated with a PBL strategy

without any task. The research subjects involved 64 pre-service science teachers in Malang, Indonesia, on chemical elements and compounds. All participants have agreed to participate as subject research in each class. Trial and control class each comprised 32 students.

The procedure to implement SMART-PBL learning strategy consists of ten phases namely: (1) attentional focusing and motivational process; (2) problem orientation; (3) student orientation; (4) fact identifications; (5) generate hypothesis; (6) identification knowledge deficiencies; (7); knowledge creation process; (8) generation process; (9) apply new knowledge; (10) abstraction (Figure 1).

### 2.2. Data Collection Tools and Analysis

The statistical test in this study carried out using statistical data processing software in the form of IBM SPSS Statistics 21 using MANOVA parametric analysis. Quantitative data obtained using MAI (*Metacognitive Awareness Inventory*) by Schraw & Denison with a range scale of 1-5. The metacognitive knowledge data obtained using the rubric by Rompayom on a range scale of 0-2. Data on problem-solving skills were collected using the problem-solving rubric by Greenstein on a range scale of 1-4.

## 3. RESULTS AND DISCUSSIONS:

The Shapiro-Wilk's normality test results showed the acquisition of a significant value of metacognitive skills of 0.06 in the experimental class and 0.12 in the control class. The acquisition of the problem-solving skills in the trial class was 0.587, while in the control class was 0.146. The overall value was more significant than the standard criteria ( $\text{sig} > 0.05$ ), so it can conclude that the data distributed. Levene's test showed the acquisition of metacognitive skills of 0.111 and problem-solving skills of 0.596. While the Box's M test was 6.784 with a significance value of 0.709, obtaining all the significance values were more significant than the standard criteria ( $\text{sig} > 0.05$ ), so the data can be said to be homogeneous and come from the same variant, so it is worth to compare.

The hypothesis test performed using; 1) Multivariate analysis to examine the effect of strategy on metacognitive and problem-solving skills simultaneously. This test aimed to assess the significance of the difference in scores between the SMART-PBL group on the metacognitive and problem-solving skills variable

due to the primary influence and interaction between the independent variables. Results showed that each learning strategy's main effect obtains a probability value smaller than the standard criteria (sig)  $0.000 < 0.005$ . The result of ASLR was  $0.705 > 0.005$ , so it concluded that ASLR does not affect metacognitive and problem-solving simultaneously.

After knowing the presence or absence of the influence from each independent variable on the dependent variable, then performed 2) Hypothesis test using a *Test of Between-Subjects Effects* to determine the effect between subjects by testing the comparison between the average scores estimated average and interactive influence analysis in Table 2.

### 3.1. Hypothesis Testing 1

Data results from table 2 showed a significant difference in metacognitive skills among learners taught using SMART-PBL. PBL strategies due to both of the acquisition of significant value were smaller than the standard criteria ( $0.000 < 0.005$ ). The addition of metacognitive awareness scores of students treated using the SMART-PBL strategy increased from 2.58 to 4.18. Whereas in the PBL class, the average value increased from 2.39 to 3.84 (Figure 2). The data analysis results showed that the gain score in the SMART-PBL was 66.04%, with quite a practical interpretation (56-76%). While the PBL class obtained a gain score of 55.37% in the correct interpretation category (40-55%). It concluded that the SMART-PBL strategy was more effective in increasing students' metacognitive awareness than the PBL strategy.

There was a significant difference between before and after implementing the SMART-PBL strategy on the acquisition of an average score of metacognitive knowledge. The increase in the average value of the metacognitive abilities of the trial class from 0.97 to 1.191 while increasing the control class from 0.60 to 1.50 (Figure 3). There was a significant value difference in the aspect of metacognitive knowledge between the SMART-PBL with higher grades than the PBL class. It means the SMART-PBL strategy could increase learners' metacognitive skills more effectively than the PBL strategy.

Several phases on the SMART-PBL strategy contributed to enhancing metacognitive skills for students, that's; **Phase 1**, (Attentional Focusing & Motivational Processes). Before learning begins, students gave generative assignments to draw a mapping concept or to summarize related to the

next meeting material. Tasks were optional according to students' learning preferences to help students collect initial information on these materials (*declarative knowledge*).

This phase was successfully improving student metacognitive skills. The study (Astriani *et al.*, 2020) reported concept mapping applied in the syntax of learning models could improve the metacognitive skills of science students. **Phase 2** (Problem Orientation). Students presented several cases caused by chemical elements in the alkali metal group and others.

At this stage, students practiced thinking about solving problems by identifying what kinds of chemical elements are involved in every case. Students also started practicing metacognitive thinking way by asked themselves how to resolve the issues (*procedural knowledge*). Problems to be solved were products from developing textual concepts became contextual concepts. It could provide a better chemistry learning experience and a positive effect on content comprehension (Silva, Daniele dos Santos; Yamaguchi, 2018).

Some assistance (scaffolding) included in every case. The latest research supports that increasing chemistry learning motivation could use experiments based on concrete evidence (Lima, Alessandra Rodrigues; Silva, Flávia Cristiane Vieira da; Simoes Neto and Euzebio, 2019). Scaffolding also improves metacognitive skills and interest in learning chemistry for learners with a profound understanding of science (Tosun and Senocak, 2013). Cases presented in Table 3.

### 3.2. Hypothesis Testing 2

Data analysis results showed no significant difference in metacognitive skill among learners who had a high level of ASLR and low level of ASLR skills; this was due to the acquisition of considerable value higher than the standard criteria ( $0.690 > 0.005$ ). Results of previous studies showed that there was an effect of one's Self Regulated Learning ability on metacognitive skills. However, in this study, ASRL skills did not significantly influence metacognitive skills. Data in Figure 4 showed learners with a low level of ASRL reached metacognitive value almost equals with high-level ASRL student groups in PBL class. Interestingly, a similar result found by (Nietfeld, 2015) the group with the low academic ability could obtain a higher value of the metacognitive ability (conditional knowledge aspect) than the group with high ones. The high level of ASLR learners described as disciplined and always

active individuals. They have a good strategy in remembering subject matter; a brief target goal should achieve, a structured plan in attaining these goals, and proper evaluation in measuring the progress of learning. They also have a high effort in seeking help for the needs of the learning process either through literature, friends, teachers, and even parents actively, make arrangements or a suitable provision of the learning environment to obtain comfort and focus during learning. They have high priority in completing school assignments and finishing as soon as possible. While the characteristics of groups of students with low ASRL levels are less active in doing these things, it concluded that a high level of ASRL students tended to have higher physical activity in regulating their learning process than the lower level of ASLR students.

The research results from the *Journal of Health Psychology* (Mcelroy, Dickinson and Dickinson, 2015) psychologically explained these findings; they reported that individuals who tend to reduce physical activity appeared to have higher thinking activity. Instead, they were more likely to use this time to think efficiently. They practiced becoming strategic thinkers who can find smart shortcuts to solve problems, save time, and generate innovative ideas. This condition happened to the groups of students with low ASRL capability. They lack physical activity in regulating the learning process, but reportedly high-value metacognitive skill.

Meanwhile, groups of students with high activity (high ASRL) said they were easily bored when they had to sit still and observe their abstract thoughts. Instead, they prefer to stimulate their minds by doing physical activities, such as doing assignments, organizing the study room to be comfortable, making a list of study plans, and other physical activities. The low level of ASRL only indicates the low physical activity in the self-regulation of learning and not as a measure of the low activity (ability) of thinking. It concluded that the low-level ASRL student group had higher thinking skills and was equivalent to the high-level ASRL group. As a result, there was no significant difference between the level of ASRL and metacognitive skills.

### 3.3 Hypothesis Testing 3

The results showed no interaction between SMART-PBL strategy and ASLR skills towards metacognitive skills; this is due to the acquisition of significant value was higher than the standard criteria ( $0,463 > 0,005$ ). These results indicated that the SMART-PBL strategy not

influenced by the ASRL skills of students in improving metacognitive skills. The findings of this study reported that in certain circumstances, SRL also found no effect on the school's academic abilities and learning outcomes (Johny and Magno, 2012). SMART-PBL not affected by ASRL to enhance metacognitive skills; this strategy emphasized training how to know what concepts to learn, how to rearranged thinking ways to solve a problem, and why to choose and use this knowledge and procedures through a series of learning steps that have developed.

### 3.4 Hypothesis Testing 4

The analysis showed a significant difference between student ability to solve problems treated using SMART-PBL and PBL strategy due to the significant value was smaller than the standard criteria ( $0,000 < 0,005$ ). The acquisition of problem-solving skills in the trial class 85.10, with a standard deviation of 1.38 (Figure 5). From the results of the analysis, the ability of the experimental class taught by using the SMART-PBL strategy obtained higher average value than the control class taught by using the PBL strategy.

Several phases in SMART-PBL designed to enhance problem-solving skills in learning, such as **Phase 3** (Students Orientation). A division of the groups has aimed to make students able to solve cases collaboratively. Many advantages if learning sets in teamwork (collaborative) will support sharing knowledge and developing communication skills. Next was **Phase 4** (Facts Identification). Students practiced to identify solutions by looking for facts can be in their prior knowledge or clues that contribute to solving cases. The information obtained at this stage was general and original (authentic) then continued in the next phase. **Phase 5** was (Generate Hypotheses). Students practiced finding the solution of the cases by predicting some of the elements involved in the given problems. In the group, students with the correct hypothesis continued to prove their hypotheses scientifically. Similar things applied to groups with false assumptions. They studied more deeply to find why their predictions cannot be accepted scientifically. At this stage, all students training their conditional knowledge to evaluate the solutions by using their critical thinking and scientific reasoning skills.

**Phase 6** (Identification Knowledge Deficiencies), at this stage, students got a new learning experience. The limited knowledge in

formulating hypotheses completed at this stage. Through the process of searching for information that still needed to build appropriate explanations for solving the problem correctly. Students used mobile Augmented Reality technology in the form of a scanner application to present the desired elements of information. The information displayed is 3D visuals represented the physical form of chemical elements (solid phase, gas phase, liquid phase), atomic number, a symbol of the elements, and the general properties of the elements accompanied by audio when the information is displayed. Data obtained through the interview method as much as 80% of the students like this media, 20% still prefer to use the periodic table element as data collection instruments. These results were similar to research findings, which reported that Augmented Reality could provide an authentic new learning experience (Suartama, Kadek Setyosari, and Ulfa, 2019).

Figures 6 - 9 showed the activities of students when involved with the mobile Augmented Reality. AR technology used in this study took the form of mobile Augmented Reality application using an application on a smartphone equipped with cards containing chemical element information. The mobile Augmented Reality chosen in this study supported by literature, which stated that the form of mobile learning media had a significant impact on learning success due to its ability to take over the role of computers in the speed of accessing information as a learning source (Ulfa, 2013).

**Phase 7, (The Knowledge Creation Processes).** This stage was crucial because students carried out the process of constructing knowledge. (Wittrock, 1992) stated that the knowledge construction process occurs when students manage to connect old information (fundamental knowledge, clues, and hypotheses) that they have with new information obtained. The success of the knowledge construction was if students can explain how to solve the problems and found the chemical elements involved in the case. They analyzed the suitability of new with old information in the form of instructions found. At this stage, students defend solutions by using their creative and critical thinking skills.

**Phase 8 (The Generation Process).** This phase also called the refinement or maturation of knowledge. Students directed to make a categorization or classification of elements been found based on group, nature, and usefulness.

**Phase 9 was (Apply New Knowledge).** This stage

tested the new knowledge that students have about elements and compounds by giving further questions about daily life problems compared to the character of chemical elements found. This phase tested whether students can use their knowledge in solving problems.

**Phase 10 (Abstractions).** Students and lecturers conducted to join evaluations related to chemical elements, and compounds learned on that day. In this last stage, students practiced maintaining their solutions by making deductive or inductive conclusions related to the case resolved. This conclusion makes ensured students had solved the problem correctly, and students have understood the concept thoroughly and anticipated the occurrence of misconceptions.

### 3.5 Hypothesis Testing 5

The analysis showed no significant differences in the problem-solving skill of students who had a high and low level of ASLR due to the acquisition of considerable value that is greater than the standard criteria ( $0,476 > 0,005$ ) (Figure 10). The addition of the ability to solve problems among high and low ASRL student groups had a small difference, so it concluded that there were differences, but otherwise not significant. Several findings reported similar things (Barış, 2018). Research of Nurhayati and Retnowati (2018) found that students with low SRL abilities could solve problems better than the high one. In other words, the high and low level of SRL was not significantly different in solving problems.

SMART-PBL strategy was not depending on how the high-low quality of self-regulation (ASRL) of students will enhance problem-solving skill, and this strategy had phases which designed to improve problem-solving ability. One of them was at the stage of the *Attentional Focusing & Motivational Process*. Pre-meeting assignments must complete before the class meeting; this task optionally gave in the form of making a general description related to the next subject matter could be to draw a concept map or make a summary. The optionally tasks done so that students were more motivated to work on tasks. Summarizing techniques make a significant contribution to students in understanding information, transferring it to long-term memory, and improving memory and knowledge by ensuring practical mental skills (Özdemir, 2018). Wammes, Meade, and Fernandes (2015) found that students who given the task to draw the word (mapping concept) can remember twice as high as those who wrote it. When it completed, unconsciously, students with high and low ASRL levels already have the



same composition of prior knowledge as a knowledge saving in the process of constructing knowledge to help them solve problems during learning. Thus, this explained why students who have high and low ASRL abilities found to have a similar ability to solve problems in this study.

### 3.6 Hypothesis Testing 6

The results showed no interaction between SMART-PBL strategy and ASLR ability to problem-solving skills due to the acquisition of significant value was higher than the standard criteria ( $0.743 > 0.05$ ). ASRL level less considered implementing the SMART-PBL strategy in the future because it was not proven to provide significantly different learning outcomes in solving problems. Following research (F Sulistyowati, B Budiyo, 2017), SRL was not effective in improving problem-solving skills. There was no interaction between SRL on students' mathematical communication and problem-solving abilities. SMART-PBL not influenced by the quality of self-regulation (ASRL) to improve problem-solving skills, but emphasized the process of motivating and focusing the attention of students before starting learning, introducing the content in the form of contextual cases, analyzing cases to collect clues, looking for facts through various learning sources, observing chemical elements in 3D, and learning to formulate hypotheses.

The main results from this study found that; (1) There was a significant difference in metacognitive skills in groups of students who taught using the SMART-PBL and PBL strategies during learning. (2) There was no significant difference in metacognitive skills in students with high ASRL levels and low ASRL levels. Student groups with low ASRL levels provide a higher value of metacognitive skills. (3) There was no significant interaction between learning strategies with ASRL's ability to metacognitive skills. (4) There was a significant difference in problem-solving skills in groups of students who taught using the SMART-PBL and PBL strategies during learning. (5) There was no significant difference in problem-solving skills in groups of students with high ASRL levels and low ASRL levels. (6) There was no significant interaction between learning strategies with ASRL's ability to problem-solving skill.

### 4. CONCLUSIONS:

SMART-PBL learning strategy has successfully improving metacognitive and

problem-solving skills in learning chemistry. Besides developing those skills, SMART-PBL also evokes other higher-order thinking skills such as creative thinking and critical thinking skills. Furthermore, communication skills, scientific reasoning skills, teamwork also appeared in students during solving chemical problems. Problem-solving skills mainly needed critical and creative thinking ability, while scientific reasoning and communication skills required for metacognitive skills.

Metacognitive thinking skills are not affected by academic-self-regulated learning but influenced by the ability; to solve real-world chemical problems; to collect prior knowledge; to identify facts; to build and prove the hypothesis. Similarly, problem-solving skills are also not affected by ASRL skills but by various efforts such as doing collaborative-teamwork, collecting more facts and clues, making hypotheses, finding new information needed, and constructing knowledge, applying new knowledge into real-world life, and concluding a solution.

Chemical augmented Reality (AR) technology can evoke student motivation for learning chemistry; students engaged in meaningful learning with a new learning experience.

### 5. REFERENCES:

1. Ahghar, G. (2013). Effect of Problem-solving Skills Education on Auto-Regulation Learning of High School Students in Tehran. *Procedia-Social and Behavioral Sciences*, pp. 688–694.
2. Armengol, E., and Plaza, E. (2005). *An Ontological Approach to Represent Molecular Structure Information*.
3. Astriani, D. et al. (2020). 'Mind Mapping in Learning Models: A Tool to Improve Student Metacognitive Skills. *International Journal of Emerging Technologies in Learning (iJET)*, 15(06).
4. Aurah, C. M. et al. (2011). The Role of Metacognition In Every Day Among Primary Students In Kenya. *Problems of education in the 21st century*, 30(9).
5. Azizah, U., and Nasrudin, H. (2019). Metacognitive Skills: A Solution in Chemistry Problem Solving Metacognitive Skills. *Journal of Physics: Conference*



Series.

6. Barış, Ç. (2018). Metacognition and Self-regulated Learning in Predicting University Students' Academic Achievement in Turkey. *Journal of Education and Training Studies*, 5(04), pp. 132–138.
7. Cai, S., Wang, X. and Chiang, F.-K. (2014) A case study of Augmented Reality simulation system application in a chemistry course. *Computers in Human Behavior*, 37, pp. 31–40.
8. Dasna, I. W. (2012). Peran Dan Tantangan Pendidikan MIPA Dalam Menunjang Arah Menuju Pembangunan Berkelanjutan. *Prosiding Seminar Nasional MIPA*. Malang.
9. Dewey, J. (1910). *How We Think*. New York: D. C. HEATH & CO, PUBLISHERS.
10. Efimova, O. V (2012). Identifying Students' Attitudes Regarding Augmented Reality Applications in Science Classes. *International Journal of Emerging Technologies in Learning (iJET)*, 14(22), pp. 45–55.
11. FS, Irwansyah. Y M, Y. (2018). Augmented Reality (AR) Technology on The Android Operating System in Chemistry Learning A. *The 2nd Annual Applied Science and Engineering*
12. F Sulistyowati, B Budiyo, and I. S. (2017). Problem Solving Reasoning and Problem Based Instruction in Geometry Learning. *International Conference on Mathematics and Science Education (ICMScE)*. Semarang: IOP Publishing.
13. Flavell, J. H. (1979). Metacognition and cognitive monitoring: A new area of cognitive-developmental inquiry. *American Psychologist*. US: American Psychological Association, 34(10), pp. 906–911.
14. Gao, S. et al. (2018). Application of problem-based learning in instrumental analysis teaching at Northeast Agricultural University', *Analytical and Bioanalytical Chemistry*, 410(16), pp. 3621–3627.
15. Gayon, E. E. P. (2003). The Problem Solving Ability of High School Chemistry Students and Its Implication in Redefining Chemistry Education.
16. Hendry, Robin, F. (2006). Elements, Compounds, and Other Chemical Kinds. *Philosophy of Science*. [The University of Chicago Press, Philosophy of Science Association], 73(5), pp. 864–875.
17. Hmelo-Silver, C. E. (2004). Problem-based learning: What and how do students learn?. *Educational Psychology Review*, 16(3), pp. 235–266.
18. Ijirana, S. (2018). Metacognitive Skills Profiles of Chemistry Education. *Jurnal Pendidikan IPA*, 7(2), pp. 239–245.
19. Isaacson, R., and Fujita, F. (2006). Metacognitive knowledge monitoring and self-regulated learning; Academic success and reflections on learning. *Journal of the Scholarship of Teaching and Learning*, 6, pp. 39–55.
20. Jauhangeer, S., Shuib, L., and Azizul Hasan, Z. (2018). Metacognitive Skillfulness of Students in Problem-Solving. *International Journal of Information Systems and Engineering*, 6, pp. 1–9.
21. Johny, L., and Magno, C. (2012). The Assessment of Academic Self-Regulation and Learning Strategies : Can they Predict School Ability ?. *Educational Measurement and Evaluation Review*, 3(July), pp. 75–86.
22. Jong, O., and Taber, K. (2007). Teaching and learning the many faces of chemistry', in S. Abell, N. L. (ed.) *Handbook of Research on Science Education*. Mahwah, NJ: Lawrence Erlbaum Publishers, pp. 631–652.
23. Jusniar, J. et al. (2020). Developing a three-tier diagnostic instrument on chemical equilibrium (TT-DICE). *Educacion Quimica*, 31, pp. 84–102.
24. Kadir, Z. A. et al. (2016). Does Problem-Based Learning Improve Problem Solving Skills?--A Study among Business Undergraduates at Malaysian Premier Technical University. *International*

*Education Studies*. ERIC, 9(5), pp. 166–172.

25. Kamdi, W. (2007). *Model-model Pembelajaran Inovatif*. Malang: Universitas Negeri Malang.
26. Kupatadze, K. (2018). The History of Chemistry and Pharmacy Development in Early and Medieval Georgia. *PERIÓDICO TCHÊ QUÍMICA*, 16(31), pp. 784–790.
27. Lee, H. W., Grabowski, B., and Lim, K. Y. (2009). Generative Learning Strategies and Metacognitive Feedback to Facilitate comprehension of Complex Science Topics and Self-Regulation. *Journal of Educational Multimedia and Hypermedia*, 18.
28. Lima, Alexsandra Rodrigues; Silva, Flávia Cristiane Vieira da; Simoes Neto, J. and Euzebio (2019). Experimental Activities and teaching by Investigation: Propose Continued Formation of Chemistry Teachers. *PERIÓDICO TCHÊ QUÍMICA*, 16(No. 31), p. 164.
29. Mcelroy, T., Dickinson, D. L., and Dickinson, C. A. (2015). The physical sacrifice of thinking: Investigating the relationship between thought and physical activity in everyday life. *Journal of Health Psychology* (January).
30. Miller, D. A. (2015). Learning How Students Learn: An Exploration of Self-Regulation Strategies in a Two-Year College General Chemistry Class. *Journal of College Science Teaching*. National Science Teachers Association, 44(3), pp. 11–16.
31. Nietfeld, J. L. (2015). A comparison of high and low achieving students on self-regulated learning variables. *Elsevier*, (December), p. 9.
32. Núñez, M. *et al.* (2008). Collaborative Augmented Reality for Inorganic Chemistry Education. *5th WSEAS / IASME International Conference on ENGINEERING EDUCATION (EE'08)*. Heraklion, Greece, pp. 271–277.
33. Nurhayati, S., and Retnowati, E. (2018). Can students develop self-regulated learning through worked examples. *International Conference on Teacher Education and Professional Development*. Jogjakarta: Routledge.
34. Özdemir, S. (2018). The Effect of Summarization Strategies Teaching on Strategy Usage and Narrative Text Summarization Success. *Universal Journal of Educational Research*, 6(10), pp. 2199–2209.
35. Özmen, H. (2004). Some Student Misconceptions in Chemistry: A Literature Review of Chemical Bonding. *Journal of Science Education and Technology*, 13, pp. 147–159.
36. Parlan. (2019). Analisis pengetahuan metakognitif dan kesadaran metakognitif peserta didik serta hubungannya dengan prestasi belajarnya. *Jurnal Pembelajaran Kimia, Universitas Negeri*, 4(1), pp. 1–13.
37. Parlan, P. *et al.* (2018). The Improvement of Metacognition of Chemistry Education Students using Metacognitive Learning Strategy. *1st Annual International Conference on Mathematics, Science, and Education (ICoMSE 2017)*. Malang, Indonesia: Atlantis Press.
38. Partington, J. R. (1948). The Concepts of Substance and Chemical Element. *JSTOR*. University of California Press, 1, pp. 109–121.
39. Pratama, A. T. (2018). Improving metacognitive skills using problem-based learning (PBL) at natural science of primary school in Deli Serdang, Indonesia. *Biosfer : Jurnal Pendidikan Biologi*, 11(2), pp. 100–105.
40. Rahman, M. (2019). 21 st Century Skill Problem Solving: Defining the Concept. *Asian Journal of Interdisciplinary Research*, 2(1), pp. 71–81.
41. Reid, A. J., and Morrison, G. R. (2014). Generative Learning Strategy Use and Self-Regulatory Prompting in Digital Text. *Journal of Information Technology Education: Research*, 13, pp. 49–72.
42. Rosli, M. S. (2018). Synergizing Augmented Reality and Chemistry for the 21 st Century Classroom', in *Seminar*

43. Salinitri, F. D. *et al.* (2015). Facilitating Facilitators: Enhancing PBL through a Structured Facilitator Development Program. *Interdisciplinary Journal of Problem-Based Learning*, 9(1).
44. Setyosari, P. (2005) *Media Pembelajaran*, Malang: Elang Mas.
45. Silva, Daniele dos Santos; Yamaguchi, K. K. de L. (2018). Drug Chemistry and Self-Medication Awareness as a Tool In Teaching Organic Function. *PERIÓDICO TCHÊ QUÍMICA*, 16(31), p. 223.
46. Simsek, A. (2010). Learning Strategies of Successful and Unsuccessful University Students. *CONTEMPORARY EDUCATIONAL TECHNOLOGY*, 1(1), pp. 36–45.
47. Steven V. Ley. (2016). *Augmented Reality for Enhanced Chemical Communication*. UK.
48. Stockwell, B. R., Stockwell, M. S., and Jiang, E. (2017). Group Problem-Solving in Class Improves Undergraduate Learning. *ACS Central Science*. American Chemical Society, 3(6), pp. 614–620.
49. Suartama, Kadek Setyosari, P., and Ulfa, S. (2019). Development of an Instructional Design Model for Mobile Blended Learning in Higher Education. *International Journal of Emerging Technologies in Learning (IJET)*, 14(16), pp. 4–22.
50. Symington, D. J. (1977). Primary school pupils' ability to see scientific problems in everyday phenomena. *Research in Science Education*, 7(1), pp. 41–49.
51. Tosun, C., and Senocak, E. (2013). The Effects of Problem-Based Learning on Metacognitive Awareness and Attitudes toward Chemistry of Prospective Teachers with Different Academic Backgrounds. *Australian Journal of Teacher Education*, 38.
52. Üce, M., and Ceyhan, İ. (2019). The misconception in Chemistry Education and Practices to Eliminate Them: Literature Analysis. 7(3), pp. 202–208.
53. Ulfa, S. (2013). Mobile Technology Integration into Teaching and Learning. *International Journal of Science and Technology (IJSTE)*, 2(1), pp. 1–7.
54. Wammes, J. D., Meade, M. E., and Fernandes, M. A. (2015). The Drawing Effect: Evidence for Reliable and Robust Memory Benefits in Free Recall. *The Quarterly Journal of Experimental Psychology*, 0218(October).
55. Widiasih. (2018). The problem-solving ability of students of distance education in science learning The pattern of the problem-solving ability of students of distance education in science learning. *4th International Seminar of Mathematics, Science and Computer Science Education*. IOP Publishing.
56. Wittrock, M. C. (1992). Generative Learning Processes of the Brain. *Educational Psychologist*, 27(4), pp. 531–541.
57. Wittrock, M. C. (1994). Generative Science Teaching. *The Content of Science: A Constructivist Approach to Its Teaching and Learning*. Psychology Press, p. 29.
58. Yiin, H. K. O. H. (2010). Misconception In The Teaching of Chemistry in Secondary Schools in Singapore & Malaysia. *Proceedings of the Sunway Academic Conference*, pp. 1–10.
59. Zheng, L. *et al.* (2017). Quality assurance of chemical ingredient classification for the National Drug File–Reference Terminology. *Journal of Biomedical Informatics*, 73, pp. 30–42.

**Table 1. Factorial Design 2x2**

| Academic-Self Regulated Learning (ASRL) Skill | Strategy of SMART-PBL (Experimental Class)<br>$X^1$ | Strategy of PBL (Control Class)<br>$X^2$ |
|---|---|--|
| High $Y^1$                                    | $X^1Y^1$  | $X^2Y^1$                                 |
| Low $Y^2$                                     | $X^1Y^2$  | $X^2Y^2$                                 |

**Table 2. Hypothesis Test Results**

| Tests of Between-Subjects Effects |                       |                         |    |             |            |             |                     |
|-----------------------------------|-----------------------|-------------------------|----|-------------|------------|-------------|---------------------|
| Source                            | Dependent Variable    | Type III Sum of Squares | df | Mean Square | F          | Sig.        | Partial Eta Squared |
| Corrected Model                   | Metacognitive Skill   | 6942.857 <sup>a</sup>   | 3  | 2314.286    | 219.452    | .000        | .916                |
|                                   | Problem Solving Skill | 1245.343 <sup>b</sup>   | 3  | 415.114     | 259.029    | .000        | .928                |
| Intercept                         | Metacognitive Skill   | 409308.833              | 1  | 409308.833  | 38812.704  | .000        | .998                |
|                                   | Problem Solving Skill | 449846.295              | 1  | 449846.295  | 280701.563 | .000        | 1.000               |
| Strategy                          | Metacognitive Skill   | 6241.527                | 1  | 6241.527    | 591.853    | <b>.000</b> | .908                |
|                                   | Problem Solving Skill | 1103.039                | 1  | 1103.039    | 688.290    | <b>.000</b> | .920                |
| ASRL                              | Metacognitive Skill   | 1.699                   | 1  | 1.699       | .161       | <b>.690</b> | .003                |
|                                   | Problem Solving Skill | .825                    | 1  | .825        | .515       | <b>.476</b> | .009                |
| Strategy * ASRL                   | Metacognitive Skill   | 5.748                   | 1  | 5.748       | .545       | <b>.463</b> | .009                |
|                                   | Problem Solving Skill | .174                    | 1  | .174        | .108       | <b>.743</b> | .002                |
| Error                             | Metacognitive Skill   | 632.745                 | 60 | 10.546      |            |             |                     |
|                                   | Problem Solving Skill | 96.155                  | 60 | 1.603       |            |             |                     |
| Total                             | Metacognitive Skill   | 471762.324              | 64 |             |            |             |                     |
|                                   | Problem Solving Skill | 512791.748              | 64 |             |            |             |                     |
| Corrected Total                   | Metacognitive Skill   | 7575.602                | 63 |             |            |             |                     |
|                                   | Problem Solving Skill | 1341.498                | 63 |             |            |             |                     |

a. R Squared = .916 (Adjusted R Squared = .912)

b. R Squared = .928 (Adjusted R Squared = .925)

**R-Square** – This is the proportion of variability in the dependent variable (useful) that can be explained by the model. It is the ratio of the model sum of squares to the total sum of squares.

**Source** – This is the source of the variability in the specified dependent variable.

**Dependent Variable** - This is the variable observed for the effect of treatment on MANOVA.

**Type III SS** – This is a type of sum-of-squares calculation. SS gives the sum of squares that would be obtained for each variable if it were entered last into the model. That is, the effect of each variable is evaluated after all other factors have been accounted for.

**df** – This is the number of degrees of freedom in the model.

**Mean Square** – This is the sum of squares divided by the degrees of freedom.

**F** – This is the approximate F statistic for the given effect and test statistic.

**Sig.** – This is the p-value associated with the F statistic and the hypothesis and error degrees of freedom of a given effect and test statistic. The null hypothesis that a given predictor has no effect on either of the outcomes is evaluated with regard to this p-value. For a given alpha level, if the p-value is less than alpha, the null hypothesis is rejected and accepted  $H_1$ . If not, then we fail to reject the null hypothesis.

**Partial Eta Squared** - The ratio of variance associated with an effect, plus that effect and its associated error variances.

Asterisk (\*) shows signs of interaction between strategy and ASRL. In this study there was no interaction occur due to significant value was higher than 0.005 as standard value (sig.0.463>0.005); (sig.0.743>0.005). as it can be seen in result & discussions of Hypothesis Testing 3 and Hypothesis Testing 6.

**Table 3.** Real-world Chemical Problems as Learning Materials

| No | Real-World Chemical Problems To be Solved  | Chemical Elements Involved That Must Be Found                 | Chemical Elements Concepts To Learn More  |
|----|--|---|---|
| 1  | Investigate the chemical elements in the form of compounds in cooking ingredients that can cause high blood pressure if consumed in excessive amounts.               | Na in the form of Sodium Chloride (NaCl)                      | Sodium (Na): atomic structure, physical properties, and chemical properties                 |
| 2  | Investigate the chemical constituents contained in bananas that can save the brain by preventing blood clots if consumed regularly.                                  | Potassium (K)   | Potassium (K): atomic structure, physical properties, and chemical properties               |
| 3  | Investigate the chemical element known as white fire, which will cause a big explosion if given water—formerly used as a war bomb during World War II.               | Magnesium (Mg)  | Magnesium (Mg): atomic structure, physical properties, and chemical properties              |
| 4  | Investigate the chemical elements in the form of carbonate compounds contained in oyster shells and can produce beach sand into pearls.                              | Calcium in the form of Calcium carbonate (CaCO <sub>3</sub> ) | Calcium (Ca): atomic structure, physical properties, and chemical properties                |
| 5  | Investigate the chemical elements that can nourish human teeth—usually contained in toothpaste at the right levels.  | Fluoride (F <sup>-</sup> )                                    | Fluorine (F <sub>2</sub> ): atomic structure, physical properties, and chemical properties  |
| 6  | Investigate the chemical elements in the gaseous form. World War I used as a yellowish-green colored poisonous gas that could attack the enemy's respiratory system. | Chlorine (Cl <sub>2</sub> )                                   | Chlorine (Cl <sub>2</sub> ): atomic structure, physical properties, and chemical properties |
| 7  | Investigate the chemical elements in seaweed and other seafood, which, if routinely consumed with the right amount, can prevent hyperthyroid disease.                | Iodine (I <sub>2</sub> )                                      | Iodine (I <sub>2</sub> ): atomic structure, physical properties, and chemical properties    |

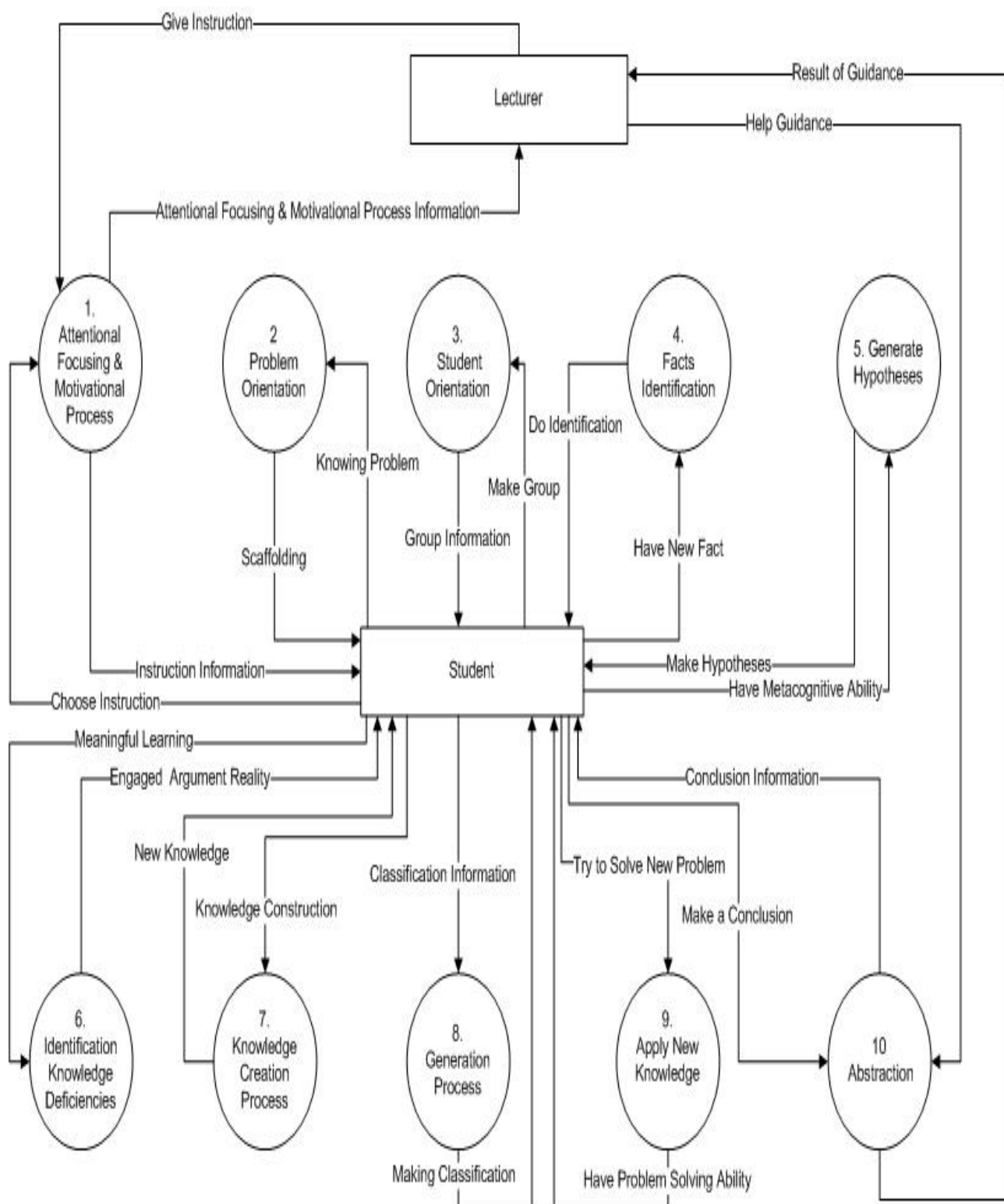


**Figure 1.** A procedural framework of lecturer and student activities in the SMART-PBL strategy during the learning process. Source: the author

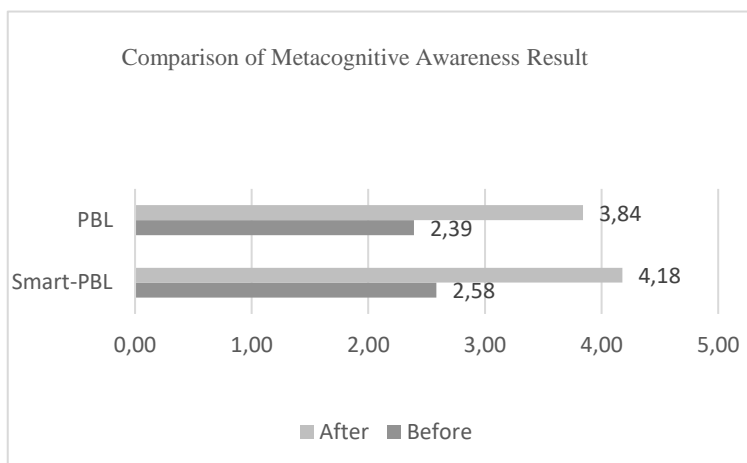


**Figure 2.** Comparison of Before-After Metacognitive Awareness Score during 11 Weeks Implementation of Learning Strategies.

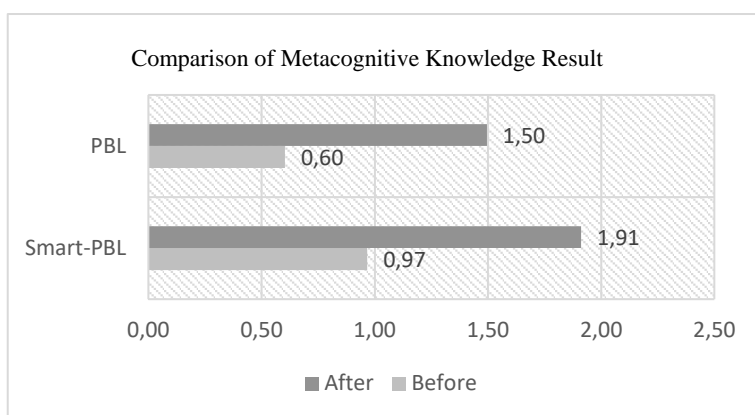


**Figure 3.** Comparison of Before-After Metacognitive Knowledge Score during 11 Weeks Implementation of Learning Strategies.

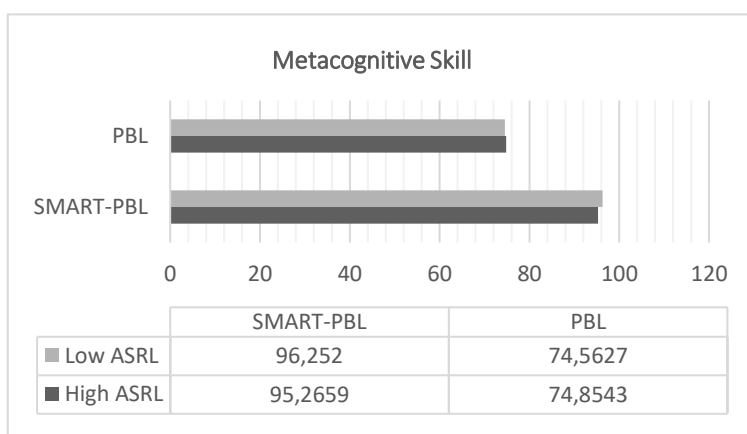


**Figure 4.** Comparison of Metacognitive Learning Outcomes between high ASLR and low ASRL students

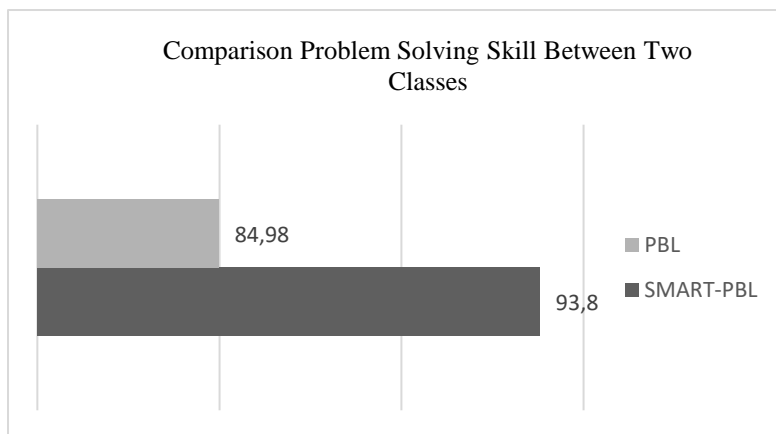


**Figure 5.** Comparison Results Problem Solving Ability in class with SMART-PBL and PBL Strategy



**Figure 6.** The scanning process uses a mobile AR application. Source: the author

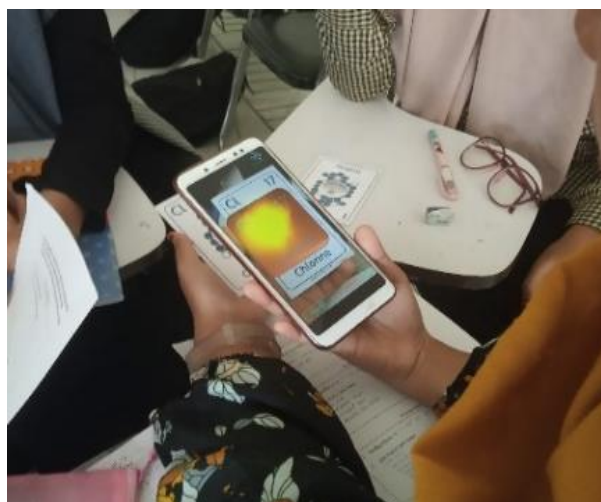


**Figure 7.** 3D visual information displayed in the form of the physical properties of Chlorine. Source: the author





**Figure 8.** Collaborative sharing knowledge to investigate the elements involved. Source: the author



**Figure 9.** Evaluation in the form of a quiz. Source: the author

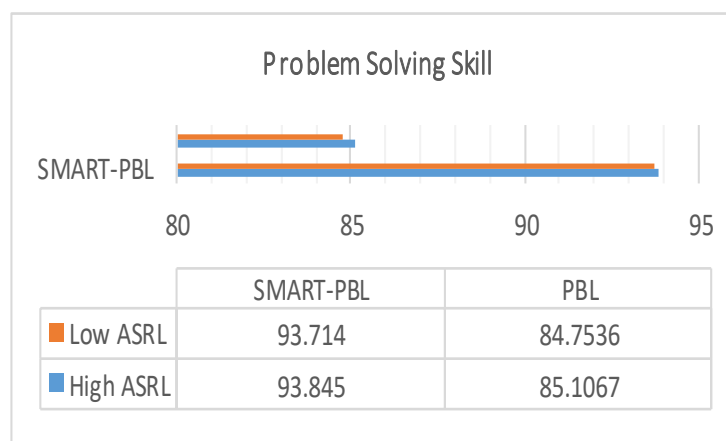


**Figure 10.** Comparative Learning Outcomes of Problem-Solving Skills between high ASLR and low ASRL' students

**HÁBITOS COMPORTAMENTAIS DE DOENÇA CARDIOVASCULAR EM PENSIONISTAS DE VÁRIOS PERFIS PROFISSIONAIS****BEHAVIORAL BACKGROUND OF CARDIOVASCULAR DISEASE IN PENSIONERS OF VARIOUS PROFESSIONAL TYPES****ПОВЕДЕНЧЕСКИЕ ПРЕДПОСЫЛКИ СЕРДЕЧНО-СОСУДИСТЫХ ЗАБОЛЕВАНИЙ У ПЕНСИОНЕРОВ РАЗЛИЧНЫХ ПРОФЕССИОНАЛЬНЫХ ТИПОВ**BEREZINA, Tatiana N.<sup>1\*</sup>; CHUMAKOVA, Elizaveta<sup>2</sup><sup>1</sup>Department of Scientific Basis of Extreme Psychology, Moscow State University of Psychology and Education, 2A/1 Shelepkhinskaya Naberezhnaya, Office 207, Moscow 123290. Russia.<sup>2</sup>State Budgetary Institution of Healthcare City Polyclinic No. 9 of the Moscow City Health Department. Russia.

\* Correspondence author  
e-mail: [tn-berezina@mail.ru](mailto:tn-berezina@mail.ru)

Received 06 May 2020; received in revised form 12 June 2020; accepted 02 July 2020

**RESUMO**

O objetivo do estudo foi examinar a influência dos padrões de comportamento no desenvolvimento de doenças cardiovasculares em diferentes perfis profissionais de pessoas em idade de aposentadoria. Métodos: a base clínica de 500 pensionistas (111 homens e 389 mulheres) ligados a uma das clínicas de Moscou foi usada no estudo. Os documentos médicos foram analisados, a avaliação de especialistas foi realizada, a experiência de vida foi pesquisada e as características comportamentais foram autoavaliadas. A gravidade das doenças cardiovasculares foi tomada como uma variável independente e os perfis profissionais foram utilizados como variáveis adicionais, como segue: perfil realista, perfil convencional e perfil social. Padrões de comportamento foram sendo utilizados como variáveis dependentes. A análise de variância (ANOVA) (um fator e dois fatores) foi usada como método de processamento dos dados. Resultados: maus hábitos (alcoolismo, tabagismo, supernutrição), e agressividade aumentam a gravidade das doenças cardiovasculares entre os aposentados, enquanto a existência de *hobbies* e otimismo diminuem. Nos pensionistas de perfil Realista, os *hobbies* esportivos aumentaram o risco, mas os passa tempos e o bordado diminuíram. Nos aposentados de perfil Social, os hobbies esportivos reduziram ainda mais o risco. Nos aposentados do tipo Convencional, a atividade profissional reduziu o risco, enquanto a presença de uma família, filhos, comunicação e vários hobbies a aumentaram. A supernutrição e a agressividade não produziram um efeito adverso significativo. Conclusão: juntamente com os pré-requisitos comportamentais gerais para a ocorrência de doenças cardiovasculares, os indivíduos dependem do perfil profissional da pessoa. Pesquisas adicionais são necessárias para refinar esses resultados.

**Palavras-chave:** *hábitos comportamentais, hobbies comportamentais, idade da aposentadoria, doenças cardiovasculares, tipos profissionais.*

**ABSTRACT**

The study has been aimed at examining the influence of behavior patterns on the development of cardiovascular diseases in different professional types of retirement-age people. Methods: the clinical base of 500 pensioners (111 men and 389 women) attached to one of the Moscow clinics has been used in the study. Medical documents have been analyzed, the expert assessment has been carried out, the life experience has been surveyed, and behavioral features have been self-assessed. The severity of cardiovascular diseases has been taken as an independent variable, and the professional types have been used as the additional variables as follows: Realistic type, Conventional type, and Social type. Behavior patterns have been used as the dependent variables. Analysis of variance (ANOVA) (one-factor and two-factor) has been used as the data processing method. Results: bad habits (alcoholism, tobacco smoking, overnutrition), aggressiveness increase the severity of cardiovascular diseases among pensioners, whereas the existence of subject hobbies and optimism reduce it. In the pensioners of the Realistic type, sports hobbies have increased the risk, but subject hobbies and needlework reduced it. In the pensioners of the Social type, sports hobbies have further reduced the risk. In the

pensioners of the Conventional type, the professional activity has reduced the risk, whereas the presence of a family, children, communication, and various hobbies have increased it. Overnutrition and aggressiveness have not produced a significant adverse effect. Conclusion: along with general behavioral prerequisites for the occurrence of cardiovascular diseases, individual ones are depending on the person's professional type. Additional research is needed to refine these results.

**Keywords:** *behavioral habits, behavioral hobbies, retirement age, cardiovascular disease, professional types.*

## АННОТАЦИЯ

Цель исследования – изучить, как влияют особенности поведения на развитие сердечно-сосудистых заболеваний у разных профессиональных типов людей пенсионного возраста. Метод: мы использовали клиническую базу пенсионеров, прикрепленных к одной из московских поликлиник – 500 человек (111 мужчин и 389 женщин). Проводился анализ медицинских документов, экспертная оценка, анкетирование жизненного пути и самооценка особенностей поведения. В качестве независимой переменной мы взяли степень сердечно-сосудистых заболеваний, дополнительными переменными являлись: профессиональные типы: Realistic type, Conventional type, Social type. Зависимыми переменными являлись: особенности поведения. Метод обработки данных – дисперсионный анализ ANOVA (однофакторный и двухфакторный). Результаты: степень сердечно-сосудистых заболеваний у пенсионеров увеличивают: вредные привычки (алкоголизм, табакокурение, переедание), агрессивность; снижают: наличие предметных увлечений и оптимизм. У пенсионеров Realistic type усиливали риск: спортивные хобби, а снижали риск предметных хобби и рукоделие. У пенсионеров Social type дополнительно снижало риск наличие спортивных хобби. У пенсионеров – Conventional type снижала риск профессиональная активность, наличие семьи, детей, общения, наличие различных хобби усиливали риск, а переедание и агрессивность не оказывали значимого негативного эффекта. Выводы: наряду с общими, существует индивидуальные поведенческие предпосылки к возникновению сердечно-сосудистых заболеваний, зависящие от профессионального типа человека. Для уточнения этих результатов необходимы дополнительные исследования.

**Ключевые слова:** *поведенческие привычки, поведенческие хобби, пенсионный возраст, сердечно-сосудистые заболевания, профессиональные типы.*

## 1. INTRODUCTION

There are behavioral traits that affect the life expectancy of all people and the development of cardiovascular diseases in them (Berezina and Mansurov, 2015). Such bad habits include alcoholism, tobacco smoking, and overnutrition. The negative effect of bad habits is manifested in all people, regardless of their psychological type or age. At the young age, the risk factors for cardiovascular diseases include excessive weight (20.06 % of cases), tobacco smoking (35.1 % of cases); the adaptive potential of the circulatory system in people with nicotine addiction and those with the excessive weight is significantly lower, systolic hypertension occurs significantly more often (1.5 times), as well as diastolic hypertension (3.1 times) (Ponomareva and Moskalenko, 2016). In the old age, bad habits lead not only to the development of coronary heart disease but also to increase the mortality of heart disease sufferers (Robert *et al.*, 2005).

There are also typological features affecting the development of the cardiovascular disease. Behavioral types with an increased risk of heart disease were identified. The study of M.

Friedman and R. Rosenman is the most famous in this area (Friedman and Rosenman, 1974). Two types of behavior were distinguished in the study: type A – "fight-or-flight" and type B – "hiding". At the same time, the predominance of type A behavior in human life correlates with the risk of cardiovascular disease. Empirical studies confirmed this pattern. In the study, including more than 3,000 people, the authors described the results of an eight-year longitude according to which there were two times more cases of coronary heart disease among the men with the type A personality (Friedman and Rosenman, 1974). In women, type A behavior also contributed to the development of coronary heart disease (Haynes, 1990).

Type A behavior is characteristic of people with the professional Enterprising type, according to John Holland (1973). Such people are set up for competition and success; they feel shortage of time, it is difficult for them to relax, and they become impatient and angry when faced with time delays or with people they consider incompetent. They seem confident, but they are constantly tormented by the feeling of insecurity; they force themselves to do more in less time (Barefoot *et al.*,

1989). It is also known that the psychological traits of a type A patient influence the efficiency of hypertension treatment for some groups of patients (Chumakova *et al.*, 2014).

However, there is no unequivocal evidence of the connection between professional Enterprising type and cardiovascular diseases. Other authors claimed that the features of the emotional sphere rather than the style of professional activity had an influence on the risk of cardiovascular diseases (Spielberger *et al.*, 1985). Moreover, the main factor in the development of cardiovascular diseases was the emotions associated with hostility but not those associated with competition (anger, irritation) (Keith *et al.*, 2017). For example, the 25-year study of 118 male lawyers revealed that those who were more hostile in a law school as per personal questionnaire were more likely to die before the age of 50 years from heart disease than their less-so-hostile fellow students (Barefoot *et al.*, 1989).

Later, another behavioral type – "distressed personality" (D) – was distinguished, which was characterized by a constant intense experience of negative emotions and a tendency to hide them from others because of the fear of being rejected. The representatives of this type are bad-tempered and moody, their attitude to themselves and the world is characterized by constant negativity, they are unable to cope with their negative emotions and cannot share them with other people, which is also considered as a pathogenic factor in the development of cardiovascular diseases (Staniute *et al.*, 2015). It can be noticed that the personal characteristics of such people are opposite to the professional Artistic type according to the John Holland's typology. The representatives of the Artistic type, on the contrary, tend to show their feelings to the whole world. It can be assumed that the risk of cardiovascular disease will be reduced in this type opposite to the "distressed personality" type.

For some other behavioral characteristics, different authors obtained different data. This applies, for example, too optimistic or pessimistic behavior, as well as lifestyle (lonely or with a wide social circle). Some researchers have noted the positive effect of optimism and a wide social circle on the functioning of the cardiovascular system. Researchers at Harvard University demonstrated a positive effect of optimism (Kim *et al.*, 2017). They studied the health data of more than 70 thousand American women of middle and old age that had been obtained as part of mass monitoring among nurses. The researchers found that the most optimistic women had died, on average, 30

% less than their peers and colleagues in a depressed spirit. Also, cancer appeared in them less than usual by 16 %, heart disease – by 38 %, stroke – by 39 %, lung disease, and infection – by 38 % and 52 %, respectively (Kim *et al.*, 2017). There is also evidence of the positive effect of a sense of humor on human health. The 15-year study of life, carried out by Norwegian researchers on 53 thousand participants, showed that the sense of humor was positively related to life expectancy, reduced the risk of death from cardiovascular and infectious diseases in women and the risk of death from infectious diseases in men (Romundstad *et al.*, 2016). Most authors also consider the person's sociability and their wide social circle to be a positive resource. As noted by American researchers, life expectancy is positively related to the frequency of socialization with neighbors, religious participation, and proposal (Cornwell *et al.*, 2008).

Other authors, on the contrary, claim the positive effect of pessimism and a lonely lifestyle. For example, the author of the monumental "The Longevity Project" Lewis Terman and his students, is based on the longitude study that had lasted more than half a century, argued that the pessimism was the key to longevity, whereas the premature death, including that from cardiovascular diseases, was more likely in particularly cheerful and humorous project participants with a wide social circle (Friedman and Martin, 2012). According to their data, hunks and skeptics are more likely to reach older age, since an optimistic view of life often leads to arrogance; optimists lose their sense of prudence: they like to drink, smoke and do not care at all about a healthy diet, and rarely visit doctors (Friedman and Martin, 2012). It turns out that optimists, especially elderly ones, harder bear their misfortune when their optimistic predictions about health turn out to be false. The results of an empirical study of the health status of optimists and pessimists showed that repeated unsatisfied health expectations could undermine motivational resources and accelerate the deterioration of physical condition at the end of life (Hamm *et al.*, 2017).

The authors believe that some of the contradictions of the literature data can be explained by the typological features of a person. Different behavioral factors are favorable for different types of people. In other words, in different types of people, different behavioral patterns can have an effect on the progression of cardiovascular diseases. Professional types are the most important types of mediating the action of

behavioral factors.

The **aim** of the study was the examination of behavioral patterns of different professional types of people (according to Holland's typology), having an effect on the progression of cardiovascular diseases in old age.

**Hypothesis.** The authors have hypothesized that in people engaged in various professional activities during life, various behavioral patterns (hobbies, life path features, attitude to life, and other people) will have an effect on the progression of cardiovascular diseases at the old age. Some behavioral features will be favorable for the specific type of people since they reduce the risk of the disease. Others will be unfavorable for this type and will increase the likelihood of the development of the diseases.

## 2. MATERIALS AND METHODS

### Methods.

1. Analysis of documents. Examination of medical records, medical books, and health certificates. Gender, age, health indicators, and diagnosis were determined based on this.

2. An expert assessment of the severity of diseases by a geriatrician based on clinical trials and data from a medical examination carried out by four experts – neurologist, ophthalmologist, cardiologist, and pulmonologist.

Three levels of severity were distinguished for cardiovascular diseases, as follows: first – low, certain symptoms of cardiovascular pathology were recorded, second – medium, with the history of acute micro-impairments of cerebral or cardiac circulation (first – the second degree of severity), and third – high, cerebrovascular or circulatory disorders of third-degree of severity, third functional class effort angina.

3. Life experience survey. Original development. The subjects were asked to name their profession, level of career achievements, the presence of family and children, religiosity, and to list their interests and hobbies that had taken place throughout life and were preserved. Further, the number of interests and hobbies was calculated in the intellectual, creative, sports, and subject (needlework, hand-made) groups.

4. The Dembo-Rubinstein method of self-assessment of personality characteristics as modified by the authors. The subjects were asked to evaluate personality characteristics, such as activity, aggressiveness, sociability, optimism, and

carefulness (the presence of an object of care). The development of these indicators during life and at the moment was assessed. Subsequently, self-assessment of indicators was reduced to three levels: low, medium, and high.

5. Mathematical statistics methods. One-factor and two-factor Anova (Statistika-12) was used. The severity of cardiovascular disease served as an independent variable. The dependent variables included personality traits and the life paths thereof, namely education, the existence of a family, children, religiosity, number of relocations, continued work at the retirement age, occupation types according to John Holland (Realistic type, Investigative type, Artistic type, Social type, Enterprising type, Conventional type) (Holland, 1973), level of career achievements, bad habits (tobacco smoking, alcoholism, overnutrition), self-assessment of personality characteristics, namely the activity, sociability, optimism, aggressiveness, and carefulness.

6. The professional type served as an additional variable in the two-factor analysis.

**Subjects.** Five hundred retirement-age people, of which 111 men over 60 years of age and 389 women over 55 years of age, all were residents of Moscow, attached to the city polyclinic of the southeastern district and regularly visiting a doctor at least once every two months; 456 subjects were in the medical follow-up due to cardiac disease, and four were not followed-up.

Table 1 presents a detailed gender and age composition of the sample.

## 3. RESULTS AND DISCUSSION

At the first stage, the authors studied how the behavioral characteristics of Russian pensioners influenced the development of cardiovascular diseases in the entire sample. The results are shown in Table 2.

As it follows from the table, all bad habits (alcoholism, tobacco smoking, overnutrition) significantly increase the severity of the cardiovascular diseases at the retirement age, and aggressiveness significantly reduces optimism.

In the second stage, the authors studied the influence of professional types on the progression of cardiovascular diseases (Table 3).

In the third stage, the authors studied the influence of the person's behavioral characteristics on the progression of cardiovascular diseases in the most numerous professional types of the

sample (Realistic type, Social type, and Conventional type).

**Realistic type.** The representatives of this type have higher severity of the cardiovascular disease than all others ( $F(1.494) = 6.7262$ ,  $p = 0.00978$ ).

For the representatives of this type, the authors discovered several additional behavioral patterns. Firstly, it is favorable for them to have substantive hobbies, both during life ( $F(2.494) = 5.4519$ ,  $p = 0.00455$ ) and at the retirement age ( $F(2.494) = 5.0469$ ,  $p = 0.00676$ ). Secondly, the presence of sports hobbies is not favorable for them (at the trend level  $F(4.490) = 2.2382$ ,  $p = 0.06390$ ). See details in Tables 4, 5, and 6.

As it follows from the table, the representatives of the Realistic type with no subject hobbies have the highest severity of cardiovascular diseases. The presence of subject hobbies reduces the severity of the diseases in the representatives of this type (in the table, these are groups 4, 6). For the other types, the presence of subject hobbies is favorable only in relation to the representatives of the Realistic type with no subject hobbies.

As it follows from the table, the same pattern is preserved. The highest severity of cardiovascular disorders was observed in the representatives of the Realistic type with no subject hobbies. The presence of subject hobbies in the representatives of the Realistic type (group 3) significantly reduces the severity of the cardiovascular disorders both in relation to other professional types having such hobbies (group 3) and in relation to their own type with no such hobbies (group 2).

As it follows from the table, the representatives of the Realistic type with many sports hobbies have the highest level of cardiovascular disorders (group 8). It is significantly higher than in many other groups. Also, the presence of sports hobbies significantly increases the severity of cardiovascular disorders in the representatives of the Realistic type (group 6) in relation to other professional types (group 5).

**Social type.** For the representatives of this type, the authors discovered several additional behavioral patterns.

Firstly, it is the link to sex. It is favorable for men to have a profession of the Social type since it reduces the severity of the cardiovascular disorders ( $F(1.496) = 4.7774$ ,  $p = 0.02930$ ). Secondly, for all representatives of the Social type, it is favorable to have sports hobbies throughout

life ( $(4.490) = 2.6221$ ,  $p = 0.03422$ ), and at the retirement age, completeness persists only as a trend. Thirdly, the availability of subject hobbies is not favorable for them at the trend level both during life ( $F(2.494) = 2.5215$ ,  $p = 0.08137$ ) and at the retirement age ( $F(1.495) = 3.3266$ ,  $p = 0.06877$ ). Reliable patterns are presented in Tables 7 and 8.

As it follows from the table, the highest severity of cardiovascular disorders is observed in the men working in other areas (non-Social type) – group 3. In the men of the Social type, the severity of cardiovascular disorders does not differ from that in the women.

As it follows from the table, the representatives of the Social type with one sports hobby (group 4) have lower severity of the cardiovascular disorders than all other groups. It is significantly lower than that of the representatives of other professional types (groups 3 and 6).

**Conventional type.** For the representatives of the Conventional type, the greatest number of patterns was found.

Firstly, for the representatives of the Conventional type, correlation with age is evident. In some age groups, they have lower severity of the cardiovascular disorders ( $F(3.492) = 2.7456$ ,  $p = 0.04249$ ).

Secondly, the existence of a family ( $F(2.494) = 4.4053$ ,  $p = 0.01270$ ), children ( $F(1.496) = 5.1180$ ,  $p = 0.02411$ ), a high level sociability throughout life ( $F(2.494) = 8.9792$ ,  $p = 0.00015$ ) and at the retirement age ( $F(2.494) = 6.8030$ ,  $p = 0.00122$ ) are favorable for the representatives of the Conventional type.

Thirdly, the presence of a variety of hobbies for this type does not have a positive effect. The presence of a large number of intellectual hobbies increases the severity of cardiovascular diseases ( $F(3.492) = 2.8606$ ,  $p = 0.03646$ ). The presence of creative hobbies increases the severity of cardiovascular diseases at the trend level ( $F(1.495) = 3.5924$ ,  $p = 0.05863$ ). In the representatives of this type, the presence of sports hobbies increases the severity of cardiovascular disorders compared to those without sports hobbies ( $F(3.491) = 3.7472$ ,  $p = 0.01106$ ).

Fourthly, some behavioral characteristics harmful to all people are less harmful to the representatives of the Conventional type. For them, the average severity of overnutrition at the retirement age does not have a harmful effect ( $F(2.493) = 3.4019$ ,  $p = 0.03409$ ). Also, a high level

of aggressiveness does not have a harmful effect ( $F(2.494) = 3.3022$ ,  $p = 0.03762$ ) for them.

The most significant differences are shown in Table 9.

As it follows from the table, social characteristics are favorable for the representatives of the Conventional type. The existence of a family, children, and social circle reduces the severity of cardiovascular disorders in the representatives of this type. Also, at the age of 75 – 85 years, cardiovascular diseases are less pronounced in the representatives of this type. A variety of hobbies does not have a positive effect on this type. The presence of intellectual, sports, and creative hobbies does not reduce the severity of cardiovascular disorders. At the same time, some harmful behavioral characteristics (overnutrition, aggressive behavior) do not increase the severity of cardiovascular diseases in the representatives of this type.

In the study, the representatives of the Realistic type, which included all working and technical specialties, turned out to be the most vulnerable to the development of cardiac pathology. In general, both negative professional factors described in the literature affected this group, namely, the work stress associated with increased requirements for work and low ability to influence something, and the imbalance between efforts and rewards. The first one is the demand-control working stress model (by R. Karasek), where the work, which requires great diligence, is the most unfavorable for the cardiovascular system, and at the same time, it has a low decision-making level (Karasek *et al.*, 1998). This applies specifically to the representatives of the Realistic type. This model is supported by the results of the longitudinal study, in which 1,928 working men had been observed for six years, where for the workers performing an unfavorable type of work, the risk of coronary death was six times higher than for the rest (Ushakov *et al.*, 2016).

The second is the effort-reward imbalance model (by J. Siegrist), where the work that requires greater returns and does not give a decent reward is the most dangerous for the development of cardiovascular diseases and atherosclerosis (Siegrist *et al.*, 2004). In summary, the authors emphasize the importance of chronic occupational stress as a factor affecting the development and course of cardiovascular diseases (Gilbert-Quimet *et al.*, 2014), especially if the work is not accompanied by career growth (Berezina and Mansurov, 2015). The professionals related to the

representatives of the Realistic type in the study were also subjected to this type of stress.

However, this study was able to find resource areas that could help the representatives of the Realistic type to reduce the risk of cardiovascular disease. Needlework is positive for this type. Therefore, the psychologists involved in the rehabilitation of retirement-age heart disease sufferers, in this case, recommend developing a person's interests and subject hobbies as a self-help measure. Sports, intellectual and creative hobbies are not associated with the risk of cardiovascular diseases in the representatives of this type. This is mainly because these are mostly the people involved in physical labor, and the positive effect of physical exercises is implemented through labor, and intellectual and creative hobbies are simply expendable.

However, for the representatives of the Social type, which include the representatives of the service sector, teachers, medical workers, a completely different scenario is observed. General psychological patterns (needlework and the development of optimism as the factors reducing the risk of cardiovascular diseases) do not work for them, and it is unlikely that the psychological rehabilitation in this direction will be favorable. However, it should be noted that the level of optimism among employees has been quite high and even slightly above the average for the sample, and it is possible that the positive strength in the representatives of this type has already been involved and an additional increase in optimism would not add anything. To reduce the risk of cardiovascular disease development among the retirees of this group (often leading a sedentary life), it is recommended to practice gymnastics and develop sports hobbies.

For the representatives of the Conventional type, the physical health of a person does not depend on whether he/she is engaged in any hobby or not. For the psychological rehabilitation of workers in this area, it may be effective to turn to their professional activities: continuing to work at the retirement age, acting as an expert or mentor, etc. For the representatives of this type, the resource area is the social one, namely the extension of social circle, increasing the time spent with family and children. In the literature, the presence of kinship at the retirement age is a traditionally favorable factor that reduces the risk of diseases and increases life expectancy (Cornwell *et al.*, 2008). Loneliness is a negative factor since people living alone are less likely to care about their health, and as a result, have a greater risk of developing cardiovascular diseases



and premature death (Jain *et al.*, 2017). The authors have shown that this is true for at least one of the professional types.

#### 4. CONCLUSION

Behavioral factors influence the onset, development, and severity of cardiovascular diseases at the retirement age. Thus, the person's bad habits (alcoholism, smoking, overnutrition), aggressiveness as a personality trait, and a profession related to the Realistic type worsen prognosis, and optimism and the presence of subject hobbies improve it.

Additional positive and negative factors have been discovered for various professional types. In the pensioners of the Realistic type, needlework has a positive effect on the development of substantive interests and hobbies. For the pensioners of the Social type, physical education, sports, and physical activity have a positive effect, whereas optimism and needlework have no effect. For the pensioners who worked with documents – office workers (Conventional type) – engaging in any hobby has no effect, and professional activity and social activity have a positive effect.

#### 5. AUTHOR CONTRIBUTIONS:

Conceptualization, BTN.; Methodology, BTN., CE.; Validation, CE.; Resources, BTN, CE.; Writing-Original Draft Preparation BTN.; Writing-Review & Editing, BTN.; Visualization, BTN.; Supervision, BTN.; Project Administration, BTN.

#### 6. ACKNOWLEDGMENTS:

This work was supported by the Russian Foundation for Basic Research 18-013-00092A.

#### 7. REFERENCES:

1. Barefoot, J. C.; Dodge, K. A.; Peterson, B. L.; Dahlstrom, W. G.; Williams, R. B.; *Psychosomatic Medicine*. **1989**, 51, 46-57.
2. Berezina, T. N.; Mansurov, E. I.; *Voprosy Psikhologii*. **2015**, 3, 73-83.
3. Chumakova, E. A.; Gaponova, N. I.; Berezina, T. N.; *Russian Journal of Cardiology*. **2014**, 2(106), 89-95.
4. Cornwell, B.; Laumann, E. O.; Schumm, L. P.; *American Sociological Review*. **2008**, 73, 185–203. DOI: 10.1177/000312240807300201.
5. Friedman, H. S.; Martin, L. R.; *The Longevity Project: Surprising Discoveries for Health and Long Life from the Landmark Eight-Decade Study*. Plume: New York, **2012**.
6. Friedman, M.; Rosenman, R.; *Type A behavior and your heart*, Knopf: New York, **1974**.
7. Gilbert-Ouimet, M.; Trudel, X.; Brisson, C.; Milot, A.; Vezina, M.; *Scand J Work Environ Health*. **2014**, 40(2), 109-132. Doi:10.5271/sjweh.3390.
8. Hamm, J. M.; Kamin, S. T.; Chipperfield, J. G.; Perry, R. P.; Lang, F. R.; *J Gerontol B Psychol Sci Soc Sci*. **2017**, Jun 13. DOI: 10.1093/geronb/gbx074.
9. Haynes, S. N. *Behavioral assessment of adults*; In Goldstein, G.; Hersen, M., eds.; *Handbook of psychological assessment*, 2nd ed., Pergamon Press: New York, **1990**.
10. Holland, John L.; *Making vocational choices: A theory of careers*, Prentice-Hall: Englewood Cliffs, N.J., **1973**.
11. Jain, A.; van Hoek, A. J.; Boccia, D.; Thomas, S. L.; *Vaccine*. **2017**, Apr. 25, 35(18), 2315-2328. Doi: 10.1016/j.
12. Karasek, R.; Brisson, C.; Kawakami, N.; Houtman, I.; Bongers, P.; Amick, B.; *J Occup Health Psychol*. **1998**, 3(4), 322-355. Doi: 10.1037/1076-8998.3.4.322.
13. Keith, F.; Krantz, D. S.; Chen, R.; Harris, K. M.; Ware, C. M.; Lee, A. K.; Bellini, P. G.; Gottlieb, S. S.; *Health Psychology*. **2017**, 36(9), 829-838. <http://dx.doi.org/10.1037/hea0000519>
14. Kim, E. S.; Hagan, K. A.; Grodstein, F.; DeMeo, D. L.; De Vivo, I.; Kubzansky, L. D.; *Am J Epidemiol*. **2017**, 185(1), 21–29.
15. Ponomareva, I. P.; Moskalenko, V. A.; *Elektronnyi nauchnyi zhurnal "Gerontologiya"*. **2016**, 3. <http://www.gerontology.su/magazines?text=265>
16. Robert, M.; Kenneth, E.; Veith, R. C.; *Psychosomatic Medicine*. **2005**, 67, 29–33.
17. Romundstad, S.; Svebak, S.; Holen, A.; Holmen, J. *Psychosom Med*. **2016**, Apr. 78(3), 345-353. Doi: 10.1097/PSY.0000000000000275.
18. Siegrist, J.; Starke, D.; Chandola, T.; Godin, I.; Marmot, M.; Niedhammer, I.; Petr, R.; *Soc Sci Med*. **2004**, 58(8), 1483-



1499. DOI: 10.1016/S0277-9536(03)00351-4.
19. Spielberger, C. D.; Johnson, E. H.; Russell, S. F.; Crane, R. J.; Jacobs, G. A.; Worden, T. J. *The experience and expression of anger: Construction and validation of an anger expression scale*; In Chesney, M. A.; Rosenman, R. H., eds.; Anger and hostility in cardiovascular and behavioral disorders; Hemisphere/McGraw-Hill: New York, **1985**.
20. Staniute, M.; Brozaitiene, J.; Burkauskas, J.; Kazukauskienė, N.; Mickuviene, N.; Bunevicius, R.; Health Qual Life Outcomes. **2015**, 13, 1. Doi: 10.1186/s12955-014-0204-2.
21. Ushakov, A. V.; Ivanchenko, V. S.; Gagarina, A. A.; *Arterial'naya gipertenziya*. **2016**, 22(2), 128-143.

**Table 1.** Gender and age composition of the sample

| Sex   | Age groups (number of people)  |                                 |                                 |   |
|-------|--------------------------------|---------------------------------|---------------------------------|---|
|       | First group<br>55-65 years old | Second group<br>66-75 years old | Third group<br>76- 85 years old | Fourth group<br>86 years old and<br>older |
| all   | 187                            | 191                             | 109                             | 13  |
| Men   | 34                             | 52                              | 23                              | 2   |
| Women | 153                            | 139                             | 86                              | 11  |

**Table 2.** Features of the personal organization of life path time influencing the severity of the cardiovascular diseases

| The severity of disease at different levels of behavioral indicator |                  |      |      | Influence | F                 | p         |
|---|------------------|------|------|-----------|-------------------|-----------|
| Indicator   | Indicator levels |      |      |           |                   |           |
|   | 1                | 2    | 3    |           |                   |           |
| Tobacco smoking   | 1.89             | 2.18 | 2.10 | increases | F(2.497) = 5.60   | p = 0.003 |
| Alcoholism  | 1.87             | 2.20 | 2.25 | increases | F(2.497) = 5.60   | p = 0.004 |
| Overnutrition   | 1.89             | 2.08 | 2.12 | increases | F(2.497) = 5.14   | p = 0.006 |
| Alcoholism at the moment  | 1.93             | 2.18 | 2.0  | increases | F(2.497) = 4.4518 | p = 0.012 |
| Aggressiveness  | 1.92             | 1.93 | 2.15 | increases | F(2.497) = 3.33   | p = 0.037 |
| Aggressiveness at the moment  | 1.89             | 1.95 | 2.19 | increases | F(2.497) = 3.99   | p = 0.019 |
| Optimism at the moment  | 2.22             | 1.95 | 1.92 | decreases | F(2.497) = 3.25   | p = 0.039 |

1. The severity of the cardiovascular disease in the patients with low behavioral indicator (arithmetic mean of the severity of the disease).

2. The severity of the cardiovascular disease in the patients with medium behavioral indicator (arithmetic mean of the severity of the disease).

3. The severity of the cardiovascular disease in the patients with high behavioral indicator (arithmetic mean of the severity of the disease).

**Table 3.** The influence of the professional type on the progression of cardiovascular diseases ( $F(5.494) = 8.3543$ ,  $p = 0.00000$ )

| No. | Professional types | Number of persons | Severity of the disease (arithmetic mean) | Standard deviation |
|-----|--------------------|-------------------|---|--------------------|
| 1   | Realistic type     | 156               | 2.108974 <sup>2, 4, 6</sup>               | 0.050506           |
| 2   | Investigative type | 4                 | 0.250000 <sup>1, 3, 4, 5, 6</sup>         | 0.315409           |
| 3   | Artistic type      | 9                 | 1.777778 <sup>2</sup>                     | 0.210272           |
| 4   | Social type        | 155               | 1.922581 <sup>1, 2</sup>                  | 0.050668           |
| 5   | Enterprising type  | 5                 | 1.600000 <sup>2</sup>                     | 0.282110           |
| 6   | Conventional type  | 171               | 1.918129 <sup>1, 2</sup>                  | 0.048240           |

<sup>1</sup>– the reliable difference with the Fisher's type 1 ( $p \leq 0.05$ )

<sup>2</sup>– the reliable difference with the Fisher's type 2 ( $p \leq 0.05$ )

<sup>3</sup>– the reliable difference with the Fisher's type 3 ( $p \leq 0.05$ )

<sup>4</sup>– the reliable difference with the Fisher's type 4 ( $p \leq 0.05$ )

<sup>5</sup>– the reliable difference with the Fisher's type 5 ( $p \leq 0.05$ )

<sup>6</sup>– the reliable difference with the Fisher's type 6 ( $p \leq 0.05$ )

**Table 4.** The severity of the cardiovascular disorders in the representatives of the Realistic type, with and without subject hobbies throughout life

| Group No. | Number of subject hobbies throughout life | Professional types | Severity of the cardiovascular disorders (arithmetic mean) | Standard deviation | Number of persons |
|-----------|---|--------------------|--|--------------------|-------------------|
| 1         | 0   | 1                  | 1.864322 <sup>2</sup>                                      | 0.045421           | 199               |
| 2         | 0   | 2                  | 2.200000 <sup>1, 3, 4, 5, 6</sup>                          | 0.058491           | 120               |
| 3         | 1   | 1                  | 1.953846 <sup>2</sup>                                      | 0.056196           | 130               |
| 4         | 1   | 2                  | 1.793103 <sup>2</sup>                                      | 0.118982           | 29                |
| 5         | 2   | 1                  | 1.733333 <sup>2</sup>                                      | 0.165438           | 15                |
| 6         | 2   | 2                  | 1.857143 <sup>2</sup>                                      | 0.242176           | 7                 |

<sup>1, 2, 3, 4, 5, 6</sup> – the significant difference with the relevant Fisher group ( $p \leq 0.05$ )

Professional types:

1- all other types

2- Realistic type

**Table 5.** The severity of the cardiovascular disorders in the representatives of the Realistic type, with and without subject hobbies at the retirement age

| Group No. | Number of subject hobbies throughout life | Professional types | Severity of cardiovascular disorders (arithmetic mean) | Standard deviation | Number of persons |
|-----------|---|--------------------|--|--------------------|-------------------|
| 1         | 0   | 1                  | 1.895833 <sup>2</sup>                                  | 0.037735           | 288               |
| 2         | 0   | 2                  | 2.157534 <sup>1</sup>                                  | 0.052998           | 146               |
| 3         | 1   | 1                  | 1.872727 <sup>2, 3</sup>                               | 0.086349           | 55                |
| 4         | 1   | 2                  | 1.444444 <sup>1, 3</sup>                               | 0.213460           | 9                 |
| 5         | 2   | 1                  | 2.000000   | 0.640380           | 1                 |
| 6         | 2   | 2                  | 1.000000   | 0.640380           | 1                 |

<sup>1, 2, 4</sup> – the significant difference with the relevant Fisher group (with  $p \leq 0.05$ )

Professional types:

1– all other types

2– Realistic type

**Table 6.** The severity of the cardiovascular disorders in the representatives of the Realistic type, with sports hobbies and without them throughout life

| Group No. | Number of sports hobbies throughout life | Professional types | Severity of the cardiovascular disorders (arithmetic mean) | Standard deviation | Number of persons |
|-----------|--|--------------------|--|--------------------|-------------------|
| 1         | 0  | 1                  | 1.866667 <sup>6, 8</sup>                                   | 0.058868           | 120               |
| 2         | 0  | 2                  | 2.023256 <sup>8</sup>                                      | 0.098341           | 43                |
| 3         | 1  | 1                  | 1.929293 <sup>6, 8</sup>                                   | 0.064811           | 99                |
| 4         | 1  | 2                  | 2.062500 <sup>7, 8</sup>                                   | 0.093078           | 48                |
| 5         | 2  | 1                  | 1.911765 <sup>6, 8</sup>                                   | 0.063851           | 102               |
| 6         | 2  | 2                  | 2.148148 <sup>1, 3, 5</sup>                                | 0.087755           | 54                |
| 7         | 3  | 1                  | 1.727273 <sup>4</sup>                                      | 0.137486           | 22                |
| 8         | 3  | 2                  | 2.555556 <sup>1, 2, 3, 4, 5</sup>                          | 0.214955           | 9                 |
| 9         | 4  | 1                  | 3.000000   | 0.644866           | 1                 |
| 10        | 4  | 2                  | 2.000000   | 0.455989           | 2                 |

1, 2, 3, 4, 5, 6, 8 – significant difference with the relevant Fisher group ( $p \leq 0.05$ )

Professional types:

1– all other types

2– Realistic type

**Table 7.** The severity of the cardiovascular disorders in the male and female representatives of the Social type

| Group No. | Sex    | Professional types | Severity of the cardiovascular disorders (arithmetic mean) | Standard deviation | Number of persons |
|-----------|--------|--------------------|--|--------------------|-------------------|
| 1         | female | 1                  | 1.848980 <sup>3</sup>                                      | 0.040475           | 245               |
| 2         | female | 2                  | 1.923077 <sup>3</sup>                                      | 0.052978           | 143               |
| 3         | male   | 1                  | 2.290000 <sup>1, 2</sup>                                   | 0.063353           | 100               |
| 4         | male   | 2                  | 1.916667   | 0.182883           | 12                |

1, 2, 3, – significant difference with the relevant Fisher group (with  $p \leq 0.05$ )

Professional types: 1– all other types. 2– Social type

**Table 8.** The severity of the cardiovascular disorders in the representatives of the Social type, with and without sports hobbies throughout life

| Group No. | Number of sports hobbies throughout life | Professional types | Severity of the cardiovascular disorders (arithmetic mean) | Standard deviation | Number of persons |
|-----------|--|--------------------|--|--------------------|-------------------|
| 1         | 0  | 1                  | 1.842593 <sup>3, 5</sup>                                   | 0.062606           | 108               |
| 2         | 0  | 2                  | 2.036364   | 0.087730           | 55                |
| 3         | 1  | 1                  | 2.049505 <sup>1, 4</sup>                                   | 0.064739           | 101               |
| 4         | 1  | 2                  | 1.804348 <sup>3, 5</sup>                                   | 0.095929           | 46                |
| 5         | 2  | 1                  | 2.035714 <sup>1, 4</sup>                                   | 0.061478           | 112               |
| 6         | 2  | 2                  | 1.886364   | 0.098085           | 44                |
| 7         | 3  | 1                  | 2.000000   | 0.138713           | 22                |
| 8         | 3  | 2                  | 1.888889   | 0.216874           | 9                 |
| 9         | 4  | 1                  | 2.000000   | 0.460059           | 2                 |
| 10        | 4  | 2                  | 3.000000   | 0.650621           | 1                 |

1, 3, 4, 5, – significant difference with the relevant Fisher group ( $p \leq 0.05$ )

Professional types: 1– all other types. 2– Social type

**Table 9.** The severity of the cardiovascular disorders in the representatives of the Conventional type and other professional types in the presence of various behavioral characteristics

| Indicators                           | Indicator levels     | Severity of the disease  |                   | Effect   |
|--------------------------------------|----------------------|--------------------------|-------------------|----------|
|                                      |                      | Other professional types | Conventional type |          |
| Age group                            | 55 – 65 years of age | 1.836207                 | 1.985507          | 0.130755 |
|                                      | 66 – 75 years of age | 2.076336                 | 1.950820          | 0.212589 |
|                                      | 76 – 85 years of age | 2.027397                 | 1.729730*         | 0.023426 |
| Family                               | Absent               | 0.500000                 | 2.000000*         | 0.011550 |
|                                      | Short marriage       | 1.931034                 | 2.032258          | 0.483059 |
|                                      | Permanent marriage   | 2.003717                 | 1.890511          | 0.096748 |
| Children                             | Absence              | 1.687500                 | 2.222222*         | 0.049352 |
|                                      | Presence             | 1.996805                 | 1.901235          | 0.130142 |
| Sociability in life                  | Low                  | 0.000000                 | 3.000000*         | 0.000147 |
|                                      | Medium               | 1.927273                 | 1.982456          | 0.597651 |
|                                      | High                 | 2.027650                 | 1.876106*         | 0.041849 |
| Sociability at the retirement age    | Low                  | 0.000000                 | 2.33333*          | 0.001899 |
|                                      | Medium               | 1.941176                 | 2.000000          | 0.544867 |
|                                      | High                 | 2.020833                 | 1.852941*         | 0.034733 |
| Overnutrition                        | Low                  | 1.914798                 | 1.933824          | 0.767105 |
|                                      | Medium               | 2.120000                 | 1.823529*         | 0.043176 |
| Aggressiveness at the retirement age | Low                  | 1.837209                 | 2.086957          | 0.100525 |
|                                      | Medium               | 2.020833                 | 1.852941*         | 0.024969 |
| Intellectual hobbies in life         | Absent               | 2.065934                 | 1.800000*         | 0.040487 |
|                                      | High level           | 1.647059                 | 2.166667*         | 0.034735 |
| Creative hobbies in life             | Absent               | 2.038298                 | 1.886179*         | 0.035511 |
|                                      | Medium level         | 1.890244                 | 2.000000          | 0.352054 |
|                                      | High level           | 1.500000                 | –                 |          |
| Sports hobbies in life               | Absent               | 2.019417                 | 1.716667          | 0.004269 |
|                                      | Low level            | 1.927083                 | 2.058824          | 0.242205 |
|                                      | High Level           | 1.880000                 | 2.333333          | 0.125241 |

– there were no subjects with this indicator level.

\* –The difference is significant between the representatives of the Conventional type and other professional types.

**ESTUDOS EXPERIMENTAIS DE TRANSFERÊNCIA DE CALOR E MASSA DE MODELOS DE PONTAS PRODUZIDOS A PARTIR DE MATERIAL COMPÓSITO DE CARBONO-CARBONO (MCCC) SOB CONDIÇÕES DE CARGA DE CALOR DE ALTA INTENSIDADE****EXPERIMENTAL STUDIES OF HEAT AND MASS TRANSFER FROM TIP MODELS MADE OF CARBON-CARBON COMPOSITE MATERIAL (CCCM) UNDER CONDITIONS OF HIGH-INTENSITY THERMAL LOAD****ЭКСПЕРИМЕНТАЛЬНЫЕ ИССЛЕДОВАНИЯ ТЕПЛОМАССОПЕРЕНОСА С МОДЕЛЕЙ НАКОНЕЧНИКОВ, ИЗГОТОВЛЕННЫХ ИЗ УГЛЕРОД-УГЛЕРОДНОГО КОМПОЗИЦИОННОГО МАТЕРИАЛА (УУКМ) В УСЛОВИЯХ ВЫСОКОИНТЕНСИВНОГО ТЕРМОСИЛОВОГО НАГРУЖЕНИЯ**

SHA, Minggong<sup>1\*</sup>; UTKIN, Yuri A.<sup>2</sup>; TUSHAVINA, Olga V.<sup>3</sup>; PRONINA, Polina F.<sup>4</sup>;

<sup>1</sup> Northwestern Polytechnical University (NPU), School of Civil Aviation, 127 West Youyi Road, Beilin District, zip code 710072, Xi'an Shaanxi – People's Republic of China.

<sup>2</sup> Moscow Aviation Institute (National Research University), Department of Perspective Materials and Technologies, 4 Volokolamskoe Highway, zip code 125993, Moscow – Russian Federation.

<sup>3,4</sup> Moscow Aviation Institute (National Research University), Institute of Aerospace, Department of Managing Exploitation of Space-Rocket Systems, 4 Volokolamskoe Highway, zip code 125993, Moscow – Russian Federation.

\* Correspondence author  
e-mail: 695792773@qq.com

Received 20 April 2020; received in revised form 26 June 2020; accepted 02 July 2020

**RESUMO**

Os materiais compósitos de carbono-carbono são caracterizados por alta resistência ao calor e estabilidade térmica, para as quais, devido a maioria de suas características físicas e mecânicas, podem ser atribuídos aos materiais mais promissores. Aproximadamente 81% de todos os materiais compósitos de carbono-carbono são utilizados na fabricação de discos de freio para aeronaves, 18% - na tecnologia de foguetes espaciais e apenas 1% - para todas as outras áreas de aplicação. Embora a necessidade de materiais compósitos para tecnologia de foguetes espaciais esteja constantemente diminuindo – o volume de produção de discos de freio para aeronaves está em constante crescimento e, portanto, estudos de propriedades dos materiais compósitos de carbono-carbono sob condições de carga térmica de alta intensidade são extremamente urgentes hoje em dia. Este artigo considera o método para a introdução de silicatos e óxidos nos MCCC, que os endurecem, com a adição de elementos químicos resistentes ao calor. Testes de pontas do MCCC foram realizados sob condições de carga de calor de alta intensidade. Os objetivos do experimento foram obter as formas queimadas do modelo de ponta e registrar a temperatura na superfície durante a ação de um jato que sai do bico do sistema de propulsão. A ponta do MCCC é soprada por meio do sistema de propulsão com um fluxo supersônico de gás contendo oxigênio de alta entalpia. Os resultados de estudos experimentais foram determinados usando gravação de vídeo com base em qual as sequências de quadros foram obtidas. De acordo com os quadros mencionados as formas queimadas foram construídas. Usando medições de imagem térmica, o campo de temperatura na superfície do modelo foi determinado durante todo o tempo em que a superfície do modelo foi exposta ao fluxo de gás supersônico.

**Palavras-chave:** material compósito de carbono-carbono, revestimento com proteção térmica, motor de foguete de propulsão líquida, modelo de ponta, características físicas e mecânicas.

**ABSTRACT**

Carbon-carbon composite materials are characterized by high heat resistance and thermostability for which they, in most of their physical and mechanical characteristics, can be attributed to the most promising

materials. Approximately 81% of all carbon-carbon composite materials are used for the manufacture of brake rotors for aircraft, 18% – in space rocket technology, and only 1% – for all other areas of application. While the need for composites for rocket and space technology is constantly decreasing – the volume of production of brake disc rotors for aircraft is steadily growing, and therefore research on the properties of carbon-carbon composite materials (CCCM) under conditions of high-intensity thermal loading is extremely urgent at the moment. In this paper, we consider a method for introducing silicates and oxides hardening them with the addition of refractory, chemical elements into CCCM. Tests of tips from CCCM were carried out under conditions of high-intensity thermo-force loading. The objectives of the experiment were to obtain scalded forms of the tip model and to record the temperature on the surface during the action of a jet flowing out of the nozzle of the propulsion system (PS). The tip of the CCCM is blown by means of a propulsion system with a supersonic flow of a highly enthalpy oxygen-containing gas. The results of experimental studies were determined using video recording on the basis of which sequences of frames were obtained on the basis of which the burning forms were built. Using thermal imaging measurements, the temperature field on the model surface was determined during the entire time the supersonic gas flow was exposed to it.

**Keywords:** *carbon-carbon structural material, thermal insulation coating, liquid rocket engine, tip model, physicomechanical characteristics.*

## АННОТАЦИЯ

Углерод-углеродные композиционные материалы характеризуются высокой жаропрочностью и термостойкостью, за что их, по большинству своих физико-механических характеристик, можно отнести к наиболее перспективным материалам. Примерно 81% всех углерод-углеродных композиционных материалов используется для производства тормозных дисков для самолетов, 18% – в ракетно-космической технике и только 1% – для всех остальных сфер применения. В то время как потребность в композитах для ракетно-космической техники постоянно снижается – объем производства тормозных дисков для самолетов стабильно растет, в связи с чем исследования свойств УУКМ в условиях высокоинтенсивного термосилового нагружения на сегодняшний момент крайне актуальны. В данной работе рассматривается метод введения в УУКМ упрочняющих их силицидов и оксидов с добавлением тугоплавких химических элементов. Проведены испытания наконечников из (УУКМ) в условиях высокоинтенсивного термосилового нагружения. Целями эксперимента являлось получение обгарных форм модели наконечника и регистрация температуры на поверхности в процессе воздействия на неё струи, истекающей из сопла двигательной установки (ДУ). Наконечник из УУКМ обдувается при помощи двигательной установки сверхзвуковым потоком высокоэнтальпийного кислородосодержащего газа. Результаты экспериментальных исследований определялись с помощью видеорегистрации на основе которой были получены последовательности кадров, на базе которых были построены обгарные формы. С помощью термовизионных измерений определялось поле температур на поверхности модели в течение всего времени воздействия на неё сверхзвукового потока газа.

**Ключевые слова:** *углерод-углеродный конструкционный материал, теплозащитное покрытие, жидкостной ракетный двигатель, модель наконечника, физико-механические характеристики.*

## 1. INTRODUCTION

Carbon-carbon composite materials for most of their physical and mechanical characteristics (FMC) can be attributed to the most promising materials. CCCM are characterized by high heat resistance and thermostability. With intense aerodynamic heating of the thermal protection of hypersonic aircraft, the properties of FMC can change (Bulychev and Kuznetsova, 2019; Ryapukhin *et al.*, 2019; Kozorez and Kruzhkov, 2019; Shen *et al.*, 2019). This is due to the processes of the dynamic interaction of a high-temperature gas flow with the surface of the material. Composite materials of the carbon-carbon system were first created in the early

1960s, simultaneously with the advent of high-strength carbon fibers (Anikin *et al.*, 2019). Obtaining CCCM is based on the principle of heating organic fibers under certain conditions, not destroying them, but turning them into carbon fibers (Kolesnikov *et al.*, 2017; Reznik *et al.*, 2017; Stepashkin *et al.*, 2018). Almost all industrial fibers, as well as a number of specially prepared fibers, were tested as feedstock for these purposes. However, most of them did not meet the requirements, the main of which were the non-meltability or ease of imparting it, the yield of the finished fiber, and its high performance. At the same time CCCM contain a carbon reinforcing element in the form of discrete fibers, continuous filaments, and bundles, as well as various

volumetric frame structures (Song, 2009; Babaytsev *et al.*, 2017; Akhmetzhanov *et al.*, 2018; Yin *et al.*, 2018; Evdokimenkov *et al.*, 2019a; Evdokimenkov *et al.*, 2019b; Formalev *et al.*, 2019; Stepashkin *et al.*, 2019).

The advantage of CCCM is that it is able to perceive various external loads due to the fact that the carbon matrix combines the reinforcing elements in a composite (Mohammed *et al.*, 2019). The properties of CCCM vary over a wide range, and its strength characteristics are especially important (Skvortsov *et al.*, 2014; Orlov *et al.*, 2003). To increase the strength of the composite, carbonization of its polymer matrix is carried out by high-temperature heat treatment in a non-oxidizing medium, and then its graphitization is carried out. It is known that the strength of CCCM based on high-strength carbon fibers is higher than the strength of a composite material based on high-modulus carbon fibers obtained at various processing temperatures. Some CCCM, especially those obtained by carbonizing carbon fiber based on organic polymers, are characterized by an increase in strength with an increase in operating temperature up to 2700 °C. At temperatures above 3000°C, CCCM are efficient for a short time, since intense graphite sublimation begins (Kabanov *et al.*, 2019; Kolotyryn *et al.*, 2019; Radyuk *et al.*, 2019).

Physico-mechanical characteristics of carbon-carbon composite materials are significantly reduced in oxygen-containing environments when exposed to relatively low temperatures (Doretta *et al.*, 2017; Volovik *et al.*, 2018; Piat *et al.*, 2019). Among the special properties of CCCM are low porosity, low coefficient of thermal expansion, maintaining a stable structure and properties, as well as product dimensions. Here, we consider the development of a method for introducing silicides and oxides hardening them with the addition of refractory, chemical elements into the CCCM, which allows us to ensure the functioning of the fired forms of the tip models and to record the temperature on the surface in the process of exposure to a high-enthalpy stream of the oxygen-containing gas.

The mechanical strength of solids is determined by the strength of the interatomic bond. Of the natural bodies, diamond has the highest hardness, in which there are carbon-carbon interatomic bonds. Carbon-carbon bonds are also present in graphite; it has a layered structure. There are strong carbon-carbon bonds inside the layers. These bonds are used to create high strength materials. One of the important problems of creating designs of aviation, aircraft

and rocket engines is the development of new materials used for the manufacture of the most loaded parts operating under high temperatures (Djugum and Sharp, 2017; Wu and Yan, 2018; Wang and Zhu, 2018; Xie *et al.*, 2019).

Carbon-carbon composite materials – a new class of structural materials designed to create heat-loaded, durable, tough products operating in aggressive environments (Chen *et al.*, 2018; Zhang *et al.*, 2019). Products from similar materials are used to create parts for aircraft, rocket devices, and engines. They have a unique ability to maintain high strength and stiffness at temperatures up to 2700 °C, and coating provides performance in an oxidizing environment. Multidimensionally reinforced CCCM are materials based on a carbon matrix and a woven frame of three- or four-dimensional carbon fiber structures. Designed for use in rocketry products operating at high temperatures. It is produced in the form of cylindrical billets and parallelepipeds using serial technologies. Antioxidant coatings are applied to parts operating under high-enthalpy flow products (Mei *et al.*, 2017; Wang *et al.*, 2019). These coatings consist of adhesive and erosion resistant antioxidative layers. The adhesive layer is made on the basis of tantalum carbide, which provides high mechanical bond strength of the erosion-resistant antioxidant coating with CCCM. The main method for testing products is to create conditions as close as possible to the conditions in which the product will work. This is gas-dynamic heat load, creation of an oxidizing environment, vacuum (Davydovich *et al.*, 2017).

## 2. MATERIALS AND METHODS

A tip model made of the composite material was manufactured for the experiment. An antioxidant coating was applied to the tip. Material characteristics are as follows:

- density, 1.67 g / cm<sup>3</sup>;
- porosity 2.5%;
- thermal conductivity 2.6 W / m;
- ultimate tensile stress at 260 MPa;
- tensile modulus 75 MPa;
- breaking stress at compression 140 MPa;
- Poisson's ratio 0.12.

To create a high-temperature free flow from the engine nozzle to the tip on the stand, a liquid rocket engine operating on liquefied oxygen-hydrogen gas is used. The engine using oxygen-

hydrogen fuel in specific impulse is approximately 30% higher than oxygen-kerosene.

The engine consists of a mixing head with pressure jet atomizers, a combustion chamber, and a nozzle. The engine uses a Laval nozzle. It represents a gas channel of a special profile having a narrowing to change the speed of the gas stream passing through it. It is an important part of modern rocket engines. For a video recording of experiments, two video cameras were used, with a recording rate of 30 frames per second, network cable, two opto-digital converters, neutral light filters.

Temperature measurements were made with a thermal imager. Thermal radiation from the surface of the cone passes through the filters and through the lenses of the lens, which forms the image of the cone on the camera matrix. Each matrix element forms a signal proportional to the perceived radiation energy. This signal is digitized and transmitted to the computer via the USB port. On a computer using software, the data is processed, and the thermal radiation of the object is visualized in real-time. Video recording was carried out with a shot breakdown of 30 frames per second, which allowed the construction of combusted forms.

The start of thermal registration was carried out before the start of the experiment. A thermogram was shown on the computer with the maximum tip temperature recorded during the experiment. Thermal registration allowed us to determine the maximum surface temperatures achieved during the experiments. The pressure in the chamber and at the nozzle exit was registered by sensors.

Additional methods using plasmotrons and other equipment were not used.

### 3. RESULTS AND DISCUSSION:

The schematic diagram of the video and thermovisual fixation of the experiment is shown in Figure 1, which shows the overtaking flow coming out from the nozzle of a propulsion system (PS) (1), the investigated model of CCCM (2), a quartz optical window (3), a VideoScan-415 camera (4), a Nikon NIKKOR-52AF lens (5), a filter package consisting of a cut-off filter LP850 and a neutral filter ND8 (6), moreover, objects 4, 5 and 6 together constitute the Tandem VS-415-V2 thermal imager, camera-controller connection 5 m long (7), a laptop with the TERMO-6 thermal imager software installed and data recorded (8), a network cable ~ 60 m long connecting the

recording and controlling laptops (9) located in the control room at a distance of ~ 50 m from the laptop from which control of a laptop connected to a thermal imager is carried out, including data logging control (10).

The video recording complex consists of a laptop, from which data of video cameras are recorded, a network cable-twisted pair (12), with which the laptop was connected to a fiber optic path, which consisted of analog-to-digital converters (13) and fiber itself (14). The cameras (16, 17) were connected to an analog-to-digital converter using network cables-twisted pairs (15). The distance from the cameras and the thermal imager to the model was ~ 4 m. Both devices were located in a separate room next to the stand on an isolated foundation, which allowed to reduce the level of equipment vibration.

Tip models were tested on a bench stand. The bench setup included: an oxygen-hydrogen chamber with a critical section diameter of 92 mm, a holder, an ignition unit, and spark plugs. The model was attached to the stand holder through a spacer. The spacer on the outside was covered with a fairing. The distance of the model from the nozzle exit before testing was  $40 \pm 0.5$  mm.

The duration of the propulsion system in a given mode was 10 s. Samples were measured after testing. The propulsion system worked at the set modes, the temperature at the cut of the chamber was 2780°C, the discharge velocity was 1742 m/s. The objective of the experiment was to obtain scalded forms of the tip model and to register the temperature at the surface during the action of a jet flowing from the remote-controlled nozzle. To achieve these goals, thermal imaging measurements and video recording of the experiment process were carried out as part of the CCCM test program.

The purpose of the video recording is to obtain a sequence of frames on the basis of which the burning forms are built. Using thermal imaging measurements, the temperature field was determined on the model surface during the entire time the jet was exposed to it. The models were a cone with spherical blunting. The half-angle of the cone solution was 7°, and the radius of the spherical blunting was 36 mm. The total length of the model was 125 mm. It should be noted that the models consisted of three parts: the tip of the CCCM material, the stern, and the conical insert along the central axis.

For a video recording of experiments, two video cameras were used. One recorded the general view of the stand during the tests (SONY),



and the second fixed the sample from the angle as close as possible to the thermal imager (JAI), which is designed for non-contact measurement of the temperature of the studied objects. The thermal imager was connected via a communication cable to a PC with the installed VS2001 controller, on which the TERMO 6 software was installed, and on which the obtained thermal images were recorded. PC data management was carried out remotely from the stand control center (Krayushkina *et al.*, 2019).

Thermal radiation from the surface of the object under study passed through the filters and through the lenses of the camera, which forms the image of the object on the CCD matrix of the camera. Each element of the CCD matrix forms a signal proportional to the perceived radiation energy. This signal is digitized and transmitted to the computer via a USB port. On a computer using the TERMO 6 software, the obtained data is processed, and the thermal radiation of the object is visualized in real-time, as well as the reproduction of single thermal images and sequences of thermal images in video mode, as well as a retrospective analysis of the obtained data. It must be clarified that after processing the signal of the TERMO 6 software, a thermogram is formed with temperatures corresponding to the brightness temperature adjusted for the degree of blackness of the test sample (Yuilin *et al.*, 2019).

Further, the term "true temperature" will be used for this temperature. In this case, the actual temperature of objects in some cases may differ from the true temperature recorded by the thermal imager. The video recording was launched by the clock signal received directly from the stand with the following parameters:

- registration speed ~ 6 frames per second;
- degree of blackness – 0.9;
- ambient temperature – 17°C;
- $\lambda$  is the specified coefficient of the medium transmittance (quartz window) – 0.93;
- distance to the sample – 4 m.

The start of thermal registration was carried out manually, before starting. Figure 2 shows a sample before starting. The initial shape of the sample and its position relative to the nozzle are clearly visible. Figure 3 shows a thermogram with temperature decoding. The temperature profile in the "Profile XY" window (3) is calculated along the horizontal line visible on the thermogram (1). In the rectangular region (2), the maximum temperature, the average value, and the number of parameters are calculated. The recorded true

temperature of the gas in the shock layer (6) reaches 1900 °C. In region (6), a jet is seen flowing out of the propulsion system nozzle.

During the experiment, video recording and thermal recording were carried out, which allowed us to construct the diagrams shown in Figure 4 and build the charred forms. Here is a diagram of the distribution of the temperature field ( $T_a$ ) and the flow velocity at the nozzle exit ( $W_a$ ) at different points in time. Figures 5-6 show the appearance of the tip model before and after the test.

As a result of the high-intensity effect of gas-dynamic and thermal loads, the material was carried away from the tip. The ablation of the material largely depends on the heat resistance, heat resistance, and mechanical strength of the tips, which largely depends on the weaving of the fabric, the number of layers of their orientation, epoxy fillers, hardening of products by coating tantalum carbide, silicon. All of the above properties affect the physical and mechanical characteristics. Thanks to video cameras, frames were sequentially obtained on the basis of which rainfed forms were built. Thermal imagers measured the temperature fields on the surface of the tips during the entire time the jet was exposed to them. Tips made of aluminum alloys, stainless steel, titanium could not withstand such loads when conducting similar experiments.

#### 4. CONCLUSIONS:

Therefore, on the basis of the experimental studies carried out in the work, the following data is obtained: experimental dependences of the burning forms of the models on time, data on the distribution of temperature and velocity of the jet outflow on the surface of the models. A diagram of the distribution of the temperature field and the flow velocity as a function of time is shown, from which it can be seen that the jumps in the temperature field are synchronized with the jumps of the velocity vector at times of 3.5 and 5 min. It also illustrated the process of ablation of the mass of the tip when exposed to high-speed high-enthalpy gas flow.

It can be seen from the experimental work that the CCCM retains high heat resistance and heat resistance at high gas-dynamic loads and high temperatures. Experiments have shown that CCCM accepts temperature and gas-dynamic loads due to the fact that the carbon matrix combines the reinforcing elements in CCCM. To increase the strength of CCCM, carbonization of its matrix was carried out, due to which the heat

resistance, heat resistance, erosion resistance of the products were significantly increased.

## 5. ACKNOWLEDGMENTS:

The work was carried out with the financial support of the state project of the Ministry of Education and Science project code "Modern technologies of experimental and digital modeling and optimization of spacecraft systems parameters", project code FSFF-2020-0016

## 6. REFERENCES:

1. Akhmetzhanov, R.V., Balashov, V.V., Bogachev, Y.A., Yelakov, A.B., Kashirin, D.A., Svotina, V.V., Spivak, O.O., and Cherkasova, M.V. (2018). An ion thruster accelerating electrode made of carbon-carbon composite material. *Thermal Engineering*, 65(13), 986-993.
2. Anikin, A.V., Berdov, R. D., Volkov, N.N., Volkova, L.I., Gurina, I.N., and Tsatsuev, S.M. (2019). Long-run testing of model nozzle extensions made of a carbon-carbon composite material in a liquid-propellant rocket engine operating on hydrogen and oxygen. *Journal of Applied Mechanics and Technical Physics*, 60(1), 80-86.
3. Babaytsev, A.V., Prokofiev, M.V., and Rabinskiy, L.N. (2017). Mechanical properties and microstructure of stainless steel manufactured by selective laser sintering. *International Journal of Nanomechanics Science and Technology*, 8(4), 359-366.
4. Bulychyev, N.A., and Kuznetsova, E.L. (2019). Ultrasonic Application of Nanostructured Coatings on Metals. *Russian Engineering Research*, 39(9), 80-812.
5. Chen, B., Wen, W., Cui, H., Zhang, H., and Xu, Y. (2018). Test on mechanics of three-dimensional four directional C/C composites at elevated temperature and oxidation environment. *Hangkong Dongli Xuebao/Journal of Aerospace Power*, 33(8), 1916-1922.
6. Davydovich, D., Dron, M., Zharikov, K., and Jordan, Y. (2017). Research of the launch vehicle design made of composite materials under the aerodynamic, thermal and acoustic loadings. *MATEC Web of Conferences*, 102, article number 01011.
7. Djugum, R., and Sharp, K. (2017). The fabrication and performance of C/C composites impregnated with TaC filler. *Carbon*, 115, 105-115.
8. Doretto, L., Longo, G.A., Mancin, S., Righetti, G., and Zilio, C. (2017). Flow boiling heat transfer on a Carbon/Carbon surface. *International Journal of Heat and Mass Transfer*, 109, 938-948.
9. Evdokimenkov, V.N., Kim, N.V., Kozorez, D.A., and Mokrova, M.I. (2019a). Control of unmanned aerial vehicles during fire situation monitoring. *INCAS Bulletin*, 11, 67-73.
10. Evdokimenkov, V.N., Kozorez, D.A., and Krasilshchikov, M.N. (2019b). Development of pre-flight planning algorithms for the functional-program prototype of a distributed intellectual control system of unmanned flying vehicle groups. *INCAS Bulletin*, 11, 75-88.
11. Formalev, V.F., Kolesnik, S.A., and Kuznetsova, E.L. (2019). Effect of components of the thermal conductivity tensor of heat-protection material on the value of heat fluxes from the gasdynamic boundary layer. *High Temperature*, 57(1), 58-62.
12. Kabanov, E.I., Korshunov, G.I., and Gridina, E.B. (2019). Algorithmic provisions for data processing under spatial analysis of risk of accidents at hazardous production facilities. *Naukovyi Visnyk Natsionalnoho Hirnychoho Universytetu*, 2019(6): 117-121.
13. Kolesnikov, S.A., Kim, L.V., Vorontsov, V.A., Protsenko, A.K., and Cheblakova, E.G. (2017). Study of thermophysical property formation of spatially reinforced carbon-carbon composite materials. *Refractories and Industrial Ceramics*, 58(4), 439-449.
14. Kolotyryn, K.P., Bogatyrev, S.A., Savon, D.Y., and Aleksakhin, A.V. (2019). Use of resource-saving technologies in fabrication and restoration of steel bushing-type components via hot plastic deformation. *CIS Iron and Steel Review*, 18, 38-41.
15. Kozorez, D.A., and Kruzhkov, D.M. (2019). Autonomous navigation of the space debris collector. *INCAS Bulletin*, 11, 89-104.
16. Krayushkina, K., Khymeryk, T., and Bieliatynskiy, A. (2019). Basalt fiber concrete as a new construction material for roads and airfields. *IOP Conference Series: Materials Science and Engineering*, 708, Article number 012088.
17. Mei, X., Zhang, X., Liu, X., and Wang, Y. (2017). Effect on structure and mechanical property of tungsten irradiated by high-

- intensity pulsed ion beam. *Nuclear Instruments and Methods in Physics Research, Section B: Beam Interactions with Materials and Atoms*, 406, 697-702.
18. Mohammed, A.S.K., Sehitoglu, H., and Rateick, R. (2019). Interface graphitization of carbon-carbon composites by nanoindentation. *Carbon*, 150, 425-435.
  19. Orlov, A.M., Skvortsov, A.A., and Litvinenko, O.V. (2003). Bending vibrations of semiconductor wafers with local heat sources. *Technical Physics*, 48(6): 736-741.
  20. Piat, R., Zuo, Y., and Megyesi, P. (2019). Numerical modeling of the 2D crack propagation in carbon-carbon composites. *Ceramic Engineering and Science Proceedings*, 39(3), 89-104.
  21. Radyuk, A.G., Gorbatyuk, S.M., Tarasov, Y.S., Titlyanov, A.E., Aleksakhin, A.V. (2019). Improvements to mixing of natural gas and hot-air blast in the air tuyeres of blast furnaces with thermal insulation of the blast duct. *Metallurgist*, 63(5-6), 433-440.
  22. Reznik, S.V., Mikhailovskii, K.V., and Prosuntsov, P.V. (2017). Heat and mass transfer in the chemical vapor deposition of silicon carbide in a porous carbon-carbon composite material for a heat shield. *Journal of Engineering Physics and Thermophysics*, 90(2), 291-300.
  23. Ryapukhin, A.V., Kabakov, V.V., and Zaripov, R.N. (2019). Risk management of multimodular multi-agent system for creating science-intensive high-tech products. *Espacios*, 40(34), 19-32.
  24. Shen, Q., Song, Q., Li, H., Xiao, C., Wang, T., Lin, H., and Li, W. (2019). Fatigue strengthening of carbon/carbon composites modified with carbon nanotubes and silicon carbide nanowires. *International Journal of Fatigue*, 124, 411-421.
  25. Skvortsov, A.A., Kalenkov, S.G., and Koryachko, M.V. (2014). Phase transformations in metallization systems under conditions of nonstationary thermal action. *Technical Physics Letters*, 40(9), 787-790.
  26. Song, M. (2009). Effects of volume fraction of SiC particles on mechanical properties of SiC/Al composites. *Transactions of Nonferrous Metals Society of China*, 19(6), 1400-1404.
  27. Stepashkin, A.A., Ozherelkov, D.Y., Sazonov, Y.B., and Komissarov, A.A. (2018). Criteria for evaluating the fracture toughness of carbon-carbon composite materials. *Metal Science and Heat Treatment*, 60(3-4), 266-272.
  28. Stepashkin, A.A., Ozherelkov, D.Y., Sazonov, Y.B., Komissarov, A.A., and Mozalev, V.V. (2019). Change in interlayer strength and fracture toughness of carbon-carbon composite material under the impact of cyclic loads. *Inorganic Materials: Applied Research*, 10(1), 155-161.
  29. Volovik, A.Y., Krylik, L.V., Kobyl'yanska, I.M., Kotyra, A., and Amirgaliyeva, S. (2018). Methods of stochastic diagnostic type observers. *Proceedings of SPIE – The International Society for Optical Engineering*, 10808, Article number 108082X.
  30. Wang, B., Xu, B., and Li, H. (2019). Fabrication and properties of carbon/carbon foam composites. *Textile Research Journal*, 89(21-22), 4452-4460.
  31. Wang, M., and Zhu, W. (2018). Pore-scale study of heterogeneous chemical reaction for ablation of carbon fibers using the lattice Boltzmann method. *International Journal of Heat and Mass Transfer*, 126, 1222-1239.
  32. Wu, Q.-J., and Yan, H. (2018). Fabrication of carbon nanofibers/A356 nanocomposites by high-intensity ultrasonic processing. *Metallurgical and Materials Transactions A: Physical Metallurgy and Materials Science*, 49(6), 2363-2372.
  33. Xie, W., Yang, Y., Meng, S., Peng, T., Yuan, J., Scarpa, F., Xu, C., and Jin, H. (2019). Probabilistic reliability analysis of carbon/carbon composite nozzle cones with uncertain parameters. *Journal of Spacecraft and Rockets*, 56(6), 1765-1774.
  34. Yin, T., Li, X., Wang, Y., He, L., and Gong, X. (2018). Effect of the meso-structure on the strain concentration of carbon-carbon composites with drilling hole. *Science and Engineering of Composite Materials*, 25(4), 825-834.
  35. Yulin, H., Beljatynskij, A., and Ishchenko, A. (2019). Non-Roundabout design of cancel the intersection signal light on horizontal plane. *E3S Web of Conferences*, 91, 1-22.
  36. Zhang, Q., Zhu, X.P., Zhang, C.C., and Lei, M.K. (2019). Comprehensive material constraints incorporation in coupled thermal-mechanical responses modelling for high-

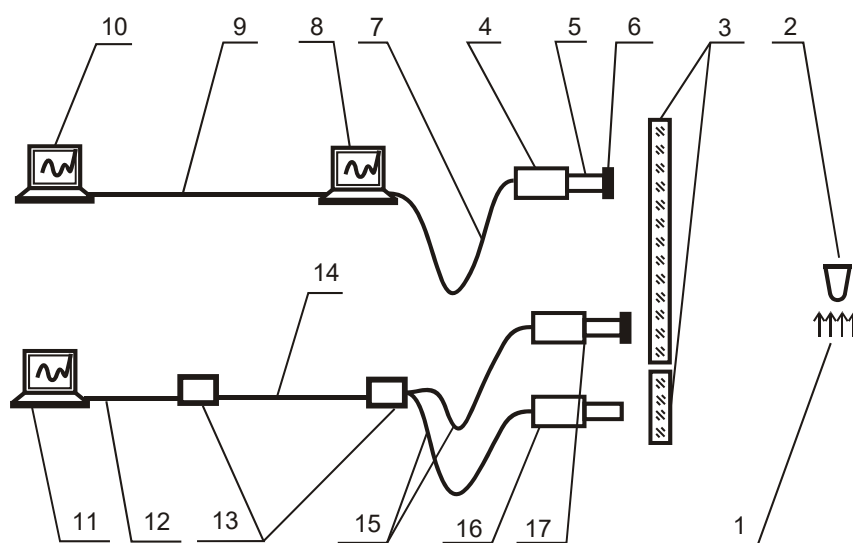


**Figure 1.** Schematic diagram of the experiment for measuring the temperature of a sample streamlined by a supersonic jet flowing out of a propulsion system

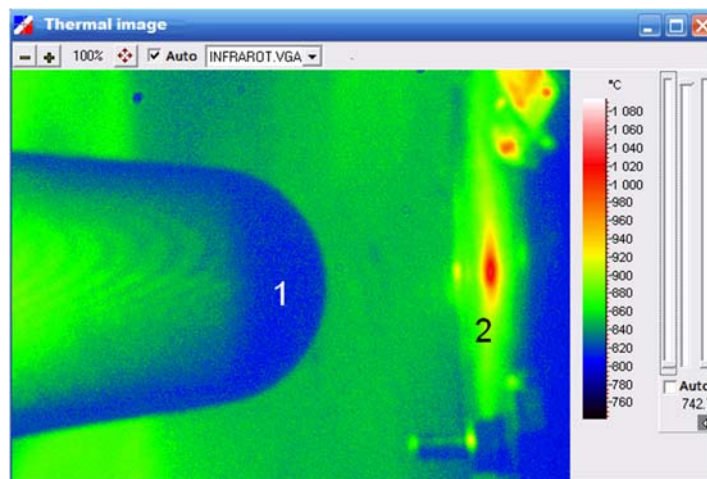


**Figure 2.** Sample before starting (1 - sample, 2 – cut-off of propulsion system nozzle)

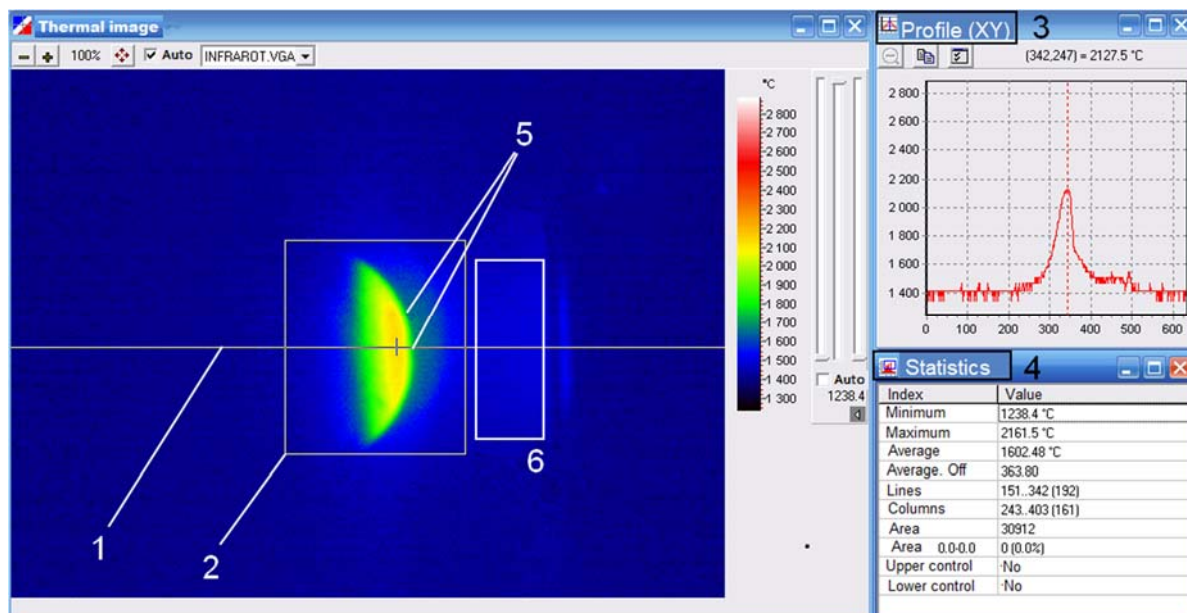


**Figure 3.** The first frame after heating of the sample

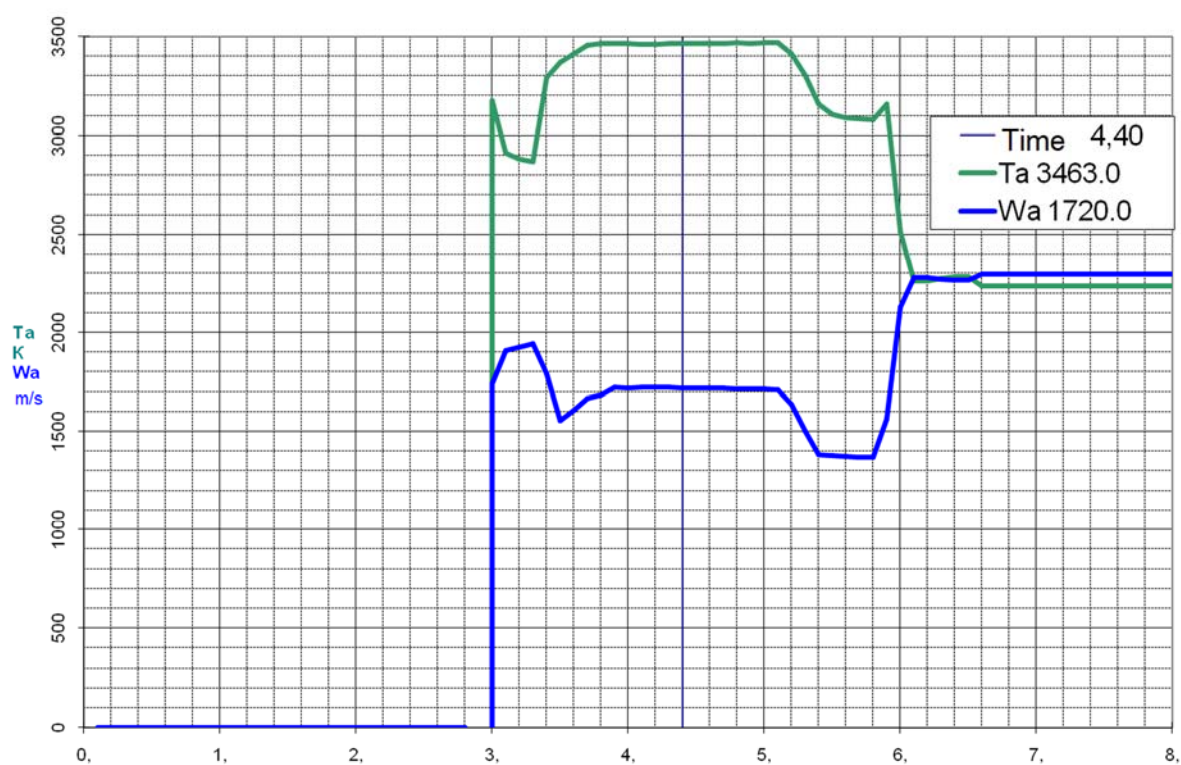


**Figure 4.** Diagram of temperature ( $T_a$ ) and jet velocity ( $W_a$ )





**Figure 5.** *Tip model view before the test*



**Figure 6.** *Tip model view after the test*

## PRODUÇÃO DE FRAÇÕES DE MIRICETINA DE PLANTA DE *LINOSYRIS VILLOSA* E ESTUDO DE SUA ATIVIDADE BIOLÓGICA

## ISOLATION OF MIRICETINE-CONTAINING FRACTIONS FROM *LINOSYRIS VILLOSA* PLANT AND THEIR APPLICATION AS ANTIANEMIC AGENT

## ВЫДЕЛЕНИЕ МИРИЦЕТИНСОДЕРЖАЩИХ ФРАКЦИЙ ИЗ РАСТЕНИЯ *LINOSYRIS VILLOSA* И ИХ ПРИМЕНЕНИЕ В КАЧЕСТВЕ АНТИАНЕМИЧЕСКОГО СРЕДСТВА

NAZAROVA, Valentina D.<sup>1</sup>; SALIKOVA, Natalya S.<sup>2\*</sup>; BEKTEMISOVA, Ainash U.<sup>3</sup>; BEGENOVA, Bahyt E.<sup>4</sup>; AUBAKIROVA, Gulsim B.<sup>5</sup>;

<sup>1,3,4,5</sup> M. Kozybayev North Kazakhstan State University; Department of Chemistry and Chemical Technology; 86 Pushkin Str.; ZIP code 150000; Petropavlovsk – Republic of Kazakhstan.

<sup>2</sup> Abay Myrzakhmetov Kokshetau University; Department of Ecology, Life Safety, and Environmental Protection; 189A Auezov Str.; ZIP code 020000; Kokshetau – Republic of Kazakhstan.

\* Correspondence author  
e-mail: natsal66@mail.ru

Received 22 March 2020; received in revised form 06 June 2020; accepted 03 July 2020

### RESUMO

Com o desenvolvimento da química, substâncias naturais foram ativamente substituídas da vida humana por produtos químicos. No entanto, apesar do enorme progresso nessa área, nas últimas décadas, os problemas de graves efeitos colaterais dos produtos químicos sintéticos no meio ambiente tornam-se cada vez mais pronunciados. Foram utilizados os métodos de cromatografia bidimensional e unidimensional de papel, cromatografia de adsorção em coluna, cromatografia gasosa e espectroscopia de infravermelho. O objetivo do artigo é estudar a composição química da planta de *Linosyris villosa* por métodos físico-químicos de análise e criar formas de dosagem baseadas nela. O problema do artigo é a busca e criação de medicamentos baseados na flora do norte do Cazaquistão. A novidade científica reside no fato de que a composição química e a atividade biológica da planta *Linosyris villosa*, que cresce no território do norte do Cazaquistão, estão sendo estudadas pela primeira vez. De acordo com os resultados da análise, em 13% dos pacientes o efeito do tratamento é insignificante e em 87% dos pacientes houve uma melhoria nas contagens sanguíneas (aumento da hemoglobina, aumento no número de glóbulos vermelhos, quase todos os pacientes retornaram a contagem normal de cores), o número de leucócitos aumentou para normal e a fórmula de leucócitos melhorou. Portanto, o medicamento “Vitin”, que é um extrato de água-álcool da planta *Linosyris villosa*, é um medicamento eficaz para o tratamento de pacientes com anemia de várias gravidades. O significado prático do trabalho é definido da seguinte forma: os compostos biologicamente ativos da planta *Linosyris villosa* foram obtidos com o objetivo de estudá-los e aplicá-los na medicina e na agricultura.

**Palavras-chave:** planta de *Linosyris villosa*, flavonóides, frações de miricetina, filmes de drogas, atividade antianêmica, pesticidas.

### ABSTRACT

With the development of chemistry, natural substances were actively supplanted from human life by chemical products. However, despite the enormous progress in this area, in recent decades, the problems of serious side effects of synthetic chemicals on the environment have become more and more pronounced. Methods of two-dimensional and one-dimensional paper chromatography, column adsorption chromatography, gas chromatography, and IR spectroscopy were used. The purpose of the article is to study the chemical composition of the *Linosyris villosa* plant by physicochemical methods of analysis. Creation of dosage forms based on it. The problem of the article is the search and creation of drugs based on the flora of Northern Kazakhstan. The scientific novelty lies in the fact that the chemical composition and biological activity of the *Linosyris villosa* plant, growing in the territory of Northern Kazakhstan, is being studied for the first time. According to the results of the analysis, in 13% of patients the treatment effect is insignificant, and in 87% of patients there was an improvement in blood values (increase in hemoglobin, an increase in the number of red blood cells, almost

all patients returned color index of blood), the number of white blood cells increased to normal, and the WBC differential improved. Therefore, the drug "Vitin", an aqueous-alcoholic extract of the *Linosyris villosa*, is an effective drug for the treatment of patients with anemia of varying severity. The practical significance of the work is defined as follows: biologically active compounds from the *Linosyris villosa* plant were obtained for the purpose of studying and applying them in medicine and agriculture.

**Keywords:** *Linosyris villosa* plant, flavonoids, myricetin fractions, medicated films, antianemic activity, pesticides.

## АННОТАЦИЯ

С развитием химии, природные вещества активно вытеснялись из жизни человека продуктами химического производства. Однако, несмотря на огромный прогресс в этой области, в последние десятилетия все настоятельнее заявляют о себе проблемы серьезных побочных воздействий синтетических химических препаратов на окружающую среду. Были использованы методы двумерной и одномерной бумажной хроматографии, адсорбционной хроматографии на колонках, газовая хроматография, ИК-спектроскопия. Целью статьи является изучение химического состава растения *Linosyris villosa* физико-химическими методами анализа. Создание на его основе лекарственных форм. Проблемой статьи является поиск и создание лекарственных препаратов на основе флоры Северного Казахстана. Научная новизна заключается в том, что химический состав и биологическая активность растения *Linosyris villosa*, произрастающего на территории Северного Казахстана, изучается впервые. По результатам анализа у 13% больных эффект лечения незначительный, а у 87% больных отмечалось улучшение показателей крови (увеличение гемоглобина прирост количества эритроцитов, почти у всех больных нормализовался цветной показатель крови), увеличилось количество лейкоцитов до нормы, улучшилась лейкоцитарная формула. Следовательно, препарат «Витин», представляющий собой водно-спиртовой экстракт растения *Linosyris villosa*, является эффективным препаратом для лечения больных с анемией различной тяжести. Практическая значимость работы определяется в следующем: получены биологически активные соединения из растения *Linosyris villosa* с целью изучения и применения их в медицине и сельском хозяйстве.

**Ключевые слова:** растение *Linosyris villosa*, флавоноиды, мирицетиновые фракции, лекарственные пленки, антианемическая активность, пестициды.

## 1. INTRODUCTION

A person uses plants not only as food but also as therapeutic agents, as well as in perfumes and as dyes. With the development of chemistry, natural substances were actively supplanted from human life by chemical products. However, despite the enormous progress in this area, in recent decades, the problems of serious side effects of synthetic chemicals on the environment have become more and more pronounced. For example, prolonged use of pesticides in agriculture has caused serious harm to nature and human health (Kumar and Kumar, 2019).

In the field of pharmacology, plants have been the basis for the creation of highly effective medicinal drugs and dietary additives that are used to correct human health. In the field of agriculture, insecticides of new generations, defoliants, attractants, many of which are of plant origin, have been obtained. Active substances from plants are necessary for various fields of industry, as well as promising for use in biotechnology (Fakheri *et al.*, 2011).

The growing amount of information on the diversity of biological activities in plants requires not only an assessment of the role of metabolites in their life and protection against biotic and abiotic stresses but also encourages a comprehensive study of the chemical composition of wild plant species, depending on their habitats. To replenish the assortment of plants, the rigorous and comprehensive studies of the chemical composition and biological properties of individual compounds and phytocomplexes are necessary. The theoretical aspects of the study of secondary plant products as growth regulators, gene expression modulators, and signal transmitters are of great interest. The study of this problem is promising from the point of view of evolutionary transformations of the molecules of secondary compounds and, possibly, the mechanisms of their action on various organisms. According to WHO, the pharmaceutical market in some countries is already 80% represented by plant preparations. Moreover, the production of herbal preparations in the world reaches 60 billion US dollars (WHO traditional..., 2002; Willcox and Bodeker, 2004). Currently, plants containing



flavonoids (biologically active compounds belonging to the class of plant polyphenols) are considered to be the most promising as a source of drug raw materials. Due to the wide variety of their structures and the wide distribution in various plants, flavonoids, and plants containing them are increasingly being studied as a source of phytopreparations in pharmacy (Harborne and Mabry, 1982; Wagner, 1993; Kurkin, 2009; Makarova and Makarov, 2010; Kurkina, 2012; Abdrakhmanova *et al.*, 2019).

Flavonoids belong to natural compounds and are part of many phytopreparations that exhibit specific biological activity of a targeted action (Abhay, 2013; Karak, 2019). Flavonoids in the human body act both on enzyme systems and immune and metabolic processes, causing various effects positive for the body (Hoensch and Oertel, 2015; Panche *et al.*, 2016). Many scientists argue that the diversity of the biological effects of flavonoids is due to their antioxidant activity (Pandey *et al.*, 2010; Kurkin *et al.*, 2013; Mishra *et al.*, 2013). Flavonoids also have antimicrobial, anti-inflammatory, wound healing, vessel-strengthening, antitumoral, antiulcerogenic, and other actions. Flavonoids can be a free radicals scavenger and inhibit lipid peroxidation (Gerdin and Srenso, 1983; Cowan, 1999; Cushnie and Lamb, 2005; Nagendra Prasad *et al.*, 2010; Zandi *et al.*, 2011). Flavonoids as antioxidants play an important role in preventing violations of the structure and functions of the liver in various pathologies, accelerating the regeneration and restoring the functional activity of hepatocytes, especially in the treatment of acute and chronic hepatitis and cirrhosis (Chen *et al.*, 2014; Sánchez-Salgado *et al.*, 2019). The most active were flavonols quercetin and myricetin, which showed high antiviral activity (Kaul *et al.*, 1985; Wu *et al.*, 2008). Currently, flavonoid preparations in the form of various dosage forms are widely used in medical practice: tablets, ointments, tinctures, extracts, powders, dragees, and capsules (Pashtetskiy *et al.*, 2020).

Modern wound coverings include films. The wound covering, as a dressing, must meet the following requirements: create an optimal microenvironment for wound healing, prevent the penetration of microorganisms into the wound, have elasticity, the ability to model surfaces with complex relief, without pyrogenic, antigenic and toxic effects, local irritating and allergic actions. Also, for artificial wound coverings, the following properties are highly desirable: transparency, the ability to observe a wound, the ability to be a drugs

vehicle (antibacterial, reparants), ease of use of films for medical personnel, easy removal of the film from the surface of the skin.

Kazakhstani scientists are also intensively searching for new effective, environmentally friendly medicines based on herbal raw materials. Northern Kazakhstan is the richest region of the medicinal flora habitat, which is represented by *Linosyris villosa*. The chemicals included in the medicinal plant *Linosyris villosa* are currently equally interesting as objects of study in phytochemistry, pharmacy, and medicine (Nazarova *et al.*, 2013; Ramilyeva *et al.*, 2019).

The object of study: *Linosyris villosa*, collected in the flowering phase in Northern Kazakhstan (Korulkin *et al.*, 2007). This is a perennial herbage plant with numerous stems and a horizontal rhizome 30-40 cm high. The leaves are oblong-linear, sessile, whole-cut. The flowers are collected in a cymose inflorescence of yellow color. The plant blooms in late July and early August. *Linosyris villosa* grows in the European part of Russia, Western Siberia, the Caucasus, Ukraine, and Kazakhstan.

The chemical composition of the plant has not been studied. In folk medicine, *Linosyris villosa* is used in the treatment of bronchial asthma, angina pectoris, toothache, and rheumatic pains (Kyusev, 2002). The following dosage forms were obtained based on *Linosyris villosa*: ointment, tinctures, adhesive plasters, which have antidermatitis, anti-inflammatory, and antiseptic effects, so further study of the plant is of extreme interest (Nazarova and Bakumova, 2015; Nevkrytaya *et al.*, 2020).

The problem of the article is the search and creation of drugs based on the flora of Northern Kazakhstan. The scientific novelty lies in the fact that the chemical composition and biological activity of the *Linosyris villosa*, growing in the territory of Northern Kazakhstan, is being studied for the first time. The practical significance of the work is defined as follows: biologically active compounds from the *Linosyris villosa* plant were obtained for the purpose of studying and applying them in medicine and agriculture.

The purpose of the article is to study the chemical composition of the *Linosyris villosa* by physicochemical methods of analysis, as well as the creation of dosage forms based on it.

## 2. MATERIALS AND METHODS

The extraction of biologically active substances from the plant was carried out in a

Soxhlet's apparatus using various solvents (96% aqueous solution, 70% aqueous solution). Extraction was carried out at a temperature of 40 °C for 7 days. Aluminium oxide and nylon as adsorbents were pre-established and used for the separation of flavonoids contained in extracts of the *Linosyris villosa* plant.

Determination of pesticides in alcohol fractions of *Linosyris villosa*. The ECD\_pesticides (HOP).M method was calibrated to detect organochlorine compounds for the following pesticides: hexachlorocyclohexane (HCH) and its isomers: alpha-HCH, beta-HCH, gamma-HCH; 4,4-dichlorodiphenyltrichloroethane (DDT) and its metabolites: 4,4-dichlorodiphenyldichloroethylene (DDE), 4,4-dichlorodiphenyldichloroethane (DDD). The calibration of the pesticide mixture was carried out at 3 levels. Calibration solutions were prepared from standard pesticide samples (pesticide solutions in hexane with a concentration of 100 µg/ml), from which calibration solutions with concentrations of 16.667 µg/ml (level 3), 8.333 µg/ml (level 2) were prepared by sequential dilution 4.167 mcg/ml (level 1). To carry out the calibration,  $5 \cdot 10^{-3}$  cm<sup>3</sup> of the solution was sequentially introduced into the chromatograph evaporator using a microsyringe for each calibration concentration. Each solution was chromatographed twice, calculating the average peak area value of the determined organochlorine pesticide in the chromatogram. The correlation coefficients for the calibration lines for all three concentrations (3 levels) were: 0.99986 for α-HCH, 0.99575 for β-HCH, 0.99942 for γ-HCH, 0.99912 for DDE, 0.99969 for DDD.

The studies were carried out on an Agilent Technologies 7890B GC System gas chromatograph with an electron capture detector (ECD) and a nitrogen phosphorus detector (NPD), on an HP-5 capillary column.

The concentration of residual amounts of organochlorine pesticides, mg/kg, in the analyzed sample, was calculated following the calibration curves. The arithmetic mean value of the results of three parallel determinations was taken as the final analysis result. The discrepancy between the parallel determinations did not exceed the repeatability limit. The repeatability limit for all determining organochlorine pesticides is 20%. The results were considered reliable if the discrepancy between parallel determinations did not exceed the repeatability limit. The repeatability limit for all detectable organochlorine pesticides on a gas chromatograph with an electron-capture and nitrogen-phosphorus

detector is 20% according to the determination method of ST RK 2011-2010 "Water, food, feed and tobacco products. Determination of organochlorine pesticides by chromatographic methods".

The toxicity of polymer films was determined using an AT-05 image toxicity analyzer. This indicator is an alternative to the "local skin irritant action" indicator and does not require the use of experimental animals during testing (Kurkin *et al.*, 2013).

The separation of the substances from the aqueous-alcoholic extract was made using the method of column adsorption chromatography. Aluminum oxide, nylon, and polysorb were used as adsorbents. The best separation results were achieved on nylon and aluminum oxide. On nylon, carbohydrates were separated as related substances, aglycones and glycosides of flavonoid nature were separated.

Aglycones were separated on an aluminum oxide column, in particular, myricetin-containing fractions were obtained. To identify the aglycon, myricetin, it was accumulated, dissolved in 96% alcohol, and rechromatographed on an aluminum oxide column. The resulting eluate was evaporated to dryness and crystallized many times from 80% ethanol in the presence of activated charcoal during which received yellowish crystals with a melting point of 318-320°C. The substance was investigated by two-dimensional paper chromatography in I R<sub>f</sub> = 0.50 and II R<sub>f</sub> = 0.00 systems (Figure 1).

During the study, 4 options for films that differ in composition and production technology were obtained.

**Option 1.** A portion of polyvinyl alcohol (PVA) weighing 1 g was poured into 40 ml of distilled water and left to swell for 24 hours. Then the PVA solution was heated on a tile with an asbestos mesh for 30 minutes. Subsequently, 1 ml of glycerol was added and heated for another 10 minutes. The resulting solution was poured onto a fat extracted base glass lubricated with glycerol. The film dried in 24 hours. The film was thin, transparent, and elastic. The main disadvantage of the film obtained is that it was not well fixed on the skin.

**Option 2.** A portion of PVA weighing 1.25 g was poured into 40 ml of distilled water and left for 24 hours to swell. Then the PVA solution was heated on the tile for 30 minutes. Subsequently, 1 ml of glycerol was added and heated for another 10 minutes. To the obtained carrier, when

heating, 1 ml of alcohol was poured and left to dry. Such a film dried longer than a film obtained from a carrier.

**Option 3.** To the carrier of the film obtained in option 2 was added 1 ml of water while heating. The resulting carrier was poured onto a base glass for drying. The film did not dry for a week. The resulting films did not meet the requirements since their drying time increased in several times.

**Option 4.** The carrier was prepared according to option 1, then, when heated, 2 ml of glycerol was added to the prepared carrier. The resulting solution was poured onto fat extracted base glass, lubricated with glycerol. The film dried in 24 hours. Such a film was thin, transparent, elastic, easily fixed on the skin and did not deform when moving.

Then, the active substance (*Linosyris villosa* extract) was added dropwise to the resulting solution while stirring. The resulting solution was poured onto a fat extracted base glass, lubricated with glycerol. The film dried in 24 hours. The addition of the active substance did not change the properties of the film. The substance was distributed evenly over the entire area of the film. It was concluded that the addition of alcohol and water to the film carrier increased the drying time of the film. Such films do not meet the requirements. The film carrier, with the addition of glycerin and the active substance, meets all the requirements for medicated films and has a prolonged effect (Smiyan *et al.*, 2018).

The test of the obtained films was carried out in an experiment on the skin of patients of the surgical department, after surgical interventions, by such indicators as drying time, film quality, and fixation on the skin (Table 1).

To verify the safety of the obtained medicated film, four aqueous extracts from a polymer film were prepared according to option No. 4, 2 aqueous extracts without an active substance and 2 aqueous extracts with the addition of an active substance with a different concentration, one for each concentration of the active substance (*Linosyris villosa* extract). Previously, it was necessary to evaluate the toxicity of the polymeric material (PVA) used to prepare the films. According to the methodology, an extract from the granules of the polymer material is prepared as follows: the M/V ratio of the PVA granules to distilled water should be 0.1 g per 1 ml of water. For testing, 100 ml of extract was prepared. 10 g of PVA was poured into 150 ml of water and kept in a thermostat at a temperature of 70 °C for 24 hours. After that, the

extract was passed through a paper filter to relieve the swollen PVA. In parallel, the same volume of distilled water was thermostated under the same conditions to obtain a control sample (K).

The obtained extracts were kept in a thermostat at a temperature of 70 °C for 24 hours. In parallel, the same volume of distilled water was thermostated under the same conditions to obtain a control sample (K). The degree of toxicity was determined by comparing the value of the selected test parameter of the test sample (solution) and the value of the same test parameter of the control sample (solution). When determining the toxicity index on the AT-05 image toxicity analyzer, the time-weighted average of the advancement of the sperm suspension was chosen as a test parameter. For the experiment, it was prepared the control and experimental solutions. The experimental solution is prepared from the calculation: 10 ml of aqueous extract, 0.4 g of glucose, 0.1 g of sodium citrate. The control solution is prepared similarly to the experimental one, but instead of the aqueous extract of the polymer film it includes 10 ml of distilled water. After preparation, the control and experimental solutions using a 0.4 ml dispenser were placed in thin section test tubes. The tubes are closed with stoppers and installed in the sample preparation unit (SPU).

The preparation of a uterine sperm suspension was carried out as follows: 1.5 ml of a control solution (solution for sperm thawing) was placed in a test tube using a dispenser. A tube with a solution for thawing is installed in the SPU and warmed up to 40 °C for at least 5 minutes. Then, we removed "straw" with sperm from the Dewar flask using surgical forceps, the end of which is cooled in liquid nitrogen. Holding the straw in the middle with forceps, we cut the polymer packaging on both sides with scissors and place the straw in a test tube. After 10-15 minutes, when the contents of the "straw" completely goes into solution, the tube was shaken several times and returned to its place for further heating. The contents of the tube were warmed for 5-7 minutes and periodically shaken. After that, 0.1 ml of the uterine sperm suspension was added to the tubes with control and experimental solutions using a dispenser. The contents of each tube were mixed. After thorough mixing, the capillaries of the device were filled with work solutions.

The capillaries were filled as follows: the capillary was taken in the right hand so as not to touch the central part of the working surface of the

capillary. The forefinger of the right-hand clamps the end of the capillary and dip the opposite end into a test tube with a work solution with cells to a depth of at least 5 mm. Then the clamped end of the capillary was released. Due to the capillary effect, the solution fills the capillary. The filling process is monitored visually. The capillary is removed from the tube, the wet end is wiped with dry gauze, and the capillary is placed in the carriage at the appropriate position. The carriage is closed with a lid and placed in the analyzer block. 5 capillaries filled with a control sample and 5 capillaries of a test sample were placed in the analyzer unit. 5 cycles of measurements were carried out. The toxicity index was calculated according to the following formula (Equation 1), where  $I_t$  is the toxicity index,  $t_{tw}^o$ ,  $t_{tw}^k$ , are the time-weighted averages of the mobility time of the sperm suspension in experimental and control capillaries with solutions, respectively.

All procedures performed in studies involving human participants were in accordance with the ethical standards of the institutional and national research committee and with the 1964 Helsinki declaration and its later amendments or comparable ethical standards. Informed consent was obtained from all individual participants included in the study.

### 3. RESULTS AND DISCUSSION:

#### 3.1. Obtaining myricetin fractions from the *Linosyris villosa* plant

The object of study was the *Linosyris villosa* plant, the aerial part of which was collected in Northern Kazakhstan during the flowering phase. The moisture content of the raw materials is 8.10%, the ash content is 4.45%. The number of extractives, depending on the type of solvent, is presented in Table 2. Subsequently, to obtain extractives, 70% ethanol was used as the best extraction solvent for the *Linosyris villosa* plant, according to the results of Table 2. In order to establish the composition of the aqueous-alcoholic extract, a qualitative analysis was carried out using specific reagents (Table 3).

Analyzing the results presented in Table 3, it should be concluded that flavonoids are contained in all extracts obtained from the *Linosyris villosa* plant. In the interaction of ammonia vapors with the extract, a yellow color develops, indicating the presence of flavonoids in the extract, the molecule of which contains a carbonyl group that reacts with ammonia to form yellow imines. When the extract interacts with an

alcoholic solution of aluminum chloride, yellow color forms, indicating the presence of flavonoids containing hydroxyl groups in 3 and 5 positions, due to which complex compounds colored in yellow forms. As a result of the interaction of a 1% aqueous solution of lead acetate with the extract, an orange-yellow precipitate forms, indicating the presence of flavones and flavanols in the aqueous-alcoholic extract. During the interaction of a 1% alcohol solution of ninhydrin with the extract, a blue-violet color develops when heated, due to the formation of a blue-violet Ruehmann purpura, indicating the presence of amino acids in the extract. During the interaction of a 1% solution of ferrous ammonium sulfates (FAS) with the extract, green color was observed, and when left to stand, a dark green precipitate formed, indicating the presence of hydrolyzable and condensed tannins in the extract.

Thus, on the basis of qualitative analysis, it can be assumed that the following classes of compounds are present in the extract: flavonoids (flavones, flavonols), tannins, amino acids, carbohydrates, and other compounds. The aqueous-alcoholic extract was also studied by two-dimensional paper chromatography (PC) in systems B:A:W (butanol-acetic acid-water) in the ratio (4:1:5) (I) and 2% acetic acid (II). According to OFS.1.2.1.2.0002.15 "Chromatography on paper", two-dimensional paper chromatography allows us to establish the authenticity, purity, and quantification of the substance sampled involves the sequential passage of the released substances on a sheet of filter paper when moving the mobile phase in two perpendicular directions along the capillaries of the paper, which allows for a clearer separation of the mixture of analytes. Five substances related to flavonoids (aglycones, glycosides), phenolic acids, as well as carbohydrates, amino acids, and traces of tannins were found on the chromatogram.

For aglycon, the IR spectrum was taken in Kbr tablets. In the IR spectrum there were absorption bands in the range of  $1650\text{ cm}^{-1}$  (C=O);  $3450\text{ cm}^{-1}$  (-OH); in the region of in the range of  $2850\text{ cm}^{-1}$ ,  $2940\text{ cm}^{-1}$  (C-H) of the E-ring; in the range of  $1480$ ,  $1520$ ,  $1610\text{ cm}^{-1}$  (C=C) of the E-ring. Thus, on the basis of identification tests, melting point, comparison with myricetin marker, literature data, and IR spectroscopy, the obtained aglycon was identified as myricetin (Figure 2).

#### 3.2. Determination of the toxicity of myricetin fractions produced from the *Lynosyris villosa* on the content of pesticides

To study myricetin fractions, pesticides were selected, which occupy one of the leading positions in terms of hazard and prevalence in the environment. The danger of HCH and its isomers, as well as DDT and its metabolites, is that they are able to persist and accumulate in environmental objects for a long time. And despite the fact that they have not been used for a long time in Kazakhstan, however, they can still be found in environmental objects due to their high persistency.

Determination of pesticides in alcohol fractions of *Linisyris villosa*. The ECD\_pesticides (HOP).M method was calibrated to detect organochlorine compounds for the following pesticides: hexachlorocyclohexane (HCH) and its isomers: alpha-HCH, beta-HCH, gamma-HCH; 4,4-dichlorodiphenyltrichloroethane (DDT) and its metabolites: 4,4-dichlorodiphenyldichloroethylene (DDE), 4,4-dichlorodiphenyldichloroethane (DDD). The studies were carried out on an Agilent Technologies 7890B GC System gas chromatograph with an electron capture detector (ECD) and a nitrogen phosphorus detector (NPD), on an HP-5 capillary column.

According to the results of three parallel studies of myricetin fractions, the organochlorine compounds were not found in the samples; there were no peaks on the chromatogram corresponding to the determined pesticides (Figure 3).

### 3.3. Study of the safety parameters of medicated films based on the *Linisyris villosa* plant

The specified interval of the toxicity index is  $70 < I_t < 120$ . Belonging to this specified interval allows the tested products to be considered non-toxic. The boundaries of the interval are established on the basis of the analysis of the results of parallel tests on animals and on the semen of a bull, which made it possible to find a range where the toxic effect is not found in animal tests. The results of the analysis of the PVA toxicity are presented in Table 4.

Calculation of the toxicity index for PVA polymer material based on the results of 5 cycles (Equation 2). Since the value is  $70 < 84.3 < 120$ , therefore, the polymer material can be considered safe for use and the manufacture of polymer films. Next, the film was prepared according to the recipe of experiment No. 4. We prepared a polymer film and an extract from it: Sample No. 1 ( $O_1$ ) is the polymer film without adding an active substance; Sample No. 2 ( $O_2$ ) is the polymer film with an active substance; Sample No. 3 ( $O_3$ ) is the

polymer film with an active substance, the dose of which is doubled.

An extract for dressings in contact with human skin is prepared as follows: S (area) of the test film is taken to V (volume) of distilled water in ratio 1/1 cm<sup>2</sup>/ml. Moreover, both surfaces of the polymer film are taken into account. To obtain the desired volume, we took 3 samples of a film measuring 10 x 10 cm and filled in a beaker with 200 ml of distilled water. A beaker was covered with a watch glass, and extraction was carried out at a temperature of 40 °C for 7 days. In parallel, the same volume of distilled water was thermostated under the same conditions to obtain a control sample. Samples were taken, and the toxicity index was measured on the 1st, 3rd, and 7th days of extraction. The results of the experiment on the toxicity of polymer extracts after extraction on day 1 are presented in Table 5.

Calculation of the toxicity index for 3 samples according to the results of 5 measurements:  $I_t(O_1) = \frac{185}{226} \times 100\% = 81.9\%$ ,  $I_t(O_2) = \frac{177}{226} \times 100\% = 78.3\%$ ,  $I_t(O_3) = \frac{177}{226} \times 100\% = 78.3\%$ . The results of toxicity after extraction on the 3rd day are presented in Table 6.

Calculation of the toxicity index for 3 samples according to the results of 5 measurements, after 3 days of extraction:  $I_t(O_1) = \frac{255}{315} \times 100\% = 80.9\%$ ,  $I_t(O_2) = \frac{251}{315} \times 100\% = 79.6\%$ ,  $I_t(O_3) = \frac{251}{315} \times 100\% = 79.6\%$ . The results of toxicity after extraction of polymer films extracts for 7 days are presented in Table 7.

The toxicity index was calculated for 3 samples according to the results of 5 measurements, after 7 days of extraction:  $I_t(O_1) = \frac{271}{348} \times 100\% = 77.9\%$ ,  $I_t(O_2) = \frac{271}{348} \times 100\% = 77.9\%$ ,  $I_t(O_3) = \frac{271}{348} \times 100\% = 77.9\%$ . The results showed that PVA-based polymer films with and without the addition of the *Linisyris villosa* extract do not exhibit toxic effects.

### 3.4. Determination of the skin irritant action of medicated films based on the *Linisyris villosa* plant

The skin irritant action of the films was tested in parallel on 3 samples:

– sample No. 1 ( $O_1$ ) is the polymer film

without adding an active substance;

- sample No. 2 (O<sub>2</sub>) is the polymer film with an active substance;

- sample No. 3 (O<sub>3</sub>) is the polymer film with an active substance, the dose of which is doubled.

The action was studied on white mice by immersion of the tails in the extract. The result was compared with a control sample (distilled water). To obtain 1200 ml of the extract, a total of 600 cm<sup>2</sup> of each sample was taken, the film was placed in a beaker covered with a porcelain dish, extraction was carried out at a temperature of 40 °C for ten days. In parallel, the same volume of distilled water was thermostatically controlled under the same conditions to obtain a control sample. Within ten days, samples were taken, and studies were conducted.

White mice were fixed in special cages so that their tails were immersed 2/3 in the solution. The exposure was carried out for 2 hours. The reaction was taken into account immediately after the end of the exposure by the presence of local skin changes (Tables 8-10).

The data showed that the polymer film does not have a skin irritant action and is safe to use.

### 3.5. Study of the drug "VITIN" regarding antianemic activity

The drug "Vitin" obtained by aqueous-alcoholic extraction of the *Linostyris villosa* plant. The following classes of natural compounds were found in the preparation by phytochemical analysis using specific reagents: flavonoids, essential oils, carbohydrates, amino acids, phenolic acids, vitamins, trace elements, and tannins in the form of traces. The drug was studied in the toxicology laboratory "Deri-Dermek" for toxicity, irritating, healing effects, and blood formation. Analysis of the data obtained indicates that Vitin is non-toxic, stimulates the healing process, has an antiseptic effect, and normalizes blood formation.

The effect of the Vitin drug on blood formation was investigated on the basis of a regional hospital on patients in the hematological department during inpatient treatment and during outpatient treatment after the discharge of patients from the hospital. More than 30 patients with anemia and diseases of the internal organs were examined (Table 11).

Studies were performed on 30 patients (22

women and 8 men) aged 17 to 70 years (mean age 40 ± 3.5 years) (Table 12). The patients were divided into 3 groups. Patients of the 1st group took Vitin as a monotherapy, patients of the 2nd group took Vitin in combination therapy with iron preparations. The control group 3 consisted of patients taking iron preparations without Vitin.

Evaluation of the drug effectiveness was carried out after a 2-3 week course of treatment according to the indicators of a complete blood count for two months. Prior to inclusion in the study protocol, at the entrance to its completion, and at the end of the study, all patients underwent a complete blood count to calculate the number of red blood cells and hemoglobin, color index, white blood cell count, and WBC differential. The treatment was stopped when achieving normal blood counts and performance status.

## 4. CONCLUSIONS:

The object of the study was the *Linostyris villosa* plant, collected in the flowering phase in Northern Kazakhstan. To establish the quality of raw materials, pharmacopoeial indicators were determined: humidity (8.10%), ash content (4.45%), and the amount of extractives (16.88%). The optimal flavonoid extractant for the *Linostyris villosa* was experimentally established, which is the aqueous-alcoholic solution (70% ethanol). Using sequential extraction methods and two-dimensional paper chromatography in systems-I (butanol-acetic acid-water) (B:A:W) in a ratio of 4:1:5 and system II (2% acetic acid) the presence of flavonoids in all extracts was observed. Using adsorption chromatography on aluminum oxide, and then distribution chromatography on nylon, a flavonoid aglycone was isolated, the structure of which was proved by physicochemical methods of analysis. Based on qualitative reactions, melting point, comparison with a marker, literature data, and IR spectroscopy, the isolated substance was identified as a flavonoid-based aglycone – myricetin.

The aqueous-alcoholic extract from the *Linostyris villosa* plant was studied for safety by the residual amount of organochlorine pesticides in the extract. There were no pesticides in the studied extract; a conclusion was drawn about the possibility of using plant materials based on *Linostyris villosa* for the manufacture of dosage forms. Polyvinyl alcohol-based medicated films were obtained with the addition of an active substance based on myricetin containing extracts from the *Linostyris villosa* plant. A study of the obtained medicated films for the presence of toxic

and skin irritant actions were conducted. The results showed that polyvinyl alcohol-based polymer films with and without the addition of *Linostyrus villosa* extract did not exhibit toxic effects. The reaction to skin irritant action was zero points (reaction – negative).

The aqueous-alcoholic extract of the *Linostyrus villosa* plant was investigated for the presence of antianemic activity. According to the results of the analysis, in 13% of patients the treatment effect is insignificant, and in 87% of patients there was an improvement in blood values (increase in hemoglobin, an increase in the number of red blood cells, almost all patients returned normal color index), the number of white blood cells increased to normal, and the WBC differential improved. The conclusion was made that the aqueous-alcoholic extract of the *Linostyrus villosa* plant is an effective drug for the treatment of patients with anemia of various severity.

## 5. REFERENCES:

1. Abdrakhmanova, S. A., Zhanzakova, Z.Z., Turganbekova, A. A., and Saduakas, Z.K. (2019). Assessment of hematopoietic stem cell molecular engraftment based on STR analysis. *Cellular Therapy and Transplantation*, 8(3), 26-27.
2. Abhay, K. (2013). Pandey chemistry and biological activities of flavonoids: An overview. *The Scientific World Journal*, 2013, article number 162750. <https://doi.org/10.1155/2013/162750>
3. Chen, X., Mukwaya, E., Wong, M.-S., and Zhang, Y. (2014). A systematic review on biological activities of prenylated flavonoids. *Pharmaceutical Biology*, 52, 655–660. <https://doi.org/10.3109/13880209.2013.853809>.
4. Cowan, M. M. (1999). Plant products as antimicrobial agents. *Clinical Microbiology Reviews*, 12(4), 564-582.
5. Cushnie, T.P.T., and Lamb, A.J. (2005). Antimicrobial activity of flavonoids. *International Journal of Antimicrobial Agents*, 26(5), 343-356.
6. Fakheri, B., Rahimi, M., Tavassoli, A., and Raissi, A. (2011). Application of biotechnology in production of medicinal plants. *American-Eurasian Journal of Agricultural and Environmental Science*, 11. Retrieved from [https://www.researchgate.net/publication/266231628\\_Application\\_of\\_Biotechnology\\_in\\_Production\\_of\\_Medicinal\\_Plants](https://www.researchgate.net/publication/266231628_Application_of_Biotechnology_in_Production_of_Medicinal_Plants).
7. Gerdin, B., and Srenssso, E. (1983). Inhibitory effect of the flavonoid on increased microvascular permeability induced by various agents in rat skin. *International Journal of Microcirculation, Clinical, and Experimental*, 2(1), 39-46.
8. Harborne, J.B., and Mabry, T.J. (Eds.). (1982). *The flavonoids: Advances in research*. London, United Kingdom; New York City, New York: Chapman and Hall.
9. Hoensch, H.P., and Oertel, R. (2015). The value of flavonoids for the human nutrition: Short review and perspectives. *Clinical Nutrition Experimental*, 3, 8-14. <https://doi.org/10.1016/j.clnex.2015.09.001>
10. Karak, P. (2019). Biological activities of flavonoids: an overview. *International Journal of Pharmaceutical Sciences and Research*, 10(4), 1567-74. DOI: 10.13040/IJPSR.0975-8232.10(4).1567-74.
11. Kaul, T., Middleton, E., and Ogra, P. (1985). Antiviral effect of flavonoids on human viruses. *Journal of Medical Virology*, 15, 71–79.
12. Korulkin, D. Yu., Abilov, J. A., Muzychikina, R.A., and Tolstikov, G.A. (2007). *Natural flavonoids*. Novosibirsk, Russian Federation: GEO.
13. Kumar, V., and Kumar, P. (2019). Pesticides in agriculture and environment: Impacts on human health. In *Contaminants in agriculture and environment: health risks and remediation, chapter: Chapter 7* (pp. 76-95). Haridwar, India: Agro Environ Media.
14. Kurkin, V. A. (2009). *Fundamentals of herbal medicine: A manual for students of pharmaceutical universities*. Samara, Russian Federation: Etching LLC, GOU VPO SamGMU of Roszdrav.
15. Kurkin, V. A., Kurkina, A.V., and Avdeeva, E.V. (2013). Flavonoids as biologically active compounds of medicinal plants. *Fundamental Research*, 11-9, 1897-1901.
16. Kurkina, A.V. (2012). *Flavonoids of pharmacopeia plants*. Samara, Russian Federation: LLC "Etching"; SBEI HPE SamSMU of the Ministry of Health and Social Development of Russia.
17. Kyusev, P.A. (2002). *A complete directory of medicinal plants*. Moscow, Russian

Federation: Eksmo.

18. Makarova, M.N., and Makarov, V.G. (2010). *Molecular biology of flavonoids (chemistry, biochemistry, pharmacology): a guide for doctors*. St. Petersburg, Russian Federation: Lema.
19. Mishra, A., Sharma, A.K., Kumar, S., Saxena, A.K., and Pandey, A.K. (2013). Bauhinia variegata leaf extracts exhibit considerable antibacterial, antioxidant and anticancer activities. *BioMed Research International*, 2013, article number 915436.
20. Nagendra Prasad, K., Xie, H., and Hao, J. (2010). Antioxidant and anticancer activities of 8-hydroxypsoralen isolated from wampee [Clausena lansium (Lour.) Skeels] peel. *Food Chemistry*, 118(1), 62-66.
21. Nazarova, V. D., and Bakumova, E. V. (2015). Flavonoids of the *Linosyris villosa* plant. *Chemical Journal of Kazakhstan*, 2, 348-353.
22. Nazarova, V. D., Bektemisova, A. U., and Bakumova, E. V. (2013). The study of polyphenols in the plant *Linosyris villosa*. *Materials of the Scientific and Practical Conference "Kozybaev Readings – 2013: Kazakhstan in the World Cultural and Civilization Processes, III*, 194-198.
23. Nevkrytaya, N. V., Pashtetskiy, V. S., Novikov, I. A., Korotkikh, I. N., and Tkhananov, R. R. (2020). Variability of component composition of melissa officinalis l. essential oil depending on the climatic conditions of the region of cultivation. *Khimiya Rastitel'nogo Syr'ya*, 1, 257-263.
24. Panche, A. N., Diwan, A. D., and Chandra, S.R. (2016). Flavonoids: an overview. *Journal of Nutritional Science*, 5, article number e47. DOI:10.1017/jns.2016.41.
25. Pandey, A. K., Mishra, A. K., Mishra, A., Kumar, S., and Chandra, A. (2010). Therapeutic potential of zeylanicum extracts: an antifungal and antioxidant perspective. *International Journal of Biological and Medical Research*, 1, 228-233.
26. Pashtetskiy, V. S., Turin, E. N., Izotov, A. M., Abdurashytov, S. F., Gongalo, A. A., and Zhenchenko, K. G. (2020). Effect of Pisum sativum L. seed treatment with the complex of microbiological preparation on the plants' growth and development under direct sowing. *IOP Conference Series: Earth and Environmental Science*, 422(1), article number 012012.
27. Ramilyeva, I. R., Burkitbaev, Zh. K., Abdrakhmanova, S. A., Turganbekova, A. A., Baimukasheva, D. K., and Zhiburt, E. B. (2019). Distribution pattern for HLA specificities in the patients with acute myeloid leukemia. *Medical Immunology (Russia)*, 21(5), 965-972.
28. Sánchez-Salgado, J. C., Estrada-Soto, S., and García-Jiménez, S. (2019). Analysis of flavonoids bioactivity for cholestatic liver disease: Systematic literature search and experimental approaches. *Biomolecules*, 9(3), article number 102. <https://doi.org/10.3390/biom9030102>
29. Smiyan, O. I., Loboda, A.M., Manko, Y.A., Bynda, T. P., Popov, S.V., Petrashenko, V.O., Sichnenko, P.I., Romaniuk, O.K., Gorbas, V.A., Zagorodnii, M.P., Smiian-Horbunova, K.O., Kosarchuk, V.V., Ovsianko, O.L., and Kolesnikova, M.V. (2018). Dynamics of content of some minerals in teenagers with cardiovascular system pathology against the background of chronic tonsillitis. *Wiadomosci lekarskie (Warsaw, Poland: 1960)*, 71(4), 861-864.
30. Wagner, H. (1993). *Pharmazeutische biologie. Drogen und ihre Inhaltsstoffe*. Stuttgart, Germany: Gustav Fischer Verlag.
31. WHO traditional medicine strategy 2002–2005 Geneva: WHO. (2002). Retrieved from <https://www.who.int/medicines/publications/traditionalpolicy/en/>.
32. Willcox, M. L., and Bodeker, G. (2004). Traditional herbal medicines for malaria. *British Medical Journal*, 329, 1156-1159.
33. Wu, D., Kong, Y., and Han, C. (2008). d-Alanine: d-alanine ligase as a new target for the flavonoids quercetin and apigenin. *International Journal of Antimicrobial Agents*, 32, 421-426.
34. Zandi, K., Teoh, B. T., Sam, S. S., Wong, P. F., Mustafa, M. R., and Abubakar, S. (2011). Antiviral activity of four types of bioflavonoid against dengue virus type-2. *Virology Journal*, 8, article number 560.



$$I_t = \frac{t_{tw}^o}{t_{tw}^k} \times 100\% \quad (\text{Eq. 1})$$

$$I_t = \frac{145}{172} \times 100\% = 84.3\%. \quad (\text{Eq. 2})$$

**Table 1.** medicinal films test results

| Film variant | Drying time | Organoleptic characteristics of films | Fixation on the skin  |
|--------------|-------------|---------------------------------------|---|
| 1            | 24 hours    | thin, transparent, elastic            | short-term fixation (for 12 hours), deformation during movement           |
| 2            | 4 days      | absence of elasticity                 | absence of fixation   |
| 3            | 6 days      | absence of elasticity                 | absence of fixation   |
| 4            | 24 hours    | thin, transparent, elastic            | long-term fixation (for 24 hours), absence of deformation during movement |

**Table 2.** Determination of the amount of extractives

| Raw material                            | The number of extractives, %, in solvents: |                                |                                |
|---|--|--------------------------------|--------------------------------|
|   | hexane                                     | ethanol (96% aqueous solution) | ethanol (70% aqueous solution) |
| Aerial part of <i>Linosyris villosa</i> | 3.79                                       | 10.10                          | 16.88                          |

**Table 3.** Qualitative study of the extract

| Extract     | Reagents               |                                       |   |                               |  |
|-------------|------------------------|---------------------------------------|---|-------------------------------|--|
|             | NH <sub>3</sub> (fume) | AlCl <sub>3</sub> 1% alcohol solution | Pb (CH <sub>3</sub> COO) <sub>2</sub> 1% aqueous solution | Ninhydrin 1% alcohol solution | Ferrous ammonium sulfate 1% aqueous solution |
| 70% ethanol | bright yellow          | yellow                                | orange-yellow   | violet                        | green  |

**Table 4.** Time-weighted average values of sperm suspension motility time

| No. of capillary | K <sub>1</sub> | K <sub>2</sub> | K <sub>3</sub> | K <sub>4</sub> | K <sub>5</sub> | $t_{tw}^k$ | K <sub>6</sub> | K <sub>7</sub> | K <sub>8</sub> | K <sub>9</sub> | K <sub>10</sub> | $t_{tw}^o$ |
|------------------|----------------|----------------|----------------|----------------|----------------|------------|----------------|----------------|----------------|----------------|-----------------|------------|
| Cycle No.        |                |                |                |                |                |            |                |                |                |                |                 |            |
| 1                | 174            | 195            | 212            | 117            | 176            | 175        | 218            | 147            | 130            | 129            | 116             | 148        |
| 2                | 161            | 207            | 186            | 163            | 179            | 179        | 226            | 151            | 232            | 144            | 108             | 151        |
| 3                | 152            | 186            | 236            | 115            | 210            | 180        | 220            | 147            | 196            | 145            | 96              | 153        |
| 4                | 140            | 175            | 184            | 192            | 156            | 170        | 200            | 104            | 156            | 120            | 118             | 140        |
| 5                | 148            | 163            | 180            | 136            | 160            | 157        | 200            | 159            | 190            | 126            | 103             | 135        |
| Average value    |                |                |                |                |                | 172        |                |                |                |                |                 | 145        |

**Table 5.** Weighted average values of the mobility time of the sperm suspension for polymer extracts after extraction in 1 day

| No. of capillary | K <sub>1</sub>  | K <sub>2</sub>  | K <sub>3</sub>  | K <sub>4</sub>  | K <sub>5</sub>  | $t_{tw}^k$   | K <sub>6</sub>  | K <sub>7</sub>  | K <sub>8</sub>  | K <sub>9</sub>  | K <sub>10</sub> | $t_{tw}^o$ 1 |
|------------------|-----------------|-----------------|-----------------|-----------------|-----------------|--------------|-----------------|-----------------|-----------------|-----------------|-----------------|--------------|
| Cycle No.        |                 |                 |                 |                 |                 |              |                 |                 |                 |                 |                 |              |
| 1                | 253             | 296             | 234             | 198             | 156             | 227          | 186             | 123             | 271             | 220             | 154             | 191          |
| 2                | 263             | 231             | 284             | 202             | 174             | 231          | 202             | 105             | 197             | 236             | 186             | 185          |
| 3                | 198             | 168             | 303             | 241             | 196             | 221          | 174             | 134             | 200             | 208             | 174             | 178          |
| 4                | 185             | 224             | 268             | 271             | 165             | 223          | 210             | 132             | 203             | 215             | 186             | 189          |
| 5                | 307             | 185             | 242             | 237             | 178             | 230          | 187             | 135             | 206             | 198             | 181             | 181          |
| Average value    | 226             |                 |                 |                 |                 |              |                 |                 |                 |                 |                 |              |
| No. of capillary | K <sub>11</sub> | K <sub>12</sub> | K <sub>13</sub> | K <sub>14</sub> | K <sub>15</sub> | $t_{tw}^o$ 2 | K <sub>16</sub> | K <sub>17</sub> | K <sub>18</sub> | K <sub>19</sub> | K <sub>20</sub> |              |
| Cycle No.        |                 |                 |                 |                 |                 |              |                 |                 |                 |                 |                 |              |
| 1                | 164             | 157             | 183             | 170             | 200             | 175          | 146             | 168             | 174             | 179             | 211             | 176          |
| 2                | 210             | 135             | 157             | 203             | 189             | 179          | 154             | 156             | 157             | 201             | 214             | 176          |
| 3                | 185             | 134             | 210             | 200             | 174             | 181          | 157             | 154             | 213             | 213             | 163             | 180          |
| 4                | 206             | 148             | 194             | 165             | 176             | 178          | 165             | 148             | 181             | 183             | 176             | 171          |
| 5                | 178             | 153             | 176             | 169             | 181             | 171          | 170             | 167             | 219             | 169             | 181             | 181          |
| Average value    | 177             |                 |                 |                 |                 |              |                 |                 |                 |                 |                 | 177          |

**Table 6.** Weighted average values of the mobility time of the sperm suspension for polymer extracts after extraction in the 3rd day

| No. of capillary | K <sub>1</sub>  | K <sub>2</sub>  | K <sub>3</sub>  | K <sub>4</sub>  | K <sub>5</sub>  | $t_{tw}^k$   | K <sub>6</sub>  | K <sub>7</sub>  | K <sub>8</sub>  | K <sub>9</sub>  | K <sub>10</sub> | $t_{tw}^o$ 1 |
|------------------|-----------------|-----------------|-----------------|-----------------|-----------------|--------------|-----------------|-----------------|-----------------|-----------------|-----------------|--------------|
| Cycle No.        |                 |                 |                 |                 |                 |              |                 |                 |                 |                 |                 |              |
| 1                | 356             | 296             | 316             | 310             | 300             | 316          | 256             | 263             | 246             | 287             | 268             | 264          |
| 2                | 302             | 316             | 299             | 326             | 325             | 314          | 254             | 234             | 248             | 254             | 277             | 253          |
| 3                | 297             | 265             | 326             | 341             | 350             | 316          | 210             | 218             | 295             | 235             | 274             | 246          |
| 4                | 307             | 325             | 330             | 289             | 325             | 315          | 269             | 257             | 231             | 245             | 278             | 256          |
| 5                | 307             | 316             | 296             | 310             | 348             | 315          | 260             | 274             | 236             | 253             | 262             | 257          |
| 5                | 356             | 296             | 316             | 310             | 300             | 316          | 256             | 263             | 246             | 287             | 268             | 264          |
| Average value    | 315             |                 |                 |                 |                 |              |                 |                 |                 |                 |                 | 255          |
| No. of capillary | K <sub>11</sub> | K <sub>12</sub> | K <sub>13</sub> | K <sub>14</sub> | K <sub>15</sub> | $t_{tw}^o$ 2 | K <sub>16</sub> | K <sub>17</sub> | K <sub>18</sub> | K <sub>19</sub> | K <sub>20</sub> | $t_{tw}^o$ 3 |
| Cycle No.        |                 |                 |                 |                 |                 |              |                 |                 |                 |                 |                 |              |
| 1                | 226             | 234             | 248             | 248             | 263             | 244          | 215             | 265             | 237             | 242             | 259             | 244          |
| 2                | 235             | 248             | 265             | 235             | 247             | 246          | 234             | 219             | 268             | 237             | 248             | 241          |
| 3                | 258             | 267             | 231             | 255             | 249             | 252          | 284             | 236             | 247             | 259             | 235             | 252          |
| 4                | 273             | 245             | 261             | 268             | 254             | 260          | 249             | 235             | 268             | 245             | 247             | 249          |
| 5                | 264             | 239             | 243             | 248             | 275             | 254          | 243             | 235             | 236             | 257             | 249             | 244          |
| Average value    | 251             |                 |                 |                 |                 |              |                 |                 |                 |                 |                 | 246          |

**Table 7.** Weighted average values of the mobility time of the sperm suspension for polymer extracts after extraction at 7 days

| No. of capillary | K <sub>1</sub>  | K <sub>2</sub>  | K <sub>3</sub>  | K <sub>4</sub>  | K <sub>5</sub>  | $t_{tw}^k$   | K <sub>6</sub>  | K <sub>7</sub>  | K <sub>8</sub>  | K <sub>9</sub>  | K <sub>10</sub> | $t_{tw}^0$ 1 |
|------------------|-----------------|-----------------|-----------------|-----------------|-----------------|--------------|-----------------|-----------------|-----------------|-----------------|-----------------|--------------|
| Cycle No.        |                 |                 |                 |                 |                 |              |                 |                 |                 |                 |                 |              |
| 1                | 395             | 356             | 326             | 321             | 374             | 354          | 248             | 301             | 274             | 236             | 286             | 269          |
| 2                | 258             | 297             | 374             | 384             | 356             | 334          | 297             | 305             | 248             | 268             | 274             | 278          |
| 3                | 358             | 367             | 314             | 325             | 387             | 350          | 247             | 295             | 287             | 263             | 248             | 268          |
| 4                | 368             | 347             | 315             | 348             | 367             | 349          | 274             | 235             | 308             | 247             | 278             | 268          |
| 5                | 374             | 310             | 359             | 362             | 348             | 351          | 263             | 310             | 258             | 267             | 265             | 273          |
|                  |                 |                 |                 |                 |                 | 348          |                 |                 |                 |                 |                 | 271          |
| No. of capillary | K <sub>11</sub> | K <sub>12</sub> | K <sub>13</sub> | K <sub>14</sub> | K <sub>15</sub> | $t_{tw}^0$ 2 | K <sub>16</sub> | K <sub>17</sub> | K <sub>18</sub> | K <sub>19</sub> | K <sub>20</sub> | $t_{tw}^0$ 3 |
| Cycle No.        |                 |                 |                 |                 |                 |              |                 |                 |                 |                 |                 |              |
| 1                | 236             | 247             | 256             | 284             | 296             | 264          | 289             | 301             | 305             | 274             | 268             | 287          |
| 2                | 239             | 254             | 261             | 247             | 254             | 251          | 258             | 234             | 314             | 287             | 277             | 274          |
| 3                | 301             | 278             | 241             | 251             | 236             | 261          | 265             | 287             | 307             | 254             | 295             | 282          |
| 4                | 270             | 265             | 248             | 264             | 275             | 264          | 274             | 269             | 268             | 283             | 298             | 278          |
| 5                | 263             | 258             | 247             | 302             | 279             | 270          | 281             | 269             | 275             | 297             | 306             | 286          |
|                  |                 |                 |                 |                 |                 | 262          |                 |                 |                 |                 |                 | 281          |

**Table 8.** The reaction of white mice to extract sample No. 1

| Extraction day | White mouse mass, g | Exposure time, hour | Reaction |
|----------------|---------------------|---------------------|----------|
| 1              | 19                  | 2                   | Negative |
| 2              | 20                  | 2                   | Negative |
| 3              | 20                  | 2                   | Negative |
| 4              | 19                  | 2                   | Negative |
| 5              | 19                  | 2                   | Negative |
| 6              | 21                  | 2                   | Negative |
| 7              | 20                  | 2                   | Negative |
| 8              | 19                  | 2                   | Negative |
| 9              | 20                  | 2                   | Negative |
| 10             | 20                  | 2                   | Negative |

**Table 9.** The reaction of white mice to extract sample No. 2

| Extraction day | White mouse mass, g | Exposure time, hour | Reaction |
|----------------|---------------------|---------------------|----------|
| 1              | 20                  | 2                   | Negative |
| 2              | 20                  | 2                   | Negative |
| 3              | 22                  | 2                   | Negative |
| 4              | 19                  | 2                   | Negative |
| 5              | 21                  | 2                   | Negative |
| 6              | 21                  | 2                   | Negative |
| 7              | 20                  | 2                   | Negative |
| 8              | 19                  | 2                   | Negative |
| 9              | 19                  | 2                   | Negative |
| 10             | 20                  | 2                   | Negative |

**Table 10.** The reaction of white mice to extract sample No. 3

| Extraction day | White mouse mass, g | Exposure time, hour | Reaction |
|----------------|---------------------|---------------------|----------|
| 1              | 22                  | 2                   | Negative |
| 2              | 22                  | 2                   | Negative |
| 3              | 20                  | 2                   | Negative |
| 4              | 18                  | 2                   | Negative |
| 5              | 19                  | 2                   | Negative |
| 6              | 19                  | 2                   | Negative |
| 7              | 20                  | 2                   | Negative |
| 8              | 20                  | 2                   | Negative |
| 9              | 21                  | 2                   | Negative |
| 10             | 22                  | 2                   | Negative |

**Table 11.** The distribution of patients by disease

| Diseases                          | Quantity | Specific gravity, % |
|-----------------------------------|----------|---------------------|
| Posthemorrhagic anemia            | 5        | 20                  |
| Anemia in GIT chronic diseases    | 16       | 64                  |
| Anemia in chronic kidney diseases | 4        | 16                  |

**Table 12.** The distribution of patients by age

| Age         | Quantity | %  |
|-------------|----------|----|
| 15-25 years | 7        | 22 |
| 26-45 years | 18       | 58 |
| 46-70 years | 5        | 20 |

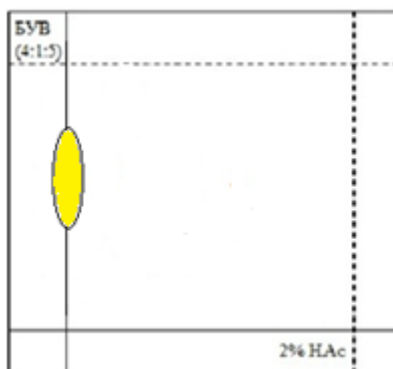


**Figure 1.** Aglycon Chromatogram

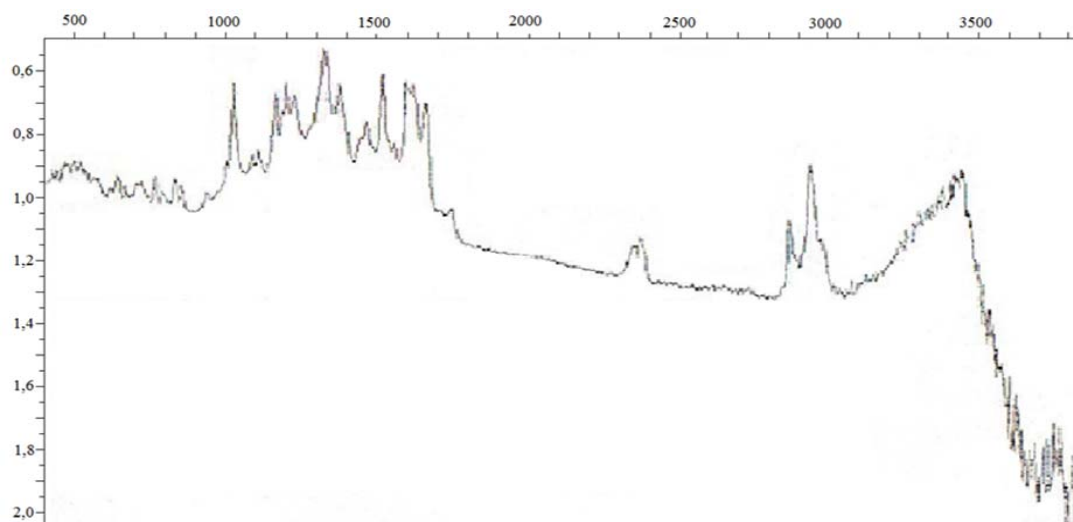


**Figure 2.** IR spectrum of myricetin fractions from the *Linosyris villosa* plant

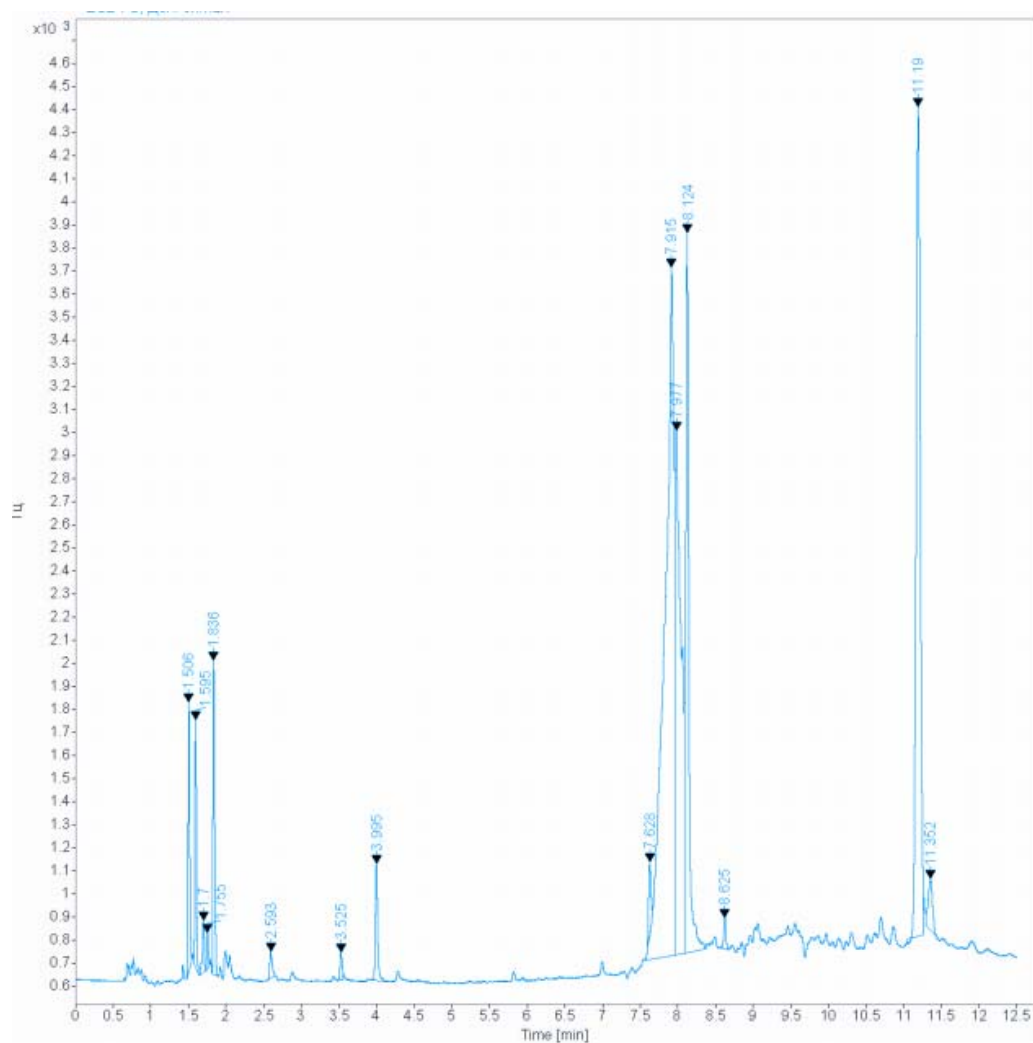


**Figure 3.** The chromatographic spectrum of the studied extract (Sample\_3)

**AVALIAÇÃO DE MARKETING DAS PREFERÊNCIAS DO CONSUMIDOR NO USO DE APLICATIVOS MÓVEIS PARA CUIDADOS DE SAÚDE PARA APOIAR A ADERÊNCIA AO MEDICAMENTO****MARKETING EVALUATION OF CONSUMER PREFERENCES IN USING MOBILE APPS FOR HEALTHCARE TO SUPPORT DRUG ADHERENCE****МАРКЕТИНГОВАЯ ОЦЕНКА ПОТРЕБИТЕЛЬСКИХ ПРЕДПОЧТЕНИЙ ИСПОЛЬЗОВАНИЯ МОБИЛЬНЫХ ПРИЛОЖЕНИЙ ЗДРАВООХРАНЕНИЯ ДЛЯ ПОДДЕРЖКИ ПРИВЕРЖЕННОСТИ К ЛЕКАРСТВЕННЫМ ПРЕПАРАТАМ**

BABASKIN, D.V.<sup>1\*</sup>; LITVINOVA, T.M.<sup>1</sup>; BABASKINA, L.I.<sup>1</sup>; OVAKIMYAN, A.K.<sup>1</sup>; KOLEVATOVA, K.Y.<sup>1</sup>

<sup>1</sup> Sechenov First Moscow State Medical University. 8-2, Trubetskaya St., Moscow, 119991, Russian Federation.

\* Correspondence author

Received 19 March 2020; received in revised form 29 May 2020; accepted 03 July 2020

**RESUMO**

O objetivo do estudo foi realizar uma pesquisa de mercado e uma avaliação das preferências do consumidor relacionadas ao uso de aplicativos móveis de saúde (mHealth) na Rússia para apoiar e promover a adesão dos pacientes aos medicamentos. Materiais e métodos. A pesquisa envolveu 1.099 consumidores de saúde móvel de dois segmentos-alvo. O primeiro segmento (S1) incluía consumidores intermediários: real (264 farmacêuticos de 22 regiões da Rússia) e potencial (293 estudantes com especialização em Farmácia). O segundo segmento (S2) incluiu 542 consumidores finais, ou membros do público em geral, de 28 regiões da Rússia. Os estudos de campo foram conduzidos usando os métodos de pesquisa oral (27%) e pesquisa baseada na web (73%) com um questionário estruturado. O método qualitativo com um gráfico de percepção bidimensional e o método quantitativo de estimativas pontuais individuais com o cálculo de indicadores integrais foram utilizados para o posicionamento. Resultados e discussão. O estudo de marketing da adesão a medicamentos revelou que mais de 50% dos entrevistados no S2 têm baixo grau de adesão. As formas mais comuns de apoiar a adesão foram tomar medicamentos como parte da rotina diária normal (87,1%) e usar aplicativos móveis de saúde (66,4%). De acordo com 98,2% dos farmacêuticos e estudantes (S1), os aplicativos mHealth poderiam ser mais amplamente recomendados para uso. As dificuldades técnicas foram a principal barreira para sua implementação (32,5% para o S1 e 59,8% para o S2). Os líderes entre aplicativos móveis para controle de drogas na Rússia foram estabelecidos como resultado do posicionamento usando métodos qualitativos e quantitativos. Foi proposto um mecanismo para promover a saúde móvel, a fim de satisfazer mais plenamente as preferências dos consumidores. Conclusão. Os resultados obtidos fornecem a base para o desenvolvimento de um conjunto de medidas estratégicas para o desenvolvimento adicional do segmento básico do mercado de aplicativos móveis de assistência médica para apoiar a adesão a medicamentos e aumentar as vantagens competitivas do mHealth, que contribuirão para o tratamento eficaz e prevenção de doenças crônicas na Rússia.

**Palavras-chave:** *mHealth, adesão a medicamentos, preferências do consumidor, aplicativos móveis, marketing.*

**ABSTRACT**

The goal of the study is to conduct a market research and an evaluation of the consumer preferences related to the use of mobile healthcare apps (mHealth) in Russia to support and promote patients' adherence to drugs. Materials and methods. The survey involved 1,099 mHealth consumers from two target segments. The first segment (S1) included intermediate consumers: real (264 pharmacists from 22 regions of Russia) and potential (293 students with major in Pharmacy). The second segment (S2) included 542 final consumers, or members of the general public, from 28 regions of Russia. Field studies were conducted using the oral survey (27 %) and web-based survey (73 %) methods with a structured questionnaire. The qualitative method with a two-dimensional perception chart and the quantitative method of individual point estimates with the calculation of integral indicators were used for positioning. Results and discussion. The marketing study of drug adherence has revealed that over 50 % of the respondents in S2 have low degree of adherence. The most common ways to

support adherence were to take medications as part of the normal daily routine (87.1 %) and to use mobile healthcare apps (66.4 %). According to 98.2 % of the pharmacists and students (S1), mHealth apps could be more widely recommended for use. The leaders among mobile apps for drug control in Russia have been established as a result of positioning using qualitative and quantitative methods. A mechanism for promoting mHealth has been proposed in order to more fully satisfy consumer preferences. Conclusion. The obtained results provide the basis for the development of a set of strategic measures for the further development of the basic segment of the mobile healthcare app market to support drug adherence and to increase the competitive advantages of mHealth, which will contribute to the effective treatment and prevention of chronic diseases in Russia.

**Keywords:** *mHealth, drug adherence, consumer preferences, mobile apps, marketing.*

## АННОТАЦИЯ

Цель – провести маркетинговое исследование и оценку потребительских предпочтений использования мобильных приложений здравоохранения (mHealth) в России для поддержки и продвижения приверженности пациентов к лекарственным препаратам. Материалы и методы. В опросе участвовали 1099 потребителей mHealth из двух целевых сегментов. Первый сегмент (S1) включал промежуточных потребителей: реальных (264 фармацевта из 22 регионов России) и потенциальных (293 студента, обучающихся по направлению подготовки «Фармация»). Ко второму сегменту (S2) были отнесены 542 конечных потребителей, или представителей широкой общественности, из 28 регионов России. Полевые исследования проводили методом устного опроса (27%) и web-опроса (73%) с использованием структурированной анкеты. Позиционирование осуществляли качественным методом с использованием двумерной карты-схемы восприятия и количественным методом индивидуальных балльных оценок с расчетом интегральных показателей. Результаты и обсуждение. Маркетинговое исследование приверженности к лекарственным препаратам показало, что более 50% респондентов сегмента S2 имеют невысокую степень приверженности. Наиболее распространенными способами поддержки приверженности являлись прием лекарств в рамках обычного ежедневного режима (87.1%) и использование мобильных приложений здравоохранения (66.4%). По мнению 98.2% фармацевтов и студентов (сегмент S1) приложения mHealth могли быть более широко рекомендованы к применению. В результате позиционирования качественным и количественным методами были установлены лидеры среди мобильных приложений по контролю приема лекарств в России. Предложен механизм продвижения mHealth с целью более полного удовлетворения потребительских предпочтений. Выводы. Полученные результаты дают основание для разработки комплекса стратегических мероприятий по дальнейшему развитию базового сегмента рынка мобильных приложений здравоохранения для поддержки приверженности к лекарственным препаратам, повышению конкурентных преимуществ mHealth, что будет способствовать эффективному лечению и профилактике хронических заболеваний в России.

**Ключевые слова:** *mHealth, приверженность к лекарственным препаратам, потребительские предпочтения, мобильные приложения, маркетинг.*

## 1. INTRODUCTION

The problem of insufficient patient adherence to therapy is among the most urgent ones in the modern medicine and society. This problem is especially acute in the treatment of chronic diseases that require a long (often lifelong) intake of drugs and compliance with a list of medical recommendations (McCabe *et al.*, 2017; Nikishchenkova and Nikiforov, 2018; Norberg and Gustafsson, 2018; Rosenberg *et al.*, 2020; Salimzadeh *et al.*, 2019; Schinköthe, 2019). It is believed that low adherence is the main reason for reducing the manifested therapeutic effect, it significantly increases the likelihood of complications of the underlying disease, and leads to a decrease in the living standards of patients and to an increase in treatment costs (Babaskin *et al.*, 2019a; Lukina *et al.*, 2017).

Today, there is no single effective strategy for increasing adherence to therapy; no method is absolutely reliable. The most common ways to support patients' adherence to medication regimens are reminder systems, including tips through written notes, diaries, special packages, smart watches, smart patches, and daily routines (Davies *et al.*, 2015; Henriksen *et al.*, 2018; Skrzypecki *et al.*, 2019). The use of mobile healthcare apps has significantly increased for these purposes in recent years (Bachiri *et al.*, 2016; Brzan *et al.*, 2016; Haase *et al.*, 2017; Sharp and O'Sullivan, 2017). According to analysts of Research and Markets and Research2Guidance, the global market for these apps annually increases by 25 % on average (Sydow, 2019). Mobile apps can give consumers a notification about taking a specific drug at a certain time, its dosage, a reminder to purchase a new drug

package, information on its use, and are also able to control physiological parameters (García *et al.*, 2019; Hansen *et al.*, 2018; Helbostad *et al.*, 2017; Hristoforova *et al.*, 2019; Istepanian and Al-Anzi, 2018; Jeffrey *et al.*, 2019; Jogova *et al.*, 2019; Kagen and Garland, 2019; Nikolaou and Lean, 2017; Peake *et al.*, 2018; Mariblanca and Cano de la Cuerda, 2017; Santo and Redfern, 2019; Stubberud and Linde, 2018). However, they are not able to solve such issues as educational barriers and medical literacy of the population. These barriers can be overcome with the support of patients by pharmacists as the most accessible public health workers (Spears *et al.*, 2020). Pharmacists play a key role in integrating mobile apps in this area. New technologies of mobile apps in healthcare can both increase patients' commitment to therapy and improve the pharmacists' work – make it more automated and effective.

It is necessary to focus primarily on meeting the needs of the population in order to successfully advance patient adherence to drugs and increase the competitiveness of mobile healthcare apps. This requires to conduct research on consumer preferences for using mobile apps to control the administration of drugs and the factors that shape these preferences.

The purpose of the study is to conduct a market research and an evaluation of the consumer preferences related to the use of mobile healthcare apps (mHealth) in Russia in order to support and promote patients' adherence to medication regimens.

## 2. MATERIALS AND METHODS

The objects of research were mHealth apps popular in Russia and used for supporting and promoting drug adherence: Course Pill - medicine intakes, Dosecast - Medication Reminder, Med Helper Pill Reminder, Medisafe Pill Reminder, Mr. Pillster - pill reminder, My pill reminder, MyTherapy Pill Reminder, Pill in Time - reminder and drug take schedule, Pill Reminder and Health Tracker, RX2 - Meds and Pill Reminder L.

A descriptive marketing research – a survey involving 1,099 mHealth consumers – was conducted to support and promote drug adherence from two target segments. The first target segment (S1) included intermediate mHealth consumers: real (264 pharmacists from 22 regions of Russia and 235 business entities with various forms of ownership) and potential

(293 students with major in Pharmacy from the I. M. Sechenov First Moscow State Medical University). It is generally accepted in pharmaceutical marketing that the intermediate consumers are persons who prescribe or recommend medicines (doctors or pharmacists, accordingly) (Skorobogatykh *et al.*, 2018; Smith *et al.*, 2002). The second target segment (S2) included 542 mHealth end users, or members of the general public, from 28 regions of Russia. Real and potential mHealth consumers older than 18 who were ready to participate in the survey, with the exception of pharmaceutical workers and medical students, were included in S2. The participation was anonymous and voluntary, and respondents were fully aware of the purpose, nature, potential benefits, and risks of the survey. The study was conducted in accordance with the principles stipulated by the Helsinki Declaration and the ICC/ESOMAR International Code on Market, Opinion and Social Research and Data Analytics (ICC and ESOMAR, 2016). The sample size of each target segment was determined by time and resource constraints.

The field study was carried out in March – June 2019 by the personal oral interview (27.2 %) and web-based survey (72.8 %) methods using a structured questionnaire (Appendix 1). The questionnaire contained 20 questions regarding the characteristics of respondents, their consumer preferences in using mobile apps to support drug adherence, factors that shaped those preferences, and evaluation of the need satisfaction. Some questions were focused only on the S1 or S2 consumers. This was due, for example, to the professional activities of pharmacists (work experience in the specialty) or the training of students (training course). In the questionnaire, such questions were noted with the words: "If you are a pharmaceutical worker ..." or "If you are a representative of the general public ...". A cover letter with information for the survey participants was attached to the questionnaire (Appendix 2). All questionnaires were coded for tracking purposes, the codes were securely stored.

The questionnaire included questions from the Morisky-Green MMAS-4 test (Morisky *et al.*, 1986) for a general evaluation of the survey participants' adherence to medication regimens: "Do you ever forget to take medications?", "Do you sometimes not pay attention to the hours of the drugs administration?", "Do you skip taking medications if you feel well?", "If you feel unwell after taking medications, do you miss the next dose?". Each negative response was rated at one point. The respondents who scored four points



were considered highly adherent to drugs, three points were medium adhered, and two points or less were low adhered.

The Likert scale was used in responses to some questions of the questionnaire: strongly agree, agree, find it difficult to respond, disagree, strongly disagree, and the "option text" field was used to better understand the opinions of the respondents.

A qualitative method with a two-dimensional perception chart (Malhotra and Birks, 1999) and a quantitative method of individual point estimates with the calculation of integral indicators (Babaskin *et al.*, 2018) were used for positioning.

The statistical data processing was performed using the SPSS.Statistics.v17.Multilingual-EQUINOX (SPSS Inc) software. The characteristics of the respondents of the studied target segments were expressed either in absolute and relative values, or in metric units, such as the median, lower (25 %) and upper (75 %) quartiles (IQR), or the mean  $\pm$  standard deviation (SD). Cross tabulations, Mann-Whitney and Kruskal-Wallis tests were used to evaluate differences between the individual groups. The critical level of significance in testing statistical hypotheses in the study was taken equal to 0.05.

### 3. RESULTS AND DISCUSSION

#### 3.1. Characteristics of the survey participants

Women predominated among 557 respondents in S1 (81.5 %). There were 229 women (86.7 %) in the cohort group of specialists in the field of pharmaceutical activity and 225 women (76.8 %) in the group of students. Their average age was  $37.8 \pm 10.2$  years (median was 38, IQR was 29 – 47) and  $21.3 \pm 3.1$  years (median was 21, IQR was 19 – 23), respectively. Of those surveyed in the group of pharmaceutical workers, 166 people had experience in their field of up to ten years (62.9 %) and 98 respondents had ten years of experience or more (37.1 %). The cohort group of students was approximately evenly distributed among the courses of study: 19.5 % for the first year, 20.1 % for the second year, 20.1 % for the third year, 19.8 % for the fourth year, and 20.5 % for the fifth year.

There were 330 women (60.9 %) and 212 men (39.1 %) among the 542 respondents in S2. Their average age corresponded to  $45.1 \pm 11.6$  years (median was 45, IQR was 34 – 56). Without

any prejudice, the survey participants in S2 were divided into age groups: 18 to 40 years old, or "young" (43.0 %); 40 to 60 years old, or "middle-aged", (35.1 %); and 60 years old and older, or "elderly" (21.9 %). According to their social status, most of the respondents in S2 were employees and workers (64.9 %), while pensioners made up only 7.9 %. It must be noted that the workers from other countries (guest workers) made up a small part of the respondent workers – 2.3 %. The predominant number of mHealth consumers in S2 had higher professional education: specialist's degree (26.2 %), master's degree (12.0 %), and bachelor's degree (32.8 %). The share of S2 respondents with secondary vocational education was 22.5 %, the share without professional training was 6.5 %. The majority of participants in the S2 survey had an average monthly income per family member (57.0 %). The ratio of the respondents from various sociodemographic groups in S2 corresponded to the consumer structure of the Russian pharmaceutical market.

#### 3.2. Consumer preferences in supporting the drug adherence

The results of a general evaluation of the survey participants' adherence to medication regimens using the Morisky-Green test indicated that 71.3 % of the respondents from pharmaceutical workers and students (S1) had high degree of drug adherence (Figure 1). This indicator amounted to 46.1 % among the members of the general public (S2). It must be noted that 83.1 % of the participants in the survey in S1 and only 37.1 % of the participants in S2 observed the regimen of taking medications, regardless of their state of health.

Various methods to support patient adherence to drug regimens are currently known. The results of the survey of the respondents in S1 and S2 about the methods that they would use or would recommend to support drug adherence are presented in Table 1.

The survey results indicated that 98.2 % of the respondents in S1 would recommend using mHealth to support and promote drug adherence. This was equally expressed both in the cohort group of pharmaceutical workers and in the group of students ( $p > 0.05$ ). The external devices (smart patches, smart watches) ranked second (67.3 %) with a slight advantage in the preferences of the student cohort group ( $p = 0.047$ ). This was followed by the methods that helped not forget about taking medications: special packaging and observance of the daily routine (42.7 % each),

according to the equivalent opinion of pharmaceutical workers and students ( $p > 0.05$ ).

The respondents in S2 gave their preference for taking medications as part of the usual daily routine (87.1 %). It must be noted that the most common methods of supporting adherence to prescribed treatment regimens among pharmacists and students (S1) were not widely used among the members of the general public (S2). For example, only 25.6 % of the respondents in S2 used external devices (smart patches, smart watches) to control the intake of drugs. mHealth apps were in demand among 66.4 % of the respondents in S2. The rest of the survey participants (33.6 %) were willing to use this method of supporting drug adherence. The young cohort group in S2 was more willing to acquire mobile apps for adherence to drug regimens compared to the middle-aged group ( $p = 0.032$ ) and the elderly one ( $p = 0.017$ ). In this regard, the respondents in S1 were asked to consider whether patients over 40 years old could use mHealth to support drug adherence. The pharmacists suggested that they completely agreed or rather agreed with a positive response (41.7 %), found it difficult to respond (33.3 %), and rather disagreed or completely disagreed (25.0 %). The data obtained suggested the need for mandatory separation of consumers into age groups for acceptance and the ability to use mHealth to support drug adherence. The opinions in the group of students were divided into exactly the opposite. For example, 36.9 % of the respondents strongly agreed or rather agreed with the capabilities of patients over 40 years old to use mobile apps to control the intake of medications, and 36.5 % of the students were more likely to disagree or completely disagree. Moreover, 43.3 % of the students enrolled in the fifth year and 41.4 % of the fourth-year students indicated that middle-aged and elderly patients could use mHealth. This indicator was reduced to 30 % in the students of the first two years ( $p < 0.05$ ). It can be assumed that there are age and educational gaps between the students with major in Pharmacy regarding their opinions on the possibility of using mobile apps by people over 40 years old to support drug adherence.

### 3.3. Barriers to using mobile apps

To identify barriers to using mHealth, the respondents in each segment were asked to answer the following question: "What factors, in your opinion, make it difficult to use mobile apps to control drug intake?". The survey results are presented in Table 2.

It was found that the current and future pharmacists (S1) considered technical difficulties (32.5 %), unreliable information (28.7 %), and limited content (27.5 %) as the main problems for using mHealth. The statements of the members of the general public (S2) were similar. Technical difficulties were a key problem in using mobile apps (59.8 %). This was especially expressed in the cohort of elderly people (72.3 %,  $p < 0.05$ ). It must be noted that the data on the most significant factors in the group of students in S1 were approximately the same: 31.1 % for technical difficulties, and 30.7 % for both unreliable information and insufficient mobile content.

### 3.4. Positioning consumer preferences in using mobile apps (qualitative method)

The consumer preferences in using mHealth were positioned by compiling two-dimensional perception charts according to two indicators: awareness and popularity (Figure 2).

The results indicated that Medisafe Pill Reminder and MyTherapy Pill Reminder apps were the most recognizable and preferred mHealth apps in S1 and S2. Mobile drug control apps were better known in the cohort group of pharmaceutical workers and students (S1) compared with the group of the members of the general public (S2). The opinions of respondents from S1 and S2 were approximately the same by the Popularity indicator. In this regard, the participants in S2 were asked to answer the question of who advised them to acquire a mobile app. The answers were distributed as follows: doctor advice – 19.6 % (mainly from the group of elderly people,  $p < 0.01$ ), pharmaceutical worker advice – 21.8 % (mainly middle-aged and elderly members of the general public,  $p < 0.05$ ), friend advice – 14.0 %, family tradition – 6.4 %, personal experience – 8.1 %, information on the Internet and reference books – 18.5 %, advertising – 11.1 %, and spontaneously – 0.5 %. It can be assumed that the leading position of pharmacists in the promotion of mHealth explains the comparability of the opinions of respondents in S1 and S2 on the popularity of mobile apps to some extent.

It is known that the level of knowledge about products largely depends on the amount of their advertising. In this case, a directly proportional dependence of the awareness and popularity of mobile apps on the level of their advertising was also observed. Although the value of advertising when choosing mHealth was low (11.1 %), according to the survey, the positioning results revealed that effective advertising support

made mobile apps recognizable and preferred by most Russian consumers.

### 3.5. Factors shaping consumer preferences in using mobile apps

Simplicity and ease of use were the main factors shaping consumer preferences in using mHealth for more than 40 % of the survey participants (ranks 11 and 12, Table 3) ( $p > 0.05$ , S1 and S2). Accessibility, reliability, and security of mobile apps were crucial for almost 30 % of the respondents (ranks 9 and 10, Table 3) ( $p > 0.05$ , S1 and S2). The leading factor in acquiring the app was mHealth quality for 10.1 % of the survey participants in S2, the volume of mobile content for 7.6 %, and 6.3 % of the respondents primarily paid attention to the purchase price. The relationship with the attending physician and/or pharmacist, as well as additional monitoring of physiological parameters were decisive when choosing mHealth for 3.1 % and 1.3 % of the consumers in S2, respectively.

### 3.6. Positioning consumer preferences in using mobile apps (quantitative method)

The positioning of consumer preferences in using mHealth using the quantitative method revealed that mobile apps Medisafe Pill Reminder ( $P_n = 4.9$ , S1;  $P_n = 4.8$ , S2), MyTherapy Pill Reminder ( $P_n = 4.8$ , S1;  $P_n = 4.7$ , S2), and Mr. Pillster – pill reminder ( $P_n = 4.7$ , S1;  $P_n = 4.6$ , S2) had higher competitive advantages (Figure 3). The factors that shaped consumer preferences were used as parameters for comparison (Table 3). The evaluation was carried out on a five-point scale. The significance of factors was taken into account when calculating the integral indicators (Table 3).

### 3.7. Overall satisfaction evaluation

The question “Are you satisfied with the use of the mobile app?” was answered by the respondents in S2 as follows: 46.5 % were completely satisfied or rather satisfied, 40.4 % found it difficult to respond, and 13.1 % were rather not satisfied. The young cohort group in S2 was more satisfied with the use of mHealth to control drug intake compared with the middle-aged group ( $p = 0.035$ ) and the elderly one ( $p = 0.022$ ).

When asked whether the respondent would use mHealth apps in the future to support drug adherence, the overwhelming majority of the respondents in S2 (73.4 %) responded “definitely will” and “rather will”, 19.0 % responded “I find it

difficult to respond”, and 7.6 % responded “probably not.” None of the survey participants was “completely dissatisfied” with the use of the mobile app and responded the question as “definitely not” about the future use of mHealth apps.

Despite the successes achieved in medicine in Russia, the main tasks of the treatment and prevention of certain chronic diseases and their complications remain unresolved (Babaskin *et al.*, 2019b; Ministry of Health of Russian Federation, 2020). This is partly due to the low patients' adherence to drugs. For example, more than 50 % of the respondents in S2 in this study had low and medium adherence (Figure 1). The increasing use of mobile healthcare apps can be a way to support and promote drug adherence. According to IMS mHealth, their global market currently exceeds 165 thous. offers, but only 36 apps account for 50 % of the market (Upatov, 2016). Research2Guidance conducted a survey of 5,000 medical app development firms from around the world (R2G, 2017). Only 2 % of the apps have been downloaded one million times or more, while 62 % have less than five thous. downloads. According to this study, only 66.4 % of the respondents in S2 were real consumers of mobile apps, while 33.6 % would like to use mHealth (Table 1). Technical difficulties were the main barrier to the implementation of mobile apps (59.8 %, S2). This factor was also key in the formation of consumer preferences in using mHealth (24.3 %, S2). Inadequate consumer awareness of mobile drug control apps was another constraint (Figure 2). The authors believe that individuals can be educated to use mobile apps in order to solve these problems in promoting adherence to drugs. This is especially relevant for the “elderly” age cohort group. Adherence to drug regimens is a very important problem for the representatives of this group, and the market capacity of this segment should be the largest. However, only 21.9 % of the respondents in this study were targeted mHealth consumers among the people aged 60 or older (S2). Only about 50 % of them were real consumers of apps. Older people can be taught how to use mHealth by pharmacists leading the way in promoting mobile drug control apps (21.8 %). In this regard, a group of pharmaceutical workers (S1) was asked to consider whether they would agree to help educate these people in using mHealth. 72.3 % of the pharmacists responded positively (“strongly agree” and “rather agree”). 75.1% of respondents from the elderly and middle-aged groups, target segment S2, indicated that they “completely agreed” or “rather agreed” to

receive training in using mobile apps to support drug adherence. They indicated that they “strongly agreed” or “rather agreed” to be educated in using mobile apps to support compliance with prescribed treatment regimens. This can be implemented in Russia at the present time as part of the Concept of Active Longevity Policy under development (TASS, 2019). A cohort group of students in S1 was asked to answer the question of whether they wanted to take an elective course at the university in order to increase their knowledge of mobile healthcare apps. In the long run, they could educate real and potential mHealth users to support drug adherence themselves. The positive response was given by 72.3 % of the students in the third to fifth year of study (“strongly agree” and “rather agree”). Junior students (69.0 %) would like to attend such a course in senior years.

#### 4. CONCLUSION:

1. The marketing study of patient adherence to drug regimens in Russia has revealed that more than 50 % of the respondents in S2 had low degree of adherence. The most common ways to support adherence were to take medications as part of the normal daily routine (87.1 %) and to use mobile health apps (66.4 %). According to 98.2 % of the pharmacists and students (S1), mHealth apps could be more widely recommended for use. The main barriers to their implementation were technical difficulties (32.5 % in S1 and 59.8 % in S2), limited mobile content (27.5 % in S1 and 53.9 % in S2), and unreliable information (28.7% in S1 and 50.2% in S2).

2. The factors shaping consumer preferences in using mobile apps have been identified. Convenience and ease of use were of decisive importance for more than 40 % of the survey participants. Accessibility, reliability, and security of mobile apps were preferred by almost 30 % of the respondents. This was followed by the quality of mHealth (10.1 %), the volume of mobile content (7.6 %), the purchase price (6.3 %), etc. The ranking of the factors allowed to calculate their weight and use these data when positioning consumer preferences.

3. The results of positioning consumer preferences in using mHealth apps using the qualitative method have revealed that mobile apps from Medisafe Pill Reminder and MyTherapy Pill Reminder are the most recognizable and preferred. The data obtained were confirmed by the method of quantitative assessment with the calculation of integral indicators. Medisafe Pill

Reminder ( $P_n = 4.9$ , S1;  $P_n = 4.8$ , S2), MyTherapy Pill Reminder ( $P_n = 4.8$ , S1;  $P_n = 4.7$ , S2), and Mr. Pillster – pill reminder ( $P_n = 4.7$ , S1;  $P_n = 4.6$ , S2) were the leaders among mobile apps. A mechanism has been proposed for promoting mobile apps to control drug intake in order to better satisfy consumer preferences.

The obtained results provide the basis for creating a set of strategic measures for the further development of the basic segment of the mobile healthcare app market to support drug adherence and increase the competitive advantages of mHealth, which will contribute to the effective treatment and prevention of chronic diseases in Russia.

#### 5. REFERENCES:

1. Babaskin, D. V., Litvinova, T. M., and Babaskina, L. I. (2019a). The Effect of the Phytocomplex Electrophoresis on the Clinical Symptomatology and Quality of Life of Patients with the Knee Joint Osteoarthritis. *Open Access Macedonian Journal of Medical Sciences*, 7(14), 2236–2241.  
<https://doi.org/10.3889/oamjms.2019.603>
2. Babaskin, D. V., Litvinova, T. M., and Babaskina, L. I. (2019b). Search Screening Algorithm of Herbal Medicines for Electro and Phonophoresis. *Research Journal of Pharmacy and Technology*, 12(12), 5860.  
<https://doi.org/10.5958/0974-360X.2019.01016.3>
3. Babaskin, D. V., Litvinova, T. M., Babaskina, L. I., Okonenko, T. I., and Rumyantsev, Y. Y. (2018). Competitive advantages of the rehabilitation methods under development as a strategic factor of their introduction efficiency (Through the example of phytocomplex SMC-electrophoresis). *Journal of Pharmaceutical Sciences and Research*, 10(5), 1292–1296.
4. Bachiri, M., Idri, A., Fernández-Alemán, J. L., and Toval, A. (2016). Mobile personal health records for pregnancy monitoring functionalities: Analysis and potential. *Computer Methods and Programs in Biomedicine*, 134, 121–135.  
<https://doi.org/10.1016/j.cmpb.2016.06.008>
5. Brzan, P. P., Rotman, E., Pajnikihar, M., and Klanjek, P. (2016). Mobile Applications for Control and Self

- Management of Diabetes: A Systematic Review. *Journal of Medical Systems*, 40(9), 210. <https://doi.org/10.1007/s10916-016-0564-8>
6. Davies, M. J., Kotadia, A., Mughal, H., Hannan, A., and Alqarni, H. (2015). The attitudes of pharmacists, students and the general public on mHealth applications for medication adherence. *Pharmacy Practice*, 13(4), 644–644. <https://doi.org/10.18549/PharmPract.2015.04.644>
  7. Ministry of Health of Russian Federation (2020). *State program of the Russian Federation "Healthcare Development", 2014 (revised on 16.06.2020)*. <https://www.rosminzdrav.ru/ministry/programms/health/info>
  8. García, J. S., Alonso, S. G., de la Torre Díez, I., García-Zapirain, B., Castillo, C., Coronado, M. L., and Salvador, J. C. (2019). Reviewing Mobile Apps to Control Heart Rate in Literature and Virtual Stores. *Journal of Medical Systems*, 43(4), 80. <https://doi.org/10.1007/s10916-019-1202-z>
  9. Haase, J., Farris, K. B., and Dorsch, M. P. (2017). Mobile Applications to Improve Medication Adherence. *Telemedicine and E-Health*, 23(2), 75–79. <https://doi.org/10.1089/tmj.2015.0227>
  10. Hansen, C., Sanchez-Ferro, A., and Maetzler, W. (2018). How Mobile Health Technology and Electronic Health Records Will Change Care of Patients with Parkinson's Disease. *Journal of Parkinson's Disease*, 8(s1), S41–S45. <https://doi.org/10.3233/JPD-181498>
  11. Helbostad, J., Vereijken, B., Becker, C., Todd, C., Taraldsen, K., Pijnappels, M., Aminian, K., and Mellone, S. (2017). Mobile Health Applications to Promote Active and Healthy Ageing. *Sensors*, 17(3), 622. <https://doi.org/10.3390/s17030622>
  12. Henriksen, A., Haugen Mikalsen, M., Woldaregay, A. Z., Muzny, M., Hartvigsen, G., Hopstock, L. A., and Grimsgaard, S. (2018). Using Fitness Trackers and Smartwatches to Measure Physical Activity in Research: Analysis of Consumer Wrist-Worn Wearables. *Journal of Medical Internet Research*, 20(3), e110. <https://doi.org/10.2196/jmir.9157>
  13. Hristoforova, I. V., Silcheva, L. V., Arkhipova, T. N., Demenkova, A. B., and Nikolskaya, E. Y. (2019). Improvement of Digital Technologies in Marketing Communications of Tourism and Hospitality Enterprises. *Journal of Environmental Management and Tourism*, 10(4), 829–834.
  14. ICC, and ESOMAR. (2016). *International code on market, opinion and social research and data analytics*. [https://www.esomar.org/uploads/pdf/professional-standards/ICCESOMAR\\_Code\\_English\\_.pdf](https://www.esomar.org/uploads/pdf/professional-standards/ICCESOMAR_Code_English_.pdf)
  15. Istepanian, R. S. H., and Al-Anzi, T. (2018). m-Health 2.0: New perspectives on mobile health, machine learning and big data analytics. *Methods*, 151, 34–40. <https://doi.org/10.1016/j.ymeth.2018.05.015>
  16. Jeffrey, B., Bagala, M., Creighton, A., Leavey, T., Nicholls, S., Wood, C., Longman, J., Barker, J., and Pit, S. (2019). Mobile phone applications and their use in the self-management of Type 2 Diabetes Mellitus: a qualitative study among app users and non-app users. *Diabetology and Metabolic Syndrome*, 11(1), 84. <https://doi.org/10.1186/s13098-019-0480-4>
  17. Jogova, M., Shaw, J., and Jamieson, T. (2019). The Regulatory Challenge of Mobile Health: Lessons for Canada. *Healthcare Policy | Politiques de Santé*, 14(3), 19–28. <https://doi.org/10.12927/hcpol.2019.25795>
  18. Kagen, S., and Garland, A. (2019). Asthma and Allergy Mobile Apps in 2018. *Current Allergy and Asthma Reports*, 19(1), 6. <https://doi.org/10.1007/s11882-019-0840-z>
  19. Lukina, Y. V., Kutishenko, N. P., and Martsevich, S. Y. (2017). Treatment adherence: modern view on a well known issue. *Cardiovascular Therapy and Prevention*, 16(1), 91–95. <https://doi.org/10.15829/1728-8800-2017-1-91-95>
  20. Malhotra, N. K., and Birks, D. F. (1999). *Marketing Research: An Applied Orientation*. Prentice Hall Inc.
  21. McCabe, C., McCann, M., and Brady, A. M. (2017). Computer and mobile technology interventions for self-management in chronic obstructive pulmonary disease. *Cochrane Database of Systematic Reviews*. <https://doi.org/10.1002/14651858.CD0114>

- 25.pub2
22. Morisky, D. E., Green, L. W., and Levine, D. M. (1986). Concurrent and Predictive Validity of a Self-reported Measure of Medication Adherence. *Medical Care*, 24(1), 67–74. <https://doi.org/10.1097/00005650-198601000-00007>
  23. Nikishchenkova, I. V., and Nikiforov, V. S. (2018). The Influence of Adherence to Treatment on Myocardial Dysfunction in Elderly and Senile Patients with Ischemic Heart Disease and Heart Failure. *The Russian Archives of Internal Medicine*, 8(1), 59–65. <https://doi.org/10.20514/2226-6704-2018-8-1-59-64>
  24. Nikolaou, C. K., and Lean, M. E. J. (2017). Mobile applications for obesity and weight management: current market characteristics. *International Journal of Obesity*, 41(1), 200–202. <https://doi.org/10.1038/ijo.2016.186>
  25. Norberg, S., and Gustafsson, M. (2018). Older Peoples' Adherence and Awareness of Changes in Drug Therapy after Discharge from Hospital. *Pharmacy*, 6(2), 38. <https://doi.org/10.3390/pharmacy6020038>
  26. Peake, J. M., Kerr, G., and Sullivan, J. P. (2018). A Critical Review of Consumer Wearables, Mobile Applications, and Equipment for Providing Biofeedback, Monitoring Stress, and Sleep in Physically Active Populations. *Frontiers in Physiology*, 9, 743. <https://doi.org/10.3389/fphys.2018.00743>
  27. R2G. (2017). *mHealth Economics 2017 – Current Status and Future Trends in Mobile Health*. <https://research2guidance.com/product/mhealth-economics-2017-current-status-and-future-trends-in-mobile-health/>
  28. Rodríguez Mariblanca, M., and Cano de la Cuerda, R. (2017). Aplicaciones móviles en la parálisis cerebral infantil. *Neurología*. <https://doi.org/10.1016/j.nrl.2017.09.018>
  29. Rosenberg, S. M., Petrie, K. J., Stanton, A. L., Ngo, L., Finnerty, E., and Partridge, A. H. (2020). Interventions to Enhance Adherence to Oral Antineoplastic Agents: A Scoping Review. *JNCI: Journal of the National Cancer Institute*, 112(5), 443–465. <https://doi.org/10.1093/jnci/djz244>
  30. Salimzadeh, Z., Damanabi, S., Kalankesh, L., and Ferdousi, R. (2019). Mobile Applications for Multiple Sclerosis: a Focus on Self-Management. *Acta Informatica Medica*, 27(1), 12–18. <https://doi.org/10.5455/aim.2019.27.12-18>
  31. Santo, K., and Redfern, J. (2019). The Potential of mHealth Applications in Improving Resistant Hypertension Self-Assessment, Treatment and Control. *Current Hypertension Reports*, 21(10), 81. <https://doi.org/10.1007/s11906-019-0986-z>
  32. Schinköthe, T. (2019). Individualized eHealth Support for Oncological Therapy Management. *Breast Care*, 14(3), 130–134. <https://doi.org/10.1159/000500900>
  33. Sharp, M., and O'Sullivan, D. (2017). Mobile Medical Apps and mHealth Devices: A Framework to Build Medical Apps and mHealth Devices in an Ethical Manner to Promote Safer Use-A Literature Review. *Studies in Health Technology and Informatics*, 235, 363–367. <https://doi.org/10.3233/978-1-61499-753-5-363>
  34. Skorobogatikh, I. I., Shishkin, A. V., Murtuzaliev, T. V., Pogorilyak, B. I., and Gorokhova, A. E. (2018). Marketing Tools for Development of the Tourist and Recreational Area. *Journal of Environmental Management and Tourism*, 9(2), 343–354. [https://doi.org/10.14505/jemt.9.2\(26\).16](https://doi.org/10.14505/jemt.9.2(26).16)
  35. Skrzypecki, J., Stańska, K., and Grabska-Liberek, I. (2019). Patient-oriented mobile applications in ophthalmology. *Clinical and Experimental Optometry*, 102(2), 180–183. <https://doi.org/10.1111/cxo.12830>
  36. Smith, M. C., Kolassa, E. M., Perkins, J. G., and Siecker, B. R. (2002). *Pharmaceutical Marketing: Principles, Environment, and Practice*. Pharmaceutical Products Press.
  37. Spears, J., Erkens, J., Misquitta, C., Cutler, T., and Stebbins, M. (2020). A Pharmacist-Led, Patient-Centered Program Incorporating Motivational Interviewing for Behavior Change to Improve Adherence Rates and Star Ratings in a Medicare Plan. *Journal of Managed Care and Specialty Pharmacy*, 26(1), 35–41. <https://doi.org/10.18553/jmcp.2020.26.1.35>
  38. Stubberud, A., and Linde, M. (2018). Digital Technology and Mobile Health in Behavioral Migraine Therapy: a Narrative Review. *Current Pain and Headache Reports*, 22(10), 66. <https://doi.org/10.1007/s11916-018-0718->

- 0
39. Sydow, L. (2019). *App Annie Report: The entire mobile app market for 2018*. <https://www.appannie.com/ru/insights/market-data/the-state-of-mobile-2019/>
40. TASS. (2019). *Concept of active longevity policy to appear in Russia*.

- <https://tass.ru/obschestvo/6873294>
41. Upatov, A. (2016). *mHealth: industry news overview*. [https://medaboutme.ru/zdorove/publikacii/stati/sovety\\_vracha/mhealth\\_obzor\\_novostey\\_v\\_industrii/](https://medaboutme.ru/zdorove/publikacii/stati/sovety_vracha/mhealth_obzor_novostey_v_industrii/)

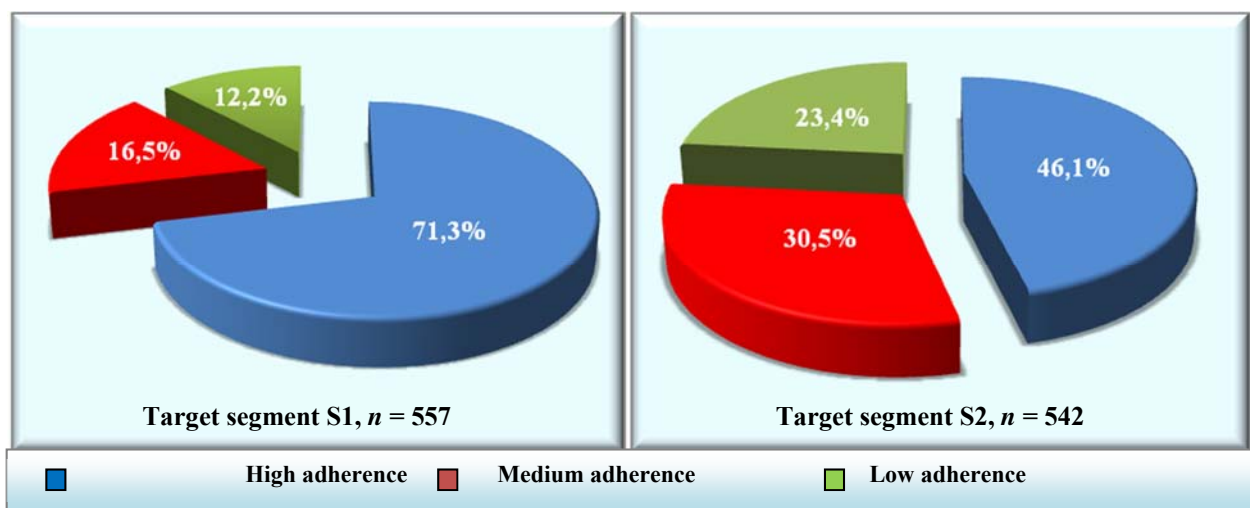


**Figure 1.** General evaluation of the respondents' adherence to drug administration in the two target segments

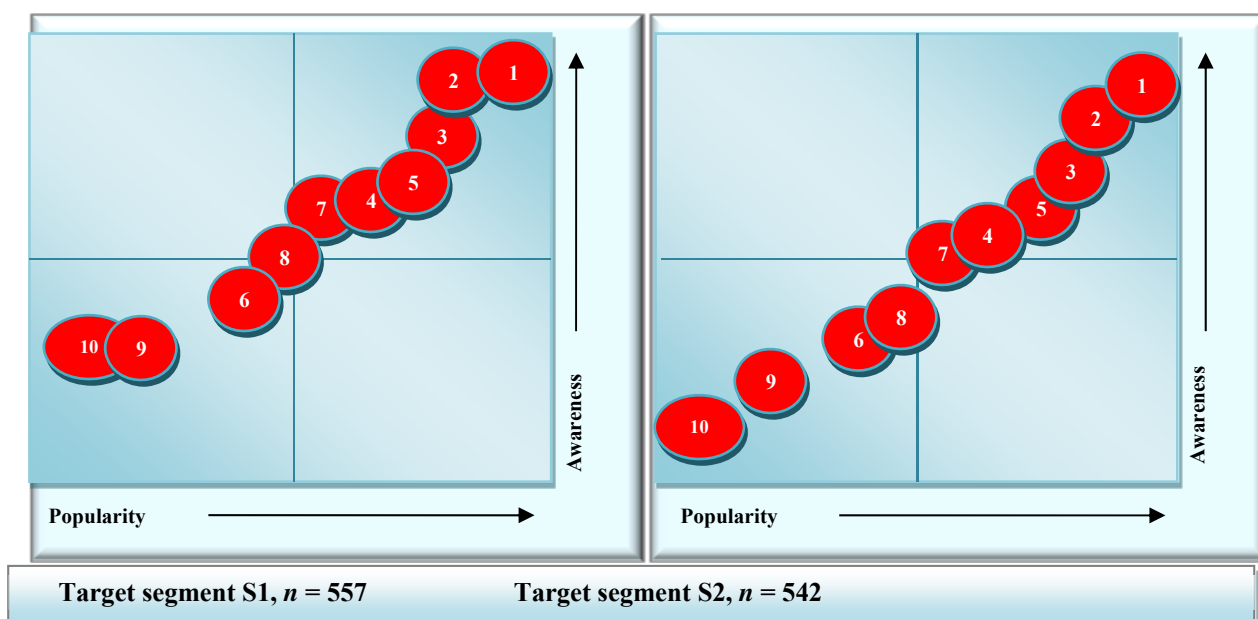


**Figure 2.** Two-dimensional charts of positioning consumer preferences in using mobile apps to support drug adherence among intermediate (S1) and final (S2) consumers in Russia (qualitative method)

Mobile apps: 1 – Medisafe Pill Reminder, 2 – MyTherapy Pill Reminder, 3 – Course Pill – medicine intakes, 4 – RX2 – Meds and Pill Reminder L, 5 – My pill reminder, 6 – Pill Reminder and Health Tracker, 7 – Mr. Pillster – pill reminder, 8 – Pill in Time – reminder and drug take schedule, 9 – Dosecast – Medication Reminder, 10 – Med Helper Pill Reminder



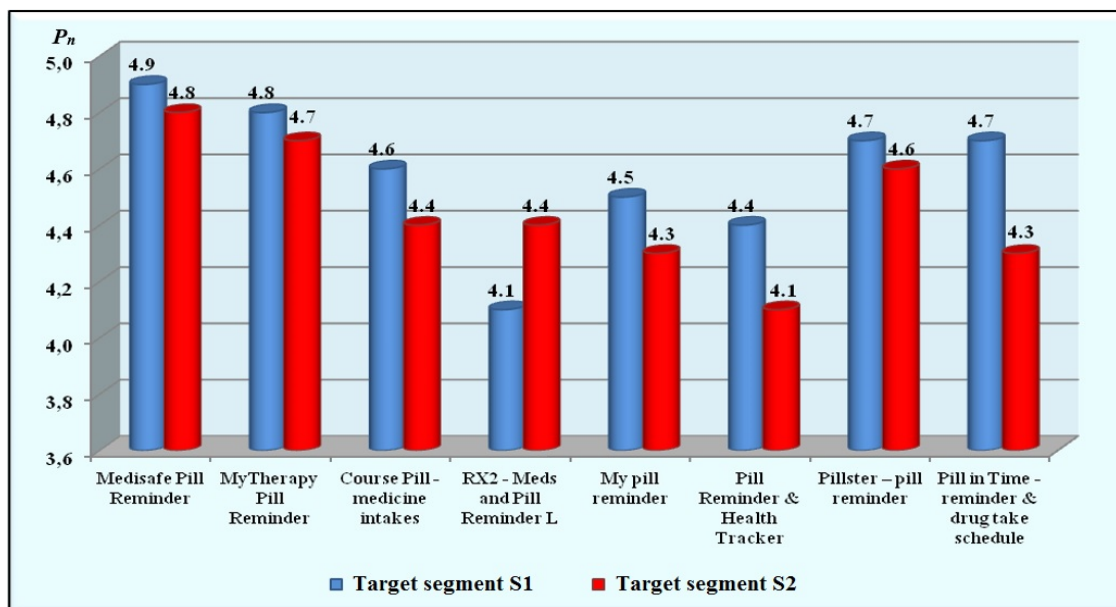


**Figure 3.** Fragment of the chart of positioning the consumer preferences in using mobile apps to support drug adherence among intermediate (S1) and final (S2) consumers in Russia (quantitative method,  $P_n$  is a composite parametric index)

**Table 1.** Consumer preferences in using various methods of supporting drug adherence among intermediate (S1) and final (S2) consumers in Russia

| Methods of supporting drug adherence                       | Share of respondents, % (one or several answer options) |              |
|--|---|--------------|
|  | S1 (n = 557)  | S2 (n = 542) |
| Written reminder or self-monitoring diary                  | 24.1  | 34.5         |
| Normal daily routine                                       | 42.7  | 87.1         |
| Health impairment  | 4.5   | 18.6         |
| Reminders from family members or colleagues                | 13.5  | 10.5         |
| Special packaging for drug control (with or without timer) | 42.7  | 21.0         |
| External devices (smart patches, smart watches)            | 67.3  | 25.6         |
| Mobile apps (mHealth)                                      | 98.2  | 66.4         |
| Phone alarm  | 1.8   | 0.9          |

**Table 2.** Barriers to using mHealth to support drug adherence among intermediate (S1) and final (S2) consumers in Russia

| Barriers to using mHealth to support drug adherence | Share of respondents, % (one or several answer options) |              |
|---|---|--------------|
|   | S1 (n = 557)  | S2 (n = 542) |
| Technical difficulties                              | 32.5  | 59.8         |
| Inadequate security                                 | 24.1  | 30.4         |
| Unreliable information                              | 28.7  | 50.2         |
| High price  | 12.4  | 19.2         |
| Inadequate regulation by professional bodies        | 15.3  | 22.3         |
| Limited mobile content                              | 27.5  | 53.9         |
| Low availability                                    | 15.6  | 16.6         |
| Lack of usability                                   | 8.4   | 11.6         |



**Table 3.** Results of determining the significance of factors shaping consumer preferences for using mHealth to support drug adherence in two target segments (S1 and S2) in Russia

| Factor  | Rank<br>( $R_i$ )* | Rank price<br>( $C$ )** | Factor weight<br>( $W_i$ ***) |
|---|--------------------|-------------------------|-------------------------------|
| Convenience   | 11                 |                         | 0.141                         |
| Reliability and security  | 9                  |                         | 0.115                         |
| Availability  | 10                 |                         | 0.128                         |
| Price   | 6                  |                         | 0.077                         |
| Volume of the mobile content  | 7                  |                         | 0.090                         |
| Developer   | 1                  |                         | 0.013                         |
| Design  | 2                  | 0.0128                  | 0.026                         |
| Ease of use   | 12                 |                         | 0.154                         |
| Quality   | 8                  |                         | 0.103                         |
| Relationship with the attending doctor,<br>pharmacist                         | 5                  |                         | 0.064                         |
| Control of physiological parameters: pressure,<br>weight, blood glucose, etc. | 4                  |                         | 0.051                         |
| Additional reminders: buying a medicine, visiting<br>a doctor, etc.           | 3                  |                         | 0.038                         |

Note. \* – direct ranking method; \*\* –  $C = 1 / \sum R_i$ ; \*\*\* –  $W_i = C \cdot R_i$ .

## APPENDIX 1. QUESTIONNAIRE

### Dear survey participant!

We are conducting a marketing research of consumer preferences in using mobile healthcare apps (mHealth) to control drug adherence. This will make apps more accessible, convenient and useful.

Please answer the questions below. Choose an answer option (one or more) or specify your own.

#### 1. Your gender:

- ☐ male
- ☐ female

#### 2. Your age: \_\_\_\_\_

#### 3. Your education:

- ☐ without vocational education
- ☐ secondary vocational education
- ☐ incomplete higher education
- ☐ higher education
- ☐ Master's degree
- ☐ Bachelor's degree

#### 4. Your social status:

- ☐ worker
- ☐ worker of other countries (guest worker)
- ☐ employee
- ☐ retiree
- ☐ student
- ☐ housewife
- ☐ temporarily unemployed
- ☐ entrepreneur

#### 5. Your average monthly income per family member:

- ☐ below average
- ☐ average
- ☐ above average

**6. You are:**

- ☐ a pharmaceutical worker
- ☐ a student with major in Pharmacy
- ☐ a representative of the general public

**7. If you are a pharmaceutical worker, then your work experience in the specialty is:**

- ☐ up to 10 years
- ☐ 10 years and more

**8. If you are a student with major in Pharmacy, then your year of study is:**

- ☐ 1
- ☐ 2
- ☐ 3
- ☐ 4
- ☐ 5

**9. Do you ever forget to take medications?**

- ☐ yes
- ☐ no

**10. Do you sometimes not pay attention to the hours of drugs administration?**

- ☐ yes
- ☐ no

**11. Do you skip taking medications if you feel well?**

- ☐ yes
- ☐ no

**12. If you feel unwell after taking medications, do you miss the next dose?**

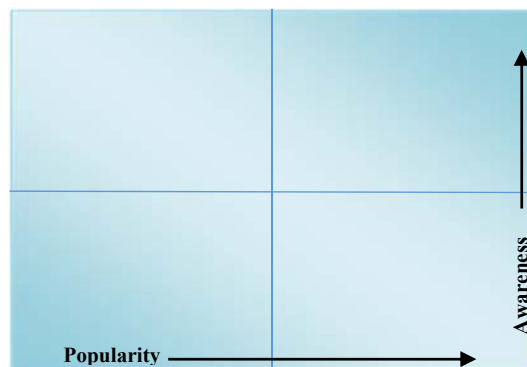
- ☐ yes
- ☐ no

**13. The method that you use or would recommend for use to control the drug intake:**

- ☐ written reminder or self-control diary
- ☐ normal daily routine
- ☐ poor health
- ☐ reminders from family members or work colleagues
- ☐ special packages for control of drug intake (with or without timer)
- ☐ external devices (smart patches, smart watches)
- ☐ mHealth apps
- ☐ phone alarm

**14. Indicate the popularity degree of the mHealth apps that you use, would like to use or would recommend to use, using the perceptual map:**

- Course Pill – medicine intakes (1)
- Dosecast – Medication Reminder (2)
- Med Helper Pill Reminder (3)
- Medisafe Pill Reminder (4)
- Mr. Pillster – pill reminder (5)
- My pill reminder (6)
- MyTherapy Pill Reminder (7)
- Pill in Time – reminder and drug take schedule (8)
- Pill Reminder and Health Tracker (9)
- RX2 – Meds and Pill Reminder L (10)
- Other \_\_\_\_\_ (11)



**15. How do you think what factors make it difficult to use mHealth apps to control medication intake?**

- ☐ technical difficulties
- ☐ inadequate security
- ☐ unreliable information
- ☐ high cost
- ☐ insufficient regulation by professional bodies
- ☐ limited mobile content
- ☐ low availability
- ☐ lack of usability
- ☐ other \_\_\_\_\_

**16. If you are a representative of general public and use mHealth apps to control drug intake, then who advised you to make a purchase:**

- ☐ advice of a doctor
- ☐ recommendation of a pharmaceutical worker
- ☐ advice of friends
- ☐ tradition in the family
- ☐ personal experience
- ☐ information on the Internet and reference literature

- ☐ advertising
- ☐ spontaneously

**17. If you are a pharmaceutical worker or a student with major in Pharmacy, indicate your opinion. Patients older than 40 years old can use mHealth apps to control medication intake:**

- ☐ totally agree
- ☐ rather agree
- ☐ difficult to answer
- ☐ rather disagree
- ☐ totally disagree

**18. Rank and evaluate (on a five-point scale) the factors that shape your preferences for use or recommendations for using mHealth apps to control drug intake (twelve is the most important factor, one is the least important factor):**

| Factor   | Rank | Mobile app name (mHealth) |  |  |
|--|------|---------------------------|--|--|
|  |      |                           |  |  |
| User-friendliness  |      |                           |  |  |
| Reliability and safety   |      |                           |  |  |
| Availability   |      |                           |  |  |
| Cost   |      |                           |  |  |
| Mobile content volume  |      |                           |  |  |
| Developer  |      |                           |  |  |
| Design   |      |                           |  |  |
| Ease of use  |      |                           |  |  |
| Quality  |      |                           |  |  |
| Contact with the doctor, pharmacist  |      |                           |  |  |
| Control of physiological parameters: blood pressure, weight, glucose, etc. |      |                           |  |  |
| Additional reminders: buying a medicine, visiting a doctor, etc.           |      |                           |  |  |

**19. Are you satisfied with the mHealth app?**

- ☐ completely satisfied
- ☐ rather satisfied
- ☐ difficult to answer
- ☐ rather unsatisfied
- ☐ completely unsatisfied

**20. Will you use mHealth apps in the future to control medication intake?**

- ☐ definitely yes
- ☐ rather yes
- ☐ difficult to answer
- ☐ rather no
- ☐ definitely no

## APPENDIX 2. INFORMATION FOR THE SURVEY PARTICIPANT

**Dear survey participant!**

**Research title:** MARKETING EVALUATION OF CONSUMER PREFERENCES IN USING MOBILE APPS FOR HEALTHCARE TO SUPPORT DRUG ADHERENCE

**The research is aimed at** studying and analyzing consumer preferences in using mobile healthcare applications (mHealth) to support and promote patients' adherence to drugs in Russia.

**Research objectives:** to establish the degree of patients' drug adherence in Russia and ways to support it; to show the main barriers to the introduction of mHealth apps for drug intake control; to identify the factors that shape consumer preferences in using mobile apps; to conduct positioning of consumer preferences in using mHealth apps popular in Russia.

**The research duration:** the field phase lasts for 4 months: March-June 2019.

**Sample size:** 1,100 people. The sample size is stipulated by time and resource constraints.

**Research methods:** personal oral survey and web-based survey using a structured questionnaire.

**Survey participation:** anonymous, voluntary.

**Characteristics of survey participants**

All respondents are divided into two target segments.

Target segment 1 (550 people) - pharmaceutical workers and students with major in Pharmacy.

Target segment 2 (550 people) - mHealth apps consumers, or members of the general public.

**Possible benefits for respondents from participating in the survey.** Survey participants can obtain additional information on the possible benefits of supporting drug adherence, on existing methods for controlling drug intake, on modern mobile healthcare apps and their characteristics, which will contribute to the effective treatment and prevention of chronic diseases.

**Possible risks associated with the survey.** The risks associated with the confidentiality of the information obtained during the survey can be mitigated by assigning a code to each profile, which will be securely stored.

**Inconvenience and additional burdens when participating in the survey.** The survey may take 20-30 minutes. Issues of ranking factors and their evaluation can present certain difficulties requiring additional clarification and assistance.

**Responsibilities of the survey participant in the course of the survey:** participation in the full volume of the survey, sincere and honest answers.

**Information on the confidentiality of survey participants' data.** Interviewers participating in the survey will be further warned of the obligation to keep the information about respondents confidential. A market researcher is required to monitor the confidentiality of information about the participants in the survey.

# CONTROLE DE ODORES EM PRODUTOS ALIMENTARES USANDO FIBRAS ALIMENTARES

## ODOR CONTROL IN FOODS USING DIETARY FIBERS

### РЕГУЛИРОВАНИЕ ЗАПАХА В ПИЩЕВЫХ ПРОДУКТАХ ИСПОЛЬЗОВАНИЕМ ПИЩЕВЫХ ВОЛОКОН

BOITSOVA, Tatyana Maryanovna<sup>1</sup>; PROKOPETS, Zhanna Georgievna<sup>2</sup>; ZHURAVLEVA, Svetlana Valerevna<sup>3</sup>; LYAKH, Vladimir Alekseevich<sup>4\*</sup>

<sup>1,3,4</sup> Far Eastern Federal University. Sukhanov Street, 8, Vladivostok, 690090, Russia.

<sup>1,2</sup> Vladivostok State University of Economics and Service. Gogol Street, 41, Vladivostok, 690014, Russia.

\* Correspondence author  
e-mail: lyah\_v@bk.ru

Received 15 March 2020; received in revised form 20 May 2020; accepted 03 July 2020

## RESUMO

O objetivo do presente trabalho é determinar a capacidade do farelo de trigo de eliminar o cheiro desagradável de peixe através da conversão de substâncias voláteis em não voláteis, bem como o efeito do farelo de trigo no valor nutricional de amostras tratadas termicamente de tecido muscular picado de peixe. Os principais métodos de pesquisa incluem o método Kjeldahl, para determinar o conteúdo de extratos nitrogenados, a cromatografia gás-líquido para determinar a composição de ácidos graxos e o organismo de teste de ciliado de *Tetrahymena pyriformis* para determinar o valor biológico relativo. Como resultado, a capacidade das fibras alimentares de eliminar um cheiro desagradável de peixe pela conversão de extrativos nitrogenados voláteis em não voláteis foi demonstrada pelo exemplo do farelo de trigo: uma série de experimentos realizada para identificar a dependência do conteúdo de óxido de trimetilamina e nitrogênio de bases voláteis em amostras de tecido muscular picado da navaga, dependendo da proporção de farelo de trigo adicionado, verificou-se que em todas as amostras há uma diminuição no conteúdo de extrativos com um aumento na fração de massa de farelo de trigo. Além disso, o farelo não moído contribui mais ativamente para o processo de neutralização do odor. Foram identificadas a composição dos ácidos graxos dos lipídios da navaga do Extremo Oriente *Eleginus gracilis*, farelo de trigo e sua mistura, e o efeito no valor biológico relativo determinado no organismo de teste de amostras experimentais após tratamento térmico (escaldamento e fervura).

**Palavras-chave:** farelo de trigo, extrativos nitrogenados, composição de lipídios dos ácidos graxos, valor biológico relativo.

## ABSTRACT

The aim of the present work is to determine the ability of wheat bran to eliminate an unpleasant fish smell by converting volatile extractive substances to nonvolatile ones, as well as the effect of wheat bran on the nutritional value of thermally treated samples of minced muscle tissue of fish. The main methods for research include the Kjeldahl's method for determining the content of nitrogenous extractives, the gas-liquid chromatography for determining the composition of fatty acids, and the test organism of *Tetrahymena pyriformis* ciliate for determining the relative biological value. As a result, the ability of dietary fibers to eliminate an unpleasant fish smell by converting volatile nitrogenous extractives into nonvolatile ones has been shown by the example of wheat bran: in a series of experiments to identify the dependence of the content of trimethylamine oxide and nitrogen of volatile bases in samples of minced muscle tissue of the navaga, depending on the proportion of added wheat bran, it has been found that in all samples there is a decrease in the content of extractives with an increase in the mass fraction of wheat bran. Moreover, unmilled bran more actively contributes to the process of neutralizing odor. The fatty acid composition of the lipids of the Far Eastern navaga *Eleginus gracilis*, wheat bran and their mixture, and the effect on the relative biological value determined on the test organism of experimental samples after thermal treatment (scalding and boiling) have been identified.

**Keywords:** wheat bran, nitrogenous extractives, fatty acid composition of lipids, relative biological value.

## АННОТАЦИЯ

Целью работы являлось определение способности пшеничных отрубей устранять неприятный рыбный запах путем перевода летучих экстрактивных веществ в нелетучие, а также влияние пшеничных отрубей на пищевую ценность термически обработанных образцов из измельченной мышечной ткани рыбы. В качестве основных методов для проведения исследований были выбраны: рекомендации Кельдаля для определения содержания экстрактивных азотистых веществ, газожидкостная хроматография для определения состава жирных кислот, тест-организм инфузория *Tetrahymena pyriformis* для определения относительной биологической ценности. В результате была показана способность пищевых волокон на примере пшеничных отрубей устранять неприятный рыбный запах путем перевода азотистых летучих экстрактивных веществ в нелетучие: в серии экспериментов по выявлению зависимости содержания триметиламинооксида и азота летучих оснований в образцах из измельченной мышечной ткани наваги, в зависимости от доли добавляемых пшеничных отрубей, было установлено, что во всех образцах наблюдается снижение содержания экстрактивных веществ с увеличением массовой доли пшеничных отрубей. Причем неизмельченные отруби более активно способствуют процессу нейтрализации запаха. Определен жирнокислотный состав липидов дальневосточной наваги *Eleginus gracilis*, пшеничных отрубей и их смеси, и влияние на относительную биологическую ценность, определенную на тест-организме, экспериментальных образцов после термической обработки (бланширование и варка).

**Ключевые слова:** пшеничные отруби, азотистые экстрактивные вещества, жирнокислотный состав липидов, относительная биологическая ценность.

## 1. INTRODUCTION

The development of the technology of products from minced fish is promoted by the wide possibilities of carrying out various modifications on its basis with the aim of regulating nutritional value and creating enriched and functional food products. The traditional raw materials for minced meat production are fish with predominantly light muscle tissue, low-fat content, and high content of myofibrillar proteins (Hagen and Johnsen, 2016; Murthy *et al.*, 2017; Gonçalves and Salas-Mellado, 2018; Cardoso *et al.*, 2019; Chen *et al.*, 2020; Gu *et al.*, 2020).

The authors had carried out the studies which allowed establishing that when using two indicators: the conditional protein coefficient ( $C_p$  – the ratio of nitrogen of the protein salt-soluble fraction to nitrogen of the water-soluble fraction) and the structure formation coefficient ( $C_{st}$  – the ratio of the nitrogen content of the salt-soluble fraction to total nitrogen), it was possible to qualify how much fish was suitable for minced meat production (Bidenko and Rambesa, 1978). With  $C_p < 1$  and  $C_{st} < 0.2$ , poorly formed minced meat with rigid consistency (e.g., pollock, blue whiting, cardinalfish) is obtained. At  $C_p 1 - 1.2$  and  $C_{st} \sim 0.2$ , the formability of minced meat increases (e.g., Baltic cod, Macrourus icefish). The best raw material for obtaining well-formed minced meat with a high ability to hold water is fish with  $C_p > 1.2$  and  $C_{st} > 0.2$ . These species include herring, ivasi,

horse mackerel, and scomber mackerel. These are just those types of objects that contain a significant amount of dark muscle tissue. Unlike light muscles, dark ones consist of thin dark fibers, the space between which is filled with sarcoplasm with a high content of glycogen, myoglobin, cytochrome C, i.e., substances that accelerate the oxidation of lipids (Kolakovskii, 1991; Lee, Seki, and Kato, 1990; Obatake, 1985). The total lipid content in dark muscles is 5 to 20 times greater than in light ones.

All this, including high iron content (up to 75 %), which is not part of the myoglobin heme, and increased enzymatic activity contribute to the susceptibility of dark muscles to rapid oxidation, and to the formation and rapid growth of an unpleasant odor. Moreover, the deeper the degree of dressing of raw materials is, the longer the contact with atmospheric oxygen is, and the more intense the oxidation processes are (Boitsova, Doroshenko, and Shipova, 2001).

At the same time, certain fish species with predominantly light muscles, low-fat content, low enzymatic activity, and practically not subject to oxidation, are also not suitable for the production of good quality minced meat. Thus, a typical representative of codfishes, pollock (*Theragra chalcogramma*), is characterized by a high content of trimethylamine oxide in the light muscles (TMAO up to 10.80 mg/g). Immediately after catching, the TMAO breaks down into trimethylamine (TMA) and formaldehyde in muscle

tissue of pollock, which have a significant effect on the specific taste and aromatic properties of minced meat (Crapo and Himelbloom, 1994; Greene and Bernatt-Byrne, 1990).

These specific features of pollock are among the reasons for the undesirable use of pollock for obtaining unwashed minced meat, and it is used only for the production of surimi.

Surimi technology involves mincing fish muscle tissue and washing it with water to remove water-soluble components: sarcoplasmic (water-soluble) proteins, enzymes, nitrogenous extractives, including TMAO, TMA, and formaldehyde. Surimi practically consists only of myofibrillar (salt-soluble) proteins, has no negative smell and taste. Surimi is the main raw material for the production of structured analog products. However, its output is only from 12 to 15 % by weight of the whole fish (Li and Chen, 2009; Filomena-Ambrosio *et al.*, 2016; Iwashita *et al.*, 2016; Li *et al.*, 2016; Konno, 2017; Houjyo *et al.*, 2017; Sipailiene, 2017; Zhang *et al.*, 2017; Ma *et al.*, 2017; Jin *et al.*, 2018; Gao *et al.*, 2018).

It is known that dietary wheat fiber, wheat bran (WB), has a sorption ability, including in relation to a number of metals (Guillon and Champ, 2000; Lin *et al.*, 2019; Zhang, Huang and Ou, 2011).

It has been suggested that substances adding an unpleasant smell to minced fish products can also be absorbed by dietary fiber. In addition, there are a number of works devoted to the introduction of dietary fiber into the composition of minced meat of surimi from other fish species: Alaska pollock (Alakhrash, Anyanwu, and Tahergorabi, 2016; Debusca, Tahergorabi, Beamer, Matak, and Jaczynski, 2014), silver carp (Yin *et al.*, 2019), bighead carp (Alipour, Rezaei, Shabanpour, and Tabarsa, 2018, 2019).

The purpose of these studies is to determine the ability of WB to eliminate an unpleasant fish smell by converting volatile extractive substances to nonvolatile ones, as well as the effect of WB on the nutritional value of thermally treated samples of minced muscle tissue of fish.

## 2. MATERIALS AND METHODS

For the model system, minced meat of the muscle tissue of the Far Eastern navaga (*Eleginus gracilis*) as an object containing light and dark muscles, up to 0.002 mg/g of formaldehyde, and 0.5 – 1.4 % of lipids, was selected. These

components, in addition to the formation of an unpleasant odor, contribute to a decrease in the water-holding ability of the protein due to the binding of amine groups and the formation of methylene-amine complexes.

WB was used as a sorbing complex, part of which had been preliminarily milled to sizes less than 250 microns, and the other part had been left to industrial production. The main part size was from 350 to 600 microns.

The content of nitrogenous extractives was determined by Kjeldahl's method (Regenstein and Regenstein, 1984). It was based on the organic matter oxidation during combustion in sulfuric acid in the presence of a catalyst, the distillation of ammonia formed by steam, trapping it with a solution of sulfuric acid and determination of the nitrogenous substances content by titration.

To determine the composition of lipid fatty acids, hydrolysis of lipids isolated by the Bligh-Dyer method (Bligh and Dyer, 1959) and methylation of higher fatty acids by the method of Metcalf and Schmitz (Metcalf and Schmitz, 1961) were performed. The obtained fatty acid methyl esters were analyzed by gas chromatography on a G-180 Yanako device (Japan) and a Shimadzu gas-liquid chromatograph using Argon gas. Identification was carried out according to the methods of Miwa (1963); Cfrreau and Dubacq (1978).

To determine the relative biological value, the test organism of the *Tetrahymena pyriformis* ciliate was used. The ciliate has small body sizes: 20 by 50 microns, the weight of one tetrahymena is  $1.8 \cdot 10^{-9}$  g. It gives 7.51 divisions per day, which is directly dependent on such vital factors as growth and stimulation of vital processes. The ciliate is cultivated on a protein nutrient medium, and the optimal cultivation temperature is 25 °C. For the analysis, 0.02 ml of a three-day culture and 1 – 3 g of the test product were used. The duration of the analysis was four days.

The relative biological value and biological activity of the ciliate were compared with the whole milk. The essence of the method for determining biological activity is to establish the moment of the growth stationary phase of the ciliate at the limiting level of samples of the studied and standard samples and to determine the rate of reproduction in the studied sample in comparison with the standard one. Exact quantitative accounting of the grown individuals was carried out in the Gorjaev's count chambers. The samples that had not shown death or other pathological changes in tetrahymena within four days were left for further

incubation for up to seven days to identify the possibility of long-term negative consequences (Ignatiev and Myagkov, 1980; Mohr, 1981; Shulgin, Shulgina, and Petrov, 2006, pp. 83-95).

The reliability of the obtained experimental data was ensured by the method of mathematical statistics. Reliability is 0.90 – 0.95 (P), and the confidence interval is  $\pm 5$  %.

### 3. RESULTS AND DISCUSSION

In a series of experiments to identify the dependence of the content of TMAO and volatile base nitrogen (VBN) in samples of minced muscle tissue of navaga, depending on the proportion of added WB, it was found that there was a decrease in the content of extractive substances with an increase in the mass fraction of WB in all samples (Figure 1, Figure 2). Moreover, unmilled bran more actively contributes to the process of neutralizing odor than milled one up to a size of 250 microns, despite the large sorption surface. Obviously, this is due to the violation in the milling process of not only physical dimensions but also the chemical structure of bran, which affects their ability to sorb volatile bases and TMA.

Wheat bran also has a positive effect on the fatty acid composition of the minced meat. The nutritional value of fish lipids is characterized by the presence of higher polyunsaturated fatty acids, which are necessary for normal human life. There are about 49 % of them in the navaga lipids (Table 1). Moreover, such types of thermal treatment as boiling in water and scalding practically do not influence the reduction of their quantity. The recorded fluctuations are within the error limits. WBs themselves also contain polyenoic acids, especially a large amount of linoleic acid (18:2 $\omega$ 6 – up to 51.88 %), which is characteristic of plant raw materials.

The addition of 5 % of WB to the minced muscle tissue of navaga leads to an increase of four times in the mass fraction of linoleic acid, and of linolenic acid (18:3 $\omega$ 3) – 1.5 times. The content of other polyunsaturated fatty acids (arachidonic 20:5 $\omega$ 3, eicosapentaenoic 22:5 $\omega$ 3, and docosahexaenoic 22:6 $\omega$ 3) is practically unchanged and does not depend on the thermal treatment method.

The presence of WB practically does not affect the content of saturated fatty acids. Their total amount decreases somewhat when scalding and, to a greater extent, when cooking in water, apparently due to the transition of the fat fraction into the broth.

Among monoenoic fatty acids, the oleic one (18:1 $\omega$ 9) and its isomer (18:1 $\omega$ 7) are the most characteristic of fish. Their ratio should be 2:1, and this ratio, despite natural minor losses during thermal treatment, remains unchanged.

Considering that the properties of odor are determined by organoleptic sensations, experimental samples of minced muscle tissue of navaga with the addition of 5 % of WB have been prepared. Products of 6x3x3 size were formed from the mixture and were thermally treated. Other components of the formulation were not involved in the experiment.

The results of the organoleptic evaluation confirmed the data of the chemical tests. Tasters noted a pleasant smell with a bread aroma and a meat-like taste.

The relative biological value of the experimental samples in comparison with the standard one (whole cow's milk), determined on the test organism, shows a slightly lower result (Table 2). However, the addition of WB only slightly reduces the relative biological value compared with the muscle tissue of fish without WB (by 2 – 6 %). At the same time, the thermal treatment of the experimental samples (scalding, frying) promotes more active cell growth.

### 4. CONCLUSION:

It has been found that wheat bran sorbs volatile extractive nitrogenous compounds (TMAO and VBN), contributing to the neutralization of fish smell. In this case, additional milling of WB is not required. Moreover, the addition of WB leads to an increase in the mass fraction of essential linoleic and linolenic fatty acids, which is characteristic of plant raw materials. In this case, the content of other polyunsaturated fatty acids is practically unchanged and does not depend on the thermal treatment method. The obtained results and the established VBN suggest that ready-made foods made from minced muscle tissue of fish with the addition of WB will have high nutritional value.

### 5. REFERENCES:

1. Alakhrash, F., Anyanwu, U., and Tahergorabi, R. (2016). Physicochemical properties of Alaska pollock (*Theragra chalcogramma*) surimi gels with oat bran. *LWT – Food Science and Technology*, 66, 41-47.
2. Alipour, J. H., Rezaei, M. E., Shabanpour, B., and Tabarsa, M. (2018). Effects of



- sulfated polysaccharides from green alga *Ulva intestinalis* on physicochemical properties and microstructure of silver carp surimi. *Food Hydrocolloids*, 74, 87-96.
3. Alipour, J. H., Rezaei, M. E., Shabanpour, B., and Tabarsa, M. (2019). Edible green seaweed, *Ulva intestinalis* as an ingredient in surimi-based product: chemical composition and physicochemical properties. *Journal of Applied Phycology*, 31(4), 2529-2539.
  4. Bidenko, M. S., and Rambesa, E. F. (1978). Vliyanie sootnosheniya rastvorimykh belkovykh fraktsii myshechnoi tkani ryby na kachestvo morozhenogo rybnogo farsha [The effect of the ratio of soluble protein fractions of muscle tissue of fish on the quality of frozen minced fish]. *Tr. AtlantNIRO*, 75, 64-69.
  5. Bligh, E.G. and Dyer, W.J.(1959). A rapid method of total lipid extraction and purification. *Canadian journal of biochemistry and physiology*, 37(8), 911-917
  6. Boitsova, T. M., Doroshenko, A. A., and Shipova, A. G. (2001). Tekhnokhimicheskie svoistva temnoi myshechnoi tkani mintaya [Technochemical properties of dark muscle pollock tissue]. *Izv. TINRO: Biotechnology for processing hydrobionts*, 129, 120–130.
  7. Cardoso, M., de Faria Barbosa, R., Torrente-Vilara, G., Guanaz, G., Oliveira de Jesus, E.F., Mársico, E.T., de Oliveira Resende Ribeiro, R., and Gusmão, F. (2019). Multielemental composition and consumption risk characterization of three commercial marine fish species. *Environmental Pollution*, 252, 1026-1034.
  8. Cfireau, J.P. and Dubacq, J.P. (1978). Adaptation of macro-scale method to the micro-scale for fatty acid methyl transesterification of biological lipid extracts. *Journal of Chromatography A*, 151(3), 384-390.
  9. Chen, Y., Xu, A., Jia, R., Zhang, J., Xu, D., and Yang, W. (2020). Myofibrillar Protein Structure and Gel Properties of *Trichiurus haumela* Surimi Subjected to High Pressure or High Pressure Synergistic Heat. *Food and Bioprocess Technology*, 13(4), 589-598.
  10. Crapo, C., and Himelbloom, B. (1994). Quality of mince from alaska pollock (*Theragra chalcogramma*) frames. *Journal of Aquatic Food Product Technology*, 3(1), 1–4.
  11. Debusca, A., Tahergorabi, R., Beamer, S. K., Matak, K. E., and Jaczynski, J. (2014). Physicochemical properties of surimi gels fortified with dietary fiber. *Food Chemistry*, 148, 70-76.
  12. Filomena-Ambrosio, A., Quintanilla-Carvajal, M.X., Ana-Puig, Hernando, I., Hernández-Carrión, M., and Sotelo-Díaz, I. (2016). Changes of the water-holding capacity and microstructure of panga and tilapia surimi gels using different stabilizers and processing methods. *Food Science and Technology International*, 22(1), 68-78.
  13. Gao, Y., Fukushima, H., Deng, S., Jia, R., Osako, K., and Okazaki, E. (2018) Effect of pH and heating conditions on the properties of Alaska pollock (*Theragra chalcogramma*) surimi gel fortified with fish oil. *Journal of Texture Studies*, 49(6), 595-603.
  14. Greene, D. H., and Bernatt-Byrne, E. I. (1990). Adenosine triphosphate catabolites as flavor compounds and freshness indicators in Pacific Cod (*Gadus macrocephalus*) and Pollock (*Theragra chalcogramma*): A Research Note. *Journal of Food Science*, 55(1), 257-258.
  15. Gonçalves, L.S., and Salas-Mellado, M.M. (2018). Evaluation of technology and sensory quality of cream cracker enriched with minced cobia (*Rachycentron canadum*). *International Food Research Journal*, 25(3), 1197-1203.
  16. Gu, S., Dai, W., Chong, Y., Lyu, F., Zhou, X., and Ding, Y. (2020). The binding of key fishy off-flavor compounds to silver carp proteins: A thermodynamic analysis. *RSC Advances*, 10(19), 11292-11299.
  17. Guillon, F., and Champ, M. (2000). Structural and physical properties of dietary fibres, and consequences of processing on human physiology. *Food Research International*, 33(3-4), 233-245.
  18. Hagen, O., and Johnsen, C.A. (2016). Flesh quality and biochemistry of light-manipulated Atlantic cod (*Gadus morhua*) and the significance of collagen cross-links on fillet firmness and gaping. *Food Chemistry*, 190, 786-792.
  19. Houjyo, K., Sugiyama, J., Kokawa, M., Fujita, K., Yuge, W., Nozaki, R., and Itoh, T. (2017). Physical properties of heated surimi gel containing emulsified high amylose rice gel. *Nippon Shokuhin Kagaku Kogaku Kaishi*, 64(3), 139-149.

20. Ignatiev, A. D., and Myagkov, A. S. (1980). *Metodicheskie ukazaniya k provedeniyu biologicheskoi otsenki kormov i pishchevykh produktov [Methodological guidelines for the biological assessment of feed and food]*. Moscow: Ministry of Higher Education of the RSFSR, USSR Ministry of Health.
21. Iwashita, K., Sumida, M., Shiota, K., and Shiraki, K. (2016). Recovery method for Surimi Wash-water protein by pH shift and heat treatment. *Food Science and Technology Research*, 22(6), 743-749.
22. Jin, R., Meng, R., Zhang, H., Yang, X., and Wu, Z. (2018). Effects of different deodorising processes on the off-odour compounds and gel properties of common carp surimi. *International Journal of Food Science and Technology*, 53(9), 2045-2053.
23. Kolakovskii, E. (1991). *Tekhnologiya pishchevogo rybnogo farsha [Technology of fish minced meat]*. Moscow: VO Agropromizdat.
24. Konno, K. (2017). Myosin denaturation study for the quality evaluation of fish muscle-based products. *Food Science and Technology Research*, 23(1), 9-21.
25. Lee, N., Seki, N., and Kato, N. (1990). Gel forming ability of myosin heavy in salted meat paste from threadfin bream. *Nippon Suisan Gakkaishi*, 56, 320-336.
26. Li, H. P., and Chen, H. H. (2009). Effect of washing and thermal treatment on gel properties of carp surimi. *Food and Fermentation Industries*, 35(3), 109-113.
27. Li, R.-Z., Wang, W., Yi, S.-M., Li, J.-R., Li, X.-P., Li, Y.-J., Li, C., Xiong, S.-B., and Huang, Q.-L. (2016). Changes in water and gel properties of silver carp (*Hypophthalmichthys molitrix*) surimi during gelation process. *Modern Food Science and Technology*, 32(5), 91-97, 198.
28. Lin, Y., Chen, K., Tu, D., Yu, X., Dai, Z., and Shen, Q. (2019). Characterization of dietary fiber from wheat bran (*Triticum aestivum* L.) and its effect on the digestion of surimi protein. *LWT – Food Science and Technology*, 102, 106-112.
29. Ma, Y.-L., Xiong, S.-B., Yin, T., You, J., and Hu, Y. (2017). Effects of Chopping Method and Sodium Chloride Concentration on the Quality Characteristics of Silver Carp Surimi. *Modern Food Science and Technology*, 33(8), 182-187.
30. Metcalf, L.D. and Schmitz, A.A. (1961). The rapid preparation of fatty acid esters for gas chromatography analysis. *Analytical Chemistry*, 33(3), 363-364.
31. Mohr, J. L. (1981). Methods for protozoa. In G. Clark (Ed.), *Staining procedures* (4th ed., pp. 281-310). Baltimore: Williams and Wilkins.
32. Miwa, T.K. (1963). Identification of peaks in gas-liquid chromatography. *Journal of the American Oil Chemists' Society*, 40(7), 309-310.
33. Murthy, L.N., Phadke, G.G., Siddaiah, V., and Boraiah, R.K. (2017). Rheological properties of washed and unwashed tilapia (*Oreochromis mossambicus*) fish meat: effect of sucrose and sorbitol. *Food Science and Biotechnology*, 26(5), 1177-1183.
34. Obatake, A. H. (1985). A rapid method to measure dark muscle content in fish. *Bull Jap. Soc. Sci. Fish*, 51(6), 1001-1004.
35. Regenstein, J. M., and Regenstein, C. E. (1984). *Food Protein Chemistry: An Introduction for Food Scientists (Food Science and Technology International)*. New York: Academic Press.
36. Shulgin, Yu. P., Shulgina, L. V., and Petrov, V. A. (2006). *Rapid Biological Assessment of the Quality and Safety of Raw Materials and Products of Living Aquatic Resources*. Vladivostok: PSEU.
37. Sipailiene, A. (2017). Advances in surimi processing (Book Chapter). *Trends in Fish Processing Technologies* (pp. 121-134 ). Boca Raton: CRC Press.
38. Yin, T., Yao, R., Ullah, I., Xiong, Sh., Huang, Q., You, J., Hu, Y., Shi, L. (2019). Effects of nanosized okara dietary fiber on gelation properties of silver carp surimi. *LWT – Food Science and Technology*, 111, 111-116.
39. Zhang, M.-L., Fan, Y., Zhang, J., Xiong, S.-B., and Liu, R. (2017). Effects of Heating Modes on the Mechanical Properties of Surimi Gels from Silver Carp (*Hypophthalmichthys molitrix*). *Modern Food Science and Technology*, 33(2), 129-135.
40. Zhang, N., Huang, C., and Ou, S. (2011). In vitro binding capacities of three dietary fibers and their mixture for four toxic elements, cholesterol, and bile acid. *Journal of Hazardous Materials*, 186(1), 236-239.

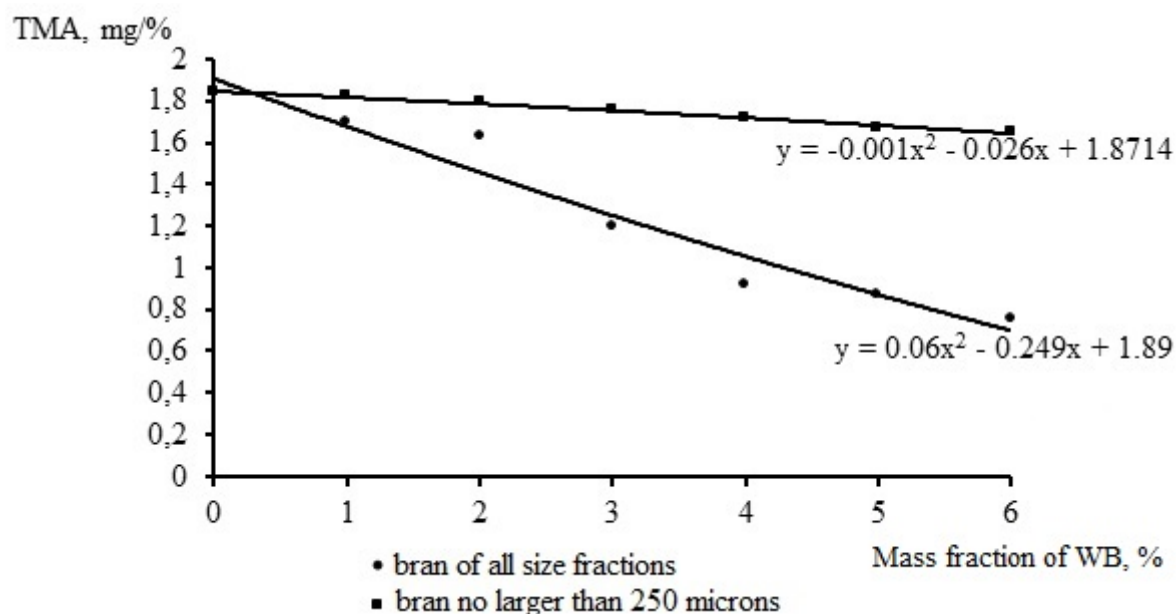


**Figure 1** - Dependence of the content of TMA in minced fish on the mass fraction of WB

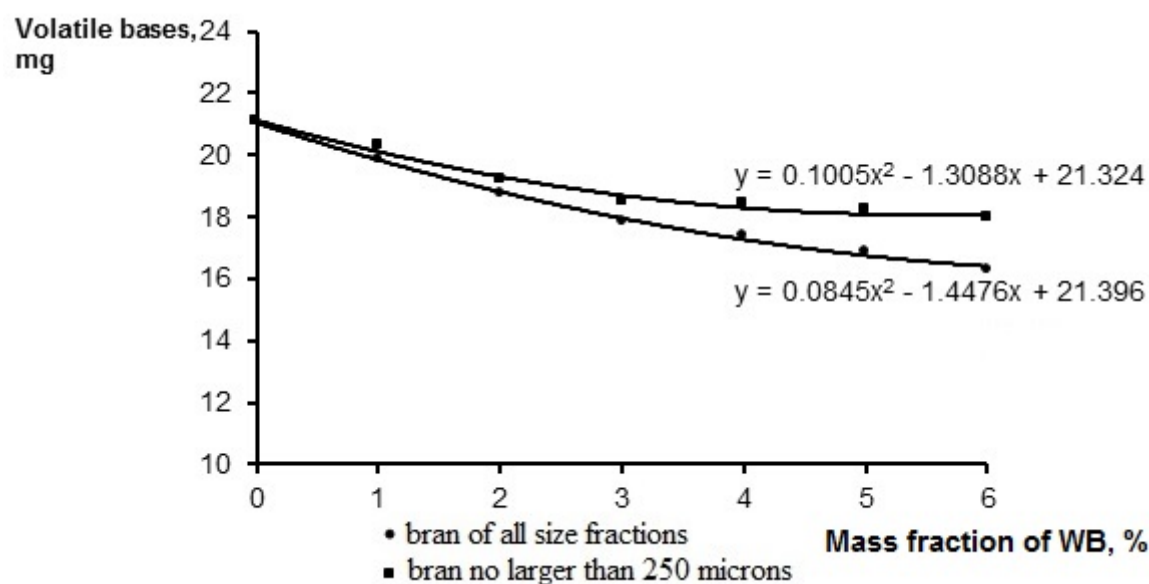


**Figure 2** - Dependence of the content of volatile bases in minced fish on the mass fraction of WB

**Table 1 - Composition of fatty acids of navaga muscle tissue (MT) and WB, in % of the total fatty acids**

| Fatty acids                            | MT           | MT after boiling | MT after scalding | MT with WB   | MT with WB after boiling | MT with WB after scalding | WB           |
|--|--------------|------------------|-------------------|--------------|--------------------------|---------------------------|--------------|
| 1                                      | 2            | 3                | 4                 | 5            | 6                        | 7                         | 8            |
| 12:0                                   | 0.11         | 0.12             | 0.10              | 0.10         | 0.10                     | 0.14                      | 0.03         |
| 14:0                                   | 1.80         | 1.94             | 1.65              | 1.38         | 1.28                     | 1.85                      | 0.12         |
| i-15:0                                 | 0.14         | 0.14             | 0.12              | 0.10         | 0.10                     | 0.12                      | 0.02         |
| 15:0                                   | 0.63         | 0.61             | 0.57              | 0.52         | 0.47                     | 0.55                      | 0.12         |
| i-16:0                                 | 0.13         | 0.14             | 0.14              | 0.12         | 0.11                     | 0.12                      | 0.01         |
| 16:0                                   | 19.69        | 19.52            | 19.31             | 19.05        | 19.03                    | 20.20                     | 16.47        |
| i-17:0                                 | 0.38         | 0.33             | 0.35              | 0.29         | 0.28                     | 0.26                      | -            |
| ai-17:0                                | 0.35         | 0.36             | 0.33              | 0.29         | 0.28                     | 0.26                      | 0.04         |
| 17:0                                   | 0.61         | 0.60             | 0.58              | 0.54         | 0.50                     | 0.51                      | 0.10         |
| i-18:0                                 | 0.19         | 0.18             | 0.17              | 0.15         | 0.15                     | 0.10                      | -            |
| 18:0                                   | 4.26         | 4.75             | 4.25              | 3.72         | 3.54                     | 4.02                      | 1.50         |
| 19:0                                   | 0.10         | 0.11             | 0.12              | 0.12         | 0.12                     | 0.12                      | 0.19         |
| 20:0                                   | 0.14         | 0.14             | 0.11              | 0.12         | 0.12                     | 0.17                      | 0.10         |
| <b>Amount of saturated</b>             | <b>28.53</b> | <b>29.04</b>     | <b>27.80</b>      | <b>26.50</b> | <b>26.08</b>             | <b>28.48</b>              | <b>18.74</b> |
| 14:1                                   | 0.14         | 0.13             | 0.10              | 0.10         | 0.10                     | 0.13                      | 0.08         |
| 15:1                                   | 0.23         | 0.12             | 0.10              | 0.10         | 0.10                     | 0.10                      | 0.05         |
| 16:1 $\omega$ 7                        | 4.75         | 4.74             | 4.50              | 3.99         | 3.68                     | 3.97                      | 0.37         |
| 16: $\omega$ 5                         | 0.28         | 0.28             | 0.26              | 0.25         | 0.24                     | 0.23                      | -            |
| 17:1                                   | 0.70         | 0.65             | 0.63              | 0.56         | 0.53                     | 0.53                      | -            |
| 18:1 $\omega$ 11                       | 0.24         | 0.27             | 0.24              | 0.23         | 0.22                     | 0.22                      | -            |
| 18:1 $\omega$ 9                        | 8.42         | 8.72             | 8.72              | 9.05         | 9.91                     | 11.35                     | 23.46        |
| 18:1 $\omega$ 7                        | 4.36         | 4.67             | 4.29              | 4.11         | 3.78                     | 3.60                      | 0.70         |
| 1                                      | 2            | 3                | 4                 | 5            | 6                        | 7                         | 8            |
| 18:1 $\omega$ 5                        | 0.21         | 0.26             | 0.20              | 0.19         | 0.18                     | 0.17                      | 0.02         |
| 19:1                                   | 0.25         | 0.12             | 0.18              | 0.17         | 0.20                     | 0.10                      | 0.03         |
| 20:1 $\omega$ 11                       | 0.29         | 0.30             | 0.23              | 0.22         | 0.18                     | 0.30                      | 0.21         |
| 20:1 $\omega$ 9                        | 0.37         | 0.36             | 0.28              | 0.36         | 0.39                     | 0.53                      | 0.34         |
| 20:1 $\omega$ 7                        | 0.21         | 0.16             | 0.19              | 0.22         | 0.16                     | 0.21                      | -            |
| 22:1 $\omega$ 11                       | 0.46         | 0.36             | 0.37              | 0.32         | 0.24                     | 0.53                      | -            |
| 24:1                                   | 0.27         | 0.26             | 0.34              | 0.25         | 0.32                     | 0.32                      | -            |
| <b>Amount of monoenoic</b>             | <b>21.18</b> | <b>21.40</b>     | <b>20.63</b>      | <b>20.12</b> | <b>20.23</b>             | <b>22.29</b>              | <b>25.26</b> |
| 16:2 $\omega$ 4                        | 0.78         | 0.79             | 0.58              | 0.67         | 0.61                     | 0.64                      | -            |
| 18:2 $\omega$ 9                        | 0.18         | 0.18             | 0.17              | 0.19         | 0.19                     | 0.21                      | -            |
| 18:2 $\omega$ 6                        | 1.17         | 1.24             | 1.06              | 4.49         | 10.94                    | 11.46                     | 51.88        |
| 18:2 $\omega$ 4                        | 0.22         | 0.23             | 0.19              | 0.22         | 0.17                     | 0.14                      | 0.04         |
| 18:3 $\omega$ 6                        | 0.10         | 0.11             | 0.10              | 0.13         | 0.18                     | 0.16                      | 0.07         |
| 18:3 $\omega$ 3                        | 0.42         | 0.46             | 0.41              | 0.66         | 1.08                     | 1.14                      | 3.82         |
| 18:4 $\omega$ 3                        | 0.48         | 0.53             | 0.49              | 0.46         | 0.41                     | 0.39                      | -            |
| 20:2 $\omega$ 6                        | 0.29         | 0.36             | 0.31              | 0.31         | 0.28                     | 0.27                      | 0.12         |
| 20:3 $\omega$ 6                        | 0.17         | 0.12             | 0.17              | 0.15         | 0.11                     | 0.10                      | -            |
| 20:4 $\omega$ 6                        | 4.07         | 4.26             | 4.20              | 4.02         | 3.60                     | 3.06                      | -            |
| 20:3 $\omega$ 3                        | 0.16         | 0.15             | 0.17              | 0.16         | 0.14                     | 0.10                      | -            |
| 20:4 $\omega$ 3                        | 0.33         | 0.33             | 0.36              | 0.31         | 0.28                     | 0.23                      | -            |
| 20:5 $\omega$ 3                        | 15.65        | 16.20            | 16.19             | 15.31        | 13.75                    | 12.09                     | -            |
| 21:5 $\omega$ 3                        | 0.19         | 0.18             | 0.22              | 0.21         | 0.16                     | 0.14                      | -            |
| 22:4 $\omega$ 6                        | 0.29         | 0.30             | 0.35              | 0.33         | 0.30                     | 0.20                      | -            |
| 22:5 $\omega$ 6                        | 0.62         | 0.54             | 0.69              | 0.64         | 0.56                     | 0.42                      | -            |
| 22:5 $\omega$ 3                        | 1.64         | 1.55             | 1.73              | 1.62         | 1.42                     | 1.21                      | -            |
| <b>Amount of polyene</b>               | <b>48.20</b> | <b>49.14</b>     | <b>50.27</b>      | <b>51.73</b> | <b>52.96</b>             | <b>48.43</b>              | <b>55.93</b> |
| <b>Amount of <math>\omega</math>6</b>  | <b>6.71</b>  | <b>6.93</b>      | <b>6.88</b>       | <b>10.52</b> | <b>15.97</b>             | <b>15.67</b>              | <b>52.07</b> |
| <b>Amount of <math>\omega</math> 3</b> | <b>40.31</b> | <b>41.01</b>     | <b>42.45</b>      | <b>40.13</b> | <b>36.02</b>             | <b>31.77</b>              | <b>3.82</b>  |

**Table 2 - Relative biological value of the samples**

| Sample for research | Number of ciliates during the transition to the stationary phase, cells | Biological activity of the object, cells/hour | Relative biological value, % |
|---------------------|---|---|------------------------------|
| Scalded             | 53 – 55   | 0.73 – 0.76                                   | 69 – 73                      |
| Fried in oil        | 48 – 50   | 0.67 – 0.69                                   | 63 – 66                      |
| Scalded with WB     | 49 – 51   | 0.68 – 0.71                                   | 65 – 68                      |
| Fried with WB       | 45 – 48   | 0.64 – 0.66                                   | 62 – 64                      |
| Whole cow's milk    | 75 – 77   | 1.04 – 1.07                                   | 100                          |

ESTUDO DA ATIVIDADE ANTIMICROBIANA DE *Tecoma stans* (L.) ex Kunth  
(BIGNONIACEAE)STUDY OF THE ANTIMICROBIAL ACTIVITY OF *Tecoma stans* (L.) ex Kunth  
(BIGNONIACEAE)GONÇALVES, Thaís Paula Rodrigues<sup>1</sup>; PARREIRA, Adriano Guimarães<sup>1</sup>;  
LIMA, Luciana Alves Rodrigues dos Santos<sup>1\*</sup><sup>1</sup>Campus Centro-Oeste Dona Lindu, Universidade Federal de São João Del Rei

\* Correspondence author

e-mail: luarsantos@ufsj.edu.br

Received 29 May 2020; received in revised form 15 June 2020; 03 July accepted 2020

## RESUMO

A resistência antimicrobiana tornou-se uma grande preocupação em todo o mundo. No presente trabalho, foi realizada a triagem fitoquímica do extrato etanólico e das frações de flores de *Tecoma stans* e avaliou-se o potencial antimicrobiano, através do ensaio de microdiluição em caldo sobre 10 isolados de interesse clínico. Também foi avaliada a interação das combinações de amostras de *T. stans* com antimicrobianos comerciais. As amostras de *T. stans* demonstraram atividade antibacteriana e potencial fungistático sobre *Proteus mirabilis*, *Proteus vulgaris*, *Staphylococcus aureus*, *Streptococcus mutans* e *Candida infanticola*, especialmente o extrato etanólico e as frações diclorometânica e acetatoetílica, com valores de Concentração Inibitória Mínima (CIM 2000 - 500 µg/mL). A combinação das amostras de *T. stans* com os antimicrobianos mostrou efeitos sinérgicos e aditivos. Nas combinações classificadas como interação sinérgica, observou-se que a CIM para o antimicrobiano, em combinação com as amostras de *T. stans*, foi reduzida de 2 a 7 vezes em comparação com a CIM para o antimicrobiano, quando utilizado isoladamente. Os melhores resultados foram encontrados para a combinação do extrato etanólico com amoxicilina sobre *P. mirabilis* e do extrato etanólico e da fração diclorometânica com tetraciclina sobre *S. aureus*. Testes de combinações do extrato e das frações de *T. stans* com antimicrobianos são inéditos, tornando esses resultados promissores. Na caracterização fitoquímica foi possível observar a presença de alguns compostos fenólicos, o que pode justificar o potencial antimicrobiano de *T. stans*. Destaca-se a importância de identificar novos agentes antimicrobianos, alguns dos quais podem estar presentes na flora inexplorada do Brasil.

**Palavras-chave:** Antimicrobiano, Extrato, Fitoquímica, Sinergismo.

## ABSTRACT

Antimicrobial resistance has become a significant concern worldwide. In the present work was performed the phytochemical screening of ethanol extract and fractions of *Tecoma stans* flowers, and evaluated the antimicrobial potential by a broth microdilution assay against 10 isolates of clinical interest. Also was assessed the interaction of combinations of *T. stans* samples with commercial antimicrobials. The samples of *T. stans* demonstrated antibacterial activity and fungistatic potential against *Proteus mirabilis*, *Proteus vulgaris*, *Staphylococcus aureus*, *Streptococcus mutans*, and *Candida infanticola*, especially the ethanol extract and the dichloromethane and ethyl acetate fractions, with Minimal Inhibitory Concentration values (MIC 2000 - 500 µg/mL). The combination of *T. stans* samples with antimicrobials showed synergistic and additive effects. In combinations classified as synergistic interaction, was observed that MIC for the antimicrobial in combination with the samples of *T. stans* was reduced by 2 to 7 times compared to the MIC for the antimicrobial when used alone. The best results were found for the combination of the ethanol extract with amoxicillin against *P.*

*mirabilis*, and the ethanol extract and the dichloromethane fraction with tetracycline against *S. aureus*. Tests of combinations of extract and fractions of *T. stans* with antimicrobials are unprecedented, making these results promising. In the phytochemical characterization, it was possible to observe the presence of some phenolic compounds, which may justify the antimicrobial potential of *T. stans*. It is important to highlight the identification of new antimicrobial agents, some of which may be present in the unexplored flora of Brazil.

**Keywords:** Antimicrobial, Extract, Phytochemistry, Synergism.

## 1. INTRODUCTION

The increasing resistance of fungi and bacteria to traditionally used antimicrobials represents one of the major concerns faced by humanity in recent times, associated with severe consequences such as an increase in microbial infections (Costa and Junior, 2017; Nikaido, 2009). Therefore, the production of drugs from natural products has been encouraged in several countries (Aumeeruddy-Elalfi *et al.*, 2015).

Higher plants may represent a promising alternative as they are capable of synthesizing compounds with antimicrobial activity, and these substances can be used against the development of infections in humans. In this sense, is highlight the phenolic compounds that are commonly associated with the antibacterial and antifungal activity of plants (Carvalho *et al.*, 2018; Lima *et al.*, 2016; Orhan *et al.*, 2010). Also, plant extracts can be combined with commercial antibiotics and present some interactions. These combinations can expand the spectrum of activity of antimicrobials, increasing their effectiveness in the treatment of infections, and reducing the minimum inhibitory concentration against resistant pathogens (Berg and Lubert, 2008; Casanova and Costa, 2017).

*Tecoma stans* (L.) ex Kunth is an exotic species found in Brazil, which is commonly used in ornamentation. In other countries, such as Mexico, this species is also used in traditional medicine to treat fungal infections and digestive problems (Singh *et al.*, 2013). However, only a few studies have reported its medicinal potential. Thus, this work evaluated the antimicrobial properties of *T. stans* flowers to confirm the medicinal potential of this species in Brazil.

## 2. MATERIALS AND METHODS

### 2.1. Plant material and extraction

The flowers of *T. stans* were collected in the Divinópolis municipality of MG state (coordinates 20°10'44"S, 44°55'6"W) in April

2018, according to the registration of botanical material collection performed at the SISBIO (no. 30006 in 20/03/2018). A voucher specimen was deposited in the institution herbarium Pesquisa e Agropecuária de Minas Gerais (EPAMIG/PAMG) and identified as *Tecoma stans* (L.) Juss. ex Kunth (PAMG 58384).

The flowers were dried in an oven at 40 °C for 7 days, crushed in a mechanical mill, and extracted with ethanol 70% in a proportion of 9:1 (ethanol/plant) by turbo extraction (Ultra-Turrax, MA-102 Plus). The solvent was removed in a rotary evaporator (IKA-HB10) to obtain the ethanol extract (EE, 37.49 g). Subsequently, 10 g of the obtained EE was solubilized in 100 mL of ethanol/water (7:3), and fractionated by a liquid-liquid partition, obtaining hexane (HEX, 0.62 g), dichloromethane (DCM, 1.19 g), ethyl acetate (AC, 5.41 g), and hydroethanol residue (HE, 2.08 g) fractions (Gonçalves, 2020).

### 2.2. Phytochemical analysis

The EE and fractions were submitted to phytochemical screening to evaluate the presence of the main classes of secondary metabolites for the identification of flavonoids, coumarins, saponin alkaloids, tannins, steroids, and triterpenoids (Matos, 2009; Silva *et al.*, 2010), characterized by chemical reactions that result in the development of staining, precipitation, and foams.

- A) Tannins: this test was performed by adding of FeCl<sub>3</sub> alcoholic solution 5% w/v (5 g/100 mL) with the formation of precipitate or not, being blue precipitate indicative of hydrolyzable tannins, and green precipitate indicative of condensed tannins (Matos, 2009; Silva *et al.*, 2010).
- B) Triterpenoids and steroids: this test was performed by the Liebermann-Buchard reaction (H<sub>2</sub>SO<sub>4</sub> + acetic anhydride). The upper phase of blue or green color indicated the presence of steroids, and red, pink, purple, or violet interphasic halo indicated the presence of triterpenes (Matos, 2009; Silva *et al.*, 2010).

- C) Saponins: the sample was shaken vigorously with distilled water for 1 minute, and the presence of persistent foam for 15 minutes indicated the presence of saponins (Matos, 2009; Silva *et al.*, 2010).
- D) Coumarins and anthraquinones: this test was performed by adding NaOH solution 1 M. The yellow color indicated the presence of coumarins, and violet to the purple color indicated the presence of anthraquinones (Silva *et al.*, 2010).
- E) Alkaloids: this test was performed by adding Drangendorff reagent with the formation of precipitate or not. The formation of insoluble and flocculent precipitate was indicative of the presence of alkaloids (Silva *et al.*, 2010).
- F) Flavonoids: this test was performed by adding of H<sub>2</sub>SO<sub>4</sub> concentrated solution. The yellow, orange or red color was indicative of flavonoids (Silva *et al.*, 2010).

### 2.3. Antimicrobial potential assay

The microorganisms used in this study originated from American Type Culture Collection (ATCC) and were provided by the microorganism reference laboratory of the Fundação Oswaldo Cruz (FIOCRUZ, Rio de Janeiro, Brasil). Eight species were used: *Klebsiella oxytoca* (ATCC 0182), *Proteus mirabilis* (ATCC 15290), *Proteus vulgaris* (ATCC 13315), *Enterobacter cloacae* (ATCC 23355), *Staphylococcus aureus* (ATCC 25923), *Staphylococcus epidermidis* (ATCC 12228), *Streptococcus mutans* (NCTC 10449), *Streptococcus agalactiae* (ATCC 13813). In antifungal tests, *Candida infanticola* (UFSJ6A), and *Candida glabrata* (ATCC 2001) were used.

The bacterial susceptibility test was performed according to the CLSI (Clinical and Laboratory Standards Institute) document guidelines M100-S25 (2015). The bacterial inoculum colonies isolated from a 24-hour growth streak were transferred to tubes containing saline solution 0.85% (p/v). Inoculum was prepared by dilution of a suspension corresponding to 0.5 on the McFarland density scale ( $DO_{530nm} = 0.19 - 0.21$ ) in Mueller-Hinton broth (MH) (1:10) to obtain a final inoculum with  $7.5 \cdot 10^5$  UFC/mL, which was used to assay. The fungal suspension was prepared in a similar way (NCCLS, 2002), to obtain a final inoculum with  $1 \cdot 10^3$  UFC/mL, which was used to assay. Stretch marks of 48 h of growth were used to obtain the suspension in saline, and later adjusted to 0.5 on the McFarland scale ( $DO_{530nm} = 0.19 - 0.21$ ), representing a cell density of approximately  $1 \cdot 10^6$  UFC/mL. To

obtain the final inoculum, two dilutions were performed, produced by transferring 20  $\mu$ L of the suspension to 980  $\mu$ L of Sabouraud dextrose (SD) broth and, subsequently, from 1 mL of the resulting suspension to 19 mL of SD broth. The samples were dissolved in water/DMSO (9:1), obtaining the initial concentration of 40 mg/mL. The MIC was carried out in 96-well polystyrene microplates containing 100  $\mu$ L of the liquid medium, 20  $\mu$ L of the samples solution (ranging from 2000 to 2  $\mu$ g/mL, dissolved in 9:1 water:dimethylsulfoxide), and 100  $\mu$ L of the different microbial inoculum in each well. After microdilution, they were incubated in a bacteriological incubator (Nova Instruments) at 37 °C for 24 h for bacteria, and at 28 °C for 48 h for yeasts, and the minimum inhibitory concentration (MIC) was defined as the lowest concentration of samples without visible growth of microorganisms. Subsequently, the minimal bactericidal concentration (MBC) was defined as the lowest concentration of samples that inhibit bacterial growth, as described by Lyu *et al.* (2016). Amoxicillin, tetracycline, and ketoconazole were used as positive controls. Water/dimethylsulfoxide (DMSO) 9:1 v/v was used as solvent control. The tests were carried out in triplicate wells, with three independent repetitions between them.

### 2.4. Evaluation of combinations

For the evaluation of synergistic, additive, or antagonistic effects between antimicrobials (amoxicillin and tetracycline), and *T. stans* samples that presented a MIC (inhibition between 1000 and 500  $\mu$ g/mL) against the tested microorganisms, the "checkerboard" method was used (Lee *et al.*, 2012; Oroojalian *et al.*, 2010). In the 96-well plates, the antimicrobial was added horizontally, and then *T. stans* samples were added vertically in concentrations of 125 to 0.9  $\mu$ g/mL, combined in a proportion of 1:1, to evaluate whether there is a combined antimicrobial effect. The resulting assay included a total of 64 combinations. After the distribution of the samples, 100  $\mu$ L of MH was added to each well with the bacterial inoculum at  $7.5 \cdot 10^5$  CFU/mL, and the plates were incubated in an oven at 35 °C for 16 to 20 hours. For the positive control, MH broth and microbial inoculum were used; only the MH broth was used for the sterility control, and water/dimethylsulfoxide (9:1) was used as the solvent control. As standards, amoxicillin and tetracycline antimicrobials were used. The MIC was determined for antimicrobials



and *T. stans* samples alone and in different combinations. After visual reading from those wells that had no microbial growth detected with the naked eye, the calculation of the fractional inhibitory concentration (FIC) of each compound was determined by Equations 1 to 3.

$$\text{FIC (antimicrobial)} = \text{MIC (antimicrobial) in combination} / \text{MIC (antimicrobial) alone} \quad (\text{Eq. 1})$$

$$\text{FIC (extract)} = \text{MIC (sample) in combination} / \text{MIC (sample) alone} \quad (\text{Eq. 2})$$

$$\text{FIC index (FICI)} = \text{FIC antimicrobial} + \text{FIC sample} \quad (\text{Eq. 3})$$

The combinations were considered synergic when  $\text{FICI} \leq 0.5$ , additive or indifferent at  $0.5 < \text{FICI} \leq 2.0$ , and antagonistic when  $\text{FICI} > 2.0$  (He and Chen, 2006; Oroojalian *et al.*, 2010; Palaniappan and Holley, 2010).

### 3. RESULTS AND DISCUSSION

The results of the phytochemical screening are presented in Table 1. In the EE, flavonoids, alkaloids, coumarins, saponins, and condensed tannins were observed. The HEX fraction contained alkaloids and steroids. The DCM, AC, and HE fractions were similar and contained alkaloids, saponins, and coumarins. In the DCM fraction, flavonoids were also observed, and the AC fraction also contained flavonoids, and condensed tannins. A previous study by Raju *et al.* (2011) confirmed the presence of flavonoids, saponins, tannins, and glycosides in the floral extracts of *T. stans*. Salvadó *et al.* (2002) showed the presence of triterpens, steroids, phenols, taninns, alkaloids, and flavonoids in dry and fresh leaves of *T. stans*.

The extract and fractions showed antimicrobial activity against *P. mirabilis*, *P. vulgaris*, *S. aureus*, *S. mutans*, and *C. infanticola*, except the HE fraction. The best results obtained in this study were for the EE, DCM, and AC fractions (Table 2). The EE and AC fraction exhibited an effect against *P. mirabilis*, and the AC fraction against *S. aureus* (MIC of 500 µg/mL and MBC of 1000 µg/mL). Some flavonoids have the ability to form antimicrobial barriers as a

response by plants to microbial infection. Thus, there has been an increase in the number of studies on flavonoids as potential antimicrobial agents (Gutiérrez-Venegas *et al.*, 2019). The presence of flavonoids in *T. stans* flowers may explain its antibacterial potential. Gutiérrez-Venegas *et al.* (2019) previously demonstrated antibacterial activity of the flavonoid apigenin against strains of *Escherichia coli*, *Enterococcus faecalis*, and *S. aureus* present in dental plaque.

The *T. stans* extract, and fractions that showed the most effective action in the MIC/MBC tests were submitted to the checkboard method to verify whether there were any interactions of these samples when combined with the commercial antimicrobials amoxicillin and tetracycline (Table 3). The samples showed synergistic and additive interactions when combined with commercial antimicrobials. In combinations classified as a synergistic interaction, we observed that the MIC for the antimicrobial in combination with *T. stans* samples was reduced by 2 to 7 times in comparison with the MIC of the antimicrobial when used alone. The best results were found for the combination of EE with amoxicillin against *P. mirabilis*, and EE and DCM fraction with tetracycline against *S. aureus*.

The association of plant extracts and antimicrobials has been observed previously. Araújo *et al.* (2014) reported the synergic potential of ethanol extracts from Lamiaceae species (*Melissa officinalis*, *Mentha* sp., *Ocimum basilicum*, *Plectranthus barbatus*, and *Rosmarinus officinalis*) with streptomycin against *E. faecalis*, *S. aureus*, *S. mutans*, *E. coli*, and *Pseudomonas aeruginosa*. The association of antimicrobials with medicinal plants or their derivatives in the treatment of microbial infections can increase the bioavailability of active substances, decrease toxicity and adverse effects, decrease resistance and increase therapeutic efficacy, allowing the use of these drugs when their effectiveness as a single agent in the treatment of infections is reduced (Chung *et al.*, 2011; Van Vuuren and Viljoen, 2011).

### 4. CONCLUSIONS

In conclusion, these results regarding the antimicrobial effect of *T. stans* flowers corroborate the data already presented in the literature, and this study is the first to report these effects in plants of this species from Brazil. The samples obtained from the flowers of *T. stans*

exhibited antimicrobial action against *P. mirabilis*, *P. vulgaris*, *S. aureus*, *S. mutans*, and *C. infanticola*, and that effect can be explained by the presence of phenolic compounds in these samples. The combination of plant samples with antimicrobials demonstrated an important interaction, potentiating the antimicrobial effects. The best results were observed for the combination of EE with amoxicillin against *P. mirabilis*, and EE and DCM fraction with tetracycline against *S. aureus*.

## 5. ACKNOWLEDGMENTS

We thank the *Universidade Federal de São João Del-Rei* (UFSJ), *Conselho Nacional de Desenvolvimento Científico e Tecnológico* (CNPq), *Fundação de Amparo à Pesquisa do Estado de Minas Gerais* (FAPEMIG), and *Coordenação de Aperfeiçoamento de Pessoal de Nível Superior* (CAPES) for all the support during the search. "This study was financed in part by the *Coordenação de Aperfeiçoamento de Pessoal de Nível Superior - Brasil* (CAPES) - Finance Code 001."

## 6. REFERENCES

- Costa, A. L. P., Junior, A. C. S. S. Resistência bacteriana aos antibióticos e saúde pública: uma breve revisão de literatura. *Estação Científica (UNIFAP)*, **2017**, 7, 45-57.
- Nikaido, H. Multidrug Resistance in Bacteria. *Annu. Rev. Biochem.*, **2009**, 78, 119-146.
- Aumeeruddy-Elalfi, Z., Gurib-Fakim, A., Mahomoodally, F. Antimicrobial, antibiotic potentiating activity, and phytochemical profile of essential oils from exotic and endemic medicinal plants of Mauritius. *Ind. Crop. Prod.*, **2015**, 71, 197-204.
- Carvalho, R. S., Carollo, C. A., De Magalhães, J. C., Palumbo, J. M. C., Boaretto, A. G., Nunes e Sá, I. C., Ferraz, A. C., Lima, W. G., de Siqueira, J. M., Ferreira, J. M. S. Antibacterial and antifungal activities of phenolic compound-enriched ethyl acetate fraction from *Cochlospermum regium* (Mart. Et. Schr.) Pilger roots: Mechanisms of action and synergism with tannin and gallic acid. *S. Afr. J. Bot.*, **2018**, 114, 181-187.
- Lima, V. N., Oliveira-Tintino, C. D. M., Santos, E. S., Morais, L. P., Tintino, S. R., Freitas, T. S., Geraldo, Y. S., Pereira, R. L. S., Cruz, R. P., Menezes, I. R. A., Coutinho, H. D. M. Antimicrobial, and enhancement of the antibiotic activity by phenolic compounds: gallic acid, caffeic acid, and pyrogallol. *Microb. Pathog.*, **2016**, 99, 56-61.
- Orhan, D. D., Özçelik, B., Özgen, S., Ergun, F. Antibacterial, antifungal, and antiviral activities of some flavonoids. *Microbiol. Res.*, **2010**, 165, 496-504.
- Berg, J. M. T., Lubert, J. *Bioquímica*. 6<sup>a</sup> ed. Guanabara Koogan, **2008**, 545p.
- Casanova, L. M., Costa, S. S. Synergistic interactions in natural products: Therapeutic potential and challenges. *Revista Virtual de Química*, **2017**, 9, 575-595.
- Singh, A., Nagori, B., Mathur, K. *Tecoma stans*: An important medicinal plant. *Int. J. Pharm.*, **2013**, 3, 13-21.
- Gonçalves, T. P. R. Estudo fitoquímico e avaliação do potencial antimicrobiano, sinérgico e antioxidante das flores de *Tecoma stans* (L.) Juss. ex Kunth (Bignoniaceae). Dissertação (Mestrado em Ciências Farmacêuticas). Universidade Federal de São João Del Rei, Divinópolis, **2020**.
- Silva, N. L. A., Miranda, F. A. A., Conceição, G. M. Triagem Fitoquímica de Plantas de Cerrado, da Área de Proteção Ambiental Municipal do Inhamum, Caxias, Maranhão. *Scientia Plena*, **2010**, 6, 1-17.
- Matos, F. J. A. Introdução à fitoquímica experimental. Edições UFC, **2009**, 150p.
- Clinical and Laboratory Standards Institute. Performance Standards for Antimicrobial Susceptibility Testing; Twenty-Fifth Informational Supplement. CLSI document M100-S25, **2015**, 35, 3-240.
- NCCLS. Reference Method for Broth Dilution Antifungal Susceptibility Testing of Yeasts; Approved Standard-Second Edition. NCCLS document M27-A2. Pennsylvania, United States, **2002**.
- Lyu, Y., Yang, Y., Lyu, X., Dong, N., Shan, A. Antimicrobial activity, improved cell selectivity, and mode of action of short PMAP-36-derived peptides against bacteria and *Candida*. *Sci Rep.*, **2016**, 6, 1-12.
- Lee, Y. S., Jang, K. A., Cha, J. D. Synergistic antibacterial effect between silibinin and antibiotics in oral bacteria. *J. Biomed. Biotechnol.*, **2012**, 1-7.

17. Oroojalian, F., Kasra-Kermanshahi, R., Azizi, M., Bassami, M.R. Phytochemical composition of the essential oils from three Apiaceae species and their antibacterial effects on food-borne pathogens. *Food Chem.*, **2010**, 120, 765-770.
18. He, L., Chen, W. Synergetic activity of nisin with cell-free supernatant of *Bacillus licheniformis* ZJU12 against food-borne bacteria. *Food Res. Int.*, **2006**, 39, 995-999.
19. Palaniappan, K., Holley, R. A. Use of natural antimicrobials to increase antibiotic susceptibility of drug-resistant bacteria. *Int. J. Food Microbiol.*, **2010**, 140, 164-168.
20. Raju, S., Kavimani, S., Uma, M. R. V., Sreeramulu, R. K. *Tecoma stans* (L.) Juss. Ex Kunth (Bignoniaceae): Ethnobotany, Phytochemistry, and Pharmacology. *J. Pharm. Biomed. Sci.*, **2011**, 8, 1-5.
21. Salvadó, A. C., Rivero, G. J., Naranjo, J. P. Droga cruda y extracto fluido de *Tecoma stans* L. *Rev. Cuba. Plantas Med.*, **2002**, 7, 138-141.
22. Gutiérrez-Venegas, G., Gómez-Mora, J. A., Meraz-Rodríguez, M. A., Flores-Sánchez, M. A., Ortiz-Miranda, L. F. Effect of flavonoids on antimicrobial activity of microorganisms present in dental plaque. *Heliyon*, **2019**, 5, 1-6.
23. Araújo, S. G., Alves, L. F., Pinto, M. E. A., Oliveira, G. T., Siqueira, E. P., Ribeiro, R. I. M. A., Ferreira, J. M. S., Lima, L. A. R. S. Volatile compounds of Lamiaceae exhibit a synergistic antibacterial activity with streptomycin. *Braz. J. Microbiol.*, **2014**, 45, 1341-1347.
24. Chung, P. Y., Navaratnam, P., Chung, L. Y. Synergistic antimicrobial activity between pentacyclic triterpenoids and antibiotics against *Staphylococcus aureus* strains. *Ann. Clin. Microbiol. Antimicrob.*, **2011**, 10, 25-31, 2011.
25. Van Vuuren, S., Viljoen, A. Plant-based antimicrobial studies - methods and approaches to study the interaction between natural products. *Planta Med.*, **2011**, 77, 1168-1182.

**Table 1.** Phytochemical analysis of flower extract and fractions of *T. stans*.

| Secondary metabolites | EE | HEX | DCM | AC | HE |
|-----------------------|----|-----|-----|----|----|
| Alkaloids             | +  | +   | +   | +  | +  |
| Anthraquinones        | -  | -   | -   | -  | -  |
| Coumarins             | +  | -   | +   | +  | +  |
| Steroids              | -  | +   | -   | -  | -  |
| Triterpenoids         | -  | -   | -   | -  | -  |
| Flavonoids            | +  | -   | +   | +  | -  |
| Saponins              | +  | -   | +   | +  | +  |
| Condensed Tannins     | +  | -   | -   | +  | -  |
| Hydrolyzable Tannins  | -  | -   | -   | -  | -  |

EE: ethanol extract; HEX: hexane fraction; DCM: dichloromethane fraction; AC: ethyl acetate fraction; HE: hydroethanol fraction; (+): Presence; (-): Absence.

**Table 2.** MIC values (MBC/MFC) in µg/mL of microorganisms when treated with the extract and fractions.

| Strains               | EE             | HEX          | DCM            | AC            | AMX          | TETRA        | KETZ          |
|-----------------------|----------------|--------------|----------------|---------------|--------------|--------------|---------------|
|                       | MIC<br>(MBC)   | MIC<br>(MBC) | MIC<br>(MBC)   | MIC<br>(MBC)  | MIC<br>(MBC) | MIC<br>(MBC) | MIC<br>(MFC)  |
| <i>P. mirabilis</i>   | 500<br>(1000)  | -            | 1000<br>(2000) | 500<br>(1000) | 7<br>(15)    | 60<br>(125)  | -             |
| <i>P. vulgaris</i>    | -              | 2000<br>(-)  | 2000<br>(-)    | 2000<br>(-)   | 125<br>(250) | 7<br>(15)    | -             |
| <i>S. aureus</i>      | 1000<br>(2000) | 2000<br>(-)  | 500<br>(1000)  | -             | 15<br>(30)   | 7<br>(15)    | -             |
| <i>S. mutans</i>      | 2000<br>(-)    | -            | -              | -             | 15<br>(30)   | 15<br>(30)   | -             |
| <i>C. infanticola</i> | -              | -            | 2000<br>(-)    | 2000<br>(-)   | -            | -            | 500<br>(1000) |

EE: ethanol extract; HEX: hexane fraction; DCM: dichloromethane fraction; AC: ethyl acetate fraction; AMX: amoxicillin; TETRA: tetracycline; KETZ: ketoconazole; MIC: minimum inhibitory concentration; MBC and MFC: minimum bactericidal and fungicidal concentration; - value not determined.

**Table 3.** FICI values of different combinations of samples of *T. stans* and commercial antibacterials on some microorganisms.

| Samples             | MIC in combination<br>µg/mL | MIC alone<br>µg/mL | FIC    | FICI   | Activity                |
|---------------------|-----------------------------|--------------------|--------|--------|-------------------------|
| <i>P. mirabilis</i> |                             |                    |        |        |                         |
| 1. EE               | 2                           | 500                | 0.0040 | 0.1325 | Synergistic             |
| 2. AMX              | 0.9                         | 7                  | 0.1285 |        |                         |
| 1. EE               | 3                           | 500                | 0.0060 | 2.0893 | Additive or Indifferent |
| 2. TETRA            | 125                         | 60                 | 2.0833 |        |                         |
| 1. DCM              | 0.9                         | 1000               | 0.0009 | 0.2866 | Synergistic             |
| 2. AMX              | 2                           | 7                  | 0.2857 |        |                         |
| 1. DCM              | 3                           | 1000               | 0.0030 | 2.0863 | Additive or Indifferent |
| 2. TETRA            | 125                         | 60                 | 2.0833 |        |                         |
| 1. AC               | 0.9                         | 500                | 0.0018 | 0.4303 | Synergistic             |
| 2. AMX              | 3                           | 7                  | 0.4285 |        |                         |
| 1. AC               | 125                         | 500                | 0.2500 | 1.2500 | Additive or Indifferent |
| 2. TETRA            | 60                          | 60                 | 1      |        |                         |
| <i>S. aureus</i>    |                             |                    |        |        |                         |
| 1. EE               | 7                           | 1000               | 0.0070 | 0.4736 | Synergistic             |
| 2. AMX              | 7                           | 15                 | 0.4666 |        |                         |
| 1. EE               | 2                           | 1000               | 0.0020 | 0.1305 | Synergistic             |
| 2. TETRA            | 0.9                         | 7                  | 0.1285 |        |                         |
| 1. DCM              | 0.9                         | 500                | 0.0018 | 0.4684 | Synergistic             |
| 2. AMX              | 7                           | 15                 | 0.4666 |        |                         |
| 1. DCM              | 3                           | 500                | 0.0060 | 0.1345 | Synergistic             |
| 2. TETRA            | 0.9                         | 7                  | 0.1285 |        |                         |

EE: ethanol extract; DCM: dichloromethane fraction; AC: ethyl acetate fraction; AMX: amoxicillin; TETRA: tetracycline.

**TECNOLOGIAS DA INFORMAÇÃO PARA DETERMINAR O PERÍODO ÓTIMO DE PREPARAÇÃO DE ALIMENTOS A PARTIR DE ERVAS DE CEREAIS PERENES****INFORMATION TECHNOLOGIES FOR DETERMINATION THE OPTIMAL PERIOD OF PREPARING FODDER FROM PERENNIAL GRASSES****ИНФОРМАЦИОННЫЕ ТЕХНОЛОГИИ ОПРЕДЕЛЕНИЯ ОПТИМАЛЬНЫХ СРОКОВ ЗАГОТОВКИ КОРМОВ ИЗ МНОГОЛЕТНИХ ЗЛАКОВЫХ ТРАВ**

KHUDYAKOVA, Elena V.<sup>1\*</sup>; KHUDYAKOVA, Hatima K.<sup>2</sup>; SHITIKOVA, Aleksandra V.<sup>3</sup>; SAVOSKINA, Olga A.<sup>4</sup>; KONSTANTINOVICH, Anastasiia V.<sup>5</sup>;

<sup>1</sup> Russian State Agrarian University – Moscow Timiryazev Agricultural Academy, Department of Applied Informatics, 49 Timiryazevskaya Str., zip code 127550, Moscow – Russian Federation

<sup>2</sup> Federal Williams Research Center of Forage Production and Agroecology, Laboratory of Physical and Chemical Research Methods, 1 Nauchnyy Gorodok, zip code 141055, Lobnya – Russian Federation

<sup>3</sup> Russian State Agrarian University – Moscow Timiryazev Agricultural Academy, Department of Crop Production and Meadow Ecosystems, 49 Timiryazevskaya Str., zip code 127550, Moscow – Russian Federation

<sup>4</sup> Russian State Agrarian University – Moscow Timiryazev Agricultural Academy, Department of Agriculture and Field Research Methods, 49 Timiryazevskaya Str., zip code 127550, Moscow – Russian Federation

<sup>5</sup> Russian State Agrarian University – Moscow Timiryazev Agricultural Academy, Department of Vegetable Growing, 49 Timiryazevskaya Str., zip code 127550, Moscow – Russian Federation

*\* Correspondence author*

*e-mail: khud.elena2017@yandex.ru*

Received 22 April 2020; received in revised form 29 June 2020; accepted 03 July 2020

**RESUMO**

A eficácia da criação de gado é amplamente determinada por uma base sólida de alimentação. Atualmente, a produtividade do gado na Federação Russa está aumentando e isso requer uma abordagem mais cuidadosa para avaliar a qualidade da alimentação. Isso, em primeiro lugar, diz respeito a tipos de alimentos como feno, silagem, haylage, que representam 60-85% da dieta diária média dos animais. O valor nutricional desses tipos de alimentos depende em grande parte do conteúdo e da proporção de proteína bruta e fibra bruta nas ervas perenes quando são colhidas. Nos estágios iniciais do desenvolvimento da planta, a proteína bruta predomina em sua composição e o teor de fibras é insuficiente. Portanto, cortar ervas perenes nesse período é irracionalmente. Com o crescimento e desenvolvimento da planta, sua transição para o estágio da emergência da espiga, o teor de proteína bruta diminui com o aumento do teor de fibras. A colheita de ervas perenes durante o período em que contêm uma grande quantidade de fibras e baixa proteína também é irracional, uma vez que o baixo teor de proteína nos alimentos não contribui para o crescimento da produtividade animal. O momento ideal para a colheita das ervas é considerado o momento em que o teor de proteína bruta é de 14 a 16% e da fibra bruta – 26 a 28%. Determinar o conteúdo desses elementos é um processo bastante trabalhoso e caro, a análise dura cerca de 3 dias. Somente grandes empresas agrícolas podem se dar ao luxo de realizar essas análises. Ao mesmo tempo, hoje existem tecnologias para exame remoto de culturas, que neste caso podem ser realizadas usando veículos aéreos não tripulados (VANTs). Atualmente, com a ajuda deles, determina-se o teor de nitrogênio nas plantas. Os autores deste artigo propõem uma técnica digital para determinação remota de fibra bruta e proteína bruta, que determina o momento ideal da preparação de alimentos.

**Palavras-chave:** *composição dos alimentos, análise remota, composição química das plantas, veículos aéreos não tripulados, sensores infravermelhos de nitrogênio.*

## ABSTRACT

The effectiveness of cattle breeding is mostly determined Forage base. Currently, cattle productivity in the Russian Federation is increasing, and this requires a more careful approach to assessing the quality of feed. This primarily applies to such types of feed like hay, silage, haylage, which make up 60-85% in the average daily diet of livestock. The nutritional value of these types of feed depends mostly on the content and ratio of crude protein and crude fiber in perennial grasses when they are harvested. In the early phases of plant development, crude protein predominates in its composition, and the fiber content is insufficient. Therefore, mowing perennial grasses in these terms is irrational. With the growth and development of the plant, its transition to the heading stage, the crude protein content decreases with increasing fiber content. Harvesting perennial grasses at a time when they contain a large amount of fiber and low protein is also irrational since the low protein content in feed does not contribute to the growth of animal productivity. The optimum time for harvesting herbs is considered to be the time when the crude protein content is 14-16%, and crude fiber – 26-28%. Determination the content of these elements is a rather laborious and expensive process, the analysis lasts about three days. Only large agricultural enterprises can afford to carry out such analyses. At the same time, today, there are technologies for remote sensing of crops, which in this case can be carried out using unmanned aerial vehicles (UAVs). Currently, with their help, the nitrogen content in plants is determined. The authors of this paper propose a digital technique for remote determination of crude fiber and crude protein, which determines the optimal timing of the harvesting herbs.

**Keywords:** *feed composition, remote analysis, chemical composition of plants, unmanned aerial vehicles, infrared nitrogen sensors.*

## АННОТАЦИЯ

Эффективность скотоводства во многом определяется прочной кормовой базой. В настоящее время продуктивность крупного рогатого скота в Российской Федерации возрастает и это требует более внимательного подхода к оценке качества кормов. Это, прежде всего, касается таких видов кормов, как сено, силос, сенаж, которые составляют в среднесуточном рационе скота 60-85%. Питательность этих видов кормов во многом зависит от содержания и соотношения сырого протеина и сырой клетчатки в многолетних травах при их заготовке. На ранних фазах развития растения в его составе преобладает сырой протеин, а содержание клетчатки недостаточно. Поэтому скашивание многолетних трав в эти сроки нерационально. С ростом и развитием растения, переходом его в фазу колошения содержание сырого протеина уменьшается при увеличении содержания клетчатки. Заготовка многолетних трав в период, когда в них содержится большое количество клетчатки и мало протеина – также нерациональна, так как низкое содержание протеина в кормах не способствует росту продуктивности животных. Оптимальными сроками заготовки трав считаются те сроки, когда содержание сырого протеина составляет 14-16%, а сырой клетчатки – 26-28%. Определение содержания данных элементов – довольно трудоемкий и дорогостоящий процесс, анализ длится около 3 дней. Только крупные сельскохозяйственные предприятия могут позволить себе производить такие анализы. В то же время сегодня существуют технологии дистанционного зондирования посевов, которые могут в данном случае осуществляться при помощи беспилотных летательных аппаратов (БПЛА). В настоящее время с их помощью определяется содержание азота в растениях. Авторы данной статьи предлагают цифровую методику дистанционного определения содержания сырой клетчатки и сырого протеина, что определяет оптимальные сроки заготовки корма.

**Ключевые слова:** *состав кормов, дистанционный анализ, химический состав растений, беспилотные летательные аппараты, инфракрасные датчики азота.*

## 1. INTRODUCTION

At the present moment, the meat and dairy cattle breeding industry in the Russian Federation continues to reduce production volumes. Among the main reasons are the long production cycle in these sub-sectors and the need to develop a related industry such as feed production with significant sown areas of fodder crops and fodder

land, a long train of equipment, which determines a significant investment and a low rate of return on investment (Khudyakova *et al.*, 2018). This reduces the food security of the Russian Federation in milk and dairy products, as well as in beef. In this regard, the search for ways to increase the efficiency of animal husbandry is very urgent, one of these ways is to strengthen the feed base – providing livestock with high-quality feed,

increasing feed output while reducing the cost of feed production (Shuai *et al.*, 2019). This can be achieved in many ways due to adherence to feeding production technology. In particular – due to the procurement of feed in optimal terms (Karydas *et al.*, 2020).

In the structure of the feed ration of livestock, a significant part (60-85%) consists of feed produced from perennial grasses – hay, silage, haylage. This paper is devoted to the chemical analysis of the quality of perennial grasses in order to determine the optimal term for their mowing. Large agricultural enterprises, agricultural holdings, which have their laboratories for the analysis of feed, analyse the content of crude protein daily to determine the optimal harvesting time (Schmidhuber and Tubiello, 2007; Misselhorn *et al.*, 2012). This is a time consuming and expensive process. About 1% of agricultural enterprises in the Russian Federation have such laboratories, which is not enough. Moreover, this issue is being resolved in the Russian Federation for significant sown areas of perennial and annual grasses. Currently, the grass area is 18.3% of the cultivated area of the Russian Federation and 90.2% of the cultivated area of fodder crops (Agriculture in Russia, 2019). Despite the determined tendency to reduce the area under forage crops in general, and forage grasses, in particular, they occupy a relatively large area – 14544 thousand hectares (Table 1).

Determining the optimal harvesting time for perennial grasses is an important task. As the herbs grow, the collection of dry matter increases. However, at the same time, their quality may deteriorate in terms of feed value (Kasakova *et al.*, 2019; Tynybekov *et al.*, 2013; Pashtetsky *et al.*, 2018). As a rule, this is expressed in a decrease in the content of crude protein and the accumulation of the fibrous fraction – crude fiber, which leads to a deterioration in the digestibility of the resulting feed and its energy value. In this regard, it is necessary to choose the harvesting dates when the quality would be high enough, at the same time, without compromising yield (Laliberte *et al.*, 2011; Astor *et al.*, 2018).

The nutritional value of perennial herbs is primarily determined by the content of crude protein and fiber. The digestibility of the feed and energy content depends on the fiber content. The productivity of animals directly depends on the amount of protein (Pashtetsky *et al.*, 2018; Pashtetskiy *et al.*, 2020). And therefore, these two criteria should be in the optimal combination to establish the timing of cleaning. It is believed that under production conditions, these parameters

correlate with each other. So, the content of crude fiber in the silage and haylage of the 1st class should not exceed 26-28 in dry matter, with a crude protein level of at least 14-16% (Stepanova, 2019).

## 2. MATERIALS AND METHODS

The main suggestion of the study is to determine protein and fiber in plants by remote sensing of perennial grass crops using unmanned aerial vehicles equipped with special nitrogen sensors. The operation of sensors for non-contact measurement of nitrogen in plant leaves is based on taking into account the degree of light or laser beams reflection from the plant leaf. The more chlorophyll in the leaf, the higher the nitrogen content and the higher the degree of reflection. Sensors can be mounted, for example, on the roof of a tractor or on an UAVs. Such sensors are widely marketed. For example, sensors such as the CropSpec™ Vegetation Level Sensor or the YARA N-Sensor (AgriCon company). And the principle of operation of the N-sensor MiniVeg N system is based on the excitation of chlorophyll by laser beams. This sensor is mounted on the front of the tractor. Sensors can also be portable and displaceable, as for example CCM-200 PLUS sensor (USA). Information technologies such as satellite navigation, unmanned vehicles, and aircraft (UAVs) equipped with all kinds of sensors, IoT-platforms, and Big Data are actively being introduced into agriculture today (Khudyakova *et al.*, 2018). In particular, in solving the problem posed above, technologies for remote sensing of crops can be used. Determination of the critical phase of growth of fodder culture can be carried out using special sensors that are mounted on static installations or UAVs. Together with the analysis of weather data carried out by other sensors mounted on the same devices, they can help determine the optimal harvesting time for forage crops concerning a specific place on the field.

This is the task of precision farming (Karydas *et al.*, 2020; Ismailova *et al.*, 2016; Tarshilova *et al.*, 2016). The International Precision Agriculture Society (ISPA) defined this term as “a management strategy that collects, processes and analyses temporal, spatial and other data, and combines them with other information to support management decisions to improve the use of resources to increase efficiency, productivity, quality, profitability and sustainability of agriculture (International society of precision..., 2019). Precision farming can

significantly increase the efficiency of agricultural production, both due to resource-saving and due to the implementation of a host of measures in optimal terms, which, as in this case, ensures the optimal content of nutrients in the feed and contributes to the growth of livestock productivity by increasing the rate of feed output (Bongiovanni and Lowenberg-DeBoer, 2004; Schmidhuber and Tubiello, 2007; Misselhorn *et al.*, 2012; Lowenberg-DeBoer and Erickson, 2019). The results of multispectral remote sensing from unmanned aerial vehicles and their application in pasture conditions, including low-flying drones, were described in (Laliberte *et al.*, 2011; Astor *et al.*, 2018). Characterisation of plant growth parameters and yield forecasting was done in (Zhou *et al.*, 2017; Shuai *et al.*, 2019; Yudaev *et al.*, 2019).

To solve the problem of non-contact determination of the crude protein content in perennial grasses, we can also use the method of reconnaissance diagnostics of plant conditions using unmanned aerial vehicles (The technique of remote..., 2011). The method involves the formation of a specific reference area of a homogeneous surface next to the field to be tested; the establishment of the boundaries of several control sites in a field with varying degrees of plant density; aerial photography of the field with UAVs with multispectral images. Next, the nitrogen content in plants is measured at control sites using a nitrogen tester, and a spectroradiometer is used to perform ground-based measurements of the spectral brightness of point objects on a reference site and the spectral brightness of a calibration panel. The ground-based spectral brightness coefficients (GSB) are determined by dividing the results of measuring the areas on the reference site with a spectroradiometer by the measurement result of the calibration panel, with the result reduced to the range 0-1 (0-100%). Further, the obtained results are transferred to a computer, where, using special processing, a multispectral orthophoto map of the diagnosed field is formed. Next, atmospheric-corrected GSBs for each pixel of the orthomosaic are calculated by regressing the initial brightness values of the pixels obtained directly during aerial photography to the GSB obtained from ground-based measurements of the reference sites included in the orthomosaic. A normalised difference vegetation index (NDVI) map is constructed, showing the nitrogen content in the plants of the diagnosed field. Calibrate the resulting maps using ground measurement data from reference sites.

To obtain images of crops of perennial grasses to determine the content of nitrogen and digestible protein in plants, UAVs of both airplane, helicopter, and multicopters types can be used. At the same time, the last two species are considered the most acceptable option, since they do not require special take-off space and are able to "hover" over the object. Specialists recommend using the following UAVs for these purposes (Table 2). Today, the market offers several dozen types of UAVs that can be used for the above purposes (Korotaev and Novopashin; 2018 RoboTrends, 2018).

The operation of sensors for non-contact measurement of nitrogen in plant leaves is based on taking into account the degree of light or laser beams reflection from the plant leaf. The more chlorophyll in the leaf, the higher the nitrogen content and the higher the degree of reflection. Such sensors are widely marketed. So, for example, Figure 1 shows the Resonon Pika-L hyperspectral sensor, which has 281 spectral channels (spectral range 400-1000 nm), a lens with a field of view of 17.6 degrees. The camera is mounted on the DJI S1000 octocopter. Sensors can also be mounted on the roof of the tractor (Figure 2).

Compared to static field stations, UAVs have a number of advantages such as high quality of collected data, high quality of image resolution, relatively low price, the ability to select and integrate various sensors. The drones are equipped with various modern technologies such as infrared cameras, GPS, and LASER. UAVs monitor the state of nitrogen to establish the adequacy of its concentration. An analysis of the ripeness of crops and grass using UAVs was carried out in (Honkavaara *et al.*, 2012; Tlesova *et al.*, 2018). The advantages of Spatio-temporal sounding of UAVs in comparison with remote sensing are shown in (Berni *et al.*, 2009; Schwarzbach *et al.*, 2009).

To determine the content of structural carbohydrates, empirical methods are usually used to ensure the separation of carbohydrates according to their digestibility in the process of animal nutrition. So, in the framework of the analysis of feed according to the Weende analysis, the level of structural substances is estimated by the content of crude fiber (CF). However, CF does not represent the sum of indigestible substances, as well as the whole amount of structural carbohydrates (SC), some of which, as well as part of lignin, are removed during its determination and enter, along with non-structural carbohydrates, in the fraction of nitrogen-free extractive substances



(NFE), which includes carbohydrates, significantly different in their digestibility. At the same time, knowledge of the entire amount of SC and its individual components is necessary for a more accurate prediction of feed consumption and digestibility. Neutral-detergent fiber (NDF), representing the total amount of SC and lignin, is one of the most important indicators of feed quality. The feed consumption (Mertens, 2010), its nutritional value (Weiss, 1998), and, ultimately, the productive effect, depending on its level and digestibility. Since the end of the last century, the assessment of feed and rations for the content of detergent forms of fiber in them has become widespread throughout the world. Analysis methods are standardised at the international and interstate levels (GOST ISO 13906-2013, 2013; GOST ISO 16472-2014, 2014). In Russian Federation, some forages and forage grasses were also examined by the level of acid-detergent fiber (ADF) and NDF in the conditions of the Moscow, Kaluga, and Orenburg regions (Vorobyova, 2002; Kharitonov *et al.*, 2008; Levakhin *et al.*, 2015) and Tatarstan (Bykova and Gibadullina, 2010), studies were carried out to study the digestion in bull calves (Levakhin *et al.*, 2007; Bykova and Gibadullina, 2010) and cows (Kharitonov and Khotmirova, 2009) depending on the content of structural carbohydrates in the diet. However, there is still insufficient information on the levels of ADF and NDF in different types of forage grasses, depending on the phase of vegetation and other conditions. Partly in connection with this, forages feed standards (GOST R 55986-2014, 2014) contain standards for CF content, but there are no requirements for levels of detergent forms of fiber.

### 3. RESULTS AND DISCUSSION:

In practical activities, the harvesting time is set based on the phase of growth of plants. For example, for preparing silage, it is recommended to mow grass in the phase of the beginning of the heading, for haylage – in the phase of the end of going booting and the beginning of heading. But the problem is that this or that phase does not occur simultaneously and can last quite a long time – depending on the type of grass. For example, the booting phase lasts up to 20 days. The heading and flowering phase is 7-10 days. During the same phase, the composition of plants changes. The composition of plants can be different in the same phase of development, depending on weather conditions. For example, with a lack of moisture in combination with adverse temperature conditions, even in the phase of the

beginning of booting, the content of crude fiber can reach the level of the earing phase - 30% or more. Therefore, the optimal harvesting time is determined by daily analyses during the harvesting period.

The crude protein content in the feed is related to the nitrogen content. Currently, the nitrogen content in herbs is determined as follows. Herbal samples are taken by a special method. Further, herbs dried at a temperature of 60-65°C in an oven with forced ventilation are grounded until they pass through a sieve with 1 mm openings. A portion of the feed is burned in concentrated sulfuric acid in the presence of a catalyst, and the amount of ammonia formed is determined in one way or another. The ammonia content is determined by the nitrogen content.

Large farms that have reached a high level of animal productivity are forced to conduct such analyses in order to procure high-quality feed daily. But it is quite laborious and expensive. Analysis by conventional chemical methods takes at least three days. Therefore, special studies are carried out in order to develop methods for optimal timing of grass harvesting without analysis. So, sometimes regression equations are used that relate the composition of the plants to their height, the sum of the temperatures, and the amount of rainfall during the growing season of grass. But this requires lengthy research over several years with field trials. The quality of the statistical prediction of the composition is poor.

Precision farming is based on information management and has been made possible thanks to many technological innovations based on information technology. These technologies allow the farmer to receive large amounts of information regarding the state of the soil (moisture content of nutrients in it), the state of crops, and the state of the environment. With this information, management decisions become more appropriate and effective. Information technologies used directly in the field make it possible to isolate from the whole set of factors precisely those whose impact will give the highest results, in particular the yield of forage crops. Ultimately, this increases the profitability of production and its stability (Plant *et al.*, 2000). In particular, remote sensing of crops can be used to determine the crude protein content in feed crops. The ability to determine crude protein (crude protein) in a plant provides a determination of its nitrogen content. It can be determined by multiplying the nitrogen content by 6.25 since the nitrogen concentration in most proteins is, on average, 16%.

Currently, the most common form of remote sensing, including for determining the nitrogen content in plant leaves, is electromagnetic radiation, which is detected by sensors installed on a variety of media - satellites, drones, agricultural machinery, various static installations in the field. Most widely used in agriculture are wavelengths, such as visible light, near-infrared, and thermal infrared. And if thermal infrared radiation is mainly used to remotely determine the stress level of a plant as a result of a lack of nutrients, moisture, etc., then near-infrared radiation can be used to test the content of nutrients in the plant.

Currently, many different sensors have been developed for smart crop production. For example, CLAAS today offers the CROP SENSOR sensor for the biomass and nitrogen index, equipped with a measuring system with four high-power LEDs (How do drones work..., 2019). The measurement frequency of such a sensor is 800 units per second, regardless of the time of day or the nature of the lighting. Such sensors are manufactured by the company for subsequent mounting on equipment traveling in the field, but similar sensors can be installed on low-flying UAVs.

The UAVs listed above and several dozen similar ones using a multispectral camera make it possible to obtain accurate maps of the vegetation index (NDVI), which can serve as the basis for determining the digestible protein content in forage grasses, in increments of up to several centimeters (Figure 3).

An interesting solution was developed by the German company Fritzmeier, which offers agricultural producers the ISARIA plant stand sensor (Sergeev, 2019). Similar tasks are performed by, for example, the Topcon CropSpec sensor system. Sensors installed on this system scan plants in order to detect chlorophyll content, since this indicator correlates with the nitrogen content in plant leaves (CropSpec™ vegetation..., 2019). Such sensors are used to determine the amount of nitrogen in plants in order to determine the doses of accurate fertilizer application. However, we propose the use of such systems to determine the optimal timing of grass harvesting for fodder storage. The flight control system communicates with an assistant installed on a personal computer (PC) via a Micro-USB cable. This allows us to configure UAVs and update their firmware (Agriculture in Russia, 2019). The architecture of a remote monitoring system for crude protein content in perennial grasses (determining the optimal mowing time for

perennial grasses) may include subsystems traditional for similar monitoring (Lupyan *et al.*, 2015): data acquisition subsystem; data processing subsystem; subsystem for maintaining data archives; subsystem of data presentation and analysis; system control and monitoring unit.

Knowing the content of nitrogen (protein) in plants, we can determine the fiber content. This term is called structural carbohydrates (SC) together with lignin, which makes up the cell walls of plants. Structural carbohydrates include pectin, hemicellulose (HC), and cellulose (C) (Bailey, 1973). They are a source of energy for ruminants, which, with the help of the microflora of the gastrointestinal tract, are able to partially digest them. It should also be noted the physiological role of structural substances, which consists in ensuring the normal functioning of the rumination and motor function of the gastrointestinal tract.

How to determine the content of crude fiber in plants? There is an inverse relationship between the crude protein content in plants and the crude fiber content. So, for example, experiments conducted at the V.R. Williams All-Russian Research Institute of Feed on alfalfa showed the following regression equation between the content of crude fiber and crude protein in alfalfa in the flowering phase (Stepanova, 2019):  $Y = -1.5x + 56.6$  (correlation coefficient  $r = -0.83 \pm 0.15$  ( $tr = 5.4$   $9 > t_{01} = 2.98$ )). In the non-chernozem zone of Russia, in the crops of perennial grasses, a significant proportion of cereal grasses such as brome, meadow fescue, and timothy grass meadow occupy a significant share. This species of grasses and feed from them occupy a high share in the feed balance of ruminants. The content of crude fiber and crude protein in these grasses in the conditions of central Russia, depending on the vegetation phase, obtained by the authors of this article, are given in Table 3.

The correlation between crude protein and crude fiber in these grasses are close (Figure 4) (Equation 1):

$$Y = 43.41 - 1.13X \quad (R^2 = 0.844), \quad (\text{Eq. 1})$$

where  $X$  – crude protein content in plants, %;  $Y$  – crude fiber content in plants, %.

#### 4. CONCLUSIONS:

Thus, the nitrogen content determined using remote technology in perennial grasses can serve as a starting point for determining the crude protein content in them, which in turn can serve as the basis for determining the amount of crude fiber

(based on the use of the above regression equation). The period of time when the crude protein content is 16-18%, and the fiber content 26-28% will be the optimal mowing period for perennial grasses.

Digital technologies are firmly entering our lives and are more often being used in field agriculture. The use of unmanned aerial vehicles equipped with powerful infrared sensors allows us to quickly, within a few hours, determine not only the nitrogen content but also the crude protein content in feed crops. Using the correlation and regression dependencies between the content of crude protein and crude fiber in plants, it is possible to determine the optimal harvesting time of perennial grasses for hay, silage, and haylage, which will increase the efficiency of feed use, reduce the unit costs of meat and dairy cattle breeding, and increase their efficiency.

## 5. REFERENCES:

1. Agriculture in Russia. (2019). Retrieved from [https://www.gks.ru/storage/mediabank/sh\\_2019.pdf](https://www.gks.ru/storage/mediabank/sh_2019.pdf).
2. Astor, T., Dayananda, S., Rao Nidamanuri, R., and Nautiyal, S. (2018). Estimation of vegetable crop parameter by multi-temporal UAV-borne images. *Remote Sensing*, 10(5), 805-817.
3. Bailey, R.W. 1973. *Chemistry and biochemistry of herbage*. New York City, New York: Academic Press.
4. Berni, J., Zarco-Tejada, P., Suárez, L., González-Dugo, V., and Fereres, E. (2009). Remote sensing of vegetation from UAV platforms using lightweight multispectral and thermal imaging sensors. *The International Archives of the Photogrammetry, Remote Sensing and Spatial Information Sciences*, 38(6), 6-20.
5. Bongiovanni, R., and Lowenberg-DeBoer, J. (2004). Precision agriculture and sustainability. *Precision Agriculture*, 5(4), 359-387.
6. Bykova, M.Yu., and Gibadullina, F.S. (2010). The content of structural carbohydrates in the feed of Tatarstan and their optimization in the diets of young cattle. *Scientific Notes of the Kazan State Academy of Veterinary Medicine named after N.E. Bauman*, 202, 50-55.
7. CropSpecTM vegetation level sensors. (2019). Retrieved from [https://agro.topcon.pro/resheniya/system-](https://agro.topcon.pro/resheniya/system-cropspec/)
8. GOST ISO 13906-2013. (2013). Animal feed. Determination of acid-detergent fiber and acid-detergent lignin. Retrieved from <http://docs.cntd.ru/document/1200105733>.
9. GOST ISO 16472-2014. (2017). Animal feed. Determination of neutral detergent fiber content using amylase. Retrieved from <http://docs.cntd.ru/document/1200110768>.
10. GOST R 55986-2014. (2014). Silage from fodder plants. General specifications. Retrieved from <http://docs.cntd.ru/document/1200110080>.
11. Honkavaara, E., Kaivosoja, J., Mäkynen, J., Pellikka, I., Pesonen, L., and Saari, H. (2012). Hyperspectral reflectance signatures and point clouds for precision agriculture by light weight UAV imaging system. *ISPRS Annals of the Photogrammetry, Remote Sensing and Spatial Information Sciences*, 7, 353-358.
12. How do drones work and what is drone technology? (2019). Retrieved from <https://russiandrone.ru/publications/kak-rabotayut-drony-i-chto-predstavlyayut-iz-sebya-tekhnologiya-dronov>.
13. International society of precision agriculture (ISPA). (2019). Retrieved from <https://www.ispag.org>.
14. Ismailova, A., Balkibayeva, A., Shahrjerdi, R., Palmieri, A., and Nukesheva, A. (2016). Overview on state support of development of agriculture in Kazakhstan (Akmola region evidence). *Economia Agro-Alimentare*, 18(1), 73-81.
15. Kanning, M., Kühling, I., Trautz, D., and Jarmer, Th. (2019). Hyperspectral imaging with UAVs to predict yield. Retrieved from [https://bespilotnik.org/info/articles/2019/giper-spektralnaya-semka\\_s\\_bpla\\_dlya\\_prognozirovaniya\\_urozhaynosti/](https://bespilotnik.org/info/articles/2019/giper-spektralnaya-semka_s_bpla_dlya_prognozirovaniya_urozhaynosti/)
16. Karydas, Ch., Iatrou, M., Kouretas, D., Patouna, A., Iatrou, G., Lazos, N., Gewehr, S., Tseni, X., Tekos, F., Zartaloudis, Z., Mainos, E., and Mourelatos, S. (2020). Prediction of antioxidant activity of cherry fruits from UAS multispectral imagery using machine learning. *Antioxidants*, 9(2), article number 156.
17. Kasakova, A.S., Yudaev, I.V., Mayboroda, S.Y., Taranov, M.A., Ksenz, N.V., and Chronyuk, V.B. (2019). Prospects for the use of stimulation by electric field of old cereal seeds. *Asia Life Sciences*, 1, 229-239.

18. Kharitonov, E.L., and Khotmirova, O.V. (2009). *Digestion processes in cows with different levels of fiber in the diet*. Moscow, Russian Federation: Federal Center for Agricultural Consulting and Retraining of Agricultural Personnel.
19. Kharitonov, E.L., Agafonov, V.I., and Kharitonov, L.V. (2008). *Methodological recommendations for the improvement and use of fodder base in dairy cattle breeding in the Kaluga region (practical recommendations)*. Kaluga, Russian Federation: All-Russian Research Institute of Physiology, Biochemistry, and Nutrition of Farm Animals.
20. Khudyakova, E.V., Gorbachev, M.I., and Nifontova, E.A. (2018, October). *Improving the efficiency of agro-industrial complex management based on digitalization and system approach//International scientific and practical conference on agrarian economy in the era of globalization and integration (AGEGI 2018)*. Paper presented at the IOP Conference Series: Earth and Environmental Science, Moscow, Russian Federation.
21. Korotaev, A.A., and Novopashin, L.A. (2018). *The use of unmanned aerial vehicles for monitoring agricultural land and sown areas in the agricultural sector*. Retrieved from <https://russiadrone.ru/publications/primeneniye-bespilotnykh-letatelnykh-apparatov-dlya-monitorirovaniya-selskokhozyaystvennykh-ugodiy-i/>
22. Laliberte, A.S., Goforth, M.A., Steele, C.M., and Rango, A. (2011). Multispectral remote sensing from unmanned aircraft: Image processing workflows and applications for rangeland environments. *Remote Sensing*, 3(11), 2529-2551.
23. Levakhin, G., Duskaev, G., and Dusaeva, H. (2015). Assessment of chemical composition of grain crops depending on vegetative stage for feeding. *Asian Journal of Crop Science*, 7, 207-213.
24. Levakhin, G.I., Airikh, V.A., Duskayev, G.K., and Breus, D.A. (2007). The degree of digestion of substances in the rumen of gobies taking into account structural carbohydrates in the diet. *Bulletin of RAAS*, 4, 79-81.
25. Lowenberg-DeBoer, J., and Erickson, B. (2019). Setting the record straight on precision agriculture adoption. *Agronomy Journal Abstract*, 111(4), 1552-1569.
26. Lupyan, E.A., Balashov, I.V., Burtsev, M.A., Efremov, V.Yu., Kashnitsky, A.V., Kobets, D.A., Krashennikova, Yu.S., Mazurov, A.A., Nazirov, R.R., Proshin, A.A., Sychugov, I.G., Tolpin, V.A., Uvarov, I.A., and Flitman, E.V. (2015). Creation of technologies for building information systems for remote monitoring. *Modern Problems of Remote Sensing of the Earth from Space*, 12(5), 53-75.
27. Mertens, D.R. (2010). *NDF and DMI – has anything changed?* Paper presented at the Cornell Nutrition Conference for Feed Manufacturers. New York City, New York.
28. Misselhorn, A., Aggarwal, P., Ericksen, P., Gregory, P., Horn-Phathanothai, L., and Ingram, J. (2012). A vision for attaining food security. *Current Opinion in Environmental Sustainability*, 4(1), 7-17.
29. Nagornyuk, K.E. (2016). UAVs will not surprise anyone: data from UAVs in ArcGIS. *GIS for Agriculture*, 3(78). Retrieved from [https://www.esri-cis.ru/news/arcreview/detail.php?ID=24061andSECTION\\_ID=1095](https://www.esri-cis.ru/news/arcreview/detail.php?ID=24061andSECTION_ID=1095)
30. Pashtetskiy, V.S., Turin, E.N., Izotov, A.M., Abdurashytov, S.F., Gongalo, A.A., and Zhenchenko, K.G. (2020). Effect of *Pisum sativum* L. seed treatment with the complex of microbiological preparation on the plants' growth and development under direct sowing. *IOP Conference Series: Earth and Environmental Science*, 422(1), article number 012012.
31. Pashtetsky, V.S., Demchenko, N.P., and Poliakova, N.Y. (2018). Flexible management of the economic activity – The Guarantee for the enterprise stability and the economy growth. *International Journal of Management and Business Research*, 8(1), 210-222.
32. Plant, R.E., Pettygrove, S., and Reinert, W.R. (2000). Precision agriculture can increase profits and limit environmental impacts. *California Agriculture*, 54(4), 66-71.
33. RoboTrends. (2018). *Choice of a drone for precision farming: opportunities and ideas*. Retrieved from <http://robotrends.ru/pub/1836/vybor-drona-dlya-tochnogo-zemledeliya-vozmozhnosti-i-idei>
34. Schmidhuber, J., and Tubiello, F.N. (2007). Global food security under climate change. *Proceedings of the National Academy of Sciences*, 104(50), 19703-19708.
35. Schwarzbach, M., Putze, U., Kirchgaessner, U., and Schoenermark, M.V. (2009).

Acquisition of high-quality remote sensing data using a UAV controlled by an open-source autopilot. In *ASME 2009 International Design Engineering Technical Conferences and Computers and Information in Engineering Conference* (pp. 595-601). New York City, New York: American Society of Mechanical Engineers.

36. Sergeev, K. (2019). Sensors for smart crop production. *Resource-Saving Agriculture*, 1. Retrieved from <http://agropraktik.ru/blog/1460.html>
37. Shuai, G., Martinez-Feria, R.A., Zhang, J., Li, Sh., Price, R., and Basso, B. (2019). Capturing maize stand heterogeneity across yield-stability zones using unmanned aerial vehicles (UAV). *Sensors (Basel)*, 19(20), article number 4446.
38. Stepanova, G. (2019). Influence of weather conditions on chemical composition of dry matter of alfalfa (*medicago varia mart.*) In the flowering phase. *Adaptive Fodder Production*, 2(38). Retrieved from <https://adaptagro.editorum.ru/en/nauka/article/29146/view>.
39. Tarshilova, L.S., Ibyzhanova, A.J., and Kazambayeva, A.M. (2016). Territorial specialization of agricultural production of the region. *International Journal of Applied Business and Economic Research*, 14(9), 5935-5950.
40. The technique of remote reconnaissance diagnostics of providing plants with nitrogen (using a multispectral camera and unmanned aerial vehicles). (2011). Retrieved from [https://yandex.ru/patents/doc/RU2693255C1\\_20190701](https://yandex.ru/patents/doc/RU2693255C1_20190701).
41. Tlesova, A., Primbetova, S., Kazambayeva, A., Yessengaliyeva, S., and Mukhambetkaliyeva, F. (2018). Reflections on sustainable development planning in the agricultural industry. *Journal of Environmental Management and Tourism*, 9(3), 591-598.
42. Tynybekov, B.M., Litvinenko, Y.A., Mukanova, G.A., Satybaldiyeva, G.K., Baimurzayev, N.B., Ablaihanova, N.T., Kuatbayev, A.T., and Sharakhmetov, S.E. (2013). Phytochemical investigation of the roots of *Rumex confertus* W. grown in the culture. *World Applied Sciences Journal*, 26(7), 941-944.
43. Vorobyova, S.V. (2002). *Guidelines for the use of neutral and acid-detergent fiber in the feeding of farm animals and methods for their determination in zootechnical analysis*. Dubrovitsy, Russian Federation: All-Russian Research Institute of Animal Husbandry named after L.K. Ernst.
44. Weiss, W.P. (1998). Estimating the available energy content of feeds for dairy cattle. *Journal of Dairy Science*, 81, 830-839.
45. Yudaev, I., Stepanchuk, G., Kaun, O., Ukraitsev, M., and Ponamareva, N. (2019). Small-sized irradiation structures for intensive year-round cultivation of green vegetable crops. *IOP Conference Series: Earth and Environmental Science*, 403(1), article number 012084.
46. Zhou, X., Zheng, H., Xu, X.Q., and He, J. (2017). Predicting grain yield in rice using multi-temporal vegetation indices from UAV-based multispectral and digital imagery. *ISPRS Journal of Photogrammetry and Remote Sensing*, 130, 246-255.

**Table 1.** The sown area of forage grasses in the Russian Federation, thous. ha.

| Forage grasses    | 2000<br>year | 2014<br>year | 2015<br>year | 2016<br>year | 2017<br>year | 2018<br>year |
|-------------------|--------------|--------------|--------------|--------------|--------------|--------------|
| Perennial grasses | 18046        | 10849        | 10760        | 10717        | 10588        | 10558        |
| Annual grasses    | 5946         | 4571         | 4536         | 4187         | 4107         | 3986         |

**Table 2.** UAVs that are best for using to take pictures of crops of perennial grasses

| Name                      | Distinctive features  |
|---------------------------|---|
| BirdsEyeView FireFLY6 Pro | the possibility of vertical take-off and landing,<br>the possibility of reverse motion<br>coverage - up to 2.42 km <sup>2</sup><br>payload weight - 0.7 kg<br>time of flight - up to 1 hour         |
| Honeycomb AgDrone         | surveying speed - 3.47 km <sup>2</sup> /h<br>speed - up to 82 km/h<br>time in the air - up to 1 hour<br>coverage radius - 344 ha/hour<br>resolution - 2.5 cm/pixel<br>flight altitude - about 130 m |
| eBee SQ, senseFly Ag 360  | coverage radius - up to 200 ha<br>time in the air - 55 minutes<br>flight altitude - 120 meters<br>resolution - 12 cm/pixel  |
| The Sentera PHX           | time in the air - 59 minutes<br>coverage radius - up to 280 ha<br>flight altitude - 130 meters<br>resolution - 3.8 cm/pixel   |

**Table 3.** The content of crude fiber and crude protein by the phases of vegetation, % of dry matter

| Culture and vegetation phase | Crude fiber content,% | Crude protein content,% |
|------------------------------|-----------------------|-------------------------|
| Brome                        |                       |                         |
| booting phase                | 20.07                 | 22.23                   |
| heading phase                | 24.8                  | 14.69                   |
| initial blossom              | 30.42                 | 8.88                    |
| Festuca                      |                       |                         |
| booting phase                | 19.67                 | 18.45                   |
| heading phase                | 29.04                 | 13.12                   |
| initial blossom              | 34.35                 | 10.81                   |
| Timothy                      |                       |                         |
| booting phase                | 23.69                 | 16.90                   |
| heading phase                | 30.98                 | 12.87                   |
| initial blossom              | 33.99                 | 8.56                    |

Source: data by Khudyakova Kh.K., V.R. Williams All-Russian Research Institute of Feed.







a)



b)

**Figure 1.** Octocopter with camera (a) and triaxial cardan-joint for camera and inertial measuring unit (IMU) (b) (Kanning et al., 2019)



**Figure 2.** Tractor roof with CropSpecTM vegetation level sensor mounted on it

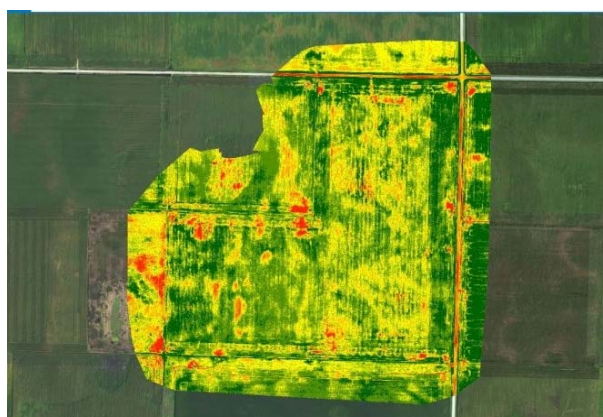


**Figure 3.** Crop monitoring (vegetation index NDVI) from UAV images converted to map in Drone2Map for ArcGIS (Nagornyuk, 2016)



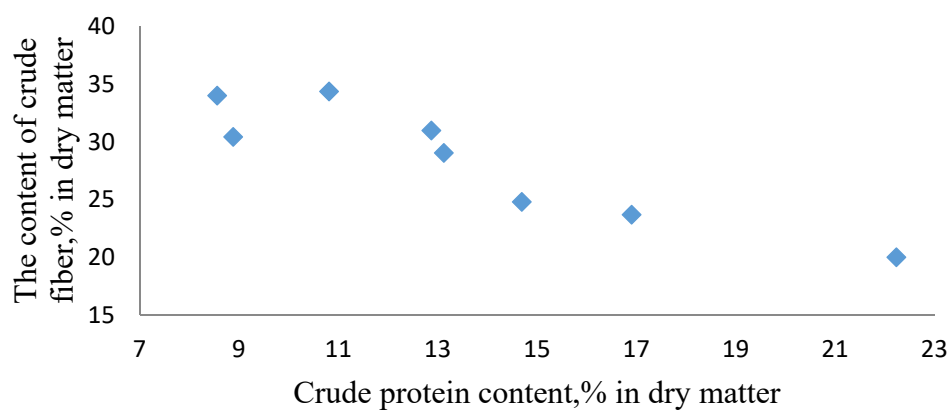


**Figure 4.** *Dependence between the content of crude protein and crude fiber in the dry matter of perennial grasses*

**POTENCIAL DE PERSISTENCIA DOS PROTOZOÁRIOS *BLASTOCYSTIS* SPP.**
**PERSISTENT POTENTIAL OF PROTOZOA *BLASTOCYSTIS* SPP.**
**ПЕРСИСТЕНТНЫЙ ПОТЕНЦИАЛ ПРОСТЕЙШИХ *BLASTOCYSTIS* SPP.**

BUGERO, Nina Vladimirovna<sup>1\*</sup>; ILYINA, Natalya Anatolyevna<sup>2</sup>;  
ALEXANDROVA, Svetlana Mikhaylovna<sup>3</sup>;

<sup>1,2,3</sup> Pskov State University, Russian Federation

\* Correspondence author  
e-mail: bugero@mail.ru

Received 12 April 2020; received in revised form 22 June 2020; accepted 03 July 2020

**RESUMO**

Nos últimos anos, o protozoário parasitário *Blastocystis* spp., que habita o trato gastrointestinal humano, começou a atrair cada vez mais atenção dos parasitologistas. Uma alta incidência de contaminação por blastocisto foi revelada em indivíduos de vários grupos populacionais. Neste artigo, os resultados do estudo mostram altas taxas de invasão de trabalhadores de fundição pelo protozoário mencionado acima, caracterizado por condições perigosas de trabalho, tanto de natureza física quanto química. A capacidade dos protozoários de habitar um nicho ecológico específico depende de suas propriedades biológicas; assim, fatores de persistência são de particular interesse. O artigo descreve o potencial persistente do *Blastocystis* spp., habitando o intestino humano. As propriedades persistentes nos procariontes são um fator fisiológico significativo para a sua existência e determinam o mecanismo de interação dos microrganismos que formam a microflora intestinal. Foi estudado o complexo de fatores de persistência (ALA, ALFA e AHA) do *Blastocystis* spp. Foi encontrada uma correlação direta entre a atividade persistente dos blastocistos e a gravidade dos distúrbios da microbiocenose intestinal. O efeito de fatores desestabilizadores da produção que levam à reestruturação do bioma intestinal foi estabelecido, contribuindo para a diminuição do grupo nativo de microrganismos e para o aumento da flora oportunista. Os dados recebidos permitem utilizar as propriedades biológicas mais importantes da sobrevivência dos microrganismos para estudar os mecanismos de formação de microsimbiocenoses no biótopo do intestino grosso e são um pré-requisito teórico para o desenvolvimento de um método de rastreamento do diagnóstico de disbiose intestinal com base na determinação de ALA, ALFA e AHA de isolados clínicos de blastocistos.

**Palavras-chave:** *microbiocenose, parasitocenose, distúrbios disbióticos, antiliscito, antilactoferrina.*

**ABSTRACT**

In recent years, the parasitic protozoan *Blastocystis* spp., inhabiting in the human gastrointestinal tract, has begun to attract more and more attention on the site of parasitologists. A high incidence of blastocyst contamination was revealed in individuals of various population groups. In this paper, the results of the study showing high rates of invasiveness of foundry workers by the above-mentioned protozoan, characterized by hazardous working conditions of both physical and chemical nature. The ability of protozoa to inhabit a particular ecological niche depends on their biological properties; thus, persistence factors are of particular interest. The article describes the persistent potential of *Blastocystis* spp., inhabiting the human intestines. Persistent properties in prokaryotes is a significant physiological factor for their existence and determine the mechanism of interaction of microorganisms that form the intestinal microflora. The complex of persistence factors (ALA, ALFA, and AHA) of *Blastocystis* spp. was studied. A direct correlation between the persistent activity of the blastocysts and the severity of intestinal microbiocenosis disorders was found. The effect of destabilizing production factors leading to the restructuring of the intestinal biome has been established, contributing to a decrease in the indigenous group of microorganisms and an increase of opportunistic flora. The received data allow using the most important biological properties of the survival of

the microorganisms to study the mechanisms of microsymbiocenoses formation of in the biotope of the large intestine and are a theoretical prerequisite for developing a method for screening diagnosis of intestinal dysbiosis based on the determination of ALA, ALFA and AHA of clinical blastocyst isolates.

**Keywords:** *microbiocenosis, parasitocenosis, dysbiotic disorders, antilysocyme, antilactoferrin.*

## АННОТАЦИЯ

В последние годы все большее внимание паразитологов стал привлекать паразитический простейший организм *Blastocystis* spp., обитающий в желудочно-кишечном тракте человека. Выявлены высокие показатели обсемененности бластоцист у лиц различных групп населения. В настоящей работе представлены результаты исследования, регистрирующие высокие показатели инвазированности данными простейшими рабочих литейного производства, характеризующиеся опасными условиями труда как физической, так и химической природы. При этом способность простейших к заселению той или иной экологической ниши зависит от наличия у них биологических свойств, в этом плане несомненный интерес представляют факторы персистенции. В статье представлена характеристика персистентного потенциала простейшего *Blastocystis* spp., населяющего кишечник человека. Наличие персистентных свойств у прокариот является чрезвычайно важным физиологическим аспектом их существования и определяет механизм взаимодействия микроорганизмов формирующих микрофлору кишечного тракта. Изучен комплекс факторов персистенции (АЛА, АЛФА и АГА) простейших *Blastocystis* spp. Обнаружена прямая корреляционная зависимость между персистентной активностью бластоцист и глубиной нарушений микробиоценоза кишечника. Установлено действие дестабилизирующих факторов производства, которые ведут к перестройке кишечного биома, способствуют уменьшению индигенной группы микроорганизмов и увеличению условно-патогенной флоры. Эти материалы позволяют использовать важнейшие биологические свойства выживания микроорганизмов для исследования механизмов формирования микросимбиоценозов в биотопе толстого кишечника и являются теоретической предпосылкой для разработки способа скрининговой диагностики кишечного дисбиоза, основанного на определении АЛА, АЛФА и АГА клинических изолятов бластоцист.

**Ключевые слова:** *микробиоценоз, паразитоценоз, дисбиотические нарушения, антилизозимная, антилактоферриновая.*

## 1. INTRODUCTION

The general transformation of the influence of environmental conditions in modern society is evident. A lot of abiotic and biotic factors, including anthropogenic ones, affect human health (Sharapov, 2012). The effects of industrial environmental factors on the body should not be ignored. Industries characterized by hazardous working conditions can be determined. This entirely concerns foundry. In a foundry, harmful factors of both physical and chemical nature are inherent (Soloviev, 2013). Physical factors include vibration, noise, high temperature, ultrasound, ionizing radiation; chemical factors include the influence of isocyanates, formaldehyde, tertiary amines such as dimethylethylamine, triethylamine, silicon dioxide, metal oxides. All of the above factors produce favorable conditions for different diseases (Lazarenkov and Khoreva, 2016).

Literature analysis showed that vibration causes changes in cardiac activity, in the nervous system, spasms of blood vessels, changes in the

joints, limiting their mobility (Turovets *et al.*, 2015). Studies of the noise effect on the human body also revealed changes in the functioning of the nervous and cardiovascular systems (Afanasova *et al.*, 2010). During the examination, workers exposed to noise, often complain of irritability, headaches, drowsiness, increased fatigue, poor sleep, dizziness. Persons constantly in contact with the noise of varying degrees and duration revealed disturbances of thermoregulation, increased pulse levels, and blood pressure (Izmerova and Denisova, 2003). Chemical factors inhibit hemopoiesis, disturbs metabolism, and causes functional changes in the nervous system and gastrointestinal tract (Denisov *et al.*, 2010).

Studying the influence of environmental factors on the human body is not a new problem. However, the influence of the entire spectrum of foundry factors on the microbiome of the worker's body is still not completely studied. Intestinal flora serves as an indicator of the microorganisms state, and when exposed to destabilizing environmental factors, its qualitative and quantitative change occurs, indigenous flora

decreases, and opportunistic pathogenic group increase (Kuvaeva and Ladodo, 1991).

In the last decade, many authors have shown the role of opportunistic microorganisms in the occurrence of intestinal infections. The epidemiological situation on parasitic diseases is especially acute; more than 1.3 million patients with various parasitoses are officially registered annually in the country. However, the incidence of parasitic infestations and their importance for public health and the country as a whole remains underestimated for a number of reasons. The reasons for the preservation of such a situation are the difficulties of specific diagnostics, lack of a clear system for recording the incidence rate, insufficient knowledge of doctors, and misunderstanding of both doctors and the population in the field of diagnosis and treatment of parasitoses.

*Blastocystis* spp is the most widespread among the parasitic microorganisms. (Abe, 2004; Dogruman, 2009). According to the classification of microorganisms, this protozoan belongs to the kingdom of Stramenopiles (synonym Chromista, Heterokonta), subdomain Chromobiota, subtype Opalinata, class Blastocystea, order Blastocystida, family Blastocystidae, genus Blastocysts (Hameed, 2011).

The growing interest of scientists and practical parasitologists in this protozoan is explained by its spread in the world. It is found in 30–50% of the inhabitants of developing countries and in 1.5–10% of developed countries (Iguchi, 2007; Jones, 2009; Meloni *et al.*, 2011). Besides, blastocysts are often present in patients with gastroenterological diseases, allergies. For example, due to Horiki *et al.* (1999), in examining a practically healthy population from Tokyo (Japan), blastocysts were found in 7.4% of cases (Horiki, 1999), and in similar studies in Perm, performed by N. M. Koza *et al.* in 1997 - 2001, the blastocystic invasion was revealed in 13.1% of cases (Koza *et al.*, 2002). In Omsk, according to the results of population surveys in 1999 – 2001, the rate of *Blastocystis hominis* detection in healthy persons was within 0.9 – 2.3% (Starostina *et al.*, 2002).

However, in clinical practice, laboratory assistants often do not register blastocysts in the test material. This is explained by the fact that the pathogenic nature of protozoan remains controversial, and, therefore, the registration of the results is not mandatory, and also by inadequate knowledge of laboratory assistants of this object.

It was established that blastocysts have a significant effect on the formation of microbiocenosis of the human intestine, accompanied by a decrease in the seeding rate of indigenous flora (bifidobacteria and lactobacilli), and an increase of opportunistic flora. It was shown that the disturbance of biocenotic relations between pathogenic bacteria and normal intestinal microflora is one of the factors affecting the development of many diseases, especially those with a chronic course. Experimental data confirm a high incidence of blastocysts in individuals with liver diseases, gastric ulcers, and dermatoses (Krasnoperova, 2009).

The discovery of microorganisms belonging to the group of protozoa in the intestinal biome does not always testify to their role in the formation of the studied biotope, and it is absolutely impossible to assess their significance for a macroorganism experiencing constant pressure from a complex of factors of an unfavorable industrial environment, which reduces the protective forces of the human body and makes him vulnerable to various forms of the disease.

Human normoflora provides non-specific resistance of a macroorganism (Tsimmerman, 2014). Microorganisms colonizing the intestine prevent contamination of the mucous membranes of the digestive tract with opportunistic microorganisms, using a large group of secreted bacterial substances as a defense against the pathogen. Conventionally pathogenic flora is present in the intestines of healthy people as additional or transient representatives in certain quantitative and qualitative indicators (Blaser and Falkow, 2014; Kuchumova, 2011).

Thus, in determining the etiological significance of the conventionally pathogenic flora, to which the group of parasitic protozoa *Blastocystis* spp can be attributed, along with their number, factors contributing to persistence must be taken into account, which are considered as a marker that determines the long-term habitation of the pathogen in the host organism. These traits include the ability of microorganisms to degrade lysozyme - antilysozyme activity (ALA), the ability to inactivate lactoferrin - antilactoferrin (ALPA), and antihistamine (AHA) activity.

The purpose of the study was to give a comparative characteristic of the persistent potential of parasitocenosis of the human intestine, under the influence of a complex of unfavorable factors in the working environment.

To achieve this purpose, the following tasks were set:

1. To study microbiocenosis characteristics in human large intestine under the influence of a complex of destabilizing factors of the working environment.
2. To determine the occurrence of protozoa *Blastocystis* spp. in the intestines in norm and in dysbiosis.
3. To study blastocysts biological properties using antilysocyme, antilactoferrin, and antihistone activities as an example.

## 2. MATERIALS AND METHODS

A series of studies on the intestinal microbiocenosis in persons working in the foundry of the Armature Plant were performed at the clinic of OJSC "Reinforcing Plant", the Helix laboratory and the research laboratory "Diagnostics" in St. Petersburg.

To assess the microbiocenosis, the method of quantitative isolation of types and variants of microorganisms that make up the microbiocenosis according to the order of the Ministry of Health of Russia of 09.06.2003 No. 231 "On approval of the industry standard "Protocol for the management of patients. Intestinal dysbiosis" (OST 91500.11.0004-2003) was used.

Cultures grown on culture media were subjected to group, generic, and species identification.

The inoculation and incubation on solid media for the isolation of lacto- and bifidumbacteria was carried out in anaerostats AE-01 (OJSC NIKI MLT, St. Petersburg) and OXOID (England) using Anaerogaz gas-generating packages. Anaerobic microorganisms were identified using ANAEROTEST 23 (Lachema, Czech Republic). Identification of opportunistic enterobacteria was carried out using general identification schemes. Identification of opportunistic enterobacteria was performed following generally accepted identification schemes using PBDE (Diagnostic Systems, Nizhny Novgorod), ENTEROTEST 24 (Lachema, Czech Republic), NEFERMtest (Lachema, Czech Republic), and Giss mediums. Yeast-like fungi, genus *Candida*, were revealed by their ability to assimilate carbohydrates using the API 20C AUX system (bioMerieux, France).

To detect protozoa, including blastocysts,

both traditional parasitological diagnostic methods (microscopy of fecal smears) and molecular biological methods (PCR) were used. Microscopy of stool smears stained with Lugol solution was carried out in compliance with all requirements for the preparing of preparations (Guidelines 4.2.735-99 "Parasitic methods of helminthism and protozoal diseases laboratory diagnostics" improved by the chief state sanitary doctor of the Russian Federation)

Pavlova and Zierdt media were used to obtain protozoa *Blastocystis* spp. cultures. Persistence factors of microorganisms were studied from 2015 to 2017 at the Institute of Cellular and Intracellular Symbiosis of the Ural Branch of the Russian Academy of Sciences, Orenburg (IKVN Ural Branch of the Russian Academy of Sciences).

Microorganisms persistence factors were studied using research methods proposed by O.V. Bukharin et al. To study microorganisms antilysocyme activity (ALA) the photometric method was used [23]. *Blastocystis* spp. test culture was grown in a liquid nutrient medium, the supernatant was separated and mixed with lysozyme, while preparing a control. The test sample and control were mixed with a suspension of the *Micrococcus lysodeikticus* test culture (strain No. 2665, L.A. Tarasevich GISK), and antilysocyme activity was determined by the optical density of the resulting mixtures, characterized in that the control used a mixture of nutrient broth with lysozyme, incubated the supernatant with lysozyme, introduced the incubated mixture into a pre-treated Trilon B test culture and measuring the optical density of the experimental sample and control in 2 and 4 hours, then calculated antilysocyme activity according to the formula:

$$K = \frac{V_K - V_L - C_L \cdot (M_{O4} - M_{O2})}{M_{K4} - M_{K2}}$$

where K is the coefficient of blastocysts antilysocyme activity;  $V_K$  - the volume of the broth culture of the studied strain;  $V_L$  is the volume of lysozyme solution in the initial concentration;  $C_L$  - lysozyme concentration;  $M_{O4}$  is the average optical density of experimental wells with a broth culture of the studied strain with lysozyme after 4 hours of incubation, units optical density;  $M_{O2}$  is the average optical density of experimental wells with a broth culture of the studied strain with lysozyme after 2 hours of incubation, units optical density;  $M_{K4}$  - the average value of the optical density of control wells with a broth culture of the studied strain without lysozyme after 4 hours of incubation, units optical density;  $M_{K2}$  - the

average optical density of the control wells with a broth culture of the studied strain without lysozyme after 2 hours of incubation, units optical density; 100 - conversion factor.

Microorganisms antilactoferrin activity (ALFA) of was studied according to the method described O.V. Bukharin et al. [24]. The amount of lactoferrin was determined by the method of enzyme-linked immunosorbent assay using sets of "Lactoferrin-strip", CJSC "Vector - Best", Novosibirsk. Test culture *Blastocystis* spp. was grown on solid nutrient medium; a microbial suspension was prepared from the grown agar culture, mixed with lactoferrin, while preparing a control., a liquid nutrient medium was added to the control instead of a microbial suspension. The test sample and control were incubated, the supernatant was separated from the simple blastocyst cells by centrifugation, determining the concentration of lactoferrin in the experimental and control samples by enzyme immunoassay and then calculate ALfa according to the formula:  $ALFA = Ck - Co$ ,

where: ALFA - antilactoferrin activity, ng of inactivated lactoferrin / ml supernatant; Ck is lactoferrin concentration in the control, ng / ml; Co - lactoferrin concentration of in the experiment, ng / ml.

The antihistone activity of the studied microorganisms was determined by the photometric method [25]. To do it histone preparation from bovine thymus manufactured by Sigma (USA) in the form of a lyophilized powder containing a total fraction of histones was used. Test *Blastocystis* spp culture. grown in a liquid nutrient medium, was treated with chloroform, the culture fluid was separated, mixed with histone solution, simultaneously preparing two control samples. Isotonic NaCl solution was added in Control 1, instead of histones solution, and in control 2 liquid nutrient medium was added instead of culture fluid. The experimental and control samples were incubated, after incubation, the meat-peptone broth and the *Micrococcus luteus* test culture (GISK 211001) were added to all samples, re-incubated, the optical density of the suspensions was measured in the experiment and controls, then antihistone activity was calculated be the formular

$$\left( \frac{oDts - oDc1}{oDc1 - oDc2} \right) * 12.84 mcg / ml$$

where: oDts -optical density of the test sample; oDc1 -optical density of control1; oDc2 – optical density of control 2.

### 3. RESULTS AND DISCUSSION

The study was performed in 129 workers of the enterprise aged from 25 to 55. The control group consisted of 50 healthy m. persons.

Analysis of outpatient cards, record cards with the results of periodic medical examinations for the period from 2013 to 2017, revealed a number of diseases in the studied group. Vibration disease was on the first place ( $78.30 \pm 2.7\%$ ), diseases of the hearing organs were registered in  $43.20 \pm 3.2\%$  of workers, diseases of the nervous and cardiovascular systems in  $32.40 \pm 3.4\%$  and  $28.6 \pm 1.3\%$ , respectively, acute respiratory infections in the mean of  $19.20 \pm 1.8\%$ , diseases of the musculoskeletal system in  $8.40 \pm 1.7\%$ . A high percentage of digestive organs diseases were registered, their rate was  $62.30 \pm 3.6\%$  (80 persons).

The gastrointestinal tract plays a significant role in the human body since the main physiological processes occur there. Therefore, the proper functioning of the human digestive system serves as the basis for normal and full life support. The question of the influence of industrial and technical factors on the microbiome of the human body, which actively performs many functions that provide homeostasis, is still not clear. So monitoring of human health under the influence of unfavorable factors of the working environment and their influence on the digestive system of the body was performed.

In this connection, studied subjects were divided into three groups, depending on the duration of contact with destabilizing industrial factors. The first group consisted of employees working at the enterprise from 1 to 5 years - 26 persons ( $32.5 \pm 2.7\%$ ,  $p < 0.03$ ), the second included those who worked at the enterprise from 5 to 10 years - 32 people ( $40.0 \pm 3.9\%$ ,  $p < 0.05$ ), the third group consisted of employees working at the enterprise 10-15 years and more - 22 persons ( $27.5 \pm 1.4\%$ ,  $p < 0.03$ ).

Diagnosis of the qualitative and quantitative composition of the intestinal microbiocenosis of the examined patients showed disturbances on the part of normoflora. Besides, a decrease in the occurrence of the representatives of obligate microflora was shown: bifidobacteria and propionic bacteria to  $85.4 \pm 3.4\%$ ,  $81.3 \pm 3.1\%$ , respectively ( $p < 0.05$ ), lactobacilli to  $77.4\% \pm 4.3$  ( $p < 0.03$ ), bacteroids up to  $87.5 \pm 3.9\%$ , ( $p < 0.05$ ), non-hemolytic *E. coli* up to  $68.3 \pm 2.9\%$ , ( $p < 0.05$ ). In the control group, these figures were within the range of 98-100% ( $p < 0.03$ ). A decrease in the density of

colonization was observed in these groups of microorganisms, for example, for bifidobacteria, it averaged  $\log 6.4 \pm 0.4$  CFU/g, for lactobacilli and bacteroids,  $\log 7.0 \pm 0.1$  CFU/g and  $\log 8.5 \pm 0.1$  CFU/g, respectively ( $p < 0.05$ ).

Depending on the duration of work in the foundry, the frequency and density of colonization of obligate endoflora representatives varied among workers of the 2nd group, reaching maximum deviations from the normocenosis in the examined from the 3rd group. The most visible disorders in the obligate group of microbes were noted among the workers with more than ten years of work experience. The seeding rate in relation to the bifidobacteria group was  $\log 5.3 \pm 0.2$  CFU/g, for lactobacilli  $\log 6.2 \pm 0.1$  CFU/g, which is significantly lower than in the comparison group. In the control group, the seeding rate for bifidobacteria and lactobacilli was  $\log 10.5 \pm 0.3$  CFU/g and  $\log 9.9 \pm 0.4$  CFU/g, respectively ( $p < 0.05$ ).

The occurrence of opportunistic flora increased depending on the duration of the technogenic factors of the production environment action. High colonization density was observed for bacteria genus *Enterococcus* spp., *Proteus* spp., *Staphylococcus* spp., and fungi genus *Candida* spp. Their dissemination rates were significantly higher in comparison with the control group and amounted on average to  $1g 10.2 \pm 0.3$  CFU/g,  $\log 2.6 \pm 0.4$  CFU/g,  $\log 5.0 \pm 0.3$  CFU/g and  $\log 4.5 \pm 0.4$  CFU/g, respectively ( $p < 0.05$ ). In the control group, these figures were as follows:  $\log 2.5 \pm 0.3$  CFU/g,  $1g 0.9 \pm 0.4$  CFU/g,  $1g 2.3 \pm 0.3$  CFU/g and  $1g 2.4 \pm 0.4$  CFU/g, respectively ( $p < 0.05$ ). The occurrence and the density of colonization of opportunistic microbes were directly dependent on the length of service at the enterprise.

A significant increase in the content of *Escherichia coli* with hemolytic activity should be stressed. This indicates their high pathogenicity compared with the control group.

At present, much attention is paid to the importance of colonic dysbiosis in parasitoses. So, besides representatives of the bacterial flora, an assessment of the intestinal parasitocenosis was performed in the subjects studied. *Blastocystis* spp. ( $62.00 \pm 5.4\%$ ), *Lambli* *intestinalis* ( $36.72 \pm 3.2\%$ ) and *Entamoeba coli* ( $16.34 \pm 1.3\%$ ) prevailed as to the frequency of their occurrence.

Studies have shown that, depending on the duration of work in the foundry, the detection of blastocysts in the feces of workers increases

from  $56.30 \pm 4.6\%$  in the first group to  $85.63 \pm 7.8\%$  in the third group.

A study of the biological properties of *Blastocystis* spp., colonizing the mucous membranes of the large intestine, will allow developing new approaches to assessing the participation of this pathogen in the development of the pathological process, explain the possible reason for the presence of blastocysts in the studied biotope and determine the participation of these protozoa in the formation of the intestinal biome in the persons under study.

Blastocyst strains isolated from the intestines of foundry workers were selected as a material for the study. All the subjects were divided into four groups depending on the severity of dysbiotic disorders (Table 1).

To date, there is no universally accepted classification of intestinal dysbiosis. Classification Intestinal flora dysbiosis, proposed by G. Kuznetsova (1972), was used in this work. It includes 4 degrees of colonic dysbiosis severity: stage I showed a decrease in the number of bifidobacteria and lactobacilli, stage II was characterized by a pronounced increase and subsequent predominance of colibacterial flora, appearance of atypical and enzymatically defective *E. Coli*, in stage III high titers of optional flora associations (staphylococci, streptococci, clostridia, fungi of the genus *Candida*, etc.) were registered while bifidobacteria and lactobacilli decreased on this background and stage IV with a predominance of *Proteus* or *Pseudomonas aeruginosa* prevalence.

With an increase in work experience from 1 to 15 years or more, the factors of dysbiotic manifestations increased, characterized by quantitative and qualitative values of microorganisms underlying the determination of dysbiosis of varying severity.

The studies performed allowed to determine the quantitative composition of the blastocyst strains isolated from the examined individuals, depending on the degree of intestinal dysbiosis (Table 1).

The greatest number of *Blastocystis* spp. was found in individuals with dysbiotic changes of the II degree of severity - 28 strains ( $47.50 \pm 1.7\%$ ,  $p < 0.03$ ).

The control group (50 people) consisted of persons undergoing outpatient treatment and not contacting the harmful factors of the working environment. The data obtained above were analyzed considering the questionnaire survey, in

which the persons of the comparison group participated. In persons from this group, dysbiosis of varying severity was observed in 4.0 0.7%,  $p < 0.03$ , blastocyst invasion in 12.0 0.2%,  $p < 0.03$  (6 people).

The study of biological properties was carried out on the example of ALA, ALPA, and AGA activities, which are quite widely represented in the group of opportunistic bacteria. However, the study of these traits in *Blastocystis* spp., isolated in individuals exposed to destabilizing factors of foundry and aggravated by gastrointestinal diseases, was not yet carried out.

The role of lysozyme in protecting the macroorganism from infection is well known. Antilysozyme activity is one of the factors that increase the tolerance of microorganisms to the action of human and animal serum lysozyme. Some authors believe that antilysozyme activity contributes to the long-term survival of microorganisms in a macroorganism and can be used in bacteriological laboratories to assess the etiological role of isolated cultures.

Of the 62 studied blastocyst strains, 56 ( $89.28 \pm 5.7\%$ ) possessed the studied trait. To analyze persistent characteristics of *Blastocystis* spp. Three groups of protozoa were chosen: the first included strains with a low ALA level - up to 2  $\mu\text{g} / \text{ml}$  inclusive, the second with a mean ALA level of 3-4  $\mu\text{g} / \text{ml}$ , and the third with a high ALA level - 5  $\mu\text{g}/\text{ml}$  or more. The proportion of strains with low ALA values was  $33.92 \pm 2.3\%$  (19 strains), with mean ALA -  $50.01 \pm 4.6\%$  (28 strains) and  $16.07.23 \pm 1.7\%$  (9 strains) with high ALA values (Table 2).

Table 3 shows that half of the blastocyst strains ( $50.01 \pm 4.6\%$ ) isolated from the workers had average antilysozyme activity values within the range of 3-4  $\mu\text{g}/\text{ml}$ . The proportion of *Blastocystis* spp. isolates with low and high values of the studied trait were  $33.92 \pm 2.3\%$  and  $16.07 \pm 1.7\%$ , respectively.

The performed studies revealed a direct dependence of the ALA blastocysts manifestation on the severity of dysbiotic changes (Table 3).

Thus, blastocysts isolated in individuals with grade I dysbiosis were characterized to a greater extent by low ALA levels, which amounted to  $2.1 \pm 0.02 \text{ mg}/\text{ml}$ , while protozoa strains with grade III and IV dysbiosis had completely no low values of the studied trait. Increased ALA levels in blastocysts were observed with more pronounced factors of

intestinal dysbiotic disorders in workers. Among the nine protozoa strains isolated in dysbiosis of the IV degree of severity, two strains were characterized by mean ( $2.3 \pm 0.02 \text{ mg}/\text{ml}$ ) and seven strains ( $2.7 \pm 0.05 \text{ mg}/\text{ml}$ ) high level of the studied property.

Such an increase in the expression of antilysozyme activity in different degrees of dysbiosis is due to the fact that during biocenosis, which is characterized by a high content of opportunistic flora and a sharp decrease in obligate representatives (IV degree of dysbiosis), an inflammatory state of the intestinal mucosa is observed, which is accompanied by the increased concentration of endogenous lysozyme, intensely secreted by exocrinocytes of the colon in response to increased colonization of the digestive tract by optional microorganisms. It can be assumed that assimilating the ecological niche of *Blastocystis* spp. they produce lysozyme, necessary for the formation of biocenosis, which can lead to a compensatory ALA increase in representatives of the obligate group.

The antilactoferrin activity (ALFA) of protozoa was studied. Data on ALFA prevalence and severity in *Blastocystis* spp., isolated in foundry workers, show that the studied protozoa are highly able to inactivate lactoferrin. Antilactoferrin activity was revealed with a frequency of  $69.35 \pm 3.7\%$  (43 strains).

Prevalence of ALFA *Blastocystis* spp. ranged from 65 to 289  $\text{ng}/\text{ml}$  (Table 4). Depending on the parameters of the studied property, all the studied strains were divided into three groups.

The first group of blastocyst cultures had low values of the studied trait, which were in the range of  $65-161 \pm 22.2 \text{ ng}/\text{ml}$ , the second - means -  $162-223 \pm 30.7 \text{ ng}/\text{ml}$  and the third high -  $224-289 \pm 49.3 \text{ ng}/\text{ml}$ . An analysis of the quantitative relations of the studied characteristic showed that almost half of the blastocyst strains were characterized by an average ALFA value ( $45.51 \pm 2.3\%$ ).  $32.56 \pm 2.7\%$  and  $20.93 \pm 3.7\%$  of the studied strains showed, respectively, high and low ALFA values.

As the studies showed, the number of blastocyst strains with high persistent properties had a low percentage of occurrence or was completely absent in dysbiosis of I and II degrees of severity (Table 5). Thus, ALFA analysis showed that protozoa strains isolated in those examined with I degree of dysbiosis had neither mean or high level of the studied trait. In this group, only one strain of blastocysts was



characterized by a low value ( $65-161 \pm 22.2$  ng/ml) of the trait.

In the III degree of intestinal dysbiosis, approximately there was the same number of strains, both with mean and low values of the trait. It should be noted that in significant disturbances of the qualitative and quantitative intestinal microflora composition, characterized by an IV degree of dysbiosis, only blastocyst strains were obtained in the experiment that inactivated lactoferrin in high concentrations of the studied persistent property in 11 isolates.

Of the 62 blastocyst strains, 32 *Blastocystis* spp. isolates, isolated from feces of workers, with the pathology of the gastrointestinal tract, had antihistone activity.

The values of antihistone activity ranged from 1.3-12.8 ng/ml, and in mean, were  $9.1 \pm 1.6$  ng/ml. The results obtained in the experiment allowed to divide all the studied blastocyst strains into three groups (Table 6).

The determination of the AHA level revealed in the vast majority of protozoa low ( $1.3-5.3 \pm 0.9$ ) and mean ( $5.7-9.1 \pm 4.3$  ng/ml) values of the studied trait. Such cultures accounted for 89.28 3.9% of the studied blastocyst strains. The third group consisted of blastocyst strains with high AHA values ( $9.2-12.8 \pm 4.6$  ng/ml) (Table 7).

The number of blastocyst strains isolated from feces of persons in contact with harmful factors of the working environment without obvious dysbiotic disturbances (I degree of dysbiosis) showed the prevalence of protozoa strains with a number of manifested AHA traits. On the contrary, a high level of antihistone activity was observed in blastocyst strains isolated in individuals with dysbiotic changes of moderate and high severity.

Thus, blastocyst strains isolated from feces of individuals exposed to destabilizing factors of the working environment are capable of inactivating certain factors of the natural anti-infection resistance of the microorganism (ALA, ALFA, and AHA). The results of the study allowed not only to reveal them but also to rank according to the degree of their information content (Figure 1).

The antilysozyme trait is the main persistent trait that determines the formation of the intestinal microbiocenosis of a given biotope. It was recorded with a frequency of  $89.28 \pm 5.7\%$ . Isolated *Blastocystis* spp. strains possess high values of the studied persistent characteristics

(ALA, ALFA, AHA) characterizing their persistent activity.

These traits contribute to the displacement of the dominant symbionts of the intestinal flora by blastocysts, colonization of mucous membranes by the protozoa studied, and leads to the formation of special parasitocenosis.

Since *Blastocystis* spp. possess a wide range of persistent symptoms, the question arises on protozoal infection of the macroorganism cell nucleus, and it is possible to confirm this at the light microscopic level, make an indirect assessment of the morbidity of the population by the occurrence rate of protozoan strains isolated from this contingent of the examined individuals, and also use them to diagnose and predict blastocystosis.

A study of the relationship between the severity of dysbiotic changes and persistent characteristics revealed an increase in the persistent characteristics of blastocysts with an increase in the severity of microecological disturbances in the intestine. The revealed relationship between persistent features of protozoa and the severity of disturbances in the intestinal microbiocenosis made it possible to consider persistence factors as markers of the dysbiotic process.

#### 4. CONCLUSION

The study of the intestinal microbiome in persons working in foundry conditions, characterized by the complex effect of the examined factors of physical and chemical nature on the body, allowed to detect qualitative and quantitative changes in the composition of the normal flora of the large intestine. A decrease in the occurrence of obligate microflora representatives and an increase in the conditionally pathogenic group were registered. Experimental data revealed four severity levels of dysbiotic disorders in individuals of the examined group, which were directly dependent on the length of service at the enterprise. In persons with an experience of 10-15 years or more, in  $73.56 \pm 2.3\%$  ( $p < 0.05$ ) of cases, there were changes in intestinal dysbiosis of the 4th degree. In the control group, no visible changes in the composition of the obliterate representatives were found ( $p < 0.05$ ).

The study of intestinal parasitocenosis of the examined biotope showed the prevalence of the protozoan group *Blastocystis* spp. ( $62.00 \pm 5.4\%$ ). The studies showed that, depending on

the duration of work in the foundry, blastocysts in the feces of workers increases from  $56.30 \pm 4.6\%$  in the first group, where the duration of work ranged from 1 year to 5 years, up to  $85.63 \pm 7.8\%$  in the examined, with experience of 10-15 years or more.

The studies performed allowed to determine the quantitative composition of the blastocyst strains isolated from the examined individuals, depending on the degree of intestinal dysbiosis.

The largest number of protozoa is *Blastocystis* spp. found in the feces of individuals with dysbiotic changes of the II degree of severity - 28 strains ( $47.50 \pm 1.7\%$ ,  $p < 0.03$ ). The data obtained can be interpreted in the context of the fact that the simplest blastocysts, together with a community of other microorganisms, participate in the formation of a special microbiocenosis of the studied biotope, characterized by a decrease in representatives of the obligate flora and a significant increase in the optional one.

The data on a high level of severity of persistent properties of strains of *Blastocystis* spp. were obtained using ALA, ALFA, and AHA as an example. The results of the study allowed not only to detect them but also to rank according to the degree of their information content. The leading persistent trait that determines the formation of the intestinal microbiocenosis of a given biotope is their antilysocyme trait.

An increase in the persistent characteristics of blastocysts with an increase in the depth of microecological disturbances in the intestine was established. The revealed relationship between persistent features of protozoa and the depth of disturbances in the intestinal microbiocenosis made it possible to consider persistence factors as markers of the dysbiotic process.

## 5. REFERENCES

1. Abe, N. Molecular and phylogenetic analysis of *Blastocystis* isolates from various hosts. *Vet Parasitol.*, **2004**, 120(3), 235-242.
2. Afanasova O.E., Poteryaeva E.L., Vereshchagina G.N. The influence of working conditions on the formation of arterial hypertension in workers at high occupational risk. *Occupational medicine and industrial ecology.* **2010**, 8, 19-22.
3. Blaser, M.J.; Falkow, S. Disappearing Microbiota. *Clinical pharmacology and therapy*, **2014**, 23(4), 7-15.
4. Bukharin, O.V. Method for determination of antilysocyme activity of microorganisms. *Journal of Microbiology*, **1984**, 2, 27-39.
5. Bukharin, O. V.; Chernov, O. L.; Matyushina, S. B. A method for determining the anticarnosine activity of microorganisms. *RF Patent No. 2132879*, Patent holder Institute of Cellular and Intracellular Symbiosis of the Ural Branch of the Russian Academy of Sciences, **1999**, Bull. Number 19.
6. Bukharin, O. V.; Nemtseva, N. V.; Yatsenko-Stepanova, T.N. Assessment of the relationship of symbionts of phytoplankton community. *Ecology*, **2010**, 1, 17-21.
7. Bukharin, O. V.; Perunova, N. B.; Chaynikova, I. N.; Ivanovam, E. V.; Smolyagin, A. I. Anticytokine activity of microorganisms. *Journal of Microbiology, Epidemiology and Immunobiology*, **2011**, 4, 56-61.
8. Denisov, E. I.; Prokopenko, L. V.; Sivochalova, O. V.; Chelishcheva, M. Yu.; Chesalin, P. V. Methodological issues of identifying and preventing diseases associated with work. Saint-Petersburg. Proceedings of the All-Russian scientific-practical conf. with international participation: "Modern problems of hygienic science and occupational medicine." Ufa, 2010.
9. Dogruman, A.; Adışen, E.; Kuştımur, S.; Gürer, M.A. The role of protozoan parasites in etiology of urticarial. *Turkiye Parazitolo Derg.*, **2009**, 33(2), 136-139.
10. Hameed, D. M.; Hassanin, O. M.; Zuel-Fakkar, N. M. Association of *Blastocystis hominis* genetic subtypes with urticarial. *Parasitol Res.*, **2011**, 108(3), 553-560.
11. Horiki, N.; Kaneda, Y.; Maruyama, M.; Fujita, Y.; Tachibana, H. Intestinal blockage by carcinoma and *Blastocystis hominis* infection. *Am. J. Trop. Med. Hyg.*, **1999**, 60(3), 400-402.
12. Iguchi, A.; Ebisu, A.; Nagata, S.; Saitou, Y.; Yoshikawa, H.; Iwatani, S.; Kimata, I. Infectivity of different genotypes of human *Blastocystis hominis* isolates in chickens and rats. *Parasitol. Int.*, **2007**, 56(2), 107-112.
13. Izmerov, N.F. *Occupational health risks for workers*: Hand-in; Izmerov, N.F.; Denisov, E. I., eds; Trent: Moscow, 2003, p. 430.

14. Jones, M. S.; Whipps, C. M.; Ganac, R. D.; Hudson, N. R. Boorom, K. Association of *Blastocystis* subtype 3 and 1 with patients from an Oregon community presenting with chronic gastrointestinal illness. *Parasitol. Res.*, **2009**, 104(2), 341-345.
15. Koza, N. M.; Sergeevnin, V. I.; Gorban, L.Ya. The spread of intestinal protozoa among the population of a large city. Materials of VIII All-Russian Congress of Epidemiologists, Microbiologists and Parasitologists; LLC "Rosinex": Moscow, 2002, 1, 339-340.
16. Krasnoperova, Yu.Yu. Characterization of changes in the pathogenic potential of symbiont microorganisms in protozoa-bacterial associations: Ph.D. thesis. biol. Sciences, Orenburg, 2009,
17. Kuchumova, S. Yu.; Poluektova, E. A.; Sheptulin, A. A.; Ivashkin, V. T. Physiological significance of intestinal microflora. *Russian Journal of Gastroenterology, Hepatology and Coloproctology*, **2011**, 5, 17-27.
18. Kuvaeva, I. B.; Ladodo, K. S. *Microecological, and immune disorders in children*; Medicine: Moscow, 1991, p. 240.
19. Lazarenkov, A. M.; Khoreva, S. A. Analysis of industrial factors of foundries. Foundry and Metallurgy, 2016. Belarus: proceedings of the 24th International Scientific and Technical Conference (Minsk, October 19–21, 2016). Minsk: Publishing House of the Belarusian National Technical University. **2016**, 117-120.
20. Meloni, D.; Sanci, G.; Poirier, P.; El Alaoui, H.; Chabé, M.; Delhaes, L.; Dei-Cas, E.; Delbac, F.; Luigi Fiori, P.; Di Cave, D.; Viscogliosi, E. Molecular subtyping of *Blastocystis* sp. isolates from symptomatic patients in Italy. *Parasitol. Res.*, **2011**, 109(3), 613-619.
21. Potaturkina-Nesterova, N.I.; Kvasova, N. A.; Nesterov, A. S. Blastocyst invasion and intestinal dysbiosis (monograph). Ulyanovsk: Ulyanovsk State University Publishers, 2003. P. 221.
22. Sharapov, R. V. Transition from technical to natural-technical systems. *Mechanical Engineering and Life Safety*. **2012**, 2 (12), 43-46.
23. Soloviev, L. P. State of the monitoring system of environmental and economic systems. *Mechanical Engineering and Life Safety*. **2013**, 1, 15-19.
24. Starostina, O. Yu.; Zapariy, S. P.; Tolmacheva, A. M. The prevalence of parasitic infestations in urban residents. Materials of VIII All-Russia. Congress of Epidemiologists, Microbiologists, and Parasitologists; Rosinex LLC: Moscow, 2002, 1, 403-404.
25. Tsimmerman, Ya. S.; Tsimmerman, I. Ya. Classification of gastroenterological diseases and clinical syndromes, 4th ed., Perm, 2014.
26. Turovets, O. G. *Organization of production and enterprise management*: Textbook; Turovets, O.G.; Bukhalkov, M.I.; Rodionov V. B., eds.; SIC INFRA-M: Moscow, 2015, p.506.

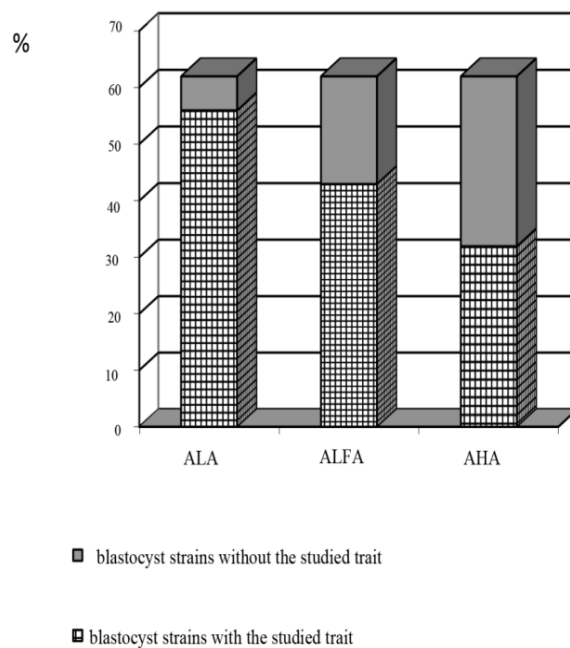


**Fig. 1.** Occurrence rate of ALA, ALFA, AHA in blastocyte strains

**Table 1.** Factors of dysbiotic disorders of the large intestine of workers invaded by *Blastocystis* spp.

| Degree of intestinal dysbiosis | Number of examined (n) | Occurrence frequency of intestinal dysbiosis (%) | Number of <i>Blastocystis</i> spp. strains |
|--------------------------------|------------------------|--|--|
| I                              | 24                     | $30.00 \pm 2.2\%$                                | 18   |
| II                             | 38                     | $47.50 \pm 1.7\%$                                | 28   |
| III                            | 11                     | $13.75 \pm 1.3\%$                                | 9  |
| IV                             | 7                      | $8.75 \pm 3.2\%$                                 | 7  |
| Total                          | 80                     | 100  | 62   |

**Table 2.** Indices of antilysocyme activity (ALA) in *Blastocystis* spp.

| Groups                    | Number of strains with ALA (abs.) | Occurrence rate (%) |
|---------------------------|-----------------------------------|---------------------|
| 1 group (low ALA values)  | 19                                | $33.92 \pm 2.3$     |
| 2 group (mean ALA values) | 28                                | $50.01 \pm 4.6$     |
| 3 group (high ALA values) | 9                                 | $16.07 \pm 1.7$     |
| Total                     | 56                                | 100                 |

**Table 3.** The relationship of the degree of intestinal dysbiosis with the severity of the *Blastocystis* spp. antilysocyme activity

| Degree of intestinal dysbiosis | Number of strains with ALA (abs) | Low ALA level (mg/ml) | Mean ALA level (mg/ml) | High ALA level (mg/ml) |
|--------------------------------|----------------------------------|-----------------------|------------------------|------------------------|
|                                |                                  | 2,1±0,02              | 2,3±0,02               | 2,7±0,05               |
| I                              | 10                               | 7                     | 3                      | -                      |
| II                             | 26                               | 10                    | 9                      | 7                      |
| III                            | 11                               | -                     | 6                      | 5                      |
| IV                             | 9                                | -                     | 2                      | 7                      |
| Total                          | 56                               | 17                    | 20                     | 19                     |
| %                              | 100                              | 30.36 ± 2.8%          | 35.71 ± 4.2%           | 33.93 ± 5.6%           |

**Table 4.** Indicators of antilactoferrin activity (ALFA) in *Blastocystis* spp.

| Groups                     | Number of strains with ALFA (abs) | Occurrence rate (%) |
|----------------------------|-----------------------------------|---------------------|
| 1 group (low ALFA levels)  | 9                                 | 20.93±3.7           |
| 2 group (mean ALFA levels) | 20                                | 45.51±2.3           |
| 3 group (high ALFA levels) | 14                                | 32.56±2.7           |
| Total                      | 43                                | 100                 |

**Table 5.** The relationship of intestinal dysbiosis degree with the severity of *Blastocystis* spp. antilactoferrin

| Degree of intestinal dysbiosis | Number of strains with ALFA (abs.) | Low ALFA level (ng/ml) | Mean ALFA level (mg/nl) | High ALFA level (ng/ml) |
|--------------------------------|------------------------------------|------------------------|-------------------------|-------------------------|
|                                |                                    | 65-161±22.2            | 162-223±30.7            | 224-289±49.3            |
| I                              | -                                  | 1                      | -                       | -                       |
| II                             | 19                                 | 9                      | 2                       | 7                       |
| III                            | 13                                 | -                      | 6                       | 7                       |
| IV                             | 11                                 | -                      | -                       | 11                      |
| Bcero                          | 43                                 | 10                     | 8                       | 25                      |
| %                              | 100                                | 23.25 ± 2.4            | 18.60 ± 3.6             | 58.15 ± 5.3             |

**Table 6.** Parameters of antihistone activity (AHA) in *Blastocystis* spp.

| Groups                     | Number of strains with AHA (abs.) | Occurrence rate (%) |
|----------------------------|-----------------------------------|---------------------|
| 1 group (low ALFA levels)  | 20                                | 62.50±2.1           |
| 2 group (mean ALFA levels) | 8                                 | 25.00±1.2           |
| 3 group (high ALFA levels) | 4                                 | 12.50±3.7           |
| total                      | 32                                | 100                 |

**Table 7.** The relationship of the intestinal dysbiosis degree with the manifestation of *Blastocystis* spp. antihistone activity

| Intestinal dysbiosis degree | Number of strains with AHA (abs) | Low AHA level (ng/ml) | Mean AHA level (ng/ml) | High AHA level (ng/ml) |
|-----------------------------|----------------------------------|-----------------------|------------------------|------------------------|
|                             |                                  | 1.3–5.3±0.9           | 5.7-9.1 ± 4.3          | 9.2-12.8 ± 4.6         |
| I                           | 15                               | 12                    | 3                      | -                      |
| II                          | 9                                | -                     | 9                      | -                      |
| III                         | 4                                | -                     | 3                      | 1                      |
| VI                          | 4                                | -                     | -                      | 4                      |
| Bcero                       | 32                               | 12                    | 15                     | 5                      |
| %                           | 100                              | 37.50 ± 5.3           | 46.88 ± 2.7            | 15.63 ± 1.3            |

**AVALIAÇÃO DA BIOEQUIVALÊNCIA EM VOLUNTÁRIOS SAUDÁVEIS DE TABLETS ORODISPERSÍVEIS COM OLANZAPINA**

**ASSESSMENT OF OLANZAPINE ORODISPERSIBLE TABLETS BIOEQUIVALENCE IN HEALTHY VOLUNTEERS**

**ОЦЕНКА БИОЭКВИВАЛЕНТНОСТИ ДИСПЕРГИРУЕМЫХ ТАБЛЕТИРОВАННЫХ ФОРМ ОЛАНЗАПИНА У ЗДОРОВЫХ ДОБРОВОЛЬЦЕВ**

LISOVSKAYA, S. B.<sup>1\*</sup>; KARGIN, V. S.<sup>1</sup>; MATYUSHIN, A. A.<sup>1</sup>; TITOVA, N. A.<sup>1</sup>; BELOV, A. V.<sup>1</sup>

<sup>1</sup> Sechenov First Moscow State Medical University. Moscow, Russia.

\* Correspondence author  
e-mail: sb.lisovskaya@bk.ru

Received 02 February 2020; received in revised form 30 June 2020; accepted 03 July 2020

**RESUMO**

A forma dispersa de comprimidos (ODT) dos medicamentos é conveniente para os pacientes; a eficácia de seu uso aumenta significativamente com o tratamento de não conformidade de transtornos mentais. Após o vencimento da patente do medicamento original, a produção de genéricos com o mesmo ingrediente farmacologicamente ativo geralmente começa. Devido a diferenças nas cargas e nas técnicas de fabricação, mesmo cópias de alta qualidade do produto original podem não ser equivalentes. Portanto, o objetivo deste estudo foi avaliar a bioequivalência da forma ODT do medicamento original e genérico com 10 mg de olanzapina. Depois de consumir o medicamento original e o genérico, em dois estágios, com o estômago vazio de voluntários saudáveis, foram coletadas amostras de sangue venoso em tubos a vácuo com heparina. O período entre as doses dos medicamentos foi de 21 dias. A extração (LLE) da olanzapina foi realizada com uma mistura de n-hexano:isopropanol (3:1) com pH 8,0, e analisada por cromatografia líquida-espectrometria de massa em tandem (armadilha de íons quadrupolo-linear). O grau de extração da olanzapina do sangue (amostras modelo, 20 ng/ml) foi de 75,2% (CV 4,6%). O limite quantitativo para a olanzapina por HPLC-MS/MS (LLOQ) foi de 0,50 ng/ml (CV 2,0%, precisão 17,6%). Os estudos conduzidos em sistema aberto randomizado mostraram um perfil de biodisponibilidade e bioequivalência satisfatório do medicamento original e olanzapina genérica. Os parâmetros farmacocinéticos calculados para os valores médios convertidos logaritmicamente, verificados com um intervalo de confiança de 90%, foram:  $C_{max}$  - 95,93-99,80% (valor médio 97,64%);  $AUC_{0-t}$  - 95,43-100,35% (valor médio 97,75%);  $C_{max} / AUC_{0-t}$  - 94,44-101,73% (valor médio 97,87%).

**Palavras-chave:** olanzapina, comprimido orodispersível, bioequivalência genérica, LC-MS / MS.

**ABSTRACT**

Dispersible tablet form (ODT) of drugs is convenient for patients to take; the effectiveness of its use increases significantly with non-compliance treatment of mental disorders. Upon the expiration of the patent for the original drug, the production of generics with the same pharmacologically active ingredient often starts. Due to differences in fillers and manufacturing techniques, even high-quality copies of the original product may not be equivalent to it. Therefore, the aim of this study was to evaluate the bioequivalence of the ODT form of the original drug and generic with 10 mg olanzapine. After taking the original drug and generic in two stages, on an empty stomach from healthy volunteers, from the vein were sampled bloods into vacuum heparin tubes. The washout period between doses of the drugs was 21 days. The extraction (LLE) of olanzapine was carried with a mixture of n-hexane:isopropanol (3:1) at pH 8.0, and analyzed by liquid chromatography-tandem mass spectrometry (quadrupole-linear ion trap). The degree of extraction olanzapine from bloods (model samples, 20 ng/ml) was 75.2% (CV 4.6%). The quantitative limit for olanzapine by HPLC-MS/MS (LLOQ) was 0.50 ng/ml (CV 2.0%, accuracy 17.6%). Conducted on an open randomized cross scheme studies showed a satisfactory bioavailability and bioequivalence profile of the original drug and generic containing olanzapine. The calculated pharmacokinetic parameters for the logarithmically converted mean values verified with a 90% confidence interval were:  $C_{max}$  - 95.93-99.80% (average value 97.64%);  $AUC_{0-t}$  - 95.43-100.35% (average value 97.75%);  $C_{max} / AUC_{0-t}$  - 94.44-101.73% (average value 97.87%).

**Keywords:** olanzapine, orodispersible tablet, bioequivalence, generic, LC-MS/MS.

## АННОТАЦИЯ

Диспергируемая таблетированная форма (ДТ) лекарственных препаратов удобна для приема пациентами; эффективность ее применения существенно возрастает при нонкомплаенсе лечения психических расстройств. По окончании срока действия патента на оригинальное лекарство часто запускается производство дженериков с тем же фармакологически активным ингредиентом. Из-за различий в наполнителях и технологиях изготовления даже высококачественные копии оригинального препарата могут быть не эквивалентны ему. Поэтому целью данного исследования было оценить биоэквивалентность ДТ формы оригинального препарата и дженерика с содержанием оланзапина 10 мг. После приема оригинального препарата и дженерика в два этапа, натошак у здоровых добровольцев из вены отбирались пробы крови в вакуумные пробирки с гепарином. Период вымывания между дозами препаратов составлял 21 день. Извлечение оланзапина проводили методом жидкостно-жидкостной экстракции смесью н-гексан: изопропанол (3:1) при pH 8,0, анализировали методом жидкостной хроматографии с тандемной масс-спектрометрией (квадруполь-линейная ионная ловушка). Степень извлечения оланзапина из крови (модельные образцы 20 нг/мл) составила 75,2% (CV 4,6%). Предел количественного определения оланзапина методом ВЭЖХ-МС/МС составил 0,50 нг/мл (CV 2,0%, точность 17,6%). Проведенные по открытой рандомизированной перекрёстной схеме исследования показали удовлетворительный профиль биодоступности и биоэквивалентности оригинального препарата и дженерика, содержащих оланзапин. Рассчитанные фармакокинетические параметры для логарифмически преобразованных средних значений верифицированные с 90%-ным доверительным интервалом составили:  $C_{max}$  - 95,93-99,80% (среднее значение 97,64%);  $AUC_{0-t}$  - 95,43—100,35% (среднее значение 97,75 %);  $C_{max}/AUC_{0-t}$  - 94,44-101,73% (среднее значение 97,87%).

**Ключевые слова:** оланзапин, диспергируемая таблетка (ДТ), биоэквивалентность, дженерик, ВЭЖХ-МС/МС.

## 1. INTRODUCTION:

Development of second generation of atypical antipsychotics, such as olanzapine (a thienobenzodiazepine derivative), provided a possibility for new, safer standards of psychiatric disorders treatment (San, Casileas, Ciudad, and Gilaberte, 2011).

Olanzapine binds to serotonin (5-HT<sub>2A/2C</sub>, 5-HT<sub>3</sub>, 5-HT<sub>6</sub>), dopamine (D<sub>1</sub>, D<sub>2</sub>, D<sub>3</sub>, D<sub>4</sub>, D<sub>5</sub>), and muscarinic (M<sub>1-5</sub>) receptors, as well as to  $\alpha_1$ -adrenoreceptors and histamine H<sub>1</sub>-receptors, which predetermines its pharmacological activity. Olanzapine  $C_{max}$  in serum is reached within 5-8 hours; the concentrations (1-20 mg) are changing linearly, proportional to the dose of the drug. The degree of plasma protein binding is high (FB 0.93) (Tolmacheva, 2019).

Orodispersible tablets (ODT) of olanzapine, manufactured using Zydis® technology, provide several advantages over traditional tablets as they increase patient compliance and more comfortable for use in patients who have difficulty swallowing (San, Casillas, and Gilaberte, 2008; Seager, 1998; Sreenivas, Dandagi, Gadad, and Godblou, 2005). It should be noted that olanzapine absorption depends heavily on the manufacturing technology and dosage form composition: particle size and excipients affect both rate and degree of API

absorption, considering that olanzapine dissolves faster in the acidic environment of the stomach than in the neutral environment of saliva (Chauhan, Kadliya, Patel, Patel, and Patel, 2014; Hobbs, Karagianis, Treuer, and Raskin, 2013; Kozlova, Zabolotnaya, and Maslova, 2015; Maher, Ali, Salem, and Abdelrahman, 2016; Sun, McDonnell, and von Moltke, 2018).

Taking into account increasing trends for wider use of generic (reproduced) drugs in the Russian Federation and worldwide, including drugs released in form of generic ODTs, obligatory tests must be performed in order to confirm their bioequivalence to the original drugs (Russian Federation. Federal Law, 2010). Robust and inexpensive, generic drugs are often preferred due to optimal combination of clinical efficacy, safety and lower costs of treatment (Shabelsky, 2015). However, the conclusion about equivalence of the generic and original drug should be based on the results of comprehensive studies (Russian federation. Ministry of Health and Social Development, 2008; Yin *et al.*, 2016; Yu, Lou, Ruon, Jiang, and Chen, 2012).

Now increasingly a highly sensitive and reproducible method liquid chromatography-tandem mass spectrometry has for the quantification olanzapine in whole blood (plasma, serum) (Cavalcanti Bedor *et al.*, 2015; Domingues *et al.*, 2016; Steuer *et al.*, 2015; Ufinovská *et al.*,



2012).

Olanzapine is a weak base (pKa1 5.0; pKa2 7.4, pKa3 14, 7), has a log P 3.0 and strongly binds to blood proteins. Various extraction variants are used to extract olanzapine from blood samples (Nielsen *and* Johansen, 2009; Poothong, Lundanes, Thomsen, *and* Haug, 2017), but the liquid-liquid extraction (LLE) method is simpler to perform and economical. Therefore, in a carried study, a used optimized variant of liquid-liquid extraction a blood sample for analysis olanzapine developed using the special program "ASD/Percepta".

Olanzapine is administered in doses of 5-40 mg / day, the level and time to reach its maximum concentration in the blood varies depending on the dosage form used, and its pharmacokinetic profile is affected by the genotype of the subject (Chen *et al.*, 2012; Citrome *et al.*, 2009; Fan *et al.*, 2020; Markowitz *et al.*, 2006; Polasek *et al.* 2018; Sathirakul *et al.*, 2003).

A critical analysis of the publications showed that patients prefer the dispersible form of the drug and studies are being conducted in different countries to study the bioequivalence of generics from various manufacturers, especially it actual for the often administered doses of olanzapine 10-20 mg/day (Cánovas *et al.*, 2011; Chatsiricharoenkul *et al.*, 2011; Chatsiricharoenkul, 2009; Du *et al.*, 2019; Elshafeey, Elsherbiny, *and* Fathallah, 2009; Sun *et al.*, 2016; Waykar *and* Kulkarni, 2012; Zakeri-Milani, Islambulchilar, Ghanbarzadeh, *and* Valizadeh, 2013).

Therefore, the aim of the study was to compare bioavailability and bioequivalence of a single, orodispersible dose of olanzapine (10 mg), manufactured by Teva Operations Poland Sp.z.o.o. (Olanzapine-DT-Teva, generic drug (T)) and by Catalent U.K. (Zyprexa® Zydis®, original drug, (R)).

## 2. MATERIALS AND METHODS:

### **Reference standards and reagents:**

Olanzapine and clozapine reference standards (RS) ( $\geq 98\%$  purity, HPLC) were purchased from Sigma-Aldrich (USA). Ascorbic acid (pharmacopoeial quality) was purchased from FARM,  $\Phi$ C-42-2668-95. Methanol (HPLC-MS grade), isopropanol, *n*-hexane, formic acid, and ammonium acetate (HPLC grade) were obtained from Merck KGaA (Germany). Deionized water for HPLC analysis was obtained using Barnstead

Easypure II, Model 7134 (Thermo Fisher Scientific, USA) water purification system.

**Instrumentation:** Atom 80 (Biotron, Spain) automatic shaker, Eppendorf 5415C (Eppendorf, Germany) centrifuge, Eppendorf Concentrator 5301 (Eppendorf, Germany). HPLC-ESI-MS/MS was conducted on a Shimadzu (Columbia, MD) HPLC system composed of two LC-20AD pumps with a CTO-20A column oven, DGU-20A3 degasser and CBM 20A controller connected to a SIL20A autosampler all interfaced with an API Sciex 3200 triple quadrupole mass spectrometer (Applied Biosystems/MDS Sciex, Foster City, CA). Analyst 1.6.3 software (AB Sciex, Foster City, CA) was utilized for instrument control, data acquisition, and analyte mass spectrometric parameter optimization.

**Volunteers:** A total of 18 healthy, non-smoking male volunteers (Caucasian, age 18-45) were included in the study after signing informed consent agreement and undergoing medical examination.

**Study design:** An open randomized crossover study was carried out in two stages: a course of original drug was followed by a 21-day washout period, then a course of generic drug. The drugs were administered on an empty stomach. Both drug products during study satisfied manufacturers' quality requirements and were within their shelf-life limits. Blood samples were withdrawn prior to drug administration and 1.0, 2.0, 3.0, 3.5, 4.0, 4.5, 5.0, 5.5, 6.0, 7.0, 8.0, 9.0, 10.0, 12.0, 16.0, 24.0, 36.0, 48.0, 72.0, 120.0, and 168.0 hours after olanzapine administration. Blood samples from cubital vein were collected into vacuum test tubes containing heparin and allowed to stand for 5-10 min before centrifugation. After centrifugation for 10 min at 2500 RPM, separated plasma was transferred into labeled plastic vials. All samples were stored at  $-40^{\circ}\text{C}$  in low-temperature freezer (Sanyo, Japan) until analysis.

**Analytical procedure:** The method of liquid-liquid extraction was developed based on calculations of the physicochemical parameters of olanzapine by the specialized ACD/Percepta program (pKa, LogP, LogD). Also, using this program "ACD/Percepta", an internal standard of clozapine (LogP 3,37) was selected, which has physico-chemical parameters similar to olanzapine (Figure 1 and 2). The selection of the internal standard is very important for the sample preparation and analysis stage, as it allows the sample preparation to rectify the effect of error on the measurement results by correcting it

mathematically (using the ratio).

The LogP distribution coefficient (octanol/water) determines the lipophilicity of the compound and its distribution between two immiscible phases, with different polarity properties. Indices of acidity (pKa) of olanzapine allow to determine optimal solution pH for its dissolution, and LogD characterizing dependence between LogP and pKa was used to achieve maximum extraction of olanzapine (Sanjivanjit, 2019). As can be seen from the figures, the non-ionized form of substances already prevails at a pH above 8, and the change Log D is insignificant. On the basis of the obtained data, a protocol of operational procedures for analysis (SOP) was developed.

In order to extract olanzapine from plasma samples, 2 mcl of clozapine methanol solution (internal standard, 225 ng/ml) were added to 100 mcl of plasma in 2 mL Eppendorf centrifuge test tubes, followed by 25 mcl of 5% ascorbic acid solution, 400 mcl of carbonate buffer (pH 8), 1 ml of n-hexane-isopropanol mixture (3:1), and 150 mg of sodium chloride. The mixture was shaken for 10 minutes using automatic shaker. After that, all samples were centrifuged for 10 min at 12500 RMP. Seven hundred microliters of organic phase were transferred into vial using automatic pipette and were evaporated until dry. Dry residue was reconstituted in 100 mcl of methanol and transferred into glass inserts, which were, in turn, placed into 1,5 ml chromatographic vials. Solutions were analyzed LC-MS/MS. Separation was carried out in gradient mode (mobile phase – 0.10% ammonium acetate (A) and methanol (B), starting with 10% A, flow rate – 0,4 ml/min) on ProntoSIL 120-5-C18 AQ (2.0 x 75 mm) chromatographic column at 40°C. Injection volume – 5 mcl. Olanzapine retention time was 5.37 min (Figure 3).

Detection was performed using M+H values and MRM transition, using main and daughter ions: 313.2/256.2 m/z for olanzapine (Figure 4) and 327.3/270.2 m/z – for clozapine (internal standard, Figure 5). Olanzapine content was determined using internal standard method with automatic integration by standard AB Sciex software (Analyst 1.6.3).

The quantification procedure was validated using several parameters presented in table 1 to prove its suitability for bioequivalence studies.

Thus, the results obtained comply with the requirements of GOST, EMA, FDA and EURASES Validation Guides (European Medicines Agency, 2011; USA. Food and drug Administration, 2018;

GOST R 56431-2015; Collegion of the eurasian economic commission, 2018) and the technique was found to be suitable for quantitative determination of olanzapine in the blood. Then concentration of olanzapine in blood samples of volunteers was determined validated method as described SOP.

**Pharmacokinetic parameters calculation and statistical data processing:** All calculations were performed using SigmaPlot 12.0 (SYSTAT Software, USA) and Microsoft Excel 2007 (Microsoft, USA).

The following pharmacokinetic parameters were calculated for each participant, using olanzapine concentrations determined after administration of original drug and generic:  $C_{max}$  (maximum measured concentration),  $T_{C_{max}}$  (time until  $C_{max}$ ),  $k_{el}$  (elimination rate constant, which was derived using slope of the final (monoexponential) part of the pharmacokinetic curve, described using non-linear regression analysis),  $T_{1/2}$  (elimination half-life, calculated as natural logarithm (ln) (2)/ $k_{el}$ ),  $AUC_{0-t}$  (area under pharmacokinetic curve from time of administration (0 hours) until final blood sample withdrawal ( $t$  hours); calculated using trapezium rule),  $AUC_{0-\infty}$  (from time of administration to infinity;  $AUC_{0-\infty} = AUC_{0-t} + C_t/k_{el}$ , where  $C_t$  is the last measured drug concentration in plasma),  $AUC_{0-t}/AUC_{0-\infty}$  (this ratio, expressed as per cent, is a measure of adequacy of blood sampling time points),  $C_{max}/AUC_{0-t}$  (relative absorption rate). Consequent analysis of pharmacokinetic data included calculation of relative olanzapine bioavailability after administration of generic drug versus administration of original product ( $f' = AUC_{0-t}(T)/AUC_{0-t}(R)$ ) and calculation of  $f'' = C_{max}(T)/C_{max}(R)$  ratio for each drug. The following descriptive statistics parameters were calculated for all pharmacokinetic values: mean ( $\bar{X}$ ), standard deviation (SD), geometric mean (G), coefficient of variation (CV), median, and maximum (Max) and minimum (Min) values. Values of main pharmacokinetic parameters ( $AUC_{0-t}$ ,  $C_{max}$ , and  $C_{max}/AUC_{0-t}$ ), after logarithmic transformation, were analyzed using ANOVA with  $p < 0,05$ . For common randomized crossover study, statistical model of dispersion analysis included the following factors, which influence observed data variability: drug administration sequence, stages of study, volunteers (within sequence). Dispersion analysis was used to test hypotheses about statistical significance of each of the mentioned factors to the overall variability. Obtained residual variance was used in calculation of 90% confidence interval (CI) for the ratio of mean values of corresponding

parameter.

The conclusion about bioequivalence of compared olanzapine products was based on the assessment of 90% CIs for the ratio of logarithmically transformed mean values of main pharmacokinetic parameters ( $AUC_{0-t}$ ,  $C_{max}$ ,  $C_{max}/AUC_{0-t}$ ). The drugs were considered bioequivalent if 90% CI limits for  $AUC_{0-t}$  and  $AUC_{0-\infty}$  were within 80–125% range. For  $C_{max}$ ,  $C_{max}/AUC_{0-t}$ , and  $C_{max}/AUC_{0-\infty}$  values, which have higher variability, the range was 75–133% (Russian federation. Ministry of Health and Social Development, 2008; Pisarev, Ulyashova, Vdovin, and Tiseyko, 2013).

The study was carried out in accordance with ethical norms, principles of good laboratory practices and good clinical practices, following SOP and study protocol, which were developed in consistence with relevant local regulatory framework (Russian Federation. Federal Law, 2010; GOST 33044-2014; GOST R 52379-2005).

### 3. RESULTS AND DISCUSSION:

Obtained averaged pharmacokinetic curves of olanzapine concentrations in plasma of health volunteers (Figure 6) suggest that the type of the dependence for both studies products is essentially the same.

Using obtained pharmacokinetic curves, individual olanzapine pharmacokinetic parameters ( $C_{max}$ ,  $AUC_{0-t}$  and  $C_{max}/AUC_{0-t}$ ) required for bioequivalence assessment were calculated for each participant. Values of  $AUC_{0-t}$ ,  $T_{C_{max}}$ ,  $k_{el}$ , and  $T_{1/2}$  were also calculated in order to obtain additional information. Mean values of calculated pharmacokinetic parameters and other descriptive statistics parameters are presented in Table 2.

Results of dispersion analysis (Table 3) allowed to accept null hypothesis that the difference in mean values of main pharmacokinetic parameters is not caused by difference in composition or manufacturing technology of the drugs under comparison: the 'Drug' factor (5% level of significance) contributed insignificantly into overall variability of olanzapine pharmacokinetic parameters ( $AUC_{0-t}$ ,  $C_{max}$ ,  $C_{max}/AUC_{0-t}$ ). The critical value for assessing the contribution of drug type factors is value  $F_{0,05;1;17}$  4,45.

The effects due to 'administration period' and 'administration sequence' were also insignificant ( $p < 0.05$ ). Factor 'Volunteer (intra-sequence)' had significant effect on all

pharmacokinetic parameters ( $p > 0.05$ ), but it indicates only intraindividual variability with the volunteer group. Comparison of the obtained data showed that studied olanzapine products do not significantly differ from each other in terms of their pharmacokinetics, and individual values dispersion is identical for both drugs. Mean value ( $\pm SD$ ) of olanzapine relative bioavailabilities ( $f'$ ) after administration of generic drug versus original products was  $0,936 \pm 0.272$  and the ratio of maximum concentrations ( $f''$ ) was  $0,950 \pm 0,099$ .

Calculated 90% CI for the ratios of mean log values of olanzapine  $AUC_{0-t}$ ,  $C_{max}$ ,  $C_{max}/AUC_{0-t}$ , and intraindividual variability coefficients of these parameters are presented in Table 4.

Confidence interval for the ratio of olanzapine log  $AUC_{0-t}$  values was 96,23 - 100,45% (mean = 98.21%); thus, calculated 90% CI is within bioequivalence criteria. Confidence intervals for logarithmically transformed  $C_{max}$  and  $C_{max}/AUC_{0-t}$  values were 95,97 - 99,61% (mean = 97,70%) and 95,83 - 101,87% (mean = 98.60%), also satisfying bioequivalence criteria (Russian federation. Ministry of Health and Social Development, 2008; Romodanovsky, Goryachev, Solovieva, and Eremenko, 2018).

### 4. CONCLUSION:

It was shown that the values of 90% CIs for the ratio of log transformed olanzapine  $AUC_{0-t}$ ,  $C_{max}$ , and  $C_{max}/AUC_{0-t}$  values were 96,23-100,45%; 95,97-99,61%, and 95,83-101,87%, respectively. These results satisfy the currently accepted criteria of bioequivalence, stated in the relevant regulatory documents of the Russian Federation. Therefore, it can be concluded that two studied olanzapine orodispersible dosage forms (10 mg, manufactured by Teva Operations Poland Sp.z.o.o. and by Catalent U.K.) are bioequivalent.

### 5. REFERENCES:

1. Cánovas, M., Torres, F., Domenech, G., Cebrecos, J., Pelagio, P., Manríquez, M., ... Cabre, F. (2011). Bioequivalence evaluation of two dosage forms of olanzapine 10 mg formulations in healthy volunteers. *Arzneimittelforschung*, 61(2), 75–79.
2. Cavalcanti Bedor, N. C., Galindo Bedor, D. C., De Sousa, C. E. M., Bonifacio, F. N., Branco, D. D. M. C., Leal, L. B., and De Santana, D. P. (2015). The development and validation of a method for quantifying

- olanzapine in human plasma by liquid chromatography tandem mass spectrometry and its application in a pharmacokinetic study. *Clinical and Experimental Pharmacology and Physiology*, 42(3), 305–313.
3. Chatsiricharoenkul, S. . (2009). In vivo bioequivalence study of 10 mg Olanzapine tablets in healthy Thai volunteers. *Basic and Clinical Pharmacology and Toxicology*, 105, 102.
4. Chatsiricharoenkul, S., Thangboonjit, W., Pongnarin, P., Konhan, K., Sathirakul, K., and Kongpatanakul, S. (2011). Bioequivalence Study of 10 mg Olanzapine Tablets in Healthy Thai Volunteers. *J Bioequiv. Availab*, 3(5), 82-85.
5. Chauhan, K. V., Kadliya, P. N., Patel, B. A., Patel, K. N., and Patel, P. A. (2014). Formulation Optimization and Evaluation of Orodispersible Tablets of an Antipsychotic Drug Using Solubility Enhancement Technique. *Journal Club for Pharmaceutical Sciences*, 1(1), 33-57.
6. Chen, Q., Zhang, M.-Q., Lui, Y.-M., Li, S.-J., Lu, Ch., Liu, G.-Y., ... Jia, J.-Y. (2012). Pharmacokinetics and bioequivalence of 2 tablet formulations of olanzapine in healthy Chinese volunteers: a randomized, open-label, single-dose study. *Arzneimittelforschung*, 62(11), 508-512.
7. Citrome, L., Stauffer, V. L., Chen, L., Kinon, B. J., Kurtz, D. L., Jacobson, J. G., and Bergstrom, R. F. (2009). Olanzapine plasma concentrations after treatment with 10, 20, and 40 mg/d in patients with schizophrenia: an analysis of correlations with efficacy, weight gain, and prolactin concentration. *Journal of Clinical Psychopharmacology*, 29(3), 278–283.
8. Collegion of the eurasian economic commission. (2018). Guidance on the validation of analytical methods for testing drugs.
9. Domingues, D., Pinto, M., De Sousa, I., Hallak, J., Crippa, J., and Queiroz, M. (2016). Determination of drugs in plasma samples by high-performance liquid chromatography-tandem mass spectrometry for therapeutic drug monitoring of schizophrenic patients. *Journal of Analytical Toxicology*, 40(1), 28-36.
10. Du, P., Li, P., Liu, H., Zhao, R., Zhao, Zh., Yu, W., ... Liu, L. (2019). Open-Label, Randomized, Single-Dose, 2-Period, 2-Sequence Crossover, Comparative Pharmacokinetic Study to Evaluate Bioequivalence of 2 Oral Formulations of Olanzapine Under Fasting and Fed Conditions. *Clinical Pharmacology in Drug Development*, Oct. 8. <https://doi.org/10.1002/cpdd.743>
11. Elshafeey, A. H., Elsherbiny, M. A., and Fathallah, M. M. (2009). A single-dose, randomized, two-way crossover study comparing two olanzapine tablet products in healthy adult male volunteers under fasting conditions. *Clinical Therapeutics*, 31(3), 600-608.
12. European Medicines Agency. (2011). Guideline on bioanalytical method validation.
13. Fan, L., Zhang, L., Zheng, H., Cheng, J., Hu, Y., Liu, J., and Fan, H. (2020). Pharmacokinetics and Bioequivalence of 2 Olanzapine Orally Disintegrating Tablet Products in Healthy Chinese Subjects Under Fed and Fasting Conditions. *Clinical Pharmacology in Drug Development*, May 15. <https://doi.org/10.1002/cpdd.765>
14. GOST 33044-2014 “Principles of Good Laboratory Practice”.
15. GOST R 52379-2005 “Good Clinical Practice”.
16. GOST R 56431-2015 “Quality Management System. Medical Products. Process Validation Guide”.
17. Hobbs, D., Karagianis, J., Treuer, T., and Raskin, J. (2013). An In Vitro Analysis of Disintegration Times of Different Formulations of Olanzapine Orodispersible Tablet: A Preliminary Report. *Drugs in RandD*, 13, 281–288.
18. Kozlova, Zh. M., Zabolotnaya, P. G., and Maslova, M. N. (2015). Bystrodispersiruemye oral'nye sistemy dostavki. *Novaya nauka: ot idei k rezul'tatu*, 2, 75–78.
19. Maher, E. M., Ali, A. M. A., Salem, H. F., and Abdelrahman, A. A. (2016). In vitro/in vivo evaluation of an optimized fast dissolving oral film containing olanzapine coamorphous dispersion with selected carboxylic acids. *Drug Delivery*, 23(8), 3088–3100.

20. Markowitz, J. S., DeVane, S. L., Malcolm, R. J., Gefroh, H. A., Wang, J.-Sh., Zhu, H.-J., and Donovan, J. L. (2006). Pharmacokinetics of olanzapine after single-dose oral administration of standard tablet versus normal and sublingual administration of an orally disintegrating tablet in normal volunteers. *J Clin Pharmacol.*, 46(2), 164–171.
21. Nielsen, M. K., and Johansen, S. S. (2009). Determination of olanzapine in whole blood using simple protein precipitation and liquid chromatography-tandem mass spectrometry. *Journal of Analytical Toxicology*, 33(4), 212-217.
22. Pisarev, V. V., Ulyashova, M. M., Vdovin, K. A., and Tiseyko, N. I. (2013). Bioequivalence study of tablet forms of risperidone, olanzapine and quetiapine in healthy volunteers. *Pharmacokinetics and Pharmacodynamics*, 1, 14–22.
23. Polasek, T. M., Tucker, G. T., Sorich, M. J., Wiese, M. D., Mohan, T., Rostami-Hodjegan, A., ... Rowland, A. (2018). Prediction of olanzapine exposure in individual patients using physiologically based pharmacokinetic modelling and simulation. *British Journal of Clinical Pharmacology*, 84(3), 462-476
24. Poonthong, S., Lundanes, E., Thomsen, C., and Haug, L. (2017). High throughput online solid phase extraction-ultra high performance liquid chromatography-tandem mass spectrometry method for polyfluoroalkyl phosphate esters, perfluoroalkyl phosphonates, and other perfluoroalkyl substances in human serum, plasma, and whole blood. *Analytica Chimica Acta*, 957, 10-19.
25. Romodanovsky, D. P., Goryachev, D. V., Solovieva, A. P., and Eremenko, N. N. (2018). Principles of Statistical Evaluation of Bioequivalence Studies in the Context of Current Regulatory Requirements and Legal Acts. *The Bulletin of the Scientific Centre for Expert Evaluation of Medicinal Products*, 8(2), 92-98.
26. Russian Federation. Federal Law "On circulation of medicines" No 61-FZ dated April 12, 2010 (as amended by Federal Law of December 27, 2018 No 511-FZ). Retrieved from <https://legalacts.ru/doc/federalnyi-zakon-ot-12042010-n-61-fz-ob/>
27. Russian Federation. Ministry of Health and Social Development. (May 12, 2008). Guidelines of the Ministry of Health and Social Development of the Russian Federation "Bioequivalence assessment of medicinal products".
28. San, L., Casileas, M., Ciudad, A., and Gilaberte, I. (2011). Dispergiruemye tabletki olanzapina: obzor effektivnosti i komplensa (referat). *Psihiatriya i psihofarmakoterapiya imeni P.B. Gannushkina*, 4, 51–58.
29. San, L., Casillas, M., and Gilaberte, I. (2008). Olanzapine orally disintegrating tablet: a review of efficacy and compliance. *CNS Neuroscience and Therapeutics*, 14(3), 203-214.
30. Sanjivanjit, K. (2019). *Bhal Lipophilicity Descriptors: Understanding When to Use LogP and LogD*. Toronto, Canada: Advanced Chemistry Development, Inc.
31. Sathirakul, K., Chan, C., Teng, L., Bergstrom, R. F., Yeo, K. P., and Wise, S. D. (2003). Olanzapine pharmacokinetics are similar in Chinese and Caucasian subjects. *Br J Clin Pharmacol*, 56(2), 184–187.
32. Seager, H. (1998). Drug-delivery Products and the Zydys Fast-dissolving Dosage Form. *Journal of Pharmacy and Pharmacology*, 50(4), 375–382.
33. Shabelsky, V. S. (2015). Original drugs and generics: is there an optimal balance on the pharmaceutical market? *Young Scientist*, 8, 684 - 689.
34. Sreenivas, S. A., Dandagi, P. M., Gadad, A. P., and Godblou, A. M. (2005). Orodispersible tablets: New-fangled drug delivery systems – A review. *Indian Journal of Pharmaceutical Education and Research*, 39(4), 177–181.
35. Steuer, A., Poetzsch, M., Koenig, M., Tingelhoff, E., Staeheli, S., Roemmelt, A., and Kraemer, T. (2015). Comparison of conventional liquid chromatography-tandem mass spectrometry versus microflow liquid chromatography-tandem mass spectrometry within the framework of full method validation for simultaneous quantification of 40 antidepressants and neuroleptics in whole blood. *Journal of Chromatography A*, 1381, 87-100.

36. Sun, L., McDonnell, D., Liu, W., Carter, D., Simmons, A., and von Moltke, L. (2016). Bioequivalence evaluation of three olanzapine-containing tablet formulations in healthy volunteers. *Clinical Pharmacology in Drug Development*, 5, 19.
37. Sun, L., McDonnell, D., and von Moltke, L. (2018). Bioequivalence of Olanzapine Given in Combination With Samidorphan as a Bilayer Tablet (ALKS 3831) Compared With Olanzapine-Alone Tablets: Results From a Randomized, Crossover Relative Bioavailability Study. *Clinical Pharmacology in Drug Development*, 8(4), 459-466.
38. Tolmacheva, E. A. (Ed.). (2019). *Vidal Reference Book "Medicinal Products in Russia"*. Moscow, Russia: Vidal Rus.
39. Uřinová, R., Brožmanová, H., Šišťík, P., Šilhán, P., Kacířová, I., Lemr, K., and Grundmann, M. (2012). Liquid chromatography-tandem mass spectrometry method for determination of five antidepressants and four atypical antipsychotics and their main metabolites in human serum. *Journal of Chromatography B: Analytical Technologies in the Biomedical and Life Sciences*, 907, 101-107.
40. USA. Food and drug Administration. (May, 2018). Bioanalytical Method Validation Guidance for Industry.
41. Waykar, R., and Kulkarni, Y. (2012). Development and bioequivalence study of olanzapine 10mg tablets. *International Journal of Pharmaceutical Sciences and Research*, 3(9), 3370-3375.
42. Yin, A., Shang, D., Wen, Y., Li, L., Zhou, T., and Lu, W. (2016). Population pharmacokinetics analysis of olanzapine for Chinese psychotic patients based on clinical therapeutic drug monitoring data with assistance of meta-analysis. *Eur J Clin Pharmacol.*, 72, 933-944.
43. Yu, L.-Y., Lou, H.-G., Ruon, Z.-R., Jiang, B., and Chen, J.-L. (2012). Pharmacokinetics and bioequivalence of domestic olanzapine tablets in healthy Chinese volunteers. *Chinese Pharmaceutical Journal*, 47(23), 1934-1936.
44. Zakeri-Milani, P., Islambulchilar, Z., Ghanbarzadeh, S., and Valizadeh, H. (2013). Single dose bioequivalence study of two brands of olanzapine 10 mg tablets in Iranian healthy volunteers. *Drug Research*, 63(7), 346-350.

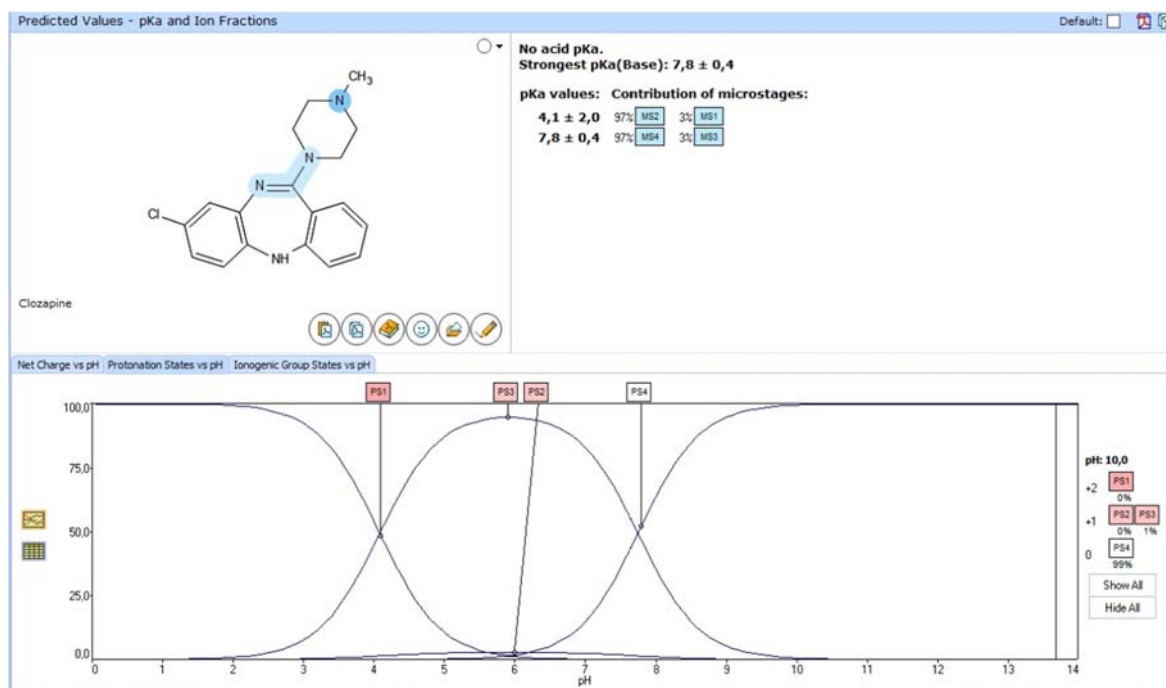
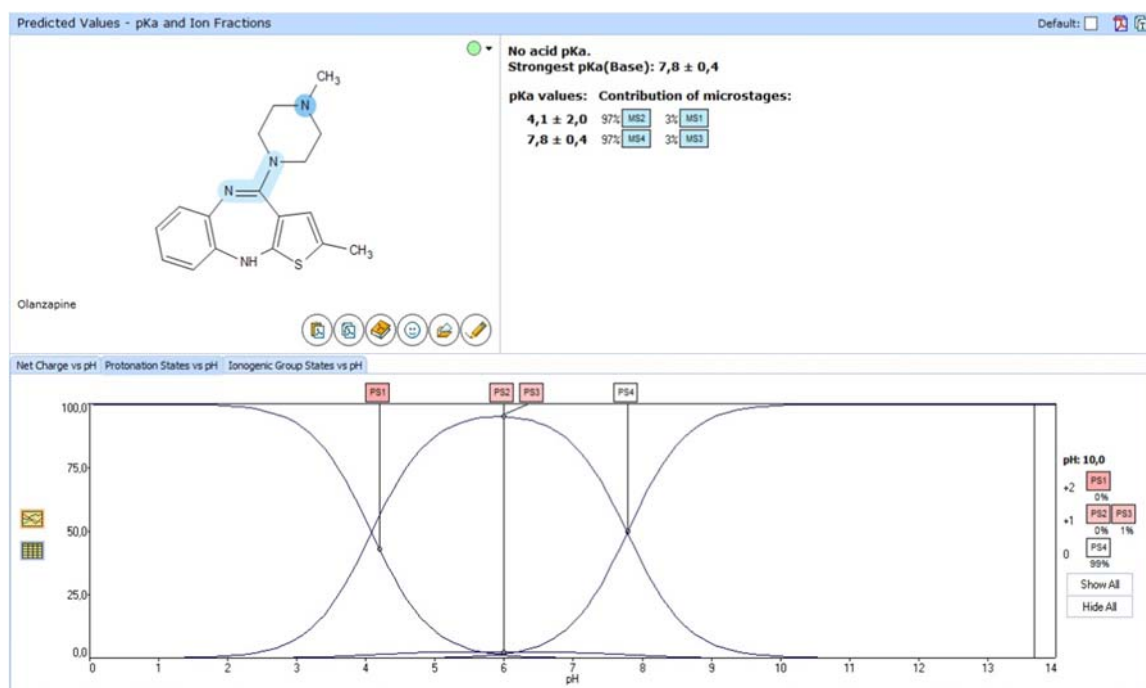


**Figure 1.** Acidity and isoelectric curve of substances



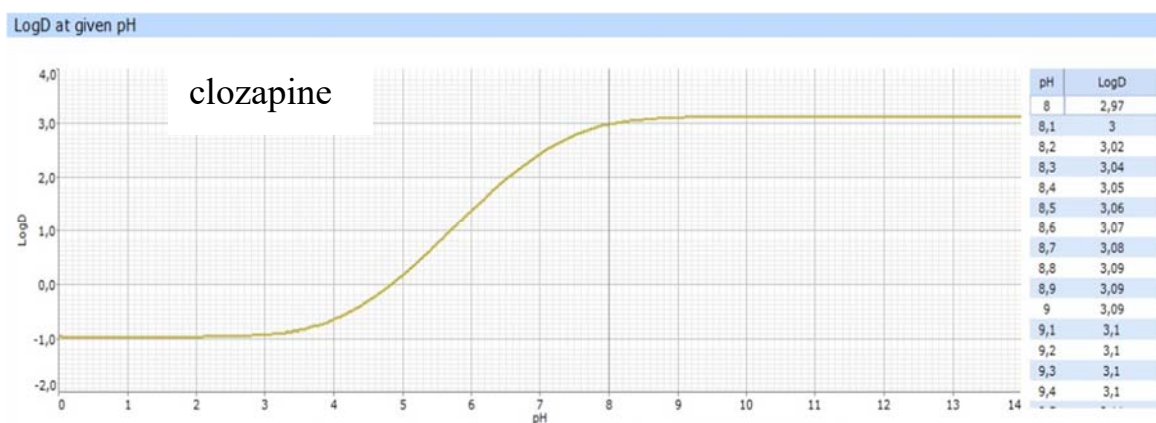
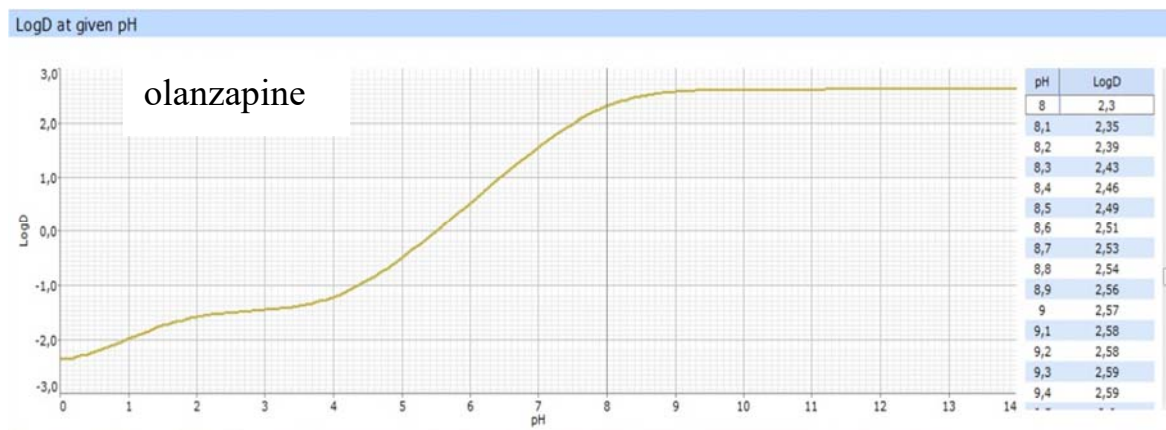


**Figure 2.** Dependence Log D from pH

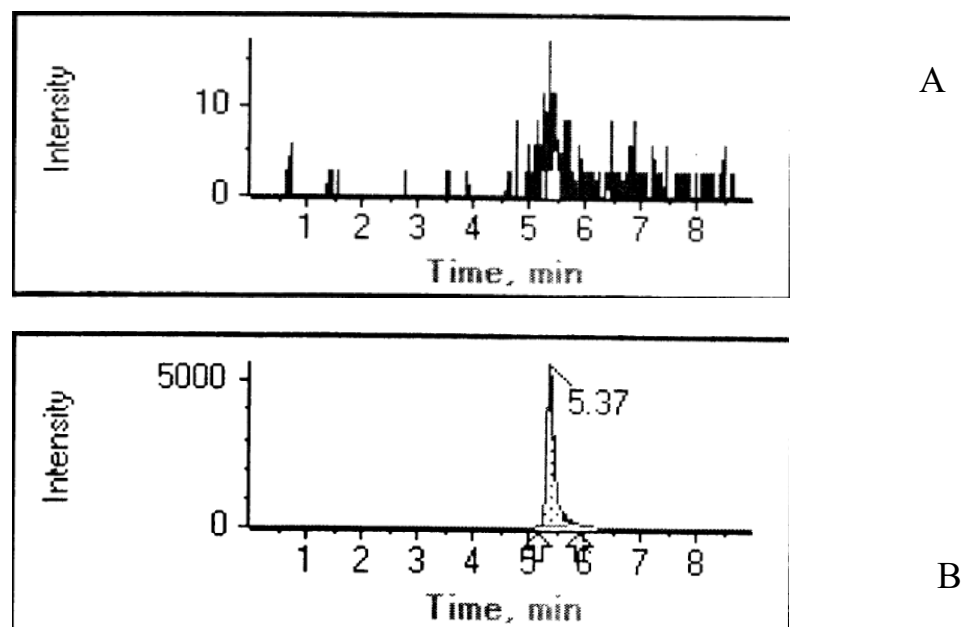


**Figure 3.** Typical blood extraction chromatogram: A-blank, B-containing olanzapine



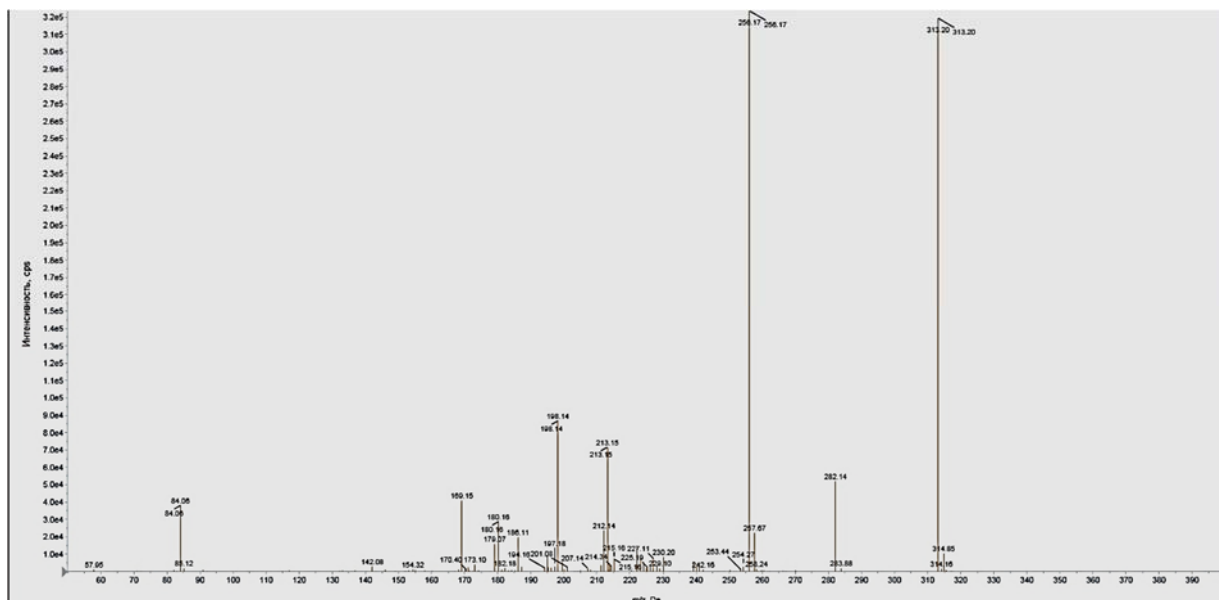


**Figure 4.** Mass spectrum of olanzapine (direct input to the MS detector in EPI mode (TIC))

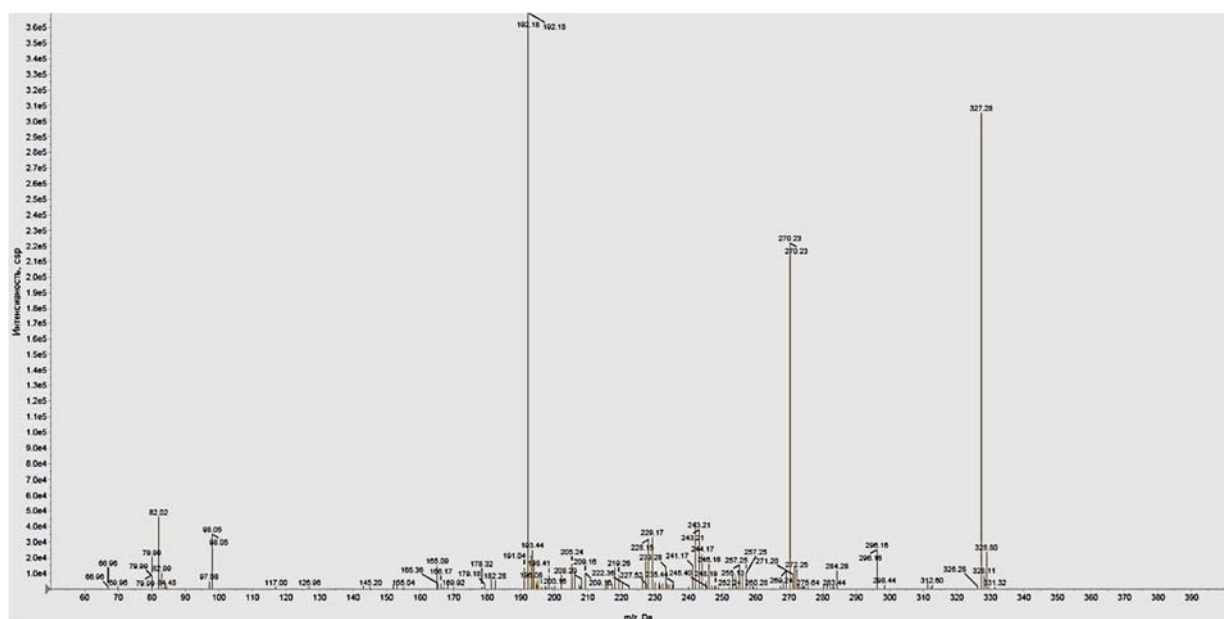


**Figure 5.** Mass spectrum of clozapine (direct input to the MS detector in EPI mode (TIC))

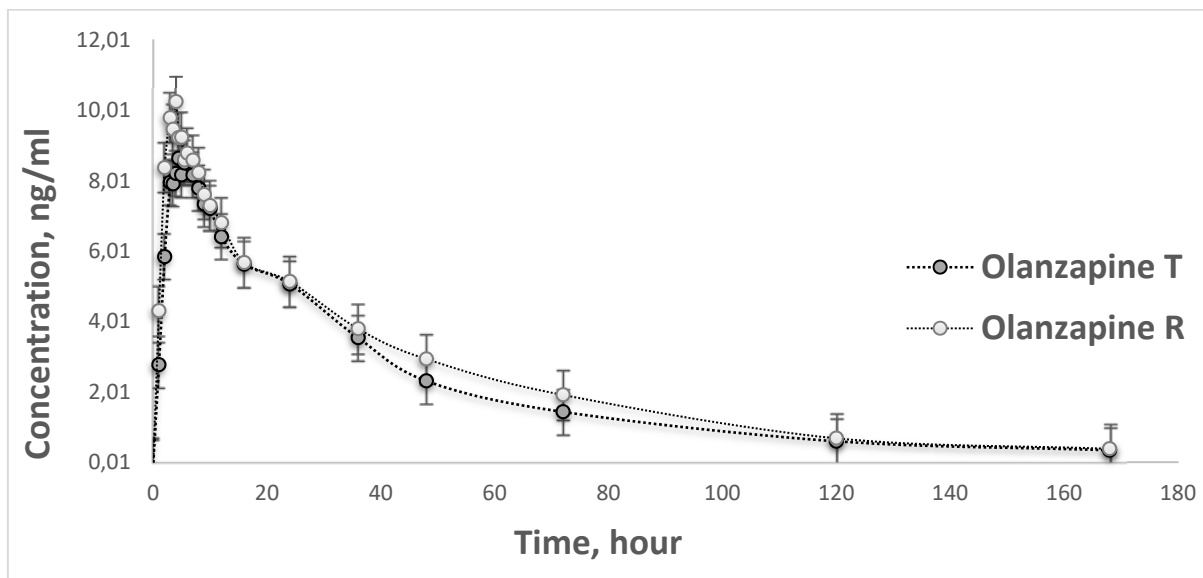


**Figure 6.** Averaged pharmacokinetic curves of olanzapine concentration in plasma of 20 volunteers after single administration of studied drugs (10 mg)

**Table 1.** Method validation

| Validation parameter                         | Testing sample                   | Results   |             | Criteria  |             |
|--|----------------------------------|---|-------------|-----------|-------------|
| Calibration curve N=3                        | Expended<br>Concentration, ng/ml | CV, %   | Accuracy, % | CV, %     | Accuracy, % |
|  | 0.25                             | -   | -           |           |             |
|  | <b>0.5</b>                       | 2,0   | 117.6       |           | <20         |
|  | 1.0                              | 2.8   | 98.2        |           | <15         |
|  | 5.0                              | 1.6   | 93.3        | <20%      | <15         |
|  | <b>10.0</b>                      | 1.0   | 91.9        |           | <15         |
|  | 15.0                             | 0.6   | 100.1       |           | <15         |
|  | 25.0                             | 1.3   | 93.7        |           | <15         |
|  | <b>50.0</b>                      | 1.0   | 105.3       |           | <15         |
| Detection Limit (LOD) 0,25 ng/ml             |                                  | Linear regression with weighting 1/x;<br>y = 0.92594x + - 0.04408 |             |           |             |
| Limit of quantification (LLOQ) 0,5 ng/ml N=9 |                                  | (0.5 ng/ml–50 ng/ml)  |             |           |             |
| Linearity                                    |                                  | r=0,99810   |             | r ≥0.9900 |             |
| Recovery, %                                  | 2.0 ng/ml                        | 92,3%   |             |           |             |
|  | 20.0 ng/ml                       | 75,2%   |             |           |             |
|  | 40.0 ng/ml                       | 75,0%   |             |           |             |
| Accuracy, %<br>N=6                           | 2.0 ng/ml                        | 99.96%  |             |           |             |
|  | 20.0 ng/ml                       | 102.22%   |             |           |             |
|  | 40.0 ng/ml                       | 104.29%   |             | 100±15%   |             |
| Precision N=6 (CV%)                          | 2.0 ng/ml                        | 2.35%   |             |           |             |
|  | 20.0 ng/ml                       | 4.61%   |             |           |             |
|  | 40.0 ng/ml                       | 6.45%   |             | <10%      |             |
| Inter day precision, %<br>N=6                | 2.0 ng/ml                        | 6.4%  |             |           |             |
|  | 20.0 ng/ml                       | 7.12%   |             |           |             |
|  | 40.0 ng/ml                       | 6.60%   |             | <10%      |             |

| Validation parameter  | Testing sample            | Results               | Criteria        |
|---|---------------------------|-----------------------|-----------------|
| Selectivity N=6<br>Calibration standard:<br>olanzapine<br>IS: closapine     | Blank,<br><br>0.5 ng/ml   | No interference       | <20%<br><br><5% |
| Carry-over (N=6), %<br>Calibration standard:<br>olanzapine<br>IS: closapine | Blank after<br>50 ng/ml   | 1,60<br><br>0,01      | <20%<br><br><5% |
| Stability, % N=3 (freeze and<br>thaw -40°C - +20°C)                         | 0.5 ng/ml<br><br>50 ng/ml | 93,93%<br><br>111,78% | <br><br>100±15% |

**Table 2.** Pharmacokinetic parameters after single administration of the studied olanzapine products

| Parameter  |   | $\bar{X}$ | Min    | Max    | Med    | SD         | G          | CV, % | C.I.<br>90% |
|--|---|-----------|--------|--------|--------|------------|------------|-------|-------------|
| C <sub>max</sub> , ng/ml                                   | T | 10,62     | 8,26   | 12,40  | 10,58  | 1,06       | 10,56      | 10,02 | 0,44        |
|  | R | 11,26     | 7,72   | 13,40  | 11,36  | 1,28       | 11,18      | 11,40 | 0,53        |
| T <sub>Cmax</sub> , h                                      | T | 5,28      | 3,00   | 10,00  | 4,50   | 1,94       | 4,98       | 36,79 | 0,80        |
|  | R | 4,33      | 2,00   | 9,00   | 4,00   | 1,76       | 4,01       | 40,70 | 0,72        |
| AUC <sub>0-t</sub> ,<br>ng•h/ml                            | T | 354,84    | 199,08 | 444,96 | 367,29 | 71,99      | 347,1<br>9 | 20,29 | 29,52       |
|  | R | 400,17    | 217,25 | 556,86 | 422,25 | 101,3<br>7 | 386,9<br>8 | 25,33 | 41,56       |
| AUC <sub>0-∞</sub> ,<br>ng•h/ml                            | T | 379,57    | 205,91 | 521,04 | 380,36 | 85,27      | 369,7<br>7 | 22,48 | 34,96       |
|  | R | 400,18    | 217,26 | 556,87 | 422,26 | 101,3<br>7 | 386,9<br>8 | 25,33 | 41,56       |
| C <sub>max</sub> /<br>AUC <sub>0-t</sub> , h <sup>-1</sup> | T | 0,03      | 0,02   | 0,05   | 0,03   | 0,01       | 0,03       | 26,40 | 0,003       |
|  | R | 0,03      | 0,02   | 0,06   | 0,03   | 0,01       | 0,03       | 27,79 | 0,003       |
| C <sub>max</sub> /<br>AUC <sub>0-∞</sub> , h <sup>-1</sup> | T | 0,03      | 0,02   | 0,05   | 0,03   | 0,01       | 0,03       | 21,48 | 0,003       |
|  | R | 0,03      | 0,02   | 0,06   | 0,03   | 0,01       | 0,03       | 26,40 | 0,003       |
| k <sub>el</sub> , h <sup>-1</sup>                          | T | 0,017     | 0,01   | 0,028  | 0,016  | 0,01       | 0,017      | 26,71 | 0,003       |
|  | R | 0,017     | 0,01   | 0,028  | 0,016  | 0,01       | 0,017      | 27,58 | 0,003       |
| T <sub>1/2</sub> , h                                       | T | 42,64     | 24,93  | 64,18  | 43,19  | 10,64      | 41,36      | 24,96 | 4,36        |
|  | R | 42,88     | 24,93  | 64,18  | 43,59  | 10,92      | 41,53      | 25,46 | 4,62        |

**Table 3.** The results of dispersion analysis of pharmacokinetic parameters  $\ln AUC_{0-t}$ ,  $\ln C_{max}$ ,  $\ln C_{max} / \ln AUC_{0-t}$  determining the bioavailability of olanzapine from dosage form

| Source of Variation         | $\ln AUC_{0-t}$               |    |        |       |
|-----------------------------|-------------------------------|----|--------|-------|
|                             | SS                            | DF | MF     | F     |
| Between Treatments/Preparat | 0,106                         | 1  | 0,106  | 1,699 |
| Between Subjects            | 1,332                         | 17 | 0,0784 | 2,287 |
| Residual                    | 0,788                         | 17 | 0,0463 | -     |
| Total                       | 2,226                         | 35 | -      | -     |
| Source of Variation         | $\ln C_{max}$                 |    |        |       |
|                             | SS                            | DF | MF     | F     |
| Between Treatments/Preparat | 0,0289                        | 1  | 0,0289 | 2,180 |
| Between Subjects            | 0,353                         | 17 | 0,0208 | 5,029 |
| Residual                    | 0,0978                        | 17 | 0,0057 | -     |
| Total                       | 0,480                         | 35 | -      | -     |
| Source of Variation         | $\ln C_{max} / \ln AUC_{0-t}$ |    |        |       |
|                             | SS                            | DF | MF     | F     |
| Between Treatments/Preparat | 0,0242                        | 1  | 0,0242 | 0,542 |
| Between Subjects            | 0,995                         | 17 | 0,0585 | 0,789 |
| Residual                    | 0,521                         | 17 | 0,0306 | -     |
| Total                       | 1,540                         | 35 | -      | -     |

Notes: SS is the sum of squared deviations; DF - the number of degrees freedom; MS is the root mean square error; F - calculated value Fisher's F-test (at a significance level of  $\alpha = 5\%$ )

**Table 4.** Values of pharmacokinetic parameters after logarithmic data transformation

| Parameter           |   | GMean  | SD     | CV, % | ratio T/R, % | CV <sub>intra</sub> , % | 90% CI<br>Lower limit<br>Upper limit, % |
|---------------------|---|--------|--------|-------|--------------|-------------------------|---|
| $C_{max}$           | T | 2,4109 | 0,1029 | 4,37  | 97,70        | 14,50                   | 95,97-99,61                             |
|                     | R | 2,3554 | 0,1262 | 5,23  |              |                         |   |
| $AUC_{0-t}$         | T | 5,8458 | 0,2224 | 3,80  | 98,21        | 28,55                   | 96,23-100,45                            |
|                     | R | 5,9523 | 0,2743 | 4,60  |              |                         |   |
| $AUC_{0-\infty}$    | T | 5,8458 | 0,2224 | 3,80  | 98,21        | 28,55                   | 96,23-100,45                            |
|                     | R | 5,9523 | 0,2743 | 4,60  |              |                         |   |
| $C_{max}/AUC_{0-t}$ | T | 3,4873 | 0,1917 | 5,49  | 98,60        | 24,54                   | 95,83-101,87                            |
|                     | R | 3,5368 | 0,2289 | 6,45  |              |                         |   |

## AVALIAÇÃO OPERACIONAL DOS PARÂMETROS DE CONTAMINAÇÃO QUÍMICA

### RAPID ASSESSMENT OF CHEMICAL CONTAMINATION PARAMETERS

### ОПЕРАТИВНА ОЦІНКА ПАРАМЕТРІВ ХІМІЧНОГО ЗАРАЖЕННЯ

MELNYK, Oleksandr V.<sup>1\*</sup>; SOVHIRA, Svitlana V.<sup>2</sup>; DUSHECHKINA, Nataliia Yu.<sup>3</sup>;  
AVRAMENKO, Oleg B.<sup>4</sup>; DUBOVA, Nataliia V.<sup>5</sup>;

<sup>1,4</sup> Pavlo Tychyna Uman State Pedagogical University; Department of Technical and Technological Disciplines, Labor Protection and Life Safety; 2 Sadova Str.; zip code 20300; Uman – Ukraine

<sup>2,3</sup> Pavlo Tychyna Uman State Pedagogical University; Department of Chemistry, Ecology and Methods of Their Training; 2 Sadova Str.; zip code 20300; Uman – Ukraine

<sup>5</sup> Pavlo Tychyna Uman State Pedagogical University; Department of Professional Education and Technology for Profiles; 2 Sadova Str.; zip code 20300; Uman – Ukraine

\* Correspondence author

e-mail: [aleksandr9949@ukr.net](mailto:aleksandr9949@ukr.net)

Received 15 April 2020; received in revised form 01 June 2020; accepted 03 June 2020

## RESUMO

O artigo descreve o risco químico que pode afetar adversamente o meio ambiente e as pessoas em caso de acidentes em instalações de alto risco, levar à poluição tecnogênica, grandes danos e mortes entre as pessoas. Foi realizada uma análise dos métodos existentes para avaliar os efeitos da contaminação química. As propriedades tóxicas de substâncias tóxicas (ST) foram reveladas. O artigo apresenta o algoritmo de cálculo e o método para prever a situação química após a emissão de ST ou derramamento acidental de substâncias altamente tóxicas (SAT) no ambiente. Mostra-se a sequência de cálculo da solução do problema de avaliação dos parâmetros químicos usando os dados iniciais condicionais. Um programa de computador foi desenvolvido para processar os parâmetros de contaminação química e calcular as perdas entre os funcionários e residentes que possam estar na área de acidentes de indústrias químicas ou emissões para o meio ambiente (de ST, SAT). A análise de cálculos realizados sem o uso do programa de computador para processamento dos parâmetros de contaminação química e de cálculos realizados com o seu uso confirma a confiabilidade do desenvolvimento com base no produto de software Microsoft Visual Studio (Visual C#). É proposto o método de cálculo e avaliação da situação química após acidentes e destruição nas instalações da indústria química. Descreve-se a aplicação prática do programa de computador desenvolvido, que permite que especialistas no campo da defesa civil (DC) realizem os cálculos mais rapidamente para determinar o grau de estabilidade vertical do ar, profundidade e área da nuvem química, tempo de sua chegada ao assentamento, perda de pessoal e população, para tomar decisões mais rapidamente, tanto em tempos de paz quanto em períodos especiais. O artigo apresenta as conclusões sobre os cálculos e os resultados obtidos na resolução de problemas de avaliação de situações químicas utilizando tecnologias modernas.

**Palavras-chave:** *exposição a substâncias perigosas, toxicidade relativa, eliminação das consequências de acidentes, características quantitativas da toxicidade, danos a objetos quimicamente perigosos.*

## ABSTRACT

The article describes a chemical hazard that can adversely affect the environment and humans in the event of accidents at high-risk facilities, lead to man-made pollution, large casualties and deaths. The existing methods of assessment of the effects of chemical contamination were analysed. The toxic properties of poisonous substances (PSs) have been revealed. The calculation algorithm has been presented and the technique for the prediction of the chemical situation after the release of explosive or emergency spills, highly toxic substances (HTS) into the environments has been disclosed. The sequence of solution calculation of the estimation of chemical parameters problem using conditional initial data has been shown. A computer program has been developed to handle the parameters of chemical contamination and to calculate losses among working personnel and residents who may end up in the accident zone of chemical industry facilities or into the environment (PS, HTS). The analysis of the calculations without the use of a computer program for processing chemical parameters

of contamination and using it confirms the reliability of its design based on the Microsoft Visual Studio software (Visual C#). The method of calculation and estimation of a chemical situation after accidents and destruction at chemical industry facilities has been offered. The practical application of the developed computer program has been described, which enables the specialists in the field of civil protection (CP) to make calculations more quickly to determine the degree of vertical stability of air, depth and area of distribution of chemical cloud, time of reaching the settlement, losses of both working personnel and population, more promptly to make decisions both in peacetime and in a special period. Conclusions were made regarding the calculations performed and the results obtained when solving the problems of chemical situation estimation using modern technologies.

**Keywords:** *impact of hazardous substances, relative toxicity, accident response, quantification of toxicity, damage to chemically hazardous objects.*

## АНОТАЦІЯ

У статті описана хімічна небезпека, яка може негативно вплинути на оточуюче середовище та людей при виникненні аварій на об'єктах підвищеної небезпеки, призвести до техногенного забруднення, великих збитків та смертельних випадків серед людей. Проведений аналіз існуючих методик оцінки наслідків хімічного зараження. Розкриті токсичні властивості отруйних речовин (ОР). Приведений алгоритм розрахунку та розкрита методика щодо прогнозування хімічної обстановки після викиду ОР або аварійного розливу, сильнодіючих отруйних речовин (СДОР) у навколишнє природне середовище. Показана послідовність розрахунку рішення задачі оцінки хімічних параметрів з використанням умовних вихідних даних. Розроблена комп'ютерна програма обробки параметрів хімічного зараження та розрахунку втрат серед працюючого персоналу та мешканців які можуть опинитися в зоні аварій об'єктів хімічної промисловості, або викиду в навколишнє середовище (ОР, СДОР). Проведений аналіз розрахунків без застосування комп'ютерної програми обробки параметрів хімічного зараження та з її використанням підтверджує про достовірність її розробки на базі програмного продукту Microsoft Visual Studio (Visual C#). Запропонована методика розрахунку та оцінки хімічної обстановки після аварій та руйнувань на об'єктах хімічної промисловості. Описане практичне застосування розробленої комп'ютерної програми, яка дає можливість фахівцям у сфері цивільного захисту (ЦЗ) більш швидше проводити розрахунки щодо визначення ступеню вертикальної стійкості повітря, глибини та площі розповсюдження хімічної хмари, часу досягнення до населеного пункту, втрат як працюючого персоналу так і населення, оперативніше приймати рішення як в мирний час так і в особливий період. Дані висновки стосовно проведених розрахунків та отриманих результатів при розв'язуванні задач з оцінки хімічної обстановки з використанням сучасних технологій.

**Ключові слова:** *вплив небезпечних речовин, відносна токсичність, ліквідація наслідків аварій, кількісна характеристика токсичності, ураження на хімічно небезпечних об'єктах.*

## 1. INTRODUCTION

In Ukraine, as in other industrial countries of the world, there are facilities where a large number of various chemicals, which are dangerous to the environment, toxic and harmful to human and animal health, are manufactured, recycled, disposed. Such substances are called HTS (highly toxic substances). Many of them are carried with transport, which in turn increases their risk during accidents. In addition, during a special period of state functioning, objects that store HTS may be deliberately destroyed (Bell *et al.*, 2017; Bourdrel *et al.*, 2017; Melnichuk *et al.*, 2020; Tyliczszak *et al.*, 2009; Talismanov *et al.*, 2018; Kosnik and Reif, 2019; Mo *et al.*, 2019; Krechetov *et al.*, 2018; Zavala *et al.*, 2020). In peacetime, in the event of accidents, catastrophes or other natural disasters, HTS can enter the environment and cause damage to humans, animals, plants, in

particular cause fatalities. In peacetime as well as in a special period to eliminate threats to life and health, civil protection is implemented through the implementation of localisation plans and the elimination of accidents or catastrophes. There are many different methods used to calculate the parameters of chemical contamination, which take into account the toxic properties of toxic substances (Steblyuk, 1998; Williams *et al.*, 2017; New Hampshire..., 2019; NTP. National Toxicology..., 2019).

Civil protection is one of the main priorities of the activity of the central state authorities, bodies of local self-government institutions and organisations throughout Ukraine. From the foregoing, it is clear that due consideration of the post-accident chemical environment at the facilities of the chemical industry needs to be given sufficient attention, in particular to study, investigate and implement both organisational and

technical measures (Manucci and Franchini, 2017).

Many well-known scientists were engaged in studying of PS and HTS, research and development of methods of chemical situation estimation at different times: V. N. Aleksandrov (Alexandrov and Emelyanov, 1990) classified the main types of poisonous substances, the nature and extent of their toxic action, V. G. Atamanyuk (Atamanyuk *et al.*, 1986) described the definition of the stability of poisonous substances, A. T. Altunin (1984) described the actions of the population in the conditions of infection with highly toxic substances, G. G. Migovich (2001) listed the general analytical formulas for determining the individual components of the chemical situation estimation, P. T. Egorov (Egorov *et al.*, 1977) characterised the chemical intelligence instruments, I. M. Mitsenko (Mitsenko and Mizentseva, 2004) disclosed the classification of toxic substances, A. P. Volkov (1988) highlighted the special treatment of objects after the influence of PS and HTS, M. I. Steblyuk (1998; 2006), V. I. Bukhtoyarov (1988), V. M. Shobotov (2006) proposed the calculation of the determination of the individual components of the chemical situation. The mentioned works describe the physicochemical and toxic properties of PS and HTS, give the general analytical formulas for determining the depth and area of chemical contamination, the calculations of determining the stability and time of an approach of the infected cloud from the emergency object to the settlement, but there are no algorithms of calculation starting from the initial data and ending with the projected loss of residents who will be affected by HTS. The writings of A. A. Zuikova (2006), A. V. Katkovsky (2015) consider increasing the effectiveness of decision-making in accidents with the release of chemically hazardous substances, pay attention to the use of computer technologies to solve environmental problems and industrial safety problems, draw attention to the use of information technology in the assessment of chemical environment after accidents on chemical facilities, however, the calculation using the software is not provided (Ring *et al.*, 2017; Casey *et al.*, 2018; Centers for Disease..., 2019; Wambaugh *et al.*, 2019).

A review and analysis of the literature in the Scopus database showed that, for example, there are works (Gervich, 2016; Jordan and Abdaal, 2013; Jordan *et al.*, 2009; Pashtetskiy *et al.*, 2020; Konyavsky and Ross, 2019; Wang and Wang, 2014) that make a comparative characterisation of socio-economic systems for better understanding

of the effects of industrial pollution on society; modern methods to support decision-making for ecological assessment of pollution in the mine territories and spatial modelling of contamination of reservoirs by processing industry have been considered; the ecological situation on water pollution after fire in chemical industry has been researched (US EPA (US Environmental..., 2018).

Currently, there are many programs for calculating chemical contamination parameters, such as ALOHA. The program is powerful, written in English. It is not adapted for the departments of the CP of Ukraine (Everything you need..., 2019; Ginsberg *et al.*, 2019; Yudaev *et al.*, 2019a; Yudaev *et al.*, 2019b; Zykova *et al.*, 2019; Rabinskiy and Tushavina, 2019). It is therefore understandable that the methodology for assessing the chemical environment should be investigated, studied, calculated and the results obtained – analysed. In order to promptly calculate the chemical situation, make timely decisions on protecting workers and residents who are affected by PS or HTS due to accidents at chemically hazardous sites, civil protection professionals need to have software that will speed up the calculation and enable them to take timely action on localisation and elimination of consequences of accidents at chemical industry facilities (Oltra *et al.*, 2017; Richmond-Bryant *et al.*, 2018; Jennifer, 2020).

The aim of the article – on the basis of the analysis of the existing methods of assessment of the chemical environment and the necessity to quickly respond to the consequences of accidents occurring at the facilities of the chemical industry, to develop an operational assessment of chemical contamination, to calculate the chemical situation without using software and with its use, to analyse the reliability of the results obtained.

#### Research objectives:

- 1) To analyse existing methods of calculating chemical contamination parameters.
- 2) To develop an algorithm for calculating the chemical post-accident assessment of a chemical facility (Figure 1).
- 3) To develop an operational assessment of chemical contamination.
- 4) To evaluate a chemical situation without the use of an operational assessment of chemical contamination and with its use, to analyse the reliability of results.
- 5) To analyse the results obtained using an operational assessment of chemical contamination.

## 2. MATERIALS AND METHODS

In order to determine the scale, nature, extent of exposure of hazardous substances to humans, animals, plants, foodstuffs, and the development of appropriate actions of the CP and the population before liquidation of chemical contamination and works on the site, chemical conditions are evaluated (Melnyk, 2013; Melnyk, 2014). The baseline data for assessing the chemical situation are:

- 1) the area and time of application of the HS or release into the environment of HTS;
- 2) type and amount of HS or HTS;
- 3) the degree of protection of humans, animals, food;
- 4) storage conditions (under pressure, without pressure) and the nature of hazardous chemicals entering the environment;
- 5) topographical conditions of the terrain, nature of development, presence of forest plantations on the way of spread of contaminated air. The configuration of the terrain, as well as all natural and artificial objects located on it (rivers, forests, shrubs, mountains, settlements, (closed terrain) affect the final result of the software calculation. This condition is taken into consideration upon entry of the initial data;
- 6) meteorological conditions: wind speed and direction in the surface layer, air and soil temperature, degree of vertical stability of air.

The degree of vertical stability of the air ground layer can be determined from the data of meteorological surveys. In addition, it can be more accurately determined by the wind speed at an altitude of 1 m and a temperature gradient (Equation 1) where  $t_{50}$  – air temperature at a height of 50 cm;  $t_{200}$  – air temperature at an altitude of 200 cm from the earth's surface. When the ratio of magnitudes  $\Delta t / v^2 \leq -0.1$  there will be inversion,  $-0.1 < \Delta t / v^2 < +0.1$  – isothermy, and  $\Delta t / v^2 \geq +0.1$  – convection. HSs are characterised by their toxicity (toxikon – poison). It is an important characteristic of HS that determines their ability to cause pathological changes in the body that lead to severe consequences or death. The quantitative characterisation of the toxicity of HS is determined by a dose (Vozza, 2017; Sarma *et al.*, 2018). The dose of a substance that causes a certain toxic effect is called the toxic dose (D). The toxic properties of HS are determined experimentally on different laboratory animals, so they are more

likely to use the concept of specific toxic dose – the dose attributed to the unit of live weight of the animal and expressed in milligrams per kilogram (mg/kg). Toxic doses (Alexandrov and Emelyanov, 1990) are divided into:

- 1) mortal;
- 2) incapacitating vital activity;
- 3) initial.

Toxic doses of HS of skin and resorption action are divided into:

- Lethal toxic dose  $LD$  (from Lat. letalis – lethal) – is the amount of HS that causes death upon penetration into the body with a certain probability, it is denoted respectively  $LD_{100}$  or  $LD_{50}$ , (100%, 50% of wounded).
- Toxic dose that incapacitates vital activity  $ID$  (from the English “incapacitate”) – is the amount of HS that infringe vital activity both temporally or lethally of a certain percentage of wounded when penetrating a body, it is denoted respectively  $ID_{100}$  or  $ID_{50}$ , (100%, 50 % of wounded).
- Initial toxic dose  $PD$  (from English “primary”) – the amount of PS that causes the initial signs of damage to an organism with a certain probability or the initial signs of damage in a certain percentage of humans and animals. Initial toxic doses are denoted  $PD_{100}$  or  $PD_{50}$ . (100%, 50% initial signs of a lesion).

It is more difficult to calculate toxic doses for PS that enters the human body as a vapour by inhalation. First of all, it is suggested that the inhalation toxic dose is directly proportional to the concentration of PS in the air,  $C$ , and the time of inhalation  $\tau$ . In addition, it is necessary to take into account the intensity of breathing  $V$ , which depends on physical activity and human condition. In a calm state, a person takes about 16 breaths per minute and absorbs 8-10 l/m of air on average. During medium exercise, the absorption of air increases to 20-30 l/m, and during heavy physical exertion is approximately 60 l/m. Thus, if a person weighing  $G$  (kg) inhales air with a concentration of PS  $C$  (mg/l) in it during  $\tau$  (min) with the intensity of breathing  $V$  (l/min), then the specific absorbed dose of PS (the amount of PS into the body) will be equal to Equation 2.

In (Alexandrov and Emelyanov, 1990), the German chemist F. Haber proposed to simplify this expression. He made the assumption that the relationship is constant for humans or a specific species of animals that are in the same conditions.



Divide both parts of the equation in this relation, he obtained the Equation 3.

F. Haber called  $C \cdot \tau$  toxicity coefficient and assumed it as a constant. Although this product is not a specific toxic dose, it does allow comparison of different PSs by inhalation toxicity. If, for example,  $C \cdot \tau$  for yperite is  $1.5 \text{ mg} \cdot \text{min/l}$  and for phosgene  $3.2 \text{ mg} \cdot \text{min/l}$ , it is clear that inhalation of yperite is about 2 times more toxic than phosgene. Notwithstanding many other factors that affect toxicity, the value  $C \cdot \tau$  is used to evaluate the inhalation toxicity of PS and is referred to as relative inhalation toxicity. For the characteristics of the lethal, life-threatening and primary toxicity of the PS, which affect the human body by inhalation in the form of steam or aerosol, use the same letters and indexes as with toxic doses of skin-resorptive action. They are denoted respectively  $LC\tau_{100}$  and  $LC\tau_{50}$ ,  $IC\tau_{100}$  and  $IC\tau_{50}$ ,  $PC\tau_{100}$  and  $PC\tau_{50}$ . The relative toxicity  $C \cdot \tau$  during inhalation depends on the physical exertion on the person. For people engaged in heavy physical labour, it will be much less than for people who are at rest. With increasing respiratory rate, the rate of action of the PSs increases. For example, for *GB* with pulmonary ventilation, the value is  $0.075 \text{ mg} \cdot \text{min/l}$  and  $0.025 \text{ mg} \cdot \text{min/l}$ , respectively, and if for phosgene the product  $C \cdot \tau$   $3.2 \text{ mg} \cdot \text{min/l}$  at respiratory rate is medium lethal, then for pulmonary ventilation  $40 \text{ l/min}$  is absolutely lethal. Table 1 shows the toxicological characteristics of HPs.

Tabular values of skin resorptive PS are valid only for infinitely large exposure, that is, for cases where PSs, that hit the skin surface, are not removed or degassed. In fact, for the manifestation of one or another toxic effect on the surface of the skin, there must be a greater amount of poison than the toxicity of toxic substances given in the table. This amount and the time during which PS is on the surface of the skin during absorption, in addition to toxicity, is largely due to the rate of absorption of the PS through the skin. Thus, according to US specialists, a substance *VX* characterised by a skin-resorptive toxic dose  $LD_{50}$   $6\text{--}7 \text{ mg}$  per humans will enter the human body if the droplet-liquid *VX* amounted at  $200 \text{ mg}$  is on the surface of the skin for 1 hour, or approximately  $10 \text{ mg}$  – for 8 hours. Due to the protective properties of the clothing, this amount is increased, and in the summer for 8 hours exposure will be approximately  $95 \text{ mg}$ .

It should be noted that the table values of the constant  $C \cdot \tau$  are valid for short exposures,

which differ significantly for different poisonous substances depending on their physical, physicochemical and chemical properties. For *AC* this value is valid if  $\tau$  – several minutes, and for *CG* – within one hour. The extent of damage caused by accidents at chemically hazardous sites depends first of all on the number of PSs, meteorological and topographic conditions of the area, the type of storage of HTSs (under pressure, without pressure). From the above it can be concluded: protective measures and, above all, the forecasting, detection and periodic monitoring of the chemical situation, alerting the personnel of the enterprise, the population and the CA forces, should be carried out with extremely high speed.

To create an operational assessment of chemical contamination and enable timely decision-making on taking measures to localise and eliminate the consequences of accidents at chemical industry facilities, it is necessary to develop an algorithm for civil protection professionals to evaluate chemical contamination parameters. It must start from the moment of receipt of the initial data on an object at which an accident occurred, its location, settlement, if any, the number of residents who live in it, ending with calculations of the consequences of chemical contamination, possible loss of working staff at this facility, a population that is projected to fall into the zone of chemical contamination.

- 1) Develop an algorithm for calculating the chemical post-accident assessment of a chemical facility (Figure 1).
- 2) Develop an operational assessment of chemical contamination.
  - a) Create a new project “Windows Form Application”.
  - b) Add software elements.
  - c) Write the program code.
  - d) Add reference material.
  - e) Run the program and enter the corresponding output data.
  - f) Calculate the problem.
  - g) Obtain the results of the calculation.

The program works in accordance with the algorithm provided in (Figure 1). Let us enter the source data. In accordance with the input data, the software determines the degree of vertical stability of the air (inversion, convection, isothermy). Considering the topographic conditions of the area (source data), the Depth (D) and the area (S) of chemical contamination are calculated (Figure 1).

The next step is the time it takes to reach and the time it takes to affect people with toxic substances. Further, the software calculates population losses by degrees of severity, taking into consideration the availability of personal protective gear. The software interface is as follows (Figure 2).

Table 2 provides statistics on past accidents. Table 2 was developed with the use of software modelling of data.

### 3. RESULTS AND DISCUSSION:

The study was conducted on the following input data (Melnyk, 2014):

1. An emergency object: Kind of HTS – chlorine; Quantity of HTS – 10 t; Type of container – unbuttoned; Number of employees – 600 people; Gas supply is 70%.

2. Settlement: Distance to the village R-3 km; Number of inhabitants 1000 persons; Gas mask security – 90%; Terrain – open; Meteorological conditions –  $V_w = 2$  m/s,  $\Delta t^\circ\text{C} = 70.1$

Calculation sequence:

1. Determine the degree of vertical stability of the air: Wind velocity  $V_w = 2$  m/s and  $\Delta t^\circ\text{C} = 0,1$  – isothermy.

2. Determine the depth of CCZ:  $D = 7$  km. Take into account the correction coefficient of wind speed:  $D = 7 \text{ km} \cdot 0.7 = 4.9 \text{ km}$ ;  $D = 4.9 \text{ km}$ .

3. Determine the width of CCZ:  $W = 0.15 \cdot G$  – isothermy.  $W = 0.15 \cdot 4.9 \text{ km} = 0.74 \text{ km}$ .  $W = 0.74 \text{ km}$ .

4. Determine the area of CCZ:  $S = 1/2 \cdot G \cdot W$ .  $S = 1/2 \cdot 4.9 \text{ km} \cdot 0.74 \text{ km} = 1.8 \text{ km}^2$ ;  $S = 1.8 \text{ km}^2$

5. Map the predicted CCZ (Figure 1).

6. Determine the  $t_{\text{reach}}$  of contaminated air to the locality:  $t_{\text{reach}} = 3000 \text{ m} / (3 \text{ m/s} \cdot 60) = 16.66$  minutes.

7. Determine the HTS  $t_{\text{affection}}$ : affection =  $1.3 \text{ h} \cdot 0.7 = 0.91 \text{ h}$ .

8. Calculate the possible losses of employees:

$600 \cdot 18\%/100\% = 108$  persons – total losses (t.l.);

$108 \cdot 25\%/100\% = 27$  persons with lesions of mild degree (m.d.);

$108 \cdot 40\%/100\% = 43$  persons of moderate and severe degree (m.s.d);

$108 \cdot 35\%/100\% = 38$  persons – fatalities (f.).

9. Calculate the possible population loss:

$1000 \cdot 9\%/100\% = 90$  persons t.l.;

$108 \cdot 25\%/100\% = 23$  persons m.s.d.;

$108 \cdot 40\%/100\% = 36$  persons m.d.;

$108 \cdot 35\%/100\% = 31$  persons f.

The results of the calculation are shown in Table 3.

### 4. CONCLUSIONS:

Comparative analysis of the results obtained from the solution of the problem of chemical post-accident assessment at a chemical industry facility conducted in two ways: without using an operational assessment of chemical contamination and with its use testify to the correctness of the developed an operational assessment of chemical contamination software product in accordance with the proposed methodology. The novelty of the obtained results is that a methodology for the assessment of the chemical situation after accidents at the chemical industry facilities is improved and an operational assessment of the parameters of chemical contamination is developed.

The existing methods of calculation of chemical contamination parameters were analysed. The algorithm of calculation of chemical contamination parameters was given. An operational assessment of chemical contamination using Microsoft Visual Studio (Visual C#) was developed. The software can be downloaded from <https://visualstudio.microsoft.com/ru/vs/express/> for calculation and estimation of a chemical situation after accidents and destruction at chemical industry facilities. The chemical situation without using an operational assessment of chemical contamination and with its use was estimated, the reliability of the obtained results was analysed. The developed operational assessment of chemical contamination will enable the specialists of city and district departments of civil protection and defence-mobilisation work to make calculations on chemical situation more promptly, to take timely measures of protection of workers, population and territories that will be under the influence of HS and HTS.

### 5. REFERENCES:

1. Alexandrov, V. N., and Emelyanov, V. I. (1990). *Poisonous substances*. Moscow, Russian Federation: Voenizdat.
2. Altunin, A. T. (Ed.). (1984). *Civil defence*. Moscow, Russian Federation: Voenizdat.
3. Atamanyuk, V. G., Shirshov, L. G., and Ekimov, N. I. (1986). *Civil defence*. Moscow, Russian Federation: Vysshaya Shkola.
4. Bell, S. M., Phillips, J., Sedykh, A., Tandon, A., Sprankle, C., Morefield, S.Q., Shapiro, A., Allen, D., Shah, R., Maull, E.A., Casey, W.M., and Kleinstreuer, N.C. (2017). An integrated chemical environment to support 21st-century toxicology. *Environmental Health Perspectives*, 125, Article number 054501. doi:10.1289/EHP1759.
5. Bourdrel, T., Bind, M.-A., Béjot, Y., Morel, O., and Argacha, J.-F. (2017). Cardiovascular effects of air pollution. *Archives of Cardiovascular Diseases*, 110, 634–642. doi:10.1016/j.acvd.2017.05.003.
6. Bukhtoyarov, V. I. (Ed.). (1988). *Textbook of a sergeant of chemical troops*. Moscow, Russian Federation: Voenizdat.
7. Casey, W. M., Chang, X., Allen, D. G., Ceger, P. C., Choksi, N. Y., Hsieh, J.-H., Wetmore, B.A., Ferguson, S.S., DeVito, M.J., Sprankle, C.S., Kleinstreuer, N.C. (2018). Evaluation and optimization of pharmacokinetic models for in vitro to in vivo extrapolation of estrogenic activity for environmental chemicals. *Environmental Health Perspectives*, 126, Article number 97001. doi:10.1289/EHP1655.
8. Centers for Disease Control and Prevention. (2019). National Health and Nutrition Examination Survey. Retrieved from <https://www.cdc.gov/nchs/nhanes/index.htm>
9. Egorov, P. T., Shlyakhov, I. A., and Alabin, N. I. (1977). *Civil defence*. Moscow, Russian Federation: Vysshaya Shkola.
10. Everything you need to know about aerosols and air pollution. (2019). Retrieved from <https://ethicalunicorn.com/2019/04/29/everything-you-need-to-know-about-aerosols-air-pollution/>.
11. Gervich, C. (2016). Social-ecological systems mapping to enhance students' understanding of community-scale conflicts related to industrial pollution. *Learner-Centered Teaching Activities for Environmental and Sustainability Studies*, 1, 233-238.
12. Ginsberg, G. L., Fedinick, K. P., Solomon, G. M., Elliott, K. C., Vandenberg, J. J., Barone, S., and Bucher, J. R. (2019). New toxicology tools and the emerging paradigm shift in environmental health decision-making. *Environmental Health Perspectives*, 127(12), Article number 125002-1-125002-7. doi:10.1289/EHP4745.
13. Jennifer, A.L. (2020). Assessment of exposures in vulnerable populations: exposure and response modelling for environmental contaminants through a lifetime. In *Good health and well-being* (pp. 38-50). Cham, Switzerland: Springer International Publishing AG. doi:10.1007/978-3-319-95681-7\_73.
14. Jordan, G., and Abdaal, A. (2013). Decision support methods for the environmental assessment of contamination at mining sites. *Environmental Monitoring and Assessment*, 185, 7809-7832.
15. Jordan, G., Van Rompaey, A., Somody, A., Fügedi, U., and Farsang, A. (2009). Spatial modelling of contamination in a catchment area impacted by mining: A case study of the Recsk copper mine, Hungary. *Land Contamination and Reclamation*, 17(3-4), 413-421.
16. Katkovsky, A. V. (2015). Use of information technology in the process of studying the discipline "Civil Protection". *Collection of the NA of Border Guard Service of Ukraine. Series: Pedagogical and Psychological Sciences*, 1(74), 111-120.
17. Konyavsky, V.A., and Ross, G.V. (2019). Secure computers of the new Harvard architecture. *Asia Life Sciences*, 28(1), 33-53.
18. Kosnik, M. B., and Reif, D. M. (2019). Determination of chemical-disease risk values to prioritize connections between environmental factors, genetic variants, and human diseases. *Toxicology and Applied Pharmacology*, 379, Article 114674. doi:10.1016/j.taap.2019.114674.
19. Krechetov, I.V., Skvortsov, A.A., Poselsky, I.A., Paltsev, S.A., Lavrikov, P.S., and Korotkovs, V. (2018). Implementation of automated lines for sorting and recycling household waste as an important goal of environmental protection. *Journal of Environmental Management and Tourism*, 9(8), 1805-1812.
20. Manucci, P. M., and Franchini, M. (2017). Health effects of ambient air pollution in

- developing countries. *International Journal of Environmental Research and Public Health*, 14(9), Article 1048. doi:10.3390/ijerph14091048.
21. Melnichuk, T.N., Abdurashytov, S.F., Andronov, E.E., Abdurashytova, E.R., Egovtseva, A.Y., Gongalo, A.A., Turin, E.N., and Pashtetskiy, V.S. (2020). The taxonomic structure of southern chernozem at the genus level influenced by microbial preparations and farming systems. *IOP Conference Series: Earth and Environmental Science*, 422(1), Article number 012101.
  22. Melnyk, O. V. (2013). *Methods of estimation of radiation and chemical situation in peacetime and wartime in case of emergencies at the facilities of nuclear power plants and chemical industry*. Uman, Ukraine: FOP Yellow O.O.
  23. Melnyk, O. V. (2014). *Civil defence*. Uman, Ukraine: Pavlo Tychyna Uman State Pedagogical University.
  24. Migovich, G. G. (2001). *Handbook of Civil defence*. Kyiv, Ukraine: Ukrainian Technology Group.
  25. Mitsenko, I. M., and Mizentseva, O. M. (2004). *Civil defense*. Chernivtsi, Ukraine: Knyga – XXI.
  26. Mo, Z., Fu, Q., Lyu, D., Zhang, L., Qin, Z., Tang, Q., Yao, K. (2019). Impacts of air pollution on dry eye disease among residents in Hangzhou, China: a case-crossover study. *Environmental Pollution*, 246, 183–189. doi:10.1016/j.envpol.2018.11.109.
  27. New Hampshire Department of Environmental Services Current and Forecasted Air Quality in New Hampshire. Environmental Fact Sheet (2019). Retrieved from <https://www.des.nh.gov/organization/commissioner/pip/factsheets/ard/documents/ard-16.pdf>.
  28. NTP. National Toxicology Program. National Institute of Environmental Health Sciences (2019) Chemical Effects in Biological Systems. Retrieved from <https://manticore.niehs.nih.gov/cebssearch/>.
  29. Oltra, C., Sala, R., Boso, A., and Asensio, S. L. (2017). Public engagement on urban air pollution: an exploratory study of two interventions. *Environmental Monitoring and Assessment*, 189(6), Article 296.
  30. Pashtetskiy, V.S., Turin, E.N., Izotov, A.M., Abdurashytov, S.F., Gongalo, A.A., and Zhenchenko, K.G. (2020). Effect of *Pisum sativum* L. seed treatment with the complex of microbiological preparation on the plants' growth and development under direct sowing. *IOP Conference Series: Earth and Environmental Science*, 422(1), Article number 012012.
  31. Rabinskiy, L.N., and Tushavina, O.V. (2019). Problems of land reclamation and heat protection of biological objects against contamination by the aviation and rocket launch site. *Journal of Environmental Management and Tourism*, 10(5), 967-973.
  32. Richmond-Bryant, J., Snyder, M.G., Owen, R.C., and Kimbrough, S. (2018). Factors associated with NO<sub>2</sub> and NOX concentration gradients near a highway. *Atmospheric Environment*, 174, 214-226. doi:10.1016/j.atmosenv.2017.11.026.
  33. Ring, C.L., Pearce, R. G., Setzer, R. W., Wetmore, B. A., and Wambaugh, J. F. (2017). Identifying populations sensitive to environmental chemicals by simulating toxicokinetic variability. *Environment International*, 106, 105–118. doi:10.1016/j.envint.2017.06.004.
  34. Sarma, A. K., Singh, V. P., Bhattacharjya, R. and Kartha, S. A. (2018). *Urban Ecology, Water Quality and Climate Change*. Dordrecht, The Netherlands: Springer Science.
  35. Shobotov, V. M. (2006). *Civil defence*. Kyiv, Ukraine: Center for educational literature.
  36. Steblyuk, M. I. (1998). *Methods of evaluation of radiation, chemical and fire conditions*. Kiev, Ukraine: UVK Printing Station.
  37. Steblyuk, M. I. (2006). *Civil defence*. Kiev, Ukraine: Znannya.
  38. Talismanov, V.S., Popkov, S.V., Zykova, S.S., Karmanova, O.G., and Bondarenko, S.A. (2018). Synthesis and cytotoxic activities of substituted N-4-[4-(1,2,4-triazol-1-ylmethyl)-1,3-dioxolan-2-yl]phenyl-N'-arylureas. *Journal of Pharmaceutical Sciences and Research*, 10(1), 152-155.
  39. Tyliczszak, B., Polaczek, J., Pielichowski, J., and Pielichowski, K. (2009). Preparation and properties of biodegradable slow-release PAA superabsorbent matrixes for phosphorus

- fertilizers. *Macromolecular Symposia*, 279(1), 236-242.
40. US EPA (US Environmental Protection Agency). (2018). Retrieved from <https://www.epa.gov/pm-pollution/particulate-matter-pm-basics>.
  41. Volkov, A. P. (1988). *A guide to special cleaning*. Moscow, Russian Federation: Voenizdat.
  42. Voza, D. (2017). Historical pollution and human rights violations: is there a role for criminal law? *Historical Pollution: Comparative Legal Responses to Environmental Crimes*, 1, 385-421. doi:10.1007/978-3-319-56937-6\_13.
  43. Wambaugh, J. F., Wetmore, B. A., Ring, C. L., Nicolas, C. I., Pearce, R. G., Honda, G. S., Dinallo R., Angus D., Gilbert J., Sierra T., Badrinarayanan A., Snodgrass B., Brockman A., Strock Ch., Setzer, R.W. (2019). Assessing Toxicokinetic Uncertainty and Variability in Risk Prioritization. *Toxicological Sciences*, 172(2), 235-251. doi:10.1093/toxsci/kfz205.
  44. Wang, Y. Y., and Wang, B. Q. (2014). Study on countermeasures of water pollution accident after chemical industry fire. *Advanced Materials Research*, 886, 219-222.
  45. Williams, A. J., Grulke, C. M., Edwards, J., McEachran, A. D., Mansouri, K., Baker, N.C., Patlewicz, G., Shah, I., Wambaugh, J.F., Judson, R.S. (2017). The CompTox Chemistry Dashboard: a community data resource for environmental chemistry. *Journal of Cheminformatics*, 9, Article 61. doi:10.1186/s13321-017-0247-6.
  46. Yudaev, I., Ivushkin, D., Belitskaya, M., and Gribust, I. (2019b). Pre-sowing treatment of *Robinia Pseudoacacia* L. seeds with electric field of high voltage. *IOP Conference Series: Earth and Environmental Science*, 403(1), Article number 012078.
  47. Yudaev, I., Stepanchuk, G., Kaun, O., Ukraitsev, M., and Ponamareva, N. (2019a). Small-sized irradiation structures for intensive year-round cultivation of green vegetable crops. *IOP Conference Series: Earth and Environmental Science*, 403(1), Article number 012084.
  48. Zavala, J., Freedman, A. N., Szilagyi, J. T., Jaspers, I., Wambaugh, J. F., Higuchi, M., and Rager, J. E. (2020). New approach methods to evaluate health risks of air pollutants: Critical design considerations for in vitro exposure testing. *International Journal of Environmental Research and Public Health*, 17(6), Article number 2124. doi:10.3390/ijerph17062124.
  49. Zuikova, A.A. (2006). *Increasing the effectiveness of decision-making in accidents with the release of hazardous chemical substances*. Tula, Russian Federation: Tula State University.
  50. Zykova S.S., Talismanov V.S., Tsaplin G.V., Bulatov I.P., Popkov S.V., Karmanova O.G., and Savinkov A.V. (2019). Study of acute toxicity and antihypoxic activity of N4-substituted 5-(1,2,4-triazole-1-ylmethyl)-1,2,4- triazole-3-thiones. *International Journal of Pharmaceutical Research*, 11(3), 1189-1192.

$$\Delta t = t_{50} - t_{200}, \quad (\text{Eq. 1})$$

$$D = \frac{C \cdot \tau \cdot V}{G} = \frac{\frac{mg}{l} \cdot \min \cdot \frac{l}{min}}{kg} = \frac{mg}{kg} \quad (\text{Eq. 2})$$

$$T = C \cdot \tau = \frac{mg \cdot min}{l} \quad (\text{Eq. 3})$$

**Table 1.** Toxicological characteristics of HP. Source: the author

| Name of poisonous substances and their code | Lesion through the respiratory system |                                   | Lesion through skin              |
|---|---------------------------------------|-----------------------------------|----------------------------------|
|   | <i>LC<sub>50</sub> (mg·min)/l</i>     | <i>IC<sub>50</sub> (mg·min)/l</i> | <i>LD<sub>50</sub> mg/person</i> |
| Sarin (GB)                                  | 0.075                                 | 0.055                             | 1480                             |
| Soman (GD)                                  | 0.05                                  | 0.025                             | 100                              |
| VX (VX)                                     | 0.01                                  | 0.005                             | 7                                |
| Yperite (AD)                                | 1.50                                  | 0.200                             | –                                |
| Nitrous yprete (HN)                         | 1.00                                  | 0.100                             | 5000                             |
| Hydrogen cyanide (AC)                       | 2.00                                  | 0.300                             | 1000                             |
| Cholorocyan (CK)                            | 11.00                                 | 7.000                             | –                                |
| Phosgene (CG)                               | 3.20                                  | 1.600                             | –                                |
| Bi-et (BZ)                                  | 110.00                                | 0.110                             | –                                |
| Chloroacetophenone (CN)                     | 85.00                                 | 0.030                             | –                                |
| Adamsite (DM)                               | 30.00                                 | 0.030                             | –                                |
| CS (CS)                                     | 25.00                                 | 0.020                             | –                                |
| CR (CR)                                     | –                                     | 0.001                             | –                                |

**Table 2.** Comparative analysis of accident development scenarios

| The statistics of accidents at chemical facilities |          |                            |                         |                                      |                               | Data calculated with the use of software |                                      |                               |
|--|----------|----------------------------|-------------------------|--------------------------------------|-------------------------------|--|--------------------------------------|-------------------------------|
| Accident location                                  | HHC type | The amount of HHC (tonnes) | Depth of affection (km) | Area of affection (km <sup>2</sup> ) | The number of people affected | Depth of affection (km)                  | Area of affection (km <sup>2</sup> ) | The number of people affected |
| 1934, Niagara Falls, (USA).                        | chlorine | 15                         | -                       | -                                    | 1                             | 10                                       | 4.5                                  | 30                            |
| 1989, Jonava (Lithuania)                           | ammonia  | 7000                       | 30                      | 37                                   | 36                            | 35                                       | 43.3                                 | 50                            |
| 1991, Mexico                                       | chlorine | 300                        | -                       | -                                    | 500                           | 30                                       | 37.1                                 | 700                           |
| 2008, Balakovo (Russia)                            | ammonia  | 0.6                        | -                       | -                                    | 2                             | 0.4                                      | 0.007                                | 10                            |

**Table 3.** Calculation of chemical contamination parameters. Source: the author

| List of tasks |   | Without an operational assessment of chemical contamination | With an operational assessment of chemical contamination |
|---------------|---|---|--|
| 1             | Determination of degree of vertical stability of air                      | isothermy   | isothermy  |
| 2             | Determination of depth of chemical contamination zone                     | 4.9 km  | 4.93 km  |
| 3             | Determination of the width of the chemical contamination zone             | 0.74 km   | 0.75 km  |
| 4             | Determination of the area of the chemical contamination zone              | 1.8 km <sup>2</sup>   | 1.8 km <sup>2</sup>                                      |
| 5             | Mapping the predicted CCZ   |   |  |
| 6             | Determination the time of reaching the contaminated air to the settlement | 16.66 min.  | 16.8 min.  |
| 7             | Determination the time of HTS lesion                                      | 0.91 h.   | 0.91 h.  |
| 8             | Calculation of possible losses of employees                               | 108 person t.l.   | 108 person t.l.  |
|               |   | 27 persons m.d.   | 27 persons m.d.  |
|               |   | 43 persons m.s.d.   | 43 persons m.s.d.  |
|               |   | 38 persons f.   | 38 persons f.  |
| 9             | Calculation of possible population losses                                 | 90 persons t.l.   | 90 persons t.l.  |
|               |   | 23 persons m.s.d.   | 23 persons m.s.d.  |
|               |   | 36 persons m.d.   | 36 persons m.d.  |
|               |   | 31 persons f.   | 31 persons f.  |

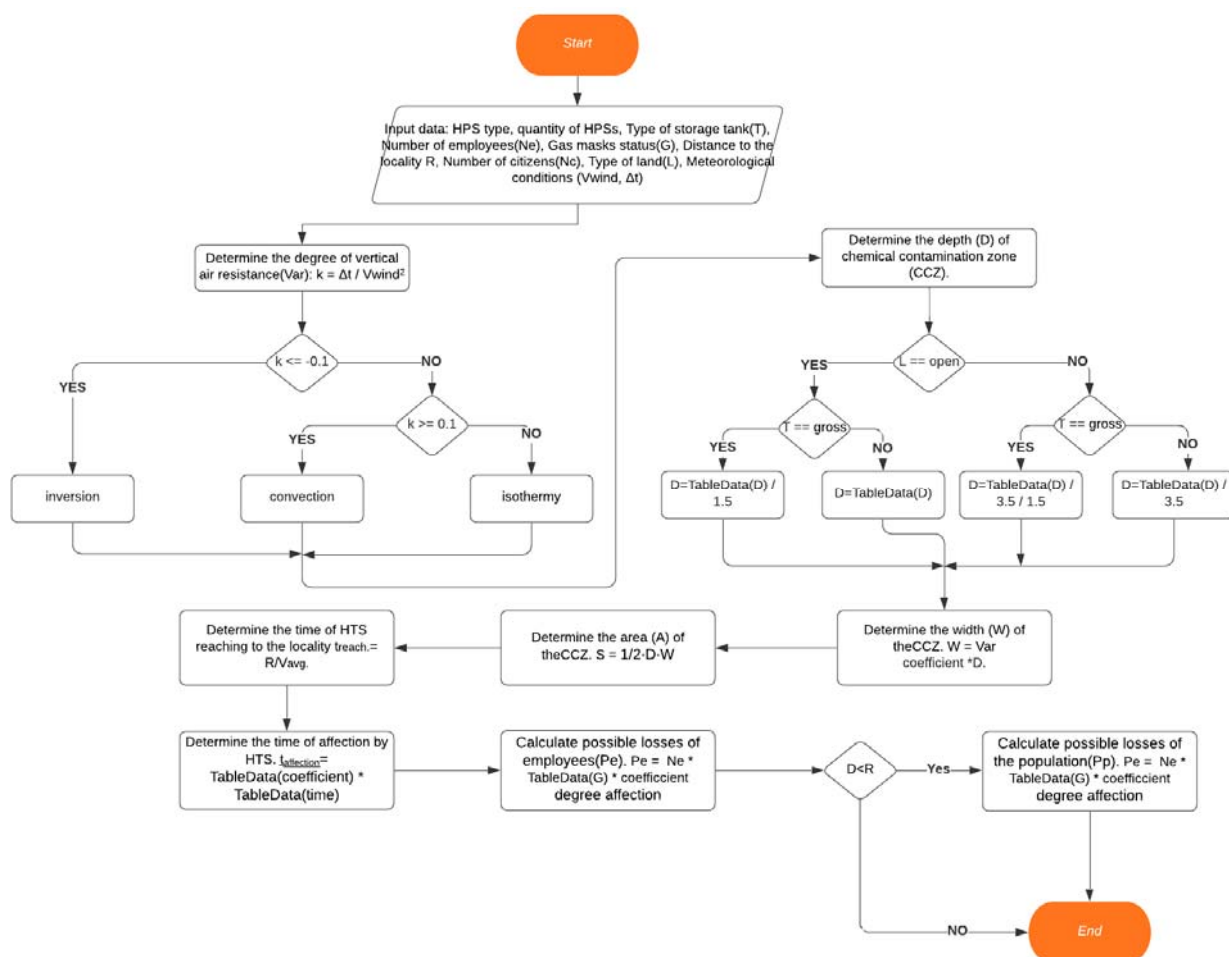


**Figure 1.** Algorithm for calculating the chemical situation evaluation after accidents at chemical facilities

Chemical situation evaluation after the emergency on the chemical industry object

Menu Help

Emergency object

Locality

1. The HPS type :

2. The quantity of HPSs:

3. Type of storage tank:

4. The number of employees :

5. Gas masks status (%):

6. Where are the employees located?

7. Distance to the locality R:

8. Number of citizens :

9. Gas masks status (%):

10. The territory:

11. Meteorological conditions V (m/s) =

Δt (°C) =

12. Where is the population located?

Clear Get result Random

**Figure 2.** Software Interface



# EXPERIÊNCIA DA INTRODUÇÃO DE TILÁPIA NAS FONTES GEOTÉRMICAS DO CAZAQUISTÃO

## EXPERIENCE OF TILAPIA INTRODUCTION AT GEOTHERMAL SOURCES OF KAZAKHSTAN

### ОПЫТ ВНЕДРЕНИЯ ТИЛАПИИ В ГЕОТЕРМИЧЕСКИЕ ИСТОЧНИКИ КАЗАХСТАНА

SYZDYKOV, Kuanysh N.<sup>1\*</sup>; NARBAYEV, Serik<sup>2</sup>; ASSYLBEKOVA, Ainur S.<sup>3</sup>; BARINOVA, Gulnaz K.<sup>4</sup>; KUANCHALEYEV, Zhaxygali B.<sup>5</sup>;

<sup>1,2,3,4,5</sup> S. Seifullin Kazakh Agro Technical University, Department of Hunting and Fisheries, 62 Zhenis Ave., zip code 010011, Nur-Sultan – Republic of Kazakhstan

\* Correspondence author  
e-mail: k\_syzydykov@mail.ru

Received 20 March 2020; received in revised form 30 June 2020; accepted 06 July 2020

## RESUMO

Nos últimos anos, muita atenção tem sido dada ao uso de fontes geotérmicas na pesca. As perspectivas para esta área são enormes, pois abrem oportunidades para o gerenciamento de processos de criação de peixes, independentemente das condições climáticas. O principal objetivo do estudo foi uma análise abrangente dos processos tecnológicos de piscicultura. Uma das reservas promissoras para o aumento da produção de peixes é o uso racional de resíduos comerciais de água quente e fontes geotérmicas. O trabalho de pesquisa foi realizado em 2019 com base na fazenda TOO Tengri Fish, localizada a 270 quilômetros da cidade de Almaty. Os materiais foram coletados e processados de acordo com os métodos geralmente aceitos em ictiologia e piscicultura e subsequentemente analisados por meio de computador pessoal. Com base nos resultados do estudo, foram determinadas as primárias tecnológicas da criação de tilápia em SRA (sistema de recirculação da aquicultura) utilizando águas geotérmicas. Durante o estudo, foi realizado um trabalho para otimizar o regime hidroquímico. Os principais indicadores de criação de peixes e indicadores biológicos de crescimento e desenvolvimento de peixes da tilápia foram estabelecidos. Foi determinada a densidade ideal da tilápia em sistemas de recirculação da aquicultura usando água geotérmica e a temperatura em que a tilápia tem um ganho médio diário mais alto. A novidade do trabalho: um estudo abrangente da biologia e a adaptação de uma nova unidade de piscicultura industrial de tilápia e peixe-gato, realizado fora da área natural e que determinou a possibilidade de adaptar tilápia e peixe-gato a fatores extremos do ambiente aquático.

**Palavras-chave:** *fonte geotérmica, desgaseificação, caviar, larva, hidroquímica.*

## ABSTRACT

Over recent years much attention has been paid to the fishery use of geothermal sources. The prospects for this area are enormous, as it opens up possibilities for managing fish-breeding processes, regardless of climatic conditions. The main objective of the research was a comprehensive study of the technological processes of growing. One of the promising reserves for increasing fish production is the rational fishery use of waste warm water and geothermal sources. Research work was carried out in 2019 based on the farm of "Tengri Fish" LLP, which is located 270 kilometers from Almaty. The collection and processing of materials were carried out according to generally accepted methods in ichthyology and fish farming, followed by their analysis on a PC. Based on the results of the research, technological primaries of growing tilapia in a RAS (Recirculating Aquaculture System) using geothermal waters were determined. During the research, work was carried out to optimize the hydrochemical regime. The main fish breeding and biological indicators for the growth and development of tilapia were established. The optimal stocking density of tilapias in recirculating aquaculture systems using geothermal waters and the temperature when tilapias have a higher average daily weight gain were found. The novelty of the research: a complex study of biology and adaptation of a new object of industrial fish farming of tilapia and clarium catfish has been carried out outside the range and determined the adaptation possibilities of tilapia and clarium catfish to extreme factors of the aquatic environment.

**Keywords:** *geothermal spring, degassing, caviar, larva, hydrochemistry.*

## АННОТАЦИЯ

В последние годы большое внимание уделяется использованию геотермальных источников в рыбном хозяйстве. Перспективы этой области огромны, так как она открывает возможности для управления процессами разведения рыбы, независимо от климатических условий. Основной целью исследования было комплексное изучение технологических процессов выращивания. Одним из перспективных резервов для увеличения производства рыбы является рациональное использование промысловых отходов теплой воды и геотермальных источников. Исследовательские работы проводились в 2019 году на базе фермы ТОО «Tengri Fish», расположенной в 270 километрах от Алматы. Сбор и обработка материалов проводились в соответствии с общепринятыми методами в ихтиологии и рыбоводстве с последующим их анализом на ПК. По результатам исследования определены технологические праймериз выращивания тилапии в РСА (рециркуляционной системе аквакультуры) с использованием геотермальных вод. В ходе исследования проводились работы по оптимизации гидрохимического режима. Установлены основные рыбоводные и биологические показатели роста и развития тилапии. Найдена оптимальная плотность посадки тилапии в рециркуляционных системах аквакультуры с использованием геотермальных вод и температура, при которой у тилапии наблюдается более высокий среднесуточный прирост веса. Новизна исследования: комплексное изучение биологии и адаптация нового объекта промышленного рыбоводства тилапии и клариумного сома, проведенного за пределами ареала, и определившего возможности адаптации тилапии и клариумного сома к экстремальным факторам водной среды.

**Ключевые слова:** геотермальный источник, дегазация, икра, личинка, гидрохимия.

---

## 1. INTRODUCTION

Over the past decades, aquaculture has become one of the fastest-growing areas of food production and plays an increasingly important role in the economic development of many countries. In terms of development, aquaculture is ahead of fish caught in the oceans and seas and today provides more than 40% of total fish production (Mamontov, 2000). One of the promising reserves for increasing fish production is the rational fishery use of waste warm water and geothermal sources. Over recent years, in our country and abroad, much attention has been paid to the fishery use of geothermal sources (Gurkina *et al.*, 2019; Lefers *et al.*, 2020). The prospects for this area are enormous, as it opens up possibilities for managing fish-breeding processes, regardless of climatic conditions (Budiasa *et al.*, 2018; Leite *et al.*, 2018).

A promising direction in fish farming is the use of not only the potential of inland water bodies but also the rational use of waste warm water and geothermal sources. Geothermal sources located on the territory of the Republic of Kazakhstan are one of the water areas where the cultivation and cultivation of new aquaculture facilities with a high growth rate and valuable taste qualities are quite promising (Beisembayeva *et al.*, 2017; Syzdykov *et al.*, 2019).

Geothermal waters in different regions of

the country and at different levels of occurrence can vary significantly. The temperature of such waters also varies from 30-40 to 80-90 °C and higher. A common characteristic feature of geothermal waters can be considered the absence of a minimum amount of dissolved oxygen, high content of carbon dioxide, and mineral salts. However, in the process of filling the ponds and their operation, the chemical composition of the water may change. In particular, it is saturated with oxygen, and the carbon dioxide content is reduced. In determining the possibility of using geothermal waters for fish farming, in each specific case, their careful chemical analysis is necessary (Tetdoyev, 2009; Tosun, 2017).

The area of application of geothermal sources in the national economy is expanding more and more and requires economic and rational use, including in fish farming (Tetdoyev, 2009; Tetdoyev and Pliyev, 2009). The chemical composition of the new, previously unknown aquatic environment, will allow establishing the degree of tolerance, adaptive plasticity, as well as their growth and development potential at different stages of cultivation when breeding fish farming objects (Tetdoyev, 2009; Tetdoyev and Pliyev, 2009).

Geothermal waters in different regions and at different levels of occurrence can vary significantly. The composition of geothermal waters is characterized by a large amplitude of

fluctuation both in chemical composition and in the number of salts and gases dissolved in it. A common characteristic feature of geothermal waters can be considered the absence or minimum amount of dissolved oxygen, high content of carbon dioxide, and minerals. However, in the process of filling the ponds and their operation, the chemical composition of the water may change. In particular, it is saturated with oxygen, and the carbon dioxide content is reduced (Boronetskaya, 1993; Mamontov, 2000; Tetdoyev, 2009; Bolotov *et al.*, 2016).

Scientists of Russia have experience in growing traditional fish farming objects (carp, wild carp), as well as new aquaculture objects (tilapia). Research on the cultivation of tilapia in ponds using geothermal water was carried out based on the fish breeding department of the Mostovskaya greenhouse complex in the Krasnodar Territory (Mamontov, 2000; Tetdoyev, 2009). Studies have shown that the geothermal water of the Mostovskoye field belongs to sulfate-sodium waters, has a temperature of 75-800 °C. Mineralization of water is low (1-1.5 g/l). Geothermal water was pre-mixed with river water and then fed into fish ponds. The ratio of geothermal and river water varied depending on the season of the year. The temperature in the ponds was also regulated due to the intensity of water exchange (Tetdoyev, 2009). Russian scientists conducted experiments on growing carp using geothermal, weakly mineralized, carbonate-chloride-sodium water from deep wells with total salinity in hatcheries from 1.9 to 3.6 g/l, and in commercial fish plots up to 12.2 g/l (Pevnev, 2000; Korentovich *et al.*, 2017).

The new economic conditions in Kazakhstan over the past decade (2010-2020) put the fisheries industry in a rather difficult position, and therefore, the per capita consumption of fish products for this period reached only 4 kg, that is, 2.5 times less than the following consumption rate (14 kg per capita), which reduced the usefulness of protein nutrition. The principal, decisive factor for solving this issue will be, first of all, the development of aquaculture in the Republic of Kazakhstan, using available water resources and the introduction of new aquaculture facilities – fish with an intensive growth and development rate, crustaceans, mollusks, aquatic plants and other aquatic organisms (Master plan of commercial..., 2011).

Growing fish in industrial fish farms has several advantages over pond farming. No more than 0.01 m<sup>2</sup> of land and 0.005 m<sup>3</sup> of water are spent on the production of 1 kg of products in

industrial fish farming, which is two orders of magnitude less than in pond fish farming. At the same time, a high yield of fish products is achieved – 100 kg or more from 1 m<sup>2</sup> of cage and pool area. One of the real ways to increase the economic efficiency of industrial fish farming is to grow more valuable fish species that have a reasonably high growth and development rate, unpretentiousness to the habitat and food, high fecundity, and high taste (Pruszyński and Pistelok, 1999; Shelton, 2002; Rothbard and Peretz, 2002; Zdanovich and Pushkar, 2007; Tetdoyev and Boronetskaya, 2008).

The main objective of the research is a comprehensive study of the technological processes of growing Nile tilapia at geothermal sources. In order to achieve the objectives, the following tasks had to be accomplished:

- to study the features of the hydrochemical regime of geothermal sources (thermal regime, gas and salt composition of water);

- study of the influence of technological factors (planting density, feeding level) on the growth and development of tilapia when kept in a water storage system using geothermal water.

The novelty of the research: a complex study of biology and adaptation of a new object of industrial fish farming of tilapia and clari catfish has been carried out outside the range and determined the adaptation possibilities of tilapia and clari catfish to extreme factors of the aquatic environment: lack of oxygen dissolved in water, high and low concentration of ions (pH), high concentration of minerals (Grande Burgos *et al.*, 2018; Billah *et al.*, 2020; Mansano *et al.*, 2020).

## 2. MATERIALS AND METHODS

Research work was carried out in 2019 based on the farm of “Tengri fish” LLP, which is located 270 kilometers from Almaty, near the village of Chunzha, on a plot of 15 hectares. This farm has two deep, self-flowing, artesian, geothermal wells. Previously, it was conducted hydrochemical studies of geothermal waters in order to determine the hydrochemical regime of water bodies for the subsequent planting of aquaculture objects in them – tilapia and Clari (African) catfish.

Aquaculture objects were grown at a planting density of 50-150 kg/m<sup>3</sup> for African catfish and 30-50 kg/m<sup>3</sup> for tilapia. Feeding was carried out with specialized Aller aqua aquaculture feeds

containing 45% protein, 15% fat, and 22% carbohydrate. The daily diet ranged from 10% for juveniles to 3% for marketable fish. Each month, fish were sorted to reduce planting density and uniform fish growth. The OxyGuard Handy Polaris Thermo Oximeter was used for daily monitoring of oxygen in the water. Water samples were taken to describe the complex hydrochemical regime in fish hatcheries. The studies were carried out in an accredited hydrochemical laboratory of the Scientific Analytical Center LLP.

To characterize the hydrochemical regime in fish hatcheries, water samples were taken. The studies were carried out according to standard methods. The control of the hydrochemical regime was carried out according to the following leading indicators (parameters) – oxygen content ( $O_2$ ), carbon dioxide ( $CO_2$ ), pH – medium, water temperature ( $t\text{ }^{\circ}C$ ), as well as the content of nitrates ( $NO_3$ ) and nitrites ( $NO_2$ ) (Semyonov, 1977; Yudin, 1980). For ichthyologic studies, generally accepted research methods used in fish farming were used. The ichthyologic analysis includes the determination of linear dimensions, weight, fatness (Pravdin, 1966). The growth rate of the studied fish was carried out according to accepted methods (Chugunova, 1959; Privezentsev, 1991). Ichthyological studies were carried out every 7 days in order to determine the growth rate and calculate the daily diet.

### 3. RESULTS AND DISCUSSION:

#### 3.1. The Features of the Hydrochemical Regime of Geothermal Sources

Geothermal waters in different regions of the country and at different levels of occurrence vary significantly. The composition of geothermal waters is characterized by a large amplitude of fluctuation both in chemical composition and in the number of salts and gases dissolved in it. A characteristic feature of geothermal sources can be considered the absence or minimum content of dissolved oxygen with a high content of carbon dioxide and minerals (Boronetskaya, 1993; Pevnev, 2000).

Studies on the cultivation of tilapia using geothermal waters were carried out based on the fish farm of "Tengry fish" LLP. This farm is located in the Almaty region, Uygur district, the village of Chunzha, for fish growing was used as a system of closed water supply systems with geothermal water. As this study shows, as well as data from foreign scientists (Boronetskaya, 1993; Pruszyński and Pistelok, 1999; Pevnev, 2000; Tetdoyev, 2009; Bolotov *et al.*, 2016; Korentovich

*et al.*, 2017), the minimum salient oxygen content at high content of carbon dioxide and mineral salts can be considered a common characteristic feature of geothermal sources. Accordingly, in the waters of geothermal sources used in this study, the hydrochemical regime corresponded to the above data. Preliminary studies of water from geothermal sources indicate that the maximum permissible concentrations of carbon dioxide (80.1 mg/l) and total nitrogen (2.86 mg/l) are exceeded. Table 1 shows the hydrochemical parameters of water of geothermal sources, and in Figure 1, the proportion of chemical components present in the geothermal source.

The negative effect of a high concentration of carbon dioxide on the vital activity of fish is that fish, being in a depressed state, use oxygen dissolved in water worse. Moreover, not only the absolute content of oxygen and carbon dioxide (carbon dioxide) in the water is essential, but their ratio. For carp, for example, the ratio of  $O_2$  and  $CO_2$  approaching 0.02 is dangerous. With a low oxygen content and an unfavorable ratio of  $O_2$  and  $CO_2$ , fish use feed much worse. The critical carbon dioxide concentration varies for different fish species.

The high content of carbon dioxide leads to a decrease in pH, as a result of which prerequisites are created for limiting the transfer of blood oxygen in the gills. As a result, signs of asphyxia in fish develop. Nitrogen is less toxic to fish. However, fodder and vital products of fish continuously get into the fish's artificial keeping water, and in the process of their decomposition, a large amount of phosphorus and nitrogen is formed in the form of ammonia. This leads to the uncontrolled growth of algae and causes intoxication of the fish organism; chronic gill lesions occur. According to hydrochemical analyzes, the concentration of iron did not exceed the MPC. However, it should be noted that iron in the water of geothermal sources is presented as divalent, which, in turn, is toxic to caviar and juvenile fish.

In order to regulate and optimize the hydrochemical regime of the waters of the geothermal spring, it is necessary to reduce the carbon dioxide content. The removal of carbon dioxide in geothermal springs was carried out by the method of degassing – by aeration of water or by stripping. Aeration is carried out by forcing air into water. With this degassing method, the turbulent contact of air bubbles and water removes gases. In this research, a more effective degassing method is stripping. In a drip filter system, gases are stripped by physical contact

between water and a plastic aggregate (bio blocks) stacked in a column. The stripping process will remove carbon dioxide and nitrogen from the water, and the aeration well will allow ferrous iron to become ferric with subsequent conversion to iron oxide, which precipitates (Figure 2). As a result of regulation by the method of degassing the hydrochemical regime in the pools, it was found that the water indicators practically corresponded to the normative indicators (Table 2). As shown in Table 2, the effective operation of the degassing unit is reflected in a decrease in carbon dioxide concentration by 20 times from the initial one and increases the concentration of dissolved oxygen by two times.

As reflected in Figure 3, when using the degassing method, the level of dissolved oxygen in closed water supply plants almost reached the maximum level and averaged 6.27 mg/dm<sup>3</sup>. This was seen in the behavioral response of fish (tilapia). At the initial stage of the experiment, when using water from geothermal springs, after degassing, the fish behaved relatively passively, inactive, sluggishly took food, and for the most part, they were at the surface of the water. Subsequently, as the concentration of dissolved oxygen increased, the activities of the fish increased, willingly and actively took food and were dispersed over the entire basin. The highest activity was observed during the periods of July-August. The method of degassing effectively reduced the concentration of carbon dioxide (Figure 4). Figure 4 shows the dynamics of decreasing carbon dioxide concentration in the recirculating aquaculture system with the content of tilapias up to 71%. In this study, the pH dependence on carbon dioxide concentration is traced. According to V. V. Tetdoyev (2009) research, low pH is "favorable" for the presence of free carbon dioxide. When pH increases to 8, the balance shifts towards the formation of bicarbonate (HCO<sub>3</sub>), resulting in a reduction in free carbon dioxide. This study notes a gradual increase in the pH value (Figure 5). As reflected in Figure 5, the pH of water in basins with tilapias was predominantly of a weakly alkaline environment.

Figure 6 reflects the general dependence of pH on carbon dioxide using geothermal waters while keeping tilapia in the recirculating aquaculture system. The inverse dependence of pH on the content of carbon dioxide becomes evident after drawing the trend lines: the higher the concentration of carbon is, the lower is the pH of the medium. A similar tendency can be observed for "the content of carbon dioxide – pH of the

medium" pair. In order to confirm that, the correlation ratio in these pairs of features was calculated. In the pair "carbon dioxide – concentration", it was  $r = -0.448$ , and in the pair "pH – ionic medium"  $r = -0.04$ . To determine the effect of the temperature on tilapia growth, in the process of growing the mint here circulating aquaculture system using geothermal waters, experiments with temperature regimes from 25 to 33 °C was conducted. The results of the experiment are represented in Table 3. The results of the experiment proved the advantages in the growth of tilapias, which had been kept at the temperatures of 29 °C and 30 °C. The tilapias kept in these temperature regimes have higher average daily weight gain rates, which indicates the high activity of fish and, consequently, feed digestion.

### **3.2. Influence of Technological Factors on Tilapia Growth and Development at Content in Recirculating Aquaculture System Using Geothermal Waters**

The main task of the conducted research was to develop technological processes of tilapia rearing and cultivation in a recirculating aquaculture system with geothermal water supply. In the course of the research, tilapias (females) were evaluated and then divided into three groups – with stocking densities of 100, 200, and 300 pcs/m<sup>3</sup>, respectively. Live weight and body indices were used as the main criteria for a comprehensive evaluation of the investigated fish population. The evaluation was also carried out in terms of secondary sexual characteristics.

Reproductive qualities were checked based on the results of two successive spawnings. The first spawning was carried out with fish kept at a water temperature of 27-29 °C in the basins. As a result of observations, it was found that the females matured 35-40 days after spawning. The results of tilapia growing at different stocking densities are presented in Table 4. The results of the studies have shown (Figures 7, 8) that tilapias grown under conditions of high stocking density are inferior in growth rate, the highest growth rate is observed in the basins with the lowest planting density.

As it can be seen in Figures 7-8, the growth rate is directly proportional to the density of fish stocking in the basins, the optimal density for growing tilapia in the basins using recirculating aquaculture system with geothermal water supply is 100 pcs/m<sup>3</sup>. At the same time, with a denser stocking, tilapia size and weight indices are close to commercial fish, and only a decrease in working fecundity and relative fecundity is noted (Table 4).

In order to determine the reproductive quality of tilapias grown under conditions of keeping in recirculating aquaculture system basins with geothermal water supply, studies were conducted (Table 5). Productive qualities of tilapias were identified during the periods of two spawnings. Assessment of tilapias productive and reproductive qualities at a specific stocking density and spawning order revealed certain differences.

The results of the performed research showed that tilapias grown in recirculating aquaculture systems using geothermal waters at a high density of stocking reflect the tendency to depend on the density level. The measurements taken at optimal stocking of tilapias with a density equal to 100 pcs/m<sup>3</sup> show that the fish had high fecundity rate rates compared to tilapias grown at stocking densities of 200 to 300 pcs/m<sup>3</sup>. When assessing the efficiency of cultivation, not only the gross yield of products was taken into account, but also their commercial and nutritional qualities, as well as the efficiency of use of the given feeds.

Expectedly, the highest growth rate was observed in the basin with the lowest stocking density (average weight 300 g). 98% of tilapia, which had been kept at a stocking density of 100 pcs/m<sup>3</sup>, was esteemed as a standard product. In the third variant of growing, with a stocking density of 300 pcs/m<sup>3</sup>, the average fish weight was about 196 g, with only 14% of the yield of standard production (above 250 g). Feed consumption is not more than 2.5 kg/kg weight gain.

Aquaculture is one of the fastest-growing areas of food production in the world market. Tilapia is one of the top contributors to the increase in aquaculture production. Tilapias are grown in more than 120 countries. The largest tilapia producers are China – 51% (897.3 thousand tons), Southeast Asian countries (Philippines, Indonesia, Thailand), Mexico, and Egypt. In Europe, tilapias are cultivated in Germany, France, Belgium, Czech Republic, Bulgaria, and some other countries.

Such a rapid spread of tilapia in world aquaculture and a significant increase in its production are associated with several valuable biological characteristics and economic benefits that are peculiar to these fish. (Boronetskaya, 1993; Pevnev, 2000; Shelton, 2002; Rothbard and Peretz, 2002; Tetdoyev, 2009; Tetdoyev and Pliyev, 2009; Boronetskaya and Privezentsev, 2011; Boronetskaya, 2012).

Tilapias are also of great interest in fish farming in Kazakhstan. In our country, the first studies related to the study of tilapia as a possible

object of domestic aquaculture have been launched quite recently. As researches have shown, the natural and climatic conditions of our country allow cultivating it in the southern regions of the republic. Also, a promising production base for tilapias is industrial fish farms that use natural and technical warm waters, including the use of geothermal sources.

The necessary condition ensuring the realization of the high genetic potential of tilapias in the knowledge of their requirements to the main water parameters – temperature, dissolved oxygen in the water and other water quality parameters, their adaptation capabilities. In this regard, the research tasks included, on the one hand, the study of the peculiarities of the hydrochemical regime of geothermal sources (thermal regime, gas and salt composition of water, etc.), and on the other hand – the study of the influence of technological factors (density of stocking, feeding level) on the growth and development of tilapia in the recirculating aquaculture system using geothermal water.

The work was carried out based on the fish farm of “Tengry fish” LLP. Several studies related to the influence of individual environmental factors were carried out in the conditions of the Research Center “Fish Industry”. When studying the technology of tilapia growing in recirculating aquaculture systems using geothermal waters, great attention was paid to studying their temperature regime. Temperature is one of the leading environmental factors determining the possibility and effectiveness of tilapia cultivation. The temperature regime in basins with geothermal water supply is practically in a controlled mode. The experience of cultivation of tilapias in conditions of keeping in ponds with geothermal water supply created essential problems in the winter period due to temperature decrease to 10-15 °C (Tetdoyev, 2009). Studies have shown that the closed water supply system provides reliable control of water quality and allows year-round reproduction and cultivation of fish.

One important indicator of water quality is the oxygen regime. Studies on tilapia growing in conditions of closed water supply using geothermal waters indicate that the oxygen regime was quite favorable for tilapia breeding. Assessing the environmental conditions for growing tilapias in conditions of closed water supply using geothermal waters, it can be concluded that they meet the requirements for tilapias. The ability to regulate several water quality indicators, in particular through degassing, will create the conditions to ensure the realization of highly

productive and reproductive qualities of these fish species.

Much attention was paid to the study of tilapia growth and development in the conditions of a recirculating aquaculture system using geothermal waters. In the course of the research, the reactions of tilapias to the technology of content (density of stocking) and, accordingly, its impact on growth and development and reproductive qualities were determined. Performed researches have shown high tolerance of tilapias to influence of adverse factors of environment, extensive adaptive possibilities and high productive qualities that confirms the possibility of cultivation of new object of aquaculture in Republic of Kazakhstan in the conditions of domestic industrial fish farms.

#### 4. CONCLUSIONS:

1. To regulate and stabilize the hydrochemical regime of geothermal sources, degasation was carried out, as a result of which the level of dissolved oxygen reached an average of 6.27 mg/dm<sup>3</sup>; pH 7.56; concentration of carbon dioxide to 2.11 mg/dm<sup>3</sup>.

2. As a result of growing tilapias at different stocking densities, it was found that the optimal stocking density of tilapias in recirculating aquaculture systems using geothermal waters is 100 and 200 pcs/m<sup>3</sup>. At the given density of stocking, higher indicators of growth rate are observed – absolute weight gain was 1603.1 g and 1357.1 g, respectively, in comparison with a stocking density of 300 pcs/m<sup>3</sup>, where absolute weight gain was 1214.2 g.

3. It has been found that reproductive qualities of tilapias grown in recirculating aquaculture system using geothermal waters at planting density from 100 to 200 pcs/m<sup>3</sup> are also higher in all parameters than those kept at planting density of 300 pcs/m<sup>3</sup>, concerning both the weight of producers and such indicators as fecundity, the mass of reproductive products, yield of larvae.

4. It has been found that at the temperature, 29-30 °C tilapias have a higher average daily weight gain and, accordingly, more efficient use of feeds.

#### 5. ACKNOWLEDGMENTS:

For successful research, we would like to express special gratitude to the Ministry of Education and Science of the Republic of Kazakhstan for the grant financing of the scientific

project on “Development of technology of cultivation of new aquaculture facilities on geothermal sources” (individual registration number No. AP05135409), “Tengry Fish” LLP for providing the base for research work.

Also, the work would be impossible without the participation of scientific, administrative, and technical personnel of Research Center “Fish economy”, at the Department of Hunting and Fisheries of S. Seifullin Kazakh Agro Technical University.

#### 6. REFERENCES:

1. Beisembayeva, L., Romanova, S., Ponomarenko, O., and Matveyeva, I. (2017). Features of chemical composition of reservoir – Cooler of Ekibastuz GRES-1 (Kazakhstan). *International Multidisciplinary Scientific GeoConference Surveying Geology and Mining Ecology Management, SGEM*, 17(31), 285-292.
2. Billah, M. K., Uddin, M. K., Samad, M. Y. A., Hassan, M. Z. B., Anwar, M. P., Kamal, A. H. M., Shahjahan, M., and Al-Asif, A. (2020). Effects of different stocking density of Nile tilapia (*Oreochromis niloticus*) and common carp (*Cyprinus carpio*) on the growth performance and rice yield in rice-fish farming system. *AACL Bioflux*, 13(2), 789-803.
3. Bolotov, I. N., Aksyonova, O. V., Besspalaya, Y. V., and Spitsyn, V.M. (2016). Endemism of freshwater fish fauna in geothermal regions: review of molecular biogeographic studies. *Vestnik SAFU. Series Natural Science*, 1, 29-50.
4. Boronetskaya, O. I. (1993). *Technology for growing tilapia in ponds with geothermal water supply*. Moscow, Russian Federation: TAA.
5. Boronetskaya, O.I. (2012). Use of tilapia (Tilapiinae) in global and domestic aquaculture. *Izvestiya TSKA*, 1, 164-173.
6. Boronetskaya, O.I., and Privezentsev, Y.A. (2011). Biological characteristics and productive qualities of tilapia fish of timiryazevskaya breed. *Izvestiya TSKA*, 4, 131-137.
7. Budiasa, I. W., Santosa, I. G. N., Ambarawati, I. G. A. A., Suada, I.K., Sunarta, I. N., and Shchegolkova, N. (2018). Feasibility study and carrying capacity of lake Batur ecosystem to preserve tilapia fish farming in Bali, Indonesia. *Biodiversitas*, 19(2), 568-575.

8. Chugunova, N. I. (1959). *A guide to the study of fish age and growth*. Moscow, Russian Federation: Academy of Sciences Press.
9. Grande Burgos, M. J., Romero, J. L., Pérez Pulido, R., Cobo Molinos, A., Gálvez, A., and Lucas, R. (2018). Analysis of potential risks from the bacterial communities associated with air-contact surfaces from tilapia (*Oreochromis niloticus*) fish farming. *Environmental Research*, 160, 385-390.
10. Gurkina, O. A., Vasiliev, A. A., Poddubnaya, I. V., Kiyashko, V. V., Suchkov, V. V., and Fadeeva, Y. D. (2019). The effect of aquatic organisms on the water quality in ponds in various fish-breeding processes. *Ecology, Environment and Conservation*, 25(3), 1180-1184.
11. Korentovich, M. A., Litvinenko, A. I., and Sirotkina, Y. A. (2017). Results and prospects of geothermal aquaculture development in valuable fish species in Southwest Siberia. In *collection of articles of the All-Russian Scientific and Practical Conference "Modern Scientific and Practical Solutions in the Agroindustrial Complex"* (pp. 307-317). Tyumen, Russian Federation: State Agrarian University of the Northern Trans-Urals.
12. Lefers, R., Alam, A., Scarlett, F., and Leiknes, T. (2020). Aquaponics water use and nutrient cycling in a seawater-cooled controlled environment agriculture system. *Acta Horticulturae*, 1271, 392-402.
13. Leite, N. K., Stolberg, J., da Cruz, S.P., Tavela, A. O., Safanelli, J. L., Marchini, H.R., Exterkoetter, R., Leite, G. M. C., Krusche, A. V., and Johnson, M.S. (2018). Hydrochemistry of shallow groundwater and springs used for potable supply in Southern Brazil. *Environmental Earth Sciences*, 77(3), article number 80.
14. Mamontov, Y. P. (2000). *Current state and prospects of aquaculture development in Russia*. Krasnodar, Russian Federation: All-Russian Research Institute of Freshwater Fisheries.
15. Mansano, C. F. M., do Nascimento, T. M. T., Peres, H., Rodrigues, F. H. F., Khan, K. U., Romaneli, R. S., Sakomura, N.K., and Fernandes, J. B. K. (2020). Determination of the optimum dietary essential amino acid profile for growing phase of Nile tilapia by deletion method. *Aquaculture*, 523, article number 735204.
16. Master plan of commercial fish farming development in the Republic of Kazakhstan in 2011-2025. (2011). Astana. <http://agroalem.kz/article/pisciculture/1329-o-programme-razvitiya-rybnogo-hozyaystva-do-2020-goda.html>
17. Pevnev, I. G. (2000). *Technological features of cultivation of fish stocking material of carp using geothermal water*. Omsk, Russian Federation: Omsk State Agrarian University.
18. Pravdin, I. F. (1966). *A manual of fish study*. Moscow, Russian Federation: Food industry.
19. Privezentsev, Y. A. (1991). *Intensive pond fish farming*. Moscow, Russian Federation: Agropromizdat.
20. Pruszyński, T., and Pistelok, F. (1999). Biological and economical evaluation of African and European catfish rearing in water recirculation systems. *Fisheries and Aquatic Life*, 7(2), 343-352.
21. Rothbard, S., and Peretz, Y. (2002). Tilapia culture in Negev. Retrieved from <http://aquafind.com/articles/TilapiaDesert.php>
22. Semyonov, A. D. (Ed.). (1977). *Chemistry guidelines for the chemical analysis of terrestrial surface water*. Leningrad, Russian Federation: Hydrometeoizdat.
23. Shelton, W. L. (2002). Tilapia culture in the 21st century. In R. D. Guerrero, and M. R. Guerrero-del Castillo (Eds.), *Proceedings of the International Forum on Tilapia Farming in the 21st Century (Tilapia Forum 2002)* (pp. 1-20). Laguna, Philippines: Philippine Fisheries Association Inc.
24. Syzdykov, K. N., Kuanchaleyev, Z. B., Assylbekova, A. S., Marlenov, E. B., and Mussin, S. E. (2019). Breeding new aquaculture objects at geothermal sources. *Ecology, Environment and Conservation*, 25(2), 907-912.
25. Tetdoyev, V. V. (2009). *Reproduction and cultivation of tilapia in water bodies with different ecological conditions*. Moscow, Russian Federation: Russian State Agrarian Correspondence University.
26. Tetdoyev, V. V., and Boronetskaya, O. I. (2008). Ecological conditions of ponds with geothermal water supply for tilapia cultivation. *Vestnik RGAZU*, 4(9), 47-51.
27. Tetdoyev, V. V., and Pliyev, T. K. (2009). Ecological conditions of various water bodies for growing tilapia. *Vestnik RUDN, Agronomy and Cattle Breeding Series*, 3, 47-51.



28. Tosun, Y. I. (2017). Ultrafiltration of saline waters in geothermal fields hot water discharge. *Lecture Notes in Civil Engineering*, 4, 639-643.
29. Yudin, F. A. (1980). *Methodology of agrochemical research*. Moscow, Russian Federation: Kolos.
30. Zdanovich, V. V., and Pushkar, V. Y. (2007). Intensification of young catfish growing under conditions of thermogradient field. *Proceedings and Reports of the International Symposium*, 14, 113-115.

**Table 1.** Hydrochemical parameters of geothermal waters

| No. | The name of indicators                       | Actual figures | Normative indicators |
|-----|--|----------------|----------------------|
| 1   | Dissolved oxygen, mg / dm <sup>3</sup>       | 2.5            | >5                   |
| 2   | pH units                                     | 7.7            | 6.5-8.5              |
| 3   | General stiffness, mg-eq/dm <sup>3</sup>     | 3.8            | <7                   |
| 4   | Carbon dioxide, mg / dm <sup>3</sup>         | 80.1           | 10-15                |
| 5   | Hydrogen sulfide, mg / dm <sup>3</sup>       | 0.002          | <0.003               |
| 6   | Permanganate oxidation, mg / dm <sup>3</sup> | 0.301          | 5                    |
| 7   | Total nitrogen, mg / dm <sup>3</sup>         | 2.86           | <1.5                 |
| 8   | Phosphorus total, mg/dm <sup>3</sup>         | 0.009          | <2                   |
| 9   | Chlorides, mg / dm <sup>3</sup>              | 69.2           | <350                 |
| 10  | Iron total, mg/dm <sup>3</sup>               | 0.030          | <0.3                 |
| 11  | Fluorine, mg / dm <sup>3</sup>               | 0.068          | 0.5-1.5              |
| 12  | Zinc, mg / dm <sup>3</sup>                   | 0.091          | <0.01                |
| 13  | Manganese, mg / dm <sup>3</sup>              | 0.009          | <0.1                 |
| 14  | Oil products, mg / dm <sup>3</sup>           | 0.073          | <0.1                 |

**Table 2.** The hydrochemical regime in a recirculating aquaculture system with the use of geothermal waters with tilapia content (maintenance time six months)

| Indicators                         | Month |       |       |        |       |        | Average index | Normative indicators |
|------------------------------------|-------|-------|-------|--------|-------|--------|---------------|----------------------|
|                                    | March | April | May   | June   | July  | August |               |                      |
| Oxygen, mg/dm <sup>3</sup>         | 6.01  | 6.09  | 6.24  | 6.28   | 6.47  | 6.58   | 6.27          | >5                   |
| pH, units                          | 7.5   | 7.5   | 7.5   | 7.6    | 7.6   | 7.7    | 7.56          | 6.5-8.5              |
| Carbon dioxide, mg/dm <sup>3</sup> | 3.8   | 2.5   | 1.6   | 2.1    | 1.6   | 1.1    | 2.11          | 10-15                |
| Iron (II), mg/dm <sup>3</sup>      | 0.003 | 0.002 | 0.002 | 0.001  | 0.001 | 0.001  | 0.001         | <0.3                 |
| Iron (III), mg/dm <sup>3</sup>     | 0.114 | 0.115 | 0.114 | 0.112  | 0.111 | 0.111  | 0.112         |                      |
| Nitrates, mg/dm <sup>3</sup>       | 4.11  | 3.28  | 3.1   | 2.84   | 2.77  | 2.71   | 3.135         | <3                   |
| Nitrites, mg/dm <sup>3</sup>       | 0.024 | 0.021 | 0.013 | 0.011  | 0.009 | 0.010  | 0.014         | <0.02                |
| Phosphates, mg/dm <sup>3</sup>     | 0.01  | 0.01  | 0.011 | 0.0094 | 0.009 | 0.009  | 0.009         | <2                   |

**Table 3.** The effect of the temperature on the growth and development of tilapia while growing them in the recirculating aquaculture system using geothermal waters

| Indicators                                | Water temperature, °C |           |          |
|---|-----------------------|-----------|----------|
|   | 25                    | 29        | 33       |
| Average stocking weight, g                |                       | 12.6±0.36 |          |
| Average fishing weight, g                 | 89.7±1.6              | 92.4±1.2  | 91.6±1.5 |
| Average daily weight gain, g              | 0.86                  | 1.14      | 1.11     |
| Consumption of feed, kg/kg of weight gain | 1.8                   | 1.8       | 1.8      |

**Table 4.** The results of growing Nile Tilapia under different conditions of keeping

| Indicators                       | Feeding level, % | Stocking density, pcs/m <sup>3</sup> |          |          |
|----------------------------------|------------------|--------------------------------------|----------|----------|
|                                  |                  | 100                                  | 200      | 300      |
| The initial weight of females, g |                  | 12.6±0.36                            |          |          |
| The final weight of females, g   | 3.5              | 202±6.3                              | 171±4.5  | 153±5.9  |
| Absolute weight gain, g          | 3.5              | 1603.174                             | 1357.142 | 1214.285 |
| Average daily weight gain, g     | 3.5              | 1.06                                 | 0.88     | 0.78     |
| Workingfecundity, pcs. eggs      | 3.5              | 603±24.9                             | 490±31.8 | 400±33.1 |
| Relativefecundity, pcs. /g       | 3.5              | 2.9                                  | 2.6      | 2.5      |

**Table 5.** Characteristics of reproductive qualities of tilapias growing in a recirculating aquaculture system using geothermal waters

| Indicators                                  | Spawning  |          |
|---|-----------|----------|
|   | 1         | 2        |
| Stocking density, 100 pcs/m <sup>3</sup>    |           |          |
| Weightoffish, g. female                     | 158±13.5  | 242±9.6  |
| Weightoffish, g. male                       | 198±10.4  | 306±10.7 |
| Feed consumption, kg/kg weight gain         | 2.5       | 2.5      |
| Absolute weight gain, g female              | -         | 84±5.8   |
| Absolute weight gain, g male                | -         | 108±9.5  |
| Average daily weight gain, g female         | -         | 2.1      |
| Average daily weight gain, g male           | -         | 2.7      |
| Fecundity: working, pcseggs relative, pcs/g | 427±9.2   | 750±10.3 |
| Weight of eggs, mg                          | 3.2±0.09  | 3.5±0.12 |
| Weight of fish larvae, mg                   | 7.7±0.14  | 7.9±0.11 |
| Larvalyield, %                              | 83.0±1.25 | 85.2±1.1 |
| Stocking density, 200 pcs/m <sup>3</sup>    |           |          |
| Weightoffish, g. female                     | 127±14.2  | 203±9.8  |
| Weightoffish, g. male                       | 154±12.2  | 250±10.4 |
| Feed consumption, kg/kg weight gain         | 2.5       | 2.5      |
| Absolute weight gain, g female              | -         | 76±5.9   |
| Absolute weight gain, g male                | -         | 96±7.1   |
| Average daily weight gain, g female         | -         | 1.9      |
| Average daily weight gain, g male           | -         | 2.4      |
| Fecundity: working, pcseggs relative, pcs/g | 317±9.8   | 528±9.7  |
| Weight of eggs, mg                          | 3.1±0.1   | 3.5±0.14 |
| Weight of fish larvae, mg                   | 7.5±0.11  | 7.7±0.12 |
| Larvalyield, %                              | 80±1.6    | 81±1.5   |
| Stocking density, 300 pcs/m <sup>3</sup>    |           |          |
| Weightoffish, g. female                     | 117±13.1  | 192±9.6  |
| Weightoffish, g. male                       | 144±11.3  | 201±10.5 |
| Feed consumption, kg/kg weight gain         | 2.5       | 2.5      |
| Absolute weight gain, g female              | -         | 71±5.5   |
| Absolute weight gain, g male                | -         | 93±7.2   |
| Average daily weight gain, g female         | -         | 1.6      |
| Average daily weight gain, g male           | -         | 2.1      |
| Fecundity: working, pcseggs relative, pcs/g | 287±9.6   | 418±8.8  |
| Weight of eggs, mg                          | 2.9±0.1   | 3.3±0.12 |
| Weight of fish larvae, mg                   | 7.1±0.1   | 7.3±0.14 |
| Larvalyield, %                              | 78±1.2    | 80±1.4   |

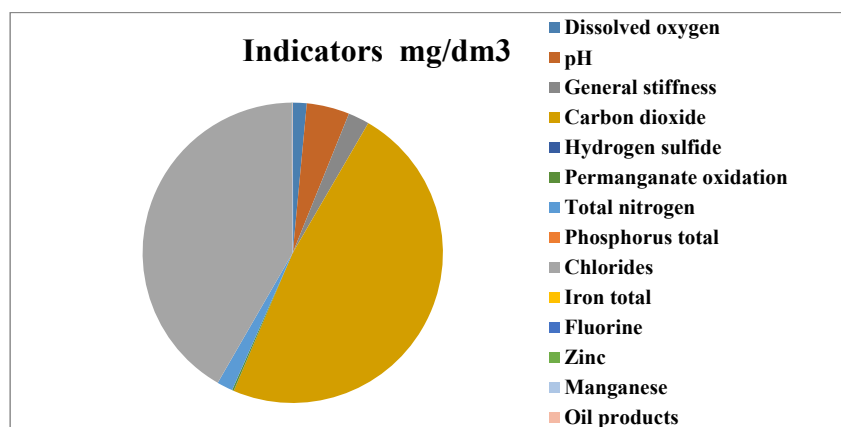


**Figure 1.** Diagram of the parameters of the hydrochemical regime of geothermal waters of fish farm Tengry fish LLP



**Figure 2.** Experimental degassing unit

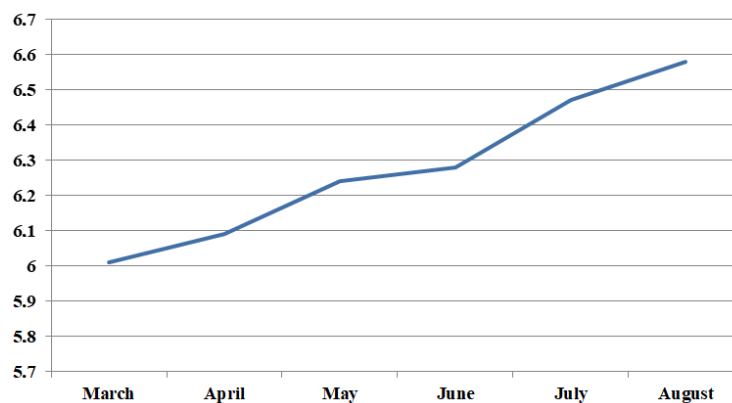


**Figure 3.** Dynamics of changes in the oxygen regime in the installation of closed water supply using geothermal waters with tilapia content for six months

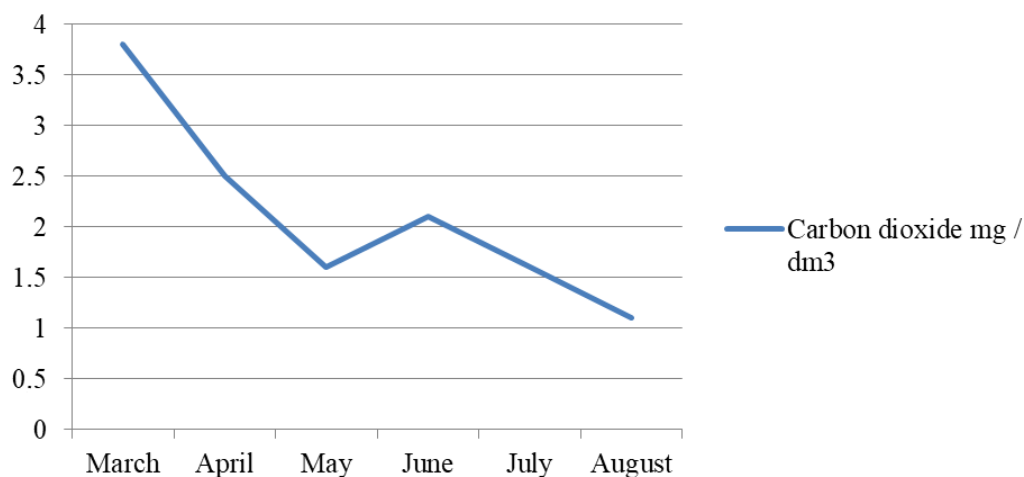


**Figure 4.** Dynamics of changes in the concentration of carbon dioxide in the installation of closed water supply using geothermal waters with tilapia content for six months

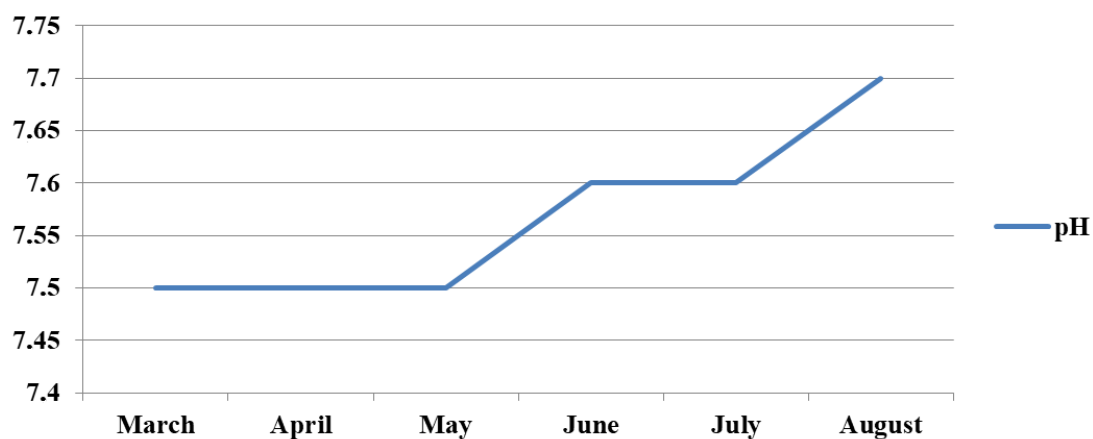


**Figure 5.** Dynamics of pH change in a recirculating aquaculture system using geothermal water keeping tilapia for six months

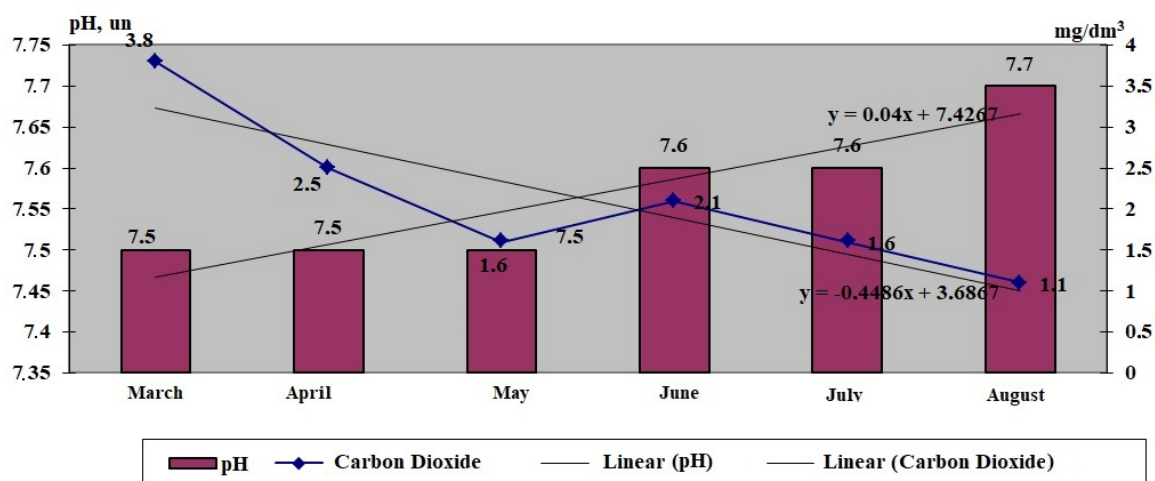


**Figure 6.** The effect of carbon dioxide on the pH of water in a recirculating aquaculture system using geothermal water while keeping tilapia for six months

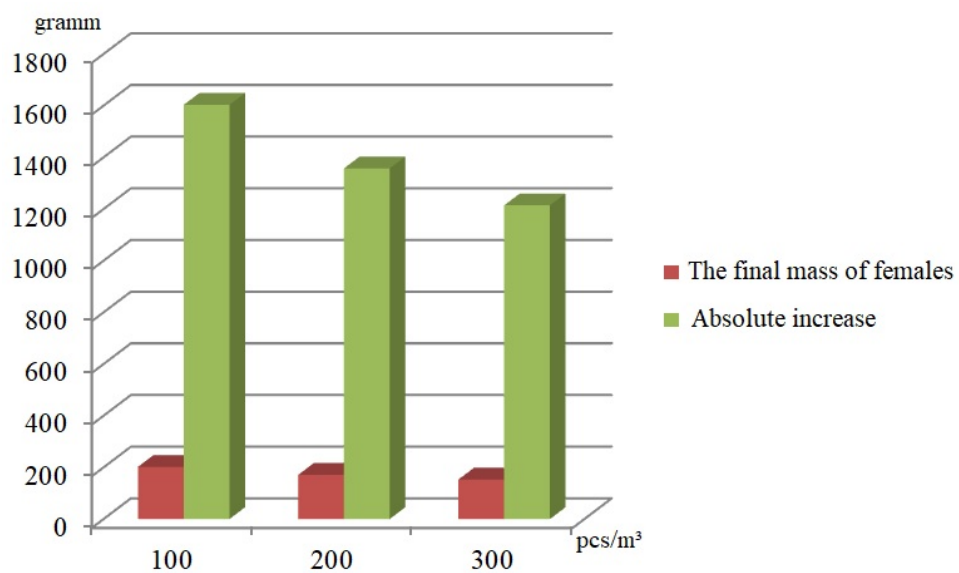


**Figure 7.** The tilapia growth rate in recirculating aquaculture system using geothermal waters with different stocking densities

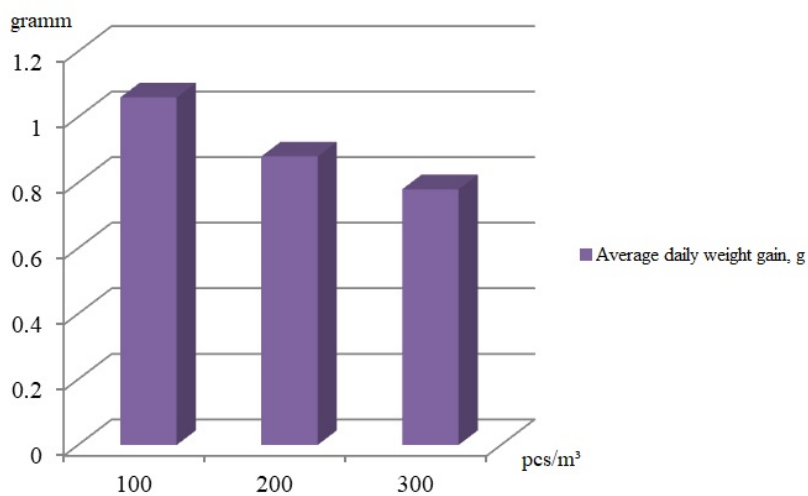


**Figure 8.** Average daily weight gain of tilapia in recirculating aquaculture system using geothermal waters with different stocking densities

## MÉTODO CAS WAVELETS PARA RESOLVER O SISTEMA DE DIFUSÃO DE REAÇÃO E COMPARAR COM O MÉTODO (G.F.E)

### CAS WAVELETS METHOD TO SOLVE REACTION-DIFFUSION SYSTEM AND COMPARE IT WITH (G.F.E) METHOD

SALIM, Badran Jasim<sup>1</sup>; JASIM, Oday Ahmed<sup>2\*</sup>

<sup>1,2</sup> University of Mosul, College of Basic Education, Department of Mathematics. Iraq.

\* Corresponding author

e-mail: odayalnoamy@uomosul.edu.iq

Received 14 May 2020; received in revised form 14 June 2020; accepted 04 July 2020

## RESUMO

A análise de Onduleta ou ondaleta (em inglês: *wavelet*) desempenha um papel de destaque em vários campos das disciplinas científicas. Particularmente, as wavelets são usadas com muito sucesso na análise de sinais para representação e segmentação de formas de onda, análise de frequência-tempo e algoritmos rápidos nas equações de propagação e reação. Esta pesquisa teve como objetivo orientar os pesquisadores a usar Cos e Sin (CAS) para aproximar a solução do sistema de equações diferenciais parciais. Este método foi aplicado com sucesso para resolver um sistema acoplado de sistemas não-lineares de difusão de reação onde foi demonstrado que o método de wavelets CAS é bastante capaz e adequado para encontrar soluções exatas uma vez que a consistência do método oferece uma aplicabilidade mais ampla onde a ideia principal é transformar equações diferenciais parciais não lineares complexas em sistemas de equações algébricas, fáceis de manusear e encontrar uma solução numérica para elas. Ao comparar as soluções numéricas dos métodos de elementos finitos CAS e Galerkin, a solução de sistemas não-lineares de difusão de reação usando as wavelets do CAS para todos os valores de  $x$  é precisa, confiável, robusta, promissora e chega rapidamente à solução exata. Quando os parâmetros  $\varepsilon_1$  e  $\varepsilon_2$  estão crescendo e com  $L$  diminuindo, o método CAS converge rapidamente para soluções em estado estacionário (quanto menos  $L$ , mais precisa é a solução). Ele está convergindo para soluções de estado estacionário mais rapidamente e perde etapas ao longo do tempo. Além disso, os resultados também mostram que a solução das wavelets CAS é mais confiável e mais rápida em comparação com os elementos finitos de Galerkin (G.F.E).

**Palavras-chave:** Sistema acoplado não-linear PDE, método de elementos finitos de Galerkin (G.F.E), solução numérica, wavelets Haar.

## ABSTRACT

Wavelet analysis plays a prominent role in various fields of scientific disciplines. Mainly, wavelets are very successfully used in signal analysis for waveform representation and segmentation, time-frequency analysis, and fast algorithms in the propagation equations and reaction. This research aimed to guide researchers to use Cos and Sin (CAS) to approximate the solution of the partial differential equation system. This method has been successfully applied to solve a coupled system of nonlinear Reaction-diffusion systems. It has been shown CAS wavelet method is quite capable and suited for finding exact solutions once the consistency of the method gives wider applicability where the main idea is to transform complex nonlinear partial differential equations into algebraic equation systems, which are easy to handle and find a numerical solution for them. By comparing the numerical solutions of the CAS and Galerkin finite elements methods, the answer of nonlinear Reaction-diffusion systems using the CAS wavelets for all  $\hat{t}$  and  $x$  values is accurate, reliable, robust, promising, and quickly arrives at the exact solution. When parameters  $\varepsilon_1$  and  $\varepsilon_2$  are growing and with  $L$  decreasing, then the CAS method converges to steady-state solutions quickly (the less  $L$ , the more accurate the solution). It is converging towards steady-state solutions faster than and loses steps over time. Moreover, the results also show that the solution of the CAS wavelets is more reliable and faster compared to the Galerkin finite elements (G.F.E).

**Keywords:** Coupled of nonlinear PDE system, Galerkin finite elements method (G.F.E), Numerical solution, Haar wavelets.

## 1. INTRODUCTION:

"Reaction-diffusion systems lead to the formation of tissue based on process simulations and nonlinear interactions, which were proposed as a model for the formation of a biological pattern. Alan Turing (1952) proposed the first chemical mechanism for calculating pattern formation in biological morphology, assuming tissue formation and chemical reaction and the amount of rate that depends on their concentration. These mechanisms are called reaction and diffusion systems" (Turing, 1952; Lepik, 2007; Qasim and Salim, 2019).

Wavelet analysis plays a prominent role in several areas of mathematics. The wavelets are utilized in the solution of all types of equations. These wavelets possess many remarkable properties. They studied intensively, and their connections with different branches of study, like convex and numerical analysis, were investigated. Furthermore, the Sin and Cos for the (CAS) wavelets used, to approximate the solution of linear integral equations (Yousefi and Banifatemi, 2006), Volterra integral equations of the second kind (Adibi and Assari, 2009), and optimal control systems by time-dependent coefficients (Abualrub et al., 2009).

Convert differential equation into an algebraic one is the main characteristic of the operational method and the integration is a core of the functional matrix starting by the integral property of the basic orthonormal matrix,  $\zeta(\hat{t})$  can write the following approximation:

$$\underbrace{\int_0^{\hat{t}} \int_0^{\hat{t}} \dots \int_0^{\hat{t}}}_{k} \psi(\hat{t})(d)^k \cong Q_{\psi}^k \psi(\hat{t}) \quad (\text{Eq.1})$$

Where  $\psi(\hat{t}) = [\bar{\psi}_0(\hat{t}) \ \bar{\psi}_1(\hat{t}) \ \dots \ \bar{\psi}_{m-1}(\hat{t})]^T$  in which the elements  $\bar{\psi}_0(\hat{t}), \bar{\psi}_1(\hat{t}), \dots, \bar{\psi}_{m-1}(\hat{t})$  are the discrete representation of essential functions which are orthogonal on the interval  $[0,1)$  and  $Q_{\psi}$  is the operational matrix for the integration of  $Q(\hat{t})$  [10] (Wu and Chen, 2003).

Yousefi and Banifatemi, 2006, suggested introducing the CAS waves first. CAS wavelets approximation method utilized to reduce the Fredholm integral equations to the solution of algebraic equations. The CAS wavelet operational matrix P of integration will be first presented, and a general procedure to generate this matrix P is given. CAS wavelet approximating method utilized

to reduce the integro-differential equation to the algebraic equations (Han and Shang, 2007). A wavelet-based method for evaluating the modal optimal control and trajectory of the bilinear system is proposed. The technique employs finite CAS wavelets to approximate modal control and state variables (Taher et al., 2009).

Presenting a computational method for solving nonlinear Fredholm integral equations: of the second kind which based on the use of Haar wavelets, for fractional-order which based on CAS (Cosine and Sine) wavelets, A new approach using CAS wavelets in combination with the collocation technique is proposed (Babolian and Shahsavaran, 2009; Saeedi et al., 2011; Ezzati and Najafalizadeh, 2012)

For fractional equations and wave waves, CAS: Using the series of CAS waves with an operational matrix to reduce fractional differential equations to the algebraic equation system. The solution to this system gives the approximate solution of the truncated finite "2K (2M + 1)" (Mingxu et al., 2013). A mathematical method is presented for the numerical solution of a class of differential equations with a weak single nucleus of a fractional system dependent on the Sin and Cos (CAS) waves and mass pulse functions (Mingxu and Jun, 2014). A novel numerical scheme for the approximate solutions of linear as well as nonlinear ordinary differential equations of fractional order with boundary conditions, this method combines Cosine and Sine (CAS) wavelets with Green function, called the Green-CAS method (Muhammad et al., 2019).

Presented a computational method for resolving integral boundary equations for singular logarithmic kernels, which occur as reformulations of a boundary value problem for Laplace's equation (Shamooshakya et al., 2014). The solution of time-varying systems obtained by using CAS wavelets, this method is based upon expanding various time functions in the system as their truncated CSA wavelets. The operational matrices of integration are utilized to reduce the resolution of time-varying systems to the solution of algebraic equations (Xiangyu, 2014). A based on CAS wavelets presented quadrature rules for the numerical solution of double and triple integrals with variable limits of integration (Rezabeyk and Maleknejad, 2015). Present a computational method for solving boundary integral equations with singular logarithmic kernels that occur as reformulations of a boundary value problem for Laplace's equation (Fathizadeh et al., 2017). Proposed a new operational matrix of differentiation using CAS wavelets, with the aid of



these matrices, the CAS wavelets method (CASWM) is developed for the integrodifferential equations (Shiralashetti and Kumbinaraiah, 2019). Solved this system numerically by finite elements method (G.F.E) method, and found that (G.F.E) method is faster than (F.D) method to reach equilibrium state for all  $\hat{t}$  and  $x$  values (Manaa and Qasim, 2019).

Therefore, this study aimed to highlight the CAS wavelets method and test the strength of this method by comparing the solution with a widely known and well-method, which is the Galerkin finite element method.

## 2. MATERIALS AND METHODS:

### 2.1. CAS wavelet method

CAS wavelets method can be written as:  $\tau_{\gamma,m}(\chi) = \tau(\rho, \gamma, m, \chi)$  Where  $\gamma = 1, 2, \dots, 2^\rho$ ,  $\rho, m$  a positive integer and  $\chi$  is the normalized time.

Orthonormal CAS wavelets are defined on the  $[0, 1]$  by:

$$\tau_{\gamma,m}(\chi) = \begin{cases} 2^{\frac{\rho}{2}} CAS_m(2^\rho \chi - \gamma + 1) & \text{for } \frac{\gamma-1}{2^\rho} \leq \chi < \frac{\gamma}{2^\rho} \\ 0 & \text{otherwise} \end{cases} \quad (\text{Eq. 2})$$

Where  $CAS_m(\chi) = \cos(2\pi m \chi) + \sin(2\pi m \chi)$ , and  $m \in \{-M, \dots, M\}$  the CAS wavelets are orthonormal for weight function  $W(x) = 1$ .

The CAS wavelets have the following form with  $m=0$ :

$$\tau_{\gamma,0}(\chi) = 2^{\frac{\rho}{2}} G_\gamma(\chi) = 2^{\frac{\rho}{2}} \begin{cases} 1 & \frac{\gamma-1}{2^\rho} \leq \chi < \frac{\gamma}{2^\rho} \\ 0 & \text{otherwise} \end{cases} \quad (\text{Eq. 3})$$

where  $\{G_\gamma(\chi)\}_{\gamma=1}^{2^\rho}$  is Block -Pulse functions (basis set) on the close interval  $[0, 1]$  (Lepik, 2007).

It can be defined as the integral of (Eq. 2) by CAS wavelets analytically as:

$$P_{2^\rho(2M+1),1}(\chi) = \int_0^\chi \tau_{\gamma,m}(\chi') d\chi' = \begin{cases} 0 & 0 \leq \chi < \frac{\gamma-1}{2^\rho} \\ \int_{\frac{\gamma-1}{2^\rho}}^\chi 2^{\frac{\rho}{2}}(\varpi) d\chi' & \frac{\gamma-1}{2^\rho} \leq \chi < \frac{\gamma}{2^\rho} \\ \int_{\frac{\gamma-1}{2^\rho}}^{\frac{\gamma}{2^\rho}} 2^{\frac{\rho}{2}}(\varpi) d\chi' & \frac{\gamma}{2^\rho} \leq \chi < 1 \end{cases}$$

Where

$$\varpi = \sin(2\pi m(2^\rho \chi' - \gamma + 1)) + \cos(2\pi m(2^\rho \chi' - \gamma + 1))$$

Then

$$P_{2^\rho(2M+1),1}(\chi) = \begin{cases} 0 & 0 \leq \chi < \frac{\gamma-1}{2^\rho} \\ 2^{\frac{\rho}{2}} \frac{1}{\varphi} (\sin(2\pi m(2^\rho \chi - \gamma + 1)) - \sin(2\pi m(\frac{\gamma-1}{2^\rho}))) & \frac{\gamma-1}{2^\rho} \leq \chi < \frac{\gamma}{2^\rho} \\ c \cos(2\pi m(2^\rho \chi - \gamma + 1)) - 2^{\frac{\rho}{2}} \frac{1}{\varphi} \cos(2\pi m(\frac{\gamma}{2^\rho})) & \frac{\gamma}{2^\rho} \leq \chi < 1 \end{cases}$$

Where  $\varphi = 2^{\rho+1} \pi m$

Founding the integration n times as:

$$P_{\lambda,u}(x) = \begin{cases} 0 & 0 \leq \chi < \frac{\gamma-1}{2^\rho} \\ 2^{\frac{\rho}{2}} \frac{(-1)^f u}{(\varphi)^u} \cos(2\pi m(2^\rho \chi - \gamma + 1)) & \frac{\gamma-1}{2^\rho} \leq \chi < \frac{\gamma}{2^\rho} \\ + 2^{\frac{\rho}{2}} \frac{(-1)^e u}{(\varphi)^u} \sin(2\pi m(2^\rho \chi - \gamma + 1)) & \frac{\gamma}{2^\rho} \leq \chi < 1 \\ - \sum_{jj=0}^{u-1} 2^{\frac{\rho}{2}} \frac{1}{jj!} \frac{(-1)^f u}{(\varphi)^{u-jj}} \left( \chi - \frac{\gamma-1}{2^\rho} \right)^{jj} & \\ \sum_{j=0}^{u-1} \frac{1}{j!} \left( \chi - \frac{\gamma}{2^\rho} \right)^j & \\ \left( 2^{\frac{\rho}{2}} \frac{(-1)^f u}{(\varphi)^u} \cos(2\pi m) + 2^{\frac{\rho}{2}} \frac{(-1)^e u}{(\varphi)^u} \sin(2\pi m) \right) & \\ - \sum_{jj=0}^{u-1} 2^{\frac{\rho}{2}} \frac{1}{jj!} \frac{(-1)^f u}{(\varphi)^{u-jj}} \left( \frac{1}{2^\rho} \right)^{jj} & \end{cases} \quad (\text{Eq. 4})$$

Where  $\varphi = 2^{\rho+1}\pi m$ , and

$$f_u = \begin{cases} 0 & \text{if } u = 3, 4, 7, 8, 11, 12, \dots \\ 1 & \text{if } u = 1, 2, 5, 6, 9, 10, \dots \end{cases}$$

And

$$e_u = \begin{cases} 0 & \text{if } u = 1, 4, 5, 8, 9, 12, \dots \\ 1 & \text{if } u = 2, 3, 6, 7, 10, 11, \dots \end{cases}$$

If  $u=0$  corresponds to CAS function  $\tau_{\gamma, m}(\chi)$  in (Eq. 2). To solve boundary value problems, substitute  $\chi = G$  in (Eq. 4). In some instances where  $u=1$ , finding (Lepik, 2007):

$$P_{\lambda, u}(x) = \begin{cases} 0 & 0 \leq \chi < \frac{\gamma-1}{2^\rho} \\ +2^{\frac{\rho}{2}} \frac{1}{\varphi} \sin(2\pi m(2^\rho G - \gamma + 1)) - \cos(2\pi m(2^\rho G - \gamma + 1)) & \frac{\gamma-1}{2^\rho} \leq \chi < \frac{\gamma}{2^\rho} \\ -2^{\frac{\rho}{2}} \frac{1}{\varphi} & \frac{\gamma}{2^\rho} \leq \chi < \frac{\gamma+1}{2^\rho} \\ 2^{\frac{\rho}{2}} \frac{1}{\varphi} (\sin(2\pi m) - \cos(2\pi m)) - 2^{\frac{\rho}{2}} \frac{1}{\varphi} & \frac{\gamma+1}{2^\rho} \leq \chi < \frac{\gamma+2}{2^\rho} \end{cases}$$

## 2.2. Approximation CAS Function

Expanded  $v(\chi)$  by CAS wavelets such that:

$$v(\chi) = \sum_{\lambda=0}^{\infty} z_{\lambda} \tau_{\lambda, m}(\chi), \quad \lambda = 0, 1, 2, 3, \dots, N$$

Hence:

$$Z_0 = \int_0^1 v(\chi) \tau_0(\chi) d\chi,$$

$$Z_{\lambda} = 2^j \int_0^1 v(\chi) \tau_{\lambda}(\chi) d\chi$$

(Eq. 5)

(Eq. 6) With the initial and boundary conditions:

$$\lambda = 2^j + \rho, \quad j \geq 0, \quad 0 \leq \rho < 2^j, \quad \chi \in [0, 1]$$

The integral square error E minimized as:

$$E = \int_0^1 \left[ v(\chi) - \sum_{\lambda=0}^{2^\rho-1} z_{\lambda} \tau_{\lambda}(\chi) \right]^2 d\chi, \quad \rho = 0, 1, 2, \dots, N \quad (\text{Eq. 7})$$

Any function  $v(\chi) \in L^2[0, 1]$  may be expanded using CAS wavelets as:

$$v(\chi) = \sum_{\lambda=0}^{2^\rho} z_{\lambda, m} \tau_{\lambda, m}(\chi) = z^T \tau(\chi) \quad (\text{Eq. 8})$$

Where  $m \in [-M, M]$  and  $Z, \tau(x)$  are matrices given by:

$$Z = [Z_{1, (-M)}, Z_{1, (-M+1)}, \dots, Z_{1, M}, Z_{2^\rho, (-M)}, Z_{2^\rho, (-M+1)}, \dots, Z_{2^\rho, M}]^T$$

$$\tau(x) = [\tau_{1, (-M)}(\chi), \tau_{1, (-M+1)}(\chi), \tau_{1, M}(\chi), \dots, \tau_{2^\rho, (-M)}(\chi), \tau_{2^\rho, (-M+1)}(\chi), \dots, \tau_{2^\rho, M}(\chi)]^T$$

; T transposes (Hariharan and Kannan, 2010).

## 2.3. Mathematical Model

Applying CAS wavelets method to solve nonlinear reaction-diffusion system which has the form (Kan-on, 1997):

$$\begin{aligned} \frac{\partial v}{\partial t_*} &= \varepsilon_1 \frac{\partial^2 v}{\partial \chi_*^2} + v[\alpha_1(\chi_*) - \beta_1 v - \delta_1 \sigma] \\ \frac{\partial \sigma}{\partial t_*} &= \varepsilon_2 \frac{\partial^2 \sigma}{\partial \chi_*^2} - \sigma[\alpha_2(\chi_*) - \delta_2 v] \end{aligned}$$

(Eq. 9)

$$v(\chi_*, 0) = v_0(\chi)$$

$$\sigma(\chi_*, 0) = \sigma_0(\chi)$$

$$\frac{\partial v}{\partial \chi_*} = \frac{\partial \sigma}{\partial \chi_*} = \frac{\partial v}{\partial \chi_*}(a, t) = \frac{\partial v}{\partial \chi}(b, t) = 0$$

$$\chi_* \in [a, b]$$

$$t \geq 0$$

(Eq. 10)

$v(\chi, \hat{t})$  represents the reaction type,  $\sigma(\chi, \hat{t})$  represents the diffusion type.  $\varepsilon_1, \varepsilon_2, \beta_1, \delta_1, \delta_2$  are positive constants.  $\alpha_1(\chi), \alpha_2(\chi)$  are the rates of growth of aspects,  $v_0$  and  $\sigma_0$  are constant interior solutions of (Eq. 9).

First normalize with regard to  $\chi_* \in [a, b]$  because CAS wavelets method defined for  $\chi \in [0, 1]$ , the variables changing as (Lou et al., 2006):

$$\chi = \frac{1}{L}(\chi_* - a), \quad \hat{t} = \hat{t}_* - 0, \quad L = b - a$$

(Eq. 9), (Eq. 10) becomes:

$$\frac{\partial v}{\partial \hat{t}} = \frac{\varepsilon_1}{L^2} \frac{\partial^2 v}{\partial \chi^2} + v[\alpha_1(L\chi + a) - \beta_1 v - \delta_1 \sigma]$$

$$\frac{\partial \sigma}{\partial \hat{t}} = \frac{\varepsilon_2}{L^2} \frac{\partial^2 \sigma}{\partial \chi^2} - \sigma[\alpha_2(L\chi + a) - \delta_2 v]$$

(Eq. 11)

And

$$v(\chi, 0) = v_0(\chi), \quad \sigma(\chi, 0) = \sigma_0(\chi)$$

$$\frac{\partial v}{\partial \chi} = \frac{\partial \sigma}{\partial \chi} = \frac{\partial v}{\partial \chi}(0, \hat{t}) = \frac{\partial v}{\partial \chi}(1, \hat{t}) = 0$$

$$\chi \in [0, 1]$$

$$\hat{t} \geq 0$$

(Eq. 12)

Suppose that,  $v_{\chi\chi}(\chi, \hat{t}), \sigma_{\chi\chi}(\chi, \hat{t})$  can extend the range of CAS waves as follows:

$$v_{\chi\chi}(\chi, \hat{t}) = \sum_{\lambda=0}^{2^p} \sum_{m=-M}^M z_s(\lambda) \tau_\lambda(x) = z_m^T \tau_m(x) \quad t \in (\hat{t}_s, \hat{t}_{s+1}]$$

$$\sigma_{\chi\chi}(\chi, \hat{t}) = \sum_{\lambda=0}^{2^p} \sum_{m=-M}^M z_s(\lambda) \tau_\lambda(x) = z_m^T \tau_m(x) \quad t \in (\hat{t}_s, \hat{t}_{s+1}]$$

(Eq. 13)

Where the elements  $z_{(m)}^T$  are constant in the subinterval

$$t_s = (s-1)\Delta\hat{t}, \Delta\hat{t} = \frac{T}{N} \quad \hat{t} \in (\hat{t}_s, \hat{t}_{s+1}]$$

$$s = 1, 2, 3, \dots, N, \hat{t} \in (0, T)$$

Integrating (Eq. 13) finding:

$$v_{\chi\chi}(\chi, \hat{t}) = (\hat{t} - \hat{t}_s) z_m^T \tau_m(\chi) + v_{\chi\chi}(\chi, \hat{t}_s)$$

$$\sigma_{\chi\chi}(\chi, \hat{t}) = (\hat{t} - \hat{t}_s) z_m^T \tau_m(\chi) + \sigma_{\chi\chi}(\chi, \hat{t}_s)$$

(Eq. 14)

$$v_\chi(\chi, \hat{t}) = (\hat{t} - \hat{t}_s) z_m^T P_{\lambda,1}(\chi) + [v_\chi(\chi, \hat{t}_s) - v_\chi(0, \hat{t}_s)] + v_\chi(0, \hat{t})$$

$$\sigma_\chi(\chi, \hat{t}) = (\hat{t} - \hat{t}_s) z_m^T P_{\lambda,1}(\chi) + [\sigma_\chi(\chi, \hat{t}_s) - \sigma_\chi(0, \hat{t}_s)] + \sigma_\chi(0, \hat{t})$$

(Eq. 15)

$$v(\chi, \hat{t}) = (\hat{t} - \hat{t}_s) z_m^T P_{\lambda,2}(\chi) + [v(\chi, \hat{t}_s) - v(0, \hat{t}_s)] + \chi[v(0, \hat{t}) - v(0, \hat{t}_s)] + v(0, \hat{t})$$

$$\sigma(\chi, \hat{t}) = (\hat{t} - \hat{t}_s) z_m^T P_{\lambda,2}(\chi) + [\sigma(\chi, \hat{t}_s) - \sigma(0, \hat{t}_s)] + \chi[\sigma(0, \hat{t}) - \sigma(0, \hat{t}_s)] + \sigma(0, \hat{t})$$

(Eq. 16)

The differential of equation (Eq.16) with respect  $\hat{t}$  can be writing:

$$\begin{aligned}v^*(\chi, \hat{t}) &= z_m^T P_{\lambda,2}(\chi) + x v_x^*(0, \hat{t}) + v^*(0, \hat{t}) \\ \sigma^*(\chi, \hat{t}) &= z_m^T P_{\lambda,2}(\chi) + \chi \sigma_\chi^*(0, \hat{t}) + \sigma^*(0, \hat{t})\end{aligned}\quad (\text{Eq. 17})$$

It can be reducing the boundary condition  $v_\chi^*(0, \hat{t})$  and  $v^*(0, \hat{t})$  in equation (Eq. 17) such that:

$$v^*(0, \hat{t}) = \frac{v(0, \hat{t}) - v(0, \hat{t}_s)}{(\hat{t} - \hat{t}_s)}$$

Then (Eq. 17) for  $v^*(\chi, \hat{t})$  becomes:

$$\begin{aligned}v^*(\chi, \hat{t}) &= z_m^T P_{\lambda,2}(\chi) + \chi \left[ \frac{v_\chi(0, \hat{t}) - v_\chi(0, \hat{t}_s)}{(\hat{t} - \hat{t}_s)} \right] \\ &\quad + \left[ \frac{v(0, \hat{t}) - v(0, \hat{t}_s)}{(\hat{t} - \hat{t}_s)} \right]\end{aligned}\quad (\text{Eq. 18})$$

Now, by substitute equations (Eq. 14) - (Eq. 18) in (Eq. 11), then get:

$$\begin{aligned}&z_m^T P_{\lambda,2}(\chi) + \frac{\chi}{\Delta t} \left[ v_\chi(0, \hat{t}) - v_\chi(0, \hat{t}_s) \right] - \frac{1}{\Delta t} \left[ v(0, \hat{t}) - v(0, \hat{t}_s) \right] \\ &= \frac{\varepsilon_1 \Delta t}{L^2} z_m^T \tau v(\chi, \hat{t}) + \frac{\varepsilon_1}{L^2} v_{\chi\chi}(\chi, \hat{t}) + v(\chi, \hat{t}_s) \\ &\quad \left[ \alpha_1(\chi L + a) - \beta_1 v(\chi, \hat{t}_s) - \delta_1 \sigma(\chi, \hat{t}_s) \right] \\ &z_m^T P_{\lambda,2}(\chi) + \frac{x}{\Delta t} \left[ \sigma_\chi(0, \hat{t}) - \sigma_\chi(0, \hat{t}_s) \right] - \frac{1}{\Delta t} \left[ \sigma(0, \hat{t}) - \sigma(0, \hat{t}_s) \right] \\ &= \frac{\varepsilon_2 \Delta t}{L^2} z_m^T \tau \sigma(\chi, \hat{t}) + \frac{\varepsilon_2}{L^2} \sigma_{\chi\chi}(\chi, \hat{t}) - \sigma(\chi, \hat{t}_s) \\ &\quad \left[ \alpha_2(\chi L + a) - \delta_2 v(\chi, \hat{t}_s) \right]\end{aligned}\quad (\text{Eq. 19})$$

The (Eq.19) is a linear system. The problem was found to be resolved (Eq. 16).

### 3. RESULTS AND DISCUSSION:

#### 3.1. Reducing the order boundary conditions:

Integrating equation (Eq. 17) to calculate

unknown term such as:

$$\begin{aligned}\int_0^1 v_\chi(\chi, t) d\chi &= \int_0^1 (\hat{t} - \hat{t}_s) z_m^T P_{\lambda,1}(\chi) d\chi + \int_0^1 v_\chi(\chi, \hat{t}_s) d\chi \\ &\quad + \int_0^1 [v_\chi(0, \hat{t}) - v_{\chi\chi}(0, \hat{t}_s)] d\chi\end{aligned}$$

$$\Rightarrow v(1, \hat{t}) - v(0, \hat{t}) = (\hat{t} - \hat{t}_s) z_m^T D_{\lambda,1}(\chi) + [v(1, \hat{t}_s) - v(0, \hat{t}_s)] + [v_\chi(0, \hat{t}) - v_\chi(0, \hat{t}_s)]$$

$$\Rightarrow [v_\chi(0, \hat{t}) - v_\chi(0, \hat{t}_s)] = -(\hat{t} - \hat{t}_s) z_m^T D_{\lambda,1}(\chi) + [v(1, \hat{t}) - v(1, \hat{t}_s)] - [v(0, \hat{t}) - v(0, \hat{t}_s)]$$

(Eq. 20)

$$\text{Where } D_{\lambda,1}(\chi) = \int_0^1 P_{\lambda,1}(\chi) d\chi$$

By substitute (Eq. 20) in equations (Eq. 14) - (Eq. 18) about  $v(\chi, \hat{t})$  we get:

$$v_{\chi\chi}(\chi, \hat{t}) = (\hat{t} - \hat{t}_s) z_m^T \tau_m(\chi) + v_{\chi\chi}(\chi, \hat{t}_s) \quad (\text{Eq. 21})$$

$$\begin{aligned}v_\chi(\chi, \hat{t}) &= (\hat{t} - \hat{t}_s) z_m^T P_{\lambda,1}(\chi) - (\hat{t} - \hat{t}_s) z_m^T D_{i,1}(\chi) \\ &\quad + [v(1, \hat{t}) - v(1, \hat{t}_s)] - [v(0, \hat{t}) - v(0, \hat{t}_s)] + v_\chi(0, \hat{t}_s)\end{aligned}$$

(Eq. 22)

$$\begin{aligned}v(\chi, \hat{t}) &= (\hat{t} - \hat{t}_s) z_m^T P_{\lambda,2}(\chi) + [v_\chi(\chi, \hat{t}_s) - v_\chi(0, \hat{t}_s)] \\ &\quad + \chi [-(\hat{t} - \hat{t}_s) z_m^T D_{i,1}(\chi) + [v(1, \hat{t}) - v(1, \hat{t}_s)] \\ &\quad - [v(0, \hat{t}) - v(0, \hat{t}_s)] + v(0, \hat{t}_s)]\end{aligned}\quad (\text{Eq. 23})$$

Now, differential (Eq. 23) by respect  $\hat{t}$ , then get:

$$\begin{aligned}v^*(\chi, \hat{t}) &= z_m^T P_{\lambda,2}(\chi) + \frac{1}{(\hat{t} - \hat{t}_s)} [v_\chi(\chi, \hat{t}_s) - v_\chi(0, \hat{t}_s)] + \frac{\chi}{(\hat{t} - \hat{t}_s)} \\ &\quad [-(\hat{t} - \hat{t}_s) z_m^T D_{\lambda,1}(\chi) + \frac{1}{(\hat{t} - \hat{t}_s)} [v(1, \hat{t}) - v(1, \hat{t}_s)] \\ &\quad - [v(0, \hat{t}) - v(0, \hat{t}_s)]]\end{aligned}$$

(Eq. 24)

Now, by substitute equations (Eq. 21) - (Eq. 24) in (Eq. 11), then get:

$$z_m^T P_{\lambda,2}(\chi) + \frac{1}{\Delta t} [v_\chi(\chi, \hat{t}_s) - v_\chi(0, \hat{t}_s)] + \frac{\chi}{\Delta t} [-\Delta t z_m^T D_{i,1}(\chi)] \\ + \frac{1}{\Delta t} [v(1, \hat{t}) - v(1, \hat{t}_s)] - [v(0, \hat{t}) - v(0, \hat{t}_s)] = \frac{\varepsilon_1 \Delta t}{L^2} z_m^T \tau_m(\chi) \\ + \frac{\varepsilon_1 \Delta t}{L^2} v_{\chi\chi}(\chi, \hat{t}_s) + v(\chi, \hat{t}_s) [\alpha_1(\chi) - \beta_1 v(\chi, \hat{t}_s) - \delta_1 \sigma(\chi, \hat{t}_s)]$$

Similarly, find  $\sigma(\chi, \hat{t}_s)$  then:

$$z_m^T P_{\lambda,2}(\chi) - x z_m^T D_{\lambda,1}(\chi) - \frac{\varepsilon_1 \Delta t}{L^2} z_m^T \tau_m(\chi) = -\frac{1}{\Delta t} [v_\chi(\chi, \hat{t}_s) \\ - v_\chi(0, \hat{t}_s)] - \frac{1}{\Delta t} [v(1, \hat{t}) - v(1, \hat{t}_s)] + [v(0, \hat{t}) \\ - v(0, \hat{t}_s)] + \frac{\varepsilon_1 \Delta t}{L^2} v_{\chi\chi}(\chi, \hat{t}_s) + v(\chi, \hat{t}_s) \\ [\alpha_1(\chi) - \beta_1 v(\chi, \hat{t}_s) - \delta_1 \sigma(\chi, \hat{t}_s)] \\ z_m^T P_{\lambda,2}(\chi) - x z_m^T D_{\lambda,1}(\chi) - \frac{\varepsilon_2 \Delta t}{L^2} z_m^T \tau_m(\chi) = -\frac{1}{\varepsilon_1 \Delta t} [\sigma_\chi(\chi, \hat{t}_s) \\ - \sigma_\chi(0, \hat{t}_s)] - \frac{1}{\Delta t} [\sigma(1, \hat{t}) - \sigma(1, \hat{t}_s)] + [\sigma(0, \hat{t}) - \sigma(0, \hat{t}_s)] \\ + \frac{\varepsilon_2 \Delta t}{L^2} \sigma_{\chi\chi}(\chi, \hat{t}_s) - \sigma(\chi, \hat{t}_s) [\alpha_2(\chi) - \delta_2 v(\chi, \hat{t}_s)]$$

(Eq. 25)

### 3.2. Numerical results and Discussion

solve (Eq. 11) by using (Eq. 25) and the exact solution such that (Lou and et al., 2006):

$$v(\chi, 0) = \frac{\alpha_1}{\beta_1} + \frac{1}{(\alpha_1 - \alpha_2)\beta_1} \delta_2 \sin(\sqrt{-\mu\varepsilon_1}\chi) \left\{ \right. \\ \sigma(\chi, 0) = \frac{1}{(\alpha_2 - \alpha_1)\delta_1} \delta_2 \sin(\sqrt{-\mu\varepsilon_1}\chi) \left. \right\}$$

(Eq. 26)

$$\text{Where } \mu = \frac{\alpha_1 - \alpha_2}{\varepsilon_1 - \varepsilon_2} < 0, \quad \alpha_1, \alpha_2 > 0$$

$$v(\chi, 0) = v_0(\chi) \\ \sigma(\chi, 0) = \sigma_0(\chi) \\ \frac{\partial v}{\partial \chi} = \frac{\partial \sigma}{\partial \chi} = \frac{\partial v}{\partial \chi}(0, \hat{t}) = \frac{\partial v}{\partial \chi}(1, \hat{t}) = 0 \\ 0 \leq \chi \leq 1 \\ t \geq 0$$

(Eq. 27)

Thus will found:

$$v(\chi, \hat{t}_s) = v(\chi, 0) = \frac{\alpha_1}{\beta_1} + \frac{1}{(\alpha_1 - \alpha_2)\beta_1} \delta_2 \sin(\sqrt{-\mu\varepsilon_1}\chi) \left\{ \right. \\ \sigma(\chi, \hat{t}_s) = \sigma(\chi, 0) = \frac{1}{(\alpha_2 - \alpha_1)\delta_1} \delta_2 \sin(\sqrt{-\mu\varepsilon_1}\chi) \left. \right\}$$

$$v_\chi(\chi, \hat{t}_s) = v_\chi(\chi, 0) = \frac{\partial}{\partial \chi} \frac{\alpha_1}{\beta_1} + \frac{1}{(\alpha_1 - \alpha_2)\beta_1} \delta_2 \sin(\sqrt{-\mu\varepsilon_1}\chi) \left\{ \right. \\ \sigma_\chi(\chi, \hat{t}_s) = \sigma_\chi(\chi, 0) = \frac{\partial}{\partial \chi} \left[ \frac{1}{(\alpha_2 - \alpha_1)\delta_1} \delta_2 \sin(\sqrt{-\mu\varepsilon_1}\chi) \right] \left. \right\}$$

$$v_{\chi\chi}(\chi, \hat{t}_s) = v_{\chi\chi}(\chi, 0) = \frac{\partial^2}{\partial \chi^2} \left[ \frac{\alpha_1}{\beta_1} + \frac{1}{(\alpha_1 - \alpha_2)\beta_1} \delta_2 \sin(\sqrt{-\mu\varepsilon_1}\chi) \right] \left\{ \right. \\ \sigma_{\chi\chi}(\chi, \hat{t}_s) = \sigma_{\chi\chi}(\chi, 0) = \frac{\partial^2}{\partial \chi^2} \left[ \frac{1}{(\alpha_2 - \alpha_1)\delta_1} \delta_2 \sin(\sqrt{-\mu\varepsilon_1}\chi) \right] \left. \right\}$$

(Eq. 28)

Comparison of the numerical solution and the exact solution by us (Lou and et al., 2006):

$$v(\chi, 0) = \frac{1}{10} \sin^2\left(\frac{24}{10} \pi \chi\right) + \sin^2\left(\frac{-5}{100} \pi \chi\right) \quad \chi \in [0, L] \\ \sigma(\chi, 0) = \frac{1}{10} \sin^2\left(\frac{24}{10} \pi \chi\right) + \sin^2\left(\frac{-5}{100} \pi \chi\right) \quad \chi \in [0, L]$$

Where L=0.5 and time step

$$\Delta t = 0.1, \varepsilon_1 = \varepsilon_2 = 0.001, \theta = 0.5, \alpha_1 = 1, \alpha_2 = 0.06,$$

$\beta_1 = \delta_1 = \delta_2 = 1$  the results are given in Table 1 and Figures 1 and 2.

Where L=0.5 is step size and time step

$$\Delta t = 0.1, \varepsilon_1 = \varepsilon_2 = 0.001, \theta = 0.5, \alpha_1 = 1, \alpha_2 = 0.01,$$

$\beta_1 = \delta_1 = \delta_2 = 0.0001$  and M=21 the results given in Table 2 and Figures 3 and 4.

Table 3 represents a comparison of the system's absolute errors (Eq. 11) between the CAS and finite element results with the exact solution. Noted the calculation of the CAS method in Table 2 We chose a value  $\beta_1, \delta_1, \delta_2$  close to zero which is,  $\beta_1 = \delta_1 = \delta_2 = 0.0001$ , while we took the value  $\beta_1 = \delta_1 = \delta_2 = 0$  in the calculation of the finite element method, because when calculating in the CAS method and when one of them  $\beta_1 = \delta_1 = \delta_2 = 0$  an appears in the solution amount is not defined.

From solving nonlinear partial differential equations for Reaction-diffusion Systems numerically by using the CAS method. "This

method found that it is better and faster for all the values for  $\hat{t}$  and  $x$ . It also found that it is converging towards steady-state solutions faster than and loses steps over time". As well, the CAS method converges to an exact solution faster when growing  $\varepsilon_1$  and  $\varepsilon_2$  and decreasing  $L$ . When  $\hat{t}$  is reduced, the solution will be quick to arrive at the real solution.

Finally, the comparison between the CAS methods and the finite elements was found the solution converged but clear preference for the CAS method on the finite element method, as shown in Tables 1 - 3 and Figures 1 - 4.

#### 4. CONCLUSIONS:

CAS wavelet method has been successfully applied to solve a coupled system of nonlinear Reaction-diffusion systems. It has been shown that the CAS wavelets method is quite capable and suited for finding exact solutions. The consistency of the method gives this method wider applicability. By comparing the numerical solution of the nonlinear Reaction-diffusion system and using the CAS wavelets and finite element methods with the exact solution, it was found that the CAS wavelets method is the most accurate and fastest way to reach the exact solution. Maple 18 was used to carry out the computations. Finally, it is worth noting that this method is clear and concise, and can be applied to nonlinear PDF equations in engineering and applied science.

#### 5. ACKNOWLEDGEMENTS:

"The authors are very grateful to the University of Mosul / College of Basic Education for their provided facilities, which helped to improve the quality of this work."

#### 6. REFERENCES:

1. Al-Rawi E. S. and Qasem, A. F., "CAS Wavelets for Solving General TwoDimensional Partial Differential Equations of Higher Order with Application", Vol. 3 Issue 3, March-2014, pp: (496-507).
2. Barzkar A., Assari P. and Mehrpouya, M.A., "Application of The CAS Wavelets in Solving Fredholm-Hammerstein Integral Equations of the Second Kind with Error Analysis", World Applied Sciences Journal 18(12), (2012); pp.1695-1704. DOI: 10.1080/09720502.2019.1602354
3. E. Babolian and A. Shamsavaran, Numerical solution of nonlinear Fredholm integral equations of the second kind using Haar wavelets, Journal of Computational and Applied Mathematics, 225 (2009) 87–95.
4. E. Fathizadeh, R. Ezzati and K. Maleknejad, CAS Wavelet Function Method for Solving Abel Equations with Error Analysis, Int. J. Res. Ind. Eng. Vol. 6, No. 4 (2017) 350–364.
5. Fathizadeh E., Ezzati R., Maleknejad K. "CAS Wavelet Function Method for Solving Abel Equations with Error Analysis", Int. J. Res. Ind. Eng. Vol. 6, No. 4, (2017); 350–364.
6. H. Adibi and P. Assari, Using CAS wavelets for numerical solution of Volterra integral equations of the second kind. Dyn. Contin. Discrete Impuls. Syst., Ser. A, Math. Anal. 16 (2009), pp. 673–685.
7. H. Saeedi, M. Mohseni Moghadam, N. Mollahasani and G.N. Chuev, A CAS wavelet method for solving nonlinear Fredholm integro-differential equations of fractional order, Vol 16, Issue, 2011, Pages 1154-1163.
8. Han Danfu and Shang Xufeng, Numerical solution of integro-differential equations by using CAS wavelet operational matrix of integration, Applied Mathematics and Computation 194 (2007) 460–466.
9. Hariharan, G. and Kannan, K., (2010), "Haar wavelet method for solving some nonlinear parabolic equations", J. Math. Chem., 48, (2017); Pp. 1044-1061.
10. Kan-on, Y. , "Fisher Wave Fronts for the Lotka-Volterra Competition Model with Diffusive, Nonlinear Analysis", TMP 28, (1997); PP. 363-340.
11. Lepik, U., "Application of the Haar Wavelet Transform to Solving Integral and Differential Equations", Proc. Estonian Acad. Sci. Phys. Math., Vol. 56, No. 1, (2007); pp.28-46.
12. Lepik, U., "Numerical Solution of Evolution Equations by the Haar Wavelet Method", Applied Mathematics and Computation, 185, (2007); Pp. 695-704.
13. Lou Y. Martinez S., Polacik P., "Loops and Branches of Coexistence States in Lotka-Volterra Companion Model. USA, (2006).

14. M. M. Shamooshakya, P. Assarib and H. Adibic, CAS Wavelet Method for the Numerical Solution of Boundary Integral Equations with Logarithmic Singular Kernels, *International Journal of Mathematical Modelling & Computations* Vol. 04, No. 04, 2014, 377- 387.
15. Manaa S. A., Qasim A. F., " Numerical solution of nonlinear prey-predator system using finite elements method" *Raf. J. of Comp. & Math's.* , Vol. 4, No. 2, 2007 113.
16. Mingxu Yi, Kangwen Sun, Jun Huang, and Lifeng Wang, Numerical Solutions of Fractional Integrodifferential Equations of Bratu Type by Using CAS Wavelets, *Applied Mathematics*, 2013. <http://dx.doi.org/10.1155/2013/801395>
17. Mingxu Yia & Jun Huang, CAS wavelet method for solving the fractional integro-differential equation with a weakly singular kernel, *International Journal of Computer Mathematics*, 2014. <http://dx.doi.org/10.1080/00207160.2014.964692>
18. Muhammad Ismail, Umer Saeed, Jehad Alzabut, and Mujeeb ur Rehman, Approximate Solutions for Fractional Boundary Value Problems via Green-CAS Wavelet Method, 2019, 7, 1164. DOI:10.3390/math7121164
19. R. Ezzati and S. Najafalizadeh, Numerical Methods for Solving Linear and Nonlinear Volterra-Fredholm Integral Equations by using CAS Wavelets, *World Applied Sciences Journal* 18 (12): 1847-1854, 2012. DOI: 10.5829/idosi.wasj.2012.18.12.198
20. S. C. Shiralashetti and S. Kumbinarasaiah, CAS wavelets analytic solution and Genocchi polynomials numerical solutions for the integral and integro-differential equations, *International Journal of Mathematical Modelling & Computations* Vol. 04, No. 04, Fall 2014, 377- 387.
21. S. Rezabeyk and K. Maleknejad, Research Article Application of CAS wavelet to construct quadrature rules for numerical integration, Available Vol. 7, No. 1, 2015.
22. S.A. Youse and A. Banifatemi, Numerical solution of Fredholm integral equations by using CAS wavelets, *Appl. Math. Comput.* 183 (2006), pp. 458–463.
23. T. Abualrub, I. Sadek, and M. Abukhaled, Optimal control system by time-dependent coefficients using CAS wavelets, *J. Appl. Math.* 2009 (2009), pp. 1–10.
24. Taher Abualrub, Ibrahim Sadek, and Marwan Abukhaled, Optimal Control Systems by Time-Dependent Coefficients Using CAS Wavelets, *Journal of Applied Mathematics*, 2009.
25. Turing. A., " The chemical basis of morphogenesis, *philosophical transactions of the royal society*" (B), 237, (1952); PP. 37-72.
26. Wu, J. L. and Chen, C. H., "A Novel Numerical Method for Solving Partial Differential Equations Via Operational Matrices", *Proceeding of the 7th World Multi-Conference on Systemic, Cybernetics and Informatics, Orlando, USA, Vol.5, (2003)*; pp.276-281.
27. Xiangyu Wang, Numerical solution of time-varying systems by CAS Wavelets, *Advances in Information Sciences and Service Sciences (AISS)*, Volume 6, Number 5, 2014).

**Table 1.** A CAS wavelets, Galerkin finite element method and the exact solution or  $\nu(\chi, \hat{t}), \sigma(\chi, \hat{t})$  when  $\hat{t}=14.5, \hat{t}=8$  and comparison between them.

| NO. | $ \text{CAS} - \text{exact} $<br>$\hat{t}=14.5$<br>$\nu(\chi, \hat{t})$ | $ \text{G.F.E} - \text{exact} $<br>$\hat{t}=14.5$<br>$\nu(\chi, \hat{t})$ | $ \text{CAS} - \text{exact} $<br>$\hat{t}=8$<br>$\sigma(\chi, \hat{t})$ | $ \text{G.F.E} - \text{exact} $<br>$\hat{t}=8$<br>$\sigma(\chi, \hat{t})$ | $ \text{CAS} - \text{exact} $<br>$\hat{t}=9.5$<br>$\nu(\chi, \hat{t})$ | $ \text{G.F.E} - \text{exact} $<br>$\hat{t}=9.5$<br>$\nu(\chi, \hat{t})$ | $ \text{CAS} - \text{exact} $<br>$\hat{t}=13.5$<br>$\sigma(\chi, \hat{t})$ | $ \text{G.F.E} - \text{exact} $<br>$\hat{t}=13.5$<br>$\sigma(\chi, \hat{t})$ |
|-----|---|---|---|---|--|--|--|--|
| 1   | 8.19E-04  | 1.01E-03  | 0.00E+00  | 1.11E-02  | 7.60E-05   | 1.00E-04   | 1.09E-05   | 8.00E-04   |
| 2   | 7.43E-04  | 8.41E-04  | 9.04E-03  | 1.11E-02  | 7.89E-05   | 9.99E-05   | 2.54E-04   | 1.10E-03   |
| 3   | 3.76E-04  | 4.11E-04  | 5.10E-04  | 6.70E-02  | 1.05E-04   | 1.29E-04   | 2.13E-04   | 3.01E-04   |
| 4   | 7.79E-05  | 1.11E-04  | 6.19E-03  | 6.54E-03  | 8.60E-05   | 8.91E-05   | 1.65E-04   | 3.00E-04   |
| 5   | 6.63E-05  | 1.11E-04  | 2.63E-03  | 6.89E-03  | 8.62E-05   | 9.68E-05   | 8.99E-05   | 3.00E-04   |
| 6   | 2.05E-04  | 2.41E-04  | 2.52E-03  | 2.89E-03  | 1.06E-04   | 7.22E-05   | 2.29E-04   | 4.00E-04   |
| 7   | 5.74E-04  | 6.11E-04  | 2.49E-03  | 2.89E-03  | 1.05E-04   | 1.00E-04   | 1.60E-04   | 2.00E-04   |
| 8   | 5.88E-04  | 4.11E-04  | 2.33E-02  | 3.02E-02  | 1.05E-04   | 1.34E-04   | 2.13E-04   | 2.00E-04   |
| 9   | 7.97E-04  | 6.11E-04  | 5.20E-03  | 9.45E-03  | 1.38E-04   | 1.53E-04   | 3.94E-04   | 4.00E-04   |
| 10  | 7.98E-04  | 6.11E-04  | 1.13E-03  | 1.11E-03  | 8.35E-05   | 1.16E-04   | 4.12E-04   | 3.00E-04   |
| 11  | 4.14E-05  | 1.62E-04  | 7.73E-04  | 2.66E-03  | 5.21E-06   | 6.00E-05   | 2.72E-04   | 3.00E-04   |
| 12  | 3.03E-04  | 1.12E-04  | 2.31E-04  | 2.88E-04  | 1.51E-05   | 3.32E-05   | 5.22E-04   | 6.00E-04   |
| 13  | 1.77E-04  | 1.11E-04  | 4.68E-05  | 4.48E-04  | 5.39E-06   | 4.17E-05   | 3.20E-04   | 5.00E-04   |
| 14  | 1.84E-04  | 1.11E-04  | 3.32E-05  | 2.10E-04  | 5.24E-06   | 3.36E-05   | 2.19E-04   | 4.00E-04   |
| 15  | 7.42E-06  | 1.69E-04  | 3.17E-04  | 4.47E-04  | 5.18E-06   | 4.00E-07   | 2.13E-04   | 3.00E-04   |
| 16  | 9.14E-05  | 1.11E-04  | 1.61E-02  | 2.37E-02  | 3.94E-06   | 1.77E-05   | 2.42E-04   | 3.00E-04   |
| 17  | 4.65E-04  | 1.11E-04  | 3.05E-03  | 7.60E-03  | 3.39E-06   | 1.42E-05   | 3.28E-04   | 4.00E-04   |
| 18  | 2.03E-05  | 1.11E-04  | 5.35E-04  | 9.89E-04  | 3.26E-06   | 3.43E-05   | 9.24E-04   | 1.10E-03   |
| 19  | 2.30E-05  | 2.11E-05  | 2.01E-03  | 2.03E-03  | 3.50E-06   | 3.98E-05   | 8.67E-04   | 1.02E-03   |
| 20  | 3.40E-05  | 9.92E-05  | 2.00E-04  | 6.19E-04  | 1.39E-05   | 4.71E-05   | 2.14E-05   | 7.69E-05   |
| 21  | 1.81E-05  | 8.57E-06  | 8.40E-04  | 3.03E-03  | 1.22E-05   | 3.00E-05   | 9.19E-05   | 1.90E-04   |



**Table 2.** A CAS wavelets, Galerkin finite element method and the exact solution for  $v(\chi, \hat{t}), \sigma(\chi, \hat{t})$  when  $\hat{t}=9.5, \hat{t}=13.5$  and comparison between them  $v_0(\chi) = \sigma_0(\chi) = \sin^2\left(\frac{12}{10}\pi\chi\right) + \sin^2\left(\frac{-1}{10}\pi\chi\right)$

| NO. | CAS Wavelets<br>$v(\chi, \hat{t})$<br>$\hat{t}=14.5$ | Galerkin Finite<br>element method<br>$v(\chi, \hat{t}), \hat{t}=14.5$ | Exact Solution<br>$v(\chi, \hat{t})$<br>$\hat{t}=14.5$ | CAS wavelets<br>$\sigma(\chi, \hat{t})$<br>$\hat{t}=8$ | Galerkin Finite<br>element method<br>$\sigma(\chi, \hat{t}), \hat{t}=8$ | Exact Solution<br>$\sigma(\chi, \hat{t})$<br>$\hat{t}=8$ |
|-----|--|---|--|--|---|--|
| 1   | 0.01676753   | 0.01695454  | 0.01594873   | 0.72826192   | 0.77554676  | 0.76443563   |
| 2   | 0.01667693   | 0.01677521  | 0.01593418   | 0.79753859   | 0.81768448  | 0.80657393   |
| 3   | 0.01629418   | 0.01632946  | 0.01591805   | 0.97969854   | 0.91319185  | 0.98020868   |
| 4   | 0.01581375   | 0.01584698  | 0.01573587   | 1.00295773   | 1.00260765  | 1.00914925   |
| 5   | 0.01552882   | 0.01557386  | 0.01546253   | 1.04908083   | 1.04482057  | 1.05170986   |
| 6   | 0.01560161   | 0.01563745  | 0.01539631   | 1.02656122   | 1.02619394  | 1.02908211   |
| 7   | 0.01593843   | 0.01597543  | 0.01536432   | 0.95641845   | 0.95602083  | 0.95890937   |
| 8   | 0.01655065   | 0.01637400  | 0.01596299   | 0.86701762   | 0.86014518  | 0.89034389   |
| 9   | 0.01677542   | 0.01658927  | 0.01597819   | 0.80473367   | 0.80048434  | 0.80993732   |
| 10  | 0.01666415   | 0.01647741  | 0.01586636   | 0.81711765   | 0.81935633  | 0.81824762   |
| 11  | 0.01594643   | 0.01606683  | 0.01590502   | 0.90812098   | 0.90468775  | 0.90734775   |
| 12  | 0.01573507   | 0.01554364  | 0.01543203   | 1.00167385   | 1.00161710  | 1.00190506   |
| 13  | 0.01522607   | 0.01515988  | 0.01504874   | 1.06219537   | 1.06259648  | 1.06214853   |
| 14  | 0.01517993   | 0.01510713  | 0.01499600   | 1.06779761   | 1.06755464  | 1.06776443   |
| 15  | 0.01558367   | 0.01542225  | 0.01559109   | 1.01728809   | 1.01715799  | 1.01760468   |
| 16  | 0.01577813   | 0.01598064  | 0.01586953   | 0.93782376   | 0.93018756  | 0.95390674   |
| 17  | 0.01600137   | 0.01657747  | 0.01646632   | 0.85042574   | 0.84587901  | 0.85347679   |
| 18  | 0.01690879   | 0.01704017  | 0.01692906   | 0.80745692   | 0.80700317  | 0.80799209   |
| 19  | 0.01730477   | 0.01730286  | 0.01728175   | 0.82319381   | 0.82317497  | 0.82520638   |
| 20  | 0.01734002   | 0.01740520  | 0.01730599   | 0.88183075   | 0.88141190  | 0.88203098   |
| 21  | 0.01739987   | 0.01742652  | 0.01741795   | 0.87604015   | 0.87991302  | 0.87688019   |

**Table 3.** The Absolute error for CAS wavelets, Galerkin finite element method with the exact solution for  $v(\chi, \hat{t}), \sigma(\chi, \hat{t})$  when  $\hat{t}=14.5, \hat{t}=8., \hat{t}=13.5, \hat{t}=9.5$

| NO. | CAS Wavelets<br>$v(\chi, \hat{t})$<br>$\hat{t}=9,5$ | Galerkin Finite<br>element method<br>$v(\chi, \hat{t}), t=9,5$ | Exact Solution<br>$v(\chi, \hat{t})$<br>$\hat{t}=9,5$ | CAS Wavelets<br>$\sigma(\chi, \hat{t})$<br>$\hat{t}=13.5$ | Galerkin Finite<br>element method<br>$\sigma(\chi, \hat{t}), \hat{t}=13,5$ | Exact Solution<br>$\sigma(\chi, \hat{t})$<br>$\hat{t}=13,5$ |
|-----|---|--|---|---|--|---|
| 1   | 0.99947887  | 0.99945457   | 0.99955488  | 0.04189611  | 0.04110720   | 0.04190700  |
| 2   | 0.99949230  | 0.99947123   | 0.99957116  | 0.04243655  | 0.04159035   | 0.04269024  |
| 3   | 0.99953581  | 0.99951240   | 0.99964123  | 0.04377317  | 0.04368605   | 0.04398658  |
| 4   | 0.99955963  | 0.99955657   | 0.99964564  | 0.04520569  | 0.04507065   | 0.04537045  |
| 5   | 0.99959187  | 0.99958132   | 0.99967812  | 0.04599862  | 0.04578861   | 0.04608850  |
| 6   | 0.99954155  | 0.99957533   | 0.99964752  | 0.04577914  | 0.04560786   | 0.04600775  |
| 7   | 0.99953912  | 0.99954407   | 0.99964439  | 0.04473945  | 0.04469978   | 0.04489967  |
| 8   | 0.99953614  | 0.99950661   | 0.99964065  | 0.04363260  | 0.04364617   | 0.04384606  |
| 9   | 0.99950048  | 0.99948520   | 0.99963851  | 0.04391755  | 0.04312346   | 0.04352335  |
| 10  | 0.99952576  | 0.99949328   | 0.99960931  | 0.04394595  | 0.04323447   | 0.04353436  |
| 11  | 0.99958324  | 0.99952845   | 0.99958845  | 0.04471332  | 0.04468572   | 0.04498561  |
| 12  | 0.99959233  | 0.99957422   | 0.99960741  | 0.04640536  | 0.04632790   | 0.04692779  |
| 13  | 0.99964551  | 0.99960918   | 0.99965090  | 0.04761359  | 0.04743364   | 0.04793353  |
| 14  | 0.99964657  | 0.99961824   | 0.99965181  | 0.04774001  | 0.04755889   | 0.04795878  |
| 15  | 0.99960512  | 0.99959954   | 0.99959994  | 0.04668060  | 0.04659355   | 0.04689344  |
| 16  | 0.99954245  | 0.99956406   | 0.99954639  | 0.04483311  | 0.04477505   | 0.04507494  |
| 17  | 0.99953946  | 0.99952862   | 0.99954285  | 0.04284865  | 0.04277671   | 0.04317660  |
| 18  | 0.99953736  | 0.99950634   | 0.99954062  | 0.04128423  | 0.04110823   | 0.04220812  |
| 19  | 0.99953650  | 0.99950015   | 0.99954000  | 0.04036414  | 0.04020614   | 0.04123103  |
| 20  | 0.99953644  | 0.99950323   | 0.99955032  | 0.03997833  | 0.03992289   | 0.03999976  |
| 21  | 0.99952353  | 0.99950576   | 0.99953576  | 0.03988845  | 0.03979043   | 0.03998032  |

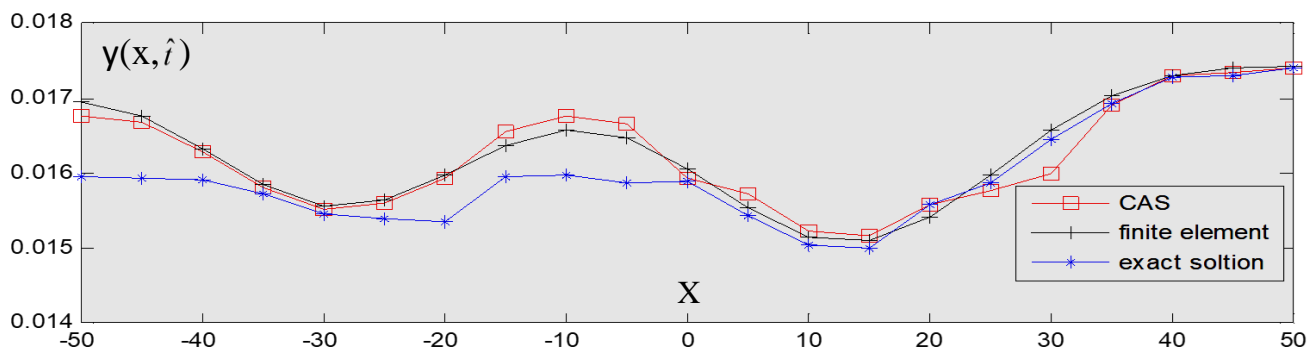


**Figure 1.** Comparison between CAS Galerkin finite elements (obtained from (Eq 11),(Eq 28 ) and Table 1) with exact solution where  $X=\{-50,-45,\dots,45,50\}$ ,  $Y=y(X,\hat{t})$ ,  $L=0.5$ ,  $\Delta\hat{t}=0.1$ ,  $\varepsilon_1=\varepsilon_2=0.001$ ,  $\theta=0.5$ ,  $\alpha_1=1$ ,  $\alpha_2=0.06$ ,  $\beta_1=\delta_1=\delta_2=1$  and  $\hat{t}=14.4$

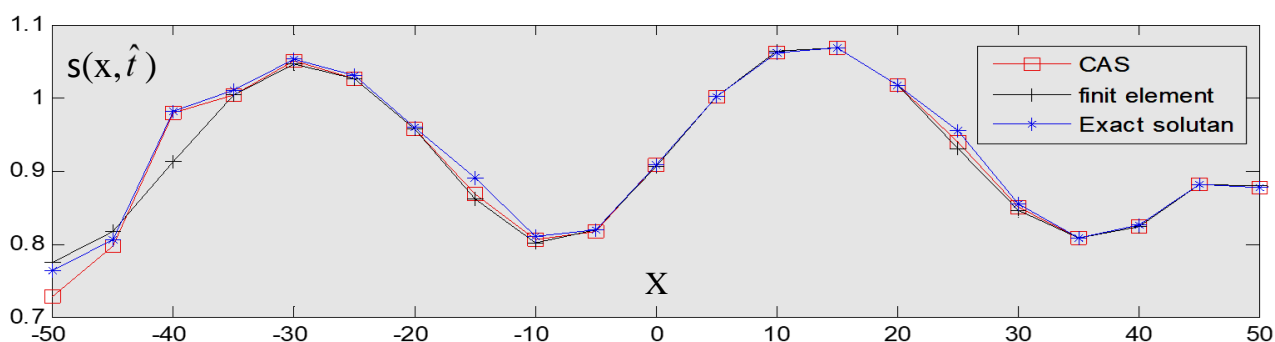


**Figure 2.** Comparison between CAS Galerkin finite elements (obtained from (Eq 11),(Eq 28 ) and Table 1) with exact solution where  $X=\{-50,-45,\dots,45,50\}$ ,  $Y=s(X,\hat{t})$ ,  $L=0.5$ ,  $\Delta\hat{t}=0.1$ ,  $\varepsilon_1=\varepsilon_2=0.001$ ,  $\theta=0.5$ ,  $\alpha_1=1$ ,  $\alpha_2=0.06$ ,  $\beta_1=\delta_1=\delta_2=1$  and  $\hat{t}=8$

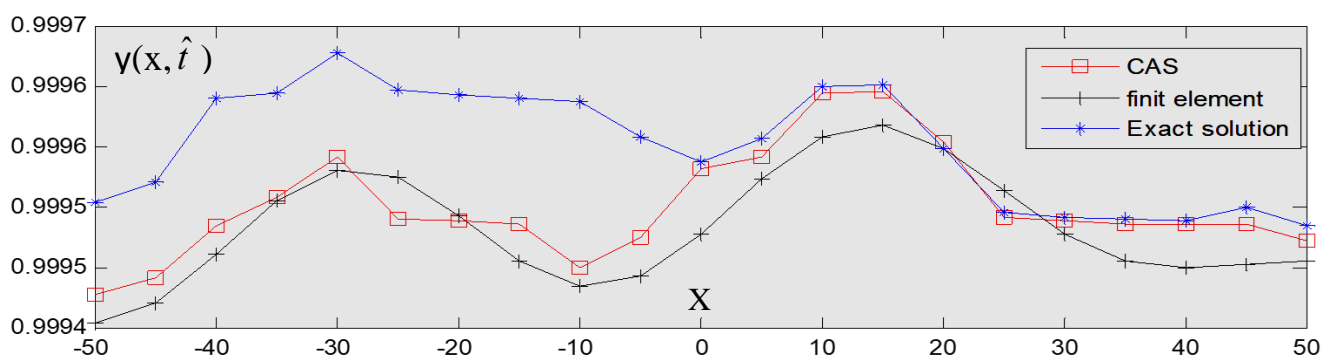


**Figure 3.** Comparison between CAS Galerkin finite elements (obtained from (Eq 11),(Eq 28 ) and Table 1) with exact solution where  $X=\{-50,-45,\dots,45,50\}$ ,  $Y=y(X,\hat{t})$ ,  $L=0.5$ ,  $\theta=0.5$ ,  $\alpha_1=1$ ,  $\Delta\hat{t}=0.1$ ,  $\varepsilon_1=\varepsilon_2=0.001$ ,  $\alpha_2=0.01$ ,  $\beta_1=\delta_1=\delta_2=0.0001$ ,  $M=21$  and  $\hat{t}=9.5$

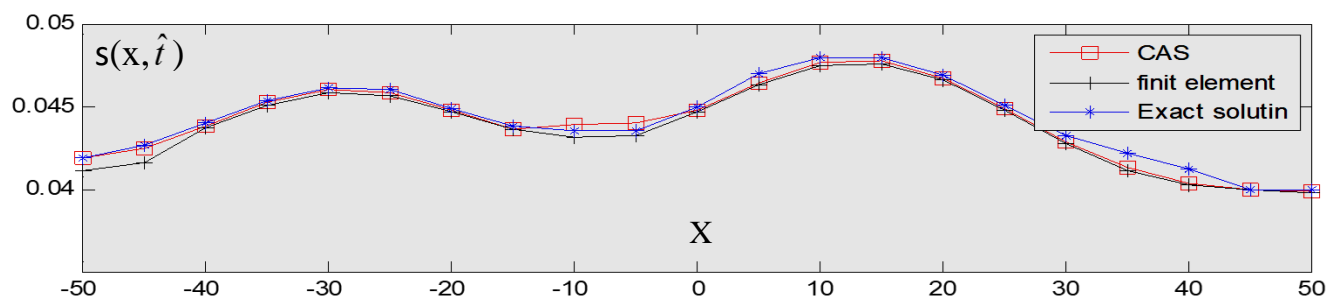


**Figure 4.** Comparison between CAS Galerkin finite elements (obtained from (Eq 11),(Eq 28) ) and Table 1) with exact solution where  $X=\{-50,-45,\dots,45,50\}$ ,  $Y=S(X,\hat{t})$ ,  $L=0.5$ ,  $\theta=0.5$ ,  $\alpha_1=1$ ,  $\Delta\hat{t}=0.1$ ,  $\varepsilon_1=\varepsilon_2=0.001$ ,  $\alpha_2=0.01$ ,  $\beta_1=\delta_1=\delta_2=0.0001$ ,  $M=21$  and  $\hat{t}=13.5$

## ENGENHARIA DE TIPIFICAÇÃO GEOLÓGICA DE TERRITÓRIOS PARA ALOCAÇÃO DE INSTALAÇÕES MUNICIPAIS DE GERENCIAMENTO DE RESÍDUOS SÓLIDOS

## ENGINEERING GEOLOGICAL TYPIFICATION OF TERRITORIES FOR ALLOCATION OF MUNICIPAL SOLID WASTE MANAGEMENT FACILITIES

KOZLIAKOVA, Irina<sup>1</sup>; KOZHEVNIKOVA, Irina<sup>2</sup>; EREMINA, Olga<sup>3\*</sup>; ANISIMOVA, Nadezhda<sup>4</sup>

<sup>1,2,3,4</sup> Russian Academy of Sciences, Sergeev Institute of Environmental Geoscience, Laboratory for Exogenous Geodynamics and Geological Risk Analysis. Russia.

\* Correspondence author  
e-mail: o\_eremina@mail.ru

Received 25 May 2020; received in revised form 18 June 2020; accepted 04 July 2020

### RESUMO

A gestão de resíduos sólidos urbanos (RSU) parece ser um dos principais problemas ecológicos atualmente. A seleção de locais para o descarte de resíduos sólidos municipais ou de instalações de utilização de resíduos é um dos aspectos mais controversos do gerenciamento de resíduos. O objetivo do presente estudo foi desenvolver uma metodologia para avaliar a proteção natural do ambiente geológico contra contaminação na implementação de grandes projetos ecológicos devido à alocação de instalações de utilização de RSU. O caso do Distrito Federal Central da Rússia (CFD) foi tomado como exemplo. A adequação dos territórios para o descarte de resíduos sólidos municipais é avaliada de acordo com a presença de depósitos pouco permeáveis na seção geológica e seu modo de ocorrência. Um “mapa de CFD de zoneamento geológico de engenharia pelas condições de alocação de locais de descarte de RSU e instalações de utilização” foi compilado na escala 1:2500000. O mapa fornece uma indicação geral da adequação dos locais planejados para a eliminação de resíduos na região considerada e mostrou que, para a maior parte do território, a alocação de instalações de manejo e descarte de RSU exige a adoção de medidas adicionais para a proteção geoambiental da contaminação.

**Palavras-chave:** *Resíduos sólidos municipais, Gerenciamento de resíduos, Instalações de armazenamento e reprocessamento de resíduos, Favorabilidade do meio ambiente, Zoneamento e mapeamento geológico da engenharia.*

### ABSTRACT

The management of municipal solid waste (MSW) appears to be one of the major ecological problems at present. Selecting sites for the disposal of municipal solid wastes or waste utilization facilities is one of the most contentious aspects of waste management. The present study aimed to develop the methodology to assess the natural protection of the geological environment from contamination upon the implementation of large ecological projects due to the allocation of MSW utilization facilities. The case of the Central Federal District of Russia (CFD) is taken as an example. The suitability of territories for municipal solid waste disposal is assessed according to the presence of weakly permeable deposits in the geological cross-section and their occurrence mode. A “map of engineering geological zoning CFD by the conditions of allocation MSW disposal sites and utilization facilities” has been compiled to a scale 1:2500000. The map gives a general indication of the suitability of the planned sites for waste disposal within the regarded region and showed that, for the bulk of territory, the allocation of MSW disposal and management facilities requires undertaking additional measures for the geoenvironmental protection from contamination.

**Keywords:** *Municipal solid waste, Waste management, Waste storage, and reprocessing facilities, Favorability of geoenvironment, Engineering geological zoning and mapping.*

### 1. INTRODUCTION:

The management of municipal solid waste appears to be one of the significant ecological problems at present. A lot is said about how to

solve the issue (Khmelchenko, 2018; Osipov, 2019). Selecting sites for the disposal of municipal solid wastes or waste utilization facilities is one of the most contentious aspects of waste management. Experts all over the world are

attracted to research aimed at providing safe and environmental-friendly waste management (Cremiato, Mastellone, Tagliaferri, Zaccariello, & Lettieri, 2018; Nakhaei, Amiri, Rezaei, & Moosaei, 2015; Ogola, Chimuka, & Tshivhase, 2011; Ogola *et al.*, 2011; Yannah, Martens, Van Camp, & Walraevens, 2019). The complexity of the municipal solid waste (MSW) storage problem results, above all, from being multidisciplinary, that is, many social, economic, technical, and environmental issues must be taken into consideration. A lot of works have proven the necessity of performing multicriteria analysis for waste disposal site selection (Ghobadi, Taheri, & Taheri, 2017; Khan & Samadder, 2014; Kontos, Komilis, & Halvadakis, 2005; Rahmat *et al.*, 2017). Lately, in many countries around the world, the multicriteria approach including the hierarchical analytical process (AHP) as well as the more complex analytic network process (ANP) combined with geo-informational system (GIS) technologies are used for waste disposal site selection, which has proved their efficiency in finding a suitable and appropriate locations (Alanbari, Al-Ansari, & Jasim, 2014; Aydi, Zairi, & Dhia, 2013; Chang, Parvathinathan, & Breeden, 2008; Charnpratheep, Zhou, & Garner, 1997; Deswal & Laura, 2018; El Maguiri, Kissi, Idrissi, & Souabi, 2016; Güler & Yomralioğlu, 2017; Khodaparast, Rajabi, & Edalat, 2018).

Engineering geological conditions are one of the criteria involved in selecting an appropriate site, and in practice is one of the last taken into consideration. Priority is given to the distance from settlements and water reservoirs (remoteness), as well as natural reserves and protected areas (The State Duma, 1998). The geological environment degrades much more slowly than surface features do. At the same time, geological environment, that is, rocks and groundwater, can accumulate hazardous components for a long time and become prerequisites for future ecological disasters for future generations. By underestimating the impacts waste disposal has on the geoenvironment now, we create danger for environmental safety in the future.

Storage at disposal sites remains to be the primary method of municipal solid waste treatment in Russia. The current waste management system cannot cope with a large amount of waste produced. The problem of waste management is most acute in the Central Federal District (CFD) of the Russian Federation, which covers an area of more than 650 thousand sq. km and includes 18 oblasts. This is one of the most densely populated and industrially developed regions of Russia. At

present, over 90 billion tons of waste have accumulated in this area (VSEGEI, 2018). Above 1000 waste disposal facilities, that is, landfills and waste disposal sites, exist there, with the bulk of them not included in the national registration list (The Government of the Russian Federation, 2016).

One of the ways to solve the waste-management issue in Central Russia has been the construction of a limited number of extensive, sophisticated engineering facilities uniting an incinerator plant, a waste-reprocessing plant, and waste disposal (Ekzaryan, 2018; Kashperiyuk, Makeeva, Akanov, Nikitina, & Podlesnykh, 2018). Such industrial complexes already exist in many well-developed countries. Sites for the allocation of such complexes are typically selected on the basis of sanitary standards, which constrain landfill allocation depending on the distance from settlements and water bodies, as well as topographic, geological and hydrogeological conditions (Djokanović, Abolmasov, & Jevremović, 2016; El Maguiri *et al.*, 2016; Ministry of Health of the Russian Federation, 2001; Zelenović Vasiljević, Srdjević, Bajčetić, & Vojinović Miloradov, 2012).

In terms of geology and hydrogeology, territories suitable for waste disposal include those where weakly permeable clay layers occur at the top of a geological massif, and the groundwater lies deeper than two meters below the surface. The presence of thick clay strata in the upper part of the geologic massif appears to be the primary condition of territory favorability for the allocation of waste management facilities because these strata prevent the permeating of contamination from the surface to the underlying aquifers. Experience demonstrates that ignorance of this requirement results in serious undesirable ecological consequences (Dzhamalov, Medovar, & Yushmanov, 2018; Khmelchenko, 2018; Zaikanov, Zaikanova, & Buldakova, 2018).

For the CFD of the Russian Federation, the conditions (parameters) of natural protection of the geological environment from contamination have been analyzed, the principal types of geological-hydrogeological conditions have been distinguished, and the criteria of assessing the favorability of the territory for the implementation of combined projects in waste management have been suggested.

The present study aimed to develop the methodology to assess the natural protection of the geological environment from contamination upon the implementation of large ecological

projects due to the allocation of MSW utilization facilities. The case of the Central Federal District of Russia is taken as an example.

## 2. MATERIALS AND METHODS:

### 2.1. Conceptual model of Engineering Geological Assessment of the Central Russia territory for the allocation of municipal solid waste treatment facilities

Engineering geological assessment of potential sites for waste disposal proceeds from the idea that the occurrence of natural barriers in the geological cross-section can prevent contaminations from penetrating the surface down to the geological strata and groundwater. This prevention significantly enables the preservation of favorable ecological conditions around waste disposal sites and waste treatment facilities. Clay strata operate as such natural barriers. Engineering geological studies consider the presence of thick clay strata in the upper part of the geological massif to be the main condition of territory suitability for the allocation of the waste treatment facilities (Goldberg, 1987).

Figure 1 lists the main steps of the methodology of territory assessment in Central Russia. In terms of structural geology, CFD is located within the Russian platform, within which the upper part of the geological cross-section is composed of various stratigraphic and lithological sedimentary rock complexes of different ages. To a depth of 50–60 m, the entire diversity of these complexes may be subdivided into several types depending on their lithology, age, and the degree of water content in the pre-Quaternary and Quaternary soils and rocks (Komarov, 1978; Leonenko, Sidorenko, & Shik, 1971).

Mapinfo computer tools were used to create two auxiliary layers; one of the layers showing the pre-Quaternary rock complexes of different permeability and water content, and the other, the complexes of Quaternary deposits. The formal superposition of these layers permitted us to reveal their possible combinations. For each combination, the typical geological cross-section (column) was built, showing the layers of different age, lithological composition, and permeability. The input data for the compilation of these information layers and cross-sections included the small-scale archive geological maps for the Central Russia territory and other publications. In this work, we used the map data from the GIS atlas "The bowels of Russia" compiled at A.P. Karpinsky Russian Geological Research Institute (VSEGEI)

and the State geologic map of the Russian Federation to a scale 1:1000000 (VSEGEI, 2019; VSEGEI & Pogrebitsky, 1999).

Each type of geological structure (a typical geological cross-section) was referred to a certain category of territory suitability (a taxon) depending on the presence of low-permeable Quaternary and pre-Quaternary layers and the depth of their occurrence. Five taxons were distinguished corresponding to favorable, conventionally favorable, conventionally unfavorable, unfavorable and very unfavorable conditions from the viewpoint of MSW treatment projects. The assessment was performed proceeding from the geological structure depending on the mode of occurrence of low-permeable deposits in the upper part of geological massif.

The resultant zoning map manifests the outlines and indices of all types of geological structure, and the regions of different suitability (favorability) categories are distinguished in color (according to the traffic light principle). Thus, the map represents a highly informative document presenting not only the estimation criteria but also the generalized geological characteristics of each taxon.

### 2.2. Assessment of natural protection of the geological environment

The natural protection of the geological environment from contamination coming from the surface was assessed depending on the presence of low-permeable deposits (capable of protecting the geological environment from contamination penetrating from the surface) in the geological cross-section of pre-Quaternary and Quaternary deposits.

The pre-Quaternary deposits are subdivided into:

- low-permeable clay layers from the Jurassic age;
- unevenly permeable chalk and marl from the Cretaceous era and aleurolite-argillite gypsiferous rocks and gypsum from the Permian and Triassic ages;
- high-permeable sand and sandstone from the Neogene, Paleogene and Cretaceous ages;
- terrigenous-carbonate rocks from the Devonian and Carboniferous ages.

The spatial position of these complexes is shown on the first auxiliary layer compiled in Mapinfo format.

The analysis of Quaternary deposits was based on the presence of low-permeable loams of different genetic types and their position in the geological massif (Kashperuk *et al.*, 2018; Kozliakova, Kozhevnikova, Anisimova, & Eremina, 2020; Kozlovskiy, Mamaev, & Stol'nikova, 2020). Among Quaternary deposits, moraine loam forms the main low-permeable complex. On the second auxiliary information layer, the territories are outlined, where these soils lie at the surface or under alluvial and fluvio-glacial sand. We have also defined the territories where mantle loam and sandy loam manifest a considerable stretch and thickness.

Superposition of the two auxiliary information layers resulted in 18 types of ground massifs depending on the stratigraphic and lithological specifics and the water-content of pre-Quaternary and Quaternary complexes. These types formed the basis for the resultant estimation zoning of territory by the degree of favorability for allocation of MSW treatment facilities and disposal sites (Table 1).

A schematic column was built for each zoning taxon (Figure 2), explaining the mode of occurrence of the distinct geological and lithological complexes differing in its permeability. It can be distinguished: water-bearing and high-permeable deposits; low water-bearing and unevenly water-saturated deposits; and aquicludes or low-permeable deposits. In the geological cross-sections, the color stands for water content and water permeability, whereas the hatch designates stratigraphy and lithology.

### 3. RESULTS AND DISCUSSION:

The typification of the Central Russian territory according to the favorability of allocating MSW treatment facilities and disposal sites is a result of the research performed (Table 2). The general small-scale (1:2500000) map of engineering geological zoning was compiled (Figure 3).

Favorable ground massifs are considered to be those that include two aquiclude strata, that is, the Quaternary moraine loam occurs close to the surface and the Jurassic clay. Thus, the quaternary and the Mesozoic water-bearing complexes are isolated from each other, and the geological environment is protected from contamination coming from the surface. These

regions are outlined locally, mainly in the northern part of the territory.

It is recognized territories as conventionally favorable if the Quaternary moraine loam occurs at the surface, being underlain by high-permeable deposits. The degree of protection of the geoenvironment from surface contamination is controlled by the moraine loam thickness at these sites. The areas of this kind are outlined in the northwest of the territory and on the interfluvial surfaces in its central part.

Conventionally unfavorable sites are those where ground massif is composed of sandy-clayey Quaternary deposits without any continuously stretching low-permeable layers underlain by the Jurassic clay strata. The groundwater aquifer is prone to pollution at such sites, and the degree of protection of deep horizons is controlled by the thickness and depth of occurrence of the Jurassic clay. These regions are registered in the northern and eastern parts of the Moscow region.

Sites are classified as unfavorable if the geological massif is composed of high-permeable Quaternary and pre-Quaternary deposits with locally spread low-permeable layers. The geological environment in these areas is virtually unprotected from contamination. These areas include the bulk of the territory in the southwest and in the east of the Central Federal district and local sites in the north.

Very unfavorable sites are those where the geological massif consists of only highly permeable and water-saturated deposits. At these sites, the geological environment is not isolated from contamination coming from the surface. These sites are usually confined to river valleys, with alluvial deposits immediately overlying Carboniferous and Devonian carbonate rocks; or to the regions where Paleogene-Neogene sand and sandstone occur.

As shown above, the geological conditions as one of the criteria for site selection of MSW facilities requires special analysis due to substantial spatial variability. When characterizing sites, it appears not enough just to mark the soil and rocks occurring at the surface in the given territory and to point out the groundwater depth, as it is usually done upon zoning for waste disposal site selection (Djokanović *et al.*, 2016; El Maguiri *et al.*, 2016).

By assessing MSW disposal sites by the presence of one or several low-permeable layers in the geological cross-section, we are able to take



into account the hazards of the contamination of the ground massif and groundwater when assessing the territory.

The map of the geological engineering zoning compiled based on the proposed typification gives a general idea about the favorability of planned sites for the allocation of MSW reprocessing facilities in the Central Federal district. It is compiled in a digital form, and it should be considered as an informational layer to be integrated into the general GIS based on the multicriteria principle for making decisions on waste disposal site selection. For the subsequent transition to the quantitative methods of multicriteria analysis, it appears easy to assign scores to taxons according to their favorability degree (Bottero & Ferretti, 2011; Chang *et al.*, 2008).

Besides, the zoning map has its own value as an individual document reflecting the present-day state of the waste-disposal problem in Central Russia. The map analysis proves that the entire territories of Kursk and Belgorod oblasts are related to very unfavorable and unfavorable categories. That means no large sites can be identified within these territories, where the ground massif manifests natural protection from the contamination coming from the surface. In Bryansk, Kaluga, Orel, Lipetsk, Tambov, Voronezh, Ryazan, Vladimir and Kostroma oblasts, unfavorable and very unfavorable regions occupy more than half of the oblast territory.

Thus, for most of the Central Federal district, the construction of waste management facilities requires additional engineering measures for the protection of the geological environment from contamination. At present, many MSW disposal sites and landfills have been arranged within this territory without taking the geological conditions into account.

To minimize the risks of contamination, the specifics of the geological environment should be analyzed at the early stages of compiling waste-management GIS. In doing so, the geological environment should be considered as a massif of a complex structure with variable properties, as it is done in our research for the Central Russian region. The existing experience in GIS compilation demonstrates that the geological block is developed inadequately as a rule (Ali Jalil Chabuk, Nadhir Al-Ansari, Hussain Musa Hussain, Sven Knutsson, & Roland Pusch, 2016; Aragonés-Beltrán, Pastor-Ferrando, García-García, & Pascual-Agulló, 2010; Ghobadi *et al.*, 2017; Khan & Samadder, 2014; Khodaparast *et al.*, 2018;

Kontos *et al.*, 2005). As proceeds from the analysis of international publications, the multicriteria approach to selecting waste disposal sites, which is commonly employed all over the world, unfortunately, underestimates the geological conditions of the territories being considered. At best, only the soil and rocks of the uppermost geological layer are taken into consideration, whereas the entire geological cross-section to a depth of anthropogenic impact is not considered (Deswal & Laura, 2018; El Maguiri *et al.*, 2016; Güler & Yomralioğlu, 2017; Rahmat *et al.*, 2017). It is suggested the typification of the geological environment according to the suitability (favorability) for the safe and reliable MSW disposal to be used at the early stage of planning the allocation of MSW treatment facilities. It permits, on the one hand, the capacity to formalize the assessment of geological conditions and, on the other hand, to take into account their variability by area and by the depth most comprehensively.

#### 4. CONCLUSIONS:

The assessment of the suitability of a territory for the allocation of MSW utilization facilities and waste disposal sites should obligatorily take into account the degree of natural protection from contamination provided by the geological environment.

The degree of natural protection of the geological environment is assessed proceeding from the presence or absence in the geological massif of one or several low permeable rock strata, preventing the penetration of contaminants from the surface to groundwater aquifers, as well as the thickness and the depth of occurrence of these strata.

Engineering geological zoning, including typifying territories by the specific features of geological and hydrogeological structures, assessing the favorability of each distinct type, and zoning territories according to the geological criteria to determine their suitability to contain MSW utilization facilities and waste disposal sites appears to be a versatile method for assessing the natural protection of geological environment in vast territories.

To conclude, it is worth noting that small-scale maps or estimation schemes of geological engineering zoning can give a general idea of the suitability of the planned places for the allocation of waste disposal complexes. They point out the possible vital sites for further investigation and give an overview of the volume of the necessary

additional measures on geoenvironment protection from contamination upon the construction and running of these engineering facilities. These maps and schemes should be used at the early stages of projecting the MSW storage and management complexes.

## 5. REFERENCES:

1. Alanbari, M. A., Al-Ansari, N., & Jasim, H. K. (2014). GIS and Multicriteria Decision Analysis for Landfill Site Selection in Al-Hashimiyah Qadaa. *Natural Science*, 06(05), 282–304. <https://doi.org/10.4236/ns.2014.65032>
2. Ali Jalil Chabuk, Nadhir Al-Ansari, Hussain Musa Hussain, Sven Knutsson, & Roland Pusch. (2016). Landfill Siting Using GIS and AHP (Analytical Hierarchy Process): A Case Study Al-Qasim Qadhaa, Babylon, Iraq. *Journal of Civil Engineering and Architecture*, 10(5), 530–543. <https://doi.org/10.17265/1934-7359/2016.05.002>
3. Aragonés-Beltrán, P., Pastor-Ferrando, J. P., García-García, F., & Pascual-Agulló, A. (2010). An Analytic Network Process approach for siting a municipal solid waste plant in the Metropolitan Area of Valencia (Spain). *Journal of Environmental Management*, 91(5), 1071–1086. <https://doi.org/10.1016/j.jenvman.2009.12.007>
4. Aydi, A., Zairi, M., & Dhia, H. (2013). Minimization of environmental risk of landfill site using fuzzy logic, analytical hierarchy process, and weighted linear combination methodology in a geographic information system environment. *Environmental Earth Sciences*, 68(5), 1375–1389. <https://doi.org/10.1007/s12665-012-1836-3>
5. Bottero, M., & Ferretti, V. (2011). An analytic network process-based approach for location problems: The case of a new waste incinerator plant in the Province of Torino (Italy). *Journal of Multi-Criteria Decision Analysis*, 17(3–4), 63–84. <https://doi.org/10.1002/mcda.456>
6. Chang, N.-B., Parvathinathan, G., & Breeden, J. B. (2008). Combining GIS with fuzzy multicriteria decision-making for landfill siting in a fast-growing urban region. *Journal of Environmental Management*, 87(1), 139–153. <https://doi.org/10.1016/j.jenvman.2007.01.011>
7. Charnpratheep, K., Zhou, Q., & Garner, B. (1997). Preliminary Landfill Site Screening Using Fuzzy Geographical Information Systems. *Waste Management & Research - WASTE MANAGE RES*, 15(2), 197–215. <https://doi.org/10.1177/0734242X9701500207>
8. Cremiato, R., Mastellone, M. L., Tagliaferri, C., Zaccariello, L., & Lettieri, P. (2018). Environmental impact of municipal solid waste management using Life Cycle Assessment: The effect of anaerobic digestion, materials recovery and secondary fuels production. *Renewable Energy*, 124, 180–188. <https://doi.org/10.1016/j.renene.2017.06.033>
9. Deswal, M., & Laura, J. S. (2018). GIS based modeling using Analytic Hierarchy Process (AHP) for optimization of landfill site selection of Rohtak city, Haryana (India). *Journal of Applied and Natural Science*, 10(2), 633–642. <https://doi.org/10.31018/jans.v10i2.1753>
10. Djokanović, S., Abolmasov, B., & Jevremović, D. (2016). GIS application for landfill site selection: A case study in Pančevo, Serbia. *Bulletin of Engineering Geology and the Environment*, 75(3), 1273–1299. <https://doi.org/10.1007/s10064-016-0888-0>
11. Dzhamaalov, R. G., Medovar, Yu. A., & Yushmanov, I. O. (2018). Vliyanie ploshchadki utilizatsii tverdykh bytovykh otkhodov na kachestvo podzemnykh i poverkhnostnykh vod (na primere Vladimirskoy oblasti) [The influence of municipal solid waste disposal site on the quality of ground- and surface water (by the example of Vladimir oblast)]. In *Sergeevskie Chteniya: Vol. issue 20. Proceedings of the Scientific conference in the framework of the IX International Forum "Ecology": Materials of the annual session of the Scientific Council of the Russian Academy of Sciences on the problems of geoecology, engineering geology and hydrogeology, March 22, 2018* (pp. 175–178). Moscow: RUDN Publ.

12. Ekzaryan, V. N. (2018). Metodologicheskiye osnovy zonirovaniya territoriy dlya vybora mest razmeshcheniya otkhodov [Methodological fundamentals of zoning territories for selecting places for the waste storage sites]. In *Sergeevskie Chteniya: Vol. issue 20. Proceedings of the Scientific conference in the framework of the IX International Forum "Ecology": Materials of the annual session of the Scientific Council of the Russian Academy of Sciences on the problems of geoecology, engineering geology and hydrogeology, March 22, 2018* (pp. 97–101). Moscow: RUDN Publ.
13. El Maguiri, A., Kissi, B., Idrissi, L., & Souabi, S. (2016). Landfill site selection using GIS, remote sensing and multicriteria decision analysis: Case of the city of Mohammedia, Morocco. *Bulletin of Engineering Geology and the Environment*, 75(3), 1301–1309. <https://doi.org/10.1007/s10064-016-0889-z>
14. Ghobadi, M. H., Taheri, M., & Taheri, K. (2017). Municipal solid waste landfill siting by using analytical hierarchy process (AHP) and a proposed karst vulnerability index in Ravansar County, west of Iran. *Environmental Earth Sciences*, 76(2), 68. <https://doi.org/10.1007/s12665-017-6392-4>
15. Goldberg, V. M. (1987). Vzaimosvyaz' zagryazneniya podzemnykh vod i prirodnoy sredy [Relationship between the contamination of groundwater and the environment]. Leningrad: Gidrometeoizdat.
16. Güler, D., & Yomralioğlu, T. (2017). Alternative suitable landfill site selection using analytic hierarchy process and geographic information systems: A case study in Istanbul. *Environmental Earth Sciences*, 76(20), 678. <https://doi.org/10.1007/s12665-017-7039-1>
17. Kashperuk, P. I., Makeeva, T. G., Akanov, A. V., Nikitina, K. V., & Podlesnykh, A. I. (2018). Nekotoryye zakonodatel'nyye i prirodookhrannyye voprosy pri organizatsii ob'yektov pererabotki i zakhroneniya TBO v Moskovskoy oblasti [Some legislative and nature-conservation issues in the arrangement of MSW reprocessing and disposal sites in the Moscow region]. In *Sergeevskie Chteniya: Vol. issue 20. Proceedings of the Scientific conference in the framework of the IX International Forum "Ecology": Materials of the annual session of the Scientific Council of the Russian Academy of Sciences on the problems of geoecology, engineering geology and hydrogeology, March 22, 2018* (pp. 71–73). Moscow: RUDN Publ.
18. Khan, D., & Samadder, S. R. (2014). Municipal solid waste management using Geographical Information System aided methods: A mini review. *Waste Management & Research*, 32(11), 1049–1062. <https://doi.org/10.1177/0734242X14554644>
19. Khmelchenko, E. G. (2018). Problemy utilizatsii tvordykh kommunal'nykh otkhodov v rossiyskoy federatsii i puti ikh resheniya [Problems of utilization of solid municipal waste in the Russian Federation and ways to solve them]. *Munitsipal'naya Akademiya [Municipal Academy]*, (2), 110–114. Retrieved from <https://elibrary.ru/item.asp?id=35311297>
20. Khodaparast, M., Rajabi, A. M., & Edalat, A. (2018). Municipal solid waste landfill siting by using GIS and analytical hierarchy process (AHP): A case study in Qom city, Iran. *Environmental Earth Sciences*, 77(2), 52. <https://doi.org/10.1007/s12665-017-7215-3>
21. Komarov, I. S. (Ed.). (1978). Inzhenernaya geologiya SSSR. Tom 1: Russkaya platforma [Engineering geology of the USSR, Volume 1: The Russian Platform]. Moscow: Moscow University Press.
22. Kontos, T. D., Komilis, D. P., & Halvadakis, C. P. (2005). Siting MSW landfills with a spatial multiple criteria analysis methodology. *Waste Management*, 25(8), 818–832. <https://doi.org/10.1016/j.wasman.2005.04.002>
23. Kozliakova, I. V., Kozhevnikova, I. A., Anisimova, N. G., & Eremina, O. N. (2020). Geologicheskie aspekty problem razmeshcheniya tverdykh kommunal'nykh otkhodov (na primere tsentral'noi Rossii) [Geological aspects of municipal solid waste disposal (by the example of central Russia)]. *Sergeevskie Chteniya: Issue 22*.

*Proceedings of the scientific conference*, 129–132. Moscow: RUDN Publ.

24. Kozlovskiy, S. V., Mamaev, Y., & Stol'nikova, P. V. (2020). Inzhenerno-geologicheskoe obosnovanie plana razmeshcheniya tverdykh kommyunal'nykh otkhodov na territorii Ruzskogo gorodskogo okruga Moskovskoi oblasti [Engineering geological substantiation of the municipal solid waste disposal in Ruza urban district, Moscow area]. *Sergeevskie Chteniya: Issue 22. Proceedings of the Scientific Conference*, 125–129. Moscow: RUDN Publ.
25. Leonenko, I. N., Sidorenko, A. V., & Shik, S. M. (Eds.). (1971). *Geologiya SSSR. Tom 4. Tsentral'noyevropeyskoy chasti SSSR. Chast' 1. Geologicheskoye opisaniye (Moskovskaya, Vladimirskaia, Ivanovskaya, Kalininskaya, Kaluzhskaya, Kostromskaya, Ryazanskaya, Tul'skaya, Smolenskaya i Yaroslavskaya oblasti)* [Geology of the USSR. Volume 4. Center of the European part of the USSR. Part 1. Geological description (Moscow, Vladimir, Ivanovo, Kalinin, Kaluga, Kostroma, Ryazan, Tula, Smolensk and Yaroslavl regions)]. Moscow: Nedra.
26. Ministry of Health of the Russian Federation. (2001). *Sanitary Rules SP 2.1.7.1038-01 Hygiene requirements for the arrangement and maintenance of solid domestic waste disposal sites*. Retrieved from <https://gostperevod.com/catalog/product/view/id/339144/s/sp-2-1-7-1038-01/category/44/>
27. Nakhaei, M., Amiri, V., Rezaei, K., & Moosaei, F. (2015). An investigation of the potential environmental contamination from the leachate of the Rasht waste disposal site in Iran. *Bulletin of Engineering Geology and the Environment*, 74(1), 233–246. <https://doi.org/10.1007/s10064-014-0577-9>
28. Ogola, J. S., Chimuka, L., & Tshivhase, S. (2011). Management of Municipal Solid Wastes: A Case Study in Limpopo Province, South Africa. *Integrated Waste Management - Volume I*. <https://doi.org/10.5772/18655>
29. Osipov, V. I. (2019). Management of solid municipal waste as the federal ecological project. *Geoecology. Engineering Geology. Hydrogeology. Geocryology*, 3, 3–11. <https://doi.org/10.31857/S0869-7809201933-11>
30. Rahmat, Z. G., Niri, M. V., Alavi, N., Goudarzi, G., Babaei, A. A., Baboli, Z., & Hosseinzadeh, M. (2017). Landfill site selection using GIS and AHP: A case study: Behbahan, Iran. *KSCE Journal of Civil Engineering*, 21(1), 111–118. <https://doi.org/10.1007/s12205-016-0296-9>
31. The Government of the Russian Federation. (2016, March 16). Postanovleniye Pravitel'stva RF N 197 "Ob utverzhdenii trebovaniy k soderzhaniyu i strukture territorial'nykh skhem obrashcheniya s otkhodami, v tom chisle tverdymi bytovymi otkhodami" [Decision of the RF Government N 197 "Adoption of requirements to the content and structure of territorial schemes of waste management, including solid municipal waste"]. Retrieved from <https://rg.ru/2016/03/25/othodi-site-dok.html>
32. The State Duma. Federal'nyy zakon ot 24.06.1998 N 89-FZ (red. ot 07.04.2020) "Ob otkhodakh proizvodstva i potrebleniya" [Federal Law of June 24, 1998 N 89-Φ3 (as amended on April 7, 2020) "On Production and Consumption Wastes"], (1998).
33. VSEGEI. (2018). GIS atlas of current geological information, Central Federal district. Retrieved from <http://atlaspacket.vsegei.ru>
34. VSEGEI. (2019). GIS atlas of current geological information, Central Federal district. Retrieved from <http://atlaspacket.vsegei.ru/#f78cf9c49e5ef7fa0>
35. VSEGEI, & Pogrebitsky, Yu. E. (1999). *State Geological Map of the Russian Federation*. St. Petersburg: VSEGEI.
36. Yannah, M., Martens, K., Van Camp, M., & Walraevens, K. (2019). Geophysical exploration of an old dumpsite in the perspective of enhanced landfill mining in Kermt area, Belgium. *Bulletin of Engineering Geology and the Environment*, 78(1), 55–67. <https://doi.org/10.1007/s10064-017-1169-2>
37. Zaikanov, V. G., Zaikanova, I. N., & Buldakova, E. V. (2018).

Geoekologicheskiy i landshaftno-ekologicheskiy analiz poligonov v Moskovskoy oblasti [Geoecological and landscape ecological analysis of landfill sites in Moscow oblast]. In *Sergeevskie Chteniya: Vol. issue 20. Proceedings of the Sci. Conference March 22, 2018* (pp. 65–73). Moscow: RUDN Publ.

<https://doi.org/10.1007/s00267-011-9792-3>

38. Zelenović Vasiljević, T., Srdjević, Z., Bajčetić, R., & Vojinović Miloradov, M. (2012). GIS and the Analytic Hierarchy Process for Regional Landfill Site Selection in Transitional Countries: A Case Study From Serbia. *Environmental Management*, 49(2), 445–458.

**Table 1.** Types of ground massifs in the map of engineering geological zoning CFD

| Quaternary deposits<br>pre-Quaternary deposits   | Sand, moraine loam, interbedding sand, and loam (1) | Sand (2) | Moraine loam, interbedding sand, and loam (3) | Loessial sandy loam and loam (4) |
|--|---|----------|---|----------------------------------|
| Mainly sand and sandstone (K, Pg, N) water-bearing<br><b>I</b>   | I-1   | I-2      | I-3   | I-4                              |
| Marl, chalk (K) low water-bearing and unevenly water-saturated<br><b>II</b>  | II-1  | II-2     | II-3  | II-4                             |
| Mainly impermeable clay (J)<br><b>III</b>  | III-1   | III-2    | III-3   | -                                |
| Argillite, aleurolite, sandstone locally gypsiferous, gypsum (P-T), weakly and unevenly water-bearing<br><b>IV</b> | IV-1  | IV-2     | IV-3  | -                                |
| Water-bearing limestone, dolomites with clay interlayers (D –C)<br><b>V</b>  | V-1   | V-2      | V-3   | V-4                              |

**Table 2.** *Typification of the Central Federal territory by its suitability for allocation of disposal sites and utilization facilities for MSW depending on geological engineering conditions*

| Types of the geological structure according to the suitability degree and corresponding indices of typical geological cross-sections | Specific features of geological engineering conditions  |
|--|---|
| Favorable<br>III-3   | Two aquiclude strata are distinguished in the cross-section, i.e., the Quaternary moraine loam at the surface and Jurassic clay dividing the Quaternary and Mesozoic water-bearing complexes. Geoenvironment is protected from the contamination coming from the surface.   |
| Conventionally favorable<br>I-3,<br>II-3,<br>IV-3,<br>V-3  | Quaternary moraine loam aquiclude is present on the top of the cross-section, which is underlain by permeable either water-bearing or unevenly and poorly water-saturated deposits of Quaternary and pre-Quaternary age. The protection of geoenvironment from contamination is controlled by the moraine layer thickness.  |
| Conventionally unfavorable<br>III-1, III-2   | Quaternary deposits are represented by sandy-clayey water-bearing or poorly and unevenly water-saturated soils. The groundwater aquifer is not protected from contamination. The Quaternary massif is underlain by the Jurassic clay aquiclude. The Mesozoic aquifer is protected from contamination.<br>The protection of geoenvironment from contamination is controlled by the depth of occurrence and the thickness of the Jurassic clay layer. |
| Unfavorable<br>I-1, I-4,<br>II-1, II-2, II-4,<br>IV-1, IV-2,<br>V-1, V-4   | Water-permeable, water-bearing, weakly water-bearing and unevenly water-saturated complexes of Quaternary and pre-Quaternary deposits are distinguished in the geological cross-section. Low-permeable aquicludes of variable thickness and depth of occurrence occur sporadically and locally. Geoenvironment is almost unprotected or poorly protected from contamination.  |
| Very unfavorable<br>I-2,<br>V-2  | Quaternary and underlying pre-Quaternary deposits are composed of water-permeable and water-bearing soil and rock complexes. Geoenvironment is not protected from contamination coming from the surface.  |

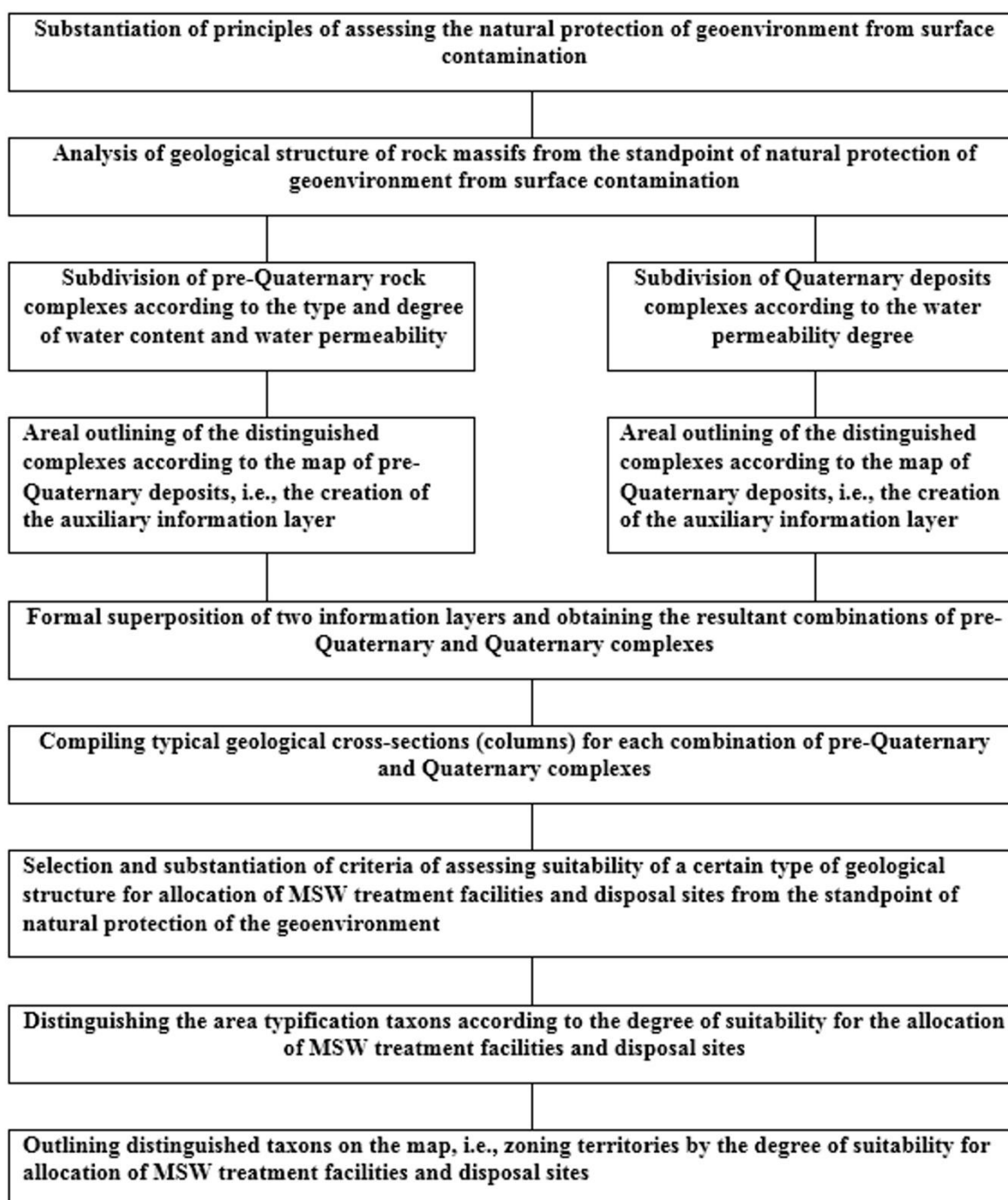


**Figure 1.** Conceptual model of engineering geological assessment of the Central Russia territory for the allocation of MSW treatment facilities and disposal sites

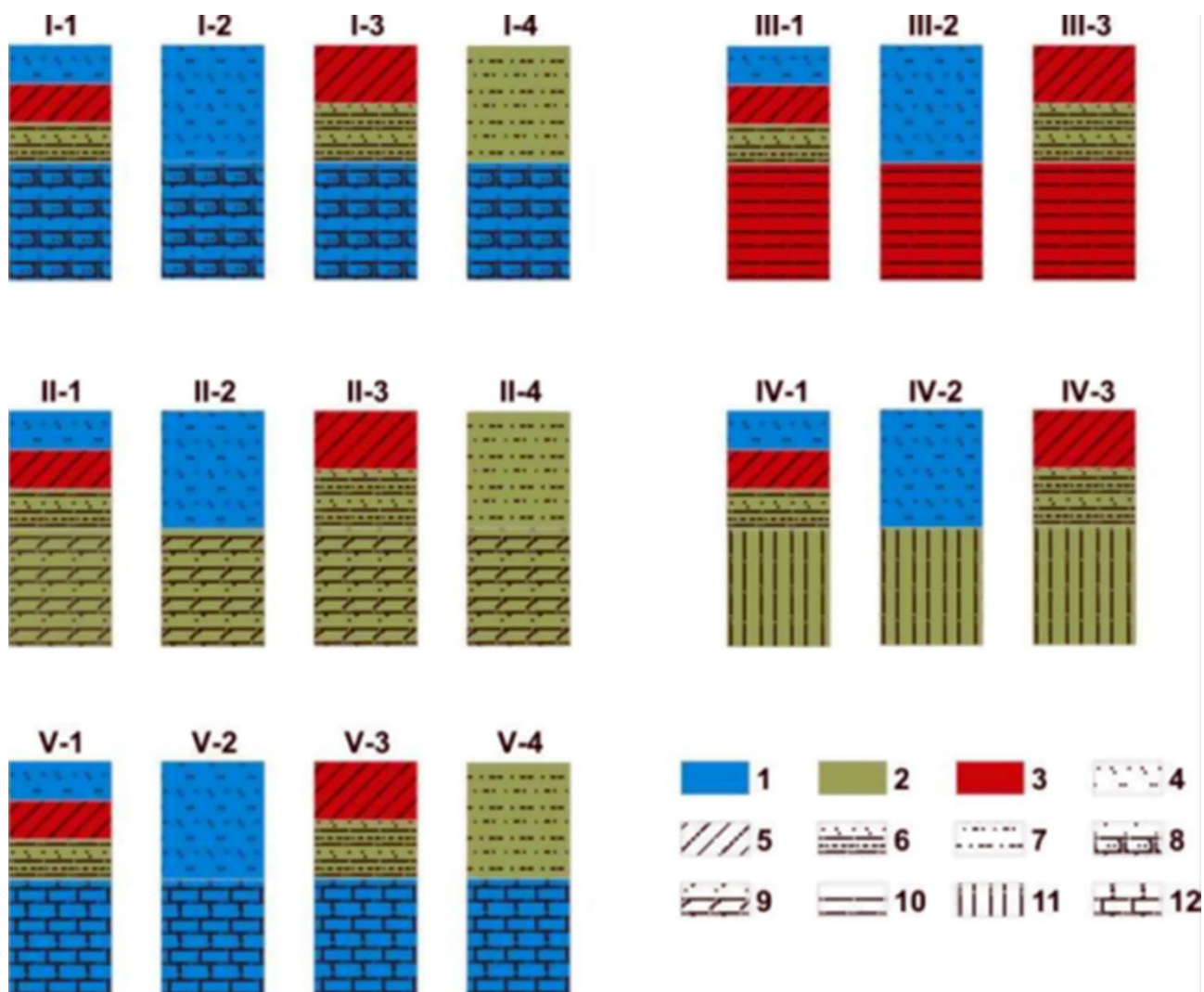


**Figure 2.** Schematic columns to the map of geological engineering zoning.

Designations: 1 – water-bearing permeable deposits, 2 – weakly water-bearing and unevenly water-saturated deposits, 3 – impermeable aquicludes. Quaternary deposits: 4 – sand, 5 – moraine loam, 6 – interbedding sand and loam, 7 – loessial sandy loam, and loam. Pre-Quaternary deposits: 8 – mainly sand and sandstone (K, Pg, N), 9 – marl and chalk (K), 10 – primarily clay (J), 11 – argillite, aleurolite, sandstone locally gypsiferous, gypsum (P-T), 12 – limestone and dolomite with clay interlayers (D-C)



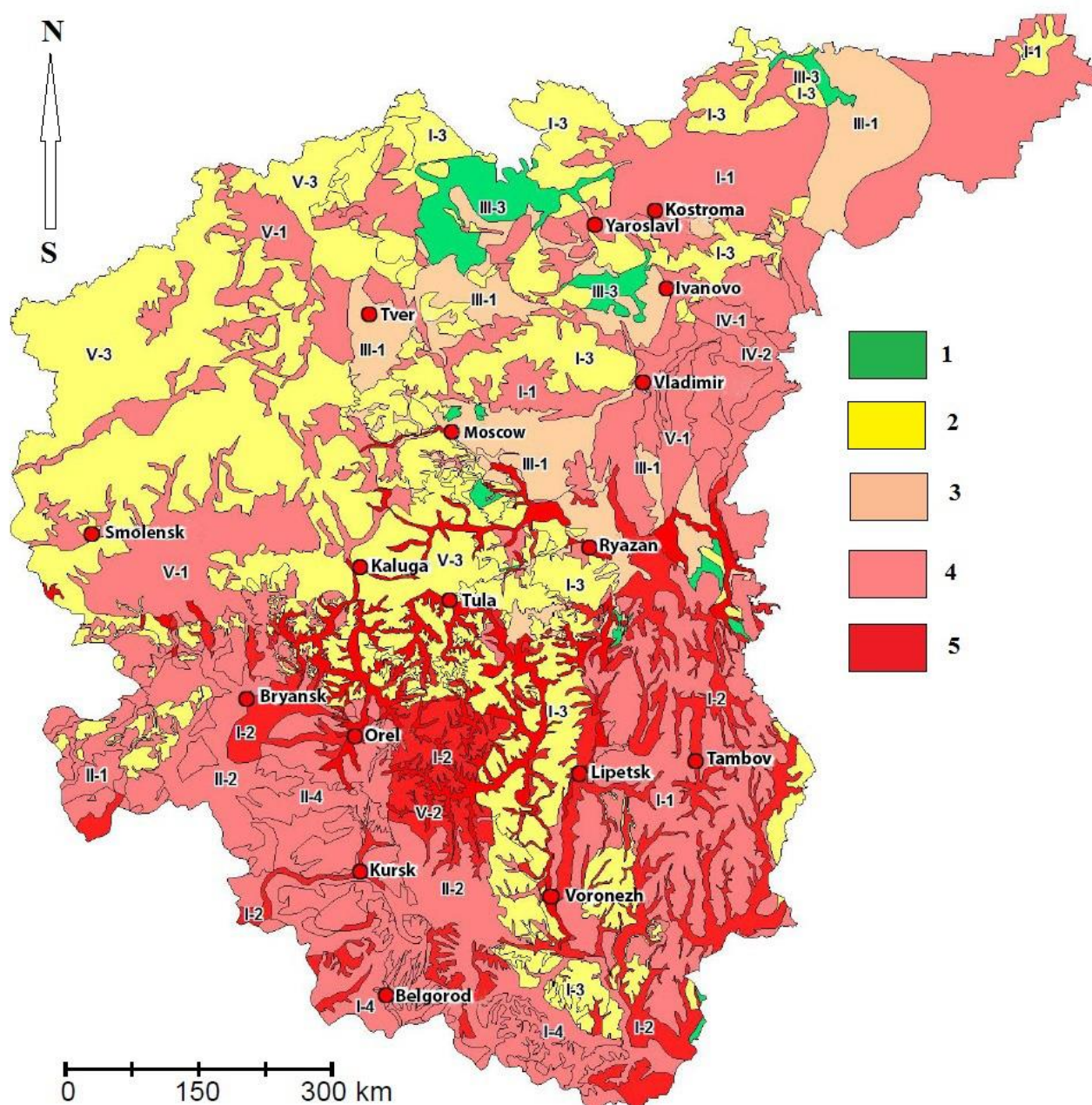


**Figure 3.** The map of geological engineering zoning of the Central Federal district in Russia by the suitability of allocating MSW disposal sites and reprocessing facilities. Suitability grades: 1 – favorable; 2 – conventionally favorable; 3 – conventionally unfavorable; 4 – unfavorable; 5 – very unfavorable.

Note: The regions are described in detail in Table 2

**ALTERAÇÕES CITOGENÉTICAS EM CRIANÇAS RESIDENTES  
EM REGIÕES ECOLÓGICAMENTE ADVERSAS DO CAZAQUISTÃO****CYTOGENETIC CHANGES IN SCHOOLCHILDREN  
RESIDING IN ECOLOGICALLY ADVERSE REGIONS OF KAZAKHSTAN**

BAKHTIYAROVA, Sholpan<sup>1</sup>; ZHAKSYMOV, Bolatbek<sup>2</sup>; KAPYSHEVA, Unzira<sup>3\*</sup>;  
CHEREDNICHENKO, Oksana<sup>4</sup>

<sup>1,2,3</sup> Republican State Enterprise "Institute of Human and Animal Physiology" Committee of Science of the Ministry of Education and Science of the Republic of Kazakhstan..

<sup>4</sup> Institute of General Genetics and Cytology of the Ministry of Education and Science of the Republic of Kazakhstan, Laboratory of Genetic Monitoring. Kazakhstan.

\* *Corresponding author*  
e-mail: [unzira@inbox.ru](mailto:unzira@inbox.ru)

Received 01 June 2020; received in revised form 18 June 2020; accepted 04 July 2020

**RESUMO**

No Cazaquistão, devido ao fortalecimento do papel geopolítico na arena internacional e ao desenvolvimento industrial ativo, os impactos ambientais negativos se intensificaram nos últimos anos. Muitas regiões são ambientalmente desfavoráveis e correm o risco de um aumento na incidência de vida nessas condições da população. Inúmeros desvios na saúde da população criam condições para o polimorfismo genético e o crescimento de certos grupos de doenças característicos de regiões com poluição ambiental. A poluição ambiental a longo prazo é a razão do aumento da taxa do processo de mutação e do volume da carga genética na população humana. O objetivo deste estudo é mostrar a influência de fatores ambientais dominantes em regiões distantes do Cazaquistão sobre distúrbios citogenéticos no corpo da geração mais jovem. Estudantes de diferentes escolas com idades entre 16 e 18 anos que moram perto do local de teste de Semipalatinsk, na região leste do Cazaquistão e na região de Aral, na região de Kyzylorda, participaram dos estudos. Os resultados do estudo mostram que as células epiteliais orais em dois terços dos adolescentes examinados que vivem em condições ambientalmente desfavoráveis, próximas ao local do teste de Semipalatinsk ou na região do Mar de Aral, no Cazaquistão, revelaram uma ampla gama de distúrbios citogenéticos. A maior porcentagem de violações, associada à formação de micronúcleos, protrusões e apoptose, foi detectada em estudantes urbanos que vivem a 150 km do local do teste de Semipalatinsk. Ao comparar os dados de estudantes urbanos e rurais, foi revelado o desenvolvimento predominante de desordens citológicas, como destruição nuclear (cariorexia, cariólise e apoptose) em adolescentes rurais, o que indica o impacto negativo contínuo do local de teste de Semipalatinsk fechado e a salinização do Mar de Aral sobre a saúde da geração mais jovem de crianças.

**Palavras-chave:** *Ecologia, Saúde do adolescente, Local de teste de Semipalatinsk, Priaralye, Distúrbios citogenéticos.*

**ABSTRACT**

In Kazakhstan, due to the strengthening of the geopolitical role in the international arena and active industrial development, negative environmental impacts have intensified in recent years. Many regions are environmentally unfavorable and carry the risk of an increase in the incidence of living in these conditions of the population. Numerous deviations in the health of the community create the conditions for genetic polymorphism and the growth of certain groups of diseases characteristic of regions with environmental pollution. Long-term environmental pollution is the reason for the increase in the rate of the mutation process and the volume of the genetic load in the human population. The purpose of this study is to show the influence of dominant environmental factors in distant regions of Kazakhstan on cytogenetic disturbances in the body of the younger generation. Students from different schools aged 16 to 18 years living near the Semipalatinsk test site of the East Kazakhstan region and in the Aral region of the Kyzylorda region took part in the studies. The results of the study show that the oral epithelial cells in two-thirds of the examined adolescents living in environmentally unfavorable conditions either near the Semipalatinsk Test Site or in the Aral Sea region of Kazakhstan revealed a wide range of cytogenetic disorders. The most significant percentage of violations associated with the formation of micronuclei, protrusions, and apoptosis, was detected in urban students living 150 km from the Semipalatinsk Test Site. When comparing the data of urban and rural students, the predominant development of cytological

disorders was revealed, such as nuclear destruction (karyorrhexis, karyolysis, and apoptosis) in rural adolescents, which indicates the ongoing negative impact of the closed Semipalatinsk Test Site and the salinization of the Aral Sea on the health of the younger generation of children.

**Keywords:** Ecology, Adolescent health, Semipalatinsk Test Site, Priaralye, Cytogenetic disorders.

## 1. INTRODUCTION:

Currently, there is an increase in the incidence of environmental pollution, with industrial waste entering the water, soil, air, and food. Changes in the quality of the living environment lead to the disruption of numerous evolutionarily established mechanisms of interaction between man and nature. Such shifts violate the ecology of the external and internal environments of a person and lead to disease (UNECE Environment Division, 2013).

In Kazakhstan, environmental problems also pose dangerous risk elements for human life and health, including the long-term effect of radioactive contamination in the area near the former Semipalatinsk Nuclear Test Site and the pollution of the environment with toxic compounds as the Aral Sea dries up. These problems, due to their significance, have a global resonance (Nazarbayev *et al.*, 2016).

The East Kazakhstan Region in Kazakhstan has existed since 1932 and includes the territories of 15 districts. The Altai and Tarbagatai mountains are located in the region, and it contains more than 885 rivers, carrying over 40% of all water reserves in Kazakhstan. About 1.5 million inhabitants of more than 15 nationalities live here (Nazarbayev *et al.*, 2016). Over the past 20 years, the mortality rate from neoplasms among the adult population in the East Kazakhstan Region has been 20-30% higher than the average national level (Yan, 2019). Radioactive pollution of the environment continues to be considered the cause for this high mortality, the sources of which are the Semipalatinsk Test Site and the enterprises of the nuclear-industrial complex. For 40 years, until 1989, about 456 nuclear tests were carried out at the abovementioned test site, including 30 ground and 86 air tests (Nazarbayev *et al.*, 2016). The consequences of such tests are a still increased level of radioactive infection and genetic mutations, with a high incidence for the population of several generations living near the landfill (Grosche *et al.*, 2017). With industry concentrated in this region, 154 industrial enterprises annually emit 294 thousand tons of toxic chemicals into the environment. For example, in the territory of

Semey, the maximum concentration of heavy metals exceeds the permissible standards for copper, lead, and chromium by 100 times, for zinc by 300 times, and for cobalt and nickel by 50 times (Gazaliev, 2016). Currently, at the state level, a number of programs have been adopted to improve the region's ecology and disease prevention measures (Nazarbayev *et al.*, 2016). As a result of sanitary and hygienic standards over the past ten years, the incidence rates of many diseases in the population have decreased in the Semipalatinsk region. Still, over the years, the level of endocrine disorders has remained 30-40% higher than both the regional average and the national average (in 2011, 1255.5 in Semey vs 954.3 in the republic; in 2017, 1389.7 in Semey vs 976.4 in the republic) (Ministry of Health of the Republic of Kazakhstan, 2011).

Regarding the Kazakhstani part of the Aral Sea region, the following problems should be highlighted. The intensive development of irrigation since 1960 in both Kazakhstan and Central Asia as a whole has led to a steady decline in the level of the Aral Sea, the deterioration of ecosystems, the development of aridization, and significant desertification in the region. As a consequence of such processes, there have emerged problems, including a high content of mineral salts in the water and soil and the depletion and pollution of water resources of the Aral Sea region (Crighton, Barwin, Small, & Upshur, 2011; Novikov & Kelly, 2017; White, 2013).

The environmental problems of the region have led to wide-scale and regional climate changes in large areas of the country due to an increase in the greenhouse effect, an increase in the concentration of carbon dioxide in the atmosphere, and salt and dust emissions, which have impacted human living conditions in the Aral Sea region. According to a number of authors, in the Kazakhstani part of the Aral Sea region, over the past 20 years, demographic processes have significantly deteriorated due to an increase in total and infant mortality. The leading causes of this mortality increase are diseases of the circulatory system and respiratory and digestive organs (Ni, Tonkobaeva, & Ilyasova, 2013; Toleutay, 2017).

In recent years, according to official statistics, in the Republic of Kazakhstan, there has been a general decrease in the incidence of disease in the population (Ministry of Health of the Republic of Kazakhstan, 2011, 2017, 2018). This has been primarily due to the widespread provision of modern equipment to medical facilities in cities and outpatient networks in districts, which has increased the diagnostic capabilities of local health care. Nevertheless, in many regions of the country, a high incidence of disease in the population remains, which can be explained by the environmental pollution of the living environment. Environmental pollution is one of the main reasons for the increase in the rate of the mutation process and the volume of the genetic load in human and animal populations, as evidenced by the growth in the number of hereditary and multifactorial diseases, congenital pathologies, and malformations, which are especially pronounced in ecologically disadvantaged regions (Landrigan & Fuller, 2015).

One of the indicators of the state of the body is cytogenetic homeostasis, which is determined using a micronucleus test, which, essentially, calculates the frequency of cells with micronuclei in the epithelial cells of the buccal epithelium. The micronuclear test is included in many manuals (Hayashi, 2016) and is actively used in many studies, in particular, to determine the environmental load that can cause damage to the genetic apparatus in humans and animals (Baranov, 2019; Yurchenko, Krivtsova, & Podolnaya, 2008). The popularity of this test is because it is fast, non-invasive, and economically viable, allows an intravital screening of the examined individuals an unlimited number of times, and does not require special equipment for cell culture or enhanced sterility.

An indicator of genetic disorders in interphase nuclei is not only the frequency of the micronuclei but also the sum of cytological disorders, such as binuclear cells, protrusions, and destructive changes in nuclei. Micronuclei are formed mainly from fragments of chromosomes lacking a centromere during the formation of chromosome aberrations or due to lagging at the anaphase stage of the total number of diverging chromosomes. During mitosis, this material enters one of the daughter cells and forms one or more micronuclei. They can also be formed by the whole chromosome as a result of the violation of the spindle of division (Kolmakova, Belik, Morgul, & Sevryukov, 2013).

Protrusions, like micronuclei, can be formed by fragments of chromosomes or due to

lagging when the fission spindle is broken by whole chromosomes, the nuclear membrane of which is connected to the membrane of the central nucleus. A broken egg protrusion looks like a micronucleus connected to the nucleus by a nucleoplasmic bridge. It is assumed that nuclear protrusion can also be formed by budding of the interphase nuclei (Sarto *et al.*, 1987).

Proliferation indicators are the presence in the sample of binuclear cells and nuclei with a circular notch (a groove that is equal to or partially shifted to one of the poles of the groove). This anomaly is likely to arise in the process of incomplete mitosis as a result of damage to the spindle of division (Holland *et al.*, 2008).

Indicators of nuclear destruction are the presence of cells with karyorrhexis, karyolysis, and apoptotic bodies. They are observed in diseases of accumulation, inflammation, as well as after exposure to chemicals and radiation (Holland *et al.*, 2008).

Determining the genetic status of the most vulnerable population – adolescents from 16 to 18 years old, living in different regions of the country according to environmental stress – will show the presence of cytological disorders at the cellular level, which can lead to various health problems in the future. Undoubtedly, under the conditions of scientific and technological progress on a global scale, there is a high probability of an increase in ecogenetic pathology, which requires strengthening the measures to prevent diseases caused by an unfavorable living environment due to the growing role of new pollution factors (Landrigan & Fuller, 2015). The research results will bring a new understanding of the problem of the deteriorating health of the younger generation according to the ecology of the living environment.

Hence, the purpose of this study is to show the influence of dominant environmental factors in distant regions of Kazakhstan on cytogenetic disorders in the bodies of the younger generation.

## 2. MATERIALS AND METHODS:

The study participants were schoolchildren living in cities and villages located 150-200 km from the Semipalatinsk Test Site and the Aral Sea region of Kazakhstan, 150-200 km from the Aral Sea. A total of 182 high school students aged 16 to 18 years were examined, of which 81 were schoolchildren living near the Semipalatinsk Test Site of the East Kazakhstan Region, and 101 were students living in the Aral Sea region of the Kyzylorda Region. At the time of the study, all

students were healthy. According to the requirements of the local ethics commission, informed consent was obtained from each participant and their parents. The cytogenetic studies carried out were comparative in nature, allowing a new understanding of the nature of their appearance, regardless of the type of dominant environmental load, and the long-term effects of the radioactive contamination or mineralization of the atmosphere and drinking water.

For an analysis of the cytogenetic smear preparations, samples of buccal epithelium were taken by scraping epithelial cells from the inner surface of the pupils' cheeks with a plastic spatula. Next, the epithelial cells were resuspended in 100 µl of phosphate buffer (AMRESCO) or saline, evenly distributed over the surface of the slide, and dried in air. Two preparations were prepared (right, left cheek) from each student. The preparations were stained with 10% Romanovsky–Giemsa solution for 10 min (Stefanović *et al.*, 2017).

The micronuclei frequency was calculated using a Zeiss Axioscop 40 microscope at a magnification of 16x10. Photo documentation of the most specific disorders of the analyzed epithelial cells was carried out. The cytogenetic analysis of the buccal epithelium was conducted for 1000 to 3000 cells in each sample. The frequency of cytogenetic disorders was calculated as a percentage per 100 cells analyzed. When conducting a cytogenetic examination, all violations of the structure of epithelial cells that differed from normal morphology were recorded. The data obtained were processed using Microsoft Office Excel software. To compare the average values, a student's t-test was conducted using the formula (Eq. 1):

$$t = \frac{M_1 - M_2}{\sqrt{\frac{m_1^2 + m_2^2}{2}}} \quad (\text{Eq. 1})$$

where  $M_1$  and  $M_2$  are the arithmetic means of the compared indicators, and  $m_1$  and  $m_2$  are the average errors of these indicators. The number of degrees of freedom was found according to the formula (Eq. 2):

$$F = (n_1 + n_2) - 2 \quad (\text{Eq. 2})$$

after which the student criterion was determined from the Table at a significance level at  $p \leq 0.01$ . (Chaliev & Ovcharov, 2007).

To examine the schoolchildren, permission was obtained from the Local Ethics Commission (LEC) of the Kazakh National Medical University, S.D. Asfendiyarova, extract from protocol No. 3 (80) of 02/27/2019.

### 3. RESULTS AND DISCUSSION:

The cytogenetic analysis of buccal epithelial cells of the oral cavities of students living in the Aral Sea region of Kazakhstan and near the Semipalatinsk Test Site of the East Kazakhstan Region showed the presence of epithelial cells containing a few micronuclei (m/i), cells with a protrusion of nuclear material, binuclear cells, and epithelial cells with apoptotic bodies and karyolysis. Figures 1 – 4, respectively, show images of normal epithelial cells and cells with various changes, namely with two nuclei, a protrusion of nuclear material, and epithelial cells with apoptotic bodies and karyolysis, as detected in the students.

When comparing the data of urban students in both regions, it was found that the frequency of cells with cytogenetic disorders in adolescents living in the city of Semey, located near (143 km) the Semipalatinsk Test Site, is 7 times higher than that of schoolchildren in the Aral Sea region (Table 1).

In rural schoolchildren living in settlements located 200 to 300 km from the Semipalatinsk Test Site, the frequency of cells with cytogenetic disorders was 1.6 times higher than in rural teenagers of the Aral Sea region living 200 km from the Aral Sea. In terms of proliferation, no significant differences were observed in both regions (Table 1). Based on the changes in the structure of the nucleus, it was found that urban schoolchildren living in the city of Semey (East Kazakhstan Region, Kazakhstan) had a 20 times higher frequency of nuclear destruction than urban pupils in the Aral Sea region. However, in rural schoolchildren living near the nuclear test site (East Kazakhstan Region, Kazakhstan), the frequency of nuclear destruction was 4 times lower than that of rural students in the Aral Sea region (Table 1).

In general, adolescents in both studied regions showed a high level of cytogenetic changes. The maximum level of micronucleus frequency was found in 90% of the examined adolescents, 2-3 nuclei were found in the genetic material of 54% of the examined schoolchildren, and protrusions were found in 41% of students, regardless of the place of residence and environmental load. Nevertheless, in the students from Semey, located near the Semipalatinsk Test Site, the cytogenetic changes associated with nuclear destruction (karyorrhexis, karyolysis, and apoptosis) were found to be significantly higher than in the adolescents in the Aral Sea region. The presence of a high frequency of such violations in



the younger generation indicates that the long-term effect of environmental pollution by radioactive contamination products has been preserved despite the fact that the nuclear test site has been closed since 1991.

It is known that buccal cells have a limited ability to recover DNA compared to peripheral blood lymphocytes and, therefore, can more accurately reflect the age-related event of genomic instability in epithelial tissue (Grewal, Jindal, & Chauhan, 2013; Ladnova, Istomin, Kurochitskaya, & Silyutina, 2016). Being in direct contact with inhaled and absorbed genotoxic agents and metabolites of various chemicals, epithelial tissues are the first to express the genotoxic effects of these agents. The frequency of occurrence of micronuclei reflects the destruction of chromosomes under the action of adverse factors long before the development of clinical symptoms of pathological disorders of the body's functions (Grewal *et al.*, 2013; Podrimaj-Bytyqi *et al.*, 2018; Thomas *et al.*, 2009; Weng & Morimoto, 2009).

As a result of a cytogenetic analysis of oral epithelial cells, various cytogenetic disorders were revealed in two-thirds of the examined adolescents from 16 to 18 years old. The most significant percentage of violations associated with the presence of micronuclei was detected in urban students living 130 km from the former Semipalatinsk Nuclear Test Site. The data obtained are consistent with the high incidence of disease among adolescents in this region, as cited by official sources. The official statistical data for the teenage population of the East Kazakhstan Region of Kazakhstan for the period 2010-2017 showed a high incidence of neoplasms as well as a cardiovascular, respiratory and nervous system, and congenital anomalies at a rate 1.5-2 times higher than the average national level (Ministry of Health of the Republic of Kazakhstan, 2011, 2017, 2018).

When comparing the results of the study of buccal epithelium samples of urban and rural students of the Aral Sea region (Kyzylorda Region, Kazakhstan), the likelihood of developing cytogenetic disorders in rural adolescents, such as micronuclei, proliferation and nuclear destruction, including karyorrhexis, karyolysis, and apoptosis, which also indicates a negative effect, is revealed concerning the impact of the ecology of the region of residence on the health of the younger generation. This is confirmed by the official statistics for the period 2010-2017 and by the total morbidity of adolescents aged 15 to 17 years in the Kyzylorda Region, which shows that the number

of sick adolescents is 45% more in rural areas (10509.4 cases) than in the city (7218.0 cases). Moreover, over the past seven years, the incidence of adolescent diseases of the blood and blood-forming organs, as well as immune disorders and iron deficiency anemia, has remained significantly high, exceeding the national average by 2 times (in 2017, 3,792.2 cases in the Republic of Kazakhstan against 7976.8 cases in the Kyzylorda Region per 100 thousand teenagers) (Ministry of Health of the Republic of Kazakhstan, 2017).

The changes in the chromosomal material of the cells of the body of the younger generation shown in this work reflect a whole set of cytogenetic changes up to the destruction of the cell nucleus, regardless of the type of pathological environmental factor. Adolescents living in places located near the former Semipalatinsk Test Site, as well as the adolescent population of the Aral Sea region, suffer from pollution and drought in the region due to the drying out of the Aral Sea, whereby identical changes in cytogenetic indices with slight deviations in one direction or another were revealed. Considering that the main period of active pollution of the ecology of the regions where the adolescents lived was in the 1970-80s (Stepanov, 2016), the revealed changes at the chromosomal level show the long-term negative effect of environmental pollution on the health of the younger generation (UNESCO, 2013).

Currently, the acceleration of technological progress is creating more zones of ecological disadvantage, which is increasing the incidence of disease among the child population. This is not only occurring in the present but will also, as our study shows, cause cytogenetic changes in the cells of the bodies of future generations. In different countries of the world, the genetic vulnerability of populations to various environmental challenges has been shown (Panico *et al.*, 2020; Zani *et al.*, 2020). Mexican researchers investigated and showed the effect of gasoline vapors contained in exhaust gases on the human genome. They revealed cytogenetic disorders such as micronucleus frequency, karyolysis, karyorrhexis, and binuclear cells in the buccal epithelium, similar to our results. The authors suggest that this can cause carcinogenic diseases (Martinez-Valenzuela *et al.*, 2017). Genomic instability in the buccal epithelial cells of children living in one of the contaminated regions of Brazil has also been shown. The authors indicated a high level of cytogenetic disorders, also similar to our data, in children under the influence of the abnormal ecology of the region,

namely the pollution of water resources (Alpire, Cardoso, Seabra Pereira, & Ribeiro, 2019). Indian researchers, assessing the health of children, also indicated genetic damage, such as damage to telomere length, micronuclei, and urothelial cells in samples of the buccal epithelium, as a result of drinking water from underground sources with increased content of heavy metals that are especially dangerous for health, such as arsenic (Chatterjee *et al.*, 2018). In Russia, in the Altai Territory, which is 500 km or more distant from the Semipalatinsk test site, an increased level of cytogenetic abnormalities and incidence of adolescent endocrine diseases and congenital anomalies has been maintained for 40 years (Kolyado, Plugin, & Konovalov, 2017; Muldagaliev & Konovalov, 2018). Increasingly, they write about the impact of climate change in Central Asia on the health and gene pool of the population (Danielyan, Nazaretyan, Kosyan, & Nersisyan, 2017; Montgomery, 2016; Mullerson, 2014).

As can be seen from the literature, the presented research results are consistent with the data of various authors on a global scale, thereby introducing a new insight into the problems of the increased incidence of disease among the child population in regions where the peak of environmental problems was observed 40-50 years ago. The revealed cytogenetic disorders in the younger generation highlight the need to reduce the environmental burden in all regions to preserve the health of children, for both current and future generations.

#### 4. CONCLUSIONS:

Ecological dysfunction of the environment has a distant negative effect on the health of the younger generation and contributes to the development of cytogenetic disorders at the cellular level:

1. The maximum level of cytogenetic disorders associated with increased micronuclei and proliferation of nuclei in cells was detected in students living 150-200 km from the Semipalatinsk nuclear test site. The data are consistent with official data for 2010-2018 on a high incidence of adolescents in this region with diseases of the cardiovascular, respiratory and nervous systems, neoplasms and congenital anomalies exceeding 1.5-2.0 times the national average.

2. An extensive spectrum of cytogenetic disorders was detected in the overwhelming majority of the Aral Sea teenagers living 150-200 km from the dried Aral Sea, the territory of which

is characterized by desertification and significant salinization of the soil and remaining water. The micronuclei, the presence of 2-3 micronuclei, the proliferation of the nucleus and the destruction of the cell nucleus in the form of karyorrhexis, karyolysis and apoptosis were revealed in the buccal epithelium of the adolescent population, which indicates the continuing negative effect of the dried Aral Sea on the genetic material of the young generation of this region.

The presented data on cytogenetic changes in children born much later than peak environmental pollution emphasize the need for constant monitoring of their health and assessment of their genetic status, since environmental and human health issues are interrelated and are one of the urgent problems of our time. Given that the current study is preliminary, further analysis with a wider selection of children from different regions of the country is of scientific interest and opens up prospects for the future.

#### 5. ACKNOWLEDGEMENTS:

The study was funded by the Science Committee of the Ministry of Education and Science of the Republic of Kazakhstan as part of grant No. AR05132033.

#### 6. REFERENCES:

1. Alpire, M. E. S., Cardoso, C. M., Seabra Pereira, C. D., & Ribeiro, D. A. (2019). Genomic instability in Buccal mucosal cells of children living in abnormal conditions from Santos-Sao Vicente Estuary. *International Journal of Environmental Health Research*, 1–7. <https://doi.org/10.1080/09603123.2019.1636004>
2. Baranov, D. Y. (2019). [Investigation of the effect of different factors on buccal cells of schoolchildren by using micronucleus test]. *Bulletin of Science and Education*, 9(63), 11–14.
3. Chaliev, A. A., & Ovcharov, A. O. (2007). *Statistika: Uchebno-metodicheskoye posobiye. Chast' 1 [Statistics: Educational-methodical manual. Part 1]*. Nizhny Novgorod: Publishing House of the Nizhny Novgorod State University.
4. Chatterjee, D., Adak, S., Banerjee, N., Bhattacharjee, P., Bandyopadhyay, A. K.,

- & Giri, A. K. (2018). Evaluation of health effects, genetic damage and telomere length in children exposed to arsenic in West Bengal, India. *Mutation Research/Genetic Toxicology and Environmental Mutagenesis*, 836, 82–88. <https://doi.org/10.1016/j.mrgentox.2018.06.012>
5. Crighton, E. J., Barwin, L., Small, I., & Upshur, R. (2011). What have we learned? A review of the literature on children's health and the environment in the Aral Sea area. *International Journal of Public Health*, 56(2), 125–138. <https://doi.org/10.1007/s00038-010-0201-0>
  6. Danielyan, K., Nazaretyan, A., Kosyan, S., & Nersisyan, L. (2017). [Children's health challenges caused by environmental degradation and climate change and main proposed solution approaches]. In *Chemical Safety* (Vol. 1, pp. 11–43). Moscow: FSBI RAS.
  7. Gazaliev, A. M. (Ed.). (2016). *Ekologiya i zdorov'ye natsii. V pomoshch' kuratoram studencheskikh grupp* [Ecology and health of the nation: To help curators of student groups] (3rd ed., revised. and add.). Karaganda: Publishing house of the Karaganda State Technical University.
  8. Grewal, H., Jindal, S., & Chauhan, I. (2013). Alteration in buccal mucosal cells due to the effect of tobacco and alcohol by assessing the silver-stained nucleolar organiser regions and micronuclei. *Journal of Cytology*, 30(3), 174–178. <https://doi.org/10.4103/0970-9371.117667>
  9. Grosche, B., Katayama, H., Hoshi, M., Apsalikov, K. N., Belikhina, T., Noso, Y., & Takeichi, N. (2017). Thyroid Diseases in Populations Residing Near the Semipalatinsk Nuclear Test Site, Kazakhstan: Results from an 11 Years Series of Medical Examinations. *SM Journal of Public Health and Epidemiology*, 3(1), 1038. Retrieved from <https://smjournals.com/public-health-epidemiology/fulltext/smjphe-v3-1038.php>
  10. Hayashi, M. (2016). The micronucleus test—Most widely used in vivo genotoxicity test —. *Genes and environment*, 38(18), 1-6. <https://doi.org/10.1186/s41021-016-0044-x>
  11. Holland, N., Bolognesi, C., Kirschvolders, M., Bonassi, S., Zeiger, E., Knasmueller, S., & Fenech, M. (2008). The micronucleus assay in human buccal cells as a tool for biomonitoring DNA damage: The HUMN project perspective on current status and knowledge gaps. *Mutation Research/Reviews in Mutation Research*, 659(1-2), 93-108. <https://doi.org/10.1016/j.mrrev.2008.03.007>
  12. Kolmakova, T. S., Belik, S. N., Morgul, E. V., & Sevryukov, A. V. (2013). Ispol'zovaniye mikroyadernogo testa dlya otsenki effektivnosti lecheniya allergii u detey: Metod. Rekomendatsi [Using a microkernel test to evaluate the efficacy of treating allergies in children: Method recommendations]. Rostov-on-Don: Publishing House of Rostov State Medical University.
  13. Kolyado, I. B., Plugin, S. V., & Konovalov, B. Y. (2017). Pokazateli zdorov'ya zhitel'ey Altayskogo kraya, podvergshikhsya vozdeystviyu radiatsii v rezul'tate yadernykh ispytaniy na Semipalatinskoy poligone [Health indicators of residents of the Altai Territory exposed to radiation as a result of nuclear tests at the Semipalatinsk test site]. *Materials 52nd scientific and practical conference "Hygiene, healthcare organization and occupational pathology. Environmental and socio-hygienic aspects of the health of the population of Siberia. Russia,"* 53–56.
  14. Ladnova, G. G., Istomin, A. V., Kurochitskaya, M. G., & Silyutina, V. V. (2016). Tsitogeneticheskiye pokazateli bukkal'nogo epiteliya shkol'nikov, prozhivayushchikh na territoriyakh s raznym urovнем zagryazneniya atmosfernogo vozdukh [Cytogenetic indices of buccal epithelium in schoolchildren residing in territories with different levels of the air pollution]. *Hygiene and Sanitation*, 95(5), 428–431. <https://doi.org/10.18821/0016-9900-2016-95-5-428-431>
  15. Landrigan, P. J., & Fuller, R. (2015). Global health and environmental pollution. *International Journal of Public Health*, 60(7), 761-762. <https://doi.org/10.1007/s00038-015-0706-7>
  16. Martinez-Valenzuela, C., Soto, F. B., Waliszewski, S. M., Meza, E., Arroyo, S. G., Martínez, L. D. O., ... Caba, M. (2017).



- Induced cytotoxic damage by exposure to gasoline vapors: A study in Sinaloa, Mexico. *Environmental Science and Pollution Research*, 24(1), 539–546. <https://doi.org/10.1007/s11356-016-7821-8>
17. Ministry of Health of the Republic of Kazakhstan (Ed.). (2011). Zdorov'ye naseleniya respubliki Kazakhstan i deyatel'nost' organizatsiy zdravookhraneniya v 2010 godu [health of the population of the Republic of Kazakhstan and the activities of healthcare organizations in 2010: Statistical digest]. Astana-Almaty: Ministry of Health of the Republic of Kazakhstan.
  18. Ministry of Health of the Republic of Kazakhstan (Ed.). (2017). Zdorov'ye naseleniya respubliki Kazakhstan i deyatel'nost' organizatsiy zdravookhraneniya v 2016 godu [health of the population of the Republic of Kazakhstan and the activities of healthcare organizations in 2016: Statistical digest]. Astana: Ministry of Health of the Republic of Kazakhstan.
  19. Ministry of Health of the Republic of Kazakhstan. (2018). Zdorov'ye naseleniya respubliki Kazakhstan i deyatel'nost' organizatsiy zdravookhraneniya v 2017 godu [health of the population of the Republic of Kazakhstan and the activities of healthcare organizations in 2017: Statistical digest]. Astana: Ministry of Health of the Republic of Kazakhstan.
  20. Montgomery, D. W. (2016). *Negotiating well-being in Central Asia*. London: Routledge.
  21. Muldagaliev, T. Zh., & Konovalov, A. P. (2018). The state of health and the problems of medical and social support for the population affected by the tests at the Semipalatinsk nuclear testing ground (results of a mass sociological study). In *Pedagogical education in Altai* (pp. 133–145). Barnaul: ASPU.
  22. Mullerson, R. A. (2014). Central Asia: A chessboard and player in the new great game. Oxon: Routledge.
  23. Nazarbayev, N. A., Shkolnik, V. S., Batyrbekov, E. G., Berezin, S. A., Lukashenko, S. N., & Skakov, M. K. (2016). *[Conducting a set of scientific, technical and engineering works to bring the former Semipalatinsk Test Site into a safe state]*. Kurchatov: National Nuclear Center of the Republic of Kazakhstan.
  24. Ni, V., Tonkobaeva, A., & Ilyasova, A. (2013). Ekologicheskaya migratsiya i yeye posledstviya dlya sotsial'noy politiki na primere Kyzylordinskoy oblasti [Ecological migration and its consequences for social policy on the example of the Kyzylorda region] (Report on the Cluster order). Almaty: UNESCO Almaty Cluster Office for Kazakhstan, Kyrgyzstan, Tajikistan and Uzbekistan.
  25. Novikov, V., & Kelly, C. (2017). Climate change and security in Central Asia. The Republic of Kazakhstan, the Kyrgyz Republic, the Republic of Tajikistan, Turkmenistan and the Republic of Uzbekistan: Regional assessment. Retrieved from Organization for Security and Co-operation in Europe (OSCE) website: <https://www.osce.org/secretariat/355471?download=true>
  26. Panico, A., Grassi, T., Bagordo, F., Idolo, A., Serio, F., Tumolo, M. R., ... De Donno, A. (2020). Micronucleus Frequency in Exfoliated Buccal Cells of Children Living in an Industrialized Area of Apulia (Italy). *International Journal of Environmental Research and Public Health*, 17(4), 1208. <https://doi.org/10.3390/ijerph17041208>
  27. Podrimaj-Bytyqi, A., Borovečki, A., Selimi, Q., Manxhuka-Kerliu, S., Gashi, G., & Elezaj, I. R. (2018). The frequencies of micronuclei, nucleoplasmic bridges and nuclear buds as biomarkers of genomic instability in patients with urothelial cell carcinoma. *Scientific Reports*, 8(1), 17873. <https://doi.org/10.1038/s41598-018-35903-5>
  28. Sarto, F., Finotto, S., Giacomelli, L., Mazzotti, D., Tomanin, R., & Levis, A. G. (1987). The micronucleus assay in exfoliated cells of the human buccal mucosa. *Mutagenesis*, 2(1), 11–17. <https://doi.org/10.1093/mutage/2.1.11>
  29. Stefanović, D., Samardžija, G., Redžek, A., Arnaut, M., Nikin, Z., & Stefanović, M. (2017). Buffered Romanowsky-Giemsa method for formalin fixed, paraffin embedded sections: Taming a traditional stain. *Biotechnic & Histochemistry*, 92(5), 299–308. <https://doi.org/10.1080/10520295.2017.1315456>

30. Stepanov, Yu. S. (2016). [Semipalatinsk Test Site. Radioactive fallout in 1949, village of Dolon]. *ANRI (Scientific-Production Enterprise "Dose")*, 4(87), 73–79.
31. Thomas, P., Holland, N., Bolognesi, C., Kirsch-Volders, M., Bonassi, S., Zeiger, E., ... Fenech, M. (2009). Buccal micronucleus cytome assay. *Nature Protocols*, 4(6), 825–837. <https://doi.org/10.1038/nprot.2009.53>
32. Toleutay, U. (2017). [Environmental pollution and the health status of the population of the Kyzylorda region: Literature review]. *Young Scientist*, 19(1), 9–12.
33. UNECE Environment Division. (2013). *Environment @ UNECE: Safeguarding the environment for future generations*. Retrieved from UNECE website: [http://www.unece.org/fileadmin/DAM/env/Brochures/Environment%40UNECE\\_English.pdf](http://www.unece.org/fileadmin/DAM/env/Brochures/Environment%40UNECE_English.pdf)
34. UNESCO. (2013). *UNESCO Country Programming Document (UCPD) for the Republic of Uzbekistan, 2014-2017 (TAS/UCPD/2013/UZB)*. Retrieved from <https://unesdoc.unesco.org/ark:/48223/pf0000226136?posInSet=16&queryId=8911dea2-27d7-4417-8e2d-8075642dd8ae>
35. Weng, H., & Morimoto, K. (2009). Differential responses to mutagens among human lymphocyte subpopulations. *Mutation Research/Genetic Toxicology and Environmental Mutagenesis*, 672(1), 1–9. <https://doi.org/10.1016/j.mrgentox.2008.10.010>
36. White, K. D. (2013). Nature–Society Linkages in the Aral Sea Region. *Journal of Eurasian Studies*, 4(1), 18–33. <https://doi.org/10.1016/j.euras.2012.10.003>
37. Yan, W. (2019). The nuclear sins of the Soviet Union live on in Kazakhstan. *Nature*, 568(7750), 22–24. <https://doi.org/10.1038/d41586-019-01034-8>
38. Yurchenko, V. V., Krivtsova, E. K., & Podolnaya, M. A. (2008). [The use of micronucleus test on the epithelium of the mucous membrane of the human cheek]. *Hygiene and Sanitation*, (6), 53 – 56.
39. Zani, C., Ceretti, E., Zerbini, I., Viola, G. C. V., Donato, F., Gelatti, U., & Feretti, D. (2020). Comet Test in Saliva Leukocytes of Pre-School Children Exposed to Air Pollution in North Italy: The Respira Study. *International Journal of Environmental Research and Public Health*, 17(9), 3276. <https://doi.org/10.3390/ijerph17093276>

**Table 1.** The average frequency of cytogenetic disorders in the buccal epithelium of the oral cavity in students aged 16 to 18 years living in the Aral Sea region (Kyzylorda Region, Kazakhstan) and 150 km from the Semipalatinsk Test Site (East Kazakhstan Region, Kazakhstan)

| Indicator / Region                         | 300 km from Lake Aral<br>Priaralye (Kyzylorda Region,<br>Kazakhstan) |                               | 130-300 km from<br>the Semipalatinsk Test Site (East<br>Kazakhstan Region, Kazakhstan) |                               |
|--|--|-------------------------------|--|-------------------------------|
|  | city<br>n <sup>a</sup> =50   | village<br>n <sup>a</sup> =51 | city<br>n <sup>a</sup> =35   | village<br>n <sup>a</sup> =46 |
| <i>Indicators of cytogenetic disorders</i> |  |                               |  |                               |
| Micronuclei, %                             | 0.85±0.06  | 0.92±0.06                     | 4.15±0.19*   | 1.29±0.05*                    |
| Protrusions, %                             | 0.02±0.01  | 0                             | 0.71±0.05*   | 0.36±0.03*                    |
| 2-3 m/i <sup>a</sup> , %                   | 0.12±0.02  | 0.18±0.01                     | 2.07±0.08*   | 0.16±0.02*                    |
| Sum  | 0.99±0.01  | 1.10±0.01                     | 6.93±0.07*   | 1.81±0.02*                    |
| <i>Proliferation rates</i>                 |  |                               |  |                               |
| Binuclear cells, %                         | 0.61±0.04  | 0.56±0.03                     | 0.66±0.05*   | 0.45±0.02*                    |
| Sum  | 0.61±0.04  | 0.56±0.03                     | 0.66±0.05*   | 0.45±0.02*                    |
| <i>Nucleus destruction indicators</i>      |  |                               |  |                               |
| Apoptosis, %                               | 0.05±0.01  | 0.24±0.01                     | 1.00±0.08*   | 0.06±0.01*                    |
| <i>Integral Evaluation</i>                 | 1.65±0.01  | 1.90±0.01                     | 8.59±0.14*   | 2.32±0.03*                    |

Note: <sup>a</sup> accordingly: n - the number of students, m/i – micronuclei;

\* p≤0.01, when compared with the data of students in the city and villages of the Aral Region.

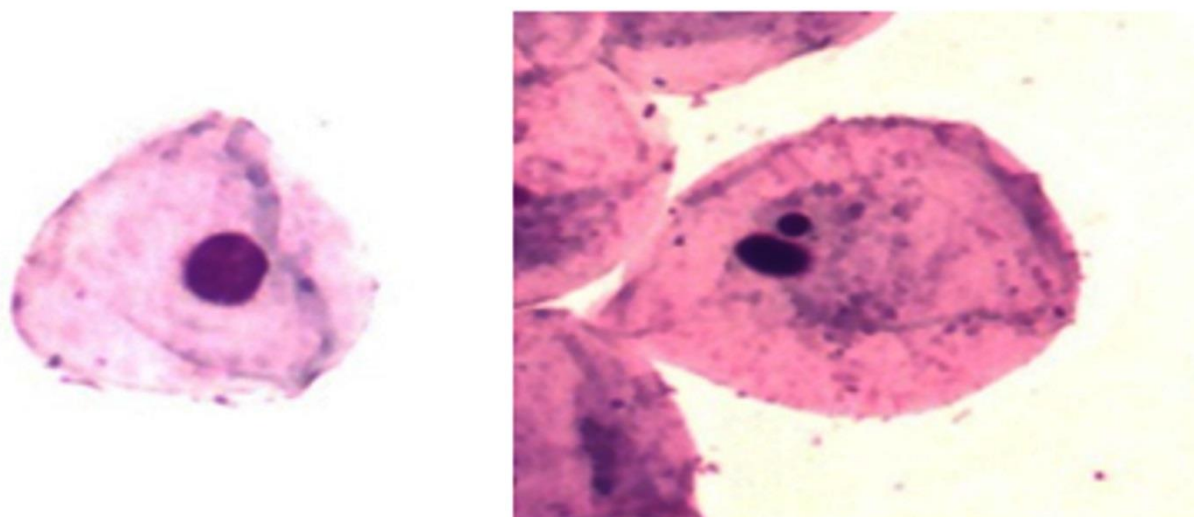


**Figure 1.** Normal cell and cell with one micronucleus of the buccal epithelium of the oral cavity (x160)

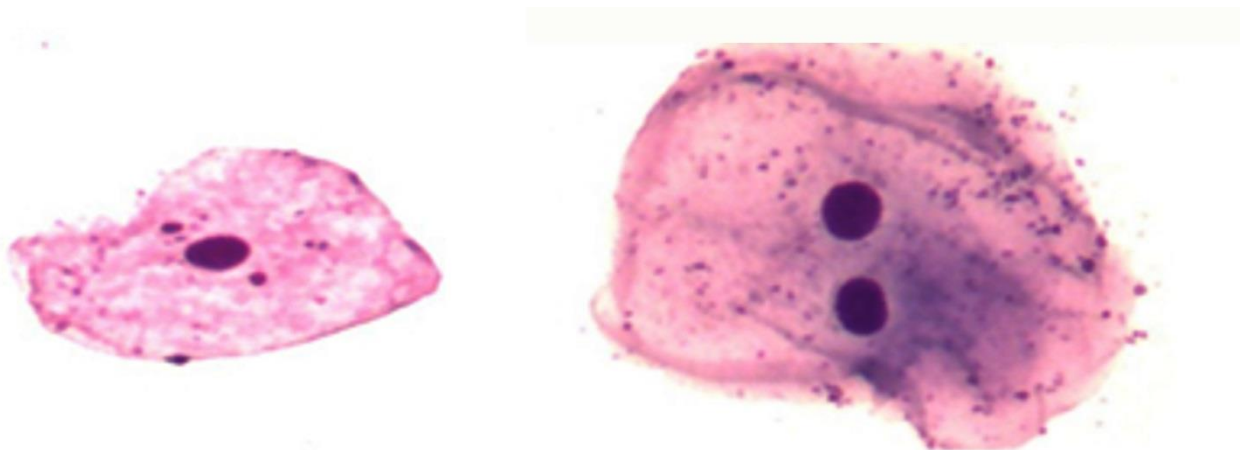


**Figure 2.** Cells of the buccal epithelium of the oral cavity with several small and two large micronuclei (x160)

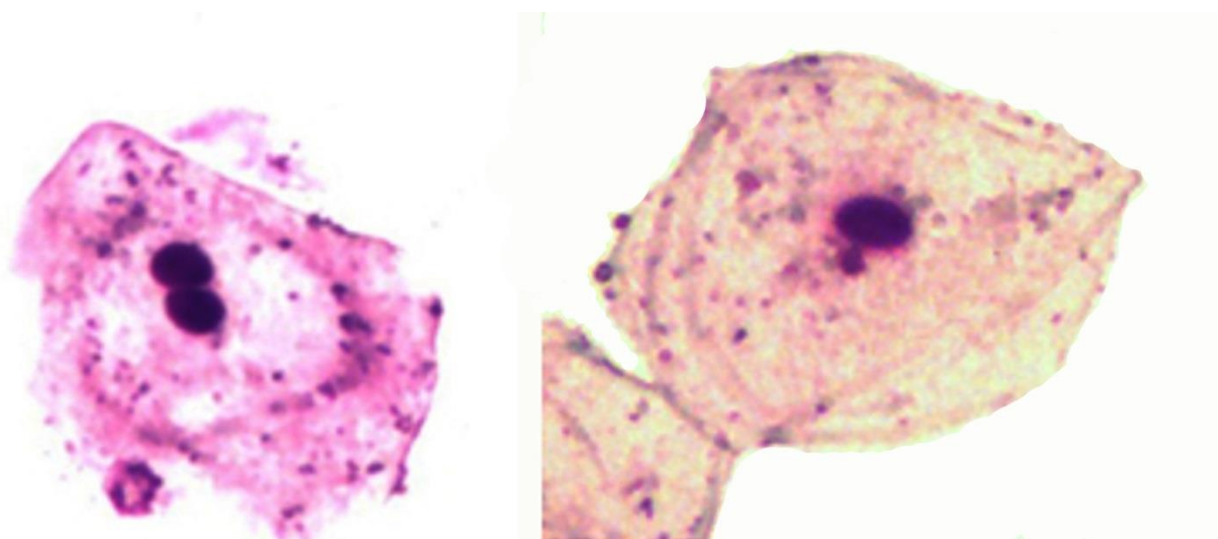


**Figure 3.** A core with a circular notch and with a protrusion of the "broken egg" type (x160)

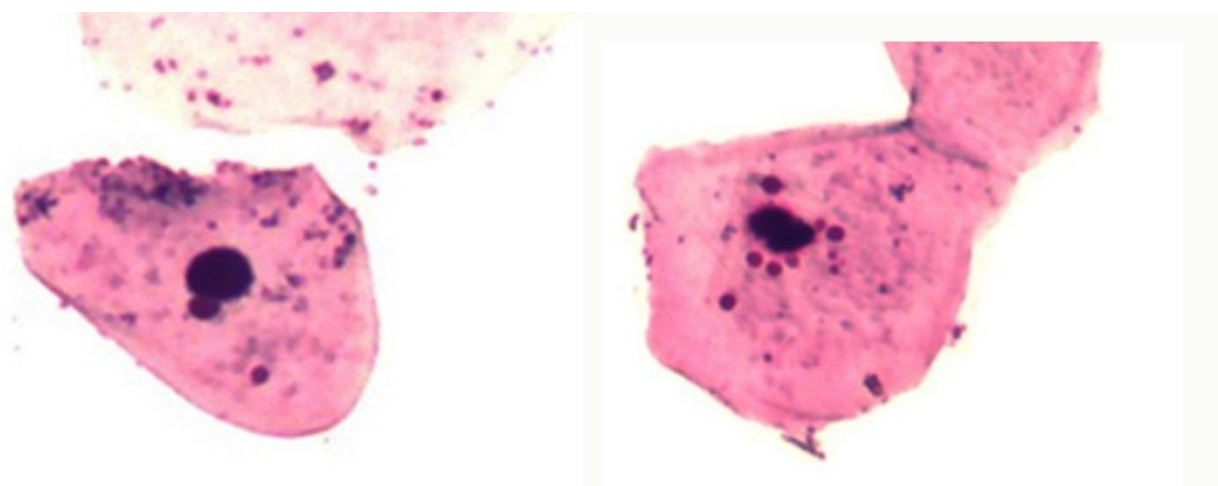


**Figure 4.** Cells of the buccal epithelium of the oral cavity with a protrusion of the "bubble" type and with apoptotic bodies (x160)

**UMA NOVA GEOMETRIA FRACTAL DOPING PARA NANOFIBRAS DE GRAFENO E A OTIMIZAÇÃO DE CRISTAL: UM ESTUDO DA TEORIA DA DENSIDADE FUNCIONAL (DFT)****A NOVEL FRACTAL GEOMETRY DOPING FOR GRAPHENE NANORIBBON AND THE OPTIMIZATION OF CRYSTAL: A DENSITY FUNCTIONAL THEORY (DFT) STUDY**JABBAR, Mohammed L.<sup>1\*</sup>; AL-SHEJAIRY, Kadhum J.<sup>2</sup><sup>1</sup> Physics Department, Science College, University of Thi- Qar, Nassiriya – Iraq.<sup>2</sup> Physics Department, Science College, University of Mustansiriyah – Iraq.*\*Corresponding Author**E-mail: mohammed25382@gmail.com*

Received 18 May 2020; received in revised form 22 June; accepted 04 July 2020

**RESUMO**

A dopagem química é uma rota promissora para projetar e controlar as propriedades eletrônicas de nanofibras de grafeno em zigue-zague (ZGNR). Utilizando os primeiros princípios dos cálculos da teoria funcional da densidade (DFT), no B3LYP / 6-31G, implementado no software Gaussian 09, várias propriedades, como a estrutura geométrica, o espectro de infravermelho DOS, HOMO, LUMO e o gap de energia do ZGNR foram investigadas com vários locais e concentrações de fósforo (P). Observou-se que o ZGNR pode ser convertido da dimensão linear para a fractal usando impurezas de fósforo (P). Também se destaca a árvore binária fractal das estruturas ZGNR e P-ZGNR. Os resultados demonstraram que a diferença de energia possui valores diferentes, localizados nessa faixa de 0,51eV a 1,158 eV para estruturas ZGNR e P-ZGNR intocadas. Essa faixa de gap de energia é variável de acordo com o uso de GNRs em qualquer aparelho. Então, o P-ZGNR tem comportamento semicondutor. Além disso, não há números de onda imaginários no espectro vibracional avaliado, confirmando que o modelo corresponde à energia mínima. Então, esses resultados fazem com que o P-ZGNR possa ser utilizado em várias aplicações, devido a essa estrutura ter se tornado mais estável e com menor reatividade.

**Palavras-chave:** *Nanofibras de grafeno, diferença de energia, Densidade de estado, espectros de infravermelho.***ABSTRACT**

Chemical doping is a promising route to engineering and controlling the electronic properties of the zigzag graphene nanoribbon (ZGNR). By using the first-principles of the density functional theory (DFT) calculations at the B3LYP/ 6-31G, which implemented in the Gaussian 09 software, various properties, such as the geometrical structure, DOS, HOMO, LUMO infrared spectra, and energy gap of the ZGNR, were investigated with various sites and concentrations of the phosphorus (P). It was observed that the ZGNR could be converted from linear to fractal dimension by using phosphorus (P) impurities. Also, the fractal binary tree of the ZGNR and P-ZGNR structures is a highlight. The results demonstrated that the energy gap has different values, which located at this range from 0.51eV to 1.158 eV for pristine ZGNR and P-ZGNR structures. This range of energy gap is variable according to the use of GNRs in any apparatus. Then, the P-ZGNR has semiconductor behavior. Moreover, there are no imaginary wavenumbers on the evaluated vibrational spectrum confirms that the model corresponds to minimum energy. Then, these results make P-ZGNR can be utilized in various applications due to this structure became more stable and lower reactivity.

**Keywords:** *Graphene Nanoribbon, energy gap, Density of State, Infrared spectra.*

## 1. INTRODUCTION:

Graphene nanoribbon (GNR) may be a sheet of graphite (monolayer) comprising of atoms  $sp^2$  hybridized C making a daily honeycomb (hexagonal) lattice. GNR has attracted considerable importance within the industry and research community thanks to its outstanding properties like structural, electronic, and optical. Recently, there has been outsized importance towards the realization, and studying of nanoribbon graphene supported devices of electronic design through the accurate structure of electronic tailoring that exploiting the electrical field effect and other fields of application as strain. In other words, the GNR has stimulated enormous outburst of experiment and theoretic fields an investigation (Aliofkhazraei *et al.* 2016); (Moghaddam *et al.* 2011); (Abbott's 2007); (Sahoo and Dutta 2012); (Banerjee and Sahoo 2013); (Bryan 2013).

Many reports (theoretical) proposed an electronic property (band structure) must appear that's presumed to account upon the shape and width (Oliveira Jr *et al.* 2015), additionally to the precise orientation for crystallographic of nanoribbon (Morozov *et al.* 2005); (Ezawa 2006); (Brey and Fertig 2006); (Shemella *et al.* 2007); (Son, Cohen, and Louie 2006a). GNRs with edges of shaped of zigzag are assumed to possess gaps of the direct band, where the gap lowers with width increasing, while edges of armchair-shape are often either semiconducting or metallic counting at widths (Nakada *et al.* 1996); (Wakabayashi *et al.* 1999); (Celis *et al.* 2016); (Neto *et al.* 2009); (Geim and Novoselov 2010); (Son, Cohen, and Louie 2006b); (Ajeel, Mohammed, and Khudhair 2019). One is aware that the stability of Hydrogen terminated GNR (Okada 2008); (Wassmann *et al.* 2008).

Benoit Mandelbrot (Mohammed Lateef Jabbar 2015); (Vass 2014); (Jebbar 2007); (Mohammed L Jabbar 2017) suggested the existence of geometries, referred to as geometry. A natural sort of fractal tree is represented by a binary fractal tree (BFT). Four factors specify a binary fractal tree ( $\theta_1$ ,  $\theta_2$ ,  $r_1$ , and  $r_2$ ). Where, the primary two factors (belong the angle) are the branching angles  $\theta_1$  and  $\theta_2$ , which may take any real values between  $0^\circ$  and  $360^\circ$  while the last two factors are the scaling ratios  $r_1$  and  $r_2$ , which may take any real values between 0 and 1 (Taylor 2005); (Pons 2013).

An intuitive explanation of a binary fractal

tree is as follows. Every tree features a trunk, which may be a closed vertical line segment of unit length. This trunk divides into two new branches at the highest. The primary branch has length  $r_1$  and makes of  $\theta_1$  angle with the affine trunk hull, and therefore the second branch has length  $r_2$  and makes of  $\theta_2$  angle with the affine trunk hull. Each of those two branches procedures the trunk of a sub-tree, i.e., it splits into two more branches, following an equivalent method. BFT is that the object obtained by applying the branching process to Infinitum (Taylor 2005); (Mandelbrot and Frame 1999); (Koch and Holthausen 2015) (Baughman, Zakhidov, and De Heer 2002) (Pons 2013). The density functional methods supply a strong instrument in quantum physics and computational nanoscience of atoms, (Parr 1980) molecules and other finite structures (Martin and Martin 2004). It proposes the density function rather than the wave function to explain the quantum systems (Wysokiński, Kuduk-Jaworska, and Michalska 2006). Born interpretation is one among methods that represent the theoretical basis of density functional theory (Tozer and De Proft 2005). It offers a chic formulation of the N electron system and computational efficiency (Young 2004). Electron density plays an important role in molecular structure, electrostatic potential, and contours (Koch and Holthausen 2015) (Koch and Holthausen 2015). Density functional theory (DFT) is additionally an approximation for the outline of the properties of the bottom state of insulators, metals, and semiconductors. The base state is unequivocally defined by the electron density (Mohammed L Jabbar 2018); (H Muzel, Alwan, and Jabbar 2017).

The main purpose of this paper was to study the binary fractal trees structure (with a scaling ratio  $r=r_1=r_2=1$  to make some structures of zigzag graphene nanoribbon (ZGNRs) doping by phosphorus atoms), and electronic properties of the graphene systems. Based on the first-principles of the density functional theory calculations, frontier orbital (highest occupied molecular orbital, HOMO, and lowest unoccupied molecular orbital, LUMO) distributions, the energy gaps, density of state and infrared spectra have been investigated.

## 2. MATERIALS AND METHODS:

Herein are hydrocarbons chains of aromatic polycyclic (PAHs) that are occupied as ZGNRs models of finite-size. The treated ZGNRs contain edges of zigzag shape on each side with passivation hydrogen to decrease the boundary



effects (Figure 1). The GNR may be a rectangular  $[n,m]$  with width  $m=4$  (in direction of armchair) and length  $n=6$  (in direction of zigzag).

## 2.1. Details of computation

All ZGNRs computations were carried out utilizing the method of DFT as applied within the Gaussian 09W software (Frisch *et al.* 2009). B3LYP (Stephens *et al.* 1994), as a functional hybrid that informs the exchange of Becke (Becke 1992) and correlation of Lee, Yang, and Parr's (Lee, Yang, and Parr 1988) the 3-21G (or 6-31G) means set of basis (Petersson and Al-Laham 1991), were utilized for the computation of quantum-chemical (H Muzel, Alwan, and Jabbar 2017); (Zandler and D'Souza 2006); (Rad 2016); (Yoosefian, Raissi, and Mola 2015). Before energy calculations for pristine ZGNR and with addition different atoms levels of P, whole systems are relaxed. This process is named geometry optimization. The GNR electronic characteristics such as DOS of analysis, energies of molecular highest occupied orbital (HOMO), molecular energies of lowest unoccupied orbital (LUMO), and gaps of energy (the eigenvalues difference the of the maximum valence band and therefore the band of minimum conduction or mathematically through express  $E_g = E_{LUMO} - E_{HOMO}$ ) are theoretically investigated along few impurities structures P by using fractal binary tree method as novel mathematically model for doping.

## 3. RESULTS AND DISCUSSION:

As a primary task, the researchers started by building a pristine, a ZGNR. It consists of 48 atoms. GNR rectangular  $[4, 6]$  (rectangular  $[n, m]$  with width equally ( $m = 4$  atoms) (in the armchair direction) and length equally ( $n = 6$  atoms)) of width adequate to 4 (in the trend of an armchair) and length appropriate to 6 (in the trend of zigzag), is GNR designated  $[4, 6]$ . The ZGNRs treated contain edges of a zigzag for a single side along with the passivation of Hydrogen to minimize the effects of the boundary. Method of DFT was used to optimize the structure geometrically along with the B3LYP functional of hybrid. The structure of the pure GNR  $[4, 6]$ , as elucidated in Figure 2, is consistent with GNRs are nowadays illustrious: their characters of electronic predicted to be considered upon the shape and width, additionally to the precise crystallographic orientation of the nanoribbon. However, it is not possible to observe the visible deformation of pure GNRs along its zigzag direction.

The model BFT can be applied in the doping process to get a new structure. An intuitive description of a BFT is as follows. Each tree features a trunk, which may be a closed vertical line segment of unit length (Figure 3a). This trunk divides into two new branches at the highest. One branch has length  $r_1$  and yields  $\theta_1$  angle with affine trunk hull, and therefore other branch has length  $r_2$  and yields  $\theta_2$  angle with affine trunk hull as illustrated in Figure 3b. Those 2 branches yields subtree trunk as elucidated in Figure 3c, i.e., it splits into two more branches, following an equivalent method., a pristine GNR was then doped with different impurities of phosphorus atom ( $P=2, 4, 8$ ). This addition of impurities obeyed to mathematically model. It's been wont to create nanostructures involving phosphorus element, theoretically, by using the geometry to urge a replacement structure to replace some carbon atoms within the pristine structure by the number of phosphorus atoms to offer the model binary fractal tree. Also, the models are geometrically optimized and need final arrangements (Figures 3 and 4).

As the fractal binary tree retains branching and splitting from 0 into 1 into 2 and so on., the binary tree is doing so, during this case, in base two and a scaling ratio  $r=r_1=r_2=1$ . The primary step of binary fractal tree does not have any value of angle with vertical line in other word, the angle value will adequate to zero. The second step branch trunk has one angle with a vertical line, while the third step has two angles on each side (Table 1).

Current surface is often expressed by high orbital's molecular occupation (HOMO) and low orbital's molecular occupation (LUMO). The abbreviations HOMO and LUMO occasionally ask the frontier orbitals in frontier molecular orbital theory. Figure 5 appears schematic HOMO, LUMO surfaces for pure GNR  $[4,6]$ , and GNR with P. The resulting orbitals could also be interpreted consistent with a molecular orbital theory, which considers the orbitals of the molecule because of the combination of linearity to the orbitals of molecule. The green color in figure 5 mentions positive a part of the function of the wave, whereas red color mentions the negative a part of the function of the wave. The energy gap may be a vital property in solids because it allows the prediction of the fabric, whether it's conductor or insulator or semiconductor. The bandgap is defined because of the difference in energy between the upper region of the valence band edge (VBE) and,

therefore, the lower region of conduction band edge (CBE).

Table 2 demonstrates the values of LUMO, HOMO, and energy gap for GNR and GNR with impurities (P=2, 4, and 8), respectively. During this work, the worth of the energy gap is calculated for pristine GNR following others obtained results (Son, Cohen, and Louie 2006a). Here energy values gap for both GNR and GNR with dopants performed by Gaussian 09 package. One note that the structures have different values of energy gap thanks to the various numbers and positions of dopants. Whereas, the electronic properties of GNR are quite different due to these different interfacial Interactions.

Figure 5 demonstrates that states density (DOS) versus energy according to the chemical structure of the material; naturally when the chemical structure is modified, at least, in theory, the DOS distribution should change. Generally, those impurities are called dopants, so the chemical composition changes by doping. The change within the energy distribution of the allowed states cannot have a general rule such as the bandgap will increase after the introduction of impurities from phosphorus.

The infrared spectral range is extensive, approximately from 12800 to 10  $\text{cm}^{-1}$  spectral region. In the IR spectrum, a molecule to be absorbed by the moment of the molecules should be expected to vary as a result of vibration and rotation frequencies. There are two sorts of stretching variations. The primary type is named symmetric stretching, which occurs when the vibration of atoms of equivalency occurred within an identical phase. The opposite last type is called stretching of asymmetric, which takes place when vibrations of bonds occur in different phases. IR spectrum shows information about the structure of a molecule. The frequencies of harmonic vibration are studied for pure P-GNRs and GNR. Figure 6a shows the peaks shape for pure GNR, while figures 6b – 6d elucidate that there is a peak replacement; a single peak denotes the bond between 2 atoms neighboring to each other. Figure 6a demonstrates some peaks in the 800-900  $\text{cm}^{-1}$  region (c-c single bond - aromatic atoms), whereas the peaks in 1200 - 1550  $\text{cm}^{-1}$  region are the (c=c double bond - aromatic atoms). The obtained results are following the experimental results (Dykstra *et al.* 2017). New bonds inform new modes of specific numbers wave, whereas spectra of infrared are effected by coordinates of geometry and topological characters. Figure 6 shows C-P and P-P bond, which is cause to point

out a replacement peak. These new peaks show thanks to strange atoms. Then the structure will become asymmetric.

#### 4. CONCLUSIONS:

The structures were extremely useful in making up apply devices because they need hetero-junction of band gap (the ability to fabricate P- and n-type regions is required). The calculations demonstrated that this work might be an example to use the mathematical model to make nanostructures involving phosphorus element by using the fractal geometry method to exchange some atoms in the pristine structure by phosphorus atoms. The model binary fractal tree can apply in doping process to get a new structure. The non-existence of imaginary wavenumbers on the evaluated vibrational spectrum confirms that the model corresponds to minimum energy.

#### 5. ACKNOWLEDGMENTS:

Authors express their appreciation because of the pc and knowledge Networking Center at Science of school for the assistance in facilities of computing of high-performance.

#### 6. REFERENCES:

1. Abbott's, In Edwin. 2007. "Graphene: Exploring Carbon Flatland." *Phys. Today* 60(8): 35.
2. Ajeel, Fouad N, Mohammed H Mohammed, and Alaa M Khudhair. 2019. "Energy Bandgap Engineering of Graphene Nanoribbon by Doping Phosphorous Impurities to Create Nano-Heterostructures: A DFT Study." *Physica E: Low-dimensional Systems and Nanostructures* 105: 105–15.
3. Aliofkhazraei, Mahmood, Ali, Nasar, Milne, William I, Ozkan, Cengiz S, Mitura, Stanislaw, and Gervasoni, Juana L. 2016. *Graphene Science Handbook: Electrical and Optical Properties*. CRC press.
4. Banerjee, D, and S Sahoo. 2013. "Energy Band Nonparabolicity and Density of States of Graphene."
5. Baughman, Ray H, Anvar A Zakhidov, and Walt A De Heer. 2002. "Carbon Nanotubes--the Route toward



- Applications." *science* 297(5582): 787–92.
6. Becke, Axel D. 1992. "Density-functional Thermochemistry. II. The Effect of the Perdew–Wang Generalized-gradient Correlation Correction." *The Journal of chemical physics* 97(12): 9173–77.
  7. Brey, Luis, and H A Fertig. 2006. "Electronic States of Graphene Nanoribbons Studied with the Dirac Equation." *Physical Review B* 73(23): 235411.
  8. Bryan, Sarah Elizabeth. 2013. "Structural and Electrical Properties of Epitaxial Graphene Nanoribbons."
  9. Celis, Arlenciu, Nair, M N, Taleb-Ibrahimi, Amina, Conrad, E H, Berger, Claire, De Heer, W A, and Tejeda, Antonio. 2016. "Graphene Nanoribbons: Fabrication, Properties and Devices." *Journal of Physics D: Applied Physics* 49(14): 143001.
  10. Dykstra, Haidee, Fisher, Ewan , Brooke, Sam, Way, Ashley, and Waterland, Mark . 2017. "Infrared and Raman Spectroscopy of Graphene Nanoribbons." *New Zealand Institute of Chemistry*. 166.
  11. Ezawa, Motohiko. 2006. "Peculiar Width Dependence of the Electronic Properties of Carbon Nanoribbons." *Physical Review B* 73(4): 45432.
  12. Frisch, MJE, Trucks, G W, Schlegel, H Bernhard, Scuseria, Gustavo E, Robb, Michael A, Cheeseman, James R, Scalmani, Giovanni, Barone, Vincenzo, Mennucci, Benedetta, and Petersson, GA. 2009. "Gaussian 09, Revision D. 01."
  13. Geim, Andre K, and Konstantin S Novoselov. 2010. "The Rise of Graphene." In *Nanoscience and Technology: A Collection of Reviews from Nature Journals*, World Scientific, 11–19.
  14. H Muzel, Maged, Abbas S Alwan, and Mohammed L Jabbar. 2017. "Electronical Properties for (C<sub>x</sub>H<sub>y</sub>Z<sub>2</sub>-NO) Nanoclusters." *Current Nanomaterials* 2(1): 33–38.
  15. Jabbar, Mohammed L. 2017. "Theoretical Study of The Transmittance Effect of Fractal Optical Modulator For CaF<sub>2</sub>." *Journal of Education for Pure Science* 7(2): 34–51.
  16. ———. 2018. "Some Electronical Properties for Coronene-Y Interactions by Using Density Functional Theory (DFT)." *Journal of Basrah Researches (Sciences)* 44(1A): 11–19.
  17. Jabbar, Mohammed Lateef. 2015. "Evaluation MTF for Output Signal from Fractal Optical Modulator Made of BaF<sub>2</sub> Material." *Journal of Education for Pure Science* 5(1): 19–28.
  18. Jebbar, M L. 2007. "Evaluation of MTF for Fractal Optical Modulator of Semiconductor." *MSc. Thesis, Al-Mustansiriyah University*.
  19. Koch, Wolfram, and Max C Holthausen. 2015. *A Chemist's Guide to Density Functional Theory*. John Wiley & Sons.
  20. Lee, Chengteh, Weitao Yang, and Robert G Parr. 1988. "Development of the Colle-Salvetti Correlation-Energy Formula into a Functional of the Electron Density." *Physical review B* 37(2): 785.
  21. Mandelbrot, Benoit B, and Michael Frame. 1999. "The Canopy and Shortest Path in a Self-Contacting Fractal Tree." *The Mathematical Intelligencer* 21(2): 18–27.
  22. Martin, Richard M, and Richard Milton Martin. 2004. *Electronic Structure: Basic Theory and Practical Methods*. Cambridge university press.
  23. Moghaddam, Nahid Shayesteh, Ahmadi, Mohammad Taghi, Rahmani, Meisam, Amin, Noraliah Aziziah, Moghaddam, Hossein Shayesteh, and Ismail, Razali. 2011. "Monolayer Graphene Nanoribbon Pn Junction." In *2011 IEEE Regional Symposium on Micro and Nano Electronics*, IEEE, 253–55.
  24. Morozov, S V, Novoselov, K S, Schedin, F, Jiang, D, Firsov, A A, and Geim, A K. 2005. "Two-Dimensional Electron and Hole Gases at the Surface of Graphite." *Physical Review B* 72(20): 201401.
  25. Nakada, Kyoko, Mitsutaka Fujita, Gene Dresselhaus, and Mildred S Dresselhaus. 1996. "Edge State in Graphene Ribbons: Nanometer Size Effect and Edge Shape Dependence." *Physical Review B* 54(24): 17954.
  26. Neto, A H Castro, Guinea, Francisco, Peres, Nuno M R, Novoselov, Kostya S, and Geim, Andre K. 2009. "The Electronic Properties of Graphene." *Reviews of*

27. Okada, Susumu. 2008. "Energetics of Nanoscale Graphene Ribbons: Edge Geometries and Electronic Structures." *Physical Review B* 77(4): 41408.
28. Oliveira Jr, Myriano H, Lopes, Joao Marcelo J, Schumann, Timo, Galves, Lauren A, Ramsteiner, Manfred, Berlin, Katja, Trampert, Achim, and Riechert, Henning. 2015. "Synthesis of Quasi-Free-Standing Bilayer Graphene Nanoribbons on SiC Surfaces." *Nature communications* 6(1): 1–7.
29. Parr, Robert G. 1980. "Density Functional Theory of Atoms and Molecules." In *Horizons of Quantum Chemistry*, Springer, 5–15.
30. Petersson, G A, and Mohammad A Al-Laham. 1991. "A Complete Basis Set Model Chemistry. II. Open-shell Systems and the Total Energies of the First-row Atoms." *The Journal of chemical physics* 94(9): 6081–90.
31. Pons, Bernat Espigule. 2013. "Generalized Self-Contacting Symmetric Fractal Trees." *Symmetry Cult Sci* 21: 333–51.
32. Rad, Ali Shokuhi. 2016. "Al-Doped Graphene as a New Nanostructure Adsorbent for Some Halomethane Compounds: DFT Calculations." *Surface Science* 645: 6–12.
33. Sahoo, S, and A K Dutta. 2012. "Graphene: A New Star in Material Science." *Int. J. Electrochem.*
34. Shemella, Philip, Zhang, Yiming, Mailman, Mitch, Ajayan, Pulickel M, and Nayak, Saroj K. 2007. "Energy Gaps in Zero-Dimensional Graphene Nanoribbons." *Applied Physics Letters* 91(4): 42101.
35. Son, Young-Woo, Marvin L. Cohen, and Steven G. Louie. 2006a. "Energy Gaps in Graphene Nanoribbons." 216803 (November): 1–4. <http://arxiv.org/abs/condmat/0611602%0A> <http://dx.doi.org/10.1103/PhysRevLett.97.216803>.
36. Son, Young-Woo, Marvin L Cohen, and Steven G Louie. 2006b. "Half-Metallic Graphene Nanoribbons." *Nature* 444(7117): 347–49.
37. Stephens, Philip J, F J Devlin, C F N Chabalowski, and Michael J Frisch. 1994. "Ab Initio Calculation of Vibrational Absorption and Circular Dichroism Spectra Using Density Functional Force Fields." *The Journal of physical chemistry* 98(45): 11623–27.
38. Taylor, Tara D. 2005. "Computational Topology and Fractal Trees."
39. Tozer, David J, and Frank De Proft. 2005. "Computation of the Hardness and the Problem of Negative Electron Affinities in Density Functional Theory." *The Journal of Physical Chemistry A* 109(39): 8923–29.
40. Vass, József. 2014. "On the Geometry of IFS Fractals and Its Applications."
41. Wakabayashi, Katsunori, Mitsutaka Fujita, Hiroshi Ajiki, and Manfred Sigrist. 1999. "Electronic and Magnetic Properties of Nanographite Ribbons." *Physical Review B* 59(12): 8271.
42. Wassmann, Tobias, Seitsonen, Ari P, Saitta, A Marco, Lazzeri, Michele, and Mauri, Francesco. 2008. "Structure, Stability, Edge States, and Aromaticity of Graphene Ribbons." *Physical review letters* 101(9): 96402.
43. Wysokiński, Rafał, Janina Kuduk-Jaworska, and Danuta Michalska. 2006. "Electronic Structure, Raman and Infrared Spectra, and Vibrational Assignment of Carboplatin. Density Functional Theory Studies." *Journal of Molecular Structure: THEOCHEM* 758(2–3): 169–79.
44. Yoosefian, Mehdi, Heidar Raissi, and Adeleh Mola. 2015. "The Hybrid of Pd and SWCNT (Pd Loaded on SWCNT) as an Efficient Sensor for the Formaldehyde Molecule Detection: A DFT Study." *Sensors and Actuators B: Chemical* 212: 55–62.
45. Young, David. 2004. *Computational Chemistry: A Practical Guide for Applying Techniques to Real World Problems*. John Wiley & Sons.
46. Zandler, Melvin E, and Francis D'Souza. 2006. "The Remarkable Ability of B3LYP/3-21G (\*) Calculations to Describe Geometry, Spectral and Electrochemical Properties of Molecular and Supramolecular Porphyrin–Fullerene Conjugates." *Comptes Rendus Chimie* 9(7–8): 960–81.

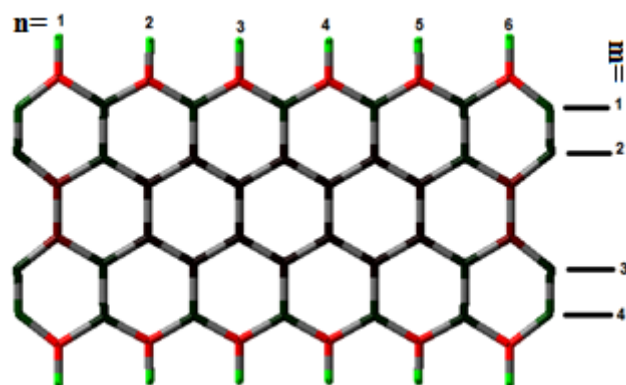


**Figure 1.** Grapheme of nanoribbon rectangular with width  $m = 4$  (in direction of armchair) and length  $n = 6$  (in direction of zigzag) of GNR designing [4, 6].

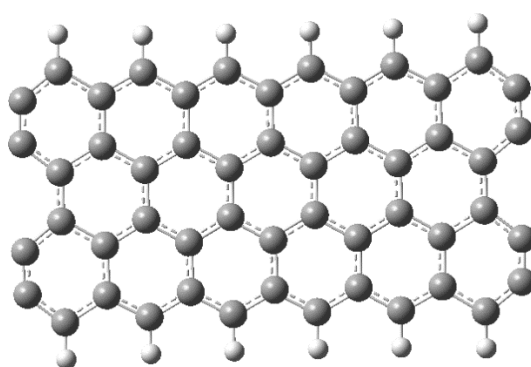


**Figure 2.** Pure GNRs structure of geometry

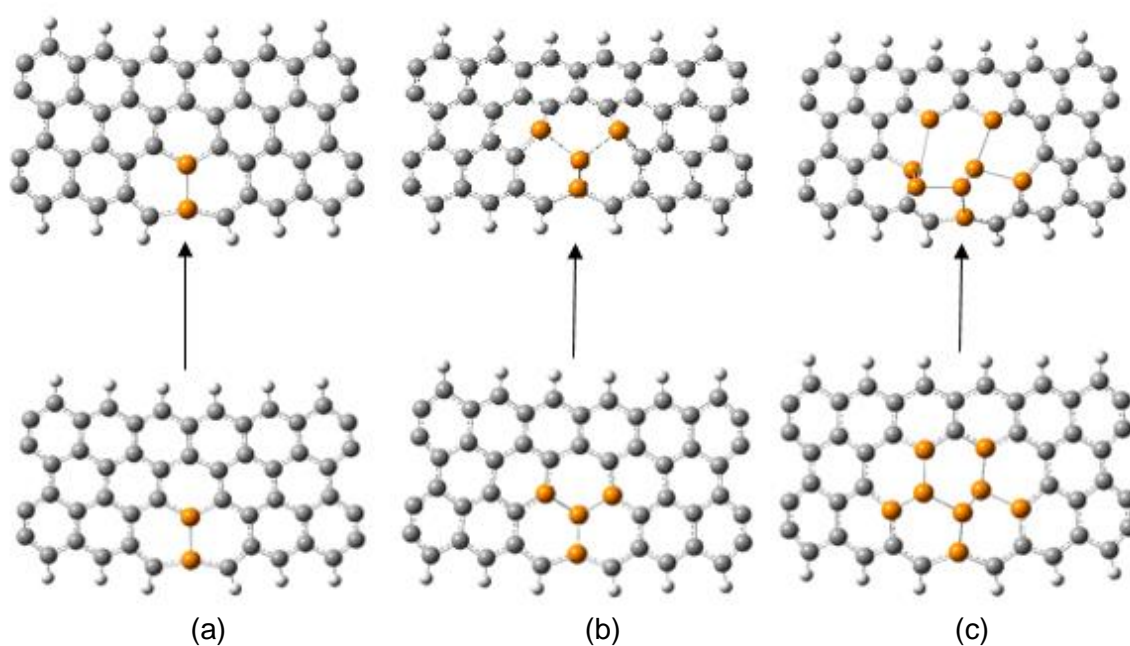


**Figure 3.** Structure of geometry after and before optimized of (a) two atoms of impurities P with GNRs (b) four atoms of impurities P with GNRs (c) eight atoms of impurities P with GNRs.

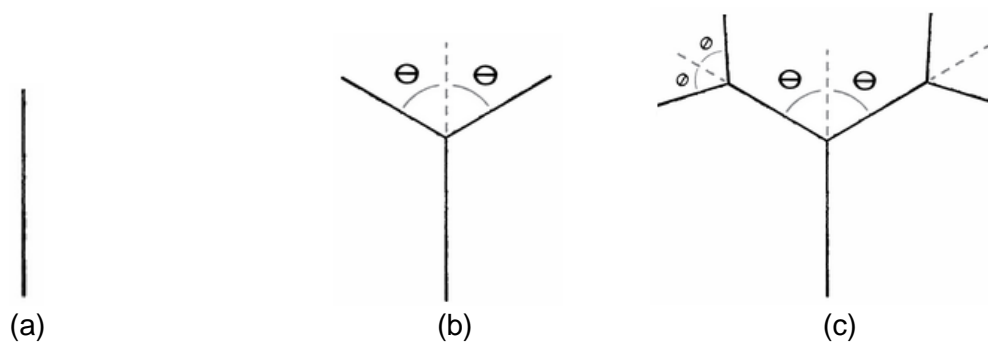
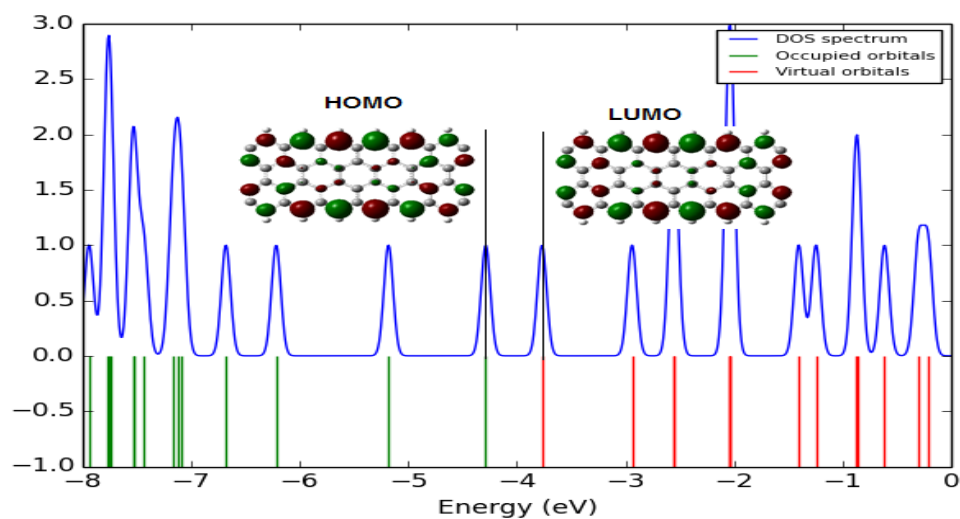
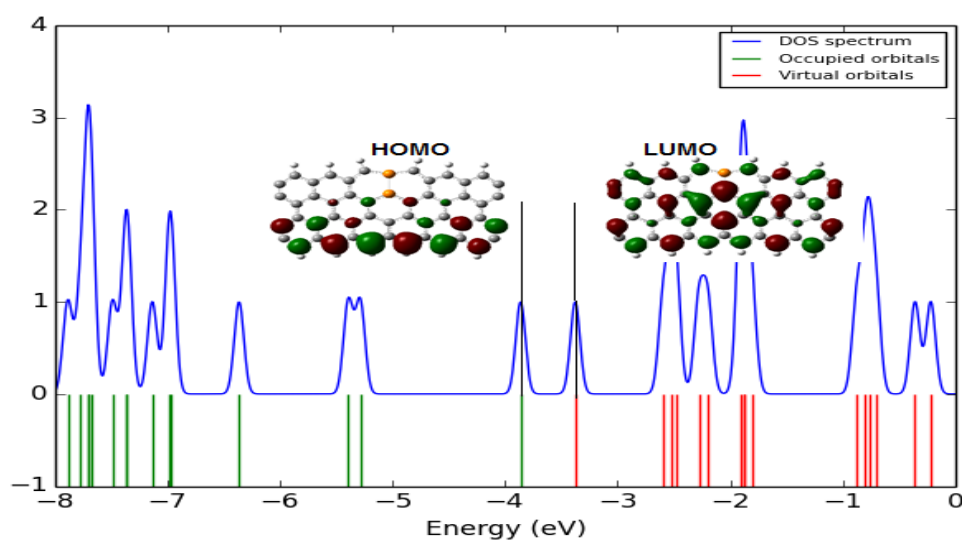


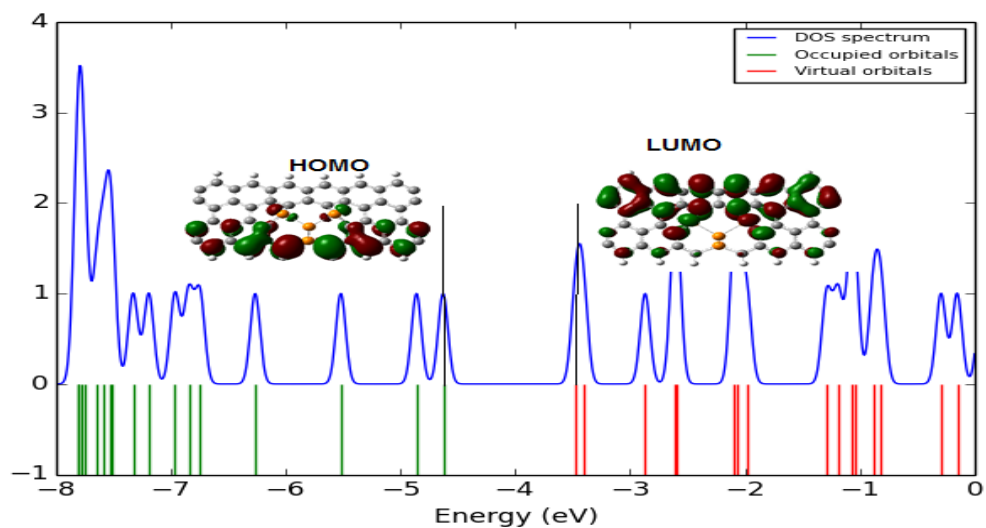
**Figure 4.** Fractal binary tree (a) the first step of doped. (b) the second step of doped. (c) the third step of doped.



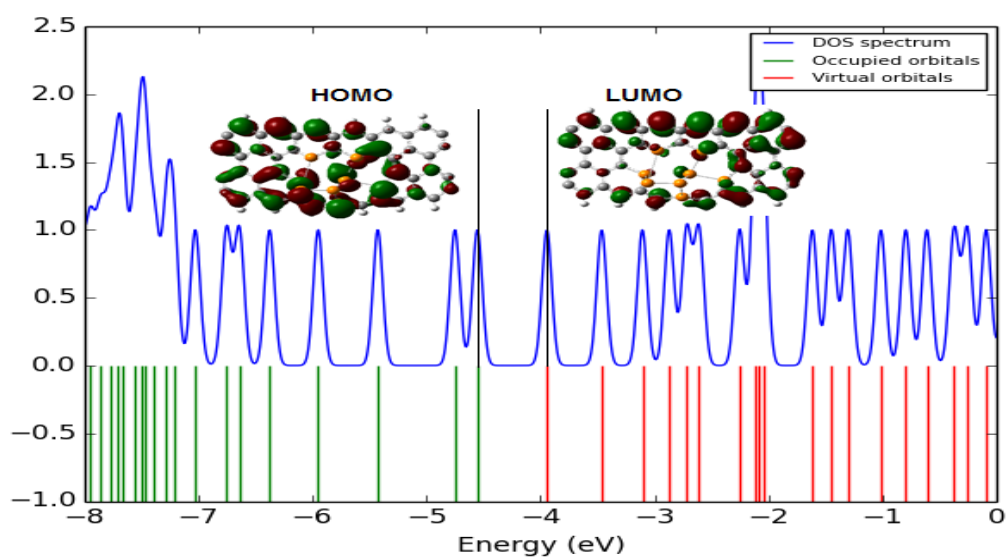
(a)



(b)

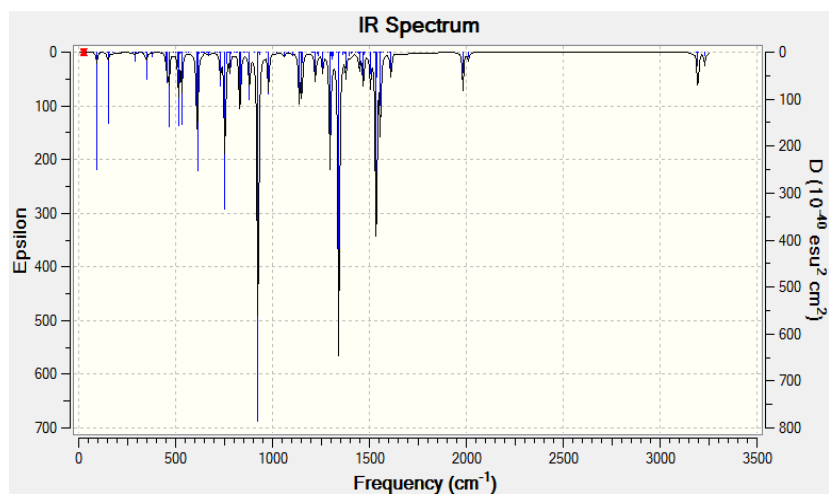


(c)

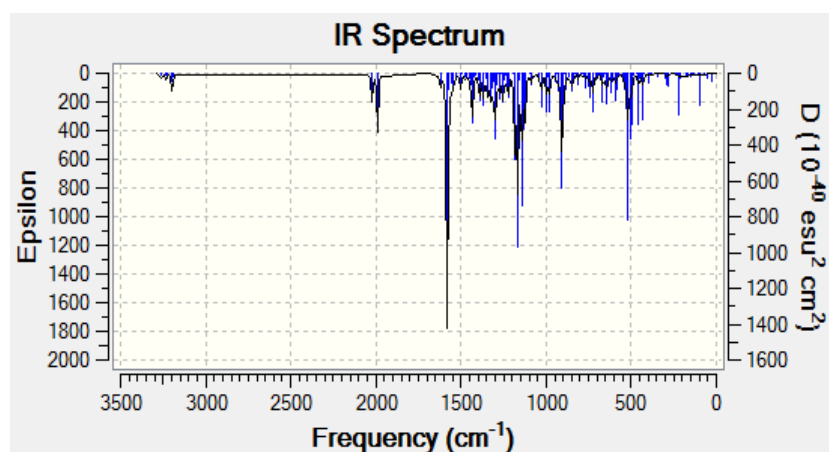


(d)

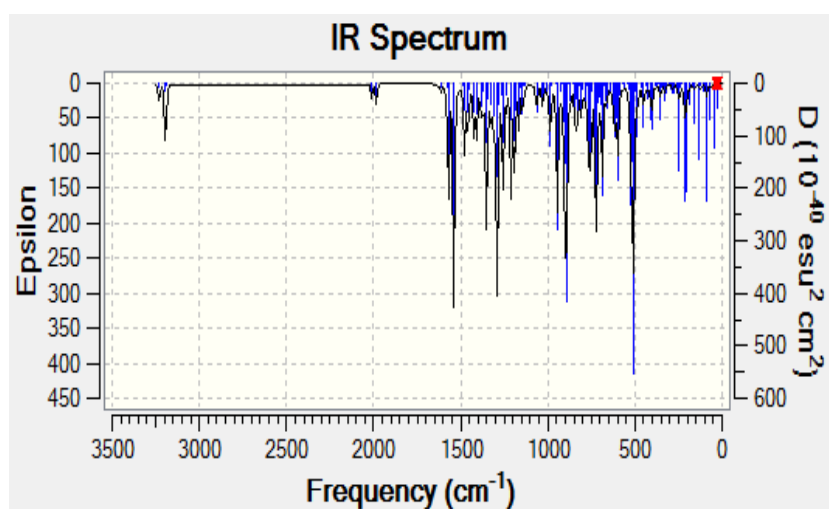
**Figure 5.** HOMOs scheme of the (left) and LUMOs (right) and density of state (DOS) of (a) pristine GNR [4, 6], (b) 2 P-GNR, (c) 4 P-GNR, and (d) 8 P-GNR.



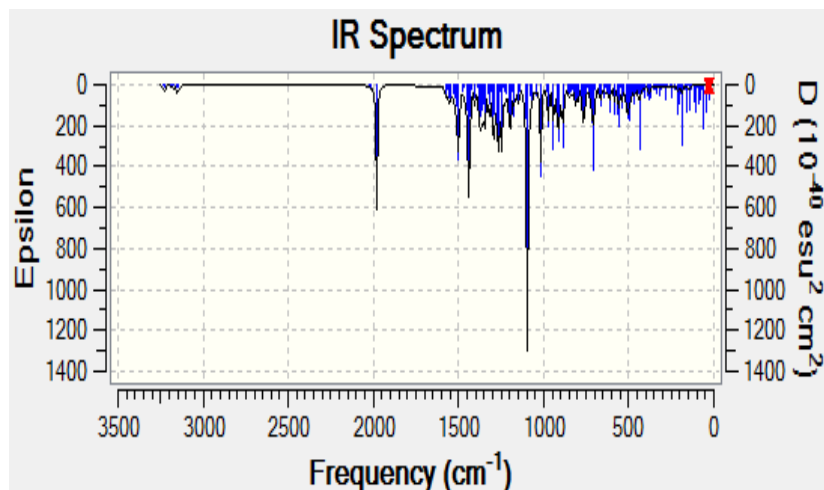
(a)



(b)



(c)



(d)

**Figure 6.** Infrared spectra of (a) pristine GNR (b) 2 P-GNR, (c) 4 P-GNR, and (d) 8 P-GNR

**Table 1.** Geometrical parameters optimized for S-GNR some selected branch order (Z) and angles (°).

| System | Branch order Z | $2^Z$ | Branch level | Angle $\theta$ (degree) |          |
|--------|----------------|-------|--------------|-------------------------|----------|
| 2-P    | 0              | $2^0$ | 1            | 0                       |          |
| 4-P    | 1              | $2^1$ | 2            | 51.181                  |          |
| 8-P    | 2              | $2^2$ | 4            | L=26.955                | R=41.371 |

Note: L: point out the left branch, and R: point out the proper branch on each side.

**Table 2.** The electronic states for pure GNR and nP- GNR (where n=2, 4, and 8)

| System       | HOMO (eV)    | LUMO (eV)    | $E_g$ (eV)  |
|--------------|--------------|--------------|-------------|
| Pristine GNR | -3.76768989  | -4.286611212 | 0.518921322 |
| 2 P- GNR     | -3.37666213  | -3.86211343  | 0.485451305 |
| 4 P- GNR     | -3.469997218 | -4.62838634  | 1.158389128 |
| 8 P - GNR    | -3.943475508 | -4.55382712  | 0.610351612 |

**EFICIÊNCIA DAS TECNOLOGIAS REMOTAS NA ABORDAGEM DO CONTEÚDO DE UM CURSO DE MATEMÁTICA E-LEARNING USANDO O SISTEMA MOODLE: ESTUDO DE CASO****EFFICIENCY OF REMOTE TECHNOLOGIES ON THE APPROACHING THE CONTENT OF A E-LEARNING MATHEMATICS COURSE USING MOODLE SYSTEM: CASE STUDY****ЭФФЕКТИВНОСТЬ ДИСТАНЦИОННЫХ ТЕХНОЛОГИЙ В РЕАЛИЗАЦИИ ЭЛЕКТРОННОГО ОБРАЗОВАТЕЛЬНОГО КУРСА ПО МАТЕМАТИКЕ, СОЗДАННОГО НА БАЗЕ LMS MOODLE: ТЕМАТИЧЕСКОЕ ИССЛЕДОВАНИЕ**

SOZONTOVA, Elena A.<sup>1\*</sup>; PRODANOVA, Natalia A.<sup>2</sup>; ZEKIY, Angelina O.<sup>3</sup>; RAKHMATULLINA, Leila V.<sup>4</sup>; KONOVALOVA, Elena V.<sup>5</sup>

<sup>1</sup> Kazan (Volga Region) Federal University, Elabuga Institute (branch), Department of Mathematics and Applied Informatics, Russian Federation.

<sup>2</sup> Plekhanov Russian University of Economics, Moscow, Russian Federation.

<sup>3</sup> Sechenov First Moscow State Medical University, Moscow, Russian Federation.

<sup>4,5</sup> Naberezhnye Chelny State Pedagogical University, Naberezhnye Chelny, Russian Federation.

\* Correspondence author  
e-mail: sozontova-elena@rambler.ru

Received 28 May 2020; received in revised form 26 June 2020; accepted 04 July 2020

**RESUMO**

No sistema de ensino superior, o ensino a distância usando cursos eletrônicos de educação está se tornando a maneira mais relevante e amplamente exigida de aprendizado. Isso se deve principalmente ao rápido processo mundial de digitalização da educação. Além disso, em conexão com a transição para um sistema educacional de dois níveis, o número de horas no currículo dedicado ao trabalho independente dos alunos aumentou significativamente. Essas tecnologias são uma boa ferramenta para organizar a independência cognitiva de um aluno. As vantagens são a capacidade de estudar a qualquer momento, em qualquer lugar, a capacidade de aprender no próprio ritmo e a capacidade de aprender sem interromper o trabalho. Por outro lado, existem algumas deficiências, como o problema de identificação do usuário e a necessidade de o aluno ter uma forte motivação. Este estudo teve como objetivo mostrar uma das opções para organizar o trabalho independente dos alunos no exemplo do curso educacional eletrônico "Matemática e fundamentos do processamento de informações matemáticas", criado com base no sistema LMS MOODLE. Participaram do experimento 30 estudantes de dois grupos acadêmicos (15 pessoas cada), com idades entre 16 e 17 anos, estudando na Universidade Federal do Instituto Elabuga de Kazan (Volga). Um dos grupos dominou a disciplina "Matemática e Fundamentos do Processamento de Informações Matemáticas" na forma tradicional, o outro grupo - na forma remota, usando o curso educacional eletrônico desenvolvido pelos autores. Depois de estudar o curso em ambos os grupos, foram realizados trabalhos de verificação e uma pesquisa. O processamento dos resultados do trabalho de controle usando métodos estatísticos possibilitou avaliar quanto o sucesso dos alunos em matemática depende da escolha da forma de treinamento. Os resultados da pesquisa permitiram aos autores formular maneiras de melhorar a qualidade da matemática do ensino a distância usando um curso educacional eletrônico.

**Palavras-chave:** *matemática, tecnologias de educação a distância, processamento de informações, avaliação de desempenho.*

**ABSTRACT**

In the higher education system, distance learning using electronic educational courses is becoming the most relevant and widely demanded way of learning. This is primarily due to the rapidly developing



worldwide process of digitalization of education. Besides, in connection with the transition to a two-level education system, the number of hours in the curriculum devoted to students' independent work has significantly increased. These technologies are a useful tool for organizing a student's cognitive independence. The advantages are the ability to study at any convenient time, anywhere, the ability to learn at one's own pace, and the ability to learn without interrupting work. On the other hand, there are some shortcomings, such as the problem of user identification and the need for the student to have strong motivation. This study aimed to show one of the options for organizing students' independent work on the example of the electronic educational course "Mathematics and Fundamentals of Mathematical Information Processing", created on the basis of the LMS MOODLE system. The experiment was attended by 30 students from two academic groups (15 people each) aged 16 to 17, studying at the Elabuga Institute of Kazan (Volga) Federal University. One of the groups mastered the discipline "Mathematics and Fundamentals of Mathematical Information Processing" in the traditional form, the other group - in the remote form using the electronic educational course developed by the authors. After studying the course in both groups, verification work and a survey were conducted. Processing the results of the control work using statistical methods made it possible to assess how much the success of students in mathematics depends on the choice of the form of training. The survey results allowed the authors to formulate ways to improve the quality of distance learning mathematics using an electronic educational course.

**Keywords:** *mathematics, distance educational technologies, information processing., performance evaluation.*

## АННОТАЦИЯ

В системе высшего образования дистанционное обучение с помощью электронных образовательных курсов становится наиболее актуальным и широко востребованным способом обучения. Это связано, в первую очередь, со стремительно развивающимся во всем мире процессом цифровизации образования. Кроме того, в связи с переходом на двухуровневую систему образования значительно возросло количество часов в учебном плане, отводимых на самостоятельную работу студента. Эти технологии являются хорошим инструментом для организации познавательной самостоятельности студента. Преимущества - способность учиться в любое удобное время и в любом месте, способность учиться в своем собственном темпе и способность учиться, не прерывая работу. С другой стороны, есть некоторые недостатки, такие как проблема идентификации пользователя и потребность в сильной мотивации учащегося. Целью данного исследования было показать один из вариантов организации самостоятельной работы студентов на примере электронного учебного курса «Математика и основы математической обработки информации», созданного на основе системы LMS MOODLE. В эксперименте приняли участие 30 студентов из двух академических групп (по 15 человек в каждой) в возрасте от 16 до 17 лет, обучающихся в Елабужском институте Казанского (Приволжского) федерального университета. Одна из групп освоила дисциплину «Математика и основы математической обработки информации» в традиционной форме, другая группа - в дистанционной форме с использованием электронного учебного курса, разработанного авторами. После изучения курса в обеих группах были проведены проверочные работы и опрос. Обработка результатов контрольной работы с использованием статистических методов позволила оценить, насколько успехи учащихся по математике зависят от выбора формы обучения. Результаты опроса позволили авторам сформулировать способы повышения качества дистанционного обучения математике с помощью электронного учебного курса.

**Ключевые слова:** *математика, дистанционные образовательные технологии, обработка информации, оценка эффективности.*

## 1. INTRODUCTION:

In connection with the transition to a two-level education system, the number of hours in the curriculum devoted to students' independent work has significantly increased. For its active organization, distance educational technologies are widely used. Also, these technologies play an essential role in the rapidly developing worldwide digitalization of education (Schmidt & Tang, 2020).

Remote educational technologies are understood to be technologies that are implemented primarily with the use of information and telecommunication networks with the indirect interaction of students and teachers (Kuderova *et al.*, 2019). There are various ways of organizing distance learning: using electronic educational resources (Anisimova & Krasnova, 2015; Akhmetshin *et al.*, 2019), digital educational resources, massive open online courses (MOOC), offering extensive interactive participation and open access through the

Internet (Kaplan & Haenlein, 2016).

Due to the intensification of the digitalization of education worldwide, not only colleges and universities but also schools pay attention to various ways of distance learning (Dawson *et al.*, 2009; Fuller, Vician, & Brown, 2006; Guri-Rosenblit, 2016; Kearsley, 2000). Online learning is gaining popularity every day, significantly expanding the educational space (Beese, 2014; Soekartawi, & Librero, 2002) and allowing students to independently study various educational programs (Aktaruzzaman & Plunkett, 2016).

In addition to the fact that distance educational technologies are an excellent tool for organizing a student's cognitive independence, there are many other advantages of their use.

Firstly, the opportunity to learn at a convenient time. Indeed, studying remotely, a student has the opportunity to build his or her own individual training schedule, determine when and how much time to spend studying a particular material (Nguyen, 2015).

Secondly, the ability to learn at one's own pace (Thoms & Eryilmaz, 2014). In the traditional form of training, the teacher, as a rule, focuses on a particular group of students – average performers. In the case of distance learning, the learning process takes place at a pace convenient for the student. He or she can always return to the study of more complex topics, re-examine the lecture material, ask questions to the teacher online.

Thirdly, the ability to learn in a convenient place (Bachmaier, 2011; So & Brush, 2008). With the remote form of training, a student can study without leaving home, which is especially important for people with disabilities, for people with small children.

Also, other significant advantages are the opportunity to learn without interrupting work; availability of training materials (with the remote form of training, all educational material, as a rule, is posted on the course);

Non less critical, it has to be considered the possibility of implementing an individual approach (Korableva *et al.*, 2019 a, b). In the traditional form of teaching, it is quite difficult for a teacher to pay attention to each student to adapt to the pace of each of them. In the case of the remote form, students have the opportunity to receive answers to their questions in a mode convenient for them.

Besides, the convenience for the teacher. With distance learning, the teacher can pay attention to each student, has the opportunity to observe the learning process, even while on a business trip. Although, at the same time, the load on the teacher increases, so it is necessary to provide the teacher with appropriate financial support, reduce his or her workload (Meyer & Barefield, 2010).

However, there are several disadvantages of this form of training, which make teachers doubt the effectiveness of the use of distance technologies in the educational process. Indeed, in the modern educational environment, the success of the introduction of distance learning largely depends on the perception of teachers.

One of the shortcomings is the need for a student to have strong motivation. Since the student learns all the material on a distance-learning basis, this requires good willpower, self-discipline, perseverance, and responsibility (Chow & Croxton, 2017).

Another topic is the bias toward theoretical knowledge. Indeed, with the remote form of training, it is rather difficult to carry out the study of disciplines that require a large number of practical classes. This is especially true for the disciplines of the natural science cycle.

The problem of monitoring the learning process is also relevant. Unfortunately, in most cases with distance learning, it is impossible to check how honestly the student is concerned with completing assignments and whether he or she performs them him/herself. Therefore, the final form of control should be carried out in the audience.

The impossibility of developing such personal qualities as sociability, teamwork, oratorical qualities (Joksimović *et al.*, 2015; Keller *et al.*, 2017; Liaw, Huang, & Chen, 2007; Xiao, 2018) might put this tool in doubt. At the same time, for people experiencing difficulties with socialization in the real world, distance learning is a definite plus, allowing one to get an education in a comfortable environment (Sazmandasfaranjan *et al.*, 2013)

Insufficient technical equipment of the teacher's and (or) student's workplace (Anderson & Dron, 2011; Hung, 2016; Rogerson-Revell, 2015) can also be faced as a disadvantage.

It is also important to remember the students' poor computer literacy (Hatlevik *et al.*,

2018; Hoffman & Vance, 2005) and insufficient degree of mastering the material compared to traditional training (Kirtman, 2009). For example, the number of students taking at least one online course increased in the USA in 2013 to 6.7 million people (Allen & Seaman, 2013). At the same time, the Pew Research Center found that, although many college leaders in America said their institutions offered online courses, only 50% agreed that these courses were at the same level as traditional study classes (Parker *et al.*, 2011).

There are also institutional and financial problems that hinder the spread of distance technologies in the educational environment. The lack of qualified teachers (Baran *et al.*, 2011), weak government support (Piña, 2010), unequal competitive conditions (Drori, 2015; Zawacki-Richter & Anderson, 2014). Even in an academic environment, such a concept as "brand" is crucial. Therefore, large universities will have a more significant competitive advantage, positioning themselves as experts in creating educational materials of the required quality. They will also be more competitive because of the economic benefits of the number of students enrolling in their courses, as large universities have more opportunities to expand the audience of their courses through, for example, opening branches and representative offices in the regions. However, in turn, this forces regional universities to focus on more innovative teaching principles.

Thus, distance learning is a rapidly developing field in the field of education, including higher education (Reese, 2015). Distance education is developing per the goals set to increase the power, speed, and accessibility of educational technologies (Conde *et al.*, 2014; Shannon & Rice, 2017).

However, despite the advantages of distance learning, there are obstacles of a personal, institutional, and financial nature for the holistic implementation of the distance learning system in the educational process (Leontyeva, 2018).

Therefore, this study aimed to show one of the options for organizing students' cognitive activity that allows students to organize their independent work as efficiently as possible (by the example of the distance course "Mathematics and Fundamentals of Mathematical Information Processing," created based on the LMS MOODLE system), to evaluate the effectiveness of the use of distance learning technologies in the study of

mathematics and formulate possible ways to improve the quality of distance learning mathematics using an electronic educational course (based on statistical data collected in the process of students' work on the indicated course).

## 2. MATERIALS AND METHODS:

First, the authors briefly describe the structure of the course "Mathematics and Fundamentals of Mathematical Information Processing," created based on the LMS MOODLE system at the Elabuga Institute (branch) of the Kazan (Volga) Federal University (KFU) and posted on the KFU website for distance education (edu.kpfu.ru), disclose the algorithm for working with it, and then reveal the essence of the pedagogical experiment conducted by the author of the article to evaluate the effectiveness of the use of distance learning technologies in the study of higher mathematics at a university.

This educational distance learning course consists of the following topics (sections):

1. The primary means of presenting information in mathematics and their use in the pedagogical activity.
2. Elements of set theory. Counts. Functions.
3. Elements of probability theory.
4. Aspects of mathematical statistics.

Each section has the following structure (see Table 1):

**Table 1. Section Structure**

| <b>№</b> | <b>Components</b>  |
|----------|--|
| 1.       | Methodical recommendations to the student on the study of the topic. |
| 2.       | Lecture material.  |
| 3.       | Questions for self-control.  |
| 4.       | Test.  |
| 5.       | Verification work.   |
| 6.       | List of references.  |
| 7.       | Glossary.  |
| 8.       | Forum.   |

The content of the course is entirely consistent with the work program of the discipline.

The study of each section should begin by reading the guidelines (see Table 2), which

allow the student to build an algorithm for his work on the topic.

Each section includes lecture notes and self-examination questions (see Table 3). After studying the lecture material, the student proceeds to questions. Questions for self-control allow the student to evaluate the success of mastering the studied material independently. If difficulties arise with the answers to them, the student can return to studying the part of the lecture material that caused the challenges. Next, the student proceeds to test (see Table 4), the results of which demonstrate the degree to which the student has mastered this material and the possibility of moving to the study of a new section. Each test contains from 5 to 10 questions. The correct answer to one question is estimated at one point. To proceed to the next step (performing verification work), it is necessary that the student have at least 50% of the correct answers. As noted above, one of the features of LMS MOODLE is the ability to customize the course so that students get access to subsequent classes only after completing previous tasks. Therefore, it is possible to open for students' access to following forms of control only after completing the previous form for a satisfactory assessment. Testing can also be repeated if the initial result does not meet the requirements established by the teacher (these attempts are visible to the teacher from his/her personal account). The final form of control for each section (except section 1, which is primarily theoretical, and involves only the execution of the test) is the verification work (typical tasks for each topic can be seen in table. 5). The completed verification work is sent to the teacher for evaluation. Based on these forms of control, an assessment is made.

After studying all the sections, it is necessary to pass the final test, the questions (tasks) of which cover all the lecture and practical material on the course. The ultimate test consists of 30 questions (see Table 4). It includes questions from all the tests that are in sections 1-4.

Each section also includes a list of references, which can be useful in the case of questions in the process of studying the material. The student can also ask a question directly to the teacher on the course using interactive forms of communication integrated into the LMS MOODLE system (forum, chat), and the student can find the basic definitions and terms encountered in the process of studying the discipline in the glossary.

As noted above, one of the drawbacks of distance learning is the fact that it is impossible to evaluate how honestly one or another student completes assignments fully, it is impossible to verify whether he or she independently completed the proposed appointments. Therefore, the course ends with a final verification work, which is conducted in the audience and includes tasks from each topic of the course (see Table 5).

The study involved 30 students aged 16 to 17 years of first year at the Faculty of History and Philology of the Elabuga Institute of Kazan (Volga Region) Federal University. Among them were 26.67 percent of boys (8) and 73.33 percent of girls (22).

The experiment was conducted from September 2018 to December 2018.

At the beginning of the 1st semester (the 2018-2019 academic year), two groups of students were selected studying in the direction of 44.03.05 – Pedagogical Education (with two training profiles). The profile of the preparation of group No. 1 is the Russian Language and Literature, that of group No. 2 is History and Social Studies. The first group mastered the discipline "Mathematics and Fundamentals of Mathematical Information Processing" in remote form using the electronic educational course described above, the second - in the traditional style.

Since distance learning is currently very relevant, it is fully implemented at the Yelabuga Institute. Each university teacher develops electronic training courses that are widely used in teaching. Students subscribe to these courses without fail and undergo training under strict supervision.

The written permissions of the subjects to use their personal data allowed us to process their exam results, verification work, and survey.

In each group, 15 students were selected (in the first group there were 12 girls, 3 boys, in the second - 10 girls, 5 boys) with the following scores for the exam in mathematics (basic level):

Group No. 1 – 11, 12, 14, 12, 15, 16, 15, 16, 14, 16, 17, 16, 13, 14, 12.

Group No. 2 – 12, 11, 16, 14, 16, 14, 16, 14, 11, 15, 16, 17, 12, 13, 15.

Students were selected in such a way that their math exam results were not significantly different from each other.

First, it is necessary to find out whether it is advisable to experiment with these students. To do this, it is necessary to find the coefficient of variation. In this case, quantitative data (exam results) will be interpreted using one of the methods of statistical information processing - correlation analysis. First, it is necessary to calculate the sample average (1):

$$\bar{x} = \frac{\sum_i x_i}{\sum_i n_i} = \frac{11 + \dots + 15}{30} = 14.17 \quad (1)$$

Next, it is needed to find the error of representativeness of the sample average (2):

$$S_x = \sqrt{\frac{\sum_i (x_i - \bar{x})^2}{n(n-1)}} \approx 0.3427 \quad (2)$$

Finally, need to find the coefficient of variation (3):

$$C_x = \frac{S_x}{\bar{x}} \cdot 100\% = \frac{0.3427}{14.17} \cdot 100\% \approx 2.42\% \quad (3)$$

These calculations were performed in MS Excel.

Since in this case, the coefficient of variation is less than 3%, therefore, the participants in the groups do not significantly differ from each other in the number of USE scores in mathematics, and research can be carried out.

As mentioned above, in group No. 1, classes were conducted in a remote format using the course described above, and group No. 2 studied in the audience. At the end of the semester after completing the course, verification work was carried out (in the audience) in both groups (see Table 5). The results of the verification work (in percent) of students selected for research are as follows:

Group No. 1: 62, 70, 80, 78, 74, 65, 75, 76, 60, 76, 60, 74, 64, 58, 78.

Group No. 2: 75, 80, 85, 82, 79, 72, 85, 88, 74, 70, 74, 88, 70, 78, 94.

It is necessary to evaluate how different the effectiveness of the test work is (and, consequently, the result of mastering the discipline as a whole) depending on the form of training. For this, it is necessary to find the coefficient of determination. At the same time, quantitative data (results of verification work) will

be interpreted using one of the methods of statistical information processing - correlation analysis.

First, find the average value and variance in each group.

Group No. 1 (4)-(5):

$$\bar{x}_1 = \frac{\sum_i x_i}{\sum_i n_i} = \frac{62 + \dots + 78}{15} = 70. \quad (4)$$

$$D_1 = \frac{\sum_i (x_i - \bar{x}_1)^2}{\sum_i n_i} = 55,067. \quad (5)$$

Group No. 2 (6)-(7):

$$\bar{x}_2 = \frac{\sum_i x_i}{\sum_i n_i} = \frac{75 + \dots + 94}{15} = 79.6. \quad (6)$$

$$D_2 = \frac{\sum_i (x_i - \bar{x}_2)^2}{\sum_i n_i} = 141,6. \quad (7)$$

It is necessary to find the average value for all students (8):

$$\bar{x} = \frac{\sum_i \bar{x}_i \cdot N_i}{\sum_i N_i} = \frac{70 \cdot 15 + 79,6 \cdot 15}{30} = 74,8. \quad (8)$$

It is needed to compute the intragroup dispersion (9):

$$D_{intragroup} = \frac{\sum_i D_i \cdot N_i}{\sum_i N_i} \approx 98,333. \quad (9)$$

Then, it is necessary to find the intergroup variance (10):

$$D_{intergroup} = \frac{\sum_i (\bar{x}_i - \bar{x})^2 N_i}{\sum_i N_i} = 23,04. \quad (10)$$

Using the two previous values, need to find the total variance (11):

$$D_{total} = 98,333 + 23,04 = 121,373. \quad (11)$$

Finally, it is necessary to calculate the coefficient of determination, which characterizes how strongly the success of mastering the

material and the result of learning the discipline as a whole depends on the choice of the form of training (12):

$$\eta^2 = \frac{D_{intergroup}}{D_{total}} \approx 0,1898. \quad (12)$$

These calculations were carried out in MS Excel.

To improve the quality of distance learning mathematics using the electronic educational course in group No. 1, in addition to the test work, a survey was conducted (see Table 6). Data was collected and then placed in a database to organize information. Quantitative data were interpreted using descriptive analysis.

**Table 6.** Questionnaire Content

| No | Question   |
|----|--|
| 1. | Did you enjoy studying math with the e-learning course?              |
| 2  | Do you think that distance learning is as effective as traditional?  |
| 3. | What are the main advantages and disadvantages of distance learning. |

### 3. RESULTS AND DISCUSSION:

The described experiment was conducted in order to assess the effectiveness of the use of an electronic educational course in the study of the discipline "Mathematics and the foundations of mathematical processing of information." For this, 30 students from two groups (15 people each) were selected. The first group during the semester studied mathematics in remote form using the electronic educational course described above, the second in the traditional form.

The processing of experimental results can be divided into three stages.

Initially, it was necessary to assess how appropriate it was to conduct an experiment among selected students. For this, based on the results of the exam in mathematics, the coefficient of variation was calculated  $C_x \approx 2,42 \%$ .

The coefficient of variation allows to determine whether the subjects differ

significantly from each other according to one or another sign.

It is generally accepted that differences between subjects in some way are insignificant if the coefficient of variation does not exceed 5%. To increase the reliability level of an experiment, this bar is sometimes reduced to 3%. Since in this case, the coefficient of variation is less than 3%, therefore, the participants in the groups do not significantly differ from each other in the number of USE scores in mathematics, and research can be carried out.

In the second stage, it was necessary to evaluate how strongly the success of mastering the discipline "Mathematics and the foundations of mathematical processing of information" depends on the choice of the form of training. To do this, at the end of the semester after studying all sections, verification work was carried out in both groups (see table. 1). Using the correlation analysis based on the results of the verification work, the coefficient of determination was calculated  $\eta^2 \approx 0,1898$ . Translating this value into percent, we have:  $0,1898 \cdot 100\% \approx 19\%$ .

The coefficient of determination allows to determine how strongly the results of the subjects are due to their belonging to a particular group.

The obtained result indicates that the success of mastering mathematics by 19% depends on the choice of the form of training. In order to determine which particular form of training is more effective, we compare the average values of the results of the test work of each group:  $\bar{x}_1 = 70$ ,  $\bar{x}_2 = 79,6$ . Since, therefore, it is traditional learning that is 19% more effective than distance learning.

At the third stage, in order to improve the quality of distance learning mathematics using an electronic educational course, a survey was conducted in group No. 1 (see Table 2).

When answering the first question, 80% (12 people) of the respondents answered in the affirmative.

When answering the second question, approximately 73% of respondents (11 people) answered in the affirmative.

In answering the third question, students identified both the advantages and disadvantages of distance learning. They noted that the advantages of distance learning are that it is possible to study material and perform tasks

anywhere, in any free time, from any electronic device with Internet access. Students also noted a wide variety of teaching and assessment materials. Besides, students indicated that the electronic course is equipped with a lot of background information.

The main disadvantages of distance learning, according to the respondents, are the lack of full communication with teachers and fellow students (80% - 12 respondents), the lack of skills necessary for working with an electronic educational course (60% - 9 respondents), the difficulty of independent study of some topics ( $\approx$  53.3% - 8 respondents), lack of video materials (20% - 3 respondents), negative attitude of parents to distance learning ( $\approx$  13.3% - 2 respondents).

Thus, the results of the survey allowed us to formulate ways to increase the effectiveness of the developed electronic course in the study of mathematics. It is necessary:

- to conduct part of the lessons in the format of a video conference (LMS Moodle does not have a video chat function, however, Moodle can be combined with other software products);
- develop a training manual with a detailed description of the functionality of LMS Moodle or conduct an introductory training session to build skills with the electronic course;
- supplement the most complex topics with video lectures;
- attend orientation lectures with students and their parents to popularize distance learning.

Further research by the authors will focus on improving the quality of distance learning mathematics using an electronic educational course and assessing the effectiveness of distance learning in the study of other academic disciplines involving more students in the experiment.

#### 4. CONCLUSIONS:

The students better assimilated the material in the traditional form of training. However, in cases where a student's presence in the audience is impossible for any reason (illness, family circumstances, etc.), distance courses, make it possible to remotely organize independent work of students and contribute to the development of self-education.

#### 5. REFERENCES

1. Aktaruzzaman, M., & Plunkett, M. (2016). An Innovative Approach toward a Comprehensive Distance Education Framework for a Developing Country. *American Journal of Distance Education*, 30(4), 211-224. <https://doi.org/10.1080/08923647.2016.1227098>
2. Akhmetshin, E. M., Bochkareva, T. N., Tikhonova, A. N. (2019). Analysis and classification of digital educational resources used in the work of a proactive teacher. Paper presented at the Proceedings - International Conference on Developments in eSystems Engineering, DeSE, October-2019, 9073282, 199-204.
3. Allen, I. E., & Seaman, J. (2017). Digital Compass Learning: Distance Education Enrollment Report 2017. *Babson Survey Research Group*.
4. Anderson, T., & Dron, J. (2011). Three generations of distance education pedagogy. *The International Review of Research in Open and Distributed Learning*, 12(3), 80-97. <https://doi.org/10.19173/irrod.v12i3.890>
5. Anisimova T.I., & Krasnova L.A. (2015). Interactive Technologies in Electronic Educational Resources. *International Education Studies*. 8(2), 186-194. <http://dx.doi.org/10.5539/ies.v8n2p186>
6. Bachmaier, R. (2011). Fortbildung Online. Entwicklung, Erprobung und Evaluation eines tutoriell betreuten Online-Selbstlernangebots für Lehrkräfte (Doctoral dissertation).
7. Baran, E., Correia, A. P., & Thompson, A. (2011). Transforming online teaching practice: Critical analysis of the literature on the roles and competencies of online teachers. *Distance Education*, 32(3), 421-439. <https://doi.org/10.1080/01587919.2011.610293>
8. Beese, J. (2014). Expanding learning opportunities for high school students with distance learning. *American Journal of Distance Education*, 28(4), 292-306. <https://doi.org/10.1080/08923647.2014.959343>

9. Chavan, A., & Pavri, S. (2004). Open-source learning management with Moodle. *Linux Journal*, 2004(128), 2.
10. Chow, A. S., & Croxton, R. A. (2017). Designing a Responsive e-Learning Infrastructure: Systemic Change in Higher Education. *American Journal of Distance Education*, 31(1), 20-42. <https://doi.org/10.1080/08923647.2017.1262733>
11. Conde, M. Á., García-Peñalvo, F. J., Rodríguez-Conde, M. J., Alier, M., Casany, M. J., & Piguillem, J. (2014). An evolving Learning Management System for new educational environments using 2.0 tools. *Interactive Learning Environments*, 22(2), 188-204. <https://doi.org/10.1080/10494820.2012.745433>
12. Dawson, S. P., Bakharia, A., & Heathcote, E. (2009). Social networks adapting pedagogical practice: SNAPP.
13. Drori, G. (2015). Branding universities: Trends and strategies. *International Higher Education*, (71), 3-5. <https://doi.org/10.6017/ihe.2013.71.6083>
14. Fuller, R. M., Vician, C., & Brown, S. A. (2006). E-learning and individual characteristics: the role of computer anxiety and communication apprehension. *The Journal of Computer Information Systems*, 46(4), 103-15.
15. Guri-Rosenblit, S. (2016). Distance higher education in the digital era: Challenges and prospects. *Distance Education in China*, 6, 16-25.
16. Hatlevik, O. E., Throndsen, I., Loi, M., & Gudmundsdottir, G. B. (2018). Students' ICT self-efficacy and computer and information literacy: Determinants and relationships. *Computers & Education*, 118, 107-119. <https://doi.org/10.1016/j.compedu.2017.11.011>
17. Hoffman, M. E., & Vance, D. R. (2005, February). Computer literacy: what students know and from whom they learned it. *In ACM SIGCSE Bulletin*, 37(1), 356-360.
18. Hung, M. L. (2016). Teacher readiness for online learning: Scale development and teacher perceptions. *Computers & Education*, 94, 120-133. <https://doi.org/10.1016/j.compedu.2015.11.012>
19. Joksimović, S., Gašević, D., Loughin, T. M., Kovanović, V., & Hatala, M. (2015). Learning at distance: Effects of interaction traces on academic achievement. *Computers & Education*, 87, 204-217. <https://doi.org/10.1016/j.compedu.2015.07.002>
20. Kaplan, A. M., & Haenlein, M. (2016). Higher education and the digital revolution: About MOOCs, SPOCs, social media, and the Cookie Monster. *Business Horizons*, 59 (4), 441-50. doi:10.1016/j.bushor.2016.03.008
21. Kearsley, G. (2000). Online education: Learning and teaching in cyberspace. *Wadsworth Publishing Company*.
22. Keller, J. M., Ucar, H., & Kumtepe, A. T. (2017). Culture and Motivation in Globalized Open and Distance Learning Spaces. *Supporting Multiculturalism in Open and Distance Learning Spaces*, 146.
23. Kirtman, L. (2009). Online Versus In-Class Courses: An Examination of Differences in Learning Outcomes. *Issues in Teacher Education*, 18 (2), 103-115.
24. Korableva, O., Durand, T., Kalimullina, O., & Stepanova, I. (2019a). Usability testing of MOOC: Identifying user interface problems. Paper presented at the ICEIS 2019 - Proceedings of the 21st International Conference on Enterprise Information Systems, 2 468-475.
25. Kuderova, I. G., Ryumshin, A. V., Gayazova, S. R., Romanova, E. V., & Erzinkyan, E. A. (2019). Entrepreneurial skills development through distance learning. *Journal of Entrepreneurship Education*, 22, 1-12.
26. Leontyeva I.A. (2018). Modern distance learning technologies in higher education: Introduction problems. *Eurasia Journal of Mathematics, Science and Technology Education*, 14(10). em1578. <https://doi.org/10.29333/ejmste/92284>
27. Liaw, S., Huang, H., & Chen, G. (2007). Surveying instructor and learner attitudes. *Computers & Education*, 49(1),



- 1066-1080.  
<https://doi.org/10.1016/j.compedu.2006.01.001>
28. Meyer, J. D., & Barefield, A. C. (2010). Infrastructure and administrative support for online programs. *Online Journal of Distance Learning Administration*, 13(3), n3.
  29. Nguyen, T. (2015). The Effectiveness of Online Learning: Beyond No Significant Difference and Future Horizons. *MERLOT Journal of Online Learning and Teaching*. 11(2), 309-319.
  30. Parker, K., Lenhart, A., & Moore, K. (2011). The digital revolution and higher education: College presidents, public differ on value of online learning. *Washington, D.C.: Pew Research Center*.
  31. Piña, A. A. (2010). Online diploma mills: Implications for legitimate distance education. *Distance Education*, 31(1), 121-126.  
<https://doi.org/10.1080/01587911003725063>
  32. Reese, S. A. (2015). Online learning environments in higher education: Connectivism vs. dissociation. *Education and information technologies*, 20(3), 579-588. <https://doi.org/10.1007/s10639-013-9303-7>
  33. Rogerson-Revell, P. (2015). Constructively aligning technologies with learning and assessment in a distance education master's programme. *Distance Education*, 36(1), 129-147. <https://doi.org/10.1080/01587919.2015.1019972>
  34. Sazmandasfaranjan, Ya., Shirzad, F., Baradari, F., Salimi, M., & Salehi, M. (2013). Alleviating the Senses of Isolation and Alienation in the Virtual World: Socialization in Distance Education. *Procedia - Social and Behavioral Sciences*, 93, 332-337.  
[doi:10.1016/j.sbspro.2013.09.199](https://doi.org/10.1016/j.sbspro.2013.09.199)
  35. Schmidt J.T., Tang M. (2020) Digitalization in Education: Challenges, Trends and Transformative Potential. In: Harwardt M., Niermann PJ., Schmutte A., Steuernagel A. (eds) *Führen und Managen in der digitalen Transformation*. Springer Gabler, Wiesbaden.
  36. Shannon, L. J. Y., & Rice, M. (2017). Scoring the Open Source Learning Management Systems. *International Journal of Information and Education Technology*, 7(6), 432-436.
  37. So, H. J., & Brush, T. A. (2008). Student perceptions of collaborative learning, social presence and satisfaction in a blended learning environment: Relationships and critical factors. *Computers & education*, 51(1), 318-336.  
<https://doi.org/10.1016/j.compedu.2007.05.009>
  38. Soekartawi, H. A., & Librero, F. (2002). Greater Learning Opportunities Through Distance Education: Experiences in Indonesia and the Philippines. *Journal of Southeast Asian Education*. 3(2), 283-320.
  39. Thoms, B., & Eryilmaz, E. (2014). How media choice affects learner interactions in distance learning classes. *Computers & Education*, 75, 112-126.  
<https://doi.org/10.1016/j.compedu.2014.02.002>
  40. Xiao, J. (2018). On the margins or at the center? Distance education in higher education. *Distance Education*, 259-274.  
<https://doi.org/10.1080/01587919.2018.1429213>
  41. Zawacki-Richter, O., & Anderson, T. (Eds.). (2014). *Online distance education: Towards a research agenda*. Athabasca University Press.

**Table 2.** *Methodical recommendations to the student on the study of the topic*

| <b>Nº</b> | <b>Step</b>  |
|-----------|--|
| 1.        | Learn the lecture material.  |
| 2.        | Answer questions for self-control. If the questions are complicated, you need to study the lecture material again.   |
| 3.        | Study the primary literature, familiarize yourself with additional literature, new publications in periodicals, and familiarize yourself with the glossary.  |
| 4.        | Run a test. Proceeding to the next step requires that there are at least 50% correct answers. If you have less than 50% of the right answers, you need to study the lecture material again and rerun the test. |
| 5.        | Perform test work. Make a report as a file and send it to the teacher for verification.  |
| 6.        | If necessary, you can ask the teacher a question in the forum that arose while studying the topic or offer a topic for discussion.   |

**Table 3. Questions for self-control**

| Topics<br>(sections)   | Questions  |
|--|--|
| The main means of presenting information in mathematics and their use in pedagogical activity. | <ol style="list-style-type: none"> <li>1. What is information?</li> <li>2. What is the axiomatic method?</li> <li>3. What is mathematical modeling?</li> <li>4. What means of presenting information models do you know?</li> <li>5. What types and methods of giving information do you know?</li> </ol>  |
| Elements of set theory. Counts. Functions.   | <ol style="list-style-type: none"> <li>1. What is a graph?</li> <li>2. What methods of defining graphs do you know?</li> <li>3. What is it «mathematical set»? What set is called empty, finite, infinite?</li> <li>4. What are the basic operations on sets?</li> <li>5. What is a function?</li> </ol>   |
| Elements of probability theory.  | <ol style="list-style-type: none"> <li>1. What events are called reliable, impossible, random?</li> <li>2. What is the probability of a random event?</li> <li>3. What are the conditions for the applicability of the theorems of addition and multiplication of probabilities?</li> <li>4. What are the conditions for the applicability of the total probability formula, the Bayes formula.</li> <li>5. What numerical characteristics of random variables do you know?</li> </ol> |
| Elements of mathematical statistics.   | <ol style="list-style-type: none"> <li>1. What is the subject of mathematical statistics?</li> <li>2. What is called the population, sample, variation series, statistical series?</li> <li>3. List measures of central tendency, measures of variability.</li> <li>4. What are the dispersion characteristics of the variational series.</li> <li>5. What criteria for testing statistical hypotheses do you know?</li> </ol>   |

**Table 4. Test tasks**

| Topics<br>(sections)   | Questions   |
|--|---|
| The main means of presenting information in mathematics and their use in pedagogical activity. | <p>1. Experimental studies give:</p> <p>a) criteria for assessing the validity and acceptability in the practice of any theories and theoretical assumptions;</p> <p>b) the approach of the provisions on the study of the assessment of the acceptability of certain conclusions;</p> <p>c) means for obtaining knowledge about the object of study;</p> <p>2. How many stages is the process of mathematical modeling divided into? Write down the answer in numerical format.</p> <p>3. Is the statement true: "The first stage of mathematical modeling is the formulation of laws linking the main objects of the model"?</p> <p>a) yes; b) no.</p> <p>4. What is a translation of text from German into Russian?</p> <p>a) information search;</p> <p>b) data structuring;</p> <p>c) changing the presentation of information;</p> <p>d) obtaining new information.</p> <p>5. The second stage of mathematical modeling is:</p> <p>a) the formulation of laws linking the main objects of the model;</p> <p>b) the study of mathematical problems that lead to a mathematical model;</p> <p>c) ascertaining whether the accepted hypothetical model meets the criteria of practice.</p>   |
| Elements of set theory. Counts. Functions.   | <p>1. Set the correspondence between the name of the set and its designation:</p> <p>1) set of natural numbers;                      a) <math>\mathbb{N}</math>;</p> <p>2) the set of integers;                              b) <math>\mathbb{Q}</math>;</p> <p>3) set of rational numbers.                      c) <math>\mathbb{Z}</math>.</p> <p>2. Were given the following sets: <math>A = \{2; 4; 6\}</math>, <math>B = \{4; 6; 8; 10\}</math>. Find <math>A \setminus B</math>. Choose one answer:</p> <p>a) <math>\{2\}</math>; b) <math>\{4;6\}</math>; c) <math>\{4;6;8;10\}</math>.</p> <p>3. Set the correspondence between the designation of the operation and its name.</p> <p>1) <math>A \Delta B</math>;    a) difference / remainder;</p> <p>2) <math>A \cup B</math>;    b) crossing;</p> <p>3) <math>A \setminus B</math>;    c) combination;</p> <p>4) <math>A \cap B</math>;    d) symmetric difference.</p> <p>4. If <math>A</math> is the set of even natural numbers, and <math>B = \{11, 22, 33, 44, 55, 66, 77\}</math>, then the number of elements of the set <math>A \cap B</math> is equal (write down the answer in numerical format): ...</p> <p>5. If <math>A</math> is a set of natural numbers less than 10, and <math>B = \{8,9,10,11,22\}</math>, then the number of elements of the set <math>A \setminus B</math> is equal (write down the answer in numerical format): ...</p> |

Elements of probability theory.

6. Many points that can be connected by lines are called ....
  7. A closed route is called ....
  8. What is called the Euler path in the graph?
    - a) a path containing all edges of the graph;
    - b) a path that can be drawn on a plane so that no two of its edges have other common points except a common vertex;
    - c) only edges of the directed graph;
    - d) a path containing all edges of the graph whose degrees of adjacent vertices are 1.
  9. The function  $f(x) = x + \sin 2x$  is given. Find  $f(0)$ .
    - a) 0; b) 2; c) 1; d) -1.
  10. Find the domain of the function  $y = \ln(1-x^2)$ .
    - a)  $(0;1]$ ; b)  $(-1;1)$ ; c)  $(-\infty;-1) \cup (1;+\infty)$ ; d)  $[-1;1]$ .
- 
1. In the task "Two shots are fired at a target. Find the probability that the target will be hit once. The test is:
    - a) the target will be hit twice;
    - b) two shots are fired at the target;
    - c) the target will be hit once.
  2. A dice is thrown. Let us designate the events: A - "loss of 6 points", B - "loss of 4 points", D - "loss of 2 points", C - "loss of an even number of points". Then event C is equal to:
    - a)  $C=A+D$ ; b)  $C=A+B+D$ ; c)  $C=A \cdot B \cdot D$ ; d)  $C=A+B$ .
  3. Match:
    - 1) Event - "the letter M is selected from the word MIR "is; a) reliable;
    - 2) Event - "from an urn containing only white balls retrieve white ball "is; b) impossible;
    - 3) Event - "the letter K is selected from the word CHALLENGE is. c) random.
  4. If the complete system consists of 2 incompatible events, then such events are called ...
  5. Two students pass the exam. Events: A - "the first student will pass the exam", B - "the second student will pass the exam" are:
    - a) joint; b) independent; c) incompatible.
  6. Test - "throw two coins." Event - "at least one of the coins will have a coat of arms". The number of elementary outcomes conducive to this event is (write down the answer in numerical format): ...
  7. The probability for a student to pass the first exam is 0.6, the second 0.4. The probability of passing at least one exam is:
    - a) 0,24; b) 0,52; c) 0,76; d) 1.

|                                      |  |
|--------------------------------------|--|
| Elements of mathematical statistics. | <p>8. There are 10 textbooks on the shelf in random order. Of these, 1 in mathematics, 2 in chemistry, 3 in biology and 4 in geography. The student randomly took 1 textbook. What is the likelihood that he will be either in mathematics or in chemistry?</p> <p>a) 0,1; b) 0,2; c) 0,3; d) 0,24.</p> <p>9. There are 2 white, 3 black balls in the urn. Two balls are taken out of the urn in a row. The probability that both balls are white is equal (write down the answer in numerical format): ...</p> <p>10. Projects from three competing firms come for examination. The probability that the project of the first company will pass the examination with a positive assessment is 0.8, the second - 0.6, the third - 0.9. For examination, only one project was chosen at random. He passed it with a good mark. What is the likelihood that this was a project of the first company? Write down the answer in numerical format.</p> <p>1. Which statement about the general and sample populations is true?</p> <p>a) the sample and the population are equal in number;</p> <p>b) the sample - part of the general;</p> <p>c) the population is part of the sample.</p> <p>2. The sum of the frequencies of the sign is equal to:</p> <p>a) 0; b) 1; c) sample size n.</p> <p>3. A polyline, the segments of which connect the points with the coordinates <math>(x_i, n_i)</math>, where <math>x_i</math> is the value of the variational series, <math>n_i</math> - is the frequency, is called ....</p> <p>4. The statistical hypothesis is called:</p> <p>a) an assumption regarding the size of the population;</p> <p>b) an assumption regarding the size of the sample;</p> <p>c) an assumption regarding the parameters or type of distribution law of the population.</p> <p>5. Is the true statement "The sample mean is the interval estimate of the mathematical expectation <math>M(X)</math>, and the sample variance is the point estimate of the variance <math>D(X)</math>"?</p> <p>a) yes; b) no.</p> |
|--------------------------------------|--|

**Table 5.** Verification task for students

| Topics<br>(sections)                                | Task   |
|---|--|
| Elements of<br>set theory.<br>Counts.<br>Functions. | <p>1. Two hundred forty applicants passed the Russian language exam, of which 170 people got a score lower than 5 points, 205 people passed this exam, i.e. got grades 3, 4 or 5. How many people got grades 3 and 4?</p> <p>2. Out of 37 students of the Faculty of Philology, 15 students received an excellent rating in Russian, 14 in literature, 18 in linguistics, 6 in Russian and literature, 9 in Russian and linguistics, in all three disciplines – 4. How many students received at least one mark of "5"?</p> <p>3. Badminton competitions are attended by ten athletes. Competitions are held according to the Olympic system, in which a participant is eliminated from the tournament after the first loss. What is the minimum number of hours that competition can be held if the organizing committee has 2 courts at its disposal and an hour is allocated for each meeting, including warm-up and relaxation?</p>  |
| Elements of<br>probability<br>theory.               | <p>4. For the exam, it was necessary to prepare answers to 30 examination papers. The student prepared only 25 of them. He takes out two examination papers in turn. Find the likelihood that he will pass the exam if it is necessary to answer at least one examination paper for this, and the first examination paper taken by the student contained unlearned questions?</p> <p>5. The same verification work was carried out in two groups. In the first group of 25 students, 8 received the "excellent" mark for their works, in the second, consisting of 30 students, there were 6 "excellent" works. What is the likelihood that the chosen random work from the randomly selected group will be "excellent"?</p>   |
| Elements of<br>mathematical<br>statistics.          | <p>6. Let a set of attribute values be given: 15; 20; 18; 20; 25; 11; 12; 13; 24; 23; 23; 24; 21; 22; 21; 23; 23; 22; 21; 14; 14; 22; 15; 16; 20; 20; 16; 16; 20; 17; 17; 17. It is necessary to compile a variational and statistical series of the distribution, to calculate the numerical characteristics.</p> <p>7. Five students were selected for participation in the programming Olympiad. A computer program records the time for solving each task (three tasks in total):<br/> the time to solve the first task (min): 24, 16, 12, 5, 6;<br/> the time to solve the second task (min): 18, 14, 10, 4, 16;<br/> the time to solve the third task (min): 22, 15, 16, 12, 8.<br/> It is necessary to determine whether there are statistically significant differences between the time of solving the tasks?</p> <p>8. Fifteen first-year students were selected. They were asked the question "How much time did you spend preparing for the standings?" Their answers (in hours): 8, 6, 3, 1, 0, 5, 9, 2, 1, 4, 6, 10, 0, 3, 6. It is necessary to find the coefficient of variation and draw an appropriate conclusion.</p> |

## PRODUTIVIDADE DE NOVOS HÍBRIDOS DE MILHO NAS CONDIÇÕES DOS URAIS

## PRODUCTIVITY OF NEW MAIZE HYBRIDS IN CONDITIONS OF THE URALS

## ПРОДУКТИВНОСТЬ НОВЫХ ГИБРИДОВ КУКУРУЗЫ В УСЛОВИЯХ ПРЕДУРАЛЬЯ

ISMAGILOV, Raphael<sup>1\*</sup>; SOTCHENKO, Elena<sup>2</sup>; AKHIYAROV, Bulat<sup>1</sup>; ISLAMGULOV, Damir<sup>3</sup>; NURLYGAJANOV, Razit<sup>3</sup>

<sup>1</sup> Federal State Budgetary Educational Institution of Higher Education "Bashkir State Agrarian University", Department of crop production, plant breeding, and biotechnology. Russian Federation

<sup>2</sup> Federal State Budgetary Scientific Institution "All-Russian Research Scientific Institute of Corn", Department of corn breeding for immunity. Russian Federation

<sup>3</sup> Federal State Budgetary Educational Institution of Higher Education "Bashkir State Agrarian University", Department of soil science, agrochemistry, and precision agriculture. Russian Federation

\* Corresponding author  
e-mail: ismagilov.raf@rambler.ru

Received 20 April 2020; received in revised form 16 June 2020; accepted 25 June 2020

### RESUMO

**Objetivos.** A pesquisa teve como objetivo identificar os híbridos mais produtivos selecionados pelo Instituto *All-Russian* de Pesquisa de Milho para cultivar pela tecnologia de sementes de cereais nas condições naturais dos Cis-Urais. **Metodologia.** O milho foi cultivado para sementes e forragem verde para animais de fazenda nas condições dos Cis-Urais. A massa verde do milho, composta principalmente por caules e folhas, geralmente contém de 88 a 90% de água. A ensilagem preparada para isso possui menos matéria seca e proteínas. Essas forragens têm baixo valor nutricional e baixo retorno dos produtos pecuários. Os alimentos mais nutritivos e de alta qualidade podem ser recebidos a partir de sementes de milho ou de sua massa acima do solo, com grãos leitosos e maduros. Selecionar híbridos de maturação precoce com alto valor nutricional é a principal preocupação do estudo. **Resultados.** Os resultados demonstram que a produtividade dos híbridos de milho varia de 2,50 a 6,76 t/ha, dependendo do solo e das condições climáticas. Quando os híbridos de milho são cultivados por tecnologia de sementes, a massa acima do solo das culturas estudadas é de 30,68-68,80 t/ha. **Conclusões.** É necessário selecionar maturação anterior e híbridos altamente produtivos para aumentar a qualidade e nutrição da ração para milho. Os híbridos recomendados para a produção de grãos são Ural 150 (5,45 t/ha), Baikal (5,38 t/ha) e Mashuk 170 MV (4,98 t/ha); K-170 (56,7 t/ha), Shihan (55,67 t/ha) e Mashuk 170 MV (54,99 t/ha) que proporcionaram uma maior produção da massa verde na maturação grãos leitosos, melhores para produção de silagem. Os dados resultantes permitem selecionar híbridos de milho com alto rendimento e valor nutricional para fazendas com condições similares de solo e clima e desenvolver dietas para gado leiteiro e de corte altamente produtivo.

**Palavras-chave:** massa acima do solo; grão; híbridos; milho; produção.

### ABSTRACT

**Objectives.** The research aimed to identify the most productive hybrids selected by the All-Russian Research Institute of Maize to cultivate by the cereal seed technology in the natural conditions of the Middle Cis-Urals. **Methodology.** Maize was cultivated for seeds and green fodder for farm animals in the conditions of the Middle Cis-Urals. The maize green mass, consisting mainly of stems and leaves, usually contains up to 88-90% water. Silage being prepared for it has less dry matter and protein. Such fodder has low nutritional value and poor return from livestock products. The most high quality and nutritious feed can be received from maize seeds or its above-ground mass with seeds of milky-wax and wax ripeness. To select early-maturing hybrids with high nutritional value is the primary concern for the studied area. **Results.** The results demonstrate that the productivity of maize hybrids ranges from 2.50 to 6.76 t/ha depending on soil and climatic conditions. When maize hybrids are grown by seed technology, the above-ground mass of the studied crops is 30.68-68.80 t/ha. **Conclusions.** It is necessary to select earlier ripening and highly productive hybrids to increase the quality and nutrition of corn feed. The recommended hybrids for grain production are Ural 150 (5.45 t/ha), Baikal (5.38 t/ha) and Mashuk 170 MV



(4,98 t/ha); K-170 (56,7 t/ha), Shihan (55,67 t/ha) and Mashuk 170 MV (54,99 t/ha) that provided a higher output of the green mass at milky-wax ripeness of grain are best for silage production. The resulting data make it possible to select maize hybrids with high yields and nutritional value for farms with similar soil and climate conditions and to develop diets for highly productive dairy and beef cattle.

**Keywords:** above-ground mass; grain; hybrids; maize; yield.

## АННОТАЦИЯ

Цели. Данное исследование имело целью выявить наиболее высокопроизводительные гибриды кукурузы для выращивания в естественных условиях Среднего Предуралья среди отобранных Всероссийским научно-исследовательским институтом кукурузы образцов. Методология. Кукурузу выращивали на семена и зеленый корм для сельскохозяйственных животных в условиях Среднего Предуралья. Зеленая масса кукурузы, состоящая в основном из стеблей и листьев, обычно содержит в своем составе до 88-90% воды. Однако, в готовом силосе сухого вещества и белка содержится меньше. Соответственно, такой корм имеет низкую пищевую ценность и его использование влечет сокращение объемов производства продукции животноводства. Наиболее качественный и питательный корм можно получить из семян кукурузы в фазе молочно-восковой и восковой спелости. Выбор для изготовления корма раннеспелых гибридов с высокой питательной ценностью является основной задачей исследуемой агропромышленной области. Результаты. Результаты данного исследования показывают, что урожайность гибридов кукурузы колеблется от 2,50 до 6,76 т/га в зависимости от почвы и климатических условий. При выращивании гибридов кукурузы в соответствии с семенной технологией, надземная масса исследуемых культур составляет 30,68-68,80 т/га. Выводы. С целью повышения качества и питательности корма, необходимо выбирать более ранние и высокопроизводительные гибриды кукурузы. Рекомендованными для производства зерна являются гибриды Уральский 150 (5,45 т/га), Байкал (5,38 т/га) и Машук 170 MB (4,98 т/га); K-170 (56,7 т/га), Шихан (55,67 т/га) и Машук 170 MB (54,99 т/га), которые обеспечивали более высокую урожайность зеленой массы для производства силоса при созревании зерна молочно-восковой спелости. Полученные данные позволяют выбирать гибриды кукурузы с высокой урожайностью и питательной ценностью для ферм с аналогичными почвенными и климатическими условиями и разрабатывать рационы для эффективного функционирования молочного и мясного скотоводства.

**Ключевые слова:** надземная масса, зерно, гибриды, кукуруза, урожайность.

## 1. INTRODUCTION:

Maize growing is a traditional source of income and subsistence for many farmers and rural populations in rainfed areas. On an industrial scale, in large countries, maize is a cash crop with diverse applications (Novák *et al.*, 2019). It is grown for food, animal feed, as well as a raw material to produce industrial goods (Akinchin and Fedorov, 2015). This crop is cultivated on nearly 150 million hectares in about 160 countries with a wide variety of soils, climate, and management practices, contributing 36% (361.1 million tons) to world grain production (Dahlan *et al.*, 2014; Huato *et al.*, 2016). The United States of America (USA) is the largest maize producer in the world, accounting for about 35% of the total maize production. Corn growing is the driving force of the American economy. The United States has the highest productivity (9.5 tons per hectare) being twice as high as that in other countries. Thus, the average yield in India is 2.5 tons per 1 hectare.

Maize is the third most important food crop after rice and wheat in this country. Almost 80% of

India's cropland is used for maize growing. Maize provides 9% of the national food basket (Adedokun *et al.*, 2018; Barry *et al.*, 2017; Ismagilov *et al.*, 2019; Ngaboyisonga *et al.*, 2012). Russia ranks the twelfth among the world producers of maize with 11.3 million tons. The share of our country in cultivating this crop is just 0.9% of the total world production. North Caucasus and the Central Non-Black Soil Zone are the most productive regions to grow maize in open fields. The plants cultivated there to get enough sunlight and provide an abundant harvest. Some areas grow maize as a fodder crop. These are the Ural, Volga-Viatka, central regions, and Siberia (Sotchenko *et al.*, 2018).

Maize is the main crop with different applications. This cereal crop plays an integral part in agriculture. It enables us to address two challenges: to replenish grain stocks and produce nutritional feed for farm animals. This crop is also used to prepare silage well digested by animals. It is a good milk-making feed. Maize is used as green fodder as well (Akhiyarov *et al.*, 2018; Araya *et al.*, 2019; Lin *et al.*, 2019). The ten largest maize

producers accounted for 79.4% of the total world production in 2018. These are the USA, China, Brazil, Argentina, Ukraine, India, Mexico, Indonesia, South Africa, Romania (Barry *et al.*, 2017; Chung *et al.*, 2019; Venkatesha *et al.*, 2019). The share of the leading 30 producers of maize totals 92.4%. In 2018 this list included Canada, Russia, Nigeria, Hungary, Italy, Serbia, Philippines, Ethiopia, Tanzania, Turkey, Egypt, Vietnam, Germany, Thailand, Pakistan, Spain, Poland, Malawi, Kenya and Zambia (Chung *et al.*, 2019). The USA is a key producer and exporter of maize in the world. In 2018 the share of the country in the global production of this cereal crop accounted for 35.3%. The output was 361.1 mln tons. China is the second-largest maize producer in the world. In 2018 the share of China in the global production of the given cereal crop amounted to 21.1%. The output was 215.6 million tons. Brazil is the third world producer of maize. In 2018 its total output was 79.9 million tons. Argentina ranks the fourth among the largest maize producers in the world, its share in the structure of the global production was 3.2%, and the total output amounted to 33.0 million tons of maize. Ukraine is the fifth in the list of top five world producers of the very cereal crop, with 28.5 million tons.

The largest producers of maize in Russia were the Krasnodar and Stavropol territories, Rostov, and Voronezh regions (see Figure 1).

The area under maize amounted to 569.3 thousand hectares (23.2% of the total area) with an average yield of 64.9 kg/ha. The Stavropol territory (the area under maize is 197.5 thousand hectares with the share in the total cropland being 8.1%) has an average yield of 63.7 C/ha. The Rostov region (189.2 thousand hectares, 7.7%) harvests an average yield of 49.1 C/ha. The Voronezh region (184.6 thousand hectares, 7.5%) has an average yield of 77.2 kg/ha. The Kabardino-Balkar Republic (141.3 thousand hectares, 5.8%) gets, on average, 62.9 C/ha. In 2018, the maize yield for seeds in Russia amounted to 47.9 C/ha, which is 2.2% (1.1 C/ha) less than in 2017. It decreased by 4.4 % (2.2 C/ha) for five years. Over ten years, the yield growth was 24.1% (9.3 C/ha). The yield increased by 166.1% (29.9 C/ha) concerning 2001. The average annual yield of this type of cereal crop in Russia was 25.0 C/ha in 1991-2000. In 2001-2010 it increased to 32.7 C/ha. In 2011-2018 the average annual yield reached 47.6 C/ha (Sotchenko *et al.*, 2018; Ismagilov *et al.*, 2019).

The Food and Agriculture Organization of the United Nations (FAO) predicts that the cultivation of this grain crop will increase from year to year world-wide. Countries with the most favorable temperate climate will have the highest yields of maize (Kedir, 2018; Venkatesha *et al.*, 2019; Xu *et al.*, 2019b).

To produce maize seeds in the northern regions of Russia, it is necessary to develop ultra-early maturing and cold-resistant hybrids that can withstand the soil temperature below the biological minimum for a long time. In the northern zone of maize cultivation, more attention should be paid to the seed quality. Using seeds with low laboratory germination and spread resulted from their long-term storage can prevent the planned stand, delay the seedling emergence. It leads to the weak initial growth of plants and, consequently, to lower yields of seeds (Barry *et al.*, 2017; Pandurovic *et al.*, 2013). To get higher yields with a given population at the optimum sowing time, it is necessary to increase the seeding rate by 10-20% in conditions of the Maize Research Institute and by 20-30% in conditions of the northern parts of the region depending on the hybrid used. It requires taking into account the biological characteristics of maize hybrids to germinate in different conditions, seed reproduction, sowing qualities, and the seeding rate adjusted to specific growing conditions. Maize hybrid Nur turned to be the best hybrid to get guaranteed seeds at earlier sowing time in conditions of the Middle Cis-Urals. The stalk fragility below the ear is primarily determined by the hybrid's genotype and growing conditions. Ear infection with *Fusarium* varies differently from year to year. However, maize hybrid Nur is found to be resistant to this disease independently of other factors (Ismagilov *et al.*, 2019).

Maize hybrid productivity trends in the U.S. prove that the estimated annual improvement rates range from 1.2 to 2.4% (Barry *et al.*, 2017). Studies on the relationship between climate and human activities often place greater emphasis on the science of climate change. The savings were mostly due to temperature and precipitation. The phase transition of economic performance was positively affected by the long-term temperature change in combination with the trigger effect of short-term precipitation changes (Ismagilov *et al.*, 2019). From a more macroeconomic perspective, the climate movement for macroeconomic cycles has been mitigated by larger and slower processes such as social memory, spatial displacement of key economic areas, and socio-technological progress (Chung *et al.*, 2019).

These genetic changes are associated with improved management practices, including fertilizer use, irrigation, tillage, weed, and pest control, as well as crop rotation (Barry *et al.*, 2017; Chavas and Mitchell, 2018; Xu *et al.*, 2019a). The use of fertilizers eliminates the lack of nutrients in the soil, as the maize yield is very sensitive to nitrogen (Lamptey *et al.*, 2018). When possible, irrigation reduces soil water scarcity and drought. Pest and weed populations can be controlled and suppressed by tillage, crop rotation, and the use of pesticides (insecticides and herbicides). For centuries, farmers have used crop rotation to reduce pest and weed infestation and to restore soil fertility (Chavas and Mitchell, 2018).

One of the significant constraints in the middle Cis-Urals is the low nutritional value of feed (Ismagilov *et al.*, 2019). This issue can be addressed by developing new elements in conventional technologies to cultivate crops, paying particular attention to grain-forage crops (Mударисов *et al.*, 2019; Omokanye *et al.*, 2013; Xu *et al.*, 2019b). The main grain crops cultivated in the Russian Federation are maize, barley, oats, wheat, rye. The high concentration of digestible carbohydrates provides high grain energy nutrition for these crops. Maize occupies a special place among other cereal crops as a source of energy (12.2-12.8 MJ of metabolizable energy per 1 kg) (Araya *et al.*, 2019; Emmanuel and Mutimura, 2012).

The climate of the Middle Cis-Urals is sharp continental; the sum of active temperatures is 2000-2200 degrees. To produce high-quality maize fodder in the conditions of this region, it is necessary to cultivate early-maturing hybrids. The crop should have time to mature in a short summer. Maize is a heat-loving plant; it is not tolerant of the temperature decline. As a result of the work performed over many years, plant breeders have created hybrids that meet the requirements of the climate in the Middle Cis-Urals. Thus, the seeds of these hybrids after being sown withstand a decrease in temperature to minus 2° C. While maize seeds germinate within eight days in a warm climatic zone, early-ripening hybrids adapted to the natural conditions of the Middle Cis-Urals germinate at relatively low temperatures for the same time. To achieve milky ripeness, maize needs a period of effective temperatures above 10° C for at least 120 days, including about 70 days with an average daily temperature above 15° C (Sotchenko *et al.*, 2018).

To ensure a sufficiently high yield under variable weather conditions, it is recommended to grow several hybrids in each farm, being different in several properties (Barry *et al.*, 2017; Chung *et al.*, 2019; Emmanuel and Mutimura, 2012). The choice of varieties suitable for cultivation in this area, the correct selection and preparation of seed material are of great importance for the Middle Cis-Urals with its sharp differences in soil and climatic conditions (Akinchin and Fedorov, 2018; Chavas and Mitchell, 2018; Ngaboyisonga *et al.*, 2012). In recent years, several early-ripening hybrids have been created. They develop a seed of milky-wax ripeness even in adverse weather conditions of the Middle Cis-Urals (Sotchenko *et al.*, 2018).

In the conditions of the Middle Cis-Urals, maize is mainly cultivated for silage and green feeding of animals (Sotchenko *et al.*, 2018). However, the green mass of maize, consisting mainly of stems and leaves without ears, usually contains up to 88-90% water. Silage, being prepared from such a mass, has less dry matter and especially protein (Kedir, 2018; Xu *et al.*, 2019b). Such fodder has low nutritional value and relatively low return on livestock products (Lubova *et al.*, 2018). Maize seeds or a groundmass with seeds of milky-wax and wax ripeness can develop the most high-quality and nutritious feed (Hisse *et al.*, 2019).

A maize seed has a high starch content (up to 70%), compared with other cereal crops, it is rich in fat (up to 7%) (Kedir, 2018; Ngeno *et al.*, 2012; Omokanye *et al.*, 2013). Maize seeds contain less calcium (3,5 times less than oats and sorghum, three times less than barley and millet, two times less than rye and 1,5 times less than wheat) (Ngeno *et al.*, 2012; Wakili, 2012). Early-maturing hybrids on their morphological features do not differ in robust development, but they have a significant share of ears in the total harvest due to lack of heat (Barry *et al.*, 2017; Chavas and Mitchell, 2018; Kätterer *et al.*, 2019). When these hybrids are grown according to the cereal seed technology, farms receive high-quality raw material and prepare silage with nutrient content of 0.25-0.32 fodder units. It is found that in the conditions of the Middle Cis-Urals, it is advisable to grow varieties and hybrids with a period of 95-100 day germination-wax ripeness. It provides high yields of dry mass with ears of milky-wax and wax ripeness. Maize fodder with a high content of ears in the phase of milky-wax ripeness of seeds is characterized by a high content of metabolic energy, starch, and fat (Lin *et al.*, 2019; Ngaboyisonga *et al.*, 2012). Maize seed

digestibility is very high and reaches 90%. Digested nutrients are complete. It is not only the seed that is well digested but other parts of the plant as well. Thus, there are 30-40% of seeds, 10% of rods, and stalks without seeds, about 50% of the rest parts of the plant (Akhiyarov *et al.*, 2018; Kätterer *et al.*, 2019; Venkatesha *et al.*, 2019).

## 2. MATERIALS AND METHODS:

### 2.1. The research place

The study of hybrids was carried out on the territory of the Republic of Bashkortostan, occupying a significant part of the Middle Cis-Urals. There are six agricultural zones in the Republic: northern forest-steppe, north-eastern forest-steppe, southern forest-steppe, Cis-Ural steppe, trans-Ural steppe, and mountain-forest zone (Barry *et al.*, 2017; Chavas and Mitchell, 2018; Ismagilov *et al.*, 2019). Field studies of maize hybrids developed by the All-Russian research institute of maize were conducted in the northern forest-steppe ("Agro Tanyp" agricultural production cooperative, located in the Tatyshly district) and southern forest-steppe (scientific training center of the Bashkir State Agrarian University (BSAU)).

In the "Agro Tanyp" farm, the soil cover is represented by dark gray forest soils with medium loamy granulometric composition. The humus horizon depth is 18-22 cm, the humus content in the arable layer is 3.7-4.1 %. The soil medium reaction is slightly acidic pH (kcl) 4.8-5.2; the bulk unit weight of the soil in the arable layer is 1.10-1.14 g/cm<sup>3</sup>. The soil contains 70-80 mg/kg of easily hydrolyzable nitrogen, 111-118 mg/kg of mobile phosphorus, and 121-125 mg/kg of exchange potassium. The frost-free period is 120-125 days. The growing season precipitation is 236-284 mm, with the average annual rainfall being 587 mm. The soil cover in the scientific training center of the Bashkir State Agrarian University is represented by leached chernozem having medium loamy granulometric composition. The humus horizon layer is 58-69 cm; the humus content in the topsoil is 9.7-9.8%. The soil medium reaction is slightly acidic pH (kcl) 4.8-5.2; the bulk unit weight of the soil in the arable layer is 1.02-1.10 g/cm<sup>3</sup>. The soil contains 135-156 mg/kg of easily hydrolyzable nitrogen, 160-166 mg/kg of mobile phosphorus, 185-187 mg/kg of exchange potassium. The frost-free period is 110-135 days. The growing season precipitation is 225-275 mm, with the average annual rainfall being 523 mm.

During the growing season of 2019, meteorological conditions in the Republic of Bashkortostan as a whole, especially in May and June, were cold. The shortage of favorable temperatures amounted to 116 0C for these two months. Though the temperature was a bit higher than usual in the subsequent maize vegetation period, the heat shortage remained.

### 2.2. Equipment

Maize was cultivated according to the following management practice in experiments of the scientific training center of the BSAU: predecessor – spring wheat, tillage – autumn plowing with PN-4-35 to a depth of 26-28 cm, spring harrowing (3BZTS-1.0) and pre-sowing cultivation (CSO-4) to a depth of 5 cm, sowing was carried out on May 10-12 by seeder UPS-8. Row spacing was 70 cm, seeding rate – 80 thousand pieces of seeds per 1 ha to a depth of 5 cm.

### 2.3. Field experiments

In "Agro Tanyp" maize in the experiments was cultivated by the technology generally accepted for this zone. The registered area of plots is 150 m<sup>2</sup>, the number of replication is fourfold. The variants are arranged in a line in the experiment. The field experience was conducted on the following hybrids: Mashuk 140, K-140, K-150, Uralskii 150, Nur, Mashuk 150, Biliar 160, K-160, K-170, Shikhan, Katerina, Baikal, Mashuk 170, Mashuk 175, Mashuk 171, Mashuk 185, Newton, Mashuk 220, Mashuk 250. The variants are arranged in a line in the experiment. The registered area of plots is 150 m<sup>2</sup>, the number of replication is fourfold. The field scheme included hybrids: Mashuk 140, K-140, K-150, Uralskii 150, Nur, Mashuk 150, Biliar 160, K-160, K-170, Shikhan, Katerina, Baikal, Mashuk 170, Mashuk 175, Mashuk 171, Mashuk 185, Newton, Mashuk 220, Mashuk 250.

### 2.4. Data analysis

During the growing season, the height and weight of plants were determined. Yield accounting was performed by the continuous harvest method and weighing the mass of plants and seeds after maize ear threshing. To conduct laboratory analysis, seed samples were chosen. Seed moisture was determined with Wile-55 electronic moisture meter and the drying method in the drying chamber. The seed protein content

was tested with Infracum FT-10 infrared analyzer.

### 3. RESULTS AND DISCUSSION:

According to the results of field studies, it was revealed that maize hybrids mostly formed a pre-harvest height at the level of 160.0-280.0 cm. Better conditions for growth were in the BSAU's scientific training center in the Ufa district (Figure 2). Three hybrids had the maximum height: Mashuk 250 MV (275 cm); Mashuk 220 MV (260 cm), and Shikhan (250 cm). The hybrid K-140 had the minimum height indicators in this experiment (175 cm). In conditions of "Agro Tany" farm, located in the Tatyshly district, the highest height of plants was in hybrids Mashuk 250 SV (260 cm), Mashuk 175MV (250 cm) and Newton (250 cm). The minimum height was found in hybrid K-140 (185 cm).

Seed yield development in maize hybrids in the conditions of two zones were studied along with finding the above-ground mass of the crop in the phase of milky-wax ripeness of seeds. When maize is grown according to the cereal seed technology, the green mass yield of the studied hybrids in the conditions of the BSAU's scientific training center of the Ufa district ranges from 33.7 to 68.8 t/ha (see Figure 3). The top three hybrids in terms of yields included: Mashuk 175 MV (68.8 t/ha), Baikal (59.6 t/ha), and Shikhan (56.7 t/ha). The minimum yield was formed in Mashuk 140 hybrid (33.7 t/ha). There is a close correlation between plant height and yield of green mass ( $r=0.823$ ). In the conditions of the "Agro Tany" farm in the Tatyshly district, the green mass yield of maize hybrids varied within 32.8-56.7 t/ha. The top three hybrids in terms of yields included: K-170 (56.7 t/ha), Shikhan (55.67 t/ha), and Mashuk 170 MV (54.99 t/ha). The K-160 hybrid had the lowest yield (32.8 t/ha).

In the conditions of the Middle Cis-Urals, it is essential to evaluate hybrids by seed moisture at the time of maize harvesting in this zone. Hybrid seeds had different moisture content depending on the group of ripeness (28-63.5%). 2 hybrids, namely Mashuk 140 and K-140, had the lowest moisture content at harvesting. Other hybrids had high moisture content (Table 1). With the standard moisture content being 14%, the seed yield of maize hybrids in the conditions of the "Agro Tany" farm ranged from 3.17 to 6.3 t/ha. The highest yield was received from the hybrid Uralskii 150 (5.45 t/ha). The yields of Baikal (5.38 t/ha) and

Mashuk 170 (4.98 t/ha) hybrids were a bit lower. Under the conditions of the BSAU's scientific training center, the seed yield of hybrids at 14 % moisture content was 2.50-6.76 t/ha. The highest grain yield was provided by the Uralskii 150 hybrid (6.76 t/ha). Relatively high productivity rates were observed for Mashuk 150 (6.57 t/ha), Baikal (6.16 t/ha), and Shikhan (5.89 t/ha) hybrids.

Thus, different soil and climatic conditions made it possible to evaluate and identify highly productive maize hybrids for the conditions of the studied farms. Nur, Uralskii 150, Mashuk 150 MV, Mashuk 170 MV short-season hybrids (FAO 150-199) are the most suitable for the conditions of the northern and southern forest-steppe of the Republic in terms of ripening and yields. To get high-quality as well as high-energy silage, it is advisable to grow short-season hybrids Mashuk 171, Mashuk 175 MV, Mashuk 185 MV, and Katerina SV.

Academician Sotchenko V.S., professor Shlapunov V.N., cytogeneticist McClintock Barbara, plant breeder Borlaug Norman Ernest argue that a higher nutritional value of feed for cows requires hybrids adapted to a particular soil and climate conditions (Barry *et al.*, 2017; Ismagilov *et al.*, 2019; Omokanye *et al.*, 2013). When there is insufficient heat, it is necessary to use early-maturing hybrids. Their yield is not high, but the nutrient content is much higher. These are hybrids of 140-150 FAO (Lin *et al.*, 2019). In conditions with heat security, hybrids of 170-200 FAO can be sown. In Northern Kazakhstan, the average yield of dry matter was 4.8 t/ha (Sotchenko *et al.*, 2018). However, there can be a sharp decline in yields in dry years and when summers are short and cold.

Maize productivity depends not only on climatic conditions but on soil factors and mineral nutrition (Falade *et al.*, 2017; Pandurovic *et al.*, 2013). Under the conditions of Ogallala Aquifer, the maize seed yield ranged from  $5.2 \pm 1.0$  t/ha to  $7.4 \pm 0.7$  t/ha with the highest value when treated with mineral fertilizer and the lowest value when composted with 100% fertilizer (Ayhan *et al.*, 2013; Barry *et al.*, 2017; Lin *et al.*, 2019). The maize productivity largely depended on the level of nutrient supply. Maize programs run by private companies typically conduct extended product testing in multiple growing environments to better recommend new hybrids, as well as providing farmers with an opportunity to evaluate their products by DuPont Pioneer in Minas Gerais and Goias States. The yield of the new hybrids was at

the standard level exceeding the control variants in some conditions (Xu *et al.*, 2019a, 2019b).

To increase the nutritional value of maize silage, there were carried out tests on adding legumes. The latter is considered to be an important element of sustainable agriculture. Legumes provide biological nitrogen fixation that increases the protein content in the diet. Thus, depending on the local conditions, it is necessary to select the elements of technology that increase the productivity of maize hybrids, thereby increasing the nutritional value of feed, taking into account their economic efficiency.

#### 4. CONCLUSIONS:

The plant height of the studied maize hybrids selected by the All-Russian Research Institute in the conditions of the Middle Cis-Urals varies from 160.0 to 280 cm. The seed yield of maize hybrids studied in two soil-climatic zones of the Middle Cis-Urals ranges from 2.50 to 6.76 t/ha. Uralskii 150 (5.45 t/ha), Baikal (5.38 t/ha), and Mashuk 170 MV (4.98 t/ha) hybrids have relatively high seed productivity.

When cultivating maize hybrids on the seed technology, they develop a green mass at the level of 30.68-68.80 t/ha. The hybrids K-170 (56.7 t/ha), Shiha (55.67 t/ha), and Mashuk 170 MV (54.99 t/ha) showed the highest productivity with the milky-wax ripeness phase of seeds. The K-160 hybrid had the lowest yield (32.8 t/ha). The received data will allow selecting maize hybrids with high yield and nutritional value for farms with similar soil and climatic conditions and to prepare diets for highly productive dairy cows and beef cattle.

#### 5. REFERENCES:

1. Adedokun, I. I., Nwokeke, B. C., Onyeneke, E. N., Ojukwu, M., and Ekemenye, I. A. (2018). Bambaranut Protein Isolate: Effect of Incorporation on Nutrient Content and Sensory Properties of Enriched Indigenous Maize Noodle 'kokoro'. *Journal of Food Technology*, 16, 7-13.
2. Akhiyarov, B. G., Ismagilov, R. R., Islamgulov, D. R., Kuznetsov, I. Y., Akhiyarova, L. M., Abdolvaleev, R. R., Alimgafarov, R. R., Pavlov, A. V., Valitov, A.V. and Sergeev, V. S. (2018). Yield and quality of table beet depending on cultivation technology elements. *Journal of Engineering and Applied Sciences*, 13(S11), 8752-8759.
3. Akinchin, A. V., and Fedorov, A. S. (2015). Effect of green-manure crops on agrophysical properties of the soil and maize productivity for grain. *Bulletin of Kursk State Agricultural Academy*, 8, 143-145.
4. Araya, A., Kisekka, I., Vara Prasad, P. V., and Gowda, P. H. (2017). Evaluating optimum limited irrigation management strategies for corn production in the Ogallala aquifer region. *Journal of Irrigation and Drainage Engineering*, 143(10), 04017041.
5. Ayhan, A., Liu, Q., Alibas, K., and Unal, H. (2013). Biogas production from maize silage and dairy cattle manure. *Journal of Animal and Veterinary Advances*, 12(5), 553-556.
6. Barry, M., Triulzi, G., and Magee, C. L. (2017). Food Productivity Trends from Hybrid Corn: Statistical Analysis of Patents and Field-test data. *arXiv preprint arXiv:1706.05911*.
7. Chavas, J. P., and Mitchell, P. D. (2018). Corn Productivity: The Role of Management and Biotechnology. Chapter 2. In Amanullah D and Fahad S (Eds), *Corn: Production and Human Health in Changing Climate* (pp. 13-26). Intech, U.K.
8. Chung, S. U., Sung, S. H., Zhang, Q. M., Jung, J. S., Oh, M., Yun, Y. S., ... and Moon, S. H. (2019). Assessment of Productivity and Vulnerability of Climate Impacts of Forage Corn (Kwangpyeongok) Due to Climate Change in Central Korea. *Journal of The Korean Society of Grassland and Forage Science*, 39(2), 105-113.
9. Dahlan, S. S., Mappigau, P., and Khaerani, S. (2014). Human Capital Specific, Entrepreneurial Behavior and Integrated Maize Crop Management Adoption. *Research Journal of Applied Sciences*, 9(8), 481-488.
10. Emmanuel, R., and Mutimura, M. (2012). Comparison of nutrient composition and in vitro digestion characteristics of four forage legumes from two agro-ecological zones of Rwanda. *Agricultural Journal*, 7(4), 264-269.
11. Falade, A. T., Buys, E. M., and Taylor, J. R. (2017). Effect of Different Non-Wheat Bread Making Methods on the Quality of Maize Bread. *Journal of Food Technology*, 15(1), 1-6.
12. Hisse, I. R., D'Andrea, K. E., and Otegui, M. E. (2019). Source-sink relations and kernel weight in maize inbred lines and hybrids: responses to contrasting nitrogen supply

- levels. *Field Crops Research*, 230, 151-159.
13. Huato, M. A. D., Arenas, O. R., Lopez-Reyes, L., Carcano-Montiel, M. G., Lezama, J. F., and Leon, A. C. (2016). Model: Producer-Innovator, Farmers Technologies, and Food Security in Rainfed Maize in Mexico Producers. *Research Journal of Biological Sciences*, 11, 98-104.
14. Ismagilov, R., Akhiyarov, B., Islamgulov, D., Ayupov, D., and Salnikov, V. (2019). Maize hybrid productivity and grain quality in conditions of the Cis-Ural forest-steppe. *AIMS Agriculture and Food*, 4(3), 604-612.
15. Kätterer, T., Roobroeck, D., Andrén, O., Kimutai, G., Karlton, E., Kirchmann, H., ... and de Nowina, K. R. (2019). Biochar addition persistently increased soil fertility and yields in maize-soybean rotations over 10 years in sub-humid regions of Kenya. *Field Crops Research*, 235, 18-26.
16. Kedir, M. (2018). Adoption and determinants adoption of improved maize in Ethiopia. *Agricultural Journal*, 13, 1-8.
17. Lamptey, S., Yeboah, S., Li, L., and Zhang, R. (2017). Dry matter accumulation and nitrogen concentration in forage and grain maize in dryland areas under different soil amendments. *Agronomy Research*, 15(4), 1646-1658.
18. Lin, H., Xie, Y., Liu, G., Zhai, J., and Li, S. (2019). Soybean and maize simulation under different degrees of soil erosion. *Field Crops Research*, 230, 1-10.
19. Lubova, T. N., Islamgulov, D. R., Ismagilov, K. R., Ismagilov, R. R., Mukhametshin, A. M., Alimgafarov, R. R., ... and Lebedeva, O. Y. (2018). Economic efficiency of sugar beet production. *Journal of Engineering and Applied Sciences*, 13(S8), 6565-6569.
20. Mudarisov, S., Khasanov, E., Rakhimov, Z., Gabitov, I., Badretdinov, I., Farchutdinov, I., ... and Jarullin, R. J. (2017). Specifying two-phase flow in modeling pneumatic systems performance of farm machines. *Journal of Mechanical Engineering Research and Developments*, 40(4), 706-715.
21. Ngaboyisonga, C., Njoroge, K., Kirubi, D., and Githiri, S. M. (2012). Quality protein maize under low N and drought environments: endosperm modification, protein and tryptophan concentrations in grain. *Agricultural Journal*, 7(5), 327-338.
22. Ngeno, V., Mengist, C., Langat, B. K., Nyangweso, P. M., Serem, A. K., and Kipsat, M. (2012). Measuring Technical Efficiency among Maize Farmers in Kenya's Bread Basket. *Agricultural Journal*, 7(2), 106-110.
23. Novák, P., Kovaříček, P., Hůla, J., and Buřič, M. (2009). Surface water runoff of different tillage technologies for maize. *Agronomy Research*, 17(3), 754-760.
24. Omokanye, A. T., Kelleher, F. M., and McInnes, A. (2013). Crop residues for mulch, feed yield and quality as influenced by low-input maize-based cropping systems and N fertilizer. *Agricultural Journal*, 8(5), 222-231.
25. Pandurovic, Z., Dragicevic, V., Glamoclija, D., and Dumanovic, Z. (2013). Possibilities of maize cropping for feed on acid soil. *Journal of Animal and Veterinary Advances*, 12(7), 813-822.
26. Sotchenko, Yu. V., Ismagilov, R. R., and Akhiyarov, B. G. (2018). Maize hybrid grain productivity and quality in conditions of the Bashkortostan Republic. *Vestnik of Bashkir State Agrarian University*, 4(48), 39-43.
27. Venkatesh, M. S., Hazra, K. K., Ghosh, P. K., and Mishra, J. P. (2019). Integrated phosphorus management in maize-chickpea rotation in moderately-alkaline Inceptisol in Kanpur, India: An agronomic and economic evaluation. *Field Crops Research*, 233, 21-32.
28. Wakili, A. M. (2012). Technical Efficiency of Maize Farmers in Gombi Local Government of Adamawa State, Nigeria. *Agricultural Journal*, 7(1), 1-4.
29. Xu, J., Han, H., Ning, T., Li, Z., and Lal, R. (2019). Long-term effects of tillage and straw management on soil organic carbon, crop yield, and yield stability in a wheat-maize system. *Field Crops Research*, 233, 33-40.
30. Xu, J., Meng, J., and Quackenbush, L. J. (2019). Use of remote sensing to predict the optimal harvest date of corn. *Field Crops Research*, 236, 1-13.



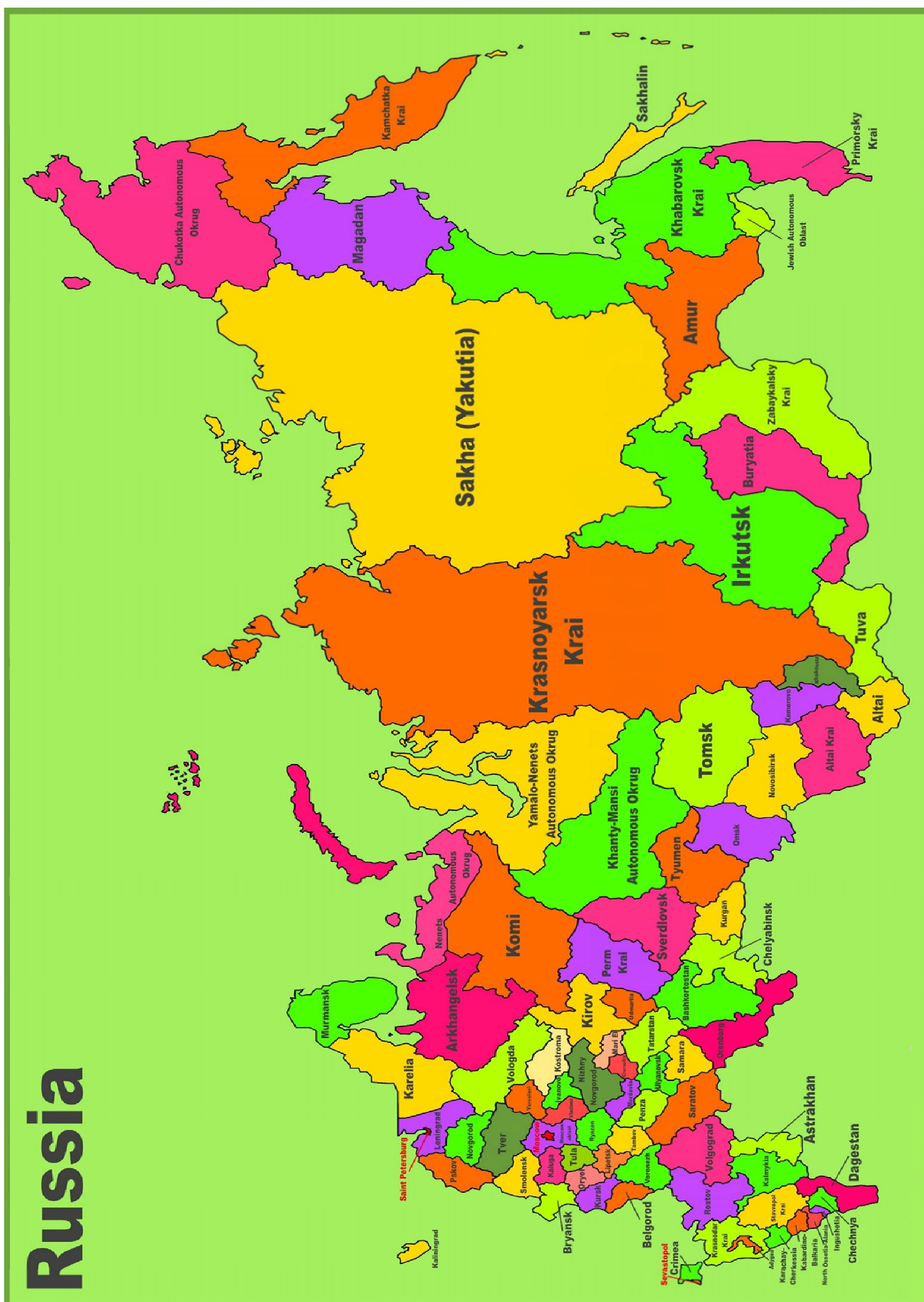
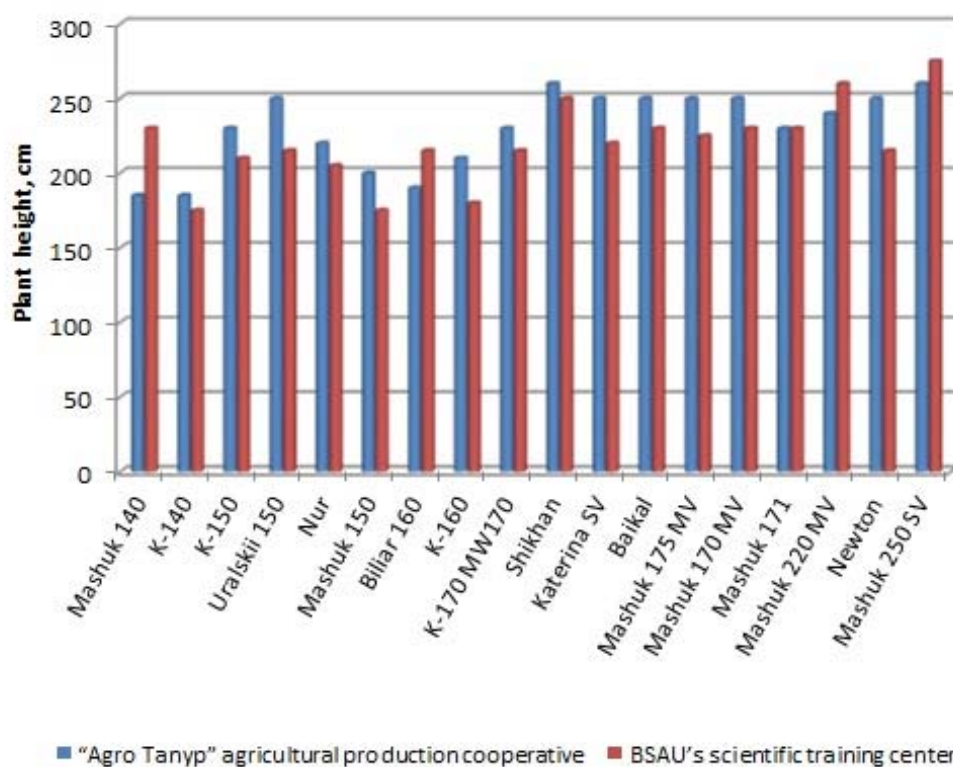
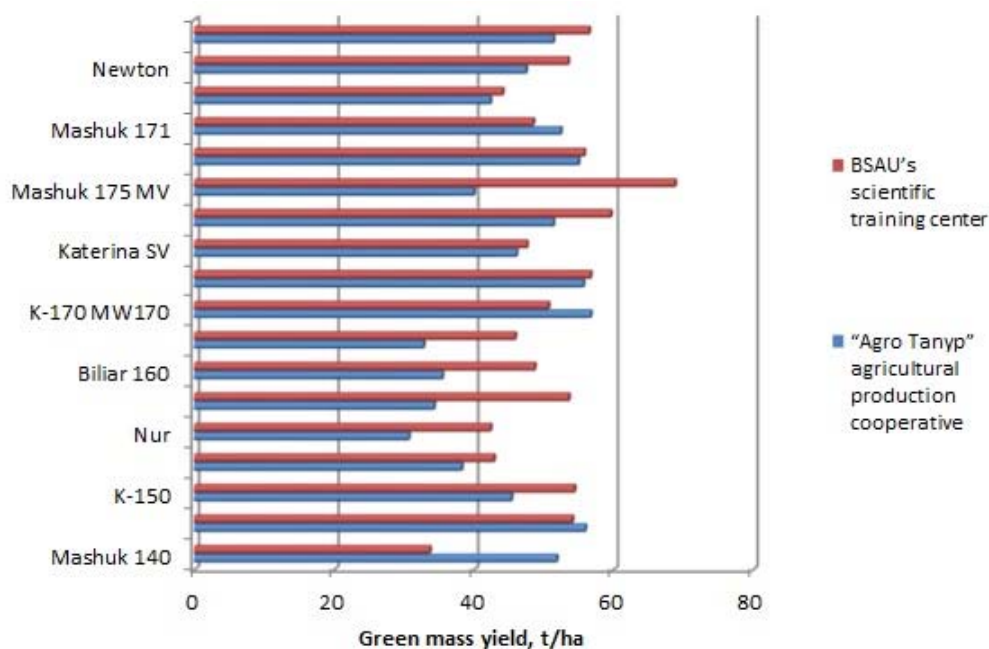


Figure 1. Map of Russian regions.





**Figure 2.** The height of maize plants in the "Agro Tany" agricultural production cooperative of the Tatyshly district and the scientific training center of the Bashkir State Agrarian University located in the Ufa district (before harvesting, 2019).



**Figure 3.** Maize green mass yield in "Agro Tany" of the Tatyshly district and the BSAU's scientific training center of the Ufa district (the milky-wax ripeness phase of seeds, 2019)

**Table 1.** Seed moisture content and yield depending on hybrids (2019)

| Hybrid            | “Agro Tanyp” agricultural production cooperative |  | the scientific training center of the BSAU |  |
|-------------------|--|--|--|--|
|                   | Seed moisture at harvesting                      | Seed yield at the standard moisture content(14%), t/ha | Seed moisture at harvesting                | Seed yield at the standard moisture content(14%), t/ha |
| Mashuk 140        | 28.00  | 4.81   | 25.00                                      | 4.43   |
| K-140             | 29.00  | 4.43   | 25.20                                      | 5.47   |
| K-150             | 32.00  | 4.24   | 29.30                                      | 5.37   |
| Uralskii 150      | 30.10  | 5.45   | 28.40                                      | 6.76   |
| Nur               | 32.20  | 3.73   | 29.20                                      | 5.68   |
| Mashuk 150        | 31.50  | 4.21   | 29.80                                      | 6.57   |
| Biliar 160        | 42.00  | 4.13   | 35.30                                      | 4.74   |
| K-160             | 43.60  | 4.12   | 36.20                                      | 5.21   |
| K-170             | 54.30  | 4.98   | 38.60                                      | 5.05   |
| Shikhan           | 54.00  | 4.53   | 38.00                                      | 5.89   |
| Katerina SV       | 55.00  | 4.04   | 45.30                                      | 5.42   |
| Baikal            | 54.30  | 5.38   | 46.20                                      | 6.16   |
| Mashuk 175 MV     | 58.60  | 3.25   | 49.10                                      | 5.23   |
| Mashuk 170 MV     | 58.40  | 4.45   | 47.60                                      | 5.27   |
| Mashuk 171        | 62.00  | 4.27   | 48.10                                      | 5.75   |
| Mashuk 220 MV     | 62.20  | 3.27   | 55.30                                      | 2.77   |
| Newton            | 62.40  | 3.17   | 59.20                                      | 5.29   |
| Mashuk 250 SV     | 63.50  | 3.43   | 59.30                                      | 2.50   |
| HCP <sub>05</sub> | 0.28   | 0.15   | 0.31                                       | 0.16   |

SISTEMA DE PROTEÇÃO DA BATATA CONTRA PRAGAS E DOENÇAS PARA  
OBTER PRODUTOS ECOLÓGICAMENTE LIMPOSSYSTEM OF PROTECTION FOR POTATO FROM PESTS AND DISEASES TO GET  
ECOLOGICALLY CLEAN PRODUCTSСИСТЕМА ЗАЩИТЫ РАСТЕНИЙ КАРТОФЕЛЯ ОТ ВРЕДИТЕЛЕЙ И БОЛЕЗНЕЙ  
ДЛЯ ПОЛУЧЕНИЯ ЭКОЛОГИЧЕСКИ ЧИСТОЙ ПРОДУКЦИИBUTOV, A. V.<sup>1</sup>; ZUBKOVA, T. V.<sup>2\*</sup><sup>1, 2</sup> Bunin Yelets State University. Russian Federation.

\* Corresponding author

e-mail: tatyana.v.zubkova@yandex.ru

Received 16 June 2020; received in revised form 26 June 2020; accepted 04 July 2020

## RESUMO

A batata compreende uma cultura alimentar estrategicamente importante na Federação Russa. A quimiocalização aprimorada da produção de batata, protegendo-a de pragas e doenças, permite obter altos rendimentos, mas ao mesmo tempo afeta significativamente a qualidade biológica dos produtos. A cadeia varejista frequentemente recebe muitos tubérculos com excesso de nitratos, enquanto contém os chamados pesticidas "de longa duração". Ao entrar no corpo humano com produtos, as substâncias tóxicas causam doenças graves. Há um problema agudo de fornecer às crianças produtos ecologicamente corretos. Essa pesquisa desenvolveu uma importante tarefa de neutralizar o acúmulo de inseticidas e fungicidas tóxicos em tubérculos pelo início da colheita ao cultivar variedades de batatas de médio porte. Isto foi conseguido quando se utiliza o inseticida Celest TOP (Tiametoxame, classe de risco 2) em normas reduzidas em 25%, em combinação com o uso de preparações biológicas Siliplant ou Albit e reduzidas em 40% em normas de fungicidas. O sistema de proteção incluiu: para tubérculos: Celestino 0,3 l/ha + Albite TPS 0,1 l/t; para os tops: Ridomil ouro MC VDG 1,5 kg / ha primeiro, segundo e terceiro tratamentos; Shirlan SK 0,24 l / ha 4-5º tratamento + Albit TPS 2 vezes para vegetação 0,05 l / ha ou Siliplant BP 2 vezes para vegetação 1,0 l / ha. As análises laboratoriais revelaram quantidades residuais de pesticidas e nitratos em tubérculos. Os produtos resultantes, com o sistema de proteção de plantas desenvolvido, atenderam às exigências de nutrição infantil e dietética. O método voltamétrico invertido foi usado para determinar a concentração de pesticidas em tubérculos. Os nitratos foram determinados usando um eletrodo seletivo de íons. Está estabelecido que o Prestige (Imidacloprid, classe de risco 1) é impraticável de usar na produção de batatas ecologicamente limpas. O uso de Celest (Thiamethoxam, classe de risco 2) em combinação com Albit ou Siliplant aumentou o rendimento e reduziu o conteúdo de substâncias tóxicas nos tubérculos.

**Palavras-chave:** *pesticidas modernos, agentes biológicos, nitratos.*

## ABSTRACT

Potatoes comprise a strategically important food crop in the Russian Federation. Enhanced chemicalization of potato production, while protecting it from pests and diseases, allows you to get high yields, but at the same time significantly affects the biological quality of products. The retail chain often receives lots of tubers with excess nitrates, while containing the so-called "long-playing" pesticides. Getting into the human body with products, toxic substances cause severe diseases. There is an acute problem of providing children with environmentally friendly products. This research developed an important task of neutralizing the accumulation of toxic insecticides and fungicides in tubers by the beginning of harvesting when cultivating medium-early varieties of potatoes. This was achieved when using the insecticide Celest TOP (Thiamethoxam, hazard class 2) in reduced by 25% norms, in combination with the use of biological preparations Siliplant or Albit and reduced by 40% norms of fungicides. The protection system included for tubers: Celestine 0.3 l/ha + Albite TPS 0.1 l/t. For tops: Ridomil gold MC VDG 1.5 kg / ha first, second and third treatments. Shirlan SK 0.24 l / ha 4-5-th treatment + Albit TPS 2 times for vegetation 0.05 l / ha or Siliplant BP 2 times for vegetation 1.0 l / ha. Laboratory analyses revealed residual amounts of pesticides and nitrates in tubers. The resulting products, with the plant protection system developed by us, meet the requirements for children's and dietary nutrition. The inversion voltammetric method was used to determine

the concentration of pesticides in tubers. Nitrates were determined using an ion-selective electrode. It is established that Prestige (Imidacloprid, hazard class 1) is impractical to use in producing ecologically clean potatoes. Using Celest (Thiamethoxam, hazard class 2) in combination with Albit or Siliplant increased the yield and reduced the content of toxic substances in tubers.

**Keywords:** *modern pesticides, biological agents, nitrates.*

## АННОТАЦИЯ

Картофель - стратегически важная продовольственная культура в Российской Федерации. Усиленная химизация производства картофеля при защите его от вредителей и болезней, позволяет получать высокие урожаи, но при этом значительно страдает биологическое качество продукции. В торговую сеть нередко поступают партии клубней с превышением нитратов, содержащие при этом, так называемые, «долгоиграющие» пестициды. Попадая в организм человека с продукцией, отравляющие вещества, вызывают тяжелые заболевания. Возникает острая проблема по обеспечению экологически чистой продукцией детей. Нашими исследованиями решена важная задача по нейтрализации накопления токсичных инсектицидов и фунгицидов в клубнях к началу уборки при возделывании среднераннего сорта картофеля. Это достигается при использовании инсектицида Селеста ТОП (по тиаметоксаму 2-й класс опасности) в уменьшенных на 25% нормах, в сочетании с применением биопрепаратов Силиплант или Альбит и сниженными на 40% нормами фунгицидов. Система защиты включала по клубням: Селест Топ 0,3 л/га + Альбит ТПС 0,1 л/т. По ботве: Ридомил Голд МЦ ВДГ 1,5 кг/га первая, вторая и третья обработки. Ширлан СК 0,24 л/га 4-5-я обработка + Альбит ТПС 2 раза за вегетацию 0,05 л/га или Силиплант ВР 2 раза за вегетацию 1,0 л/га. Лабораторными анализами выявлены остаточные количества пестицидов и нитратов в клубнях. Полученная продукция, при разработанной нами системе защиты растений, отвечает требованиям предъявляемым к детскому и диетическому питанию. Для определения концентрации пестицидов в клубнях использовали инверсионный вольтамперометрический метод. Определение нитратов проводили с помощью ионоселективного электрода. Установлено, что Престиж (по имidakлоприду 1-ый класс опасности) нецелесообразно применять в производстве экологически чистой продукции. Применение инсектофунгицида Селест (по тиаметоксаму 2-й класс опасности) в сочетании с биопрепаратами Альбит или Силиплант повышало урожайность и уменьшало содержания токсических веществ в клубнях.

**Ключевые слова:** *современные пестициды, биопрепараты, нитраты.*

## 1. INTRODUCTION:

Potatoes comprise a strategically important food crop in the Russian Federation. The population even calls it a "second bread". Pests and diseases may severely damage potatoes. The fight against some of them has become a routine in potato cultivation. These dangers primarily include the Colorado potato beetle, wireworm (elaterid larva), dangerous fungal diseases (late blight), bacterial rot, and various viral diseases. The annual under-harvest of potatoes because of these factors depends on the variety and ranges from 20 to 30%. In adverse years, the under-harvest can be exceeded by 50% (Tulcheev and Yagforov, 2014). An integrated system for the protection of potatoes from diseases, pests, and weeds is a set of measures, among which the chemical method is the primary one (Zeyruk *et al.*, 2019b). The enhanced chemicalization of potato production allows for getting high yields, but the biological quality of the product can suffer greatly (Butov, Zakharov, and Zubkova,

2019). Often the over-nitrated tubers containing so-called "long-lasting" pesticides arrive at shops and markets (Damodaran, Tarkin, and Fennema, 2012). These pesticides may cause serious illnesses in human beings when consumed (Kaplin, 2007). They also have an allergenic and carcinogenic effect and may destroy human immunity (Chernikov and Sokolov, 2014). Chemophobia is becoming more popular among the population. People are wary of products grown industrially and they do not tend to learn more about the technological processes, it is enough for them to know about the use of pesticides and fertilizers in agriculture (Edelev, Grebenkin, Baranov, and Royev, 2013). This may undermine not only the physical but also the spiritual health of a person (Lysenko and Dogadina, 2015). Another urgent problem is the poor preservation of tubers in the post-growing season (Simakov, Starovoitov, and Anisimov, 2013). A complete rejection of pesticides at the current level of agronomic science development is impossible. However, it is quite possible to reduce significantly their

negative impact (Fokina, Ogorodnikova, Olkova, Skugoreva, and Lyalina, 2015). Potato cultivation in the Central black-earth region of the Russian Federation is becoming increasingly complex from year to year and requires serious measures and financial influx to control pests and diseases (Fedotov, Butov, and Goncharov, 2005). The most dangerous is the Colorado potato beetle (*Leptinotarsa decemlineata*) and late blight disease. Without proper measures on protecting, these pests and diseases can cause huge damage to the yield of the crop. They may reduce the yield by 60-70%, and destroy it (Zeyruk *et al.*, 2019a). Recently, there appeared modern, highly effective pesticides with a hazard class lower than the previous generation. There is a need to develop a new system for protecting potato plants from diseases and pests with a reduced rate of pesticides in combination with biological agents (Zeyruk *et al.*, 2019a; Rabinovich and Fomicheva, 2018). Around thirty years ago, there was outstripping growth in population demand for ecologically clean products in Western Europe and North America (Kochurko, Abarova, and Zuev, 2013). Russian Federation does not have legislation, certification, and policy of financial support for ecologically clean products. Producers of biologically high-quality potatoes need clear recommendations for guaranteed production of a sufficiently good, ecologically clean tuber crop (Butov and Boeva, 2013).

The purpose of the study was to establish methods of effective protection of potato plants from pests and diseases. It is needed to reduce pesticides and get ecologically clean products. Besides, it was aimed to substantiate the methods of using Celest (with a hazard class lower than the previously used agent Prestige) in combination with Albit and Siliplant.

The scope of the research included the development of an effective and environmentally friendly system for the comprehensive protection of potatoes from economically significant pests and pathogens in the black-earth forest-steppe of the Russian Federation using modern plant protection products and methods.

The scientific novelty of the research is the development of combining Celest (a modern insectofungicide) with Albit, Siliplant at reduced pesticide rates to obtain ecologically clean, a good level of the potato harvest.

## 2. MATERIALS AND METHODS:

Field experiments were carried out in 2015-2017 at the educational experimental farm of Bunin Yelets State University (Lipetsk region, Russian Federation). The soil of the plots was leached black-earth, medium loamy with a 5.8% humus content (according to Tyurin). The area of the experimental plot was 54 m<sup>2</sup>, and the repetition of the experimental cases was 4-fold/ Potato variety is mid-season Nevsky. The planting density of tubers is 54–55 thousand/ha at potato spacing - 75 cm. Mineral fertilizers in a dose of N<sub>75</sub>P<sub>150</sub>K<sub>120</sub> were applied in the general background in spring, after separating the experiments following the research program. Nitrogen dose (N<sub>75</sub>) in full mineral fertilizer was reviewed in the previous studies on nitrates in experiments with fertilizers (Butov *et al.*, 2019). In the spring, the soil underwent the pre-planting treatment upon the onset of its physical ripeness. Potato planting during the years of the experiments depended on weather conditions and occurred from May 11 to May 14. Harvesting and accounting of the crop were in the third decade of August.

The inversion voltammetric method (GOST R 51301–99) was used to determine the concentration of pesticides in tubers. Nitrates were determined according to the procedure based on the extraction of nitrates from the analyzed material with a solution of aluminum-potassium alum, followed by measuring their concentration in the resulting extract using an ion-selective electrode (Mineev, 2011). The analysis-of-variance method by Dospekhov (2012) was applied to process the crops mathematically.

In the experiments, the following agents were applied: Ridomil Gold MZ (Mancozeb), which is a systemic fungicide against potato diseases, Revus (Mandipropamide + Difenconazole), which is a translaminar fungicide, Shirlan (Fluazinam), which is a contact fungicide, and Prestige SC (Imidacloprid + Pentacuron), which is an insectofungicidal agent. The Imidacloprid pesticide has the highest, first hazard class. Celest TOP, SC (Thiamethoxam + Fludioxonil + Difenconazole) has the second hazard class, which is less than that of Prestige. Prestige SC and Celest TOP are combined insecticidal fungicide protectants for seed potato tubers. Albit is an effective complex biological agent, a universal plant growth regulator, with the properties of a fungicide and

complex fertilizer. Siliplant is a complex fertilizer; its active substance is bioactive silicon in chelated form, supplemented with trace elements (iron, zinc, magnesium, copper, boron).

Spraying seed tubers with dressing agents was done directly in the combined seed planter "Grimme" during planting. Following the research scheme, knapsack sprayers were used to treat the studied agents in vegetating plants. Tuber samples were analyzed for residual fungicides in case 3, where full pesticide rates were applied.

### 3. RESULTS AND DISCUSSION:

Economically significant pests and pathogens of diseases can significantly reduce the potential yield of potatoes (Zeyruk *et al.*, 2019a). Account of the tuber yield in the harvesting experiment showed that the modern means and methods of plant protection had a noticeable effect on its value (Table 1). Thus, the first control case with plant protection only against the Colorado potato beetle (*Leptinotarsa decemlineata*) (fungicides were not used) delivered a yield of 23.5 t/ha. The yield increased to 34.1 and 34.9 t/ha respectively with an intensive system of plant protection against pests and diseases in combination at full rates of pesticides and new biological agents for cases 4 and 6. All other cases, except for the control case, envisage measures to control the Colorado potato beetle (*Leptinotarsa decemlineata*) by applying insectofungicides to tubers (in the planter's opener) when planting.

The modern insectofungicide Celest Top was more effective than Prestige. The yield increase in case 3 (Celest) was 1.7 t/ha compared with case 2 (Prestige). Adding Albit at full pesticide rates to the plant protection system in case 4 increased the yield by 3.4 t/ha, compared to the similar case 3, which did not have biological agents. Case 6 with Siliplant demonstrated a slightly higher yield (0.8 t/ha) than with Albit (case 4). However, this difference did not exceed the experimental error (1.6 t/ha) i.e. it is not reliable. The cases 5 and 7 with reduced by 40% rates of fungicides and Celest Top demonstrated yield decrease by 25%. The case 5 with Albit demonstrated yield decrease (in comparison with the case 4) by 2.6 t/ha. The case 7 with the Siliplant demonstrated

yield decrease by 1.8 t/ha (in comparison with the case 6).

However, despite a significant decrease, the yield level at reduced pesticide rates, but in combination with Albit or Siliplant biological agents, remained at a fairly high level - 31.5-33.1 t/ha against 23.5 t/ha for the control case. A slight decrease in yield can be neglected, when the production will be tasked with obtaining ecologically clean from pesticides potato products for baby and diet nutrition. The results of laboratory studies showed that the residual amount of insecticide in the tubers of the first (control) case was not detected when processing only on tops 40 days after the last spraying (Table 1).

Analyzes of the residual pesticide content in the tubers, according to the test cases, were done 4 times during the growing season with an interval of 10 days. The previously widely used Prestige (case 2), due to the Imidacloprid content, belongs to the first, highest class of danger. Besides, when determining Imidacloprid residual amounts in tubers, it turned out that its content was significantly higher in all cases of determination than the Thiamethoxam (Celest) content, which was used in case 3.

Thus, when determining 65-75 days after the treatment of tubers in the samples from the case 2, the content of Imidacloprid was 16.1% and 15.8% more than in the same periods for Thiamethoxam in the case 2 (Celest). In 95 days after the treatment of the tubers, at the end of the growing season and before harvesting, the content of Imidacloprid (case 2) in the samples was small, but it was 3 times higher than the content of Thiamethoxam in the case 3. This means that Prestige, in comparison with Celest, not only initially belongs to the first, highest hazard class, but it also significantly exceeds the toxicants content in tubers compared to cases with Celest throughout the growing season. This indicates that the Prestige (Imidacloprid) is a "long-lasting" pesticide. It is impractical to use it in the cultivation of potatoes to get ecologically clean products. Adding Celest, Albit, and Siliplant to the plant protection system effected positively not only by increased yields but also by a reduced content of toxic substances in tubers. Albit and Siliplant in combination with Celest effectively neutralized the level of toxic substances accumulation in tubers. This is especially noticeable when Celest's doses are reduced by 25% and when fungicides of various

classes are reduced by 40%. When treating seed tubers with Albit RP and then using it during the following two treatments at the vegetating plants as in the case 4, the level of the residual amount of Thiamethoxam decreased compared to the case 3, without Albit. Thus, Thiamethoxam content decreased by 2.7% on the 65th day after the treatment of tubers; and its content decreased by 15.4% on the 75th day after the treatment of the tops. Before harvesting on the 95th day after the completion of treatments with biological agents, the insecticide concentration in case 4 decreased by 47.8% compared to case 3, without Albit. A decrease in pesticide rates (by 25% of insecticide and by 40% of fungicides) in case 5 with Albit contributed to a more significant decrease in Thiamethoxam content in potato tubers. In the first stages of determination, 65 and 75 days after the treatment of tubers in the case 5, Thiamethoxam content was 25.4-25.9% less than with the full rate of insecticides in the same period in the case 4. A similar trend continued further in terms of determination. Thiamethoxam was not found in the tubers on the 95th day in case 5 with reduced Thiamethoxam rates. At reduced pesticide rates and with Albit RP, a complete absence of the Thiamethoxam insecticide in the potatoes is achieved at the time of harvesting. This fully complies with strict requirements (*SanPin 2.3.2.1078-01*, 2002) for ecologically clean potato products intended for children and medical institutions.

The plant protection system in cases 6 and 7 with Siliplant was the most successful, not only in terms of yield but also in terms of the lowest content of harmful substances in tubers at all times of determination. In case 7 with Siliplant and at reduced pesticide rates as well as in case 5, the insecticide in the tubers was reliably absent before harvesting (95 days after). As for case 6 with Celest and at full rates of pesticides, only traces of the Thiamethoxam insecticide were found in 2015 on the 95th day before harvesting. In 2016 and 2017, there was no insecticide in tubers in case 6 before harvesting. It should be noted that starting from a period of 75 days after the treatment of tubers with pesticides, the residual amount of insecticides (from 0.038-0.032 to 0.028-0.017 mg/kg) in almost all (2-7) cases did not exceed Maximum permissible level (MAL) of 0.05 mg/kg in raw tubers. However, before harvesting, their concentrations in cases 2, 3, and 4 were significantly lower than MAL - from

0.007 to 0.0012 mg/kg. The yield of crops obtained on the indicated cases corresponds to sanitary and hygienic requirements and standards (*SanPin 2.3.2.1078-01*, 2002), as ecologically clean potatoes suitable for the nutrition of the adult population. Toxic substances were not found by the time of harvesting in cases 5, 6, and 7. Therefore, the system of plant protection from pests and diseases studied in these cases can be recommended for the production of ecologically clean potatoes.

Figure 1 shows the dynamics of Thiamethoxam decomposition in tops and tubers when using Celest TOP. Figure 1 shows that Thiamethoxam persists in the tops of potatoes after processing the tubers when planted with Celest TOP at the level of 0.069-0.031 mg/kg for 85-95 days. This provides a long-term protective effect of Thiamethoxam against an economically significant pest - the Colorado potato beetle (*Leptinotarsa decemlineata*). Such protection of vegetating plants from the pest is quite enough for the medium early variety Nevsky.

At the same time, two fungicides that are part of Celest TOP protect young seeds from black speck and other crop diseases starting from the date of planting tubers. The dynamics of Thiamethoxam decomposition, as follows from Figure 1, was parallel to the toxicant's decomposition in the tops, although not strictly proportionally. Thus, for example, on day 95, the tops of case 6 demonstrated the presence of 0.031 mg/kg. However, it was already absent from the tubers.

In the first period of determination, 65 days after planting in the case 6 with full pesticide rates, the content of insecticide in tubers was 28.6% higher than the MAL values (0.05 mg/kg). At the same time, in the case 7 with the reduced by 25% Celest rate, the residual amount of Thiamethoxam (exceeding MAL only by 2%) was actually at the maximum allowable level (MAL). A positive difference towards a lower content of residual insecticide with reduced Celest rates (case 7) persisted throughout the growing season. When analyzing samples 95 days after treatment, Thiamethoxam was not found in the tubers in the cases presented in Figure 1, which indicates complete decomposition of the toxicant. Thus, the present studies have solved the important task of neutralizing the accumulation of toxic insecticides in tubers by harvesting time when cultivating a medium

early variety of potato. This is achieved by using Celest TOP in rates reduced by 25%, in combination with Siliplant or Albit and fungicide in rates reduced by 40%. Production of ecologically clean potatoes is guaranteed with the most acceptable plant protection system in cases 5 and 7.

During the growing season, three types of fungicides were used in the recommended (*Directory of pesticides ...*, 1917, 2015, 2016) and reduced by 40% rates following the experimental design to protect plants from diseases on tops. These included Ridomil Gold MZ WDG (systemic product), Revus SC (translaminar product), and Shirlan SC (contact product). Ridomil Gold MZ WDG is a toxic fungicide because of Mancozeb content: the second hazard class for humans and the third hazard class for bees. The residual amount of Mancozeb (Ridomil Gold MZ WDG) in the samples of tubers taken 5 days after the treatment of potato plants amounted to 0.024 mg. After 10 days, it amounted to 0.002 mg, and after 20 days, this fungicide was not found. In this case, the acceptable value for Mancozeb is 0.1 mg/kg. Revus fungicide containing two active Mandipropamide 25% and Difenconazole 25% is not dangerous for the environment, humans, and bees because of low toxicity. The hazard class for mammals is three and for bees is also three. There are no restrictions on using it in the sanitary zone around fisheries. It quickly decomposes in plants (7-10 days) (*Directory of pesticides ...*, 1917, 2015, 2016). No residual amount of this fungicide was tested due to its low toxicity and rapid decomposition. Shirlan with the active substance of Fluazinam (500 g/l) is hazard class 2 for humans and hazard class 3 for bees. However, the agent is harmful to the inhabitants of water bodies. MAL for potatoes is 0.05 mg/kg. In the present studies, the tuber samples were taken 5 days after treatment contained 0.031 mg/kg of Fluazinam, 10 days after - 0.003 mg/kg, 20 days after - no fungicide was found. The results of analyzes on the residual amount of fungicides indicate a relatively rapid decomposition in tubers. Already 10 days after the last treatment, the amount of fungicides is only 0.002-0.003 mg/kg, and after 20 days, they are completely absent. Besides, the fungicides, which were studied, belong to medium or low toxic hazard classes (2 and 3). As a result, the fungicides used in the experiments did not create an obvious strain in fulfilling the task of obtaining ecologically clean potatoes. However, for guaranteed quality of

products supplied to children and medical institutions, it is advisable to reduce the rates of fungicides by 40%, as it is done in cases 5 and 7. In general, the level of chemicalization of cultivation should be significantly reduced when performing such a task to avoid inconsistencies and errors arising in large-scale production.

Nitrates are a significant hazard to human and animal health. Nitrites are formed from nitrates in the gastrointestinal tract of humans and warm-blooded animals. Nitrites cause severe illness in people due to the formation of methemoglobin in the blood. This is especially dangerous for children. The approved MAL of nitrates in potatoes for children and medical institutions set by the Russian Federation standards is not more than 80 mg/kg per raw tubers. MAL for adults is set at 250 mg/kg (*SanPin 2.3.2.1078-01*, 2002). The World Health Organization (WHO) has established the maximum non-dangerous daily dose of nitrates for humans with their systematic intake in the range of 3.65 mg per 1 kg of body weight (Edelev *et al.*, 2013). Developed countries of the European Union set the maximum allowable level of nitrates in potatoes for baby food within 3 mg% (30 mg/kg) (Damodaran *et al.*, 2012). Some researchers predict in advance nitrate accumulation in tubers by analyzing their content in potato leaves during the growing season (Dreyer, Bohm, and Dresow, 2011). Tubers were sampled in the experiment for analyzing nitrate content along the diagonal of the plot. This related to the general background of mineral fertilizers in the experiments, which was the dose of  $N_{75}P_{150}K_{120}$ . In 2015, the average experimentally observed nitrate content was 71.7 mg, in 2016 - 65.4 mg, in 2017 - 78.5 mg/kg of raw tubers. On average, over three years, with a predominance of 2 times in the proportion of phosphorus and of 1.6 times in potassium over nitrogen in the mineral fertilizer ( $N_{75}P_{150}K_{120}$ ), the nitrate content in tubers was 71.9 mg/kg at MAL equaling to 80 mg/kg for children and medical institutions. The predominance of the proportion of phosphorus and potassium over nitrogen in the fertilizer in a ratio of N:P:K equal to 1:2:1.6 inhibits the accumulation of nitrates in potato tubers. This fact underlines the importance of introducing increased doses of phosphorus to obtain potatoes with low nitrate content. If being guided by the standards of the European Union in terms of the nitrates content in potato products intended for children and diet food, when the content should not exceed 3 mg% (30



mg/kg), it is recommended to follow the previous studies (2011-2013). These studies found that only the dose of  $N_{30}P_{90}K_{60}$  with a nitrate content of 20.8 mg/kg meets the EU requirements. Since the subsequent dose of  $N_{60}P_{90}K_{60}$  results in 47.7 mg/kg of nitrates (Butov *et al.*, 2019).

#### 4. CONCLUSIONS:

1. There is a system in the Central Black Earth region of the Russian Federation, which has been developed to protect plants from pests and diseases for the medium-early variety of potatoes and which ensures a good level of yield and ecologically clean products. This goal can be achieved by using modern plant protection agents, a hazard class lower than the previous ones, in combination with new Albit and Siliplant, and reduced pesticide rates.

2. The protection system should include the treatment of tubers when planted with Celest TOP insectofungicide at a rate of 0.3 l/t reduced by 25% in combination with Albit RP 0.1 l/t or Silipant WS 0.04 l/t. For vegetative plants, fungicide rates are reduced by 40%, in combination with biological agents, including Ridomil Gold MZ WDG 1.5 kg/ha - the 1st treatment; Revus SC 0.36 l/ha - 2nd and 3rd treatments; Shirlan SC 0.24 l/ha - 4th and 5th treatments; Siliplant 2 times during the growing season 1.0 l/ha or Albit 2 times during the growing season 1.0 l/t. Such a plant protection system is guaranteed to ensure the production of medium early potato products, which are ecologically clean from pesticides and which are intended for children and medical institutions.

3. A good yield of 31.5-33.1 t/ha, with a nitrate content of 71.9 mg/kg, not exceeding the MAL for children and dietary nutrition of 80 mg/kg, was obtained against the background of the application rate of mineral fertilizers in a dose of  $N_{75}P_{150}K_{120}$  kg/ha with a ratio of N:P:K equal to 1:2:1.6. Reducing the nitrate content in tubers to EU standards of 3 mg % (30 mg/kg) can be successfully achieved by reducing the dose of nitrogen ( $N_{75}$ ) in full mineral fertilizer by at least two times.

#### 5. REFERENCES:

1. Butov, A.V. & Boeva, O.Yu. (2013). Ecologically clean potatoes. *Potato and Vegetables*, 5, 25-26.

2. Butov, A., Zakharov, V. & Zubkova, T. (2019). Biological quality and preservation of Potato under drip irrigation and different fertilizers. *Bulgarian Journal of Agricultural Science*, 25(Suppl. 2), 37-44.
3. Chernikov, V.A. & Sokolov, V.A. (2014). The strategy of obtaining ecologically clean products. *Agroecology*, 1, 13-18.
4. Damodaran, S., Tarkin, K.L. & Fennema, O.R. (Eds.). (2012). *Chemistry of food products*. St. Petersburg, Russia: Profession.
5. *Directory of pesticides and agrochemicals approved for use in the Russian Federation*. (1917, 2015, 2016). Moscow, Russia: Publishing House of Agrus.
6. Dospekhov, B.A. (2012). *Methods of field experience (with the basics of statistical processing of research results)*. Moscow, Russia: Book on Demand.
7. Dreyer, W., Bohm, W. & Dresow, J.F. (2011). Fruchtfolgestellung und N-Versorgung von Kartoffeln im Ökologischen Landbau sowie Möglichkeiten der Überprüfung des N-Versorgungsstatus. *Landbauforschung - Braunschweig*, 348, 43-54.
8. Edelev, D.A., Grebenkin, N.N., Baranov, A.N. & Royev, N.N. (2013). *Fundamentals of ecology and ecotoxicology*. Ryazan, Russia: Ryazan Publishing House.
9. Fedotov, V.A., Butov, A.V. & Goncharov, S.V. (2005). *Potato in the Black Earth forest-steppe*. Voronezh, Russia: Publishing House of the Voronezh State University.
10. Fokina, A.I., Ogorodnikova, S.Yu., Olkova, A.S., Skugoreva, S.G. & Lyalina, E.I. (2015). *Chemical fundamentals of ecotoxicology*. Kirov, Russia: LLC "Loban".
11. Kaplin, V.G. (2007). *Fundamentals of ecotoxicology*. Moscow, Russia: Koloss.

12. Kochurko, V.I., Abarova, E.E. & Zuev, V.N. (2013). *Fundamentals of organic farming: a practical guide*. Minsk, Belarus: Donarit.
13. Lysenko, N.N. & Dogadina, M.A. (2015). *Fundamentals of ecotoxicology*. Oryol, Russia: Oryol State Agrarian University.
14. Mineev, V.G. (Ed.). (2011). *Workshop on agrochemistry*. Moscow, Russia: Publishing House of Moscow University.
15. Rabinovich, G.Y. & Fomicheva, N.V. (2018). Efficacy of the liquid biological product on the growth and development of potatoes. *Indian Journal of Agricultural Research*, 52(2), 182-186.
16. SanPin 2.3.2.1078-01. (2002). *Hygienic requirements for safety and nutrition value of food products. Health and hygiene rules and standards*. Moscow, Russia: FSUE «InterSAN».
17. Simakov, E.A., Starovoitov, V.I. & Anisimov, B.V. (2013). *Potato industry*. Moscow, Russia: NPF AgroNif.
18. Tulcheev, V.V. & Yagforov, O.M. (2014). World potato market. *AIC: Economics and Management*, 5, 57-64.
19. Zeyruk, V.N., Vasiliev, S.V., Derevyagina, M.K., Belov, G.L., Novikova, I.I. & Belyakova, N.A. (2019a). Ecological problems of the protection of potatoes from diseases and pests. In *Phytosanitary technologies in ensuring the independence and competitiveness of the Russian agro-industrial complex: Collection of abstracts*. St. Petersburg, Russia: All-Russian Research Institute for Plant Protection.
20. Zeyruk, V.N., Vasilieva, S.V., Novikova, I.I., Belyakova, N.A., Derevyagina, M.K. & Belov, G.L. (2019b). Prospects for the development of environmental methods of protecting potatoes from diseases and pests. *Agricultural Science*, S3, 54-59.

**Table 1.** Yields and residual insecticides in potato tubers at a different system of plant protection from pests and diseases. Background –  $N_{75}P_{150}K_{120}$ . 2015-2017. Source: the authors

| Case   | Yield<br>t/ha | The residual amount of insecticides in tubers.<br>Numerator: the number of days from treatment.<br>Denominator: insecticide content in tubers, mg/kg<br>(MAL = 0.05 mg/kg). |           |            |              |
|--|---------------|---|-----------|------------|--------------|
|  |               | Thiamethoxam (Actara)   |           |            |              |
| 1. <i>Control</i> : Without treating tubers and tops with fungicides. Actara SC only, 0.06 l/ha was applied to tops 2-3 times during the growing season to protect from Colorado potato beetle ( <i>Leptinotarsa decemlineata</i> ), if necessary.   | 23.5          | 10 /0.081   | 20 /0.028 | 30 /0.0027 | 40/not found |
| 2. <i>Prestige SC</i> : Full pesticide rates, old agent. Prestige SC 0.7 l/t to tops. To vegetation. Ridomil Gold MZ WDG was applied at a rate of 2.5 kg/ha at the 1st treatment, Revus SC was applied at a rate of 0.6 l/ha at the 2nd and 3rd treatments, Shirlan, SC was applied at a rate of 0.4 l/ha at the 4th and 5th treatments. Hazard class - 1.   | 29.0          | Imidacloprid (Prestige)   |           |            |              |
|  |               | 65 /0.087   | 75 /0.038 | 85 /0.016  | 95 /0.007    |
| 3. <i>Celest Top</i> : Full rates. New agent Celest Top SC was applied at a rate of 0.4 l/t to tubers To vegetation: Ridomil Gold MZ WDG, 2.5 was applied at a rate of kg/ha at the 1st treatment, Revus SC was applied at a rate of 0.6 l/ha at the 2nd and 3rd treatments. Shirlan SC was applied at a rate of 0.4 l/ha at the 4th and 5th treatments. Hazard class - 2.   | 30.7          | Thiamethoxam (Celest)   |           |            |              |
|  |               | 65 /0.073   | 75 /0.032 | 85 /0.017  | 95 /0.0023   |
| 4. <i>Albit (+)</i> : Full rates. Celest Top was applied at a rate of 0.4 l/t + Albit RP was applied at a rate of 0.1 l/t to tubers. To vegetation: Ridomil Gold MZ WDG was applied at a rate of 2.5 kg/ha at the 1st treatment, Revus SC was applied at a rate of 0.6 l/ha at the 2nd and 3rd treatments. Shirlan SC was applied at a rate of 0.4 l/ha at the 4th and 5th treatments + Albit RP was applied 2 times during the growing season at a rate of 1.0 l/ha | 34.1          | Thiamethoxam (Celest)   |           |            |              |
|  |               | 65 /0.071   | 75 /0.027 | 85 /0.015  | 95 /0.0012   |
| 5. <i>Reduced rates of pesticides</i> to tubers and tops. To tubers: Celest Top was applied at a rate of 0.3 l/ha + Albit RP was applied at a rate of 0.1 l/t. To tops: Ridomil Gold MZ WDG was applied at a rate of 1.5 kg/ha at the 1st, 2nd, and 3rd treatments. Shirlan SC was applied at a rate of 0.24 l/ha at the 4th and 5th treatments + Albit RP was applied 2 times during the growing  | 31.5          | Thiamethoxam (Celest)   |           |            |              |
|  |               | 65 /0.053   | 75 /0.020 | 85 /0.011  | 95/not found |

|   |      |                       |           |           |              |
|---|------|-----------------------|-----------|-----------|--------------|
| season at a rate of 0.05 l/ha   |      |                       |           |           |              |
| 6. <i>Siliplant</i> (+): Full rates. To tubers: Celest Top was applied at a rate of 0.4 l/t + Siliplant WS was applied at a rate of 0.04 l/t. To vegetation: Ridomil Gold MZ WDG was applied at a rate of 2.5 kg/ha at the 1st treatment, Revus SC was applied at a rate of 0.6 l/ha at the 2nd and 3rd treatments, Shirlan SC was applied at a rate of 0.4 l/ha at the 4th and 5th treatments + Siliplant WS was applied 2 times during the growing season at a rate of 1.0 l/ha.        | 34.9 | Thiamethoxam (Celest) |           |           |              |
|   |      | 65 /0.070             | 75 /0.028 | 85 /0.013 | 95/not found |
| 7. <i>Reduced rates of pesticides</i> : To tubers: Celest Top SC was applied at a rate of 0.3 l/t + Siliplant WS was applied at a rate of 0.04 l/t. To vegetation: Ridomil Gold MZ WDG was applied at a rate of 1.5 kg/ha at the 1st treatment. Revus SC was applied at a rate of 0.36 l/ha at the 2nd and 3rd treatments. Shirlan SC was applied at a rate of 0.24 l/ha at the 4th and 5th treatments, Siliplant WS was applied 2 times during the growing season at a rate of 1.0 l/ha. | 33.1 | Thiamethoxam (Celest) |           |           |              |
|   |      | 65 /0.051             | 75 /0.017 | 85 /0.010 | 95/not found |
| Least significant difference <sub>05</sub> (average) t/ha.  | 1.6  |                       |           |           |              |

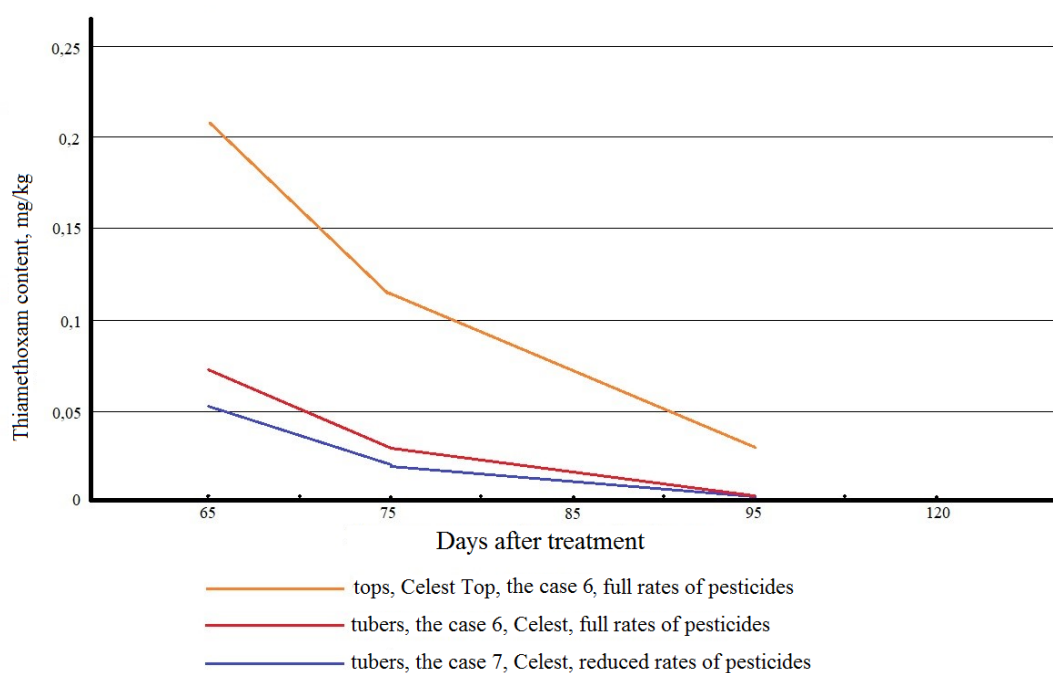


**Figure 1.** The dynamics of Thiamethoxam decomposition (Celest TOP) in tops and tubers. MAL is 0.05 mg/kg

**CARACTERÍSTICAS MORFOLÓGICAS E ANATÔMICAS DOS ESTADOS ETÁRIOS DE *Scutellaria stevenii* Juz. (*Scutellaria orientalis* subsp. *orientalis*) EM FITOCENOSES DA CRIMEIA DE ENCOSTAS****MORPHOLOGICAL AND ANATOMICAL FEATURES OF AGE STATES OF *Scutellaria stevenii* Juz. (*Scutellaria orientalis* subsp. *orientalis*) IN PHYTOCOENOSES OF THE CRIMEA FOOTHILLS****МОРФОЛОГИЧЕСКИЕ И АНАТОМИЧЕСКИЕ ОСОБЕННОСТИ ВОЗРАСТНЫХ СОСТОЯНИЙ *Scutellaria stevenii* Juz. (*Scutellaria orientalis* subsp. *Orientalis*) В ФИТОЦЕНОЗАХ ПРЕДГОРИЙ КРЫМА**

VAKHRUSHEVA, Lyudmila P.<sup>1\*</sup>; ABDULGANIEVA, Elvira F.<sup>2</sup>; AKHKIYAMOVA, Guzeliya R.<sup>3</sup>, SHICHIYAKH, Rustem A.<sup>4</sup>; AVDEEV, Yuri M.<sup>5</sup>

<sup>1,2</sup> V.I. Vernadsky Crimean Federal University, Faculty of Biology and Chemistry.

<sup>3</sup> Naberezhnye Chelny State Pedagogical University, Naberezhnye Chelny, Russian Federation.

<sup>4</sup> Kuban State Agrarian University named after I.T. Trubilin, Russian Federation.

<sup>5</sup> Vologda State University, Vologda. Russian Federation.

\* Corresponding author  
e-mail: vakhl@inbox.ru

Received 08 June 2020; received in revised form 26 June 2020; accepted 05 July 2020

**RESUMO**

Os recursos de implementação do ciclo de vida para a maioria das plantas são específicos da espécie, o que se reflete em uma mudança nas esferas morfológicas, anatômicas e fisiológicas da planta. Um estudo da ontogenese das plantas permite uma compreensão mais profunda das características coenóticas da população e do grau de influência do meio ambiente na implementação da ontomorfogênese das plantas. Este trabalho é dedicado ao estudo do ciclo de vida de uma das espécies taxonomicamente controversas de Crimeia - *Scutellaria stevenii* Juz. O estudo da ontogênese de *Scutellaria stevenii* foi realizado na natureza e para mudas e indivíduos jovens em laboratório. Os princípios de identificação e contabilização de critérios qualitativo-quantitativos foram utilizados para identificar características morfológicas características de vários estados etários. O estudo da estrutura anatômica dos órgãos vegetativos (raiz, caule, brotação) foi realizado com preparações temporárias de um tecido vivo, com métodos padrão. Nesse estudo, o ciclo de vida de *Scutellaria stevenii* contém 4 períodos ontogenéticos e 10 estados etários, que são realizados na ontogenese total ou parcial. No caso de desenvolvimento normal, a ontogênese dos genetes dura de 10 a 16 anos. Em indivíduos virgens que crescem em ecótopos móveis, foi encontrado um tipo de desenvolvimento polivariável. Indivíduos polvariantes formam o arbusto primário com xilorzomas de diferentes comprimentos que exercem a função de fixação adicional no solo e a formação de arbustos parciais que perdem sua conexão com o indivíduo primário pela idade geradora. A capacidade de indivíduos pré-regenerativos de se estabelecer vegetativamente pode ser considerada como adaptação compensatória devido à alta morte de mudas em fitocenoses naturais. As características anatômicas do caule e da raiz de várias idades indicam a partição incompleta morfológicamente não expressa. Esses critérios são uma adição importante à identificação morfológica da idade.

**Palavras-chave:** ciclo de vida, tipo de desenvolvimento polivariável, Crimeia.

**ABSTRACT**

The life cycle implementation features for most plants are species-specific, which is reflected in a change in the morphological, anatomical and physiological spheres of the plant. A study of plant ontogenesis allows a deeper understanding of both the coenotic features of the population and the degree of influence of the environment on the implementation of plant ontomorphogenesis. This work is devoted to the study of the life cycle of one of the taxonomically controversial species for Crimea - *Scutellaria stevenii* Juz. Ontogenesis study of

*Scutellaria stevenii* was carried out in nature and for seedlings and juvenile individuals in a laboratory. The concept of a discrete description of ontogenesis was used to describe the life cycle of *Scutellaria stevenii*, under which to revealed a group of anatomical and morphological features characteristic of each ontogenetic state. The study of the anatomical structure of the vegetative organs (root, stem, flower-bearing shoot) was carried out using temporary preparations of a living tissue with standard methods. In this study the life cycle of *Scutellaria stevenii* contains 4 ontogenetic periods and 10 age states, which are realized in full or partial ontogenesis. In the case of normal development, ontogenesis of genets lasts 10-16 years. In virginal individuals growing on mobile ecotopes, a polyvariant type of development have been found. Polyvariant individuals form the primary bush with xylorizomes of different lengths which carry the function of additional fixation in the soil and the formation of partial bushes that lose their connection with the primary individual by the generative age. The ability of pregenerative individuals to vegetatively established in our study can be considered as compensatory adaptation due to the high death of seedlings in natural phytocoenoses. The anatomical features of the stem and root of various age states to identify morphologically unexpressed incomplete partition. These criteria is an important addition to the morphological identification of age.

**Keywords:** *life cycle, polyvariant type of development, Crimea.*

## АННОТАЦИЯ

Особенности реализации жизненного цикла для большинства растений видоспецифичны, что отражается в изменении морфологической, анатомической и физиологической сферах растения. Изучение онтогенеза растений проводится с целью более глубокого понимания, как ценотических черт популяции, так и для выяснения степени влияния среды обитания на реализацию онтоморфогенеза растения. Данное исследование посвящено изучению жизненного цикла одного из таксономически спорных для Крыма видов – *Scutellaria stevenii* Juz. Изучение онтогенеза *Scutellaria stevenii* проводилось в природе и частично (проростков и ювенильных особей) в лаборатории. Для описания жизненного цикла шлемника Стевена использована концепция дискретного описания онтогенеза, согласно которой выявляется группа анатомо-морфологических признаков, характерных для каждого онтогенетического состояния. Исследование анатомической структуры проводилось с помощью временных препаратов, изготовленных вручную с использованием живых растений стандартными методами. В жизненном цикле *Scutellaria stevenii* выделено 4 онтогенетических периода и 10 возрастных состояний, которые реализуются в форме полного или частичного онтогенеза; в случае нормального развития онтогенез генеты длится 10-16 лет. У виргинильных особей, произрастающих на подвижных экотопах, обнаружен поливариантный тип развития, при котором первичный куст образует различной длины ксилоризомы, несущие функцию дополнительного закрепления в почве и образования парциальных кустов, которые к генеративному возрасту теряют связь с материнской особью. Установленная в нашем исследовании способность особей прегенеративного периода к вегетативному размножению, может рассматриваться как компенсаторная адаптация, обусловленная высокой гибелью проростков в естественных фитоценозах. В анатомическом строении корня и побега наблюдается неполная, морфологически невыраженная партикуляция, ограниченная, главным образом, зоной корневой шейки и базальной части главного корня. Эти критерии являются важным дополнением к морфологической идентификации возраста.

**Ключевые слова:** *жизненный цикл, поливариантность развития, Крым.*

## 1. INTRODUCTION:

*Scutellaria* L. - the numerous polymorphic genus of the family Lamiaceae (Labiatae) has more than 460 species according to the APG II system (The Plant List, 2019). *Scutellaria* genus presented to 5 species *S. albida* L. subsp. *albida*, *S. albida* subsp. *colchica* (Rech. f.) J.R. Edm., *S. altissima* L., *S. galericulata* L. and *S. orientalis* L. subsp. *orientalis* in the Crimea (2,3). Species composition of the genus *Scutellaria* has always had controversial issues, some of which continue to the present, especially regarding the intraspecific structure of *S. orientalis* L. (Pichugin, 2011; Yena, 2012).

Five Crimea endemic species *S. heterochroa* Juz., *S. hypopolia* Juz., *S. hirtella* Juz., *S. taurica* Juz. and *S. stevenii* Juz. were described by S. Yuzepchuk independent of *S. orientalis* based on morphological differences in the structure of the leaf blade and the pubescent character (Komarov, 1954). Such an opinion was supported and reflected in the summary of the flora of the Crimea peninsula by E. V. Wulf (1966) and V. Golubev (1996). The opposite view was expressed by D. Dobrochaeva, M. Kotov (Mosyakin, Fedoronchuk, 1999), according to which, described by S. Yuzepchuk, species

should be considered a different geographical race of *S. orientalis* (Yena, 2012). A similar trend is also incorporated in the last review of the flora of Crimea, in which the species is listed as *S. orientalis* L. subsp. *orientalis*. However, recent studies have shown a more complicated composition of *S. orientalis* distributed in the peninsula and the possibility of isolating distinct species. Such disagreements indicate the need for detailed research of the genus *Scutellaria* in the Crimea and the search for more "strong" keys for the differentiation of species (Pichugin, 2012).

Biomorphological features act as additional taxonomic criteria for distinguishing species (Savinykh et al.; Notov and Kusnetzova, 2004). At present, the life cycles of *Scutellaria* species growing on the territory of the Russian Federation have been described for *S. baicalensis* Georgi (Banaeva, 2000), *S. tuvensis* Juz., *S. galericulata* L., *S. supina* L., *S. tuvensis* Juz. (Guseva, 2013a,b,c,d).

The goal of this study was to identify the anatomical and morphological features of the age states of the life cycle of a well-differentiated species *S. stevenii*. The data on this ornamental plant is scarce and mainly concerns its distribution on the peninsula (Pichugin, 2012). The keys proposed by V. Pichugin for identifying 6 disputed subtaxa, among which *S. stevenii* is also included, are not sufficiently convincing and need further clarification.

## 2. MATERIALS AND METHODS:

The classification of life forms of higher plants by I. G. Serebryakova (1954; 1964) and Savinykh (2015) was adopted as the basis for the identification of types of biomorphs. The definition of the type of ontogenesis and variants of polyvariant development was carried out according to the classifications proposed by L. A. Zhukova (1983; 1995; 2001; 2013). At the heart of the allocation of age groups was the idea of T.A. Rabotnov (1950) about the division of the life cycle into four periods: latent (dormant seed time); virginal (from seed germination to reproduction of an individual in a generative way); generative; senile (senile). Rabotnov's ideas were supplemented by Uranov (1975) and his followers (Coenopopulations of plants ..., 1976, 1988; Nukhimovsky 1997; Ontogenetic Atlas ..., 1997, 2000, 2002, 2004; Zlobin (2012) as a result the modern periodization of the life cycle includes 4 periods, 2 subperiods

(embryonic and latent) and 12 ontogenetic ages: seeds (se), juvenile (j), immature (im), virgin (v), early ( $g_1$ ), mature ( $g_2$ ), later ( $g_3$ ) generative states, subsenile (ss) and senile (s) states).

The life cycle of *S. stevenii* was monitored at the 3 years in two natural populations growing in the foothill Crimea. The sample of plants for each age group was 30 individuals. Morphological parameters were measured in the natural population (Cheremisina et al., 2017, 2018). Seedlings and partially juvenile plants were observed in conditions of artificial cultivation.

Before germination, the seeds were sterilized in 3% hydrogen peroxide solution for 10 min and 70% ethanol for 1 min and then washed in 3 times 45 minutes in sterile distilled water. Then the seeds were transferred to a moistened filter paper, 50 pieces each, in sterile Petri dishes, and placed in a thermostat at 20-30. Seed germination was conducted in 2-fold repetition. Seed germination was determined on the seventh day (GOST, 2011; Zaripova, 2016).

Conclusions about the age of plants were taken based on the degree of xylem development and the number of annual rings of the primary root and stem. Anatomical cuts were carried out on live drugs (preparations) with 3-5 multiples for each age condition. Floroglucin dye was used to stain xylem tissues (Lotova, 2001; Barikina, 2004; Serebryakova, 2006). The microscopy of permanent and temporary preparations was carried out using the Olympus CX31RTSF microscope. The objects were photofixed by the Olympus digital camera (Industrial Digital Camera TOUPCAMTM U3CMOS10000KPA).

## 3. RESULTS AND DISCUSSION:

*Scutellaria stevenii* is a erosulate dwarf-shrub growing in tomillars and petrophytic steppes of the foothills, where it can perform the function of a dominant, and often determining the structure of phytocoenoses (Abdulganieva, 2013). In the spatial and ecological distribution, this species is mainly found to sloping calcareous gravelly and marl ecotopes. *S. stevenii* is morphologically close to the species *S. taurica* and different from it short tomentose pubescence of the stem and petioles. The upper side of leaves is rarely tomentose gray-green and densely white-tomentose with completely hidden veins in the underside. Leaf margins have



shorter and broader straight teeth (Komarov, 1954).

### 3.1. Latent and Pre-generative periods

In connection with the arisen difficulties of finding the seedlings in the natural environment, observation of this age was carried out in artificial conditions. **Seeds (se)** are small (2x1 mm), oval in shape, compressed laterally. Seed peel densely pubescent with short hairs due to the seeds are gray. Seed germination was determined on the seventh day, and it averaged 10%, which explains the difficulty of finding the seedlings in the natural phytocenosis. This low percent of germination can be attributed to the lack of endosperm in the seeds of the Lamiaceae family. The **seedlings (p)** have rounded cotyledons (at the time of opening 0.4 x 0.4 cm), are painted green. The development of the 2nd pair of leaves occurs at 4-5 days after planting in the soil. They, in contrast to the cotyledons, have a peristolped form with 3 lobes on each side (Figure 1).



**Figure 1.** Seedlings of *S. stevenii*.

In seedlings formed 1-5 leaves of similar shape. The emergence of seedlings in nature is timed to the end of February - March of the spring period or the end of September - October of the autumn period of germination.

In the case of normal development, by the end of the first month, the seedlings acquire the features of a **juvenile age (j)**. Their distinctive feature is the absence of cotyledons and the active appearance of leaves with 3 toothed lobes, which then die off successively, and well-marked scars remain in their place. The duration of this age from 2.5 to 3 months (Figure 2).



**Figure 2.** *S. stevenii* juvenile individuals.

Plants of **immature age (im)** are distinguished by the appearance of leaves with 4 toothed lobes on each side of the leaf blade (Figure 3). The position of the epicotyl and hypocotyl is typically perpendicular to the soil surface, but they can greatly change the angle of inclination due to the peculiarities of the microrelief of the territory. At immature age the individuals of *S. stevenii* leave for the 1st wintering period.



**Figure 3.** *S. stevenii* immature individual.

At 2-3 years of the life cycle of the plant enters a **virginal age (v)**, (Figure 4).





**Figure 4.** Virgin *S. stevenii*.

In this age, all the vegetative features of the adult plant are already formed: the leaves are ovate, along the edge are deeply crenate-toothed, with wide, straight, 5-7 teeth on each side. Lateral growth branch are develop at this age - usually after winter (less often summer) dormancy. The first leaves of lateral branches are morphologically similar to the leaves of a seedling or juvenile plant.

There are signs of polyvariant development of life cycle. Individuals growing on a horizontal surface of the relief go through 2 stages of morphogenesis: 1) primary shoot ( $p \rightarrow j \rightarrow im$ ); 2) the primary bush ( $v \rightarrow g_1 \rightarrow g_2 \rightarrow g_3 \rightarrow ss \rightarrow s$ ). With the growth of individuals on movable soils of the slopes, virginal plants form different lengths (from 5-30 cm) xylorrhizoma, on which developing secondary bushes. In this type of life cycle, an individual has 3 stages of development: 1) primary shoot ( $p \rightarrow j \rightarrow im$ ); 2) primary bush ( $v$ ), 3) secondary bush ( $g_1 \rightarrow g_2 \rightarrow g_3 \rightarrow ss \rightarrow s$ ), resulting from the destruction of xylorrhizoma between primary and secondary bushes (Figure 5).

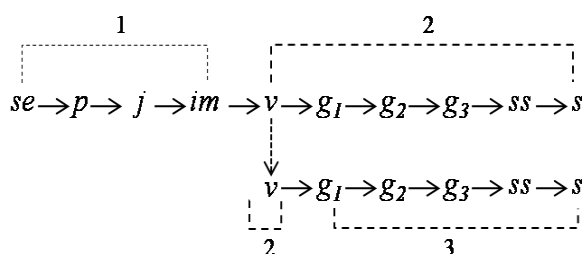


**Figure 5.** *S. stevenii* life cycle scheme  
1 – primary shoot; 2 – primary bush; 3 – partial bush.

The formation of this kind of rhizomes and secondary bushes provides a more vigorous fixation plant in the soil, the conquest of free

space. It compensates for the almost complete absence of sexual reproduction associated with the mass death of seedlings in a natural ecotope.

The general scheme of development of the pregenerative stage is shown in Figure 6, 7.

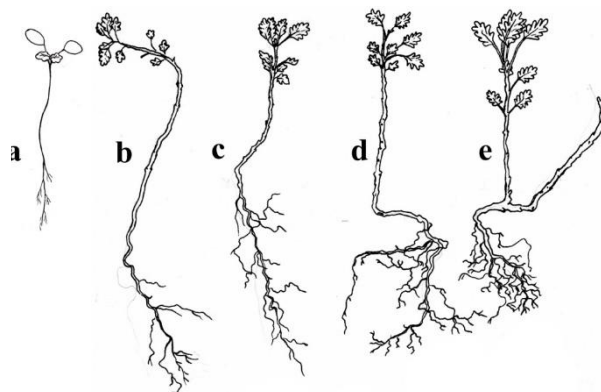


**Figure 6.** The scheme of the pregenerative period *S. stevenii*. a – seedling; b – juvenile plant; c – immature; d, e – virginal.

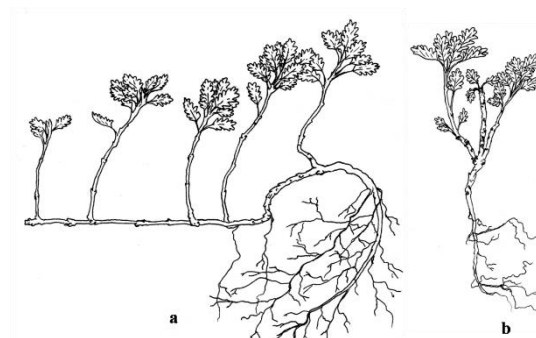


**Figure 7.** Variants of development of *S. stevenii* virginal individuals. a - formation of partial bushes on xylorrhizoma; b - virginal individual, preserving the structure of the primary bush.

### 3.2. Generative period

**Young generative plants ( $g_1$ )** are characterized by such an important feature as the loss of the connection of the parent plant with young bushes (particulas) that were formed in the virginal period of the life cycle.  $G_1$  usually has 2-3 woody branches of renewal, which can form 1-2 generative shoots (second-order growth axis). After flowering, the grassy part of generative shoots dies, and their woody bases begin to branch, giving the 3rd order growth axes.

*S. stevenii* generative shoots are monocyclic, and by the next spring, they die entirely until the lateral shoot but remain in contact with the parent plant. Therefore, in  $g_1$  individuals, shoots of the 2nd and 3rd orders remain capable of flowering, but the flowering shoots number is small (1-3). The flowers number in the inflorescence is 4-7. The main root is thickened, and the first signs of partitioning are noted in the anatomical structure. A large number of adventitious roots are formed. The root systems of young bushes are intensively developed, creating the secondary root system. The generative shoots formation and their transition to flowering in young bushes occur 1-2 years later than the primary individual. The duration of this age phase is 2-3 years (Figure 8).



**Figure 8.** Young generative individual.

**Mature generative (middle-aged) individuals ( $g_2$ )** are represented by a compact dwarf-shrub, composed of 18–20 mixed-age renewal growth axes, of which 1/3 (sometimes 1/2) are represented by generative shoots with 9–11 flowers. The lower parts of the perennial shoots begin to form the plagiotropic part, but at the same time, the compactness of the general structure of the dwarf-shrub is preserved. The function of the plagiotropic part is provided by dwarf-shrub regeneration and construction of the new above-ground growth axes. The fourth growth axes begin to appear. Some of the second-order shoots, in the basal part, acquires an oblique orthotropic position. On this part, a large number of renewal buds appear, from which can develop generative shoots or new renewal axes. The observed anatomical structure of the root shows the beginning of the particleon process in the mature generative plant. In this age, phase plant remains 2-4 years (Figure 9).



**Figure 9.** Mature generative (middle-aged) individual.

**Older generative plants ( $g_3$ )** are generally losing dwarf-shrub. At the base of vegetative and generative shoots, there is a distinctly pronounced plagiotropic part; therefore, spatially shoots acquire an ascending structure. The number of generative shoots decreases (less than 1/4 of the total), and the number of dead shoots of previous years increases, especially in the central part of the caudex. Also, the number of flowers in the inflorescence is reduced to 5-7. The degree of branching decreases only occasionally shoots of the 4th order of branching occur. The growth of shoots occurs mostly on the periphery of the dwarf-shrub. The bush becomes less dense, the main root twists along the central axis. In the root, anatomical partition processes continue. In this age phase, the plant remains 2-4 years (Figure 10).

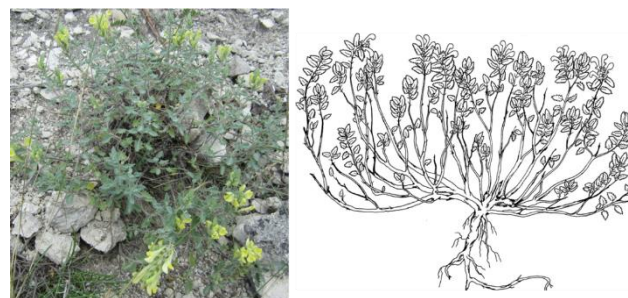


**Figure 10.** Older generative plants individual.

In **sub-senile plants (ss)**, primary growth axes are intensively dying. Plant height is 15–20 cm. In this phase, dwarf-shrub is preserved by 4–6 principal axes along the periphery of the bush, branching only in the upper part (3–4 shoots). There are 1-3 generative shoots; buds contain no more than 2-3 flowers. The adventitious roots do not develop, which reduces the ability of reproduction of the new lateral roots. The particleoning process in the anatomical structure of the primary root is more progressive. The



duration of this age phase is 1-2 years (Figure 11).

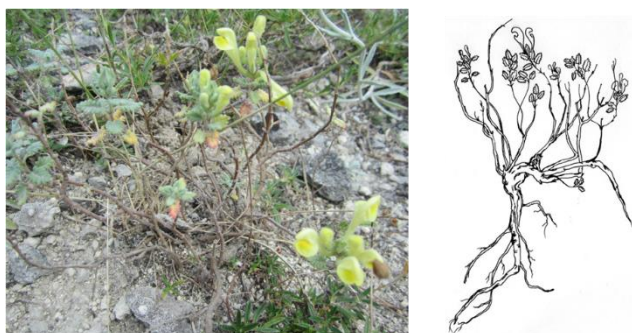


**Figure 11.** Sub-senile individual.

In individuals of the **senile age (s)**, generative shoots are not formed. In this phase, processes of the elimination of primary aerial axes and lateral roots increase. A perennial woody base, up to 3-5 cm in diameter, is formed from the basal parts of dead shoots. The height of the aboveground portion is 8-12 cm. The size of the leaf blade is significantly reduced, but the number of teeth (5-7 tooth), which is typical for adult generative plants, remains the same (Figure 12). The duration of this age phase is 1 year.



**Figure 12.** Senile individual.

### 3.3. The anatomical structure of the stem and root.

The lower ligneous part of the generative shoot is covered with secondary dermal tissue - periderm. Phellem (cork cells) has longitudinal gaps and consists of 3-4 layers of dead cells. Under periderm, there are 5-6 layers of parenchymal cells of the cortex. Phloem with poorly developed mechanical tissue surrounds the xylem in a continuous layer. The conducting elements of xylem are represented by radial rows of vessels separated by thin medullary rays and xylem fibers. In the center - the pith with a well-

defined perimedullary zone, including elements of the primary xylem (Figure 13).

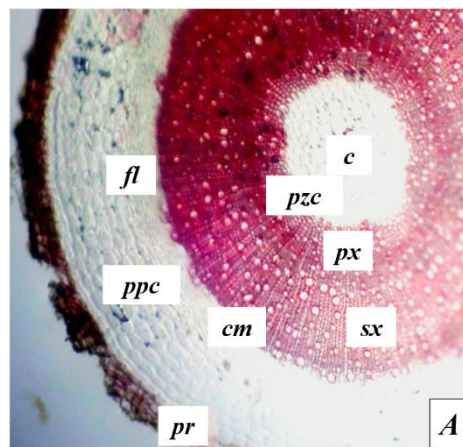


**Figure 13.** A – cross-section of the generative shoot of *S. stevenii*. sx – secondary xylem; cm – cambium; c – core, px – primary xylem; ppc – parenchyma of the primary cortex; pzc – perimedullary zone of the core; pr – periderm; fl – phloem, (15x20).

The main root is covered with a multilayer periderm of subepidermal origin, (Figure 14).

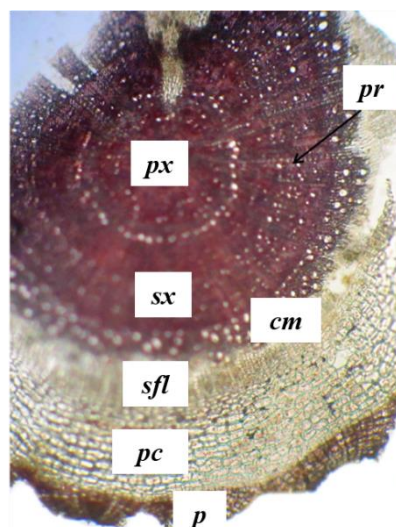


**Figure 14.** Cross-section of the main root of the generative individual *S. stevenii*. sx-secondary xylem; sfl – secondary phloem; cm – cambium; pc – primary cortex; px – primary xylem; pr – parenchymal ray; p – periderm (15x20).

The outer layers of the cork are formed of 3-6 rows of cells. Under the periderm, there are remnants of the cortex, formed by thin-walled cells elongated in the tangential direction (5-7 rows). After the inner layer of the cortex is functioning phloem. Narrow single-row rays

separate the xylem vessels in the radial direction. Between the conducting elements are located with non-woody fibers of the libriform

In the anatomical structure of the root of generative plants, signs of partition were found, the initial stages of which can be observed at 5-7 years of age in young generative individuals. In this age, the central cylinder in the cross-section becomes asymmetric, acquiring lobed outlines (Figure 15, A). The processes of xylem separation continue intensively along with the radial rays, and in the old generative individuals, they reach the middle of the stele. (Figure 15, B). The distance between the xylem segments is filled with parenchymal tissue. In some cases, the xylem is completely separating, forming small islands surrounded by parenchymal tissue (Figure 15, D). The processes of destruction of living tissues begin in the center of the cylinder and continue in the centrifugal direction, capturing the wood parenchyma and the parenchyma of radial rays. Dead tissue areas are don't coloring (Figure 15, C, E).

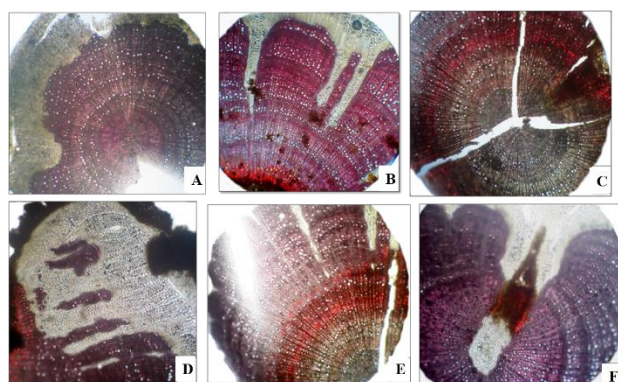


**Figure 15.** Anatomical features of root (A-E) and shoot (F) *S. stevenii* partition, (15x40).

Particle starts as a result of the spreading of traces of dead shoots to the root collar and further to the taproot. Partition of the shoot is visible in Figure 15 (F). The abundance of mechanical elements in the wood of the root and the long-term functioning of the growth axes determine the incomplete, morphologically unexpressed particularization, mainly limited by the root neck area and the basal part of the main root.

#### 4. CONCLUSIONS:

The leaf morphology and the teeth number of *S. stevenii* leaf blade are the main features of differentiation the preregenerative

period into 5 age states; the three age states ( $g_1$ ,  $g_2$  and  $g_3$ ) of generative period are differentiated by habitus, branch axes of 2-4th orders, the ratio of generative and vegetative shoots, and the number of flowers. In the senile period included two age-related states (s, ss) are differentiate according to the intensity of branching, partition and dying of the aboveground skeletal axes; the early stages of shrubs partition are clearly correspond to the anatomical features. The vegetative reproduction in the preregenerative period is a compensatory adaptation respond to the high flexibility of seedlings in natural phytocoenoses. This indicates a high ecological and morphological plasticity of the species due to a change in realization of ontogenesis. The primary taxonomic criteria for intraspecific differences between *S. stevenii* and *S. orientalis* are the presence of xylorizome, vegetative reproduction at virgin age and differences in the teeth number of leaf margin.

#### 5. REFERENCES:

1. Abdulganieva, E. F. (2013). Phytocoenotic confinement of *Scutellaria stevenii* Juz. in the Belogorsk district (AR Crimea). *Mater. VIII Intern. conf. young scientists "Biology: from a molecule to the biosphere"* [Mater. VIII mezhdunar. konf. molodykh uchenykh "Biologiya: ot molekuly do biosfery"]. Kharkov, p. 201.
2. Banaeva, Yu. A. (2000). Ontogenesis of Baikal skullcap. *Ontogenetic Atlas of Plants* [Ontogeneticheskii atlas rastenii]. pp. 180-185 (in Russian)
3. Barikina, R. P., Veselova, T.D., Devyatov, A. G., Dzhalilova, H. H., Iliina, G. M., Chubatova, N. V. (2004) *Spravochnik po botanicheskoy mikrotekhnike. Osnovy i metody* [Handbook of Botanical Microtechnology. Basics and Methods], Moscow, Publishing house of the Moscow State University, 312 p. (in Russian)
4. Cheremisina, O., Sergeev, V., Alabusheva, V., Fedorov, A., & Iliyna, A. (2018). The efficiency of strontium-90 desorption using iron (III) solutions in the decontamination process of radioactive soils. *Journal of Ecological Engineering*, 19(2), 149-153. doi:10.12911/22998993/81838

5. Cheremisina, O., Sergeev, V., Fedorov, A., & Ilyina, A. (2017). Problems of protection of urban areas from radionuclides strontium-90 and caesium-137 after technological disasters. *Journal of Ecological Engineering*, 18(3), 97-103. doi:10.12911/22998993/70201
6. Dobrochaeva, D. N. [et. all] (1987). *Opredelitel vysshikh rastenii Ukrainy* [The determinant of higher plants of Ukraine]. Kiev, Naukova dumka Publ., 548p.
7. Fedorov, A. A. (ed.). (1978). *Flora Evropeiskoi chasti SSSR* [Flora European part of the USSR]. Leningrad, Nauka Publ., vol. 20, 259 p. (in Russian)
8. Golubev, V. N. (1996). *Biologicheskaya flora Kryma* [The biological flora of the Crimea]. Yalta, GNBS, 126 p. (In Russian)
9. GOST 12038-84 [State Standard] *Agricultural seeds. Methods for determination of germination* (with changes No. 1, 2), Moscow, Standartinform, 2011, 30 p (in Russian)
10. Guseva, A .A. (2013) Ontogenesis of *Scutellaria tuvensis* Juz. *Ontogenetic Atlas of Plants* [Ontogeneticheskii atlas rastenii]. vol. 7, pp. 125-127. (in Russian)
11. Guseva, A. A. (2013). Ontogenesis of *Scutellaria supina* L. *Ontogenetic Atlas of Plants* [Ontogeneticheskii atlas rastenii]. vol. 7, pp. 117-120. (in Russian)
12. Guseva, A. A. (2013). Ontogeneticheskaya struktura *Scutellaria tuvemis* Juz. [Ontogenetic structure of *Scutellaria tuvemis* Juz.] *Botanicheskoe obrazovanie v Rossii: proshloe, nastoyashchee, budushchee: materialy I Vserossiiskoi nauchno-prakticheskoi konferentsii, Novosibirsk, 13-15 maya 2013* [Botanical Education in Russia: Past, Present, Future: Proceedings of the First All-Russian Scientific Practical Conference, Novosibirsk, May 13-15, 2013]. Novosibirsk, pp. 21-22. (in Russian)
13. Guseva, A. A. (2013). Ontogeneticheskaya struktura *Scutellaria galericulata* L. [Ontogenetic structure of *Scutellaria galericulata* L.] *Printsipy i sposoby sokhraneniya bioraznootvornosti: materialy V Mezhdunar. nauch. konf. (Yoshkar-Ola, 9-13 dek. 2013 g.)* [Principles and methods of biodiversity conservation: Proceedings of the V Intern. scientific conf. (December 9-13, 2013)]. Yoshkar-Ola, Ch. 1, pp. 243-245. (in Russian)
14. Komarov, V. L. (ed.). (1954). *Flora SSSR* [Flora of USSR]. Moscow, AN SSSR Publ., vol. 20, 555 p. (In Russian)
15. Lotova, L. I. (2001) *Morfologiya i anatomiya vysshikh rastenij* [Morphology and anatomy of higher plants], Moscow, Editorial URSS, 528 p. (in Russian)
16. Mosyakin, S. L.; Fedoronchuk M.M. (1999). Vascular plants of Ukraine: a nomenclatural checklist. Kiev, M.G. Kholodny Inst. of Botany Publ., 346 p.
17. Notov, A. A.; Kusnetzova, T. V. (2004). Architectural units axially and their taxonomic implications in Alchemillinae. *Wulfenia*, vol. 11, pp. 85–130.
18. Nukhimovsky, E. L. (1997) *Osnovy biomorfologii semennykh rastenij. Teoriya organizatsii biomorf* [Fundamentals of biomorphology of seed plants. Theory of biomorph organization] Moscow, Nedra, Vol. 1, 630 p.
19. Ontogenetic Atlas of Medicinal Plants (Ed. L. A. Zhukova) Vol. 1, Yoshkar-Ola, 1997, 239 p. (in Russian)
20. Ontogenetic Atlas of Medicinal Plants (Ed. L. A. Zhukova) Vol. 2, Yoshkar-Ola, 2000, 267 p. (in Russian)
21. Ontogenetic Atlas of Medicinal Plants (Ed. L. A. Zhukova) Vol. 3, Yoshkar-Ola, 2002, 284 p. (in Russian)
22. Ontogenetic Atlas of Medicinal Plants (Ed. L. A. Zhukova) Vol. 4, Yoshkar-Ola, 2004, 239 p. (in Russian)

23. Pichugin, V. S. (2011). Distribution of *Scutellaria orientalis* in the Crimea. *Optimization and Protection of Ecosystems* [Ekosistemy, ikh optimizatsiya i okhrana]. iss. 4, pp. 65-70. (in Russian)
24. Pichugin, V. S. (2012). The Crimean endemics of the genus *Scutellaria* (Lamiaceae). *Optimization and Protection of Ecosystems* [Ekosistemy, ikh optimizatsiya i okhrana]. iss. 6, pp. 109–114. (in Russian)
25. Rabotnov, T. A. (1950). The Life Cycle of Perennial Herbaceous Plants in Meadow Cenoses *Trudy BIN AN SSSR* [Trudy BIN AN SSSR]. Seriya 3, issue 6, pp. 7-204. (in Russian)
26. Savinykh, N. P., Cheryomushkina, V. A. (2015). Biomorphology: Current status and prospects. *Contemporary Problems of Ecology*. Iss. 8, pp. 541-549.
27. Savinykh, N. P.; Cheryomushkina, V. A. (2015). Biomorphology: Current status and prospects. *Contemporary Problems of Ecology*, iss. 8, pp. 541-549. DOI: 10.1134/S1995425515050121
28. Serebryakov, I. G. (1954) Biological-morphological and phylogenetic analysis of life forms of angiosperms. *Scientists notes of the Moscow State Pedagogical Institute* [Uchen. zap Mosk. mountains ped. Inst.]. vol. 37, iss. 2, p. 21-89. (in Russian).
29. Serebryakov, I. G. (1964) Life forms of higher plants and their study. *Polevaya geobotanika* [Field geobotany]. Vol. 3, pp. 146-205. (in Russian)
30. Serebryakova T. I., Sokolova T.G. (Resp. ed.) *Cenopopulyacii rastenij (oчерki populyacionnoj biologii)* [Coenopopulations of plants (essays on population biology)]. Moscow, Publishing House of Science, 1988, 184 p.
31. Serebryakova, T. I., Voronin, N. S., Elenevsky. A. G. *et al.* (2006) *Botanika s osnovami fitocenologii* [Botany with the basics of phytocenology]. Moscow, Akademkniga, 543 p. (in Russian)
32. The Plant List [Electronic resource]. URL: <http://www.theplantlist.org/> (reference date: 20.04.2019).
33. Uranov, A. A. (1975). Age range of coenopopulations as a function of time and energy wave processes. *Biological Sciences* [Biologicheskie nauki]. no 2, pp. 7-34. (in Russian)
34. Uranov, A. A.; Serebryakova, T. I. and all (ed.) (1976). *Cenopopulyacii rastenij rastenii (osnovnye ponyatiya i struktury)* [Coenopopulations of plants: General Concepts and Structure]. Moscow, Nauka Publ., 217 p. (in Russian)
35. Wulf, E.V. (1966) *Flora of Crimea. Vol. 3. Issue. 2. Convolvulaceae-Solanaceae* (Ed. I. N. Rubtsova), Yalta City Printing House, Kolos, 257 p.
36. Yena, An. V. (2012). *Prirodnaya flora Krymskogo poluostrova* [Spontaneous Flora of the Crimean Peninsula]. Simferopol, N. Orianda, 232 p. (In Russian)
37. Zaripova, A. A. (2016) Introduction to *in vitro* culture of *Scutellaria baicalensis*. *Bulletin of Botanic Garden of Saratov State University*, Vol. 24, iss. 1, pp. 94-98. (in Russian)
38. Zhukova L. A., Polyanskaya T. A. (2013) About some approaches to forecasting prospects of development coenopopulation. *Herald of Tver State University. Series: Biology and Ecology*, No 31, pp. 160-171. (in Russian)
39. Zhukova, L. A. (1983) Ontogenesis and plant reproduction cycles. *ZHurnal Obshchej biologii* [Journal of General Biology], Vol. 44, No 3, pp. 361-374. (in Russian)
40. Zhukova, L. A. (1995) *Populyacionnaya zhizn' lugovyh rastenij* [Population life of meadow plants.]. Yoshkar-Ola, Lanar, 224 p. (in Russian)
41. Zhukova, L. A.; Glotov, N. V. (2001). Morphological polyvariation of ontogenesis in natural plant populations.



Ontogenez [Ontogenesis]. vol. 32 (6), pp. 455-461. (in Russian)

42. Zlobin, A. Yu. (2012). Rare plant species: Floristic, phytocenotic, and population approaches. *Biology Bulletin Reviews*, vol. 2, iss. 3, pp. 226–237. DOI: 10.1134/S2079086412030073.

## MACRÓFAGOS REGENERATIVOS: UMA NOVA ESPERANÇA PARA CARDIOMIOPATIA

## REGENERATIVE MACROPHAGES: A NEW HOPE FOR CARDIOMYOPATHY

PUTRANTO, Terawan Agus<sup>1\*</sup>, IKRAR, Taruna<sup>2</sup>., WASKITO, Pujo<sup>3</sup><sup>1</sup> The Indonesia Army Medical Sciences Institute (THIAMS), Central Jakarta, Indonesia.<sup>2,3</sup> RSPAD Gatot Subroto, Central Jakarta, Indonesia.

\* Corresponding author  
e-mail: terawan@rspadgs.net

Received 13 June 2020; received in revised form 29 June 2020; accepted 06 July 2020

## RESUMO

Globalmente, as doenças cardiovasculares (DCV) são a principal causa de morte. Prevê-se que 23,6 milhões de pessoas morrerão em 2030 tendo como causa principalmente derrames e ataques cardíacos. Este estudo teve como objetivo investigar o novo tratamento da cardiomiopatia, uma doença cardiovascular que dificulta o fornecimento de sangue do coração para o corpo e pode causar insuficiência cardíaca. Embora o tratamento tradicional se concentre na reabilitação cardíaca, incluindo exercícios de aconselhamento e prescrições de estilo de vida, cirurgia na artéria coronária e medicamentos para aumentar o fluxo sanguíneo, o uso de células terapêuticas é uma nova forma para lidar com doenças cardiovasculares e infarto do coração. Pretende substituir efetivamente ou regenerar as células cardíacas mortas ou danificadas, de forma eficaz, como a principal vantagem deste tratamento. O uso de método alternativo para tratar as doenças cardiovasculares tem alto valor potencial, conforme encontrado no método de imunoterapia através do uso de "macrófagos regenerativos". Trata-se de um estudo qualitativo de pesquisa de relato de caso em que fornece uma exploração do fenômeno ou oportunidade de compartilhar esforços para intervir anteriormente na saúde de um único paciente com recursos de saúde não relatados. O resultado deste estudo mostrou que um homem de 71 anos foi hospitalizado no Hospital Central do Exército de Gatot Soebroto, em Jacarta, na Indonésia, pelo diagnóstico de doença arterial coronariana. Ele apresentou tosse crônica e edema periférico. Negava síncope, dispnéia, náusea, vômito e diaforese. A aplicação da ecocardiografia referente ao tratamento anterior indicou disfunção diastólica, hipocinesia do ventrículo esquerdo e hipertrofia ventricular esquerda com 44% de baixa ejeção na fração. Após a vacinação da terapia com Macrófagos Regenerativos (ReM), foram observadas melhorias significativas nos parâmetros ecocardiográficos, com cinética normal, fração de ejeção melhorada e disfunção diastólica que aumentou para 56%. Significativamente, os macrófagos regenerativos podem ser uma opção de imunoterapia em pacientes com cardiomiopatias com baixo risco de tratamento eficaz.

**Palavras-chave:** *Macrófagos Regenerativos, Cardiomiopatia, Ecocardiografia, Fração de Ejeção.*

## ABSTRACT

Globally, cardiovascular diseases (CVD) are the number one cause of death. It is predicted that 23.6 million people will die from it by 2030, mainly caused by strokes and heart attacks. This study aimed to investigate the new treatment of cardiomyopathy, a cardiovascular disease that hinders blood supply from the heart to the body and can cause heart failure. While the traditional treatment focus on cardiac rehabilitation, including lifestyle counseling and prescription exercise, surgery on coronary bypass artery, and medication of increasing the flow of blood, the use of therapeutic cells is a new way to deal with cardiovascular diseases and heart infarction. It intends to effectively replace or regenerate dead or damaged heart cells, as the main advantage of this treatment. The use of alternative methods to treat cardiovascular diseases has high potential value, as found in the immunotherapy method through the use of "regenerative macrophages." This study is a qualitative case report research study which provides an exploration of phenomenon or opportunity of sharing efforts to intervene single patient's health with unreported health features previously. The result of this study showed that a 71 years old man was hospitalized in Gatot Soebroto Central Army Hospital Jakarta, Indonesia, by the diagnosis of coronary artery disease. He presented for chronic cough and peripheral edema. He denied syncope, dyspnea, nausea, vomiting, and diaphoresis. The application of echocardiography regarding the previous treatment indicated diastolic dysfunction, left ventricle hypokinesis and left ventricular hypertrophy with 44% of low ejection on the fraction. After the vaccines of Regenerative Macrophages (ReM) therapy were given to the patient, significant improvements in the echocardiography parameters were observed, with normal kinetics, improved ejection fraction, and diastolic dysfunction increased to 56%. Significantly, regenerative macrophages could be an option of immunotherapy in patients with cardiomyopathies with low risk of effective treatment further.



## 1. INTRODUCTION:

As the leading cause in over budgeting for universal coverage in terms of health blanket insurance in developing countries, cardiovascular disease (CVD) gets its vital concern for years. Its symptoms appear mostly at middle age along with pathological features called atherosclerosis. Acute coronary and cerebrovascular events frequently suddenly occur, and are often fatal before medical care can be given. Modification of treatment risk factors has been shown to reduce mortality and morbidity in people with diagnosed and undiagnosed cardiovascular disease (CVD). Cardiovascular disease is characterized by its high prevalence as the leading cause of early morbidity in the population (Apetrei-Corduneau, Fildan, Radu, Statescu, Nemteanu, Lupusoru., 2020., Diaconu, 2019).

The devitalizing impediment found in CVD is usually seen in middle-aged or older adults and women. However, atherosclerosis, the principal pathological process leading to coronary artery disease, cerebral artery disease, and peripheral artery disease, begins early in life and progresses gradually through adolescence and early adulthood (Berenson *et al.*, 1989., Zieske, Malcom, & Strong, 2002., Mendis *et al.*, 2005).

Several factors cause an increased risk of the threat of someone suffering from cardiovascular disease, one of which is the rate of development of atherosclerosis. It is exacerbated by smoking habits, improper dietary patterns without being balanced with physical activity, diabetes, dyslipidemia, and hypertension which are risk factors as triggers for the blockage of blood flow, and narrowing of blood vessels because of continued effects of the development of atherosclerosis which can trigger severe illness such as; myocardial infarction, stroke, transient cerebral ischemic attacks, and angina.

There are some ways of therapy to halt cerebral, peripheral vascular, and coronary events without putting aside aspects of intensity and particular aversive action to predict any risks of vascular features as the guidance leading for decision.

The most current treatment applied for most patients with cardiovascular diseases is by having healthy living behavior continued by taking medicine when needed to reduce the occurrence of strokes and heart attacks which directly affect

the reduction in mortality, morbidity, and premature disability. Nearly most people are unaware or aware of their status against potential CVD attacks. With self-screening, it will be able to detect several risk factors that arise, such as blood pressure, blood glucose, and blood lipids (Tunstall-Pedoe, 2003). By the result of screening for the risk of their status in CVD, it can be used as a guide for further action, whether in the form of a healthy lifestyle program related to the type of food intake, or physical exercise that can cure patients at an affordable cost. (World Health Organization, 2003).

The pattern of prevention of CVD by being associated with existing risk factors will be very significant in the accuracy of the diagnosis and clinical action taken on patients. Other considerations, such as the type of food intake and physical body processing, should also not be ruled out because it is related to the type, dose, and time of medication given to patients for continued risk control. Efficiency and effectiveness in managing patients become a necessity amid limited resources through a risk stratification approach (Integrated cardiovascular management, 2002). Administration of drugs in patients with diastolic blood pressure above 90 mmHg, systolic levels above 150 mmHg, and blood cholesterol levels above 5.0 mmol/l can reduce the risk of cardiovascular disease by one third to a quarter (Lewington., & Clarke, 2005; Baigent *et al.*, 2005., Turnbull, 2003., Sever, 2003., Lewington *et al.*, 2002., Lawes *et al.*, 2003., & LaRosa, He, Vupputuri, 1999). To anticipate cardiovascular disease contributed by blood compulsion is in proceeding toward of overall risk of 5-8 mmHg (diastolic), 10-15 mmHg (systolic) and included blood cholesterol at approximately 20% integrated medication with antihypertensive and statins, then cardiovascular disease morbidity and mortality would be reduced by up to 50% (Wald ., & Law, 2003). People at very high CVD risk would bring more positive and significant results in the perspective of total circumstances as the declining risk of CVD toward higher diagnostic risk (MacMahon., & Rodgers, 1993).

However, the disadvantages of this regular or traditional treatment are at the cost of medicines. It is a significant component of total preventive health care costs, and particularly relevant to base drug treatment decisions on an individual's risk level, and not on arbitrary criteria, such as the ability to pay, or on comprehensive

preventive strategies. Also, the cumulative risk of CVD, which uses risk scoring methods, has been shown to be both expensive and less effective.

For people or patients who have a history or record of transient ischemic attacks, myocardial infarction, a stroke, which generally begins with atherosclerosis symptoms, it becomes an essential record in efforts to obtain other treatment methods. This is crucial because there is a very high risk of coronary, peripheral, and cerebral artery stability. The patient's history of the tendency of CVD symptoms will affect the type of care given to reduce mortality and or the cost of care for patients who recover. Stratification risk charts are unnecessary to arrive at treatment decisions for these categories of patients. They require another option of medical treatment, which not only to have healthy food but also an intervention in how to stop smoking, achieve ideal weight and have regular body exercise, which is highly cost and consuming much time (World Health Organization, 2003; Tunstall-Pedoe, 2003).

Therefore, this study aimed to investigate the new treatment of cardiovascular disease as occurred in cardiomyopathy in a less expensive and complicated procedure to reduce the risk of death to respond to the patients' needs for medication.

## 2. REVIEW OF LITERATURE:

### 2.1. Macrophages

Macrophages were first discovered by Ilya Metchnikoff in the late 19th century and are conserved phagocytes evolutionary that evolved more than 500 million years ago as the system against occurred injury (Yonggang, Merry., *et al.*, 2018). They belong to white blood cell digests cancer cells, foreign substances, cellular debris, and microbes, and any other substances that have specific proteins for the body's health on its surface, namely as phagocytosis.

They are found basically in all tissues by amoeboid movements to patrol for potential pathogens. The forms of these macrophages are varied (with various names) along the body (for example, Kupffer cells, microglia, histiocytes, alveolar macrophages) as part of the system in mononuclear phagocyte. They keep up their essential role as the protection by the mechanism of defense both in innate immunity and adaptive immunity by involving other immune cells such as lymphocytes (Yonggang, Merry., *et al.*, 2018., Gordon, 2007., Epelman, Lavine, Randolph, 2014).

In addition, to improve stimulation and inflammation towards the immune system, they can be functioned as reducing reactions on immunity and anti-inflammatory by releasing cytokines Ben-Mordechai., Palevski., Glucksan-Galnoy., Elron-Gross., Margalit., Leor, 2015). Macrophages which can lead into inflammation are labeled as M1, while others heading to declining on inflammation and supporting the repair on tissues are tagged as M2.10 The main difference between two of them are found in their metabolism where M1 includes unique ability to metabolize arginine into nitric oxide "killer" molecules. At the same time, M2 can metabolize arginine into ornithine "repair" molecules (Gombozhapova, Rogovskaya, Shurupov., *et al.*, 2017., Martine., Sica, Mantovani., & Locati, 2008).

### 2.2. Physical Examination

It is exposed that around 21 micrometers (0,00083 in) in the diameter of human macrophages are resulted by the categorization of monocytes' tissue (Gombozhapova, Rogovskaya, Shurupov., *et al.*, 2017., Martinez., Sica, Mantovani., & Locati, 2008). By applying cytometry flow or immune histochemical staining with a particular expression of their proteins such as lysozyme M, MAC-1 / MAC-3, and CD68, CD14, CD40, CD11b, CD64, F4 / 80 (rat) / EMR1 (human) (Pelegrin., & Surprenant, 2009). These characteristics are mentioned in table 1 (Bai, Adriani, Dang., *et al.*, 2009., Colin, Chinetti-Gbaugidi., & Staels, 2014). M2a and M2c macrophages are mainly undertaking to coordinate the response of adaptive, while M2b macrophages suppress (inflammation, fibrosis) and tissue remodeling (Lindset., & Saucerman, 2016).

### 2.3. Parameters Checked

The parameter or macrophages are the total number of viable cells, proportion of viable cells, proportion of TLR 2- Positive cells, the proportion of CD 274 positive cells, the balance of CD 80 positive cells, the proportion of CD11c positive cells. The required review result of each: the total number of viable cells  $\geq 1 \times 10^6$  cells proportion of viable cells  $> 50\%$  proportion of TLR 2- Positive cells  $\leq 40\%$ , the proportion of CD 274 positive cells  $\geq 50\%$ , the proportion of CD 80 positive cells  $\leq 75\%$ , the proportion of CD11c positive cells  $\geq 90\%$ .

Cardiomyopathy patient that refused CABG and PCI come to cell cure. The doctor that cell-cure qualified takes a medical history and do

a physical examination. Physical examination consists of head to toe checking and vital sign. After that, the patient received a series of examinations in the laboratory, such as complete blood count, liver function, renal function, and immunoserology (HIV, Hep B, and Hep C). After that, the cell cure takes whole blood with two techniques. First, it was done manually (without the device). The whole blood had been taken as much as 9 cc x 23 tubes. Total whole blood is 207 cc. Second, it was used leukapheresis to get monocyte from the leukocyte. After that, it was processed in a clean-room. To get the monocyte cell, a labeling system was used with a flow cytometer. Similar things to the monocyte that manipulated become macrophages were done. It was also used as a labeling system with flow cytometry until it gets macrophages that were wanted.

In contrary to recently used treatments, Therapeutic methods immunotherapy have the significant possibility to encourage and promote endogenous mechanisms of cardiac repair and give the main element for full regeneration of damaged heart tissue (Lemcke., Voronina., Steinhoff., *et al.*, 2018).

Most of the macrophages are located in the strategic point where the accumulation of microbial invasion may take place along together in the mononuclear phagocyte system. Each type of macrophage, determined by its location, has a specific name (Kara, Spiller., & Timothy, 2017). Macrophages can express the function of paracrine within an organ that is specific to the role of that organ. The viable cells of ReM that needed to stimulate a robust inflammation immune response is  $\geq 1 \times 10^6$  cells). ReM was administrated by intravenous therapy (IV) (Figure 1).

Macrophages are widely distributed in the human body. Macrophages play a role in the inflammatory process as the body's reaction to foreign matter or microbes. In neoplastic growth, macrophages are found in the extracellular space. These macrophages in the extracellular space are known as tumor-associated macrophages (TAMs). For years it has been known that TAMs are the main cellular component of cancer in humans. However, it is still difficult to understand how the process and mechanism. Macrophages phagocytose pathogens, dead cells, and some elements in the matrix extracellular. Macrophages also function to regulate organ and homeostasis remodeling. During tissue regeneration or healing, macrophages stimulate angiogenesis and facilitate tissue remodeling by protease secreting

and growth factors. Macrophages in tissue can be identified by the expression of several markers; in humans, the marker is CD68. The majority of macrophages are in the area perivascular wound healing area

In some cases, the pathogenesis of cardiomyopathy remains unknown and thus is classified into idiopathic cardiomyopathy. Previously, ischemic cardiomyopathy was also included in the category of cardiomyopathy but the current consensus separates it into coronary heart disease. The causes of cardiomyopathy are various, but the most common is inherited genetic factors, both autosomal dominant and recessive, and related to sex chromosomes. Other causes include toxins related to alcohol use disorder, cocaine and amphetamine use disorder, or the use of chemotherapy drugs.

The patient wanted an advance therapy, but he refused coronary artery bypass graft (CABG). The doctors want to increase survival rate with gave especially regenerative macrophages vaccine therapy. After this intervention approach, the patient had been checked by echocardiography. The result was significantly changed and increased. Echocardiography showed diastolic dysfunction, left ventricular hypertrophy, ejection fraction, and normokinetic, from 44% became 56 %.

Macrophages can migrate out of the vascular system by crossing cell membranes from capillaries and entering the area between cells that are being targeted by pathogens. Neutrophils are the most efficient phagocytes followed by macrophages and can digest large amounts of bacteria or other cells. Binding of bacterial molecules to the surface receptors of macrophages triggers the process of swallowing and destroying bacteria through "respiratory attack", causing the release of reactive oxygen species (ROS). The pathogen also stimulates macrophages to produce chemokines, which call other phagocytic cells around the infected area to give influence on the development of chronic inflammatory diseases such as cardiomyopathy.

### 3. MATERIALS AND METHODS:

It is a qualitative case report research study where provides an exploration of phenomenon or opportunity of sharing efforts to intervene single patient's health with unreported health features previously. As a qualitative methodology, it encompasses a great deal more complexity and incorporates of data combined in creative ways. It provides richness and depth description that helps

to understand the situation and whether findings from the case are applicable of a report from a 71 years old man by the diagnosis of coronary artery disease as the sample to be reported. The patient presented for chronic cough and peripheral edema of left ventricular diastolic function.

His parents and/or relatives in this participant study were informed related to the nature of the study and signed a consent for taking part in the study. It was approved by the Ethics and Bioethics Committee of the National Health Ministry of Indonesia and according to Helsinki Declaration (1975).

#### 4. RESULTS AND DISCUSSIONS:

According to the survey in 2013 to 2016 by National Health and Nutrition Examination, the generality of cardiovascular diseases (CVD), adjusting stroke, coronary heart disease (CHD), hypertension, and heart failure (HF) in  $\geq 20$  years of age by category of adults is 48.0% (121.5 million in 2016) and uplifting with progressing age in both men and women. Using Healthcare Cost and Utilization Project (HCUP) data for cardiomyopathy in 2014, there were 16,000 hospitalizations in America. Its system to be not transparent and understudied as underlying the changes that occurred (Roytberg, Sharkhun, Platonova., & Stepanova, 2020).

It showed that cardiomyopathy became the main diagnosis of 966.000 cardiovascular diseases, mostly found. Data from the National Heart, Lung, and Blood Institute, sponsored by some institutions covering; Chicago Heart Association Detection Project in Industry, ARIC (Atherosclerosis Risk in Communities Study), and CHS (Cardiovascular Health Study) indicate that incidence of HF approaching population to 21 per 1000 after the age of 65 years old (Benjamin. *et al*, 2019).

The cells in heart muscle cells or myocardiocytes are muscle cells that form heart's muscle consisting of sarcomeres. They expose something in common as found in skeletal muscle cells that may have as many as four nucleus producing adenosine triphosphate quickly, making it very resistant to fatigue.

The necrosis in cardiomyocyte is caused by external factors of cells or tissues, such as infection, toxins, or trauma that result in irregular digestion of cell components. Cellular death due to necrosis does not follow the apoptotic signal transduction pathway; various activated receptors result in loss of cell membrane integrity and

uncontrolled release of cell death products into the extracellular space. This event triggers an inflammatory response in the surrounding tissue, attracting leukocytes and phagocytes that are close to killing death cells with phagocytosis. However, destructive microbial agents released by leukocytes will create additional damage to the surrounding tissue. This extra damage is excessively inhibiting the healing process. Thus, untreated necrosis results in piles of tissue and debris that decompose dead cells at or near the location of cell death.

Macrophages originate from monocytes found in the blood circulation, which become mature and differentiated then migrate to the tissue. They can be found in large numbers, especially in connective tissue, such as those connected to the digestive tract, in the lungs (in body fluids or alveoli), and along certain blood vessels in the liver such as Kupffer cells, and in the entire spleen where the cells are damaged blood is recycled out of the body. This type of macrophage is called a resident who is fully differentiated. They are an integral part of innate immune response and leads to the main interest of research scientifically. As the key to respond inflammation, macrophages perform antigens on the surface on their cell by major histocompatibility complex II (MHC II) that result in cellular debris on resorption, anti and pro factors on inflammatory, and formation of granule tissue. They could also function as healing and remodeling the cardiac through growth factors, apoptosis, proteases, and proliferation (Gombazhapova, Rogovskaya, Shurupov., *et al*, 2017., Yona, Kim, Wolf, Mildner, Varol, Breker., *et al*, 2013).

The plasticity of myocardial infarction in macrophages and monocytes' function plays an essential role to control cardiac remodeling, inflammation, and acute coronary healing (Furth., & Cohn, 1968., Takahashi, 1994., Yona, Kim, Wolf, Mildner, Varol, Breker., *et al*, 2013., Sica., & Mantovani, 2012).

A 71 years old man was taken to Gatot Soebroto Central Army Hospital Jakarta, Indonesia, by the diagnosis of coronary artery disease. The patient presented for chronic cough and peripheral edema. He denied syncope, dyspnea, nausea, vomiting, and diaphoresis. His medical history was notable for hypertension and diabetes mellitus type II. On admission, the patient was afebrile; his heart rate was 86 beats per minute, respiratory rate was 20 breaths per minute, blood pressure was 140/90 mmHg, oxygen saturation was 98% on room air. He was alert and in no acute distress, without notable

jugular distension. Cardiac examination revealed normal S1 and S2, with no murmur or extra heart sounds. His lungs are clear to auscultation bilaterally. Peripheral edema was noted.

The patient performed a series of investigations covering; echocardiography, chest X-ray, and electrocardiography. Chest X-ray was abnormal with CTR 50% (Cardiothoracic ratio), fibrosis in right basal lung, without infiltrate, and haziness in the costophrenic angle, with differential diagnosis of pleuritis. The electrocardiogram showed multiple ventricular extrasystoles. The echocardiography performed diastolic dysfunction (impaired relaxation type), hypertrophy on left ventricular, and hypokinetic on the left ventricle with low ejection fraction 44% (Figure 1). The diagnosis of hypertrophic cardiomyopathy was established.

The patient refused the coronary artery bypass graft (CABG). Furthermore, the doctors want to increase survival rate with gave especially Regenerative Macrophages vaccines therapy. After this intervention approach, the patient had been checked by echocardiography. The result was significantly changed. Echocardiography showed left ventricular hypertrophy, normokinetic, diastolic dysfunction, and ejection fraction became 56 %.

In this case, the patient treated by the method of immunotherapy was chosen by regenerative macrophages of human origin from the patient. In regenerative macrophages of human origin vaccine therapy, blood's monocytes were split out from others' components and programmed as regenerative macrophages of human origin. The human macrophages cultures were established by treating peripheral blood monocytes and complete for four days.

The measurement of pulse wave Doppler sample volume on the transmittal inflow shows an E / A ratio, a marker of the function of the left ventricle of the heart. It represents the ratio of peak velocity blood flow from left ventricular relaxation in early diastole (the E wave) to peak velocity flow in late diastole caused by atrial contraction (the A wave), of less than 1, showing a grade 1 diastolic dysfunction (Figure 2).

Visualization of the left ventricle in PLAX, Mmode at the mitral tips level that works by transducing image marker directed toward the patient's right ear and the sound beam directed to the spine. Slight adjustments in angle and rotation maybe necessary to demonstrate all the structures for this view optimally, quantify LVEF with the Teicholz equation is 44%, with myocardial

thickening as measured by interventricular septum was 13.4 mm at diastolic and 16.6 mm at systolic and also 267 g/m<sup>2</sup> in LV mass (Figure 3).

Quantitative assessment of Right Ventricular function with Tricuspid Annular Plane Systolic Excursion (TAPE) was 23.7 mm, reveal the normal value of RV function (>20mm means RV EF >50%) (Figure 4). The left ventricular ejection fraction increased with the calculation of the Teicholz formula obtained by 56% (Figure 5).

By using RPMI-1640 (Lonza), adherent cells were accomplished with additives with 5% CO<sub>2</sub> at 37°C. The recombinant of human macrophage colony-stimulating factor (50 ng/mL) was used to gain M2-like macrophages and the deprivation conditions of its serum (autologous plasma in low percentage). PBS (Phosphate Buffer Saline) is used to have macrophages in four days, followed by EDTA (Lonza), washed with Triple Express Tripsine (Gibco), and counted in 4 days (Table 1). M2-like macrophages were generated and resuspended in 2 mL of 3x 10<sup>7</sup> sodium chloride 0.9% plus Albumin 20% and the end infused into IV of the patient. Therapeutic methods immunotherapy and their combination are the major promising strategies. The modes of immunotherapy were classified as conventional and rush immunotherapies. In contrast to currently applied treatments, immunotherapy has the potential to stimulate and support endogenous mechanisms of cardiac (Table 2).

## 5. CONCLUSIONS:

CVD is characterized by its high prevalence as the leading cause of early morbidity in the population. The suffered patient with cardiomyopathy found no alternative for medication recovery performed positive progress on echocardiography and clinical after treated with immunotherapy by the Regenerative Macrophages vaccine. In some pathological conditions, it has the function to force tissue homeostasis and innate immunity. Macrophages degrade and ingest foreign materials, dead cells, and debris. They support homeostasis by responding to external and internal changes within the body. It is not only as phagocytes, but also repair functions, regulatory, and trophic.

## 6. REFERENCES:

1. Apetrei-Corduneau, O., Fildan, P. A., Radu, R., Stănescu, C., Nemteanu, R., Lupusoru, C. E. (2020). Cardiovascular Side Effects of

- Neuropsychiatric Medication: An Update. Archives of the Balkan Medical Union, 55(1), 138–145.
2. Bai, J., Adriani, G., Dang, T. M., *et al.* (2015). Contact-dependent carcinoma aggregate dispersion by M2a macrophages via ICAM-1 and  $\beta 2$  integrin interactions. *Oncotarget*, 6(28):25295–25307.
  3. Baigent, C *et al.*, (2005). Cholesterol Treatment Trialists' (CTT) Collaborators. Efficacy and safety of cholesterol-lowering treatment: prospective meta-analysis of data from 90,056 participants in 14 randomised trials of statins. *Lancet*, 366(9493):1267–78
  4. Berenson, G. S. *et al.* (1989). Risks factor in early life as predictors of adult heart disease: the Bogalusa heart study. *American Journal of Medical Science*, 298(3), 213–237.
  5. Benjamin, *et al.* (2019). Statistic update Heart Disease and Stroke Statistics. American Heart Association. Report number: 139.
  6. Ben-Mordechai, T., Palevski, D., Gluksam-Galnoy, Y., Elron-Gross, I., Margalit, R., Leor, J. (2015). Targeting macrophage subsets for infarct repair. *J Cardiovasc Pharmacol Ther*, 20(4): 36–51.
  7. Colin, S., Chinetti-Gbaguidi, G., Staels, B. (2014). Macrophage phenotypes in atherosclerosis. *Immunol Rev*, 262(1):153–166.
  8. Diaconu, C. (2019). Is the Implication of Intestinal Microbiota in Cardiovascular. Archives of the Balkan Medical Union, 54(4), 609–611.
  9. Epelman, S., Lavine, K. J., & Randolph, G. J. (2014). Origin and functions of tissue macrophages. *Immunity*, 41(10): 21–35.
  10. Furth, R., Cohn, Z. A. (1968). The origin and kinetics of mononuclear phagocytes. *J Exp Med*, 128(4): 15–35.
  11. Gombazhapova, A., Rogovskaya, Y., Shurupov V, *et al.* (2017). Macrophage activation and polarization in post-infarction cardiac remodeling. *Journal of Biomedical Science*, 24(6): (13–19). Available from: doi: 10.1186/s12929.017.0322.3.
  12. Gombozhapova, A., Rogovskaya, Y., Shurupov, V., *et al.* (2017). Macrophage activation and polarization in post-infarction cardiac remodeling. *J Biomed Sci*, 8(24):13–19.
  13. Gordon, S. (2007). The macrophage: past, present and future. *Eur J Immunol*, 37(2): 9–17.
  14. Integrated Management of Cardiovascular risk. (2002). Report of a WHO meeting. Geneva, World Health Organization.
  15. Kara, L., Spiller & Timothy, J. Ko. (2017). Macrophage-based therapeutic strategies in regenerative medicine. *Adv Drug Deliv Rev*, 122(7): 74–83. Available from: doi :10.1016/j.addr.2017.05.010.
  16. Lawes, C. M. *et al.*, (2003). Asia Pacific Cohort Studies Collaboration. Blood pressure and cardiovascular disease in the Asia Pacific region. *J Hypertens*, 21(4):707–716.
  17. Lemcke, H., Voronina, N., Steinhoff, G., *et al.* (2018). Recent Progress in Stem Cell Modification for Cardiac Regeneration. *Hindawi Stem Cells International*, 3(6): 1–22. Available from: doi: org/10.1155/2018/1909346.
  18. LaRosa, J. C., He, J., & Vupputuri, S. (1999). Effect of statins on risk of coronary disease: a meta-analysis of randomized controlled trials. *JAMA*, 282(24):2340–2346.
  19. Lewington, S. *et al.*, (2002). Prospective Studies Collaboration. Age-specific relevance of usual blood pressure to vascular mortality: a meta-analysis of individual data for one million adults in 61 prospective studies. *Lancet*, 360(9349):1903–1913.
  20. Lewington, S., & Clarke, R. (2005). Combined effects of systolic blood pressure and total cholesterol on cardiovascular disease risk. *Circulation*, 112:3373–3374.
  21. Lindsey, M. L., Saucerman, J. J., DeLeon-Pennell, K.Y. (2016). Knowledge gaps to understanding cardiac macrophage polarization following myocardial infarction. *Biochim Biophys Acta*, 186(222): 88–92.
  22. MacMahon, S., & Rodgers, A. (1993). The effects of blood pressure reduction in older patients: an overview of five randomized controlled trials in elderly hypertensives. *Clin Exp Hypertens*, 15(6):967–978.
  23. Martinez, F. O., Sica, A., Mantovani, A., Locati, M. (2015). Macrophage activation and polarization. *Front Biosci*, 13(4): 53–61.
  24. Mendis, S. *et al.* (2005). For the pathobiological determinants of atherosclerosis in Youth (PBDAY) research group. Atherosclerosis in children and young adults: an overview of the World Health

- Organizations (WHO and International Society and Federation of Cardiology Study on Pathobiological Determinants of Artherosclerosis in Youth Study (1985-1995). Prevention and Control, 1, 3-15.
25. Pelegrin, P., & Surprenant, A. (2009). Dynamics of macrophage polarization reveal new mechanism to inhibit IL-1 $\beta$  release through pyrophosphates. *EMBO J*, 28(21):14–27.
  26. Roytberg, G. E., Sharkhun, O. O., Platonova, O. E., & Stepanova, A. A. (2020). The positron emission tomography in early diagnostics transtornos metabolic myocardial disorders in insulin-resistant patient with non-alcoholic fatty liver disease, *Periodico Tchê Química*, 17(34), 1026-1032.
  27. Sica, A., & Mantovani, A. (2012). Macrophage plasticity and polarization: in vivo veritas. *J Clin Invest*, 8(122): 87–95.
  28. Sever, P. S. *et al.*, (2003). ASCOT investigators. Prevention of coronary and stroke events with atorvastatin in hypertensive patients who have average or lower-than-average cholesterol concentrations, in the Anglo-Scandinavian Cardiac Outcomes Trial – Lipid Lowering Arm (ASCOT–LLA): a multicentre randomised controlled trial. *Lancet*, 361(9364):1149–1158.
  29. Takahashi, K. (1994). Development and differentiation of macrophages and their related cells. *Hum Cell*, 7(10): 9–15.
  30. Tunstall-Pedoe, H. (2003). For the WHO MONICA project, MONICA monograph and multimedia sourcebook. World largest study of heart disease, stroke, risk factors and populations trends. 1979-2002. Geneva. World Health Organization.
  31. Turnbull, F. (2003). Blood pressure lowering treatment trialists' collaboration. Effects of different blood-pressurelowering regimens on major cardiovascular events: results of prospectively-designed overviews of randomised trials. *Lancet*. 362(9395):1527–1535.
  32. Wald, N. J., & Law, M. R. (2003). A strategy to reduce cardiovascular disease by more than 80%. *BMJ*. 2003 Jun 28;326(7404):1419. Erratum in: *BMJ*. 2003 Sep 13;327(7415):586. *BMJ*. 2006 Sep;60(9):823.
  33. World Health Organization. (2003). Prevention of recurrent heart attacks and strokes in low and middle income populations. Evidence-based recommendations for policy makers and health professionals. Geneva
  34. Yona, S., Kim, K. W., Wolf, Y., Mildner, A., Varol, D., Breker, M., *et al.* (2013). Fate mapping reveals origins and dynamics of monocytes and tissue macrophages under homeostasis, *immunity*. 6(38): 79–91.
  35. Yonggang, M. A., Alan, J., Merry, L. *et al.* (2018). Cardiac macrophage biology in the steady-state heart, the aging heart, and following myocardial infarction. *HHS Public Access*, 20(191): 15– 28. Available on: doi: 10.1016/j.trsl.2017.10.001.
  36. Zieske, A. W., Malcom, G. T., & Strong, J. P. (2002). Natural history and risk factors of atherosclerosis in children and youth: the PDYA study. *Pediatr Pathol Mol Med*, 21(2), 213-237.



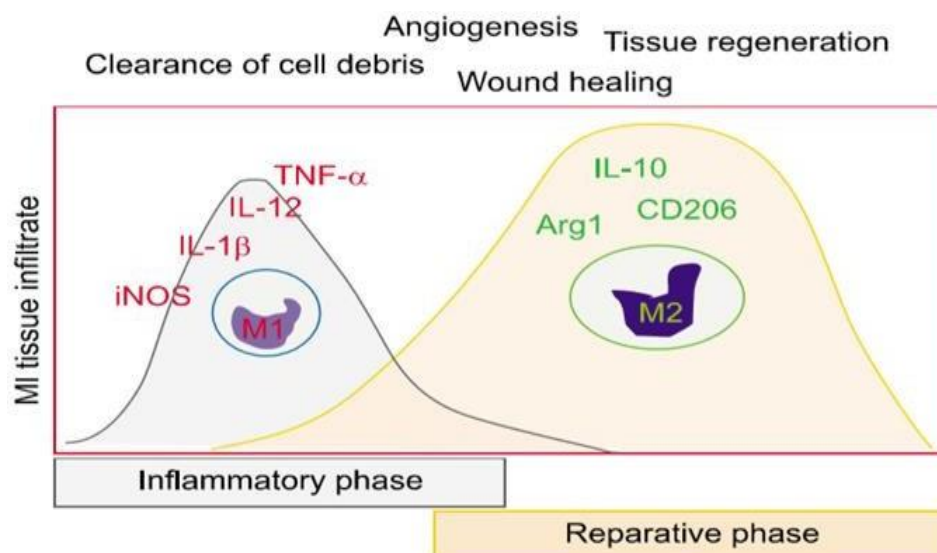


**Figure 1.** Macrophages function.

**Source:** Macrophages Clinical and Diagnostic Laboratory Test Result of Gatot Soebroto Central Army Hospital

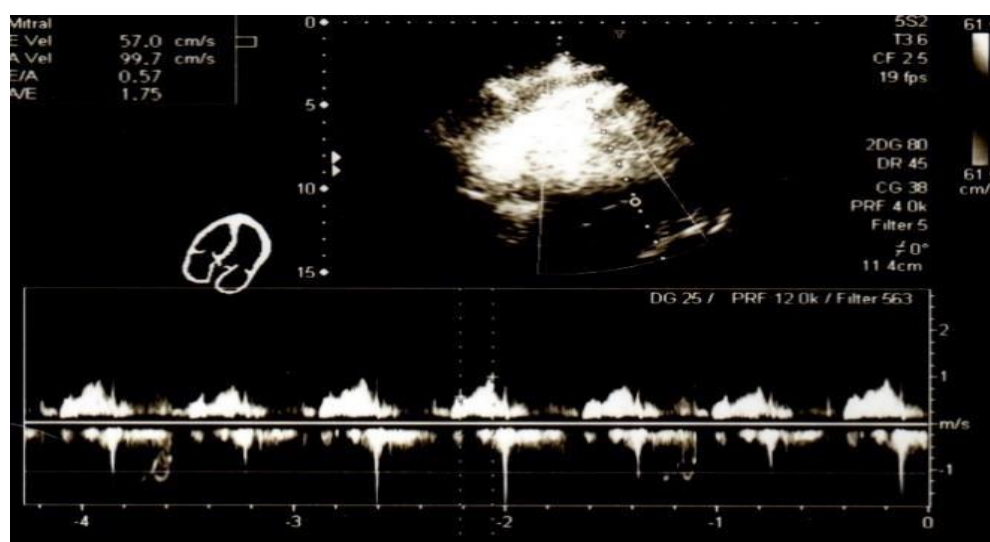


**Figure 2.** Assessment of left ventricular diastolic function

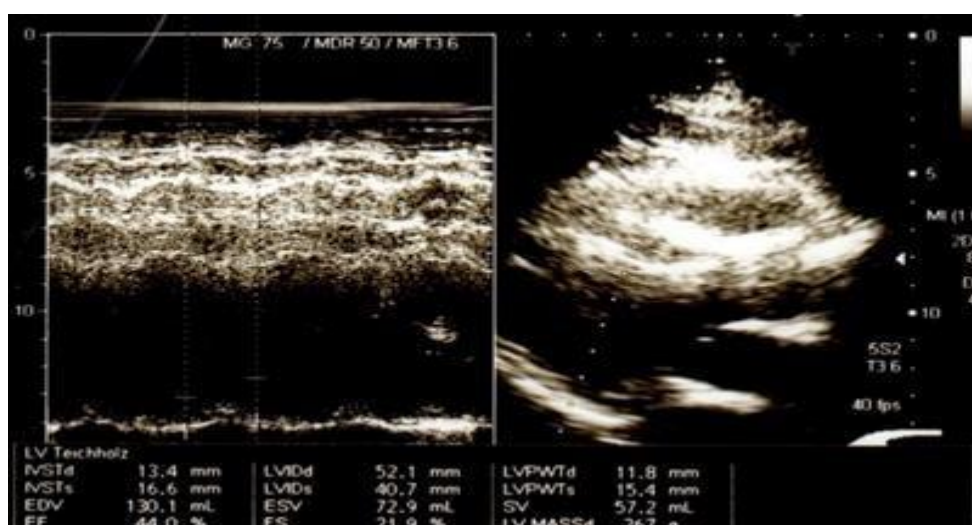


**Figure 3.** Assessment of left ventricular function



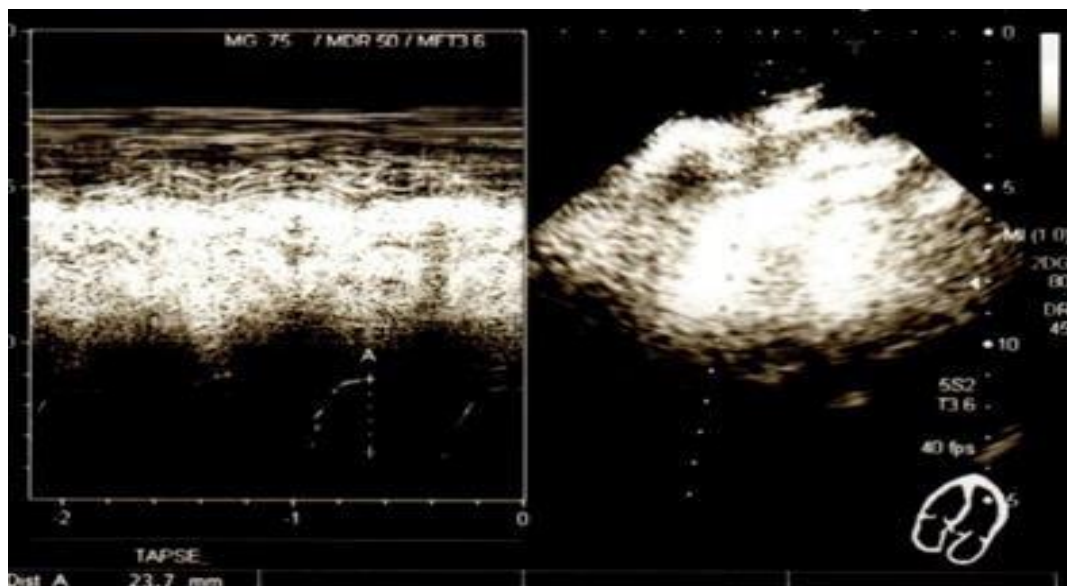


**Figure 4.** Quantitative assessment of right ventricular function before Cellcure.

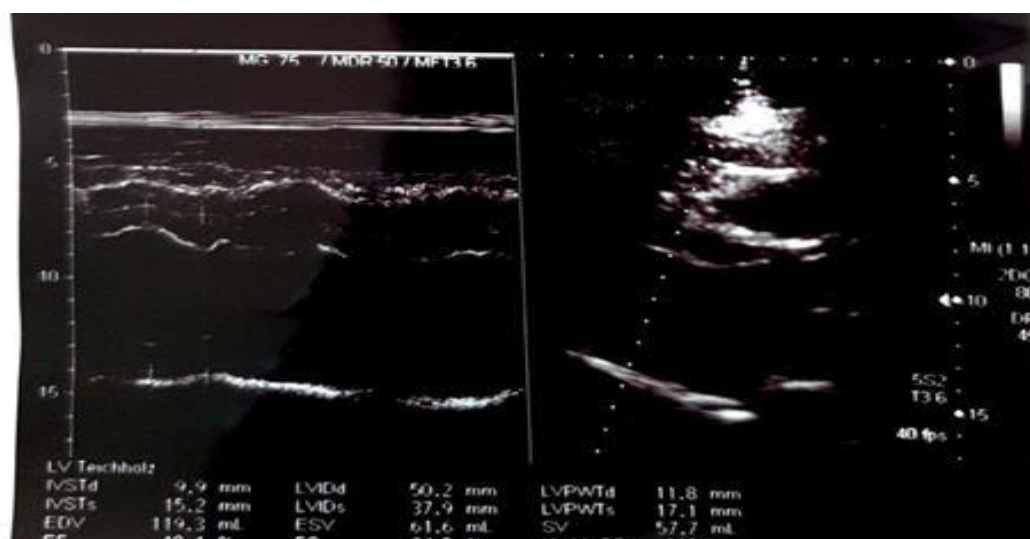


**Figure 5.** Assessment of left ventricular function after Cellcure.

**Table 1.** Report of Echo/ Doppler

| REPORT OF ECHO/DOPPLER                         |  |
|--|--|
| Name   | : DA   |
| Date Birth                                     | : 14-05-1948                                 |
| Date Assessment: 11-04-2019 and 28-05-2019     |  |
| 11-04-2019                                     | 28-05-2019                                   |
| EF: 44 %                                       | EF: 56,49 %                                  |
| EDD: 52,1 %                                    | EDD: 42%                                     |
| ESD: 40,7 %                                    | ESD: 29,7 %                                  |
| LVH (+); LV Hypokinetic; Diastolic Dysfunction | LVH (+); Normokinetic, Diastolic Dysfunction |
| Hyperthrophy Cardiomyopathy                    | LVH, Diastolic Dysfunction                   |

**Notes:** EF = Ejection fraction; EDD = End-diastolic diameter; ESD = End Systolic diameter; LVH = Left ventricular hypertrophy;

**Table 2.** Characteristics and molecular release from activated macrophages

| Subtypes | Inducers                      | Cell markers                        | Cytokines                      | Chemokines        | Function                        |
|----------|-------------------------------|-------------------------------------|--------------------------------|-------------------|---------------------------------|
| M1       | Ifn- $\gamma$ , LPS, Bacteria | CCR7, CD25, CD86,                   | TNF- $\alpha$ , IL-1 $\beta$ , | RANTES,           | Proinflammatory function        |
|          | GM-CSF, oxidative             | CD127, MHCII, ROS,                  | NO, IP-10.                     | CCL-8/15/19/20.   | Pathogen clearance, tissue      |
|          | fatty acid/LDL, HMGBI         | Inos, arginase-2                    | IL-6/8/12/15/17/23             | CXCL-9/10/11/13   | damage                          |
| M2a      | IL-4, IL13, M-CSF,            | CD206, CD209, Fizzl,                | IL-4/10/13/33/35,              | CCL-8/13/14       | Allergic inflammation           |
|          | NLRP3                         | YmL/2, RELM- $\alpha$ , arginase-I  | MMP-9, MMP-14, IGF-I           | CCL-17/18/23/26   |                                 |
| M2b      | LPS, IL-1 $\beta$ ,           | CD206, CD209, Fizzl,                | IL-10, TGF- $\beta$ ,          | CCL-1/20          | Tissue remodeling, fibrosis     |
|          | Immune complex/IL-1ra         | YmL/2, RELM- $\alpha$ , arginase-I  | CCL-I/20, CXCL-1/2/3           | CXCL-1/2/3        |                                 |
| M2c      | TGF- $\beta$ , IL-10, PGE2,   | CD163, CD206, Fizzl,                | IL-10, TGF- $\beta$ , IGF- I,  | CCL-8/17/18/22/24 | Anti-inflammatory function      |
|          | Tregs, BM-MSC,                | YmL/2, RELM- $\alpha$ , arginase-I, | PGE-2                          |                   | Phagocytosis tissue remodeling, |
|          | ADSCs, IDO                    | PPAR- $\delta$ , SRA-I TLRI/8       |                                |                   | Fibrosis                        |

**Notes:** M1 cells are classically activated macrophages; alternatively activated macrophages (M2 cells) can be divided into subtypes of M2a, M2b, and M2c. Abbreviations: LPS, lipopolysaccharide; GM-CSF, granulocyte-macrophage colony-stimulating factor; LDL low-density lipoprotein; HMGBI, high-mobility group box I; iNOS, inducible nitric oxide synthase; Tregs, regulatory T cells; ADSCs, adipose tissue-derived stromal cells; IDO, indoleamine 2,3-dioxygenase; PPAR, peroxisome proliferator-activated receptor  $\alpha$ -I; pge2, prostaglandin E2.

**Source:** Macrophages Clinical and Diagnostic Laboratory Test Result of Gatot Soebroto Central Army Hospital

## AVALIAÇÃO DA FORÇA DE UM PACOTE COMPOSTO COM DEFEITOS INTERNOS DE ACORDO COM VÁRIOS CRITÉRIOS DE FALHAS SOB A INFLUÊNCIA DE CARGA INDEPENDENTE

### ASSESSMENT OF THE STRENGTH OF A COMPOSITE PACKAGE WITH INTERNAL DEFECTS ACCORDING TO VARIOUS FAILURES CRITERIA UNDER THE INFLUENCE OF UNSTEADY LOAD

MEDVEDSKIY, Aleksandr L.<sup>1\*</sup>; MARTIROSOV, Mikhail I.<sup>2</sup>; KHOMCHENKO, Anton V.<sup>3</sup>; DEDOVA, Darina V.<sup>4</sup>;

<sup>1</sup> Central Aerohydrodynamic Institute, 1 Zhukovsky Str., zip code 140180, Zhukovsky – Russian Federation

<sup>2,4</sup> Moscow Aviation Institute (National Research University); Department of Resistance of Materials, Dynamics, and Strength of Machines; 4 Volokolamskoe Highway; zip code 125993; Moscow – Russian Federation

<sup>3</sup> JSC “Irkut Corporation”, Design Bureau of the Engineering Center, 68 Leningradsky Ave., zip code 125315, Moscow – Russian Federation

\* Correspondence author  
e-mail: mdv66@mail.ru

Received 22 March 2020; received in revised form 29 June 2020; accepted 07 July 2020

## RESUMO

Uma das tarefas prioritárias para a indústria aeronáutica moderna é elevar a eficiência econômica das aeronaves. No contexto da solução deste problema, ao criar novas aeronaves, os materiais compostos de polímeros (PCM) são cada vez mais utilizados. É dada especial atenção aos elementos estruturais, cujos danos podem levar a diminuição da resistência geral da estrutura. Portanto, uma tarefa essencial no projeto, manutenção e operação do teste é estudar o efeito de defeitos entre camadas na resistência e no comportamento das estruturas de PCM sob a influência de cargas instáveis. Este trabalho foi dedicado a análise numérica do comportamento de uma placa feita de material compósito de polímero (PCM) sob carga instável, considerando defeitos intercamadas de forma elíptica, bem como uma avaliação da resistência de uma embalagem compósita de acordo com várias fraturas critério. O problema foi resolvido pelo método dos elementos finitos usando o pacote de *software* LS-DYNA. Em seguida, utilizando o método de modelagem matemática, analisou-se a separação entre camadas de uma forma elíptica, que permitiu avaliar a resistência da placa e da fibra de acordo com os critérios de Hashin, Puck, Chang-Chang e LaRC03 e comparar os resultados. Verificou-se no estudo que os índices de falha e os fatores de segurança, obtidos através de vários critérios (Hashin e Chang-Chang), têm a mesma distribuição, desde a dependência do modo de fratura implementado (compressão da fibra na direção longitudinal) foi idêntico. Os materiais de análise podem ser levados em consideração ao desenvolver requisitos técnicos e montar estruturas de aeronaves.

**Palavras-chave:** *placa composta, critérios de falha em compósitos, defeito interlaminar, método dos elementos finitos (MEF), material compósito polimerico.*

## ABSTRACT

One of the priority tasks of the modern aviation industry is to increase the economic efficiency of aircrafts. In the context of solving this problem, when creating new aircrafts, polymer composite materials (PCM) are increasingly used. Particular attention is paid to structural elements, damage to which can lead to a decrease in the strength of an airframe as a whole. Therefore, an essential task in the design, maintenance, and operation of the test is to study the effect of interlayer defects on the strength and behavior of PCM structures under the influence of unsteady loads. This work is devoted to a numerical analysis of the behavior of a plate made of a polymer composite material (PCM) under unsteady load considering interlayer defects of an elliptical shape, as well as an assessment of the strength of a composite package according to various fracture criteria. The problem is solved by the finite element method using the LS-DYNA software package. Then, using the method of mathematical modeling, the interlayer separation of an elliptical shape was analyzed, which allowed to evaluate the strength of the plate and fiber according to the criteria of Hashin, Puck, Chang-Chang, and LaRC03 and

compare the results. It was found in the study, that the failure indices and safety factors, which were obtained using various criteria (Hashin and Chang-Chang), have the same distribution, since the dependence of the implemented fracture mode (fiber compression in the longitudinal direction) is identical. Analysis materials can be taken into account when developing technical requirements and assembling aircraft structures.

**Keywords:** *composite plate, composites failure criteria, interlaminar defect, finite element method (FEM), polymer composite material.*

---

## 1. INTRODUCTION

Appropriate calculations and full-scale tests must support the structural strength of the PCM in the aviation industry. Particular attention is given to the structural elements, damage which can lead to a decrease in airframe structural strength in general. The result of such damages may be interlayer defects such as bundles (Nia *et al.*, 2020; Shen *et al.*, 2020; Tian *et al.*, 2020).

Interlaminar defects can occur at various stages, both at the production stage and during operation. Among the main reasons that can cause defects, we can distinguish the following: a collision with a bird, hit stones on takeoff, non-localized dispersion of the engine rotor, hit fragments pneumatics, hit hail, collision when towing or steering with aerodrome infrastructure facilities, falling tool or replacement part (Koh and Madsen, 2018; Valverde *et al.*, 2020).

The resulting defects at selected non-destructive testing methods (including ultrasonic flaw detection, x-ray, current-vortex, optical holography, acoustic monitoring) are divided into undetectable, detectable with any form of control, reliably detected within several flights by technical personnel and evident to the crew (Miranda Guedes, 2019). The presence of defects in the structure of the PCM elements can lead to cracking of the binder, fiber destruction, and loss of strength of the composite packet (CP) (Kulkarni *et al.*, 2020). It follows that an essential task for the design, maintenance, and operation of the test is to study the influence of interlaminar defects on the strength and behavior of PCM constructions under the influence of unsteady loads (Ershova *et al.*, 2018; Medvedskiy *et al.*, 2019; Medvedsky *et al.*, 2019a; Medvedsky *et al.*, 2019b; Medvedsky *et al.*, 2019c; Medvedsky *et al.*, 2019d; Medvedsky *et al.*, 2019e). This paper shows the results of numerical simulation of the behavior of a rectangular plate made of a layered composite in the presence of interlayer defects of the bundle type. The impact of a spherical blast wave formed after the detonation of a point source is considered as an external non-stationary load. In solving the problem, we used the finite element method (FEM)

implemented in the LS-DYNA software package using an explicit time integration scheme for the complete system of FEM equations (Bento Rebelo and Cismaşiu, 2017; Trajkovski, 2017a; Trajkovski, 2017b; Erdik and Uçar, 2018; Teng, 2018; Bisyk *et al.*, 2019). The distribution of pressure on the outer surface of the plate, deflections in the zone of defects at different times were obtained, as well as the analysis of the operating stresses and deformations in the layers of the plate, and based on this analysis, the maximum failure indices and minimum safety factors in the most loaded layer were determined according to various failure criteria for composite materials (Chen *et al.*, 2020; Rena *et al.*, 2020). A comparison of the considered failure criteria for a point with a minimum safety factor is performed, and a graph of changes in the failure indices at various points in time is presented. A quantitative assessment of the degree of reduction of the minimum safety factor in the presence of multiple elliptic defects between the layers of the plate is made. The proposed method allows us to take into account the presence of interlayer defects of various shapes, sizes and layouts between the layers of the package under the action of a wide range of non-stationary loads: the action of pressure fields distributed according to different laws, the impact of a striker with different speed and energy, the action of acoustic and explosive waves generated by different sources, the impact of temperature fields.

The consideration of interlayer effects with allowance for temperature factors was considered. This work is devoted to the numerical analysis of the behavior of the plate of a polymer composite material (PCM) under unsteady load considering interlayer defects elliptical shape, as well as evaluating the strength of the composite package according to various failure criteria.

## 2. MATERIALS AND METHODS

The object of this research is a rectangular plate made of PCM length  $a = 500$  mm and a width  $b = 200$  mm (Figure 1). The plate is made of carbon fiber using autoclave technology based on

prepreg HexPly M21/34%/UD194/IMA (IMA carbon tape-based high-strength fiber HexTow IMA-12K and modified epoxy binder M21) manufactured by Hexcel Composites (USA). The thickness of the mono-layer is assumed to be equal to  $h = 0.184$  mm. Laying plate has the following scheme:  $[+45^\circ/-45^\circ/90^\circ/0^\circ/+45^\circ/-45^\circ/-45^\circ/+45^\circ/0^\circ/90^\circ/-45^\circ/+45^\circ]$  (total of 12 mono-layer, 2.208 mm total thickness of the package).

The problem is solved by the finite element method (FEM) in the software package LS-DYNA. Each mono-layer modeled a separate set of finite elements with the wording "16: Fully integrated shell element" and property "COMPOSITE". It is assumed that between all layers, there are defects in the form of interlaminar delamination of elliptical shape with axes of 60 and 40 mm. The layers, except for the defect zones, are connected by a glue contact "Automatic One-Way Surface to Surface Tiebreak". The "Automatic Surface to Surface" contact is taken into account between defects.

As an external unsteady load, an explosive impact with a spherical blast wave is used, which is modeled using the "Load Blast Enhanced" function based on the Kingery-Bulmash model (Le Blanc *et al.*, 2005; Tabatabaei and Volz, 2012; Schwer *et al.*, 2015). The epicenter of the explosion is located above the defects at a distance of 300 mm, and the detonation energy is  $E = 33.47$  kJ. As boundary conditions, the hinge support along the long edges of the plate is used. To assess the strength of a PCM plate, the following failure criteria are used to evaluate the strength of the matrix and the fiber separately: Hashin (1980), Puck (Puck and Schurmann, 1998), Chang and Chang (1987), LaRC03 (Sebaey *et al.*, 2011; Muizemnek and Kartashova, 2017). Appropriate depending is shown below. Criteria Hashin. Fiber strength for plane stress state is determined by the following Equations (1)-(2).

The strength of the matrix (Equations 3-4), where  $f_f$  – fiber failure index,  $f_m$  – matrix failure Index,  $\sigma_1$  – normal stress acting in the longitudinal direction,  $\sigma_2$  – normal stress acting in the lateral direction,  $\tau_{12}$  – shear stress acting in the plane,  $X_T$  – tensile strength in the longitudinal direction at a stretching,  $X_C$  – tensile strength in the longitudinal direction at a compression,  $Y_T$  – tensile strength in the transverse direction at a stretching,  $Y_C$  – tensile strength in the transverse direction under compression,  $S_{12}$  – shear strength in the plane. Failure occurs when one of the Equations (1)-(4) becomes equal to unity. Hashin failure index can be written as (Equation 5).

2. Criterion Puck. Fiber strength is determined by the following Equations (6)-(7). The strength of the matrix (Equations 8-13), where (Equations 12-13),  $f_{mA}$ ,  $f_{mB}$ ,  $f_{mC}$  – form of failure of the matrix. For carbon fiber reinforced plastics  $p_{12}^{(+)} = 0.3$ ,  $p_{12}^{(-)} = 0.35$ ,  $p_{22}^{(+)} = p_{22}^{(-)} = 0.25-0.3$ .

3. Criterion Chang-Chang. Strength fibers for plane stress state are determined by the following Equations (14)-(18). Fiber strength was determined using Equations (14), (15). The strength of the matrix was determined using Equations (16)-(18), where  $\beta$  – taken equal to 0.1.

4. Criterion LaRC03 (Chen *et al.*, 2018) Equations (19)-(25), where  $\varepsilon_1$  – the deformation is exerted in the longitudinal direction by stretching;  $\varepsilon_1^T$  – limiting deformation in the longitudinal direction at a stretching,  $\sigma_{22}^m$ ,  $\tau_{12}^m$  – stresses in areas of misalignment,  $\eta^L$  – longitudinal friction coefficient,  $Y_{is}^T$ ,  $S_{is}^L$  – the limits of local strength,  $g$ ,  $(G_{IC}/G_{IIC})$  – fracture stiffness coefficient,  $\tau_{eff}^T$ ,  $\tau_{eff}^L$  – effective shear stress in compression of the matrix calculated based on the Mohr-Coulomb criterion, which binds effective shear stress in the disk Mora failure plane (Equation 26), where  $\alpha_0 = 53$  – fracture angle.

Material mono-layer has the following mechanical characteristics:  $X_T = 2830$  MPa,  $X_C = 1500$  MPa,  $Y_T = 54$  MPa,  $Y_C = 271$  MPa,  $S_{12} = 96$  MPa,  $E_1 = 178$  GPa,  $E_2 = 8.6$  GPa,  $G = 3.0$  GPa,  $\mu_{12} = 0.32$ ,  $\rho = 1580$  kg / m<sup>3</sup>. Here  $\mu_{12}$  – Poisson ratio, which characterizes the lateral contraction in the longitudinal direction,  $G$  – shear modulus in the plane of the sheet,  $\rho$  – density,  $E_1$  – elasticity module in the longitudinal direction,  $E_2$  – modulus of elasticity in the transverse direction. Characteristics mono-layer received PKM manufacturer experimentally according to European standards EN samples for RTD mode (Room Temperature Dry): normal temperature +23 °C and the humidity – in the delivery state (Antufev *et al.*, 2019; Kuznetsova and Rabinskiy, 2019).

### 3. RESULTS AND DISCUSSION:

Figure 2 shows the variation of the external pressure on the surface of the plate in the center location of the defects as a result of the detonation wave. Figures 3-4 shows the stress distribution in the longitudinal direction and shear stresses in the layer No. 10 (90°) at a time 0.59 ms in cases of presence and absence of defects between the layers. Figures 5-7 show the distribution of safety factors in layer 10 (90°) at the time of 0.59 m s for

cases of presence and absence of defects between layers according to various failure criteria. Figure 8 shows the distribution of pressure from the blast wave action on the surface of the plate at a time 0.59 ms. Figures 9-10 show displacement along the major axis of the defect in the layer No. 10 at different time points for the plate in the presence and absence of defects, respectively. Figures 9-10 show that for layer 10, the maximum displacement values differ slightly, but the behavior is different. This is due to the presence of defects between layers. Figure 11 shows the variation of failure index at the point with a minimum safety factor for any failure criteria.

Thus, from Figures 3-7, it is seen that in case of a defect, the maximum-acting guides longitudinal stresses above about 1.68 times compared with the case of absence of defects. Analysis of the distribution failure indexes and safety factors obtained by different failure criteria showed that criteria Hashin and Chang-Chang have the same distribution because the dependence of the realized form of destruction (fiber compression in the longitudinal direction) is the same. The minimum safety factor was calculated from LaRC03 criterion (" $\eta = 0.87$ ") decrease in strength of the structure in case of the presence of defects LaRC03 criterion is 2.46 times.

#### 4. CONCLUSIONS:

Thus, the behavior of a laminate plate made of a polymer composite material under non-stationary load taking into account interlayer defects of an elliptical shape was studied, as well as the strength of the composite package according to various fracture criteria was assessed. The pressure distribution on the outer surface of the plate under the influence of an air blast wave is determined. The deflections of the plate along the defect are also determined in the presence and absence of interlayer defects. The analysis of these dependencies shows a difference in the behavior of the plate in the defect zone. The dependences of the failure indices on the considered failure criteria at various moments in time are determined. An analysis of distribution failure indices and safety factors obtained using different failure criteria showed that the Hashin and Chang-Chang criteria have the same distribution since the dependence of the realized fracture shape (longitudinal compression of the fiber) is the same. For the design under consideration, the presence of a defect reduces the strength by 2.46 times, the minimum safety factor is implemented using the LaRC03 criterion

and is 0.87. The results of the analysis can be taken into account when developing technical requirements and assembling the structures of an aircraft including when exposed to temperature fields.

#### 5. ACKNOWLEDGMENTS:

The work was conducted at the Moscow Aviation Institute with financial support from the Russian Foundation for Basic Research, project No. 18-08-01153.

#### 6. REFERENCES:

1. Antufev, B. A., Kuznetsova, E. L., Rabinskiy, L. N., and Tushavina, O. V. (2019). Complex stressed deformed state of a cylindrical shell with a dynamically destructive internal elastic base under the action of temperature fields of various physical nature. *Asia Life Sciences*, 2, 775-782.
2. Bento Rebelo, H., and Cismaşiu, C. (2017). *A comparison between three air blast simulation techniques in LS-DYNA*. Paper presented at the 11th European LS-DYNA Conference 2017, Salzburg, Austria.
3. Bisyk, S., Davydovskyi, L. S., Hutov, I., Slyvins'kyi, O. A., Aristarkhov, O. M., and Lilov, I. (2019). Comparison of numerical methods for modeling the effect of explosion on protective structures. *International Scientific Journal "Trans Motauto World"*, 4(1), 20-23.
4. Chang, F. K., and Chang, K. Y. (1987). A progressive damage model for laminated composites containing stress concentration. *Journal of Composite Materials*, 21, 834-855.
5. Chen, M., Zhang, D., and Gong, J. (2018). Predictions of transverse thermal conductivities for plain weave ceramic matrix composites under in-plane loading. *Composite Structures*, 202, 59-767.
6. Chen, Y., Zhao, Y., He, C., Ai, S., Lei, H., Tang, L., and Fang, D. (2020). Yield and failure theory for unidirectional polymer-matrix composites. *Composites Part B: Engineering*, 164, 612-619.
7. Erdik, A., and Uçar, V. (2018). On evaluation and comparison of blast loading methods used in numerical simulations. *Sakarya University Journal of Science*, 22(5), 1385-1391.
8. Ershova, A. Y., Kuznersova, E. L., Martirosov,

- M. I., and Rabinsky, L. N. (2018). Experimental determination of characteristics of crack-resistance of disperse-strengthened composites based on non-saturated polyesters. *Journal of Mechanical Engineering Research and Developments*, 41(3), 33-36.
9. Hashin, Z. (1980). Failure Criteria for unidirectional fiber composites. *Journal of Applied Mechanics*, 47, 329-334.
10. Koh, R., and Madsen, Bo. (2018). Strength failure criteria analysis for a flax fibre reinforced composite. *Mechanics of Materials*, 124, 26-32.
11. Kulkarni, P., Mali, K. D., and Singh, S. (2020). An overview of the formation of fibre waviness and its effect on the mechanical performance of fibre reinforced polymer composites. *Composites Part A: Applied Science and Manufacturing*, 137, Article number 106013.
12. Kuznetsova, E. L. and Rabinskiy, L. N. (2019). Heat transfer in nonlinear anisotropic growing bodies based on analytical solution. *Asia Life Sciences*, 2, 837-846.
13. Le Blanc, G., Adoum, M., and Lapoujade, V. (2005). External blast load on structures – Empirical approach. Retrieved from <https://www.dynalook.com/conferences/european-conf-2005/Leblanc.pdf>.
14. Medvedskiy, A. L., Rabinskiy, L. N., Martirosov, M. I., Ershova, A. Yu., and Khomchenko, A. V. (2019). The study of changes in strength of polymer composite panels with interlayer defects under the action of unsteady load. *The Asian International Journal of Life Sciences*, 21(1), 565-576.
15. Medvedsky, A. L., Martirosov, M. I., and Khomchenko, A. V. (2019a). Behavior of the shallow composite panel with initial defects at strike influence. *Izvestiya TulGU. Technical Science*, 12, 159-163.
16. Medvedsky, A. L., Martirosov, M. I., and Khomchenko, A. V. (2019b). Dynamic of reinforced composite panel with mono-layer combined stacking with inner damages at non-stationary impacts. *Bulletin of Bryansk State Technical University*, 7, 35-41.
17. Medvedsky, A. L., Martirosov, M. I., and Khomchenko, A. V. (2019c). Numerical analysis of layered composite panel behavior with interlaminar defects subject to dynamic loads. *Structural Mechanics of Engineering Construction and Buildings*, 15(2), 127-134.
18. Medvedsky, A. L., Martirosov, M. I., and Khomchenko, A. V. (2019d). Numerical research of failure of the plane panel made polymer composite material with internal defects under action of non-stationary load. *Aviation Industry. Quarterly Scientific and Technical Magazine*, 1, 52-56.
19. Medvedsky, A. L., Martirosov, M. I., and Khomchenko, A. V. (2019e). Numerical study of the behavior of a composite plate with multiple damages under dynamic loads. *Collection of Works of the XII All-Russian Congress on Fundamental Problems of Theoretical and Applied Mechanics*, 3, 552-554.
20. Miranda Guedes, R. (2019). *Creep and fatigue in polymer matrix composites*. Sawston, England: Woodhead Publishing.
21. Muizemnek, A. Yu., and Kartashova, E. D. (2017). *Mechanics of deformation and destruction of polymer layered composite materials*. Penza, Russian Federation: Publishing House PSU.
22. Nia, X., Furtado, C., Fritz, N.K., Kopp, R., Camanho, P.P., and Wardle, B.L. (2020). Interlaminar to intralaminar mode I and II crack bifurcation due to aligned carbon nanotube reinforcement of aerospace-grade advanced composites. *Composites Science and Technology*, 190, Article number 108014.
23. Puck, A., and Schurmann, H. (1998). Failure analysis of FRP laminates by means of physically based phenomenological models. *Composites Science and Technology*, 58, 1045-1067.
24. Rena, Zh., Liu, L., Liu, Y., and Leng, J. (2020). Damage and failure in carbon fiber-reinforced epoxy filament-wound shape memory polymer composite tubes under compression loading. *Polymer Testing*, 85, Article number 106387.
25. Schwer, L., Teng, H., and Souli, M. (2015). *LS-DYNA air blast techniques: Comparisons with experiments for close-in charges*. Paper presented at the 10th European LS-DYNA Conference, Würzburg, Germany.
26. Sebaey, T. A., Blanco, N., Lopes, C. S., and Costa, J. (2011). Numerical investigation to prevent crack jumping in Double Cantilever Beam test of multidirectional composite laminates. *Composites Science and Technology*, 71, 1587-1592.
27. Shen, L., Liu, L., Zhou, Y., and Wu, Z. (2020). Thickness effect of carbon nanotube interleaves on free-edge delamination and

ultimate strength within a symmetric composite laminate. *Composites Part A: Applied Science and Manufacturing*, 132, Article number 105828.

28. Tabatabaei, Z. S., and Volz, J. S. (2012). A comparison between three different blast methods in LS-DYNA: LBE, MM-ALE, coupling of LBE and MM-ALE. Retrieved from <https://www.dynalook.com/conferences/12th-international-ls-dyna-conference/blast-impact20-d.pdf>.
29. Teng, H. (2018). Scalability study of particle method with dynamic load balancing. Retrieved from <https://www.semanticscholar.org/paper/Scalability-Study-of-Particle-Method-with-Dynamic-Teng/f78f0f20a5ce1d2620a8bd191207fbaa028244db>.
30. Tian, K., Pan, Q., Deng, H., and Fu, Q. (2020). Shear induced formation and destruction behavior of conductive networks in nickel/polyurethane composites during strain sensing. *Composites Part A: Applied Science and Manufacturing*, 130, Article number 105757.
31. Trajkovski, J. (2017a). *Comparison of MM-ALE and SPH methods for modelling blast wave reflections of flat and shaped surfaces*. Paper presented at the 11th European LS-DYNA Conference 2017, Salzburg, Austria.
32. Trajkovski, J. (2017b). MM-ALE Modelling Technique for Blast Response Analysis of Light Armoured Vehicles (LAV) According to AEP-55 Standard: Pros and Cons. *Key Engineering Materials*, 755, 159-169.
33. Valverde, M. A., Kupfer, R., Wollmann, T., Kawashita, L. F., Gude, M., and Hallett, S. R. (2020). Influence of component design on features and properties in thermoplastic overmolded composites. *Composites Part A: Applied Science and Manufacturing*, 132, Article number 105823.



$$f_f = \left(\frac{\sigma_1}{X_T}\right)^2 + \left(\frac{\tau_{12}}{S_{12}}\right)^2 = 1 \text{ at } \sigma_1 \geq 0 \quad (\text{Eq. 1})$$

$$f_f = \left(\frac{\sigma_1}{X_C}\right)^2 = 1 \text{ at } \sigma_1 < 0 \quad (\text{Eq. 2})$$

$$f_m = \left(\frac{\sigma_2}{Y_T}\right)^2 + \left(\frac{\tau_{12}}{S_{12}}\right)^2 = 1 \text{ at } \sigma_2 \geq 0 \quad (\text{Eq. 3})$$

$$f_m = \left(\frac{\sigma_2}{Y_T}\right)^2 + \left(\frac{\tau_{12}}{S_{12}}\right)^2 = 1 \text{ at } \sigma_2 < 0 \quad (\text{Eq. 4})$$

$$f = \max(f_m, f_f) \quad (\text{Eq. 5})$$

$$f_f = \frac{|\sigma_1|}{X_T} \text{ at } \sigma_1 \geq 0 \quad (\text{Eq. 6})$$

$$f_f = \frac{|\sigma_1|}{X_C} \text{ at } \sigma_1 \leq 0 \quad (\text{Eq. 7})$$

$$f_{mA} = \frac{1}{S_{12}} \left[ \sqrt{\left(\frac{S_{12}}{Y_T} - p_{12}^{(+)}\right)^2 \sigma_2^2 + \tau_{12}^2} + p_{12}^{(+)} \sigma_2 \right] \text{ at } \sigma_2 \geq 0 \quad (\text{Eq. 8})$$

$$f_{mB} = \frac{1}{S_{12}} \left[ \sqrt{\tau_{12}^2 + (p_{12}^{(-)} \sigma_2)^2} + p_{12}^{(-)} \sigma_2 \right], \text{ if } \sigma_2 < 0, 0 \leq \left| \frac{\sigma_2}{\tau_{12}} \right| \leq \frac{Y^A}{\tau_{12C}} \quad (\text{Eq. 9})$$

$$f_{mC} = \left( \left( \frac{\tau_{12}}{2(1+p_{12}^{(-)} S_{12})} \right)^2 + \left( \frac{\sigma_2}{Y_C} \right)^2 \right) \frac{Y_C}{|\sigma_2|}, \text{ if } \sigma_2 < 0, 0 \leq \left| \frac{\tau_{12}}{\sigma_2} \right| \leq \frac{\tau_{12C}}{Y^A} \quad (\text{Eq. 10})$$

$$f = \max(f_{mA}, f_{mB}, f_{mC}, f_f) \quad (\text{Eq. 11})$$

$$\tau_{12C} = S_{12} \sqrt{1 + 2p_{22}^{(-)}}, p_{22}^{(-)} = p_{12}^{(-)} \frac{Y^A}{S_{12}} \quad (\text{Eq. 12})$$

$$Y^A = \frac{S_{12}}{2p_{22}^{(-)}} \left[ \sqrt{1 + 2p_{12}^{(-)} \frac{Y_C}{S_{12}}} - 1 \right] \quad (\text{Eq. 13})$$

$$f_f = \left(\frac{\sigma_1}{X_T}\right)^2 + \beta \left(\frac{\tau_{12}}{S_{12}}\right)^2 = 1 \text{ at } \sigma_1 \geq 0 \quad (\text{Eq. 14})$$

$$f_f = \left(\frac{\sigma_1}{X_C}\right)^2 = 1 \text{ at } \sigma_1 < 0 \quad (\text{Eq. 15})$$

$$f_m = \left(\frac{\sigma_2}{Y_T}\right)^2 + \left(\frac{\tau_{12}}{S_{12}}\right)^2 = 1 \text{ at } \sigma_2 \geq 0 \quad (\text{Eq. 16})$$

$$f_m = \left(\frac{\sigma_2}{2S_{12}}\right)^2 + \left[ \left(\frac{\sigma_2}{2S_{12}}\right)^2 - 1 \right] \frac{\sigma_2}{Y_C} + \left(\frac{\tau_{12}}{S_{12}}\right)^2 = 1 \text{ at } \sigma_2 < 0 \quad (\text{Eq. 17})$$

$$f = \max(f_m, f_f) \quad (\text{Eq. 18})$$

$$f_f = \frac{\varepsilon_1}{\varepsilon_T} \text{ at } \sigma_1 \geq 0 \quad (\text{Eq. 19})$$

$$f_f = \frac{\varepsilon_1}{\varepsilon_1} \text{ at } \sigma_1 \leq 0 \quad (\text{Eq. 20})$$

$$f_f = \frac{|\tau_{12}^m| + \eta_L \sigma_{22}^m}{S_{is}^L} \text{ at } \sigma_1 < 0 \text{ and } \sigma_{22}^m < 0 \quad (\text{Eq. 21})$$

$$f_f = g \left( \frac{\sigma_{22}^m}{Y_{is}^T} \right)^2 + \left( \frac{\tau_{12}^m}{S_{is}^T} \right)^2 + (1 - g) \left( \frac{\sigma_{22}^m}{Y_{is}^T} \right) \text{ at } \sigma_1 < 0 \text{ and } \sigma_{22}^m \geq 0 \quad (\text{Eq. 22})$$

$$f_m = g \left( \frac{\sigma_2}{Y_{is}^T} \right)^2 + \left( \frac{\tau_{12}}{S_{is}^T} \right)^2 + (1 - g) \left( \frac{\sigma_2}{Y_{is}^T} \right) \text{ at } \sigma_2 \geq 0 \quad (\text{Eq. 23})$$

$$f_m = g \left( \frac{\tau_{eff}^T}{S^T} \right)^2 + \left( \frac{\tau_{eff}^L}{S_{is}^L} \right)^2 \text{ at } \sigma_1 \geq -Y_C \text{ and } \sigma_2 < 0 \quad (\text{Eq. 24})$$

$$f_m = g \left( \frac{\tau_{eff}^{mT}}{S^T} \right)^2 + \left( \frac{\tau_{eff}^{mL}}{S_{is}^L} \right)^2 \text{ at } \sigma_1 < -Y_C \text{ and } \sigma_2 < 0 \quad (\text{Eq. 25})$$

$$S^T = Y_C \cos(\alpha_0) \left( \sin(\alpha_0) + \frac{\cos(\alpha_0)}{\tan(2\alpha_0)} \right) \quad (\text{Eq. 26})$$

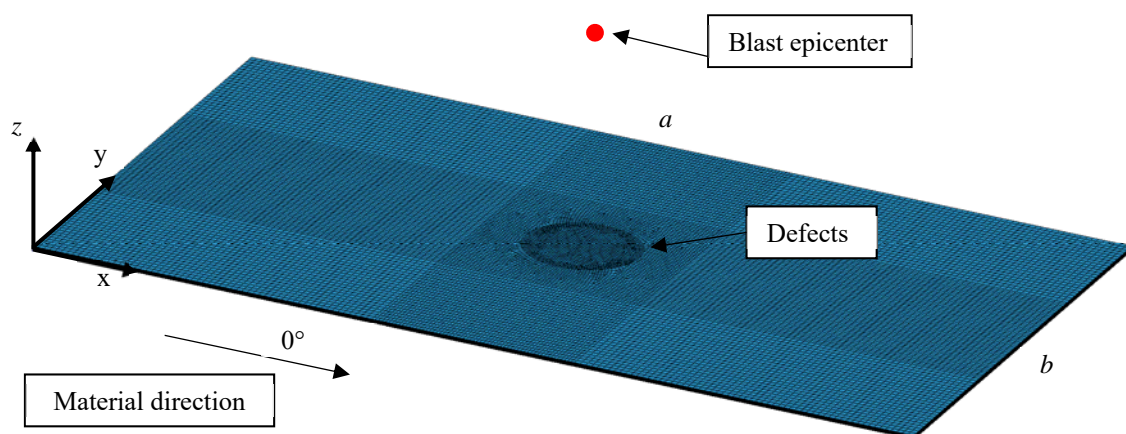


**Figure 1.** Rectangular composite plate

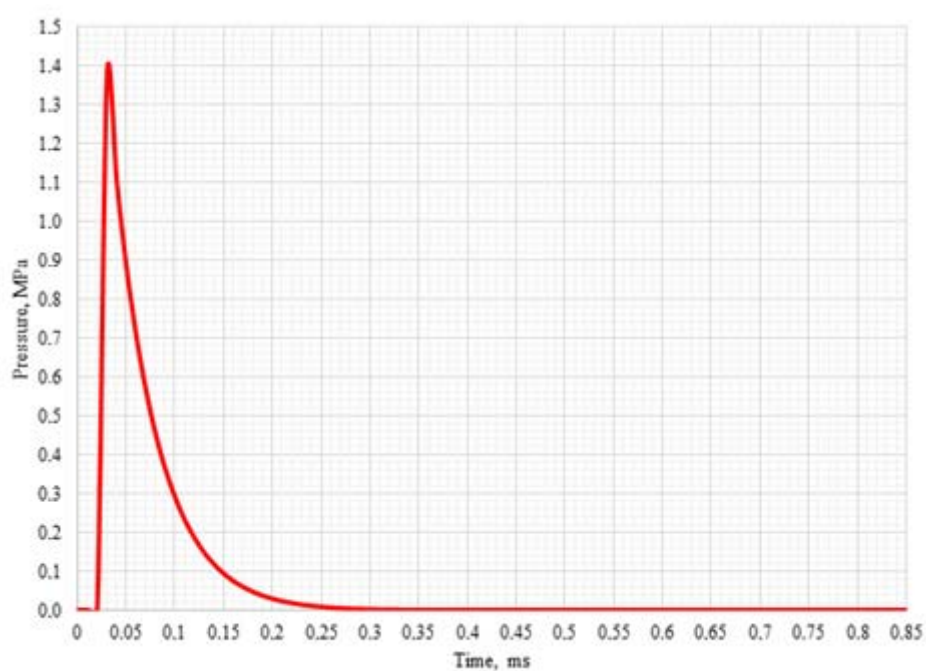


**Figure 1.** Pressure change

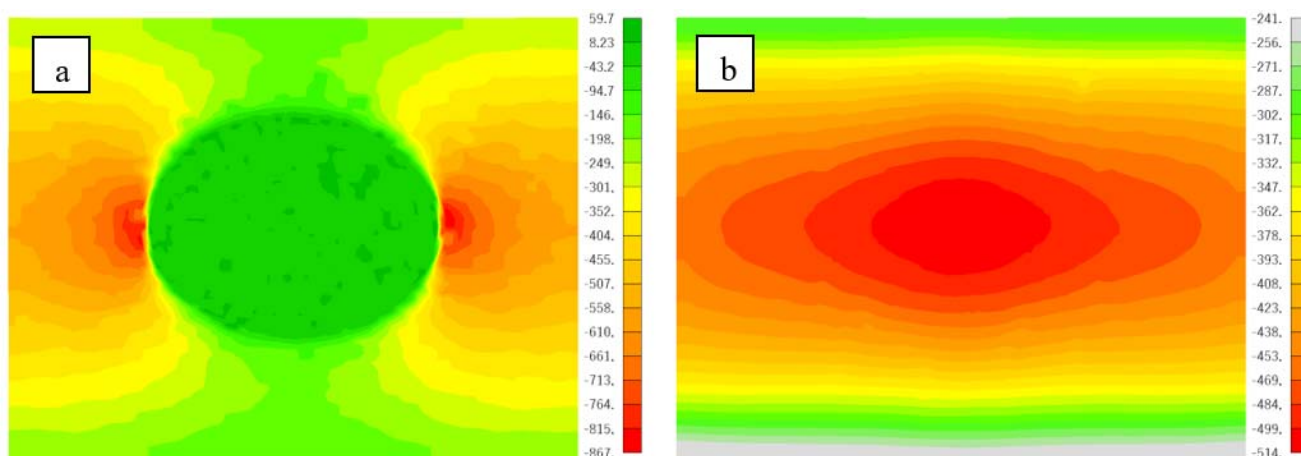


**Figure 2.** Normal longitudinal stresses at 0.59 ms, MPa: a – with defects; b – without defects

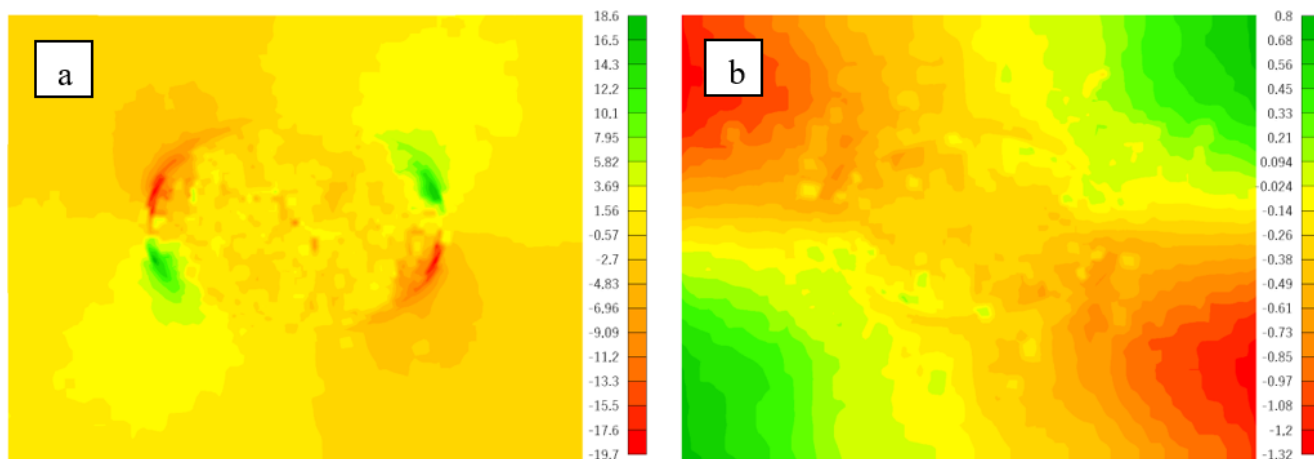


**Figure 3.** Shear stresses at 0.59 ms, MPa: a – with defects; b – without defects

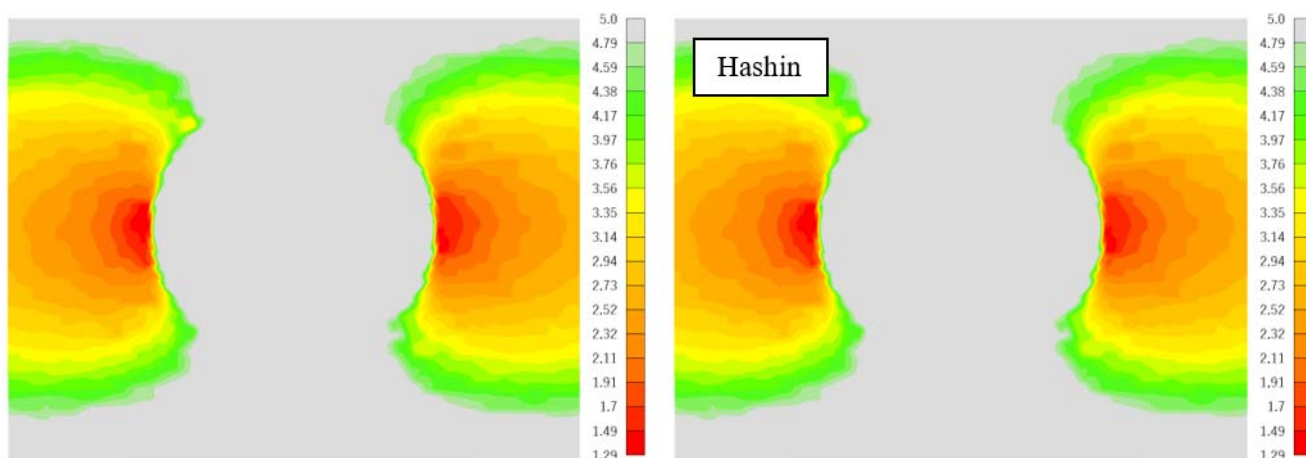


**Figure 4.** Safety factors at 0.59 ms for the plate with defects

Source: Hashin (1980), Chang and Chang (1987).

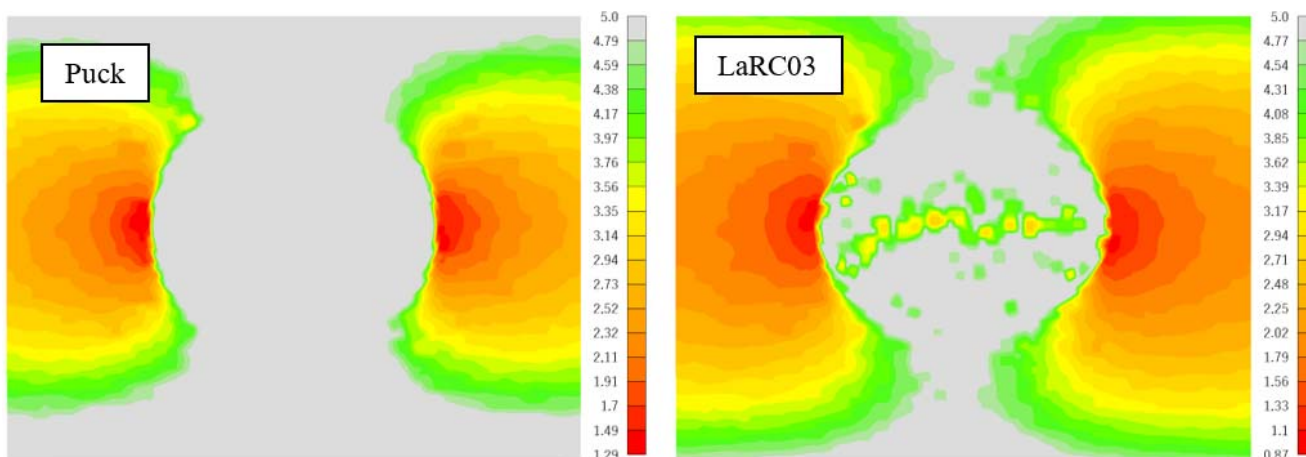


**Figure 5.** Safety factor at 0.59 ms for plate with defects

Source: Puck and Schurmann (1998).

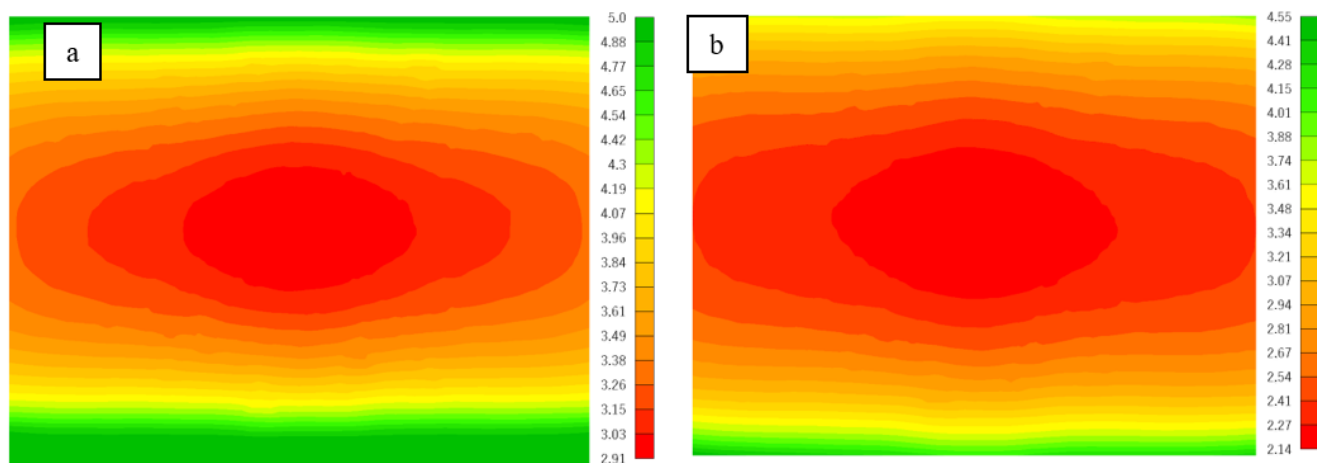


**Figure 6.** Safety factor at 0.59 ms (without defects): a – a progressive damage model for laminated composites containing stress concentration, Failure criteria for unidirectional fiber composites, Failure analysis of FRP laminates by means of physically based phenomenological models; b – LaRC03

Source: Hashin (1980), Chang and Chang (1987); Puck and Schurmann (1998).

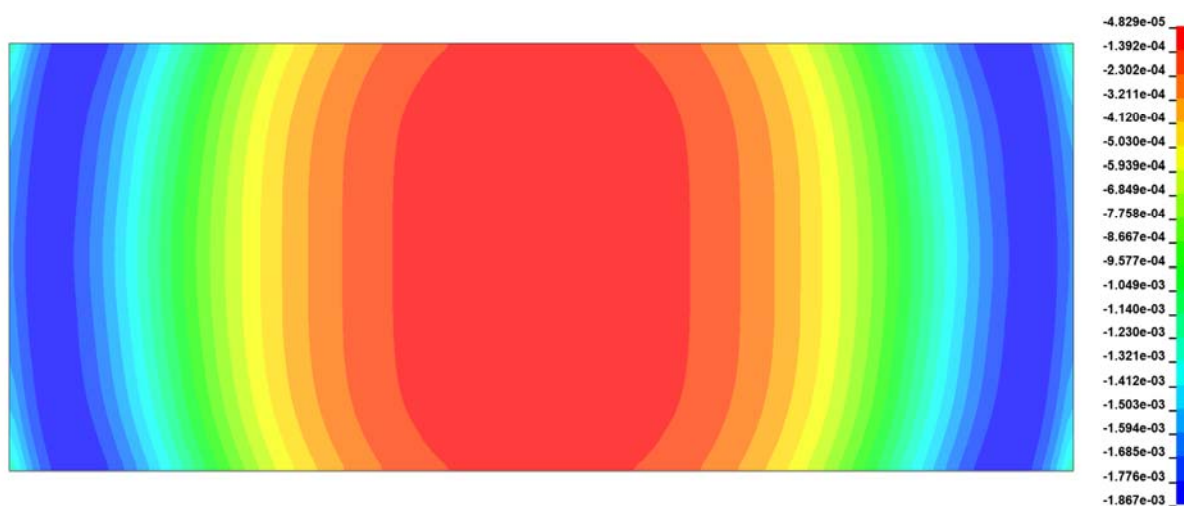


**Figure 7.** Blast pressure on the plate at time 0.59 ms

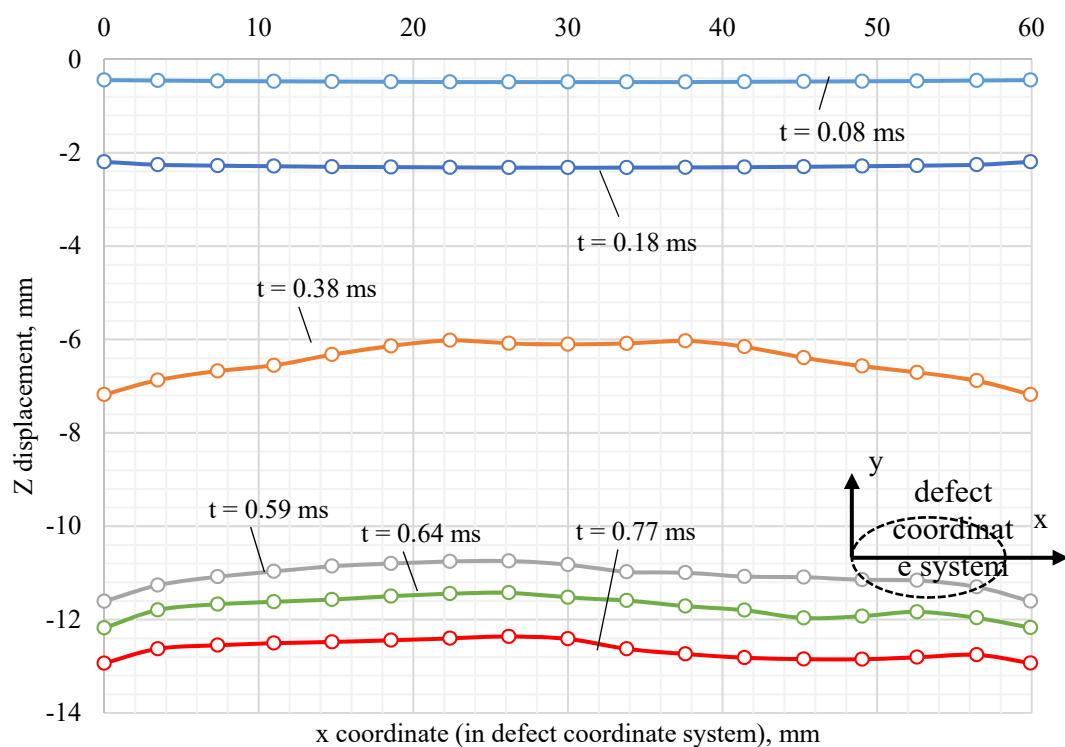


**Figure 8.** Displacement of ply No. 10 in defect zone (plate with defects)

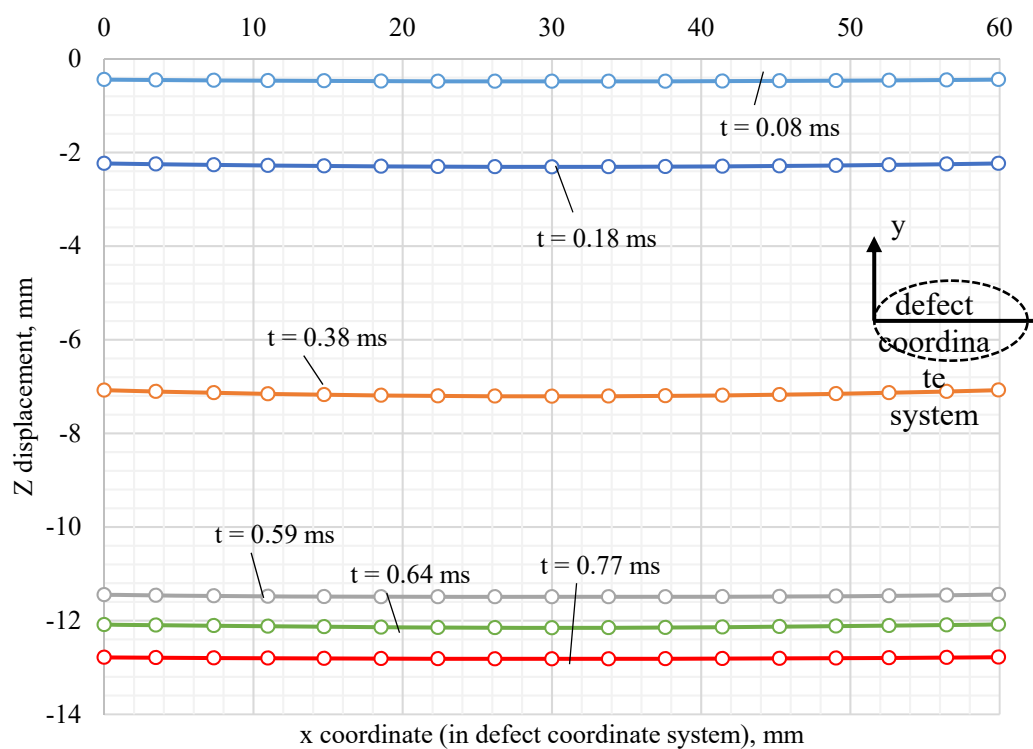


**Figure 9.** Displacement of ply No. 10 in defect zone (plate without defects)

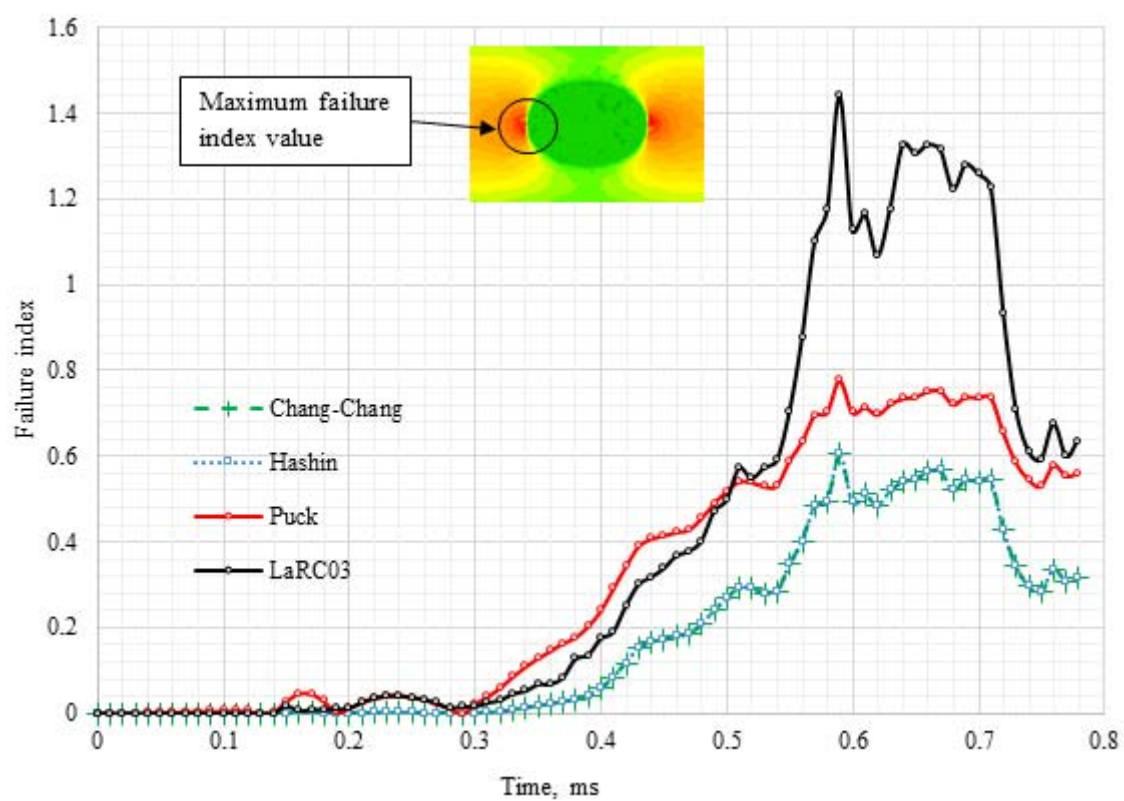


**Figure 10.** Failure index



## INSTRUCTIONS FOR AUTHORS

We ask authors always to visit the online instructions for the use of the latest instructions available. Manuscripts must be submitted using the template available on the Journal's website.

## PREPARATION OF MANUSCRIPTS

1. PREPARATION OF MANUSCRIPTS
2. THE FIRST PAGE OF THE MATERIAL
3. THE CENTRAL TEXT PART OF THE MATERIAL
4. GUIDELINES FOR REFERENCES
5. FIGURES
6. TABLES
7. MATHEMATICAL EXPRESSIONS
8. SUPPLEMENTARY MATERIAL

---

1. PREPARATION OF MANUSCRIPTS (TEMPLATE):

Please, observe the following points in preparing manuscripts. Papers not conforming strictly to these instructions may be returned to their authors for appropriate revision or may be delayed in the review process.

**Readability:** Manuscripts should be written in clear, concise, and grammatically correct English (British or American English throughout). The editors can not undertake wholesale revisions of poorly written papers. Every paper must be free of unnecessary jargon and readable by any specialist of the related field. The abstract should be written in an explanatory style that will be comprehensible also to readers who are not experts in the subject matter.

**General format:** The complete paper has to be written, preferably in Rich Text Format either in an MS-Word (.doc) or a Br.Office (.odt) compatible file. Page size: A4, margins: 2 cm on each side, line spacing: single, font type: Arial. Please leave headers and footers unchanged, since the editors should fill it. Please check guidelines for accurate information based on all different categories (review articles, technical notes, etc.) available. A single file of the whole manuscript should then be submitted through TQJ's email (journal.tq@gmail.com). The Journal no longer accepts submissions in any other form.

The order of the material should be as follows: Title, Author(s), Abstract, Keywords, Main text (Introduction, Review of Literature, Definitions (if any), Materials and Methods, Results, Discussion), Acknowledgements (if any), References, Appendix (if any). This structure of the main text is not obligatory, but the paper must be logically presented. Footnotes should be avoided. The main text must be written with font size 11, Arial, justify. Within each main section, three levels of subheadings are available, and the titles must be bold, bold, and italic, italic, respectively.

The manuscript should contain the whole text, figures, tables, and explanations according to the followings (we suggest using the template file):

---

2. THE FIRST PAGE OF THE MATERIAL SHOULD BE AS FOLLOWS:

**Title:** (both in Portuguese and English). The editors can provide the title in Portuguese for those whose Portuguese is not the first language. It should be brief and informative. The title should reflect



the essential aspects of the article, in a preferably concise form of not more than 100 characters and spaces. Font size 12, Arial, capital letters, center alignment.

**By-line:** Names (size 12, Arial, small capital) of the authors. No inclusion of scientific titles is necessary. In the case of two or more authors, place their names in the same row, separate them with a semicolon (;) and please indicate the corresponding author with \* in superscript. The corresponding author should be the one submitting the article online and an e-mail given (only one e-mail) below the addresses of all authors. Authors from different institutions must be labeled with numbers in superscript after the names. Addresses of the authors, phone, and fax number should also be given (size 10). Authors should be grouped by address.

**Abstract:** (both in Portuguese and English). The editors can provide the translation of the abstract to Portuguese for those whose Portuguese is not the first language. Required for all manuscripts in which the problem, the principal results, and conclusions are summarized. The abstract must be self-explanatory, preferably typed in one paragraph, and limited to max. 200 words. It should not contain formulas, references, or abbreviations. The name ABSTRACT should be written in capital letters, Arial, size 12, bold, left alignment. The abstract should be written font Arial, size 10, justify.

**Keywords:** (both in Portuguese and English. The editors can provide the keywords in Portuguese for those who Portuguese is not the first language). Keywords should not exceed five, not including items appearing in the title. The keywords should be supplied, indicating the scope of the paper. Size 10, italic, justify, only the word Keywords must be bold, left alignment.

The authors should include Abbreviations and Nomenclature listings when necessary.

---

### 3. THE CENTRAL TEXT PART OF THE MATERIAL SHOULD BE AS FOLLOWS:

The words Introduction, Materials, and Methods, Results and Discussion, Conclusion, Acknowledgements, and References must be written in capital letters, Arial, font size 12, left alignment, bold.

**Introduction:** The introduction must clearly state the problem, the reason for doing the work, the hypotheses or theoretical predictions under consideration, and the essential background. It should not contain equations or mathematical notation. A brief survey of the relevant literature so that a non-specialist reader could understand the significance of the presented results.

**Materials and Methods:** Provide sufficient details to permit repetition of the experimental work. The technical description of methods should be given when such methods are new.

**Results and Discussion:** Results should be presented concisely. Also, point out the significance of the results and place the results in the context of other work and theoretical background.

**Conclusion:** Summarize the data discussed in the Results and Discussion showing the relevance of the work and how different it is from other researches. Also, point out the benefits and improvements that can be observed to develop new scientific standards that can change something in the related field.

**Acknowledgments:** (if any) These should be placed in a separate paragraph at the end of the text, immediately before the list of references. It may include funding information too.

**References:** In the text, references should be cited in Harvard style (Author, year). Alternatively, the author's surname may be integrated into the text, followed by the year of publication in parentheses. Cite only essential resources, avoid citing unpublished material. References to papers "in press" must mean that the article has been accepted for publication, at the end of the paper list references alphabetically by the last name of the first author. Please, list only those references that are cited in the text and prepare this list as an automatically numbered list. The word References with size 12, Arial,

bold, capital letters, left alignment.

---

#### 4. GUIDELINES FOR REFERENCES:

- The Journal uses the APA (American Psychological Association) FORMAT CITATION as follows:

**Author's surname, initial(s).** **(Date Published).** **Title of Source.** **Location of publisher:**  
**publisher.** Retrieved from URL

##### Author Rules:

1. Initials are separated and ended by a period.

Examples: Goldani, E.  
De Boni, L.A.B.

2. Multiple authors are separated by commas and an ampersand.

Examples: Goldani, E. & De Boni, L.A.B.  
Goldani, E., De Boni, L.A.B. & Casanova, K.

3. Multiple authors with the same surname and initial: add their name in square brackets.

Example: Goldani, E. [Eduardo]

##### Date Rules:

1. Date refers to date of publishing
2. If the date is unknown 'n.d' is used in its place.

Example: De Boni, L.A.B (n.d)

##### Title Rules:

1. The format of this changes depending on what is being referenced

##### Publisher Rules:

1. If in the US: the city and two letter state code must be stated.

Examples: San Diego, CA  
Houston, TX  
New York, NY

2. If not in the US: the city and country must be stated.

Examples: Sydney, Australia  
Lisbon, Portugal  
Rome, Italy

**Retrieved from URL:** This is used if the source is an online source

- ✓ The Journal recommend to visit the websites below for a more detailed information.

< <https://www.mendeley.com/guides/apa-citation-guide> >  
< <https://libguides.murdoch.edu.au/APA6/all> >  
< <https://aut.ac.nz.libguides.com/APA6th/referencelist> >

---

## 5. FIGURES:

The number of pictures (including graphs, diagrams, etc.) should not exceed 10 and should be submitted either in JPG or PNG formats. All photographs, charts, and diagrams should be numbered consecutively (e.g., Figure 1) in the order in which they are referred in the text. Caption must appear below the figure (size 11, bold, italic) and should be sufficiently detailed to enable us to understand apart from the text. Explanation of lettering and symbols should be also given in the caption and only exceptionally in the figures. Figures should be of good quality and preferably in black and white. (Color figures will appear in the downloadable files, but all papers will be printed in black and white.) Scanned figures should be at a resolution of 800 dpi/bitmap for line graphs. Diagrams containing chemical structures should be of high graphical quality and always be of the same size so that they can be uniformly reduced. Figures should have a maximum width of one Journal column (8.5 cm) to be inserted on the body of the text so that they can be applied to the standards of the Journal. If the figures exceed 8.5 cm, they will be placed at the end of the article. Also, authors may be requested to submit each figure also as an image file in one of the following formats: jpg or png. For pictures, graphs, diagrams, tables, etc., identical to material already published in the literature, authors should seek permission for publication from the companies or scientific societies holding the copyrights and send it to the editors of TQ along with the final form of the manuscript.

---

## 6. TABLES:

Tables should be self-explanatory. They should be mentioned in the text, numbered consecutively (e.g., Table 1) and accompanied by title at the top (size 11, bold, italic). Please insert all the tables in the text, do not enclose huge tables which cannot be fit within the page margins.

---

## 7. MATHEMATICAL EXPRESSIONS:

In general, minimize unusual typographical requirements, use solidus, built-up fractions. Avoid lengthy equations that will take several lines (possibly by defining terms of the equation in separate displays). For drawing equations, please use the Equation Editor of Word, if possible. Make subscripts and superscripts clear. Display only those mathematical expressions that must be numbered for later reference or that need to be emphasized. Number displayed equations consecutively throughout the paper. The numbers should be placed in parentheses to the right of the equation, e.g. (Eq. 1).

---

## 8. SUPPLEMENTARY MATERIAL:

Any Supplementary material (other figures, tables, diagrams, etc.) should be placed at the end of the manuscript and indicated as such. A single.PDF - document, including the supplementary material, should be submitted.

**Editors, at any time of the editing process, may ask authors to split off part of the manuscript, presenting it as supplementary material.**

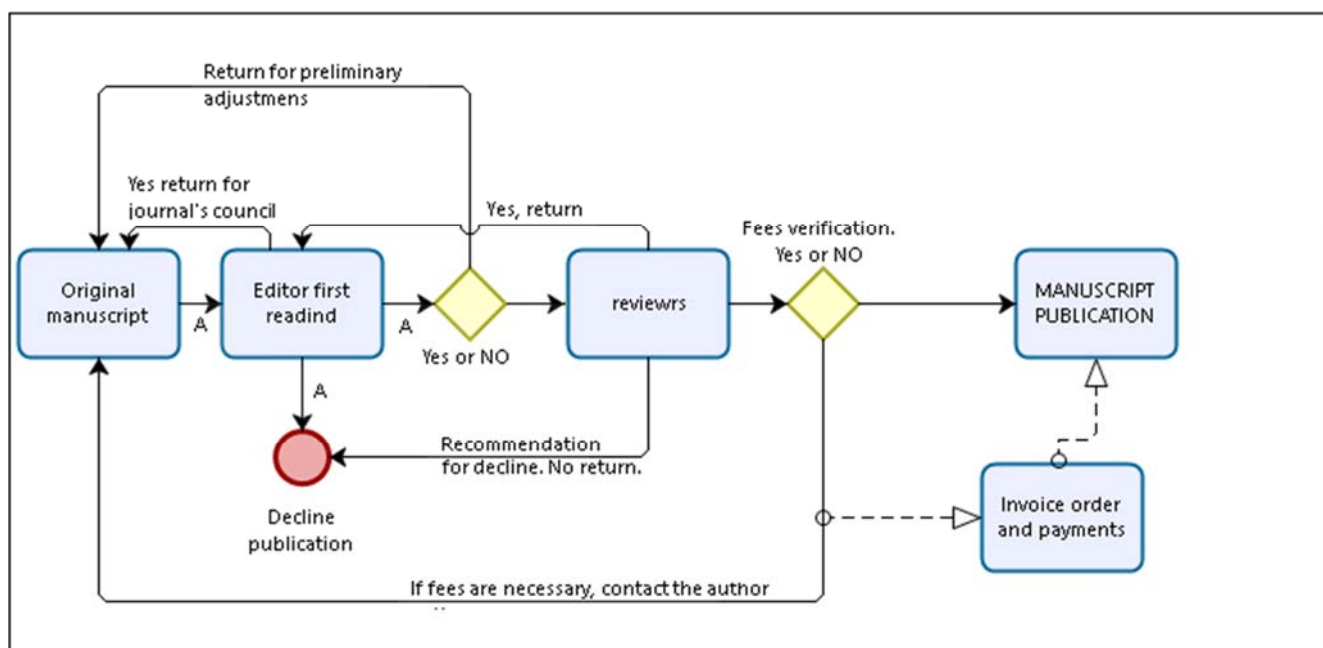
---

## PUBLICATION FEES (1), ADDITIONAL FEES FOR PUBLICATION (2), DISCOUNTS (3), AND FREE PUBLICATION OPPORTUNITIES (4)

Authors are required to pay a publication fee to share in the costs of production. The fee will be asked **if, and only if, the article is accepted for publication**. Once full payment has been made (PayPal, Bank Transfer, or Western Union Services), the paper will be published at the Ahead of Print and scheduled for the next available issue.

All waivers (as well as the publication fee requests) are **applied to the accepted papers after successful peer-review only**.

Please observe the flowchart below to understand how we work.



### 1. PUBLICATION FEES

\*Brazilian authors, USD 200

\*Other countries income groups:

High income (or nuclear-capable countries) - USD 300

Upper middle-income USD 250

Lower middle-income USD 120

Lower middle income (Heavily indebted poor countries (HIPC)) USD 100

Low-income USD 100

Low income (Heavily indebted poor countries (HIPC)) USD 80

- ✓ In order to improve the services of the journal, starting from the NOVEMBER issue of 2020, the Journal will adjust the scope in the area of Education. In this area, we will publish only Chemistry Education manuscripts. The publication fee for approved manuscripts will be unique for all nations, USD 300.
- ✓ (\*) Classification according to the World Bank list of economies (June 2017)
- ✓ \*\* Optional page formatting fee + USD 80. If you don't have time or the proper conditions to execute the formatting of your manuscript, we will find someone to do it for you.

## 2. ADDITIONAL FEES FOR PUBLICATION

### a) Proofreading and / or plagiarism

If the submitted manuscript has more than 100 grammatical errors or plagiarism greater than 5%, a fee of USD 200 will be charged. This fee does not guarantee publication of the manuscript and is non-refundable.

### b) Alteration of PDF files

After undergoing the final check of the manuscript file and Pre-Print PDF generation, a USD 100 will be charged with the authors in case they want to change something. For each new change, the fee is charged again.

### c) Acceptance Letter for article publication

The acceptance letter is an optional service of the Journal. If the authors need a document to prove that their article has been peer-reviewed and accepted for publication, they may request, upon payment of an additional fee of USD 40, an acceptance letter for publication of the article.

NOTE 1: THE LETTER OF ACCEPTANCE may be issued if, and only if, the article has undergone a complete peer-review and is considered ACCEPTED for publication. Letters will NOT be issued for newly sent articles that have not yet been appropriately evaluated and peer-reviewed.

NOTE 2: The Journal does not agree with the trade-in documents that can attest to the publication of articles that have not gone through the due process of peer-review and are legitimately considered approved for publication in the subsequent edition.

NOTE 3: Bearing in mind that the pre-printing PDF is generally already considered as proof of publication, authors must, via e-mail, justify the request for a letter of acceptance for purposes of general registration by the Journal.

- If there is no need, additional fees are not charged.

## 3. DISCOUNTS

a) **50% discount** for authors who support other journals from the team (*Southern Brazilian Journal of Chemistry* (this is a 100% free journal)), with 1 manuscript approved for publication;

b) **100% discount** for authors who support other journals from the team (*Southern Brazilian Journal of Chemistry* (this is a 100% free journal)), with 2 manuscripts approved for publication;

c) **Volume discount**, if you are an author/collaborator of the journal, that has published with us 4 manuscripts (paid your full corresponded price), your fifth manuscript will be free of charge. Later the counting cycle restart.

#### 4. FREE PUBLICATION OPPORTUNITIES

- a) Young scientists publishing the first manuscript of their career with us. Requirements: Copy of the curriculum with no publications; maximum of 2 authors;
- b) All personal related to the production of the journals, from Brazil and abroad;
- c) Longtime collaborators. Authors who have published four (4) articles with us during the past decade will be rewarded with one (1) free publication. After that, this cycle starts again, that is, for every 5 articles published, one will be free of publication fees. Thank you for choosing and trusting the Journal to publish your research.
- d) Paper considered by the Editors of high quality, priority, and relevance for the development of the society shall pay no fees. Note that this condition is a small recognition prize, not something that you may request. Thank you for your comprehension.